British Journal of Pharmacology

December 1994

Volume 113 Number 4 pages 1079–1574

Br. J. Pharmacol. (1994), **113**, 1079–1080 © Macmillan Press Ltd, 1994

OBITUARY

Sir William Paton, CBE DM FRCP FRS

Bill Paton (sometimes addressed as Sir William but never to my knowledge as William), was a member of the Society for 45 years, joining in 1948, and being elected an Honorary Member in 1981. He served both as Chairman of the Editorial Board (1965–74) and as Chairman of the Committee (1978–81).

He was one of the relatively small band of those who worked during what I think of as the transition phase of pharmacology. The early years, the era of smoked drums, string and sealing wax pharmacology, personified in Britain by the towering figures of Dale, Brown, Feldberg and Gaddum, were coming to an end with the advent of the more sophisticated recording apparatus made possible by electronics, the age of pharmacology based on molecular biology and computer simulation had not yet dawned. The challenges of the transition were special. New technology allowed exploration at the cellular level but still without the advantages of micro-electrodes reading from inside the cell. During this transition phase Bill Paton was at his best, and a very good best it was. I worked at a desk facing his in F4, the physiology-pharmacology lab at the NIMR in Hampstead for several years, during which time we did a number of studies together. Bill was the most brilliant analyst of the results of an experiment I ever came across. At the end of a long day when I was ready only for a drink, a meal and bed he would set off home with the notes of the experiment and come back in the morning with a complete analysis, what it all meant and precisely what we should do in the next one. It was wholly logical and crystal clear. I realised later when working with Feldberg that Bill had none of the intuition, the mysticism, that led Feldberg sometimes to do wholly irrational things which occasionally bore fruit. Bill never did anything irrational.

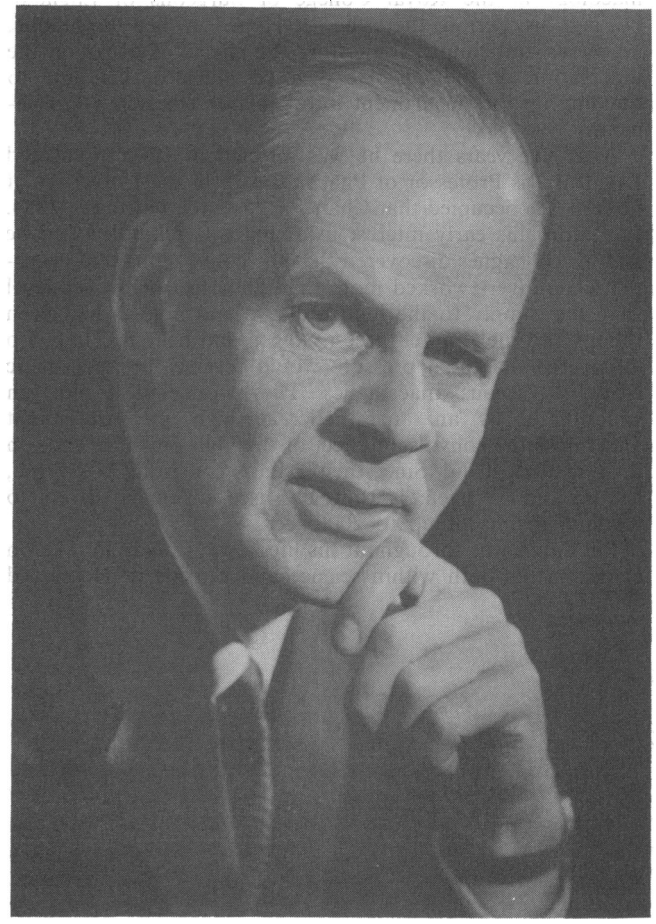
He was a son of the manse, born on May 5th, 1917 to the Rev William Paton and his wife, Grace MacKenzie Paton. He was a natural scholar. After schooling at Winchester House, Brackley and at Repton, he entered New College, Oxford. He won the Theodore Williams, Christopher Welch and Jesse Therese Rowden scholarships and completed a first-class honours degree in physiology in 1938. He then went to University College Hospital in London, won the Goldsmid exhibition there in 1939 and the Gold Medal in clinical medicine in 1941 and qualified BM BCh (Oxon) in 1942.

Bill was never wholly fit. He had chronic trouble with his lungs which kept him out of the services and which prevented his active participation in games.

It was probably another factor that intensified his natural scholarly bent. In 1942 he married Phoebe Margaret Rooke and began work as a pathologist in the King Edward VII sanatorium; but two years later took the decisive step in his career when he was recruited by G.L. Brown who had succeeded Dale as Head of Physiology and Pharmacology in F4 at the NIMR in Hampstead. There he was to spend eight of his most productive research years.

His first interest was in the physiological problems of diving which was the wartime activity of the department. There was a decompression chamber at Hampstead where G.L. Brown, aided by J.B.S. Haldane, K.W. Donald, and others were already working, and Bill's attention was fairly caught, but his contribution to that field was to come later.

After the war Bill had, as his main colleagues in F4, G.L. Brown, F.C. McIntosh, John Gray, Nora Zaimis and myself. F4 was a sort of Mecca for physiologists, including the most distinguished of them, so that there was a constant stream of visitors from all over the world. Working in that atmosphere there was nothing to blame except oneself if research did not go well. Bill Paton's went very well; Paton and Zaimis on the methonium drugs (1951) and on the different type of neuromuscular block (1952), McIntosh and Paton on the histamine liberators (1952) and Paton and Perry on different types of ganglion block (1953) were all seminal papers. They were all to have profound effects in clinical medicine. Although tubocurarine was already in use as a muscle relaxant in surgery, the advent of decamethonium with a wholly different mode of action, sparked off a series of studies on other muscle relaxants which have been of great value both in surgery and in intensive care to allow artificial ventilation. Hexamethonium, a ganglion blocking agent was the very first drug that reduced blood pressure specifically and safely. Since then the search for other and better drugs with this action has been intense and successful.



Sir William Paton *© copyright Godfrey Argent Studio*

Life in F4 in those days was very hard work tempered with quite a bit of play. There were lots of excuses for evening parties when the experiments were finished. We produced a film (now in the BPS archives) called 'Let's get an effect' which lampooned each of the staff; and we produced spoof papers for meetings, Bill playing a major part in several, one on 'perfusion of the isolated Id with a solution of ectoplasm.' Bill had a very pretty wit and wrote extremely amusing minutes when he was Secretary of the Physiological Society. He was kind and sympathetic but reserved and sometimes

withdrawn. Although he took a full part in all the activities in F4 he was never quite 'one of the boys' and I suspect that stemmed as much from his lack of complete physical fitness as from a distaste for the more plebian activities.

In 1952 he became Reader in Pharmacology and Therapeutics at University College, London but after only two years there he was appointed to a new Chair of Pharmacology at the Royal College of Surgeons of England. During his period there he developed a new technique, ingenious and simple, for testing the effects of drugs on the innervation of the gut. He devoted much of his time to building up the department into a major research establishment.

After five years there he was selected in 1959 to succeed J.H. Burn as Professor of Pharmacology in the University of Oxford. He occupied that Chair for 25 years, retiring in 1984. In Oxford his early interest in diving was rekindled and he and his colleagues discovered that the convulsions that occurred when divers worked more than 2000 feet below sea level were due simply to the high pressure and not, as had been thought, to the respired gases, oxygen and helium. They also discovered that high pressure would reverse the anaesthetic effect of gaseous anaesthetics. They wondered if nitrogen which acts as an anaesthetic at high pressure might antagonise the convulsant effect of the high pressure, and, on investigation, it did. Since then Trimix, consisting of oxygen, helium and nitrogen, is routinely used to enable divers to work at depths of up to 2000 feet.

Bill Paton was throughout his life, always ready to take on commitments both within science and outside it. He served on the Medical Research Council, the Wellcome Trust, the Research Defence Society and as Director of the Wellcome Institute for the History of Medicine and the Chairman of the Rhodes Trust. He was a JP from 1956, the same year that he was elected FRS, and was Chairman of the Committee for the Suppression of Doping set up by the Joint Racing Board.

I would especially mention his services to the Research Defence Society. He was Chairman of the Council from 1972 to 1978 and, in 1978, delivered a memorable Paget Lecture. He developed his thoughtful ideas about the ethics of animal experimentation over the next few years and, in 1984, published them in his book 'Man & Mouse' which is remarkable for its clarity, its humanity and its total lack of prejudice.

His work in all these fields brought many honours, a CBE in 1968 and a knighthood in 1979; the Cameron Prize (jointly with E Zaimis) in 1956, the Gold Medal of the Society of Apothecaries in 1976, the Baly medal of the Royal College of Physicians in 1983 and the British Pharmacological Society's Wellcome Gold Medal in 1991.

He was only 42 when he went to Oxford. He had become, all too early, one of the father figures of pharmacology. Holding as he did the premier Chair in England he was as we have seen almost immediately in demand to undertake public duties of many different kinds. His natural reserve emphasised a gravitas that led some to consider him pompous. Those who knew him saw that his gravitas merely concealed his kindness, his humour and his wisdom.

Walter Perry, Edinburgh

Br. J. Pharmacol. (1994), **113**, 1081–1082

SPECIAL REPORT

© Macmillan Press Ltd., 1994

Prevention by dexamethasone of the marked antiarrhythmic effects of preconditioning induced 20 h after rapid cardiac pacing

*Agnes Vegh, *Julius Gy Papp & †James R. Parratt

*Department of Pharmacology, Szent György Medical University, Dom ter 12, Szeged, Hungary and †Department of Physiology & Pharmacology, University of Strathclyde, Glasgow G1 1XW

Dogs were paced, via a pacing electrode in the right ventricle, for four 5 min periods at a rate of 220 beats min^{-1}. On the following day they were reanaesthetized, thoracotomized and the left anterior descending coronary artery occluded for 25 min. Pacing markedly reduced the severity of ischaemia-induced arrhythmias (e.g. reduction in VF from 45% in unpaced dogs to 10% in paced dogs; $P<0.05$), an effect reversed by dexamethasone (4 mg kg^{-1} i.v., 45 min prior to pacing). This protection may be due to the induction of nitric oxide synthase or cyclo-oxygenase.

Keywords: Ischaemic preconditioning; second window of protection; rapid cardiac pacing; ventricular arrhythmias; antiarrhythmic effect of cardiac pacing; dexamethasone; nitric oxide

Introduction Brief periods of either regional or global myocardial ischaemia (e.g. as a result of coronary artery occlusion or rapid ventricular pacing) markedly reduce the effects of a subsequent prolonged coronary artery occlusion. A particularly significant effect of ischaemic preconditioning is a marked suppression of those ventricular arrhythmias that result from coronary artery occlusion and reperfusion (Vegh *et al.*, 1990; 1992a). Unfortunately, this antiarrhythmic effect of preconditioning, which can also be induced by rapid cardiac pacing (Vegh *et al.*, 1991) as well as by short periods of coronary artery occlusion, is relatively short lived. For example, if the time between the preconditioning period and the prolonged coronary artery occlusion is increased to between 1 and 2 h, the antiarrhythmic effect is lost (Vegh *et al.*, 1992a).

Recently, it has been demonstrated that the protective effects of ischaemic preconditioning return many hours after the initial preconditioning stimulus, a phenomenon known as the 'second window of protection'. Thus, prolonged coronary artery occlusion 24 h after the initial preconditioning stimulus results in a marked reduction in infarct size (Yamashita *et al.*, 1992; Baxter *et al.*, 1993) and in life-threatening ventricular arrhythmias (Vegh *et al.*, 1994). We now show that this marked protection is abolished by the prior administration of dexamethasone, suggesting that the induction of a nitric oxide synthase and/or a cyclo-oxygenase may be responsible for this protection.

Methods Adult mongrel dogs of either sex and with a mean body weight of 39.1 ± 2.0 kg were anaesthetized by the intravenous administration of sodium pentobarbitone and a pacing electrode was inserted, via the right jugular vein, into the right ventricle. The correct placing of this electrode was confirmed by recording the endocardial electrocardiogram. The dogs were allowed to breathe spontaneously and blood pressure was monitored from a carotid artery using methods previously described in detail by Vegh *et al.* (1992a). The dogs were then paced for four 5 min periods at a rate of 220 beats min^{-1} with 5 min intervals between the pacing stimuli.

Eight dogs were given dexamethasone 4 mg kg^{-1} by slow intravenous injection, 45 min prior to the initial 5 min pacing period. The controls for this series of dogs were those in which the Cordat F4 bipolar electrode was introduced into the right ventricle, left for a period of 45 min and then withdrawn. These dogs were not paced.

The catheters were then removed and the dogs were allowed to recover from the anaesthetic. The following day they were re-anaesthetized with a mixture of chloralose and urethane (60 and 200 mg kg^{-1}), thoracotomized and prepared for a 25 min occlusion of the left coronary artery (Vegh *et al.*, 1992a). One of the dexamethasone-treated dogs was not occluded because of haemorrhage around the occlusion site. The measured parameters and analysis of arrhythmias were as described in full by Vegh *et al.* (1992b).

Results In both groups of paced dogs the increase in heart rate was a mean of 70 beats min^{-1} above a resting heart rate of 146 ± 6 beats min^{-1}. Pacing resulted, in both groups, in a reduction in mean arterial blood pressure (from 126 ± 4 to 79 ± 6 mmHg), an increase in LVEDP and, 5 s after terminating pacing, in marked endocardial ST-segment elevation. This was more pronounced, 5 s after the initial pacing stimulus, in the dogs given dexamethasone (7.4 ± 1.4 mV) than in those not given dexamethasone (3.3 ± 1.3 mV).

When the coronary artery was occluded a mean of 20 h after the pacing protocol, the severity of the arrhythmias was much less than in those dogs not previously subjected to pacing (Vegh *et al.*, 1994). However, this protection was completely lost in those dogs given dexamethasone (Figure 1). In particular, the marked reduction in occlusion-induced VF in the paced dogs (10% v 45% in the controls) was completely reversed by dexamethasone (VF during occlusion 57%). None of these dogs survived reperfusion, in contrast to a 60% survival in those paced without dexamethasone. An analysis of epicardial ST-segment changes during the prolonged occlusion (Figure 2) demonstrated that, whereas pacing 20 h previously reduced this index of ischaemia, it was not reduced in those dogs administered dexamethasone, where the changes were similar to those in the controls.

Discussion There has been considerable recent interest in the marked protective effects of ischaemic preconditioning many hours after the initial preconditioning stimulus. This so-called 'second window of protection' has been demonstrated both for a reduction in infarct size (Yamashita *et al.*, 1992), where it seems to be dependent upon adenosine receptor activation (Baxter *et al.*, 1993) and has now been demonstrated for a reduction in those life-threatening arrhythmias

[1] Author for correspondence.

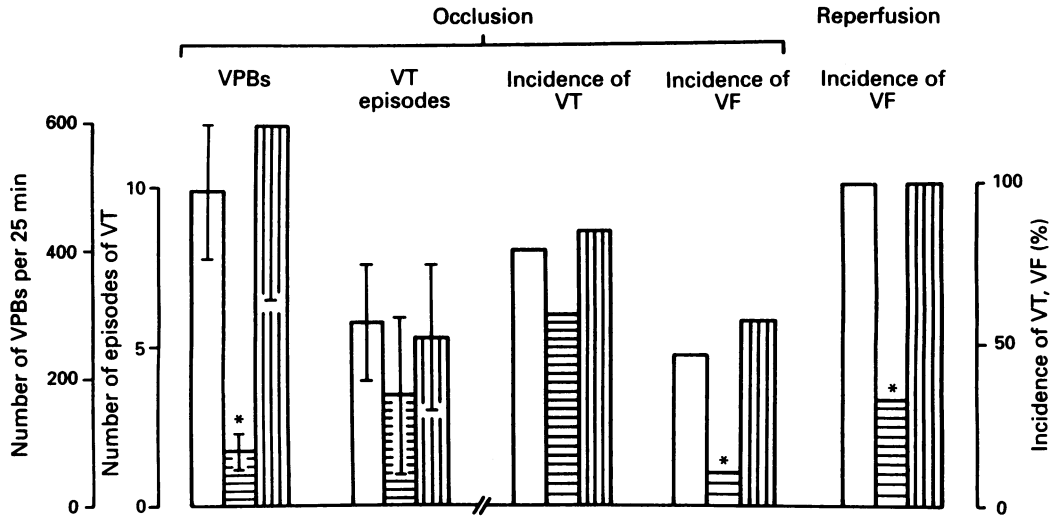


Figure 1 Ventricular arrhythmias during a 25 min occlusion of the left anterior descending coronary artery in anaesthetized dogs subjected, 20 h previously, to four 5 min periods of global ischaemia induced by rapid cardiac pacing (columns with horizontal stripes) and subjected to the same protocol but given dexamethasone 4 mg kg^{-1} 45 min previously (columns with vertical stripes). The control dogs (open columns) had a pacing catheter in place in the lumen of the left ventricle but were not subjected to pacing. Pacing markedly reduced the severity of ventricular arrhythmias but this was abolished by the prior administration of dexamethasone. VPBs = ventricular premature beats, VT = ventricular tachycardia, VF = ventricular fibrillation. The values given are the means ± s.e.mean from 20 control, 10 paced dogs and 7 dogs paced in the presence of dexamethasone. $*P<0.05$.

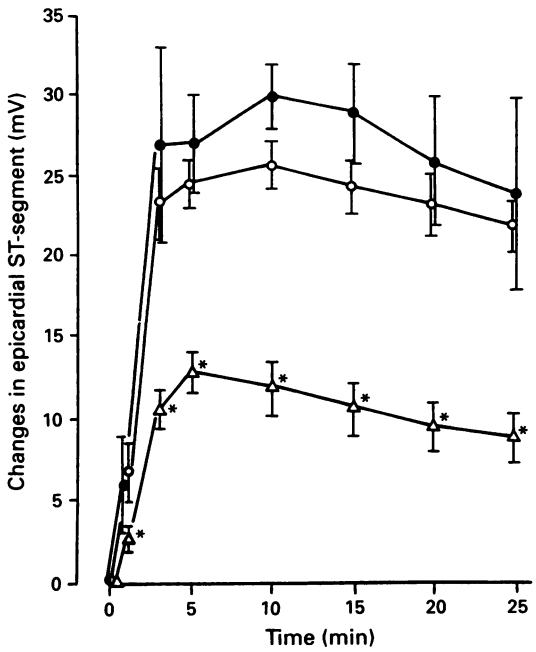


Figure 2 Changes in the epicardial ST-segment elevation during a 25 min occlusion of the left anterior descending coronary artery in dogs subjected to ventricular pacing 20 h previously (Δ, $n = 10$), in dogs also subjected to pacing but in the presence of dexamethasone (●, $n = 7$) and in control dogs in which the pacing electrode was positioned in the right ventricle but the dogs were not paced (○, $n = 20$). The marked attenuation of this index of myocardial ischaemia which resulted from prior cardiac pacing was abolished if dogs were subjected to the same pacing protocol after dexamethasone administration. $*P<0.05$.

which result from ischaemia and reperfusion (Vegh *et al.*, 1994). Presumably, the mechanism of this protection is distinct from that of 'classical' preconditioning (Vegh *et al.*, 1992a) and appears to depend upon enzyme induction. Our present results, demonstrating that dexamethasone abolishes this protection, suggests that either nitric oxide synthase or a cyclo-oxygenase is involved. There is evidence that both nitric oxide and cyclo-oxygenase products contribute to the early antiarrhythmic effects of ischaemic preconditioning (Vegh *et al.*, 1990; 1992b) and more recently, Sessa *et al.* (1994) have demonstrated that prolonged periods of pacing, induce nitric oxide synthase in the myocardium.

We acknowledge the financial support of the Hungarian State Government (OTKA) and of the British Council/HNCTD.

References

BAXTER, G.F., MARBER, M.S., PATEL, V.C. & YELLON, D.M. (1993). A 'second window of protection' 24 hours after ischemic preconditioning may be dependent upon adenosine receptor activation. *Circulation*, **88** (Suppl. 1), 101.

SESSA, W.C., PRITCHARD, K., SEYEDI, N., WANG, J. & HINTZE, T.H. (1993). Chronic exercise in dogs increases coronary vascular nitric oxide production and endothelial cell nitric oxide synthase gene expression. *Circ. Res.*, **74**, 349–353.

VEGH, A., KOMORI, S., SZEKERES, L. & PARRATT, J.R. (1992a). Antiarrhythmic effects of preconditioning in anaesthetised dogs and rats. *Cardiovasc. Res.*, **26**, 486–495.

VEGH, A., PAPP, J.GY., KASALA, K. & PARRATT, J.R. (1994). Cardiac pacing in anaesthetised dogs preconditions the heart against arrhythmias when ischaemia is induced 24 h later. *J. Physiol.*, **480**, 89P.

VEGH, A., SZEKERES, L. & PARRATT, J.R. (1990). Protective effects of preconditioning of the ischaemic myocardium involves cyclooxygenase products. *Cardiovasc. Res.*, **24**, 1020–1023.

VEGH, A., SZEKERES, L. & PARRATT, J.R. (1991). Transient ischaemia induced by rapid cardiac pacing results in myocardial preconditioning. *Cardiovasc. Res.*, **25**, 1051–1053.

VEGH, A., SZEKERES, L. & PARRATT, J.R. (1992b). Preconditioning of the ischaemic myocardium; involvement of the L-arginine nitric oxide pathway. *Br. J. Pharmacol.*, **107**, 448–452.

YAMASHITA, N., KUZUYA, T., HOSHIDA, S., FUJI, H., OE, H., KITABATAKE, A., TADA, M. & KAMADA, T. (1992). Relationship between time interval from preconditioning to sustained ischemia and its effect on limiting infarct size. *J. Mol. Cell. Cardiol.*, **24** (Suppl. 1), S150.

(Received August 5, 1994
Accepted September 5, 1994)

Br. J. Pharmacol. (1994), **113**, 1083–1084

SPECIAL REPORT

© Macmillan Press Ltd., 1994

Attenuation by dexamethasone of endotoxin protection against ischaemia-induced ventricular arrhythmias

Wu Song, Brian L. Furman & [1]James R. Parratt

Department of Physiology & Pharmacology, Royal College, University of Strathclyde, Glasgow, G1 1XW

Ventricular arrhythmias from a 30 min occlusion of the left coronary artery were assessed in Langendorff perfused isolated hearts removed from rats administered either saline, or endotoxin derived from *Escherichia coli* (2.5 mg kg^{-1} i.p.) given either 2, 4, 8, 24 or 48 h previously. Arrhythmia severity was markedly reduced in those hearts removed from rats administered endotoxin with a maximum protection at 8h; there was a marked reduction in the incidence of ventricular fibrillation (from 54% to 4%) and in the number of ventricular premature beats during the occlusion period (e.g. from 1165 ± 144 to 37 ± 19; $P<0.01$). Dexamethasone (3 mg kg^{-1}, given 1 h prior to endotoxin or saline) markedly attenuated the protection afforded by endotoxin.

Keywords: Endotoxin; ventricular arrhythmias; dexamethasone; nitric oxide

Introduction Because endotoxin administration leads to the induction of a calcium-independent nitric oxide synthase (iNOS) both in blood vessels (Fleming *et al.*, 1990; Knowles *et al.*, 1990; Rees *et al.*, 1990) and in the heart (Schulz *et al.*, 1992), and because nitric oxide has been implicated in the protective (antiarrhythmic) effects of ischaemic preconditioning (Vegh *et al.*, 1992) we have examined whether endotoxin administration can protect the heart against one of the most severe consequences of ischaemic injury, life-threatening ventricular arrhythmias.

Methods Hearts were removed from male Sprague-Dawley rats weighing between 250 and 300 g which had been given endotoxin derived from *Escherichia coli* (Boivin preparation, Difco, 2.5 mg kg^{-1}) or an equivalent volume of saline, by intraperitoneal injection 2, 4, 8, 24 or 48 h previously. This dose of endotoxin reduces the vascular responsiveness to noradrenaline which is due to the induction of iNOS (Fleming *et al.*, 1990; Julou-Schaeffer *et al.*, 1990). Hearts were rapidly removed and transferred to a Langendorff apparatus where they were perfused with Krebs-Henseleit solution at a constant flow of 8–10 ml min^{-1} (Piacentini *et al.*, 1993). Perfusion pressure was monitored via a side-port situated immediately above the aorta using a Gould P23 ID transducer and, before coronary artery occlusion, was typically 30–40 mmHg.

Fine platinum electrodes were placed on the right atrium and the apex of the left ventricle allowing an epicardial electrogram to be recorded. The main left coronary artery was occluded for 30 min. This resulted in an increase in perfusion pressure and in ventricular arrhythmias which were analysed by counting the total number of premature beats (VPBs), and the incidence and (duration) of both ventricular tachycardia (VT) and ventricular fibrillation (VF) as defined previously (Vegh *et al.*, 1992; Piacentini *et al.*, 1993).

Dexamethasone (3 mg $kg,^{-1}$ i.p.) was given 1 h before the administration of either endotoxin or saline.

To compare the number of VPBs between the groups, the Kruskal-Wallis nonparametric test was used and for comparison of incidences of events, the Fisher exact probability test.

Results In isolated hearts removed from saline-treated rats, coronary artery occlusion led to marked ventricular ectopic activity over the 30 min occlusion period (Table 1). There were more than 1,000 VPBs in each of the 4 control saline groups, all the rats exhibited VT lasting between 1 and 2 min and there was a 53% incidence of VF. In contrast, there was a time-dependent reduction in the severity of these arrhythmias in rats administered endotoxin with maximum protection at 8 h; indeed, the reduction in the severity of arrhythmias was very marked at this time. Perhaps of particular significance is the fact that only 1 of 24 hearts removed from rats given endotoxin 4, 8 or 24 h earlier exhibited ventricular fibrillation in contrast to 13 out of 24 rats administered saline at these respective times.

The protection at 8 h was greatly attenuated by the prior administration of dexamethasone (Figure 1) which itself had no significant effect on arrhythmias resulting from coronary artery occlusion. For example, there were 575 ± 99 VPBs on occlusion (cf. 37 ± 19 without dexamethasone; $P<0.01$, Table 1) and 1218 ± 126 in hearts removed from rats given only dexamethasone (cf. 1165 ± 144 in those given only saline). The duration of VT (which occurred in all hearts) was 83 ± 20s (cf. 1.5s in the 1/8 hearts in the endotoxin group without dexamethasone; Table 1).

There was no significant difference between resting coronary artery perfusion pressure in rats given saline

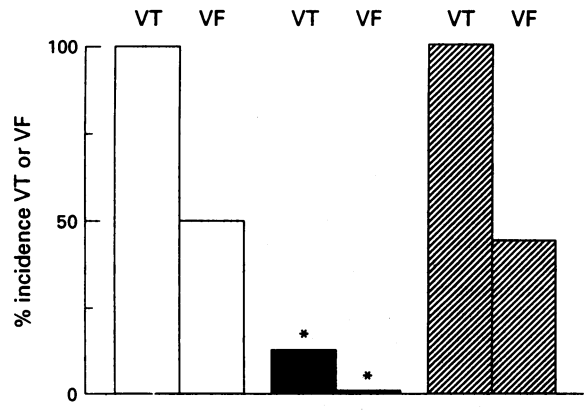


Figure 1 The incidence of ventricular tachycardia (VT) and of ventricular fibrillation (VF) in hearts removed from hearts administered either saline (open columns), endotoxin (solid columns) or a combination of endotoxin and dexamethasone (hatched columns) 8 h previously and subjected to coronary artery occlusion. There is a marked reduction in the incidence of these arrhythmias in hearts removed from rats given endotoxin. This protection is abolished by the prior administration of dexamethasone. The values are means or 8 or 9 experiments. *$P<0.05$ compared to saline controls.

[1] Author for correspondence.

Table 1 The effect of endotoxin (*E. coli*, lipopolysaccharide; LPS, 2.5 mg kg^{-1}, i.p.) or of an equivalent volume of saline, given at 2, 4, 8, 24 or 48 h prior to removal of the heart, on the arrhythmias resulting from a 30 min occlusion of the left coronary artery when the hearts were perfused according to Langendorff

		Total VPBs	*Arrhythmia incidence*				*Arrhythmia duration*	
	n	(beats)	VT	Rev VF	Irrev VF	Total VF	VT (s)	Rev VF (s)
Saline 2 h	8	1129 ± 242	8/8	1/8	3/8	4/8	76.0 ± 10.6	14.0 ± 14.0
LPS 2 h	8	911 ± 154	8/8	1/8	2/8	3/8	57.8 ± 8.9	9.2 ± 9.2
Saline 4 h	8	999 ± 185	8/8	3/8	1/8	4/8	93.7 ± 22.2	14.3 ± 7.1
LPS 4 h	8	209 ± 53*	5/8	0/8	0/8	0/8*	12.0 ± 4.5*	0
Saline 8 h	8	1165 ± 144	8/8	3/8	1/8	4/8	103.2 ± 17.5	6.7 ± 4.7
LPS 8 h	8	37 ± 19**	1/8**	0/8	0/8	0/8*	1.5	0
Saline 24 h	8	1049 ± 205	8/8	3/8	2/8	5/8	68.8 ± 16.8	28.3 ± 12.8
LPS 24 h	8	342 ± 66*	7/8	1/8	0/8	1/8	20.8 ± 5.9	8.0
LPS 48 h	8	1015 ± 153	8/8	2/8	2/8	4/8	74.4 ± 18.9	23.7 ± 17.6

VPBs = ventricular premature beats, VT = ventricular tachycardia, VF = ventricular fibrillation (reversible or irreversible).
*$P<0.05$; **$P<0.01$.

(31 ± 2 mmHg) and those given endotoxin 2, 4, 8 or 24 h previously (31 ± 3 mmHg); neither was there any difference in the increase in perfusion pressure which occurred following coronary artery occlusion (to 58 ± 9 mmHg and 57 ± 6 mmHg, respectively 15 min into the occlusion time) in hearts removed from rats given saline or endotoxin 8 h previously. There were no significant changes in heart rate on coronary artery occlusion; neither did endotoxin administration influence this parameter.

Discussion These results demonstrate, for the first time, that the administration of endotoxin markedly reduces the severity of life-threatening ischaemia-induced ventricular arrhythmias that occur when a major coronary artery is occluded. The time course of this pronounced protection is significant and follows almost precisely the induction of nitric oxide synthase (Knowles *et al.*, 1990) which results from endotoxin administration and which is most pronounced between 3 and 10 h. The protection is not apparent 2 h after administration, is maximum at 8 h, and is much reduced at 24 and 48 h. The fact that this protection is not seen in hearts removed from rats given dexamethasone 1 h prior to endotoxin administration again suggests a likely role for iNOS. Although a possible role of protective prostanoids resulting from the induction of a cyclo-oxygenase enzyme cannot be discounted, there is little evidence that cyclo-oxygenase products significantly modify ischaemia-induced arrhythmias in this model (reviewed by Parratt, 1989). To confirm this would require experiments using selective inhibitors of nitric oxide and prostanoid production both alone and in combination.

These results are a good example of a phenomenon known as 'cross tolerance', that is, the protection by one form of injurious stimulus (endotoxin) against those of another, quite different form of acute injury (ischaemia). Paradoxically, endotoxin has been shown previously to have several beneficial effects (Nowotny, 1983). Although this is the first evidence of a marked protection against a particularly important consequence of ischaemic injury (life-threatening ventricular arrhythmias), recently Yao *et al.* (1993) have demonstrated that a non-toxic analogue of the lipid A component of endotoxin reduces infarct size in a canine model of ischaemia. Arrhythmias were not assessed in this study.

This work was supported by the EEC (Biomed I) and by an ORS studentship to W.S.

References

FLEMING, I., GRAY, G.A., JULOU-SCHAEFFER, G., PARRATT, J.R. & STOCLET, J.-C. (1990). Incubation with endotoxin activates the L-arginine pathway in vascular tissue. *Biochem. Biophys. Res. Commun.*, **171**, 562–568.

JULOU-SCHAEFFER, G., GRAY, G.A., FLEMING, I., SCHOTT, C., PARRATT, J.R. & STOCLET, J.-C. (1990). Loss of vascular responsiveness induced by endotoxin involves the L-arginine pathway. *Am. J. Physiol.*, **259**, H1038–H1043.

KNOWLES, R.G., SALTER, M., BROOKS, S.L. & MONCADA, S. (1990). Anti-inflammatory glucocorticoids inhibit the induction by endotoxin of nitric oxide synthase in the lung, liver and aorta of the rat. *Biochem. Biophys. Res. Commun.*, **172**, 1042–1048.

NOWOTNY, A. (1983). *Beneficial Effects of Endotoxin*. New York: Plenum.

PARRATT, J.R. (1989). Eicosanoids and arrhythmogenesis. In *Antiarrhythmic Drugs*, (Handbook of Experimental Pharmacology, volume 89), ed. Vaughan Williams, E.M. pp 569–589. Berlin: Springer.

PIACENTINI, L., WAINWRIGHT, C.L. & PARRATT, J.R. (1993). The antiarrhythmic effect of ischaemic preconditioning in isolated rat heart involves a pertussis toxin sensitive mechanism. *Cardiovasc. Res.*, **27**, 674–680.

REES, D.D., SELLEK, S., PALMER, R.M.J. & MONCADA, S. (1990). Dexamethasone prevents the induction by endotoxin of a nitric oxide synthase and the associated effects on vascular tone. An insight into endotoxin shock. *Biochem. Biophys. Res. Commun.*, **173**, 541–547.

SCHULZ, R., SMITH, J.A., LEWIS, M.J. & MONCADA, S. (1991). Nitric oxide synthase in cultured endocardial cells of the pig. *Br. J. Pharmacol.*, **104**, 21–24.

VEGH, A., SZEKERES, L. & PARRATT, J.R. (1992). Preconditioning of the ischaemic myocardium; involvement of the L-arginine nitric oxide pathway. *Br. J. Pharmacol.*, **107**, 648–652.

YAO, Z., AUCHAMPACH, J.A., PIEPER, G.M. & GROSS, G.J. (1993). Cardioprotective effects of monophosphoryl lipid A, a novel endotoxin analogue, in the dog. *Cardiovasc. Res.*, **27**, 832–838.

(Received August 5, 1994
Accepted September 7, 1994)

Br. J. Pharmacol. (1994), **113**, 1085–1087

SPECIAL REPORT

© Macmillan Press Ltd., 1994

Modulation by endogenous ATP of the light-evoked release of ACh from retinal cholinergic neurones

[1]Michael Neal & Jo Cunningham

Department of Pharmacology, UMDS, St Thomas' Hospital, London, SE1 7EH

The retina is an area of the central nervous system that possesses intrinsic cholinergic neurones which release acetylcholine (ACh) in response to stimulation with flickering light. Using an eye-cup preparation in anaesthetized rabbits we found that when the retina was exposed to the P_2-purinoceptor antagonist, PPADS, the light-evoked release of ACh was strikingly increased (by over 40%). In contrast, ATP reduced the light-evoked release of ACh by 20%. The inhibitory effect of ATP was not due to its catabolism to adenosine because it was not affected by the A_1-adenosine receptor antagonist, DPCPX, in combination with adenosine deaminase. The actions of both ATP and PPADS were completely blocked by strychnine. We conclude that during physiological stimulation of the retina with light, ATP is co-released with ACh and partially inhibits ACh release by activating (with ACh) an inhibitory glycinergic feedback loop.

Keywords: ATP release; retina; cholinergic neurones; ACh release; purinergic transmission; P_2-purinoceptors

Introduction Adenosine is co-located with acetylcholine (ACh) in displaced amacrine cells in the retina (Blazynski, 1989) and since adenosine in the retina is rapidly phosphorylated to ATP (Perez *et al.*, 1986), it is highly probable that ACh and ATP are co-localized in these central neurones. In the present study we provide evidence that co-released ATP modulates the light-evoked release of ACh from cholinergic neurones by stimulating (together with ACh) a glycinergic inhibitory feedback loop.

Methods The methods have been described previously (Cunningham & Neal, 1985). Briefly, rabbits were anaesthetized with urethane (1.5g kg^{-1}, i.p.) and an eye-cup prepared which was filled, for 30 min, with Krebs Ringer bicarbonate containing [^{3}H]-Ch (0.5 μM). After washing with fresh medium containing physostigmine (30 μM), a syringe was used to place 0.5 ml of medium in the eye-cup, and this was replaced at 5 min intervals. The total radioactivity in the resulting samples was measured by liquid scintillation counting. The retina was stimulated for 5 min periods by flickering light (3Hz). [^{3}H]-ACh represented 95–100% of the increase in total radioactivity evoked by light flashes (Cunningham & Neal, 1985).

Pyridoxalphosphate -6- azophenyl -2', 4'- disulphonic acid (PPADS) was obtained from Cookson Chemicals.

Results When the retina was stimulated with flickering light in the absence of drugs (controls) the release of ACh was increased 2.1 ± 0.3 fold (mean ± s.e.mean, $n = 24$) compared with the spontaneous resting release. The effect of exposing the retina to medium containing ATP (1 mM) is illustrated in Figure 1a. On average ATP reduced the light-evoked release of ACh by 19.5 ± 3.5% ($n = 4$) (Figure 1b). The inhibitory effect of ATP was not due to its catabolism to adenosine because it produced the same effect on ACh release in the presence of the A_1-adenosine receptor antagonist, 8-cyclopentyl-1,3-dipropylxanthine (DPCPX) (0.1 μM) in combination with adenosine deaminase (1 u ml^{-1} (Figure 1b). Either of these agents alone completely blocks the effects of adenosine on retinal ACh release (Blazynski *et al.*, 1992). In contrast, the P_2-purinoceptor antagonist, PPADS, (Lambrecht *et al.*, 1992) (100 μM) completely blocked the effects of ATP on the light-evoked release of ACh (Figure 1b). When

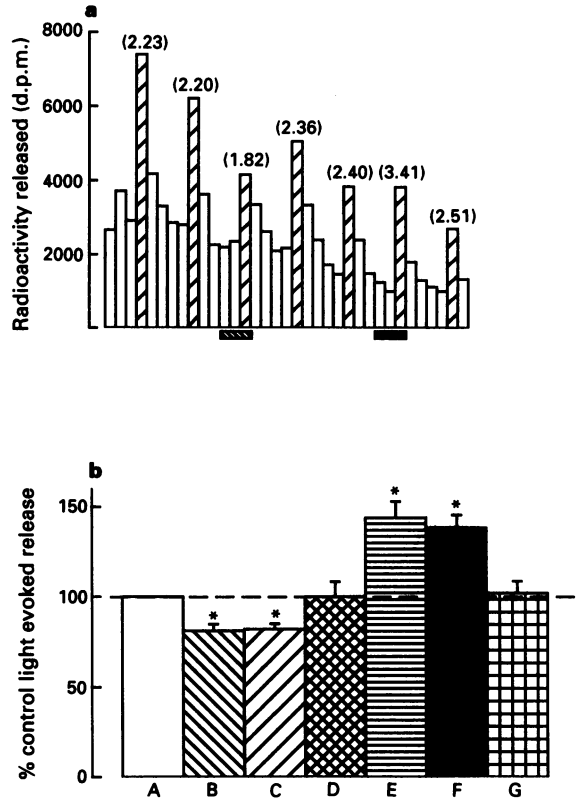


Figure 1 (a) Typical rabbit eye-cup experiment illustrating the effect of ATP (1 mM) (hatched horizontal bar) and PPADS (100 μM) (solid horizontal bar) on the light-evoked release of ACh. Each column is a 5 min collection period. Hatched columns indicate stimulation with flickering light (3Hz). Figures in parentheses indicate stimulated release/resting release and are taken as a measure of 'light-evoked release of ACh'. (b) Summary of effects of drugs on the light-evoked release of ACh. The results are expressed as (light-evoked release in presence of drug/control light-evoked release) × 100: (A) control; (B) ATP 1 mM; (C) ATP + DPCPX 0.1 μM + adenosine deaminase 1 u ml^{-1}; (D) ATP + strychnine 20 μM; (E) ATP + PPADS 100 μM; (F) PPADS 100 μM; (G) PPADS + strychnine 20 μM. Each column is the mean ± s.e.mean of 3–6 separate rabbit experiments. *Indicates significantly different from control $P < 0.01$, Student's *t*-test. For abbreviations, see text.

[1] Author for correspondence.

the retina was exposed to PPADS alone, there was no significant effect on the spontaneous resting release of ACh (mean release of 2 collection periods in presence or absence of drug: mean release of preceding 2 collection periods = 0.64 ± 0.04 and 0.54 ± 0.03 respectively, $n = 5$). However, PPADS strikingly increased the light-evoked release of ACh (Figure 1a) and on average, PPADS increased the light-evoked release of ACh by 45.1 ± 5.6% ($n = 6$) (Figure 1b) suggesting that endogenous ATP modulates the light-evoked release of ACh.

PPADS (100 μM) did not affect ACh release by activating $GABA_B$ receptors (Figure 2) because CGP 35348 (3-aminopropyl(diethoxymethyl) phosphinic acid) (0.5 mM) did not alter the enhancing effect of PPADS on the light-evoked release of ACh (light-evoked release as % of control: PPADS alone 142 ± 8.2% ($n = 4$); PPADS + CGP 35348 148.1 ± 8.2% ($n = 4$)). Also PPADS did not antagonize the inhibitory effect of muscarine (10 μM) on the light-evoked release of ACh from the retina (light-evoked release as % of control: muscarine 61.3 ± 6.3%, muscarine + PPADS 60 ± 7.1% ($n = 4$)), confirming its lack of antimuscarinic activity (Lambrecht *et al.*, 1992).

We tested the possibility that ATP co-released with ACh might be stimulating the release of glycine from inhibitory neurones by examining the effect of strychnine on the actions of ATP and PPADS. Both drugs were completely blocked by strychnine (Figure 1b) at a concentration (20 μM) that itself did not affect ACh release and that specifically blocks glycine receptors in the retina (Neal & Cunningham, 1994).

Discussion The present study shows that ATP decreases and PPADS increases the light-evoked release of ACh from the retina. The finding that PPADS enhances the light-evoked release of ACh suggests that endogenous ATP modulates ACh release in the rabbit retina. Our concentration of PPADS was higher than that usually reported but high concentrations of drugs are sometimes required in the eye-cup preparation, perhaps because of the glial barrier formed by the end-feet of the Müller cells (see Neal & Cunningham, 1994). Since we ruled out effects of PPADS at muscarinic receptors and $GABA_B$ receptors that might have enhanced the light-evoked release of ACh (Figure 2), the effects of PPADS on ACh release seem most likely to be due to antagonism of ATP at P_{2x}-purinoceptors.

We do not yet know the cellular location of the P_2-purinoceptors in the retina. However, the actions of both ATP and PPADS were blocked by strychnine suggesting that P_2-purinoceptors are present on glycinergic amacrine cells. Our experiments suggest that when the retina is stimulated physiologically with flickering light, ACh and ATP are released and together stimulate glycinergic neurones which provide inhibitory feedback to the cholinergic amacrines (Figure 2).

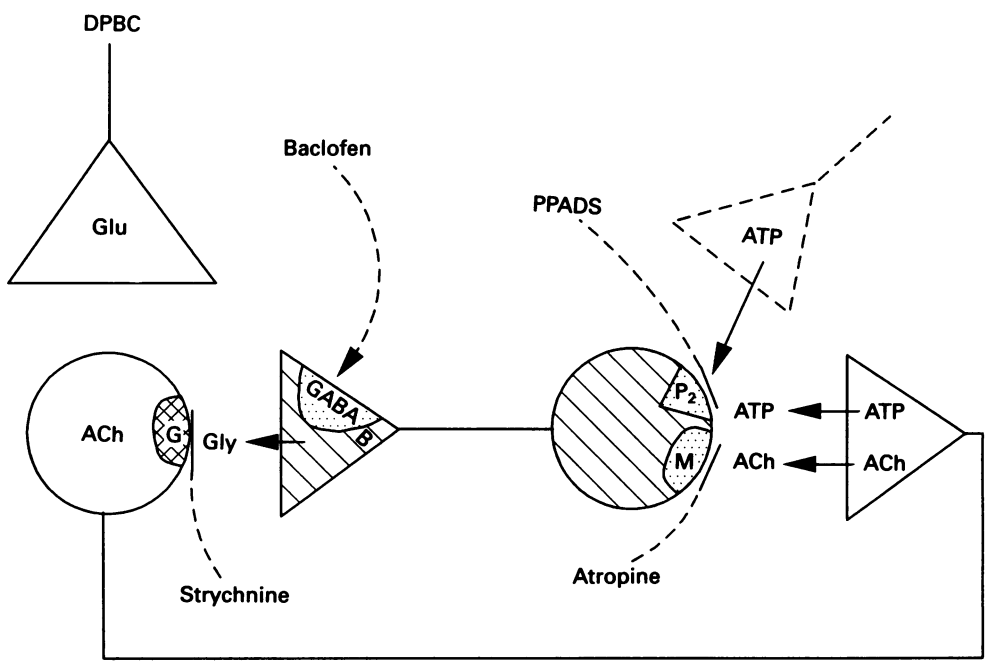


Figure 2 Diagram showing possible sites of action of ATP and PPADS in the retina. The depolarizing (ON) bipolar cell (DBPC) releases glutamate which activates kainate receptors (Cunningham & Neal, 1985) on the cholinergic amacrine cells (ACh). ACh and ATP from these cells activates muscarinic (M) and purinoceptors (P_2) respectively on the glycinergic amacrine cells (shaded) which in turn releases glycine (Gly) onto the cholinergic amacrine cells. Activation of strychnine-sensitive glycine receptors (G) partially inhibits ACh release. Drugs that interupt the feedback loop (Neal & Cunningham, 1994) (atropine, baclofen, strychnine, PPADS?) enhance the light-evoked release of ACh, whilst drugs that stimulate the glycinergic neurones (muscarine, ATP) reduce the evoked-ACh release. The present results are most simply explained if ATP is co-released with ACh from cholinergic neurones but we cannot rule out the possibility that ATP is released from other neurones (dashed).

References

BLAZYNSKI, C. (1989). Displaced cholinergic, GABAergic amacrine cells in the rabbit retina also contain adenosine. *Visual Neurosci.*, **3**, 425–431.

BLAZYNSKI, C., WOODS, C. & MATHEWS, G.C. (1992). Evidence for the action of endogenous adenosine in the rabbit retina: modulation of the light-evoked release of acetylcholine. *J. Neurochem.*, **58**, 761–767.

CUNNINGHAM, J.R. & NEAL, M.J. (1985). Effect of excitatory amino acids and analogues on [^{3}H]-acetylcholine release from amacrine cells of the rabbit retina. *J. Physiol.*, **366**, 47–62.

LAMBRECHT, G., FRIEBE, T., GRIMM, U., WINDSCHEIF, U., BUNGARDT, E., HILDEBRANDT, C., BAUMERT, H.G., SPATZ-KUMBEL, G. & MUTSCHLER, E. (1992). PPADS, a novel functionally selective antagonist of P_2 purinoceptor-mediated responses. *Eur. J. Pharmacol.*, **217**, 217–219.

NEAL, M.J. & CUNNINGHAM, J.R. (1994). Baclofen enhances acetylcholine release from amacrine cells in the rabbit retina by reducing glycinergic inhibition. *J. Physiol.*, (in press).

PEREZ, M.T.R., EHINGER, B.E., LINDSTROM, K. & FREDHOLM, B.B. (1986). Release of endogenous and radioactive purines from the rabbit retina. *Brain Res.*, **398**, 106–112.

(Received September 2, 1994
Accepted September 12, 1994).

Br. J. Pharmacol. (1994), **113**, 1088–1092 © Macmillan Press Ltd, 1994

Smooth muscle relaxing effects of NO, nitrosothiols and a nerve-induced relaxing factor released in guinea-pig colon

[1]*†H.H. Iversen, *†L.E. Gustafsson, **A.M. Leone & *††N.P. Wiklund

*Department of Physiology and Pharmacology, †Institute of Environmental Medicine, ††Department of Urology, Karolinska Institute, S-171 77 Stockholm, Sweden and **Wellcome Research Laboratories, Langley Court, Beckenham, Kent BR3 3BS

1 The aim of the present study was to compare the biological activity of S-nitroso-L-cysteine (CYSNO), S-nitrosoglutathione (GSNO), S-nitroso-N-acetyl-D,L-penicillamine (SNAP) and hydroxylamine to that of nitric oxide (NO) and a vascular relaxing factor released by nerve stimulation in the guinea-pig intestine. The biological activity was examined in a bioassay system with guinea-pig colon as donor tissue and a series of spiral strips of rabbit aorta without endothelium as detector tissues.

2 Electrical stimulation of the guinea-pig colon released a vascular relaxing factor. The half-life of the relaxing factor down the bioassay cascade was the same as exogenously applied NO. N^{ω}-nitro-L-arginine (L-NOARG) inhibited the release of bioactivity.

3 The relaxations of the assay tissues caused by exogenous CYSNO also declined during the passage down the cascade. However, in the presence of L-cysteine (10^{-5} M) the half-life of CYSNO increased and there was no significant breakdown through the cascade. In contrast, the half-life of applied NO and the vascular relaxing factor released by nerve stimulation was unaffected by the presence of L-cysteine.

4 Exogenously applied GSNO (20–50 nM), SNAP (2–4 nM) and hydroxylamine (300–600 nM) caused relaxations that did not decline during the passage down the cascade.

5 In summary, the relaxation of the bioassay tissues during nerve stimulation was indistinguishable from the relaxation induced by NO, whereas relaxations induced by CYSNO, GSNO, SNAP and hydroxylamine showed different pharmacological profiles. The released bioactivity is thus likely to be NO itself.

Keywords: Non-adrenergic non-cholinergic; nitric oxide; S-nitroso-L-cysteine; bioassay; smooth muscle

Introduction

Nitric oxide (NO) is formed enzymatically from L-arginine in mammalian tissue (Palmer *et al.*, 1988), where it has roles in cell-to-cell signalling and in host-defence reactions (Moncada *et al.*, 1991). NO released from neurones has been suggested as a non-adrenergic non-cholinergic (NANC) mediator of relaxation in intestinal smooth muscle (Bult *et al.*, 1990; Desai *et al.*, 1991). In support, NO synthase is present within enteric neurones (Bredt *et al.*, 1991; Belai *et al.*, 1992; Ward *et al.*, 1992) and nerve-stimulation elicits the release of a factor with similar biological activity to NO (Bult *et al.*, 1990; Wiklund *et al.*, 1993). Furthermore, nerve-stimulation induces a frequency-dependent release of the NO-metabolites, nitrite and nitrate in guinea-pig intestine (Wiklund *et al.*, 1993). Inhibitors of NO synthase reduce NANC relaxations of the anococcygeus muscle (Gillespie *et al.*, 1989; Li & Rand, 1989), canine duodenum (Toda *et al.*, 1990) and guinea-pig caecum (Shuttleworth *et al.*, 1991), but evidence on the effect of the inhibitors on bioactivity- or metabolite-overflow is often lacking.

It has been suggested that NO, a highly reactive and unstable molecule is stabilized in tissues by a reaction with a carrier molecule R-SH, thus prolonging its half-life *in vivo* and preserving its biological activity (Myers *et al.*, 1990; Stamler *et al.*, 1992a). Accordingly, the NO-like factor released by NANC-nerves, as well as the endothelium-derived relaxing factor (EDRF), has been propsed to be a NO-containing molecule from which NO is subsequently released to the target cells (Myers *et al.*, 1990). Different S-nitrosothiols have been suggested as possible endogenous NO-donors, such as S-nitroso-L-cysteine (CYSNO; Myers *et al.*, 1990), dinitrosyl-iron-cysteine complex (DNIC; Vanin, 1991), and S-nitrosoglutathione (GSNO). Another suggested endogenous compound is hydroxylamine or an analogue thereof (Thomas & Ramwell, 1989). If NO can be stored as a nitrosothiol compound in nerve-terminal vesicles it may be able to function as a classical neurotransmitter, stored and released from vesicles (Thornbury *et al.*, 1991; Sanders & Ward, 1992). Cysteine is the most abundant source of free sulphydryl groups in mammalian tissue (Jocelyn, 1972), and at normal extracellular pH, CYSNO has a biological half-life similar to that of NO. Thus, CYSNO has been a favoured candidate for an alternative, endogenously released NO-like compound (Myers *et al.*, 1990). L-Cysteine recently has been shown to prolong the half-life of CYSNO, but not of NO or EDRF, released from vascular tissue (Feelisch *et al.*, 1994).

The aim of the present study was to compare the biological activity of NO, CYSNO, GSNO, S-nitroso-N-acetyl-D,L-penicillamine (SNAP) and hydroxylamine to that of a vascular relaxing factor released by stimulation of nerves in the guinea-pig intestine, in order to elucidate whether NO is released as a free radical or in a more stabilized form.

Methods

Bioassay

Guinea-pigs (250–400 g) of either sex were stunned and bled. The mesenteric artery was cannulated and the large intestine perfused with saline. The distal part of the colon was removed and a 25 cm long strip of longitudinal muscle, together with the underlying myenteric plexus was isolated, folded five times and used as donor tissue. The preparation was mounted in a heated (37°C) glass chamber and superfused (5 ml min^{-1}) with Tyrode solution (concentration in mM: Na^+ 161, K^+ 2.8, Ca^{2+} 1.8, Mg^{2+} 0.5, Cl^- 144, HCO_3^- 24, $H_2PO_4^-$ 0.4 and glucose 5.6) heated to 37°C and continuously gassed with 5% CO_2 in O_2. Transmural nerve

[1] Author for correspondence at: Department of Physiology 1, Karolinska Institutet, 171 77 Stockholm, Sweden

stimulation (20 Hz, 1.0 ms, 1200 pulses) was applied by needle-shaped silver electrodes. New Zealand White rabbits (1.5–2.5 kg) of either sex were anaesthetized with sodium pentobarbitone (50 mg kg^{-1}, i.v.) and the aorta was removed and cut into 3–4 cm long spiral strips. The endothelium was removed by gentle rubbing and the detector arteries (RbAs) were mounted in glass chambers arranged in a cascade as previously described (Gryglewski *et al.*, 1986a). The effluent from the donor tissue was used to superfuse the detector arteries and reached detector artery 1 at 2 s, artery 2 at 5 s and artery 3 at 8 s delay. The superfusate also contained guanethidine 3×10^{-6} M and L-arginine 3×10^{-5} M. The detector arteries were in addition superfused with atropine (10^{-6} M), N^{ω}-nitro-L-arginine methyl ester (L-NAME) (5×10^{-5} M) and phenylephrine (5×10^{-7} M); phenylephrine was used to increase smooth muscle tone.

Glyceryl trinitrate (GTN), applied by 20 s injection of 5–50 pmol, caused submaximal relaxations of the detector arteries. The relaxations by GTN did not decline down the cascade, and were used to calibrate the relative sensitivity of the detector arteries to guanylyl cyclase-mediated relaxation. Only detector arteries with less than 10% variability in the relaxation to GTN were used. All experiments were made in the presence of 10 units ml^{-1} superoxide dismutase (SOD; Gryglewski *et al.*, 1986b).

Mechanical muscular activity of the donor tissue was recorded isometrically by a Grass FT03 transducer (Grass Instruments, Quincy, MA, U.S.A.) at a load of 10 mN. Responses of the detector arteries were monitored isotonically from a load of 30 mN by Harvard Bioscience transducers type 52-9511 (Harvard Apparatus Company, Inc., Millis, MA, U.S.A.). Recordings were displayed by a Grass Polygraph (mod. 7P1).

Drugs

Nitric oxide solutions were prepared as previously described (Palmer *et al.*, 1987). Solutions of S-nitroso-L-cysteine (CYSNO) were synthesized according to Gibson *et al.* (1992) and were prepared immediately before application. L-Arginine, atropine chloride, N^{ω}-nitro-L-arginine (NOARG), N^{ω}-nitro-L-arginine methyl ester (L-NAME), L-cysteine, guanethidine, phenylephrine, tetrodotoxin (TTX), hydroxylamine and superoxide dismutase (SOD) (3900 units mg^{-1} solid) were purchased from Sigma Co (St Louis, MO, U.S.A.). S-nitroso-N-acetyl-D,L-penicillamine (SNAP) and S-nitrosoglutathione (GSNO) were purchased from Alexis Co (Läufelfingen, Switzerland) and were prepared on ice and diluted with deoxygenated H_2O immediately before use.

Statistics

Experimental data were expressed as mean values ± s.e.mean. Statistical significance was tested according to Student's *t* test for paired observations.

Results

Electrical stimulation (20 Hz, 1.0 ms, 1200 pulses) of the guinea-pig colon elicited a contraction (35 ± 3 mN, $n = 4$) that was blocked by tetrodotoxin (10^{-6} M; $n = 3$) (not shown). Furthermore, there was a concomitant release of a vascular relaxing factor. The bioactivity of this factor rapidly declined during the passage down the cascade. When the relaxation in detector artery 1 was defined as 100% there was 13 ± 7% of the relaxing bioactivity left in the superfusate at detector artery 2 and 8 ± 7% left at detector artery 3 ($n = 6$–7, $P < 0.001$; Figures 1a and 2a). L-NOARG (5×10^{-5} M) almost completely inhibited the nerve-induced vascular relaxing activity (16 ± 7% left at detector artery 1 and no activity left at detector artery 2 or 3, $n = 3$, $P < 0.005$). Concomitantly, L-NOARG (5×10^{-5} M) increased the nerve-induced contractile responses in the donor tissue by 39 ± 13% ($P < 0.05$, $n = 4$). TTX (10^{-6} M) totally abolished the stimulation-induced vascular relaxing activity ($n = 3$).

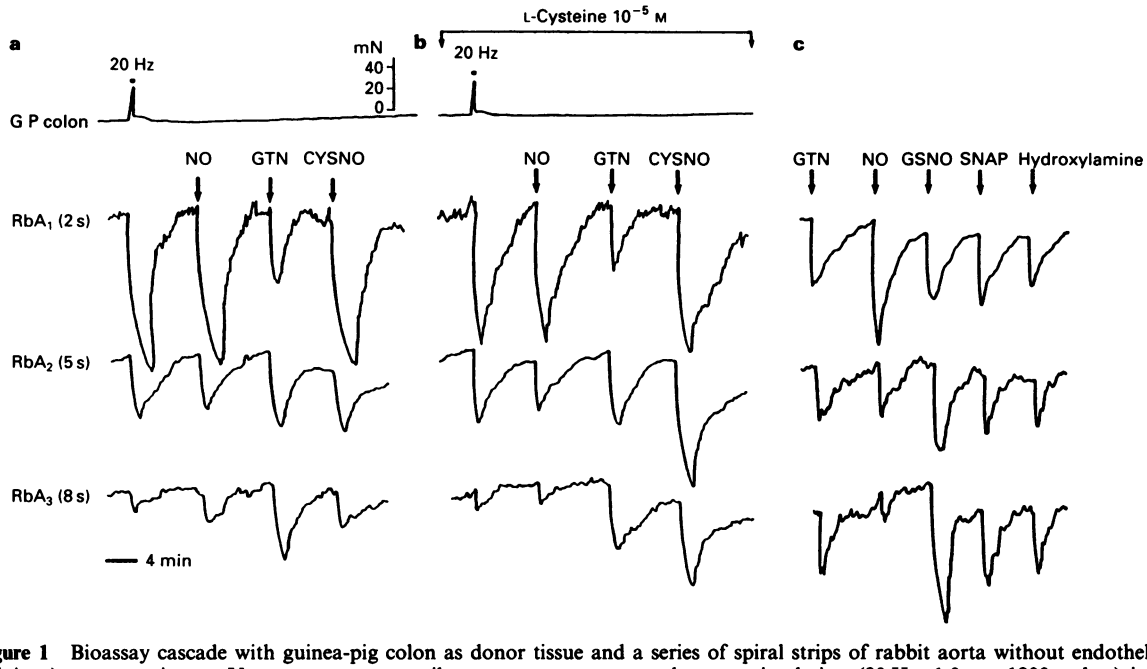


Figure 1 Bioassay cascade with guinea-pig colon as donor tissue and a series of spiral strips of rabbit aorta without endothelium (RbA_{1-3}) as assay tissues. Upper trace: contractile response to transmural nerve stimulation (20 Hz, 1.0 ms, 1200 pulses) in the donor tissue. Lower traces: inhibitory responses in the assay tissues, induced by a factor released during nerve stimulation of the donor tissue, or by application of exogenous compounds. (a) The inhibitory effect of glyceryl trinirate (GTN) was unaffected down the cascade while the inhibitory effects of the nerve-induced factor, nitric oxide (NO) and S-nitroso-L-cysteine (CYSNO) were degraded down the cascade at approximately the same rate. (b) In the presence of 10^{-5} M L-cysteine there was a significant prolongation of the relaxing bioactivity by CYSNO down the cascade, while the vascular relaxing bioactivity released by nerve stimulation, or NO was still rapidly degraded down the cascade. (c) Application of GTN, nitrosoglutathione (GSNO), S-nitroso-N-acetyl-D,L-penicillamine (SNAP) and hydroxylamine by injection over the assay tissues caused relaxations in the rabbit aortic strips that did not decline down the cascade while the inhibitory effect of exogenous NO was degraded down the cascade.

When NO (10–50 pmol) was applied by 20 s injection over the assay tissues, the detector arteries relaxed with the same time course as previously observed for the vascular relaxing factor released by nerve stimulation (Figure 1a and Table 1). NO was applied at a dose that caused a relaxation in detector artery 1 of the same size as that elicited by nerve stimulation. When the relaxation in detector artery 1 was defined as 100% there was 17 ± 13% left at detector artery 2 and 2 ± 2% left at detector artery 3 (Figures 1a and 2c).

Exogenous application of CYSNO (25–75 pmol), by 20 s injection, resulted in relaxations in the detector arteries, that declined down the cascade ($n = 4$, $P < 0.005$). The amount of CYSNO applied was chosen to cause a relaxation in detector artery 1 of the same magnitude as those elicited by nerve stimulation and NO. When the relaxation in detector artery 1 was defined as 100% there was 63 ± 19% left at detector artery 2 and 35 ± 11% left at detector artery 3 (Figures 1a and 2e, and Table 1).

In the presence of L-cysteine (10^{-5} M) there was no change in biological half-life of the vascular relaxing bioactivity induced by nerve stimulation or exogenous NO (Table 1). When the relaxation to nerve stimulation in detector artery 1 was defined as 100% there was 19 ± 9% remaining in superfusate at detector artery 2 and 5 ± 4% left at detector artery 3 (Figures 1b and 2b). When the relaxation to NO in detector artery 1 was defined as 100% there was 20 ± 9% of bioactivity left at detector artery 2 and 8 ± 6% at detector artery 3 (Figures 1b and 2d). In contrast, there was in the presence of 10^{-5} M L-cysteine, a significant increase in half-life of the relaxing effect caused by CYSNO ($P < 0.01$, $n = 4$) and there was no longer a breakdown during its passage down the cascade (Table 1). When the relaxation in detector artery 1 was defined as 100% there was 104 ± 18% of bioactivity remaining at detector artery 2 and 110 ± 18% remaining at detector artery 3 (Figures 1b and 2f).

Application of GSNO (40–80 pmol), SNAP (3–7 pmol) or

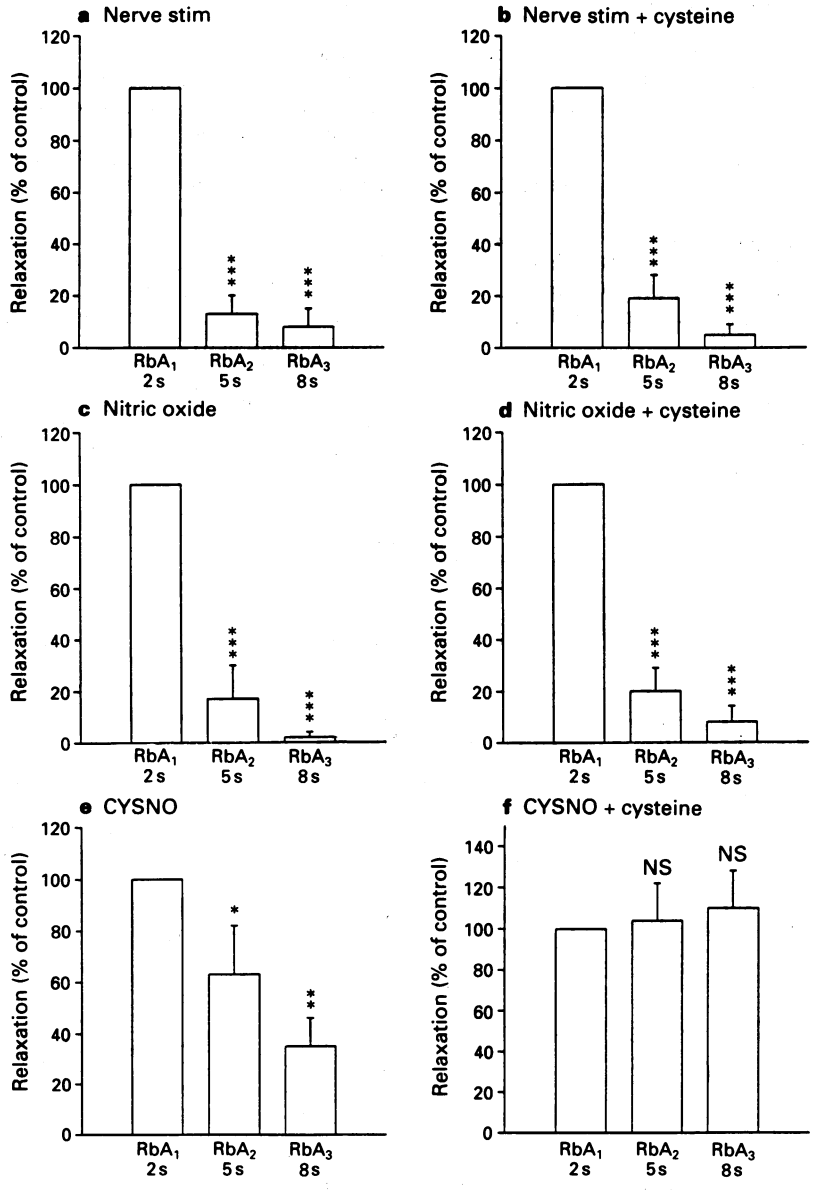


Figure 2 Diagrams illustrating the vascular relaxing activities of a nitric oxide (NO)-like factor released by nerve stimulation, and by exogenous NO and by S-nitroso-L-cysteine (CYSNO), in a bioassay cascade where the donor tissue was guinea-pig colon and the assay tissues were rabbit aortic strips. The superfusate reached detector artery 1 (RbA1) at 2 s, RbA2 at 5 s and RbA3 at 8 s delay. The relaxations in RbA1 were defined as 100%. (a) Relaxing activity released by nerve stimulation of the donor tissue. (b) Relaxing activity released by nerve stimulation of the donor tissue, in the presence of 10^{-5} M L-cysteine. (c) Relaxing effect of exogenous NO applied over the detector arteries. (d) Relaxing effect of exogenous NO applied over the detector arteries, in the presence of 10^{-5} M L-cysteine. (e) Relaxing effect of exogenous CYSNO applied over the detector arteries. (f) Relaxing effect of exogenous CYSNO, in the presence of 10^{-5} M L-cysteine. The half-life of the relaxing effect by CYSNO increased significantly in the presence of L-cysteine. (*$0.05 > P > 0.01$; **$0.01 > P > 0.001$; ***$P < 0.001$).

Table 1 Characteristics of a NANC-factor, released from guinea-pig colon and of some candidate molecules for this entity

Compound	*Half-life in bioassay cascade* (s)	*Half-life in bioassay cascade in the presence of* L-*cysteine (s)*
NANC factor	~2	~2
NO	~2	~2
CYSNO	5–6	>>NANC factor*
GSNO	>>NANC factor*	ND
SNAP	>>NANC factor*	ND
Hydroxylamine	>>NANC factor*	ND

*There was no detectable loss of vascular relaxing activity during passage down the cascade. ND = not determined. CYSNO: S-nitroso-L-cysteine; GSNO: S-nitrosoglutathione; SNAP: S-nitroso-N-acetyl-D,L-penicillamine.

hydroxylamine (0.5–1.0 nmol) by 20 s injection caused relaxations of the rabbit aortic strips. However, there were no measurable losses of vascular relaxing activity down the cascade when they were administered at concentrations causing relaxations, in detector artery 1, of the same magnitude as those elicited by nerve stimulation ($n = 4$) (Figure 1c and Table 1).

Discussion

NANC inhibitory nerves in the colon are likely to mediate the inhibitory component of the peristaltic reflex (Sanders & Ward, 1992). In the present study, contractile responses to nerve stimulation in the guinea-pig colon were studied. However, when the muscle tone is increased transmural stimulation elicits NANC relaxations which are inhibited by L-NOARG (Iversen *et al.*, 1994).

This study has shown that S-nitroso-L-cysteine (CYSNO) presents certain pharmacological properties in a bioassay-system that distinguish it from the arginine-derived NANC inhibitory factor in the guinea-pig colon. Thus, the half-life of the vascular relaxing activity of CYSNO in our bioassay system was significantly prolonged in the presence of L-cysteine, which was not the case for exogenous NO or the arginine-derived inhibitory factor released from the guinea-pig colon. The prolongation of CYSNO-mediated relaxation by cysteine is in agreement with previous observations on EDRF/NO released from rabbit aorta endothelium cells (Feelisch *et al.*, 1994), in which the half-life of EDRF/NO bioactivity from these cells was in fact found to be shortened by L-cysteine. This has also been observed in intact aortic strips (Jia & Furchgott, 1993), where SOD treatment largely attenuated the shortening effect of L-cysteine on EDRF and NO. The shortening effect is thought to be due to auto-oxidation of L-cysteine, with generation of O_2^-, and this might well explain why in our experiments, where SOD was present throughout, L-cysteine did not shorten the half-life of NO or the released bioactivity. The present data thus indicate a resemblance in bioactivity between authentic nitric oxide (NO) and the arginine-derived NANC inhibitory factor, providing further evidence that, during activation of NANC-nerves, NO is released as a free molecule, rather than as a S-nitrosothiol.

The biological activities of the NO-generating compounds GSNO, SNAP and hydroxylamine were examined in the bioassay cascade. The half-lives of these compounds were found to be much longer than those of NO and the nerve-induced vascular relaxing factor, with no loss of activity down the cascade. This is consistent with previous studies on hydroxylamine and DNIC (Feelisch *et al.*, 1994), and on GSNO and S-nitrosomercaptoethanol (Myers *et al.*, 1990), thereby making them unlikely candidates for the inhibitory principle of intestinal NANC-neuroeffector transmission.

The relatively short-lasting biological activity of exogenous CYSNO in the bioassay cascade (in the absence of L-cysteine) is consistent with the previous observation that CYSNO spontaneously liberates substantially more NO than other S-nitrosothiols, when measured by headspace during 10 min in oxygenated Krebs buffer (Kowaluk & Fung, 1990). This spontaneous liberation of NO does not seem to account for the major part of *in vitro* vascular relaxation by S-nitrosothiols (Kowaluk & Fung, 1990). It has been suggested that metal ion catalysis is the predominant pathway for the release of NO from S-nitrosothiols (McAninly *et al.*, 1993). The stabilization by L-cysteine of CYSNO is proabably due to the ability of thiols to complex metal ions present in the buffer solution (Feelisch *et al.*, 1994).

Conversion of NO to other oxidation states (NO^+ or NO^-) has recently been suggested (Stamler *et al.*, 1992b). However NO^+ as such is not active as a dilator, and NO^- is only relaxant at very high concentrations and is considerably more stable than NO in a bioassay cascade (Feelisch *et al.*, 1994).

In conclusion, the relaxation of bioassay tissues to nerve stimulation of a donor tissue from guinea-pig colon was indistinguishable from the relaxation induced by NO, whereas relaxations by CYSNO, GSNO, SNAP and hydroxylamine showed different pharmacological profiles. The data suggest that intact NO is a major nerve-induced relaxing principle in the guinea-pig colon.

Supported by The Swedish Medical Research Council (proj 11199 and 7919), the Tore Nilson, Magn Bergvall and Maud and Birger Gustafsson Foundations, the Swedish National Environmental Protection Board. The authors would like to thank Dr Salvador Moncada for valuable discussions.

References

BELAI, A., SCHMIDT, H.H.H.W., HOYLE, C.H., HASSALL, C.J., SAFFREY, M.J., MOSS, J., FÖRSTERMANN, U., MURAD, F. & BURNSTOCK, G. (1992). Colocalization of nitric oxide synthase and NADPH-diaphorase in the myenteric plexus of the rat gut. *Neurosci. Lett.*, **143**, 60–64.

BREDT, D.S., HWANG, P.H. & SNYDER, S.H. (1991). Localization of nitric oxide synthase indicating a neural role for nitric oxide. *Nature*, **351**, 714–718.

BULT, H., BOECKXSTAENS, G.E., PELCKMANS, P.A., JORDAENS, F.H., VAN MAERCKE, Y.M. & HERMAN, A.G. (1990). Nitric oxide as an inhibitory non-adrenergic non-cholinergic neurotransmitter. *Nature*, **345**, 346–347.

DESAI, K.M., SESSA, W.C. & VANE, J.R. (1991). Involvement of nitric oxide in the reflex relaxation of the stomach to accommodate food or fluid. *Nature*, **351**, 477–479.

FEELISCH, M., TE POEL, M., ZAMORA, R., DEUSSEN, A. & MONCADA, S. (1994). Understanding the controversy over the identity of EDRF. *Nature*, **368**, 62–65.

GIBSON, A., BABBEDGE, R., BRAVE, S.R., HART, S.L., HOBBS, A.J., TUCKER, J.F., WALLACE, P. & MOORE, P.K. (1992). An investigation of some S-nitrosothiols, and of hydroxy-arginine, on the mouse anococcygeus. *Br. J. Pharmacol.*, **107**, 715–721.

GILLESPIE, J.S., LIU, X. & MARTIN, W. (1989). The effects of L-arginine on the response of the rat anococcygeus muscle to NANC nerve stimulation. *Br. J. Pharmacol.*, **98**, 1080–1082.

GRYGLEWSKI, R.J., MONCADA, S. & PALMER, R.M.J. (1986a). Bioassay of prostacyclin and endothelium-derived relaxing factor (EDRF) from porcine aorthic endothelial cells. *Br. J. Pharmacol.*, **87**, 685–694.

GRYGLEWSKI, R.J., PALMER, R.M.J. & MONCADA, S. (1986b). Superoxide anion is involved in the breakdown of endothelium-derived vascular relaxing factor. *Nature*, **320**, 454–456.

IVERSEN, H.H., WIKLUND, N.P. & GUSTAFSSON, L.E. (1994). Nitric oxide-like activity in guinea-pig colon as determined by effector responses, bioassay and chemiluminescence analysis. *Acta Physiol. Scand.*, (in press).

JIA, L. & FURCHGOTT, R.F. (1993). Inhibition by sulfhydryl compounds of vascular relaxation induced by nitric oxide and endothelium-derived relaxing factor. *J. Pharmacol. Exp. Ther.*, **267**, 371–378.

JOCELYN, P.C. (1972). *Biochemistry of the SH group*. New York: Academic Press.

KOWALUK, E.A. & FUNG, H.-L. (1990). Spontaneous liberation of nitric oxide cannot account for in vitro vascular relaxation by S-nitrosothiols. *J. Pharmacol. Exp. Ther.*, **255**, 1256–1264.

LI, C.G. & RAND, M.J. (1989). Evidence for a role of nitric oxide in the neurotransmitter system mediating relaxation of the rat anococcygeus muscle. *Clin. Exp. Pharmacol. Physiol.*, **16**, 933–938.

MCANINLY, J., WILLIAMS, D.L.H., STUART, C.A., BUTLER, A.R. & RUSSEL, C. (1993). Metal Ion Catalysis in Nitrosothiol (RSNO) Decomposition. *J. Chem. Soc. Chem. Commun.*, **23**, 1758–1759.

MONCADA, S., PALMER, R.M.J. & HIGGS, E.A. (1991). Nitric oxide: physiology, pathophysiology and pharmacology. *Pharmacol. Rev.*, **43**, 109–142.

MYERS, P.R., MINOR, R.L., GUERRA, R., BATES, J.N. & HARRISON, D.G. (1990). Vasorelaxant properties of the endothelium-derived relaxing factor more closely resemble S-nitrosocysteine than nitric oxide. *Nature*, **345**, 161–163.

PALMER, R.M.J., ASHTON, D.S. & MONCADA, S. (1988). Vascular endothelial cells synthesize nitric oxide from L-arginine. *Nature*, **333**, 664–666.

PALMER, R.M.J., FERRIGE, A.G. & MONCADA, S. (1987). Nitric oxide release accounts for the biological activity of the endothelium-derived relaxing factor. *Nature*, **327**, 524–526.

SANDERS, K.M. & WARD, S.M. (1992). Nitric oxide as a mediator of nonadrenergic noncholinergic neurotransmission. *Am. J. Physiol.*, **262**, G379–G392.

SHUTTLEWORTH, C.W.R., MURPHY, R. & FURNESS, J.B. (1991). Evidence that nitric oxide participates in non-adrenergic inhibitory transmission to intestinal muscle in the guinea-pig. *Neurosci. Lett.*, **130**, 77–80.

STAMLER, J.S., SIMON, D.I., OSBORNE, J.A., MULLINS, M.E., JARAKI, O., MICHEL, T., SINGEL, D.J. & LOSCALZO, J. (1992a). S-nitrosylation of proteins with nitric oxide: synthesis and characterization of biologically active compounds. *Proc. Natl. Acad. Sci. U.S.A.*, **89**, 444–448.

STAMLER, J.S., SINGEL, D.J. & LOSCALZO, J. (1992b). Biochemistry of nitric oxide and its redox-activated forms. *Science*, **258**, 1898–1902.

THOMAS, G. & RAMWELL, P.W. (1989). Vascular relaxation mediated by hydroxylamines and oximes: their conversion to nitrites and mechanism of endothelium dependent vascular relaxation. *Biochem. Biophys. Res. Commun.*, **164**, 889–893.

THORNBURY, K.D., WARD, S.M., DALZIEL, H.H., CARL, A., WESTFALL, D.P. & SANDERS, K.M. (1991). Nitric oxide and nitrosocysteine mimic non-adrenergic, non-cholinergic hyperpolarization in canine proximal colon. *Am. J. Physiol.*, **261**, G553–G557.

TODA, N., BABA, H. & OKAMURA, T. (1990). Role of nitric oxide in non-adrenergic, non-cholinergic nerve-mediated relaxation in dog duodenal longitudinal muscle strips. *Jpn. J. Pharmacol.*, **53**, 281–284.

VANIN, A. (1991). Endothelium-derived relaxing factor is a nitrosyl iron complex with thiol ligands. *FEBS Letts*, **289**, 1–3.

WARD, S.M., XUE, C., SHUTTLEWORTH, C.W., BREDT, D.S., SNYDER, S.H. & SANDERS, K.M. (1992). NADPH diaphorase and nitric oxide synthase colocalization in enteric neurons of the canne proximal colon. *Am. J. Physiol.*, **263**, G277–G284.

WIKLUND, N.P., LEONE, A.M., GUSTAFSSON, L.E. & MONCADA, S. (1993). Release of nitric oxide evoked by nerve stimulation in guinea-pig intestine. *Neuroscience*, **53**, 607–611.

(Received May 4, 1994
Revised June 13, 1994
Accepted June 16, 1994)

Br. J. Pharmacol. (1994), **113**, 1093–1098 © Macmillan Press Ltd, 1994

Pharmacological reactivity of human epicardial coronary arteries: phasic and tonic responses to vasoconstrictor agents differentiated by nifedipine

Andrew P. Stork & [1]Thomas M. Cocks

Baker Medical Research Institute, Commercial Road, Prahran, Victoria 3181, Australia

1 Human epicardial coronary artery rings, freshly obtained from cardiac transplantation patients, commonly exhibited phasic contractile activity *in vitro*. This activity occurred either spontaneously or in response to vasoconstrictor stimulation.

2 Nifedipine pretreatment (1 nM–0.1 μM) reduced both types of phasic contractions in a concentration-dependent manner. At 0.1 μM nifedipine, spontaneous contractions were completely abolished, as were phasic contractions induced by U46619, endothelin-1 or 5-hydroxytryptamine (5-HT).

3 For U46619 (0.1–100 nM), the largest phasic contractions (amplitude peak to trough) occurred over the mid-range of concentrations used (1–10 nM). At higher concentrations (30–100 nM), phasic activity was reduced as the response reached a maximum. Estimated pEC_{50} values for the upper phasic and lower phasic curves were significantly different (8.71 ± 0.13 versus 7.90 ± 0.11; $P<0.05$; $n = 10$). In the presence of nifedipine (0.1 μM), the purely tonic contraction curve to U46619 was similar to the lower phasic curve in the absence of nifedipine ($pEC_{50} = 8.14 \pm 0.06$, $n = 10$). Similar results were obtained for endothelin-1 (0.1–100 nM).

4 Responses to 5-HT (1 nM–3 μM) were more variable. The largest phasic contractions were spread unevenly throughout the concentration-response curve. In the presence of nifedipine (0.1 μM), the curve to 5-HT was significantly depressed in range but not sensitivity (pEC_{50}) when compared with the phasic curves.

5 In conclusion, activation of dihydropyridine-sensitive voltage-operated Ca^{2+} channels mediated the phasic contractions commonly observed in human epicardial coronary arteries. These contractions amplified the contractile responses to low concentrations of vasoconstrictors. Inhibition of phasic activity by the Ca^{2+} channel antagonist, nifedipine, allowed the tonic vasoconstrictor profile of human isolated coronary artery to be determined which is important information for the accurate quantitative assessment of vasodilator responses in this tissue *in vitro*.

Keywords: Human coronary artery; nifedipine; 5-HT; endothelin; thromboxane A_2; spontaneous phasic contractions; cromakalim

Introduction

Spontaneous phasic contractile activity in human isolated coronary artery has been reported by many researchers over the past fifteen years (Golenhofen, 1978; Ross *et al.*, 1980; Kalsner, 1985; Kimura *et al.*, 1989). Phasic activity is present in tissues of both cadaver and transplantation origin (Ginsburg *et al.*, 1980, 1984; Godfraind *et al.*, 1984; Verdernikov, 1986).

Whilst the mechanisms controlling tone in the human coronary artery are complex (see Ginsburg, 1984 for an overview), the phasic contractions are known to be dependent on Ca^{2+} entry (Ginsburg *et al.*, 1984). They are sensitive to various Ca^{2+} channel antagonists, including nifedipine, verapamil and diltiazem (Weinheimer *et al.*, 1983; Sjögren *et al.*, 1986; Kimura *et al.*, 1989) which abolish the phasic activity.

The occurrence of phasic activity, however, makes quantitative analysis of concentration-response curves to both vasoconstrictor and vasodilator agents in human isolated coronary arteries difficult (Verdernikov, 1986; Sjögren *et al.*, 1986). Therefore, the aim of this study was to use nifedipine to remove spontaneous phasic activity and to determine for the first time the tonic vasoconstrictor profile of human isolated coronary artery to the thromboxane A_2-mimetic U46619, endothelin-1 and 5-hydroxytryptamine (5-HT). A preliminary account of this study was presented at the 25th annual meeting of the Australian Society of Clinical and Experimental Pharmacologists and Toxicologists (Stork *et al.*, 1991).

[1] Author for correspondence at present address: Department of Pharmacology, University of Melbourne, Parkville, Victoria 3052, Australia.

Methods

Human coronary arteries

Epicardial coronary arteries were obtained from the explanted hearts of 15 patients (12 male, 3 female) involved in the Alfred Hospital Heart & Lung Transplant Service who signed consent forms prior to surgery. Patients were diagnosed as having dilated cardiomyopathy ($n = 7$), ischaemic heart disease ($n = 5$), congenital heart disease ($n = 1$) or mitral valve disease ($n = 1$). One donor heart, unsuitable for transplantation, was also used. Average age was 45 years with a median age of 48 years (range 15–61).

Epicardial coronary arteries were dissected from hearts within 20 min of excision and taken to the laboratory in cold Krebs solution (4°C, see below for composition). Arteries were then further dissected free of any surrounding myocardium and fatty tissue and cut into 3 mm long ring segments. Only rings of arteries without gross macroscopic evidence of atherosclerosis were included. In total, 86 rings from 5 circumflex, 9 left anterior descending and 5 right coronary arteries, 2 primary circumflex and 3 primary left anterior descending coronary artery branches were used. Endothelium was left intact in all cases.

The vessel segments were set up in 30 ml organ baths containing Krebs solution [consisting of (in mM): Na^+ 144, K^+ 5.9, Ca^{2+} 2.5, Mg^{2+} 1.2, Cl^- 128.7, HCO_3^- 25, $H_2PO_4^-$ 1.2, SO_4^{2-} 1.2 and glucose 11] at 37°C and aerated with a 95% O_2/5% CO_2 gas mixture. Two L-shaped wire hooks (355 μm in diameter) were passed through the vessel lumen. One wire was attached to a stationary support leg attached to a manually-driven micrometer, while the other wire was attached to an isometric force transducer (Grass Instruments, model FT03C) to measure force development. Force was recorded on either single (Rikadenki) or dual (W&W Scientific Instruments) flat bed pen recorders.

The arterial rings were allowed to equilibrate for 60 min before being subjected to two passive stretches to 5 g force at 30 min intervals (as per Chester *et al.*, 1990), which gives an resting tension optimal for contraction responses. Test drugs were then added and allowed to equilibrate for 30 min before cumulative concentration-response curves to the various vasoconstrictor agents were constructed at half-log unit intervals. Only one protocol and curve per ring per patient was performed.

Drugs

The following drugs were used: 5-hydroxytryptamine creatinine sulphate (5-HT), N^G-nitro-L-arginine (L-NOARG) (Sigma); U46619 [1,5,5-hydroxy-11α,9α (epoxymethano) prosta-E 2,13-dienoic acid] (Upjohn); endothelin-1 (Peninsula Laboratories, U.S.A.), (−)-nifedipine (Bayer) and cromakalim (Beecham).

Nifedipine (10 mM) was made up in 100% ethanol, and 5-HT (10 mM) in distilled water on the day of the experiment. L-NOARG-stock solution (0.1 M) was made up in 1 M $NaHCO_3$. All other drugs were from stock solutions made up in distilled water. All dilutions were in distilled water.

Statistics and data analysis

Contractile responses were measured and expressed in g force. In control vessels, where phasic activity occurred, both the top and bottom of the phasic contraction were measured separately for each agonist concentration (upper phasic and lower phasic, respectively). The individual concentration-response curves were computer-fitted to the sigmoidal logistic equation

$$Y = P_1 + P_2/[1 + e^{P_3(\log X - P_4)}],$$

where X = agonist concentration, P_1 = lower plateau response, P_2 = range between the lower and the maximal plateau of the concentration response curve, P_3 = a negative curvature index indicating the slope independently of the range and P_4 = log dose required to produce a half-maximal response (EC_{50}) (Elghozi & Head, 1990). These calculations were used to determine pEC_{50} values. All values are presented as the mean ± standard error of the mean (s.e.mean) for the given number of experiments (n).

One-way analysis of variance with Scheffe's test was used to make comparisons between the three individual groups (upper phasic, lower phasic and nifedipine-treated; Wallenstein *et al.*, 1980). The level of significance was set at $P \leqslant 0.05$.

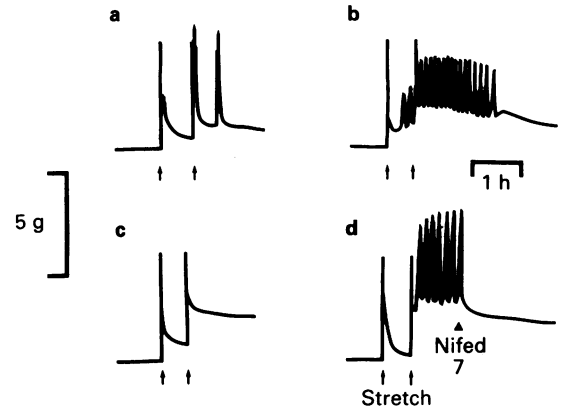


Figure 1 Traces of representative chart recordings of phasic contractile activity in human coronary artery; (a) irregular phasic contractions; (b) phasic activity with a regular rhythm; (c) quiescent arterial ring and (d) regular contractions abolished by nifedipine (Nifed, in − log M). Arrows indicate 5 g passive stretches.

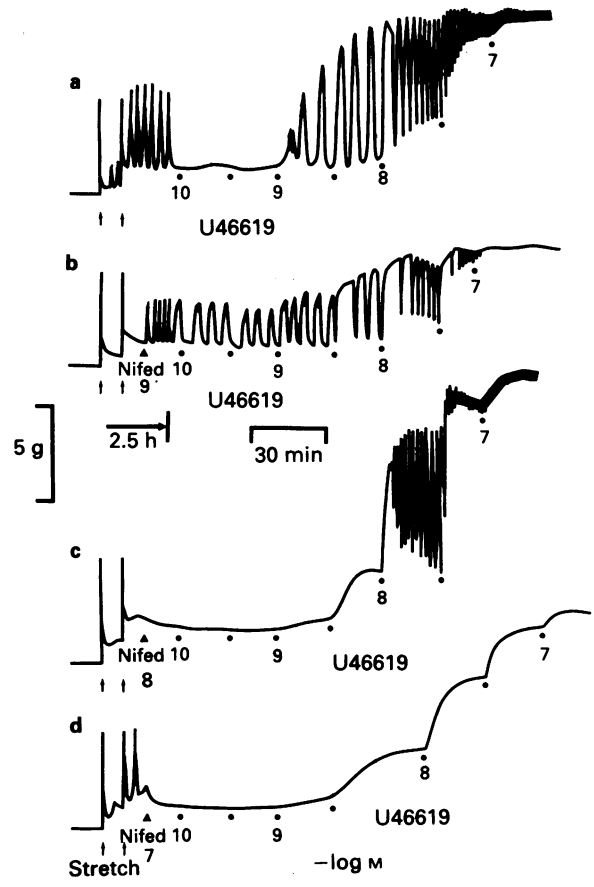


Figure 2 Effect of increasing concentrations of nifedipine on phasic activity and the concentration-response curve to U46619 in human coronary artery. Arterial rings were treated with concentrations (in − log M) of (a) nil; (b) 9; (c) 8 and (d) 7 nifedipine (Nifed). Traces are of chart recordings from 4 consecutive rings of a circumflex coronary artery from a 42 year old male. The recordings are representative of 4 separate experiments.

Results

Spontaneous phasic activity

Human isolated epicardial coronary artery ring segments commonly exhibited phasic contractile activity. These contractions occurred in nearly all ring segments, either spontaneously after the vessel was stretched or in response to vasoconstrictor stimulation (Figures 1, 2). The incidence, rhythm and amplitude of the spontaneous phasic contractions varied considerably, even between consecutive ring segments taken from the same artery. The amplitude of phasic contraction ranged between 1 and 7 g force and was observed to be independent of the level of passive force. Phasic activity was readily and rapidly removed by the addition of nifedipine (0.1 μM, Figures 1, 2).

Vasoconstrictor profiles

U46619 Tonic contractions to U46619 were masked by phasic contractile activity which was induced in quiescent arterial rings and enhanced in those which were already phasically active (Figure 2). Increasing concentrations of U46619 increased both the frequency (see Figure 2) and amplitude (see Figure 3) of the phasic contractions. At the higher concentrations (30–100 nM, U46619), the amplitude of the phasic contractions was reduced as the tonic contraction approached an apparent maximal response, but the frequency of phasic activity was increased to seconds per cycle (Figure 2). These U46619-induced phasic contractions were greatest in amplitide range (peak to trough) at 1–10 nM concentration (Figures 2a, 3b) and were blocked in a concentration-dependent manner by nifedipine (Figure 2).

In four separate experiments, consecutive arterial rings were exposed to either zero, 1, 10 or 100 nM nifedipine after which a cumulative concentration-response curve to the thromboxane A_2-mimetic U46619 was constructed (Figure 2). At zero and 1 nM nifedipine, phasic activity was seen in the U46619 curve on all occasions. In two experiments, 10 nM nifedipine completely abolished the phasic contractions, whilst in the other two experiments, the appearance of the phasic contractions was substantially delayed. In all four experiments, however, only tonic contractions were observed to U46619 stimulation in the presence of 0.1 μM nifedipine (Figure 2). Thus the amount of tonic contraction to U46619 was revealed in the presence of nifedipine (0.1 μM, Figure 3a). The tonic contraction curve for U46619 was superimposed on the curve for the lower level of the phasic contractions compared with the upper level curve, with all three curves (upper phasic, lower phasic and nifedipine-treated) converging at the highest concentration used (maximum response = 8.88 ± 1.16 g, 8.49 ± 1.28 g and 10.27 ± 1.54 g respectively, Figure 3a). Calculated pEC_{50} values for the lower phasic and nifedipine-treated curves were similar. The estimated value for the upper phasic curve, however, was significantly less ($P<0.05$, Table 1).

Sensitivity to U46619 did not differ between the main coronary vessels (circumflex and left anterior descending artery pEC_{50}s = 8.24 ± 0.10 and 8.15 ± 0.06; $n=3$ and 6, respectively) and their primary branches (pEC_{50} = 8.16 ± 0.17, $n=6$). Differences in maximum contractile force between the two groups of arteries were observed, but these could be attributed to differences in muscle mass (data not shown).

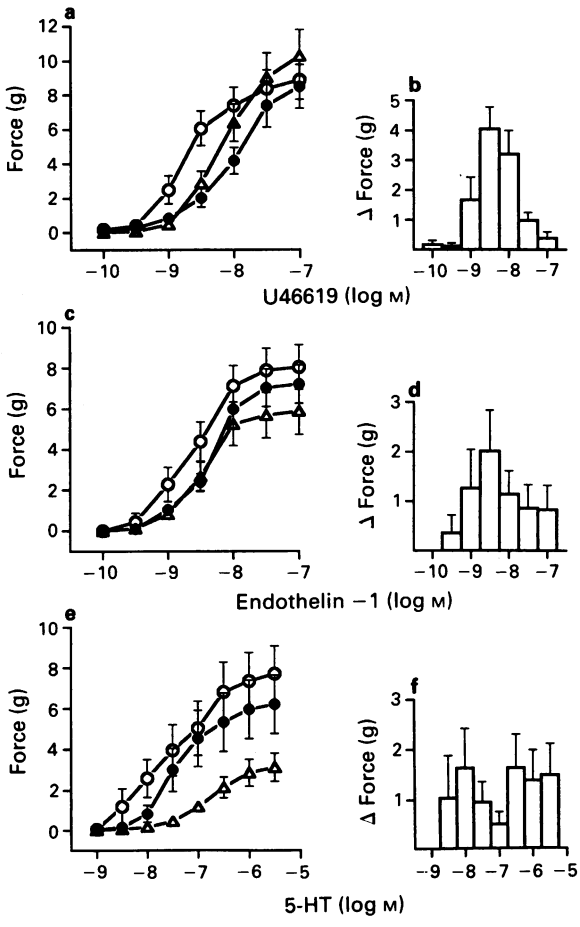


Figure 3 Response of human coronary artery to U46619, endothelin-1 and 5-hydroxytryptamine (5-HT). Mean cumulative concentration-response curves and the mean range of phasic contractions for each concentration were determined for (a) and (b) U46619; (c) and (d) endothelin-1 and (e) and (f) 5-HT in control [upper (○) and lower (●) levels of phasic contraction] and nifedipine-treated (0.1 μM, Δ) arterial rings. Mean pEC_{50} values for the curves are given in Table 1. Results are the mean ± s.e.mean of 10, 7 and 10 separate experiments for U46619, endothelin-1 and 5-HT, respectively

Endothelin-1 Results for endothelin-1 closely resembled those for U46619. Endothelin-1 induced phasic contractions in arterial rings not treated with nifedipine, which again made determination of the tonic contraction curve difficult (Figure 3c). Again, the amplitude of the phasic activity was greatest in the mid-range of concentrations; 1–10 nM (Figure 3d). Nifedipine (0.1 μM)-treated tissues contracted only tonically to endothelin-1. The concentration-tonic contraction curve in the presence of nifedipine closely followed the lower phasic curve in the phasically active tissues. There was a small but significant reduction in the maximal response between the upper phasic and nifedipine-treated curves (7.90 ± 1.08 g vs. 5.70 ± 1.12 g, $P<0.05$). There was also a significant difference between the pEC_{50} estimates for the upper phasic and lower phasic curves ($P<0.05$, Table 1).

5-HT Responses to 5-HT were the most variable. In the absence of nifedipine, phasic contractions reached a peak amplitude of 7.69 ± 1.08 g at 3 μM 5-HT (Figure 3e). The maximum contraction in the presence of nifedipine (0.1 μM) was significantly less (3.10 ± 0.69 g, $P<0.05$). The range in amplitude of the phasic contractions did not follow the pattern seen with U46619 and endothelin-1 where the greatest responses occurred in the mid-range concentrations. Rather, they were spread throughout the 5-HT concentration-response curve (Figure 3f). There was no significant difference between the pEC_{50} values for the three groups (upper phasic, lower phasic and nifedipine-treated) ($P<0.05$, Table 1).

Other drugs The ability of the ATP-sensitive K^+ channel opener, cromakalim and the L-arginine analogue N^G-nitro-L-arginine (L-NOARG) to abolish the phasic contractile activity was also examined.

Cromakalim (0.3 μM, in preliminary studies found to be a submaximal concentration for relaxation) initially removed any spontaneous phasic activity from the arterial ring segments but failed to stop induction of phasic contractions by vasoconstrictor stimulation with U46619 ($n=4$).

Table 1 Calculated pEC_{50} values for three vasoconstrictor drugs in human coronary artery

	Upper phasic	*Lower phasic*	*Nifedipine*
U46619	8.71 ± 0.13* (9)	7.90 ± 0.11 (10)	8.14 ± 0.06 (10)
Endothelin-1	8.75 ± 0.16 (7)†	8.34 ± 0.14 (7)†	8.45 ± 0.10 (7)
5-HT	7.31 ± 0.27 (8)	7.16 ± 0.18 (9)	6.80 ± 0.11 (9)

Values are mean ± s.e.mean for (n) experiments. *Indicates values significantly different from all others; †indicates values significantly different from each other ($P<0.05$, ANOVA).

Cromakalim pretreatment did not significantly affect the U46619 concentration-response curve (data not shown).

L-NOARG (0.1 mM) had no effect on either phasic contractile activity or U46619-induced tone ($n = 4$, data not shown).

Discussion

Human isolated epicardial coronary arteries commonly exhibited phasic contractile activity either spontaneously upon stretch or with vasoconstrictor stimulation. These contractions were abolished by nifedipine in a concentration-dependent manner but were not removed by cromakalim or the L-arginine analogue N^G-nitro-L-arginine (L-NOARG). Thus nifedipine (0.1 μM) allowed the determination of the vasoconstrictor profile of the thromboxane A_2-mimetic U46619, endothelin-1 and 5-HT in this tissue.

It could be argued that the phasic contractions observed in this and previous studies (see Introduction for references) are indicative of diseased hearts. However, in this study and others we have performed (Cocks *et al.*, 1993) vessels obtained from unused donor hearts have also been observed to display phasic contractile activity. The observation of a wide variation in phasic contractions amongst arterial rings, even within the same artery, has been previously reported by both Ross *et al.* (1980) and Verdernikov (1986). The reason for the variability in phasic activity, however, remains unknown.

Nifedipine, a dihydropyridine, voltage-operated Ca^{2+} channel antagonist, which acts by preventing the opening of the ion channel in response to depolarization of the smooth muscle membrane, removed phasic activity and unmasked stable, tonic contractions to vasoconstrictor stimulation. Golenhofen (1978) and Weinheimer *et al.* (1983) have previously reported that spontaneous activity in human isolated coronary artery was reduced and rhythmic fluctuations abolished by nifedipine in the range of 1 nM–1 μM. Similar results have been reported for two other Ca^{2+} channel antagonists, verapamil (Ross *et al.*, 1980; Verdernikov, 1986; Sjögren *et al.*, 1986) and diltiazem (Ginsburg *et al.*, 1980; Kimura *et al.*, 1989). All three Ca^{2+} antagonists are also effective against rhythmic contractions in monkey isolated coronary arteries (Ishii *et al.*, 1985), in concentrations similar to those required in human tissue.

Sjögren *et al.* (1986) noted that '. . . rhythmic activity in the human coronary arteries *in vitro* to some extent renders pharmacological experiments impossible'. In the present study we were able to determine the vasoconstrictor profile of U46619, endothelim-1 and 5-HT in the presence and absence of nifedipine (0.1 μM). In the absence of nifedipine, the phasic contractions appeared to be added on top of the tonic contractions for all three agonists. This was previously noticed by Godfraind *et al.* (1984) for 5-HT, but seemingly not followed up. Addition of the phasic contractions on the tonic contractions was confirmed by the fact that in the presence of nifedipine, the tonic contraction curves to U46619 and endothelin-1, at least, were superimposed on the curves for the lower level of phasic activity.

The results for U46619 closely matched those for the stable analogue carbocyclic thromboxane A_2 in similar preparations (Toda, 1984). The reason for the difference in pEC_{50} values for U46619 between the upper phasic curves and the lower phasic and nifedipine-treated curves is unclear but may indicate that the phasic contractions are more sensitive than tonic contractions to this vasoconstrictor stimulus.

Endothelin-1 also caused contraction of human coronary artery, possibly via receptors located predominantly on the adventitial side of the tunica media (Chester *et al.*, 1989), with a maximal contraction of 0.1 μM. The maximal contraction to endothelin-1 was 6.56 ± 0.77 g (64.35 ± 7.55 mN, n = 14, combining our results for the lower phasic and nifedipine-treated curves), approximately double that of Chester *et al.* (1989; 38.7 ± 6.4 mN, $n = 34$). Estimates for pEC_{50} values for endothelin-1 also differ between the two studies. Whilst not documented, the data of Chester *et al.* (1989) indicates a pEC_{50} value of approximately 7.7, about an order of magnitude lower than that found here (8.45 in the presence of nifedipine, 0.1 μM). Our pEC_{50} value for endothelin-1 in the human coronary artery is similar to pEC_{50} estimates in human internal mammary artery (8.60, Lüscher *et al.*, 1990; 8.01, Costello *et al.*, 1990), human saphaneous vein (8.40, Lüscher *et al.*, 1990; 8.12, Costello *et al.*, 1990) and porcine coronary artery (approximately 9.3, Yanagisawa *et al.*, 1988). As with U46619, the difference in pEC_{50} values for endothelin-1 between the phasic curves probably reflects the relative sensitivity of phasic activity to vasoconstrictors.

The reduction of the maximal contraction to endothelin-1 by nifedipine (and nicardipine, see Chester *et al.*, 1989) may be due to a decrease in Ca^{2+} entry via voltage-operated Ca^{2+} channels, since Yanagisawa *et al.* (1988) showed the responses to endothelin-1 are sensitive to Ca^{2+} channel antagonists. Endothelin-1, however, also activates the phosphatidylinositol second messenger system which has also been implicated in the contraction responses to this peptide (Pang *et al.*, 1989; Kasuya *et al.*, 1989).

5-HT stimulates both 5-HT_1-like and 5-HT_2 receptors to contract the human coronary artery and is the most efficacious of a range of 5-HT receptor antagonists in this tissue (Connor *et al.*, 1989; Chester *et al.*, 1990; Angus, 1990; Cocks *et al.*, 1993; Bax *et al.*, 1993). Both receptor subtypes appear to be important in mediating the hyperreactivity to 5-HT associated with coronary artery disease (Chester *et al.*, 1990; Cocks *et al.*, 1993; McFadden *et al.*, 1991). The 5-HT responses in the presence of nifedipine (3.10 ± 0.69 g at 3 μM) were generally equal to, or greater in contractile strength than those seen in previous studies (Chester *et al.*, 1990; Kalsner & Richards, 1984; Kalsner, 1985).

In the absence of nifedipine, the maximum force developed was significantly greater than the maximum contractile response in the presence of nifedipine. This may indicate that the response to 5-HT was not only augmented by the phasic activity, but also that part of the tonic contraction of 5-HT was blocked by nifedipine. Angus & Brazenor (1983) have shown that nifedipine is a more selective relaxant of submaximal 5-HT- then U46619-induced tone in dog large coronary artery, while in rabbit basilar artery, the contractile but not the depolarization response to 5-HT is sensitive to voltage-operated Ca^{2+} antagonists (Clark & Garland, 1993).

Phasic contractions of a similar magnitude developed to 5-HT over the whole range of the concentration-response curve. This contrasts with the pattern of the phasic contractions seen to U46619 and endothelin-1, where there was a bell-shaped distribution of the amplitude of phasic contractions and the phasic activity was added on top of the tonic contractions. Such amplification of the contractile responses to vasoconstrictor agonists by phasic activity may be important clinically in cases of arterial spasm. Maseri *et al.* (1990) suggested that segmental arterial spasm is caused by local hyperresponsiveness to a range of vasoconstrictors, including ergonovine (a 5-HT receptor agonist). Functional synergy may also be involved as we have previously demonstrated that in human epicardial coronary arteries *in vitro*, low concentrations of U46619 increase the contractile response to 5-HT and other 5-HT agonists (sumatriptan, ergometrine and methysergide) but do not affect the sensitivity to these agonists (Cocks *et al.*, 1993, see also Chester *et al.*, 1993). The synergistic interaction also occurs with noradrenaline (Cocks and Kemp, unpublished data) and for both noradrenaline and 5-HT with threshold concentrations of endothelin-1 (Yang *et al.*, 1990).

Our results in this study indicate that phasic activity can also augment the contractile response to a range of vasoconstrictors, particularly at low and medium concentrations. The mechanism behind this synergy remains to be elucidated,

although it would appear to be at a second messenger level, rather than the receptor level, since a range of agonists, and therefore receptor mechanisms, are implicated. In the case of amplification by phase activity, it is likely that the changing intracellular Ca^{2+} levels 'prime' the contractile processes to respond, hence increasing responsiveness, particularly to low vasoconstrictor concentrations. Clinically, our results implicate phasic activity in arterial spasm and indicate the use of nifedipine or other voltage-operated Ca^{2+} channel antagonists in both prophylactic and acute treatment.

In summary, phasic contractile activity was commonly seen in human coronary arterial rings *in vitro*. This activity involved activation of voltage-operated Ca^{2+} channels. Nifedipine removed the phasic contractions in a concentration-dependent manner and allowed determination of tonic vasoconstrictor profiles in the human coronary arteries for the thromboxane A_2-mimetic U46619, endothelin-1 and 5-HT. These results suggest that, under appropriate *in vivo* conditions, phasic activity could amplify contractile responses to low concentrations of vasoconstrictor drugs, such as 5-HT and thromboxane A_2, which are implicated in coronary artery spasm (see Kalsner, 1982; Maseri *et al.*, 1990; McFadden *et al.*, 1991; Cocks *et al.*, 1993; Chester *et al.*, 1993). This study has also established conditions under which vasodilator responses can be studied optimally (see Stork & Cocks, 1994).

We gratefully acknowledge the assistance of Mr Don Esmore, Mr Robin McEgan, Mr Arthur Preovolos and all the team of the Alfred Hospital Heart & Lung Transplant Service. Cromakalim was a gift from Beecham and Dr Grant McPherson. This work was supported by institute grants from the National Health and Medical Research Council of Australia and Glaxo Australia.

References

ANGUS, J.A. (1990). 5-HT receptors in the coronary circulation. *Trends Pharmacol. Sci.*, **10**, 89–90.

ANGUS, J.A. & BRAZENOR, R.M. (1983). Relaxation of large coronary artery by verapamil, D600, and nifedipine is constrictor selective: comparison with glyceryl trinitrate. *J. Cardiovasc. Pharmacol.*, **5**, 321–328.

BAX, W.A., RENZENBRINK, G.J., VAN HEUVEN-NOLSEN, D., THIJSSEN, E.J.M., BOS, E. & SAXENA, P.R. (1993). 5-HT receptors mediating contractions of the isolated human coronary artery. *Eur. J. Pharmacol.*, **239**, 203–210.

CHESTER, A.H., ALLEN, S.P., TADJKARIMI, S. & YACOUB, M.H. (1993). Interaction between thromboxane A_2 and 5-hydroxytryptamine receptor subtypes in human coronary arteries. *Circulation*, **87**, 874–880.

CHESTER, A.H., DASHWOOD, M.R., CLARKE, J.G., LARKIN, S.W., DAVIES, G.J., TADJKARIMI, S., MASERI, A. & YACOUB, M.H. (1989). Influence of endothelin on human coronary arteries and localisation of its binding sites. *Am. J. Cardiol.*, **63**, 1395–1398.

CHESTER, A.H., MARTIN, G.R., BODELSSON, M., ARNEKLO-NOBIN, B., TADJKARIMI, S., TORNEBRANDT, K. & YACOUB, M.H. (1990). 5-Hydroxytryptamine receptor profile in healthy and diseased human epicardial coronary arteries. *Cardiovasc. Res.*, **24**, 932–937.

CLARK, A.H. & GARLAND, C.J. (1993). Ca^{2+} channel antagonists and inhibition of protein kinase C each block contraction but not depolarization to 5-hydroxytryptamine in the rabbit basilar artery. *Eur. J. Pharmacol.*, **235**, 113–116.

COCKS, T.M., KEMP, B.K., PRUNEAU, D. & ANGUS, J.A. (1993). Comparison of contractile responses to 5-hydroxytryptamine and sumatriptan in human isolated coronary artery: synergy with the thromboxane A_2-receptor agonist, U46619. *Br. J. Pharmacol.*, **110**, 360–368.

CONNOR, H.E., FENIUK, W. & HUMPHREY, P.P.A. (1989). 5-hydroxytryptamine contracts human coronary arteries predominantly via 5-HT_2 receptor activation. *Eur. J. Pharmacol.*, **161**, 91–94.

COSTELLO, K.B., STEWART, D.J. & BAFFOUR, R. (1990). Endothelin is a potent constrictor of human vessels used in coronary revascularization surgery. *Eur. J. Pharmacol.*, **186**, 311–314.

ELGHOZI, J.-L. & HEAD, G.A. (1990). Spinal noradrenergic pathways and pressor responses to central angiotensin II. *Am. J. Physiol.*, **258**, H240–H246.

GINSBURG, R.C. (1984). Myogenic tone of the isolated human epicardial artery: regulatory controls. *Acta Med. Scand.*, **694**, Suppl. 29–37.

GINSBURG, R., BRISTOW, M.R., HARRISON, D.G. & STINSON, E.B. (1980). Studies with isolated human coronary arteries – some general observations, potential mediators of spasm, role of calcium antagonists. *Chest*, **78**, Suppl. 180–186.

GINSBURG, R., BRISTOW, M.R., DAVIS, K., DIBIASE, A. & BILLINGHAM, M.E. (1984). Quantitative pharmacologic responses of normal and atherosclerotic isolated human epicardial coronary arteries. *Circulation*, **69**, 430–440.

GODFRAIND, T., FINET, M., LIMA, J.S. & MILLER, R.C. (1984). Contractile activity of human coronary arteries and human myocardium *in vitro* and their sensitivity to calcium entry blockade by nifedipine. *J. Pharmacol. Exp. Ther.*, **230**, 514–518.

GOLENHOFEN, K. (1978). Activation mechanisms in smooth muscle of human coronary arteries and their selective inhibition. *Naunyn-Schmied. Arch. Pharmacol.*, **302**, Suppl. R36.

ISHII, K., YANAGISAWA, T., SATOH, K. & TAIRA, N. (1985). Abolition of spontaneous rhythmic contractions of isolated monkey coronary arteries by diltiazem, nifedipine, verapamil and nicorandil but not by nitroglycerine. *Tohoku J. Exp. Med.*, **145**, 85–90.

KALSNER, S. (1982). Vasoconstrictors, spasm and acute myocardial events. In *The Coronary Artery*. ed. Kalsner, S. pp. 551–595. London: Croom Helm.

KALSNER, S. (1985). Coronary artery reactivity in human vessels: some questions and answers. *Fed. Proc.*, **44**, 321–325.

KALSNER, S. & RICHARDS, R. (1984). Coronary arteries of cardiac patients are hyperreactive and contain stores of amines: a mechanism for coronary spasm. *Science*, **223**, 1435–1437.

KASUYA, Y., TAKUWA, Y., YANAGISAWA, M., KIMURA, S., GOTO, K. & MASAKI, T. (1989). Endothelin-1 induces vasoconstriction through two functionally distinct pathways in porcine coronary artery: contribution of phosphoinositide turnover. *Biochem. Biophys. Res. Commun.*, **161**, 1049–1055.

KIMURI, T., YASUE, H., SAKAINO, N., ROKUTANDA, M. JOUGASAKI, M. & ARAKI, H. (1989). Effects of magnesium on the tone of isolated human coronary arteries – comparison with diltiazem and nitroglycerin. *Circulation*, **79**, 1118–1124.

LÜSCHER, T.F., YANG, Z., TSCHUDI, M., VON SEGESSER, L., STULZ, P., BOULANGER, C., SIEBENMANN, R., TURINA, M. & BÜHLER, F.R. (1990). Interaction between endothelin-1 and endothelium-derived relaxing factor in human arteries and veins. *Circ. Res.*, **66**, 1088–1094.

MCFADDEN, E.P., CLARKE, J.G., DAVIES, G.J., KASKI, J.C., HAIDER, A.W. & MASERI, A. (1991). Effect of intracoronary serotinin on coronary vessels in patients with stable angina and patients with variant angina. *N. Engl. J. Med.*, **324**, 648–654.

MASERI, A., DAVIES, G., HACKETT, D. & KASKI, J.C. (1990). Coronary artery spasm and vasoconstriction: the case for a distinction. *Circulation*, **81**, 1983–1991.

PANG, D.C., JOHNS, A., PATTERSON, K., BOTELHO, L.H.P. & RUBANYI, G. (1989). Endothelin-1 stimulates phosphatidylinositol hydrolysis and calcium uptake in isolated canine coronary arteries. *J. Cardiovasc. Pharmacol.*, **13**, Suppl. 5 S75–S79.

ROSS, G., STINSON, E., SCHROEDER, J. & GINSBURG, R. (1980). Spontaneous phasic activity of isolated human coronary arteries. *Cardiovasc. Res.*, **14**, 613–618.

SJÖGREN, A., EDVISSON, L. & OTTOSEN, A. (1986). Vasomotor responses of isolated human coronary arteries to magnesium, nitroglycerin and verapamil: a comparison with coronary arteries from cat and rat. *Acta Pharmacol. Toxicol.*, **59**, 195–203.

STORK, A.P. & COCKS, T.M. (1994). Pharmacological reactivity of human epicardial coronary arteries: characterization of relaxation responses to endothelium-derived relaxing factor. *Br. J. Pharmacol.*, **113**, 1099–1104.

STORK, A.P., KEMP, B.K. & COCKS, T.M. (1991). Nifedipine abolishes spontaneous phasic contractile activity in human coronary artery. *Clin. Exp. Pharmacol. Physiol.*, Suppl. 18, 59.

TODA, N. (1984). Responses of human, monkey and dog coronary arteries *in vitro* to carbocyclic thromboxane A_2 and vasodilators. *Br. J. Pharmacol.*, **83**, 399–408.

VERDERNIKOV, Y.P. (1986). Mechanisms of coronary spasm of isolated human epicardial coronary segments excised 3 to 5 hours after sudden death. *J. Am. Coll. Cardiol.*, **8**, Suppl. 42A–49A.

WALLENSTEIN, S., ZUCKER, C.L. & FLEISS, J.L. (1980). Some statistical methods useful in circulation research. *Circ. Res.*, **47**, 1–9.

WEINHEIMER, G., GOLENHOFEN, K. & MANDREK, K. (1983). Comparison of the inhibitory effects of nifedipine, nitroglycerin and nitroprusside sodium on different types of activation in canine coronary arteries, with comparative studies in human coronary arteries. *J. Cardiol. Pharmacol.*, **5**, 989–997.

YANAGISAWA, M., KURIHARA, H., KIMURA, S., TOMOBE, Y., KOBAYASHI, M., MITSUI, Y., YAZAKI, Y., GOTO, K. & MASAKI, T. (1988). A novel potent vasoconstrictor peptide produced by vascular endothelial cells. *Nature*, **332**, 411–415.

YANG, Z., RICHARD, V., VON SEGESSER, L., BAUER, E., STULZ, P., TURINA, M. & LÜSCHER, T.F. (1990). Threshold concentrations of endothelin-1 potentiate contractions to norepinephrine and serotonin in human arteries. *Circulation*, **82**, 188–195.

(Received September 20, 1993
Revised February 16, 1994
Accepted February 17, 1994)

Br. J. Pharmacol. (1994), **113**, 1099–1104 © Macmillan Press Ltd, 1994

Pharmacological reactivity of human epicardial coronary arteries: characterization of relaxation responses to endothelium-derived relaxing factor

Andrew P. Stork & [1]Thomas M. Cocks

Baker Medical Research Institute, Commercial Road, Prahran, Victoria 3181, Australia

1 Human epicardial coronary artery rings, freshly obtained from cardiac transplant patients, were examined for their responses to endothelium-derived relaxing factor (EDRF)-releasing agents.

2 Functional antagonism profoundly influenced relaxation responses in this tissue. Increasing force with concentrations of U46619 above 3 nM (40% of maximum contraction response) resulted in a reduction of the maximum response to four vasorelaxants which relax vascular smooth muscle via different mechanisms: the EDRF-releasing agents, substance P and bradykinin; the endothelium-independent nitro-vasodilator, sodium nitroprusside (SNP); and the β-adrenoceptor agonist, isoprenaline.

3 Substance P, histamine, bradykinin and the Ca^{2+} ionophores ionomycin and A23187 all caused concentration- and endothelium-dependent relaxation in vessels pre-contracted with the thromboxane A_2-mimetic, U46619 (3 nM) to an active force optimal for relaxation responses. Nifedipine (0.1 μM), added to prevent spontaneous contractions, had no effect on relaxation responses to substance P, bradykinin and histamine.

4 Substance P was the most potent of the EDRF-releasing agents examined and all agents except for bradykinin caused near-maximal relaxation. Bradykinin caused only 46.2% ± 7.3% relaxation. Responses were abolished when the endothelium was removed and, except for histamine, were not significantly affected by indomethacin (3–10 μM, $P > 0.05$). Histamine (0.1–10 μM) caused a concentration-dependent contraction of arterial rings without endothelium.

5 The L-arginine analogues N^G-nitro-L-arginine (L-NOARG, 0.1 mM) and N^G-monomethyl-L-arginine (L-NMMA, 0.1 mM) both caused no further contraction in arteries precontracted with U46619 (3 nM) and were in general, poor inhibitors of responses to EDRF agonists. L-NMMA, but not L-NOARG, caused small but significant decreases in the maximum responses to substance P, bradykinin (18.5 ± 6.9% and 27.6 ± 10.9% relaxation with L-NMMA and L-NOARG, respectively), histamine and A23187 ($P < 0.05$). The analogues had no effect on SNP responses.

6 In conclusion, EDRF release in human isolated coronary artery is only poorly antagonized by the nitric oxide synthase inhibitors L-NOARG and L-NMMA. These results indicate that either the nitric oxide transduction pathway present in human coronary artery is different from that in other tissues or that another factor(s) (e.g. endothelium-derived hyperpolarizing factor) is also released in response to EDRF-releasing agents and augments the relaxation to nitric oxide.

Keywords: Human coronary artery; endothelium-derived relaxing factor; nitric oxide; substance P; bradykinin; L-arginine analogues; Ca^{2+} ionophores; isoprenaline; functional antagonism

Introduction

The importance of endothelium-derived relaxing factor (EDRF) in the regulation of vascular reactivity has been of interest since Furchgott & Zawadzki (1980) first described the role of the endothelium in mediating relaxation responses to some vasodilator agents.

Investigations in human coronary artery *in vivo* for evaluation of endothelial dysfunction in association with atherosclerosis have revealed that substance P (Crossman *et al.*, 1989; Kushwaha *et al.*, 1991; Yamamoto *et al.*, 1992) and to some extent, acetylcholine (Ludmer *et al.*, 1986; Yasue *et al.*, 1990) cause potent vasodilatation of human epicardial coronary arteries. Acetylcholine has been shown to be a sensitive marker of endothelial dysfunction with early atheroma (Vita *et al.*, 1990; Zeiher *et al.*, 1991), whilst substance P is a powerful vasodilator agent which can increase arterial diameter by up to 30% (Crossman *et al.*, 1989).

Toda (1987) demonstrated a relaxation response to substance P in human coronary artery helical strips *in vitro*, and release of EDRF by histamine in the same tissue. Bradykinin, the calcium ionophore A23187 and, occasionally, acetylcholine, have also been shown to relax human coronary artery *in vitro* (Förstermann *et al.*, 1988).

Palmer *et al.* (1987) showed that the response of EDRF was identical to that seen to nitric oxide (NO). The source for EDRF (NO) is the guanidino nitrogen atom of arginine (Palmer *et al.*, 1988). Since these discoveries, various L-arginine analogues have been used experimentally in a number of tissues to block activity in the enzyme which converts L-arginine to NO, nitric oxide synthase (see Moncada *et al.*, 1991): N^G-nitro-L-arginine methyl ester (L-NAME), N^G-nitro-L-arginine (L-NOARG), N^G-methyl-L-arginine (L-NMA) and N^G-monomethyl-L-arginine (L-NMMA), amongst others (see Moncada *et al.*, 1991 for an overview). In human coronary arteries, however, only the effect of L-NMMA on the EDRF response to substance P has been examined, with the L-arginine analogue reported to decrease the maximum relaxation response from 89.1 ± 8.5% to 34.0 ± 10.5% of the glyceryl trinitrate response (Chester *et al.*, 1990a,b).

The first part of this study was designed to establish optimal conditions in human isolated epicardial coronary

[1] Author for correspondence at present address: Department of Pharmacology, University of Melbourne, Parkville, Victoria 3052, Australia.

artery in order to examine the effects of endothelium-dependent vasorelaxing agents. Some of these conditions were described in the preceding paper, where we found that nifedipine abolished spontaneous phasic contractile activity, but tonic contractions to the thromboxane A_2-mimetic U46619 were unaffected by the calcium channel antagonist (Stork & Cocks, 1994). The importance of any functional (physiological) antagonism of relaxation responses via increasing levels of U46619-induced active force, and the effect of nifedipine on release of EDRF were determined. Once optimal conditions for EDRF-mediated relaxations were established, the response to the EDRF (NO)-releasing agents substance P, bradykinin, histamine, ionomycin and A23187 (the latter two being Ca^{2+} ionophores) were characterized. The effect of the L-arginine analogues L-NOARG and L-NMMA on these responses, as well as on basal or U46619-induced active force, were also investigated.

A preliminary account of this study was presented at the 26th annual meeting of the Australian Society of Clinical and Experimental Pharmacologists and Toxicologists (Stork & Cocks, 1992).

Methods

Human coronary arteries

Epicardial coronary arteries were obtained from the explanted hearts of 31 patients (21 male, 10 female) involved in the Alfred Hospital Heart & Lung Transplant Service who signed consent forms prior to surgery. Patients were diagnosed as having dilated cardiomyopathy ($n = 17$), ischaemic heart disease ($n = 9$), congenital heart disease ($n = 1$) or mitral valve disease ($n = 1$). Three donor hearts from primary pulmonary hypertensive patients, unsuitable for transplantation, were also used. Average age was 46.5 years with a median age of 52 years (range 19–66).

Epicardial coronary arteries were dissected from hearts within 20 min of excision and taken to the laboratory in cold Krebs solution (4°C, see below for composition). Arteries were then further dissected free of any surrounding myocardium and fatty tissue and cut into 3 mm long ring segments. Only rings of arteries without gross macroscopic evidence of atherosclerosis were included. In total, 373 rings from nine circumflex, 15 left anterior descending and 13 right coronary arteries, six primary circumflex, six primary left anterior descending and eight primary right coronary artery branches were used. Endothelium was left intact in most cases and was removed from a few rings by mechanical rubbing with a tapered wooden stick to check for endothelium-dependency of the responses.

The vessel segments were set up in 30 ml organ baths containing Krebs solution [consisting of (in mM): Na^+ 144, K^+ 5.9, Ca^{2+} 2.5, Mg^{2+} 1.2, Cl^- 128.7, HCO_3^- 25, $H_2PO_4^-$ 1.2, SO_4^{2-} 1.2 and glucose 11] at 37°C and aerated with a 95% O_2/5% CO_2 gas mixture. Two L-shaped wire hooks (355 μm in diameter) were passed through the vessel lumen. One wire was attached to a stationary support leg attached to a manually-driven micrometer, while the other wire was attached to an isometric force transducer (Grass Instruments, model FT03C) to measure force development. Force was recorded on either single (Rikadenki) or dual (W&W Scientific Instruments) flat bed pen recorders.

The arterial rings were allowed to equilibrate for 60 min before being subjected to two passive stretches to 5 g force at 30 min intervals (resulting in an optimal passive tension). Nifedipine (0.1 μM) was then added to remove and prevent phasic contractile activity (see Stork & Cocks, 1994). Where the effect of the L-arginine analogues on the agonists were examined, the analogues were added and allowed to equilibrate for 30 min. The vessels were then precontracted with the thromboxane A_2-mimetic, U46619 (1–30 nM) and cumulative concentration-response curves to various vasorelaxant drugs were constructed at half-log unit intervals once a steady level of active force was obtained. In some experiments, nifedipine was not used and the vessels were contracted with 1 nM U46619 due to the increased sensitivity of the phasically active tissue (Stork & Cocks, 1994). Only one protocol and curve per ring per patient was performed.

Drugs

The following drugs were used: histamine dihydrochloride, ionomycin free acid and A23187 free acid (Calbiochem); substance P acetate, bradykinin acetate, (−)-isoprenaline bitartrate and N^G-nitro-L-arginine (L-NOARG) (Sigma); N^G-monomethyl-L-arginine (L-NMMA, International Drug Technology, Melbourne, Australia); sodium nitroprusside (SNP, Roche); U46619 [1,5,5-hydroxy-11α,9α(epoxymethano) prosta-E 2,13-dienoic acid] (Upjohn); endothelin-1 (Peninsula Labs, USA) and (−)-nifedipine (Bayer).

Nifedipine (10 mM) was made up in 100% ethanol on the day of the experiment. Stock solutions of L-NOARG (0.1 M) and the Ca^{2+} ionophores, ionomycin and A23197 (both 1 mM), were made up in 1 M $NaHCO_3$ and 100% ethanol, respectively. All other drugs were from stock solutions made up in distilled water and all dilutions were in distilled water.

Statistics and data analysis

Individual relaxation responses to the agonists were converted to percentages of the maximum possible relaxation, as assessed by the level of active force developed to U46619. The constrictor effects of the L-arginine analogues, L-NOARG and L-NMMA, were measured in g force, due to wide variation when converted to percentage values of the initial contraction to U46619.

The individual concentration-response curves were then computer-fitted to the sigmoidal logistic equation

$$Y = P_1 + P_2/[1 + e^{P_3(\log X - P_4)}],$$

where X = agonist concentration, P_1 = lower plateau response, P_2 = range between the lower and the maximal plateau of the concentration response curve, P_3 = a negative curvature index indicating the slope independently of the range and P_4 = log dose required to produce a half-maximal response (EC_{50}) (Elghozi & Head, 1990). These calculations were used to determine pEC_{50} (− log M) values. All values are presented as the mean ± standard error of the mean (s.e. mean) for the given number of experiments (n).

Student's unpaired t test was used to compare two independent groups of data and one-way analysis of variance (ANOVA) with Scheffe's test was used to make comparisons between multiple individual groups (Wallenstein *et al.*, 1980). The level of significance was set at $P \leqslant 0.05$.

Results

Optimal conditions

Concentration-relaxation response curves to substance P ($n = 5$), bradykinin ($n = 5$), and histamine ($n = 2$, data not shown) were determined in vessels which held a stable contraction to U46619 (1 nM) in the absence of nifedipine (Figure 1). In the absence of nifedipine, substance P caused 89.7 ± 4.8% relaxation ($pEC_{50} = 10.02 \pm 0.13$) and bradykinin caused 47.2 ± 12.6% relaxation ($pEC_{50} = 8.48 \pm 0.13$). The presence of nifedipine (0.1 μM) abolished phasic contractions and did not affect the relaxation responses to these agents ($P > 0.05$, see below for data in the presence of nifedipine). Consequently, nifedipine (0.1 μM) was routinely used in all following experiments to abolish phasic activity and ensure a steady level of active force to U46619.

The magnitude of relaxation responses to substance P, bradykinin, sodium nitroprusside (SNP) and isoprenaline

depended on the amplitude of contractions to U46619 (Figure 2). At 1, 3, 10 and 30 nM, U46619 caused contractions of approximately 15%, 40%, 70% and 85%, respectively, of the constrictor-maximum in this tissue (Stork & Cocks, unpublished data). In arterial rings contracted with 1 and 3 nM U46619, the relaxation curves to all relaxant agents were superimposable, with similar pEC_{50} values and maximum responses [pEC_{50} values in 3 nM U46619-contracted tissues = 9.93 ± 0.15 (substance P); 8.45 ± 0.17 (bradykinin); 7.85 ± 0.12 (SNP) and 6.40 ± 0.21 (isoprenaline); $n = 5$ for each agonist]. At 10 nM U46619, maximum responses were decreased, although this just failed to reach statistical significance ($P > 0.05$, ANOVA). At 30 nM U46619 there was a significant decrease in the maximum response for all four relaxant agents when compared with the responses in rings contracted with 1 and 3 nM U46619 ($P < 0.05$) and a significant decrease in the pEC_{50} value for SNP with similar comparisons ($pEC_{50} = 6.40 \pm 0.31$, $P < 0.05$). Relaxation responses to bradykinin were abolished at 30 nM U46619 (Figure 2b). Consequently, all relaxation experiments were performed in vessels contracted with 3 nM U46619.

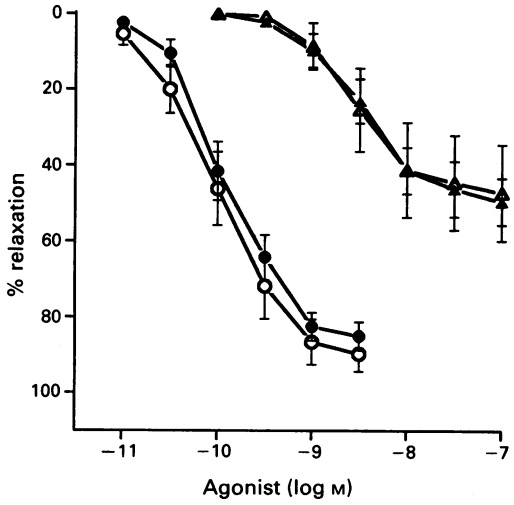


Figure 1 Absence of effect of nifedipine (0.1 μM) on the relaxation response to substance P (○, ●) and bradykinin (△, ▲) in human coronary artery. Concentration-response curves were performed in the absence (○, △, $n = 5$ for both agonists) and presence of nifedipine (●, ▲, $n = 11$ and 10 for substance P and bradykinin, respectively).

EDRF

The EDRF-releasing agents substance P, bradykinin, histamine, ionomycin and A23187 all caused concentration- and endothelium-dependent relaxation responses in U46619-precontracted human coronary artery rings.

Substance P was the most potent of the endothelium-dependent relaxants examined. Threshold responses occurred at 10–30 pM with an estimated pEC_{50} value of 9.94 ± 0.10 ($n = 11$, Table 1). The maximum relaxation response to substance P was 85.2% ± 3.7% at 3 nM ($n = 11$, Table 1, Figure 3a). Addition of 10 μM SNP caused complete relaxation of the tissue (data not shown).

Bradykinin was more potent than histamine (Table 1) but histamine was more effective, causing a maximum relaxation

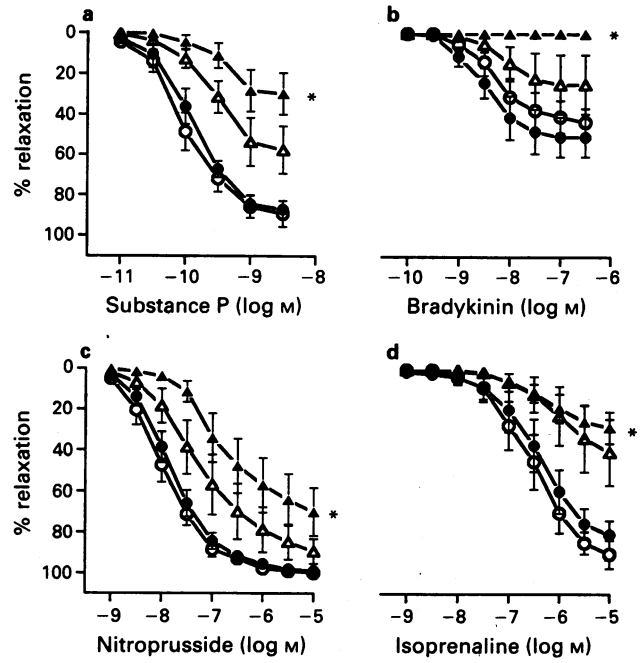


Figure 2 Effect of functional antagonism on relaxation responses in human coronary artery. Arterial rings were contracted with (○) 1 nM, (●) 3 nM, (△) 10 nM and (△) 30 nM U46619. Mean cumulative concentration-relaxation curves are shown for (a) substance P, (b) bradykinin, (c) sodium nitroprusside and (d) isoprenaline. Values are the mean ± s.e.mean of 4–6 experiments. *Indicates $P < 0.05$ (ANOVA) for maximum response in 30 nM- vs 1 nM- and 3 nM-contracted rings.

Table 1 Estimated pEC_{50} values and relaxation maxima (% R) for EDRF agonists in human coronary arteries in the absence and presence of N^G-nitro-L-arginine (L-NOARG, 0.1 mM) and N^G-monomethyl-L-arginine (L-NMMA, 0.1 mM)

		Control	*L-NOARG*	*L-NMMA*
Substance P	(pEC_{50})	9.94 ± 0.10 (11)	9.63 ± 0.08 (9)	9.69 ± 0.12 (7)
	(%R)	85.2 ± 3.7% (11)	69.5 ± 7.3% (10)	58.7 ± 7.2% (7)†
Bradykinin	(pEC_{50})	8.42 ± 0.10 (9)	8.26 ± 0.21 (6)	8.01 ± 0.25 (5)
	(%R)	46.2 ± 7.3% (7)	27.6 ± 10.9% (7)	18.5 ± 6.9% (7)†
Histamine	(pEC_{50})	7.20 ± 0.12 (7)	6.79 ± 0.14 (7)	7.11 ± 0.10 (7)
	(%R)	81.5 ± 2.6% (7)	72.8 ± 7.2% (5)	69.6 ± 11.7% (5)†
Histamine + indomethacin	(pEC_{50})	6.48 ± 0.14 (5)	5.98 ± 0.20 (4)	6.47 ± 0.32 (4)
	(%R)	75.3 ± 8.6% (5)	63.6 ± 3.1% (4)	70.3 ± 8.3% (4)
Ionomycin	(pEC_{50})	7.76 ± 0.11 (7)	7.28 ± 0.15 (6)	7.36 ± 0.18 (7)
	(%R)	87.5 ± 8.6% (7)	52.8 ± 12.3% (7)*	80.2 ± 5.4% (7)
A23187	(pEC_{50})	7.12 ± 0.15	6.63 ± 0.17 (7)	6.71 ± 0.21 (7)
	(%R)	92.8 ± 2.0% (8)	75.2 ± 5.3% (7)	68.4 ± 7.3% (7)†
SNP	(pEC_{50})	7.90 ± 0.16 (6)	7.87 ± 0.20 (4)	8.03 ± 0.27 (4)
	(%R)	100.0 ± 0.0% (6)	100.0 ± 0.0% (4)	100.0 ± 0.0% (4)

Values are mean ± s.e.mean for (n) experiments. *Indicates values significantly different from all others; †indicates values significantly different from control ($P < 0.05$, ANOVA).

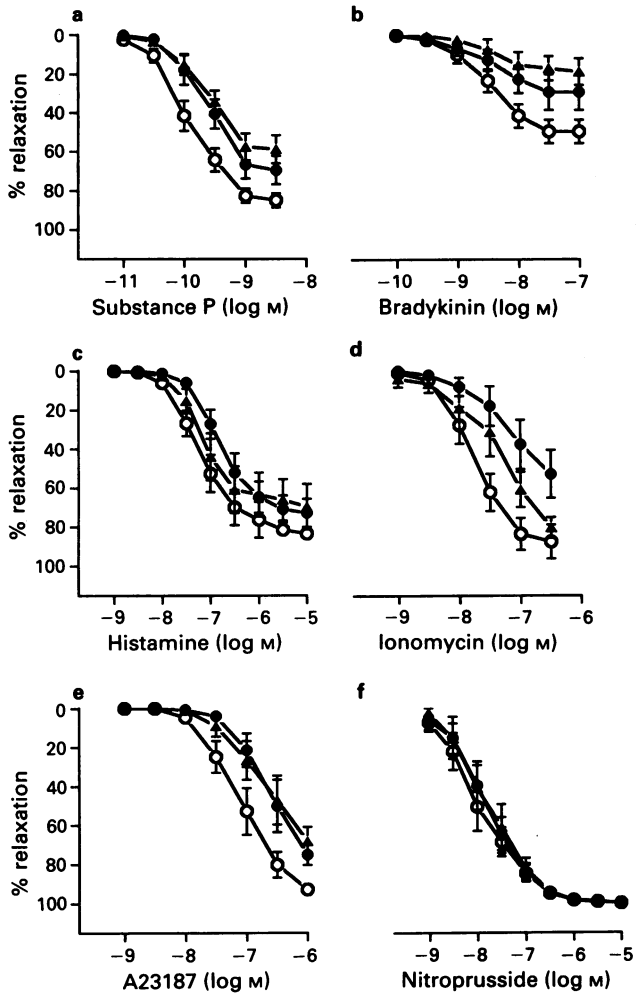


Figure 3 Mean cumulative concentration-relaxation curves for EDRF-releasing agents in human coronary artery. Arterial rings were: (○) control; (●) N^G-nitro-L-arginine-treated (0.1 mM) and (△) N^G-monomethyl-L-arginine-treated (0.1 mM). Agents examined were (a) substance P, (b) bradykinin, (c) histamine, (d) A23187, (e) ionomycin and (f) the endothelium-independent dilator, sodium nitroprusside. Mean pEC_{50} and maximum relaxation values are given in Table 1.

equal to that for substance P (Figure 3c). Bradykinin, on the other hand, caused only 46.2% ± 7.3% relaxation at 0.1 μM (Figure 3b, $n = 10$). Addition of 1 nM substance P after the bradykinin concentration-response curve caused further relaxation, resulting in a total endothelium-dependent response of 84.1% ± 4.6% relaxation ($n = 6$, data not shown). Threshold responses were obtained at concentrations of 0.3–1 nM for bradykinin and 3–10 nM for histamine.

Pretreatment of arterial rings with indomethacin (3–10 μM) did not significantly alter the responses to substance P or bradykinin ($n = 5$ and 4, respectively, data not shown) but the pEC_{50} value for histamine was significantly increased from 7.20 ± 0.12 to 6.48 ± 0.14 ($n = 5$, Table 1, $P < 0.05$, t test). The maximum response to histamine, however, was not affected by indomethacin (Table 1).

The Ca^{2+} ionophores, ionomycin and A23187, also caused near-maximal relaxation of U46619-precontracted arterial rings (Figure 3d,e). Ionomycin was more potent than A23187, with threshold responses at 3 nM, compared with 10 nM for A23187, and a greater pEC_{50} value (Table 1).

Possible release of EDRF by endothelin-1 was also examined. No relaxation responses, however, were seen over the concentration range 0.1–100 pM and at 300 pM, further contraction occurred (data not shown).

Relaxation responses to substance P, bradykinin and histamine were abolished by removal of the endothelium ($n = 2$ for each drug; data not shown). Histamine, in concentrations above 0.1 μM, caused further contraction of U46619 precontracted endothelium-denuded rings (data not shown).

SNP (10 μM) caused maximal (100%) relaxation of all arterial rings. Threshold responses were between 1–3 nM with a pEC_{50} value of 7.90 ± 0.15 nM ($n = 6$, Table 1, Figure 3f).

L-Arginine analogues

The L-arginine analogues L-NOARG and L-NMMA (both 0.1 mM) caused no contraction responses when added to uncontracted rings. Similarly, cumulative addition of either analogues (1–100 μM) following establishment of stable contractions to U46619 (3 nM) caused no significant further increases in active force compared with time controls (from 5.0 ± 1.2 g to 5.1 ± 1.2 g with 100 μM L-NOARG and from 6.8 ± 1.5 g to 7.4 ± 1.6 g with 100 μM L-NMMA; $P > 0.05$ for both, t test). In further experiments, haemoglobin (1 μM, $n = 3$) and methylene blue (10 μM, $n = 3$) also had little or no further contractile effect on the contraction to U46619.

In general, both L-NOARG and L-NMMA were poor inhibitors of relaxation responses to all EDRF-releasing agents (Table 1, Figure 3a–e). L-NMMA caused a small but significant ($P < 0.05$, ANOVA) inhibition of the maximum responses to all agents except ionomycin, which was the only agent against which L-NOARG caused a small but significant depression of the maximum response (Table 1).

Whilst L-NOARG and L-NMMA appeared to cause rightward shifts of the concentration-response curves of some of the EDRF-releasing agents, on statistical analysis, the changes in the pEC_{50} values were not significant ($P > 0.05$, ANOVA, (Table 1). The concentration-relaxation curve for SNP was unaffected by either analogue (Figure 3f).

Both the degree and pattern of inhibition by the L-arginine analogues on relaxation responses to susbtance P and bradykinin were unaffected by pretreatment with indomethacin (3–10 μM; $P > 0.05$, t test). Even with histamine responses in the presence of indomethacin, L-NOARG and L-NMMA still had no significant further inhibitory effects on either pEC_{50} values or the maximum responses (Table 1, $P > 0.05$, ANOVA, $n = 4$ for both analogues).

Discussion

This study has defined the optimal conditions for examining relaxation responses in human coronary artery *in vitro*. The two major determinants for these conditions were removal of phasic contractile activity and avoidance of functional antagonism by the agent used to precontract the tissues. Phasic contractile activity, particularly that which occurs in response to contractile agents like U46619, is characteristic of this tissue (Cocks *et al.*, 1993; Stork & Cocks, 1994). We have shown that nifedipine not only abolishes this activity, but also, importantly, has no effect on tonic contractions to U46619 (Stork & Cocks, 1994). Thus nifedipine allowed us to determine full concentration-dependent relaxation-response curves to various relaxing agents and evaluate the importance of the level of precontraction on these responses. Nifedipine had no inhibitory effect on relaxation responses to any EDRF-releasing agents used in this tissue, in agreement with previous studies in dog coronary artery (Angus & Cocks, 1989) and rat aorta (Schoeffter & Miller, 1986).

Functional antagonism was found to be an important factor in determining the maximum response to endothelium-dependent and independent vasorelaxants. There is little uniformity in the literature on the constrictors used, their concentrations and the level of active force present when determining relaxation responses in human isolated coronary artery (compare Förstermann *et al.*, 1986; 1988;

Chester *et al.*, 1990a,b). We found that above approximately 40% of the U46619-maximum in this tissue, functional antagonism became an increasingly influential factor. The pattern of relaxant curve shifts in response to increasing levels of active force appeared to fit the type IIb model of functional antagonism proposed by Mackay (1981): i.e. depression of the maximum response, but no shift in the location of the curve.

With the optimal conditions for measuring relaxation responses in the human coronary artery defined, we were in a position to clarify possible roles for NO in relaxations to various EDRF-releasing agents.

Substance P was the most potent EDRF-releasing agent examined in this study. The results obtained for this neuropeptide correlate well with those of Chester *et al.* (1990a) in similar preparations, although in our study, substance P was more potent (by approximately a half- to one log unit). Indeed, substance P appears to be the most potent of all dilators in human coronary artery, including the related neuropeptide, calcitonin gene-related peptide (CGRP; McEwan *et al.*, 1986; Franco-Cereceda & Lundberg, 1987) and has been found not to be affected by cyclosporin treatment (O'Neil *et al.*, 1991a,b).

Histamine, although less potent, was as effective in relaxing human coronary artery as substance P, as indicated by similar maximum responses. Toda (1987) suggested that relaxation to histamine was mediated by both H_1 receptors on the endothelium and H_2 receptors in the smooth muscle, but that the response was complicated by contraction via H_1 receptors on the muscle at high concentrations of histamine (0.1 μM and above). Consequently, biphasic curves have often been reported (Toda, 1987; Toda & Okamura, 1989). In this study, however, no contraction responses were observed, even at high concentrations of histamine (1–10 μM), except in the absence of endothelium, indicating that EDRF release (via endothelial H_1 receptors) and stimulation of the (relaxing) H_2 receptors was overriding the direct constrictor effect on the smooth muscle.

Bradykinin, whilst relaxing the arterial rings, caused less than 50% relaxation. This result confirms previous work by Förstermann *et al.* (1988) and Chester *et al.* (1990b) but contradicts the findings of Toda & Okamura (1989), who reported near-maximal relaxation responses to bradykinin. The ability of substance P to cause further relaxation after the maximum response to bradykinin was obtained, indicated that the decreased response with bradykinin was probably not due to factors influencing the release and action of EDRF but that bradykinin is less effective at releasing EDRF in this tissue than the other EDRF agonists (see Martin *et al.*, 1992).

The L-arginine analogues L-NOARG and L-NMMA surprisingly had no effect on either uncontracted or U46619-contracted vessels. Similarly, haemoglobin and methylene blue (two EDRF inhibitors with different mechanisms of action; see Angus & Cocks, 1989) also had little or no contractile effect. This indicates that in the human coronary artery, basal or tonic release of EDRF is poor, at least under *in vitro* conditions. The use of the L-arginine analogues to determine basal release of EDRF, however, has been questioned (Cocks & Angus, 1991).

More surprisingly, L-NOARG and L-NMMA had little antagonistic effects on the relaxation responses to a variety of EDRF-releasing agents, including bradykinin, which had the lowest relative efficacy. Previous findings in other vascular tissues show L-NOARG and L-NMMA to be effective blockers of EDRF release, with L-NOARG or its metabolic precursor L-NAME more potent and effective than L-NMMA (Mülsch & Busse, 1990; Rees *et al.*, 1990). However, this was not demonstrated in our study and in fact, the trend was reversed, with L-NMMA being more effective than L-NOARG in decreasing the maximum response to most of the relaxants.

Martin *et al.* (1992) pointed out that there are a number of factors which influence the release of EDRF, its blockade by the L-arginine analogues and the final, observed effect. Cell entry and enzyme affinity (which could be affected by isoform differences) obviously characterize the analogues and influence their effectiveness. Levels of intracellular L-arginine can also influence the effectiveness of the L-arginine analogues at inhibiting the enzyme, as they compete for the same site. Agonist-receptor coupling and enzyme activation characteristics of the EDRF-releasing agent used also affect the observed response, as do target cell activation characteristics (see Martin *et al.*, 1992).

The model of Martin *et al.* (1992) for EDRF release and action, together with L-arginine analogue interaction and pharmacokinetics, predicts parallel displacement of high-efficacy agonists and combination of curve-shifts with maxima depression for low-efficacy agonists. In our study, however, only depressed maxima were observed for all EDRF-releasing agonists examined, probably indicating low-efficacy agonists. This is supported by a small displacement to the right and a significant reduction in the maximum of the relaxation curves to substance P and bradykinin with functional antagonism. Correspondingly, the L-arginine analogues could be expected to be effective blockers of EDRF release in this tissue. Nevertheless, the response to bradykinin, the least-effective agent in this tissue, could not be abolished in the presence of L-NOARG and L-NMMA, which, if bradykinin-induced relaxation were mediated by nitric oxide, suggests ineffective blockade of the enzyme. Further, decreasing the pEC_{50} for histamine with indomethacin also failed to increase the ability of the L-arginine analogues to shift the histamine curve or depress the maximum response. These results support the idea that human coronary artery may either possess a different isoform of nitric oxide synthase or a different transduction pathway, or other factors apart from nitric oxide may contribute to the endothelium-dependent relaxation response.

The involvement of prostacyclin in the relaxation response to the EDRF-releasing agents used here was found to be minor. Only responses to histamine, a known releaser of prostacyclin, were affected by cyclo-oxygenase inhibition with indomethacin, confirming previous work which found no evidence for a role for prostacyclin in human coronary artery *in vitro* (Chester *et al.*, 1990a; Toda, 1987). This is despite using the constrictor agent on which prostacyclin and EDRF are at their most effective (U46619; Noll *et al.*, 1991). The possibility that another factor, endothelium-derived hyperpolarizing factor (EDHF; Taylor & Weston, 1988) contributes to the relaxation response cannot be ruled out and its role in human coronary artery requires further research.

The physiological role of EDRF remains uncertain, although according to Moncada *et al.* (1991) '... the cardiovascular system is in a constant state of active vasodilatation dependent on the generation of [nitric oxide].' Our results indicate that in human coronary artery, at least *in vitro*, EDRF is released by a number of vasodilator agents and is relatively unaffected by the L-arginine analogues L-NOARG and L-NMMA. If nitric oxide is the EDRF released in response to these agonists, then the possibility of a different transduction pathway in this tissue may account for the poor inhibition of the responses by the L-arginine analogues.

We gratefully acknowledge the assistance of Mr Don Esmore, Mr Robin McEgan, Mr Arthur Preovolos and all the team of the Alfred Hospital Heart & Lung Transplant Service. This work was supported by institute grants from the National Health and Medical Research Council of Australia and from Glaxo Australia.

References

ANGUS, J.A. & COCKS, T.M. (1989). Endothelium-derived relaxing factor. *Pharmacol. Ther.*, **41**, 303–351.

CHESTER, A.H., O'NEIL, G.S., TADJKARIMI, S., PALMER, R.M.J., MONCADA, S. & YACOUB, M.H. (1990a). The role of nitric oxide in mediating endothelium dependent relaxations in the human epicardial coronary artery. *Int. J. Cardiol.*, **29**, 305–309.

CHESTER, A.H., O'NEIL, G.S., MONCADA, S., TADJKARIMI, S. & YACOUB, M.H. (1990b). Low and basal release of nitric oxide in atherosclerotic epicardial coronary arteries. *Lancet*, **336**, 897–900.

COCKS, T.M. & ANGUS, J.A. (1991). Evidence that contractions of isolated arteries by L-NMMA and NOLA are not due to inhibition of basal EDRF release. *J. Cardiovasc. Pharmacol.*, **17**, Suppl. 3, S159–S164.

COCKS, T.M., KEMP, B.K., PRUNEAU, D. & ANGUS, J.A. (1993). Comparison of contractile responses to 5-hydroxytryptamine and sumatriptan in human isolated coronary artery: synergy with thromboxane A_2-receptor agonist, U46619. *Br. J. Pharmacol.*, **110**, 260–368.

CROSSMAN, D.D., LARKIN, S.W., FULLER, R.W., DAVIES, G.J. & MASERI, A. (1989). Substance P dilates epicardial coronary arteries and increases coronary blood flow in humans. *Circulation*, **80**, 475–484.

ELGHOZI, J.-L. & HEAD, G.A. (1990). Spinal noradrenergic pathways and pressor response to central angiotensin II. *Am. J. Physiol.*, **258**, H240–H246.

FÖRSTERMANN, U., MÜGGE, A. & FRÖLICH, J.C. (1986). Endothelium-dependent relaxation of human epicardial coronary arteries: frequent lack of effect of acetylcholine. *Eur. J. Pharmacol.*, **128**, 277–281.

FÖRSTERMANN, U., MÜGGE, A., ALHEID, U., HAVERICH, A. & FRÖLICH, J.C. (1988). Selective attenuation of endothelium-mediated vasodilation in atherosclerotic human coronary arteries. *Circ. Res.*, **62**, 185–190.

FRANCO-CERECEDA, A. & LUNDBERG, J.M. (1987). Potent effects of neuropeptide Y and calcitonin gene-related peptide on human coronary vascular tone *in vitro*. *Acta Physiol. Scand.*, **131**, 159–160.

FURCHGOTT, R.F. & ZAWADZKI, J.V. (1980). The obligatory role of endothelial cells in the relaxation of arterial smooth muscle by acetylcholine. *Nature*, **288**, 373–376.

KUSHWAHA, S.S., CROSSMAN, D.C., BUSTAMI, M., DAVIES, G.J., MITCHELL, A.G., MASERI, A. & YACOUB, M.H. (1991). Substance P for evaluation of coronary endothelial function after cardiac transplantation. *J. Am. Coll. Cardiol.*, **17**, 1537–1544.

LUDMER, P.L., SELWYN, A.P., SHOOK, T.L., WAYNE, R.P., MUDGE, G.H., ALEXANDER, R.W. & GANZ, P. (1986). Paradoxical vasoconstriction induced by acetylcholine in atherosclerotic coronary arteries. *New Engl. J. Med.*, **315**, 1046–1051.

MCEWAN, J., LARKIN, S., DAVIES, G., CHIERCHIA, S., BROWN, M., STEVENSON, J., MACINTYRE, I. & MASERI, A. (1986). Calcitonin gene-related peptide: a potent dilator of human epicardial coronary arteries. *Circulation*, **6**, 1243–1247.

MACKAY, D. (1981). An analysis of functional antagonism and synergism. *Br. J. Pharmacol.*, **73**, 127–134.

MARTIN, G.R., BOLOFO, M.L. & GILES, H. (1992). Inhibition of endothelium-dependent vasorelaxation by arginine analogues: a pharmacological analysis of agonist and tissue dependence. *Br. J. Pharmacol.*, **105**, 643–652.

MONCADA, S., PALMER, R.M.J. & HIGGS, E.A. (1991). Biosynthesis and endogenous roles of nitric oxide. *Pharmacol. Rev.*, **43**, 109–142.

MÜLSCH, A. & BUSSE, R. (1990). N^G-nitro-L-arginine (N^5-[imino (nitroamino)methyl]-L-ornithine) impairs endothelium-dependent dilations by inhibiting cytosolic nitric oxide synthesis from L-arginine. *Naunyn-Schmied. Arch. Pharmacol.*, **341**, 143–147.

NOLL, G., BÜHLER, F.R., YANG, Z. & LÜSCHER, T.F. (1991). Different potency of endothelium-derived relaxing factors against thromboxane, endothelin, and potassium chloride in intramyocardial porcine coronary arteries. *J. Cardiovasc. Pharmacol.*, **18**, 120–126.

O'NEIL, G.S., CHESTER, A.H., KUSHWAHA, S., ROSE, M., TADJKARIMI, S. & YACOUB, M.H. (1991a). Cyclosporin treatment does not impair the release of nitric oxide in human coronary arteries. *Br. Heart J.*, **66**, 212–216.

O'NEIL, G.S., CHESTER, A.H., ROSE, M., TADJKARIMI, S. & YACOUB, M.H. (1991b). The effect of cyclosporine on the release of endothelium-derived relaxing factor from isolated human epicardial coronary arteries. *Transplant.*, **51**, 736–738.

PALMER, R.M.J., ASHTON, D.S. & MONCADA, S. (1988). Vascular endothelial cells synthesize nitric oxide from L-arginine. *Nature*, **333**, 664–666.

PALMER, R.M.J., FERRIGE, A.G. & MONCADA, S. (1987). Nitric oxide release accounts for the biological activity of endothelium-derived relaxing factor. *Nature*, **327**, 524–526.

REES, D.D., PALMER, R.M.J., HODSON, H.F. & MONCADA, S. (1990). Characterization of three inhibitors of endothelial nitric oxide synthase *in vitro* and *in vivo*. *Br. J. Pharmacol.*, **101**, 746–752.

SCHOEFFTER, P. & MILLER, R.C. (1986). Role of sodium-calcium exchange and effects of calcium entry blockers on endothelial-mediated responses in rat isolated aorta. *Mol. Pharmacol.*, **30**, 53–57.

STORK, A.P. & COCKS, T.M. (1992). Endothelium-derived relaxing factor (EDRF) in human coronary artery *in vitro*. *Clin. Exp. Pharmacol. Physiol.*, Suppl. 21, 68.

STORK, A.P. & COCKS, T.M. (1994). Pharmacological reactivity of human epicardial coronary arteries: phasic and tonic responses to vasoconstrictor drugs differentiated by nifedipine. *Br. J. Pharmacol.*, **113**, 1093–1098.

TAYLOR, S.G. & WESTON, A.H. (1988). Endothelium-derived hyperpolarizing factor: a new endogenous inhibitor from the vascular endotheliu. *Trends Pharmacol. Sci.*, **9**, 272–274.

TODA, N. (1987). Mechanism of histamine actions in human coronary arteries. *Circ. Res.*, **61**, 280–286.

TODA, N. & OKAMURA, T. (1989). Endothelium-dependent and -independent responses to vasoactive substances of isolated human coronary arteries. *Am. J. Physiol.*, **257**, H988–H995.

VITA, J.A., TREASURE, C.B., NAGEL, E.G., MCLENACHAN, J.M., FISH, R.D., YEUNG, A.C., VEKSHTEIN, V.I., SELWYN, A.P. & GANZ, P. (1990). Coronary vasomotor response to acetylcholine relates to risk factors for coronary artery disease. *Circulation*, **81**, 491–497.

WALLENSTEIN, S., ZUCKER, C.L. & FLEISS, J.L. (1980). Some statistical methods useful in Circulation Research. *Circ. Res.*, **47**, 1–9.

YAMAMOTO, H., YOSHIMURA, H., NOMA, M., KAI, H., SUZUKI, S., TAJIMI, T., SUGIHARA, M. & KIKUCHI, Y. (1992). Preservation of endothelium-dependent vasodilation in the spastic segment of the human epicardial coronary artery by substance P. *Am. Heart J.*, **123**, 298–303.

YASUE, H., MATSUYAMA, K., MATSUYAMA, K., OKUMARA, K., MORIKAMI, Y. & OGAWA, H. (1990). Responses of angiographically normal human coronary arteries to intracoronary injection of acetylcholine by age and segment. *Circulation*, **81**, 482–490.

ZEIHER, A.M., DREXLER, H., WOLLSCHLÄGER, H. & JUST, H. (1991). Modulation of coronary vasomotor tone in humans: progressive endothelial dysfunction with different early stages of coronary atherosclerosis. *Circulation*, **83**, 391–401.

(Received September 20, 1993
Revised February 16, 1994
Accepted February 17, 1994)

Br. J. Pharmacol. (1994), **113**, 1105–1112 © Macmillan Press Ltd, 1994

Blockade of noradrenaline-induced constrictions by yohimbine and prazosin differs between consecutive segments of cutaneous arteries in guinea-pig ears

J.L. Morris

Centre for Neuroscience, and Department of Anatomy & Histology, School of Medicine, Flinders University of South Australia, G.P.O. Box 2100, Adelaide, S.A. 5001, Australia

1 The study has examined the receptors mediating constriction produced by brief local application of noradrenaline (NA) to cutaneous arteries and arterioles in the ear vasculature of anaesthetized guinea-pigs. The innervation of the corresponding vascular segments has been examined immunohistochemically at the conclusion of the pharmacological experiments.

2 Small arteries of branch order 4 (4°, 40–110 μm internal diameter) were more sensitive to the vasoconstrictor action of NA than were more proximal arteries of branch order 3 (3°, 60–150 μm internal diameter), or more distal arteries and arterioles of branch orders 5 to 7 (5°–7°, 18– 85 μm internal diameter). This higher sensitivity of 4° arteries was maintained after blockade of neuronal uptake with desipramine (1 μM), and after blockade of β-adrenoceptors with propranolol (1 μM).

3 NA-induced vasoconstrictions of distal arterioles (5°–7°) were abolished or greatly reduced by yohimbine (1 μM). The blockade by yohimbine decreased progressively with increasing vessel diameter of proximal arteries, while the blockade by prazosin (1 μM) increased progressively in arteries >40 μm diameter.

4 In 3° and 4° arteries, a substantial component (approximately 50%) of NA-induced vasoconstrictions remained after combined treatment with yohimbine and prazosin, in the presence or absence of desipramine. These constrictions were not further reduced by benextramine (1–10 μM), but were abolished by dihydroergotamine (1–10 μM). Constrictions induced by ATP (0.1–1 mM) were not affected by dihydroergotamine.

5 5-Hydroxytryptamine (3–100 μM) had a variable effect on 3° and 4° arteries including: concentration-dependent constrictions ($n = 3$); small constrictions at some concentrations, and dilatations or no change in diameter at other concentrations ($n = 6$); concentration-dependent dilatations only ($n = 3$). The 5-HT_2 receptor antagonist, ketanserin (0.1–0.3 μM), did not affect NA-induced constrictions.

6 In 16 arterial segments ranging from 3° arteries to 6° arterioles, there was a significant correlation between the presence of neuropeptide Y-immunoreactive (NPY-IR) sympathetic axons and the degree of blockade of NA-induced constrictions by yohimbine, prazosin and dihydroergotamine.

7 These results demonstrate marked differences in the postsynaptic adrenoceptors mediating vasoconstriction to a bolus of NA applied briefly to the adventitial surface of different segments of the cutaneous vasculature of the guinea-pig ear. Furthermore, the presence or absence of adrenoceptors sensitive to blockade by yohimbine or prazosin is related to the proportion of sympathetic axons innervating each vascular segment which contain NPY-IR.

Keywords: Adrenoceptors; vasoconstriction; cutaneous arteries; microcirculation; video microscopy; noradrenaline; prazosin; yohimbine; 5-hydroxytryptamine; dihydroergotamine

Introduction

The cutaneous vasculature supplying the ears and feet of guinea-pigs is innervated by several different populations of sympathetic neurones, which vary in the neuropeptides which are co-localized with noradrenaline (NA). In particular, neuropeptide Y (NPY) is co-localized with NA and dynorphin-related peptides in sympathetic neurones supplying proximal cutaneous arteries, but NPY is absent from sympathetic neurones supplying distal arterioles and arteriovenous anastomoses (Gibbins & Morris, 1990). Recent pharmacological studies from this laboratory have shown that NA constricts all arterial segments in the guinea-pig ear, but NPY constricts only those arterial segments which are innervated by NPY-containing sympathetic neurones (Morris, 1994a). Thus, there appears to be some relationship between the type of neurone innervating a vascular segment, and the type of receptors present on the postsynaptic smooth muscle membrane.

Previous studies on cutaneous arteries from laboratory animals and man have demonstrated that both α_1- and α_2-adrenoceptors may be present, although α_1-adrenoceptors seem to predominate in proximal cutaneous arteries while α_2-adrenoceptors become more prominent in distal cutaneous arteries (Flavahan *et al.*, 1987; Medgett & Ruffolo, 1988; Nielsen *et al.*, 1989; Parkinson *et al.*, 1992; Stephens *et al.*, 1992). A recent study from this laboratory has demonstrated that α_1-adrenoceptors mediate constriction produced by NA in the guinea-pig main ear artery (Morris, 1994b). The present study set out to investigate the adrenoceptors mediating NA constrictions of medium to small diameter cutaneous arteries, and of distal arterioles, in an *in vivo* preparation of the guinea-pig ear. Furthermore, the innervation of different vascular segments has been studied immunohistochemically at the conclusion of the pharmacological studies, to examine directly whether a correlation exists between the characteristics of NA receptors and the subpopulations of sympathetic axons present in each arterial segment of this cutaneous vascular bed.

Methods

White-eared guinea-pigs of either sex (250–350 g body weight), were anaesthetized initially with a mixture of ketamine (40 mg kg^{-1}, i.m.), xylazine (8 mg kg^{-1}, i.m.) and diazepam (2.5 mg kg^{-1}, i.p.). Animals were treated preoperatively with atropine (0.14 mg kg^{-1}) to reduce secretion in the airways. Animals were ventilated (SAR-830P Small Animal Ventilator, CWE Inc., U.S.A.) via a tracheal cannula at a rate of 58–60 cycles min^{-1} and tidal volume of 2 ml, with room air plus sufficient oxygen to maintain arterial P_{O_2} at 90–110 mmHg (see below). Neuromuscular blockade was not used. Surgical anaesthesia was maintained throughout the experiments by continuous infusion of ketamine (30–40 mg kg^{-1} h^{-1}, i.m.), and was monitored by frequent testing of limb-withdrawal and corneal-blink reflexes and continuous monitoring of arterial blood pressure via a femoral artery cannula. Blood gases were tested approximately every 2 h after withdrawl of 150 µl of blood from the femoral artery cannula (Department of Clinical Biochemistry, Flinders Medical Centre). This volume of blood was replaced with buffered saline. Experiments were included in the present analysis only if cardiovascular parameters stayed stable throughout the experimental period. Core temperature was maintained at 37°C by a homeothermic blanket with a rectal temperature probe (Harvard).

The left cervical sympathetic nerve trunk was resected at the mid-cervical level, to remove tonic sympathetic effects on the ear vasculature, as well as any indirect effects of the agonists in altering tonic sympathetic constriction. The left cervical vagus also was resected, which helped maintain a steady heart rate and pulse pressure.

Regions of the dorsal ear vasculature were exposed by removing the hair with depilatory cream (active ingredient, thioglycollate), then peeling off small areas of the dorsal skin using fine forceps (see Morris, 1994a). Animals were placed on a microscope stage with the left ear submerged in a jacketed perspex bath. The left ear was superfused with HEPES-buffered balanced salt solution (composition in mM: NaCl 146, KCl 4.7, $MgSO_4$ 0.6, $NaHCO_3$ 1.6, NaH_2PO_4 0.13, $CaCl_2$ 2.5, glucose 7.8, N-2-hydroxyethylpiperazine-N-2-ethanesulphonic acid (HEPES) 20; ascorbic acid 0.1) bubbled with 100% O_2 at pH 7.40 and 28°C (the mean surface temperature of the right ear). Animals were left to stabilize for 1–2 h before experiments were started.

Arterial vessels were imaged with a Nikon × 10 water immersion lens, or an Olympus × 20 water immersion lens, attached to a Leitz Laborlux microscope, using transillumination. In some experiments up to four different arterial segements in the same ear were examined. The position of each vessel in the arterial tree was mapped carefully, and designated a branching order, with the main ear artery being the first order artery (1°, see Morris, 1994a). Images were transmitted to a high resolution video screen (National WV-54100) by a Panasonic CCD WV-BL600 camera, and were recorded on S-VHS tape using a Panasonic 7750 video recorder. The internal diameter (i.d.) of arterial segments was determined on line by the DIAMTRAK DTVIVO programme (developed and kindly supplied by Dr T.O. Neild; see Morris, 1994a). In the absence of sympathetic tone, and with superfusion, the resting arterial diameter of arterial vessels in animals with stable blood pressure and blood gases, was 75–100% of the maximum (determined by addition of $NaNO_2$ at the conclusion of experiments). Percentage decreases in diameter were determined by expressing the peak decrease in diameter as a proportion of the average diameter in the 2 min period prior to agonist application. When arteries exhibited regular oscillations in diameter (vasomotion), the diameter before and after addition of an agonist was determined from the mid point of each oscillation.

Superfusion of the experimental ear was stopped 3 min before addition of an agonist, to allow equilibration of the bath fluid (3 ml volume). Small volumes (32–70 nl) of agonists were then applied to the adventitial surface of restricted regions of the ear vasculature by delivery from a micropipette (20–30 µm tip diameter) using a Drummond 'Nanoject' motorized injector. The pipette tip was angled at approximately 45°, and was positioned precisely by means of a motorized micromanipulator with calibrated step size (Märzhäuser MS314). Agonists were diluted to a known concentration in HEPES-buffered balanced salt solution containing the food dye GREEN S142 (CI 44090; sodium 5-[4-dimethylamino-α-(4-dimethylaminio-cyclohexa-2,5-dienylidene) benzyl]-6-hydroxy-7-sulphonatonaphthalene-2-sulphonate; 6.5 mg ml^{-1}). This allowed verification of the area of vascular bed reached by each delivery of agonist. The green agonist solution appeared to displace the clear HEPES solution at the site of application for a period of 3–5 s, and thus the peak concentration of agonist reaching the postsynaptic receptors was likely to be only slightly less than that in the pipette. For arteries of all sizes, the solution covered the full width of the vessel for a length of approximately 100 µm. Application of this concentration of the green dye alone had no effect on arterial diameter and did not alter the magnitude of constrictions produced by a range of agonists (noradrenaline, neuropeptide Y, adenosine 5'-triphosphate).

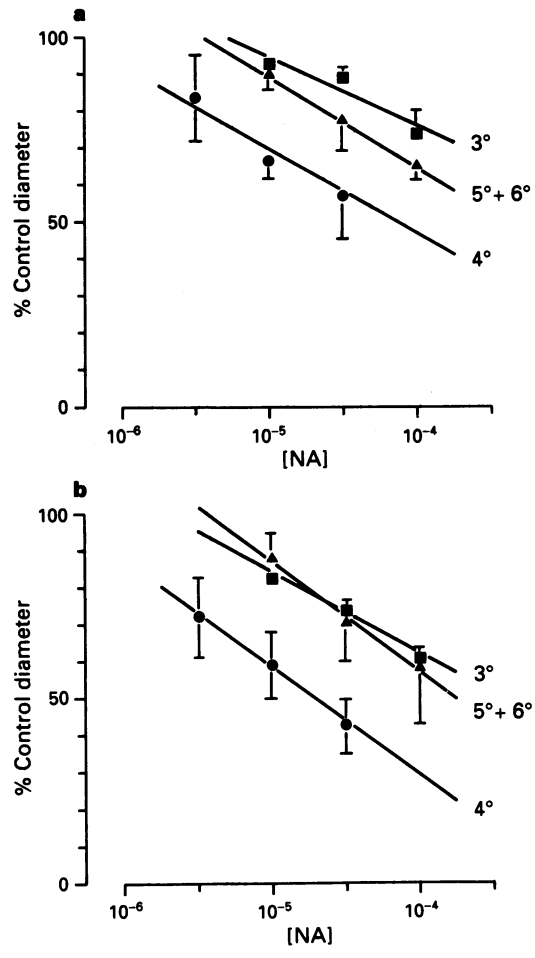


Figure 1 Constrictions produced by local application of 50 nl of a range of noradrenaline (NA) concentrations to 12 vessels from 10 animals. Data points represent the mean (± s.e.mean) percentage of resting (control) diameter after application of each concentration of NA to 3 or 4 arteries; points without s.e.mean indicate individual values. Each vessel was tested with the same concentrations of NA both before (a) and after (b) 1 µM desipramine: (■) 3° arteries; (●) 4° arteries; (▲) pooled values for 5° and 6° arteries. Three-way ANOVA showed significant effect of arterial branch order ($F_{(2,30)} = 13.57$, $P = 0.0001$), significant effect of desipramine ($F_{(1,30)} = 15.7$, $P = 0.02$), and no interaction between arterial branch order and desipramine treatment ($F_{(2,30)} = 0.55$, $P = 0.6$).

Non cumulative concentration-response curves were constructed by changing the concentration of agonist solution in the micropipette. At least 20 min was left between successive applications of agonists to the same arterial segment. At least 2 control concentration-response curves were performed on each vessel, to confirm that responses were not changing with time alone. Antagonist drugs were added to the reservoir of HEPES solution used to superfuse the ear for at least 30 min before retesting agonists. No changes in arterial blood pressure were observed after addition of agonists or antagonists to the exterior of the ear vasculature, indicating that significant amounts of these agents did not enter the general circulation.

Drugs used were: adenosine-5'-triphosphate (ATP); benextramine hydrochloride; desipramine hydrochloride; dihydroergotamine tartrate; 5-hydroxytryptamine sulphate (5-HT); noradrenaline hydrochloride (NA; arterenol); prazosin hydrochloride; propranolol hydrochloride; yohimbine hydrochloride, all obtained from Sigma Chemical Company, St. Louis, MO, U.S.A.; and ketanserin, a gift from Janssen-Cilag Pty. Ltd.

At the conclusion of experiments, a lethal dose of ketamine was injected, animals were disconnected from the ventilator and were exsanguinated via the femoral artery cannula. These experiments have been approved by the Flinders University Animal Ethics Committee.

Some arterial vessels subsequently were fixed in Zamboni's solution and processed for double-labelling immunohistochemistry to demonstrate immunoreactivity to tyrosine hydroxylase (TH) and neuropeptide Y (NPY) (see Gibbins & Morris, 1990). The preparations were examined with high magnification using an Olympus Vanox microscope fitted with appropriate filters for double-labelling immunofluorescence. The proportion of perivascular axons with immunoreactivity (IR) to TH which also had NPY-IR was estimated, and was classified semi-quantitatively as 'very few' (no axons, or only one TH-IR axon with NPY-IR), 'some' (about half of the TH-IR axons with NPY-IR) or 'most or all' (more than 75% of TH-IR axons with NPY-IR).

Groups of data were compared by 1-, 2- or 3-way analysis of variance (ANOVA) using the GLM procedure, followed by contrast analysis (SAS, Release 6.04, SAS Institute, Cary, N.C., U.S.A.) on a personal computer.

Results

Responses to noradrenaline

Arterial segments were constricted by brief local application of 50 nl of noradrenaline (NA) in the concentration range 1–100 μM. These NA concentrations were 10–100 times greater than those needed to produce constriction in response to bath application of NA to the whole ear (see Morris, 1994a). There was a consistent difference in the sensitivity of different segments to NA. Arterial vessels of branch order 4 (4°) were constricted to a greater degree by NA (3–100 μM) than were more proximal (3°), or more distal (5°, 6°, 7°), arterial segments. In a goup of 11 arterial segments from 10 animals, where NA partial concentration-response curves were constructed, a 3 to 10 times higher concentration of NA was required to produce a given percentage decrease in diameter of 3° arteries, or 5° and 6° arteries, than was required to constrict 4° arteries (Figure 1a). This was confirmed in a larger sample of 67 vessels where there was a significant effect of branch order on the magnitude of cons-

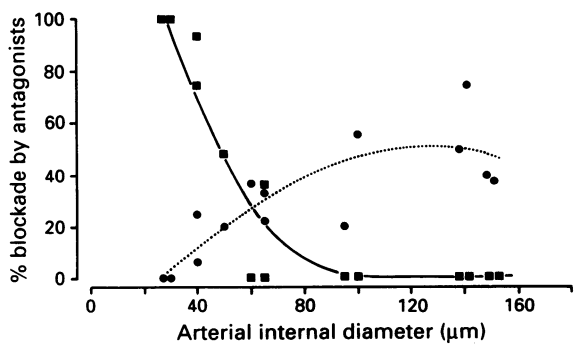


Figure 2 Data from 14 arterial vessels of various resting internal diameters, showing the percentage reduction in a control constriction produced by 50 nl of 10 μM noradrenaline (NA) after treatment with 1 μM yohimbine (■), and subsequent treatment of the same vessels with 1 μM prazosin (●). Lines of best fit for yohimbine data (solid line) and prazosin data (dotted line) were determined by curvilinear regression.

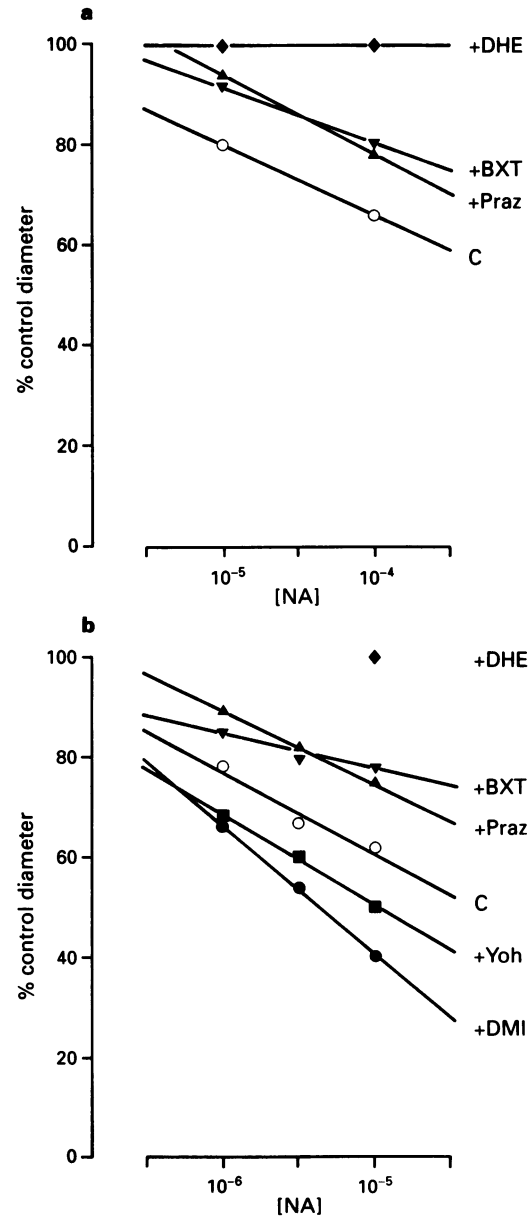


Figure 3 Representative partial concentration-response curves for noradrenaline (NA)-induced constrictions of (a) a 3° artery and (b) a 4° artery, showing effects of sequential addition of a range of blocking drugs. Control NA (C) constrictions shown (○), expressed as % of resting (C) diameter. (a) NA constrictions after addition of 1 μM prazosin (+ Praz, ▲), plus 1 μM benextramine (+ BXT, ▼), plus 10 μM dihydroergotamine (+ DHE, ◆). (b) NA constrictions after addition of 1 μM desipramine (+ DMI, ●), plus 1 μM yohimbine (+ Yoh, ■), plus 1 μM prazosin (Praz, ▲), plus 1 μM benextramine (+ BXT, ▼), plus 10 μM dihydroergotamine (+ DHE, ◆).

trictions produced by 50 nl of 10 μM NA (1-way ANOVA, $F_{(3,63)} = 3.16$, $P = 0.03$). The constriction of 4° arteries was significantly greater than constriction of 6° and 7° vessels (Tukey's test for multiple comparisons, $P < 0.05$).

Pretreatment with the neuronal uptake blocker, desipramine (1 μM), produced a significant leftward shift in NA concentration-response curves in all 4° and 3° arteries (Figure 1). The effect of desipramine was inconsistent in 5° and 6° arterial vessels ($n = 4$). NA constrictions were reduced in 2 vessels, unchanged in one vessel and enhanced in another. However, the higher sensitivity of 4° arteries to NA compared with 3°, or 5° and 6° arteries, was not altered by desipramine treatment (Figure 1b). Because desipramine may have had some α-blocking action, particularly in arterioles where NA constrictions were sometimes reduced, it was not routinely added to the bathing solution. Subsequent addition of propranolol (1 μM) produced no further change in the constrictions produced by NA ($n = 8$), therefore the higher sensitivity of 4° arteries to NA also was maintained after blockade of β-adrenoceptors.

Effects of yohimbine and prazosin

The adrenoceptor antagonists, yohimbine and prazosin, were tested for their relative potencies in blocking NA-induced constrictions in different arterial segments in a group of 14 vessels, in the absence of desipramine. Addition of antagonists did not produce systematic changes in resting arterial diameter (see Figures 4,5). Yohimbine (1 μM) treatment virtually abolished NA constrictions in distal arterioles < 40 μm i.d. (Figures 2,4,6). sometimes revealing a very small dilatation (Figure 4b). Yohimbine produced progressively less blockade in more proximal arteries of increasing diameter (Figures 2,4,6). Cumulative addition of 1 μM prazosin produced progressively greater reductions of yohimbine-resistant constrictions in arterial vessels of decreasing branch order (ie. increasing diameter; Figures 2,3,5). However, a combination of yohimbine and prazosin never abolished constrictions produced by NA (1–10 μM) in arteries > 40 μm i.d. (3° and 4° arteries; Figures 2,3,5,6). Furthermore, these high concentrations of receptor antagonists produced only small, parallel shifts to the right in NA concentration-response curves (Figure 3). Qualitatively similar results were obtained in a further set of 8 experiments testing yohimbine and prazosin in the presence of desipramine (eg. Figure 3b).

The immunohistochemical localization of immunoreactivity (IR) to tyrosine hydroylase (TH) and NPY was investigated in 16 arterial segments from 11 animals at the conclusion of pharmacological experiments quantifying the effects of yohimbine and prazosin (Figures 4,5). Vessels were placed in one of three groups according to semi-quantitative estimates of the proportion of TH-IR perivascular axons containing NPY-IR (see Methods). The mean percentage reduction in the initial constriction produced by yohimbine, and then subsequent reduction produced by prazosin, was calculated for each group. The percentage of the initial constriction resistant to blockade by yohimbine and prazosin also was calculated for each vessel. This analysis showed a clear inverse relationship between the presence of NPY-IR axons and the presence of postsynaptic adrenoceptors sensitive to yohimbine (1-way ANOVA, $F_{(2,13)} = 100.6$, $P = 0.0001$). In contrast, there was a positive relationship between the presence of NPY-IR axons, and the presence of prazosin-sensitive adrenoceptors ($F_{(2,13)} = 14.4$, $P = 0.0005$) and of adrenoceptors resistant to yohimbine and prazosin ($F_{(2,13)} = 11.7$, $P = 0.001$; Figure 6).

Effects of dihydroergotamine

Attempts were made to produce further blockade of NA-induced constrictions resistant to yohimbine and prazosin by use of the non-competitive α-adrenoceptor antagonist, benextramine (1–10 μM). In 7 experiments performed on 3° and 4° arteries, benextramine reduced NA constrictions remaining after yohimbine and prazosin in only one artery (reduced by 25%); no further reduction was obtained in the other 6 arteries (Figure 3). The only antagonist tested which pro-

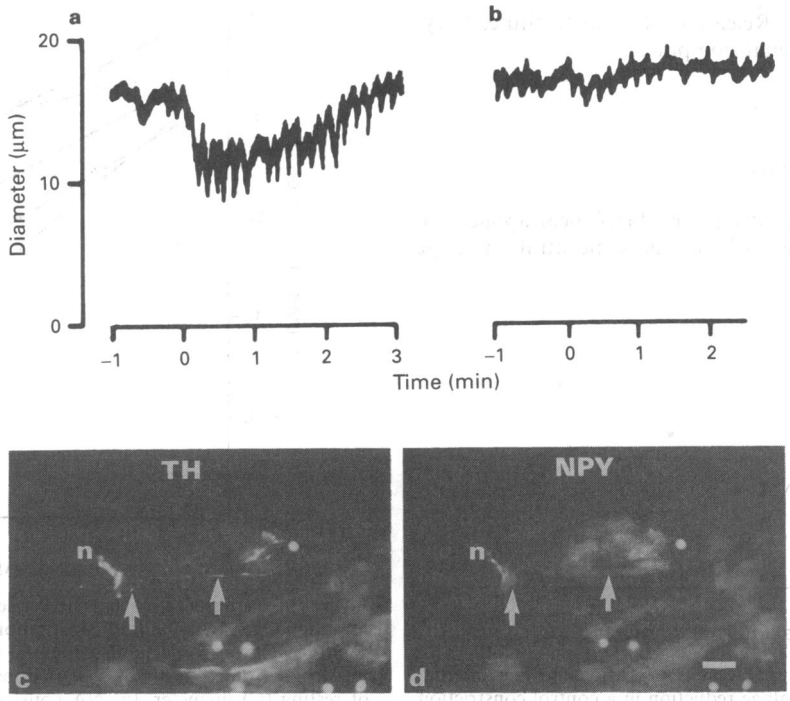


Figure 4 Correlated pharmacology and immunohistochemistry of 6° arteriole near the margin of the ear. Top panel shows traces of diameter after local applications of 50 nl of 10 μM noradrenaline (NA) (at time 0) in the absence of antagonists (a) and 30 min after addition of 1 μM yohimbine to the superfusate (b). Lower panel shows immunoreactivity to tyrosine hydroxylate (TH) (c) and neuropeptide Y (NPY) (d) in a double-labelled section through the same arteriole. Note the absence of NPY-IR in the TH-IR axon running along the arteriole (arrows). A nearby nerve bundle (n) contains axons with both TH-IR and NPY-IR. Scale bar = 20 μm.

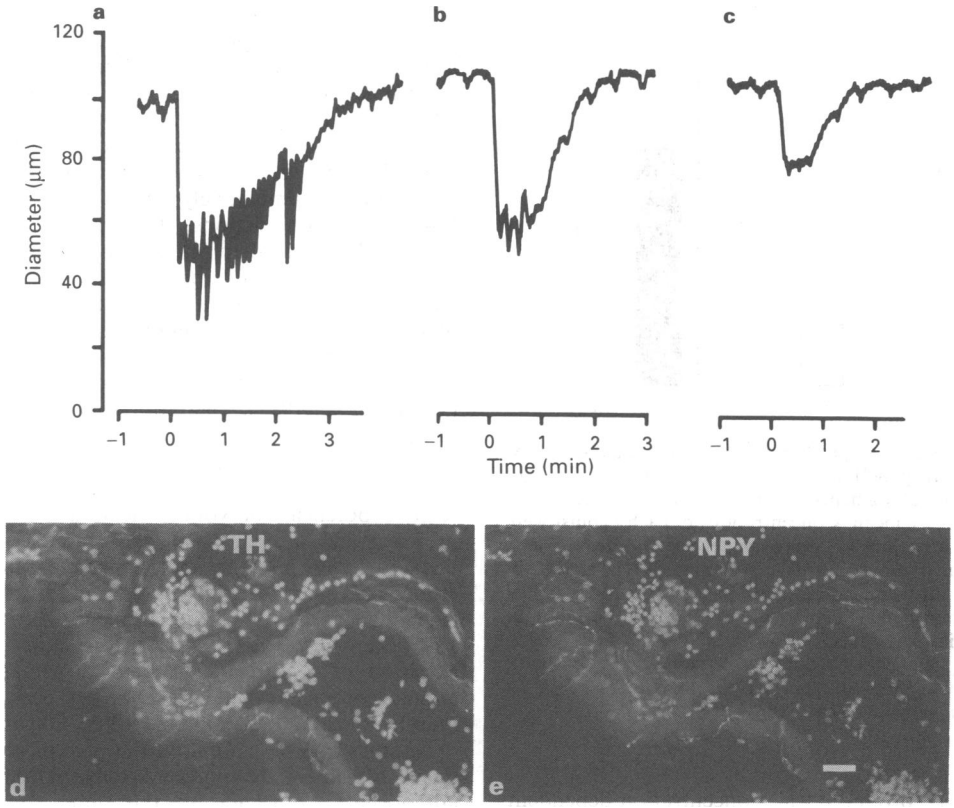


Figure 5 Correlated pharmacology and immunohistochemistry of a 4° artery from the ear. Top panel shows traces of diameter changes produced by local applications of 50 nl of 10 μM noradrenaline (NA) (at time 0) in the absence of antagonists (a) 30 min after addition of 1 μM yohimbine to the superfusate (b), and 30 min after treatment with both yohimbine and 1 μM prazosin (c). Lower panel shows immunoreactivity to tyrosine hydroxylate (TH) (d) and neuropeptide Y (NPY) (e) in oblique section through the same artery. Almost all axons with TH-IR also have NPY-IR. The fluorescence of the blood cells is non-specific. Scale bar = 40 μm.

duced substantial blockade of NA-constrictions remaining after yohimbine and prazosin, was dihydroergotamine (1–10 μM). In 9 experiments, dihydroergotamine produced no change in resting diameter, but abolished NA-induced constrictions (1–100 μM) remaining after treatment with a combination of prazosin, and yohimbine or benextramine (Figure 3).

The specificity of dihydroergotamine in antagonizing NA-induced constrictions was tested in a series of 7 experiments, in which consistent constrictions to alternating applications of NA (30–100 μM) and ATP (0.1–1 mM) were obtained. NA-induced constrictions were abolished in 6 arteries, and were substantially reduced in the 7th after addition of dihydroergotamine (1–10 μM) to the superfusion solution (Figure 7). This antagonism was only slowly reversible (Figure 7). In contrast, ATP-induced constrictions were not significantly reduced by dihydroergotamine (Figure 7).

Effects of 5-hydroxytryptamine and ketanserin

To test whether the dihydroergotamine-sensitive constrictions produced by NA might be due to occupation of 5-hydroxytryptamine receptors, increasing concentrations of 5-HT (3 μM–0.1 mM) were applied to 3° or 4° arterial segments, and responses were compared with those produced by similar concentrations of NA. Furthermore, the 5-HT_2 receptor antagonist, ketanserin (Van Nueten *et al.*, 1981), was tested against the NA-induced constrictions, and against 5-HT constrictions when they occurred. 5-HT (3–100 μM) had variable effects on the diameter of 3° and 4° arteries ($n = 12$). In three arteries, 5-HT produced concentration-dependent constrictions with a similar time course and magnitude as NA constrictions of the same arteries. In two of these experiments,

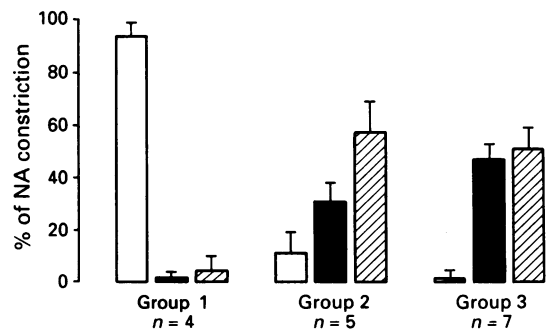


Figure 6 Histograms showing mean percentage (± s.e.mean) of initial constrictions produced by 50 nl of 10 μM noradrenaline (NA), which were reduced by 1 μM yohimbine (open columns), were reduced by subsequent addition of 1 μM prazosin (solid columns), and which were resistant to blockade by yohimbine and prazosin (hatched columns). Arterial segments have been separated into 3 groups according to the proportion of tyrosine hydroxylase (TH)-IR axons containing neuropeptide Y (NPY)-IR: group 1, few or none; group 2, about 50%; group 3, most or all (>75%). See text for statistical details.

5-HT constrictions were not affected by 1 μM prazosin, but were abolished by 1 μM dihydroergotamine. In the third experiment, the constriction produced by 10 μM 5-HT was abolished by 0.1 μM ketanserin. However, ketanserin (0.1–0.3 μM) did not affect constrictions produced by 10 μM NA ($n = 6$; 1-way ANOVA, $F_{(1,5)} = 4.46$, $P = 0.09$). In the remaining experiments, 5-HT either had a slight constrictor or dilator effect at some concentrations and no effect at

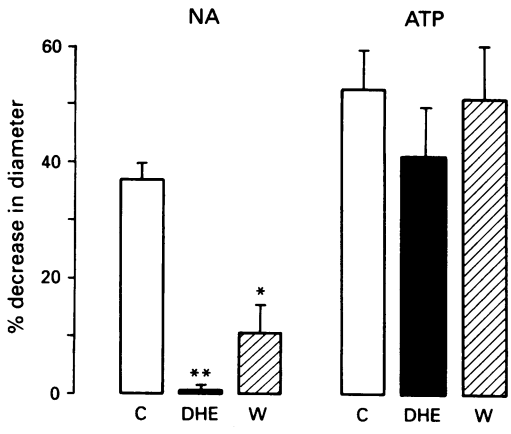


Figure 7 Vasoconstrictions produced by noradrenaline (NA, 30–100 μM, $n = 7$, left panel) and ATP (0.1–1 mM, $n = 7$, right panel) in the same arterial segments. Columns show mean percentage decrease in diameter ± s.e.mean. Concentrations of each agonist were chosen that gave constrictions of approximately equal size. C (open columns), control constrictions; dihydroergotamine (DHE) (solid column), constrictions 40–60 min after DHE (1–10 μM); W (hatched columns), constrictions 30–60 min after washout of DHE. **significant reduction by DHE, 1-way ANOVA, $F_{(2,5)} = 67.2$, $P = 0.0002$; *still significant reduction after DHE washout, $F_{(1,6)} = 20.5$, $P = 0.004$. DHE did not have a significant effect on ATP constrictions: $F_{(2,5)} = 2.7$, $P = 0.16$.

others ($n = 6$), or produced a concentration-dependent vasodilatation ($n = 3$).

Discussion

This study has demonstrated consistent differences in the potency of a bolus of exogenous noradrenaline applied to the adventitial surface in producing constriction of different segments of the cutaneous arterial system in the guinea-pig ear studied *in vivo*. Furthermore, adrenoceptors with differing sensitivities to blockade by yohimbine and prazosin appear to mediate the noradrenaline-induced constrictions in consecutive arterial segments.

All arterial vessels in this vascular bed are innervated by sympathetic catecholamine-synthesizing neurones, but the density of innervation tends to decrease in more distal arterioles (see Morris, 1994a). Furthermore, sympathetic neurones innervating different arterial segments belong to distinct neuronal subpopulations which differ in their neuropeptide content (Gibbins & Morris, 1990; Morris, 1994a). Thus, one possible explanation for the differential sensitivity to NA seen here is that differential neuronal uptake by the distinct populations of sympathetic neurones leads to variations in the concentration of NA reaching postsynaptic adrenoceptors in different arterial segments. Indeed, use of desipramine in the present study indicates that neuronal uptake can lead to significant changes in the concentrations of NA available to produce vasoconstriction after brief local application of the agonist. As would be predicted from the different densities of innervation in the larger versus the smaller arterial segments, neuronal uptake seemed to have a greater effect in larger than in smaller vessels. However, the greater sensitivity of 4° arteries to NA compared with 3°, or 5° and 6° arteries, was maintained after desipramine, and thus cannot be explained by differences in neuronal uptake in different arterial segments. Furthermore, although the presence of β-adrenoceptors on these cutaneous arterial segments cannot be ruled out, especially in smaller arterioles, the higher sensitivity of 4° arteries to NA was also unchanged after treatment with propranolol and thus is unlikely to be due primarily to differential distribution of β-adrenoceptors in different arterial segments.

It is likely that the differential sensitivity to NA at least partly reflects the presence of different subpopulations of adrenoceptors mediating NA constriction in consecutive arterial segments of this vascular bed (see also Bevan *et al.*, 1987). Detailed characterization of receptor subtypes in each vascular segment was not carried out in this study, where NA was added briefly in non-equilibrium conditions and could not be added cumulatively due to the transient nature of the NA-induced constrictions. However, the cumulative addition of yohimbine and then prazosin in the present study demonstrated striking differences in the characteristics of adrenoceptors present in consecutive arterial segments. The high concentrations of yohimbine and prazosin used in this study in order to achieve maximal blockade of α_1- and α_2-adrenoceptors are non-selective for α-adrenoceptor subtypes (Wilson *et al.*, 1991). Therefore, it is not possible at this stage to draw a conclusion about which receptor subtypes mediate NA-induced constrictions of distal arterioles and proximal cutaneous arteries in the guinea-pig ear. However, the relative potencies of yohimbine and prazosin found in the present study, are consistent with findings in proximal versus distal arteries in other cutaneous vascular beds, both in laboratory animals (Medgett & Ruffolo, 1988) and in man (Flavahan *et al.*, 1987; Nielsen *et al.*, 1989; Parkinson *et al.*, 1992; Stephens *et al.*, 1992). Furthermore, a preferential distribution of α_1-adrenoceptors in proximal arteries and α_2-adrenoceptors in distal arterioles has been found in skeletal muscle vascular beds (Faber, 1988; Ohyanagi *et al.*, 1991).

Another notable finding in the present study was the selective location of NA-induced constrictions resistant to α-adrenoceptor blockade in the more proximal 3° and 4° arterial segments. These constrictions were not substantially reduced by subsequent addition of the non-competitive α-adrenoceptor antagonist, benextramine. Thus, it is unlikely that the failure of a combination of yohimbine and prazosin to produce more substantial antagonism of NA-induced constrictions in 3° and 4° arteries is due to the inability of these competitive antagonists to block the effects of high local concentrations of NA.

The one antagonist found to date which abolishes the non-α-adrenoceptor mediated constrictions in the guinea-pig ear vasculature is the non-selective antagonist, dihydroergotamine. This agent has a long history as a blocker of sympathetic vasoconstriction (Barcroft & Swan, 1953), and is well-known to antagonise both α-adrenoceptors and 5-hydroxytryptamine receptors mediating vasoconstriction (Müller-Schweinitzer & Weidman, 1978). 5-HT-induced vasoconstrictions were present in at least some of the ear arteries examined here, and may have been obscured by 5-HT-induced vasodilations in other vessels. Previous studies indicate that both α_1-adrenoceptors and 5-HT_2 receptors can mediate 5-HT-induced constrictions (Purdy *et al.*, 1987; Xu *et al.*, 1990). However, as the 5-HT_2 receptor antagonist, ketanserin, blocked constrictions of guinea-pig ear arteries produced by 5-HT in the one experiment where it could be tested, but did not reduce NA-induced constrictions, non-α-adrenoceptor mediated constrictions do not seem to be due to NA acting on postsynaptic 5-HT receptors.

It is most likely that the dihydroergotamine-sensitive constrictions in the present study were mediated by NA acting on a population of unusual adrenoceptors. Dihydroergotamine previously has been shown to antagonise chronotropic effects of applied adrenaline and sympathetic nerve stimulation which are resistant to α- and β-adrenoceptor antagonists (Bramich *et al.*, 1990). Furthermore, there have been several earlier reports of NA-induced vasoconstrictions which are resistant to α-adrenoceptor blockade (Duckles & Bevan, 1976; Hirst & Neild, 1980a,b; 1981; Bevan *et al.*, 1987). In cerebral arteries, non-α-receptor mediated vasoconstrictions are mediated by higher concentrations of NA than are required to produce the maximum α-adrenoceptor-mediated constriction (Duckles & Bevan, 1976; Laher *et al.*, 1986). In rat basilar artery, high concentrations of NA produce mem-

brane depolarizations without associated constriction, which are resistant to adrenoceptor blockade (Hirst *et al.*, 1982). In contrast, α-adrenoceptor-resistant constrictions produced by NA in the present study occurred in the same concentration range (1–100 μM) that produced NA-induced constrictions which were sensitive to yohimine or prazosin. Thus, the receptors revealed in the present study may well be distinct from the previously described 'gamma' receptors (Hirst & Neild, 1980b; Hirst *et al.*, 1982), or 'extraceptors' (Laher *et al.*, 1986; Bevan *et al.*, 1987). Both of these previously-described non-α-adrenoceptors have been implicated in mediating a component of the vasoconstriction mediated by NA released from sympathetic neurones (Hirst & Neild, 1981; Hirst *et al.*, 1982; Laher *et al.*, 1986).

In conclusion, this study has demonstrated the differential localization of three populations of postsynaptic receptors mediating NA constrictions throughout the guinea-pig ear arterial tree: NA constricts proximal arteries within the ear (3°) via α-adrenoceptors sensitive to prazosin and via non-α-adrenoceptors; 4° and 5° arteries are constricted via a combination of receptors sensitive to yohimbine, receptors sensitive to prazosin, and non-α-adrenoceptors; NA constricts distal arterioles (6°, 7°) almost exclusively via adrenoceptors sensitive to yohimbine. Furthermore, the location of these different receptor types in the arterial tree can be correlated with the differential distribution of different populations of sympathetic neurones. As the proportion of sympathetic neurones containing NPY increased in more proximal arteries, so did the proportion of NA-induced constrictions mediated by adrenoceptors sensitive to prazosin, and by non-α-adrenoceptors. A similar correlation between the presence of NPY-IR sympathetic neurones and the presence of postsynaptic NPY receptors has been found previously in this vascular bed (Morris, 1994). Edwards *et al.* (1989) found that non-α, non-β (gamma) adrenoceptors were located selectively on cerebral arteries which received a sympathetic innervation. It is not yet known whether some or all of the postsynaptic NA receptor types found in the present study are located close to the sympathetic nerve terminals (junctional receptors), or are located more diffusely on the smooth muscle membrane (extrajunctional receptors, see Hirst & Neild, 1981). The present results suggest that there may be very discrete trophic interactions between different populations of sympathetic neurones and between different arterial segments in the same vascular bed (cf. Danielsson *et al.*, 1982; Creazzo *et al.*, 1983; Hill *et al.*, 1983).

This study was supported by grants from the National Health and Medical Research Council of Australia, the Flinders Medical Centre Research Foundation, the Flinders University Research Budget, and the Clive and Vera Ramaciotti Foundations. I am extremely grateful to Dr Tim Neild for valuable advice, and for development and supply of the DIAMTRAK DTVIVO programme: to Prof. David Hirst for a generous gift of dihydroergotamine; to Prof. Ian Gibbins for help with statistical analyses; and to Pat Vilimas, Rachel Perry and Wendy Hodgson for expert technical assistance.

References

BARCROFT, H. & SWAN, H.J.C. (1953). *Sympathetic Control of Human Blood Flow. Monographs of the Physiological Society*, Number 1. ed. Bayliss, L.E., Feldberg, W. & Hodgkin, A.L. London: Edward Arnold.

BEVAN, J.A., DUCKWORTH, J., LAHER, I., ORIOWO, M.A., McPHERSON, G.A. & BEVAN, R.A. (1987). Sympathetic control of cerebral arteries: specialization in receptor type, reserve, affinity, and distribution. *FASEB J.*, **1**, 193–198.

BRAMICH, N.J., EDWARDS, F.R. & HIRST, G.D.S. (1990). Sympathetic nerve stimulation and applied transmitters on the sinus venosus of the toad. *J. Physiol.*, **429**, 349–375.

CREAZZO, T.L. & SOHAL, G.S. (1983). Neural regulation of embryonic acetylcholine receptor and skeletal muscle. *Cell Tissue Res.*, **228**, 1–12.

DANIELSSON, A., HENRIKSSON, R., LINDSTROM, P. & SEHLIN, J. (1982). The importance of an intact sympathetic innervation for the differentiation of the β-adrenoceptor subtypes in the rat parotid gland. *Acta Physiol. Scand.*, **115**, 377–379.

DUCKLES, S.P. & BEVAN, J.A. (1976). Pharmacological characterization of adrenergic receptors of a rabbit cerebral artery *in vitro*. *J. Pharmacol. Exp. Ther.*, **197**, 371–378.

EDWARDS, F.R., HARDS, D., HIRST, G.D.S. & SILVERBERG, G.D. (1989). Noradrenaline (gamma) and ATP responses of innervated and non-innervated rat cerebral arteries. *Br. J. Pharmacol.*, **96**, 785–788.

FABER, J.E. (1988). In situ analysis of α-adrenoceptors on arteriolar and venular smooth muscle in rat skeletal muscle microcirculation. *Circ. Res.*, **62**, 37–50.

FLAVAHAN, N.A., COOKE, J.P., SHEPHERD, J.T. & VANHOUTTE, P.M. (1987). Human postjunctional alpha-1 and alpha-2 adrenoceptors: differential distribution in arteries of the limbs. *J. Pharmacol. Exp. Ther.*, **241**, 361–365.

GIBBINS, I.L. & MORRIS, J.L. (1990). Sympathetic noradrenergic neurons containing dynorphin but not neuropeptide Y innervate small cutaneous blood vessels of guinea-pigs. *J. Autonom. Nerv. Syst.*, **29**, 137–149.

HILL, C.E., HIRST, G.D.S. & VAN HELDEN, D.F. (1983). Development of sympathetic innervation to proximal and distal arteries of the rat mesentery. *J. Physiol.*, **338**, 129–147.

HIRST, G.D.S. & NEILD, T.O. (1980a). Evidence for two populations of excitatory receptors for noradrenaline on arteriolar smooth muscle. *Nature*, **283**, 767–768.

HIRST, G.D.S. & NEILD, T.O. (1980b). Noradrenergic transmission – a reply to McGrath. *Nature*, **288**, 301–302.

HIRST, G.D.S. & NEILD, T.O. (1981). Localization of specialized noradrenaline receptors at neuromuscular junctions on arterioles of the guinea-pig. *J. Physiol.*, **313**, 343–350.

HIRST, G.D.S., NEILD, T.O. & SILVERBERG, G.D. (1982). Noradrenaline receptors on the rat basilar artery. *J. Physiol.*, **328**, 351–360.

LAHER, I., KHAYAL, M.A. & BEVAN, J.A. (1986). Norepinephrine sensitive, phenoxybenzamine-resistant receptor sites associated with contraction in rabbit arterial but not venous smooth muscle: possible role in adrenergic neurotransmission. *J. Pharmacol. Exp. Ther.*, **237**, 364–368.

MEDGETT, I.C. & RUFFOLO, R.R. (1988). Alpha adrenoceptor-mediated vasoconstriction in rat hindlimb: innervated alpha-2 adrenoceptors in the saphenous arterial bed. *J. Pharmacol. Exp. Ther.*, **246**, 240–254.

MORRIS, J.L. (1994a). Selective constriction of small cutaneous arteries by NPY matches distribution of NPY in sympathetic axons. *Regul. Pep.*, **49**, 225–236.

MORRIS, J.L. (1994b). Roles of noradrenaline and ATP in sympathetic vasoconstriction of the guinea-pig main ear artery. *J. Autonom. Nerv. Syst.*, (in press).

MÜLLER-SCHWEINITZER, E. & WEIDMAN, H. (1978). Basic pharmacological properties. In *Ergot Alkaloids and Related Compounds*. ed. Berde, B. & Schild, H.O. pp. 87–232. Berlin, Heidelberg, New York: Springer-Verlag.

NIELSEN, H., THOM, S.McG., HUGHES, A.D., MARTIN, G.N., MULVANY, M.J. & SEVER, P.S. (1989). Postjunctional α_2-adrenoceptors mediate vasoconstriction in human subcutaneous resistance vessels. *Br. J. Pharmacol.*, **97**, 829–834.

OHYANAGI, M., FABER, J.E. & NISHIGAKI, K. (1991). Differential activation of α_1- and α_2-adrenoceptors on microvascular smooth muscle during sympathetic nerve stimulation. *Circ. Res.*, **68**, 232–244.

PARKINSON, N.A., THOM, S.McG., HUGHES, A.D., SEVER, P.S., MULVANY, M.J. & NIELSEN, H. (1992). Neurally evoked responses of human isolated resistance arteries are mediated by both α_1- and α_2-adrenoceptors. *Br. J. Pharmacol.*, **106**, 568–573.

PURDY, R.E., MURRAY, D.L. & STUPECKY, G.L. (1987). Receptors for 5-hydroxytryptamine in rabbit blood vessels: activation of alpha adrenoceptors in rabbit thoracic aorta. *J. Pharmacol. Exp. Ther.*, **240**, 535–541.

STEPHENS, N., BUND, S.J., FARAGHER, E.B. & HEAGERTY, A.M. (1992). Neurotransmission in human resistance arteries: contribution of α_1- and α_2-adrenoceptors but not P_2-purinoceptors. *J. Vasc. Res.*, **29**, 347–352.

VAN NUETEN, J.M., JANSSEN, P.A.J., VAN BEEK, J., XHONNEUX, R., VERBEUREN, T.J. & VANHOUTTE, P.M. (1981). Vascular effects of ketanserin (R 41 468), a novel antagonist of 5-HT_2 serotonergic receptors. *J. Pharmacol. Exp. Ther.*, **218**, 217–229.

WILSON, V.G., BROWN, C.M. & MCGRATH, J.C. (1991). Are there more than two types of α-adrenoceptors involved in physiological responses? *Exp. Physiol.*, **76**, 317–346.

XU, Z., MONDAL, G., SONG, J.P. & PURDY, R.E. (1990). Effect of ouabain on the rabbit ear artery contraction to serotonin: enhanced response by serotonergic rather than alpha adrenergic receptors. *J. Pharmacol. Exp. Ther.*, **253**, 668–675.

(Received March 18, 1994
Revised June 6, 1994
Accepted June 9, 1994)

Br. J. Pharmacol. (1994), **113**, 1113–1120 © Macmillan Press Ltd, 1994

Effects of tenoxicam and aspirin on the metabolism of proteoglycans and hyaluronan in normal and osteoarthritic human articular cartilage

[1]*†Daniel Henri Manicourt, *Anne Druetz-Van Egeren, **Ludo Haazen & †Charles Nagant de Deuxchaisnes

ICP, *Connective Tissue Group and †Department of Rheumatology, Saint-Luc University Hospital, University of Louvain in Brussels, Brussels, Belgium and the **Produits Roche S.A., Brussels, Belgium

1 As nonsteroidal anti-inflammatory drugs may impair the ability of the chondrocyte to repair its damaged extracellular matrix, we explored the changes in the metabolism of newly synthesized proteoglycan (PG) and hyaluronan (HA) molecules produced by tenoxicam and aspirin in human normal cartilage explants and in osteoarthritic (OA) cartilage from age-matched donors.

2 Explants were sampled from the medial femoral condyle and were classified by use of Mankin's histological-histochemical grading system. Cartilage specimens were normal in 10 subjects, exhibited moderate OA (MOA) in 10 and had severe OA (SOA) in 10.

3 Cartilage explants were pulsed with [^{3}H]-glucosamine and chased in the absence and in the presence of either aspirin (190 $\mu g\,ml^{-1}$) or tenoxicam (4–16 $\mu g\,ml^{-1}$). After papain digestion, the labelled chondroitin sulphate ([^{3}H]-PGs) and HA([^{3}H]-HA) molecules present in the tissue and media were purified by anion-exchange chromatography.

4 In normal cartilage as well as in explants with MOA and SOA aspirin reduced more strongly PG and HA synthesis than the loss of [^{3}H]-HA and [^{3}H]-PGs.

5 In normal cartilage, tenoxicam did not affect PG metabolism whereas it reduced HA synthesis in a dose-dependent manner and did not change or even increased the net loss of [^{3}H]-HA. In contrast, in OA cartilage, tenoxicam produced a stronger reduction in the loss of [^{3}H]-PGs than in PG synthesis and this decrease occurred at lower concentrations in cartilage with SOA (4–8 $\mu g\,ml^{-1}$) than in cartilage with MOA (8–16 $\mu g\,ml^{-1}$). In cartilage with MOA, the metabolic balance of HA was unaffected by tenoxicam whereas in cartilage with SOA, the drug decreased the loss of [^{3}H]-HA and concomitantly did not change or even increased HA synthesis.

6 The data obtained in short-term *in vitro* cultures indicate that aspirin may produce OA-like changes in normal cartilage and is likely to worsen the disease process in OA tissue. On the other hand, although tenoxicam may reduce the HA content of normal cartilage, and, in so doing, may produce OA-like lesions, this drug should not *per se* accelerate joint failure in OA.

Keywords: Nonsteroidal anti-inflammatory drugs; aspirin; tenoxicam; aggrecan; hyaluronan; normal cartilage; osteoarthritic cartilage

Introduction

Proteoglycans (PGs) and hyaluronan (HA) play an important role in the macromolecular organization and in the biomechanical properties of articular cartilage. PGs provide the articular tissue with its elasticity and stiffness in compression whereas the long strands of HA interact specifically with PG molecules to form supramolecular aggregates of very large size which are firmly immobilized within the collagen meshwork (Lohmander, 1988). PG aggregation also increases dramatically the rheological properties of PG molecules and, in so doing, affects the dynamic behaviour of cartilage in compression (Hardingham *et al.*, 1987). Therefore, any decrease in the tissue concentration of PG and HA, as occurs in osteoarthritis (OA), compromises the functional properties of cartilage.

Nonsteroidal anti-inflammatory drugs (NSAIDs) are widely prescribed in patients suffering from rheumatological disorders and they undeniably produce relief of pain and improvement of joint mobility. The use of these drugs might however be detrimental to the joints. Effective pain relief could indeed lead to overuse of a disabled joint. Further *in vitro* and *in vivo* studies have shown that some NSAIDs inhibit the synthesis of articular cartilage PGs whereas others do not (Brandt, 1987; Muir *et al.*, 1988; Howell *et al.*, 1991). This differential effect of NSAIDSs on cartilage metabolism are most relevant to clinical practice as any drug, that suppresses PG synthesis and impairs the ability of the chondrocyte to repair its damaged extracellular matrix, could potentially accelerate the breakdown of the articular tissue. On the other hand, although HA plays a central structural role in the macromolecular organization of PGs, the possible effects of NSAIDs on the metabolism of this glycosaminoglycan have not yet focussed any investigative attention.

Tenoxicam is a thienothrazine derivative of the oxicam class. Although this drug displays good efficacy and tolerability in therapy for rheumatic disorders (Kirchheimer *et al.*, 1982; Gonzalez & Todd, 1987), knowledge of its possible effects on the metabolism of articular cartilage is still fragmentary (Franchimont *et al.*, 1989). We therefore investigated the action of tenoxicam on the metabolism of newly synthesized PGs and HA molecules in explant cultures from human normal and OA cartilage. Results were compared with those obtained with aspirin.

[1] Author for correspondence at: Department of Rheumatology, UCL 53.90, Avenue Mounier, 1200 Bruxelles, Belgium.

Methods

Patients' evaluation and cartilage tissue sampling

Thirty subjects were included in the study. Exclusion criteria were septicaemia, connective tissue disorders, rheumatoid arthritis, crystal deposition diseases, known hereditary or congenital defects, immobilization for several weeks as well as treatment with corticosteroids and cytotoxic drugs.

Full thickness cartilage was sampled from the medial femoral condyle of the knee within 24 h postmortem and cartilage specimens were brought into sterile phosphate-buffered saline solutions (PBS) for transport to culture facilities.

For each individual, 3 cartilage slices were taken at random from the pool of sampled tissue and processed for the histological-histochemical grading system devised by Mankin *et al.* (1971). The mean score of the 3 cartilage slices was retained for each donor.

Articular cartilage was normal in 10 subjects whose mean ± s.d. age was 53.9 ± 4.8 years (range 46–61). Mankins's grading system ranged from 2–5 in 10 other individuals who were classified as having moderate osteoarthritis (MOA): their mean ± s.d. age was 54.4 ± 4.7 years (range 49–65) and none of the donors were known to have overt clinical manifestations of OA. In contrast Mankin's grading system ranged from 6–9 in 10 other subjects who were labelled as having severe OA (SOA). Their mean ± s.d. age was 56.8 ± 5.4 years (range 51–65): 8 out of these 10 donors had clinical manifestations of OA and were taking either analgesics (paracetamol in 2, dextropropoxyphen HCl in 2) and/or NSAIDs (diclofenac in 3, ibuprofen in 2, Naproxen in 2) on an irregular basis.

General culture procedures

Tissue specimens obtained from each donor were cut into pieces of 3–6 mg in Dulbecco's modified Eagle's medium (DMEM) supplemented with penicillin (5,000 i.u. ml^{-1}) and streptomycin (5,000 $\mu g\ ml^{-1}$). The tissue was washed 3 times with this culture medium and aspirated free from liquid. Cartilage pieces were taken at random, weighed and distributed into the different wells of multiwell culture plates (typically between 30 and 60 mg tissue/well). Extra pieces were not cultured but stored at −20°C in order to assess the initial PG and HA contents of the cartilage. Culture medium supplemented with 20% (v/v) foetal calf serum (culture medium A) was then added to each well and the culture plates were placed in a 90%:10% (v/v) air:CO_2 humidified incubator for 48 h at 37°C.

For each experiment the cartilage from one individual was used and tissue cultures were conducted in triplicate: that is, for the control culture as well as for each NSAID concentration, 3 cartilage explants were cultured separately. Reported values are the mean of the triplicate cultures.

Pulse studies

After 2 days of culture, the culture medium was aspirated and the explants were washed 3 times with 1 ml of DMEM. Explants were resuspended in culture medium A (1 ml 50 mg^{-1} tissue) supplemented with [^{3}H]-glucosamine (50 $\mu Ci\ ml^{-1}$) (culture medium B). To each well, a solution of NSAID dissolved in dimethylsulphoxide (DMSO) was added (10 $\mu l\ ml^{-1}$ in culture medium) to achieve the following final concentrations: 4, 8 and 16 $\mu g\ ml^{-1}$ for tenoxicam and 190 $\mu g\ ml^{-1}$ for aspirin. Control cultures received DMSO that did not contain any NSAID (10 $\mu l\ ml^{-1}$). Culture wells were then incubated for 12 h.

Chase studies

After one day of culture in medium A, the cartilage pieces were aspirated free of medium, washed 3 times with 1 ml of DMEM, resuspended in culture medium B (1 ml 50 mg^{-1} tissue) and cultured for 12 h. After pulse labelling, the cartilage pieces were washed with DMEM and resuspended in culture medium A. DMSO alone or the appropriate NSAID dissolved in DMSO was added to each well (10 $\mu l\ ml^{-1}$) as stated above and a non-radioactive chase period was conducted for 24 h.

Isolation and purification of hyaluronan and proteoglycans

At the end of the pulse labelling and non-radioactive chase periods, the culture media were removed and the cartilage pieces were washed with 0.15 M sodium chloride/0.05 M sodium acetate, pH 6.0 (buffer A). Media and corresponding washes were combined. Bovine nasal A1D1D1 PGs (500 $\mu g\ ml^{-1}$) and hyaluronan (10 $\mu g\ ml^{-1}$) were added. The mixtures were dialyzed against buffer A and then incubated with papain (10 $\mu g\ ml^{-1}$) for 24 h at 60°C. Cartilage specimens were resuspended in buffer A; papain was added to each vial (0.1 mg ml^{-1}) and the tissues were digested for 24 h at 60°C. Aliquots were sampled for hydroxyproline determinations or subjected to ion-exchange chromatography on Econo-Pak Q cartridge.

The Econo-Pak Q column (5 ml) was pre-equilibrated in buffer A at a flow rate of 2 ml min^{-1}. Aliquots of papain-digested samples (100–200 μl for tissue digests and 0.5–1 ml for medium digests) were adjusted to 2 ml with buffer A and applied to the column that was then washed with 6 column volumes of buffer A. Anionic macromolecules were eluted from the column at 2 ml min^{-1} with the following NaCl gradient (0.15–0.23 M over 2 min run, 0.23–0.23 M over 15 min, 0.23–1.5 M over 15 min) in 0.05 M Na acetate pH 6.0. Fractions of 2 ml were collected and assayed for radioactivity. The yield of radioisotope in the combined breakthrough and gradient fractions was >90%.

Two ^{3}H-radiolabelled peaks were consistently eluted from the column: peak A at 0.23 M NaCl and peak B at about 1 M NaCl. For each specimen (tissues and media) fractions containing radiolabelled peaks were separately pooled, heated at 80°C for 10 min and applied to a column (0.7 × 50 cm) of Sephadex G-50 equilibrated in 0.1 M ammonium bicarbonate buffer, pH 8.5. In each case more than 90% of the radiolabelled material present in both peaks A and B eluted at the excluded volume of the G-50 column. Therefore, aliquots of peaks A and B were digested with *Streptomyces* hyaluronidase (0.1 u/aliquot in 0.05 M Na acetate pH 5.0, 6 h at 60°C and chondroitinase ABC (0.5 u/aliquot in 0.1 M Tris-fluoride, pH 8.0, 6 h at 37°C) and the digestion products were applied to the G-50 column. Indeed *Streptomyces* hyaluronidase has an absolute specificity for HA and produces tetra- and hexasaccharides which are eluted in the included volume of the G-50 column. On the other hand, the digestion products of chondroitinase ABC are also included into the G-50 column but, in contrast to *Streptomyces* hyaluronidase, chrondroitinase ABC digests both HA and chrondroitin chains. Accordingly, the amount of [^{3}H]-HA present in each peak was calculated by multiplying the total radioactivity of the peak by the relative percentage of radiolabelled material that was sensitive to *Streptomyces* hyaluronidase whereas the amount of [^{3}H]-PG present in each peak was calculated by multiplying the total radioactivity of the peak by the relative percentage of radiolabelled material that was resistant to digestion with *Streptomyces* hyaluronidase and susceptible to digestion with chrondroitinase ABC.

Analytical methods

Hydroxyproline was determined by the method of Woessner (1961) and hexuronate acid by the method of Bitter & Muir (1962). HA was quantified by a specific radiosorbent assay technique (Tengblad, 1980).

Materials

[^{3}H]-glucosamine was from New England Nuclear Corporation (Brussels, Belgium). The scintillation liquid Hi-Safe-Optiphase II, purified hyaluronan (Healon) and Sephadex G-50 were from LKB-Pharmacia (Brussels, Belgium). Culture plates and media were from Gibco (Gent, Belgium). Chondroitin ABC lyase, *Streptomyces* hyaluronidase, twice crystallized papain and acetylsalicylic acid (aspirin) were from Sigma Chemical Company (St Louis, MO, U.S.A.). Econo-Pac Q cartridges were from Bio-Rad (Nazareth, Belgium). Dialysis membranes (mol. wt. cutoff: 3,500) were from Spectrum (Los Angeles, CA, U.S.A.). Tenoxicam was a gift from Roche (Basel, Switzerland). All other reagents were from Merck (Darmstadt, Germany).

Expression of results and statistics

The rate of biosynthesis of PG and HA was determined by the summation of [^{3}H]-PG and [^{3}H]-HA desintegrations per min (d.p.m.) found in papain-digested tissues and media at the end of the 12 h pulse labelling period and expressed as d.p.m. [^{3}H]-PG and [^{3}H]-HA per h and per mg of hydroxyproline. Indeed, the loss of hydroxyproline (and thus of collagen) from the normal and OA tissue specimens into the medium over a 72-h culture period was less than 5% of the amount present in cartilage pieces before culture.

At the end of the 24-h non-radioactive chase period, the total incorporation of [^{3}H]-glucosamine into HA and PGs was determined by the summation of [^{3}H]-HA and [^{3}H]-PGs d.p.m. found in the media and corresponding papain-digested tissue specimens. The radiolabelled material that accumulated in the medium during this non-radioactive chase period represents not only degraded HA and PG molecules but also intact HA and PG molecules that were being synthesized at the end of the pulse period and that were not incorporated into the matrix and lost in the medium during the subsequent chase period. As the material present in the chase medium was not characterized in the present study, it is difficult to assess the respective proportion of these 2 processes and, accordingly, the radiolabelled material recovered in the medium during the 24-h chase period was not described as the result of catabolism but rather as net loss. This net loss was expressed as the percentage of total incorporated d.p.m. found in the medium samples of the 24-h period.

The statistical significance of the differences observed

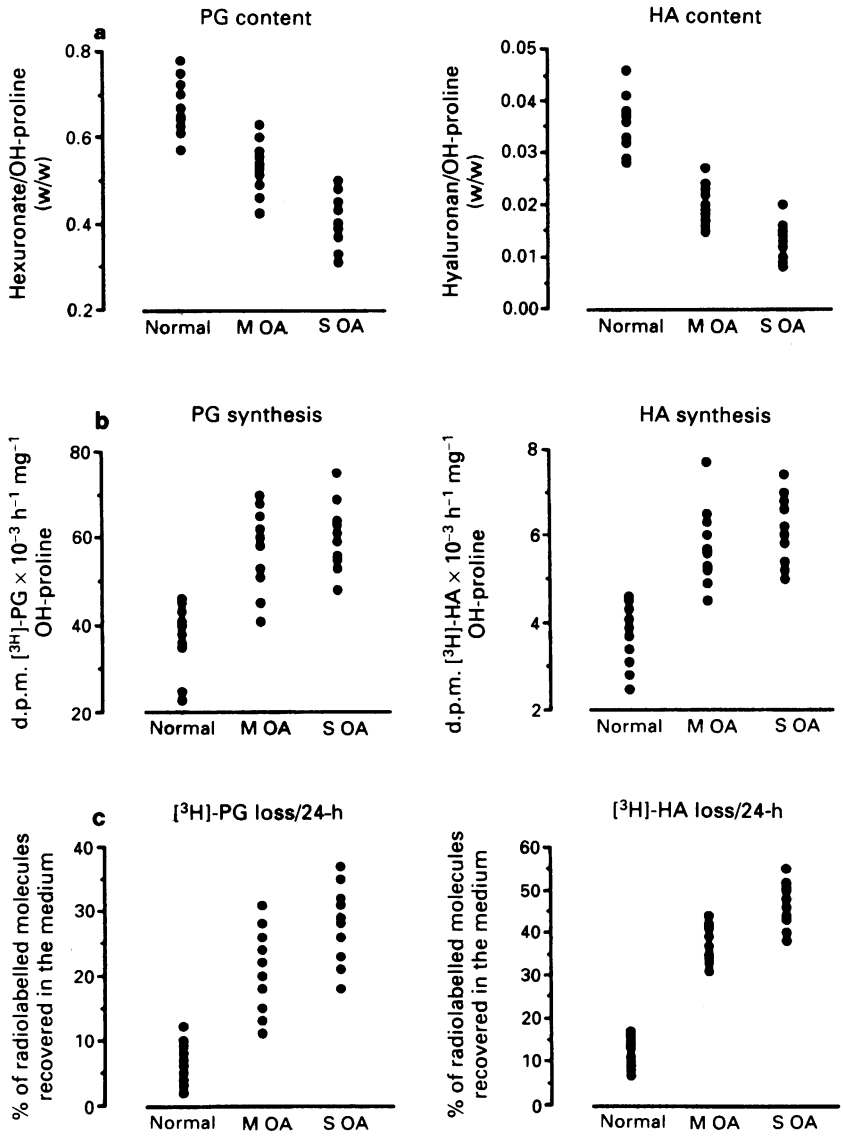


Figure 1 Distribution of values of total proteoglycan (PG) content, total hyaluronan (HA) content (a), rates of PG and HA synthesis (b) and net loss of newly synthesized PG ([^{3}H]-PG) and HA ([^{3}H]-HA) molecules (c) over a 24-h non-radioactive chase period in normal cartilage explants and in cartilage explants with moderate (M) and severe (S) osteoarthritis (OA) that were cultured in the absence of nonsteroidal anti-inflammatory drugs.

between groups was evaluated by the Mann-Whitney U test whereas in each group the significance of the differences in PG and HA metabolism in the presence of different NSAID concentrations were evaluated by the Wilcoxon signed-ranks test. P values <0.05 were considered as statistically significant.

Results

Biochemical and metabolic characterization of cartilage explants

The proteoglycan (PG) and hyaluronan (HA) contents of cartilage specimens were distributed over a wide range of values in the normal group and in the groups with moderate osteoarthritis (MOA) and severe osteoarthritis (SOA), as well (Figure 1, upper panels). Values found in normal explants (mean ± s.d. = 0.67 ± 0.07 and 0.04 ± 0.01 for the PG and HA contents, respectively) are in close agreement with those observed by Holmes *et al.* (1988) in normal articular tissue from the knee of age-matched subjects. The mean ± s.d. values of the PG and HA content were significantly higher in the normal group than in both OA groups ($P<0.001$). Further, the group with MOA had a significantly higher content of PG and HA than the group with SOA (0.53 ± 0.06 versus 0.41 ± 0.06 respectively for the PG content; U = 8; $P<0.002$; and 0.02 ± 0.01 versus 0.01 ± 0.01 respectively for the HA content; U = 7.5; $P<0.002$). This overall cartilage chemistry was not significantly affected by standard culture conditions and treatment with the NSAIDs examined over the 72-h period of culture (results not shown).

In the different pulse and chase experiments conducted in the absence and in the presence of NSAIDs, analysis of tissue and medium samples from normal and OA cartilage gave the following results: 50–70% of the labelled material present in peak A was sensitive to *Streptomyces* hyaluronidase and was thus identified as [^{3}H]-HA. On the other hand, all the labelled material present in peak B was identified as chondroitin sulphate (and thus as proteoglycans) as it was consistently resistant to digestion with *Streptomyces* hyaluronidase and susceptible to complete digestion with chondroitinase ABC.

In the absence of NSAID, the rates of PG and HA synthesis were distributed over a wide range of values in the 3 groups (Figure 1, middle panels). There was no statistically significant difference in the rate of PG and HA synthesis between the group with moderate OA and the group with severe OA (57.30 ± 9.66 versus 60.30 ± 7.93, respectively for PG synthesis; U = 42.5; $P>0.10$ and 5.77 ± 0.92 versus 6.14 ± 0.81, respectively for HA synthesis; U = 36; $P>0.10$). The rates of PG and HA synthesis were however significantly higher ($P<0.001$) in the 2 OA groups than in the normal group (37.20 ± 7.83 for PG synthesis and 3.69 ± 0.72 for HA synthesis).

When labelled cartilage explants were cultured in the absence of drug the net loss of [^{3}H]-HA and [^{3}H]-PG molecules was distributed over a wide range of values in the 3 groups (Figure 1, bottom panels). Although the loss of [^{3}H]-HA was significantly higher in the group with SOA than in the group with MOA (46.56 ± 5.79 versus 36.90 ± 4.41, respectively; U = 8.5; $P<0.002$) both OA groups did not differ in their loss of [^{3}H]-PG (20.80 ± 6.61 for the group with MOA versus 28.00 ± 6.09 for the group with SOA). On the other hand, the loss of both [^{3}H]-HA and [^{3}H]-PG was significantly higher ($P<0.001$) in the 2 OA groups than in the normal group (12.0 ± 3.5 for the loss of [^{3}H]-HA and 6.6 ± 3.2 for the loss of [^{3}H]-PG).

These wide variations in composition and metabolism that, in each group, were displayed by the cartilage explants cultured in the absence of drug were likely to hamper the assessment of the effect of NSAIDs on PG and HA metabolism. Therefore, for each cartilage specimen of the 3 groups, the rates of PG and HA metabolism that were obtained in the presence of different concentrations of NSAID were divided by the values observed in the absence of drug to yield percentage changes.

Effects of texonicam and aspirin on the total synthesis of PG and HA

As shown in Figure 2a aspirin inhibited dramatically the total amounts (tissue + medium) of newly synthesized PG molecules in both normal and OA cartilage explants, whereas the effect of tenoxicam differed between normal and OA cartilage. Indeed in normal cartilage, there was no significant inhibition of PG synthesis over the range of tenoxicam concentrations examined. On the other hand, a significant reduction in PG synthesis was observed at a tenoxicam concentration of 8 μg ml^{-1} in cartilage with moderate OA and of 4 μg ml^{-1} in cartilage with severe OA. The strongest inhibition of PG synthesis induced by tenoxicam was however mild when compared to that observed in the presence of aspirin (84% versus 20% of control values, respectively).

In both normal and OA cartilage, tenoxicam inhibited the total amounts (tissue + medium) of newly synthesized HA molecules in a relatively dose-dependent manner over the range of concentrations examined (Figure 2b). The maximum inhibition produced by tenoxicam approximated 77% of control values. In contrast, the inhibition caused by 190 μg ml^{-1}

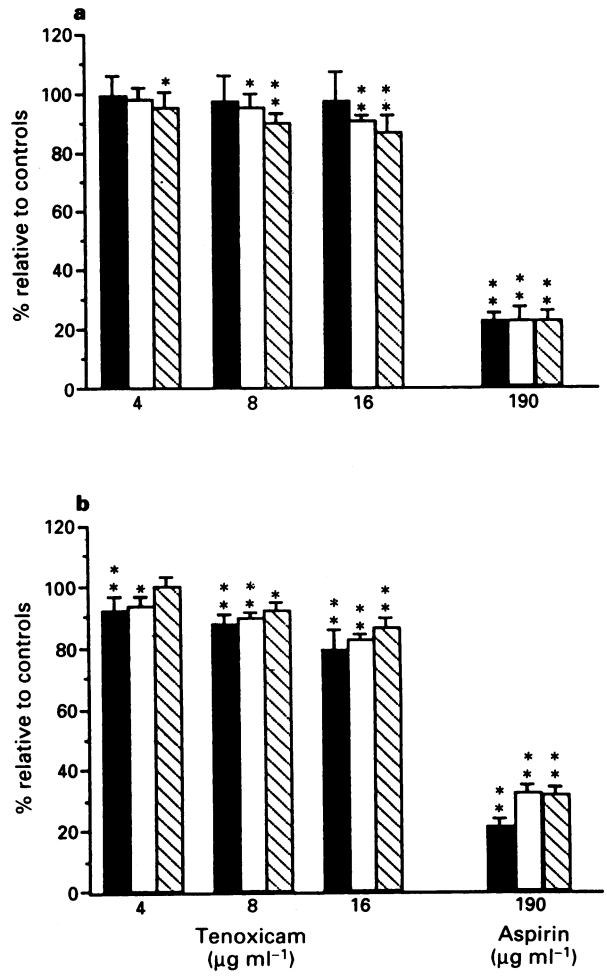


Figure 2 Effects of different concentrations (μg ml^{-1}) of tenoxicam and aspirin on the synthesis of proteoglycans (PG) (a) and hyaluronan (HA) (b) in normal articular cartilage explants (solid columns) as well as in cartilage explants with moderate (open columns) and severe (hatched columns) osteoarthritis. Results are expressed as the relative percentage of values observed in corresponding explants cultured in the absence of drug. Comparison by the Wilcoxon signed-rank test: *$P<0.05$; **$P<0.001$.

of aspirin was quite stronger and ranged from 20% of control values in normal tissue to 32% of control values in OA specimens.

Effects of tenoxicam and aspirin on the relative amounts of newly synthesized PG and HA molecules incorporated within the cartilage matrix

During the pulse studies of normal and OA explants conducted in the absence of drug a relative proportion of newly synthesized PG and HA molecules were not incorporated within the extracellular matrix and were lost into the culture medium. Further, in both normal and OA groups, this relative loss of labelled molecules varied from one donor to another. Therefore, in each experiment the amounts of radiolabelled PG and HA (as expressed in d.p.m. h^{-1} mg^{-1} hydroxyproline) found in the explants at the end of the pulse-labelling period conducted in the presence of different concentrations of NSAIDs were divided by the content of corresponding labelled molecules observed in the control explants pulse-labelled in the absence of drug to yield percentage changes.

The changes in the tissue content of labelled PG obtained at each NSAID concentration are illustrated in Figure 3 (open columns). In normal cartilage the relative amounts of newly synthesized PGs remaining within the matrix at the end of the pulse labelling period were unaffected by tenoxicam over the range of concentration studied whereas a significant reduction was observed at a tenoxicam concentration of 16 $\mu g\ ml^{-1}$ in cartilage with moderate OA and of 8 $\mu g\ ml^{-1}$ in cartilage with severe OA. The maximum reduction in the cartilage content of labelled PG induced by tenoxicam approximated 85% of control values in contrast to the 12% of control values observed in the presence of aspirin.

The changes in the tissue content of labelled HA observed at each NSAID concentration are shown in Figure 4 (open columns). Tenoxicam had a quite different effect in normal and OA tissue. In normal cartilage 4 $\mu g\ ml^{-1}$ of tenoxicam had already produced a small but statistically significant reduction in the tissue content of labelled HA. This reduction became stronger with higher tenoxicam concentrations and reached approximately 76% of control values at a concentration of 16 $\mu g\ ml^{-1}$. In contrast, in cartilage with moderate OA the tissue content of newly synthesized HA was unaffected by a tenoxicam concentration of 4 $\mu g\ ml^{-1}$. Higher tenoxicam concentrations were however able to reduce the labelled HA content of explants with moderate OA. This reduction was nevertheless significantly smaller ($P<0.05$) than that observed in normal explants at similar drug concentration. On the other hand, over the range of tenoxicam concentrations tested, there was no significant reduction in the content of labelled HA molecules remaining within the matrix of explants with severe OA and one could even

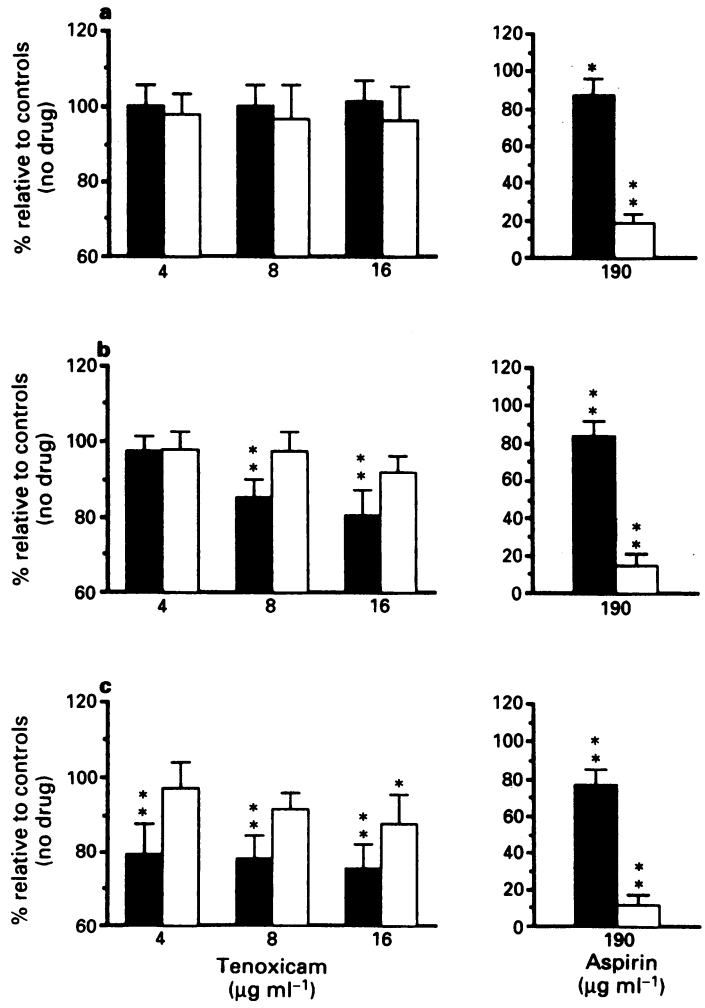


Figure 3 Effects of different concentrations of tenoxicam and aspirin on the net loss of labelled proteoglycans (PGs) from the tissue during the 24-h non-radioactive chase period (solid columns) and on the relative amounts of newly synthesized PG molecules remaining within the matrix at the end of the pulse labelling period (open columns) in normal cartilage (a) and in explants with moderate (b) and severe (c) osteoarthritis. Results are expressed as the relative percentage of values found in explants cultured in the absence of drug. Comparison by the Wilcoxon signed-rank test: $*P<0.05$; $**P<0.001$.

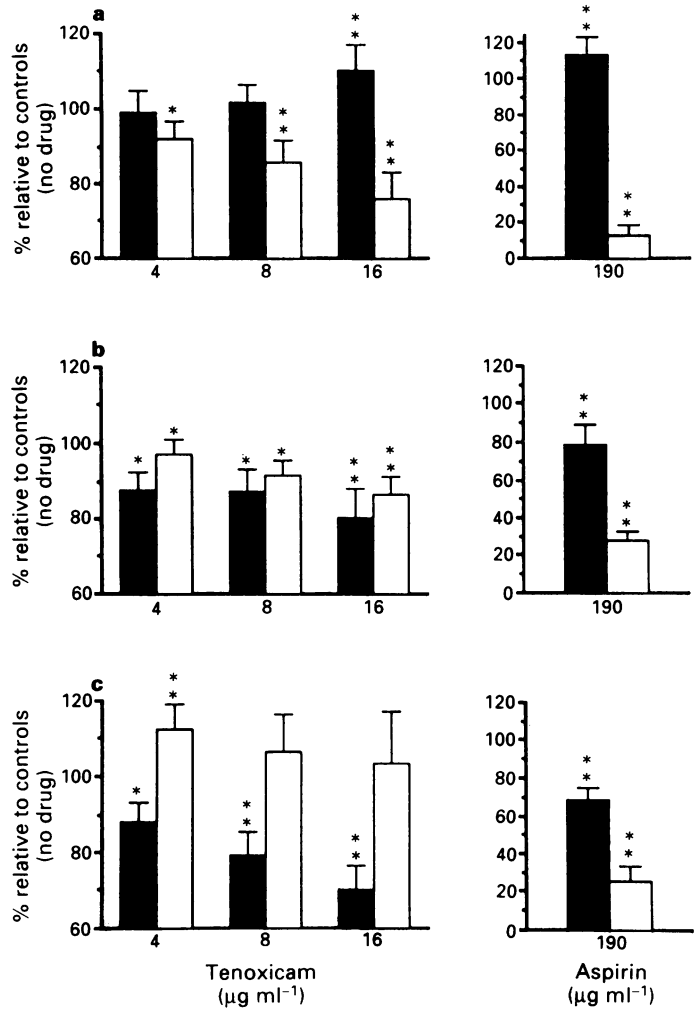


Figure 4 Effects of different concentrations of tenoxicam and aspirin on the net loss of labelled hyaluronan (HA) from the tissue during the 24-h non-radioactive chase period (solid columns) and on the relative amounts of newly synthesized HA molecules remaining within the matrix at the end of the pulse labelling period (open columns) in normal cartilage (a) and in explants with moderate (b) and severe (c) osteoarthritis. Results are expressed as the relative percentage of values found in explants cultured in the absence of drug. Comparison by the Wilcoxon signed-rank test: $*P<0.05$; $**P<0.001$.

observe a significant increase at a concentration of 4 μg ml^{-1}.

Aspirin at a concentration of 190 μg ml^{-1} reduced dramatically the tissue levels of labelled HA in both normal and OA explants. Although the levels observed in OA tissue were significantly higher than those observed in normal tissue ($P<0.001$), the values were nevertheless quite lower than those obtained in the presence of tenoxicam 16 μg ml^{-1}.

Effects of tenoxicam and aspirin on the net loss of newly synthesized PG and HA

In contrast to aspirin, tenoxicam did not induce any significant change in the net loss of labelled PGs from normal cartilage during the 24-h chase period (Figure 3, closed columns). On the other hand, in OA cartilage the reduction in the loss of labelled PGs varied with the concentration of tenoxicam and the severity of OA. Indeed, a significant reduction was observed at a concentration of 4 μg ml^{-1} in explants with severe OA and of 8 μg ml^{-1} in explants with moderate OA. Further, at each concentration examined, the effect of tenoxicam was always stronger in cartilage with severe OA than in cartilage with less advanced OA lesions.

In normal cartilage there was a significant increase in the loss of labelled HA at an aspirin concentration of 190 μg ml^{-1} and at a tenoxicam concentration of 16 μg ml^{-1} (Figure 4, closed columns). In contrast, in cartilage with moderate OA, 4 and 8 μg ml^{-1} of tenoxicam reduced significantly the net loss of labelled HA and this reduction became even stronger ($P<0.001$) at a concentration of 16 μg ml^{-1}. In cartilage with severe OA, tenoxicam also inhibited the loss of labelled HA in a dose-dependent manner as there was a statistically significant difference ($0.008<P<0.02$) between the values obtained at the different drug concentrations. In both OA groups, 16 μg ml^{-1} of tenoxicam reduced the loss of labelled HA to values similar to those found with 190 μg ml^{-1} of aspirin.

Discussion

The present investigation is the first to describe the effect of tenoxicam and aspirin on the metabolism of proteoglycans (PGs) and hyaluronan (HA) in explants of human normal and osteoarthritic (OA) cartilage.

Cartilage composition and metabolism vary widely in the different topographical areas of the same joint, between the different joints of an individual, and between individuals, and both composition and metabolism change with age (Muir, 1986; Holmes *et al.*, 1988). Accordingly, variations in the concentration and metabolism of both PG and HA were restricted by sampling the articular tissue from the same region of both normal and OA knees. Further, in the normal and OA groups, the donors had a very similar range of age distribution so that differences observed in response to

NSAIDs could be more closely related to the OA disease process rather than aging.

The aspirin and tenoxicam concentrations used in our culture system are similar to the synovial fluid levels of these drugs that have been observed in patients with OA of the knee (Palmoski & Brandt, 1979; 1980; Day *et al.*, 1991). It is however difficult to assess the actual effective concentration of drug acting on the tissue since this depends upon various factors such as the pH of the synovial fluid, the integrity of the surface of the cartilage, the partition coefficient of the drug and protein binding. Further, the final albumin concentration was lower in our culture system than in synovial fluid. Therefore it is likely that, at a tenoxicam level of 16 $\mu g\,ml^{-1}$, the concentration of the free drug in our culture media was greater than that present in the synovial fluid bathing cartilage *in vivo*.

Our study provides for the first time evidence that in normal articular cartilage both aspirin and tenoxicam are able concomitantly to reduce HA synthesis and increase the loss of newly synthesized HA molecules from the tissue. This negative metabolic balance of HA could eventually lead to OA like changes in the normal articular tissue as the OA cartilage matrix is characterized by a progressive depletion of its content in HA (Sweet *et al.*, 1977; Manicourt & Pita, 1988; Rizkalla *et al.*, 1992). It should be however pointed out that the action of aspirin was considerably stronger than that of tenoxicam.

On the other hand, the 2 NSAIDs exhibited a quite different action on the HA metabolism of OA cartilage. Indeed, aspirin is likely to increase the HA depletion of the OA tissue as this drug reduced HA synthesis much more than the net loss of newly synthesized HA molecules. In contrast, in cartilage with severe OA, tenoxicam uncoupled HA synthesis from the loss of HA and produced a positive balance in HA metabolism. This specific effect on the chondrocyte is likely to decrease the HA depletion of the OA tissue and its exact mechanism should be elucidated in further studies as it might be of great biological and therapeutic significance in OA.

In agreement with previous reports (Palmoski & Brandt, 1979; 1980; Muir *et al.*, 1988), aspirin inhibited less strongly the net loss of PG than PG synthesis and the inhibition of PG synthesis was greater in OA cartilage than in normal cartilage. The reduction in the ability of chondrocytes to synthesize PGs was however more marked in the present study (15–25% of control values) than in previous investigations (60–70% of control values) conducted at similar drug concentrations (Brandt, 1987; Muir *et al.*, 1988). It is possible that this difference reflects the fact that, in contrast to the present investigation, the previous studies were conducted on canine articular cartilage.

In contrast to aspirin, tenoxicam had no significant effect on the overall metabolism of PG in normal cartilage whereas in OA cartilage this NSAID produced a positive balance of PG metabolism. Indeed the reduction in the net loss of labelled PG molecules was always greater than the reduction in PG synthesis and cartilage with severe OA was more susceptible to this effect of tenoxicam than cartilage with moderate OA. This heightened susceptibility of pathological articular tissue has already been observed *in vitro* and *in vivo* with other NSAIDs (Brandt, 1987). Although its exact mechanism is unknown at present, data in the literature suggest that it is independent of the inhibition of the cyclooxygenase pathway by the drug and that the uptake of NSAID by cartilage is inversely related to the PG content of the matrix (Brandt, 1987). Accordingly, the decrease in the concentration of negatively charged PGs, which is proportional to the gravity of the OA process, would increase the permeability of the matrix to the acidically charged NSAID.

The reduction in the net loss of PG produced by tenoxicam is quite consistent with a recent report (Vignon *et al.*, 1992) showing that the proteoglycanase activity present in the cartilage of human OA femoral heads sampled at the time of total hip replacement was markedly reduced in the presence of this NSAID at a concentration of 4 $\mu g\,ml^{-1}$. It remains to determine whether this suppressive effect of tenoxicam on the loss of PGs is due either to an inhibition of the production of superoxide anions (Minta & Williams, 1985), or to a reduction in the synthesis and/or activation of proteolytic enzymes or to a stimulation of the synthesis and secretion of tissue inhibitors of proteolytic enzymes (Dean, 1991).

Although it remains to be established whether changes observed in cartilage metabolism over short-term *in vitro* cultures would also occur *in vivo* as a result of long-term administration, the present study suggests that, in contrast to aspirin, tenoxicam at the concentrations found in synovial fluid exerts a favourable effect on the overall metabolism of PG and HA in cartilage with advanced OA lesions. Accordingly, tenoxicam should not *per se* accelerate joint failure in OA. Tenoxicam, however, did not normalize the changes in cartilage metabolism observed in the OA tissue.

We thank Mr Marchand for his excellent secretarial work. This work was supported by the FRSM grant 3.4553.90 and the Belgian State Prime Minister's Office, Science Policy Programming (interuniversity attraction poles, grant 7bis, and concerted actions, grant 88/93.122).

References

BITTER, T. & MUIR, H. (1962). A modified uronic acid carbazole reaction. *Anal. Biochem.*, **4**, 330–334.

BRANDT, K.D. (1987). Effects of nonsteroidal anti-inflammatory drugs on chondrocyte metabolism *in vitro* and *in vivo*. *Am. J. Med.*, **83** Suppl.5A, 29–34.

DAY, R.O., WILLIAMS, K.M., GRAHAM, S. & HANDEL, H. (1991). The pharmacokinetics of total and unbound concentrations of tenoxicam in synovial fluid and plasma. *Arthritis Rheum.*, **34**, 751–760.

DEAN, D.D. (1991). Proteinase-mediated cartilage degradation in osteoarthritis. *Sem. Arthritis Rheum.*, **20** Suppl.2, 2–11,

FRANCHIMONT, P., BASSLEER, C. & HENROTIN, Y. (1989). Effects of hormones and drugs on cartilage repair. *J. Rheumatol.*, **16** Suppl. 18, 5–9.

GONZALEZ, J.P. & TODD, P.A. (1987). Tenoxicam: a preliminary review of its pharmacodynamic and pharmacokinetic properties and therapeutic efficacy. *Drugs*, **34**, 289–310.

HARDINGHAM, T.E., MUIR, H., KWAN, M.K., LAI, W.M. & MOW, V.C. (1987). Viscoelastic properties of proteoglycan solutions with varying proportions present as aggregates. *J. Orthop. Res.*, **5**, 36–46.

HOLMES, M.W., BAYLISS, M.T. & MUIR, H. (1988). Hyaluronic acid in human articular cartilage. Age-related changes in content and size. *Biochem. J.*, **250**, 435–441.

HOWELL, D.S., PITA, J.C., MULLER, F.J., MANICOURT, D.H. & ALTMAN, R.D. (1991). Treatment of osteoarthritis with tiaprofenic acid: biochemical and histological protection against cartilage breakdown in the Pond-Nuki canine model. *J. Rheumatol.*, **18** Suppl. 27, 138–142.

KIRCHHEIMER, B., HOLM, P., JENSEN, E.M., KRYGER, J., ROMBERG, O. & SALVESON, A. (1982). A new long-acting anti-inflammatory agent tenoxicam (tilcotil) in osteoarthritis of the knee and the hip: a randomized comparison with indomethacin. *Curr. Ther. Res.*, **32**, 627–632.

LOHMANDER, S. (1988). Proteoglycan of joint cartilage. Structure, function, turnover and role as markers of joint disease. *Baillière's Clin. Rheum.*, **2**, 37–62.

MANICOURT, D.H. & PITA, J.C. (1988). Progressive depletion of hyaluronic acid in early experimental osteoarthritis in dogs. *Arthritis Rheum.*, **31**, 538–544.

MANKIN, H.J., DORFMAN, H., LIPPIELLO, L. & ZARINS, A. (1971). Biochemical and metabolic abnormalities in articular cartilage from osteoarthritic hips. II. Correlation of morphology with biochemical and metabolic data. *J. Bone Jt. Surg.*, **53A**, 523–537.

MINTA, J.O. & WILLIAMS, M.D. (1985). Some nonsteroidal antiinflammatory drugs inhibit the generation of superoxide anions by activated polymorphs by blocking ligand-receptor interactions. *J. Rheumatol.*, **12**, 751–757.

MUIR, H. (1986). Current and future trends in articular cartilage research and osteoarthritis. In *Articular Cartilage Biochemistry*. ed. Kuettner, K., Scheyerbach, D.U.M. & Hascall, V.C. pp. 423–440. New York: Raven Press.

MUIR, H., CARNEY, S.L. & HALL, L.G. (1988). Effects of tiaprofenic acid and other NSAIDs on proteoglycan metabolism in articular cartilage explants. *Drugs*, **35** Suppl. 1, 15–23.

PALMOSKI, M.J. & BRANDT, K.D. (1979). Effect of salicylate on proteoglycan metabolism in normal canine articular cartilage *in vitro*. *Arthritis Rheum.*, **22**, 746–754.

PALMOSKI, M.J. & BRANDT, K.D. (1980). Effects of some nonsteroidal antiinflammatory drugs on proteoglycan metabolism and organization in canine articular cartilage. *Arthritis Rheum.*, **23**, 1010–1020.

RIZKALLA, G., REINER, A., BOGOCH, E. & POOLE, A.R. (1992). Studies of the articular cartilage proteoglycan aggrecan in health and osteoarthrosis. Evidence for molecular heterogeneity and extensive molecular changes in disease. *J. Clin. Invest.*, **90**, 2268–2277.

SWEET, M.B.E., THONAR, E.J.M., IMMELMAN, A.R. & SOLOMON, L. (1977). Biochemical changes in progressive osteoarthritis. *Ann. Rheum. Dis.*, **36**, 387–398.

TENGBLAD, A. (1980). Quantitative analysis of hyaluronate in nanograms amounts. *Biochem. J.*, **185**, 101–105.

VIGNON, E., MATHIEU, P., LOUIZOT, P. & RICHARD, M. (1992). *In vitro* effect of nonsteroidal antiinflammatory drugs on proteoglycanase and collagenase activity in human osteoarthritic cartilage. *Arthritis Rheum.*, **34**, 1332–1335.

WOESSNER, J.F. Jr. (1961). The determination of hydroxyproline in tissue and protein samples containing a small portion of this amino acid. *Arch. Biochem. Biophys.*, **93**, 440–447.

(Received December 22, 1993
Revised May 5, 1994
Accepted June 17, 1994)

Br. J. Pharmacol. (1994), **113**, 1121–1126 © Macmillan Press Ltd, 1994

Neutral endopeptidase (NEP) inhibition in rats with established pulmonary hypertension secondary to chronic hypoxia

[1]J.S. Thompson, W. Sheedy & A.H. Morice

Department of Medicine and Pharmacology, University of Sheffield, Royal Hallamshire Hospital, Glossop Road, Sheffield, S10 2JF

1 Atrial natriuretic peptide (ANP) causes vasorelaxation in the pulmonary vasculature. ANP levels are elevated in conditions characterized by pulmonary hypertension and it has been hypothesized that ANP may be autoregulatory in the pulmonary circulation.

2 One route of ANP metabolism *in vivo* is by the action of the enzyme neutral endopeptidase (NEP). We have studied the effects of the NEP inhibitor, SCH 42495, in rats with established pulmonary hypertension secondary to chronic hypoxia.

3 Rats ($n = 32$) were divided into 4 groups. Normoxic controls were kept in air for 10 days (NC10) and all other animals were placed in a normobaric hypoxic chamber (Fi O_2 10%). Chronic hypoxic controls were studied at 10 days (CHC10). After 10 days hypoxia the two remaining groups received oral treatment for a further 10 days, consisting of either SCH 42495 (30 mg kg^{-1}, twice daily CHT20) or methyl cellulose vehicle (0.4%, twice daily, CHV20).

4 Animals were anaesthetized and blood collected for measurement of plasma ANP. Hearts were dissected and ventricles weighed and the histology of the pulmonary vasculature examined.

5 CHC10 rats had significant right ventricular hypertrophy (0.53 ± 0.08) and pulmonary vascular remodelling ($29.0 \pm 0.01\%$) and had gained significantly less body weight (33.2 ± 5.5 g) than NC10 rats (0.31 ± 0.04, $10.9 \pm 0.01\%$, and 59.2 ± 11.9 g respectively). CHC10 rats had significantly elevated plasma ANP levels (58.4 ± 9.9 pM) compared with NC10 rats (23.9 ± 32 pM). Treatment with SCH 42495 caused a significant reduction in pulmonary vascular remodelling ($25.0 \pm 0.01\%$) and right ventricular hypertrophy (0.52 ± 0.09) in CHT20 rats compared with CHV20 controls ($33.0 \pm 0.02\%$ and 0.61 ± 0.09 respectively). Pulmonary vascular remodelling was also significantly lower in CHT20 rats than CHC10 animals.

6 Thus, short term inhibition of NEP causes regression of established pulmonary vascular remodelling and may be a useful therapeutic strategy in pulmonary hypertension.

Keywords: Atrial natriuretic peptide; neutral endopeptidase inhibitor; chronic hypoxic pulmonary hypertension; remodelling

Introduction

Atrial natriuretic peptide (ANP) is a 28 amino acid hormone of cardiac origin which exhibits vasoactive, diuretic and natriuretic properties (Adams, 1987). ANP is released in response to an increase in pulmonary artery pressure because of right atrial and ventricular distension. In disease states characterized by an increased pulmonary artery pressure, such as primary pulmonary hypertension (Morice *et al.*, 1990), chronic obstructive airways disease (COAD) (Winter *et al.*, 1989), acute respiratory distress syndrome (Eison *et al.*, 1988), and chronic thromboembolism (Noll *et al.*, 1990), ANP synthesis and secretion is increased and plasma levels are elevated.

ANP is a potent vasodilator in the pulmonary vasculature. Jansen *et al.* (1987) showed that ANP was more potent in isolated pulmonary, as opposed to renal, vessels of the pig. We have demonstrated that ANP causes a dose-dependent relaxation in preconstricted isolated perfused lungs (Stewart *et al.*, 1991b), and isolated pulmonary resistance vessels (Rogers *et al.*, 1992) in the rat and that relaxation appears to be particularly potent against hypoxic vasoconstriction (Rogers *et al.*, 1992).

Chronic pulmonary hypertension causes remodelling of the pulmonary vasculature, with neomuscularization of pulmonary vessels towards the periphery of the lung. Infusion of ANP with osmotic minipumps has been shown to reduce the cardio-pulmonary remodelling associated with the development of hypoxic pulmonary hypertension in rats (Zhao *et al.*, 1991), as has chronic elevation of ANP in mice that have been genetically engineered to over-express ANP (Klinger *et al.*, 1993a). However, the therapeutic potential of ANP is limited by rapid *in vivo* metabolism with a plasma half life of ANP of less than 3 min in the rat (Hollister *et al.*, 1989). The metabolic action of the enzyme neutral endopeptidase 24.11 (NEP) and clearance receptor binding are the two identified mechanisms of ANP clearance. Because of this dual pathway of clearance, attempts to elevate plasma ANP solely by inhibiting NEP have met with limited success. However, NEP inhibition does prolong the half life of ANP, elevate plasma ANP levels, and cause diuresis on volume loading in rats (Watkins *et al.*, 1993), normal human volunteers (Danielwicz *et al.*, 1989) and patients in chronic heart failure (Northridge *et al.*, 1989).

We and others have previously found that NEP inhibition caused a significant reduction in the cardio-pulmonary remodelling associated with the development of pulmonary hypertension in rats exposed to chronic hypoxia (Winter *et al.*, 1991; Stewart *et al.*, 1992; Klinger *et al.*, 1993b; Thompson *et al.*, 1994). Unfortunately, these models are of limited clinical relevance in that they study the development of pulmonary hypertension. Of more interest is the effect of NEP inhibition on established pulmonary hypertension. In the present study therefore, we have investigated the effects of the NEP inhibitor SCH 42495 on rats with established cardio-pulmonary remodelling secondary to chronic hypoxia.

Methods

Litters of male Wistar rats (Royal Hallamshire Hospital) were obtained at 21 days of age and allowed to acclimatize to

[1] Author for correspondence.

the laboratory for 5 days. Animals were maintained in 12 h/12 h dark/light cycle with free access to standard rat chow and water. The litters were divided into four groups, two of 6 rats and two of 10 rats. One group of 6 animals were placed in the normobaric, hypoxic chamber at an Fi O_2 of 10% for 10 days (chronic hypoxic controls; CHC10), while the other group of 6 rats were kept in the same room but exposed to air for 10 days (normoxic controls; NC10).

The two remaining groups of 10 rats were placed in the normobaric, hypoxic chamber at an Fi O_2 of 10% for 20 days. After 10 days, one group (chronic hypoxic drug-treated; CHT20) received SCH 42495 (30 mg kg^{-1}, 1 to 2 ml) while the other group (chronic hypoxic vehicle-treated; CHV 20) received aqueous methyl cellulose vehicle (0.4%, 1 to 2 ml) at 12 hourly intervals by oral gavage. All animals were weighed daily prior to the morning dose. Treatment resulted in rats in the hypoxic chamber being exposed to room air for approximately 30 min twice daily. Groups of rats were anaesthetized with pentobarbitone (60 mg kg^{-1}, i.p.) and blood samples were collected in a heparinized syringe from the main pulmonary artery via the right ventricle. Blood was immediately transferred to chilled EDTA tubes, centrifuged (3000 r.p.m., 15 min), and plasma stored at − 40°C for subsequent radioimmunoassay of ANP (Stewart et al., 1991a) (intra-assay coefficient of variation, 16.3%; inter-assay coefficient of variation, 14.6%; assay sensitivity, 8.9 pM; and limit of detection, 2.0 pM).

The heart was carefully removed from the animal and the atria cut away and discarded. The right ventricle (RV) was dissected from the left ventricle plus septum (LV + S) and post-mortem blood removed by blotting on a piece of tissue paper. The ventricles were weighed on a chemical balance (Ohaus Analytical Plus) and the ratio of RV to LV + S determined. The trachea was cannulated and lungs inflated and fixed with 10% buffered formol saline (pH 7.4) at a pressure of 20 cm water. Blocks (3 mm) were cut from the left lung just below the hilum and vacuum embedded in paraffin wax; 5 μm sections were cut and stained with Miller's solution. Slides were examined under an optical microscope (× 40 magnification) without prior knowledge of their identity. All vessels less than 50 μm diameter with an elastic coat, situated adjacent to an alveolar duct or alveoli, were counted. The proportion of these vessels with a double elastic lamina (DEL) around at least 50% of the vessels' internal wall were calculated, as previously described (Leach et al., 1977).

Results were expressed as mean ± standard error of the mean (s.e.mean). Groups were compared by Student's two-tailed unpaired t test.

Results

Body weight

After 10 days exposure to a normobaric, hypoxic environment, the CHC10 animals had gained significantly ($P<0.001$) less weight (g) than the NC10 controls (33.2 ± 5.5 and 59.2 ± 11.9 respectively). There was no significant difference in change in body weight between the CHV20 group, which received vehicle for a further 10 days in the hypoxic environment, and the CHT20 group, which received SCH 42495 for a further 10 days in the hypoxic environment (84.4 × 10.2 and 87.6 ± 13.1 respectively). Results are shown graphically in Figure 1.

RV/[LV + S]

The CHC10 rats had developed significant ($P<0.001$) right ventricular hypertrophy when compared with NC10 controls (0.53 ± 0.08 and 0.31 ± 0.04 respectively) after 10 days in the hypoxic chamber. Treatment with SCH 42495 for 10 days arrested any further development of ventricular hypertrophy, the ventricular ratio for the CHT20 animals was similar to the ratio of the CHC10 animals (0.52 ± 0.09 and 0.53 ± 0.08 respectively). Those animals receiving vehicle for 10 days (CHV20) demonstrated continued progression of right ventricular hypertrophy, the ratio being significantly greater ($P<0.05$) than the CHC10 animals (0.61 ± 0.09 and 0.53 ± 0.08 respectively). Results are shown graphically in Figure 2.

Pulmonary vascular remodelling

Ten days exposure to normobaric hypoxia resulted in significant remodelling of the pulmonary vasculature (Figure 3). The proportion of vessels < 50 μm that had developed a DEL in CHC10 animals was significantly greater ($P<0.005$) than the NC10 rats (29.0 ± 0.01% and 10.9 ± 0.01% respectively). Treatment with SCH 42495 caused an attenuation in the development of DEL. Not only was the degree of pulmonary vascular remodelling in the CHT20 rats less than that in the CHV20 animals (25.0 ± 0.01% and 33.0 ± 0.02% respectively, $P<0.05$), but it was also significantly less ($P<0.05$) than the degree of pulmonary vascular remodelling observed after 10 days exposure to hypoxia in the CHC10 rats (29.0 ± 0.01%). Results are shown graphically in Figure 4.

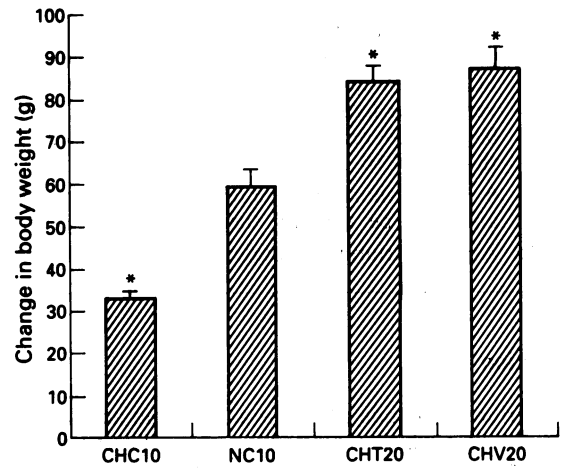


Figure 1 Change in body weight (g) in untreated, control rats exposed to chronic hypoxia for 10 days (CHC10) and normoxia for 10 days (NC10), and in rats treated with SCH 42495 (CHT20) or vehicle (CHV20) during a further 10 days in the chronic hypoxic environment. *$P<0.001$ compared with NC10. Results are as mean ± s.e.mean.

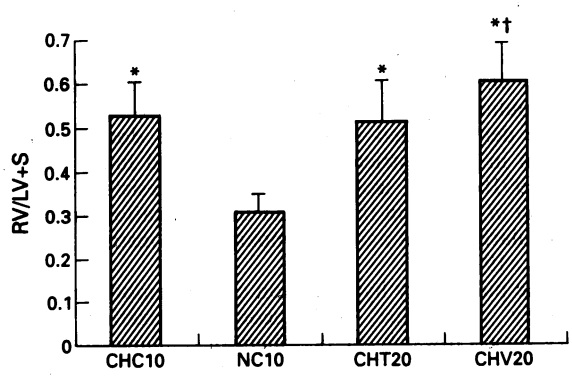


Figure 2 Ventricular ratios in untreated, control rats exposed to chronic hypoxia for 10 days (CHC10) and normoxia for 10 days (NC10), and in rats treated with SCH 42495 (CHT20) or vehicle (CHV20) during a further 10 days in the chronic hypoxic environment. *$P<0.001$ compared with NC10. †$P<0.05$ compared with CHC10. Results are as mean ± s.e.mean.

ANP levels

Plasma ANP levels (pM) were significantly ($P<0.05$) elevated after 10 days in CHC10 rats (58.4 ± 9.9) compared with NC10 controls (23.9 ± 3.2). Treatment with SCH 42495 did not result in any further elevation of plasma ANP levels in CHT20 rats (23.9 ± 5.7). Indeed, treatment with SCH 42495 caused a significant decrease in plasma ANP levels towards levels observed in the NC10 rats. Vehicle-treated animals (CHV20) continued to demonstrate significantly elevated plasma ANP levels (47.4 ± 11.2 pM). Results are shown graphically in Figure 5.

Discussion

Chronic alveolar hypoxia, whether it is normobaric or hypobaric, is a well-documented model of man at high altitude and of hypoxic lung disease. Rats exposed to low inspired oxygen tensions develop pulmonary hypertension (Rabinovitch *et al.*, 1979) which is associated with pulmonary vascular remodelling, right ventricular hypertrophy, and an increase in haematocrit secondary to the renal response to hypoxia (Abraham *et al.*, 1971; Leach *et al.*, 1977). The development of pulmonary hypertension is closely correlated with the morphological changes seen in the cardio-pulmonary system, particularly the pulmonary vascular remodelling (Rabinovitch *et al.*, 1979).

In the pulmonary vascular bed remodelling is characterized by a thickening of the vessel wall predominantly by hyperplasia of smooth muscle. These changes occur primarily in the small, non-muscularized, precapillary pulmonary arteries and result in the apparent duplication of the elastic laminae (Rabinovitch *et al.*, 1979). The structural changes in the pulmonary vascular tree caused by chronic exposure to hypoxia are largely reversible on return to air. In the rat, pulmonary vascular remodelling begins after about 2 days exposure and is complete after about 10 days (Hunter *et al.*, 1974).

In this study we examined pulmonary vessels less than 50 μm internal diameter following exposure to normobaric hypoxia using the development of a double elastic lamina as a marker for pulmonary vascular remodelling. Hypoxia caused a threefold increase in the proportion of small vessels

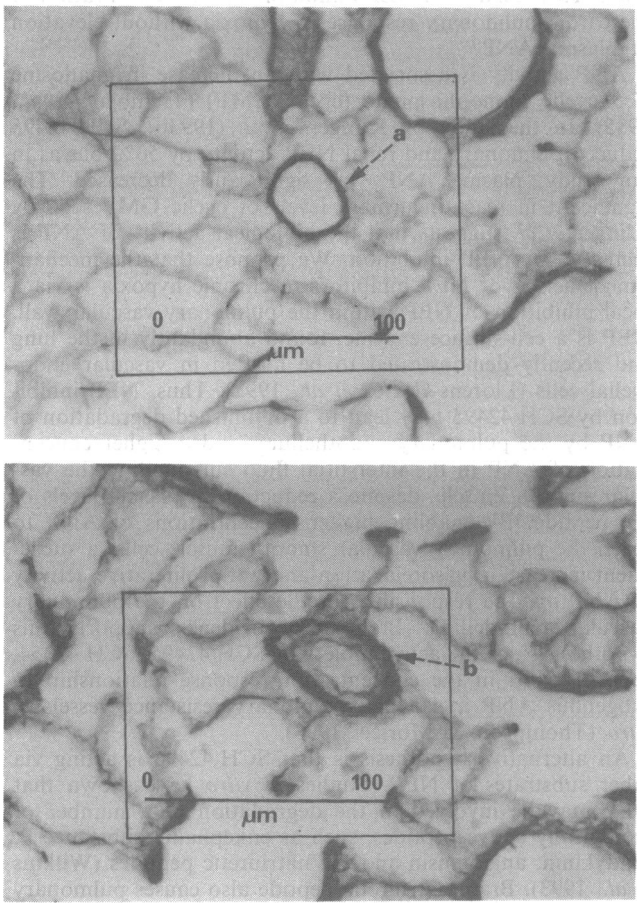


Figure 3 The light microscopical appearance of (a) a normal pulmonary vessel (< 50 μm external diameter) from a littermate kept in room air and (b) a remodelled rat pulmonary vessel (< 50 μm external diameter) after 10 days exposure to chronic, normobaric hypoxia. Sections were stained with Miller's solution and viewed under a magnification of × 40. Treatment (SCH 42495, 30 mg kg^{-1}) or rats with established pulmonary vascular remodelling for a further 10 days (CHT20) resulted in significant ($P<0.05$) fewer pulmonary vessels which had developed a DEL around at least 50% of the internal circumference compared with vehicle-treated, chronic hypoxic rats (CHV20).

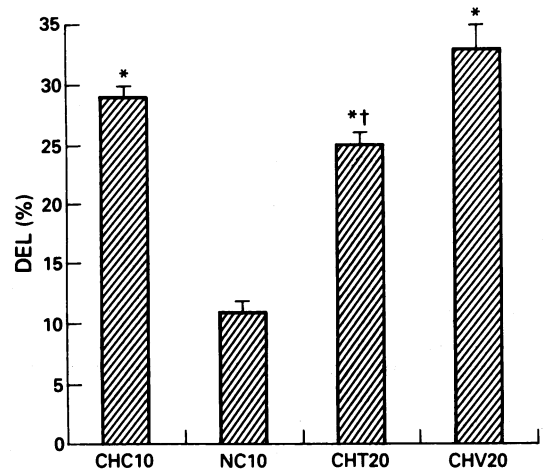


Figure 4 Proportion of vessels (< 50 μm internal diameter) which had developed a double elastic lamina (DEL, %) around at least 50% on the internal circumference in the four groups of rats, were compared. Groups were untreated, control rats exposed to chronic hypoxia for 10 days (CHC10) and normoxia for 10 days (NC10), and in rats treated with SCH 42495 (CHT20) or vehicle (CHV20) during a further 10 days in the chronic hypoxic environment. *$P<0.005$ compared with NC10. †$P<0.05$ compared with CHC10 and CHV20. Results are as mean ± s.e.mean.

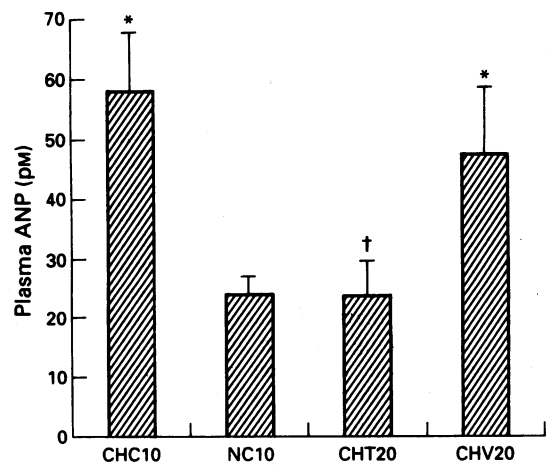


Figure 5 Plasma ANP levels (pM) in untreated, control rats exposed to chronic hypoxia for 10 days (CHC10) and normoxia for 10 days (NC10), and in rats treated with SCH 42495 (CHT20) or vehicle (CHV20) during a further 10 days in the chronic hypoxic environment. *$P<0.05$ compared with NC10. †$P<0.05$ compared with CHC10 and CHV20. Results are as mean ± s.e.mean.

exhibiting a double elastic lamina, an effect which was established after 10 days. Animals also demonstrated significant right ventricular hypertrophy, the ratio of RV/LV + S increasing by two thirds after 10 days hypoxia. Unlike the changes of pulmonary vascular remodelling, right ventricular hypertrophy progressed with continued hypoxic exposure, the RV/LV + S ratio doubling after 20 days exposure.

On return to normoxia, the pathophysiological changes which develop during chronic hypoxia in this rat model resolve at different rates. Right ventricular hypertrophy takes approximately 12 weeks to resolve whereas pulmonary vascular remodelling is still evident after 20 weeks and never fully resolves (Hunter *et al.*, 1974; Leach *et al.*, 1977). In man, descent from high altitude to sea level leads to similar resolution of cardio-pulmonary remodelling, but with a much slower time course (Heath & Williams, 1981).

In patients with COAD, pulmonary vascular resistance is elevated (Matthay *et al.*, 1990), due in part to remodelling of the small pulmonary arteries and arterioles (Singer *et al.*, 1987). The only treatment available to date which has altered mortality in COAD is long-term oxygen therapy, which has been suggested to act by inhibiting the further development of pulmonary vascular remodelling secondary to hypoxia. Thus, treatment that causes a reduction in the degree of vascular remodelling, as opposed to simple pulmonary vasodilatation, may be preferable in diseases characterized by hypoxic pulmonary hypertension, since studies investigating the use of vasodilators in COAD have so far failed to demonstrate any effect on prognosis (Howard, 1989).

In animal models, the majority of studies looking at pulmonary vascular remodelling have examined the effect of therapy on the development of remodelling during exposure to a stimulus (usually hypoxia). Whilst this is a good screening test for potential activity, in the clinical situation the patient presents with established pulmonary hypertension and ideally therapy should reverse established pulmonary vascular remodelling.

It has been hypothesized that ANP may be involved in a homeostatic feedback loop to protect the pulmonary vasculature from pulmonary hypertension. In support of this, plasma levels of ANP have been shown to be elevated in response to increased pulmonary artery pressure both in animal models (McKenzie *et al.*, 1986; Jin *et al.*, 1990) and in man (Winter *et al.*, 1989; Morice *et al.*, 1990). The vasodilatation caused by ANP is particularly potent in the pulmonary circulation (Jansen *et al.*, 1987) with hypoxic vasoconstriction being preferentially inhibited (Rogers *et al.*, 1992). In a recent study we have shown that an acute infusion of ANP in patients with COAD and pulmonary hypertension caused specific pulmonary vasodilatation without adversely effecting systemic haemodynamics or ventilation perfusion matching (Rogers *et al.*, 1994).

The effect of ANP on pulmonary vascular remodelling in response to chronic hypoxia has been studied by continuous infusion of exogenous ANP and a reduction of DEL has been demonstrated (McKenzie *et al.*, 1986; Zhao *et al.*, 1991). Similarly, transgenic mice that overexpress ANP have reduced remodelling in chronic hypoxia (Klinger *et al.*, 1993a). The mechanism by which ANP reduces the cardio-pulmonary remodelling associated with chronic hypoxic pulmonary hypertension is undefined. It is most likely to be a combination of vasodilatation leading to a reduction in the stimulus for remodelling, and an antiproliferative action on vascular smooth muscle, as studies have demonstrated inhibition of vascular smooth muscle cell growth by ANP *in vitro* (Abell *et al.*, 1989; Itoh *et al.*, 1990).

ANP is rapidly cleared from the circulation by clearance receptor binding and the metabolic action of the membrane-bound enzyme, neutral endopeptidase (NEP) EC 24.11. ANP therefore has a relative short half life *in vivo* (Hollister *et al.*, 1989), and has little therapeutic potential. Attempts to prolong the bioavailability of ANP *in vivo* have included ANP clearance receptor blockade, and inhibition of NEP. Studies using NEP inhibitors *in vivo* have demonstrated an increase in the half-life and natriuretic effect of exogenous ANP (Lafferty *et al.*, 1989; Sybertz *et al.*, 1990a). This is a specific effect since ANP antisera blocks the activity of NEP inhibitors (Shepperson *et al.*, 1991). We have previously demonstrated an attenuation in the development of pulmonary hypertension secondary to chronic hypoxia in rats by the NEP inhibitor, SCH 42495 (Thompson *et al.*, 1994), although no significant elevation in plasma ANP levels were observed. Similar results have also been reported with the less potent (Watkins *et al.*, 1993) compound, SCH 34826 (Stewart *et al.*, 1992), and the structurally unrelated drug, Candoxatrilat (Winter *et al.*, 1991). However, in this latter study, Winter *et al.* observed a significant elevation of plasma ANP levels in rats treated with Candoxatrilat during seven days exposure to hypoxia and proposed that the mechanism by which NEP inhibition reduced pulmonary vascular remodelling was by elevation of plasma ANP levels.

In the present study, NEP inhibition with SCH 42495 led to significant reduction in the progression of pulmonary vascular remodelling, which was clearly not attributable to elevations in plasma ANP levels, as we observed a significant fall in plasma ANP with drug treatment. Similarly, Klinger *et al.* (1993b) showed that rats treated with the less potent NEP inhibitor, SCH 34826 (90 mg kg^{-1}; twice daily) during 3 weeks of chronic hypoxia had a significantly lower degree of right ventricular hypertrophy, and less pulmonary vascular remodelling, despite a significant reduction in plasma ANP levels. How then does NEP inhibition lead to modification of the cardio-pulmonary response to hypoxia without elevation of plasma ANP?

ANP activity is associated with an increase in guanosine 3':5'-cyclic monophosphate (cyclic GMP) (Tremblay *et al.*, 1985). In the study by Klinger *et al.* (1993b), SCH 42495 reduced pulmonary and renal NEP activity by 50% but as in our study, plasma ANP was significantly decreased. The significant increase in urinary levels of cyclic GMP seen by Klinger *et al.* suggests that the biological activity of ANP is increased by NEP inhibition. We propose that the mechanism of action of NEP inhibitors in chronic hypoxia is via a local inhibition of NEP within the pulmonary vascular wall. NEP is a cell-surface enzyme, found abundantly in the lung and recently demonstrated to be located in vascular endothelial cells (Llorens-Cortez *et al.*, 1992). Thus, NEP inhibition by SCH 42495 may lead to a diminished degradation of ANP by the pulmonary endothelium, and a higher concentration of ANP in the interstitial fluid surrounding the vascular smooth muscle, despite a reduction in plasma levels of the peptide. By enabling higher concentrations of ANP to reach the pulmonary vascular smooth muscle cells, a subsequent increase in vasorelaxation and antiproliferative activity of ANP may be responsible for the effect on the pulmonary vascular remodelling. Preliminary evidence supports this hypothesis since the active moiety of SCH 42495, SCH 42354, causes a shift in the concentration-response relationship to exogenous ANP in isolated pulmonary resistance vessels *in vitro* (Thompson & Morice, 1993).

An alternative hypothesis is that SCH 42495 is acting via other substrates of NEP. Studies *in vitro* have shown that NEP may be involved in the degradation of a number of biologically active peptides, such as enkephalin, substance P, bradykinin, angiotensin and the natriuretic peptides (Wilkins *et al.*, 1993). Brain natriuretic peptide also causes pulmonary vasodilatation (Rogers *et al.*, 1993), and C-type natriuretic peptide has vasorelaxant and antiproliferative actions (Furuya *et al.*, 1991; Stingo *et al.*, 1992).

SCH 42495 appears to be relatively specific to NEP, with little activity against other peptidases. Watkins *et al.* (1993) demonstrated that the *in vivo* hypotensive response to SCH 42495 (3 and 30 mg kg^{-1}), seen in volume expanded rats, was not affected by intravenous administration of two substrates of ACE, bradykinin or angiotensin II. Similarly, Sybertz *et al.* (1990b) showed that, whilst the antihypertensive response

to SCH 42495 in DOCA-salt hypertensive rats was abruptly reversed by ANP antibodies, intravenous administration of a bradykinin antagonist had no effect.

Treatment with the NEP inhibitor, SCH 42495, partially reversed the proportion of DEL and attenuated the further development of right ventricular hypertrophy, in rats in which pulmonary vasculature had already been remodelled by exposure to 10 days hypoxia. To date only two studies have demonstrated a reduction in pulmonary vascular remodelling in established pulmonary hypertension, both using calcium channel blockade (Stanbrook *et al.*, 1984; Michael *et al.*, 1986). In man, calcium channel blockade is used in the treatment of primary pulmonary hypertension and may affect prognosis (Rich *et al.*, 1992). In pulmonary hypertension secondary to COAD, calcium channel blockade has proven less successful (Howard, 1989). Thus, the demonstration that inhibitors of NEP cause a reduction in established pulmonary vascular remodelling may have important implications for the treatment of this disease.

In summary, we have demonstrated that treatment with the NEP inhibitor, SCH 42495, reduced the established cardio-pulmonary changes associated with pulmonary hypertension secondary to chronic hypoxia in rats. However, this occurred despite a reduction in plasma ANP levels suggesting that elevated tissue, rather than plasma, levels of the peptide are involved in the action of this NEP inhibitor.

Research was supported by Schering-Plough and The British Heart Foundation.

References

ABELL, T.J., RICHARDS, A.M., IKRAM, H., ESPINER, E.A. & YANDLE, T. (1989). Atrial natriuretic factor inhibits proliferation of vascular smooth muscle cells stimulated by platelet-derived growth factor. *Biochem. Biophys. Res. Commun.*, **160**, 1392–1396.

ABRAHAM, A.S., KAY, J.M., COLE, R.B. & PINCOCK, A.C. (1971). Haemodynamic and pathological study of the effect of chronic hypoxia and subsequent recovery of the heart and pulmonary vasculature of the rat. *Cardiovasc. Res.*, **5**, 95–102.

ADAMS, S.P. (1987). Structure and biologic properties of the atrial natriuretic peptides. *Endocrinol. Metab. Clin. N. Am.*, **16**, 1–17.

DANIELEWICZ, J.C., BARCLAY, P.L., BARNISH, I.T., BROWN, D., CAMPBELL, S.F., JAMES, K, SAMUELS, G.M.R., TERRETT, N.K. & WYTHES, M.J. (1989). UK 69,578, a novel inhibitor of EC 3.4.24.11 which increases endogenous ANF levels and is natriuretic and diuretic. *Biochem. Biophys. Res. Commun.*, **164**, 58–65.

EISON, H.B., ROSEN, M.J., PHILLIPS, R.A. & KRAKOFF, L.R. (1988). Determinants and atrial natriuretic factor in the adult respiratory distress syndrome. *Chest*, **94**, 1040–1045.

FURUYA, M., YOSHIDA, M., HAYASHI, Y., OHNUMA, N., MINAMINO, N., KANGAWA, K. & MATSUO, H. (1991). C-type natriuretic peptide is a growth inhibitor of vascular smooth muscle cells. *Biochem. Biophys. Res. Commun.*, **177**, 927–931.

HEATH, D. & WILLIAMS, D.R. (1981). *Man at High Altitude*. London: Churchill Livingstone.

HOLLISTER, A.S., ROEDEHEFFER, R.J., WHITE, F.J., POTTS, J.R., IMADA, T. & INAGAMI, T. (1989). Clearance of atrial natriuretic factor by lung, liver and kidney in human subjects and the dog. *J. Clin. Invest.*, **83**, 623–628.

HOWARD, P. (1989). Vasodilator drugs in chronic obstructive airways disease. *Eur. Respir. J.*, Suppl. 7, 678s–681s.

HUNTER, C., BARER, G.R., SHAW, J.W. & CLEGG, E.J. (1974). Growth of the heart and lungs in hypoxic rodents: a model of human hypoxic disease. *Clin. Sci. Mol. Med.*, **46**, 375–391.

ITOH, H., PRATT, R.E. & DZAU, V.J. (1990). Atrial natriuretic polypeptide inhibits hypertrophy of vascular smooth muscle cells. *J. Clin. Invest.*, **86**, 1690–1697.

JANSEN, T.L., MORICE, A.H. & BROWN, M.J. (1987). A comparison of the vasodilator responses to atrial peptides in the pulmonary and renal arteries of the pig *in vitro*. *Br. J. Pharmacol.*, **91**, 687–691.

JIN, H., YANG, R.H., CHEN, Y.F., JACKSON, R.M. & OPARIL, S. (1990). Atrial natriuretic peptide attenuates the development of pulmonary hypertension in rats adapted to chronic hypoxia. *J. Clin. Invest.*, **85**, 115–120.

KLINGER, J.R., PETIT, R.D., CURTIN, L.A., WARBURTON, R., WRENN, D.S., STEINHELPER, M.E., FIELD, L.J. & HILL, N.S. (1993a). Cardiopulmonary responses to chronic hypoxia in transgenic mice that overexpress ANP. *J. Appl. Physiol.*, **75**, 198–205.

KLINGER, J.R., PETIT, R.D., WARBURTON, R.R., WRENN, D.S., ARNAL, J.-F. & HILL, N.S. (1993b). Neutral endopeptidase inhibition attenuates the development of hypoxic pulmonary hypertension in rats. *J. Appl. Physiol.*, **75**, 1615–1623.

LAFFERTY, H.M., GUNNING, M., SILVA, P., ZIMMERMAN, M.B., BRENNER, B.M. & ANDERSON, S. (1989). Enkephalinase inhibition increases plasma atrial natriuretic peptide levels, glomerular filtration rate, and urinary sodium excretion in rats with reduced renal mass. *Circ. Res.*, **65**, 640–646.

LEACH, E., HOWARD, P. & BARER, G.R. (1977). Resolution of hypoxic changes in the heart and pulmonary arterioles of rats during intermittent correction of hypoxia. *Clin. Sci. Mol. Med.*, **52**, 153–162.

LLORENS-CORTEZ, C., HUANG, H., VICAR, P., GASE, J.M., PAULIN, D., CORVOL, P. (1992). Identification and characterization of neutral endopeptidase in endothelial cells from venous and arterial origins. *J. Biol. Chem.*, **267**, 14012–14018.

MATTHAY, R.A., NIEDERMAN, M.S. & WIEDEMANN, M.D. (1990). Cardiovascular-pulmonary interaction in chronic obstructive pulmonary disease with special reference to the pathogenesis and management of cor pulmonale. *Med. Clin. N. Am.*, **74**, 571–618.

MCKENZIE, J.C., TANAKA, I., INAGAMI, T., MISONO, K.S. & KLEIN, R.M. (1986). Alterations in atrial and plasma atrial natriuretic factor (ANF) content during development of hypoxia-induced pulmonary hypertension in the rat. *Proc. Soc. Exp. Biol. Med.*, **181**, 459–463.

MICHAEL, J.R., KENNEDY, T.P., BUESCHER, P.C., FARRUKH, I.S., LODATO, R.F., ROCK, P.C., GOTTLIEB, J.E., GURTNER, G.H., DE LA MONTE, S.M. & HUTCHINS, G.M. (1986). Nitrendipine attenuates the pulmonary vascular remodelling and right ventricular hypertrophy caused by intermittent hypoxia in rats. *Am. Rev. Respir. Dis.*, **133**, 375–379.

MORICE, A.H., PEPKE-ZABA, J., BROWN, M.J., THOMAS, P.S. & HIGENBOTTAM, T.W. (1990). Atrial natriuretic peptide in primary pulmonary hypertension. *Eur. Resp. J.*, **3**, 910–913.

NOLL, B., HEIN, H., MAISCH, B. & VON WICHERT, P. (1990). Changes in atrial natriuretic peptide in patients with lung embolism and obstructive respiratory tract disease. [German]. *Pneumologie*, **44**, 70–73.

NORTHRIDGE, D.B., JARDINE, A.G., ALABASTER, C.T., BARCLAY, P.L., CONNELL, J.M., DARGIE, H.J., DILLY, S.G., FINDLAY, I.N., LEVER, A.F. & SAMUELS, G.M. (1989). Effects of UK 69 578: a novel atriopeptidase inhibitor. *Lancet*, **ii**, 591–593.

RABINOVITCH, M., GAMBLE, W., NADAS, A.S., MIETTINEN, O.S. & REID, L. (1979). Rat pulmonary circulation after chronic hypoxia haemodynamic and structural features. *Am. J. Physiol.*, **236**, 818–827.

RICH, S., KAUFMANN, E. & LEVY, P.S. (1992). The effect of high doses of calcium-channel blockers on survival in primary pulmonary hypertension. *New Engl. J. Med.*, **327**, 76–81.

ROGERS, T.K., JONES, Q.T.G. & MORICE, A.H. (1993). Inhibition of hypoxic vasoconstriction by brain natriuretic peptide. *Thorax*, **48**, 466.

ROGERS, T.K., SHEEDY, W., WATERHOUSE, J., HOWARD, P. & MORICE, A.H. (1994). Haemodynamic effects of Atrial Natriuretic Peptide in hypoxic chronic obstructive pulmonary disease. *Thorax*, **49**, 233–239.

ROGERS, T.K., STEWART, A.G. & MORICE, A.H. (1992). Effect of chronic hypoxia on rat pulmonary resistance vessels: vasodilatation by atrial natriuretic peptide. *Clin. Sci.*, **83**, 723–729.

SHEPPERSON, N.B., BARCLAY, P.L., BENNETT, J.A. & SAMUELS, G.M. (1991). Inhibition of neutral endopeptidase (EC 3.4.24.11) leads to an atrial natriuretic factor-mediated natriuretic, diuretic and antihypertensive response in rodents. *Clin. Sci.*, **80**, 265–269.

SINGER, D.R., DEAN, J.W., BUCKLEY, M.G., SAGNELLA, G.A. & MACGREGOR, G.A. (1987). Secretion of atrial natriuretic peptide from the heart in man. *Br. Heart J.*, **58**, 24–28.

STANBROOK, H.S., MORRIS, K.G. & McMURTRY, I.F. (1984). Prevention and reversal of hypoxic pulmonary hypertension by calcium antagonists. *Am. Rev. Resp. Dis.*, **130**, 81–85.

STEWART, A.G., BARDSLEY, P.A., BAUDOUIN, S.V., WATERHOUSE, J.C., THOMPSON, J.S., MORICE, A.H. & HOWARD, P. (1991a). Changes in atrial natriuretic peptide concentrations during intravenous saline infusion in hypoxic cor pulmonale. *Thorax*, **46**, 829–834.

STEWART, A.G., THOMPSON, J.S., ROGERS, T.K. & MORICE, A.H. (1991b). Atrial natriuretic peptide-induced relaxation of preconstricted isolated rat perfused lungs: a comparison in control and hypoxia-adapted animals. *Clin. Sci.*, **81**, 201–208.

STEWART, A.G., SHEEDY, W., THOMPSON, J.S. & MORICE, A.H. (1992). Effects of SCH 34826, a neutral endopeptidase inhibitor, on hypoxic pulmonary vascular remodelling. *Pulm. Pharmacol.*, **5**, 111–114.

STINGO, A.J., CLAVELL, A.L., AARHUS, L.L. & BURNETT, J.C. (1992). Cardiovascular and renal actions of C-type natriuretic peptide. *Am. J. Physiol.*, **262**, H308–H312.

SYBERTZ, E.J., CHIU, P.J., VEMULAPALLI, S., WATKINS, R. & HASLANGER, M.F. (1990a). Atrial natriuretic factor-potentiating and antihypertensive activity of SCH 34826. An orally active neutral metalloendopeptidase inhibitor. *Hypertension*, **15**, 152–161.

SYBERTZ, E.J., CHIU, P.J.S., WATKINS, R.W. & VEMULAPALLI, S. (1990b). Neutral metalloendopeptidase inhibition: a novel means of circulatory modulation. *J. Hypertens.*, **8**, S161–S167.

THOMPSON, J.S., SHEEDY, W. & MORICE, A.H. (1994). The effects of the neutral endopeptidase inhibitor, SCH 42495, on the cardiovascular remodelling secondary to chronic hypoxia in rats. *Clin. Sci.*, **87**, 109–114.

THOMPSON, J.S. & MORICE, A.H. (1993). SCH 42354 increases potency of ANP in rat pulmonary resistance vessels in vitro. *Am. Rev. of Respir. Dis.*, **147**, A141.

TREMBLAY, J., GERZER, R. & VINAY, S. (1985). The increase of cGMP by atrial natriuretic factor correlates with the distribution of particulate guanylate cylase. *Febs. Lett.*, **181**, 17–22.

WATKINS, R.W., VEMULAPALLI, S., CHIU, P.J.S., FOSTER, C., SMITH, E.M., NEUSTADT, B., HASLANGER, M. & SYBERTZ, E.J. (1993). Atrial natriuretic factor potentiating and haemodynamic effects of SCH 42495, a new, neutral metalloendopeptidase inhibitor. *Am. J. Hypertens.*, **6**, 357–368.

WILKINS, M.R., NUNEZ, D.J. & WHARTON, J. (1993). The natriuretic peptide family: turning hormones into drugs. *J. Endocrinol.*, **137**, 347–359.

WINTER, R.J., DAVIDSON, A.C., TREACHER, D., RUDD, R.M., ANDERSON, J.V., MELEAGROS, L. BLOOM, S.R. (1989). Atrial natriuretic peptide concentrations in hypoxic secondary pulmonary hypertension: relation to haemodynamic and blood gas variables and response to supplemental oxygen. *Thorax*, **44**, 58–62.

WINTER, R.J., ZHAO, L., KRAUSZ, T. & HUGHES, J.M. (1991). Neutral endopeptidase 24.11 inhibition reduces pulmonary vascular remodelling in rats exposed to chronic hypoxia. *Am. Rev. Respir. Dis.*, **144**, 1342–1346.

ZHAO, L., WINTER, R.J., KRAUSZ, T. & HUGHES, J.M. (1991). Effects of continuous infusion of atrial natriuretic peptide on the pulmonary hypertensin induced by chronic hypoxia in rats. *Clin. Sci.*, **81**, 379–385.

(Received April 7, 1994
Revised June 17, 1994
Accepted June 22, 1994)

Br. J. Pharmacol. (1994), **113**, 1127–1130 © Macmillan Press Ltd, 1994

Dissociation of castor oil-induced diarrhoea and intestinal mucosal injury in rat: effect of N^G-nitro-L-arginine methyl ester

[1]Francesco Capasso, Nicola Mascolo, Angelo A. Izzo & *Timothy S. Gaginella

Department of Experimental Pharmacology, University of Naples Federico II, via D. Montesano 49, 80131 Naples, Italy and *Aphton Corporation, P.O. Box 1049, Woodland CA 95776, U.S.A.

1 Castor oil (2 ml orally) produced diarrhoea in rats 1–7 h after challenge, which was associated with gross damage to the duodenal and jejunal mucosa.

2 The injury was accompanied by release of acid phosphatase into the gut lumen, indicating cellular injury.

3 Intraperitoneal injection of the nitric oxide (NO) synthase inhibitor N^G-nitro-L-arginine methyl ester (L-NAME, 2.5–50 mg kg^{-1} twice), prevented the diarrhoea. The dose of L-NAME (50 mg kg^{-1}) completely blocked the diarrhoea but increased the release of acid phosphatase and worsened the gross damage.

4 The NO donating compound, isosorbide-5-mononitrate (IMN, 150 mg kg^{-1} twice) reversed the effects of L-NAME (50 mg kg^{-1}) on castor oil-induced diarrhoea, gross damage and acid phosphatase release.

5 The apparent dissociation of the diarrhoeal and intestinal mucosal damaging effects of castor oil suggest that NO has a protective effect on the rat duodenal and jejunal mucosa, but that NO mediates, in part, the diarrhoea effect of this laxative.

Keywords: Castor oil; ricinoleic acid; nitric oxide, N^G-nitro-L-arginine methyl ester (L-NAME); isosorbide-5-monitrate (IMN); diarrhoea; laxative; duodenum; jejunum; acid phosphatase

Introduction

Castor oil (ricinoleic acid) affects electrolyte transport and smooth muscle contractility in the intestine (Gullikson & Bass, 1984; Nell & Rummel, 1984; Binder, 1977; Izzo *et al.*, 1993b; Gaginella, 1994). The precise mechanism of action of this common laxative remains elusive, partly because of its multiple effects on the gut. It inhibits intestinal Na,K-ATPase activity (Phillips *et al.*, 1965; Gaginella & Bass, 1978; Nell & Rummel, 1984), interferes with oxidative metabolism (Nakao, 1963; Gaginella *et al.*, 1975) and has effects on adenylate cyclase or mucosal adenosine 3':5'-cyclic monophosphate (cyclic AMP) content (Gaginella *et al.*, 1978; Racusen & Binder, 1979; Simon & Kather, 1980).

Castor oil is cytotoxic to intestinal epithelial cells (Valette & Salvanet, 1936; Gaginella *et al.*, 1977a; Bretagne *et al.*, 1981), and causes histological abnormalities with enhanced mucosal permeability (Cline *et al.*, 1976; Gaginella *et al.*, 1977b; Saunders *et al.*, 1977; 1978). These effects may be related to the release of eicosanoids (Beubler & Juan, 1979; Capasso *et al.*, 1986) and platelet activating factor (PAF) by the intestinal mucosa (Pinto *et al.*, 1989; 1992). Whether or not these alterations are essential for the laxative effect of castor oil or are merely epiphenomena remains to be clarified.

Nitric oxide (NO) is protective against endotoxin-induced intestinal damage in the rat (Boughton-Smith *et al.*, 1990; 1993a; Laszlo *et al.*, 1994) and is also a mediator of gastric protection (Konturek *et al.*, 1993). However, N^G-nitro-L-arginine methyl ester (L-NAME), an NO synthase inhibitor, prevents castor oil-induced diarrhoea (Mascolo *et al.*, 1992; 1993; 1994). In order to determine whether castor oil-induced diarrhoea and intestinal mucosal damage are independent events we have studied the effects of L-NAME, and the NO donating compound, isosorbide-5-mononitrate (IMN) in rats treated with castor oil.

[1] Author for correspondence.

Methods

Male Wistar rats (Morini, Italy), 160–180 g, were used after acclimatization for a week (23 ± 2°C; 60% humidity). Food was withheld 12 h before experiments but there was free access to drinking water. Castor oil (2 ml per rat) was given orally and 1–7 h later the individual rat cages were inspected (by an observer unaware of the particular treatment) for the presence of characteristic diarrhoeal droppings; their absence indicated protection from diarrhoea. Some animals were pretreated with L-NAME (2.5–50 mg kg^{-1}, i.p. Sigma, Milan) 15 min before and 3 h after castor oil and/or IMN (150 mg kg^{-1} p.o.; Astra, Milan), 45 min before and 3 h after castor oil.

Acid phosphatase measurements

Intraluminal release of the lysosomal enzyme, acid phosphatase was determined as previously described (Pinto *et al.*, 1989; Izzo *et al.*, 1993a). Rats were killed and 8 cm segments of duodenum and jejunum were excised. The segment was rinsed with saline to remove food and mucus. A ligature was placed at one end of the segment and isotonic saline (1 ml, 0.9% w/v) was instilled into the segment by a polyethylene cannula introduced into the other end. The segment was placed in an organ bath containing Tyrode solution (37°C) gassed with 95% O_2, 5% CO_2. The tissue was incubated for 30 min. After 15 min the fluid inside the segment was carefully removed by syringe and was replaced with 1 ml of fresh saline. Immediately after the incubation period the intraluminal solution was removed and the acid phosphatase activity measured by a spectrophotometric assay.

Damage injury assessment

Rats were killed and two segments from standardized regions of duodenum and jejunum were visibly evaluated for macroscopical damage by an observer unaware of the particular treatment. Mucosal injury was graded as follow: 0 (normal), 1 (hyperaemia), 2 (hyperaemia with evidence of haemorrhage into the lumen), 3 (severe haemorrhage into the lumen).

Statistics

The Chi-Square test was used to determine the significance between groups with diarrhoea. The visual score and the intraluminal release of acid phosphatase are expressed as mean ± s.e.mean and were compared by Student's t test. A P value less than 0.05 was considered significant.

Results

Castor oil (2 ml per rat) produced diarrhoea in 40% of animals after 1 h and copious diarrhoea in all animals 3, 5 and 7 h after challenge (Figure 1). Macroscopic damage was produced throughout the duodenum and jejunum, characterized mainly by vasocongestion (Table 1,2). The injury was mild (hyperaemia) by 1 h, severe 3 and 5 h after castor oil administration and less severe 7 h after challenge (Table 1,2). No injury was observed at 0.5 h or at 9 h after castor oil administration and the tissue appeared normal by visual examination.

L-NAME dose-dependently prevented diarrhoea (Figure 1) but markedly ($P<0.01$) enhanced macroscopic injury (Table 1), causing extensive hyperaemia and haemorrhage into the small intestinal lumen. The effect of L-NAME (50 mg kg^{-1}) on castor oil-induced damage (Table 2) and diarrhoea was abolished by orally administered IMN (150 mg kg^{-1}): diarrhoea in 40% of animals after 1 h, in 80% after 3 h and in 90% after 5–7 h (c.f. Figure 1) $n=10$, $P<0.01$ at 3–7 h. IMN (150 mg kg^{-1}) given alone did not modify the diarrhoea due to castor oil (diarrhoea in 40% of animals after 1 h, in 100% of animals after 3–7 h, $n=10$). In contrast, IMN (150 mg kg^{-1}) reduced castor oil-induced damage (mean ± s.e., $n=10$, $P<0.01$ at 3–7 h; duodenum 1 h, 0.2 ± 0.1; 3 h, 0.5 ± 0.1; 5 h, 0.6 ± 0.2; 7 h, 0.3 ± 0.1; jejunum, 1 h, 0.2 ± 0.1; 3 h, 0.4 ± 0.1; 5 h, 0.4 ± 0.2; 7 h, 0.2 ± 0.1; compare to Table 1) but was devoid of any effect in rats untreated with castor oil (normal rats). L-NAME (50 mg kg^{-1}) itself caused mild mucosal congestion after 1 h (duodenum 0.4 ± 0.1; jejunum 0.4 ± 0.1).

The macroscopic changes in the mucosa indicating injury were accompanied by significant increases ($P<0.05$–0.001) in release of the acid phosphatase (Table 2). L-NAME (50 mg kg^{-1}) enhanced this effect, especially at the 3 and 5 h time points. IMN (150 mg kg^{-1}) partially negated this additive effect of L-NAME ($P<0.05$).

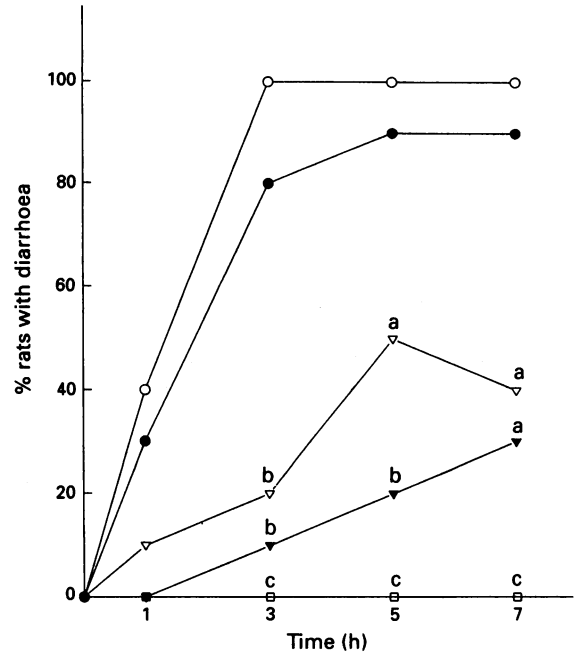


Figure 1 Effect of graded doses of N^G-nitro-L-arginine methyl ester (L-NAME) on castor oil-induced diarrhoea. Ten animals were used for each group. L-NAME was given i.p. 15 min before and 3 h after castor oil. Results were analysed by Chi-Square test. $^aP<0.05$; $^bP<0.01$; $^cP<0.001$ vs. castor oil (CO). Symbols; (○) castor oil (CO); (●) CO + L-NAME 2.5 mg kg^{-1}; (△) CO + L-NAME 10 mg kg^{-1}; (▼) CO + L-NAME 25 mg kg^{-1}; (□) CO + L-NAME 50 mg kg^{-1}.

Table 1 Effect of N^G-nitro-L-arginine methyl ester (L-NAME 2.5–50 mg kg^{-1}, i.p. twice) on macroscopic intestinal damage (scored 0–3) induced by castor oil (2 ml, p.o.).

Time (h)	*Castor oil*	*Castor oil + L-NAME* 2.5	10	25	50 mg kg^{-1}
			Duodenum		
1	0.5 ± 0.1	0.6 ± 0.2	0.7 ± 0.2	0.9 ± 0.3	1.2 ± 0.1**
3	1.4 ± 0.2	1.6 ± 0.3	1.7 ± 0.3	2.2 ± 0.3*	2.7 ± 0.3**
5	1.3 ± 0.2	1.5 ± 0.3	1.7 ± 0.3	2.0 ± 0.3*	2.5 ± 0.3**
7	1.0 ± 0.2	1.2 ± 0.2	1.3 ± 0.2	1.6 ± 0.2*	1.9 ± 0.3**
			Jejunum		
1	0.4 ± 0.1	0.5 ± 0.2	0.6 ± 0.2	0.6 ± 0.2	0.7 ± 0.1
3	1.2 ± 0.2	1.6 ± 0.3	1.9 ± 0.2	2.1 ± 0.3*	2.5 ± 0.3**
5	1.2 ± 0.2	1.4 ± 0.2	1.7 ± 0.3	2.0 ± 0.3*	2.2 ± 0.2**
7	0.7 ± 0.1	0.9 ± 0.2	1.0 ± 0.2	1.2 ± 0.2*	1.5 ± 0.2**

Results are the mean ± s.e.mean for 10 rats per experimental group.
*$P<0.05$ and $P<0.01$ vs. castor oil group

Table 2 Isosorbide 5-mononitrate (IMN 150 mg kg^{-1}, p.o. twice) reverses the effect of N^G-nitro-L-arginine methyl ester (L-NAME 50 mg kg^{-1}, i.p. twice) on castor oil (2 ml)-induced macroscopic damage (scored 0–3)

	Castor oil		*Castor oil + L-NAME*			
			No IMN	*IMN*	*No IMN*	*IMN*
Time	*Duodenum*	*Jejunum*	*Duodenum*		*Jejunum*	
1	0.5 ± 0.1	0.4 ± 0.1	1.2 ± 0.1*	0.6 ± 0.2†	0.7 ± 0.1	0.4 ± 0.1
3	1.4 ± 0.2	1.2 ± 0.2	2.7 ± 0.3*	1.3 ± 0.2†	2.5 ± 0.3*	1.1 ± 0.3†
5	1.3 ± 0.2	1.2 ± 0.2	2.5 ± 0.3*	1.2 ± 0.3†	2.2 ± 0.2*	1.0 ± 0.2†
7	1.0 ± 0.2	0.7 ± 0.1	1.9 ± 0.3*	0.9 ± 0.2†	1.5 ± 0.2*	0.7 ± 0.1†

Results are the mean ± s.e.mean for 10 rats per experimental group.
*$P<0.01$ vs. castor oil group
†$P<0.01$ vs. castor oil + L-NAME group (No IMN)

Table 3 Intraluminal release of acid phosphatase by intestinal tissue of rats treated with castor oil (2 ml/rat) and pretreated with or not with N^G-nitro-L-arginine methyl ester (L-NAME 50 mg kg^{-1} i.p., twice) and isosorbide 5-mononitrate (IMN 150 mg kg^{-1}, i.p. twice)

	Castor oil		*Castor oil + L-NAME*			
			No IMN	*IMN*	*No IMN*	*IMN*
Time	*Duodenum*	*Jejunum*	*Duodenum*		*Jejunum*	
0	724 ± 140	680 ± 113	720 ± 120	700 ± 135	685 ± 102	695 ± 136
1	1430 ± 180[a]	1118 ± 264[a]	2730 ± 201[b,d]	1620 ± 160[a,e]	2520 ± 384[b,d]	1433 ± 173[a,e]
3	2591 ± 383[b]	2480 ± 226[b]	5024 ± 403[c,d]	2980 ± 303[b,e]	4341 ± 428[c,d]	2822 ± 293[b,e]
5	2368 ± 325[b]	2124 ± 296[b]	4820 ± 413[c,d]	794 ± 93[b,e]	4003 ± 395[c,d]	774 ± 101[b,e]
7	1629 ± 290[a]	1499 ± 273[a]	3354 ± 280[c,d]	704 ± 79[a,e]	3243 ± 287[c,d]	731 ± 84[a,e]

Results [μg substrate transformed (g dry wt)$^{-1}$)] are the mean ± s.e.mean for 10 rats per experimental group.
[a]$P<0.05$, [b]$P<0.01$ and [c]$P<0.001$ vs control (time 0) [d]$P<0.01$ vs castor oil [e]$P<0.05$ vs castor oil + L-NAME (No IMN)

Discussion

Our results show that castor oil produced concurrent diarrhoea and gross evidence of mucosal damage. The latter effect was exacerbated by the NO synthase inhibitor, L-NAME, suggesting that NO serves in a protective capacity. The fact that L-NAME blocked the diarrhoeal effect of castor oil while worsening the apparent injury to the mucosa, suggests that these two events are not related in cause and effect. The augmentation of the damaging effect to the epithelium with L-NAME is supported by the enhanced release of acid phosphatase. Furthermore, the NO-donating compound IMN, prevented the deleterious action of L-NAME, reducing the injury scores and the acid phosphatase values nearly to the level of the castor oil controls (see Tables 2,3).

The effects of castor oil on fluid transport have been previously associated with, but not proved to be due to, mucosal injury. In 1936 Valette & Salvanet noted the damaging effects of ricinoleic acid on the rat intestine, followed by a report of 'chemical gastroenteritis' in rats fed castor oil (Raynell & Spray, 1958). More recent studies have demonstrated potentially detrimental metabolic (Nakao, 1963; Gaginella *et al.*, 1975) and cytotoxic effects of ricinoleic acid on intestinal cells *in vitro* (Gaginella *et al.*, 1977b) and *in vivo* (Bretagne *et al.*, 1981). Increased intestinal epithelial permeability (sometimes with cytomorphological changes) is associated with intraluminal fluid accumulation in response to ricinoleic acid (Dobbins & Binder, 1976; Cline *et al.*, 1976; Gaginella *et al.*, 1977a; Gullikson *et al.*, 1977). We have previously demonstrated that castor oil-induced mucosal hyperaemia and haemmorhage is associated with intraluminal release of acid phosphatase and PAF, two markers of cellular injury (Pinto *et al.*, 1989; 1992).

In our study, NO generated in response to the castor oil could have several actions. We believe it contributed to the diarrhoea because of the stimulatory effect of NO-donating compounds (McNaughton, 1993; Wilson *et al.*, 1993) and NO itself (Tamai & Gaginella, 1993), and the inhibitory action of L-NAME (Mascolo *et al.*, 1993; 1994) on water and electrolyte transport. This response may be related to interference with cellular metabolism, but not be due to gross mucosal damage. Tepperman *et al.* (1993) showed that induction of NO synthase is associated with decreased viability of rat enterocytes. The diphenylmethane laxatives (phenolphthalein and bisacodyl) increase the activity of inducible NO synthase (Gaginella *et al.*, 1994), increase mucosal permeability and injure the mucosa (Saunders *et al.*, 1977), but, it is not known if L-NAME worsens the mucosal injury. When the rat jejunum and colon were exposed to endotoxin, vascular permeability and leakage of plasma proteins were increased; this was reversed by inhibition of inducible NO synthase (Boughton-Smith *et al.*, 1993a). Induction of colonic nitric oxide synthase was also detected in a trinitrobenzene colitis model (Boughton-Smith *et al.*, 1993b). Other authors have likewise concluded that NO promotes mucosal injury in chronic ileitis (Miller *et al.*, 1992).

Alternatively, there is evidence for protective effects of NO on the gastric and intestinal mucosa. The healing of chronic gastric ulcers in rats is delayed by inhibition of NO synthesis (Konturek *et al.*, 1993). Furthermore, NO synthase inhibition increases intestinal permeability, probably through activation of mucosal mast cells (Kanwar *et al.*, 1994). In models of ileitis in rodents, NO may enhance the restitutive capacity of the epithelium (Miller *et al.*, 1993). The significance of the present results lies in the apparent dual action of NO in response to castor oil, illustrating that it is possible to dissociate the laxative effect from intestinal mucosal damage.

This work was supported by CNR (Rome) and MURST 60%

References

BEUBLER, E. & JUAN, H. (1979). Effect of ricinoleic acid and other laxatives on net water flux and prostaglandin E release by the rat colon. *J. Pharm. Pharmacol.*, **31**, 681–685.

BINDER, H.J. (1977). Pharmacology of laxatives. *Annu. Rev. Pharmacol. Toxicol.*, **17**, 355–367.

BOUGHTON-SMITH, N.K., EVANS, S.M., LASZLO, F., WHITTLE, B.J.R. & MONCADA, S. (1993a). The induction of nitric oxide synthase and intestinal vascular permeability by endotoxin in the rat. *Br. J. Pharmacol.*, **110**, 1189–1195.

BOUGHTON-SMITH, N.K., EVANS, S.M., WHITTLE, B.J.R. & MONCADA, S. (1993b). Induction of nitric oxide synthase in rat intestine and its association with tissue injury. *Agents Actions*, **38**, C125–C126.

BOUGHTON-SMITH, N.K., HUTCHESON, I.R., DEAKIN, A.M., WHITTLE, B.J.R. & MONCADA, S. (1990). Protective effect of S-nitroso-N-acetyl-penicillamine in endotoxin-induced acute intestinal damage in the rat. *Eur. J. Pharmacol.*, **191**, 585–588.

BRETAGNE, J.F., VIDON, N., L'HIRONDEL, C. & BERNIER, J.J. (1981). Increased cell loss in the human jejunum induced by laxatives (ricinoleic acid, dioctyl sodium sulphosuccinate, magnesium sulphate, bile salts). *Gut*, **22**, 264–269.

CAPASSO, F., MASCOLO, N., AUTORE, G. & ROMANO, V. (1986). Laxatives and the production of autocoids by rat colon. *J. Pharm. Pharmacol.*, **38**, 627–629.

CLINE, W.S., LORENZSONN, V., BENZ, L., BASS, P. & OLSEN, W.A. (1976). The effects of sodium ricinoleate on small intestinal function and structure. *J. Clin. Invest.*, **58**, 380–390.

DOBBINS, J.W. & BINDER, H.J. (1976). Effect of bile salts and fatty acids on the colonic absorption of oxalate. *Gastroenterology*, **70**, 1096–1100.

GAGINELLA, T.S. (1994). Laxative drugs. In *Textbook of Basic and Clinical Pharmacology*. ed. Munson, P., Mueller, R. & Breese, G. New York: Chapman & Hall (in press).

GAGINELLA, T.S. & BASS, P. (1978). Laxatives: an update on mechanism of action. *Life Sci.*, **23**, 1001–1010.

GAGINELLA, T.S., BASS, P., OLSEN, W. & SHRUG, A. (1975). Fatty acid inhibition of water absorption and energy production in the hamster jejunum. *FEBS Lett.*, **53**, 347–350.

GAGINELLA, T.S., CHADWICK, V.S. DEBONGNIE, J.C., LEWIS, J.C. & PHILLIPS, S.F. (1977a). Perfusion of rabbit colon with ricinoleic acid: dose related mucosal injury, fluid secretion and increased permeability. *Gastroenterology*, **73**, 95–101.

GAGINELLA, T.S., HADDAD, A.C., GO, V.L.W. & PHILLIPS, S.F. (1977b). Cytotoxicity of ricinoleic acid (castor oil) and other intestinal secretagogues on isolated intestinal epithelial cells. *J. Pharmacol. Exp. Ther.*, **201,** 259–266.

GAGINELLA, T.S., MASCOLO, N., IZZO, A.A., AUTORE, G. & CAPASSO, F. (1994). Nitric oxide is a mediator of bisacodyl and phenolphthalein laxative action: induction of nitric oxide synthase. *J. Pharmacol. Exp. Ther.*, (in press).

GAGINELLA, T.S., PHILLIPS, S.F., DOZOIS, R.R. & GO, V.L.W. (1978). Stimulation of adenylate cyclase in homogenates of isolated intestinal epithelial cells from hamsters. Effects of gastrointestinal hormones, prostaglandins, and deoxycholic and ricinoleic acid. *Gastroenterology*, **74,** 11–15.

GULLIKSON, G.W. & BASS, P. (1984). In *Pharmacology of Intestinal Permeation*, II. pp. 419–459. Berlin: Springer-Verlag.

GULLIKSON, G.W., CLINE, S.W., LORENZSONN, V., BENZ, L., OLSEN, W.A. & BASS, P. (1977). Effects on anionic surfactants on hamster small intestine membrane structure and function: relationship to surface activity. *Gastroenterology*, **73,** 501–511.

IZZO, A.A., MASCOLO, N., AUTORE, G., DI CARLO, G. & CAPASSO, F. (1993a). Increased ex-vivo colonic generation of PAF induced by diphenylmethane stimulant laxatives in rats, mice, guinea-pigs and rabbits. *J. Pharm. Pharmacol.*, **45,** 916–918.

IZZO, A.A., MASCOLO, N., VIOLA, P. & CAPASSO, F. (1993b). Inhibitors of nitric oxide synthase enhance rat ileum contractions induced by ricinoleic acid in vitro. *Eur. J. Pharmacol.*, **243,** 87–90.

KANWAR, S., WALLACE, J.L., BEFUS, D. & KUBES, P. (1994). Nitric oxide synthesis inhibition increases epithelial permeability via mast cells. *Am. J. Physiol.*, **266,** G.

KONTUREK, S.J., BRZOZOWSKI, T., MAJKA, J., PYTKO-POLONCZYK, J. & STACHURA, J. (1993). Inhibition of nitric oxide synthase delays healing of chronic gastric ulcers. *Eur. J. Pharmacol.*, **239,** 215–217.

LASZLO, F., WHITTLE, B.J.R. & MONCADA, S. (1994). Time-dependent enhancement or inhibition of endotoxin-induced vascular injury in rat intestine by nitric oxide synthase inhibitors. *Br. J. Pharmacol.*, **111,** 1309–1315.

MACNAUGHTON, W.K. (1993). Nitric oxide-donating compounds stimulate electrolyte transport in the guinea pig intestine in vitro. *Life Sci.*, **53,** 585–593.

MASCOLO, N., IZZO, A.A., AUTORE, G., BARBATO, F. & CAPASSO, F. (1994). Nitric oxide and castor oil-induced diarrhea. *J. Pharmacol. Exp. Ther.*, **268,** 291–295.

MASCOLO, N., IZZO, A.A., BARBATO, F. & CAPASSO, F. (1993). Inhibitors of nitric oxide synthetase prevent castor-oil-induced diarrhoea in the rat. *Br. J. Pharmacol.*, **108,** 861–864.

MASCOLO, N., IZZO, A.A. & CAPASSO, F. (1992). Castor oil induced diarrhoea: involvement of nitric oxide. In *Natural Drugs and the Digestive Tract*, ed. Capasso, F. & Mascolo, N. pp. 121–128. Rome: EMSI.

MILLER, M.J.S., SADOWSKA-KROWICKA, H., CHOTINARUEMOL, S., KAKKIS, J.L. & CLARK, D.A. (1992). Amelioration of chronic ileitis by nitric oxide synthase inhibition. *J. Pharmacol. Exp. Ther.*, **264,** 11–16.

MILLER, M.J.S., ZHANG, X.-J., SADOWSKA-KROWICKA, H., CHOTINARUEMOL, S., MCINTYRE, J.A., CLARK, D.A. & BUSTAMANTE, S.A. (1993). Nitric oxide release in response to gut injury. *Scand. J. Gastroenterol.*, **28,** 149–154.

NAKAO, S. (1963). The effect of ricinoleic acid and phenolphthalein on creatine phosphate levels in the rat intestine in vitro. *Biochem.*, **12,** 216–217.

NELL, G. & RUMMEL, W. (1984). Action mechanism of secretagogue drugs. In *Pharmacology of Intestinal Permeation*, II. ed. Csaky, T.-Z. pp. 461–508. Berlin: Springer-Verlag.

PHILLIPS, R.A., LOVE, A.H.G., MITCHELL, T.G. & NEPTUNE, E.M. (1965). Cathartics and the sodium pump. *Nature*, **206,** 1367–1368.

PINTO, A., AUTORE, G., MASCOLO, N., SORRENTINO, R., BIONDI, A., IZZO, A.A. & CAPASSO, F. (1992). Time course of PAF information by gastrointestinal tissue in rats after caster oil challenge. *J. Pharm. Pharmacol.*, **44,** 224–226.

PINTO, A., CALIGNANO, A., MASCOLO, N., AUTORE, G. & CAPASSO, F. (1989). Castor oil increases intestinal formation of platelet-activating factor and acid phosphatase release in the rat. *Br. J. Pharmacol.*, **96,** 872–874.

RACUSEN, L.C. & BINDER, H.J. (1979). Ricinoleic acid stimulation of active anion secretion in colonic mucosa of the rat. *J. Clin. Invest.*, **63,** 743–749.

RAYNELL, D.R. & SPRAY, G.H. (1958). Chemical gastroenteritis in the rat. *Gastroenterology*, **72,** 849–856.

SAUNDERS, D.R., SILLERY, J., RACHMILEWITZ, D., RUBEN, C.E. & TYTGAT, G.N. (1977). Effect of bisacodyl on the structure and function of rodent and human intestine. *Gastroenterology*, **72,** 849–856.

SAUNDERS, D.R., SILLERY, J., SURUWICA, C. & TYTGAT, G.N. (1978). Effect of phenolphthalein on the function and structure of rodent and human intestine. *Dig. Dis. Sci.*, **23,** 909–913.

SIMON, B. & KATHER, H. (1980). Interaction of laxatives with enzymes of cyclic AMP metabolism from human colonic mucosa. *Eur. J. Clin. Invest.*, **10,** 231–234.

TAMAI, H. & GAGINELLA, T.S. (1993). Direct evidence for nitric oxide stimulation of electrolyte secretion in the rat colon. *Free Rad. Res. Comms.*, **19,** 229–239.

TEPPERMAN, B.L., BROWN, J.F. & WHITTLE, B.J.R. (1993). Nitric oxide synthase induction and intestinal epithelial cell viability in rats. *Am. J. Physiol*, **265,** G214–G218.

VALETTE, G. & SALVANET, R. (1936). Les causes de l'action de l'huile de ricin. *Bull. Sci. Pharmacol.*, **43,** 1–11.

WILSON, K.T., XIE, Y., MUSCH, M.W. & CHANG, E.B. (1993). Sodium nitroprusside stimulates anion secretion and inhibits sodium chloride absorption in rat colon. *J. Pharmacol. Exp. Ther.*, **266,** 224–230.

(Received February 28, 1994
Revised May 12, 1994
Accepted June 23, 1994)

Br. J. Pharmacol. (1994), **113**, 1131–1136 © Macmillan Press Ltd, 1994

Interactions of constitutive nitric oxide with PAF and thromboxane on rat intestinal vascular integrity in acute endotoxaemia

F. László, [1]B.J.R Whittle & S. Moncada

Department of Pharmacology, Wellcome Research Laboratories, Langley Court, Beckenham, Kent BR3 3BS

1 The involvement of endogenous platelet activating factor (PAF) and thromboxane A_2 in the acute microvascular damage in the ileum and colon induced by the nitric oxide (NO) synthase inhibitor, N^G-nitro-L-arginine methyl ester (L-NAME) following endotoxin administration was investigated in the rat over a 1 h period.

2 Administration of L-NAME (1–10 mg kg^{-1}, s.c.) concurrently with *E. coli* lipopolysaccharide (LPS; 3 mg kg^{-1}, i.v.) dose-dependently increased vascular permeability in the ileum and colon, as determined by the leakage of radiolabelled albumin, and caused macroscopic mucosal damage in the ileum determined 1 h later. Neither LPS administration nor L-NAME (5 mg kg^{-1}) alone affected resting vascular permeability.

3 Infusion of phenylephrine (10 μg kg^{-1} min^{-1}, i.v. for 1 h) caused an elevation in blood pressure similar to that found following L-NAME administration (5 mg kg^{-1}, i.v. or s.c.), but did not increase intestinal vascular permeability, when administered with LPS (3 mg kg^{-1}, i.v.).

4 The increased vascular permeability in the ileum and colon and macroscopic damage in the ileum, induced by L-NAME (5 mg kg^{-1}, s.c.) and LPS (3 mg kg^{-1}, i.v.) was dose-dependently inhibited following s.c. pretreatment (15 min before challenge) with the thromboxane synthase inhibitors, OKY 1581 (5–25 mg kg^{-1}) or 1-benzyl-imidazole (1–50 mg kg^{-1}), or with the thromboxane receptor antagonist, BM 13177 (0.2–2 mg kg^{-1}).

5 Pretreatment with the cyclo-oxygenase inhibitor, indomethacin (2–5 mg kg^{-1}, s.c., 15 min before challenge) reduced the microvascular injury in the ileum and colon and macroscopic lesions in the ileum, observed after the concurrent administration of L-NAME and LPS.

6 Pretreatment (15 min) with the PAF-receptor antagonists, WEB 2086 (0.5–1 mg kg^{-1}, s.c.) or BN 52021 (2.5–10 mg kg^{-1}, s.c.) likewise attenuated this intestinal vascular injury.

7 Combined administration of low doses of 1-benzyl-imidazole (1 mg kg^{-1}) with WEB 2086 (0.5 mg kg^{-1}) 15 min before L-NAME and LPS challenge, abolished this vascular damage and macroscopic injury.

8 These results suggest that PAF and thromboxane A_2 are released acutely following challenge with a low dose of endotoxin. However, these mediators do not appear to injure the intestinal microvascular bed unless NO synthase is concurrently inhibited. Such findings support the protective role of constitutively-formed NO, counteracting the injurious vascular actions of cytotoxic mediators released under pathological conditions.

Keywords: Nitric oxide; PAF; thromboxanes; intestinal mucosal injury; intestinal vascular permeability; N^G-nitro-L-arginine methyl ester

Introduction

Nitric oxide (NO), formed from L-arginine, plays an important role in the maintenance of gastrointestinal microvascular and mucosal integrity (Whittle *et al.*, 1990; Kubes & Granger, 1992; Whittle, 1993). The beneficial action of endogenous NO, synthesized by the Ca^{2+}-dependent constitutive enzyme in the early phase of endotoxaemia, has been suggested from the findings that administration of the NO synthase inhibitor, N^G-monomethyl-L-arginine (L-NMMA) augmented the acute mucosal damage in the gastrointestinal tract provoked by high doses of endotoxin (Hutcheson *et al.*, 1990). Moreover, L-NMMA or the more potent NO synthase inhibitor, N^G-nitro-L-arginine methyl ester (L-NAME) induces an acute substantial increase of vascular permeability in the rat small and large intestine following the intravenous injection of low doses of endotoxin (László *et al.*, 1994a).

The mechanism of the acute effects of endotoxin on the gastrointestinal integrity are not fully understood and may result from a direct injurious action on the vascular endothelium (Harlan *et al.*, 1983; Meyrick *et al.*, 1986). However, following exposure to high doses of lipopolysaccharide (LPS), such intestinal injury appears to cause the early release of tissue damaging secondary mediators, including platelet-activating factor (PAF) or thromboxane A_2 (Wallace *et al.*, 1987; Boughton-Smith *et al.*, 1989). An injurious role or PAF as a mediator of gastrointestinal mucosal damage is supported by the observation that PAF induces gastric haemorrhagic necrosis (Rosam *et al.*, 1986) and causes significant microvascular injury in the gastrointestinal tract (Wallace *et al.*, 1987; Boughton-Smith *et al.*, 1992; Filep & Földes-Filep, 1993). Furthermore, the immediate hypotension following the administration of high doses of endotoxin can be prevented by the PAF-receptor antagonist, WEB 2086 (Casals-Stenzel, 1987; Szabó *et al.*, 1993). In other studies, the increased survival rate after the treatment with thromboxane synthase inhibitors and thromboxane receptor antagonists indicates a pathological involvement of thromboxane A_2 in endotoxaemic states (Wise *et al.*, 1980; Halushka *et al.*, 1983; Olanoff *et al.*, 1985).

The aim of the present study was to evaluate the possible

[1] Author for correspondence.

role of PAF and thromboxanes in the acute intestinal mucosal damage and microvascular injury provoked by inhibition of NO synthesis with L-NAME following challenge by a low dose of endotoxin in the rat. Thus, the effects of two structurally unrelated PAF-receptor antagonists, BN 52021 and WEB 2086 (Casals-Stanzel, 1987; Koltai et al., 1991a,b) have been investigated. Likewise, the actions of the thromboxane synthase inhibitor, 1-benzyl-imidazole and the non-imidazole compound OKY 1581, along with the thromboxane receptor antagonist BM 13177 (Hamid-Bloomfield & Whittle, 1989; Boughton-Smith et al., 1989) and the cyclooxygenase inhibitor, indomethacin, have been evaluated.

Part of this work has been presented to the British Pharmacological Society (László et al., 1994b).

Methods

Experimental protocol

Male Wistar rats (225–275 g) were fasted overnight, but received water *ad libitum*. Under halothane anaesthesia *E. coli* lipopolysaccharide (3 mg kg^{-1}, i.v.) ^{125}I-labelled human serum albumin ([^{125}]-HSA; 2 μCi kg^{-1}, i.v.) and L-NAME (1–10 mg kg^{-1}, s.c.) were injected. Indomethacin (2 and 5 mg kg^{-1}), OKY 1581 (5–25 mg kg^{-1}), 1-benzyl-imidazole (BZI; 1–50 mg kg^{-1}), BM 13177 (0.2–2 mg kg^{-1}), BN 52021 (2.5–10 mg kg^{-1}) or WEB 2086 (0.1–1 mg kg^{-1}) were administered s.c. 15 min prior to LPS and L-NAME (5 mg kg^{-1}, s.c.) treatment. The doses of these agents were selected on the basis of previous studies in the rat (Casals-Stanzel, 1987; Wallace et al., 1987; Boughton-Smith et al., 1989; Hamid-Bloomfield & Whittle, 1989; Martinez-Cuesta et al., 1992).

In further studies, BZI (1 mg kg^{-1}, s.c.) and WEB 2086 (0.5 mg kg^{-1}, s.c.) were injected concurrently, 15 min before challenge with LPS (3 mg kg^{-1}, i.v.) and L-NAME (5 mg kg^{-1}, s.c.). Plasma leakage in the ileum and colon, and mucosal damage in the ileum was determined after 1 h.

For the evaluation of intestinal macroscopic injury and vascular permeability changes, tissue was removed 1 h after endotoxin injection.

Plasma leakage

As a measure of vascular endothelial damage, plasma leakage of [^{125}I]-HSA was determined in the ileum and colon. Under halothane anaesthesia, blood was collected from the abdominal aorta into syringes containing trisodium citrate (final concentration 0.318%) and centrifuged (10,000 *g*, 10 min, 4°C). The [^{125}I]-HSA content of the plasma and segments of the ileum and colon was determined in a gamma-spectrometer (Nuclear Enterprises NE 1600) and the albumin content in intestinal tissue was calculated as described previously (Boughton-Smith et al., 1993). Values from control tissue were subtracted from the values of treated tissue and the data were expressed as change in (Δ) plasma leakage, μl plasma g^{-1} tissue.

Evaluation of macroscopic lesions

Segments of the ileum were photographed and the gross macroscopic damage to the ileum was assessed by an observer unaware of the experiment, using a scoring system 0–IV, where 0 was the normal tissue; I = mild hyperaemia; II = more severe hyperaemia with one or two vasocongested streaks; III = vasocongested streaks and IV = confluent vasocongestion. It was not, however, possible to grade macroscopic mucosal injury in the colon, since although the colonic tissue appeared oedematous, well-demarcated damage was not clearly apparent.

Comparison of the effect of phenylephrine infusion and L-NAME on blood pressure and plasma leakage

Systemic arterial blood pressure was measured over a 1 h period from the right carotid artery of rats under pentobarbitone anaesthesia (60 mg kg^{-1}, i.p.) using a blood pressure transducer (Elcomatic) connected to a Grass Polygraph. L-NAME (5 mg kg^{-1}) was administered s.c. or intravenously as a bolus injection and phenylephrine was infused into the tail vein (10 μg kg^{-1} min^{-1}).

In a separate study, the phenylephrine infusion (10 μg kg^{-1} min^{-1}, i.v.) was initiated concurrently with LPS administration (3 mg kg^{-1}, i.v.) in pentobarbitone-anaesthetized rats. Plasma leakage in the ileum and colon were determined 1 h later. Likewise, the action of L-NAME (5 mg kg^{-1}, s.c.) administered concurrently with LPS on intestinal plasma leakage in pentobarbitone-anaesthetized rats was determined after 1 h.

Materials

E. coli lipopolysaccharide (0111:B4), indomethacin (dissolved in 1.25% sodium bicarbonate), phenylephrine and L-NAME (dissolved in isotonic saline) were obtained from Sigma Chemical Co. (Poole, Dorset). ^{125}I-labelled human serum albumin was from Amersham International (U.K.). OKY 1581 (sodium (E)-3[4-(3-pyridylmethyl)phenyl]-2-methylacrylate) was a gift from ONO Pharmaceuticals, 1-benzylimidazole and BM 13177 (4-[2-benzyenesulphonamide)-ethyl]-phenoxyacetic acid) were synthesized in the Wellcome Research Laboratories, BN 52021 (ginkgolide B, 9H-1,7a-(epoxymethanol)-1H,6aH, cyclopenta[c][2-3-b]furo-[3,2′:3,4] cyclopenta-[1,2-d]furan 5,9,12-[4H]trione, 3 *tert*-butylhexahydro 4,7b,11,hydroxy-8-methyl) and WEB 2086 ((3-[4-(2-chlorophenyl)-9-methyl-6H-thieno[3,2-f][1,2,4]triazolo-[4,3-a] [1,4]diazepine-2-yl]-1-(4-morpholinyl)-1-propanone) were supplied by IHB-IPSEN Research Laboratories and by Boehringer Ingelheim K.G., respectively. The compounds were dissolved in isotonic saline or in the case of BN 52021, in the supplied vehicle, which was used in control studies.

Statistics

Data are expressed as mean ± s.e.mean of (*n*) observations. For statistical comparisons, analysis of variance with the Bonferroni test was utilised. $P < 0.05$ was taken as significant.

Results

Effect of L-NAME on endotoxin-induced intestinal plasma leakage and mucosal damage

Administration of LPS (3 mg kg^{-1}, i.v.) did not cause plasma leakage in the ileum or colon (Figure 1), or macroscopic injury in the ileum (Table 1) when determined 1 h after challenge. Concurrent administration of L-NAME (1–10 mg kg^{-1}, s.c.) with LPS, however, dose-dependently induced plasma leakage in the intestine with a maximum increase of Δ430 ± 59 and Δ315 ± 40 μl g^{-1} tissue in the ileum and in the colon, respectively ($P < 0.001$), as shown in Figure 1. The combination of LPS and L-NAME (5 mg kg^{-1}, s.c.) also provoked macroscopic injury in the ileum over a 1 h period (Table 1). Administration of L-NAME (5 mg kg^{-1}, s.c.) alone did not cause plasma leakage in the ileum and colon ($n = 8$ and 11).

Effect of thromboxane synthase inhibitors and receptor antagonist on intestinal plasma leakage and macroscopic damage

The administration of the thromboxane synthase inhibitors, OKY 1581 (5–25 mg kg^{-1}, s.c.) and BZI (1–50 mg kg^{-1}, s.c.)

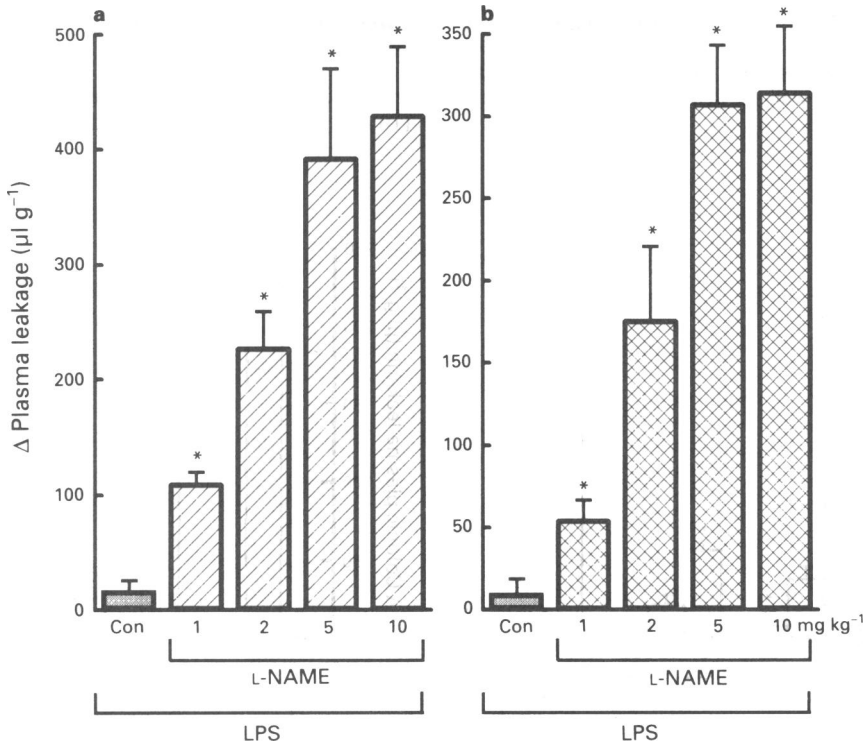


Figure 1 Potentiation of lipopolysaccharide (LPS, 3 mg kg^{-1}, i.v.)-induced vascular leakage of plasma, determined using radiolabelled albumin, in (a) rat ileum and (b) colon by concurrent administration of N^G-nitro-L-arginine methyl ester (L-NAME, 1–10 mg kg^{-1}, s.c.) after 1 h. The columns show the leakage of plasma (Δ μl g^{-1} tissue) 1 h after injection of LPS alone (stippled column) or LPS with L-NAME (hatched columns). Data are given as the mean ± s.e.mean of 12 (control) and 8, 8, 10, 8 rats per group, respectively; statistical significance is shown as $*P < 0.05$ compared to the LPS-alone group (Con).

Table 1 Macroscopic injury induced by concurrent administration of lipopolysaccharide (LPS, 3 mg kg^{-1}, i.v.) and N^G-nitro-L-arginine methyl ester (L-NAME, 5 mg kg^{-1}, s.c.) in the mucosa of the rat ileum: inhibition by pretreatment (15 min, s.c.) with the thromboxane synthase inhibitors, OKY 1581 and 1-benzyl-imidazole (BZI), the thromboxane receptor antagonist, BM 13177 and the platelet-activating factor receptor antagonists, WEB 2086 and BN 52021

Treatment	*Dose* (mg kg^{-1})	*Damage index*
Saline		0.13 ± 0.13
LPS		0.54 ± 0.22
LPS + L-NAME		2.57 ± 0.30*
+ OKY 1581	5.0	1.75 ± 0.31
	10.0	1.50 ± 0.19*
	25.0	0.88 ± 0.13*
+ BZI	5.0	1.08 ± 0.18*
	50.0	0.50 ± 0.19*
+ BM 13177	0.2	2.60 ± 0.24
	2.0	0.60 ± 0.24*
+ WEB 2086	0.1	3.13 ± 0.23
	1.0	1.22 ± 0.22*
+ BN 52021	2.5	2.80 ± 0.29
	10.0	1.05 ± 0.25*

Data are expressed as a damage index (on a 0–4 scale) and calculated as mean ± s.e.mean of at least 4 rats per group, where statistical significance is shown as $*P < 0.05$ compared with the LPS group, $*P < 0.05$ vs. LPS + L-NAME group.

dose-dependently attenuated plasma leakage in the ileum and colon (Figures 2 and 3), and prevented the macroscopic injury in the ileum induced by LPS and L-NAME (Table 1).

The thomboxane receptor antagonist, BM 13177 (0.2–2 mg kg^{-1}, s.c.) also dose-dependently inhibited ileal and colonic plasma leakage (Figures 2 and 3), and protected the ileum against macroscopic injury induced by LPS and L-NAME (Table 1).

Effects of PAF antagonists on intestinal plasma leakage and macroscopic damage

The plasma leakage in the ileum and colon, caused by LPS and L-NAME was dose-dependently diminished by pretreatment with the PAF-receptor antagonists, WEB 2086 (0.1–1 mg kg^{-1}, s.c.) or BN 5202 (2.5–10 mg kg^{-1}, s.c.) as shown in Figure 4. These agents also significantly reduced the macroscopic injury in the ileum (Table 1).

Effect of indomethacin on intestinal plasma leakage and mucosal injury

Indomethacin (2 and 5 mg kg^{-1}, s.c.) reduced the intestinal plasma leakage induced by the concurrent administration of LPS and L-NAME (by 93 ± 3% and 100% in the ileum, and 88 ± 6% and 100% in the colon, respectively, $P < 0.001$; $n = 4–8$), and also protected the ileum against macroscopic damage (by 68 ± 16% and 93 ± 5%, respectively; $P < 0.001$).

Interaction between BZI and WEB 2086 on intestinal plasma leakage and mucosal injury

Administration of a low dose of BZI (1 mg kg^{-1}, s.c.) had no effect on plasma leakage induced by the concurrent administration of LPS and L-NAME in the ileum and colon, and did not protect the ileal mucosa against macroscopic lesions (Figure 5). Administration of WEB 2086 (0.5 mg kg^{-1}, s.c.) reduced L-NAME and LPS-induced plasma leakage in the ileum and colon (by 59 ± 6% and 62 ± 5%, respectively; $P < 0.01$; $n = 8$ and 10), but did not reduce significantly ileal

macroscopic injury. By contrast, when BZI (1 mg kg^{-1}, s.c.) and WEB 2086 (0.5 mg kg^{-1}, s.c.) were injected together prior to the administration of LPS and L-NAME, ileal and colonic plasma leakage as well as ileal macroscopic damage was abolished (Figure 5).

Effect of phenylephrine infusion on blood pressure and intestinal plasma leakage

In pentobarbitone-anaesthetized rats, phenylephrine infusion (10 μg kg^{-1} min^{-1}, i.v.) caused a similar elevation in blood

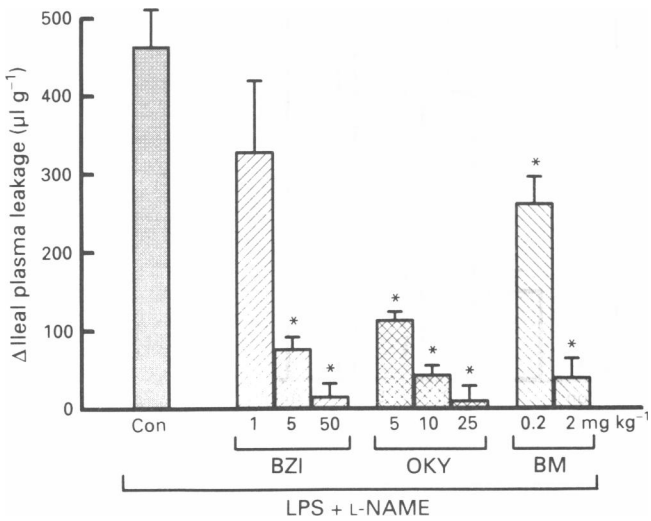


Figure 2 Inhibition by OKY 1581 (OKY, 5–25 mg kg^{-1}, s.c.), 1-benzyl-imidazole (BZI, 1–50 mg kg^{-1}, s.c.) and BM 13177 (BM, 0.2–2 mg kg^{-1}, s.c.) pretreatment (15 min before endotoxin) of vascular leakage of radiolabelled albumin induced by concurrent administration of lipopolysaccharide (LPS, 3 mg kg^{-1}, i.v.) and N^{G}-nitro-L-arginine methyl ester (L-NAME, 5 mg kg^{-1}, s.c.) in the ileum. Albumin leakage (expressed as plasma leakage, Δ μl g^{-1} tissue) was determined 1 h after challenge. Data are shown as the mean ± s.e.mean of 12 (control) and 6, 10, 8, 6, 7, 7, 4, and 4 rats per group, respectively; statistical significance is shown as $*P < 0.05$ compared to the LPS + L-NAME group (Con).

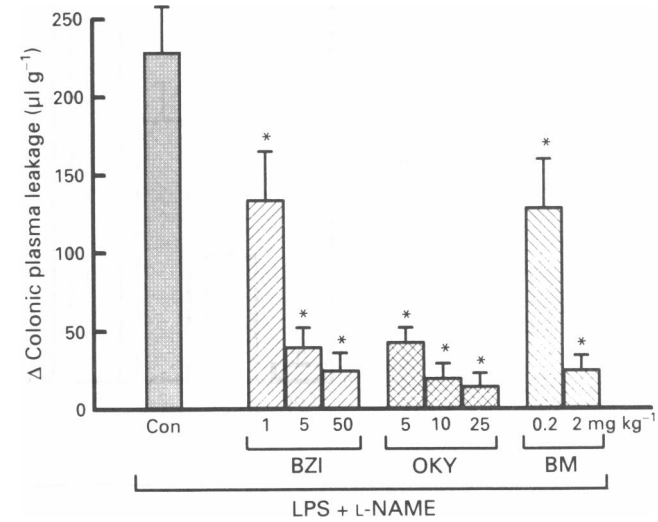


Figure 3 Inhibition by OKY 1581 (OKY, 5–25 mg kg^{-1}, s.c.), 1-benzyl-imidazole (BZI, 1–50 mg kg^{-1}, s.c.) and BM 14177 (BM, 0.2–2 mg kg^{-1}, s.c.) pretreatment (15 min before endotoxin) of vascular leakage of radiolabelled albumin induced by concurrent administration of lipopolysaccharide (LPS, 3 mg kg^{-1}, i.v.) and N^{G}-nitro-L-arginine methyl ester (L-NAME, 5 mg kg^{-1}, s.c.) in the colon. Albumin leakage (expressed as plasma leakage, Δ μl g^{-1} tissue) was determined 1 h after challenge. Data are shown as the mean ± s.e.mean of 12 (control) and 6, 10, 8, 6, 7, 7, 4, and 4 rats per group, respectively; statistical significance is shown as $*P < 0.05$ compared to the LPS + L-NAME group (Con).

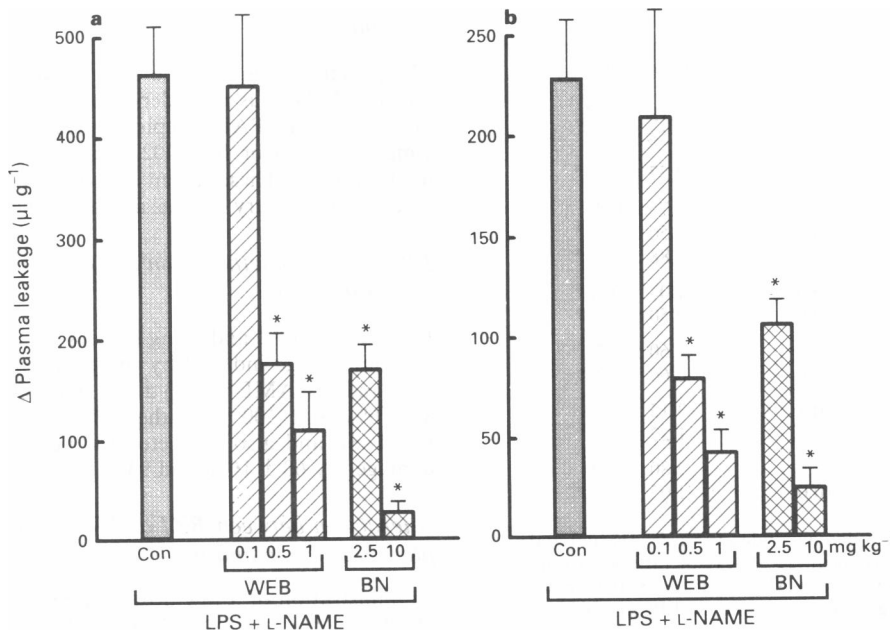


Figure 4 Inhibition by WEB 2086 (WEB, 0.1–1.0 mg kg^{-1}, s.c.) and BN 52021 (BN, 2.5–10 mg kg^{-1}, s.c.) pretreatment (15 min before endotoxin) of vascular leakage of radiolabelled albumin induced by concurrent administration of lipopolysaccharide (LPS, 3 mg kg^{-1}, i.v.) and N^{G}-nitro-L-arginine methyl ester (L-NAME, 5 mg kg^{-1}, s.c.) in the ileum (a) and colon (b). Albumin leakage (expressed as plasma leakage, Δ μl g^{-1} tissue) was determined 1 h after challenge. Data are shown as the mean ± s.e.mean of 12 (control) and 7, 12, 9, 6 and 8 rats per group, respectively; statistical significance is shown as $*P < 0.05$ compared to the LPS + L-NAME group (Con).

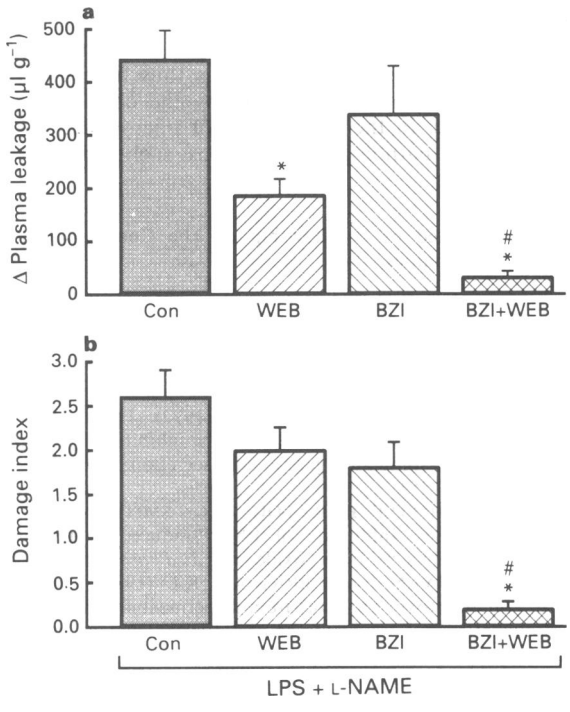


Figure 5 Effect of WEB 2086 (WEB, 0.5 mg kg^{-1}, s.c.) and 1-benzyl-imidazole (BZI, 1 mg kg^{-1}, s.c.) pretreatment (15 min before endotoxin) on vascular leakage (a) and macroscopic damage (b) induced by concurrent administration of lipopolysaccharide (LPS, 3 mg kg^{-1}, i.v.) and N^G-nitro-L-arginine methyl ester (L-NAME, 5 mg kg^{-1}, s.c.) in the ileum. Albumin leakage (expressed as plasma leakage, μl g^{-1} tissue) and macroscopic damage (damage index: 0–4) were determined 1 h after challenge. Data are shown as the mean ± s.e.mean of 10 (control) and 8, 8 and 10 rats per group, respectively; statistical significance is shown as $^*P < 0.05$ compared to the LPS + L-NAME group (Con), $^\#P < 0.05$ vs. WEB or BZI groups.

pressure (BP) to that observed following the bolus administration of L-NAME (5 mg kg^{-1}, i.v.) over a 1 h period. Thus, the BP changes were Δ 46 ± 11 and Δ 41 ± 6 mmHg after 15 and 60 min of phenylephrine infusion, compared with Δ 48 ± 11 and Δ 43 ± 5 mmHg at similar times after L-NAME administration ($P < 0.001$ for each compared with values from control, untreated rats; $n = 4$ and 5). Administration of LPS (3 mg kg^{-1}) had no significant effect on BP over the experimental period (Δ − 7 ± 11 mmHg after 1 h). In LPS challenged rats, the increase in BP, determined 15 min following intravenous administration of L-NAME (5 mg kg^{-1}) or infusion of phenylephrine (10 μg kg^{-1} min^{-1}), was Δ 37 ± 9 and Δ 52 ± 6 mmHg, respectively ($n = 4$; $P < 0.01$ from control, untreated rats), while after 1 h, the BP values were Δ 24 ± 8 and Δ 22 ± 2 mmHg, respectively ($n = 4$). Likewise, the increase in BP following subcutaneous administration of L-NAME (5 mg kg^{-1}) in LPS-treated rats was Δ 36 ± 7 mmHg after 15 min and Δ 23 ± 6 mmHg after 1 h ($n = 5$). Thus, following LPS administration, the changes in BP caused by these doses of L-NAME (either by the i.v. or s.c. route) were not significantly different from those of the intravenous infusion of phenylephrine at either time-point during the 1 h observation period.

Phenylephrine infusion (10 μg kg^{-1} min^{-1}, i.v.) had no effect on plasma leakage in the ileum and colon of LPS-treated pentobarbitone-anaesthetized rats during the 1 h investigation period (Δ 0 ± 5 and Δ 0 ± 4 μl g^{-1} in ileal and colonic tissue in the LPS alone group, and Δ 0 ± 19 and Δ 0 ± 3 μl g^{-1} tissue in the LPS and phenylephrine group, respectively; $n = 4$ and 6). By contrast, administration of L-NAME (5 mg kg^{-1}, s.c.) and LPS in pentobarbitone-anaesthetized rats increased plasma leakage in the ileum and colon by Δ 473 ± 16 and Δ 329 ± 45 μl g^{-1} tissue, respectively ($n = 5$, $P < 0.001$).

Discussion

This study confirms our recent observations that the administration of a low dose of LPS does not cause any acute vascular or mucosal damage of the intestine (Boughton-Smith *et al.*, 1993), whereas extensive acute injury can be provoked by concurrent administration of the NO synthase inhibitor, L-NAME (László *et al.*, 1994a). The increased plasma leakage in the ileum and colon following concurrent administration of L-NAME and endotoxin over a 1 h period appears unrelated to elevation of systemic arterial blood pressure and a consequent increase in microvascular hydrostatic pressure, since phenylephrine infusion, in a dose that increased blood pressure to a similar extent to L-NAME, did not affect intestinal vascular permeability following endotoxin administration. It is possible however, that there are differences in the local changes in intestinal blood flow with these two agents, but interpretation of comparative studies on the mucosal microcirculation would be complex. These acute actions of L-NAME have previously been shown to be abolished by L-arginine (László *et al.*, 1994a) and thus appear to reflect inhibition of constitutive NO synthase, expression of the inducible NO synthase in rat intestinal tissue not being detected until 3 h after endotoxin challenge (Salter *et al.*, 1991; Boughton-Smith *et al.*, 1993).

Administration of high doses of endotoxin acutely elevates the tissue concentration of both PAF and thromboxane A_2 in the rat intestine, and these mediators may be involved the associated damage in the intestinal vasculature and mucosa (Whittle *et al.*, 1987; Boughton-Smith *et al.*, 1989). In the present study, low doses of endotoxin in combination with L-NAME were used to induce intestinal injury and unlike a previous study over 15 min using high doses of endotoxin and L-NMMA (Hutcheson *et al.*, 1990), plasma leakage was observed in the colon as well as in the ileum after 1 h. Under these conditions the PAF-receptor antagonists, WEB 2086 and BN 52021 reduced plasma leakage and mucosal damage in both intestinal tissues during this early phase of endotoxaemia. Furthermore, the thromboxane synthase inhibitors, 1-benzyl-imidazole and OKY 1581, as well as the thromboxane receptor antagonist, BM 13177 inhibited such plasma leakage and mucosal damage. The reduction by indomethacin of the plasma leakage and mucosal injury is likely to reflect inhibition of thromboxane formation, as seen previously when endotoxin alone was used (Boughton-Smith *et al.*, 1989), and suggests that cyclo-oxygenase products do not play a key role in the maintenance of microvascular integrity in the early phase of endotoxaemia.

The potent vasodilator actions of endogenous NO may protect the intestinal microvascular bed and the consequent mucosal injury by effectively opposing the vasoconstrictor actions of thromboxane A_2 (Whittle, 1993). Furthermore, NO may prevent microthrombotic occlusion of the microvasculature provoked by thromboxane, as it can inhibit platelet aggregation and the adhesion of platelets to the vascular endothelium (Radomski *et al.*, 1987a,b). Since PAF-induced microvascular stasis and mucosal damage appears to involve the aggregation of neutrophils and other inflammatory cells in the microcirculation (Wallace & Whittle, 1986; Whittle *et al.*, 1986) and neutrophil adhesion is implicated in vascular injury (Kubes *et al.*, 1990), NO could also maintain intestinal microcirculatory perfusion by preventing such neutrophil aggregation and adhesion (McCall *et al.*, 1988; Kubes *et al.*, 1991). Indeed, S-nitroso-*N*-acetyl-penicillamine, a spontaneous generator of NO, inhibits gastrointestinal plasma leakage induced by endotoxin and by PAF (Boughton-Smith *et al.*, 1990; 1992) and PAF-induced increase of vascular permeability in the gut can be potentiated by L-NAME (Filep & Földes-Filep, 1993).

The present study suggests that PAF and thromboxanes are released following the administration of low doses of endotoxin, but do not cause acute injury to the intestinal microvasculature unless there is concurrent inhibition of NO synthase. The pronounced inhibitory effect of the combination of PAF-receptor antagonist and thromboxane synthase inhibitor could suggest interactions between the damaging effects of these endogenous mediators. It therefore appears that the maintenance of intestinal microvascular and mucosal integrity during the acute phase of endotoxaemia depends on complex regulatory mechanisms, involving the balance between the release of aggressive mediators and the beneficial actions of NO. These present findings thus further support the protective role of NO, formed by the constitutive NO synthase enzyme, in the modulation of microvascular integrity under acute pathological conditions, such as in the early phase of sepsis.

F.L. was supported by a fellowship of The Commission of the European Communities.

References

BOUGHTON-SMITH, N.K., DEAKIN, A.M. & WHITTLE, B.J.R. (1992). Actions of nitric oxide on the acute gastrointestinal damage induced by PAF in the rat. *Agents Actions, Special Conference Issue*, C3–C9.

BOUGHTON-SMITH, N.K., EVANS, S.M., LÁSZLÓ, F., WHITTLE, B.J.R. & MONCADA, S. (1993). The induction of nitric oxide synthase and intestinal vascular permeability by endotoxin in the rat. *Br. J. Pharmacol.*, **110**, 1189–1195.

BOUGHTON-SMITH, N.K., HUTCHESON, I.R., DEAKIN, A.M., WHITTLE, B.J.R. & MONCADA, S. (1990). Protective effect of S-nitroso-N-acetyl-penicillamine in endotoxin-induced acute intestinal damage in the rat. *Eur. J. Pharmacol.*, **191**, 485–488.

BOUGHTON-SMITH, N.K., HUTCHESON, I. & WHITTLE, B.J.R. (1989). Relationship between paf-acether and thromboxane A_2 biosynthesis in endotoxin-induced intestinal damage in the rat. *Prostaglandins*, **38**, 319–333.

CASALS-STENZEL, J. (1987). Protective effect of WEB 2086, a novel antagonist of platelet-activating factor, in endotoxin shock. *Eur. J. Pharmacol.*, **135**, 117–122.

FILEP, J.G. & FÖLDES-FILEP, É. (1993). Modulation by nitric oxide of platelet-activating factor-induced albumin extravasation in the conscious rat. *Br. J. Pharmacol.*, **110**, 1347–1352.

HALUSHKA, P.V., COOK, J.A. & WISE, W.C. (1983). Beneficial effects of UK 37248, a thromboxane synthetase inhibitor, in experimental endotoxic shock in the rat. *Br. J. Clin. Pharmacol.*, **15**, Suppl. 1, 133S–139S.

HAMID-BLOOMFIELD, S. & WHITTLE, B.J.R. (1989). Antagonism of PGD_2 vasodepressor responses in the rat in vivo by the novel, selective antagonist, BW A868C. *Br. J. Pharmacol.*, **96**, 307–312.

HARLAN, J.M., HARKER, L.A., RIEDY, M.A., GAJDUSEK, C.M., SCHWARTZ, S.M. & STRIKER, G.E. (1983). Lipopolysaccharide-mediated bovine endothelial cell injury in vitro. *Lab. Invest.*, **48**, 269–274.

HUTCHESON, I.R., WHITTLE, B.J.R. & BOUGHTON-SMITH, N.K. (1990). Role of nitric oxide in maintaining vascular integrity in endotoxin-induced acute intestinal damage in the rat. *Br. J. Pharmacol.*, **101**, 815–820.

KOLTAI, M., HOSFORD, D., GUINOT, P., ESANU, A. & BRAQUET, P. (1991a). Platelet activating factor (PAF). A review of its effects, antagonists and possible future clinical implications (Part I). *Drugs*, **42**, 9–29.

KOLTAI, M., HOSFORD, D., GUINOT, P., ESANU, A. & BRAQUET, P. (1991b). Platelet activating factor (PAF). A review of its effects, antagonists and possible future clinical implications (Part II). *Drugs*, **42**, 174–204.

KUBES, P. & GRANGER, D.N. (1992). Nitric oxide modules microvascular permeability. *Am. J. Physiol.*, **262**, H611–H615.

KUBES, P., SUZUKI, M. & GRANGER, D.N. (1990). Modulation of PAF-induced leukocyte adherence and increased microvascular permeability. *Am. J. Physiol.*, **259**, G859–G864.

KUBES, P., SUZUKI, M. & GRANGER, D.N. (1991). Nitric oxide: an endogenous modulator of leukocyte adhesion. *Proc. Natl. Acad. Sci. U.S.A.*, **88**, 4651–4655.

LASZLÓ, F., WHITTLE, B.J.R. & MONCADA, S. (1994a). Time-dependent enhancement and inhibition of endotoxin-induced vascular injury in rat intestine by nitric oxide synthase inhibitors. *Br. J. Pharmacol.*, **111**, 1309–1315.

LASZLÓ, F., WHITTLE, B.J.R. & MONCADA, S. (1994b). Interactions between endogenous nitric oxide, platelet-activating factor and thromboxanes during endotoxin-induced acute vascular injury in rat intestine. *Br. J. Pharmacol.*, **112**, 68P.

MARTINEZ-CUESTA, M.A., BARRACHINA, M.D., PIQUE, J.M., WHITTLE, B.J.R. & ESPLUGUES, J.V. (1992). The role of nitric oxide and platelet-activating factor in the inhibition by endotoxin of pentagastrin-stimulated gastric acid secretion. *Eur. J. Pharmacol.*, **218**, 351–354.

MCCALL, T.B., WHITTLE, B.J.R., BOUGHTON-SMITH, N.K. & MONCADA, S. (1988). Inhibition of FMLP-induced aggregation of rabbit neutrophils by nitric oxide. *Br. J. Pharmacol.*, **95**, 571P.

MEYRICK, B.O., RYAN, U.S. & BRIGHAM, K.L. (1986). Direct effect of E. coli endotoxin on structure and permeability of pulmonary endothelial monolayers and the endothelial layer of intimal explants. *Am. J. Pathol.*, **122**, 140–151.

OLANOFF, L.S., COOK, S.A., ELLER, T., KNAPP, D.R. & HALUSHKA, P.V. (1985). Protective effects of trans-13-APT, a thromboxane receptor antagonist, in endotoxaemia. *J. Cardiovasc. Pharmacol.*, **7**, 114–120.

RADOMSKI, M.W., PALMER, R.M.J. & MONCADA, S. (1987a). Endogenous nitric oxide inhibits human platelet adhesion to vascular endothelium. *Lancet*, **ii**, 1057–1058.

RADOMSKI, M.W., PALMER, R.M.J. & MONCADA, S. (1987b). The anti-aggregating properties of vascular endothelium: interactions between prostacyclin and nitric oxide. *Br. J. Pharmacol.*, **92**, 639–646.

ROSAM, A.-C., WALLACE, J.L. & WHITTLE, B.J.R. (1986). Potent ulcerogenic actions of platelet-activating factor on the stomach. *Nature*, **319**, 54–56.

SALTER, M., KNOWLES, R.G. & MONCADA, S. (1991). Widespread tissue distribution, species distribution and changes in activity of Ca^{2+}-dependent and Ca^{2+}-independent nitric oxide synthases. *FEBS Lett.*, **291**, 145–149.

SZABÓ, C., MITCHELL, J.A., GROSS, S.S., THIEMERMANN, C. & VANE, J.R. (1993). An antagonist of platelet-activating factor (WEB 2086) inhibits the induction of nitric oxide synthase by bacterial lipopolysaccharide. *Br. J. Pharmacol.*, **109**, 11P.

WALLACE, J.L., STEEL, G., WHITTLE, B.J.R., LAGENTE, V. & VARGAFTIG, B. (1987). Evidence for platelet-activating factor as a mediator of endotoxin-induced gastrointestinal damage in the rat. Effects of three platelet-activating factor antagonists. *Gastroenterology*, **93**, 765–773.

WALLACE, J.L. & WHITTLE, B.J.R. (1986). Picomole doses of platelet-activating factor predispose the gastric mucosa to damage by topical irritants. *Prostaglandins*, **31**, 989–998.

WHITTLE, B.J.R. (1993). Nitric oxide and the gastrointestinal tract. In *Immunopharmacology of the Gastrointestinal System*. ed. Wallace, J.L. pp. 155–167. London: Academic Press.

WHITTLE, B.J.R., BOUGHTON-SMITH, N.K., HUTCHESON, I.R., ESPLUGUES, J.V. & WALLACE, J.L. (1987). Increased intestinal formation of Paf in endotoxin-induced damage in the rat. *Br. J. Pharmacol.*, **92**, 3–4.

WHITTLE, B.J.R., LOPEZ-BELMONTE, J. & MONCADA, S. (1990). Regulation of gastric mucosal integrity by endogenous nitric oxide: interactions with prostanoids and sensory neuropeptides in the rat. *Br. J. Pharmacol.*, **99**, 607–611.

WHITTLE, B.J.R., MOROSHITA, T., OHYA, Y., LEUNG, F.W. & GUTH, P.H. (1986). Microvascular actions of platelet-activating factor on rat gastric mucosa and submucosa. *Am. J. Physiol.*, **251**, G772–G778.

WISE, W.C., COOK, J.A., HALUSHKA, P.V. & KNAPP, D.R. (1980). Protective effects of thromboxane synthase inhibitors in rats in endotoxic shock. *Circ. Res.*, **46**, 845–849.

(Received April 19, 1994
Revised June 28, 1994
Accepted July 15, 1994)

Br. J. Pharmacol. (1994), **113**, 1137–1140 © Macmillan Press Ltd, 1994

Antianginal effects of FK409, a new spontaneous NO releaser

[1]Yasuhiro Kita, *Reiko Ozaki, *Shigeru Sakai, Toshiko Sugimoto, Yoshimi Hirasawa, *Minoru Ohtsuka, Hachiro Senoh, Keizo Yoshida & Kazuhiro Maeda

Department of Pharmacology, New Drug Research Laboratories and *Pharmacological Research Laboratories, Fujisawa Pharmaceutical Co., Ltd., 1-6, 2-chome, Kashima Yodogawa-ku, Osaka 532, Japan

1 The aim of this study was to compare antianginal effects of (±)-(E)-ethyl-2-[(E)-hydroxyimino]-5-nitro-3-hexeneamide (FK409), a new spontaneous nitric oxide releaser, with those of isosorbide dinitrate (ISDN). We used two types of rat angina model; methacholine- and arginine vasopressin (AVP)-induced coronary vasospasm models.

2 In the *in vitro* study, FK409 showed 80 times more potent vasorelaxant effect in dog isolated coronary artery than ISDN (EC_{50} = 16.7 ± 4.8 and 1340 ± 320 nM, respectively).

3 In the rat methacholine-induced coronary vasospasm model, FK409 suppressed the elevation of ST segment dose-dependently and significantly at 0.1 mg kg^{-1}, i.d. On the other hand, ISDN suppressed it significantly at 3.2 mg kg^{-1}, i.d. In addition, the efficacy of 3.2 mg kg^{-1} ISDN in the model was almost the same as that of 0.1 mg kg^{-1} FK409.

4 In the above experiments, FK409 and ISDN decreased mean blood pressure significantly at the maximum dose tested (1.0 mg kg^{-1}, i.d. and 3.2 mg kg^{-1}, i.d., respectively) but did not change heart rate at these doses. Therefore, the hypotensive effect of FK409 was 10 times weaker than the antianginal effect of the compound, while those of ISDN were almost the same.

5 In the rat AVP-induced coronary vasospasm model, 32 mg kg^{-1} FK409 significantly inbibited the depression of ST segment 60 min after oral administration. On the other hand, 32 mg kg^{-1} ISDN did not inhibit it at 60 and 120 min after oral administration.

6 In conclusion, FK409 inbibits coronary vasospasm more potently in two types of rat angina models than ISDN. In addition, FK409 shows an antianginal effect more selectively that a hypotensive effect, compared with ISDN.

Keywords: FK409; isosorbide dinitrate; nitric oxide; angina

Introduction

(±)-(E)-ethyl-2-[(E)-hydroxyimino]-5-nitro-3-hexeneamide (FK409) (Figure 1) is a structurally unique compound, which has been discovered from the fermentation products of *Streptomyces griseosporeus*, with vasorelaxant and antiplatelet activities (Hino *et al.*, 1989). FK409 produces a potent vasorelaxation mediated by the elevation of guanosine 3':5'-cyclic monophosphate (cyclic GMP) in the isolated coronary artery of the dog (Yamada *et al.*, 1991) and rabbit aorta (Shibata *et al.*, 1991) and rat aorta (Isono *et al.*, 1993). From these facts, FK409 seems to have a mode of action similar to that of organic nitrates reported by Katsuki *et al.* (1977) and Schultz *et al.* (1977). We have shown that biological actions such as vasorelaxation and inhibition of platelet aggregation of FK409 are due to nitric oxide (NO), which is generally accepted as endothelium derived relaxing factor (EDRF) (Palmer *et al.*, 1987), released spontaneously from the compound (Kita *et al.*, 1994a).

Recently we have reported that FK409 inhibits thrombus formation in a rat extracoporeal model (Kita *et al.*, 1994b) and suppresses myocardial infarction following ischaemia and reperfusion in rat coronary artery (Kita *et al.*, 1994c). In addition, these effects of FK409 are superior to those of isosorbide dinitrate (ISDN) (Figure 1), which is an organic nitrate and the most popular orally active drug for treatment of ischaemic cardiovascular diseases. Owing to these facts, FK409 seems to be a very useful compound for studying the role of NO in ischaemic cardiovascular diseases.

The aim of this work was to evaluate the antianginal effects of FK409, using two types of rat angina model; methacholine- and arginine vasopressin (AVP)-induced coronary vasospasm models. In addition, we compared these effects of FK409 with those of ISDN.

[1] Author for correspondence.

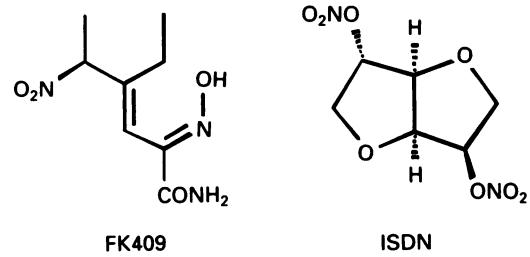
Methods

Animals

Sprague-Dawley rats, Donryu rats and beagle dogs were supplied from Nihon SLC Co. (Sizuoka, Japan), Charles River Japan Co. (Tokyo, Japan) and Keari Co. (Osaka, Japan), respectively. In methacholine-induced coronary vasospasm model, Sprague-Dawley rats were fasted for 24 h and were given each drug dissolved in saline in a volume of 5 ml kg^{-1}. In the AVP-induced coronary vasospasm model, Donryu rats were fasted for 24 h and were given each drug suspended in 0.5% methylcellulose in a volume of 5 ml kg^{-1}.

In vitro *vasorelaxation*

Beagle dogs, weighing 8–10 kg, were anaesthetized with sodium pentobarbitone (35 mg kg^{-1}, i.p.) and were bled from the femoral artery to obtain the vascular preparation. The coronary artery was dissected from the myocardium and was cut into a helical strip after removal of excess fat and connec-



FK409 ISDN

Figure 1 Chemical structure of FK409 and isosorbide dinitrate (ISDN).

tive tissues. The strip was mounted vertically in an organ bath containing 25 ml of Tyrode solution of the following composition (mM): NaCl 136.9, KCl 2.7, $CaCl_2$ 1.8, $MgCl_2$ 1.0, $NaHCO_3$ 11.9, NaH_2PO_4 0.4 and dextrose 5.6. Isometric tension was measured with a force-displacement transducer (UL-10GR, Shinkoh Co., Tokyo, Japan) connected to an amplifier (AP-630G, Nihon Koden Co., Tokyo, Japan) and was recorded with a polygraph (Recti-Horiz-8K, Nihon Denki Sanei Co., Tokyo, Japan). The tissue bath solution was maintained at 37°C and bubbled with a 95% O_2 and 5% CO_2 gas mixture. After the 60 min equilibrium period with a resting tension of 1.0 g, the strip was contracted by 0.25 ml of KCl (final concentration: 35 mM). After the contraction reached a plateau, each drug dissolved in distilled water was added to the organ bath cumulatively. In concentration-relaxation curves for FK409 and ISDN, the resting tension (1.0 g) and 35 mM KCl-produced tension were taken as 100 and 0% relaxation, respectively. The EC_{50} value was computed by regression analysis logistically.

Rat methacholine-induced coronary vasospasm model

The rat methacholine-induced coronary vasospasm model was prepared as described previously (Sakai *et al.*, 1981). Briefly, male Sprague-Dawley rats, weighing 350–420 g, were anaesthetized with urethane (1.25 g kg^{-1}, s.c.) dissolved in saline. The trachea, duodenum and left femoral artery were cannulated with polyethylene tubing. For selective bolus injection of methacholine into the ostia of the coronary artery, a double walled cannula was introduced through the exposed right carotid artery to a point near the aortic valve. Mean blood pressure and heart rate were measured through a cannula in the femoral artery with a pressure transducer (TP-400T, Nihon Kohden Co.) connected to an amplifier (AP-601G, Nihon Kohden Co.) and a heart rate counter (AT-600G, Nihon Kohden Co.), respectively, and they were recorded on a polygraph. Single doses of methacholine (8 μg) in a volume of 0.01 ml were injected into the aorta over a 1 s interval in microsyringes before and 5, 35 and 65 min after intraduodenal administration of vehicle or each drug. The standard limb lead II of the electrocardiogram was recorded with an electrocardiograph (LABO SYSTEM ZS-501, Fukuda ME Kogyo Co., Tokyo, Japan). The difference in the amplitudes of ST segment after and just before administration of methacholine is presented as elevation of the ST segment. Effects on ST elevation, mean blood pressure and heart rate are expressed as a percentage of pre-administration values of each drug.

Rat AVP-induced coronary vasospasm model

Male Donryu rats, weighing 175–225 g, were anaesthetized with sodium pentobarbitone (60 mg kg^{-1}, i.p.) dissolved in saline 15 min before intravenous administration of AVP and a polyethylene tubing filled with saline was inserted into the left femoral vein. By using the method of Hiramatsu *et al.* (1970), coronary vasospasm was induced with 1 ml kg^{-1} of AVP (0.2 iu kg^{-1}) dissolved in saline through the cannula in the femoral vein. Each drug was administered orally 60 and 120 min before the administration of AVP. The standard limb lead II of the electrocardiogram was recorded with an electrocardiograph. As previously described (Hatano *et al.*, 1980), the difference in the amplitudes of the ST segment after and just before the administration of AVP is presented as the depression of ST segment (ΔST). The amplitudes of ST segment were measured at intervals of 0.5 min for 5 min after administration of AVP. The mean of ΔST from 1.0 to 5.0 min is expressed as IΔSTI.

Drugs

FK409 and ISDN were synthesized by the Fujisawa Pharmaceutical Co. (Osaka, Japan). Methacholine chloride and AVP were purchased from Wako Pure Chemical Co. (Osaka, Japan) and Sigma Chemical Co. (St. Louis, MO, USA), respectively.

Statistical analysis

Data were presented as the mean ± s.e.mean for the number of experiments as indicated. For multiple comparisons, data were analyzed by one-way analysis of variance followed by Dunnett's test.

Results

In vitro *vasorelaxation*

In dog isolated coronary artery strips contracted with 35 mM KCl, cumulative administrations of FK409 (0.465–465 nM) or ISDN (42.4–42,400 nM) induced a concentration-dependent relaxation and the maximum relaxation produced by each drug was about 100%. Concentration-relaxation curves for both drugs are shown in Figure 2. EC_{50} values of FK409 and ISDN were 16.7 ± 4.8 and 1340 ± 320 nM, respectively. Thus, in producing a vasorelaxant effect, FK409 was about 80 times more potent than that of ISDN.

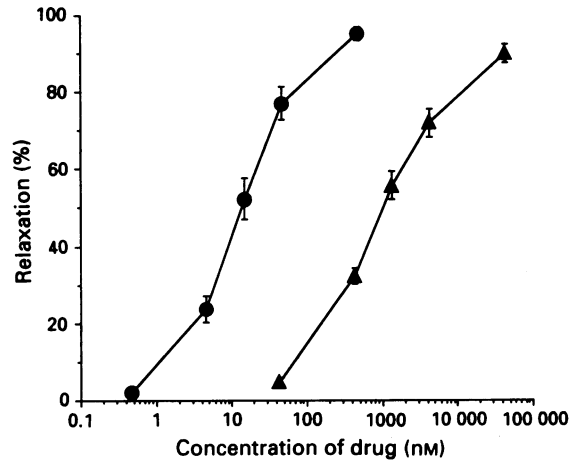


Figure 2 Vasorelaxant effects of FK409 (●) and isosorbide dinitrate (ISDN) (▲) on 35 mM KCl-induced contraction in dog isolated coronary artery. The resting tension (1.0 g) and KCl-produced tension were taken as 100 and 0% relaxation, respectively. Each value represents the mean ± s.e.mean of five experiments for FK409 and four experiments for ISDN.

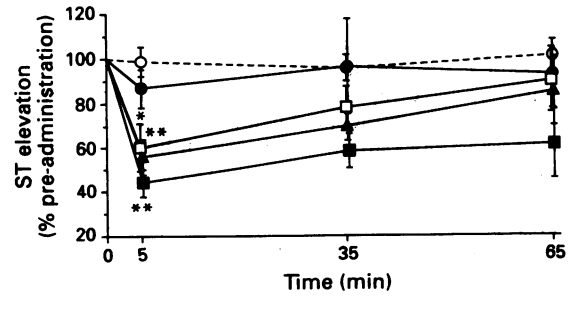


Figure 3 The effects of vehicle (○), FK409 (●; 0.01, ▲; 0.1, and ■; 1.0 mg kg^{-1}) and isosorbide dinitrate (ISDN, □; 3.2 mg kg^{-1}) on methacholine-induced ST elevation in rats. Methacholine was injected into the ostia of the coronary artery before and 5, 35 and 65 min after intraduodenal administration of each drug. The effect on ST elevation is expressed as a percentage of the pre-administration value of each drug. Each value represents the mean ± s.e. mean for six experiments. *$P<0.05$, **$P<0.01$ compared with vehicle-treated group.

Effects in methacholine-induced coronary vasospasm model

Figure 3 shows the effects of FK409 and ISDN on methacholine-induced coronary vasospasm. The elevation values of ST segment before intraduodenal administration of vehicle, FK409 (0.01, 0.1 and 1.0 mg kg^{-1}) and ISDN (3.2 mg kg^{-1}) were 0.364 ± 0.078, 0.369 ± 0.081, 0.362 ± 0.077, 0.352 ± 0.046 and 0.397 ± 0.072 mV, respectively. These values were not significantly different. FK409 inhibited the ST elevation dose-dependently from 0.01 mg kg^{-1} and significantly at 0.1 mg kg^{-1}, 5 min after administration. At 0.1 and 1.0 mg kg^{-1}, FK409 inhibited the ST elevation 35 and 65 min after administration, respectively. On the other hand, ISDN showed significant inhibition of the ST elevation at 3.2 mg kg^{-1}, 5 min after administration. The time course of inhibition of the ST elevation was like that of 0.1 mg kg^{-1} FK409.

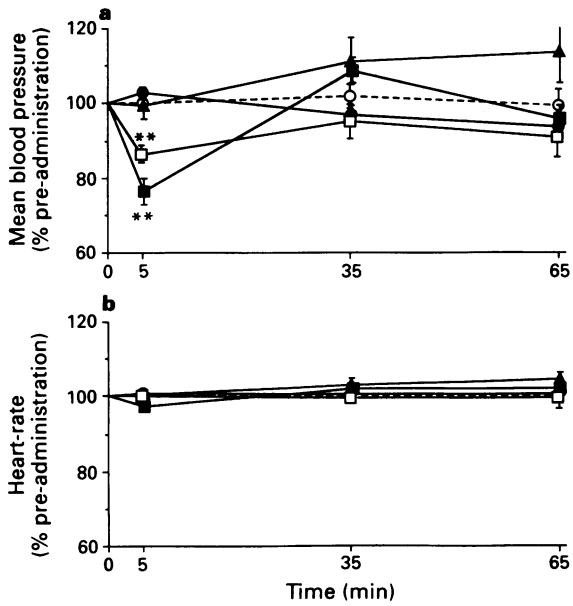


Figure 4 The effects of vehicle (○), FK409 (●; 0.01, ▲; 0.1, and ■; 1.0 mg kg^{-1}) and isosorbide dinitrate (ISDN, □; 3.2 mg kg^{-1}) on (a) mean blood pressure and (b) heart rate. Effects on mean blood pressure and heart rate were expressed as percentages of pre-administration values of each drug. Each value represents the mean ± s.e.mean for six experiments. $^{**}P < 0.01$ compared with vehicle-treated group.

Figure 4 shows the effects of FK409 and ISDN on mean blood pressure and heart rate. The pre-administration values of mean blood pressure and heart rate were not significantly different among all groups. At 1.0 mg kg^{-1} and 3.2 mg kg^{-1} respectively, FK409 and ISDN decreased mean blood pressure significantly 5 min after intraduodenal administration. However, the compounds did not change heart rate at the maximum doses tested at any time.

Effect in AVP-induced coronary vasospasm model

In the vehicle-treated group, depression of the ST segment was observed from 0.5 min after administration of AVP. One minute later the ST depression (ΔST) reached the maximum level (about -0.175 ± 0.016 mV; $n = 12$) and 5 min later, ΔST returned to -0.019 ± 0.006 mV ($n = 12$) (data not shown). As shown in Figure 5, oral FK409 inhibited the ST depression (IΔSTI) dose-dependently. At 32 mg kg^{-1}, FK409 produced about 93% and 37% inhibition vs. vehicle-treated group, 60 and 120 min after administration, respectively. This inhibitory effect of FK409 was significant 60 min after administration, while 32 mg kg^{-1} ISDN did not inhibit the ST depression significantly, 60 and 120 min after oral administration.

Discussion

In the present study, we evaluated antianginal effects of FK409 in two models of rat coronary vasospasm. We used methacholine and AVP to induce coronary vasospasm. Methacholine produced an elevation of the ST segment on the electrocardiogram whereas AVP produced depression of ST segment. The ST elevation represents transmural ischaemia caused by transient total occlusion of a large epicardial artery. The ST depression, however, represents subendocardial artery ischaemia occlusion of a major artery, with collaterals from an uninvolved artery (Rothman & Khan, 1991).

In the methacholine-induced coronary vasospasm model (*in vivo* study), FK409 and ISDN showed rapid and significant antianginal effects at 0.1 and 3.2 mg kg^{-1}, i.d., respectively. In addition, the efficacies of 0.1 mg kg^{-1} FK409 and 3.2 mg kg^{-1} ISDN in the model were almost the same at all time points tested. Thus, the pharmacokinetic profiles of FK409 and ISDN seem to be closely similar. FK409 is thought to be about 30 times more potent in the model than ISDN. In the *in vitro* study, FK409 was about 80 times more potent in producing a vasorelaxant effect in the dog isolated coronary artery than ISDN. From these results, the diffe-

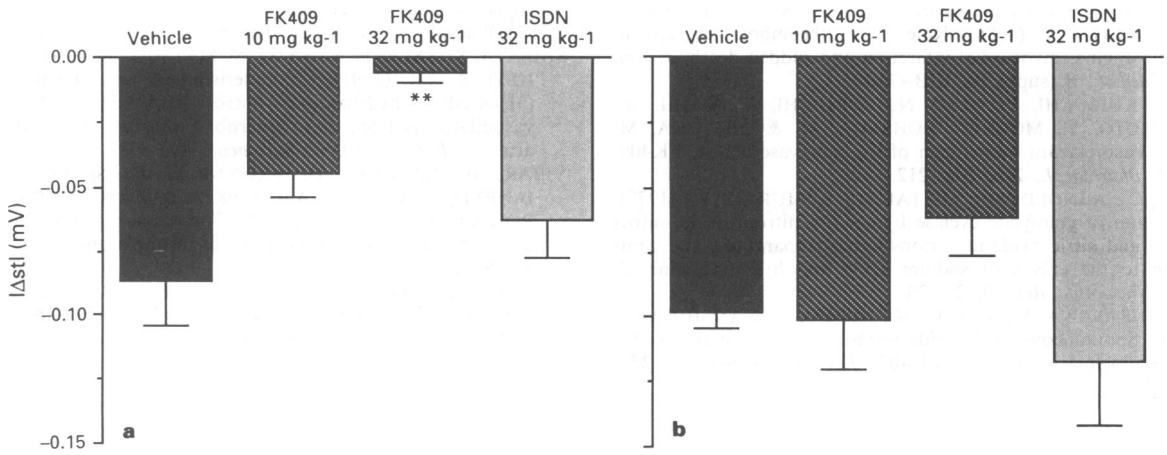


Figure 5 The effects of FK409 and isosorbide dinitrate (ISDN) on arginine vasopressin (AVP)-induced ST depression in rats. Each drug was administered orally (a) 60 and (b) 120 min before intravenous administration of AVP. The IΔSTI expresses the mean of the depression of ST segment from 1.0 to 5.0 min. Each value represents the mean ± s.e.mean for six experiments. $^{**}P < 0.01$ compared with vehicle-treated group.

rence in the potencies of FK409 and ISDN in the *in vivo* study closely reflects that in the *in vitro* study.

In the above experiments, FK409 and ISDN significantly decreased mean blood pressure at 1.0 and 3.2 mg kg^{-1}, i.d., respectively. Taking account of the potencies of the above antianginal effects, FK409 produces the suppression of methacholine-induced coronary vasospasm more selectively than the decrease in mean blood pressure, whereas ISDN does not produce the selective suppression of the coronary vasospasm.

In the AVP-induced coronary vasospasm model, 32 mg kg^{-1} FK409 significantly inhibited the coronary vasospasm, 60 min after oral administration whereas 32 mg kg^{-1} ISDN did not show a significant inhibitory effect either at 60 or 120 min after oral administration. Recently we have reported that the oral absorption of FK409 is rapid and almost complete (Kita *et al.*, 1994a). That of ISDN is also rapid (Morrison & Fung, 1984) and almost complete (Kita *et al.*, 1994a). As described above, the pharmacokinetic profiles of FK409 and ISDN are closely similar. From these data, oral FK409 is considered to have more potent antianginal activity in the AVP-induced coronary vasospasm model than oral ISDN. We have reported recently that the dose-dependency of suppression of myocardial infarction by oral FK409 coincided with that of the increase in the plasma cyclic GMP level (Kita *et al.*, 1994c); the dose-dependency of the present antianginal effect of FK409 in AVP-induced coronary vasospasm model also coincides with that of the increase in the plasma cyclic GMP level, whereas oral ISDN does not inhibit AVP-induced coronary vasospasm or the increase in the plasma cyclic GMP level at 32 mg kg^{-1} (Kita *et al.*, 1994c). The increase in plasma cyclic GMP level induced by FK409 is thought to be due to copious production of intracelluar cyclic GMP mediated by NO, which is released spontaneously from FK409 in contrast with ISDN (Kita *et al.*, 1994a). Therefore, the superior antianginal effect of FK409 is probably due to the different NO-releasing profile of FK409 from that of ISDN.

Recently we have reported that FK409 inhibits thrombus formation in the rat extracoporeal shunt model more potently than ISDN (Kita *et al.*, 1994b). The antiplatelet action could play an important role in the prevention of acute coronary syndromes such as unstable angina pectoris and acute myocardial infarction (Fitzgerald *et al.*, 1986; Hjemdahl-Monsen *et al.*, 1986; Fuster *et al.*, 1988; Vejar *et al.*, 1990). In the present study, FK409 suppressed coronary vasospasms induced by methacholine and AVP more potently than ISDN. Considered together with our recent report that FK409 suppresses myocardial infarction following ischaemia and reperfusion in the rat coronary artery (Kita *et al.*, 1994c). FK409 seems to be a very useful compound to study the role of NO in ischaemic cardiovascular diseases.

In conclusion, FK409 has a more potent vasorelaxant effect in dog coronary artery than ISDN. In both methacholine- and AVP-induced rat coronary vasospasm models, FK409 inhibits the coronary vasospasms more potently than ISDN. The different potencies of the antianginal effects of FK409 and ISDN are probably due to the different NO-releasing profiles of the compounds.

References

FITZGERALD, D.J., ROY, L., CATELLA, F. & FITZGERALD, G.A. (1986). Platelet activation in unstable coronary disease. *N. Engl. J. Med.*, **315**, 983–989.

FUSTER, V., BADIMON, L., COHEN, M., AMBROSE, J.A., BADIMON, J.J. & CHESEBRO, J. (1988). Insight into the pathogenesis of acute ischemic syndromes. *Circulation*, **77**, 1213–1220.

HATANO, N., NAKATSUJI, K., NOSE, I. & SHIMIZU, M. (1980). Effect of antianginal agents on electrocardiographic change induced with vasopressin in rats. *Pharmacometrics*, **19**, 311–317.

HINO, N., IWAMI, M., OKAMOTO, M., YOSHIDA, K., HARUTA, H., OKUHARA, M., HOSODA, J., KOHSAK, M., AOKI, H. & IMANAKA, H. (1989). FK409, a novel vasodilator isolated from the acid-treated fermentation broth of *Streptomyces griseosporeus*. I. Taxonomy, fermentation, isolation and physio-chemical and biological characteristics. *J. Antibiotics*, **42**, 1578–1583.

HIRAMATSU, Y., IZUMI, A., TEZUKA, T. & KUROSAWA, Y. (1970). Antagonizing substances obtained from whale heart extract to vasopressin induced myocardial hypoxia. *Jpn. J. Pharmacol.*, **20**, 313–324.

HJEMDAHL-MONSEN, C.E., LEWIS, H.D., CAIRNS, J., CHESEBRO, J.H. & FUSTER, V. (1986). Role of antithrombotic therapy in unstable angina, myocardial infarction and sudden death. *J. Am. Coll. Cardiol.*, **8** (suppl. B), 67B–75B.

ISONO, T., KOIBUCHI, Y., SATO, N., FURUICHI, A., NISHII, M., YAMAMOTO, T., MORI, J., KOHSAKA, M. & OHTSUKA, M. (1993). Vasorelaxant mechanism of the new vasodilator, FK409. *Eur. J. Pharmacol.*, **246**, 205–212.

KATSUKI, C., ARNOLD, W., MITTAL, C. & MURAD, F. (1977). Stimulation of guanylate cyclase by sodium nitroprusside, nitroglycerin and nitric oxide in various tissue preparations and comparison to the effects of sodium azide and hydroxylamine. *J. Cyclic Nucleotide Res.*, **3**, 23–25.

KITA, Y., HIRASAWA, Y., MAEDA, K., NISHIO, E. & YOSHIDA, K. (1994a). Spontaneous nitric oxide release accounts for the potent pharmacological actions of FK409. *Eur. J. Pharmacol.*, **257**, 123–130.

KITA, Y., HIRASAWA, Y., YOSHIDA, K. & MAEDA, K. (1994b). Antiplatelet activites of FK409, a new spontaneous NO releaser. *Br. J. Pharmacol.*, (in press).

KITA, Y., SUGIMOTO, T., HIRASAWA, Y., YOSHIDA, K. & MAEDA, K. (1994c). Close correlation of the cardioprotective effect of FK409, a spontaneous NO releaser, with an increase in plasma cyclic GMP level. *Br. J. Pharmacol.*, **113**, 5–6.

MORRISON, R.A. & FUNG, H.-L. (1984). Isosorbide dinitrate disposition in the rat: metabolite pgarmacokinetics and interactions. *J. Pharmacol. Exp. Ther.*, **231**, 124–130.

PALMER, R.M.J., FERRIGE, A.G. & MONCADA, S. (1987). Nitric oxide release accounts for the biological activity of endothelium-derived relaxing factor. *Nature*, **327**, 524–526.

ROTHMAN, M.T. & KHAN, B. (Summer 1991). Coronary artery spasm. *Br. J. Clin. Pract.*, **45**, 129–134.

SAKAI, K., AKIMA, M. & AONO, J. (1981). Evaluation of drug effects in a new experimental model of angina pectoris in the intact anesthetized rat. *J. Pharmacol. Methods*, **5**, 325–336.

SCHULTZ, K.D., SCHULTZ, K. & SCHULTZ, G. (1977). Sodium nitroprusside and other smooth muscle relaxants increase cyclic GMP levels in rat ductus deferens. *Nature*, **265**, 750–751.

SHIBATA, S., SATAKE, N., SATO, N, MATSUO, M., KOIBUCHI, Y. & HESTER, R.K. (1991). Characteristics of vasorelaxing action of (3E)-4-ethyl-2-hydroximino-5-nitro-3-hexamide FK409, a new vasodilator isolated from microbial sources, in isolated rabbit arteries. *J. Cardiovasc. Pharmacol.*, **17**, 508–518.

VEJAR, M., HACKETT, D., BRUNNELLI, C., SPALLAROSSA, P., IANETTI, M., GALASSI, A.R., LIPKIN, D., CAPONNETTO, S., PATRONO, C. & MASERI, A. (1990). Comparison of low dose aspirin and coronary vasodilators in acute unstable angina. *Circulation*, **81** (Suppl. 1), 4–11.

YAMADA, H., YONEYAMA, F., SATOH, K. & TAIRA, N. (1991). Comparison of the effects of the novel vasodilator FK409 with those of nitroglycerin in isolated coronary artery of the dog. *Br. J. Pharmacol.*, **103**, 1713–1718.

(Received July 5, 1994
Accepted July 18, 1994)

Br. J. Pharmacol. (1994), **113**, 1141–1146 © Macmillan Press Ltd, 1994

Effects of RP 67580, a tachykinin NK_1 receptor antagonist, on a primary afferent-evoked response of ventral roots in the neonatal rat spinal cord

[1]Rumiko Hosoki, Mitsuhiko Yanagisawa, Jian-Zhong Guo, Koichi Yoshioka, *Taketoshi Maehara & Masanori Otsuka

Departments of Pharmacology and *Neurosurgery, Faculty of Medicine, Tokyo Medical and Dental University, Tokyo 113, Japan

1 The pharmacological characteristics of RP 67580, a non-peptide tachykinin NK_1 receptor antagonist, and its effects on a reflex response evoked by stimulation of primary afferent fibres, were examined in isolated neonatal spinal cord preparations of the rat. Potentials were recorded extracellularly from a lumbar ventral root and drugs were bath-applied in normal artificial cerebrospinal fluid (CSF) or in the presence of tetrodotoxin (TTX).

2 In normal artificial CSF, RP 67580 (0.1–0.3 μM) caused rightward shifts of the concentration-response curves for substance P (SP), neurokinin A (NKA) and substance P methyl ester (SPOMe), an NK_1-selective agonist, with pA_2 values of 7.25, 7.47 and 7.49, respectively.

3 In the presence of TTX (0.3 μM), RP 67580 also caused rightward shifts of the concentration-response curves for SPOMe and NKA. The pA_2 value of RP 67580 against SPOMe (6.75) was significantly lower than that against NKA (7.22). RP 67580 (0.3–1 μM) did not cause a clear parallel shift of the concentration-reponse curves for SP, and it depressed the depolarizations induced by low concentrations of SP, but slightly potentiated those induced by high concentrations of SP.

4 RP 67580 (1 μM) did not depress the depolarizing responses to bombesin, L-glutamate, γ-aminobutyric acid (GABA), thyrotropin-releasing hormone and muscarine. RP 67580 (1 μM), however, depressed the response to acetylcholine in the presence of atropine and the response to nicotine. RP 68651 (1 μM), the enantiomer of RP 67580 devoid of activity at tachykinin NK_1 receptors, also depressed the response to acetylcholine in the presence of atropine.

5 RP 67580 (1 μM) did not induce GABA release from the rat spinal cord.

6 In the neonatal gerbil spinal cord, the antagonist effects of RP 67580 (0.3–1 μM) against SPOMe were much less potent than in the neonatal rat spinal cord.

7 In the rat spinal cord-saphenous nerve preparation, electrical stimulation of the saphenous nerve at C-fibre strength evoked a prolonged depolarization of the ipsilateral L3 ventral root (slow VRP). RP 67580 (0.1–1 μM) depressed the saphenous nerve-evoked slow VRP. In contrast, RP 68651 (0.3 μM) had no effect on the slow VRP.

8 The results of the present study indicate that RP 67580 acts as a high affinity NK_1 receptor antagonist in the neonatal rat spinal cord, although it also possesses an antinicotinic action. This study further suggests the existence of a subpopulation of tachykinin NK_1 receptors that are activated by NKA and SPOMe, as well as by low concentrations of SP, and are sensitive to the antagonist action of RP 67580 in the neonatal rat spinal cord. This study also provides further evidence for the involvement of SP and NKA in the slow VRP evoked by C-fibre stimulation in the neonatal rat spinal cord.

Keywords: Tachykinin NK_1 receptor; RP 67580; tachykinins; spinal cord; tachykinin receptor antagonist

Introduction

There is evidence that the tachykinin neuropeptides, substance P (SP) and neurokinin A (NKA), present in a subpopulation of primary afferent fibres play a role in pain transmission in the spinal cord (for review, see Otsuka & Yoshioka, 1993). We have previously reported that in the isolated spinal cord preparations of neonatal rats, electrical stimulation of primary afferent C-fibres and chemical noxious stimulation of peripheral tissues, such as tail and skin, induce prolonged depolarizations of ventral roots, hereafter referred to as slow ventral root potentials (VRPs), and that the slow VRPs were markedly depressed by tachykinin receptor antagonists, [D-Arg[1], D-Pro[2], D-Trp[7,9], Leu[11]]SP, spantide and GR71251 (Yanagisawa *et al.*, 1982; Akagi *et al.*, 1985; Otsuka & Yanagisawa, 1988; Nussbaumer *et al.*, 1989; Yanagisawa *et al.*, 1992a; Guo *et al.*, 1993). These results, together with other lines of evidence (Otsuka & Yanagisawa, 1987; Yanagisawa *et al.*, 1992b), strongly suggest the involvement of tachykinins in the slow VRPs. However, these tachykinin receptor antagonists, which are all peptide analogues of tachykinins with similar pharmacological characteristics, are still not entirely satisfactory with regard to affinity, selectivity, metabolic stability and the problem of transmitter releasing action (see below).

Recently, Garret *et al.* (1991) described a high affinity, non-peptide tachykinin NK_1 receptor antagonist, RP 67580. This compound not only inhibited competitively the binding of [^{3}H]-SP to rat brain membranes, but also, when injected intravenously in low doses, blocked plasma extravasation induced by SP in the rat urinary bladder or that induced by antidromic electrical stimulation of the saphenous nerve in the rat hind paw skin. Moreover, RP 67580 exhibited higher affinity versus NK_1 receptors in the mouse and rat than in the dog, guinea-pig and man. In contrast, CP-96,345, another recently described non-peptide NK_1 receptor antagonist (Snider *et al.*, 1991) displayed higher affinity versus NK_1

[1] Author for correspondence.

receptors present in the latter group of species (Fardin *et al.*, 1992; 1993; Barr & Watson, 1993). In the present study, we have examined the pharmacological profile of RP 67580 in the neonatal rat spinal cord and its effects on a primary afferent-evoked slow VRP.

Methods

Electrophysiological experiments

The isolated spinal cord preparation and spinal cord-saphenous nerve preparation of newborn rats were used (Akagi *et al.*, 1985; Nussbaumer *et al.*, 1989). Spinal cords below thoracic segments were isolated from 1–3 day old Wistar rats of either sex. The hemisected spinal cord preparation was used in the experiments to examine depolarizing actions of various agonists and the effects of RP 67580 thereupon. The preparation was placed in a chamber of 0.2–0.5 ml volume and perfused with artificial cerebrospinal fluid (CSF) at a rate of 4 ml min^{-1}. The temperature of the chamber was kept at 27°C. The composition of artificial CSF was (mM): NaCl 138.6, KCl 3.35, $CaCl_2$ 1.26, $MgCl_2$ 1.15, $NaHCO_3$ 21.0, NaH_2PO_4 0.58, and glucose 10.0. In the experiments in which the effects of RP 67580 on the action of exogenous agonists were examined in normal artificial CSF, the concentration of $MgCl_2$ was increased from 1.15 to 2 mM in order to reduce spontaneous electrical activity. The perfusion medium was saturated with a gas mixture of 95% O_2 and 5% CO_2 before perfusion. Potentials were recorded extracellularly from a lumbar ventral root (L3–5) with a tightly fitting suction electrode and displayed via preamplifier on an oscilloscope and a d.c. pen-recorder.

To examine the effects of RP 67580 on the actions of bombesin and other agonists, these agonists were applied by perfusion for 30 s at concentrations that were close to EC_{70} values determined from their concentration-response curves.

Effects of RP 67580, together with its enantiomer RP 68651, on the saphenous nerve-evoked slow VRP were investigated in the spinal cord-saphenous nerve preparation (Nussbaumer *et al.*, 1989). Electrical stimulation with two shocks (40 V intensity, 100 μs duration at 20 Hz) was given to the saphenous nerve every 3 min with a suction electrode and the resulting reflex responses were recorded extracellularly from the ipsilateral L3 ventral root. The average areas (mV × s) under the curves of three consecutive responses were measured before and after adding RP 67580 or RP 68651, and expressed as percentages of the control responses just before adding RP 67580 or RP 68651.

To investigate species selectivity of RP 67580 as tachykinin receptor antagonist, the isolated spinal cord preparation of the neonatal gerbil was also used. Spinal cords were isolated from 1–4 day-old gerbils of either sex. Other experimental details were the same as described for rat spinal cords.

Estimation of pA_2 values

Tachykinin receptor agonists were bath-applied for 30 s at 10 min intervals to spinal cord preparations. The concentration-response curves were constructed in normal or tetrodotoxin (TTX)-containing artificial CSF and then after equilibration of the preparation for 25 min with RP 67580 at two increasing concentrations. The pD_2 value of each agonist in normal or TTX-containing medium was estimated as the negative logarithm of the molar concentration giving 50% amplitude of that of the maximal response. The pA_2 values of RP 67580 were calculated from Schild plots (Arunlakshana & Schild, 1959).

GABA release from the neonatal rat spinal cord

GABA release from the neonatal rat spinal cord was measured as described previously (Sakuma *et al.*, 1991). Briefly, one hemisected spinal cord was placed in a 1 ml perfusion chamber and continuously perfused at a rate of 0.7 ml min^{-1} with artificial CSF. After washing the spinal cord with artificial CSF for 2 h, 3 min fractions of the perfusate were collected and GABA contents determined using h.p.l.c.

Drugs

RP 67580, (3a**R**, 7a**R**)-7,7-diphenyl-2-[1-imino-2-(2-methoxyphenyl)-ethyl]perhydroisoindol-4-one and RP 68651, (3a**S**, 7a**S**)-7,7-diphenyl-2-[1-imino-2-(2-methoxyphenyl)-ethyl]perhydroisoindol-4-one, were kindly donated by Dr C. Garret of Rhône-Poulenc Rorer, Centre de Recherches de Vitry-Alfortville, Vitry-sur-Seine, France. Bombesin, SP, neurokinin A and thyrotropin releasing hormone (TRH) were purchased from Peptide Institute Inc., Japan; substance P methyl ester (SPOMe) from Peninsula Laboratories, U.S.A.; acetylcholine chloride and muscarine chloride from Sigma, U.S.A.; atropine sulphate and sodium L-glutamate from Wako, Japan; dihydro-β-erythroidine hydrobromide from Merck Sharp & Dohme Research Lab, U.S.A.: GABA from Tokyo Kasei, Japan; nicotine tartrate from Nakalai Tesque Inc., Japan; and TTX from Sankyo Co. Ltd., Japan.

Statistical analysis

Data are expressed as means ± s.e.mean. Student's *t* test was used to determine the statistical significance and *P* values less than 0.05 were considered significant.

Results

Effects of RP 67580 on the depolarizations evoked by tachykinin receptor agonists in normal artificial CSF

Bath applications of the tachykinin receptor agonists, SP, NKA and SPOMe, to neonatal rat spinal cords in normal artificial CSF produced concentration-dependent depolarizations of lumbar ventral roots (Figure 1a,c and e). In normal artificial CSF, the ventral root responses induced by these tachykinin receptor agonists are mainly due to transsynaptic action through spinal interneurones and partly through direct action on motoneurones (Yanagisawa & Otsuka, 1990). The pD_2 values and maximum responses of the agonists are given in Table 1. The rank order of potencies was SP≈SPOMe> NKA. The three tachykinin receptor agonists induced similar maximum responses (1.7–2.1 mV), which were not significantly different from the maximal response obtained with L-glutamate at 3 mM in normal and TTX-containing medium (1.9–2.6 mV).

RP 67580 alone did not alter the d.c. potential of ventral roots over the concentration range 0.1–1 μM. RP 67580 (0.1–0.3 μM) caused rightward shifts of the concentration-response curves for SP, NKA and SPOMe. After removal of RP 67580, recovery of the depolarizations from the action of the antagonist was slow, being incomplete even after 1 h of washing (data not shown). The pA_2 values of RP 67580 against SP, NKA and SPOMe are given in Table 2. The slopes of Schild plots for RP 67580 against SP, NKA and SPOMe were close to unity (Table 2), suggesting competitive antagonism.

Effects of RP 67580 on the depolarizations evoked by tachykinin receptor agonists in the presence of TTX

The effects of RP 67580 on the responses of spinal motoneurones to the three tachykinin receptor agonists were examined after eliminating transsynaptic action by TTX at 0.3 μM (Yanagisawa & Otsuka, 1990). The rank order of potencies of the agonists expressed as pD_2 values was NKA≈SPOMe>SP and the amplitudes of the maximum

responses were almost identical (Table 1). Addition of RP 67580 at 0.3–1 μM caused parallel rightward shifts of the concentration-response curves for NKA and SPOMe in a concentration-dependent manner (Figure 1d, f). The pA_2 value of RP 67580 against SPOMe, however, was significantly smaller than that against NKA (Table 2). In contrast, RP 67580 did not cause a clear parallel shift of the concentration-response curve for SP, but rather it depressed the depolarizations induced by low concentrations of SP and slightly potentiated those induced by high concentrations of SP (Figure 1b). RP 68651 at 1 μM did not alter the concentration-response curve for SPOMe in the presence of TTX ($n = 3$).

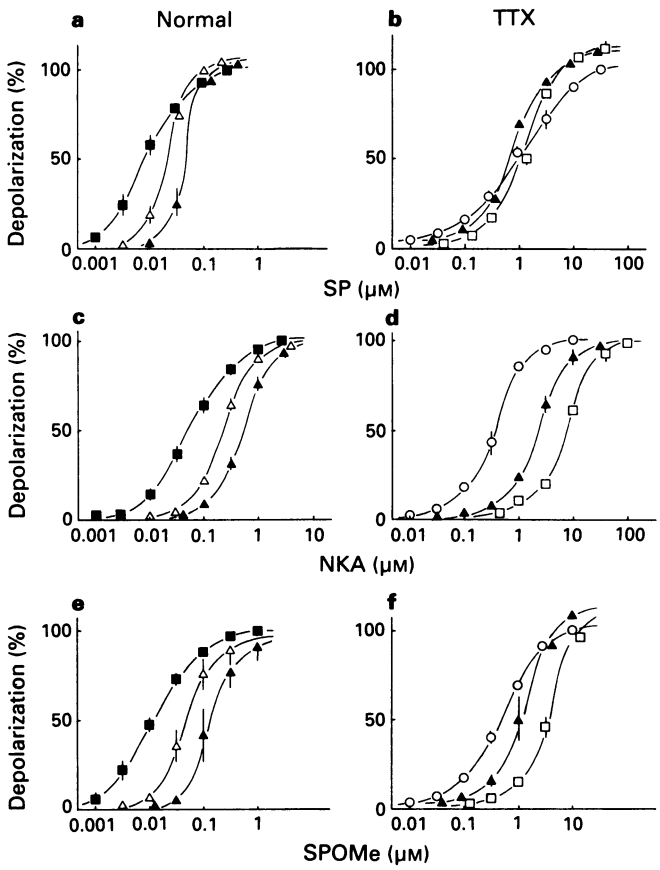


Figure 1 Effects of RP 67580 on the concentration-response curves for substance P (SP), neurokinin A (NKA) and substance P methyl ester (SPOMe) in the neonatal rat spinal cord in normal or tetrodotoxin (TTX)-containing artificial CSF. Ordinate scales: peak height of agonist-induced depolarization of ventral roots expressed as percentages of maximum control response to each agonist. Abscissa scale: logarithm of molar concentration of each agonist. Each symbol represents the mean ± s.e.mean ($n = 3$–4). For some symbols, standard errors are smaller than the symbols and therefore not shown. Some symbols are displaced horizontally to avoid overlapping. (a) and (b), Concentration-response curves for SP; (c) and (d), concentration-response curves for neurokinin A (NKA); (e) and (f), concentration-response curves for SPOMe. (a), (c) and (e), In normal artificial CSF; (b), (d) and (f), in the presence of TTX (0.3 μM). (■) Control in normal artificial CSF; (○) control in the presence of TTX; (△), (▲) and (□), after addition of RP 67580 at 0.1, 0.3, 1 μM, respectively.

Specificity of RP 67580

The effects of RP 67580 on the depolarizing responses of ventral roots to various agonists were examined (Table 3). RP 67580 at 1 μM, a concentration which depressed the response to NKA (1 μM) to 12.6% of the control, did not alter the depolarizing responses to L-glutamate (3 mM), GABA (1 mM) and TRH (0.4 μM) in the presence of TTX (0.3 μM). Moreover, RP 67580 at 1 μM did not affect the depolarizing responses to bombesin (70 nM) in normal artificial CSF (Table 3). However, this antagonist depressed the response to acetylcholine (ACh, 2 mM) to 54% in the presence of TTX. The depolarizing response to ACh (2 mM) in the presence of atropine (0.1 μM) and TTX was similarly depressed by RP 67580 to 46%, whereas the response to muscarine in the presence of TTX was unaffected (Table 3). RP 67580 caused a parallel rightward shift of the concentration-repsonse curves to ACh in the presence of atropine and TTX with pA_2 of 6.27 (Table 2). In addition, RP 67580 depressed the depolarizing response to nicotine (1 μM) in the presence of TTX to 56.5% ($n = 2$). RP 68651 (1 μM), the enantiomer of RP 67580 not possessing activity at NK_1 tachykinin receptors (Garret *et al.*, 1991), also depressed the depolarizing response to ACh (2 mM) in the presence of atropine and TTX to 47 ± 2% ($n = 3$). These results suggest that both RP 67580 and RP 68651 exhibit an antinicotinic action in the neonatal rat spinal cord.

Effects of RP 67580 on the ventral root depolarizations evoked by tachykinin receptor agonists in the neonatal gerbil spinal cord

Since species differences have been reported in the affinities of non-peptide NK_1 receptor antagonists for NK_1 receptors between rodents and other species, including the gerbil (Beresford *et al.*, 1991; Snider *et al.*, 1991; Gitter *et al.*, 1991; Fardin *et al.*, 1992), the effects of RP 67580 on the ventral root depolarizations evoked by tachykinin receptor agonists were examined in the neonatal gerbil spinal cord. Compared with its potent action in the neonatal rat spinal cord (Figure 1e and f), in the neonatal gerbil spinal cord RP 67580 (up to 1 μM) exerted almost no antagonistic action against SPOMe in the absence and presence of TTX (Figure 2a and b).

Effects of RP 67580 on GABA release from the neonatal rat spinal cord

Bath application of SP to neonatal rat spinal cords caused an increase in the GABA release (Figure 3a). In contrast,

Table 1 pD_2 values and maximum effects of tachykinin receptor agonists at inducing depolarizations of ventral roots in the neonatal rat spinal cord

	Normal artificial CSF		*In the presence of TTX* (0.3 μM)	
Agonist	pD_2	*Maximum action*	pD_2	*Maximum action*
SP	8.10 ± 0.10**	1.04 ± 0.02	5.99 ± 0.09**	0.94 ± 0.01
NKA	7.25 ± 0.10	1	6.43 ± 0.06	1
SPOMe	7.92 ± 0.06**	1.02 ± 0.04	6.31 ± 0.05†	0.98 ± 0.03

All agonists were bath applied for 30 s. pD_2: negative logarithm of the molar concentration giving 50% of the maximum amplitude of depolarization and expressed as mean ± s.e.mean ($n = 3$–5). Maximum action: ratio of the maximum amplitude of depolarization induced by each tachykinin receptor agonist to the maximum amplitude of response to neurokinin A (NKA, 1.77 ± 0.27 mV at 3 μM in normal artificial CSF and 2.07 ± 0.44 mV at 10 μM in tetrodotoxin (TTX)-containing artificial CSF). **$P < 0.01$, when compared with the corresponding values for NKA; †$P < 0.05$, when compared with the corresponding values for substance P (SP). SPOMe: substance P methyl ester.

Table 2 pA_2 values and slopes of the Schild plot for RP 67580 against the ventral root depolarizing actions of tachykinin receptor agonists and acetylcholine (ACh) in the neonatal rat spinal cord in normal or tetrodotoxin (TTX)-containing artificial CSF

	Normal artificial CSF		*TTX (0.3 μM)*	
Agonists	*pA_2*	*Slope*	*pA_2*	*Slope*
SP	7.25 ± 0.05	0.97 ± 0.05		
NKA	7.47 ± 0.08†	0.98 ± 0.03	7.22 ± 0.03	1.06 ± 0.03
SPOMe	7.49 ± 0.16††	1.00 ± 0.04	6.75 ± 0.04***	1.06 ± 0.06
ACh			6.27 ± 0.17	1.16 ± 0.09

The pA_2 values were determined from Arunlakshana-Schild plots. Each value is mean ± s.e.mean ($n = 3-4$). ***$P<0.001$, when compared with the value for neurokinin A (NKA) in the presence of TTX. †$P<0.05$ and ††$P<0.01$, when compared with the corresponding values for NKA and substance P methyl ester (SPOMe) in the presence of TTX, respectively. The experiments with ACh were carried out in the presence of atropine (0.1 μM) and TTX.

Table 3 Effects of RP 67580 (1 μM) on the ventral root depolarizing actions of various agonists in the neonatal rat spinal cord

Agonists	*% of control*
NKA (1 μM)	12.6 ± 0.4***
Bombesin (70 nM)	103 ± 3
ACh (2 mM)	54 ± 4**
L-Glutamate (3 mM)	103 ± 6
GABA (1 mM)	117 ± 7
TRH (0.4 μM)	91 ± 5
Muscarine (30 μM)	101 ± 3
ACh (2 mM) in atropine (0.1 μM)	46 ± 1***

Each value represents the amplitude of depolarization evoked by an agonist at a concentration close to EC_{70} in the presence of RP 67580 (1 μM) expressed as a percentage of the amplitude of the control response before adding RP 67580. The effect of RP 67580 on the action of bombesin was examined in normal artificial CSF and on the actions of other agonists in the presence of tetrodotoxin (TTX, 0.3 μM). Each value is mean ± s.e.mean ($n = 3$). **$P<0.01$ and ***$P<0.001$, when compared with 100%. For abbreviations, see text.

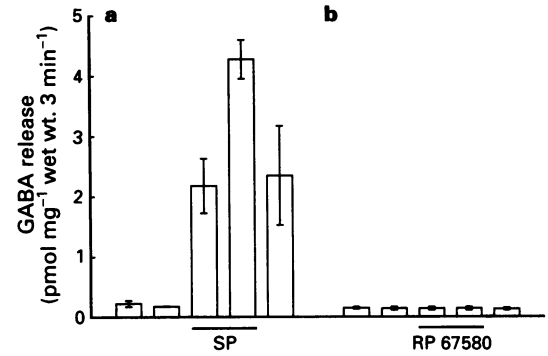


Figure 3 Effects of substance P (SP) and RP 67580 on γ-aminobutyric acid (GABA) release from neonatal rat isolated spinal cords. In each experiment, 5 successive 3 min fractions were collected, and SP at 10 μM (a) or RP 67580 at 1 μM (b) was applied by perfusion for 6 min during the period indicated by the horizontal bar under the abscissa. Ordinate scale represents the amount of GABA in each 3 min fraction of the perfusate. Each column and vertical bar represent the mean ± s.e.mean ($n = 3$).

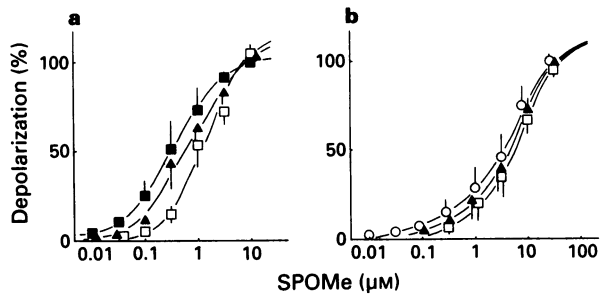


Figure 2 Effects of RP 67580 on the concentration-response curves for substance P methyl ester (SPOMe) in normal artificial CSF and in the presence of tetrodotoxin (TTX, 0.3 μM) in the neonatal gerbil spinal cord. Peak amplitudes of ventral root depolarizations were plotted against logarithmic concentrations of SPOMe. Each symbol represents the mean ± s.e.mean ($n = 3$). (a), In normal artificial CSF; (b), in the presence of TTX (0.3 μM). (■), Control in normal artificial CSF: (○), control in the presence of TTX; (▲) and (□) after addition of RP 67580 at 0.3 and 1 μM, respectively.

RP 67580 (1 μM) did not alter GABA release from spinal cords (Figure 3b).

Effects of RP 67580 on the saphenous nerve-evoked slow ventral root potential in the neonatal rat spinal cord

In the spinal cord-saphenous nerve preparation of the neonatal rat, electrical stimulation of the saphenous nerve at a strength sufficient to activate C fibres evokes a slow depolarizing potential of approximately 30 s duration in the L3 ventral root and this slow VRP is depressed by spantide and GR71251 (Nussbaumer *et al.*, 1989; Guo *et al.*, 1993). RP 67580 (0.1–1 μM) likewise depressed the saphenous nerve-evoked slow VRP in a concentration-dependent manner (Figure 4a). The inhibitory effect of RP 67580 reached a plateau at 0.3 μM (Figure 4b). Figure 5 shows the time course of the depressant effect of RP 67580 on the sapheous nerve-evoked slow VRP. The depressant effect of RP 67580 (0.3 μM) reached a plateau in about 20 min after adding the antagonist and the effect lasted for about 1.5 h after its removal. In contrast, RP 68651 (0.3 μM) had no effect on the slow VRP (Figure 5).

Discussion

The present study demonstrates that RP 67580 acts as a high affinity tachykinin NK_1 receptor antagonist in the neonatal rat spinal cord and possesses some properties that are superior to other tachykinin receptor antagonists. Thus, RP 67580 has the highest affinity for the NK_1 receptor among the antagonists so far examined in the neonatal rat spinal cord; the pA_2 values of RP 67580 against various tachykinin receptor agonists to induce ventral root depolarizations were in the range 7.2–7.5 (Table 2), which are much higher than the values obtained for the peptide NK_1 receptor antagonist GR71251 (6.1–6.7; Guo *et al.*, 1993). Unlike spantide (Sakuma *et al.*, 1991) and GR71251 (Guo *et al.*, unpublished observation), RP 67580 did not cause GABA release from the spinal cord, and unlike spantide (Otsuka & Yanagisawa, 1988; Guo *et al.*, 1993) it did not antagonize the

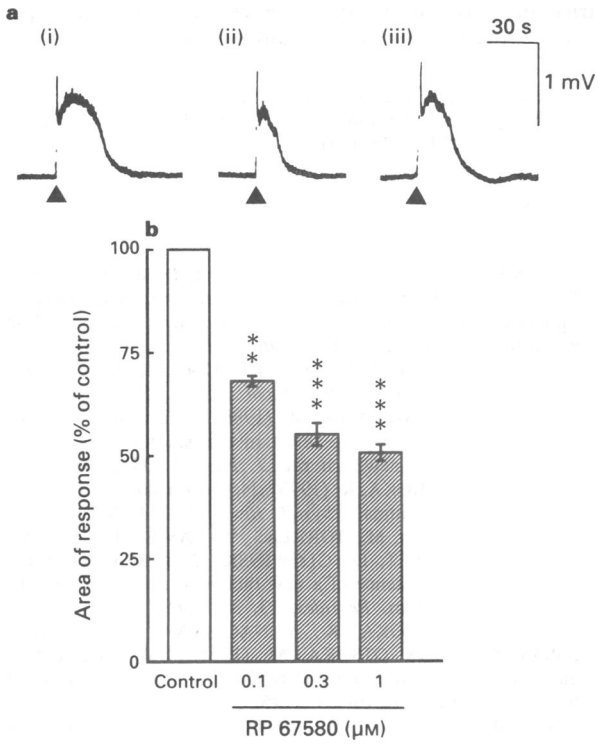


Figure 4 Effects of RP 67580 on the saphenous nerve-evoked slow VRP. (a) Sample records from an isolated spinal cord-peripheral nerve preparation of a 1 day old rat. The saphenous nerve was stimulated every 3 min at (▲) with 2 shocks (40 V intensity and 100 μs duration at 20 Hz) and the potentials were recorded from the ipsilateral L3 ventral root. (i) Control response; (ii) 44 min after addition of RP 67580 at 0.3 μM; (iii) 120 min after removal of RP 67580. (b) Concentration-dependent effect of RP 67580 on saphenous nerve-evoked slow VRPs. Areas under the curves of responses in mV × s were measured and expressed as percentages of the averages of control responses. The open column represents control response; hatched columns, after addition of RP 67580 at 0.1, 0.3 and 1 μM. Each column represents the mean ± s.e.mean ($n = 3-4$). $^{**}P<0.01$ and $^{***}P<0.001$, when compared with the control.

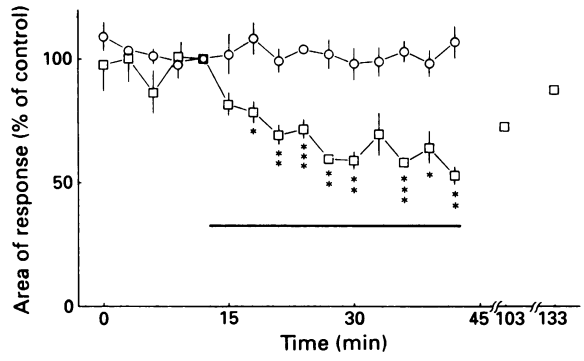


Figure 5 Time courses of actions of RP 67580 and RP 68651 on the saphenous nerve-evoked slow VRP in the neonatal rat spinal cord. Areas under the curves of responses were expressed as percentages of the control response just before the addition of RP 67580 or RP 68651. Each point represents the mean ± s.e.mean ($n = 3-4$, except for the points at 103 and 133 min, which were from one preparation). These two points show an incomplete recovery afer the removal of RP 67580. RP 68651 at 0.3 μM (○) or RP 67580 at 0.3 μM (□) was added to perfusion medium during the period indicated by the horizontal bar. $^{*}P<0.05$, $^{**}P<0.01$ and $^{***}P<0.001$, when compared with the values derived from the experiments with RP 68651 at corresponding times. Other details are the same as in Figure 4.

action of bombesin. RP 67580, however, depressed the depolarizing action of ACh. Since it did not antagonize the action of muscarine, but antagonized the action of ACh in the presence of atropine and that of nicotine, RP 67580 seems to have an antinicotinic action in the neonatal rat spinal cord. RP 68651 exhibited a similar antinicotinic action, but was inactive as a tachykinin NK_1 receptor antagonist. These results further confirmed the stereospecificity of RP 67580 as a tachykinin NK_1 receptor antagonist (Garret *et al.*, 1991).

Our previous study showed that spantide (Sakuma *et al.*, 1991) and GR71251 (Guo *et al.*, unpublished observation) evoked GABA release from neonatal rat spinal cords. It is conceivable, therefore, that the depressant effects of these tachykinin receptor antagonists on primary afferent-evoked slow VRPs, as observed in our previous studies (Nussbaumer *et al.*, 1989; Guo *et al.*, 1993), might be due to their ability to evoke a release of GABA or other neurotransmitters (Surprenant *et al.*, 1987). In the present study, however, RP 67580 was found to be devoid of the GABA releasing action, yet still depressed the saphenous nerve-evoked slow VRP to about 50% of the control. This maximal depressant action of RP 67580 was similar to those of spantide and GR71251 (Guo *et al.*, 1993). The possibility that the depressant action of RP 67580 on the slow VRP is due to its antinicotinic action appears unlikely, because RP 68651, which has a similar antinicotinic action, did not depress the slow VRP (Figure 5). Furthermore, in a preliminary experiment we observed that the slow VRP was not depressed by dihydro-β-erythroidine (5 μM), which acts as a nicotinic antagonist in this preparation (Jahr & Yoshioka, 1986). The present study, therefore, provides further evidence for the involvement of tachykinins in this C-fibre response (Nussbaumer *et al.*, 1989; Guo *et al.*, 1993).

In confirmation of previously discussed data which indicate the existence of species variants of the NK_1 receptor, RP 67580 was found to be more potent in antagonizing the ventral root depolarizing action of SPOMe, an NK_1-selective agonist (Watson *et al.*, 1983), in the spinal cord of the neonatal rat than in the neonatal gerbil.

In the neonatal rat spinal cord, the depressant effects of RP 67580 on the tachykinin receptor agonist-induced ventral root depolarizations varied depending on the agonists and on the presence or absence of TTX. Thus, the actions of SPOMe, NKA and SP in the presence of TTX were less sensitive to the antagonist than that in the absence of TTX (Figure 1, Table 2). Furthermore, in the presence of TTX, the pA_2 value of RP 67580 against SPOMe was significantly lower than that determined against NKA (Table 2). These results raise the possibility that more than one tachykinin NK_1 recepteor subtype may be present in the neonatal rat spinal cord, as suggested in the guinea-pig ileum (Chassaing *et al.*, 1992; Petitet *et al.*, 1992; Maggi *et al.*, 1993) and the rat superior cervical ganglion (Hawcock *et al.*, 1993).

The pA_2 values of RP 67580 against SPOMe and NKA in normal artificial CSF were almost identical (Table 2). This suggests that the antagonist and both agonists bind to a single population of tachykinin NK_1 receptor subtype present on spinal interneurones. We have previously reported similar results using the antagonists, spantide and GR71251, and the agonists, NKA and [acetyl-Arg^6]septide (Yanagisawa & Otsuka, 1990; Guo *et al.*, 1993). Furthermore, we found that NK_2-selective agonists showed almost no agonistic actions on neonatal rat spinal interneurones (Guo *et al.*, 1993). These results suggest that NKA acts on NK_1 rather than NK_2 receptors in the neonatal rat spinal cord. The possibility that NKA acts on NK_1 receptors has also been suggested in other preparations (Kunitomo *et al.*, 1993; Zhao *et al.*, 1993).

The depolarizing action of SP and the effects of tachykinin receptor antagonists thereupon in the presence of TTX are complex. The slope of concentration-response curves for SP

became steeper in the presence of RP 67580. Similar change was also observed with spantide and GR71251 (Yanagisawa & Otsuka, 1990; Guo *et al.*, 1993). Likewise, the concentration-response curves for SP in normal artificial CSF and that for SPOMe in the presence of TTX also became steeper under RP 67580 (Figure 1). Further studies are needed to clarify the mechanisms of these changes of dose-response curves in the presence of the antagonists.

This work was supported by grants-in-aid for scientific research from the Ministry of Education, Science and Culture, Japan (Nos. 04255101, 05557117, 05454147).

References

AKAGI, H., KONISHI, S., OTSUKA, M. & YANAGISAWA, M. (1985). The role of substance P as a neurotransmitter in the reflexes of slow time courses in the neonatal rat spinal cord. *Br. J. Pharmacol.*, **84**, 663–673.

ARUNLAKSHANA, O. & SCHILD, H.O. (1959). Some quantitative uses of drug antagonists. *Br. J. Pharmacol. Chemother.*, **14**, 48–58.

BARR, A.J. & WATSON, S.P. (1993). Non-peptide antagonists, CP-96,345 and RP 67580, distinguish species variants in tachykinin NK_1 receptors. *Br. J. Pharmacol.*, **108**, 223–227.

BERESFORD, I.J.M., BIRCH, P.J., HAGAN, R.M. & IRELAND, S.J. (1991). Investigation into species variants in tachykinin NK_1 receptors by use of the non-peptide antagonist, CP-96,345. *Br. J. Pharmacol.*, **104**, 292–293.

CHASSAING, G., LAVIELLE, S., BRUNISSEN, A., CARRUETTE, A., GARRET, C., PETITET, F., SAFFROY, M., BEAUJOUAN, J.C., TORRENS, Y. & GLOWINSKI, J. (1992). [Pro^9]SP and [$pGlu^6$,Pro^9]SP(6-11) interact with two different receptors in the guinea-pig ileum as demonstrated with new SP antagonist. *Neuropeptides*, **23**, 73–79.

FARDIN, V., FOUCAULT, F., BOCK, M.D. & GARRET, C. (1992). Binding profile of RP 67580, a nonpeptide substance P antagonist: comparison with CP-96,345. *Br. J. Pharmacol.*, **105**, 80P.

FARDIN, V., FOUCAULT, F., BOCK, M.D., JOLLY, A., FLAMMAND, O., CLERC, F. & GARRET, C. (1993). Variations in affinities for the NK_1 receptor: differences between the non-peptide substance P antagonists RP 67580 and CP-96,345 and the agonist septide. *Regul. Pept.*, **46**, 300–303.

GARRET, C., CARRUETTE, A., FARDIN, V., MOUSSAOUI, S., PEYRONEL, J.F., BLANCHARD, J.C. & LADURON, P.M. (1991). Pharmacological properties of a potent and selective nonpeptide substance P antagonist. *Proc. Natl. Acad. Sci. U.S.A.*, **88**, 10208–10212.

GITTER, B.D., WATERS, D.C., BRUNS, R.F., MASON, N.R., NIXON, J.A. & HOWBERT, J.J. (1991). Species differences in affinities of non-peptide antagonists for substance p receptors. *Eur. J. Pharmacol.*, **197**, 237–238.

GUO, J.-Z., YOSHIOKA, K., YANAGISAWA, M., HOSOKI, R., HAGAN, R.M. & OTSUKA, M. (1993). Depression of primary afferent-evoked responses by GR71251 in the isolated spinal cord of the neonatal rat. *Br. J. Pharmacol.*, **110**, 1142–1148.

HAWCOCK, A.B., MARSHALL, F.H., BERESFORD, I.J.M. & HAGAN, R.M. (1993). Two NK_1 agonist responses in the rat superior cervical ganglion. *Neuropeptides*, **24**, 110P.

JAHR, C.E. & YOSHIOKA, K. (1986). Ia afferent excitation of motoneurones in the *in vitro* new-born rat spinal cord is selectively antagonized by kynurenate. *J. Physiol.*, **370**, 515–530.

KUNITOMO, M., IMAIZUMI, N., SAMESHIMA, E. & FUJIWARA, M. (1993). Pharmacological analysis of receptors involved in the late, tachykininergic contractile response to electrical stimulation in isolated rabbit iris sphincter muscle. *Jpn. J. Pharmacol.*, **62**, 257–261.

MAGGI, C.A., PATACCHINI, R., MEINI, S. & GIULIANI, S. (1993). Evidence for the presence of a septide-sensitive tachykinin receptor in the circular muscle of the guinea-pig ileum. *Eur. J. Pharmacol.*, **235**, 309–311.

NUSSBAUMER, J.-C., YANAGISAWA, M. & OTSUKA, M. (1989). Pharmacological properties of a C-fibre response evoked by saphenous nerve stimulation in an isolated spinal cord-nerve preparation of the newborn rat. *Br. J. Pharmacol.*, **98**, 373–382.

OTSUKA, M. & YANAGISAWA, M. (1987). Does substance P act as a pain transmitter? *Trends Pharmacol. Sci.*, **8**, 506–510.

OTSUKA, M. & YANAGISAWA, M. (1988). Effect of a tachykinin antagonist on a nociceptive reflex in the isolated spinal cord-tail preparation of the newborn rat. *J. Physiol.*, **395**, 255–270.

OTSUKA, M. & YOSHIOKA, K. (1993). Neurotransmitter functions of mammalian tachykinins. *Physiol. Rev.*, **73**, 229–308.

PETITET, F., SAFFROY, M., TORRENS, Y., LAVIELLE, S., CHASSAING, G., LOEUILLET, D., GLOWINSKI, J. & BEAUJOUAN, J.C. (1992). Possible existence of a new tachykinin receptor subtype in the guinea pig ileum. *Peptides*, **13**, 383–388.

SAKUMA, M., YOSHIOKA, K., YANAGISAWA, M., ONISHI, Y., KOBAYASHI, N. & OTSUKA, M. (1991). Substance P-evoked release of gamma-aminobutyric acid from isolated spinal cord of the newborn rat. *Neuroscience*, **45**, 323–330.

SNIDER, R.M., CONSTANTINE, J.W., LOWE, J.A., III, LONGO, K.P., LEBEL, W.S., WOODY, H.A., DROZDA, S.E., DESAI, M.C., VINICK, F.J., SPENCER, R.W. & HESS, H.-J. (1991). A potent nonpeptide antagonist of the substance P (NK_1) receptor. *Science*, **251**, 435–437.

SURPRENANT, A., NORTH, R.A. & KATAYAMA, Y. (1987). Observations on the actions of substance P and [D-Arg^1,D-Pro^2, D-$Trp^{7,9}$,Leu^{11}]substance P on single neurons of the guinea pig submucous plexus. *Neuroscience*, **20**, 189–199.

WATSON, S.P., SANDBERG, B.E.B., HANLEY, M.R. & IVERSEN, L.L. (1983). Tissue selectivity of substance P alkyl esters: suggesting multiple receptors. *Eur. J. Pharmacol.*, **87**, 77–84.

YANAGISAWA, M., HOSOKI, R. & OTSUKA, M. (1992a). The isolated spinal cord-skin preparation of the newborn rat and effects of some algogenic and analgesic substances. *Eur. J. Pharmacol.*, **220**, 111–117.

YANAGISAWA, M. & OTSUKA, M. (1990). Pharmacological profile of a tachykinin antagonist, spantide, as examined on rat spinal motoneurones. *Br. J. Pharmacol.*, **100**, 711–716.

YANAGISAWA, M., OTSUKA, M., KONISHI, S., AKAGI, H., FOLKERS, K. & ROSELL, S. (1982). A substance P antagonist inhibits a slow reflex response in the spinal cord of the newborn rat. *Acta Physiol. Scand.*, **116**, 109–112.

YANAGISAWA, M., YOSHIOKA, K., KURIHARA, T., SAITO, K., SENO, N., SUZUKI, H., HOSOKI, R. & OTSUKA, M. (1992b). Enzymatic inactivation of tachykinin neurotransmitters in the isolated spinal cord of the newborn rat. *Neurosci. Res.*, **15**, 289–292.

ZHAO, F.-Y., SAITO, K., KONISHI, S., GUO, J.-Z., MURAKOSHI, T., YOSHIOKA, K. & OTSUKA, M. (1993). Involvement of NK_1 receptors in synaptic transmission in the guinea pig coeliac ganglion. *Neurosci. Res.*, **18**, 245–248.

(Received May 6, 1994
Revised July 18, 1994
Accepted July 19, 1994)

Br. J. Pharmacol. (1994), **113**, 1147–1152 © Macmillan Press Ltd, 1994

Evidence for reduction of bradykinin-induced bronchoconstriction in guinea-pigs by release of nitric oxide

Fabio L.M. Ricciardolo, *Jay A. Nadel, Shigemi Yoishihara & [1]Pierangelo Geppetti

Cardiovascular Research Institute and *Departments of Medicine and Physiology, University of California, San Francisco, San Francisco, CA 94143-0130, U.S.A.

1 In this study the influence of nitric oxide (NO) on the bronchoconstriction induced by bradykinin in anaesthetized and artifically ventilated guinea-pigs pretreated with atropine was investigated.

2 Aerosol administration of bradykinin (0.1–1 mM, 40 breaths) caused a dose-dependent increase in lung resistance (R_L): maximum increase in R_L was 2.5 fold the baseline value. Pretreatment with aerosolized N^G-nitro-L-arginine methyl ester (L-NAME) or N^G-monomethyl-L-arginine (L-NMMA) (1 mM, 10 breaths every 5 min for 30 min), NO synthase inhibitors, markedly increased the bronchoconstrictor response to bradykinin. L-Arginine, but not D-arginine, (3 mM, 10 breaths every 5 min for 30 min) reversed the hyperresponsiveness to aerosolized bradykinin caused by L-NAME and L-NMMA.

3 L-NAME (1 mM, 10 breaths every 5 min for 30 min) increased the bronchoconstriction induced by intravenous bradykinin (1–10 nmol kg^{-1}). L-Arginine, but not D-arginine, (10 breaths every 5 min for 30 min) reversed the hyperresponsiveness to intravenous bradykinin caused by L-NAME.

4 The increase in R_L induced by capsaicin, either aerosol (10 μM, 10 breaths) or i.v. (20 nmol kg^{-1}) was not affected by L-NAME (1 mM, 10 breaths every 5 min for 30 min). Acute resection of the vagi did not affect the bronchoconstriction evoked by bradykinin in guinea-pigs, either in the absence or presence of L-NAME (1 mM, 10 breaths every 5 min for 30 min).

4 These results suggest that, irrespective of the route of administration, bradykinin releases NO or a related molecule which exerts a bronchodilator action that opposes the bronchoconstrictor mechanisms activated by bradykinin itself.

Keywords: Bradykinin; nitric oxide; capsaicin; guinea-pig airways; bronchoconstriction; epithelium; N^G-nitro-L-arginine methyl ester (L-NAME); N^G-monomethyl-L-arginine (L-NMMA); nitric oxide synthase inhibitors

Introduction

The nonapeptide, bradykinin and the decapeptide, kallidin are kinins released from plasma and tissue precursors during inflammation (Regoli & Barabe, 1980). Kinins exert a variety of inflammatory responses which in the airways include increases in plasma protein extravasation and bronchoconstriction. Bradykinin given by aerosol to anaesthetized guinea-pigs increases plasma extravasation mainly by releasing the tachykinins substance P (SP) and neurokinin A (NKA) from sensory nerve endings and also it appears, albeit in a smaller contribution, by a direct action on endothelial cells of post-capillary venules (Lundberg & Saria, 1983; Saria *et al.*, 1983; Bertrand *et al.*, 1993a). The atropine-insensitive component of the bronchoconstriction induced by local application of bradykinin into the guinea-pig airways is mediated by similar mechanisms: most of the response is due to tachykinin release and a minor component is mediated by a direct action on tracheobronchial smooth muscle cells (Ichinose *et al.*, 1990). Capsaicin, the hot component of the plants of the genus *Capsicum*, stimulates selectively a subpopulation of sensory nerves and causes the release of neuropeptides, including tachykinins (Holzer, 1991). In the airways of anaesthetized guinea-pigs, capsaicin increases plasma extravasation an causes an atropine-insensitive bronchoconstriction, effects that are entirely due to tachykinins released from sensory nerve endings (Ballati *et al.*, 1992; Bertrand *et al.*, 1993b; Saria *et al.*, 1983).

In the first part of this study we observed that aerosolized capsaicin is more potent than aerosolized bradykinin in causing bronchoconstriction in anaesthetized guinea-pigs pretreated with atropine and phosphoramidon. In contrast, we found that aerosolized bradykinin is almost equipotent to aerosolized capsaicin in causing plasma extravasation in the trachea of these animals. Furthermore, the dose of bradykinin that caused half maximal plasma extravasation was not sufficient to cause any bronchoconstriction. The mechanism by which bradykinin and capsaicin induce bronchoconstriction and plasma extravasation in the experimental conditions mentioned above is similar and mostly due to tachykinin release from sensory nerves (Ichinose *et al.*, 1990; Bertrand *et al.*, 1993b). Nevertheless, bradykinin, in contrast to capsaicin, is a less potent agent in causing bronchoconstriction than in increasing plasma extravasation. We hypothesizd that one possible explanation for the apparent discrepancy was that bradykinin, like capsaicin, induces the release of tachykinins which cause bronchoconstriction and increase plasma protein extravasation, but that bradykinin, in contrast to capsaicin, also releases a bronchodilator agent.

Bradykinin releases a variety of prostaglandins (Leikauf *et al.*, 1985). However, the observation that bronchoconstriction following bradykinin applied locally to the guinea-pig airways is not affected by indomethacin (Ichinose *et al.*, 1990) rules out the possibility that a bronchodilator prostaglandin released by bradykinin opposes markedly bronchoconstriction induced of bradykinin. Activation of bronchodilator β-adrenoceptors, probably due to catecholamines released from the adrenal medulla, occurs following intravenous administration by bradykinin (Piper *et al.*, 1967). However, this bronchodilator mechanism has not been reported after aerosolized bradykinin. More recently, it has been proposed that the L-arginine-nitric oxide (NO) pathway plays a role in the regulation of bronchomotor tone (Belvisi *et al.*, 1991; Li

[1] Author for correspondence at present address: Institute of Internal Medicine and Therapeutics IV, Laboratory of Clinical Pharmacology, University of Florence, Viale Pieraccini 6, 50139 Florence, Italy.

& Rand, 1991; Lei et al., 1993; Sekizawa et al., 1993). Therefore, we tested the hypothesis that bradykinin causes the release of NO or a related molecule from the airways of guinea-pigs and by this mechanism reduces its bronchoconstrictor action. The present data indicate that NO or a related molecule released by bradykinin markedly inhibits the bronchoconstrictor response to bradykinin. An attempt to determine the neural or non-neural source of NO released by bradykinin was also performed. The present data and recent studies (Nijkamp et al., 1993; Schempler & Calixto, 1994) suggest that bradykinin does not release NO from neural elements, but more probably from the epithelium.

Methods

Animals

Male Hartley guinea-pigs (Simonsen Laboratories, Inc., Gilroy, CA, U.S.A.) weighing 350–400 g at the time of housing, were used in this study. They were kept in a temperature-controlled environment with standard laboratory food and water freely available.

Measurement of total pulmonary resistance (R_L)

Animals were anaesthetized with sodium pentobarbitone (45 mg kg^{-1}, i.p.; Anthony Product Corp., Arcadia, CA, U.S.A.) and then ventilated artificially through a tracheal cannula, using a constant-volume ventilator (model 683; Harvard Apparatus Co., Inc) at a frequency of 80 breaths min^{-1}. The tidal volume was adjusted to maintain normal arterial blood gases as described previously (Dusser et al., 1988). Airflow was monitored coninuously with a pneumotachograph A. Fleisch, Medical Inc.) connected to a differential pressure transducer (model DP45; Validyne Engineering Corp.). A fluid-filled polyethylene catheter was introduced into the oesophagus to measure the oesophageal pressure as an approximation of pleural pressure. Intratracheal pressure was measured with a polyethylene catheter inserted into a short tube connecting the tracheal cannula to the pneumotachograph. The transpulmonary pressure (defined as the pressure difference between the intratracheal and the oesophageal pressures) was measured with a differential pressure transducer (model DP7; Valdyne Engineering Corp.). Output signals representing transpulmonary pressure and airflow were amplified with an amplifier (model CD19; Validyne Engineering Corp.) and recorded on a polygraph recorder (model 1508 B Visicorder; Honeywell, Inc.). R_L was calculated as previously described (Dusser et al., 1988). The right jugular vein and the left carotid artery were cannulated to permit administration of drugs and to withdraw a sample of blood for arterial blood gas measurement, respectively.

Measurement of plasma extravasation

Evans blue dye (3% solution in 0.9% saline; Polysciences, Inc., Warrington, PA, U.S.A.) was injected immediately before the use of the aerosol. Five minutes after injection of the tracer, the chest was opened, a cannula was inserted into the ascending aorta through the left ventricle, and the circulation was perfused for 2 min with phosphate buffer (pH 5; Sigma Chemical Co., St Louis MO, U.S.A.) at a pressure of 120 mmHg. The trachea was dissected and opened along the ventral midline, blotted, weighed, and then incubated in 3 ml of formamide (Fisher Scientific, Santa Clara, CA) at 50°C for 18 h to extract the extravasated Evans blue dye. The extravasation of Evans blue-labelled macromolecules from the microcirculation in different tissues was quantified by measuring the optical density of the formamide extracts at a wavelength of 620 nm with a spectrophotometer (Model UV160U, Shimatzu Scientific Instruments, Inc., Columbia, MD, U.S.A.). The amount of Evans blue dye extravasated in the tissues, expressed in nanograms per milligram of wet weight, was interpolated from a standard curve of Evans blue concentrations (0.1 to 5 μg ml^{-1}).

Measurement of arterial blood pressure

A polyethylene catheter (i.d. 0.8 mm, length 2.5 cm; Angiocath, Deseret Medical) was inserted into the left carotid artery and then connected to a pressure transducer (model 1270A, Hewlett-Packard) for measurement of arterial pressure. The amplified signal from the transducer (module M2102B, Electronics for Medicine) was displayed continuously on a video monitor (model OM, Electronics for Medicine) and recorded with an oscillographic recorder (model DASH-8, Astro-Med). Heart rate was derived from the pressure pulse signal by a cardiotachometer coupler.

Experimental design

Baseline R_L remained stable for at least 2 h, and no significant changes were produced by aerosol administration (5 breaths) or i.v. injection (1 ml kg^{-1}) of saline (0.9% NaCl) after a stabilization period of 30 min. Aerosols of saline or drugs were generated from an ultrasonic nebulizer (Pulmo-Sonic model 25, DeVilbiss Co., Somerset, PA, U.S.A.) and were delivered into the airways by the respirator via the tracheal cannula (aerosol delivery rate, 0.2 ml min^{-1}). To deliver NO synthase inhibitors, we used the protocol used previously (Nijkamp et al., 1993): guinea-pigs inhaled 10 breaths of an aerosol containing 0.9% saline (controls), N^G-nitro-L-arginine methyl ester (L-NAME, 1 mM) or N^G-monomethyl-L-arginine (L-NMMA, 1 mM). This procedure was repeated every 5 min for 30 min (total 60 breaths). Five minutes after the last inhalation, bradykinin or capsaicin were given. A single dose of bradykinin or capsaicin was given to each animal. Ten breaths of an aerosol containing L-arginine (L-Arg, 3 mM), D-arginine (D-Arg, 3 mM) or 0.9% saline were administered every 5 min for 30 min to L-NAME pretreated animals. All animals were pretreated with atropine (1.4 μmol kg^{-1}, i.v., 15 min before the stimulus). To increase the tachykinin-mediated bronchoconstriction, 5 min before the bradykinin aerosol, guinea-pigs received phosphoramidon (4.5 μmol kg^{-1}, i.v.). To block the effect of bronchodilator catecholamines released by i.v. bradykinin, guinea-pigs were also treated with propranolol (3.4 μmol kg^{-1}, i.v., 15 min before bradykinin i.v.). To maintain identical experimental conditions, propranolol was also given to guinea-pigs treated with capsaicin i.v. and phosphoramidon was also given to guinea-pigs treated with capsaicin aerosol. Vagotomy was performed by a standard procedure by exposing both cervical vagus nerves and sectioning them below the nodose ganglion 10 min before the delivery of the stimulus. Drugs given by i.v. route were diluted in saline (1 ml kg^{-1}).

Drugs

L-Arg, D-Arg, L-NAME, L-NMMA, capsaicin, propranolol, atropine and histamine were obtained from Sigma Chemical (St. Louis, MO, U.S.A.). Phosphoramidon and bradykinin were purchased from Peninsula Laboratories, Inc. (Belmont, CA, U.S.A.). All drugs were dissolved in 0.9% saline. Capsaicin was dissolved in a solution containing 10% ethanol, 5% Tween 80 and 85% 0.9% NaCl. Further dilutions were made in saline (0.9% NaCl).

Statistical analysis

Values in the text and figures are the mean ± standard error of the mean (s.e.mean). Statistical comparisons were performed by one way analysis of variance and Dunnett's test or Student's bilateral unpaired t tests, when appropriate. In all cases, a P value of less than 0.05 was considered significant.

Results

Plasma extravasation

In guinea-pigs pretreated with 0.9% saline (10 breaths every 5 min for 30 min), atropine (1.4 μmol kg^{-1}, i.v.) and phosphoramidon (4.5 μmol kg^{-1}, i.v.) baseline plasma extravasation in the trachea was 19.6 ± 2.3 ng mg^{-1} of tissue ($n = 4$). Bradykinin aerosol (40 breaths) and capsaicin aerosol (10 breaths) caused a dose-dependent increase in the extravasation of the Evans blue dye in the guinea-pig trachea (Figure 1b). The two drugs were equipotent in increasing plasma extravasation (Figure 1b).

Bradykinin aerosol

In guinea-pigs pretreated with 0.9% saline (10 breaths every 5 min for 30 min), atropine (1.4 μmol kg^{-1}, i.v.) and phosphoramidon (4.5 μmol kg^{-1}, i.v.), baseline R_L was 0.18 ± 0.012 mmH$_2$O ml^{-1} min^{-1} ($n = 6$). Aerosolization of 0.9% NaCl, L-NAME (1 mM) or L-NMMA (1 mM) (all, 10 breaths every 5 min for 30 min) did not change the baseline value of R_L (data not shown). Aerosolized bradykinin (0.1–1 mM, 40 breaths) induced a dose-dependent increase in R_L (Figures 1 and 2). The maximum increase obtained with 1 mM bradykinin was approximately 2.5 fold higher than the baseline value. After administration of L-NAME (1 mM, 10 breaths every 5 min for 30 min) the bronchoconstrictor response to each dose of bradykinin was markedly increased (Figure 2). The administration of L-Arg (3 mM, 10 breaths every 5 min for 30 min), but not the administration of D-Arg (3 mM, 10 breaths every 5 min for 30 min), after the aerosolization of L-NAME, reversed the potentiating effect of L-NAME on bradykinin-induced bronchospasm (Figure 2). Pretreatment with L-NMMA (1 mM, 10 breaths every 5 min for 30 min) increased the bronchoconstriction induced by aerosolized bradykinin (1 mM, 40 breaths) (Figure 3). Pretreatment with L-Arg (3 mM, 10 breaths every 5 min for 30 min), but not the administration of D-Arg (3 mM, 10 breaths every 5 min for 30 min), abolished the L-NMMA-induced increase in the bronchoconstriction evoked by bradykinin (Figure 3).

Intravenous bradykinin

In guinea-pigs pretreated with atropine (1.4 μmol kg^{-1}, i.v.) and propranolol (34 μmol kg^{-1}, i.v.) baseline R_L was 0.20 ± 0.024 mmH$_2$O ml^{-1} min^{-1} ($n = 6$). Bradykinin (1–10 nmol kg^{-1},

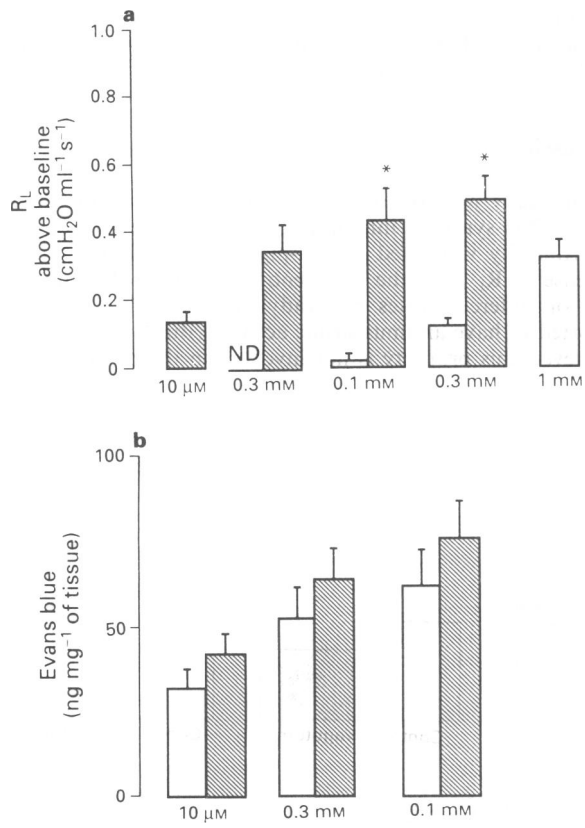


Figure 1 Increase in total pulmonary resistance (R_L) (a) and Evans blue dye extravasation (b) in the trachea induced by increasing doses of aerosolized bradykinin (open columns) or capsaicin (hatched columns) in anaesthetized and artifically ventilated guinea-pigs in the presence of atropine (1.4 μmol kg^{-1}, i.v.) and phosphoramidon (4.5 μmol kg^{-1}, i.v.). Each column is the mean ± s.e.mean of at least four experiments. ND, not detectable. *$P < 0.01$.

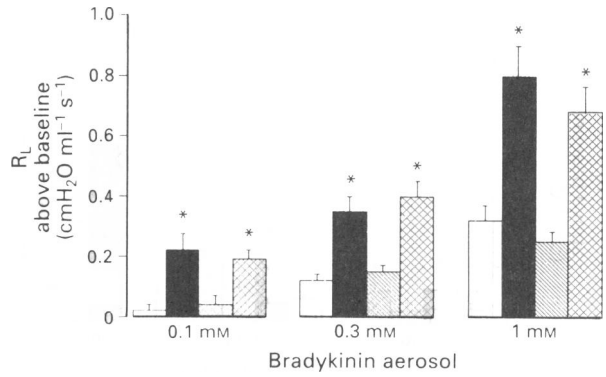


Figure 2 Effect of aerosolized 0.9% saline (open columns), N^G-nitro-L-arginine methyl ester (L-NAME, 1 mM) (solid columns), L-NAME (1 mM) plus L-arginine (L-Arg, 3 mM) (hatched columns), L-NAME (1 mM) plus D-arginine (D-Arg, 3 mM) (cross-hatched columns) on the increase in total pulmonary resistance (R_L), induced by different doses of aerosolized bradykinin in anaesthetized and artificially ventilated guinea-pigs in presence of atropine (1.4 μmol kg^{-1}, i.v.) and phosphoramidon (4.5 μmol kg^{-1}, i.v.). Saline and L-NAME were administered by giving 10 breaths every 5 min for 30 min. L-Arg and D-Arg (3 mM, 10 breaths every 5 min for 30 min) were given 5 min after the last administration of L-NAME. Each column is the mean ± s.e.mean of five experiments. *$P < 0.05$ versus saline group.

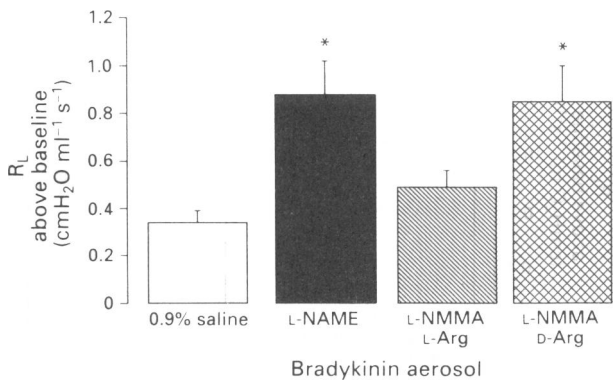


Figure 3 Effect of aerosolized 0.9% saline (open column), N^G-monomethyl-L-arginine (L-NMMA, 1 mM, solid column), L-NMMA (1 mM) plus L-arginine (L-Arg, 3 mM, hatched column), L-NMMA (1 mM) plus D-arginine (D-Arg, 3 mM, cross-hatched column) on the increase in total pulmonary resistance (R_L), induced by aerosolized bradykinin (1 mM, 40 breaths) in anaesthetized and artificially ventilated guinea-pigs in presence of atropine (1.4 μmol kg^{-1}, i.v.) and phosphoramidon (4.5 μmol kg^{-1}, i.v.). Saline and L-NAME were administered by giving 10 breaths every 5 min for 30 min. L-Arg and D-Arg (3 mM, 10 breaths every 5 min for 30 min) were given 5 min after the last administration of L-NAME. Each column is the mean ± s.e.mean of five experiments. *$P < 0.05$ versus saline group.

i.v.) induced a dose-dependent increase in R_L (Figure 4). The maximum increase obtained with 10 nmol kg^{-1} was approximately 2.5 fold higher than the baseline value. In guinea-pigs pretreated with L-NAME (1 mM, 10 breaths every 5 min for 30 min) bronchoconstrictor response to each dose of bradykinin were significantly increased. L-Arg (3 mM, 10 breaths every 5 min for 30 min), but not D-Arg (3 mM, 10 breaths every 5 min for 30 min), abolished the potentiation induced by L-NAME of the bronchoconstrictor response to i.v. bradykinin (Figure 4).

Capsaicin and vagotomy

In guinea-pigs pretreated with atropine (1.4 μmol kg^{-1}, i.v.) and phosphoramidon (4.5 μmol kg^{-1}, i.v.) baseline R_L was 0.19 ± 0.016 mmH_2O ml^{-1} min^{-1} ($n = 5$). Aerosolization of capsaicin (10 breaths) increased R_L in a dose-dependent manner (Figure 1a). Capsaicin caused a much higher bronchoconstrictionr than bradykinin at any concentration tested (Figure 1a). Pretreatment with L-NAME (1 mM, 10 breaths every 5 min for 30 min) did not affect the bronchoconstrictor response to capsaicin (10 μM, 10 breaths). In guinea-pigs pretreated with atropine (1.4 μmol kg^{-1}, i.v.) and propranolol (3.4 μmol kg^{-1}, i.v.) the bronchoconstriction induced by intravenous injection of 20 nmol of capsaicin was not affected by pretreatment with L-NAME (1 mM, 10 breaths every 5 min for 30 min) (Figure 5).

In guinea-pigs pretreated with atropine (1.4 μmol kg^{-1}, i.v.) and phosphoramidon (4.5 μmol kg^{-1}, i.v.) acute resection of both vagus nerves slightly, but not significantly, reduced the bronchoconstrictor response to bradykinin (1 mM, 40 breaths). In guinea-pigs pretreated with L-NAME (1 mM, 10 breaths every 5 min for 30 min) vagotomy had no effect on the potentiating effect of L-NAME on bradykinin-induced bronchoconstriction (Figure 6).

Cardiovascular measurements

Baseline heart beat frequency and arterial blood pressure were not changed after aerosolization of 0.9% saline (10 breaths every 5 min for 30 min). Aerosolized L-NAME or L-NMMA (1 mM, 10 breaths every 5 min for 30 min) did not affect baseline heart beat frequency and arterial blood pressure (Table 1). L-Arg and D-Arg (3 mM, 10 breaths every 5 min for 30 min) did not alter basal arterial pressure (Table 1). Bradykinin aerosol (1 mM) did not change blood pressure and heart rate (Table 1). Intravenous administration of bradykinin dose-dependently decreased blood pressure and heart beat frequency. The effect of bradykinin was short-lived and blood pressure and heart rate returned to baseline values within 60–120 s. Maximum changes induced by bradykinin 10 nmol kg^{-1} are reported in Table 1. Capsaicin aerosol did not affect cardiovascular parameters. Capsaicin i.v. caused a transient (20–40 s) decreases in blood pressure and a transient (20–40 s) increase in heart rate (Table 1).

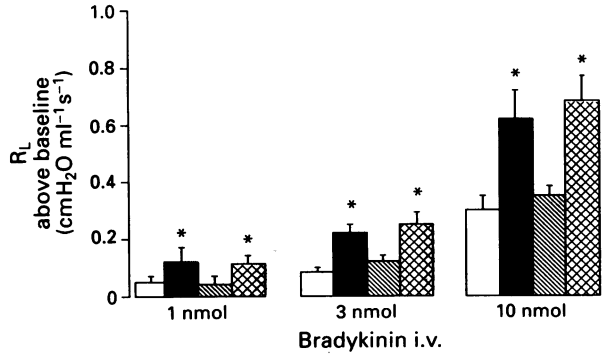


Figure 4 Effect of aerosolized 0.9% saline (open columns), N^G-nitro-L-arginine methyl ester (L-NAME, 1 mM, solid columns), L-NAME (1 mM) plus L-arginine (L-Arg, 3 mM, hatched columns) and L-NAME (1 mM) plus D-arginine (D-Arg, 3 mM, cross-hatched columns) on the increase in total pulmonary resistance (R_L), induced by intravenous administration of bradykinin at different doses in anaesthetized and artifically ventilated guinea-pigs in presence of atropine (1.4 μmol kg^{-1}, i.v.) and propranolol (3.4 mmol kg^{-1}, i.v.). Saline and L-NAME were administered by giving 10 breaths every 5 min for 30 min. L-Arg and D-Arg (3 mM, 10 breaths every 5 min for 30 min) were given 5 min after the last administration of L-NAME. Each column is the mean ± s.e.mean of five experiments. $*P < 0.05$ versus saline group.

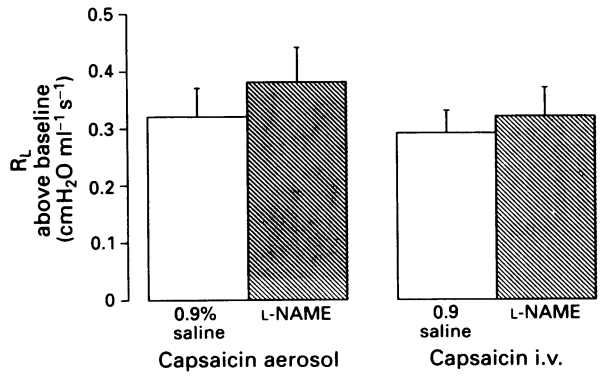


Figure 5 Effect of aerosolized 0.9% saline and N^G-nitro-L-arginine methyl ester (L-NAME, 1 mM, hatched column) on the increase in total pulmonary resistance (R_L), induced by aerosol (10 μM, 10 breaths) and intravenous (20 nmol) administration of capsaicin in anaesthetized and artifically ventilated guinea-pigs. Capsaicin aerosol was given to guinea-pigs pretreated with atropine (1.4 μmol kg^{-1}, i.v.) and phosphoramidon (4.5 mmol kg^{-1}, i.v.). Capsaicin i.v. was given to guinea-pigs pretreated with atropine (1.4 μmol kg^{-1}, i.v.) and propranolol (3.4 mml kg^{-1}, i.v.). Saline and L-NAME were administered by giving 10 breaths every 5 min for 30 min. Each column is the mean ± s.e.mean of five experiments. $*P < 0.05$ versus saline group.

Discussion

In this study we have demonstrated that aerosol administration of NO-synthase inhibitor, L-NAME (Rees *et al.*, 1990) to artificially ventilated giunea-pigs resulted in a significant increase in R_L after the intravenous and aerosol administration of different doses of bradykinin. L-NAME has been reported to have antimuscarinic activity (Buxton *et al.*, 1993). However, this property is not involved in the potentiation of

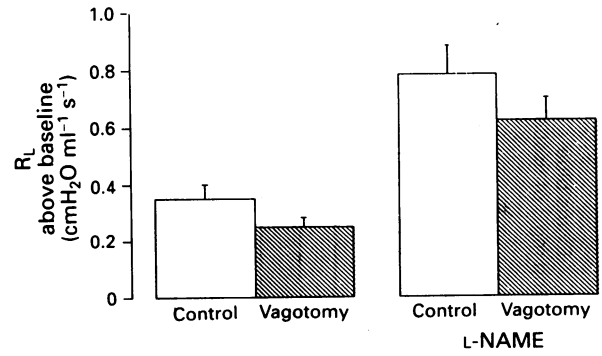


Figure 6 Effect of aerosolized 0.9% saline and N^G-nitro-L-arginine methyl ester (L-NAME, 1 mM) and vagotomy (hatched column) on the increase in total pulmonary resistance (R_L), induced by aerosolized bradykinin (1 mM, 40 breaths) in anaesthetized and artifically ventilated guinea-pigs pretreated with atropine (1.4 μmol kg^{-1}, i.v.) and phosphoramidon (4.5 μmol kg^{-1}, i.v.). Saline and L-NAME were administered by giving 10 breaths every 5 min for 30 min. Each column is the mean ± s.e.mean of five experiments. $*P < 0.05$ versus saline group.

Table 1 Mean arterial blood pressure and heart beat frequency before and after administration of the indicated drugs in one pentobarbitone anaesthetized guinea pigs

Treatment	*Blood pressure* (mmHg)	*Heart beat* (beats min^{-1})
Baseline	82 ± 5	283 ± 7
Bradykinin 1 mM (40 breaths, aerosol)	72 ± 6	288 ± 7
Capsaicin 10 μM (10 breaths, aerosol)	78 ± 4	286 ± 8
Baseline	85 ± 4	282 ± 8
Bradykinin 10 nmol, i.v.	40 ± 3*	210 ± 11*
Capsaicin 20 nmol, i.v.	54 ± 3*	320 ± 11*
Baseline	89 ± 5	280 ± 3
L-NAME	83 ± 5	273 ± 8
L-NMMA	85 ± 3	285 ± 6
L-NAME + L-Arg	85 ± 3	279 ± 4
L-NAME + D-Arg	83 ± 4	279 ± 5
L-NMMA + L-Arg	84 ± 5	283 ± 6
L-NMMA + D-Arg	85 ± 3	279 ± 5

Values are mean ± s.e.mean of at least five experiments. Guinea-pigs receiving i.v. drugs were pretreated with propranolol (3.4 μmol kg^{-1}) and atropine (1.4 μmol kg^{-1}); guinea-pigs receiving aerosol drugs were pretreated with phosphoramidon (4.5 μmol kg^{-1}) and atropine (1.4 μmol kg^{-1}). N^G-nitro-L-arginine methyl ester (L-NAME), N^G-monomethyl-L-arginine (L-NNMA), L-arginine (L-Arg) and D-Arg were administered by aerosol according to the protocol and doses reported in the text.
*$P < 0.05$ vs baseline.

the bradykinin-induced increase in R_L as the experiments were performed in the presence of atropine. Furthermore, L-NMMA, a NO-synthase inhibitor which does not have significant affinity for muscarinic receptors (Buxton *et al.*, 1993), also potentiated the bronchoconstrictor response to bradykinin. Finally, administration of the NO precursor, L-Arg, but not the inactive enantiomer D-Arg (Moncada & Higgs, 1993), given after the administration of L-NAME or L-NMMA reversed the increased airway responsiveness to bradykinin induced by the NO-synthase inhibitors. Therefore, these findings provide evidence that bradykinin administration releases NO or a related molecule which counteracts the bronchoconstrictor response to bradykinin.

Administration of bradykinin causes bronchoconstriction in guinea-pigs by multiple mechanisms which depend on the route of administration of the peptide (Ichinose *et al.*, 1990). Most of the response to aerosolized bradykinin is due to activation of neural pathways, e.g. cholinergic reflexes and axon reflexes and the subsequent release of tachykinins (Ichinose *et al.*, 1990). A minor component is apparently due to the direct action of bradykinin on smooth muscle cells (Ichinose *et al.*, 1990). After intravenous administration, bradykinin causes bronchoconstriction by activating cholinergic reflexes and by releasing prostanoids. Furthermore, bronchodilator catecholamines are released from the adrenal medulla following intravenous bradykinin (Piper *et al.*, 1967). The present results indicate that the bronchodilator agent, NO, is released by bradykinin, irrespective of the method of administration of the peptide. Thus, L-NAME increased the response to both aerosol and i.v. bradykinin.

NO released by bradykinin may originate from the airways or from a tissue outside the airways. Bradykinin aerosol, even at the highest dose, did not affect baseline blood pressure and heart rate. This observation suggests that bradykinin does not reach the systemic circulation and its action is confined to the airways. Hence, we postulate that the source of the NO released by bradykinin aerosol is located within the airway tissue. Decreases in arterial blood pressure and in heart rate were caused by i.v. bradykinin administration, thus indicating that systemic effects were produced by bradykinin given by this route of administration. However, it is possible that the source of NO released by i.v. and aerosol bradykinin is the same.

NO-synthase is present in different anatomical structures of the airways, which include non-cholinergic non-adrenergic nerves (Li & Rand, 1991; Lei *et al.*, 1993), macrophages and other inflammatory cells (Jorens *et al.*, 1993), and endothelial and epithelial cells (Fischer *et al.*, 1993; Kobzik *et al.*, 1993). To determine whether NO released by bradykinin derives from neural or non-neural elements, we studied the effect of L-NAME on the bronchoconstrictor response to capsaicin and to bradykinin after resection of the vagus nerves. Bronchoconstriction evoked by aerosolized capsaicin is due entirely to activation of cholinergic reflexes and release of tachykinins from sensory nerves (Ballati *et al.*, 1992; Bertrand *et al.*, 1993b). Bradykinin-induced bronchoconstriction is largely due to these two mechanisms (Ichinose *et al.*, 1990; Geppetti, 1993). We found that in guinea-pigs pretreated with atropine and phosphoramidon, capsaicin is more potent than bradykinin in causing bronchoconstriction, whereas the two drugs were equipotent in causing plasma extravasation. In these experimental conditions bradykinin and capsaicin cause bronchoconstriction and plasma extravasation by a common mechanism, e.g. tachykinin release from sensory nerves (Ichinose *et al.*, 1990; Bertrand *et al.*, 1993b). These observations support the hypothesis that bradykinin, but not capsaicin, releases bronchodilator agents. In addition, the present and previous (Lei *et al.*, 1993) observations that capsaicin-induced bronchoconstriction was not increased by L-NAME indicate that sensory nerves are not the source of NO released by bradykinin. Bradykinin and capsaicin seem to stimulate the same type of afferent fibres of the guinea-pig vagus nerve, e.g. C-fibres, but not Aδ-fibres (Fox *et al.*, 1993). This observation and the fact that acute vagotomy did not affect the bronchoconstrictor response to bradykinin and that L-NAME did not affect the response to capsaicin suggest that activation of neural cholinergic reflexes is not involved in the release of NO by bradykinin and that NO released by bradykinin does not originate from postganglionic cholinergic nerves. However, the present experimental data cannot exclude the possibility that bradykinin releases NO from neural elements by a direct action on NANC nerves containing NO-synthase and releasing NO.

An alternative hypothesis is that bradykinin releases NO from non-neural elements. The airway epithelium is a possible candidate as the site of NO release based on the following rationale: bradykinin B_2 receptors have been identified in guinea-pig airway epithelial cells (Proud *et al.*, 1993); bradykinin increases the mobilization and intracellular Ca^{2+} in bronchial epithelial cells (Geppetti *et al.*, 1994); increased intracellular Ca^{2+} concentration is required to activate constitutive NO-synthase (Moncada *et al.*, 1991); and the epithelium of various species (Fischer *et al.*, 1993; Kobzik *et al.*, 1993), including guinea-pig, is positively stained for NO-synthase. Recently, Nijkamp *et al.* (1993) reported that in anaesthetized spontaneously breathing guinea-pigs, histamine i.v. causes a bronchoconstrictor response which was potentiated by NO-synthase inhibitors. Potentiation by L-NAME and L-NMMA also was observed *in vitro* when histamine was administered to the guinea-pig trachea through the luminal surface and was abolished in tracheae in which the epithelium was removed. These data led the authors to suggest that histamine releases the bronchodilator agent, NO, from the epithelium. We propose that bradykinin, delivered either from the intravascular space or from the airway lumen, releases NO from the airway epithelium and by this mechanism opposes its own bronchoconstrictor action. This hypothesis is supported by the recent observation by Schlemper & Calixto (1994), who reported that the epithelium-dependent relaxant effect of bradykinin in strips of guinea-pig trachea is largely mediated by release of NO. However, further study is needed to test definitively the hypothesis that bradykinin releases NO from the airway epithelium of guinea-pigs *in vivo*.

Bradykinin aerosol does not substantially affect the bronchomotor tone in healthy volunteers. However, bradykinin causes bronchoconstriction in asthmatic patients (Herxheimer & E., 1961; Simonsson *et al.*, 1973; Fuller *et al.*, 1987). Histamine does not produce more than 20% reduction in FEV_1 in healthy subjects, whereas asthmatic patients exhibit hyperresponsiveness to histamine (Woolcock *et al.*, 1984). The ability of bradykinin and histamine to release the bronchodilator agent, NO, leads to the speculation that NO-synthase activity may be diminished in the airway epithelium of asthmatic patients and this reduction may contribute to the hyperresponsiveness to these mediators. The possibility that airway epithelial cells contain NO-synthase that is activated by bradykinin and other mediators adds further support to the view that these cells are a major pathophysiological component of asthma (Bertrand & Tschirhart, 1993).

Supported in part by Program Project HL-24136 from the National Institute of Health and Progetto Bilaterale from the Consiglio Nazionale delle Ricerche.

References

BALLATI, L., EVANGELISTA, S., MAGGI, C.A. & MANZINI, S. (1992). Effects of selective tachykinin receptor antagonists on capsaicin- and tachykinin-induced bronchoconspasm in anaesthetized guinea-pigs. *Eur. J. Pharmacol.*, **214**, 215–221.

BELVISI, M.G., STRETTON, D. & BARNES, P.J. (1991). Nitric oxide as an endogenous modulator of cholinergic neurotransmission in guinea pig airways. *Eur. J. Pharmacol.*, **198**, 219–221.

BERTRAND, C., GEPPETTI, P., BAKER, J., PETERSSON, G., PIEDIMONTE, G. & NADEL, J.A. (1993a). Role of peptidase and NK_1 receptors in vascular extravasation induced by bradykinin in rat nasal mucosa. *J. Appl. Physiol.*, **74**, 2456–2461.

BERTRAND, C., NADEL, J.A., GRAF, P.D. & GEPPETTI, P. (1993b). Capsaicin increases airflow resistance in guinea pigs in vivo by activating both NK2 and NK1 tachykinin receptors. *Am. Rev. Respir. Dis.*, **148**, 909–914.

BERTRAND, C. & TSCHIRHART, E. (1993). Epithelial factors: modulation of the airway smooth muscle tone. *Fundam. Clin. Pharmacol.*, **7**, 261–273.

BUXTON, I.L.O., CHEEK, D.J., ECKMAN, D., WESTFALL, D.P., SANDERS, K.M. & KEEF, K.D. (1993). N^G-nitro L-arginine methyl ester and other alkyl esters of arginine are muscarinic receptor antagonists. *Circ. Res.*, **72**, 387–395.

DUSSER, D.J., UMENO, E., GRAPH, P.D., DJOKIC, T.D., BORSON, D.B. & NADEL, J.A. (1988). Airway netural endopeptidase-like enzyme modulates tachykinin-induced bronchoconstriction in vivo. *J. Appl. Physiol.*, **65**, 2585–2591.

FISCHER, A., MUNDEL, P., MAYER, B., PREISSLER, U., PHILIPPIN, B. & KUMMER, W. (1993). Nitric oxide synthase in guinea pig lower airway innervation. *Neurosci. Lett.*, **149**, 157–160.

FOX, A.J., BARNES, P.J., URBAN, L. & DRAY, A. (1993). An in vitro study of the properties of the single vagal afferents innervating guinea-pig airways. *J. Physiol.*, **469**, 21–35.

FULLER, R.W., DIXON, C.M.S., CUSS, F.M.C. & BARNES, P.J. (1987). Bradykinin-induced bronchoconstriction in humans. Mode of action. *Am. Rev. Respir. Dis.*, **135**, 176–180.

GEPPETTI, P. (1993). Sensory neuropeptide release by bradykinin: mechanisms and pathophysiological implications. *Regul. Pept.*, **47**, 1–23.

GEPPETTI, P., RICCIARDOLO, F.M.L., GARLAND, A.D., LOVETT, M., HALLIDAY, D.A., NADEL, J.A., HESS, J.F., KANEKO, T. & BUNNETT, N.W. (1994). Characterization of bradykinin B2 receptors in human bronchial epithelial cells. *Am. Rev. Respir. Crit. Care Med.*, **149**, Suppl., A989.

HERXHEIMER, H. & E.S. (1961). The effect of bradykinin aerosol in guinea pigs and in man. *J. Physiol.*, **158**, 38–39.

HOLZER, P. (1991). Capsaicin: cellular targets, mechanisms of actions, and selectivity for thin sensory neurons. *Pharmacol. Rev.*, **43**, 143–201.

ICHINOSE, M., BELVISI, M.G. & BARNES, P.J. (1990). Bradykinin-induced bronchoconstriction in guinea pig in vivo: role of neural mechanism. *J. Pharmacol. Exp. Ther.*, **253**, 594–599.

JORENS, P.G., VERMEIRE, P.A. & HERMAN, A.G. (1993). L-arginine-dependent nitric oxide synthase: a new metabolic pathway in the lung and airways. *Eur. Respir. J.*, **6**, 258–266.

KOBZIK, L., BREDT, D.S., LOWENSTEIN, C.J., DRAZEN, J., GASTON, B., SUGARBAKER, D. & STAMLER, J.S. (1993). Nitric oxide synthase in human and rat lung: Immunocytochemical and histochemical localization. *Am. J. Respir. Cell. Mol. Biol.*, **9**, 371–377.

LEI, Y.-H., BARNES, P.J. & ROGERS, D.F. (1993). Regulation of NANC neural bronchoconstriction *in vivo* in the guinea-pig: involvement of nitric oxide, vasoactive intestinal peptide and soluble guanylyl cyclase. *Br. J. Pharmacol.*, **108**, 228–235.

LEIKAUF, G.D., UEKI, I.F., NADEL, J.A. & WIDDICOMBE, J.H. (1985). Bradykinin stimulates Cl secretion and prostaglandin E2 release by canine tracheal epithelium. *Am. J. Physiol.*, **248**, F48–F55.

LI, C.G. & RAND, M.J. (1991). Evidence that part of the NANC relaxant response of guinea-pig trachea to electrical field stimulation is mediated by nitric oxide. *Br. J. Pharmacol.*, **102**, 91–94.

LUNDBERG, J.M. & SARIA, A. (1983). Capsaicin induced desensitization of the airway muscosa to cigarette smoke, mechanical and chemical irritants. *Nature*, **302**, 251–253.

MONCADA, S. & HIGGS, A. (1993). The L-arginine nitric oxide pathway. *New Engl. J. Med.*, **329**, 2002–2012.

MONCADA, S., PALMER, R.M.J. & HIGGS, E.A. (1991). Nitric oxide: physiology, pathophysiology and pharmacology. *Pharmacol. Rev.*, **443**, 109–142.

NIJKAMP, F.P., VAN DER LINDE, H.J. & FOLKERTS, G. (1993). Nitric oxide synthesis inhibitors induce airway hyperresponsiveness in the guinea pig in vivo and in vitro. Role of the epithelium. *Am. Rev. Respir. Dis.*, **148**, 727–734.

PIPER, P.J., COLLIER, H.O. & VANE, J.R. (1967). Release of catecholamines in the guinea pig by substances involved in anaphylaxis. *Nature*, **223**, 838–840.

PROUD, D., REYNOLDS, C.J., BROOMFIELD, J., GOLDMAN, D.W. & BATHON, J.M. (1993). Bradykinin effects in guinea-pig tracheal epithelial cells are mediated through a B2 kinin receptor and can be inhibited by the selective antagonist HOE 140. *J. Pharmacol. Exp. Ther.*, **264**, 1124–1131.

REES, D.D., PALMER, R.M.J., SCHULTZ, R., HODSON, H.F. & MONCADA, S. (1990). Characterization of three inhibitors of endothelial nitric oxide synthase *in vitro* and *in vivo*. *Br. J. Pharmacol.*, **101**, 746–752.

REGOLI, D. & BARABE, J. (1980). Pharmacology of bradykinin related kinins. *Pharmacol. Rev.*, **32**, 1–46.

SARIA, A., LUNDBERG, J.M., SKOFITSCH, G. & LEMBECK, F. (1983). Vascular protein leakage in various tissues induced by substance P, capsaicin, bradykinin, serotonin, histamine and by antigen challenge. *Naunyn Schmied. Arch. Pharmacol.*, **324**, 212–218.

SCHEMPLER, V. & CALIXTO, J.B. (1994). Nitric oxide pathway-mediated relaxant effect of bradykinin in the guinea-pig isolated trachea. *Br. J. Pharmacol.*, **111**, 83–88.

SEKIZAWA, K., FUKUSHIMA, T., IKARASHI, Y., MARUYAMA, Y. & SASAKI, H. (1993). The role of nitric oxide in cholinergic neurotransmission in rat trachea. *Br. J. Pharmacol.*, **110**, 816–820.

SIMONSSON, B.G., SKOOGH, B.-E., BERGH, N.P., ANDERSON, R. & SVEDMYR, N. (1973). In vivo and in vitro effects of bradykinin on bronchial motor tone in normal subjects and patients with airways obstruction. *Respiration*, **30**, 378–388.

WOOLCOCK, A.J., SALOME, C.M. & YAN, K. (1984). The shape of the response curve to histamine in normal and asthmatic subject. *Am. Rev. Respir. Dis.*, **130**, 71–75.

(Received April 5, 1994
Revised July 7, 1994
Accepted July 21, 1994)

Br. J. Pharmacol. (1994), **113**, 1153–1158 © Macmillan Press Ltd, 1994

Participation of tumour necrosis factor and nitric oxide in the mediation of vascular dysfunction in splanchnic artery occlusion shock

[1]Francesco Squadrito, Domenica Altavilla, Patrizia Canale, Mariapatrizia Ioculano, Giuseppe M. Campo, Letteria Ammendolia, Marcella Ferlito, Basilia Zingarelli, *Giovanni Squadrito, *Antonino Saitta & Achille P. Caputi

Institute of Pharmacology and Department of *Internal Medicine, School of Medicine, University of Messina, Italy

1 Splanchnic artery occlusion (SAO) shock is characterized by irreversible circulatory failure. Tumour necrosis factor (TNF-α) may affect the L-arginine/nitric oxide (NO) pathway, thus contributing to the cardiovascular derangements of circulatory shock.

2 We investigated the contribution of both TNF-α and the L-arginine/nitric oxide pathway to the vascular dysfunction of SAO shock. Anaesthetized rats, subjected to total occlusion of the superior mesenteric artery and the coeliac trunk for 45 min developed a severe shock state (SAO shock) resulting in a fatal outcome within 75–90 min after the release of occlusion. Sham operated animals were used as controls. SAO shocked rats had also a marked hypotension and enhanced macrophage and serum levels of TNF-α. Furthermore, aortic rings from shocked rats showed a marked hyporeactivity to phenylephrine (PE 1 nM–10 μM) and reduced responsiveness to acetylcholine (ACh 10 nM–10 μM). Endothelium-denuded aortic rings had also a marked hyporeactivity to phenylephrine, which was restored to control values by *in vitro* administration of N^G nitro-L-arginine-methyl ester (L-NAME 10 μM).

3 *In vivo* administration of cloricromene (2 mg kg^{-1}, i.v.), an inhibitor of TNF-α biosynthesis, increased survival, enhanced mean arterial blood pressure and reduced macrophage and serum levels of TNF-α. Furthermore, aortic rings from shocked rats treated with cloricromene exhibited a greater contractile response to phenylephrine and improved responsiveness to ACh when compared to aortic rings from vehicle-treated SAO shocked rats.

4 Our results suggest that TNF-α alters both endothelial and muscular L-arginine/nitric oxide pathways which in turn produce vascular dysfunction in SAO shock.

Keywords: Cytokine; impaired vascular reactivity; endothelium; L-arginine-NO pathway

Introduction

Splanchnic artery occlusion (SAO) shock is an experimental type of circulatory shock which is the consequence of a prolonged ischaemia of the splanchnic region (Sturniolo *et al.*, 1988). SAO shock is characterized by impaired activity of the reticuloendothelial system (Sturniolo *et al.*, 1989), elevated macrophage and plasma levels of thromboxane B_2 (Squadrito *et al.*, 1992c) increased plasma levels of platelet activating factor (Squadrito *et al.*, 1991b; Zingarelli *et al.*, 1992b) and enhanced macrophage and serum levels of tumour necrosis factor (TNF-α) (Squadrito *et al.*, 1992b). Furthermore, SAO shock produces an irreversible circulatory failure which leads to the death of the animals within 75–90 min after the release of the occlusion (Squadrito *et al.*, 1989).

Acute splanchnic ischaemia induced by SAO shock may, therefore, induce an impaired vascular reactivity, but the mechanisms underlying these cardiovascular derangements are not yet well known.

It has been proposed that the L-arginine/nitric oxide pathway may play a key role in the regulation of vascular tone (Vane *et al.*, 1990). The biosynthesis of nitric oxide (NO) from L-arginine is a pathway for the regulation of cell function and communication (Moncada *et al.*, 1991). In all cell types so far studied NO is generated following oxidation and cleavage of the terminal nitrogen atom(s) of L-arginine by an enzyme, NO synthase. At least two types of NO synthase have been identified (Palmer *et al.*, 1987). The enzyme found in the endothelial cells (Pollock *et al.*, 1991) and in the brain (Bredt *et al.*, 1990) is constitutive, Ca^{2+}-dependent and releases picomolar amounts of NO for a short period following receptor stimulation. In contrast, the enzyme found in the macrophages is induced following stimulation with cytokines or endotoxin, is Ca^{2+}-independent, and releases nanomolar amounts of NO for a long period (Knowles *et al.*, 1990). Furthermore, the presence of a Ca^{2+}-independent NO synthase in vascular smooth muscle cells has been shown (Busse *et al.*, 1990).

These findings, taken together, suggest that vascular tone results from a cooperative participation of both endothelial and smooth muscle L-arginine/nitric oxide pathways.

TNF-α is a pleiotropic cytokine that plays an important role in nonseptic ischaemic states (Squadrito *et al.*, 1993) and that causes a marked impairment in vascular reactivity (Takahashi *et al.*, 1992). Since TNF-α has been shown to play an important role in the pathogenesis of SAO shock, we investigated the contribution of TNF-α and L-arginine/nitric oxide pathway to the vascular dysfunction of SAO shock. To investigate the role of TNF-α we used a pharmacological tool and, more specifically cloricromene. This coumarin derivative inhibits both *in vivo* and *in vitro* TNF-α production, an effect that appears to be the consequence of an increase in intracellular adenosine 3',5'-cyclic monophosphate (cyclic AMP) (Squadrito *et al.*, 1991a).

Methods

Surgical procedures

Male Sprague-Dawley rats weighing 250–300 g were permitted access to food and water *ad libitum*. The rats were anaesthetized with urethane (1.3 g kg^{-1}, i.p.). During the

[1] Author for correspondence.

experiment, no supplemental dose of anaesthetic was administered. After anaesthesia, catheters were placed in the carotid artery and jugular vein. Blood pressure was monitored continuously with a Statham pressure transducer. After midline laparotomy, the coeliac and superior mesenteric arteries were isolated near their aortic origins. During this procedure, the intestinal tract was maintained at 37°C by placing it between gauze pads soaked with warmed 0.9% NaCl solution.

Rats were given heparin (1,000 u kg^{-1}, i.v.) and were observed for a 30 min stabilization period prior to either splanchnic ischaemia or sham ischaemia. SAO shock was induced by clamping both the superior mesenteric artery and the coeliac trunk resulting in total occlusion of these arteries for 45 min. After this period of occlusion the clamps were removed. Following reperfusion the rats were observed for 240 min. Sham shocked rats were subjected to all the same surgical procedures as SAO shocked rats except that the arteries were not occluded.

Survival evaluation

Five minutes before the splanchnic artery occlusion shock procedures, treated rats received intravenously cloricromene (2 mg kg^{-1}) dissolved in NaCl saline solution and control rats received the vehicle. Survival was evaluated for 4 h.

Arterial blood pressure

Animals were anaesthetized with urethane (1.3 g kg^{-1}, i.p.) and a cannula (PE 50) was inserted into the left common carotid artery as described elsewhere (Caputi *et al.*, 1980). The arterial catheter was connected to a pressure transducer. The pressure pulse triggered a cardiotachometer, and arterial blood pressure was displayed on a polygraph. Arterial blood pressure is reported as mean arterial pressure (MAP) in mmHG. Rats were subjected to the same experimental protocol as described above.

Biological assay for tumour necrosis factor-α activity

Killing of L929 mouse tumour cells was used to measure TNF-α levels in serum and in the supernatants of peritoneal macrophages by use of a standard assay (Ruff & Gifford, 1980). Animals were killed 80 min after the onset of reperfusion. Peritoneal macrophages were obtained by peritoneal lavage with RPMI 1640 (Altavilla *et al.*, 1989), counted and diluted to 10^6 ml^{-1}. The cells were then incubated in Petri dishes at 37°C in a humidified CO_2 atmosphere for 1 h. L929 cells in RPMI 1640 medium containing 5% foetal calf serum were seeded at 3×10^4 cells per well in 96-well microdilution plates and incubated overnight at 37°C in an atmosphere of 5% CO_2 in air. Serial dilutions of serum and supernatants of peritoneal macrophages, collected as previously described (Squadrito *et al.*, 1991b) were made in a medium containing actinomycin D, 1.0 μg ml^{-1}, and 100 μl of each dilution was added to the wells. On the next day, cell survival was assessed by fixing and staining the cells with crystal violet (0.2% methanol) and 0.1 ml of 1% sodium dodecyl sulphate was added to each well to solubilize the stained cells. The absorbance of each well was read at 490 nm with a model BT-100 Microelisa Autoreader. The percentage of cytotoxicity was calculated as [1 − (490 of sample/A490 of control)] × 100. One unit of TNF-α was defined as the amount giving 50% cell cytotoxicity. TNF-α content in the sample was calculated by comparison with a calibration curve performed with recombinant murine TNF-α (Nuclear Laser Medicine, Italy). To verify if the cytotoxicity tested was due to the presence of TNF-α or to other factors, we preincubated our samples for 2 h at 37°C with an excess of rabbit anti-recombinant murine TNF-α polyclonal antibodies (Nuclear Laser Medicine, Milan, Italy) or with control rabbit serum. Our results showed that cytotoxicity against L929 cells was completely neutralized by rabbit anti-recombinant TNF-α polyclonal antibodies but not by control rabbit serum.

Isolated aortic rings

Animals were killed 80 min after the onset of reperfusion. Thoracic aortae were removed and placed in cold Krebs solution of the following composition (mM): NaCl 118.4, KCl 4.7, $MgSO_4$ 1.2, $CaCl_2$ 2.5, KH_2PO_4 1.2, $NaHCO_3$ 25.0 and glucose 11.7. Then aortae were cleaned of adherent connective and fat tissue and cut into rings of approximately 2 mm in length. In some rings the vascular endothelium was removed mechanically by gently rubbing the luminal surface with a thin wooden stick. Rings were then placed under 1 g of tension in an organ bath containing 10 ml Krebs solution at 37°C and bubbled with 95% O_2 and 5% CO_2 (pH 7.4). All experiments were carried out in the presence of indomethacin (10 μM) in order to exclude the involvement of prostaglandins and their metabolites. Developed tension was measured with an isometric force transducer and recorded on a polygraph (Ugo Basile, Torino, Italy). After an equilibration period of 60 min during which time the rings were washed with fresh Krebs solution at 15–20 min intervals and basal tension was readjusted to 1 g, the tissue was exposed to phenylephrine (PE, 100 mM). When the contraction was stable, the functional integrity of endothelium was assessed by a relaxant response to acetylcholine (ACh, 100 nM). The tissues were then washed occasionally for 30 min.

Endothelium-dependent relaxation was evaluated with cumulative concentrations of ACh (10 nM–1 μM) in aortic rings precontracted with PE (100 nM). Relaxation of the rings was calculated as the percentage decrease in contractile force.

Concentration-response curves were obtained by cumulative concentrations of PE (1 nM–10 μM) in intact or endothelium-denuded aortic rings.

In some experiments L-NAME (10 μM), L-arginine (300 μM) or their dextro-isoforms, D-NAME (10 μM) and D-arginine (300 μM) were added to the organ bath 1 h before the rings were contracted with cumulative concentrations of PE. The results (mean ± s.d.) are expressed as g of tension per mg of tissue.

Drugs

Acetylcholine chloride, phenylephrine hydrochloride, indomethacin, L-arginine hydrochloride, D-arginine hydrochloride, N^G-nitro-L-arginine methyl ester hydrochloride and N^G-nitro-D-arginine methyl ester hydrochloride were obtained from Sigma. Cloricromene (8-monochloro-3-β-diethylaminoethyl-4-methyl-7-ethoxycarbonylmethoxycoumarin) was obtained from Fidia Research Laboratories. We used the dose of 2 mg kg^{-1} in keeping with previous studies that have shown that this dose is the most effective for *in vivo* studies (Squadrito *et al.*, 1991a).

Statistical analysis

The difference between the means of two groups was evaluated with an ANOVA followed by Bonferroni's test and was considered significant when $P < 0.05$.

Results

Relaxant response to acetylcholine

Addition of PE (100 nM) to the organ bath contracted intact aortic rings (80–90% of the maximum response). These rings were relaxed in a concentration-dependent manner by ACh (10 nM–10 μM). The relaxant effect of ACh in aortic rings from shocked rats was significantly lower in SAO shocked rats than in Sham shocked rats. The maximum relaxation

induced by 1 μM ACh was 36 ± 2% and 90 ± 2% respectively ($P < 0.001$; Figure 1).

Contractile response to phenylephrine

Figure 2 shows the contractile force induced by PE (1 nM–10 μM) in intact aortic rings from Sham and SAO shocked rats. SAO shock markedly reduced the contractile response to PE (1 nM–10 μM) of intact aortae. The maximum force of contraction (g tension per mg tissue) induced 10 μM PE in aortic rings from Sham rats was 1.8 ± 0.08 whereas it was 1.06 ± 0.04 in rings from SAO shocked rats ($P < 0.001$; Figure 2).

Removal of endothelium increased slightly but not significantly the vasconstrictor potency of PE in the aortae from sham-shocked rats (Figure 3). In contrast, when PE was tested in denuded aortae from shocked rats, it produced overlapping effects in aortic rings with (Figure 2) or without endothelium (Figure 3). Therefore, removal of endothelium in aortae from SAO shocked animals did not restore the PE-induced contractile response to the values of the Sham group. These results indicated that smooth muscle cells are involved in the hyporesponsiveness to PE. In endothelium-denuded aortic rings from shocked rats, N^G-nitro-L-arginine-methyl ester (L-NAME 10 μM), an inhibitor of NO synthase,

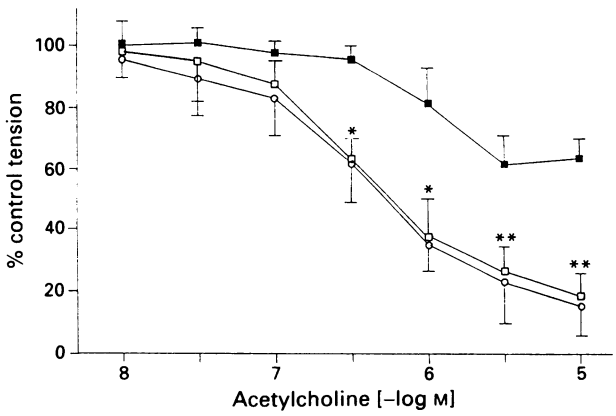


Figure 1 Relaxant effect of acetylcholine in aortic rings (contracted with phenylephrine, 100 nM) of sham-shocked rats and splanchnic artery occlusion (SAO) shocked rats treated either with vehicle (1 ml kg^{-1}, i.v. of a 0.9% NaCl saline solution) or cloricromene (2 mg kg^{-1}, i.v., 5 min before SAO: (○) Sham + vehicle; (■) SAO + vehicle; (□) SAO + cloricromene. Each point represents the mean ± s.d. from seven experiments. *$P < 0.05$ vs SAO + vehicle; **$P < 0.001$ vs SAO + vehicle.

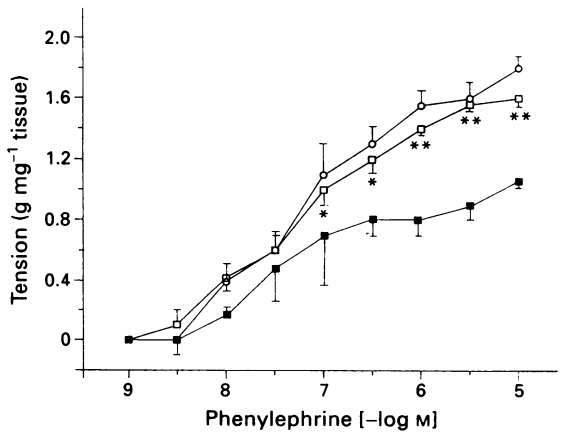


Figure 2 Contractile response to cumulative concentrations of phenylephrine in aortic rings from sham-shocked rats and splanchnic artery occlusion (SAO) shocked rats treated either with vehicle (1 ml kg^{-1}, i.v. of a 0.9% NaCl saline solution) or cloricromene (2 mg kg^{-1}, i.v., 5 min before SAO). Each point represents the mean ± s.d. from seven experiments. (○) Sham + vehicle; (■) SAO + vehicle; (□) SAO + cloricromene. *$P < 0.05$ vs SAO + vehicle; **$P < 0.001$ vs SAO + vehicle.

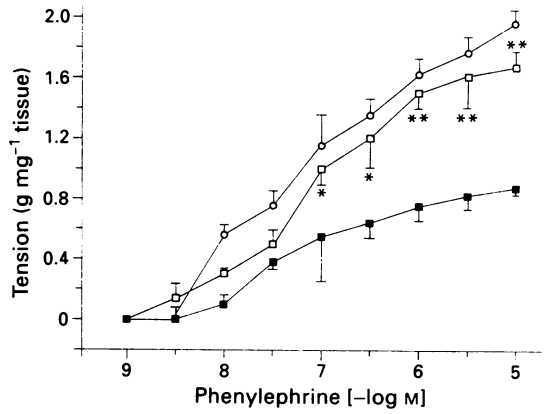


Figure 3 Effect of N^G-nitro-L-arginine methyl ester (L-NAME, 10 μM) on contractile response to cumulative concentrations of phenylephrine in aortic rings without endothelium from sham or splanchnic artery occlusion (SAO) shocked rats. L-NAME was added to the bath 1 h before phenylephrine. (○) Sham + vehicle; (■) SAO + vehicle; □ SAO + L-NAME. Each point represents the mean ± s.d. from six experiments. *$P < 0.05$ vs SAO + vehicle; **$P < 0.001$ vs SAO shocked rats.

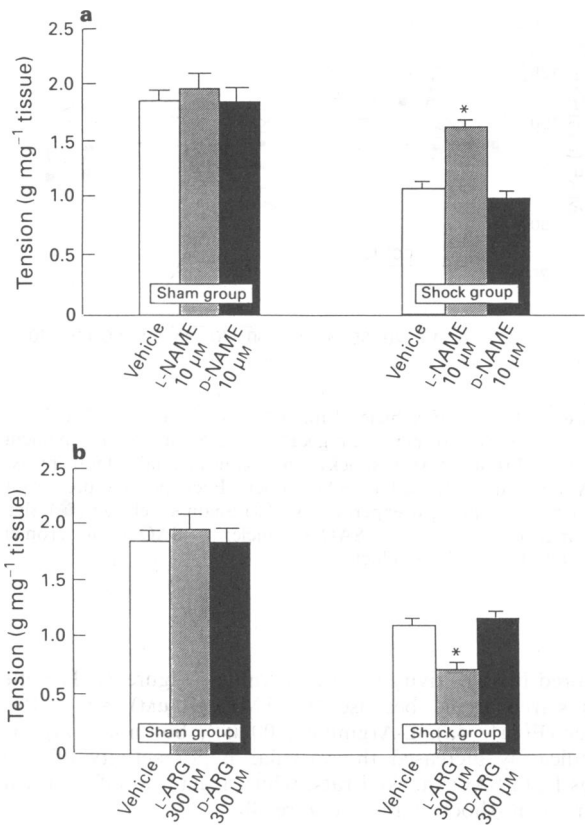


Figure 4 (a) Effects of N^G-nitro-L-arginine methyl ester (L-NAME, 10 μM) or D-NAME (10 μM) on maximal contractile response to phenylephrine in aortic rings without endothelium from sham and splanchnic artery occlusion (SAO) shocked rats. Each point represents the mean ± s.d. from six experiments. $P < 0.001$ vs shock- + vehicle. (b) Effects of L-arginine (300 μM) or D-arginine (300 μM) on maximal contractile response to phenylephrine in aortic rings without endothelium from sham and SAO-shocked rats. Each point represents the mean ± s.d. from six experiments. $P < 0.05$ vs shock- + vehicle.

Table 1 Effect of cloricromene on survival rate, percentage survival and survival time in splanchnic artery occlusion (SAO) shocked rats

	Hours after SAO				
	2		*4*		*Survival*
Treatment	*Surviving*	(%)	*Surviving*	(%)	*time* (min)
Sham + vehicle	10/10	100	10/10	100	>240
Sham + cloricromene	10/10	100	10/10	100	>240
SAO + vehicle	0/10	0	0/10	100	83 ± 15
SAO + cloricromene	10/10*	100*	8/10*	80*	235 ± 12*

Animals received cloricromene (2 mg kg^{-1}) or vehicle (1 ml kg^{-1} of a 0.9% NaCl solution) as a bolus 5 min before inducing SAO shock. $P < 0.001$ vs SAO + vehicle. Survival rate was monitored for 4 h.

Table 2 Effects of cloricromene on serum and macrophage tumour necrosis factor-α (TNF-α) in splanchnic artery occlusion (SAO) shocked rats

Treatment	*Serum TNF-α* (u ml^{-1})	*Macrophage TNF-α* (u ml^{-1})
Sham + vehicle	ND	ND
Sham + cloricromene	ND	ND
SAO + vehicle	345 ± 21	110 ± 12
SAO + cloricromene	18 ± 1*	9 ± 2

Serum and macrophages were collected 80 min after clamp removal. Each point represents mean ± s.d. from six experiments. Animals received cloricromene (2 mg kg^{-1}) or vehicle (1 ml kg^{-1} of a 0.9% NaCl solution) as a bolus 5 min before inducing SAO shock. $P < 0.001$ vs SAO + vehicle. ND = not detectable.

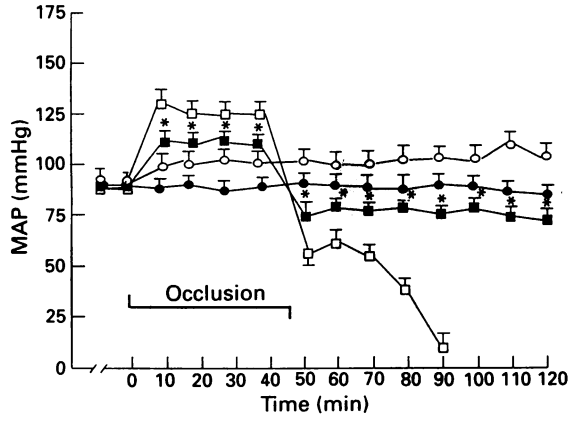


Figure 5 Effects of vehicle (1 ml kg^{-1}, i.v. of a 0.9% NaCl saline solution) or cloricromene (2 mg kg^{-1}, i.v., 5 min before splanchnic artery occlusion (SAO) shock) on mean arterial blood pressure (MAP) in rats subjected to SAO shock. Each point represents the mean ± s.d. from eight experiments. (○) Sham + vehicle; (●) Sham + cloricromene; □ SAO + vehicle; SAO + Cloricromene. *$P < 0.001$ vs SAO + vehicle.

restored PE-sensitivity to control values (Figure 3). The effect was stereospecific because D-NAME (10 μM) was without effect (Figure 4a). L-Arginine (300 μM), but not D-arginine, significantly increased the vascular hyporeactivity of aortic rings from SAO shocked rats, whilst it had no effect in rings from sham-shocked rats (Figure 4b).

Effect of in vivo *cloricromene pretreatment*

Survival rate Table 1 summarizes survival rate, percentage survival and survival time for the groups of rats subjected to splanchnic artery occlusion shock or sham shock. All sham shocked rats survived the entire 4 h observation period. In contrast, in rats treated with vehicle, SAO shock produced a profound shock state characterized by a high lethality: no rat survived at 2 h (survival time 83 ± 15 min). Treatment with cloricromene significantly increased survival rate and time in shocked rats when compared with rats treated with vehicle (Table 1).

Macrophage and serum TNF-α Macrophage and serum levels of TNF-α were undetectable in sham shocked rats treated with vehicle or cloricromene. TNF-α was significantly increased in the serum and in the supernatants of peritoneal macrophages collected from SAO shocked rats (Table 2). Treatment with cloricromene decreased the macrophage and serum TNF-α levels in SAO shocked rats (Table 2).

Mean arterial blood pressure SAO shock caused a sustained increase in mean arterial blood pressure. Subsequently pressure decreased sharply upon release of the clamps (Figure 5). Administration of cloricromene significantly improved these cardiovascular changes (Figure 5).

Relaxant response to ACh and contractile response to PE

Administration of cloricromene, an inhibitor of TNF-α production, significantly improved responsiveness to ACh (Figure 1; 80 ± 5%). The treatment with the drug also succeeded in partially restoring the contractile response to PE (Figure 2; 1.63 ± 0.2 g mg^{-1} tissue).

Discussion

Acute splanchnic ischaemia results in an irreversible circulatory failure and death (Squadrito *et al.*, 1991b; 1992c). The mechanisms underlying these cardiovascular derangements of SAO shock are not yet well known and therefore we carried out experiments to investigate the various components which together produce the severe vascular dysfunction of SAO shock.

It has been suggested that during SAO shock endothelial NO is reduced and administration of NO donors in this type of experimental shock increased short term survival and improves endothelial dysfunction (Carey *et al.*, 1992). In concurrence with this hypothesis our present data show that aortic rings from SAO shocked rats had a marked reduced

responsiveness to vasorelaxant effects of ACh. Indeed our present data and those of Carey *et al.* (1992) would indicate that in SAO shock a reduced NO production might be present and therefore these findings would justify the use of NO enhancing drugs in circulatory shock.

However, these results are in disagreement with data from both our laboratory (Zingarelli *et al.*, 1992a; 1994) and other research groups (Rees *et al.*, 1990; Thiemermann *et al.*, 1993) that, in contrast, claim an overproduction of NO as responsible for the vascular dysfunction observed in other types of circulatory shock such as haemorrhagic or septic shock. Previous studies on vascular reactivity in SAO shock (Aoki *et al.*, 1990; Carey *et al.*, 1992) have not been complete and conclusive; for example, in those studies a dose-response curve to vasoconstrictor agents in vessels with or without endothelium was not performed.

We therefore investigated the contractile response to phenylephrine. Our results demonstrate that a reduced vascular sensitivity to phenylephrine also occurs in aortic rings from SAO shocked rats. In addition, no difference between the aortae with or without endothelium was observed in the responses to phenylephrine.

The mechanism responsible for vascular dysfunction seems to be due to an overproduction of the potent vasodilator NO. In fact L-NAME, an inhibitor of NO synthase, restored the contractile responses to phenylephrine in aortic rings from SAO-shocked rats to control values. The stereospecificity of this effect was shown by the lack of effect of the dextro-enantiomer D-NAME which is not able to affect NO syntheses (Palmer *et al.*, 1988). Furthermore, our findings suggest that, even in the absence of endothelium, a continuous production of NO persists, probably due to the expression of the inducible NO synthase in the vascular smooth muscle (Busse *et al.*, 1990).

Therefore all these data, taken together, would suggest that both endothelial (reduced production of NO) and muscular (overproduction of NO) L-arginine/nitric oxide pathways are significantly, even if differently, affected by SAO shock.

The subsequent question that we raised was: is TNF-α, a pleiotropic cytokine, involved in mediating the vascular dysfunction of SAO shock? As far as this aspect is concerned it has been suggested that TNF-α may impair the release of NO from endothelial cells (Aoki *et al.*, 1989), thus leading to decreased production of endothelial-derived relaxing factor. On the other hand, TNF-α administration in conscious rats has been reported to induce a decrease in mean arterial blood pressure and to produce vascular hyporesponsiveness to contractile agents that is reversed by inhibitors of NO synthesis (Takahashi *et al.*, 1992). Furthermore, it has been shown that TNF-α is able to induce production of the Ca^{2+}-independent NO synthase in vascular smooth muscle cells (Busse *et al.*, 1990). These apparently conflicting results may be interpreted as follows: TNF-α might either inhibit the constitutive and endothelial NO synthase or stimulate the inducible form of NO synthase at the smooth muscle level and, finally, vascular dysfunction produced by this pleiotropic cytokine would result from the sum of these events.

To test this hypothesis we performed experiments using cloricromene, a previously reported inhibitor of TNF-α synthesis (Squadrito *et al.*, 1991a; 1992a). Our results indicate that cloricromene reduced macrophage and serum TNF-α, significantly increased survival and mean arterial blood pressure, and succeeded in restoring both the contractile response to phenylephrine and the vasorelaxant effects of ACh.

Therefore these findings, taken together, strongly suggest that TNF-α is deeply involved in the pathogenesis of vascular dysfunction that occurs in SAO shock. However (an)other factor(s) might also contribute to producing the irreversible circulatory failure of SAO shock.

In conclusion, our data suggest that in SAO shock: (a) endogenous NO generated by the constitutive NO synthase is blunted; (b) endogenous NO produced by the inducible NO synthase is increased; (c) these opposite effects on the two forms of NO synthase are probably induced by TNF-α.

This work was supported by Ministero Pubblica Istruzione, Fondi 40% and 60%. We gratefully acknowledge the skilful assistance of Carole Campbell in the preparation of the manuscript.

References

ALTAVILLA, D., BERLINGHIERI, M.C., SEMINARA, S., IANNELLO, D., FOCA' & MASTROENI, P. (1989). Different effects of bacterial lypopolysaccharide on superoxide anion production by macrophages from normal and tumor bearing rats. *Immunopharmacol.*, **17**, 99–106.

AOKI, N., JOHNSON III, G. & LEFER, A.M. (1990). Beneficial effects of two forms of NO administration in feline splanchnic artery occlusion shock. *Am. Physiol. Soc.*, **321**, G275–G281.

AOKI, N., SIEGFRIED, M. & LEFER, A.M. (1989). Anti-EDRF effect of tumor necrosis factor in isolated perfused cat carotid arteries. *Am. J. Physiol.*, **256**, H1509–H1512.

BREDT, D.S. & SNYDER, S.H. (1990). Isolation of nitric oxide synthetase, a calmodulin-requiring enzyme. *Proc. Natl. Acad. Sci. U.S.A.*, **87**, 682–685.

BUSSE, R. & MULSCH, A. (1990). Induction of nitric oxide synthase by cytokines in vascular smooth muscle cells. *FEBS Lett.*, **275**, 87–90.

CAPUTI, A.P., ROSSI, F., CARNEY, K. & BREZENOFF, H.E. (1980). Modulatory effect of brain acetylcholine on reflex-induced bradycardia and tachycardia in conscious rats. *J. Pharmacol. Exp. Ther.*, **215**, 309–316.

CAREY, C., SIEGFRIED, M.R., MA, C., WEYRICH, A.S & LEFER, A.M. (1992). Antishock and endothelial protective actions of a NO donor in mesenteric ischaemia and reperfusion. *Circ. Shock*, **38**, 209–216.

KNOWLES, R.G., MERRETT, M., SALTER, M. & MONCADA, S. (1990). Anti-inflammatory glucocorticods inhibit the induction by endotoxin of nitric oxide in the lung, liver and aorta of the rat. *Biochem. Biophys. Res. Commun.*, **172**, 1042–1048.

MONCADA, S., PALMER, R.M.J. & HIGGS, E.A. (1991). Nitric oxide: physiology, pathophysiology, and pharmacology. *Pharmacol. Rev.*, **43**, 109–142.

PALMER, R.M.J., FERRIGE, A.G. & MONCADA, S. (1987). Nitric oxide release accounts for the biological activity of endothelium-derived relaxing factor. *Nature*, **327**, 524–526.

PALMER, R.M.J., REES, D.D, ASHTON, D.S. & MONCADA, S. (1988). L-Arginine is the physiological precursor for the formation of nitric oxide in endothelium-dependent relaxation. *Biochem. Biophys. Res. Commun.*, **153**, 1251–1256.

POLLOCK, J.S., FORSTERMANN, U., MITCHELL, J.A., WARNER, T.D., SCHMIDT, H.H.H.W., NAKANE, M. & MURAD, F. (1991). Purification and characterization of particulate endothelium-derived relaxing factor synthase from cultured and native bovine aortic endothelial cells. *Proc. Natl. Acad. Sci. U.S.A.*, **88**, 10480–10484.

REES, D.D., CELLEK, S., PALMER, R.M.J. & MONCADA, S. (1990). Dexamethasone prevents the induction by endotoxin of a nitric oxide synthase and the associated effects on vascular tone. An insight into endotoxin shock. *Biochem. Biophys. Res. Commun.*, **173**, 541–547.

RUFF, M.R. & GIFFORD, G.E. (1980). Purification and physicochemical characterization of rabbit tumor necrosis factor. *J. Immunol.*, **125**, 1671–1675.

SQUADRITO, F., ALTAVILLA, D., CAMPO, G.M., CALAPAI, G., IOCULANO, M.P., ZINGARELLI, B., SAITTA, A., PROSDOCIMI, M. & CAPUTI, A.P. (1992a). Cloricromene, a coumarine derivative, protects against lethal endotoxin shock in rats. *Eur. J. Pharmacol.*, **210**, 107–113.

SQUADRITO, F., ALTAVILLA, D., IOCULANO, M., CALAPAI, G., ZINGARELLI, B., SAITTA, A., CAMPO, G.M., RIZZO, A. & CAPUTI, A.P. (1992b). Passive immunization with antibodies against tumor necrosis factor (TNF-α) protects from the lethality of splanchnic artery occlusion shock. *Circ. Shock*, **37**, 236–244.

SQUADRITO, F., ALTAVILLA, D., ZINGARELLI, B., IOCULANO, M., CALAPAI, G., CAMPO, G.M., MICELI, A. & CAPUTI, A.P. (1993). Tumor necrosis factor involvement in myocardial ischaemia-reperfusion injury. *Eur. J. Pharmacol.*, **237,** 223–230.

SQUADRITO, F., ALTAVILLA, D., ZINGARELLI, B., IOCULANO, M., CAMPO, G.M., SAITTA, A., URNA, G., SPIGNOLI, G. & CAPUTI, A.P. (1992c). Protective effects of G 619, a dual thromboxane synthase inhibitor and thromboxane A_2 receptor antagonist, in splanchnic artery occlusion shock. *J. Cardiovasc. Pharmacol.*, **19,** 115–119.

SQUADRITO, F., PROSDOCIMI, M., ALTAVILLA, D., ZINGARELLI, B. & CAPUTI, A.P. (1991a). Cloricromene. Cardiovasc. *Drug Rev.*, **9,** 357–371.

SQUADRITO, F., STURNIOLO, R., ALTAVILLA, D., CAMPO, G.M., TRIMARCHI, G.R., SCURI, R. & CAPUTI, A.P. (1989). Effects of fructose 1,6 diphosphate on splanchnic artery occlusion shock in the rat. *Resuscitation,* **18,** 299–307.

SQUADRITO, F., STURNIOLO, R., ALTAVILLA, D., SANTORO, G., CAMPO, G.M., ARENA, A. & CAPUTI, A.P. (1991b). Platelet activating factor involvement in splanchnic artery occlusion shock in rats. *Eur. J. Pharmacol.*, **192,** 47–53.

STURNIOLO, R., ALTAVILLA, D., BERLINGHIERI, M.C., SQUADRITO, F. & CAPUTI, A.P. (1988). Splanchnic artery occlusion shock in the rat: effects of calcium entry blockers nimodipine and verapamil. *Circ. Shock*, **24,** 43–53.

STURNIOLO, R., SQUADRITO, F., ALTAVILLA, D., TRIMARCHI, G.R., PROSDOCIMI, M. & CAPUTI, A.P. (1989). Cloricromene improves survival rate and macrophage function in splanchnic artery occlusion shock in rats. *Circ. Shock*, **28,** 267–277.

TAKAHASHI, K., ANDO, K., ANO, A., SHIMOSAWA, T., OGATA, E. & FUJITA, T. (1992). Tumor necrosis factor-α induces vascular hyporesponsiveness in Sprague-Dawley rats. *Life Sci.*, **50,** 1437–1444.

THIEMERMANN, C., SZABO', C., MITCHELL, J.A. & VANE, J.R. (1993). Vascular hyporeactivity to vasconstrictor agents and hemodynamic decompensation in hemorrhagic shock is mediated by nitric oxide. *Proc. Natl. Acad. Sci. U.S.A.*, **90,** 267–271.

VANE, J.R., ANGGARD, E.E. & BOTTING, R.M. (1990). Regulatory functions of the vascular endothelium. *N. Engl. J. Med.*, **323,** 27–36.

ZINGARELLI, B., SQUADRITO, F., ALTAVILLA, D., CALAPAI, G., CAMPO, G.M., CALO' M., SAITTA, A. & CAPUTI, A.P. (1992a). Evidence for a role of nitric oxide in hypovolemic hemorrhagic shock. *J. Cardiovasc. Pharmacol.*, **19,** 982–986.

ZINGARELLI, B., SQUADRITO, F., IOCULANO, M., ALTAVILLA, D., BUSSOLINO, F., CAMPO, G.M. & CAPUTI, A.P. (1992b). Platelet activating factor interaction with tumor necrosis factor and myocardial depressant factor in splanchnic artery occlusion shock. *Eur. J. Pharmacol.*, **222,** 13–19.

ZINGARELLI, B., SQUADRITO, F., ALTAVILLA, D., CALAPAI, G., DI ROSA, M. & CAPUTI, A.P. (1994). Role of tumor necrosis factor-α in acute hypovolemic hemorrhagic shock in rats. *Am. J. Physiol.*, **266,** H1512–H1515.

(Received March 24, 1994
Revised July 15, 1994
Accepted July 26, 1994)

Br. J. Pharmacol. (1994), **113**, 1159–1166 © Macmillan Press Ltd, 1994

The effects of administration of monoamine oxidase-B inhibitors on rat striatal neurone responses to dopamine

[1]M.D. Berry, E. Scarr, M.-Y. Zhu, I.A. Paterson & A.V. Juorio

Neuropsychiatric Research Unit, A114 Medical Research Building, University of Saskatchewan, Saskatoon, Saskatchewan, Canada, S7N 0W0

1 (−)-Deprenyl has been shown to potentiate rat striatal neurone responses to dopamine agonists at doses not altering dopamine metabolism. Since there are a number of effects of (−)-deprenyl which could result in this phenomenon, we have investigated the effects of MDL 72,145 and Ro 19-6327, whose only common effect with (−)-deprenyl is an inhibition of monoamine oxidase-B (MAO-B), on rat striatal neurone responses to dopamine and on striatal dopamine metabolism.

2 Using *in vivo* electrophysiology, i.p. injection of either MDL 72,145 or Ro 19-6327 was found to produce a dose-dependent potentiation of striatal neurone responses to dopamine but not γ-aminobutyric acid.

3 Neurochemical investigations revealed that this occurred at doses (0.25–1 mg kg^{-1}) which, while not affecting levels of dopamine or its metabolites, 3,4-dihydroxyphenylacetic acid or homovanillic acid, did cause a significant, dose-dependent, elevation in striatal levels of the putative neuromodulator, 2-phenylethylamine (PE).

4 Inhibition of PE synthesis by i.p. injection of the aromatic L-amino acid decarboxylase inhibitor, NSD 1015, produced a reversal of the effects of MDL 72,145 and Ro 19-6327.

5 Neurochemical analysis revealed this to occur at a dose of NSD 1015 (10 mg kg^{-1}) selective for reduction of elevated PE levels.

6 These results suggest that PE can act as a neuromodulator of dopaminergic responses and that MAO-B inhibitors may potentiate neuronal responses to dopamine via the indirect mechanism of elevation of PE following MAO-B inhibition.

Keywords: Dopamine; monoamine oxidase-B inhibitors; 2-phenylethylamine; neuromodulation

Introduction

(−)-Deprenyl, a selective inhibitor of monoamine oxidase (E.C. 1.4.3.4; MAO)-B (Knoll & Magyar, 1972), which is useful in the treatment of Parkinson's disease (Birkmayer *et al.*, 1975; Tetrud & Langston, 1989), has previously been shown to produce a potentiation of rat striatal neurone responses to the two dopamine agonists, apomorphine and (±)2-(N-phenethyl-*N*-propyl)amino-5-hydroxytetralin (PPHT) (Paterson *et al.*, 1991). This effect was seen at doses which did not alter levels of dopamine or its metabolites 3,4-dihydroxyphenylacetic acid (DOPAC) and homovanillic acid (HVA) (Paterson *et al.*, 1991). It was suggested that this effect may be indirect in nature, through an elevation of the endogenous brain amine, 2-phenylethylamine (PE), since the effect observed with (−)-deprenyl was similar to that observed following administration of low levels of PE. Further, PE is a selective substrate for MAO-B (Yang & Neff, 1973), and the endogenous levels are markedly elevated following inhibition of MAO-B (Philips & Boulton, 1979).

However, (−)-deprenyl has a number of other pharmacological actions in addition to inhibition of MAO-B (Knoll, 1983; Heinonen & Lammintausta, 1991) which could conceivably have resulted in the increased dopaminergic sensitivity observed. In order to confirm that these effects of (−)-deprenyl were due to an elevation of endogenous PE levels following MAO-B inhibition, we have examined the effects of two other MAO-B inhibitors, (E)-2-(3',4'-dimethoxyphenyl)-3-fluoroallylamine (MDL 72,145) and N-(2-aminoethyl)-5-chloro-2-pyridine carboxamide (Ro 19-6327). Both MDL 72,145, an irreversible inhibitor (Bey *et al.*, 1984), and Ro 19-6327, a reversible inhibitor (Da Prada *et al.*, 1987), share only an inhibition of MAO-B in common with (−)-deprenyl. The effects of these two compounds have been examined electrophysiologically and neurochemically in order to confirm that the effects previously observed with (−)-deprenyl were a function of MAO-B inhibition. Further, the effects of the aromatic-L-amino acid decarboxylase (EC 4.1.1.28; AADC) inhibitor *m*-hydroxybenzyl hydrazine (NSD 1015) (Bartholini & Pletscher, 1969) have also been examined in order to determine the role that PE may play in any response observed.

Methods

Animals

Male Wistar rats obtained from Charles River (Montréal, Canada), weighing 250–400 g, were used in all experiments. Animals were housed five to a cage on a 12 h light-dark cycle, at a temperature of 19–21°C, and allowed food and water *ad libitum*. All procedures were in accordance with the Canadian Council on Animal Care and National Institutes of Health guidelines for the use of experimental animals.

Microelectrode preparation

Five-barrelled glass microelectrodes were used in all electrophysiological experiments. The electrode tip was broken back to a diameter of 6–10 μm under a light microscope immediately prior to use. The central recording barrel contained 3 M NaCl, and had a resistance of 4–7 MΩ. One other barrel also contained 3 M NaCl, this being used for current balancing during iontophoresis. Of the other three barrels, one contained 10 mM monosodium glutamate (pH 8.0–8.6) dissolved in 10 mM NaCl, another 50 mM dopamine hydro-

[1] Author for correspondence at present address: Department of Pharmacology, Ohio State University College of Medicine, 333, West Tenth Avenue, Columbus, Ohio 43210-1239, U.S.A.

chloride (pH 6.0–6.5) dissolved in distilled water, and the final barrel 50 mM γ-aminobutyric acid (GABA) hydrochloride (pH 3.5–4.0) dissolved in 0.1 M hydrochloric acid. Throughout the course of the experiments, drugs were prevented from diffusing from individual barrels by the application of a 10–15 nA retaining current of the appropriate polarity.

Electrophysiology

Anaesthesia was induced with a combination of chloral hydrate (400 mg kg^{-1}, i.p.) and urethane (1 g kg^{-1}, s.c.), and maintained throughout the experiment with urethane (100 mg kg^{-1}, i.p.) as required. Depth of anaesthesia was tested by the absence or presence of foot withdrawal reflex following application of pressure and eye blink reflex to gentle touching of the corneal surface. Animals were placed in a stereotaxic frame and following exposure of the brain surface 2–3 mm lateral to bregma, a 5-barrelled glass microelectrode was lowered to the level of the striatum using co-ordinates from the rat brain atlas of Paxinos & Watson (1986) and a microelectrode manipulator (Narishige Scientific Instruments Laboratory, Tokyo, Japan). Between a depth of 3 and 6 mm below the pial surface, extracellular recordings of all spontaneously active and glutamate driven cells were obtained. Where cells were glutamate-driven, glutamate was either applied continuously at an ejection current of between − 5 nA and − 10 nA, or on a rapidly repeating cycle (ejection − 40 nA to − 60 nA for 6 s; retention + 10 nA to + 15 nA for 6 s). Action potentials were counted using a SPS 801 dynamic template-matching waveform analyser (Signal Processing Systems, Prospect, Australia), and neuronal firing rates recorded on a model 7D polygraph (Grass Instruments, Scarborough, Canada) and MacIntosh computer fitted with MacLab interface.

Following detection of a cell, control responses were obtained to the randomized, alternating iontophoretic administration of dopamine and GABA. On demonstrating stable responses to both, a cumulative dose-response curve was constructed for the intraperitoneal administration of either MDL 72,145 (0.125–1.0 mg kg^{-1}) or Ro 19-6327 (0.125–1.0 mg kg^{-1}). Successive doses of the MAO-B inhibitor were administered at 15 min intervals, and 15 min following the final dose, the AADC inhibitor NSD 1015 (10 mg kg^{-1}, i.p.) was administered. This was followed 15 min later by a further injection of NSD 1015 to give a cumulative dose of 100 mg kg^{-1}, i.p., and responses to dopamine and GABA recorded for a further 15 min.

Electrophysiological analysis

Neuronal responses were quantified by calculating the IT_{50} value (De Montigny & Aghajanian, 1977), as previously described (Paterson *et al.*, 1991). Individual IT_{50} values represent the average of three successive responses. In order to aid interpretation, IT_{50} values were converted into neuronal sensitivities by transforming to the reciprocal and expressing these as a fraction of control values.

Determination of MAO activity

Rats were divided into two groups and pretreated 2 h before they were killed, one group with MDL 72,145 (0.0625 to 2 mg kg^{-1}, i.p.) and the other with Ro 19-6327 (0.0625 to 2 mg kg^{-1}, i.p.). The animals were killed by stunning followed by decapitation and the striata rapidly dissected on ice. The tissues were homogenized in ice cold 0.01 M potassium phosphate buffer (pH 7.5) and the resultant suspension centrifuged at 40,000 *g* for 30 min. The pellet was re-suspended in 20 ml of 0.01 M potassium phoshate buffer and centrifuged as before. The resulting pellet was re-suspended in ice-cold distilled water and a portion removed for protein determination with bovine serum albumin used as a standard (Lowry *et al.*, 1951).

The activities of MAO-A and MAO-B were determined by a modification of the method of Wurtman & Axelrod (1963), using [^{14}C]-5-hydroxytryptamine (5-HT) bioxalate and [^{14}C]-PE hydrochloride as substrates for MAO-A and MAO-B respectively, as previously described (Paterson *et al.*, 1991).

Determination of dopamine, DOPAC and HVA

Rats were again divided into two groups and pretreated 2 h before they were killed, one with MDL 72,145 (0.125 to 4 mg kg^{-1}, i.p.) and the other with Ro 19-6327 (0.125 to 4 mg kg^{-1}, i.p.). The animals were killed and the striata rapidly dissected on ice. Left and right striata from individual animals were pooled and homogenized in 0.1 N perchloric acid containing 0.25 mM EDTA, 0.1 mM sodium metabisulphite and 100 ng ml^{-1} isoprenaline as an internal standard. Dopamine, DOPAC and HVA were determined by high performance liquid chromatography (h.p.l.c.) with electrochemical detection as previously described (Kwok & Juorio, 1986).

Determination of PE

Rats and tissues were prepared as described for the determination of dopamine, DOPAC and HVA. Following homogenization, a portion of the sample was combined with 50 ng of tetradeutero-phenylethylamine as the internal standard. The samples were derivatised with dansyl chloride and the amines extracted into toluene:ethylacetate (9:1, v/v). The derivatives were isolated using two unidirectional thin layer chromatograms (Juorio & Kazakoff, 1984). The isolated derivatives were then determined for PE by a high resolution mass spectrometric selected ion monitoring method (Durden *et al.*, 1973).

The effect of NSD 1015 on dopamine and PE levels

The levels of dopamine and PE were also determined in rats pretreated with the AADC inhibitor, NSD 1015. Rats were divided into four groups, the first received NSD 1015 (10 mg kg^{-1}, i.p.) 2 h before they were killed, the second pargyline (75 mg kg^{-1}, i.p.), the third pargyline (75 mg kg^{-1}, i.p.) followed 1 h later by NSD 1015 (10 mg kg^{-1}, i.p.) and the fourth saline. Striatal dopamine and PE levels were then determined as described above.

Determination of AADC activity

Rats were pretreated 2 h before they were killed with NSD 1015 (0.1 to 100 mg kg^{-1}, i.p.) and, following stunning and decapitation, the striata were rapidly dissected on ice. The preparation and assay of AADC was performed as described elsewhere (Zhu *et al.*, 1992). Briefly, striata were homogenized in 5 ml of ice-cold 0.25 M sucrose solution. The homogenate was centrifuged at 12,000 *g* for 10 min and 50 µl of the resultant supernatant transferred to the incubation medium. This consisted of 50 mM sodium phosphate buffer (pH 7.2), 0.01 mM pyridoxal-5-phosphate, 0.1 mM pargyline, 1 mM 2-mercaptoethanol and 0.1 mM EDTA. The reaction was started by the addition of 0.04 mM L-DOPA containing 0.17 mM ascorbic acid to prevent auto-oxidation and allowed to proceed at 37°C for 20 min; 600 µl of ice-cold 0.1 M perchloric acid containing 0.1 mM sodium metabisulphite, 0.25 mM EDTA and 100 ng ml^{-1} isoprenaline as an internal standard was added to terminate the reaction. The activity of the enzyme was determined by calculating the amount of dopamine formed by h.p.l.c. with electrochemical detection.

Drugs and chemicals

Dopamine hydrochloride, GABA hydrochloride, monosodium glutamate, NSD 1015, pargyline hydrochloride, 5-HT

creatinine sulphate, phenylethylamine hydrochloride and isoprenaline hydrochloride were all obtained from Sigma Chemicals (St. Louis, MO, U.S.A.). (−)-Deprenyl hydrochloride was obtained from Research Biochemicals (Natwick, MA, U.S.A.), clorgyline hydrochloride was a generous gift from May and Baker Ltd. (Essex, U.K.). [^{14}C]-Phenylethylamine hydrochloride and [^{14}C]-5-HT bioxalate were obtained from NEN (Boston, MA, U.S.A.). MDL 72,145 was a generous gift from Marion Merrel Dow Inc. (Cincinnati, Ohio, U.S.A.) and Ro 19-6327 a generous gift from Hoffmann La Roche Ltd. (Etobicoke, Ont., Canada). All other reagents and solvents were of analytical grade.

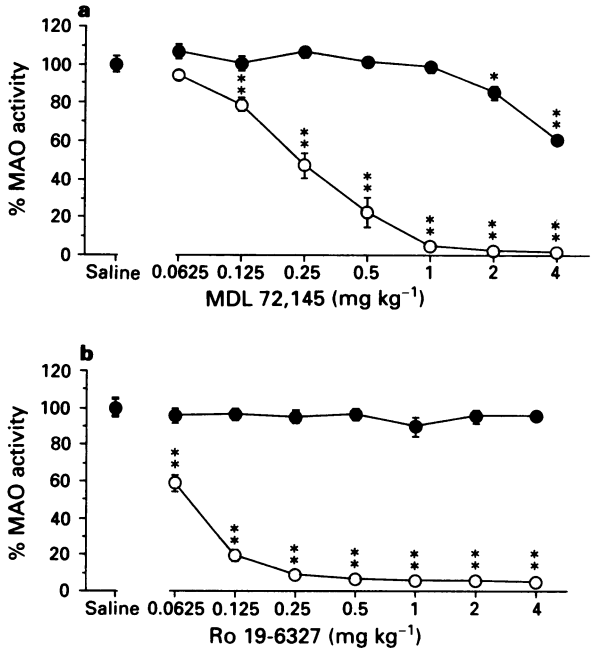


Figure 1 Effect of various doses of (a) MDL 72,145 and (b) Ro 19-6327 on striatal monoamine oxidase (MAO) activity. Drugs were injected i.p. 2 h prior to killing: (●) MAO-A activity: (○) MAO-B activity. Values represent means ± s.e. of at least five observations. $*P<0.05$, $**P<0.01$, Newman-Keuls test with respect to saline.

Statistics

Results were subjected to a one-way analysis of variance with the Newman-Keuls test for statistical significance. Statistical significance was taken at values of $P<0.05$.

Results

Inhibition of striatal MAO-A and MAO-B activity by MDL 72,145 and Ro 19-6327

Administration of MDL 72,145 resulted in a highly selective inhibition of MAO-B (Figure 1a). At a dose of 1 mg kg^{-1} an almost complete inhibition of MAO-B was obtained while MAO-A activity remained unaffected. Only at doses of 2 mg kg^{-1} and greater was a significant inhibition of MAO-A observed (Figure 1a).

At the doses employed in the current study Ro 19-6327 was completely selective towards inhibition of MAO-B. While a dose of 0.5 mg kg^{-1} produced an almost complete inhibition of MAO-B, no inhibition of MAO-A was produced at doses up to 4 mg kg^{-1} (Figure 1b).

The effect of MDL 72,145 and Ro 19-6327 on striatal dopamine, DOPAC, HVA and PE levels

At doses of 0.5 mg kg^{-1} and greater, MDL 72,145 produced a dose-dependent, statistically significant, increase in striatal levels of PE (Figure 2a). There was no maximum effect evident even at the highest dose (4 mg kg^{-1}, i.p.) employed. A statistically significant, dose-related increase in striatal PE levels was observed at all doses of Ro 19-6327 tested, with again, no maximum effect evident (Figure 3a).

In contrast, neither MDL 72,145 nor Ro 19-6327 caused a

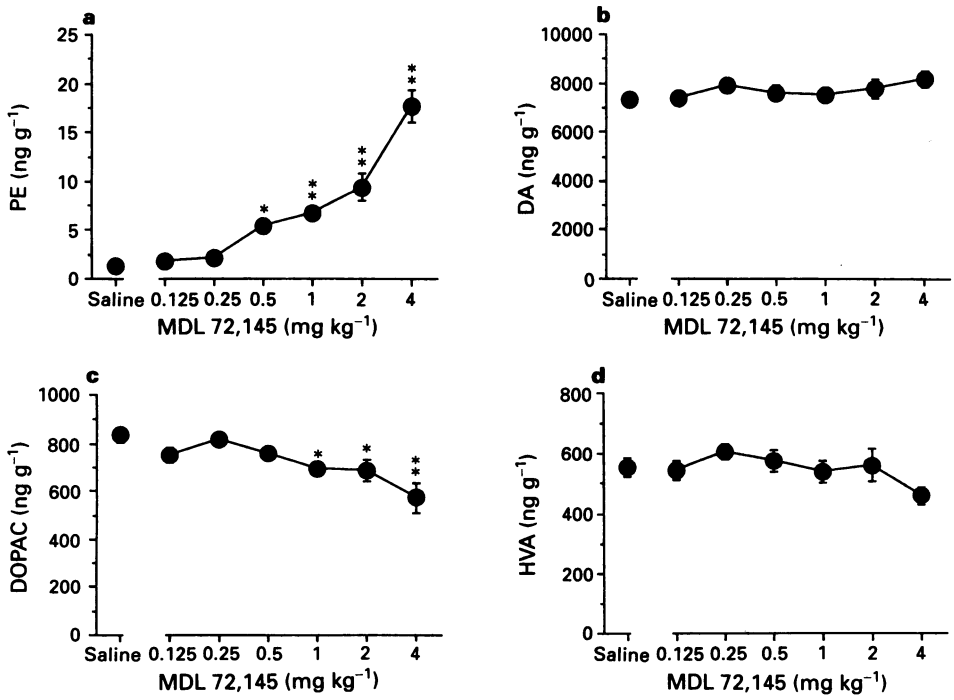


Figure 2 The effects of different doses of MDL 72,145 on the striatal concentrations of (a) 2-phenylethylamine (PE), (b) dopamine (DA), (c) 3,4-dihydroxyphenylacetic acid (DOPAC) and (d) homovanillic acid (HVA). MDL 72,145 or saline was administered by i.p. injection 2 h before death. Each point represents the mean ± s.e. of at least seven determinations. $*P<0.05$, $**P<0.01$, Newman-Keuls test with respect to saline.

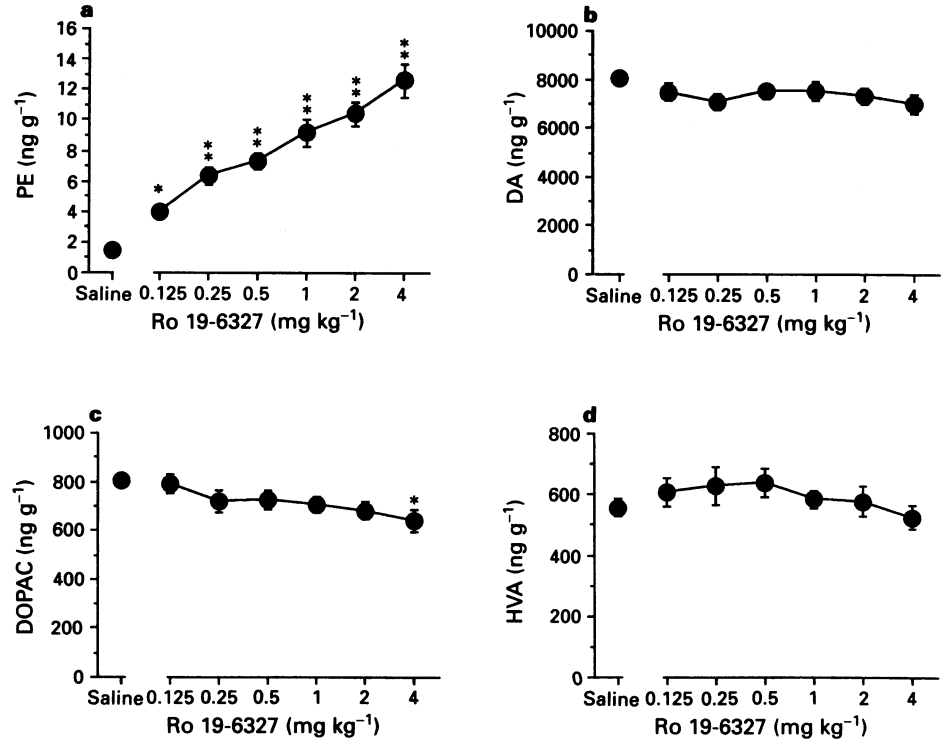


Figure 3 The effects of different doses of Ro 19-6327 on the striatal concentrations of (a) 2-phenylethylamine (PE), (b) dopamine (DA), (c) 3,4-dihydroxyphenylacetic acid (DOPAC) and (d) homovanillic acid (HVA). Ro 19-6327 was administered by i.p. injection 2 h before death. Each point represents the mean ± s.e. of at least eight determinations. $*P<0.05$, $**P<0.01$, Newman-Keuls test with respect to saline.

significant change in striatal levels of dopamine or HVA at any dose employed (Figures 2b, 2d, 3b and 3d). Levels of DOPAC were reduced to a significant extent only at MDL 72,145 doses of 1 mg kg^{-1} or greater (Figure 2c) and at the highest dose (4 mg kg^{-1}) of Ro 19-6327 employed (Figure 3c).

The effect of MDL 72,145 and Ro 19-6327 on striatal neurone responses to dopamine and GABA

Intraperitoneal administration of MDL 72,145 resulted in a dose-dependent potentiation of neuronal responses to dopamine but not GABA (Figures 4 and 5a), which reached statistical significance at a dose of 0.5 mg kg^{-1}. A maximum effect of a doubling of neuronal sensitivity to dopamine was seen at a dose of 0.5 mg kg^{-1} (Figure 5a). There was no difference in response to MDL 72,145 between spontaneously active and glutamate driven cells.

A dose-dependant potentiation of neuronal responses to dopamine but not GABA, was also observed following intraperitoneal administration of Ro 19-6327 (Figure 5b). This reached statistical significance at a dose of 0.5 mg kg^{-1}, with a doubling in neuronal sensitivity to dopamine observed at 1.0 mg kg^{-1} (Figure 5b). Again, spontaneously active and glutamide driven neurones responded in the same manner to Ro 19-6327.

In all responsive cells, dopamine resulted in an inhibition of neuronal firing and neither MAO-B inhibitor alone altered the basal neuronal activity (Figure 4).

The effect of NSD 1015 on striatal dopamine and PE levels

Administration of 10 mg kg^{-1} NSD 1015 did not result in a statistically significant alteration in striatal levels of either PE or dopamine (Table 1). A significant effect was observed with NSD 1015 only following pargyline pretreatment. Pargyline (75 mg kg^{-1}, i.p.) resulted in a significant elevation of both PE and dopamine levels within the striatum (Table 1). Under these conditions, a significant decrease in striatal PE, but not dopamine levels were observed following NSD 1015 (10 mg kg^{-1}, i.p.) administration (Table 1).

Inhibition of striatal AADC activity by NSD 1015

At doses of 1 mg kg^{-1} and greater, a significant, dose-dependent reduction in striatal AADC activity was observed following NSD 1015 administration (Figure 6).

The effect of NSD 1015 on striatal neurone responses to MDL 72,145 and Ro 19-6327

The administration of NSD 1015 (10 mg kg^{-1}, i.p.) resulted in a reversal of the potentiation of dopamine responses observed with MDL 72,145 and Ro 19-6327 (Figure 7). Increasing the dose to 100 mg kg^{-1} had no further effect on responses to dopamine and at neither dose was an effect on GABA responses observed (Figure 7). NSD 1015 alone did not alter neuronal responses to either dopamine or GABA (data not shown).

Discussion

At doses selective for inhibition of MAO-B, both MDL 72,145 and Ro 19-6327 resulted in a steady increase in the endogenous levels of PE (Figures 2a and 3a), but no change in the concentrations of dopamine or HVA (Figures 2b, 2d, 3b and 3d), consistent with results previously reported for (−)-deprenyl (Azzaro *et al.*, 1985; Hovevey-Sion *et al.*, 1989; Butcher *et al.*, 1990; Paterson *et al.*, 1991). Slight decreases were observed in the striatal levels of DOPAC at the higher doses of both drugs (Figures 2c and 3c), which corresponded to an approximate 95% inhibition of MAO-B (Figures 1a

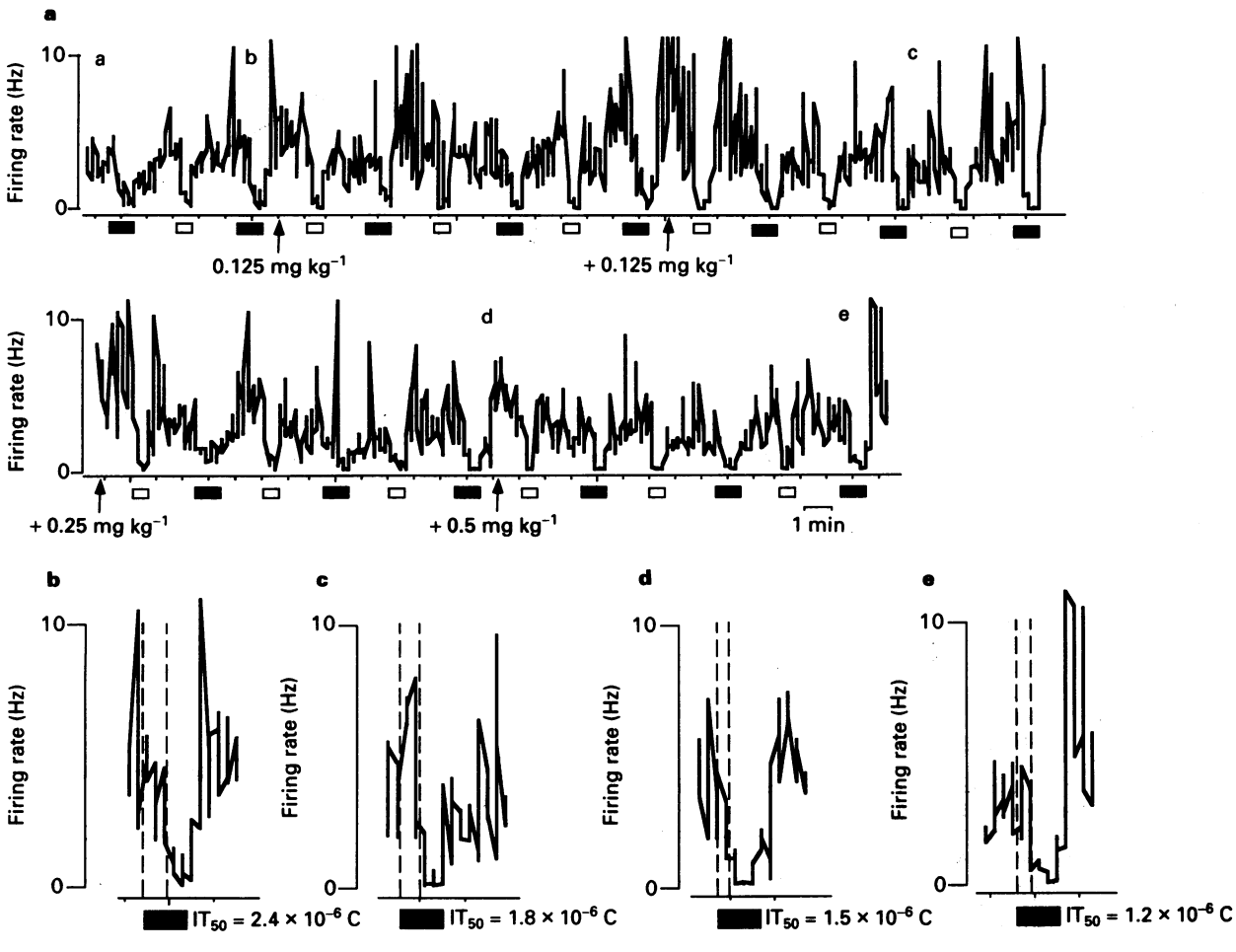


Figure 4 (a) Ratemeter record of the effect of MDL 72,145 on neuronal responses to dopamine (DA) and γ-aminobutyric acid (GABA). Neuronal activity was driven by the application of glutamate (ejection − 25 nA, 6.5 s, retain + 12 nA, 6.5 s). Dopamine was applied at an ejection current of 100 nA for 60 s (solid horizontal bars) GABA at 5 nA for 30 s, (open horizontal bars) 105 s following termination of dopamine application. This cycle was repeated every 5 min. Increasing doses of MDL 72,145 were administered i.p. at 15 min intervals, up to a final cumulative dose of 1 mg kg^{-1}. Responses were then followed for a further 15 min. Individual responses to dopamine (marked b–e), following each dose of MDL 72,145, are shown in expanded forms in (b), (c), (d) and (e) respectively. Here, dotted lines indicate the point at which application of dopamine was begun and the point at which a 50% inhibition of firing was obtained.

and 1b). Interestingly, in contrast to previous studies with (−)-deprenyl (Azzaro *et al.*, 1985; Hovevey-Sion *et al.*, 1989; Butcher *et al.*, 1990; Paterson *et al.*, 1991), this reduction in DOPAC levels was seen at doses of both MDL 72,145 and Ro 19-6327 which were selective for MAO-B inhibition (Figures 1a and b). This demonstrates that at least part of the metabolism of dopamine under normal conditions occurs via MAO-B in the rat. However, the lack of effect observed on dopamine and HVA levels would indicate that this normally only comprises a small proportion of dopamine metabolism. The majority, due to active neuronal re-uptake (Holz & Coyle, 1974; Iversen, 1974), will occur intraneuronally, where MAO-A appears to be the sole isozyme present, although there may be trace quantities of MAO-B (Westlund *et al.*, 1988), which could explain the small amount of metabolism observed by MAO-B in the present study. It is probable that this small amount of dopamine metabolism by MAO-B in the rat was not detected previously with (−)-deprenyl due to a lack of selectivity. Thus, at doses sufficient to cause a 95% inhibition of MAO-B, (−)-deprenyl also results in a significant inhibition of MAO-A (Paterson *et al.*, 1991). As such, the small MAO-B component of dopamine metabolism will tend to be masked by progressive MAO-A inhibition.

Results from electrophysiological studies reveal that, at doses which selectively inhibit MAO-B, elevate PE levels, but do not alter dopamine, DOPAC or HVA levels, both MDL 72,145 and Ro 19-6327 cause a potentiation of neuronal responses to dopamine. Similar results were previously obtained with (−)-deprenyl (Paterson *et al.*, 1991). Both MDL 72,145 and Ro 19-6327 resulted in a doubling of neuronal sensitivity to dopamine but not GABA. A doubling of dopamine sensitivity was observed with MDL 72,145 at a dose of 0.5 mg kg^{-1} (Figure 5a). This corresponds to an 80% inhibition of MAO-B (Figure 1a) and a 3–4 fold increase of PE levels (Figure 2a). With Ro 19-6327, a doubling of neuronal sensitivity to dopamine was observed at a dose of 1.0 mg kg^{-1} (Figure 5b). This corresponds to approximately a 95% inhibition of MAO-B (Figure 1b) and a 4–5 fold increase in PE levels (Figure 3a).

Thus, there appears to be a discrepancy between MDL 72,145 and Ro 19-6327 for the degree of MAO-B inhibition and PE elevation required for potentiation of neuronal responses to dopamine. However, this apparent discrepancy can be explained by examining the nature of the inhibition produced by these compounds. MDL 72,145 is an irreversible and as such, time-independent, inhibitor (Bey *et al.*, 1984). In contrast, Ro 19-6327 is a reversible, and hence time-dependent, inhibitor of MAO-B (Da Prada *et al.*, 1987). While this difference is unlikely to be of importance in the neurochemical analyses where animals were treated 2 h before determinations were performed, it may be of impor-

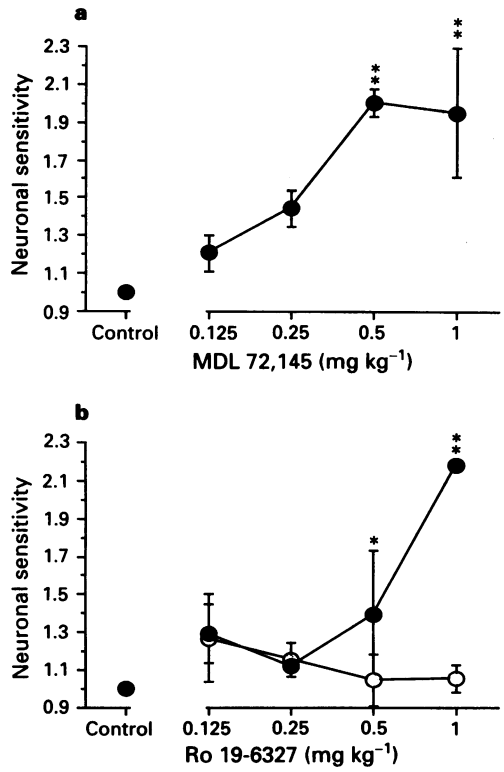


Figure 5 Cumulative dose-response curves for the administration of (a) MDL 72,145 and (b) Ro 19-6327 on striatal neurone sensitivity to dopamine (DA) and γ-aminobutyric acid (GABA). Successive doses of MDL 72,145 and Ro 19-6327 were given at 15 min intervals: (○) GABA sensitivity; (●) dopamine sensitivity. All values are mean ± s.e. of three observations. $*P<0.05$, $**P<0.01$, Newman-Keuls test with respect to control responses.

Table 1 The effect of the administration of NSD 1015 on the striatal concentration of 2-phenylethylamine (PE) and dopamine (DA) of pargyline-treated rats

Treatment	*PE* (ng g^{-1})	*DA* (ng g^{-1})
Saline	2.1 ± 0.5 (10)	8340 ± 360 (11)
NSD 1015	1.3 ± 0.4 (10)	8230 ± 310 (11)
Pargyline	53.9 ± 3.3 (9)	10820 ± 590 (9)
Pargyline + NSD 1015	23.9 ± 1.6 (8)**	10320 ± 400 (9)

Rats were first injected with pargyline (75 mg kg^{-1}) and 1 h later given NSD 1015 (10 mg kg^{-1}) and killed 2 h after the beginning of the experiment. Values are means ± s.e. with the number of determinations in parentheses. $**P<0.01$, Neuman-Keuls test with respect to the pargyline-treated controls. In all cases pargyline increases amine concentrations ($P<0.01$).

tance in the electrophysiological determinations where only a 15 min period could be allowed between successive doses. As such, the apparent lower potency of Ro 19-6327 may be due to the reversible nature of the inhibition, which, combined with the short time period allowed between each dose, may not allow a full expression of MAO-B inhibition in the presence of elevated PE levels. Thus, although the reversible nature of the inhibition produced by Ro 19-6327 is a complicating factor, it is apparent that dopaminergic neuronal responses are potentiated by three chemically unrelated compounds (MDL 72,145, Ro 19-6327 and (−)-deprenyl) whose only common effect is an inhibition of MAO-B, resulting in an elevation of PE levels.

Previously, it was suggested that this effect of (−)-deprenyl was due to an elevation of PE following MAO-B inhibition

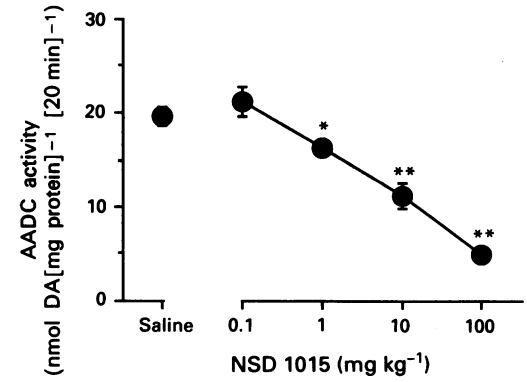


Figure 6 Dose-response effects of NSD 1015 on striatal aromatic-L-amino acid decarboxylase (AADC) activity in the rat. AADC activity is expressed in nmol of dopamine (mg protein) (20 min)$^{-1}$. The values of each experimental group are means ± s.e. obtained from seven determinations. $*P<0.05$, $**P<0.01$, Newman-Keuls test with respect to saline group.

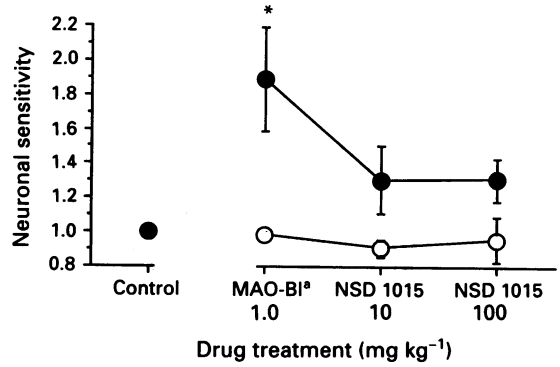


Figure 7 Striatal neurone sensitivity to dopamine and γ-aminobutyric acid (GABA) following NSD 1015 administration. Following a cumulative dose of 1.0 mg kg^{-1} i.p. of either of the MAO-B inhibitors, NSD 1015 was administered i.p. at 15 min intervals: (○) GABA sensitivity; (●) dopamine sensitivity. All values are mean ± s.e. of three observations. $*P<0.05$, Newman-Keuls test with respect to control responses. *MAO-BI = MAO-B inhibitor.

(Paterson *et al.*, 1991). PE appears to be synthesized in dopaminergic neurones (Greenshaw *et al.*, 1986; Juorio *et al.*, 1991), but unlike classical monoamines, is thought to exist in a steady state, the concentration being dependent on the relative rates of synthesis by AADC and degradation via MAO-B (Paterson *et al.*, 1990). Thus, the role that PE elevation plays in the responses observed to MAO-B inhibitors can be studied by subsequent inhibition of PE synthesis with an AADC inhibitor.

On administration of NSD 1015, a reversal of the potentiatory effects of both MDL 72,145 and Ro 19-6327 on dopaminergic responses was obtained (Figure 7). Again, no change in neuronal sensitivity to GABA was observed (Figure 7). This reversal was observed at a dose of 10 mg kg^{-1}. Increasing the dose to 100 mg kg^{-1} had no further effect on neuronal sensitivity (Figure 7), although AADC inhibition was increased (Figure 6). A similar reversal was previously observed for NSD 1015 (100 mg kg^{-1}) following potentiation of neuronal responses to DA agonists by (−)-deprenyl (Berry & Paterson, unpublished observations).

That inhibition of NSD 1015 was causing a reduction in PE levels was confirmed in neurochemical analyses (Table 1). Although only a trend for a decrease in PE levels following NSD 1015 alone was observed, this is not too surprising, since the levels of PE present under normal physiological conditions approach the detection limits of the mass spectro-

metric technique employed. As such, the errors present in the determination of PE levels will tend to mask any decreases in concentration. Following elevation of PE levels, however, a reduction can be demonstrated following administration of NSD 1015. By administering a non-selective dose (75 mg kg^{-1}, i.p.) of the mixed MAO inhibitor pargyline, an elevation of both dopamine and PE levels in the striatum can be obtained (Table 1). Under these conditions, NSD 1015 (10 mg kg^{-1}, i.p.) caused a decrease in the levels of PE but not dopamine (Table 1). Although AADC is involved in the synthesis of both PE and dopamine, it is only rate limiting for PE synthesis (Brodie *et al.*, 1962). For dopamine synthesis the rate limiting step involves the enzyme tyrosine hydroxylase, AADC appearing to be present in a large excess. Therefore, following 10 mg kg^{-1} NSD 1015, which gives around 50% inhibition of AADC (Figure 6), the large excess of AADC will result in dopamine synthesis not being compromised. In contrast, AADC is the sole enzyme required for PE synthesis and as such, a 50% inhibition of activity will result in a marked reduction in PE levels.

In conclusion, these results demonstrate that rat striatal neurone responses to dopamine are potentiated by MAO-B inhibitors at doses which selectively elevate PE levels. Further, this is reversed by NSD 1015 at a dose which selectively decreases elevated PE levels. These results are in agreement with the hypothesis that PE can act as a neuromodulator of dopaminergic functioning, and that inhibition of MAO-B results in a potentiation of neuronal responses due to an elevation of endogenous PE levels (Paterson *et al.*, 1990). Further, these results suggest that endogenous PE is normally present in sufficient quantities to modulate dopaminergic responses following mild MAO-B inhibition. These results are in agreement with the suggestion that acute treatment with (−)-deprenyl leads to an increase in the sensitivity of neurones to dopaminergic responses (Knoll, 1983), without altering the firing rate of nigro-striatal neurones (Knoll, 1983; Engberg *et al.*, 1991). It is interesting to note that recent results have demonstrated that chronic administration of (−)-deprenyl or PE causes a down-regulation of D_1 receptors, with a trend for a similar decrease in D_2 receptors (Paetsch & Greenshaw, 1993). Further, the effects of (−)-deprenyl and PE were additive, suggesting a common mechanism (Paetsch & Greenshaw, 1993). Such an effect following chronic administration would be expected from the results presented here, where acute elevation of PE levels results in an increased responsiveness to dopamine. The mechanism by which PE exerts this action is at present unknown, although it probably involves a regulation of dopamine receptors. A receptor site was previously described for PE (Hauger *et al.*, 1982), although it now appears that this site is in fact MAO-B (Li *et al.*, 1992). Studies aimed at elucidating the mechanism of interaction between PE and dopamine are currently in progress.

While the data presented here are consistent with the responses being mediated via changes in PE levels, it cannot be ruled out that the changes in neuronal sensitivity observed could reflect changes in local dopamine concentrations. Thus, although whole tissue levels of dopamine are not altered, MDL 72,145, Ro 19-6327 and NSD 1015 may result in changes in dopamine concentration in individual cellular compartments. Further, these treatments may also have resulted in changes in striatal levels of 'trace' amines other than PE, such as tyramine, which may have contributed to the observed effects. All of these other amines, however, are metabolized to a significant degree by MAO-A, unlike PE which appears to be a very selective substrate for MAO-B. Since the observed effects appeared maximal at MAO-B selective doses, we believe that the responses observed are most probably due to changes in striatal PE concentrations.

Although this has been demonstrated only in the rat, it is likely that a similar situation also applies in man, where PE is present in similar concentrations to those found in the rat (Philips *et al.*, 1978). As such, an elevation of PE following MAO-B inhibition may contribute to the beneficial effects of MAO-B inhibitors observed in various disorders, such as Parkinson's disease.

The authors would like to thank L. Evered-Epp, E.P. Zarycki, M, Lang and S. Ambrose for their technical assistance, Dr B.A. Davis for synthesis of deuterated 2-phenylethylamine, Dr D.A. Durden for supervision of mass spectrometric analyses and Dr A.A. Boulton for helpful discussions. At the time of writing, M.-Y.Z. was the recipient of the Laura Chapman Award and a Schizophrenia Society of Saskatchewan Scholarship and M.D.B. the recipient of a University of Saskatchewan Scholarship. E. S. was supported by a grant from the National Sciences and Engineering Research Council of Canada. We would also like to thank Saskatchewan Health, Saskatchewan Health Research Board, Deprenyl Research Ltd., Toronto and The Medical Research Council of Canada for their financial support.

References

AZZARO, A.J., KING, J., KOTZUK, J., SCHOEPP, D.D., FROST, J. & SCHOCHET, S. (1985). Guinea-pig striatum as a model of human dopamine deamination: the role of monoamine oxidase isozyme ratio, localisation and affinity for substrate in synaptic dopamine metabolism. *J. Neurochem.*, **45**, 949–956.

BARTHOLINI, G. & PLETSCHER, A. (1969). Effects of various decarboxylase inhibitors on the cerebral metabolism of dihydroxyphenylalanine. *J. Pharm. Pharmacol.*, **21**, 323–324.

BEY, P., FOZARD, J., MCDONALD, I., PALFREYMAN, M.G. & ZREIKA, M. (1984). MDL 72145: a potent and selective inhibitor of MAO type B. *Br. J. Pharmacol.*, **81**, 50P.

BIRKMAYER, W., RIEDERER, P., YOUDIM, M.B.H. & LINAUER, W. (1975). The potentiation of the anti-akinetic effect after l-dopa treatment by an inhibitor of MAO-B, deprenyl. *J. Neural. Transm.*, **36**, 303–326.

BRODIE, B.B., KUNTZMAN, R., HIRCH, C.W. & COSTA, E. (1962). Effects of decarboxylase inhibition on the biosynthesis of brain monoamines. *Life Sci.*, **1**, 81–84.

BUTCHER, S.P., FAIRBROTHER, I.S., KELLY, J.S. & ARBUTHNOTT, G.W. (1990). Effects of selective monoamine oxidase inhibitors on the in vivo release and metabolism of dopamine in the rat striatum. *J. Neurochem.*, **55**, 981–988.

DA PRADA, M., KETTLER, R., KETTLER, H.H., KYBURZ, E. & BURKARD, W.P. (1987). Ro 19-6327: a novel highly selective and reversible MAO-B inhibitor. *Pharmacol. Toxicol.*, **60** Suppl 1, 10.

DE MONTIGNY, C. & AGHAJANIAN, G.K. (1977). Preferential action of 5-methoxytryptamine and 5-methoxydimethyltryptamine on presynaptic serotonin receptors: A comparative iontophoretic study with LSD and 5-HT. *Neuropharmacol.*, **16**, 811–818.

DURDEN, D.A., PHILIPS, S.R. & BOULTON, A.A. (1973). Identification and distribution of β-phenylethylamine in the rat. *Can. J. Biochem.*, **51**, 995–1002.

ENGBERG, G., ELEBRING, T. & NISSBRANDT, H. (1991). Deprenyl (selegiline), a selective MAO-B inhibitor with active metabolites; effects on locomotar activity, dopaminergic neurotransmission and firing rate of nigral dopamine neurones. *J. Pharmacol. Exp. Ther.*, **259**, 841–847.

GREENSHAW, A.J., JUORIO, A.V. & NGUYEN, T.V. (1986). Depletion of striatal β-phenylethylamine following dopamine but not 5-HT denervation. *Brain Res. Bull.*, **17**, 477–484.

HAUGER, R.L., SKOLNICK, P. & PAUL, S.M. (1982). Specific [^{3}H]β-phenylethylamine binding sites in rat brain. *Eur. J. Pharmacol.*, **83**, 147–148.

HEINONEN, E.H. & LAMMINTAUSTA, R. (1991). A review of the pharmacology of selegiline. *Acta Neurol. Scand.*, **84** Suppl. 136, 44–59.

HOLZ, R.W. & COYLE, J.T. (1974). The effects of various salts, temperature and the alkaloids veratridine and batrachotoxin on the uptake of [^{3}H]dopamine into synaptosomes from rat striatum. *Mol. Pharmacol.*, **10**, 746–758.

HOVEVEY-SION, D., KOPIN, I.J., STULL, R.W. & GOLDSTEIN, D.S. (1989). Effects of monoamine oxidase inhibitors on levels of catechols and homovanillic acid in striatum and plasma. *Neuropharmacol.*, **28,** 791–797.

IVERSEN, L.L. (1974). Uptake mechanisms for neurotransmitter amines. *Biochem. Pharmacol.*, **23,** 1927–1935.

JUORIO, A.V., GREENSHAW, A.J., ZHU, M.-Y. & PATERSON, I.A. (1991). The effects of some neuroleptics and *d*-amphetamine on striatal 2-phenylethylamine levels in the mouse. *Gen. Pharmacol.*, **22,** 407–413.

JUORIO, A.V. & KAZAKOFF, C.W. (1984). The presence of β-phenylethylamine, *p*—tyramine, *m*-tyramine and tryptamine in ganglia and foot muscle in the garden snail (*Helix aspersa*). *Experentia*, **40,** 549–551.

KNOLL, J. (1983). Deprenyl (selegiline): the history of its development and pharmacological action. *Acta Neurol. Scand.*, Suppl. 95, 57–80.

KNOLL, J. & MAGYAR, K. (1972). Some puzzling pharmacological effects of monoamine oxidase inhibitors. In *Monoamine Oxidases-New Vistas.* ed. Costa, E. & Sandler, M. pp. 393–408. New York: Raven Press.

KWOK, R.P.S. & JUORIO, A.V. (1986). The concentration of striatal tyramine and dopamine metabolism in diabetic rats and the effect of insulin administration. *Neuroendocrinology*, **43,** 590–596.

LI, X.-M., JUORIO, A.V., PATERSON, I.A. & BOULTON, A.A. (1992). Absence of 2-phenylethylamine binding after monoamine oxidase inhibition in rat brain. *Eur. J. Pharmacol.*, **210,** 189–193.

LOWRY, O.H., ROSEBROUGH, N.J., FARR, A.L. & RANDALL, R.J. (1951). Protein measurement with the folin phenol reagent. *J. Biol. Chem.*, **193,** 265–271.

PAETSCH, P.R. & GREENSHAW, A.J. (1993). Down-regulation of β-adrenergic and dopaminergic receptors induced by 2-phenylethylamine. *Cell Mol. Neurobiol.*, **13,** 203–216.

PATERSON, I.A., JUORIO, A.V., BERRY, M.D. & ZHU, M.-Y. (1991). Inhibition of monoamine oxidase-B by (−)deprenyl potentiates neuronal responses to dopamine agonists but does not inhibit dopamine catabolism in the rat striatum. *J. Pharmacol. Exp. Ther.*, **258,** 1019–1026.

PATERSON, I.A., JUORIO, A.V. & BOULTON, A.A. (1990). 2-Phenylethylamine: a modulator of catecholamine transmission in the mammalian central nervous system? *J. Neurochem.*, **55,** 1827–1837.

PAXINOS, G. & WATSON, C. (1986). *The Rat Brain in Stereotaxic Co-ordinates* (2nd ed.). Toronto: Academic Press.

PHILIPS, S.R. & BOULTON, A.A. (1979). The effect of monoamine oxidase inhibitors on some arylalkylamines in the rat striatum. *J. Neurochem.*, **33,** 159–167.

PHILIPS, S.R., ROZDILSKY, B. & BOULTON, A.A. (1978). Evidence for the presence m-tyramine, p-tyramine, tryptamine and phenylethylamine in the rat brain and several areas of the human brain. *Biol. Psychiat.*, **13,** 51–57.

TETRUD, J.W. & LANGSTON, J.W. (1989). The effect of deprenyl (selegiline) on the natural history of Parkinson's Disease. *Science*, **245,** 519–522.

WESTLUND, K.N., DENNEY, R.M., ROSE, R.M. & ABELL, C.W. (1988). Localization of distinct monoamine oxidase A and monoamine oxidase B cell populations in human brainstem. *Neurosci.*, **25,** 439–456.

WURTMAN, R.J. & AXELROD, J. (1963). A sensitive and specific assay for the estimation of monoamine oxidase. *Biochem. Pharmacol.*, **12,** 1439–1441.

YANG, H.-Y.T. & NEFF, N.H. (1973). β-Phenylethylamine: a specific substrate for type B monoamine oxidase of brain. *J. Pharmacol. Exp. Ther.*, **187,** 365–371.

ZHU, M.-Y., JUORIO, A.V., PATERSON, I.A. & BOULTON, A.A. (1992). Regulation of aromatic L-amino acid decarboxylase by dopamine receptors in the rat brain. *J. Neurochem.*, **58,** 636–641.

(Recevied July 21, 1993
Revised July 25, 1994
Accepted July 27, 1994)

Br. J. Pharmacol. (1994), **113**, 1167-1172 © Macmillan Press Ltd, 1994

Attenuation of the antiarrhythmic effects of ischaemic preconditioning by blockade of bradykinin B_2 receptors

Agnes Vegh, Julius Gy Papp & [1]*James Parratt

Department of Pharmacology, Albert Szent-Gyorgyi Medical University, Dom ter 12, Szeged, Hungary and *Department of Physiology and Pharmacology, University of Strathclyde, Glasgow G1 1XW

1 The possibility that bradykinin is involved in the pronounced antiarrhythmic effects of ischaemic preconditioning in anaesthetized mongrel dogs was examined with the use of the selective B_2 antagonist, icatibant (Hoe-140).

2 Preconditioning, achieved by two 5 min occlusions of the left anterior descending coronary artery, followed 20 min later by a 25 min occlusion of the same artery resulted, during this prolonged occlusion, in less severe arrhythmias (VF 0% versus 47% in control non-preconditioned dogs), reductions in the incidence and number of episodes of ventricular tachycardia (VT) and in the number of ventricular premature beats and increased survival following reperfusion (50% versus 0% in the controls).

3 Hoe-140 was given in a dose of 300 $\mu g\,kg^{-1}$ either before the preconditioning procedure or after preconditioning but before the prolonged occlusion. This dose of Hoe-140 had insignificant haemodynamic effects and failed to modify the increase in coronary blood flow that occurred in the circumflex coronary artery when the anterior descending branch was occluded.

4 It was difficult to precondition dogs in the presence of Hoe-140. There were more ventricular arrhythmias during the initial 5 min occlusion (44 ± 12 versus 10 ± 3) and a higher incidence of ventricular fibrillation (50% versus 21%) during the preconditioning procedure. There was also a more pronounced ST-elevation (recorded from epicardial electrodes) during the preconditioning occlusions in those dogs given Hoe-140.

5 In those dogs that survived to the long (25 min) occlusion, Hoe-140 prevented the antiarrhythmic effects of preconditioning (reduction in ventricular premature beats and in VT) although all the dogs survived the occlusion period. However on reperfusion, survival in the preconditioned dogs given Hoe-140 was less than in those dogs preconditioned without the B_2 antagonist.

6 Changes in the degree of inhomogeneity of conduction within the ischaemic area, which were markedly suppressed by preconditioning, were attenuated in those dogs preconditioned in the presence of Hoe-140.

7 These results suggest that bradykinin acts as both a 'trigger' for preconditioning and as one of the mediator protective (antiarrhythmic) substances generated by the myocardium under these conditions. Since the protection afforded both by preconditioning and by local intracoronary infusions of bradykinin is markedly attenuated by an inhibitor of the L-arginine nitric oxide pathway, we suggest that much of the protection afforded by ischaemic preconditioning results from the generation of nitric oxide, and that bradykinin, released early during ischaemia, acts as a stimulant for this generation.

Keywords: Ischaemic preconditioning; ventricular arrhythmias; bradykinin; Hoe-140 (icatibant); nitric oxide

Introduction

Apart from the reduction in myocardial ischaemic damage (Murry *et al.*, 1986), one of the most pronounced consequences of ischaemic preconditioning is a marked reduction in the severity of those ventricular arrhythmias that occur soon (i.e. minutes) after coronary artery occlusion (Vegh *et al.*, 1990; 1992a; Lawson *et al.*, 1993a,b; Piacentini *et al.*, 1993; Parratt & Vegh, 1994) and reperfusion. Particularly impressive in the canine model is the complete abolition of ventricular fibrillation and a marked reduction in the incidence and number of episodes of ventricular tachycardia (Vegh *et al.*, 1992a). The most likely mechanisms of this protection, recently reviewed by Lawson & Downey (1993) and by Parratt (1994a) would appear to be a reduction in the severity of ischaemia and its metabolic consequences, a reduction in the release of substances such as noradrenaline which induce arrhythmias under ischaemic conditions, and the production of some endogenous myocardial protective substance.

We have recently suggested that nitric oxide plays an important role in the antiarrhythmic effects of preconditioning, at least in dogs. The evidence for this is the marked attenuation of this protection by an inhibitor of the L-arginine nitric oxide pathway (Vegh *et al.*, 1992b) and by methylene blue (Vegh *et al.*, 1992c), which is both an inhibitor of the pathway and of soluble guanylyl cyclase. Because bradykinin is antiarrhythmic in this model (Vegh *et al.*, 1991), an effect which, since it is prevented by an inhibitor of the L-arginine nitric oxide pathway is presumably mediated by nitric oxide (NO) release (Vegh *et al.*, 1993), we investigated whether bradykinin might be the trigger for the generation of nitric oxide under conditions of ischaemic preconditioning. We have therefore examined whether an antagonist of bradykinin B_2 receptors, activation of which is responsible for the release of prostacyclin and the generation of nitric oxide by bradykinin (Hecker *et al.*, 1992), modifies the antiarrhythmic effects of ischaemic preconditioning in anaesthetized open-chest mongrel dogs. A preliminary account of these results was presented at the joint meeting of the Italian and British Pharmacological Societies in Rome (Vegh *et al.*, 1994a).

Methods

These were similar to those already described in detail (Vegh *et al.*, 1992a,b). In brief, we used mongrel dogs, of either sex,

[1] Author for correspondence.

with a body weight in excess of 17 kg (mean 26.6 ± 2.4 kg). They were anaesthetized with a mixture of chloralose and urethane (60 and 200 mg kg^{-1}, i.v. respectively), and ventilated with room air using a Harvard Respirator at a rate and volume sufficient to maintain arterial blood gases and pH within normal limits (Vegh *et al.*, 1992a). The animals were thoracotomised at the fifth intercostal space and the anterior descending branch of the left coronary artery (LAD) was prepared for occlusion just proximal to the first main diagonal branch. This gives an area at risk, as assessed by infusing patent blue V dye into the occluded artery at the end of the experiment, of between 34 and 42%.

Blood flow was measured on both the LAD (Doppler flow probe; Triton, U.S.A.) and left circumflex (LCX) coronary arteries (2.0 mm electromagnetic flow probe and a Statham SP 2202 flow meter). Epicardial ST-segment changes and the degree of inhomogeneity of electrical activation were measured from the left ventricular wall distal to the occlusion site using a 'composite' electrode described previously (Williams *et al.*, 1974; Vegh *et al.*, 1987; 1992a). This gives a summarised recording of R-waves from 30 epicardial measuring points. In the adequately perfused and oxygenated myocardium all sites are activated simultaneously, resulting in a single large spike. However, following occlusion, widening and fractionation of the summarized R-waves occurs indicating that adjacent fibres are not simultaneously activated because of inhomogeneity of conduction. We expressed this as the greatest delay in activation (ms) within the ischaemic area. This reflects, in part, local changes in myocardial blood flow.

All these parameters, together with a limb lead electrocardiogram, systemic arterial and left ventricular (LV) systolic (S) and end-diastolic (ED) pressures (Statham P23 Dp transducers) and LV$dP/dt$ were recorded on an eight channel Medicor R81 recorder.

Ventricular arrhythmias during ischaemia and reperfusion were assessed and analysed as outlined previously (Vegh *et al.*, 1992a) i.e. total ventricular premature beats (VPBs), the incidence and number of episodes of ventricular tachycardia (VT) and the incidence of ventricular fibrillation (VF). All the data were analysed statistically as previously described (Vegh *et al.*, 1992a) i.e. data are expressed as means (± s.e.mean) and differences between means were compared by a Student's t test corrected for multiple comparisons or, for arrhythmias, by the Mann-Whitney U-test. For comparison of the incidences of arrhythmias the chi-squared test for independence in a 2 × 2 table was used. Differences between groups was considered significant when $P<0.05$.

Although these experiments were carried out in Szeged the protocol complied with U.K. Home Office regulations (Project Licence No. 60/00307).

There were four groups of animals. Some dogs were preconditioned as previously described (Vegh *et al.*, 1992a) by occluding the LAD for two 5 min periods, with a 20 min reperfusion period between. Twenty min later, in fourteen of these dogs, the artery was reoccluded at the same site for 25 min and the ventricular arrhythmias assessed during this period; the myocardium was then reperfused by re-opening the occlusion. The second group of dogs ($n = 20$) were control animals which were subjected only to a 25 min coronary artery occlusion i.e. without preconditioning. Two other separate groups of dogs were preconditioned as described above but, in addition, received the bradykinin B_2 antagonist, Hoe-140 (icatibant; Wirth *et al.*, 1991), in a dose (300 μg kg^{-1}, i.v.) chosen on the basis of unpublished studies from this laboratory in conscious dogs and which blocks the vasodepressor responses to injected bradykinin in doses of up to 10 μg kg^{-1} for a period of between 30 and 60 min. Icatibant was given either 10 min prior to the first preconditioning occlusion ($n = 10$) or after preconditioning but 10 min prior to the long (25 min) occlusion ($n = 10$).

Results

Haemodynamic effects of coronary artery occlusion and of icatibant

The haemodynamic effects of coronary artery occlusion are summarised in Table 1. There was a transient decrease in mean arterial pressure, an increase in LVEDP and reductions in both positive and negative LV$dP/dt$. These changes were not significantly modified by the prior administration of the B_2 antagonist, Hoe-140.

When the LAD is occluded there is invariably a compensatory increase in blood flow in the LCX coronary artery. This too was unchanged by icatibant (Figure 1). The only significant haemodynamic effect of icatibant itself was a slight reduction in mean arterial pressure (Table 1), which was slightly greater in those dogs which had been subjected to the preconditioning procedure (i.e. from 114 ± 12 to 104 ± 10 mmHg, $P<0.05$).

Ventricular arrhythmias during the initial preconditioning coronary artery occlusions and the effects of the prior administration of icatibant

In normal dogs there are relatively few ventricular premature beats during a 5 min coronary artery occlusion. For example, in a total of 29 dogs subjected to preconditioning, including those used in the present study, there were less than a mean of 10 VPBs over the entire 5 min occlusion period. There was little difference between the number of VPBs during the first and second preconditioning occlusions (Figure 2). However, 6 out of 29 dogs fibrillated during reperfusion following the first occlusion (21%). Those dogs that were given icatibant

Table 1 Haemodynamic effects of Hoe-140 (0.3 mg kg^{-1}, i.v.) and of the subsequent occlusion of the LAD coronary artery (first preconditioning occlusion)

	Pre Hoe-140	*Hoe-140*	Δ	*Pre-occlusion*	*5 min post-occlusion*	Δ
Arterial blood pressure (systolic; mmHg)	152 ± 10	145 ± 1	−7 ± 3	155 ± 10	146 ± 11	−9 ± 2
Arterial blood pressure (diastolic: mmHg)	103 ± 7	97 ± 7	−6 ± 3	102 ± 7	96 ± 7	−6 ± 4
Arterial blood pressure (mean; mmHg)	119 ± 8	113 ± 9	−6 ± 2	119 ± 8	114 ± 8	−5 ± 3
LV systolic pressure (mmHg)	165 ± 11	159 ± 12	−6 ± 4	169 ± 11	156 ± 12	−12 ± 2
LVEDP (mmHg)	7 ± 0.8	8 ± 0.8	1 ± 0.6	8 ± 0.8	28 ± 0.9	20 ± 0.8*
Heart rate (beats min^{-1})	166 ± 6	164 ± 7	−2 ± 2	165 ± 7	170 ± 8	5 ± 1
LV$dP/dt_{max}$ (+ve; mmHg min^{-1})	2962 ± 200	2791 ± 206	−126 ± 97	3088 ± 253	2324 ± 208	−632 ± 129*
LV$dP/dt_{max}$ (−ve; mmHg min^{-1})	2470 ± 185	2726 ± 188	256 ± 108	2724 ± 188	2168 ± 181	−557 ± 65*

*$P<0.05$; $n = 10$–12.

were much more difficult to precondition. There was an increased number of VPBs during the initial occlusion (44 ± 12; Figure 2) and a higher incidence of VF both during the initial occlusion and following reperfusion (50%). In each case VF was preceded by a brief period of VT. In those dogs that survived the initial occlusion in the presence of icatibant, the changes induced by a second occlusion were similar to those in control preconditioned dogs (Figure 2).

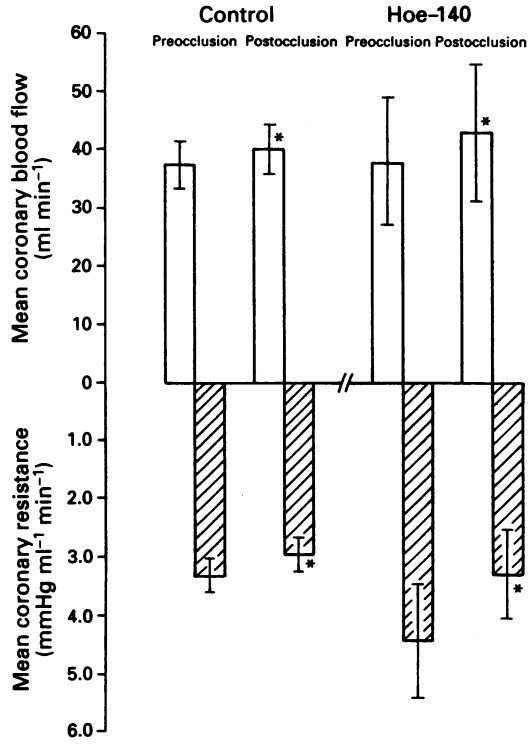


Figure 1 Changes in mean coronary blood flow and in coronary resistance in the left circumflex coronary artery which occur when the left anterior descending branch of that same artery is occluded for 5 min. Under control conditions there is a compensatory vasodilatation (increase in flow; decrease in resistance) which, since it is unaffected by Hoe-140, is unlikely to be due to the release of bradykinin.

Changes induced by icatibant on the antiarrhythmic effects of ischaemic preconditioning, on the degree of inhomogeneity of conduction within the ischaemic area and on the epicardial electrocardiogram

As we have shown previously (e.g. Vegh *et al.*, 1992a) ischaemic preconditioning markedly decreased the severity of the early, ischaemia-induced ventricular arrhythmias that results from coronary artery occlusion in this species. This is illustrated in Figure 3. Preconditioning markedly reduced the number of VPBs, and the incidence and duration of VT during the 25 min occlusion period. Ventricular fibrillation was reduced from 47% in control dogs to 0% in those subjected to the preconditioning protocol ($P<0.05$) and 7/14 of these dogs survived reperfusion at 25 min. Those dogs that survived reperfusion had significantly fewer VPBs during the 25 min occlusion (20 ± 4) than those that did not (109 ± 27; $P<0.05$). This protection was markedly attenuated by icatibant both when given prior to the preconditioning protocol and when given after preconditioning but before the

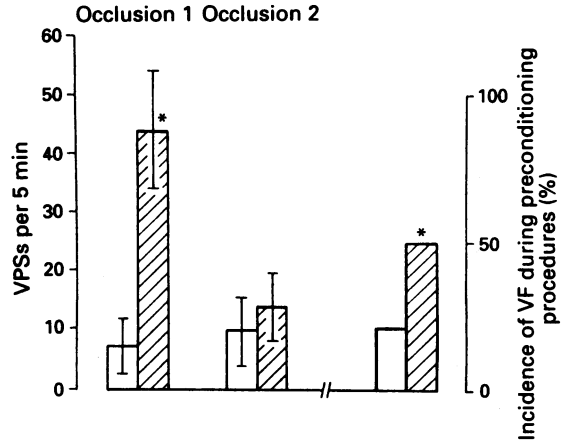


Figure 2 Ventricular premature beats during the two 5 min preconditioning coronary artery occlusion periods in dogs in the absence (open columns, $n = 29$) and presence (hatched columns, $n = 12$) of the bradykinin B_2 antagonist, Hoe-140. On the right is shown the incidence of ventricular fibrillation which occurred during this preconditioning procedure in the two groups of dogs.

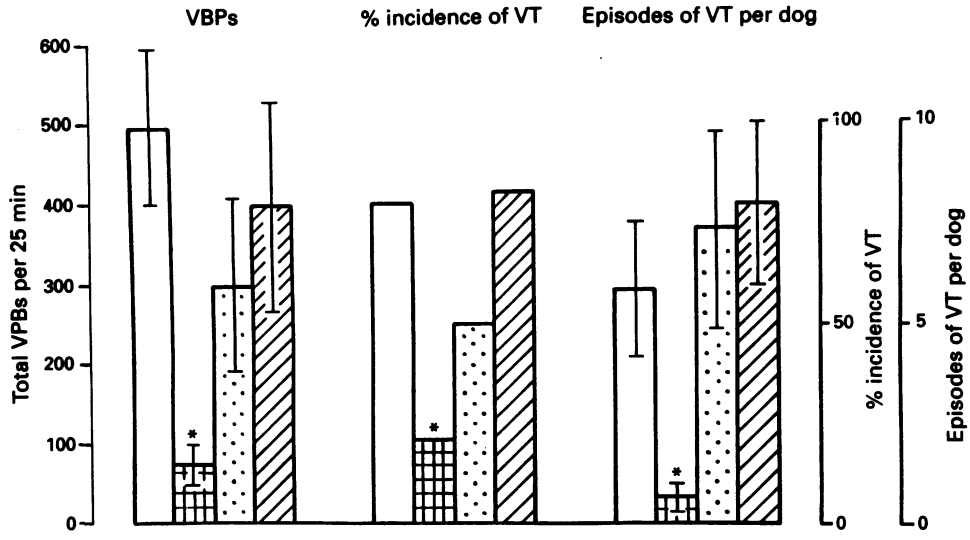


Figure 3 The number of ventricular premature beats (VPBs), the incidence of ventricular tachycardia (VT) and the number of episodes of ventricular tachycardia which occurred during a 25 min occlusion of the left anterior descending coronary artery in control dogs (open columns, $n = 20$) and in preconditioned dogs (cross hatched columns, $n = 14$) in the absence, or presence, of the bradykinin B_2 antagonist Hoe-140. Hoe-140 was given either *before* the preconditioning procedures (hatched columns, $n = 6$) or *after* preconditioning but prior to the prolonged (25 min) occlusion (stippled columns, $n = 8$).

prolonged occlusion (Figure 3). Further, survival from the combined ischaemia/reperfusion insult was reduced, especially when icatibant was given before the start of the preconditioning protocol. This is illustrated in Figure 4.

Under conditions of myocardial ischaemia there is a marked inhomogeneity of conduction within the area supplied by the occluded vessel. This is greatly attenuated during the entire 25 min occlusion period in dogs that have been preconditioned (Figure 5). However, this inhomogeneity was markedly increased in those dogs given icatibant either before the preconditioning protocol or after the preconditioning protocol but before the prolonged occlusion. This too is illustrated in Figure 5. Because the local intracoronary infusion of bradykinin also reduces the degree of inhomogeneity of conduction during ischaemia (Vegh *et al.*, 1991), we presume that this is due to the blockade of endogenous bradykinin.

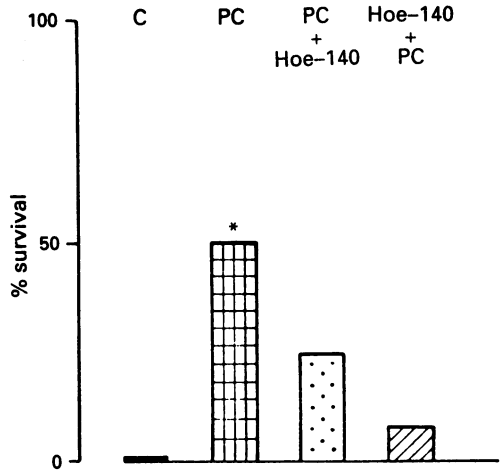


Figure 4 Survival from a combined 25 min occlusion period followed by reperfusion in control dogs (C) and in dogs subjected to preconditioning (PC) in the absence or presence of Hoe-140 given either before preconditioning (Hoe-140 + PC) or after preconditioning (PC + Hoe-140). The marked increase in survival from the combined ischaemia-reperfusion insult following preconditioning is attenuated by Hoe-140.

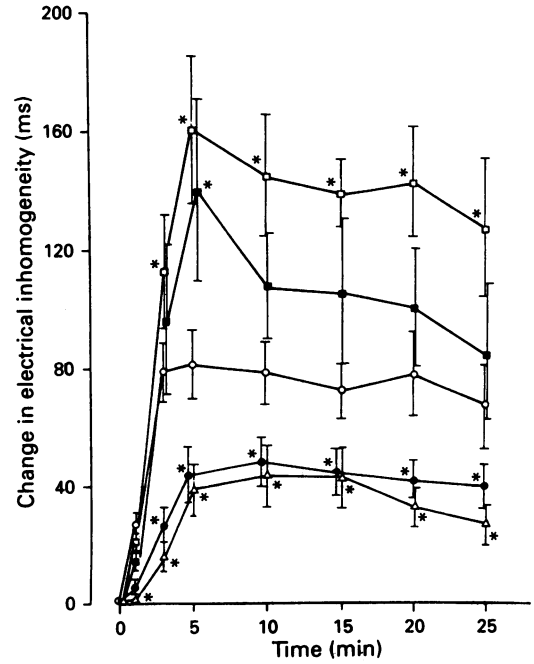


Figure 5 Changes in the inhomogeneity of activation in the ischaemic area during a 25 min coronary artery occlusion in control dogs (○), in dogs administered bradykinin by intracoronary infusion (●), in preconditioned dogs (△) and in preconditioned dogs in the presence of the bradykinin B_2 antagonist Hoe-140: (□) Hoe-140 after preconditioning; (■) Hoe-140 before preconditioning. The bradykinin results are taken from Vegh *et al.* (1991).

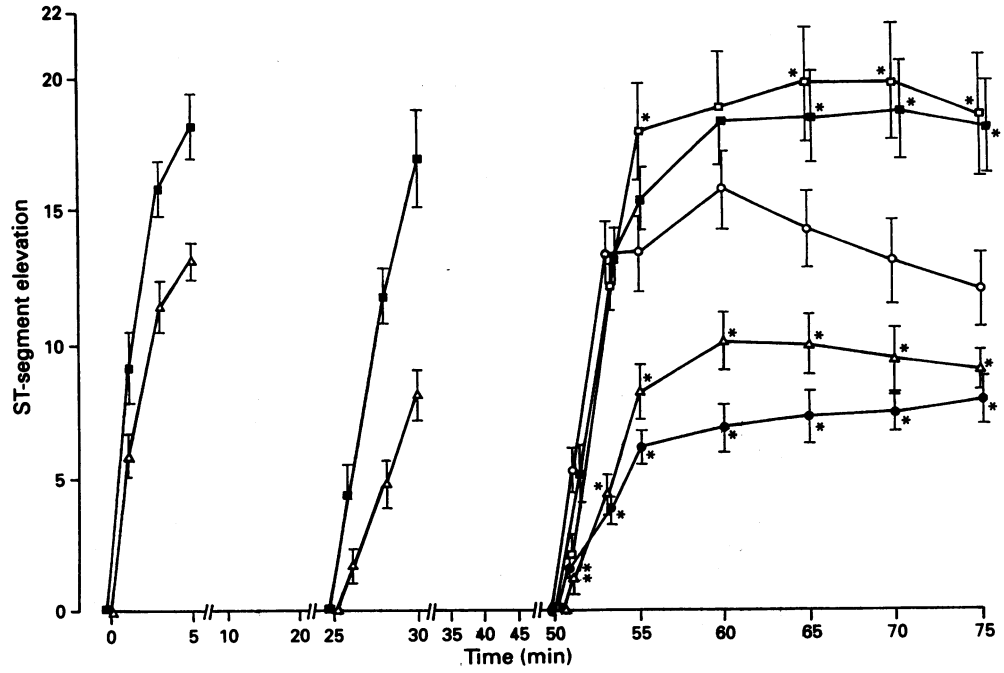


Figure 6 Changes in ST-segment elevation, recorded from epicardial electrodes, during the two 5 min preconditioning coronary artery occlusions and during the subsequent prolonged (25 min) occlusion of that same artery. ST-segment elevation following preconditioning during the prolonged occlusion is markedly reduced (△) compared with control, non-preconditioned dogs (○). This reduction in this particular index of ischaemia is attenuated by the administration of Hoe-140 (300 $\mu g\ kg^{-1}$, i.v.) either before the preconditioning procedure (■) or after preconditioning but before the prolonged occlusion (□). Also included in the figure are results obtained following the local intracoronary administration of bradykinin (●), data obtained from Vegh *et al.* (1991).

Coronary artery occlusion leads to ST-segment elevation, as recorded from epicardial electrodes. This is less pronounced during a subsequent occlusion (Figure 6) and during a local intracoronary infusion of bradykinin (Vegh *et al.*, 1991). However, following icatibant administration, ST-segment elevation was significantly greater both during the two brief (5 min) preconditioning occlusions and during the prolonged (25 min) occlusion. This is also illustrated in Figure 6.

Discussion

The results from our previous studies using a similar experimental model (Vegh *et al.*, 1992b,c) suggested that the generation of nitric oxide is involved in the pronounced antiarrhythmic effects of ischaemic preconditioning in the canine. The present experiments were designed to explore the possibility that one stimulus for NO generation under these conditions might be bradykinin. The evidence that bradykinin should be considered as an endogenous myocardial protective substance has been recently reviewed (Parratt, 1993). This evidence includes: (a) its rapid generation under conditions of myocardial ischaemia; (b) that various indices of the severity of ischaemia are reduced by bradykinin and (c) that locally infused bradykinin, in doses too small to influence coronary blood flow, exerts a profound antiarrhythmic effect against the early, life-threatening ventricular arrhythmias that result from coronary artery occlusion. Since this antiarrhythmic effect of locally infused bradykinin is prevented by an inhibitor of the L-arginine nitric oxide pathway (Vegh *et al.*, 1993) it seemed at least possible that bradykinin 'triggers' the release of nitric oxide during ischaemic preconditioning. With the availability of a selective and potent antagonist at the relevant (B_2) bradykinin receptor we were able to investigate this possibility and the present results strongly suggest a primary role for bradykinin in mediating this protection. The evidence is that the reduction in arrhythmia severity and in the degree of inhomogeneity of conduction within the ischaemic area resulting from ischaemic preconditioning are both attenuated following blockade of B_2 bradykinin receptors, whether this achieved before or after the preconditioning procedures.

The effects of the initial preconditioning coronary artery occlusion were more marked if bradykinin B_2 receptors had first been blocked; ST-segment changes were accentuated (Figure 6) and arrhythmia severity was markedly increased (Figure 2). This suggests that bradykinin is generated during very short periods of ischaemia and has a protective role. Although it was not possible to sample coronary sinus blood in these particular experiments we do have data, from patients with coronary artery disease undergoing coronary angioplasty, that bradykinin levels in coronary sinus blood are elevated by up to 50 times during a 1 min balloon inflation (Oldroyd, Cobbe, Koide, Parratt and Zeitlin, unpublished observations), suggesting that this generation is extremely rapid. These levels are of a similar order of magnitude to those required to reduce arrhythmia severity during ischaemia when infused locally into a branch of the LAD coronary artery in anaesthetized dogs (Vegh *et al.*, 1991). We do not know how the rapid generation of bradykinin occurs but the precursor (kininogen) is present in or on the surface of vascular endothelial cells (Busse & Lamontagne, 1991) and we have described an acid-optimum kinin forming enzyme in the coronary vessels which can generate bradykinin from human kininogen (Zeitlin *et al.*, 1989) and which is depleted following ischaemia (Koide *et al.*, 1993).

These studies were designed to examine whether bradykinin acted as the 'trigger' for ischaemic preconditioning i.e. that it was released during the preconditioning period with the possibility that other protective mediators, such as nitric oxide and prostacyclin, might then be released as mediators of the protection afforded by preconditioning when the same coronary artery was occluded some time later. The present experiments show that whether icatibant is given before the preconditioning protocol or after it, the protection afforded by preconditioning was attenuated (e.g. Figures 3, 4, 5 and 6). This would suggest that bradykinin is both the 'trigger' and also one of the mediators of preconditioning, together with nitric oxide and prostacyclin. These results with a bradykinin B_2 antagonist are therefore quite different from those obtained with the non-selective adenosine receptor blocking agent 8-sulphophenyltheophylline (8-SPT) (Vegh *et al.*, 1994b). In the studies with 8-SPT, the severity of arrhythmias during the initial preconditioning occlusion, like those following the administration of icatibant, were much more severe than in dogs preconditioned in the absence of the drug. However, the protection afforded by preconditioning itself was not modified by 8-SPT whereas it clearly was with icatibant. This suggests that whereas both adenosine and bradykinin are potential endogenous myocardial protective (antiarrhythmic) agents (Parratt, 1993) it is only bradykinin that takes part in the protection afforded by ischaemic preconditioning. It would seem then that although the myocardium is able to generate a variety of potentially antiarrhythmic substances under conditions of ischaemia (including adenosine, bradykinin, nitric oxide and prostacyclin) it is only bradykinin, and the mediators released by it (nitric oxide, prostacyclin) that takes part in the protection afforded by ischaemic preconditioning, at least with regard to protection afforded against life-threatening ischaemia-induced ventricular arrhythmias.

As yet, we have no direct evidence that any of these potential mediators are released in increased amounts following a preconditioning protocol. Neither have we any clear explanation as to why the generation of nitric oxide, presumably from endothelial cells, results in such a marked attenuation of arrhythmia severity. One possibility might be through elevation of guanosine 3':5'-cyclic monophosphate (cyclic GMP) levels. This might influence arrhythmogenesis in several ways. First, nitric oxide depresses myocardial contractility (Brady *et al.*, 1992) which would improve the myocardial oxygen supply demand ratio and hence lead to 'energy sparing', which is a significant feature of preconditioning (Vander Heide *et al.*, 1993). Second, elevation of cyclic GMP inhibits calcium influx through L-type channels in the sarcolemma (Tohse & Sperelakis, 1991). Third, stimulation of a cyclic-GMP dependent cyclic-AMP phosphodiesterase should lead to a decrease in myocardial cyclic AMP levels, which would also result following direct stimulation of bradykinin B_2 receptors (Parratt, 1994a).

In conclusion, we would like to emphasize that these studies relate only to a possible mechanism of ischaemic preconditioning in reducing the severity of ventricular arrhythmias in one particular animal model. We cannot draw the conclusion that bradykinin is a 'universal trigger' for ischaemic preconditioning, although there is experimental evidence that inhibition of bradykinin breakdown with inhibitors of angiotensin converting enzyme has cardioprotective effects on the myocardium including suppression of ventricular arrhythmias (Parratt, 1994b). This may well have clinical implications.

This work was supported by grants from the Wellcome Trust, the British Council (in collaboration with the Hungarian National Committee for Technical Development) and the Hungarian State Government (OTKA). We are grateful to Professor Bernward Scholkens for a generous supply of icatibant.

References

BRADY, A.J.B., POOLE-WILSON, P.A., HARDING, S.E. & WARREN, J.B. (1992). Nitric oxide production within cardiac myocytes reduces their contractility in endotoxemia. *Am. J. Physiol.*, **263**, H1963–H1966.

BUSSE, R. & LAMONTAGNE, D. (1991). Endothelium-derived bradykinin is responsible for the increase in calcium produced by angiotensin-converting enzyme inhibitors in human endothelial cells. *Naunyn Schmeid. Arch. Pharmacol.*, **344**, 126–129.

HECKER, M., DAMBACHER, T. & BUSSE, R. (1992). Role of endothelium-derived bradykinin in the control of vascular tone. *J. Cardiovasc. Pharmacol.*, **20**, (Suppl. 9), 555–561.

KOIDE, A., ZEITLIN, I.J. & PARRATT, J.R. (1993). Kinin formation in ischaemic heart and aorta of anaesthetised rats. *J. Physiol.*, **467**, 125P.

LAWSON, C.S., AVKIRAN, M., SHATTOCK, M.J., COLTART, D.J. & HEARSE, D.J. (1993a). Preconditioning and reperfusion arrhythmias in the isolated rat heart: true protection or temporal shift in vulnerability? *Cardiovasc. Res.*, **27**, 2274–2281.

LAWSON, C.S., COLTART, D.J. & HEARSE, D.J. (1993b). 'Dose-dependency' and temporal characteristics of protection by ischaemic preconditioning against ischaemia-induced arrhythmias in rat hearts. *J. Mol. Cell. Cardiol.*, **25**, 1391–1402.

LAWSON, C.S. & DOWNEY, J.M. (1993). Preconditioning: state of the art in myocardial protection. *Cardiovasc. Res.*, **27**, 542–550.

MURRY, C.E., JENNINGS, R.B. & REIMER, K.A. (1986). Preconditioning with ischemia: a delay of lethal cell injury in ischaemic myocardium. *Circulation*, **74**, 1124–11136.

PARRATT, J.R. (1993). Endogenous myocardial protective (antiarrhythmic) substances. *Cardiovasc. Res.*, **27**, 693–702.

PARRATT, J.R. (1994a). Protection of the heart by ischaemic preconditioning: mechanisms and possibilities for pharmacological exploitation. *Trends Pharmacol. Sci.*, **15**, 19–25.

PARRATT, J.R. (1994b). Cardioprotection by angiotensin converting enzyme inhibitors. *Cardiovasc. Res.*, **28**, 183–189.

PARRATT, J.R. & VEGH, A. (1994). Pronounced antiarrhythmic effects of ischaemic preconditioning: a brief review. *Cardioscience*, **5**, 9–18.

PIACENTINI, L., WAINWRIGHT, C.L. & PARRATT, J.R. (1993). The antiarrhythmic effect of ischaemic preconditioning in isolated rat hearts involves a pertussis toxin sensitive mechanism. *Cardiovasc. Res.*, **27**, 674–680.

TOHSE, N. & SPERELAKIS, N. (1991). Inhibition of L-type calcium channels by cyclic GMP. *Circ. Res.*, **69**, 325–331.

VANDER HEIDE, R.S., REIMER, K.A. & JENNINGS, R.B. (1993). Adenosine slows ischaemic metabolism in canine myocardium in vitro; relationship to ischaemic preconditioning. *Cardiovasc. Res.*, **27**, 669–673.

VEGH, A., KOMORI, S., SZEKERES, L. & PARRATT, J.R. (1992a). Antiarrhythmic effects of preconditioning in anaesthetised dogs and rats. *Cardiovasc. Res.*, **26**, 487–495.

VEGH, A., PAPP, J.G.Y., SZEKERES, L. & PARRATT, J.R. (1992c). The local intracoronary administration of methylene blue prevents the pronounced antiarrhythmic effect of ischaemic preconditioning. *Br. J. Pharmacol.*, **107**, 910–911.

VEGH, A., PAPP, J.G.Y., SZEKERES, L. & PARRATT, J.R. (1993). Prevention by an inhibitor of the L-arginine-nitric oxide pathway of the antiarrhythmic effects of bradykinin in anaesthetised dogs. *Br. J. Pharmacol.*, **110**, 18–19.

VEGH, A., PAPP, J.G.Y., SZEKERES, L. & PARRATT, J.R. (1994a). Evidence that bradykinin contributes to the pronounced antiarrhythmic effects of ischaemic preconditioning. *Br. J. Pharmacol.*, **111**, 193P.

VEGH, A., PAPP, J.G.Y., SZEKERES, L. & PARRATT, J.R. (1994b). Blocking adenosine receptors fails to modify the pronounced antiarrhythmic effect of ischaemic preconditioning in the canine myocardium. *Br. J. Pharmacol.*, **112**, 399P.

VEGH, A., SZEKERES, L. & PARRATT, J.R. (1990). Protective effects of preconditioning of the ischaemic myocardium involve cyclooxygenase products. *Cardiovasc. Res.*, **24**, 1020–1023.

VEGH, A., SZEKERES, L. & PARRATT, J.R. (1991). Local coronary infusions of bradykinin profoundly reduce the severity of ischaemia-induced arrhythmias in anaesthetised dogs. *Br. J. Pharmacol.*, **104**, 294–295.

VEGH, A., SZEKERES, L. & PARRATT, J.R. (1992b). Preconditioning of the ischaemic myocardium; involvement of the L-arginine nitric oxide pathway. *Br. J. Pharmacol.*, **107**, 648–652.

VEGH, A., SZEKERES, L. & UDVARY, E. (1987). Effect of the blood supply to the normal noninfarcted myocardium on the incidence and severity of early post-occlusion arrhythmias in dogs. *Basic Res. Cardiol.*, **82**, 159–171.

WILLIAMS, D.C., SHERLAG, B.J., HOPE, R.R., EL-SHERIF, N. & NAZZARA, R. (1974). The pathophysiology of malignant ventricular arrhythmias during acute myocardial ischaemia. *Circulation*, **50**, 1163–1172.

WIRTH, K., HOCK, F.J., ALBUS, U., LINZ, W., ALPERMANN, H.G., ANAGNOSTOPOULOS, H., HENKE, S., BREIPHOL, G., KONIG, W., KNOLLE, J. & SCHOLKENS, B.A. (1991). Hoe 140 a new potent and long acting bradykinin-antagonist; *in vivo* studies. *Br. J. Pharmacol.*, **102**, 774–777.

ZEITLIN, I.J., FAGBEMI, S.O. & PARRATT, J.R. (1989). Enzymes in normally perfused and ischaemic dog hearts which release a substance with kinin like activity. *Cardiovasc. Res.*, **23**, 91–97.

(Received April 5, 1994
Revised July 2, 1994
Accepted July 27, 1994)

Br. J. Pharmacol. (1994), **113**, 1173–1182 © Macmillan Press Ltd, 1994

The effects of a novel vasodilator, LP-805, on cytosolic Ca^{2+} concentrations and on tension in rabbit isolated femoral arteries

Masuko Ushio-Fukai, Katsuya Hirano & [1]Hideo Kanaide

Division of Molecular Cardiology, Research Institute of Angiocardiology, Faculty of Medicine, Kyushu University, Fukuoka 812, Japan

1 LP-805, 8-tert-butyl-6,7-dihydropyrrolo-[3,2-e]-5-methylpyrazolo-[1,5a]-pyrimidine-3-carbonitrile, is a newly synthesized potent vasodilator. To investigate the cellular mechanisms of vasorelaxation induced by LP-805, we simultaneously determined the effects of LP-805 on cytosolic Ca^{2+} concentrations ($[Ca^{2+}]_i$) and on tension of smooth muscle of rabbit femoral arterial strips, with or without the endothelium, using front-surface fluorometry and fura-2.

2 In the absence of the endothelium, LP-805, in a concentration-dependent manner, decreased $[Ca^{2+}]_i$ and tension during the contraction induced by K^+-depolarization, at relatively low concentrations ($[K^+]_o \leqslant 30$ mM). The decreases in $[Ca^{2+}]_i$ and tension were fully antagonized by treatment with 2×10^{-6} M glibenclamide. The $[Ca^{2+}]_i$-tension relationship in the LP-805-induced relaxation was similar to that of K^+-depolarization-induced contractions.

3 LP-805, in a concentration-dependent manner (IC_{50} for inhibition of tension; 1.7×10^{-6} M), decreased both $[Ca^{2+}]_i$ and tension during the steady-state of contractions induced by 1×10^{-7} M noradrenaline (NA) in the strips without the endothelium. Glibenclamide completely inhibited these reductions of $[Ca^{2+}]_i$ and tension. At the steady-state of relaxation induced by LP-805 during NA-induced contraction, $[Ca^{2+}]_i$-tension relation was shifted to the left of that obtained with high K^+-induced contraction.

4 NA induced transient increases in $[Ca^{2+}]_i$ and tension in the absence of extracellular Ca^{2+}. LP-805 (up to 3×10^{-6} M) had no effect on these intracellular Ca^{2+} mobilisation and tension development induced by NA.

5 In strips with an intact endothelium, LP-805 decreased both $[Ca^{2+}]_i$ and tension during contraction induced by 1×10^{-7} M NA. The concentration-response curve for inhibition of $[Ca^{2+}]_i$ and tension obtained in the presence of the endothelium was shifted to the left from that obtained in the absence of endothelium. IC_{50} for the inhibition of tension obtained in the strips with the endothelium was 4.0×10^{-7} M. Treatment with 1×10^{-4} M N^G-nitro-L-arginine (L-NOARG) attenuated reductions of both $[Ca^{2+}]_i$ and tension induced by LP-805 and the concentration-response curve shifted to the right and overlapped that obtained in the absence of the endothelium. Treatment with glibenclamide almost fully overcame the reduction of $[Ca^{2+}]_i$ induced by LP-805, while the reversion of tension was 50% at most.

6 In the presence of the endothelium with L-NOARG, LP-805 reduced the tension to the extent of that expected from the reduction of $[Ca^{2+}]_i$, as based on the $[Ca^{2+}]_i$-tension relationship obtained with LP-805 in the absence of endothelium. On the contrary, in the presence of the endothelium without L-NOARG, LP-805 induced a greater reduction of tension than expected from the reduction of $[Ca^{2+}]_i$. This effect became more apparent after treatment with glibenclamide.

7 These results suggest that: (1) LP-805 relaxes smooth muscle mainly by activating ATP-sensitive K^+ channels of smooth muscle and by releasing endothelium-derived relaxing factor (EDRF). (2) Activation of ATP-sensitive K^+ channels decrease $[Ca^{2+}]_i$ and thereby relax smooth muscle with no effect on Ca^{2+}-sensitivity of the contractile apparatus of smooth muscle or on the agonist-induced Ca^{2+}-release process. (3) EDRF induced by LP-805 relaxes smooth muscle not only by decreasing $[Ca^{2+}]_i$ but also decreasing Ca^{2+}-sensitivity of the contractile apparatus of smooth muscle. In the presence of an intact endothelium, a decrease in Ca^{2+}-sensitivity of the contractile apparatus may play an important role in LP-805-induced relaxation.

Keywords: ATP-sensitive K^+ channel; endothelium-derived relaxing factor; cytosolic Ca^{2+} concentration; LP-805; cromakalim; vascular smooth muscle; rabbit femoral artery

Introduction

LP-805, 8-tert-butyl-6,7-dihydropyrrolo-[3,2-e]-5-methylpyrazolo-[1,5a]-pyrimidine-3-carbonitrile, is a newly synthesized potent vasodilator. LP-805 was shown to hyperpolarize the resting membrane and induce vasodilatation (Nakashima *et al.*, 1992; Kamouchi *et al.*, 1993). These events were antagonized by glibenclamide, an ATP-sensitive K^+ channel blocker (Cook, 1989), in the rabbit coronary artery. In vascular smooth muscle, K^+ channel openers in general are considered to hyperpolarize membrane potential by increasing permeability of the cell membrane to K^+ (Hamilton *et al.*, 1986), which in turn inactivates voltage-operated Ca^{2+} channels and may decrease cytosolic Ca^{2+} concentration, $[Ca^{2+}]_i$, and induce vasodilatation. However, the precise mechanism of vasorelaxation by K^+ channel openers remains an open question. Cromakalim and lemakalim (BRL38227), an active enantiomer of cromakalim (Hof *et al.*, 1988), may inhibit intracellular Ca^{2+} mobilization by decreasing the syn-

[1] Author for correspondence.

thesis of inositol 1,4,5-trisphosphate induced by noradrenaline (NA) (Ito *et al.*, 1991; Quast & Baumlin, 1991) and by U46619, a thromboxane A_2 analogue, (Yamagishi *et al.*, 1992) via membrane hyperpolarization. Lemakalim was also shown to reduce Ca^{2+} sensitivity of the contractile apparatus by membrane hyperpolarization (Okada *et al.*, 1993).

LP-805 was shown to release endothelium-derived relaxing factor (EDRF) (Furchgott & Zawadzki, 1980) from vascular endothelial cells *in vitro* (Kishii *et al.*, 1992a; Nakashima *et al.*, 1992) and *in vivo* (Inazu & Tsujitani, 1993). Endothelial cells of vascular tissues release not only EDRF but also prostaglandin I_2 and endothelium-derived hyperpolarizing factor (for review, Vanhoutte, 1993). An essential component of EDRF is thought to be nitric oxide (NO), a compound synthesized from L-arginine (Ignarro *et al.*, 1987). NO/EDRF increases guanosine 3':5'-cyclic monophosphate (cyclic GMP) in the cytosol of smooth muscles and decreases Ca^{2+} sensitivity of the contractile apparatus during endothelium-dependent relaxation (Sato *et al.*, 1990; Hirano & Kanaide, 1993).

To investigate the mechanism of action of various vasoconstrictors (Kodama *et al.*, 1989; Hirano *et al.*, 1991) and vasodilators (Abe *et al.*, 1990; Hirano *et al.*, 1990; Ushio-Fukai *et al.*, 1993), we simultaneously determined the effects of these agents on $[Ca^{2+}]_i$ and tension and evaluated $[Ca^{2+}]_i$-tension relationship, using front-surface fluorometry and fura-2 loaded vascular strips. In the present work, we used this technique to determine the cellular mechanisms of vasorelaxation induced by LP-805.

Methods

Tissue preparation

The study protocol was approved by the Animal Care and Committe of Research Institute of Angiocardiology, Faculty of Medicine, Kyushu University. Japanese white rabbits (male, 16–20 weeks old, body weight 2.5–3.0 kg) were killed with sodium pentobarbitone (100 mg kg^{-1}, intravenously) and femoral arteries were immediately excised. Fat and adventitia were removed by dissection under a binocular microscope. The preparations were opened longitudinally and then cut into approximately 1 × 3 mm circular strips, 0.2 mm thick. To obtain strips without the endothelium, the intraluminal surface was rubbed with a cotton swab.

Fura-2 loading

Vascular strips with or without the endothelium were loaded with the $[Ca^{2+}]_i$ indicator dye, fura-2 by incubation in medium containing 50 μM fura-2/AM (an acetoxymethyl ester form of fura-2) and 2.5% foetal bovine serum for 3–4 h at 37°C. Subsequently, the strips were washed with physiological salt solution (PSS) containing 1.25 mM Ca^{2+} at 37°C to remove the dye from the extracellular space and were then equilibrated in normal PSS for at least 1 h before initiation of the measurements. Strips thus treated showed the specific peak of the fluorescence emission spectrum for fura-2 (500 nm) and the specific peak and valley of the fluorescence excitation spectrum for fura-2, 340 nm and 380 nm, respectively, determined by use of a fluorescence spectrophotometer (model 650-40, Hitachi, Toyko, Japan). Loading the vascular strips with fura-2 did not alter the time course or the maximum levels of force development during 118 mM K^+ depolarizing (data not shown), thereby suggesting that no tissue damage occurred by possible acidification of the cells due to formaldehyde release on AM-ester hydrolysis (Hirano *et al.*, 1990).

Measurement of tension

A strip of the femoral artery was mounted vertically in a quartz organ bath with one end connected to a force-transducer (strain gauge TB-612T, Nihon Koden, Japan). During a 1 h equilibration period, the strips were stimulated with 118 mM K^+-depolarization every 15 min, and the resting tension was increased in a stepwise manner. After equilibration, the resting tension was adjusted to 350 mg. The tension development was expressed as a percentage, assuming the values in normal (5.9 mM K^+) and 118 mM K^+ PSS to be 0% and 100%, respectively.

Measurement of $[Ca^{2+}]_i$

Changes in the fluorescence intensity of the fura-2-Ca^{2+} complex were simultaneously monitored during measurement of the tension, using a front-surface fluorometer specially designed for fura-2 fluorometry (CAM-OF-1) (Abe *et al.*, 1990; Hirano *et al.*, 1991; Ushio-Fukai *et al.*, 1993). In brief, the strips were illuminated by guiding the alternating (400 Hz) 340 nm and 380 nm excitation light from a Xenon light source through quartz optic fibres arranged in a concentration inner circle (diameter = 3 mm). Surface fluorescence of the strips was collected by glass optic fibres arranged in an outer circle (diameter = 7 mm) and introduced through a 500 nm band-pass filter (full width at half maximum transmission = 10 nm) into a photon-counting photomultiplier. The ratio of the 500 nm fluorescence intensity at 340 nm excitation to that at 380 nm excitation was also recorded and expressed as a percentage assuming the values in normal (5.9 mM K^+) and 118 mM K^+ PSS to be 0% and 100%, respectively. The absolute values of $[Ca^{2+}]_i$ in normal and 118 mM K^+ PSS were determined in the separate measurements, using the equation given by Grynkiewicz *et al.* (1985) for a dye using intensity values at one wavelength (340 nm) and the K_d value of 224 nM at 37°C. Since we used % fluorescence ratio, not $[Ca^{2+}]_i$ values, throughout the experiments, we did not discuss the way to calculate $[Ca^{2+}]_i$ in detail. The mean values of $[Ca^{2+}]_i$ at normal PSS (at rest; 0% and 118 mM K^+-depolarization (100%) of the strips without the endothelium were 115.5 ± 3.1 nM (n = 10) and 716.8 ± 2.2 nM (n = 10), respectively, and those of the strips with an intact endothelium were 99.5 ± 10.1 nM (n = 5) and 699.4 ± 12.2 nM (n = 5), respectively. The levels of $[Ca^{2+}]_i$ were not significantly different between the strips with and without the endothelium, as reported by Hirano & Kanaide (1993). Since in this procedure, it is necessary to permeabilize the cell membrane with ionomycin (25 μM), which enlarges the margin of the error of $[Ca^{2+}]_i$ values, we used percentage changes of the fluorescence ratio to express $[Ca^{2+}]_i$ levels in the measurements, taking the response to 118 mM K^+-depolarization to be 100%. When measuring the fluorescence intensity of vascular strips with an intact endothelium, the fura-2 signal may becoming from either the smooth muscle or the endothelium, or both (Sato *et al.*, 1990). However, we found that the fluorescence of endothelial cells, if any, is negligible when measurements of fluorescence were carried out from the adventitial surface of the strips with an intact endothelium (data not shown), and that changes in fluorescence in the strip indicate changes in $[Ca^{2+}]_i$ in the smooth muscle cells, as reported by Kuroiwa *et al.* (1993).

Since high concentrations of LP-805 disturbed the recordings of fura-2-Ca^{2+} fluorescence signals, the limit of LP-805 concentrations was 3×10^{-6} M, under the present experimental conditions.

Drugs and solutions

The millimolar composition of the normal physiological salt solution (normal PSS) was: NaCl 123, KCl 4.7, $NaHCO_3$ 15.5, KH_2PO_4 1.2, $MgCl_2$ 1.2, $CaCl_2$ 1.25 and D-glucose 11.5. The Ca^{2+}-free solution (Ca^{2+}-free PSS) contained 2 mM EGTA instead of 1.25 mM $CaCl_2$. High K^+ PSS was made by equimolar substitution of KCl for NaCl. All solutions were gassed with a mixture of 5% CO_2 and 95% O_2 (pH 7.4 at 37°C). The chemicals used in the experiments were cromaka-

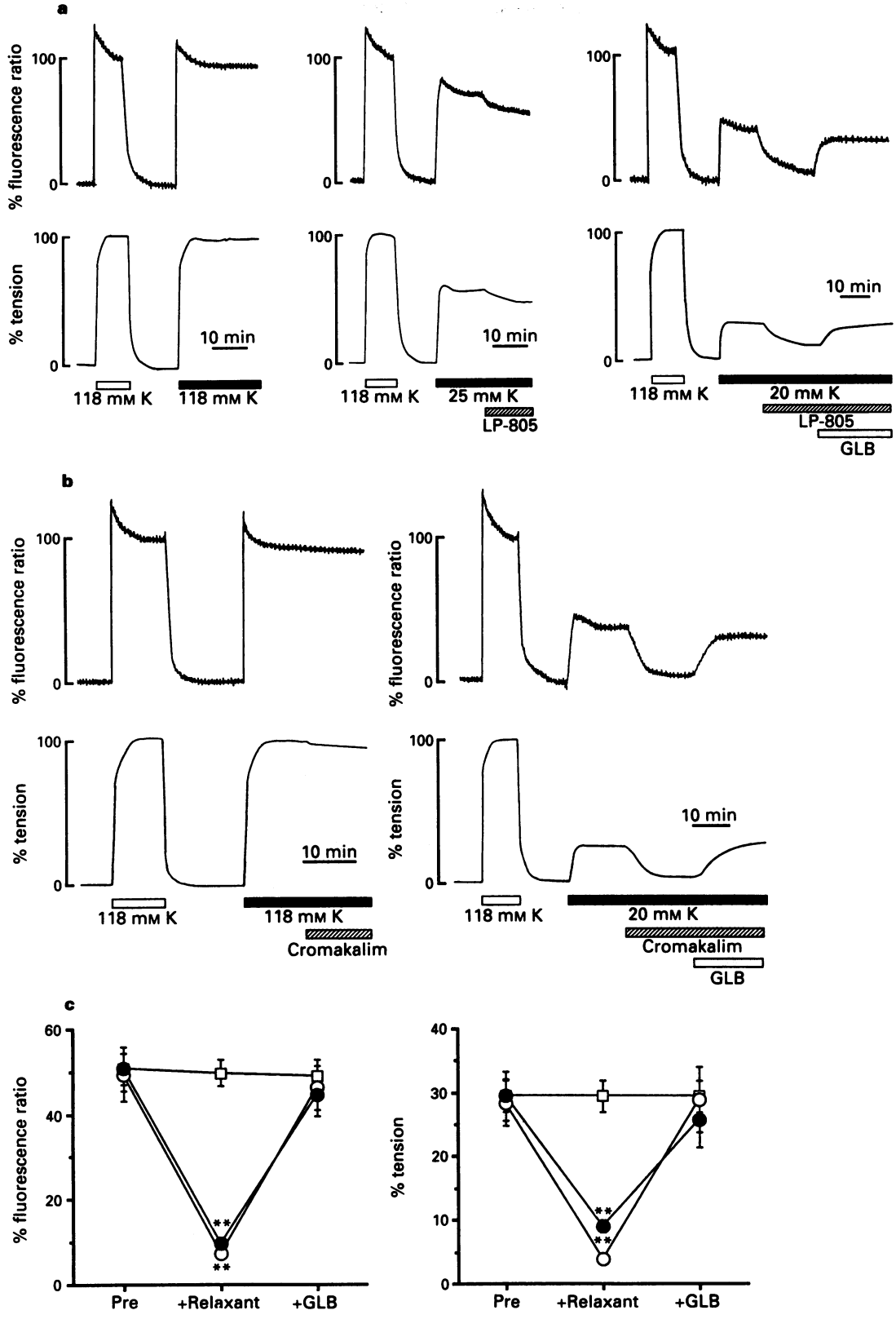


Figure 1 Representative recordings of the effects of 3×10^{-6} M LP-805 (a) and of 3×10^{-7} M cromakalim (b) on the elevations of $[Ca^{2+}]_i$ (upper trace) and tension (lower trace) induced by various concentrations of extracellular K^+, and the effects of 2×10^{-6} M glibenclamide (GLB) on LP-805- or cromakalim-induced relaxation. LP-805 or cromakalim was applied after the contraction induced by high K^+-depolarization reached a steady-state, and GLB was applied after LP-805- or cromakalim-induced relaxation reached a steady-state. Responses of fluorescence ratio and tension to 118 mM K^+ were recorded before each experiment, as a control, 100%. (c) Summary of the results of the experiments carried out with the protocols shown in (a) and (b). $[Ca^{2+}]_i$ (left panel) and tension development (right panel) induced by 20 nM K^+-depolarization in the presence of LP-805 (●) or cromakalim (○). (□) Time matched control of 20 mM K^+-induced increases in $[Ca^{2+}]_i$ and tension. (Pre): $[Ca^{2+}]_i$ and tension development induced by 20 mM K^+ just before the applications of LP-805 or cromakalim. (+ Relaxant): the steady-state levels of $[Ca^{2+}]_i$ and tension development in the presence of LP-805 or cromakalim. (+ GLB): $[Ca^{2+}]_i$ and tension development after application of GLB in the presence of LP-805 or cromakalim. Data are means ± s.e.mean ($n = 6$). $^{**}P < 0.01$ compared with time matched control values.

lim (provided by Chugai Pharmaceutical Co. Tokyo, Japan), noradrenaline hydrochloride and glibenclamide (Sigma Chemical Co. U.S.A.), N^G-nitro-L-arginine (Aldrich Chemical Co., U.S.A.) and indomethacin (Wako Pure Chemical Co., Osaka, Japan). LP-805 was provided by POLA Pharmaceutical R&D Laboratory (Tokyo, Japan) and was dissolved in 0.1 N HCl as a stock solution (0.1 M) and diluted in the distilled water, just before use. Fura-2/AM was purchased from Dojindo Laboratories (Kumamoto, Japan), and was dissolved in dimethyl sulphoxide (DMSO) as a stock solution and diluted in the medium, just before loading the dye. The final concentration of DMSO was 5%. At this concentration, DMSO had no effect on the contraction of vascular smooth muscle (Hirano *et al.*, 1990).

Statistical analysis

Values are expressed as mean ± standard error. Student's *t* test was used to determine the statistical significance. $P<0.05$ as considered to be significant. Statistical analysis of the shift of the $[Ca^{2+}]_i$-tension curves was carried out by an analysis of covariance. $P<0.05$ as considered to be significant.

The EC_{50} (or IC_{50}) values, the concentration that increased (or decreased) fluorescence ratio and tension to 50% of the maximum response, were determined from the concentration-response curve fitted according to a four-parameter logistic model (De Lean *et al.*, 1987).

Results

Effects of LP-805 on high K^+-induced increases in $[Ca^{2+}]_i$ and tension of the strips without the endothelium

When the external bathing solution was changed from normal PSS (rest) to 118 mM K^+ solution to depolarize smooth muscle cells, $[Ca^{2+}]_i$ and tension rapidly increased and reached the steady-state levels in 5 min and 10 min, respectively; these levels were maintained for at least 30 min (Figure 1a). The extent of increases in $[Ca^{2+}]_i$ and tension depended on the concentration of external K^+; EC_{50} for $[Ca^{2+}]_i$ and tension were 19.8 mM and 23.8 mM, respectively. When the strips were depolarized with high K^+ at concentrations higher than 30 mM, 3×10^{-6} M LP-805 had no effects on $[Ca^{2+}]_i$ and tension (Figure 1a). However, when 3×10^{-6} M LP-805 was applied during 20–25 mM K^+-depolarization, $[Ca^{2+}]_i$ and tension decreased to a lower steady-state level within 20 min. During the 25 mM K^+-induced contraction, 3×10^{-6} M LP-805 decreased $[Ca^{2+}]_i$ and tension to 55.6 ± 4.3% ($n = 6$) and 46.7 ± 5.9% ($n = 6$), respectively, and during the 20 mM K^+-induced contraction, application of 3×10^{-6} M LP-805 decreased $[Ca^{2+}]_i$ and tension to 9.9 ± 1.1% ($n = 6$) and 9.1 ± 0.9% ($n = 6$), respectively (Figure 1a). Cromakalim (K^+ channel opener) showed effects on $[Ca^{2+}]_i$ and tension during K^+-depolarization-induced contraction similar to those seen with LP-805 (Figure 1b). When the strips were depolarized with K^+ concentrations higher than 30 mM, 3×10^{-7} M cromakalim had no effects on $[Ca^{2+}]_i$ and tension, as shown by LP-805. When 3×10^{-7} M cromakalim was applied during 20 mM K^+-depolarization, $[Ca^{2+}]_i$ and tension decreased to a lower steady-state level within 15 min; 7.5 ± 1.4% and 5.1 ± 0.6% ($n = 6$), respectively. Glibenclamide (2×10^{-6} M), a specific blocker of ATP-sensitive K^+ channel, overcame the decreased levels of $[Ca^{2+}]_i$ and tension induced by cromakalim and reverted to the control levels (Figure 1b and c), as reported earlier (Yoshitake *et al.*, 1991). Similarly, reductions of $[Ca^{2+}]_i$ and tension induced by LP-805 were restored by 2×10^{-6} M glibenclamide (Figure 1a and c).

To evaluate the $[Ca^{2+}]_i$-tension relationships (Figure 2), the effects of LP-805 on Ca^{2+}-sensitivity of the contractile apparatus were determined. The $[Ca^{2+}]_i$-tension relation of

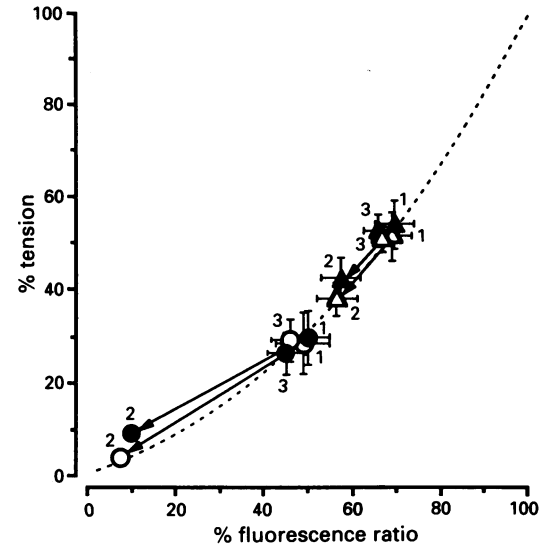


Figure 2 Effects of 3×10^{-6} M LP-805 and 3×10^{-7} M cromakalim on the $[Ca^{2+}]_i$-tension relationships during contractions induced by 20 mM K^+ or 30 mM K^+. Broken line: control $[Ca^{2+}]_i$-tension relationship of the steady-state of the contractions obtained with various concentrations of extracellular K^+ (5.9, 20, 25, 30, 60 and 118 mM) in separate measurements. The individual points represent the $[Ca^{2+}]_i$-tension relationship induced by 20 mM K^+ (●; LP-805, ○; cromakalim) or 30 mM K^+ (▲; LP-805, △; cromakalim) observed before (1) and after (2) the applications of LP-805 or cromakalim, and then, application of 2×10^{-6} M glibenclamide (3). Data are obtained from Figure 1c. The arrows indicate the direction of (1) to (2). Measurements were performed at a time when LP-805- or cromakalim-induced relaxation reached a steady-state. Data are means ± s.e.mean ($n = 6$).

the relaxation induced by LP-805 during the K^+-depolarization-induced contraction overlapped the control $[Ca^{2+}]_i$-tension relation curve obtained at the steady-state of contractions induced by various concentration of extracellular K^+ in the absence of LP-805, regardless of whether glibenclamide was applied or not. This was also the case with cromakalim-induced relaxation during K^+-depolarization-induced contraction. Thus, the extent of relaxation induced by LP-805 or cromakalim was much as expected from the reduction of $[Ca^{2+}]_i$ based on the control $[Ca^{2+}]_i$-tension relationship of K^+-induced contractions.

Effects of LP-805 on the noradrenaline-induced increases in $[Ca^{2+}]_i$ and tension of the strips without the endothelium

When the vascular strip was exposed to 1×10^{-7} M NA in the presence of extracellular Ca^{2+}, $[Ca^{2+}]_i$ rapidly increased to reach the first transient peak at 1 min, then declined to reach a lower, fairly steady-state level within 10 min; this level was gradually and slightly lowered during the application (Figure 3a). The levels of $[Ca^{2+}]_i$ at the peak and 10 min after 1×10^{-7} M NA exposure were 95.5 ± 9.6% ($n = 6$) and 77.5 ± 4.3% ($n = 6$) of that seen with 118 mM K^+-depolarization, respectively. Tension also developed rapidly and reached a maximum at 2 min, then declined to a lower, fairly steady-state level within 10 min, and this level was maintained or was gradually and slightly lowered. The extents of tension development at the maximum and at 10 min after NA application were 116.5 ± 8.3% ($n = 6$) and 109.8 ± 4.9% ($n = 6$) of that seen with 118 mM K^+-depolarization, respectively. For a similar tension development, NA required smaller increase in $[Ca^{2+}]_i$ than did K^+-depolarization. Thus, the $[Ca^{2+}]_i$-tension curve at the steady-state of the NA-induced contraction obtained with various concentrations of NA was shifted to the left of that obtained with K^+-de-

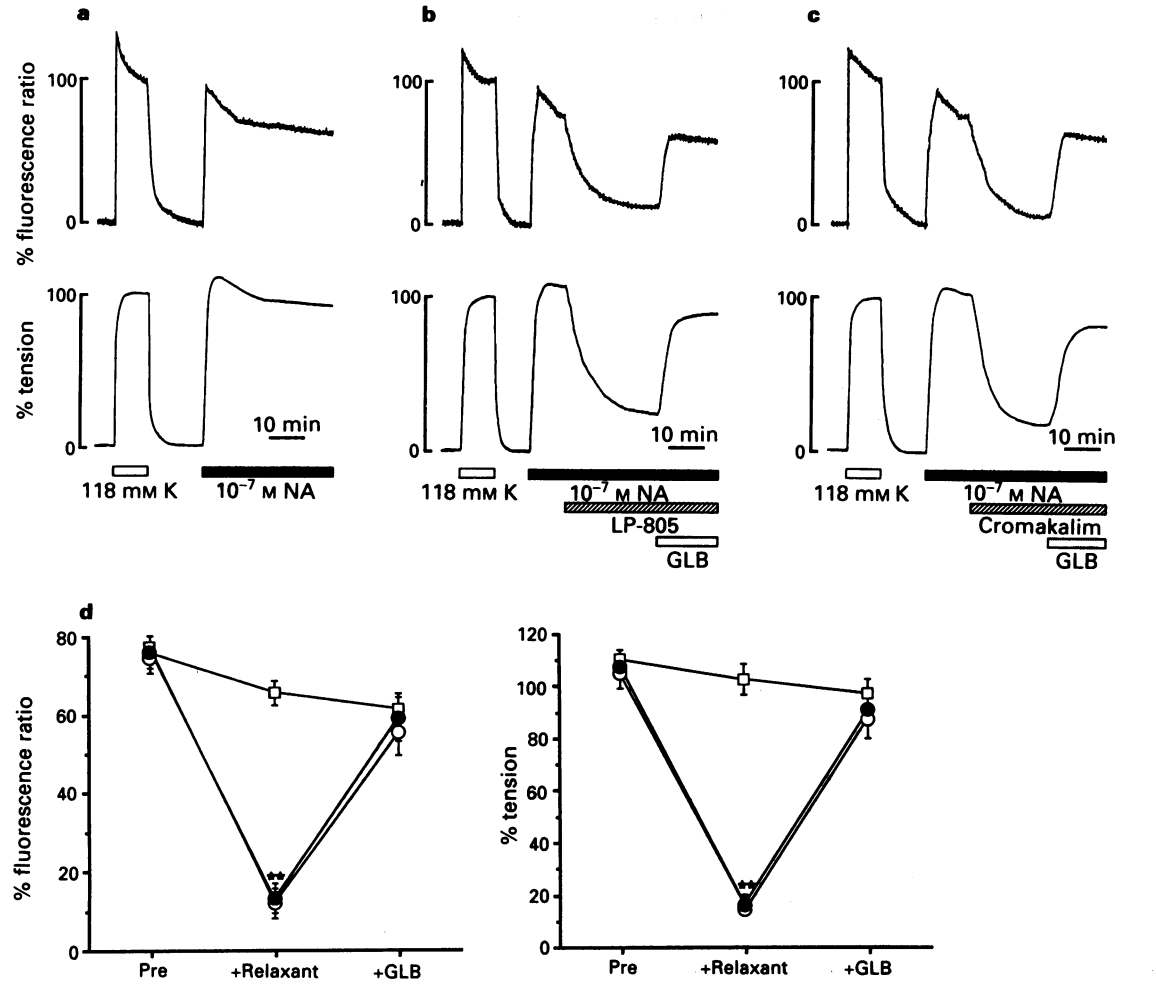


Figure 3 Effects of 3×10^{-6} M LP-805 and 3×10^{-7} M cromakalim on the increases in $[Ca^{2+}]_i$ and tension induced by 10^{-7} M noradrenaline (NA) in normal PSS (1.25 mM Ca^{2+}), and the effects of 2×10^{-6} M glibenclamide (GLB) on LP-805- or cromakalim-induced relaxation. Representative recordings of changes in $[Ca^{2+}]_i$ (upper trace) and tension (lower trace) induced by NA (a, control) and the effects of LP-805 (b) or cromakalim (c) on these changes. LP-805 or cromakalim was applied after the contraction induced by NA reached almost a steady-state, and GLB was applied after LP-805- or cromakalim-induced relaxation reached a steady-state. Response of fluorescence ratio and tension to 118 mM K^+ was recorded before each experiment to determine 100% levels. (d) Summary of the results of the experiments carried out with the protocols shown in (b) and (c). $[Ca^{2+}]_i$ (left panel) and tension development (right panel) induced by 10^{-7} M NA in the presence of LP-805 (●) or cromakalim (○), (□): Time matched control of NA-induced increases in $[Ca^{2+}]_i$ and tension. (Pre): $[Ca^{2+}]_i$ and tension development induced by NA just before the applications of LP-805 or cromakalim. (+ Relaxant): the steady-state of $[Ca^{2+}]_i$ and tension development in the presence of LP-805 or cromakalim. (+ GLB): $[Ca^{2+}]_i$ and tension development after application of GLB in the presence of LP-805 or cromakalim. Data are means ± s.e.mean ($n = 6$). $^{**}P < 0.01$ compared with time matched control values.

polarization (Figure 4) ($P < 0.05$, by analysis of covariance). Thus, NA contracts the rabbit femoral artery by increasing both $[Ca^{2+}]_i$ and the sensitivity of the contractile apparatus to $[Ca^{2+}]_i$.

When 3×10^{-6} M LP-805 was applied during the NA-induced contraction, $[Ca^{2+}]_i$ and tension gradually decreased to 13.3 ± 3.8% ($n = 6$) and 16.3 ± 3.7% ($n = 6$), respectively, within 30 min (Figure 3b). Similarly, 3×10^{-7} M cromakalim gradually decreased $[Ca^{2+}]_i$ and tension to 12.1 ± 3.8% ($n = 6$) and 16.1 ± 3.6% ($n = 6$), respectively, within 20 min (Figure 3c). At the steady-state of relaxation induced by LP-805 (30 min) and cromakalim (20 min) during the NA-induced contraction, the $[Ca^{2+}]_i$-tension relation was shifted to the left of that for the high K^+-induced contraction (Figure 4) ($P < 0.05$, by analysis of covariance). This may mean that LP-805 had negligible effects on sensitivity of the contractile apparatus to $[Ca^{2+}]_i$, which was increased by NA. As shown in Figure 3b, c and d, both LP-805- and cromakalim-induced reductions of $[Ca^{2+}]_i$ and tension were antagonized by 2×10^{-6} M glibenclamide, as in case of K^+-depolarization-induced contraction. Therefore, the leftward shift of the $[Ca^{2+}]_i$-tension relations of 1×10^{-7} M NA-induced contraction in the presence of LP-805 and cromakalim were reversed by glibenclamide to the control $[Ca^{2+}]_i$-tension relation of NA-induced contractions in their absence.

Effect of LP-805 on increases in $[Ca^{2+}]_i$ and tension induced by noradrenaline in Ca^{2+}-free solution

When the vascular strips were exposed to Ca^{2+}-free PSS, $[Ca^{2+}]_i$ gradually declined to − 27.9 ± 2.9% ($n = 6$) with no change in resting tension within 15 min (Figure 5a). Treatment with LP-805 or cromakalim had no effect on the decrease in $[Ca^{2+}]_i$ induced by depletion of extracellular Ca^{2+} or on tension (Figure 5b and c). When 1×10^{-5} M NA was applied 15 min after incubation of the vascular strip in Ca^{2+}-free PSS, $[Ca^{2+}]_i$ and tension increased to reach a peak ($[Ca^{2+}]_i$ = 7.2 ± 2.8%, and tension = 62.2 ± 5.7%, $n = 6$) due to the release of Ca^{2+} from intracellular storage sites, then rapidly declined to the pre-stimulation levels within 8 min (Figure 5a). Transient elevations of $[Ca^{2+}]_i$ and tension

induced by 1×10^{-5} M NA were not significantly inhibited by 3×10^{-6} M LP-805 ($[Ca^{2+}]_i = 3.0 \pm 2.1\%$, and tension = $52.2 \pm 8.1\%$, $n = 6$). In the presence of 3×10^{-7} M cromakalim, transient elevations of $[Ca^{2+}]_i$ and tension were also not significantly inhibited ($[Ca^{2+}]_i = 4.6 \pm 1.9\%$, and tension = $54.0 \pm 8.8\%$, $n = 6$). Furthermore, prolonged exposure to LP-805 or cromakalim for 30 min also could not significantly inhibit the intracellular Ca^{2+} mobilization induced by NA (data not shown).

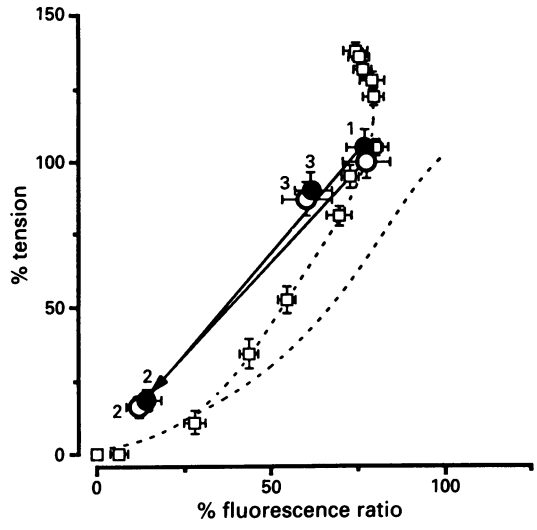


Figure 4 Effects of 3×10^{-6} M LP-805 (●) and 3×10^{-7} M cromakalim (○) on the $[Ca^{2+}]_i$-tension relationship during 10^{-7} M noradrenaline (NA)-induced contraction. Broken line without symbols indicates the control $[Ca^{2+}]_i$-tension relationship obtained with various concentrations of extracellular K^+ (5.9, 20, 25, 30, 60 and 118 mM), being similar to that in Figure 2. Broken line with (□) indicates $[Ca^{2+}]_i$-tension relationship obtained by cumulative applications of NA (10^{-9}–10^{-5} M). The individual points represent the $[Ca^{2+}]_i$-tension relationship induced by 10^{-7} M NA before (1) and after (2) applications of 3×10^{-6} M LP-805 (●) and 3×10^{-7} M cromakalim (○), and then, application of 2×10^{-6} M glibenclamide (3). Data are obtained from Figure 3d. The arrows indicate the direction of (1) to (2). Measurements were performed at the time when LP-805- and cromakalim-induced relaxation reached a steady-state. Data are means ± s.e.mean ($n = 6$).

Effects of LP-805 on the noradrenaline-induced increases in $[Ca^{2+}]_i$ and tension of the strips with endothelium

To eliminate the involvement of prostanoid relaxing factors possibly released from endothelium, all measurements were performed in the presence of 1×10^{-5} M indomethacin (indomethacin was applied 80 min before measurement), unless otherwise specified. In the strip with an intact endothelium, NA induced increases in $[Ca^{2+}]_i$ and tension similar to findings in case of no endothelium. When the strip was exposed to 1×10^{-6} M LP-805 during steady-state of 1×10^{-7} M NA-induced contraction, $[Ca^{2+}]_i$ and tension gradually decreased to near resting level; $4.4 \pm 5.5\%$ and $4.0 \pm 1.9\%$ ($n = 6$), respectively (Figure 6a). These reductions of $[Ca^{2+}]_i$ and tension induced by 1×10^{-6} M LP-805 in the presence of the endothelium were greater than those obtained with the same concentration of LP-805 in the absence of the endothelium (Figure 3b), thereby suggesting the involvement of EDRF, in addition to the glibenclamide-sensitive relaxation, in LP-805-induced relaxations in the strips with endothelium (Nakashima *et al.*, 1992). Since LP-805 reduced $[Ca^{2+}]_i$ and tension in the absence of indomethacin to a similar extent as seen in the presence of indomethacin (data not shown), the involvement of prostanoid relaxing factors, if any, can be excluded in the LP-805-induced relaxation. When strips were treated with 1×10^{-4} M N^G-nitro-L-arginine (L-NOARG), an inhibitor of NO synthesis (Mülsch & Busse, 1990), tension development in the vascular strips by K^+-depolarization or by NA was slightly (<5%), but significantly, enhanced (data not shown), thereby indicating a basal release of EDRF which continuously reduced the tension. In strips with the endothelium and in the absence of L-NOARG, cumulative applications of LP-805 (1×10^{-7} M–3×10^{-6} M) reduced $[Ca^{2+}]_i$ and tension during the 1×10^{-7} M NA-induced contraction, in a concentration-dependent manner (Figure 6c). The IC_{50} for inhibition of $[Ca^{2+}]_i$ and tension was about $4.0 \pm 0.2 \times 10^{-7}$ M. On the other hand, in the presence of 1×10^{-4} M L-NOARG, the concentration-response curves shifted to the right and overlapped those

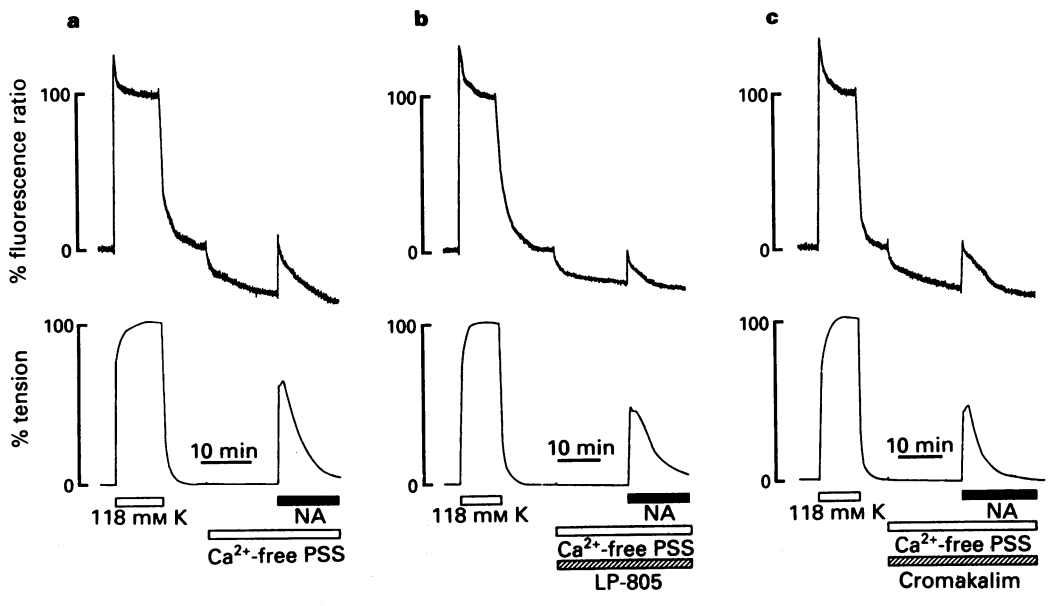


Figure 5 Effects of 3×10^{-6} M LP-805 and 3×10^{-7} M cromakalim on the increases in $[Ca^{2+}]_i$ and tension induced by 10^{-5} M noradrenaline (NA) in Ca^{2+}-free (2 mM EGTA) PSS. Representative recordings of changes in $[Ca^{2+}]_i$ (upper trace) and tension (lower trace) induced by NA in Ca^{2+}-free PSS in the absence (a, control) and the presence of LP-805 (b) or cromakalim (c). In (b) and (c), LP-805 and cromakalim were applied 15 min before and during application of NA.

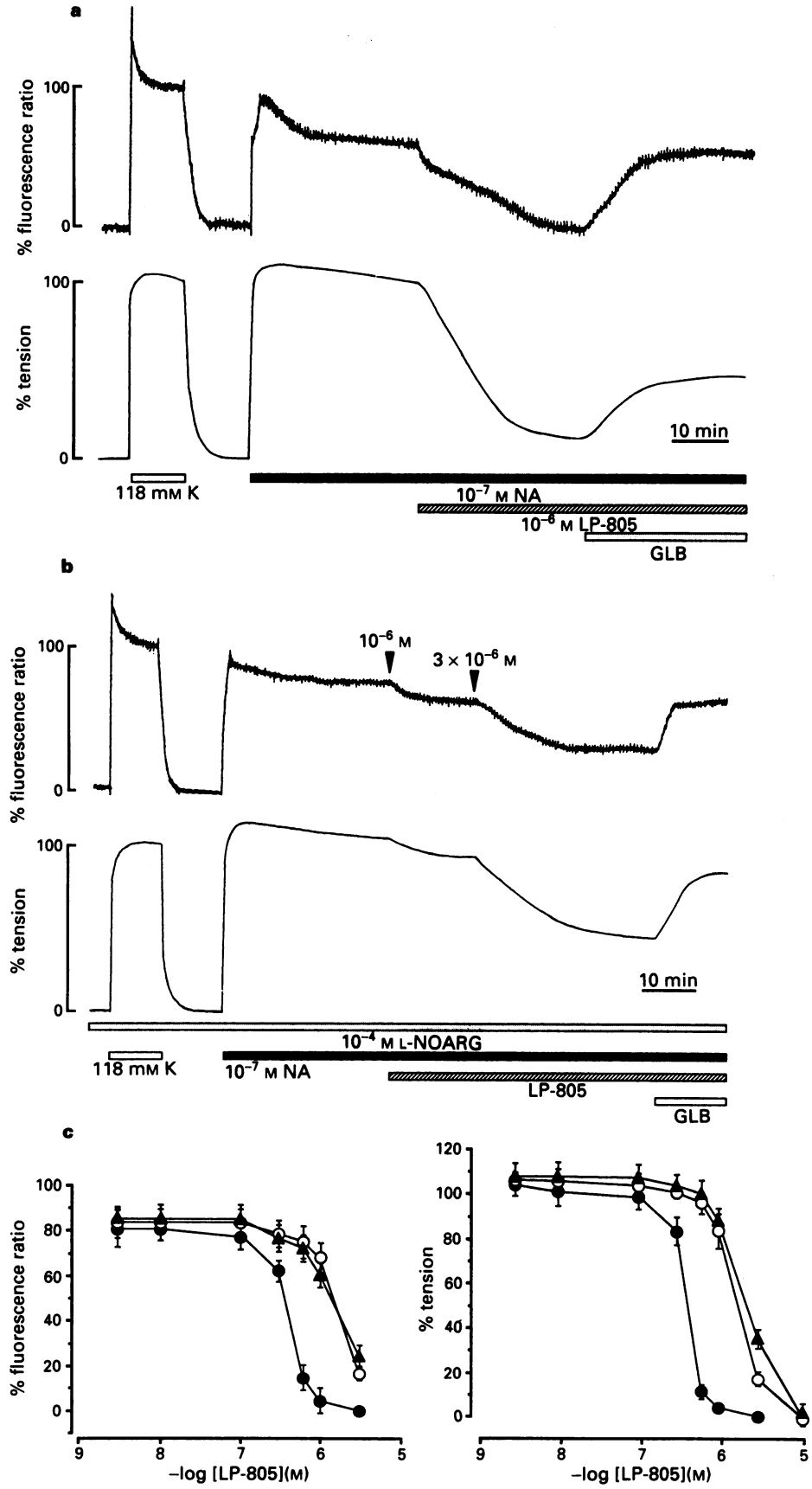


Figure 6 Effects of LP-805 on the elevations of $[Ca^{2+}]_i$ and tension induced by 10^{-7} M noradrenaline (NA) in strips with an intact endothelium. Representative recordings of changes in $[Ca^{2+}]_i$ (upper trace) and tension (lower trace) during LP-805-induced relaxation in the absence (a) and presence (b) of 10^{-4} M N^G-nitro-L-arginine (L-NOARG). LP-805 (10^{-6} M) was applied after the contraction induced by NA reached a steady-state. Glibenclamide (GLB, 2×10^{-6} M) was applied after LP-805-induced relaxation reached a steady-state. In (b), L-NOARG was applied at the end of the equilibration period and 10^{-6} M and 3×10^{-6} M LP-805 were applied at the point indicated by arrow head. Responses of fluorescence ratio and tension to 118 mM K^+ were recorded before each experiment, as a control, 100%. (c) Concentration-response curves for LP-805-induced reductions of $[Ca^{2+}]_i$ (left panel) and tension (right panel) during 10^{-7} M NA-induced contraction in strips with (●) or without (○) the endothelium in the absence of L-NOARG. (▲): Strips with the endothelium in the presence of L-NOARG. LP-805 was cumulatively applied during steady-state of NA-induced contraction. Abscissa scale: final concentration of LP-805. Data are means ± s.e.mean ($n = 6$).

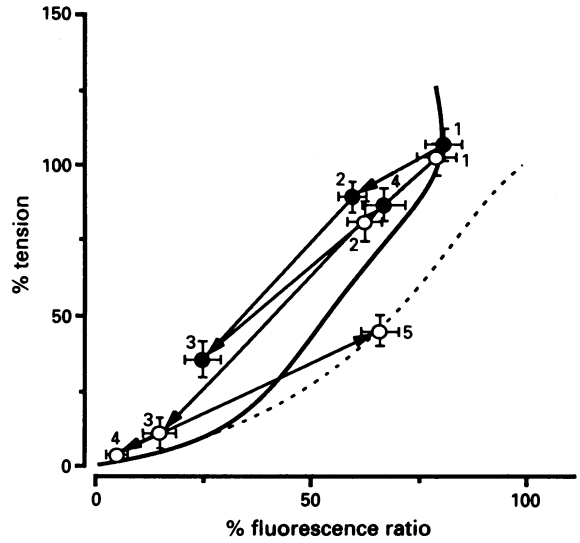


Figure 7 Effects of LP-805 on the $[Ca^{2+}]_i$-tension relationship during 10^{-7} M noradrenaline (NA)-induced contraction in strips with an intact endothelium in the absence (○) and presence (●) of 10^{-4} M N^G-nitro-L-arginine (L-NOARG). Experiments were carried out with the protocols shown in Figure 6a and b. The broken and thick solid lines indicate the control $[Ca^{2+}]_i$-tension relationships obtained with various concentrations of extracellular K^+ (5.9, 20, 25, 30, 60 and 118 mM) and by cumulative applications of NA (10^{-9}–10^{-5} M), respectively. In the absence of L-NOARG, the individual points represent the $[Ca^{2+}]_i$-tension relationship induced by 10^{-7} M NA before (○1) and after applications of 3×10^{-7} M (○2), 6×10^{-7} M (○3) and 10^{-6} M (○4) LP-805, and then, application of 2×10^{-6} M glibenclamide (○5). In the presence of L-NOARG, the individual points represent the $[Ca^{2+}]_i$-tension relationship induced by 10^{-7} M NA before (●1) and after application of 10^{-6} M (●2) and 3×10^{-6} M (●3) LP-805, and then, application of 2×10^{-6} M glibenclamide (●4). The arrows indicate the direction of time. Measurements were performed at the time when LP-805-induced relaxation reached steady-state. Data are means ± s.e.mean ($n = 6$).

obtained for the strips without the endothelium. The IC_{50} for inhibition of tension obtained in the strips with the endothelium and in the presence of L-NOARG were $2.0 \pm 0.2 \times 10^{-6}$ M and $2.0 \pm 0.3 \times 10^{-6}$ M, respectively. The IC_{50} for $[Ca^{2+}]_i$ inhibition could not be estimated because fura-2 measurements were not carried out at concentrations higher than 3×10^{-6} M, thus, the maximum inhibition was not obtained. The IC_{50} for the inhibition of tension obtained in the absence of the endothelium (without L-NOARG) was $1.7 \pm 0.3 \times 10^{-6}$ M. Therefore, in the strips with an intact endothelium, LP-805 induced relaxation during NA-induced contraction, not only by activating the glibenclamide-sensitive K^+ channels of smooth muscle but also by releasing EDRF from the endothelial cells.

After obtaining steady-state of relaxation induced by 1×10^{-6} M LP-805 in strips with an intact endothelium, 2×10^{-6} M glibenclamide was applied to eliminate the component of relaxation due to activation of ATP-sensitive K^+-channels. Glibenclamide reversed the decreases in $[Ca^{2+}]_i$ and tension induced by LP-805 (Figure 6a). $[Ca^{2+}]_i$ returned to the level close to that observed before relaxation (68.4 ± 11.1%, $n = 6$), while reversion of the tension was half-way (46.4 ± 8.9%, $n = 6$). Conversely, when strips were treated with both 1×10^{-4} M L-NOARG (this treatment completely eliminated the contribution of EDRF to the LP-805-induced relaxation) and glibenclamide, both $[Ca^{2+}]_i$ and tension reverted to levels close to those obtained before LP-805 application (Figure 6b).

Figure 7 summarizes the effects of LP-805 on the relationship between $[Ca^{2+}]_i$ and tension during the 1×10^{-7} M NA-induced contraction in strips with an intact endothelium. The control $[Ca^{2+}]_i$-tension relation curves of NA- and K^+-depolarization-induced contractions in strips with an intact endothelium were similar to those obtained in strips without the endothelium. In the presence of 1×10^{-4} M L-NOARG, the levels of tension at the relaxations induced by LP-805 were higher than those expected from the levels of $[Ca^{2+}]_i$, based on the $[Ca^{2+}]_i$-tension relationship of control contractions induced by K^+-depolarization. This alteration of $[Ca^{2+}]_i$-tension relationship, (leftward shift), observed with LP-805 in the presence of L-NOARG in endothelium-intact strips was similar to that observed in strip without the endothelium (Figure 4). This finding supports the argument that in the presence of L-NOARG, LP-805 relaxed strips with the endothelium by activating glibenclamide-sensitive K^+-channels in smooth muscle. The $[Ca^{2+}]_i$-tension relationship obtained during the LP-805-induced relaxation in the absence of L-NOARG was slightly, but significantly, shifted to the right of that obtained in the presence of L-NOARG ($P < 0.05$, by analysis of covariance), indicating LP-805 induced a greater reduction of tension than expected from the reduction of $[Ca^{2+}]_i$ in strips with an intact endothelium. This effect became more apparent by the treatment with glibenclamide, because glibenclamide further shifted the $[Ca^{2+}]_i$-tension curve of LP-805-induced relaxation to the right of that obtained in the absence of glibenclamide. This finding suggests that LP-805 markedly decreases Ca^{2+}-sensitivity of the contractile apparatus of vascular smooth muscle cells by releasing EDRF from endothelial cells.

Discussion

LP-805 was shown to activate ATP-sensitive K^+ channels of smooth muscle cells and to induce release of EDRF from the endothelial cells (Nakashima *et al.*, 1992). In the present study, we characterized the relaxation induced by LP-805, especially with regard to modulation of $[Ca^{2+}]_i$, tension development and the $[Ca^{2+}]_i$-tension relationship in intact vascular tissue, both in the presence and absence of the endothelium.

The reductions in $[Ca^{2+}]_i$ and tension induced by LP-805 in strips without the endothelium depended on extracellular K^+ concentrations and were antagonized by glibenclamide. These characteristics were similar to those obtained with cromakalim. These findings were consistent with the theory that LP-805 relaxes vascular strips by activating the ATP-sensitive, glibenclamide-sensitive K^+ channel, despite the fact that the chemical structure of LP-805 is distinct from those of existing K^+ channel openers, such as cromakalim and pinacidil (Edwards & Weston, 1990). LP-805 was shown to hyperpolarize the resting membrane potential (Nakashima *et al.*, 1992; Kamouchi *et al.*, 1993) and to increase K^+ efflux (Kishii *et al.*, 1992b) of smooth muscle, effects of which were antagonized by glibenclamide. Thus, it is suggested that in the absence the endothelium, LP-805 relaxes vascular strips by directly activating the ATP-sensitive K^+ channels of smooth muscle cells to reduce $[Ca^{2+}]_i$.

The effect of K^+ channel openers on Ca^{2+}-sensitivity of the contractile apparatus varies with agents. The K^+ channel openers such as cromakalim (Yanagisawa *et al.*, 1990) are considered to relax smooth muscle by hyperpolarizing the membrane potential of smooth muscle which inactivates voltage-dependent Ca^{2+} channels, the result being decrease in $[Ca^{2+}]_i$. This K^+ channel opener had no effect on Ca^{2+}-sensitivity of the contractile apparatus, as shown in the present study. Thus, the intracellular mechanisms of relaxation induced by a K^+ channel opener may be similar to those for Ca^{2+}-channel blockers (Hirano *et al.*, 1990). On the other hand, pinacidil, nicorandil (Yanagisawa *et al.*, 1990) and lemakalim, an active enantiomer of cromakalim (Okada *et al.*, 1993), were shown to reduce Ca^{2+}-sensitivity of the contractile apparatus. In the present study, LP-805 had no direct effect on the Ca^{2+}-sensitivity of the contractile apparatus.

Kishii *et al.* (1992c) showed that LP-805 inhibited the Ca^{2+} release from ryanodine-sensitive stores induced by NA, but at high concentration of 1×10^{-5} M. Cromakalim (1×10^{-6} M) and lemakalim ($> 1 \times 10^{-7}$ M) were also shown to inhibit Ca^{2+} release by inhibiting the synthesis of inositol 1,4,5-trisphosphate induced by NA (Ito *et al.*, 1991; Quast & Baumlin, 1991) and by U-46619 (Yamagishi *et al.*, 1992). We reported that diltiazem, at a very high concentration ($> 1 \times 10^{-5}$ M), inhibited the histamine (1×10^{-5} M)-induced Ca^{2+} release from intracellular store sites in the porcine coronary artery, and this effect correlated with inhibition of histamine binding to its receptors (Hirano *et al.*, 1990). However, in the concentration-range (1×10^{-7} M–3×10^{-6} M) used in this study, LP-805 had no apparent effect on the Ca^{2+} release induced by NA.

In the presence of an intact endothelium, we found that LP-805 relaxed vascular strips both by activating ATP-sensitive K^+ channels of smooth muscle and by releasing EDRF from endothelial cells. This finding is consistent with previous reports (Kishii *et al.*, 1992a; Nakashima *et al.*, 1992). NO/EDRF activates guanylate cyclase in soluble fractions and increases the concentrations of intracellular cyclic GMP (Ignarro *et al.*, 1987). Vasodilators which increase cellular cyclic GMP such as nitroglycerin (Abe *et al.*, 1990) and sodium nitroprusside (Karaki *et al.*, 1988) were shown to relax smooth muscle, not only by reducing $[Ca^{2+}]_i$ but also by decreasing Ca^{2+}-sensitivity of the contractile apparatus (Karaki *et al.*, 1988; Abe *et al.*, 1990). In α-toxin permeabilized smooth muscle, cyclic GMP relaxed smooth muscle and the Ca^{2+} concentration remained constant (Nishimura & van Breemen, 1989). In the absence of glibenclamide in strips with an intact endothelium, the decrease in Ca^{2+}-sensitivity of the contractile apparatus during LP-805-induced relaxation was observed. This effect became more apparent during treatment with glibenclamide (eliminating activation of ATP-sensitive K^+ channels by LP-805 but the effect on the endothelium remaining intact). LP-805 induced a greater reduction in tension than expected from the reduction of $[Ca^{2+}]_i$, based on the $[Ca^{2+}]_i$-tension relationship observed during LP-805-induced relaxation in strips without the endothelium, where LP-805 relaxed the strips by activating ATP-sensitive K^+ channels. When the strips were treated with L-NOARG to remove any effect of the endothelium, LP-805 relaxed strips as seen in the absence of the endothelium and induced a reduction of tension to the extent expected from the reduction of $[Ca^{2+}]_i$. Thus, in the presence of an intact endothelium, LP-805 relaxes smooth muscle by acting both on smooth muscle and on the endothelium to reduce $[Ca^{2+}]_i$ and Ca^{2+}-sensitivity of the contractile apparatus. The decrease in Ca^{2+}-sensitivity of the contractile apparatus is induced by EDRF and is one of the major mechanisms of LP-805-induced relaxation seen in the presence of an intact endothelium.

Although LP-805 activates ATP-sensitive K^+-channels of smooth muscle (Kishii *et al.*, 1992b; Nakashima *et al.*, 1992; Kamouchi *et al.*, 1993), the mechanism by which LP-805 stimulates the release of NO/EDRF from endothelial cells has yet to be clarified. NO synthase was purified from bovine aortic endothelial cells (Mr = 135,000 Da) and its cDNA was cloned and sequenced. The NO synthase (constitutive isoform) requires Ca^{2+} and calmodulin for its activity (for review, Marletta, 1993). $[Ca^{2+}]_i$ therefore can be a primary determinant of the enzyme activity. Production and secretion of EDRF were shown to be mainly Ca^{2+}-dependent (Busse *et al.*, 1991). Thus, increase in $[Ca^{2+}]_i$ of endothelial cells could be the first event when LP-805 induces a release of NO/EDRF. Voltage-gated Ca^{2+} channels have not been detected in large-vessel endothelium, although they have been reported on capillary endothelial cells (Revest & Abbott, 1992). Therefore, hyperpolarization would augment the electrical driving force on Ca^{2+} and increase Ca^{2+} entry into cells (Adams *et al.*, 1989). Schilling (1989) showed that bradykinin-induced Ca^{2+}-influx was decreased with membrane depolarization. Lückhoff & Busee (1990) showed that pinacidil and cromakalim had little effect on $[Ca^{2+}]_i$ of unstimulated endothelial cells, while these drugs elevated $[Ca^{2+}]_i$ up to about 600 nM when Ca^{2+} influx was stimulated by bradykinin or thimerosal. It has also been reported that rat aorta and brain microvascular endothelial cells express ATP-sensitive K^+ channels (Janigro *et al.*, 1993). Therefore, the possibility exists that LP-805 might also activate K^+ channels of endothelial cells and hyperpolarize membrane potential to increase K^+ influx, thereby elevating $[Ca^{2+}]_i$ of endothelial cells. However, we also found that cromakalim did not release NO/EDRF in strips with the endothelium (data not shown). Thus, LP-805 might stimulate the release of NO/EDRF through different mechanisms from activating K^+ channels.

In summary, we found that LP-805 relaxes the rabbit femoral artery by directly activating ATP-sensitive, glibenclamide-sensitive K^+ channels of smooth muscle and indirectly by releasing NO/EDRF from endothelial cells. LP-805 had no direct effect on Ca^{2+}-sensitivity of the contractile apparatus of smooth muscle or agonist-induced Ca^{2+} release process. Thus, in the absence of the endothelium, LP-805 decreases $[Ca^{2+}]_i$ by hyperpolarizing the membrane potential due to activation of K^+ channels and relaxes smooth muscle to the extent expected from the reduction of $[Ca^{2+}]_i$, based on the $[Ca^{2+}]_i$-tension relationship of high K^+-induced contractions. However, in the presence of an intact endothelium, LP-805 relaxes smooth muscle not only by decreasing $[Ca^{2+}]_i$ due to direct hyperpolarization or EDRF but also by decreasing Ca^{2+}-sensitivity of the contractile apparatus. If the endothelium is intact, Ca^{2+}-desensitization by EDRF is one of the major mechanism related to LP-805-induced relaxation.

We thank M. Ohara for helpful comments. This study was supported in part by Grants-in-Aid for Developmental Scientific Research (No. 03557043), for General Scientific Research (No. 04454268) from the Ministry of Education, Science and Culture, Japan.

References

ABE, S., KANAIDE, H. & NAKAMURA, M. (1990). Front-surface fluorometry with fura-2 and effects of nitroglycerin on cytosolic calcium concentrations and on tension in the coronary artery of the pig. *Br. J. Pharmacol.*, **101**, 545–552.

ADAMS, D.J., BARAKEH, J., LASKEY, R. & VAN BREEMEN, C. (1989). Ion channels and regulation of intracellular calcium in vascular endothelial cells. *FASEB J.*, **3**, 2389–2400.

BUSSE, R., LÜCKHOFF, A. & MÜLSCH, A. (1991). Cellular mechanisms controlling EDRF/NO formation in endothelial cells. *Basic Res. Cardiol.*, **86**, S7–S16.

COOK, N.S. (1989). The pharmacology of potassium channels and their therapeutic potential. *Trends Pharmacol. Sci.*, **9**, 21–28.

DE LEAN, A., MUNSON, P.J. & RODBARD, D. (1987). Simultaneous analysis of families of sigmoidal curves: application to bioassay, radioligand assay, and physiological dose-response curves. *Am. J. Physiol.*, **235**, E97–102.

EDWARDS, G. & WESTON, A.H. (1990). Structure-activity relationships of K^+ channel openers. *Trends Pharmacol. Sci.*, **11**, 417–422.

FURCHGOTT, R.F. & ZAWADZKI, J.V. (1980). The obligatory role of endothelial cells in the relaxation of arterial smooth muscle by acetylcholine. *Nature*, **288**, 373–376.

GRYNKIEWICZ, G., POENIE, M. & TSIEN, R.Y. (1985). A new generation of Ca^{2+} indicators with greatly improved fluorescence properties. *J. Biol. Chem.*, **260**, 3440–3450.

HAMILTON, T.C., WEIR, S.W. & WESTON, A.H. (1986). Comparison of the effects of BRL-34915 and verapamil on electrical and mechanical activity in rat portal vein. *Br. J. Pharmacol.*, **88**, 103–111.

HIRANO, K. & KANAIDE, H. (1993). Cytosolic Ca^{2+} transients in endothelium-dependent relaxation of pig coronary artery, and effects of captopril. *Eur. J. Pharmacol.*, **250**, 439–446.

HIRANO, K., KANAIDE, H., ABE, S. & NAKAMURA, M. (1990). Effects of diltiazem on calcium concentrations in the cytosol and on force of contractions in porcine coronary arterial strips. *Br. J. Pharmacol.*, **101**, 273–280.

HIRANO, K., KANAIDE, H., ABE, S. & NAKAMURA, M. (1991). Temporal changes in the calcium-force relation during histamine-induced contractions of the strips of the coronary artery of the pig. *Br. J. Pharmacol.*, **102**, 27–34.

HOF, R.P., QUAST, U., COOK, N.S. & BLARER, S. (1988). Mechanism of action and systemic regional hemodynamics of the potassium channel activator BRL34915 and its enantiomers. *Circ Res.*, **62**, 679–686.

IGNARRO, L.J., BUGA, G.M., WOOD, K.S., BYRNS, R.E. & CHAUDHURI, G. (1987). Endothelium-derived relaxing factor produced and released from artery and vein is nitric oxide. *Proc. Natl. Acad. Sci. U.S.A.*, **84**, 9265–9269.

INAZU, M. & TSUJITANI, M. (1993). Effect of LP-805, a releaser of endothelium-derived nitric oxide, on systemic vasodilation in vivo. *Naunyn-Schmied. Arch. Pharmacol.*, **348**, 178–183.

ITO, S., KAJIKURI, J., ITOH, T. & KURIYAMA, H. (1991). Effects of lemakalim on changes in Ca^{2+} concentration and mechanical activity induced by noradrenaline in the rabbit mesenteric artery. *Br. J. Pharmacol.*, **104**, 227–233.

JANIGRO, D., WEST, G.A., GORDON, E.L. & WINN, H.R. (1993). ATP-sensitive K^+ channels in rat aorta and brain microvascular endothelial cells. *Am. J. Physiol.*, **265**, C812–C821.

KAMOUCHI, M., KAJIOKA, S., SAKAI, T, KITAMURA, K. & KURIYAMA, H. (1993). A target K^+ channel for the LP-805-induced hyperpolarization in smooth muscle cells of the rabbit portal vein. *Naunyn-Schmied. Arch. Pharmacol.*, **347**, 329–335.

KARAKI, H., SATO, K., OZAKI, H. & MURAKAMI, K. (1988). Effects of sodium nitroprusside on cytosolic calcium level in vascular smooth muscle. *Eur. J. Pharmacol.*, **156**, 259–266.

KISHII, K., MORIMOTO, T., NAKAJIMA, N., TSUJITANI, M. & TAKAYANAGI, I. (1992a). Endothelium-dependent vasodilation by LP-805, a novel vasodilating agent, on rat thoratic aorta. *Gen. Pharmacol.*, **23**, 343–346.

KISHII, K., MORIMOTO, T., NAKAJIMA, N., YAMAZAKI, K., TSUIJITANI, M. & TAKAYANAGI, I. (1992b). Effects of LP-805, a novel vasorelaxant agent, a potassium channel opener, on rat thoracic aorta. *Gen. Pharmacol.*, **23**, 347–353.

KISHII, K., INAZU, M., MORIMOTO, T., TSUJITANI, M. & TAKAYANAGI, I. (1992c). Effects of LP-805, a new vasodilator agent, on cytosolic Ca^{2+} and contraction in vascular smooth muscle of rat aorta. *Gen. Pharmacol.*, **23**, 355–363.

KODAMA, M., KANAIDE, H., ABE, S., HIRANO, K., KAI, H. & NAKAMURA, M. (1989). Endothelin-induced Ca^{2+}-independent contraction of the porcine coronary artery. *Biochem. Biophys. Res. Commun.*, **160**, 1302–1308.

KUROIWA, M., AOKI, H., KOBAYASHI, S., NISHIMURA, J. & KANAIDE, H. (1993). Role of GTP-protein and endothelium in contraction induced by ethanol in pig coronary artery. *J. Physiol.*, **470**, 521–537.

LÜCKHOFF, A. & BUSSE, R. (1990). Activators of potassium channels enhance calcium influx into endothelial cells as a consequence of potassium currents. *Arch Pharmacol.*, **342**, 94–99.

MARLETTA, M.A. (1993). Nitric oxide synthase structure and mechanism. *J. Biol. Chem.*, **268**, 12231–12234.

MÜLSCH, A. & BUSSE, R. (1990). N^G-nitro-L-arginine (N^G-[imino (nitroamino)methyl]-L-ornithine) impairs endothelium-dependent dilations by inhibiting cytosolic nitric oxide synthesis from L-arginine. *Naunyn-Schmied. Arch. Pharmacol.*, **341**, 143–147.

NAKASHIMA, M., AKATA, T. & KURIYAMA, H. (1992). Effects on the rabbit coronary artery of LP-805, a new type of releaser of endothelium-derived relaxing factor and a K^+ channel opener. *Circ Res.*, **71**, 859–869.

NISHIMURA, J. & VAN BREEMEN, C. (1989). Direct regulation of smooth muscle contractile elements by second messengers. *Biochem. Biophys. Res. Commun.*, **163**, 929–935.

OKADA, Y., YANAGISAWA, T. & TAIRA, N. (1993). BRL38227 (levcromakalim)-induced hyperpolarization reduces the sensitivity to Ca^{2+} of contractile elements in canine coronary artery. *Naunyn-Schmied. Arch. Pharmacol.*, **347**, 438–444.

QUAST, U. & BAUMLIN, V. (1991). Cormakalim inhibits contraction of rat isolated mesenteric bed induced by noradrenaline but not caffeine in Ca^{2+}-free medium: evidence for interference with receptor-mediated Ca^{2+} mobilization. *Eur. J. Pharmacol.*, **200**, 239–249.

REVEST, P.A. & ABBOTT, N.J. (1992). Membrane ion channels of endothelial cells. *Trends Pharmacol. Sci.*, **13**, 404–407.

SATO, K., OZAKI, H. & KARAKI, H. (1990). Differential effects of carbachol on cytosolic calcium levels in vascular endothelial and smooth muscle. *J. Pharmacol. Exp. Ther.*, **246**, 294–300.

SCHILLING, W.P. (1989). Effect of membrane potential on cytosolic calcium on bovine aortic endothelial cells. *Am. J. Physiol.*, **257**, H778–H784.

USHIO-FUKAI, M., ABE, S., KOBAYAHI, S., NISHIMURA, J. & KANAIDE, H. (1993). Effects of isoprenaline on cytosolic calcium concentrations and on tension in the porcine coronary artery. *J. Physiol.*, **462**, 679–696.

VANHOUTTE, P.M. (1993). Other endothelium-derived vasoactive factors. *Circulation*, **87**, [suppl V], V9–V17.

YAMAGISHI, T., YANAGISAWA, T. & TAIRA, T. (1992). Activation of phospholipase C by the agonist U-46619 is inhibited by cromakalim-induced hyperpolarization in porcine coronary artery. *Biochem. Biophys. Res. Commun.*, **187**, 1517–1522.

YANAGISAWA, T., TESHIGAWARA, T. & TAIRA, N. (1990). Cytoplasmic calcium and the relaxation of canine coronary arterial smooth muscle produced by cromakalim, pinacidil and nicorandil. *Br. J. Pharmacol.*, **101**, 157–165.

YOSHITAKE, K., HIRANO, K. & KANAIDE, H. (1991). Effects of glibenclamide on cytosolic calcium concentrations and on contraction of the rabbit aorta. *Br. J. Pharmacol.*, **102**, 113–118.

(Received February 7, 1994
Revised July 6, 1994
Accepted July 29, 1994)

Br. J. Pharmacol. (1994), **113**, 1183–1190 © Macmillan Press Ltd, 1994

'Sensory-efferent' neural control of mucus secretion: characterization using tachykinin receptor antagonists in ferret trachea *in vitro*

Sean I. Ramnarine, Yoshitaka Hirayama, Peter J. Barnes & [1]Duncan F. Rogers

Department of Thoracic Medicine, National Heart & Lung Institute, Dovehouse Street, London SW3 6LY

1 We characterized the tachykinin receptor(s) mediating 'sensory-efferent' neural control of release of $^{35}SO_4$-labelled macromolecules (mucus) from ferret trachea *in vitro* in Ussing chambers using selective tachykinin antagonists. Secretion was induced by substance P (SP), neurokinin A (NKA), capsaicin, the NK_1 tachykinin receptor agonist [Sar^9, Met$(O_2)^{11}$]substance P ([Sar^9]SP), or acetylcholine (ACh), or by electrical stimulation of nerves. Antagonists used were FK888 and L-668,169, selective for the NK_1 receptor, SR 48968, selective for the NK_2 receptor, and FK224, a dual antagonist at NK_1 and NK_2 receptors. The selectivity of FK888 and SR 48968 was examined on NKA-induced contraction of ferret tracheal smooth muscle *in vitro*.

2 SP (1 μM) increased mucus secretion by 695% above vehicle controls. FK888 (0.1 μM–30 μM) inhibited SP-induced secretion in a dose-dependent manner, with complete inhibition at 10 μM and an IC_{50} of 1 μM. L-668,169 (1 μM) also completely inhibited SP-induced secretion.

3 NKA (1 μM) significantly increased mucus secretion by 271% above baseline, a response which was completely inhibited by FK888 (10 μM) or L-668,169 (μM). Secretion induced by ACh (10 μM: 317% above baseline) was not inhibited by FK888 but was inhibited by atropine. Capsaicin (10 μM)-induced secretion (456% above vehicle controls) was significantly inhibited by FK888 and by L-668,169 (111% and 103% inhibition respectively).

4 Electrical stimulation (50 V, 10 Hz, 0.5 ms, 5 min) increased mucus output above baseline (increased by 12 to 26 fold), a response blocked by tetrodotoxin (0.1 μM). FK888 (10 μM) inhibited the increase in secretion due to electrical stimulation by 47%. Atropine, propranolol and phentolamine in combination (APP) inhibited the response to electrical stimulation by 48%. The remaining NANC response, i.e. in the presence of APP, was further reduced by 66% with FK888. FK224 (10 μM) inhibited neurally-evoked secretion by 73%. SR 48968 (0.1 μM) had no effect on electrically-stimulated or [Sar^9]SP-induced secretion.

5 NKA (10 nM–10 μM: in the presence of DMSO control vehicle) induced tracheal smooth muscle contraction in a concentration-dependent manner with a maximal contraction of 30% of the maximal response to ACh (10 mM) and an EC_{50} of 0.3 μM. SR 48968 (0.1 μM in DMSO) inhibited the NKA-induced contraction whereas FK888 did not. Neither antagonist had any inhibitory effect on ACh-induced contraction.

6 We conclude that 'sensory-efferent' neurogenic mucus secretion in ferret trachea *in vitro* is mediated via tachykinin NK_1 receptors with no involvement of NK_2 receptors. Potent and selective tachykinin antagonists may have therapeutic potential in bronchial diseases such as asthma and chronic bronchitis in which neurogenic mucus hypersecretion may be aetiologically important.

Keywords: NK_1 receptors; NK_2 receptors; FK888; FK224; SR 48968; mucus secretion; tachykinin antagonists; tachykinin receptors; mucus; sensory nerves

Introduction

Secretion of high molecular weight mucous glycoproteins (mucus) onto the internal surface of the airways is a protective mechanism which can be induced by irritants and by humoral and neuronal mechanisms. Electrical stimulation of nerves both *in vivo* and *in vitro* induces mucus secretion in the airways of a number of animal species and a proportion of the secretion persists despite adrenoceptor and cholinoceptor blockade (Peatfield & Richardson, 1983; Borson *et al.*, 1984; Fung *et al.*, 1992a,b). Two principle neural pathways mediate the latter non-adrenergic, non-cholinergic (NANC) component of neurogenic secretion (Ramnarine & Rogers, 1994). The first pathway comprises an orthodromic system of adrenergic and cholinergic nerves which contain neuropeptides colocalized with the classical neurotransmitter including vasoactive intestinal peptide (VIP) and neuropeptide Y (NPY), both of which may increase or decrease mucus secretion or modulate stimulus-evoked secretion, depending upon preparation. The second pathway comprises a system of capsaicin-sensitive nerves which subserve a motor function and may be termed 'sensory-efferent' nerves (Maggi & Meli, 1987). The neurotransmitters of the latter neural system are collectively termed sensory neuropeptides and include calcitonin gene-related peptide (CGRP) and the tachykinins substance P (SP) and neurokinin A (NKA) and NKB. Of these, the tachykinins elicit significant mucus secretion (Lundgren *et al.*, 1989; Mizoguchi & Hicks, 1989; Rogers *et al.*, 1989; Webber, 1989; Gentry, 1991), whereas CGRP is a weak secretagogue (Webber *et al.*, 1991). In the absence of selective receptor antagonists for VIP or NPY, the relevance of these peptides to NANC neural control of mucus secretion is difficult to assess. In contrast, potent and selective tachykinin receptor antagonists are now available, and we investigated a number of these in the present study.

Currently three classes of tachykinin receptor are recognised and are designated NK_1, NK_2 and NK_3 according to

[1] Author for correspondence.

their preferential affinities for SP, NKA and NKB respectively (Guard & Watson, 1991). The order of potency of the natural tachykinins (i.e. SP > NKA > NKB: Lundgren *et al.*, 1989; Mizoguchi & Hicks, 1989; Rogers *et al.*, 1989; Webber, 1989; Gentry, 1991), and of synthetic agonists selective for the three classes of tachykinin receptor (Geppetti *et al.*, 1993; Meini *et al.*, 1993) in inducing mucus secretion indicate that tachykinin NK_1 receptors mediate tachykinin-induced secretion. However, the relevance of tachykinins to control of mucus secretion induced by stimulation of sensory-efferent nerves and the tachykinin receptor(s) involved in the response is not reported. Consequently, in the present study we determined the effects of selective tachykinin antagonists not only on agonist-induced secretion, but more particularly on secretion induced by electrical stimulation of nerves. We used the selective NK_1 receptor antagonists, FK888 (Fujii *et al.*, 1992; Hirayama *et al.*, 1993) and L-668,169 (McKnight *et al.*, 1988; Williams *et al.*, 1988), the NK_2 receptor antagonist SR 48968 (Advenier *et al.*, 1992a,b; Edmonds-Alt *et al.*, 1992; Martin *et al.*, 1992), and the dual NK_1/NK_2 receptor antagonist FK224 (Morimoto *et al.*, 1992; Murai *et al.*, 1992; Hirayama *et al.*, 1993). We used the ferret trachea to study sensory-efferent neural control of mucus secretion because: (a) mucus secretion can be induced in this preparation via NANC neural mechanisms (Borson *et al.*, 1984); (b) the source of mucus is identifiable because the trachea of this species contains abundant submucosal glands and very few epithelial goblet cells (Robinson *et al.*, 1986; Meini *et al.*, 1993); (c) the ferret trachea is supplied by axons containing sensory neuropeptides (Luts & Sundler, 1989); and (d) the airway submucosal glands express SP receptors (Meini *et al.*, 1993). We used $^{35}SO_4$ as the mucus label, because it is a marker predominately for tracheal submucosal gland mucous glycoprotein in the ferret (Gashi *et al.*, 1987). The selectivity of FK888 and SR 48968 in the ferret was investigated by determining their activity on NKA-induced tracheal smooth muscle contraction *in vitro*, a preparation which synthetic agonists indicate as essentially an NK_2 receptor system (Geppetti *et al*, 1993; Meini *et al.*, 1993). The selectivity of SR 48968 was further investigated against secretion induced by [$Sar^9Met(O_2)^{11}$] substance P ([Sar^9]), a synthetic agonist selective for the NK_1 receptor (Maggi *et al.*, 1990) which induces secretion in the ferret trachea (Meini *et al.*, 1993). Some of these results have been published in abstract form (Ramnarine *et al.*, 1993).

Methods

Tissue preparation for secretory studies

Male ferrets (Regal Rabbits, Great Bookham, Surrey) weighing 1.0–2.0 kg were anaesthetized with pentobarbitone sodium (Sagatal: 60 mg kg^{-1}, i.p.). The tracheae were removed, bathed in aerated (95% O_2 + 5% CO_2) Krebs-Henseleit solution of the following composition (mM): NaCl 118, KCl 5.9, $MgSO_4$ 1.2, $CaCl_2$ 2.5, $NaHCO_2$ 25.5 and glucose 5.05, and cut longitudinally through the dorsal membrane, opened flat and cut transversely to give four segments. Each segment was pinned and clamped across the aperture separating the two halves of perspex Ussing-type chambers so that the tissue divided the chambers into a 'luminal' (i.e. mucus-producing) and 'submucosal' side. The chambers were rectangular in cross-section to ensure optimal use of the tissue. The exposed surface area of each segment was 1.12 cm^2. Each side of the tissue was bathed with 9 ml warmed (37°C) Krebs-Henseleit solution which was oxygenated (95% O_2:5% CO_2) and circulated with gas-lift pumps. The tracheal segments could be subjected to an electrical current (not alternating in polarity) to stimulate excitable tissues (e.g. nerves). Two pins piercing the tissue on either side were connected via outlet wires through the chambers to a Grass stimulator (model S88; Grass Instruments, Quincy, U.S.A.) (Borson *et al.*, 1984). Tissues were stimulated at 10 Hz, 50 V and 0.5 ms for the first 5 min of a 15 min collection period.

We have previously established optimal conditions under which collections are taken in order to define baseline secretion and to maximize detection of the secretory response to drug addition (Meini *et al.*, 1993). At time 0 h, $Na_2{}^{35}SO_4$ (0.1 mCi; Amersham International plc, Aylesbury, Bucks.) was added to the submucosal half-chambers, in order to label newly-synthesised intracellular mucus, where it remained throughout the experiment. At unit time intervals, the fluid in the luminal side of the chamber (containing secretions) was collected and replaced with fresh Krebs-Henseleit solution. Baseline stability of spontaneous output of $^{35}SO_4$-labelled macromolecules was achieved by taking four 30 min collections followed by two 15 min collections (i.e. over 2.5 h following addition of radiolabel). After stabilisation, drugs or control solutions were added and the tissues were electrically stimulated (see *Protocols for secretory studies* below).

Measurement of $^{35}SO_4$-labelled macromolecule secretion

Luminal fluid, approximately 9 ml and comprising secretions in Krebs-Henseleit solution, was drained into tubes containing 5 g guanidine hydrochloride, to dissolve the mucus. The final concentration of guanidine hydrochloride in the fluid was 6 M. Following this, each sample was exhaustively dialysed against distilled water containing excess Na_2SO_4 and sodium azide (10 mg l^{-1}) using cellulose tubing (Medicell International Ltd., London) which allowed molecules of 12000–14000 Da or less to pass through. The sodium azide was used to limit bacterial contamination. The samples were recovered after at least six changes of distilled water when the radioactive count of the dialysis water was the same after dialysis as before dialysis (~20 disintegrations per minute [d.p.m.]). The recovered samples were weighed and the remaining radioactivity in 1 ml duplicates of each sample mixed with 2 ml scintillant (Ultima Gold XR, Canberra Packard Ltd., Pangbourne, Berks.) was determined by scintillation spectometry (model 1900CA Spectrophotometer, Canberra Packard Ltd.). The total radioactivity of each sample was estimated by multiplying the radioactivity present in a 1 ml aliquot of that sample by the total weight of the sample (assuming a 1 ml sample weighs 1 g).

Protocols for secretory studies

To examine the effects of antagonists on baseline and stimulated secretion, drugs were added to the luminal half chambers for varying times before stimulation: atropine, phentolamine and propranolol (APP) in combination (all 10 μM) for 45 min (i.e. present for three 15 min collections), SR 48968 (0.1 μM) for 45 min prior, and FK888 (0.1 μM–30 μM), FK224 (10 μM) or L-668,169 (1 μM) for 30 min prior to stimulation (i.e. present for two 15 min collections). Antagonists were also present in the chambers during the period of stimulation.

We have found previously that there is no significant tachyphylaxis of secretion to consecutive additions of SP and methacholine when additions are separated by 1.25 h (Meini *et al.*, 1993). In the present study we determined whether there was tachyphylaxis between consecutive electrical stimulations. We found that using at least a 1 h interval there was no significant difference in magnitude of secretory response to consecutive stimulations: mean increase (and s.e.mean) above baseline in radiolabel output for the first stimulation was 106.1% ± 52.6% ($n = 8$) and for the second stimulation was 118.9% ± 38.8% ($n = 8$). Thus, for the four chambers, eight possible combinations of stimulations could be carried for each experiment.

The effect of FK888 or L-668,169 on SP-induced secretion was tested to establish inhibitory concentrations for the antagonists. At time 3 h, SP was added at a final concentra-

tion of 1 μM to tissues pretreated with either FK888 (0.1 μM–30 μM), L-668,169 (1 μM), or their vehicle, dimethylsulphoxide (DMSO), the latter given at a concentration equivalent to the highest concentration of antagonist used. Collections were made so that data for baseline secretion, the effect of DMSO, FK888 or L-668,169 on baseline, the effect of SP, and the effects of DMSO, FK888 or L-668,169 on the response to SP were assessed.

The effects of single concentrations of FK888 (10 μM) or L-668,169 (1 μM) on secretion induced by NKA (1 μM) or capsaicin (10 μM) were also examined, as were those of FK888 and atropine (10 μM) on ACh-evoked mucus secretion. In addition, the effect of SR 48968 (0.1 μM) on secretion induced by [Sar^9]SP (10 μM) was determined.

Single concentrations of FK888 or SR 48968 upon secretion induced by electrical stimulation of the tissues was investigated. The effect of each tachykinin antagonist was investigated on secretion induced both in the absence of autonomic receptor blockade and in the presence of autonomic blockade by APP (the latter representing the remaining NANC neural response). Responses to six combinations of treatment were obtained, namely (1) sham stimulation (i.e. collections in the absence of electrical stimulation but at the same time-point as other tissues were electrically stimulated); (2) electrical stimulation alone (i.e. without antagonist or vehicle, DMSO); (3) electrical stimulation with antagonist vehicle (i.e. to determine the effect of vehicle on the magnitude of the secretory response); (4) electrical stimulation with FK888 or SR 48968 (i.e. to determine the effect of the antagonists on the total secretory response to cholinergic, adrenergic and NANC stimulation); (5) electrical stimulation with APP (to determine the magnitude of the NANC neurogenic component of secretion); and (6) electrical stimulation with APP and either FK888 or SR 48968 (to determine how much of the NANC response is reduced by these antagonists). The neural composition of the electrically-induced increase in secretion was investigated by use of tetrodotoxin, 0.1 μM given for 45 min before stimulation.

Contractility studies

Studies of smooth muscle contraction in ferret tracheal strips were performed in order to assess the specificity of SR 48968 and FK888. Ferret tracheae were cut longitudinally through the cartilage and then cut transversely into 3–4 mm segments (approximately 6 cartilage rings). On each day of experimentation, three segments from each of two animals were suspended from isometric force transducers connected to a six channel polygraph (model 7D, Grass Instruments Co., Quincy, U.S.A.) in 5 ml organ baths containing warmed (37°C), aerated (95% O_2 + 5% CO_2) Krebs-Henseleit solution (composition as for secretory studies) containing 10 μM indomethacin to inhibit the effects on tracheal tension of spontaneously-released prostaglandins. The polygraph was calibrated to record a 4 g resting tension on the segments for equilibration during which time the Krebs solution was changed every 5–10 min until a stable baseline was established (approximately 1 h). A supramaximal dose of ACh (10 mM) was added to all tissues to establish tissue viability and responsiveness. Once the contraction peak to ACh had plateaued the tissues were washed repeatedly until baseline tension was restored. Following this a cumulative concentration-response to NKA (10 μM–10 mM) for smooth muscle contraction was carried out, with each sequential addition of the tachykinin added after the effect of the previous addition had plateaued. Tissues were then washed again until baseline tension was restored after which they were incubated with either drug vehicle (DMSO) or the tachykinin antagonists before carrying out a second dose-response to NKA (in the same concentration-range as used in the initial dose-response determination). Thus, the effect of vehicle or tachykinin antagonist on NKA-induced tracheal contraction was investigated for each animal. Incubation with DMSO or FK888 was for 45 min before NKA. With SR 48968, preincubation was for either 120 min ($n = 2$) or 45 min ($n = 4$). Where incubation with SR 48968 was for 120 min before the second administration of NKA, the two remaining tracheal strips from that animal were left untreated for the additional 75 min before administration of either DMSO or FK888. Finally, ACh (10 mM) was added again to the tissues to assess the responsiveness of the tissue at the end of the experiment compared with the initial response to ACh.

Drugs

The following drugs were used: SP, NKA, capsaicin, indomethacin, tetrodotoxin and DMSO (Sigma Chemical Company Ltd., Poole, Dorset), atropine sulphate (Phoenix Pharmaceuticals Ltd., Pharma Hameln, G.m.b.H., Germany), phentolamine mesylate (Ciba Laboratories, Horsham, West Sussex), propranolol hydrochloride (Imperial Chemical Industries Ltd., Macclesfield, Cheshire), pentobarbitone sodium B.P. (Sagatal; RMB Animal Health Ltd., Dagenham, Essex), [Sar^9]SP (Bachem (UK) Ltd., Saffron Waden, Essex).

Tachykinin receptor antagonists were kind gifts from the Fujisawa Pharmaceutical Co. Ltd., Osaka, Japan (FK888 and FK224), Cambridge Research Biochemicals Limited, Northwich, Cheshire (L-668,169), and Sanofi Recherche, Montpellier, France (SR 48968). FK888 is a synthetic dipeptide with the structure N^2-[(4**R**)-4-hydroxy-1-(1-methyl-1*H*-indol-3-yl)carbonyl-L-prolyl]-*N*-benzyl-*N*-methyl-*N*-phenylmethyl-3-(2-napthyl)-L-alaninamide). FK224 is a modified cyclic peptide with the structure N-(N^2-(*N*-(*N*-(*N*-(2,3-didehydro-*N*-methyl-*N*-(*N*-(3-(2-penthlyphenyl)-propionyl)-L-threonyl]tyrosyl-L-leucynyl]-D-phenylalanyl)-L-*allo*-threonyl)-L-asparaginyl-L-serine-*v*-lactone. L-668,169 is a cyclic dimer: cyclo(Gln-D-Trp(NMe)Phe(R)Gly[ANC-2]LeuMet)$_2$. SR 48968 is a non-peptide with the structure (S)-N-methyl-N[4-(4-acetylamino-4-phenylpiperidino)-2-(3,4-dichlorophenyl)butyl] benzamide.

FK888, FK224 and L-668,169 were dissolved in DMSO (stock solutions of 10 mM), SR 48968 was dissolved in distilled water (stock of 100 μM), and SP, NKA, ACh and [Sar^9]SP were dissolved in distilled water (stock solutions of 10 mM). These stock solutions were divided into aliquots, stored at − 20°C. Capsaicin was dissolved in ethanol (stock solution of 10 mg ml^{-1}), stored at 4°C. All stock solutions were diluted in Krebs-Henseleit on each day of experimentation. Indomethacin was prepared in phosphate buffer (pH 7.8) of composition: 20 mM KH_2PO_4 and 120 mM Na_2HPO_4.

Data analysis

Data in Results are the arithmetic mean and one standard error of the mean (s.e.mean), with *n*-values being the number of animals. Responses obtained from individual tissue segments were calculated to give percentage changes in radiolabel output for the differences between response to drug or electrical stimulation and the preceding collection. The latter are presented in Results as mean ± s.e.mean, whereas changes compared with another group are given only as a percentage. Drug-induced changes in tension were calculated as a percentage of the contraction to ACh (10 mM). The concentration of antagonist causing 50% inhibition (IC_{50}) in secretion or contraction was calculated by non-linear regression. Significance of changes in secretion pre and post-drug or electrical stimulation were assessed with the Wilcoxon sign-rank sum test. The significance of differences between groups were assessed by the Mann-Whitney U-test. The null hypothesis was rejected at $P < 0.05$ (two-tail). Inhibition of stimulated secretion by an antagonist was considered complete when the value for stimulations with

antagonist were significantly different from stimulations without antagonist and were not significantly different from the value for sham stimulation.

Results

Effects of tachykinin NK_1 antagonists on SP-induced secretion

Median baseline radioactivity in this series of experiments was 51 d.p.m. (range 10–57 d.p.m.; $n = 14$) and median SP-stimulated radioactivity was 184 d.p.m. (range 57–382 d.p.m.; $n = 5$). SP (1 μM) increased radiolabel output by 695% above vehicle controls (Figure 1). FK888 inhibited this response in a concentration-dependent manner with an IC_{50} of 1 μM ($pIC_{50} = 6$), and abolished the secretory response at concentrations 3 μM and greater (Figure 1). FK888 alone caused minimal changes in basal secretion (range of − 4% to + 18% change in radiolabel output compared to baseline at 0.1 μM–3 μM FK888) which were not significantly different from the response to DMSO (7.5% ± 3.7% increase). L-688,169 (10 μM) had no significant effect on baseline secretion (increased by 9.0% ± 10.8%, $n = 5$) but inhibited SP-induced secretion by 125% (i.e. reduced below baseline values: baseline value was a 9.0% ± 10.4% increase above previous collection, $n = 8$; response to SP was 58.0% ± 9.7% increase above previous collection, $n = 8$, L-668,169 reduced the response to SP to − 14.5% ± 15.1% below baseline value, in separate tracheal segments).

Effects of NK_1 antagonists on NKA-, acetycholine- or capsaicin-induced secretion

Median baseline radioactivity in this series of experiments was 47 d.p.m. (range 7–143 d.p.m.; $n = 13$). Median stimulated radioactivity was similar in all three agonist groups (combined median of 88 d.p.m., range 42–382 d.p.m.; $n = 16$). The DMSO vehicle increased secretion by 15% ± 9% above baseline, although this was not significant ($P = 0.14$; Figure 2). NKA (1 μM), capsaicin (10 μM) or ACh (10 μM) induced significant increases above vehicle controls in radiolabel output (271%, 456% and 317% increases respectively) (Figure 2). FK888 (10 μM) completely inhibited NKA-induced and capsaicin-induced increases in secretion (by 103% and 111% respectively), whereas the ACh-evoked secretion was not significantly inhibited by FK888 (reduced by 8%: Figure 2). Increase in radiolabel output due to ACh was significantly inhibited by atropine (by 87%). L-668,169 also significantly ($P < 0.05$) inhibited the secretion evoked by both NKA and capsaicin by 107% and 103% for each stimulant respectively ($n = 5$, for NKA, and $n = 6$).

Effects of tachykinin antagonists on secretion induced by electrical stimulation

The magnitude of the response to electrical stimulation differed by 127% between the two series of experiments. Median baseline radioactivity in the first series of experiments was 146 d.p.m. (range 52–330 d.p.m.; $n = 7$) which was not significantly different ($P = 0.6$) from that of 69 d.p.m. (range 7–378 d.p.m.; $n = 8$) in the second series of experiments. The median stimulated radioactivity was 402 d.p.m. (range 67–624 d.p.m.; $n = 7$) in the first series of experiments and 134 d.p.m. (range 31–443 d.p.m.; $n = 8$) in the second series of experiments.

In the first series of experiments (Figure 3), electrical stimulation of the tissue at 50 V, 10 Hz, 0.5 ms for 5 min resulted in a 26 fold increase in radiolabel output over sham-stimulated values. The antagonist vehicle (DMSO) had no significant effect on the stimulated increase in radiolabel output. Adrenoceptor and cholinoceptor blockade with APP

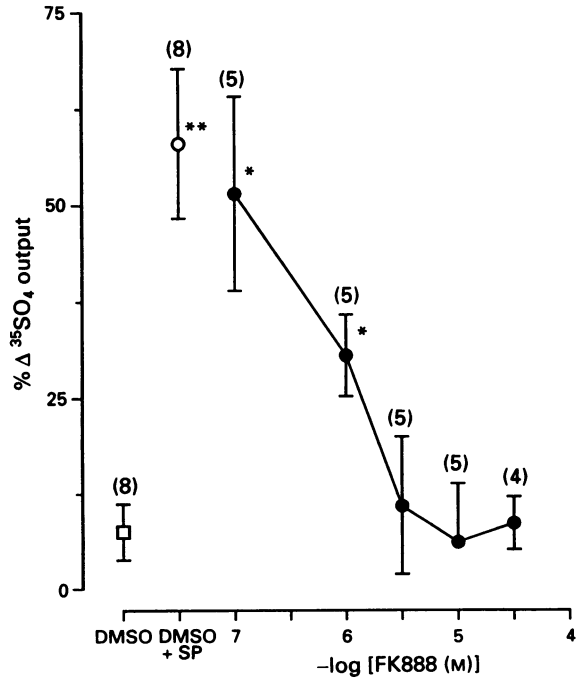


Figure 1 Effect of a tachykinin NK_1 receptor antagonist, FK888 (●), on mucus secretion induced by substance P (SP: 1 μM; O) in ferret trachea *in vitro*. Data are mean percentage changes in output of macromolecules labelled *in situ* with $^{35}SO_4$ (representing mucus) for the number of animals indicated in parentheses for each group; s.e.mean are shown. $*P < 0.05$, $**P < 0.01$ compared with DMSO group (dimethylsulphoxide, the vehicle for FK888, □).

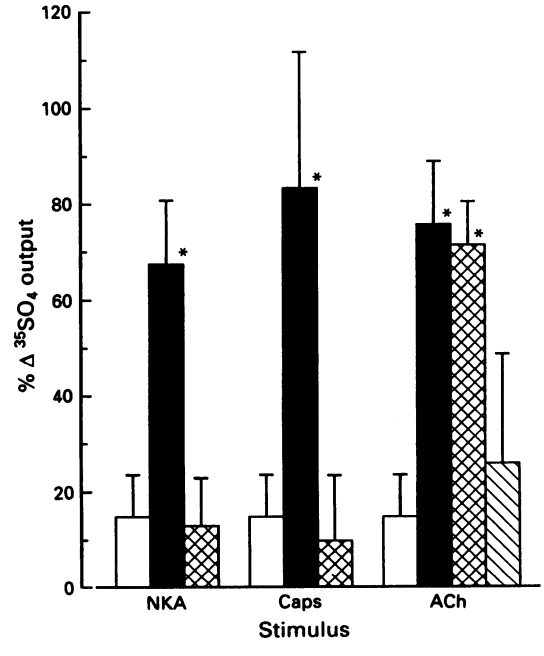


Figure 2 Effects of a tachykinin NK_1 receptor antagonist, FK888 (10 μM), on mucus secretion induced *in vitro* in ferret trachea by neurokinin A (NKA, 1 μM), capsaicin (Caps. 1 μM) or acetylcholine (ACh 10 μM). Data are mean percentage change in output of macromolecules labelled *in situ* with $^{35}SO_4$ (representing mucus); s.e.mean are shown. Open columns: DMSO (vehicle for FK888; $n = 11$ for all three sets); solid colums: DMSO = mucus stimulant ($n = 5$ for NKA and ACh, $n = 6$ for capsaicin); cross-hatched columns: effect of FK888 on stimulated secretion ($n = 5$ for NKA and ACh, $n = 6$ for capsaicin); hatched column: atropine (10 μM) + ACh ($n = 5$). $*P < 0.05$ compared with DMSO group.

in combination significantly though partially inhibited the latter increase in secretion by 48% leaving 52% of the response due to NANC innervation. FK888 (10 μM) alone significantly inhibited the total neurogenic response by 47%. In combination with adrenoceptor and cholinoceptor blockade, FK888 significantly inhibited the remaining NANC response by 66% (Figure 3): thus, blockade of adrenoceptors, cholinoceptors and tachykinin NK_1 receptors accounted for 83% of the total secretory response to electrical stimulation, leaving 17% of the response which was insensitive to blockade of the latter autonomic receptors. FK888 had no significant effect on baseline secretion (mean increase of 17.9% ± 6.4% above baseline, $n = 7$). FK224 (10 μM) significantly inhibited NANC neurogenic secretion by 73%.

In the second series of experiments (Figure 4), electrical stimulation (50 V, 10 Hz, 0.5 ms for 5 min) resulted in a 12 fold increase in radiolabel output. The antagonist vehicle (DMSO) had no significant effect on the stimulated increase in radiolabel output. Adrenoceptor and cholinoceptor blockade significantly reduced the latter response by 70%. SR 48968 (0.1 μM) did not inhibit the total neurogenic response nor did it inhibit the remaining NANC neurogenic response. SR 48968 had no significant effect on baseline secretion (5.4% increase, $n = 7$). In this series of experiments, tetrodotoxin (0.1 μM) significantly ($P < 0.01$) reduced electrically-stimulated secretion from 114% ± 20.8% (a significant increase above baseline, $n = 10$) to 27.3% ± 8.2%, the latter value not being a significant increase above baseline ($P = 0.06$, $n = 5$).

The lack of effect on tachykinin-induced secretion of SR 48968 was further investigated with [Sar^9]SP. [Sar^9]SP (1 μM) evoked a 42.3% ± 8.4% ($n = 6$) increase above baseline in radiolabel output, which was not inhibited by SR 48968 (increase of 53.8% ± 12.5% above baseline, $n = 8$).

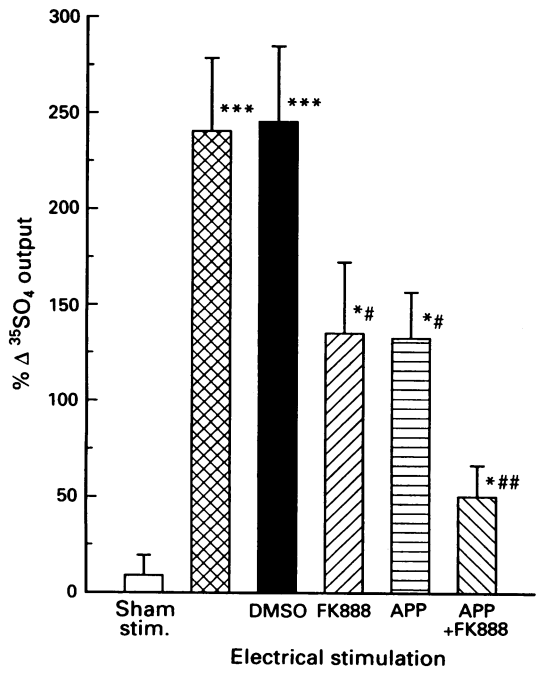


Figure 3 Effect of a tachykinin NK_1 receptor antagonist, FK888 (10 μM), on mucus secretion induced in ferret trachea *in vitro* by electrical stimulation (50 V, 10 Hz, 0.5 ms, 5 min). Data are mean percentage change in output of macromolecules labelled *in situ* with $^{35}SO_4$ (representing mucus); s.e.mean are shown ($n = 8-10$ for each experimental group). APP = adrenoceptor and cholinoceptor inhibition with atropine, propranolol and phentolamine in combination (all at 10 μM); DMSO = dimethylsulphoxide (vehicle for FK888). $^*P < 0.05$, $^{***}P < 0.001$ compared with sham stimulation; $^\#P < 0.05$, $^{\#\#}P < 0.01$ compared with DMSO and electrical stimulation respectively.

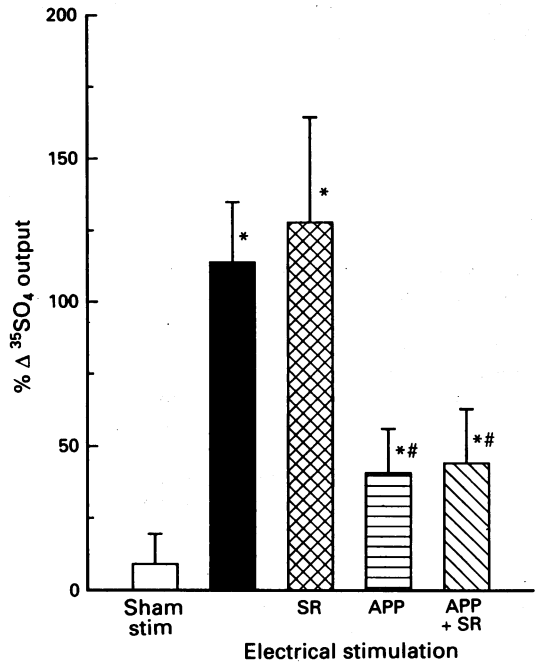


Figure 4 Effects of an NK_2 tachykinin receptor antagonist, SR 48968 (0.1 μM), on mucus secretion induced in ferret trachea *in vitro* by electrical stimulation (50 V, 10 Hz, 0.5 ms, 5 min). Data are mean percentage change in output of macromolecules labelled *in situ* with $^{35}SO_4$ (representing mucus); s.e.mean are shown. Open column: sham stimulation ($n = 8$); solid column: electrical stimulation ($n = 10$); cross-hatched column: effect of SR 48968 on stimulated secretion ($n = 5$); lined column: effect of adrenoceptor and cholinoceptor inhibition with atropine, propranolol and phentolamine in combination (APP, all at 10 μM) on stimulated secretion ($n = 10$); hatched column: effect of adrenoceptor, cholinoceptor and NK_2 receptor inhibition on stimulated secretion ($n = 12$). $^*P < 0.05$ compared with sham stimulation; $^\#P < 0.05$ compared with electrical stimulation without receptor antagonists.

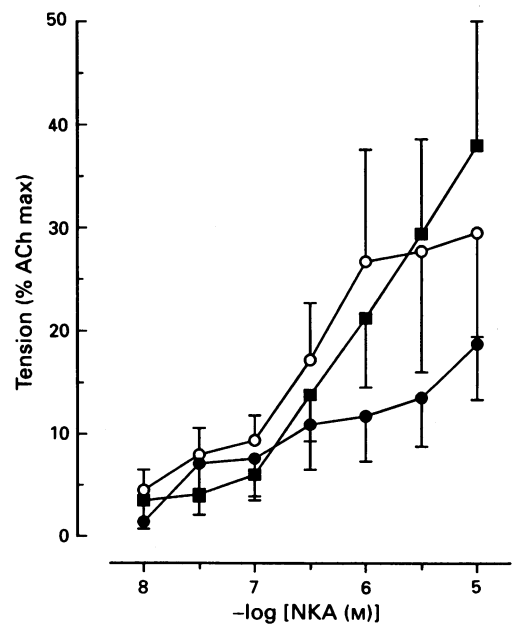


Figure 5 Effect of a tachykinin NK_1 receptor antagonist, FK888 (■; 10 μM) or a tachykinin NK_2 receptor antagonist, SR 48968 (●; 0.1 μM), on ferret tracheal smooth muscle contraction induced by neurokinin A (○) *in vitro*. All drugs were dissolved in dimethylsulphoxide (DMSO). Data are mean tension developed expressed as a percentage of the contraction to 10 mM ACh (ACh max) for $n = 6$ per group; s.e.mean are shown.

Effect of FK888 and SR 48968 on tracheal smooth muscle contraction

NKA (10 nM–10 μM), given after tension had returned to baseline following contraction to a supramaximal concentration of ACh, concentration-relatedly increased tracheal smooth muscle tone (maximal contraction of 45% of the ACh maximum and an EC_{50} of 0.47 μM). The second dose-response to NKA, although reduced, was not significantly affected following 45 min preincubation with DMSO, the drug vehicle (maximal contraction of 30% of the ACh maximum and an EC_{50} of 0.31 μM). No evidence was obtained for a difference in magnitude of inhibition by SR 48968 (0.1 μM) when tissues were incubated for 45 min ($n = 4$) or 120 min ($n = 2$) and the data for the two groups were pooled. SR 48968 (0.1 μM) inhibited NKA-induced tracheal contraction at concentrations of NKA above 0.3 μM (Figure 5). FK888 (10 μM) had no significant effect on the contractile response over the concentration-range of NKA used (Figure 5). None of the treatments had any significant effect on the magnitude of contraction to ACh before or after drug administration: mean percentage differences between initial and final administrations of acetylcholine were 14.4% (s.e.mean 5.2%) for the DMSO group, −2.2% (s.e.mean 4.3%) for the FK888 group, and −7.7% (s.e.mean 4.7%) for the SR 48968 group ($n = 6$ each).

Discussion

In the present study, electrical stimulation *in vitro* of ferret trachea increased secretion of $^{35}SO_4$-labelled macromolecules. The increased output of $^{35}SO_4$ is consistent with increased mucus secretion from submucosal glands because: (1) ferret trachea has few surface epithelial goblet cells (Robinson *et al.*, 1986; Meini *et al.*, 1993) indicating that the main source of mucus is the submucosal glands; (2) $^{35}SO_4$ is relatively selective for labelling intracellular mucin in submucosal glands of cat trachea (Davies *et al.*, 1990); and (3) autoradiographic localisation of $^{35}SO_4$ demonstrates preferential loss of label from ferret tracheal glands in response to neuromimetic drugs (Gashi *et al.*, 1987).

The secretory response observed herein was blocked by tetrodotoxin indicating that the increase in $^{35}SO_4$ output was via stimulation of nerves associated with submucosal glands. A proportion of the secretory response (30%–50%) remained after inhibition of cholinergic and adrenergic influences, an observation consistent with previous studies (Fung *et al.*, 1992a,b; Peatfield & Richardson, 1983; Borson *et al.*, 1984). Partial inhibition of neurogenic mucus secretion in the present study in unlikely to be due to use of insufficiently high concentrations of autonomic receptor antagonists (10 μM) because in a similar preparation concentrations of 1–100 μM of these antagonists gave comparable degrees of partial inhibition of neurogenic secretion (Borson *et al.*, 1984). In the present study the sensory nerve stimulant capsaicin (Holzer, 1991) induced mucus secretion. Capsaicin also induces mucus secretion in human bronchi *in vitro* (Rogers & Barnes, 1989). Thus, a portion of the remaining NANC response may be due to activation of sensory-efferent nerves and release of tachykinins.

In the present study, the NK_1 receptor antagonist, FK888, partially inhibited secretion evoked by electrical stimulation. In rodents, binding assays, bioassays and *in vivo* functional studies demonstrate that FK888 has a high degree of selectivity for the tachykinin NK_1 receptor (Fujii *et al.*, 1992; Hirayama *et al.*, 1993; Miyayasu *et al.*, 1993; Wang *et al.*, 1994). In the present study, FK888 inhibited SP-induced mucus secretion with a pIC_{50} of 6. The concentration of SP used is submaximal for secretion under the present experimental conditions (Meini *et al.*, 1993). The pIC_{50} found herein is higher than the K_i of 0.69 nM or pA_2 of 9.3 reported for inhibition of [^{3}H]-SP binding to guinea-pig lung membranes or SP-induced contraction of guinea-pig ileum *in vitro* (Fujii *et al.*, 1992). However, it is consistent with the pIC_{50} of 6.6 for inhibition of electrically-evoked contraction of rabbit iris sphincter (Wang *et al.*, 1994). The reasons for the discrepancy between data in the guinea-pig and the data in the rabbit and ferret are unclear but may be due to the recently-reported species and tissue differences in affinities of NK_1 receptor antagonists (Maggi *et al.*, 1993; Hall *et al.*, 1993). In the present study the selectivity of FK888 was established for the NK_1 receptor in the ferret trachea. It has been demonstrated previously that only the selective synthetic tachykinin NK_1 receptor agonist [Sar^9]SP induces mucus secretion in this preparation (Geppeti *et al.*, 1993, Meini *et al.*, 1993). In the present study, FK888 inhibited SP-induced mucus secretion in a dose-dependent manner with maximal inhibition at 10 μM. The selectivity of FK888 at this concentration was investigated further in ferret tracheal smooth muscle *in vitro* where only a synthetic selective NK_2 agonist induces contraction. FK888 did not inhibit NKA-induced tracheal contraction which indicates that FK888 does not interact with NK_2 receptors in this preparation. FK888 did not exhibit non-selective activity in inhibiting stimulated secretion because it did not inhibit ACh-induced mucus output, a response which was blocked by atropine. Another NK_1 antagonist, L-668,169 (McKnight *et al.*, 1988; Williams *et al*, 1988), inhibited $^{35}SO_4$ labelled macromolecule secretion evoked by SP which is further evidence for the involvement of the NK_1 receptor in tachykinin-induced mucus secretion. Both FK888 and L-688,169 blocked secretion evoked by capsaicin and NKA, the latter indicating that NKA interacts with NK_1 receptors in the *in vitro* ferret tracheal preparation. The concentration of NKA used is submaximal for secretion *in vitro* in ferret trachea (Mizoguchi & Hicks, 1989, Webber, 1989). It should be noted that in the isolated submucosal gland of the cat trachea, secretion and glandular contraction induced by SP are not blocked by peptide SP receptor antagonists (Shimura *et al.*, 1987). The reasons why the latter antagonists failed to block SP-induced responses whereas SP-induced secretion in the present study was blocked by two different tachykinin NK_1 receptor antagonists is unclear but may be related to the activity of the drugs used, to a species difference, or to differences in use of an isolated glandular preparation compared with the present intact preparation.

In contrast to previous studies using natural and synthetic tachykinins (see above), a preliminary report on isolated cat tracheal submucosal glands found an order of potency of NKA > NKB > SP in inducing secretion of trichloroacetic acid-predictable glycoconjugates (Nagaki *et al.*, 1991) which indicated that the tachykinin NK_2 receptor mediated secretion. In the present study, SR 48968 failed to inhibit neurally-evoked secretion, either in the absence or presence of adrenoceptor and cholinoceptor inhibition. In rodent binding assays, bioassays and *in vivo* functional studies, and in human airway smooth muscle *in vitro*, SR 48968 exhibits a high degree of selectivity for the NK_2 receptor (Advenier *et al.*, 1992a,b; Edmonds-Alt *et al.*, 1992; Martin *et al.*, 1992). In the present study, SR 48968, at a dose of 0.1 μM which inhibits NK_2-mediated but not NK_1-mediated responses (Advenier *et al.*, 1992b; Edmonds-Alt *et al.*, 1992), inhibited NKA-induced tracheal smooth muscle contraction (NK_2 receptor system: see above). In the guinea-pig, SR 48968 has activity at tachykinin NK_3 receptors and μ-opioid receptors (Boyle *et al.*, 1993). The involvement of the latter two receptors in NKA-induced tracheal contraction is unlikely because of the minimal effect of a selective NK_3 agonist in inducing contraction in this preparation (Geppetti *et al.*, 1993; Meini *et al.*, 1993) and because a μ-opioid antagonist does not inhibit SP-induced contraction of guinea-pig airway smooth muscle (Belvisi *et al.*, 1990). In contrast to inhibition of NKA-induced tracheal contraction, SR 48968 did not inhibit ACh-induced contraction or [Sar^9]SP-induced mucus secretion. The latter observations provide further evidence for the

selectivity of SR 48968 for the ferret tracheal NK_2 receptor.

In the present study, a small secretory response remained ($\sim$17%) after inhibition of adrenoceptors, cholinoceptors and tachykinin NK_1 receptors. The neurotransmitter(s) of the response are unknown. It is unlikely to be due to activation of tachykinin NK_2 receptors because the magnitude of the inhibition by FK224, a tachykinin antagonist which is active at both NK_1 and NK_2 receptors (Morimoto *et al.*, 1992; Murai *et al.*, 1992; Hirayama *et al.*, 1993), was not greater than that induced by the NK_1 antagonist (FK888). The remaining response may be mediated by vasoactive intestinal polypeptide (VIP) and related peptides, or NPY (Ramnarine & Rogers, 1994). The relevance of these and other neuropeptides to NANC neural control of mucus secretion awaits development of selective antagonists.

In the present study, we found variability in secretion of $^{35}SO_4$-labelled mucins. Variation in secretion is related to uptake of label and its incorporation into mucus, to the amount of gland present in different tissue segments, and to the tenacity of the mucus, which affects its release from the luminal surface and dispersion into the bathing medium. The basal condition of the tissue does not appear to contribute greatly to variability because baseline absolute counts of released radioactivity did not differ significantly between experimental groups. Variation in secretory response to capsaicin has been noted previously (Rogers & Barnes, 1989). The reasons for this are unclear but relate to accessibility of capsaicin to the submucosa (the drug is applied luminally), and to variation in distribution of sensory-efferent nerves, tachykinin receptors and degradative enzymes between tissue segments. Difference in magnitude of secretion between the two nerve-stimulated groups is most probably due to variability between batches of ferrets because baseline secretion was not different between the groups.

The present data have clinical implications. Although sensory-efferent neural control of mucus secretion can be readily demonstrated in the airways of a number of non-human animal species (Ramnarine & Rogers, 1994), the involvement of these nerves in control of mucus secretion in human airways is difficult to demonstrate (Baker *et al.*, 1985) and any increase in secretion is comparatively small (Rogers & Barnes, 1989). It is possible that sensory-efferent neural pathways become important in control of mucus secretion in certain diseases of the airways. In asthmatics, the number of SP-immunoreactive nerves associated with airway submucosal glands is increased above that in non-asthmatics (Ollerenshaw *et al.*, 1991) and mRNA levels for NK_1 receptors are increased in asthmatic airways (Adcock *et al.*, 1993), although this increase is not associated with increased receptor number (Goldie, 1990). SP immunoreactivity is increased in sputum of patients with asthma and chronic bronchitis compared with healthy subjects (Tomaki *et al.*, 1993). The dual NK_1/NK_2 antagonist, FK224, has been found to reduce sputum production and cough in patients with chronic bronchitis (Ichinose *et al.*, 1993). Clarification of whether NK_1 receptors are relevant to human bronchial hypersecretory disease requires information on whether reduction in sputum represents a reduction in mucus production and the dual activity of FK224 requires that inhibition of sputum production be confirmed using a selective NK_1 antagonist.

In conclusion, the present study provides evidence that sensory-efferent neural control of mucus secretion *in vitro* in ferret trachea is via activation of tachykinin NK_1 receptors whereas the involvement of NK_2 receptors is minimal. Use of selective and potent tachykinin antagonists will be invaluable in elucidating the involvement of tachykinins in secretory processes in the airways. However, the activity of the dual antagonist FK224 demonstrates that although of value in determining the role of tachykinins in disease, selective tachykinin antagonists may be of limited use therapeutically whereas development of compounds with multiple antagonism at selected receptors may have greater therapeutic potential.

We thank Pfizer Central Research (Sandwich, Kent), the Fujisawa Pharmaceutical Co. Ltd. (Osaka, Japan), and the Clinical Research Committee of the Royal Brompton National Heart & Lung Hospitals for financial support. We wish to acknowledge the technical skill of Mr Bill Clack in modifying the Ussing chambers for electrical stimulation. We also thank Susie Lee for her assistance with the secretory studies during her work experience placement from North East Surrey College of Technology(NESCOT), and Drs. M.A. Giembycz and M.G. Belvisi for helpful discussion concerning the contractility studies.

References

ADCOCK, I.M., PETERS, M., GELDER, C., SHIRASAKI, H., BROWN, C.R. & BARNES, P.J. (1993). Increased tachykinin receptor gene expression in asthmatic lung and its modulation by steroids. *J. Mol. Endocrinol.*, **11**, 1–7.

ADVENIER, C., NALINE, E., TOTY, L., HAYASSAM, B., EDMONDS-ALT, X., VILAIN, P., BRELIÈRE, J.-C. & LE FUR, G. (1992a). Effects on the isolated human bronchus of SR 48968, a potent and selective nonpeptide antagonist of the neurokinin A (NK_2) receptors. *Am. Rev. Respir. Dis.*, **146**, 1177–1181.

ADVENIER, C., ROUISSI, N., NGUYEN, Q.T., EDMONDS-ALT, X., BRELIÈRE, J.-C., NELIAT, G., NALINE, E., & REGOLI, D. (1992b). Neurokinin A (NK_2) receptor revisited with SR 48968, a potent non-peptide antagonist. *Biochem. Biophys. Res. Commun.*, **184**, 1418–1424.

BAKER, B., PEATFIELD, A.C. & RICHARDSON, P.S. (1985). Nervous control of mucin secretion into human bronchi. *J. Physiol.*, **365**, 297–305.

BELVISI, M.G., STRETTON, C.D. & BARNES, P.J. (1990). Modulation of cholinergic neurotransmission in guinea-pig airways by opioids. *Br. J. Pharmacol.*, **100**, 131–137.

BORSON, D.B., CHARLIN, M., GOLD, B.D. & NADEL, J.A. (1984). Neural regulation of $^{35}SO_4$-macromolecule secretion from tracheal glands of ferrets. *J. Appl. Physiol.*, **57**, 457–466.

BOYLE, S.J., MANLEY, S., TANG, K.-W., MEECHAM, K., GUARD, S., WATLING, K.J., WOODRUFF, G.M. & MCKNIGHT, A.T. (1993). Affinity of the NK_2 antagonist SR 48968 at NK_3-tachykinin and μ-opioid receptors. *Br. J. Pharmacol.*, **108**, 24P.

COLES, S.J., NEILL, K.H. & REID, L.M. (1984). Potent stimulation of glycoprotein secretion in canine trachea by substance *P. J. Appl. Physiol.*, **57**, 1323–1327.

DAVIES, J.R., CORBISHLEY, C.M., RICHARDSON, P.S. (1990). The uptake of radiolabelled precursors of mucus glycoconjugates by secretory tissues in the feline trachea. *J. Physiol.*, **420**, 19–30.

EDMONDS-ALT, X., VILAIN, P., GOULAOUIC, P., PROIETTO, V., VAN BROECK, D., ADVENIER, C., NALINE, E., NELIAT, G., LE FUR, G. & BRELIÈRE, J.C. (1992). A potent and selective non-peptide antagonist of the neurokinin A (NK_2) receptor. *Life Sci.*, **50**, PL–101–PL–106.

FUJII, T., MURAI, M. MORIMOTO, H., MAEDA, Y., YAMAOKA, M., HAGIWARA, D., MIYAKE, H., IKARI, N. & MATSUO, M. (1992). Pharmacological profile of a high affinity dipeptide NK_1 receptor antagonist, FK888. *Br. J. Pharmacol.*, **107**, 785–789.

FUNG, D.C.K., ALLENBY, M.I. & RICHARDSON, P.S. (1992a). NANC nerve pathways controlling mucus glycoconjugate secretion into feline trachea. *J. Appl. Physiol.*, **73**, 625–630.

FUNG, D.C.K., BEACOCK, D.J. & RICHARDSON, P.S. (1992b). Vagal control of mucus glycoconjugate secretion into the feline trachea. *J. Physiol.*, **453**, 435–447.

GASHI, A.A., BORSON, D.B., FINKBEINER, W.E., NADEL, J.A. & BASBAUM, C.B. (1987). Neuropeptides degranulate serous cells of ferret tracheal glands. *Am. J. Physiol.*, **251**, C2223–C2229.

GENTRY, S.E. (1991). Tachykinin receptors mediating airway macromolecular secretion. *Life Sci.*, **48**, 1609–1618.

GEPPETTI, P., BERTRAND, C., BACCI, E., HUBER, O. & NADEL, J. (1993). Characterisation of tachykinin receptors in ferret trachea by peptide agonists and nonpeptide antagonists. *Am. J. Physiol.*, **265**, L164–L169.

GOLDIE, R.G. (1990). Receptors in asthmatic airways. *Am. Rev. Respir. Dis.*, **141**, S151–S156.

GUARD, S. & WATSON, S.P. (1991). Tachykinin receptor types: classification and membrane signalling mechanisms. *Neurochem. Int.*, **13**, 149–165.

HALL, J.M., CAULFIELD, M.P., WATSON, S.P. & GUARD, S. (1993). Receptor subtypes or species homologues: relevance to drug discovery. *Trends Pharmacol. Sci.*, **14**, 376–383.

HIRAYAMA, Y., LEI, Y.-H., BARNES, P.S. & ROGERS, D.F. (1993). Effects of two novel tachykinin antagonists, FK224 and FK888, on neurogenic airway plasma exudation, bronchoconstriction and systemic hypotension in guinea-pigs *in vivo*. *Br. J. Pharmacol.*, **108**, 844–851.

HOLZER, P. (1991). Capsaicin: cellular targets, mechanisms of action, and selectivity for thin sensory neurons. *Pharmacol. Rev.*, **43**, 143–201.

ICHINOSE, M., KATSUMATA, U., KIKUCHI, R., FUKUSHIMA, T., ISHII, M., INOUE, C., SHIRATO, K. & TAKISHIMA, T. (1993). Effect of tachykinin antagonist on chronic bronchitis patients. *Am. Rev. Respir. Dis.*, **147** (Suppl.), A318.

LUNDGREN, J.D., WIEDERMAN, C.J., LOGUN, C., PLUTCHOK, J., KALINER, M. & SHELHAMER, J.H. (1989). Substance P receptor-mediated secretion of respiratory glycoconjugate from feline airways in vitro. *Exp. Lung Res.*, **15**, 17–29.

LUTS, A. & SUNDLER, F. (1989). Peptide-containing nerve fibres in the respiratory tract of the ferret. *Cell Tissue Res.*, **258**, 259–267.

MAGGI, C.A. & MELI, A. (1987). The sensory-efferent function of capsaicin-sensitive sensory neurones. *Gen. Pharmacol.*, **19**, 1–43.

MAGGI, C.A., PATACCHINI, R, QUARTARA, L., ROVERO, P. & SANTICIOLLI, P. (1990). Tachykinin receptors in the guinea-pig isolated bronchi. *Eur. J. Pharmacol.*, **197**, 167–174.

MAGGI, C.A., PATACCHINI, R., ROVERO, P. & GIACHETTI, A. (1993). Tachykinin receptors and tachykinin receptor antagonists. *J. Auton. Pharmacol.*, **13**, 23–93.

MARTIN, C.A.E., NALINE, E., EDMONDS-ALT, X. & ADVENIER, C. (1992). Influence of (±)-CP-96,345 and SR 48968 on electrical field stimulation of the isolated guinea-pig main bronchus. *Eur. J. Pharmacol.*, **224**, 137–143.

MCKNIGHT, A.T., MAGUIRE, J.J., WILLIAMS, B.J., FOSTER, A.C., TRIDGETT, R. & IVERSEN, L.L. (1988). Pharmacological specificity of synthetic peptides as santagonists at tachykinin receptors. *Regul. Pept.*, **22**, 127.

MEINI, S., MAK, J.C.W., ROHDE, J.A.L. & ROGERS, D.F. (1993). Tachykinin control of ferret airways: mucus secretion, bronchoconstriction and receptor mapping. *Neuropeptides*, **24**, 81–89.

MIYAYASU, K., MAK, J.C.W., NISHIKAWA, M. & BARNES, P.J. (1993). Characterisation of guinea-pig pulmonary neurokunin type 1 receptors using a novel antagonist ligand, [^{3}H]FK888. *Mol. Pharmacol.*, **44**, 539–544.

MIZOGUCHI, H. & HICKS, C.R. (1989). Effects of neurokinins on ion transport and sulphated macromolecule release in the isolated ferret trachea. *Exp. Lung. Res.*, **15**, 837–848.

MORIMOTO, H., MURAI, M., MAEDA, Y., YAMAOKA, M., NISHIKAWA, M., KIYOTOH, S. & FUJII, T. (1992). FK224, a novel cyclopeptide substance P antagonist with NK_1 and NK_2 receptor selectivity. *J. Pharmacol. Exp. Ther.*, **262**, 398–402.

MURAI, M., MORIMOTO, H., MAEDA, Y., KIYOTOH, S., NISHIKAWA, M. & FUJII, T. (1992). Effects of FK224, a novel compound NK_1 and NK_2 receptor antagonist, on airway constriction and airway edema induced by neurokinins and sensory nerve stimulation in guinea-pigs. *J. Pharmacol. Exp. Ther.*, **262**, 402–408.

NAGAKI, M., ISHIHARA, H., SHIMURA, S., SATOH, M., SASAKI, H. & TAKISHIMA, T. (1991). Tachykinins evoke mucus glycoprotein secretion from feline submucosal glands via NK-2 receptors mediating $[Ca^{++}]_i$ as a second messenger. *Am. Rev. Respir. Dis.*, **143** (suppl.), A620.

OLLERENSHAW, S.L., JARVIS, D., SULLIVAN, C.E. & WOOLCOCK, A.J. (1991). Substance P immunoreactive nerves in airways from asthmatics and non asthmatics. *Eur. Respir. J.*, **4**, 673–682.

PEATFIELD, A.C. & RICHARDSON, P.S. (1983). Evidence for non-cholinergic, non-adrenergic nervous control of mucus secretion into the cat trachea. *J. Physiol.*, **342**, 335–345.

RAMNARINE, S.I., HIRAYAMA, Y., LEE, S., BARNES, P.J. & ROGERS, D.F. (1993). Tachykinin NK_1 receptors mediate neurogenic mucus secretion in ferret trachea *in vitro*. *Am. Rev. Respir. Dis.*, **147** (suppl.), A711.

RAMNARINE, S.I. & ROGERS, D.F. (1994). Non-adrenergic, non-cholinergic neural control of mucus secretion in the airways. *Pulmonary Pharmacol.*, **7**, 19–33.

ROBINSON, N.P., VENNING, L., KYLE, H. & WIDDICOMBE, J.H. (1986). Quantification of secretory cells of the ferret tracheobronchial tree. *J. Anat.*, **145**, 173–188.

ROGERS, D.F., AURSUDKIJ, B. & BARNES, P.J. (1989). Effects of tachykinins on mucus secretion in human bronchi in vitro. *Eur. J. Pharmacol.*, **174**, 283–286.

ROGERS, D.F. & BARNES, P.J. (1989). Opioid inhibition of neurally mediated mucus secretion in human bronchi. *Lancet*, **i**, 930–932.

SHIMURA, S., SASAKI, T., OKAYAMA, H., SASAKI, H. & TAKISHIMA, T. (1987). Effect of substance P on mucus secretion of isolated submucosal gland from feline trachea. *J. Appl. Physiol.*, **63**, 646–653.

TOMAKI, M., ICHINOSE, M., NAKAJIMA, N., MIURA, M., YAMAUCHI, H., INOUE, H. & SHIRATO, K. (1993). Elevated substance P concentration in sputum after hypertonic saline inhalation in asthma and chronic bronchitis patients. *Am. Rev. Respir. Dis.*, **147** (suppl.), A478.

WANG, Z-Y., TUNG, S.R., STRICHARTZ, G.R. & HAKANSON, R. (1994). Investigation of the specificity of FK888 as a tachykinin NK_1 receptor antagonist. *Br. J. Pharmacol.*, **111**, 1342–1346.

WEBBER, S.E. (1989). Receptors mediating the effects of substance P and neurokinin A on mucus secretion and smooth muscle tone of the ferret trachea: potentiation by an enkephalinase inhibitor. *Br. J. Pharmacol.*, **98**, 1197–1206.

WEBBER, S.E., LIM, J.C.S. & WIDDICOMBE, J.G., (1991). The effects of calcitonin gene-related peptide on submucosal gland secretion and epithelial albumin transport in the ferret trachea *in vitro*. *Br. J. Pharmacol.*, **102**, 79–84.

WILLIAMS, B.J., CURTIS, N.R., MCKNIGHT, A.T., MAGUIRE, J., FOSTER, A. & TRIDGETT, R. (1988). Development of NK-2 selective antagonists. *Regul. Pept.*, **22**, 189.

(Received January 17, 1994
Revised July 20, 1994
Accepted July 29, 1994)

Br. J. Pharmacol. (1994), **113**, 1191-1196 © Macmillan Press Ltd, 1994

Contractile effects of uridine 5'-triphosphate in the rat duodenum

C. R. Johnson & [1]S.M.O. Hourani

Receptors & Cellular Regulation Research Group, School of Biological Sciences, University of Surrey, Guildford, Surrey GU2 5XH

1 Previous studies have shown that the rat duodenum relaxes to adenosine and adenosine 5'-triphosphate (ATP) via P_1 and P_{2Y} purinoceptors respectively, but in preliminary studies uridine 5'-triphosphate (UTP) was found to contract this tissue. The non-selective P_2 antagonist suramin and a number of nucleotides were therefore used to investigate this response further.

2 ATP, UTP, adenosine 5'-diphosphate (ADP), adenosine 5'-*O*-(3-thiotriphosphate) (ATP-γ-S), guanosine 5'-triphosphate (GTP) and uridine 5'-diphosphate (UDP) each relaxed the duodenum, with an agonist potency order of ATP = ADP > ATP-γ-S >> GTP >> UTP = UDP, consistent with the presence of a P_{2Y} purinoceptor mediating relaxation.

3 ATP-γ-S, UTP and UDP each contracted the duodenum with an agonist potency order of ATP-γ-S > UTP > UDP, although maximal responses to these agonists were not obtained at a concentration of 267 μM (ATP-γ-S) and 300 μM (UTP and UDP). No contractions were observed with any of the other agonists at concentrations up to 300 μM.

4 Indomethacin (25 μM) did not inhibit the contractions induced by UTP, indicating that they were not mediated via production of prostaglandins.

5 Suramin (100 μM and 1 mM) inhibited relaxations induced by ATP, shifting the concentration-response curve to the right, with the maximal response to ATP being decreased by the higher concentration of suramin (1 mM). Suramin (1 mM) inhibited relaxations induced by ATP-γ-S, shifting the concentration-response curve to the right, and completely abolished contractions induced by ATP-γ-S. In contrast, suramin (100 μM and 1 mM) had no effect on contractions induced by UTP. Contractions induced by UTP were, however, less sustained in the presence of suramin, which also affected the basal tone of some tissues when precontracted with carbachol (0.1 μM). In the presence of suramin (1 mM), no contractions to ATP were observed.

6 These results confirm that in the rat duodenum there is a P_{2Y} purinoceptor that mediates relaxation in response to a number of purine nucleotides, and at which the pyrimidine nucleotides UTP and UDP are almost inactive. There are also receptors at which UTP and ATP-γ-S act to cause contraction. Suramin discriminates between the contractile effects of these two agonists, which may indicate the presence of a suramin-insensitive pyrimidinoceptor as well as a suramin-sensitive receptor for ATP-γ-S. An alternative explanation is that the differential effects of suramin are via its actions as an antagonist in addition to its action as an ectonucleotidase inhibitor.

Keywords: ATP; UTP; ATP-γ-S; rat duodenum; suramin; P_2 purinoceptors; pyrimidinoceptors.

Introduction

Adenosine and adenine nucleotides act via P_1 and P_2 purinoceptors respectively to elicit relaxation or contraction of smooth muscle. P_1 purinoceptors are subdivided into A_1, A_{2a}, A_{2b} and A_3 subtypes (reviewed by Collis & Hourani, 1993), and P_2 purinoceptors on smooth muscle were divided initially into P_{2X} and P_{2Y} (Burnstock & Kennedy), 1985; reviewed by Fredholm *et al.*, 1994). The most useful P_2 purinoceptor antagonist to date is suramin, but it is not selective between P_{2X} and P_{2Y} subtypes (Hoyle *et al.*, 1990) and is also an inhibitor of ectonucleotidases (Hourani & Chown, 1989), which degrade adenosine 5'-triphosphate (ATP) and its analogues to their corresponding nucleosides, which can then act at P_1 purinoceptors (Bailey & Hourani, 1990). Degradation may lead to decreased potency of ATP and some of its analogues in some tissues (Welford *et al.*, 1987), which will affect agonist potency orders.

Although adenosine and adenine nucleotides have been most investigated to date, other purines and pyrimidines are also active in eliciting responses in many tissues. There is increasing interest in uridine 5'-triphosphate (UTP), which has been shown to elicit similar responses to ATP in some tissue preparations but not in others. UTP may act via P_{2X} purinoceptors in the mouse vas deferens (Von Kügelgen *et al.*, 1990) and via P_{2Y} purinoceptors in the rat colon muscularis mucosae (Hourani *et al.*, 1993), as cross-desensitization is seen between ATP analogues and UTP. However, evidence in a number of other tissues suggests that, although UTP is active, it is not acting via a P_{2X} or P_{2Y} purinoceptor but by a different receptor. In a number of blood vessels which contract to ATP, in addition to a P_{2X} purinoceptor at which ATP is active, evidence indicates that separate UTP receptors are also present (Von Kügelgen *et al.*, 1987; Saïag *et al.*, 1987; 1990; Von Kügelgen & Starke, 1990). In fact, the term pyrimidinoceptor has been proposed for a receptor at which pyrimidines are active in place of purines (reviewed by Seifert & Schultz, 1989). A number of cells contain a receptor which is coupled to phospholipase C and at which ATP and UTP show equal potency, but at which P_{2Y} purinoceptor-selective agonists such as 2-methylthioadenosine 5'-triphosphate (2-MeSATP) show little or no activity. These receptors have been proposed to be nucleotide receptors for which the agonist potency order is ATP = UTP >> 2-MeSATP (O'Connor *et al.*, 1991). Nucleotide receptors are equivalent to P_{2U} receptors, a name that has also been given to receptors at which ATP and UTP

[1] Author for correspondence.

are equipotent and which are coupled to phospholipase C (Dubyak & El-Moatassim, 1993). In confirmation of the suggestion that there are P_{2U} receptors distinct from P_{2Y} purinoceptors, receptors with the characteristics of these subtypes have now been cloned (Lustig *et al.*, 1993; Webb *et al.*, 1993).

The rat duodenum contains P_1 (A_1 and A_2 subtypes) (Nicholls *et al.*, 1992) and P_{2Y} purinoceptors (Nicholls *et al.*, 1990), which mediate relaxation to adenosine and ATP respectively. However, preliminary studies with UTP revealed that this nucleotide causes contraction rather than relaxation of this tissue. Suramin and a number of nucleotides were therefore used to investigate further this contractile response.

Methods

Pharmacological studies

Non-starved adult male Wistar Albino rats (University of Surrey strain) (200–250 g) were killed by cervical dislocation. The duodenum was dissected out by cutting at the base of the pylorus and at 1.5 cm from this point, cleared of any connective tissue and washed thoroughly with Krebs solution. Cotton thread was tied round each end of the segment of duodenum so that the lumen was sealed, and the tissues then mounted in 4 ml organ baths containing Krebs solution aerated with 95% O_2/5% CO_2 and maintained at 35–36°C. The Krebs solution had the following composition (mM): NaCl 118, KCl 4.8, $MgSO_4$ 1.2, $CaCl_2$ 2.5, KH_2PO_4 1.2, $NaHCO_3$ 25 and glucose 11. A resting tension of 1 g was applied to the tissues and isometric responses were recorded with a Grass FT03 transducer and displayed on a Grass 79D polygraph. Tissues were allowed to equilibrate for 45 min, with washes at 15 min intervals, before the addition of drugs.

The potency of the agonists was expressed as the EC_{50}, calculated by linear regression analysis of the linear portions of the individual log concentration–response curves. As a maximum contractile response was not obtained for all of the agonists, relative agonist potency was measured at a level equal to 50% of the response to carbachol (0.1 μM). For statistical analysis of results the pD_2 values (the negative log of these EC_{50} values) were compared using Student's *t*-test. Concentration–response curves to only one agonist were carried out on any single tissue. Relaxations were first measured, followed by contractile responses on the same piece of tissue. Relaxations were quantified by precontracting the duodenum with carbachol (0.1 μM) with a contact time of 1.5 min and challenging with agonist (contact time 1 min). Contractions to carbachol (approximately 1.4 g tension) were measured from the centre of spontaneous baseline activity to the highest point of carbachol contraction. Relaxations were measured as the reduction in the height of the rhythmic contractions, relative to the time immediately before addition of the relaxant agonist and expressed as per cent reversal of carbachol contraction [per cent relaxation = (BC/AB) × 100 in Figure 3a]. Contractions were observed by adding agonist (contact time 1 min) without precontracting the tissue and contractions were expressed as a percentage of the contraction caused by carbachol (0.1 μM) (determined as the mean value of all the doses of carbachol (0.1 μM) used in determining relaxation). Where agonists induced contractions with marked spontaneous activity, contractions were measured as the centre point of this activity (DE in Figure 3b). Atropine (0.1 μM) was administered following the relaxation concentration–response curve and prior to determination of the contraction concentration–response curve, incubated for 15 min and then readded after each washout. Atropine was used to suppress spontaneous activity in the tissue, and thus allow a more accurate measurement of contractions to agonists. Atropine did not affect the response to any of the nucleotides. A 10 min dosecycle was used and a 30–60 s washout following each dose of test agonist. Concentration–response curves were obtained non-cumulatively using tissues from four animals, and results were expressed graphically as the mean and standard error of the mean (s.e. mean) of the responses obtained.

Relaxation and contraction concentration–response curves to ATP, UTP and adenosine 5′-*O*-(3-thiotriphosphate) (ATP-γ-S) were also determined in the presence of suramin (100 μM or 1 mM) preincubated for 1 h, in separate experiments. Suramin was observed to affect the basal tone of the tissue in some preparations when precontracted with carbachol (0.1 μM), making the spontaneous contractions more variable, and thus making quantification of relaxant responses difficult on some of these preparations. When this was observed the experiment was repeated rather than use these data. A relaxation and contraction concentration–response curve to UTP was also determined in the presence of indomethacin (25 μM), preincubated for 45 min. Inhibition of cyclo-oxygenase by indomethacin was confirmed by the ability of indomethacin (25 μM) to inhibit contractions induced by arachidonic acid (100 μM).

ATP-γ-S and UTP were used in an attempt to desensitize the receptors at which they act to cause contraction. A 100 μM concentration of the agonist was administered repeatedly over 90 min with a contact time of 5–10 min and 1–2 min between washing and readdition of the agonist. The agonists were tested on separate tissues, and the percentage contraction for each dose of agonist was determined from the mean of three doses of carbachol (0.1 μM) given prior to the administration of ATP-γ-S or UTP.

Purification of adenosine 5′-O-(3-thiotriphosphate)

High performance liquid chromatographic analysis of adenosine 5′-*O*-(3-thiotriphosphate) (ATP-γ-S) as obtained from the supplier showed an 11% impurity of ADP to be present. Relaxation and contraction concentration–response curves were therefore obtained for ATP-γ-S both in the presence of the ADP impurity and also for ATP-γ-S enzymically treated to degrade the ADP impurity to inosine. Different pieces of tissue were used for the experiments with enzymically and non-enzymically treated ATP-γ-S. The enzyme mixture was also given on its own to ensure that it did not cause relaxation or contraction of the tissue. For 100 μM ATP-γ-S containing the ADP impurity, 10 units of alkaline phosphatase (AP) and 10 units of adenosine deaminase (ADA) in Tris buffer (0.1 M, pH 8.0) were added for 5 min at room temperature and then kept on ice until use. Solutions of ATP-γ-S were made at concentrations of 10^{-5} M, 10^{-4} M, 10^{-3} M and 10^{-2} M, and to these the enzymes were added at the appropriate concentrations, being diluted in the same ratio. Each dilution of ATP-γ-S had enzymes added immediately prior to use for two consecutive concentrations. Aliquots were taken of the enzymically treated ATP-γ-S during the experiment and stored at −20°C, then analysed by h.p.l.c. at a later date. Analysis was carried out using a Waters chromatograph with a Techsphere 5 μm ODS C_{18} column eluted with 0.1 M KH_2PO_4/8 mM tetrabutylammonium hydrogen sulphate (pH 6.0) (solvent A) and a 60:40 mixture of solvent A and acetonitrile (pH 6.73) (solvent B), using a non-linear gradient (0–2.5 min, 0% B; 2.5–5 min, 0–20% B; 5–10 min, 20–40% B; 10–13 min, 40–100% B; 13–18 min, 100% B), at a flow rate of 1.3 ml min^{-1}. The purines were detected by u.v. absorbence at 259 nm and quantified from the height of their absorbence peaks, which was linearly related to the concentration. Where ATP-γ-S is mentioned in the text, this refers to the enzymically treated nucleotide unless otherwise stated, and the true concentrations were calculated by subtracting the concentration of ADP initially present.

Materials

ATP, UTP, adenosine 5'-diphosphate (ADP), uridine 5'-triphosphate (UDP), adenosine 5'-(α,β-methylene) triphosphonate (AMPCPP), guanosine 5'-triphosphate (GTP), inosine, carbachol, indomethacin, alkaline phosphatase, adenosine deaminase, arachidonic acid and tetrabutylammonium hydrogen sulphate were obtained from Sigma (Poole, Dorset, U.K.), 2-MeSATP was obtained from Research Biochemicals, Semat Ltd (St. Albans, U.K.), ATP-γ-S was obtained from Boehringer Mannheim (Lewes, East Sussex, U.K.) and buffer salts and solvents were of analytical or h.p.l.c. grade and were obtained from BDH (Poole, Dorset, U.K.). Suramin was a generous gift from Bayer, U.K.

Indomethacin was initially dissolved in ethanol and made up in 1:19 (v/v) ethanol–phosphate buffer. The pH of this solution was approximately 7.4 and the indomethacin should therefore be stable for 24 h (Curry & Brown, 1982), but a fresh solution was prepared for immediate use before each experiment. Arachidonic acid was freshly made up in 0.1 M Na_2CO_3 before the experiment.

Results

ATP, ADP, ATP-γ-S and GTP each relaxed the rat duodenum in a concentration-dependent manner with mean pD_2 values of 5.93 ± 0.03 ($EC_{50} = 1.2\ \mu M$), 5.87 ± 0.15 ($EC_{50} = 1.4\ \mu M$), 5.43 ± 0.17 ($EC_{50} = 3.7\ \mu M$) and 4.09 ± 0.32 ($EC_{50} = 82\ \mu M$) respectively. UDP and UTP ($> 30\ \mu M$) only caused very small and inconsistent relaxations, and no EC_{50} value could be obtained. The agonist potency order for relaxation was ATP = ADP > ATP-γ-S >> GTP >> UTP = UDP (Figure 1a; see Figure 3a for representative traces).

UDP, UTP and ATP-γ-S each contracted the rat duodenum in a concentration-dependent manner, whereas the other agonists used (2-MeSATP, ATP, ADP, AMPCPP and GTP, at concentrations of up to 300 μM) did not. At concentrations of up to 300 μM (UDP and UTP) and 267 μM (ATP-γ-S) maximal responses were not obtained. The agonist potency order for contracting the duodenum was ATP-γ-S > UTP > UDP, with mean pD_2 values of 4.76 ± 0.06 ($EC_{50} = 17\ \mu M$), 4.26 ± 0.16 ($EC_{50} = 55\ \mu M$) and 3.57 ± 0.07 ($EC_{50} = 270\ \mu M$) respectively (Figure 1b). The contractile response to UDP, UTP and to ATP-γ-S consisted of an increase in both the basal tone and the spontaneous activity of contractions at concentrations up to 300 μM (UDP and UTP) and 26.7 μM (ATP-γ-S), whereas at higher concentrations the increase in spontaneous activity was not so marked (see Figure 3b for representative traces).

Pretreatment with suramin (100 μM or 1 mM) shifted the relaxation concentration–response curve for ATP to the right, and this shift was statistically significant in each case ($p < 0.01$), resulting in mean pD_2 values of 5.27 ± 0.06 ($EC_{50} = 5.4\ \mu M$) and 4.86 ± 0.14 ($EC_{50} = 14\ \mu M$) and a dose ratio of 4.5 and 12 respectively. The maximal responses to ATP were also depressed in the presence of 1mM but not 100 μM suramin (Figure 2a). In the presence of 100 μM and 1 mM suramin no contractions to ATP were observed. Pretreatment with suramin (1 mM) also shifted the relaxation concentration–response curve for ATP-γ-S to the right, and this shift was statistically significant ($P < 0.01$), resulting in a mean pD_2 value of 4.43 ± 0.09 ($EC_{50} = 37\ \mu M$), and a dose ratio of 10 (Figure 2b). Contractions to ATP-γ-S were abolished in the presence of 1 mM suramin (Figure 2d). In contrast, pretreatment with suramin (100 μM or 1mM) had little effect on the contractions to UTP (Figure 2c). Even with 1mM suramin there was less than a two-fold shift to the right of the concentration–response curve (mean pD_2 value of 4.03 ± 0.19 ($EC_{50} = 94\ \mu M$), and this shift was not statistically significant ($P > 0.01$). In the presence of suramin (100 μM or 1 mM) the UTP-induced contractions were less sustained and fell off more rapidly, and the spontaneous contractions were suppressed (see Figure 3b for representative traces). Pretreatment with indomethacin (25 μM for 45 min) had no effect on contractions induced by UTP (results not shown). No desensitization was observed to ATP-γ-S or UTP (100 μM) when contractions were induced by these agonists repeatedly over a period of 90 min, the contraction remaining constant over this period (results not shown).

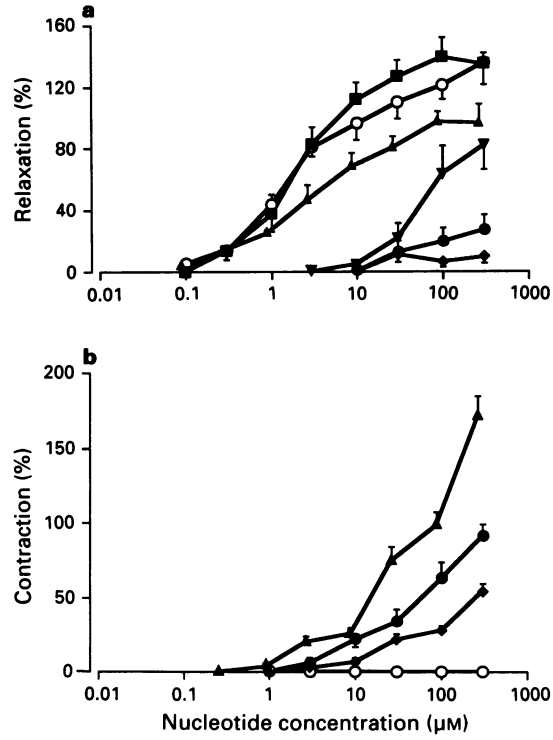


Figure 1 (a) Relaxation of the rat duodenum by adenosine 5'-diphosphate (ADP) (■), adenosine 5'-triphosphate (ATP) (○), adenosine 5'-*O*-(3-thiotriphosphate) (ATP-γ-S) (▲), guanosine 5'-triphosphate (GTP) (▼), uridine 5'-triphosphate (UTP) (●) or uridine 5'-diphosphate (UDP) (◆), expressed as per cent reversal of carbachol (0.1 μM)-induced contraction. (b) Contraction of the rat duodenum by ATP-γ-S (▲), UTP (●) UDP (◆) or ATP (○) expressed as a percentage of the contraction induced by carbachol (0.1 μM). Each point is the mean of four determinations, and the vertical bars show s.e. mean.

ATP-γ-S as obtained from suppliers contained approximately 11% ADP. After enzymatic treatment with AP and ADA this ADP impurity was degraded to inosine, whereas the ATP-γ-S was not degraded (results not shown). Inosine was inactive at concentrations of up to 100 μM for both relaxation and contraction (results not shown). After enzymatic degradation of the ADP impurity, relaxations to ATP-γ-S were slightly reduced, resulting in approximately a twofold shift in the concentration–response curve, with a decrease in the pD_2 value from 5.77 ± 0.10 ($EC_{50} = 1.7\ \mu M$) to 5.43 ± 0.17 ($EC_{50} = 3.7\ \mu M$), whereas contractions to ATP-γ-S were slightly enhanced, resulting in approximately a twofold shift in the concentration–response curve, with an increase in the pD_2 value from 4.48 ± 0.09 ($EC_{50} = 34\ \mu M$) to 4.76 ± 0.06 ($EC_{50} = 17\ \mu M$) respectively (Figure 2b and d). However, these shifts were not statistically significant ($P > 0.01$).

Discussion

Our previous studies have shown that relaxation is mediated via a P_{2Y} purinoceptor in this tissue with an agonist potency order of 2-MeSATP > ATP > AMPCPP (Nicholls *et al.*,

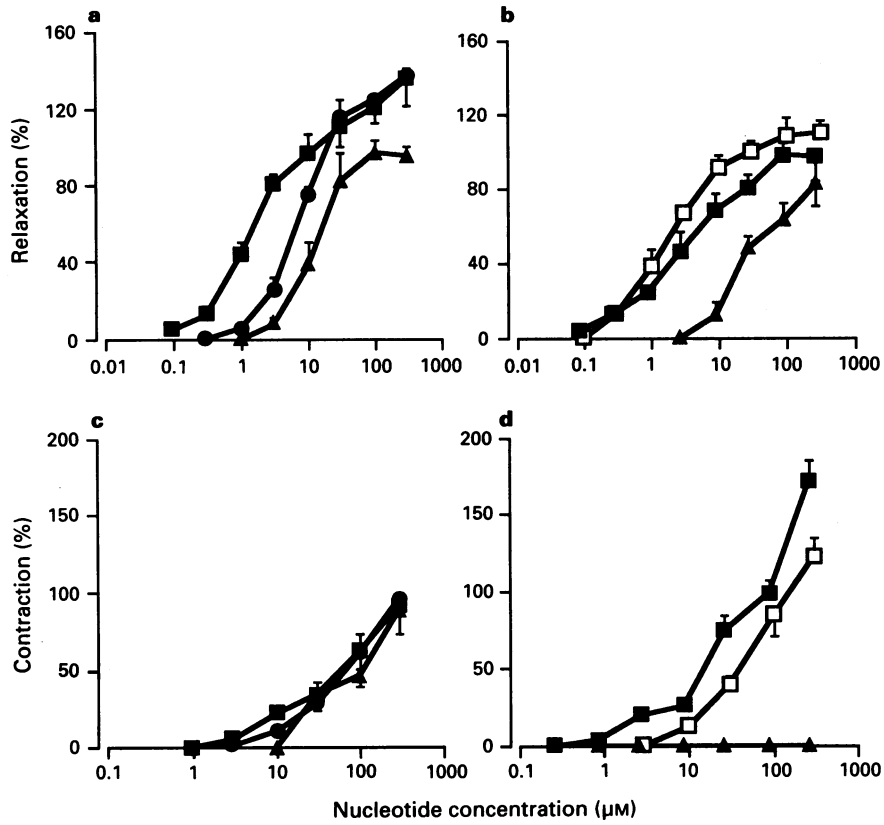


Figure 2 Effect of suramin on responses to nucleotides of the rat duodenum. (a) Relaxation by ATP; (b) relaxation by ATP-γ-S; (c) contraction by UTP and (d) contraction by ATP-γ-S in the absence (■) or presence of suramin (100 μM) (●) or (1 mM)(▲). Relaxation or contraction by ATP-γ-S as obtained from the supplier is shown as open squares in (b) and (d) respectively. Relaxation was expressed as per cent reversal of carbachol (0.1 μM)-induced contraction, and contraction was expressed as a percentage of the contraction induced by carbachol (0.1 μM). Each point is the mean of four determinations, and the vertical bars show s.e. mean. Abbreviations used are given in the caption to Figure 1.

1990), and the additional agonist potency order obtained in the present study of ATP = ADP > ATP-γ-S >> GTP >> UTP = UDP is consistent with this conclusion. In contrast, UDP and UTP, which were almost inactive in relaxing precontracted duodenum, brought about a marked contraction of this tissue. As indomethacin did not block contractions to UTP, but did those to arachidonic acid (results not shown), contractions induced by UTP were not mediated by prostaglandins. ATP-γ-S, in addition to relaxing the duodenum, also caused marked contraction of this tissue, and was more potent than either of the pyrimidine nucleotides. As no contraction was observed in response to AMPCPP, which is a potent agonist at P_{2X} purinoceptors, or to 2-MeSATP, a potent agonist at P_{2Y} purinoceptors, contraction of the rat duodenum does not appear to be mediated by a purinoceptor of the P_{2X} or P_{2Y} subtypes.

The terms nucleotide receptor or P_{2U} receptor have been proposed for a receptor which is linked to phospholipase C and at which the agonist potency order is UTP = ATP > ATP-γ-S > ADP > 2-MeSATP > AMPCPP (O'Connor *et al.*, 1991; O'Connor, 1992). There have been a number of tissues which have been shown to contain either P_{2U} receptors, such as human airway epithelial cells (Brown *et al.*, 1991) or a mixed population of P_{2Y} and P_{2U} receptors, such as bovine aortic endothelial cells (Wilkinson *et al.*, 1993). However, as ATP does not cause contraction in the rat duodenum, our results indicate that these contractions are not mediated by P_{2U} receptors as defined in previous literature. Although the relaxations induced by ATP could possibly mask any contractions, ATP-γ-S clearly caused contraction in spite of being a potent relaxant agonist, and suramin (1 mM), which inhibited ATP-induced relaxations, did not reveal any contractile response.

Another type of receptor termed pyrimidinoceptors, which respond to uracil nucleotides instead of adenine nucleotides, has been proposed to exist largely on the basis of differences in the responses of ATP and UTP in some tissues (reviewed by Seifert & Schulz, 1989). In a number of blood vessels such as the rabbit ear artery (Von Kügelgen *et al.*, 1987), rat tail and femoral arteries and dog saphenous vein (Saïag *et al.*, 1987; 1990) and rabbit basilar artery (Von Kügelgen & Starke, 1990), both ATP and UTP elicit vasoconstriction, but on the basis of data such as desensitization it has been proposed that ATP and UTP act via different receptors, the receptor at which UTP acts having been termed a pyrimidinoceptor. In the rabbit basilar artery in which ATP-γ-S was used, prolonged exposure to this agonist reduced subsequent responses to ATP, whereas those to UTP were slightly increased (Von Kügelgen & Starke, 1990), suggesting that the purines ATP and ATP-γ-S act at a different receptor from the pyrimidine UTP. In the rat duodenum, however, desensitization was not observed to either ATP-γ-S or UTP, so this approach could not be used to investigate whether these agonists acted at a common receptor. However, the antagonist suramin abolished the contractile response to ATP-γ-S but did not affect that of UTP. This suggests that ATP-γ-S and UTP may be acting via different receptors to elicit contraction. UDP, which is a potent agonist at the proposed pyrimidinoceptors in the rabbit ear artery (Von Kügelgen *et al.*, 1987) and basilar artery (Von Kügelgen & Starke, 1990), was also a potent agonist in eliciting contraction in the rat duodenum.

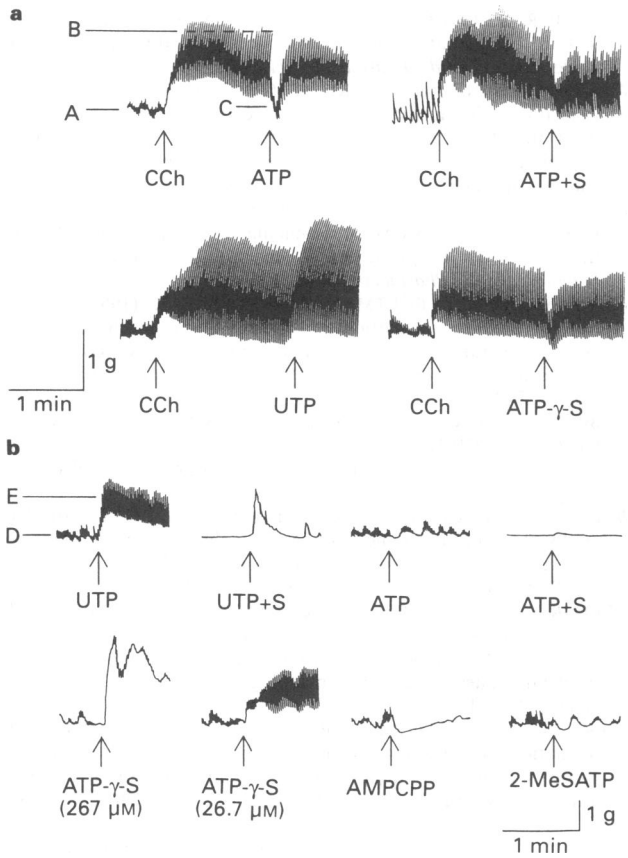


Figure 3 Representative traces showing results from rat duodenum. (a) Effect of ATP (10 μM), ATP (10 μM) in the presence of suramin (1 mM) (ATP+S), UTP (100 μM) or ATP-γ-S (8.9 μM), following contraction with carbachol (CCh) (0.1 μM). (b) Effect of UTP, UTP in the presence of suramin (1 mM) (UTP+S), ATP, ATP+S, ATP-γ-S (267 μM or 26.7 μM), AMPCPP or 2-MeSATP. All drugs were at a concentration of 300 μM unless otherwise indicated. Vertical arrows indicate administration of drug. Abbreviations used are given in the caption to Figure 1. The trace in (a) showing relaxation to ATP shows the method of quantification of relaxation, and the trace in (b) showing contraction to UTP shows the method of quantification of contraction in the presence of spontaneous activity (see Methods).

The lack of truly selective antagonists for the P_2 purinoceptor subtypes has limited classification of these receptors to date, and the non-selective suramin is probably the best antagonist available. Our results show that suramin shifted the ATP relaxation concentration–response curve to the right, as expected for a P_{2Y} purinoceptor. In contrast, suramin did not affect the UTP contraction concentration–response curve. This indicates that the receptor at which UTP is acting to elicit contraction is not blocked by suramin, and further supports the suggestion that it is not of the P_{2X} or P_{2Y} subtypes. However, suramin completely abolished the contractions to ATP-γ-S, and this could suggest that, in addition to a suramin-insensitive pyrimidinoceptor, there is a further suramin-sensitive receptor causing contraction of the rat duodenum, which can be activated only by the purine nucleotide ATP-γ-S, and not by the other nucleotides tested. Alternatively, there could be one receptor at which both UTP and ATP-γ-S act, and the effect of suramin on contractions could be explained in terms of its action as an ectonucleotidase inhibitor (Hourani & Chown, 1989). Degradation by ectonucleotidases has been shown to lead to decreased potency of ATP and some of its analogues in some tissues, and ATP-γ-S has been shown to be relatively resistant to ectonucleotidase activity, unlike UTP, which is rapidly degraded (Welford *et al.*, 1987). Thus the dual effect of suramin in inhibiting ectonucleotidase activity and antagonizing the receptor could result in differential inhibition of the agonists. The effect on ATP-γ-S would be simple antagonism, whereas in the case of UTP the enhanced potency due to inhibition of ectonucleotidases would oppose any shift in its observed concentration–response curve. Indeed, a similar mechanism has been proposed recently to explain variable effects of suramin against agonists degraded at different rates in the rabbit ear artery (Crack *et al.*, 1994).

A complication which should be borne in mind when ATP-γ-S is used is the presence of ADP as an impurity in the ATP-γ-S as obtained from the supplier. As ADP is a potent P_{2Y} purinoceptor agonist but has little activity at P_{2U} receptors, this could affect the observed potency of ATP-γ- S. In addition, ADP is readily dephosphorylated by ectonucleotidases to its corresponding nucleoside adenosine (Welford *et al.*, 1986; 1987), which can then act at P_1-purinoceptors (Bailey & Hourani, 1990). In this study, enzymatic degradation of the ADP impurity to inosine, which was inactive in this tissue, slightly shifted both relaxation and contraction concentration–response curves to ATP-γ-S, enhancing the contractile responses while depressing the relaxations.

In conclusion, our data indicate that in the rat duodenum in addition to P_{2Y} purinoceptors causing relaxation, there are receptors causing contraction at which UTP and ATP-γ-S act and which are neither P_{2X} nor P_{2Y}. Because of the differential inhibition by suramin of these agonists, these results could be interpreted as indicating the presence of a suramin-insensitive pyrimidinoceptor as well as a suramin-sensitive receptor for ATP-γ-S. An alternative explanation for the differential effects of suramin, however, is that its actions as an antagonist are compromised in the case of rapidly degraded nucleotides such as UTP by its action as an ectonucleotidase inhibitor.

We thank the MRC for a studentship for C.R.J. and the Wellcome Trust for financial support.

References

BAILEY, S.J. & HOURANI, S.M.O. (1990). A study of the purinoceptors mediating contraction in the rat colon. *Br. J. Pharmacol.*, **100,** 753–756.

BROWN, H.A., LAZAROWSKI, E.R., BOUCHER, R.C. & HARDEN, T.K. (1991). Evidence that UTP and ATP regulate phospholipase C through a common extracellular 5'-nucleotide receptor in human airway epithelial cells. *Mol. Pharmacol.*, **40.** 648–655.

BURNSTOCK, G. & KENNEDY, C. (1985). Is there a basis for distinguishing two types of P_2-purinoceptor? *Gen. Pharmacol.*, **16,** 433–440.

COLLIS, M.G. & HOURANI, S.M.O. (1993). Adenosine receptor subtypes. *Trends Pharmacol. Sci.*, **14,** 360–366.

CRACK, S.E., BEUKERS, M.W., IJZERMAN, A.P., McKECHNIE, K.C.W. & LEFF, P. (1994). Inhibition of ATP degradation by L-2-methylthio-β,γ-dibromomethylene-ATP and suramin. *Drug Dev. Research*, **31,** 259.

CURRY, S.H. & BROWN, E.A. (1982). Preparation and stability of indomethacin solutions. *Can. J. Physiol. Pharmacol.*, **60,** 988–992.

DUBYAK, G.R. & EL-MOATASSIM, C. (1993). Signal transduction via P_2-purinergic receptors for extracellular ATP and other nucleotides. *Am. J. Physiol.*, **265,** C577–C606.

FREDHOLM, B.B., ABBRACCHIO, M.P., BURNSTOCK, G., DALY, J.W., HARDEN, T.K., JACOBSON, K.A., LEFF, P. & WILLIAMS, M. (1994). Nomenclature and classification of purinoceptors. *Pharmacol. Rev.*, **46**, 143–156.

HOURANI, S.M.O. & CHOWN, J.A. (1989). The effects of some possible inhibitors of ectonucleotidases on the breakdown and pharmacological effects of ATP in the guinea-pig urinary bladder. *Gen. Pharmacol.*, **20**, 413–416.

HOURANI, S.M.O., JOHNSON, C.R. & BAILEY, S.J. (1993) Desensitization of the P_2-purinoceptors on the rat colon muscularis mucosae. *Br. J. Pharmacol.*, **110**, 501–505.

HOYLE, C.H.V., KNIGHT, G.E. & BURNSTOCK, G. (1990). Suramin antagonizes responses to P_2-purinoceptor agonists and purinergic nerve stimulation in the guinea-pig urinary bladder and taenia coli. *Br. J. Pharmacol.*, **99**, 617–621.

LUSTIG, K.D., SHIAU, A.K., BRAKE, A.J. & JULIUS, D. (1993). Expression cloning of an ATP receptor from mouse neuroblastoma cells. *Proc. Natl. Acad. Sci. U.S.A.*, **90**, 5113–5117.

NICHOLLS, J., HOURANI, S.M.O. & KITCHEN, I. (1990). The ontogeny of purinoceptors in rat urinary bladder and duodenum. *Br. J. Pharmacol.*, **100**, 874–878.

NICHOLLS, J., HOURANI, S.M.O. & KITCHEN, I. (1992). Characterization of P_1purinoceptors on rat duodenum and urinary bladder. *Br. J. Pharmacol.*, **105**, 639–642.

O'CONNOR, S.E. (1992). Recent developments in the classification and functional significance of receptors for ATP and UTP, evidence for nucleotide receptors. *Life Sci.*, **50**, 1657–1664.

O'CONNOR, S.E., DAINTY, I.A. & LEFF, P. (1991). Further subclassification of ATP receptors based on agonist studies. *Trends Pharmacol. Sci.*, **12**, 137–141.

SAÏAG, B., MILON, D., GUELOU, M.C., VAN DEN DRIESSCHE, J. & RAULT, B. (1987). Pharmacological evidence for the existence of P2 purinoceptors different from 'pyrimidinoceptors' on arterial and venous smooth muscle. In *Abstracts of the 10th International Congress of Pharmacology, Sydney*, 1987, p.959.

SAÏAG, B., MILON, D., ALLAIN, H., RAULT, B., & VAN DEN DRIESSCHE, J. (1990). Constriction of the smooth muscle of rat tail and femoral arteries and dog saphenous vein is induced by uridine triphosphate via 'pyrimidinoceptors', and by adenosine triphosphate via P2X purinoceptors. *Blood Vessels*, **27**, 352–364.

SEIFERT, R. & SCHULTZ, G. (1989). Involvement of pyrimidinoceptors in the regulation of cell functions by uridine and by uracil nucleotides. *Trends Pharmacol. Sci.*, **10**, 365–369.

VON KÜGELGEN, I. & STARKE, K. (1990). Evidence for separate vasoconstriction-mediating nucleotide receptors, both distinct from the P_{2X}-receptor, in rabbit basilar artery: a receptor for pyrimidine nucleotides and a receptor for purine nucleotides. *Naunyn-Schmied. Arch. Pharmacol.*, **341**, 538–546.

VON KÜGELGEN, I., HÄUSSINGER, D. & STARKE, K. (1987). Evidence for a vasoconstriction-mediating receptor for UTP, distinct from the P_2 purinoceptor, in rabbit ear artery. *Naunyn-Schmied. Arch. Pharmacol.*, **336**, 556–560.

VON KÜGELGEN, I., BÜLTMAN, R. & STARKE, K. (1990). Interaction of adenine nucleotides, UTP and suramin in mouse vas deferens: suramin-sensitive and suramin-insensitive components in the contractile effect of ATP. *Naunyn-Schmied. Arch. Pharmacol.*, **342**, 198–205.

WEBB, T.E., SIMON, J., KRISHEK, B.J., BATESON, A.N., SMART, T.G., KING, B.F., BURNSTOCK, G. & BARNARD, E.A. (1993). Cloning and functional expression of a brain G-protein-coupled ATP receptor. *FEBS Lett.*, **324**, 219–225.

WELFORD, L.A., CUSACK, N.J. & HOURANI, S.M.O. (1986) ATP analogues and the guinea-pig taenia coli: a comparison of the structure-activity relationships of ectonucleotidases with those of the P_2-purinoceptor. *Eur. J. Pharmacol.*, **129**, 217–224.

WELFORD, L.A., CUSACK, N.J. & HOURANI, S.M.O. (1987). The structure-activity relationships of ectonucleotidases and of excitatory P_2-purinoceptors: evidence that dephosphorylation of ATP analogues reduces pharmacological potency. *Eur. J. Pharmacol.*, **141**, 123–130.

WILKINSON, G.F., PURKISS, J.R. & BOARDER, M.R. (1993). The regulation of aortic endothelial cells by purines and pyrimidines involves co-existing P_{2Y}-purinoceptors and nucleotide receptors linked to phospholipase C. *Br. J. Pharmacol.*, **108**, 689–693.

(Received February 16, 1994
Revised July 25, 1994
Accepted August 1, 1994)

Br. J. Pharmacol. (1994), **113**, 1197–1202 © Macmillan Press Ltd, 1994

Nitric oxide, and not vasoactive intestinal peptide, as the main neurotransmitter of vagally induced relaxation of the guinea pig stomach

[1]*K.M. Desai, †T.D. Warner, ‡A.E. Bishop, ‡J.M. Polak & †J.R. Vane

*Department of Pharmacology, Boyer Center for Molecular Medicine, Yale University, Box 9812, 295 Congress Avenue, New Haven, CT 06536-0812, U.S.A; †William Harvey Research Institute, St. Bartholomew's Hospital Medical College, Charterhouse Square, London EC1M 6BQ and ‡Department of Histochemistry, Royal Postgraduate Medical School, Hammersmith Hospital, Du Cane Road, London W12 0NN

1 Nitric oxide synthase (NOS) was localized in the guinea pig stomach by immunocytochemistry. *In vitro* experiments were carried out on the isolated stomach of the guinea pig to study any possible links between nitric oxide (NO) and vasoactive intestinal peptide (VIP) in mediating relaxations induced by vagal stimulation.

2 NOS was localized to nerve cell bodies and nerve fibre varicosities of the myenteric plexus in wholemounts of the longitudinal muscle–myenteric plexus of the stomach fundus. The NOS-positive cells had a Dogiel type I morphology characteristic of motor neurones.

3 The cross-sections of the stomach wall showed NOS-positive neurones mainly in the myenteric plexus ganglia and NOS-positive nerve fibre varicosities in the circular muscle layer.

4 Relaxations induced by vagal stimulation were almost completely prevented by L-NAME with an IC_{50} value of 5.5×10^{-6}M. This inhibition was reversed by L-arginine (2 mM).

5 VIP (100 nM) induced reproducible relaxations of the stomach. These were unaffected by tetrodotoxin (2 μM) or N^{ω}-nitro-L-arginine methyl ester (L-NAME, 100 μM).

6 Desensitization to the relaxant effect of VIP partially reduced relaxations induced by vagal stimulation, glyceryl trinitrate or sodium nitroprusside but not noradrenaline.

7 These results show that NO has a neuronal origin in the guinea pig stomach, and support NO, and not VIP, as the major neurotranmitter of vagally induced gastric relaxation in the guinea pig.

Keywords: Nitric oxide; vasoactive intestinal peptide; myenteric plexus; NANC mediator; guinea pig stomach

Introduction

Nitric oxide (NO) is an inhibitory non-adrenergic, non-cholinergic (NANC) mediator at various sites in the gastrointestinal (GI) tract and is widely believed to be released from neurones (Gillespie *et al.*, 1989; Gibson *et al.*, 1990; Li & Rand, 1990; Desai *et al.*, 1991a,b; Boeckxstaens *et al.*, 1992; Meulemans *et al.*, 1993). This has been confirmed in a number of studies by immunocytochemical localization of nitric oxide synthase (NOS), the enzyme catalysing the formation of NO from endogenous L-arginine, to neurones of the myenteric plexus in the guinea pig and rat ileum, rat stomach, duodenum, canine proximal colon and the human gut (Bredt *et al.*, 1990; Schmidt *et al.*, 1992; Springall *et al.*, 1992; Ward *et al.*, 1992; Forster & Southam, 1993). In the guinea pig ileum, NOS-immunoreactive neurones in the myenteric plexus synapse with other neurones and innervate the circular muscle (Llewellyn-Smith *et al.*, 1992). In the rat duodenum and canine proximal colon the NOS-positive neurones have a Dogiel type I morphology and axons going towards the muscle, which is characteristic of motor neurones (Ward *et al.*, 1992; Aimi *et al.*, 1993). In addition, NOS has been localized to the vagal efferent fibres innervating the rat stomach (Forster & Southam, 1993). Histochemistry also suggests that NO is a neurotransmitter with paraneuronal actions in the brain (Schmidt *et al.*, 1992), and recently NO release has been shown from isolated ganglia of the myenteric plexus of the guinea pig ileum (Grider & Jin, 1993). Thus, NO is now established as a neurotransmitter in the brain and the periphery. Vasoactive intestinal peptide (VIP) has also been proposed as a mediator of gastric relaxation in the guinea pig, rat, cat and ferret (Grider *et al.*, 1985; De Beurme & Lefebvre, 1988; D'Amato *et al.*, 1988, 1992; Kamata *et al.*, 1988; Grundy *et al.*, 1993). For instance, electrical field stimulation of muscle strips from the guinea-pig and rat gastric fundus causes release of VIP-like immunoreactivity (Grider & Makhlouf, 1987; D'Amato *et al.*, 1992). It has also been suggested that VIP and NO are co-transmitters of gastric relaxation in the guinea pig, rat and ferret (Li & Rand, 1990; Boeckxstaens *et al.*, 1992; Grider *et al.*, 1992; Said, 1992; Grider & Jin, 1993; Grundy *et al.*, 1993) and internal anal sphincter in the opossum (Chakder & Rattan, 1993). One possibility is that VIP acts partly through stimulation of NO formation, as has been suggested in the smooth muscle cells of the guinea pig stomach (Grider *et al.*, 1992). To examine this possibility we have localized NOS by immunocytochemistry to confirm that it is present in neurones and determined if there is any involvement of VIP in mediating vagally induced relaxation of the guinea pig stomach.

Some of the results of this study were reported earlier to the British Pharmacological Society as an abstract (Desai *et al.*, 1993).

Methods

Immunocytochemical studies

These studies were carried out on wholemount preparations of the longitudinal muscle–myenteric plexus (LM–MP) and

[1] Author for correspondence.

on cross-sections of the stomach fundus of the guinea pig. Male Hartley guinea pigs (300–350 g) were killed by cervical dislocation and exsanguination. The stomach was removed, cut open along the lesser curvature and the contents washed out with Krebs' solution NaCl, 118 mM; KCl, 4.7 mM; $NaHCO_3$, 25 mM; KH_2PO_4, 1.17 mM; $MgSO_4$, 2.5 mM; $CaCl_2$, 2.5 mM; glucose, 5.6 mM; pH 7.4). For wholemounts (Costa *et al.*, 1980) the fundal portion was cut as a flat sheet and pinned, slightly stretched, on to a thin board with the mucosal surface facing down. It was then fixed by immersion for 16–18 h in Zamboni's solution (2% paraformaldehyde in 0.1 M phosphate buffer, pH 7.2, plus saturated picric acid solution in a ratio of 85:15). The tissue was removed from the board and washed in 80% ethanol. It was dehydrated through 95% and 100% ethanol, cleared in xylol and rehydrated through 100%, 80% and 50% ethanol (30 min each) and stored in phosphate-buffered saline (PBS, 0.1 M, pH 7.2) at 4°C until use. The LM–MP was separated as a sheet by separating the mucosal and circular muscle layers with watchmakers' forceps under a dissecting microscope, and incubated for 16–18 h at room temperature with rabbit antibody to NOS, diluted 1:5000 and 1:10,000 in 0.01 M PBS (pH 7.2) with 0.1% bovine serum albumin (BSA) and 0.01% sodium azide. It was then washed in PBS (3 × 5 min) and incubated with fluorescein isothiocyanate (FITC)-conjugated goat anti-rabbit serum diluted 1:40 for 1 h at room temperature and washed in PBS (3 × 5 min). The preparation was then mounted in PBS–glycerine (1:9, v/v) and examined under a confocal microscope. Photographs were taken using FP4 black and white film (speed 100 ASA) (Ilford).

For cross-sections of the stomach wall, the stomach fundus was fixed as before and washed in PBS containing 15% sucrose and 0.01% sodium azide. Cryostat blocks were prepared from small pieces of tissue (2 × 1 cm) and 7–8 μm sections were cut at −20°C, transferred to poly-L-lysine-coated slides and allowed to dry for 1 h. They were immunostained for NOS using the indirect avidin–biotin complex (ABC) immunoperoxidase method (Polak, 1988). The sections were immersed in 0.03% (v/v) hydrogen peroxide in PBS for 30 min to remove the endogenous peroxidase activity. Possible background staining was reduced by incubation for 30 min at room temperature with normal goat serum, diluted 1:30. The sections were then incubated with the primary rabbit antibody to NOS, diluted 1:5000 and 1:10,000, for 16–18 h at room temperature in a humid chamber. For the second layer, biotinylated goat anti-rabbit antibody, diluted 1:100, was applied for 30 min at room temperature. The final layer consisted of Elite Vector reagents A and B (5 μl each of A and B diluted in 90 μl of diluent) incubated for 1 h at room temperature. The reaction was visualized by the nickel-enhanced diaminobenzidine method (Graham & Karnovsky, 1976). When developed, the sections were counterstained with neutral red, dehydrated with absolute alcohol and Inhibisol and mounted. The sections were observed under a transmitted light microscope (Reichert-Jung).

The rabbit polyclonal antibody against the rat brain constitutive NOS had been characterized for specificity (Springall *et al.*, 1992). For negative controls only the diluent was used for first-layer incubation. Antibody against the general neuronal marker protein gene product 9.5 (PGP 9.5, human, 1:4000) (Gulbenkian *et al.*, 1987) was used to confirm neuronal staining with NOS antibody.

In vitro *functional studies on the isolated stomach*

The isolated stomach of the guinea pig was prepared as described previously (Desai *et al.*, 1991b). Briefly, the guinea pig stomach with the vagus nerves was isolated and immersed in oxygenated (95% O_2, 5% CO_2) Krebs' solution and the pyloric end was cannulated. The oesophagus was ligated and the contents of the stomach were flushed out. It was then placed in an isolated organ bath in 100 ml of gassed (95% O_2 + 5% CO_2) Krebs' (37°C) solution containing atropine (3 μM) and guanethidine (5 μM) to study the non-adrenergic, non-cholinergic (NANC) inhibitory effects of vagal stimulation. Bacitracin (3 μg ml^{-1}), thiorphan (1 μM) and captopril (1 μM) were also added to the Krebs' solution to inhibit the endogenous peptidases and angiotensin-converting enzyme and prevent metabolism of VIP. The pyloric cannula was connected to a reservoir (2 l) containing 1 l of Krebs' solution. The reservoir was placed on a movable rack so that it could be moved up or down to increase or decrease the pressure of fluid entering the stomach (Paton & Vane, 1963). Intragastric pressure was measured with a Statham pressure transducer. The reservoir was sealed and connected to a float recorder to measure intragastric volume changes with a Harvard isotonic transducer. The volume and pressure changes were recorded on a Graphtec WR 3310 recorder. The vagus was stimulated with a pair of ring electrodes connected to a Grass S 88 stimulator. Experiments were started after a 45–60 min equilibration period. The threshold pressure for a NANC adaptive response (Paton & Vane, 1963; Desai *et al.*, 1991a) was determined first and the intragastric pressure was elevated to 1–2 cmH_2O below it, usually to 3 cmH_2O, to give an elevated intragastric volume from which to measure subsequent relaxant responses to drugs or vagal stimulation (supramaximal voltage, 10–16 Hz, 1 ms, 50–60 s). After a response the fluid in the stomach was emptied via a side cannula and the next response was recorded after 10 min. Under these conditions the vagally induced responses were reproducible. Since the electrodes were immersed in Krebs' solution surrounding the vagus nerves, supramaximal voltage was used to eliminate variations in the electrical current reaching the nerves for stimulation. In previous experiments, a stimulation frequency of 10–16 Hz gave optimal reproducible monophasic relaxant responses in the presence of atropine (3 μM) and guanethidine (5 μM), and these frequencies were used here for stimulation. Stimulation frequencies between 0.1 and 8 and between 32 and 256 Hz gave monophasic relaxation responses smaller than with 10 and 16 Hz. In those experiments vagal responses at all frequencies from 0.1 to 256 Hz were completely prevented by inhibition of NOS.

To study the effects of tetrodotoxin (TTX), N^{ω}-nitro-L-arginine methyl ester (L-NAME) or L-arginine (L-Arg) on the relaxant responses, the stomach was incubated, both intra- and extraluminally, with the drug(s) for the required time before eliciting a response.

Statistical analysis

The volume changes due to relaxation induced by vagal/drug stimulation are expressed as a percentage of the total gastric volume. All results are expressed as the mean ± s.e. mean of n observations. The data were analysed for statistical significance by analysis of variance and post-hoc Bonferroni test or Student's unpaired two-tailed t-test, with a P-value <0.05 taken as significant.

Drugs used

Noradrenaline bitartrate, atropine sulphate, bacitracin, bovine serum albumin, captopril, glucose oxidase (type III), guanethidine sulphate, L-arginine hydrochloride, N^{ω}-nitro-L-arginine methyl ester, sodium nitroprusside (sodium ferricyanide), *dl*-thiorphan and vasoactive intestinal peptide (VIP) were purchased from Sigma Chemical Co. Glyceryl trinitrate (GTN) (Nitronal) was purchased from Lipha Pharmaceuticals, U.K. The NOS antibody was kindly provided by The Wellcome Research Laboratories, Beckenham, Kent, U.K. All other reagents used were of the highest commercially available purity and were purchased from either BDH or Sigma. The drug solutions were made in distilled water. The stock solution of VIP was made in 0.1% BSA in distilled water and stored at −20°C until used.

Results

Immunohistochemical localization of NOS in wholemounts of LM–MP

Wholemounts of the LM–MP of the stomach fundus showed NOS localized to neuronal cell bodies (confirmed by PGP 9.5 staining) of the myenteric plexus and to nerve fibre varicosities of internodal strands and fibres going to the muscle. The NOS-positive cells were grouped towards the periphery of the ganglia (Figure 1) and had a Dogiel type I morphology (Figure 2) with multistellate shape, 4–5 short broad lamellar processes and a long axon, which is characteristic of motor neurones innervating the muscle. There was no staining of the muscle fibres.

Cross-sections of the stomach fundus wall

The cross-sections of the stomach fundus showed NOS localized mainly to nerve cell bodies in the myenteric plexus ganglia with occasional NOS-positive nerve cells in the submucosa. NOS-positive nerve fibres were seen running parallel to circular smooth muscle fibres and very few fibres in the longitudinal muscle layer. There was no immunostaining of smooth muscle cells or mucosal cells.

Tetrodotoxin prevents vagus-but not VIP-induced gastric relaxation

Vagal stimulation induced reproducible monophasic gastric relaxations. Exogenous VIP in lower concentrations (1, 3, 10 and 30 nM, 4–5 min) failed to induce consistent and reproducible relaxations. However, VIP in a concentration of 100 nM (3–4 min) induced at least three reproducible relaxations (VIP first exposure, 24.2 ± 6%; second exposure, 21.3 ± 1.3%; third exposure, 22.9 ± 2.2%; $n = 3$, $P > 0.05$ between each group). A higher concentration of 200 nM VIP (3–4 min) did not increase the magnitude of relaxation and was subsequently not used to avoid desensitization. Incubation of the stomach with tetrodotoxin (TTX, 2 μM, 20 min) completely prevented gastric relaxation induced by vagal stimulation (control, 36.1 ± 3.3%; + TTX, 0.1 ± 0%; $n = 3$, $P < 0.001$), but did not affect that induced by VIP (100 nM; control, 32.7 ± 5.0%; + TTX, 33.4 ± 3.5%; $n = 3$, $P > 0.05$); or by GTN (2 μM, 1–1.5 min; control, 41.6 ± 4.0%; + TTX, 34.5 ± 6.1%; $n = 3$, $P > 0.05$).

L-NAME inhibits relaxations of the stomach induced by vagal stimulation

A dose–response curve (Figure 3) was obtained for the inhibitory effect of L-NAME (0.1, 1, 3, 10, 30, 100 μM, 20 min each, $n = 4$) on gastric relaxations induced by vagal stimulation in the presence of atropine (3 μM) and guanethidine (5 μM). After control reproducible responses to vagal stimulation the lowest concentration of L-NAME was incubated, intra- and extraluminally simultaneously, for the specified time. After recording a response to vagal stimulation the stomach was emptied and washed. The next higher concentration of L-NAME was then incubated for the same time and a response was recorded. This sequence was repeated. L-NAME had an IC_{50} value of 5.5×10^{-6} M. In subsequent experiments gastric relaxation induced by vagal stimulation was almost completely inhibited by L-NAME (100 μM, 20 min). This inhibition was partially reversed after washout of L-NAME and incubation with L-arginine (L-Arg, 2 mM, 30 min; Figure 4) (control, 46.4 ± 1.4%; + L-NAME, 5.7 ± 1.0%; + L-Arg, 36.8 ± 3.5%; $n = 4$, $P < 0.001$). Washout of L-NAME with L-Arg was attempted since co-incubation of L-NAME (100 μM) with L-Arg (0.5–2 mM) does not reverse the inhibitory effect of L-NAME (Desai *et al.*, 1991a), which could be because L-NAME is an irreversible inhibitor of NOS (Dwyer *et al.*, 1991).

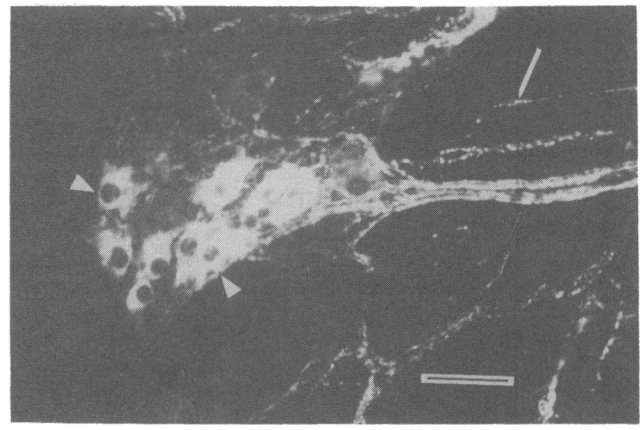


Figure 1 Immunocytochemical localization of nitric oxide synthase (NOS) in a wholemount of the longitudinal muscle–myenteric plexus of the guinea pig stomach fundus. Immunostaining for NOS was by the indirect immunofluorescence method. This figure shows a myenteric plexus ganglion with NOS-positive nerve cells (arrowheads) grouped towards the periphery and surface of the ganglion. NOS-positive nerve fibre varicosities can also be seen (arrow) in internodal fibres and tertiary fibres going to muscle cells. Scale bar = 50 μm.

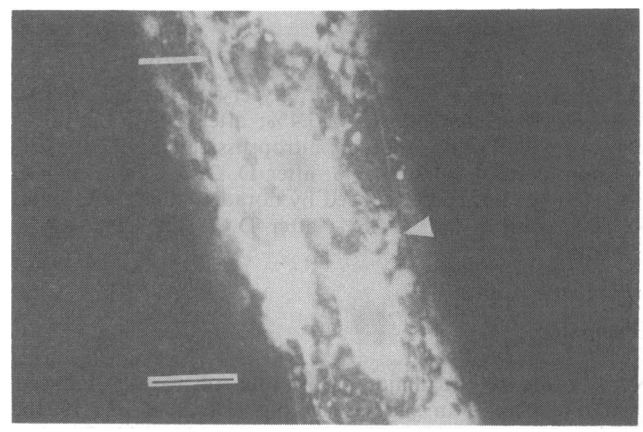


Figure 2 A wholemount preparation of the myenteric plexus of the guinea pig stomach fundus immunostained for nitric oxide synthase (NOS) using the indirect immunofluorescence method. NOS-positive nerve cells in a ganglion can be seen. The cells show a Dogiel type I morphology with a multistellate shape, short broad lamellar processes (arrowhead) and a single long axon (arrow), which is characteristic of motor neurones. Scale bar = 25 μm.

L-NAME does not affect relaxation of the stomach induced by exogenous VIP

VIP (100 nM, 3–4 min) induced relaxation of the stomach which was not affected by incubation with L-NAME (100 μM, 20 min) or L-Arg (2 mM, 30 min) (Figure 4) (control, 30.5 ± 1.9%; + L-NAME, 31.0 ± 1.7%; + L-Arg, 27.9 ± 3.2%; $n = 6$, $P > 0.05$).

Desensitization to the relaxant effect of VIP reduces gastric relaxations induced by vagal stimulation, glyceryl trinitrate or sodium nitroprusside

Desensitization to the relaxant effect of VIP was induced by repeatedly (4–5 times) exposing the stomach to VIP (100 nM) for 90–150 min. Desensitization was evident as a reduced response to VIP (100 nM) (VIP first exposure, 41.9 ± 3.5%; VIP after desensitization, 23.6 ± 3.1%; $n = 9$, $P < 0.01$). This desensitization (D) also reduced the relaxations induced by vagal stimulation (VS; control, 39.3 ± 1.1%; after D,

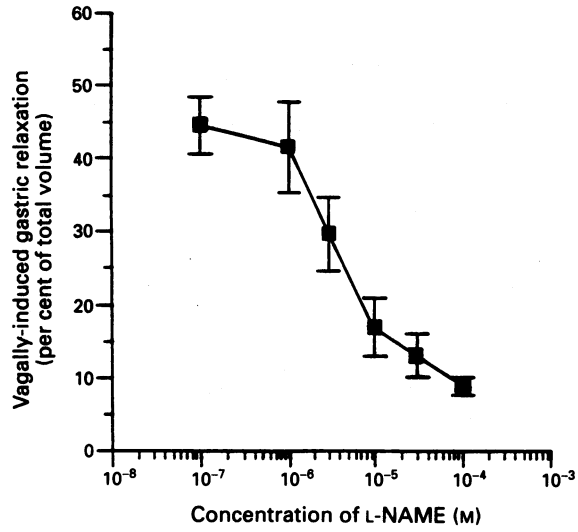


Figure 3 Dose–response relationship of the inhibitory effect of L-NAME. This graph shows the inhibitory effect of increasing concentrations of L-NAME on vagally induced relaxations of the isolated stomach of the guinea pig in the presence of atropine (3 μM) and guanethidine (5 μM). Values are mean ± s.e. mean from four experiments.

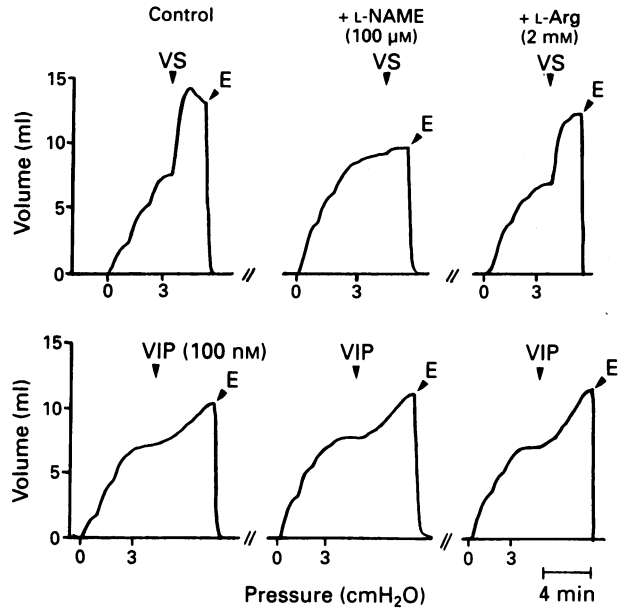


Figure 4 L-NAME inhibits gastric relaxation induced by vagal stimulation but not by VIP. The intragastric pressure was elevated to 3 cmH_2O and the vagus was stimulated (VS, 1 min) (upper panel) or VIP (100 nM lower panel) given to induce relaxation. Incubation with L-NAME (100 μM, 20 min) prevented the relaxation to VS but did not affect that to VIP. Washout of L-NAME with L-Arg (2 mM, 30 min) reversed the inhibition of vagally induced relaxation, whereas VIP-induced relaxation remained unaffected. E denotes emptying of the stomach. This figure is representative of at least five experiments.

23.5 ± 1.9%; $n = 9$, $P < 0.001$), glyceryl trinitrate (GTN, 2 μM, 60–90 s; control, 46.7 ± 3.4%; after D, 31.1 ± 1.6%; $n = 6$, $P < 0.01$), or sodium nitroprusside (SNP, 0.5 μM, 2–3 min; control, 34.5 ± 4.3%; after D, 21.5 ± 2.4%; $n = 4$, $P < 0.05$) but not those induced by noradrenaline (NA, 2 μM, 60–90 s; control, 30.7 ± 4.6%; after D, 29.2 ± 3.2%; $n = 7$, $P > 0.05$).

Discussion

Nitric oxide is the major transmitter of vagally induced gastric relaxation in the guinea pig (Desai *et al.*, 1991b; Meulemans *et al.*, 1993). Here we have localized NOS, using immunocytochemistry, to nerve cell bodies in the myenteric plexus and nerve fibre varicosities in the circular muscle layer. This strongly supports our view that NO is released from efferent neurones upon vagal stimulation and that NO is responsible for adaptive and receptive relaxation. No NOS was detected in muscle cells by this antibody. Thus any NOS present in muscle cells must be different from neuronal NOS.

VIP has also been proposed as the main NANC neurotransmitter of gastric relaxation in the guinea pig (Grider *et al.*, 1985; 1992). However, in our functional studies we found that vagal stimulation induced a rapid relaxation that faded rapidly when stimulation was stopped (Figure 5). This is consistent with the short half-life of NO (Palmer *et al.*, 1987). Glyceryl trinitrate and sodium nitroprusside, both of which induce relaxation through liberation of NO (Noack & Feelisch, 1991), produced similar responses. VIP, on the other hand, induced a different pattern of relaxation which developed slowly and also faded very slowly (Figure 5). Lefebvre *et al.* (1992) also observed a more sustained relaxation that developed slowly in response to VIP (10^{-9} to 10^{-7} M) in circular muscle strips of guinea pig gastric fundus.

Experiments using L-NAME also support NO as being the main neurotransmitter mediating these gastric relaxations. Vagally induced relaxation was prevented by L-NAME, an inhibitor of NO formation and reversed by L-arginine, the substrate for NO formation, whereas the relaxation induced by VIP was unaffected by L-NAME or L-arginine. In

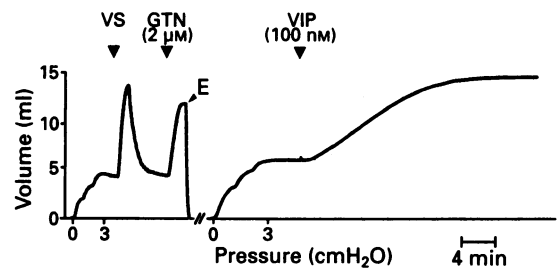


Figure 5 Comparison of the relaxant effects of vagal stimulation (VS), glyceryl trinitrate (GTN) and VIP on the isolated stomach. The intragastric pressure was elevated to 3 cmH_2O and then the relaxant responses to either VS, GTN (2 μM) or VIP (100 nM) were recorded. VS induced a relaxation which developed rapidly to a peak in about 45 s, when stimulation was stopped, and faded rapidly to the baseline within 4–5 min. GTN induced a response which developed rapidly to a peak within 90 s, at which time the stomach was emptied (E). The relaxation induced by VIP developed slowly, reaching a peak in about 3–4 min, and was sustained for 20–30 min. This figure is representative of responses seen in at least four experiments.

previous studies L-NAME inhibited relaxations induced by vagal stimulation even at high frequencies between 32 and 256 Hz (unpublished). Meulemans *et al.* (1993) also obtained a maximal amplitude of relaxation at 20 Hz vagal stimulation in the guinea pig stomach. They reported a virtually complete abolition of this relaxation by N^G-nitro-L-arginine (10^{-4} M). Similarly, Lefebvre *et al.* (1992) showed that in circular muscle strips of guinea pig gastric fundus N^G-nitro-L-arginine (10^{-5} and 10^{-4} M) inhibited relaxations elicited with short-lasting frequency-dependent as well as continuous electrical stimulation with cumulative increase in frequency from 0.125 to 16 Hz, but did not affect relaxations induced by VIP (10^{-9}

to 10^{-7} M). This is in contrast to other reports which have shown that inhibition of NOS only partially prevents gastric relaxation in the rat and ferret (Li & Rand, 1990; Boeckxstaens *et al.*, 1992; Grundy *et al.*, 1993), findings that could be due variations in the relative importance of NO and VIP as inhibitory transmitters in different species and tissues. For instance, even though NO and VIP have been reported to be co-transmitters in the guinea pig trachea (Tucker *et al.*, 1990; Li & Rand, 1991), NO is the main transmitter in feline and human trachea (Belvisi *et al.*, 1992; Fisher *et al.*, 1993). The lack of effect of tetrodotoxin on relaxations induced by VIP confirms a direct action and shows that the latter is not activating neurones causing release of a mediator such as NO for its relaxant effect. This is because we have localized NOS to neurones and not to smooth muscle cells. The most important evidence that VIP does not act through NO is that L-NAME prevented relaxations induced by vagal stimulation but did not affect those induced by VIP. Thus, even if VIP is released by vagal stimulation, it does not act through stimulation of NO production from neurones or smooth muscle cells, as has been suggested (Grider *et al.*, 1992). This would hold even if these tissues contain isoforms of NOS not detected by our antibody staining.

When densensitization was induced to the relaxant effect of VIP it also reduced the relaxant effects of vagal stimulation, glyceryl trinitrate and sodium nitroprusside, but not that of noradrenaline. Since glyceryl trinitrate and sodium nitroprusside cause release of NO (Noack & Feelisch, 1991), which directly induces relaxation, this suggests that desensitization to the relaxant effect of VIP interferes with the action of NO. Thus, this interference could be at the level of second messengers cGMP and cAMP, which mediate relaxations induced by NO (Arnold *et al.*, 1977) and VIP (Bitar & Makhlouf, 1982) respectively. Interactions between cAMP and cGMP and the protein kinases activated by them have been reported (see Jiang *et al.*, 1992). However, it could be argued that NO is causing relaxation through the release of VIP, but this seems unlikely since the vagally induced relaxation is mimicked by glyceryl trinitrate and sodium nitroprusside but not by VIP. Thus, the effect of desensitization to VIP on NO-induced relaxation requires further study, especially at the second-messenger level.

In conclusion, NO seems to be the major neurotransmitter of gastric relaxation induced by vagal stimulation in the guinea pig, and the role of VIP in this response, if any, seems minor.

We wish to thank Drs S. Moncada and V. Riveros-Moreno, who developed the antibodies in conjunction with Professor Polak. This work was supported by Glaxo Group Research Ltd, U.K.

References

AIMI, Y., KIMURA, H., KINOSHITA, T., MINAMI, Y., FUJIMURA, M. & VINCENT, S.R. (1993). Histochemical localization of nitric oxide synthase in rat enteric nervous system. *Neuroscience*, **53**, 553–560.

ARNOLD, P.W., MITTAL, C.K., KATSUKI, S. & MURAD, F. (1977). Nitric oxide activates guanylate cyclase and increases gaunosine 3′:5′-cyclic monophosphate levels in various tissue preparations. *Proc. Natl. Acad. Sci. USA*, **74**, 3203–3207.

BELVISI, M.G., STRETTON, C.D., YACOUB, M. & BARNES, P.J. (1992). Nitric oxide is the endogenous neurotransmitter of brochodilator nerves in humans. *Eur. J. Pharmacol.*, **210**, 221–222.

BITAR, K.N. & MAKHLOUF, G.M. (1982). Relaxation of isolated smooth muscle cells by vasoactive intestinal peptide. *Science*, **216**, 531–533.

BOECKXSTAENS, G.E., PELCKMANS, P.A., DE MAN, J.G., BULT, H., HERMAN, A.G. & VAN MAERCKE, Y.M. (1992). Evidence for a differential release of nitric oxide and vasoactive intestinal polypeptide by nonadrenergic noncholinergic nerves in the rat gastric fundus. *Arch. Intern. Pharmacodyn. Ther.*, **318**, 107–115.

BREDT, D.S., HWANG, P.M. & SNYDER, S.H. (1990). Localization of nitric oxide synthase indicating a neural role for nitric oxide. *Nature*, **347**, 768–770.

CHAKDER, S. & RATTAN, S. (1993). Involvement of cAMP and cGMP in relaxation of internal anal sphincter by neural stimulation, VIP, and NO. *Am. J. Physiol.*, **264**, G702–G707.

COSTA, M., BUFFA, R., FURNESS, J.B. & SOLCIA, E. (1980). Immunohistochemical localization of polypeptides in peripheral autonomic nerves using wholemount preparations. *Histochemistry*, **65**, 157–165.

D'AMATO, M., DE BEURME, F.A. & LEFEBVRE, R.A. (1988). Comparison of the effect of vasoactive intestinal polypeptide and non-adrenergic non-cholinergic neurone stimulation in the cat gastric fundus. *Eur. J. Pharmacol.*, **152**, 71–82.

D'AMATO, M., CURRO, D., MONTUSCHI, P., CIABATTONI, G., RAGAZZONI, E. & LEFEBVRE, R.A. (1992). Release of vasoactive intestinal polypeptide from the rat gastric fundus. *Br. J. Pharmacol.*, **105**, 691–695.

DE BEURME, F.A. & LEFEBVRE, R.A. (1988). Vasoactive intestinal polypeptide as possible mediator of relaxation in the rat gastric fundus. *J. Pharm. Pharmacol.*, **40**, 711–715.

DESAI, K.M., SESSA, W.C. & VANE, J.R. (1991a). Involvement of nitric oxide in the reflex relaxation of the stomach to accomodate food and fluid. *Nature*, **351**, 477–479.

DESAI, K.M., ZEMBOWICZ, A., SESSA, W.C. & VANE, J.R. (1991b). Nitroxergic nerves mediate vagally induced relaxation in the isolated stomach of the guinea pig. *Proc. Natl. Acad. Sci. USA*, **88**, 11490–11494.

DESAI, K.M., WARNER, T.D., BISHOP, A.E., POLAK, J.M. & VANE, J.R. (1993). *In vitro* and immunohistochemical studies suggest that nitric oxide, and not VIP, mediates vagally-induced gastric relaxation in the guinea-pig. *Br. J. Pharmacol.*, **110** (Suppl.), 50P.

DWYER, M.A., BREDT, D.S. & SNYDER, S.H. (1991). Nitric oxide synthase: irreversible inhibition by L-N^G-nitroarginine in brain *in vitro* and *in vivo*. *Biochem. Biophys. Res. Commun.*, **176**, 1136–1141.

FISHER, J.T., ANDERSON, J.W. & WALDRON, M.A. (1993). Nonadrenergic noncholinergic neurotransmitter of feline trachealis: VIP or NO? *J. Appl. Physiol.*, **74**, 31–39.

FORSTER, E.R. & SOUTHAM, E. (1993). The intrinsic and vagal extrinsic innervation of the rat stomach contains nitric oxide synthase. *Neuroreport*, **4**, 275–278.

GIBSON, A., MIRZAZADEH, S., HOBBS, A.J. & MOORE, P.K. (1990). L-N^G-monomethylarginine and L-N^G-nitroarginine inhibit non-adrenergic, non-cholinergic relaxation of the mouse anococcygeus muscle. *Br. J. Pharmacol.*, **99**, 602–606.

GILLESPIE, J.S., LIU, X.R. & MARTIN, W. (1989). The effects of L-arginine and N^G-monomethyl L-arginine on the response of rat anococcygeus muscle to NANC nerve stimulation. *Br. J. Pharmacol.*, **98**, 1080–1082.

GRAHAM, R.C. & KARNOVSKY, M.J. (1976). The early stages of absorption of injected horse-radish peroxidase in the proximal tubules in the mouse kidney. *J. Histochem. Cytochem.*, **14**, 291–302.

GRIDER, J.R. & JIN, J.-G. (1993). Vasoactive intestinal peptide release and L-citrulline production from isolated ganglia of the myenteric plexus: evidence for regulation of vasoactive intestinal peptide release by nitric oxide. *Neuroscience*, **54**, 521–526.

GRIDER, J.R. & MAKHLOUF, G.M. (1987). Prejunctional inhibition of vasoactive intestinal peptide release. *Am. J. Physiol.*, **253**, G7–G12.

GRIDER, J.R., CABLE, M.B., SAID, S.I. & MAKHLOUF, M. (1985). Vasoactive intestinal peptide as a neural mediator of gastric relaxation. *Am. J. Physiol.*, **248**, G73–G78.

GRIDER, J.R., MURTHY, K.S., JIN, J.-G. & MAKHLOUF, G.M. (1992). Stimulation of nitric oxide from muscle cells by VIP: prejunctional enhancement of VIP release. *Am. J. Physiol.*, **262**, G774–G778.

GRUNDY, D., GHARIB-NASERI, M.K. & HUTSON, D. (1993). Role of nitric oxide and vasoactive intestinal polypeptide in vagally mediated relaxation of the gastric corpus in the anaesthetized ferret. *J. Auton. Nerv. Sys.*, **43**, 241–246.

GULBENKIAN, S., WHARTON, J. & POLAK, J.M. (1987). The visualization of cardiovascular innervation in the guinea-pig using an antiserum to protein gene product 9.5 (PGP 9.5). *J. Auton. Nerv. Syst.*, **18**, 235–247.

JIANG, H., SHABB, J.B. & CORBIN, J.D. (1992). Cross activation: overriding cAMP/cGMP selectivities of protein kinases in tissues. *Biochem. Cell Biol.*, **70**, 1283–1289.

KAMATA, K., SAKAMOTO, A. & KASUYA, Y. (1988). Similarities between the relaxations induced by vasoactive intestinal peptide and by stimulation of the non-adrenergic non-cholinergic neurons in the rat stomach. *Naunyn-Schmiedeberg's Arch. Pharmacol.*, **338**, 401–406.

LEFEBVRE, R.A., BAERT, E. & BARBIER, A.J. (1992). Influence of N^G-nitro-L-arginine on non-adrenergic non-cholinergic relaxation in the guinea-pig gastric fundus. *Br. J. Pharmacol.*, **106**, 173–179.

LI, C.G. & RAND, M.J. (1990). Nitric oxide and vasoactive intestinal polypeptide mediate non-adrenergic, non-cholinergic inhibitory transmission to smooth muscle of the rat gastric fundus. *Eur. J. Pharmacol.*, **191**, 303–309.

LI, C.G. & RAND, M.J. (1991). Evidence that part of the NANC relaxant response of guinea-pig trachea to electrical field stimulation is mediated by nitric oxide. *Br. J. Pharmacol.*, **102**, 91–94.

LLEWELYN-SMITH, I.J., SONG, Z.-M., COSTA, M., BREDT, D.S. & SNYDER, S.H. (1992). Ultrastructural localization of nitric oxide synthase immunoreactivity in guinea-pig enteric neurones. *Brain Res.*, **577**, 337–342.

MEULEMANS, A.L., HELSEN, L.F. & SCHUURKES, J.A.J. (1993). Role of NO in vagally-mediated relaxations of guinea-pig stomach. *Naunyn-Schmiedeberg's Arch. Pharmacol.*, **347**, 225–230.

NOACK, E. & FEELISCH, M. (1991). Molecular mechanisms of nitrovasodilator bioactivation. *Basic Res. Cardiol.*, **86** (Suppl. 2), 37–50.

PALMER, R.M.J., FERRIGE, A.G. & MONCADA, S. (1987). Nitric oxide release accounts for the biological activity of endothelium-derived relaxing factor. *Nature*, **327**, 524–526.

PATON, W.D.M. & VANE, J.R. (1963). An analysis of the responses of the isolated stomach to electrical stimulation and to drugs. *J. Physiol.*, **165**, 10–46.

POLAK, J.M. (1988). Appendix: technical notes. In *An Introduction to Immunocytochemistry: Current Techniques and Problems*, ed. Polak, J.M. & Van Noorden, S. pp. 45–48. Oxford: Oxford University Press.

SAID, S.I. (1992). Nitric oxide and vasoactive intestinal peptide: cotransmitters of smooth muscle relaxation. *News Physiol. Sci.*, **7**, 181–183.

SCHMIDT, H.H.H.W., GAGNE, G.D., NAKANE, M., POLLOCK, J.S., MILLER, M.F. & MURAD, F. (1992). Mapping of neural nitric oxide synthase in the rat suggests frequent co-localization with NADPH diaphorase but not with soluble guanylyl cyclase, and novel paraneural functions for nitrinergic signal transduction. *J. Histochem. Cytochem.*, **40**, 1439–1456.

SPRINGALL, D.R., RIVEROS-MORENO, V., BUTTERY, L., SUBURO, A., BISHOP, A.E., MERRETT, M., MONCADA, S. & POLAK, J.M. (1992). Immunological detection of nitric oxide synthase(s) in human tissues using heterologous antibodies suggesting different isoforms. *Histochemistry*, **98** (4), 259–266.

TUCKER, J.F., BRAVE, S.R., CHARALAMBOUS, L., HOBBS, A.J. & GIBSON, A. (1990). L-N^G-nitroarginine inhibits non-adrenergic non-cholinergic relaxations of guinea-pig isolated tracheal smooth muscle. *Br. J. Pharmacol.*, **100**, 663–664.

WARD, S.M., XUE, C., SHUTTLEWORTH, C.W., BREDT, D.S., SNYDER, S.H. & SANDERS, K.M. (1992). NADPH diaphorase and nitric oxide synthase colocalization in enteric neurones of the canine proximal colon. *Am. J. Physiol.*, **263**, G277–G284.

(Received September 30, 1993
Revised July 1, 1994
Accepted August 1, 1994)

Br. J. Pharmacol. (1994), **113**, 1203–1208 © Macmillan Press Ltd, 1994

In vitro studies of release of adenine nucleotides and adenosine from rat vascular endothelium in response to α_1-adrenoceptor stimulation

[1]*K. Shinozuka, †M. Hashimoto, †S. Masumura, ‡R.A. Bjur, ‡D.P. Westfall & *K. Hattori

*Department of Pharmacology and †Department of Physiology, Shimane Medical University, Izumo 693, Japan, and ‡Department of Pharmacology, University of Nevada School of Medicine, Reno, Nevada 89557-0046, U.S.A.

1 Noradrenaline-induced release of endogenous adenine nucleotides (ATP, ADP, AMP) and adenosine from both rat caudal artery and thoracic aorta was characterized, using high-performance liquid chromatography with fluorescence detection.

2 Noradrenaline, in a concentration-dependent manner, increased the overflow of ATP and its metabolites from the caudal artery. The noradrenaline-induced release of adenine nucleotides and adenosine from the caudal artery was abolished by bunazosin, an α_1-adrenoceptor antagonist, but not by idazoxan, an α_2-adrenoceptor antagonist. Clonidine, an α_2-adrenoceptor agonist, contracted caudal artery smooth muscle but did not induce release of adenine nucleotides or adenosine.

3 Noradrenaline also significantly increased the overflow of ATP and its metabolites from the thoracic aorta in the rat; however, the amount of adenine nucleotides and adenosine released from the aorta was considerably less than that released from the caudal artery.

4 Noradrenaline significantly increased the overflow of ATP and its metabolites from cultured endothelial cells from the thoracic aorta and caudal artery. The amount released from the cultured endothelial cells from the aorta was also much less than that from cultured endothelial cells from the caudal artery. In cultured smooth muscle cells from the caudal artery, a significant release of ATP or its metabolites was not observed.

5 These results suggest that there are vascular endothelial cells that are able to release ATP by an α_1-adrenoceptor-mediated mechanism, but that these cells are not homogeneously distributed in the vasculature.

Keywords: ATP; rat thoracic aorta; rat caudal artery; endothelial cells; ATP release; α_1-adrenoceptor; noradrenaline

Introduction

Adenosine triphosphate (ATP), in addition to its known functions in intracellular metabolism, is increasingly being recognized for its extracellular functions in various tissues, including blood vessels (Gordon, 1986; White, 1988; Burnstock, 1991). Recently, it has been suggested that one endogenous source of extracellular ATP is vascular endothelium (Pearson & Gordon, 1979; Buxton *et al.*, 1990; Milner *et al.*, 1990; Sedaa *et al.*, 1990). We also observed a large release of ATP and its metabolites induced by methoxamine, an α_1-adrenoceptor agonist from the caudal artery of rats (Shinozuka *et al.*, 1991); however, details of the release have not been revealed.

In the present study, we measured the release of endogenous adenine nucleotides (ATP, ADP, AMP) and adenosine from both rat caudal artery and thoracic aorta to characterize the release of ATP.

Methods

Tissue preparations

Male Wistar rats (SLC, Japan), ranging from 20 to 25 weeks of age, were anaesthetized with pentobarbital sodium (50 mg kg^{-1} i.p.) and exsanguinated. The caudal arteries and thoracic aortas were removed, immersed in a continuously oxygenated Krebs–Henseleit buffer solution and cleaned of connective tissue. The composition of the Krebs solution was as follows (mM): NaCl 118.4, KCl 4.7, $CaCl_2$ 2.2, KH_2PO_4 1.2, $MgSO_4$ 1.2, $NaHCO_3$ 25.0 and glucose 5.6. In the release experiments, the caudal arteries (approximately 11 cm in length and 10 mg wet weight) were either cut open lengthwise (open preparation) or tied at both ends (closed preparation). For the measurement of contractile activity, the caudal artery was cut into small rings 2–3 mm in length.

Release experiments

The caudal artery and thoracic aorta preparations were suspended in water-jacketed organ chambers containing 2.0 ml of the Krebs solution at 37°C, then allowed to equilibrate for 1 h. The medium was replaced every 3 min during the second half of the equilibration period. After a 60 min equilibration period, the bathing solution was rapidly collected by draining the organ chamber every 3 min. After the first samples were taken (basal overflow), the tissues were stimulated with noradrenaline (1.0 μM) for 3 min, and the bathing solutions (noradrenaline-induced overflow) were collected. The details of the experimental protocol have been described previously (Ishii *et al.*, 1993).

To obtain data for the concentration-release curve in response to noradrenaline, caudal arteries were removed from Wistar rats. Each artery was divided into four segments, which were then opened lengthwise. After the first samples were taken, each of the four open-preparation segments was stimulated with noradrenaline at four concentrations (0.1, 1.0, 10.0 and 100.0 μM), for 3 min each in a random sequence.

[1] Author for correspondence.
Present address: Department of Pharmacology, Faculty of Pharmaceutical Sciences, Mukogawa Women's University, 11-68, Koshien Kyuban-cho, Nishinomiya 663, Japan.

Contraction experiments

The ring preparations of the caudal artery were suspended under a resting tension of 0.5 g in a water-jacketed micro-organ chamber containing 2.0 ml of the Krebs solution at 37°C and then allowed to equilibrate for 1 h. The tension was measured isometrically with a force-displacement transducer (Iwashiya Kishimoto Medical Instruments, Japan) and recorded with a Hitachi Recorder (Model 561, Japan). The details of the method for measuring the tension changes have been described previously (Shinozuka *et al.*, 1992). A concentration–contraction curve for noradrenaline was generated in a cumulative manner, and each successive concentration was added after the response to the previous concentration had reached its peak.

To compare the contractions induced by noradrenaline and by clonidine, caudal arteries from four rats were stimulated, first with noradrenaline and then with clonidine, at 30 min intervals. Another four arteries were stimulated first with clonidine and then with noradrenaline. The values were expressed as a percentage of the maximum contraction induced in each artery by a 3 min treatment with 1.0 μM noradrenaline.

Cell cultures

Endothelial and smooth muscle cells in primary cultures from either the thoracic aorta or caudal artery of the rat were prepared by methods previously described (Ohoka *et al.*, 1990; Hashimoto *et al.*, 1992). Briefly, after excising caudal arteries and thoracic aortas from the 5–6 rats anaesthetized with ether, ranging from 20 to 25 weeks of age, the vessels were rinsed in Dulbecco's modified Eagle medium (DMEM) containing antibiotics (100 U ml^{-1} penicillin, 100 μg ml^{-1} streptomycin) and an antifungal agent (0.25 μg ml^{-1} fungizone).

To obtain endothelial cells for the primary culture, vessels were cut into flat segments of approximately 2 mm^2. Each segment was placed endothelial side down on a well of a collagen culture plate (Celltight C-1, Sumitomo Bakelite, Osaka, Japan), to which just enough growth medium [50 μg ml^{-1} ECGF, endothelial cell growth factor and 3% fetal bovine serum (FBS) in Opti-MEM®1] was added to keep the tissue moist. The segments were incubated in a humidified incubator at 37°C in a 95% air and 5% CO_2 atmosphere. Within 48 h, the segments were removed from the culture plates, and the growth medium was exchanged for a renewal medium (25 μg ml^{-1} ECGF, 3% FBS and 5U ml^{-1} heparin in DMEM). The remaining cells were cultivated for a further 3–5 days, during which time the renewal medium was changed every 2–3 days, and the cells were subjected to release experiments of adenine nucleotides and adenosine after growing to confluent monolayers.

To obtain smooth muscle cells for the primary culture of rat caudal arteries, the artery was opened longitudinally, and the adventitia and intima were carefully removed from the media. The media was cut into segments of 1–2 mm^2 and explanted to dishes containing DMEM with 10% FBS. The dishes were incubated for approximately 2 weeks in a humidified incubator at 37°C in a 95% air and 5% CO_2 atmosphere. After cultivation for 2 weeks, the cells grew into clumps like those observed in smooth muscle cells cultured from guinea-pig vas deferens (Chamley *et al.*, 1974). This suggests that the cultured smooth muscle cells in the present experiments are predominantly of the contractile phenotype, which is characteristic of the cells in normal physiological conditions.

To identify endothelial cells and smooth muscle cells in primary culture, immunocytochemical characterization was performed using monoclonal antibodies against factor VIII-related antigen (a Biomeda Histo Scan Kit, COSMO BIO, Tokyo, Japan) and smooth muscle α-actin (Sigma, St Louis, MO, U.S.A.) and also using acetylated low-density lipoprotein labelled with the fluorescent probe 1,1′-dioctadecyl-1-3,3,3′,3′-tetramethyl-indocarbocyanine perchlorate (Dil-Ac-LDL; Biomedical Technologies, Stoughton, MA, U.S.A.), as previously described (Hashimoto *et al.*, 1992). Endothelial cells showed positive staining for factor VIII-related antigen but undetectable staining for α-actin and also showed uptake of Dil-Ac-LDL, while smooth muscle cells were negative for factor VIII-related antigen and positive for α-actin (data not shown).

In the release experiments, the cells in the primary cultures were incubated on culture dishes in 2 ml of Krebs solution for 60 min at 37°C in an atmosphere of 95% air and 5% CO_2 ($20-25 \times 10^4$ cells per 35 mm dish for endothelial cells, $25-30 \times 10^4$ cells per 35 mm dish for smooth muscle cells). After 60 min of equilibration, 200 μl of the bathing solution was collected (basal overflow), after which cells were stimulated with noradrenaline (10.0 μM) for 3 min, followed by another 200 μl collection (stimulated overflow). The collected samples were then processed for the measurement of adenine nucleotides and adenosine as described above.

Measurement of ATP and its metabolites

The collected sample solutions were immediately acidified to pH 4 with 0.36 ml of citrate–phosphate buffer solution and placed on ice. Chloroacetaldehyde and internal standard (9-β-D-arabinofuranosyl adenine) were added to each acidified sample, which was then incubated in a dry bath at 80°C for 40 min. The reaction was terminated by placing the samples on ice. The resulting ethenonucleotides and ethenoadenosine were analysed by high-performance liquid chromatography (HPLC) with fluorescence detection as described by Mohri *et al.*, (1993).

The HPLC system consisted of a reversed-phase Ultron-N-phenyl HPLC column (Shinowa-Kakoh, Japan), a delivery pump (LC-9A, Shimadzu, Japan) equipped with a fluorescence monitor (RF-535, Shimadzu, Japan), a sample processor (AS-8010, Tosoh, Japan) and a chromatopac computing integrator (C-R4A, Shimadzu, Japan).

Drugs

Clonidine hydrochloride, α,β-methylene ADP, idazoxan hydrochloride and [−] noradrenaline bitartrate were obtained from Sigma, U.S.A. Bunazosin was kindly supplied by Eisai Pharmaceutical, Japan. The DMEM was obtained from Nissui Pharmaceutical, (Japan). The ECGF was purchased from Boehringer Mannheim (Mannheim, Germany). Opti-MEM1 and FBS were purchased from Gibco Laboratories (U.S.A.).

Statistics

All data were expressed as means ± standard error of the mean. The significance of difference between the amounts of purine overflow before and after treatment with noradrenaline was analysed by paired *t*-test. The other data were evaluated for statistical significance by using Student's *t*-test, the Cochran–Cox test or Duncan's multiple range test where appropriate. The 0.05 level of probability was accepted as significant.

Results

In the rat caudal artery, noradrenaline, at a concentration of 1 μM, significantly increased the overflow of ATP, ADP, AMP and adenosine from the caudal artery segments which were opened lengthwise (Figure 1). Adenosine (4.41 ± 0.72 pmol mg^{-1}, $n = 4$) was present in the greatest amount, which was approximately equal to the sum of those of the nucleotides: ATP, ADP and AMP (3.74 ± 0.37 pmol mg^{-1}, $n = 4$). α,β-methylene ADP, a nucleotidase inhibitor, at

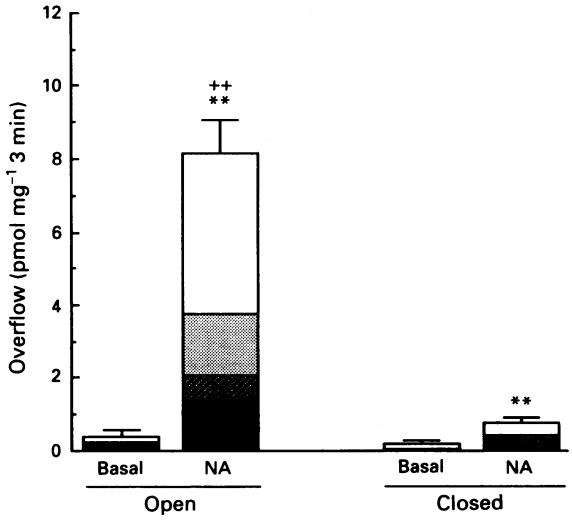


Figure 1 Effect of 1.0 μM noradrenaline (NA) on the overflow of adenine nucleotides [ATP (solid column), ADP (diagonal hatched column), AMP (dotted column)] and adenosine (ADO, open columns) from rat caudal artery. Noradrenaline significantly (**$P<0.01$, paired t-test) increased the total overflow of adenine nucleotides and adenosine in both preparations. The total amount of adenine nucleotides and adenosine overflow induced by noradrenaline from open preparations was significantly larger (++$P<0.01$) than that from closed preparations. Each column represents the mean of four experiments. The vertical bar on each column indicates standard error of the mean of the total amount of purines released.

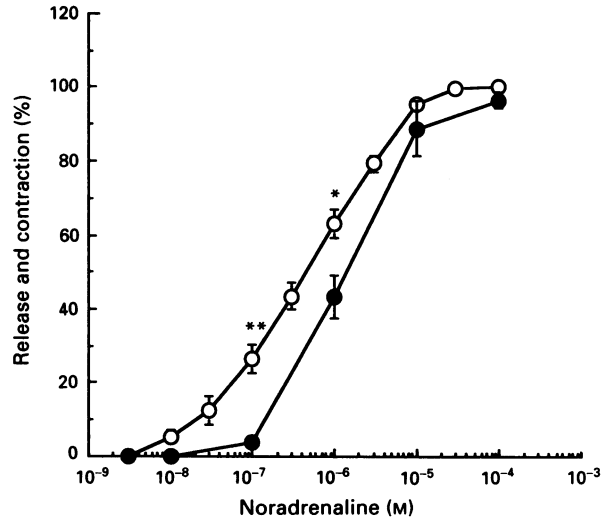


Figure 2 Noradrenaline-induced release of adenine nucleotides and adenosine and noradrenaline-induced contraction curves for rat caudal artery. The release curve (●) represents the relationship between the total amount of adenine nucleotides and adenosine released (per cent of the mean of the maximal release) and the concentration of noradrenaline used to induce release from open caudal artery preparations. The amount released is the difference between the amounts present in basal and in noradrenaline-induced overflow. The second curve (○) is the per cent contraction induced by specified concentrations of noradrenaline in ring preparations of the rat caudal artery. Each point represents the mean of six experiments. The single and double asterisks indicate significant differences (*$P<0.05$ and **$P<0.01$ respectively) between the per cent release and per cent contraction.

0.1 μM significantly ($P<0.05$, $n=4$) increased the noradrenaline-induced overflow of ATP from 1.606 ± 0.120 to 3.007 ± 0.124 pmol mg^{-1}. In intact arteries that had been tied closed at both ends, noradrenaline (1.0 μM) also increased the overflow of adenine nucleotides and adenosine. However, the total amount of adenine nucleotides and adenosine released, which was the difference between the overflow in the absence (basal) and presence of noradrenaline, from closed preparations (0.57 ± 0.09 pmol mg^{-1}) was significantly less ($P<0.01$) than that from open preparations (7.76 ± 0.86 pmol mg^{-1}).

The noradrenaline-induced release of adenine nucleotides and adenosine was concentration-dependent from 0.1 to 100.0 μM. Noradrenaline at a concentration of 100.0 μM produced maximal release of adenine nucleotides and adenosine, which amounted to 22.02 ± 2.20 pmol mg^{-1}, and at 0.01 μM produced no release. The concentration–response curve for purine release induced by noradrenaline was shifted slightly to the right in comparison with the concentration–response curve for contraction induced by noradrenaline in the caudal artery (Figure 2). However, the EC_{50} values for release and contraction were 1.81 ± 0.73 μM ($n=6$) and 0.49 ± 0.10 μM ($n=6$) respectively, and there was no significant difference between these two EC_{50} values.

The increase in adenine nucleotides and adenosine overflow in response to 1 μM noradrenaline (control, 9.90 ± 2.14 pmol mg^{-1}, $n=5$) was significantly ($P<0.05$) reduced to 0.81 ± 0.31 pmol mg^{-1} ($n=4$) by 30.0 nM bunazosin, an α_1-adrenoceptor antagonist, but was not affected by 0.1 μM idazoxan (9.39 ± 1.31 pmol mg^{-1}, $n=4$), an α_2-adrenoceptor antagonist. Clonidine, an α_2-adrenoceptor agonist, produced a contraction of the caudal artery when administered at a final concentration of 10 μM, the magnitude and time course of which was almost identical to that produced by 1.0 μM noradrenaline (Figure 3a). However, neither 1.0 nor 10.0 μM clonidine caused any significant increase in purine overflow (Figure 3b).

In rat thoracic aorta, noradrenaline also increased the overflow of adenine nucleotides and adenosine (Figure 4a). However, the total amount of adenine nucleotides and adenosine released (noradrenaline-induced overflow minus basal overflow) from the thoracic aorta (0.22 ± 0.04 pmol mg^{-1}) was significantly less ($P<0.01$) than that obtained from the caudal artery (7.91 ± 0.77 pmol mg^{-1}). When the amount of release was compared on the basis of area (mm^2) instead of weight (mg) of tissue, the release of purines from aorta (0.06 ± 0.02 pmol mm^{-2}, $n=4$) was still significantly ($P<0.01$) less than that obtained from the caudal artery (1.59 ± 0.14 pmol mm^{-2}, $n=4$).

In cultured endothelial cells that had been obtained from either the caudal artery or the thoracic aorta, noradrenaline, at a concentration of 10.0 μM, significantly increased the overflow of total purines (Figure 4b). There was no significant difference between the basal overflow levels of adenine nucleotides and adenosine from cultured endothelial cells from the aorta and caudal artery. However, the total amount of noradrenaline-induced release of adenine nucleotides and adenosine from endothelial cells of the caudal artery (3.45 ± 1.12 pmol per 10,000 cells) was significantly greater ($P<0.05$) than that from the aorta (0.21 ± 0.06 pmol per 10,000 cells), with that of the former approximately 16 times that of the latter. The amount of nucleotides (3.41 ± 1.14 pmol per 10,000 cells, $n=6$) released from primary cultures of endothelial cells from the caudal artery by 10 μM noradrenaline was significantly greater ($P<0.05$) than that of adenosine (0.03 ± 0.02 pmol per 10,000 cells, $n=5$), as shown in Figure 4b. In a primary culture of rat caudal artery smooth muscle cells, we did not detect a significant release of purines induced by 10 μM noradrenaline (Figure 4b).

Discussion

In the present study, we have shown that noradrenaline induced the release of ATP, ADP, AMP and adenosine from the caudal artery segments that had been opened lengthwise.

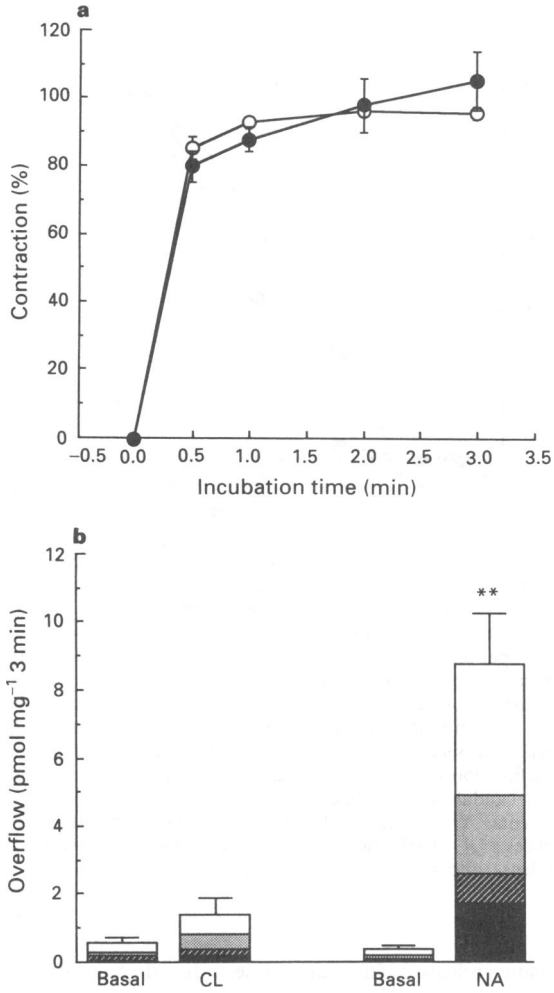


Figure 3 Comparison of the effects of noradrenaline (NA) and clonidine (CL) on both contraction and purine overflow in rat caudal artery. (a) Magnitude and time course of the contractile responses induced by noradrenaline (○, 1.0 μM) and clonidine (●, 10.0 μM) for 3 min with ring preparations of the rat caudal artery. The values are expressed as the per cent of the maximal contraction induced by a 3-min treatment of noradrenaline in each artery. Each point represents the mean of eight experiments. (b) Comparison of the effects of 10.0 μM clonidine and 1.0 μM noradrenaline on the overflow of adenine nucleotides and adenosine from open preparations of rat caudal artery. Noradrenaline significantly ($*P<0.05$, paired t-test) increased the total overflow of adenine nucleotides and adenosine. Each column represents the mean of four experiments. Vertical bars on each column indicate standard error of the mean of the total amounts of adenine nucleotides and adenosine present in each experimental group. Columns as in Figure 1.

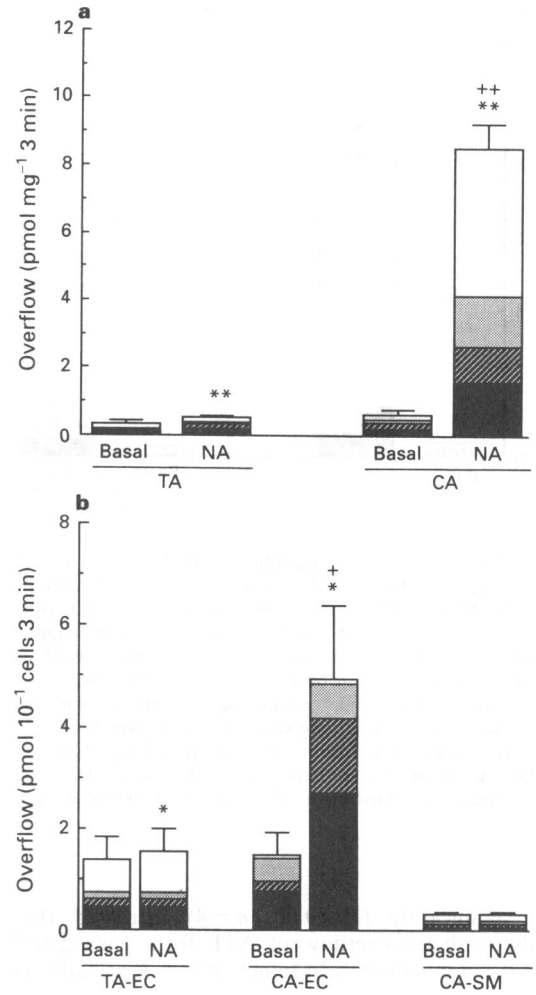


Figure 4 Comparison of the effects of noradrenaline (NA) on the overflow of adenine nucleotides and adenosine from the thoracic aorta and caudal artery of the rat. (a) Effects of 1.0 μM noradrenaline on the overflow of adenine nucleotides and adenosine from open preparations of the thoracic aorta (TA) and caudal artery (CA). Noradrenaline significantly ($**P<0.01$, paired t-test) increased the total overflow of adenine nucleotides and adenosine in both tissues. The total amount of adenine nucleotides and adenosine overflow induced by noradrenaline from the caudal artery was significantly greater ($^{++}P<0.01$) than that obtained from the thoracic aorta. Each column represents the mean of five experiments. Vertical bars on each column indicate standard error of the mean of the total amounts of adenine nucleotides and adenosine present in each experimental group. (b) Effect of 10.0 μM noradrenaline on the overflow of adenine nucleotides and adenosine from isolated endothelial cells in primary cultures which were obtained from the thoracic aorta (TA-EC) and caudal artery (CA-EC) and smooth muscle cells in primary cultures which were obtained from the caudal artery (CA-SM). Noradrenaline significantly ($*P<0.05$, paired t-test) increased the total overflow of adenine nucleotides and adenosine from the endothelial cells. The total amount of noradrenaline-induced overflow of adenine nucleotides and adenosine from endothelial cells of the caudal artery was much greater ($^{+}P<0.05$) than that from the aorta. Data were obtained from 5–6 rats. Each column represents the mean of the values averaged in two or three observations in different dishes of cells per rat. Vertical bars on each column indicate standard error of the mean of the total amount of adenine nucleotides and adenosine present in each group. Columns as in Figure 1.

In intact arteries that had been tied closed at both ends, noradrenaline also induced the release of adenine nucleotides and adenosine, but the total amount of adenine nucleotides and adenosine released by closed arteries was only 7% of that released by open arteries. This indicates that most (approximately 93%) of the adenine nucleotides and adenosine released by noradrenaline in the open arteries comes from the intimal side of the artery, most probably from the endothelium. Indeed, we observed that the release of purines was considerably reduced in a rat caudal artery that had been denuded of endothelium by rubbing the lumen of the vessel (data not shown). This is consistent with our previous results (Sedaa *et al.*, 1990) with rabbit thoracic aorta, in which the release of purines by methoxamine, an α_1-adrenoceptor agonist, was reduced by 90% by removal of the endothelium.

Very recently, work in our laboratory has shown that a variety of vasoactive agents, including bradykinin, acetylcholine, serotonin and ADP, cause purine release from primary cultures of endothelial cells obtained from guinea pig heart (Yang *et al.*, 1994). This suggests that agonist-induced release of adenine nucleotides and adenosine may not be

restricted to α_1-receptor agonists. It is possible that noradrenaline activates α_2- or β_2-adrenoceptors in additon to α_1-adrenoceptors. However, the noradrenaline-induced release of purines was almost abolished by bunazosin, an α_1-adrenoceptor antagonist (Shoji, 1981), but was not affected by idazoxan, an α_2-adrenoceptor antagonist. Clonidine, an α_2-adrenoceptor agonist, produced a contraction of the caudal artery, the magnitude and time course of which were almost identical to that produced by noradrenaline. However, clonidine did not cause any significant increase in purine overflow. Also, isoproterenol (1.0 μM), a β-adrenoceptor agonist, did not affect the overflow of purines (data not shown). From these results, the α-adrenoceptor that mediates purine release appears to be the α_1-receptor, a finding that is consistent with our previously reported observations (Buxton *et al.*, 1990; Sedaa *et al.*, 1990).

It is well known that the release of EDRF, endothelium-derived relaxing factor, from endothelial cells can be elicited by mechanical and physical stimulation, such as flow shear stress (Rubanyi *et al.*, 1986) and stretch (Ohno *et al.*, 1990). Furthermore, Milner *et al.*, (1990) demonstrated that endothelin and ATP release can be induced from rabbit aortic endothelial cells by shear stress. In the present study, the concentration–response curve for purine release was similar to the concentration–response curve for contraction of the caudal artery, and the EC_{50} values for release and contraction were not significantly different. This suggests the possibility that mechanical contraction may induce the release of adenine nucleotides and adenosine. However, the release of ATP that was observed in the present study seems not to be induced by mechanical stimulation, such as contraction, because clonidine produced a contraction but did not induce release. These findings taken together suggest that adenine nucleotides and adenosine are released by an α_1-adrenoceptor-coupled mechanism that is present in endothelial cells.

In rat thoracic aorta, noradrenaline also increased the overflow of adenine nucleotides and adenosine, but the amount of release was only approximately 3% of that obtained from the caudal artery, despite there being no significant difference between the basal total purine overflow levels from the aorta and caudal artery. When the amount of release was compared on the basis of area instead of weight of tissue, as described previously (Shinozuka *et al.*, 1993), the release of adenine nucleotides and adenosine from aorta was still significantly less than that from the caudal artery. Thus, there appears to be a marked difference between the amount of purines released from the aorta and that from the caudal artery.

In cultured endothelial cells from either the caudal artery or the thoracic aorta, noradrenaline induced the release of total purines. There was no significant difference between the basal overflow levels of adenine nucleotides and adenosine from cultured endothelial cells from the aorta and those from the caudal artery. However, the noradrenaline-induced release of adenine nucleotides and adenosine from cultured endothelial cells from the aorta was again much less than that from cells from the caudal artery, with the former approximately 6% of the latter. This release of purines from specific endothelial cell populations, therefore, agrees with the results from intact caudal artery and thoracic aorta. Thus, these experimental results suggest that a functional role exists for an α_1-adrenoceptor-mediated release of purines on the endothelial cells which is regionally differentiated in the vasculature.

The amount of nucleotides released by noradrenaline from primary cultures of endothelial cells from the caudal artery was significantly greater than that of adenosine. However, in intact caudal artery preparations, the amount of adenosine released was greater than that of nucleotides. Pearson & Gordon (1979) also showed that the quantity of adenine nucleotides released from cultured endothelial cells was greater than that of adenosine, and Gordon *et al.* (1986) suggested that the degradation of ATP to adenosine by endothelial cell ectonucleotidases is not very rapid. In contrast, these investigators showed that ATP is rapidly degraded to adenosine by cultured smooth muscle cells from pig aorta (Gordon *et al.*, 1989). Indeed, we observed that the amount of ATP released by noradrenaline from the opened caudal artery of rat was increased approximately 2-fold by the 5′-nucleotidase inhibitor, α,β-methylene ADP. Thus, most of the ATP released from endothelial cells by α_1-adrenoceptor stimulation may be rapidly hydrolysed to adenosine by ectonucleotidase on the surface of smooth muscle cells in the caudal artery of the rat.

In a primary culture of rat caudal artery smooth muscle cells, we did not detect a significant release of adenine nucleotides or adenosine induced by noradrenaline. Bodin *et al.*, (1991) also reported that shear stress did not evoke ATP release in cultured vascular smooth muscle cells. These results suggest that vascular smooth muscle cells do not possess a significant ATP-releasing function, but are important in the metabolic conversion of ATP to adenosine.

Extracellular ATP and its metabolites are known to produce a number of biological and pharmacological effects in blood vessels by acting on specific cell-surface purinoceptors on adrenergic nerves (Shinozuka *et al.*, 1988; 1991; Yokoyani *et al.*, 1992; Ishii *et al.*, 1993), smooth muscles (Burnstock, 1991) and endothelium (Burnstock, 1987; Ando *et al.*, 1991; Vials & Burnstock, 1993). Although it is not possible to calculate from our present data the exact concentration of endogenous ATP released from the endothelium that is then available to interact with tissue-specific purinoceptors, a reasonable approximation of the amount of purines per tissue volume can be made and is in the neighbourhood of 20 μM. Based on literature values, this concentration of ATP is in the range to effectively interact with purinoceptors of vascular tissues. From both the present results and these approximations, it is proposed that ATP and its metabolites that are released from the endothelium have important physiological or pathophysiological functions in the vasculature.

In conclusion, the present results strongly suggest that (1) an α_1-adrenoceptor-mediated mechanism for ATP release exists on the vascular endothelial cells and (2) functional heterogeneity involving this α_1-adrenoceptor-mediated release of ATP exists in the vasculature. A heterogeneous anatomical distribution of α_1-adrenoceptors on vascular endothelial cells may well explain the differences in the noradrenaline-induced ATP release in the rat caudal artery and thoracic aorta. In addition, the functions of ATP and its metabolites may be more important in the lower resistance blood vessels rather than in larger vessels, such as the aorta.

The authors are deeply indebted to Yoko Tanabe for her technical assistance and Keiko Shimoura for her secretarial assistance. This study was supported in part by grants from the Ministry of Education, Science and Culture of Japan; the Smoking Research Foundation of Japan; the Takeda Medical Research Foundation of Japan and the National Institutes of Health (HL38126).

References

ANDO, J., OHTSUKA, A., KORENAGA, R. & KAMIYA, A. (1991). Effect of extracellular ATP level on flow-induced Ca^{2+} response in cultured vascular endothelial cells. *Biochem. Biophys. Res. Commun.*, **179**, 1192–1199.

BODIN, P., BAILEY, D. & BURNSTOCK, G. (1991). Increased flow-induced ATP release from isolated vascular endothelial cells but not smooth muscle cells. *Br. J. Pharmacol.*,**103**, 1203–1205.

BURNSTOCK, G. (1987). Local control of blood pressure by purines. *Blood Vessels*, **24**, 156–160.

BURNSTOCK, G. (1991). Distribution and roles of purinoceptor subtypes. *Nucleosides Nucleotides*, **10**, 917–930.

BUXTON, I.L.O., WALTHER, J. & WESTFALL, D.P. (1990). α-Adrenergic receptor-stimulated release of ATP from cardiac endothelial cells in primary culture. In *Biological Actions of Extracellular ATP*. ed. Dubyak, G.R. & Fedan J.S. pp. 503–506, *Ann. NY Acad. Sci.*, **603**.

CHAMLEY, J.H., CAMPBELL, G.R. & BURNSTOCK, G. (1974). Dedifferentiation, redifferentiation and bundle formation of smooth muscle cells in tissue culture: the influence of cell number and nerve fibres. *J. Embryol. Exp. Morphol.*, **32**, 297–323.

GORDON, J.L. (1986). Extracellular ATP: effects, sources and fate. *Biochem. J.*, **233**, 303–319.

GORDON, E.L., PEARSON, J.D. & SLAKEY, L.L. (1986). The hydrolysis of extracellular adenine nucleotides by cultured endothelial cells from pig aorta. *J. Biol. Chem.*, **261**, 15496–15504.

GORDON, E.L., PEARSON, J.D., DICKINSON, E.S., MOREAU, D. & SLAKEY, L.L. (1989). The hydrolysis of extracellular adenine nucleotides by arterial smooth muscle cells: regulation of adenosine production at the cell surface. *J. Biol. Chem.*, **264**, 18986–18992.

HASHIMOTO, M., HARA, T., HONDA, M., ISHINAGA, Y., MORIYAMA, K. & MASUMURA, S. (1992). Metabolic aspects of endothelial cells cultured from rat aortae. *Artery*, **19**, 284–296.

ISHII, R., SHINOZUKA, K., KOBAYASHI, Y., HATTORI, K., HASHIMOTO, T. & TAKEUCHI, K. (1993). Methoxamine enhances the release of endogenous noradrenaline from rabbit ear artery: possible involvement of ATP. *Naunyn-Schmied. Arch. Pharmacol.*, **348**, 46–52.

MILNER, P., BODIN, P., LOESCH, A. & BURNSTOCK, G. (1990). Rapid release of endothelin and ATP from isolated aortic endothelial cells exposed to increased flow. *Biochem. Biophys. Res. Comm.*, **170**, 649–656.

MOHRI, K., TAKEUCHI, K., SHINOZUKA, K., BJUR, R.A. & WESTFALL, D.P. (1993). Simultaneous determination of nerve-induced adenine nucleotides and nucleosides released from rabbit pulmonary artery. *Anal. Biochem.*, **210**, 262–267.

OHNO, M., OCHIAI, M., TAGUCHI, J., HARA, K., AKASTUKA, N. & KUROKAWA, K. (1990). Stretch may enhance the release of endothelium derived relaxing factor in rabbit aorta. *Biochem. Biphys. Res. Commum.*, **173**, 1038–1042.

OHOKA, M., HONDA, M., MORIOKA, S., ISHINAGA, S., NAKAYAMA, K., YAMORI, Y. & MORIYAMA, K. (1990). Effects of E-1020, a new cyclic AMP-specific phosphodiesterase inhibitor, on cyclic AMP and cytosolic free calcium of cultured vascular smooth muscle cells. *Jpn. Circ. J.*, **54**, 679–687.

PEARSON, J.D. & GORDON, J.L. (1979). Vascular endothelial and smooth muscle cells in culture selectively release adenine nucleotides. *Nature*, **281**, 384–386.

RUBANYI, G.M., ROMERO, J.C. & VANHOUTTE, P.M. (1986). Flow-induced release of endothelium-derived relaxing factor. *Am. J. Physiol.*, **250**, H1145–1149.

SEDAA, K.O., BJUR, R.A., SHINOZUKA, K.& WESTFALL, D.P. (1990). Nerve and drug-induced release of adenine nucleotides and nucleosides from rabbit aorta. *J. Pharmacol. Exp. Ther.*, **252**, 1060–1067.

SHINOZUKA, K., BJUR, R.A. & WESTFALL, D.P. (1988). Characterization of prejunctional purinoceptors on adrenergic nerves of the rat caudal artery. *Naunyn-Schmied. Arch. Pharmacol.*, **338**, 221–227.

SHINOZUKA, K., SEDAA, K.O., BJUR, R.A. & WESTFALL, D.P. (1991). Participation by purines in the modulation of norepinephrine release by methoxamine. *Eur. J. Pharmacol.*, **192**, 431–434.

SHINOZUKA, K., KOBAYASHI, Y., SHIMOURA, K. & HATTORI, K. (1992). Role of nitric oxide from the endothelium on the neurogenic contractile response of rabbit pulmonary artery. *Eur. J. Pharmacol.*, **222**, 113–120.

SHINOZUKA, K., TANABE, Y., KOBAYASHI, Y., SHIMOURA, K., TAKAORI, S., TAKEUCHI, K., BJUR, R.A., WESTRALL, D.P. & HATTORI, K. (1993). Comparison of endogenous adenine nucleotides and adenosine release from aorta and caudal artery of rat. *Proc. West. Pharmacol. Soc.*, **36**, 89–93.

SHOJI, T. (1981). Comparison of pre- and postsynaptic α-adrenoceptor blocking effect of E-643 in the isolated vas deferens of the rat. *Jpn. J. Pharmacol.*, **31**, 361–368.

VIALS, A. & BURNSTOCK, G. (1993). A_2-purinoceptor-mediated relaxation in the guinea pig coronary vasculature: a role for nitric oxide. *Br. J. Pharmacol.*, **109**, 424–429.

WHITE, T.D. (1988). Role of adenine compounds in autonomic neurotransmission. *Pharmacol. Ther.*, **38**, 129–168.

YANG, S., CHEEK, D.J., WESTFALL, D.P. & BUXTON, I.L.O. (1994). A purinergic axis in cardiac blood vessels: agonist mediated release of ATP from cardiac endothelial cells. *Circ. Res.*, **74**, 401–407.

YOKOTANI, K., OKUMA, Y. & OSUMI, Y. (1992). Release of endogenous noradrenaline from the vascularly perfused rat stomach in vitro: modulation by pre- and postsynaptic adrenoceptors. *J. Pharmacol. Exp. Ther.*, **260**, 728–733.

Received May 9, 1994
Revised July 21, 1994
Accepted August 4, 1994)

Br. J. Pharmacol. (1994), **113**, 1209–1214 © Macmillan Press Ltd, 1994

Antithrombotic actions of argatroban in rat models of venous, 'mixed' and arterial thrombosis, and its effects on the tail transection bleeding time

[1]Christopher N. Berry, Denise Girard, Sylvette Lochot & Catherine Lecoffre

Blood and Vessels Pharmacology Group, Pre-Clinical Research Department, Synthélabo Recherche (LERS), 31, avenue Paul Vaillant Couturier, 92220 Bagneux, France

1 The antithrombotic action of argatroban, a synthetic thrombin inhibitor, was studied in three models of thrombosis in the rat, and in the tail transection bleeding time test. Heparin was studied as a reference anticoagulant.

2 In the model of venous thrombosis induced by thromboplastin followed by stasis of the abdominal vena cava, argatroban had an ED_{50} of 125 $\mu g\ kg^{-1}$, when administered as an i.v. bolus 5 min prior to the thromboplastin injection: the ED_{50} of heparin was 42 $\mu g\ kg^{-1}$, where ED_{50} is the dose which reduces the weight of the thrombus by 50% compared with that of the control animals. When the two compounds were administered by continuous i.v. infusion, argatroban ($ED_{50} = 1.5\ \mu g\ kg^{-1}\ min^{-1}$) had the same potency as heparin ($ED_{50} = 1.2\ \mu g\ kg^{-1}\ min^{-1}$).

3 Argatroban was active in the arterio-venous shunt model with an ED_{50} of 0.6 $mg\ kg^{-1}$ when the compound was given as a bolus. The ED_{50} of herapin was 0.04 $mg\ kg^{-1}$ under the same conditions. The two compounds had ED_{50} values of 6 $\mu g\ kg^{-1}\ min^{-1}$(argatroban) and 3 $\mu g\ kg^{-1}\ min^{-1}$(heparin), when administered by continuous i.v. infusion.

4 When tested against occlusive arterial thrombus formation by electrical stimulation of the left carotid artery, both compounds given as either an i.v. bolus or a continuous infusion led to dose-dependent increases in the duration of post-lesion vessel patency. Heparin bolus was more active than argatroban on a weight basis, in that 2 $mg\ kg^{-1}$ gave a similar increase in the time to occlusion as 8 $mg\ kg^{-1}$ argatroban. As in the other models, when given as continuous infusions, argatroban (111% increase in time to occlusion at 20 $\mu g\ kg^{-1}, min^{-1}$) had similar activity to that of heparin (180% increase at 25 $\mu g\ kg^{-1}\ min^{-1}$) on a weight basis. Hoever, the antithrombotic effects of argatroban were accompanied by only moderate changes in the coagulation parameters (thrombin time and activated partial thromboplastin time, APTT), whereas, even at a subthreshold dose of heparin (12.5 $\mu g\ kg^{-1}\ min^{-1}$), both the thrombin time and the APTT were greater than 150 s.

5 Infusions of both compounds caused dose-dependent increases in the tail transection bleeding time, with the dose of argatroban that doubles the bleeding time (11 $\mu g\ kg^{-1}\ min^{-1}$) being five times greater than that of heparin ($ED_{100} = 2.2\ \mu g\ kg^{-1}\ min^{-1}$).

6 These data show that, when administered as an intravenous infusion, argatroban is a potent antithrombotic agent in rat models of venous 'mixed' and arterial thrombosis, this effect can be obtained with a lower degree of systemic anticoagulation than with heparin in the arterial model, and argatroban has a lower haemorrhagic potential than that of heparin.

Keywords: Argatroban; heparin; rat venous thrombosis; rat arteriovenous shunt; arterial thrombosis; bleeding time

Introduction

Argatroban ((2*R*,4*R*)4-methyl-{N^2-[(3-methyl-1,2,3,4, tetrahydro-8-quinolyl) sulphonyl]-L-arginyl}-2-piperidinecarboxylic acid monohydrate) is a potent and selective synthetic thrombin inhibitor with K_i values against thrombin ranging from 5 to 39 nM (Okamoto *et al.*, 1981; Kikumoto *et al.*, 1984; Taparelli *et al.*, 1993). It is also a potent anticoagulant *in vitro*, where a concentration of 60 nM is sufficient to double (approximately) the thrombin time in human, rabbit and rat plasma (Tamao *et al.*, 1986a). In addition, argatroban has been shown to inhibit the platelet aggregatory and vasoconstrictor actions of thrombin, which are dependent upon the proteolytic properties of this enzyme (Nakamura *et al.*, 1985; Hara *et al.*, 1986).

Argatroban has antithrombotic properties in a wide variety of animal models of both platelet-rich and erythrocyte-rich thrombosis (see Bush, 1991, for review), and, as expected for an active site inhibitor, its action is independent of the presence of antithrombin III, unlike heparin (Kumada & Abiko, 1981). However, to our knowledge, no systemic study has been performed on the actions of argatroban in purely erythrocyte-rich venous, 'mixed' (platelet- and erythrocyte-rich), and arterial thrombosis models in the same species. Moreover, unlike heparin, argatroban has a short duration of action both in animals and in man (Iida *et al.*, 1986; Verstraete, 1990; Clarke *et al.*, 1991); thus, in order to ascertain its real antithrombotic efficacy, it is necessary to administer the compound by intravenous infusion. We therefore studied the antithrombotic action of intravenous argatroban, both as a bolus and as an infusion, in three models of thrombosis in the rat: the Wessler model (Wessler *et al.*, 1959), transposed to the rat by Freund *et al.* (1990), which is a model of venous thrombosis; an arteriovenous shunt containing a thrombogenic surface where thrombus formation depends upon both platelet and coagulation activation ('mixed' thrombus; Peters *et al.*, 1991); and a model of platelet-rich thrombosis induced by deep intimal lesion of the left common carotid artery. In addition the effects of i.v. infusions of argatroban on tail transection bleeding time were studied. In all cases, calcium heparin was studied in parallel as a reference anticoagulant. Part of this work was presented at the IBC conference on Advances in Anticoagulant, Antithrombotic

[1] Author for correspondence.

and Thrombolytic Drugs, Boston, MA, 26–29 September 1993, and at the meeting of the French Study Group on Haemostasis and Thrombosis, Paris, 15–16 October 1993.

Methods

Animals

Non-fasted male CD rats (Charles River, France) anaesthetized with sodium pentobarbital (Sanofi, 60 mg kg^{-1} i.p., 0.1 ml 100 g^{-1} body weight) were used in all the studies.

Venous thrombosis model

The left jugular vein of animals weighing 350–450 g was cannulated for the intravenous injection of drugs and thromboplastin. The abdominal vena cava was exposed for the placing of vessel clamps. Thrombus formation was induced by the injection 20 $\mu g\ kg^{-1}$ rabbit brain thromboplastin (Stago) followed 10 s later by stasis of a 1-cm segment of the abdominal vena cava. Stasis was maintained for 15 min, after which time the thrombus was removed and immediately weighed. Test compounds or vehicle were administered either as a single bolus injection (2 ml kg^{-1} body weight) 5 min before the injection of thromboplastin or as continuous infusions (0.1 ml min^{-1}) starting 30 min before the thromboplastin injection and continuing throughout the experiment (i.e. 45 min). For each treatment group the mean thrombus weight ± s.e. mean was determined, and tests for statistical significance between the treatment and control groups were performed by one-way analysis of variance followed by Dunnett's test using RS1 software. The percentage inhibition of thrombus formation was determined for each treatment group, and ED_{50} values (dose which produced 50% inhibition of thrombus formation) were estimated.

Arteriovenous shunt model

Rats weighing 350–450 g were anaesthetized as above. The left jugular vein and the right common carotid artery were cannulated with 8-cm-long polyethylene cannulae (Biotrol no. 3) mounted on 25/8 needles. The shunt was assembled by connecting the two cannulae with a slightly curved 6-cm-long plastic tube (internal diameter = 3 mm) containing a 5-cm-long nylon filament (diameter = 0.25 mm) which had been scraped with a scalpel blade to render it more thrombogenic. The extracorporeal circulation is maintained for 15 min, during which time a thrombus adheres to the nylon thread. The shunt is then removed and the thread with its associated thrombus is withdrawn and immediately weighed. The thrombus wet weight is determined by subtracting the average weight (3.3 mg) of a 5-cm-long nylon monofilament from the value obtained. The compounds were administered either as an i.v. bolus 5 min before shunt assembly or as continuous infusions (0.1 ml min^{-1}) starting 30 min before shunt assembly and continuing throughout the experiment (i.e. 45 min). The results are expressed as described above.

Arterial thrombosis model

Rats (450–500 g) were anaesthetized as above. The right jugular vein was cannulated for i.v. drug administration. Thrombosis was induced using the method described by Hladovec (1971). A segment (approximately 2 cm long) of the left carotid artery was exposed and dissected free of the vagus and surrounding tissue and fitted on the distal end with an appropriately sized Doppler flow probe (Triton Technology, San Diego, CA, USA). A bipolar Dastre electrode was placed 1 cm proximal to the probe. Blood flow was measured with a Triton pulsed Doppler flowmeter (system 6, model 200) and recorded on a Gould TA4000 chart recorder. A mechanical zero flow was determined by momentarily clamping the artery between the probe and the electrode. Thrombus formation was induced by the application of an electrical current (3 mA d.c.) for 5 min (with the flowmeter turned off during current application) to the external arterial surface by means of a d.c. stimulator (Service Electronique, Synthélabo Recherche). Blood flow was recorded for 60 min post stimulation. When the flow declined to the predetermined zero flow (mechanical zero, see above), the time in minutes to thrombus formation was noted. Test compounds were administered as above except that the infusions were started 45 min before thrombus induction (i.e. 110 min total drug administration). For each treatment group the mean time to occlusion ± s.e.mean was determined, and tests for statistical significance between the treatment and control groups were performed as above. The percentage increase in the time to occlusive thrombus formation was determined for each treatment group. If the vessels were still patent at the end of the observation period, a value of 60 min was ascribed for the sake of statistical analysis. Additionally, in the i.v. infusion studies, a 5 ml blood sample was taken at the end of the observation period for the determination of the thrombin time and the activated partial thromboplastin time (APTT). Blood was taken from the right carotid artery using 3.8% trisodium citrate (one volume of citrate to 9 volumes of blood) as anticoagulant. The blood samples were centrifuged at 1000 *g* for 15 min, and the plasmas were stored at −20°C until use. Thrombin times were determined using a Behring Fibrintimer as follows. Plasma (200 μl) was incubated for 2 min at 37°C prior to the addition of 0.75 NIH units ml^{-1} (final concentration) bovine thrombin. The time to coagulation in seconds was then noted. APTT values were obtained using commercially available kits and by following the manufacturer's instructions (Diagnostica Stago, Asnières, France).

Tail transection bleeding time

The animals used weighed from 310 to 390 g. The right jugular vein was cannulated for i.v. drug administration. Bleeding was induced by section of the extremity of the tail 3 mm from the tip; the tails were gently blotted with tissue paper every 30 s, and the time in minutes to cessation of bleeding was noted. Care was taken that no pressure was exerted on the tail tips which could affect haemostasis. The compounds were administered as continuous intravenous infusions starting 60 min before tail transection and continuing throughout the experiment (i.e. 150 min total treatment duration). For each treatment group the mean bleeding time ± s.e.mean was determined, and tests for statistical significance between the treatment and control groups were performed as above. If bleeding was still present at the end of the 90 min observation period, a value of 90 min was ascribed for the sake of statistical analysis.

Drugs

Argatroban was obtained from Mitsubishi Kasei Corporation, and heparin (calcium salt) was purchased from Sigma, France.

Results

Venous thrombosis model

The injection of thromboplastin followed by 15 min stasis leads to the formation of a red thrombus weighing approximately 20 mg wet weight. Table 1 shows the results obtained when argatroban and heparin were given as an i.v. bolus 5 min before the injection of thromboplastin. Argatroban dose-dependently prevented thrombus formation with an estimated ED_{50} of 125 $\mu g\ kg^{-1}$ in this test. Under the same conditions, heparin was found to be a more potent inhibitor

of thrombus formation with an estimated ED_{50} of approximately 42 $\mu g\ kg^{-1}$. When the compounds were given as i.v. infusions starting 30 min before the injection of thromboplastin (Table 2). argatroban had an estimated ED_{50} of 1.5 $\mu g\ kg^{-1}\ min^{-1}$ and heparin had an ED_{50} of 1.2 $\mu g\ kg^{-1}\ min^{-1}$.

Arteriovenous shunt model

In this model, placing of a plastic shunt between the carotid artery and the jugular vein led to the formation of a thrombus weighing between 122 and 194 mg. There was very little variation between individual control animals in that the standard errors in the two studies were $\leqslant 5\%$ of the mean values. When argatroban was administered as a single bolus injection 5 min before thrombus induction, there was a dose-dependent reduction in thrombus wet weight, and the ED_{50} value obtained was 0.6 mg kg^{-1} with significant inhibition of thrombus formation as from 0.3 mg kg^{-1}. Heparin was more active than argatroban under these conditions with an ED_{50} of 0.04 mg kg^{-1}. These results are summarized in Figure 1. When the two compounds were administered as a continuous i.v. infusion starting 30 min before shunt assembly and maintained throughout the experiment, the difference in antithrombotic activity of the two compounds was considerably less marked (Figure 2). Once again, both compounds dose-dependently inhibited thrombus formation; argatroban had an ED_{50} of 6 $\mu g\ kg^{-1}\ min^{-1}$, and heparin had an ED_{50} of 3 $\mu g\ kg^{-1}\ min^{-1}$.

Table 1 Effects of intravenous bolus injections of argatroban and heparin on thromboplastin- and stasis-induced venous thrombosis in the rat

Compound	Dose (mg kg^{-1})	Thrombus weight (mg)		Decrease (%)
Vehicle	-	22.0 ± 1.8	(6)	-
Heparin	0.025	15.9 ± 2.2	(6)	27
	0.050	8.8 ± 2.3**	(6)	60
Argatroban	0.050	18.5 ± 1.7	(6)	16
	0.100	12.5 ± 2.5*	(6)	43
	0.200	7.6 ± 1.5**	(6)	65

Compounds were administered as i.v. bolus injections 5 min before the injection of 20 $\mu g\ kg^{-1}$ thromboplastin followed by stasis of the abdominal vena cava. The results show the mean (±s.e.mean) thrombus wet weight. Statistical significance compared with control values is denoted by asterisks where $*P<0.05$, $**P<0.01$ versus controls, Dunnett's test. The number of animals per treatment group is shown in parentheses.

Table 2 Effects of intravenous infusions of argatroban and heparin on thromboplastin- and stasis-induced venous thrombosis in the rat

Compound	Dose ($\mu g\ kg^{-1}\ min^{-1}$)	Thrombus weight (mg)		Decrease (%)
Vehicle	-	21.8 ± 1.5	(12)	-
Argatroban	0.25	21.2 ± 4.7	(6)	3
	0.50	14.7 ± 1.9	(6)	33
	1.00	15.7 ± 1.8	(12)	28
	2.00	8.1 ± 2.2**	(6)	63
	4.00	6.9 ± 1.6**	(6)	68
Heparin	0.25	15.8 ± 4.9	(6)	28
	0.50	19.7 ± 3.4	(6)	10
	1.00	11.1 ± 1.5**	(12)	49
	2.00	8.4 ± 1.7**	(6)	61
	4.00	5.2 ± 1.0**	(6)	76

Compounds were administered as i.v. infusions starting 30 min before the injection of 20 $\mu g\ kg^{-1}$ thromboplastin followed by stasis of the abdominal vena cava. The results show the mean (±s.e.mean) thrombus wet weight. Statistical significance compared with control values is denoted by asterisks where $*P<0.05$, $**P<0.01$ versus controls, Dunnett's test. The number of animals per treatment group is shown in parentheses.

Arterial thrombosis model

Application of an electric current to the adventitial surface of the carotid artery leads to the formation of a stable occlusive thrombus denoted by zero blood flow, which occurred at 10.6 ± 0.79 and 12.5 ± 1.25 min (mean ± s.e.mean) after the end of the period of electrical stimulation for the bolus and infusion studies respectively. When argatroban was administered as an i.v. bolus 5 min before thrombus induction, there was a dose-dependent increase in the time to occlusion with statistically significant effects observed as from 4 mg kg^{-1} (Figure 3). Heparin was also active under these circumstances with a significant increase in the delay to occlusion at 2 mg kg^{-1}, which was roughly equivalent to the antithrombotic effect observed with 8 mg kg^{-1} argatroban. When the compounds were given as i.v. infusions, the difference in potency between the two compounds on a weight basis seen above was no longer present (Figure 4). Both compounds produced dose-dependent increases in the time to occlusion. Moreover, the vessels remained patent throughout the observation period at the highest doses used (40 $\mu g\ kg^{-1}\ min^{-1}$ argatroban and 50 $\mu g\ kg^{-1}\ min^{-1}$ heparin). However, there was a marked difference between the two compounds concerning their effects on thrombin time and APTT (Tables 3 and 4). Argatroban produced a dose-dependent increases in the thrombin time with a 511% inc-

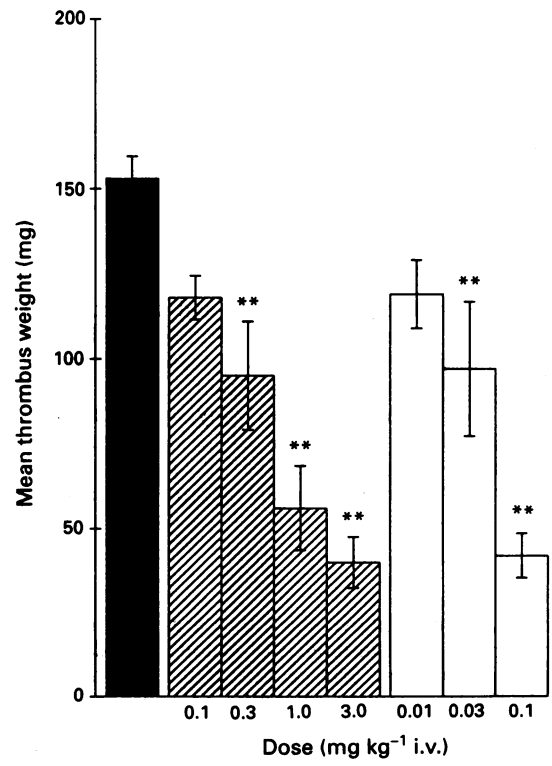


Figure 1 Effects of intravenous bolus injections of argatroban (hatched columns) and heparin (open columns) on thrombus formation in the rat arteriovenous shunt preparation. Each bar shows the mean (±s.e.mean) thrombus weight for each treatment group ($n = 7$, except controls, where $n = 9$). The compounds were administered 5 min before shunt assembly. Statistical significance compared to control values (filled columns) is denoted by asterisks where $*P<0.05$, $**P<0.01$ versus controls, Dunnett's test.

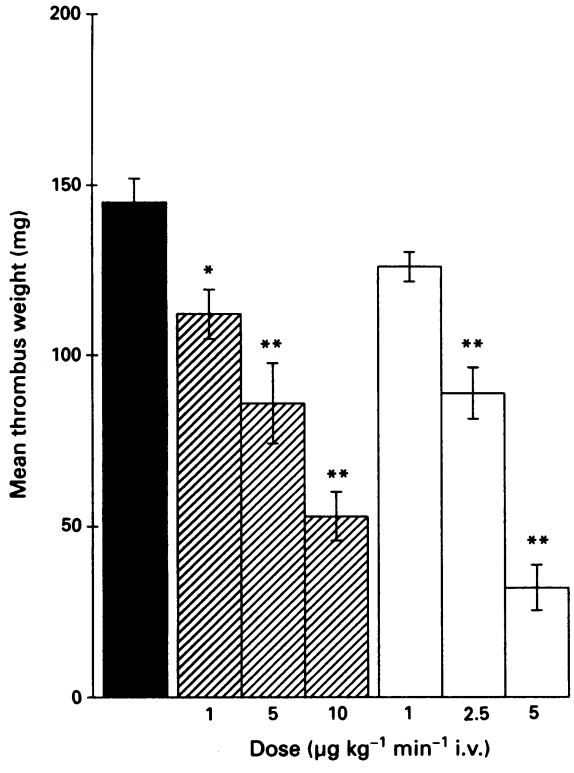


Figure 2 Effects of intravenous infusions of argatroban (hatched columns) and heparin (open columns) on thrombus formation in the rat arteriovenous shunt preparation. Each bar shows the mean (±s.e.mean) thrombus weight for each treatment group ($n = 7$, except controls, where $n = 9$). The infusions were started 30 min before shunt assembly. Statistical significance compared with control values (filled columns) is denoted by asterisks where $*P < 0.05$, $**P < 0.01$ versus controls, Dunnett's test.

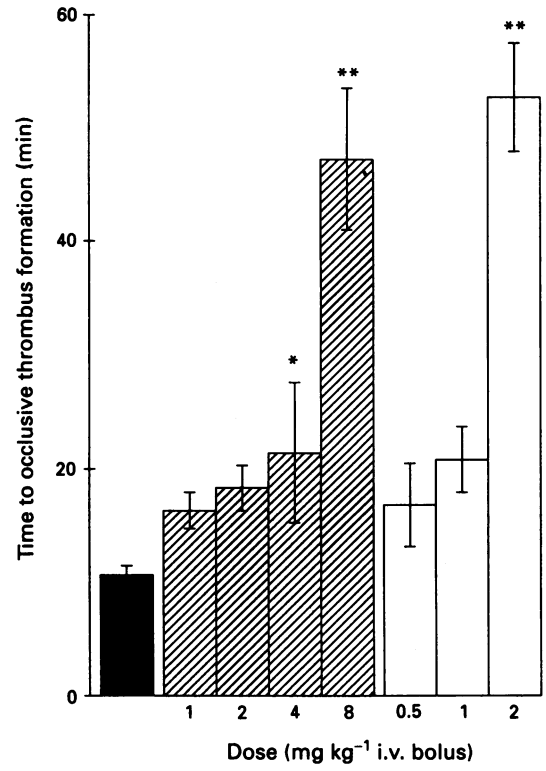


Figure 3 Effects of intravenous bolus injections of argatroban (hatched columns) and heparin (open columns) on thrombus formation induced by a 3 mA d.c. electric current applied to the left carotid artery. Each bar shows the mean (±s.e.mean) time in minutes to the formation of an occlusive thrombus as denoted by zero flow for each treatment group ($n = 8$, except controls, where $n = 14$). The compounds were administered 5 min before thrombus induction. Statistical significance compared with control values (filled columns) is denoted by asterisks where $*P < 0.05$, $**P < 0.01$ versus controls, Dunnett's test.

rease at the highest dose used with only a 73% increase in the APTT at this dose. On the other hand, no coagulation was observed in both tests (>150 s) in any of the samples taken from animals receiving heparin at all the doses tested.

Tail transection bleeding time

Table 5 shows that both heparin and argatroban caused dose-dependent increases in the tail transection bleeding time. In the case of the former, significant increases were noted at $3\,\mu g\,kg^{-1}\,min^{-1}$, whereas a significant increase in bleeding time was seen with argatroban only at the highest dose studied ($30\,\mu g\,kg^{-1}\,min^{-1}$). The ED_{100} value for each compound was estimated to be $2.2\,\mu g\,kg^{-1}\,min^{-1}$ and $11\,\mu g\,kg^{-1}\,min^{-1}$ for heparin and argatroban respectively.

Discussion

The data presented above show that argatroban is a potent antithrombotic agent in models of venous, mixed and arterial thrombosis in the rat. Irrespective of the thrombosis model studied, argatroban was less active on a weight basis than heparin when given as i.v. bolus. However, when the two compounds were administered as continuous infusions, this difference in activity disappears in two out of the three models studied and is reduced to a factor of 2 in the shunt model. These observations are consistent with the differential elimination rates of the two compounds as mentioned above, and underlines the need to take into account the duration of action of test compounds when comparing efficacy in animal models in which the pathogenic stimulus may still be present when the compound is not longer present in the circulation. Indeed, when argatroban has been evaluated in models of thrombosis as an i.v. bolus, its antithrombotic effects are seen at relatively high doses. For example, Morishita *et al.* (1991) showed that bolus injections of greater than $1\,mg\,kg^{-1}$ were necessary to confer greater than 50% protection of rat jugular veins in an endothelial damage model.

In the case of the Wessler model, this is the first study to our knowledge performed with argatroban in a purely coagulation-based model of localised thrombus formation. The two published studies (Morishita *et al.*, 1991; Imura *et al.*, 1992) on the effects of argatroban in venous thrombosis both include a platelet component, and it is therefore difficult to compare our data with the literature. Nevertheless, the antithrombotic efficacy of argatroban given as an i.v. bolus is of the same order of magnitude as that obtained with recombinant hirudins, low molecular weight thrombin active site and anion-binding exosite inhibitors in other published rat models of venous thrombosis (Freund *et al.*, 1990; Gray *et al.*, 1991; Schumacher *et al.*, 1993).

Argatroban is a potent inhibitor of thrombus formation in the rat arteriovenous shunt. This model has been described as a mixed thrombosis model, in that both activation of platelets and the coagulation cascade are determinants of thrombus formation. Morphometric studies in a similar model (using a cotten thread rather than a nylon fibre) have shown this to be the case (Peters *et al.*, 1991). Nevertheless, the present results with heparin suggest that the two compounds are acting primarily on fibrin formation at the doses used, since Peters *et al.* (1991) have shown that the reduction in the platelet content of such shunts is only achieved at doses of thrombin inhibitor (in this case recombinant

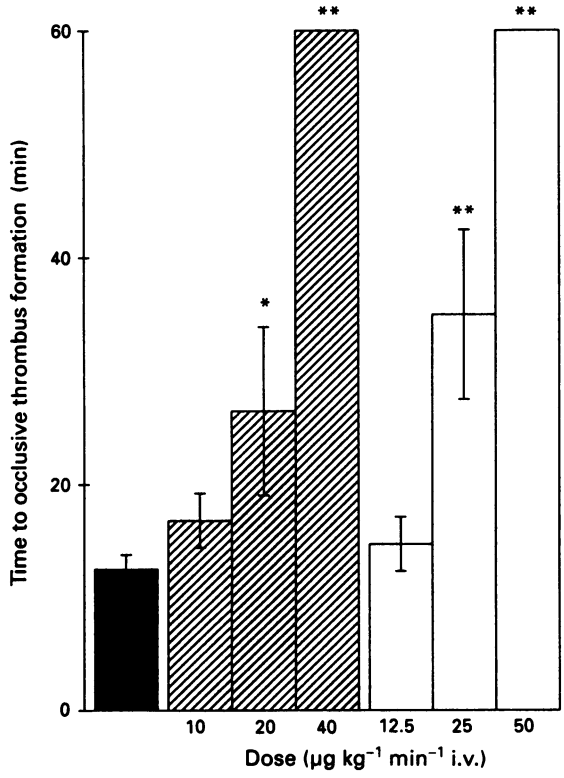


Figure 4 Effects of intravenous infusions of argatroban (hatched columns) and heparin (open columns) on thrombus formation induced by a 3 mA d.c. electric current applied to the left carotid artery. Each bar shows the mean (±s.e.mean) time in minutes to the formation of an occlusive thrombus as denoted by zero flow for each treatment group ($n = 8$, except controls, where $n = 14$). The infusions started 45 min before thrombus induction. Statistical significance compared to control values (filled columns) is denoted by asterisks where $*P<0.05$, $**P<0.01$ versus controls, Dunnett's test.

Table 3 Effects of argatroban and heparin infusions on the thrombin times in the carotid arterial thrombosis model in the rat

Compound	Dose ($\mu g\ kg^{-1}\ min^{-1}$)	Thrombin time (s)		Increase (%)
Vehicle	–	12.1 ± 0.3	(14)	–
Argatroban	10.0	28.1 ± 2.3*	(8)	132
	20.0	36.8 ± 7.2**	(7)	204
	40.0	73.9 ± 6.3**	(8)	511
Heparin	12.5	>150	(8)	>1140
	25.0	>150	(6)	>1140
	50.0	>150	(8)	>1140

Compounds were administered as i.v. infusions starting 45 min before the application of electrical current (3 mA d.c., 5 min) to the outer wall of the left carotid artery. The results show the mean (±s.e.mean) thrombin time in plasmas taken at the end of the observation period.. Statistical significance compared with control values is denoted by asterisks where $*P<0.05$, $**P<0.01$ versus controls, Dunnett's test. The number of animals per treatment group is shown in parentheses.

hirudin) which reduce the thrombus weight by more than 80%.

The doses of argatroban or heparin (whether by i.v. bolus or infusion) required to inhibit arterial thrombosis are at least ten times greater than those required to inhibit venous thrombosis. These observations support the observations that, as the platelet contribution to thrombus increases, more argatroban is required to inhibit thrombus formation (as reviewed by Bush, 1991) to the extent that Jang *et al.* (1990) used a dose of 100 $\mu g\ kg^{-1}\ min^{-1}$ argatroban to prevent arterial occlusion in 9 out of 13 animals in their rabbit femoral arterial eversion model, which is resistant to heparin. Given the high specificity of argatroban towards both the amidolytic and platelet-aggregating actions of thrombin (Kikumoto *et al.*, 1984; Hara *et al.*, 1986; Tamao *et al.*, 1986b), this reinforces the hypothesis that more thrombin is activated in platelet-rich thrombi, and that thrombin is a central mediator of arterial thrombosis, based on similar results obtained with the hirudins (see Talbot *et al.*, 1991, for review) and the tripeptide irreversible thrombin inhibitor PPACK (Hanson & Harker, 1988).

Table 4 Effects of argatroban and heparin infusions on the APTT in the carotid arterial thrombosis model in the rat

Compound	Dose ($\mu g\ kg^{-1}\ min^{-1}$)	APTT (s)		Increase (%)
Vehicle	–	19.8 ± 0.8	(14)	–
Argatroban	10.0	27.1 ± 2.6*	(8)	37
	20.0	25.0 ± 1.1**	(7)	26
	40.0	34.3 ± 2.7**	(8)	73
Heparin	12.5	>150	(8)	>723
	25.0	>150	(6)	>723
	50.0	>150	(8)	>723

Compounds were administered as i.v. infusions starting 45 min before the application of electrical current (3 mA d.c., 5 min) to the outer wall of the left carotid artery. The results show the mean (±s.e.mean) APTT in plasmas taken at the end of the observation period.. Statistical significance compared with control values is denoted by asterisks where $*P<0.05$, $**P<0.01$ versus controls, Dunnett's test. The number of animals per treatment group is shown in parentheses.

Table 5 Effects of intravenous argatroban and heparin infusions on the tail transection bleeding time in the rat

Compound	Dose ($\mu g\ kg^{-1}\ min^{-1}$)	Bleeding time (min)		Increase (%)
Vehicle	–	17.8 ± 0.9	(22)	–
Argatroban	3.0	25.2 ± 5.6	(10)	39
	10.0	32.3 ± 3.6	(10)	78
	30.0	80.8 ± 5.0**	(10)	350
Heparin	1.0	22.1 ± 2.9	(10)	22
	3.0	42.4 ± 7.6**	(10)	133
	10.0	64.0 ± 7.3**	(10)	256
	30.0	>90.0	(8)	>400

Compounds were administered as i.v. infusions starting 60 min before tail transection. The results show the mean (±s.e.mean) bleeding time. Statistical significance compared with control values is denoted by asterisks where $*P<0.05$, $**P<0.01$ versus controls, Dunnett's test. The number of animals per treatment group is shown in parentheses.

The degree of systemic anticoagulation (thrombin time and APTT prolongation) in the arterial thrombosis model required to inhibit thrombus formation is much lower for argatroban than for heparin. In fact, even the dose of heparin which did not inhibit thrombus formation gave an APTT of >150 s. Similar results were obtained with heparin by Schumacher *et al.* (1993) in their rat arterial thrombosis model, and by other groups in pig and baboon models of arterial thrombosis (Cadroy *et al.*, 1989; Heras *et al.*, 1990). The fact that heparin is relatively inactive or only active at 'supramaximal' anticoagulant doses could be due to several factors. Heparin is inhibited by platelet factor 4, to which it binds with a higher affinity than to antithrombin III (Levine & Wohl, 1976). The formation of the prothrombinase complex, with binding of factor Xa to the activated platelet in association with factor Va protects factor Xa from inactiva-

tion by the heparin–antithrombin III complex (Miletich *et al.*, 1978). In addition, clot-bound thrombin is resistant to the inhibitory effects of the heparin–antithrombin III complex (Mirshahi *et al.*, 1989; Weitz *et al.*, 1990). Argatroban is a potent inhibitor of clot-associated thrombin with only a 3-fold shift to the right of the log-concentration inhibition curve compared with its effects on fluid phase thrombin, compared with 16- and 228-fold shifts to the right for recombinant hirudin and heparin respectively (Berry *et al.*, 1994). In the context of our rat model, where the end-point is total occlusion, the thrombin bound to the mural thrombus could play an important role in thrombus growth, and such clot-associated thrombin could be resistant to heparin but not to argatroban, hence the lower degree of systemic anticoagulation necessary for antithrombotic efficacy.

Finally, on a weight basis, argatroban was considerably less active than heparin in increasing the rat tail transection bleeding time. This supports the data on the coagulation parameters described above and suggests that argatroban would have a better therapeutic margin than that of heparin. Moreover, this results contributes to the growing mass of evidence which suggests that direct acting thrombin inhibitors have a lower haemorrhagic potential of thrombin inhibitors than heparin.

In conclusion, the results in this study suggest that argatroban has a potential as a potent antithrombotic agent, particularly in the context of arterial thrombosis in the light of its activity at a very low degree of systemic anticoagulation, at least in the rat.

References

BERRY, C.N., GIRADOT, C., LECOFFRE, C. & LUNVEN, C. (1994). Effects of the synthetic thrombin inhibitor argatroban on fibrin- or clot-incorporated thrombin: comparison with heparin and recombinant hirudin. *Thrombos. Haemostas.* (in press).

BUSH, L.R. (1991). Argatroban, a selective, potent thrombin inhibitor. *Cardiovasc. Drug Rev.*, **9**, 247–263.

CADROY, Y., HARKER, L.A. & HANSON, S.R. (1989). Inhibition of platelet-dependent thrombosis by low molecular weight heparin (CY222); comparison with standard heparin. *J. Lab. Clin. Med.*, **114**, 349–359.

CLARKE, R.J., MAYO, G., FITZGERALD, G.A. & FITZGERALD, D.J. (1991). Combined administration of aspirin and a specific thrombin inhibitor in man. *Circulation*, **83**, 1510–1518.

FREUND, M., CAZENAVE, J.-P., COURTNEY, M., DEGRYSE, E., ROITSCH, C., BERNAT, A., DELEBASSEE, D., DEFREYN, G. & MAFFRAND, J.-P. (1990). Inhibition by recombinant hirudins of experimental venous thrombosis and disseminated intravascular coagulation induced by tissue factor in rats. *Thrombos. Haemostas.*, **63**, 187–192.

GRAY, E., WATTON, J., CESMELI, S., BARROWCLIFFE, T.W. & THOMAS, D.P. (1991). Experimental studies on a recombinant hirudin CGP 39393. *Thrombos. Haemostas.*, **65**, 355–391.

HANSON, S.R. & HARKER, L.A. (1988). Interruption of acute platelet-dependent thrombosis by the synthetic antithrombin D-phenylalanyl-L-prolyl-L-arginyl chloromethyl ketone. *Proc. Natl. Acad. Sci. USA*, **85**, 3184–3188.

HARA, H., TAMAO, Y. & KIKUMOTO, R. (1986). Effect of argatroban (MD-805) on platelet function. *Jpn. Pharmacol. Ther.*, **14** (Suppl 5), 13–19.

HERAS, M., CHESEBRO, J.H., WEBSTER, M., MRUK, J.S., GRILL, D.E., PENNY, W.J., BOWIE, E.J.W., BADIMON, L. & FUSTER, V. (1990). Hirudin, heparin and placebo during deep arterial injury in the pig. *Circulation*, **82**, 1476–1484.

HLADOVEC, J. (1971). Experimental thrombosis in rats with continuous registration. *Thrombos. Haemostas.*, **26**, 407–410.

IIDA, S., KOMATSU, T., HIRANO, T., FUJIMURA, Y., NAKAI, H., KITAZAWA, K., KUMAGAI, Y., SATO, T., HAYASHI, K. & INOKUCHI, K. (1986). Pharmacokinetic studies of argatroban (MD-805) in dogs and rabbits. Blood or plasma level profile, metabolism, excretion and accumulation after single or consecutive intravenous administration of argatroban. *Oyo Yakuri (Pharmacometrics)*, **32**, 1117–1127.

IMURA, Y., STASSEN, J.-M. & COLLEN, D. (1992). Comparative antithrombotic effects of heparin, recombinant hirudin and argatroban in a hamster femoral vein platelet-rich mural thrombosis model. *J. Pharmacol. Exp. Ther.*, **261**, 895–898.

JANG, I.-K., GOLD, H.K., ZISKIND, A.A., LEINBACH, R.C., FALLON, J.T. & COLLEN, D. (1990). Prevention of platelet-rich arterial thrombosis by selective thrombin inhibition. *Circulation*, **81**, 219–225.

KIKUMOTO, R., TAMAO, Y., TEZUKA, T., TONOMURA, S., HARA, H., NINOMIYA, K., HIJIKATA, A. & OKAMOTO, S. (1984). Selective inhibition of thrombin by (2r,4r)-4-methyl-l-[n^2-[(3-methyl-1, 2, 3, 4-tetrahydro-8-quinolinyl)sulfonyl]-arginyl]-2-piperidinecarboxylic acid. *Biochemistry*, **23**, 85–90.

KUMADA, T. & ABIKO, Y. (1981). Comparative study of heparin and a synthetic thrombin inhibitor no. 805 (MD-805) in experimental antithrombin III-deficient animals. *Thrombosis Res.*, **24**, 285–298.

LEVINE, S.P. & WOHL, H. (1976). Human platelet factor 4 (PF_4) purification and characterization by affinity chromatography. *J. Biol. Chem.*, **251**, 324–328.

MILETICH, J.P., JACKSON, C.M. & MAJERUS, P.W. (1978). Properties of the factor Xa binding site on human platelets. *J. Biol. Chem.*, **253**, 6908–6916.

MIRSHAHI, M., SORIA, J., SORIA, C., FAIVRE, R., LU, H., COURTNEY, M., ROITSCH, C., TRIPIER, D. & CAEN, J.P. (1989). Evaluation of the inhibition by heparin and hirudin of coagulation activation during r-t-PA-induced thrombolysis. *Blood*, **74**, 1025–1030.

MORISHITA, K., WADA, M., KUMADA, T., TANAKA, T., TOMIKAWA, M. & IWAMOTO, M. (1991). Effect of ticlopidine and other antithrombotics on the venous thrombosis induced by endothelial damage of jugular vein in rats. *Thrombosis Res.*, **63**, 373–384.

NAKAMURA, K., HATANO, Y. & MORI, K. (1985). Thrombin-induced vasoconstriction in isolated cerebral arteries and the influence of a synthetic thrombin inhibitor. *Thrombosis Res.*, **40**, 715–720.

OKAMOTO, S., HIJIKATA, A., KIKUMOTO, R., TONOMARA, S., HARA, H., NINOMIYA, K., MARUYAMA, A., SUGANO, M. & TAMAO, Y. (1981). Potent inhibition of thrombin by the newly synthesized arginine derivative no. 805. The importance of stereostructure of its hydrophobic carboxamide portion. *Biochem. Biophys. Res. Commun.*, **101**, 440–446.

PETERS, R.F., LEES, C.M., MITCHELL, K.A., TWEED, M.F., TALBOT, M.D. & WALLIS, R.B. (1991). The characterisation of thrombus development in an improved model of arterio-venous shunt thrombosis in the rat and the effects of recombinant desulphatohirudin (CGP 39393), heparin and iloprost. *Thrombos. Haemostas.*, **65**, 268–274.

SCHUMACHER, W.A., STEINBACHER, T.E., HERAN, C.L., SEILER, S.M., MICHEL, N.M. & OGLETREE, M.L. (1993). Comparison of thrombin active site and exosite inhibitors and heparin in experimental models of arterial and venous thrombosis and bleeding. *J. Pharmacol. Exp. Ther.*, **267**, 1237–1242.

TALBOT, M.D., AMBLER, J.A., BUTLER, K.D., LEES, C.M., MITCHELL, K.A., PETERS, R.F., TWEED, M.F. & WALLIS, R.B. (1991). The effects of recombinant desulphatohirudin on arterial thrombosis in rats. *Haemostasis*, **21** (Suppl. 1), 73–79.

TAMAO, Y., YAMAMOTO, T., HIRATA, T., KINUGASA, M. & KIKUMOTO, R. (1986a). Effect of argatroban (MD-805) on blood coagulation. *Jpn. Pharmacol. Ther.*, **14**, (Suppl. 5), 7–12.

TAMAO, Y., YAMAMOTO, T., KIKUMOTO, R., HARA, H., ITOH, J., HIRATA, T., MINEO, K. & OKAMOTO, S. (1986b). Effect of a selective thrombin inhibitor MCI-9038 on fibrinolysis in vitro and in vivo. *Thrombos. Haemostas.*, **56**, 28–34.

TAPPARELLI, C., METTERNICH, R., EHRHARDT, C., ZURINI, M., CLAESON, G., SCULLY, M.F. & STONE, S.R. (1993). *In vitro* and *in vivo* characterization of a neutral boron-containing thrombin inhibitor. *J. Biol. Chem.*, **268**, 4724–4741.

VERSTRAETE, M. (1990). Pharmacotherapeutic aspects of unfractionated and low molecular weight heparins. *Drugs*, **40**, 498–530.

WEITZ, J.I., HUDOBA, M., MASEL, D., MARAGANORE, J. & HIRSH, J. (1990). Clot bound thrombin is protected from inhibition by heparin-antithrombin III but is susceptible to inactivation by antithrombin III independent inhibitors. *J. Clin. Invest.*, **86**, 385–391.

WESSLER, S., REIMER, S.M. & SHEPS, M.C. (1959). Biologic assay assay of a thrombosis inducing activity in human serum. *J. Appl. Physiol.*, **14**, 943–946.

(Received July 7, 1994
Accepted August 5, 1994)

Br. J. Pharmacol. (1994), **113**, 1215–1220 © Macmillan Press Ltd, 1994

Effect of activity at metabotropic, as well as ionotropic (NMDA), glutamate receptors on morphine dependence

†Marian E. Fundytus & [1]†‡Terence J. Coderre

*Pain Mechanisms Laboratory, Clinical Research Institute of Montreal, †Department of Psychology, McGill University and ‡Centre de recherche en sciences neurologiques et Département de médecine, Université de Montréal, Montreal, Canada

1 The contribution of various excitatory amino acid (EAA) receptors (NMDA, AMPA/kainate and metabotropic) in the brain to the development of morphine dependence was examined. This was performed by measuring the severity of the precipitated withdrawal syndrome following chronic subcutaneous (s.c.) morphine and intracerebroventricular (i.c.v.) EAA antagonist treatment.

2 Continuous subcutaneous (s.c.) treatment with morphine sulphate (36.65 μmol day^{-1}) produced an intense and reliable naloxone-precipitated withdrawal syndrome.

3 Chronic i.c.v. treatment with antagonists selective for metabotropic and NMDA receptors, but not AMPA/kainate receptors, significantly attenuated abstinence symptoms. Conversely, EAA antagonists had very little effect on non-withdrawal behaviours.

4 These results suggest that, as well as changes elicited by activation of NMDA receptors, metabotropic receptors and intracellular changes in the phosphatidylinositol (PI) second-messenger system or the cyclic adenosine 3′,5′-monophosphate (cAMP) second messenger system, to which EAA metabotropic receptors are linked, may be involved in the development of opioid dependence with chronic morphine treatment.

Keywords: Opioid; morphine; dependence; glutamate; metabotropic glutamate receptor; AMPA; kainate; NMDA; abstinence syndrome; excitatory amino acids

Introduction

Although opioid drugs such as morphine are widely used for the management of pain, their clinical usefulness is limited by the development of tolerance and dependence that occurs with their chronic use. Tolerance is indicated by a decreased efficacy of the drug with repeated administration, and results in a need to increase the morphine dose in order to achieve the desired analgesic effect. Dependence is a continued need for the drug to maintain a state of physiological equilibrium, and leads to an aversive withdrawal or abstinence syndrome when morphine administration is terminated. Recently, it has been demonstrated that co-administration of *N*-methyl-D-aspartate (NMDA) receptor antagonists attenuates the development of morphine tolerance and dependence (Marek *et al.*, 1991a,b; Trujillo & Akil, 1991). Since the endogenous excitatory amino acid (EAA) glutamate activates NMDA receptors, it is likely that glutamate contributes to the development of these phenomena. In addition to NMDA receptors, glutamate acts at at least two other types of ionotropic receptors: receptors at which α-2-amino-3-(hydroxy-5-methylisoxazol-4yl)propanoic acid (AMPA) is a selective agonist and receptors at which kainate is a selective agonist; and metabotropic receptors (Mayer & Westbrook, 1987a; Monaghan *et al.*, 1989). While a role for the NMDA receptor has already been suggested, the specific contribution of these other receptors to behavioural indices of opioid tolerance and dependence has not been investigated.

The NMDA receptor gates a cation channel that is permeable to Ca^{2+} and Na^{+} (MacDermott *et al.*, 1986; Mayer *et al.*, 1987) and is gated in a voltage-dependent fashion by Mg^{2+}(Mayer *et al.*, 1984; Nowak *et al.*, 1984). It is the voltage-dependent Ca^{2+} permeability of the NMDA receptor that is thought to be necessary for use-dependent synaptic plasticity (Cotman *et al.*, 1988) and may be critical for the development of neuronal changes that mediate opioid tolerance and dependence (Marek *et al.*, 1991a,b; Trujillo & Akil, 1991). AMPA and kainate receptors gate cation channels that are permeable to Na^{+}, but for the most part have negligible permeability to Ca^{2+} (Mayer & Westbrook, 1987b; Murphy & Miller, 1989). However, AMPA/kainate receptors that exhibit Ca^{2+} permeability have recently been cloned (Miller, 1991; Sommer & Seeburg, 1992). Traditionally, AMPA/kainate receptors are thought to be involved in the mediation of rapid excitatory responses to EAA transmitters (Kiskin *et al.*, 1986; Jonas & Sakmann, 1992) and may contribute to neuronal plasticity by relieving the NMDA receptor of its voltage-dependent block by Mg^{2+}. Unlike ionotropic receptors, metabotropic glutamate receptors are not linked to cation channels. Instead they are coupled directly to the cell membrane by a G protein (Sladeczek *et al.*, 1985; Sugiyama *et al.*, 1987). Several subtypes of metabotropic glutamate receptors have recently been cloned. Some subtypes affect phosphatidylinositol (PI) hydrolysis (mGluR1α, mGluR1β and mGluR5), while others affect the production of adenosine 3′,5′-cyclic monophosphate (cAMP) (mGluR2, mGluR3, mGluR4) (Schoepp & Conn, 1993). Activity at metabotropic receptors coupled to the PI system activates phospholipase C, which catalyses phosphatidylinositol hydrolysis, leading to the production of inositol 1,4,5-trisphosphate (IP3) and diacylglycerol (DAG) (Ambrosini & Meldolesi, 1989; Manzoni *et al.*, 1990; Schoepp & Conn, 1993). Activity at metabotropic receptors coupled to the cAMP second messenger system generally leads to decreased production of cAMP, although activation of mGluR1α stimulates an increase in cAMP (Schoepp & Conn, 1993). Through the increased production of intracellular messengers associated with PI hydrolysis, or decreased production of cAMP, metabotropic receptor activation may play an important role in the long-term effects mediated by glutamate (Nicoletti *et al.*, 1991), and like NMDA receptors may be critical to the development of neuronal changes mediating opioid tolerance and dependence.

In the present study we have investigated the contribution of various EAA receptor subtypes in the brain to the

[1] Author for correspondence at Pain Mechanisms Laboratory, Clinical Research Institute of Montreal, 110 Pine Ave. West, Montreal (Quebec), Canada H2W 1R7.

development of opioid dependence. This purpose was achieved by examining the effects of the intracerebroventricular (i.c.v.) administration of selective EAA receptor antagonists concurrently with the chronic subcutaneous (s.c.) administration of morphine. NMDA receptors were antagonized with the non-competitive antagonist 5-methyl-10,11-dihydro-5H-dibenzocycloheptene-5,10-imine hydrogen maleate (MK-801) (Wong *et al.*, 1986); AMPA/kainate receptors were antagonized with 1-(4-aminophenyl)-4-methyl-7,8-methylenedioxy-5H-2,3-benzodiazepine-hydrochloride (GYKI 52466) (Donevan & Rogawski, 1993). Although distinct families of high-affinity AMPA and kainate receptors have been isolated, the functional distinction between these receptors is not entirely clear (Barnard & Henley, 1990). Consequently, pharmacological investigations with receptor antagonists are limited to investigations of non-selective AMPA/kainate receptor effects. Metabotropic receptors were antagonized with the highly selective antagonist (*S*)-4-carboxyphenylglycine [(*S*)-4C-PG] (Birse *et al.*, 1993; Eaton *et al.*, 1993) and a more commonly used, yet less selective antagonist, L-2-amino-3-phosphonopropanoic acid (L-AP3) (Schoepp *et al.*, 1990; Birse *et al.*, 1993).

Methods

Subjects and surgery

Subjects were male Long Evans rats (280–350 g). The rats were housed 2–3 per cage, on a 12:12 h light–dark cycle (lights on at 06:00 h), with food and water available *ad libitum*.

On day 0 rats were anaesthetized with sodium pentobarbital (Somnotol, MTC Pharmaceuticals, 60 mg kg^{-1}), and 23 gauge stainless steel cannulae, attached to model 2001 Alzet osmotic mini-pumps filled with one of the EAA antagonist solutions or saline, were implanted stereotaxically in the lateral ventrical (AP = −1.3 mm and L = −1.8 mm from bregma and V = −3.8 mm from the top of the skull; Paxinos & Watson, 1986). While the rats were still under pentobarbital anaesthesia, one unprimed (i.e. not yet pumping) model 2ML1 Alzet pump containing 60 mg ml^{-1} morphine sulphate solution was implanted s.c. on the back. These morphine-containing pumps started pumping the morphine solution approximately 2–4 h following implantation. On the following day, day 1, rats were briefly anaesthetized with halothane and a second unprimed model 2ML1 Alzet pump containing 60 mg ml^{-1} morphine sulphate solution was implanted s.c. on the back. This two day pump implantation procedure was used to reduce the risk of mortality resulting from the accumulation of lethal systemic morphine concentrations prior to any tolerance development. To assess the effects of chronic i.c.v. EAA antagonist treatment on behaviour in rats not dependent on morphine, some rats were given vehicle or 40 nmol day^{-1} L-AP3, (*S*)-4C-PG, MK-801 or GYKI 52466 without concurrent morphine treatment.

Drugs

MK-801, L-AP3 and GYKI 52466 were obtained from Research Biochemicals, (Natick, MA, U.S.A.), while (*S*)-4C-PG was purchased from Tocris Neuramin (Bristol, U.K.). EAA antagonists were continuously infused at a rate of 1 μl h^{-1} in the following concentrations: 1.6 nmol day^{-1}, 8 nmol day^{-1} and 40 nmol day^{-1}. Morphine sulphate (Sabex, Montreal, Canada) was continuously delivered at a rate of 10 μl h^{-1} for a total dose of 36.65 μmol day^{-1} morphine sulphate.

Withdrawal measurement

Precipitated abstinence symptoms were assessed on the seventh day of treatment (while all pumps were still delivering antagonists and morphine) after injection of naloxone (1 mg kg^{-1} s.c.). For 10 min before and 40 min after naloxone injection, the withdrawal symptoms were assessed by measuring the amount of time spent teeth chattering and writhing, as well as by counting jumps and wet dog shakes (Bläsig *et al.*, 1973). The time spent in non-withdrawal behaviours (ambulating, rearing, grooming and resting) was also measured for comparison, for 10 min before and after the injection of naloxone, in rats treated with i.c.v. EAA antagonists either alone or with s.c. morphine.

Statistical analysis

Timed withdrawal behaviours (teeth chattering, writhing) were analysed using ANOVA, followed by *post hoc* tests on significant main effects. Counted withdrawal behaviours (number of jumps and wet dog shakes) were analysed using a Kruskal–Wallis ANOVA for non-parametric data, followed by Mann–Whitney *U*-tests on significant main effects.

The effect of EAA antagonist treatment on non-withdrawal behaviours (ambulating, rearing, grooming and resting) was assessed by comparing the first two time blocks (i.e. 10 min prior to naloxone injection and 10 min after naloxone injection) for rats in each treatment group. Planned comparisons were used to analyse differences in the proportion of time spent in each timed non-withdrawal and the two timed withdrawal behaviours during these two time blocks across the different treatment conditions.

Results

Administration of 36.65 μmol day^{-1} s.c. morphine sulphate by Alzet pump produced an intense and reliable naloxone-precipitated abstinence syndrome which was evidenced by the occurrence of teeth chattering, writhing, jumping and wet dog shaking. As indicated in Figure 1a, the metabotropic receptor antagonists (*S*)-4C-PG and L-AP3 significantly decreased the occurrence of timed abstinence symptoms (teeth chattering and writhing). The effect for (*S*)-4C-PG appeared to be dose dependent, with the highest dose, 40 nmol day^{-1}, producing the greatest reduction in teeth chattering and writhing. L-AP3 was most effective at 8 nmol day^{-1}. Figure 1b shows the amount of time spent teeth chattering and writhing for rats treated with MK-801 and GYKI 52466. The NMDA receptor antagonist MK-801 significantly decreased the time spent in withdrawal at all doses used. The AMPA/kainate receptor antagonist GYKI 52466 did not affect the amount of time spent in withdrawal at any of the doses used.

Figure 2 illustrates the frequency of the counted abstinence symptoms, jumps and wet dog shakes. Although MK-801 tended to *increase* the number of jumps and wet dog shakes at the high dose (40 nmol day^{-1}), none of the i.c.v. EAA antagonist treatments *significantly* affected the number of jumps and wet dog shakes.

Figure 3 shows the percentage of time spent in each of the timed behaviours during the 10 min prior to naloxone administration and during the 10 min following naloxone for rats in each i.c.v. treatment group either with or without concurrent morphine treatment. As can be seen in Figure 3a and b, prior to the injection of naloxone, rats in all i.c.v. treatment groups, with or without morphine, behaved very similarly, with the only differences being more grooming in L-AP3 treated rats than in saline treated rats. In addition, saline-treated rats that were also given morphine reared more that rats given i.c.v. saline alone. Although activity levels (ambulating and rearing) were lower and resting was generally higher after the injection of naloxone, rats given i.c.v. EAA antagonists without morphine still behaved very similarly to rats given i.c.v. saline without morphine. The only differences observed were an increase in grooming in L-AP3-treated rats and increased activity in GYKI 52466-

treated rats, as evidenced by increased ambulating, rearing and grooming and decreased resting. As expected, rats dependent on morphine showed significantly more naloxone-precipitated withdrawal, with a resultant decrease in non-withdrawal behaviours, than rats given i.c.v. treatments alone. In morphine-dependent rats, time in withdrawal was significantly less in L-AP3-, (*S*)-4C-PG- and MK-801-treated rats, which coincided with an increase in ambulation in (*S*)-4C-PG- and MK-801-treated rats.

Discussion

The present results demonstrate that concurrent treatment of rats with various EAA antagonists and chronic morphine leads to a decrease in various symptoms of morphine withdrawal. The NMDA receptor antagonist MK-801 and the metabotropic receptor antagonists (*S*)-4C-PG and L-AP3 were all effective at decreasing the amount of time spent exhibiting the withdrawal symptoms of teeth chattering and writhing, while the AMPA/kainate receptor antagonist GYKI 52466 had no effect. Although all but the AMPA/kainate receptor antagonist significantly reduced the timed withdrawal symptoms, none of the EAA antagonists significantly affected the counted withdrawal symptoms (i.e. jumping and wet dog shakes). It has been suggested that withdrawal symptoms such as jumping are mediated primarily by structures around the fourth ventricle, as evidenced by focal brain micro-injections of naltrexone and levallorphan in morphine-dependent rats (Laschka *et al.*, 1976; Koob *et al.*, 1992). In the present study, EAA antagonists were infused in very small volumes into the lateral ventricle, thus it is possible that the counted symptoms were not affected because the drugs were unable to diffuse to the appropriate brain structures around the fourth ventricle.

There was very little effect of i.c.v. EAA antagonist treatment on non-withdrawal behaviours, except for a general increase in grooming in rats given L-AP3 and increased activity in GYKI 52466-treated rats given naloxone. In general, rats given i.c.v. treatment alone rested more during the second 10 min (i.e. after naloxone), with concurrent decreases in ambulation and rearing. This is probably *not* an effect of naloxone, but rather because they had adequately explored the test box and were comfortable in the environment (a phenomenon common in untreated rats). Rats treated chronically with morphine exhibited withdrawal following the injection of naloxone, which caused a subsequent decrease in other timed behaviours. L-AP3, (*S*)-4C-PG and MK-801 all decreased withdrawal compared with saline in morphine-treated rats, with a resultant increase in ambulation in rats given MK-801 + morphine and (*S*)-4C-PG + morphine. The decrease in withdrawal allows for more time to be spent in other behaviours.

Although we have no explanation for why L-AP3 would increase grooming, it appears to be a robust effect since it occurred in every condition except in rats going through withdrawal (i.e. morphine + naloxone). The increase in activity produced by GYKI 52466 appears to be less robust since it occurred only in the group also treated with naloxone. Nonetheless, it is not expected that these behavioural effects of L-AP3 or GYKI 52466 alter our conclusions about the effects of EAA antagonists on withdrawal behaviour. GYKI 52466 did not significantly affect withdrawal, and the effects of the metabotropic receptor antagonist L-AP3 were confirmed by another metabotropic antagonist (*S*)-4C-PG, which did not significantly influence non-withdrawal behaviours. Therefore, we propose that EAA antagonist treatment affects the development of dependence directly, and not indirectly by interfering with the measurement of the withdrawal behaviours.

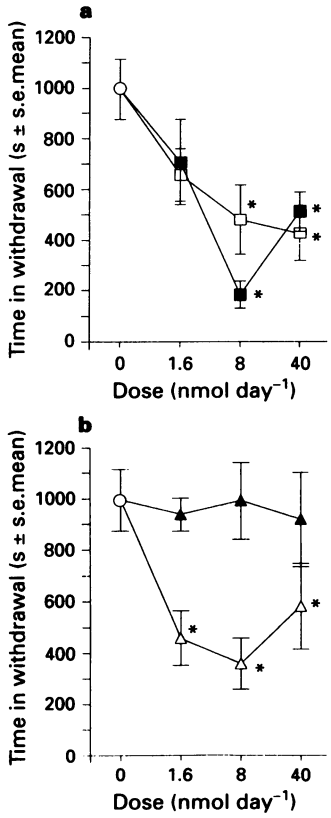


Figure 1 Mean time spent exhibiting withdrawal (teeth chattering and writhing) during the 40 min withdrawal period in rats given chronic s.c. morphine and i.c.v. treatment with the metabotropic receptor antagonists (*S*)-4C-PG (□) ($n = 5-10$ per dose) and L-AP3 (■) ($n = 4-10$ per dose) (a), the NMDA receptor antagonist MK-801 (△) ($n = 4-10$ per dose) (b), and the AMPA/kainate receptor antagonist GYKI 52466 (▲) ($n = 4-10$ per dose) (b). ANOVA indicated significant effects of (*S*)-4C-PG [$F_{(3,22)} = 5.124$, $P < 0.001$], L-AP3 [$F_{(3,23)} = 12.107$, $P < 0.001$] and MK-801 [$F_{(3,21)} = 6.222$, $P < 6.222$, $P < 0.01$], but not GYKI 52466 [$F_{(3,20)} = 0.071$, $P > 0.05$]. Significant differences from the control group are indicated by asterisks (*$P < 0.05$, LSD *t*-test).

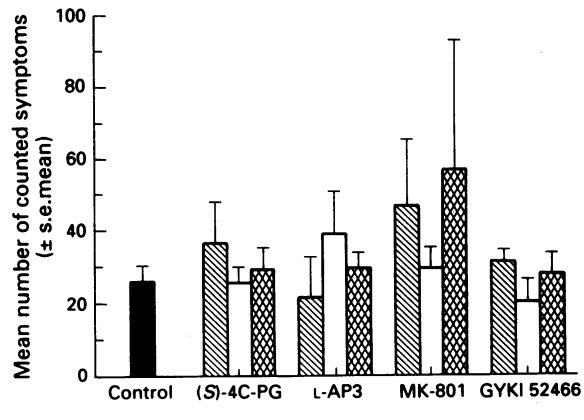


Figure 2 Frequency of counted symptoms (jumps and wet dog shakes) during the 40 min withdrawal period for rats given chronic s.c. morphine and i.c.v. treatment with the metabotropic receptor antagonists (*S*)-4C-PG ($n = 5-10$ per dose) or L-AP3 ($n = 4-10$ per dose), the NMDA receptor antagonist MK-801 ($n = 4-10$ per dose) or the AMPA/kainate receptor antagonist GYKI 52466 ($n = 4-10$ per dose). Kruskal-Wallis ANOVA for non-parametric data revealed no significant effects of any of the EAA antagonists. (*S*)-4C-PG, $H_{(3,22)} = 0.803$, $P > 0.05$; MK-801, $H_{(3,21)} = 0.747$, $P > 0.05$; GYKI 52466, $H_{(3,20)} = 2.580$, $P > 0.05$; L-AP3, $H_{(3,23)} = 2.142$, $P > 0.05$. Solid columns, 0 nmol day^{-1}; diagonal hatched columns, 1.6 nmol day^{-1}; open columns, 8 nmol day^{-1}; cross-hatched columns, 40 nmol day^{-1}.

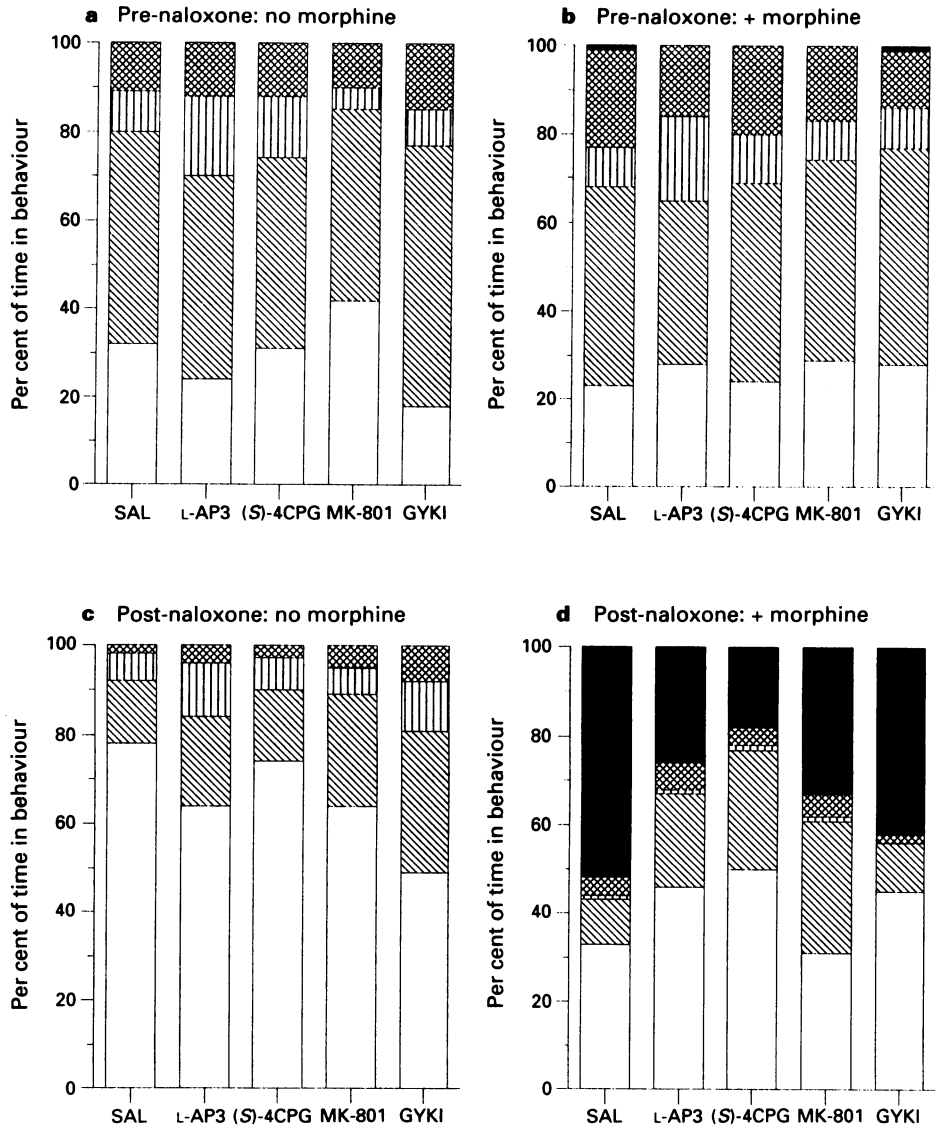


Figure 3 Percentage of time in non-withdrawal and withdrawal behaviours in rats treated chronically with either saline or 40 nmol day^{-1} L-AP3, (*S*)-4C-PG, MK-801 or GYKI 52466 (EAA antagonists) i.c.v. alone (i.e. no s.c. morphine; $n = 6-8$ per i.c.v. treatment) (a) or with s.c. morphine ($n = 4-10$ per i.c.v. treatment) (b) during the 10 min *prior* to the injection of naloxone; and in rats given chronic i.c.v. saline or EAA antagonists alone (c) or with s.c. morphine (d) during the 10 min *after* the injection of naloxone. Prior to the injection of naloxone, rats in all i.c.v. treatment groups, with or without morphine, behaved very similarly, with the only differences being increased grooming in L-AP3-treated rats (planned comparison$_{(1,52)}$, $P<0.05$) (a and b). With the addition of morphine, saline-treated rats exhibited more rearing than rats not treated with morphine (planned comparison$_{(1,52)}$, $P<0.05$) (b). After the injection of naloxone, rats not dependent on morphine generally rested more than in the first 10 min. Non-dependent rats in all i.c.v. treatment groups behaved similarly, with the only differences being more grooming in L-AP3-treated rats (planned comparison$_{(1,52)}$, $P<0.05$) (c) and more activity in GYKI 52466-treated rats as evidenced by significantly more ambulating (diagonal hatched columns), rearing (cross-hatched columns) and grooming (vertically hatched columns) and significantly less resting (open columns) (planned comparison$_{(1,52)}$, $P<0.05$) (c). Morphine-dependent rats showed a significant increase in withdrawal behaviours (solid columns) regardless of i.c.v. treatment after the injection of naloxone (planned comparison$_{(1,52)}$, $P<0.05$) (d). However, L-AP3, (*S*)-4C-PG and MK-801 all significantly decreased the percentage of time spent in withdrawal behviours, with a concurrent increase in ambulation in (*S*)-4C-PG- and MK-801-treated rats (planned comparison$_{1,52)}$, $P<0.05$) (d).

Previously, it has been observed that concurrent treatment of rats with the non-selective EAA antagonist kynurenic acid (Marek *et al.*, 1991a) or the non-competitive NMDA antagonist MK-801 (Marek *et al.*, 1991b; Trujillo & Akil, 1991) with daily injections of morphine attenuated the development of tolerance to morphine's analgesic effects. MK-801 also alleviated the severity of some symptoms of the precipitated withdrawal syndrome (Trujillo & Akil, 1991). Furthermore, some investigators have found that acute treatment with kynurenic acid and MK-801 only on the day of testing (i.e. not concurrently with morphine) is effective in decreasing the severity of some withdrawal symptoms (Rasmussen *et al.*, 1991a,b; Tanganelli *et al.*, 1991), while others did not find this acute administration effective (Trujillo & Akil, 1991). While each of these above studies assessed the effects of *systemically* administered EAA antagonists, in additional experiments (unpublished data), we have found that acute *i.c.v.* injections of EAA antagonists on day 7 prior to precipitation of withdrawal failed to attenuate severity of abstinence symptoms, lending support to the latter group.

Hyperactivity in the locus coeruleus (LC) has been shown to be correlated with the morphine withdrawal syndrome (Aghajanian, 1978; Valentino & Wehby, 1989). Central administration of non-specific, NMDA-selective and AMPA/

kainate-selective EAA antagonists into either the lateral ventricle or the locus coeruleus has been found to decrease the hyperactivity of locus coeruleus neurones during precipitated morphine withdrawal (Akaoka & Aston-Jones, 1991), with the best effects produced by the non-specific EAA antagonist. Conversely, systemic administration of selective NMDA receptor antagonists was unable to affect the hyperactivity of locus coeruleus neurones during precipitated morphine withdrawal (Rasmussen *et al.*, 1991a).

The present data indicate that chronic i.c.v. administration of the selective metabotropic EAA receptor antagonists (*S*)-4C-PG and L-AP3 was at least as effective in attenuating the severity of the morphine withdrawal syndrome as antagonists selective for the NMDA receptors. It is noteworthy that the most effective treatment was 8 nmol day^{-1} L-AP3. This strong effect of L-AP3 may have resulted from a possible additive effect of L-AP3 at both metabotropic and NMDA receptors. There is evidence that L-AP3 may have non-selective effects at the NMDA receptor as well as its proposed major action at the metabotropic receptor (Birse *et al.*, 1993). The significant dose-dependent effects of the highly selective metabotropic receptor antagonist (*S*)-4C-PG, however, do suggest an important role of metabotropic glutamate receptors in the development of morphine dependence. The failure of GYKI 52466 to influence precipitated withdrawal suggests that AMPA/kainate receptors do not play an important role in morphine dependence. Although it is possible that GYKI 52466's ineffectiveness could be explained by rapid metabolism *in vivo*, this is unlikely because the drug was chronically infused. Furthermore, it has been demonstrated, using an osmotic pump infusion method similar to that used in the present study, that GYKI 52466 is as effective at attenuating excitatory amino acid induced seizures on the 14th day of infusion as it is on the third day of infusion (Steppuhn & Turski, 1993).

Activity at specific metabotropic receptor subtypes stimulates phosphatidylinositol (PI) hydrolysis and leads to the production of the intracellular messengers inositol 1,4,5-trisphosphate (IP3) and diacylglycerol (DAG) (Ambrosini & Meldolesi, 1989; Manzoni *et al.*, 1990; Schoepp & Conn, 1993). Chronic opioid use may alter production of these intracellular messengers and thus elicit long-term changes which contribute to opioid tolerance and dependence. There is evidence that acute morphine treatment stimulates PI hydrolysis (Raffa & Martinez, 1992), while chronic morphine treatment inhibits PI hydrolysis (Dixon *et al.*, 1990). (*S*)-4C-PG and L-AP3 antagonism of the metabotropic glutamate receptor during morphine treatment may prevent cellular changes associated with persistent phosphatidylinositol hydrolysis, and consequently reduce withdrawal symptoms that are associated with these cellular changes. Other metabotropic receptor subtypes inhibit production of cAMP (Schoepp & Conn, 1993). It is well established that both acute and chronic opioid use also affect the production of cAMP (Collier, 1980, 1983; Sharma *et al.*, 1975). Thus it is possible that (*S*)-4C-PG and L-AP3 antagonism of metabotropic receptors prevented changes in the cAMP system associated with chronic opioid use. Currently, we are determining whether changes in the PI system or changes in the cAMP system associated with activation of metabotropic receptors are important for the development of tolerance and dependence with chronic opioid use.

Thus, the present study indicates that both NMDA and metabotropic glutamate receptors may be involved in the development of dependence with chronic morphine use. Both NMDA and metabotropic glutamate receptors are associated with changes in intracellular second messenger systems. It is therefore hypothesized that NMDA and metabotropic glutamate antagonists are effective because they prevent changes in second-messenger systems associated with chronic opioid use.

This work was supported by grants from The Medical Research Council of Canada (MT-11045) and Fonds de la Recherche en Santé du Québec (900051) to T.J.C.

References

AGHAJANIAN, G.K. (1978). Tolerance of locus coeruleus neurones to morphine and suppression of withdrawal response by clonidine. *Nature*, **267**, 186–189.

AKAOKA, H. & ASTON-JONES, G. (1991). Opiate withdrawal-induced hyperactivity of locus coeruleus neurones is substantially mediated by augmented excitatory amino acid input. *J. Neurosci.*, **11**, 3830–3839.

AMBROSINI, A. & MELDOLESI, J. (1989). Muscarinic and quisqualate receptor-induced phosphoinositide hydrolysis in primary cultures of striatal and hippocampal neurones. Evidence for differential mechanisms of activation. *J. Neurochem.*, **53**, 825–833.

BARNARD, E.A. & HENLEY, J.M. (1990). The non-NMDA receptors: types, protein structure and molecular biology. In *The Pharmacology of Excitatory Amino Acids, a TiPS Special Report*, Ed. Lodge, D. & Collingridge, G. pp. 82–89. Amsterdam: Elsevier.

BIRSE, E.F., EATON, S.A., JANE, D.E., JONES, P.L., PORTER, R.H., POOK, P.C., SUNTER, D.C., UDVARHELYI, P.M., WHARTON, B., ROBERTS, P.J., SALT, T.E. & WATKINS, J.C. (1993). Phenylglycine derivatives as new pharmacological tools for investigating the role of metabotropic glutamate receptors in the central nervous system. *Neuroscience*, **52**, 481–488.

BLÄSIG, J., HERZ, A., REINHOLD, K. & ZIEGLGÄNSBERGER, S. (1973). Development of physical dependence on morphine in respect to time and dosage quantification of the precipitated withdrawal syndrome in rats. *Psychopharmacology*, **33**, 19–38.

COLLIER, H.O.J. (1980). Cellular site of opiate dependence. *Nature*, **283**, 625–629.

COLLIER, H.O.J. (1983). Physiological basis of opiate dependence. *Drug Alcohol Dep.*, **111**, 15–21.

COTMAN, C.W., MONAGHAN, D.T., & GANONG, A.H. (1988). Excitatory amino acid neurotransmission: NMDA receptors and Hebb-type synaptic plasticity. *Ann. Rev. Neurosci.*, **11**, 61–80.

DIXON, W., TING, Y.-W. & CHANG, P.L. (1990). The effects of morphine on norepinephrine-stimulated phosphatidylinositol response in rat cerebral cortex. *Prog. Clin. Biol. Res.*, **328**, 279–282.

DONEVAN, S.D. & ROGAWSKI, M.A. (1993). GYKI 52466, a 2,3-benzodiazepine, is a highly selective, non-competitive antagonist of AMPA/kainate receptor responses. *Neuron*, **10**(1), 51–59.

EATON, S.A., JANE, D.E., JONES, P.L., PORTER, R.H., POOK, P.C., SUNTER, D.C. & UDVARHELYI, P.M. (1993). Competitive antagonism at metabotropic glutamate receptors by (*S*)-4-carboxyphenylglycine and (RS)-alpha-methyl-4-carboxyphenylglycine. *Eur. J. Pharmacol.*, **244**, 195–197.

JONAS, P. & SAKMANN, B. (1992). Glutamate receptor channels in isolated patches from CA1 and CA3 pyramidal cells of rat hippocampal slices. *J. Physiol.*, **455**, 143–171.

KISKIN, N.I., KRISHTAL, O.A. & TSYNDRENKO, A.Y. (1986). Excitatory amino acid receptors in hippocampal neurons: kainate fails to desensitize them. *Neurosci. Lett.*, **63**, 225–230.

KOOB, G.F., MALDONADO, R. & STINUS, L. (1992). Neural substrates of opiate withdrawal. *Trends Neurosci.*, **15**, 186–191.

LASCHKA, E., TESCHEMACHER, H.J., MEHRAEIN, P. & HERZ, A. (1976). Sites of action of morphine involved in the development of physical dependence in rats. *Psychopharmacologia*, **46**, 141–147.

MACDERMOTT, A.B., MAYER, M.L., WESTBROOK, G.L., SMITH, S.J. & BARKER, J.L. (1986). NMDA-receptor activation increases cytoplasmic calcium concentration in cultured spinal cord neurones. *Nature*, **321**, 519–522.

MANZONI, O.J.J., FINIELS-MARLIER, F., SASSETTI, I., BLOCKAERT, J., LE PEUCH, C. & SLADECZEK, F.A.J. (1990). The glutamate receptor of the Q_p-type activates protein kinase C and is regulated by protein kinase C. *Neurosci. Lett*, **109**, 146–151.

MAREK, P., BEN-ELIYAHU, S., GOLD, M. & LIEBESKIND, J.C. (1991a). Excitatory amino acid antagonists (kynurenic acid and MK-801) attenuate the development of morphine tolerance in rats. *Brain Res.*, **547**, 77–81.

MAREK, P., BEN-ELIYAHU, S., VACCARINO, A.L. & LIEBESKIND, J.C. (1991b). Delayed application of MK-801 attenuates development of morphine tolerance in rats. *Brain Res.*, **558**, 163–165.

MAYER, M.L. & WESTBROOK, G.L. (1987a). The physiology of excitatory amino acids in the vertebrate central nervous system. *Prog. Neurobiol.*, **28**, 197–276.

MAYER, M.L. & WESTBROOK, G.L. (1987b). Permeation and block of N-methyl-D-aspartic acid receptor channels by divalent cations in mouse cultured central neurones. *J. Physiol.*, **394**, 501–527.

MAYER, M.L., WESTBROOK, G.L. & GUTHRIE, P.B. (1984). Voltage-dependent block by Mg^{2+} of NMDA responses in spinal cord neurones. *Nature*, **309**, 261–263.

MAYER, M.L., MACDERMOTT, A.B., WESTBROOK, G.L., SMITH, S.J. & BARKER, J.L. (1987). Agonist- and voltage-gated calcium entry in cultured mouse spinal cord neurons under voltage clamp measured using Arsenazo III. *J. Neurosci.*, **7**, 3230–3244.

MILLER, R.J. (1991). The revenge of the kainate receptor. *Trends Neurosci.*, **14**, 477–479.

MONAGHAN, D.T., BRIDGES, R.J. & COTMAN, C.W. (1989). The excitatory amino acid receptors: their classes, pharmacology and distinct properties in the function of the central nervous system. *Ann. Rev. Pharmacol. Toxicol.*, **29**, 365–402.

MURPHY, S.N. & MILLER, R.J. (1989). Regulation of Ca^{++} influx into striatal neurons by kainic acid. *J. Pharmacol. Exp. Ther.*, **249**, 184–193.

NICOLETTI, F., CONDORELLI, D.F., DELL'ALBANI, P., ARONICA, E., CATANIA, M.V., SORTINO, M.A. & REYMANN, K.G. (1991). Metabotropic glutamate receptors and neuroplasticity. In *Excitatory Amino Acids, Fidia Research Foundation Symposium Series*, Vol. 9, ed. R.P. Simon, pp. 167–170. New York: Thieme Medical Publishers.

NOWAK, L., BREGESTOVSKI, P., ASCHER, P., HERBERT, A. & PROCHIANTZ, A. (1984). Magnesium gates glutamate-activated channels in mouse central neurones. *Nature*, **307**, 462–465.

PAXINOS, G. & WATSON, C. (1986). The rat brain in stereotaxic coordinates. Academic Press: San Diego.

RAFFA, R.B. & MARTINEZ, R.P. (1992). Morphine antinociception is mediated through a LiCl-sensitive, IP_3-restorable pathway. *Eur. J. Pharmacol.*, **215**, 357–358.

RASMUSSEN, K., FULLER, R.W., STOCKTON, M.E., PERRY, K.W., SWINFORD, R.M. & ORNSTEIN, P.L. (1991a). NMDA receptor antagonists suppress behaviors but not norepinephrine turnover or locus coeruleus unit activity induced by opiate withdrawal. *Eur. J. Pharmacol.*, **197**, 9–16.

RASMUSSEN, K., KRYSTAL, J.H. & AGHAJANIAN, G.K. (1991b). Excitatory amino acids and morphine withdrawal: differential effects of central and peripheral kynurenic acid administration. *Psychopharmacology*, **105**, 508–512.

SCHOEPP, D.D. & CONN, P.J. (1993). Metabotropic glutamate receptors in brain function and pathology. *Trends Pharmacol. Sci.*, **14**, 13–25.

SCHOEPP, D.D., JOHNSON, B.G., SMITH, E.C.R. & MCQUAID, L.A. (1990). Stereo selectivity and mode of inhibition of phosphoinositide-coupled excitatory amino acid receptors by 2-amino-3-phosphonopropanoic acid. *Mol. Pharmacol.*, **38**, 222–228.

SHARMA, S.K., NIRENBERG, M. & KLEE, W.A. (1975). Morphine receptors as regulators of adenylate cyclase activity. *Proc. Natl. Acad. Sci. USA*, **72**, 590–594.

SLADECZEK, F., PIN, J.P., RÉCASENS, M., BOCKAERT, J. & WEISS, S. (1985). Glutamate stimulates inositol phosphate formation in striatal neurones. *Nature*, **317**, 717–719.

SOMMER, B. & SEEBURG, P.H. (1992). Glutamate receptor channels: novel properties and new clones. *Trends Pharmacol. Sci.*, **13**, 291–296.

STEPPUHN, K.G. & TURSKI, L. (1993). Diazepam dependence prevented by glutamate antagonists. *Proc. Natl. Acad. Sci. USA*, **90**, 6889–6893.

SUGIYAMA, H., ITO, I. & HIRONO, C. (1987). A new type of glutamate receptor linked to inositol phospholipid metabolism. *Nature*, **325**, 531–533.

TANGANELLI, S., ANTONELLI, T., MORARI, M., BIANCHI, C. & BEANI, L. (1991). Glutamate antagonists prevent morphine withdrawal in mice and guinea pigs. *Neurosci. Lett.*, **122**, 270–272.

TRUJILLO, K.A. & AKIL, H. (1991). Inhibition of morphine tolerance and dependence by the NMDA receptor antagonist MK-801. *Science*, **251**, 85–87.

VALENTINO, R.J. & WEHBY, R.G. (1989). Locus coeruleus discharge characteristics of morphine-dependent rats: effects of naltrexone. *Brain Res.*, **488**, 126–134.

WONG, E.H.F., KEMP, J.A., PRIESTLEY, T., KNIGHT, A.R., WOODRUFF, G.N. & IVERSEN, L.L. (1986). The anticonvulsant MK-801 is a potent N-methyl-D-aspartate antagonist. *Proc. Natl. Acad. Sci. USA*, **83**, 7104–7108.

(Received June 17, 1994
Revised August 1, 1994
Accepted August 5, 1994)

Br. J. Pharmacol. (1994), **113**, 1221–1230 © Macmillan Press Ltd, 1994

β-Adrenoceptors mediate inhibition of [^{3}H]-acetylcholine release from the isolated rat and guinea-pig trachea: role of the airway mucosa and prostaglandins

[1]*Ignaz Wessler, *Torsten Reinheimer, †Gernot Brunn, ‡Gary P. Anderson, §Jennifer Maclagan & †Kurt Racké

*Department of Pharmacology, University of Mainz, Obere Zahlbacher Strasse 67, D-55101 Mainz, Germany, †Department of Pharmacology, University of Frankfurt, Theodor-Stern-Kai 7, D-60596 Frankfurt, Germany, ‡Research Department, Ciba-Geigy AG, CH-4002 Basle, Switzerland, and §William Harvey Research Institute, London EC1M 6BQ, UK

1 Rat or guinea pig isolated tracheae were labelled with [^{3}H]-choline to measure evoked tritium outflow, which reflects neuronal release of [^{3}H]-acetylcholine. Tritium outflow was evoked either by electrical stimulation of the extrinsic vagal nerve (rat tracheae) or by 27 mM potassium (guinea pig tracheae).

2 In rat tracheae isoprenaline (0.01, 0.1 μM) inhibited evoked [^{3}H]-acetylcholine release, whereas β_2-adrenoceptor-selective agonists (fenoterol, formoterol, salbutamol) were ineffective.

3 The inhibitory effect of isoprenaline was abolished under the following conditions: (i) presence of propranolol (1 μM) or of the β_1-selective antagonist CGP 20712 A (0.1 μM); (ii) removal of the mucosa at the start of the experiments; (iii) blockade of cyclooxygenase activity by 3 μM indomethacin.

4 In rat isolated tracheae prelabelled with [^{3}H]-arachidonic acid, isoprenaline (0.1 μM) but not formoterol (0.01 μM) enhanced the outflow of [^{3}H]-prostaglandins (PGD_2, PGE_2). This effect was blocked by 0.1 μM CGP 20712 A.

5 In guinea pig tracheae electrical stimulation of the extrinsic vagal nerve did not cause a constant release of [^{3}H]-acetylcholine, but 27 mM potassium elicited a reproducible release of [^{3}H]-acetylcholine. In this species both isoprenaline (0.1 μM) and formoterol (0.01 μM) inhibited evoked [^{3}H]-acetylcholine release. Inhibition was abolished under the following conditions: (i) presence of propranolol (1 μM) or of the β_2-selective antagonist ICI 118551 (0.3 μM); (ii) removal of the mucosa at the start of the experiments; (iii) blockade of cyclooxygenase activity by 3 μM indomethacin.

6 In conclusion, the present experiments have demonstrated that activation of β-adrenoceptors localized in the mucosa mediates inhibition of [^{3}H]-acetylcholine release from the neuroeffector junctions of the pulmonary, parasympathetic nerves most probably by the liberation of inhibitory prostaglandins from the airway mucosa. The adrenoceptor subtype involved differs in rat (β_1 subtype) and guinea pig ($\beta_2$subtype) airways.

Keywords: Rat and guinea pig tracheae; inhibition of [^{3}H]-acetylcholine release; airway mucosa; β-adrenoceptors; prostaglandins

Introduction

Presynaptic interactions between cholinergic and adrenergic pulmonary nerves are still a matter of debate. The close proximity of adrenergic and cholinergic varicosities found in some species (baboon, cat, dog, guinea pig, monkey) suggests presynaptic communication between both nervous systems (Silva & Ross, 1974; Jones *et al.*, 1980; Knight *et al.*, 1981). In human airways adrenergic innervation is less extensive, but the smaller human bronchi have been found to receive also adrenergic innervation (Daniel *et al.*, 1986). Evidence for a presynaptic communication between the two branches of the autonomic nervous system has been found in functional studies. Using the innervated tube preparation of the guinea pig trachea evidence was found for presynaptic inhibition by acetylcholine or noradrenaline release from adjacent sympathetic nerves (Pendry & Maclagan, 1991). In contrast, β-adrenoceptor agonists have been found to inhibit contractions evoked by vagal stimulation more effectively than those evoked by bath-applied acetylcholine (Vermeire & Vanhoutte, 1979; Danser *et al.*, 1987; Ito, 1988; Aizawa *et al.*, 1991). This observation may indicate a presynaptic inhibitory action of β-adrenoceptor agonists on the release of acetylcholine from the adjacent cholinergic nerves.

However, the only study in which the release of acetylcholine was measured directly (canine trachea) failed to obtain evidence for an inhibitory action of noradrenaline (Martin & Collier, 1986). In this study, acetylcholine release was measured after blockade of cholinesterase, a condition which is known to affect presynaptic mechanisms (Kilbinger & Wessler, 1980; Pendry & Maclagan, 1991; Wessler, 1992; Wessler *et al.*, 1992). Recently, we have reported a radiotracer method for the measurement of the release of newly synthesized [^{3}H]-acetylcholine from the rat or guinea pig isolated trachea in the absence of cholinesterase inhibitors (Wessler *et al.*, 1990; 1991). In an attempt to further elucidate cholinergic–adrenergic interactions, we have investigated the effects of β-adrenoceptor agonists on the release of [^{3}H]-acetylcholine from isolated rat and guinea pig tracheae. In addition, the effect of β-adrenoceptors on the metabolism of arachidonic acid has been tested. Some of these results have been communicated to the German Society of Pharmacology and Toxicology (Reinheimer *et al.*, 1993).

Materials and methods

Tissue preparation

Rats (Sprague–Dawley, 200–250 g) and guinea pigs (Dunkin–Hartley, 300–400 g) of either sex (Charles River Wiga, Sulzfeld, Germany) were kept at a constant temperature

[1] Author for correspondence.

(21°C) and a regular light (06.30–19.30 h) dark (19.30–06.30 h) cycle with food and water *ad libitum*. The animals were killed by stunning followed by exsanguination. Tracheae (from the larynx to the carina) together with the left recurrent laryngeal nerve and the right vagal nerve (proximal to the origin of the right recurrent laryngeal nerve) were dissected. The preparation was transferred into a Petri dish filled with a physiological salt solution of the following composition (given in mM): NaCl 125, KCl 2.7, $CaCl_2$ 1.8, $MgCl_2$ 1.0, NaH_2PO_4 0.4; $NaHCO_3$ 24, D-glucose 5.1, choline 0.00001). The medium was gassed with 5% CO_2 (v/v) in O_2. The pH of the gassed solution was 7.30. The trachea was opened longitudinally by cutting through the cartilage. In some experiments the mucosa was removed mechanically before starting the incubation/perfusion protocol. The opened trachea was fixed by means of small needles with its luminal surface facing upwards. The mucosa was removed by gently rubbing ten times with a pipe cleaner along the whole length of the trachea. Removal of the mucosa was confirmed by microscopic inspection of histological sections stained with haematoxylin and eosin. The trachea was fixed onto an electrode holder vertically under a tension of 1 g by means of cotton threads and the nerves were threaded through two platinium ring electrodes (internal diameter 1 mm). Thereafter the electrode holder together with the tissue was transferred into a 2 ml organ bath containing the salt solution described above, warmed to a constant temperature of 36°C and bubbled with 5% CO_2 in O_2 (v/v).

Incubation and superfusion protocol ([^{3}H]-choline)

The experimental protocol reported previously was used (Wessler *et al.*, 1991; 1993). In short, the tissues were allowed to equilibrate for a 30 min period of superfusion (2 ml min^{-1}). During the last 10 min of this equilibration period the cut ends of the left recurrent laryngeal nerve and of the right thoracic vagal nerve (proximal to the origin of the right recurrent nerve) were stimulated electrically (0.2 ms, 20 V, 20 mA, 1 Hz; current flow was determined by the voltage drop across a resistance by use of an oscilloscope). Thereafter, superfusion was stopped and the trachea was incubated in 1.5 ml of the salt solution containing in addition 0.01 μM [^{3}H]-choline with a specific activity of 1.2 GBq $nmol^{-1}$. During the incubation with [^{3}H]-choline the cut ends of the nerves were stimulated continuously at 10 Hz. Guinea pig tracheae were stimulated transmurally during the incubation with [^{3}H]-choline (biphasic pulses of 1 ms, 100 V, 250 mA). Labelling was followed by a 75 min washout (perfusion rate 8 ml min^{-1}) to remove excess radioactivity. From the washout period onwards, 10 μM hemicholinium-3 was added to the medium and the concentration of unlabelled choline was raised to 1 μM. At the end of the washout period superfusion was stopped (time zero) and the bath fluid was exchanged every 3 min. Tritium content in each individual sample was measured by liquid scintillation spectrometry (Packard TriCarb 1900 CA); external standardization was used to correct for counting efficiency.

Stimulation of tritium outflow

Release of [^{3}H]-acetylcholine was elicited by two periods (S_1, S_2) of either electrical nerve stimulation (cut ends of both parasympathetic nerves) or chemical stimulation (elevation of extracellular potassium to 27 mM; equimolar reduction of sodium). S_1 and S_2 started 12 and 42 min after the end of the washout period respectively. During each stimulation period (S_1, S_2) four trains of 20 s duration at 15 Hz were applied with 10 s intervals between the trains. β-Adrenoceptor agonists were added 18 min before S_2 to the bath medium; in each experiment the antagonists were present from 30 min before S_1 onwards. When high potassium was used as release stimulus, extracellular potassium was increased from 13–15 min (S_1) and 43–45 min (S_2) after the end of the washout. At the end of the experiments tracheae were blotted and weighed.

Separation of the radioactive compounds (acetylcholine, choline, phosphorylcholine) by reversed-phase high-performance liquid chromatography (h.p.l.c.)

In the present experiments β_2-adrenoceptor agonists enhanced the basal tritium outflow immediately after application to the organ bath. To identify the underlying radioactive compound responsible for this effect, acetylcholine, choline and phosphorylcholine were separated by reversed-phase h.p.l.c. and quantified by measuring the radioactive content of the collected eluate by β-scintillation spectrometry (see Wessler & Werhand, 1990).

[^{3}H]-Arachidonic acid metabolism in rat isolated tracheae

After a 30 min equilibration period, during which the medium was changed every 10 min, the tracheae were incubated for 2 h in medium containing 10 μCi of [^{3}H]-arachidonic acid. Thereafter, the tracheae were washed ten times within 10 min followed by eight consecutive 10 min periods of incubation (see Figure 5, upper part). The medium was collected into plastic vials, frozen immediately and kept at −60°C until analysed by h.p.l.c. (see below). Test stimuli were added to the medium from the 40th min of incubation onwards. In the corresponding interaction experiments, the β-adrenoceptor antagonist CGP 20712 A was added to the incubation medium from the onset of incubation. At the end of incubation each trachea was blotted, weighed, minced and extracted in 2 ml of methanol for 1–2 h at 0–4°C. The extracts were centrifuged at 20,000 g × min and the supernatants were stored at −60°C until analysed.

Arachidonic acid and its metabolites were separated by reversed-phase gradient h.p.l.c. The h.p.l.c. system used was from Waters/Millipore (Waters 600 E Powerline), equipped with a Rheodyne injection valve (1000 μl loop) and a reversed-phase column (250 mm length, 4.6 mm inner diameter, prepacked with Shandon ODS-Hypersil 5 μm). The mobile phase was continuously pumped through the column at a rate of 1 ml min^{-1}. The effluent was collected in 1 min fractions directly into counting vials for the determination of radioactivity (see below). A methanol–glacial acid gradient solvent system which had been shown to allow the separation of all classes of eicosanoids (van Scott *et al.*, 1990) was used. Two solvents, A (100% methanol) and B (10% methanol adjusted to pH 5.05 with glacial acetic acid and ammonium hydroxide), were mixed to yield four gradients over 120 min (52, 62, 71 and 100% solvent A, starting with 52% and changing at 27, 52 and 77 min). ^{14}C- or ^{3}H-labelled standards were run consecutively with samples to identify specific peaks. Radioactivity in the incubation media, tissue extracts or h.p.l.c. fractions was determined after addition of a commercial scintillation cocktail (Zinsser aqua safe) by liquid scintillation spectrometry in a Packard TR 1900a. External standardization was used to correct for counting efficiency and background was subtracted automatically.

Analysis of results

Tritium outflow ([^{3}H]-choline) is expressed as d.p.m. g^{-1} 3 min^{-1}. Stimulated tritium outflow was calculated by subtracting the basal tritium outflow from the total (see Wessler *et al.*, 1991; 1993). Tritium outflow ([^{3}H]-arachidonic acid) is expressed as a percentage of the corresponding tissue radioactivity or is normalized to the outflow observed during 30–40 min of incubation (i.e. fourth period) in each individual experiment (see Figure 5). The radioactivity of individual peaks in the radiochromatograms were quantified as d.p.m. per incubation samples and were also expressed as percentage of that observed during the fourth incubation period.

The results are given as means ± s.e.mean. The significance of differences was evaluated by Student's *t*-test (for paired and unpaired data); for multiple comparison the modified *t*-test according to Bonferroni was used (see Wallenstein *et al.*, 1980). *P*-values<0.05 were regarded as significant. To evaluate the effects of test compounds on evoked [^{3}H]-acetylcholine release the stimulated tritium outflow elicited by S_2 was related to that elicited by S_1 and the S_2/S_1 ratio was then compared with the control ratio obtained in the absence of test compounds.

Drugs and special chemicals

The following drugs were used: [^{3}H]-arachidonic acid (Amersham Buchler, Frankfurt, Germany; 5.5–8 TBq mmol^{-1}); bradykinin (Sigma Chemie, Munich, Germany); CGP 20712 A (±[2-(3-carbamoyl-4-hydroxyphenoxy)ethylamino]-3[4-(1-methyl-4-trifluoromethyl-2-imidazolyl)phenoxy]-2-propanol-methanesulphonate, Ciba-Geigy, Basle, Switzerland); choline chloride (Sigma Chemie); fenoterol hydrobromide (Boehringer Ingelheim, Germany); formoterol hydrochloride (Ciba-Geigy); hemicholinium-3 bromide (Sigma Chemie); methyl-[^{3}H]-choline (3 TBq mmol^{-1}; NEN, Dreieich, Germany); ICI-118551 (±1[(2,3-dihydro-7-methyl-1H-inden-4-yl)oxy]-3[(1-methylethyl)amino]-2-butanol hydrochloride, RBI, Natick, U.S.A.); isoprenaline hydrochloride (Boehringer Ingelheim); neostigmine methylsulphate (Merck, Darmstadt, Germany); propranolol hydrochloride (Sigma Chemie); and salbutamol hemisulphate (Sigma Chemie).

Results

Effects of β-adrenoceptor agonists on evoked tritium outflow ([^{3}H]-choline) from mucosa-intact and mucosa-denuded rat tracheae

Effect of isoprenaline in the absence of indomethacin Tritium outflow from radiolabelled tracheae was measured during 3 min periods (see Figure 1). In the absence of test substances (control, mucosa-intact) two subsequent periods of electrical stimulation of the extrinsic vagal nerves caused a similar increase in tritium outflow, resulting in a ratio S_2/S_1 of 1.00 ± 0.07 (n = 10). The electrically stimulated increase in tritium outflow was abolished by removal of extracellular calcium (Wessler *et al.*, 1991), whereas this manipulation did not reduce tritium outflow stimulated by high potassium (27 mM) in mucosa-intact rat tracheae (S_2/S_1 ratio, 1.10 ± 0.10; n = 4; experiments not shown). For this reason, electrical stimulation was used in all succeeding experiments in the rat trachea.

Isoprenaline, added 18 min before S_2, reduced the evoked tritium outflow in a concentration-related manner (Figures 1 and 2). A concentration as low as 0.01 μM isoprenaline was effective. The maximal effect (54% inhibition) occurred in the presence of 0.1 μM isoprenaline, whereas a 10-fold higher concentration was ineffective, i.e. a bell-shaped concentration-response curve was found (see Figure 2). The non-selective β-adrenoceptor antagonist propranolol (1 μM) and the β_1-selective antagonist CGP 20712 A (0.1 μM) prevented the inhibitory effect of 0.1 μM isoprenaline (Figure 1 and Table 1); the antagonists were applied from 30 min before S_1 onwards. Propranolol alone, added 18 min before S_2 to the bath medium, did not significantly affect the stimulated tritium outflow (Wessler *et al.*, 1993). When, in the present experiments, propranolol was present in the medium throughout S_1 and S_2, a small not significant reduction of the ratio S_2/S_1 was obtained (Table 1).

In mucosa-denuded tracheae electrical stimulation of the vagal nerves caused a substantially higher increase in tritium outflow during S_1 and the control ratio S_2/S_1 was lower than in mucosa-intact tracheae (Table 1). Isoprenaline (0.1 μM), however, did not inhibit the stimulated tritium outflow in mucosa-denuded preparations, even when a very high concentration of 1 μM was used (Table 1).

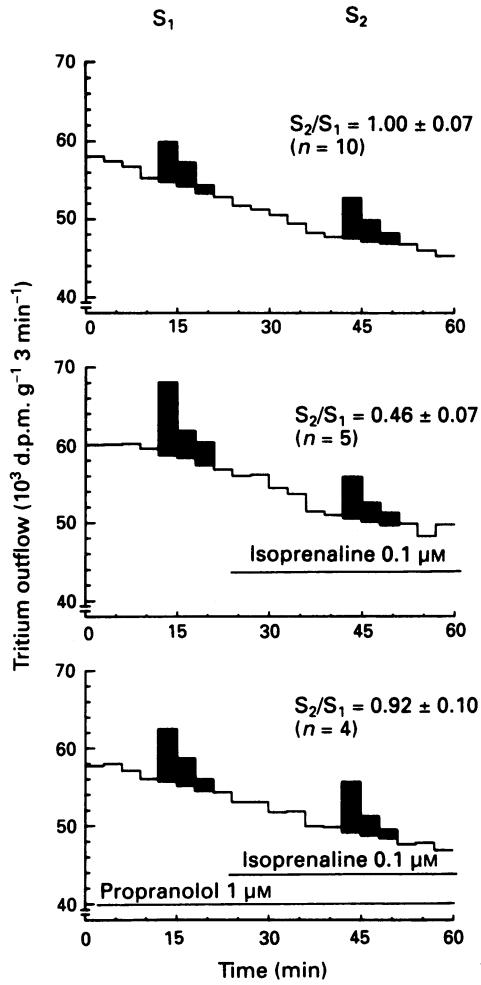


Figure 1 Rat, mucosa-intact trachea: effect of isoprenaline, alone or in the presence of propranolol, on basal and electrically stimulated tritium outflow. After the labelling and washout period (time zero) tritium outflow was measured in 3 min intervals. The extrinsic vagal nerves were electrically stimulated (four 20 s trains at 15 Hz with 10 s intervals) at the times indicated (S_1, S_2). Isoprenaline (0.1 μM) was added 15 min before S_2 and when indicated the β-adrenoceptor antagonist propranolol 30 min before S_1. The filled columns represent evoked tritium outflow. Given are the means of 5–10 experiments (for each series), s.e.mean was 6–15%.

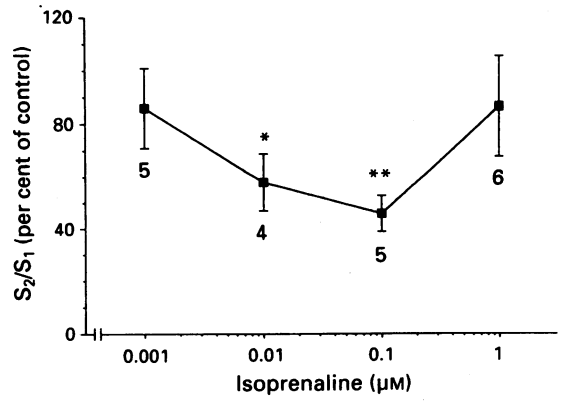


Figure 2 Concentration response curve for isoprenaline on the stimulated tritium outflow from rat isolated tracheae with intact mucosa. The experimental protocol is shown in Figure 1. Given are the means ± s.e.mean of the number of experiments indicated. Significance of difference from control: *P<0.05, **P<0.01.

Table 1 Effects of isoprenaline (iso), formoterol (for) and salbutamol (sal) on the stimulated tritium outflow from rat isolated tracheae

Agonist (μM)	*Antagonist* (μM)	S_1 (d.p.m. g^{-1})	S_2/S_1	n
Mucosa-intact				
–	–	10,000 ± 1500	1.00 ± 0.07	10
–	propranolol (1)	10,100 ± 2100	0.85 ± 0.08	4
–	CGP 20712A (0.1)	12,100 ± 3000	0.88 ± 0.10	5
iso (0.01)	–	8500 ± 1600	0.58 ± 0.11*	4
iso (0.1)	–	17,800 ± 5200	0.46 ± 0.07**	5
iso (0.1)	propranolol (1)	11,600 ± 1900	0.92 ± 0.10	4
iso (0.1)	CGP 20712A (0.1)	14,300 ± 24200	0.85 ± 0.06	6
fen (0.1)	–	15,100 ± 1700	0.95 ± 0.12	4
for (0.01)	–	12,100 ± 3100	1.14 ± 0.07	6
sal (0.1)	–	12,100 ± 2400	0.93 ± 0.13	7
sal (1)	–	11,500 ± 1400	0.86 ± 0.35	5
Mucosa-denuded				
–	–	23,200 ± 3500	0.74 ± 0.04	7
iso (0.1)	–	18,700 ± 3000	0.67 ± 0.04	7
iso (1)	–	20,000 ± 3000	0.68 ± 0.03	4
for (0.001)	–	35,600 ± 3100	0.95 ± 0.11	6
for (0.01)	–	25,800 ± 4300	0.65 ± 0.06	7
for (0.1)	–	26,800 ± 9000	0.89 ± 0.08	4

After the labelling and washout period tritium outflow was measured in 3 min periods. In each experiment mucosa was removed before the start of the perfusion/incubation protocol. Tritium outflow was elicited by electrical nerve stimulation (four 20-s trains at 15 Hz with a 10 s interval). The β-receptor agonists were added 18 min before the second stimulation period (S_2) and the antagonist 30 min before S_1. Given are the means ± s.e.mean of the number of experiments indicated. Significance of differences from the respective control: $*P<0.05$, $**P<0.01$.

Effect of isoprenaline in the presence of indomethacin Indomethacin (3 μM) was added 30 min before S_1 to block cyclooxygenase activity and left in contact. In the presence of indomethacin isoprenaline (0.1 μM) lost its inhibitory effect on stimulated tritium outflow (see Figure 3).

Effects of β_2-adrenoceptor agonists Neither the short-acting β_2-adrenoceptor agonists fenoterol (1 μM) and salbutamol (0.1 and 1 μM) nor the long-acting β_2-agonist formoterol (0.01 μM) modified evoked tritium outflow from mucosa-intact rat tracheae (Table 1). Also in mucosa-denuded rat tracheae formoterol failed to modify stimulated tritium outflow significantly; the ratios S_2/S_1 are given in Table 1.

Effect of β-adrenoceptor agonists on basal tritium outflow from rat tracheae Formoterol enhanced the basal tritium outflow after its application to the organ bath (Figure 4). Likewise, fenoterol and salbutamol facilitated the basal tritium outflow (experiments not shown). In contrast, in most experiments, isoprenaline did not affect basal tritium outflow (see Figure 1); however, in some experiments (1 μM isoprenaline) a slight increase was also observed (experiments not shown).

The facilitatory effect of formoterol on basal tritium outflow was (i) more pronounced in mucosa-denuded than in mucosa-intact preparations (Table 2), (ii) abolished by propranolol (1 μM) in the rat (Figure 4 and Table 2) and by the β_2-selective antagonist ICI 118551 (0.3 μM) in the guinea pig (see Figure 7), (iii) unaffected by a 40 min pre-exposure of rat tracheae with 0.1 μM isoprenaline (to induce receptor desensitization; $n = 4$, experiments not shown) and (iv) unaffected by removal of extracellular calcium (incubation in nominally calcium-free medium containing in addition 1000 μM EDTA for 30 min before the addition of formoterol; experiments not shown; $n = 4$). Analysis of the tritium outflow by reversed-phase h.p.l.c. showed that the formoterol-induced increase in the basal tritium outflow was caused by an enhanced outflow of [^{3}H]-phosphorylcholine and to a smaller extent by that of [^{3}H]-choline, whereas the outflow of [^{3}H]-acetylcholine remained unchanged (Table 2).

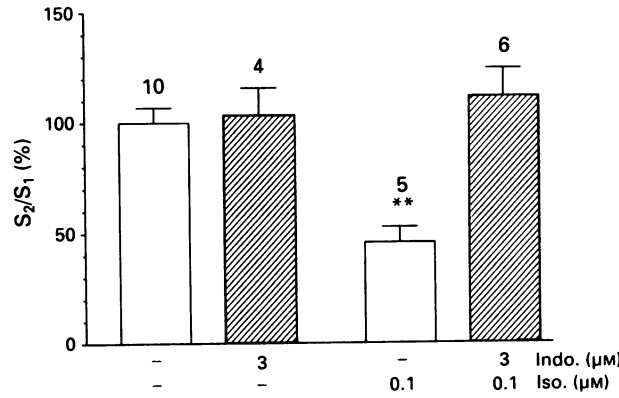


Figure 3 Effect of indomethacin on the isoprenaline-induced inhibition in mucosa-intact rat trachea. The experimental protocol is shown in Figure 1. In each experiment indomethacin was present from 30 min before S_1 onwards and isoprenaline from 18 min before S_2. Given are means ± s.e.mean of the number of experiments indicated. Significance of difference (comparison with the untreated control): $P<0.01$.

Effect of β-adrenoceptor agonists on [^{3}H]-arachidonic acid metabolism in rat tracheae Total tritium outflow from rat tracheae labelled with [^{3}H]-arachidonic acid amounted to 0.134 ± 0.003% 10 min^{-1} of the tissue radioactivity ($n = 30$) during the first 10 min incubation period (starting after the washout; see Methods) and slightly, but continuously declined during the subsequent 70 min of incubation (Figure 5, upper tracing). Application of 0.1 μM isoprenaline prevented the decline of the outflow of total tritium, i.e. it had a marginal stimulatory effect on total tritium outflow (Figure 5, upper tracing).

When the radioactivity of the incubation samples (collected during 30–40 min and 40–50 min) was separated by h.p.l.c.,

two peaks were consistently observed (see examples of radiochromatogramms in Figure 6), one co-eluting with arachidonic acid and the other with the prostaglandins PGE_2 and PGD_2 (which were not separated by the current conditions). In the sample collected during 30–40 min of incubation in the absence of drugs the [^{3}H]-prostaglandin peak amounted to 237 ± 33 d.p.m. and the [^{3}H]-arachidonic acid peak to 2870 ± 380 d.p.m. ($n = 18$). In control experiments the outflow of prostaglandins determined in the subsequent (40–50 min) sample was reduced by about 35% (Figure 5, lower part). However, isoprenaline (0.1 μM) caused a clear increase in the outflow of [^{3}H]-prostaglandins (Figure 5), without affecting that of [^{3}H]-arachidonic acid (not shown). For comparison, the effect of bradykinin, a mediator which is well known to cause release of prostaglandins in the airways (Bramley *et al.*, 1990), was also tested. In the present

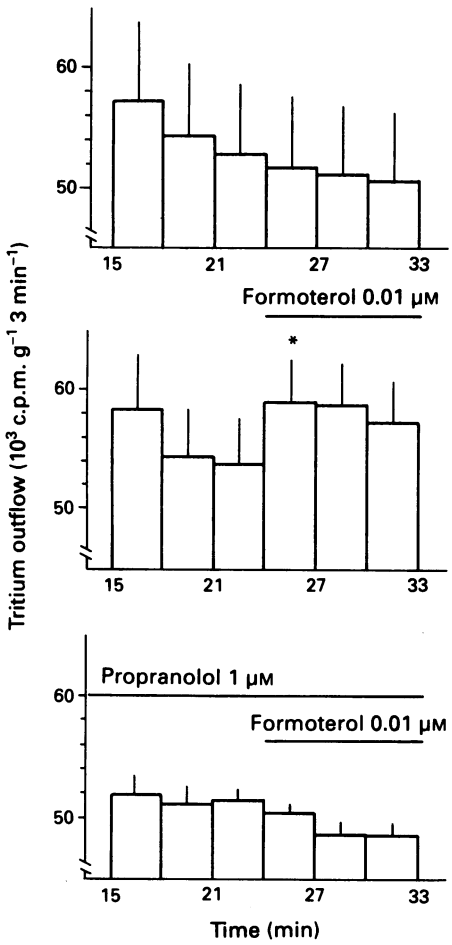


Figure 4 Effect of formoterol on the basal tritium outflow in the absence and presence of propranolol. Formoterol (10 nmol l^{-1}) was added to mucosa-intact, isolated rat tracheae preincubated with [^{3}H]-choline. In one group of experiments propranolol was present 42 min before the addition of formoterol (bars indicate the presence of the test compounds). Formoterol enhanced the basal tritium outflow (middle part) and the effect was abolished by propranolol (lower part). Propranolol by itself did not affect the basal tritium outflow (not shown). Given are the means ± s.e.mean of 4–10 experiments (for each series). Significance of difference: $P < 0.01$ (paired t-test)

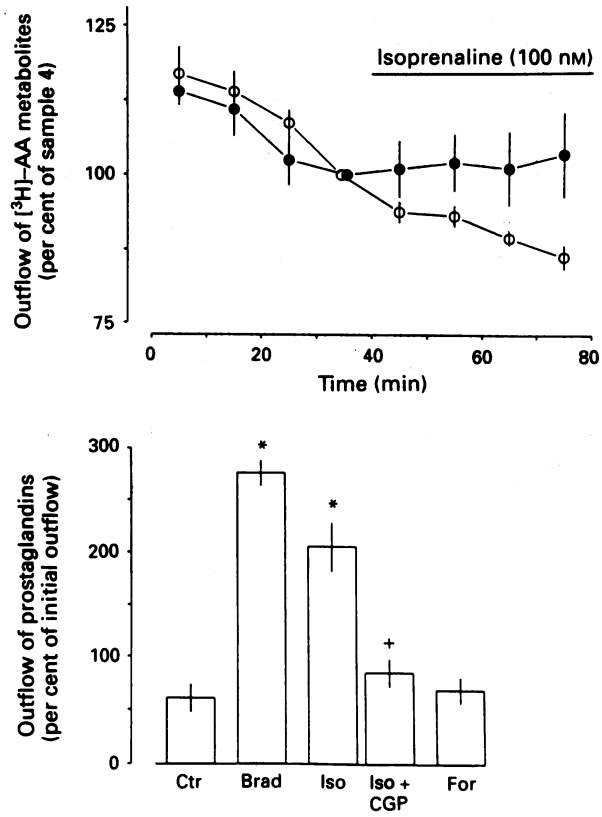


Figure 5 Effects of isoprenaline on the outflow of total tritium (upper part) and effects of 0.1 μM bradykinin (Brad), 0.1 μM isoprenaline in the absence (Iso) and presence of 0.1 μM CGP 20712 A (Iso + CGP) or 0.01 μM formoterol (For) on the outflow of [^{3}H]-prostaglandins (lower part) from isolated rat tracheae preincubated with [^{3}H]-arachidonic acid for 2 h. Upper part, ordinate: Outflow of total tritium, expressed as a percentage of that observed during 30–40 min of incubation in the individual experiments, means ± s.e.mean of three (filled symbols, isoprenaline) or 12 (open symbols, controls) experiments. Lower part, height of columns: Outflow of [^{3}H]-prostaglandins observed during 40–50 min of incubation expressed as a percentage of that observed during 30–40 min of incubation in the individual experiments, means ± s.e.mean of 3–6 experiments. Significance of differences: $^*P < 0.01$ from the controls (Ctr.); $\dagger P < 0.01$ from the experiments 'Iso' alone

Table 2 Effect of formoterol (0.01 μM) on the basal tritium outflow (d.p.m. 3 min^{-1} per trachea) in mucosa-intact and mucosa-free rat tracheae

	Total tritium	*PCH*	*CH*	*ACH*
Mucosa-free				
before	2800 ± 300	1000 ± 100	1300 ± 150	240 ± 100
after	3600 ± 160*	1650 ± 60**	1600 ± 240	230 ± 50
Mucosa-intact				
before	2600 ± 120	1470 ± 220	800 ± 140	120 ± 50
after	2900 ± 120	1700 ± 170	880 ± 140	70 ± 20

After the labelling and washout period (time zero), tritium outflow was measured in 3 min periods. Aliquots (200 μl) of the incubation medium obtained before (24–26 min) and after (27–29 min) the application of formoterol were injected into the h.p.l.c. system to separate phosphorylcholine (PCH), choline (CH) and acetylcholine (ACH). Given are means ± s.e.mean of four experiments in each series. Significance of difference from the value obtained before the application of formoterol: $^*P < 0.05$; $^{**}P < 0.01$.

experiments 0.1 μM bradykinin also enhanced the outflow of the [^{3}H]-prostaglandins, and the effect was slightly larger than that of isoprenaline (Figure 5). In addition, bradykinin increased the outflow of other metabolites (see Figure 6) which appeared earlier in the chromatogram and which might represent 6-keto-PGF$_{1\alpha}$ (see van Scott *et al.*, 1990). The stimulatory effect of isoprenaline on the outflow of [^{3}H]-prostaglandins was prevented by the β_1-selective antagonist CGP 20712 A (Figure 5). When the concentration of isoprenaline was enhanced to 1 μM the stimulatory effect on the outflow of [^{3}H]-prostaglandins was vanished: after application of 1 μM isoprenaline the outflow of [^{3}H]-prostaglandins amounted to 86 ± 15% (n = 3) of the predrug period only, a value which did not differ from the control (see Figure 5, lower part), whereas 0.1 μM isoprenaline increased the [^{3}H]-prostaglandin outflow to 205 ± 24% of the predrug level (Figure 5, lower part). Correspondingly, evoked [^{3}H]-acetylcholine release was not inhibited in the presence of 1 μM isoprenaline (see Figure 2). In rat tracheae formoterol (0.01 μM) had no effect on the outflow of total tritium (not shown) or on the outflow of [^{3}H]-prostaglandins (Figure 5).

Effects of isoprenaline and formoterol on evoked tritium outflow ([^{3}H]-choline) from mucosa-intact and mucosa-denuded guinea pig tracheae

In mucosa-intact guinea pig tracheae electrical stimulation of the extrinsic, parasympathetic nerves caused a small and variable increase in tritium outflow, even when the stimulation period was prolonged (1800 instead of 1200 pulses; experiments not shown; n = 15). Transmural stimulation of mucosa-intact tracheae has already been found to trigger mainly an outflow of [^{3}H]-phosphorylcholine (Wessler *et al.*, 1990). Thus, it was not possible to investigate the effect of β-adrenoceptor agonists on electrically-stimulated release of [^{3}H]-acetylcholine from guinea pig tracheae with intact mucosa. Therefore high potassium was used as the release stimulus in the following experiments with the guinea pig trachea.

Elevation of extracellular potassium (27 mM) caused a substantial and reproducible increase in tritium outflow from mucosa-intact guinea pig tracheae (see Figure 7). The potassium-evoked increase in tritium outflow was nearly abolished by removal of extracellular calcium (S_2/S_1 ratio: 0.16 ± 0.12, n = 4; experiments not shown) indicating a calcium-dependent release mechanism. Isoprenaline (0.1 μM) or formoterol (0.01 μM) reduced the potassium-stimulated tritium outflow significantly (see Figure 7 and Table 3). Salbutamol also reduced the stimulated tritium outflow, but a considerably higher concentration was required (3 μM, see Table 3; $P<0.1$). The inhibitory action of formoterol was prevented by propranolol or by ICI 118551, whereas formoterol maintained its inhibitory effect in the presence of the β_1-selective antagonist CGP 20712 A (Table 3). Formoterol

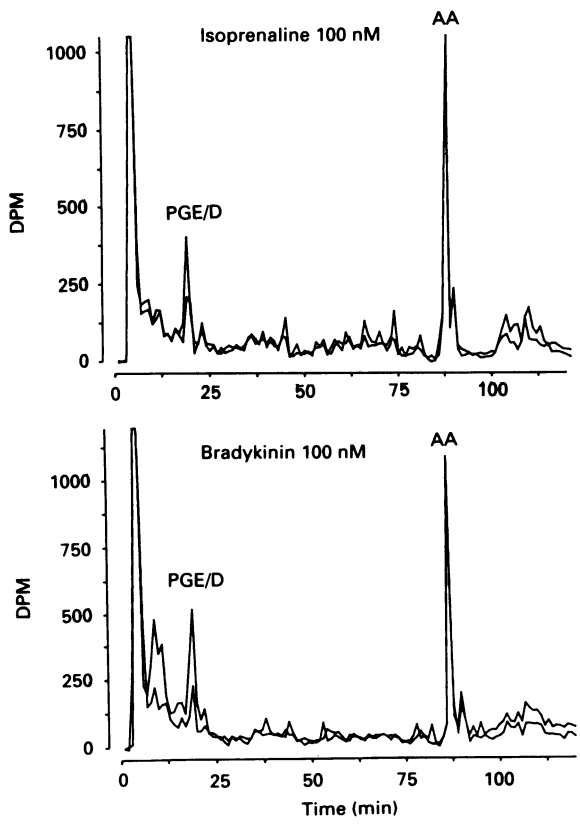


Figure 6 Examples of radiochromatograms of incubation samples of the experiments described in Figure 5. Each tracing shows two chromatograms superimposed: one collected during 30–40 min of incubation in the absence and the other during 40–50 min of incubation in the presence of the test drug. For further details see Figure 5 and Methods.

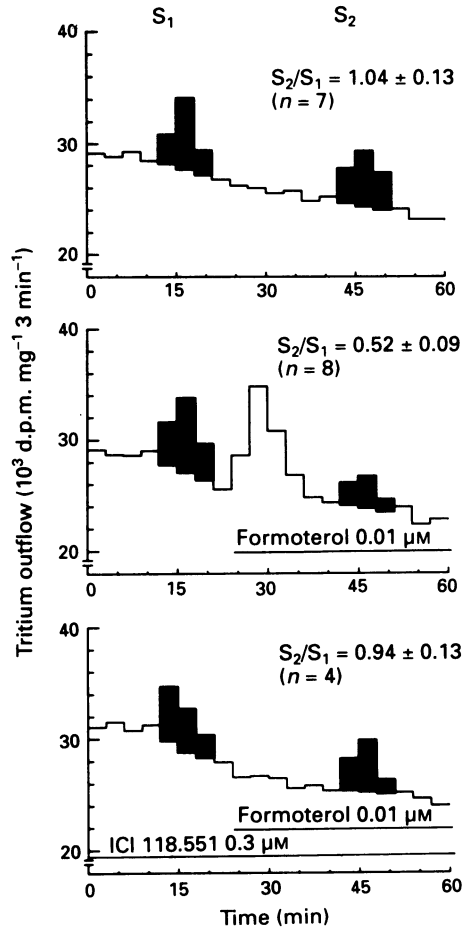


Figure 7 Guinea pig, mucosa-intact trachea: effect of formoterol, alone or in the presence of ICI 118551, on basal and high potassium-stimulated tritium outflow. After the labelling and washout period (time zero) tritium outflow was measured in 3 min intervals. Tritium outflow was stimulated by high potassium: extracellular potassium was increased to 27 mM (equimolar reduction of sodium chloride) for two (S_1 S_2) 3 min periods as indicated. Formoterol was added 18 min befoe S_2 and ICI 115881 30 min before S_1. Given are the means of 5–7 experiments (for each series), s.e.mean was 6–10% of the means. The filled columns represent evoked tritium outflow. Isoprenaline did not enhance the basal tritium outflow but caused similar inhibition of the stimulated tritium outflow to the data seen with formoterol (see Table 2)

Table 3 Effects of isoprenaline (iso), formoterol (for) and salbutamol (sal) on the stimulated tritium outflow from guinea pig isolated tracheae

Agonist (μM)	*Antagonist* (μM)	S_1 (d.p.m. g^{-1})	S_2/S_1	n
Mucosa-intact				
–	–	10,000 ± 2300	1.04 ± 0.13	7
–	propranolol (0.1)	16,000 ± 1100	0.69 ± 0.10	6
–	ICI 118551 (0.3)	13,400 ± 2500	0.60 ± 0.06*	6
–	CGP 20712 (0.3)	11,800 ± 900	0.86 ± 0.03	4
iso (0.01)	–	17,700 ± 3200	0.53 ± 0.09*	6
sal (0.1)	–	14,100 ± 2500	0.85 ± 0.13	6
sal (1)	–	18,000 ± 5000	0.82 ± 0.13	4
sal (3)	–	12,000 ± 4500	0.58 ± 0.30	4
for (0.01)	–	13,700 ± 1400	0.52 ± 0.09*	8
for (0.01)	propranolol (0.1)	12,300 ± 5700	1.11 ± 0.29	4
for (0.01)	ICI 118551 (0.3)	10,800 ± 1700	0.94 ± 0.13	4
for (0.01)	CGP 20712 (0.3)	13,300 ± 1700	0.60 ± 0.07†	4
Mucosa-denuded				
–	–	27,300 ± 5200	0.81 ± 0.09	4
for (0.01)	–	26,800 ± 8000	0.85 ± 0.04	4

After the labelling and washout period tritium outflow was measured in 3 min periods. Tritium outflow was elicited by 27 mM potassium. The β-receptor agonists were added 18 min before the second stimulation period (S_2) and the antagonist 30 min before S_1. Given are the means ± s.e.mean of the number of experiments indicated. Significance of differences from the controls: control experiments without test compounds, $*P<0.01$; control experiments with CGP 20712 A alone, $\dagger P<0.01$.

failed to cause inhibition in mucosa-denuded tracheae (see Table 3), whereas the agonist still enhanced the basal tritium outflow in mucosa- denuded tracheae (see Table 2). As before, indomethacin prevented the inhibitory effect of β-adrenoceptor activation as shown by the following data: in control experiments (indomethacin present throughout) a ratio S_2/S_1 of 0.70 ± 0.06 ($n = 4$) was found and a similar ratio was obtained, when 0.01 μM formoterol was additionally added 18 min before S_2 (0.72 ± 0.09; $n = 5$).

When the β-receptor antagonist propranolol or ICI 118551 was added already 30 min before S_1, considerably lower ratios S_2/S_1 were obtained in control experiments (see Table 2), indicating a slowly developing, depressant effect on evoked [^{3}H]-acetylcholine release. The underlying mechanism is unknown, but a similar effect was not observed when electrical nerve stimulation was used to selectively excite the extrinsic vagal nerves in the rat trachea (see Table 1).

Discussion

The airway mucosa of mammals contains a dense population of β-adrenoceptors of unknown physiological functions (Xue *et al.*, 1983; Davis *et al.*, 1990; see also Nijkamp *et al.*, 1992). In the present experiments β-adrenoceptors mediate inhibition of the stimulated release of [^{3}H]-acetylcholine in isolated rat and guinea pig tracheae. This effect was prevented by propranolol, indicating a specific, receptor-mediated effect. Most importantly, the inhibition could not be demonstrated in mucosa-denuded tracheae or when cyclooxygenase activity was blocked by indomethacin. Isoprenaline stimulated the liberation of prostaglandins (PGD_2, PGE_2) from the isolated trachea, and β-adrenoceptor agonists have already been reported by others to enhance phospholipase A_2 activity in guinea pig lung (Blackwell *et al.*, 1978; Suzuki *et al.*, 1987). Our data suggest the existance of a previously uncharacterized regulatory mechanism controlling cholinergic transmission in the airways: β-adrenoceptors localized at the mucosa mediate the liberation of prostanoids inhibitory to the release of newly synthesized acetylcholine (see scheme in Figure 8). Although less likely, a permissive role of the mucosa and of prostaglandins on neuronal effects of presumably presynaptically localized β-adrenoceptors cannot be excluded. However, classical presynaptic receptors (for instance α_2- or muscarinic receptors) produce their effects directly at nerve terminals without the involvement of surrounding tissue, whereas in the present study isoprenaline was inefffective in mucosa-denuded preparations. In rat cava an indirect regulatory pathway similar to the present one has been described: β_2-adrenoceptors assumed to be localized on subendothelial cells facilitate noradrenaline release by the generation of angiotensin II, which activates facilitatory angiotensin receptors present on the adrenergic nerves (Göthert & Kollecker, 1986).

In the airways an inhibitory role of β-adrenoceptors on cholinergic neurotransmission has already been postulated on the basis of functional experiments (for references see Barnes, 1992; Nijkamp *et al.*, 1992). β-Adrenoceptor agonists inhibited nerve-evoked contractions in the canine and human bronchial tissue more effectively than those evoked by bath-applied acetylcholine; this difference was considered to indicate a neuronal effect (Vermeire & Vanhoutte, 1979; Danser *et al.*, 1987; Ito, 1988; Rhoden *et al.*, 1988; Janssen & Daniel, 1990; Aizawa *et al.*, 1991). β-Adrenoceptor agonists, however, have direct effects on smooth muscle tone, and it may be difficult to discriminate between both sites of action. The present release experiments clearly support the concept that β-adrenoceptors mediate inhibition of cholinergic transmission. Inhibition was observed after preganglionic stimulation (rat) or after chemical stimulation with 27 mM potassium (guinea pig). Thus, the post-ganglionic neuro-effector junction is the target of the inhibitory, mucosa-dependent mechanism. This conclusion is in line with the results drawn from functional experiments (guinea pig trachea) in which transmural electrical stimulation was applied (Ito, 1988; Aizawa *et al.*, 1991).

There are, however, important differences between the present results and those obtained in functional experiments. For instance, Ito (1988) reported the 'presynaptic' inhibitory effect of procaterol to occur in the presence of indomethacin. Danser *et al.* (1987) found 'prejunctional' β_1-adrenoceptors to inhibit canine bronchial contraction evoked by electrical transmural stimulation in the absence of the airway mucosa. In this study tyramine was used to displace noradrenaline from neuronal stores and tyramine was found to inhibit contractile responses evoked by transmural stimulation of canine bronchial tissue even in epithelium-denuded preparations and in the presence of 10 μM indomethacin. Species

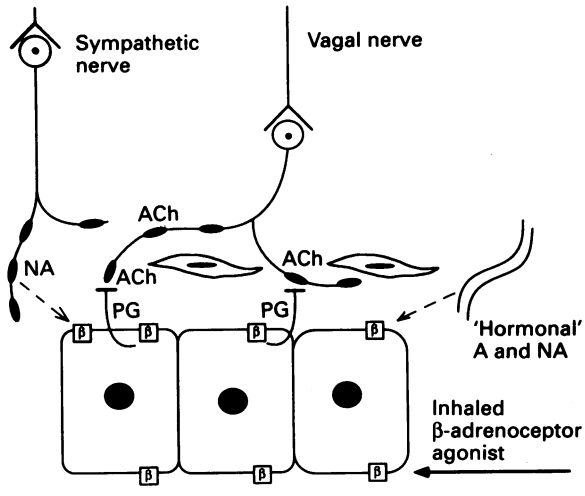


Figure 8 Scheme of β-adrenoceptor-mediated inhibition of cholinergic transmission in rat or guinea pig tracheae. Varicosities of postganglionic parasympathetic and sympathetic pulmonary nerves are localized close to the airway mucosa. Mucosally localized β-adrenoceptors may be activated by neuronally released noradrenaline (depending on species), by circulating hormones (noradrenaline and adrenaline) and by inhaled drugs. Upon stimulation prostaglandins are liberated from the mucosa and inhibit release of acetylcholine from neuroeffector junctions. Evidence for a direct, β-adrenoceptor-mediated inhibition of ganglionic transmission has not been obtained in the present experiments, because isoprenaline did not inhibit [^{3}H]-acetylcholine release evoked by stimulation of extrinsic vagal nerve in mucosa-denuded rat tracheae.

differences may account for the differences between these results and the present study. In addition, one cannot exclude the possibility that there are different regulatory mechanisms for newly-synthesized [^{3}H]-acetylcholine and endogenous, stored acetylcholine. Nevertheless, even in the study reported by Danser *et al.* (1987), removal of the mucosa nearly halved the inhibitory action of tyramine, an observation that suggests a mucosa-dependent pathway, as concluded from the results of the present study.

In control experiments lower S_2/S_1 ratios were obtained in mucosa-denuded than in mucosa-intact tracheae (see Table 1 and 3), indicating some fading of evoked [^{3}H]-acetylcholine release in the former. It had been shown that mechanical removal of the mucosa, as applied in the present study, disrupts mast cells and causes release of their content (Franconi *et al.*, 1990). Possibly, mast cell products are inhibiting [^{3}H]-acetylcholine release over the time. Alternatively, fading of [^{3}H]-acetylcholine release may also be explained by the limitation of the releasable [^{3}H]acetylcholine pool; in mucosa-denuded tracheae release of [^{3}H]-acetylcholine evoked by S_1 was doubled and therewith the amount of [^{3}H]-acetylcholine available for S_2 reduced.

β-Receptor subtype

In rat tracheae isoprenaline but not β_2-adrenoceptor-selective agonists inhibited evoked [^{3}H]-acetylcholine release, indicating involvement of a β_1-adrenoceptor subtype. This conclusion is confirmed by the effect of the antagonist CGP 20712 A, which prevented the isoprenaline-mediated inhibition at a concentration which is known to be β_1-subtype specific. Corroborative evidence was found in the experiments in which [^{3}H]-arachidonic acid metabolism was studied: isoprenaline but not formoterol caused enhanced liberation of prostaglandins and the effect was prevented by a subtype-specific concentration of CGP 20712 A. Also, binding studies have confirmed the existence of β_1-receptors in rat lung (Rugg *et al.*, 1978). In conclusion, in rat tracheae adrenoceptors of the β_1-subtype are involved in the liberation of prostaglandins and the inhibition of [^{3}H]-acetylcholine release.

Different results about the adrenoceptor subtype involved were obtained in guinea pig trachea. In this species both isoprenaline and formoterol inhibited potassium-evoked release of [^{3}H]-acetylcholine, an effect that was prevented by the β_2-selective antagonist ICI 118551 but maintained in the presence of CGP 20712 A. These results confirm that a β_2-subtype is invovled in guinea pig airways. However, as different stimuli were used in the two species studied in these experiments, one might argue that acetylcholine released by different stimuli may be regulated by different receptor subtypes. Unfortunately, it was not possible to use the same stimuli in both species because in rat tracheae high potassium caused a calcium-independent increase in tritium outflow which made it impossible to measure potassium-induced [^{3}H]-acetylcholine release in the rat. Nevertheless, in rat tracheae β_2-adrenoceptors cannot inhibit high potassium-evoked [^{3}H]-acetylcholine release in a way similar to that found with electrical nerve stimulation, because formoterol did not trigger the liberation of prostaglandins and the effect of isoprenaline was exclusively mediated by β_1-adrenoceptors.

A bell-shaped concentration–response curve was obtained for isoprenaline; 0.1 μM isoprenaline caused a maximal inhibition, whereas 1 μM was ineffective. The same concentration dependency was found for the effect of isoprenaline to mediate the liberation of prostaglandins. So far, a conclusive explanation cannot be given. It is, however, known that β_1-adrenoceptor-mediated effects can rapidly desensitize. Possibly, the high concentration of 1 μM isoprenaline may have desensitized the mucosally localized β-adrenoceptors and therewith cut the response.

Effect on basal tritium outflow

The β_2-selective adrenoceptor agonists formoterol, salbutamol and fenoterol, immediately after their application to the organ bath, enhanced the basal tritium outflow, whereas isoprenaline was rather ineffective. The facilitatory effect was prevented by propanolol or by the β_2-selective antagonist ICI 115881, i.e. was related to the binding at β_2-adrenoceptors. Separation of the radioactive compounds by reversed-phase h.p.l.c. showed that formoterol increased mainly the outflow of [^{3}H]-phosphorylcholine and to a smaller extent that of [^{3}H]-choline. This observation suggests a breakdown of phosphatidylcholine by activation of phospholipase C, however the effect was maintained in the absence of extracellular calcium. Therefore, it is also possible that β_2-adrenoceptor agonists displace [^{3}H]-phosphorylcholine and [^{3}H]-choline from the outer leaflet of the cell membrane when penetrating and binding to the β_2-receptor (see also Anderson, 1992). The difference between β_1- and β_2-adrenoceptor agonists may indicate a difference of the microenvironment in which both receptor subtypes are embedded.

Formoterol failed to cause inhibition of evoked [^{3}H]-acetylcholine release in mucosa-denuded tracheae, whereas the agonist still enhanced the basal tritium outflow in mucosa-denuded tracheae (see Tables 2 and 3). This clearly indicates that both the enhancement of basal tritium outflow and the inhibition of evoked [^{3}H]-acetylcholine release are independent mechanisms. The same conclusion can also been drawn from the experiments with isoprenaline which did not

enhance basal tritium efflux but caused inhibition of evoked [^{3}H]-acetylcholine release (see Figure 1).

Underlying inhibitory mechanism

Blockade of cyclooxgenase prevented the inhibitory effect of isoprenaline on evoked [^{3}H]-acetylcholine release, indicating involvement of prostaglandins either directly or indirectly in the inhibitory pathway. The present experiments have also shown that isoprenaline liberates prostaglandins from the rat airways. Prostaglandin E_2 inhibits cholinergic transmission in canine trachea (Deckers *et al.*, 1989) and indomethacin enhances evoked [^{3}H]-acetylcholine in guinea pig, mucosa-intact tracheae (Wessler *et al.*, 1990). Thus, it is suggested that mucosally localized β-adrenoceptors stimulate the liberation of prostanoids, which diffuse to the submucosa and mediate inhibition of acetylcholine release (see proposed scheme in Figure 8). A prior condition of the proposed regulatory pathway is that prostanoids released from the mucosa can gain access to cholinergic nerve endings. Indirect experimental evidence for this assumption has already been obtained as mentioned above: in guinea pig tracheae indomethacin enhances evoked [^{3}H]-acetylcholine release only in mucosa-intact but not in mucosa-denuded preparations (Wessler *et al.*, 1990). In addition, tissue content of endogenous acetylcholine is markedly reduced by removal of the mucosa (rat trachea, I. Wessler, unpublished observation), indicating cholinergic nerve terminals to be located very close to or even within the airway mucosa, at least in the rat trachea.

It is an undecided question whether mucosally localized β-adrenoceptors are innervated. In rat tracheae the tissue content of noradrenaline was substantially lower in mucosa-denuded than in mucosa-intact preparations (Racké *et al.*, 1992), an observation which favours a localization of adrenergic nerve fibres very close to the airway mucosa. If this is so, activation of mucosally localized β-adrenoceptors could also occur in response to the transmitter noradrenaline in the rat trachea. The airway mucosa is also an important target for therapeutic interventions; mucosally localized β-adrenoceptors can be very effectively activated by inhaled β-adrenoceptor agonists and can thus inhibit evoked acetylcholine release by the indirect pathway which is shown in this study. Such a mechanism would have a beneficial effect in the treatment of bronchial asthma. Most importantly, the inhibitory effect depends on the presence of an intact airway mucosa and the generation of prostaglandins.

The gift of fenoterol by Boehringer Ingelheim, Germany is gratefully acknowledged. This paper contains parts of the Dr. rer. nat. thesis of T.R. This paper was supported by a research grant from Ciba Geigy, Basle, Switzerland.

References

AIZAWA, H., INOUE, H., IKEDA, T., HIROSE, T. & ITO, Y. (1991). Effects of procaterol, a beta-2-adrenoceptor stimulant, on neuroeffector transmission in human bronchial tissue. *Respiration*, **58**, 163–166.

ANDERSON, G.P. (1992). Formoterol: Pharmacology, molecular basis of agonism, and mechanism of long duration of highly potent and selective β2-adrenoceptor agonist bronchodilator. *Life Sci.*, **52**, 2145–2160.

BARNES, P.J. (1992). Modulation of neurotransmission in airways. *Physiol. Rev.*, **72**, 699–729.

BLACKWELL, G.J., FLOWER, R.J., NIJKAMP, F.P. & VANE, J.R. (1978). Phospholipase A_2 activity of guinea pig isolated perfused lungs: stimulation, and inhibition by anti-inflammatory steroids. *Br. J. Pharmacol.*, **62**, 79–89.

BRAMLEY, A.M., SAMHOUN, M.N. & PIPER, P.J. (1990). The role of the epithelium in modulating the responses of guinea pig trachea induced by bradykinin in vitro. *Br. J. Pharmacol.*, **99**, 762–766.

DANIEL, E.E., KANNAN, M., DAVIS, C. & POSEY-DANIEL, V. (1986). Ultrastructural studies on the neuromuscular control of human tracheal and bronchial muscle. *Resp. Physiol.*, **63**, 109–128.

DANSER, A.H.J., VAN DEN ENDE, R., LORENZ, R.R., FLAVAHAN, N.A. & VANHOUTTE, P.M. (1987). Prejunctional β_1-adrenoceptors inhibit cholinergic transmission in canine bronchi. *J. Appl. Physiol.*, **62**, 785–790.

DAVIS, P.B., SILSKI, C.L., KERCSMAR, C.M. & INFIELD, M. (1990). β-Adrenergic receptors on human tracheal epithelial cells in primary culture. *Am. J. Physiol.*, **258**, C71–C76.

DECKERS, I.A., RAMPART, M., BULT, H. & HERMAN, A.G. (1989). Evidence for the involvement of prostaglandins in modulation of acetylcholine release from canine bronchial tissue. *Eur. J. Pharmacol.*, **167**, 415–418.

FRANCONI, G.M., RUBINSTEIN, I., LEVINE, E.H., IKEDA, S. & NADEL, J.A. (1990). Mechanical removal of airway epithelium disrupts mast cells and releases granules. *Am. J. Physiol.*, **259**, L372–L377.

GÖTHERT, M. & KOLLECKER, P. (1986). Subendothelial β2-adrenoceptors in the rat vena cava: facilitation of noradrenaline release via local stimulation of angiotensin II synthesis. *Naunyn-Schmied. Arch. Pharmacol.*, **334**, 156–165.

ITO, Y. (1988). Pre- and post-junctional actions of procaterol, a β2-adrenoceptor stimulant, on dog tracheal tissue. *Br. J. Pharmacol.*, **95**, 268–274.

JANSSEN, L.J. & DANIEL, E.E. (1990). Characterization of the prejunctional *beta* adrenoceptors in canine bronchial smooth muscle. *J. Pharmacol. Exp. Ther.*, **254**, 741–749.

JONES, T.R., KANNAN, M.S. & DANIEL, E.E. (1980). Ultrastructural study of guinea pig tracheal smooth muscle and its innervation. *Can. J. Physiol. Pharmacol.*, **58**, 974–983.

KILBINGER, H. & WESSLER, I. (1980). Inhibition by acetylcholine of the stimulation-evoked release of [^{3}H]acetylcholine from the guinea pig myenteric plexus. *Neuroscience*, **5**, 1331–1340.

KNIGHT, D.S., HYMAN, A.L. & KADOWITZ, P.J. (1981). Innervation of intrapulmonary airway smooth muscle of the dog, monkey and baboon. *J. Autonom. Nerv. Syst.*, **3**, 31–43.

MARTIN, J.G. & COLLIER, B. (1986). Acetylcholine release from canine isolated airway is not modulated by norepinephrine. *J. Appl. Physiol.*, **61**, 1025–1030.

NIJKAMP, F.P., ENGELS, F., HENRICKS, P.A.J. & VAN OOSTERHOUT, A.J.M. (1992). Mechanisms of β-adrenergic receptor regulation in lungs and its implications for physiological responses. *Physiol. Rev.*, **72**, 323–367.

PENDRY, Y.D. & MACLAGAN, J. (1991). Evidence for inhibition of sympathetic neurotransmission by endogenously released acetylcholine in the guinea pig trachea. *Br. J. Pharmacol.*, **104**, 817–822.

RACKÉ, K., BÄHRING, J., LANGER, C., BRÄUTIGAM, M. & WESSLER, I. (1992). Prostanoids inhibit release of endogenous norepinephrine from rat isolated trachea. *Am. Rev. Respir. Dis.*, **146**, 1182–1186.

REINHEIMER, T., ANDERSON, G., MACLAGAN, J., RACKÉ, K. & WESSLER, I. (1993). Stimulation of β1-adrenoceptors inhibits evoked [^{3}H]acetylcholine (ACh) release from the isolated rat trachea by an epithelium derived mechanism. *Naunyn-Schmied. Arch Pharmacol.*, **347**, (Suppl), R113.

RHODEN, K.J., MELDRUM, L.A. & BARNES, P. (1988). Inhibition of cholinergic neurotransmission in human airways by β_2-adrenoceptors. *J. Appl. Physiol.*, **65**, 700–705.

RUGG, E.L., BARNETT, D.B. & NAHORSKI, S.R. (1978). Coexistence of $beta_1$ and $beta_2$ adrenoceptors in mammalian lung: evidence from direct binding studies. *Mol. Pharmacol.*, **14**, 996–1005.

SILVA, D.G. & ROSS, G. (1974). Ultrastructural and fluorescence histochemical studies on the innervation of the tracheo bronchial muscle of normal cats and cats treated with 6-hydroxydopamine. *J. Ultrastruct. Res.*, **47**, 310–328.

SUZUKI, K., SUGIYAMA, S., TAKAGI, K., SATAKE, T. OZAWA, T. (1987). The role of phospholipase in β-agonist-induced down regulation in guinea pug lungs. *Biochem. Med. Metab. Biol.*, **37**, 157–166.

VAN SCOTT, M.R., MCINTIRE, M.R. & HENKE, D.C. (1990). Arachidonic acid metabolism and regulation of ion transport in rabbit Clara cells. *Am. J. Physiol.*, **259**, L213–L221.

VERMEIRE, P.A. & VANHOUTTE, P.M. (1979). Inhibitory effects of catecholamines in isolated canine bronchial smooth muscle. *J. Appl. Physiol.*, **46**, 787–791.

WALLENSTEIN, S., ZUCKER, C.L. & FLEISS, J.I. (1980). Some statistical methods useful in circulation research. *Circ. Res.*, **47**, 1–9.

WESSLER, I. (1992). Acetylcholine at motor nerves: storage, release and presynaptic modulation by autoreceptors and adrenoceptors. *Int. Rev. Neurobiol.*, **34**, 283–384.

WESSLER, I. & WERHAND, J. (1990). Evaluation by reverse phase HPLC of [^{3}H]acetylcholine release evoked from the myenteric plexus of the rat. *Naunyn-Schmied. Arch. Pharmacol.*, **431**, 510–516.

WESSLER, I., HELLWIG, D. & RACKÉ, K. (1990). Epithelium-derived inhibition of [^{3}H]acetylcholine release from the isolated guinea pig trachea. *Naunyn-Schmied. Arch. Pharmacol.*, **342**, 387–393.

WESSLER, I., KLEIN, A., POHAN, D., MACLAGAN, J. & RACKÉ, K. (1991). Release of [^{3}H]acetylcholine from the isolated rat or guinea pig trachea evoked by preganglionic nerve stimulation, a comparison with transmural stimulation. *Naunyn-Schmied. Arch. Pharmacol.*, **344**, 403–411.

WESSLER, I., WAGNER, D. & WALCZOK, A. (1992). Suppression by cholinesterase inhibition of a Ca^{2+}-independent outflow of [^{3}H]acetylcholine from the neuromuscular junction of the isolated rat diaphragm. *Eur. J. Pharmacol.*, **221**, 371–376.

WESSLER, I., HÖLZ, C., MACLAGAN, J., POHAN, D., REINHEIMER, T. & RACKÉ, K. (1993). Cromakalim inhibits electrically-evoked [^{3}H]acetylcholine release from a tube-preparation of the rat isolated trachea by an epithelium-dependent mechanism. *Naunyn-Schmied. Arch. Pharmacol.*, **348**, 14–20.

XUE, Q.F., MAURER, R. & ENGEL, G. (1983). Selective distribution of beta- and alpha$_1$-adrenoceptors in rat lung visualized by autoradiography. *Arch. Int. Pharmacodyn.*, **266**, 308–314.

Br. J. Pharmacol (1994), **113**, 1231–1236 © Macmillan Press Ltd, 1994

Potentiation of the anti-obesity effect of the selective β_3-adrenoceptor agonist BRL 35135 in obese Zucker rats by exercise

[1]Eriika Santti, *Risto Huupponen, Juha Rouru, Virve Hänninen, Ullamari Pesonen, †Meena Jhanwar-Uniyal & Markku Koulu

Department of Pharmacology, University of Turku, Turku, Finland, *Department of Clinical Pharmacology, Turku University Hospital, Turku, Finland, and †Department of Neuroendocrinology, The Rockefeller University, New York, NY, U.S.A.

1 The effects of chronic treatments with a selective β_3-adrenoceptor agonist and a selective α_2-adrenoceptor antagonist and their interactions with physical exercise training were studied in experimental obesity.

2 BRL 35135 (β_3-agonist, 0.5 mg kg^{-1} day^{-1} p.o.), atipamezole (α_2-antagonist, 4.0 mg kg^{-1} day^{-1} p.o.) and placebo were given to genetically obese male Zucker rats. Half of the rats were kept sedentary whereas the other half were subjected to moderate treadmill exercise training. Body weight gain, cumulative food intake, the neuropeptide Y content of the hypothalamic paraventricular nucleus, brown adipose tissue thermogenic activity (measured as GDP binding), plasma insulin and glucose levels were measured after 3 weeks' treatment and exercise.

3 Treatment with BRL 35135 reduced weight gain by 19%, increased brown adipose tissue thermogenic activity 45-fold and reduced plasma insulin by 50%. Atipamezole slightly increased food intake and neuropeptide Y content in the paraventricular hypothalamic nucleus but had no effect on the other measured parameters. Exercise alone had no effect on weight gain, food intake or thermogenic activity, whereas it reduced plasma insulin and glucose levels.

4 The effect of BRL 35135 on weight gain and thermogenic activity was significantly potentiated by exercise; the reduction in weight gain was 56% in comparison with 19% in sedentary animals. Food intake was significantly reduced in the BRL 35135-treated–exercise-trained animals, although neither β_3-agonist nor exercise alone affected it.

5 Based on the present results in genetically obese Zucker rats, combination of β_3-agonist treatment with a moderate physical training may offer a new feasible approach to the therapy of obesity.

Keywords: BRL 35135; atipamezole; β_3-adrenoceptor agonism; α_2-adrenoceptor antagonism; brown adipose tissue; thermogenesis; genetic obesity; Zucker rat; exercise; neuropeptide Y

Introduction

The rat adipocyte β-adrenergic receptor subtype mediating lipolysis was originally classified as the β_1-adrenoceptor (Lands *et al.*, 1967), but this view was challenged when atypical β_3-adrenoceptors were found in rat brown adipose tissue (BAT) (Arch *et al.*, 1984). At least three β-adrenoceptor subtypes (β_1, β_2 and β_3 subtypes) seem to coexist in both white and brown adipose tissue of several mammalian species (Arch *et al.*, 1984; Langin *et al.*, 1991). The β_3-receptor has been cloned from rat BAT (Granneman *et al.*, 1991; Muzzin *et al.*, 1991); the human β_3-adrenoceptor, having 80–90% homology with the rat and mouse receptors (Emorine *et al.*, 1994) was initially characterized after transfection and expression of the corresponding gene in Chinese hamster ovary cells (Emorine *et al.*, 1989). There is now ample evidence that activation of β_3-adrenergic receptors in adipose tissue stimulates both lipolysis (Arch *et al.*, 1984; Hollenga *et al.*, 1990) and thermogenesis (Milner *et al.*, 1988; Cawthorne *et al.*, 1992).

Treatment with selective β_3-adrenoceptor agonists results in favourable effects on energy balance in genetically obese mice and rats (Cawthorne *et al.*, 1992; Holloway *et al.*, 1992), suggesting that these compounds have potential as thermogenic anti-obesity drugs (Arch *et al.*, 1984). Thus BRL 35135 (R*,R*-(±)-methyl-4-[2-[2-hydroxy-2-(3-chlorophenyl) ethylamino]-propyl]-phenoxyacetate hydrobromide), a selective β_3-adrenoceptor agonist which is de-esterified rapidly *in vivo* to its active metabolite BRL 37344, produces a dose-dependent increase in energy expenditure, reduces weight gain and improves insulin sensitivity in obese animals (Cawthorne *et al.*, 1992). Preliminary studies in obese patients suggests that β_3-agonists may be useful clinically as well; BRL 35135 improves insulin sensitivity (Mitchell *et al.*, 1989), and another β_3-agonist, BRL 26830, increases energy expenditure and reduces weight gain (Connacher *et al.*, 1988).

Brown adipose tissue is the major site for non-shivering thermogenesis in rodents (Ricquier & Mory, 1984). Drugs activating BAT thermogenesis via β-adrenoceptors cause uncoupling of oxidative phosphorylation from electron transport (Arch *et al.*, 1984). The binding of the nucleotide guanosine diphosphate (GDP) to BAT mitochondrial membrane protein, the uncoupling protein, is an established indicator of the thermogenic activity of BAT (Milner *et al.*, 1988). The sympathetic nervous system (SNS) seems to be the primary pathway in the regulation of BAT thermogenesis (Seydoux & Girardier, 1978), but other peripheral and central mechanisms are also involved. Although the activity of sympathetic nervous system is increased during exercise (Richard *et al.*, 1992), the effect of exercise on BAT thermogenesis is still unclear. Swimming exercise studies in mice and rats have demonstrated increased BAT thermogenesis after training (Hirata, 1982; Bell *et al.*, 1984) but the effect was not found in animals trained on a treadmill (Rivest *et al.*, 1989). Other studies also failed to detect any effect of an acute exercise bout (Arnold *et al.*, 1986) or a longer exercise on BAT GDP binding (McDonald *et al.*, 1988). Since cold exposure is a well-known stimulus for BAT thermogenesis (Smith & Roberts, 1964), the results from swimming experiments may actually reflect a temperature rather than an exercise effect.

[1] Author for correspondence.

α_2-Adrenoceptor antagonists may facilitate SNS activity through increased presynaptic noradrenaline release (Taouis *et al.*, 1988). However, data on the effects of α_2-adrenoceptor antagonists on BAT thermogenesis are scarce. In the dog an acute administration of yohimbine, a rather selective α_2-adrenoceptor blocking agent, enhances lipid mobilization and thermogenesis (Galitzky *et al.*, 1991). In humans α_2-antagonism increases lipolysis, presumably through increased synaptic noradrenaline concentration (Berlan *et al.*, 1991). Peripheral α_2-antagonism seems to potentiate the lipolytic and plasma noradrenaline increasing effects of exercise in man (Sciberras *et al.*, 1994), suggesting that the combination of physical training with an α_2-antagonist might be advantageous when activation of fat tissue metabolism is required.

Hypothalamic neuropeptide Y (NPY) is a potent stimulator of feeding (Leibowitz, 1991). This peptide is found in many central and peripheral neurones, mostly co-localized with catecholamines (Michel, 1991), and its concentration in hypothalamus increases after intense physical exercise in rats (Lewis *et al.*, 1993).

Earlier studies demonstrated important beneficial interactions between cold exposure and physical activity on BAT thermogenesis (LeBlanc & Diamond, 1988; Richard *et al.*, 1992). However, no data on the combined effects of a β_3-receptor agonist or an α_2-antagonist treatment and exercise on BAT thermogenesis are available. We therefore performed an experiment in which sedentary and exercise-trained obese Zucker rats were given atipamezole and BRL 35135 for 3 weeks and the effects on weight gain, feeding behaviour, BAT thermogenesis and hypothalamic paraventricular NPY content were recorded. Obese Zucker rats were chosen since they have lowered sympathetic tone, resting metabolic rate and BAT thermogenic activity (Godbole *et al.*, 1978), while their SNS is activated by exercise in a similar manner to lean animals (Scheurink *et al.*, 1992).

Materials and methods

Animals

Sixty obese male Zucker rats were purchased from Iffa Credo (L'Arbresle, France). In the beginning of the experiment they weighed 382 ± 3 g (mean ± s.e.mean). The animals were individually housed and maintained under a constant light–dark cycle (light on from 06.00 to 20.00 h). They had free access to water *ad libitum* and normal laboratory rat chow (R36, Lactam, Stockholm, Sweden) containing 12.6 MJ kg^{-1} metabolizable energy.

Experimental protocol

The rats were divided into two groups. One group was exercise trained on a treadmill whereas the other was sedentary. These groups were further divided into three treatment groups. One group received atipamezole 2 mg kg^{-1} twice daily, one BRL 35135 0.5 mg kg^{-1} in the evening and saline (0.9%) in the morning and one saline (0.9%) 1 ml kg^{-1} twice daily. The dose of atipamezole was selected in preliminary studies in which this dose effectively antagonized the sedative effect of the selective α_2-agonist dexmedetomidine (Kallio *et al.*, 1989) during chronic treatment in obese Zucker rats (E. Santti *et al.*, unpublished data). The dose of BRL 35135 was based on previous studies in which it was found to have significant anti-obesity activity in obese Zucker rats (Cawthorne *et al.*, 1992). All six groups were matched with body weight and food intake at the beginning of the experiment. All groups (except control exercise and atipamezole exercise groups, which contained nine rats) consisted of ten rats each. The drugs were dissolved in saline and dosed at 1 ml kg^{-1} orally using a gastric cannula at 08:00 and 16:00 h by trained investigators. The rats were accustomed to oral administration of drugs for 2 days before the experiment. The 48 h food intake was measured every other day by placing a weighed amount of pelleted food in the cage and calculating the amount consumed. Body weights were also measured every other day.

The exercise protocol was modified from a previous study performed with obese Zucker rats (Cortez *et al.*, 1991). The rats were trained on a motor-driven treadmill for rodents up an 8° incline for 30 min twice a day, 5 days a week for 3 weeks. The speed was increased gradually from 9 m min^{-1} to 18 m min^{-1} by the third week and was maintained at 18 m min^{-1} during the last week. The physical exercise training sessions started at 08:00 and 16:00 h and the drugs were dosed immediately before the exercise.

For technical reasons the rats were decapitated in a balanced order on three consecutive days starting on the 21st day of treatment. The food was withdrawn at 17:00 h at the previous night in order to minimize the confounding effects of food digestion on plasma glucose and insulin. The last drug doses were given at 17:00 on the day before the decapitation (i.e. 16–19 h earlier). Blood was collected into prechilled EDTA tubes, whereafter plasma was separated and stored at −70°C until analysed. Interscapular brown adipose tissue was quickly dissected from surrounding tissues and was used for the preparation of mitochondrial cell fraction in order to analyse the GDP binding. The brains were removed, frozen in isopentane on solid carbon dioxide and stored at −70°C until analysed. The epididymal and intraperitoneal white adipose tissues were removed and weighed.

[^{3}H]-GDP binding

The method utilized is based on the assay described originally by Nicholls (1976). In brief, the BAT was minced, diluted with 250 mM sucrose and homogenized with a Potter S homogenizer (B. Braun Melsungen, Germany). The homogenate was centrifuged for 10 min at 8500 *g*. The pellet was diluted with 250 mM sucrose and centrifuged at 700 *g* for 10 min. The supernatant was collected and centrifuged at 8500 *g* for 10 min. Bovine serum albumin (BSA) at 0.2% was added to the wash resuspension of the pellet, which now consisted of mitochondria. After centrifugation (8500 *g*) the resulting pellet was suspended in albumin-free sucrose buffer. The binding of [^{3}H]-GDP to mitochondria of single rats was determined by incubating mitochondria in a basic medium containing 100 mM sucrose, 20 mM TES, 1 mM EDTA, 10 mM choline chloride, 2 μM rotenone, [^{14}C]-sucrose (0.125 μCi ml^{-1}) and 10 μM [^{3}H]-GDP (0.53 Ci $mmol^{-1}$) at room temperature. Non-specific binding was assessed in the presence of excess unlabelled GDP (1 mM). After 10 min of incubation, the reaction was terminated by filtrating the mixture through Thomas A/E glassfibre filters (Gelman Sciences MI, U.S.A.) by using a Brandel cell harvester (Biomedical Research Devices, Gaithersburg, MD, U.S.A.). The radioactivity was measured with the Opti Phase 'High Safe' II scintillation cocktail (FSA Lab. Supplies, Loughborough, U.K.) and the liquid scintillation counter (LKB Wallac 1219, Turku, Finland), enabling the samples to be counted for both ^{3}H and ^{14}C. GDP binding was assessed from ^{3}H radioactivity with a correction for trapped medium using [^{14}C]-sucrose. The protein content of mitochondrial suspensions was assayed according to the method of Peterson (1977).

Measurement of hypothalamic neuropeptide Y content

Brains were cut into coronal sections of 300 μm at −12°C, and paraventricular nuclei (PVN) was micropunched following the coordinates given in stereotaxic atlas of König & Klippel (1974). Bilateral tissue samples were placed in 100 μl of cold aprotinin in microfuge tubes and were stored at −70°C until assayed. The tissue samples were homogenised in cold 0.2 N HCl. An aliquot was taken for protein analysis and the remainder of the homogenate was centrifuged at

2500 g for 30 min at 4°C, and the supernatant (50 µl) was then lyophilized and taken for determination of NPY concentration.

NPY was measured by a specific radioimmunoassay kit using the double antibody method (Peninsula laboratories, U.S.A.). Standard (porcine NPY) or lyophilized extract reconstituted with 0.04 M phosphate buffer (pH 7.4) was incubated with specific NPY antiserum and ^{125}I-labelled NPY for 48 h including a 24 h preincubation period without labelled NPY. Bound and free fractions were separated by the addition of a goat anti-rabbit IgG serum. The samples were measured in duplicate and the values are presented as pg per mg of protein. The protein determination was performed by the method of Bradford (1976).

Fasting plasma insulin and glucose

Plasma insulin was measured with rat insulin RIA kit supplied by Novo Nordisk, Bagsvaerd, Denmark. Plasma glucose was analysed with glucose oxidase method with an Analox GM 7 measuring device (Analox Instruments, London, U.K.).

Drugs and chemicals

BRL 35135 was a generous gift from SmithKline Beecham Pharmaceuticals, Surrey, U.K. and atipamezole from Farmos Oy, Turku, Finland. Sucrose and EDTA (ethylendinitrilotetraacetic acid) were purchased from Merck, TES (*N*-tris-[hydroxymethyl]-methyl-2-aminoethane-sulphonic acid), choline chloride, rotenone, GDP (guanosine 5'-diphosphate) from Sigma, [^{14}C]-sucrose from Amersham (Buckinghamshire, U.K.), [^{3}H]-GDP from DuPont NEN (Boston, MA, U.S.A.) and aprotinin from Iniprol, Laboratorie Choay (Paris, France).

Statistical analysis

A two-way analysis of variance (ANOVA) combining all groups was performed first. This gave a *P*-value for treatment effect (placebo, atipamezole, BRL 35135), exercise effect and treatment–exercise interaction. When the *P*-value was significant, contrasts were used as *post-hoc* test to reveal which groups differed from each other.

Depending if there was a significant interaction between treatment and exercise, the drug effect *per se* was tested using two different approaches. If both the treatment effect and the treatment–exercise interaction were significant, contrasts were formed only in the sedentary group between the atipamezole and vehicle-treated rats on one hand and between BRL 35135-and vehicle-treated rats on the other hand. If no interaction was present (meaning that the drug effects were similar in sedentary and exercised animals), these groups were handled together in the contrast analysis.

If there was a significant interaction between treatment and exercise (meaning that at least one drug had a different effect in sedentary and exercised animals), contrasts were formed between the placebo-corrected drug effects of sedentary and exercised animals.

The calculations were performed using the BMDP software programs 7D and 4V (BMDP Statistical Software, Los Angeles, CA, U.S.A.). A *P*-value less than 0.05 was considered statistically significant.

Results

Weight gain

Sedentary animals When compared with rats receiving the vehicle only, BRL 35135 significantly reduced weight gain ($P<0.05$), whereas atipamezole had no effect (Figure 1).

Exercise-trained animals Exercise alone did not affect weight gain of the vehicle-treated animals. However, comparison with sedentary animals revealed that exercise markedly potentiated the weight gain reducing effect of BRL 35135 ($P<0.01$). In fact, in the exercised, BRL 35135-treated animals a plateau of the weight gain was reached after 12 days, whereafter the animals actually lost weight (data not shown). The lack of any atipamezole effect was also seen in exercise-trained rats.

Cumulative food intake

Sedentary animals Atipamezole ($P<0.05$) slightly increased cumulative food intake during the treatment, whereas BRL 35135 had no statistically significant effect (Figure 2).

Exercise-trained animals Exercise itself had no effect on food intake. However, combination of BRL 35135 treatment and physical exercise significantly reduced food intake of the animals ($P<0.05$). There was no difference in the effect of atipamezole on food intake between sedentary and exercise-trained rats.

Neuropeptide Y content in paraventricular nucleus

The NPY content of PVN was somewhat higher in atipamezole-treated rats than in control animals (0.05<

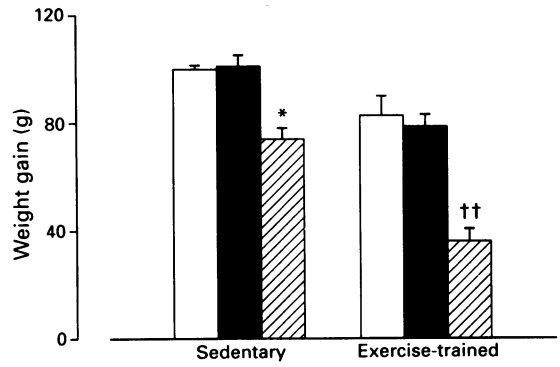


Figure 1 Weight gain (mean ± s.e.mean; $n = 9-10$) during the treatment in sedentary and exercise-trained rats receiving vehicle only (open columns), atipamezole 4 mg kg^{-1} day^{-1} (closed columns) or BRL 35135 0.5 mg kg^{-1} day^{-1} (hatched columns) for 3 weeks. *$P = 0.012$ compared with vehicle-treated sedentary group; ††$P = 0.002$ placebo-corrected effect significantly different from corresponding sedentary group.

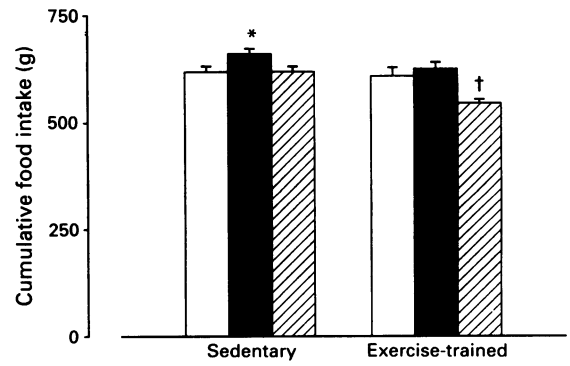


Figure 2 Cumulative food intake (mean ± s.e.mean; $n = 9-10$) in sedentary and exercise-trained rats receiving vehicle only (open columns), atipamezole 4 mg kg^{-1} day^{-1} (closed columns) or BRL 35135 0.5 mg kg^{-1} day^{-1} (hatched columns) for 3 weeks. *$P = 0.027$ compared with vehicle-treated sedentary group; †$P = 0.021$ placebo-corrected effect significantly different from corresponding sedentary group.

$P<0.1$, Table 1), whereas BRL 35135 or exercise training had no significant effect.

GDP binding and BAT protein content

Sedentary animals Treatment with BRL 35135 significantly increased GDP-binding to BAT mitochondria ($P<0.001$) and mitochondrial protein content ($P<0.001$), whereas atipamezole had no effect on GDP binding (Figure 3) or protein content (Table 1).

Exercise-trained animals Exercise training further increased the effect of BRL 35135 on GDP binding ($P<0.05$), but atipamezole and exercise alone had no effect (Figure 3). Exercise had no effect on BAT mitochondrial protein content.

Epididymal and intraperitoneal white fat

Treatment with BRL 35135 significantly reduced both the intraperitoneal ($P<0.001$) and epididymal ($P<0.001$) fat tissue weight in both sedentary and exercised animals, but atipamezole had no effect (Table 1). Exercise training *per se* tended to decrease the weight of epididymal ($0.05<P<0.1$) but not that of intraperitoneal fat.

Plasma glucose and insulin

In both sedentary and exercised rats, treatment with BRL 35135 significantly reduced plasma insulin ($P<0.001$, Figure 4), whereas atipamezole had no significant effect. Neither of the drugs had any effect on plasma glucose. Both plasma glucose ($P<0.05$) and insulin ($P<0.01$) levels were lowered by exercise.

Discussion

In accordance with earlier studies (Cawthorne *et al.*, 1992) we found a clear reduction in weight gain after BRL 35135 treatment in sedentary animals. Since BRL 35135 had no effect on food intake in sedentary rats, the stimulation of BAT thermogenesis during chronic BRL 35135 administration is the most evident contributing factor leading to increased energy expenditure and reduced weight gain in obese Zucker rats. An important new finding with potential therapeutic implications is that physical exercise training markedly potentiates the antiobesity effect of BRL 35135. This suggests that the combination of a moderate exercise with a β_3-receptor agonist may be a useful approach in the treatment of obesity, although clinical studies are required to prove it. In contrast, the present study does not provide evidence that combination of physical training with an α_2-receptor antagonist would have anti-obesity effects in genetically obese Zucker rats.

The present data suggest that the potentiation of the anti-obesity effect of BRL 35135 by physical exercise training is due partly to a greater activation of BAT thermogenesis and partly to a reduction in food intake in the exercise-trained BRL 35135 treated rats. A reduction in weight gain has been described earlier in exercised male Wistar rats (Rivest *et al.*, 1989). Interestingly, in the present study exercise alone did not enhance BAT thermogenesis or affect feeding and weight gain. The insensitivity of Zucker rats to exercise-induced

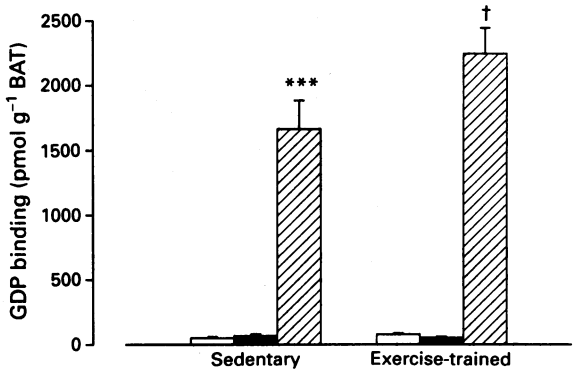


Figure 3 GDP binding to BAT mitochondria (mean ± s.e.mean; $n = 9-10$) in sedentary and exercise-trained rats receiving vehicle only (open columns), atipamezole 4 mg kg^{-1} day^{-1} (closed columns) or BRL 35135 0.5 mg kg^{-1} day^{-1} (hatched columns) for 3 weeks. ***$P<0.001$ compared with vehicle-treated sedentary group; †$P = 0.042$ placebo-corrected effect significantly different from corresponding sedentary group.

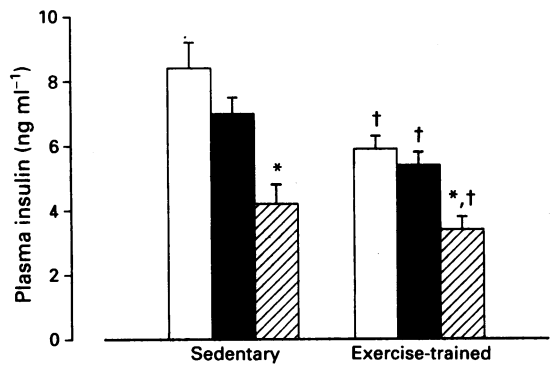


Figure 4 Plasma insulin (mean ± s.e.mean; $n = 9-10$) in sedentary and exercise-trained rats receiving vehicle only (open columns), atipamezole 4 mg kg^{-1} day^{-1} (closed columns) or BRL 35135 0.5 mg kg^{-1} day^{-1} (hatched columns) for 21 days. *$P<0.001$ compared with vehicle-treated sedentary group (since interaction between treatment and exercise was non-significant sedentary and exercised rats were handled together); †$P = 0.001$ exercise-trained rats compared with sedentary rats.

Table 1 Brown adipose tissue mitochondrial protein content, concentration of neuropeptide Y in the hypothalamic paraventricular nucleus, weight of the epididymal and intraperitoneal white fat pads and plasma glucose concentrations in sedentary and exercise-trained rats receiving vehicle only, atipamezole 4 mg kg^{-1} day^{-1}, or BRL 35135 0.5 mg kg^{-1} day^{-1} for 21 days. Values are means ± s.e.mean, $n = 9-10$

	Sedentary			*Exercise*		
	Control	*Atipamezole*	*BRL 35135*	*Control*	*Atipamezole*	*BRL 35135*
BAT protein (mg per lobe)	0.3 ± 0.1	0.3 ± 0.1	6.4 ± 0.6[a]	0.3 ± 0.04	0.2 ± 0.03	6.7 ± 0.6[a]
NPY content (pg mg^{-1} protein)	1.7 ± 0.6	3.3 ± 0.8	1.4 ± 0.3	2.4 ± 0.8	3.1 ± 0.7	1.3 ± 0.29
Epididymal fat (g)	7.8 ± 0.4	8.0 ± 0.4	7.2 ± 0.2[a]	7.9 ± 0.2	7.4 ± 0.2	6.3 ± 0.3[a]
Intraperitoneal fat (g)	13.3 ± 0.5	12.3 ± 0.7	8.7 ± 0.3[a]	12.6 ± 0.6	13.5 ± 1.1	7.2 ± 0.8[a]
Plasma glucose (mmol l^{-1})	7.3 ± 0.2	7.9 ± 0.2	7.3 ± 0.1	7.2 ± 0.1[b]	7.1 ± 0.3[b]	7.1 ± 0.1[b]

[a]$P<0.001$ compared with vehicle-treated rats (sedentary and exercise-trained rats handled together); [b]$P = 0.011$ when compared with sedentary animals.

weight reduction has been noted earlier in female animals (Cortez *et al.*, 1991).

Physical training increases sympathetic activity in obese Zucker rats as evidenced by increased plasma adrenaline and noradrenaline concentrations during exercise (Scheurink *et al.*, 1992). It is obvious that exercise sessions of moderate strength as performed here cannot alone lead to the stimulation of BAT thermogenesis (Figure 3), although the sympathetic nervous system is the major regulator of its activity. The thermogenic effects of unselective sympatomimetics are partly mediated through β_1-adrenoceptors (Arch & Kaumann, 1993). It is possible that the treatment with the β_3-receptor agonist BRL 35135, which markedly stimulates BAT thermogenesis, renders the tissue more sensitive towards catecholamines released during exercise.

The mechanism leading to reduced food intake in the exercise-trained–BRL 35135-treated animals, while neither of these alone had any effect on food intake, remains speculative. In the present study the intensity of the exercise was gradually increased to a level which the grossly obese animals could tolerate. The effect of exercise on food intake may be dependent on the intensity and duration of exercise. It has been concluded previously that there is only little change in energy intake following light exercise of long duration, whereas exercise of high intensity and short duration tend to decrease food intake (Thompson *et al.*, 1982). The regulation of food intake involves complex interrelated neural, metabolic and endocrine signals which are coordinated mainly at the hypothalamic level. It is possible that multiple peripheral mechanism, such as activation of lipolysis, reduced plasma insulin levels or improved insulin sensitivity of the peripheral tissues may have contributed to reduced food intake. The present study was not designed to clarify these interrelationships, and therefore it does not provide evidence regarding which if any of these factors are involved. Further studies are clearly warranted to elucidate this interesting observation.

Atipamezole, a new potent and selective α_2-adrenoceptor antagonist having similar affinities to all three α_2-adrenoceptor subtypes (Harrison *et al.*, 1991; Marjamäki *et al.*, 1993), was used in the present study to investigate possible beneficial effects of α_2-receptor antagonism in the treatment of genetic obesity. Theoretically, at least two possible mechanisms of action of atipamezole could be implemented. First, since the activity of noradrenaline release from the nerve terminals is partly controlled by presynaptic α_2-receptors, atipamezole may increase noradrenaline release as shown in humans (Karhuvaara *et al.*, 1990). Since the activity of sympathetic tone is low in obese Zucker rats, as well as in human obesity, α_2-receptor antagonists might thus be able to improve low sympathetic activity. Second, antagonism of the α_2-adrenoceptors in BAT may stimulate BAT thermogenesis by facilitating β-receptor-mediated adenylate cyclase formation. There are some experimental data suggesting that α_2-adrenoceptor antagonists may have a beneficial effect on energy balance. In dogs, yohimbine increases lipolysis and thermogenesis (Galitzky *et al.*, 1991). In rats α_2-adrenoceptor agonists decrease resting energy expenditure, which can be reversed by α_2-antagonists, suggesting that α_2-adrenergic receptors are invovled in the regulation of energy expenditure in rats (Gazzola, 1993). In the present study the administration of atipamezole, either alone or in combination with exercise, in doses which according to our earlier experiments effectively blocked the sedative effects of the α_2-agonist dexmedetomidine in obese Zucker rats (see Materials and methods) failed to modify BAT thermogenesis or weight gain in genetically obese rats.

Acute administration of 1 mg kg^{-1} atipamezole to dogs was found to have a short-lasting (2 h) reducing effect on food intake (Berlan *et al.*, 1991). On the other hand, we found a slight, but statistically significant, increase in the cumulative food intake in the atipamezole-treated rats. Food intake is regulated by complex mechanisms in which various hypothalamic neurotransmitters and particularly NPY play a prominent role (Morley, 1987; Blundell, 1991; Leibowitz, 1991). Acute and chronic injections of NPY into PVN elicit a long-lasting hyperphagic effect, and NPY has been regarded as the most potent naturally occurring orexigenic agent (Leibowitz, 1991; Sahu & Kalra, 1993). Since atipamezole-treated rats had an approximately 2-fold higher NPY content in the PVN than control animals (Table 1), hypothalamic NPY neurones may be involved in the hyperphagic effect of chronic atipamezole treatment. Our finding is supported by the results from an *in vitro* experiment in which α_2-antagonist yohimbine was found to increase the potassium-evoked release of NPY from rat hypothalamus (Ciarleglio *et al.*, 1993).

The plasma insulin levels were reduced in all exercise-trained animals. As in previous studies (Cawthorne *et al.*, 1992) BRL 35135 treatment alone also decreased plasma insulin levels. The reduction in plasma insulin concentration with lowered or unchanged concentration of plasma glucose suggests an improved glucose utilization in peripheral tissues.

It is concluded that the combination of exercise training and β_3-adrenoceptor agonist BRL 35135 significantly potentiates the BAT thermogenesis-stimulating and weight gain-reducing properties of BRL 35135 in genetically obese Zucker rats. Furthermore, the present data suggest that atipamezole, a selective and potent α_2-antagonist, may not have beneficial effects in the treatment of obesity. The combination of β_3-agonist treatment with a moderate physical training is potentially important improvement in the therapy of obesity which needs to be evaluated clinically.

The study was financially supported by the Medical Research Council of the Academy of Finland and Nordisk Insulin Foundation Committee, which are gratefully acknowledged. The visit of Dr Meena Jhanwar-Uniyal to the University of Turku was financed by Turku University Foundation. Ms Elina Kahra, Ms Taina Lehti and Ms Ulla Heikonen are acknowledged for their skilful technical assistance. BRL 35135 was a generous gift from Dr Michael A. Cawthorne, SmithKline Beecham Pharmaceuticals, and atipamezole from Dr Raimo Virtanen, Farmos Oy.

References

ARCH, J.R.S. & KAUMANN, A.J. (1993). β_3 and atypical β-adrenoceptors. *Med. Res. Rev.*, **13**, 663–729.

ARCH, J.R.S., AINSWORTH, A.T., CAWTHORNE, M.A., PIERCY, V., SENNITT, M.V., THODY, V.E., WILSON, C. & WILSON, S. (1984). Atypical β-adrenoceptor on brown adipocytes as target for anti-obesity drugs. *Nature*, **309**, 163–165.

ARNOLD, J., LEBLANC, J., CÔTE, J., LALONDE, J. & RICHARD, D. (1986). Exercise suppression of thermoregulatory thermogenesis in warm- and cold-acclimated rats. *Can. J. Physiol. Pharmacol.*, **64**, 922–926.

BELL, R.R., MCGILL, T.J., DIGBY, P.W. & BENNETT, S.A. (1984). Effects of dietary protein and exercise on brown adipose tissue and energy balance in experimental animals. *J. Nutr.*, **114**, 1900–1908.

BERLAN, M., GALITZKY, J., TRAN, M.A. & MONTASTRUC, P. (1991). Anorectic effect of alpha 2-antagonists in dog: effect of acute and chronic treatment. *Pharmacol. Biochem. Behav.*, **39**, 313–320.

BLUNDELL, J.E. (1991). Pharmacological approaches to appetite suppression. *Trends Pharmacol. Sci.*, **12**, 147–157.

BRADFORD, M.M. (1976). A rapid and sensitive method for the quantitation of microgram quantities of protein utilizing the principle of protein–dye binding. *Anal. Biochem.*, **72**, 248–254.

CAWTHORNE, M.A., SENNITT, M.V., ARCH, J.R.S. & SMITH, S.A. (1992). BRL 35135, a potent and selective atypical β-adrenoceptor agonist. *Am. J. Clin. Nutr.*, **55**, 252S–257S.

CIARLEGLIO, A.E., BEINFELD, M.C. & WESTFALL, T.C. (1993). Pharmacological characterization of the release of neuropeptide Y-like immunoreactivity from the rat hypothalamus. *Neuropharmacology*, **32**, 819–825.

CONNACHER, A.A., JUNG, R.T. & MITCHELL, P.E.G. (1988). Weight loss in obese subjects on a restricted diet given BRL 26830A, a new atypical β-adrenoceptor agonist. *Br. Med. J.*, **296**, 1217–1220.

CORTEZ, M.Y., TORGAN, C.E., BROZINICK, JR, J.T. & IVY, J.L. (1991). Insulin resistance of obese Zucker rats exercise trained at two different intensities. *Am. J. Physiol.*, **261**, E613–E619.

EMORINE, L.J., MARULLO, S., BRIEND-SUTREN, M.-M., PATEY, G., TATE, K., DELAVIER-KLUTCHKO, C. & STROSBERG, A.D. (1989). Molecular characterization of the human β_3-adrenergic receptor. *Science*, **245**, 1118–1121.

EMORINE, L., BLIN, N. & STROSBERG, A.D. (1994). The human β_3-adrenoceptor: the search for a physiological function. *Trends Pharmacol. Sci.*, **15**, 3–7.

GALITZKY, J., VERMOREL, M., LAFONTAN, M., MONTASTRUC, P. & BERLAN, M. (1991). Thermogenic and lipolytic effect of yohimbine in the dog. *Br. J. Pharmacol.*, **104**, 514–518.

GAZZOLA, C. (1993). α_2-adrenoceptor-mediated effects on resting energy expenditure. *Int. J. Obes.*, **17**, 637–641.

GODBOLE, V., YORK, D.A. & BLOXHAM, D.P. (1978). Developmental changes in the fatty (fa/fa) rat: Evidence for defective thermogenesis preceding the hyperlipogenesis and hyperinsulinaemia. *Diabetologia*, **15**, 41–44.

GRANNEMAN, J.G., LAHNERS, K.N. & CHAUDHRY, A. (1991). Molecular cloning and expression of the rat β_3-adrenergic receptor. *Mol. Pharmacol.*, **40**, 895–899.

HARRISON, J.K., D'ANGELO, D.D., ZENG, D. & LYNCH, K.R. (1991). Pharmacological characterization of rat α_2-adrenergic receptors. *Mol. Pharmacol.*, **40**, 407–412.

HIRATA, K. (1982). Enhanced calorigenesis in brown adipose tissue in physically trained rat. *Jpn. J. Physiol.*, **32**, 647–653.

HOLLENGA, C., HAAS, M. DEINUM, J.T. & ZAAGSMA, J. (1990). Discrepancies in lipolytic activities induced by β-adrenoceptor agonists in human and rat adipocytes. *Horm. Metabol. Res.*, **22**, 17–21.

HOLLOWAY, B.R., HOWE, R., RAO, B.S. & STRIBLING, D. (1992). ICI D7114: a novel selective adrenoceptor agonist of brown fat and thermogenesis. *Am. J. Clin. Nutr.*, **55**, 262S–264S.

KALLIO, A., SCHEININ, M., KOULU, M., PONKILAINEN, R., RUSKOAHO, H., VIINAMÄKI, O. & SCHEININ, H. (1989). Effects of dexmedetomidine, a selective α_2-adrenoceptor agonist, on hemodynamic control mechanisms. *Clin. Pharmacol. Ther.*, **46**, 33–42.

KARHUVAARA, S., KALLIO, A., SCHEININ, M., ANTTILA, M., SALONEN, J.S. & SCHEININ, H. (1990). Pharmacological effects and pharmacokinetics of atipamezole, a novel α_2-adrenoceptor antagonist–a randomized, double-blind cross-over study in healthy male volunteers. *Br. J. Clin. Pharmacol.*, **30**, 97–106.

KÖNIG, J.F.R. & KLIPPEL, R.A. (1974). *The Rat Brain, A Stereotactic Atlas of the Forebrain and Lower Parts of the Brain Stem*. New York: Williams & Wilkins.

LANDS, A.M., ARNOLD, A. MCAULIFF, J.P., LUDUENA, F.P. & BROWN, Jr, T.G. (1967). Differentiation of receptor systems activated by sympathomimetic amines. *Nature*, **214**, 597–598.

LANGIN, D., PORTILLO, M.P., SAULNIER-BLACHE, J.-S. & LAFONTAN, M. (1991). Coexistence of three β-adrenoceptors subtypes in white fat cells or various mammalian species. *Eur. J. Pharmacol.*, **199**, 291–301.

LEBLANC, J. & DIAMOND, P. (1988). Interaction between exercise training and cold acclimation in rats. *Eur. J. Appl. Physiol.*, **57**, 89–92.

LEIBOWITZ, S.F. (1991). Brain neuropeptide Y: an integrator of endocrine, metabolic and behavioral processes. *Brain Res. Bull.*, **27**, 333–337.

LEWIS, D.E., SHELLARD, L., KOESLAG, D.G., BOER, D.E., MCCARTHY, H.D., MCKIBBIN, P.E., RUSSELL, J.C. & WILLIAMS, G. (1993). Intense exercise and food restriction cause similar hypothalamic neuropeptide Y increases in rats. *Am. J. Physiol.*, **264**, E279–284.

MCDONALD, R.B., HORWITZ, B.A. & STERN, J.S. (1988). Cold-induced thermogenesis in younger and older Fischer 344 rats following exercise training. *Am. J. Physiol.*, **254**, (6 Part 2), R908–R916.

MARJAMÄKI, A., LUOMALA, K., ALA-UOTILA, S. & SCHEININ, M. (1993). Use of recombinant human α_2-adrenoceptors to characterize subtype selectivity of antagonist binding. *Eur. J. Pharmacol.*, **246**, 219–226.

MICHEL, M.C. (1991). Receptors for neuropeptide Y: multiple subtypes and multiple second messengers. *Trends Pharmacol. Sci.*, **12**, 389–394.

MILNER, R.E., WILSON, S. ARCH, J.R.S. & TRAYHURN, A. (1988). Acute effects of a β-adrenoceptor agonist (BRL 26830A) on rat brown-adipose-tissue mitochondria. *Biochem. J.*, **249**, 759–763.

MITCHELL, T.H., ELLIS, R.D.M., SMITH, S.A., ROBB, G. & CAWTHORNE, M.A. (1989). Effects of BRL 35135, a β-adrenoceptor agonist with novel selectivity, on glucose tolerance and insulin sensitivity in obese subjects. *Int. J. Obes.*, **13**, 757–766.

MORLEY, J.E. (1987). Neuropeptide regulation of appetite and weight. *Endocrinol. Rev.*, **8**, 256–287.

MUZZIN, P., REVELLI, J.-P., KUHNE, F., GOCAYNE, J.D., MCCOMBIE, W.R., VENTER, J.G., GIACOBINO, J.-P. & FRASER, C.M. (1991). An adipose tissue-specific β-adrenergic receptor. *J. Biol. Chem*, **266**, 24053–24058.

NICHOLLS, D.G. (1976). Hamster brown-adipose-tissue mitochondria. Purine nucleotide control of the inner membrane, the nature of the nucleotide control of the inner membrane, the nature of the nucleotide binding site. *Eur. J. Biochem.*, **62**, 223–228.

PETERSON, G.L. (1977). A simplification of the protein assay method of Lowry *et al.* which is generally more applicable. *Anal. Biochem.*, **83**, 346–356.

RICQUEIR, D. & MORY, G. (1984). Factors affecting brown adipose tissue activity in animals and man. *Endocrinol. Metab. Clin. N. Am.*, **13**, 501–521.

RICHARD, D., LABRIE, A. & RIVEST, S. (1992). Tissue specificity of SNS response to exercise in mice exposed to low temperatures. *Am. J. Physiol.*, **262**, R921–R925.

RIVEST, S., LANDRY, J. & RICHARD, D. (1989). Effect of exercise training on energy balance of orchidectomized rats. *Am. J. Physiol.*, **257**, R550–R555.

SAHU, A. & KALRA, S.P. (1993). Neuropeptidergic regulation of feeding behavior: neuropeptide Y. *Trends Endocrinol. Metab.*, **4**, 217–224.

SCHEURINK, A.J., STEFFENS, A.B., ROOSSIEN, B. & BALKAN, B. (1992). Sympathoadrenal function in genetically obese Zucker rats. *Physiol. Behav.*, **52**, 679–685.

SCIBERRAS, D.G., REED, J.W., ELLIOTT, G. BLAIN, P.G. & GOLDBERG, M.R. (1994). The effect of a peripherally selective α_2-antagonist, MK-467, on the metabolic and cardiovascular response to exercise in healthy man. *Br. J. Clin. Pharmacol.*, **37**, 39–44.

SEYDOUX, J. & GIRARDIER, L. (1978). Control of brown fat thermogenesis by the sympathetic nervous system. *Experientia*, **32** (Suppl.), 153–167.

SMITH, R.E. & ROBERTS, J.C. (1964). Thermogenic activity of BAT in cold acclimated rats. *Am. J. Physiol.*, **206**, 143–148.

TAOUIS, M., BERLAN, M., MONTASTRUC, P. & LAFONTAN, M. (1988). Mechanism of the lipid-mobilizing effect of alpha-2 adrenergic antagonists in the dog. *J. Pharmacol. Exp. Ther.*, **247**, 1172–1180.

THOMPSON, J.K., JARVIE, G.J., LAHEY, B.B. & CURETON, K.J. (1982). Exercise and obesity: etiology, physiology and intervention. *Psychol. Bull.*, **91**, 55–79.

(Received May 20, 1994
Revised August 9, 1994
Accepted August 10, 1994)

Br. J. Pharmacol. (1994), **113**, 1237–1242 © Macmillan Press Ltd, 1994

Differences in sensitivity to the specific protein kinase C inhibitor Ro31-8220 between small and large bronchioles of the rat

[1]L.C. Chopra, C.H.C. Twort & J.P.T. Ward

Respiratory Research Laboratories, UMDS Smooth Muscle Group, UMDS, St Thomas' Campus, London SE1 7EH

1 The involvement of protein kinase C (PKC) in constriction of small bronchioles has never been investigated. In this study we have examined the effects of the specific PKC inhibitors Ro31-8220 and Ro31-7549 and the non-specific inhibitor H7 on carbachol-, 5-hydroxytryptamine (5-HT)- and 4β-phorbol dibutyrate (4β-PDBu)-induced contractions in large and small bronchioles.

2 The study was performed on isolated bronchioles of the rat with internal diameters of 574 μm ± 11 (small, $n = 128$), and 1475 μm ± 32 (large, $n = 93$), using a Mulvaney–Halpen small vessel myograph.

3 In these preparations 4β-PDBu had no effect if added on its own. However, after precontracting with 30 mM K^+, 0.5 μM 4β-PDBu caused a contractile response of 110.4 ± 7.0% T_K (T_K = maximum response to 75 mM K^+ in small and 69.3 ± 6.5% T_K in large bronchioles. Ro31-8220, Ro31-7549 and H7 all showed concentration-dependent inhibition of this response.

4 In small bronchioles 10 μM Ro31-8220 shifted both the carbachol and 5-HT concentration– response curves to the right, and reduced the maximum response. In contrast, 10 μM Ro31-8220 had no significant effect on the EC_{50} to carbachol of larger bronchioles, although the maximum response was reduced, and had no significant effect on the 5-HT concentration– response curve. 200 μM H7 shifted the carbachol concentration– response curve to the right as well as reducing the maximal response in both small and large bronchioles.

5 Large bronchioles exhibited a greater rate of decay of carbachol-induced contraction than did small bronchioles. Pretreatment with Ro31-8220 accelerated the rate of decay.

6 Pretreatment with 10 μM Ro31-8220 caused a small reduction in the response to 75 mM K^+ in both small and large bronchioles (small: to 87.8 ± 3.0% T_K; large: to 94.1 ± 0.8% T_K). H7 at 200 μM caused a much larger reduction in both preparations (small: to 75.1 ± 3.0% T_K); large: to 82.7 ± 0.6% T_K).

7 Small bronchioles were more sensitive than larger bronchioles to agonists and phorbol ester. The protein kinase inhibitor Ro31-8220 could reduce agonist-induced constriction in small and large bronchioles, as well as reducing or abolishing phorbol ester-induced contractions. Small bronchioles were more sensitive than large bronchioles to Ro31-8220. These results suggest that there is a significant PKC involvement in constriction of bronchioles to carbachol and 5-HT, and that the proportion of the contractile response that can be attributed to PKC is greater in smaller than larger bronchioles.

Keywords: Airway smooth muscle; bronchioles; contraction; protein kinase C; Ro31-8220, H7

Introduction

Protein kinase C (PKC) plays a crucial role in signal transduction for the activation of many cellular functions (Nishizuka, 1986). It is activated endogenously by diacylglycerol, which is generated by the hydrolysis of membrane polyphosphoinositides by phospholipase C after stimulation of specific cell membrane receptors (Berridge & Irvine, 1984). Phorbol esters such as 4β-phorbol dibutyrate (4β-PDBu) can intercalate into the plasma membrane and activate PKC by mimicking the stimulant action of diacylglycerol (Castagna *et al.*, 1982). There have been several reports on the effects of phorbol esters on the response to spasmogenic agents in airway smooth muscle; in brief, whereas low concentrations of phorbol ester ($\leqslant 1$ μM) can augment contraction induced by spasmogens (Schramm & Grunstein, 1989), high concentrations ($\geqslant 1$ μM) tend to inhibit the response (Menkes *et al.*, 1986).

An alternative approach for investigations into the role of PKC has been the use of inhibitors of the kinase. Staurosporine, 1-(5-isoquinolinesulphonyl)-2-methylpiperazine (H7), and related compounds have been found to be potent inhibitors of PKC (Savineau *et al.*, 1991; Souhrada & Souhrada, 1993). However, these inhibitors act at the catalytic domain of PKC, which carries a high degree of sequence homology with other protein kinases, and they are therefore relatively unselective for PKC itself (Shinamoto *et al.*, 1993). In contrast, several potent and selective inhibitors of PKC have now been described (Davis *et al.*, 1989). Two of these, namely Ro31-8220 and Ro31-7549, have been demonstrated to be more selective for PKC than for cAMP-dependent protein kinase and Ca^{2+}/calmodulin-dependent protein kinase, even though they are structured on staurosporine and inhibit PKC by competition with ATP for the co-substrate site.

Most studies in airway smooth muscle have been performed in large airways such as the trachea (e.g. Schramm & Grunstein, 1989; Morrison & Vanhoutte, 1991). However, it has been reported that contractions evoked by histamine or high [K^+] give a smaller response in the trachea than in the bronchus of the rabbit, with further variations down to the fourth branch of the bronchial tree (Fujiwara *et al.*, 1988). This suggests that there are regional differences in the functional properties of the airways analogous to those demonstrated in the pulmonary vascular tree (Leach *et al.*, 1992), and which could be of clinical relevance. In this study we have compared the response to agonists of small (~575 μm; fourth to fifth branch) and large (~1500 μm; second branch) bronchioles. The involvement of PKC in augmenting the

[1] Author for correspondence.

contractile response was examined by using the specific inhibitors of PKC, Ro31-8220 and Ro31-7549, to inhibit 4β-PDBu- and agonist-induced contractions. The action of Ro31-8220 was also compared with the non-selective PKC inhibitor, H7. Part of this work has been communicated to the British Pharmacological Society (Chopra et al., 1994).

Methods

Tissue preparations

Male Wistar rats (200–300 g) were anaesthetized with ether and the heart and lungs removed. Bronchioles of two sizes of internal diameter (small, 574 ± 11 μm, branch 4–5, $n = 128$: large, 1475 ± 32 μm, branch 2, $n = 93$) were dissected free of connective tissue and mounted on a Mulvaney–Halpen small vessel myograph using a technique modified from that previously described for small vessels (Leach et al., 1992). The tissues were bathed in a physiological saline solution (PSS) of composition (in mM): 118 NaCl, 24 $NaHCO_3$, 4 KCl, 1.8 $CaCl_2$, 1 $MgSO_4$, 0.43 NaH_2PO_4, 5 sodium-pyruvate and 5.56 glucose. The bath was aerated with a 95%O_2. 5%CO_2 gas mixture, pH 7.4, and the temperature held at 37°C. The degree of stretch was normalized for bronchiole size by setting each preparation to the peak of the length–tension curve using the following protocol. The bronchioles were incrementally stretched and challenged with PSS containing 75 mM K^+ (KPSS; equimolar substitution for Na^+). The bronchioles were stretched to the point where the maximum response to KPSS was achieved. Overstretching resulted in a decrease in the response.

Experimental protocol

At the start of each experimental procedure, KPSS was applied successively on three occasions, by which time the contractions were of similar magnitude. Results are expressed as a percentage of the last KPSS (T_K) reponse unless otherwise stated.

As previously reported (Chopra et al., 1993) 4β-PDBu (1 nM to 1 μM) alone had no effect on tension. However, after precontracting with 30 mM K^+ (equimolar substitution for Na^+), 0.5 μM 4β-PDBu did cause a contractile response. The inhibitory action of Ro31-8220 (1 nM to 10 μM) and H7 (1 μM–200 μM) on bronchioles precontracted with 30 mM K^+ + 0.5 μM 4β-PDBu was studied. After precontraction with 30 mM K^+ + 0.5 μM 4β-PDBu, the bronchioles were allowed to stabilize for 30 min. Thereafter, increasing concentrations of inhibitor were added every 30 min. The degree of relaxation was compared with time-matched controls. The effect of the non-active enantiomer of PDBu, 4α-PDBu, on tissues precontracted with 30 mM K^+ was also studied.

The contractile response to carbachol or 5-HT was investigated in both sizes of preparation by adding cumulative concentrations of carbachol (0.01–20 μM) or 5-HT (0.01–20 μM). Each concentration was left for 10 min, by which time the maximum contractile effect was observed. The effect of Ro31-8220, Ro31-7549 and H7 on the concentration–response curves was examined by pretreating the tissues with inhibitor for 20 min before the addition of agonist.

In other experiments the inhibitory action of Ro31-8220 (1 nM to 10 μM) on preparations precontracted with 0.5 μM carbachol was examined. After precontraction with carbachol the bronchioles were left for 30 min, by which time a stable contraction was achieved. Each concentration of inhibitor was then left for 30 min. The degree of relaxation was again compared with time-matched controls.

For three concentrations of carbachol (0.5, 1, 5 μM) the rate of decay of tension 30 min after addition of agonist was compared with tissues that had been pretreated with 10 μM Ro31-8220.

The effect of Ro31-8220 and H7 on the response to KPSS alone (75 mM K^+) were examined in preparations that had been pretreated with inhibitor for 15 min before challenge with KPSS.

Chemicals

Carbachol, 5-HT, H7, 4α-PDBu and 4β–PDBu were obtained from Sigma (UK). Ro31-8220 and Ro31-7549 were gifts from Roche Products Ltd. 4α-PDBu, 4β-PDBu, Ro31-8220 and Ro31-7549 were dissolved in dimethyl sulphoxide (DMSO). The maximum final concentration of DMSO was less than 0.1%, and in separate preliminary experiments was shown to have no effect on the contractility of either preparation.

Analysis of results

Results are expressed as arithmetic mean ± s.e.mean or geometric mean (95% confidence limits), and were tested for significance using Student's t-test for unpaired values or analysis of variance as appropriate. Differences were considered significant for $P \leqslant 0.05$. EC_{50} values were obtained from individual concentration–response curves as the concentration at which half-maximal tone occurred. These values were converted to logarithmic values (pD_2) for statistical analysis.

Results

Inhibition of the contractile response induced by 4β-PDBu by Ro31-8220, Ro31-7549 and H7

After precontracting with 30 mM K^+ (small: 38.5 ± 3.0% T_K; large: 24.3 ± 2.4% T_K, 0.05 μM 4β-PDBu caused a maximum contractile response of 110.4 ± 7.0% T_K ($n = 24$) in the small bronchioles and 69.3 ± 6.5% T_K ($n = 17$) in the large bronchioles. The inactive enantiomer 4α-PDBu had no effect on small or large bronchioles precontracted with 30 mM K^+ ($n = 4$). Ro31-8220 caused a concentration-dependent inhibition of the 30 mM K^+ + 0.5 μM 4β-PDBu response in both sizes of preparation. Ro31-8220 at 10 μM completely inhibited the phorbol ester response ($n = 8$) in small bronchioles (Figure 1a). In large bronchioles, 10 μM Ro31-8220 caused a large reduction but did not completely inhibit the response to 4β-PDBu ($n = 8$) (Figure 1b). The effect of Ro31-7549 was also examined in small bronchioles only, and had a similar effect to Ro31-8220 ($n = 8$) (Figure 1a).

H7 caused a concentration-dependent inhibition of the 30 mM K^+ + 0.5 μM 4β-PDBu response in both sizes of preparation. H7 at 200 μM completely inhibited the phorbol ester response in small and large bronchioles, but showed no signs of reaching a maximum effect ($n = 6$) (Figure 2a and b).

Ro31-8220, Ro31-7549 and H7 had no effect on basal tension in small and large bronchioles ($n = 16$).

Effect of PKC inhibitors on carbachol and 5-HT concentration–response curves

Concentration–response curves to carbachol (0.01–20 μM) and 5-HT (0.01–20 μM) were carried out in the absence and presence of Ro31-8220. In small bronchioles carbachol showed an EC_{50} of 0.500 (0.380–0.657) μM, with a maximal contraction of 161.8 ± 3.0% T_K at 10 μM ($n = 9$; Figure 3a). Large bronchioles had a similar EC_{50} of 0.582 (0.389–0.870) μM (Ns, $n = 8$), but a significantly small maximum response of 140.5 ± 4.6% T_K ($P < 0.01$; Figure 3b). In small bronchioles 1 μM Ro31-8220 reduced the maximal carbachol response to 110.8 ± 3.9% T_K ($P < 0.001$), with no significant change in EC_{50} [0.618 (0.483–0.789) μM], whereas 10 μM Ro31-8220 caused a significant shift to the right of the carbachol concentration–response curve [EC_{50} 0.976 (0.881–1.080) μM, $P < 0.001$] and further reduced the maximum response to 102.0 ± 4.5% T_K ($P < 0.001$) ($n = 8$; Figure

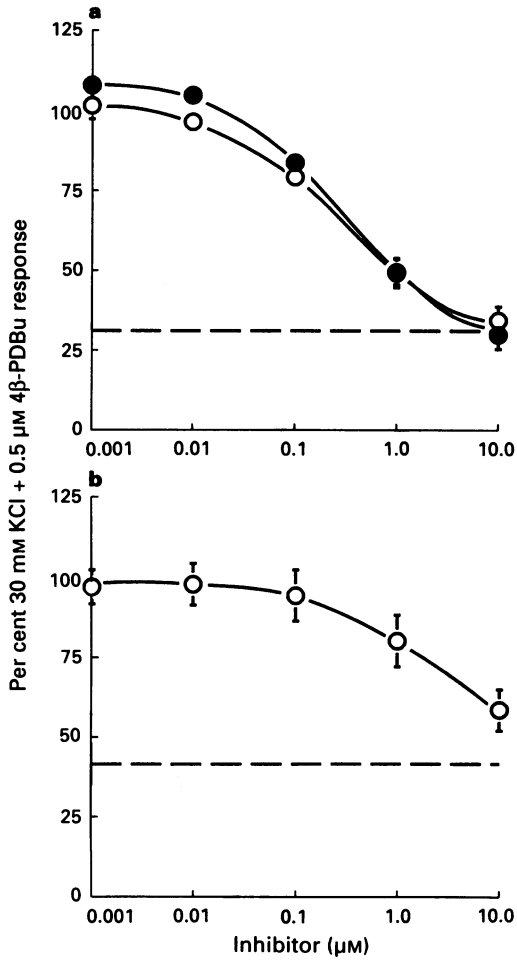


Figure 1 Inhibition of the contractile response to 30 mM K^+ + 0.5 μM 4β-PDBu using Ro31-8220 (○) and Ro31-7549 (●) in small (a) and large (b) bronchioles. The mean initial tone elicited by 30 mM K^+ before addition of 4β-PDBu or inhibitor is shown by the dotted line. Symbols represent the mean ± s.e.mean ($n = 8$). Where no error bars are shown the s.e.mean is smaller than the symbol size.

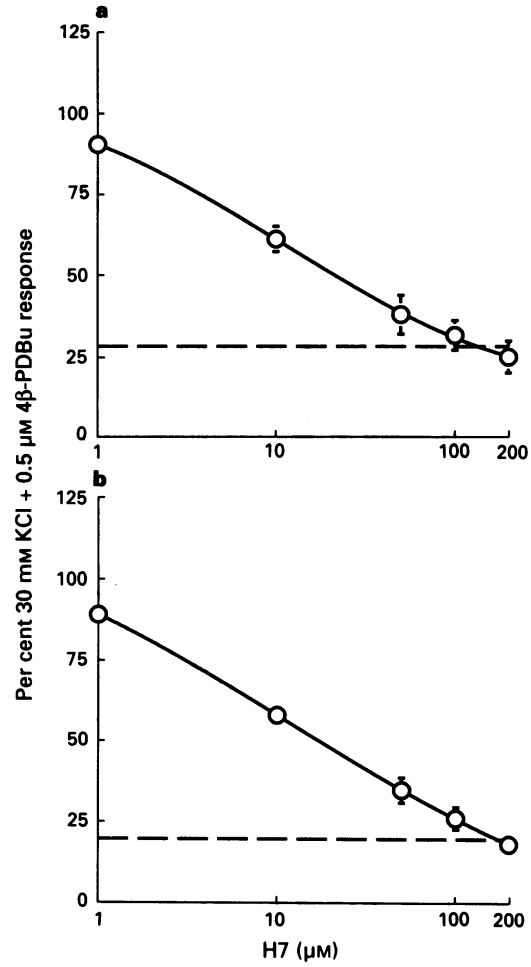


Figure 2 Inhibition of the contractile response to 30 mM K^+ + 0.5 μM 4β-PDBu using H7 in small (a) and large (b) bronchioles. The mean initial tone elicited by 30 mM K^+ before addition of 4β-PDBu or inhibitor is shown by the dotted line. Symbols represent the mean ± s.e.mean ($n = 6$). Where no error bars are shown the s.e.mean is smaller than the symbol size.

3a). In large bronchioles 1 μM Ro31-8220 had no significant effect on the response to carbachol, but 10 μM Ro31-8220 reduced the maximal carbachol response at 10 μM to 106.1 ± 5.2% T_K ($P<0.001$), although the shift in the EC_{50} did not reach significance [0.879 (0.732–1.055) μM, $n = 8$; Figure 3b].

Concentration–response curves to carbachol were also performed in the presence of H7. In both small and large bronchioles 200 μM H7 caused a shift to the right in the carbachol concentration–response curve [EC_{50}, small: 2.69 (2.41–3.00) μM, $P<0.001$; large: 2.20 (1.85–2.63) μM, $P<0.001$; $n = 6$] and altered the maximum response (small: 104.1 ± 2.1% T_K, $P<0.001$; large: 92.8 ± 5.3% T_K, $P<0.001$, $n = 6$) (Figure 3a and b).

Concentration–response curves to 5-HT (0.01–20 μM) were performed in the absence and presence of Ro31-8220. The maximum contraction to 10 μM 5-HT in small bronchioles was significantly greater than that in large bronchioles (small: 89.4 ± 6.7% T_K, $n = 6$; large: 69.3 ± 5.2% T_K, $P<0.05$, $n = 6$). The EC_{50} was greater in large bronchioles [small: 0.699 (440–1.120) μM; large: 1.18 (1.09–1.29) μM; $P<0.02$] (Figure 4a and b). In small bronchioles Ro31-8220 (10 μM) caused both a shift to the right in the concentration–response curve (EC_{50}, 1.23 (1.07–1.41) μM, $P<0.05$, and reduced the maximum response to 52.2 ± 4.7% T_K, $P<0.01$, $n = 6$) (Figure 4a), whereas in large bronchioles 10 μM Ro31-8220 had no significant effect on either the maximal 5-HT response or the EC_{50}, [52.3 ± 6.0% T_K, 1.12 (1.00–1.25) μM; $n = 6$] (Figure 4b).

Inhibition of the response to 0.5 μM carbachol by Ro31-8220 and Ro31-7549

Ro31-8220 and Ro31-7549 caused a concentration-dependent relaxation of pre-existing tone induced by 0.5 μM carbachol. In small bronchioles 10 μM Ro31-8220 decreased the tone by 58.5 ± 9.4% ($n = 9$) and 10 μM Ro31-7549 decreased it by 41.3 ± 7.5% ($n = 10$) (Figure 5). By way of comparison, in large bronchioles 1 μM Ro81-8220 only reduced the response to 0.5 μM carbachol by 8.1 ± 6.4% and 10 μM Ro31-8220 only by 12.2 ± 5.4% ($n = 6$) (data for large bronchioles not shown on figure).

Effect of Ro31-8220 on the rate of decay of the contraction to carbachol

Small bronchioles showed no reduction in contractile tone after 30 min following contraction with 0.5 μM carbachol, but there was a small yet significant relaxation following contraction with 1 and 5 μM carbachol; carbachol-induced tone in large bronchioles showed a more rapid rate of decay, with a significant reduction in tone after 30 min at all concentrations (Figure 6). In small bronchioles pretreated with 10 μM Ro81-8220 the rate of decay was more rapid at all three

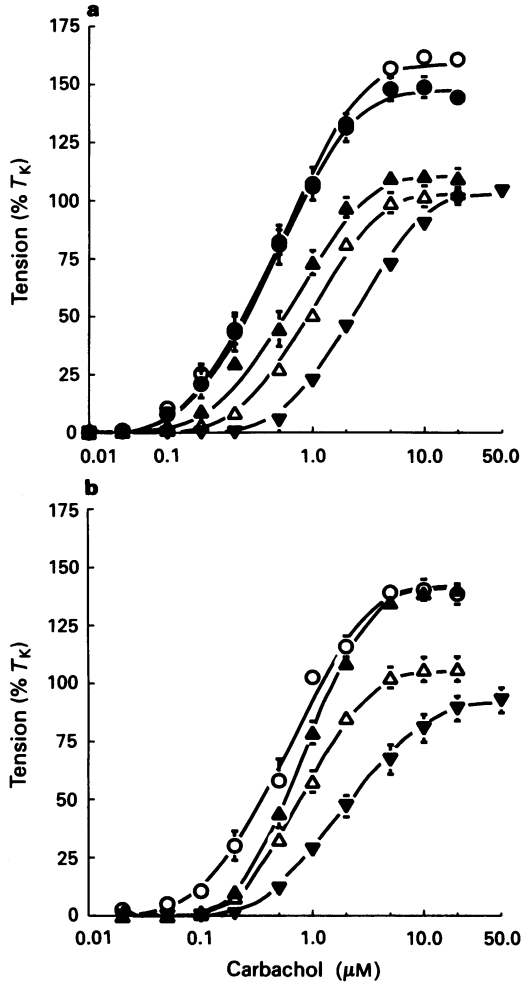


Figure 3 Effect of Ro31-8220 and H7 on the concentration-response curve to carbachol in small (a) and large bronchioles (b). The concentration response for carbachol alone (○) and in the presence of 0.1 μM Ro31-8220 (●), 1 μM Ro31-8220 (▲), 10 μM Ro31-8220 (△) and 200 μM H7 (▼). Symbols represent the mean ± s.e.mean ($n = 6-8$). Where no error bars are shown the s.e.mean is smaller than the symbol size.

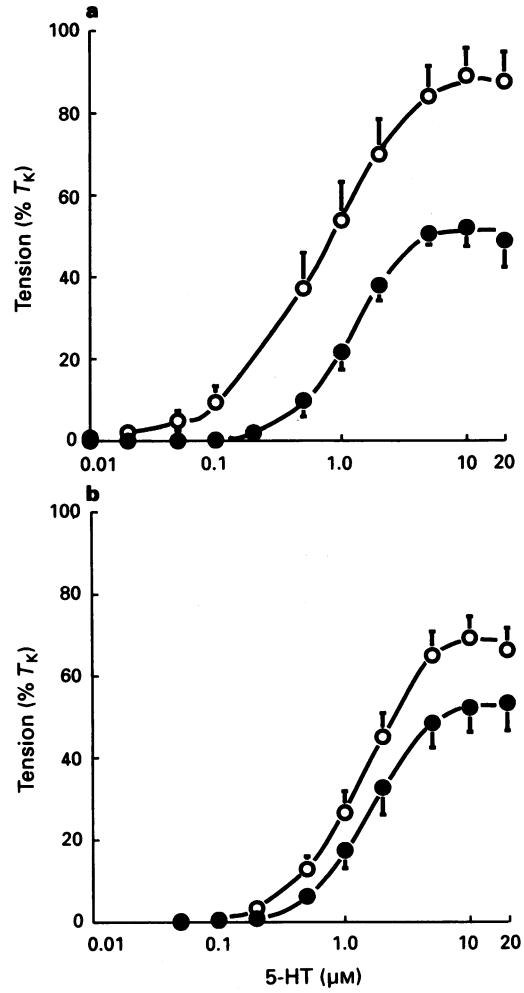


Figure 4 Effect of Ro31-8220 on the concentration response curve to 5-HT in small (a) and large bronchioles (b). Control concentration response to 5-HT (○). Concentration-response curve in the presence of 10 μM Ro31-8220 (●). Symbols represent the mean ± s.e.mean ($n = 6$). Where no error bars are shown the s.e.mean is smaller than the symbol size.

concentrations of carbachol studied (0.5, 1, 5 μM), but the difference between the rate of decay in control and pretreated tissues decreased with increasing concentration of carbachol ($n = 6$; Figure 6). In large bronchioles there was a significance difference between the rate of decay in control preparations and those pretreated with 10 μM Ro31-8220 following constriction with 0.5 μM carbachol, but not with 1 or 5 μM carbachol ($n = 6$; Figure 6).

Effect of Ro31-8220 and H7 on the response to KPSS

Pretreatment with 10 μM Ro31-8220 caused a small reduction in the response to KPSS in both small and large bronchioles (small: 87.8 ± 3.0% T_K, $n = 7$; large: 94.1 ± 0.8% T_K, $n = 6$). H7 caused a concentration-dependent inhibition of the response to KPSS, which was similar in small and large bronchioles. H7 at 200 μM reduced the response to 24.9 ± 3.0% T_K ($n = 8$) in small bronchioles and to 17.3 ± 0.6% T_K ($n = 6$) in large bronchioles.

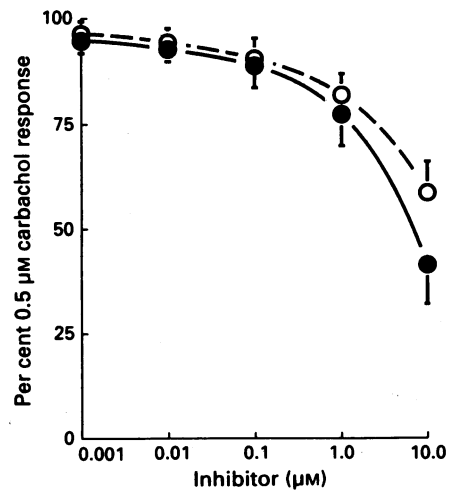


Figure 5 Inhibition of the contractile response to 0.5 μM carbachol using Ro31-8220 (○) and Ro31-7549 (●) in small bronchioles. Symbols represent the mean ± s.e.mean ($n = 9-10$).

Discussion

We have demonstrated in these experiments that there is a difference in some pharmacological responses between large (second branch) and small (fourth to fifth branch) bronchioles. Smaller bronchioles showed a greater sensitivity to carbachol and 5-HT as well as the phorbol ester 4β-PDBu,

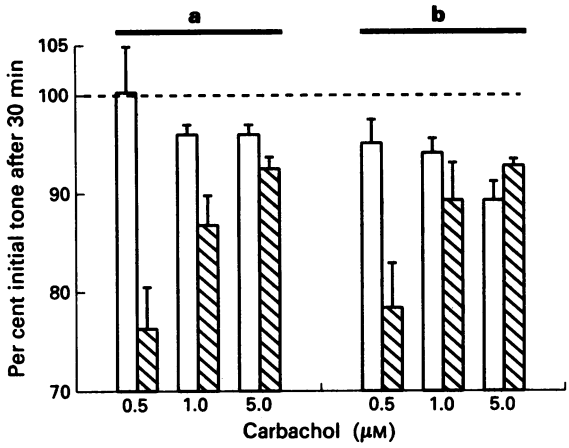


Figure 6 Decay in carbachol-induced tension after 30 min in small (a) and large (b) bronchioles under control conditions (open columns) compared with those pretreated with 10 μM Ro31-8220 (hatched columns). Tension is expressed in terms of the initial tension at zero time in the absence or presence of Ro31-8220 respectively. Bars represent the mean ± s.e.mean ($n = 6$ for each bar).

and were also found to have a slower rate of decay following contraction with carbachol than large bronchioles. We have also shown that the involvement of PKC in agonist-induced contraction is greater in small bronchioles than it is in large bronchioles.

In order for 4β-PDBu to have any effect in these preparations the bronchioles had to be precontracted with 30 mM K^+;thereafter 0.5 μM 4β-PDBu induced a large contraction. This is not unexpected as it has been established that an increased intracellular Ca^{2+} concentration can augment PKC sensitivity (Schramm & Grunstein, 1992). The results imply that the normal 'resting' intracellular [Ca^{2+}] in these preparations is too low for PKC activation on its own to have any contractile effect. This is in contrast to studies on vascular smooth muscle, in which phorbol esters can induce contraction without any prior depolarization (e.g. Savineau *et al.*, 1991).

As would be expected of PKC inhibitors, Ro31-8220, Ro31-7549 and H7 all showed concentration-dependent inhibition of the phorbol ester induced component of the 30 mM K^+ + 0.5 μM 4β-PDBu-induced contraction. However whereas H7 was equipotent in large and small bronchioles, such that 200 μM H7 completely abolished the 4β-PDBu response in both preparations, maximally effective Ro31-8220 (10 μM) only inhibited the response completely in small bronchioles; in large bronchioles it was not so effective. The actions of Ro31-8220 and Ro31-7549 were very similar; Ro31-7549 is closely structurally related to Ro31-8220 and would therefore be expected to show similar inhibitory properties (Davis *et al.*, 1992; Nixon *et al.*, 1992).

Ro31-8220 also shifted the carbachol and 5-HT concentration–response curves to the right as well as reducing the maximum response achieved. Small bronchioles were more sensitive to the inhibitor than were the larger preparations. After precontraction with carbachol, Ro31-8220 and Ro31-7549 induced a large relaxation in small bronchioles. However, 10 μM Ro31-8220 had only a limited effect in large bronchioles. These results suggest that a significant proportion of the constrictor effect of both carbachol and 5-HT is mediated via a mechanism that involves PKC. This was most apparent in the small bronchioles, in which 10 μM Ro31-8220 reduced the maximum contraction by approximately 40% for both agents (see Figures 3 and 4).

The differential effects between Ro31-8220 and H7 are to be expected as it is becoming increasingly apparent that H7 has a very poor selectivity for PKC (Bradshaw *et al.*, 1993; Shimamoto *et al.*, 1993). Whereas Ro31-8220 caused a small but significant inhibition of the response to KPSS, preincubation with H7 resulted in a profound depression. Depolarization of smooth muscle with high concentrations of K^+ induces contraction by increasing Ca^{2+} influx through voltage-operated Ca^{2+} channels, followed by activation of myosin light chain kinase. An increase in intracellular Ca^{2+} concentration is able to induce the translocation of PKC to the membrane without activating phosphoinositide hydrolysis (Takuwa *et al.*, 1986). The small reduction in the response to KPSS observed after pretreatment with Ro31-8220 may therefore be due to a component of the response being related to PKC translocation. Alternatively, it could be argued that this small inhibition is due to a non-selective action of Ro31-8220, although at the concentrations used Ro31-8220 has been shown to be very selective for PKC over other protein kinases (Wilkinson *et al.*, 1993). Whatever the mechanism, the effect is greater in small bronchioles than large bronchioles. Pretreatment with H7 clearly caused additional effects, indicating action sites other than PKC, and re-emphasizing the non-selective nature of H7.

As previously stated, small bronchioles had a slower rate of decay after constriction with carbachol than large bronchioles. PKC is thought to play a major role in the maintenance of agonist-induced tone, and the results shown in Figure 6 would be consistent with this, as the rate of decay following preincubation with Ro31-8220 was very much more rapid, at least for the lower concentrations of carbachol. However, carbachol undoubtedly also acts by mechanisms additional to those involving PKC (discussed below). At higher concentrations of carbachol these PKC-independent (Ro31-8220-insensitive) mechanisms may be responsible for a proportionally greater part of the constrictor response, as seen by comparing the control and 10 μM Ro31-8220 curves in Figure 3 for example. This may be reflected in the decreasing ability of Ro31-8220 to enhance the rate of decay at the higher concentrations of carbachol.

The increased sensitivity to Ro31-8220 in small bronchioles compared with large bronchioles could be attributed to either a difference in the contribution of PKC between the two sizes of preparation or a difference in the relative distributions of PKC isoenzymes. In smooth muscle α,β,ε and ξ isoenzymes have been identified (Andrea & Walsh, 1992). Ro31-8220 has been shown to preferentially inhibit PKC-α over PKC-β, -γ and -ε; it is equipotent for PKC-β, -γ and -ε (Wilkinson *et al.*, 1993). It could therefore be argued that the results reflect a difference in the spatial distribution of these PKC isoenzymes. However, various factors suggest that this is not the case. Firstly specific isoenzymes are thought to be activated by different agonists. In this study small bronchioles were more sensitive to Ro31-8220 than large bronchioles for all three agonists used: phorbol ester, carbachol and 5-HT. Secondly, the response to 4β-PDBu itself is larger in the smaller bronchioles. Thirdly, small bronchioles have a slower rate of decay after constriction with carbachol than large bronchioles; PKC-activated mechanisms are thought to play a major role in the maintenance of contraction. It is therefore likely that small bronchioles have a larger component of the contractile response that is dependent on PKC-dependent mechanisms.

As expected, neither Ro31-8220 nor the non-selective inhibitor H7 could completely inhibit the response to carbachol or 5-HT in either size of bronchiole. There is strong evidence that various agonists of airway smooth muscle cause both a release of Ca^{2+} from intracellular stores and Ca^{2+} entry across the membrane, resulting in a transient rise in intracellular [Ca^{2+}], followed by a smaller sustained plateau. Murray & Kotlikoff (1991) have demonstrated that histamine and bradykinin promote Ca^{2+} entry via receptor-operated mechanisms in human tracheobronchial smooth muscle, and it has been postulated that the opening of L-type-like Ca^{2+} channels induced by acetylcholine stimulation in dog tracheal smooth muscle contributes to the maintenance of the internal

Ca^{2+} store during agonist-induced contraction (Bourreau *et al.*, 1991). It is likely that refilling and cycling of Ca^{2+} in intracellular stores plays a major role in the response to agonists.

It has recently been proposed that phorbol esters may also directly affect Ca^{2+} stores. Stores in guinea pig trachea have shown that phorbol 12,13-diacetate (PDA) augments spasmogenic activity of methylxanthines and ryanodine (Cortijo *et al.*, 1994), and it was suggested that this was due to the phorbol ester facilitating release of Ca^{2+} from intracellular stores rather than stimulation of PKC. Although the current studies were on tonic rather than phasic tone, it is notable that 10 μM Ro31-8220 could completely inhibit 4β-PDBu induced tone in small, but not large bronchioles. There is also evidence that receptor agonists in vascular smooth muscle can activate a PKC-*independent* pathway which leads to Ca^{2+} sensitization (Hori *et al.*, 1993), although there have been no equivalent studies in airway smooth muscle. An investigation of this pathway using different kinase inhibitors is planned for future studies.

In conclusion, these results confirm that PKC is of major importance in the contractile mechanisms of airway smooth muscle. They also strongly suggest that there are significant differences in the pharmacological profile of large and small bronchioles, including the degree to which PKC is involved in agonist-induced contraction. This variation between small and large bronchioles should be taken into account when extrapolating from results obtained in large airway tissue such as trachea.

We thank the Wellcome Trust (Grant Ref: 034503) and the Special Trustees of St Thomas' Hospital for support, and Roche Products Ltd for the gifts of Ro31-8220 and Ro31-7549.

References

ANDREA, J.E. & WALSH, M.P. (1992). Protein kinase C of smooth muscle. *Hypertension*, **20**, 585–595.

BERRIDGE, M.J. & IRVINE, R.F. (1984). Inositol trisphosphate, a novel second messenger in cellular signal transduction. *Nature*, **312**, 315–321.

BOURREAU, J.-P., ABELA, A.P., KWAN, C.Y. & DANIEL, E.E. (1991). Acetylcholine Ca^{2+} stores refilling directly involves a dihydropyridine-sensitive channel in dog trachea. *Am. J. Physiol.*, **261**, C497–C505.

BRADSHAW, D., HILL, C.H., NIXON, J.S. & WILKINSON, S.E. (1993). Therapeutic potential of protein kinase C inhibitors. *Agents Action*, **38**, 135–147.

CASTAGNA, M., TAKAI, Y., KAIBUCHI, U., SANO, K., KIKKAWA, U. & NISHIZUKA, Y. (1982). Direct activation of calcium-activated, phospholipid-dependent protein kinase by tumour-promoting phorbol esters. *J. Biol. Chem.*, **257**, 7847–7851.

CORTIJO, J., SANZ, C.M., VILLAGRASA, V., MORCILLO, E.J. & SMALL, R.C. (1994). The effects of phorbol 12,13-diacetate on responses of guinea-pig isolated trachea to methylxanthines, isoprenaline and ryanodine. *Br. J. Pharmacol.*, **111**, 769–776.

CHOPRA, L.C., TWORT, C.H.C. & WARD, J.P.T. (1993). Investigation of the action of phorbol ester on small bronchioles using a small vessel myograph. *Am. Rev. Respir. Dis.*, **147** (4), A54.

CHOPRA, L.C., TWORT, C.H.C. & WARD, J.P.T. (1994). Inhibition of contraction by PKC inhibitors, Ro31-8220 and Ro31-7549 in small and large bronchioles of the rat. *Br. J. Pharmacol.*, **112**, 80P.

DAVIS, P.D., HILL, C.H., KEECH, E., LAWTON, G., NIXON, J.S., SEDGWICK, A.D., WADSWORTH, J., WESTMACOTT, D. & WILKINSON, S.E. (1989). Potent selective inhibitors of protein kinase C. *FEBS Lett.*, **259**, 61–63.

DAVIS, P.D., ELLIOT, L.H., HARRIS, W., HILL, C.H., HURST, S.A., KEECH, E., HARI KUMAR, M.K., LAWTON, G., NIXON, J.S. & WILKINSON, S.E. (1992). Inhibitors of protein kinase C. 2. Substituted bisindolylmaleimides with improved potency and selectivity. *J. Med. Chem.*, **35**, 994–1001.

FUJIWARA, T., ITOH, T. & KURIYAMA, H. (1988). Regional differences in the mechanical properties of rabbit airway smooth muscle. *Br. J. Pharmacol.*, **94**, 389–396.

HORI, M., SATO, K., MIYAMOTO, S., OZAKI, H. & KARAKI, H. (1993). Different pathways of calcium sensitization activated by receptor agonists and phorbol ester in vascular smooth muscle. *Br. J. Pharmacol.*, **110**, 1527–1531.

LEACH, R.M., TWORT, C.H.C., CAMERON, I.R. & WARD, J.P.T. (1992). A comparison of the pharmacological and mechanical properties *in vitro* of large and small pulmonary arteries of the rat. *Clin. Sci.*, **82**, 55–62.

MENKES, H., BARABAN, J.M. & SNYDER, S.H. (1986). Protein kinase C regulates smooth muscle tension in guinea-pig trachea and ileum. *Eur. J. Pharmacol.*, **122**, 19–27.

MORRISON, K.J. & VANHOUTTE, P.M. (1991). Inhibition of airway smooth muscle tone by a phorbol ester in the Guinea pig trachea: role of epithelium and receptor reserve of the contractile agent. *J. Pharmacol. Exp. Ther.*, **259**, 198–204.

MURRAY, R.K. & KOTLIKOF, M.J. (1991). Receptor activated calcium influx in human airway smooth muscle cells. *J. Physiol.*, **435**, 123–144.

NISHIZUKA, Y. (1986). Studies and perspectives of protein kinase C. *Science*, **233**, 305–312.

NIXON, J.S., BISHOP, J., BRADSHAW, D., DAVIS, P.D., HILL, C.H., ELLIOTT, L.H., KUMAR, H., LAWTON, G., LEWIS, E.J., MULQUEEN, M., WESTMACOTT, D., WADSWORTH, J. & WILKINSON, S.E. (1992). The design and biological properties of potent and selective inhibitors of protein kinase C. *Biochem. Soc. Trans.*, **20**, 419–425.

SAVINEAU, J.-P., MARTHAN, R. & CREVEL, H. (1991). Contraction of vascular smooth muscle induced by phorbol 12,13 dibutyrate in human and rat pulmonary arteries. *Br. J. Pharmacol.*, **104**, 639–644.

SCHRAMM, C.M. & GRUNSTEIN, M.M. (1989). Mechanisms of protein kinase C regulation of airway contractility. *J. Appl. Physiol.*, **66** (4), 1935–1941.

SCHRAMM, C.M. & GRUNSTEIN, M.M. (1992). Assessment of signal transduction mechanisms regulating airway smooth muscle contractility. *Am. J. Physiol.*, **262**, L119–L139.

SHIMAMOTO, Y., SHIMAMOTO, H., KWAN, C.-Y. & DANIEL, E.E. (1993). Differential effects of putative protein kinase C inhibitors on contraction of rat aortic smooth muscle. *Am. J. Physiol.*, **264**, H1300–H1306.

SOUHRADA, M. & SOUHRADA, J.F. (1993). Inhibitory effect of staurosporine on protein kinase C stimulation of airway smooth muscle cells. *Am. Rev. Respir. Dis.*, **148**, 425–430.

TAKUWA, Y., TAKUWA, N. & RASMUSSEN, H. (1986). Carbachol induces a rapid and sustained hydrolysis of polyphosphoinositide in bovine tracheal smooth muscle measurements of the mass of polyphosphoinositides, 1,2,-diacylglycerol and phosphatidic acid. *J. Biol. Chem.*, **261**, 14670–14675.

WILKINSON, S.E., PARKER, P.J. & NIXON, J.S. (1993). Isoenzyme specificity of bisindolylmaleimides, selective inhibitors of protein kinase C. *Biochem. J.*, **294**, 335–337.

(Received May 9, 1994
Accepted August 11, 1994)

Br. J. Pharmacol. (1994), **113**, 1243–1248 © Macmillan Press Ltd, 1994

Calcitonin gene-related peptide receptors in human gastrointestinal epithelia

[1]H.M. Cox & I.R. Tough

Department of Pharmacology, The Royal College of Surgeons of England, 35–43, Lincoln's Inn Fields, London WC2A 3PN

1 The secretory responses to calcitonin gene-related peptide (CGRP) receptor agonists have been characterized in two human adenocarcinoma cell lines, namely HCA-7 and Colony-29 (Col-29) epithelia. These cells form polarized epithelial layers when grown on permeable supports and allow changes in electrogenic ion transport in response to agonists to be monitored continuously.

2 α-CGRP (rat and human sequences), rat β-CGRP and human [Tyr^0]CGRP applied to the basolateral surface were found to be full agonists, causing prolonged increases in short-circuit current. Concentration–response curves exhibited EC_{50} values of 0.6–1.5 nM in HCA-7 cells. The same agonists were less effective in Col-29 epithelia, the EC_{50} values ranging from 1 to 10 nM in these cells. [Cys(ACM)^{2,7}]CGRP was effective in both cell lines and was more potent in HCA-7 cells.

3 CGRP receptors were preferentially located on the basolateral surface in both cell types. Addition of rα-CGRP to the apical domain produced significantly smaller secretory responses (8.1% in HCA-7 and 29.2% in Col-29) compared with those produced following basolateral application (100%).

4 In both cell lines rα-CGRP-elevated short-circuit current was inhibited by the loop diuretic piretanide (200 μM) and by somatostatin (100 nM). Pretreating epithelia with the cyclo-oxygenase inhibitor, piroxicam (5 μM) had no significant effect upon CGRP responses in either cell line.

5 Rat α-CGRP (0.2 nM) responses in HCA-7 epithelia were inhibited by the C-terminal fragment CGRP(8–37) (1 μM). Pretreatment of Col-29 cells with CGRP(8–37) did not, however, alter the size or profile of responses to rα-CGRP (1 nM).

6 We conclude that high-affinity CGRP receptors exist on the basolateral surface of both cell lines, however they differ in their sensitivity to CGRP(8–37) and agonist orders of potency. Thus different CGRP receptor subtypes appear to predominate in these two epithelial cell types.

Keywords: Calcitonin gene-related peptide; CGRP receptors; colonic epithelia; ion transport

Introduction

Calcitonin gene-related peptide (CGRP) is an enteric neuropeptide found in cell bodies present in both the myenteric and the submucous ganglia, and in varicose nerve fibres located in the mucosa and circular smooth muscle but not the outer longitudinal smooth muscle of the rat colon (Ekblad *et al.*, 1988). Differential peptide expression has been observed in the rat alimentary canal, α-CGRP being preferentially expressed by sensory neurones while β-CGRP is present predominantly in intrinsic enteric neurones (Mulderry *et al.*, 1988). The presence of CGRP-like immunoreactivity in the colonic mucosa (where a subpopulation of CGRP-positive submucous neurones also contain somatostatin; Ekblad *et al.*, 1988) suggested a role for these peptides in the control of epithelial function. Earlier studies with α- and β-CGRP identified a bifunctional concentration–response curve in preparations of rat colon mucosa (Cox *et al.*, 1989). At low concentrations (pM), both peptides produced antisecretory responses that were abolished by tetrodotoxin (TTX) and at higher concentrations (nM) a secretory epithelial effect was observed which was insensitive to TTX. In the guinea pig colon, in contrast, the secretory effects observed with human (h) αCGRP were predominantly mediated via myenteric neurones (McCulloch & Cooke, 1989).

In order to study epithelial CGRP receptors in the absence of other mucosal cell types we have used two adenocarcinoma cell lines which, when grown to confluence on permeable supports, respond to a range of secretory (Cuthbert *et al.*, 1987; MacVinish *et al.*, 1993) and antisecretory (H.M. Cox, unpublished observations) agonists. The two stable cell lines used were the parent primary human colonic adenocarcinoma (HCA) line (HCA-7, Kirkland, 1985) and a subpopulation isolated from this cell line called Colony-29 (Col-29). Both epithelial cell lines responded to CGRP peptides with an increase in short-circuit current (s.c.c.; Cox & Tough, 1994), the profile of which was similar to CGRP responses observed in rat colon mucosa in the presence of TTX (Cox *et al.*, 1989). The aim of this study was to characterize pharmacologically epithelial CGRP receptors, establish their basolateral and/or apical location and, in so doing, identify the cell line most similar to normal epithelia with respect to CGRP receptor type.

[1] Author for correspondence.

Methods

Cell culture and short-circuit current (s.c.c.) measurement

Cells were seeded into culture flasks (25 cm^2) suspended and subsequently maintained in Dulbecco's modified Eagle medium (DMEM, Gibco, Paisley, U.K.) containing fetal calf serum (10%) kanamycin (100 μg ml^{-1}) and amphotericin B (1.2 μg ml^{-1}). Once confluent, cells were treated with trypsin (0.5%, w/v) and versene and seeded ($4–6 \times 10^5$ cells in 100 μl) onto collagen-coated millipore filters (as described in detail by Cuthbert *et al.*, 1987). HCA-7 and Col-29 epithelia reached confluence within 7–10 days when grown on filters, and both cell lines were used within passages 20–25 for HCA-7 and 18–30 for Col-29. Confluent epithelia on filters were gently positioned between two halves of Ussing chambers and bathed in oxygenated (95% O_2/5% CO_2) Krebs–Henseleit (KH) solution, pH 7.4, at 37°C. All

preparations were voltage clamped at zero potential (WP Instruments, Sarasota, FL, U.S.A.) and the resultant s.c.c. was continuously recorded on pen recorders (Cuthbert *et al.*, 1987). Each side of the epithelial layers were bathed in 15 ml of KH and peptides and other drugs were added to either the basolateral or apical reservoir to provide the final concentrations quoted. When cell layers were pretreated with inhibitors the pretreatment drug was added 15 min prior to addition of rα-CGRP without intermediate washing, and subsequent responses to rα-CGRP were compared with controls obtained in the absence of inhibitor. Changes in s.c.c. are given as $\mu A\,cm^{-2}$ and concentration–response curves constructed from single additions of peptide per filter were analysed using the iterative curve-fitting program, Graphpad. Unpaired Student's *t*-test was used for statistical analysis of data and a *P*-value of less than 0.05 was considered statistically significant.

Materials

KH solution had the following composition (in mM): NaCl 118, KCl 4.7, $CaCl_2$ 2.5, $MgSO_4$ 1.2, $NaHCO_3$ 25.0 and glucose 11.1. All peptides were purchased from Peninsula, and stock solutions in sterile water were diluted, frozen as aliquots and stored at −20°C. Piroxicam, collagen and forskolin were supplied by Sigma, and piretanide was a generous gift from Hoechst Pharmaceuticals. Trypsin was purchased from Worthington Biochemical Corporation.

Results

Agonist concentration–response relationships

The transepithelial baseline s.c.c. and resistance values for the epithelial layers were, for HCA-7, $6.0 \pm 0.9\,\mu A\,cm^{-2}$ ($n = 24$) and $117.1 \pm 10.1\,\Omega\,cm^2$ ($n = 24$) respectively, and for Col-29 values $8.8 \pm 0.8\,\mu A\,cm^{-2}$ ($n = 24$) and $61.5 \pm 2.7\,\Omega\,cm^2$ ($n = 24$) respectively. The secretory responses stimulated by rat (r) and human (h) α-CGRP and rβ-CGRP in both epithelial cell lines were initially rapid, reaching a maximum within 5 min of addition of peptide to the basolateral surface (Figures 1 and 2). All agonist responses were long-lasting, the s.c.c. staying elevated above the original baseline for more than 1 h after peptide addition. Representative traces of different CGRP analogues are shown in Figure 1 for HCA-7 and in Figure 2 for Col-29 epithelia. The concentration–response relationships with each agonist were different in the two cell lines (Figure 3a–f). HCA-7 epithelia were significantly more sensitive than Col-29 cells to rα- and rβ-CGRP and hα-CGRP, but not to h[Tyr^0]CGRP. The maxima from each concentration–response curve were higher for all four agonists in HCA-7 than in Col-29 epithelia. Salmon (s) calcitonin and h[$Cys(ACM)^{2,7}$]CGRP were also more potent in HCA-7 than in Col-29 cells. The maxima from s-calcitonin response curves in both cell lines were lower than those obtained with other agonists. The EC_{50} values calculated from each agonist concentration–response curve are shown in Table 1.

Sidedness of rα-CGRP responses

Responses to apically applied rα-CGRP (3 nM with HCA-7 and 30 nM with Col-29) were significantly smaller ($1.0 \pm 0.2\,\mu A\,cm^{-2}$, $n = 4$, and $2.7 \pm 0.5\,\mu A\,cm^{-2}$, $n = 6$, respectively) than those to basolaterally applied agonist ($12.4 \pm 1.3\,\mu A\,cm^{-2}$, $n = 15$, in HCA-7 and $9.4 \pm 0.7\,\mu A\,cm^{-2}$, $n = 20$, in Col-29). The peak heights of responses to basolateral rα-CGRP were not significantly altered by apical rα-CGRP pretreatment in HCA-7 cells, though there was a significant inhibition ($P < 0.01$) observed in Col-29 epithelia (Figure 4a and b). Responses to apical rα-CGRP were significantly attenuated in both cell lines following basolateral peptide pretreatment (Figure 4a and b).

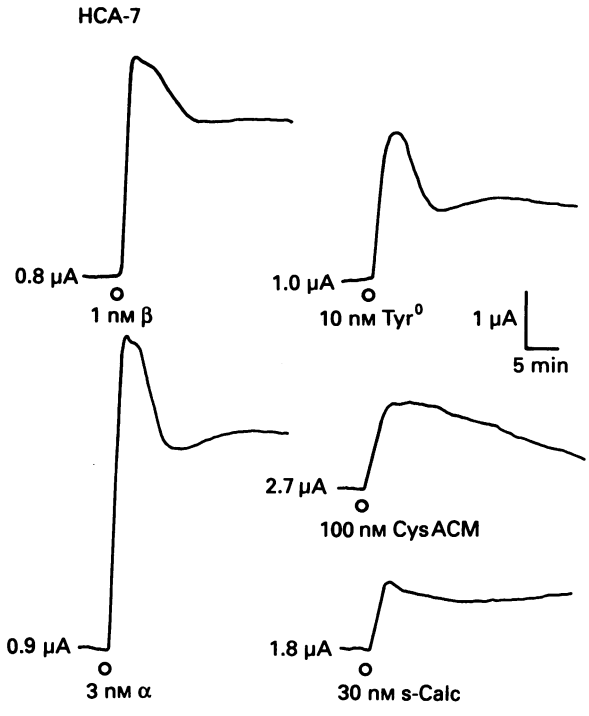


Figure 1 Representative traces from HCA-7 epithelia following basolateral addition of five different agonists, namely: rβ-CGRP (1 nM, β) rα-CGRP (3 nM, α) h[Tyr^0]CGRP (10 nM, Tyr^0) h[$Cys(ACM)^{2,7}$]CGRP (100 nM, CysACM) and s-calcitonin (30 nM, s-Calc). The concentrations chosen were those at, or close to, the maximum for each peptide–response curve. The baseline s.c.c. values are shown to the left of each trace and were obtained from epithelial layers covering an area of $0.2\,cm^2$.

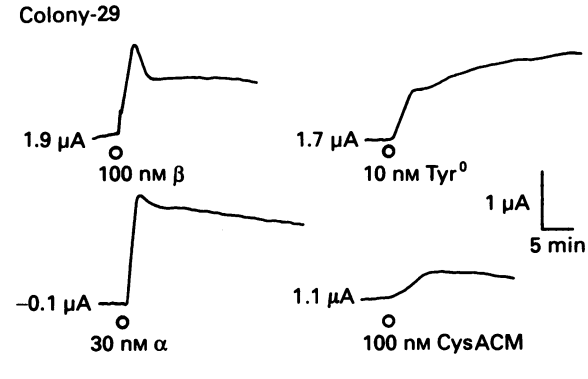


Figure 2 Representative traces from Col-29 epithelia following basolateral addition of four different agonists, namely: rβ-CGRP (100 nM, β) h[Tyr^0]CGRP (10 nM, Tyr^0) rα-CGRP (30 nM, α) and h[$Cys(ACM)^{2,7}$]CGRP (100 nM, CysACM). The concentrations chosen were those at the maximum of each peptide–response curve. The baseline s.c.c. values are shown to the left of each trace.

Effect of piroxicam and somatostatin upon basal s.c.c.

Pretreating cells with the cyclo-oxygenase inhibitor, piroxicam (5 μM added to both surfaces) resulted in minor reductions in the basal s.c.c. ($-0.3 \pm 0.05\,\mu A\,cm^{-2}$ in HCA-7, $n = 5$; and $-1.8 \pm 0.7\,\mu A\,cm^{-2}$ in Col-29, $n = 6$). Somatostatin 14–28 (100 nM, basolaterally) reduced basal s.c.c. by $-1.7 \pm 0.5\,\mu A\,cm^{-2}$ ($n = 5$, from a baseline of $3.2 \pm 1.3\,\mu A\,cm^{-2}$) in HCA-7 and by $-2.9 \pm 0.5\,\mu A\,cm^{-2}$ ($n = 6$, from a baseline of $9.9 \pm 3.2\,\mu A\,cm^{-2}$) in Col-29 cells.

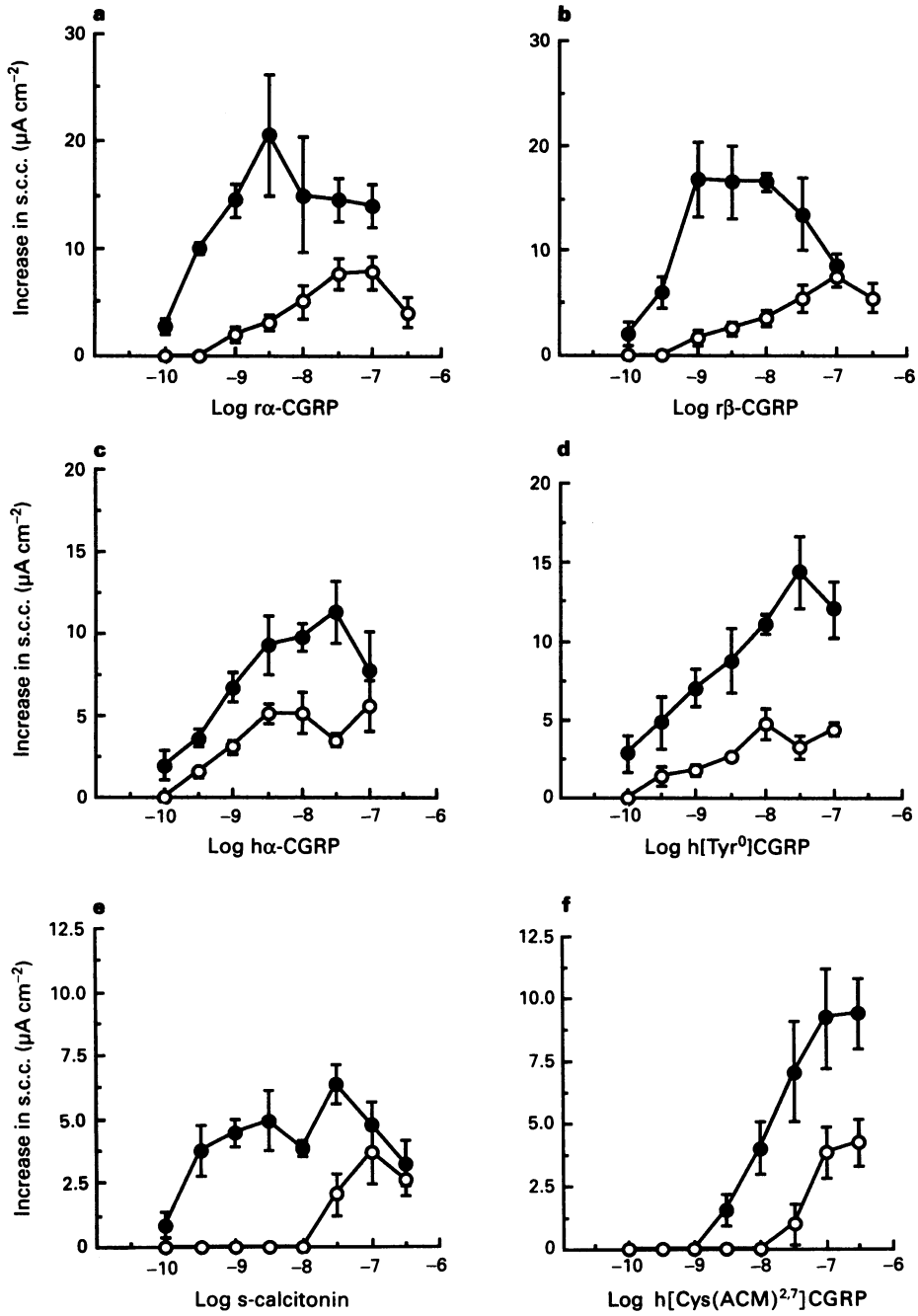


Figure 3 Concentration–response curves in HCA-7 (●) and Col-29 (○) epithelia in response to (a) rα-CGRP, (b) rβ-CGRP, (c) hα-CGRP, (d) h[Tyr^0]CGRP, (e) s-calcitonin and (f) h[Cys-(ACM)^{2,7}]CGRP. Each point represents the mean ± s.e.mean and n values were between 4 and 12 for each concentration of peptide.

Effects of piretanide, piroxicam and somatostatin upon responses to rα-CGRP

The stimulated s.c.c. levels achieved following either apical or basolateral rα-CGRP (3 nM in HCA-7 and 30 nM in Col-29 cells) were reduced by the loop diuretic piretanide (200 μM) applied to the basolateral surface. In HCA-7 epithelia, piretanide reduced the elevated s.c.c. by $-1.8 \pm 0.3\ \mu A\ cm^{-2}$ ($n = 8$) and in Col-29 cells by $-2.1 \pm 0.7\ \mu A\ cm^{-2}$ ($n = 8$) from baselines of $4.5 \pm 0.8\ \mu A\ cm^{-2}$ ($n = 8$) and $7.9 \pm 1.8\ \mu A\ cm^{-2}$ ($n = 8$) respectively. In piroxicam-pretreated epithelia rα-CGRP-stimulated responses were not significantly altered from controls ($13.5 \pm 2.4\ \mu A\ cm^{-2}$, in HCA-7, $n = 4$; and $10.2 \pm 1.1\ \mu A\ cm^{-2}$, in Col-29, $n = 12$, Figure 5a and b). Similarly, pretreatment with somatostatin (100 nM, basolateral) did not alter rα-CGRP responses in either cell line (Figure 5a and b). However, basolateral addition of rα-CGRP (at the same concentrations used above) potentiated the s.c.c. responses to somatostatin in HCA-7 cells ($-6.7 \pm 1.1\ \mu A\ cm^{-2}$, $n = 6$, $P < 0.01$, from an elevated s.c.c. of $19.6 \pm 3.1\ \mu A\ cm^{-2}$) but inhibited the response to this agonist in Col-29 epithelia ($-1.4 \pm 0.4\ \mu A\ cm^{-2}$, $n = 9$, $P < 0.05$, from an elevated s.c.c. level of $14.6 \pm 3.5\ \mu A\ cm^{-2}$).

Effects of CGRP(8–37) on rα-CGRP and forskolin responses

The C-terminal fragment of hα-CGRP, CGRP(8–37), was tested in both cell lines. When added to the basolateral surface at 500 nM the fragment reduced the basal s.c.c. by $-1.8 \pm 0.7\ \mu A\ cm^{-2}$ ($n = 8$) in HCA-7 and by $-1.6 \pm 0.7\ \mu A\ cm^{-2}$ ($n = 7$) in Col-29. If each epithelial layer was

pretreated with basolateral rα-CGRP (3 nM to HCA-7 and 30 nM to Col-29) subsequent CGRP(8–37) (500 nM) responses were significantly enhanced in HCA-7 (-3.7 ± 0.5 μA cm^{-2}, $n = 7$, $P < 0.02$) but not altered in Col-29 cells (-0.8 ± 0.3 μA cm^{-2}, $n = 10$, $P > 0.05$). At the higher concentration of 1 μM, CGRP(8–37) significantly inhibited responses to rα-CGRP (0.2 nM) in HCA-7 ($P < 0.001$) but had no effect upon responses to rα-CGRP (1 nM) in Col-29 ($P > 0.3$, Figure 6a and b). CGRP(8–37) at 1 μM had no significant effect upon forskolin-induced increases in s.c.c. in either cell line (Figure 6).

Table 1 Order of agonist potencies for CGRP analogues in HCA-7 in Col-29 epithelia

Analogue	EC_{50} (nM) *HCA-7*	*Col-29*
rα-CGRP	0.6	4.4
rβ-CGRP	0.5	9.8
hα-CGRP	0.7	4.0
h[Tyr^0]CGRP	1.5	1.4
h[Cys(ACM)^{2,7}]CGRP	134.0	>300.0
s-Calcitonin	0.3*	>300.0*
hCGRP(8–37)	–	–

Concentration-response curves (Figures 1 and 2) were constructed from single applications of peptide made to the basolateral surface of epithelial cell layers. The maximum increase in s.c.c. obtained within 15 min of peptide addition was taken as the response and the results averaged for each peptide concentration (where n values were between 4 and 12). Data were analysed using the iterative curve fitting program, Graphpad. The species of origin of each peptide is included; r, rat; h, human and s, salmon. An asterisk identifies response curves where the maxima were reduced compared with r- and hα- rβ-CGRP and h[Tyr^0]CGRP.

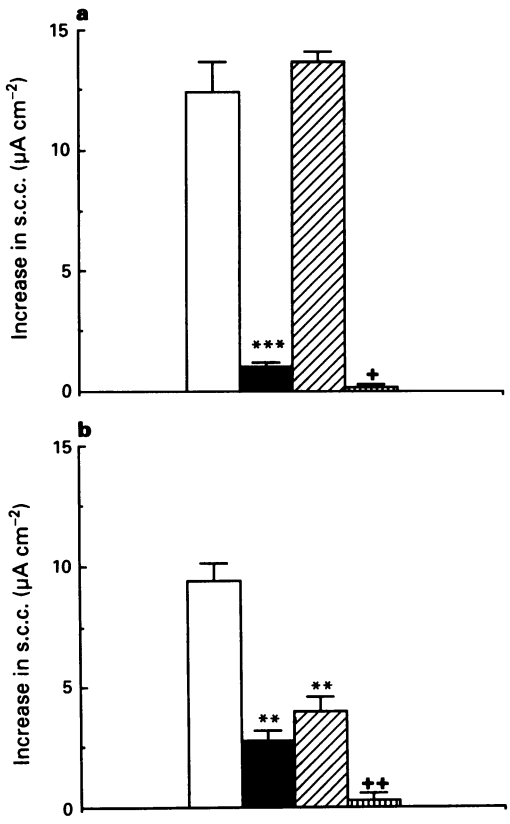


Figure 4 Peak increases in s.c.c. following either basolateral or apical addition of rα-CGRP in (a) HCA-7 and (b) Col-29 cells. The concentration of rα-CGRP was 3 nM for HCA-7 and 30 nM for Col-29 epithelia. Each column represents the mean with 1 s.e.mean. Open columns are basolateral controls ($n = 15$ in a and 20 in b). Solid columns are apical rα-CGRP responses ($n = 4$ in a and 6 in b). Cross-hatched columns are basolateral responses obtained from apically pretreated cells ($n = 4$ in a and 6 in b), while vertical hatched columns are apical rα-CGRP responses after basolateral pretreatment ($n = 4$ in a and 5 in b). Significant differences compared with control basolateral CGRP responses are, $^{***}P < 0.001$ and $^{**}P < 0.01$. Comparison of control apical and apical following basolateral rα-CGRP were also significantly different: $^{+}P < 0.05$ and $^{++}P < 0.01$.

Discussion

α- and β-CGRP (and their analogues) produced prolonged increases in s.c.c. in two epithelial cell lines, and these responses resembled the changes in s.c.c. observed in mucosal preparations from the rat descending colon in the presence of TTX (Cox *et al.*, 1989). The raised s.c.c. levels obtained following basolateral rα-CGRP were attenuated by basolateral addition of piretanide, in a manner analogous to that observed for piretanide inhibition of vasoactive intestinal polypeptide responses in HCA-7 epithelia (Cuthbert *et al.*, 1987). The loop diuretic inhibited rα-CGRP elevated s.c.c. in both cell lines by blocking Cl^- entry via the basolateral co-transporter and, consequently, indirectly inhibiting Cl^- secretion through apical channels. This process is, we presume, primarily responsible for the electrogenic responses recorded. The potencies of r- and hα- and rβ-CGRP used in this study were all greater in HCA-7 than Col-29 epithelia. The latter are a subpopulation of cells derived from HCA-7 and thus the parent cell line probably expresses the CGRP receptor subtype present in Col-29 together with another

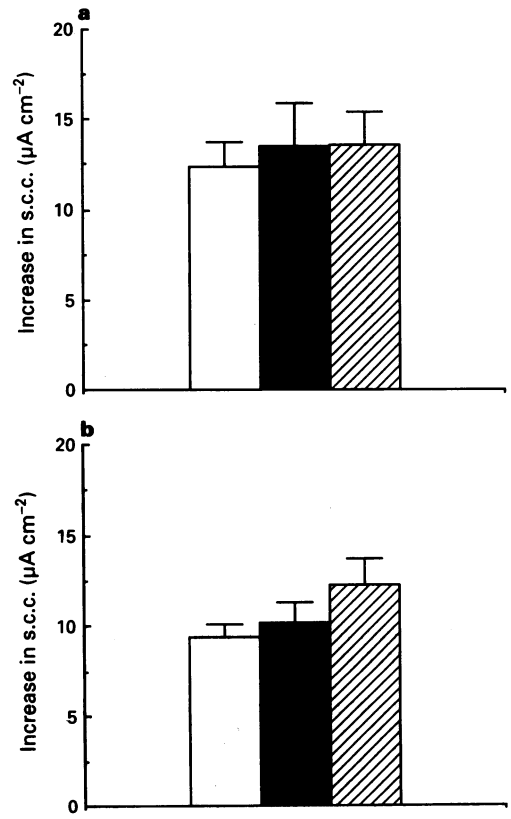


Figure 5 The effect of piroxicam (5 μM, added to both sides) and basolateral somatostatin 14–28 (100 nM) pretreatment upon rα-CGRP responses (3 nM and 30 nM respectively) in HCA-7 (a) and Col-29 cells (b). Each column represents the mean ± s.e.mean, and open columns are control rα-CGRP responses ($n = 15$ and 20 in a and b respectively). Solid columns represent CGRP responses following piroxicam ($n = 4$ and 12) and cross-hatched columns following somatostatin pretreatment ($n = 5$ and 6).

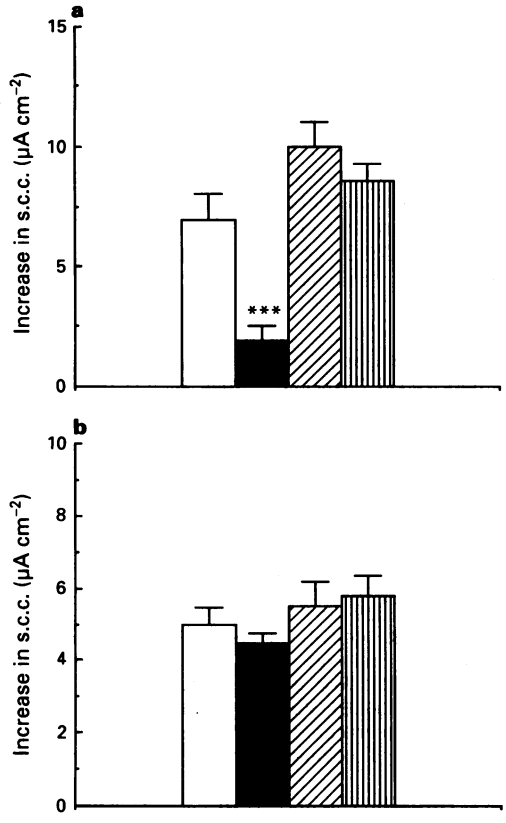


Figure 6 The effect of pretreating HCA-7 (a) and Col-29 (b) epithelia with 1 μM CGRP(8–37) upon either rα-CGRP (0.2 nM in HCA-7 or 1 nM in Col-29) or forskolin-mediated secretory responses (10 μM, basolateral). Each column represents the mean ± s.e.mean, and open and cross-hatched columns represent control rα-CGRP ($n = 5$ and 4 in a and b) and forskolin ($n = 5$ and 4) respectively. Solid and vertical hatched columns are CGRP(8–37) pretreated, rα-CGRP and forskolin responses ($n = 6$ and 4) respectively. ***$P < 0.001$.

predominant subtype. h[Tyr^0]CGRP exhibited similar EC_{50} values in HCA-7 and Col-29 (1.5 and 1.4 nM respectively). In HCA-7 epithelia the order agonist potency was rβ-CGRP ≥ rα-CGRP ≥ hα-CGRP > h[Tyr^0]CGRP >> h[Cys(ACM)^{2,7}]CGRP, whereas in Col-29 it was h[Tyr^0]CGRP > hα-CGRP ≥ rα-CGRP ≥ rβ-CGRP >> h[Cys(ACM)^{2,7}]CGRP. The linear peptide h[Cys(ACM)^{2,7}]CGRP was also more potent in HCA-7 than Col-29 epithelia, as was s-calcitonin. s-Calcitonin could either be stimulating specific calcitonin receptors (if these are present in both cell lines) or, alternatively, could be acting as a partial agonist upon HCA-7 and Col-29 cells (since both maxima were lower than those obtained with other agonists). It is possible that the two cell lines may express different peptidases which may result in differential agonist degradation. This may in turn contribute to slight differences in the order of agonist potency and could be investigated using specific peptidase inhibitors. Nevertheless, the more likely explanation for the different orders of potency is that the receptor type in Col-29 epithelia is different from that predominating in the parent cell line, HCA-7, and this conclusion is strengthened by the results obtained with CGRP(8–37).

According to Dennis *et al.* (1989), type 2 CGRP receptors exhibit affinity for [Cys(ACM)^{2,7}]CGRP, while the C-terminal fragments of CGRP inhibit full-length peptide binding to type 1 receptors. In preliminary studies with the C-terminal fragment, CGRP(8–37) (Cox & Tough, 1994) we did not observe any significant effect in either cell line. Further investigation, however, has allowed us to identify both minor reductions in basal s.c.c. in both cell lines and an inhibition of rα-CGRP responses in one of the lines. rα-CGRP responses in HCA-7 were sensitive to CGRP(8–37) pretreatment, however they were not significantly altered in Col-29 epithelia. Taken in isolation, pretreatment with CGRP(8–37) indicates that Col-29 epithelia may express type 2 CGRP receptors whereas type 1 receptors predominate in HCA-7. However, the relatively increased activity of [Cys-(ACM)^{2,7}]CGRP in HCA-7 compared with Col-29 cells does not support this tentative classification, and in the absence of other selective antagonists we must conclude: (i) that the CGRP receptor subtypes are different in the two cell lines and (ii) that these epithelial receptors are pharmacologically different from those described in brain and smooth muscle (Dennis *et al.*, 1989). Col-29 epithelia more closely resemble rat colon mucosal preparations in so far as the agonist orders of potency (H.M. Cox, unpublished) and CGRP(8–37) insensitivity (Cox & Tough, 1994) are concerned.

The sidedness of CGRP responses indicated that the receptors are preferentially located on the basolateral surface in both cell lines. Apical responses to rα-CGRP were relatively larger in Col-29 than in HCA-7 epithelia when compared with their respective basolateral controls. This, together with the fact that apical rα-CGRP reduced subsequent responses to basolateral peptide in Col-29, may be explained by the reduced resistance of Col-29 compared with HCA-7 epithelial layers, the peptide therefore passing to the basolateral compartment more readily in the former and, in so doing, causing a degree of receptor desensitization. The prolonged elevation in s.c.c. observed with CGRP peptides in both cell lines is a hallmark of cAMP-dependent secretory responses (rather than an indication of the apparent extent of receptor desensitization). In preliminary studies (Poyner *et al.*, 1993) we have identified cAMP as the intracellular transducer involved in secretory responses in HCA-7 and Col-29 epithelia, showing similar time-dependent, sustained increases in cAMP production in response to rα-CGRP. Elevation of adenylate cyclase activity is the most common transduction mechanism observed following CGRP stimulation (Poyner *et al.*, 1992; Stangl *et al.*, 1993), though there is evidence in skeletal muscle cells of an increase in inositol phosphate production (Laufer & Changeux, 1989). Type 1-like CGRP receptors have been identified in rat epididymal cells in culture, in which CGRP increases the s.c.c. by a Cl^--dependent mechanism involving increased intracellular cAMP (Leung *et al.*, 1992). In human ocular ciliary epithelia, CGRP-stimulated cAMP production occurs via a protein kinase C-dependent mechanism (Crook & Yabu, 1992).

The electrogenic secretory responses to rα-CGRP in the present study were not significantly altered by pretreating either cell line with the cyclo-oxygenase inhibitor piroxicam at a concentration which inhibits secretagogue-induced (in the same cell lines; MacVinish *et al.*, 1993) and basal secretion in other gastrointestinal epithelial preparations (Cox & Cuthbert, 1988; Ferrar *et al.*, 1990). Thus, the absence of piroxicam sensitivity in HCA-7 and Col-29 indicates that eicosanoid production is not involved in CGRP responses in these epithelia. In contrast, the secretory response stimulated in Col-29 cells by lysylbradykinin (MacVinish *et al.*, 1993) is mediated by both a Ca^{2+}-and prostaglandin-dependent mechanism, the latter providing for cAMP-mediated Cl^- secretion. In our studies pretreatment with the anti-secretory neuropeptide, somatostatin also failed to have any significant effect upon rα-CGRP-mediated ion secretion in either cell line, whereas in rat colonic mucosa somatostatin inhibits rα- and rβ-CGRP-mediated secretion (Ferrar *et al.*, 1990). An interesting divergence in somatostatin responsiveness was also observed between the two cell lines following CGRP pretreatment. As seen in rat colonic mucosal preparations (Ferrar *et al.*, 1990), somatostatin produces prolonged sustained reductions in s.c.c., and these responses (primarily a result of inhibition of epithelial cAMP production) were enhanced by prior addition of cAMP-dependent

secretagogues. Somatostatin responses in HCA-7 cells are similar to the interactions observed in rat colon, however their attenuation following rα-CGRP treatment in Col-29 epithelia was unexpected. Perhaps a partial explanation lies with the predominating transduction mechanism observed in each of these cell lines. In HCA-7 cells cAMP-mediated Cl^- secretion is more pronounced than Ca^{2+}-dependent Cl^- secretion, while the reverse is true of Col-29 cells (Cuthbert *et al.*, 1987; MacVinish *et al.*, 1993). It is possible therefore that relatively small changes in intracellular cAMP levels are not transduced as readily into changes in s.c.c. in Col-29 epithelia.

In conclusion, we describe two types of CGRP receptor expressed in HCA-7 and Col-29 epithelia. The EC_{50} values for CGRP agonists were all lower in HCA-7 than in Col-29 epithelia. Peptide responses in both cell lines were significantly larger following basolateral application, and both electrogenic responses were due primarily to an increase in Cl^- secretion. Use of the 8–37 C-terminal fragment of hα-CGRP and the linear peptide, [Cys(ACM)^{2,7}]CGRP leads us to conclude that the receptor subtypes are different not only between HCA-7 and Col-29 epithelia but also between these and other previously described CGRP receptor subtypes. We await the availability of novel selective antagonists to verify this differential characterization. The CGRP receptors expressed in Col-29 epithelia most closely resemble those found in rat colon mucosa.

This work was supported in part by the Medical Research Council. We thank Drs David Poyner and Mick Bahkle for helpful discussions during the preparation of this manuscript.

References

COX, H.M. & CUTHBERT, A.W. (1988). Neuropeptide Y antagonises secretagogue evoked chloride transport in rat jejunal epithelium. *Pfliigers Arch.*, **413**, 38–42.

COX, H.M. & TOUGH, I.R. (1994). Comparison of responses to calcitonin gene-related peptide in cultured epithelial and rat colon mucosa. *Br. J. Pharmacol.*, **112**, 238P.

COX, H.M. FERRAR, J.A. & CUTHBERT, A.W. (1989). Effects of α- and β-calcitonin gene-related peptides upon ion transport in rat descending colon. *Br. J. Pharmacol.*, **97**, 996–998.

CROOK, R.B. & YABU, J.M. (1992). Calcitonin gene-related peptide stimulates intracellular cAMP via a protein kinase C-controlled mechanism in human ocular ciliary epithelial cells. *Biochem. Biophys. Res. Commun.*, **188**, 662–670.

CUTHBERT, A.W., EGLEME, C., GREENWOOD, H., HICKMAN, M., KIRKLAND, S.C. & MACVINISH, L.J. (1987). Calcium- and cyclic AMP-dependent chloride secretion in human colonic epithelia. *Br. J. Pharmacol.*, **91**, 503–515.

DENNIS, T., FOURNIER, A., ST. PIERRE, S. & QUIRION, R. (1989). Structure–activity profile of calcitonin gene-related peptide in peripheral and brain tissues. Evidence for receptor multiplicity. *J. Pharmacol. Exp. Therap.*, **251**, 718–725.

EKBLAD, E., EKMAN, R., HÅKANSON, R. & SUNDLER, F. (1988). Projections of peptide-containing neurones in rat colon. *Neuroscience*, **27**, 655–674.

FERRAR, J.A., CUTHBERT, A.W. & COX, H.M. (1990). The antisecretory effects of somatostatin and analogues in rat descending colon mucosa. *Eur. J. Pharmacol.*, **184**, 295–303.

KIRKLAND, S.C. (1985). Dome formation by a human colonic adenocarcinoma cell line (HCA-7). *Cancer Res.*, **45**, 3790–3795.

LAUFER, R. & CHANGEUX, J.P. (1989). Calcitonin gene-related peptide and cAMP stimulate phosphoinositide turnover in skeletal muscle cells. *J. Biol. Chem.*, **264**, 2683–2689.

LEUNG, A.Y.H., LEUNG, P.Y., CHENG-CHEW, S.B. & WONG, P.Y.D. (1992). The role of calcitonin gene-related peptide in the regulation of anion secretion by the rat and human epididymis. *J. Endocrinol.*, **133**, 259–268.

MCCULLOCH, C.R. & COOKE, H.J. (1989). Human α-calcitonin gene-related peptide influences colonic secretion by acting on myenteric neurones. *Reg. Peptides*, **24**, 87–96.

MACVINISH, L.J., PICKLES, R.J. & CUTHBERT, A.W. (1993). Cyclic AMP and Ca^{2+} interactions affecting epithelial chloride secretion in human cultured colonic epithelia. *Br. J. Pharmacol.*, **108**, 462–468.

MULDERRY, P.K., GHATEI, M.A., SPOKES, R.A., JONES, P.M., PIERSON, A.M., HAMID, Q.A., KANSE, S., AMARA, S.G., BURRIN, J.M., LEGON, S., POLAK, J.M. & BLOOM, S.R. (1988). Differential expression of α-CGRP and β-CGRP by primary sensory neurons and enteric autonomic neurones of the rat. *Neuroscience*, **25**, 195–205.

POYNER, D.R., ANDREW, D.P., BROWN, D., BOSE, C. & HANLEY, M.R. (1992). Pharmacological characterisation of a receptor for calcitonin gene-related peptide on rat L6 myocytes. *Br. J. Pharmacol.*, **105**, 441–447.

POYNER, D.R., TOMLINSON, A.E., GOSLING, M., TOUGH, I.R. & COX, H.M. (1993). Stimulation of chloride secretion and adenylate cyclase in human colonic derived cell lines by calcitonin gene-related peptide. *Biochem. Soc. Trans.*, **21**, 434S.

STANGL, D., MUFF, R., SCHMOLCK, C. & FISCHER, J.A. (1993). Photoaffinity labeling of rat CGRP receptors and adenylate cyclase activation: identification of receptor subtypes. *Endocrinology*, **132**, 744–750.

(Received June 8, 1994
Revised August 11, 1994
Accepted August 11, 1994)

Br. J. Pharmacol. (1994), **113**, 1249–1256 © Macmillan Press Ltd, 1994

The binding of 1,3-[^{3}H]-dipropyl-8-cyclopentylxanthine to adenosine A_1 receptors in rat smooth muscle preparations

J.A. Peachey, [1]S.M.O. Hourani & I. Kitchen

Receptors and Cellular Regulation Research Group, School of Biological Sciences, University of Surrey, Guildford, Surrey GU2 5XH

1 The binding of 1,3-[^{3}H]-dipropyl-8-cyclopentylxanthine ([^{3}H]-DPCPX), an antagonist radioligand selective for adenosine A_1 receptors, was studied in rat duodenum, colon muscularis mucosae and longitudinal muscle, urinary bladder and vasa deferentia.

2 [^{3}H]-DPCPX bound with high affinity to a single site in all membrane preparations studied with the exception of the rat urinary bladder in which no specific binding was detected. The affinity (K_d) of the binding site for [^{3}H]-DPCPX was similar in all membrane preparations, the colon longitudinal muscle (1.18 ± 0.47 nM), colon muscularis mucosae (0.84 ± 0.15 nM), duodenum (1.59 ± 0.18 nM) and vasa deferentia (0.93 ± 0.17 nM). The density of [^{3}H]-DPCPX binding sites was similar in the duodenum (38.8 ± 4 fmol mg^{-1} protein), muscularis mucosae (43 ± 3.5 fmol mg^{-1} protein) and vasa deferentia (43.3 ± 12.2 fmol mg^{-1} protein), but in the longitudinal muscle 6–7 fold more binding sites (295 ± 70 fmol mg^{-1} protein) were identified.

3 Inhibition studies using DPCPX (0.1–100 nM), N^6-cyclopentyladenosine (CPA) (0.1–100 nM), 5'-N-ethylcarboxamidoadenosine (NECA) (2 nM–10 μM) and (**R**)-N^6-phenylisopropyladenosine (**R**-PIA) (1 nM–1 μM) to displace the binding of [^{3}H]-DPCPX at a concentration around the K_d value (1 nM), demonstrated an order of potency of displacement in all tissues of DPCPX ≥ CPA > **R**- PIA > NECA. This potency order is characteristic of an A_1 receptor, indicating that [^{3}H]-DPCPX binds to adenosine A_1 receptors in the rat duodenum, colon and vasa deferentia. Two site analysis revealed that the agonists bind to both a high and low affinity state of the receptor.

4 The existence of A_1 binding sites in the rat vasa deferentia, colon muscularis mucosae and duodenum, and their absence in the urinary bladder, is consistent with previous functional studies. However, in contrast to the findings of the [^{3}H]-DPCPX binding assay, no functional response mediated by adenosine A_1 receptors could be detected by measuring contractile or relaxant responses to CPA in the colon longitudinal muscle. The functional significance of the binding sites in this tissue has therefore yet to be determined.

Keywords: Rat smooth muscle preparations; [^{3}H]-DPCPX; radioligand binding; adenosine A_1 receptor; purinoceptors

Introduction

The P_1-purinoceptors mediating the action of extracellular adenosine were originally divided into two major subclasses, A_1 and A_2, on the basis of their differential selectivity for adenosine and adenosine analogues and because of their opposite effects on adenylate cyclase, with A_1 inhibiting and A_2 stimulating enzyme activity (Van Calker *et al.*, 1979). On A_1 receptors N^6 substituted adenosine analogues such as N^6-cyclopentyladenosine (CPA) and (**R**)-N^6-phenylisopropyladenosine (**R**-PIA) are more potent than 5' substituted analogues such as 5'-N-ethylcarboxamidoadenosine (NECA), whereas on A_2 receptors the reverse is true. Xanthines such as 8-sulphophenyltheophylline (8-SPT) are antagonists at both A_1 and A_2 receptors, whereas the antagonist 1,3-dipropyl-8-cyclopentylxanthine (DPCPX) has nanomolar affinity at A_1 receptors and micromolar affinity at A_2 receptors and thus effectively discriminates between the two types of receptor. A_2 receptors have been further subdivided into high and low affinity subtypes A_{2a} and A_{2b} based on their affinity for [^{3}H]-NECA in radioligand binding studies (Bruns *et al.*, 1986). A_{2a} receptors can be distinguished from A_{2b} on the basis of the selective activity of some 2-substituted adenosine analogues such as 2-[*p*-(carboxyethyl)-phenylethylamino]-5'-*N*-ethylcarboxamidoadenosine (CGS 21680) at A_{2a} receptors. More recently, a xanthine-insensitive A_3 receptor has been cloned from rat striatum and has also been shown to be negatively linked to adenylate cyclase (Zhou *et al.*, 1992). For a recent review of adenosine receptor subtypes see Collis & Hourani (1993).

[1] Author for correspondence.

Numerous agonist radioligands are available for A_1 binding studies and binding affinity at A_1 sites has commonly been assessed by use of [^{3}H]-N^6-cyclohexyladenosine (CHA) or [^{3}H]-CPA as the ligand and brain membrane preparations as a source of binding sites (Bruns *et al.*, 1980; Williams *et al.*, 1986). Until recently, the lack of highly selective A_2 agents has generally meant that specific A_2 binding has been determined by the use of a ligand such as [^{3}H]-NECA, which binds to both A_1 and A_2 receptors, with the binding study carried out in the presence of an A_1 agonist and rat striatum being used as a source of tissue (Bruns *et al.*, 1986; Stone *et al.*, 1988). More recently [^{3}H]-CGS 21680 has been used to identify A_{2a} binding sites in various regions of the brain of both human and rat (Wan *et al.*, 1990), though no agent specific for the low affinity A_{2b} site has yet been developed. The affinity of agonist radioligands used in receptor classification, however, may be subject to complications which can be overcome by the use of selective antagonists. Antagonist radioligands bind with high affinity to both agonist defined coupling states of a given receptor and are thus preferable. To this end [^{3}H]-DPCPX has superseded tritiated A_1 selective agonists, such as [^{3}H]-CPA, for the study of the binding affinity of A_1 receptors. Indeed, [^{3}H]-DPCPX has been shown to bind to a single site commensurate with an A_1 receptor, in rat whole brain membranes (Bruns *et al.*, 1987).

Much of the interest in adenosine receptors has focused on its effects in the central nervous system and has involved the use of radioligand binding assays to characterize receptor subtypes. Studies of the peripheral effects of adenosine have

in contrast, used mainly functional studies and very few successful binding studies for adenosine receptors in peripheral tissues have been reported, although binding has been shown to A_1 receptors in the heart (Leid *et al.*, 1988; Martens *et al.*, 1988; Musser *et al.*, 1993), testis (Cushing *et al.*, 1988), uterus (Schiemann *et al.*, 1990; 1991; Smith *et al.*, 1988), human fat cell (Larrouy *et al.*, 1991) and to A_2 receptors in some vascular tissues (Diocee & Souness, 1987; Moritoki *et al.*, 1990).

We have attempted to develop a receptor binding assay in a number of rat peripheral tissues using the antagonist [^{3}H]-DPCPX to identify the A_1 adenosine receptor, and to study the distribution of these receptors in various smooth muscle preparations. The rat duodenum, vas deferens and colon muscularis mucosae were chosen as these tissues have previously been shown in functional studies to contain A_1 receptors (Nicholls *et al.*, 1992; Bailey *et al.*, 1992; Hourani *et al.*, 1993). The rat urinary bladder and the longitudinal muscle of the colon were chosen as negative controls as these tissues have been shown in functional studies to contain A_{2b} receptors (Nicholls *et al.*, 1992; Bailey & Hourani, 1992).

Some of our findings have previously been published in abstract form (Peachey *et al.*, 1994).

Methods

Membrane preparation

Adult male Wistar albino rats (200–300g), University of Surrey strain, were killed by cervical dislocation. The duodenum and urinary bladder were dissected out as described in Nicholls *et al.* (1990), the distal colon and the vasa deferentia were rapidly removed and placed in ice-cold 50 mM Tris HCl buffer (pH 7.4). The longitudinal muscle and the muscularis mucosae of the colon were separated, as described by Bailey & Hourani (1992). Tissues from 25 animals were pooled, all tissues were cleaned and blotted dry to remove any excess buffer, weighed and roughly scissor chopped. Homogenization was performed with a Polytron homogenizer (three 10 s bursts, mid-speed setting), followed by a Potter homogenizer (15 strokes at 1300 r.p.m.). The homogenates were centrifuged for 20 min at 1000*g*, the pellets discarded and the supernatants recentrifuged at 50,000*g* for 20 min. The resulting pellets were resuspended in 50 mM Tris HCl buffer and incubated with 5 u ml^{-1} adenosine deaminase at room temperature for 30 min before use. Protein estimations were performed according to the method of Lowry *et al.* (1951).

Binding assays

Saturation experiments were performed in triplicate in polypropylene tubes using a total assay volume of 250 µl. A range of [^{3}H]-DPCPX (specific activity 88.2 Ci mmol^{-1}) concentrations (0.05–10 nM) were used and the non-specific binding defined by 1 µM CPA. The reaction was initiated by the addition of homogenate and the mixture incubated for 30 min at temperatures determined to be optimal in pilot studies (duodenum 0°C, colon muscularis mucosae and longitudinal muscle 25°C and vas deferens 35°C). The reaction was terminated by the addition of ice-cold 50 mM Tris HCl buffer followed by three 2.5 ml washes under vacuum filtration over Whatman GF/B filters using a Brandel Cell Harvester. The filters were removed and placed in scintillation vials, solubilised with 20% Triton in toluene, scintilla-

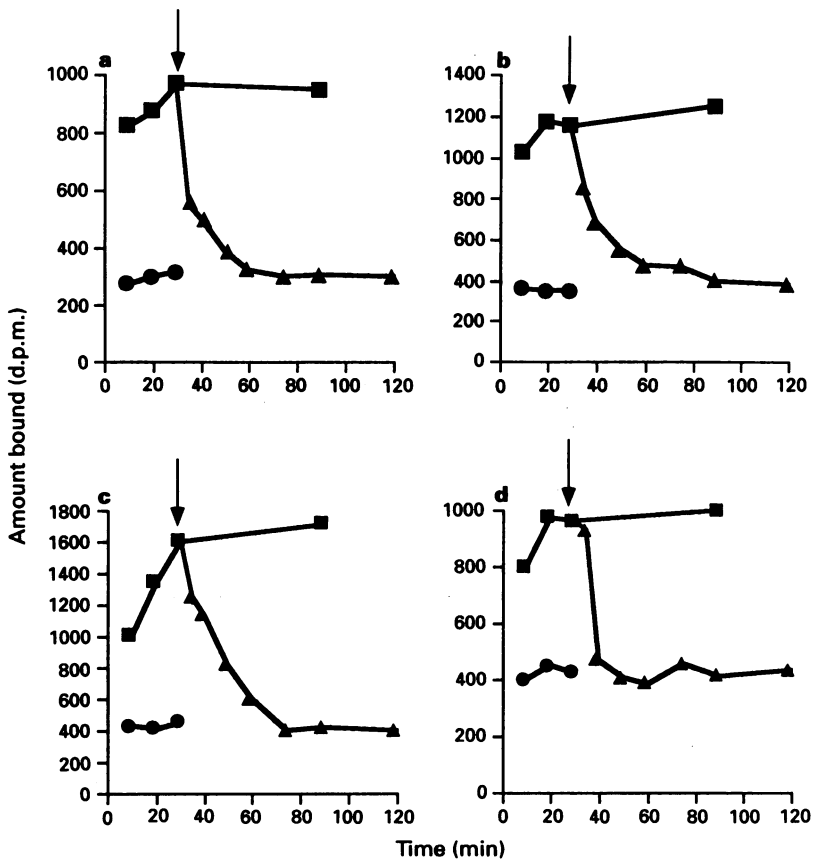


Figure 1 Representative time course experiments on (a) colon longitudinal muscle, (b) colon muscularis mucosae, (c) duodenum and (d) vasa deferentia performed at optimal temperatures (colon 25°C, vasa deferentia 35°C and duodenum on ice), showing total binding (■) and non-specific binding (●) determined in the presence of 1µM CPA; reversibility of binding is shown by the addition of 1µM CPA (↓) at 30 min and the subsequent dissociation (▲) of [^{3}H]-DPCPX. For abbreviations in this and subsequent figure legends, see text.

tion fluid (Unisolve E) added and the tubes left overnight to reduce chemiluminescence prior to counting on a Wallac LKB scintillation counter. The results were analysed using LIGAND (Munson & Rodbard, 1980) and the specific binding was subjected to Scatchard transformation for estimation of B_{max} and K_d. Inhibition studies were performed with a single concentration (1 nM) of [^{3}H]-DPCPX in the presence of increasing concentrations of competing ligands, DPCPX 0.1–100 nM, CPA 0.1–100 nM, **R**-PIA 1 nM–1 μM and NECA 2 nM–10 μM, and the same procedure was followed as outlined above.

Functional assays

Adult male Wistar albino rats (200–250 g), University of Surrey strain, were killed by cervical dislocation and the distal colon rapidly excised and placed in Tyrode buffer (ionic composition, mM: Na^+ 149.1, K^+ 2.8, Ca^{2+} 1.8, Mg^{2+} 2.1, Cl^- 147.5, $H_2PO_4^-$ 0.3, HCO_3^- 11.9 and glucose 5.6), pregassed with 95% O_2, 5% CO_2. The dissection of the longitudinal muscle was carried out as described in Bailey & Hourani (1992). The longitudinal muscle was suspended with the lumen closed, under a resting tension of 1g, in 3.5 ml glass organ bath in gassed Tyrode solution at 32–35°C. Contractions were measured isometrically via an FTO3 force displacement transducer and displayed on a Grass 79D polygraph. The tissues were allowed to equilibrate for 90 min with frequent washing, before the addition of any drugs. Carbachol (CCh) 1 μM was used to contract the tissue and this response was used as a reference contractile response against which the effects of CPA (1 nM–1 μM) in the absence and presence of DPCPX (1 nM) were assessed. The tissues were dosed non-cumulatively and an interval between doses of 15 min was maintained in all cases. To determine whether CPA had any inhibitory or stimulatory effect on the CCh-induced response, the tissues were treated with CPA either for 1 min prior to the addition of CCh, or when the CCh-induced contraction had achieved a stable plateau. The effects of CPA on field stimulation of the longitudinal muscle by trains of pulses (Grass S48 stimulator, train rate 0.03, duration 10 s, stimulation rate 10 Hz for 1 ms, 70 V) via parallel platinum electrodes (0.3 mm diameter, 0.5 cm apart) were also investigated. In experiments to determine the effects of DPCPX on the CPA-induced response, a control concentration-response curve was carried out, after which the tissues were incubated with 1 nM DPCPX for 30 min and then a second concentration-response curve to CPA was obtained.

Materials

CPA, **R**-PIA, NECA and adenosine deaminase (ADA) (Type VI) were obtained from Sigma UK. Ltd, Poole, Dorset; DPCPX from Research Biochemicals, Natick, MA (U.S.A.) and [^{3}H]-DPCPX from NEN DuPont UK. Ltd., Stevenage, Hertfordshire. NECA (10 mM) was dissolved in distilled water, CPA (10 mM), DPCPX (10 mM) and **R**-PIA (10 mM) were dissolved in 20% ethanol and diluted in buffer for use.

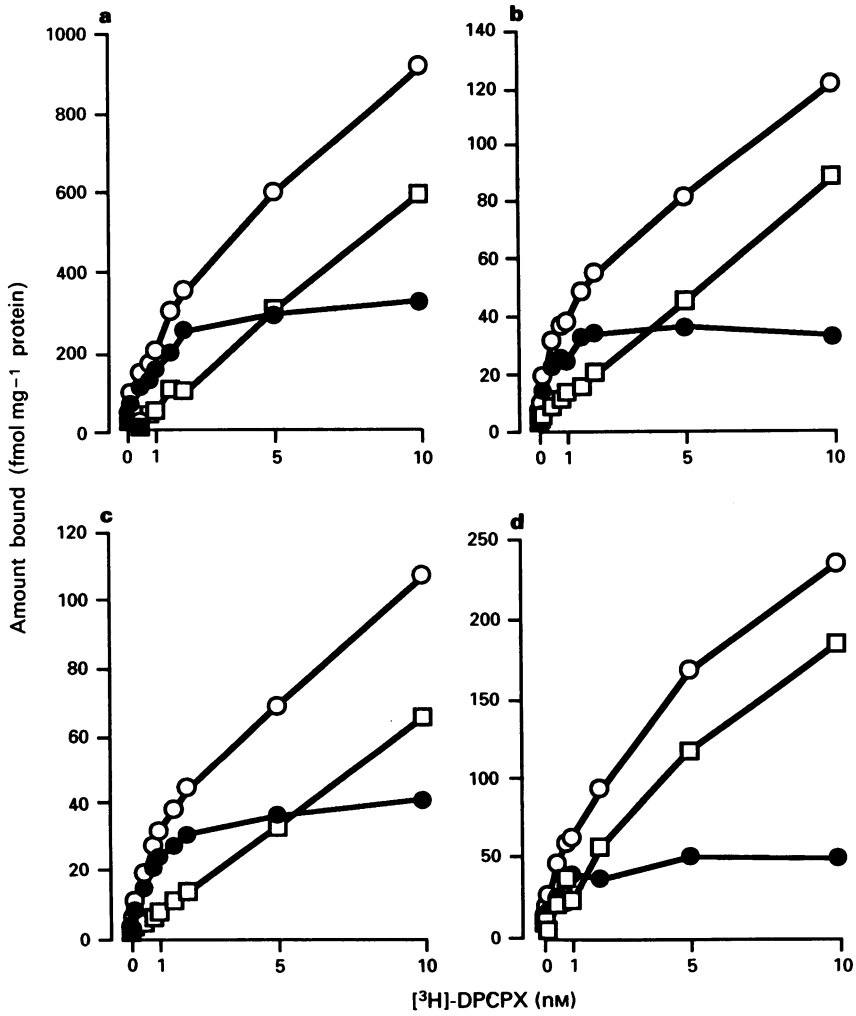


Figure 2 Representative saturation plots performed on (a) colon longitudinal muscle, (b) colon muscularis mucosae, (c) duodenum and (d) vasa deferentia, showing total binding (○), non-specific binding (□) (determined in the presence of 1 μM CPA) and specific binding (●).

All stock solutions were stored frozen at − 18°C. The ADA solution was supplied in 50% glycerol-0.01 M potassium phosphate solution at a concentration of 1000 units in 0.6 ml.

Results

Pilot studies

Pilot studies were undertaken to determine the optimal temperature at which to perform the binding assay on each tissue preparation (results not shown). The optimal temperature for binding was 25°C for the colon, 35°C for the vas deferens and on ice (0°C) for the duodenum. In the duodenum, at higher temperatures the ligand demonstrated a very rapid binding, followed by an immediate loss of binding. At 0°C the reaction was slower but the binding of the radioligand remained at a steady state. A similar loss of binding was observed in the colon at 35°C, but to a lesser extent, allowing the binding assay to be carried out at 25°C. The reason for the loss of binding at 35°C in these tissues in not known, but could be due to some degradation of the radioligand by the gut tissues, which are known to degrade rapidly other purinoceptor ligands (Bailey & Hourani, 1990; 1992; Hourani *et al.*, 1991). Time course studies showed the binding of [^{3}H]-DPCPX to be rapid and reach a steady state within 30 min for each tissue preparation; 30 min was therefore used as the incubation time in the rest of the experiments. On addition of unlabelled CPA (1 μM), [^{3}H]-DPCPX dissociated rapidly from its binding site, with the total amount of [^{3}H]-DPCPX bound returning to a level equivalent to the non-specific binding after 30 min in each tissue (Figure 1). Reproducible binding was obtained only in fresh tissue preparations, freezing homogenate preparations resulted in a decrease in the density of [^{3}H]-DPCPX binding sites.

Saturation experiments

[^{3}H]-DPCPX bound saturably, reversibly and with high affinity to all tissue preparations studied (Figure 2) with the exception of the rat urinary bladder, in which no specific binding of the radioligand was detected (data not shown). Scatchard transformation of specific binding generated monophasic plots (Figure 3) and Hill coefficients were not significantly different from unity, indicating that [^{3}H]-DPCPX binds to an apparently homogenous population of binding sites. The affinity (K_d) of the ligand for each tissue prepara-

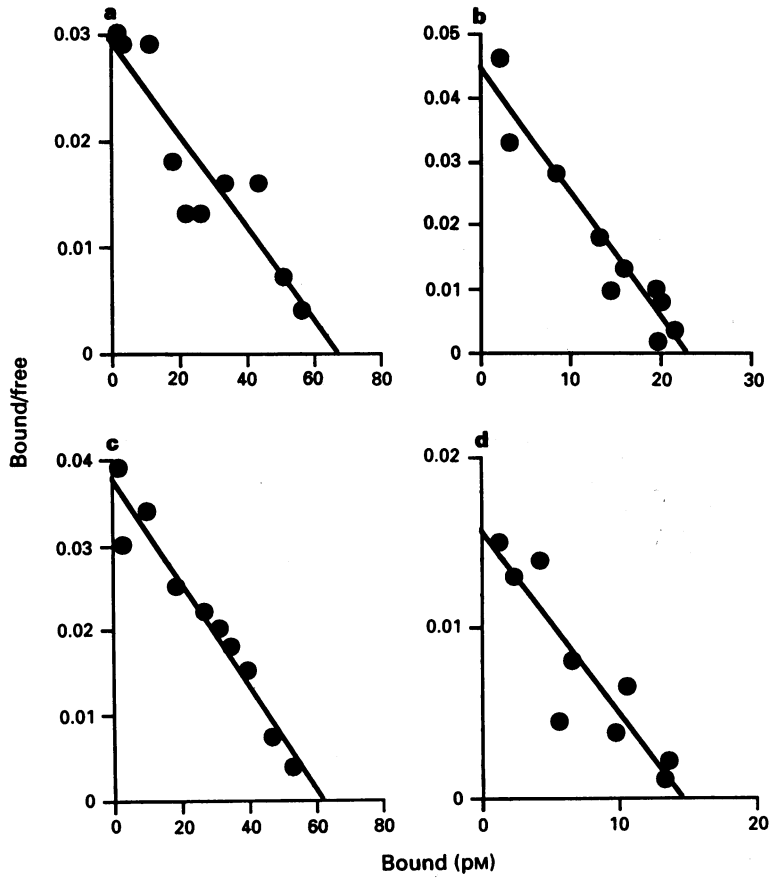


Figure 3 Representative Scatchard plots showing the transformation of the data shown in Figure 2 for the specific binding (●) of [^{3}H]-DPCPX in (a) colon longitudinal muscle, (b) colon muscularis mucosae, (c) duodenum and (d) vasa deferentia.

Table 1 Binding affinity (K_d) and capacity (B_{max}) for 1,3-[^{3}H]-dipropyl-8-cyclopentylxanthine in various membrane preparations

	Colon LM	*Colon MM*	*Duodenum*	*Vas deferens*
B_{max} (fmol mg^{-1} protein)	295 ± 70	43 ± 3.5	38.8 ± 4	43.3 ± 12.2
K_d (nM)	1.18 ± 0.47	0.84 ± 0.15	1.59 ± 0.18	0.93 ± 0.17

Values are the mean ± s.e.mean of at least 3 observations.
LM, longitudinal muscle; MM, muscularis mucosae.

tion and the density of binding sites (B_{max}) were determined from individual Scatchard plots (Scatchard, 1949). The affinity of [^{3}H]-DPCPX binding was similar in all membrane preparations with a K_d of ~1 nM (Table 1). The density of binding sites (B_{max}) did not differ significantly between the duodenum, vas deferens and colon muscularis mucosae (Table 1). In the longitudinal muscle of the colon however, there were 6–7 fold more binding sites (Table 1).

Inhibition studies

Inhibition studies were performed with 1 nM [^{3}H]-DPCPX and increasing concentrations of displacing ligands as previously described. Binding was inhibited in a dose-dependent manner by various adenosine receptor ligands, with a rank order of potency of DPCPX ≥ CPA > **R**-PIA > NECA (Figure 4 and Table 2). This rank order of potency is indicative of binding to an A_1 receptor. Concentration-inhibition curves for unlabelled DPCPX versus [^{3}H]-DPCPX were steep with slope factors near unity, whereas the agonists CPA, **R**-PIA and NECA presented with slope factors ranging from 0.8–0.6, suggesting the presence of more than one binding site. Where a better fit was obtained with a two site model than with a one site model, the agonist concentration-inhibition curves were fitted to a two site model using LIGAND (Table 3), resulting in K_d and B_{max} estimates for both a high and low affinity binding site.

Functional assays

Various attempts were made to demonstrate some functional response mediated by A_1 receptors in the longitudinal muscle of the colon (see Figure 5 for representative traces). CPA (1 nM–1 μM) added alone had no direct effect on the longitudinal muscle. Preincubating the tissue with CPA (1 nM–1 μM) for 1 min before the addition of CCh (1 μM) had no effect on the CCh-induced response either in the absence or presence of DPCPX (1 nM). Addition of CPA following contraction of the tissue by CCh was also without effect, except at the higher concentration of CPA (10 μM) when a small relaxation was observed. DPCPX (1 nM) did not modify this effect. Field stimulation of the longitudinal muscle by trains of pulses did not induce contractions but after precontracting the tissue with CCh, field stimulation caused relaxations which were neurogenic in origin as they were inhibited by tetrodotoxin (TTX, 1 μM). Addition of CPA (1 nM–1 μM),

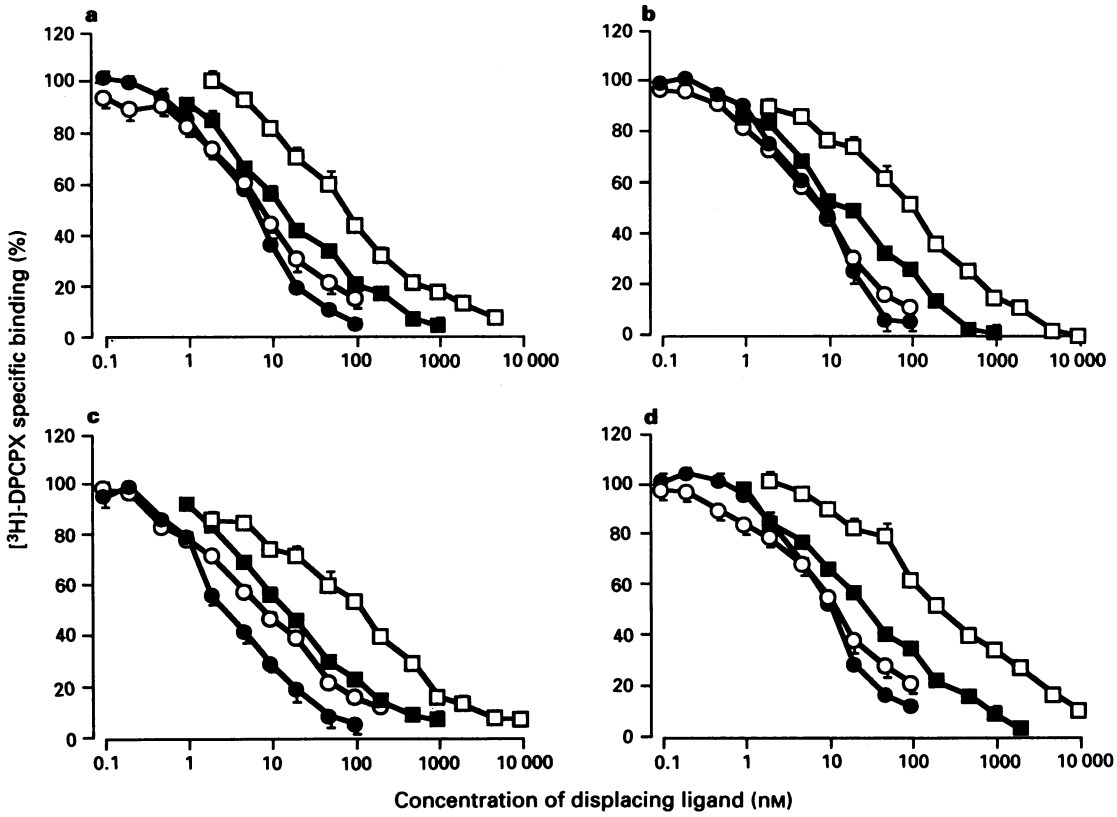


Figure 4 Inhibition of specific [^{3}H]-DPCPX (1nM) binding by (●) DPCPX, (○) CPA, (■) **R**-PIA or (□) NECA in (a) colon longitudinal muscle, (b) colon muscularis mucosae, (c) duodenum and (d) vasa deferentia. Each point is the mean with s.e.mean of at least 5 observations.

Table 2 K_i values (nM) for the inhibition of 1,3-[^{3}H]-dipropyl-8-cyclopentylxanthine ([^{3}H]-DPCPX) binding by various adenosine receptor ligands

	DPCPX		*CPA*		***R**-PIA*		*NECA*	
	K_i	Hill slope	K_i	Hill slope	K_i	Hill slope	K_i	Hill slope
Colon LM	2.95 ± 0.26	1.06 ± 0.03	2.96 ± 0.36	0.81 ± 0.08	9.4 ± 1.67	0.72 ± 0.04	50.09 ± 3.48	0.69 ± 0.04
Colon MM	2.8 ± 0.35	0.99 ± 0.03	3.07 ± 0.62	0.82 ± 0.08	12.22 ± 3.34	0.73 ± 0.05	56.37 ± 12.42	0.62 ± 0.04
Duodenum	1.69 ± 0.28	0.97 ± 0.04	4.45 ± 1.02	0.63 ± 0.02	9.19 ± 1.13	0.69 ± 0.02	67.45 ± 8.4	0.59 ± 0.05
Vas deferens	3.58 ± 0.4	1.09 ± 0.05	3.28 ± 0.64	0.74 ± 0.09	13.62 ± 1.98	0.64 ± 0.03	64.48 ± 9.21	0.58 ± 0.06

Values are the mean ± s.e.mean of at least 5 observations, calculated using a one site model.
LM, longitudinal, MM, muscularis mucosae.

Table 3 Two-site analysis of concentration-inhibition curves for agonists in displacing 1,3-[^{3}H]-dipropyl-8-cyclopentylxanthine binding: K_i values (nM) are given for high (K_H) and low (K_L) affinity sites

	CPA			*R-PIA*			*NECA*		
	K_H	K_L	% K_H	K_H	K_L	% K_H	K_H	K_L	% K_H
Colon LM	0.25	41.99	45.52	2.63 ± 0.75	370 ± 270	62.6 ± 4.9	22.62 ± 3.82	4110 ± 1700	74.7 ± 2.3
Colon MM	0.93 ± 0.56	10.84 ± 1.45	55.2 ± 8.5	1.52 ± 0.04	88.1 ± 45.6	55.7 ± 5.7	10.97 ± 6.18	2190 ± 1560	44 ± 7.5
Duodenum	0.17 ± 0.06	31.58 ± 21.46	36.9 ± 6.6	1.97 ± 0.33	43.9 ± 1.4	50.2 ± 12	11.22 ± 6.32	509.6 ± 205.8	51 ± 10.4
Vas deferens	0.43	9.82	37.7	3.04 ± 0.93	30.25 ± 9.07	58.6 ± 12	18.49 ± 7.8	5350 ± 3500	40.7 ± 5.8

% K_H shows the percentage of receptors in the high affinity state.
Not all the competition inhibition experiments with CPA were best described by a two site fit, consequently the number of determinations presented for this agonist are reduced compared with Table 2; Colon LM $n = 1$, Colon MM $n = 3$, duodenum $n = 4$ and vas deferens $n = 2$.

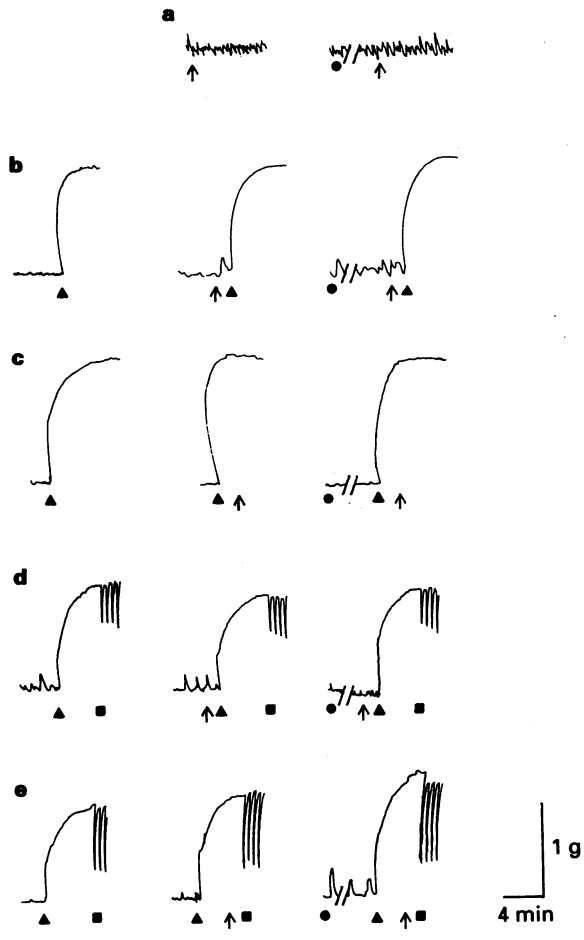


Figure 5 Representative traces showing the responses of the rat colon longitudinal muscle to CPA (↑) (10 nM) in the absence and presence of DPCPX (1 nM) (●); (a) the effects of CPA alone; (b) the effect of preincubation with CPA (1 min) followed by contraction induced by CCh (1 μM) (▲); (c) the effect of precontraction with CCh followed by administration of CPA; (d) the effect on nerve stimulation (■) of CPA added before contraction with CCh (1 μM); (e) the effect on nerve stimulation of CPA added after contraction with CCh (1 μM).

however, had no effect on the nerve induced response either in the absence or in the presence of DPCPX (1 nM).

Discussion

Much of the interest in adenosine binding sites has concentrated on the central nervous system, with binding sites commensurate with adenosine A_1 receptors identified in the brains of a variety of different species including rat, sheep, guinea-pig and cattle (Bruns *et al.*, 1987; Klotz *et al.*, 1991; Leung *et al.*, 1990; Williams & Valentine, 1985). However, limited attention has been paid to adenosine A_1 binding sites in peripheral tissues, although such sites have been identified in myocardial tissue (Leid *et al.*, 1988; Musser *et al.*, 1993), bovine testicular tissue (Cushing *et al.*, 1988), guinea-pig uterus (Schiemann *et al.*, 1990; 1991) and human adipocyte membranes (Larrouy *et al.*, 1991). The limited information regarding adenosine A_1 binding sites in peripheral tissues led us to attempt to develop a radioligand binding assay for A_1 receptors in a variety of rat smooth muscle preparations for which we already had functional data (Bailey *et al.*, 1992; Nicholls *et al.*, 1992; Hourani *et al.*, 1993; Hourani & Jones, 1994). [^{3}H]-DPCPX is an antagonist radioligand with 700 fold A_1 over A_2 selectivity (Bruns *et al.*, 1987), and was thus the ligand of choice to characterize the adenosine A_1 binding sites in smooth muscle.

The present study demonstrated [^{3}H]-DPCPX binding sites on all membrane preparations studied, with the exception of the rat urinary bladder where no specific [^{3}H]-DPCPX binding was detected. However, such a finding was not unexpected as previous functional assays have demonstrated the existence of A_2 receptors only (Nicholls *et al.*, 1992), and furthermore provided a useful method of validation for the assay protocol used. [^{3}H]-DPCPX bound with high affinity to the rat duodenum, colon muscularis mucosae and longitudinal muscle and vasa deferentia and in all cases the affinity of the adenosine A_1 binding site for [^{3}H]-DPCPX was similar, with K_d values in the low nM range. This is consistent with previous studies in a number of tissue preparations where the K_d values have ranged from 0.45 nM for rat brain membranes (Klotz *et al.*, 1990), 1.6 nM for pregnant guinea-pig myometrium (Schiemann *et al.*, 1990) to 3.01 nM for guinea-pig ventricular preparations (Musser *et al.*, 1993). The K_d values for [^{3}H]-DPCPX derived for the duodenum, colon muscularis mucosae and vasa deferentia are also consistent with values previously derived with DPCPX used an an antagonist in functional studies. In these tissues, K_B values in the region of 1 nM were obtained, although Schild plots were not carried out in the duodenum and vas deferens and the slope of the Schild plot was not unity in the colon muscularis mucosae (Nicholls *et al.*, 1992; Bailey *et al.*, 1992; Hourani *et al.*, 1993). The density of binding sites in these tissues was similar with B_{max} values ranging from 38–43 fmol mg^{-1} protein, and this is again consistent with our previous functional studies, where the potency of the A_1 agonist CPA was similar with EC_{50} values of around 0.1 μM for each tissue (Nicholls *et al.*, 1992; Bailey *et al.*, 1992; Hourani *et al.*, 1993). These findings provide evidence that the [^{3}H]-DPCPX binding sites do indeed correspond to A_1 receptors.

Further evidence that [^{3}H]-DPCPX binds to A_1 receptors was established by inhibition experiments using CPA, DPCPX, NECA and R-PIA. In all tissue preparations studied the order of potency of the competing ligands was DPCPX ≥ CPA > R-PIA > NECA, with K_i values in good agreement with those previously reported (Bruns *et al.*, 1987;

Leid *et al.*, 1988) and this order of potency is characteristic of an A_1 receptor (Collis & Hourani, 1993). Competition for binding of [^{3}H]-DPCPX resulted in shallower curves for the agonists than for unlabelled DPCPX suggesting the existence of receptors in both high and low affinity states for the agonists. Indeed when subjected to a two site fit the agonists did display both a high and low affinity binding component of the receptor (Table 3), and such findings are consistent with previous reports demonstrating the existence of multiple affinity binding states for agonists versus [^{3}H]-DPCPX binding, in the brain (Bruns *et al.*, 1987; Klotz *et al.*, 1991), adipocyte membranes (Larrouy *et al.*, 1991) and myocardial tissue (Leid *et al.*, 1988).

Species, tissue and ligand differences, in combination with variations in membrane preparations, make it difficult to compare directly the published binding parameters, such as receptor density (B_{max}), of radioligands for the adenosine A_1 receptor. Porcine brain has a significantly lower density of A_1 binding sites labelled with [^{3}H]-DPCPX than both hamster and sheep brain (Klotz *et al.*, 1991); pregnant guinea-pig myometrium has half the number of A_1 binding sites compared to non-pregnant guinea-pig myometrium (Schiemann *et al.*, 1990; 1991). The density of A_1 binding sites, labelled by [^{3}H]-DPCPX, in the rat duodenum, colon muscularis mucosae and vasa deferentia is less than the B_{max} values reported for brain membranes (0.19–4.09 pmol mg^{-1} protein) (Klotz *et al.*, 1991; Oliveira *et al.*, 1991), but is in agreement with the density of A_1 binding sites in myocardial tissue (8.5–75.9 fmol mg^{-1} protein) (Musser *et al.*, 1993), thereby suggesting that peripheral tissues have a lower density of A_1 receptors. Further evidence for the diversity in density of A_1 receptors between peripheral and central tissues has been provided by Williams & Valentine (1985), who demonstrated a greater number of high affinity A_1 binding sites labelled with [^{3}H]-CHA in the brain membranes than the ileal membranes of guinea-pigs. Surprisingly, we found the highest density of A_1 binding sites in the outer thin walled longitudinal muscle of the rat colon, seven fold higher than the density of binding sites situated on the thick walled inner muscularis mucosae, thereby indicating a heterogeneous density of A_1 binding sites within the structure of the distal colon. Such interstructure variations have been reported elsewhere, as Musser *et al.* (1993) found that in guinea-pig myocardial tissue, the density of A_1 binding sites differed between the atria and ventricles, with the higher density of A_1 binding sites found in the atria.

The presence of A_1 receptors in the rat duodenum, colon muscularis mucosae and vasa deferentia has previously been confirmed by functional assays. We have shown the existence of inhibitory A_1 receptors in the rat duodenum (Nicholls *et al.*, 1992), excitatory A_1 receptors in the colon muscularis mucosae (Bailey *et al.*, 1992) and both inhibitory prejunctional and excitatory postjunctional A_1 receptors in the vasa deferentia (Hourani *et al.*, 1993; Hourani & Jones, 1994). However, the binding of [^{3}H]-DPCPX to the longitudinal muscle of the rat colon was unexpected as we have previously shown the existence of relaxant A_2 receptors only in this tissue preparation (Bailey & Hourani, 1992). The possible existence of previously undetected postjunctional A_1 receptors was explored using the A_1 agonist CPA and the antagonist DPCPX at a concentration (1 nM) selective for A_1 receptors. The finding that CPA had no direct effect on the tissue preparation and no effect on the CCh-induced contractile response, either in the absence or presence of DPCPX, demonstrated the lack of postjunctional A_1 receptors in this smooth muscle preparation. The presence of any prejunctional A_1 receptors was also ruled out, as CPA was without effect on the nerve stimulated responses, again both in the absence and presence of DPCPX. The apparent lack of a functional response to A_1 receptor stimulation is in direct contrast to the findings of the [^{3}H]-DPCPX binding assay performed on this tissue preparation, where a large number of A_1 binding sites were identified. This suggests that the [^{3}H]-DPCPX binding sites identified in the longitudinal muscle of the rat colon correspond to A_1 receptors which cannot be detected by measuring contractile or relaxant responses.

In conclusion, we have successfully developed a [^{3}H]-DPCPX radioligand binding assay using smooth muscle tissue preparations and have demonstrated high affinity, saturable binding of the A_1-selective antagonist [^{3}H]-DPCPX to rat duodenum, vasa deferentia and colon muscularis mucosae, which we have previously shown in functional studies (Nicholls *et al.*, 1992; Bailey *et al.*, 1992; Hourani *et al.*, 1993) to contain A_1 receptors. A high density of binding sites for [^{3}H]-DPCPX was also detected in the longitudinal muscle of the rat colon, although the functional significance of these binding sites has yet to be determined.

We would like to thank the Wellcome Trust (Grant ref. 030318/Z/93/Z/1.5) for financial support.

References

BAILEY, S.J., HICKMAN, D. & HOURANI, S.M.O. (1992). Characterisation of the P_1-purinoceptors mediating contraction of the rat colon muscularis mucosae. *Br. J. Pharmacol.*, **105**, 400–404.

BAILEY, S.J. & HOURANI, S.M.O. (1990). A study of the purinoceptors mediating contraction in the rat colon. *Br. J. Pharmacol.*, **100**, 753–756.

BAILEY, S.J. & HOURANI, S.M.O. (1992). Effects of purines on the longitudinal muscle of the rat colon. *Br. J. Pharmacol.*, **105**, 885–892.

BRUNS, R.F., DALY, J.W. & SNYDER, S.H. (1980). Adenosine receptors in brain membranes: binding of N^6-cyclohexyl[^{3}H]adenosine and 1,3-diethyl-8-[^{3}H]phenylxanthine. *Proc. Natl. Acad. Sci. USA*, **77**, 5547–5551.

BRUNS, R.F., FERGUS, J.H., BADGER, E.W., BRISTOL, J.A., SANTAY, L.A., HARTMAN, J.D., HAYS, S.J. & HUANG, C.L. (1987). Binding of the A_1 selective adenosine antagonist 8-cyclopentyl-1,3-dipropylxanthine to rat brain membranes. *Naunyn-Schmied. Arch. Pharmacol.*, **335**, 59–63.

BRUNS, R.F., LU, G.H. & PUGSLEY, T.A. (1986). Characterization of the A_2 adenosine receptor labeled by [^{3}H]NECA in rat striatal membranes. *Mol. Pharmacol.*, **29**, 331–346.

COLLIS, M.G. & HOURANI, S.M.O. (1993). Adenosine receptor subtypes. *Trends Pharmacol. Sci.*, **14**, 360–366.

CUSHING, D.J., MCCONNAUGHEY, M.M. & MUSTAFA, S.J. (1988). Characterization of adenosine binding sites in bovine testicular tissue using 8-cyclopentyl-1,3-[^{3}H]dipropylxanthine. *Eur. J. Pharmacol.*, **152**, 353–356.

DIOCEE, B.K. & SOUNESS, J.E. (1987). Characterization of 5'-N-ethylcarboxamido[^{3}H]adenosine binding to pig aorta smooth muscle membranes. *Biochem. Pharmacol.*, **36**, 3621–3627.

HOURANI, S.M.O., BAILEY, S.J., NICHOLLS, J. & KITCHEN, I. (1991). Direct effects of adenylyl 5'-(β,γ-methylene)diphosphonate, a stable ATP analogue, on relaxant P_1-purinoceptors in smooth muscle. *Br. J. Pharmacol.*, **104**, 685–690.

HOURANI, S.M.O., NICHOLLS, J., LEE, S.B.S., HALFHIDE, E.J. & KITCHEN, I. (1993). Characterisation and ontogeny of P_1-purinoceptors in rat vas deferens. *Br. J. Pharmacol.*, **108**, 754–758.

HOURANI, S.M.O. & JONES, D.A.D. (1994). Post-junctional excitatory adenosine A_1 receptors in the rat vas deferens. *Gen. Pharmacol.*, **25**, 417–420.

KLOTZ, K.-N., KEIL, R., ZIMMER, F.J. & SCHWABE, U. (1990). Guanine nucleotide effects on 8-cyclopentyl-1,3-[^{3}H]dipropylxanthine binding to membrane bound and solubilized A_1 adenosine receptors of rat brain. *J. Neurochem.*, **54**, 1988–1994.

KLOTZ, K.-N., VOGT, H. & TAWFICK-SCHLIEPER, H. (1991). Comparison of A_1 adenosine receptors in brain from different species by radioligand binding and photoaffinity labelling. *Naunyn Schmied. Arch. Pharmacol.*, **343**, 196–201.

LARROUY, D., GALITZKY, J. & LAFONTAN, M. (1991). A_1 adenosine receptors in the human fat cell: tissue distribution and regulation of radioligand binding. *Eur. J. Pharmacol.*, **206**, 139–147.

LEID, M. FRANKLIN, P.H. & MURRAY, T.F. (1988). Labeling of A_1 adenosine receptors in porcine atria with the antagonist radioligand 8-cyclopentyl-1,3-[^{3}H]dipropylxanthine. *Eur. J. Pharmacol.*, **147**, 141–144.

LEUNG, E., JACOBSON, K.A. & GREEN, R.D. (1990). Analysis of agonist-antagonist interactions at A_1 receptors. *Mol. Pharmacol.*, **38**, 72–83.

LOWRY, O.H., ROSEBROUGH, N.J., FARR, A.L. & RANDALL, R.J. (1951). Protein measurement with the Folin phenol reagent. *J. Biol. Chem.*, **193**, 265–275.

MARTENS, D., LOHSE, M.J. & SCHWABE, U. (1988). [^{3}H]-8-cyclopentyl-1,3-dipropylxanthine binding to A_1 adenosine receptors of intact rat ventricular myocytes. *Circ. Res.*, **63**, 613–620.

MORITOKI, H., MATSUGI, T., TAKASE, H., UEDA, H. & TANIOKA, A. (1990). Evidence for the involvement of cyclic GMP in adenosine induced, age dependent vasodilatation. *Br. J. Pharmacol.*, **100**, 569–575.

MUNSON, P.J. & RODBARD, D. (1980). LIGAND: A versatile computerised approach for the characterisation of ligand binding systems. *Anal. Biochem.*, **107**, 220–239.

MUSSER, B., MORGAN, M.E., LEID, M., MURRAY, T.F., LINDEN, J. & VESTAL, R.E. (1993). Species comparison of adenosine and β-adrenoceptors in mammalian atrial and ventricular myocardium. *Eur. J. Pharmacol.*, **246**, 105–111.

NICHOLLS, J., HOURANI, S.M.O. & KITCHEN, I. (1990). The ontogeny of purinoceptors in rat urinary bladder and duodenum. *Br. J. Pharmacol.*, **100**, 874–878.

NICHOLLS, J., HOURANI, S.M.O. & KITCHEN, I. (1992). Characterization of P_1-purinoceptors on rat duodenum and urinary bladder. *Br. J. Pharmacol.*, **105**, 639–642.

OLIVEIRA, J.C., SEBASTIAO, A.M. & RIBEIRO, J.A. (1991). Solubilized rat brain adenosine receptors have two high affinity binding sites for 1,3-dipropyl-8-cyclopentylxanthine. *J. Neurochem.*, **57**, 1165–1171.

PEACHEY, J.A., HOURANI, S.M.O. & KITCHEN, I. (1994). Adenosine A_1 binding sites in rat smooth muscle preparations. *Br. J. Pharmacol.*, **111**, 323P.

SCATCHARD, G. (1949). The attraction of proteins for small molecules and ions. *Ann. NY. Acad. Sci.*, **51**, 660–672.

SCHIEMANN, W.P., DOGGWILER, K.O. & BUXTON, I.L.O. (1991). Action of adenosine in estrogen-primed non-pregnant guinea-pig myometrium: characterization of the smooth muscle receptor and coupling to phosphoinositide metabolism. *J. Pharmacol. Exp. Ther.*, **258**, 429–437.

SCHIEMANN, W.P., WALTHER, J.M. & BUXTON, I.L.O. (1990). On the ability of endogenous adenosine to regulate purine nucleoside receptor binding of antagonists in smooth muscle membranes. *J. Pharmacol. Exp. Ther.*, **265**, 886–892.

SMITH, M.A., BUXTON, I.L.O. & WESTFALL, D.P. (1988). Pharmacological classification of receptors for adenyl purines in guinea-pig myometrium. *J. Pharmacol. Exp. Ther.*, **247**, 1059–1063.

STONE, G.A., JARVIS, M.F., SILLS, M.A., WEEKS, B., SNOWHILL, E.W. & WILLIAMS, M. (1988). Species differences in high affinity adenosine A_2 binding sites in striatal membranes from mammalian brain. *Drug. Dev. Res.*, **15**, 31–46.

VAN CALKER, D., MÜLLER, M. & HAMPRECHT, B. (1979). Adenosine regulates via two different types of receptor, the accumulation of cyclic AMP in cultured brain cells. *J. Neurochem.*, **33**, 999–1005.

WAN, W., SUTHERLAND, G.R. & GEIGER, J.D. (1990). Binding of the adenosine A_2 receptor ligand [^{3}H]CGS 21680 to human and rat brain: evidence for multiple affinity sites. *J. Neurochem.*, **55**, 1763–1771.

WILLIAMS, M., BRAUNWALDER, A. & ERICKSON, T.J. (1986). Evaluation of the A_1 selective adenosine radioligand, cyclopentyladenosine (CPA) to rat brain tissue. *Naunyn Schmied. Arch. Pharmacol.*, **332**, 179–183.

WILLIAMS, M. & VALENTINE, H.L. (1985). Binding of [^{3}H]cyclohexyladenosine to adenosine recognition sites in guinea-pig ileal membranes: comparison with binding in brain membranes. *Neurosci. Letts.*, **57**, 79–83.

ZHOU, Q.-Y., LI, C., OLAH, M.E., JOHNSON, R.A., STILES, G.L. & CIVELLI, O. (1992). Molecular cloning and characterization of an adenosine receptor: the A_3 adenosine receptor. *Proc. Natl. Acad. Sci. USA*, **89**, 7432–7436.

(Received May 25, 1994
Revised July 21, 1994
Accepted August 15, 1994)

Br. J. Pharmacol. (1994), **113**, 1257–1262 © Macmillan Press Ltd, 1994

Block of Endothelin-1-induced release of thromboxane A_2 from the guinea pig lung and nitric oxide from the rabbit kidney by a selective ET_B receptor antagonist, BQ-788

[1]Pedro D'Orléans-Juste, Audrey Claing, Sabine Télémaque, Marie-Claude Maurice, Mitsuo Yano* & Jean-Philippe Gratton

Department of Pharmacology, Medical School, Université de Sherbrooke, Sherbrooke (Québec) J1H 5N4, Canada, and *Banyu Pharmaceutical Co., Ltd., Tsukuba Research Institute, Okubo 3, Tsukuba 300-33, Japan

1 The present study characterizes the receptors responsible for endothelin-1-induced release of thromboxane A_2 from the guinea pig lung and of endothelium-derived nitric oxide from the rabbit perfused kidney, by the use of the selective ET_A receptor antagonist, BQ-123, and a novel selective ET_B receptor antagonist, BQ-788.

2 In the guinea pig perfused lung, endothelin-1 (ET-1) (5 nM) induced a marked increase of thromboxane A_2 which was reduced by 17 ± 5.0, 70 ± 1.0 and 93 ± 1.2% by BQ-788 infused at concentrations of 1, 5 and 10 nM respectively. In contrast, BQ-123 (0.1 and 1.0 μM) had little or no effect on the ET-1-induced release of thromboxane A_2.

3 In the same perfused model, the selective ET_B agonist, IRL 1620 (50 nM), stimulated the release of thromboxane A_2, but not prostacyclin. The eicosanoid-releasing properties of IRL 1620 were abolished by BQ-788 at 10 nM, yet were unaffected by BQ-123 (1 μM).

4 In the rabbit perfused kidney, BQ-788 (10 nM) potentiated the increase of perfusion pressure induced by endothelin-1 (1, 5 and 10 nM) by approximately 90%, but not that induced by angiotensin II (1 μM). Furthermore, the selective ET_B receptor antagonist did not reduce the release of prostacyclin triggered by either peptide.

5 In another series of experiments, pretreatment of the perfused kidney with a nitric oxide synthase inhibitor, L-NAME (100 μM), potentiated the pressor responses to both endothelin-1 and angiotensin II. Under L-NAME treatment, BQ-788 did not further potentiate the pressor response to endothelin-1.

6 Our results illustrate the predominant role of ET_B receptor activation in the release of thromboxane A_2 and nitric oxide triggered by endothelin-1 in the guinea pig perfused lung and rabbit kidney respectively.

Keywords: Endothelin; eicosanoids, ET_A and ET_B receptor antagonists; nitric oxide; guinea pig lung; rabbit kidney; L-NAME; BQ-788; BQ-123; IRL 1620

Introduction

Endothelin-1 is a potent releaser of prostacyclin and thromboxane A_2 from the guinea pig perfused lung (de Nucci *et al.*, 1988). Furthermore, the bronchoconstriction induced by intravascularly administered endothelin-1 may be mediated by the release of thromboxane A_2, for this effect is abolished by indomethacin (Whittle *et al.*, 1989a) and blocked by a thromboxane receptor antagonist (Noguchi *et al.*, 1993).

Noguchi *et al.* (1993) also showed that BQ-123 (2 mg kg^{-1}), a selective ET_A receptor antagonist (Ihara *et al.*, 1992a), is inactive against endothelin-1-induced bronchoconstriction and suggested that the increase in airway resistance induced by endothelin-1 in the guinea pig *in vivo* may be mostly due to the activation of ET_B receptors responsible for the release of thromboxane A_2. As the levels of thromboxane A_2 were not measured by Whittle *et al.* (1989a) or Noguchi *et al.* (1993), a definite contribution of that particular eicosanoid in the ET_B receptor-mediated bronchoconstrictive properties of endothelins in the guinea pig remained to be investigated. Conversely, we have shown that endothelin-1 triggers the release of prostacyclin in the rat perfused lung via the activation of ET_A receptors (D'Orléans-Juste *et al.*, 1992). Interestingly, Hay *et al.* (1993) have also demonstrated that BQ-123 abolishes the release of eicosanoids from human bronchus.

The pharmacological characterization of the endothelin-1-induced release of eicosanoids in the guinea pig perfused lung is rendered more difficult by the presence of distinct functional receptor populations. Indeed, Hay *et al.* (1993) have shown that the presence of ET_A receptors in the guinea pig pulmonary artery and ET_B receptors in the guinea pig bronchus. Furthermore, the complex interactions of the two receptor types in airway reactivity have been described by Battistini *et al.* (1994) using BQ-123 and the mixed ET_A/ET_B antagonist PD 145065 (Cody *et al.*, 1993). Thus, to date, it has been difficult to dissociate ET_A receptor- from ET_B receptor-linked phenomena in the guinea pig lungs by the sole use of either ET_A receptor antagonists, such as BQ-123 (Ihara *et al.*, 1992a), or mixed ET_A/ET_B receptor antagonists, such as Ro 46-2005 or PD 145065 (Clozel *et al.*, 1993; Cody *et al.*, 1993).

In order to discriminate clearly between similar pharmacological effects of endothelins mediated via distinct receptor populations, the use of a selective ET_B receptor antagonist is now essential. To that effect, Ishikawa *et al.* (1994) have recently reported that a novel compound, BQ-788 (*N*, *cis*-2,6-dimethylpiperidinocarbonyl-L-γ-methylleucyl-D-1-methoxycarbonyltryptophanyl-D-norleucine), competitively antagonizes the vasoconstriction induced by a selective ET_B receptor agonist, BQ-3020, in rabbit pulmonary arteries with a pA_2 of 8.4. Furthermore, it has been shown by binding assays that BQ-788 has a 1000-fold higher affinity in ET_B than ET_A receptor-containing preparations (Ishikawa *et al.*, 1994). With the advent of this new and potent selective ET_B receptor antagonist, we have attempted, in the first part of our

[1] Author for correspondence.

study, to characterize the receptors responsible for the release of thromboxane A_2 in the guinea pig perfused lung.

On the other hand, Rae *et al.* (1989) have shown that endothelin-1 is a potent vasoconstrictor and enhancer of prostacyclin release from the renal circulation of the rabbit, and that the pressor response of this perfused organ to the peptide is sharply potentiated by indomethacin. In addition, by the use of the order of potency of natural agonists (endothelins-1, -2 and -3) as well as the selective ET_A receptor antagonist, BQ-123, we were able to confirm that the increase in perfusion pressure and the release of prostacyclin induced by endothelin-1, were solely mediated via the activation of ET_A receptors in that particular organ (Télémaque *et al.*, 1992; 1993). Therefore, in order to validate pharmacologically the selectivity of the ET_B antagonist, BQ-788, we verified if it would alter the ET_A receptor-mediated pressor and prostanoid-releasing properties of endothelin-1 in the rabbit perfused kidney.

Finally, it is known that endothelins trigger the release of nitric oxide in endothelial cells via the activation of ET_B receptors (Sakurai *et al.*, 1990), as initially suggested by Warner *et al.* (1989). Indeed, nitric oxide has been shown to interfere with the pressor effects of endothelin-1 *in vivo* (de Nucci *et al.*, 1988; Whittle *et al.*, 1989b) and in the rat arterial mesentery (D'Orléans-Juste *et al.*, 1993). The availability of BQ-788 provided us with the opportunity to explore the vasomodulatory role of the ET_B receptor-mediated release of nitric oxide in the pressor response to endothelin-1 in the rabbit perfused kidney.

Methods

Measurements of eicosanoids from isolated perfused guinea pig lungs

Duncan Hartley guinea pigs (250–350 g) (Charles River, St-Constant, Canada) of either sex were killed by cervical dislocation. Following thoracotomy, the pulmonary artery was cannulated for perfusion of the pulmonary circulation with a heparinized Krebs' solution (100 units ml^{-1}). The lungs were then removed and immediately suspended in a heated chamber (37°C) and perfused (5 ml min^{-1}) with an oxygenated (95% O_2, 5% CO_2) Krebs' solution. The lungs were left to stablize for 60 min before 3 min infusions of endothelin-1 (5 nM) or IRL 1620 (50 nM), either alone or in presence of BQ-123 (0.1 and 1 μM) or BQ-788 (1, 5 and 10 nM), infusion starting 15 min beforehand. The effluent from the lungs was collected (1 min samples) before, during and after infusion of the various peptides. The samples were then stored (−20°C) until the stable, hydrolytic metabolites of prostacyclin (6-keto-prostaglandin $F_{1\alpha}$; 6-keto-$PGF_{1\alpha}$) and thromboxane A_2 (thromboxane B_2; TxB_2) were determined by radioimmunoassay (Salmon, 1978).

Measurements of eicosanoid-releasing and pressor properties from rabbit perfused kidneys

Experiments were performed on kidneys taken from rabbits (New Zealand White, 2.0–2.5 kg) (St-Valérien, Canada) of either sex. Briefly, the rabbits were anaesthetized with ketamine/xylazine (40/10 mg kg^{-1} i.m.) and sacrificed by spinal transection. A polyethylene catheter (Portex, tube size 6FG) was placed in the right renal artery and the kidney was excised while being continuously perfused (5 ml min^{-1}) with heparinized (100 units ml^{-1}) Krebs' solution. The kidney was then rapidly placed in a heated chamber (37°C) and perfused at 5 ml min^{-1} with oxygenated (95% O_2, 5% CO_2) protein-free Krebs' solution. After an equilibration period of 60 min, the pressor and prostanoid-releasing effects of endothelin-1, angiotensin II and IRL 1620 were evaluated in absence or in presence of BQ-788 (10 nM). In some experiments, L-NAME (100 μM) was infused for 30 min prior to the administration of the peptides. The samples were collected and stored as before, and 6-keto-$PGF_{1\alpha}$ was later determined by radioimmunoassay.

In order to monitor oedema formation, the kidneys were weighed before being placed in the heated chamber and again at the end of each experiment, which lasted for a maximum time of 180 min. The mean value for the weight of the kidneys was 10.8 ± 0.2 g before and 13.2 ± 0.3 g at the end of the experiments ($n = 40$, $P < 0.01$).

Drugs and solutions

Synthetic endothelin-1 was purchased from Peninsula (Belmont, CA, U.S.A.). BQ-123 and BQ-788 were synthesized at Banyu Pharmaceuticals (Tsukuba, Japan). IRL 1620 was synthesized at Ciba-Geigy (Takarazuka, Japan) and generously supplied by Dr M. Takai. Angiotensin II was synthetized in the laboratory of Dr D. Regoli (Department of Pharmacology, Université de Sherbrooke, Canada). Heparin, phosphate-buffered saline, 6-keto-$PGF_{1\alpha}$, TxB_2 and the 6-keto-$PGF_{1\alpha}$ and TxB_2 antisera were purchased from Sigma (St Louis, Mo, U.S.A.). Tritiated 6-keto-$PGF_{1\alpha}$ and TxB_2 were purchased from Amersham (Oakville, Canada). The TxB_2 antiserum has been reported to display 100% cross-reactivity with TxB_2, less than 2% cross-reactivity with PGD_2 and $PGF_{2\alpha}$ and less than 0.1% cross-reactivity with 6-keto-$PGF_{1\alpha}$, PGE_1 and PGE_2, whereas 6-keto-$PGF_{1\alpha}$ antiserum shows 100% cross-reactivity with 6-keto-$PGF_{1\alpha}$, 23% with PGE_1, less than 10% with PGE_2 and $PGF_{2\alpha}$, and less than 1% with TxB_2 (Sigma). The eicosanoid antisera did not cross-react with endothelin-1, BQ-123, BQ-788, IRL 1620 or angiotensin II. All peptides were dissolved in phosphate-buffered saline (pH 7.4) except IRL 1620, which was dissolved in 0.01 N NaOH and then diluted with phosphate-buffered saline.

Statistics

Data used in the text and figures are expressed as mean ± s.e.mean of n observations. Statistical comparisons between groups were made by paired Student's t-test. P-values of <0.05 were considered to be statistically significant.

Results

BQ-788, but not BQ-123, blocks endothelin-1-induced release of thromboxane A_2 in the guinea pig perfused lung

A 3 min infusion of endothelin-1 (5 nM) through the pulmonary artery triggered a marked increase in the release of thromboxane A_2 (maximal release 7.9 ± 0.8 ng ml^{-1}, $n = 14$) as well as prostacyclin (3.2 ± 0.5 ng ml^{-1}, $n = 7$) from the perfused lungs. A second infusion of endothelin-1 (5 nM) triggered the same release of thromboxane A_2 from the lungs (7.6 ± 1.1 ng ml^{-1}, $n = 8$), whereas the release of prostacyclin was reduced by about 46% (1.7 ± 0.5 ng ml^{-1}, $n = 7$). In another series of experiments, 15 min infusions of BQ-788 (1, 5 and 10 nM) prior to a second administration of endothelin-1 (5 nM) reduced the release of thromboxane A_2 by 17 ± 2.5, 70 ± 5.0 and 93 ± 2.1% respectively (Figure 1a), the last two concentrations of the antagonist significantly reducing the maximal secretion.

Secondly, the release of thromboxane A_2 induced by endothelin-1 was monitored in absence or presence of BQ-123 (100 nM and 1 μM, Figure 1b). BQ-123 at 100 nM did not affect the release of thromboxane A_2, yet a higher concentration (1 μM) significantly reduced the endothelin-1-induced release of the eicosanoid only at the 2 min time period (Figure 1b).

In a third series of experiments, the selective ET_B receptor agonist, IRL 1620, infused at 50 nM also triggered a marked

release of thromboxane A_2 (from a basal of 0.6 ± 0.1 to 10.4 ± 1.0 ng ml^{-1}, $n = 5$) (Figure 2), but did not significantly increase the basal release of prostacyclin from the guinea pig perfused lung [basal (control), 0.6 ± 0.1; in presence of IRL 1620 (maximal release), 1.3 ± 0.3 ng ml^{-1}, $n = 4$]. The release of eicosanoid induced by IRL 1620 was abolished by BQ-788 at 10 nM, but remained unaffected by BQ-123 (1 μM) (Figure 2).

BQ-788 and L-NAME potentiate the perfusion pressure increase induced by endothelin-1 in the rabbit perfused kidney

In a series of control experiments, two successive infusions of endothelin-1 (10 nM) induced similar increases of perfusion pressure (first infusion, 53 ± 2.5 mmHg; second infusion, 57 ± 3.0 mmHg, $n = 3$, results not shown). Figure 3 illustrates the concentration-dependent increase in perfusion pressure triggered by endothelin-1 (0.5, 1 and 10 nM). BQ-788 (10 nM), infused for 15 min prior to the second administration of endothelin-1, markedly enhanced by approximately 90% the pressor responses to the three concentrations of the agonist.

Furthermore, a 30 min infusion of L-NAME (100 μM) markedly potentiated the pressor response induced by endothelin-1 (10 nM) (control, 53.5 ± 6.7 mmHg; in presence of L-NAME, 133.4 ± 7.9 mmHg; $n = 6$, $P < 0.01$). In kidneys pretreated with L-NAME (100 μM), endothelin-1 (10 nM) induced a protracted pressor effect which was not significantly increased by BQ-788 (10 nM) (L-NAME, 133.2 ± 12.6 mmHg; in the presence of BQ-788 and L-NAME, 148.6 ± 10.1 mmHg; $n = 5$) (Figure 3). Finally, to ascertain that the maximal vasoconstrictive capacity was not reached with endothelin-1 (10 nM) in kidneys treated with L-NAME, the agonist was infused at a concentration of

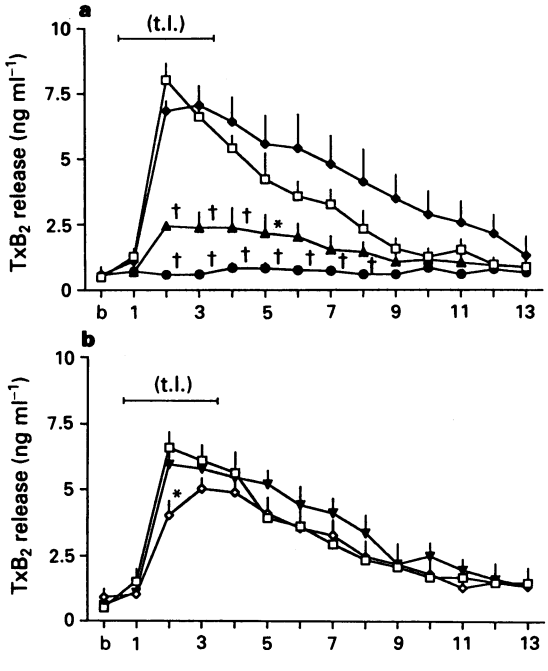


Figure 1 Profile of thromboxane A_2 release (measured as TxB_2) from the isolated perfused guinea pig lung induced by ET-1 (5 nM) in the absence (□) or in the presence of BQ-788 at 1 nM (◆), 5 nM (▲) and 10 nM (●) (a) and BQ-123 at 100 nM (▼) and 1 μM (◇) (b). Thromboxane B_2 was monitored for 10 min after the interruption of a 3 min infusion of the peptide through the lung (t.l.) arterial vasculature. (b) Basal levels of thromboxane measured before the infusion of the peptide. Each point represents the mean ± s.e.mean of 4–6 experiments. $*P < 0.05$ and $\dagger P < 0.01$ when compared with levels of thromboxane B_2 from lungs without added antagonist at each time point.

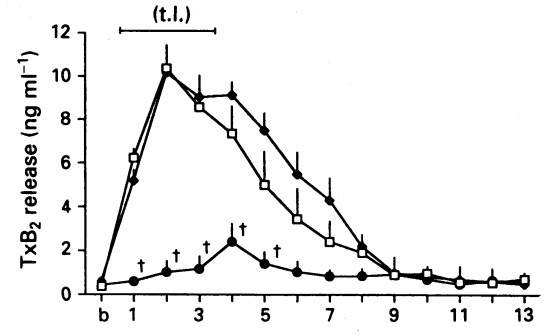


Figure 2 Profile of thromboxane A_2 release (measured as TxB_2) from the perfused guinea pig lung induced by IRL 1620 (50 nM) in the absence (□) and in the presence of BQ-788 (10 nM; ●) and BQ-123 (1 μM; ◆). Thromboxane B_2 was monitored for 10 min after the interruption of a 3 min infusion of the peptide through the lung (t.l.) arterial vasculature. (b) Basal levels of thromboxane measured before the infusion of the peptide. Each point represents the mean ± s.e.mean of five experiments. $\dagger P < 0.01$ when compared with levels of thromboxane B_2 from lungs without added antagonist at each time point.

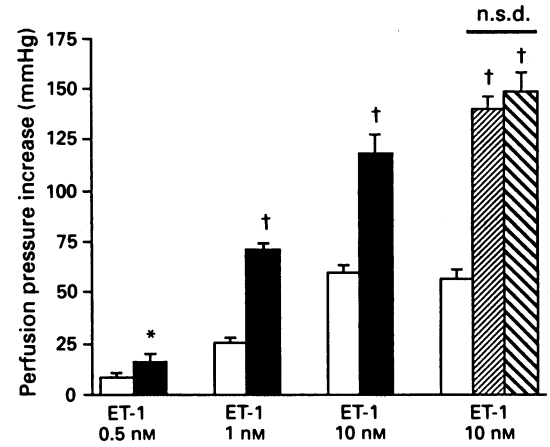


Figure 3 Effect of endothelin-1 on the perfusion pressure of the perfused rabbit kidney in the absence (□) and in the presence of BQ-788 (10 nM; ■), L-NAME (100 μM; ▨) and BQ-788 (10 nM)+L-NAME (100 μM) (▩). Each point represents the mean ± s.e.mean of 5–6 experiments. $*P < 0.05$ and $\dagger P < 0.01$ when compared with control values. n.s.d.; non significantly different.

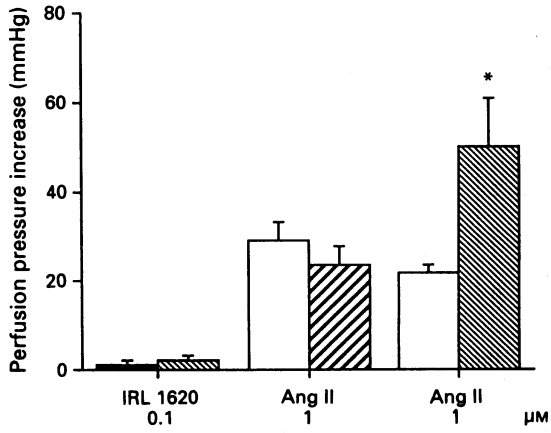


Figure 4 Effect of IRL 1620 (0.1 μM; ■) and angiotensin II (Ang II; 1 μM; □) on the perfusion pressure of the perfused rabbit kidney in the absence and in the presence of BQ-788 (10 nM; ▨) and L-NAME (100 μM; ▩). Each point represents the mean ± s.e.mean of 4–6 experiments. $*P < 0.01$ when compared with control values.

100 nM in untreated kidneys [maximal increase, 170 ± 7 mmHg ($n = 3$, $P < 0.01$) when compared with endothelin-1 (10 nM) in presence of L-NAME].

In another series of experiments, an infusion (i.a.) of IRL 1620 (0.1 μM) did not increase the perfusion pressure in the rabbit kidney in absence or presence of L-NAME (100 μM) (Figure 4). Furthermore, the increase in perfusion pressure induced by angiotensin II (1 μM) was unaffected by the ET_B antagonist BQ-788 (10 nM), yet was markedly potentiated by L-NAME (100 μM) (Figure 4).

Lack of effect of BQ-788 and L-NAME on the release of prostacyclin induced by endothelin-1 in the rabbit perfused kidney

Figure 5 shows the release of prostacyclin triggered by a 5 min infusion of endothelin-1 (10 nM) in the rabbit perfused kidney. Subsequently, infusion of BQ-788 (10 nM) for 15 min did not reduce the release of prostacyclin induced by endothelin-1 or angiotension II (1 μM); in fact, the release of the prostanoid was potentiated by the ET_B receptor antagonist at the three latest time points (13–15 min). Furthermore, L-NAME (100 μM) did not significantly increase the release of the prostanoid induced by endothelin-1 (maximal control release, 2.9 ± 0.4 ng ml^{-1}; in presence of L-NAME, 2.8 ± 1.0 ng ml^{-1}, $n = 6$). IRL 1620 (0.1 μm), in absence or presence of L-NAME, did not enhance the basal level of prostacyclin (results not shown).

Discussion

By the use of two highly selective antagonists, one for ET_A (BQ-123) and one for the ET_B receptors (BQ-788), we have been able, in the present study, to characterize the receptors responsible for the release of thromboxane A_2 in the guinea pig pulmonary vasculature. Our results support the observations made by Noguchi *et al.* (1993), who have suggested that the bronchoconstrictive properties of endothelin-1 *in vivo* in the guinea pig are predominantly mediated by thromboxane A_2 released following the activation of ET_B receptors.

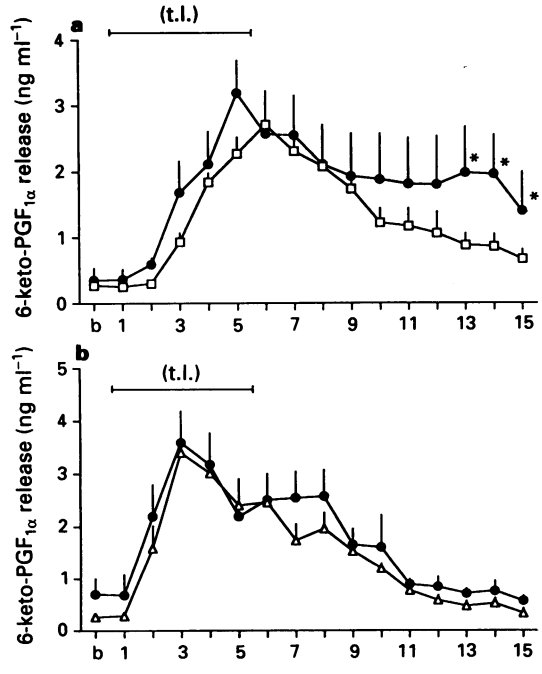


Figure 5 Profile of prostacyclin release (measured as 6-keto-$PGF_{1\alpha}$) from the rabbit perfused kidney induced by endothelin-1 (10 nM; □) (a) and angiotensin II (1 μM; Δ) (b) in the absence and in the presence of BQ-788 (10 nM; ●). Prostacyclin was monitored for 10 min after the interruption of a 5 min infusion of the peptide through the kidney (t.k.) arterial vasculature. (b) Basal levels of prostacyclin measured before the infusion of the peptide. Each point represents the mean ± s.e.mean of 6–8 experiments. *$P < 0.05$ when compared with level of 6-keto-$PGF_{1\alpha}$ in kidneys without added antagonist at each time point.

In the current study, we observed that, although the selective ET_A receptor antagonist BQ-123 moderately reduced the release of thromboxane A_2 induced by endothelin-1, it did not affect the release of the same eicosanoid stimulated by the selective ET_B receptor agonist, IRL 1620. Furthermore, the new selective ET_B receptor antagonist, BQ-788, at a concentration 100-fold lower than that of BQ-123, inhibited endothelin-1-induced thromboxane A_2 release by 90% and abolished the release triggered by IRL 1620. The larger release of TxB_2 by IRL 1620 than by ET-1 may be due to the lack of PGI_2-releasing properties of the selective ET_B receptor agonist, as it did not alter the basal level of that prostanoid in the guinea pig pulmonary vasculature. In contrast, ET-1-induced release of TxB_2 may be hampered by the concomitant release of PGI_2, which may act as a physiological antagonist of the endothelin-triggered vasoconstriction and bronchoconstriction in the guinea pig lung. Hence, there is a predominant contribution of ET_B receptor activation in the release of thromboxane A_2 in the guinea pig perfused lung. Nonetheless, one cannot exclude a relatively small proportion of ET_A receptor-dependent release of the same eicosanoid from the guinea pig perfused lung, as illustrated by the significant effect of BQ-123 in that phenomenon. Moreover, this suggests that the antagonism of the bronchoconstrictive properties of endothelin-1 in the guinea pig *in vivo* by BQ-123 at 30 but not at 2 mg kg^{-1}, as demonstrated by Noguchi *et al.* (1993), may be due not only to the limited selectivity of the ET_A receptor antagonist, but also to a relatively minor proportion of ET_A receptors involved in the release of the same eicosanoid *in vivo*. Indeed, Ihara *et al.* (1992b) have shown that ET_A receptors account for 15% of the total endothelin-1 binding in the guinea pig lung.

Our observations would also support the conclusion drawn by Battistini *et al.* (1994), who have suggested a possible ET_A receptor-dependent release of prostanoids from epithelial cells derived from the guinea pig trachea. On the other hand, the cells involved in the ET_B receptor-mediated release of thromboxane A_2 remain to be identified. However, we suggest that the bronchial smooth muscle may be involved in the release of eicosanoids following endothelin-1 administration, for ET_B receptors have been identified in this tissue (Hay *et al.*, 1993). Also, resident inflammatory cells may participate significantly in this process, as leucocytes not only can produce endothelin-1 (Ehrenreich *et al.*, 1990; Sessa *et al.*, 1991; Kaw *et al.*, 1992), but are also activated by the peptide to release several mediators including eicosanoids (Ninomiya *et al.*, 1992).

Because of the poor reproducibility of the release of prostacyclin caused by two successive infusions of endothelin-1 in the guinea pig perfused lung, we were unable to assess the effects of BQ-788 against the endothelin-1-induced release of that prostanoid. However, it is unlikely that ET_B receptors mediate prostacyclin release from this organ, as basal levels of this prostanoid were not modified by the selective ET_B receptor agonist IRL 1620. Thus, in the guinea pig perfused lung, as seen in the rat perfused lung, rabbit kidney and human bronchi (D'Orléans-Juste *et al.*, 1992; Télémaque *et al.*, 1993; Hay *et al.*, 1993), the receptors responsible for the release of prostacyclin are not of the ET_B receptor type.

The distinct pharmacological properties of BQ-788 and BQ-123 were further illustrated with our results obtained in the rabbit kidney. In this preparation, we have previously established that BQ-123 selectively blocks the release of prostacyclin as well as the increase in perfusion pressure induced by endothelin-1 (Télémaque *et al.*, 1993). Interestingly, we were now able to detect the presence of functional ET_B receptors in the renal vasculature of the rabbit with BQ-788.

In our hands, blockade of the ET_B receptors markedly enhanced, via a L-NAME-sensitive mechanism, the pressor response to endothelin-1. This result suggests that this latter response induced by endothelin-1 in the rabbit perfused kidney is strongly modulated by the concomitant release of nitric oxide via the activation of ET_B receptors, as initially suggested by Warner *et al.* (1989). Furthermore, our results illustrate that ET_A and ET_B receptor activation by exogenously administered endothelin-1 may lead to a physiological antagonism of the vasoactive properties of the peptide in the rabbit renal vasculature.

This observation is of interest when considering that the kidney is highly sensitive to endothelin-1 (King *et al.*, 1989; Denton & Anderson, 1990). The blockade of ET_B receptors responsible for the release of modulatory nitric oxide may, therefore, increase the sensitivity of the renal vasculature to the potent vasoconstrictor peptide. Furthermore, the use of antagonists interfering with ET_B receptor-mediated activities may be deleterious to the renal homeostasis, as this would potentiate ET_A receptor-mediated constriction of that organ.

The fact that BQ-788 was unable to reduce the pressor responses to endothelin-1 in the rabbit kidney treated with L-NAME strongly suggests that only ET_A receptors are involved in the renal vasoconstrictive properties of the peptide. This suggestion is further reinforced by the fact that the selective ET_B receptor agonist, IRL 1620, remained inactive as a pressor or eicosanoid releasing-agent in untreated (Télémaque *et al.*, 1993) or L-NAME-treated kidneys. It is also of interest to note that inhibition of nitric oxide release, either by blockade of nitric oxide synthase or by antagonism of ET_B receptor activation, did not alter the prostacyclin-releasing properties of endothelin-1. This suggests that modulation of the mechanical properties of the renal vasculature by nitric oxide does not influence the release of eicosanoid induced by the peptide. The exact location of the ET_A receptors responsible for the release of prostacyclin from the rabbit kidney remains to be identified. Nonetheless, we suggest that those particular receptors are located mostly on the renal vascular smooth muscle, as outlined by Télémaque *et al.* (1993).

However, irrespectively of ET_B receptor activation, simple flow-induced release of nitric oxide may indeed modulate the effect of vasoconstrictors such as endothelin-1 and angiotensin II in the rabbit kidney, as L-NAME sharply potentiated the response of the organ to the two peptides. On the other hand, the fact that the vasoconstrictive properties of angiotensin II were not affected by BQ-788 illustrates the characteristic of specificity of the ET_B receptor antagonist.

In summary, the use of a selective and specific ET_B receptor antagonist, BQ-788, has allowed us to distinguish between the receptor types involved in the pharmacological properties of endothelin-1 in the guinea pig pulmonary vasculature and has furthered our knowledge on the contribution of ET_B receptors in the rabbit renal vasculature. It is also important to point out that the mixed ET_A/ET_B receptor antagonist Ro 46-2005, but not BQ-123, has been shown to increase the circulating plasma levels of endothelin-1 in the rat, suggesting that ET_B receptor activation suppresses the release of endothelium-derived immunoreactive endothelin-1 (Löffler *et al.*, 1993). In this regard, and considering the higher sensitivity of the renal, as opposed to the systemic, vasculature to endothelins (King *et al.*, 1989; Denton & Anderson, 1990), selective blockade of ET_B receptors may be particularly deleterious to the kidneys, as this may well lead to increased plasma levels of endothelin-1 allied to reduced ET_B receptor-mediated vasodilation. Hence, the ET_B receptor blockade afforded by mixed ET_A/ET_B receptor antagonists may undermine their beneficial properties in conditions in which endogenous endothelin-1 may influence systemic or renal vascular resistance.

The authors are grateful to H. Morin for her secretarial assistance. The present study was financially supported by the Heart and Stroke Foundation of Québec and the Medical Research Council of Canada. A.C., S.T. and P.D.J. are in receipt of a studentship, a fellowship and a scholarship, respectively, of the Heart and Stroke Foundation of Canada.

References

BATTISTINI, B., WARNER, T.D., FOURNIER, A. & VANE, J.R. (1994). Characterization of ET_B receptors mediating contractions induced by endothelin-1 or IRL 1620 in guinea pig isolated airways: effects of BQ-123, FR139317 or PD145065. *Br. J. Pharmacol.*, **111**, 1009–1016.

CLOZEL, M., BREU, V., BURRI, K., CASSAL, J.-M., FISCHLI, W., GRAY, G.A., HIRTH, G., LÖFFLER, B.M., MÜLLER, M., NEIDHART, W. & RAMUZ, H. (1993). Pathophysiological role of endothelin revealed by the first orally active endothelin receptor antagonist. *Nature*, **365**, 759–761.

CODY, W.L., DOHERTY, A.M., HE, J.X., DEPUE, P.L., WAITE, L.A., TOPLISS, J.G., HALEEN, J.J., LADOUCEUR, K.E., FLYNN, M.A. & HILL, D.M. (1993). The rational design of a highly potent combined ET_A and ET_B receptor antagonist (PD 14065) and related analogues. *Med. Chem. Res.*, **3**, 154–162.

D'ORLÉANS-JUSTE, P., TÉLÉMAQUE, S., CLAING, A., IHARA, M. & YANO, M. (1992). Human big-endothelin-1 and endothelin-1 release prostacyclin via the activation of ET_1 receptors in the rat perfused lung. *Br. J. Pharmacol.*, **105**, 773–775.

D'ORLÉANS-JUSTE, P., CLAING, A., WARNER, T.D., YANO, M. & TÉLÉMAQUE, S. (1993). Characterization of receptors for endothelins in the perfused arterial and venous mesenteric vasculatures of the rat. *Br. J. Pharmacol.*, **110**, 687–692.

DENTON, K.M. & ANDERSON, W.P. (1990). Vascular actions of endothelin in the rabbit kidney. *Clin. Exp. Pharmacol. Physiol.*, **17**, 861–872.

DE NUCCI, G., THOMAS, R., D'ORLÉANS-JUSTE, P., ANTUNES, E., WALDER, C., WARNER, T.D. & VANE, J.R. (1988). Pressor effects of circulating endothelin are limited by its removal in the pulmonary circulation and by the release of prostacyclin and endothelium-derived relaxing factor. *Proc. Natl. Acad. Sci. USA*, **85**, 9797–9800.

ENRENREICH, H., ANDERSON, R.W., FOX, C.H., RIECKMANN, P., HOFFMAN, G.S., TRAVIS, W.D., COLIGAN, J.E., KEHRL, J.H. & FAUCI, A.S. (1990). Endothelins, peptides with potent vasoactive properties, are produced by human macrophages. *J. Exp. Med.*, **177**, 1741–1748.

HAY, D.W.P., LUTTMANN, M.A., HUBBARD, W.C. & UNDEM, B.J. (1993). Endothelin receptor subtypes in human and guinea pig pulmonary tissues. *Br. J. Pharmacol.*, **110**, 1175–1183.

IHARA, M., NOGUCHI, K., SAEKI, T., FUKURODA, T., TSUCHIDA, S., KIMURA, S., FUKAMI, T., ISHIKAWA, K., NISHIKIBE, M. & YANO, M. (1992a). Biological prolifes of highly potent novel endothelin antagonists selective for the ET_A receptor. *Life Sci.*, **50**, 247–255.

IHARA, M., ISHIKAWA, K., FUKURODA, T., SAEKI, T., FUNABASHI, K., FUKAMI, T., SUDA, H. & YANO, M. (1992b). *In vitro* biological profile of a highly potent novel endothelin (ET) antagonist, BQ-123, selective for the ET_A receptor. *J. Cardiovasc. Pharmacol.*, **20**, 511–514.

ISHIKAWA, K., IHARA, M., NOGUCHI, K., MASE, T., MINO, N., SAEKI, T., FUKURUDA, T., FUKAMI, T., OZAKI, S., NAGASE, T., NISHIKIBE, M. & YANO, M. (1994). Biochemical and pharmacological profile of a newly-developed, potent and selective endothelin B receptor antagonist, BQ-788. *Proc. Natl. Acad. Sci. USA*, **20**, 4892–4896.

KAW, S., HECKER, M. & VANE, J.R. (1992). The two-step conversion of big-endothelin-1 to endothelin-1 and degradation of endothelin-1 by subcellular fractions from human polymorphonuclear leukocytes. *Proc. Natl. Acad. Sci. USA*, **89**, 6886–6890.

KING, A.J., BRENNER, B.M. & ANDERSON, S. (1989). Endothelin: a potent renal and systemic vasoconstrictor peptide. *Am. J. Physiol.*, **256**, F1051–F1058.

LÖFFLER, B.M., BREU, V. & CLOZEL, M. (1993). Effect of different endothelin receptor antagonists and of the novel non-peptide antagonist, Ro 46-2005, on endothelin levels in rat plasma. *FEBS Lett.*, **333**, 108–110.

NOGUCHI, K., NOGUCHI, Y., HIROSE, H., NISHIKIBE, M., IHARA, M., ISHIKAWA, K. & YANO, M. (1993). Role of endothelin ET_B receptors in bronchoconstrictor and vasoconstrictor responses in guinea pigs. *Eur. J. Pharmacol.*, **233**, 47–51.

NINOMIYA, H., YU, X.Y., HASEGAWA, S. & SPANNHAKE, E.W. (1992). Endothelin-1 induces stimulation of prostaglandin synthesis in cells obtained from canine airways by bronchoalveolar lavage. *Prostaglandins*, **43**, 401–411.

RAE, G.A., TRYBULEC, M., DE NUCCI, G. & VANE, J.R. (1989). Endothelin-1 releases eicosanoids from rabbit isolated perfused kidney and spleen. *J. Cardiovasc. Pharmacol.*, **13**, S89–S92.

SAKURAI, T., YANAGISAWA, M., TAKUWA, Y., MIYAZAKI, M., KIMURA, S., GOTO, K. & MASAKI, T. (1990). Cloning of a cDNA encoding a non-isopeptide-selective subtype of the endothelin receptor. *Nature*, **348**, 732–735.

SALMON, J.A. (1978). A radioimmunoassay for 6-keto-prostaglandin $F_{1\alpha}$. *Prostaglandins*, **15**, 383–387.

SESSA, W.C., KAW, S., HECKER, M. & VANE, J.R. (1991). The biosynthesis of endothelin-1 by human polymorphonuclear leukocytes. *Biochem. Biophys. Res. Commun.*, **174**, 613–618.

TÉLÉMAQUE, S., LEMAIRE, D., CLAING, A. & D'ORLÉANS-JUSTE, P. (1992). Phosphoramidon-sensitive effects of big endothelins in the perfused rabbit kidney. *Hypertension*, **20**, 518–523.

TÉLÉMAQUE, S., GRATTON, J.-P., CLAING, A. & D'ORLÉANS-JUSTE, P. (1993). Endothelin-1 induces vasoconstriction and prostacyclin release via the activation of endothelin ET_A receptors in the perfused rabbit kidney. *Eur. J. Pharmacol.*, **237**, 275–281.

WARNER, T.D., DE NUCCI, G. & VANE, J.R. (1989). Rat endothelin is a vasodilator in the isolated perfused mesentery of the rat. *Eur. J. Pharmacol.*, **159**, 325–326.

WHITTLE, B.J., PAYNE, A.N. & ESPLUGUES, J.V. (1989a). Cardiopulmonary and gastric ulcerogenic actions of endothelin-1 in the guinea pig and rat. *J. Cardiovasc. Pharmacol.*, **13**, S103–S107.

WHITTLE, B.J., LOPEZ-BELMONTE, J. & REES, D.D. (1989b). Modulation of the vasodepressor actions of acetylcholine, bradykinin, substance P and endothelin in the rat by a specific inhibitor of nitric oxide formation. *Br. J. Pharmacol.*, **98**, 646–652.

(Received June 2, 1994
Accepted August 11, 1994)

Br. J. Pharmacol. (1994), **113**, 1263–1268 © Macmillan Press Ltd, 1994

Interactions of chloroethylclonidine with rauwolscine- and prazosin-sensitive adrenoceptors in dog saphenous vein

[1]A.M. Low, D.M. Bowdish, T.R. Prashad & V. Gaspar

Department of Biomedical Sciences, McMaster University, Hamilton, Ontario L8N 3Z5, Canada

1 α_1-Adrenoceptors have been classified pharmacologically into four subtypes (α_{1A}, α_{1B}, α_{1C} and α_{1D}) on the basis of their differential affinity for novel antagonists such as chloroethylclonidine (CEC). While CEC is considered an α_{1B}-adrenoceptor antagonist, our earlier studies revealed that it also acted like an agonist in the dog saphenous vein (DSV). The present study characterized the contraction induced by CEC in endothelium-denuded rings from DSV.

2 Concentration–response curves for CEC were constructed in the absence (EC_{50} value of $11.13 \pm 3.6\,\mu M$, $n = 8$) and presence of propranolol (β-adrenoceptor antagonist, 30 nM), rauwolscine (α_2-adrenoceptor antagonist, 30 nM), prazosin (α_1-adrenoceptor antagonist, 30 nM) or methysergide ($5HT_2$ antagonist, 30 nM) or both prazosin and rauwolscine. Pretreatment with methysergide ($9.83 \pm 5.14\,\mu M$, $n = 4$) or propranolol ($23.78 \pm 12.32\,\mu M$, $n = 4$) had no consistent effect. In the presence of rauwolscine, the concentration–response curve for CEC was significantly shifted to the right with an EC_{50} value of $48.82 \pm 13.2\,\mu M$ ($n = 8$). In the presence of prazosin, the CEC concentration–response curve had an EC_{50} value of $29.12 \pm 6.42\,\mu M$ ($n = 8$). Pretreatment with both prazosin and rauwolscine shifted the concentration–response curve for CEC to the right with an EC_{50} value of $72.67 \pm 10.69\,\mu M$ ($n = 8$, $P < 0.05$). Maximum responses were significantly reduced only in tissues that were treated with both prazosin and rauwolscine.

3 CEC ($100\,\mu M$) pretreatment abolished prazosin binding sites and reduced the B_{max} for rauwolscine by 50% without affecting the K_d value or the Hill slope.

4 In Ca^{2+}-free Krebs solution containing $50\,\mu M$ EGTA, CEC produced a small transient contraction, suggesting that it can mobilize internally-stored Ca^{2+}. Pretreatment with rauwolscine abolished the CEC-induced contraction in Ca^{2+}-free medium; prazosin pretreatment reduced but did not abolish CEC response in Ca^{2+}-free medium.

5 Restoring Ca^{2+} (0.5–2.5 mM) to the extracellular solution increased CEC contraction in a concentration-dependent manner, reaching a plateau at around 1.5 mM Ca^{2+}. The contraction was insensitive to nicardipine ($1\,\mu M$), a voltage-operated Ca^{2+}channel blocker, but was blocked in a concentration-dependent manner by the putative receptor-operated Ca^{2+}channel blockers, SK&F 96365 ($1–10\,\mu M$) and genistein, also a tyrosine kinase inhibitor ($10–100\,\mu M$).

6 We conclude that CEC acts on rauwolscine- and, to a less extent, prazosin-sensitive adrenoceptors in DSV to release internally stored Ca^{2+} and to open receptor-operated Ca^{2+} channels. The inhibitory effect on CEC-induced contraction that depended on external Ca^{2+} by genistein suggests a role for tyrosine kinase in the regulation of dihydropyridine-insensitive Ca^{2+} entry.

Keywords: Vascular; SK&F 96365; genistein; Ca^{2+} entry; Ca^{2+} release; radioligand binding

Introduction

Pharmacological classification of α_1-adrenoceptor subtypes into α_{1A}, α_{1B}, α_{1C} and α_{1D} is based on differential affinity of receptors for novel receptor antagonists such as 5-methylurapidil (5-MU), WB4101 and chloroethylclonidine (CEC) (Han *et al.*, 1987; Minneman, 1988; Hicks *et al.*, 1991). While 5-MU or WB4101 displays high affinity for the α_{1A}, α_{1C} and α_{1D} adrenoceptor subtypes, CEC shows preferential inactivation of the α_{1B}-adrenoceptor subtype (Han *et al.*, 1987; Watson & Girdlestone, 1994).

CEC, given as a bolus injection, has been reported to inhibit the pressor response to intravenous injections of phenylephrine in unanaesthetized rats without affecting the mean arterial pressure and heart rate (Vargas *et al.*, 1993). In rat aortic rings, CEC causes an irreversible blockade of noradrenaline-induced contraction (Vargas *et al.*, 1993). Although there is evidence for antagonism by CEC of noradrenergic action *in vivo* and *in vitro*, other investigations have reported that CEC pretreatment does not affect noradrenaline contraction, for example, in the rat portal vein (Sayet *et al.*, 1993). Han *et al.* (1990) suggested that noradrenaline-induced contraction that is not antagonized by CEC is mediated by the α_{1A}-adrenoceptor subtype, whereas contraction that is blocked by CEC occurs via the α_{1B}-adrenoceptor subtype.

Furthermore, it has also been reported that CEC on its own can act like a partial agonist. In the rat portal vein, CEC increases tonic contraction but inhibits phasic contractions (Schwietert *et al.*, 1991). Apart from the post-junctional effects of CEC, there is evidence for its action on prejunctional adrenoceptors (Bultmann & Starke, 1993). In the rat vas deferens, CEC reduces the release of [^{3}H]-noradrenaline that is prevented by pretreatment with rauwolscine. The authors concluded that CEC causes irreversible activation of prejunctional α_2-adrenoceptors (Bultmann & Starke, 1993).

In the dog saphenous vein (DSV), the residual phenylephrine contraction after CEC pretreatment is insensitive to WB4101 or rauwolscine added after the contraction has developed. Subsequently, it became evident to us that this contraction is that of CEC. Moreover, Nunes & Guimaraes (1993) have reported α_2-agonist effects of CEC in the same tissue. In this study, we characterized the mechanisms of contractions caused by CEC in DSV.

[1] Author for correspondence.

Methods

Animals and tissue preparation

Mongrel dogs (10–30 kg) were used. They were killed with an overdose of sodium pentobarbitone (100 mg kg^{-1}, i.v.) using a procedure which was approved by our university Animal Care Committee. The subcutaneous DSV was removed and placed in cold bubbled Krebs solution composed of (mM): NaCl 119, KCl 5, $CaCl_2$ 2.5, $MgCl_2$ 2, $NaHCO_3$ 25, NaH_2PO_4 1 and glucose 11. Fat and connective tissue were removed under a dissecting microscope and 3–4 mm rings were prepared. The endothelium was gently removed with the teeth of a pair of forceps and the rings were mounted on a 15 ml organ bath connected to a force transducer (Grass FT03C) and a chart recorder (Gould 2800). The presence or absence of the endothelial cells was tested functionally using 1 μM carbachol.

The organ baths and Krebs solution were bubbled continuously with 95%O_2/5%CO_2 and warmed to 37°C. The rings were equilibrated for 20 min before they were stretched to their optimal resting force of around 3 g for active contractile responses. Stimulation of the arteries with 100 mM K^+ added hypertonically was repeated every 15–20 min until reproducible contractions were obtained. For Ca^{2+}-free Krebs, $CaCl_2$ was replaced by 50 μM EGTA.

In some experiments, agonist-induced mobilization of internally stored Ca^{2+} and Ca^{2+} entry were studied in the following manner. The preparation was washed with Ca^{2+}-free Krebs solution. The agonist was added to the medium following 5 min of preincubation in Ca^{2+}-free Krebs solution to evaluate contraction due to Ca^{2+} release. Ca^{2+} in increasing concentrations up to 2.5 mM was subsequently added to the bath; the resultant contractions were taken to reflect agonist-stimulated Ca^{2+} entry.

Membrane isolation

For [^{3}H]-rauwolscine binding experiments, the tissues were transferred from bubbled Krebs solution to ice-cold sucrose–MOPS buffer solution (0.25 M sucrose and 10 mM MOPS, pH 7.2) and trimmed as previously reported (Kwan *et al.*, 1983).

The trimmed vascular tissues were minced in 10 ml of ice-cold sucrose–MOPS buffer solution and homogenized with a Polytron PT-20 homogenizer at 15,000 r.p.m. for 15 s The crude tissue homogenate was centrifuged at 1000 *g* for 10 min to remove cell debris, nuclei, collagen fibres, sheets of elastin and basement membranes. The post-nuclear supernatant was filtered through four layers of gauze and centrifuged at 10,000 *g* for 10 min to remove mitochondria. The post-mitochondrial supernatant was further centrifuged at 105,000 *g* for 40 min to remove the fragmented mitochondria. The pellet was resuspended in ice-cold sucrose–MOPS buffer solution with seven up and down strokes using a hand-held glass homogenizer. The suspension was subjected to a final centrifugation of 10,000 *g* for 10 min to remove any trapped mitochondrial membrane. The final turbid supernatant (MIC II) was the partially purified plasma membrane-enriched microsomal fraction used in binding experiments.

Binding study

Radioligand–receptor binding was done in triplicate using [^{3}H]-rauwolscine. Mg^{2+}–MOPS buffer (50 mM MOPS and 10 mM $MgCl_2$, pH 7.2) was used as the incubation medium. [^{3}H]-rauwolscine (77–83 μCi $nmol^{-1}$; New England Nuclear, Boston, MA, U.S.A.) was used as the radioligand and was diluted from stock solution with cold Mg^{2+}–MOPS buffer solution. The incubation medium contained 100 μl of Mg^{2+}–MOPS buffer solution, 25 μl of sucrose–MOPS buffer solution and 25 μl of diluted radioligand. The reaction was started by adding 100 μl of membrane suspension to make a final volume of 250 μl. Incubation was carried out at 25°C for 30 min. The reaction was terminated by addition of ice-cold Mg^{2+}–MOPS buffer solution (4 ml) to the incubation mixture and filtration through Schleicher & Schuell GR 20 glass fibre filters (Mandel) on Millipore filtration manifolds followed by three additional rinses with 4 ml of the same buffer solution. Filters were dried at room temperature and placed in 4 ml of liquid scintillation cocktail (Beckman Instruments, Fullerton, CA, U.S.A.). Non-specific binding ran in parallel for the estimation of total binding, defined as radioactive material not displaced by 10 μM phentolamine. Specific binding was the difference between total and non-specific binding. The radioactivity on the filters was counted in a Beckman (LS-3133T) liquid scintillation counter with a counting efficiency of 40%.

CEC pre-treatment

The microsomal fraction was incubated for 15 min with 100 μM CEC at 37°C. The treatment was terminated by addition of 20 ml of ice-cold sucrose–MOPS buffer. After high-speed centrifugation (105,000 *g* for 40 min), the pellet was resuspended again in sucrose–MOPS buffer with only two strokes in Teflon glass homogenizer. Control experiments with these membranes were conducted in parallel and underwent similar procedures with the ommission of CEC.

Statistical analysis

Results are represented as the mean ± standard error of the mean. Each concentration–response curve was fitted with the Sigmoidal (Logistic) fit using a graphic package named MicroCal Origin (v2.94). An EC_{50} value was obtained for each curve. One-way analysis of variance was performed, and when *F*-ratios were significant appropriate comparisons between the pairs were made. For statistically significant differences, a probability of less than 0.05 was required.

Drugs

CEC was purchased from Research Biochemicals (Natick, MA, U.S.A.) and dissolved in double-distilled deionized water to make a stock solution of 10 mM. Since it degrades rapidly, the stock solution was aliquoted and stored at −20°C. A fresh aliquot was used each time. Prazosin (Sigma, St Louis, MO, U.S.A.), methysergide (Sigma), genistein (Sigma) and SK&F 96365 (Smith-Kline Beecham, Frythe, Welwyn, U.K.) were dissolved in dimethylsulphoxide (DMSO) to make stock solutions of 10 mM. Nicardipine (Sigma), a light-insensitive L-type Ca^{2+} channel antagonist, was dissolved in 100% ethanol to a stock of 10 mM. Propranolol (Ayerst Lab, Montreal, Canada), phentolamine (Sigma) and rauwolscine (Roth, D75 Karlsruhe1, Germany) were dissolved in water.

Results

CEC causes contraction in DSV via prazosin- and rauwolscine-sensitive adrenoceptors

Concentration–response curves for CEC were constructed in the absence and presence of receptor antagonists such as propranolol (30 nM), rauwolscine (30 nM), prazosin (30 nM), methysergide (30 nM) and both prazosin and rauwolscine. Figure 1 shows these curves constructed in DSV expressed as a percentage of 100 mM K^+ contraction. CEC caused a concentration-dependent contraction and the EC_{50} value was determined to be 11.13 ± 3.6 μM ($n = 8$, Table 1). Pretreatment with propranolol (EC_{50} 9.83 ± 5.14 μM, $n = 4$, $P > 0.05$) or methysergide (EC_{50} 23.78 ± 13.24 μM, $n = 4$, $P > 0.05$) had no significant effect on the concentration–response curve for

Table 1 Effects of receptor antagonists on EC_{50} values estimated from CEC concentration response curves and on CEC maximum responses

Receptor antagonists (30 nM)	*EC_{50}* (μM)	*Maximum responses* (percent 100 mM K^+ contraction)	*Number of observations*
Control	11.13 ± 3.6	134.5 ± 21.7	8
Propranolol	9.83 ± 5.14 NS	143.9 ± 41.9 NS	4
Methysergide	23.78 ± 13.24 NS	150.4 ± 23.7 NS	4
Prazosin	29.12 ± 6.42 NS	120.3 ± 12.7 NS	8
Rauwolscine	48.82 ± 13.24*	98.9 ± 15.7 NS	8
Prazosin + Rauwolscine	72.67 ± 10.69*	73.1 ± 5.6*	8

NS, not significantly different from control * Significantly different from control.

CEC. In the presence of prazosin, the CEC concentration-response curve had an EC_{50} value of 29.12 ± 6.42 μM ($n = 8$, $P > 0.05$). When the tissues were pretreated with rauwolscine, the CEC concentration response curve was shifted to the right with an EC_{50} of 48.82 ± 13.24 μM ($n = 8$, $P < 0.05$). In the presence of both prazosin and rauwolscine, the concentration-response curve to CEC was shifted to the right with an EC_{50} value of 72.67 ± 10.69 μM ($n = 8$, $P < 0.05$). The EC_{50} values in the presence of rauwolscine or both prazosin and rauwolscine were all significantly different from the EC_{50} value of control. The responses of the prazosin-treated group were significantly different from the group treated with both prazosin and rauwolscine, although there was no difference between the rauwolscine-treated group and that treated with both rauwolscine and prazosin.

Table 1 also shows the effects of the various receptor antagonists on the maximum responses elicited by CEC. The maximum responses obtained in the presence of propranolol, methysergide, rauwolscine and prazosin were not significantly different from controls ($P > 0.05$). In the presence of both prazosin and rauwolscine, the maximum responses were significantly inhibited ($P < 0.05$).

CEC mobilizes internal Ca^{2+} store

In order to determine whether CEC mobilizes internally stored Ca^{2+}, the rings were stimulated with CEC in Ca^{2+}-free Krebs solution. Under these conditions, CEC (50 μM) caused a transient contraction (17.1 ± 3.5% of 100 mM K^+ contraction, $n = 6$). In the presence of rauwolscine (30 nM), CEC contraction in Ca^{2+}-free medium was abolished ($n = 5$). Contraction in Ca^{2+}-free medium when the tissues were pretreated with prazosin (4.7 ± 0.5% of 100 mM K^+ contraction, $n = 5$, $P < 0.05$) were significantly reduced compared with controls.

CEC causes contraction that is insensitive to nicardipine but blocked by putative receptor-operated Ca^{2+} channel blockers

The contraction caused by CEC was not easily reversed upon washing in Ca^{2+}-containing Krebs solution. In Ca^{2+}-free solution, it caused a small, transient contraction. Restoring Ca^{2+} to the external solution in increasing concentrations (0.5, 1, 1.5, 2 and 2.5 mM) in its presence caused a concentration-dependent increase in the size of contractions which plateaued when external Ca^{2+} reached a concentration of around 1.5 mM (Figure 2).

The data summarized in Figure 2 suggest that a large portion of the tonic contraction induced by CEC depended on extracellular Ca^{2+}. The Ca^{2+} channel that is opened by CEC was investigated. Nicardipine (1 μM), an L-type Ca^{2+} channel blocker, was added to the bath at the plateau of CEC concentration. Figure 3 shows that the addition of nicardipine did not significantly reduce the contraction caused by CEC.

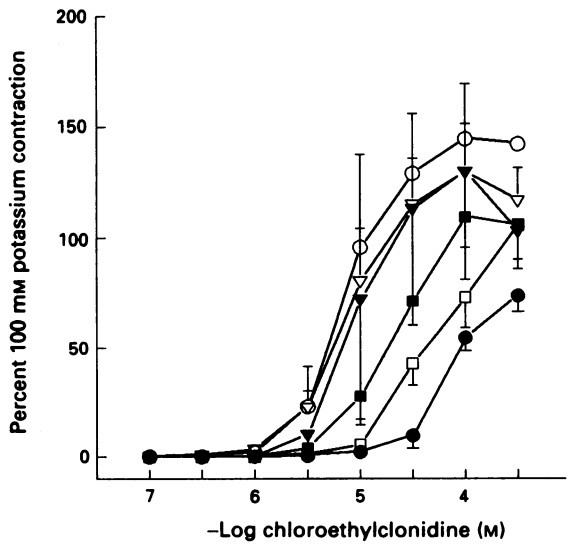


Figure 1 Concentration-response curves were constructed for CEC in the absence (▽, $n = 4-8$) and presence of propranolol (30 nM, ▼, $n = 3-4$), rauwolscine (30 nM, □, $n = 6-8$), prazosin (30 nM, ■, $n = 4-8$), methysergide (30 nM, ○, $n = 1-4$) or both prazosin and rauwolscine (●, $n = 6-8$). Responses were expressed as a percentage of 100 mM K^+ contraction.

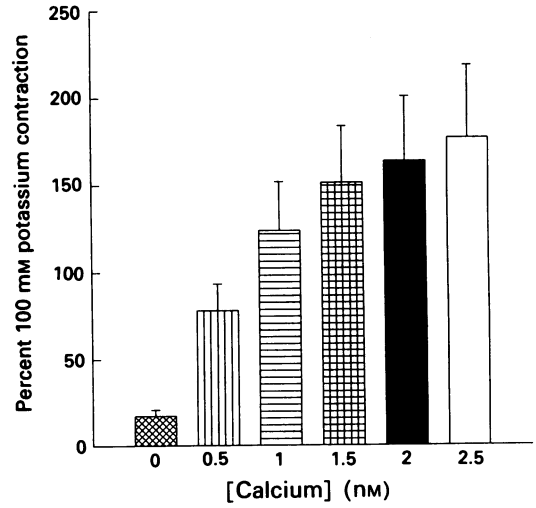


Figure 2 When external Ca^{2+} was replaced with 50 μM EGTA, a Ca^{2+}-chelating agent, CEC (50 μM) caused a transient contraction (0 [Ca^{2+}] mM), albeit significantly smaller than in the presence of external Ca^{2+}. Addition of Ca^{2+} to the external medium caused a concentration-dependent increase in the size of the contraction which was expressed as a percentage of 100 mM K^+ contraction from 4-6 experiments. The CEC contraction appeared to reach a plateau when external Ca^{2+} was 1.5 mM.

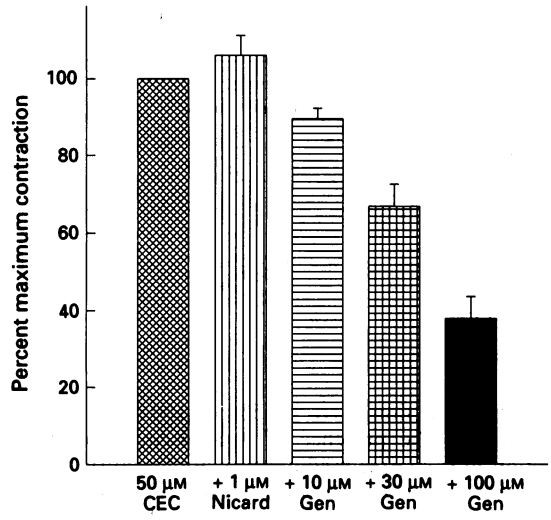


Figure 3 Contraction caused by CEC depended on Ca^{2+} entry from the extracellular space. Nicardipine (Nicard, 1 μM), an L-type Ca^{2+} channel block, did not inhibit contraction induced by CEC (50 μM). Genistein (Gen), a naturally occurring tyrosine kinase inhibitor, caused reversible concentration-dependent reduction in CEC-induced contraction, Responses were expressed as a percentage of CEC contraction from 11 experiments.

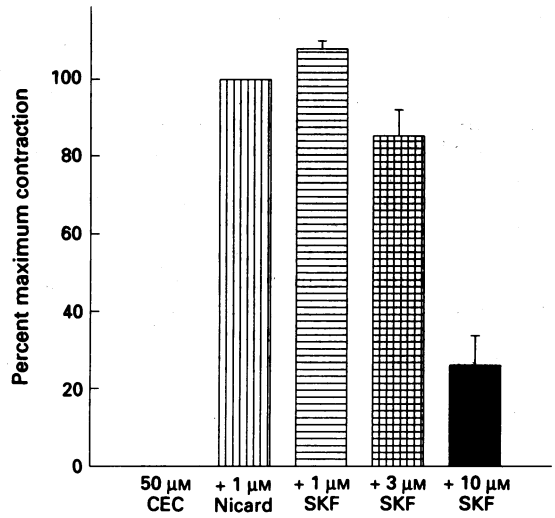


Figure 4 Addition of SK&F 96365 (SKF), a putative Ca^{2+} channel blocker, in a concentration-dependent manner relaxed CEC (50 μM)-induced contraction in the presence of 1 μM nicardipine (Nicard). Responses are expressed as a percentage of CEC responses in the presence of nicardipine from 10 experiments. The effect of SK&F 96365 was irreversible upon washing.

Ca^{2+} from the extracellular space can also enter the cell via receptor-operated Ca^{2+} channels. Putative inhibitors of these channels have recently been identified and become available. These are SK&F 96365 (Merritt *et al.*, 1990; Sage *et al.*, 1990; Schilling *et al.*, 1992) and genistein, also a tyrosine kinase inhibitor (Saifeddine *et al.*, 1992; Lee *et al.*, 1993; Sargeant *et al.*, 1993). Figure 3 shows the concentration-dependent inhibition of CEC-induced contraction by genistein, whose action was reversed upon washing. This experiment was performed in the presence of nicardipine since genistein has been shown to block voltage-operated Ca^{2+} channels (Wijetunge *et al.*, 1992). Figure 4 shows that addition of SK&F 96365, in a concentration-dependent manner in the presence of nicardipine (since SK&F 96365, like genistein, also blocks voltage-operated Ca^{2+} channels; Merritt *et al.*, 1990), caused inhibition of the CEC-induced contraction. The effect of SK&F 96365 was irreversible.

Table 2 [^{3}H]-Rauwolscine or [^{3}H]-prazosin saturation of DSV and the effects of CEC (100 μM) after 15 min preincubation at 37°C

	Control	*+CEC*
[^{3}H]-Rauwolscine		
K_d (nM)	5.35 ± 0.93	5.44 ± 1.37
B_{max} (fmol mg^{-1})	832.4 ± 168.2	407.4 ± 111*
Hill coefficient	0.925 ± 0.02	0.95 ± 0.03
Percent binding	100	44.6 ± 0.79
No. of experiments	3	3
[^{3}H]-Prazosin		
K_d (nM)	2.6 ± 1.24	
B_{max} (fmol mg^{-1})	385.07 ± 106.72	No binding
Hill coefficient	0.909 ± 0.06	
Percent binding	100	0
No. of experiments	3	4

*$P < 0.05$ compared with control.

CEC abolishes prazosin binding sites and reduces B_{max} for rauwolscine

Since functional studies suggested that CEC interacts with both prazosin- and rauwolscine-sensitive receptors, we evaluated the effects of CEC pretreatment on saturation binding of these two antagonists. Table 2 shows that CEC (100 μM) abolished prazosin binding and reduced B_{max} for rauwolscine by about 50% without affecting the K_d value or the Hill slope (near 1.0 with or without CEC treatment).

Discussion

The findings from this study indicated that CEC causes contractions mainly by stimulating rauwolscine-sensitive adrenoceptors and, to a lesser extent, prazosin-sensitive adrenoceptors. While CEC mobilizes internally stored Ca^{2+}, it also causes contractions that were insensitive to L-type Ca^{2+} channel blockade. The contractions, however, were inhibited by putative receptor-operated Ca^{2+} channel antagonists, SK&F 96365 and genistein, which is also a tyrosine kinase inhibitor.

Interestingly, to date, there is no definitive evidence for the coupling of α_2-adrenoceptors to phospholipase C. Therefore, it is unlikely that the blockade of CEC-induced release of internally stored Ca^{2+} and Ca^{2+} influx by rauwolscine occurred via α_2-adrenoceptors. In an earlier study, Matthews *et al.* (1984) reported that under Ca^{2+}-free conditions responses to B-HT 920, an α_2-adrenoceptor agonist, in DSV were abolished, whereas phenylephrine responses in Ca^{2+}-free medium were still present, albeit much reduced compared with its responses in Ca^{2+}-containing medium. The responses to phenylephrine were blocked by yohimbine, an isomer analogue of rauwolscine (Hicks *et al.*, 1991). In the same tissue (DSV), our earlier studies showed that B-HT 920 did cause small contractions in Ca^{2+}-free Krebs (Guan *et al.*, 1989). The discrepancy may be due to the use of a higher concentration (2 mM versus 50 μM) of the Ca^{2+} -chelating agent, EGTA, by Matthews *et al.* (1984).

In addition, Hicks *et al.* (1991) also showed that α_1-agonists such as phenylephrine and cirazoline cause concentration-dependent increases above baseline in the total [^{3}H]-inositol phosphate production, while BHT-920 causes only weak inositol phosphate production which is not concentration-dependent but which may explain the small BHT-920-induced contraction in Ca^{2+}-free solution reflecting Ca^{2+} release from the internal Ca^{2+} stores (Guan *et al.*, 1989).

α_2-Adrenoceptors have been recognized functionally by their selectivity towards certain agonists (e.g. UK14,304, B-HT 920) and certain antagonists (e.g. yohimbine or rauwolscine). α_1-Adrenoceptors have been distinguished by their

selective interactions with different agonists (e.g. phenylephrine or methoxamine) and antagonists (e.g. prazosin). Although these selective functional interactions have retained their validity over many tissues, there has been less certainty that different affinities of agonists in binding to α_1- and α_2-adrenoceptors account for their functional selectivities (Daniel *et al.*, 1991). Indeed, in the DSV, there has been an unexplained ability of yohimbine or rauwolscine to antagonize competitively phenylephrine-induced contractions (reviewed in Hicks *et al.*, 1991; unpublished observations) but not those of methoxamine (unpublished observations). Therefore, with regard to the nature of the α-adrenoceptors in the DSV upon which CEC acts to cause a contraction, it is unclear as to whether these adrenoceptors can be easily classified as α_1- or α_2-adrenoceptors. They are, therefore, better described as rauwolscine-sensitive adrenoceptors or unusual α-adrenoceptors. Furthermore, Nunes & Guimaraes (1993) have clearly (based on the differential temperature dependence of the contractile responses of CEC, phenylephrine and UK-14,304) shown that the adrenoceptors upon which CEC acts on in the DSV are different from those upon which UK-14,304 or phenylephrine acts.

The contractions mediated by CEC, which persisted for many minutes and were not easily reversed by washing, depended to a large extent on extracellular Ca^{2+}. This finding is consistent to that of Nunes & Guimaraes (1993). The Ca^{2+} entry induced by CEC occurred by way of the SK&F 96365-sensitive receptor-operated Ca^{2+} channels (Merritt *et al.*, 1990; Sage *et al.*, 1990; Schilling *et al.*, 1992) and not through the nicardipine-sensitive voltage-operated Ca^{2+} channels. These observations may only be partially explained by Putney's (1986) model of Ca^{2+} entry: that Ca^{2+} release and subsequent depletion of the internal Ca^{2+} stores promotes a capacitative route for Ca^{2+} entry since CEC-induced Ca^{2+} release as indicated by the transient contraction in Ca^{2+}-free Krebs solution is relatively small compared with those observed using phenylephrine. Furthermore, subsequent additional of phenylephrine (10 μM) in the presence of CEC in Ca^{2+}-free medium caused larger transient contractions (unpublished observations). These observations suggest that there are additional mechanisms involved in the regulation of agonist-induced Ca^{2+} entry since stimulation with CEC alone did not completely deplete the internal stores but still caused extracellular-dependent Ca^{2+} contraction.

Recent evidence suggests a role for tyrosine kinase in the regulation of Ca^{2+} entry. Receptor tyrosine kinases are cell-surface glycoproteins with extracellular ligand-binding domains and transmembrane and intracellular tyrosine kinase domains. They can be activated by endocrine, paracrine or autocrine growth factors (Levitzki, 1992). In contrast, non-receptor protein tyrosine kinases, such as those in the *src* and *abl* subfamilies, lack extracelular and transmembrane domains and membrane signal sequences (Maness, 1992). Since protein tyrosine kinase inhibitors have been reported to block responses that are activated independent of receptor tyrosine kinase, this suggests that non-receptor tyrosine kinases can interact with the intracellular signal transduction cascade of G-protein-coupled receptor agonists. The observation that genistein, a tyrosine kinase inhibitor, also blocks the CEC contraction in a concentration-dependent manner suggests that tyrosine kinase has a role in the regulation of this route of Ca^{2+} entry (Saifeddine *et al.*, 1992; Lee *et al.*, 1993; Sargeant *et al.*, 1993) as originally hypothesized by Vostal *et al.* (1991); these investigators observed that thrombin elevated cytosolic Ca^{2+} and caused tyrosine phosphorylation of a 130 kDa protein in human platelets. They further showed that chelation of cytosolic Ca^{2+} decreased the thrombin-induced tyrosine phosphorylation. In addition, inhibition of agonist- and thapsigargin-induced Ca^{2+} entry by tyrosine kinase inhibitors such as genistein and tyrphostin has been observed in fura-2-loaded human foreskin fibroblast cells (Lee *et al.*, 1993) and human platelets (Sargeant *et al.*, 1993).

The ability to CEC to abolish 50% of rauwolscine binding sites while eliminating prazosin binding provides additional insight into its mode of action. In this tissue, there is a much lower density of prazosin than rauwolscine binding sites (Shi *et al.*, 1989), and in this study we confirmed that the B_{max} for prazosin binding was 385 fmol mg^{-1} vs 832 fmol mg^{-1} for rauwolscine binding. The number of rauwolscine binding sites eliminated by CEC approximately equalled the total number of prazosin binding sites. These findings suggest that CEC interacts in DSV with the α_{1B} (prazosin-sensitive)-adrenoceptors to abolish them and also interacts with rauwolscine binding sites, most or all of which must be unrelated to the prazosin binding sites. Moreover, after CEC pretreatment, phenylephrine still causes contraction in this tissue (unpublished observations), presumably by acting at rauwolscine-sensitive binding sites. The binding sites abolished by CEC may be involved in the CEC-induced contractile responses, as suggested by the ability of prazosin and/or rauwolscine to antagonize them.

In conclusion, the findings of this study provided evidence that CEC not only irreversibly inactivates α_{1B}-adrenoceptor subtype, but also acts on certain α-adrenoceptors in DSV sensitive to rauwolscine. Identification of this adrenoceptor subtype requires the use of more selective pharmacological agonists and antagonists. CEC opens a route for Ca^{2+} entry, sensitive to SK&F 96365 but not nicardipine, which appears to be regulated by a tyrosine kinase.

The authors are grateful to Dr E.E. Daniel (McMaster University) and Dr C.Y. Kwan (University of Hong Kong) for constructive criticisms of the manuscript and for resources made available to authors through grants to them from the Medical Research Council and the Ontario Heart and Stroke Foundation of Canada. A.M.L. is an MRC post-doctoral fellow. D.M.B. and T.R.P. are Hill Park Secondary School Co-op students.

References

BULTMANN, R. & STARKE, K. (1993). Chloroethylclonidine: an irreversible agonist at prejunctional α_2-adrenoceptors in rat vas deferens. *Br. J. Pharmacol.*, **108**, 336–341.

DANIEL, E.E., SHI, A.G., WANG, Z.L., GUAN, Y.Y., HOO, K.H., CRAGOE, E.J. & KWAN, C.Y. (1991). Alpha-adrenoceptors in vascular smooth muscle: all is not well. *Blood Vessels*, **28**, 104–114.

GUAN, Y.Y., KWAN, C.Y. & DANIEL, E.E. (1989). Does *in vitro* activation of postsynaptic α_2-adrenoceptor utilize intracellular Ca^{2+} for contraction in dog saphenous vein? *Can. J. Physiol. Pharmacol.*, **67**, 1086–1091.

HAN, C., LI, J. & MINNEMAN, K.P. (1990). Subtypes of α_1-adrenoceptors in rat blood vessels. *Eur. J. Pharmacol.*, **190**, 97–104.

HAN, C., ABEL, P.W. & MINNEMAN, K.P. (1987). Heterogeneity of α_1-adrenergic receptors revealed by chloroethylclonidine. *Mol. Pharmacol.*, **32**, 505–510.

HICKS, P.E., BARRAS, M., HERMAN, G., MAUDUIT, P., ARMSTRONG, J.M. & ROSSIGNOL, B. (1991). α-Adrenoceptor subtypes in dog saphenous vein that mediate contraction and inositol phosphate production. *Br. J. Pharmacol.*, **102**, 151–161.

KWAN, C.Y., TRIGGLE, C.R., GROVER, A.K., LEE, R.M.K.W. & DANIEL, E.E. (1983). An analytical approach to the preparation and characterization of subcellular membranes from canine mesenteric arteries. *Preparative Biochem.*, **13**, 275–314.

LEE, K.-M., TOSCAS, K. & VILLEREAL, M.L. (1993). Inhibition of bradykinin- and thapsigargin-induced Ca^{2+} entry by tyrosine kinase inhibitors. *J. Biol. Chem.*, **268**, 9945–9948.

LEVITZKI, A. (1992). Tyrphostins: tyrosine kinase blockers as novel antiproliferative agents and dissectors of signal transduction. *FASEB J.*, **6**, 3275–3282.

MANESS, P.F. (1992). Nonreceptor protein tyrosine kinases associated with neuronal development. *Dev. Neurosci.*, **14**, 257–270.

MATTHEWS, W.D., JIM, K.F., HIEBLE, J.P. & DEMARINIS, R.M. (1984). Postsynaptic α-adrenoceptors on vascular smooth muscle. *Fed. Proc. Am. Exp. Soc.*, **43**, 2923–2928.

MERRITT, J.E., ARMSTRONG, W.P., BENHAM, C.D., HALLAM, T.J., JACOB, R., JAXA-CHAMIEC, A., LEIGH, B.K., MCCARTHY, S.A., MOORES, K.E. & RINK, T.J. (1990). SK&F 96365, a novel inhibitor or receptor-mediated Ca^{2+} entry. *Biochem. J.*, **271**, 515–522.

MINNEMAN, K.P. (1988). α_1-Adrenergic receptor subtypes, inositol phosphates and source of cell Ca^{2+}. *Pharmacol. Rev.*, **40**, 87–119.

NUNES, J.P. & GUIMARAES, S. (1993). Chloroethylclondine irreversibly activates postjunctional alpha$_2$-adrenoceptors in the dog saphenous vein. *Naunyn-Schmied. Arch. Pharmacol.*, **348**, 264–268.

PUTNEY JR, J.W. (1986). A model for receptor-regulated Ca^{2+} entry. *Cell Calcium*, **7**, 1–12.

SAIFEDDINE, M., LANIYONU, A., YANG, S.-G. & HOLLENBERG, M.D. (1992). Tyrosine kinase inhibitors and the contractile action of angiotensin-II in vascular tissue. *Pharmacol. Comm.*, **1**, 177–184.

SAGE, S.O., REAST, R. & RINK, T.J. (1990). ADP evokes biphasic Ca^{2+} influx in fura-2 loaded human platelets. Evidence for Ca^{2+} entry regulated by the intracellular Ca^{2+} store. *Biochem. J.*, **265**, 675–680.

SARGEANT, P., FARNDALE, R.W. & SAGE, S.O. (1993). ADP- and thapsigargin-evoked Ca^{2+} entry and protein-tyrosine phosphorylation are inhibited by the tyrosine kinase inhibitors genistein and methyl-2,5-dihydroxycinnamate in fura-2-loaded human platelets. *J. Biol. Chem.*, **268**, 18151–18156.

SAYET, I., NEUILLY, G., RAKOTOARISOA, L., MIRONNEAU, C. & MIRONNEAU, J. (1993). Relation between α_1-adrenoceptor subtypes and noradrenaline-induced contraction in rat portal vein smooth muscle. *Br. J. Pharmacol.*, **110**, 207–212.

SCHILLING, W.P., CABELLO, O.A. & RAJAN, L. (1992). Depletion of the inositol 1,4,5-trisphosphate-sensitive intracellular Ca^{2+} store in vascular endothelial cells activates the agonist-sensitive Ca^{2+}-influx pathway. *Biochem. J.*, **284**, 521–230.

SCHWIETERT, H.R., GOUW, M.A.M., WILHELM, D., WILFFERT, B. & VAN ZWIETEN, P.A. (1991). The role of α_1-adrenoceptor subtypes in the phasic and tonic responses to phenylephrine in the longitudinal smooth muscle of the rat portal vein. *Naunyn-Schmied. Arch. Pharmacol.*, **343**, 463–471.

SHI, A.G., KWAN, C.Y. & DANIEL, E.E. (1989). Relation between density (Bmax) of alpha adrenoceptor binding sites and contractile response in four canine vascular tissues. *J. Pharmacol. Exp. Ther.*, **250**, 1119–1124.

VARGAS, H.M., CUNNINGHAM, D., ZHOU, L., HARTMAN, H.B. & GORMAN, A.J. (1993). Cardiovascular effects of chloroethylclonidine, an irreversible α_{1B}-adrenoceptor antagonist, in the unanaesthetized rat: a pharmacological analysis *in vivo* and *in vitro*. *J. Pharmacol. Exp. Ther.*, **266**, 864–871.

VOSTAL, J.G., JACKSON, W.L. & SCHULMAN, N.R. (1991). Cytosolic and stored Ca^{2+} antagonistically control tyrosine phosphorylation of specific platelet proteins. *J. Biol. Chem.*, **266**, 16911–16916.

WATSON, S. & GIRDLESTONE, D. (1994). 1994 receptor & ion channel nomenclature supplement. *Trends Pharmacol. Sci.* (Suppl).

WIJETUNGE, S., AALKJAER, C., SCHACHTER, M. & HUGHES, A.D. (1992). Tyrosine kinase inhibitors block Ca^{2+} channel currents in vascular smooth muscle cells. *Biochem. Biophys. Res. Commun.*, **189**, 1620–1623.

(Received April 12, 1994
Revised July 26, 1994
Accepted August 15, 1994)

Br. J. Pharmacol. (1994), **113**, 1269–1274 © Macmillan Press Ltd, 1994

Effect of type A and B monoamine oxidase selective inhibition by Ro 41-1049 and Ro 19-6327 on dopamine outflow in rat kidney slices

[1]M. Pestana & [2]P. Soares-da-Silva

Institute of Pharmacology and Therapeutics, Faculty of Medicine, 4200 Porto, Portugal

1 The influence of pargyline and of selective inhibitors of type A and B monoamine oxidase (MAO), Ro 41-1049 and Ro 19-6327 respectively, on the outflow of dopamine and 3,4-dihydroxyphenylacetic acid (DOPAC) in slices of rat renal cortex loaded with exogenous L-3,4-dihydroxyphenylalanine (L-DOPA) was examined. Dopamine and DOPAC in the tissues and in the effluent were assayed by means of h.p.l.c. with electrochemical detection.

2 The levels of newly-formed dopamine and DOPAC in the perifusate decreased progressively with time. In control conditions, DOPAC/dopamine ratios in the perifusate were 3 to 5 fold those in the tissue and were found to increase progressively with time. The addition of pargyline (100 μM), produced a marked decrease in the outflow levels of DOPAC (45 to 54% reduction) and significantly increased the levels of dopamine in the effluent (102 to 158% increase); DOPAC/dopamine ratios in the perifusate remained stable throughout the perifusion and were similar to those found in the tissues. The addition of the MAO-A inhibitor Ro 41-1049 to the perifusion fluid also significantly decreased DOPAC outflow (41% to 54% reduction) and increased dopamine outflow (19% to 80% increase). In the presence of Ro 41-1049 DOPAC/dopamine ratios in the perifusate were lower ($P<0.01$) than in controls; in contrast with the effect of pargyline, this ratio was found to increase ($P<0.01$) throughout the perifusion period. Ro 19-6327 did not reduce the outflow of DOPAC, but significantly increased (by 40–60%) that of dopamine. In the presence of Ro 19-6237, the proportion of DOPAC to dopamine in the perifusate was similar to that of controls and significantly increased throughout the perifusion; however, this increase was less than that observed in the control group.

3 When benserazide (50 μM) was added to the perifusion fluid, the levels of both dopamine and DOPAC in the effluent were similar to those observed in the absence of benserazide. However, in the presence of benserazide, DOPAC/dopamine ratios in the perifusate did not increase with time. In conditions of decarboxylase inhibition, the effects of pargyline, Ro 41-1049 and Ro 19-6327 on dopamine and DOPAC outflow were less pronounced than in experiments conducted in the absence of benserazide.

4 In conclusion, the results presented here show that the fraction of newly-formed dopamine which leaves the compartment where the synthesis has occurred is a constant source for deamination into DOPAC. The results provide evidence favouring the view that MAO-A is the main form of the enzyme involved in this process; however, the data described here suggest that dopamine would also have access to MAO-B.

Keywords: Dopamine; 3,4-dihydroxyphenylacetic acid (DOPAC); monoamine oxidase; kidney; pargyline; Ro 41-1049; Ro 19-6327; benserazide

Introduction

Evidence accumulated in recent years has favoured the view that locally formed dopamine may play a considerable role in the regulation of tubular sodium reabsorption. The inhibitory effect of dopamine on tubular sodium reabsorption has been demonstrated to be dependent on the activation of specific receptors for the amine, resulting in inhibition of both Na^+-K^+ ATPase and Na^+-H^+ antiport activities (Aperia *et al.*, 1987; Felder *et al.*, 1990). The source of dopamine responsible for the natriuretic effects of the amine is believed to reside in epithelial cells of the proximal convoluted tubules. These cells are endowed with a high aromatic L-amino acid decarboxylase (AAAD) activity and L-3,4-dihydroxyphenylalanine (L-DOPA) in the tubular filtrate represents the major source of the precursor for the amine. After being taken up into the tubular epithelial cell, L-DOPA has been shown to undergo rapid decarboxylation to dopamine. It has also been suggested that the tubular epithelial cells in which the synthesis occurs may be endowed with or be located near those endowed with dopamine receptors, leading to the possibility that dopamine in the kidney may act as a paracrine and/or autocrine substance (Siragy *et al.*, 1989).

In order to be active, however, the dopamine originating in tubular epithelial cells must leave the cellular compartment where the synthesis has occurred. This is a matter of considerable importance since the receptors on which the amine is supposed to act are located on the external surface of the cell membrane (Jose *et al.*, 1992). On the other hand, the amount of dopamine that is available for the activation of dopamine receptors may depend not only on the activity of AAAD and on the levels of L-DOPA in the tubular filtrate, but also on the magnitude of the metabolism to which dopamine is submitted. In fact, renal tissues are endowed with one of the highest monoamine oxidase (MAO) activities in the body (Kopin, 1985) and deamination of newly-formed dopamine into 3,4-dihydroxyphenylacetic acid (DOPAC) represents a major pathway for the inactivation of the amine (Soares-da-Silva & Fernandes, 1990).

Both the A and B forms of MAO, (MAO-A and MAO-B), have been shown to be involved in the deamination of newly-

[1]On leave from the Dept. of Nephrology, Faculty of Medicine, 4200 Porto, Portugal
[2]Author for correspondence

formed dopamine in rat kidney slices loaded with exogenous L-DOPA (Fernandes & Soares-da-Silva, 1990); however, it has been suggested that the deamination of newly-formed dopamine by these two types of MAO occurs in different compartments. Indirect evidence has suggested that MAO-A is predominantly active in the compartment where the synthesis of dopamine takes place, whereas MOA-B is thought to be mainly active outside this compartment (Fernandes & Soares-da-Silva, 1990; Fernandes *et al.*, 1991). However, the different behaviour of types A and B MAO on the deamination of newly-formed dopamine may only reflect the cellular compartmentalization of the two forms of the enzyme.

The aim of the present study was to define whether deamination of newly-formed dopamine by MAO-A or by MAO-B reflects the preferential access of the amine to one of the enzymes during the cell outflow process. For this purpose we have studied the influence of pargyline, a non-selective MAO inhibitor, and of two selective MAO-A and MAO-B inhibitors, Ro 41-1049 and Ro 19-6327 respectively (Da Prada *et al.*, 1990), on the outflow of newly-formed dopamine and of its deaminated metabolite DOPAC in slices of rat renal cortex loaded with exogenous L-DOPA. A preliminary account of some of these findings has been presented previously (Pestana & Soares-da-Silva, 1992).

Methods

Male Wistar rats (Biotério do Instituto Gulbenkian de Ciência, Oeiras, Portugal) 30–60 days old and weighing 200–250 g were used in the experiments. Animals were kept three per cage under controlled environmental conditions (12 h light/dark cycle and room temperature 24°C). Food and tap water were allowed *ad libitum* and the experiments were all carried out during daylight hours.

Rats were killed by decapitation under ether anaesthesia and both kidneys removed and rinsed free from blood with saline (NaCl 0.9%). The kidneys were placed on an ice-cold glass plate and the kidney poles removed; thereafter, slices approximately 1.5 mm thick were obtained with a scalpel and four cortical fragments weighing about 60 mg were prepared and preincubated for 30 min in warm (37°C) and gassed (95% O_2 and 5% CO_2) Krebs solution. After preincubation, renal fragments were incubated for 15 min in 2 ml of warm and gassed Krebs solution with added L-DOPA (100 μM). Thereafter, the cortical slices were transferred to individual glass perifusion chambers, perifused with warm and gassed Krebs solution at a rate of 350 μl min^{-1} by means of a Gilson pump (Minipulse 2) and allowed a 30 min stabilization period. After the washing period, five consecutive 10 min perifusate samples were collected into glass tubes kept on ice and containing 500 μl of 2 M perchloric acid. The composition of the Krebs solution used in the experiments was as follows (in mM): NaCl 118; KCl 4.7; $CaCl_2$ 2.4; $MgSO_4$ 1.4; $NaHCO_3$ 25; KH_2PO_4 1.2; EDTA 0.4 and glucose 11; tropolone (50 μM) was added to the Krebs solution in order to inhibit the enzyme catechol-*O*-methyltransferase (COMT). In experiments performed with the aim of testing the influence of MAO inhibition on the outflow of dopamine and DOPAC, the MAO inhibitor pargyline (100 μM), Ro 41-1049 (250 nM) or Ro 19-6327 (250 nM) was added to the perifusion fluid. The concentration of pargyline, Ro 41-1049 and Ro 19-6327 used here was selected in the light of previous studies in renal tissues and have been shown to produce maximal inhibitory effects (Fernandes & Soares-da-Silva, 1990; Fernandes *et al.*, 1991); at high concentrations, both Ro 41-1049 and Ro 19-6327 may lose selectivity (Da Prada *et al.*, 1990; Guimarães & Soares-da-Silva, 1994). In some experiments, renal slices were perifused in the presence of 50 μM benserazide, in order to prevent the formation of dopamine during the perifusion period. At the end of the incubation period, tissues were collected and immediately placed in perifusion chambers and perifused from then onwards in the presence of benserazide. In some of these experiments, the effect of pargyline, Ro-41-1049 and Ro 19-6327 was also tested.

The assay of dopamine and DOPAC in renal slices and perifusate samples was performed by means of high pressure liquid chromatography (h.p.l.c.) with electrochemical detection, as previously described (Soares-da-Silva *et al.*, 1992). The lower limits for detection of dopamine and DOPAC were 8 and 14 pmol g^{-1}, respectively.

Dopamine hydrochloride, L-β-3,4-dihydroxyphenylalanine (L-DOPA), 3,4-dihydroxyphenylacetic acid (DOPAC), pargyline hydrochloride and tropolone hydrochloride were purchased from the Sigma Chemical Company (St Louis, MO, U.S.A.). Ro 41-1049 ((N-(2-aminoethyl)-5-(*m*-fluoro-phenyl)-4-thiazolecarboxamide hydrochloride), Ro 19-6327 ((N-(2-aminoethyl)-5-chloro-2-pyridine carboxamide hydrochloride) and benserazide were kindly donated by Prof. Mosé Da Prada, Hoffmann-La Roche (Basle, Switzerland).

Statistics

Results are means ± s.e. mean of values for the indicated number of experiments. Statistical significance was determined by the Tuckey-Kramer method (Sokal & Rohlf, 1981). A P value less than 0.05 was assumed to denote a significant difference.

Results

The levels of endogenous dopamine in the rat renal cortex (0.024 ± 0.006 nmol g^{-1}) were found to be lower than in renal cortical fragments incubated in the presence of L-DOPA (100 μM); levels of endogenous DOPAC were below the detection limit of the method (14 pmol g^{-1}). As shown in Table 1, the tissue concentration of newly-formed dopamine and DOPAC in renal cortical fragments perifused with pargyline, Ro 41-1049 and Ro 19-6327 did not differ significantly from those of corresponding controls (i.e., loaded with L-DOPA and perifused in the absence of MAO inhibitors); however, DOPAC/dopamine ratios in renal tissues perifused in the presence of Ro 41-1049 were found to be lower ($P<0.01$) than those of controls.

The outflow of dopamine and DOPAC in renal tissues loaded with L-DOPA (100 μM) was found to decrease progressively with time (Figure 1), but did not exhibit a monophasic decline, as evidenced by their upward concave shape when the levels of dopamine (from 0.84 ± 0.10 to 0.16 ± 0.03 nmol g^{-1} 10 min^{-1}) and DOPAC (0.80 ± 1.0 to 0.24 ± 0,02 nmol g^{-1} 10 min^{-1}) in the perifusate were logarithmically transformed and plotted against the time of perifusion (not shown, but see Pestana & Soares-da-Silva, 1994). Under control conditions, however, the decline of DOPAC outflow throughout the perifusion period did not follow that of dopamine; this is shown by the progressive increase of DOPAC/dopamine ratios in the perifusate (from 0.95 ± 0.07 to 1.77 ± 0.25, $n=8$, Figure 2). It is interesting to note that DOPAC/dopamine ratios in the perifusate were 3 to 5 fold those in the tissue. The addition of pargyline (100 μM), produced a marked decrease in the outflow levels of DOPAC (45 to 54% reduction) and significantly increased the levels of dopamine in the effluent (102 to 158% increase). In the presence of pargyline, in contrast to observations in controls, DOPAC/dopamine ratios in the perifusate remained stable throughout the perifusion (from 0.26 ± 0.02 to 0.33 ± 0.02) and were similar to those found to occur in the tissues (0.27 ± 0.02). As shown in Figure 1, the addition of the MAO-A inhibitor Ro 41-1049 to the perifusion fluid also significantly decreased DOPAC outflow (41% to 54% reduction) and increased dopamine outflow (19% to 80% increase). In the presence of Ro 41-1049 DOPAC/dopamine ratios in the perifusate were lower ($P<0.01$) than in controls, but, in contrast to results with pargyline, this ratio was

found to increase ($P<0.01$) throughout the perifusion period from 0.33 ± 0.04 to 0.66 ± 0.10 (Figure 2). As shown in Figure 1, Ro 19-6327 did not reduce the outflow of DOPAC, but significantly increased by 40–60% that of dopamine. In the presence of Ro 19-6327, the proportion of DOPAC to dopamine in the perifusate was similar to that of controls, and significantly increased from 0.86 ± 0.06 to 1.19 ± 0.13 throughout the perifusion; this increase was, however, less than that observed in the control group.

Table 1 Tissue levels (in nmol g^{-1}) of dopamine and dihydroxyphenylacetic acid (DOPAC), and DOPAC/ dopamine ratios at the end of perifusions performed in the absence (**A**) and in the presence of benserazide (50 μM) (**B**)

A

	Dopamine (nmol g^{-1})	*DOPAC* nmol g^{-1})	*DOPAC/dopamine*	(*n*)
Control	3.39 ± 0.39	1.05 ± 0.15	0.31 ± 0.02	8
Pargyline	3.85 ± 0.43	1.12 ± 0.23	0.27 ± 0.03	7
Ro 41-1049	3.67 ± 0.53	0.71 ± 0.10	0.20 ± 0.02*	8
Ro 19-6327	4.07 ± 0.38	1.37 ± 0.17	0.33 ± 0.02	7

B

	Dopamine (nmol g^{-1})	*DOPAC* nmol g^{-1})	*DOPAC/dopamine*	(*n*)
Control	3.60 ± 0.37	1.13 ± 0.11	0.32 ± 0.03	4
Pargyline	4.91 ± 1.02	0.91 ± 0.32	0.17 ± 0.03*	4
Ro 41-1049	7.20 ± 2.56	1.41 ± 0.68	0.20 ± 0.04*	4
Ro 19-6327	4.42 ± 0.23	1.11 ± 0.04	0.25 ± 0.01	4

Significantly different from values of corresponding controls, *$P<0.01$.

Results are shown for observations in control conditions and in the presence of pargyline (100 μM), Ro 41-1049 (250 nM) and Ro 19-6327 (250 nM). Each value represents the mean ± s.e.mean of *n* experiments per group.

Figure 3 shows the outflow of dopamine and DOPAC in experiments carried out in the presence of benserazide (50 μM); the AAAD inhibitor was added to the perifusion fluid from the beginning of the perifusion period. In this set of experiments, the levels of both dopamine and DOPAC in the perifusate under control conditions were similar to those observed in the absence of benserazide. However, in the presence of benserazide DOPAC/dopamine ratios in the perifusate failed to show a tendency to increase with time (0.77 ± 0.12 to 1.01 ± 0.11) (Figure 4). Under conditions of AAAD inhibition, pargyline produced a marked reduction of DOPAC outflow (60% decrease) and only a slight increase (20 to 30% increase) in the outflow of dopamine (Figure 3). DOPAC/dopamine ratios in the perifusate were also markedly reduced by pargyline (Figure 4), as was observed in the absence of benserazide. The changes in the outflow levels of dopamine and DOPAC during selective MAO-A inhibition with Ro 41-1049 in the presence of benserazide, were similar to those observed with pargyline (Figures 3 and 4). DOPAC/dopamine ratios in the perifusate were reduced to an extent similar to that observed with pargyline and did not show a tendency to increase with time (Figure 4). In the presence of benserazide, Ro 19-6327 was found not to change the outflow levels of both dopamine and DOPAC, but DOPAC/dopamine ratios in the perifusate were found to be similar to those in controls, which contrasts with those observed in experiments performed in the absence of benserazide (Figure 4).

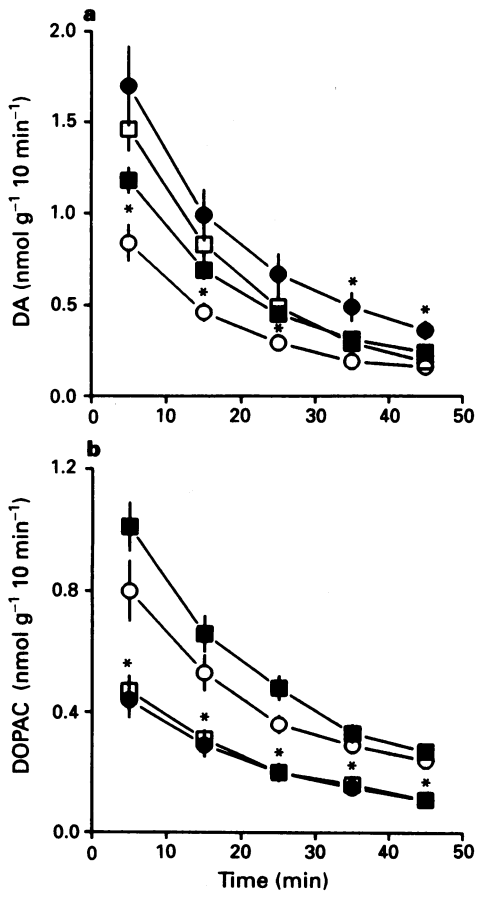


Figure 1 Dopamine (a) and DOPAC (b) outflow levels (in nmol g^{-1} 10 min^{-1}) in 10 min perifusate samples of renal cortical fragments in control conditions (○) and in the presence of pargyline (100 μM; ●), Ro 41-1049 (250 nM; □) or Ro 19-6327 (250 M; ■). Each point represents the mean ± s.e.mean of 7 to 8 experiments per group. Significantly different from corresponding control values, *$P<0.05$.

Discussion

The results presented here are in agreement with previous observations showing that renal tissues are endowed with a high capacity to synthesize dopamine from L-DOPA and that MAO plays a major role in the inactivation of the amine (Stöker & Hempel, 1976; Kopin, 1985; Fernandes *et al.*, 1991). The analysis of the outflow of dopamine and DOPAC suggests that the amine released from tubular epithelial cells is a constant source for deamination into DOPAC and that MAO-A is the main form of enzyme involved in the

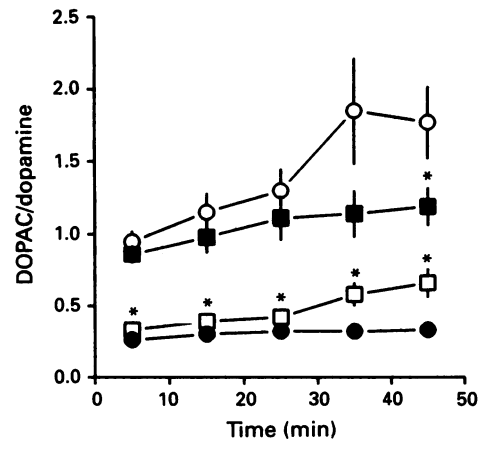


Figure 2 DOPAC/dopamine ratios in 10 min perifusate samples collected from renal cortical fragments in control conditions (○) and in the presence of pargyline (100 μM; ●), Ro 41-1049 (250 nM; □) or Ro 19-6327 (250 nM; ■). Each point represents the mean ± s.e.mean of 7 to 8 experiments per group. Significantly different from corresponding control values, *$P<0.05$.

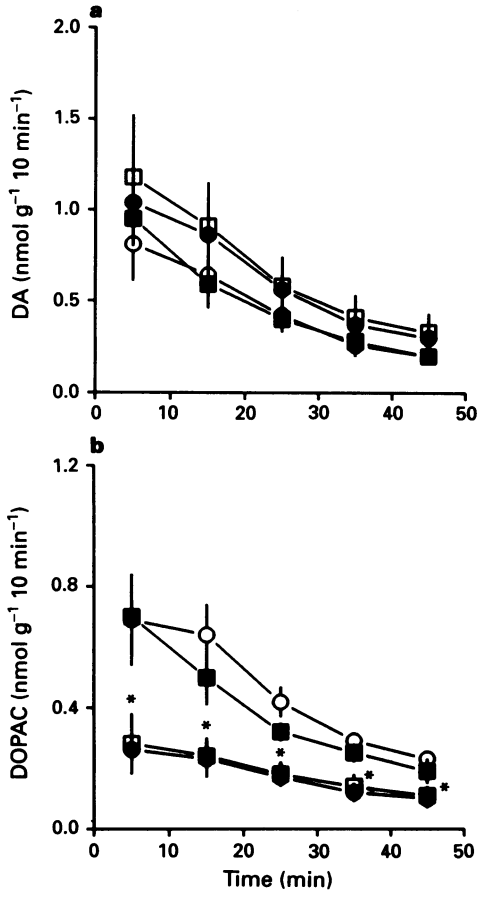


Figure 3 Dopamine (a) and DOPAC (b) outflow levels (in nmol g^{-1} 10 min^{-1}) in 1 min perifusate samples of renal cortical fragments in the presence of benserazide (50 μM). Results are shown for observations in control conditions (○), and in the presence of pargyline (100 μM; ●), Ro 41-1049 (250 nM; □) or Ro 19-6327 (250 nM; ■). Each point represents the mean ± s.e.mean of 4 experiments per group. Significantly different from corresponding control values, $*P<0.05$.

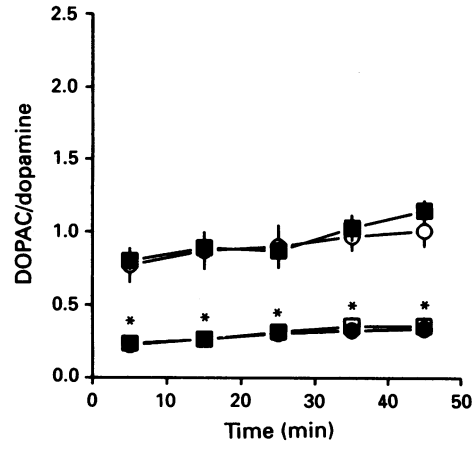


Figure 4 DOPAC/dopamine ratios in 10 min perifusate samples collected from renal cortical fragments in the presence of benserazide. Results are shown for observations in control conditions (○) and in the presence of pargyline (100 μM; ●), Ro 41-1049 (250 nM; □) or Ro19-6327 (250 nM; ■). Each point represents the mean ± s.e.mean of 4 experiments per group. Significantly different from corresponding control values, $*P<0.05$.

deamination of newly-formed dopamine, although the amine might also have a limited access to MAO-B.

Most probably, the formation of the dopamine and DOPAC present in kidney slices loaded with exogenous L-DOPA occurred during the incubation period and not during the subsequent period of perifusion. The main argument favouring this suggestion is that dopamine and DOPAC outflow and the levels of both compounds in renal tissues perifused in the presence of benserazide were similar to those obtained in experiments performed in the absene of AAAD inhibition. The effect of benserazide (added to the perifusion fluid) was mainly a reduction in DOPAC/dopamine ratios in the last two collection periods. This, as discussed below, suggests that a minor amount of the dopamine appearing in the effluent was formed during the perifusion period, after the incubation with L-DOPA and this dopamine has an easy access to MAO. Another argument favouring the view that a considerable amount of the DOPAC in the effluent (up to 50%) was formed during the incubation period is that neither pargyline nor Ro 41-1049 decreased the tissue levels of the metabolite, but significantly decreased DOPAC outflow. In agreement with this suggestion are the results of previous work from our laboratory where it has been consistently shown that a significant amount (up to 30%) of the toal dopamine formed in kidney slices loaded with L-DOPA undergoes rapid deamination to DOPAC (Fernandes & Soares-da-Silva, 1990; Fernandes *et al.*, 1991; Fernandes & Soares-da-Silva, 1993). Of course it could be argued also that the lack of effect of MAO inhibitors in reducing the tissue accumulation of DOPAC is a concentration-related problem. In our hands, however, when added to the incubation medium before loading with L-DOPA, all the three MAO inhibitors, at these very same concentrations, were found to decrease DOPAC formation (100 μM pargyline, 84% reduction; 250 nM Ro 41-1049, 86% reduction; 250 nM Ro 19-6327, 79% reduction) (Fernandes & Soares-da-Silva, 1990; Fernandes *et al.*, 1991).

The deamination of newly-formed dopamine in kidney slices loaded with exogenous L-DOPA is rather unlikely to occur in a neuronal compartment. In fact, previous studies have shown that renal denervation does not affect the deamination of dopamine to DOPAC in rat kidney slices loaded with L-DOPA (Soares-da-Silva *et al.*, 1992). this also agrees with the evidence that renal denervation does not affect both MAO-A and MAO-B activities, suggesting that in the kidney, most MAO is located extraneuronally (Caramona & Soares-da-Silva, 1990, Soares-da-Silva *et al.*, 1992). Although this does not completely rule out the possibility that some of the renal dopamine might have access to neuronal MAO, there is evidence to suggest that the neuronal uptake of newly-formed dopamine in kidney slices is most probably an irrelevant process. When levels of dopamine in kidney slices increase up to 480 nmol g^{-1} (i.e., 6000 fold the levels of endogenous dopamine), as has found to occur in the presence of 2.5 mM L-DOPA, the levels of endogenous noradrenaline (1.3 nmol g^{-1}) in kidney slices do not change (Fernandes *et al.*, 1991).

The suggestion that dopamine is intensely deaminated to DOPAC before reaching the perifusion medium is supported by the findings that: (1) DOPAC/dopamine ratios in the perifusate were significantly higher than those in the tissues (0.95 vs 0.30) and (2) this ratio progressively increased with time (from 0.95 to 1.77). Non selective inhibition of MAO with pargyline was found to increase the levels of dopamine in the effluent and to reduce the outflow of DOPAC. However, the tissue levels of both dopamine and DOPAC in the presence of pargyline did not significantly differ from those of controls. This would suggest that pargyline inhibits mainly the deamination of that dopamine leaving the compartment where the synthesis has occurred or the deamination of that dopamine which crosses a compartment rich in MAO activity before reaching the perifusion medium. This conclusion is further reinforced by the finding that the proportion of DOPAC to dopamine in the effluent, in the presence of

pargyline, was drastically reduced and did not differ from that found in the tissues. It can be hypothesized that the cellular compartment crossed by the amine before reaching the perifusate is the very same in which dopamine is synthesized; however, this would imply that the amine would be taken up into the original cellular structure, after being released. Considering that the luminal cell border has been shown not to take up dopamine (Chan, 1976) and this cell border has been found to be collapsed when renal slices are used (Wedeen & Weiner, 1973), it might then be suggested that the released dopamine would be taken up into tubular epithelial cells through the basolateral membrane. This hypothesis might explain why the proportion of DOPAC to dopamine is significantly higher in the perifusate than that found in the tissues and would also support the results presented here on the influence of selective and non selective MAO inhibitors in the outflow levels of dopamine and DOPAC.

The changes in the outflow of both dopamine and DOPAC produced by the selective MAO-A inhibitor, Ro 41-1049, were similar to those observed with pargyline. In addition, the significant reduction in DOPAC/dopamine ratios in the perifusate produced by Ro 41-1049 was similar to that observed with pargyline. These results suggest that MAO-A is the form of the enzyme located in the compartment where the synthesis of dopamine has occurred and in the cellular compartment rich in MAO crossed by the amine before it has reached the perifusion medium. However, the finding that the increase with time of DOPAC/dopamine ratios in the perifusate was found to be abolished by pargyline, but not by Ro 41-1049, suggests that MAO-B would be the form of the enzyme responsible for the increased deamination of dopamine taking place in the last two collection periods. In agreement with this suggestion are the results that Ro 19-6327 does, in fact, reduce the increase with time of DOPAC/dopamine ratios in the perifusate.

This raises the question of the relative importance of the two forms of MAO, types A and B, in the deamination of renal dopamine. Previous studies in kidney slices loaded with L-DOPA have shown that both MAO-A and MAO-B are involved in the deamination of newly-formed dopamine and that MAO-B would be particularly involved in the deamination of the amine outside the compartment where the synthesis takes place (Fernandes & Soares-da-Silva, 1990; Fernandes *et al.*, 1991). In these experimental conditions, the cellular structures potentially involved in the handling of renal dopamine may theoretically include all those present in the renal cortical slices of the rat kidney: glomeruli, tubules, vascular tissues and support connective tissue. The renal handling of dopamine is expected, however, to involve mainly tubular epithelial cells, namely those of proximal convoluted tubules. These are the cells involved in the synthesis of renal dopamine as a result of the decarboxylation of circulating L-DOPA (Baines & Chan, 1980; Lee, 1982; Suzuki *et al.*, 1984) and a major area in cortical slices is occupied by the renal tubules. The presence of type A and type B MAO in different cellular compartments has been suggested in radioautographic studies showing that MAO-A is homogenously distributed in both the cortex and the medulla, while MAO-B is heterogenously distributed throughout the renal cortex (Saura *et al.*, 1992). Although it could be hypothesized that some of the released dopamine might have been deaminated by MAO-B in non tubular epithelial cellular structures, rat proximal convoluted renal tubules were shown recently to be endowed with both MAO-A and MAO-B activities and 250 nM Ro 19-6327 was found to reduce by 70% the deamination of [^{14}C]-β-phenylethylamine, a specific substrate of MAO-B (Guimarães & Soares-da-Silva, 1994). Therefore, our hypothesis, considering all data available on this matter, is that in rat epithelial cells of cortical renal tubules, newly-formed dopamine is mainly deaminated by MAO-A.

The released dopamine appears to be taken up into a MAO-A rich compartment, whereas the deamination of newly-formed dopamine by MAO-B is dictated by a slow diffusion of the amine towards the enzyme. There is evidence indicating that MAO-B is located in renal tubular cells endowed with the ability to synthesize dopamine (Guimarães & Soares-da-Silva, 1994), but the data presented here cannot exclude the presence of a multi-compartment system where the MAO-B involved in this process might be located also in non-tubular cells. In fact, the analysis of the outflow of dopamine and DOPAC does not reveal the presence of a monocompartmental system with MAO activity, as indicated by the upward concave shape of the efflux curves, and, therefore, is not in a steady state of efflux (Pestana & Soares-da-Silva, 1994). This may be, however, of minor metabolic importance as indicated by the results that in both man (Freestone *et al.*, 1993) and rat (Vieira-Coelho *et al.*, 1993), inhibition of MAO-B was shown not to affect the urinary excretion of sodium, the main renal effect of tubular dopamine (Lee, 1993).

In some experiments renal slices were perifused in the presence of benserazide, a well-known inhibitor of the enzyme AAAD. After incubation with L-DOPA, renal tissues were immediately placed in the perifusion chambers and perifused onwards in the presence of 50 μM benserazide. These experiments were performed with the aim of preventing the synthesis *de novo* of dopamine during the perifusion period; under these experimental conditions the amount of dopamine available for release is, therefore, only that which has been synthesized during the incubation period. The synthesis *de novo* of dopamine during the perifusion appears, however, not to be of great importance, since benserazide failed to decrease the outflow of both dopamine and DOPAC. The most relevant results obtained in the presence of benserazide were the following: (1) inhibition of the increase of DOPAC/dopamine ratios in the perifusate and (2) inhibition of the increase of the outflow levels of dopamine, as induced by pargyline, Ro 41-1049 and Ro 19-6327. This suggests that the dopamine formed during the perifusion period has easy access to both forms of MAO, especially that of type B.

In conclusion, the results presented here show that the fraction of newly-formed dopamine which leaves the compartment where the synthesis has occurred is a constant source for deamination into DOPAC and also provide evidence favouring the view that MAO-A is the main form of the enzyme involved in this process; however, the data reported here suggest that dopamine also has acces to MAO-B, although this may be a minor metabolic pathway.

This work was supported by grant number PBIC/C/CEN 1139/92 from the JNICT.

References

APERIA, A., BERTORELLO, A. & SERI, I. (1987). Dopamine causes inhibition of Na^+-K^+-ATPase activity in rat proximal convoluted tubule segments. *Am. J. Physiol.*, **252**, F39–F45.

BAINES, A.D. & CHAN, W. (1980). Production of urine free dopamine from dopa: a micropuncture study. *Life Sci.*, **26**, 253–259.

CARAMONA, M.M. & SOARES-DA-SILVA, P. (1990). Evidence for an extraneuronal location of monoamine oxidase in renal tissues. *Naunyn-Schmied. Arch. Pharmacol.*, **341**, 411–413.

CHAN, Y.L. (1976). Cellular mechanisms of renal tubular transport of L-DOPA and its derivatives in the rat: microperfusions studies. *J. Pharmacol. Exp. Ther.*, **199,** 17–24.

DA PRADA, M., KETLER, R., KELLER, H.H., CESURA, A.M., RICHARDS, J.G., MARTI, J.S., MUGGLI-MANIGLIO, D., KYBURZ, E. & IMHOF, R. (1990). From moclobemide to Ro 19-6327 and Ro 41-1049: The development of a new class of reversible, selective MAO-A and MAO-B inhibitors. *J. Neural. Trans.* [Suppl], **29,** 279–292.

FELDER, C.C., CAMPBELL, T., ALBRECHT, F. & JOSE, P.A. (1990). dopamine inhibits Na^+-H^+ exchanger activity in renal BBMV by stimulation of adenylate cyclase. *Am. J. Physiol.*, **259,** F297–F303.

FERNANDES, M.H., PESTANA, M. & SOARES-DA-SILVA, P. (1991). Deamination of newly-formed dopamine in rat renal tissues. *Br. J. Pharmacol.*, **102,** 778–782.

FERNANDES, M.H. & SOARES-DA-SILVA, P. (1990). Effects of MAO-A and MAO-B selective inhibitors Ro 41-1049 and Ro 19-6327 on the deamination of newly-formed dopamine in the rat kidney. *J. Pharmacol. Exp. Ther.*, **255,** 1309–1313.

FERNANDES, M.H. & SOARES-DA-SILVA, P. (1992). Type A and B monoamine oxidase activities in the human and rat kidney. *Acta Physiol. Scand.*, **145,** 363–367.

FERNANDES, M.H. & SOARES-DA-SILVA, P. (1993). Sequential involvement of monoamine oxidase and catechol-O-methyltransferase in the metabolism of newly-formed dopamine in rat renal tissues. In *Cardiovascular and Renal Actions of Dopamine* ed. Soares-da-Silva, P. *Advances in Biosciences*, Vol. 88, pp. 21–30. Oxford: Pergamon Press.

FREESTONE, S., LI KAM, T.C. & LEE, M.R. (1993). Further studies on gludopa in man: The effect of the monoamine oxidase inhibitor selegiline. In *Cardiovascular and Renal Actions of Dopamine* ed. Soares-da-Silva, P. *Advances in Biosciences*, Vol. 88, pp. 195–202. Oxford: Pergamon Press.

GUIMARÃES, J.T. & SOARES-DA-SILVA, P. (1994). Selective inhibition of type A and B monamine oxidase in isolated rat proximal convoluted tubules. *Br. J. Pharmacol*, **112,** 375P.

JOSE, P.A., RAYMOND, J.R., BATES, M.D., APERIA, A., FELDER, R.A. & CAREY, R.M. (1992). The renal dopamine receptors. *J. Am. Soc. Nephrol.*, **2,** 1265–1278

KOPIN, I.J. (1985). Catecholamine metabolism: basic aspects and clinical significance. *Pharmacol. Rev.*, **37,** 33–364.

LEE, M.R., (1993). dopamine and the kidney: ten years on. *Clin.Sci.*, **84,** 357–375.

PESTANA, M. & SOARES-DA-SILVA, P. (1992). Influence of type A and B monamine oxidase in the outflow of newly-formed dopamine in the rat kidney. *Nephrol. Dial. Transp.*, **7,** 660.

PESTANA, M. & SOARES-DA-SILVA, P. (1994). The renal handling of dopamine originating from L-DOPA and γ-glutamyl-L-DOPA. *Br. J. Pharmacol.*, **112,** 417–422.

SAURA, J., KETTLER, M., DA PRADA, M. & RICHARDS, J.G. (1992). Quantitative enzyme radioautography with ^{3}H-Ro 41-1049 and ^{3}H-Ro 19-6327 in vitro: localization and abundance of MAO-A and MAO-B in rat CNS, peripheral organs, and human brain. *J. Neuroscience*, **12,** 1977–1999.

SIRAGY, H.M., FELDER, R.A., HOWELL, N.L., CHEVALIER, R.L., PEACH, M.J. & CAREY, R.M. (1989). Evidence that intrarenal dopamine acts as a paracrine substance at the renal tubule. *Am. J. Physiol.*, **257,** F469–F477.

SOKAL, R.R. & ROHLF, F.J. (1981). *Biometry. The Principles and Practice of Statistics in Biological Research*; New York: Freeman and Company.

SOARES-DA-SILVA, P. & FERNANDES, M.H. (1990). Synthesis and metabolism of dopamine in the kidney. Effects of sodium chloride, monamine oxidase inhibitors and α-human atrial natriuretic peptide. *Am. J. Hypertens.*, **3,** 7S–10S.

SOARES-DA-SILVA, P., FERNANDES, M.H., ALBINO-TEIXEIRA, A., AZEVEDO, I. & PESTANA, M. (1992). Brief transient ischemia induces long-term depletion of norepinephrine without affecting the aromatic amino acid decarboxylase and monamine oxidase activities in the rat kidney. *J. Pharmacol. Exp. Ther.*, **260,** 902–908.

SUZUKI, H., NAKANE, N., KAWAMURA, M., YOSHIZAWA, E. TAKESHITA, E. & SARURA, T. (1984). Excretion and metabolism of dopa and dopamine by isolated perfused rat kidney. *Am. J. Physiol.*, **247,** E285–E290.

STÖKER, W. & HEMPEL, K. (1976). Inactivation and excretion of dopamine by the cat kidney in vitro. *Naunyn-Schmied. Arch. Pharmacol.*, **295,** 123–126.

VIEIRA-COELHO, M.A., FERNANDES, M.H., PESTANA, M. & SOARES-DA-SILVA, P. (1993). Effect of type A and b monamine oxidase inhibitors on the urinary excretion of dopamine, 5-hydroxytryptamine and amine metabolites. *Br. J. Clin. Pharmacol.*, **36,** 153P.

WEDEEN, R.P. & WEINER, B. (1973). The distribution of p-aminohippuric acid in rat kidney slices. I. Tubular localization. *Kidney Int.*, **3,** 205–213.

(Received October 28, 1993
Revised August 11, 1994
Accepted August 18, 1994)

Br. J. Pharmacol. (1994), **113**, 1275–1280 © Macmillan Press Ltd, 1994

The relative importance of nitric oxide and nitric oxide-independent mechanisms in acetylcholine-evoked dilatation of the rat mesenteric bed

Sarah J.W. Parsons, *Anthony Hill, Gareth J. Waldron, [1]Frances Plane & Christopher J. Garland

Department of Pharmacology, University Walk, Bristol BS8 1TD and *Department of Physiology and Pharmacology, University of Southampton, Southampton SO9 3TU

1 The relative contribution of nitric oxide (NO) to acetylcholine-induced smooth muscle relaxation was investigated in the rat perfused mesenteric vasculature and in isolated segments of second, third and fourth order arterial branches.

2 The EC_{50} values and maximal relaxation to acetylcholine were not significantly different in the sequential arterial branches, being approximately 0.05 μM and 85%, respectively.

3 The NO synthase inhibitor L-N^G-nitro-L-arginine methyl ester (L-NAME; 100 μM) reduced acetylcholine-evoked endothelium-dependent dilatation and relaxation in the perfused mesenteric bed and in isolated arterial segments. The maximum response to acetylcholine in both preparations was reduced by between 35% to 40% while the EC_{50} values were increased by 5–6 fold. L-NAME had no effect on basal smooth muscle tone in either case.

4 In contrast, endothelium-dependent dilatation of the perfused mesenteric bed evoked by A23187 (0.002–20 nmol), was unaffected by exposure to L-NAME. The EC_{50} values and maximal responses elicited by A23187 (20 nmol) before and after exposure to L-NAME were 0.96 ± 0.5 nmol and $67.0 \pm 7.0\%$ ($n = 4$), and 0.7 ± 0.4 nmol and $70.0 \pm 5.0\%$ ($n = 4$; $P > 0.01$), respectively.

5 Perfusion of the isolated mesenteric bed with raised K^+-Krebs buffer (25 mM) had no effect on basal tone, but reduced the amplitude of both acetylcholine- and A23187-evoked dilatation. The maximum responses to acetylcholine (2 μmol) and A23187 (20 nmol) were reduced from $67.5 \pm 7.3\%$ and $65.4 \pm 8.2\%$ to $18.9 \pm 11.0\%$ ($n = 5$; $P < 0.01$) and $13.5 \pm 12.0\%$ ($n = 4$; $P < 0.01$), respectively.

6 Exposure of the mesenteric bed to L-NAME in the presence of raised K^+-Krebs further reduced the maximal response elicited by acetylcholine to only $8.9 \pm 2.8\%$ ($n = 4$; $P < 0.01$).

7 These results indicate that acetylcholine-evoked vasodilatation of the rat mesenteric vasculature is mediated by both NO-dependent and -independent mechanisms. The relative contribution made by these mechanisms does not appear to differ in sequential branches of the mesenteric artery. In contrast, A23187-evoked vasodilatation appears to be mediated predominantly by a NO-independent mechanism which is sensitive to increases in the extracellular potassium concentration and may reflect the action of endothelium-derived hyperpolarizing factor (EDHF).

Keywords: Acetylcholine; nitric oxide; rat mesenteric bed; endothelium; EDHF; N^G-nitro-L-arginine methyl ester (L-NAME)

Introduction

Endothelium-derived relaxing factor (EDRF) has been identified as nitric oxide (NO), or a closely related molecule, which is synthesized from L-arginine by the enzyme NO synthase (reviewed by Moncada *et al.*, 1991). Structural analogues of L-arginine such as N^G-nitro-L-arginine (L-NOARG) and N^G-nitro-L-arginine methyl ester (L-NAME) have been used to block this pathway and inhibit relaxation mediated by the release of endothelium-derived NO (Rees *et al.*, 1989). However, in several blood vessels, such as the porcine coronary artery and rabbit femoral artery, endothelium-dependent relaxations are not inhibited by NO synthase inhibitors, indicating that other endothelium-derived factors, distinct from NO, may contribute to the local regulation of smooth muscle tone (Chen *et al.*, 1988; Taylor & Weston, 1988; Nagao & Vanhoutte, 1992; Plane *et al.*, 1992).

Endothelium-dependent relaxation evoked by agents such as acetylcholine is accompanied by smooth muscle hyperpolarization. Although exogenous NO can evoke smooth muscle hyperpolarization in some vessels under certain conditions, there is now considerable evidence that a separate endothelium-derived hyperpolarizing factor (EDHF) is also released and contributes to reductions in smooth muscle tone, accounting for the relaxation not mediated by NO (Chen *et al.*, 1988; Tare *et al.*, 1990; Garland & McPherson, 1992; Nagao & Vanhoutte, 1992). Furthermore, when endothelium-dependent hyperpolarization is abolished by increased extracellular potassium concentration, the remaining relaxation is completely blocked by inhibitors of NO synthase (Nagao & Vanhoutte, 1992; Waldron *et al.*, 1993).

The relative contribution of NO and EDHF to endothelium-dependent relaxation appears to vary with both different vessels and agonists (Palmer *et al.*, 1988; Rees *et al.*, 1989; Plane *et al.*, 1992). A comparison of various isolated arteries from the rat indicates that the NO-independent component of relaxation may be more prominent in small arteries. In contrast, NO is probably the predominant factor released from the endothelium in large conduit arteries (Nagao *et al.*, 1992). Several investigations in the microcirculation also suggest a heterogeneous distribution of endothelial cell function, with the contribution made by NO varying along the vascular network (Tang & Joyner, 1992; Hester *et al.*, 1993).

In the perfused rat mesenteric bed, acetylcholine-evoked relaxations have been reported to be completely inhibited by L-arginine analogues such as L-NOARG and L-NAME, suggesting that the reductions in tone are mediated solely by

[1] Author for correspondence.

endothelium-derived NO (Moore et al., 1990). However, this contrasts with studies in isolated arterial segments from this vascular bed, where acetylcholine-evoked relaxations were found to be largely resistant to NO synthase inhibitors (Garland & McPherson, 1992; Bennett et al., 1992; Waldron et al., 1993). In third order arterial branches from Wistar-Kyoto rats, both the relaxation and hyperpolarization induced by acetylcholine were found to be insensitive to L-arginine analogues, suggesting a major contribution from EDHF (Garland & McPherson, 1992; Waldron et al., 1993). The membrane potential change evoked by acetylcholine, and a substantial component of the relaxation, are inhibited by 25 mM potassium, a concentration which has no effect on relaxation to exogenous or endothelium-derived NO (Parsons et al., 1991; Plane & Garland, 1993; Waldron et al., 1993). In the absence of a change in membrane potential, the remaining component of the relaxation to acetylcholine can be blocked by L-NAME. These observations show that increasing the external potassium concentration to 25 mM in the mesenteric circulation can be used to inhibit the tension change to hyperpolarization, and presumably to differentiate between the relative contribution made by each of these mechanisms.

In the present study, we have attempted to resolve the apparently conflicting observations made in the perfused mesenteric preparation and in isolated arterial segments. We have investigated the relative importance of NO-dependent and -independent mechanisms in endothelium-dependent dilatation of the isolated, perfused mesenteric bed of the rat to acetylcholine and the calcium ionophore A23187. In addition, the possibility that the relative contribution from NO and NO-independent mechanisms varied between second, third and fourth order branch arteries from this vascular bed was also examined. Some of these results have been presented in preliminary form to the British Pharmacological Society (Parsons et al., 1993).

Methods

Rat isolated mesenteric arteries

Endothelium-dependent relaxations of isolated segments of rat mesenteric arteries were studied as previously described (Garland & McPherson, 1992). Briefly, arterial segments (2 mm in length) from either second, third or fourth order branches from the superior mesenteric artery were mounted in a small vessel myograph (model 400A, J.P. Trading, Denmark) and tension changes displayed via a Kipp & Zonen pen recorder. Vessels were allowed to equilibrate under zero force for 30 min before the construction of a passive diameter-tension curve (Mulvany & Halpern, 1977). From this curve the effective transmural pressure was calculated. The vessels were set at tensions equivalent to those generated at 0.9 times the diameter of the vessel at 100 mmHg. Non-linear curve fitting of the passive diameter-tension curve was achieved using a custom written programme for the IBM PC (NORMALIZE, G.A. McPherson). Vessel diameters at an equivalent transmural pressure of 100 mmHg (D_{100}) are given in the text.

After an initial equilibration period of 60 min, tissues were pre-contracted with a submaximal concentration of noradrenaline (1–10 μM) and relaxed to cumulative concentrations of acetylcholine (1 nM–30 μM). Following washout, NO synthase inhibitors were pre-incubated in the organ bath for 30–60 min before the contraction-relaxation cycle was repeated.

Rat isolated perfused mesentery

Rat mesentery preparations were isolated as described by Moore et al. (1990). Briefly, the mesenteric vascular bed was cannulated via the superior mesenteric artery, separated from the intestine, and perfused at 5 ml min^{-1} with warmed (37°C) Krebs buffer which had been bubbled with 95% O_2/CO_2. Perfusion pressure was monitored continuously by a Bell & Howell pressure transducer connected to a pen recorder.

To induce tone, noradrenaline (10–50 μM) was added to the Krebs reservoir at a concentration sufficient to increase perfusion pressure by 80–90 mmHg, representing approximately 70–80% of the maximum response. Bolus doses of acetylcholine (0.02 nmol–2 μmol), A23187 (0.002–20 nmol) or sodium nitroprusside (0.002 nmol–2 μmol) were injected in a small volume (100 μl) to prevent injection artifacts. In some experiments, preparations were perfused for 1 min with 3-(3-cholamidopropyl) 1-propanesulphonate (CHAPS; 4.7 mg ml^{-1}) to remove the endothelial cell layer. Following exposure to CHAPS, responses to acetylcholine were abolished, whereas dilatation evoked by sodium nitroprusside was unaltered. Inhibitors of NO biosynthesis were added to the Krebs reservoir and allowed to perfuse the tissues for at least 30 min before pre-constriction.

Solutions and drugs

Tissues were maintained in Krebs buffer of the following composition (mM): NaCl 119, $NaHCO_3$ 25.0, KCl 4.7, $MgSO_4$ 1.2, $CaCl_2$ 2.5, KH_2PO_4 1.18, disodium EDTA 0.027, and glucose 11.0. Raised K^+-Krebs solution (25 mM KCl) was prepared by direct replacement of NaCl with KCl.

Drugs used were A23187 (Sigma), acetylcholine chloride (BDH), L-NAME (Sigma), L-NOARG (Sigma), noradrenaline bitartrate (arterenol, Sigma) and sodium nitroprusside (Sigma). All drugs were dissolved in Krebs buffer except A23187, the stock solution of which was dissolved in dimethylsulphoxide (DMSO).

Analysis of data

In all experiments, relaxations were expressed as a percentage decrease in the induced level of tone. All data are expressed as mean ± s.e.mean. The significance between mean values was calculated by Student's t test, with rejection of the null hypothesis at the 5% level ($P<0.05$). In some experiments, analysis of variance (ANOVA) was used to compare the effects of L-NAME and raised K^+ when used together.

In experiments on isolated arterial segments, EC_{50} values are expressed as $-\log$ M whereas in the perfused preparation, where bolus doses of drugs were added, EC_{50} values are quoted in μmol.

Results

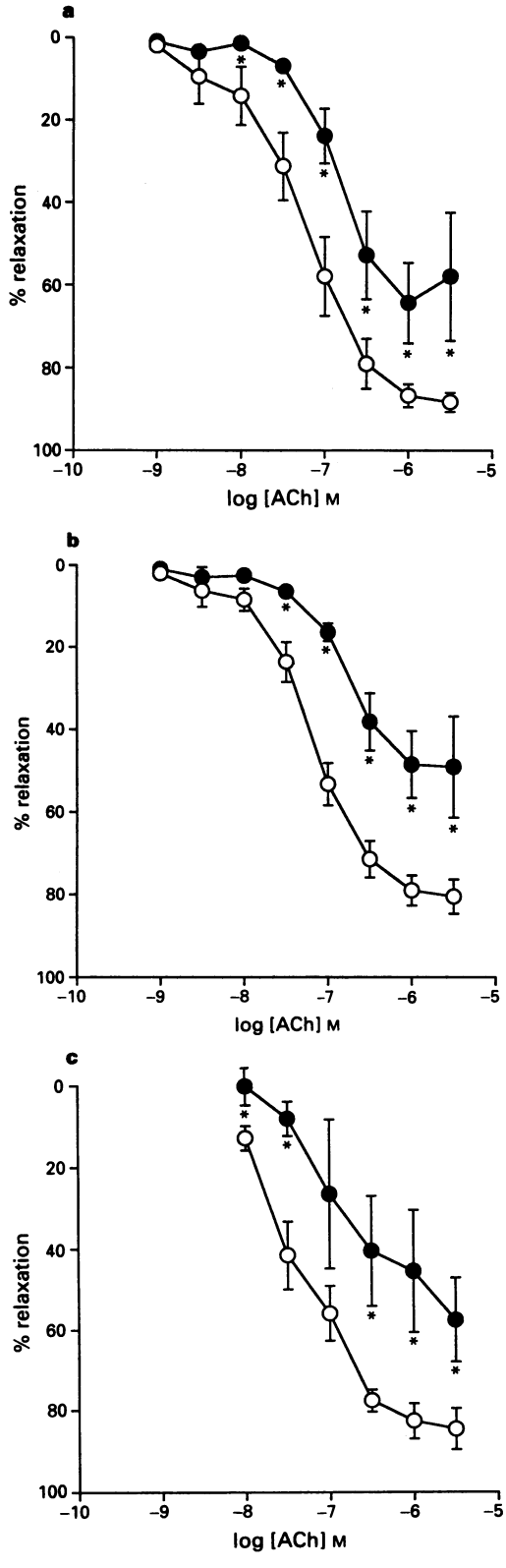
Acetylcholine-evoked relaxation of isolated segments from the mesenteric bed

Acetylcholine (1 nM–10 μM) evoked dose-dependent relaxation in noradrenaline-contracted segments of second (D_{100} = 454 ± 15 μm; n = 7), third (D_{100} = 349 ± 18 μm; n = 14) and fourth (D_{100} = 316 ± 12 μm; n = 6) order branches of rat mesenteric arteries. The EC_{50} values and maximal relaxation evoked by acetylcholine were not significantly different between the arterial segments from the different branches (Table 1). Concentration-response curves for acetylcholine-evoked relaxations in the different arterial branches are shown in Figure 1 (a, b and c).

Pre-incubation of tissues with L-NAME (100 μM; 30 min) did not alter the resting tension of any of the segments from the different arterial branches. However, following exposure to L-NAME, acetylcholine-evoked relaxations were depressed to a similar extent in each arterial branch (Figure 1). In each case there was a 5 to 6 fold increase in the EC_{50} concentration and the maximal response was reduced by approximately 40% (Table 1). Increasing the incubation time with

Table 1 Comparison of % maximal relaxation of induced tone (R_{max}) and EC_{50} values (−log M) for acetylcholine in isolated arterial segments in the presence and absence of N^G-nitro-L-arginine methyl ester (L-NAME, 100 μM)

Branch	D_{100} (μm)	*Control* R_{max}	*Control* EC_{50}	*L-NAME* (100 μM) R_{max}	*L-NAME* (100 μM) EC_{50}
2nd	454 ± 15	88.3 ± 2.3	7.15 (7.34–6.96)	58.0 ± 15.5	6.72 (6.86–6.57)
3rd	349 ± 18	80.6 ± 4.2	7.25 (7.57–6.97)	49.2 ± 12.0	6.74 (6.98–6.49)
4th	316 ± 12	84.7 ± 5.0	7.44 (7.76 ± 7.11)	57.7 ± 10.4	6.83 (7.25–6.41)



L-NAME to 60 min did not further depress the acetylcholine-evoked responses (data not shown).

Indomethacin (10 μM) was without effect on acetylcholine-evoked relaxations in the presence or absence of L-NAME ($n = 3$).

Effect of L-NAME on endothelium-dependent dilatation of the isolated perfused mesenteric bed

Bolus injections of acetylcholine (0.2 nmol–2 μmol), evoked transient, dose-dependent decreases in perfusion pressure of tissues pre-constricted with noradrenaline (10–50 μM). These responses were abolished following removal of the endothelium with CHAPS. The maximal response evoked by acetylcholine (2 μmol) was 77.2 ± 7.6% ($n = 12$) relaxation of induced tone and the EC_{50} value was 32.7 ± 13.1 nmol ($n = 12$).

When added to tissues pre-constricted with noradrenaline, L-NAME (100 μM) and L-NOARG (100 μM) caused a small, rapid, endothelium-dependent increase in perfusion pressure of 11.8 ± 2.4 mmHg ($n = 4$), which then declined to the previous level within 8–10 min. In the absence of induced tone, infusion of the L-arginine analogues for up to 30 min had no effect on basal perfusion pressure, and did not enhance the contractions evoked by noradrenaline. Acetylcholine-evoked responses were significant depressed in 80% of preparations following exposure to the NO synthase inhibitors. In the remainder, relaxation was not modified. In the tissues in which NO synthase inhibitors reduced relaxation, the maximum response to acetylcholine (2 μmol) was reduced by 35.4 ± 3.0% ($n = 6$; $P < 0.01$). A similar reduction was observed in the presence of L-NOARG. Dose-response curves for acetylcholine-induced dilatation in the presence and absence of L-NAME are shown in Figure 2. Removal of L-NAME from the Krebs buffer did not restore acetylcholine-evoked dilatation over the 45 min recovery period of the experiments, although responses were partially restored by the infusion of 100 μM L-arginine (71% of maximal response; $n = 2$).

Bolus injections of A23187 (0.002–20 nmol) also evoked transient, dose-dependent reductions in the perfusion pressure of noradrenaline-constricted preparations which were abolished by removal of the endothelium. The maximal response evoked by A23187 (0.02 μmol) was 65.44 ± 8.2% ($n = 4$) relaxation of induced tone and the EC_{50} value was 0.96 ± 0.48 nmol ($n = 4$). However, in contrast to acetylcholine, A23187-evoked responses were not depressed and in some cases were increased, by prior exposure to L-NAME (100 μM) for up to 60 min. The maximal response evoked by A23187 in the presence of L-NAME was 68.14 ± 5.1% ($n = 4$; $P > 0.05$) and the EC_{50} value was 0.7 ± 0.4 nmol

Figure 1 Mean concentration-response curves for acetylcholine-evoked relaxation in isolated segments of second (a), third (b) and fourth (c) order branches of the rat mesenteric bed, in the presence (●) and absence (○) of N^G-nitro-L-arginine methyl ester (100 μM). Points are the mean with s.e.mean from 3 or 4 separate experiments, *$P < 0.01$.

($n = 4$; $P > 0.05$). Figure 3 shows dose-response curves for A23187-induced relaxation of noradrenaline-constricted tissues in the presence and absence of L-NAME.

Indomethacin (10 μM) was without effect on responses to either acetylcholine or A23187, in either the presence or the absence of L-NAME (data not shown).

The nitrovasodilator agent, sodium nitroprusside (0.002–20 nmol), evoked dose-dependent reductions in noradrenaline-induced tone, and these relaxations were unaffected by removal of the endothelium or exposure to L-NAME (100 μM; 30 min). The maximal response evoked by sodium nitroprusside in the presence and absence of L-NAME was 77.5 ± 3.9% and 79.0 ± 5.0% ($n = 3$; $P > 0.01$).

Effect of raised K^+ Krebs buffer on endothelium-dependent dilatation of the isolated, perfused mesenteric bed

Perfusion of isolated mesenteric preparations with raised K^+-Krebs buffer had no effect on basal perfusion pressure and did not enhance noradrenaline-evoked constriction. However, in the presence of raised K^+-Krebs buffer, the dilatation of noradrenaline-induced tone evoked by acetylcholine or A23187 was significantly reduced.

In the presence of raised K^+-Krebs buffer, the responses to low doses of acetylcholine were not significantly inhibited, but the maximal response was reduced from 77.2 ± 9.2 to 18.9 ± 11.1% ($n = 5$; $P < 0.01$) compared to control. Subsequent exposure to L-NAME (100 μM), in the continued presence of raised K^+-Krebs buffer, did not further depress the acetylcholine-evoked dilatation (maximal response 8.9 ± 2.8%; $n = 4$; ANOVA). Dose-response curves for acetylcholine-evoked responses in the presence of raised K^+-Krebs buffer, alone or together with L-NAME, are shown in Figure 4.

In the presence of raised K^+-Krebs buffer, the responses to all doses of A23187 (0.002–20 nmol) were significantly inhibited by 80–90%, compared to control responses in normal Krebs buffer. The maximal response to A23187 (20 nmol) in the presence of raised K^+-Krebs buffer was

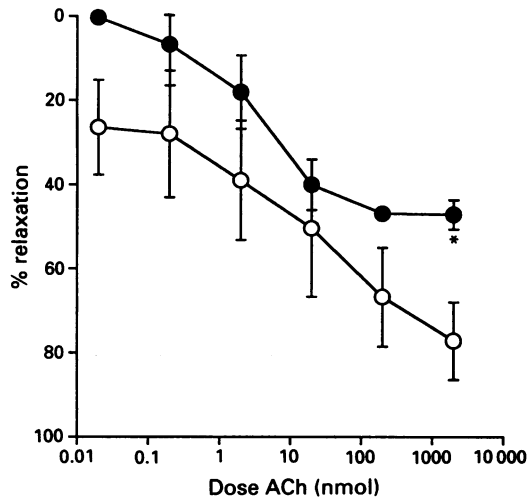


Figure 2 Mean dose-response curves for acetylcholine-evoked dilatation of the rat isolated perfused mesenteric bed pre-constricted with noradrenaline (1–10 μM). Points show dilatation in the presence (●) and absence (○) of N^G-nitro-L-arginine methyl ester (100 μM), and are the mean with s.e.mean from 6 separate experiments.

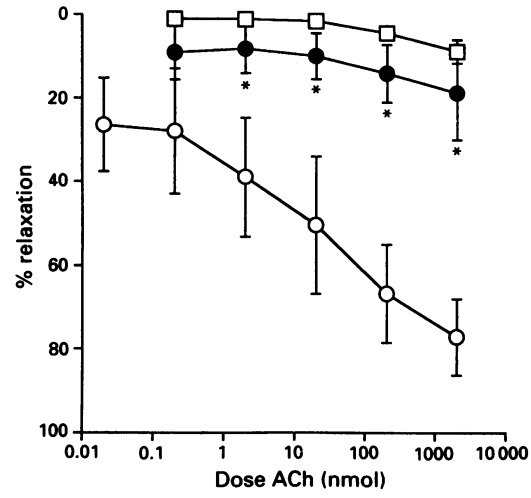


Figure 4 Mean dose-response curves for acetylcholine-evoked dilatation of the rat isolated perfused mesenteric bed pre-constricted with noradrenaline (1–10 μM). Points show dilatation in the absence (○) and presence of 25 mM K^+-Krebs buffer (●), or 25 mM K^+-Krebs buffer and N^G-nitro-L-arginine methyl ester (100 μM; □). Points are the mean with s.e.mean from 4 separate experiments, $*P < 0.01$.

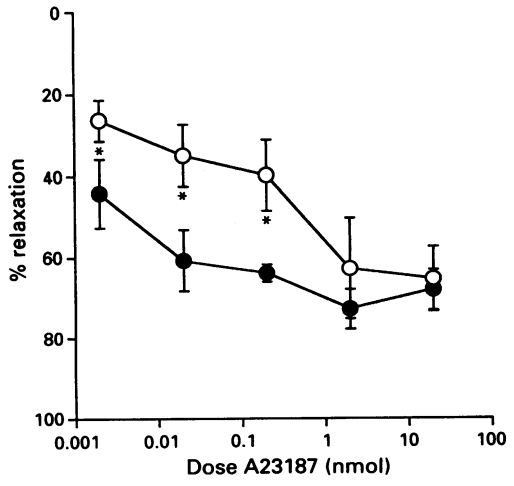


Figure 3 Mean dose-response curves for A23187-evoked dilatation of the rat isolated perfused mesenteric bed pre-constricted with noradrenaline (1–10 μM). Points show dilatation in the presence (●) and absence (○) of N^G-nitro-L-arginine methyl ester (100 μM), and are the mean with s.e.mean from 4 separate experiments, $*P < 0.01$.

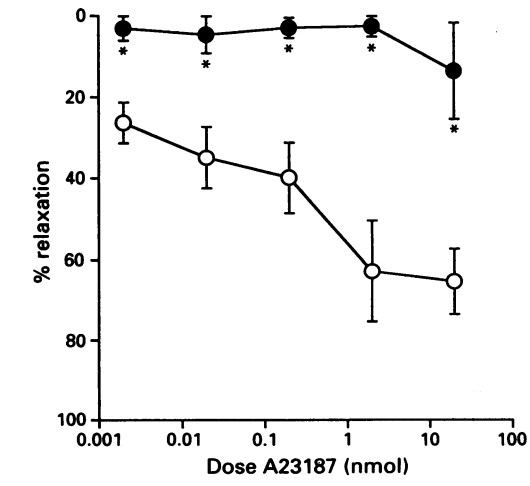


Figure 5 Mean dose-response curves for A23187-evoked dilatation of the rat isolated perfused mesenteric bed pre-constricted with noradrenaline (1–10 μM). Points show dilatation in the absence (○) and presence of 25 mM K^+-Krebs buffer (●), and are the mean with s.e.mean from 4 separate experiments, $*P < 0.01$.

13.5 ± 11.9% ($n = 4$; $P < 0.01$). Dose-response curves for A23187 in normal and raised K^+-Krebs buffer are shown in Figure 5. Relaxations evoked by the nitrovasodilator, sodium nitroprusside, were unaltered in the presence of high K^+-Krebs buffer (results not shown), and the cyclo-oxygenase inhibitor, indomethacin (10 μM) did not alter responses to either acetylcholine or A23187.

Discussion

These data indicate that endothelium-dependent dilatation of the rat mesenteric vasculature is mediated by both NO-dependent and -independent mechanisms. The relative contribution made by these separate mechanisms appears to vary with acetylcholine or A23187, and as in studies of other arteries, the NO-independent mechanisms appear to make a larger contribution in the responses evoked by A23187 (Nagao & Vanhoutte, 1992; Plane *et al.*, 1992).

In the rat perfused mesenteric vasculature, L-NAME and L-NOARG attenuated the reversal of noradrenaline-induced tone evoked by the muscarinic agonist, acetylcholine, reducing the maximum response by around 35% and shifting the concentration-response curve to the right. However, in the presence of raised K^+-Krebs buffer, the maximum response to acetylcholine was reduced by 72% and, subsequent exposure to L-NAME almost abolished the relaxation to acetylcholine. These results are in agreement with previous observations on isolated third order branches of the mesenteric bed, which indicated that acetylcholine-evoked relaxation was mediated by the release of NO and, at higher concentrations, a hyperpolarizing factor distinct from NO and inhibited by 25 mM potassium (Waldron *et al.*, 1993). As in the isolated segments, the potassium-sensitive pathway appears to make a very significant contribution to acetylcholine-evoked smooth muscle relaxation.

In contrast, A23187-evoked dilatation was not inhibited by exposure to the L-arginine analogue L-NAME, indicating that NO is probably not important in smooth muscle relaxation to this agent in the rat mesenteric vasculature. Interestingly, at some doses of A23187 the dilatation was increased following exposure to L-NAME. We do not have an explanation for this observation and it was not investigated further.

However, as with acetylcholine, the relaxation to A23187 was significantly reduced in the presence of a raised concentration of potassium, suggesting that A23187 may induce relaxation by a mechanism which is dependent on increased potassium conductance.

Previous studies have also demonstrated that factors distinct from NO contribute to endothelium-dependent relaxation in this vascular bed. For example, methylene blue and oxyhaemoglobin are much less effective in blocking acetylcholine-evoked dilatation in the perfused mesentery, in concentrations which completely inhibit equivalent responses in other arteries such as the rabbit aorta (Khan *et al.*, 1992). In addition, oxyhaemoglobin and methylene blue were found to inhibit completely relaxation to low concentrations of acetylcholine in the rat mesenteric bed, but were less effective against higher concentrations, when up to 58% relaxation persisted (Khan *et al.*, 1992). This profile was very similar to the responses to acetylcholine obtained in the presence of L-NAME in the present study, and imply that relaxation to low concentrations of acetylcholine predominantly reflects the release of NO, while at higher concentrations, an additional factor, probably EDHF, makes a major contribution.

The identity of the mediator of NO-independent relaxation is unclear although, in some vessels, such as the rabbit and bovine pulmonary artery, endothelium-dependent relaxation is mediated by the release of both NO and products of arachidonic acid metabolism (Chand *et al.*, 1987; Ignarro *et al.*, 1987). In the rabbit coronary artery, bradykinin-evoked relaxation which persists in the presence of L-NOARG is mediated by prostacyclin acting through glibenclamide-sensitive potassium channels (Jackson *et al.*, 1993). A role for prostanoids in the NO-independent responses to acetylcholine and A23187 in the rat mesentery is unlikely, as indomethacin was without effect in this and a previous study (Garland & McPherson, 1992).

L-NAME and L-NOARG did not affect the resting tone in either the perfused mesenteric preparation or in isolated arteries, indicating that the basal release of NO is low in the mesenteric bed. A transient endothelium-dependent contraction was observed when L-NAME was added to perfused preparations stimulated with noradrenaline, which may suggest that NO release is stimulated during arterial contraction. However, following exposure to the NO synthase inhibitor, noradrenaline-induced contractions were not enhanced indicating that NO release does not have an important modulatory role in this vascular bed. Another recent study has also reported that L-NAME increased the basal perfusion pressure in this bed, but only in the presence of increased extracellular potassium (Adeagbo & Triggle, 1993). These workers suggested that EDHF rather than NO is the principle regulator of basal perfusion pressure, the contribution of NO only becoming apparent after the action of EDHF had been abolished (Adeagbo & Triggle, 1993).

In the rabbit aorta, elevated potassium concentrations have been shown to inhibit the relaxation to both acetylcholine and sodium nitroprusside, by inhibiting the formation and action of guanosine 3':5'-cyclic monophosphate (cyclic GMP) in the vascular smooth muscle (Collins *et al.*, 1988). As vasodilatation of the perfused mesenteric bed evoked by the nitrovasodilator, sodium nitroprusside, was unaltered in the presence of 25 mM potassium in the mesenteric bed, it is unlikely that this potassium concentration has a significant inhibitory action on the formation or the cellular actions of cyclic GMP. This is in agreement with other studies which have also found that this concentration of potassium does not inhibit either the release or actions of endothelium-derived NO or the smooth muscle responses to exogenous NO (Parsons *et al.*, 1991; Plane & Garland, 1993; Waldron *et al.*, 1993).

In other studies, higher concentrations of potassium (up to 60 mM) had no effect on the size of relaxation to endothelium-derived NO, indicating that inhibition of either the release or the actions of NO are unlikely to account for the reduced relaxation to acetylcholine and A23187 observed in the presence of 25 mM K^+-Krebs buffer (Parsons *et al.*, 1991; Plane *et al.*, 1992; Plane & Garland, 1993). In fact, in the perfused preparation, the presence of 25 mM K^+ had little effect on the relaxation to the lowest dose of acetylcholine, but significantly depressed vasodilatation stimulated by higher doses of either acetylcholine or A23187. This supports the idea that the release of an additional factor, which is sensitive to increases in the extracellular potassium concentration, depends on the level of intracellular calcium within the endothelium. If this is the case, then it appears that EDHF production is more sensitive to calcium influx than is the synthesis of NO.

In a previous study on the perfused mesenteric bed, L-NOARG (200 μM) was found to abolish acetylcholine-evoked dilatation (Moore *et al.*, 1990). In contrast, in our experiments L-NAME (100 μM) and L-NOARG (100 μM) reduced the maximum response to acetylcholine in both the perfused preparation and isolated arterial segments by only 35%. This inhibition was not improved by increasing the concentration of the NO synthase inhibitors to 200 μM, or by increasing the exposure time to 60 min. Furthermore, in 20% of the perfused preparations, acetylcholine-evoked responses were totally resistant to the blocking action of NO synthase inhibitors. The reasons for the discrepancy between these studies is unclear, but in the light of our observations, it does not appear to be due to a variation in the relative contribution of NO to relaxation down the vascular bed, as L-NAME reduced acetylcholine-evoked relaxation to a similar extent in

each of the second, third and fourth order branches of the mesenteric artery.

In conclusion, these data indicate that in the rat mesenteric vasculature, endothelium-dependent vasodilatation is mediated by the release of both NO and an additional factor which is probably EDHF. The relative contribution made by these two mechanisms to the overall relaxation appears to vary with different agonists. Relaxation to low doses of acetylcholine appears to be mediated by NO, whereas higher concentrations activate an additional mechanism. Relaxation to A23187 appears to be independent of NO production, and mediated by a potassium-sensitive mechanism alone, implying a major role for EDHF.

This work was made possible by financial support from the Wellcome Trust.

References

ADEAGBO, A.S.O. & TRIGGLE, C.R. (1993). Varying extracellular [K^+]: a functional approach to separating EDHF- and EDNO-related mechanisms in perfused rat mesenteric arterial bed. *J. Cardiovasc. Pharmacol.*, **21**, 423–429.

BENNETT, M.A., WATT, P.A.C. & THURSTON, H. (1992). Endothelium-dependent modulation of resistance vessel contraction: studies with N^G-nitro-L-arginine methyl ester and N^G-nitro-L-arginine. *Br. J. Pharmacol.*, **107**, 616–621.

CHAND, N., MAHONEY, T.P., DIAMANTIS, W. & SOFIA, R.D. (1987). Pharmacological modulation of bradykinin-, acetylcholine- and calcium ionophore A23187-induced relaxation of rabbit pulmonary arterial segments. *Eur. J. Pharmacol.*, **137**, 173–177.

CHEN, G., SUZUKI, H. & WESTON, A.H. (1988). Acetylcholine releases endothelium-derived hyperpolarizing factor and EDRF from rat blood vessels. *Br. J. Pharmacol.*, **95**, 1165–1174.

COLLINS, P., HENDERSON, A.H., LANG, D. & LEWIS, M.J. (1988). Endothelium-derived relaxing factor and nitroprusside compared in noradrenaline and K^+-contracted rabbit and rat aortae. *J. Physiol.*, **400**, 395–400.

GARLAND, C.J. & MCPHERSON, G.A. (1992). Evidence that nitric oxide does not mediate the hyperpolarization and relaxation to acetylcholine in the rat small mesenteric artery. *Br. J. Pharmacol.*, **105**, 429–435.

HESTER, R.L., ERASLAN, A. & SAITO, Y. (1993). Differences in EDNO contribution to arteriolar diameters at rest and during functional dilation in striated muscle. *Am. J. Physiol.*, **256**, H146–H151.

IGNARRO, L.J., BYRNS, R.E., BUGA, G.M. & WOOD, K.S. (1987). Mechanisms of endothelium-dependent vascular smooth muscle relaxation elicited by bradykinin and VIP. *Am. J. Physiol.*, **253**, H1074–H1082.

JACKSON, W.F., KÖNIG, A.M., DAMBACHER, T. & BUSSE, R. (1993). Prostacyclin-induced vasodilation in the rabbit heart is mediated by ATP-sensitive potassium channels. *Am. J. Physiol.*, **264**, H238–243.

KHAN, M.T., JOTHIANANDAN, D., MATSUNAGA, K. & FURCHGOTT, R.F. (1992). Vasodilation induced by acetylcholine and by glyceryl trinitrate in rat aortic and mesenteric vasculature. *J. Vasc. Res.*, **29**, 20–28.

MONCADA, S., PALMER, R.M.J. & HIGGS, E.A. (1991). Nitric oxide: physiology, pharmacology and pathophysiology. *Pharmacol. Rev.*, **43**, 109–142.

MOORE, P.K., AL-SWAYEH, O.A., CHONG, N.W.S., EVANS, R.A. & GIBSON, A. (1990). L-N^G-nitro arginine (L-NOARG), a novel, L-arginine-reversible inhibitor of endothelium-dependent vasodilatation *in vitro*. *Br. J. Pharmacol.*, **99**, 408–412.

MULVANY, M.J. & HALPERN, W. (1977). Contractile responses of small resistance vessels in spontaneously hypertensive and normotensive rats. *Circ. Res.*, **41**, 19–26.

NAGAO, T., ILLIANO, S. & VANHOUTTE, P.M. (1992). Heterogeneous distribution of endothelium-dependent relaxations resistant to N^G-nitro-L-arginine in rats. *Am. J. Physiol.*, **263**, H1090–H1094.

NAGAO, T. & VANHOUTTE, P.M. (1992). Hyperpolarization as a mechanism for endothelium-dependent relaxation in the porcine coronary artery. *J. Physiol.*, **445**, 355–367.

PALMER, R.M.J., REES, D.D., ASHTON, D.S. & MONCADA, S. (1988). L-arginine is the physiological precursor for the formation of nitric oxide in endothelium-dependent relaxation. *Biochem. Biophys. Res. Commun.*, **153**, 1251–1256.

PARSONS, A.A., SCHILLING, L. & WAHL, M. (1991). Analysis of acetylcholine-induced relaxation of rabbit isolated middle cerebral artery: effects of inhibitors of nitric oxide synthesis, Na,K-ATPase and ATP-sensitive K channels. *J. Cereb. Blood Flow Metab.*, **11**, 700–704.

PARSONS, S., GARLAND, C.J. & PLANE, F. (1993). The role of nitric oxide in acetylcholine-evoked dilatation of the rat isolated mesenteric bed. *Br. J. Pharmacol.*, **110**, 86P.

PLANE, F. & GARLAND, C.J. (1993). Differential effects of acetylcholine, nitric oxide and levcromakalim on smooth muscle membrane potential and tone in the rabbit basilar artery. *Br. J. Pharmacol.*, **110**, 651–656.

PLANE, F., PEARSON, T. & GARLAND, C.J. (1992). Differences between endothelium-dependent relaxation to acetylcholine and A23187 in the rabbit isolated femoral artery. *Br. J. Pharmacol.*, **107**, 201P.

REES, D.D., PALMER, R.M.J., HODSON, H.F. & MONCADA, S. (1989). A specific inhibitor of nitric oxide formation from L-arginine attenuates endothelium-dependent relaxation. *Br. J. Pharmacol.*, **96**, 418–424.

TANG, T. & JOYNER, W.L. (1992). Differential role of endothelial function on vasodilator responses in series-arranged arterioles. *Microvasc. Res.*, **44**, 61–72.

TARE, M., PARKINGTON, H.C., COLEMAN, H.A., NEILD, T.O. & DUSTING, G.J. (1990). Hyperpolarization and relaxation of arterial smooth muscle caused by nitric oxide derived from the endothelium. *Nature*, **346**, 69–71.

TAYLOR, S.G. & WESTON, A.H. (1988). Endothelium-derived hyperpolarizing factor: a new endogenous inhibitor from the vascular endothelium. *Trends Pharmacol. Sci.*, **9**, 272–274.

WALDRON, G.J., MCPHERSON, G.A. & GARLAND, C.J. (1993). Acetylcholine-induced relaxation in the rat isolated mesenteric artery: relative importance of smooth muscle hyperpolarization *Br. J. Pharmacol.*, **108**, 3P.

(Received March 31, 1994
Revised July 21, 1994
Accepted August 18, 1994)

Br. J. Pharmacol. (1994), **113**, 1281–1288 © Macmillan Press Ltd, 1994

Voltage- and time-dependent inhibitory effects on rat aortic and porcine coronary artery contraction induced by propafenone and quinidine

[1]Francisco Pérez-Vizcaíno, *Buensuceso Fernández del Pozo, *Francisco Zaragozá & Juan Tamargo

Department of Pharmacology, School of Medicine, Universidad Complutense, 28040 Madrid, Spain and *Department of Pharmacognosy, School of Pharmacy, Universidad de Alcalá de Henares, Madrid, Spain

1 Class I antiarrhythmic drugs (e.g. Na^+ channel blockers) such as propafenone and quinidine also inhibit voltage-gated Ca^{2+} and K^+ channels. In the present paper the voltage- and time-dependent inhibitory effects of propafenone and quinidine were studied on depolarization-induced vascular contractions and $^{45}Ca^{2+}$ uptake in isolated endothelium denuded rat aorta and pig left descending coronary artery.

2 Quinidine and propafenone (10^{-7} M–5×10^{-5} M) produced a concentration-dependent relaxation of the contractions induced by 80 mM KCl. Propafenone was significantly more potent ($P<0.05$) than quinidine in both rat aorta and pig coronary arteries but both drugs were more potent ($P<0.05$) in relaxing rat aorta than pig coronary arteries. In rat aortic rings, the relaxant effects of propafenone were unaffected by pretreatment with the Na^+ channel blocker, tetrodotoxin.

3 The degree of inhibition produced after prolonged exposure (40 min) to propafenone and quinidine differed as the time of depolarization with 80 mM KCl was increased. Quinidine (3×10^{-6} M, 10^{-5} M and 3×10^{-5} M) not only produced an inhibition at the very early stage of contraction, but also a time-dependent inhibition was observed. In contrast, propafenone (10^{-6} M, 3×10^{-6} M and 10^{-5} M) produced a more marked concentration-dependent early block but only a mild time-dependent inhibition.

4 The voltage-dependence of propafenone- and quinidine-induced inhibition, was studied in rat aorta and coronary arteries which had been incubated in 5 or 40 mM KCl Ca^{2+}-free solution and then contracted by changing the bath solution to 100 mM KCl and 2 mM $CaCl_2$ solution. The inhibitor effects of quinidine were significantly enhanced ($P<0.05$) when the preparations were preincubated in 40 mM KCl (depolarizing) solution. In contrast, the effects of propafenone were quite similar in 5 or in 40 mM KCl solution.

5 Quinidine, 10^{-5} M, produced a greater inhibition ($P<0.05$) of 100 mM KCl-stimulated $^{45}Ca^{2+}$ uptake in aortic rings preincubated in depolarizing as compared to normal solution. In contrast, the inhibition produced by 3×10^{-6} M propafenone was similar in aortic rings incubated in 5 or 40 mM KCl solution.

6 It is concluded that both quinidine and propafenone inhibited vascular smooth muscle contraction which could be attributed to reduced Ca^{2+} entry. The voltage- and time-dependent inhibitory effects of quinidine may reflect an increased binding of the drug to Ca^{2+} channels at depolarized potentials.

Keywords: Propafenone; quinidine; rat aorta; pig coronary

Introduction

Although the main antiarrhythmic mechanism of action of class I antiarrhythmic drugs results from the inhibition of cardiac voltage-gated Na^+ channels (Hondeghem & Katzung, 1984; Grant *et al.*, 1984; Tamargo *et al.*, 1992), other voltage-gated cation channels can also be blocked by these drugs which may influence their antiarrhythmic actions (Colatsky *et al.*, 1990; Nattel, 1991; Tamargo *et al.*, 1992). Quinidine and propafenone are two class I antiarrhythmic agents widely used for the treatment of cardiac arrhythmias. Both drugs inhibit the inward cardiac Na^+ current (I_{Na}) in a voltage- and use-dependent manner and thus, they are considered as Na^+ channel blockers (Hondeghem & Katzung, 1984; Nattel, 1991; Tamargo *et al.*, 1992). In addition, they also inhibit Ca^{2+} (Satoh & Hashimoto, 1984; Salata & Wasserstrom, 1988; Scamps *et al.*, 1989; Delgado *et al.*, 1993; Fei *et al.*, 1993) and K^+ cardiac currents (Satoh & Hashimoto, 1984; Balser *et al.*, 1991; Duan *et al.*, 1993; Delpón *et al.*, 1993) and exert indirect effects on the cardiovascular system, including anticholinergic and α-adrenoceptor blockade (quinidine, Schmid *et al.*, 1974; Motulsky *et al.*, 1984) or β-adrenoceptor blocking properties (propafenone, Funk-Brentano *et al.*, 1990).

Systemic administration of quinidine causes mild hypotension, forearm vasodilatation and attenuates the vasoconstrictor response to sympathetic nerve stimulation (Schmid *et al.*, 1974; Nelson *et al.*, 1974; Walsh & Horwitz, 1979; Mariano *et al.*, 1992). This vasodilator response persisted in denervation tissues, suggesting that it is mediated both by a direct effect and by inhibition of α-adrenoceptor-mediated vasoconstriction (Schmid *et al.*, 1974). Ca^{2+} entry through voltage-gated L-type channels is the main mechanism that controls long-term vascular smooth muscle tone. In cardiac tissues both quinidine (Salata & Wasserstrom, 1988; Scamps *et al.*, 1989) and propafenone (Satoh & Hashimoto, 1984; Delgado *et al.*, 1993; Fei *et al.*, 1993) inhibit L-type Ca^{2+} channels. However, information on the inhibitory effect of antiarrhythmic drugs in vascular smooth muscle is sparse. Recently, it has been found that the inhibitory effect exerted by two class Ic antiarrhythmic drugs, propafenone and flecainide, in rat isolated aorta was accompanied by inhibition of $^{45}Ca^{2+}$ influx (Carrón *et al.*, 1991; Pérez-Vizcaíno *et al.*, 1991). Thus, it is possible that the hypotensive effect of these antiarrhythmic agents may be related to the inhibition

[1] Author for correspondence.

of vascular smooth muscle Ca^{2+} channels. The blockade of Ca^{2+} channels (Bean *et al.*, 1986; Nelson & Worley, 1989) as well as the vasodilator effect (Morel & Godfraind, 1987; Nelson & Worley, 1989; Salomone & Godfraind, 1993) of some dihydropyridine Ca^{2+} channel blockers (CCBs) have been shown to be voltage- and time-dependent. Therefore, the aim of the present paper was to study the voltage- and time-dependent inhibitory effects of propafenone and quinidine on depolarization-induced vascular contractions in endothelium-denuded rat aorta and pig coronary artery.

Methods

Tissue preparation

Male Sprague-Dawley rats (300–350 g) from Interfauna (Barcelona) and young pigs (5–7 kg) from the local abattoir were used for these experiments. Porcine hearts, still beating, were immersed in cold (4°C) physiological saline solution (PSS) of the following composition (mM): NaCl 118, KCl 5, $NaHCO_3$ 25, $MgSO_4$ 1.2, $HCaCl_2$ 2, KH_2PO_4 1.2 and glucose 11, previously bubbled with 95% O_2:5% CO_2 gas mixture. The left descending coronary artery was dissected in PSS and transported immediately to the laboratory. Rats were killed by a blow on the head and exsanguinated. The descending thoracic aorta was rapidly dissected and placed in PSS. After excess fat and surrounding tissue had been removed, the aorta and coronary arteries were cut into rings (3–4 mm in length) as described elsewhere (Pérez-Vizcaíno *et al.*, 1991; Tejerina *et al.*, 1992; Pérez-Vizcaíno *et al.*, 1993). Endothelium was removed by gentle rubbing of the internal surface of the vessels with a small metal rod. At the beginning of the experiments, the absence of functional endothelium was confirmed by the inability of the preparation precontracted with 10^{-7} M noradrenaline to relax in response to 10^{-6} M acetylcholine.

Mechanical force recording

Arterial rings were mounted in 5 ml organ baths containing PSS under tension (2 g for the aorta and 0.5 g for coronary rings) by two parallel L-shaped stainless-steel holders (diameter 0.8 mm for aorta and 0.2 mm for coronary rings) inserted into the lumen. Holders were attached to force-displacement transducers (Grass FT03, Grass, Quincy, MA, U.S.A.) and connected to a polygraph (Grass Model 7) to measure isometric contractile force as previously described (Pérez-Vizcaíno *et al.*, 1991, 1993). Tissue baths were filled with PSS maintained at 37°C and bubbled with 95% O_2:5% CO_2 gas mixture. Each preparation was allowed to equilibrate for 90 min prior to initiation of experimental procedures and during this period the incubation medium was changed every 30 min.

Depolarization-induced responses

After equilibration, aortic and coronary rings were exposed to 80 mM KCl. When the contractile responses to KCl reached steady state, concentration-response curves were obtained for quinidine and propafenone by cumulative addition of the drugs. The relaxant effect of each concentration was allowed to reach a stable level (normally after 25–35 min) before the next concentration was added. In parallel time controls, contractile force decreased by less than 5% during the study.

Time-dependence of drug-induced inhibition

To study the time-dependent inhibitory effect of propafenone and quinidine on KCl-induced contractions, following the equilibration period rat aortic rings were contracted with 80 mM KCl PSS. The contractile response was recorded for 40 min and then the preparations were washed in normal PSS. Thereafter, rings were exposed to propafenone (10^{-6} M, 3×10^{-6} M or 10^{-5} M), quinidine (3×10^{-6} M, 10^{-5} M or 3×10^{-5} M) or vehicle (PSS) for 40 min and finally rings were again contracted by addition of 80 mM KCl PSS for another 40 min in the continuous presence or absence of the drug. The contractile responses evoked during the second application of 80 mM KCl were expressed as a percentage of either the maximal tension (Figures 2a and 3a) or the tension at the corresponding time interval (Figures 2b and 3b) obtained in the same ring during the first contraction.

Voltage-dependence of drug-induced inhibition

To examine the pattern of voltage-dependence of propafenone- and quinidine-induced inhibition, in rat aorta and coronary artery the effect of the drugs was studied at different membrane potentials which were controlled by changing the extracellular concentration of KCl (i.e., 'potassium clamp'; Burges *et al.*, 1987; Nelson & Worley,1989; Godfraid & Salomone, 1991; Salomone & Godfraind, 1993). Aortic and coronary rings were incubated for 30 min in Ca^{2+}-free (5 mM KCl) or in Ca^{2+}-free depolarizing (40 mM KCl) PSS (with isotonic replacement of NaCl by KCl). Then the preparations were contracted by a short-duration (2 min) depolarizing pulse by changing the bath solution to a solution containing 100 mM KCl and 2 mM $CaCl_2$. The duration of the pulse was short enough to avoid the drugs coming into equilibrium with the Ca^{2+} channels at the membrane potential set by 100 mM KCl (Nelson & Worley, 1989). The preparations were then incubated for 30 min in PSS containing 5 or 40 mM. Three control contractile responses to 100 mM KCl PSS containing 2 mM $CaCl_2$ were obtained at the beginning of the experiment at 30 min intervals. This was followed by exposure to propafenone (10^{-6} M, 3×10^{-6} M and 10^{-5} M) or quinidine (3×10^{-6} M, 10^{-5} M and 3×10^{-5} M) for 40 min. Thereafter, the contractile response to 100 mM KCl was elicited in the presence of the drug. In each preparation only one drug and one concentration (5 or 40 mM) of KCl were tested. In parallel time controls, responses were in the range of 94 to 108% of the initial contractions. The results of these experiments were expressed as a percentage of the initial control contractile responses.

Measurement of $^{45}Ca^{2+}$ influx

The effect of the drugs on the $^{45}Ca^{2+}$ influx in aortic rings was quantified by means of the fraction of $^{45}Ca^{2+}$ uptake resistant to displacement by La^{3+} (Pèrez-Vizcaíno *et al.*, 1991). Rings weighing between 6–10 mg were equilibrated for 90 min in PSS bubbled with a 95% O_2:5% CO_2 gas mixture. All the solutions employed afterwards contained no Ca^{2+} or phosphates in order to minimize $^{45}Ca^{2+}$ precipitation. After equilibration, rings were transferred to a 5 or 40 mM KCl PSS in the presence or absence of propafenone (3×10^{-6} M), quinidine (10^{-5} M) or verapamil (10^{-4} M) for 40 min. At this time both experimental and control rings were incubated for 2 min in 100 mM KCl PSS containing $^{45}Ca^{2+}$ (specific activity 2 μCi ml^{-1}) in the presence or absence of quinidine, propafenone or verapamil and then washed for 5 min in an ice-cold lanthanum solution (composition in mM: NaCl 122, KCl 5.9, $MgCl_2$ 1.25, glucose 11, $LaCl_3$ 50 and Tris maleate 15; pH 6.8 at 0°C). Afterwards the rings were removed, dried between two sheets of filter paper, weighed and digested in a perchloric acid (35%)-H_2O_2 (33 volumes) mixture (1:1, v/v) at 75°C for 20 min. Radioactivity of the samples was assayed in a liquid scintillation counter as previously described (Pérez-Vizcaíno *et al.*, 1991).

Drugs

The following drugs were used: propafenone hydrochloride (Knoll AG, Ludwigshafen, Germany), quinidine sulphate,

(−)-noradrenaline bitartrate, acetylcholine chloride, tetrodotoxin (Sigma Ltd. Co., London). All drugs were dissolved in distilled deionized water to prepare a 1 mM stock solution and further dilutions were made in PSS. Ascorbic acid (Merk) 0.1 mM was added to the solution of noradrenaline. $^{45}CaCl_2$ was obtained from Amersham International plc (Buckinghamshire, England).

Statistics

Throughout the paper, values are expressed as mean ± s.e.mean. Statistical analysis was performed with Student's unpaired *t* test. The differences between control and experimental values were considered significant when $P<0.05$. The negative logarithm of the half-maximal effective concentration (pD_2) was calculated from the concentration-response curves by fitting the experimental data to a logistic equation by non-linear regression analysis.

Results

Concentration-response curves

Figure 1 shows the relaxant effects of quinidine and propafenone when added at the plateau of the contractile responses evoked by 80 mM KCl. Addition of 80 mM KCl to rat aortic and pig coronary rings gradually induced a contractile response which averaged 2793 ± 208 ($n = 16$) and 2101 ± 268 mg ($n = 12$), respectively. Cumulative increases of quinidine and propafenone (10^{-7} M–5×10^{-5} M) resulted in a concentration-dependent relaxation. The pD_2 values for the relaxant effects of quinidine and propafenone are shown in Table 1. It can be observed that propafenone was significantly more potent ($P<0.05$) than quinidine in both rat aorta and pig coronary arteries but both drugs were more potent ($P<0.05$) in relaxing rat aorta than pig coronary arteries.

In rat aortic rings, the Na^+ channel blocker tetrodotoxin (3×10^{-5} M), when added at the plateau of the KCl-induced contraction had no effect on tension. Furthermore, in these preparations the relaxant effects of propafenone were unaffected by the pretreatment with tetrodotoxin (Table 1).

Time-dependent effects in rat aorta

To study the time-dependent of the effects of propafenone and quinidine, aortic rings were contracted with 80 mM KCl and the evoked contraction was monitored for 40 min. Then the rings were incubated for a 40 min period in the absence or presence of the drugs and finally, contracted with 80 mM KCl for another 40 min. Figures 2 and 3 show the time course of the contractions induced by 80 mM KCl after the incubation for 40 min with vehicle, propafenone (10^{-6} M, 3×10^{-6} M and 10^{-5} M) and quinidine (3×10^{-6} M, 10^{-5} M and 3×10^{-5} M), respectively. The contractile response recorded in the presence of each drug was compared to that obtained before the addition of propafenone or quinidine. In the presence of propafenone (Figure 2a) and quinidine (Figure 3a) the contraction was inhibited in a concentration-dependent manner, but propafenone was more potent than quinidine ($P<0.05$). More interestingly, Figure 2b and 3b show that the degree of inhibition produced by propafenone and quinidine differ as the time of depolarization was prolonged. At 3×10^{-6} M, quinidine did not produce any inhibition at the very early stage of contraction but it progressively developed reaching steady-state after 20 min depolarization, whereas in the presence of 10^{-5} M and 3×10^{-5} M the drug not only produced a marked early block but a great time-dependent inhibition was also observed (Figure 3b). Thus, the percentage of inhibition produced by the three concentrations of quinidine was significantly greater ($P<0.01$) after 20 min than after 15 s. In contrast, propafenone (10^{-6} M, 3×10^{-6} M and 10^{-5} M) produced a more marked concentration-dependent early block but only a mild time-

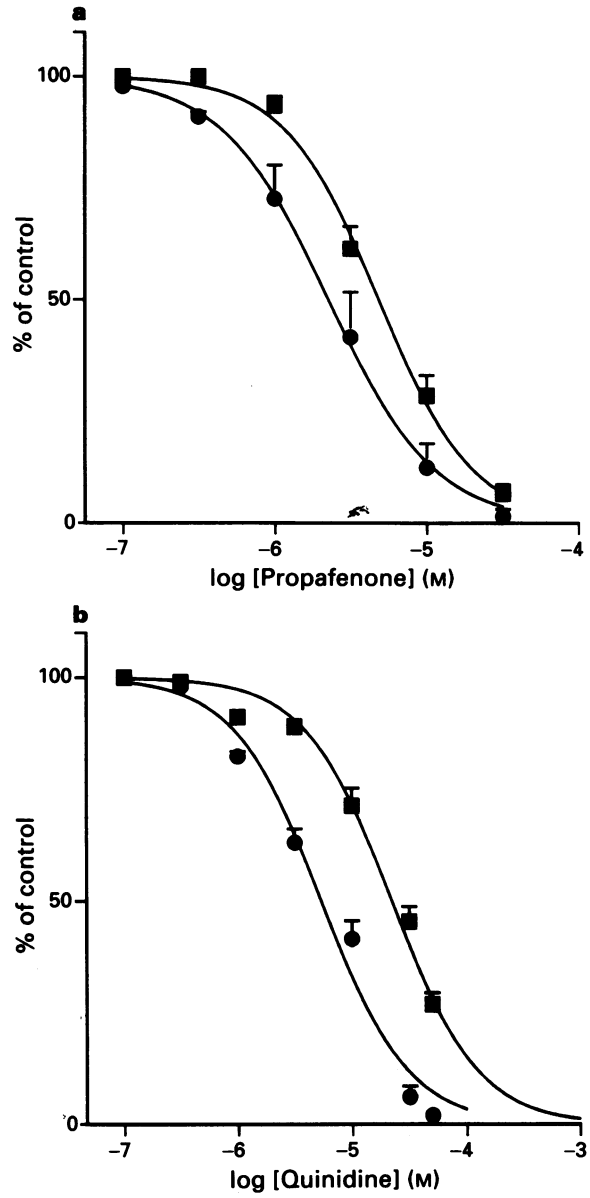


Figure 1 Effects of (a) propafenone and (b) quinidine in rat aortic (●) and pig coronary arterial rings (■) precontracted with KCl 80 mM. After the contraction induced by 80 mM KCl reached its plateau, concentration-response curves were performed by cumulative addition of the drugs. Results are expressed as a percentage of the initial control tension. Each symbol represents the mean ± s.e.mean of 6–7 rings from different animals.

Table 1 pD_2 values for the relaxant response of propafenone and quinidine on 80 nM KCl-induced contractions in rat aorta and pig coronary arteries

		Propafenone	*Quinidine*
Rat aorta	−TTX	5.64 ± 0.02 (6)	5.26 ± 0.05* (7)
	+TTX	5.49 ± 0.01 (3)	ND
Pig coronary		5.34 ± 0.06 (6)	4.65–0.03* (6)

TTX = 3×10^{-5} M tetrodotoxin, *$P<0.05$ vs propafenone, the number of experiments is shown in parenthesis; ND not determined.
Results (mean ± s.e.mean) were calculated from the experiments shown in Figure 1.

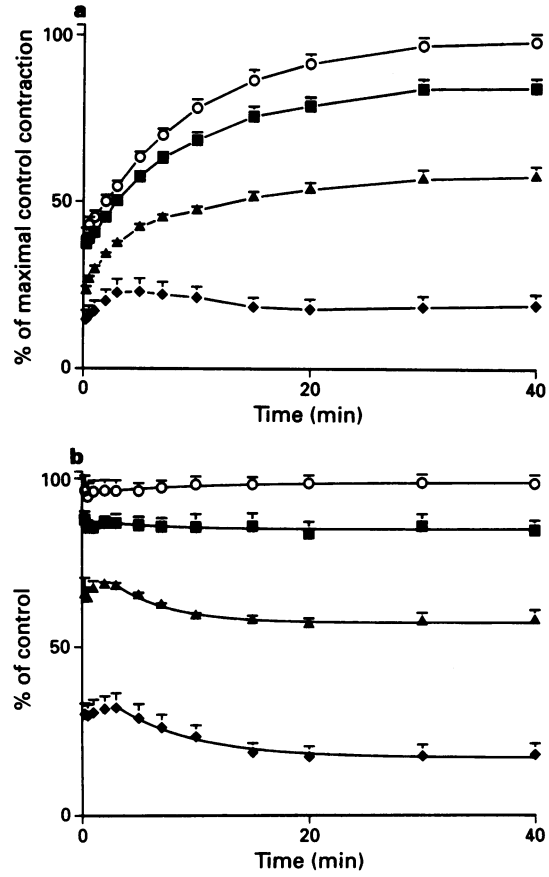


Figure 2 Time-dependent inhibition of 80 mM KCl-induced contraction produced by propafenone in rat isolated aorta. A first control contraction was elicited for 40 min. Then the rings were incubated for a 40 min period in the absence (○) or in the presence of 10^{-6} M (■), 3×10^{-6} M (▲) and 10^{-5} M (◆) propafenone and, finally, contracted by KCl in the presence of the drug for another 40 min. In (a) results are expressed as a percentage of the maximal tension during the first contraction and in (b) as a percentage of the tension of the first contraction at each time interval. Each symbol represents the mean ± s.e.mean of 5–7 rings from different animals.

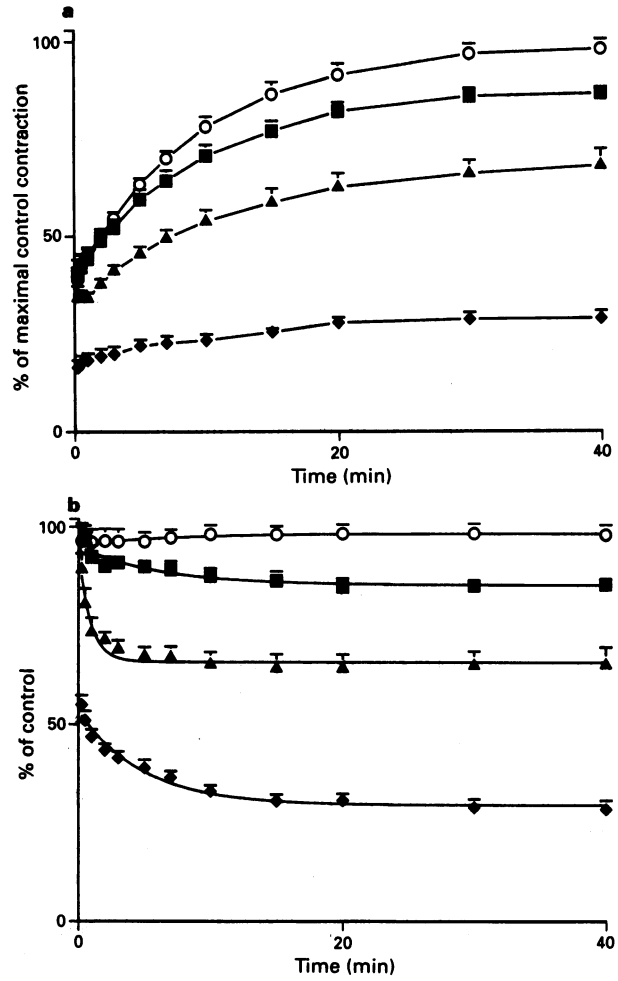


Figure 3 Time-dependent inhibition of 80 mM KCl-induced contraction produced by quinidine in rat isolated aorta. Results were obtained in the absence (○) or in the presence of 3×10^{-6} M (■), 10^{-5} nM (▲) and 3×10^{-5} M (◆) quinidine. Controls were the same as in Figure 2. Each symbol represents the mean ± s.e.mean of 5–7 rings from different animals. See Figure 2 for explanation.

dependent inhibition, which began with a delay of 3 min, was observed (Figure 2b). Thus, only at the highest concentration of propafenone tested the percentage of inhibition observed after 20 min was significantly greater ($P<0.05$) than after 15 s.

The time course of the inhibition for the two concentrations of quinidine which did not produce a high early block (3×10^{-6} M and 10^{-5} M) could be fitted by a non linear analysis to the equation:

$$B = B_{max}\ (1 - e^{-(K_1[D] + K_{-1})t})$$

where B_{max} is the steady-state inhibition, B is the level of inhibition at the time t of depolarization and [D] is the drug concentration. The estimated values for the association (K_1) and dissociation (K_{-1}) constants were $0.13\ \mu M^{-1}\ min^{-1}$ and $0.19\ min^{-1}$, respectively, and the calculated value of $K_D(K_{-1}/K_1 = 1.47 \times 10^{-6}$ M) was in the range of the observed pD_2 values.

Voltage-dependence of drug-induced inhibition

In order to test if the effects of propafenone and quinidine were modified by depolarizing the membrane potential, aortic and coronary rings were incubated for 40 min in the continuous presence of the drugs and the membrane potential was controlled by changing the KCl concentration (5 or 40 mM) in the bathing media. Thereafter, the preparations were contracted by changing for 2 min to a 100 mM KCl-depolarizing solution containing quinidine or propafenone. The previous concentration of KCl in the bathing media did not influence the amplitude of the contractile response induced by the 100 mM KCl in both, aortic (792 ± 82 and 708 ± 40 mg in 5 and 40 mM KCl, respectively. $n = 19$) or coronary rings (800 ± 104 and 759 ± 74 mg in 5 and 40 mM KCl, respectively. $n = 19$). Propafenone and quinidine inhibited these contractions in a concentration-dependent manner in rat aorta (Figure 4) and pig coronary artery (Figure 5). Furthermore, the inhibitory effects of quinidine in rat aorta (Figure 4b) and pig coronary arteries (Figure 5b) were significantly enhanced ($P<0.05$ for all concentrations) when the preparations were preincubated in depolarizing (40 mM KCl) as compared to normal (5 mM KCl) PSS. For propafenone, a similar trend was also observed in normal and in depolarizing PSS (Figures 4a and 5a). However, differences for the inhibitory effects at 5 and 40 mM KCl were significant only at 10^{-5} M propafenone in pig coronary arteries. The pD_2 values for the inhibitory effects of quinidine and propafenone are summarized in Table 2.

Inhibition of $^{45}Ca^{2+}$ influx

To determine whether the inhibitory effects of quinidine and propafenone on aortic contractility and its voltage-

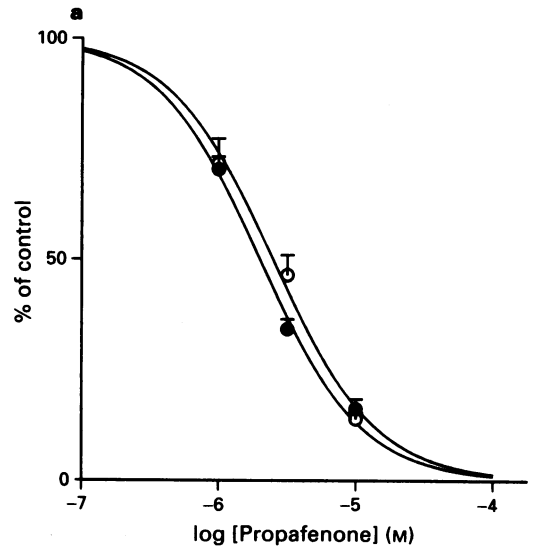


Figure 4 Voltage-dependence of the effects of (a) propafenone (10^{-6} M, 3×10^{-6} M and 10^{-5} M) and (b) quinidine (3×10^{-6} M, 10^{-5} M and 3×10^{-5} M) in aortic rings. Preparations were initially incubated for 40 min in either 5 (○) or 40 mM KCl (●) Ca^{2+}-free PSS and then, contracted by changing the solution to 100 mM KCl, 2 mM Ca^{2+} PSS for 2 min in the continuous presence of the drugs. Results are expressed as a percentage of the control contractile response induced by 100 mM KCl, 2 mM Ca^{2+} PSS. Each symbol represents the mean ± s.e.mean of 6–7 contractions in different rings expressed as a percentage of the initial control in the absence of the drug. *$P<0.05$ vs 5 mM KCl.

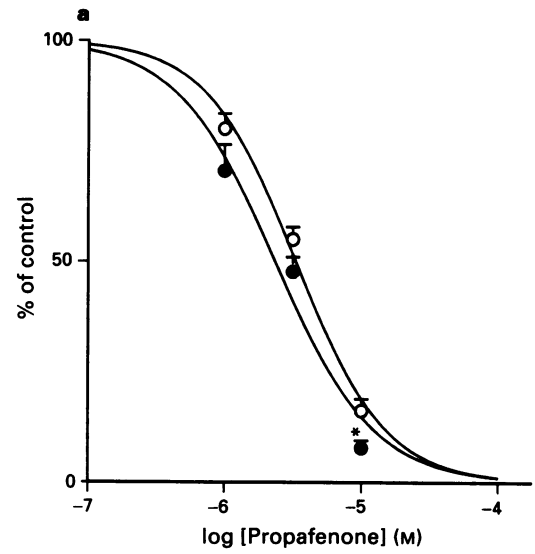


Figure 5 Voltage-dependence of the effects of (a) propafenone (10^{-6} M, 3×10^{-6} M and 10^{-5} M) and (b) quinidine (3×10^{-6} M, 10^{-5} M and 3×10^{-5} M) in coronary artery rings. The rings were incubated in either 5 (○) or 40 mM KCl (●) Ca^{2+}-free PSS and then contracted by changing the solution 100 mM KCl, 2 mM Ca^{2+} PSS for 2 min. Each symbol represents the mean ± s.e.mean of 6–7 contractions in different rings expressed as a percentage of the initial control in the absence of the drug. *$P<0.05$ vs 5 mM KCl.

Table 2 pD_2 values for the inhibitory effect of propafenone and quinidine incubated in 5 or 40 mM KCl PSS on 100 mM KCl-induced contractions in rat aorta and pig coronary arteries

	[KCl] (mM)	*Propafenone*	*Quinidine*
Rat aorta	5	5.60 ± 0.03 (6)	4.79 ± 0.01 (7)
	40	5.69 ± 0.02 (6)	5.12 ± 0.03 (6)*
Pig coronary	5	5.47 ± 0.03 (6)	4.80 ± 0.01 (6)
	40	5.63 ± 0.07 (7)	5.11 ± 0.03 (7)*

*$P<0.05$ vs 5 mM KCl, the number of experiments is shown in parenthesis.
Results (mean ± s.e.mean) were calculated from the experiments shown in Figures 4 and 5.

dependence were due to reduced Ca^{2+} entry, we measured the 100 mM KCl-stimulated $^{45}Ca^{2+}$ influx using a protocol similar to that described above to study the voltage-dependence of drug-induced inhibition of contractile responses. Concentrations of propafenone (3×10^{-6} M) and quinidine (10^{-5} M) producing about 50% inhibition of contraction were chosen for this study. $^{45}Ca^{2+}$ uptake remaining in the presence of 10^{-4} M verapamil was considered as the maximal Ca^{2+} antagonist insensitive Ca^{2+} entry. As shown in Figure 6, $^{45}Ca^{2+}$ uptake was similar in control aorta previously incubated in 5 or 40 mM KCl. Both 3×10^{-6} M propafenone and 10^{-5} M quinidine significantly inhibited $^{45}Ca^{2+}$ uptake ($P<0.05$) in preparations previously incubated in 5 or 40 mM KCl. However, quinidine produced a greater inhibition ($P<0.05$) of $^{45}Ca^{2+}$ uptake in aortic rings incubated in depolarizing (40 mM KCl) PSS as compared to normal PSS. In contrast, the inhibition of $^{45}Ca^{2+}$ uptake produced by 3×10^{-6} M propafenone was not different in aortic rings incubated in 5 or 40 mM KCl PSS.

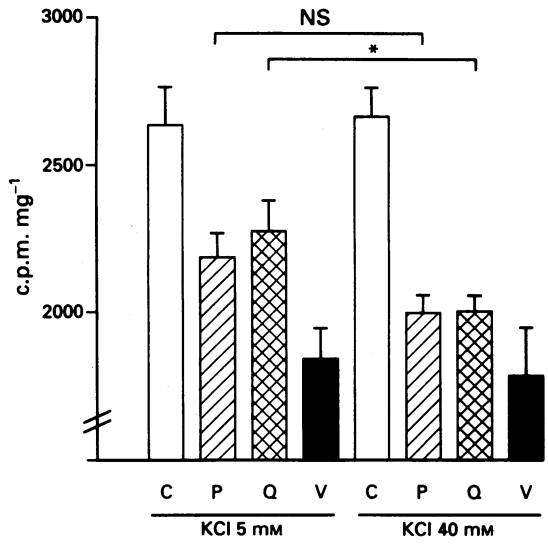


Figure 6 Voltage-dependent inhibition of $^{45}Ca^{2+}$ uptake in rat aortic rings. Rings were incubated in 5 or 40 mM KCl Ca^{2+}-free PSS in the absence (C, open columns) or in the presence of 3×10^{-6} M propafenone (P, hatched columns), 10^{-5} M quinidine (Q, cross-hatched columns) or 10^{-4} M verapamil (V, solid columns) for 40 min. Then rings were stimulated by 100 mM KCl PSS in the presence of 2 μCi ml^{-1} $^{45}Ca^{2+}$ for 2 min. The $^{45}Ca^{2+}$ uptake in the presence of 10^{-4} M verapamil was considered as the maximal Ca^{2+} antagonist-insensitive $^{45}Ca^{2+}$ entry. Ordinate scale: c.p.m. mg^{-1} of dry tissue. Each column represents the mean ± s.e.mean of 14–16 rings. $*P<0.05$, ns = not significant 5 vs 40 mM KCl.

Discussion

In the present paper we have analysed the effects of two Na^+ channel blockers, propafenone and quinidine, on contractions and $^{45}Ca^{2+}$ influx induced by membrane depolarization (high KCl concentration) in endothelium-denuded rat aorta and pig coronary artery. Tonic contractions induced by depolarization with high concentrations of KCl are associated with Ca^{2+} entry through voltage-gated L-type Ca^{2+} channels because they can be selectively blocked by Ca^{2+} channel blockers (CCBs) and are suppressed in Ca^{2+}-free solution (Cauvin *et al.*, 1983; Godfraind *et al.*, 1986). In the present experiments propafenone and quinidine inhibited the contractile responses and the increase in $^{45}Ca^{2+}$ influx induced by high KCl, propafenone being more potent than quinidine. Since Ca^{2+} ions play a determinant role in vascular contractions, these results strongly suggest that inhibition of arterial contractions induced by quinidine and propafenone may result from their inhibitory effect on Ca^{2+} entry through L-type channels. Moreover, they confirmed previous evidence suggesting that in rat isolated aorta the vasodilator effects of two class Ic antiarrhythmic drugs, propafenone and flecainide, can be attributed to their ability to inhibit Ca^{2+} entry through voltage-gated channels (Carrón *et al.*, 1991; Pérez-Vizcaíno *et al.*, 1991). The pD_2 values for inhibition of vascular contractions in the present experiments are very similar to those previously reported for inhibiting L-type Ca^{2+} channels in isolated cardiac myocytes using the patch-clamp technique for propafenone ($pD_2 = 5.3–5.8$. Delgado *et al.*, 1993; Fei *et al.*, 1993) and quinidine ($pD_2 = 5.0$. Scamps *et al.*, 1989). The existence of Na^+ channels either sensitive or relatively insensitive to tetrodotoxin in vascular smooth muscle have rarely been reported (Sturek & Hermsmeyer, 1986). In the present experiments, 3×10^{-5} M tetrodotoxin did not affect aortic contractile force under depolarizing conditions or the relaxant reponse to propafenone. Therefore, a possible role for Na^+ channel inhibition in the observed inhibitory effects can be excluded.

In *in vitro* experiments, CCBs inhibit high KCl-induced contractions in vascular smooth muscle in a voltage- and time-dependent manner (Godfraind *et al.*, 1986). According to the modulated receptor hypothesis, binding of a drug to a receptor site located within the channel is modulated by the conformational state of the channel (rested, activated, inactivated) which is determined by the membrane potential (Hondeghem & Katzung, 1984). Radioligand binding (Burges *et al.*, 1987; Godfraind & Salomone, '1991; Triggle, 1991; Salomone & Godfraind, 1993) and electrophysiological studies (Uehara & Hume, 1985; Bean *et al.*, 1986; Nelson & Worley, 1989) have found that most CCBs bind with greater affinity under depolarizing conditions. Since depolarization of the membrane potential shifts the conformation of Ca^{2+} channels into the activated and inactivated states, the voltage-dependence has been attributed to a preferential binding to these states of the channel (Uehara & Hume, 1985; Bean *et al.*, 1986; Tamargo & Delpón, 1991).

In the present experiments, after prolonged exposure (40 min) to quinidine at normally polarized membrane potentials the degree of inhibition increased as the time of depolarization was prolonged (i.e., time-dependent inhibition), reaching a steady-state within 20 min of depolarization. Similar behaviour has been described previously with some CCBs of the dihydropyridine family (Morel & Godfraind, 1987; Wibo *et al.*, 1988; Godfraind & Salomone, 1991). Since depolarization shifts Ca^{2+} channels into the inactivated state, this time-dependent effect has been proposed to reflect an increased drug affinity for this state of the channel (Wibo *et al.*, 1988). The voltage-dependence of the inhibitory effects of CCBs on vascular smooth muscle have been reported in functional studies where the membrane potential is controlled by changing the extracellular concentration of KCl (i.e., 'potassium clamp'; Burges *et al.*, 1987; Nelson & Worley, 1989; Godfraind & Salomone, 1991; Salomone & Godfraind, 1993). The voltage-dependence of the inhibitory effect of quinidine on contractions and $^{45}Ca^{2+}$ influx was confirmed by the significant increase in the inhibition observed in depolarized (40 mM KCl PSS) as compared to normally polarized arteries (5 mM KCl) when a short-duration depolarizing pulse (100 mM KCl PSS) was applied. Therefore, the voltage-dependence of the inhibitory effects of quinidine may reflect an increased binding of the drug to Ca^{2+} channels under depolarizing conditions. Because in preparations incubated in 5 mM KCl most of the Ca^{2+} channels will be in the resting state, wherease under depolarizing conditions (40 mM KCl) some channels will be in the inactivated and/or activated state we can speculate that quinidine preferentially binds to these states of the channel. In fact, in isolated ventricular myocytes, quindine decreased L-type Ca^{2+} current in a voltage- and use-dependent manner and shifted the steady state inactivation curves towards hyperpolarization (Salata & Wasserstrom, 1988; Scamps *et al.*, 1989). However, at high concentration (3×10^{-5} M) quinidine significantly reduced the amplitude of the Ca^{2+} current of the first clamp step after a prolonged resting period, i.e. it also produced a tonic block (Salata & Wasserstrom, 1988; Scamps *et al.*, 1989).

Peak Ca^{2+} current through L-type channels occurs within milliseconds whereas the contractions in vascular smooth muscle take much longer to develop. Thus, during prolonged depolarization at least some of the Ca^{2+} channels must be in a conducting state implying that either a component of the current never inactivates or alternatively, that drug-free inactivated channels return to the conducting (activated) state (Imaizumi *et al.*, 1989). In fact, KCl-induced contractions are sustained, depend on extracellular Ca^{2+} and are selectively inhibited by CCBs (Cauvin *et al.*, 1983). After exposure to depolarizing (40 mM KCl) PSS a higher portion of Ca^{2+} channels would be in the inactivated (non-conducting) state and it could be expected that during the depolarizing pulse (100 mM KCl, 2 mM $CaCl_2$) there would be less Ca^{2+} influx and contraction. The finding that the amplitude of the contractions and $^{45}Ca^{2+}$ uptake stimulated by 100 mM KCl were

similar in arteries preincubated in 5 or 40 mM KCl PSS suggests that the contraction is dependent on this dihydropyridine-sensitive, non inactivating component of the Ca^{2+} current (Imaizumi *et al.*, 1989).

Propafenone also inhibited in a concentration-dependent manner the contractions induced by high KCl. However, and in contrast to quinidine, its inhibitory effect which was quite evident within the first 2 min, increased only slightly during prolonged depolarization. Furthermore, the inhibitory effects of propafenone on the contractions evoked by 100 mM KCl and 2 mM Ca^{2+} PSS were quite similar in aorta or coronary arteries preincubated in 5 or 40 mM KCl Ca^{2+}-free PSS. Thus, the affinity of propafenone for Ca^{2+} channels does not seem to depend on membrane potential.

The possible clinical relevance of the vasodilator effects and the inhibition of Ca^{2+} entry described in this paper for quinidine and propafenone in patients with cardiac arrhythmias is uncertain. However, these effects appeared at the same range of concentrations at which both antiarrhythmics exert their inhibitory effects on inward (Na^+ and Ca^{2+} currents) and outward K^+ currents in cardiac myocytes (Colatsky *et al.*, 1990; Nattel, 1991; Balser *et al.*, 1991; Tamargo *et al.*, 1992; Duan *et al.*, 1993; Delpón *et al.*, 1993). A decrease in systemic vascular resistance may reduce ventricular afterload, while a decrease in coronary vascular resistance might increase coronary blood flow. Thus, it is possible that in some patients these vasodilator actions may improve cardiac performance, overriding the cardiodepressant effects of propafenone and quinidine. In fact, the intravenous quinidine infusion is associated with a decrease in systemic vascular resistance and in cardiac filling pressure (Mariano *et al.*, 1992). Furthermore, the inhibition of Ca^{2+} entry may explain the previously described direct vasodilator effect of quinidine that together with its α-adrenoceptor blocking action (Schmid *et al.*, 1974; Motulsky *et al.*, 1984) is responsible for the hypotensive response observed following the parenteral administration of the drug (Hirschfield *et al.*, 1977; Mariano *et al.*, 1992).

The authors are grateful to Dr E. Delpón and Dr C. Valenzuela for helpful discussions. This study was supported by a CICYT Grant SAF92-0157.

References

BALSER, J.R., BENNET, P.B., HONDEGHEM, L.M. & RODEN, D.M. (1991). Suppression of time-dependent outward current in guinea-pig ventricular myocytes. Actions of quinidine and amiodarone. *Circ. Res.*, **69**, 519–529.

BEAN, B.P., STUREK, M., PUGA, A. & HERMSMEYER, K. (1986). Calcium channels in muscle cells isolated from rat mesenteric arteries: modulation of dihydropyridine drugs. *Circ. Res.*, **59**, 229–235.

BURGES, R.A., GARDINER, D.G., GWILT, M., HIGGINS, A.J., BLACKBURN, K.J., CAMPBELL, S.F., CROSS, P.E. & STUBBS, J.K. (1987). Calcium channel blocking properties of amlodipine in vascular smooth muscle and cardiac muscle in vitro: evidence for voltage modulation of vascular dihydropyridine receptors. *J. Cardiovasc. Pharmacol.*, **9**, 110–119.

CARRON, R., PEREZ-VIZCAINO, F., DELPON, E. & TAMARGO, J. (1991). Effects of propafenone on ^{45}Ca movements and contractile responses in vascular smooth muscle. *Br. J. Pharmacol.*, **103**, 1453–1457.

CAUVIN, C., LOUTZENHISER, R. & VAN BREEMEN, C. (1983). Mechanisms of calcium antagonist-induced vasodilation. *Annu. Rev. Pharmacol. Toxicol.*, **23**, 373–396.

COLATSKY, T.J., FOLLMER, C.H. & STARMER, C.F. (1990). Channel specificity in antiarrhythmic drug action. *Circulation*, **82**, 2235–2242.

DELGADO, C., TAMARGO, J., HENZEL, D. & LORENTE, P. (1993). Effects of propafenone on calcium currents in guinea-pig ventricular myocytes. *Br. J. Pharmacol.*, **108**, 721–727.

DELPON, E., VALENZUELA, C., CASIS, O., PEREZ, O. & TAMARGO, J. (1993). Effects of propafenone on $I_{K,r}$ and $I_{K,s}$ in guinea-pig ventricular myocytes. *Biophys. J.*, **64**, A314.

DUAN, D., FERMINI, B. & NATTEL, S. (1993). Potassium channel blocking properties of propafenone in rabbit atrial myocytes. *J. Pharmacol. Exp. Ther.*, **264**, 1113–1123.

FEI, L., GILL, J.S., MCKENNA, N.J. & CAMM, A.J. (1993). Effects of propafenone on calcium currents in single ventricular myocytes of guinea-pig. *Br. J. Pharmacol.*, **109**, 178–182.

FUNK-BRENTANO, C., KROEMER, H.K., LEE, J.T. & ROSEN, D.M. (1990). Propafenone. *N. Engl. J. Med.*, **322**, 518–526.

GODFRAIND, T., MILLER, R. & WIBBO, M. (1986). Calcium antagonism and calcium entry blockade. *Pharmacol. Rev.*, **38**, 324–416.

GODFRAIND, T. & SALOMONE, S. (1991). Functional interaction of lacidipine with calcium channels in vascular smooth muscle. *J. Cardiovasc. Pharmacol.*, **18**, (Suppl II) S1–S6.

GRANT, A.O., STARMER, C.F. & STRAUSS, H.C. (1994). Antiarrhythmic drug action. Blockade of the inward sodium current. *Circ. Res.*, **55**, 427–438.

HIRSCHFIELD, D.S., UEDA, C.T., ROWLAND, M. & SCHEINMAN, M.M. (1977). Clinical and electrophysiological effects of intravenous quinidine in man. *Br. Heart J.*, **39**, 309–316.

HONDEGHEM, L.M. & KATZUNG, B.G. (1984). Antiarrhythmic agents: the modulated receptor mechanism of action of sodium and calcium channel-blocking drugs. *Annu. Rev. Pharmacol. Toxicol.*, **24**, 387–423.16.

IMAIZUMI, Y., MURAKI, K., TAKEDA, M. & WATANABE, M. (1989). Measurements and simulation of noninactivating Ca current in smooth muscle cells. *Am. J. Physiol.*, **256**, C880–C885.

MARIANO, D.J., SCHOMER, S.J. & REA, R.F. (1992). Effects of quinidine on vascular resistance and sympathetic nerve activity in humans. *J. Am. Coll. Cardiol.*, **20**, 1411–1416.

MOREL, N. & GODFRAIND, T. (1987). Prolonged depolarization increases the pharmacological effect of dihydropyridines and their binding affinity for calcium channels of vascular smooth muscle. *J. Pharmacol. Exp. Ther.*, **243**, 711–715.

MOTULSKY, H., MAISEL, A., SNAVELY, M. & INSEL, P. (1984). Quinidine is a competitive antagonist at alpha$_1$- and alpha $_2$-adrenergic receptors. *Circ. Res.*, **55**, 376–381.

NATTEL, S. (1991). Antiarrhythmic drug classifications. *Drugs*, **41**, 672–701.

NELSON, L.D., SCHMID, P.G., HOLMSTEN, D., MARK, A.L., HEIDSTAD, D.D. & ABBOUD, F.M. (1974). Effects of quinidine on venous responses to adrenergic and nonadrenergic constrictor stimuli: indirect evidence of two sites of action in vascular smooth muscle. *Proc. Soc. Exp. Biol. Med.*, **146**, 409–413.

NELSON, M. & WORLEY, J. (1989). Dihydropyridine inhibition of single calcium channels and contraction in rabbit mesenteric artery depends on voltage. *J. Physiol.*, **412**, 65–91.

PEREZ-VIZCAINO, F., CARRON, R., DELPON, E., DUARTE, J. & TAMARGO, J. (1993). Effects of (S)-nafenodone on $^{45}Ca^{2+}$ fluxes and contraction in rat isolated vascular smooth muscle. *Eur. J. Pharmacol.*, **232**, 105–111.

PEREZ-VIZCAINO, F., DUARTE, J. & TAMARGO, J. (1991). Effects of flecainidine on isolated vascular smooth muscles of rat. *Br. J. Pharmacol.*, **104**, 726–730.

SALATA, J.J. & WASSERSTROM, J.A. (1988). Effects of quinidine on action potentials and ionic currents in isolated canine ventricular myocytes. *Circ. Res.*, **62**, 324–337.

SALOMONE, S. & GODFRAIND, T. (1993). Radioligand and functional estimates of the interaction of the 1,4-dihydropyridines, isradipine and lacidipine, with calcium channels in smooth muscle. *Br. J. Pharmacol.*, **109**, 100–106.

SATOH, H. & HASHIMOTO, K. (1984). Effects of propafenone on the membrane currents of rabbit sino-atrial node cells. *Eur. J. Pharmacol.*, **99**, 185–191.

SCAMPS, F., UNDROVINAS, A. & VASSORT, G. (1989). Inhibition of I_{Ca} in single frog cardiac cells by quinidine, flecainide, ethmozin, and ethacizin. *Am. J. Physiol.*, **256**, C549–C559.

SCHMID, P.G., NELSON, L.D., HOLMSTEN, D. & MARK, A.L. (1974). Inhibition of adrenergic vasoconstriction by quinidine. *J. Pharmacol. Exp. Ther.*, **188**, 124–134.

STUREK, M. & HERMSMEYER, K. (1986). Calcium and sodium channels in spontaneously contracting vascular muscle cells. *Science*, **233**, 475–478.

TAMARGO, J. & DELPON, E. (1991). Dihydropyridines and vascular diseases. *Z. Kardiol.*, **80** (Suppl 7), 106–111.

TAMARGO, J., VALENZUELA, C. & DELPON, E. (1992). New insights into the pharmacology of sodium channel blockers. *Eur. Heart J.*, **13** (Suppl F), 2–13.

TEJERINA, T., CAUVIN, C. & TAMARGO, J. (1992). Effects of oxodipine on isolated rabbit aorta and mesenteric resistance vessels. *Eur. J. Pharmacol.*, **219**, 279–288.

TRIGGLE, D. (1991). Sites, mechanisms of action, and differentiation of calcium channel antagonists. *Am. J. Hypertens.*, **4**, 422S–429S.

UEHARA, A. & HUME, J.R. (1985). Interactions of organic calcium channel antagonists with calcium channels in single frog atrial cells. *J. Gen. Physiol.*, **85**, 621–647.

WALSH, R.A. & HORWITZ, L.D. (1979). Adverse hemodynamic effects of intravenous disopyramide compared with quinidine in conscious dogs. *Circulation*, **60**, 1053–1058.

WIBO, M., DEROTH, L. & GODFRAIND, T. (1988). Pharmacological relevance of dihydropyridine binding sites in membranes from rat aorta: kinetic and equilibrium studies. *Circ. Res.*, **62**, 91–96.

(Received March 3, 1994
Revised July 15, 1994
Accepted August 18, 1994)

Br. J. Pharmacol. (1994), **113**, 1289–1294 © Macmillan Press Ltd, 1994

The role of myoendothelial cell contact in non-nitric oxide-, non-prostanoid-mediated endothelium-dependent relaxation of porcine coronary artery

Elisabeth Kühberger, Klaus Groschner, Walter R. Kukovetz & [1]Friedrich Brunner

Institut für Pharmakologie und Toxikologie, Universität Graz, Universitätsplatz 2, A-8010 Graz, Austria

1 Experiments were designed to analyse the requirement of myoendothelial junctions by bradykinin-induced endothelium-dependent relaxations resistant to N^G-nitro-L-arginine (L-NOARG) and indomethacin in porcine coronary arteries.

2 Rings of porcine coronary arteries were contracted with the thromboxane receptor agonist, U46619 and relaxations to bradykinin recorded isometrically. All experiments were performed in the presence of indomethacin. Nitric oxide (NO)-mediated effects were blocked by the NO synthase inhibitor L-NOARG (250 μM) and myoendothelial contacts inhibited by treatment with hypertonic solution containing D-mannitol or sucrose (each 180 mM) or the gap junctional uncoupling agent 1-heptanol (2 mM). High [K^+] solutions (40 mM) were used to probe a possible contribution of endothelium-derived hyperpolarizing factor (EDHF).

3 In the presence of endothelium, bradykinin induced concentration-dependent relaxations with a mean EC_{50} of 3.2 nM and a maximum response of 95 ± 1% of papaverine-induced relaxation (control curve).

4 In the absence of endothelium, bradykinin failed to induce relaxations. Addition of cultured porcine aortic endothelial cells to the organ bath resulted in some relaxation and restored in part the relaxant effect of bradykinin. This endothelial cell-mediated relaxant effect was completely abolished in the presence of 250 μM L-NOARG.

5 Bradykinin-induced relaxations in endothelium-preserved rings were only slightly suppressed by L-NOARG (86% of control). In vessels partially depolarized by high extracellular [K^+] (40 mM) relaxation was reduced to 72% of control. In the presence of L-NOARG, bradykinin failed to relax partially depolarized vessels.

6 In the presence of 2 mM 1-heptanol, 180 mM mannitol or 180 mM sucrose maximum relaxation to bradykinin was reduced to ~70%, i.e. to the same extent as in the presence of high [K^+]. The remaining relaxation was sensitive to blockade by L-NOARG.

7 Tissue cyclic GMP content which reflects NO activity, was increased about 4 fold by bradykinin (300 nM). This increase was unaffected by high [K^+], heptanol or sucrose but blocked by L-NOARG.

8 Our results suggest that non-nitric oxide- and non-prostanoid-mediated endothelium-dependent relaxation of porcine coronary artery requires functionally intact myoendothelial junctions.

Keywords: Endothelium-dependent relaxation; porcine coronary artery; myoendothelial contact; EDHF; EDRF

Introduction

Since the discovery of endothelium-dependent relaxation (Furchgott & Zawadzki, 1980) the role of endothelial cells in the regulation of vascular tone has been of great pharmacological interest. A predominant part of these endothelial functions is mediated by the endothelium-derived relaxing factor (EDRF), a labile compound that acts by a direct stimulation of the soluble guanylate cyclase in vascular smooth muscle cells. EDRF appears to be nitric oxide (NO) or a closely related compound derived from the metabolism of L-arginine by a constitutive NO synthase (Moncada *et al.*, 1991). Furthermore, evidence now exists that the endothelium releases at least one non-prostanoid relaxing factor not derived from L-arginine. For example, bradykinin has recently been shown to cause relaxation of porcine coronary artery independently of NO or guanosine 3′:5′-cyclic monophosphate (cyclic GMP) accumulation (Bény & Brunet, 1988; Richard *et al.*, 1990; Cowan & Cohen, 1991). One possible mechanism for this NO- and prostanoid-independent relaxation is membrane hyperpolarization caused by an endothelium-derived hyperpolarizing factor (EDHF) generated in various isolated vessels (Taylor & Weston, 1988; Bény & von der Weid, 1991; Vanhoutte, 1993).

Exogenous nitric oxide is without effect on membrane potential in most arteries studied, including pig coronary artery (Bény & Brunet, 1988; Komori *et al.*, 1988; Brayden, 1990). EDHF-mediated relaxation is unaffected by haemoglobin or methylene blue, which indicates that endothelium-dependent hyperpolarization is independent of the nitric oxide pathway (Chen *et al.*, 1988; Huang *et al.*, 1988). However, the exact nature of this endothelium-derived hyperpolarizing factor (EDHF) is still unknown. An important question to be answered in this respect is whether a direct communication between the endothelium and smooth muscle cells is involved, or a paracrine factor which would diffuse from the endothelium to the extracellular space.

The present study was made to evaluate the contribution of myoendothelial junctions in bradykinin-induced non-prostanoid and non-NO-mediated endothelium-dependent relaxations of porcine coronary arteries. Myoendothelial cell contact was blocked by the gap junctional uncoupling agent 1-heptanol (heptanol) or by use of hypertonic solutions containing mannitol or sucrose which cause simple cell shrinkage. To evaluate the relative contribution of endothelium-dependent hyperpolarization (presumably mediated by EDHF) and endothelium-derived NO (EDRF) to bradykinin-induced relaxations, experiments were performed in the presence of 40 mM K^+ to prevent membrane

[1] Author for correspondence.

hyperpolarization and/or in the presence of N^G-nitro-L-arginine (L-NOARG) to inhibit generation of NO.

Methods

Tissue preparation

Porcine hearts were obtained from the local slaughterhouse and immediately transported to the laboratory in closed plastic sacs. Left and right coronary arteries were prepared without touching the intimal surface (endothelium-preserved vessels) or by gently rubbing the intimal surface with a wooden stick in order to remove the endothelium. Vessels were stored at 6°C in Krebs-Henseleit solution for up to two days.

Functional studies

Vessels were cut into rings (3–4 mm wide) which were mounted in 5 ml organ baths containing Krebs-Henseleit physiological salt solution of the following composition (mM): NaCl 118, KCl 4.7, KH_2PO_4 1.2, $CaCl_2$ 2.5, $MgCl_2$ 1.2, $NaHCO_3$ 25 and glucose 10.1, maintained at 37°C, pH 7.4 and gassed with carbogen. Tension was recorded isometrically by means of F 30 force transducers connected to a Watanabe multichannel recorder (Hugo Sachs Elektronik, Freiburg, Germany). Rings were stretched to an initial tension of 2 g, and allowed to equilibrate for approximately 1 h.

All experiments were performed in the presence of indomethacin (10 μM) to block the formation of vasoactive prostanoids. Tissues were precontracted with the thromboxane receptor agonist U46619 (9,11-dideoxy-11α,9α-epoxymethanoprostaglandin $F_{2\alpha}$ (10–300 nM). Pretreatment with L-NOARG (250 μM), hypertonic solution (180 mM mannitol or sucrose), heptanol (2 mM) or KCl (40 mM) was performed 5 min (15 min for KCl) prior to precontraction. When using 40 mM K^+-containing solutions, osmolarity was adjusted by reducing Na^+ by 40 mM. In some experiments, Na^+ was kept constant (118 mM) to exclude possible effects due to Na^+ removal. Concentration-response curves for relaxing effects were obtained by cumulative addition of bradykinin (0.1–300 nM) in endothelium-preserved tissue or isoprenaline (0.1 nM–3 μM) and sodium nitroprusside (0.1 nM–10 μM) in endothelium-denuded arteries. Effects were expressed as percentages of the maximum relaxation response obtained by addition of 260 μM papaverine at the end of experiment. Basal tone was affected differently by the various agents: L-NOARG, mannitol and sucrose increased basal tone by 0.5–1.5 g (5–15% of control), and heptanol reduced basal tone by ~1.5–2 g. K^+ (40 mM) increased basal tone up to 4 g. To achieve a similar degree of precontraction, the concentration of U46619 was varied between 10–300 nM. The actual values of tone so achieved are listed in Table 1. The inhibitory effect of heptanol was only partially overcome by a maximal concentration of U46619, resulting in a ~30% lower level of precontraction, which had to be accepted.

In a second series of experiments. endothelium-denuded rings were contracted with U46619 and, once a stable tone had developed, a suspension of cultured porcine aortic endothelial cells was added to the organ bath (~3.5×10^6 cells ml^{-1}). The effects of bradykinin (100 nM) were monitored in the absence and presence of L-NOARG (250 μM). All experiments were performed in the presence of superoxide dismutase (SOD; 30 U ml^{-1}) to protect NO from inactivation by superoxide anion (Mayer *et al.*, 1993).

Cell culture

Porcine aortic endothelial cells were cultured as described previously (Graier *et al.*, 1992). Briefly, endothelial cells were isolated by 20 min of enzymatic digestion (200 U ml^{-1} collagenase), centrifuged for 5 min at 500 *g*, resuspended in Opti-Minimum Essential Medium containing 3% foetal calf serum and antibiotics and seeded in plastic Petri dishes. Confluent cells were split by a ratio of 1:5 and subcultured for up to two passages. On the day of experiment cells were harvested by treatment with 0.025% trypsin and 0.02% EDTA, centrifuged and resuspended in Krebs-Henseleit physiological salt solution at ~20×10^6 cells ml^{-1}.

Measurement of cyclic nucleotides

Cyclic GMP content was measured by radioimmunoassay in freeze clamped coronary artery rings as described earlier (Kukovetz *et al.*, 1979). Samples were taken under similar conditions as in the mechanical experiments either during control periods or after maximum stimulation with bradykinin (300 nM).

Data analysis

Concentration-response curves were analysed with the Allfit programme package (De Lean *et al.*, 1978). Fitting of individual curves yielded EC_{50} values and maximum effect values (E_{max}). EC_{50} values are expressed as geometric means with 95% confidence intervals, calculated as the product of s.e.mean × Student's *t* values, E_{max} values were calculated as arithmetic means ± s.e.mean. *n* represents the number of tissues studied. Means were compared by Student's *t* test. Differences were considered statistically significant at $P \leqslant 0.05$.

Table 1 Level of precontraction of porcine coronary artery obtained after equilibration of rings, followed by induction of tone with U46619 in the absence and presence of agents indicated

Agent (s)	*Developed tension* (g)	*U46619 used (nM)*	n
Control	10.2 ± 0.7	100	9
+ L-NOARG	11.4 ± 0.8	50–100	10
+ Heptanol	7.0 ± 1.4	300	5
+ Heptanol and L-NOARG	7.5 ± 1.1	300	5
+ Sucrose	9.8 ± 0.8	50–100	9
+ Sucrose and L-NOARG	10.5 ± 0.5	50–100	9
+ Mannitol	9.6 ± 1.1	50–100	5
+ Mannitol and L-NOARG	11.5 ± 0.9	50–100	5
+ KCl	11.2 ± 0.7	10–30	5
+ KCl and L-NOARG	11.8 ± 0.9	10–30	5

Means ± s.e.mean of *n* tissues.

Materials

Bradykinin, N^G-nitro-L-arginine, U46619 (9,11-dideoxy-11α,9α-epoxymethanoprostaglandin $F_{2\alpha}$), D-mannitol, collagenase (Type II), trypsin and EDTA (ethylenediaminetetracetic acid) were purchased from Sigma (Munich, Germany). Indomethacin sodium trihydrate was from Merck, Sharp & Dohme (Munich, Germany). All other chemicals were obtained from Merck (Darmstadt, Germany), and tissue culture media from sources described previously (Graier *et al.*, 1992).

Results

Endothelium-preserved rings of porcine coronary artery contracted with the thromboxane receptor agonist, U46619 were potently relaxed by bradykinin (0.1–300 nM) with an EC_{50} value of 3.2 (1.8–5.6) nM (geometric mean with 95% confidence interval) and a maximum response of 95 ± 1% (arithmetic mean ± s.e.mean; $n = 9$). Pretreatment of rings with the NO synthase inhibitor, L-NOARG (250 μM), shifted the concentration-response curve to the right ($EC_{50} = 11.5$ (5.2–25.6) nM and diminished E_{max} to 86% of controls ($n = 10$) (Figure 1).

In endothelium-free preparations no relaxation to bradykinin was observed. Addition of cultured porcine aortic endothelial cells in the presence of SOD (30 U ml^{-1}) resulted in some relaxation and partly restored the relaxant effect to bradykinin (100 nM, $n = 4$). This endothelium-mediated relaxant effect was completely blocked by 250 μM L-NOARG ($n = 4$). A representative experiment is shown in Figure 2.

In vessels depolarized by high extracellular $[K^+]$ (40 mM), the bradykinin relaxation curve was shifted even further to the right than in the presence of L-NOARG ($EC_{50} = 28.8$ (9.2–90.0) nM) and E_{max} was reduced to 72% of control ($n = 5$). In the combined presence of L-NOARG and high $[K^+]$, however, relaxations to bradykinin were almost completely abolished (8% of control, $n = 5$) (Figure 3). The experiments of this group were carried out in isotonic (low Na^+) solutions (see Methods). When Na^+ was kept constant resulting in a slightly (20%) hypertonic solution, similar results were obtained ($n = 3$, data not shown).

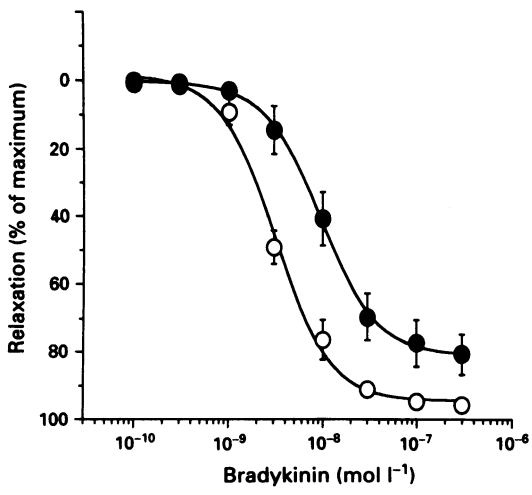


Figure 1 Bradykinin-induced relaxant effects in U46619-contracted rings of endothelium-preserved porcine coronary artery in the absence (control curve: ○) or presence of 250 μM N^G-nitro-L-arginine (●). Results are expressed as percentage of the maximum relaxation obtained by addition of 260 μM papaverine at the end of the experiment. Data points represent the mean ± s.e.mean of 9–10 individual experiments.

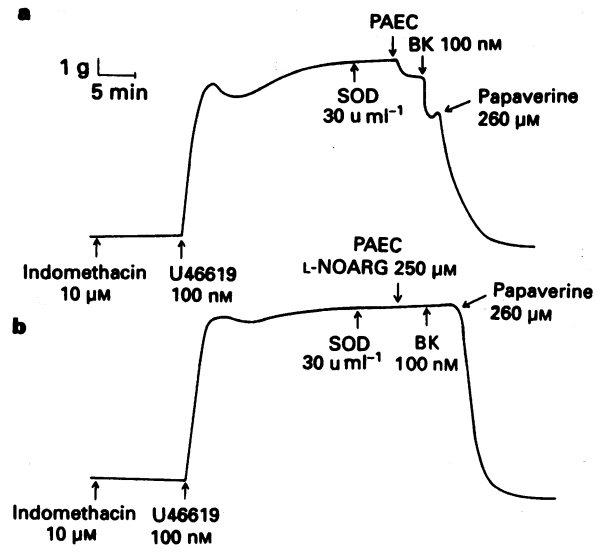


Figure 2 Effects of addition of porcine aortic endothelial cells (PAEC) to coronary artery rings without endothelium. (a) Rings were precontracted with U46619, and ~10×10^6 PAECs (~3.5×10^6 cells ml^{-1} final concentration) were then added to the organ bath, followed by bradykinin (BK, 100 nM) and, finally, papaverine (260 μM). (b) Same experimental set-up, but in the presence of 250 μM N^G-nitro-L-arginine (L-NOARG). Superoxide dismutase (SOD, 30 U ml^{-1}) was added to protect NO from inactivation.

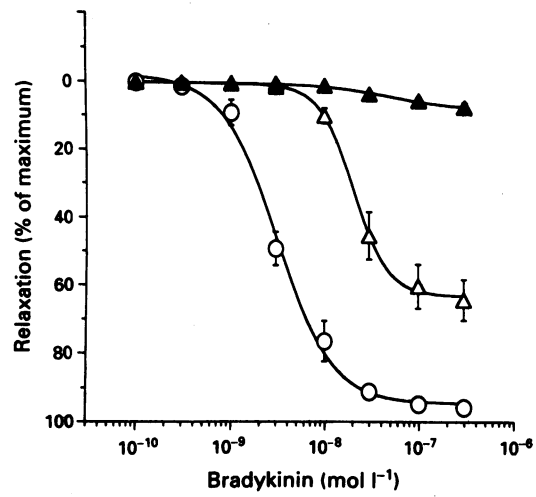


Figure 3 Bradykinin-induced relaxant effects in U46619-contracted rings of endothelium-intact porcine coronary artery in the absence (control curve: ○) and presence of 40 mM KCl (△) or 40 mM KCl plus 250 μM N^G-nitro-L-arginine (▲). Results are expressed as percentage of the maximum relaxation obtained by addition of 260 μM papaverine at the end of the experiment. Data points represent the mean ± s.e.mean of 5 individual experiments.

In the presence of the gap junctional uncoupling agent, heptanol (2 mM), E_{max} was reduced to 71%, i.e. to the same extent as in the presence of high $[K^+]$, and the EC_{50} was not significantly affected ($EC_{50} = 4.2$ (1.7–10.3) nM, $n = 5$). The remaining relaxation was sensitive to blockade by L-NOARG resulting in a suppression of E_{max} to 27% of control in the combined presence of heptanol and L-NOARG ($n = 5$) (Figure 4).

In vessels treated with hypertonic solution containing either 180 mM mannitol (Figure 5) or sucrose (Figure 6), relaxations to bradykinin were shifted to the right with an EC_{50} of 12.0 (4.1–34.9) nM (mannitol) and 19.5 (10.3–36.9) nM (sucrose). Maximum relaxations were reduced to 70%

(mannitol, $n = 5$) and 73% (sucrose, $n = 9$) of control, i.e. to the same extent as in the presence of high [K^+]. The remaining relaxations were again sensitive to blockade by L-NOARG. In the combined presence of hypertonic solution and L-NOARG, relaxations were reduced to 48% of control (mannitol, $n = 5$) and 47% (sucrose, $n = 9$), respectively.

Endothelium-independent relaxations to isoprenaline were unaffected by heptanol, sucrose, or mannitol. Control EC_{50} values were 60.3 (28.4–128) nM in the absence of inhibitors, and in their presence 66.1 (37–118) nM (heptanol), 54 (23.0–128) nM (mannitol), and 39.0 (13.5–81.5) nM (sucrose), respectively. E_{max} values ranged from 96–99% of controls ($n = 6$, data not shown). Similar results were obtained with sodium nitroprusside ($n = 7$, data not shown).

The effects of L-NOARG, heptanol, sucrose and K^+ on tissue cyclic GMP content of porcine coronary arteries are summarized in Table 2. Basal cyclic GMP content was 34.0 ± 4.9 pmol g^{-1} wet weight under control conditions, and increased to 129.8 ± 18.8 pmol g^{-1} wet weight (3.8 fold, $n = 10$) at maximum effective concentrations of bradykinin. A similar increase was seen in the presence of a depolarizing concentration of K^+, heptanol or sucrose ($n = 5$), whereas in the presence of L-NOARG or in the combined presence of L-NOARG plus heptanol, sucrose or K^+, both basal and stimulated cyclic GMP levels were reduced ($n = 5$) (Table 2).

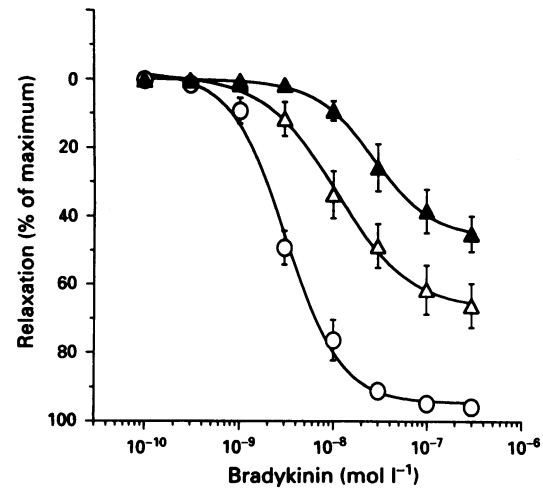


Figure 5 Bradykinin-induced relaxant effects in U46619-contracted rings of endothelium-intact porcine coronary artery in the absence (control curve: O) and presence of 180 mM mannitol (Δ) and 180 mM mannitol plus 250 μM N^G-nitro-L-arginine (▲). Results are expressed as percentage of the maximum relaxation obtained by addition of 260 μM papaverine at the end of the experiment. Data points represent the mean ± s.e.mean of 5 individual experiments.

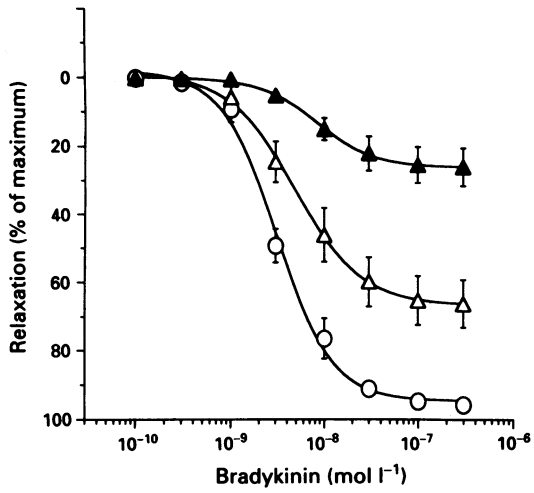


Figure 4 Bradykinin-induced relaxant effects in U46619-contracted rings of endothelium-preserved porcine coronary artery in the absence (control curve: O) and presence of 2 mM heptanol (Δ) or 2 mM heptanol plus 250 μM N^G-nitro-L-arginine (▲). Results are expressed as percentage of the maximum relaxation obtained by addition of 260 μM papaverine at the end of the experiment. Data points represent the mean ± s.e.mean of 5 individual experiments.

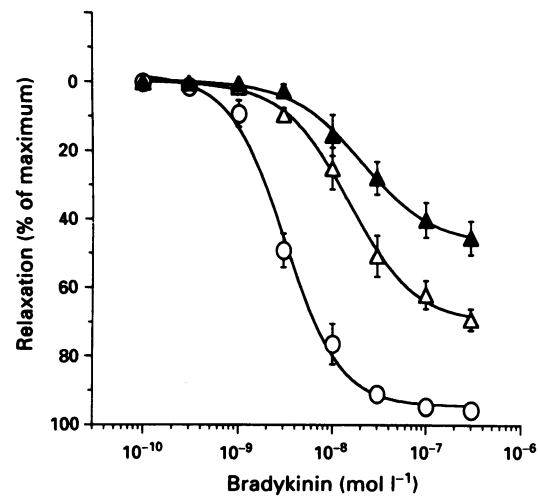


Figure 6 Bradykinin-induced relaxant effects in U46619-contracted rings of endothelium-intact porcine coronary artery in the absence (control curve: O) and presence of 180 mM sucrose (Δ) or 180 mM sucrose plus 250 μM N^G-nitro-L-arginine (▲). Results are expressed as percentage of the maximum relaxation obtained by addition of 260 μM papaverine at the end of the experiment. Data points represent the mean ± s.e.mean of 9 individual experiments.

Table 2 Cyclic GMP levels (pmol g^{-1} wet weight) during basal conditions and after stimulation with bradykinin (300 nM)

	Basal	*Bradykinin*	*-fold increase over basal*
Control	34.0 ± 4.9	129.8 ± 18.8	3.8
+ L-NOARG (250 μM)	9.6 ± 0.9	11.6 ± 1.5	
+ Heptanol (2 mM)	25.9 ± 4.2	137.5 ± 22.6	5.3
+ Heptanol (2 mM) and L-NOARG (250 μM)	10.2 ± 1.7	13.7 ± 4.3	
+ Sucrose (180 mM)	28.7 ± 4.7	110.1 ± 19.5	3.8
+ Sucrose (180 mM) and L-NOARG (250 μM)	8.4 ± 1.9	10.3 ± 1.5	
+ KCl (40 mM)	34.4 ± 9.2	99.3 ± 21.3	2.9
+ KCl (40 mM) and L-NOARG (250 μM)	7.5 ± 0.9	8.4 ± 1.3	

Cyclic GMP content was measured by radioimmunoassay in freeze clamped coronary artery rings as described in Methods. Samples were taken under similar conditions as in the mechanical experiments either during control periods (basal condition) or after stimulation with 300 nM bradykinin when maximum relaxation had developed. Values are given as arithmetic means ± s.e.mean of 5–10 individual experiments.

Discussion

The present study demonstrates that in porcine isolated coronary arteries bradykinin elicits endothelium-dependent relaxations that, (i) are not mediated by NO or prostacyclin, (ii) require close myoendothelial contact, and (iii) are inhibited to the same extent by either blockade of myoendothelial junctions or membrane depolarization with high [K^+].

A number of studies demonstrate that in porcine coronary arteries, bradykinin induces endothelium-dependent relaxations insensitive to blockade by L-NOARG and indomethacin (Kauser & Rubanyi, 1992; Nagao & Vanhoutte, 1992; Pacicca *et al.*, 1992). This observation shows that in porcine coronary arteries an endothelium-derived relaxing factor distinct from NO or prostacyclin may mediate the relaxation to bradykinin and thereby contribute to the local regulation of vascular tone. In the present study, experiments were designed to determine whether this L-NOARG-insensitive component is mediated by a diffusible factor and/or requires the existence of an intact junctional communication between endothelium and vascular smooth muscle cells.

Coronary artery rings with endothelium intact showed L-NOARG-sensitive relaxation which amounted to ~15% of the maximum inducible by bradykinin. In the absence of endothelium, no relaxation was observed which is in agreement with published data. Addition of endothelial cells to arteries without endothelium, however, resulted in a relaxation which was entirely inhibited by L-NOARG. The extent of this relaxation was similar to that mediated by NO in intact artery rings (~15%). Hence, the larger part of the total relaxation observed was mediated by a mechanism independent of NO- and prostanoids which apparently require cell-to-cell-contact. Simple addition of cultured endothelial cells, however, did not restore such NO- and/or prostanoid-independent relaxation in endothelium-denuded arteries. This may be explained if the active mediator of this relaxant component is either extremely labile and is ineffective in the present experimental set-up or if this relaxation requires tight electrical coupling between endothelial and vascular smooth muscle cells.

In our study we have blocked myoendothelial communication by the well-known gap junctional uncoupling agent, heptanol. Electrophysiological and optical imaging techniques have shown that heptanol as well as other long chain alcohols are able to block reversibly junctional transfer of current-carrying ions, second messenger molecules and fluorescent dyes in diverse cell types (Bennett *et al.*, 1991; Christ *et al.*, 1992). Moreover, gap junctions can be split by treating intact tissues with hypertonic solution (Loewenstein, 1981).

Our results clearly show that the gap junction inhibitors heptanol, mannitol, and sucrose are able to antagonize endothelium-dependent relaxations resistant to NO and prostanoids. This effect was rather specific since these blockers did not affect endothelium-independent relaxation induced by isoprenaline or sodium nitroprusside. The extent of blockade induced by these uncoupling agents was similar in all three cases (~30% reduction of maximum effect). Accordingly, close myoendothelial contact is paramount for the transfer of the relaxation signal from the endothelium to the smooth muscle.

It is of note that the gap junction blockers at the concentrations used did not entirely suppress non-NO relaxations. This may be due to the nature of these blockers which, although used at standard concentrations, may not entirely disrupt myoendothelial contact. Although we have no proof of this at present, we consider this as the probable cause for the remaining relaxation observed. Failing this, an additional hypothetical relaxant component may have to be postulated.

The nature of the physical contact between endothelial and smooth muscle layer necessary for bradykinin-induced relaxation is presently unknown. Cytoplasmatic bridges passing through fenestrations of internal elastic lamina connecting endothelium to smooth muscle cells of arteries of various calibres have been detected which could be involved in vasorelaxation, either independent of or in concert with endothelial humoral factors such as NO (Davies *et al.*, 1988). According to this hypothesis, the two tissues would function as a coupled system allowing smooth muscle responses to secondary signals generated in the endothelium and transferred through such junctions. However, it is still unclear whether the endothelial and smooth muscle cells in arteries and small arterioles are electrically coupled via gap junctions because dyes fail to diffuse via myoendothelial junctions between these cells *in situ* (Bény, 1990), although coupling between smooth muscle cells and endothelial cells was observed in co-culture (Davies *et al.*, 1985).

Another suggestion as to how endothelium-dependent agonists might mediate vasorelaxation resistant to NO and prostanoids concerns a paracrine hyperpolarizing factor (EDHF) (Feletou & Vanhoutte, 1988; Kauser *et al.*, 1989; Chen *et al.*, 1991). Consistent with this proposal, hyperpolarization of the smooth muscle layer has been observed repeatedly (Bolton *et al.*, 1984; Komori & Suzuki, 1987; Bény & Brunet, 1988; Chen *et al.*, 1988; Feletou & Vanhoutte, 1988; Nagao & Vanhoutte, 1992). To determine if hyperpolarization might be involved in this junctional transfer of the relaxant signal, we used high extracellular [K^+] which permits the differentiation between endothelium-dependent relaxations mediated by NO (EDRF) and hyperpolarization (EDHF) (Nagao & Vanhoutte, 1992; Adeagbo & Triggle, 1993). Most interestingly, use of high extracellular [K^+] resulted in a similar inhibition (i.e., to 70% of control) of bradykinin-induced relaxation as blockade of myoendothelial junctions by gap junction blockers. Thus, hyperpolarization, although not measured in this study, makes an important contribution to bradykinin-induced relaxation of porcine coronary artery as shown before (Bény & Brunet, 1988; Nagao & Vanhoutte, 1992). The present data strongly suggest that the endothelium-derived signal requires junctional cell-to-cell communication. Whether this signal is chemical (EDHF) or electrical in nature, remains to be shown.

Elevation of extracellular [K^+] above 40 mM is known to depolarize markedly smooth muscle and to antagonize the effects of various hyperpolarizing agents, including those of EDHF. We cannot exclude the possibility that part of the effects of high extracellular [K^+] is due to depolarization of endothelial cells, particularly since EDHF release is a Ca^{2+}-dependent phenomenon (Vanhoutte, 1993) and endothelial Ca^{2+} signals are depressed by K^+-depolarization (Groschner *et al.*, 1992). Such an effect is, however, unlikely, since endothelial NO-production which is also Ca^{2+}-dependent, was unaffected as evident from cyclic GMP levels measured in tissue rings (Table 2).

Endothelium-dependent relaxation of vascular smooth muscle is known to be associated with an increase in tissue cyclic GMP levels (Kukovetz *et al.*, 1979). In the present study bradykinin-stimulated accumulation of cyclic GMP was completely inhibited by L-NOARG, a specific blocker of NO production but unaffected by the blockers of myoendothelial junctions, heptanol, sucrose and mannitol, and by high [K^+]. Thus, NO and cyclic GMP are not critical for complete bradykinin-induced relaxation in porcine coronary artery, and there is at least one relaxing component which acts independently of cyclic GMP, and is blocked by depolarization of the cell membrane, or by inhibiting myoendothelial communication.

In summary, the present study demonstrates that bradykinin-induced endothelium-dependent relaxation in porcine coronary arteries requires close myoendothelial contact. This component of relaxation is independent of NO production and cGMP accumulation and is not mediated by vasoactive prostanoids. The data are compatible with EDHF or any other messenger mediating the NO-insensitive component of relaxation, providing that functional myoendothelial junctions are present.

The authors wish to thank Dr W.F. Graier for stimulating discussions. The excellent technical assistance of Miss Sandra Chraust and Mrs Christa Kern is also acknowledged. Supported by the Austrian Research Council (Österreichischer Fonds zur Förderung der wissenschaftlichen Forschung), projects 8581 and 9601.

References

ADEAGBO, A.S.O. & TRIGGLE, C.R. (1993). Varying extracellular [K^+]: A functional approach to separating EDHF- and EDNO-related mechanisms in perfused rat mesenteric arterial bed. *J. Cardiovasc. Pharmacol.*, **21**, 423–429.

BENNETT, M.V.L., BARRIO, L.C., BARGIELLO, T.A., SPRAY, D.C., HERTZBERG, E. & SÁEZ, J.C. (1991). Gap junctions: new tools, new answers, new questions. *Neuron*, **6**, 305–320.

BÉNY, J.-L. (1990). Endothelial and smooth muscle cells hyperpolarized by bradykinin are not dye coupled. *Am. J. Physiol.*, **258**, H836–H841.

BÉNY, J.-L. & BRUNET, P.C. (1988). Neither nitric oxide nor nitroglycerin accounts for all the characteristics of endothelially mediated vasodilatation of pig coronary arteries. *Blood Vessels*, **25**, 308–311.

BÉNY, J.-L. & VON DER WEID, P.-Y. (1991). Hyperpolarizing factors. *Coron. Art. Dis.*, **2**, 300–306.

BOLTON, T.B., LANG, R.J. & TAKEWAKI, T. (1984). Mechanisms of action of noradrenaline and carbachol on smooth muscle of guinea-pig anterior mesenteric artery. *J. Physiol.*, **351**, 549–572.

BRAYDEN, J.E. (1990). Membrane hyperpolarization is a mechanism of endothelium-dependent cerebral vasodilation. *Am. J. Physiol.*, **259**, H668–H673.

CHEN, G., SUZUKI, H. & WESTON, A.H. (1988). Acetylcholine releases endothelium-derived hyperpolarizing factor and EDRF from rat blood vessels. *Br. J. Pharmacol.*, **95**, 1165–1174.

CHEN, G., YAMAMOTO, Y., MIWA, K. & SUZUKI, H. (1991). Hyperpolarization of arterial smooth muscle induced by endothelial humoral substances. *Am. J. Physiol.*, **260**, H1888–H1892.

CHRIST, G.J., MORENO, A.P., MELMAN, A. & SPRAY, D.C. (1992). Gap junction-mediated intercellular diffusion of Ca^{2+} in cultured human corporal smooth muscle cells. *Am. J. Physiol.*, **263**, C373–C383.

COWAN, C.L. & COHEN, R.A. (1991). Two mechanisms mediate relaxation by bradykinin of pig coronary artery: NO-dependent and -independent responses. *Am. J. Physiol.*, **261**, H830–H835.

DAVIES, P.F., GANZ, P. & DIEHL, P.S. (1985). Reversible microcarrier-mediated junctional communication between endothelial and smooth muscle cell monolayers: an in vitro model of vascular cell interactions. *Lab. Invest.*, **85**, 710–718.

DAVIES, P.F., OLESEN, S.-P., CLAPHAM, D.E., MORREL, E.M. & SCHOEN, F.J. (1988). Endothelial communication. *Hypertension*, **11**, 563–572.

DE LEAN, A., MUNSON, P.J. & RODBARD, D. (1978). Simultaneous analysis of families of sigmoidal curves: application to bioassay, radioligand assay, and physiological dose-response curves. *Am. J. Physiol.*, **235**, E97–E102.

FELETOU, M. & VANHOUTTE, P.M. (1988). Endothelium-dependent hyperpolarization of canine coronary smooth muscle. *Br. J. Pharmacol.*, **93**, 515–524.

FURCHGOTT, R.F. & ZAWADZKI, J.V. (1980). The obligatory role of endothelial cells in the relaxation of arterial smooth muscle by acetylcholine. *Nature*, **288**, 373–376.

GRAIER, W.F., GROSCHNER, K., SCHMIDT, K. & KUKOVETZ, W.R. (1992). Increases in endothelial cyclic AMP levels amplify agonist-induced formation of endothelium-derived relaxing factor (EDRF). *Biochem. J.*, **288**, 345–349.

GROSCHNER, K., GRAIER, W.F. & KUKOVETZ, W.R. (1992). Activation of a small-conductance Ca^{2+}-dependent K^+ channel contributes to bradykinin-induced stimulation of nitric oxide synthesis in pig aortic endothelial cells. *Biochim. Biophys. Acta*, **1137**, 162–170.

HUANG, A.H., BUSSE, R. & BASSENGE, E. (1988). Endothelium-dependent hyperpolarization of smooth muscle cells in rabbit femoral arteries is not mediated by EDRF (nitric oxide). *Naunyn-Schmied. Arch. Pharmacol.*, **338**, 438–442.

KAUSER, K. & RUBANYI, G.M. (1992). Bradykinin-induced, N^{ω}-nitro-L-arginine-insensitive endothelium-dependent relaxation of porcine coronary arteries is not mediated by bioassayable relaxing substances. *J. Cardiovasc. Pharmacol.*, **20** (Suppl. 12), S101–S104.

KAUSER, K., STEKIEL, W.J., RUBANYI, G. & HARDER, D.R. (1989). Mechanism of action of EDRF on pressurized arteries: effects on K^+ conductance. *Circ. Res.*, **65**, 199–204.

KOMORI, K., LORENZ, R.R. & VANHOUTTE, P.M. (1988). Nitric oxide, ACh, and electrical and mechanical properties of canine arterial smooth muscle. *Am. J. Physiol.*, **255**, H207–H212.

KOMORI, K. & SUZUKI, H. (1987). Electrical responses of smooth muscle cells during cholinergic vasodilation in the rabbit saphenous artery. *Circ. Res.*, **61**, 586–593.

KUKOVETZ, W.R., HOLZMANN, S., WURM, A. & PÖCH, G. (1979). Evidence for cyclic GMP-mediated relaxant effects of nitrocompounds in coronary smooth muscle. *Naunyn-Schmied. Arch. Pharmacol.*, **310**, 129–138.

LOEWENSTEIN, W.R. (1981). Junctional intercellular communication: The cell-to-cell membrane channel. *Physiol. Rev.*, **61**, 829–913.

Mayer, B., Brunner, F. & Schmidt, K. (1993). Inhibition of nitric oxide synthesis by methylene blue. *Biochem. Pharmacol.*, **45**, 367–374.

MONCADA, S., PALMER, R.M.J. & HIGGS, E.A. (1991). Nitric oxide: Physiology, pathophysiology, and pharmacology. *Pharmacol. Rev.*, **43**, 109–142.

NAGAO, T. & VANHOUTTE, P.M. (1992). Hyperpolarization as a mechanism for endothelium-dependent relaxations in the porcine coronary artery. *J. Physiol.*, **445**, 355–367.

PACICCA, C., VON DER WEID, P.-Y. & BÉNY, J.-L. (1992). Effect of nitro-L-arginine on endothelium-dependent hyperpolarizations and relaxations of pig coronary arteries. *J. Physiol.*, **457**, 247–256.

RICHARD, V., TANNER, F.C., TSCHUDI, M. & LÜSCHER, T.F. (1990). Different activation of L-arginine pathway by bradykinin, serotonin, and clonidine in coronary arteries. *Am. J. Physiol.*, **259**, H1433–H1439.

TAYLOR, S.G. & WESTON, A.H. (1988). Endothelium-derived hyperpolarizing factor: a new endogenous inhibitor from the vascular endothelium. *Trends Pharmacol Sci.*, **9**, 272–274.

VANHOUTTE, P.M. (1993). Other endothelium-derived vasoactive factors. *Circulation*, **87** (Suppl. V), V9–V17.

(Received February 28, 1994
Revised May 25, 1994
Accepted August 23, 1994)

Br. J. Pharmacol. (1994), **113**, 1295–1302 © Macmillan Press Ltd, 1994

Intracerebral microdialysis combined with recording of extracellular field potential: a novel method for investigation of depolarizing drugs *in vivo*

[1]T.P. Obrenovitch, *J. Urenjak & E. Zilkha

Gough-Cooper Department of Neurological Surgery, Institute of Neurology, Queen Square, London WC1N 3BG and *Department of Discovery Biology, Pfizer Central Research, Sandwich CT13 9NJ

1 The purpose of this study was to examine whether depolarizations evoked by excitatory amino acids can be recorded quantitatively, *in vivo*, with a microelectrode incorporated within a microdialysis probe.

2 Microdialysis probes incorporating a chlorided silver wire were implanted in the striatum of anaesthetized rats and perfused with artificial cerebrospinal fluid (ACSF). Increasing concentrations of excitatory amino acids were applied for 2 min via the microdialysis probe, and the extracellular direct current (d.c.) potential was recorded between the microdialysis electrode and a reference electrode placed under the scalp.

3 N-methyl-D-aspartate (NMDA, 25–500 μM), α-amino-3-hydroxy-5-methyl-4-isoxazole propionic acid (AMPA, 5–1000 μM), kainate (5–500 μM), and glutamate (0.25–100 mM) evoked concentration-dependent depolarizations with maxima ranging from 7 to 10 mV, i.e. 3 to 10 times larger than those recorded from brain slices *in vitro*. Depolarizations evoked by glutamate receptor agonists applied by microdialysis shared several features with those recorded from brain slices. The most characteristic were: steep onset and recovery of NMDA and glutamate responses; marked post-depolarization hyperpolarization with NMDA; and very slow recovery after kainate application. At high concentrations (500 μM), NMDA occasionally initiated spreading depression. The relative potency of glutamate and NMDA was of the same order of magnitude to that obtained with the cortical wedge and hippocampal slices, glutamate being 100 to 400 times less potent than NMDA.

4 Two consecutive series of NMDA-stimuli within the same procedure evoked comparable depolarizations, indicating that reliable quantitative analysis of drug action can be performed, with each animal serving as its own control. This is relevant to the study of drugs acting on glutamate receptors especially antagonists. The remarkable inter-animal reproducibility is also a valuable feature.

5 Pretreatment with dizocilpine maleate (MK-801, 2 mg kg^{-1}, i.p.) reduced by 65% the responses evoked by NMDA (500 μM). The non-NMDA antagonist 6,7-dinitroquinoxaline-2,3-dione (DNQX, 100 μM) applied via the microdialysis probe reduced by around 78% the responses to AMPA and kainate (250 μM). The fact that drugs, especially antagonists, can be administered either systemically, or directly through the dialysis probe to by-pass the blood-brain barrier or avoid peripheral effects, is especially relevant for neuropharmacological studies.

6 Intracerebral microdialysis combined with *in vivo* recording of extracellular field potential is a novel and valuable method for the quantitative analysis of the action of drugs acting on glutamate receptors. This method should prove especially useful for comparing the sensitivitiy of specific brain structures to selective glutamate receptor agonists under normal conditions and when the neuronal microenvironment is altered. It should also be useful for investigating the action of other depolarizing agents, such as veratridine, and their antagonists.

Keywords: Microdialysis; glutamate; N-methyl-D-aspartate; excitatory amino acids; field potential; d.c. potential; depolarization

Introduction

Glutamic acid receptors remain one of the most attractive targets for developing relevant neuroactive agents. Firstly, because glutamate is the principal excitatory neurotransmitter in the mammalian central nervous system (CNS), subserving rapid postsynaptic excitatory responses in many cortical efferent systems and in intrahippocampal pathways (Collingridge & Lester, 1989). Secondly, because excessive activation of glutamate-operated ionic channels plays a major role in neuronal death associated with a wide range of neurological disorders. These include status epilepticus (Dingledine *et al.*, 1990), ischaemia (Meldrum, 1990), neurodegenerative diseases (Meldrum & Garthwaite, 1990; Beal *et al.*, 1991), and intoxication with natural excitotoxins (Teitelbaum *et al.*, 1990). Finally, the diversity of glutamate receptor subtypes (Nakanishi, 1992; Seeburg, 1993), their interrelations (Kelso *et al.*, 1992), and the complexity of their modulation (Lodge & Johnson, 1991) may favour the development of agents with selective actions and good therapeutic index.

Until now, the recording of cell population responses evoked by drugs acting on glutamate ionotropic receptors has been obtained from brain slices with the grease-gap preparation (Harrison & Simmonds, 1985; Garthwaite *et al.*, 1986; Evans, 1989; Martin & Nadler, 1991). With this method, slices are placed across a two-compartment bath, and one side of the tissue is depolarized relative to the other by superfusion with high K^+ or glutamate receptor agonists. As *in vivo* quantitative studies of drug-receptor interactions are essential for the development of novel neuroactive compounds, the purpose of this study was to assess whether similar cell population responses can be obtained, from the intact brain, using a microelectrode incorporated within a microdialysis probe.

Microdialysis is a method used routinely in neurochemistry and neuropharmacology for monitoring changes in the extracellular fluid (ECF) composition, especially neurotransmit-

[1] Author for correspondence.

ter release (Benveniste & Hüttemeier, 1990). It requires implantation of a probe with a dialysis membrane through which artifical cerebrospinal fluid (ACSF) is perfused. Low molecular weight compounds diffuse along their concentration gradient, from the extracellular fluid to the perfusate where they are analysed. By changing the perfusion medium, one can also produce controlled alterations of the ECF composition, or local application of drugs. We have previously demonstrated that an electrode placed within the input tubing of a microdialysis probe enables the recording of changes in the extracellular field or direct current (d.c.) potential of the cell populations surrounding the dialysis membrane (Obrenovitch *et al.*, 1993). This method has proved very useful for correlating electrophysiological changes with neurotransmitter effluxes associated with epileptic seizures (Millan *et al.*, 1991), cerebral ischaemia (Obrenovitch *et al.*, 1993) and cortical spreading depression (Obrenovitch & Zilkha, 1994). Here, we describe changes in the d.c. potential evoked in the rat striatum by glutamate receptor agonists applied through a microdialysis probe, under normal conditions, with Mg^{2+}-free medium, and after pretreatment with glutamate receptor antagonists.

Some of these results were presented at a meeting of the British Pharmacological Society (Obrenovitch *et al.*, 1994).

Methods

Microdialysis probe construction

Concentric microdialysis probes were made from 15 mm lengths of 24 grade stainless steel tubing (Cooper's Needle Works, Birmingham, UK). Inlet and outlet tubes were of fused silica (0.19 mm o.d., 0.075 mm i.d.; SGE Ltd., Milton Keynes, UK) sleeved with polythene tubing (0.61 mm o.d., 0.28 mm i.d.; Portex Ltd., Hythe, UK). Microdialysis electrodes were prepared by soldering 8 mm lengths of silver wire (0.125 mm diameter; Goodfellows Metals Ltd., Cambridge, UK) to 8 mm gold pin contacts (476-817, RS Components Ltd., Corby, UK). The wires were chlorided as the anode, in 0.1 M hydrochloric acid, using a potential rising at 10 mV s^{-1} to 610 mV, the latter being then held for 60–80 s (Obrenovitch *et al.*, 1993). The pin electrode was inserted alongside the inlet tube, with the connector bent at an angle of 90° to the probe body. After trimming the exposed inlet tube to a length of 2 mm, the dialysis fibre (0.25 mm o.d., AN69 Hospal Medical, New Brunswick, NY, U.S.A.) was passed over the tubing, into the body of the probe, and cut to a length 0.5 mm longer than the inlet tube. Epoxy resin (554-850, RS Components Ltd., Corby, UK) was used to seal the tip of the fibre, the joint between dialysis membrane and steel body, and the assembly at the head of the probe.

Animal preparation and intracerebral microdialysis

Male Sprague-Dawley rats (weight, 341 ± 10 g, mean ± s.e.mean; Bantin & Kingman, Grimston, Hull, UK) were used, with food and water available *ad libitum*. All animal use procedures were in strict accordance with the Home Office guidelines, and specifically licensed under the Animals (Scientific Procedures) Act 1986. Anaesthesia was induced and maintained during surgery with halothane (2.5% and 1.5–2.0%, respectively) in O_2:N_2O (30:70). Microdialysis probes were implanted in the dorsolateral striatum (coordinates: 0.8 mm anterior to bregma, 3 mm lateral, and 6 mm deep from the dural surface; Paxinos & Watson, 1982). Unless otherwise stated, they were perfused with ACSF (composition in mmol l^{-1}: NaCl 125, KCl 2.5, $MgCl_2$ 1.18, $CaCl_2$ 1.26, NaH_2PO_4 0.2; pH 7.3 adjusted with 1 M NaOH), at 1 µl min^{-1} with a syringe pump (CMA/100; CMA/Microdialysis, Stockholm, Sweden). A femoral artery and vein were catheterised for continuous monitoring of arterial blood pressure and induction of cardiac arrest, respectively. In order to minimize any possible interference of halothane anaesthesia with the processes under study, once the surgical procedure had been completed, the depth of anaesthesia was carefully controlled by monitoring electroencephalogram (EEG) and blood pressure, and the concentration of halothane in the breathing mixture kept to a minimum (0.8 to 1.2%). Body temperature was maintained at 37.5–38°C throughout the experiment.

Recording of extracellular d.c. potential and EEG

The EEG and d.c. potential were derived from the potential between the electrode built into the probe, and a Ag/AgCl reference electrode placed under the scalp. The reference was made of a pellet of Ag/AgCl (Type E255; 0.8 mm o.d.; Clark Electromedical Instruments, Reading, UK), inserted into polythene tubing (0.76 mm i.d.; 1.22 mm o.d.; Portex Ltd., Hythe, UK) and sealed with epoxy resin (554-850, RS Components Ltd., Corby, UK). The potential between the electrode in the probe and the reference was first amplified (× 10) with a high impedance input pre-amplifier (NL 102G, Neurolog System, Digitimer Ltd., Welwyn Garden City, UK). The alternating current component in the 1–30 Hz window, amplified 6,000–8,000 times, provided EEG, and the d.c. component, the d.c. potential. The antenna effect of the tubing between the syringes and the microdialysis probe was eliminated by grounding the metal needle of the syringes with wires incorporating 0.01 µF capacitors. A dedicated application programme allowed all parameters to be continuously acquired, displayed and stored (Obrenovitch *et al.*, 1988). Linear spectra of consecutive EEG data sections (4 s epoch) were computed on-line using the Fast Fourier Transformation. The d.c. potential was converted to absolute values (mV) from prior calibration.

Experimental procedure

After a 2 h period of stabilisation/control, increasing concentrations of glutamate receptor agonists were perfused for 2 min [NMDA 25–500 µM, $n = 6$; (**RS**)-α-amino-3-hydroxy-5-methyl-4-isoxazole proprionic acid (AMPA) 5–1000 µM, $n = 3$; kainate 5–500 µM; $n = 3$; and glutamate 0.25–100 mM, $n = 3$], with 20 min of recovery between each agonist application. Changes from normal ACSF to the medium containing the agonist under study were made with a liquid switch (CMA/110; CMA/Microdialysis, Stockholm, Sweden). In order to test the reproducibility of two separate sets of concentration-dependent responses, in 6 experiments with NMDA, a second set of 2 min stimuli was repeated 30 min after completion of the first series of NMDA applications. The effect of Mg^{2+}-free medium on NMDA responses was also tested ($n = 7$), using the same paradigm, except that a further 45 min of perfusion with Mg^{2+}-free ACSF separated the two series of NMDA applications, and Mg^{2+} was omitted from the perfusing medium during the rest of the procedure. No attempt was made to determine the maximum responses because of the initiation of spreading depression (i.e. a sudden and transient further depolarization) that we observed with NMDA (see Results), and the well known neurotoxic effects of these compounds, especially kainate. The suitability of this method for studying the action of glutamate receptor antagonists was also examined. At the end of the Mg^{2+}-free ACSF experiments with NMDA, MK-801 was administered (2 mg kg^{-1}, i.p.) 10 min before an additional application of 500 µM NMDA ($n = 7$). In the experiments with AMPA and kainate, the non-NMDA antagonist DNQX was perfused via the microdialysis probe, for at least 10 min before an additional stimulation with 250 µM of the corresponding agonist.

Drugs

The following drugs were used: AMPA and DNQX (Tocris, Neuramin, Bristol, UK); glutamic acid, kainate and NMDA

(Sigma Chemicals, Poole, UK); MK-801 (Research Biochemical Inc., Natick, MA, U.S.A.). All other chemicals were of analytical grade (BDH, Poole, UK). All drugs, except MK-801 and DNQX were dissolved in ACSF and pH adjusted to 7.3. MK-801 (1 mg ml^{-1}) was prepared in sterile saline (0.9% w/v NaCl) solution. DNQX was dissolved in dimethylsulphoxide at 33 mM and subsequently diluted with ACSF to 100 μM.

Data presentation and analysis

The polarity of the d.c. potential in Figures 1, 5 and 6 was defined so that depolarizing agents produce upwards voltage deflection and traces were aligned by setting the 2 min preceding the agonist application to 0 mV. Although the receptors of the cell populations surrounding the microdialysis probe were exposed to a much lower agonist concentration than that in the perfusing medium (Benveniste & Hüttemeier , 1990), preliminary analysis showed that conventional models of agonism fitted our experimental data well. Therefore, as maximum responses could not be determined experimentally, they were determined, together with the estimated EC_{50}, from the log concentration-responses relationships fitted by the Gauss-Newton method (ASYST, Keithley, Reading, UK) to the function:

$$y = \frac{R_{max}}{1 + (\log\ 'EC_{50}'/\log\ x)^n}$$ (Horne & Simmonds, 1989)

where x = *dialysate concentration* of agonist producing responses amplitude y, R_{max} = maximal responses, 'EC_{50}' = estimated EC_{50} (i.e. agonist *concentration in the ACSF* producing half-maximal response) and n = slope parameter.

Responses were then expressed as a fraction of the estimated R_{max}, which allowed the Hill coefficients to be determined as the slope of the Hill plots (Simmonds, 1990).

All values in Results are mean ± s.e.mean. Statistical analysis was by Student's *t* test (paired or unpaired).

Results

Control period

Even though the d.c. potential typically stabilized within 30 min of electrode implantation, pharmacological analysis was always performed after a 2 h period of stabilization. The oscillations superimposed onto the d.c. potential trace (Figures 1, 5 and 6) originated from the EEG slow waves, and increased with the depth of anaesthesia (Figure 5). They never impaired the quantitative analysis of drug-evoked responses, even with Mg^{2+}-free medium.

NMDA-evoked responses

NMDA applied to the rat striatum produced clear concentration-dependent depolarizations, with a threshold concentration of around 25 μM (Figure 1a). Responses were short lasting with a steep onset. The recovery was multiphasic, with an initial slow reduction of depolarization starting as NMDA was still applied (Figure 1a, 250 μM), a faster decrease immediately after the switch to normal ACSF, and a marked hyperpolarization with progressive normalisation. The post-depolarization hyperpolarization (PDH) was a consistent feature, observed even when the response was modest (Figure 1a, 25 μM). At high concentrations (500 μM) NMDA occasionally initiated spreading depression. In such cases, the 'normal' response was masked and its amplitude could not be measured (Figure 1a, 500 μM). When the NMDA applications (25–500 μM) were repeated, the second concentration-dependent responses were identical to the first (Figure 2; $n = 6$), even when spreading depression had occurred. Omission of Mg^{2+} in the ACSF resulted in a slight increase in the amplitude of NMDA-induced depolarizations, but this difference was not significant (Figure 3) (Obrenovitch *et al.*, 1994). There was no sign of depolarizing epileptiform activity under these conditions.

Responses to AMPA and kainate

Measurable effects were obtained with concentrations of AMPA or kainate as low as 5 μM. AMPA produced depolarizations which were slower in onset and decline (Figure 1b) than responses of equal amplitude evoked by NMDA (Figure 1a). With AMPA, the maximum of the concentration-response curve was around 500 μM, since doubling this concentration (1 mM) did not increase further the depolarization amplitude (7.1 ± 0.3 mV and 7.5 ± 0.4 mV, respectively) (Figure 4). Responses to kainate were even slower in onset and decline; more than 15 min being necessary for the d.c. potential to normalize after a 2 min application of 500 μM kainate (Figure 1c). This was a clear feature of kainate-evoked depolarization. No PDH followed AMPA- nor kainate-stimuli. Spreading depression was not initiated in the striatum by these compounds under these experimental conditions.

Responses to L-glutamate

The threshold concentration of glutamate for a detectable response was around 1 mM, i.e. 40 to 200 times higher than with the other agonists studied. At high concentrations, glutamate-evoked depolarizations were rapid and recovered quickly (Figure 1d). Responses to glutamate were sometimes followed by a hyperpolarization, but its amplitude was much smaller than with NMDA. At the highest concentration tested (100 mM), glutamate initiated spreading depression (Figure 1d, 100 mM) but this phenomenon was also less marked than with NMDA.

Concentration-response relationships

Depolarizations induced by glutamate agonists applied through the microdialysis probe were remarkably reproducible, within the same preparation (Figure 2) and between experiments (Figure 4). The logarithm concentration-response representation clearly brings out the much lower potency of glutamate, and also a more progressive increase of the depolarization with the concentration of glutamate applied via the microdialysis probe. Conventional modelling of agonism fitted our experimental data well. The maxima obtained with AMPA and NMDA appeared slightly smaller than those obtained with kainate and glutamate, but the small number of experiments precluded a rigorous statistical analysis (Table 1). For the same reason, the estimated EC_{50} of AMPA, kainate and NMDA cannot be accurately compared, but glutamate clearly had a much lower potency. The slopes of the concentration-response curves were close to one for AMPA, kainate and glutamate, and around 2 for NMDA (Table 1).

Effects of glutamate-receptor antagonists

Pretreatment with MK-801 (2 mg kg^{-1}, i.p.) reduced responses to 500 μM NMDA by 65% (3.2 ± 1.2 mV versus 9.1 ± 1.1 mV; $n = 7$; $P < 0.001$) (Figure 5). Note the persistence of the PDH under MK-801 inhibition, and the increased amplitude of the signal oscillations, which actually corresponded to an increase of the low frequencies of the EEG reflecting potentiation of anaesthesia by MK-801. The non-NMDA antagonist DNQX (100 μM applied via the microdialysis probe) reduced by around 78% responses to 250 μM AMPA (Figure 5) and kainate ($n = 2$ for each agonist).

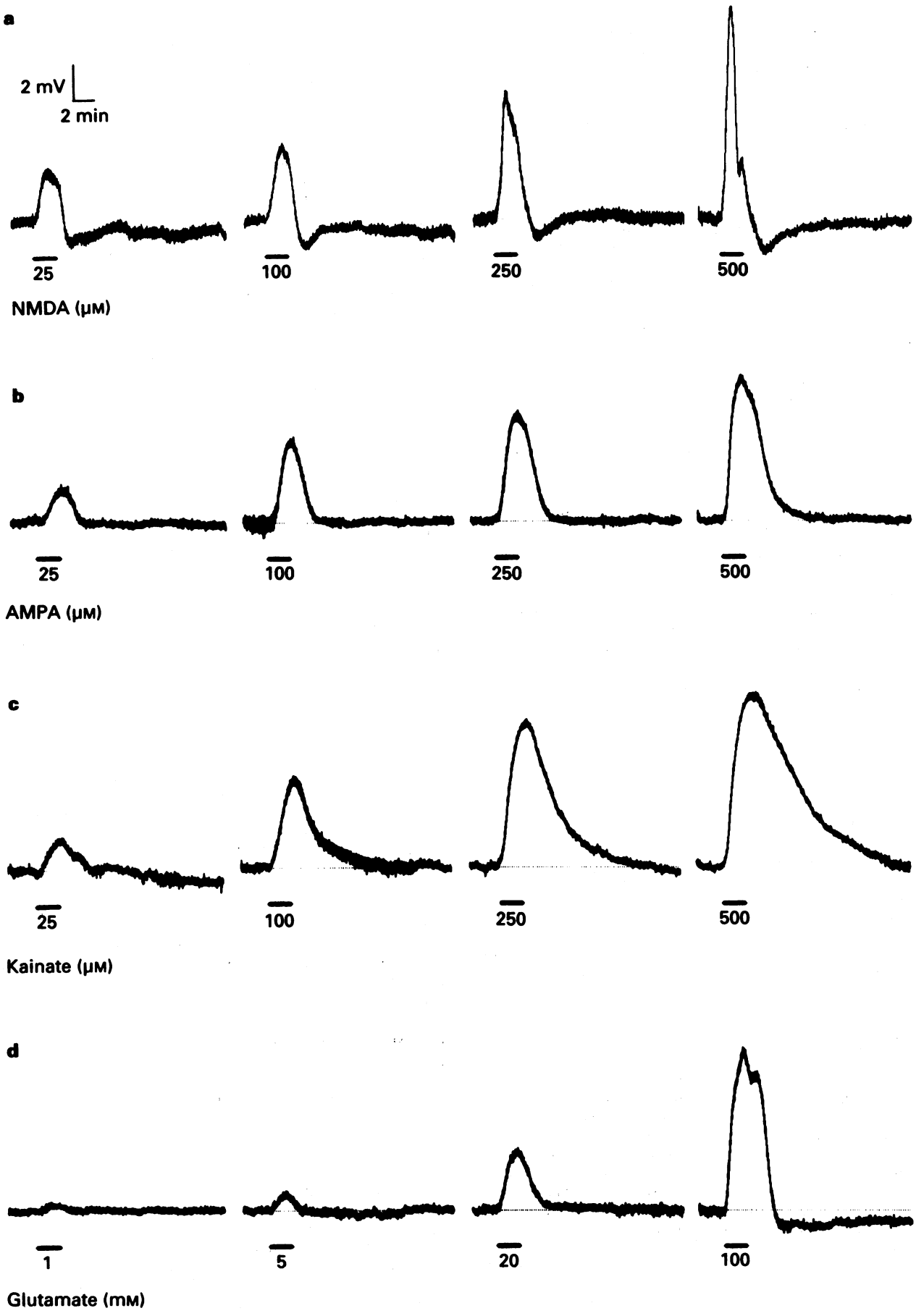


Figure 1 Representative changes in the d.c. potential produced by glutamate receptor agonists in the rat striatum *in vivo*. Increasing concentrations of N-methyl-D-aspartate (NMDA) (a), α-amino-3-hydroxy-5-methyl-4-isoxazole propionic acid (AMPA) (b), kainate (c) and glutamate (d) were applied for 2 min via a microdialysis probe, with 20 min of recovery between each challenge.

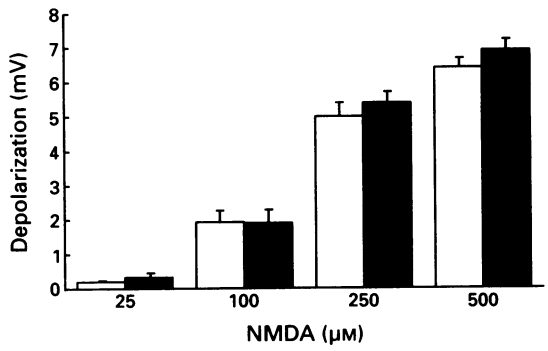


Figure 2 Comparison of the effect of repeated N-methyl-D-aspartate (NMDA) applications (25–500 μM) on the d.c. potential recorded from the rat striatum *in vivo*. Increasing concentrations of NMDA (25–500 μM) were applied for 2 min via a microdialysis probe with 20 min of recovery between each application (open columns). A second series of 2 min NMDA stimuli was repeated (solid columns), 30 min after completion of the first. Columns represent mean ± s.e.mean ($n = 6$). There was no statistical differences between the responses produced by the two series of NMDA applications.

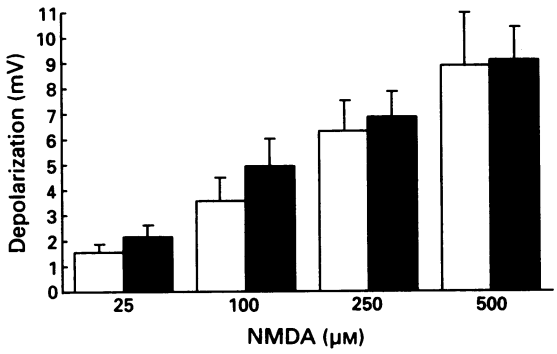


Figure 3 Effect of perfusing the microdialysis probe with Mg^{2+}-free ACSF on depolarizations evoked by N-methyl-D-aspartate (NMDA) in the rat striatum. Increasing concentrations of NMDA (25–500 μM) were applied for 2 min via a microdialysis probe with 20 min recovery between each application (open columns). After 45 min of perfusion with Mg^{2+}-free ACSF, a second series of NMDA challenges was started (solid columns). Mg^{2+} was omitted from the perfusion medium during the rest of the procedure. Columns represent mean ± s.e.mean ($n = 6$). Perfusion with Mg^{2+}-free medium slightly potentiated the average action of NMDA, but this difference was not statistically significant ($P > 0.10$ to 0.85).

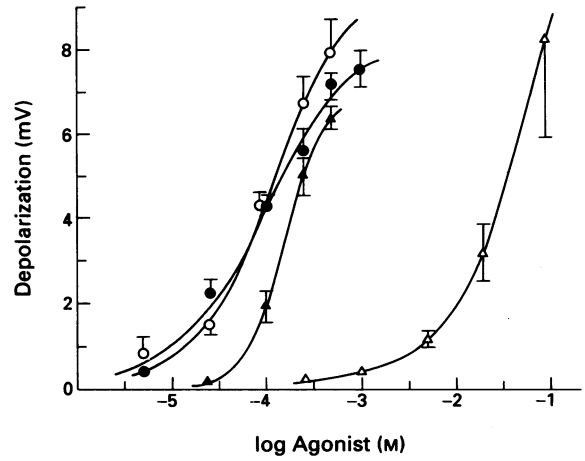


Figure 4 Logarithm concentration-response curves obtained for N-methyl-D-aspartate (NMDA) (▲), α-amino-3-hydroxy-5-methyl-4-isoxazole propionic acid (AMPA) (●), kainate (○) and glutamate (×) applied via a microdialysis probe implanted into the rat striatum. Data (mean ± s.e.mean) are from 6 experiments for NMDA, and 3 experiments for the other agonists. With the lowest concentration of AMPA, NMDA and glutamate, the s.e.mean was too small to be represented. Logarithm concentration-response relationships were fitted by the Gauss-Newton method to the conventional model for agonism (see Methods). Note the low potency of glutamate in comparison to the other agonists.

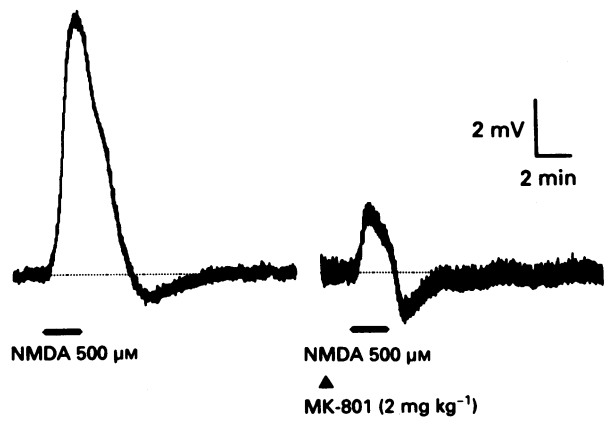


Figure 5 Inhibition of N-methyl-D-aspartate (NMDA)-evoked depolarization by MK-801 in the rat striatum. The left trace shows a representative response to NMDA (500 μM) applied for 2 min via the implanted microdialysis probe perfused with Mg^{2+}-free ACSF. After 20 min of recovery, MK-801 (2 mg kg^{-1}) was administered i.p. (arrow), and the NMDA stimulus repeated 10 min later (right trace). Note the persistence of the post-depolarization hyperpolarization under MK-801 inhibition, and the increased 'noise' of the d.c. signal which actually corresponded to an increase in the amplitude of the EEG low frequencies, reflecting a potentiation of anaesthesia by MK-801.

Discussion

Penetration injury associated with electrode implantation into the brain produces local depolarization and marked neurotransmitters effluxes, but these changes are rapidly reversed (Obrenovitch *et al.*, 1993). In most of the experiments reported here, the d.c. potential was stable within 30 min after implantation. A slight drift of the signal was observed in a few experiments, but this probably originated from alterations of either the microdialysis electrode or reference.

Although the number of cells exposed to a drug *in vitro* is certainly much larger, depolarizations evoked and measured through microdialysis probes had an amplitude 3 to 10 times larger than those recorded from brain slices in grease-gap preparations, and a better signal-to-noise ratio (Harrison & Simmonds, 1985; Garthwaite *et al.*, 1986; Blake *et al.*, 1988; Horne & Simmonds, 1989; Martin & Nadler, 1991). These features are not due to the high impedance of the microdialysis electrode since we have previously shown that the d.c. potential recorded with a microdialysis electrode is equivalent to that obtained with a glass capillary (i.e. with a much lower impedance) whose tip is positioned next to the outer surface of the dialysis membrane (Obrenovitch *et al.*, 1993). Rather, the quality of the signal probably results from the fact that, as with glass capillaries, the microdialysis electrode is very close to, and surrounded by the tissue exposed to the agonist (see below, the discussion on the origin of the recorded signal). Responses to agonists applied through microdialysis probes appeared also more reproducible than those obtained in grease-gap and brain slice experiments. This may result from the fact that, with microdialysis, the cells contributing to the recorded signal (i.e. adjacent to the microdialysis membrane) are exposed to more rapid changes in the agonist concentration: (a) abrupt increase at the beginning of the stimulus; and (b) rapid decrease when the per-

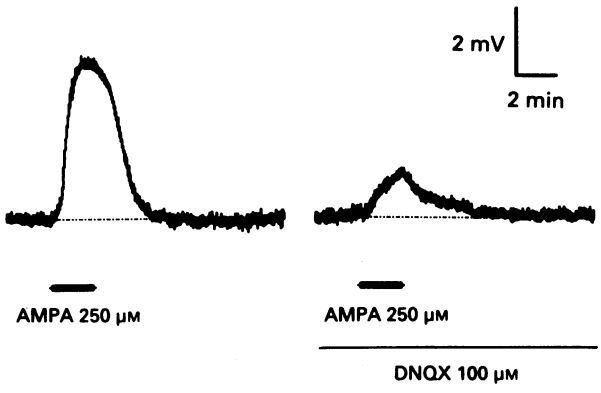


Figure 6 Inhibition of α-amino-3-hydroxy-5-methyl-4-isoxazole propionic acid (AMPA)-evoked depolarization by 6,7-dinitroquinoxaline-2,3-dione (DNQX) in the rat striatum. The left trace shows a representative response to AMPA (250 μM) applied for 2 min via the implanted microdialysis probe. After 20 min of recovery, DNQX (100 μM) was continuously perfused via the microdialysis probe and a second identical AMPA stimulus repeated 10 min later (right trace).

fusion medium is switched back to normal ACSF, because the drug is cleared both through the probe and by diffusion in the surrounding tissue.

The superimposition of the EEG slow waves onto the d.c. potential trace (Figure 1) did not impair the quantitative analysis of drug-induced responses. The amplitude of depolarization could be measured accurately, either directly on the paper recording, or using the digitized signal without any need for low pass filtering. In fact, as the amplitude of the EEG slow waves increased with the depth of anaesthesia (Figure 6), they were a helpful index for the maintenance of halothane anaesthesia to a constant and low level. This electrode configuration, however, is not suitable for the study of the effects of a drug applied through the microdialysis probe on the 'local' electrical activity because, in contrast to the d.c. potential, the EEG recorded with a microdialysis electrode includes activities from remote structures (Obrenovitch *et al.*, 1993). The effects of tetrodotoxin (TTX) illustrate this feature well: TTX applied through the microdialysis probe does not markedly modify the 'local' electrical activity, but it blocks effectively veratridine-induced depolarization (data not shown).

It is generally considered that changes in the d.c. potential recorded with a conventional glass capillary electrode reflect changes in the average membrane potential of the cells adjacent to the electrode tip, including both neurones and glia (Caspers *et al.*, 1984). Recent data obtained with a model of stroke further suggested that most of the d.c. signal recorded with a microdialysis electrode is recorded from surrounding cells, located at the level of the tip of the input flow capillary (Wahl *et al.*, 1994). These data imply that the depolarizations recorded in the present study originated locally, from changes in the membrane potential of the surrounding cells, and independently of any special axonal projection. This contrasts with the grease-gap preparation which may require a dense projection of axons within the tissue slice to pass through the grease barrier separating the two compartments of the bath (Evans, 1989; Simmonds, 1990).

Despite a possible difference in the electrogenesis of the recorded signal, and although the present study was performed in the striatum, the time course of NMDA-, AMPA-, kainate- and glutamate-evoked depolarizations were very similar to those recorded with cortical wedges (Harrison & Simmonds, 1985; Horne & Simmonds, 1989; Urenjak, unpublished data), and hippocampal (Blake *et al.*, 1988; Martin & Nadler, 1991) and cerebellar slices (Garthwaite *et al.*, 1986). Common marked features included: steep onset

Table 1 Parameters of concentration-response relationships of excitatory amino acids

Agonist	R_{max} (mV)	*Estimated* EC_{50} (mM)	*Hill coefficient*
NMDA	7.3 ± 0.3	0.188 ± 0.02	1.95 ± 0.12
AMPA	7.9 ± 0.5	0.107 ± 0.01	1.07 ± 0.09
Kainate	9.8 ± 2.0	0.135 ± 0.04	1.16 ± 0.17
Glutamate	10.1 ± 2.2	42 ± 7.6*	0.89 ± 0.19

Maximum response (R_{max}), estimated EC_{50} (agonist concentration in the ACSF producing half-maximal response) and Hill coefficient for each agonist are given as mean ± s.e.mean ($n = 6$ for NMDA; $n = 3$ for the other agonists). *$P < 0.05$ (comparison with N-methyl-D-aspartate (NMDA), α-amino-3-hydroxy-5-methyl-4-isoxazole propionic acid (AMPA) and kainate; Student's unpaired t test).

and recovery of NMDA and glutamate responses; marked PDH with NMDA; and the very slow recovery after kainate application. On the other hand, we did not observe any PDH with AMPA (Horne & Simmonds, 1989; Davies *et al.*, 1993). The threshold concentrations and estimated EC_{50} for NMDA, AMPA and glutamate were around 10–20 times higher than those previously reported with cortical (Harrison & Simmonds, 1985; Horne & Simmonds, 1989) and hippocampal slices (Blake *et al.*, 1988; Martin & Nadler, 1991). The latter difference was anticipated since the diffusion of the drugs to the tissue is limited by the dialysis membrane (see below). In contrast, the relative potency of glutamate and NMDA was of the same order of magnitude as that obtained with the cortical wedge (Harrison & Simmonds, 1985) and hippocampal slices (Martin & Nadler, 1991), glutamate being 100 to 400 times less potent than NMDA. There was no statistical difference between the EC_{50} of AMPA, kainate and NMDA, but this may be due to the small number of experiments with kainate and AMPA ($n = 3$).

The fact that two consecutive series of NMDA-stimuli evoked comparable depolarizations indicated that reliable quantitative analysis of drug action can be performed with this method, with each animal being its own control. This is especially appropriate for investigations into the effect of putative glutamate receptor antagonists. The remarkable inter-animal reproducibility is also favourable (Figure 4); the large s.e.mean for high concentrations of glutamate was due to an unusual small response in one animal.

This new application of intracerebral microdialysis offers several key advantages for investigations into the action of depolarizing drugs: (i) quantitative data can be obtained, *in vivo*, with minimal trauma; (ii) studies can be performed in specific brain regions, under physiological conditions, or during controlled alterations such as extracellular acidosis, application of metabolic blockers, ionic changes, etc.; (iii) drugs (antagonists) can be administered either systemically (Figure 5), or directly through the dialysis probe (Figure 6), thus by-passing the blood-brain barrier and avoiding possible undesirable peripheral side-effects; (iv) information on neurotransmitter release or drug metabolism can be obtained during the same procedure as the analysis of microdialysate samples remains possible. These advantages by far, outweight the few limitations discussed below.

NMDA-evoked responses in brain slices are selectively potentiated in Mg^{2+}-free medium with small depolarizations often increased to a greater extent (Harrison & Simmonds, 1985; Blake *et al.*, 1988). In contrast, omission of Mg^{2+} from the ACSF in microdialysis enhanced only slightly the action of NMDA. This was expected since, in comparison to brain slice preparations, the volume of perfusate is much smaller than that of the surrounding tissue. As a consequence, microdialysis cannot reduce markedly the extracellular levels of endogenous species. This explains why the presence of glucose in the ACSF is not prerequisite, and why it is neces-

sary to supplement Ca^{2+}-free ACSF with high Mg^{2+} and EGTA to block Ca^{2+}-dependent neurotransmitter release (Paulsen & Fonnum, 1989; Obrenovitch *et al.*, 1990). In contrast, there is no obstacle to increasing locally the ECF concentration of any low molecular weight compounds.

It is obvious that the estimated EC_{50}s given throughout the text (i.e. agonist *concentration in the ACSF* producing half-maximal responses) are much larger than the true EC_{50}, since the concentration of the drug in the ACSF is not that to which receptors are exposed. Comparison with data taken from the literature suggests that our EC_{50} estimates are 10 to 20 times higher than those measured in brain slices. However, the fact that the d.c. signal recorded with this electrode configuration mainly originates from cell populations *adjacent* to the probe, may allow modelling of the concentration gradient of the drug across the microdialysis membrane and, therefore, calculation of the true EC_{50}. This possibility is supported by the good fitting of our experimental data with conventional models of agonism (Figure 4). In order to avoid spreading depression and possible neurotoxic effects, the maximum responses were not determined, but this is a classical problem in pharmacology (Simmonds, 1990) which can be circumvented by using mathematical models (Black & Leff, 1983). A poor diffusion of the drug through the dialysis probe may also contribute to the kinetic of the response recorded. If required, this could be tested by a comparative analysis of the extraction/recovery coefficients *in vitro* (Tao & Hjorth, 1992). Finally, rapid desensitization with high concentrations of agonists is a mechanism which might also interfere by limiting the responses. Investigation of this phenomenon requires either long-lasting stimuli, or repeated drug applications separated by short intervals.

The technique described here has so far only been applied to anaesthetized rats, but it may be possible to perform similar studies in conscious animals, and certainly in rats semi-restrained in a hammock.

In conclusion, our data demonstrated that intracerebral microdialysis combined with recording of extracellular field potential is a novel and valuable method for the quantitative analysis of the action of drugs acting on glutamate receptors in any regions of the living brain. It is the *in vivo* counterpart of the grease-gap preparation. Recording the d.c. potential via a microdialysis probe should prove especially useful for comparing the sensitivity of specific brain structures to selective glutamate receptor agonists, under normal conditions and when the neuronal microenvironment is altered. It should also be useful for investigations into other depolarizing agents, such as veratridine, and their antagonists.

We wish to thank Dr Douglas R. Richards of the School of Pharmacy (London) for editing the manuscript, and Mr Wael El Deredy for helping with the analysis of the concentration–response relationships.

References

BEAL, M.F., FERRANTE, R.J., SWARTZ, K.J. & KOWALL, N.W. (1991). Chronic quinolinic acid lesions in rats closely resemble Huntington's disease. *J. Neurosci.*, **11**, 1649–1659.

BENVENISTE, H. & HÜTTEMEIER, P.C. (1990). Microdialysis – theory and application. *Prog. Neurobiol.*, **35**, 195–215.

BLACK, J.W. & LEFF, P. (1983). Operational models of pharmacological agonism. *Proc. R. Soc. B.*, **220**, 141–162.

BLAKE, J.F., BROWN, M.W. & COLLINGRIDGE, G.L. (1988). A quantitative study of the actions of excitatory amino acids and antagonists in rat hippocampal slices. *Br. J. Pharmacol.*, **95**, 291–299.

CASPERS, H., SPECKMANN, E.-J. & LEHMENKÜHLER, A. (1984). Electrogenesis of slow potentials of the brain. In *Self-Regulation of the Brain and Behavior*. ed. Elbert, T., Rockstroh, B., Lutzenberger, W. & Birbaumer, N. pp. 26–41. Berlin: Springer Verlag.

COLLINGRIDGE, G.L. & LESTER, A.J. (1989). Excitatory amino acids receptors in the vertebrate central nervous system. *Pharmacol. Rev.*, **40**, 143–209.

DAVIES, S.N., FANNING, G.R. & GANESALINGHAM, N. (1993). Origin of post-depolarization hyperpolarizations evoked by excitatory amino acids in a grease-gap recording preparation of the rat hippocampal slice. *Br. J. Pharmacol.*, **109**, 29P.

DINGLEDINE, R., MCBAIN, C.J. & MCNAMARA, J.O. (1990). Excitatory amino acid receptors in epilepsy. *Trends Pharmacol. Sci.*, **11**, 334–338.

EVANS, R.H. (1989). *In vitro* preparations of spinal cord or brain which can be used for grease gap electrical recording of excitatory amino acid action. In *The NMDA Receptor*. ed. Watkins, J.C. & Collingridg, G.L. pp. 65–75. Oxford: Oxford University Press.

GARTHWAITE, J., GARTHWAITE, G. & HAJOS, F. (1986). Amino acid neurotoxicity: relationship to neuronal depolarization in rat cerebellar slices. *Neurosci.*, **18**, 449–460.

HARRISON, N.L. & SIMMONDS, M.A. (1985). Quantitative studies on some antagonists of N-methyl-D-aspartate in slices of rat cerebral cortex. *Br. J. Pharmacol.*, **84**, 381–391.

HORNE, A.L. & SIMMONDS, M.A. (1989). The pharmacology of quisqualate and AMPA in the cerebral cortex of the rat *in vitro*. *Neuropharmacol.*, **28**, 1113–1118.

KELSO, S.R., NELSON, T.E. & LEONARD, J.P. (1992). Protein kinase C-mediated enhancement of NMDA currents by metabotropic glutamate receptors in Xenopus oocytes. *J. Physiol.*, **449**, 705–718.

LODGE, D. & JOHNSON, K.M. (1991). Noncompetitive excitatory amino acid receptor antagonists. *Trends Pharmacol. Sci.*, (Special Report), 13–18.

MARTIN, D. & NADLER, V.J. (1991). Grease-gap methods for studying pharmacology of excitatory amino acids on central nervous system neurons. In *Methods in Neurosciences*, Volt. 4. ed. Conn, M.P. pp. 349–373. London: Academic Press.

MELDRUM, B.S. (1990). Protection against ischaemic neuronal damage by drugs acting on excitatory neurotransmission. *Cerebrovasc. Brain Metab. Rev.*, **2**, 27–57.

MELDRUM, B.S. & GARTHWAITE, J. (1990). Excitatory amino acid neurotoxicity and neurodegenerative disease. *Trends Neurosci.*, **11**, 379–387.

MILLAN, M.H., OBRENOVITCH, T.P., SARNA, G.S., LOK, S.-Y., SYMON, L. & MELDRUM, B.S. (1991). Changes in rat brain extracellular glutamate concentration during seizures induced by systemic picrotoxin or focal bicuculline injection: an *in vivo* dialysis study with on-line enzymatic detection. *Epilepsy Res.*, **9**, 86–91.

NAKANISHI, S. (1992). Molecular diversity of glutamate receptors and implications for brain function. *Science*, **258**, 597–603.

OBRENOVITCH, T.P. & ZILKHA, E. (1994). High extracellular potassium, not glutamate, is the prerequiste for the propagation of spreading depression. In *New Advances in Headache Research*, Vol. 4, ed. Rose, F.C. pp. 71–75. London: Smith-Gordon.

OBRENOVITCH, T.P., MATSUMOTO, T. & SYMON, L. (1989). Multiparametric monitoring of the rat cerebral cortex subjected to transient ischaemia: a powerful tool for assessing 'anti-ischemic' drugs. *J. Cereb. Blood Flow Metab.*, **9** (Suppl 1), S630.

OBRENOVITCH, T.P., SARNA, G.S., MILLAN, M.H., LOK, S.-Y., KAWAUCHI, M., UEDA, Y. & SYMON, L. (1990). Intracerebral dialysis with on-line enzyme fluorometric detection: a novel method to investigate the changes in the extracellular concentration of glutamic acid. In *Pharmacology of Cerebral Ischemia*. ed. Krieglstein, J. & Oberpichler, H. pp. 23–31. Stuttgart: Wiss. Verlag.

OBRENOVITCH, T.P., URENJAK, J., RICHARDS, D.A., UEDA, Y., CURZON, G. & SYMON, L. (1993). Extracellular neuroactive amino acids in the rat brain striatum during moderate and severe transient ischaemia. *J. Neurochem.*, **61**, 178–186.

OBRENOVITCH, T.P., URENJAK, J., RICHARDS, D.A., SWAYNE, G.T.G. & SYMON, L. (1994). Intracerebral microdialysis combined with recording of extracellular field potential: a novel method for investigation of depolarizing drugs *in vivo*. *Br. J. Pharmacol.*, **112**, 482P.

PAULSEN, R.E. & FONNUM, F. (1989). Role of glial cells for the basal and Ca^{2+}-dependent K^+-evoked release of transmitter amino acids investigated by microdialysis. *J. Neurochem.*, **52**, 1823–1829.

PAXINOS, G. & WATSON, C. (1986). *The Rat Brain in Stereotaxic Coordinates*. 2nd ed. London: Academic Press.

SEEBURG, P. (1993). The molecular biology of mammalian glutamate receptor channels. *Trends Neurosci.*, **16**, 359–365.

SIMMONDS, M.A. (1990). Use of slices for quantitative pharmacology. In *Preparations of Vertebrate Central Nervous System In Vitro*. ed. Jahnsen, H. pp. 49–76. Chichester: John Wiley & Sons Ltd.

TAO, R. & HJORTH, S.J. (1992). Differences in the *in vitro* and *in vivo* 5-hydroxytryptamine extraction performance among three common microdialysis membranes. *J. Neurochem.*, **59**, 1778–1785.

TEITELBAUM, J.S., ZATORRE, R.J., CARPENTER, S., GENDRON, D., EVANS, A.C., GJEDDE, A. & CASHMAN, N.R. (1990). Neurologic sequelae of domoic acid intoxication due to ingestion of contaminated mussels. *N. Engl. J. Med.*, **322**, 1781–1787.

WAHL, F., OBRENOVITCH, T.P., HARDY, A.M., PLOTKINE, M., BOULU, R. & SYMON, L. (1994). Extracellular glutamate during focal cerebral ischaemia in rats: time course and calcium-dependency. *J. Neurochem.*, **63**, 1003–1011.

(Received May 11, 1994
Revised July 25, 1994
Accepted August 23, 1994)

Br. J. Pharmacol. (1994), **113**, 1303–1310 © Macmillan Press Ltd, 1994

[^{125}I]-PD151242: a selective ligand for endothelin ET_A receptors in human kidney which localizes to renal vasculature

[1]Anthony P. Davenport, Rhoda E. Kuc, Sarah L. Hoskins, Fiona E. Karet & *Fiona Fitzgerald

Clinical Pharmacology Unit, University of Cambridge, Addenbrooke's Hospital, Cambridge, CB2 2QQ and *Amersham International plc, Amersham, Bucks

1 The linear tetrapeptide radioligand, [^{125}I]-PD151242 was used to characterize ET_A receptors in human kidney which is an ET_B-rich tissue. Saturation binding assays with [^{125}I]-PD151242 revealed a single population of high affinity endothelin receptors: $K_D = 0.75 \pm 0.07$ nM and $B_{max} = 48.4 \pm 1.6$ fmol mg^{-1} protein ($n = 3$ individuals ± s.e.mean). Hill slopes were close to unity and a one site fit was preferred to a two site model.

2 ET_A-receptor-selective ligands competed for [^{125}I]-PD151242 binding with sub-nanomolar affinity: BQ123 $K_D = 0.43 \pm 0.10$ nM, $B_{max} = 46.6 \pm 7.9$ fmol mg^{-1} protein; FR139317, $K_D = 0.37 \pm 0.06$ nM, $B_{max} = 39.5 \pm 6.5$ fmol mg^{-1} protein ($n = 3$ individuals ± s.e.mean). In each case, monophasic inhibition curves were obtained and a one site fit was preferred to a two site model. The ET_B-selective agonist, BQ3020 at the highest concentration tested (10 μM) inhibited binding by only 50%. The non-selective RO462005 competed for the binding of [^{125}I]-PD151242: $K_D = 1.31 \pm 1.38$ μM, $B_{max} = 33.0 \pm 9.7$ fmol mg^{-1} protein. Endothelin-2 and sarafotoxin S6B inhibited [^{125}I]-PD151242 binding to renal tissue whereas ET-3 and sarafotoxin S6C were less effective. Non-endothelin and non-sarafotoxin peptides did not compete.

3 No degradation of [^{125}I]-PD151242 was detected following incubation of the ligand with renal tissue under the conditions of the binding assay.

4 Polymerase chain reaction products corresponding to the expected size for mRNA encoding ET_A and ET_B receptor sub-types were detected in cortex and medulla in each of the five individuals examined.

5 Autoradiographical studies showed that ET_A receptors visualised with [^{125}I]-PD151242 were mainly localized to blood vessels including interlobular and arcuate arteries, arterioles and adjacent arcuate veins. ET_B receptors localized with [^{125}I]-BQ3020 were concentrated in the medulla and the density of binding to vessels was low.

6 These data suggest [^{125}I]-PD151242 is selective for ET_A receptors in human kidney and this sub-type is mainly localized to the renal vasculature. The results provide further evidence that the human vasculature mainly expresses the ET_A receptor.

Keywords: Endothelin; PD151242; FR139317; BQ123; BQ3020; ET_A receptor; ET_A mRNA; ET_B mRNA; kidney; autoradiography; polymerase chain reaction

Introduction

Exogenously applied endothelin-1 (ET-1) has a number of important actions on the kidney *in vitro* and *in vivo* including vasoconstriction and natriuresis (see Simonson, 1993). Evidence is emerging that in some animal species these two actions may be mediated by different ET receptor sub-types. The renal vasculature is particularly sensitive to the constrictor action of this peptide (Firth *et al.*, 1988; Davis *et al.*, 1991; Bigaud & Pelton, 1992; Clozel *et al.*, 1992; Cristol *et al.*, 1993; Battistini *et al.*, 1993; Pollock & Opgenorth, 1993; 1994; Gardiner *et al.*, 1989; 1990; 1994; Wellings *et al.*, 1994). As a result of this vascular action, there are falls in plasma flow, glomerular filtration rate and urine production. The ET receptor sub-type mediating ET-induced vasoconstriction in renal vessels varies between animal species. In most animals studied, renal vasoconstriction is via ET_A receptors. However, for example in rat and pig there is a significant ET_B component (Davenport & Maguire, 1994; Cirino *et al.*, 1992). Studies in animals also indicate that ET may have a role in salt and water balance by interacting with receptors located on the tubule and collecting duct (see Karet & Davenport, 1994). In some animals these actions appear to be mediated via the ET_B sub-type.

ET antagonists have been shown to be effective in some animal models of renal disease (Benigni *et al.*, 1993; Fogo *et al.*, 1992) including ischaemia-induced acute renal failure. BQ123 (Mino *et al.*, 1992) and the non-peptide non-selective receptor antagonist RO462005 (Clozel *et al.*, 1993) were able to prevent experimentally induced vasospasm of the rat renal artery which develops following prolonged renal hypoperfusion.

In man, plasma levels of ET-like immunoreactivity are increased in patients with acute and chronic renal failure (Tomita *et al.*, 1989; Totsune, *et al.*, 1989; Koyama *et al.*, 1989; Davenport *et al.*, 1990; Suzuki *et al.*, 1990; Stockenhuber *et al.*, 1992). While the kidney is thought to be partly responsible for excreting ET in man, evidence is emerging that ET is also synthesized within the kidney, suggesting a role as an endogenously generated locally-acting renal peptide. Messenger RNA encoding ET-1, ET-2 and ET-3 has been detected in medulla and cortex by reverse-transcriptase polymerase chain reaction assays from histologically normal human kidneys whereas ET-1 was the predominant peptide detected by reverse-phase high performance liquid chromatography (Karet & Davenport, 1993).

As expected from animal studies, ET-1 is a potent vasoconstrictor in human kidney (Maggi *et al.*, 1990; Weitzberg *et al.*, 1991; Sorensen *et al.*, 1994). For example, constant intravenous infusion of ET-1 (0.4 pmol kg^{-1} min^{-1}) into healthy human volunteers decreased renal plasma flow by about 30% and increased vascular resistance by 50%

[1] Author for correspondence.

(Gasic et al., 1992). However, in contrast to rat renal vessels, ET-1 induced vasoconstriction in human isolated renal arteries and veins is mediated mainly via the ET_A sub-type (Maguire et al., 1994a). High affinity ET receptors have been detected in human kidney (Davenport et al., 1989a,b; Grone et al., 1990; Waeber et al., 1990; Rebibou et al, 1992; Nambi et al., 1992, Karet et al., 1993). We have previously localized the anatomical distribution of binding sites for [^{125}I]-ET-1, [^{125}I]-ET-2, [^{125}I]-ET-3 and [^{125}I]-sarafotoxin S6B in kidney (Davenport et al., 1989a,b; 1991) and established that there was a different distribution in human renal tissue compared with animals. Sub-type selective ligands competed for the binding of [^{125}I]-ET-1 in a biphasic manner with a ratio of about 70% ET_B: 30% ET_A in both cortex and medulla (Karet et al., 1993). The ET_B-selective radioligand, [^{125}I]-BQ3020 has been used to characterize the ET_B sub-type in human tissue (Molenaar et al., 1992; Davenport et al., 1993) including kidney (Karet et al., 1993). An [^{125}I]-ET_A selective ligand has not until now been characterized in renal tissue. The linear tetrapeptide radioligand, [^{125}I]-PD151242, has been shown to bind with high, nanomolar affinity and selectivity to ET_A receptors in the human vasculature which contains predominantly the ET_A sub-type (Davenport et al., 1994a). The unlabelled compound was a competitive antagonist, causing a parallel rightward shift of the ET-1 concentration-response curve in isolated epicardial coronary arteries. Our aim was to characterize the [^{125}I]-PD151242 in this ET_B rich tissue and compare the ability of ET ligands to inhibit binding of the iodinated peptide since pharmacological studies have suggested the presence of atypical ET_A receptors in animal tissues such as rat kidney (Pierre & Clarke, 1994). We used autoradiography to compare the distribution of ET_A and ET_B receptors and reverse-transcriptase polymerase chain reaction assays were used to confirm the identity of ET_A and ET_B mRNA in this tissue. A preliminary account of this work has been presented at the British Pharmacological Society (Davenport et al., 1994b).

Methods

Renal tissue

Normal renal tissue was obtained at the time of operation from adult males (age range 32–74 years) undergoing nephrectomy for non-obstructing tumours. Tissue was snap frozen in liquid nitrogen and stored at −70°C until use. In each case, the kidney was of normal size and biochemical function, with no evidence of hydronephrosis. Sections (10 μm thick) from the opposite pole to the tumour site were cut on a cryostat microtome and mounted onto gelatin-coated microscope slides. Light microscopy of haematoxylin and eosin stained sections confirmed the presence of normal glomerular and tubular structures.

Receptor binding assays

For saturation experiments, tissue sections were pre-incubated for 15 min in HEPES buffer as previously described (Davenport et al., 1994a). Briefly, sections were then incubated with increasing concentrations (8 pM–8 nM) of [^{125}I]-PD151242 in incubation buffer for 2 h at 23°C. Non-specific binding was defined using 1 μM unlabelled PD151242. Sections were rinsed in Tris-HCl buffer (0.05 M, pH 7.4) at 4°C (3 × 5 min) and the amount of radioactivity measured in a gamma counter. In competition assays, sections were incubated with 100 pM [^{125}I]-PD151242 and increasing concentrations of unlabelled compounds (typically over the concentration range, 20 pM-100 μM). Non-specific binding was defined using 1 μM unlabelled PD151242.

The results of binding experiments were analysed with EBDA and LIGAND programmes as previously described (Molenaar et al., 1992; 1993; Davenport et al., 1994a). The presence of 1 or 2 sites was tested using the *F*-ratio test in LIGAND. The model adopted was that which provided the best fit ($P<0.05$).

Specificity of ligand

The ability of unlabelled isoforms of ET or sarafotoxin and unrelated peptides to compete for the binding of 0.1 nM [^{125}I]-PD151242 was measured under the assay conditions described above. The ability of 1 μM·BQ123, FR139317 and BQ3020 to compete for 0.1 nM [^{125}I]-PD151242 binding to coverslips containing confluent cultures of rat A10 aortic smooth muscle cells, was also carried out under conditions described above, except that at the end of the incubation period, coverslips were apposed to radiation-sensitive film (see below).

Autoradiography

Autoradiography was used to compare the distribution and density of ET_A and ET_B receptors. Kidney sections (a total of 12 from each of three individuals) were incubated in buffer containing either 0.1 nM [^{125}I]-ET-1 to visualize all ET receptors, [^{125}I]-PD151242 to visualize ET_A or [^{125}I]-BQ3020 to detect the ET_B sub-type. Non-specific binding was determined by incubating adjacent consecutive sections in the presence of 1 μM of the corresponding unlabelled peptides. Sections were exposed to radiation-sensitive film (Hyperfilm βmax) as previously described (Davenport et al., 1988).

Reverse phase high performance liquid chromatography

Reverse phase high performance liquid chromatography (r.p.-h.p.l.c.) was used to assess the stability of [^{125}I]-PD151242 under the receptor binding assay conditions. Binding assays were carried out as described above; 8 nM [^{125}I]-PD151242 was incubated with cryostat sections from three separate kidneys for 2 h at room temperature. A similar volume was also analysed that was not exposed to tissue. The samples were run on a reverse phase Vydac C18 column, (250 mm × 4.6 mm diameter). The gradient consisted of 100% water and 0.1% v/v trifluoroacetic acid at time 0 to 100% propan-1-ol and 0.1% TFA over 25 min with flow rate of 1 ml min^{-1}. The radioactive profile was measured by an on-line flow-through radioactivity monitor. The elution position of unlabelled PD-151242 was detected with a u.v. monitor.

Reverse-transcriptase polymerase chain reaction assays (RT-PCR)

Extraction of total RNA, cDNA synthesis and RT-PCR assays were carried out by previously described methods (O'Reilly et al., 1992, 1993a,b; Karet et al., 1994). Briefly, total RNA was extracted by a single step guanidinium isothiocyanate method. First strand cDNA was synthesized from 2.5 μg RNA using avian myoblastosis virus reverse transcriptase. Nested oligonucleotide primers were designed from published nucleotide sequences:

(A) ET_A, ET_B forward, external TATCACAGAAACTAA-AGTGCTATG (Bases 379–396)

(B) ET_A, ET_B reverse, external CAAGCAAGCAAGCAAC-GTAAGAGCA (Bases 1214–1198)

(C) ET_A forward, internal CCTTTTGATCACAATGAC-TTT (Bases 439–459)

(D) ET_A reverse, internal TTTGATGTGGCATTGAGCA-TACAG (Bases 737–714)

(E) ET_B forward, internal ACTGGCCATTTGGAGCTGA-GAT (Bases 497–519)

(F) ET_B reverse, internal CTGCATGCCACTTTTCTTTC-TCAA (Bases 924–901)

Briefly, nested PCR amplification was carried out using 1 μl cDNA template, 5 μl reaction buffer (100 nM Tris-HCl, pH 8.3 at 25°C, 500 mM KCl and 15 mM $MgCl_2$), 5 μl dNTPs

(2 mM), 5 µl of each of the appropriate oligonucleotide primer pairs (10 µM) and 2.5 u Taq DNA polymerase.

PCR products were separated by agarose gel electrophoresis and the bands stained with ethidium bromide. These previously cloned and sequenced PCR products show 100% homology with published sequences for ET_A or ET_B (O'Reilly *et al.*, 1992).

Drugs

PD151242,(N-[(hexahydro-1-azepinyl)carbonyl])L-Leu(1-Me)-D-Trp-D-Tyr (Davenport *et al.*, 1994a); FR139317, (N-[(hexahydro-1-azepinyl)carbonyl])L-Leu(1-Me)D-Trp-3(2-pyridyl)-D-Ala (Nirei *et al.*, 1993); BQ123, cyclo [D-Asp-L-Pro-D-Val-L-Leu-D-Trp-] (Ihara *et al.*, 1992) and BQ3020, [Ala^{11,15}]Ac-ET-1$_{(6-21)}$ (Molenaar *et al.*, 1992) were synthesized by solid phase t-Boc chemistry. Peptide concentration was determined by u.v. spectrophotometry. RO462005, 4-tert-butyl-N[6-(2-hydroxy-ethoxy)-5-(3-methoxy-phenoxy)-4-pyrimidinyl]-benzenesulphonamide) (Clozel *et al.*, 1993). [^{125}I]-PD151242,

Table 1 **A** Saturation binding experiments: dissociation constants (K_D), maximal density of receptors (B_{max}) and Hill coefficients (nH) for [^{125}I]-PD151242 binding to human kidney

n	K_D (nM)	B_{max} (fmol mg^{-1} protein)	*nH*
3	0.75 ± 0.07	48.4 ± 1.6	0.89 ± 0.07

B Competition binding experiments: comparison of ET_A, ET_B and non-selective ligands competing for the binding of [^{125}I]-PD151242 to human kidney

	n	K_D	B_{max} (fmol mg^{-1} protein)
ET_A			
BQ123	3	0.43 ± 0.10 nM	46.6 ± 7.9
FR139317	3	0.37 ± 0.06 nM	39.5 ± 6.5
ET_B			
BQ3020	3	> 10 µM	-
Non-selective			
RO462005	3	1.31 ± 1.38 µM	33.0 ± 9.7

Values are the mean ± s.e.mean of three individuals in **A** and **B**.

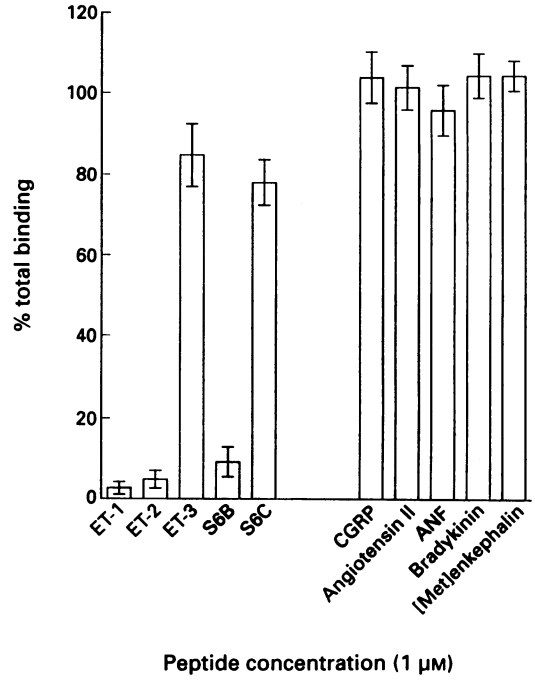


Figure 2 Inhibition of 0.1 nM [^{125}I]-PD151242 binding to slide mounted sections of renal tissue by isoforms of endothelin or sarafotoxin tested at concentrations of 1 µM. Non-selective peptides ET-1, ET-2 and S6B almost completely inhibited binding, whereas the ET_B-selective ET-3 or S6C competed for only 20% of the binding. Unrelated peptides, calcitonin gene-related peptide (CGRP), angiotensin II, atrial natriuretic factor (ANF), bradykinin and [Met]enkephalin did not compete. Each value represents the mean ± s.e.m. of three individuals.

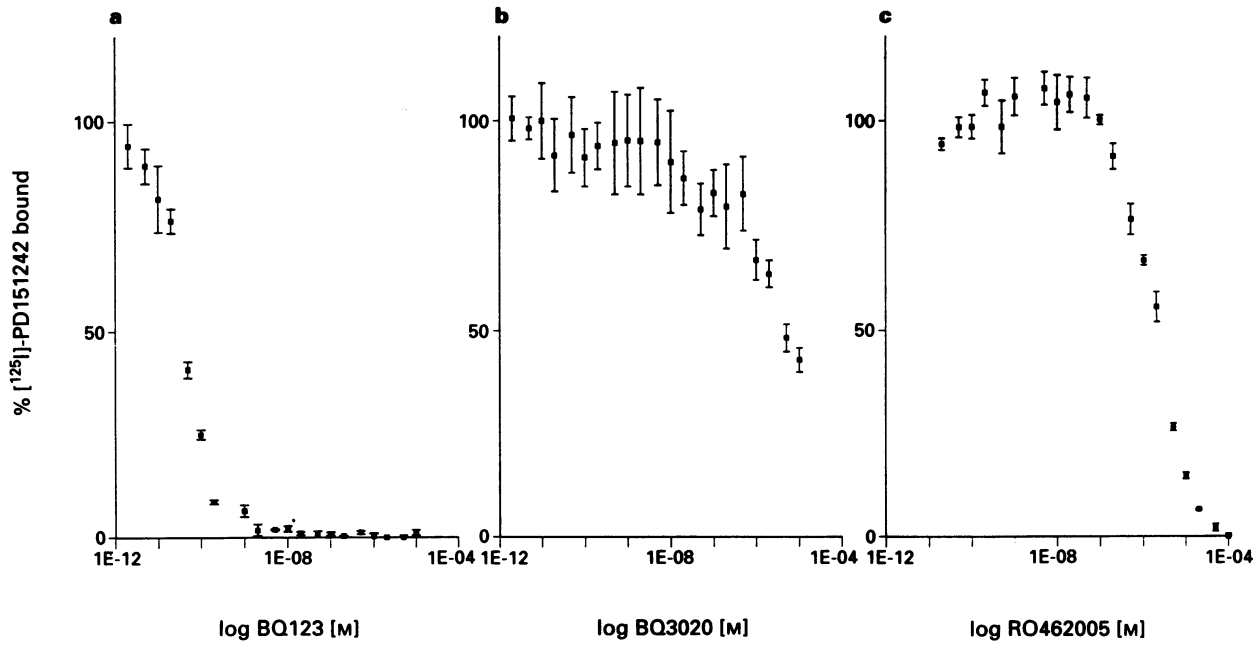


Figure 1 Graphs showing the inhibition of 0.1 nM [^{125}I]-PD151242 binding to slide mounted sections of renal tissue by (a) ET_A-selective BQ123; (b) ET_B-selective BQ3020 and (c) the non-peptide non-selective RO462005. In each case, competition curves were monophasic but BQ123 competed in the nM range whereas BQ3020 at the highest concentration tested reduced binding by only 50%. Each value represents the mean ± s.e.m. of three individuals.

[^{125}I]-ET-1, [^{125}I]-BQ3020 (Amersham International plc, Amersham, Bucks); unlabelled peptides were from the Peptide Institute (Osaka, Japan), Novabiochem (Nottingham) or Peninsula (St. Helens). Taq polymerase was from Perkin-Elmer Cetus (London), reverse-transcriptase from Anglian Biotech (Essex). H.p.l.c. reagents were from Rathburn (Livingstone, Scotland). All other reagents were from Sigma Chemical Co. (Poole, Dorset), BDH (Poole, Dorset) or Fisons (Loughborough, Leicester).

Results

In the kidney, saturation binding assays using [^{125}I]-PD151242 revealed a single population of high affinity ET

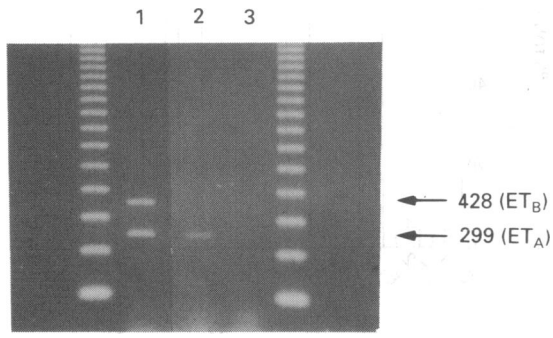


Figure 3 Agarose gel electrophoresis of RT-PCR products from a confluent culture of rat A10 aortic vascular smooth muscle cells shows the presence of PCR bands corresponding to the predicted size for ET_A (299 base pairs) but not ET_B (428 base pairs) mRNA (lane 2). Bands corresponding to the expected positions for ET_A and ET_B mRNA were detected in the positive control (human placenta, lane 1) but not in the negative control (lane 3) where cDNA template had been omitted. Markers are 100 base pair ladders.

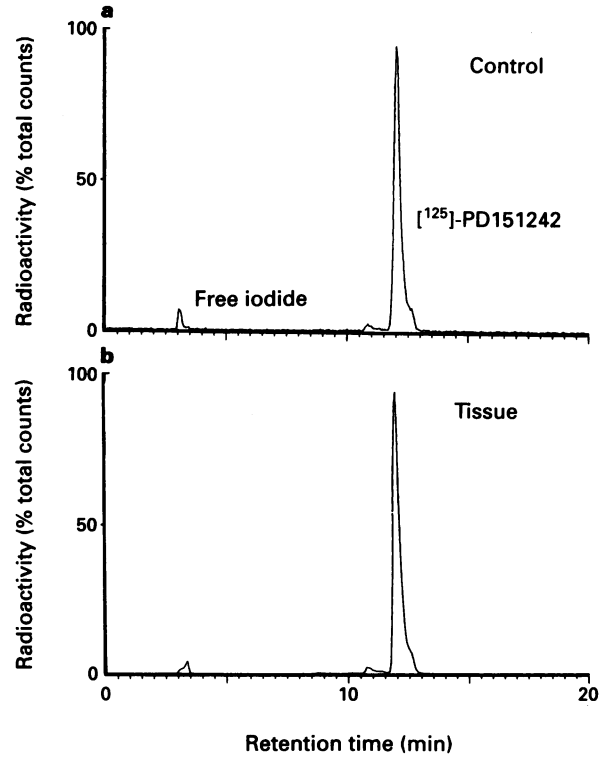


Figure 5 Reverse-phase high performance liquid chromatography analysis (r.p.-h.p.l.c.) of [^{125}I]-PD151242. An example of the radiochemical profile of [^{125}I]-PD151242 following incubation with 2 h at room temperature as in the assay buffer as described in the Methods in the absence (a) or presence (b) of tissue. More than 95% of the radioactivity eluted at the expected position for [^{125}I]-PD151242. A small peak (less than 5%) was detected at the position corresponding to free iodine. R.p.-h.p.l.c. analyses were carried out on three separate kidneys.

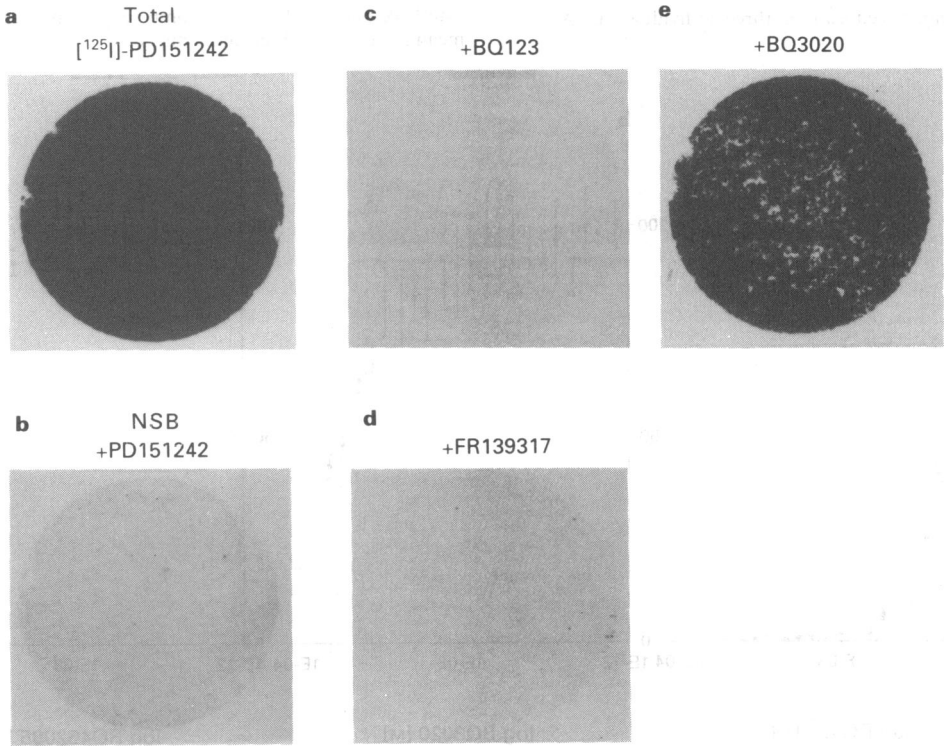


Figure 4 Examples of autoradiograms showing the total binding of 0.1 nM [^{125}I]-PD151242 to coverslips containing confluent cultures of rat A10 aortic vascular smooth muscle cells (a) and in the presence of 1 μM unlabelled PD151242 to measure non-specific binding (b). One μM of BQ123 (c) and FR139317 (d) reduced binding to non-specific levels whereas BQ3020 (e) did not compete.

receptors (Table 1), over the concentration-range tested. Hill slopes were close to unity and a one site fit was preferred to a two site model. In competition binding assays, the ET_A selective ligands BQ123 (Figure 1a) and FR139317 competed for [^{125}I]-PD151242 binding in a monophasic manner with subnanomolar affinity (Table 1). A one site fit was preferred to a two site model. In contrast, the ET_B selective ligand BQ3020 at the highest concentration tested (10 μM), competed for only 50% of the binding and K_D value could not be calculated (Figure 1b). The non-peptide but non-selective ligand RO462005 also competed for [^{125}I]-PD151242 binding in human kidney but only in the μM range (Figure 1c, Table 1).

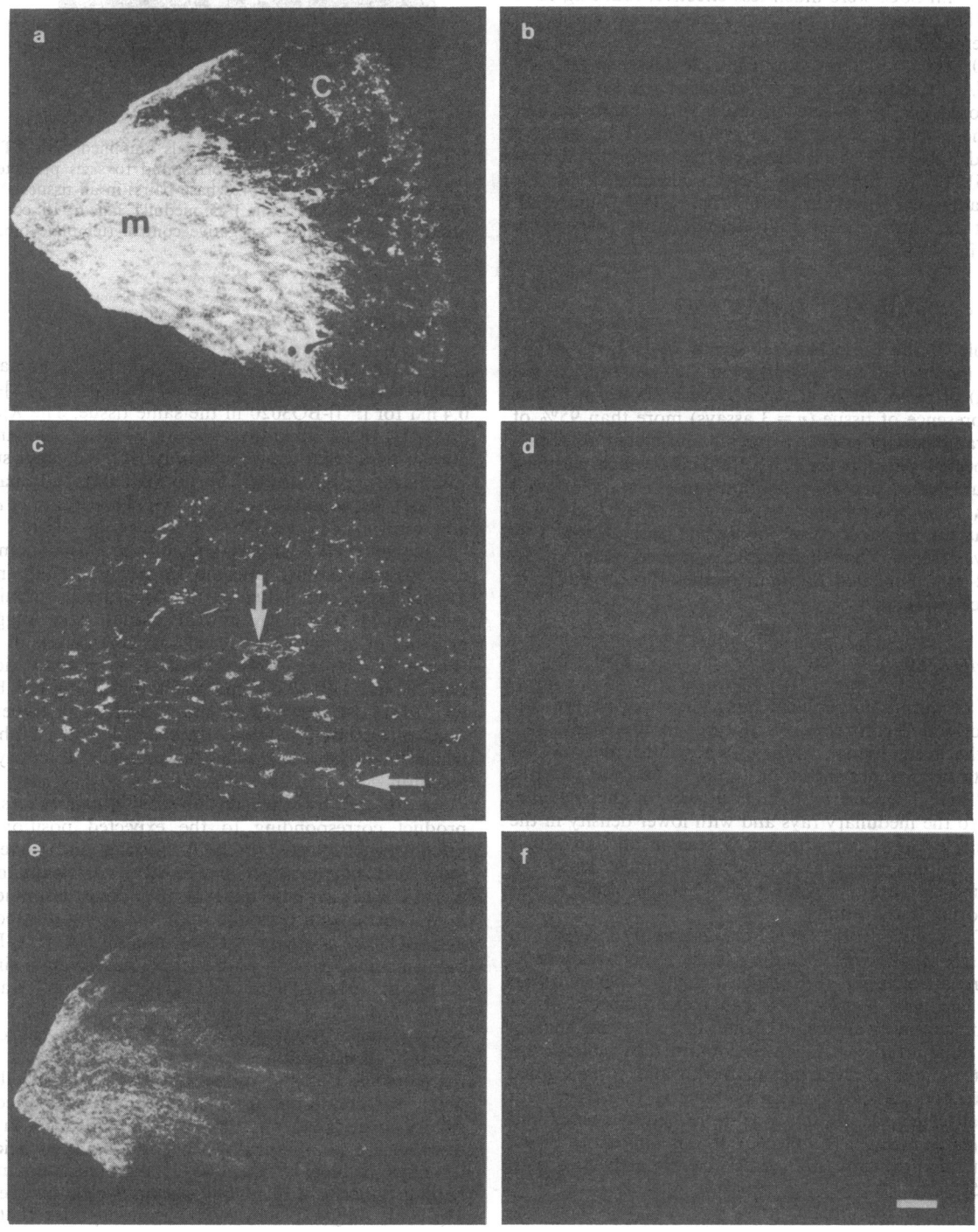


Figure 6 Autoradiographical localisation of ET receptors in consecutive sections from the same human kidney following incubation with iodinated ligands as described in Methods. Sections were apposed to the same radiation-sensitive film and therefore were exposed and developed identically. (a) Total [^{125}I]-ET-1 binding showing the distribution of all ET receptors. High densities of receptors are present in the medulla (m) especially on medullary rays, with lower densities in the cortex (c). [^{125}I]-ET-1 labelled blood vessels in both cortex and medulla and epithelial structures. (b) ET_A receptors localized using [^{125}I]-PD151242 were mainly present on intra-renal blood vessels including the arcuate arteries and adjacent veins (indicated by arrows). (c) ET_B receptors localized with [^{125}I]-BQ3020. Binding was more heterogeneous and concentrated in medulla to non-vascular structures. It was difficult to detect binding of this ligand to renal vessels clearly delineated with [^{125}I]-PD151242. Non-specific binding determined by incubating adjacent sections in the presence of 1 μM of unlabelled ET-1 (b), PD151242 (d), or BQ3020 (f). (scale bar = 2 mm).

Specificity

To confirm further the specificity of [^{125}I]-PD151242 binding, 0.1 nM of the iodinated peptide was incubated with 1 μM of unlabelled ET and sarafotoxin peptides (Figure 2). ET and sarafotoxin peptides that were not selective for either subtype (ET-2 and sarafotoxin S6B) reduced [^{125}I]-PD151242 binding to non-specific levels measured by incubating adjacent sections with 1 μM ET-1. ET_B-selective peptides, ET-3 and sarafotoxin S6C, were much less effective, reducing total [^{125}I]-PD151242 binding by less than 20% whereas unrelated, non-ET peptides did not compete.

Rat A10 aortic vascular smooth muscle cells express only ET_A mRNA; PCR products of the expected size for the ET_B receptor could not be detected (Figure 3). In confluent cultures of these cells growing on coverslips, the ET_A-selective BQ123 and FR139317 (1 μM) reduced the binding of 0.1 nM [^{125}I]-PD151242 to non-specific levels determined by incubating adjacent coverslips with 1 μM ET-1 (Figure 4). BQ3020 at the same concentration did not cause a detectable reduction in binding.

R.p.-h.p.l.c. analysis of [^{125}I]-PD151242

An example of the radiochemical profile of [^{125}I]-PD151242 following incubation for 2 h at room temperature in the absence (a) or presence (b) of renal tissue is shown in Figure 5. In the presence of tissue ($n = 3$ assays) more than 95% of the total radioactivity added to the column eluted at 12 min at the expected position for [^{125}I]-PD151242 which was just after the unlabelled peptide (retention time 11 min). A small peak (less than 5% of the total) eluted after 7 min was detected at the position corresponding to free iodine. This pattern was similar to the profile obtained when [^{125}I]-PD151242 was incubated at room temperature in buffer in the absence of tissue.

Autoradiography

Examples of autoradiographical images comparing the distribution of endothelin receptor sub-types in consecutive sections of the same human kidney, exposed to film for the same length of time, are shown in Figure 6. The non-selective ligand [^{125}I]-ET-1 bound with high density in the medulla, especially to the medullary rays and with lower density in the cortex (Figure 6a). This pattern was seen in all individuals examined. Binding to glomeruli was of a similar density to the surrounding cortex. [^{125}I]-ET-1 also labelled blood vessels in both cortex and medulla.

The ET_A-selective [^{125}I]-PD151242 was mainly localized to blood vessels (Figure 6c) including those in the medulla as well as arcuate arteries and adjacent veins at the corticomedullary junction. Vessels with a diameter down to about 0.2 mm could also be delineated which are of a size characteristic of renal arterioles. This was confirmed by comparison of the autoradiograms with haematoxylin and eosin stained sections. In contrast, the pattern of binding visualized with the ET_B-selective [^{125}I]-BQ3020 was more heterogeneous and concentrated in medulla (Figure 6e). It was difficult to detect binding of this ligand to renal vessels clearly delineated with [^{125}I]-PD151242.

Molecular biology

Agarose gels showing the presence of PCR products of the expected size corresponding to mRNA coding for the ET_A receptor (299 base pairs) and ET_B receptor (428 bases pairs) are shown in Figure 7. Message for both sub-types was detected in cortex and medulla in each of the five individuals. Similar bands were detected in the positive control (human placenta) but not in the negative control lane in which the template had been omitted.

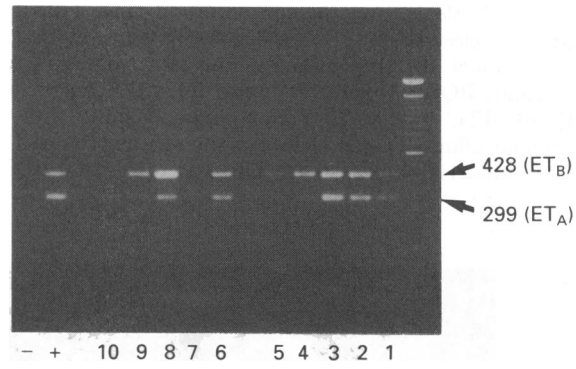


Figure 7 Agarose gel showing products of RT-PCR from renal cortex and medulla of 5 individuals amplified with ET_A and ET_B specific primers. The bands correspond to sizes predicted for ET_A (299 base pairs) and ET_B (428 base pairs) in all tissues. Markers are 100 base pair ladders. Lane 1–5: medulla; lane 6–10: cortex; lane +: positive control; lane –: negative control (template omitted).

Discussion

[^{125}I]-PD151242 binds with high affinity to human kidney. This compares with K_D values of 0.2 nM for [^{125}I]-ET-1 and 0.4 nM for [^{125}I]-BQ3020 in the same tissue. The K_D value for [^{125}I]-PD151242 in kidney was in a range similar to other human tissue that contains mainly ET_A receptors such as the vasculature and heart: aorta (0.8 nM), coronary artery (0.5 nM), pulmonary artery (1.8 nM, Davenport *et al.*, 1994a) and ventricle (1.1 nM Peter & Davenport, 1994).

Unlabelled ET_A- or ET_B- selective ligands all competed in a monophasic manner but the former with high nanomolar affinity and the latter with micromolar affinity. Pharmacological studies in animal tissues have suggested the presence of atypical ET_A receptors, for example in rat kidney (Pierre & Clarke, 1994). However, in human kidney both BQ123 and FR139317 competed for all of the binding of [^{125}I]-PD151242 to ET_A receptors and using these combinations of ligands, there was no evidence for a biphasic curve which might have suggested the presence of an atypical ET_A receptor.

As expected from the ligand binding studies, a single PCR product corresponding to the expected position for ET_A mRNA was detected in both medulla and cortex of each individual examined. A single band corresponding to ET_B mRNA was also detectable in all kidneys examined. This is in agreement with previous studies showing that both BQ123 and BQ3020 compete for the binding of [^{125}I]-ET-1 in a biphasic manner, with both compounds giving a similar ratio of about 70% ET_B to 30% ET_A receptors (Karet *et al.*, 1993).

As a linear tetrapeptide, [^{125}I]-PD151242 has one of the shortest amino-acid sequences for a radioligand. However, there was no evidence for metabolism of the labelled peptide under the conditions used in binding assays. Reduced sensitivity to peptides might be expected since the Trp and Tyr residues are non-naturally occurring D-amino acids, the N-terminus is blocked and the C-terminus is iodinated. The peptide appears to be highly specific for the ET_A receptor. As expected, only ET and sarafotoxin peptides that are non-selective for the two sub-types were able to abolish binding of [^{125}I]-PD151242 to renal tissue. Unrelated peptides had no effect on binding.

Autoradiography demonstrated that ET_A receptors visualized with [^{125}I]-PD151242 were mainly localized to the vasculature with intra-renal resistance vessels down to a diameter of about 200 μm being clearly delineated. ET_B binding to vessels was difficult to detect and was most dense on non-vascular structures particularly the tubules and collecting ducts. This is in agreement with previous results suggesting

arterioles supplying the glomerulus expressed mainly the ET_A sub-type (Karet *et al.*, 1993). Similar results have been obtained with cross sections of large renal arteries (these were not present in the samples of kidney used in this study) which also expressed a majority of ET_A receptors (Maguire *et al.*, 1994a). This was confirmed in functional studies; ET-1 potently constricted renal arteries and veins with EC_{50} values of 4 and 1 nM respectively. A response to the ET_B agonist derived from snake venom, sarafotoxin S6C, was obtained in some individuals but the endogenous ligand, ET-3, showed little or no response (Maguire *et al.*, 1994a). In large renal vessels, ET-1-induced vasoconstriction is mediated by ET_A receptors and similar results have been obtained in all other human isolated vessels. (Maguire & Davenport, 1993). The results provide further evidence in support of our hypothesis (Davenport & Maguire, 1994) that unlike some animal species, ET-1 induced vasoconstriction is mediated by the ET_A sub-type: an ET_A selective antagonist is required to produce beneficial vasodilatation in diseases associated with over-expression of ET or its receptors.

At present, orally active and therefore potentially therapeutic antagonists available, such as RO462005 (Clozel *et al.*, 1993), are not selective for either sub-type.

Though these agents block the vasoconstrictor action of ET-1 which in human isolated vessels is mainly via the ET_A receptor (Maguire *et al.*, 1994b), the differential distribution of ET_A and ET_B in human kidney strongly suggests they have different functions. For example, the peptide may affect sodium balance in man via the non-vascular ET_B sub-type and this could be exploited by the development of sub-type-selective antagonists.

We thank the surgeons and theatre staff of Addenbrookes and Hinchingbrooke Hospitals for their co-operation in obtaining tissue and Dr A.M. Doherty, Parke-Davis Pharmaceutical Division, Ann Arbor, Michigan, U.S.A. for synthesizing FR139317 and RO462005. Supported by grants from the British Heart Foundation, Royal Society, BBSRC, Isaac Newton Trust and Wellcome Trust (S.L.H.). F.E.K. is an NKRF Training Fellow.

References

BATTISTINI, B., ALLCOCK, G.H., WARNER, T.D. & VANE, J.R. (1993). ET_A and ET_B receptors mediate the release of eicosanoids from the rat kidney induced by endothelin/sarafotoxin peptides. *Br. J. Pharmacol.*, **110**, 46P.

BENIGNI, A., ZOJA, C., CORNA, D., ORISIO, S., LONGARETTI, L., BERTANI, T. & REMUZZI, G. (1993). A specific endothelin subtype A receptor antagonist protects against injury in renal disease progression. *Kidney Int.*, **44**, 440–445.

BIGAUD, M. & PELTON, J.T. (1992). Discrimination between ET_A- and ET_B- receptor mediated effects of endothelin-1 and [$Ala^{1,3,11,15}$]endothelin-1 by BQ123 in the anaesthetised rat. *Br. J. Pharmacol.*, **107**, 912–917.

CIRINO, M., MOTZ, C., MAW, J., FORDHUTCHINSON, A.W. & YANO, M. (1992). BQ-153, a novel endothelin (ET)(A) antagonist, attenuates the renal vascular effects of endothelin-1. *J. Pharm. Pharmacol.*, **44**, 782–785.

CLOZEL, M., BREU, V., BURRL, K., CASSAL, J.-M., FISCHLI, W., GRAY, G.A., HIRTH, G., LOFFLER, B.-M., MULLER, M., NEIDHART, N. & RAMUZ, H. (1993). Pathophysiological role of endothelin revealled by the first orally active endothelin receptor antagonist. *Nature*, **365**, 759–761.

CLOZEL, M., GRAY, G.A., BREU, V., LÖFFLER, B.-M. & OSTERWALDER, R. (1992). The endothelin ET_B receptor mediates both vasodilation and vasoconstriction *in vivo*. *Biochem. Biophys. Res. Commun.*, **186**, 867–873.

CRISTOL, J.-P., WARNER, T.D., THIEMERMANN, C. & VANE, J.R. (1993). Mediation via different receptors of the vasoconstrictor effects of endothelins and sarafotoxins in the systemic circulation and renal vasculature of the anaesthetised rat. *Br. J. Pharmacol.*, **108**, 776–779.

DAVENPORT, A.P., ASHBY, M.J., EASTON, P., ELLA, S., BEDFORD, J., DICKERSON, C., NUNEZ, D.J., CAPPER, S.J. & BROWN, M.J. (1990). A sensitive radioimmunoassay measuring endothelin-like immunoreactivity in human plasma: comparison of levels in essential hypertension and normotensive controls. *Clin. Sci.*, **78**, 261–264.

DAVENPORT, A.P., BERESFORD, I.J.M., HALL, M.D., HILL, R. G. & HUGHES, J. (1988). Quantitative autoradiography in *Molecular Neuroanatomy*, Vol. III, pp. 121–145 Ed. van Leeuwen, F.W., Buijs, R.M., Pool, C.W. Pach, O. Amsterdam: Elsevier

DAVENPORT, A.P., KUC, R.E., FITZGERALD, F., MAGUIRE, J. J., BERRYMAN, K. & DOHERTY, A.M. (1994a). [^{125}I]-PD151242: a selective radioligand for human ET_A receptors. *Br. J. Pharmacol.*, **111**, 4–6.

DAVENPORT, A.P., KUC, R.E., HOSKINS, S.L. & KARET, F.E. (1994b). [^{125}I]-PD151242 is a selective endothelin ET_A receptors in human kidney and localises to the vasculature. *Br. J. Pharmacol.*, **112**, 554P.

DAVENPORT, A.P. & MAGUIRE, J.J. (1994). Is endothelin-induced vasoconstriction mediated only by ET_A receptors in humans? *Trends Pharmacol. Sci.*, **15**, 9–11.

DAVENPORT, A.P., MORTON, A.J. & BROWN, M.J. (1991). Localisation of endothelin (1–3), mouse VIC and sarafotoxin S6b binding sites in mammalian heart and kidney. *J. Cardiovasc. Pharmacol.*, **17,7**, S152–S155.

DAVENPORT, A.P., NUNEZ, D.J., & BROWN, M.J. (1989a). Quantitative autoradiography reveals binding sites for [125] endothelin-1 kidneys with a differential distribution among rat, pig and man. *Clin. Sci.*, **77**, 129–131.

DAVENPORT, A.P., NUNEZ, D.J., HALL, J.A., KAUMANN, A.J. & BROWN, M.J. (1989b). Autoradiographical localisation of binding sites for [125I] endothelin-1 in humans, pigs and rats: functional relevance in man. *J. Cardiovasc. Pharmacol.*, **13,5**, S166–170.

DAVENPORT, A.P., O'REILLY, G., MOLENAAR, P., MAGUIRE, J.J., KUC, R.E., SHARKEY, A., BACON, C.R. & FERRO, A. (1993). Human endothelin receptors characterised using reverse transcriptase-polymerase chain reaction, *in situ* hybridization and sub-type selective ligands BQ123 and BQ3020: evidence for expression of ET_B receptors in human vascular smooth muscle. *J. Cardiovasc. Pharmacol.*, **22(S8)**, 22–25.

DAVIS, L.S., LADOUCEUR, D.M., KEISER, J.A. & HALEEN, S.J. (1991). Relative vasodilator and vasoconstrictor activity of endothelin-1 (ET-1), endothelin-3 (ET-3) and sarafotoxin 6c (SFTX-6c) on regional arterial beds of the anaesthetized rat: relationship to ET_A and ET_B receptor agonist activity. *FASEB*, **6(4)**, 391.

FIRTH, J.D., RAINE, A.E.G., RATCLIFFE, P.J. & LEDINGHAM, J.G.G. (1988). Endothelin: an important factor in acute renal failure? *Lancet*, **8621**, 1179–1182.

FOGO, A., HELLINGS, S.E., INAGAMI, T. & KON, V. (1992). Endothelin receptor antagonism is protective in rats with cyclosporine A-induced nephrotoxicity. *Kidney Int.*, **42**, 770–774.

GARDINER, S.M., COMPTON, A.M. & BENNETT, T. (1989). Regional hemodynamic effects of endothelin-1 in conscious, unrestrained, Wistar rats. *J. Cardiovasc. Pharmacol.*, **13,5**, S202–204.

GARDINER, S.M., COMPTON, A.M. & BENNETT, T. (1990). Regional haemodynamic effects of endothelin-1 and endothelin-3 in conscious Long Evans and Brattleboro rats. *Br. J. Pharmacol.*, **99**, 107–112.

GARDINER, S.M., KEMP, P.A., MARCH, J.E., BENNETT, T., DAVENPORT, A.P. & EDVINSSON, L. (1994). Effects of an ET_1-receptor antagonist, FR139317 on regional haemodynamic responses to endothelin-1 and [$Ala^{11,15}$] Ac-endothelin-1(6–21) in conscious rats. *Br. J. Pharmacol.*, **112**, 477–486.

GASIC, S., WAGNER, O.F., VIERHAPPER, H., NOWOTNY, P. & WALDHAUSL, W. (1992). Regional hemodynamic effects and clearance of endothelin-1 in humans: Renal and peripheral tissues may contribute to the overall disposal of the peptide. *J. Cardiovac. Pharmacol.*, **19**, 176–180.

GRONE, H.J., LAUE, A., & FUCHS, E. (1990). Localization and quantification of (1251)-endothelin binding sites in human fetal and adult kidneys -Relevance to renal ontogeny and pathophysiology. *Klinische Wochenschrift*, **68**, 758–767.

IHARA, M., NOGUCHI, K., SAEKI, T., FUKURODA, T., TSUCHIDA, S., KIMURA, S., FUKAMI, T., ISHIKAWA, K., NISHIKIBE, M. & YANO, M. (1992). Biological profiles of highly potent novel endothelin antagonists selective for the ETA receptor. *Life Sci.*, **50**, 247–255.

KARET, F.E. & DAVENPORT, A.P. (1993). Human kidney: endothelin isoforms revealed by HPLC with radioimmunoassay, and receptor sub-types detected using ligands BQ123 and BQ3020. *J. Cardiovas. Pharmacol.*, **22(S8)**, 29–33.

KARET, F.E. & DAVENPORT, A.P. (1994). Endothelin and the human kidney: a potential target for new drugs. *Nephrol. Dialysis Transpl.*, **9**, 465–468.

KARET, F.E., CHARNOCK-JONES, D.S.C., HARRISON-WOOLRYCH, M.R., O'REILLY, G., DAVENPORT, A.P. & SMITH, S.K. (1994). Validation of mRNA quantification using a novel fluorescent nested reverse transcriptase polymerase chain reaction. *Anal. Biochem.*, **220**, 384–390.

KARET, F.E., KUC, R.E. & DAVENPORT, A.P. (1993). Novel ligands BQ123 and BQ3020 characterize endothelin receptor subtypes ET_A and ET_B in human kidney. *Kidney Int.*, **44**, 36–42.

KOYAMA, H., NISHZAWA, Y., MORII, H., TABATA, T., INOUE, T. & YAMAJI, T. (1989). Plasma endothelin levels in patients with uraemia. *Lancet*, **1**, 991–992.

MAGGI, C.A., GIULIANI, S., PATACCHINI, R., BARBANTI, G., TURINI, D. & MELI, A. (1990). Contractile responses on the human urinary bladder, renal pelvis and renal artery to endothelins and sarafotoxin S6b. *Gen. Pharmacol.*, **21**, 247–249.

MAGUIRE, J.J. & DAVENPORT, A.P. (1993). Endothelin-induced vasoconstriction in human isolated vasculature is mediated predominantly via activation of ET_A receptors. *Br. J. Pharmacol.*, **110**, 47P.

MAGUIRE, J.J., KUC, R.E., O'REILLY, G. & DAVENPORT, A.P. (1994a). Vasoconstrictor endothelin receptors characterised in human renal artery and vein *in vitro*. *Br. J. Pharmacol.*, **113**, 49–54.

MAGUIRE, J.J., KUC, R.E., O'REILLY, G. & DAVENPORT, A.P. (1994b). Potency of the novel orally active antagonist Ro46–2005 for endothelin receptors in human vascular smooth muscle. *Br. J. Pharmacol.*, **112**, 552P.

MINO, N., KOBAYASHI, M., KANAJIMA, A., AMANO, H., SHIMAMOTO, K., ISHIKAWA, K., WATANABE, K., NISHIKIBE, M., YANO, M., & IKEMOTO, F. (1992). Protective effect of a selective endothelin receptor antagonist, BQ-123, in ischemic acute renal failure in rats. *Eur. J. Pharmacol.*, **221**, 77–83.

MOLENAAR, P., KUC, R.E. & DAVENPORT, A.P. (1992). Characterization of two new ET_B selective radioligands, [^{125}I]-BQ3020 and [^{125}I]-[Ala^{1,3,11,15}]ET-1 in human heart. *Br. J. Pharmacol.*, **107**, 637–639.

MOLENAAR, P., O'REILLY, G., SHARKEY, A., KUC, R.E., HARDING, D.P., PLUMPTON, P., GRESHAM, G.A. & DAVENPORT, A.P. (1993). Characterization and localization of endothelin receptor sub-types in the human atrioventricular conducting system and myocardium. *Circ. Res.*, **72**, 526–538.

NAMBI, P., PULLEN, M., WU, H.L., AIYAR, N., OHLSTEIN, E.H. & EDWARDS, R.M. (1992). Identification of endothelin receptor subtypes in human renal cortex and medulla using subtype-selective ligands. *Endocrinol.*, **131**, 1081–1086.

NIREI, H., HAMADA, K., SHOUBO, M., SOGABE, K., NOTSU, Y. & ONO, T. (1993). An endothelin ET(A) receptor antagonist, FR 139317, ameliorates cerebral vasospasm in dogs. *Life Sci.*, **23**, 1869–1874.

O'REILLY, G., CHARNOCK-JONES, D.S., CAMERON, I.T., SMITH, S.K. & DAVENPORT, A.P. (1993a). Endothelin-2 mRNA splice variants detected by RT-PCR in cultured human vascular smooth muscle and endothelial cells. *J. Cardiovasc. Pharmacol.*, **22(S8)**, 18–21.

O'REILLY, G., CHARNOCK-JONES, D.S., DAVENPORT, A.P., CAMERON, I.T. & SMITH, S.K. (1992). Presence of mRNA for endothelin-1, endothelin-2, and endothelin-3 in human endometrium, and a change in the ratio of ET_A and ET_B receptor subtype across the menstrual cycle. *J. Clin. Endocrinol. Metab.*, **75**, 1545–1549.

O'REILLY, G., CHARNOCK-JONES, D.S., MORRISON, J.J., CAMERON, I.T., DAVENPORT, A.P. & SMITH, S.K. (1993b). Alternatively spliced mRNAs for human endothelin-2 and their tissue distribution. *Biochem. Biophys. Res. Commun.*, **193**, 834–840.

PETER, M.G. & DAVENPORT, A.P. (1994). [^{125}I]-PD151242 as an endothelin ET_A selective radioligand in the human, rat and porcine heart. *Br. J. Pharmacol.*, **112**, 494P.

PIERRE, L. & CLARK, K.L. (1994). Charactertistics of endothelin receptors in rat main branch renal artery. *Br. J. Pharmacol.*, **112**, 163P.

POLLOCK, D.M. & OPGENORTH, J. (1993). Evidence for endothelin-induced renal vasoconstriction independent of ET_A receptor activation. *Am. J. Physiol.*, **264**, R222–R226.

POLLOCK, D.M. & OPGENORTH, J. (1994). ET_A receptor-mediated responses to endothelin-1 and big endothelin-1 in the rat kidney. *Br. J. Pharmacol.*, **111**, 729–732.

REBIBOU, J., H.E., C., DELARUE, F., PERALDI, M., ADIDA, C., RONDEAU, E. & SRAER, J. (1992). Functional ET-1 receptors on human glomerular podocytes and mesangial cells. *Nephrol. Dial. Transplant.*, **7**, 288–292.

SIMONSON, M.S. (1993). Endothelins: Multifunctional renal peptides. *Physiol. Rev.*, **73**, 375–412.

SORENSEN, S.S., MADSEN, J.K. & PEDERSEN, E.B. (1994). Systemic and renal effect of intravenous infusion of endothelin-1 in healthy human volunteers. *Am. J. Physiol.*, **266**, F411–F418.

STOCKENHUBER, F., GOTTSAUNER-WOLF, M., MAROSI, L., LIEBISCH, B., KURZ, R.W. & BLACKE, P. (1992). Plasma levels of endothelin in chronic renal failure and after renal transplantation: impact on hypertension and cyclosporine A-associated nephrotoxicity. *Clin. Sci.*, **82**, 255–258.

SUZUKI, N., MATSUMOTO, H., MIYAUCHI, T., GOTO, K., MASAKI, T., TSUDA, M. & FUJINO, M. (1990). Endothelin-3 concentration in human plasma: the increased concentrations in patients undergoing haemodialysis. *Biochem. Biophys. Res. Commun.*, **169**, 809–815.

TOMITA, K., UJIIE, K., NAKANISHI, T., TOMITA, S., MATSUDA, O., ANDO, K., SHICHIRI, M., HIRATA, Y. & MARUMO, F. (1989). Plasma endothelin levels in patients with acute renal failure. *New Engl. J. Med.*, **324**, 1127.

TOTSUNE, K., MOURI, T., TAKAHASHI, K., OHNEDA, M., SONE, M., SAITO, T. & YOSHINAGA, K. (1989). Detection of immunoreactive endothelin in plasma of haemodialysis patients. *FEBS Lett.*, **249**, 239–242.

WAEBER, C., HOYER, D. & PALACIOS, J.M. (1990). Similar distribution of (125I)sarafotoxin-6b and (125I)endothelin-1,-2,-3 binding sites in the human kidney. *Eur. J. Pharmacol.*, **176**, 233–236.

WEITZBERG, E., AHLBORG, G. & LUNDBERG, J.M. (1991). Long-lasting vasconstriction and efficient regional extraction of endothelin-1 in human splanchnic and renal tissues. *Biochem. Biophys. Res. Commun.*, **180**, 1298–1303.

WELLINGS, R.P., CORDER, R., WARNER, T.D., CRISTOL, J.-P., THIEMERMANN, C. & VANE, J.R. (1994). Evidence from receptor antagonists for an important role for ET_B-mediated vasoconstrictor effects of endothelin-1 in the rat kidney. *Br. J. Pharmacol.*, **111**, 515–520.

(Received June 15, 1994
Revised August 17, 1994
Accepted August 23, 1994)

Br. J. Pharmacol. (1994), **113**, 1311–1316 © Macmillan Press Ltd, 1994

The effects of β-adrenoceptor stimulation on adhesion of human natural killer cells to cultured endothelium

[1]Robert J. Benschop, *Frans P. Nijkamp, †Rudy E. Ballieux & **Cobi J. Heijnen

[1]Department of Immunology, University Hospital, Utrecht, The Netherlands; *Department of Pharmacology, Faculty of Pharmacy, Utrecht University, Utrecht, The Netherlands; †Janus Jongbloed Research Centre, Psychoimmunophysiology section, Utrecht, The Netherlands and **Department of Immunology, University Hospital for Children and Youth 'Het Wilhelmina Kinderziekenhuis', Utrecht, The Netherlands

1 The circulation of natural killer (NK) cells *in vivo* is influenced by physical exercise, mental stress, and infusion of β-adrenoceptor agonists. We have previously presented *in vitro* data, showing that β_2-adrenoceptor agonists induce detachment of NK cells from endothelial cells (EC), supporting the hypothesis that NK cells can be recruited from the marginating pool in blood vessels.

2 Because NK cells as well as EC express β_2-adrenoceptors, the present study was conducted to investigate whether stimulation of the β-adrenoceptors on NK cells, EC or both cell types is required to induce detachment from EC.

3 Cells were pretreated (15 min) with a selective β_2-adrenoceptor antagonist, GR81706, at various concentrations. The duration of β-adrenoceptor blockade was tested by determining the adenosine 3',5'-cyclic monophosphate (cyclic AMP) production induced by terbutaline (a β_2-adrenoceptor specific agonist). This receptor-mediated response was effectively inhibited for at least 4 h, whereas the cyclic AMP production in response to forskolin (a direct activator of adenylate-cyclase) was not affected.

4 Functional adhesion assays were then performed to determine the role of β-adrenoceptors on the different cell types involved (NK and EC) in catecholamine-induced detachment. Peripheral blood mononuclear cells were allowed to adhere for 1 h to monolayers of unstimulated EC in the presence or absence of cyclic AMP inducing agents, and the percentage of NK cells in the adhering lymphocyte fraction was determined by flow cytometry.

5 Both adrenaline (10^{-5} M) and forskolin (10^{-5} M) caused detachment of NK cells from EC. After blockade of the β_2-adrenoceptors on NK cells by pretreatment with GR81706 (10^{-6} M), the effect of adrenaline on NK cells adhesion was pretented; after blockade of the β_2-adrenoceptors on EC, NK cell adhesion was still significantly reduced by adrenaline. In all cases, forskolin caused detachment of NK cells.

6 To establish further that stimulation of β-adrenoceptors on NK cells is sufficient to cause detachment, we showed that adrenaline also reduced adhesion of NK cells to monolayers of Chinese hamster ovary cells, which do not express β-adrenoceptors.

7 Together, these results show that stimulation of β_2-adrenoceptors on NK cells negatively influences their capacity to adhere to EC, and that β_2-adrenoceptors on EC play a negligible role in this phenomenon.

Keywords: Catecholamines; adhesion; natural killer cells; β-adrenoceptor blockade

Introduction

Mental stress and physical exercise cause a redistribution of natural killer (NK) cells in the human body (Landmann *et al.*, 1984; Kappel *et al.*, 1991; Naliboff *et al.*, 1991; Brosschot *et al.*, 1992; Schedlowski *et al.*, 1993b). For a limited period of time, the number and function of NK cells in the circulation is increased. Catecholamines are held responsible for this redistribution, since similar alterations are observed after infusion of β-adrenoceptor agonists (Crary *et al.*, 1983; van Tits *et al.*, 1990; Schedlowski *et al.*, 1993a). Moreover, both mental and physical stress are associated with increases in catecholamine levels (Dimsdale & Moss, 1980; Kappel *et al.*, 1991). β-Adrenoceptors are directly involved in this phenomenon, because administration of β-adrenoceptor antagonists prior to exercise or mental stress inhibits the redistribution of NK cells (Murray *et al.*, 1992; Benschop *et al.*, 1994).

In the body, leucocytes are equally distibuted in a circulating and a marginating pool and these two cell populations are in dynamic exchange with each other (Vejlens, 1938; Athens *et al.*, 1961; Peters *et al.*, 1985). The majority of NK cells reside in peripheral blood, spleen, and lung interstitium (Perussia *et al.*, 1983; Weissler *et al.*, 1987). To date, it is not known whether newly appearing NK cells in the circulation are recruited from one or several of these sites. Because infusion of β-adrenoceptor agonists in splenectomized patients also leads to an increase in the numbers of NK cells (van Tits *et al.*, 1990), we have to assume that NK cells can be recruited from the marginating pool into the circulating pool without the involvement of the spleen. Thus, these cells could either be recruited from specific sites in the lung (Hogg, 1987; Lien *et al.*, 1987) or from the marginal zone in blood vessels, where they are rolling along the vessel wall (Vejlens, 1938; Atherton & Born, 1972; Peters *et al.*, 1985), in close contact with the endothelial cells (EC). Several authors have suggested that catecholamines interfere with this leucocyte rolling (McCarthy & Dale, 1988; Lawrence & Springer, 1991; Ottaway & Husband, 1992), resulting in the observed increase in NK cell numbers in the circulation.

We recently reported *in vitro* evidence to support the latter hypothesis: adhering NK cells lose their preference for adhering to monolayers of EC after the addition of catecholamines (Benschop *et al.*, 1993). We also found that the catecholamine-induced detachment of NK cells from EC is

[1] Author for correspondence at: Hannover Medical School, Department of Clinical Immunology, Konstanty-Gutschow-Str. 8, 30625 Hannover, Germany.

mediated via β_2-adrenoceptors (Benschop *et al.*, 1993). However, since both NK cells as well as EC express β_2-adrenoceptors (Buonassisi & Venter, 1976; Maisel *et al.*, 1989; Ahmad *et al.*, 1990), the effect of catecholamines on adhesion of NK cells can be mediated by β_2-adrenoceptors on either one, or on both of these cell types. This issue is explored in the present paper, by analyzing the effect of pretreatment of NK cells and EC with a selective, long-acting β_2-adrenoceptor antagonist. In addition, the effect of adrenaline on NK cell adhesion to Chinese Hamster ovary (CHO) cells, that do not express β-adrenoceptors (Samama *et al.*, 1993), is studied.

Methods

Cells

Peripheral blood mononuclear cells (PBMC) were isolated from heparinized whole blood obtained by venepuncture from healthy adults and isolated as described by Benschop *et al.*, (1993). After isolation, cells were resuspended in RPMI 1640 culture medium (Gibco, U.K.) supplemented with penicillin (100 iu ml^{-1}), streptomycin (100 $\mu g\ ml^{-1}$), and L-glutamine (2 mM) and containing 1% heat-inactivated pooled human serum, and counted in a haemocytometer. Viability of the isolated cells always exceeded 95% as determined by trypan blue exclusion.

The EA-hy-926 cell line is a hybrid cell of human umbilical cord vein endothelial cells with the lung tumour cell line A549 (Edgell *et al.*, 1983) and was kindly provided by Dr C.-J. Edgell (North Carolina, U.S.A.). CHO-K1 cells were purchased from the American Type Culture Collection (U.S.A., Cat. No. CCL61). Both cell lines were routinely cultured in Dulbecco's Modified Eagle's Medium (DMEM, Gibco), supplemented with penicillin (100 iu ml^{-1}), streptomycin (100 $\mu g\ ml^{-1}$), 5×10^{-5} M β-mercaptoethanol, and 5% foetal calf serum (hereafter referred to as DMEM).

EC cultures

EC were isolated from human umbilical cord vein and cultured in fibronectin-coated 80 cm^2 tissue culture flasks (NUNC, Denmark) in culture medium supplemented with 15% heat-inactivated pooled human serum. Cell yield at confluency was 1.5 to 3×10^6 cells per tissue culture flask. For the adhesion assay, cells were detached with 0.25% trypsin and 0.01% EDTA at 37°C and transferred to 24 well tissue culture plates (NUNC) precoated with fibronectin. Cells were seeded at 20,000 cells per well and used in the fourth or fifth passage.

Adhesion assay

Adhesion of NK cells to EC was measured by means of flow cytometry, as previously described (Benschop *et al.*, 1992; 1993). Confluent monolayers of unstimulated EC in 24-well plates were rinsed twice with PBS before adding 1 ml of PBMC (5×10^5 cells per well). Cells were allowed to adhere for 1 h (37°C, 5% CO_2). Non-adhering cells were removed by carefully rinsing the wells with PBS. After the third and final wash, 250 µl of trypsin/EDTA solution was added to each well to obtain a single cell suspension containing EC and PBMC. After 2 min of incubation (37°C, 5% CO_2) plates were put on ice and 50 µl of foetal calf serum (FCS) was added. The cells were washed in PBS, containing 0.1% NaN_3 and 0.5% BSA and stained with mAb for phenotypic analysis of the adhering cell population by flow cytometry. As previously shown, scatter properties can be used to distinguish lymphocytes from monocytes and EC (Benschop *et al.*, 1992), and the percentage of cells positive for NK cells markers (CD16 and CD56) in the lymphocyte population was calculated. Specific NK cell adhesion (and changes therein) was detected by comparing the percentage of NK cells in the adhering fractions with the percentage in PBMC prior to adhesion (i.e. 100% NK cell adhesion is the difference between the percentage of NK cells in the adhering lymphocyte fraction and the percentage of NK cells in PBMC). NK cells adhere with preference to EC, as indicated by a higher percentage of NK cells in the adhering lymphocyte fractions as compared to the percentage in PBMC (Bender *et al.*, 1987; Benschop *et al.*, 1993). This specific NK cell adhesion was manipulated by adding the various reagents to the wells during the adhesion assay, and all tests were performed in triplicate. Adhesion of PBMC to monolayers of CHO cells was performed similarly, but more PBMC were added per well (10^6).

Determination of β-adrenoceptor function and effectiveness of blockade

β_2-Adrenoceptor function was tested by inducing cyclic AMP in EA-hy-926 or CHO cells. In general, monolayers of cells were detached with trypsin/EDTA, resuspended in cold culture medium, and put on ice. Next, cells were incubated with either medium, forskolin (10^{-5} M), or a β-adrenoceptor agonist (10^{-5} M), at 37°C for 5 min. The reaction was terminated by freezing the samples instantly in liquid nitrogen. Samples were subsequently stored at − 80°C. Before determination of cyclic AMP levels, samples were heated for 5 min. A commercial radioimmunoassay (RIA) was used to assess cyclic AMP concentration (Amersham, U.K.) and the concentration was expressed as pmol cyclic AMP per 10^6 cells.

Efficiency of β-adrenoceptor blockade was tested by incubating monolayers of EA-hy-926 cells with GR81706 (various concentrations) or nadolol (10^{-5} M) in DMEM for 15 min (37°C, 5% CO_2). Next, the monolayers were washed three times with PBS, thus removing excessive β-adrenoceptor antagonist. Receptor function was assessed at once ($t = 0$) or DMEM was added and the cells were put back in the incubator for the time indicated in the text, before testing receptor function.

Materials

The following reagents were used: adrenaline (Brocacef, The Netherlands), terbutaline (β_2-selective adrenoceptor agonist; Astra, The Netherlands), nadolol (non-specific β-adrenoceptor antagonist), and forskolin (both Sigma, U.S.A.). A new, long-acting β_2-adrenoceptor blocking drug, GR81706 (1-[(1-naphthalenyl)oxy]-3-[[6-[2-(2-pyridinyl)ethoxy]hexyl]amino]-2-propanol hydrochloride, (Coleman *et al.*, 1994)), was manufactured and generously provided by Glaxo (U.K.). For the identification of NK cells, a combination of directly conjugated mAb directed against CD16 (Leu-11a) and CD56 (Leu-19) was used (Becton-Dickinson, U.S.A.). Fibronectin was a gift from Dr Ph. de Groot (Department of Haematology, University Hospital, Utrecht, The Netherlands).

Statistical analysis

For statistical analysis Student's t tests (two-tailed) were performed; P values below 0.05 were considered significant.

Results

Effectiveness and duration of β-adrenoceptor blockade by GR81706

For a proper interpretation of the results obtained with GR81706-treated cells in the functional adhesion assays (see below), it was essential to know that receptor function was inhibited for the duration of the adhesion experiment. To

investigate the efficacy of GR81706, we determined the capacity of the antagonist to inhibit terbutaline-induced cyclic AMP production in EA-hy-926 cells. These cells were chosen, because a marked, concentration-dependent increase in cyclic AMP was observed after incubation with terbutaline (Table 1), which is more pronounced than in lymphocytes (data not shown).

Experiments were performed to assess the duration of blockade after a short pretreatment with GR81706. Monolayers of EA-hy-926 cells were incubated for 15 min with GR81706 (10^{-6} M), washed three times with PBS, and β_2-adrenoceptor function was tested 0, 1, 2, 3, and 4 h after washing of the cells. For a period of up to 4 h after washing of the cells, terbutaline-induced cyclic AMP production was still blocked, demonstrating the long-acting effect of GR81706 (Figure 1a). The cyclic AMP response of GR81706-treated cells stimulated with forskolin remained unaffected. The minimal concentration of GR81706 that could effectively inhibit terbutaline-induced cyclic AMP production was determined 2 h after washing the cells. Complete receptor blockade was achieved only with 10^{-6} M GR81706, whereas partial blockade was observed with 10^{-8} M (Figure 1b). Lower concentrations of GR81706 were ineffective. Again, the cyclic AMP response to forskolin remained similar under all conditions. Based on these results, 10^{-6} M GR81706 was chosen to pretreat PBMC and EC in the following experiments.

Table 1 Induction of cyclic AMP in EA-hy-926 cells

		Cyclic AMP (pmol/10^6 cells)	*Fold increase*
Medium		38.0 ± 10.0	-
Terbutaline	10^{-5} M	435.7 ± 48.3	11.5
	10^{-6} M	335.5 ± 60.9	8.8
	10^{-7} M	150.7 ± 43.8	4.0
Forskolin	10^{-5} M	196.8 ± 54.1	5.2

Cells were incubated at 37°C for 5 min after which the reaction was stopped and cyclic AMP concentration determined (see Methods). Results of three independent experiments (mean ± s.e.mean) are shown.

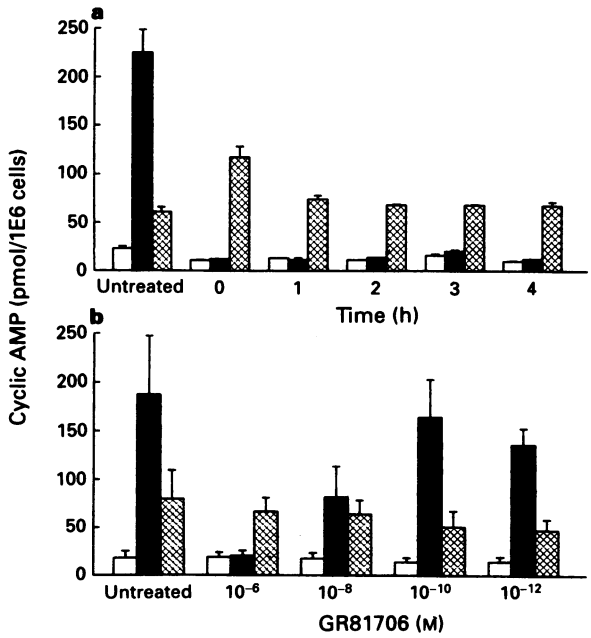


Figure 1 Assessment of β-adrenoceptor function in EA-hy-926 cells, after pretreatment (15 min) with GR81706. Cyclic AMP concentrations were determined after incubation with medium (open columns), terbutaline (10^{-5} M solid columns) or forskolin (10^{-5} M cross-hatched columns) for 5 min. (a) Shows the time course of the duration of blockade with 10^{-6} M GR81706 (results are representative for three experiments). In (b) the effectiveness of GR81706 is shown, 2 h after washing the cells; results are the mean (± s.e.mean) of three independent experiments.

Antagonistic effects of GR81706 in adhesion assays

The ability of GR81706 to inhibit the adrenaline-induced detachment of NK cells from EC was tested in adhesion assays. PBMC were allowed to adhere to monolayers of EC for 30 min. At this time, GR81706 (10^{-6} M) was added to the well simultaneously with adrenaline (10^{-5} M) or forskolin (10^{-5} M) for another 30 min. At the end of the incubation, non-adhering cells were removed and the percentage of NK cells in the adhering population determined. As reported earlier (Benschop *et al.*, 1993), the percentage of NK cells was higher in the adhering lymphocyte fraction than in PBMC (data not shown). This increase in NK cells in the adhering population was completely abolished by adrenaline or forskolin in the absence of GR81706 (100% adhesion reduction; Figure 2). Addition of GR81706 completely inhibited the action of adrenaline. The effect of forskolin on the other hand did not change significantly in the presence of GR81706. These results show that GR81706 effectively inhibits β-adrenoceptor-mediated detachment of NK cells.

Detachment of NK cells after pretreatment with GR81706

Next, it was determined whether the effects of adrenaline on NK cell adhesion to EC were mediated via β_2-adrenoceptors on NK cells, EC or on both cell types. Therefore, PBMC and/or EC were separately pretreated with the β-adrenoceptor antagonist GR81706 and the effects of adrenaline on NK cell adhesion were determined. EC or PBMC were incubated with GR81706 (10^{-6} M, 15 min, 37°C) and washed before use in the adhesion assay. Untreated and GR81706-treated PBMC were allowed to adhere to either GR81706-treated or untreated EC for 30 min, at which time adrenaline (10^{-5} M) or forskolin (10^{-5} M) was added. Thirty min later, non-adhering cells were removed and the percentage of NK cells in the adhering population determined (Table 2). The mean percentage of relative reduction of NK cell adhesion was calculated from these NK cell percentages and shown in the last two columns of Table 2. A reduction of NK cell adhesion of 71.5% and 75.6% was observed with adrenaline and forskolin respectively (both $P<0.01$), when PBMC and EC were treated with medium alone (control condition). Blocking of the β-adrenoceptors on NK cells completely abrogated the effect of adrenaline, whereas fors-

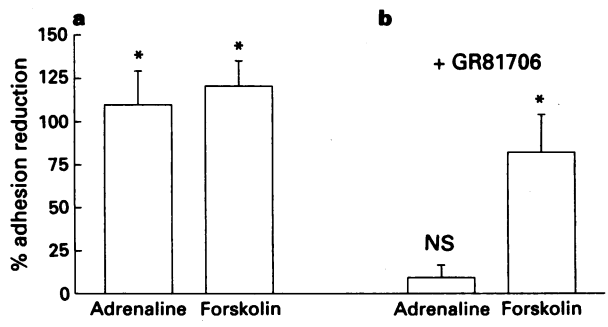


Figure 2 Effect of adrenaline (10^{-5} M) and forskolin (10^{-5} M) on NK adhesion, in the absence (a) or presence (b) of the β-adrenoceptor antagonists, GR81706 (10^{-6} M). The mean % adhesion reduction (± s.e.mean) of four independent experiments is shown. *$P<0.05$; NS, not significant.

Table 2 Effect of pretreating either peripheral blood mononuclear cells (PBMC) or endothelial cells (EC) with GR81706 (10^{-6} M) on the effect of adrenaline and forskolin on natural killer (NK) cell adhesion

GR81706 treatment			*% NK cells*		*Mean relative reduction*	
PBMC	*EC*	*Control*	*Adrenaline*	*Forskolin*	*Adrenaline*	*Forskolin*
−	−	18.7 ± 4.1	14.8 ± 3.5**	14.5 ± 4.0**	71.5	75.6
+	−	18.3 ± 4.0	18.4 ± 4.1 NS	14.5 ± 3.5**	−1.0	74.5
−	+	20.5 ± 4.5	18.0 ± 3.9*	17.3 ± 5.3*	34.7	43.4
+	+	21.0 ± 4.7	20.4 ± 4.6 NS	16.8 ± 4.9*	7.5	54.3

The mean results (± s.e.mean) of 8 independent experiments are shown. The mean percentage NK cells in PBMC was 13.2 ± 3.4 **$P<0.01$; *$P<0.05$; NS, not significant, compared to % NK cells in the control condition.

kolin still reduced 74.5% of the NK cell adhesion. Conversely, adrenaline significantly reduced adhesion of medium-treated NK cells to GR81706-treated EC ($P<0.05$), although the effect was less pronounced than in the control condition (a reduction of 34.7% and 71.5% respectively). The effect of forskolin on NK cell adhesion to GR81706-treated EC was also reduced from 74.5% to 43.4%. GR81706-treatment of both cell types resulted in an absence of the effect of adrenaline, whereas the effect of forskolin was comparable to that seen in the condition where EC had been treated with GR81706 (54.3%). These results show that blockade of β-adrenoceptors on NK cells completely abolishes adrenaline-induced detachment from EC. Pretreatment of EC results in a reduced, but still significant effect of adrenaline on NK cell adhesion.

Detachment of NK cells from CHO cells by adrenaline

An additional strategy was used to investigate via which cell type the catecholamine-induced detachment of NK cells from EC is mediated. In this approach, adhesion of NK cells to monolayers of CHO cells was studied. These cells do not express β-adrenoceptors, but cyclic AMP can be induced with forskolin (Table 3). Compared to the percentage in PBMC, the percentage NK cells in the adhering population increased ≈1.6 fold, from 10.4% (± 2.4) to 17.2% (± 3.7) ($P<0.01$). This is comparable with the increase found for adhesion to EC (Table 2). Addition of adrenaline and forskolin significantly reduced the percentage of NK cells in the adhering fraction (with 39.4% and 50.5% respectively, both $P<0.01$; Figure 3). Nadolol (a non-specific β-adrenoceptor antagonist) was included as a negative control and did not affect NK cell adhesion to EC. These results prove that stimulation of β-adrenoceptors on the NK cell is sufficient to reduce the adhesive interaction between NK cells and EC.

Table 3 Induction of cyclic AMP in CHO cells

	Cyclic AMP (pmol/10^6 cells)	*Fold increase*
Medium	21.7 ± 8.8	-
Terbutaline 10^{-5} M	19.1 ± 7.6	0.88
Adrenaline 10^{-5} M	22.4 ± 9.5	1.03
Forskolin 10^{-5} M	195.7 ± 27.4	9.04

Cells were incubated at 37°C for 5 min after which the reaction was stopped and cyclic AMP concentration determined (see Methods). Results of three independent experiments (mean ± s.e.mean) are shown.

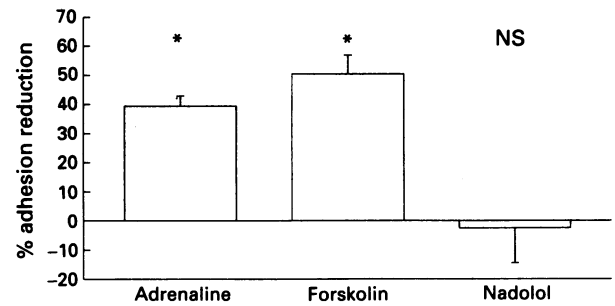


Figure 3 Effect of adrenaline, forskolin, and nadolol (all 10^{-5} M) on adhesion of NK cells to CHO cells. Mean percentage adhesion reduction (± s.e.mean) of six independent experiments is shown. *$P<0.01$; NS, not significant.

Discussion

In previous work, we have presented evidence for a catecholamine-induced detachment of NK cells from EC *in vitro* (Benschop *et al.*, 1993). The results of the present paper expand on these findings, by demonstrating that this phenomenon is mediated via β-adrenoceptors on the NK cell. The β-adrenoceptors on EC play a negligible (if any) role in this process. These results suggest that events occurring after β-adrenoceptor stimulation modulate adhesive interactions of NK cells.

In this paper we have used a new, long-acting β-adrenoceptor antagonist, GR81706, to block β-adrenoceptors. In competition assays, GR81706 completely inhibited adrenaline-induced detachment of NK cells, indicating its capacity to compete with adrenaline for β-adrenoceptors. The results of the cyclic AMP-induction experiments further indicate that a short preincubation with GR81706 is sufficient to obtain a long lasting blockade of the β-adrenoceptor. For comparison, similar pretreatment with the non-specific β-adrenoceptor antagonist, nadolol (10^{-5} M), resulted in an inhibition of only ≈50% of the cyclic AMP production to terbutaline (R.J. Benschop, unpublished observations). This emphasizes the importance of using β-adrenoceptor antagonists that have long-acting blocking properties like GR81706.

Two lines of evidence suggest that the adrenaline-induced detachment of NK cells from EC is mediated via the β-adrenoceptors on the NK cell. First, GR81706-treatment of NK cells results in a complete blockade of adrenaline-induced detachment. Although pretreatment of EC with GR81706 partially reduced the effect of adrenaline, this is probably related to non-specific effects of GR81706 on EC (see below). Second, the experiments with CHO cells, that do not express β-adrenoceptors (Samama *et al.*, 1993), support the notion that stimulation of the β-adrenoceptors of the NK cell is sufficient to reduce NK cell adhesion. Based on these data, we conclude that catecholamine-induced detachment of NK cells from EC is mediated via the β-adrenoceptor on the NK cell, and that the β-adrenoceptors on EC play a negligible (if any) role in this process.

The results from the experiments in which GR81706-treated EC were used indicate that this antagonist has some

non-specific effects on these cells. This is concluded from two observations. First, a higher percentage of NK cells adhered to GR81706-treated EC (Table 2), although this did not reach statistical significance. This finding may be explained by GR81706-induced alterations in membrane-fluidity, and it has been shown that a decrease in EC-membrane fluidity enhances monocyte adherence (Pritchard *et al.*, 1991). Although GR81706 has not actually been shown to demonstrate membrane stabilizing activity, it is an analogue of propranolol for which such activity is well-known. The second, and more important indication for non-specific effects of GR81706 on EC, pertains to the observation that the effect of forskolin on NK cell adhesion is reduced only when EC is pretreated with GR81706, and not after GR81706-treatment of PBMC (Table 2). It does not seem likely that binding of GR81706 to EC impairs the effect of forskolin on adenylate cyclase, since the forskolin-induced increase in cyclic AMP concentration in GR81706-treated cells was comparable to that observed in untreated cells. Therefore, the non-specific effect of GR81706 on EC probably involves other events, necessary for adhesion of NK cells. The reason for the different sensitivity of EC and NK cells for non-specific effects of GR81706-treatment remains unclear.

NK cells are important effector cells in the first line of immunological defence and establishing close cell-cell interactions is a crucial step in NK cell functioning. Various adhesion molecules may be involved in this process (Trinchieri, 1989; Springer, 1990). Moreover, from NK-target cell binding studies it is known that binding of an NK cell to a target cell results in phosphoinositide turnover, followed by protein kinase activation in the NK cell (Windebank *et al.*, 1988). Protein phosphorylation signals may result in further adhesion strengthening by increasing the affinity of an adhesion molecule for its ligand. It has been shown that phosphorylation of the α_6 subunit of VLA-6 increases adhesion of NK cells to laminin (Gismondi *et al.*, 1992) and that triggering through CD2 increases NK-target cell binding (Schmidt *et al.*, 1988). On the other hand, increasing intracellular cyclic AMP concentrations in NK cells inhibits phosphoinositide turnover (Windebank *et al.*, 1988), and will thus interfere with the described activation events. It is well established that cyclic AMP-inducing agents (e.g. prostaglandin E_2, β-adrenoceptor agonists, forskolin) negatively influence NK cell activity (Katz *et al.*, 1982; Goto *et al.*, 1983; Ullberg *et al.*, 1983; Steele & Brahmi, 1988; Windebank *et al.*, 1988; Whalen & Bankhurst, 1990). Indeed, the percentage of NK-target conjugates is reduced after induction of cyclic AMP (Ullberg *et al.*, 1983; Whalen & Bankhurst, 1990), although conflicting reports exist (Katz *et al.*, 1982; Steele & Brahmi, 1988). These results suggest that an increase in the cellular cyclic AMP content interferes with adhesion and adhesion-strengthening activation signals and our observations are compatible with these data.

It is still an open question which adhesion molecule(s) is (are) subject to β-adrenergic modulation and how this is accomplished. The observations that β-adrenoceptor stimulation reduces the adhesion of NK cells to EC, CHO cells, and target cells may indicate that the same adhesion molecule(s) is (are) involved. We have previously shown that T cell adhesion to EC is not affected by adrenaline (Benschop *et al.*, 1993), suggesting that we have to look for NK cell-specific adhesion molecules, although it is also possible that adhesion molecules are negatively coupled to β-adrenoceptors only in NK cells, and not in T lymphocytes. A reduction of adhesion can be achieved via (i) down-regulation of expression or (ii) a decrease in affinity of the adhesion structure for its ligand via e.g., phosphorylation events. Currently we can only speculate which of these two possibilities actually occurs. NK cells express a wide array of adhesion receptors (Trinchieri, 1989) and several of these structures are involved in NK cell adhesion to EC (Allavena *et al.*, 1991). Clearly, more work is needed to solve this issue.

In conclusion, we have shown that stimulation of β-adrenoceptors on NK cells leads to a reduction in adhesion to EC. Future studies have to reveal how exactly this decrease in adhesion is accomplished. The results of the present study prompt a detailed analysis of adhesion molecules on NK cells and the modulatory effects of β-adrenergic agents on these structures. In view of the biological implications of alterations in NK cell circulation and functioning, we think that this issue merits further investigations.

The authors thank Anne-Marie van der Hoeven for isolation of endothelial cells and Glaxo (U.K.) for supplying GR81706.

References

AHMAD, S., CHRETIEN, P., DANIEL, E.E. & SHEN, S.H. (1990). Characterization of beta adrenoceptors on cultured endothelial cells by radioligand binding. *Life Sci.*, **47**, 2365–2370.

ALLAVENA, P., PAGANIN, C., MARTIN-PADURA, I., PERI, G., GABOLI, M., DEJANA, E., MARCHISIO, P.C. & MANTOVANI, A. (1991). Molecules and structures involved in the adhesion of natural killer cells to vascular endothelium. *J. Exp. Med.*, **173**, 439–448.

ATHENS, J.W., HAAB, O.P., RAAB, S.O., MAUER, A.M., ASHENBRUCKER, H., CARTWRIGHT, G.E. & WINTROBE, M.M. (1961). Leukokinetic studies. IV. The total blood, circulating and marginal granulocyte pools and the granulocyte turnover rate in normal subjects. *J. Clin. Invest.*, **40**, 989–995.

ATHERTON, A. & BORN, G.V.R. (1972). Quantitative investigations of the adhesiveness of circulating polymorphonuclear leucocytes to blood vessel walls. *J. Physiol.*, **222**, 447–474.

BENDER, J.R., PARDI, R., KARASEK, M.A. & ENGLEMAN, E.G. (1987). Phenotype and functional characterization of lymphocytes that bind human microvascular endothelial cells in vitro. *J. Clin. Invest.*, **79**, 1679–1688.

BENSCHOP, R.J., DE SMET, M.B.M., BLOEM, A.C. & BALLIEUX, R.E. (1992). Adhesion of subsets of human blood mononuclear cells to endothelial cells in vitro, as quantified by flow cytometry. *Scand. J. Immunol.*, **36**, 793–800.

BENSCHOP, R.J., OOSTVEEN, F.G., HEIJNEN, C.J. & BALLIEUX, R.E. (1993). β2-Adrenergic stimulation causes detachment of natural killer cells from cultured endothelium. *Eur. J. Immunol.*, **23**, 3242–3247.

BENSCHOP, R.J., NIEUWENHUIS, E.E.S., TROMP, E.A.M., GODAERT, G.L.R., BALLIEUX, R.E. & VAN DOORNEN, L.J.P. (1994). Effects of β-adrenergic blockade on immunologic and cardiovascular changes induced by mental stress. *Circulation*, **89**, 762–769.

BROSSCHOT, J.F., BENSCHOP, R.J., GODAERT, G.L.R., DE SMET, M.B.M., OLFF, M., HEIJNEN, C.J. & BALLIEUX, R.E. (1992). Effects of experimental psychological stress on distribution and function of peripheral blood cells. *Psychosom. Med.*, **54**, 394–406.

BUONASSISI, V. & VENTER, J.C. (1976). Hormone and neurotransmitter receptors in an established vascular endothelial cell line. *Proc. Natl. Acad. Sci. U.S.A.*, **73**, 1612–1616.

COLEMAN, R.A., NIALS, A.T. & JOHNSON, M. (1994). Potency, selectivity and duration of action of aralkyloxyalkyl analogues of β-adrenoceptor blocking drugs: parallels with salmeterol. *Br. J. Pharmacol.*, **112**, 595P.

CRARY, B., HAUSER, S.L., BORYSENKO, M., KUTZ, I., HOBAN, C., AULT, K.A., WEINER, H.L. & BENSON, H. (1983). Epinephrine-induced changes in the distribution of lymphocyte subsets in peripheral blood of humans. *J. Immunol.*, **131**, 1178–1181.

DIMSDALE, J.E. & MOSS, J. (1980). Plasma catecholamines in stress and exercise. *J. Am. Med. Ass.*, **243**, 340–342.

EDGELL, C-J.S., MCDONALD, C.C. & GRAHAM, J.B. (1983). Permanent cell line expressing human factor VIII-related antigen established by hybridization. *Proc. Natl. Acad. Sci. U.S.A.*, **80**, 3734–3737.

GISMONDI, A., MAINIERO, F., MORRONE, S., PALMIERI, G., PICCOLI, M., FRATI, L. & SANTONI, A. (1992). Triggering through CD16 or phorbol esters enhances adhesion of NK cells to laminin via very late antigen 6. *J. Exp. Med.*, **176**, 1251–1257.

GOTO, T., HERBERMAN, R.B., MALUISH, A. & STRONG, D.M. (1983). Cyclic AMP as a mediator of prostaglandin E-induced suppression of human natural killer cell activity. *J. Immunol.*, **130**, 1350–1355.

HOGG, J.C. (1987). Neutrophil kinetics and lung injury. *Physiol. Rev.*, **67**, 1249–1295.

KAPPEL, M., TVEDE, N., GALBO, H., HAAHR, P.M., KJAER, M., LINSTOW, M., KLARLUND, K. & PEDERSEN, B.K. (1991). Evidence that the effect of physical exercise on NK cell activity is mediated by epinephrine. *J. Appl. Physiol.*, **70**, 2530–2534.

KATZ, P., ZAYTOUN, A.M. & FAUCI, A.S. (1982). Mechanisms of human cell-mediated cytotoxicity I. Modulation of natural killer cell activity by cyclic nucleotides. *J. Immunol.*, **129**, 287–296.

LANDMANN, R.M.A., MÜLLER, F.B., PERINI, C.H., WESP, M., ERNE, P. & BÜHLER, F.R. (1984). Changes of immunoregulatory cells induced by psychological and physical stress: relationship to plasma catecholamines. *Clin. Exp. Immunol.*, **58**, 127–135.

LAWRENCE, M.B. & SPRINGER, T.A. (1991). Leukocytes roll on a selectin at physiological flow rates: distinction from and prerequisite for adhesion through integrins. *Cell*, **65**, 859–873.

LIEN, D.C., WAGNER, JR, W.W., CAPEN, R.L., HASLETT, C., HANSON, W.L., HOFMEISETER, S.E., HENSON, P.M. & WORTHEN, G.S. (1987). Physiological neutrophil sequestration in the lung: visual evidence for localization in capillaries. *J. Appl. Physiol.*, **62**, 1236–1243.

MAISEL, A.S., FOWLER, P., REARDEN, A., MOTULSKY, H.J. & MICHEL, M.C. (1989). A new method for isolation of human lymphocyte subsets reveals differential regulation of β-adrenergic receptors by terbutaline treatment. *Clin. Pharmacol. Ther.*, **46**, 429–439.

MCCARTHY, D.A. & DALE, M.M. (1988). The leucocytosis of exercise. A review and model. *Sports Med.*, **6**, 333–363.

MURRAY, D.R., IRWIN, M., REARDEN, C.A., ZIEGLER, M., MOTULSKY, H. & MAISEL, A.S. (1992). Sympathetic and immune interactions during dynamic exercise. Mediation via a β2-adrenergic-dependent mechanism. *Circulation*, **86**, 203–213.

NALIBOFF, B.D., BENTON, D., SOLOMON, G.F., MORLEY, J.E., FAHEY, J.L., BLOOM, E.T., MAKINODAN, T. & GILMORE, S.L. (1991). Immunological changes in young and old adults during brief laboratory stress. *Psychosom. Med.*, **53**, 121–132.

OTTAWAY, C.A. & HUSBAND, A.J. (1992). Central nervous system influences on lymphocyte migration. *Brain Behav. Immun.*, **6**, 97–116.

PERUSSIA, B., STARR, S., ABRAHAM, S., FANNING, V. & TRINCHIERI, G. (1983). Human natural killer cells analyzed by B73.1, a monoclonal antibody blocking Fc receptor functions. *J. Immunol.*, **130**, 2133–2141.

PETERS, A.M., SAVERYMUTTU, S.H., BELL, R.N. & LAVENDER, J.P. (1985). Quantification of the distribution of the marginating granulocyte pool in man. *Scand. J. Haematol.*, **34**, 111–120.

PRITCHARD, K.A., SCHWARZ, S.M., MEDOW, M.S. & STEMERMAN, M.B. (1991). Effect of low-density lipoprotein on endothelial cell membrane fluidity and mononuclear cell attachment. *Am. J. Physiol.*, **260**, C43-C49.

SAMAMA, P., COTECCHIA, S., COSTA, T. & LEFKOWITZ, R.J. (1993). A mutation-induced activated state of the β2-adrenergic receptor. *J. Biol. Chem.*, **268**, 4625–4636.

SCHEDLOWSKI, M., FALK, A., ROHNE, A., WAGNER, T.O.F., JACOBS, R., TEWES, U. & SCHMIDT, R.E. (1993a). Catecholamines induce alterations of distribution and activity of human NK cells. *J. Clin. Immunol.*, **13**, 344–351.

SCHEDLOWSKI, M., JACOBS, R., STRATMANN, G., RICHTER, S., HÄDICKE, A., TEWES, U., WAGNER, T.O.F. & SCHMIDT, R.E. (1993b). Changes of natural killer cells during acute psychological stress. *J. Clin. Immunol.*, **13**, 118–126.

SCHMIDT, R.E., CAULFIELD, J.P., MICHON, J., HEIN, A., KAMADA, M.M., MACDERMOTT, R.P., STEVENS, R.L. & RITZ, J. (1988). T11/CD2 activation of cloned human natural killer cells results in increased conjugate formation and exocytosis of cytolytic granules. *J. Immunol.*, **140**, 991–1002.

SPRINGER, T.A. (1990). Adhesion receptors of the immune system. *Nature*, **346**, 425–434.

STEELE, T.A. & BRAHMI, Z. (1988). Phosphatidylinositol metabolism accompanies early activation events in tumor target cell-stimulated human natural killer cells. *Cell. Immunol.*, **112**, 402–413.

TRINCHIERI, G. (1989). Biology of natural killer cells. *Adv. Immunol.*, **47**, 187–376.

ULLBERG, M., JONDAL, M., LANEFELT, F. & FREDHOLM, B.B. (1983). Inhibition of human NK cell cytotoxicity by induction of cyclic AMP depends on impaired target cell recognition. *Scand. J. Immunol.*, **17**, 365–373.

VAN TITS, L.J.H., MICHEL, M.C., GROSSE-WILDE, H., HAPPEL, M., EIGLER, F.-W., SOLIMAN, A. & BRODDE, O.-B. (1990). Catecholamines increase lymphocyte β2-adrenergic receptors via a β2-adrenergic, spleen-dependent process. *Am. J. Physiol.*, **258**, E191–E202.

VEJLENS, G. (1938). The distribution of leucocytes in the vascular system. *Acta Pathol. Microbiol. Scand.*, Suppl. **33**, 11–33.

WEISSLER, J.C., NICOD, L.P., LIPSCOMB, M.F. & TOEWS, G.B. (1987). Natural killer cell function in human lung is compartmentalized. *Am. Rev. Respir. Dis.*, **135**, 941–949.

WHALEN, M.M. & BANKHURST, A.D. (1990). Effects of β-adrenergic receptor activation, cholera toxin and forskolin on human natural killer cell function. *Biochem. J.*, **272**, 327–331.

WINDEBANK, K.P., ABRAHAM, R.T., POWIS, G., OLSEN, R.A., BARNA, T.J. & LEIBSON, P.J. (1988). Signal transduction during human natural killer cell activation: inositol phosphate generation and regulation by cyclic AMP. *J. Immunol.*, **141**, 3951–3957.

(Received March 17, 1994
Revised August 24, 1994
Accepted August 28, 1994)

Br. J. Pharmacol. (1994), **113**, 1317-1327 © Macmillan Press Ltd, 1994

A pharmacological profile of the novel, peripherally-selective κ-opioid receptor agonist, EMD 61753

[1]A. Barber, G.D. Bartoszyk, *H.M. Bender, R. Gottschlich, H.E. Greiner, J. Harting, F. Mauler, K.-O. Minck, R.D. Murray, **M. Simon & C.A. Seyfried

Preclinical Pharmaceutical Research, E. Merck, 64271 Darmstadt, Germany; *Institute of Pharmacokinetics and Metabolism, E. Merck, 85567 Grafing, Germany and **Merck-Clevenot S.A., 5/9 Rue Anquetil, F-94731 Nogent-sur-Marne, France

1 The pharmacological properties of the novel diarylacetamide κ-opioid receptor agonist, EMD 61753, have been compared with those of ICI 197067 (a centrally-acting κ agonist) and ICI 204448 (a peripherally-selective κ agonist).

2 EMD 61753 binds with high affinity (IC_{50} 5.6 nM) and selectivity (κ:μ:δ:σ binding ratio 1:536:125:> 1,786) to κ-opioid receptors and is a full and potent (IC_{50} 54.5 nM) agonist in an *in vitro* assay for κ-opioid receptors (rabbit vas deferens preparation).

3 Systemically-applied [^{14}C]-EMD 61753 is found in high concentrations in the lungs, liver, adrenal glands and kidneys. Considerably less radioactivity is detected in the whole brain, and this radioactivity is concentrated in the region of the cerebral ventricles in the choroid plexuses. EMD 61753 penetrates only poorly into the CNS.

4 EMD 61753 was weakly effective in pharmacological tests of central activity. This compound reversed haloperidolol-induced DOPA accumulation in the nucleus accumbens of the rat only at a dose of 30 mg kg^{-1}, s.c., (doses of 0.1, 1.0 and 10 mg kg^{-1}, s.c., and 1.0, 10 and 100 mg kg^{-1}, p.o., were inactive). Hexobarbitone-induced sleeping in mice was prolonged by EMD 61753 at threshold doses of 10 mg kg^{-1}, s.c., and 100 mg kg^{-1}, p.o., whereas the motor performance of rats in the rotarod test was impaired by EMD 61753 with an ID_{50} value of 453 mg kg^{-1}, s.c.

5 EMD 61753 produced dose-dependent, naloxone-reversible antinociception in the mouse formalin test (1st phase ID_{50} 1.9 mg kg^{-1}, s.c., and 10.4 mg kg^{-1}, p.o.; 2nd phase ID_{50} 0.26 mg kg^{-1}, s.c., and 3.5 mg kg^{-1}, p.o.) and rodent abdominal constriction test (ID_{50} mouse 1.75 mg kg^{-1}, s.c., and 8.4 mg kg^{-1}, p.o.; ID_{50} rat 3.2 mg kg^{-1}, s.c., and 250 mg kg^{-1}, p.o.). EMD 61753 was inactive, or only weakly effective, in the rat pressure test under normalgesic conditions. After the induction of hyperalgesia with carrageenin, however, this compound elicited potent, dose-dependent (ID_{50} 0.08 mg kg^{-1}, s.c., and 6.9 mg kg^{-1}, p.o., after remedial application, and 0.2 mg kg^{-1}, s.c., and 3.1 mg kg^{-1}, p.o., after prophylactic application) and naloxone-reversible antinociception. The antinociceptive action of systemically-applied (50 mg kg^{-1}, p.o.) EMD 61753 in the hyperalgesic pressure test was completely inhibited by injection of the κ-opioid antagonist norbinaltorphimine (100 μg) into the inflamed tissue, a result which indicates that this opioid effect is mediated peripherally.

6 Cutaneous plasma protein extravasation produced by antidromic electrical stimulation of the rat saphenous nerve was dose-dependently inhibited by systemically-applied EMD 61753 (ID_{50} values 3.7 mg kg^{-1}, s.c., and 35.8 mg kg^{-1}, p.o.), and this effect was completely antagonized by intraplantar application of norbinaltorphimine (50 μg). Extravasation elicited by the intraplantar application of substance P (10 μg) was not influenced by the administration of EMD 61753.

7 EMD 61753 produced dose-dependent diuresis in non-hydrated rats at doses of and above 1.0 mg kg^{-1}, s.c., and 10 mg kg^{-1}, p.o., and in saline-loaded rats at doses of and above 10 mg kg^{-1}, s.c., and 30 mg kg^{-1}, p.o.

8 The prostaglandin-mediated fall in mean arterial blood pressure elicited in anaesthetized rats by i.v. application of arachidonic acid was not inhibited by prior treatment with EMD 61753 (10 mg kg^{-1}, p.o.). Thus, a blockade of prostaglandin synthesis via inhibition of cyclo-oxygenase activity does not contribute to the *in vivo* effects of EMD 61753 and its metabolites.

9 The present experiments therefore indicate that EMD 61753 is a potent, selective and orally-effective full κ-opioid receptor agonist which has a limited ability to penetrate the blood-brain barrier and elicit centrally-mediated sedation, putative aversion, diuresis, and antinociception. The inhibitory actions of systemically-applied EMD 61753 against hyperalgesic pressure nociception and neurogenic inflammation are mediated peripherally, probably by opioid receptors on the endings of sensory nerve fibres.

Keywords: EMD 61753; ICI 197067; ICI 204448; κ-opioid agonist; peripherally-selective; hyperalgesia; antinociception

Introduction

A successful strategy for improving the side-effect profile of peripherally-acting drugs has been to restrict the access of such compounds to the CNS. For example, a new generation of antihistamines are now available which have peripheral antiallergic effects without the drowsiness and impaired performance associated with centrally-acting antihistamines. They achieve this by virtue of their chemical structure, which prevents easy crossing of the blood-brain barrier (Nicholson, 1987).

Similar considerations have led to attempts to develop peripherally-selective κ-opioid receptor agonists. These compounds should be able to produce peripherally-mediated analgesia against pain of inflammatory origin (see Barber & Gottschlich, 1992, and Stein, 1993, for recent reviews) with-

[1] Author for correspondence.

out eliciting the unpleasant side effects of psychotomimesis/dysphoria and sedation found with centrally-acting κ agonists (Pfeiffer et al., 1986; Peters & Gaylor, 1989).

Various chemical approaches have been used in attempts to make a particular molecule less accessible to the brain without simultaneously reducing κ agonist activity. The introduction of zwitterionic groups led to the development of the highly polar hydrophilic κ-opioid receptor agonist, ICI 204448 (Shaw et al., 1989). Another strategy has been to introduce one or more moderately hydrophilic groups; GR 94839 (Rogers et al., 1992), BRL 52974 (Brooks et al., 1993), and EMD 60400 (Barber et al., 1994) are examples of such κ-opioid receptor agonists. However, while these hydrophilic compounds may be more or less peripherally selective in their actions (Shaw et al., 1989; Rogers et al., 1992; Barber et al., 1994) little has been revealed about some other important pharmacological properties, such as their bioavailability ofter oral application.

We now describe the pharmacological characteristics of the new κ-opioid receptor agonist, EMD 61753. This κ agonist is structurally novel since it contains the hydro*phobic* diphenylmethyl group in combination with a hydrophilic hydroxy group (Figure 1). This amphiphilic molecule therefore possesses the hydrophobic structural element found in the peripherally-selective antihistamines terfenadine and ebastine (Moragues & Roberts, 1990). We here compare the pharmacological properties of EMD 61753 with those of ICI 204448 and ICI 197067 (Costello et al., 1988), the latter being a κ-opioid receptor agonist which readily penetrates the blood-brain barrier (Shaw et al., 1989; Barber et al., 1994). Some of these results have been published previously in a preliminary form (Gottschlich et al., 1993; Barber et al., 1993).

Methods

Those experimental procedures which have been recently described (Barber, 1993; Barber et al., 1994) will be dealt with only briefly here.

In vitro *tests*

Binding Receptor binding was carried out in the presence of 1.6 nM [^{3}H]-U 69593 (κ), 0.5 nM [^{3}H]-PL 017 (μ), 1 nM [^{3}H]-[D-Pen^{2,5}]enkephalin (δ), or 4 nM [^{3}H]-SKF 10047 (σ) in 50 mM Tris (2-amino-2-hydroxymethyl-propan-1,3-diol) buffer (pH 7.7) using membranes prepared from guinea-pig cerebellum (κ), rat cerebrum (μ and δ) or guinea-pig whole brain (σ). Assays were run for 30 (μ and δ) or 40 (κ and σ) min at 25°C and non-specific binding was established by the use of 10 μM naloxone (κ), 0.3 μM morphine (μ), 1 μM [D-Ala^2, D-Leu^5]enkephalin (δ), or 10 μM haloperidol (σ).

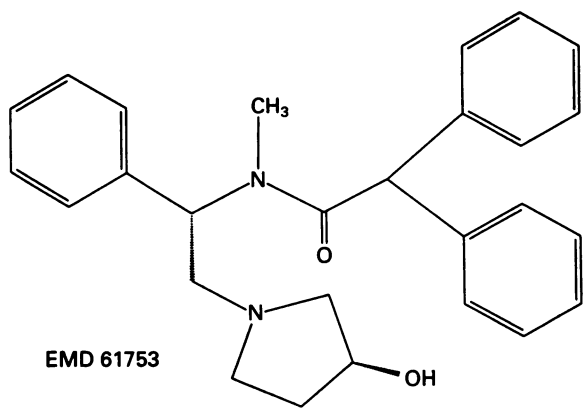


Figure 1 Structure of EMD 61753.

Rabbit vas deferens Male New Zealand rabbits (2.5–3 kg) were stunned and exsanguinated. The vasa deferentia were isolated and mounted in organ baths containing 50 ml of oxygenated (95% O_2/5% CO_2) physiological salt solution. The tissue was stimulated electrically with square-wave pulses (0.1 Hz, 2 ms, 20–40 V) via platinum field-stimulating electrodes. Contractions were recorded isometrically under a load of 0.5 g. After 60 min equilibrium a concentration-response curve to U 69593 was constructed and, after a 60 min washout period, a further curve was constructed for EMD 61753.

Central effects of EMD 61753

Studies with [^{14}C]-EMD 61753 In the macroautoradiography experiments, male Wistar rats (220–290 g) were injected i.v. with a radioactive dose of approximately 4 MBq kg^{-1} [^{14}C]-EMD 61753 (chemical dose 1 mg kg^{-1}). Five minutes later the rats were anaesthetized with ether, frozen and embedded in 3% carboxymethyl cellulose (Henkel, Düsseldorf, Germany). Sections of 20 μm thickness were then cut in a cryomicrotome (Type 450 MB, LKB, Sweden) and exposed at − 80°C for 25 to 64 days against X-ray film (Osray M3, Agfa Gevaert). The X-ray films were then developed in a modified X-ray developer (OP 22, Agfa) and fixed.

In the quantitive distribution studies, animals received a radioactive dose of approximately 2 MBq kg^{-1} [^{14}C]-EMD 61753 (chemical doses were 1 mg kg^{-1}, i.v., and 10 mg kg^{-1}, p.o.). At predetermined times after administration the animals were laparotomised under ether anaesthesia, exsanguinated by puncture of the abdominal aorta and the organs removed. Heparinised blood samples were centrifuged to separate plasma, while the organs were homogenized, dried, oxidized in a Tri-Carb 306 B oxidizer (Packard, Frankfurt) and counted in a TriCarb 460 CD or 4640 liquid scintillation spectrometer (Packard, Frankfurt).

Reversal of haloperidol-induced 3, 4-dihydroxyphenylalanine (DOPA) accumulation Male Wistar rats (175–250 g) received 0.3 mg kg^{-1} haloperidol, p.o., or vehicle (methocel; E. Merck, Darmstadt). One hour later the animals were treated s.c. or p.o. with the test compound or vehicle. Twenty-five minutes later the animals were injected i.p. with 100 mg kg^{-1} of the DOPA-decarboxylase inhibitor, NSD 1015. After a further 35 min the animals were decapitated and the N. accumbens were dissected and processed for determination of DOPA content using high performance liquid chromatography (h.p.l.c.) (Seyfried et al., 1986).

Hexobarbitone-induced sleeping time Male NMRI mice (20–30 g) were treated s.c. or p.o. with test compounds or vehicle. Thirty minutes later the mice were injected with hexobarbitone (Serva, Heidelberg, Germany; 100 mg kg^{-1}, i.p.) and the time necessary for the recovery of the righting reflex was measured.

Rotarod Male Wistar rats (190–270 g) were tested for their ability to balance on a rotating rod (diameter 9 cm; rate of rotation 7 revolutions per min). Selected rats were then injected s.c. or i.v. with test compounds. The rats were tested again 30 min after treatment; a rat falling off the bar more than twice within 2 min was considered to be showing motor impairment.

Antinociceptive tests

Pressure nociception Male Wistar rats (280–310 g) were fitted with a cuff at the base of the tail and treated with different doses of test compound by the s.c. or p.o. routes of administration. Thirty minutes later the proportion of animals in each treatment group which responded to painful pressure (4 bar, 5 s) delivered to the tail via a blunt pin built into the cuff was measured. This level of pressure produces a

behavioural response (vocalisation, turning and/or biting the cuff) in 100% of animals tested which have not received an analgesic.

Experiments were also carried out on rats in which hyperalgesia had been induced by the injection of a 1% solution of carrageenin (Marine Colloids Inc., Springfield, N.J., U.S.A.) into the tail tissue under the cuff. In this case a pressure of 2.5 bar was sufficient to produce a 100% response from untreated animals. All measurements were made 3 h after the application of carrageenin. Opiates were applied either 30 min or 3 h before testing (i.e., remedial and prophylactic application, respectively). The effect of naloxone on the remedial antinociceptive action of EMD 61753 was examined by applying naloxone 20 min before testing. Local effects of systemically-applied EMD 61753 in inflamed tissue were demonstrated by injecting the κ-opioid receptor antagonist norbinaltorphimine dissolved in 25 μl saline into the tail 5 min before testing.

Formalin test Male NMRI mice (27–33 g) were treated s.c. or p.o. with test compound or vehicle. Thirty minutes later 20 μl of a 3% solution of formalin (E. Merck, Darmstadt) was injected into the dorsal surface of the right hind paw. The amount of time spent licking the injected paw was measured 0–10 and 20–30 min after the injection of formalin (i.e., in the non-inflammatory first phase and the inflammatory second phase of the reaction, respectively; Hunskaar & Hole, 1987) and expressed as % inhibition compared to the respective vehicle group. In tests of naloxone antagonism naloxone was injected s.c. 10 min before the application of formalin.

Abdominal constriction (writhing) test Male NMRI mice (20–30 g) and Wistar rats (115–240 g) were injected s.c. or p.o. with test compound or vehicle. Thirty or 180 min later the animals were injected i.p. with a saturated aqueous solution of 2-phenyl-1,4-benzoquinone (1 ml 100 g^{-1}; E. Merck, Darmstadt). The number of abdominal constriction movements made in the subsequent 20 min were counted and expressed as % inhibition compared to the respective vehicle group. Naloxone antagonism of the action of EMD 61753 in the mouse abdominal constriction test was performed by applying naloxone at the same time as EMD 61753. Peripheral effects of EMD 61753 in the rat abdominal constriction test were looked for by applying this substance i.p. together with the irritant.

Other in vivo *tests*

Neurogenic inflammation Male Wistar rats (270–330 g) which had been pretreated s.c. or p.o. with test compound or vehicle were anaesthetized with pentobarbitone sodium (Sanofi, Paris; 60 mg kg^{-1}, i.p.) and their saphenous nerves were exposed and sectioned at the level of the thigh. Evans blue (E. Merck, Darmstadt; 50 mg kg^{-1}) was dissolved in a 0.9% solution of NaCl and applied i.v. through a catheter in a tail vein. One hour after application of the test substance or vehicle, and 15 min after the injection of Evans blue, the right saphenous nerve was stimulated antidromically with square-wave electrical pulses (5 mA, 1 ms, 2 Hz) for 10 min, after which the rat was killed with an overdose of anaesthetic. Dye was extracted by incubating hind paw skin in formamide (E. Merck, Darmstadt) and was measured spectrophotometrically at 620 nm. The dye level resulting from neurogenic extravasation was taken to be the mean difference between the stimulated and unstimulated paws in each dose group and was expressed as % inhibition in comparison to the respective vehicle group.

Plasma extravasation was also elicited by 10 μg substance P dissolved in 25 μl saline. This was injected into the paw 15 min after the application of Evans blue and was allowed to act for 10 min before the experiment was terminated. Local inhibitory actions of systemically-applied EMD 61753 were tested for by injecting norbinaltorphimine dissolved in 25 μl saline into the paw 10 min after the application of Evans blue and 5 min before the beginning of nerve stimulation. The control side was injected with 25 μl saline at the same time.

Diuresis in conscious rats Male Wistar rats (180–250 g) received water *ad libitum* and were deprived of food for 18 h before the start of the experiments. Groups of rats had their urinary bladders emptied by light pressure and were placed in metabolism cages (three rats in each cage) for 6 h. EMD 61753 or vehicle was given s.c. or p.o. just before the rats were placed in their cages. In experiments with volume-loaded rats, a 0.6% solution of NaCl (10 ml per 100 g, i.p.) was also injected at this time.

In vivo *inhibition of prostaglandin synthesis* These experiments were performed as described by Damas & Mousty (1978). Briefly, male Wistar rats (330–380 g) which had been pretreated orally with either vehicle, indomethacin or EMD 61753 were anaesthetized with pentobarbitone sodium (Sanofi, Paris; 50 mg kg^{-1}, i.p. and 40 mg kg^{-1}, s.c.). Blood pressure was recorded from a carotid artery by means of a Statham pressure transducer. Following a stabilisation period, arachidonic acid (Sigma, Deisenhofen, Germany) was applied i.v. at a dose of 5 mg kg^{-1}. In the vehicle-treated group this led to a fall in mean arterial blood pressure caused by the synthesis of prostaglandin from arachidonic acid by cyclo-oxygenase.

Substances

The following substances were synthesized at E. Merck, Darmstadt, unless otherwise indicated. [D-Ala^2, D-Leu^2]enkephalin acetate (Bachem, Basel, Switzerland), EMD 61753 (N-methyl-*N*-[(1S)-1-phenyl-2-((3S)-3-hydroxypyrrolidine-1-yl)-ethyl]-2,2-diphenylacetamide HCl; Figure 1), haloperidol HCl, ICI 197067 ((2S)-N-[2-(N-methyl-3,4-dichlorphenylacetamido)-3-methylbutyl]-pyrrolidine HCl), ICI 204448 (2-[3-(1-(3, 4-dichlorphenyl-N-methylacetamido)-2-pyrrolidonoethyl) - phenoxy] acetic acid HCl), indomethacin (Research Biochemicals International, Cologne, Germany), morphine HCl, naloxone HCl (Sigma, Deisenhofen, Germany), substance P tetratrifluracetate (Bachem, Basel, Switzerland) and U 69593 ((5-α, 7-α, 8-β)-(−)-N-methyl-N-(7-(1-pyrrolidinyl)-1-oxaspiro-(4,5)-dec-8-yl)-phenylacetamide; Research Biochemicals International, Cologne, Germany). For *in vivo* applications these compounds were dissolved in physiological saline or distilled water, or were suspended in gum arabic or methocel (for p.o. application). The ligands [^{3}H]-U 69593, [^{3}H]-PL 017 ([N-MePhe^3, D-Pro^4]morphiceptin), [^{3}H]-[D-Pen^{2,5}]enkephalin and [^{3}H]-SKF 10047 ((+)-(2S, 6R, 11S)-3-allyl-1, 2, 3, 4, 5, 6-hexahydro-6, 11-dimethyl-2, 6-methanobenzo(D)azocine-8-ol) were from NEN Research Products (Dreieich, Germany), while [^{14}C]-EMD 61753 was synthesized at the Institute of Pharmacokinetics and Metabolism of E. Merck (Grafing, Germany).

Statistics

The Dunnett test for multiple comparisons with control was used to determine statistical significance. Ninety five percent confidence intervals were calculated by the method of Litchfield & Wilcoxon (1949), except in the case of the pressure nociception and rotarod tests, where the staircase method of Dixon & Mood (1948) was applied.

Results

In vitro *tests*

Binding EMD 61753 binds to κ-opioid receptors with an IC_{50} value (mean ± s.d.) of 5.6 ± 1.4 nM ($n = 3$). The binding

Table 1 ^{14}C-concentrations (ng-eq g^{-1} and for plasma ng-eq ml^{-1}) in selected organs and tissues after single administration of [^{14}C]-EMD 61753 to male Wistar rats

	Time after application			
EMD 61753 (1 mg kg^{-1}, i.v.)	5 min	1 h	6 h	24 h
Plasma	595 ± 64	131 ± 10	22 ± 3	7 ± 1
Whole brain	242 ± 3	48 ± 4	49 ± 9	4 ± 0.4
Pituitary	2110 ± 189	480 ± 152	52 ± 4	10 ± 4
Lung	13700 ± 688	1940 ± 290	115 ± 14	13 ± 0.8
Liver	4030 ± 441	2470 ± 226	758 ± 44	401 ± 32
Kidney	3470 ± 287	757 ± 77	275 ± 4	175 ± 4
Adrenals	6630 ± 382	871 ± 103	123 ± 5	33 ± 6
Muscles	873 ± 52	107 ± 7	11 ± 0.2	2 ± 0.4
EMD 61753 (10 mg kg^{-1}, p.o.)	1 h	3 h	6 h	24 h
Plasma	353 ± 85	391 ± 17	369 ± 39	62 ± 9
Whole brain	168 ± 21	170 ± 20	190 ± 14	33 ± 8
Pituitary	888 ± 320	969 ± 211	798 ± 83	151 ± 23
Lung	4250 ± 1477	2540 ± 601	1540 ± 193	82 ± 4
Liver	9140 ± 1909	9820 ± 561	9840 ± 711	2340 ± 148
Kidney	1640 ± 403	1850 ± 198	1530 ± 144	431 ± 9
Adrenals	2010 ± 674	2350 ± 310	1620 ± 140	211 ± 28
Muscles	228 ± 47	236 ± 24	162 ± 23	18 ± 1.6

Values are mean ± s.e.mean, $n = 3$.

affinity of EMD 61753 to μ-opioid, δ-opioid, and σ-receptors was much weaker, with IC_{50} values of 3000 ± 900, 700 ± 120, and > 10,000 nM (all $n = 3$), respectively.

Rabbit vasa deferentia EMD 61753 was a full and potent κ-opioid receptor agonist, which produced concentration-dependent inhibition of electrically-induced contractions of rabbit isolated vasa deferentia. The IC_{50} value (with 95% confidence interval) of this effect was 54.5 (37.6–79) nM ($n = 4$), a value very simiar to that of the κ-opioid agonist, U 69593 (57.7 (47.6–70) nM; $n = 4$).

Central actions of EMD 61753

In vivo *distribution of [^{14}C]-EMD 61753* The distribution of radioactivity at various times following the application of [^{14}C]-EMD 61753 to male Wistar rats at a dose of 1 mg kg^{-1}, i.v., is shown in Table 1. The plasma concentration of 595 ng eq ml^{-1} found 5 min after i.v. administration (Table 1) indicates an initial distribution volume of 1.7 l kg^{-1}, which means that the substance is distributed rapidly to organs and tissues. The radioactivity in the plasma and brain at this timepoint represents unmetabolized substance, as indicated by radio-h.p.l.c. measurements (not shown). Initial concentrations were highest in the lungs, but relatively high concentrations were also measured in the adrenal glands, liver and kidneys (Table 1). Considerably less radioactivity, in comparison to the above organs, was found at all timepoints in the whole brain, although noticeably higher concentrations were detected in the pituitary (Table 1). Autoradiographs taken from rats 5 min after i.v. application (Figure 2) revealed that the radioactivity measured in the whole brain was highly concentrated in the region of the cerebral ventricles (3rd, 4th and lateral). These regions of high radioactivity were identified histologically as choroid plexus.

The distribution pattern of [^{14}C]-EMD 61753 following application at a dose of 10 mg kg^{-1}, p.o., was comparable to that after i.v. administration (Table 1). Comparisons of plasma concentrations of unmetabolised EMD 61753 over time after i.v. and p.o. application indicate a bioavailability of EMD 61753 of 13%; EMD 61753 was eliminated from the

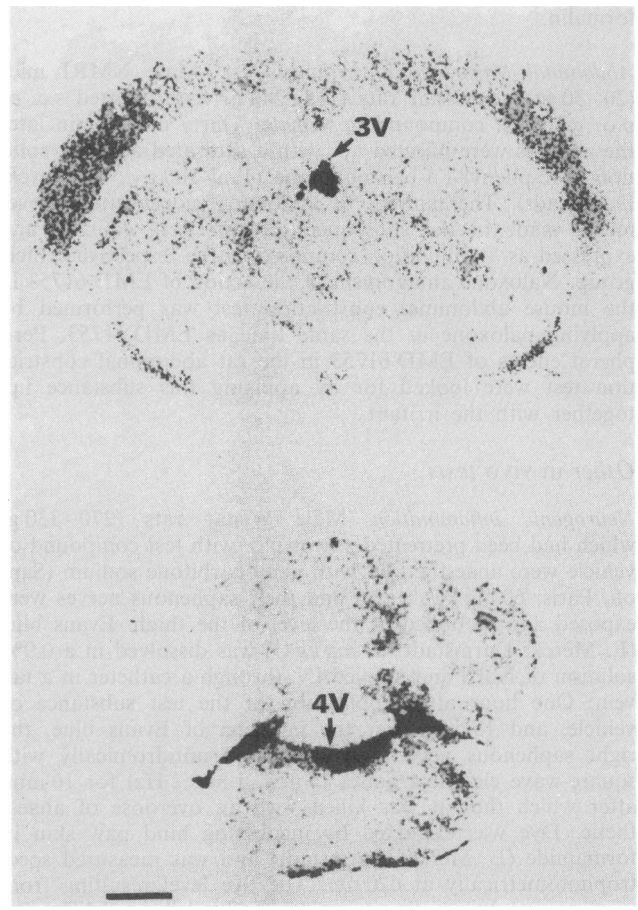


Figure 2 Autoradiographs of coronal sections of a rat brain showing the distribution of ^{14}C radioactivity 5 min after i.v. administration of 1 mg kg^{-1} [^{14}C]-EMD 61753. Radioactivity was concentrated in the ventricular system in the choroid plexuses (cf. Figure 1 of Risau & Wolburg, 1990, and Figure 56 of Paxinos & Watson, 1982). The calibration bar indicates 150 μm. 3V: 3rd ventricle; 4V: 4th ventricle.

plasma with a half life of 0.67 h (H.M. Bender, unpublished observations).

Haloperidol-induced DOPA accumulation In a first series of experiments the accumbal DOPA level (mean ± s.e.mean) in the vehicle-treated control group was 1565 ± 266 ($n = 4$), in the haloperidol-treated control group was 4012 ± 205 ($n = 6$), and in the animals treated with EMD 61753 at doses of 0.1, 1 and 10 mg kg^{-1}, s.c. was 3448 ± 414, 4322 ± 215, and 3607 ± 363 (all $n = 4$) ng g^{-1} fresh weight, respectively. These values for the EMD 61753-treated groups were not significantly different from haloperidol-treated controls. In the next set of experiments control and haloperidol-treated control animals had DOPA values of 2143 ± 71 ($n = 4$) and 6070 ± 496 ($n = 6$) ng g^{-1}, respectively, whereas rats treated with 30 mg kg^{-1} EMD 61753, s.c., had accumbal DOPA concentrations of 3969 ± 305 ng g^{-1} ($n = 4$). The latter represents a statistically significant ($P < 0.05$) reversal of the haloperidol effect by EMD 61753 (Table 2). The corresponding values after oral application were 2616 ± 139 ($n = 3$) and 6396 ± 277 ($n = 5$) ng g^{-1} for the control and haloperidol-treated control, respectively, and 6582 ± 527 ($n = 4$), 6239 ± 275 ($n = 4$) and 5117 ± 469 ($n = 3$) ng g^{-1} in animals given 1, 10 and 100 mg kg^{-1} EMD 61753, p.o., respectively. None of these levels in the EMD 61753-treated groups was significantly different from the haloperidol-treated control (Table 2).

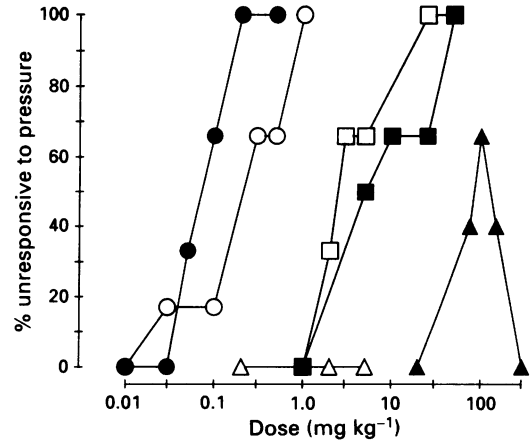


Figure 3 Effect of EMD 61753 on pressure nociception in the rat. Measurements were either made in rats without inflammation 30 min after application s.c. (△) or p.o. (▲) or animals with inflammation after s.c. (○, ●) or p.o. (□, ■) administration. Pressure testing in rats with inflammation was carried out either 3 h after the application of carrageenin and EMD 61753 (i.e. prophylactic application; □ and ○) or 3 h after the application of carrageenin and 30 min after the application of EMD 61753 (i.e. remedial application; ■ and ●). Each point represents the % of animals ($n = 3$–6) which did not respond to standard noxious pressure.

Table 2 Summary of effectiveness in tests of central activity

Test	*EMD 61753* (s.c.)	*EMD 61753* (p.o.)	*ICI 204448*[a] (s.c.)	*ICI 197067*[a] (s.c.)
DOPA accumulation[b]	30	>100	>30	0.3
Hexobarbitone sleeping[b]	10	100	>30	1.0
Rotarod[c]	453 (237–750)	–	>100	0.71 (0.45–1.12)

[a]From Barber *et al.* (1994).
[b]Threshold dose (mg kg^{-1}) for statistically significant effect.
[c]ID_{50} value (with 95% confidence intervals) in mg kg^{-1}.

Table 3 Summary of ID_{50} values (with 95% confidence intervals) in antinociceptive and related tests

Test	*EMD 61753* (s.c.)	*EMD 61753* (p.o.)	*ICI 204448* (s.c.)	*ICI 204448* (p.o.)	*ICI 197067* (s.c.)
Pressure nociception					
Normalgesic	5.0	c.100[a]	30[b]	100	0.08[b]
	inactive		inactive	inactive	(0.02–0.2)
Hyperalgesic	0.2[c]	3.1[c]	0.8[b,c]	30[c]	0.004[b,c]
	(0.08–0.46)	(1.8–5.2)	(0.3–2.4)	inactive	(0.001–0.01)
	0.08[d]	6.9[d]	0.4[d]	30[d]	0.004[d]
	(0.05–0.12)	(2.6–18.4)	(0.2–0.9)	inactive	(0.001–0.01)
Formalin					
1st phase	1.9	10.4	18.9[b]	>100	0.04[b]
	(0.4–9.5)	(2.1–52)	(7.3–49.1)		(0.02–0.1)
2nd phase	0.26	3.5	12.6[b]	77.7	0.02[b]
	(0.06–1.2)	(1.3–9.1)	(8.4–18.9)	(23.5–256.4)	(0.01–0.04)
Abdominal constriction					
Mouse	1.75	8.4	1.9[b]	22[c]	0.02[b]
	(1.4–2.3)	(6.2–11.3)	(0.6–5.9)		(0.01–0.03)
Rat	3.2	250	4.5[b]	200	0.04[b]
	(0.8–12.0)	(89.3–700)	(0.6–31.5)	inactive	(0.01–0.11)
Neurogenic inflammation	3.7	35.8	5.2	100	3.1
	(1.2–11.1)	(13.8–93.6)	(1.7–15.6)	inactive	(0.9–10.85)

All values expressed in mg kg^{-1}.
[a]Bell-shaped dose-response curve; [b]From Barber *et al.* (1994); [c]Prophylactic application, i.e., rats tested 180 min after application of opiates and carrageenin; [d]Remedial application, i.e., rats tested 180 min after application of carrageenin and 30 min after receiving opiates; [e]No 100% effect. Maximum effect 56% after 100 mg kg^{-1}, p.o.

Sleeping time Control sleeping times (mean ± s.e.mean) were 74.7 ± 4.8 ($n = 30$) and 70.8 ± 6.3 ($n = 15$) min in mice which had received vehicle s.c. and p.o., respectively. Sleeping times were 72.3 ± 4.8, 133.9 ± 14.3, 175.5 ± 13.9, and 211.3 ± 8.0 min (all $n = 10$) in mice injected with 3, 10, 30 or 100 mg kg^{-1} EMD 61753, s.c., respectively. The sleeping times after the last three of these doses represent statistically significant ($P < 0.01$) potentiation of narcosis (Table 2). Mice treated with EMD 61753 at doses of 10, 30 and 100 mg kg^{-1}, p.o., had sleeping times of 88.5 ± 9.4, 89.9 ± 11.7 and 169.2 ± 5.0 min (all $n = 10$), respectively, of which only the latter was significantly different ($P < 0.01$) from control (Table 2).

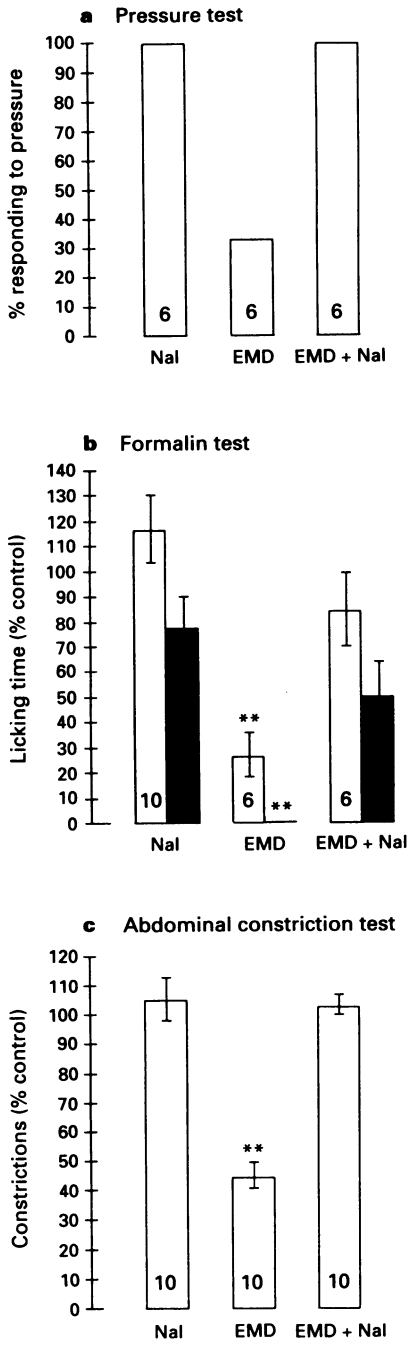


Figure 4 Effects of naloxone on the antinociceptive action of EMD 61753. (a) Pressure test: the proportion of animals responding to noxious pressure on the inflamed tail after the application of 0.5 mg kg^{-1} naloxone, s.c. (Nal), 10 mg kg^{-1} EMD 61753, p.o. (EMD), or EMD 61753 and naloxone (EMD + Nal) are shown. (b) Formalin test: licking times in the 1st (open columns) and 2nd (solid columns) phases of the response to formalin are expressed as % control (absolute licking times in the control group were 64.7 ± 6.0 and 103.7 ± 11.0 s (mean ± s.e.mean, $n = 10$), respectively). Responses after naloxone (Nal) applied at a dose of 1.0 mg kg^{-1}, s.c., EMD 61753 (EMD) at 30 mg kg^{-1}, p.o., and EMD 61753 and naloxone (EMD + Nal) are displayed. (c) Abdominal constriction test: constrictions are expressed as % of the control group, in which the absolute number of constrictions was 60.5 ± 2.8 (mean ± s.e.mean; $n = 15$). Responses after 1 mg kg^{-1} naloxone, s.c., (Nal), 2 mg kg^{-1} EMD 61753, s.c., (EMD), and EMD 61753 and naloxone (EMD + Nal) are shown. The number of animals used is shown in each column. (**$P < 0.01$).

Rotarod The ID_{50} value (with 95% confidence intervals) of EMD 61753 after administration by the s.c. route was 453 (237–750) mg kg^{-1} (Table 2). Motor performance was not affected by EMD 61753 at doses of 1 and 3 mg kg^{-1}, i.v., but the ability to balance on the rotarod was completely inhibited 2 and 10 (but not 20) min after the application of 10 mg kg^{-1} EMD 61753, i.v.

Antinociceptive actions of EMD 61753

Pressure test EMD 61753 was ineffective against pressure nociception in normalgesic rats after s.c. application at doses between 0.2 and 5.0 mg kg^{-1} (Figure 3; Table 3). Oral administration of EMD 61753 in this test revealed a bell-shaped dose-response relationship (Figure 3; Table 3), with a maximum effect (66% antinociception) after the application of a dose of 100 mg kg^{-1}.

EMD 61753 was considerably more potent following the induction of inflammatory hyperalgesia. Dose-dependent antinociception was found after prophylactic and remedial application via both oral and s.c. routes of administration (Figure 3; see Table 3 for ID_{50} values). In contrast, ICI 204448 was inactive in this test at a dose of 30 mg kg^{-1}, p.o. ($n = 3$; Table 3).

The antinociceptive action of EMD 61753 (remedial application of 10 mg kg^{-1}, p.o.) against pressure nociception under hyperalgesic conditions could be completely inhibited by systemic application of the opioid-receptor antagonist naloxone (0.5 mg kg^{-1}, s.c.; Figure 4a).

Formalin-induced paw licking EMD 61753 elicited dose-dependent antinociception against both early and late phase nociception after s.c. and p.o. administration in the mouse (Figure 5; see Table 3 for ID_{50} values). ICI 204448 was only weakly active after oral application (Figure 5; Table 3).

Systemic naloxone (1.0 mg kg^{-1}, s.c.) was able to antagonize the action of EMD 61753 (30 mg kg^{-1}, p.o.) in this test (Figure 4b).

Rodent abdominal constriction EMD 61753 produced an antinociceptive action in this test, although this effect showed some species-dependency. In rats the dose-response curve to EMD 61753 was not as steep as in the mouse, and EMD 61753 was only very weakly active after oral application (Figure 6; Table 3). Another finding in the rat was that EMD 61753 had an ID_{50} value (with 95% confidence interval) of 3.06 (1.1–8.6) mg kg^{-1} when applied i.p. simultaneously with phenylbenzoquinone. ICI 204448 was inactive in the rat abdominal constriction test at a dose of 200 mg kg^{-1}, p.o. ($n = 5$; Table 3), and was active but unable to produce 100% inhibition of abdominal constriction in the mouse following its oral administration (Figure 6).

The opioid nature of the antinociceptive action of EMD 61753 (2 mg kg^{-1}, s.c.) in the mouse abdominal constriction test was demonstrated by antagonism with naloxone (1 mg kg^{-1}, s.c.; Figure 4c).

Other in vivo *effects*

Neurogenic inflammation Neurogenic plasma extravasation was dose-dependently inhibited by s.c. or oral application of EMD 61753 (Figure 7; see Table 3 for ID_{50} values). ICI

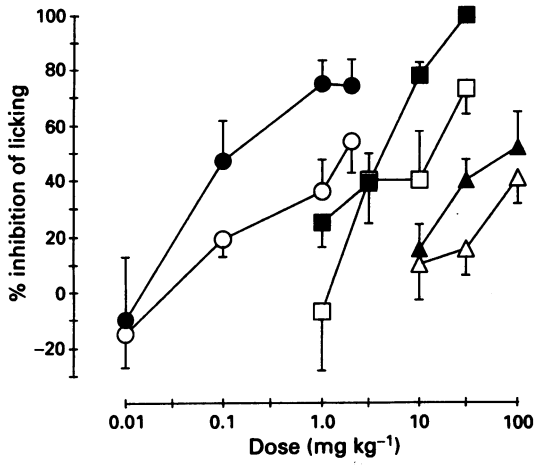


Figure 5 Effects of EMD 61753 and ICI 204448 on formalin-induced paw licking observed 0–10 (○, □, △) and 20–30 (●, ■, ▲) min after the intraplantar injection of formalin. EMD 61753 was applied s.c. (○, ●) and p.o. (□, ■), and ICI 204448 was applied p.o. (△, ▲), 30 min before formalin. Absolute licking times (mean ± s.e.mean; 1st phase/2nd phase) in the vehicle-treated groups were 73.1 ± 8.4/107 ± 11.7 (n = 17), 77.4 ± 8.3/153.7 ± 18.0 (n = 10), and 66.7 ± 6.0/105.3 ± 14.5 (n = 14) s for EMD 61753 s.c., EMD 61753 p.o., and ICI 204448 p.o., respectively. Each point in the figure represents the mean ± s.e.mean of measurements from 5 or 6 mice.

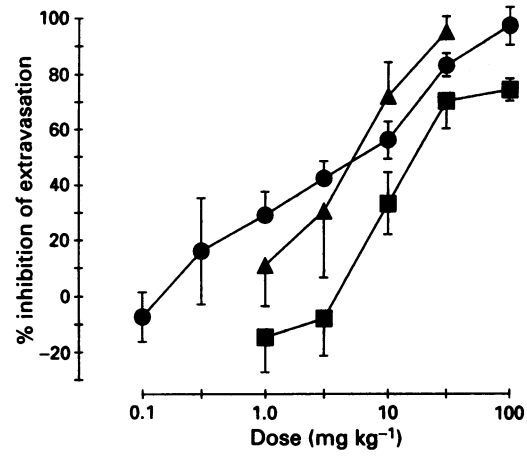


Figure 7 Effect of EMD 61753 and ICI 204448 on neurogenic plasma extravasation elicited by 10 min antidromic electrical stimulation of the rat saphenous nerve. EMD 61753 s.c. (●), EMD 61753 p.o. (■), and ICI 204448 s.c. (▲) were applied 60 min before the beginning of nerve stimulation. Mean dye levels (± s.e.mean) resulting from electrical stimulation (i.e. the difference between stimulated and control paws) were 7.1 ± 0.7 (n = 19), 5.4 ± 0.5 (n = 10), and 5.9 ± 0.9 (n = 6) μg dye per 100 mg skin in the EMD 61753 s.c., EMD 61753 p.o., and ICI 204448 s.c. vehicle-treated control groups, respectively. Each point in the figure represents the mean ± s.e.mean from 5–12 animals.

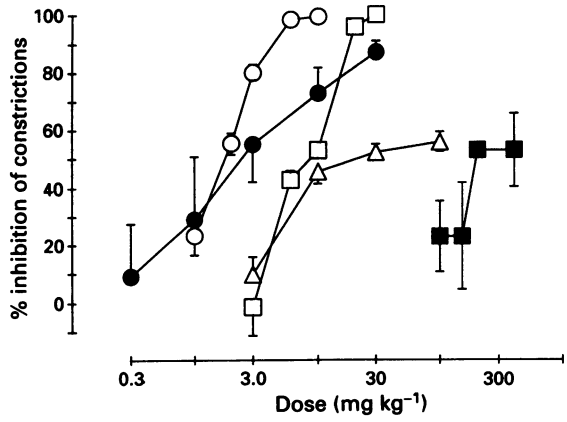


Figure 6 Effects of EMD 61753 and ICI 204448 on constriction movements measured 0–20 min after the i.p. injection of 2-phenyl-1,4-benzoquinone. EMD 61753 was applied s.c. (○, ●) 30 min, or p.o. (□, ■) 30 min (mouse) or 180 min (rat), before 2-phenyl-1,4-benzoquinone, whereas ICI 204448 (△) was allowed to act for 30 min p.o. before injection of the irritant. The numbers of constriction movements (mean ± s.e.mean) in the vehicle-treated groups in mice were 45.3 ± 3.2, 42.5 ± 3.7 and 50.9 ± 3.3 (all n = 15) and in rats were 42.9 ± 2.5 (n = 25) and 46.7 ± 3.1 (n = 20) for EMD 61753 s.c., EMD 61753 p.o., ICI 204448 p.o., EMD 61753 s.c. and EMD 61753 p.o., respectively. Each point in the figure represents the mean ± s.e.mean of measurements from 5 rats (●, ■) or 10 mice (○, □, △).

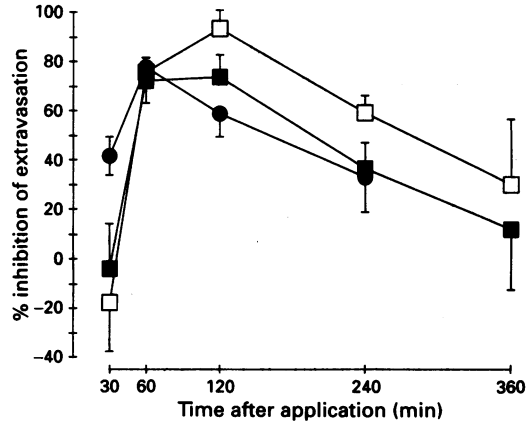


Figure 8 Time course of the inhibitory effect of EMD 61753 on neurogenic plasma extravasation. EMD 61753 was applied at doses of 4 mg kg^{-1}, s.c., (●), 30 mg kg^{-1}, p.o. (■), and 100 mg kg^{-1}, p.o., (□), and nerve stimulation was begun at various times thereafter. The mean (± s.e.mean) amounts of dye in the control groups (measured 60 min after application of vehicle) were 6.8 ± 0.5 (n = 24) and 5.8 ± 0.5 (n = 20) μg dye per 100 mg skin in the s.c. and p.o. groups, respectively. Each point represents mean ± s.e.mean from 5–11 animals.

204448 was also effective via the s.c. route of administration (Figure 7), but was inactive in this test at a dose of 100 mg kg^{-1}, p.o. (n = 5).

Levels of Evans blue (mean ± s.e.mean) after the injection of 10 μg substance P, i.pl., were 14.6 ± 1.2 μg dye per 100 mg skin (n = 5) in rats treated with vehicle p.o., and 11.2 ± 1.1 μg dye per 100 mg skin (n = 5) in animals treated with 100 mg kg^{-1} EMD 61753, p.o. This difference was not statistically significant ($P > 0.05$). Dye levels in paws injected with 25 μl saline were 5.6 ± 0.3 (n = 5) and 5.0 ± 0.62 (n = 5) μg per 100 mg skin in the vehicle- and EMD 61753-treated groups, respectively.

Eliciting neurogenic extravasation at various times after the application of EMD 61753 revealed that at single doses of 4.0 mg kg^{-1}, s.c., and 30 mg kg^{-1}, p.o. (i.e. approximate ID_{50} doses s.c. and p.o.), this compound still had a statistically significant ($P < 0.01$) inhibitory effect 2 but not 4 h after administration (Figure 8). After a dose of 100 mg kg^{-1}, p.o., the action of EMD 61753 was undetectable after 6 h (Figure 8).

Diuresis EMD 61753 elicited dose-dependent diuresis after its s.c. or oral administration in non-hydrated (Figure 9) and hydrated (data not shown) rats. A statistically significant

diuretic effect ($P<0.05$) of EMD 61753 was observed at doses of and greater than 1.0 mg kg^{-1}, s.c., and 10 mg kg^{-1}, p.o., in non-hydrated animals and at doses of 10 mg kg^{-1}, s.c., and 30 mg kg^{-1}, p.o., in hydrated rats. An antidiuretic action of EMD 61753 at low doses was not observed in either non-hydrated or hydrated animals.

Effects on prostaglandin biosynthesis The i.v. administration of 5 mg kg^{-1} arachidonic acid in anaesthetized rats produced a hypotensive response due to the *in vivo* formation of prostaglandins. Arterial blood pressure (mean ± s.e.mean) was reduced from 112.4 ± 2.5 to 48.8 ± 1.2 mmHg ($n = 12$) in rats pretreated with vehicle p.o. These values were changed from 91.2 ± 3.1 to 53.0 ± 1.5 mmHg ($n = 6$) in animals given 10 mg kg^{-1} EMD 61753, p.o., and from 103.5 ± 5.1 to 114.3 ± 6.6 mmHg ($n = 6$) in animals which had received 1 mg kg^{-1} indomethacin, p.o.

Peripheral effects of systemically-applied EMD 61753

The antinociceptive action of 50 mg kg^{-1} EMD 61753, p.o. in the hyperalgesic pressure test was completely antagonized by the application of 100 μg of the κ-opioid receptor antagonist norbinaltorphimine directly into the inflamed portion of the tail (Figure 10a). The action of the antagonist appeared to be a local inhibitory effect, since norbinaltorphimine at this dose did not produce a systemic antagonism of the action of EMD 61753 (Figure 10a).

The action of 50 mg kg^{-1} EMD 61753, p.o. against neurogenic inflammation was also inhibited by the local application of norbinaltorphimine (Figure 10b), in this case into the paw. On the other hand, the systemic application of the same dose of norbinaltorphimine had no effect on the systemic action of EMD 61753 (Figure 10b).

Discussion

EMD 61753 has been shown in the present *in vitro* experiments to be a selective, potent and full κ-opioid receptor agonist. The binding affinity of EMD 61753 for the κ-opioid receptor as indicated by the IC_{50} value (5.6 nM) is equivalent to that of other established κ agonists, such as ICI 197067 (6.3 nM, Costello *et al.*, 1988; 1.19 nM, Shaw *et al.*, 1989; 1.5 nM, Barber *et al.*, 1994), ICI 204448 (33.2 nM, Shaw *et al.*, 1989; 13 nM, Barber *et al.*, 1994), EMD 60400 (2.8 nM, Barber *et al.*, 1994), and U 69593 (9.5 nM, Lahti *et al.*, 1985). EMD 61753 also binds selectively to κ receptors with a κ:μ:δ binding ratio of 1:536:125. For ICI 197067 and EMD 60400 these ratios were 1:67:800 and 1:179:119, respectively (Barber *et al.*, 1994), and U 69593 has a κ:μ binding ratio of 1:484 (Lahti *et al.*, 1985). ICI 204448, on the other hand, is relatively unselective in its binding affinity (κ:μ:δ binding ratio 1:17.9:12.8, Barber *et al.*, 1994). The IC_{50} value of EMD 61753 in the rabbit vas deferens test of functional κ agonist potency (54.5 nM) is also comparable to that of EMD 60400 (41.8 nM), ICI 197067 (15.7 nM) and ICI 204448 (15 nM; Barber *et al.*, 1994).

The distribution of a radioactively labelled compound after i.v. injection occurs without distortion through absorption or first-pass metabolism. In the case of [^{14}C]-EMD 61753 it was shown that radioactivity in plasma and brain 5 min after i.v. administration represents exclusively the parent drug and not radioactive metabolites. EMD 61753 distributes rapidly from plasma, although its concentration in the whole brain was found to be low at all timepoints relative to that in other organs (Table 1). Moreover, these measurements from the whole brain include the high concentrations in the choroid plexus revealed on autoradiographs (Figure 2); the actual concentrations of EMD 61753 in nervous tissue will thus be less than those given in Table 1. These results therefore indicate that EMD 61753 penetrates poorly into the CNS and so can be termed peripherally-selective in its distribution after systemic application.

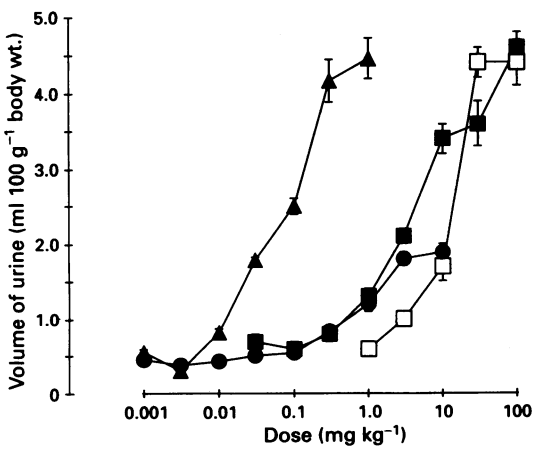


Figure 9 Effect of κ agonists on urinary volume in non-hydrated rats in the 6 h following s.c. application of ICI 197067 (▲), ICI 204448 (●), and EMD 61753 (■), and the p.o. application of EMD 61753 (□). The mean (± s.e.mean) amounts of urine in the vehicle-treated groups were 0.49 ± 0.03 ($n = 20$ cages), 0.44 ± 0.03 ($n = 30$ cages), 0.6 ± 0.1 ($n = 15$ cages), and 0.8 ± 0.1 ($n = 10$ cages) ml per 100 g body weight, respectively. Each point in the figure represents the mean ± s.e.mean of 5 or 10 cage measurements. The data with ICI 197067 and ICI 204448 are from Barber *et al.* (1994).

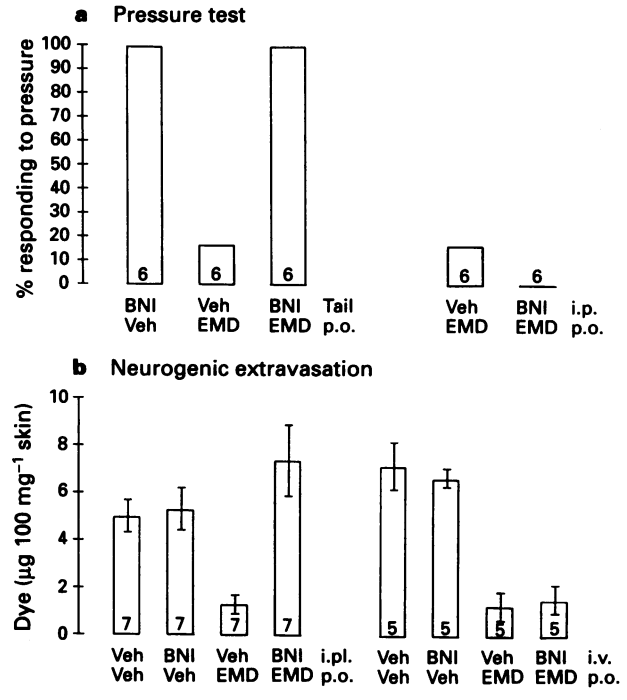


Figure 10 Demonstration of the peripheral action of systemically-applied EMD 61753. (a) Pressure test: the proportion of animals responding to noxious pressure on the inflamed tail after the application of 100 μg norbinaltorphimine (BNI) into the tail, 50 mg kg^{-1} EMD 61753, p.o. (EMD), and EMD 61753 and norbinaltorphimine are shown. Also displayed are the proportion of animals responding to pressure after administration of 10 mg kg^{-1} EMD 61753, p.o., and after EMD 61753 together with 100 μg norbinaltorphimine, i.p. (b) Neurogenic extravasation: the amount of dye extravasated after treatment with vehicle (Veh), with 50 μg norbinaltorphimine after intraplantar (i.pl.) application, with 50 mg kg^{-1} EMD 61753, p.o., and EMD 61753 and norbinaltorphimine are shown. Also indicated are the results obtained when this experiment was repeated with the same doses of the test compounds but the i.v. route of administration for norbinaltorphimine. The number of animals used is indicated in each column.

The pharmacological profile of EMD 61753 is consistent with that of a κ-opioid receptor agonist which has only weak central activity (Table 2). The major central side effects of κ agonists are sedation and aversive psychotomimesis/dysphoria (Pfeiffer *et al.*, 1986; Peters & Gaylor, 1989). Sedation was detected in the rotarod and narcosis potentiation models at much higher doses with EMD 61753 and the peripherally-selective κ-opioid receptor agonist ICI 204448 than with the centrally-active κ-agonist, ICI 197067 (Table 2). The same was true in our animal model of 'putative aversion', that is, the detection of the inhibitory effect of κ agonists on dopamine turnover in the nucleus accumbens as measured by DOPA accumulation (Table 2). κ agonists are known to inhibit the activity of mesolimbic dopaminergic neurones in this model (Manzanares *et al.*, 1991), and this characteristic is believed to be the physiological basis of their aversive action (Di Chiara & Imperato, 1988; Spanagel *et al.*, 1990; Shippenberg *et al.*, 1993).

Rank order of potency comparisons between various κ ligands in the diuresis, rodent abdominal constriction, formalin and normalgesic pressure tests indicate that activity in these models is probably due to penetration of the blood-brain barrier and activation of central κ-opioid receptors. Although the κ agonists tested all have a similar functional κ agonistic activity, the effectiveness of these substances after s.c. application (ICI 197067 > EMD 60400 > EMD 61753 and ICI 204448 in the normalgesic pressure, abdominal constriction, and diuresis tests and ICI 197067 > EMD 60400 > EMD 61753 > ICI 204448 in the formalin test; Barber *et al.*, 1994; Table 3; Figure 9) corresponds much better to their ability to produce central actions following systemic administration (Barber *et al.*, 1994; Table 2).

Our observation that the ability of a κ agonist to elicit diuresis corresponds to its effectiveness in stimulating central κ-opioid receptors confirms the findings of Brooks *et al.* (1993), who concluded that diuresis is mediated by κ receptors located beyond the blood-brain barrier. Furthermore, diuresis induced by the centrally-acting κ ligands ethylketazocine, spiradoline or CI 977 is found in the same dose-range as central discriminative stimulus properties in Rhesus monkeys (Dykstra *et al.*, 1987) and aversive and subjective effects in man (Peters *et al.*, 1987; Reece *et al.*, 1989), all of which indicates that water diuresis is a sensitive indicator of the activation of central κ-opioid receptors.

By this measure EMD 61753 compares favourably with other peripherally-selective κ-opioid receptor agonists. ICI 204448 elicits diuresis at doses of and above 0.3 mg kg^{-1},s.c., (Figure 9) while BRL 52974, which has an IC_{50} value of 42 nM in the rabbit vas deferens assay and an ID_{50} value > 10 mg kg^{-1}, s.c., in the rat rotarod test, elicits diuresis in the rat at doses above 0.03 mg kg^{-1}, i.v. (Brooks *et al.*, 1993). The threshold dose of EMD 61753 for the induction of diuresis (1.0 mg kg^{-1}, s.c., and 10 mg kg^{-1}, p.o., in non-hydrated rats) is relatively low in comparison to other measures of central activity (Table 2), possibly because EMD 61753 may have preferential access (see Table 1 for radioactivity levels in the pituitary) to hypothalamo-neurohypophysial κ-opioid receptors (Rossi & Brooks, 1993).

Peripheral antinociceptive effects of systemically- (Smith *et al.*, 1985; Follenfant *et al.*, 1988) and locally-applied (Bentley *et al.*, 1981) opioid receptor agonists have been claimed in the abdominal constriction test, although we, like Hayes & Hayward (1988) found no difference in ID_{50} values when our κ agonist was given by the i.p. or s.c. routes of administration. Moreover, since the action of systemically-applied EMD 61753 could not be inhibited by i.p. injection of norbinaltorphimine (100 μg; F. Mauler, unpublished observations) our findings are consistent with the contention of Rogers *et al.* (1992) that activity in this test is due to penetration into the CNS and activation of central κ receptors. This would further imply that there are species differences in the ability of EMD 61753 to activate central κ-opioid receptors since, in contrast to EMD 60400, ICI 197067, and ICI 204448 (Barber *et al.*, 1994), the dose-response curve of EMD 61753 in the abdominal constriction test is much shallower in the rat than in the mouse (Figure 6).

The ability of EMD 61753 to produce what is probably centrally-mediated antinociception in the normalgesic pressure test after p.o. but not s.c. application (Figure 3) was surprising. First-pass metabolism in the liver could generate active metabolites which are able to penetrate the blood-brain barrier more easily than the parent compound. The decreased potency of EMD 61753 in this test after very high oral doses (150 and 300 mg kg^{-1}; Figure 3) may reflect altered metabolism in the liver compared to that at lower doses. This must remain speculative, however, because activity of EMD 61753 after only oral but not s.c. administration was not observed in any other central test applied here.

In contrast to the weak central effects of EMD 61753, antinociception in the hyperalgesic pressure test was observed at relatively low doses (threshold doses in this test were approximately 0.03 mg kg^{-1}, s.c., and 1.0 mg kg^{-1}, p.o.; Figure 3). It seems likely that systemically-applied EMD 61753 is producing its antinociceptive effect in this test in the periphery. This is because the action of EMD 61753 was completely inhibited by local injection of the κ-opioid receptor antagonist norbinaltorphimine into the inflamed tissue at a dose (100 μg) which produced no systemic inhibition of κ-mediated antinociception (Figure 10a). Another indication that the actions of EMD 61753 in this model are peripherally mediated is that the rank order of potency of different κ ligands in this test under hyperalgesic conditions (EMD 60400 > ICI 197067 > EMD 61753 > ICI 204448; Table 3; Barber *et al.*, 1994) does not correlate with their ability to produce activation of central κ-opioid receptors (Table 2; Barber *et al.*, 1994). The difference in the activity of EMD 61753 in the pressure test under normalgesic and hyperalgesic conditions (Figure 3) confirms that the presence of an inflammatory response is important for the manifestation of peripheral antinociceptive effects (Stein, 1993).

The inhibitory action of EMD 61753 on neurogenic inflammation (Figure 7) is also likely to be peripheral in nature since the actions of opiates in this test are known to be largely independent of their CNS and systemic effects (Barber, 1993). As in the hyperalgesic pressure test, the effect of systemically-applied EMD 61753 in this model was antagonized by the local application of norbinaltorphimine (50 μg; Figure 10b). Moreover, EMD 61753, ICI 204448 and ICI 197067 were equipotent after s.c. application (Table 3; ICI 204448 and ICI 197067 are also equipotent after i.v. administration; Barber, 1993; Barber *et al.*, 1994), although they have very different tendencies to cross the blood-brain barrier. The observation that plasma extravasation elicited by the injection of substance P, the putative neurotransmitter mediating neurogenic inflammation (Lembeck & Holzer, 1979), was not influenced by treatment with EMD 61753 indicates that this compound has a presynaptic site of action.

The peripheral mechanism of action of EMD 61753 in the neurogenic inflammation test is likely to be presynaptic inhibition of the release of substance P and other inflammatory mediators from the nerve endings of sensory C fibres (Yonehara *et al.*, 1992). In the case of the hyperalgesic pressure model, on the other hand, the most important peripheral action of EMD 61753 is probably an inhibition of the sensory impulse flow from the inflamed area (Russell *et al.*, 1987; Haley *et al.*, 1990; Meßlinger *et al.*, 1993). Opioid receptors which could mediate these actions have been detected on the peripheral terminals of sensory neurones (see Stein, 1993). The lower potency of EMD 61753 in the neurogenic inflammation model in comparison to the hyperalgesic pressure test (Table 3) may be related to the different nature of the inflammatory stimuli used in these tests (electrical stimulation vs. carrageenin, respectively) or the different lengths of time between initiation of the inflammatory reaction and testing (0–10 min and 3 h, respectively).

The present experiments indicate that EMD 61753 is a compound which despite its lipophilic diphenylmethyl group (Figure 1) has a low tendency to penetrate into the CNS. EMD 61753 has, like terfenadine and astemizole, a high binding affinity to plasma proteins (97% in the rat; R. Kunert, unpublished observations) which will not facilitate crossing of the blood-brain barrier endothelial membrane (Seelig *et al.*, 1994). A further possibility is that free EMD 61753 may be trapped in the hydrophobic interior membrane of blood-brain barrier endothelial cells and so be unable to reach the extracellular fluid of the brain (Seelig *et al.*, 1994). One of the advantages of amphiphilic structures such as EMD 61753 is their generally improved oral activity in comparison to hydrophilic compounds (Kuschinsky & Lüllmann, 1981). This was confirmed in the present study; the hydrophilic molecule, ICI 204448, was in contrast to EMD 61753 only very poorly active after oral application (Table 3).

To summarise, EMD 61753 is a potent and selective, orally-active κ-opioid receptor agonist which has a low propensity to cross the blood-brain barrier and produce unwanted side effects (sedation and putative aversion) through activation of central κ-opioid receptors. The strong antinociceptive actions of EMD 61753 against pressure nociception under inflammatory conditions are mediated peripherally, possibly by opioid receptors on the endings of sensory nerve fibres. EMD 61753 therefore represents progress towards the development of a new class of analgesic compounds with which pain of inflammatory origin may be alleviated without evoking unacceptable central side effects.

References

BARBER, A. (1993). μ- and κ-opioid receptor agonists produce peripheral inhibition of neurogenic plasma extravasation in rat skin. *Eur. J. Pharmacol.*, **236**, 113–120.

BARBER, A., BARTOSZYK, G.D., GREINER, H.E., MAULER, F., MURRAY, R.D,. SEYFRIED, C.A., SIMON, M., GOTTSCHLICH, R., HARTING, J. & LUES, I. (1994). Central and peripheral actions of the novel κ-opioid receptor agonist, EMD 60400. *Br. J. Pharmacol.*, **111**, 843–851.

BARBER, A., BARTOSZYK, G.D., GOTTSCHLICH, R., MAULER, F. & SEYFRIED, C.A. (1993). *In vivo* effects of the peripherally-selective, orally-active, κ-opioid receptor agonist EMD 61753. *Soc. Neurosci. Abstr.*, **19**, 577.15.

BARBER, A. & GOTTSCHLICH, R. (1992). Opioid agonists and antagonists: an evaluation of their peripheral actions in inflammation. *Med. Res. Rev.*, **12**, 525–562.

BENTLEY, G.A., NEWTON, S.H. & STARR, J. (1981). Evidence for an action of morphine and the enkephalins on sensory nerve endings in the mouse peritoneum. *Br. J. Pharmacol.*, **73**, 325–332.

BROOKS, D.P., GIARDINA, G., GELLAI, M., DONDIO, G., EDWARDS, R.M., PETRONE, G., DEPALMA, P.D., SBACCHI, M., JUGUS,M., MISIANO, P., WANG, Y.X. & CLARKE, G.D. (1993). Opiate receptors within the blood-brain barrier mediate kappa agonist-induced water diuresis. *J. Pharmacol. Exp. Ther.*, **266**, 164–171.

COSTELLO, G.F., MAIN, B.G., BARLOW, J.J., CARROLL, J.A. & SHAW, J.S. (1988). A novel series of potent and selective agonists at the opioid κ-receptor. *Eur. J. Pharmacol.*, **151**, 475–478.

DAMAS, J. & MOUSTY, J.-C. (1978). Inhibition de l'âction hypotensive de l'ácide arachidonique chez le rat. *J. Pharmacol. (Paris)*, **9**, 13–23.

DI CHIARA, G. & IMPERATO, A. (1988). Drugs abused by humans preferentially increase synaptic dopamine concentrations in the mesolimbic system of freely moving rats. *Proc. Natl. Acad. Sci. U.S.A.*, **85**, 5274–5278.

DIXON, W.J. & MOOD, A.M. (1948). A method for obtaining and analyzing sensitivity data. *J. Am. Stat. Ass.*, **43**, 109–126.

DYKSTRA, L.A., GMEREK, D.E., WINGER, G. & WOODS, J.H. (1987). Kappa opioids in Rhesus monkeys. I. Diuresis, sedation, analgesia and discriminative stimulus effects. *J. Pharmacol. Exp. Ther.*, **242**, 413–420.

FOLLENFANT, R.L., HARDY, G.W., LOWE, L.A., SCHNEIDER, C. & SMITH, T.W. (1988). Antinociceptive effects of the novel opioid peptide BW 443C compared with classical opiates; peripheral versus central actions. *Br. J. Pharmacol.*, **93**, 85–92.

GOTTSCHLICH, R., ACKERMANN, A., BARBER, A., BARTOSZYK, G.D., GREINER, H.E. & STOHRER, M. (1993). EMD 61753 is a unique representative of the diarylacetamides, a novel class of κ-opiate agonists. *Soc. Neurosci. Abstr.*, **19**, 577.14.

HALEY, J., KETCHUM, S. & DICKENSON, A. (1990). Peripheral κ-opioid modulation of the formalin response: an electrophysiological study in the rat. *Eur. J. Pharmacol.*, **191**, 437–446.

HAYES, A.G. & HAYWARD, N.J. (1988). Can the mouse abdominal constriction test be used as a model for peripheral opioid antinociceptive activity? *Br. J. Pharmacol.*, **93**, 173P.

HUNSKAAR, S. & HOLE, K. (1987). The formalin test in mice: dissociation between inflammatory and non-inflammatory pain. *Pain*, **30**, 103–114.

KUSCHINSKY, G. & LÜLLMANN, H. (1981). *Kurzes Lehrbuch der Pharmakologie und Toxikologie*. Stuttgart: G. Thieme.

LAHTI, R.A., MICKELSON, M.M., MCCALL, J.M. & VON VOIGTLANDER, P.F. (1985). [^{3}H]U-69593: a highly selective ligand for the opioid κ receptor. *Eur. J. Pharmacol.*, **109**, 281–284.

LEMBECK, F. & HOLZER, P. (1979). Substance P as neurogenic mediator of antidromic vasodilation and neurogenic plasma extravasation. *Naunyn-Schmied. Arch. Pharmacol.*, **310**, 175–183.

LITCHFIELD, J.T. & WILCOXON, F. (1949). A simplified method of evaluating dose-effect experiments. *J. Pharmacol. Exp. Ther.*, **96**, 99–113.

MANZANARES, J., LOOKINGLAND, K.J. & MOORE, K.E. (1991). Kappa opioid receptor-mediated regulation of dopaminergic neurons in rat brain. *J. Pharmacol. Exp. Ther.*, **256**, 500–505.

MEßLINGER, K., PAWLAK, M., LUKAS, A. & SCHMIDT, R.F. (1993). Peripheral action of EMD 60400, a new kappa-opioid agonist, on the activity of slowly conducting afferents in the inflamed knee joint of the cat. Abstract 42 *7th World Congress on Pain, Paris*, Seattle: IASP Publications.

MORAGUES, J. & ROBERTS, D.J. (1990). Ebastine. *Drug Fut.*, **15**, 674–679.

NICHOLSON, A.N. (1987). New antihistamines free of sedative side-effects. *Trends Pharmacol. Sci.*, **8**, 247–249.

PAXINOS, G. & WATSON, C. (1982). *The Rat Brain in Stereotaxic Coordinates*. Sydney: Academic Press.

PETERS, G. & GAYLOR, S. (1989). Human central nervous system effects of a selective kappa opioid agonist. *Clin. Pharmacol. Ther.*, **51**, PPF-5.

PETERS, G.R., WARD, N.J., ANTAL, E.G., LAI, P.Y. & DEMAAR, E.W. (1987). Diuretic actions in man of a selective kappa opioid agonist: U-62,066E. *J. Pharmacol. Exp. Ther.*, **240**, 128–131.

PFEIFFER, A., BRANTL, V., HERZ, A. & EMRICH, H.M. (1986). Psychotomimesis mediated by κ opiate receptors. *Science*, **233**, 774–776.

REECE, P.A., DAWKINS, R., WRIGHT, S., RAJAGOPALAN, R. & SEDMAN, A.J. (1989). Dose proportionality and pharmacodynamics of intramuscular CI-977. *Clin. Pharmacol. Ther.*, **51**, PIII–75.

RISAU, W. & WOLBURG, H. (1990). Development of the blood-brain barrier. *Trends Neurosci.*, **13**, 174–178.

ROGERS, H, BIRCH, P.J., HARRISON, S.M., PALMER, E., MANCHEE, G.R., JUDD, D.B., NAYLOR, A., SCOPES, D.I.C. & HAYES, A.G. (1992). GR 94839, a κ-opioid agonist with limited access to the central nervous system, has antinociceptive activity. *Br. J. Pharmacol.*, **106**, 783–789.

ROSSI, N.F. & BROOKS, D.P. (1993). Kappa agonist BRL 52656 inhibits osmotically-stimulated vasopressin secretion preferentially at hypothalamic sites. *Soc. Neurosci. Abstr.*, **19**, 478.9.

RUSSELL, N.J.W., SCHAIBLE, H.-G. & SCHMIDT, R.F. (1987). Opiates inhibit the discharges of fine afferent units from inflamed knee joint of the cat. *Neurosci. Lett.*, **76**, 107–112.

SEELIG, A., GOTTSCHLICH, R. & DEVANT, R.M. (1994). A method to determine the ability of drugs to diffuse through the blood-brain barrier. *Proc. Natl. Acad. Sci. U.S.A.*, **91**, 68–72.

SEYFRIED, C.A., ADAM, G. & GREVE, T. (1986). An automated direct-injection HPLC-method for the electrochemical/fluorimetric quantitation of monoamine and related compounds for the screening of large numbers of animals. *Biomed. Chromatogr.*, **1**, 78–88.

SHAW, J.S., CARROLL, J.A., ALCOCK, P. & MAIN, B.G. (1989). ICI 204448: a κ-opioid agonist with limited access to the CNS. *Br. J. Pharmacol.*, **96**, 986–992.

SHIPPENBERG, T.S., BALS-KUBIK, R. & HERZ, A. (1993). Examination of the neurochemical substrates mediating the motivational effects of opioids: role of the mesolimbic dopamine system and D-1 vs. D-2 dopamine receptors. *J. Pharmacol. Exp. Ther.*, **265**, 53–59.

SMITH, T.W., FOLLENFANT, R.L. & FERREIRA, S.H. (1985). Antinociceptive models displaying peripheral opioid activity. *Int. J. Tiss. Reac.*, **7**, 61–67.

SPANAGEL, R., HERZ, A. & SHIPPENBERG, T.S. (1990). The effect of opioid peptides on dopamine release in the nucleus accumbens: an *in vivo* microdialysis study. *J. Neurochem.*, **55**, 1734–1740.

STEIN, C. (1993). Peripheral mechanisms of opioid analgesia. *Anesth. Analg.*, **76**, 182–191.

YONEHARA, N., IMAI, Y., CHEN, J.-Q., TAKIUCHI, S. & INOKI, R. (1992). Influence of opioids on substance P release evoked by antidromic stimulation of primary afferent fibers in the hind instep of the rat. *Regul. Pept.*, **38**, 13–22.

(Received April 18, 1994
Revised July 6, 1994
Accepted July 25, 1994)

Br. J. Pharmacol. (1994), **113**, 1328–1332 © Macmillan Press Ltd, 1994

The interaction of α-human atrial natriuretic peptide (ANP) with salbutamol, sodium nitroprusside and isosorbide dinitrate in human bronchial smooth muscle

[1]Jane E. Nally, Robert A. Clayton, *Neil C. Thomson & †John C. McGrath

Autonomic Physiology Unit and †Clinical Research Initiative Institute of Physiology, Glasgow University, Glasgow G12 8QQ and *Department of Respiratory Medicine, Western Infirmary, Glasgow, G11 6NT

1 Contractions in human bronchial rings evoked by methacholine (10^{-6} M) were reversed by single contractions of α-human atrial natriuretic peptide (10^{-6} M), salbutamol (10^{-6} M), sodium nitroprusside (10^{-6} M) or isosorbide dinitrate (4.2×10^{-5} M) and the extent of the relaxations compared. The activity of combinations of ANP with salbutamol, sodium nitroprusside and isosorbide dinitrate were compared with those for each agonist alone.

2 ANP and salbutamol were equipotent in reversing methacholine-evoked contraction and, in combination these agonists evoked an additive response. ANP and sodium nitroprusside also evoked similar degrees of relaxation and were additive, as were ANP and isosorbide dinitrate; however, with isosorbide dinitrate a higher concentration was required to evoke the same degree of relaxation as ANP, sodium nitroprusside or salbutamol.

3 Cumulative concentration-response curves to methacholine (10^{-9}–3×10^{-4} M) were examined in the presence and absence of the above bronchodilator substances, alone and in combination allowing their abilities to protect against contraction to be compared. ANP (10^{-6} M) and salbutamol (10^{-6} M) each attenuated subsequent contractions evoked by methacholine, an ability not shared with sodium nitroprusside (10^{-6} M) or isosorbide dinitrate (4.2×10^{-5} M). Indeed at lower concentrations of methacholine ($<3 \times 10^{-7}$ M), sodium nitroprusside evoked a paradoxical enhancement of methacholine-evoked contractions.

4 In combination, ANP and salbutamol attenuated contractions evoked by methacholine to a significantly greater degree than that seen with either agonist alone, whilst a combination of ANP and sodium nitroprusside evoked no greater effect than that seen with ANP alone. By contrast, isosorbide dinitrate and ANP together evoked a greater inhibition than ANP alone.

5 These results suggest that a combination of agents such as ANP and salbutamol evokes a greater effect than either alone, both in reversing and protecting against methacholine-evoked contractions. Such combinations may be of benefit in the treatment of patients, allowing lower doses of drug to be used. Combinations of ANP and isosorbide dinitrate may likewise be of interest; however, the mechanism underlying the enhancement of ANP responses by isosorbide dinitrate requires further study.

Keywords: Atrial natriuretic peptide; salbutamol; sodium nitroprusside; isosorbide dinitrate

Introduction

α-Human atrial natriuretic peptide (ANP) is a naturally occurring 28 amino acid peptide, released from the atria (Sagnella *et al.*, 1984) and from isolated lung tissue (Gutkowska & Nemer, 1989). Its mechanism of action has been postulated as being via activation of particulate guanylate cyclase leading to elevation of guanosine 3':5'-cyclic monophosphate (cyclic GMP) (Ishii & Murad, 1989) and it has been shown to have vasodilator (Sagnell *et al.*, 1984) natriuretic (Gutkowska & Nemer, 1989) and diuretic (Anderson *et al.*, 1986) properties. More recently, studies *in vitro* and *in vivo* have shown that ANP may have activity in the lungs. Infused ANP evokes a bronchodilator effect in asthmatic patients (Hulks *et al.*, 1989; Angus *et al.*, 1993) and confers protection against subsequent histamine challenge (Hulks *et al.*, 1991) or the effects of nebulised distilled water (McAlpine *et al.*, 1992). Inhalation of ANP has been demonstrated to produce a small bronchodilatation (Hulks & Thomson, 1994) and to protect against subsequent histamine (Hulks & Thomson, 1992) or methacholine (Angus *et al.*, 1994a) challenge. *In vitro*, ANP evokes reversal of methacholine-evoked contraction as well as protecting against subsequent challenge with this agonist. Each of these effects was greatly enhanced by the presence of the neutral endopeptidase inhibitor, phosphoramidon, (Angus *et al.*, 1994b). As a result of the above studies, the possible therapeutic use of ANP in asthma has been postulated, possibly as an adjunct to current therapy. Its relative effectiveness compared to currently available bronchodilators has not however been established, nor has the ability of ANP to interact with such therapies been studied.

In this present study, a direct comparison of ANP with other bronchodilators has been undertaken *in vitro*, to examine further the possible usefulness of this peptide in asthma. The initial bronchodilator chosen for comparison was the β_2-adrenoceptor agonist salbutamol, which is thought to act via K^+channel opening (Miura *et al.*, 1992) as well as via adenosine 3':5'-cyclic monophosphate (cyclic AMP) activation (Rinard *et al.*, 1983). In addition, the effects of sodium nitroprusside and isosorbide dinitrate, each of which is thought to act as a nitric oxide donator (Feelisch & Noack, 1987), resulting in activation of soluble, rather than particulate guanylate cyclase, have been compared to ANP. The extent to which ANP interacts with each of these dilators has been evaluated.

Methods

Tissue collection and preparation

Macroscopically normal human bronchi (3rd to 6th order) were obtained from patients undergoing thoracic surgery.

[1] Author for correspondence.

Tissues were dissected free of connective tissue and fat and stored overnight at 4°C in oxygenated Krebs-Henseleit solution of the following composition (mM): NaCl 118.4, KCl 4.7, $CaCl_2$ 2.5, $MgSO_4$ 1.2, $NaHCO_3$ 24.9, KH_2PO_4 1.2 and glucose 11.1. Published data (Brink *et al.*, 1980) have shown that overnight storage of this tissue does not alter its reactivity.

Measurement of contractile responses

Contractile responses were measured from rings of human bronchi (3–5 mm) in vertical organ baths (10 ml) at 37 ± 0.5°C in oxygenated (95% O_2, 5% CO_2) Krebs-Henseleit solution. Tension (2 g wt.) was applied by inserting two platinum wires into the lumen. One wire was anchored and the other attached to a force displacement transducer (Grass FT03T). After pre-incubation of tissues with methacholine (10^{-6} M), cumulative concentration-response curves were constructed to ANP (10^{-8}–3×10^{-6} M), salbutamol (10^{-8}–10^{-5} M), sodium nitroprusside (10^{-8}–10^{-5} M) and isosorbide dinitrate (4.2×10^{-7}–4.2×10^{-4} M) in order to establish pD_2 values for these dilators. These concentrations of agonists were subsequently used to reverse contractions evoked by methacholine (3×10^{-6} M). In this and in all subsequent experiments where ANP was used, the neutral endopeptidase inhibitor phosphoramidon (3.67×10^{-5} M) was present to prevent ANP's breakdown. Combinations of ANP with each of these agonists were then compared with the agonists alone.

In a second set of experiments, cumulative concentration-response curves were constructed to methacholine in the presence and absence of ANP, salbutamol, sodium nitroprusside and isosorbide dinitrate, alone and in combination. Drugs were added directly to the organ bath.

Materials

The following chemicals were used; α-human atrial natriuretic peptide 28 amino acid (ANP, Bachem), isosorbide dinitrate (Isoket, Schwarz Pharma Ltd.), methacholine chloride (Sigma), N-(α-rhamnopyranosyloxyhydroxy-phosphinyl)-L-leucyl-L-tryptophan (Phosphoramidon, Sigma), salbutamol (Sigma), sodium nitroprusside (Sigma). Concentration in text refers to the salts, with the exception of salbutamol which is expressed as the base. Stock solutions of drugs were prepared in distilled water and subsequent dilutions made in Krebs-Henseleit solution.

Analysis of results

Results are expressed as mean ± s.e. mean. Statistical significance between data samples was tested by two-way analysis of variance. Significance between pD_2 values (the negative log of the concentration evoking 50% of the maximum response) was calculated by Student's *t* test. A probability level of $P<0.05$ was considered significant. Number of observations (*n*) refers to the number of animals used.

Results

After pre-constriction of tissues with methacholine (10^{-6} M, the EC_{50} for methacholine in this tissue), cumulative concentration-response curves were constructed to ANP (10^{-8}–3×10^{-6} M, in the presence of phosphoramidon (3.67×10^{-5} M)) (Figure 1), to salbutamol (10^{-8}–10^{-5} M) (Figure 1), to sodium nitroprusside (10^{-8}–10^{-5} M) and to isosorbide dinitrate (4.2×10^{-7}–4.2×10^{-4} M) from which pD_2 values of 5.91 ± 0.1, 6.27 ± 0.18, 6.05 ± 0.2 and 4.8 ± 0.3 respectively were calculated.

In order to examine additive effects of bronchodilators, without reaching maximal dilatation in these tissues, methacholine 3×10^{-6} M was used to pre-constrict tissues in subsequent experiments rather than the 10^{-6} M used in the calculation of pD_2 values. The use of the higher concentrations of methacholine resulted in small relaxations being evoked by the dilators, since there is an inverse relationship between the level of airway tone and the potency of relaxant agonists (Van den Brink, 1973; Angus *et al.*, 1994b). Contractions of the bronchial rings evoked by single concentrations of methacholine (3×10^{-6} M) were reversed by ANP (16.4 ± 2.8% inhibition, $n=6$) and salbutamol (23.8 ± 13.4% inhibition, $n=6$) each at 10^{-6} M. A combination of ANP and salbutamol (each at 10^{-6} M) evoked an additive (43.3 ± 8.7%, $n=6$) inhibition of methacholine-evoked tone compared with these agonists alone (Figure 2a). Phosphoramidon alone (3.67×10^{-5} M) did not evoke any reversal of methacholine-evoked tone in these tissues. ANP (10^{-6} M) alone and in combination with either sodium nitroprusside (10^{-6} M) or isosorbide dinitrate (4.2×10^{-5} M) was also examined. A combination of ANP and sodium nitroprusside similarly evoked a relaxation (36.9 ± 8.6%, $n=6$) which was significantly greater than that evoked by sodium nitroprusside (16.4 ± 7.6%, $n=6$) or ANP (22.6 ± 4.7%, $n=6$) alone (Figure 2b) as did a combination of ANP and isosorbide dinitrate (40.1 ± 6, compared with 15.6 ± 2.8 and 19.3 ± 2.1% respectively, Figure 2c, $n=6$).

Cumulative concentration-response curves were constructed to methacholine (10^{-9}–3×10^{-4} M) in the presence and absence of phosphoramidon (3.67×10^{-5} M) alone and ANP (10^{-6} M, in the presence of phosphoramidon as previously described), salbutamol (10^{-6} M), sodium nitroprusside, (10^{-6} M) and isosorbide dinitrate (4.2×10^{-5} M), either alone or in combination. Phosphoramidon alone did not alter subsequent methacholine challenge; however, the presence of either ANP or salbutamol attenuated (each $P<0.001$) the contractions evoked by methacholine (pD_2 values; methacholine alone; 6.01 ± 0.09, $n=6$; methacholine plus ANP; 5.68 ± 0.15, $n=6$; methacholine plus salbutamol; 5.43 ± 0.17, $n=6$, $P<0.05$ compared to control in each case. Figure 3). ANP, but not salbutamol evoked a significant ($P<0.005$) decrease in maximum response. Neither the presence of sodium nitroprusside ($n=9$, Figure 4) nor of isosorbide dinitrate ($n=6$, Figure 5) alone significantly altered the contractions to methacholine. ANP and salbutamol in combination evoked a significant attenuation ($P<0.001$) of the methacholine responses compared with either agonist alone (Figure 3). In this case, the pD_2 value in

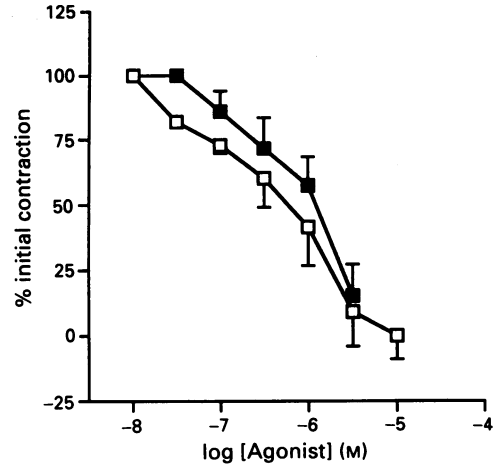


Figure 1 Concentration-response curves (CRCs) evoked by atrial natriuretic peptide (ANP 3×10^{-8}–3×10^{-6} M), in the presence of phosphoramidon (3.67×10^{-5} M, ■) and salbutamol (10^{-8}–10^{-5} M, □) after pre-constriction of human bronchial rings with methacholine (10^{-6} M). ANP (+phosphoramidon) and salbutamol each evoked concentration-dependent relaxations of evoked tone. Number of observations (n) = 6 in each case.

the presence of a combination of these agonists (5.48 ± 0.2), was not significantly different from that evoked by either agonist alone, however there was a decrease in the magnitude of contraction at each methacholine concentration, with the decrease in maximum response being 43%

ANP and sodium nitroprusside combined were no more effective than ANP alone (pD_2 for methacholine alone, 5.99 ± 0.1, plus ANP, 5.59 ± 0.18 ($P<0.05$ compared with control), plus sodium nitroprusside, 6.07 ± 0.23 plus both, 5.71 ± 0.17, $n = 9$, Figure 4).

ANP and isosorbide dinitrate in combination evoked a greater attenuation of the methacholine-evoked curve than did ANP alone ($P<0.005$). This was not reflected in a rightward shift in the concentration-response curves (pD_2 for methacholine alone, 5.97 ± 0.09, plus ANP, 5.68 ± 0.22, plus isosorbide dinitrate 5.82 ± 0.18 and plus both, 5.78 ± 0.11), but rather in suppression of the magnitude of the responses evoked by methacholine at concentrations above 10^{-5} M. The maximum response in the presence of such a combination was decreased by 48% compared with control (Figure 5).

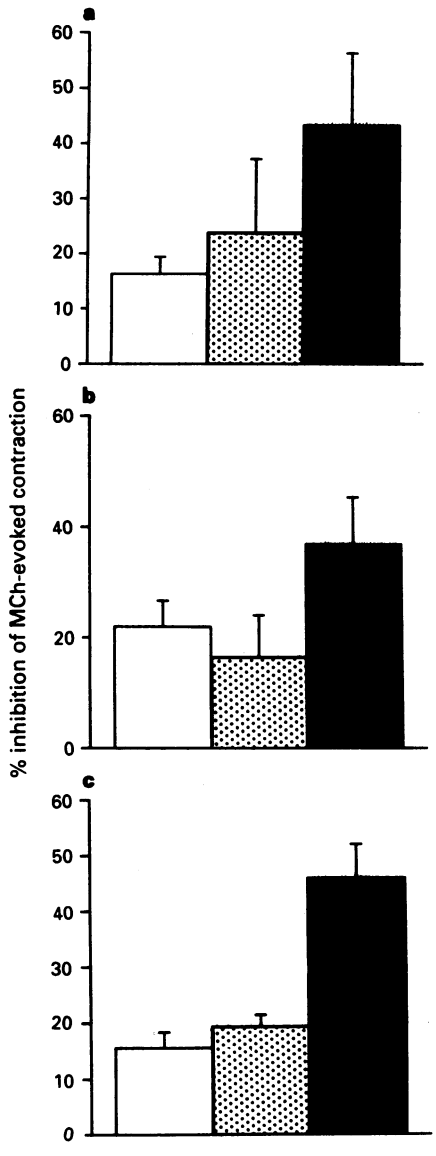


Figure 2 Relaxations of methacholine-evoked contractions (3×10^{-6} M), evoked by (a) atrial natriuretic peptide (ANP 10^{-6} M, open column) and salbutamol (10^{-6} M, stippled column) alone and in combination (solid column); (b) ANP (10^{-6} M, open column) and sodium nitroprusside (10^{-6} M, stippled column) alone and in combination (solid column) and (c) ANP (10^{-6} M, clear column) and isosorbide dinitrate (4.2×10^{-5} M, stippled column) alone and in combination (solid column). In each case where ANP was used, phosphoramidon (3.67×10^{-5} M) was present to inhibit its degradation. Alone, each of these agonists evoked similar relaxations at the concentrations used, while combinations of ANP with salbutamol, sodium nitroprusside or isosorbide dinitrate evoked additive responses. Number of observations (n) = 6 in each case.

Discussion

These results suggest for the first time, that, at the concentration chosen, ANP and salbutamol can evoke similar relaxa-

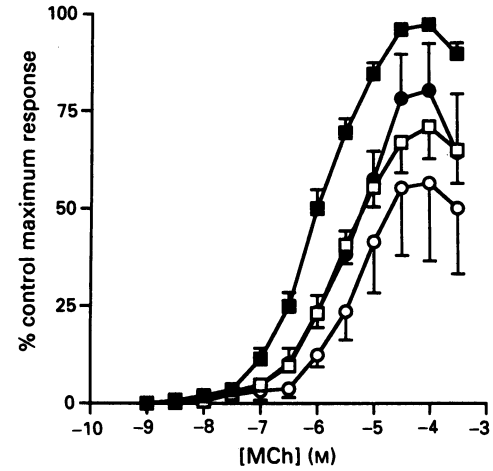


Figure 3 Concentration-response curves (CRCs) evoked by methacholine (MCh, 10^{-9}-3×10^{-4} M) were constructed in human bronchial rings in the absence (■, $n = 12$) and in the presence of atrial natriuretic peptide (ANP) (□, 10^{-6} M, $n = 6$) or salbutamol (●, 10^{-6} M, $n = 6$) alone and (○) in combination ($n = 6$). Where ANP was used, phosphoramidon (3.67×10^{-5} M) was present to inhibit its degradation. ANP and salbutamol each evoked similar rightward shifts of the MCh-evoked concentration-response curve. A combination of these agonists evoked a significantly greater attenuation than that evoked by either alone.

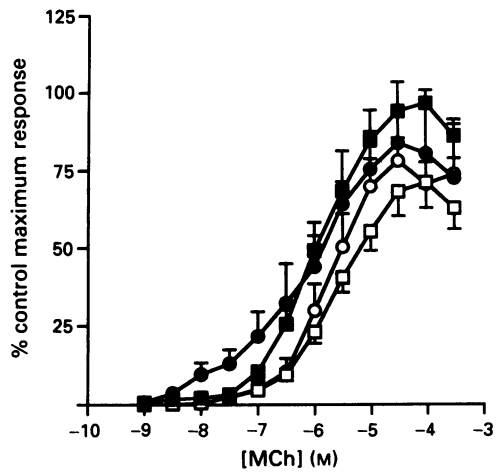


Figure 4 Concentration-response curves (CRCs) evoked by methacholine (10^{-9}-3×10^{-4} M) were constructed in human bronchial rings in the absence (■, $n = 15$) and in the presence of atrial natriuretic peptide (ANP, □, 10^{-6} M, $n = 6$) or sodium nitroprusside (●, 10^{-6} M, $n = 9$) alone and (○) in combination ($n = 6$). Where ANP was used, phosphoramidon (3.67×10^{-5} M) was present to inhibit its degradation. In contrast to ANP, sodium nitroprusside did not evoke any rightward shift of the methacholine-evoked concentration-response curve and indeed enhanced lower concentrations of methacholine. A combination of these agonists evoked no greater attenuation than that evoked by ANP alone.

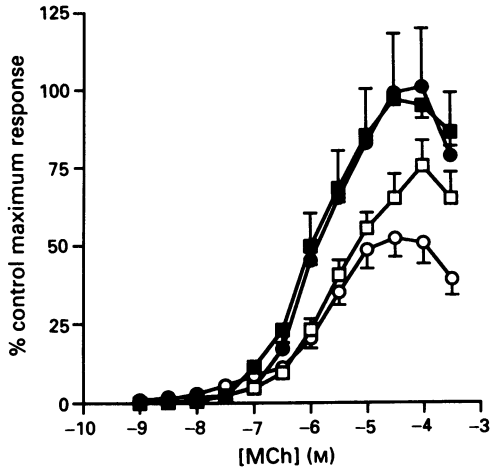


Figure 5 Concentration-response curves (CRCs) evoked by methacholine (10^{-9}–3×10^{-4} M) were constructed in human bronchial rings in the absence (■, $n = 12$) and in the presence of atrial natriuretic peptide (ANP, □, 10^{-6} M, $n = 6$) or isosorbide dinitrate (●, 4.2×10^{-5} M, $n = 6$) alone and (○) in combination ($n = 6$). Where ANP was used, phosphoramidon (3.67×10^{-5} M) was present to inhibit its degradation. In contrast to ANP, isosorbide dinitrate did not evoke any rightward shift of the methacholine-evoked concentration-response curve, however, a combination of these agonists evoked a greater reduction of the maximum response than that evoked by ANP alone.

tion of methacholine-evoked contraction, with a combination of these agonists evoking an approximately additive effect in human bronchi. The possibility exists that this represents synergy between cyclic GMP and cyclic AMP elevation, or K^+ channel opening, however further study would be required to confirm that this is the mechanism. A similar pattern of interaction is seen when ANP is compared with the nitric oxide donor, sodium nitroprusside, however, with isosorbide dinitrate a higher concentration was required to evoke the same degree of relaxation as ANP. Isosorbide dinitrate and ANP nevertheless had an additive effect when used in combination. Previous studies in bovine airway smooth muscle (Gruetter *et al.*, 1989) suggested that isosorbide dinitrate was ineffective in bovine bronchi up to a concentration of 10^{-5} M, and indeed, in this present study, a higher concentration was used. This might be expected to limit its usefulness *in vivo*; however it has been shown to protect against some forms of asthma (e.g. exercise-induced asthma; Tullet & Patel, 1983). Isosorbide dinitrate is a compound currently used in the treatment of angina and it is thought to release nitric oxide after first forming an intermediary complex (Ignarro *et al.*, 1981). The requirement to form such an intermediary may explain the difference in potency between isosorbide dinitrate and sodium nitroprusside.

When these bronchodilator substances were pre-incubated, ANP (in the presence of phosphoramidon) showed an ability to confer protection against methacholine-induced contraction, which is in keeping with our previous studies in human and bovine bronchi (Angus *et al.*, 1994b). Salbutamol likewise attenuated subsequent methacholine-challenge, which is at variance with a number of studies which have shown little (Advenier *et al.*, 1988) or no (Gustaffson & Persson, 1991; Advenier *et al.*, 1991) pre-protectant effect of this drug. Clinical studies (e.g. Tattersfield, 1987; Britton *et al.*, 1988) have however shown an ability of salbutamol to inhibit bronchial reactivity and our studies appear to indicate a similar effect against methacholine-challenge. The combination of these two agonists evoked an additive effect, again suggesting a possible role for the use of these agonists in combination.

Interactions between these drugs have not, to the best of our knowledge, been studied in airway smooth muscle before, although interactions between other bronchodilators has been evaluated. For example, theophylline and the β-adrenoceptor agonist, isoprenaline (Karlsson & Persson, 1981) demonstrated no additive effect in dilating pre-constricted guinea-pig trachea, whilst in human isolated bronchus (Advenier *et al.*, 1988), a combination of fenoterol and the muscarinic antagonist, ipratropium, produced an additive effect in attenuating subsequent challenge. In rat blood vessels a synergistic interaction in inhibiting phenylephrine-induced challenge has been demonstrated between the atrial natriuretic peptide, atriopeptin II and the non-selective β-agonist, isoprenaline (Jang *et al.*, 1993). This result was attributed to an inhibitory action of cyclic GMP on cyclic nucleotide phosphodiesterase type III and, while this is one possible explanation of our results, it is not possible from the present study to evaluate whether this mechanism underlies the interaction seen here between ANP and salbutamol, either in reversing or preventing methacholine-evoked contraction. Our results do however suggest that a combination of agonists, such as ANP with salbutamol, might be of benefit in the treatment of such conditions as acute severe asthma, allowing lower doses of β-agonist to be given.

The combinations of ANP with the other two agonists, sodium nitroprusside and isosorbide dinitrate, demonstrated some interesting dissimilarities between these two putative nitric oxide donor compounds. Sodium nitroprusside, at the concentration used, appears to have no ability to protect against subsequent methacholine-evoked contraction, despite evoking bronchodilatation at this level. Indeed at concentrations of methacholine less than 3×10^{-7} M, the presence of sodium nitroprusside evoked a significant enhancement of contractions, for which we have no explanation. This is in contrast with studies in vascular tissue, (e.g. rat aorta; Maurice *et al.*, 1991) where sodium nitroprusside inhibited subsequent contractions. Sodium nitroprusside likewise did not alter the ability of ANP to protect against subsequent contraction, suggesting perhaps that only activation of the particulate form of guanylate cyclase, as is thought to occur with ANP, leads to protection of these tissues against methacholine-evoked contraction. Isosorbide dinitrate did not enhance any methacholine-evoked contractions in the manner of sodium nitroprusside and, although it was ineffectual alone, it did enhance the ANP effect at higher concentrations of methacholine. Sodium nitroprusside and isosorbide dinitrate are proposed to (Feelisch & Noack, 1987) share a common mechanism, nitric oxide release stimulating intracellular cyclic GMP elevation, albeit with an intermediary step involved in the case of isosorbide dinitrate. It is thus tempting to speculate that nitric oxide production is not the mechanism by which isosorbide dinitrate is exerting its pre-protective effect when combined with ANP in human bronchial smooth muscle. Alternatively, the higher concentration of isosorbide dinitrate used, although required to evoke the same relaxation as that evoked by lower concentrations of sodium nitroprusside, might explain the differences seen between these two compounds in the present study.

The inability of sodium nitroprusside and isosorbide dinitrate to protect against contractions, despite evoking bronchodilatation, is in keeping with other studies. Gustafsson & Persson (1991), for example, found similar results using β_2-agonists and xanthines in guinea-pig isolated trachea. These findings suggest that 'functional antagonism' might not simply be the mechanism by which bronchodilators exert a pre-protective effect. It has been proposed (Persson *et al.*, 1982), that β_2-agonists, for example, have effects on cells other than airway smooth muscle and that this may contribute to their protective effects in human asthmatic subjects (Britton *et al.*, 1988).

In conclusion, in their capacities as both bronchodilators and as agents which, in the present study, attenuate subse-

quent challenge, ANP and salbutamol have an additive effect which may suggest their concurrent use may be of benefit in the treatment of asthma. Sodium nitroprusside and isosorbide dinitrate similarly evoke a bronchodilator effect; however, this is not accompanied by a pre-protecting ability. Nevertheless, in the case of isosorbide dinitrate, enhancement of the ANP response can be demonstrated and the differences in activity between sodium nitroprusside and isosorbide dinitrate remain to be fully explained.

This work was supported by the National Asthma Campaign and Chest Heart and Stroke Association (Scotland). We are grateful to the following for their assistance in providing human bronchial samples: Mr D. Prakash and Mr A.N. Jilaihawi and staff, theatre 6 and Dr A.L.C. Maclay and Dr H. Kamel and staff, Pathology department, Hairmyres Hospital, East Kilbride, Scotland.

References

ADVENIER, C., NALINE, E., MATRAN, R.M., TOTY, L. & BAKDASH, H. (1988). Interaction between fenoterol, ipratropium and acetylcholine on human isolated bronchus. *J. Allergy. Clin. Immunol.*, **82**, 40–46.

ADVENIER, C., CANDENAS, M.-L., NALINE, E. & DE VOS, C. (1991). The effect of cetrizine on the human isolated bronchus: interaction with salbutamol. *J. Allergy Clin. Immunol.*, **88**, 104–113.

ANDERSON, J., STRUTHERS, A., CHRISTOFIDES, N. & BLOOM, S. (1986). Atrial natriuretic peptide: an exogenous factor enhancing sodium excretion in man. *Clin. Sci.*, **70**, 327–331.

ANGUS, R.M., MCCALLUM, M.J.A., HULKS, G. & THOMSON, N.C. (1993). The bronchodilator and cardiovascular response to high dose infused atrial natriuretic peptide in asthma. *Am. Rev. Respir. Dis.*, **147**, 1122–1125.

ANGUS, R.M., MCCALLUM, M.J.A., HULKS, G. & THOMSON, N.C. (1994a). Effect of inhaled atrial natriuretic peptide on methacholine induced bronchoconstriction in asthma. *Clin. Exp. Allergy*, (in press).

ANGUS, R.M., NALLY, J.E., MCCALL, R., YOUNG, L.C., MCGRATH, J.C. & THOMSON, N.C. (1994b). Modulation of the effect of atrial natriuretic peptide in human and bovine bronchi by phosphoramidon. *Clin. Sci.*, **86**, 291–295.

BRINK, C., GRIMAUD, C., GUILLOT, C. & OREHEK, J. (1980). The interaction between indomethacin and contractile agents on human isolated airway muscle. *Br. J. Pharmacol.*, **69**, 383–388.

BRITTON, J.R., HANLEY, S.P., GARRETT, H., HADFIELD, A.E. & TATTERSFIELD, A.E. (1988). Dose related effects of salbutamol and ipratropium bromide on airway calibre and reactivity in subjects with asthma. *Thorax*, **43**, 300–305.

FEELISCH, M. & NOVAK, E.A. (1987). Correlation between nitric oxide formation during degradation of organic nitrates and activation of guanylate cyclase. *Eur. J. Pharmacol.*, **139**, 19–30.

GRUETTER, C.A., CHILVERS, C.E., BOSSERMAN, M.K., LEMKE, M., BALL, J.G. & VALENTOVIC, M.A. (1989). Comparison of relaxation induced by glyceryltrinitrate, isosorbide and dinitrate and sodium nitroprusside in bovine airways. *Am. Rev. Respir. Dis.*, **139**, 1192–1197.

GUSTAFSSON, B. & PERSSON, C.G.A. (1991). Effect of different bronchodilators on airway smooth muscle responsiveness to contractile agents. *Thorax*, **46**, 360–365.

GUTKOWSKA, J. & NEMER, M. (1989). Structure, expression and function of atrial natriuretic factor in extra atrial tissues. *Endocr. Rev.*, **10**, 519–536.

HULKS, G., JARDINE, A., CONNELL, J.M.C. & THOMSON, N.C. (1989). Bronchodilator effect of atrial natriuretic peptide in asthma. *Br. J. Med.*, **299**, 1081–1082.

HULKS, G., JARDINE, A., CONNELL, J.M.C. & THOMSON, N.C. (1991). Influence of elevated plasma levels of atrial natriuretic factor on bronchial reactivity in asthma. *Am. Rev. Resp. Dis.*, **143**, 778–782.

HULKS, G. & THOMSON, N. (1992). Inhaled atrial natriuretic peptide and asthmatic airways. *Br. J. Med.*, **304**, 1156.

HULKS, G. & THOMSON, N.C. (1994). High dose inhaled atrial natriuretic peptide is a bronchodilator in asthmatic subjects. *Eur. Respir. J.*, (in press).

IGNARRO, L.J., LIPPTON, H. EDWARDS, J.C., BARICOS, W.C., HYMAN, A.L., KADOWITZ, P.J. & GREUTTER, C.A. (1981). Mechanisms of vascular smooth muscle relaxation by organic nitrates, nitrites, nitroprusside and nitric oxide: evidence for the involvement of s-nitrosothiols as active intermediates. *J. Pharmacol. Exp. Ther.*, **218**, 739–749.

ISHII, K. & MURAD, F. (1989). ANP relaxes bovine tracheal smooth muscle and increases cGMP. *Am. J. Physiol.*, **256**, C495–C500.

JANG, E.K., DAVIDSON, M.M.L., CRANKSHAW, D. & HASLAM, R.J. (1993). Synergistic inhibitory effects of atriopeptin II and isoproterenol on contraction of rat aortic smooth muscle: roles of cGMP and cAMP. *Eur. J. Pharmacol.*, **250**, 477–481.

KARLSSON, J.A. & PERSSON, C.G.A. (1981). Influence of tracheal contraction on relaxant effects *in vitro* of theophylline and isoprenaline. *Br. J. Pharmacol.*, **74**, 73–79.

MAURICE, D.H., CRANKSHAW, D. & HASLAM, R.J. (1991). Synergistic actions of nitrovasodilators and isoprenaline on rat smooth muscle. *Eur. J. Pharmacol.*, **192**, 235–242.

MCALPINE, L.G., HULKS, G. & THOMSON, N.C. (1992). The effect of intravenous infusion of atrial natriuretic factor on fog inhaled bronchoconstriction in patients with asthma. *Am. Rev. Respir. Dis.*, **146**, 912–915.

MIURA, M., BELVISI, M.G., STRETTON, C.D., YACOUB, M.H. & BARNES, P.J. (1992). Role of potassium channels in bronchodilator responses in human airways. *Am. Rev. Respir. Dis.*, **146**, 132–136.

PERSSON, C.G.A., ERJEFÄLT, I., GREGA, G.J. & SVENSÖ, E. (1982). The role of β-receptor agonists in the inhibition of pulmonary edema. *Ann. N.Y. Acad. Sci.*, **384**, 544–557.

RINARD, G.A., JENSEN, A. & PLUNKETT, M.A. (1983). Hydrocortisone and isoproterenol effects on trachealis cAMP and relaxation. *J. Appl. Physiol.*, **55**, 1609–1613.

SAGNELLA, G.A. & MCGREGOR, G.A. (1984). Cardiac peptides and the control of sodium excretion. *Nature*, **309**, 666–669.

TATTERSFIELD, A.E. (1987). Beta agonists and anti-cholinergic drugs: effect on bronchial reactivity. *Am. Rev. Resp. Dis.*, **136**, S64–S68.

TULLET, W.M. & PATEL, K.R. (1983). Isosorbide dinitrate and isoxsuprine in exercise induced asthma. *Brit. Med. J.*, **286**, 1934–1935.

VAN DEN BRINK, F.G. (1973). The model of functional interaction II. Experimental verification of a new model: the antagonism of β-adrenoceptor stimulants and other antagonists. *Eur. J. Pharmacol.*, **22**, 279–286.

(Received April 20, 1994
Revised July 11, 1994
Accepted July 26, 1994)

Br. J. Pharmacol. (1994), **113**, 1333–1343 © Macmillan Press Ltd, 1994

Prevention of thrombosis and rethrombosis and enhancement of the thrombolytic actions of recombinant tissue-type plasminogen activator in the canine heart by DMP728, a glycoprotein IIb/IIIa antagonist

[1]Benedict R. Lucchessi, [a]William E. Rote, Edward M. Driscoll & [b]Dun-Xue Mu

Department of Pharmacology, The University of Michigan Medical School, Ann Arbor, MI 48109-0632, U.S.A.

1 We studied DMP728, a non-peptide glycoprotein (GP) IIb/IIIa receptor antagonist, for prevention of coronary artery thrombosis or rethrombosis in a chronic canine model subjected to arterial injury.

2 In protocol I, DMP728 (1.0 mg kg^{-1}, i.v., $n = 8$) or saline ($n = 8$) was administered and a 150 μA anodal current was applied to the intimal surface of the left circumflex coronary artery (LCX). Dogs were monitored for 6 h and again on each of 5 subsequent days.

3 *Ex vivo* platelet aggregation was inhibited but returned to baseline 1 day after drug administration. Thrombus weight was reduced (saline, 20.7 ± 5.0 mg; DMP728 1.7 ± 0.4 mg; $P < 0.05$), as was infarct size [saline, 27.5 ± 4.3; DMP728, 1.6 ± 0.7 (per cent left ventricle); $P < 0.05$]. All control animals died by day 3, while all but one of the treated dogs survived the entire protocol ($P < 0.05$).

4 In protocol II, an LCX thrombus was induced and thrombolytic therapy was initiated 30 min later. DMP728 (1.0 mg kg^{-1}, i.v., $n = 8$) or saline ($n = 8$) was administered 5 min after recombinant tissue-type plasminogen activator infusion had begun. The incidence of reocclusion was reduced by DMP728 (saline, 4/8; DMP728, 1/8). One day after thrombolysis, 7/8 DMP728-treated animals were alive compared with 1/8 in the control group ($P = 0.01$).

5 DMP728 inhibited *ex vivo* platelet aggregation, prevented primary and secondary occlusive thrombus formation, reduced thrombus weight and infarct size and increased survival in a chronic canine model of coronary artery thrombus formation. DMP728 is an effective anti-platelet intervention when used as the singular adjunctive agent in association with thrombolytic therapy.

Keywords: Fibrinogen receptor; anti-platelet agent; thrombolysis; integrin receptor; DMP728

Introduction

Pharmacological modulation of platelet reactivity is effective clinically in the secondary prevention of stroke, myocardial infarction and vascular death in patients with atherosclerosis exhibiting symptoms related to impaired perfusion of the cerebral, coronary or peripheral vasculature (Antiplatelet Trialists Collaboration, 1988; Harrison, 1990; Cairns *et al.*, 1992). When used as the sole adjunctive antithrombotic therapy, conventional platelet-modifying agents are less effective in preventing platelet-dependent thrombosis associated with mechanical interventions or thrombolytic therapy in the management of patients with acute arterial thrombotic occlusion (Harker, 1986; Schwartz *et al.*, 1988; Grines, 1992). In the latter instances, failure to prevent arterial reocclusion despite adjunctive therapy with aspirin and/or heparin suggests the persistence of a residual lesion capable of exerting an intense thrombogenic stimulus leading to the continued recruitment of platelets and activation of the coagulation cascade (Harker, 1987; Becker & Gore, 1991; Chesebro & Fuster, 1991).

The beneficial effects of thrombolytic therapy for myocardial infarction are well documented (GISSI Trial, 1986; ISIS-2 1988; TAMI Study Group, 1989; GUSTO Investigators, 1993). However, thrombolytic therapy with either recombinant tissue-type plasminogen activator (rt-PA) or streptokinase is associated with reocclusion rates of 5–30% and a rate of reinfarction of about 4% in the absence of adjunctive therapy (Cairns, 1990; Cairns *et al.*,; 1992). The stated percentages represent reocclusive events in patients who are receiving concomitant aspirin and/or heparin as adjunctive therapy. The relatively high incidence of reocclusion raises a question about the efficacy of heparin and aspirin for the prevention of reocclusion and suggests the need to develop more effectve pharmacological interventions to be used in conjunction with thrombolytic therapy and/or coronary angioplasty.

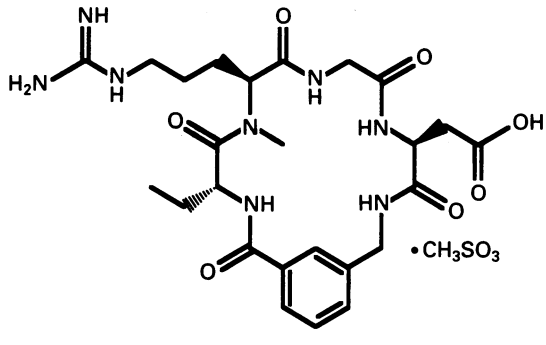
The present experimental study examines the *in vivo* antithrombotic effectiveness of DMP728 [cyclo(D-2-aminobutyrate-N-methyl-L-arginyl-glycyl-L-aspartyl- 3-aminomethylbenzoic acid) methanesulphonate; Figure 1], a glycoprotein (GP) IIb/IIIa antagonist with a high affinity and specificity for the human and the canine platelet GPIIb/IIIa receptor (Mousa *et al.*, 1994). The results in two experimental models demonstrate the efficacy of DMP728 as the sole adjunctive treatment for the prevention of either occlusive primary thrombus formation in response to severe vessel wall injury or secondary thrombus formation occurring after successful thrombolysis.

Methods

Animal investigation

The studies conform to the Position of the American Heart Association on Research Animal Use adopted 11 November 1984. The procedures were in accordance with the guidelines of the University of Michigan (Ann Arbor) University Committee on the Use and Care of Animals. Veterinary care was provided by the University of Michigan Unit for Laboratory

[1] Author for correspondence.
[a] W.E.R. is now with Corvas International, San Diego, CA 92121, U.S.A.
[b] D.X.M. is now with Du Pont Merck Research & Development, Wilmington, DE 19880, U.S.A.



DMP728

Figure 1 Chemical structure of DMP728 [(cyclo(D-2-aminobutyrate-*N*-methyl-L-arginyl-glycyl-L-aspartyl-3-aminomethylbenzoic acid) methanesulphonate]. The molecular weight is 656.7 and its water solubility exceeds 150 mg ml^{-1}. DMP728 is stable in solution at pH 7.4 and 4.5 when at room temperature. The purity of the research sample used in this study was certified as being >99.0%.

Animal Medicine. The University of Michigan is accredited by the American Association of Accreditation of Laboratory Animal Care, and the animal care and use programme conforms to the standards in '*The Guide for Care and Use of Laboratory Animals*', Department of Health, Education and Welfare Publication no. NIH 78-23.

Model of coronary occlusion

The experimental model used in this investigation is a modification of one developed by our laboratory for the study of experimentally induced coronary artery thrombosis. The experimental procedure results in the formation of a platelet-rich intravascular thrombus at the site of an electrolytically induced endothelial lesion in proximity to a distal arterial stenosis. In each of the models studied, occlusive coronary artery thrombosis developed in response to vascular injury resulting from application of an anodal current to the intimal surface of the left circumflex coronary artery. The model facilitated the evaluation of DMP728 for the prevention of primary occlusive arterial thrombosis as well as prevention of secondary thrombosis (rethrombosis) after administration of rt-PA under conditions in which the antiplatelet agent was the only adjunctive drug used in conjunction with the thrombolytic agent. Neither heparin nor aspirin was employed at any time in the experimental protocols present in this report.

Surgical preparation and experimental protocol

The surgical procedures described in this study were conducted using aseptic techniques. Male mongrel dogs weighing 14–20 kg were anaesthetized with sodium pentobarbital (30 mg kg^{-1}, i.v.), intubated and ventilated with room air and positive pressure at a stroke volume of 30 ml kg^{-1} and a frequency of 12 breaths min^{-1} (Harvard Apparatus, South Natick, MA, U.S.A.). Cannulae were placed in the left carotid artery for monitoring arterial blood pressure (Statham P23 pressure transducer, Gould, Oxnard, CA, U.S.A.) and in the right jugular vein for obtaining blood samples. The jugular venous cannula was flushed thoroughly with 0.9% sodium/chloride solution for injection after drug administration or after obtaining blood samples. The heart was exposed by a left thoracotomy through the fifth intercostal space and was suspended in a pericardial cradle. A 2–3 cm segment of the left circumflex coronary artery was isolated from surrounding tissue by blunt dissection. The artery was instrumented with a Doppler flow probe (Model 100, Triton Technology, San Diego, CA, U.S.A.), and indwelling electrode, and a ligature stenosis formed by tying a suture around an 18 gauge needle and the left circumflex coronary artery and then withdrawing the hypodermic needle. The intracoronary electrode consisted of a 30 gauge, Teflon-insulated, silver-coated, copper wire attached to the tip of a 25 gauge hypodermic needle. The wire and needle tip assembly were inserted through the wall of the left circumflex coronary artery and positioned in a manner that allowed the uninsulated region of the electrode to remain in contact with the intimal surface of the wall of the vessel. Proper positioning of the electrode in the coronary artery was confirmed by visual inspection at the end of each experiment. The external portion of the stimulating electrode and the flow probe wires were secured to the myocardium with a suture.

The intravascular electrode was connected to the positive pole (anode) of a dual-channel stimulator (Grass S88 stimulator and a Grass Constant Current Unit, Model CCU1A, Grass Instrument, Quincy, MA, U.S.A.). The cathode was connected to a distant subcutaneous site. Application of an anodal d.c. current to the intimal surface of the circumflex coronary artery results in a deep, thrombogenic, vascular lesion (Bates *et al.*, 1992). The current delivered to the circumflex coronary artery was monitored continuously with an ammeter and maintained at 150 μA.

Recordings of blood pressure, limb lead II electrocardiogram and mean and phasic blood flow velocity from the left circumflex coronary artery were obtained on a model 7 polygraph recorder (Grass Instrument). The electrocardiogram was examined for evidence of ST-segment alterations coinciding with the fluctuations in coronary artery blood flow velocity.

Protocol 1: prevention of coronary artery thrombus formation

The protocol for studies designed to determine the efficacy of DMP728 for the prevention of primary occlusive coronary artery thrombosis is shown in Figure 2a. The experimental protcol was initiated after completion of the surgical instrumentation and closure of the thoracotomy incision. The previously instrumented animals were maintained under anaesthesia, as described above. The animals were allocated to receive either saline or DMP728 1.0 mg kg^{-1}, i.v. intravenously over a period of 5 min. Fifteen minutes later, the anodal current was applied (150 μA) to the intimal surface of the left circumflex coronary artery for a maximum period of 3 h or was terminated 10 min after blood flow velocity in the coronary vessel remained stable at zero flow velocity to verify having achieved formation of a stable occlusive thrombus. Blood pressure, heart rate, coronary artery blood flow velocity and *ex vivo* platelet aggregation were monitored over the initial 6 h experimental period. The animals were returned to their housing facilities in the Unit for Laboratory Medicine upon completion of the protocol on each of the days. On the subsequent 5 days, surviving dogs were returned to the laboratory. The animals were allowed to rest in quiet surroundings without the use of anaesthesia or sedation. Recordings of coronary artery blood flow velocity were obtained to confirm the presence or absence of flow in the left circumflex coronary artery and the limb lead II electrocardiogram was monitored for electrocardiographic changes suggestive of ischaemic injury. Blood was withdrawn for cell counts and aggregation studies. The dogs were returned to the holding rooms each day after completion of the daily recordings and data acquisition.

Survivors were euthanized on the sixth study day. After spontaneous death or euthanasia, the chest was opened and the heart was removed. The left circumflex coronary artery was dissected free as far as possible and opened longitudinally. The intracoronary position of the electrode was verified and the thrombus was removed and weighed on an analytical balance. The heart was sectioned from apex to base in 1.0 cm-thick sections that were incubated, without agitation, in triphenyltetrazolium chloride for 5 min at 37°C.

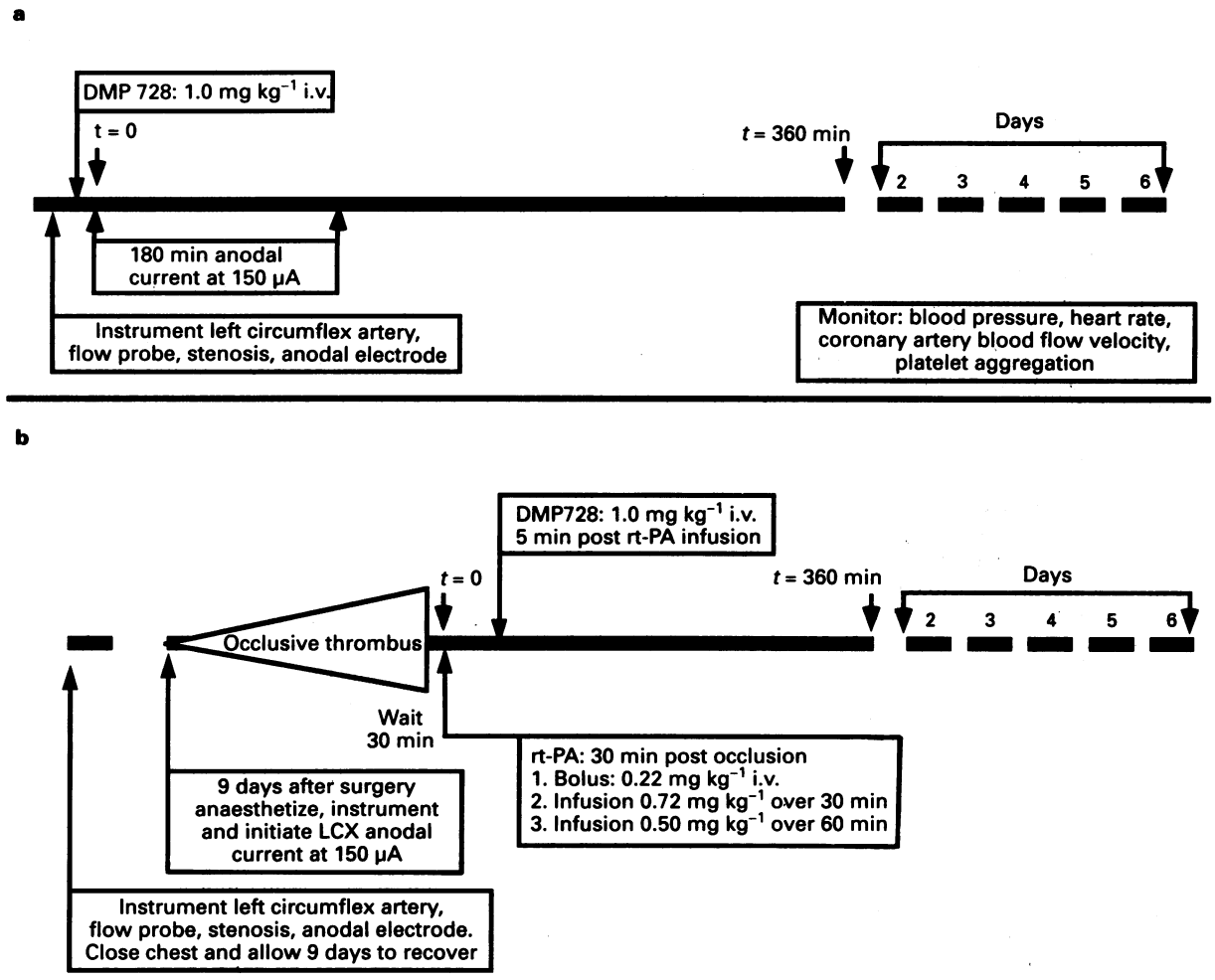


Figure 2 (a) Diagrammatic representation of the experimental protocol used to determine the ability of DMP728 to prevent primary coronary artery thrombosis in response to electrolytic current-induced injury to the vessel wall. Heart rate, coronary artery blood flow velocity, whole blood cell counts and platelet aggregation were monitored throughout the study. The period of the study is represented in the figures with the heavy dark line for day 1 and the broken dark lines representing days 2–6. DMP728 or saline was administered on day 1 before the initiation of anodal current application to the left circumflex coronary artery (LCX). (b) A protocol diagram for studies conducted to determine the ability of DMP728 to prevent secondary thrombus formation (rethrombosis) after rt-PA-induced thrombolysis of a preformed occlusive thrombus in the left circumflex coronary artery (LCX). The LCX was instrumented with a stimulating electrode, a flow probe and a critical stenosis. The dogs were allowed 9 days to recover from surgery. Dogs were returned to the laboratory and a thrombus was formed in the LCX. The coronary thrombus was allowed to age for 30 min and thrombolytic therapy with rt-PA was begun. Five mintues after the start of the graded rt-PA infusion, either DMP728 or saline was administered as an adjunctive agent. The dogs were monitored for 6 h after the start of thrombolytic therapy and then daily for 1 h on each of the five subsequent days. Heart rate, coronary artery blood flow velocity, whole blood cell counts and platelet aggregation were monitored throughout the study.

The transverse ventricular sections were weighed and traced onto clear acetate sheets. The red pigmented tissue containing the precipitated formazan complex was considered to represent viable tissue, whereas tissue that remained pallid was considered to be irreversibly injured or infarcted. The demarcated areas were scanned on a flatbed scanner and digitized using a Macintosh IIci microcomputer (Apple Computer, Cupertino, CA, U.S.A.) and appropriate software (MacDraft, Innovative Data Design, Concord, CA, U.S.A.). Infarct size was expressed as a percentage of total ventricular mass.

Protocol 2: prevention of rethrombosis after lysis

The protocol for studies designed to determine the efficacy of DMP728 for the prevention of rethrombosis is shown in Figure 2b. Animals were instrumented as described previously and were allowed 9 days to recover from the surgical procedure to ensure adequate wound healing. The animals were returned to the laboratory and anaesthetized with intravenous sodium pentobarbital (30 mg kg^{-1}, i.v.). A cannula was placed into the left jugular vein for obtaining blood samples and the injury current (150 μA) was applied to the left circumflex coronary artery for a maximum period of 3 h or was terminated 10 min after blood flow in the vessel had remained stable at zero velocity to certify formation of a stable occlusive thrombus. The thrombus was allowed to age for 30 min before initiating thrombolytic therapy. The thrombolytic agent, recombinant tissue plasminogen activator (rt-PA), was administered as a graded intravenous infusion according to the following regimen: 0.22 mg kg^{-1}, i.v. bolus, followed by 0.72 mg kg^{-1}, i.v. infused over 30 min and, finally, 0.50 mg kg^{-1}, i.v. infused over 90 min. The total intravenous dose of rt-PA was 1.44 mg kg^{-1}. DMP728 (1.0 mg kg^{-1}, i.v.) was administered as a slow intravenous injection given over 5 min and commencing 5 min after beginning the rt-PA infusion. Reperfusion was defined as the restoration of blood flow velocity to 20% of baseline values. Blood pressure, heart rate and coronary artery blood flow velocity were monitored for the remainder of the 6 h observation period, after which the animals were placed in their housing facilities until returned to the laboratory on each of the next 5 days.

Haematological measurements

Blood (20 ml) was withdrawn for platelet studies from the jugular cannula into a plastic syringe containing 3.2% sodium citrate as the anticoagulant [1:10 citrate–blood (v/v)]. Blood was taken for platelet aggregation and whole blood cell counts at baseline and 60, 240 and 360 min after the administration of DMP728 and again on each subsequent day of the protocol. The platelet count was determined with an H-10 cell counter (Texas International Laboratories, Houston, TX, U.S.A.). Platelet-rich plasma (PRP), the supernatant present after centrifugation of anticoagulated whole blood at 1000 r.p.m. for 5 min (140 g), was diluted with platelet-poor plasma (PPP) to achieve a platelet count of 200 000 mm^{-3}. PPP was prepared after the PRP was removed by centrifuging the remaining blood at 2000 *g* for 10 min and discarding the bottom cellular layer. *Ex vivo* platelet aggregation was measured by established spectrophotometric methods with a four-channel aggregometer (BioData-PAP-4, BioData Corp., Hatboro, PA, U.S.A.) by recording the increase in light transmission through a stirred suspension of PRP maintained at 37°C. Aggregation was induced with arachidonic acid (0.65 mM and 0.325 mM) and ADP (20 μM and 5 μM). A subaggregatory dose of adrenaline (550 nM) was used to prime the platelets before stimulation (Romson *et al.*, 1980). Values were expressed as percentage of aggregation, representing the percentage of light transmission standardized to PRP and PPP samples yielding 0% and 100% light transmission respectively.

Inclusion criteria

Animals to be included in the final protocol satisfied the following pre-established criteria: (a) a circulating platelet count of not less than 100,000 mm^{-3}; b) demonstrated ability for platelets to aggregate in response to arachidonic acid before administration of DMP728; and (c) absence of heart worms upon final post-mortem examination.

Drugs

DMP728 used in this study was provided by Du Pont Merck Pharmaceutical Company, Wilmington, DE, U.S.A. The recombinant tissue plasminogen activator, rt-PA (Activase), was purchased from the University of Michigan Hospital Pharmacy of the University of Michigan Medical Center, Ann Arbor, MI, U.S.A. All other chemicals used in this study were obtained from Sigma (St Louis, MO, U.S.A.)

Statistical analysis

The data are expressed as mean ± s.e.mean. *Ex vivo* platelet aggregation in response to arachidonic acid and to ADP was assessed before and after DMP728. The data were analysed by either paired or group analysis using Student's *t* test when applicable; differences were considered significant if $P<0.05$.

Results

Protocol 1: prevention of primary coronary artery thrombus formation

A total of 16 dogs was entered into protocol 1. Each of the 16 animals met the criteria for inclusion in the protocol. Eight of the dogs were assigned to each of the treatment groups, either saline of DMP728. Blood pressure, heart rate and coronary artery flow velocity were not different between groups at baseline. The administration of DMP728 had no effect on either mean arterial blood pressure or heart rate.

Circulating blood cells The effect of DMP728 (1 mg kg^{-1}, i.v.) on whole blood cell counts, haemoglobin and haematocrit are shown in Table 1. No changes were noted in red blood cell count or haematocrit over the 6 days of the study. Over the acute post-operative period, white blood cell counts increased on days 3–6 out of the range of normal laboratory values, but did not become statistically different from baseline values. Haemoglobin values were decreased on days 5 and 6 and platelet counts were significantly increased 6 days after the administration of DMP728. The importance of these changes are unclear at this time. None of the animals showed evidence of infection related to the surgical procedure or abnormal values in body temperature.

Platelet aggregation studies *Ex vivo* platelet aggregation in response to adenosine diphosphate (ADP) and arachidonic acid was determined at baseline and again at 60, 240 and 360 min after DMP728 administration. *Ex vivo* platelet aggregation determinations were repeated on the subsequent days 2 through 6 (Figure 3). Aggregation to each of the agonists was inhibited significantly on day 1 among those animals given DMP728, but remained unaltered from baseline responses in the saline-treated controls. *Ex vivo* platelet aggregation responses to arachidonic acid and ADP were consistent in the surviving control animals on each of the subsequent days. Among the animals treated with DMP728, *ex vivo* platelet aggregation returned to baseline within the first 24 h and remained consistent over the next 5 days in the surviving animals.

Thrombus formation and vessel patency Coronary artery blood flow velocity was monitored daily with the use of a chronically implanted Doppler flow probe on the left circumflex coronary artery. The data are presented graphically in Figures 4a and 4b. Blood flow velocity in the saline-treated group (Figure 4a) declined to zero within the 180 min period of anodal current application and was accompanied by char-

Table 1 Effects of DMP728 (1 mg kg^{-1}, i.v.) on whole blood cell counts in the dog

Time after DMP728	*Red cell count* ($\times 10^6$ mm^{-3})	*White cell count* ($\times 10^3$ mm^{-3})	*Platelet count* ($\times 10^3$ mm^{-3})	*Haematocrit* (%)	*Heamoglobin* (g dl)
Baseline	6.0 ± 0.6	16.4 ± 2.3	215 ± 22	34.4 ± 3.2	17.2 ± 2.9
60 min	5.8 ± 0.3	17.3 ± 2.3	242 ± 25	34.8 ± 2.6	14.8 ± 2.7
240 min	6.0 ± 0.4	14.9 ± 1.7	227 ± 19	34.5 ± 2.0	15.5 ± 2.8
360 min	6.1 ± 0.4	16.3 ± 2.2	228 ± 24	34.0 ± 2.7	15.0 ± 2.9
Day 2	5.7 ± 0.4	16.2 ± 2.5	220 ± 25	33.4 ± 2.3	15.1 ± 3.1
Day 3	6.1 ± 0.3	19.2 ± 2.9†	304 ± 46	36.9 ± 2.2	13.3 ± 2.1
Day 4	6.3 ± 0.5	19.4 ± 3.2†	265 ± 43	36.2 ± 3.2	13.4 ± 2.3
Day 5	6.3 ± 0.3	25.6 ± 4.4†	286 ± 39	35.9 ± 1.9	11.4 ± 0.5†
Day 6	6.0 ± 0.5	21.3 ± 3.4†	313 ± 39*	36.4 ± 3.6	11.5 ± 0.8†

Each value represents the mean ± s.e.mean, $n = 8$ in each group; *$P<0.05$ *vs* baseline values; †signifies out of normal range, but not statistically different from baseline values. Normal ranges (canine): red cell count 4.4–6.4, white cell count 5.8–17.8 platelet count 200–300, haematocrit 26.0–42.0, haemoglobin 12.6–24.6.

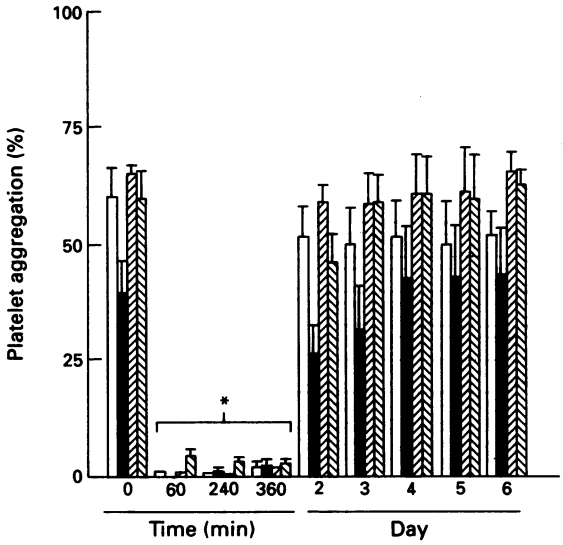


Figure 3 Adenosine diphosphate (ADP)-and arachonic acid-induced *ex vivo* platelet aggregations (mean ± s.e.mean; $n = 8$) from animals that received DMP728 (1.0 mg kg^{-1} i.v.). Platelet aggregation studies were performed at baseline and again at 60, 240 and 360 min after DMP728 administration. Aggregations also were measured on subsequent days 2–6. *$P<0.05$ *vs* baseline. □, ADP, 20 μM; ■, ADP, 5 μM; ▨, arachidonic acid, 0.650 mM; ▩, arachidonic acid, 0.32 M.

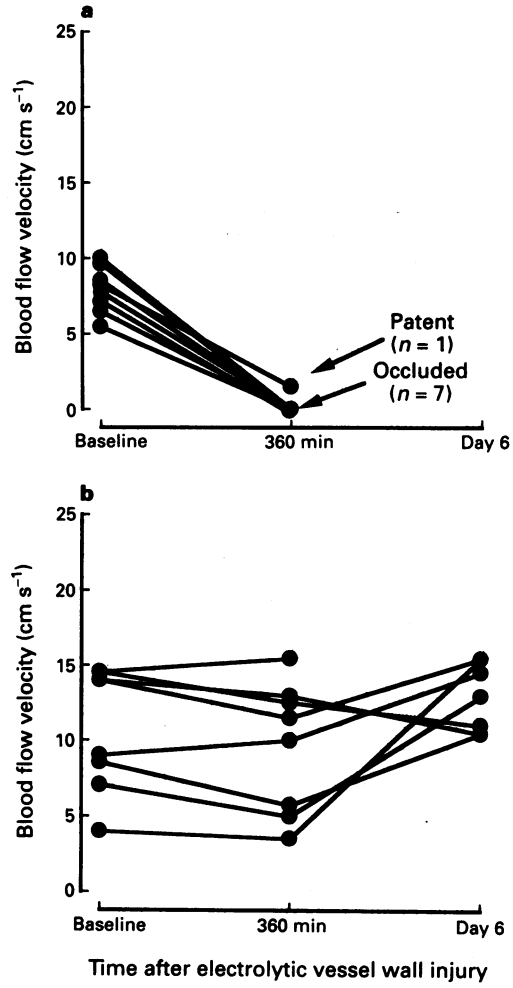


Figure 4 (a) The blood flow velocity measured in left circumflex coronary arteries in animals that received saline before application of the anodal current (180 min, 150 μA) to the intimal surface of the artery. Values are shown for each animal at baseline and 360 min after application of the electrolytic current and induction of vessel wall injury. Occlusive thrombus formation developed in seven of eight dogs before the end of the 360 min protocol on day 1. None of the control dogs survived on the day 6 time point. (b) Coronary artery blood flow velocity for dogs given DMP728 (1 mg kg^{-1}, i.v.) before the induction of vessel wall injury. Platelet inhibition with DMP728 limited thrombus formation and prevented the subsequent reduction in blood flow. Flow was maintained during the next 5 days in all but one dog, which died suddenly in the early hours of day 5.

acteristic changes in the lead II electrocardiogram showing initial depression and then persistent elevation in ST segment. In seven of the eight saline-treated control animals, the left circumflex coronary artery remained occluded for the remainder of the day, with one animal showing slight, but measurable, blood flow velocity. By day 6, all control animals had died, suddenly and without warning.

The administration of the platelet GPIIb/IIIa receptor antagonist, DMP728, limited the extent of intracoronary thrombus formation and prevented the subsequent reduction in coronary artery blood flow velocity as well as the electrocardiographic changes suggestive of regional myocardial ischaemia and/or injury. In seven of the eight animals assigned to receive DMP728, coronary artery blood flow velocity was present on each of the subsequent 5 days. The one remaining DMP728-treated animal died suddenly and unexpectedly during the evening of day 5 after being returned to its holding facilities.

The patency status of individual animals over the 6 day experimental period is summarized in Figure 5 (a and b). The open bars signify that the relevant coronary artery is patent. The hatched bars represent thrombotic occlusion of the coronary artery as determined by the absence of blood flow velocity and the presence of initial ST-segment changes and evolving Q-waves on the subsequent days of observation. The absence of a bar or lack of representation in the chart indicates that the animal has expired. Anodal current vessel wall injury resulted in complete thrombotic occlusion of the left circumflex coronary artery in each of eight animals in the control saline treatment group on day 1 of the experimental protocol. The mean time to occlusion was 90.4 ± 13.9 min in the saline-treated dogs. In contrast, those animals receiving DMP728 maintained patent coronary arteries throughout the initial 6 h period of observation. Each of the animals treated with DMP728 was alive on day 2 of the protocol as compared with three of eight (38%) animals in the saline-treated group. Among the survivors in the control group, one animal had a measurable blood flow velocity on day 2, but exhibited electrocardiographic signs of myocardial infarction. The remaining two animals had persistent thrombotic occlusion accompanied by electrocardiographic signs of myocardial injury and/or infarction. Only one of the saline-treated animals was alive on day 3, but by day 4 had expired suddenly. In contrast, each of the animals in the DMP728 group had patent coronary arteries on each of the subsequent days. One dog died suddenly between day 4 and 5, and this was the only death in the DMP728-treated animals. Survival over the course of the 6 day protocol was 88% for the DMP728 treatment group, which different significantly from the control group ($P<0.05$, Fisher's exact).

Thrombus weight Thrombus weight was reduced significantly in the group of animals treated with DMP728 when compared with the thrombi removed from the control animals (DMP728 = 1.7 ± 0.4 mg and controls = 20.7 ± 5.0 mg). The thrombi were removed either after spontaneous death of the animal or at the time of euthanasia on the sixth day. The data with respect to thrombus weights should be interpreted with caution, however, because the age of the individual thrombi differs from animal to animal and the contribution of the endogenous fibrinolytic system to further

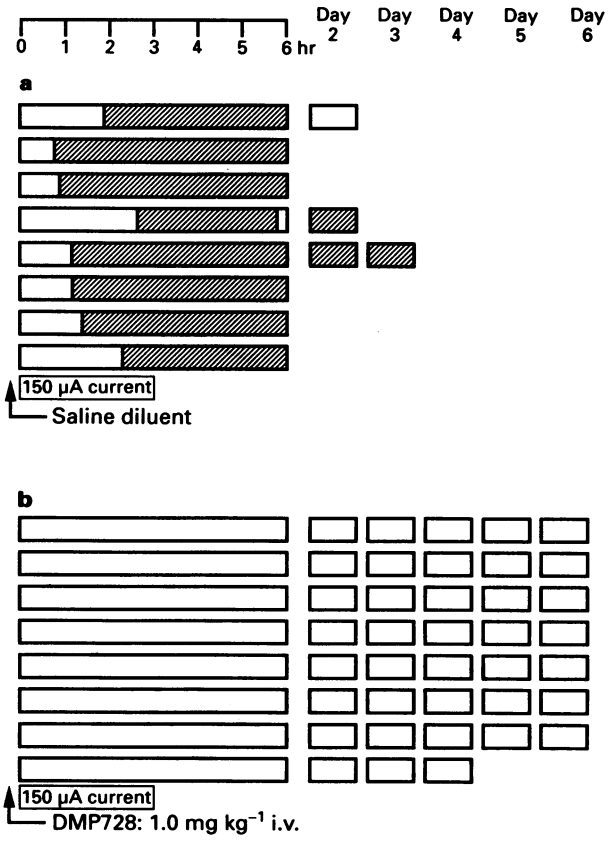


Figure 5 Diagram representing the patency status of left circumflex coronary arteries during the experimental protcol. Each horizontal bar represents one dog over 36 min on day 1; individual boxes signify patency status on days 2–6. (a) Dogs in the control group given saline. The animals shown in (b) received DMP728 (1.0 mg kg^{-1}, i.v.) before the start of anodal current application. Open or white bars represent patent arteries; hatched bars signify thrombotic occlusion; the absence of a bar indicates that the dog has died.

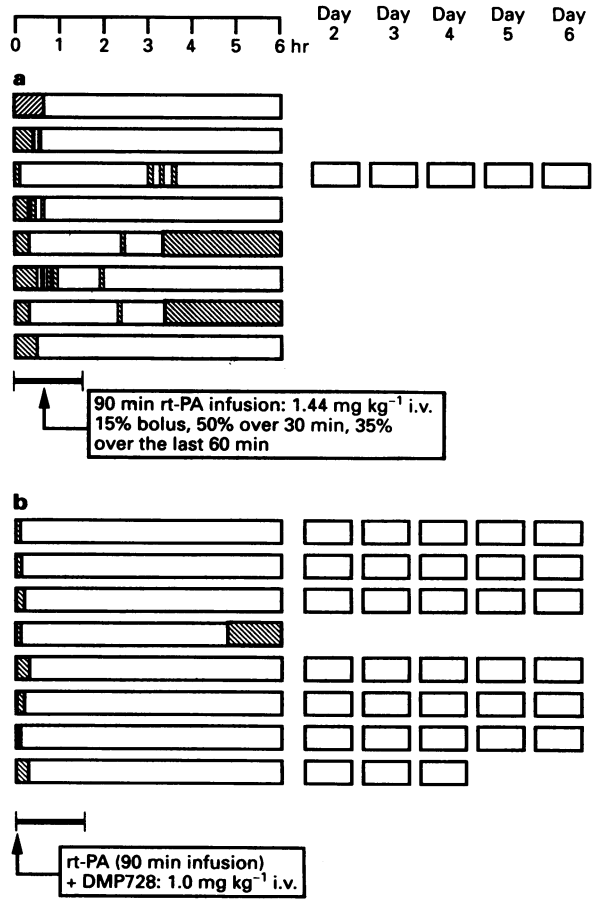


Figure 6 Diagram representing the patency status of left circumflex coronary arteries during the experimental period. Each horizontal bar represents one dog over 360 min on day 1 with zero time equal to the start of rt-PA infusion. Individual boxes indicate the patency status on days 2–6. (a) Dogs receiving rt-PA + saline. The animals shown in (b) received DMP728 (1.0 mg kg^{-1}, i.v.) as adjunctive therapy with rt-PA. Open or white bars represent patent arteries; hatched bars signify thrombotic occlusion; the absence of a bar indicates that the animal had expired.

modification of the residual thrombus is uncertain. The thrombi removed from dogs receiving DMP728 were obtained on the sixth day with the exception of one animal which died suddenly on the fourth day of the protocol.

Infarct size Each of the eight dogs in the control group exhibited evidence of extensive irreversible myocardial injury as determined by the tetrazolium method. Evidence of myocardial infarction was absent in three of the eight DMP728-treated animals, and overall infarct size was reduced significantly compared with the control group. Infarct size expressed as a percentage of the left ventricle was $1.7 \pm 0.8\%$ in the DMP728-treated group *vs* $27.5 \pm 4.5\%$ in the control group. The observations correlate with the results reported for thrombus weight and the incidence of mortality. Infarct size was expressed as a percentage of the total left ventricle. Therefore, caution should be used when interpreting the results on infarct size since determination of neither collateral blood flow nor area at risk was made owing to the limitations imposed as a result of the experimental protocol.

Protocol 2: prevention of rethrombosis after rt-PA-induced thrombolysis

A total of 17 dogs was used in this arm of the study. Eight of the dogs were assigned to each of the treatment groups, either saline or DMP728. One animal from the control group was excluded owing to the presence of heart worms upon post-mortem examination. Blood pressure, heart rate and coronary artery blood flow velocity were not different between groups at baseline. The administration of DMP728 had no effect on either mean arterial blood pressure or heart rate.

Platelet aggregation studies *Ex vivo* platelet aggregation in response to adenosine diphosphate (ADP) or arachidonic acid was determined at baseline and again at 30 and 300 min after DMP728 or saline administration. Aggregations were repeated on the subsequent days 2–6. Aggregation to each agonist was prevented on day 1 among the animals receiving DMP728. As in protocol 1, *ex vivo* platelet aggregation responses returned to baseline values within 24 h and remained consistent over the subsequent study days. The *ex vivo* platelet aggregation responses in PRP from the saline-treated animals did not differ from baseline at any time point in the study.

Thrombosis/thrombolysis/rethrombosis The patency status of the left circumflex coronary artery of individual animals in each group over the 6 day experimental period is represented in Figure 6 (a and b). As before, open bars signify that the coronary artery is patent. The hatched bars represent thrombotic occlusion of the coronary artery as indicated by the absence of a Doppler flow signal and the presence of electrocardiographic ST-segment changes or evolution of Q-

waves indicative of myocardial ischaemia or cell death respectively. The absence of a bar signifies that the animal expired suddenly and unexpectedly. All vessels became occluded in response to anodal current application and all arteries became patent with a restoration of blood flow after administration of rt-PA (1.44 mg kg^{-1}, i.v.) Reocclusions, characterized by oscillatory patterns of blood flow, of varying durations occurred in six of the eight saline-treated control animals. In contrast, oscillatory blood flow did not occur in the drug-treated animals and occlusive rethrombosis developed in only one of the dogs receiving DMP728. On day 2, only one of eight saline-treated animals had survived, whereas seven of eight dogs in the DMP728-treated group ($P<0.05$, Fisher's exact) were alive. Of the remaining animals in the DMP728-treated group, all but one survived to the end of the sixth day. One animal died suddenly between day 4 and day 5.

Time to thrombolysis The time to thrombolysis, defined as the restoration of coronary artery blood flow velocity to 20% of the baseline, was determined in each of the animals. Treatment with DMP728 during the administration of rt-PA was associated with a decrease in the time to reperfusion when compared with the group of animals receiving rt-PA plus saline (rt-PA + DMP728 (1.0 mg kg^{-1}, i.v. = 9.9 ± 2.2 min *vs* rt-PA + saline = 18.4 ± 2.3 min; $P<0.05$).

Residual thrombus size GPIIb/IIIa receptor antagonism with DMP728 showed a trend towards reduced residual thrombus weight. The thrombi were removed either after spontaneous death of the animal or at the time of euthanasia on day 6. Thrombus weights in the DMP728 group were smaller, but the difference was not significant (saline = 7.1 ± 1.8 mg; DMP728 = 2.8 ± 1.0 mg, P = NS). The comparison of thrombus weights, however, should be viewed with caution when interpreting data from these measurements owing to the varying time points at which the thrombi were recovered relative to the time of thrombus formation.

Infarct size Myocardial infarct size, expressed as a percentage of left ventricular mass averaged, 17.9 ± 2.9% in the controls *vs* 6.6 ± 1.7% in the DMP728-treated group ($P<0.05$). Adjunctive therapy with DMP728 was associated with a reduction in the extent of irreversible myocardial damage as compared with animals in the saline-treated control group.

Discussion

Interruption in the continuity of the endothelial surface of a normal blood vessel initiates the primary haemostatic response to injury invoking platelet activation accompanied by a localized vasoconstriction (Marcus, 1991) and cyclic flow variations in stenosed and endothelium-injured vessels mediated by platelet aggregates (Yao *et al.*, 1993). Endothelial cell injury leads to the exposure of subendothelial collagen fibrils that serve as an agonist for platelet activation and release of additional agonists including adensoine diphosphate, thromboxane and serotinin (Kroll & Schafer, 1989). The recruitment of additional platelets to the primary layer of adherent platelets forms the haemostatic plug. Concomitant with the activation and adhesion of platelets there is initiation of the coagulation cascade and generation of thrombin at the site of vessel injury. Thrombin is the catalyst for conversion of fibrinogen to fibrin. In addition, thrombin is a potent agonist for platelet activation (Marcus & Safier, 1993). The response to the agonistic potential of a deep vascular lesion differs from that occurring in response to normal haemostasis in injured, but otherwise healthy, vessels. Pathological or occlusive arterial thrombi that form in response to a severe arterial lesion may have the morphological features of a haemostatic plug, but involve far more platelet adhesion, activation, recruitment and consolidation (Marcus & Safier, 1993). Development of pathological arterial thrombi is the result of multiple factors required for induction, assembly and stabilization of the occlusive mass at the site of extensive vessel wall injury. The difficulty in preventing occlusive arterial lesions may be the result of the multifactorial nature of the arterial thrombotic process.

A further complication arises from the fact that thrombolytic agents activate platelets (Fitzgerald *et al.*, 1988a,b) as a result thrombin activation (Fitzgerald *et al.*, 1988b) or the effects of plasmin generation (Guccione *et al.*, 1985; Schafer *et al.*, 1986). The outcome of thrombolytic therapy is determined, in part, by the relative influences of the local proaggregatory and antiaggregatory factors exerted upon the circulating platelets and the residual vascular lesion. The circulating platelets have an important role in rethrombosis owing to their ability to be activated by the residual thrombus as well as by local thrombin and plasmin generation in response to lytic therapy (Guccione *et al.*, 1985; Schafer *et al.*, 1986; Fitzgerald *et al.*, 1988a). The final common pathway in the formation of a platelet aggregate is the cross-linking of adjacent activated platelets by binding of fibrinogen to the platelet GPIIb/IIIa receptor complex (referred to in the integrin nomenclature, as αIIbβ3) (Phillips *et al.*, 1987; Gatter *et al.*, 1988; Keiffer & Phillips, 1990; Kieffer *et al.*, 1992). Theoretically, the prevention of occlusive arterial lesions may be achived by modulating the reactivity of the blood platelet by inhibiting interaction of the GPIIb/IIIa receptor with its ligand.

GPIIb/IIIa is the most abundant of the platelet integrins and is found only on platelets and cells of megakaryoblastic potential. GPIIb/IIIa becomes a receptor for a number of soluble adhesive proteins (fibrinogen, von Willebrand factor, vitronectin, fibronectin) via interaction with the Arg-Gly-Asp (RGD) recognition sequence (Ginsbger *et al.*, 1988a,b).

There is compelling evidence that adhesive proteins binding to the GPIIb/IIIa complex and that platelet aggregates are integral components of thrombus formation *in vivo* (Coller, 1990; 1992). The GPIIb/IIIa complex provides a logical site for pharmacological interventions directed towards an inhibition of platelet aggregation and arterial thrombus formation. Several RGD-containing peptides, either synthetic or derived from snake venoms (disintegrins), are known to block fibrinogen binding and to prevent the formation of platelet thrombi (Cadroy *et al.*, 1989; Dennis *et al.*, 1990; Gould *et al.*, 1990; Tschopp *et al.*, 1993). Furthermore, blockade of the GPIIb/IIIa receptor with monoclonal antibodies has proved to be antiaggregatory in experimental (Mickelson *et al.*, 1990a,b; Bates *et al.*, 1991; Rote *et al.*, 1994a) and clinical studies (Coller, 1990; 1992; Gold *et al.*, 1990; Kleiman *et al.*, 1993). More recently, peptidomimetic and non-peptide RGD mimetics have been developed in an effort to achieve greater antithrombotic potency and selectivity at the site of the GPIIb/IIIa receptor (Kouns *et al.*, 1992; Peerlinck *et al.*, 1993; Rote *et al.*, 1993; Roux *et al.*, 1993). The present study provides experimental findings with DMP728, a non-peptidomimetic antagonist of the platelet GPIIb/IIIa integrin receptor. The intravenous administration of a single 1.0 mg kg^{-1}, dose of DMP728 prevented primary thrombus formation in response to deep arterial wall injury as well as rethrombosis after successful thrombolysis in a chronic canine model. The comparison between the control and drug-treated animals subjected to primary thrombosis or rethrombosis demonstrates the importance of modulating platelet reactivity by virtue of inhibiting the platelet GPIIb/IIIa receptor.

The first experimental protocol was designed to determine if DMP728 could prevent occlusive thrombus formation in response to severe arterial wall injury (primary thrombosis). The study was initiated in the instrumented, closed-chest, anaesthetized dog in which electrolytic injury of the left circumflex coronary artery was induced in either control saline-treated animals or in animals pretreated with DMP728 administered as a single intravenous dose of 1.0 mg kg^{-1}. The

dose of DMP728 was selected on the basis of previous studies in which it was found to prevent rethrombosis in a canine model of arterial thrombosis and thrombolysis (Mousa *et al.*, 1994; Rote *et al.*, 1994a,b). The animals were monitored continuously for 6 h on the first day of the protocol and on each of the subsequent 5 days. The results indicate that DMP728 prevented primary thrombus formation. The protective effect persisted for the duration of the protocol despite the presence of a deep arterial wall lesion and the return to control values of *ex vivo* platelet reactivity within 24 h after drug administration. The results in the saline-treated control are in marked contrast. Each of the control animals developed an occlusive thrombus in response to electrolytic injury of the arterial wall. The occurrence of sudden death due to ventricular fibrillation within the first 24 h was more common in the control group than in the DMP728-treated animals. Overall survival at the end of the 6 day protocol was improved significantly in the DMP728-treated animals as compared with the saline-treated controls. The observed long-term beneficial effects of DMP728 were obtained despite the fact that platelet reactivity, as assessed by *ex vivo* aggregation, was not inhibited beyond the first 24 h after drug administration. Thus, thrombus formation did not develop over the subsequent 5 days in the DMP728-treated animals, suggesting that the injured vessel wall had lost its potential as a thrombogenic site. As would be expected, thrombus weight and, in particular, infarct size were reduced significantly in animals receiving DMP728 as compared with the saline-treated control group.

The results of the present study are in accord with our earlier observations (Bates *et al.*, 1992) demonstrating that temporary, but complete, inhibition of the platelet GPIIb/IIIa receptor for several hours after deep arterial wall injury significantly reduced later intravascular thrombus formation and thrombotic occlusion. The long-term prevention of primary thrombus formation by selective inhibition of the GPIIb/IIIa receptor in a chronic model of severe vessel wall injury illustrates the important role of the platelet glycoprotein receptor as a mediator of thrombus formation. Temporary inhibition of the GPIIb/IIIa receptor prevents thrombus formation in contrast to merely delaying the development of the occlusive lesion. Inhibition of platelet deposition for 8 h with dipyridamole or prostacyclin after percutaneous balloon de-endothelization rendered rabbit aortae non-reactive to circulating blood platelets (Groves *et al.*, 1986). *In vivo* studies using a reperfusion model demonstrated that the vessel wall lost the ability to initiate thrombus formation within 40 min after endothelial injury, thus emphasizing that platelet deposition and thrombus formation are time-limited phenomena (Baumgartner, 1973). The existence of a specific time window in which the injured vessel wall remains thrombogenic is an important consideration in designing appropriate dosing regimens and schedules for prevention of arterial occlusive events, as might develop after invasive procedures likely to be associated with vessel wall damage and increased thrombogenicity at the site of injury. The time-limited duration of the 'window of thrombogenicity' may provide a reasonable explanation for why a single dose of DMP728 was able to prevent primary occlusive thrombus formation. Whether or not the same 'window of thrombogenicity' will apply to clinical situations of coronary artery thrombolysis or coronary angioplasty remains to be determined, especially in light of recent information suggesting the need for prolonged platelet inhibition by the chimeric 7E3-Fab antibody after thrombolytic therapy (Kleiman *et al.*, 1993).

The second phase of our study evaluated the ability of DMP728 to prevent rethrombosis after successful thrombolysis in a chronic canine model. Thrombolysis and recanalization of the affected vessel was achieved readily in all animals after the intravenous administration of rt-PA. As observed in previous studies (Mickelson *et al.*, 1990a), using the same experimental procedure, thrombolysis with rt-PA, in the absence of adjunctive therapy, was accompanied by repetitive episodes of oscillatory variations in coronary artery blood flow. The erratic flow pattern was characterized by periods of total cessation of blood flow followed by periods of reactive hyperaemia, eventually culminating in sudden arrhythmic death or total thrombotic occlusion within the first 24 h. In the present study, only one of eight saline-treated control animals undergoing thrombolysis maintained a patent circumflex coronary artery and survived the subsequent 5 days of the study protocol. Seven of the eight DMP728-treated animals maintained patent vessels and survival was improved significantly as compared with the control group.

The present study was not designed to assess the influence of DMP728 upon rt-PA-induced thrombolysis. It became apparent, however, that the administration of the GPIIb/IIIa receptor antagonist 5 min after completion of the rt-PA infusion, but before recanalization had occurred, significantly decreased the time needed to achieve thrombolysis. Therefore, the treatment regimen consisting of rt-PA followed by the intravenous administration of 1.0 mg kg^{-1} of DMP728 accelerated recanalization of the occluded vessel and significantly reduced both the incidence of reocclusion and death. Furthermore, the extent of irreversible myocardial tissue injury was reduced significantly in the animals treated with DMP728. In addition to being involved in thrombus formation, aggregating platelets can initiate intense vasoconstriction after the activation and release of potent vasoactive mediators (Saldeen *et al.*, 1993; Yao *et al.*, 1993). Infarct size expansion is related to the extent of platelet accumulation in myocardium that has undergone reperfusion in the presence of a critical stenosis (Rousseau *et al.*, 1993). The beneficial effect on the salvage of myocardial tissue, after inhibition of the GPIIb/IIIa receptor, may derive, in part, from the fact that coronary artery blood flow is maintained and not compromised by repetitive episodes of oscillatory blood flow commonly observed after thrombolysis in the absence of adjunctive anti-platelet therapy.

A recent study (Kohmura *et al.*, 1993) assessed the effect of an initial single intravenous bolus injection of chimeric 7E3-Fab followed by repeated bolus injections of rt-PA on reperfusion and reocclusion in heparinized baboons with a femoral arterial thrombosis with superimposed high-grade stenosis. The presence of the platelet GPIIb/IIIa receptor antagonist, chimeric 7E3-Fab, decreased the time to recanalization and sustained femoral artery blood flow in contrast to control animals receiving saline or aspirin as the adjunctive treatment. In addition, it has been reported that concomitant systemic therapeutic heparin anticoagulation is required for the maximal effect of 7E3 (Yasuda *et al.*, 1990). A major difference between the previous study (Kohmura *et al.*, 1993) and the present investigation is that we did not use heparin. Despite the absence of heparin in the present study, DMP728 was capable of decreasing the time to clot lysis. Whether or not heparin is necessary for attaining beneficial effects with other inhibitors of the platelet glycoprotein IIb/IIIa receptor requires further investigation. With the exception of enhancing the apparent time to clot lysis, DMP728 provided beneficial effects identical to those observed in a previous study (Mickelson *et al.*, 1990a) in which 7E3 $F(ab')_2$ was administered after rt-PA in a chronic canine model of coronary artery thrombosis and thrombolysis. As in the present study, 7E3 $F(ab')_2$ administration resulted in a preservation of vessel patency and abolition of repetitive oscillatory flow in the severely injured circumflex coronary artery. The present results complement the recent observations (Mousa *et al.*, 1994) and provide additional insight into the efficacy of DMP728 as an antithrombotic agent in a chronic model of vessel wall injury. DMP728 in a dose of 1.0 mg kg^{-1} prevented both primary and secondary thrombus formation when used as the sole anti-platelet agent and was fully effective in the absence of heparin or antithrombins. The dose of DMP728 was the same as that used by Mousa *et al.*

(1994), who reported that the drug's duration of action and efficacy in preventing thrombus formation was decreased at lower doses. A similar dose–response relationship with respect to the prevention of primary and secondary thrombosis was reported by Rote *et al.* (1994).

The ability of inhibitors of the platelet glycoprotein IIb/IIIa receptor to maintain vessel patency when used as the sole adjunctive agent in combination with thrombolytic therapy provides compelling evidence that the platelet plays a major role in rethrombosis. Platelets are activated during thrombolysis (Coller, 1990), and the residual thrombus along with the stenotic lesion present a thrombogenic substrate for recruitment of new platelets and fibrin deposition leading to rethrombosis. Thrombolysis therefore, is accompanied by a dynamic interaction in which local lytic and thrombogenic activity occur simultaneously. Inhibition of the platelet GPIIb/IIIa receptor shifts the equilibrium so that lytic activity predominates, thereby maintaining blood flow and permitting time for the residual thrombus and injured vessel to become non-thrombogenic.

Critique of the experimental model

The original electrically induced coronary artery thrombosis model in the canine heart employed alternating current delivered to the vascular lumen through a catheter electrode positioned in the coronary artery under fluoroscopic control (Salazar, 1961). The experimental model used in this study was described previously (Romson *et al.*, 1980). Since it was first described, the model has been used by several investigators to examine a variety of anti-platelet interventions for the prevention of primary thrombus formation (Fitzgerald *et al.*, 1986; Mickelson *et al.*, 1990b; Rote *et al.*, 1993) or prevention of rethrombosis after successful thrombolysis (Mickelson *et al.*, 1990a; Rote *et al.*, 1993; 1994a; Saldeen *et al.*, 1993; Tschopp *et al.*, 1993). The arterial wall lesion and subsequent formation of an occlusive thrombus result from direct application of an anodal direct current to the endothelial surface of the vessel, leading to exposure of proaggregatory subendothelial elements (Mickelson *et al.*, 1990b; Bates *et al.*, 1992). The resulting thrombus consists of a platelet–fibrin mass adherent to the vessel wall at the site of intimal injury (Romson *et al.*, 1980) and possess the morphological features of acutely formed thrombi found in patients with acute myocardial infarction (Falk, 1985). The cellular composition of the arterial thrombus is an important consideration in the interpretation of data derived from experimental studies. Erythrocyte-rich coronary arterial thrombi are consistently lysed after an intravenous infusion of rt-PA, whereas platelet-rich thrombi are relatively resistant to lysis even in the presence of high doses of a thrombolytic agent (Fitzgerald *et al.*, 1988a). It is recognized, however, that the experimental model lacks the atherosclerotic lesions that are prominent in most, if not all, diseased human arteries in which thrombus formation occurs. The inability to replicate the entire human clinical pathophysiological state may suggest that prevention of rethrombosis in a diseased human artery with atherosclerosis may not be prevented to the same degree as in the experimental animal.

An important feature of the experimental model is that it permits an extended period of observation in contrast to an acute animal model. During the subsequent days, one can evaluate the efficacy of a selective intervention with respect to preventing thrombus formation and determine the duration for maintaining inhibition of the GPIIb/IIIa receptor during which time the thrombogenic focus undergoes resolution and becomes non-thrombogenic. A minor limitation in the chronic animal model is the inability to evaluate bleeding times by the Simplate method owing to the humane concerns for the welfare of the experimental animal.

Summary

DMP728 is among the first of a new series of non-peptide, low molecular weight compounds designed to inhibit the platelet GPIIb/IIIa receptor. The present study, conducted in the chronically instrumented canine, demonstrates that DMP 728 is effective in preventing occlusive arterial thrombosis in response to severe vessel wall injury and to prevent rethrombosis after successful thrombolytic therapy. In both instances, DMP728 was administerd once as an intravenous dose of 1.0 mg kg^{-1}. DMP728, as the singular adjunctive agent, provided prolonged protection in terms of maintaining vessel patency and reducing mortality. Although the platelet GPIIb/IIIa receptor may appear to be a logical target site for therapeutic intervention in thromboembolic disease, the safety and efficacy of this class of agent will be determined by the outcome of well-designed clinical trials in man. The recently reported clinical results (Kleiman *et al.*, 1993) with a platelet GPIIb/IIIa receptor antagonist (monoclonal antibody 7E3-Fab) administered after thrombolytic therapy suggest that inhibition of the platelet integrin receptor has therapeutic potential. DMP728 provides an alternative intervention by which the concept can be evaluated further in both basic and clinical studies.

This study was supported by a grant from the National Institutes of Health, Heart, Lung and Blood Institute, Grant No. HL19782-16. The authors thank Dr Shaker A. Mousa and Dr Thomas Reilly from DuPont-Merck Pharmaceutical Company for the generous supply of DMP728.

References

ANTIPLATELET TRIALISTS COLLABORATION (1988). Secondary prevention of vascular disease by prolonged antiplatelet treatment. *Br. Med. J.*, **296**, 320–321.

BATES, E.R., MCGILLEM, M.J., MICKELSON, J.K., PITT, B. & MANCINI, G.B.J. (1991). A monoclonal antibody to the platelet receptor GPIIb/IIIa prevents platelet aggregation and thrombosis in a canine model of coronary artery angioplasty. *Circulation*, **84**, 2463–2469.

BATES, E.R., WALSH, D.G., MU, D.-X., ABRAMS, G.D. & LUCCHESI, B.R. (1992). Sustained inhibition of the vessel wall–platelet interaction after deep coronary artery injury by temporary inhibition of the platelet glycoprotein IIb/IIIa receptor. *Coronary Artery Dis.*, **3**, 67–76.

BAUMGARTNER, H.R. (1973). The role of blood flow in platelet adhesion, fibrin deposition and formation of mural thrombi. *Microvasc. Res.*, **5**, 167–179.

BECKER, R.C. & GORE, J.M. (1991). Adjuvant antiplatelet strategies in coronary thrombolysis. *Circulation*, **83**, 1115–1117.

CADROY, Y., HOUGHGEN, R.A. & HANSON, S.R. (1989). RGDV peptide selectively inhibits platelet-dependent thrombus formation in vivo. Studies using a baboon model. *J. Clin. Invest.*, **84**, 939–944.

CAIRNS, J.A. (1990). Reperfusion adjunctive therapy: heparin. *J. Interven. Cardiol.*, **3**, 217–223.

CAIRNS, J.A., HIRSH, J., LEWIS, H.D. Jr., RESNEKOV, L. & THEROUX, P. (1992). Antithrombotic agents in coronary artery disease. *Chest*, **102**, 456S–481S.

CHESEBRO, J.H. & FUSTER, V. (1991). Dynamic thrombosis and thrombolysis: role of antithrombins. *Circulation*, **83**, 1815–1817.

COLLER, B.S. (1990). Platelets and thrombolytic therapy. *N. Engl. J. Med.*, **322**, 333–342.

COLLER, B.S. (1992). Antiplatelet agents in the prevention and therapy of thrombosis. *Annu. Rev. Med.*, **43**, 171–180.

DENNIS, M.S., HENZEL, W.J., PITTI, R.M., LIPARI, M.T., NAPIER, M.A., DEISHER, T.A., BUNTING, S. & LAZARUS, R.A. (1990). Platelet GPIIb/IIIa from snake venoms: evidence for a family of platelet aggregation inhibitors. *Proc. Natl. Acad. Sci. U.S.A.*, **87**, 2471–2475.

FALK, E. (1985). Unstable angina with fatal outcome dynamic coronary thrombosis leading to infarction and/or sudden death: autopsy evidence of recurrent mural thrombosis with peripheral embolization culminating in total vascular occlusion. *Circulation*, **71**, 699–708.

FITZGERALD, D.J., DORAN, J., JACKSON, E. & FITZGERALD, G.A. (1986). Coronary vascular occlusion mediated via thromboxane A2-prostaglandin endoperoxide receptor activation in vivo. *J. Clin. Invest.*, **77**, 496–502.

FITZGERALD, D.J., CATELLA, R., ROY, L. & FITZGERALD, G.A. (1988a). Marked platelet activation *in vivo* after intravenous streptokinase in patients with acute myocardial infarction. *Circulation*, **77**, 142–150.

FITZGERALD, D.J., WRIGHT, R. & FITZGERALD, C.A. (1988b). Thrombin-mediated platelet activation during thrombolysis (abstract). *Circulation*, **78** (Suppl. 2), 120.

GATTER, K.C., CORDELL, J.L., TURLEY, H., HERYET, A., KIEFFER, N., ANSTEE, D.J. & MASON, D.Y. (1988). The immunohistological detection of platelets, megakaryocytes and thrombi in routinely processed specimens. *Histopathology*, **13**, 257–267.

GINSBERG, M.H., LOFTUS, J.C. & PLOW, E.F. (1988a). Cytoadhesions, integrins and platelets. *Thromb. Haemost.*, **59**, 1–6.

GINSBERG, M.H., LOFTUS, J.C. & PLOW, E.F. (1988b). Platelets and the adhesion receptor superfamily. *Prog. Clin. Biol. Res.*, **283**, 171–195.

GISSI TRIAL (GRUPPO ITALIANO PER LO STUDIO DELLA STREPTOCHINASE NELL'INFARTO MIOCARDICO) (1986). Effectiveness of intravenous thrombolytic treatment in acute myocardial infarction. *Lancet*, **1**, 397–402.

GOLD, H.K., GIMPLE, L.W., YASUDA, T., LEINBACH, R.C., WERNER, W., HOLT, R., JORDAN, R., BERGER, H., COLLEN, D. & COLLER, B.S. (1990). Pharmacodynamic study of F(ab')2 fragments of murine monoclonal antibody 7E3 directed against human platelet glycoprotein IIb/IIIa in patients with unstable angina pectoris. *J. Clin. Invest.*, **86**, 651–659.

GOULD, R.J., POLOKOFF, M.A., FRIEDMAN, P.A., HUANG, T.-F., HOLT, J.C., COOK, J.J. & NIEWIAROWSKI, S. (1990). Disintegrins: a family of integrin inhibitory proteins from viper venoms. *Proc. Soc. Exp. Biol. Med.*, **195**, 168–171.

GRINES, C.L. (1992). Thrombolytic, antiplatelet, and antithrombotic agents. *Am. J. Cardiol.*, **70**, 18-I–26-I.

GROVES, H.M., KINLOUGH-RATHBONE, R.L. & MUSTARD, J.F. (1986). Development of nonthrombogenicity of injured rabbit aortas despite inhibition of platelet adherence. *Atherosclerosis*, **6**, 189–195.

GUCCIONE, M.A., KINLOUGH-RATHBONE, R.L., PACKHAM, M.A., HARFENIST, E.J., RAND, M.L., GREENBERG, J.P., PERRY, D.W. & MUSTARD, J.F. (1985). Effect of plasmin on rabbit platelets. *Thromb. Haemost.*, **53**, 8–14.

GUSTO INVESTIGATORS (1993). An international randomized trial comparing four thrombolytic strategies for acute myocardial infarction. *N. Engl. J. Med.*, **329**, 673–682.

HARKER, L.A. (1986). Clinical trials evaluating platelet-modifying drugs in patients with atherosclerotic cardiovascular disease and thrombosis. *Circulation*, **73**, 206–223.

HARKER, L.A. (1987). Role of platelets and thrombosis in mechanisms of acute occlusion and restenosis after angioplasty. *Am. J. Cardiol.*, **60**, 20B–28B.

HARRISON, M.J.G. (1990). Role of platelets and antiplatelet agents in cerebrovascular disease: clues from trials. *Circulation*, **81** Suppl. I), 120–121.

ISIS-2 (SECOND INTERNATIONAL STUDY OF INFARCT SURVIVAL COLLABORATIVE GROUP) (1988). Randomized trial of intravenous streptokinase, oral aspirin, both or neither among 17,187 cases of suspected myocardial infarction: ISIS-2. *J. Am. Coll. Cardiol.*, **12** (Suppl. A), 3A–13A.

KIEFFER, N. & PHILLIPS, D.R. (1990). Platelet membrane glycoproteins: functions in cellular interactions. *Annu. Rev. Cell. Biol.*, **6**, 329–357.

KIEFFER, N., GUICHARD, J. & BRETON-GORIUS, J. (1992). Dynamic redistribution of major platelet surface receptors after contact-induced platelet activation and spreading. Immunoelectron microscopy study. *Am. J. Pathol.*, **140**, 57–73.

KLEIMAN, N.S., OHMAN, E.M., CALIFF, R.M., GEORGE, B.S., KEREIAKES, D., AGUIRRE, F.V., WEISMAN, H., SCHAIBLE, T. & TOPOL, E.J. (1993). Profound inhibition of platelet aggregation with monoclonal antibody 7E3 Fab after thrombolytic therapy. Results of the Thrombolysis and Angioplasty in Myocardial Infarction (TAMI) 8 Pilot Study. *J. Am Coll. Cardiol.*, **22**, 381–389.

KOHMURA, C., GOLD, H.K., YASUDA, T., HOLT, R., NEDELMAN, M.A., GUERRERO, J.L., WEISMAN, H.F. & COLLEN, D. (1993). A chimeric murine/human antibody Fab fragment directed against the platelet GPIIb/IIIa receptor enhances and sustains arterial thrombolysis with recombinant tissue-type plasminogen activator in baboons. *Arteroscler. Thromb.*, **13**, 1837–1842.

KOUNS, W.C., KIRCHHOFER, D., HADVARY, P., EDENHOFER, A., WELLER, T., PFENNINGER, G., BAUMGARTNER, H.R., JENNINGS, L.K. & STEINER, B. (1992). Reversible conformational changes in glycoprotein IIb/IIIa by a potent and selective peptidomimetic inhibitor. *Blood*, **180**, 2539–2547.

KROLL, M.H. & SCHAFER, A.I. (1989). Biochemical mechanisms of platelet activation. *Blood*, **74**, 1181–1195.

MARCUS, A.J. (1991). Platelets and their disorders. In *Disorders of Hemostasis*. ed. Ratnoff, O.D. & Forbes, C.D. pp. 75–140. New York: Grune & Stratton.

MARCUS, A.J. & SAFIER, L.B. (1993). Thromboregulation: multicellular modulation of platelet reactivity in hemostasis and thrombosis. *FASEB J.*, **7**, 516–522.

MICKELSON, J.K., SIMPSON, P.J., CRONIN, M., HOMEISTER, J.W., LAYWELL, E., KITZEN, J. & LUCCHESI, B.R. (1990a). Antiplatelet antibody [7E3 F(ab')2] prevents rethrombosis after recombinant tissue-type plasminogen activator-induced coronary artery thrombolysis in a canine model. *Circulation*, **81**, 617–627.

MICKELSON, J.K., SIMPSON, P.J. & LUCCHESI, B.R. (1990b). Antiplatelet monoclonal F(ab')2 antibody directed against the platelet GP IIb/IIIa receptor complex prevents coronary artery thrombosis in the canine heart. *J. Mol. Cell. Cardiol.*, **21**, 293–405.

MOUSA, S.A., BOZARTH, J.M., FORSYTHE, M.S., JACKSON, S.A., LEAMY, A., DIEMER, M.J., KAPIL, R.P., KNABB, R.M., MAYO, M.C., PIERCE, S.K., DEGRADO, W.F., THOOLEN, M.J. & REILLY, T.M. (1994). Antiplatelet, antithrombotic efficacy of DMP728, a novel platelet GPIIb/IIIa receptor antagonist. *Circulation*, **89**, 3–12.

PEERLINCK, K., DE LEPELEIRE, I., GOLDBERG, M., FARRELL, D., BARRETT, J., HAND, E., PANEBIANCO, D., DECKMYN, H., VERMYLEN, J. & ARNOUT, J. (1993). MK-383 (L-700,462), a selective nonpeptide platelet glycoprotein IIb/IIIa antagonist is active in man. *Circulation*, **88**, 1512–1517.

PHILLIPS, D.R., FITZGERALD, L.A., CHARO, I.F. & PARISE, L.V. (1987). The platelet membrane glycoprotein IIb/IIIa complex; structure, function, and relationship to adhesive protein receptors in nucleated cells. *Ann. N Y Acad. Sci.*, **509**, 177–187.

ROMSON, J.L., HAACK, D.W. & LUCCHESI, B.R. (1980). Electrical induction of coronary artery thrombosis in the ambulatory canine: a model for *in vivo* evaluation of anti-thrombotic agents. *Thromb. Res.*, **17**, 841–853.

ROTE, W.E., WERNS, S.W., DAVIS, J.H., FEIGEN, L.P., KILGORE, K.S. & LUCCHESI, B.R. (1993). Platelet GPIIb/IIIa receptor inhibition prevents thrombosis and rethrombosis in the canine carotid artery. *J. Cardiovasc. Res.*, **27**, 500–507.

ROTE, W.E., MU, D.-X., BATES, E.R., NEDELMAN, M.A. & LUCCHESI, B.R. (1994a). Prevention of rethrombosis in a chronic canine model. I. Adjunctive therapy with monoclonal antibody 7E3-F(ab')2 fragment. *J. Cardiovasc. Pharmacol.*, **23**, 194–202.

ROTE, W.E., DAVIS, J.H., MOUSA, S.A., REILLY T.M. & LUCCHESI, B.R. (1994b). Antithrombotic effects of DMP728, a platelet GPIIb/IIIa receptor antagonist, in a canine model of arterial thrombosis. *J. Cardiovasc. Pharmacol.*, **23**, 681–689.

ROUSSEAU, G., HEBERT, D., LIBERSAN, D., KHALIL, A., ST-JEAN, G. & LATOUR, J.-G. (1993). Importance of platelets in myocardial injury after reperfusion in the presence of residual coronary stenosis in dogs. *Am. Heart J.*, **125**, 1553–1563.

ROUX, S.P., TSCHOPP, T.B., KUHN, H., STEINER, B. & HADVARY, P. (1993). Effects of heparin, aspirin and a synthetic platelet glycoprotein IIb/IIIa receptor antagonist (Ro 43-5054) on coronary artery reperfusion and reocclusion after thrombolysis with tissue type plasminogen activator in the dog. *J. Pharmacol. Exp. Ther.*, **264**, 501–508.

SALAZAR, A.E. (1961). Experimental myocardial infarction, induction of coronary thrombosis in the intact closed-chest dog. *Circ. Res.*, **9**, 135–136.

SALDEEN, T.G.P., SALDEEN, P., NICHOLS, W.W., LAWSON, D.L., NICOLINI, F.A. & MEHTA, J.L. (1993). Increased production of thromboxane A2 by coronary arteries after thrombolysis. *Am. Heart J.*, **125**, 277–284.

SCHAFER, A.L., MAAS, A.K., WARE, J.A., JOHNSON, P.C., RITTENHOUSE, S.E. & SALZMAN, E.W. (1986). Platelet protein phosphorylation, elevation of cytosolic calcium, and inositol phospholipid breakdown in platelet activation induced by plasmin. *J. Clin. Invest.*, **78**, 73–79.

SCHWARTZ, L., BOURASSA, M.G., LESPERANCE, J., ALDRIDGE, H.E., KAZIM, F., SALVATORI, V.A., HENDERSON, M., BONAN, R. & DAVID, P.R. (1988). Aspirin and dipyridamole in the prevention of restenosis after percutaneous transluminal angioplasty. *N. Engl. J. Med.*, **318**, 1714–1719.

TAMI STUDY GROUP (1989). A randomized controlled trial of intravenous tissue plasminogen activator and early intravenous heparin in acute myocardial infarction. *Circulation*, **79**, 281–286.

TSCHOPP, J.F., DRISCOLL, E.M., MU, D.-X., BLACK, S.C., PIERSCHBACHER, M.D. & LUCCHESI, B.R. (1993). Inhibition of coronary artery reocclusion after thrombolysis with an RGD-containing peptide with no significant effect on bleeding time. *Coronary Art. Dis.*, **4**, 809–817.

YAO, S.-K., OBER, J.C., GONENNE, A., CLUBB, Jr., F.J., KLRISHNASWAMI, A., FERGUSON, J.J., ANDERSON, H.V., GORECKI, M., BUJA, L.M. & WILLERSON, J.T. (1993). Active oxygen species play a role in mediating platelet aggregation and cyclic flow variations in severely stenosed and endothelium-injured coronary arteries. *Circ. Res.*, **73**, 952–967.

YASUDA, T., GOLD, H.K., YAOITA, H., LEINBACH, R.C., GUERRERO, J.L., JANG, I.-K., HOLT, R., FALLON, J.T. & COLLEN, D. (1990). Comparative effects of aspirin, a synthetic thrombin inhibitor and a monoclonal antiplatelet glycoprotein IIb/IIIa antibody on coronary artery reperfusion, reocclusion and bleeding with recombinant tissue-type plasminogen activator in a canine preparation. *J. Am. Coll. Cardiol.*, **16**, 714–722.

(Received June 14, 1994
Accepted August 1, 1994)

Br. J. Pharmacol. (1994), **113**, 1344–1348 © Macmillan Press Ltd, 1994

Peripheral and central sites of action of GABA-B agonists to inhibit the cough reflex in the cat and guinea pig

[1]Donald C. Bolser, Frances C. DeGennaro, Sandra O'Reilly, Richard W. Chapman, William Kreutner, Robert W. Egan & John A. Hey

Schering-Plough Research Institute, Kenilworth, NJ 07033, U.S.A.

1 The GABA-B receptor agonists baclofen and 3-aminopropylphosphinic acid (3-APPi) have antitussive activity in the cat and guinea pig. The purpose of this study was to investigate the sites of action of these GABA-B receptor agonists to inhibit the cough reflex.

2 Single intracerebroventricular (i.c.v.) cannulas were placed in the lateral ventricles of anaesthetized guinea pigs. Approximately 1 week later, the animals were exposed to aerosols of capsaicin (0.3 mM) to elicit coughing. Coughs were detected with a microphone and counted.

3 Cough was produced in anaesthetized cats by mechanical stimulation of the intrathoracic trachea and was recorded from electromyograms of respiratory muscle activity. Cannulas were placed for intravenous (i.v.) or, in separate groups of animals, intravertebral arterial (i.a.) administration of baclofen, 3-APPi, the centrally active antitussive drug codeine or the peripherally active antitussive drug BW443c. Dose–response relationships for i.v. and i.a. administration of each drug were generated to determine a ratio of i.v. ED_{50} to i.a. ED_{50}, known as the effective dose ratio (EDR). The EDR will be 20 or greater for a centrally acting drug.

4 In the guinea pig, baclofen (3 mg kg^{-1}, s.c.) and 3-APPi (10 mg kg^{-1}, s.c.) inhibited capsaicin-induced cough by 50% and 35% respectively. The antitussive activity of baclofen was completely blocked by i.c.v. administration of the GABA-B receptor antagonist CGP 35348 (10 μg). Conversely, the antitussive effect of 3-APPi was unaffected by i.c.v. CGP 35348. However, systemic administration of CGP 35348 (30 mg kg^{-1}, s.c.) completely blocked the antitussive activity of 3-APPi (10 mg kg^{-1}, s.c.). In separate experiments baclofen alone (1 μg, i.c.v.) inhibited capsaicin-induced cough by 78%. 3-APPi (10 and 100 μg, i.c.v.) had no effect on capsaicin-induced cough in the guinea pig.

5 In the cat, potencies (ED_{50}) of the standards and GABA-B agonists by the i.v. route were: codeine (0.34 mg kg^{-1}), BW443C (0.17 mg kg^{-1}), baclofen (0.63 mg kg^{-1}) and 3-APPi (2.3 mg kg^{-1}). Potencies of these drugs by the i.a. route were: codeine, 0.013 mg kg^{-1}; BW443C, 0.06 mg kg^{-1}; baclofen, 0.016 mg kg^{-1}; and 3-APPi, 0.87 mg kg^{-1}. The EDRs for each drug were: codeine, 26; BW443C, 3; baclofen, 39; and 3-APPi, 3.

6 We conclude that in both the cat and guinea pig baclofen inhibits cough by a central site of action, while 3-APPi inhibits cough by a peripheral site of action.

Keywords: Cough; antitussive; GABA-B receptors; baclofen; 3-aminopropylphosphinic acid

Introduction

The selective GABA-B receptor agonists baclofen and 3-aminopropylphosphinic acid, (3-APPi) have recently been shown to have antitussive activity in the cat and guinea pig (Bolser *et al.*, 1993a). These effects are specific to activation of GABA-B receptors because the antitussive effects of baclofen were blocked by the GABA-B receptor antagonists CGP 35348 and 3-aminopropylphosphonic acid (Bolser *et al.*, 1993a). Possible sites of action of antitussive drugs include the inhibition of one or more components of the central reflex pathway for cough located primarily in the medulla (Chou & Wang, 1975; Korpas & Tomori, 1979; Adcock, 1991) or inhibition of the responsiveness of sensory receptors involved in the generation of cough (Adcock, 1991; Korpas & Tomori, 1979). For example, the well-known antitussive drug codeine inhibits cough at central sites (Chou & Wang, 1975), whereas other antitussive drugs, such as the opioid μ-receptor agonist BW443C, have only a peripheral site of action (Adcock *et al.*, 1988).

In this study, we investigated the sites of action of baclofen and 3-APPi in inhibiting the cough reflex. For GABA-B agonists, it is likely that baclofen acts centrally to inhibit the cough reflex, because this drug readily penetrates the CNS and can alter the discharge of spinal respiratory neurones (Lalley, 1983). Conversely, 3-APPi would be expected to have a peripheral site of action in inhibiting cough, because this drug does not penetrate the CNS (Hills & Howson, 1992). We established the central or peripheral site of action of these agents in guinea pigs by evaluating the ability of intracerebroventricular administration of the GABA-B antagonist CGP 35348 to block the antitussive effects of baclofen or 3-APPi. Furthermore, antitussive potencies were compared in cats after intravenous or intra-arterial injection of GABA-B agonists. A preliminary account of this work has been published (Bolser *et al.*, 1993b).

Methods

Capsaicin-induced cough in the guinea pig

Male unanaesthetized Dunkin–Hartley guinea pigs (500–800 g) were placed in a cylindrical transparent chamber and individually exposed to capsaicin aerosols (0.3 mM) to elict cough (Bolser *et al.*, 1993a). The dimensions of the chamber were 12" × 4". The capsaicin aerosol was produced by a jet nebulizer at an airflow of 4 l min^{-1}. The volume of capsaicin nebulized was approximately 1.6 ml. A microphone was placed in the chamber to detect coughs, and this microphone was connected to a chart recorder. The animals were exposed

[1] Author for correspondence.

to capsaicin for 4 min and the number of coughs elicited during this period was counted by visual inspection of the chart record.

Intracerebroventricular (i.c.v) administration of the GABA-B receptor antagonist, 3-aminopropyl(diethoxymethyl)phosphinic acid (CGP 35348), was used to evaluate the central antitussive action of systemically administered baclofen and 3-APPi. Single i.c.v. cannulae were placed into the lateral ventricle of anaesthetized (ketamine, 30 mg kg^{-1}; xylazine, 5 mg kg^{-1} i.m.) guinea pigs and anchored in place with dental cement. Coordinates for cannula placement were: 0.5 mm anterior (A), 2.0 mm lateral (L), and 4.5 mm ventral (V) relative to bregma (McLeod *et al.*, 1991). The animals were allowed to recover and approximately 1 week later were used for cough experiments. Baclofen (3.0 mg kg^{-1} s.c.) or 3-APPi (10 mg kg^{-1} s.c.) was administered 30 min before exposure to capsaicin. These doses were chosen on a previous study that demonstrated antitussive activity of baclofen and 3-APPi in guinea pigs (Bolser *et al.*, 1993a). CGP 35348 (10 μg in 10 μl) or artificial CSF (10 μl) was given i.c.v. 10 min before exposure to capsaicin. This dose of CGP 35348 was selected because it is much lower than the minimally active systemic dose of 3 mg kg^{-1} (Bolser *et al.*, 1993a) and preliminary experiments showed that it does not alter the cough reflex. In separate deperiments, baclofen (1 μg in 10 μl) and 3-APPi (10 and 100 μg in 10 μl) were given i.c.v. 5 min before exposure to capsaicin.

Additional experiments were conducted to verify that the antitussive effects of 3-APPi could be antagonized by systemic administration of CGP 35348. CGP 35348 (30 mg kg^{-1} s.c.) was administered 40 min before capsaicin challenge. 3-APPi (10 mg kg^{-1} s.c.) was then administered 30 min before capsaicin challenge.

Mechanically induced cough in cats

Cats (2.5–5.0 kg) were anaesthetized with pentobarbital sodium (35 mg kg^{-1} i.p.) and given supplemental anaesthetic as necessary (5 mg kg^{-1} i.v.). Atropine sulphate (1.0 mg kg^{-1} i.v.) was administered to block reflex tracheal secretions. The trachea, femoral vein and femoral artery were cannulated. In some animals, a catheter was inserted into the left axillary artery and advanced until the catheter tip was at the branch of the left vertebral artery (Chou & Wang, 1975). The omocervical, pericardiophrenic and costocervical branches were ligated. Evans blue dye was injected into the catheter at the end of the experiment and proper placement of this catheter was confirmed post mortem.

Bipolar silver wire electrodes were placed in the diaphragm and rectus abdominis muscles by the technique of Basmajian & Stecko (1962). Electromyograms (EMGs) from these muscles were amplified, filtered (0.5–10 kHz), and integrated with a resistance–capacitance circuit (100 ms time constant). The integrated EMGs were displayed on a chart recorder.

Cough was defined as a burst of EMG activity in the diaphragm immediately followed by a burst of EMG activity in the rectus abdominis muscle (Bolser *et al.*, 1993a). Coughing was produced by probing the intrathoracic trachea with a thin flexible polyethylene cannula continuously for approximately 10 s per trial. Control values were generated by averaging the number of coughs during five consecutive probing trials obtained after vehicle administration. One minute elapsed between probing trials. Probing trials were applied at 1-min intervals after each dose of drug for a total of five stimulus trials between doses. The cough response after each dose of drug was determined by averaging the number of coughs observed during these five probing trials. Five minutes elapsed between each dose of drug.

The antitussive activities of codeine, the peripheral μ-opioid agonist BW443C, baclofen and 3-APPi were evaluated from cumulative dose–response relationships after intravenous (i.v.) administration and, in separate groups of animals, after intra-arterial (i.a.) administration of each drug. An effective dose ratio (EDR) was generated for each drug. The EDR was defined as the ED_{50} for i.v. activity divided by the ED_{50} for i.a. activity of the drug. This ratio will be 20 or greater for a centrally acting antitussive drug and less than 20 for a peripheral antitussive drug (Chou & Wang, 1975).

Compounds

Compounds used in this study included atropine sulphate and capsaicin (Sigma Chemical Co., St Louis, MO, U.S.A.), codeine sulphate (Mallinkrodt, St Louis, MO, U.S.A.), BW443C (L-tyrosyl-D-arginylglycyl-4-nitrophenylalanyl-L-proliamide diacetate) (a kind gift from Wellcome Research Laboratories, Beckenham, Kent, U.K.), (±) baclofen (Research Biochemicals, Natick, MA, U.S.A.), CGP 35348 and 3-APPi (prepared at Schering-Plough Research Institute, Kenilworth, NJ, U.S.A.). Capsaicin was dissolved in 1% ethanol, 1% Tween 20 and 0.9% physiological saline. All other drugs were dissolved in physiological saline. Doses were calculated as their free base.

Statistics

All data are expressed as mean ± s.e. mean. Student's *t*-test or one-way analysis of variance was used to evaluate differences between means. Effective doses (ED_{50}) for 50% inhibition were obtained by regression analysis of dose–response relationships. Differences between means were considered significant if $P<0.05$.

Results

Influence of i.c.v. CGP 35348 on the antitussive effects of baclofen and 3-APPi in the guinea pig

Baclofen (3.0 mg kg^{-1} s.c.) inhibited capsaicin-induced cough by approximately 50% in the animals treated with i.c.v. artificial CSF (Figure 1). This antitussive effect of baclofen was completely blocked by i.c.v. administration of 10 μg of CGP 35348 (Figure 1).

3-APPi (10 mg kg^{-1} s.c.) inhibited capsaicin-induced cough by approximately 35% in the animals treated with i.c.v. artificial CSF (Figure 2). However, i.c.v. administration of CGP 35348 (10 μg) did not block the antitussive activity of 3-APPi (Figure 2). Intracerebroventricular administration of CGP 35348 alone had no significant effect on the cough reflex (i.c.v. artificial CSF 12 ± 1 coughs, $n = 22$; i.c.v. CGP 35348 11 ± 1 coughs, $n = 18$).

Influence of systemic CGP 35348 on the antitussive effect of 3-APPi in the guinea pig

3-APPi (10 mg kg^{-1} s.c.) inhibited capsaicin-induced cough by 57% (Table 1). Pretreatment with CGP 35348 (30 mg kg^{-1} s.c.) completely blocked the antitussive effects of 3-APPi (Table 1).

Influence of i.c.v. baclofen and 3-APPi on capsaicin-induced cough in the guinea pig

Baclofen (1 μg i.c.v.) inhibited capsaicin-induced cough by approximately 70% (Table 2). However, i.c.v. administration of 3-APPi at doses of 10 and 100 μg had no antitussive effect.

Intravenous and intra-arterial administration of baclofen, 3-APPi, codeine and BW443C in the cat

In animals that received drugs i.v., mechanical stimuli applied to the trachea elicited 7.3 ± 0.3 coughs per stimulus trial after saline administration ($n = 22$). In animals that

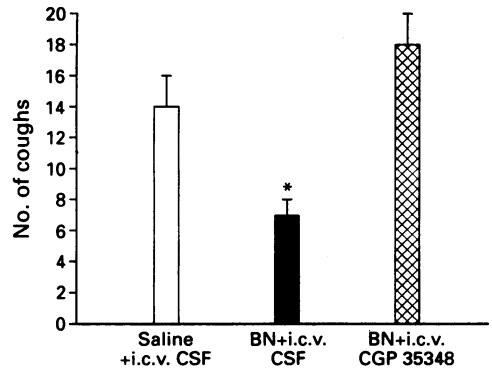


Figure 1 Influence of i.c.v. CGP 35348 on the antitussive activity of systemic baclofen in the guinea pig. Saline or baclofen (3.0 mg kg^{-1} s.c.) were given 30 min before capsaicin challenge. Artificial CSF (10 μg in 10 μl i.c.v.) or CGP 35348 (10 μl i.c.v.) was given 10 min before capsaicin challenge. *$P<0.05$, $n=4-11$ per group.

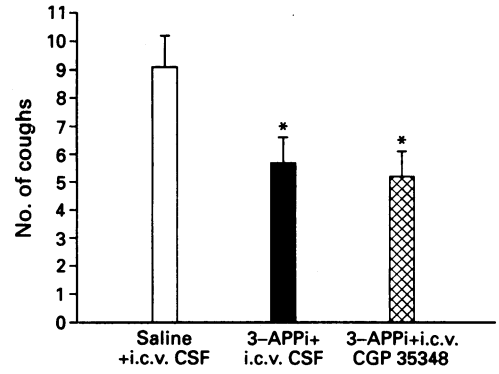


Figure 2 Influence of i.c.v. CGP 35348 on the antitussive activity of systemic 3-APPi in the guinea pig. Saline or 3-APPi (10 mg kg^{-1} s.c.) was given 30 min before capsaicin challenge. Artificial CSF (10 μl i.c.v.) or CGP 35348 (10 μg in 10 μl i.c.v.) was given 10 min before capsaicin challenge. *$P<0.05$, $n=9-13$ per group.

received drugs i.a., mechanical stimuli applied to the trachea elicited 8.8 ± 0.4 coughs per stimulus trial after saline administration ($n=23$). Figure 3 shows cumulative dose–response relationships for antitussive activity after i.v. and i.a. administration of codeine (Figure 3a), BW443C (Figure 3b), baclofen (Figure 3c) and 3-APPi (Figure 3d). Each dose–response relationship was generated from a separate group of animals.

Codeine was much more potent when given by the i.a. route ($ED_{50}=0.013$ mg kg^{-1}) than by the i.v. route ($ED_{50}=0.34$ mg kg^{-1}). The EDR for codeine was 26. The peripherally acting opioid BW443C was slightly more potent when given by the i.a. route ($ED_{50}=0.06$ mg kg^{-1}) than by the i.v. route ($ED_{50}=0.17$ mg kg^{-1}1) and had an EDR of 3.0. Baclofen was much more potent when given by the i.a. route ($ED_{50}=0.016$ mg kg^{-1}) than by the i.v. route ($ED_{50}=0.63$ mg kg^{-1}). The EDR for baclofen was 39. Conversely, 3-APPi was only slightly more potent by the i.a. ($ED_{50}=0.87$ mg kg^{-1}) route than by the i.v. route ($ED_{50}=2.3$ mg kg^{-1}) and had an EDR of 3.0. 3-APPi also was less efficacious than the other drugs, producing a maximum inibition of cough frequency of approximately 60%.

Discussion

The major findings of this study were that central administration of a GABA-B antagonist, CGP 35348, reversed the antitussive effect of systemically administered baclofen, but not that of 3-APPi in the guinea pig. Furthermore, i.c.v. administration of baclofen, but not 3-APPi, inhibited cough in the guinea pig. In the cat, the EDR for i.v. and i.a. administration of baclofen was similar to that of the central antitussive drug, codeine. However, the EDR for i.v. and i.a. 3-APPi was similar to that of BW443C, a peripheral antitussive drug.

Central administration of antagonists is a standard approach to evaluate the site of action of systemically administered drugs. The antagonist must be administered at doses that are inactive when given systemically. In this study, CGP 35348 (10 μg i.c.v.) completely blocked the antitussive activity of baclofen. This dose of CGP 35348 was at least 300-fold smaller than the effective systemic dose to block baclofen (Bolser *et al.*, 1993a). This indicates that baclofen inhibited capsaicin-induced cough in the guinea pig by a central site of action and that there was no peripheral component to the action of this GABA-B agonist. Conversely, while i.c.v. CGP 35348 did not reverse the antitussive action of 3-APPi, systemic administration of this antagonist did block the antitussive effects of 3-APPi. There are two alternative interpretations of these observations. First, 3-APPi had solely a peripheral site of action so its antitussive activity was unaffected by central administration of CGP 35348. Second, in addition to a peripheral action 3-APPi acted at a central GABA-B receptor subtype that was insensitive to CGP 35348. To resolve these two alternative interpretations, we administered baclofen and 3-APPi i.c.v. in the guinea pig. While baclofen (1 μg) inhibited cough when given i.c.v., 3-APPi was inactive at doses up to 100 μg. These data indicate that 3-APPi did not have a central action to inhibit cough in the guinea pig. However, the failure of i.c.v. CGP 35348 to block the antitussive effects of 3-APPi cannot be attributed to a lack of central penetration by this GABA-B agonist. Even if a systemic dose of 3-APPi penetrated the CNS in our

Table 1 Influence of systemic CGP 35348 on the antitussive effect of 3-APPi

Treatment[a]			
First	*Second*	n	*No. of coughs (mean ± s.e.mean)*
Saline	Saline	10	14 ± 1
Saline	3-APPi	10	6 ± 2*
CGP 35348	3-APPi	10	15 ± 2

[a]The first treatment was administered 40 min before capsaicin challenge. The second treatment was administered 30 min before capsaicin challenge. All treatments were administered by the subcutaneous route. The dose of 3-APPi was 10 mg kg^{-1} and the dose of CGP 35348 was 30 mg kg^{-1}.
*$P<0.05$ relative to either the saline/saline or the CGP 35348/3-APPi group.

Table 2 Influence of intracerebroventricular 3-APPi and baclofen on capsaicin-induced cough in the guinea pig

Treatment[a]	Dose (μg)	n	*No. of coughs (mean ± s.e.mean)*	
CSF	–	6	13 ± 2	*
Baclofen	1	5	3 ± 1	
CSF	–	9	10 ± 2	NS
3-APPi	10	9	9 ± 1	
CSF	–	6	8 ± 1	NS
3-APPi	100	5	8 ± 1	

[a]Compounds administered i.c.v. in 10 μl of artificial CSF 5 min before capsaicin challenge.
NS, not significant. *$P<0.05$.

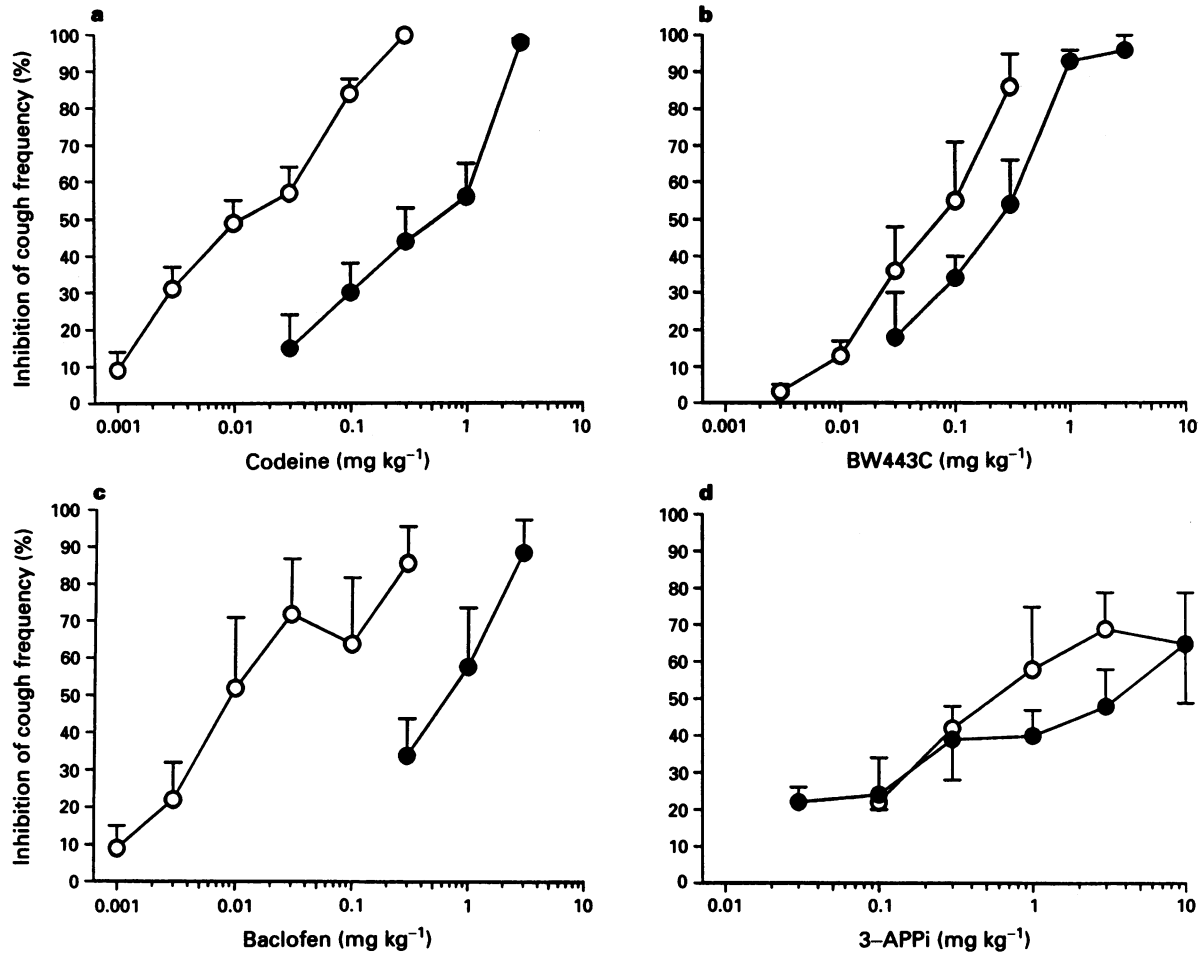


Figure 3 Effect of i.v. or i.a. GABA-B agonists and selected standards on cough frequency in the cat. Cumulative dose–response relationships for i.v. (●) and i.a. (○) administration of codeine (a), BW 443C (b), baclofen (c) and 3-APPi (d) are shown.

model, it probably would not have an antitussive effect. These results are consistent with baclofen preferentially acting at a central site that is unrecognized by 3-APPi. Our results indicate that, when 3-APPi and baclofen are given systemically, 3-APPi inhibits cough at a peripheral site of action that is relatively insensitive to baclofen. Conversely, baclofen inhibits cough at a central site that is relatively insensitive to 3-APPi.

The use of effective dose ratios generated from i.v. and i.a. (vertebral artery) dose–response relationships has been demonstrated to differentiate between centrally and peripherally active antitussive drugs (Chou & Wang, 1975). The EDR for centrally active antitussive drugs is generally high (greater than 20) because very small doses of these drugs are necessary to inhibit cough when injected into the vertebral artery. This artery supplies the brain stem, which is the primary site where the central neural elements generating cough are located (Chou & Wang, 1975). In contrast, much larger doses of peripheral antitussive drugs are necessary to inhibit cough when given in the vertebral artery because these drugs must recirculate in the venous system to reach their site of action. EDRs for peripheral antitussive drugs are less than 20 (Chou & Wang, 1975). In these studies, the EDR for baclofen was 39 and that of codeine was 26. This observation indicates that baclofen had a central site of action to inhibit the cough in the cat. The EDR for 3-APPi was only 3, the same as that of BW443C. These findings indicate that the antitussive activity of 3-APPi in the cat is also through a peripheral site of action.

Taken together, the results of this study indicate that in more than one species the antitussive activity of baclofen has a central component and that of 3-APPi is due to a peripheral site of action. These conclusions confirm and extend a previous suggestion that baclofen inhibits cough at a central site and that 3-APPi inhibits cough at a peripheral site (Chapman *et al.*, 1993). However, this suggestion was based primarily on the idea that 3-APPi penentrates the CNS to a limited extent (Hills & Howson, 1992). The data presented are the first direct evidence to support the conclusion that baclofen can inhibit cough by a central site of action and that 3-APPi inhibits cough solely by a peripheral site of action. The mechanism by which baclofen elicits its central antitussive effect is probably inhibition of one or more components of the central reflex pathway for cough. Conversely, 3-APPi probably elicits its peripheral antitussive effect by inhibition of sensory afferent responsiveness to inhaled capsaicin in the guinea pig or to mechanical stimulation of the trachea in the cat. In the guinea pig, inhaled capsaicin is thought to stimulate the C-fibers to elicit cough (Forsberg *et al.*, 1988). Pulmonary rapidly adapting receptors (RARs) have long been associated with the production of cough and are thought to be primarily responsible for cough elicited by mechanical stimuli applied to the intrapulmonary airway (Karlsson *et al.*, 1988). Based on this evidence, it is likely that 3-APPi can inhibit the responsiveness of more than one type of vagal afferent to mechanical and chemical stimuli. Similar mechanisms have been suggested for the peripheral antitussive drugs BW443C (Adcock *et al.*, 1988) and benzonatate (Korpas & Tomori, 1979).

We thank Carol Battle for typing the manuscript.

References

ADCOCK, J.J. (1991). Peripheral opioid receptors and the cough reflex. *Respir. Med.*, **85** (Suppl. A), 43–46.

ADCOCK, J.J., SCHNEIDER, C. & SMITH, T.W. (1988). Effects of codeine, morphine and a novel pentapeptide BW433C, on cough, nociception and ventilation in the unanaesthetized guinea pig. *Br. J. Pharmacol.*, **93**, 93–100.

BASMAJIAN, J.V. & STECKO, G.A. (1962). A new bipolar indwelling electrode for electromyography. *J. Appl. Physiol.*, **7**, 203–215.

BOLSER, D.C., AZIZ, S.M., DEGENNARO, F.C., KREUTNER, W., EGAN, R.W., SIEGEL, M.I. & CHAPMAN, R.W. (1993a). Antitussive effects of GABA-B agonists in the cat and guinea pig. *Br. J. Pharmacol.*, **110**, 491–495.

BOLSER, D.C., DEGENNARO, F.C. & CHAPMAN, R.W. (1993b). Central and peripheral actions of GABA-B agonists and selected standards in the cat. *Am. Rev. Resp. Dis.*, **174**, A713.

CHAPMAN, R.W., HEY, J.A., RIZZO, C.A. & BOLSER, D.C. (1993). GABA-B receptors in the lung. *Trends Pharmacol. Sci.*, **14**, 26–29.

CHOU, D.T. & WANG, S.C. (1975). Studies on the localization of central cough mechanism: site of action of antitussive drugs. *J. Pharmacol. Exp. Ther.*, **194**, 499–505.

FORSBERG, K., KARLSSON, J.-A., THEODORSSON, E., LUNDBERG, J.M. & PERSSON, C.G.A. (1988). Cough and bronchoconstriction mediated by capsaicin-sensitive sensory neurons in the guinea pig. *Pulm. Pharmacol.*, **1**, 33–39.

HILLS, J.M. & HOWSON, W. (1992). The GABA-B profile of a series of phosphinic acids-agonist and antagonist activity in a range of peripheral tissues. In *GABA Outside the CNS*, ed. Erdö, S.L. pp. 249–260. Berlin: Springer.

KARLSSON, J.-A., SANT'AMBROGIO, G. & WIDDICOMBE, J.G. (1988). Afferent neural pathways in cough and reflex bronchoconstriction. *J. Applied Physiol.*, **65**, 1007–1023.

KORPAS, J. & TOMORI, Z. (1979). *Cough and other Respiratory Reflexes*. New York: Karger.

LALLEY, P.M. (1983). Biphasic effects of baclofen on phrenic motoneurons: possible involvement of two types of γ-aminobutyric acid (GABA) receptors. *J. Pharmacol. Exp. Ther.*, **226**, 616–624.

MCLEOD, R.L., GENTNER, S.B. & HEY, J.A. (1991). Modulation of cardiovascular function by central histamine H_3 receptors in conscious guinea pigs. *Eur. J. Pharmacol.*, **209**, 141–142.

(Received January 17, 1994
Revised July 18, 1994
Accepted August 3, 1994)

Br. J. Pharmacol. (1994), **113**, 1349–1357 © Macmillan Press Ltd, 1994

Effects of the non-NMDA antagonists NBQX and the 2,3-benzodiazepine GYKI 52466 on different seizure types in mice: comparison with diazepam and interactions with flumazenil

[1]Wolfgang Löscher & Dagmar Hönack

Department of Pharmacology, Toxicology, and Pharmacy, School of Veterinary Medicine, Bünteweg 17, 30559 Hannover, Germany

1 GYKI 52466 is a benzodiazepine derivative that has muscle relaxant and anticonvulsant properties thought to be mediated by highly selective, noncompetitive antagonism of non-NMDA receptors. However, recent electrophysiological data showed that, in addition to non-NMDA receptors, the $GABA_A$-receptor associated benzodiazepine site is involved in the depressant effect of GYKI 52466 on spinal reflex transmission. In view of the structural similarities between the 2,3 benzodiazepine derivative GYKI 52466 and 1,4-benzodiazepines such as diazepam, the benzodiazepine site of $GABA_A$ receptor complex could also be involved in the anticonvulsant activity of GYKI 52466, which has not yet been proven. This prompted us to study the effect of the benzodiazepine receptor antagonist, flumazenil, on anticonvulsant and adverse effects of GYKI 52466 in different seizure models in mice. The non-NMDA antagonist, NBQX and diazepam were used for comparison.

2 Seizure threshold models for different types of generalized seizures were used. The threshold for maximal (tonic) electroshock seizures (MES) was significantly increased by GYKI 52466 (10–20 mg kg^{-1}), NBQX (80–120 mg kg^{-1}) and diazepam (5 mg kg^{-1}) shortly after i.p. drug administration. The same dose-range of the non-NMDA antagonists also significantly increased the threshold for myoclonic and clonic seizures induced by i.v. infusion of pentylenetetrazol (PTZ), although the magnitude of threshold increases obtained with the respective drugs, differed, at least in part, from that seen in the MES experiments. GYKI 52466 was clearly less potent in increasing PTZ thresholds for myoclonic and clonic seizures than on the MES threshold, while NBQX exerted about the same potency in both models. In contrast to the non-NMDA antagonists, diazepam was capable of increasing the myoclonic and clonic PTZ seizure threshold at much lower doses than the MES threshold. The PTZ threshold for tonic seizures was markedly increased by GYKI 52466, while NBQX and diazepam were clearly less potent in this respect.

3 With respect to adverse effects, GYKI 52466 and NBQX induced significant seizure threshold increases in the different seizure models only at doses which caused sedation and ataxia, while diazepam increased the myoclonic and clonic PTZ seizure threshold at doses below those inducing motor impairment.

4 Flumazenil (5–20 mg kg^{-1}) antagonized the anticonvulsant and adverse effects of diazepam but not GYKI 52466. Instead, the anticonvulsant effect of GYKI 52466 was potentiated by flumazenil in some experiments. The anticonvulsant activity of NBQX was slightly reduced by flumazenil in the MES model but not in the PTZ test.

5 The data indicate that the $GABA_A$ receptor-associated benzodiazepine site is not critically involved in anticonvulsant or adverse effects of GYKI 52466. However, both GYKI 52466 and NBQX were unable to increase seizure thresholds at doses below those inducing sedation and motor impairment, thus demonstrating that non-NMDA antagonists lack a selective anticonvulsant action in standard models of generalized seizures.

Keywords: Seizures; AMPA; NMDA; GABA; epilepsy; muscle relaxation; GYKI 52466; diazepam; flumazenil; NBQX

Introduction

Whereas the pharmacology of drugs which block glutamate receptors of the N-methyl-D-aspartate (NMDA) subtype has been well documented during the last 10 years (Willetts *et al.*, 1990; Rogawski, 1992), selective antagonists of non-NMDA receptors became available only recently. These include the quinoxaline, NBQX (2,3-dihydroxy-6-nitro-7-sulphamoyl-benzo (F)quinoxaline), a competitive inhibitor at the AMPA (α-amino-3-hydroxy-5-phenyl-4-isoxazolepropionate) type of non-HNMDA glutamate receptors, and the 2,3-benzodiazepine, GYKI 52466 (1-(4-aminophenyl)-4-methyl-7,8-methylendioxy-5*H*-2,3-benzodiazepine), a noncompetitive AMPA/kainate antagonist, which is thought to act via a benzodiazepine recognition site associated with the non-NMDA glutamate receptor (cf., Rogawski, 1993). Both compounds are effective in experimental models of ischaemia and epilepsy, although, only in doses which impair motor functions (Sheardown, 1989; Chapman *et al.*, 1991; Smith *et al.*, 1991; Taylor & Vartanian, 1992; Turski *et al.*, 1992; Löscher *et al.*, 1993; Yamaguchi *et al.*, 1993; Zorumski *et al.*, 1993; Dürmüller *et al.*, 1994). Interestingly, in seizure models the potency and spectrum of activity of GYKI 52466 differed from NBQX, and it was suggested that noncompetitive AMPA/kainate receptor antagonists such as GYKI 52466 could have advantages over competitive antagonists such as NBQX (Rogawski 1993). It is generally assumed that GYKI 52466 is a highly selective AMPA/kainate antagonist which does not affect NMDA, metabotropic glutamate or $GABA_A$

[1] Author for correspondence.

receptor-mediated responses (Rogawski, 1993). However, some of the pharmacodynamic characteristics, e.g. the muscle relaxant action and the wide spectrum of anticonvulsant activity, of the 2,3-benzodiazepine GYKI 52466 resemble those of 1,4-benzodiazepines such as diazepam, which act via selective benzodiazepine binding sites at the $GABA_A$ receptor-chloride ionophore complex (Macdonald & McLean, 1986). Although it has repeatedly been stated that the effects of GYKI 52466 are not attributable to a $GABA_A$ receptor-mediated mechanism (e.g. Donevan & Rogawski, 1993; Rogawski, 1993; Zorumski *et al.*, 1993), direct data on this possibility are scanty. Tarnawa *et al.*, (1989) noted that GYKI 52466 has some affinity towards 'central' benzodiazepine (i.e. GABA receptor-associated) receptors, although several orders of magnitude weaker than that of diazepam, but no details were given. Furthermore, the same authors noted that the benzodiazepine receptor antagonist, flumazenil (Ro 15-1788), failed to alter the effects of GYKI 52466 in some electrophysiological spinal reflex tests (Tarnawa *et al.*, 1989), but again no detailed data were shown. More recently, Block & Schwarz (1994) reported that the depressant effect of GYKI 52466 on spinal reflex transmission is partially block by flumazenil, thus indicating that GYKI 52466 acts on the $GABA_A$ receptor-associated benzodiazepine receptor. This prompted us to investigate whether flumazenil affects the anticonvulsant and adverse effects of GYKI 52466 in different seizure models in mice. NBQX and diazepam were used for comparison.

Methods

Animals

Male NMRI-mice were received in groups of 150–200 from a commercial breeder (Harlan-Winkelmann, Borchen, Germany) at the age of 4 weeks (body weight 19–27 g) and were adapted to laboratory conditions for 1 week before the experiments were started. All experiments with the respective group of mice were then carried out within the next 1–2 weeks to minimize the effect of increasing age on seizure susceptibility. Each mouse was used for only one experiment. The mice were kept in groups of 10 in plastic cages at controlled temperature (25°C) and humidity (about 40%) with a 12 h light cycle beginning at 06 h 00 min. They received standard diet (Altromin, Lage Germany) and tap water *ad libitum*. All experiments were carried out between 08 hr 00 min and 12 h 00 min at an ambient temperature of 23–25°C.

Seizure threshold determinations

In order to obtain quantitative data on anticonvulsant effects of test compounds and alterations of these effects by flumazenil, seizure threshold tests for different types of generalized seizures were used (cf., Löscher & Schmidt, 1988). Selection of doses and pretreatment times of diazepam, NBQX and GYKI 52466 were based on previous studies in mice (Chapman *et al.*, 1991; Löscher *et al.*, 1991a,b; Smith *et al.*, 1991; Yamaguchi *et al.*, 1993). According to these previous studies, all drugs were tested at the time of maximal anticonvulsant activity, which is about 15 min for all drugs after i.p. injection. Flumazenil was used in a dose-range previously shown to antagonize the anticonvulsant and muscle relaxant effect of diazepam or related 1,4-benzodiazepines (Hunkeler *et al.*, 1981; Bonetti *et al.*, 1982; Clineschmidt, 1982; Le Gal La Salle & Feldblum, 1983). In view of the rapid onset but very short duration of action of flumazenil (Bonetti *et al.*, 1982), the drug was given 5 min prior to diazepam, NBQX, or GYKI 52466. Several preliminary experiments (not shown in this paper) were done to justify the selection of doses and pretreatment times.

The threshold for maximal (tonic hindlimb extension) electroconvulsions in mice was determined via transcorneal electrodes by means of a stimulator (BMT Medizintechnik GmbH, Berlin, Germany) which delivered a constant current (adjustable from 1–200 mA regardless of impedance of the test object; self-adjusting stimulus voltage max. 7000 V) with sinusoidal pulses (50 s^{-1}) for 0.2 s. The stimulus intensity was varied by an up-and-down method in which the current was lowered or raised by 0.1-log intervals if the preceding animal did or did not exert hind limb extension, respectively (for details see Löscher *et al.*, 1991a). The data thus generated in groups of 20 mice were used to calculate the threshold current inducing hindlimb extension in 50% of the mice (CC_{50} with confidence limits for 95% probability) by the method of Kimball *et al.*, (1957). Control groups, which received the vehicle (saline) used for drug administration, were tested together with each drug experiment, using the same pretreatment time at which the drug was tested.

The threshold for different types of pentylenetetrazol (PTZ)-induced seizures was determined by infusion of a 1% solution of PTZ into the tail vein of unrestricted freely moving mice at a rate of 0.3 ml min^{-1} with an infusion pump (for details see Löscher *et al.*, 1991b). Groups of 10–12 mice were used per threshold determination. In untreated control mice, the following seizure types occurred during PTZ infusion (described in order of appearance): (1) one or more generalized myoclonic twitches of the whole body, (2) repeated clonic seizures of fore- and/or hindlimbs without loss of righting reflexes, (3) a generalized clonus with repeated clonic seizures of fore- and hindlimbs, during which animals fell onto their side, i.e. exhibited loss of righting reflexes, (4) clonic seizures with loss of righting reflexes followed by backward extension of forelimbs (forelimb tonus), often but not always followed by (5) tonic hindlimb extension. In the present experiments, the following endpoints were used for quantification of drug effects: (1) the initial myoclonic twitch, (2) the first generalized clonus with loss of righting reflexes, (3) the forelimb tonus. The threshold for each endpoint was calculated in mg kg^{-1} PTZ inducing this endpoint during infusion. The threshold for tonic hindlimb seizures could not be quantitated in all animals since infusion was generally terminated after 2.5 min and not all control animals exhibited tonic hindlimb seizures during this period of infusion. Increase of infusion time did not resolve this problem, since several mice of a group died without showing hindlimb tonus. However, all control animals showed forelimb tonus within 2.5 min and this seizure type proved to be a more reliable endpoint with less variation than hindlimb tonus. All drug-treated groups were compared with vehicle-treated groups on each day. If following drug injection no forelimb tonus was seen during 2.5 min of PTZ infusion, the amount of PTZ infused over the 2.5 min period (7.5 mg per mouse) was used for calculation of forelimb seizure threshold.

Several MES and PTZ seizure threshold experiments were repeated once to prove the reproducibility of findings with the different drugs. Since all findings were reproducible, data from both experiments were averaged for illustration.

Determination of sedation and motor impairment

Prior to seizure threshold determinations, behavioural alterations observed after drug administration were noted in the cage and by placing the animals in an open field. Muscle tone was estimated by palpation of abdominal tone. The extent of sedation and ataxia after drug administration (immediately prior to seizure threshold determination) was scored by a rating system as described previously for rats (Löscher *et al.*, 1987). In short, animals were taken out of the cage, placed on a table for observation and sedation and ataxia were rated separately (abdominal muscle tone was evaluated by palpation at the end of the period of observation): Sedation: 1 slightly reduced forward locomotion; 2,

reduced locomotion with rest periods in between (partly with closed eyes); 3, reduced locomotion with more frequent rest periods; 4, no forward locomotion, animal sits quietly with closed eyes. Ataxia: 1, slight ataxia in hind legs (tottering of the hind quarters); 2, more pronounced ataxia with dragging of hind legs; 3, further increase of ataxia and more pronounced dragging of hind legs; 4, marked ataxia, animals lose balance during forward locomotion; 5, very marked ataxia with frequent loss of balance during forward locomotion. Behavioural alterations other than sedation and ataxia were recorded separately.

Statistics

All data are given as means ± s.e. Significance of differences in seizure thresholds between drug-treated and individual control groups was calculated by Student's *t* test.

Drugs

NBQX (used as sodium salt) was kindly provided by Novo-Nordisk (Malov, Denmark) and diazepam and flumazenil by Hoffmann-La Roche (Basle, Switzerland). GYKI 52466 (used as hydrochloride) was purchased from RBI/Biotrend (Köln, Germany). NBQX, GYKI 52466, and diazepam were freshly dissolved in distilled water prior to each experiment (diazepam by means of dilute HCl). Flumazenil was dissolved in polyethylene glycol 400 (PEG 400), which was then diluted by distilled water to a final PEG concentration of 10–20%. All drugs were injected i.p. at a volume of 10-15 ml kg^{-1}. Controls received the same injection volume of saline (as control for NBQX, diazepam or GYKI 52466) or 10–20% PEG (as control for flumazenil). In all experiments with two drug applications, controls also received two applications of the respective vehicles.

Results

Drug effects on MES threshold

As shown in Figure 1, NBQX, GYKI 52466, and diazepam significantly increased the threshold for electrically induced tonic hindlimb seizures, but the drugs differed in their anticonvulsant potency in this model. The most potent drug was diazepam which doubled the threshold at 5 mg kg^{-1}, while GYKI 52466 was ineffective at this dosage. At 10 mg kg^{-1}, GYKI 52466 increased the MES threshold by about 60%. When the dose was further increased to 20 mg kg^{-1}, no tonus could be induced by stimuli up to 40 mA, indicating that the threshold had been increased by at least 250% above control (not illustrated). NBQX was the least potent compound. It was ineffective in increasing the MES threshold at 5 and 40 mg kg^{-1} and increased the threshold by only about 40% at 80 mg kg^{-1} (Figure 1). Increase of dosage to 120 mg kg^{-1} resulted in about the same threshold elevation as obtained with 80 mg kg^{-1}, indicating a truncated dose-response.

Flumazenil did not significantly alter the MES threshold at doses of 5, 10 or 20 mg kg^{-1} (Figure 1). Pretreatment with

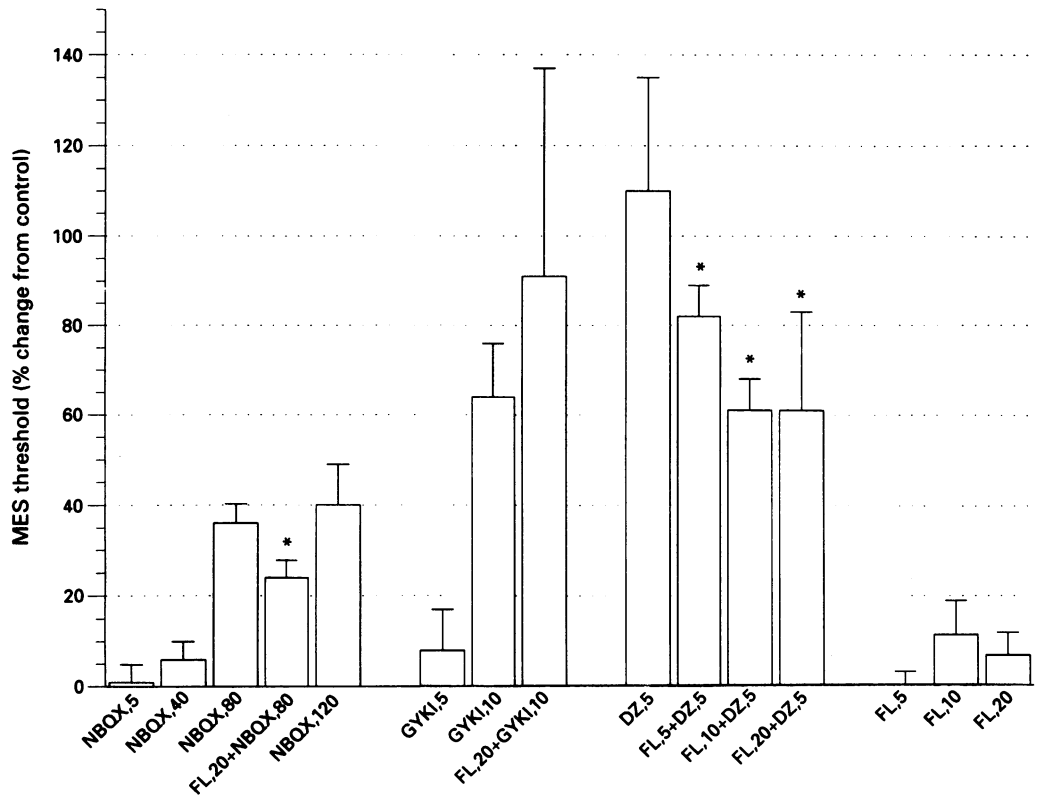


Figure 1 Effect of NBQX, GYKI 52466 and diazepam (DZ), either administered alone or after pretreatment with flumazenil (FL), on the maximal electroshock seizures (MES) threshold in mice. All data shown as mean percent change (+s.e.) from control. Per drug and dose, 20 animals were used; several experiments were repeated once and data from 40 mice were then used for the mean data shown in the figure. Doses of drugs (in mg kg^{-1}) are indicated below the column. NBQX, GYKI 52466 and diazepam were administered 15 min before threshold determination, while flumazenil was administered 20 min before threshold determination. Asterisks indicate significant differences between treatment with NBQX, GYKI 52466 and diazepam alone and after pretreatment with flumazenil (P at least<0.05). All threshold increases were significantly different from individual controls (P at least <0.05) except in case of 5 and 40 mg kg^{-1} NBQX and 5 mg kg^{-1} GYKI 52466, respectively. Flumazenil alone did not significantly alter seizure threshold. The average control MES threshold (CC_{50} with confidence limits for 95% probability) was 11.3 (10.5–12.2) mA (mean of 11 control threshold determinations in groups of 20 mice each).

flumazenil resulted in a decreased anticonvulsant potency of diazepam. However, although doses up to 20 mg kg^{-1} flumazenil were used, the antagonism of the effect of diazepam in the MES threshold test was only partial (Figure 1). A maximum antagonism of about 40% was obtained at 10 mg kg^{-1} flumazenil. The same effect was seen at 20 mg kg^{-1} flumazenil, indicating that no more than 40% reduction of the effect of diazepam could be achieved in this seizure model.

The anticonvulsant effect of GYKI 52466 on tonic electroconvulsions was not significantly altered by pretreatment with flumazenil, 20 mg kg^{-1}, although a trend to higher anticonvulsant potency compared to treatment with the AMP/kainate antagonist alone was seen (Figure 1). In case of NBQX, a slight but significant reduction of anticonvulsant activity was obtained after pretreatment with flumazenil.

Drug effects on PTZ threshold

Similar to the data with tonic electroconvulsions, NBQX, GYKI 52466 and diazepam increased significantly the threshold for myoclonic siezures induced by PTZ infusion (Figure 2). However, the anticonvulsant drug potencies in this test markedly differed from potencies in the MES threshold tests. Thus, diazepam was about 5 times more potent in increasing the myoclonic PTZ threshold than the MES threshold, while GYKI 52466 was less potent against myoclonic PTZ seizures than against tonic electroconvulsions. Significant threshold increases of 17 and 33% were seen at 10 and 15 mg kg^{-1}, respectively, while no significant effect was determined at 20 mg kg^{-1} of GYKI 52466, indicating a truncated dose-response (Figure 1). NBQX significantly increased the myoclonic PTZ seizure threshold at 80 and 120 mg kg^{-1}, the maximum increase being about 40% above control. Both GYKI 52466 (20 mg kg^{-1}) and NBQX (120 mg kg^{-1}) were also tested after 30 instead of 15 min to examine if the onset of peak activity was retarded after these relatively high doses. With NBQX, significant threshold increases of 46% and 25% were determined after 15 and 30 min, respectively, indicating that the maximum effect was reached after 15 min (not illustrated). With GYKI 52466, the effect seen after 20 mg kg^{-1} at either 15 or 30 min was lower than the effect determined after 15 mg kg^{-1}, thus substantiating that the decreased anticonvulsant activity at the higher dose was due to a truncated dose-response and not to retarded absorption.

Flumazenil did not alter the PTZ threshold at 10 mg kg^{-1}, but a significant threshold decrease was seen at 20 mg kg^{-1} (Figure 2). Therefore, 10 mg kg^{-1} flumazenil was used for most of the combination studies in this seizure model. Flumazenil dose-dependently reduced the anticonvulsant effect of diazepam against myoclonic PTZ seizures (Figure 2). In contrast, flumazenil exerted no effect on the anticonvulsant activity of 15 mg kg^{-1} GYKI 52466, but significantly increased the anticonvulsant effect of 20 mg kg^{-1} of the non-NMDA antagonist (Figure 2). The seizure threshold increase obtained with NBQX was not altered by pretreatment with flumazenil.

The data obtained for the clonic PTZ seizure threshold (Figure 3) were very similar to the data on the myoclonic

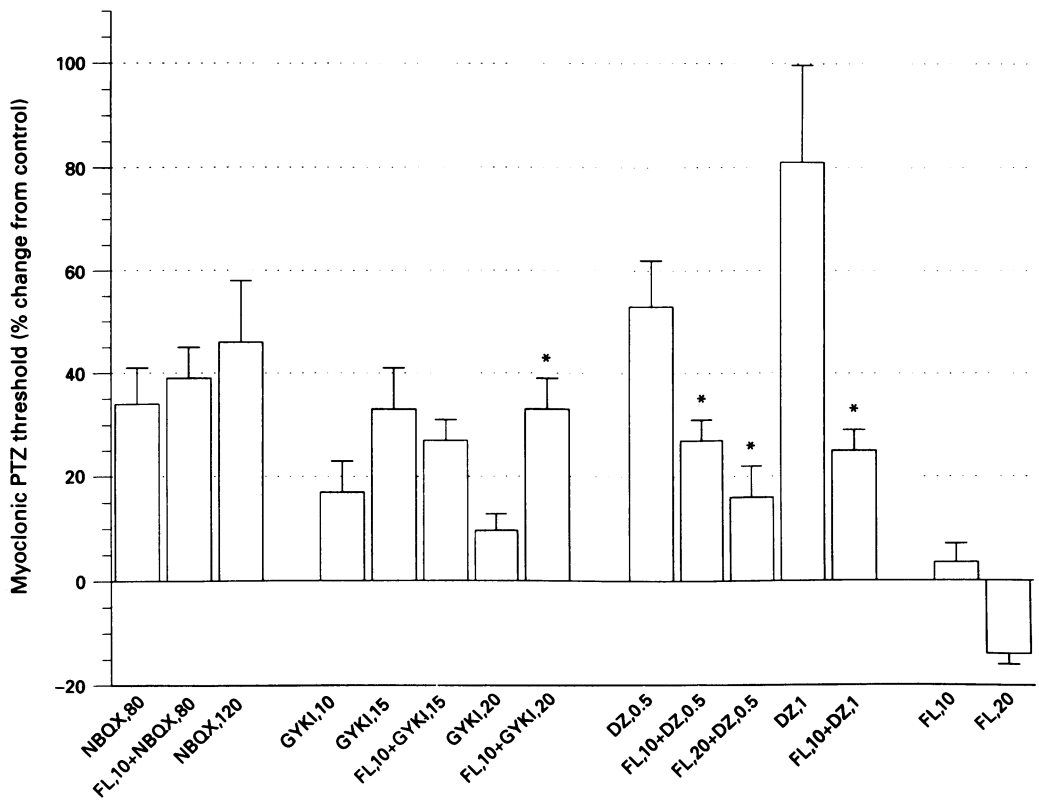


Figure 2 Effect of NBQX, GYKI 52466 and diazepam (DZ), either administered alone or after pretreatment with flumazenil (FL), on the pentylenetetrazol (PTZ) threshold for myoclonic seizures in mice. All data are shown as mean percentage change (+s.e.) from control. Per drug and dose, 10 animals were used; several experiments were repeated once and data from 20 mice were then used for the mean data shown in the figure. Doses of drugs (in mg kg^{-1}) are indicated below the columns. NBQX, GYKI 52466 and diazepam were administered 15 min before threshold determination, while flumazenil was administered 20 min before threshold determination. Asterisks indicate significant differences between treatment with NBQX, GYKI 52466 and diazepam alone and after pretreatment with flumazenil (P at least <0.05). All threshold increases were significantly different from individual controls (P at least <0.05) except in case of 20 mg kg^{-1} GYKI 52466 (injected alone). Flumazenil alone did not significantly alter seizure threshold at 10 mg kg^{-1}, but caused a significant reduction at 20 mg kg^{-1}. The average control threshold for myoclonic seizures (in mg kg^{-1} PTZ ± s.e.) was 32.1 ± 0.7 mg kg^{-1} (mean of 7 control threshold determinations in groups of 10 mice each.).

seizure threshold. Flumazenil almost totally prevented the anticonvulsant effect of diazepam on this seizure type, but had no effect or increased the anticonvulsant activity in experiments with GYKI 52466 and NBQX.

Drug activities on the threshold for tonic PTZ seizures (Figure 4) differed markedly from respective activities seen with the myoclonic and clonic seizure types. Diazepam was ineffective in increasing the tonic PTZ seizure threshold at 0.5 mg kg^{-1}, and only non-significantly increased the threshold at 1 mg kg^{-1}. In contrast, GYKI 52466 was more potent against this seizure type than against myoclonic or clonic seizures, causing threshold increases of more than 100% at 15 or 20 mg kg^{-1} (Figure 4). NBQX did not significantly increase the tonic PTZ seizure threshold at 80 mg kg^{-1}, but caused an increase of about 70% at 120 mg kg^{-1}. Flumazenil did not alter the tonic seizure threshold when given alone. In combination with GYKI 52466, flumazenil did not change or increased the anticonvulsant effect of the AMPA/kainate antagonist. The effect of NBQX was not altered by pretreatment with flumazenil (Figure 4).

Adverse effects

Diazepam, GYKI 52466 and NBQX induced sedation, ataxia and muscle relaxation (as judged by reduced abdominal muscle tone) in the dose-range of drugs used in this study although respective potencies differed. Following administration of diazepam, no adverse effects were seen at 0.5 mg kg^{-1} and only slight ataxia (with scores of 1–2) at 1 mg kg^{-1}, i.e. the effective dose-range of diazepam in the PTZ threshold experiments, while more marked ataxia (score 3–4) and sedation (score 3) were seen at 5 mg kg^{-1} of diazepam, NBQX induced ataxia and sedation at doses equal or above 40 mg kg^{-1}. At 80 mg kg^{-1}, i.e. an effective anticonvulsant dose against most seizure types, ataxia scores of 2–3 and sedation scores of 1–2 were rated. GYKI 52466 induced the most pronounced adverse effects at anticonvulsant effective doses. Scores for ataxia and sedation were 3–4 and 4 at 10 and 15 mg kg^{-1}, and up to 5 at 20 mg kg^{-1}, respectively. At the latter dose, severe ataxia and muscle relaxation with loss of righting occurred within 3 min after i.p. injection and was still present at time of threshold determinations.

Flumazenil, while not inducing any behavioural effects alone, totally prevented ataxia/muscle relaxation and sedation in response to diazepam. In contrast, flumazenil did not alter the adverse effects induced by NBQX or GYKI 52466.

Discussion

The main findings of this study are as follows. (1) The AMPA/kainate receptor antagonists NBQX and GYKI 52466 increase the threshold for different types of generalized seizures in mice. However, although seizure threshold determinations are much more sensitive to anticonvulsant drug effects than the standard MES and PTZ tests with fixed (supramaximal) seizure stimuli (Löscher & Schmidt, 1988; Löscher *et al.*, 1991a,b), anticonvulsant effects of NBQX and GYKI 52466 on seizure thresholds were only determined at

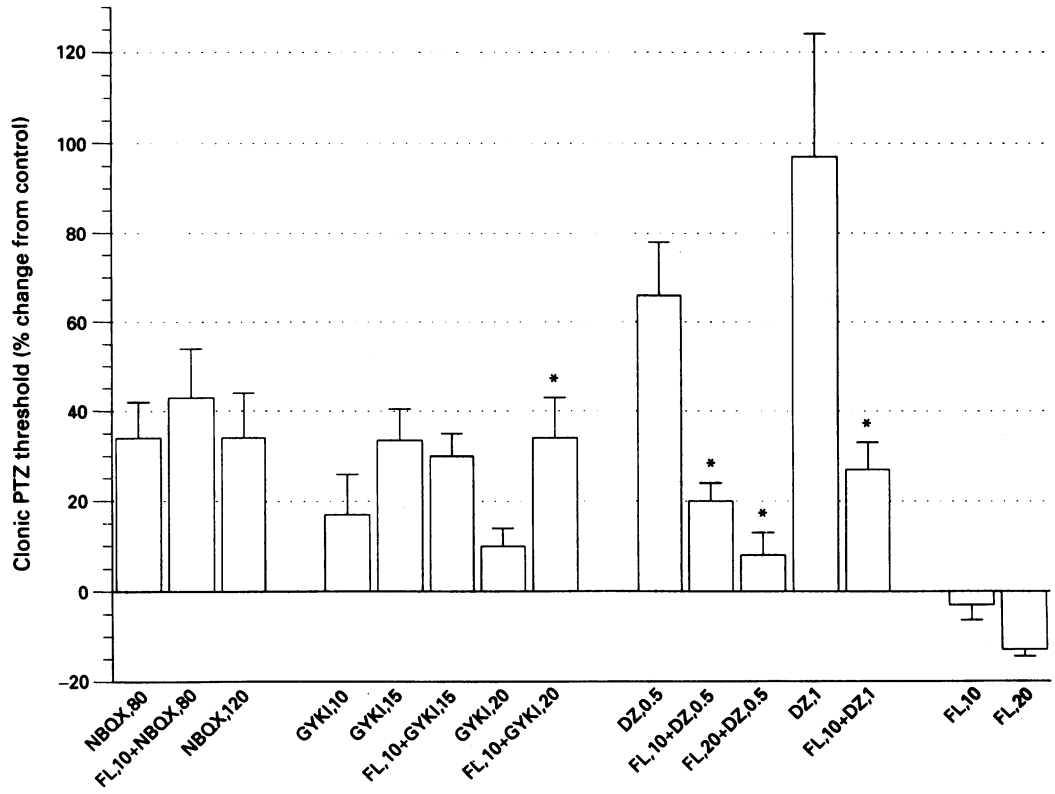


Figure 3 Effect of NBQX, GYKI 52466 and diazepam (DZ), either administered alone or after pretreatment with flumazenil (FL), on the pentylenetetrazol (PTZ) threshold for clonic seizures in mice. All data are shown as mean percentage change (+s.e.) from control. Per drug and dose, 10 animals were used; several experiments were repeated once and data from 20 mice were then used for the mean data shown in the figure. Doses of drugs (in mg kg^{-1}) are indicated below the columns. NBQX, GYKI 52466 and diazepam were administrered 15 min before threshold determination, while flumazenil was administered 20 min before threshold determination. Asterisks indicate significant differences between treatment with NBQX, GYKI 52466 and diazepam alone and after pretreatment with flumazenil (P at least <0.05). All threshold increases were significantly different from individual controls (P at least <0.05) except in case of 10 and 20 mg kg^{-1} GYKI 52466 (injected alone). Flumazenil alone did not significantly alter seizure threshold at 10 mg kg^{-1}, but caused a significant reduction at 20 mg kg^{-1}. The average control threshold for clonic seizures (in mg kg^{-1} PTZ ± s.e.) was 38.2 ± 0.9 mg kg^{-1} (mean of 7 control threshold determinations in groups of 10 mice each).

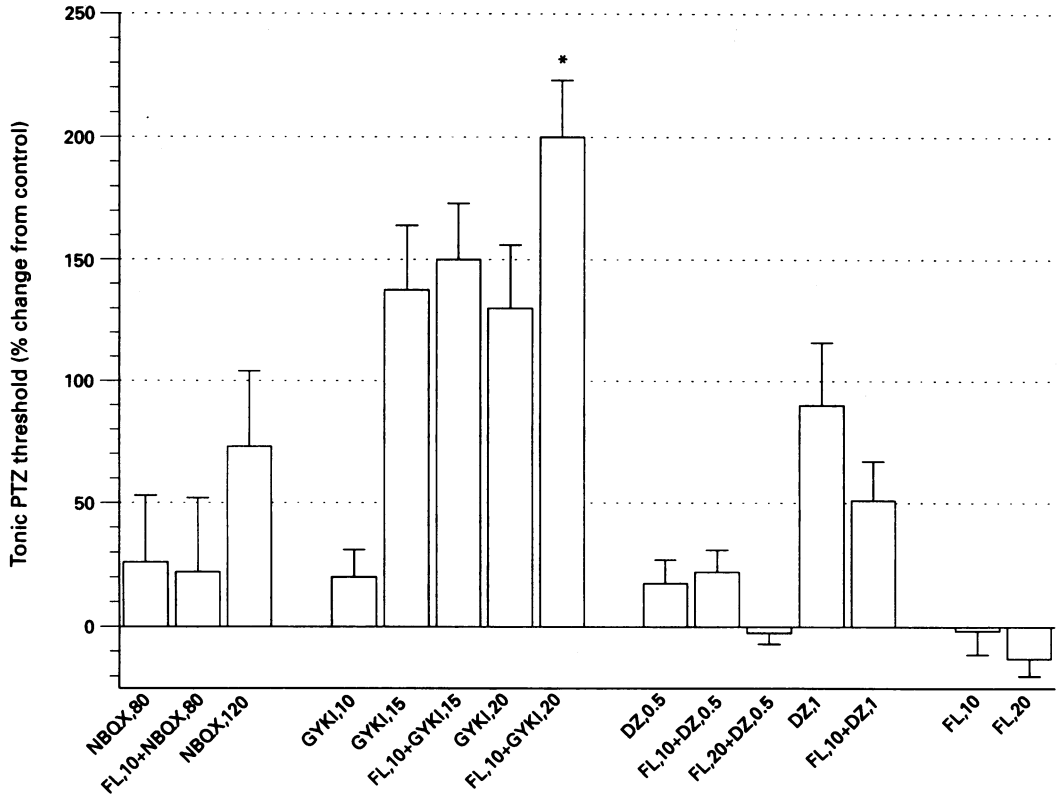


Figure 4 Effect of NBQX, GYKI 52466 and diazepam (DZ), either administered alone or after pretreatment with flumazenil (FL), on the pentylenetetrazol (PTZ) threshold for tonic forelimb seizures in mice. All data are shown as mean percentage change (+s.e.) from control. Per drug and dose, 10 animals were used; several experiments were repeated once and data from 20 mice were then used for the mean data shown in the figure. Doses of drugs (in mg kg^{-1}) are indicated below columns. NBQX, GYKI 52466 and diazepam were administered 15 min before threshold determination, while flumazenil was administered 20 min before threshold determination. Asterisks indicate significant differences between treatment with NBQX, GYKI 52466 and diazepam alone and after pretreatment with flumazenil (P at least <0.05). All threshold increases were significantly different from individual controls (P at least <0.05) except in case of 80 mg kg^{-1} NBQX (without or without flumazenil), 10 mg kg^{-1} GYKI 52466, and all experiments with diazepam. Flumazenil alone did not significantly alter seizure threshold. The average control threshold for tonic forelimb seizures (in mg kg^{-1} PTZ ± s.e.) was 83.4 ± 3.6 mg kg^{-1} (mean of 7 control threshold determinations in groups of 10 mice each).

doses inducing pronounced ataxia and muscle relaxation. Furthermore, the anticonvulsant effect of GYKI 52466 on myoclonic and clonic seizures was lost at higher doses. (2) NBQX and GYKI 52466 differed in their relative potencies against different seizure types. GYKI 52466 was clearly more effective against tonic than myoclonic or clonic seizures, while NBQX was about equally effective against all seizure types. In comparison, diazepam was much more potent against myoclonic and clonic seizures than against tonic seizures. (3) The benzodiazepine receptor antagonist, flumazenil, antagonized the anticonvulsant and adverse effects of the 1,4-benzodiazepine, diazepam but not the 2,3-benzodiazepine, GYKI 52466, strongly indicating that the $GABA_A$ receptor-associated benzodiazepine receptor is not critically involved in these effects of the AMPA/kainate antagonist. Unexpectedly, flumazenil increased the anticonvulsant activity of GYKI 52466 in some experiments. In case of NBQX, the adverse effects and the anticonvulsant action on PTZ seizure thresholds were not affected by flumazenil, while a moderate reduction of anticonvulsant activity was seen in the MES threshold experiments.

We have previously shown that competitive and uncompetitive NMDA receptor antagonists, in contrast to standard antiepileptic drugs, increase seizure thresholds in standard models of epilepsy only in doses inducing ataxia and muscle relaxation (Löscher *et al.*, 1988; Löscher & Hönack, 1991). In line with these findings, Carter (1994) recently demonstrated that various compounds which antagonize the NMDA receptor, irrespective of whether they are a noncompetitive, competitive or glycine site antagonist, disturb motor coordination at anticonvulsant doses. The first clinical trial with a competitive NMDA receptor antagonist had to be prematurely terminated because of adverse effects, particularly ataxia and sedation (Sveinsbjornsdottir *et al.*, 1993). The present data indicate that AMPA/kainate receptor antagonists have no advantages in terms of separation between anticonvulsant and motor impairing effects compared to NMDA receptor antagonists. Initial reports on the anticonvulsant effect of NBQX and GYKI 52466 found a separation between anticonvulsant and motor impairing effects when models such as AMPA-induced or sound-induced seizures in rodents were used (Chapman *et al.*, 1991; Smith *et al.*, 1991). Similarly, NBQX attenuated photically induced myoclonus in baboons in doses below those inducing muscle relaxation (Smith *et al.*, 1991). However, animal models of reflex epilepsy, such as audiogenic seizure susceptible mice or photosensitive baboons, appear to be particularly sensitive to glutamate receptor antagonists, which may lead to false positive data with respect to prediction of clinical efficacy (Löscher & Schmidt, 1994). When standard models of epileptic seizures such as the MES and PTZ tests were used, both NBQX and GYKI 52466 produced motor impairment at doses similar or below to those that were protective in these seizure tests (Yamaguchi *et al.*, 1993). The latter authors concluded that neurological adverse effects may be an impediment to the clinical use of AMPA/kainate antagonists in seizure therapy. This conclusion of Yamaguchi *et al.* (1993) from data of MES and PTZ tests with fixed

(supramaximal) seizure stimuli is substantiated by the present data from more sensitive seizure threshold tests in mice. Interestingly, in view of the potent muscle relaxant effect of AMPA/kainate receptor antagonists, it has been proposed that such drugs may offer a new approach to the treatment of spasticity (Turski *et al.*, 1992).

The muscle relaxant effect of AMPA/kainate antagonists is due to an action on spinal reflexes. While NBQX only blocks the monosynaptic Hoffmann (H)-reflex, but not the polysynaptic flexor reflex (Turski *et al.*, 1993), GYKI 52466 was shown to block both mono- and polysynaptic spinal reflexes in cats and rats (Tarnawa *et al.*, 1989; Block & Schwarz, 1994), which cannot be fully explained by its antagonistic action on non-NMDA receptors. Both GABA and glutamate receptors are involved in spinal transmission (Watkins, 1984; Bowery *et al.*, 1989). In rodents, it is suggested that non-NMDA receptors may be involved in the monosynaptic H-reflex, while NMDA receptors are thought to be engaged in the regulation of the polysynaptic flexor reflex (Turski *et al.*, 1988, 1990; 1992). Both reflexes are also affected by drugs which act on GABA receptors, including therapeutically active antispastic drugs such as the 1,4-benzodiazepines, which preferentially depress flexor reflexes, and the $GABA_B$ receptor agonist, baclofen, which preferentially affects monosynaptic reflexes (Davidoff, 1985). The depressant effect of 1,4-benzodiazepines such as diazepam on the flexor reflex can be blocked by flumazenil (e.g., Block & Schwarz, 1994). Similarly, the depressant action of the 2,3-benzodiazepine GYKI 52466, 10 mg kg^{-1}, on the flexor reflex was reduced by coadministration of flumazenil, 5 mg kg^{-1}, whereas flumazenil did not significantly reduce the depressant action of GYKI 52466 on the H-reflex in rats (Block & Schwarz, 1994). In contrast to the effects of flumazenil, the AMPA receptor agonist, ATPA (α-amino-3-hydroxy-5-tertbutyl-4-isoxazole-propionic acid) did antagonize the action of GYKI 52466 on the H-reflex but not the flexor reflex (Block & Schwarz, 1994). The depressant effects of GYKI 52466 on both reflexes were not affected by NMDA or the $GABA_B$ receptor antagonist, phaclofen, so that the experiments of Block & Schwarz (1994) strongly indicate that the action of GYKI 52466 on spinal reflex transmission is mediated by AMPA (H-reflex) *and* flumazenil-sensitive benzodiazepine (flexor reflex) receptors, respectively (Block & Schwarz, 1994).

In the present study, flumazenil did not antagonize the anticonvulsant or muscle impairing and sedative effects of GYKI 52466 but instead increased its anticonvulsant potency in some experiments. The effect of flumazenil is thought to be highly specific for the central benzodiazepine receptor associated with the $GABA_A$ receptor (Haefely, 1983). It has previously been shown that flumazenil did not affect the anticonvulsant action of the noncompetitive NMDA receptor antagonist, dizocilpine against seizures induced by bicuculline (Clineschmidt, 1982). The unexpected increase in anticonvulsant potency of GYKI 52466 after pretreatment with flumazenil is difficult to explain at present, particularly since pharmacokinetic interactions cannot be ruled out. In view of the finding that the anticonvulsant activity of GYKI 52466 on PTZ-induced myoclonic and clonic seizure was lost at a high dose (20 mg kg^{-1}) and that this loss of anticonvulsant activity was prevented by pretreatment with flumazenil (see Figures 2 and 3), one may speculate that $GABA_A$ receptors were involved in this observation. Theoretically, the loss of anticonvulsant action at high doses of GYKI 52466 and prevention of this loss by flumazenil could either be due to a direct (e.g. an inverse agonist) effect of GYKI 52466 on $GABA_A$ receptor-associated benzodiazepine receptors or an indirect effect on GABAergic activity mediated by blockade of non-NMDA receptors. Both NMDA and non-NMDA receptors tonically activate GABAergic neurones and/or increase GABA release from neurones of different brain regions (Weiss, 1988; Perouansky & Grantyn, 1990; Weiss, 1990; Giovannini *et al.*, 1994). As a consequence of blockade of this glutamate-mediated effect on GABA release, uncompetitive NMDA receptor antagonists decrease GABA release (Weiss, 1990; Giovannini *et al.*, 1994) which could be involved in the loss of anticonvulsant activity or induction of proconvulsant effects observed with these drugs at high doses (Löscher & Schmidt, 1994). Similarly, non-NMDA receptor antagonists have been reported to depress GABA release in response to kainate and quisqualate (Drejer & Honoré, 1988; Sheardown, 1989) so that inhibition of glutamate-induced GABA release could be involved in the present observations of loss of anticonvulsant activity with a high dose of GYKI 52466 in the PTZ model, particularly because the PTZ seizure threshold critically depends on GABA function (Löscher, 1982; 1989). A truncated dose-response was also seen with NBQX but, in contrast to GYKI 52466, the anticonvulsant effect of NBQX on the PTZ seizure threshold was not increased by flumazenil. However, with respect to differences between findings on GYKI 52466 and NBQX it should be noted that NBQX is less selective for non-NMDA receptors than generally thought. For instance, Pullan & Powel (1992) reported that NBQX displaces [^{3}H]-strychnine binding to the glycine-gated chloride channel of spinal cord and brainstem at low concentrations (IC_{50} 11 μM), which could be involved in its anticonvulsant and muscle relaxant effects.

The pharmacological effects of diazepam were differentially affected by flumazenil. While flumazenil totally prevented ataxia and sedation in response to diazepam and markedly reduced its anticonvulsant effect on the myoclonic and clonic PTZ seizure threshold, the antagonist only partially counteracted the effect of diazepam on the MES threshold. With respect to the doses of flumazenil and diazepam used, it should be considered that flumazenil is about half as potent as diazepam in displacing a radiolabelled benzodiazepine from central benzodiazepine receptors in mice *in vivo* (ED_{50} values 4.0 and 1.7 mg kg^{-1}, respectively) (Hunkeler *et al.*, 1981). As shown by the present data, even at a flumazenil: diazepam dose ratio of 4:1, flumazenil reduced the activity of diazepam on the MES threshold by not more than 40%. The finding that 20 mg kg^{-1} of flumazenil was not more effective than 10 mg kg^{-1} in this respect suggest that a part of the action of diazepam on tonic electroconvulsions is independent of central benzodiazepine receptors. In addition to their effect on the $GABA_A$ receptor-associated benzodiazepine binding site, benzodiazepines such as diazepam are known to exert effects unrelated to the $GABA_A$ receptor, particularly when administered at high doses (Macdonald & McLean, 1986; DeLorenzo, 1988). For instance, benzodiazepines reduce repetitive firing of action potentials in neurones, possibly by direct effects on calcium and/or sodium conductances, and it has been suggested that this action might be involved in blockade of MES in animals and generalized tonic-clonic seizures and status epilepticus in patients (Macdonald & McLean, 1986; DeLorenzo, 1988). Furthermore, experimental observations indicated that the muscle relaxant effect of benzodiazepines is mediated by flumazenil-sensitive but GABA-independent benzodiazepine receptors (Schwarz *et al.*, 1983). Consistent with the present data on diazepam, flumazenil was previously reported to inhibit only partially (even at 100 mg kg^{-1}) the anticonvulsant effect of clonazepam in the standard MES test (Petersen *et al.*, 1983) thus supporting the idea of non-GABA receptor-mediated effects of benzodiazepines in this paradigm.

In conclusion, the present data indicate that flumazenil-sensitive benzodiazepine receptors are not critically involved in the anticonvulsant effect of GYKI 52466, which is thus in contrast to the recent findings on spinal reflexes (Block & Schwarz, 1994). Whereas the present data show that AMPA/kainate receptor antagonists increase seizure thresholds only at doses which cause motor impairment, recent studies demonstrated that the anticonvulsant efficacy of such drugs can be dramatically enhanced by combination with NMDA receptor antagonists, both in models of generalized (Shear-

down, 1989) and focal seizures (Löscher *et al.*, 1993; Löscher & Hönack, 1994). Furthermore, Zarnowski *et al.* (1993) reported that low doses of NBQX (10 mg kg^{-1})potentiated the anticonvulsant effect of standard antiepileptics on the MES threshold without increasing their adverse effect potential. Thus, in addition to their potential utility as neuroprotective and antispasticity agents (Turski *et al.*, 1992; Rogawski, 1993), AMPA/kainate receptor antagonists might prove useful as adjuncts of either NMDA receptor antagonists or common antiepileptic drugs (Löscher *et al.*, 1993; Zarnowski *et al.*, 1993; Löscher & Hönack, 1994).

We thank Mrs Doris Pieper for skilful technical assistance. The study was supported by a grant (Lo 274/3-3) from the Deutsche Forschungsgemeinschaft.

References

BLOCK, F. & SCHWARZ, M. (1994). The depressant effect of GYKI 52466 on spinal reflex transmission in rats is mediated via non-NMDA and benzodiazepine receptors. *Eur. J. Pharmacol.*, **256**, 149–153.

BONETTI, E.P., PIERI, L., CUMIN, R., SCHAFFNER, R., PIERI, M., GAMZU, E.R. MÜLLER, R.K.M. & HAEFELY, W. (1982). Benzodiazepine antagonist Ro 15-1788: neurological and behavioural effects. *Psychopharmacology*, **78**, 8–18.

BOWERY, N.G., HILL, D.R., MORATALLA, R., PRICE, G.W. & WILLIAMS, L.C. (1989). GABA receptor characterization and localization in mammalian brain. In *GABA: Basic Research and Clinical Applications* ed. Bowery, N.G. & Nisticò, G., pp. 24–58. Rome: Pythagora Press.

CARTER, A.J. (1994). Many agents that antagonize the NMDA receptor-channel complex *in vivo* also cause disturbances of motor coordination. *J. Pharmacol. Exp. Ther.*, **269**, 573–580.

CHAPMAN, A.G., SMITH, S.E. & MELDRUM, B.S. (1991). The anticonvulsant effect of the non-MNDA antagonists, NBQX and GYKI 52466, in mice. *Epilepsy Res.*, **9**, 92–96.

CLINESCHMIDT, B.V. (1982). Effect of the benzodiazepine receptor antagonist Ro 15-1788 on the anticonvulsant and anticonflict actions of MK-801. *Eur. J. Pharmacol.*, **84**, 119–121.

DAVIDOFF, R.A. (1985). Antispasticity drugs: mechanisms of action. *Ann. Neurol.*, **17**, 107–116.

DELORENZO, R.J. (1988). Mechanisms of action of anticonvulsant drugs. *Epilepsia.*, **29**, (Suppl. 2), S35–S47.

DONEVAN, S.D. & ROGAWSKI, M.A. (1993). GYKI 52466, a 2,3-benzodiazepine, is a highly selective, noncompetitive antagonist of AMPA/kainate receptor responses. *Neuron.*, **10**, 51–59.

DREJER, J. & HONORÉ, T. (1988). New quinoxalinediones show potent antagonism of quisqualate responses in cultured mouse cortical neurons. *Neurosci. Lett.*, **87**, 104–108.

DÜRMÜLLER, N., GRAGGS, M. & MELDRUM, B.S. (1994). The effect of the non-NMDA receptor antagonists GYKI 52466 and NBQX and the competitive NMDA receptor antagonist D-CPPene on the development of amygdala kindling and on amygdala-kindled seizures. *Epilepsy Res.*, **17**, 167–174.

GIOVANNINI, M.G., MUTOLO, D., BIANCHI, L., MICHELASCI, A. & PEPEU, G. (1994). NMDA receptor antagonists decrease GABA outflow from the spectrum and increase acetylcholine outflow from the hippocampus: a microdialysis study. *J. Neurosci.*, **14**, 1358–1365.

HAEFELY, W. (1983). Antagonists of benzodiazepines: functional aspects. In *Benzodiazepine Recognition Site Ligands: Biochemistry and Pharmacology*. ed. Biggio, G. & Costa, E. pp. 73–79. New York: Raven Press.

HUNKELER, W., MÖHLER, H., PIERI, L., POLC, P., BONETTI, E.P., CUMIN, R., SCHAFFNER, R. & HAEFELY, W. (1981). Selective antagonists of benzodiazepines. *Nature*, **290**, 514–516.

KIMBALL, A.W., BURNETT, W.T. & DOHERTY, D.G. (1957). Chemical protection against ionizing radiation. I. Sampling methods for screening compounds in radiation protection studies with mice. *Radiation Res.*, **7**, 1–12.

LE GAL LA SALLE, G. & FELDBLUM, S. (1983). Reversal of the anticonvulsant effects of diazepam on amygdaloid-kindled seizures by a specific benzodiazepine antagonist: Ro 15-1788. *Eur. J. Pharmacol.*, **86**, 91–93.

LÖSCHER, W. (1982). Relationship between GABA concentrations in cerebrospinal fluid and seizure excitability. *J. Neurochem.*, **38**, 293–295.

LÖSCHER, W. (1989). GABA and the epilepsies. Experimental and clinical considerations. In *GABA: Basic Research and Clinical Applications*. ed. Bowery, N.G. & Nisticò, G., pp. 260–300. Rome: Pythagora Press.

LÖSCHER, W., FASSBENDER, C.P. & NOLTING, B. (1991a). The role of technical, biological and pharmacological factors in the laboratory evaluation of anticonvulsant drugs. II. Maximal electroshock seizure models. *Epilepsy Res.*, **8**, 79–94.

LÖSCHER, W. & HÖNACK, D. (1991). Anticonvulsant and behavioural effects of two novel competitive N-methyl-D-aspartic acid receptor antagonists, CGP 37849 and CGP 39551, in the kindling model of epilepsy. Comparison with MK-801 and carbamazepine. *J. Pharmacol. Exp. Ther.*, **256**, 432–440.

LÖSCHER, W. & HÖNACK, D. (1994). Over-additive anticonvulsant effect of memantine and NBQX in kindled rats. *Eur. J. Pharmacol.*, **259**, R3–R5.

LÖSCHER, W., HÖNACK, D., FASSBENDER, C.P. & NOLTING, B. (1991b). The role of technical, biological and pharmacological factors in the laboratory evaluation of anticonvulsant drugs. III. Pentylenetetrazol seizure models. *Epilepsy Res.*, **8**, 171–189.

LÖSCHER, W., HÖNACK, D. & HASHEM, A. (1987). Anticonvulsant efficacy of clonazepam and the β-carboline ZK 93423 during chronic treatment in amygdala-kindled rats. *Eur. J. Pharmacol.*, **143**, 403–414.

LÖSCHER, W., NOLTING, B. & HÖNACK, D. (1988). Evaluation of CPP, a selective NMDA antagonist, in various models of epilepsy. Comparison with other NMDA antagonists, and with diazepam and phenobarbital. *Eur. J. Pharmacol.*, **152**, 9–17.

LÖSCHER, W., RUNDFELDT, C. & HÖNACK, D. (1993). Low doses of NMDA receptor antagonists synergistically increase the anticonvulsant effect of the AMPA receptor antagonist NBQX in the kindling model of epilepsy. *Eur. J. Neurosci.*, **5**, 1545–1550.

LÖSCHER, W. & SCHMIDT, D. (1988). Which animal models should be used in the search for new antiepileptic drugs? A proposal based on experimental and clinical considerations. *Epilepsy Res.*, **2**, 145–181.

LÖSCHER, W. & SCHMIDT, D. (1994). Strategies in antiepileptic drug development: is rational drug design superior to random screening and structural variation? *Epilepsy Res.*, **17**, 403–414.

MACDONALD, R.L. & MCLEAN, M.J. (1986). Anticonvulsant drugs: mechanisms of action. In *Basic Mechanisms of the Epilepsies, Molecular and Cellular Approaches*. ed. Delgado-Escueta, A.V., Ward, Jr. A.A., Woodbury, D.M. & Porter, R.J. pp. 713–736. New York: Raven Press.

PEROUANSKY, M. & GRANTYN, R. (1990). Is GABA release modulated by presynaptic excitatory amino acid receptors? *Neurosci. Lett.*, **113**, 292–297.

PETERSEN, E.N., JENSEN, L.H., HONORÉ, T. & BRAESTRUP, C. (1983). Differential pharmacological effects of benzodiazepine inverse agonists. In *Benzodiazepine Recognition Site Ligands: Biochemistry and Pharmacology*. ed. Biggio, G. & Costa, E. pp. 57–64. New York, Raven Press.

PULLAN, L.M. & POWEL, R.J. (1992). Comparison of binding at strychnine-sensitive (inhibitory glycine receptor) and strychnine-insensitive (N-methyl-D-aspartate receptor) glycine binding sites. *Neurosci. Lett.*, **148**, 199–201.

ROGAWSKI, M.A. (1992). The NMDA receptor, NMDA antagonists and epilepsy therapy. *Drugs*, **44**, 279–292.

ROGAWSKI, M.A. (1993). Therapeutic potential of excitatory amino acid antagonists: channel blockers and 2,3-benzodiazepines. *Trends Pharmacol. Sci.*, **14**, 325–331.

SCHWARZ, M., TURSKI, L., JANISZEWSKI, W. & SONTAG, K.-H. (1983). Is the muscle relaxant effect of diazepam in spastic mutant rats mediated through GABA-independent benzodiazepine receptors? *Neurosci. Lett.*, **36**, 175–180.

SHEARDOWN, M.J. (1989). The quinoxalinediones, a new series of potent and selective non-NMDA receptor antagonists. *Drugs Future*, **14**, 667–674.

SMITH, S., DÜRMÜLLER, N. & MELDRUM, B.S. (1991). The non-N-methyl-D-aspartate receptor antagonists, GYKI 52466 and NBNQX are anticonvulsant in two animal models of reflex epilepsy. *Eur. J. Pharmacol.*, **201**, 179–183.

SVEINBJORNSDOTTIR, S., SANDER, J.W.A.S., UPTON, D., THOMPSON, P.J., PATSALOS, P.N., HIRT, D., EMRE, M., LOWE, D. & DUNCAN, J.S. (1993). The excitatory amino acid antagonist D-CCP-ene (SDZ EAA-494) in patients with epilepsy. *Epilepsy Res.*, **16**, 165–174.

TARNAWA, I. FARKAS, S., BERZSENYI, P., PATAKI, A. & ANDRÁSI, F. (1989). Electrophysiological studies with a 2,3-benzodiazepine muscle relaxant: GYKI 52466. *Eur. J. Pharmacol.*, **167**, 193–199.

TAYLOR, C.P. & VARTANIAN, M.G. (1992). Probenecid pretreatment enhances anticonvulsant action of NBQX in mice. *Eur. J. Pharmacol.*, **213**, 151–153.

TURSKI, L., BESSLER, K., KLOCKGETHER, T. & STEPHENS, D.N. (1990). Differential effects of the excitatory amino acid antagonists, 6-cyano-7-nitroquinoxaline-2,3,-dione (CNQX) and 3-((±)-2-carboxypiperazin-4-yl)-propyl-1-phosphonic acid (CCP), on spinal reflex activity in mice. *Neurosci. Lett.*, **113**, 66–71.

TURSKI, L., JACOBSEN, P., HONORÉ, T. & STEPHENS, D.N. (1992). Relief of experimental spasticity and anxiolytic/anticonvulsant actions of the *alpha*-amino-3-hydroxy-5-methyl-4-isoxazolepropionate antagonist 2,3-dihydroxy-6-nitro-7-sulfamoyl-benzo(F)-quinoxaline. *J. Pharmacol. Exp. Ther.*, **260**, 742–747.

TURSKI, L., KLOCKGETHER, T., TURSKI, W.A., IKONOMIDOU, C., SCHWARZ, M. & SONTAG, K.-H. (1988). Muscle relexant action of excitatory amino acid antagonists: Site of action. In *Frontiers in Excitatory Amino Acid Research*. ed. Cavalheiro, E.A., Lehmann, J. & Turski, L., pp. 343–350. New York: Alan R. Liss.

WATKINS, J.C. (1984). Excitatory amino acids and central synaptic transmission. *Trends Neurosci.*, **7**, 373–392.

WEISS, S. (1988). Excitatory amino acid-evoked release of γ-[^{3}H]aminobutyric acid from striatal neurons in primary culture. *J. Neurochem.*, **51**, 435–441.

WEISS, S. (1990). Pharmacological properties of the N-methyl-D-aspartate receptor system coupled to the evoked release of γ-[^{3}H]aminobutyric acid from striatal neurons in primary culture. *J. Pharmacol.*, **252**, 380–386.

WILLETTS, J., BALSTER, R.L. & LEANDER, J.D. (1990). The behavioural pharmacology of NMDA receptor antagonists. *Trends Pharmacol. Sci.*, **11**, 423–428.

YAMAGUCHI, S.-I., DONEVAN, S.D. & ROGAWSKI, M.A. (1993). Anticonvulsant activity of AMPA/kainate antagonists: comparison of GYKI 52466 and NBQX in maximal electroshock and chemoconvulsant seizure models. *Epilepsy Res.*, **15**, 179–184.

ZARNOWSKI, T., KLEINROK, Z., TURSKI, W.A. & CZUCZWAR, S.J. (1993). 2,3-Dihydroxy-6-nitro-7-sulfamoylbenzo(F)quinoxaline enhances the protective activity of common antiepileptic drugs against maximal electroshock-induced seizures in mice. *Neuropharmacology*, **32**, 895–900.

ZORUMSKI, C.F., YAMADA, K.A., PRICE, M.T. & OLNEY, J.W. (1993). A benzodiazepine recognition site associated with the non-MNDA glutamate receptor. *Neuron.*, **10**, 61–67.

(Received May 9, 1994
Revised July 11, 1994
Accepted July 22, 1994)

Br. J. Pharmacol. (1994), **113**, 1358–1362 © Macmillan Press Ltd, 1994

Inhibitory 5-hydroxytryptamine receptors involved in pressor effects obtained by stimulation of sympathetic outflow from spinal cord in pithed rats

A. Morán, C. Velasco, T. Salvador, [1]M.L. Martín & L. San Román

Laboratoratorio de Farmacognosia y Farmacodinamia, Departamento de Fisiología y Farmacología, Facultad de Farmacia, Universidad de Salamanca, E-37007 Salamanca, Spain

1 A study was made of the effects of 5-hydroxytryptamine (5-HT) on pressor response induced *in vivo* by electrical stimulation of the sympathetic outflow from the spinal cord of pithed rats. All animals had been pretreated with atropine. Intravenous infusion of 5-hydroxytryptamine at doses of 10 and 20 $\mu g\,kg^{-1}\,min^{-1}$ reduced the pressor effects obtained by electrical stimulation at intervals of 10 min over the 1 h of infusion.

2 This inhibitory action of 5-HT was depressed by cyproheptadine and methiothepin but was not modified by ketanserin or MDL-72222. By contrast, the inhibitory action of 5-HT was lost in pithed rats that had been pretreated with exogenous noradrenaline.

3 The 5-HT_1 receptor agonist 5-carboxamidotryptamine (5-CT) caused an inhibition of the pressor response, whereas the 5-HT_3 receptor agonist, 1-phenylbiguanide, produced a variable but significant increase in the pressor response. The 5-HT_2 receptor agonist, *m*-CPP, did not modify the pressor sympathetic response.

4 Our results suggest that 5-hydroxytryptamine interferes with sympathetic neurotransmission by inhibiting pressor effects as a result of stimulation of the complete sympathetic outflow, and that this inhibition is mainly through a presynaptic 5-HT_1 mechanism.

Keywords: 5-Hydroxytryptamine; 5-hydroxytryptamine receptor agonists; blood pressure; sympathetic; pithed rats; 5-HT_1 mechanisms

Introduction

Many studies conducted under different experimental conditions have shown that 5-hydroxytryptamine (5-HT) has a direct vasoconstrictor action and can also enhance the vasoconstrictor effects of other vasoactive agents. These actions are believed to be mediated via the 5-HT_2 receptor subtype (Fozard, 1984a; Medgett *et al.*, 1984; Vanhoutte, 1985; Saxena *et al.*, 1987; Bagdy *et al.*, 1988; 1989; Leysen *et al.*, 1988; Saxena & Villalon, 1991). 5-HT also has vasodilatory/inhibitory actions, thought to be mediated through the preferential involvement of the 5-HT_1 receptor subtype, although the participation of other mechanisms in these actions is evident (Feniuk *et al.*, 1981; Vanhoutte, 1985; 1987).

5-HT has been reported to have stimulatory actions on the heart, although the mechanisms involved remain to be elucidated fully (Martinez & Lokhandwala, 1980; Göther *et al.*, 1986; Bom *et al.*, 1989). The participation of 5-HT in the control of blood pressure (Cohen, 1984; Grading *et al.*, 1985; Saxena *et al.*, 1987; Dabiré, 1990) and the modulation of cardiac and vascular sympathetic transmission has also been demonstrated. For this modulation, potentiating and inhibitory actions have been proposed, however in both cases there is a disparity between mechanisms postulated to account for such actions (Fozard & Mwaluko, 1976; Fozard, 1984b; Coote *et al.*, 1987; Docherty, 1988; Bom *et al.*, 1989; Shepheard *et al.*, 1991; Done & Sharp, 1992).

Our aim was to study both the effects of 5-HT on vascular sympathetic neurotransmission and the influence of peripherally administered antagonists on such effects. Using pithed rats pretreated with atropine, we studied the effects of i.v.-infused 5-HT on the pressor effects obtained by either electrical stimulation of the sympathetic outflow at the spinal cord, or by exogenously applied (i.v.) noradrenaline.

[1] Author for correspondence.

Intravenous administrations of 5-CT, 1-phenylbiguanide and *m*-CPP allowed for a qualitative investigation of the 5-HT receptor mechanisms involved in the pressor effects of electrical sympathetic stimulation in the pithed rat.

Methods

Experimental protocol

Male Wistar rats weighing 270–300 g were used. The animals were kept and supplied by the Animalarium of the Faculty of Pharmacy of the University of Salamanca.

The animals were anaesthetized with sodium pentobarbital (60 $mg\,kg^{-1}$, i.p.). A tracheal cannulation was performed and the animals were then ventilated using a Harvard respiratory pump (1 ml air 100 g^{-1}, 45 strokes min^{-1}). Pithing was performed as described by Gillespie & Muir (1967). A steel rod (1.5 mm diameter) was inserted through the orbit and foramen magnum, and down the vertebral foramen. The rod was advanced until the tip had reached the level of S1, which corresponded to a total distance of approximately 15 cm.

The right jugular vein and the left carotid artery were cannulated. These allowed for the intravenous administration of drugs and the measurement and recording of blood pressure respectively. Blood pressure was monitored using a Letica pressure transducer connected to a PRS 205 amplifier, and displayed on one channel of a Letica Polygraph 4000. Heart rate was measured by analysis of the blood pressure data, by a CAR 1000 tachograph connected to the same PRS 205 amplifier.

The entire sympathetic outflow from the spinal cord was stimulated by the use of a Cibertec Stimulator CS-9. Two electrodes were employed: one was connected to the pithing rod (the stimulating electrode), while the other electrode (the

indifferent electrode) was inserted subcutaneously into a leg.

Prior to electrical stimulation, the animals were pretreated with *d*-tubocurarine (2 mg kg^{-1} i.v.) and atropine (1 mg kg^{-1} i.v.) and left for 10 min until the blood pressure and heart rate levels had completely stabilized.

Two initial stimulations, 10 min apart, were made (15 ± 3 V, 5 Hz, 0.1 ms, 25 s). The mean increase in mean blood pressure obtained after these two stimulations was used as the control value (E_0). After the second stimulation intravenous infusion of saline (1 ml h^{-1}), 5-HT (10, 20, 30 and 40 μg kg^{-1} min^{-1}, 1 ml h^{-1}), 5-CT, 1-phenylbiguanide or *m*-CPP (10 μg kg^{-1} min^{-1}, 1 ml h^{-1}) was performed. Each infusion was continuous over 1 h. Stimulations were performed under the above conditions every 10 min during the infusion. These stimulations were designated E_1, E_2, E_3, E_4, E_5 and E_6.

In order to analyse the mechanism of action of 5-HT, different antagonists were administered intravenously. These antagonists – ketanserin (0.5 mg kg^{-1}), cyproheptadine (1 mg kg^{-1}), methiothepin (0.1 mg kg^{-1}), and MDL-72222 (2 mg kg^{-1}) – were administered 5 min before the infusion of 20 μg kg^{-1} min^{-1} 5-HT. Two of the antagonists, methiothepin and MDL-72222, were also administered i.v. 5 min before the infusion of 10 μg kg^{-1} min^{-1} 5-CT or 1-phenylbiguanide respectively.

In another set of experiments, the pressor effects were obtained by the intravenous administration of noradrenaline (0.5 μg kg^{-1} every 15 min). A control group received i.v. noradrenaline and saline (1 ml h^{-1}), and a second group received both noradrenaline and 20 μg kg^{-1} min^{-1} 5-HT.

Drugs employed

The following drugs were used in our experiments: pentobarbital sodium (Claudio Barcia), heparin sodium (Roche), *d*-tubocurarine hydrochloride (Sigma), 5-HT–creatinine sulphate (Sigma), atropine sulphate (Scharlau), ketanserin (Janssen), cyproheptadine hydrochloride (Fides), methiothepin mesylate (RBI), 3-tropanyl-3,5-dichlorobenzoate (MDL-72222, RBI), 1-phenylbiguanide (RBI), carboxamidotryptamine maleate, 5-CT (RBI),1-(3-chlorophenyl)piperazine dihydrochloride, *m*-CPP dihydrochloride (RBI), noradrenaline bitartrate (Sigma).

All drugs used were dissolved in distilled water at the time of the experiments, with the exception of ketanserin, which was dissolved in 0.04 mol l^{-1} lactic acid, and MDL-72222 and *m*-CPP, which were both dissolved in 0.01 N HCl.

Expression and analysis of results

Modifications in blood pressure were expressed as mmHg above the mean control blood pressure, measured both before electrical stimulation and as the stabilized maximum post stimulation.

All data were expressed as the mean value ± s.e.mean of at least five experiments. The statistical significance was determined using Student's *t*-test for grouped data ($*P<0.05$; $**P<0.01$ and $***P<0.001$). The figures show the values that proved to be statistically significant when compared with the corresponding ones in the control group with the exception of Figure 2, in which they are compared with the corresponding values in the 5-HT perfused group.

Results

The mean resting blood pressure in these studies was 41.6 ± 0.7 mmHg ($n = 156$). Electrical stimulation of the entire sympathetic outflow from the spinal cord of pithed rats elicited increases in the mean blood pressure (46 ± 3.4 mmHg, $n = 40$) with no appreciable changes in heart rate. This observation is consistent with results reported by other authors (Gillespie & Muir, 1967; Borkowski & Quinn, 1983; Zukowska-Grojec *et al.*, 1983; Roquebert *et al.*, 1990). The rises in blood pressure remained stable in the animals receiving 1 ml kg^{-1} i.v. saline infusion (Figure 1).

With respect to the control group and its own E_0, intravenous infusion of 5-hydroxytryptamine led to a reduction in the blood pressure increases resulting from stimulations E_1 to E_6. This reduction was observed at the 10 μg kg^{-1} min^{-1} dose of 5-HT, although the magnitude of the reduction only became significant with the 20 μg kg^{-1} min^{-1} dose. Thereafter, smaller and more variable reductions were observed when 40 μg kg^{-1} min^{-1} 5-HT were perfused (Figure 1).

The selective 5-HT_2 receptor antagonist, ketanserin (Van Nueten *et al.*, 1981; Cohen, 1984; Petterson *et al.*, 1984), at doses that did not modify the pressor response by α-adrenergic blockade, did not alter the inhibitory action of 5-HT (Figure 2). Similarly, the 5-HT_3 receptor antagonist, MDL-72222, was not effective in blocking the inhibitory action of 5-HT (Figure 2). Cyproheptadine, a 5-HT_1 and

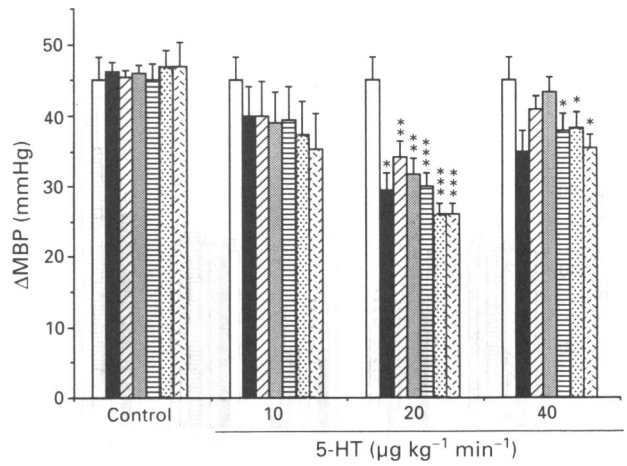


Figure 1 Influence of i.v. infusion of 5-HT on blood pressure modifications (ΔMBP) caused by electrical stimulation of the complete sympathetic outflow from the spinal cord of pithed rats. Control: saline solution 1 ml h^{-1}; 5-HT: 10, 20 and 40 μg kg^{-1} min^{-1}. □, E_0; ■, E_1; ▨, E_2; ▩, E_3; ▤, E_4; ▦, E_5; ▧, E_6.

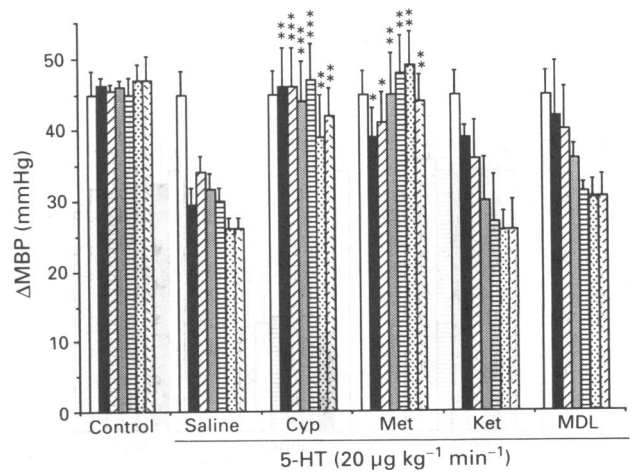


Figure 2 Effect of saline (1 ml kg^{-1}), cyproheptadine (Cyp, 1 mg kg^{-1}), methiothepin (Met, 0.1 mg kg^{-1}), ketanserin (Ket, 0.5 mg kg^{-1}) and MDL-72222 (MDL, 2 mg kg^{-1}) on 5-hydroxytryptamine-induced inhibition of the mean blood pressure increases (Δ MBP) caused by electrical stimulation of the complete sympathetic outflow. Control: saline (1 ml h^{-1}). □, E_0; ■, E_1; ▨, E_2; ▩, E_3; ▤, E_4; ▦, E_5; ▧, E_6.

5-HT_2 antagonist (Stone *et al.*, 1961), did not alter the pressor response achieved by stimulation of the entire sympathetic outflow in the control group perfused with saline, although it did abolish the inhibition exerted by 5-HT (Figure 2). With methiothepin, a preferential 5-HT_2 antagonist which also blocks 5-HT_1 receptors (Saxena & Villalon, 1990), the action of 20 $\mu g\,kg^{-1}\,min^{-1}$ 5-HT was also abolished (Figure 2).

Intravenous infusion of 5-CT (10 $\mu g\,kg^{-1}\,min^{-1}$) resulted in a significant, higher degree of pressor response inhibition than 5-HT (Figure 3). This inhibitory effect was blocked by pretreatment with methiothepin (Figure 4).

The selective 5-HT_2 receptor agonist, *m*-CPP (Humphrey *et al.*, 1993), was without effect on the pressor responses evoked by sympathetic stimulation (Figure 3). Increases in blood pressure after sympathetic stimulation were significantly potentiated in the 1-phenylbiguanide-perfused group. This enhancement was inhibited by pretreatment with MDL-72222 (Figure 5).

5-HT failed to inhibit any of the measured physiological parameters in those animals in which pressor response was evoked by the i.v. administration of noradrenaline (Figure 6).

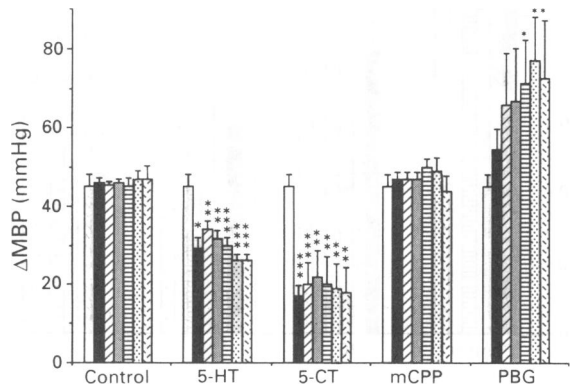


Figure 3 Mean blood pressure modifications (Δ MBP) caused by electrical stimulation of the total sympathetic outflow of pithed rats, and influence of i.v. infusion of 5-HT (20 $\mu g\,kg^{-1}\,min^{-1}$), 5-CT (10 $\mu g\,kg^{-1}\,min^{-1}$), *m*-CPP (10 $\mu g\,kg^{-1}\,min^{-1}$) and 1-phenylbiguanide (10 $\mu g\,kg^{-1}\,min^{-1}$) on these modifications. Control: saline (1 $ml\,h^{-1}$). □, E_0; ■, E_1; ▨, E_2; ▩, E_3; ▤, E_4; ▦, E_5; ▧, E_6.

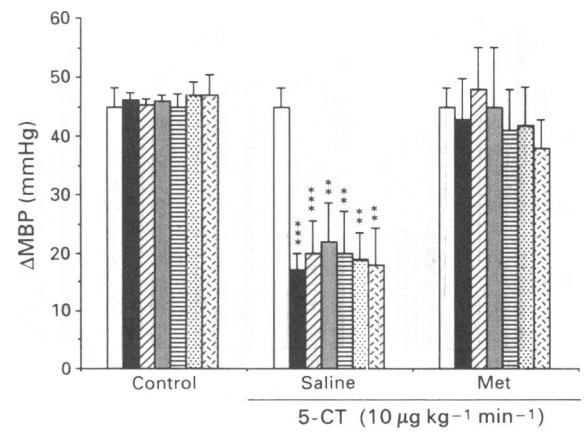


Figure 4 Abolition of the inhibitory effects of 5-carboxamidotryptamine (10 $\mu g\,kg^{-1}\,min^{-1}$) on the mean blood pressure modifications (Δ MBP) caused by electrical stimulation of the total sympathetic outflow of pithed rats, by methiothepin (0.1 $mg\,kg^{-1}$). Control: saline (1 $ml\,h^{-1}$). □, E_0; ■, E_1; ▨, E_2; ▩, E_3; ▤, E_4; ▦, E_5; ▧, E_6.

Discussion

As suspected from previous studies carried out in our laboratory (unpublished results) and from studies published by other workers (Martinez & Lokhandwala, 1980; Feniuk *et al.*, 1981; Vanhoutte, 1983; 1985; Grading *et al.*, 1985; Saxena *et al.*, 1987; Hollenberg, 1988; Saxena & Villalon, 1991; Shepheard *et al.*, 1991; Done & Sharp, 1992), 5-HT interferes with adrenergic neurotransmission and reduced the increase in mean blood pressure achieved by sympathetic stimulation. However, it did not affect the increases in blood pressure elicited by the exogenous administration of noradrenaline.

This inhibition is only observed at low doses of 5-HT (10 and 20 $\mu g\,kg^{-1}\,min^{-1}$), whereas at a dose of 40 $\mu g\,kg^{-1}$

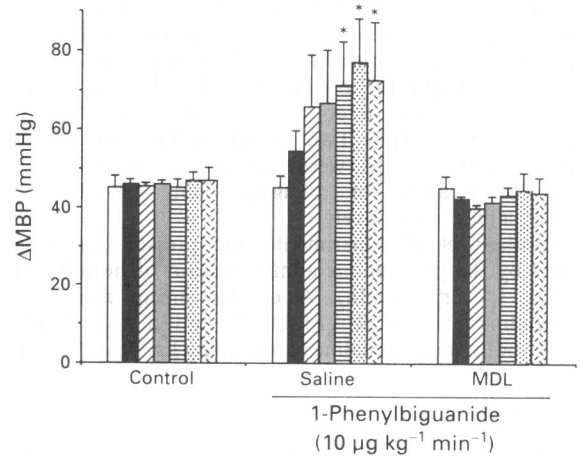


Figure 5 Block by MDL-72222 (2 $mg\,kg^{-1}$) of the enhancing effect of 1-phenylbiguanide (10 $\mu g\,kg^{-1}\,min^{-1}$) on the mean blood pressure modifications (Δ MBP) caused by electrical stimulation of the total sympathetic outflow of pithed rats. Control: saline (1 $ml\,h^{-1}$). □, E_0; ■, E_1; ▨, E_2; ▩, E_3; ▤, E_4; ▦, E_5; ▧, E_6.

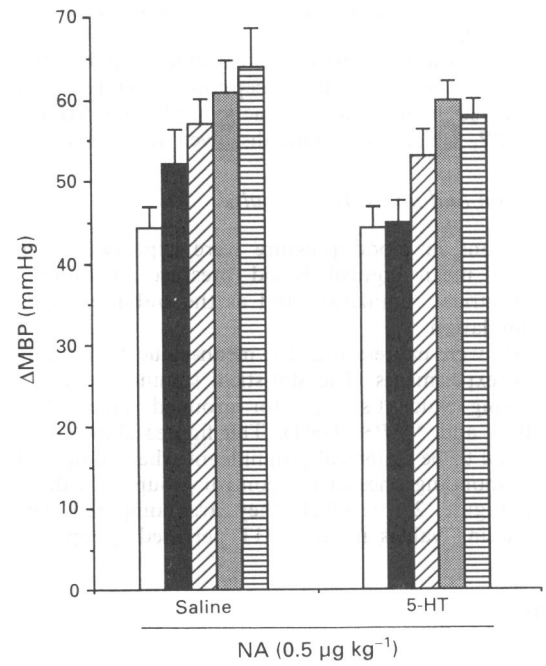


Figure 6 Influence of i.v. infusion of saline (1 $ml\,h^{-1}$) and 5-HT (20 $\mu g\,kg^{-1}\,min^{-1}$) on blood pressure modifications (Δ MBP) caused by i.v. exogenous administration of noradrenaline (0.5 $\mu g\,kg^{-1}$) in pithed rats. □, E_0; ■, E_1; ▨, E_2; ▩, E_3; ▤, E_4.

min^{-1} there is no clear reduction. These initial results seem to show that, under our experimental conditions, 5-HT only inhibits adrenergic neurotransmission at doses below $40\,\mu g\,kg^{-1}\,min^{-1}$.

Possibly, this biogenic amine could exert a double effect on the sympathetic nervous system, which would be inhibitory at low doses and perhaps potentiating at elevated doses (above $40\,\mu g\,kg^{-1}\,min^{-1}$). Under different experimental conditions and working with species other than the rat, other authors have obtained results leading them to propose similar effects of 5-HT: inhibiting or potentiating sympathetic actions. The nature, inhibitory or stimulatory, being dependent on the dose of 5-HT or on the level of sympathetic tone (Martinez & Lokhandwala, 1980; Van Nueten *et al.*, 1984).

The inhibitory effect was reproduced by the administration of the selective 5-HT_1 receptor agonist, 5-CT. The possible potentiating effect was obtained by administration of 1-phenylbiguanide, a selective 5-HT_3 receptor agonist.

This evidence, together with the results achieved with a dose of $20\,\mu g\,kg^{-1}\,min^{-1}$ 5-HT in the presence of different antagonists, implies that no 5-HT_2 serotonergic mechanisms participate in this inhibitory effect. The reasoning behind this is that $0.5\,mg\,kg^{-1}$ ketanserin, a 5-HT_2 receptor antagonist, does not modify the effect of 5-HT. *In vivo* studies by other authors have established that the inhibitory effect of 5-HT on adrenergic neurotransmission is not affected by 5-HT_2 receptor antagonists (McGrath, 1977; Van Nueten *et al.*, 1981).

In the light of the results obtained with cyproheptadine and methiothepin, this inhibitory effect of 5-HT must involve serotonergic mechanisms acting via 5-HT_1 receptors. Cyproheptadine and methiothepin blocked the inhibitory effects of 5-HT on the responses to sympathetic stimulation, and methiothepin also resulted in a dis-inhibition of 5-CT effects.

The results obtained from utilizing stimulation of the entire sympathetic outflow would, therefore, suggest that low doses of 5-HT inhibit pressor responses by a 5-HT_1-mediated mechanism that is perhaps presynaptic in nature. This inhibition might be due to a decrease in noradrenaline release. With respect to this, in 1990 Dabiré, working with the 5-HT_{1A} agonist 8-OH-DPAT reported that peripheral stimulation of 5-HT_1 receptors could reduce blood pressure by a presynaptic effect able to decrease the release of sympathetic noradrenaline.

Higher doses of 5-HT however, resulted in an enhancement of the effects of sympathetic stimulation. No such enhancement was seen upon exogenous noradrenaline administration, and it is probable that this enhancement is due to presynaptic 5-HT_3 activation. In this way, 5-HT_3 activation could elicit noradrenaline release, thereby causing the observed enhancement.

In summary, the effects of 5-HT and the serotonergic mechanisms involved in cardiovascular sympathetic neurotransmission in the pithed rat are mainly presynaptic in nature. These presynaptic mechanisms act to inhibit or facilitate the release of noradrenaline from sympathetic nerve terminals. The inhibitory mechanisms involve the activation of the 5-HT_1 receptor subtype, whereas those that enhance noradrenaline release involve the 5-HT_3 receptor subtype.

The authors would like to thank Juan Carlos Villoria for technical assistance.

References

BAGDY, G., SZEMEREDI, K., HILL, J.L. & MURPHY, D.L. (1988). The serotonin agonist, M-chlorophenylpiperazine, markedly increases levels of plasma catecholamines in the conscious rat. *Neuropharmacology*, **27** (10), 975–980.

BAGDY, G., SZEMEREDI, K. & MURPHY, D.L. (1989). Marked increases in plasma catecholamine concentrations precede hypotension and bradycardia caused by 8-hydroxy-2-(di-n-propylamino) tetralin (8-OH-DPAT) in conscious rats. *J. Pharm. Pharmacol.*, **41**, 270–272.

BOM, A.H., VERDOUW, P.D. & SAXENA, P.R. (1989). Carotid haemodynamics in pigs during infusions of 8-OH-DPAT: reduction in arteriovenous shunting is mediated by 5-HT_1-like receptors. *Br. J. Pharmacol.*, **96**, 125–132.

BORKOWSKI, K.R. & QUINN, P. (1983). The effect of bilateral adrenal demedullation on vascular reactivity and blood pressure in spontaneously hypertensive rats. *Br. J. Pharmacol.*, **80**, 429–437.

COHEN, M.L. (1984). Vascular serotonin receptors and blood pressure regulation. *Drug Dev. Res.*, **4**, 301–313.

COOTE, J.M., DALTON, D.W., FENIUK, W. & HUMPHREY, P.P. (1987). The central site of the sympathoinhibitory action of 5-HT in the cat. *Neuropharmacology*, **26** (2–3), 147–154.

DABIRÉ, H. (1990). Récepteurs serotoninergiques$_{1A}$ (5-HT_{1A}) et régulation de la pression artérielle. *Therapie*, **45**, 183–186.

DOCHERTY, J.R. (1988). Investigations of cardiovascular 5-hydroxytryptamine receptor subtypes in the rat. *Naunyn-Schmied. Arch. Pharmacol.*, **337**, 1–8

DONE, C.J.G. & SHARP, T. (1992). Evidence that 5-HT_2 receptor activation decreases noradrenaline release in rat hippocampus in vivo. *Br. J. Pharmacol.*, **107**, 240–245.

FENIUK, W., HARE, J. & HUMPHREY, P.P.A. (1981). An analysis of the mechanism of 5-hydroxytryptamine-induced vasopressor responses in ganglion-blocked anaesthetized dogs. *J. Pharm. Pharmacol.*, **33**, 155–160.

FOZARD, J.R. (1984a). MDL 72222: a potent and highly selective antagonist at neuronal 5-hydroxytryptamine receptors. *Naunyn-Schmied. Arch. Pharmacol.*, **326**, 36–44

FOZARD, J.R. (1984b). Neuronal 5-HT receptors in the periphery. *Neuropharmacology*, **23**, 1473–1486.

FOZARD, J.R. & MWALUKO, G.M.P. (1976). Mechanism of the indirect sympathomimetic effect of 5-hydroxytryptamine on the isolated heart of the rabbit. *Br. J. Pharmacol.*, **57**, 115–125.

GILLESPIE, J.S. & MUIR, J.C. (1967). A method of stimulating the complete sympathetic outflow from the spinal cord to blood vessel in the pithed rat. *Br. J. Pharmacol. Chemother.*, **30**, 78–87.

GÖTHER, M., SCHLICKER, E. & KOLLECKER, P. (1986). Receptor-mediated effects of serotonin and 5-metoxytryptamine on noradrenaline release in the rat vena cava and in the heart of the pithed rat. *Naunyn-Schmied. Arch. Pharmacol.*, **336**, 124–130.

GRADING, K., PETTERSSON, A., HJORTH, S., HEDNER, T., ARVIDSSON, L.E. & PERSSON, B. (1985). Cardiovascular effects in the Sprague–Dawley rat of 8-hydroxy-2(di-N-propylamino) tetralin, a selective 5-hydroxytryptamine receptor agonist. *J. Pharm. Pharmacol.*, **37**, 263–265.

HOLLENBERG, N.K. (1988). Serotonin and vascular responses. *Annu. Rev. Pharmacol. Toxicol.*, **28**, 41–59.

HUMPHREY, P.P.A., HARTIG, P. & HOYER, D. (1993). A proposed new nomenclature for 5-HT receptors. *Trends Pharmacol. Sci.*, **14**, 233–236.

LEYSEN, J.E., VAN GOMPEL, P. & GOMMEREN, W. (1988). Distinction between adrenergic and serotonergic receptor subtypes: specificity of drugs and absence of cooperative interactions between adrenergic and serotonergic receptor binding sites. *J. Cardiovasc. Pharmacol.*, **11** (1), S78–S87.

MCGRATH, M.A. (1977). 5-hydroxytryptamine and neurotransmitter release in canine blood vessels. *Circ. Res.*, **41** (4), 428–435.

MARTINEZ, A.A. & LOKHANDWALA, M.F. (1980). Evidence for a presynaptic inhibitory activity of 5-hydroxytryptamine on sympathetic neurotransmission to the myocardium. *Eur. J. Pharmacol.*, **63**, 303–311.

MEDGETT, I.C., FEARN, H.J. & RAND, M.J. (1984). Serotonin enhances sympathetic vasoconstrictor responses in rat isolated perfused tail artery by activation of postjunctional serotonin-2 receptors. *Clin. Exp. Pharmacol. Physiol.*, **11**, 343–346.

PETTERSSON, A., PERSSON, B., HENNING, M. & HEDNER, T. (1984). Antihypertensive effects of chronic 5-hydroxytryptamine (5-HT_2) receptors blockade with ketanserin in the spontaneously hypertensive rat. *Naunyn-Schmied. Arch. Pharmacol.*, **327**, 43–47.

ROQUEBERT, K., ALAOUI, K. & MORAN, A. (1990). Cardiovascular effects of bromocriptine in rats: role of peripheral adrenergic and dopaminergic receptors. *J. Auton. Pharmacol.*, **10**, 85–96.

SAXENA, P.R. & VILLALON, C.M. (1990). Cardiovascular effects of serotonin agonists and antagonists. *J. Cardiovasc. Pharmacol.*, **15** (7), S17.

SAXENA, P.R. & VILLALON, C.M. (1991). 5-hydroxytryptamine: a chameleon in the heart. *Trends Pharmacol. Sci.*, **12**, 223–227.

SAXENA, P.R., BOLT, G.R. & DHASMANA, K.M. (1987). Serotonin agonists and antagonists in experimental hypertension. *J. Cardiovasc. Pharmacol.*, **10 (3)**, S12–S18.

SHEPHEARD, S.L., JORDAN, D. & RAMAGE, A.G. (1991). Investigation of the effects of IVth ventricular administration of the 5-HT_2 agonist, 1-(2,5-dimethoxy-4-iodephenyl)-2-aminopropane (DOI), on autonomic outflow in the anaesthetized cat. *Br. J. Pharmacol.*, **104**, 367–372.

STONE, C.A., WENGER, H.C., LUDDEN, C.T., STAVORSKI, J.M. & ROSS, C.A. (1961). Antiserotonin-antihistamine properties of cyproheptadine. *J. Pharmacol. Exp. Ther.*, **131**, 73–84.

VANHOUTTE, P.M. (1983). 5-Hydroxytryptamine and vascular disease. *Fed. Proc.*, **42**, 233–237.

VANHOUTTE, P.M. (1985). Can peripheral serotonergic blockade explain the hypotensive effect of ketanserin. *J. Cardiovasc. Pharmacol.*, **7** (7), S105–S109.

VANHOUTTE, P.M. (1987). Cardiovascular effects of serotonin. *J. Cardiovasc. Pharmacol.*, **10** (3), S8–S11.

VAN NUETEN, J.M., JANSSEN, P.A.J., VAN BEEK, J., XHONNEUX, A., VERBEUREN, T.J. & VANHOUTTE, P.M. (1981). Vascular effects of ketanserin (R 41 468), a novel antagonist of 5-HT_2 serotonergic receptors. *J. Pharmacol. Exp. Ther.*, **218**, 217–230.

VAN NUETEN, J.M., LEYSEN, J.E., DE CLERCK, F. & VANHOUTTE, P.M. (1984). Serotonergic receptor subtypes and vascular reactivity. *J. Cardiovasc. Pharmacol.*, **6**, S564–S574.

ZUKOWSKA-GROJEC, Z., BAYORH, M.A. & KOPIN, I.I. (1983). Effect of desipramine on the effects of α-adrenoceptor inhibitors on pressor responses and release of norepinephrine into plasma of pithed rats. *J. Cardiovasc. Pharmacol.*, **5**, 297–301.

(Received April 5, 1994
Revised July 15, 1994
Accepted August 4, 1994)

Br. J. Pharmacol. (1994), **113**, 1363–1371 © Macmillan Press Ltd, 1994

Studies on the mechanisms involved in the inflammatory response in a reversed passive Arthus reaction in guinea-pig skin: contribution of neutrophils and endogenous mediators

[1]M.M. Teixeira, S.M. Fairbairn, K.E. Norman, T.J. Williams, A.G. Rossi & P.G. Hellewell

Department of Applied Pharmacology, National Heart and Lung Institute, Dovehouse Street, London SW3 6LY

1 Mediators of inflammation can increase vascular permeability in at least two different ways: by acting directly on endothelial cells or, indirectly, through an incompletely understood mechanism, dependent on circulating neutrophils. Neutrophil-dependent oedema formation has been described in the skin of rabbits, rats, hamsters, mice and man. In contrast, we presented evidence in a previous study that local oedema formation induced by i.d. injection of chemoattractants in guinea-pig skin was neutrophil-independent. In the present study, we sought evidence of neutrophil-dependent oedema formation in immune-complex-mediated vasculitis, the reversed passive Arthus (RPA) reaction, in guinea-pig skin. We also investigated whether haemorrhage in the RPA reaction was neutrophil-dependent (as it is in other species) and the role of endogenous mediators of inflammation (prostaglandins, nitric oxide, histamine, PAF and leukotrienes) in contributing to the local inflammatory response.

2 In the RPA reaction, most oedema formation occurred over the first 60 min whereas ^{111}In-neutrophil accumulation was still increasing from 60 to 240 min. The different kinetics of these two events suggested that they may be dissociated.

3 Oedema formation was partially inhibited by a long-acting PAF antagonist (UK-74,505) and an H_1 histamine receptor antagonist (mepyramine) but not by a 5-lipoxygenase inhibitor (ZM 230487). A nitric oxide synthesis inhibitor (N^G-nitro-L-arginine methyl ester, L-NAME) suppressed oedema formation by 68% whereas a cyclo-oxygenase inhibitor suppressed oedema by 27%.

4 ^{111}In-neutrophil accumulation in the RPA reaction was partially suppressed by UK-74,505. In contrast, ZM 230487 was without effect at doses which abrogated arachidonic acid-induced ^{111}In-neutrophil accumulation.

5 The anti-CD18 monoclonal antibody, (mAb) 6.5E $F(ab')_2$, effectively inhibited ^{111}In-neutrophil accumulation induced by PAF, zymosan-activated plasma (ZAP) and in the RPA reaction. However, oedema formation measured in the same sites was not altered. In contrast, oedema formation in the RPA reaction was partially suppressed by 6.5E whole mAb which was 2.5 times more potent than 6.5E $F(ab')_2$ at inhibiting guinea-pig neutrophil adhesion to protein-coated plastic. Haemorrhage induced by PAF and in the RPA reaction was significantly inhibited by 6.5E $F(ab')_2$ pretreatment.

6 We conclude that in the RPA reaction in guinea-pig skin, oedema formation is partially neutrophil-dependent as assessed by using an anti-CD18 mAb, whereas ZAP-induced oedema formation is neutrophil-independent. Haemorrhage was also dependent on neutrophil accumulation. In addition, our studies support a role for PAF in mediating both oedema formation and ^{111}In-neutrophil accumulation in the RPA reaction. Endogenous release of histamine also appears to be important in mediating oedema formation suggesting that mast cells play a critical role in increases of vascular permeability in inflammatory reactions in guinea-pig skin. Moreover, our results confirm previous findings which suggest a dominant role for nitric oxide in maintaining cutaneous blood flow in the guinea-pig.

Keywords: Reversed passive Arthus reaction; type III hypersensitivity; CD18 integrin; neutrophil; oedema formation; PAF; leukotrienes; histamine; nitric oxide; prostaglandins

Introduction

The generation and release of chemical mediators at sites of inflammation leads to increased permeability of the endothelial cell barrier lining microvessels, allowing the passage of molecules of high molecular weight from the blood into the tissues. This enhanced vascular permeability will facilitate the extravasation of molecules such as complement factors and immunoglobulin which protect the responding organism against injurious stimuli. Mediators of inflammation can increase vascular permeability in at least two ways: by acting directly on endothelial cells (direct-acting mediators, e.g. bradykinin) or indirectly, through an incompletely understood mechanism which is dependent on circulating neutrophils (neutrophil-dependent mediators, e.g. C5a, FMLP, interleukin-8) (Wedmore & Williams, 1981a; Collins *et al.*, 1991). These two mechanisms were initially described in rabbit skin (Wedmore & Williams, 1981a) but were later found to occur in hamsters (Bjork & Smedegard), 1983), rats (Mulligan *et al.*, 1992b), mice (Perretti *et al.*, 1993) and also in man (Williamson *et al.*, 1986).

The reversed passive Arthus (RPA) reaction, a model of type III hypersensitivity, is an example of immune complex-mediated vasculitis which can be elicited in the skin of experimental animals by the intradermal (i.d.) injection of an antiserum followed by intravenous (i.v.) injection of the specific antigen (Cochrane & Janoff, 1974; Crawford *et al.*, 1982). In rabbit skin, depletion of circulating neutrophils with nitrogen mustard or anti-neutrophil serum effectively inhibits the extravasation of albumin and the consequent oedema formation (Stetson, 1951; Humphrey, 1955a). Similarly, the blockade of CD11/CD18 integrins on the neutrophil surface using R15.7, a monoclonal antibody (mAb) which abrogates neutrophil accumulation in rabbit skin (Rampart *et al.*, 1991), inhibits both the extravasation of

[1] Author for correspondence.

albumin and red blood cells in the rabbit RPA reaction (Norman et al., 1994). In rat skin, another anti-CD11/CD18 mAb also suppresses oedema formation and haemorrhage in a RPA reaction (Mulligan et al., 1992b). Taken together these results suggest that, in RPA reactions in different animal species, both oedema formation and haemorrhage are dependent on circulating neutrophils and on their adhesive interaction with microvascular endothelial cells.

We recently showed that i.v. administration of $F(ab')_2$ fragments of an anti-CD18 mAb (6.5E) effectively inhibited neutrophil accumulation induced by zymosan-activated plasma (ZAP, a source of C5a des arg) but had little effect on oedema formation in guinea-pig skin (Teixeira et al., 1994). In agreement with this observation is the lack of oedema forming activity of leukotriene B_4 (LTB_4), interleukin-8 or FMLP (all neutrophil-dependent mediators of increased vascular permeability in rabbit skin) when injected i.d. in guinea-pig skin (Faccioli et al., 1991; Collins et al., 1993; Teixeira & Hellewell, 1994). In contrast to the lack of correlation between neutrophil accumulation and oedema formation in this species, an H_1 receptor antagonist was very effective in suppressing oedema formation in response to i.d. injection of ZAP (Teixeira et al., 1994). Thus, in guinea-pig skin, there is little evidence for neutrophil-dependent oedema and it is suggested that the liberation of histamine as a result of mast cell degranulation is more important for the control of cutaneous vascular permeability induced by different inflammatory stimuli.

In this study, we have further investigated whether there is any evidence for neutrophil-dependent oedema and/or haemorrhage in immune complex vasculitis in guinea-pig skin using a RPA reaction. We have addressed this by assessing the inhibitory effects of the anti-CD18 mAb (6.5E) on the accumulation of ^{111}In-neutrophils, ^{51}Cr-red blood cells (RBC) and ^{125}I-human serum albumin (HSA) in the RPA reaction. We have previously analyzed the mediators involved in RPA reactions in rabbit skin (Hellewell & Williams, 1986; Hellewell, 1990; Rossi et al., 1992) and the reliance of neutrophil-dependent oedema on CD18 (Norman et al., 1994). In this paper, we have also investigated the possible role of endogenous mediators of inflammation (prostaglandins, nitric oxide, histamine, PAF and leukotrienes) in inducing oedema formation and neutrophil accumulation in immune complex vasculitis in guinea-pig skin. The role of these mediators was investigated using the cyclo-oxygenase inhibitor, ibuprofen, the nitric oxide synthesis inhibitor (N^G-nitro-L-arginine methyl ester, L-NAME), the H_1 receptor antagonist mepyramine, the PAF antagonist UK-74,505 (Alabaster et al., 1991), and the 5-lipoxygenase inhibitor ZM 230487 (Crawley et al., 1993).

Animals

Dunkin-Hartley guinea-pigs were purchased from Banting and Kingman (300–400 g, Grimsby, Humberside) and Harlan (ex-breeders, Bicester, Oxfordshire). New Zealand White rabbits (2.5 to 3.0 kg) were purchased from Regal Group, Surrey.

Preparation of zymosan-activated plasma (ZAP)

ZAP was used as a source of guinea-pig C5a des Arg. Guinea-pig heparinized (10 iu ml^{-1}) plasma was incubated with zymosan (5 mg ml^{-1}) at 37°C. After 30 min, zymosan was removed by centrifugation (2 × 10 min at 3000 g). ZAP was then desalted with a PD-10 Sephadex G-25M column and stored in aliquots at −20°C.

Generation of antiserum for the Arthus reaction

The serum used in this series of experiments was raised in rabbits as described elsewhere (Hellewell & Williams, 1986). Briefly, subcutaneous injections (4 × 0.25 ml) of bovine gamma globulin (BGG, 2 mg ml^{-1} in saline) emulsified with an equal volume of Freund's complete adjuvant were administered. Fourteen days later, the animals received booster subcutaneous injections (4 × 0.25 ml) of the same concentration of BGG in Freund's incomplete adjuvant. At day 28, a subcutaneous injection of alum-precipitated BGG (300 μg per rabbit) was given. Blood was collected at day 38, the serum from 5 animals pooled, heat-activated at 56°C for 30 min and stored at −20°C until use.

Induction, purification and radiolabelling of guinea-pig neutrophils

Neutrophils were elicited in the peritoneal cavity of naive ex-breeders guinea-pigs by the i.p. injection of 15 ml of a 5% (w/v) solution of casein as previously described (Teixeira et al., 1993). After 12 to 16 h, the animals were killed and the peritoneal cavity washed with heparinized saline (10 iu ml^{-1}). The cells were layered onto a discontinuous Percoll-Hank's balanced salt solution (HBSS; calcium- and magnesium-free) gradient followed by centrifugation (1500 g, 25 min at 20°C). Neutrophils (>99% pure, >98% viable) were collected from the 1.090/1.095 and 1.095/1.100 g ml^{-1} density interfaces. The purified neutrophils were radiolabelled by incubation with $^{111}InCl_3$ (100 μCi in 10 μl) chelated to 2-mercaptopyridine-N-oxide (40 μg in 0.1 ml of 50 mM phosphate buffered saline (PBS), pH 7.4) for 15 min at room temperature. The cells were then washed twice in HBSS (calcium- and magnesium-free) containing 10% guinea-pig platelet-poor plasma and resuspended at a final concentration of 10^7 cells ml^{-1} prior to injection.

Radiolabelling of red blood cells

Guinea-pig blood obtained by cardiac puncture of anaesthetized animals was collected into tri-sodium citrate (0.38%, w/v) and centrifuged at 250 g for 20 min. One ml of the red blood cell pellet was added to $Na_2{}^{51}CrO_4$ (0.5 mCi in 500 μl) for 30 min at room temperature. Following incubation, the red blood cell pellet was washed three times in HBSS (calcium- and magnesium-free) and resuspended in a final volume of 2 ml. Each animal received 0.5 ml of ^{51}Cr-labelled RBC.

Measurement of local oedema formation, leukocyte accumulation and haemorrhage in guinea-pig skin

Radiolabelled leukocyte infiltration and oedema formation were measured simultaneously in the skin. [^{125}I]HSA (5 μCi) was added to the ^{111}In-labelled neutrophils prior to i.v. injection (5 × 10^6 cells per animal) into recipient guinea-pigs (350–400 g) anaesthetized with Hypnorm (0.2 ml, i.m.). Five min later, dilutions of rabbit anti-BGG antiserum (6.25 to 100%) or inflammatory stimuli were injected i.d. Antigen (BGG, 5 mg kg^{-1}) was injected i.v. after 5 min. In some experiments, ^{51}Cr-labelled RBC were injected i.v. together with BGG. The PAF antagonist, UK-74,505 (2.5 mg kg^{-1}) or 6.5E $F(ab')_2$ (2.4 mg kg^{-1}) were injected i.v. 15 min prior to i.d. injections. 6.5E whole mAb (2.4 mg kg^{-1}) or an isotype matched control IgG, MOPC21 (2.4 mg kg^{-1}), were given 15 min before i.d. injections and only oedema formation was measured in these experiments. For local treatments, inflammatory stimuli and antagonists/inhibitors were mixed just prior to i.d. injections. Each animal received a duplicate of each treatment following a randomized injection plan and the inflammatory response (^{111}In-labelled neutrophil accumulation, oedema formation and ^{51}Cr-RBC extravasation) was assessed after 4 h. At this time, blood was obtained by cardiac puncture and the animals were killed by an overdose of sodium pentobarbitone. The dorsal skin was removed, cleaned free of excess blood and the skin sites punched out with a 17 mm punch. The samples were counted in an automatic 5-head gamma-counter (Canberra Packard Ltd,

Pangbourne, Berks), and the counts were cross-channel corrected for the two isotopes (^{111}In and ^{125}I). In the experiments in which all three isotopes were used, samples were initially counted for ^{111}In and ^{125}I and then allowed to decay for 22 days (approximately eight ^{111}In half-lives) after which they were counted for ^{51}Cr and ^{125}I.

For the time-course experiments, antigen (BGG), radiolabelled neutrophils and ^{125}I-HSA were injected i.v. followed by i.d. injection of anti-BGG antiserum at the same time, and then at 2 h, 3 h, 3.5 h and 3.75 h later. Thus, cell accumulation and oedema formation were measured for 240, 120, 60, 30 and 15 min, respectively.

The number of leukocytes accumulating in each site was expressed as ^{111}In-labelled neutrophils per skin site and oedema formation as the ratio of ^{125}I counts of the skin sample divided by the ^{125}I counts in 1 μl of plasma. Haemorrhage (^{51}Cr-RBC extravasation) was assessed by dividing the number of ^{51}Cr counts of the skin sample by the ^{51}Cr counts in 1 μl of blood.

Adhesion of ^{111}In-neutrophils to serum-coated plastic

The wells of microtitre tissue culture plates (Nunc, Life Technologies Ltd.) were coated with serum by incubation for at least 2 h at 37°C with RPMI containing 10% foetal calf serum. Plates were washed twice before the addition of 100 μl of ^{111}In-neutrophils (2×10^6 cells ml^{-1}) in PBS containing 0.25% BSA (w/v). This was followed by whole 6.5E or 6.5E F(ab')$_2$ (final concentration 0.1–30 μg ml^{-1}) or MOPC21 (30 μg ml^{-1}). Fifteen min later the cells were stimulated with phorbol myristate acetate (PMA, 10^{-8} M) since this is known to be a potent and effective activator of leukocyte β_2 integrins (Figdor & Van Kooyk, 1992). After incubation for 30 min at 37°C, the medium was removed and the plate washed 3 times with PBS containing 2.5% heat-activated newborn calf serum. Adherent ^{111}In-neutrophils were solubilized with neat formic acid and an aliquot counted for radioactivity. Results are expressed as the percentage of the total ^{111}In-neutrophils added which were adherent per well. Experiments were carried out with four replicates on cells from each animal.

Reagents

The following compounds were purchased from Sigma Chemical Company (Poole, Dorset): arachidonic acid (AA), bradykinin, BGG, dimethyl sulphoxide (DMSO), histamine, N^G-nitro-L-arginine-methyl ester (L-NAME), mepyramine, phorbol myristate acetate and zymosan. Hank's solutions, HEPES buffer and horse serum were purchased from Life Technologies Ltd (Paisley, Scotland). Percoll was purchased from Pharmacia (Milton Keynes, Bucks) and PAF (C16) from Bachem (Saffron Walden, Essex). ^{125}I-HSA, $Na_2{}^{51}CrO_4$ and $^{111}InCl_3$ were obtained from Amersham international plc (Amersham, Bucks). The 5-lipoxygenase inhibitor ZM 230487 (1-ethyl-6-[fluoro-5-(4-methoxy-3,4,5,6-tetrahydro-2H-pyran-4-yl) phenoxy]methyl-quinol-2-one) was a gift from Zeneca Pharmaceuticals (Macclesfield, Cheshire) and UK-74,505 (4-(2-chlorophenyl)-1,4-dihydro-3-ethoxycarbonyl-6-methyl-2-[4-(2-methylimidazo[4,5-c]pyrid-1-yl)phenyl]-5-[N-(2-pyridyl)carbamoyl]pyridine) was a gift from Dr J. Parry (Pfizer Central Research, Sandwich, Kent). Ibuprofen was a gift from Boots Chemical Company plc (Nottingham, Notts.). The mouse anti-human CD18 mAb 6.5E (IgG$_1$) and F(ab')$_2$ fragments were generated and kindly provided by Dr M. Robinson (Celltech Limited, Slough). The mouse myeloma protein MOPC21 (IgG$_1$), used as an isotype matched control for 6.5E whole mAb, was from Celltech Limited. The endotoxin content of the stock mAb solutions was less than 1 Eu mg^{-1}.

Statistical analysis

Data were analyzed by analysis of variance on normally distributed data (log transformed). Duplicate skin responses were averaged and the mean ± s.e.mean of these responses in 4–6 animals was calculated. Significant differences ($P<0.05$) between groups were determined by the Neuman-Keuls procedure. Percentage inhibition was calculated after subtracting background values.

Results

Four hours after the i.v. injection of radiolabelled neutrophils, 6.7 ± 0.8% ($n = 19$) of the cells were circulating. None of the systemic treatments used in this study affected the percentage of ^{111}In-neutrophils that were circulating after 4 h (data not shown).

Time course of ^{111}In-neutrophil accumulation and oedema formation

Figure 1 shows the time-course of ^{111}In-neutrophil accumulation and oedema formation in the RPA reaction (25% antiserum in saline). Whereas most oedema formation occurred over the first 60 min (Figure 1a), ^{111}In-neutrophil accumulation appeared to be still increasing from 60 to 240 min (Figure 1b).

Mediators of oedema formation in the RPA reaction

The role of prostaglandins and nitric oxide in mediating oedema formation in a RPA reaction was evaluated by using the cyclo-oxygenase inhibitor, ibuprofen and the nitric oxide synthesis inhibitor, L-NAME. At a dose (10^{-7} mol per site) which completely inhibited the potentiation of bradykinin (10^{-10} mol per site)-induced oedema formation by

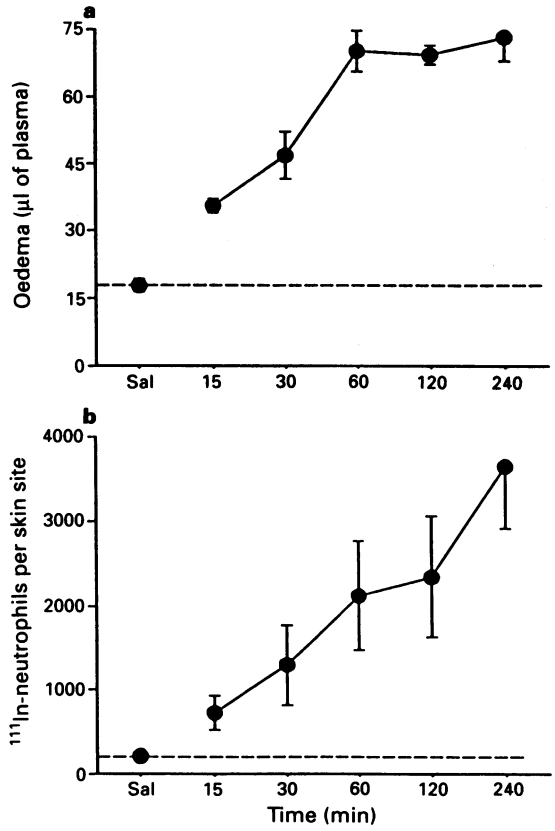


Figure 1 Time course of oedema formation (a) and ^{111}In-neutrophil accumulation (b) in a RPA reaction in guinea-pig skin. Antigen (BGG), ^{111}In-neutrophils and ^{125}I-HSA were injected i.v. followed by i.d. injection of anti-BGG antiserum (25%) at the same time, and then at 2 h, 3 h, 3.5 h and 3.75 h later. Inflammatory responses were assessed 4 h after i.v. injections. Results are the mean ± s.e.mean for 4 animals.

arachidonic acid (bradykinin, 61.3 ± 3.4 μl; bradykinin + arachidonic acid 1.5×10^{-9} mol per site, 72.3 ± 4.6 μl; bradykinin + arachidonic acid + ibuprofen, 54.4 ± 3.3 μl of plasma, $n = 6$), ibuprofen suppressed oedema formation in the RPA reaction (25% dilution in saline) by 27% (Table 1). Similarly, L-NAME (10^{-6} mol per site) also inhibited oedema formation in the RPA reaction but it was more effective (68% inhibition) (Table 1). In the same experiments, L-NAME inhibited bradykinin-induced oedema formation by 72% (bradykinin, 61.3 ± 3.4 μl; bradykinin + L-NAME, 29.3 ± 2.3 μl; saline, 11.4 ± 1.0 μl, $n = 6$). Ibuprofen has no effect on bradykinin-induced oedema formation (Teixeira *et al.*, 1993).

In order to assess the role of histamine in mediating oedema formation in the RPA reaction, increasing concentrations of antiserum (6.25 to 100% in saline) were co-injected i.d. with an H_1 histamine receptor antagonist, mepyramine (2.5×10^{-8} mol per site). In these experiments, mepyramine inhibited oedema formation induced by exogenous histamine (2.5×10^{-8} mol per site) by 92%, whereas oedema formation in the RPA in response to i.d. injection of 6.25%, 25% and 100% antiserum was inhibited by 48%, 32% and 30% respectively (Figure 2). A higher dose of mepyramine (2.5×10^{-7} mol per site) further inhibited oedema formation in the RPA reaction (e.g. RPA 25%, 83.4 ± 2.6 μl; RPA + mepyramine, 45.1 ± 1.6 μl ($P < 0.01$); saline, 17.8 ± 1.5 μl; $n = 4$).

Table 1 Effect of i.d. injection of ibuprofen and N^G-nitro-L-arginine methyl ester (L-NAME) on oedema formation in a RPA reaction in guinea-pig skin

	Oedema (μl of plasma)		
	Control	*Ibuprofen*	*L-NAME*
Saline	11.4 ± 1.0	13.3 ± 1.2	15.3 ± 1.8
RPA	73.4 ± 2.8	58.8 ± 3.5*	35.2 ± 4.2*

Rabbit anti-BGG antiserum (RPA, 25% dilution in saline) was injected alone (control) or with ibuprofen (10^{-7} mol per site) or L-NAME (10^{-6} mol per site) and oedema formation assessed after 4 h. In the same experiments, L-NAME inhibited bradykinin (10^{-10} mol per site)-induced oedema formation by 72% and ibuprofen completely inhibited the potentiation of bradykinin-induced oedema formation by arachidonic acid (1.5×10^{-9} mol per site). Results are mean ± s.e.mean for 6 animals. *$P < 0.01$ when compared to control values.

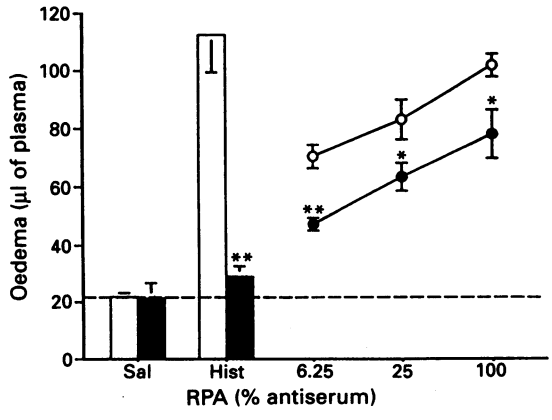


Figure 2 Effect of local treatment with mepyramine on oedema formation in a RPA reaction in guinea-pig skin. Saline (Sal), histamine (Hist, 2.5×10^{-8} mol per site) or rabbit anti-BGG antiserum (RPA, 6.25 to 100%) were injected alone (open columns or symbols) or with mepyramine (2.5×10^{-8} mol per site, solid columns or symbols) and oedema formation assessed after 4 h. The dashed line across the graph represents background values in response to i.d. injection of saline. Results are mean ± s.e.mean for 4 animals. *$P < 0.05$ and **$P < 0.01$ when compared to control values.

The 5-lipoxygenase inhibitor, ZM 230487 (10^{-8} mol per site) (Figure 3a) had no significant effect on oedema formation in the RPA reaction (6.25 to 100% antiserum). It is notable that i.d. injection of arachidonic acid (AA 3×10^{-8} mol per site) induced no significant oedema formation above saline (data not shown) although it did induce ^{111}In-neutrophil accumulation that was abrogated by ZM 230487 (Figure 3b). In contrast, i.v. administration of the long-acting PAF receptor antagonist, UK-74,505 (2.5 mg kg^{-1}), suppressed oedema responses in the RPA reaction by up to 43%, while inhibiting PAF-induced oedema formation in the same animals by up to 95% (Figure 4a).

Mediators of ^{111}In-neutrophil accumulation in the RPA reaction

Leukotrienes have been shown previously to activate neutrophils potently and cause their accumulation *in vitro* (Ford-Hutchinson *et al.*, 1980; reviewed in Nourshargh, 1992). However, local administration of ZM 230487 had no significant effect on the ^{111}In-neutrophil accumulation in the RPA reaction (6.25 to 100% antiserum) as shown in Figure 3b. In contrast to the lack of effect of ZM 230487, systemic administration of UK-74,505 (2.5 mg kg^{-1}) inhibited ^{111}In-neutrophil accumulation in the RPA reaction by up to 41% (Figure 4b). In the same experiments, PAF-induced ^{111}In-neutrophil accumulation was almost totally suppressed by UK-74,505 (Figure 4b). Since histamine induced no significant accumulation of ^{111}In-neutrophils above saline back-

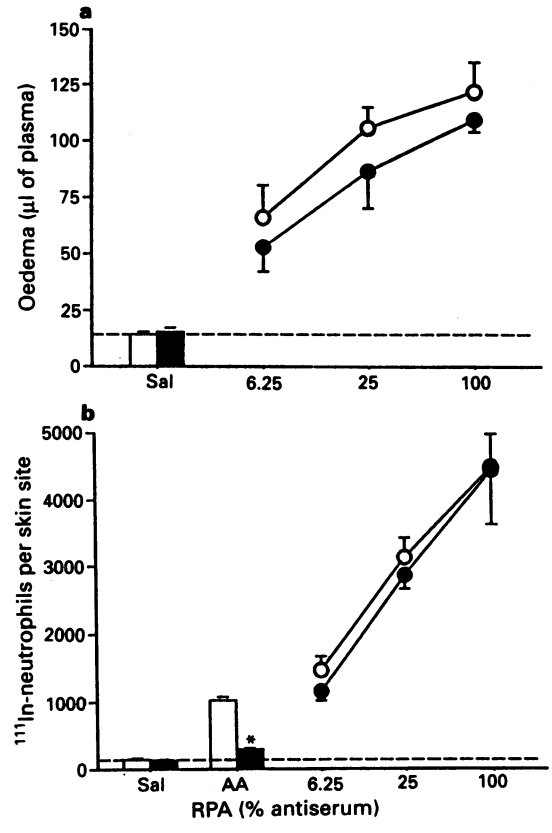


Figure 3 Effect of local treatment with ZM 230487 on oedema formation (a) and ^{111}In-neutrophil accumulation (b) in a RPA reaction in guinea-pig skin. Saline (Sal), arachidonic acid (AA, 3×10^{-8} mol per site) or rabbit anti-BGG antiserum (RPA, 6.25 to 100%) were injected alone (open columns or symbols) or with ZM 230487 (10^{-8} mol per site, solid columns or symbols) and inflammatory responses assessed after 4 h. The dashed line across the graphs represent background values in response to i.d. injection of saline. Results are mean ± s.e.mean for 4 animals. *$P < 0.05$ when compared to control values.

ground (data not shown), the effect of mepyramine on ^{111}In-neutrophil accumulation in the RPA reaction was not investigated.

Effect of an anti-CD18 mAb on ^{111}In-neutrophil accumulation in the RPA reaction

For these studies, we used a dose (2.4 mg kg^{-1}) of 6.5E F(ab')$_2$ which has previously shown to inhibit ^{111}In-neutrophil accumulation effectively in guinea-pig skin (Teixeira *et al.*, 1994). 6.5E F(ab')$_2$ significantly suppressed ^{111}In-neutrophil accumulation induced by PAF (10^{-10} to 10^{-9} mol per site) and ZAP (Figure 5a). Oedema formation measured in the same sites was unaltered by the mAb pre-treatment (Figure 5b) whereas PAF-induced haemorrhage (^{51}Cr-RBC extravasation) was significantly suppressed by 6.5E F(ab')$_2$ (Figure 5c). ZAP did not induce any significant haemorrhage over the 4 h measurement period (Figure 5c). Also in Figure 5, it is noticeable that PAF-induced haemorrhage was greater at the dose of 10^{-10} mol per site than at 10^{-9} mol per site although the reverse was observed with oedema formation. PAF-induced ^{111}In-neutrophil accumulation did not differ significantly between the two doses.

The effects of 6.5E F(ab')$_2$ on inflammatory responses in the RPA reaction are shown in Figure 6. Accumulation of ^{111}In-neutrophils in the RPA reaction was effectively inhibited by 6.5E F(ab')$_2$, although at higher doses of RPA antiserum the inhibition was not complete (e.g. 85% inhibition at 100% antiserum injection) (Figure 6a). In contrast, oedema formation in the same skin sites in response to all antiserum dilutions was unaltered by 6.5E F(ab')$_2$ treatment (Figure 6b). Haemorrhage was also detected in the RPA reaction but only at 50 and 100% antiserum (Figure 6c). Treatment with 6.5E F(ab')$_2$ abrogated haemorrhage in sites injected with 50% antiserum and significantly reduced by 29% the response in sites injected with 100% antiserum (Figure 6c).

Since ^{111}In-neutrophil accumulation was not totally suppressed by 6.5E F(ab')$_2$, we tested whether 6.5E whole mAb used at the same dose (2.4 mg kg^{-1}) had any inhibitory effect on oedema formation in RPA reactions. 6.5E whole mAb

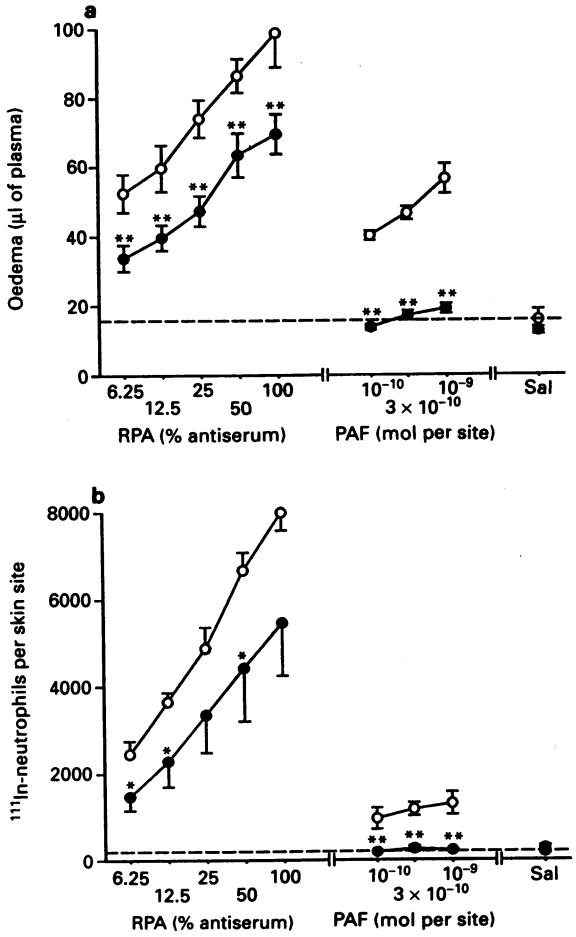


Figure 4 Effect of i.v. administration of UK-74,505 (2.5 mg kg^{-1}) on oedema formation (a) and ^{111}In-neutrophil accumulation (b) in a RPA reaction in guinea-pig skin. Saline (Sal), PAF (10^{-10} to 10^{-9} mol per site) or increasing concentrations of rabbit anti-BGG antiserum (6.25 to 100%) were injected i.d. in control (open symbols) or UK-74,505 treated (solid symbols) animals and inflammatory responses assessed after 4 h. The dashed line across the graphs represents background values in response to i.d. injection of saline in control animals. Results are mean ± s.e.mean for 5 pairs of animals. $*P<0.05$ and $**P<0.01$ when compared to values in control animals.

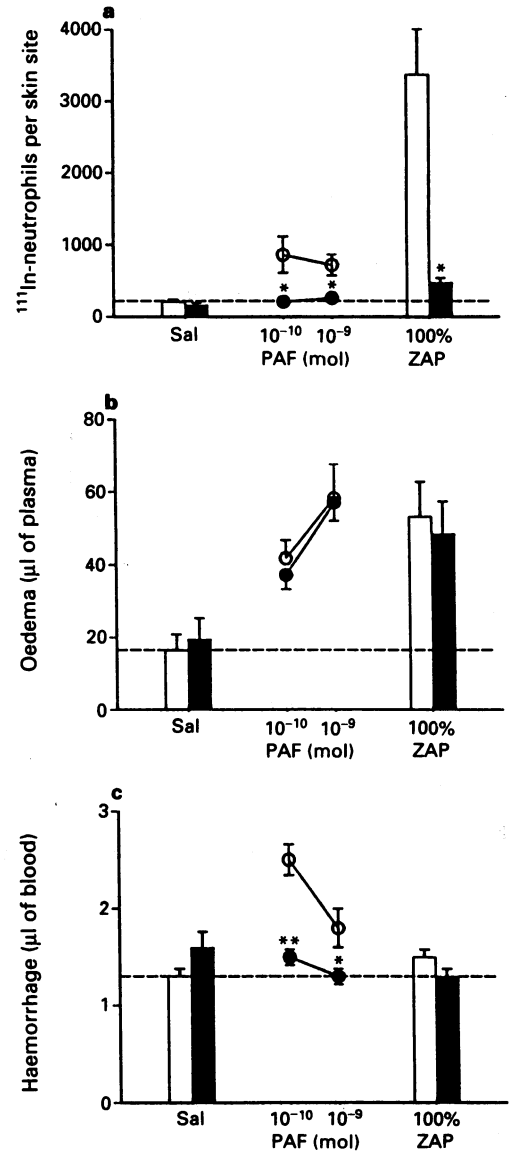


Figure 5 Effect of i.v. administration of 6.5E F(ab')$_2$ (2.4 mg kg^{-1}) on ^{111}In-neutrophil accumulation (a), oedema formation (b) and haemorrhage (c) induced by PAF and ZAP in guinea-pig skin. Saline (Sal), PAF (10^{-10} and 10^{-9} mol per site) and ZAP (100%) were injected i.d. in control (open columns or symbols) or antibody treated (solid columns or symbols) animals and inflammatory responses assessed after 4 h. The dashed line across the graph represents background values in response to i.d. injection of saline control animals. Results are mean ± s.e.mean for 6 pairs of animals. $*P<0.05$ and $**P<0.01$ when compared to values in control animals.

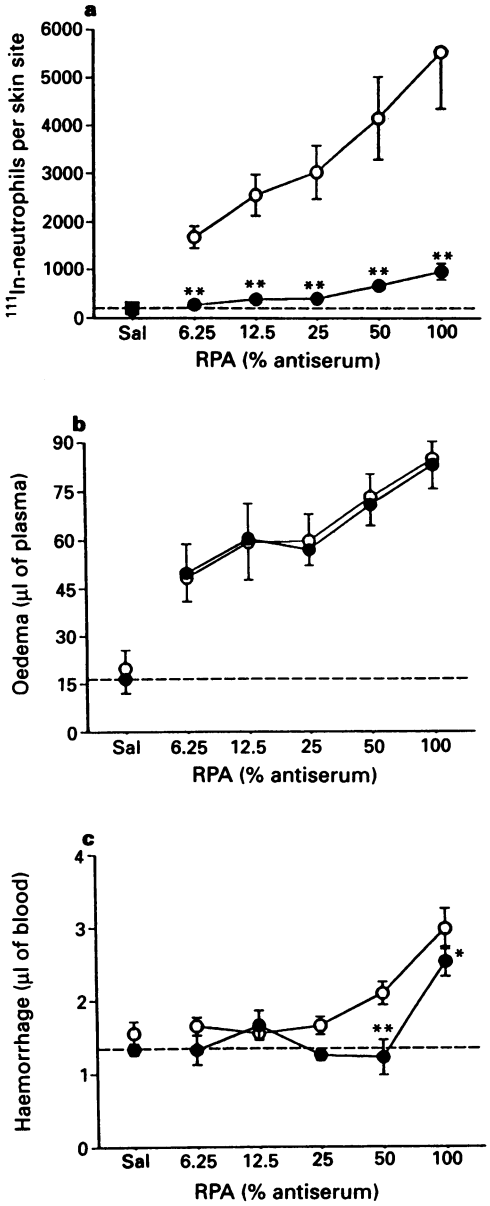


Figure 6 Effect of i.v. administration of 6.5E F(ab')$_2$ (2.4 mg kg^{-1}) on ^{111}In-neutrophil accumulation (a), oedema formation (b) and haemorrhage (c) in a RPA reaction in guinea-pig skin. Saline (Sal) or increasing concentration of rabbit anti-BGG antiserum (6.25 to 100%) were injected i.d. in control (open symbols) or antibody treated (solid columns) animals and inflammatory responses assessed after 4 h. The dashed line across the graph represents background values in response to i.d. injection of saline control animals. Results are mean ± s.e.mean for 6 pairs of animals. *$P<0.05$ and **$P<0.01$ when compared to values in control animals.

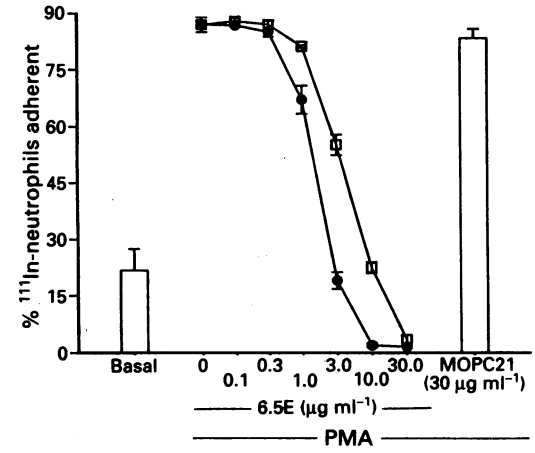


Figure 7 Effect of 6.5E whole mAb and F(ab')$_2$ fragments on adhesion of ^{111}In-neutrophils to serum-coated plastic. The whole mAb (0.1 to 30 μg ml^{-1}, ●) or the F(ab')$_2$ fragments (0.1 to 30 μg ml^{-1}, □) were pre-incubated with ^{111}In-neutrophils for 15 min. Adhesion was stimulated by phorbol myristate acetate (PMA, 10^{-8} M) and quantified after 30 min at 37°C. Unstimulated (basal) adhesion and the effects of MOPC21 (30 μg ml^{-1}) are shown for comparison. Values are means ± s.e.mean of 3 experiments.

Table 2 Effect of i.v. administration of 6.5E whole mAb on oedema formation in a RPA reaction in guinea-pig skin

		Oedema (μl of plasma	
		MOPC21	*6.5E whole mAb*
RPA	6.25%	29.3 ± 5.3	23.8 ± 5.2
	12.5%	39.3 ± 7.6	31.2 ± 6.6
	25%	40.9 ± 4.5	32.5 ± 5.7
	50%	50.5 ± 4.5	39.3 ± 7.6*
	100%	49.3 ± 5.0	30.4 ± 4.0**
Hist	2.5×10^{-9}	22.3 ± 4.4	31.5 ± 5.5
	2.5×10^{-8}	43.5 ± 3.5	42.1 ± 4.3
BK	10^{-10}	40.6 ± 3.6	42.9 ± 9.3
ZAP	10%	18.9 ± 2.6	21.2 ± 2.6
	30%	25.7 ± 2.8	25.4 ± 3.4
	100%	24.7 ± 2.3	21.8 ± 4.6

Increasing concentrations of rabbit anti-BGG antiserum (6.25 to 100% dilution in saline), histamine (Hist, 2.5×10^{-9} and 2.5×10^{-8} mol per site), bradykinin (BK 10^{-10} mol per site) and zymosan-activated plasma (ZAP, 10% to 100% in saline) were injected i.d. in control (MOPC21, 2.4 mg kg^{-1}) or antibody treated (6.5E whole mAb, 2.4 mg kg^{-1}) animals and oedema formation assessed after 4 h. Saline values have been subtracted from the results and the mean ± s.e.mean for 5 pairs of animals are shown. Saline values in MOPC21- and 6.5E-treated animals were 14.7 ± 0.6 μl and 18.0 ± 3.5 μl of plasma, respectively. *$P<0.05$ and **$P<0.01$ when compared to control values.

was approximately 2.5 times ($P<0.01$; Student's t test) more potent than 6.5E F(ab')$_2$ at inhibiting PMA-induced ^{111}In-neutrophil adhesion to serum-coated plates (Figure 7). At the dose used, 6.5E whole mAb significantly inhibited oedema formation at 50% and 100% RPA reactions by 22% and 38%, respectively (Table 2). Examination of histological sections of skin tissue confirmed that total neutrophil accumulation was inhibited by 6.5E whole mAb. The whole antibody had no inhibitory effect on oedema formation induced by histamine (2.5×10^{-9} and 2.5×10^{-8} mol per site), bradykinin (10^{-10} mol per site) and ZAP (10 to 100% in saline) (Table 2) and did not significantly alter total or differential blood cell counts (data not shown).

Discussion

The i.d. injection of inflammatory mediators such as FMLP or C5a in rabbit skin induces oedema formation which is abrogated when circulating neutrophils are depleted (Wedmore & Williams, 1981b; Hellewell *et al.*, 1989) or when neutrophil accumulation is inhibited by pretreatment with mAbs that recognize the CD11/CD18 integrins on the surface of the neutrophil (Afors *et al.*, 1987; Norman *et al.*, 1994). Similarly, in rat and rabbit skin, oedema formation and haemorrhage in a cutaneous RPA reaction are dependent on neutrophils (Mulligan *et al.*, 1992b; Norman *et al.*, 1994).

Our results obtained in investigating the neutrophil-

dependency and the mechanisms involved in a RPA reaction in guinea-pig skin can be summarized as follows: (1) Most oedema formation in the RPA reaction occurred over the first 60 min whereas ^{111}In-neutrophil accumulation was still rising from 60 to 240 min. The difference in the kinetics of oedema formation and ^{111}In-neutrophil accumulation suggests that these events may be dissociated; (2) Oedema formation was partially inhibited by a PAF antagonist (UK-74,505) or an H_1 receptor antagonist (mepyramine) but we found no evidence for a role of leukotrienes in mediating this response: (3) The nitric oxide synthesis inhibitor L-NAME inhibited oedema formation by 68% whereas the cyclo-oxygenase inhibitor ibuprofen inhibited oedema formation by 27%; (4) ^{111}In-neutrophil accumulation was suppressed by a PAF antagonist but not by a 5-lipoxygenase inhibitor; (5) The anti-CD18 mAb 6.5E F(ab')$_2$ effectively suppressed ^{111}In-neutrophil accumulation induced by PAF and in the RPA reaction, but it had no effect on oedema formation. However, haemorrhage, measured in the same sites, was inhibited by 6.5E F(ab')$_2$; (6) When used at the same dose as 6.5E F(ab')$_2$, 6.5E whole mAb partially inhibited oedema formation in the RPA reaction.

PAF has been previously described as a mediator of increased vascular permeability (Vargaftig & Ferreira, 1981; Wedmore & Williams, 1981b; Morely *et al.*, 1983) and neutrophil accumulation in different animal species (Humphrey *et al.*, 1982; Hellewell, 1990; Faccioli *et al.*, 1991). However, in contrast to mediators such as C5a, FMLP, LTB_4 and interleukin-8 which have similar inflammatory activity, PAF-induced oedema formation does not seem to be neutrophil-dependent (Wedmore & Williams, 1981b; Hellewell, 1990). In rabbit skin, PAF receptor antagonists partially inhibit oedema formation, neutrophil accumulation and platelet deposition in a RPA reaction (Hellewell & Williams, 1986; Hellewell, 1990; Rossi *et al.*, 1992; Pons *et al.*, 1993). Similarly, in guinea-pig skin, PAF receptor antagonists have been previously shown to suppress oedema formation in a RPA reaction by approximately 50% (Handley *et al.*, 1987). In the current study, we have tested the potent and specific PAF receptor antagonist, UK-74,505 (Alabaster *et al.*, 1991), in our RPA model in the guinea-pig. Systemic treatment with UK-74,505 suppressed both oedema formation and ^{111}In-neutrophil accumulation in the RPA reaction. We have not tested UK-74,505 locally since it was not possible to achieve a sufficiently high local concentration without inducing non-specific inflammation due to the diluent (0.1 M HCl, data not shown). Thus, our results using systemic UK-74,505 suggest that PAF plays an important role in mediating both ^{111}In-neutrophil accumulation and oedema formation in a RPA reaction in guinea-pig skin. In this part of the study, an unexpected effect was observed with PAF-induced haemorrhage, which decreased at the higher PAF dose (Figure 5). This result is unexplained, but it is possible that lower doses of PAF induce the formation of large gaps in the endothelium and that higher doses induce activation of platelets which plug these gaps. Smaller gaps appear not to be plugged as oedema formation did not show the same pattern.

The inhibitory effect of mepyramine on oedema formation in the RPA reaction strongly suggests a role for endogenous histamine as shown by Taichman *et al.*, (1971). In addition, we have assessed the role of endogenous leukotrienes in mediating oedema formation in the RPA reaction. The potent and effective 5-lipoxygenase inhibitor ZM 230487 (Crawley *et al.*, 1993; Teixeira & Hellewell, 1994) had no inhibitory effect on oedema formation in the RPA reaction. Thus, oedema formation in a RPA reaction in guinea-pig skin is dependent on local synthesis/release of PAF and histamine, but not of leukotrienes.

Oedema formation is dependent not only on agents which increase vascular permeability, but also on agents which induce vasodilatation by acting on the arterial side of the microcirculation. Synergism between these classes of agents led to the two mediator hypothesis (Williams & Peck, 1977). We have therefore assessed the role of the vasodilators prostaglandins and nitric oxide in mediating oedema formation in the RPA reaction. L-NAME, used at a dose which has been previoulsy shown to inhibit oedema formation effectively in guinea-pig skin (Teixeira *et al.*, 1993), suppressed by 68% oedema formation in the RPA reaction. L-NAME inhibited not only oedema formation in a RPA reaction but also mediator-induced oedema formation, suggesting that endogenously released nitric oxide plays an important role in maintaining cutaneous blood flow in the guinea-pig (see also Teixeira *et al.*, 1993). In rat skin, L-NAME (and other nitric oxide synthesis inhibitors) inhibited oedema formation and haemorrhage, but not neutrophil accumulation (as assessed by tissue MPO content), in the RPA reaction (Mulligan *et al.*, 1991; 1992a). The suggestion was that the effects of L-NAME (and other inhibitors) could not be attributed to inhibition of neutrophil emigration or production of superoxide anion but were possibly due to inhibition of direct tissue damage by locally released nitric oxide (Mulligan *et al.*, 1991; 1992a). However, an effect of nitric oxide synthesis inhibitors on blood flow and inflammation induced by known mediators of inflammation was not investigated. As previously shown, the inhibitory effect of L-NAME on cutaneous blood flow may explain its inhibitory effect on oedema formation induced by various inflammatory stimuli in guinea-pig skin (Teixeira *et al.*, 1993). The cyclo-oxygenase inhibitor, ibuprofen, also suppressed oedema formation in the RPA reaction in our model but to a much lesser extent (27%). In contrast, we have previously reported the lack of effect of ibuprofen in inhibiting oedema formation in a passive cutaneous anaphylatic reaction and induced by different mediators of inflammation, with the exception of histamine which was inhibited by 30% (Teixeira *et al.*, 1993). Thus, our results suggest that in guinea-pig skin, arteriolar tone is mostly under the control of nitric oxide but under some circumstances (e.g. RPA reaction) vasodilator prostaglandins may also play a role.

Although leukotrienes are potent neutrophil activators *in vitro* (e.g. Ford-Hutchinson *et al.*, 1980; Rossi *et al.*, 1993) and effective in causing their accumulation *in vivo* (reviewed in Nourshargh, 1992), ZM 230487 had no inhibitory effect on the ^{111}In-neutrophil accumulation in the RPA reaction although it did inhibit the response to a high dose of arachidonic acid. The dose of ZM 230487 used in the present study has been previously shown to inhibit the accumulation of eosinophils induced by arachidonic acid and in a passive cutaneous anaphylactic reaction in guinea-pig skin (Teixeira & Hellewell, 1994) suggesting that effective inhibition of 5-lipoxygenase was achieved. Thus, it is unlikely that leukotrienes, in particular LTB_4, have a major role in mediating the accumulation of neutrophils in a RPA reaction in this species. In addition, a specific LTB_4 antagonist (LY-255283), whilst blocking LTB_4-induced oedema formation, had no effect on leakage in the RPA reaction in rabbit skin (Rossi *et al.*, 1992).

There have been some studies in the literature addressing the question of whether oedema formation in a RPA reaction in guinea-pig skin is dependent on circulating neutrophils. Taichman & Movat (1966) and Taichman *et al.* (1971) studying IgG_2-mediated reactions have suggested that oedema formation in these reactions was dependent on circulating neutrophils, as judged by depleting these cells using both a rabbit anti-guinea-pig neutrophil antiserum (Taichman *et al.*, 1971) or nitrogen mustard (Taichman & Movat, 1966). However, the anti-neutrophil antiserum also induced a fall in circulating complement levels (Taichman *et al.*, 1971) and there is much evidence which supports the essential involvement of the complement system in mediating inflammation in the RPA reaction (Maillard & Zarco, 1968; Cochrane *et al.*, 1970; Rossi *et al.*, 1992). Experiments using nitrogen mustard could not be performed by Humphrey (1955b) who described the drug as too toxic for guinea-pigs. Humphrey (1955b) also

used an anti-neutrophil antiserum, which did not lead to a fall in complement levels, but was unable to find a significant inhibition of increased vascular permeability (measured by Evans Blue dye leakage) in the RPA reaction in guinea-pig skin during the first 5.5 h after inducing the reaction (Humphrey, 1955b). However, skin thickness, the measure of late oedema formation, was inhibited when determined in reactions that were 7, 24 and 48 h old (Humphrey, 1955b). In our study, the $F(ab')_2$ fragment of a CD18 mAb effectively inhibited ^{111}In-neutrophil accumulation induced by PAF and ZAP and in the RPA reaction. Haemorrhage induced by PAF and in RPA sites at 50% antiserum dilution was also effectively inhibited by 6.5E $F(ab')_2$ although, at the largest RPA reactions, haemorrhage was only partially suppressed. Oedema formation induced by all inflammatory stimuli was unaltered. However, when whole 6.5E mAb was used, oedema formation in the RPA reaction was partially inhibited and histological sections confirmed that the total neutrophil count in the skin was reduced. Blood leukocyte counts were unaltered (data not shown). The observation that 6.5E whole mAb was 2.5 times more potent than 6.5E $F(ab')_2$ *in vivo* may explain its inhibitory effects on oedema formation in the RPA reaction. In fact, at the dose used (2.4 mg kg^{-1}), one would expect a blood level of the antibodies of approximately 30 μg ml^{-1} (assuming a blood volume of 70 ml kg^{-1}). As can be seen from Figure 7, this antibody concentration is just enough for the $F(ab')_2$ fragment to achieve complete inhibition of neutrophil adhesion to protein-coated plastic. Furthermore, when compared with whole antibody, the antibody fragment is likely to have a shorter half-life *in vivo*. We could not measure ^{111}In-neutrophils in experiments with 6.5E whole mAb since it has been previously shown to enhance the clearance of radiolabelled leukocytes from the circulation (Teixeira *et al.*, 1994). Similarly, anti-CD18 treatment in rabbits and rats has been shown to inhibit not only neutrophil accumulation and haemorrhage, but also oedema formation (Mulligan *et al.*, 1992b; Norman *et al.*, 1994). Thus, in guinea-pig skin, oedema formation in a RPA reaction is partially neutrophil-dependent, at least measured over 4 h. It is possible that oedema formation measured at later periods (7 to 48 h) may also be dependent on neutrophils as suggested by Humphrey (1955b). However, further studies are necessary to evaluate this issue more carefully since skin thickness is not a sensitive or specific measure of interstitial oedema.

The experiments described here give further support to our previous findings of a lack of neutrophil-dependent oedema in response to i.d. injection of ZAP in guinea-pig skin (Teixeira *et al.*, 1994). Nevertheless, oedema formation and haemorrhage appeared to be partially neutrophil-dependent in a RPA reaction as judged by the effect of an anti-CD18 mAb. They also further demonstrate the importance of mast cells in mediating increases of vascular permeability in response to i.d. injection of different inflammatory mediators or inflammatory reactions in guinea-pig skin.

We are grateful to The National Asthma Campaign, Sandoz (Switzerland), The Wellcome Trust, The British Lung Foundation and ONO Pharmaceuticals for support.

References

ALABASTER, V.A., KEIR, R.F., PARRY, M.J. & DE SOUZA, R.N. (1991). UK-74,505 a novel and selective PAF antagonist, exhibits potent and long lasting activity *in vivo*. *Agents Actions*, **34**, S221–S227.

ARFORS, K.-E., LUNDBERG, C., LINDOM, L., LUNDBERG, K., BEATTY, P.G. & HARLAN, J.M. (1987). A monoclonal antibody to the membrane glycoprotein complex CD18 inhibits polymorphonuclear leukocyte accumulation and plasma leakage in vivo. *Blood*, **69**, 338–340.

BJORK, J. & SMEDEGARD, G. (1983). Acute microvascular effects of PAF-acether as studied by intravital microscopy. *Eur. J. Pharmacol.*, **96**, 87–94.

COCHRANE, C.G. & JANOFF, A. (1974). The Arthus reaction: A model of neutrophil and complement-mediated injury. In *The Inflammatory Process*. ed. Zweifach, B.W., Grant, L. & McCluskey, R.T. pp. 85–162. New York: Academic Press.

COCHRANE, C.G., MULLER-EBERHARD, H.J. & AIKIN, B.S. (1970). Depletion of plasma complement in vivo by a protein of cobra venom: its effect on various immunologic reactions. *J. Immunol.*, **105**, 55–69.

COLLINS, P.D., JOSE, P.J. & WILLIAMS, T.J. (1991). The sequential generation of neutrophil chemoattractant proteins in acute inflammation in the rabbit in vivo: relationship between C5a and a protein with the characteristics of IL-8. *J. Immunol.*, **146**, 677–684.

COLLINS, P.D., WEG, V.B., FACCIOLI, L.H., WATSON, M.L., MOQBEL, R. & WILLIAMS, T.J. (1993). Eosinophil accumulation induced by human interleukin-8 in the guinea pig in vivo. *Immunology*, **79** 312–318.

CRAWFORD, J.P., MOVAT, H.Z., NARENDRANATH, S.R. & HAY, J.B. (1982). Pathways to inflammation induced by immune complexes: development of the Arthus reaction. *Fedn. Proc.*, **41**, 2583–2587.

CRAWLEY, G.C., BRIGGS, M.T., DOWELL, R.I., EDWARDS, P.N., HAMILTON, P.M., KINGSTON, J.F., OLDHAM, K., WATERSON, D. & WHALLEY, D.P. (1993). 4-methoxy-2-methyltetrahydropyans: Chiral leukotriene biosynthesis inhibitors, related to ICI D2138, which display enantioselectivity. *J. Med. Chem.*, **36**, 295–296.

FACCIOLI, L.H., NOURSHARGH, S., MOQBEL, R., WILLIAMS, F.M., SEHMI, R., KAY, A.B. & WILLIAMS, T.J. (1991). The accumulation of ^{111}In-eosinophils induced by inflammatory mediators in vivo. *Immunology*, **73**, 222–227.

FIGDOR, C.G. & VAN KOOYK, Y. (1992). Regulation of cell adhesion. In *Adhesion: its Role in Inflammatory Disease*. ed. Harlan, J.M. & Liu, D.Y. pp. 151–182. New York: W.H. Freeman and Company.

FORD-HUTCHINSON, A.W., BRAY, M.A., DOIG, M.V., SHIPLEY, M.E. & SMITH, M.J.H. (1980). Leukotriene B, a potent chemokinetic and aggregating substance released from polymorphonuclear leukocytes. *Nature*, **286**, 264–265.

HANDLEY, D.A., ANDERSON, R.C. & SAUNDERS, R.N. (1987). Inhibition by SRI 63-072 and SRI 31-119 of PAF-acether and immune complex effects in the guine-pig. *Eur. J. Pharmacol.*, **141**, 409–416.

HELLEWELL, P.G. (1990). The contribution of platelet-activating factor to immune complex-mediated inflammation. In *Platelet-activating Factor in Endotoxin and Immune Diseases*. ed. Handley, D.A., Saunders, R.N., Houlihan, W.J. & Tomesch, J.C. pp. 367–386. New York: Marcel Dekker Inc.

HELLEWELL, P.G. & WILLIAMS, T.J. (1986). A specific antagonist of platelet-activating factor suppresses oedema formation in an Arthus reaction but not oedema induced by leukocyte chemoattractants in rabbit skin. *J. Immunol.*, **137**, 302–307.

HELLEWELL, P.G., YARWOOD, H. & WILLIAMS, T.J. (1989). Characteristics of oedema formation induced by FMLP in rabbit skin. *Br. J. Pharmacol.*, **97**, 181–189.

HUMPHREY, D.M., HANAHAN, D.J. & PINCKARD, R.N. (1982). Induction of leukocytic infiltrates in rabbit skin by acetyl glyceryl ether phosphorycholine. *Lab. Invest.*, **47**, 227–234.

HUMPHREY, J.H. (1955a). The mechanism of Arthus reactions. I. The role of polymorphonuclear leucocytes and other factors in reversed passive Arthus reactions in rabbits. *Br. J. Exp. Pathol.*, **36**, 268–282.

HUMPHREY, J.H. (1955b). The mechanism of Arthus reactions. II. The role of polymorphonuclear leucocytes and platelets in reversed passive reactions in the guinea-pig. *Br. J. Exp. Pathol.*, **36**, 283–285.

MAILLARD, J.L. & ZARCO, R.M. (1968). Decomplementation par un facteur extrait du venin de cobra. Effet sur plusieurs reactions immunes du cobaye et du rat. *Ann. Inst. Pasteur*, **114**, 756–774.

MORLEY, J., PAGE, C.P. & PAUL, W. (1983). Inflammatory actions of platelet activating factor (Paf-acether) in guinea-pig skin. *Br. J. Pharmacol.*, **80**, 503–509.

MULLIGAN, M.S., HEVEL, J.M., MARLETTA, M.A. & WARD, P.A. (1991). Tissue injury caused by deposition of immune complexes is L-arginine dependent. *Proc. Natl. Acad. Sci. U.S.A.*, **88**, 6338–6342.

MULLIGAN, M.S., MONCADA, S. & WARD, P.A. (1992a). Protective effects of nitric oxide synthase inhibitors in immune complex-mediated vasculitis. *Br. J. Pharmacol.*, **107**, 1159–1162.

MULLIGAN, M.S., VARANI, J., WARREN, J.S., TILL, G.O., SMITH, C.W., ANDERSON, D.C., TODD, R.F. & WARD, P.A. (1992b). Role of β_2 integrins of rat neutrophils in complement and oxygen radical-mediated acute inflammatory injury. *J. Immunol.*, **148**, 1847–1857.

NORMAN, K.E., ARGENBRIGHT, L.W., WILLIAMS, T.J. & ROSSI, A.G. (1994). Role of adhesion glycoproteins CD18 and ICAM-1 in inflammatory reactions of rabbit skin. *Br. J. Pharmacol.*, **111**, 117–122.

NOURSHARGH, S. (1992). Mechanisms of LTB_4-induced neutrophil accumulation in vivo. In *Advances in Rheumatology and Inflammation*. Vol 2. ed. Fritsch, J. & Muller-Peddinghaus, R. pp. 39–48. Basel: Eular Publishers.

PERRETTI, M., AHLUWALIA, A., HARRIS, J.G., GOULDING, N.J. & FLOWER, R.J. (1993). Lipocortin-1 fragments inhibit neutrophil accumulation and neutrophil-dependent oedema in the mouse. A qualitative comparison with an anti-CD11b monoclonal antibody. *J. Immunol.*, **151**, 4306–4314.

PONS, F., ROSSI, A.G., NORMAN, K.E., WILLIAMS, T.J. & NOURSHARGH, S. (1993). Role of platelet-activating factor in platelet accumulation in rabbit skin. Effect of the novel long-acting PAF antagonist, UK-74,505. *Br. J. Pharmacol.*, **109**, 234–242.

RAMPART, M., VAN OSSELAER, N. & HERMAN, A.G. (1991). ICAM-1 (CD54)-mediated neutrophil emigration is not associated with increased vascular permeability. *J. Leuk. Biol.*, Suppl. 2, 46.

ROSSI, A.G., MACINTYRE, D.E., JONES, C.J.P. & MCMILLAN, R.M. (1993). Stimulation of human polymorphonuclear leukocytes by leukotriene B_4 and platelet-activating factor: an ultrastructural and pharmacological study. *J. Leuk. Biol.*, **53**, 117–125.

ROSSI, A.G., NORMAN, K.E., DONIGI-GALE, D., SHOUPE, T.S., EDWARDS, R. & WILLIAMS, T.J. (1992). The role of complement, platelet-activating factor and leukotriene B_4 in the reversed passive Arthus reaction. *Br. J. Pharmacol.*, **107**, 44–49.

STETSON, C.A. (1951). Similarities in the mechanisms determining the Arthus and Schwartzman phenomena. *J. Exp. Med.*, **94**, 347–358.

TAICHMAN, N.S. & MOVAT, H.Z. (1966). Do polymorphonuclear leucocytes play a role in passive cutaneous anaphylaxis reaction of the guinea pig? *Int. Arch. Allergy*, **30**, 97–102.

TAICHMAN, N.S., MOVAT, H.Z., GLYNN, M.F. & BRODER, I. (1971). Further studies on the role for neutrophils in passive cutaneous anaphylaxis of the guinea pig. *Immunology*, **21**, 623–635.

TEIXEIRA, M.M. & HELLEWELL, P.G. (1994). Effect of a 5-lipoxygenase inhibitor, ZM 230487, on cutaneous allergic inflammation in the guinea-pig. *Br. J. Pharmacol.*, **111**, 1205–1211.

TEIXEIRA, M.M., REYINA, S., ROBINSON, M., SHOCK, A., WILLIAMS, T.J., WILLIAMS, F.M., ROSSI, A.G. & HELLEWELL, P.G. (1994). Role of CD18 in the accumulation of eosinophils and neutrophils and local oedema formation in inflammatory reactions in guinea pig skin. *Br. J. Pharmacol.*, **111**, 811–818.

TEIXEIRA, M.M., WILLIAMS, T.J. & HELLEWELL, P.G. (1993). Role of prostaglandins and nitric oxide in acute inflammatory reactions in guinea pig skin. *Br. J. Pharmacol.*, **110**, 1515–1521.

VARGAFTIG, B.B. & FERREIRA, S.H. (1981). Blockade of the inflammatory effects of PAF by cyclo-oxygenase inhibitors. *Braz. J. Med. Res.*, **14**, 187–189.

WEDMORE, C.V. & WILLIAMS, T.J. (1981a). Control of vascular permeability by polymorphonuclear leukocytes in inflammation. *Nature*, **289**, 646–650.

WEDMORE, C.V. & WILLIAMS, T.J. (1981b). Platelet-activating factor (PAF), a secretory product of polymorphonuclear leukocytes, increases vascular permeability in rabbit skin. *Br. J. Pharmacol.*, **74**, 916–917P.

WILLIAMS, T.J. & PECK, M.J. (1977). Role of prostaglandin-mediated vasodilation in inflammation. *Nature*, **270**, 530–532.

WILLIAMSON, L.M., SHEPPARD, K., DAVIES, J.M. & FLETCHER, J. (1986). Neutrophils are involved in the increased vascular permeability produced by activated complement in man. *Br. J. Haematol.*, **64**, 375–384.

(Received April 22, 1194
Revised July 15, 1994
Accepted July 22, 1994)

Br. J. Pharmacol. (1994), **113**, 1372–1376

© Macmillan Press Ltd, 1994

Modulation of morphine antinociception in the mouse by endogenous nitric oxide

Giovanni Brignola, [1]Antonio Calignano & Massimo Di Rosa

Department of Experimental Pharmacology, University of Naples 'Federico II', Via Domenico Montesano 49, 80131 Naples, Italy

1 L-Arginine (100–1000 mg kg^{-1}) administered orally (p.o.) or intraperitoneally (i.p.), but not intracerebroventricularly (i.c.v., 0.08 mg per mouse), reduced the antinociceptive effect of morphine (0.5–10 mg kg^{-1} s.c.) assessed in mice using three different tests: hot plate, tail-flick and acetic acid-induced writhing. D-Arginine (up to 1000 mg kg^{-1} p.o. or i.p.) was ineffective.

2 N^G-Monomethyl-L-arginine (L-NMMA, 5–50 mg kg^{-1} i.p.) and N^G-nitro-L-arginine methyl ester (L-NAME, 5– 30 mg kg^{-1} i.p.), but not N^G-nitro-D-arginine methyl ester (D-NAME, 30 mg kg^{-1} i.p.), reversed in all assays the effect of L-arginine on morphine-induced antinociception.

3 Morphine (10 mg kg^{-1} s.c.), L-arginine (1000 mg kg^{-1} p.o.) or L-NAME (30 mg kg^{-1} i.p.), either alone or in combination, did not produce changes in locomotor activity or sensorimotor performance of animals.

4 These results suggest that the L-arginine–nitric oxide pathway plays a modulating role in the morphine-sensitive nociceptive processes.

Keywords: Antinociception; L-arginine; morphine; nitric oxide

Introduction

The biosynthesis of nitric oxide (NO) from L-arginine is a pathway for the regulation of cell function and communication (Moncada *et al.*, 1991). In all cell types so far studied NO is generated following oxidation and cleavage of the terminal nitrogen atom(s) of L-arginine by an enzyme, NO synthase. This enzyme is competitively inhibited by some L-arginine analogues including N^G-nitro-L-arginine methyl ester (L-NAME) and N^G-monomethyl-L-arginine (L-NMMA) (Rees *et al.*, 1990).

Histochemical studies using antibodies to the constitutive NO synthase have shown that this enzyme occurs widely in brain and in peripheral nerves (Bredt *et al.*, 1990). There is now considerable evidence that NO modulates synaptic transmission in both the central and peripheral nervous system (Meller & Gebhart, 1993), and it has been suggested that NO is involved in nociceptive processes either in the periphery or within the spinal cord (Haley *et al.*, 1992). It has been shown in mouse and rat that NO mediates the *N*-methyl-D-aspartate (NMDA)-produced facilitation of the nociceptive tail-flick reflexes which depends on the activity of spinal cord neurones (Kitto *et al.*, 1992; Meller *et al.*, 1992a). Furthermore, it has been reported that L-NAME enhances morphine antinociception in rats (Przewlocki *et al.*, 1993).

In this study we have investigated in mice the interaction between the L-arginine–NO pathway and the antinociceptive effect of morphine using three experimental models: hot plate, tail-flick and acetic acid-induced writhing.

Methods

Animals

Male Swiss mice (25–30 g, Nossan, Italy) were used. Animals were housed in a room maintained at 22 ± 1°C with an alternating 12 h light–dark cycle. Food and water were available *ad libitum*. All experiments were carried out between 09.00 and 12.00 h.

[1] Author for correspondence.

Drugs

Morphine hydrochloride was obtained from SALARS (Italy), *N*-methylmorphine iodide was synthetized in our laboratory, N^G-nitro-D-arginine methyl ester (hydrochloride-D-NAME) was obtained from Bachem (Switzerland), N^G-monomethyl-L-arginine acetate (L-NMMA) was kindly donated by Dr S. Moncada (Wellcome Research Laboratories, U.K.), and L-arginine hydrochloride, D-arginine hydrochloride and N^G-nitro-L-arginine methyl ester hydrochloride (L-NAME) were purchased from Sigma (U.S.A.). Drugs were dissolved in saline and administered by various routes: morphine and *N*-methylmorphine were given subcutaneously (s.c., 10 ml kg^{-1}); L-arginine orally (p.o., 0.1 ml per mouse), intraperitoneally (i.p., 10 ml kg^{-1}) or intracerebroventricularly (i.c.v., 0.005 ml per mouse): D-arginine p.o. (0.1 ml per mouse); and L-NMMA, L-NAME and D-NAME i.p. (10 ml kg^{-1}).

Hot plate

Mice were placed on a hot plate (55.5 ± 0.5°C) according to the procedure described by Eddy and Leimback (1953). The reaction time(s) measured was either jumping off the plate or hind paw licking. The cut-off imposed was 60 s to avoid tissue damage (Porreca *et al.*, 1984). Each mouse was tested twice before administration of drugs and the reaction times were averaged to obtain a baseline. The reaction time was subsequently assessed 30 min after morphine administration or 60 min after other drugs which were given either alone or in combination. Control mice received saline instead of drugs. The antinociceptive response of each mouse was expressed as the maximum percentage effect (MPE), which was calculated as:

$$\frac{\text{Post-drug reaction time} - \text{baseline reaction time}}{\text{Cut-off value} - \text{baseline reaction time}} \times 100$$

(Hong *et al.*, 1993).

Tail flick

The tail-flick was evoked by a source of radiant heat, which was focused on the dorsal surface of the tail (D'Amour &

Smith, 1941, modified by Dewey *et al.*, 1970). Each mouse was tested twice before drug administration and the reaction times were averaged to obtain a baseline. The intensity of heat stimulus was adjusted so that the mouse flicked its tail after 2–4 s. Each mouse was then tested 30 min after morphine administration or 60 min after other drugs, which were given either alone or in combination. Control mice received saline instead of drugs. The cut-off imposed was 10 s to prevent tissue damage. The antinociceptive response of each mouse was calculated as MPE.

Acetic acid-induced writhing

Writhing was induced by the i.p. injection of 0.5 ml per mouse of acetic acid [0.6% (v/v) in saline] and the abdominal constrictions were counted for 20 min thereafter. Results were expressed as number of abdominal constrictions per mouse. Morphine and all the other drugs used were administered, respectively, 30 min and 60 min before acetic acid. Control animals received appropriate volumes of saline by different routes (i.p., p.o., s.c.). Saline was given by single or multiple administrations according to the drug treatment schedule. Since the number of abdominal constrictions in these groups did not differ significantly, the corresponding data were cumulated and shown as controls in the Results section (see Figures 4 and 5).

Locomotor activity

Locomotor activity was recorded for 20 min in an activity cage (Basile, Italy). Mice were acclimatized to the activity cage at least once prior to starting the experimental session. Morphine and all other drugs used were administered, respectively, 30 and 60 min before the session.

Sensorimotor performance

To evaluate the muscle-relaxing and sedative effects of drugs, the mice were tested on a Rotarod (Rosland *et al.*, 1990). Briefly, the Rotarod apparatus (Basile, Italy) consists of a rod 30 cm long and 3.0 cm in diameter, subdivided into five compartments by discs 24 cm in diameter. The rod rotated at a constant speed of 16 r.p.m. Sensorimotor performance was assessed 30 min after morphine administration or 60 min after L-NAME or L-arginine, which were given either alone or in combination. Results are expressed as percentage of animals that succeeded in remaining on the rod for 45 s, which was the cut-off time.

Statistical analysis

Results are expressed as mean ± s.e.mean of 6–18 animals. Statistical comparisons were made using the Student's *t*-test. *P*-values less than 0.05 were considered statistically significant.

Results

Hot plate

L-Arginine or D-arginine, up to 1000 mg kg^{-1} p.o., did not modify mouse nociception. Thus the MPEs in these groups were respectively 0.5 ± 2.6 and 3.8 ± 2.1 ($n = 6$ for each group) and were similar to those observed in control mice (1.7 ± 2.0, $n = 6$).

Morphine caused a dose-dependent increase in the reaction time (Figure 1). The MPEs after 5 and 10 mg kg^{-1} morphine were 47.0 ± 3.5 ($n = 18$, $P<0.01$) and 82.8 ± 6.4 ($n = 18$, $P<0.01$) respectively.

L-Arginine (100–1000 mg kg^{-1} p.o.), but not D-arginine (up to 1000 mg kg^{-1}) reduced, in a dose-related manner, morphine-induced antinociception. Similar results were obtained when L-arginine was administered i.p. (data not shown). In contrast, L-arginine when given i.c.v. (0.08 mg per mouse) was ineffective in reducing the effect of 5 or 10 mg kg^{-1} morphine (MPEs 50.3 ± 6.8 and 85.7 ± 7.0 respectively, $n = 6$ for each group).

L-NAME (10, 30 mg kg^{-1}), but not D-NAME (30 mg kg^{-1}), produced a slight antinociceptive effect which was significant at the highest dose (MPE 19.5 ± 5.0, $n = 12$, $P<0.01$). This effect was reversed by 1000 mg kg^{-1} p.o. L-arginine (MPE 2.4 ± 1.3, $n = 6$, $P<0.01$).

A combined treatment of L-arginine (p.o.) and L-NAME, depending on the dose ratio of these two drugs, reduced (dose ratio 1000:10), did not modify (dose ratio 300:10) or increased (dose ratio 300:30) the antinociceptive effect induced by 5 mg kg^{-1} morphine (Figure 2).

The ability of L-arginine (300 mg kg^{-1} p.o.) to reduce the antinociception induced by 5 mg kg^{-1} morphine was significantly antagonized by the administration of 50 mg kg^{-1} L-NMMA (MPE 45.8 ± 9.1, $n = 6$, $P<0.01$).

Tail-flick

No changes in tail-flick response were observed in mice treated with L-arginine or D-arginine (each group up to

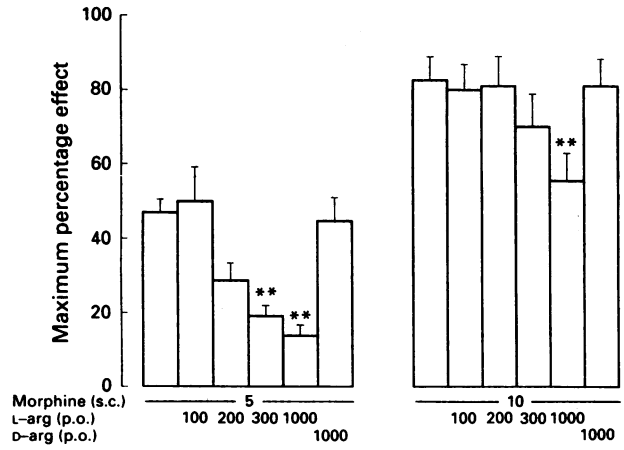


Figure 1 Effect of L-arginine (L-arg) and D-arginine (D-arg) on morphine-induced antinociception in mice assessed by the hot plate test. Doses are expressed in mg kg^{-1}. Each column represents the mean ± s.e.mean (vertical bar) of 6–18 animals. $^{**}P<0.01$ vs. morphine alone.

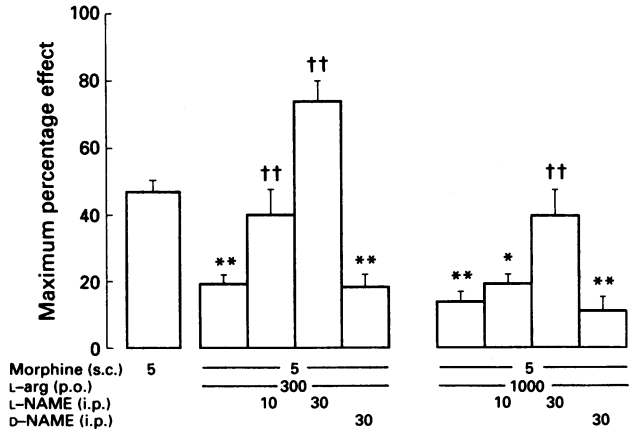


Figure 2 N^G-nitro-L-arginine methyl ester (L-NAME), but not N^G-nitro-D-arginine methyl ester (D-NAME), modulates the effect of L-arginine (L-arg) on morphine-induced antinociception in mice assessed by the hot plate test. Doses are expressed in mg kg^{-1}. Each column represents the mean ± s.e.mean (vertical bar) of 6–18 animals. $^{*}P<0.05$, $^{**}P<0.01$, vs. morphine alone; $\dagger\dagger P<0.01$, vs. morphine + L-arg.

1000 mg kg^{-1} p.o., $n = 6$). Thus the MPEs in these groups were respectively 2.4 ± 5.6 and 4.3 ± 3.1 and were not significantly different from those observed in control mice (3.5 ± 3.1, $n = 6$).

Morphine caused a dose-dependent increase in the reaction time (Figure 3). The MPEs after 2.5 or 5 mg kg^{-1} morphine were respectively 68.3 ± 12.4 ($n = 12$, $P<0.01$) and 91.2 ± 8.8 ($n = 6$, $P<0.01$).

L-Arginine (100–1000 mg kg^{-1} p.o.), but not D-arginine (1000 mg kg^{-1}), dose-dependently reduced the morphine effect on the tail-flick reflex.

The ability of L-arginine (300 mg kg^{-1} p.o.) to reduce the antinociception induced by 2.5 mg kg^{-1} morphine was significantly antagonized by the administration of 10 mg kg^{-1} L-NAME (MPE 74.5 ± 9.8, $n = 6$, $P<0.01$) or 30 mg kg^{-1} L-NMMA (MPE 65.2 ± 10.7, $n = 6$, $P<0.05$).

Acetic acid-induced writhing

Administration of 0.6% acetic acid (0.5 ml per mouse i.p.) in mice ($n = 18$) induced 51.0 ± 1.3 abdominal constrictions per mouse in the 20 min test period. L-Arginine or D-arginine treatment (up to 1000 mg kg^{-1} p.o.) did not modify the incidence of abdominal constrictions (53.2 ± 2.6 and 52.4 ± 4.1 respectively, $n = 6$ for each group). Morphine (0.5 mg kg^{-1}) significantly reduced by 55.9 ± 6.5% the number of abdominal constrictions ($P<0.01$, Figure 4). L-Arginine (100–1000 mg kg^{-1} p.o.), but not D-arginine (1000 mg kg^{-1}), dose-dependently reduced the effect of morphine. L-NAME (5 mg kg^{-1}) on its own did not modify the number of abdominal constrictions, whereas it was able to antagonize the L-arginine (300 mg kg^{-1} p.o.) effect on morphine-induced antinociception (Figure 5). Similar results were observed with L-NMMA (data not shown). *N*-Methylmorphine (5 mg kg^{-1}) significantly reduced the number of abdominal constrictions (25.4 ± 4.7, $n = 6$, $P<0.01$). L-Arginine (300 mg kg^{-1} p.o.) reversed the antinociceptive effect of this quaternarized morphine analogue (48.5 ± 4.8, $n = 6$, $P<0.01$).

Locomotor activity and sensorimotor performance

Locomotor activity of control mice was 730 ± 20 counts per session ($n = 6$). The administration of morphine (10 mg kg^{-1}), L-arginine (1000 mg kg^{-1} p.o.) or L-NAME (30 mg kg^{-1}), either alone or in combination, did not modify spontaneous activity. In fact, in these groups the locomotor activity ranged between 720 ± 23 counts and 746 ± 25 ($n = 6$ for each group).

The sensorimotor performance of control mice was 95.2 ± 4.8% ($n = 6$). The administration of morphine (10 mg kg^{-1}), L-arginine (1000 mg kg^{-1} p.o.) or L-NAME (30 mg kg^{-1}), either alone or in combination, did not modify sensorimotor performance. In fact, in these groups the percentage of animals with success in the Rotarod test ranged between 90.3 ± 6.7% and 97.4 ± 2.6% ($n = 6$ for each group).

Discussion

In this study we have shown that oral or intraperitoneal administration of L-arginine dose-dependently and stereospecifically reduces the antinociceptive effect of morphine assessed in mice using three different tests: hot plate, tail-flick and acetic acid-induced writhing.

L-Arginine is a substrate for NO synthase, the enzyme that releases NO from the terminal nitrogen atom(s) of the guanidino group of this amino acid (Moncada *et al.*, 1991). Since the L-arginine effect was reversed by concomitant

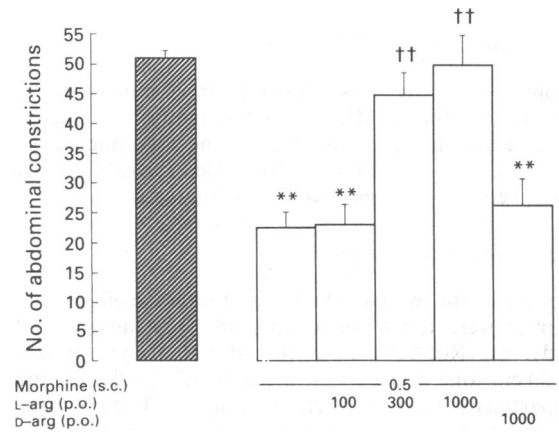


Figure 4 Effect of L-arginine (L-arg) and D-arginine (D-arg) on morphine-induced antinociception in mice assessed by the acetic acid-induced abdominal constrictions test. Doses are expressed in mg kg^{-1}. Each column represents the mean ± s.e.mean (vertical bar) of 6–18 animals. **$P<0.01$ vs. control (hatched column); ††$P<0.01$ vs. morphine alone.

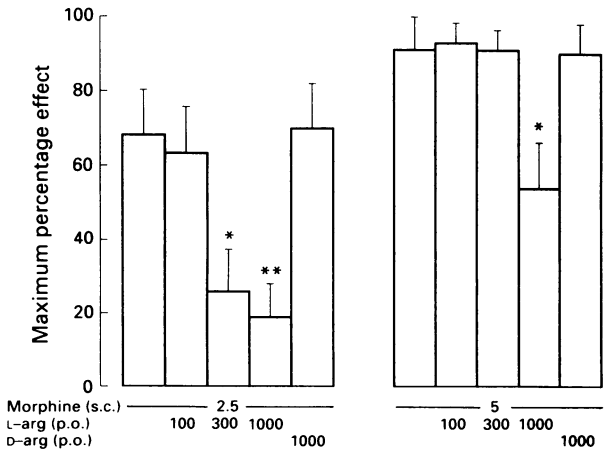


Figure 3 Effect of L-arginine (L-arg) and D-arginine (D-arg) on morphine-induced antinociception in mice assessed by the tail-flick test. Doses are expressed in mg kg^{-1}. Each column represents the mean ± s.e.mean (vertical bar) of 6–12 animals. *$P<0.05$, **$P<0.01$ vs. morphine alone.

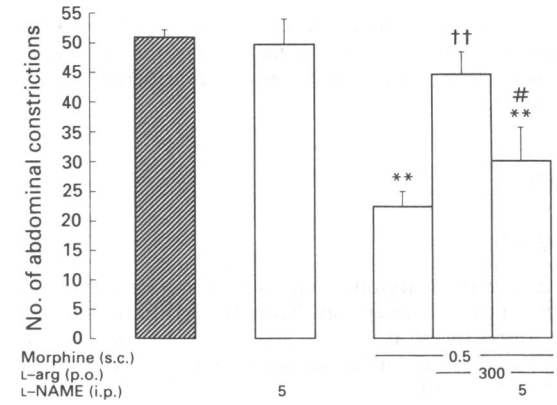


Figure 5 N^G-nitro-L-arginine methyl ester (L-NAME) modulates the effect of L-arginine (L-arg) on morphine-induced antinociception in mice assessed by the acetic acid-induced abdominal constrictions test. Doses are expressed in mg kg^{-1}. Each column represents the mean ± s.e.mean (vertical bar) of 6–18 animals. **$P<0.01$ vs. control (hatched column); ††$P<0.01$ vs. morphine alone; #$P<0.05$ vs. morphine + L-arg.

administration of competitive inhibitors of NO synthase such as L-NAME or L-NMMA (Rees *et al.*, 1990), our results strongly suggest that the reduction in morphine-induced antinociception by L-arginine is dependent on NO formation. This hypothesis is strengthened by the observation that neither D-arginine, which is not a substrate for NO synthase, nor D-NAME, which does not inhibit the NO synthase, was able to modify the antinociceptive effect of morphine.

Interestingly we have shown that following combined treatment with L-arginine and L-NAME, depending on the dose ratio of the two drugs, the antinociceptive effect of morphine was either unchanged, reduced or enhanced. Most likely, since both drugs compete for the active site of NO synthase, when a balanced dose combination of L-arginine and L-NAME was used the morphine effect was not modified, whereas when the dose ratio was shifted towards L-arginine the effect of the amino acid prevailed and the morphine effect was reduced. On the other hand, when the dose ratio was shifted towards L-NAME, this drug, even in the presence of L-arginine, was able to exhibit its own antinociceptive action and the morphine effect was increased. In this light it is interesting that low doses (1–2 mg kg^{-1} i.p.) of the NO synthase inhibitor N^G-nitro-L-arginine did not modify the antinociceptive effect of morphine (Kolesnikov *et al.*, 1992; Elliott *et al.*, 1994).

The involvement of NO in the nociceptive process is also supported by our results showing that L-NAME not only reversed the L-arginine effect, but produced a slight antinociceptive effect on its own, which is in agreement with previous reports (Moore *et al.*, 1991; Mustafa, 1992). We have also shown that the antinociceptive effect of L-NAME may be reversed by L-arginine.

L-NAME is a selective inhibitor of NO biosynthesis in a variety of mammalian tissue and cells, including both peripheral (Gibson *et al.*, 1990) and central neurones (Murad *et al.*, 1990). Although it has been suggested that L-NAME produces antinociception by a direct effect within the central nervous system (Moore *et al.*, 1991), L-NAME may also act on peripheral nerves where, according to our results, the interaction with L-arginine may take place.

It is important to point out that L-arginine also antagonizes the antinociceptive effect of *N*-methylmorphine in the acetic acid writhing test. This morphine derivative does not cross the blood–brain barrier and is therefore devoid of central effects.

The existence of a peripheral antinociceptive action of opiates is supported by several studies on the effects of quaternary analogues of opiates. It has been reported that *N*-methylmorphine induces an antinociceptive effect in the writhing test and in the hyperalgesia induced by prostaglandin E_2 in the rat paw (Smith *et al.*, 1982; Lorenzetti & Ferreira, 1982). Furthermore, Bentley *et al.*, (1981) have shown that opiate receptors are present in the mouse peritoneum. Our results clearly suggest that the L-arginine–NO pathway modulates both the central and peripheral antinociceptive effects of morphine and that this modulation operates at peripheral sites. In fact, the interaction between L-arginine and morphine does not occur at supraspinal sites because in the hot plate test, which is widely believed to be sensitive solely to drugs acting supraspinally (Yaksh & Rudy, 1977), the amino acid was ineffective when given i.c.v. Furthermore we have shown that morphine-induced constipation in the mouse, which mainly depends on action(s) within the central nervous system (Schulz *et al.*, 1979), is modulated by L-arginine acting at peripheral sites (Calignano *et al.*, 1991). However, a spinal interaction cannot be ruled out. Indeed, an involvement of NO in spinally mediated hyperalgesia has been described (Kitto *et al.*, 1992; Meller *et al.*, 1992a,b). Our results showing that L-arginine reverses the antinociceptive effect of *N*-methylmorphine in acetic acid-induced writhing suggest that endogenous NO may well play a role in the modulation of peripheral pain mechanism(s).

It has been reported that NO mediates both the peripheral and central antinociceptive effects of morphine evaluated using a modification of the Randall–Sellitto rat paw pressure test (Ferreira *et al.*, 1991; Duarte & Ferreira, 1992). The reason for the discrepancy may be related to differences between species or nociceptive stimuli.

Since animal models of nociception may be influenced by factors such as muscle relaxation, sedation or behaviour of the animals, we also investigated the possible sedative and behavioural effects of the drugs used. At the maximum doses used in the nociceptive assays, morphine, L-NAME and L-arginine, either alone or in combination, did not modify the spontaneous locomotor activity of animals or their performances in the Rotarod test.

We have previously shown that L-arginine modulates other morphine effects in mice. Thus, morphine-induced constipation is reduced by L-arginine, whereas this amino acid increases the effects of morphine on locomotor activity and food intake (Calignano *et al.*, 1991; 1993). Therefore it appears that L-arginine reduces morphine-induced antinociception by mechanisms other than interference with the absorption/distribution of the opioid. In conclusion, our results further support the hypothesis that NO is involved in the modulation of morphine effects and suggest that the L-arginine–NO pathway modulates morphine-sensitive nociceptive processes. Further studies will clarify the possible mechanism(s) of the modulatory role played by L-arginine in morphine-induced effects.

References

BENTLEY, G.A., NEWTON, S.H. & STARR, J. (1981). Evidence for an action of morphine and the enkephalins on sensory nerve endings in the mouse peritoneum. *Br. J. Pharmacol.*, **73**, 325–332.

BREDT, D.S., HWANG, P.M. & SNYDER, S.H. (1990). Localization of nitric oxide synthase indicating a neural role for nitric oxide. *Nature*, **347**, 768–770.

CALIGNANO, A., MONCADA, S. & DI ROSA, M. (1991). Endogenous nitric oxide modulates morphine-induced constipation. *Biochem. Biophys. Res. Comm.*, **181**, 889–893.

CALIGNANO, A., PERSICO, P., MANCUSO, F. & SORRENTINO, L. (1993). Endogenous nitric oxide modulates morphine-induced changes in locomotion and food intake in mice. *Eur. J. Pharmacol.*, **231**, 415–419.

D'AMOUR, F.E. & SMITH, D.L. (1941). A method for determination of pain sensation. *J. Pharmacol. Exp. Ther.*, **72**, 74–79.

DEWEY, W.L., HARRIS, L.S., HOWES, J.F. & NUITE, J.A. (1970). The effect of various neurohumoral modulators on the activity of morphine and the narcotic antagonists in the tail-flick and phenylquinone tests. *J. Pharmacol. Exp. Ther.*, **175**, 435–442.

DUARTE, I.D.G. & FERREIRA, S.H. (1992). The molecular mechanism of central analgesia induced by morphine or carbachol and the L-arginine-nitric oxide-cGMP pathway. *Eur. J. Pharmacol.*, **221**, 171–174.

EDDY, N.B. & LEIMBACK, D. (1953). Synthetic analgesics. II. Dithienylbutenyl and dithienylbutylamines. *J. Pharmacol. Exp. Ther.*, **107**, 385–393.

ELLIOTT, K., MINAMI, N., KOLESNIKOV, Y.A., PASTERNAK, G.W. & INTURRISI, C.E. (1994). The NMDA receptor antagonists, LY274614 and MK-801, and the nitric oxide synthase inhibitor, N^G-nitro-L-arginine, attenuate analgesic tolerance to the mu-opioid morphine but not to kappa opioids. *Pain*, **56**, 69–75.

FERREIRA, S.H., DUARTE, I.D.G. & LORENZETTI, B.B. (1991). The molecular mechanism of action of peripheral morphine analgesia: stimulation of the cGMP system via nitric oxide release. *Eur. J. Pharmacol.*, **201**, 121–122.

GIBSON, A., MIRZAZADEH, S., HOBBS, A.J. & MOORE P.K. (1990). L-N^G-Monomethyl arginine and L-N^G-nitroarginine inhibit non-adrenergic, non-cholinergic relaxation of the mouse anococcygeus. *Br. J. Pharmacol.*, **99**, 602–606.

HALEY, J.E., DICKENSON, A.H. & SCHACTER, M. (1992). Electrophysiological evidence for a role of nitic oxide in prolonged chemical nociception in the rat. *Neuropharmacology*, **31**, 251–258.

HONG, M., SUTAK, M. & JHAMANDAS, K. (1993). Inhibition of spinal opioid antinociception by intrathecal β-endorphin$_{1-27}$ in the rat. *Br. J. Pharmacol.*, **108**, 1137–1142.

KITTO, K.F., HALEY, J.E. & WILCOX, G.L. (1992). Involvement of nitric oxide in spinally mediated hyperalgesia in the mouse. *Neurosci. Lett.*, **148**, 1–5.

KOLESNIKOV, Y.A., PICK, C.G., & PASTERNAK, G.W. (1992). N^G-Nitro-L-arginine prevents morphine tolerance. *Eur. J. Pharmacol.* **221**, 399–400.

LORENZETTI, B.B. & FERREIRA, S.H. (1982). The analgesic effect of quaternary analogues of morphine and nalorphine. *Brazil. J. Med. Biol. Res.*, **15**, 285–290.

MELLER, S.T. & GEBHART, G.F. (1993). Nitric oxide (NO) and nociceptive processing in the spinal cord. *Pain*, **52**, 127–136.

MELLER, S.T., DYKSTRA, C. & GEBHART, G.F. (1992a). Production of endogenous nitric oxide and activation of soluble guanylate cyclase are required for *N*-methyl-D-aspartate-produced facilitation of the nociceptive tail-flick reflex. *Eur. J. Pharmacol.*, **214**, 93–96.

MELLER, S.T., PECHMAN, P.S., GEBHART, G.F. & MAVES, T.J. (1992b). Nitric oxide mediates the thermal hyperalgesia produced in a model of neuropathic pain in the rat. *Neuroscience*, **50**, 7–10.

MONCADA, S., PALMER, R.M.J. & HIGGS, E.A. (1991). Nitric oxide: physiology, patophysiology, and pharmacology. *Pharmacol. Rev.*, **43**, 109–142.

MOORE, P.K., OLUYOMI, A.O., BABBEDGE, R.C., WALLACE, P. & HART, S.L. (1991). L-N^G-Nitro arginine methyl ester exhibits antinociceptive activity in the mouse. *Br. J. Pharmacol.*, **102**, 198–202.

MURAD, F., POLLOCK, J.S., SCHMIDT, H.H.H.W., FORSTERMANN, U., ISHII, K., HEILER, M. & GORSKY, I.D. (1990). Characterization and purification of a rat brain enzyme which catalyses the formation of an EDRF-like factor from L-arginine. *Eur. J. Pharmacol.*, **183**, 647–648.

MUSTAFA, A.A. (1992). Mechanisms of L-N^G-nitro arginine methyl ester-induced antinociception in mice: a role for serotonergic and adrenergic neurons. *Gen. Pharmacol.*, **23**, 1117–1182.

PORRECA, F., MOSBERG, H.I., HURST, R., HRUBY, V.J. & BURKS, T.F. (1994). Roles of mu, delta and kappa opioid receptors in spinal and supraspinal mediation of gastrointestinal transit effects and hot-plate analgesia in the mouse. *J. Pharmacol. Exp. Ther.*, **230**, 341–348.

PRZEWLOCKI, R., MACHELSKA, H. & PRZEWLOCKA, B. (1993). Inhibition of nitric oxide synthase enhances morphine antinociception in the rat spinal cord. *Life Sci.*, **53**, PL 1–5.

REES, D.D., PALMER, R.M.J., SCHULZ, R., HODSON, H.F. & MONCADA, S. (1990). Characterization of three inhibitors of endothelial nitric oxide synthase *in vitro* and *in vivo*. *Br. J. Pharmacol.* **101**, 746–752.

ROSLAND, J.H., HUNSKAAR, S. & HOLE, K. (1990). Diazepam attenuates morphine antinociception test-dependently in mice. *Pharmacol. Toxicol.*, **66**, 382–386.

SCHULZ, R., WUSTER, M. & HERZ, A. (1979). Centrally and peripherally mediated inhibition of intestinal motility by opioids. *Naunyn Schmied. Arch. Pharmacol.*, **308**, 255–260.

SMITH, T.W., BUCHAN, P., PARSONS, D.N. & WILKINSON, S. (1982). Peripheral antinociceptive effects of N-methyl morphine. *Life Sci.*, **31**, 1205–1208.

YAKSH, T.L. & RUDY, T.A. (1977). Studies on the direct spinal action of narcotics on the production of analgesia in the rat. *J. Pharmacol. Exp. Ther.*, **202**, 411–428.

(Received May 24, 1994
Revised August 3, 1994
Accepted August 9, 1994)

Br. J. Pharmacol. (1994), **113**, 1377–1385 © Macmillan Press Ltd, 1994

Mechanism of the cardiovascular activity of laudanosine: comparison with papaverine and other benzylisoquinolines

Susana Chuliá, M. Dolores Ivorra, *Claire Lugnier, †Elisabeth Vila, M. Antonia Noguera & [1]Pilar D'Ocon

Laboratorio de Farmacognosia y Farmacodinamia, Departamento de Farmacologia, Facultad de Farmacia, Universitat de Valencia, Spain; *Laboratoire de Pharmacologie Cellulaire et Moléculaire, Faculté de Pharmacie, Université Louis Pasteur de Strasbourg, CNRS URA 600, BP 24, 67401 Illkirch, France and †Laboratorio de Farmacologia, Departament de Farmacologia i Psiquiatria, Universitat Autònoma de Barcelona, Bellaterra, Spain

1 The activity of (±)-laudanosine, a benzyltetrahydroisoquinoline alkaloid, was investigated in pithed rats and rat isolated aorta. Its effects on [^{3}H]-prazosin, [^{3}H]-(+)-*cis*-diltiazem and [^{3}H]-nitrendipine binding to rat cerebral cortical membranes, and on the different molecular forms of cyclic nucleotide phosphodiesterases (PDE) isolated from bovine aorta were investigated.

2 The dose-response curve to methoxamine (3–300 μg kg^{-1}, i.v.) in normotensive pithed rats was shifted to the right by (±)-laudanosine, 3 and 6 mg kg^{-1}.

3 (±)-Laudanosine inhibited in a concentration-dependent manner the contractile responses evoked by noradrenaline (NA 1 μM), depolarizing solution (KCl 80 mM) or depolarizing solution plus phentolamine (10 μM) in rat isolated aorta. The alkaloid appeared to be more potent against NA-induced contractions.

4 In Ca^{2+}-free solution, (±)-laudanosine (100 μM) inhibited the contraction evoked by NA and did not modify the phasic contractile response evoked by caffeine. The alkaloid did not modify the refilling of the intracellular Ca^{2+}-stores sensitive to NA or caffeine.

5 (±)-Laudanosine inhibited [^{3}H]-prazosin binding to cortical membranes and also inhibited [^{3}H]-(+)-*cis*-diltiazem but with a lower potency. [^{3}H]-nitrendipine binding was not affected by laudanosine.

6 (±)-Laudanosine does not have a significant effect on the different forms of PDEs isolated from bovine aorta. In contrast, compounds structurally related to this alkaloid such as papaverine and its derivatives, had a non-selective or more specific inhibitory effect on these PDE forms. These differences can be explained on the basis of their structural features: the planarity of the isoquinoline ring (papaverine) facilitates the interaction with receptor sites, and the different position of the benzyl group does not modify the activity unless this position leads to the presence of a chiral centre (laudanosine).

7 These results suggest that (±)-laudanosine has a selective activity as an α_1-adrenoceptor blocker. Its lack of action on different PDE forms provides us with information about a group of benzylisoquinolines that with small structural changes show a different effect on PDE-forms isolated from vascular smooth muscle.

Keywords: Pithed rat; rat aorta; calcium antagonists; α_1-adrenoceptors blocking agents; benzyltetrahydroisoquinolines; phosphodiesterase inhibitors

Introduction

Recently, new structural classes of compounds related to the benzyltetrahydroisoquinoline structure have been reported to be Ca^{2+} channel blockers (King *et al.*, 1988; Triggle *et al.*, 1989; D'Ocon *et al.*, 1989; 1991; Ming Lu & Quing Lu, 1990; Lacroix *et al.*, 1991). Some of them, such as tetrandrine, laudanosine, glaucine and cularines, show a mechanism of uterine smooth muscle relaxant activity which is different from papaverine in spite of their structural relationship (D'Ocon *et al.*, 1991; Anselmi *et al.*, 1992). Papaverine acts at the intracellular level by a non-specific mechanism, whereas benzyltetrahydroisoquinolines relax smooth muscle by a more specific mechanism, including Ca^{2+} entry blocking activity, and have no effect on contractile machinery, Ca^{2+}-release or Ca^{2+}-redistribution from intracellular storage sites. This different interaction might be attributed to the geometry as well as to differences in the basicity of the heteroatom and could be responsible for the different behaviour of these compounds.

[1] Author for correspondence at: Departament de Farmacologia, Laboratorio de Farmacognosia i Farmacodinamia, Facultat de Farmacia, Universitat de Valencia, Avda Vincent Andrés Estelles s/n, 46100 Burjassot, Valencia, Spain.

The aim of the present work was to investigate the mechanism of the relaxant action of a benzyltetrahydroisoquinoline, laudanosine, in vascular smooth muscle and compare it to the relaxant action of papaverine.

Our previous studies with rat aorta showed that some aporphines with a benzyltetrahydroisoquinoline structure such as glaucine, boldine and apomorphine, possess not only Ca^{2+} entry blocking properties but also α_1-adrenoceptor antagonist activity, and therefore inhibit [^{3}H]-(+)-*cis*-diltiazem and [^{3}H]-prazosin binding, relax rat aorta previously contracted by addition of noradrenaline or KCl and inhibit some forms of cyclic AMP-phosphodiesterases (Ivorra *et al.*, 1992a,c). The present work includes *in vivo* experiments in pithed rats and functional studies on rat isolated aorta contracted by addition of noradrenaline, caffeine or KCl. In order to assess whether laudanosine interacts directly with Ca^{2+} channel receptors or α-adrenoceptors, we examined the effects of the alkaloid on [^{3}H]-nitrendipine, [^{3}H]-(+)-*cis*-diltiazem and [^{3}H]-prazosin binding to rat cerebral cortical membranes.

The present study also examines the question of whether laudanosine has any effects on cyclic nucleotide phosphodiesterase (PDE) activity, as papaverine does. In mammalian tissue cells, several distinct molecular forms of PDE exist (for

review see Beavo, 1988). Accordingly, we examined the ability of laudanosine to inhibit separate PDE enzymes isolated from bovine smooth muscle, and compared the results obtained to the action of a series of isoquinolines, structurally related to laudanosine, on PDE activity.

Methods

Pithed rat preparation

Rats (300–340 g) received atropine (1 mg kg^{-1}, i.p.) to prevent muscarinic activation; 15 min later they were pithed under diethyl ether anaesthesia by inserting a blunt steel rod (diameter 1.5 mm) through the orbit and foramen magnun down into the spinal canal (Shipley & Tilden, 1947). The trachea was cannulated and the animals were ventilated with room air (60 strokes min^{-1}, 20 ml kg^{-1} body wt.) the left jugular vein was cannulated for drug administration and arterial blood pressure was measured by a cannula placed in the right carotid artery. Bilateral vagotomy was also performed. The rats were allowed to stabilize for 15 min before the experiment was begun. Methoxamine (3–300 μg kg^{-1}), a selective α_1-adrenoceptor agonist (Kobinger & Pichler, 1980) was injected in single doses and sufficient time was allowed between them for blood pressure to return to preinjection levels. Dose-response curves induced by methoxamine before and 7 min after drug infusion (2 min) were determined.

Values are expressed as means ± s.e.mean. The statistical significance between groups was assessed by ANOVA followed by a Student's t test. A value of $P < 0.05$ was taken as significant.

Functional study

Helically cut strips from the thoracic aorta of male Wistar rats (200–220 g) were prepared and mounted as described by Furchgott & Zawadzki (1980). Each preparation was suspended in a 10 ml organ bath containing Krebs-bicarbonate solution (KBS), maintained at 37°C and gassed with 95% O_2 and 5% CO_2. An initial load of 1 g was applied to each preparation and maintained throughout a 75–90 min equilibration period before agonist addition. Tension was recorded isometrically on a polygraph (Grass M7) via force-displacement transducers (Grass FT03).

KBS had the following composition (mM): NaCl 118, KCl 4.75, $CaCl_2$ 1.8, $MgCl_2$ 1.2, KH_2PO_4 1.2, $NaHCO_3$ 25 and glucose 11. Ca-free solution had the same composition except that $CaCl_2$ was omitted and EDTA (0.1 mM) was added.

The absence of relaxant response after 100 μM acetylcholine addition in preparations previously contracted with noradrenaline 1 μM indicated the absence of a functional endothelium (Furchgott & Zawadzki, 1980).

Concentration-relaxation response curves were obtained by the addition of cumulative concentrations of laudanosine (0.1 μM–100 μM) once the sustained contractions had been reached with KCl (80 mM) in the presence or absence of phentolamine (10 μM) and noradrenaline (1 μM). Relaxations were expressed as a percentage of the maximum tension obtained by agonist addition. E_{max} values representing the maximal relaxation obtained after addition of the highest dose of the alkaloid were calculated. The concentration needed to produce 50% inhibition (IC_{50}) was also calculated for each preparation from a least squares regression analysis of all points between 20–80% of the maximal response.

Figure 1a shows the experimental procedure used to study the action of laudanosine on noradrenaline-induced contraction in the absence of extracellular calcium at 37°C. In order to clarify the intracellular action of laudanosine similar experimental procedures were performed but NA was replaced by caffeine (Figure 1b). In Ca-free medium, caffeine yielded a contraction only at 25°C but not at 37°C, so in protocols using caffeine as agonist, the temperature was decreased to 25°C.

After incubation for 1 h in KBS to stabilize the preparation, 1 μM noradrenaline or 10 mM caffeine was administered to contract the muscle, and the amplitude of the resulting contraction was monitored as a reference. The solution was then replaced by Ca^{2+}-free solution and left for 15 min before 1 μM noradrenaline or 10 mM caffeine was added and the contractile response monitored as a measure of the amount of Ca^{2+} released from the store sensitive to the agonist. After washing, a new addition of the agonist, noradrenaline or caffeine, did not elicit any contractile response. The solution was then replaced by normal KBS and left for 20 min to refill the depleted Ca^{2+} stores. Noradrenaline or caffeine were again administered after 15 min in Ca^{2+}-free solution and a new response to agonist was obtained similar in magnitude to the first one in Ca^{2+}-free medium. The effect of alkaloids was tested on the last agonist-induced contraction (Figure 1) or on the refilling process (Figure 2).

Contractile responses in Ca-free KBS were expressed as a percentage of the noradrenaline- or caffeine-induced contraction in normal KBS.

Results are expressed as the mean ± s.e.mean of n preparations obtained from different animals. Statistical significance of differences between the means was assessed by Student's t test. P-values of less than 0.05 were considered to represent significant differences.

Radioligand binding experiments

Membranes were prepared from cerebral cortex of male Wistar rats as previously described (Schott et al., 1988). Briefly, the tissue was homogenized in 10 vol (w/v) of ice-cold buffer (50 mM Tris-HCl, pH 7.5) in an ultra-turrax (twice, 15 s). The homogenate was centrifuged at 40,000 g at 4°C for 10 min and the resulting pellet was washed by resuspension and centrifugation under the same conditions. The final pellet

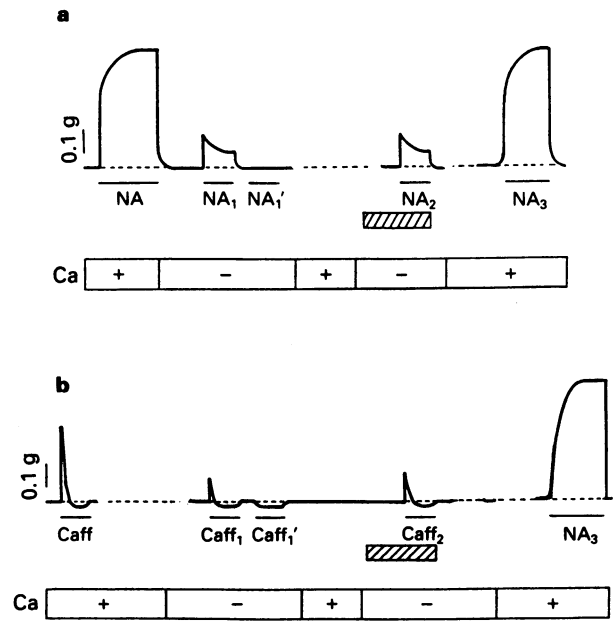


Figure 1 Experimental procedure used to study the effect of laudanosine or papaverine in the absence of extracellular calcium on noradrenaline-induced (NA) contraction (a) or caffeine-induced (Caff) contraction (b) in the absence of extracellular Ca^{2+}. NA_1 or $Caff_1$: addition of the agonist after 15 min incubation in Ca^{2+}-free medium. NA_1' or $Caff_1'$: second addition of the agonist after washing (W) in Ca^{2+}-free medium. NA_2 or $Caff_2$: addition of the agonist in presence or absence of the alkaloid 3×10^{-5} M, after 20 min resting period in KBS (Ca^{2+} 1.8 mM) and 15 min in Ca^{2+}-free solution. NA_3: addition of the agonist after a resting period in KBS (20 min).

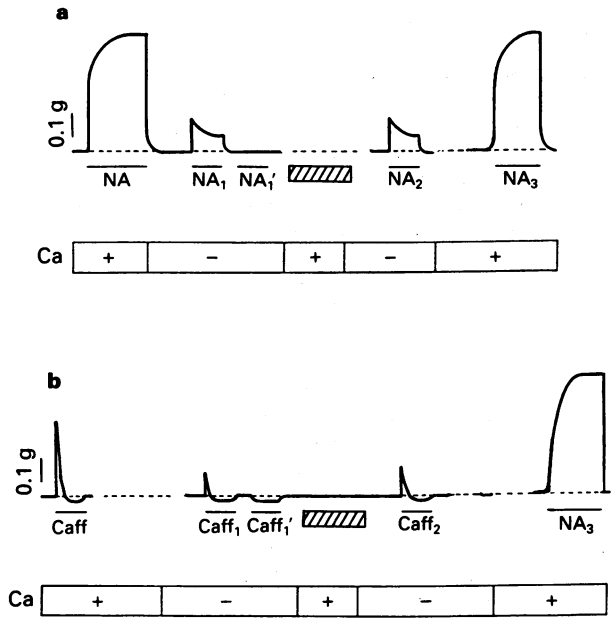


Figure 2 Experimental procedure used to study the effect of laudanosine or papaverine on the refilling of intracellular calcium stores previously depleted by noradrenaline (NA) (a) or caffeine (Caff) (b). NA_1 or $Caff_1$: addition of the agonist after 15 min incubation in Ca^{2+}-free medium. NA_1' or $Caff_1'$: second addition of the agonist after washing (W) in Ca^{2+}-free medium. NA_2 or $Caff_2$: addition of the agonist after 20 min resting period in KBS (Ca^{2+} 1.8 mM) in presence or absence of the alkaloid 3×10^{-5} M, and 15 min in Ca^{2+}-free solution.

was resuspended in incubation buffer to give a final protein concentration of about 1 mg ml^{-1}. Membrane aliquots (250 µl) were incubated in a final volume of 500 µl in 50 mM Tris-HCl (pH 7.5) with [^{3}H]-prazosin (0.1–0.2 nM) or [^{3}H]-nitrendipine (0.3–0.4 nM) or in 50 mM Tris-HCl pH 7.5 containing bovine serum albumin (BSA) 1 mg ml^{-1} with [^{3}H]-(+)-*cis*-diltiazem (3–4 nM), in the absence or in the presence of drugs at various concentrations.

Incubations were carried out at 25°C for 30 min ([^{3}H]-prazosin), 90 min ([^{3}H]-nitrendipine) or 120 min ([^{3}H]-(+)-*cis*-diltiazem), after which the reaction was terminated by the addition of 3.0 ml ice-cold buffer and rapid filtration over Whatman GF/B filters that were washed with 9 ml (3 × 3 ml) of ice-cold buffer. For [^{3}H]-(+)-*cis*-diltiazem binding experiments, filters were pretreated for 120 min with polyethylenimine 0.3%. The radioactivity bound to the filters was determined by liquid scintillation counting. Non-specific binding was determined in the presence of phentolamine (10^{-6} M) nifedipine (10^{-6} M) or diltiazem (10^{-5} M), respectively. All determinations were performed in triplicate.

Displacement curves were analysed by a computerized non-linear curve-fitting program (Graph-Pad) and K_i values were calculated from the formula of Cheng & Prusoff (1973).

Phosphodiesterase inhibition

Cytosolic cyclic nucleotide phosphodiesterases (PDE) were isolated from the media layer of bovine aorta by a modification of the methods of Lugnier *et al.* (1986). Briefly, the tissue was homogenized in 10 vol (w/v) isotonic buffer A (25 mM sodium phosphate pH 6.6; 250 mM saccharose; 2 mM magnesium acetate (MgAc); 1 mM dithiothreitol; 5 mM ethylene glycol *bis* (β-aminoethylether) *N,N,N',N'* tetraacetic acid (EGTA); 2000 u ml^{-1} aprotinin; 10 µg ml^{-1} soya bean trypsin inhibitor and 10 µg ml^{-1} leupeptin) using an ultraturrax (six times, 10 s) and a glass pestle homogenizer, and then centrifuged at 105,000 *g* for 60 min. The resulting supernatant fraction was applied to a diethylaminoethyl (DEAE)-Sephacel ion-exchange column and eluted by buffer B (25 mM phosphate pH 6.6; MgAc 2 mM and dithiothreitol 1 mM) until no absorbance was detected in the eluate at 280 nm. Elution was then continued with a linear gradient of 0–0.55 M of NaCl in buffer B (flow rate 25 ml h^{-1}). Each fraction was tested for PDE activity.

Since DEAE-Sephacel did not allow the separation of calmodulin-PDE (type I) from cyclic GMP-PDE (type V) as did DEAE-Trisacryl chromatography (Lugnier *et al.*, 1986), a further high performance liquid chromatography (h.p.l.c.) repurification was done. The first peak was then injected into an h.p.l.c. column (TSK-DEAE-5PW), washed for 20 min with elution buffer (25 mM phosphate pH 6.6) and eluted (0.8 ml min^{-1}) by a linear NaCl gradient (0.05–0.3 M) in elution buffer. Fractions under each PDE activity peak were pooled, dialyzed against buffer (20 mM Tris-HCl, 2 mM MgAc pH 7.5) and stored in aliquots at – 80°C with bovine serum albumin (BSA).

PDE activities were measured by the two-stage assay described by Wells *et al.* (1975) at a substrate ([^{3}H]-cyclic AMP or [^{3}H]-cyclic GMP) concentration of 1 µM, in the following buffer: 50 mM Tris-HCl pH 7.5, 2 mM MgAc, 1 mg ml^{-1} BSA and in the presence of 10 µM $CaCl_2$ and 18 nM calmodulin or in the absence of Ca^{2+} and calmodulin but with 1 mM EGTA. To prevent the influence of cross-contamination between CGI-PDE (Type III) and cyclic AMP-PDE (Type IV), the studies performed with these forms were always carried out in the presence of 100 µM rolipram or 100 µM cyclic GMP, respectively.

The IC_{50} (concentration which produced 50% inhibition of substrate hydrolysis) for the compounds studied was determined from the concentration-response curves obtained with five concentrations of inhibitor and calculated by a non-linear regression. The apparent K_i values were obtained according to Cheng & Prusoff (1973). Results are expressed as mean ± s.e.mean of three determinations made in duplicate using three different enzymatic preparations.

Drugs and solutions

The following drugs were used: atropine sulphate, (–)-noradrenaline L-tartrate and acetylcholine (Merck); anhydrous caffeine, laudanosine, papaverine, cyclic AMP and cyclic GMP (Sigma Chemical Co); phentolamine methanesulphonate (Ciba-Geigy), methoxamine HCl (Gayoso Wellcome), diethyl ether (Panreac).

[^{3}H]-prazosin (20.2 Ci mmol^{-1}), [^{3}H]-nitrendipine (70 Ci mmol^{-1}), [8-^{3}H]cyclic AMP (30–50 Ci mmol^{-1}) and [8-^{3}H]-cyclic GMP (5–15 Ci mmol^{-1}) were purchased from the New England Nuclear. [^{3}H]-(+)-*cis*-diltiazem (154 Ci mmol^{-1}) was obtained from Amersham.

Other reagents were of analytical grade.

Caffeine was dissolved in Ca-free KBS. The other drugs were dissolved in saline adjusted to pH 7.

Results

Pithed rats

The resting diastolic blood pressure of normotensive pithed rats was 47 ± 3.9 mmHg, $n = 15$. Intravenous administration of methoxamine (3 to 300 µg kg^{-1}) to control rats caused a dose-dependent increase in diastolic blood pressure (DBP) (Figure 3a and b). Injection of papaverine but not laudanosine at 3 and 6 mg kg^{-1} induced a transient decrease of blood pressure (10–15 mmHg) with a return to basal levels in 2–3 min. The dose-response curve induced by methoxamine was shifted to the right (Figure 3a) by 3 and 6 mg kg^{-1} laudanosine. Lower doses (0.3–1 mg kg^{-1}) were without effect on methoxamine-induced DBP responses. Systemic administration of papaverine (3–6 mg kg^{-1}) diminished in a

dose-dependent manner the methoxamine (100–300 μg kg^{-1})-induced DBP increases without affecting the pressure responses to lower doses of the α_1-adrenoceptor agonist. However, the decrease by papaverine (3 mg kg^{-1}) of the pressor response to methoxamine (100 μg kg^{-1}) did not reach statistical significance. In addition, papaverine (0.3 and 1 mg kg^{-1}) did not modify the pressor responses to methoxamine (results not shown).

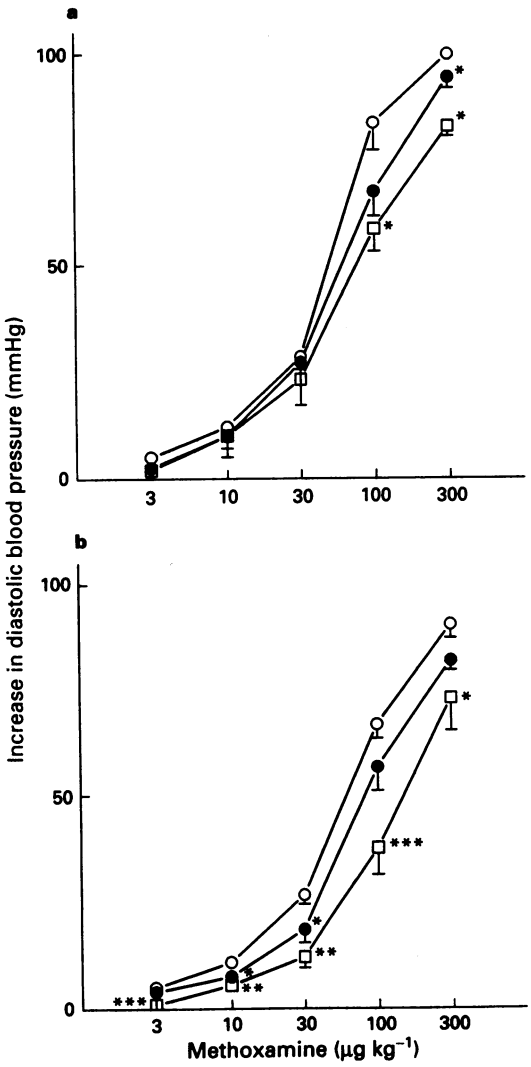


Figure 3 Increases in diastolic blood pressure in pithed rats induced by administration of single doses of methoxamine (3–300 μg kg^{-1}) before (○) and 7 min after: (a) papaverine 3 mg kg^{-1} (●) or 6 mg kg^{-1} (□); (b) laudanosine 3 mg kg^{-1} (●) or 6 mg kg^{-1} (□). Papaverine has been evaluated on 4 animals and laudanosine on 6–11 animals. s.e.mean are shown by vertical bars. ***$P < 0.001$, **$P < 0.01$, *$P < 0.05$.

Functional study

Effects of laudanosine and papaverine on noradrenaline- or KCl-induced contractions in KBS The contractile response of rat aorta elicited by depolarizing solution (KCl 80 mM) at 37°C was 792.9 ± 34.3 mg ($n = 7$). The same contraction elicited in the presence of phentolamine (10^{-5} M) at 37°C was smaller (590.8 ± 43.1 mg, $n = 7$, 74.3 ± 3.8% of the control).

Noradrenaline (1 μM) produced a sustained contraction in rat isolated thoracic aorta incubated in KBS at 37°C (735.4 ± 90.6 mg, $n = 8$). This dose of noradrenaline has proved to be maximal for contraction in rat aorta (Noguera & D'Ocon, 1992).

Laudanosine (0.1–300 μM) produced concentration-dependent relaxations of KCl-depolarized rat aorta at 37°C both in the presence and absence of phentolamine, but the parameters (E_{max} and IC_{50}) of the concentration-response curves showed significant differences (Table 1) suggesting that the relaxant action of this alkaloid depends both on α-adrenoceptor blocking activity and a decrease in the Ca^{2+} entry through voltage-dependent channels.

Addition of cumulative concentrations of laudanosine (0.1–100 μM) to the aorta contracted by noradrenaline (1 μM) in KBS induced concentration-dependent relaxations confirming results obtained with the KCl-induced contraction but the IC_{50} was lower against NA-induced contraction (Table 1).

Papaverine caused relaxation of the KCl-, KCl plus phentolamine- or NA-induced contractile response of rat aorta and the E_{max} or IC_{50} were similar in each case (Table 1).

Effects of laudanosine and papaverine on noradrenaline- or caffeine-induced contractions in a Ca^{2+}-free medium After 15 min in Ca^{2+}-free solution, addition of noradrenaline (1 μM) induced a phasic contraction followed by a tonic one (NA_1). The addition of noradrenaline for a second time in Ca^{2+}-free solution (NA_2) induced a significantly lower contractile response in the presence of laudanosine and this response was totally abolished in the presence of papaverine (100 μM) (Table 2, Figure 1a).

At 25°C, caffeine 10 mM induced a rapid transient contraction in Ca^{2+} 1.8 mM solution (210.1 ± 21.6 mg, $n = 16$). Addition of caffeine after 15 min of exposure to a Ca^{2+}-free solution yielded a phasic contraction ($Caff_1$). After washing, addition of caffeine did not induce any contractile response. After a loading period (20 min) in KBS to refill the intracellular Ca^{2+}-stores, caffeine-induced contraction in Ca^{2+}-free medium (15 min) was restored ($Caff_2$). Preincubation (10 min) with laudanosine (100 μM) did not modify the phasic contractile response induced by caffeine in Ca^{2+}-free medium whereas papaverine (100 μM) decreased this contraction ($Caff_2$; Table 2; Figure 1).

Effects of laudanosine and papaverine on the refilling of intracellular Ca^{2+} stores sensitive to noradrenaline or caffeine In order to clarify the intracellular action of laudanosine and

Table 1 Inhibitory potencies of alkaloids on contractions induced by noradrenaline 1 μM (NA), KCl (80 mM) or KCl (80 mM) plus phentolamine (10 μM) in rat aorta

		NA	*KCl*	*KCl + pH*	*IC_{50} (KCl + Ph)/IC_{50} (NA)*
Papaverine	E_{max} (%)	111.5 ± 8.3	104.8 ± 8.5	100.1 ± 3.4	
		$n = 7$	$n = 6$	$n = 4$	
	IC_{50} (μM)	3.7 ± 0.9	5.6 ± 0.9	3.2 ± 0.4	0.865
Laudanosine	E_{max} (%)	94.4 ± 2.9	69.8 ± 3.0*	56.5 ± 2.9*	
		$n = 5$	$n = 6$	$n = 7$	
	IC_{50} (μM)	11.5 ± 2.3	37.2 ± 5.1*	80.6 ± 8.0*	7.009

Values are means ± s.e.mean.
*Significant difference ($P < 0.001$) from the corresponding values on NA-induced contraction.
n = number of experiments.

Table 2 Effects of agents (10^{-4} M) on noradrenaline (NA) or caffeine (Caff) induced contraction of rat aorta in Ca^{2+}-free medium (experimental protocol see Figure 1)

Agonist		*NA*		*Caff*	
A_1	*phasic*	21.8 ± 2.3	23.2 ± 2.6	32.9 ± 4.9	44.0 ± 2.6
	tonic	10.3 ± 1.3	10.7 ± 2.5	–	–
		Laudanosine	*Papaverine*	*Laudanosine*	*Papaverine*
A_2 + alkaloid	*phasic*	7.9 ± 0.9*	0	38.1 ± 5.7	11.0 ± 1.1*
	tonic	5.6 ± 1.1*	0	–	–
		$n = 7$	$n = 4$	$n = 5$	$n = 3$

% are calculated from the initial contraction by agonist in Krebs solution.
Values are mean ± s.e.mean.
n = number of experiments.
*$P < 0.001$ from A1.

Table 3 Effects of agents (10^{-4} M) on the refilling of intracellular Ca^{2+}-stores sensitive to noradrenaline (NA) or caffeine (Caff) (experimental protocol see Figure 2)

Agonist		*NA*		*Caff*	
A_1	*phasic*	24.3 ± 2.2	27.5 ± 3.6	47.7 ± 8.4	39.2 ± 1.5
	tonic	8.6 ± 1.2	11.4 ± 3.4	–	–
Refilling		*Laudanosine*	*Papaverine*	*Laudanosine*	*Papaverine*
A_2	*phasic*	21.3 ± 1.1	0	42.2 ± 9.8	
	tonic	7.1 ± 1.1	0	–	–
		$n = 6$	$n = 4$	$n = 6$	$n = 3$

% are calculated from the initial contraction by agonist in Krebs solution.
Values are mean ± s.e.mean.
n = number of experiments.

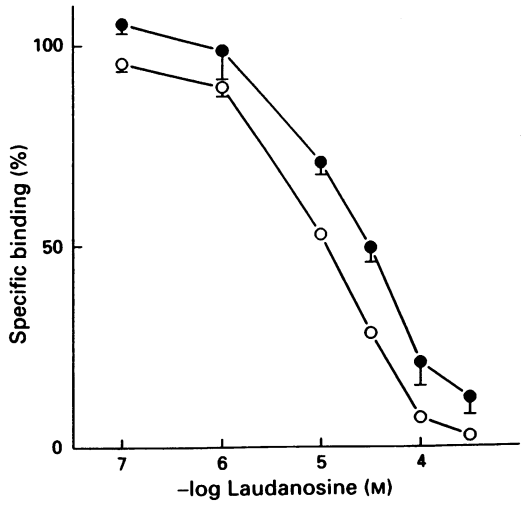


Figure 4 Displacement curves of [^{3}H]-prazosin (○) or [^{3}H]-(+)-*cis* diltiazem specific binding (●) by laudanosine. Each point is the mean from three experiments made in triplicate with s.e.mean shown by vertical bars.

papaverine, similar experimental procedures were carried out but the alkaloids were added during the loading period in Ca^{2+}-containing KBS (20 min) after depletion of the intracellular stores sensitive to noradrenaline or caffeine (Figure 2). In these experimental conditions, subsequent addition of noradrenaline or caffeine in Ca^{2+}-free solution (NA_2 or $Caff_2$) induced no contraction after papaverine treatment but similar contractile responses after loading in the presence of laudanosine (Table 3).

Binding assays

The interactions of laudanosine with [^{3}H]-prazosin and [^{3}H]-(+)-*cis*-diltiazem binding are shown in Figure 4. Laudanosine fully inhibited [^{3}H]-prazosin binding to cortical membranes, with an inhibition constant of 5.92 ± 0.69 μM. The fact that the pseudo-Hill coefficient (slope factor) was not significantly different from unity ($n_H = 0.95 \pm 0.04$) suggests direct competition between laudanosine and the radioligand for a single common binding site. In addition, laudanosine inhibited binding of [^{3}H]-(+)-*cis*-diltiazem but with a lower potency ($K_i = 26.29 \pm 4.96$ μM) and with a similar pseudo-Hill slope ($n_H = 0.91 \pm 0.13$). This suggests that the interaction between laudanosine and [^{3}H]-(+)-*cis*-diltiazem is also a simple competition for a single common binding site.

[^{3}H]-nitrendipine binding was not affected by laudanosine in concentrations up to 100 μM (results not shown).

Inhibition of bovine aorta cyclic nucleotide phosphodiesterase enzymes

As shown in Table 4, laudanosine does not have a significant effect on the different forms of PDEs. In contrast, papaverine exerted a relatively non-selective inhibitory effect on all PDE forms although the inhibition of the calmodulin-sensitive form (PDE I) appeared weaker than that of the others.

Discussion

Papaverine, a benzylisoquinoline alkaloid, is a well-known spasmolytic agent and its action is ascribed to inhibition of phosphodiesterases (Lugnier *et al.*, 1972; Bolton, 1979; Cumiskey & Feigenson, 1983), the subsequent increase in cyclic AMP and cyclic GMP levels and modification of intracellular Ca^{2+} distribution. Furthermore, there is evidence that it may also antagonize Ca^{2+} influx (Schneider *et al.*, 1975; Reinhardt *et al.*, 1977) and act on α-adrenoceptors (Ivorra *et al.*, 1992c).

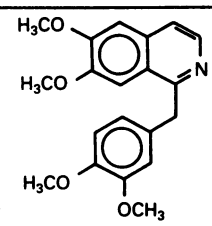
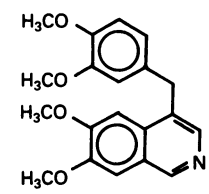
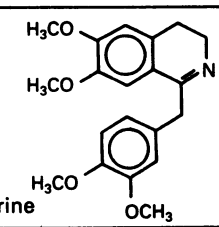
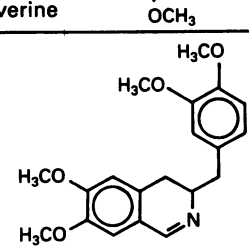
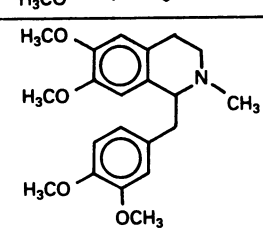
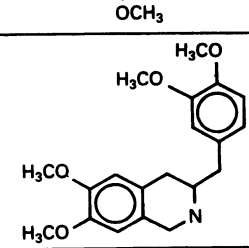
The results of our previous work on the structure-activity relationship of benzylisoquinoline alkaloids has made it possible to divide them into two groups, the first one containing those that have an unsaturated heterocyclic ring, like papaverine, and the second one formed by compounds with a

tetrahydroisoquinoline ring. The latter group exhibits a more specific activity (Cortes *et al.*, 1990; D'Ocon *et al.*, 1991; Anselmi *et al.*, 1992) and the selectivity implies that these tetrahydroisoquinoline alkaloids, unlike papaverine, act mainly on the Ca^{2+} influx from the extracellular medium without producing changes in the intracellular distribution of this ion. This more specific action on calcium entry, was accompanied by a loss in the activity of these alkaloids as PDEs inhibitors.

The above observations prompted us to examine the potential activity of laudanosine, an alkaloid with a benzyltetrahydroisoquinoline ring, and we assayed this alkaloid in the present study on different experimental models including *in vivo* and *in vitro* preparations.

Our *in vivo* experiments were carried out in the pithed rat which is devoid of central cardiovascular reflexes and has been proved to be a suitable model for studying the effects of drugs on α-adrenoceptors in the periphery. The results

Table 4 Inhibition constants (K_i μM) of agents on cyclic nucleotide phosphodiesterases isolated from bovine aorta

		CaM-PDE type I	*cGMP-PDE type V*	*cAMP-PDE type IV*
BIQ	 Papaverine	27.5	1.08	0.89
	 Compound 1	20	0.5	1.37
BDHIQ	 Dihydropapaverine	>100	18.9	8.2
	 Compound 2	>100	33.6	>100
BTHIQ	 Laudanosine	>100	>100	>100
	 Compound 3	>100	>100	95.0

Values are given as mean ± s.e.mean from three determinations obtained on different enzymatic preparations. Apparent K_i values were calculated from IC_{50} values according to Cheng & Prusoff (1973). Phosphodiesterase activity was assessed with 1 μM of [^{3}H]-cyclic GMP + 10 μM $CaCl_2$ + 18 nM calmodulin for CaM-PDE; [^{3}H]-cyclic GMP + 1 mM EGTA for cGMP-PDE and [^{3}H]-cyclicAMP + 1 mM EGTA for cAMP-PDE

BIQ = benzylisoquinoline; BDHIQ = benzyldehydroisoquinoline; BTHIQ = benzyltetrahydroisoquinoline.

obtained in this study with methoxamine, a selective α_1-adrenoceptor agonist, suggest that laudanosine has α_1-adrenoceptor antagonist activity in the pithed rat, results that agree with those obtained in rat isolated aorta (present study). However, when we studied the effect of papaverine on methoxamine-induced pressor responses the alkaloid behaved as a non-competitive antagonist.

We assayed the action of laudanosine on contractions of the rat aorta which are mediated by: (1) Ca^{2+}-entry through potential operated channels (KCl-induced contraction); (2) Ca^{2+}-entry induced by α-adrenoceptor activation (noradrenaline-induced contraction); (3) release of intracellular Ca^{2+} (EDTA-resistant response to noradrenaline or caffeine).

KCl has been shown to produce a biphasic contraction in the rat aorta (Sakata & Karaki, 1991) depending exclusively upon extracellular Ca^{2+} (Marriott, 1988). The fact that in the presence of phentolamine the contractile response induced by KCl is smaller also indicates participation of catecholamine release in the contraction elicited by depolarization in rat aorta.

Contractions induced by high concentrations of noradrenaline are also biphasic: the early fast component of contraction depends upon release of intracellular Ca^{2+}, while the slowly developing sustained phase of contraction depends upon influx of extracellular Ca^{2+} (Marriott, 1988). Accordingly, under Ca^{2+}-free conditions, a smaller contraction may be induced in the rat aorta by noradrenaline and this must be mediated by intracellular Ca^{2+}-release from internal stores (Noguera & D'Ocon, 1992, 1993). On repeated exposure to noradrenaline, this contraction was not observed, which suggests that the Ca^{2+} store was of limited size and that re-sequestration of released Ca^{2+} was relatively inefficient.

A similar contraction has been observed after addition of caffeine in Ca^{2+}-free medium, but different mechanisms are evoked. The noradrenaline-induced release of intracellular Ca^{2+} is attributable to α_1-adrenoceptor activation (Chiu *et al.*, 1987; Daly *et al.*, 1990), whereas caffeine releases Ca^{2+} from the same intracellular store as noradrenaline does (Noguera & D'Ocon, 1992), but through a different mechanism (Itoh *et al.*, 1983; Sato *et al.*, 1988).

Laudanosine and papaverine relax the contractile responses of rat aorta to noradrenaline or KCl in KBS solution, but analysis of the E_{max} and $IC_{50}(KCl)/IC_{50}(NA)$ ratios provides information on selectivity (Table 1) and indicates that laudanosine exhibits greater inhibition of the contractile response induced by NA than KCl, whereas papaverine relaxes both agents in a non-selective way, as described in an earlier paper (Ivorra *et al.*, 1992c). The fact that the IC_{50} of laudanosine on the contractile response induced by KCl was different in the presence and absence of phentolamine indicates that the relaxant action shown by this alkaloid is complex and depends both on α-adrenoceptor blocking activity and a decrease in the Ca^{2+} entry through voltage-dependent channels.

The selectivity shown by laudanosine on NA-induced contraction in KBS was checked in experiments carried out in a Ca^{2+}-free medium. In these conditions, papaverine inhibited the contractile response induced by NA or caffeine, thus confirming its non-specific relaxant activity. Furthermore, when this alkaloid was added during the loading period that permits the refilling of intracellular Ca^{2+}-stores previously depleted by NA or caffeine, posterior addition of these agonists does not induce any contractile response. This indicates that stores cannot be refilled in the presence of papaverine.

Results were different with laudanosine: this alkaloid inhibits NA-induced contractile responses in Ca^{2+}-free medium, but this effect is not attributable to direct inhibition of the smooth muscle contractile elements or release of the intracellular Ca^{2+}-stores because the same concentration of alkaloid did not inhibit caffeine-induced contraction. This confirms the selectivity of laudanosine as an α-adrenoceptor blocking agent. Moreover, laudanosine does not inhibit the refilling of intracellular stores sensitive to NA or caffeine, which suggests a lack of activity on Ca^{2+}-entry pathways depending on previous depletion of internal Ca^{2+} pools.

Results obtained in the functional study suggest that the inhibitory effect of laudanosine on NA-induced contraction may be due to antagonism of α_1-adrenoceptors or inhibition of receptor-mediated signal transduction. The relaxation induced by this alkaloid on KCl-induced contraction in the presence of phentolamine suggests a direct inhibition of calcium entry as other benzylisoquinolines does (Ivorra *et al.*, 1992a,c). In order to ascertain whether there is an interaction between laudanosine and the α_1-adrenoceptor or a receptor site at the Ca^{2+} channel, we studied this possible interaction by radioligand binding techniques. The results obtained indicate that laudanosine interacts with [^{3}H]-prazosin and [^{3}H]-(+)-*cis*-diltiazem binding to rat cerebral cortex, although it showed a higher affinity for the α_1-adrenoceptor binding site than for the benzothiazepine receptor site. Laudanosine does not interact with the [^{3}H]-nitrendipine binding site.

Analysis of the action of laudanosine on the [^{3}H]-prazosin binding site, shows that the K_i is in the same range as the IC_{50} obtained from concentration-response curves of laudanosine on NA-induced contraction. These findings provide us with experimental evidence that laudanosine acts as an α_1-adrenoceptor antagonist with a lower action as calcium entry blocker. Papaverine showed similar specificity to act by both mechanisms.

It is known that the mechanism of the relaxant action of papaverine is related to inhibition of PDEs. In order to determine whether inhibition of PDE is involved in the relaxant response to laudanosine, we tested the effect of this compound on PDE activities isolated from bovine aorta.

There are several molecular forms of PDE identified in smooth muscle. In vascular smooth muscle, four types of cyclic nucleotide phosphodiesterases (PDE) have been isolated: types I and V, which selectively hydrolyze cyclic GMP, and types III and IV, with a high affinity for cyclic AMP (Lugnier *et al.*, 1986; Lindgren *et al.*, 1990; Komas *et al.*, 1991; Ivorra *et al.*, 1992b). Papaverine is a relatively non-selective inhibitor of these PDE forms and our results show that laudanosine does not exhibit any potent inhibitory action on the different PDE forms differing from papaverine. Present findings clearly suggest that laudanosine has a relaxant effect on rat aorta, which is mediated by interaction with the α_1-adrenoceptor and the benzothiazepine receptor site at the Ca^{2+} channel, but the inhibition of PDE shown by other benzylisoquinolines like papaverine does not in this case explain the relaxation induced by laudanosine. We must therefore conclude that there are differences between the mechanisms of the relaxant action of the two alkaloids in spite of their structural similarity.

In this context, previous studies (Lugnier *et al.*, 1992; 1994) tested different benzylisoquinoline derivatives as inhibitors of the three PDE forms, and the results obtained indicated that papaverine and its analogues (Compound 1, Table 4) containing an unsaturated heterocyclic ring are the most potent inhibitors of all PDE-forms. The presence of a tetrahydroisoquinoline ring (Compound 4 and laudanosine) implies a loss of activity as PDE-inhibitors. This different behaviour can be explained on the basis of their structural features. The benzyltetrahydroisoquinoline (BTHIQ) alkaloids such as laudanosine, have an sp^3-like hybridized nitrogen atom, a partially flexible tetrahydroisoquinoline ring and a chiral centre. Papaverine, a benzylisoquinoline (BIQ) has an sp^2-like nitrogen atom, a planar isoquinoline ring and no chiral centre. The benzyldihydroisoquinolines (BDHIQ) analysed have an sp^2-like nitrogen like papaverine, a partially unsaturated isoquinoline ring and no chiral centre (3,4 dihydropapaverine) or just one (compound 2). These structural features define the geometry of the molecules and can explain the existence of different types of interactions between these agents and the receptor site in the different PDE forms.

Table 4 illustrates how the presence of a chiral centre leads to a loss of effect of the compounds tested on all PDE-forms. The planarity of the isoquinoline ring facilities the interaction with receptor sites because the more active compounds were benzylisoquinolines with a totally or partially unsaturated heterocyclic ring (benzylisoquinolines or benzyldehydroisoquinolines). The different position of the benzyl group does not modify the activity unless this difference determines the presence of a chiral centre (compound 2).

These results provide us with information about a group of compounds that with small structural changes showed a selective action on each PDE-form isolated from vascular smooth muscle. Further investigations using these compounds could identify the physiological role of each PDE-form in smooth muscle contractile process.

We would like to thank Ms C. Schott for her excellent technical assistance in the binding experiments and Mr A. Le Bec for helpful contribution in the PDE isolation. This work was supported by a research grant from the Spanish Comisión Interministerial de Ciencia y Tecnología (SAF92-0647).

References

ANSELMI, E., FAYOS, G., BLASCO, R., CANDENAS, M.L., CORTES, D. & D'OCON, M.P. (1992). Selective inhibition of calcium entry induced by benzylisoquinolines in smooth muscle. *J. Pharm. Pharmacol.*, **44**, 337–343.

BEAVO, J.A. (1988). Multiple isozymes of cyclic nucleotide phosphodiesterase. In: *Advances in Second Messenger and Phosphoprotein Research*. Vol. 22, ed. Greengard, P. & Robinson, G.A. pp. 1–38. New York: Raven Press.

BOLTON, T.B. (1979). Mechanism of action of transmitters and other substances on smooth muscle. *Physiol. Rev.*, **85**, 606–719.

CHENG, Y.C. & PRUSOFF, W.H. (1973). Relationship between the inhibition constant (K_i) and the concentration of inhibitor which causes 50 per cent inhibition (I_{50}) of an enzymatic reaction. *Biochem. Pharmacol.*, **22**, 3099–3108.

CHIU, A.T., BOARTH, J.M. & TIMMERMANS, P. (1987). Relationship between phosphatidylinositol turnover and Ca mobilization induced by α_1-adrenoceptor stimulation in the rat aorta. *J. Pharmacol. Exp. Ther.*, **240**, 123–127.

CORTES, D., TORRERO, M.Y., D'OCON, M.P., CANDENAS, M.L., CAVE, A. & HADI, A.H.A. (1990). Norstephalagine et atherospermidine, deux aporphines d'*Artabotrys maingayi* relaxantes du muscle lisse. *J. Nat. Prod.*, **53**, 503–508.

CUMISKEY, W.R. & FEIGENSON, M.E. (1983). Spasmolitic activity of cinnamedrine and papaverine in isolated rat uterine muscle. *Arch. Int. Pharmacodyn. Ther.*, **263**, 113–119.

DALY, C.J., DUNN, W.R., MCGRATH, C.J., MILLER, D.J. & WILSON, V.G. (1990). An examination of sources of calcium for contractions mediated by postjunctional α_1- and α_2-adrenoceptors in several blood vessels isolated from the rabbit. *Br. J. Pharmacol.*, **99**, 253–260.

D'OCON, M.P., BLASCO, R., CANDENAS, M.L., IVORRA, M.D., LOPEZ, S., VILLAVERDE, C., CASTEDO, L. & CORTES, D. (1991). Inhibition of calcium entry induced by cularines and isocrasifoline in uterine smooth muscle. *Eur. J. Pharmacol.*, **196**, 183–187.

D'OCON, M.P., CANDENAS, M.L., ANSELMI, E., ZAFRA-POLO, M.C. & CORTES, D. (1989). Antioquine: a new bisbenzylisoquinoline alkaloid with calcium antagonist activity. *Arch. Int. Pharmacodyn. Ther.*, **297**, 205–216.

FURCHGOTT, R.F. & ZAWADZKI, J.V. (1980). The obligatory role of endothelial cells in the relaxation of arterial smooth muscle by acetylcholine. *Nature*, **288**, 373–376.

ITOH, T., KURIYAMA, H. & SUZUKI, H. (1983). Differences and similarities in the noradrenaline- and caffeine-induced mechanical responses in the rabbit mesenteric artery. *J. Physiol.*, **337**, 609–629.

IVORRA, M.D., CHULIA, S., LUGNIER, C. & D'OCON, M.P. (1992a). Selective action of two aporphines at α_1-adrenoceptors and potential-operated calcium channels. *Eur. J. Pharmacol.*, **231**, 165–174.

IVORRA, M.D., LE BEC, A. & LUGNIER, C. (1992b). Characterization of membrane-bound cyclic nucleotide phosphodiesterases from bovine aortic smooth muscle. *J. Cardiovasc. Pharmacol.*, **19**, 532–540.

IVORRA, M.D., LUGNIER, C., SCHOTT, C., CATRET, M., NOGUERA, M.A., ANSELMI, E. & D'OCON, M.P. (1992c). Multiple actions of glaucine on cyclic nucleotide phosphodiesterases, α_1-adrenergic receptor and benzothiazepine receptor site at the calcium channel. *Br. J. Pharmacol.*, **106**, 387–394.

KING, V.F., GARCIA, M.L., HIMMEL, D., REUBEN, J.P., LAM, Y.T., PAN, J., HAN, G. & KACZOROWSKI, G.J. (1988). Interaction of tetrandrine with slowly inactivating calcium channels. *J. Biol. Chem.*, **263**, 2238–2244.

KOBINGER, W. & PICHLER, L. (1980). Investigation into different types of post and presynaptic α-adrenoceptors at cardiovascular site in rats. *Eur. J. Pharmacol.*, **65**, 393–402.

KOMAS, N., LUGNIER, C. & STOCLET, J.C. (1991). Endothelium dependent and independent relaxation of the rat aorta by cyclic nucleotide phosphodiesterase inhibitors. *Br. J. Pharmacol.*, **104**, 495–503.

LACROIX, P., LINEE, P. & FOREST, M.C. (1991). Diproteverine (BRL 40015): a new type of calcium antagonist with potential antianginal properties. *Eur. J. Pharmacol.*, **192**, 317–327.

LINDGREN, S., RASCON, A., DEGERMAN, E., BELFRAGE, P., MANGIANELLO, V. & ANDERSSON, K.E. (1990). Identification of the cyclicGMP-inhibited low Km cyclicAMP phosphodiesterase in rat aortic smooth muscle. *Eur. J. Pharmacol.*, **183**, 806–811

LUGNIER, C., BERTRAND, Y. & STOCLET, J.C. (1972). Cyclic nucleotide phosphodiesterase inhibition and vascular smooth muscle relaxation. *Eur. J. Pharmacol.*, **19**, 134–136.

LUGNIER, C., DORE, J.CH., STOCLET, J.C. & VIEL, C. (1992). Utilisation de techniques multiparamétriques pour analyser la spécificité de différents inhibiteurs vis-à-vis de plusieurs formes de phosphodiestérases des nucléotides cycliques. *Pharmazie*, **47**, 46–49.

LUGNIER, C., DORE, J.C. & VIEL, C. (1994). Inhibition of cyclic nucleotide phophodiesterases from bovine aorta by papaverine analogues: a multivariate approach. *Eur. J. Med. Chem.* (in press).

LUGNIER, C., SCHOEFFTER, P., LE BEC, A., STROUTHON, E. & STOCLET, J.C. (1986). Selective inhibition of cyclic nucleotide phosphodiesterases of human, bovine and rat aorta. *Biochem. Pharmacol.*, **35**, 1743–1751.

MARRIOTT, J.F. (1988). A comparison of the effects of the calcium entry blockers, verapamil, diltiazem and flunarizine against contractions of the rat isolated aorta and portal vein. *Br. J. Pharmacol.*, **95**, 145–154.

MING LU, Y. & QUING LU, G. (1990). The effects of (−)daurisoline on Ca^{2+} influx in presynaptic nerve terminals. *Br. J. Pharmacol.*, **101**, 45–48.

NOGUERA, M.A. & D'OCON, M.P. (1992). Different and common intracellular calcium-stores mobilized by noradrenaline and caffeine in vascular smooth muscle. *Naunyn-Schmied. Arch. Pharmacol.*, **435**, 333–341.

NOGUERA, M.A. & D'OCON, M.P. (1993). Evidence that depletion of internal stores sensitive to noradrenaline elicits a contractile response dependent on extracellular calcium in rat aorta. *Br. J. Pharmacol.*, **110**, 861–867.

REINHARDT, D., ROGGENBACH, W., SCHMIDT, U. & SCHUMANN, H.J. (1977). Effects of papaverine on the frequency-force relationship in guinea-pig left atria. *Eur. J. Pharmacol.*, **41**, 123–126.

SAKATA, K. & KARAKI, H. (1991). Effects of a novel smooth muscle relaxant, KT-362, on contraction and cytosolic Ca^{2+} level in the rat aorta. *Br. J. Pharmacol.*, **102**, 174–178.

SATO, K., OZABE, H. & KARAKI, H. (1988). Multiple effects of caffeine on contractions and cytosolic free Ca levels in vascular smooth muscle of rat aorta. *Naunyn-Schmied. Arch. Pharmacol.*, **333**, 443–448.

SCHNEIDER, J.A., BROOKER, G. & SPERELAKIS, N. (1975). Papaverine blockade of an inward Ca^{2+} current in guinea-pig heart. *J. Mol. Cell. Cardiol.*, **7**, 867–871.

SCHOTT, C., TETSI, L., HEITZ, C., STAMBACH, J.F., JUNG, L. & STOCLET, J.C. (1988). Stereoselective blockade of α-adrenoceptors by berbine derivatives. *Arzneim-Forsch. Drug. Res.*, **38**, 11, 1567–1571.

SHIPLEY, R. & TILDEN, J.H. (1947). A pithed rat preparation suitable for assaying pressor substances. *Proc. Soc. Exp. Biol.*, **64**, 453–455.

TRIGGLE, D.J., LANGS, D.A. & JANIS, R.A. (1989). Ca-channels ligands: structure-function relationships of the 1,4-dihydropyridines. *Med. Res. Rev.*, **9**, 123–180.

WELLS, J.W., BAIRD, C.E., WU, V.J. & HARDMAN, J.G. (1975). Cyclic nucleotide phosphodiesterase activity of pig coronary arteries. *Biochem. Biophys. Acta*, **384**, 430–442.

(Received February 11, 1994
Revised July 20, 1994
Accepted July 27, 1994)

Br. J. Pharmacol. (1994), **113**, 1386–1390 © Macmillan Press Ltd, 1994

Characterization of the adenosine receptors mediating hypothermia in the conscious mouse

[1]R. Anderson, M.J. Sheehan & P. Strong

Department of Cellular Sciences, Glaxo Research and Development Ltd., Park Road, Ware, Hertfordshire SG12 0DP

1 The effects of a range of adenosine receptor-selective ligands on body temperature were investigated following intracerebroventricular (i.c.v.) and intraperitoneal (i.p.) injection in conscious mice. The compounds tested were the non-selective adenosine receptor agonist 5'-N-ethyl-carboxamidoadenosine (NECA), the adenosine A_1 receptor-selective agonists cyclopentyl-adenosine (CPA), N^6-(9**R**-phenyl-isopropyl)-adenosine (**R**-PIA) and N-(1S,*trans*)-[2-hydroxycyclopentyl]-adenosine (GR79236), the A_{2a} receptor selective agonist 2-[*p*-(2-carboxyethyl)phenethylamino]-5'-N-ethylcarboxamidoadenosine (CGS-21680), the A_{2b} receptor agonist N-[(2-methylphenyl)methyl]adenosine (metrifudil) and the A_3 receptor agonist N^6-(4-aminophenylethyl)adenosine (APNEA).

2 NECA (0.01–1 μg, i.c.v.), all of the A_1-selective agonists (0.01–1 μg, i.c.v.) and APNEA (0.1–3 μg i.c.v.) produced profound and dose-related hypothermia and sedation. However, CGS-21680 (0.1–10 μg i.c.v.) and metrifudil (0.01–1 μg i.c.v.), produced only mild hypothermia at the highest doses tested.

3 The hypothermic response to the A_1 receptor-selective agonists, GR79236 and **R**-PIA was dose-dependently antagonized by peripheral administration of either the non-selective adenosine receptor antagonist, 8-phenyltheophylline (8-PT, approximately 40 and 30 fold rightward shifts of the dose-response curves respectively at 10 mg kg^{-1}, i.p.), or the adenosine A_1 receptor-selective antagonist, 8-cyclopentyl-1,3-dipropylxanthine (DPCPX, approximately 20 fold shift of the GR79236 dose-response curve at 1 mg kg^{-1}, i.p.). The hypothermic response to APNEA was similarly dose-dependently antagonized by the A_1 receptor-selective antagonist, DPCPX (5 fold shift at 0.1 mg kg^{-1}, i.p.).

4 8(*p*-Sulphophenyl)theophylline (8-SPT, 10 and 30 mg kg^{-1}, i.p.), a non-selective adenosine receptor antagonist that penetrates the blood brain barrier poorly, produced only modest antagonism (approximately 2 fold shift at 30 mg kg^{-1}, i.p.) of the hypothermic response to GR79236.

5 These data suggest that hypothermia induced by adenosine analogues in the conscious mouse is mediated via adenosine A_1 receptors, which are probably located in the CNS.

Keywords: Hypothermia; adenosine receptors; mouse; N-(1S,*trans*)-[2-hydroxycyclopentyl]adenosine (GR79236), N^6-(4-aminophenylethyl)adenosine (APNEA)

Introduction

Adenosine is an endogenous purine that plays an important role in regulating neuronal excitability. It is released from nerves under conditions of prolonged activity or hypoxia to act at specific cell membrane receptors to modify neuronal activity (Fredholm & Hedqvist, 1980). Adenosine inhibits neurotransmitter release from many neurones including cholinergic, adrenergic and dopaminergic cells through a combination of effects on intracellular adenosine 3':5'-cyclic monophosphate (cyclic AMP) accumulation, calcium and potassium ion fluxes (Fredholm & Dunwiddie, 1988). The actions of adenosine are mediated via distinct extracellular receptors. These receptors have been classified into two major categories, A_1 and A_2, based on their opposing actions on adenylate cyclase, tissue distribution and structure-activity relationships (Hamprecht & Van Calker, 1985). Generally, activation of A_1 receptors inhibits adenylate cyclase via inhibitory G-proteins, and receptors are located in high densities in the cerebral cortex, hippocampus and striatum (Fastbom *et al.*, 1987) and in lower densities in the periphery. In contrast, activation of A_2 receptors stimulates adenylate cyclase activity, and receptors are highly localized in the striatal region, nucleus accumbens and olfactory tubercle (Jarvis & Williams, 1989). The development of the agonist CGS-21680 (2-[*p*-(2-carboxyethyl)phenethylamino]-5'-*N*-ethylcarboxamido adenosine) has facilitated adenosine A_2 receptor sub-classification into two subtypes, A_{2a} receptors with high affinity for CGS-21680 and A_{2b} receptors with low affinity for this compound (Jarvis & Williams, 1989; Hutchison *et al.*, 1990; Gurden *et al.*, 1993). More recently, techniques in molecular biology have identified an adenosine A_3 receptor subtype (Zhou *et al.*, 1992) at which N^6-(4-aminophenylethyl) adenosine (APNEA) acts as an agonist.

Administration of adenosine analogues in mice produces a cluster of physiological effects which include reduced locomotor activity (Barraco *et al.*, 1983), sedation and hypothermia (Yarbrough & McGuffin-Clineschmidt, 1981; Zarrindast & Heidari, 1993). The hypothermic effects of peripherally administered adenosine and 2-chloroadenosine were blocked by the non-selective adenosine antagonists, caffeine and theophylline (Mehta & Kulkarni, 1983). To our knowledge, the specific adenosine receptors mediating this response have not been identified. Accordingly, in the present study the effects of a range of adenosine receptor-selective ligands on body temperature have been investigated in the conscious mouse in order to characterize further the adenosine receptors involved in this response.

Methods

All experiments were performed on conscious male, 8–12 g, weanling CRH mice bred by Glaxo Research and Development Ltd. Agonists or vehicle were administered by intracerebroventricular (i.c.v.) injection at the area fontanelle by means of Hamilton Gas Tight Syringes (Lot No 1704) with

[1] Author for correspondence.

Luer-Lock fitting hypodermic needles (1/8"). The dose volume was 3 μl. Once dosed, the animals were housed individually in observation beakers and monitored for 30 min. Antagonist compounds were administered as intraperitoneal injections in 0.1 ml dose volume, 10 min prior to agonist dosing. Body (core) temperature was measured 30 min post dose with an oesophageal probe and thermocouple (Digiton Instruments Ltd.) 8-Phenyltheophylline (8-PT), 8(*p*-sulphophenyl)theophylline (8-SPT) and 8-cyclopentyl-1,3-dipropylxanthine (DPCPX) had no direct effect on body temperature at the doses used in this study.

Statistical analysis

Data points are the mean ± s.e.mean of at least six animals at each dose level. The statistical significance of agonist-induced variations from the control temperatures of vehicle-treated animals at 30 min post-dose was determined by one way analysis of variance followed by Dunnett's test. For antagonist studies, data points obtained in the presence of antagonist were compared with the agonist control curve. Sedation was quantified on an observer rating scale as either mild (reduced exploratory behaviour compared to control mice), moderate (only occasional movement around the observation beaker, lowered body posture) or severe (completely flattened body posture, low muscle tone, no movement around the beaker).

Drugs

The following drugs were used: 5'N-ethyl-carboxamidoadenosine (NECA), N-(1S,*trans*)-[2-hydroxycyclopentyl]-adenosine (GR79236, Glaxo Research and Development Ltd.), N^6-(9R-phenyl-isopropyl)-adenosine (R-PIA, Research Biochemicals Inc., batch PW-688B), cyclopentyladenosine (CPA, Glaxo Research and Development Ltd.), 2-[*p*-(2-carboxyethyl)phenethylamino]-5'-N-ethylcarboxamidoadenosine (CGS-21680, Research Biochemicals Inc., batch TB-791D), N-[(2-methylphenyl)methyl]adenosine (Metrifudil, Glaxo Research and Development Ltd), 8-phenyltheophylline (8-PT, Research Biochemicals Inc., batch PW-191C), N^6-(4-aminophenylethyl)adenosine (APNEA, Glaxo Research and Development Ltd.) 8(*p*-sulphophenyl)theophylline, (8-SPT, Research Biochemicals Inc., batch PW-190C), 8-cyclopentyl-1,3-dipropylxanthine (DPCPX, Cookson Chemicals Ltd., batch 1442). Agonist compounds were initially dissolved in a small volume of 1 M HCl and made up to volume with 0.9% (w/v) sodium chloride solution (saline). All further dilutions were made in saline. The final concentration of HCl in the injection fluid was 8 mM in experiments with metrifudil, and less than 1 mM for all other compounds. Control animals were injected with the same volume of the highest concentration of HCl in saline. The non-selective adenosine receptor antagonists, 8-PT and 8-SPT, were dissolved in 2 M sodium hydroxide, partially neutralized with 1 M HCl and made to volume with 0.9% sodium chloride solution to form stock solution concentrations of 1 and 3 mg ml^{-1} respectively. The adenosine A_1 receptor-selective antagonist DPCPX was dissolved in dimethylsulphoxide to form a stock solution concentration of 0.1 mg ml^{-1}.

Results

Time-course of hypothermia

Figure 1 shows the time-course of the hypothermic effects of the adenosine A_1 receptor-selective agonist GR79236 (0.3 μg, i.c.v.). GR79236 produced a rapid fall in body temperature in the first 10 min following injection which reached a minimum by 30 min post-dose and was maintained for at least 1 h. The sedative effect appeared to follow the same time-course. In view of this result, body temperature was routinely measured 30 min post-dose in subsequent studies. In contrast, the body temperature of mice injected with the most acidic vehicle used in this study did not vary significantly from the pre-dose value (Figure 1).

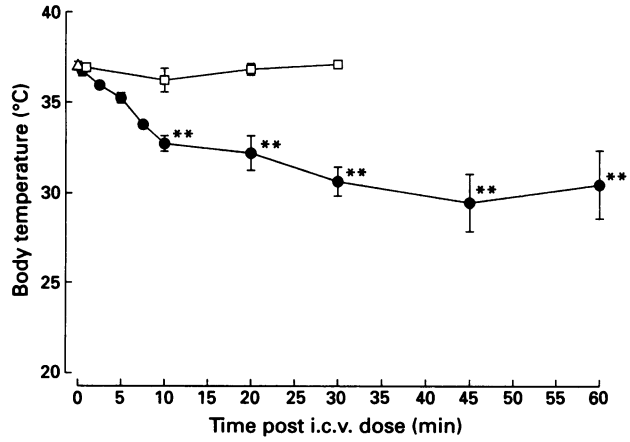


Figure 1 Time course of the hypothermic effects of GR79236 (●, 0.3 μg) and vehicle (□, 8 mM HCl) compared with pre-dose temperature (Δ) following i.c.v. injection in the conscious mouse. Data points are expressed as mean ± s.e.mean of 6 mice per dose group. Statistically significant (**$P<0.01$) reductions in body temperature were determined by one-way analysis of variance followed by Dunnett's test.

Agonist studies

In order to investigate the thermoregulatory effect of adenosine in mice, a range of adenosine analogues were tested over a dose range of 0.01–3 μg, i.c.v. (Figure 2). The non-selective adenosine receptor agonist, NECA, produced dose-dependent and profound hypothermia (Figure 2), and sedation which was rated as mild after 0.03 μg NECA, i.c.v., moderate after 0.1 μg and severe after 0.3 μg. The effects of NECA were mimicked by three adenosine A_1 receptor-selective agonists, CPA, GR79236 and R-PIA, and by the A_3 receptor agonist, APNEA. All five agonists produced a fall in body temperature of at least 6.5°C over a similar (100 fold) dose-range with an apparent molar rank order of agonist activity of NECA > GR79236 > CPA > R-PIA > APNEA. Each agonist also caused sedation in parallel with the degree of hypothermia.

In contrast, the adenosine A_{2a} receptor-selective agonist, CGS-21680 (0.1–10 μg) and the adenosine A_{2b} receptor agonist, metrifudil (0.01–1 μg) produced only mild sedation and hypothermia at the highest doses tested (Figure 2). For example CGS-21680, tested at 10 μg, produced a mean fall of 3.4°C (± 0.7°C; $n = 6$), whereas NECA, tested at 1 μg in the same experiment, produced a mean fall of 11.3°C (± 0.3°C; $n = 6$).

In a further study, GR79236 was administered peripherally as an i.p. injection over a dose-range of 0.1–3 mg kg^{-1}. GR79236 produced falls in body temperature of 0.1 ± 0.4, 3.3 ± 2.0, 12.8 ± 0.1 and 12.0 ± 0.4°C at 0.1, 0.3, 1.0 and 3.0 mg kg^{-1} i.p. respectively ($n = 6$ per dose group).

Antagonist studies

In order to investigate the specific adenosine receptors involved in the hypothermic action of adenosine, the effects of a range of adenosine receptor antagonists on agonist-induced hypothermia were investigated.

The sedative and hypothermic effects of the adenosine A_1 receptor-selective agonists GR79236 (Gurden *et al.*, 1993) and R-PIA were dose-dependently antagonized by peripheral administration of the non-selective adenosine receptor

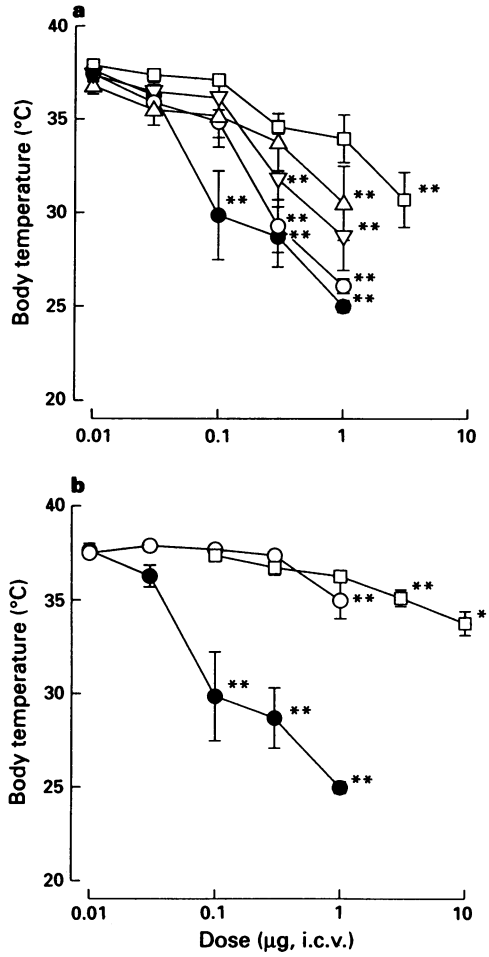


Figure 2 (a) Effects on body temperature of NECA (●), GR79236 (○), CPA (▽), R-PIA (△) and APNEA (□) 30 min following i.c.v. injection in the conscious mouse. Data points are expressed as mean ± s.e.mean of 6 mice at each dose level. Statistically significant (**$P<0.01$) reductions in body temperature were determined by one-way analysis of variance followed by Dunnett's test. (b) Effects on body temperature of NECA (●) metrifudil (○) and CGS-21680 (□) 30 min following i.c.v. injection in the conscious mouse. Data points are expressed as mean ± s.e.mean of 6 mice at each dose level. Statistically significant (**$P<0.01$) reductions in body temperature were determined by one-way analysis of variance followed by Dunnett's test. For abbreviations, see text.

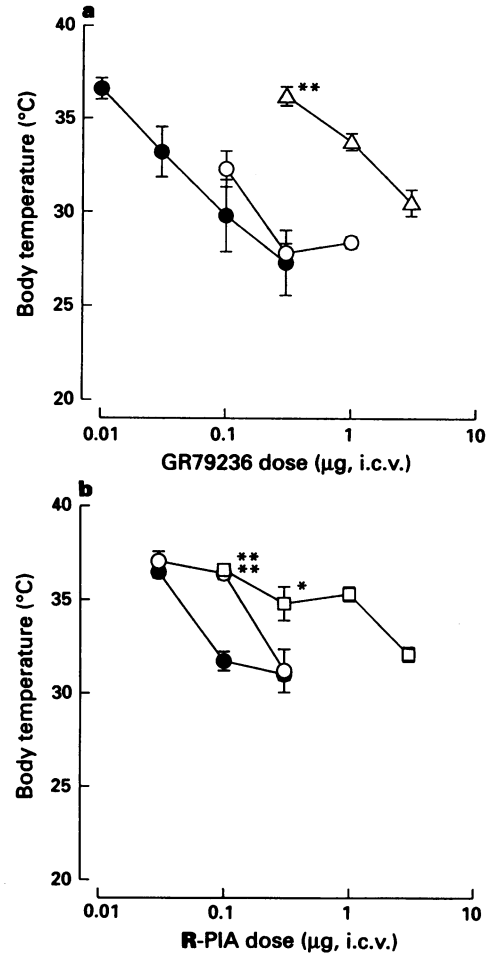


Figure 3 (a) Antagonism of the hypothermic effects of GR79236 i.c.v. (●) by 8-PT at 1.0 (○) and 10 (△) mg kg^{-1} i.p. Data points are expressed as the mean ± s.e.mean of 6 mice at each dose level. Statistically significant (*$P<0.01$) antagonism was determined by one-way analysis of variance followed by Dunnett's test. Vehicle control temperatures were 37.3 ± 0.11°C ($n = 6$). (b) Antagonism of the hypothermic effects of R-PIA i.c.v. (●) by 8-PT at 1 (○) and 10 (□) mg kg^{-1}, i.p. Data points are expressed as the mean of 6 mice at each dose level. Statistically significant (*$P<0.05$, **$P<0.01$) antagonism was determined by one-way analysis of variance followed by Dunnett's test. Vehicle control temperatures were 37 ± 0.15°C ($n = 6$). For abbreviations, see text.

antagonist 8-PT (1–10 mg kg^{-1}, i.p.). For example, there was a 40 fold rightward shift of the GR79236 dose-response curve at 10 mg kg^{-1} (Figure 3). All antagonist shifts were determined at IC_{50} levels. The effects of GR79236 were also antagonized by the potent and selective adenosine A_1 receptor-selective antagonist DPCPX (0.1–1 mg kg^{-1}, i.p.). For example, there was a 16 fold rightward shift at 1 mg kg^{-1} (Figure 4). In addition, the sedative and hypothermic response to APNEA was dose-dependently antagonized by peripheral administration of DPCPX (0.1–1 mg kg^{-1} i.p., Figure 4).

In contrast, the peripherally-acting non-selective antagonist 8-SPT (Daly *et al.*, 1985; 10–30 mg kg^{-1}, i.p.) produced only modest antagonism of the hypothermic response to GR79236 (Figure 5).

Discussion

The aim of the present study was to investigate and characterize the receptors that mediate the hypothermic effects of adenosine in the conscious mouse.

Central administration of the non-selective adenosine receptor agonist, NECA, produced profound, dose-dependent hypothermia and sedation which was mimicked by the adenosine A_1 receptor-selective agonists, CPA, GR79236 and R-PIA and the A_3 receptor agonist, APNEA (Zhou *et al.*, 1992; Gurden *et al.*, 1993). The hypothermic and sedative effects appeared at similar doses for each agonist, although the apparent molar rank order of agonist activity was NECA > GR79236 > CPA > R-PIA > APNEA. This order of potency is somewhat different from that obtained at A_1 receptors *in vitro* (Gurden *et al.*, 1993). However, variations in the lipophilicity of the drugs may partly underlie the variation in activity by modifying access to or removal from the site of action, since we have assumed that all drugs other than GR79236 had achieved equally-effective concentrations 30 min after dosing. The adenosine A_{2a} receptor-selective agonist, CGS-21680, and the modestly selective adenosine A_{2b} receptor agonist, metrifudil, were unable to evoke the same hypothermic effects over a similar dose-range. Indeed these compounds produced only mild responses at much higher doses at which their receptor selectivity may have been compromised. Adenosine A_{2a} receptors present in the nucleus

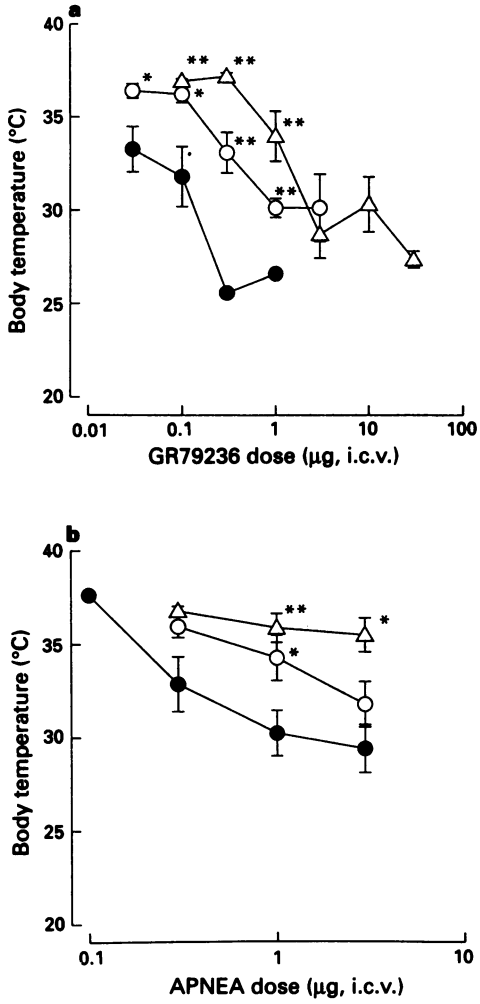


Figure 4 (a) Antagonism of the hypothermic effects of GR79236 i.c.v. (●) by DPCPX at 0.1 (○) and 1.0 (△) mg kg^{-1}, i.p. Data points are expressed as the mean ± s.e.mean of 6 mice at each dose level. Statistically significant (*$P<0.05$, **$P<0.01$) antagonism was determined at each dose level by one-way analysis of variance followed by Dunnett's test. Vehicle control temperatures were (37.4 ± 0.24 $n=6$). (b) Antagonism of the hypothermic effects of APNEA i.c.v. (●) by DPCPX at 0.1 (○) and 1.0 (△) mg kg^{-1}, i.p. Data points are expressed as the mean ± s.e.mean of ($n=6$) mice at each dose level. Statistically significant (*$P<0.05$, **$P<0.01$) antagonism determined by one-way analysis of variance followed by Dunnett's test. Vehicle control temperatures were 36.8 ± 0.28°C ($n=6$). For abbreviations, see text.

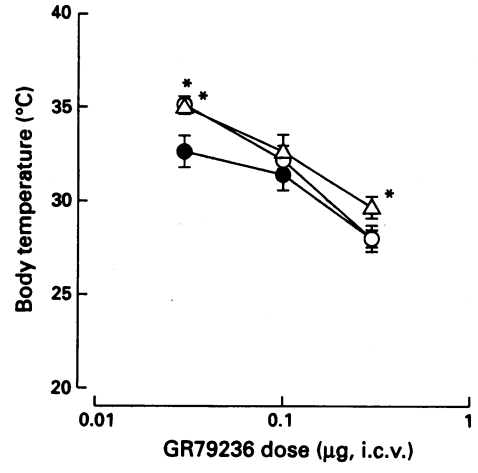


Figure 5 Antagonism of the hypothermic effects of GR79236 i.c.v. (●) by 8-SPT at 10 (○) and 30 (△) mg kg^{-1}, i.p. Data points are expressed as the mean ± s.e.mean of 6 mice at each dose level. Statistically significant (*$P<0.05$) antagonism was determined by one-way analysis of variance followed by Dunnett's test. Vehicle control temperatures were 37.1 ± 0.37°C ($n=6$).

accumbens have been reported to mediate locomotor depression (Barraco *et al.*, 1993) and catalepsy (Ferré *et al.*, 1991) in mice and rats respectively. Presumably, CGS-21680 did not diffuse into the nucleus accumbens at high enough concentrations to evoke these effects in the present study. These results suggest that hypothermia is unlikely to be mediated via activation of either A_{2a} or A_{2b} receptors. Rather they suggest that activation of adenosine A_1 and/or A_3 receptors is likely to be the mechanism involved.

The hypothermic and sedative effects of GR79236 were antagonized by the non-selective adenosine receptor antagonist 8-PT and also by low doses of the adenosine A_1 receptor-selective antagonist, DPCPX. The adenosine receptor agonist, APNEA, has been used to activate the recently-discovered adenosine A_3 receptor although it also has high affinity for A_1 receptors (Zhou *et al.*, 1992). APNEA caused hypothermia and sedation at doses of 0.3–3 μg. However, these effects were antagonized by DPCPX which has been reported to lack affinity for the A_3 receptor (Zhou *et al.*, 1992). There is thus no evidence from our study that the A_3 receptor can mediate either response. These results therefore suggest that adenosine A_1 receptors mediate the hypothermic response. A previous study has described the indirect involvement of adenosine A_1 receptors in neurotensin-induced hypothermia (Jolicoeur & Menard, 1992).

In a recent study (Zarrindast & Heidari, 1993) it was reported that intraperitoneal administration of NECA, CHA and R-PIA reduced core body temperature in mice. Furthermore, the hypothermic effects of R-PIA were potentiated by 8-PT. The latter results are clearly in conflict with our own and further work may be required to clarify the discrepancy.

The mechanism of hypothermia has not been established but may be at a peripheral site (e.g. inhibition of sympathetic nerves or reduction in heart rate), or a central site, or both. In order to investigate whether central or peripheral adenosine receptors were responsible for the hypothermic response, a further antagonist study was undertaken. In contrast to 8-PT, the sulphated analogue, 8-SPT, is a non-selective adenosine receptor antagonist that poorly penetrates the blood brain barrier (as little as 5% penetration occurs as measured by *ex vivo* binding; Baumgold *et al.*, 1992), so preferentially blocking peripheral adenosine receptors. After systemic administration, 8-SPT produced only modest antagonism of the hypothermic effects of GR79236, suggesting that the A_1 receptors responsible for mediating hypothermia are located in the CNS. In addition, the doses of GR79236 which were active on i.c.v. administration were much lower than those which were active peripherally. In the unlikely event of the whole of a maximally effective central dose of GR79236 (1 μg) leaching into the periphery, this would be equivalent to a dose of 0.1 mg kg^{-1}, i.p., which in the present study clearly had no effects on body temperature. Furthermore, Phillis *et al.* (1986) have shown that central (hypoactivity) and peripheral (hypotensive) effects of adenosine analogues could be dissociated by using an intracerebroventricular route of administration. Taken together, these data suggest that central adenosine A_1 receptors mediate the hypothermic effects of adenosine in the mouse.

We gratefully acknowledge the expert technical assistance of Roy Gray and Hilary Davidson.

References

BARRACO, R.A., COFFIN, V.L., ALTMAN, H.J. & PHILLIS, J.W. (1983). Central effects of adenosine analogues on locomotor activity in mice and antagonism of caffeine. *Brain Res.*, **272**, 392–395.

BARRACO, R.A., MARTENS, K.A., PARIZON, M. & NORMILE, H.J. (1993). Adenosine A_{2a} receptors in the nucleus accumbens mediate locomotor depression. *Brain Res. Bull.*, **31**, 397–404.

BAUMGOLD, J., NIKODIJEVIC, O. & JACOBSON, K.A. (1992). Penetration of adenosine antagonists into mouse brain as determined by *ex vivo* binding. *Biochem. Pharmacol.*, **43**, 889–894.

DALY, J.W., PADGETT, W., SHAMIM, M.T., BUTTS-LAMB, P. & WATERS, J. (1985). 1,3-Dialkyl-8-(p-sulfophenyl)xanthines: potent water-soluble antagonists for A_1 and A_2 adenosine receptors. *J. Med. Chem.*, **28**, 487–492.

FASTBOM, J., PAZOS, A., PROBST, A. & PALACIOS, J.M. (1987). Adenosine A_1 receptors in the human brain: a quantitative autoradiographic study. *Neurosci.*, **22**, 827–839.

FERRÉ, S., RUBIO, A. & FUXE, K. (1991). Stimulation of adenosine A_2 receptors induces catalepsy. *Neurosci. Lett.*, **130**, 162–164.

FREDHOLM, B.B. & DUNWIDDIE, T.V. (1988). How does adenosine inhibit transmitter release? *Trends Pharmacol. Sci.*, **9**, 130–134.

FREDHOLM, B.B. & HEDQVIST, P. (1980). Modulation of neurotransmission by nucleotides and nucleosides. *Biochem. Pharmacol.*, **29**, 1635–1643.

GURDEN, M.F., COATES, J., ELLIS, F., EVENS, B., FOSTER, M., HORNBY, E., KENNEDY, I., MARTIN, D.P., STRONG, P., VARDEY, C.J. & WHEELDON, A. (1993). Functional characterisation of three adenosine receptor types. *Br. J. Pharmacol.*, **109**, 693–698.

HAMPRECHT, B. & VAN CALKER, D. (1985). Nomenclature of adenosine receptors. *Trends Pharmacol. Sci.*, **6**, 153–154.

HUTCHISON, J., WILLIAMS, M., DE JESUS, R., YOKOYAMA, R., OEI, H.H., GHAI, G.R., WEBB, L., ZOGANAS, H.C., STONE, G.A. & JARVIS, M.F. (1990). 2-(Arylalkylamino)adenosine-5'-uronamides: a new class of highly selective adenosine A_2 receptor ligands. *J. Med. Chem.*, **33**, 1919–1924.

JARVIS, M.F. & WILLIAMS, M. (1989). Direct autoradiographic localization of adenosine A_2 receptors in the rat brain using the A_2-selective agonist [^{3}H]CGS 21680. *Eur. J. Pharmacol.*, **168**, 243–246.

JOLICOEUR, F.B. & MENARD, D. (1992). Evidence for involvement of A_1 adenosine receptors in neurotensin-induced hypothermia. *Ann. N.Y. Acad. Sci.*, **668**, 353–355.

MEHTA, A.K. & KULKARNI, S.K. (1983). Effect of purinergic substances on rectal temperature in mice: involvement of P_1-purinoceptors. *Arch. Int. Pharmacodyn.*, **264**, 180–186.

PHILLIS, J.W., BARRACO, R.A. DELONG, R.E. & WASHINGTON, D.O. (1986). Behavioural characteristics of centrally administered adenosine analogs. *Pharmacol. Biochem. Behav.*, **24**, 263–270.

YARBROUGH, G.G. & MCGUFFIN-CLINESCHMIDT, J.C. (1981). *In vivo* behavioural assessment of central nervous system purinergic receptors. *Eur. J. Pharmacol.*, **76**, 137–144.

ZARRINDAST, M.R. & HEIDARI, M.R. (1993). Involvement of adenosine receptors in mouse thermoregulation. *J. Psychopharmacol.*, **7**, 365–370.

ZHOU, Q.-Y., LI, C., OLAH, M.E., JOHNSON, R.A., STILES, G.L. & CIVELLI, O. (1992). Molecular cloning and characterization of a novel adenosine receptor: the A_3 adenosine receptor. *Proc. Natl. Acad. Sci. U.S.A.*, **89**, 7432–7436.

(Received May 9, 1994
Revised August 11, 1994
Accepted August 15, 1994)

Br. J. Pharmacol. (1994), **113**, 1391–1399 © Macmillan Press Ltd, 1994

Regional effects of amphetamine, cocaine, nomifensine and GBR 12909 on the dynamics of dopamine release and metabolism in the rat brain

[1]Farouk Karoum, Stanislaw J. Chrapusta, Raymond Brinjak, Ana Hitri & Richard J. Wyatt

Neuropsychiatry Branch, Intramural Research Program, NIMH Neuroscience Center at St. Elizabeths, 2700 M.L. King Jr. Avenue, Washington, D.C. 20032, U.S.A.

1 The effects of single-dose regimens of amphetamine, cocaine, nomifensine and GBR 12909 on the dynamics of dopamine (DA) release and metabolism were evaluated in the frontal cortex, hypothalamus, nucleus accumbens and striatum. The regimens selected are known to produce substantial behavioural effects.

2 3-Methoxytyramine (3MT) and 3,4-dihydroxyphenylacetic acid (DOPAC) rates of formation were used to assess DA metabolism by catechol-*O*-methyltransferase and monoamine oxidase respectively. The rate of formation of 3MT was used as an index of synaptic DA. The ratio and sum, respectively, of 3MT and DOPAC rates of formation were used to assess DA reuptake inhibition and turnover.

3 The effects of amphetamine on 3MT production and DOPAC steady-state levels were similar in all regions, suggesting similar pharmacodynamic actions. Amphetamine increased 3MT formation and steady-state levels, and reduced DOPAC steady-state levels. DOPAC formation was significantly reduced only in the nucleus accumbens and striatum. Total DA turnover remained unchanged except in the nucleus accumbens. Apparently, the amphetamine-induced increase in DA release occurred at the expense of intraneuronal DA metabolism and did not require stimulation of synthesis.

4 Nomifensine elevated 3MT formation in all regions. A similar effect was produced by cocaine except in the nucleus accumbens. GBR 12909 elevated 3MT production only in the hypothalamus, the striatum and the nucleus accumbens.

5 Cocaine selectively reduced DOPAC formation in the frontal cortex. Nomifensine increased and reduced, respectively, DOPAC formation in striatum and hypothalamus. GBR 12909 elevated DOPAC formation in all regions except the cortex, where pargyline did not reduce DOPAC levels in GBR 12909-treated rats.

6 Ratios and sum of 3MT and DOPAC rates of formation also exhibited wide regional variations for each drug. In contrast to the other drugs, the ratio was not increased after GBR 12909. Apparently, the DA uptake properties of this drug are poorly related to its *in vivo* effects on the ratio of 3MT production to that of DOPAC, which should increase when DA reuptake is inhibited.

7 Total DA turnover was increased by GBR 12909 in the hypothalamus, nucleus accumbens and striatum, while cocaine and nomifensine increased it only in the nucleus accumbens and striatum respectively.

8 It is concluded that:

(a) 3MT and DOPAC rates of formation provide better indices of DA release and metabolism than do their steady-state concentrations.

(b) Some effects of DA uptake blockers on DA transmission, especially those of nomifensine and cocaine, may be attributed to increased DA release.

(c) Patterns of regional effects of psychostimulants on the dynamics of DA release and metabolism may be better biochemical correlates of stimulant-induced behaviours than would changes in any single region.

Keywords: Dopamine release, uptake and metabolism; 3-methoxytyramine; amphetamine; cocaine; nomifensine; GBR 12909

Introduction

Many of the diverse and often unique behavioural (Andén, 1970; Snyder *et al.*, 1974; Ross & Kelder, 1979), electrophysiological (German *et al.*, 1979; Sanghera *et al.*, 1979) and pharmacological (Gerhards *et al.*, 1974; Braestrup, 1977; Ross, 1977; Ross & Kelder, 1979) characteristics of psychostimulants are not adequately explained by their broad classification into amphetamine- [drugs that primarily release dopamine (DA)] and non-amphetamine-like (drugs that inhibit DA reuptake) substances. Many of the biochemical changes produced by amphetamine in the DA terminal regions are not similarly produced at the cell bodies (Elverfors & Nissbrandt, 1992). Further, DA reuptake inhibitors do not always produce parallel effects on DA metabolism in different brain regions (Nissbrandt *et al.*, 1991; Kuczenski & Segal, 1992), suggesting regional heterogeneity in the pharmacodynamic action of these drugs. To specifically address these inconsistencies and to assess their relationship to drug-induced behaviours, many studies have compared regional (Kuczenski & Segal, 1992) and subregional (Glynn & Yamamoto, 1989) effects of psychostimulants on DA disposition.

Psychostimulants have been reported to preferentially elevate extracellular DA in the nucleus accumbens compared with the striatum (Carboni *et al.*, 1989; Kuczenski & Segal, 1992; Cass *et al.*, 1993; Di Chiara *et al.*, 1993). This effect may contribute to the earlier emergence of behaviours

[1] Author for correspondence.

mediated by mesolimbic/mesocortical DA systems (locomotor and reinforcement) than those mediated by the nigrostriatal systems (stereotypies) (Kuczenski, 1983; Kuczenski et al., 1991). However, while in vivo voltammetry measures of DA in the nucleus accumbens (Cass et al., 1992, 1993) have been reported to parallel behaviours produced by cocaine, behaviours induced by a number of psychostimulants including cocaine do not quantitatively parallel the changes in extracellular DA levels as measured by microdialysis (Westerink et al., 1987; Callaway et al., 1989; Kuczenski & Segal, 1989; Kuczenski et al., 1991). This calls into question the significance of dialysable DA as a suitable marker of receptor-relevant changes in synaptic DA. There is therefore a need for other biochemical correlates of behaviour. With these thoughts in mind, we have examined and compared the regional effects of amphetamine and three potent DA reuptake inhibitors on DA release and metabolism. Our objective was to test the hypothesis that, if the unique effects of different psychostimulants (Kuczenski, 1983) on the behavioural and endocrine systems can be attributed to regional differences in their effects on DA transmission, then their effects on DA release and metabolism should also exhibit regional differences.

In this communication we report on the regional effects of GBR 12909 (1-{2-[bis(4-fluorophenyl)methosy]ethyl}-4-(3-phenylpropyl)piperazine), nomifensine (1,2,3,4-2-methyl-4-phenyl-8-isoquinolinamine), cocaine and amphetamine on the steady-state concentrations and rates of formation of 3MT and DOPAC in four dopaminergic brain regions. The uptake inhibitors employed here were selected because they either are or can potentially be abused, and because of their different biochemical (Gerhards et al., 1974; Nomikos et al., 1990), pharmacological (Hunt et al., 1974; Kuczenski, 1983) and electrophysiological effects (Bunney & Aghajanian, 1978). Thus, while the behavioural effects of amphetamine and, to a certain extent, nomifensine (Braestrup & Scheel-Kruger, 1976; Broch, 1979; Hunt et al., 1979; Schacht et al., 1982; Kruk & Stamford, 1985; Hurd & Ungerstedt, 1989) have been attributed to stimulation of DA release as well as to its reuptake inhibition, those behavioural effects exhibited by cocaine and GBR 12909 are believed to result primarily from their potent DA reuptake inhibitory effects (Heikkila et al., 1975; Van der Zee et al., 1980; Heikkila & Manzino, 1984; Ritz et al., 1987). As will be demonstrated, at behaviourally affective doses, each of the four psychostimulants produced changes in 3MT and DOPAC production that are different in different regions, and the pattern of changes are characteristic for each drug.

Methods

Animals

Male Sprague-Dawley rats (Zivic-Miller, Allison Park, PA, U.S.A.) weighing initially about 200 g were used. The rats were housed (three per cage) in a room with a 12 h light period (7 a.m. to 7 p.m.), and had free access to food and water. All rats were acclimatized for 1 week before the experiment. The procedures used were in accordance with the NIH Guide for the Care and Use of Laboratory Animals and were approved by the local Animal Care Committee.

Drug schedules and brain tissue analyses

D-Amphetamine sulphate (5 mg kg^{-1}, equivalent to 3.7 mg kg^{-1} or 27.4 μmol kg^{-1} of the free base), cocaine hydrochloride (10 mg kg^{-1}, equivalent to 8.9 mg kg^{-1} or 20.4 μmol kg^{-1} of the free base), nomifensine maleate (10 mg kg^{-1}, equivalent to 6.7 mg kg^{-1} or 28.2 μmol kg^{-1} of the free base), and GBR 12909 dihydrochloride (20 mg kg^{-1}, equivalent to 17.6 mg kg^{-1} or 33.5 μmol kg^{-1} of the free base) were used. These drugs were purchased from Research Biochemical (Natick, MA, U.S.A.). The dose of pargyline hydrochloride (Aldrich Chemical Company, Milwaukee, WI, U.S.A.) used was 75 mg kg^{-1}. Physiological saline solutions of the above drugs, or vehicle, were administered intraperitoneally (i.p., 1 ml kg^{-1}).

The treatment schedules were as follows. Five groups of rats were used; one group was given saline and the other four groups were injected with one psychostimulant each at 0 min. One-third of the rats in each group received pargyline, 75 mg kg^{-1}, at 30 min, and another one-third at 45 min. All rats were sacrificed at 60 min by focused beam microwave irradiation of the brain with an output power of 7 kW for a period of 1.3 s employing a model NJ-2603-10 kW microwave instrument (New Japan Radio, Japan).

The frontal cortex, hypothalamus, nucleus accumbens and striatum were dissected and analysed by mass fragmentography essentially as previously described (Karoum, 1985; Karoum et al., 1990; Karoum & Egan, 1992).

Estimation of 3MT and DOPAC rates of formation

Concentrations of 3MT have been shown to increase linearly in the striatum (Kehr, 1981; Saller & Salama, 1986), nucleus accumbens (Wood & Altar, 1988) and frontal cortex (Wood et al., 1987a) for at least 20 min after monoamine oxidase inhibition with pargyline. This DA metabolite is not conjugated and cannot easily exit the brain (Wood & Altar, 1988). Further, the 3MT concentrations at the three time points (0, 15 and 30 min after pargyline) after all treatments had linear correlation coefficients of $r > 0.95$. Therefore, linear regression analysis was used to calculate 3MT rates of formation from 3MT accumulation after pargyline.

The rate of DOPAC formation (at steady-state conditions) is assumed to be equal to its initial rate of elimination following pargyline administration. The initial rate of elimination was estimated from the decline in DOPAC concentrations 0, 15 and 30 min after the i.p. administration of pargyline (Karoum et al., 1977; Westerink & Spaan, 1982a; Westerink et al., 1984). For each treatment schedule (saline or psychostimulants), individual concentrations of DOPAC were computer fitted to the exponential curve $y = ae^{-bt}$, where y is the concentration at time t, a is the initial concentration and b is the rate constant. The rate constant was multiplied by each of the appropriate individual baseline concentrations of DOPAC to obtain the individual initial DOPAC rates of formation (Tozer et al., 1966; Karoum et al., 1977; Westerink et al., 1984; Westerink & Kikkert, 1986).

Estimation of the ratio of 3MT to DOPAC rates of formation and their sum

The ratios of 3MT to DOPAC rates of formation were calculated by dividing the average regional 3MT rates of formation by the corresponding average DOPAC rates of formation. The standard error of the ratios were estimated by a Taylor series expansion (Kendall & Stuart, 1958). The sums of 3MT and DOPAC rates of formation (total DA turnover rates) were obtained by adding the means of the two rates. The standard errors of the sums were calculated as the square root of the sum of squares of the corresponding standard errors of the mean.

Statistics

One-way ANOVA followed by Dunnett's tests was used to examine the effects of the stimulants on 3MT and DOPAC steady-state concentrations as well as on DOPAC rates of formation. The effects of the drugs on 3MT rate of formation obtained by linear regression analysis were tested by t-tests. The ratios and sums of 3MT and DOPAC rates of formation were compared with z-tests.

Results

3MT and DOPAC steady state concentrations after psychostimulants

Sixty minutes after the administration of amphetamine, 3MT concentrations were increased and DOPAC concentrations decreased in all four brain regions analysed. (While the amphetamine effect was not significant by Dunnett's test in the frontal cortex, a strong tendency for the decrease in DOPAC steady-state concentrations was revealed by a *t*-test: $t=5.64$, $P=0.03$.) In contrast, the regional effects of the three DA reuptake blockers were inconsistent (compare results in Tables 1 and 2). GBR 12909 significantly reduced DOPAC in the frontal cortex.

3MT and DOPAC rates of formation after psychostimulants

Amphetamine and nomifensine increased the 3MT rate of formation in all four brain regions (Table 3). The 3MT rate of formation was increased after cocaine in all regions except the nucleus accumbens, while GBR 12909 increased it only in the hypothalamus nucleus accumbens and striatum.

Unlike its effects on DOPAC steady-state concentrations in the frontal cortex and hypothalamus, amphetamine did not affect DOPAC rates of formation in these two regions. It significantly reduced DOPAC steady-state levels and rates of formation in the nucleus accumbens and striatum. The regional effects of the DA reuptake blockers on DOPAC rates of formation (Table 4) were prominent when compared with the corresponding effects on DOPAC steady-state concentrations (Table 2). The effect of cocaine was characteristic in that it markedly reduced DOPAC rate of formation in the frontal cortex. A reciprocal relationship between DOPAC rates of formation was found in the hypothalamus (a decrease) and striatum (an increase) after nomifensine. GBR 12909 significantly increased DOPAC rates of formation in the hypothalamus, nucleus accumbens and striatum. DOPAC rate of formation in the frontal cortex could not be estimated after GBR 12909, because DOPAC concentrations did not

Table 1 The effects of D-amphetamine sulphate (5 mg kg^{-1}), cocaine hydrochloride (10 mg kg^{-1}), nomifensine maleate (10 mg kg^{-1}) and GBR 12909 dihydrochloride (20 mg kg^{-1}) on 3MT steady-state concentrations

Brain region	*Saline* Mean (s.e.mean) [*n*]	*Amphetamine* Mean (s.e.mean) [*n*]	*Cocaine* Mean (s.e.mean) [*n*]	*Nomifensine* Mean (s.e.mean) [*n*]	*GBR 12909* Mean (s.e.mean) [*n*]
Frontal cortex	117 (6) [19]	194 (22)* [3]	126 (116) [5]	227 (14)* [5]	129 (11) [5]
Hypothalamus	246 (15) [7]	443 (63)* [5]	244 (9) [4]	186 (21) [5]	271 (52) [5]
Nucleus accumbens	586 (35) [20]	1693 (260)* [4]	800 (125) [5]	723 (75)* [4]	889 (102)* [5]
Striatum	1239 (48) [20]	2756 (388)* [4]	1500 (52) [5]	2150 (176)* [5]	2402 (207)* [5]

Results are expressed in fmol mg^{-1} protein.
*$P<0.05$ compared with saline-treated controls by one-way ANOVA followed by Dunnett's two-tailed test.

Table 2 The effects of D-amphetamine sulphate (5 mg kg^{-1}), cocaine hydrochloride (10 mg kg^{-1}), nomifensine maleate (10 mg kg^{-1}) and GBR 12909 dihydrochloride (20 mg kg^{-1}) on DOPAC steady-state concentrations

Brain region	*Saline* Mean (s.e.mean) [*n*]	*Amphetamine* Mean (s.e.mean) [*n*]	*Cocaine* Mean (s.e.mean) [*n*]	*Nomifensine* Mean (s.e.mean) [*n*]	*GBR 12909* Mean (s.e.mean) [*n*]
Frontal cortex	2.38 (0.11) [19]	1.74 (0.24) [a] [4]	1.52 (0.24)* [5]	2.03 (0.25) [5]	1.57 (0.22)* [5]
Hypothalamus	8.00 (0.22) [19]	5.63 (0.28)* [5]	7.41 (0.60) [4]	6.21 (0.24)* [5]	7.62 (0.19) [5]
Nucleus accumbens	62.7 (3.1) [18]	34.0 (5.9)* [4]	63.6 (10.1) [5]	6.50 (4.5) [5]	60.8 (5.9) [5]
Striatum	64.5 (3.1) [19]	31.32 (3.4)* [5]	61.5 (5.7) [5]	79.9 (6.1) [5]	71.0 (4.0) [5]

Results are expressed in pmol mg^{-1} protein.
[a]$P<0.05$ compared to saline by two tailed t-test (see Results section).
*$P<0.05$ compared with saline-treated controls by one-way ANOVA followed by two-tailed Dunnett's test.

Table 3 The effects of D-amphetamine sulphate (5 mg kg^{-1}), cocaine hydrochloride (10 mg kg^{-1}), nomifensine maleate (10 mg kg^{-1}) and GBR 12909 dihydrochloride (20 mg kg^{-1}) on 3MT rate[a] of formation

Brain region	*Saline* Mean (s.e.mean) [d.f.]	*Amphetamine* Mean (s.e.mean) [d.f.]	*Cocaine* Mean (s.e.mean) [d.f.]	*Nomifensine* Mean (s.e.mean) [d.f.]	*GBR 12909* Mean (s.e.mean) [d.f.]
Frontal cortex	39 (3) [56]	66 (9) [12]**	63 (16) [14]**	50 (5) [5]*	52 (8) [12]
Hypothalamus	102 (8) [48]	224 (31) [14]**	185 (13) [10]**	185 (17) [13]**	103 (8) [14]
Nucleus accumbens	241 (8) [56]	893 (116) [13]**	290 (53) [13]	544 (54) [11]**	324 (49) [13]*
Striatum	548 (21) [56]	1227 (128) [13]**	793 (51) [12]**	1020 (80) [13]**	742 (79) [13]*

Results are expressed in fmol mg^{-1} protein min^{-1}.
[a]3MT rate of formation was estimated by regression analysis employing the least-squares method.
d.f., degrees of freedom.
*$P<0.05$, **$P<0.005$ compared with saline by *t* test.

decline after pargyline in these rats. We cannot currently explain this phenomenon.

The effects of amphetamine and the three DA reuptake blockers on the ratio of 3MT to DOPAC rates of formation (Table 5) demonstrated a heterogeneity in the regional effects of these drugs. The ratio was significantly increased in all regions after amphetamine, in the frontal cortex, hypothalamus and nucleus accumbens after cocaine, and in the hypothalamus and the nucleus accumbens after nomifensine. GBR 12909 significantly reduced the ratio in the hypothalamus, but did not change it in the nucleus accumbens and striatum.

Changes in DA turnover rate as determined from the sum of 3MT and DOPAC rates of formation are summarized in Table 6. Clear differences were observed between amphetamine and the three uptake inhibitors as well as among the inhibitors. In contrast to its clear effect on DOPAC steady-state levels in all four brain regions, amphetamine reduced DA turnover only in the nucleus accumbens (by about 30%) DA turnover was significantly increased in the nucleus accumbens after cocaine, and reduced and increased, respectively, in the hypothalamus and striatum after nomifensine. GBR 12909 increased DA turnover in all regions except the frontal cortex, where it could not be estimated because of the failure of pargyline to reduce DOPAC levels at the times selected.

Discussion

The 3MT and DOPAC rates of formation were affected by the psychostimulant treatments more than the steady-state levels of these metabolites (compare Tables 1 and 2 with Tables 3 and 4). Since the steady-state levels can be influenced by a variety of factors (changes in catabolic enzymes after drug treatment, egress of the metabolites, etc.) (Westerink *et al.*, 1984; Westerink & Kikkert, 1986), steady-state measures after drug treatment should be interpreted with caution. On the other hand, since pargyline does not affect the egress of DOPAC and homovanillic acid (Westerink & Kikkert, 1986), changes in the rate measures of 3MT and DOPAC should primarily represent changes in the production of the metabolites. For these reasons, we assume that rates of 3MT and DOPAC formation are more accurate representatives of DA release and turnover than are the basal concentrations.

Table 4 The effects of D-amphetamine sulphate (5 mg kg^{-1}), cocaine hydrochloride (10 mg kg^{-1}), nomifensine maleate (10 mg kg^{-1}) and GBR 12909 dihydrochloride (20 mg kg^{-1}) on DOPAC rate of formation

Brain region	*Saline* Mean (s.e.mean) [*n*]	*Amphetamine* Mean (s.e.mean) [*n*]	*Cocaine* Mean (s.e.mean) [*n*]	*Nomifensine* Mean (s.e.mean) [*n*]	*GBR 12909* Mean (s.e.mean) [*n*]
Frontal cortex	73.1 (3.6) [19]	58.5 (7.9) [4]	30.0 (5.0)* [5]	69.6 (8.6) [5]	N/A[a]
Hypothalamus	335 (9) [19]	298 (15) [5]	311 (25) [4]	216 (8)* [5]	428 (11)* [5]
Nucleus accumbens	3233 (249) [18]	1631 (285)* [4]	4003 (638) [5]	3397 (233) [5]	5672 (547)* [5]
Striatum	2958 (141) [19]	2029 (148)* [5]	3230 (301) [5]	4638 (356)* [5]	4104 (173)* [5]

Results are expressed in fmol mg^{-1} protein min^{-1}.
DOPAC rate of formation was calculated by multiplying the rate constant of decline in DOPAC concentration (during the 30 min after pargyline) by each of the appropriate baseline concentrations.
[a]DOPAC concentration did not decline after pargyline.
*$P<0.05$ compared with saline-treated controls by one-way ANOVA followed by two-tailed Dunnett's test.

Table 5 The effects of D-amphetamine sulphate (5 mg kg^{-1}), cocaine hydrochloride (10 mg kg^{-1}), nomifensine maleate (10 mg kg^{-1}) and GBR 12909 dihydrochloride (20 mg kg^{-1}) on ratio[a] of 3MT to DOPAC rate of formation

Brain region	*Saline*	*Amphetamine*	*Cocaine*	*Nomifensine*	*GBR 12909*
Frontal cortex	0.534 (0.050)	1.119 (0.183)*	2.100 (0.638)*	0.714 (0.116)	N/A[b]
Hypothalamus	0.304 (0.035)	0.752 (0.117)**	0.595 (0.064)**	0.856 (0.085)**	0241 (0.020)**
Nucleus accumbens	0.075 (0.013)	0.548 (0.125)**	0.072 (0.015)	0.160 (0.019)**	0.057 (0.009)
Striatum	0.185 (0.018)	0.605 (0.050)**	0.246 (0.032)	0.220 (0.026)	0.181 (00.21)

Results are means (s.e.).
[a]The ratio was obtained by dividing the mean 3MT rate of formation by the corresponding mean DOPAC rate of formation. The standard error of the ratios was calculated by a Taylor series expansion (Kendall & Stuarts, 1958).
[b]Pargyline failed to reduce DOPAC in the frontal cortex.
*$P<0.05$, **$P<0.01$ compared with saline-treated controls by z statistics.

Table 6 The effects of D-amphetamine sulphate (5 mg kg^{-1}), cocaine hydrochloride (10 mg kg^{-1}), nomifensine maleate (10 mg kg^{-1}) and GBR 12909 dihydrochloride (20 mg kg^{-1}) on total DA turnover [sum of 3MT and DOPAC rates of formation]

Brain region	*Saline*	*Amphetamine*	*Cocaine*	*Nomifensine*	*GBR 12909*
Frontal cortex	112 (5)	125 (12)	93 (17)	120 (10)	N/A[a]
Hypothalamus	437 (19)	522 (34)	496 (28)	401 (19)	531 (14)**
Nucleus accumbens	3474 (249)	2524 (308)*	4293 (640)*	3941 (239)	5996 (549)**
Striatum	3506 (143)	3256 (190)	4023 (968)	5658 (876)**	4846 (190)**

Results are means (s.e.mean) in fmol mg^{-1} protein min^{-1}.
[a]DOPAC concentration did not decline after pargyline.
*$P<0.01$, **$P<0.001$ compared with saline-treated controls by z statistics.

One concern about the use of 3-MT measurements following pargyline has been that monoamine oxidase inhibition could affect DA synthesis and release, and induce a spill-over into the extracellular space of newly synthesized DA (see Sharp *et al.*, 1986). That view, however, is based on data from rats which were probably suffering from acute brain trauma as a result of probe implantation followed by either no or a short post-surgical recovery, (deduced from Sharp *et al.*, 1986; Westerink & De Vries, 1988; Reiriz *et al.*, 1989; Butcher *et al.*, 1990; Cumming *et al.*, 1992). While tissue damage may affect both microdialysis and voltammetry data, this argument is not applicable to the present study because no surgery was involved.

The absence of a clear pargyline effect on behaviours related to stimulation of post-synaptic DA receptors (Spector *et al.*, 1963; Pani *et al.*, 1990; also our own unpublished observation) and on tissue levels of DA (Sharp *et al.*, 1986) suggests the reported elevations in extracellular DA (Sharp *et al.*, 1986) and 3MT (Cumming *et al.*, 1992) after pargyline are exaggerated effects resulting from leakage of DA from traumatized tissue rather than from increased synaptic DA. In this context, it should be noted that the accumulation of DA, both intra- and extraneuronally, should, at least theoretically, have some effect on DA synthesis and release. For this reason, the estimated rates of 3MT and DOPAC productions should be viewed as relative rather than absolute measures of the true rates.

Since 3MT concentrations and rates of production as measured here were obtained from rats sacrificed by microwave irradiation of the intact brain, they may more closely reflect the changes in synaptic DA concentrations (Kehr, 1976; Wood *et al.*, 1987a,b; Karoum & Egan, 1992) than would DA concentrations as measured by either microdialysis or voltammetry. However, as all three approaches relate to events taking place at perisynaptic sites, information rendered from their use should be complementary. Furthermore, since 3MT can only originate from released DA (Kehr, 1981; Wood & Altar, 1988), changes in its tissue and extracellular concentrations should be closely correlated. Accepting this to be the case, and considering that extracellular DA and 3MT are well correlated under a wide variety of experimental conditions (Wood *et al.*, 1987b; Brown *et al.*, 1991; Cumming *et al.*, 1992; Kuczenski & Segal, 1992), changes in tissue 3MT concentrations and/or rates of production are expected to parallel the changes in extracellular DA.

Applying the above rationale, the effects of the four psychostimulants on tissue 3MT concentrations (Table 1) and rates of formation (Table 3) were expected to parallel the changes reported in dialysate DA and 3MT. This, however, was not the case. For instance, while the observed preferential increase in tissue 3MT concentrations in the nucleus accumbens relative to the striatum after amphetamine is consistent with some reports on extracellular DA (Carboni *et al.*, 1989; Di Chiara *et al.*, 1993), it is at odds with the effects reported by others (Robinson & Camp, 1990; Kuczenski *et al.*, 1991; Kuczenski & Segal, 1992; Cass *et al.*, 1993). Differences between microdialysis and tissue measures are also evident in the changes in 3MT levels after DA reuptake inhibition. For example, the inter-regional differences in the relative increases in dialysable 3MT after cocaine and nomifensine in the nucleus accumbens compared with the striatum (Kuczenski & Segal, 1992) were not reflected in steady-state tissue 3MT (Table 1) or 3MT rates of formation (Table 3). These inconsistencies between tissue and extracellular 3MT may be attributed to the location of the probe (Di Chiara *et al.*, 1993) and/or to leakage of DA from damaged DA terminals. In this context, the possibility that interstitial DA may represent non-synaptic or non-functional DA as reported after certain treatments (Pani *et al.*, 1990) should be considered. Whether or not the same argument also applies to tissue 3MT is a subject that warrants investigation. The increase in 3MT steady-state concentrations and rates of formation in the striatum and nucleus accumbens we observed after GBR 12909 is consistent with an earlier report (Nissbrandt *et al.*, 1991). In that study, a slight increase in 3MT accumulation was also observed in cortical hemispheres, a finding that is generally in line with the present study (see Table 3).

Although knowing the dose–response effects of the four drugs on 3MT and DOPAC rates of production is desirable, performing this task is impractical because it involves the use of at least 30 rats to evaluate the effects of one dose. Furthermore, since these dynamic measures require the evaluation of the metabolites' concentrations at several time points, time course studies would require many multiples of the present number of rats. However, since the main purpose of the present study was to compare the regional effects of the same drug treatment on DA release and metabolism, we have selected regimens that are known to produce substantial behavioural and biochemical changes.

At doses similar to those employed here, the effects of amphetamine, cocaine, nomensifine and GBR 12909 on extracellular DA were reported to peak between 20 and 40 min after treatment and to remain elevated at 60 min, with concentrations ranging between 50% and 80% of the maximal levels (Church *et al.*, 1987; Westerink *et al.*, 1987; Carboni *et al.*, 1989; Callaway *et al.*, 1989; Pettit *et al.*, 1990; Kuczenski & Segal, 1992). Time course studies on the effects of 5 mg kg^{-1} of amphetamine on striatal 3MT and DOPAC demonstrated maximal effects of the drug at 60 min. Further, 25 and 30 mg kg^{-1} doses of nomifensine were reported to produce similar maximal elevations in striatal 3MT 20, 25 and 60 min after treatment (Ponzio *et al.*, 1981; Westerink & Spaan, 1982b). Striatal DOPA accumulation after inhibition of its decarboxylation, decline in tissue DA concentration after inhibition of tyrosine hydroxylase, and changes in the steady-state concentrations of DA and its metabolites, were also reported to reach a maximum at 60 min after GBR 12909 and amphetamine (Nissbrandt *et al.*, 1991; Elverfors & Nissbrandt, 1992). Again, the similar time course of amphetamine, nomifensine or cocaine effects on extracellular DA and its metabolites in the striatum and nucleus accumbens (Carboni *et al.*, 1989; Kuczenski & Segal, 1992) suggests that the distribution and pharmacokinetic of these drugs in these two brain regions are similar. Additionally, the behavioural effects of the four psychostimulants on a number of DA-related behaviours were reported to be fully developed 60 min after the administration of doses similar to those employed here (Segal & Mandell, 1974; Westerink *et al.*, 1987; Callaway *et al.*, 1989; Kuczenski *et al.*, 1991; Vaugeois *et al.*, 1993). When all the above are considered, we believe the 30–60 min period during which 3MT and DOPAC rates of formation were estimated corresponds to a period of substantial drug-induced behavioural and neurochemical changes.

The observed regional differences in DA release and metabolism are more likely to result from regional differences in the interaction of DA neurons with the four drugs (pharmacodynamic effects) than from differences in the drugs' metabolism and clearance (pharmacokinetic effects). Nevertheless, the possibility exists that different treatment regimens will produce changes hitherto not produced by the present regimens. However, the mere presence of regional differences at any dose suggests the existence of regional variations in the sensitivities of DA neurons to the drug effects. The proposed use of regional differences in DA release and metabolism as behaviour correlates should therefore not be affected.

The effects of psychostimulants on hypothalamic 3MT appeared intermediate between those found in the frontal cortex and the nucleus accumbens or the striatum. This may be related to the fact that many hypothalamic DA neurons project beyond the hypothalamus or release DA into the bloodstream (Moore, 1987; Goudreau *et al.*, 1992). Thus a significant portion of hypothalamic 3-MT most likely represents somatodendritic DA release. This, as indicated by

the results of studies on DA release and 3MT levels in the substantia nigra and ventral tegmentum, is less responsive to different pharmacological manipulations then DA release in the terminals (Westerlink, 1979; Nissbrandt *et al.*, 1989, 1991; Kalivas, 1993).

A parameter that could be of some use is the ratio of 3MT to DOPAC rates of formation. Owing to the omnipresence of monoamine oxidase and the absence of catechol-*O*-methyltransferase in catecholamine neurons, pure inhibition of DA reuptake, as is expected from the three reuptake blockers examined, should increase the ratio of 3MT to DOPAC rate of formation. Stimulation of DA release in addition to reuptake inhibition should elevate the ratio even more. The fact that DA turnover was markedly elevated after GBR 12909 indicates that the drug or its active metabolite(s) has gained access to the brain. The lack of increase in the ratio after GBR 12909 compared with the elevations in the ratio after cocaine and nomifensine (compare results in Table 5) suggests that the effects of these two drugs on the metabolic fate of DA release are different from those of GBR 12909. Additionally, because of the similarities in the effects of amphetamine, nomifensine and cocaine on the above ratio, 3MT rates of formation and total DA turnover, some of the effects of nomifensine and cocaine may be attributed to stimulation of DA release. This view is supported by a number of observations which suggest an ability of nomifensine to stimulate DA release (Braestrup & Scheel-Kruger, 1976; Broch, 1979; Kruk & Stamford, 1985; Hurd & Ungerstedt, 1989), especially when administered at relatively high doses (Hunt *et al.*, 1979). These observations, together with the recent report of reduced cocaine- and amphetamine-induced spontaneous activity in rats pretreated with putative inhibitors of DA release (Calcagnetti & Schechter, 1992), provide additional support to the notion that some of the behavioural and neurochemical effects of cocaine and nomifensine can be attributed to stimulation of DA release.

The lack of increase in the ratio of 3MT to DOPAC rates of formation after GBR 12909 (Table 5) suggests that, although GBR 12909 is a potent DA uptake blocker *in vitro* (Van der Zee *et al.*, 1980; Heikkila & Manzino, 1984; Nomikos *et al.*, 1990) and apparently also *in vivo* (Vaugeois *et al.*, 1993), its *in vivo* effects on synaptic DA metabolism and perhaps behaviour may not be entirely related to DA reuptake inhibition. This view is consistent with observations in which voltammetry was used to compare the effects of GBR 12909 with those of amphetamine and nomifensine on extracellular DA content in the nucleus accumbens and striatum (May *et al.*, 1988). Poor correlation between the locomotor effects and occupancy of DA uptake sites *in vivo* by different GBR analogues, cocaine and nomifensine was recently reported (Vaugeois *et al.*, 1993). In that report, similar occupancy of the DA uptake transporter complex by different drugs did not produce similar locomotor activities, suggesting the involvement of other effects in addition to DA reuptake inhibition. A dissociation between the effects of DA reuptake blockers on behaviour and dialysable DA was previously reported (Westerink *et al.*, 1987), and 3MT formation was proposed to be a more accurate index of receptor-relevant DA concentration than dialysable DA (Kuczenski & Segal, 1992). Therefore, it is possible that rate of formation of 3MT is a better correlate of behaviour than interstitial DA. On the other hand, compared with cocaine and nomifensine, stimulation of intraneuronal DA metabolism is apparently a prominent effect of systematically administered GBR 12909.

Since the behavioural effects of psychostimulants are directly related to stimulation of post-synaptic targets, the extent to which synaptic DA, and hence 3MT production, is elevated is perhaps more relevant to drug-induced behaviours than are the presynaptic mechanisms involved. Because the changes in 3MT production were more prominent after cocaine and nomifensine than after GBR 12909 (see Table 3), we would expect the behavioural effects of this drug to be similar or weaker than those produced by cocaine and nomifensine. This assertion is consistent with a number of recent reports. At doses similar to those employed here, GBR 12909, cocaine and nomifensine were reported to produce similar motor activities and reinforcement (Rothman *et al.*, 1992; Roberts, 1993), while cross-tolerance studies suggest that GBR 12909 is less potent than either nomifensine or cocaine (Katz *et al.*, 1993; Baker *et al.*, 1993). In this context biochemical characteristics and relatively weak behavioural effects of GBR 12909 may qualify it as one of the so-called type 2 DA reuptake inhibitors which, in spite of their potency as powerful uptake blockers *in vitro*, are weak euphoric and addictive agents (Rothman, 1990). Compared with cocaine and nomifensine, stimulation of intraneuronal DA metabolism is apparently a prominent effect of systematically administered GBR 12909.

The reductions in DOPAC steady-state concentrations after amphetamine are consistent with previous reports from this (Speciale *et al.*, 1980; Chuang *et al.*, 1982; Karoum *et al.*, 1982) and other laboratories (Braestrup, 1977; Elverfors & Nissbrandt, 1992). In these reports, DA concentrations were reported to either remain unchanged or increase after the administration of amphetamine. These findings, together with the ones reported here, can be used to draw a clearer picture of the effects of amphetamine in the terminal regions of ventral tegmental and nigrostiatal DA neurons. Thus, although enhanced egress of DOPAC after amphetamine may partly contribute towards the low DOPAC steady-state concentrations after amphetamine (Westerink & Kikkert, 1986), reduced intraneuronal metabolism of newly synthesized DA is probably the major factor responsible for this effect. This conclusion is suggested by the observation that although the rate constants of DOPAC formation after pargyline tended to increase in the striatum after amphetamine (from about 0.050 to 0.065 min^{-1}, suggesting enhanced egress), they did not change in the frontal cortex, nucleus accumbens and hypothalamus. Furthermore, while nomifensine and GBR 12909 did not affect DOPAC steady-state concentrations in the nucleus accumbens and striatum, they, like amphetamine, tended to elevate the rate constant of striatal DOPAC formation. Reduced intraneuronal metabolism of unreleased DA after amphetamine administration, at least in the nucleus accumbens and striatum, is supported by the failure of DA reuptake inhibitors to block the ability of amphetamine to lower DOPAC concentrations in the brain (Fuller & Snoddy, 1979). This view is also indirectly supported by the inability of DA reuptake inhibitors to attenuate DA release by amphetamine (Ross, 1977; Hunt *et al.*, 1979). Therefore, accelerated efflux of newly synthesized DA and competition for DA reuptake sites by amphetamine (Fischer & Cho, 1979; Kuczenski, 1983; Sulzer *et al.*, 1993) appear to be the primary mechanisms involved in its effects on DA transmission in the brain.

While most of the behavioural effects of psychostimulants are dopaminergic in nature (Kuczenski, 1983; Wise, 1984), the contributions of other factors, either direct or indirect, should not be overlooked. Among these, one may consider the involvement of phenylethylamine, whose formation is increased after amphetamine (Karoum *et al.*, 1982), stimulation of sigma receptors by GBR 12909 (Ross, 1991), serotonin and noradrenaline reuptake inhibition by cocaine (Reith *et al.*, 1986), and noradrenaline reuptake inhibition by nomifensine (Schacht *et al.*, 1982). Dopamine uptake into noradrenergic terminals constitutes a prominent mechanism for DA removal in the frontal cortex (Carboni *et al.*, 1990). Therefore blockade of DA uptake into noradrenegic terminals in the frontal cortex may significantly contribute to the increase in 3MT formation after nomifensine and cocaine. On the other hand, inhibition of DA reuptake into dopaminergic terminals but not into noradrenegic terminals

in this region (Pozzi *et al.*, 1994) by GBR 12909 may be responsible for its more potent effects on DOPAC steady-state concentration and rates of production than those of 3MT.

In summary, not only did the regional effects of amphetamine on the dynamics of DA release and metabolism differ from those exhibited by the uptake inhibitors, but the inhibitors themselves showed marked heterogeneity in their patterns of regional effects. Compared with their steady-state concentrations, 3MT and DOPAC rates of formation were more responsive to psychostimulant treatments. The sum and ratio of 3MT and DOPAC rates of formation can offer useful information on the mechanisms underlying the effects of these drugs on DA reuptake. It is concluded that, while similar mechanisms appear to mediate the effects of amphetamine on brain DA, the pharmacodynamic of DA reuptake inhibitors are in all likelihood region specific. The profile of regional effects on the dynamics of DA release and metabolism may offer better biochemical correlates of psychostimulant-induced behaviours than would changes produced in any single region.

References

ANDÉN, N.E. (1970). Effects of amphetamine and some other drugs on central catecholamine mechanisms. In *Amphetamine and Related Compounds*. ed. Costa, E. & Garattini, S. pp. 447–462. New York: Raven Press.

BAKER, L.E., RIDDLE, E.E., SAUNDERS, R.B. & APPEL, J.B. (1993). The role of monoamine uptake in discriminative stimuli effects of cocaine and related compounds. *Behav. Pharmacol.*, **4**, 69–79.

BRAESTRUP, C. (1977). Biochemical differentiation of amphetamine vs. methylphenidate and nomifensine in rats. *J. Pharm. Pharmacol.*, **29**, 463–470.

BRAESTRUP, C. & SCHEEL-KRUGER, J. (1976). Methylphenidate-like effects of the new antidepressant drug nomifensine (HOE 984). *Eur. J. Pharmacol.*, **38**, 305–312.

BROCH, O.J., (1979). In vivo effects of benztropine and nomifensine on dopamine and noradrenaline terminals in rat brain. *Eur. J. Pharmacol.*, **58**, 419–424.

BROWN, E.E., DAMSMA, G., CUMMING, P. & FIBIGER, C., (1991). Interstitial 3-methoxytyramine reflects striatal dopamine release: an in vivo microdialysis study. *J. Neurochem.*, **57**, 701–707.

BUNNEY, B.S. & AGHAJANIAN, G.K. (1978). d-Amphetamine induced depression of dopamine neuron: evidence for mediation by both autoreceptors and striatonigral feed back pathways. *Naunyn-Schmied. Arch. Pharmacol.*, **304**, 225–261.

BUTCHER, S.P., FAIRBROTHER, I.S., KELLY, J.S. & ARBUTHNOTT, G.W. (1990). Effects of selective monoamine oxidase inhibitors on the in vivo release and metabolism of dopamine in the rat striatum. *J. Neurochem.*, **55**, 981–988.

CALCAGNETTI, D.J. & SCHECHTER, M.D. (1992). Psychostimulant-induced activity is attenuated by two putative dopamine release inhibitors. *Pharmacol. Biochem. Behav.*, **43**, 1023–1031.

CALLAWAY, C.W., KUCZENSKI, R. & SEGAL, D.S. (1989). Reserpine enhances amphetamine stereotypies without increasing amphetamine-induced changes in striatal dialysate dopamine. *Brain Res.*, **505**, 83–90.

CARBONI, E., IMPERATO, A., PEREZZANI, L. & DI CHIARA, G. (1989). Amphetamine, cocaine phencyclinidine and nomifensine increase extracellular dopamine concentrations preferentially in the nucleus accumbens of freely moving rats. *Neuroscience*, **28**, 653–661.

CARBONI, E., TANDA, G.L., FRAU, R. & DI CHIARA, G. (1990). Blockade of the noradrenaline carrier increases extracellular dopamine concentrations in the prefrontal cortex: evidence that dopamine is taken up in vivo by noradrenergic terminals. *J. Neurochem.*, **55**, 1067–1070.

CASS, W.A., GERHARDT, G.A., MAYFIELD, R.D., CURELLA, P. & ZAHNISER, N.R. (1992). Differences in dopamine clearance and diffusion in rat striatum and nucleus accumbens following systemic cocaine administration. *J. Neurochem.*, **59**, 259–266.

CASS, W.A., ZAHNISER, N.R., FLACH, K.A. & GERHARDT, G.A. (1993). Clearance of exogenous dopamine in rat dorsal striatum and nucleus accumbens: role of metabolism and effects of local applied uptake inhibitors. *J. Neurochem.*, **61**, 2269–2278.

CHUANG, L., KAROUM, F. & WYATT, R.J. (1982). Different effects of behaviourally equipotent doses of amphetamine and methamphetamine on brain biogenic amines: specific increase by amphetamine. *Eur. J. Pharmacol.*, **81**, 385–392.

CHURCH, W.H., JUSTICE, J.B. & BYRD, L.D. (1987). Extracellular dopamine in rat striatum following uptake inhibition by benztropine. *Eur. J. Pharmacol.*, **139**, 345–348.

CUMMING, P., BROWN, E., DAMSMA, G. & FIBIGER, H. (1992). Formation and clearance of interstitial metabolites of dopamine and serotonin in the rat striatum: an in vivo microdialysis study. *J. Neurochem.*, **59**, 1905–1914.

DI CHIARA, G., TANDA, G., FRAU, R. & CARBONI, E. (1993). On the preferential release of dopamine in the nucleus accumbens by amphetamine – further evidence obtained by vertically implanted concentric dialysis probes. *Psychopharmacology*, **112**, 398–402.

ELVERFORS, A. & NISSBRANDT, H. (1992). Effects of d-amphetamine on dopamine neurotransmission between the substantia nigra and striatum. *Neuropharmacology*, **32**, 661–670.

FISCHER, J.F. & CHO, A.K. (1979). Chemical release of dopamine from striatal homogenates: evidence for exchange diffusion model. *J. Pharmacol. Exp. Ther.*, **208**, 203–209.

FULLER, R.W. & SNODDY, H.D. (1979). Inability of methylphenidate or mazindol to prevent the lowering or 3,4-dihydroxyphenylacetic acid in rat brain by amphetamine. *J. Pharm. Pharmacol.*, **31**, 183–184.

GERHARDS, H.J., CARENZI, A. & COSTA, E. (1974). Effects of nomifensine on motor activity, dopamine turnover and cyclic 3′,5′-adenosine monophosphate concentrations of rat striatum. *Naunyn-Schmied. Arch. Pharmacol.*, **286**, 49–63.

GERMAN, D.C., HARDEN, H., SANGHERA, M.K., MANN, D., KISER, R.S., MILLER, H.H. & SHORE, P.A. (1979). Dopamine neuronal responses to a non-amphetamine CNS stimulant. *J. Neural Transm.*, **44**, 39–49.

GLYNN, G.E. & YAMAMOTO, B.Y. (1989). In vivo neurochemical and anatomical heterogeneity of the dopamine uptake system in the rat caudate putamen. *Brain Res.*, **481**, 235–241.

GOUDREAU, J.L., LINDLEY, S.E., LOOKINGLAND, K.J. & MOORE, K.E. (1992). Evidence that hypothalamic periventricular dopamine neurons innervate the intermediate lobe of the rat pituitary. *Neuroendocrinology*, **56**, 100–105.

HEIKKILA, R.E. & MANZINO, L. (1984). Behavioral properties of GBR 12909, GBR 13069 and GBR 13908: specific inhibition of dopamine uptake. *Eur. J. Pharmacol.*, **103**, 241–248.

HEIKKILA, R.E., ORLANSKY, H. & COHEN, G. (1975). Studies on the distinction between uptake inhibition and release of dopamine in rat brain slices. *Biochem. Pharmacol.*, **24**, 847–852.

HUNT, P., KANNENGIESSER, M.H. & RAYNAUD, J. (1974). Nomifensine: a potent new inhibitor of dopamine uptake into synaptosomes from rat brain corpus striatum. *J. Pharm. Pharmacol.*, **26**, 370–371.

HUNT, P., RAYNAUD, J., LEVEN, M. & SCHACHT, V. (1979). Dopamine uptake inhibitors and releasing agents differentiated by use of synaptosomal and field-stimulated brain slices in vitro. *Biochem Pharmacol.*, **28**, 2011–2016.

HURD, Y.L. & UNGERSTEDT, U. (1989). In vivo neurochemical profile of dopamine uptake inhibitors and releasers in rat caudate-putamen. *Eur. J. Pharmacol.*, **166**, 251–260.

KALIVAS, P.W. (1993). Neurotransmitter regulation of dopamine neurons in the ventral tegmental areas. *Brain Res. Rev.*, **18**, 75–113.

KAROUM, F. (1985). Combined gas chromatography–mass spectrometry in the analysis of biogenic amines in humans. in *Neuromethods*, Vol. 2. ed. Baker, G.B., Boulton, A.A. & Baker, J.M. pp 305–323, Clifton, NJ: Humana Press.

KAROUM, F. & EGAN, M.F. (1992). Dopamine release and metabolism in the rat frontal cortex, nucleus accumbens, and striatum: a comparison of acute clozapine and haloperidol. *Br. J. Pharmacol.*, **105**, 703–707.

KAROUM, F., NEFF, N.H. & WYATT, R.J. (1977). The dynamics of dopamine metabolism in various regions of the rat brain. *Eur. J. Pharmacol.*, **44**, 311–318.

KAROUM, F., SPECIALE J.R., S.G., CHUANG, L. & WYATT, R.J. (1982). Selective effects of phenylethylamine on central catecholamines: a comparative study with amphetamine. *J. Pharmacol. Exp. Ther.*, **223**, 432–439.

KAROUM, F., SUDDATH, R.L. & WYATT, R.J. (1990). Chronic cocaine and rat brain catecholamines: long-term reduction in hypothalamic and frontal cortex dopamine metabolism. *Eur. J. Pharmacol.*, **186**, 1–8.

KAROUM, F., CHRAPUSTA, S.J. & EGAN, M.F. (1994). 3-Methoxytyramine is the major metabolite of released dopamine in the rat frontal cortex: reassessment of the effects of antipsychotics on the dynamics of dopamine release and metabolism in the frontal cortex, nucleus accumbens and striatum by a simple two pool model. *J. Neurochem.*, **63**, 972–979.

KATZ, J.L., GRIFFITHS, J.W., SHARPE, L.G., DE SOUZA, E.B. & WITKIN, J.M. (1993). Cocaine tolerance and cross-tolerance. *J. Pharmacol. Exp. Ther.*, **264**, 183–192.

KEHR, W. (1976). 3-Methoxytyramine as an indicator of impulse-induced dopamine release in rat striatum in vivo. *Naunyn-Schmied. Arch. Pharmacol.*, **293**, 209– 215.

KEHR, W. (1981). 3-Methoxytyramine and normetanephrine as indicators of dopamine and norepinephrine release in mouse brain in vivo. *J. Neural. Transm.*, **50**, 165–178.

KENDALL, M.G. & STUART, A. (1958). *The Advanced Theory of Statistics*, Vol 1. New York: Hafner.

KRUK, Z.L. & STAMFORD, J.A. (1985). Nomifensine increases stimulated dopamine release in vivo by an action on the dopamine storage pool: in vivo voltammetric evidence. *Br. J. Pharmacol.*, **86**, P635.

KUCZENSKI, R. (1983). Biochemical actions of amphetamine and other stimulants. In *Stimulants: Behavior and Clinical Properties*. ed. Creese, I. pp. 31–61. New York: Raven Press.

KUCZENSKI, R. & SEGAL, D.S. (1989). Concomitant characterization of behavioral and striatal neurotransmitter response to amphetamine using in vivo microdialysis. *J. Neurosci.*, **9**, 2051–2065.

KUCZENSKI, R. & SEGAL, D.S. (1992). Differential effects of amphetamine and dopamine uptake blockers (cocaine, nomifensine) on caudate and accumbens dialysate dopamine and 3-methoxytyramine. *J. Pharmacol. Exp. Ther.*, **262**, 1085–1094.

KUCZENSKI, R., SEGAL, S.D. & AIZENSTEIN, M.L. (1991). Amphetamine, fencamfamine, and cocaine: Relationship between locomotor and stereotypy response profiles and caudate accumbens dopamine dynamics. *J. Neurosci.*, **11**, 2703–2712.

MAY, L.J., KUHR, W. & WIGHTMAN, R.M. (1988). Differentiation of dopamine overflow and uptake processes in the extracellular fluid of the rat caudate nucleus with fast-scan in vivo voltammetry. *J. Neurochem.*, **51**, 1060–1069.

MOORE, K.E. (1987). Hypothalamic dopaminergic neuronal systems. In *Psychopharmacology: The Third Generation of Progress*, ed. Meltzer, H.Y., pp. 127–139, New York, NY: Raven Press.

NISSBRANDT, H., SUNDSTRÖM, E., JONSSON, G., HJORTH, S. & CARLSON, A. (1989). Synthesis and release of dopamine in rat brain: comparison between substantia nigra pars compacta, pars reticulata, and striatum. *J. Neurochem.*, **52**, 1170–1182.

NISSBRANDT, H., ENGBERG, G. & PILEBLAD, E. (1991). The effects of GBR 12909, a dopamine re-uptake inhibitor, on monoaminergic neurotransmission in rat striatum, limbic forebrain, cortical hemispheres and substantia nigra. *Naunyn-Schmied. Arch. Pharmacol.*, **334**, 16–28.

NOMIKOS, G.G., DAMSMA, G., WENKSTERN, D. & FIBIGER, H.C. (1990). In vivo characterization of locally applied dopamine uptake inhibitors by striatal microdialysis. *Synapse*, **6**, 106–112.

PANI, L., GESSA, G.L., CARBONI, S., PORTAS, C.M. & ROSSETTI, Z.L. (1990). Brain dialysis and dopamine: Does the extracellular concentration reflect synaptic release? *Eur. J. Pharmacol.*, **180**, 85–90.

PETTIT, H.O., HWAI-TZONG, P., PARSONS, L.H. & JUSTICE Jr., J.B. (1990). Extracellular concentrations of cocaine and dopamine are enhanced during chronic cocaine administration. *J. Neurochem.*, **55**, 798–804.

PONZIO, I., ACHILLIC, G., PEREGO, C. & ALGERI, S. (1981). Different effects of certain dopaminergic drugs on the striatal concentration of dopamine metabolites, with special reference to 3-methoxytyramine. *Neurosci. Lett.*, **27**, 61–67.

POZZI, L., INVERNIZZI, R., CERVO, L., VALLEBUONA, F. & SAMANIN, R. (1994). Evidence that extracellular concentrations of dopamine are regulated by noradrenegic neurons in the frontal cortex of rats. *J. Neurochem.*, **63**, 195–200.

REIRIZ, J., MENA, M.A., BAZAN, E., MURADAS, V., LERMA, J., DELGADO, J.M.R. & DE YEBENES, J.G. (1989). Temporal profile of levels of monoamines and their metabolites in striata of rats implanted with dialysis tubes. *J. Neurochem.*, **53**, 789–792.

REITH, M.E.A., MEISLER, B.E., SERSHEN, H. & LAJTHA, A. (1986). Structural requirements for cocaine congeners to interact with dopamine and serotonin uptake sites in mouse brain and to induce stereotyped behaviour. *Biochem. Pharmacol.*, **35**, 1123–1129.

RITZ, M.C., LAMB, R.J., GOLDBERG, S.R. & KUHAR, M.J. (1987). Cocaine receptors on dopamine transporters are related to self-administration of cocaine. *Science*, **237**, 1219–1223.

ROBERTS, D.C.S. (1993). Self-administration of GBR-12909 on fixed-ratio and progressive ration schedule in rats. *Psychopharmacology*, **111**, 202–206.

ROBINSON, T.E. & CAMP, D.M. (1990). Does amphetamine preferentially increase the extracellular concentration of dopamine in the mesolimbic system of freely moving rats? *Neuropsychopharmacology*, **13**, 163–173.

ROSS, S.B. (1977). On the mode of action of central stimulatory agents. *Acta Pharmacol. Toxicol.*, **41**, 392–396.

ROSS, S.B. (1991). Heterogeneous binding of sigma radioligands in the rat brain and liver: possible relationship to subforms of cytochrome P-450. *Acta Pharmacol. Toxicol.*, **68**, 293-301.

ROSS, S.B. & KELDER, D. (1979). Inhibition of ^{3}H-dopamine accumulation in reserpinized and normal rat striatum. *Acta Pharmacol. Toxicol.*, **44**, 329–335.

ROTHMAN, R.B. (1990). High affinity reuptake inhibitors as potential cocaine antagonists: a strategy for drug development. *Life Sci.*, **46**, PL-17–PL-21.

ROTHMAN, R.B., GRIEG, N., KIM, A., RICE, K.C., CARROL, F.I. & PERT, A. (1992). Cocaine and GBR12909 produce equivalent motoric responses at different occupancy of dopamine transporter. *Pharmacol. Biochem. Behav.*, **43**, 1135–1142.

SALLER, C.F. & SALAMA, A.I. (1986). 3-Methoxytyramine accumulation: effects of typical neuroleptics and various atypical compounds. *Naunyn-Schmied. Arch. Pharmacol.*, **334**, 125–132.

SANGHERA, M.K., GERMAN, D.C., KISER, R.S. & SHORE, P.A. (1979). Differences in norepinephrine and dopamine neurotransmitter storage systems. *Brain Res. Bull.*, **4**, 217–21.

SCHACHT, U., LEVEN, M., GERHARDS, H.J., HUNT, P. & RAYNAUD, J.P. (1982). Recent investigations on the mechanism of action of nomifensine. *Int. Pharmacopsychiatr.*, **17**, 21–34.

SEGAL, D.S. & MANDELL, A. (1974). Long-term administration of amphetamine progressive augmentation of motor activity and stereotypy. *Pharmacol. Biochem. Behav.*, **2**, 249–255.

SHARP, T., ZETTERSTRÖM, T. & UNGERSTEDT, U. (1986). An in vivo study of dopamine release and metabolism in rat brain regions using intracerebral dialysis. *J. Neurochem.*, **47**, 113-122.

SNYDER, S.H., BANERJEE, S.P., YAMAMURA, H.I. & GREENBERG, D. (1974). Drugs, neurotransmitters and schizophrenia. *Science*, **184**, 1243–1253.

SPECIALE Jr, S.G., KAROUM, F. & WYATT, R.J. (1980). Different effects of amphetamine and amfonelic acid on peripheral and central catecholamine metabolism. *Eur. J. Pharmacol.*, **62**, 297–307.

SPECTOR, S., HIRSCH, C.W. & BRODIE, B.B. (1963). Association of behavioral effects of pargyline, a non-hydrazine MAO inhibitor, with increased in brain norepinephrine. *J. Neurochem.*, **2**, 81–93.

SULZER, D., MAIDMENT, N.T. & RAYPORT, S. (1993). Amphetamine and other weak bases action to promote reverse transport of dopamine in ventral midbrain neurons. *J. Neurochem.*, **60**, 527–535.

TOZER, T.N., NEFF, N.H. & BRODIE, B.B. (1966). Application of steady state kinetics to the synthesis rate and turnover time of serotonin in the brain of normal and reserpine treated rats. *J. Pharmacol. Exp. Ther.*, **153**, 177–182.

VAN DER ZEE, P., KOGER, H.S., GOOTJES, J. & HESPE, W. (1980). Aryl 1,2,-dialk(en)yl-piperazines as selective and very potent inhibitors of dopamine uptake. *Eur. J. Pharmacol.*, **15**, 363–370.

VAUGEOIS, J.M., BONNET, J.J., DUTERTE-BOUCHER, D. & COSTENTIN, J. (1993). In vivo occupancy of striatal dopamine complex by various inhibitors does not predict their effects on locomotion. *Eur. J. Pharmacol.*, **230**, 195–201.

WESTERINK, B.H.C. (1979). Effects of drugs on the formation of 3-methoxytyramine, a dopamine metabolite, in the substantia nigra, striatum, nucleus accumbens and tuberculum olfactorium of the rat. *J. Pharm. Pharmacol.*, **31**, 94–99.

WESTERINK, B.H.C. & DE VRIES, J.B. (1988). Characterization of in vivo dopamine release as determined by brain microdialysis after acute and subchronic implantations: methodological aspects. *J. Neurochem.*, **51**, 683–687.

WESTERINK, B.H.C. & KIKKERT, R.J. (1986). Effects of various centrally acting drugs on the efflux of dopamine metabolites from the rat brain. *J. Neurochem.*, **46**, 1145–1152.

WESTERINK, B.H.C. & SPAAN, S.J. (1982a). Simultaneous determination of the formation rate of dopamine and its metabolite 3,4-dihydroxyphenylacetic acid (DOPAC) in various rat brain areas. *Brain Res.*, **252**, 239–245.

WESTERINK, B.H.C. & SPAAN, S.J. (1982b). On the significance of endogenous 3-methoxytyramine for the effects of centrally acting drugs on dopamine release in the rat brain. *J. Neurochem.*, **36**, 680–686.

WESTERINK, B.H.C., BOSKER, F.J. & WIRIX, E. (1984). Formation and metabolism of dopamine in nine areas of the rat brain: Modifications by haloperidol. *J. Neurochem.*, **42**, 1321–1327.

WESTERINK, B.H.C., DAMSMA, G., DE VRIES, J.B. & KONING, H. (1987). Dopamine re-uptake inhibitors show inconsistent effects on the in vivo release of dopamine as measured by intracerebral dialysis in the rat. *Eur. J. Pharmacol.*, **135**, 123–128.

WISE, R.A. (1984). Neural mechanisms of the reinforcing action of cocaine. In *Cocaine: Pharmacology, Effects, and Treatment of Abuse, NIDA Research Monograph 50.* ed Grabowski, J.A. pp.15–33, Washington DC:U.S. Government Printing Office.

WOOD, P.L. & ALTAR, A. (1988). Dopamine release in vivo from nigrostriatal, mesolimbic and mesocortical neurons: utility of 3-methoxytyramine measurements. *Pharmacol. Rev.*, **40**, 163–187.

WOOD, P.L., KIM, H.S. & ALTAR, C.A. (1987a). In vivo assessment of dopamine and norepinephrine release in rat neocortex: gas chromatography–mass spectometry measurement of 3-methoxytyramine and normetanephurine. *J. Neurochem.*, **48**, 574–579.

WOOD, P.L., KIM, H.S. & MARIEN, M.R. (1987b). Intracerebral dialysis: direct evidence for the utility of 3-MT measurements as an index of dopamine release. *Life Sci.*, **41**, 1–5.

(Received March 7, 1994
Revised July 20, 1994
Accepted August 2, 1994)

Br. J. Pharmacol (1994), **113**, 1400–1406 © Macmillan Press Ltd, 1994

Differential sensitivity of ^{3}H-agonist binding to pre- and postsynaptic 5-HT_{1A} receptors in bovine brain

Lawrence G. Iben, Cathy D. Mahle & [1]Frank D. Yocca

CNS Drug Discovery, Psychobiological Disorders, Bristol-Myers Squibb Pharmaceutical Research Institute, 5 Research Parkway, Wallingford, CT 06492, U.S.A.

1 The full and weak partial 5-HT_{1A} agonist ligands [^{3}H]-8-OH-DPAT and [^{3}H]-BMY-7378 were used to characterize the binding parameters of pre- and postsynaptic 5-HT_{1A} binding sites in bovine dorsal raphe and hippocampal membranes, respectively. The K_d and B_{max} values for the individual radioligands were indistinguisable across the regions tested, as were the K_i values generated by a series of agents acting at 5-hydroxytryptamine (5-HT) receptors.

2 The concentration-dependent allosteric attenuation of [^{3}H]-8-OH-DPAT and [^{3}H]-BMY-7378 binding produced by the nonhydrolyzable guanyl nucleotide, Gpp(NH)p, generated similar IC_{50} values within a particular region; however, these were significantly different between regions. While the maximal attenuation of [^{3}H]-8-OH-DPAT and [^{3}H]-BMY-7378 binding was similar in dorsal raphe, Gpp(NH)p produced a significantly greater attenuation of [^{3}H]-8-OH-DPAT binding in hippocampal membranes when compared to [^{3}H]-BMY-7378. The maximal attentuation of [^{3}H]-8-OH-DPAT binding by Gpp(NHp) in hippocampus was also significantly greater than that seen with either radioligand in dorsal raphe.

3 Although exposure to Gpp(NH)p had no effect on the affinity constants of either radioligand in either region, it produced a concentration-dependent reduction in the maximal number of binding sites for both radioligands in both regions. While the percentage reduction in B_{max} values were similar for both radioligands in the dorsal raphe, Gpp(NH)p reduced the B_{max} of [^{3}H]-8-OH-DPAT in hippocampus significantly more than that of [^{3}H]-BMY-7378.

4 These results suggest that while pre- and postsynaptic 5-HT_{1A} receptors may share similar pharmacological recognition properties, a region-dependent difference in the coupling of the 5-HT_{1A} receptor to G-proteins may exist.

Keywords: 5-Hydroxytryptamine 5-HT_{1A} receptors; 8-OH-DPAT; BMY-7378; hippocampus; raphe nucleus; presynaptic; postsynaptic; bovine brain

Introduction

Autoradiographic and membrane homogenate receptor binding studies in brain tissue were instrumental in determining the existence of dense populations of 5-HT_{1A} receptors on 5-hydroxytryptaminergic neurones in the raphe nuclei and on cells residing postsynaptic to 5-hydroxytryptamine (5-HT) containing neurones in the hippocampus of numerous species (Pazos & Palacios, 1985). While somatodendritic 5-HT_{1A} receptors act as autoreceptors and regulate the firing (Sprouse & Aghajanian, 1988) and transmitter release of 5-HT containing neurones (Hjorth & Magnusson, 1988), its postsynaptic counterpart mediates the inhibition of adenylylcyclase in rat hippocampal membrane homogenates (DeVivo & Maayani, 1986) and hippocampal pyramidal cell membrane hyperpolarization due to opening of potassium channels (Colino & Hallivell, 1987). Both receptors mediate their physiological effects through coupling to a G_i protein (Innis *et al.*, 1988; Harrington *et al.*, 1988).

Electrophysiological studies have clearly defined regional differences in 5-HT_{1A} receptor sensitivity to and modulation by 5-HT_{1A} agonists and partial agonists; namely, compounds such as LSD, buspirone and gepirone which appear as partial agonists at postsynaptic 5-HT_{1A} receptors in hippocampus and exert greater agonist activity at the somatodendritic 5-HT_{1A} autoreceptors residing on 5-HT-containing cell bodies in the dorsal raphe nucleus (Sprouse & Aghajanian, 1987; 1988). Additionally, while presynaptic 5-HT_{1A} receptors undergo desensitization after chronic administration of 5-HT_{1A} agonists, postsynaptic receptors residing in hippocampal pyramidal regions are unaffected (Blier & deMontigny, 1987).

Interestingly, a similar discrepancy in pharmacological activity of dopamine agonists has been explained by the presence of a receptor reserve at the presynaptic (terminal) striatal dopamine D_2 receptor while no receptor reserve exists at the D_2 receptor residing postsynaptic to dopamine containing neurones (Meller *et al.*, 1987; 1988). The demonstration of a large receptor reserve for agonists at the somatodendritic 5-HT_{1A} autoreceptor (Meller *et al.*, 1990) explains the ability of numerous 5-HT agonists to display equivalent intrinsic activities for agonist inhibition of 5-HT synthesis. We have recently demonstrated (Yocca *et al.*, 1992), a lack of receptor reserve at postsynaptic 5-HT_{1A} receptors coupled to the inhibition of adenylylcyclase activity. This finding accounts for the ability of 5-HT receptor agonists to demonstrate similar intrinsic activities at somatodendritic 5-HT_{1A} receptors presynaptically, yet elicit partial agonist activity at their postsynaptic counterparts.

Given the differences between pre- and postsynaptic 5-HT_{1A} receptor function, we sought to determine whether regionally distinct 5-HT_{1A} receptors which display varying degrees of receptor reserve possess different pharmacological properties. While molecular biological techniques have yet to detect additional subtypes of 5-HT_{1A} receptors, the observed region-dependent variations in drug efficacy have introduced the possibility of either a heterogeneity in 5-HT_{1A} receptors or in differential coupling of a single subtype of 5-HT_{1A} receptor to a signal transducing G-protein(s). Utilizing the radioligand binding of a full ([^{3}H]8-hydroxy-2-(di-n-propylamino)-tetralin, [^{3}H]-8-OH-DPAT; Middlemiss & Fozard, 1983) and the weak partial agonist ([^{3}H]-7, 9-dioxo-8-[2-(4-o-methoxyphenylpiperazinyl) ethyl]-8-azaspiro[4,5] decane dihyrochloride, [^{3}H]-BMY-7378; Yocca *et al.*, 1987) we

[1] Author for correspondence.

have investigated the affinity-related binding parameters of both pre- and postsynaptic 5-HT$_{1A}$ binding sites in bovine brain and their coupling to G-proteins. We have concluded that pre- and postsynaptic 5-HT$_{1A}$ receptors appear pharmacologically similar; however, a region-dependent difference in the coupling of the 5-HT$_{1A}$ receptor to the same and different G-proteins may exist.

Methods

Tissue preparation

Bovine hippocampus and dorsal raphe nucleus were obtained from a local slaughterhouse, where immediately after the animals were killed tissue was dissected on ice and frozen on dry ice. The tissue was stored at −80°C until use. On the day of assay, whole tissue sections were defrosted in 20 ml of ice cold wash buffer (50 mM Tris HCl and 1 mM EGTA, pH 7.4 at 21°C), and homogenized in a Brinkman polytron. The homogenate was diluted to a final volume of 40 ml and centrifuged at 39,000 *g* for 10 min at 4°C. The supernatant was discarded and the resulting pellet resuspended in 40 ml wash buffer in a polytron and centrifuged as before. The pellet was resuspended in 40 ml of assay buffer (50 mM Tris HCl, containing 5 mM $MgSO_4$, 2 mM EGTA, 10 μM pargyline, and 0.1% (w/v) ascorbic acid, pH 7.7 at 21°C), incubated at 37°C for 10 min to remove endogenous 5-HT (Nelson *et al.*, 1978) and centrifuged as above. The final pellet was resuspended in 100 volumes of assay buffer and the homogenate used immediately.

Radioligand binding assay

Binding assays ([^{3}H]-8-OH-DPAT and [^{3}H]-BMY-7378) were carried out by minor modification of the method we have previously described (Mahle *et al.*, 1992). Briefly, the binding assay was performed in duplicate in an assay volume of 1 ml consisting of 800 μl membrane homogenate (approximately 350 μg protein/tube), 100 μl assay buffer, competitor or masking ligand and 100 μl of radioligand. Guanyl nucleotide effects on agonist binding parameters were determined by the addition of 50 μl Gpp(NH)p with either 50 μl buffer or masking ligand. For saturation analyses, the radioligand concentration varied from 0.0625–6.0 nM. Competition experiments were performed using 0.5 nM [^{3}H]-8-OH-DPAT or 0.375 nM [^{3}H]-BMY-7378. Displacement of radiolabelled agonist by Gpp(NH)p was performed using 2 nM radioligand (approximately 50% receptor occupancy). Non-specific binding for both radioligands was defined by the addition of 1 μM 5-HT. Incubations were initiated by the addition of membrane preparation and were conducted at 37°C for 10 min. Binding reactions were terminated by rapid filtration through Whatman GF/B filters using a Brandel cell harvester (Gaithersburg, MD). Unbound radioactivity was removed by three 5 ml washes with ice cold wash buffer. Filters were placed in 20 ml borosillicate glass scintillation vials containing 10 ml of scintillation cocktail (Beckman Ready Safe), mixed for 5 min and kept in the dark for 4 h. Filters were counted by liquid scintillation spectrometry using either a Packard CA2200 (42% efficiency) or Beckman LS5801 (55% efficiency) scintillation counter. Protein was measured according to the method of Lowry *et al.* (1951) with bovine serum albumin used as the standard.

Materials

[^{3}H]-8-OH-DPAT (229 Ci mmol^{-1}) was purchased from Amersham and [^{3}H]-BMY-7378 (76.5 Ci mmol^{-1}) was synthesized by New England Nuclear. 8-OH-DPAT and 5-carboxamidotryptamine (5-CT) were purchased from Research Biochemicals, Inc. (Natick, MA, U.S.A.) and methiothepin from BIOMOL Research Laboratories (Plymouth Meeting, PA, U.S.A.). Ketanserin and spiperone were generously provided by Janssen Pharmaceuticals and ICS 205-930 by Sandoz. Buspirone and BMY-7378 were synthesized locally. Guanyl nucleotides, pargyline and all other buffer reagents of the highest grade were purchased from Sigma Chemical Co. (St. Louis, MO, U.S.A.).

Data analysis

Saturation data were analyzed by the non-linear regression analysis programme, LIGAND (Munson & Rodbard, 1980). Binding curves were best fitted to a one site model, yielding the equilibrium dissociation constant (K_d), the maximal number of binding sites (B_{max}), and the Hill coefficient (nH). Displacement curves were analyzed by non-linear regression analysis, LIGAND (Munson & Rodbard, 1980) initially assuming a one-site model of ^{3}H-agonist binding, followed by analysis according to a two-site model. An *F* test ($P \leq 0.01$) was then used to determine whether the data were best described by the two-site model.

Correlation curves for the affinity values (pK_i) of the various agonists and antagonists determined with both [^{3}H]-8-OH-DPAT and [^{3}H]-BMY-7378 were constructed as a function of brain region (hippocampus vs. dorsal raphe) and fitted by linear regression, generating correlation coefficients.

Displacement of ^{3}H-agonist by Gpp(NH)p was analyzed by non-linear regression analysis, LIGAND (Munson & Rodbard, 1980) as described for the pharmacological displacement studies. All other statistical analyses were done using Student's paired *t* test with the accepted level of significance being $P \leq 0.05$).

Results

BMY-7378 was previously shown to demonstrate high affinity, selectivity and low intrinsic activity at the 5-HT$_{1A}$ receptor negatively coupled to adenylylcyclase in rat and guinea-pig hippocampal membranes (Yocca *et al.*, 1987). In rat hippocampal membrane homogenates, pharmacologically, the binding sites radiolabelled by [^{3}H]-8-OH-DPAT and [^{3}H]-BMY-7378 appear indistinguishable (Table 1). A linear correlation exists between the affinities of drugs for specific [^{3}H]-8-OH-DPAT and [^{3}H]-BMY-7378 binding ($r = 0.99$, data not shown) suggesting these radioligands recognize a common population of binding sites.

In both bovine hippocampus (Figure 1) and dorsal raphe nucleus (Figure 2), [^{3}H]-8-OH-DPAT and [^{3}H]-BMY-7378 bound in a concentration-dependent (approximately 0.0625 to 6 nM) and saturable manner, and displayed high affinity (K_d, nM, [^{3}H]-8-OH-DPAT: 1.08 ± 0.10, 1.57 ± 0.11, [^{3}H]-BMY-7378: 1.30 ± 0.14, 1.64 ± 0.12 nM, hippocampus and dorsal raphe respectively, $n = 9$), and relatively low non-specific binding. The linear Scatchard transformations of the saturation isotherms suggested that each radioligand labelled a homogeneous population of binding sites in both hippocampus and dorsal raphe membrane homogenates. While in bovine dorsal raphe membrane homogenates [^{3}H]-BMY-7378 labelled an equivalent number of binding sites to [^{3}H]-8-OH-DPAT (58 ± 4, 55 ± 4 fmol mg^{-1} protein, respectively), in bovine hippocampal membrane homogenates, [^{3}H]-BMY-7378 appeared to label a slightly greater ($P \leq 0.05$) maximal number of binding sites than [^{3}H]-8-OH-DPAT (372 ± 22, 304 ± 19 fmol mg^{-1} protein, respectively).

The affinity constants (K_i) of various 5-HT receptor agonists and antagonists for [^{3}H]-BMY-7378 and [^{3}H]-8-OH-DPAT binding sites in bovine hippocampal and dorsal raphe homogenates were determined (Table 2). As with rat hippocampus, in both bovine hippocampus and dorsal raphe nucleus, a linear correlation ($r = 0.99$, data not shown) exists between the affinities of drugs for specific [^{3}H]-8-OH-DPAT and [^{3}H]-BMY-7378 binding. A significant correlation

Table 1 Displacement of [^{3}H]-8-OH-DPAT (0.5 nM) and [^{3}H]-BMY-7378 (0.375 nM) binding by various 5-HT receptor ligands in rat hippocampal membrane homogenates

	Rat hippocampus	
	[^{3}H]-8-OH-DPAT K_i(nM)	*[^{3}H]-BMY-7378* k_i (nM)
5 CT	0.74 ± 0.06	0.32 ± 0.04
BMY-7378	0.97 ± 0.29	1.29 ± 0.38
8-OH-DPAT	1.16 ± 0.04	1.40 ± 0.12
Buspirone	16.6 ± 0.1	16 ± 1
Methiothepin	21 ± 3	14 ± 2
Spiperone	30 ± 2	17 ± 2
Ketanserin	1907–620	845 ± 113

Results are the mean ± s.e.mean of three separate experiments performed in duplicate. The data were analyzed by non-linear regression analysis as described in Methods. For abbreviations, see text.

($r = 0.99$) was also obtained for each radioligand between brain regions (Figure 3a and b), as well as with the full and partial ^{3}H-agonist between brain regions (Figure 3c and d). Spearman's rank correlation indicates that the rank order potency of the compounds tested was conserved between regions.

The non-hydrolyzable guanine nucleotide, Gpp(NH)p, caused a concentration-dependent attenuation of both [^{3}H]-8-OH-DPAT and [^{3}H]-BMY-7378 binding (2 nM, Figure 4a and b). The data were fitted to a four-parameter logistic equation, which within either brain region, yielded shallow displacement of both [^{3}H]-8-OH-DPAT and [^{3}H]-BMY-7378 binding (slope index: hippocampus, 0.34 ± 0.01, 0.39 ± 0.05, dorsal raphe 0.67 ± 0.19, 0.54 ± 0.06). In dorsal raphe nucleus, Gpp(NH)p caused a similar maximal displacement (E_{max}) of either [^{3}H]-8-OH-DPAT or [^{3}H]-BMY-7378 binding (55.4 ± 0.6%, 51.7 ± 2.0%, respectively) and produced comparable IC_{50} values for either radioligand (0.33 ± 0.89 μM, 0.67 ± 0.22 μM, respectively). However, in hippocampus,

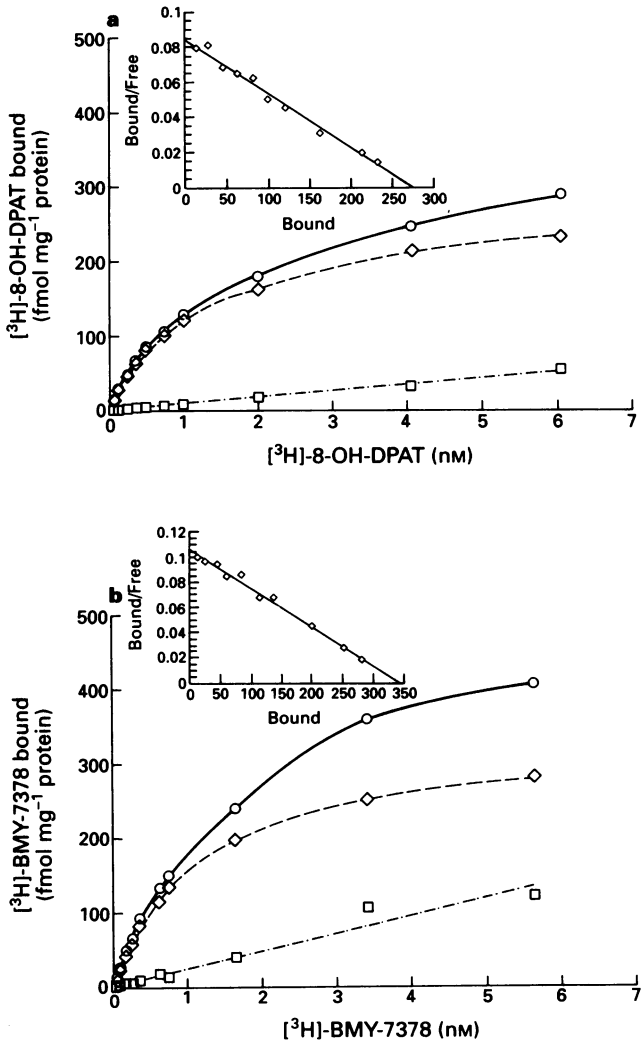


Figure 1 Representative concentration-binding curves (total binding, O; non-specific binding, □; and specific binding, ◇; and Scatchard transformations (inset) of [^{3}H]-8-OH-DPAT (a) and [^{3}H]-BMY 7378 binding (b) in a common bovine hippocampal membrane homogenate. Non-specific binding was defined by 1 μM 5-HT. Data points shown represent the mean of duplicate determination, with the range less than 5% of the mean. Estimates of K_d [^{3}H]-8-OH-DPAT, 1.23 nM; [^{3}H]-BMY-7378, 1.24 nM) and B_{max} ([^{3}H]-8-OH-DPAT, 274 fmol mg^{-1} protein; [^{3}H]-BMY-7378, 348 fmol mg^{-1} protein) values were obtained from non-linear regression analysis as described in Methods. This experiment was performed an additional eight times with similar results.

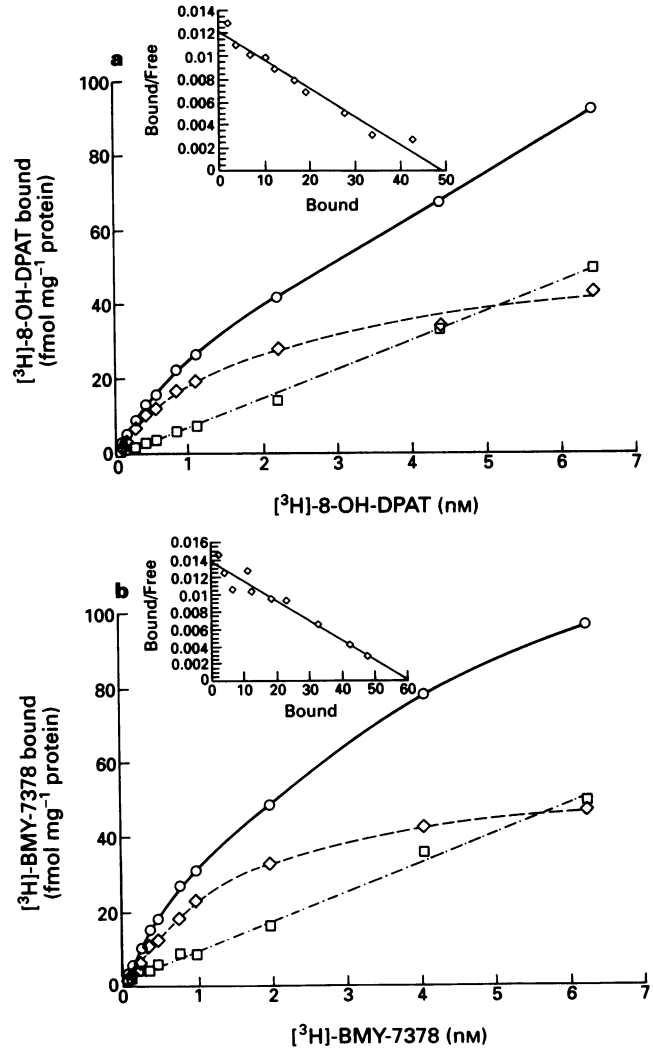


Figure 2 Representative concentration-binding curves (total binding, O; non-specific binding, □; and specific binding, ◇), and Scatchard transformations (inset) of [^{3}H]-8-OH-DPAT (a) and [^{3}H]-BMY 7378 binding (b) in a common bovine raphe nuclei membrane homogenate. Non-specific binding was defined by 1 μM 5-HT. Data points shown represent the mean of duplicate determination, with the range less than 5% of the mean. Estimates of K_d ([^{3}H]-8-OH-DPAT, 1.57 nM; [^{3}H]-BMY-7378, 1.73 nM) and B_{max} ([^{3}H]-8-OH-DPAT, 49 fmol mg^{-1} protein; [^{3}H]-BMY-7378, 61 fmol mg^{-1} protein) values were obtained from non-linear regression analysis as described in Methods. This experiment was performed an additional eight times with similar results.

Gpp(NH)p caused a significantly greater ($P \leqslant 0.01$) maximal attenuation of the specific binding of [^{3}H]-8-OH-DPAT and [^{3}H]-BMY-7378 (79.5 ± 3.3%, 60.8 ± 1.5%, respectively). While the IC_{50} values obtained with [^{3}H]-8-OH-DPAT were not significantly different from those obtained with [^{3}H]-BMY-7378 (84 ± 19 μM, 120 ± 34 μM, respectively) in hippocampus, they were significantly different ($P \leqslant 0.01$) from that obtained for both radioligands in dorsal raphe.

To determine the effect of Gpp(NH)p on affinity-related binding parameters (K_d and B_{max}), complete saturation isotherms were constructed in the absence or presence of Gpp(NH)p (1, 10, and 100 μM). In both bovine hippocampus and dorsal raphe nucleus, Gpp(NH)p did not alter the dissociation constant for either radioligand. However, a concentration-dependent attenuation in the B_{max} for both [^{3}H]-8-OH-DPAT and [^{3}H]-BMY-7378 binding (Figure 5a and b) was observed. In bovine hippocampus (Figure 5a), the above concentrations of Gpp(NH)p reduced the B_{max} of [^{3}H]-8-OH-DPAT binding by 11 ± 1%, 27 ± 3% and 42 ± 5%, respectively, while that of [^{3}H]-BMY-7378 was reduced by 5 ± 3%. 12 ± 2% and 22 ± 1%. At 10 and 100 μM Gpp(NH)p, the reduction in the B_{max} of [^{3}H]-8-OH-DPAT binding was significantly greater ($P \leqslant 0.02$) than that obtained with [^{3}H]-BMY-7378. However, in the dorsal raphe (Figure 5b), a similar B_{max} reduction ([^{3}H]-8-OH-DPAT: 17 ± 3%, 40 ± 4%, and 36 ± 8%; [^{3}H]-BMY-7378: 19 ± 2%,

Table 2 Displacement of [^{3}H]-8-OH-DPAT (0.5 nM) and [^{3}H]-BMY 7378 (0.375 nM) binding by various 5-HT receptor ligands in bovine hippocampus and dorsal raphe membrane homogenates

	Bovine hippocampus				*Bovine dorsal raphe*			
	[^{3}H]-8-OH-DPAT		*[^{3}H]-BMY 7378*		*[^{3}H]-8-OH-DPAT*		*[^{3}H]-BMY 7378*	
	K_i (nM)	nH	K_i (nM)	nH	K_i (nM)	nH	K_i (nM)	nH
5-CT	0.22 ± 0.02	1.08 ± 0.02	0.23 ± 0.003	1.04 ± 0.05	0.28 ± 0.02	0.95 ± 0.07	0.33 ± 0.02	1.08 ± 0.08
BMY-7378	1.2 ± 0.2	0.83 ± 0.10	0.94 ± 0.03	0.99 ± 0.10	1.24 ± 0.20	0.76 ± 0.20	3.02 ± 1.54	1.31 ± 0.12
8-OH-DPAT	0.96 ± 0.06	1.01 ± 0.01	1.01 ± 0.02	1.02 ± 0.04	1.37 ± 0.06	0.91 ± 0.06	1.65 ± 0.13	1.15 ± 0.25
Buspirone	10.6 ± 0.7	0.97 ± 0.01	10.1 ± 0.7	0.98 ± 0.04	12.4 ± 0.4	0.95 ± 0.05	19.6 ± 3.3	1.11 ± 0.17
Methiothepin	68 ± 8	0.90 ± 0.07	60 ± 1	0.91 ± 0.03	93 ± 8	0.86 ± 0.05	69.9 ± 3.2	1.14 ± 0.13
Spiperone	101 ± 15	0.71 ± 0.02	63 ± 10	0.64 ± 0.04	114 ± 13	0.64 ± 0.05	65.5 ± 15.2	0.68 ± 0.08
Ketanserin	2076 ± 160	1.18 ± 0.06	1886 ± 173	1.13 ± 0.05	3007 ± 564	1.22 ± 0.08	4466 ± 270	1.78 ± 0.17
ICS 205-930	3143 ± 803	1.17 ± 0.25	3400 ± 559	1.45 ± 0.05	5387 ± 646	1.26 ± 0.03	6358 ± 580	1.29 ± 0.17

Results are the mean ± s.e.mean of three separate experiments performed in duplicate. The data was analyzed by non-linear regression analysis as described in Methods.

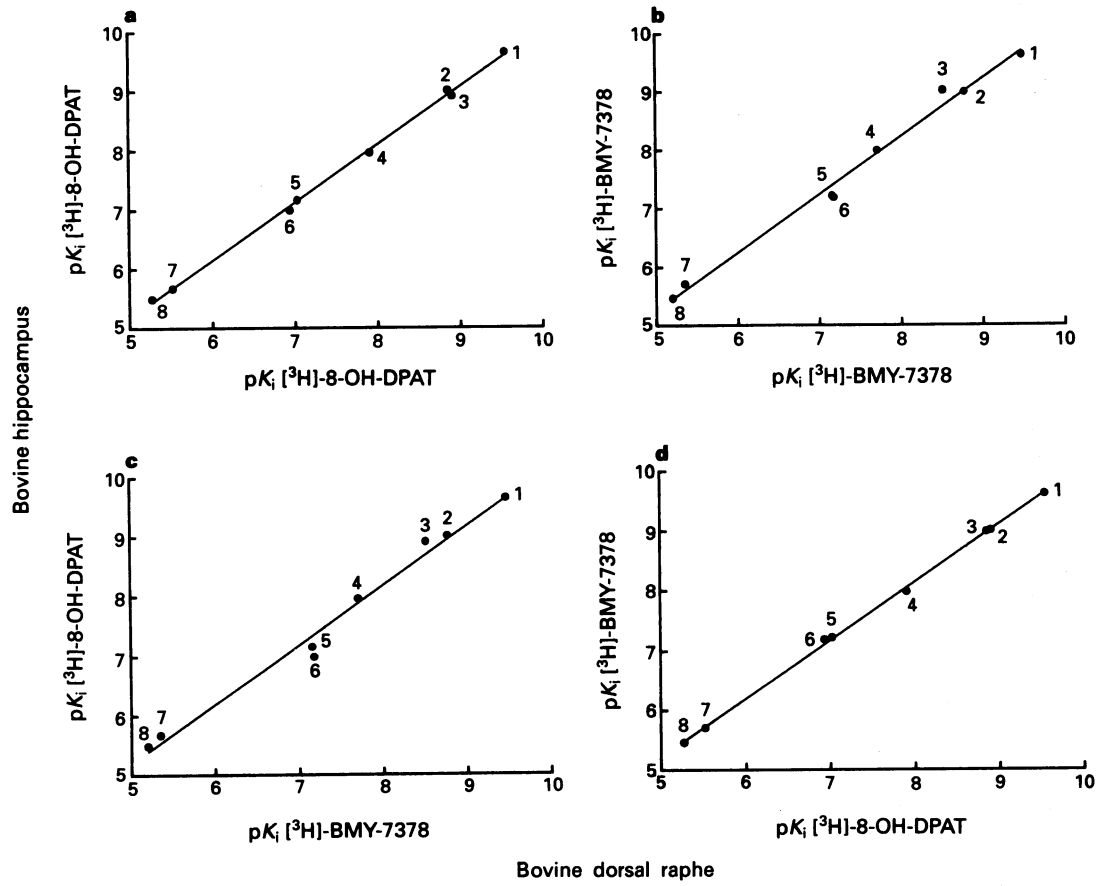


Figure 3 Correlation of the affinity values (pK_i) of various 5-HT receptor ligands for [^{3}H]-8-OH-DPAT (0.5 nM) and [^{3}H]-BMY 7378 (0.375 nM) binding in bovine hippocampal and dorsal raphe nuclei membrane homogenates. Each point represents the mean of three separate experiments. (1)= 5 CT, (2)= BMY-7378, (3)= 8-OH-DPAT, (4)= buspirone, (5)= methiothepin, (6)= spiperone, (7)= ketanserin and (8)= ICS 205-930. The data were fitted by linear regression where r was (a)= 0.9993, (b)= 0.9947, (c)= 0.9925, (d)= 0.9996.

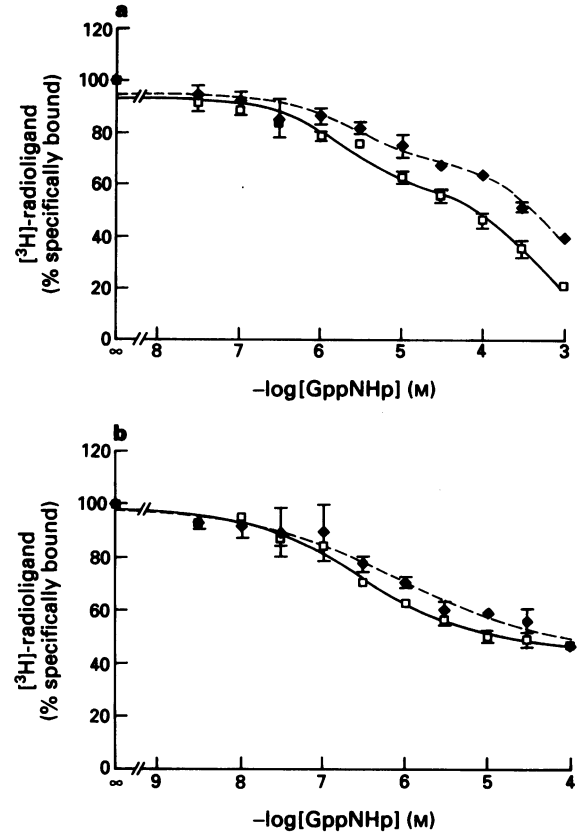


Figure 4 Attenuation of either [^{3}H]-8-OH-DPAT (□) or [^{3}H]-BMY 7378 (◆; 2 nM) binding by Gpp(NH)p in bovine hippocampal (a) and dorsal raphe nucleus (b) membrane homogenates. Data are expressed as percentage of ^{3}H-agonist binding in the absence of Gpp(NH)p and are the mean ± s.e. mean for three individual experiments performed in duplicate, and were fit to a four-parameter logistic equation which generated response parameters as described in the results section.

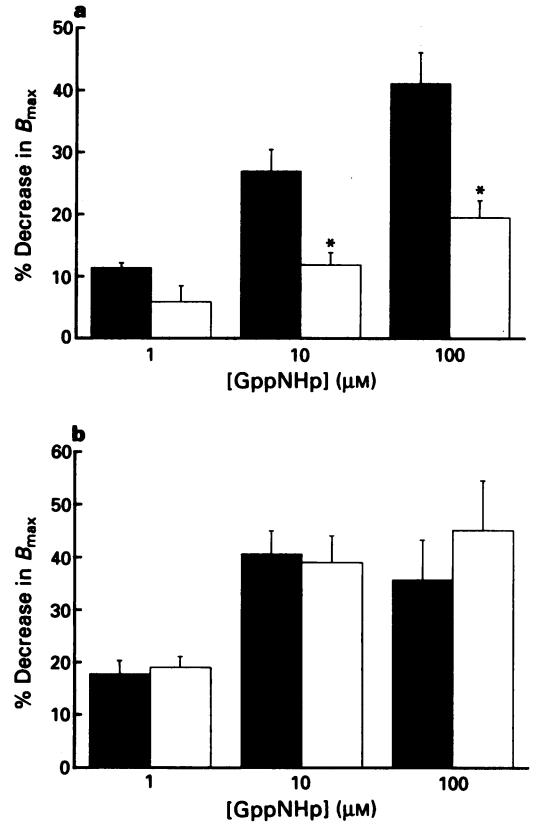


Figure 5 The effect of Gpp(NH)p (1, 10, and 100 μM) on the B_{max} values of either [^{3}H]-8-OH-DPAT (■) or [^{3}H]-BMY-7378 (□) binding in bovine hippocampus (a) and dorsal raphe nucleus (b). Each column represents the mean ± s.e. mean of three experiments, compared to the control values described in the results section. In hippocampus, [^{3}H]-8-OH-DPAT binding was reduced by 11 ± 1, 27 ± 3, and 42 ± 5%, while [^{3}H]-BMY-7378 binding was reduced by 6 ± 3, 12 ± 2, and 22 ± 1%. At 10 and 100 μM Gpp(NH)p, the effect on [^{3}H]-8-OH-DPAT binding was significantly greater than on [^{3}H]-BMY-7378 ($P<0.02$). In bovine dorsal raphe, [^{3}H]-8-OH-DPAT binding was reduced by 17 ± 3, 40 ± 4, and 36 ± 8%, while [^{3}H]-BMY-7378 was reduced by 19 ± 2, 38 ± 5, and 47 ± 11%.

38 ± 5% and 47 ± 11%) was observed with both radioligands.

Discussion

While pharmacological differences in regionally distinct 5-HT_{1A} receptors have been suggested (Blier & de Montigny, 1987; Sprouse & Aghajanian, 1988), molecular biological techniques have yet to provide evidence for multiple subtypes of 5-HT_{1A} receptors. Although the existence of distinct receptor subtypes may account for a heterogeneity in binding or functional responses, pharmacologically identical receptors may exhibit heterogeneity which can be accounted for by differences in the receptor system. These differences may occur at the level of the receptor and be influenced by large differences in receptor density (Varrault *et al.*, 1992). Variation in the availability or coupling of a particular receptor to the G-protein(s) or effector within a particular region may also occur (Ghodsi-Housepian *et al.*, 1990). In this study, the question of putative differences amongst the recognition properties of regionally distinct 5-HT_{1A} receptors was addressed by comparing the pharmacological profiles of 5-HT sensitive [^{3}H]-8-OH-DPAT and [^{3}H]-BMY-7378 binding at a 5-HT_{1A} presynaptic (dorsal raphe) and postsynaptic (hippocampus) recognition sites in the bovine brain.

The correlation of the p$K_i$values for 5-HT agonists and antagonists compared between regions as well as between ligands within the same region indicate that the 5-HT_{1A} receptor binding sites localized in the dorsal raphe are pharmacologically indistinguishable from those found in the hippocampus (Figure 3). A comparison of the K_i values obtained in either region of bovine brain with those obtained in rat hippocampus (Table 1) indicates that no significant differences between the binding profiles of rat and bovine 5-HT_{1A} receptor binding sites exists, suggesting that the recognition component of the 5-HT_{1A} receptor is conserved in different species.

While for other receptor systems it has been postulated that the affinity constant (K_d) generated from ligand binding studies represents a high affinity state parameter, and the EC_{50} generated from functional studies represents a low affinity state parameter (Nathanson, 1983), it was recently demonstrated (Chamberlain *et al.*, 1993), that [^{3}H]-8-OH-DPAT could be used to label a receptor demonstrating nanomolar affinity and a second site demonstrating lower affinity. Further analysis determined that the high affinity site correlated with the high affinity state of the 5-HT_{1A} receptor and the site displaying lower affinity correlated with the low affinity state of the 5-HT_{1A} receptor. We have previously demonstrated in rat hippocampal membrane homogenates (Mahle *et al.*, 1992), that the ratio of the EC_{50}, determined by the inhibition of forskolin-stimulated adenylylcyclase, and the K_d, determined by saturation analysis, was significantly greater for the full agonist 8-OH-DPAT and would fit the model in which this ratio was suggested to be proportional to

drug relative efficacy (Kent *et al.*, 1980). Thus compounds displaying a lesser ratio in EC_{50}/K_d values would be likely to fall more toward the antagonist end of the spectrum of intrinsic activity, and hence probably also radiolabel receptors in the low affinity state. However, in a region where R/G ratios were similar and fewer low affinity receptors exist, differences in B_{max} values would not be expected.

Saturation analysis using both a full and partial ^{3}H-agonist yielded linear scatchard plots, suggesting a homogeneity in receptor binding sites. Interestingly, similar dissociation constants were obtained between regions with both radioligands, further suggesting that both radioligands recognize a common population of sites in both regions. While we have previously shown (Mahle *et al.*, 1992), using conditions known to label primarily the high affinity state of the receptor in rat hippocampal membrane homogenates, [^{3}H]-BMY-7378 labelled fewer sites than did the full agonist [^{3}H]-8-OH-DPAT. In this study using bovine hippocampus and slightly different binding conditions, the partial agonist [^{3}H]-BMY-7378 labelled a slightly greater density of binding sites. However, in raphe nucleus, both radioligands label a similar number of binding sites.

The ability of an agonist to display differing efficacies between regions may indicate the same receptor coupling to different G-proteins or coupling to the same G-protein(s) with a different efficiency. This possibility was explored by examining the allosteric inhibition of ^{3}H-agonist binding by Gpp(NH)p. Similar to what has been previously reported in rat hippocampal membrane homogenates (Mahle *et al.*, 1992), Gpp(NH)p allosterically attenuates binding of both the full and partial ^{3}H-agonist in bovine hippocampal and dorsal raphe nuclei membrane homogenates and produced a shallow displacement curve. The shallow displacement may reflect a complex binding stoichiometry between the 5-HT$_{1A}$ receptor and G-protein(s). In the opioid system, similar shallow displacements are attributed to a high-affinity component caused by the nucleotide binding to the G-protein $\alpha\beta\gamma$ holocomplex, and a low affinity portion caused by nucleotide binding to the free α subunit (Ott & Costa, 1989).

That the maximal amount of binding displaced by Gpp(NH)p was greater for [^{3}H]-8-OH-DPAT in the hippocampus, suggested that a component of the [^{3}H]-BMY-7378 binding represented that bound to the low affinity state of the receptor, and thus was not sensitive to the presence of guanine nucleotide. This further substantiates the likelihood that the greater density of [^{3}H]-BMY-7378 binding sites in hippocampus was most likely due to a larger proportion of receptors in the low affinity state. This phenomenon was, however, not observed in the raphe nucleus, suggesting as did saturation analysis, that both ligands bound to an equivalent number of high affinity receptors, and hence was affected to the same extent by the presence of Gpp(NH)p. This raises the intriguing possibility that a lesser amount of G-protein(s) exists for formation of a high affinity ternary complex in bovine hippocampus. Thus, in dorsal raphe nucleus where postsynaptic partial agonists behave as full agonists (Sprouse & Aghajanian, 1988) in addition to a 'receptor reserve', a 'G protein reserve' may also exist (Bohmaker *et al.*, 1992).

While within a particular region, Gpp(NH)p produces comparable IC_{50} values for both radioligands, they differ significantly between regions, demonstrating that the affinity of Gpp(NH)p for the ^{3}H-agonist/receptor/G-protein complex is different between regions, and suggests that if the receptor is identical, then it may couple to different G-proteins or couple to the same G-protein with differing efficacies. Ghodsi-Housepian *et al.* (1990) demonstrated that in rat brain, a regional difference in the efficiency of coupling occurs between muscarinic receptors and G-proteins. The possibility of a heterogeneous population of G-proteins within one or both regions should not be ignored, as Sen-ogles *et al.* (1990), in examining D_2 dopamine receptor/G-protein coupling, demonstrated variations in the affinities between subtypes of G_i proteins and the receptor in a reconstituted system. Another possibility for regional differences in receptor/G-protein coupling may lie in the existence of dissimilar membrane mileus in the different brain regions.

In conclusion, while the existence of a structural heterogeneity in pre- and postsynaptic 5-HT$_{1A}$ receptors cannot be totally eliminated, the results of this study suggest a pharmacological homogeneity exists between the 5-HT$_{1A}$ receptor binding sites in bovine hippocampus and dorsal raphe nucleus. Although prior studies have shown a large receptor reserve to exist for the 5-HT$_{1A}$ receptor in the rat raphe nuclei, but not in the hippocampus, the present paper demonstrates that in similar regions of the bovine brain, a marked regional difference in 5-HT$_{1A}$ receptor coupling to G protein(s) exist. Thus, a portion of the functional differences observed with agonists at pre- and postsynaptic 5-HT$_{1A}$ receptors may therefore be attributable to the interaction of these receptors and their associated G-proteins.

References

BLIER, P. & DEMONTIGNY, C. (1987). Modification of 5-HT neuron properties by sustained administration of the 5-HT$_{1A}$ agonist gepirone: electrophysiological studies in the rat brain. *Synapse*, **1**, 470–480.

BOHMAKER, K., BORDI, F. & MELLER, E. (1992). The effects of pertussis toxin on dopamine D_2 and serotonin 5-HT$_{1A}$ autoreceptor-mediated inhibition of neurotransmitter synthesis: relationship to receptor reserve. *Neuropharmacology*, **31**, 451–459.

CHAMBERLAIN, J., OFFORD, S.J., WOLFE, B.B., TYAU, L.S., WANG, H. & FRAZER, A. (1993). Potency of 5-hydroxytryptamine$_{1A}$ agonists to inhibit adenyl cyclase activity is a function of affinity for the 'low affinity' state of [^{3}H]8-hydroxy-N-N-dipropylaminotetralin ([^{3}H]8-OH-DPAT) binding. *J. Pharmacol. Exp. Ther.*, **266**, 618–625.

COLINO, A. & HALLIVELL, J.V. (1987). Differential modulation of three separate K-conductances in hippocampal CA1 neurons by serotonin. *Nature*, **328**, 73–76.

DEVIVO, M. & MAYAANI, S. (1986). Characterization of the 5-hydroxytyptamine$_{1A}$ receptor-mediated inhibition of forskolin-stimulated adenylatecyclase activity in guinea pig and rat hippocampal membranes. *J. Pharmacol. Exp. Ther.*, **238**, 248–253.

GHODSI-HOUSEPIAN, S., MESSER, Jr, W.S. & HOSS, W. (1990). Differential coupling between muscarinic receptors and G-proteins in regions of the rat brain. *Biochem. Pharmacol.*, **39**, 1385–1391.

HARRINGTON, M.A., OKSENBERG, D. & PEROUTKA, S.J. (1988). 5-HT$_{1A}$ receptors are linked to a G_i-adenylate cyclase complex in rat hippocampus. *Eur. J. Pharmacol.*, **154**, 95–98.

HJORTH, S. & MAGNUSSON, T. (1988). The 5-HT$_{1A}$ receptor agonist, 8-OH-DPAT, preferentially activates cell body 5-HT autoreceptors in rat brain *in vivo*. *Naunyn Schmied Arch. Pharmacol.*, **338**, 463–471.

INNIS, R.B., NESTLER, E.J. & AGHAJANIAN, G.K. (1988). Evidence for G-protein mediation of serotinin- and GABA$_B$-induced hyperpolarization of rat dorsal raphe neurons. *Brain Res.*, **459**, 27–36.

KENT, R.S., DELEAN, A. & LEFKOWITZ, R.J. (1980). A quantitative analysis of beta-adrenergic receptor interactions: Resolution of high and low affinity states of the receptor by computer modeling of ligand binding states. *Mol. Pharmacol.*, **17**, 14–23.

LOWRY, O.H., ROSEBROUGH, N.J., FARR, A.L. & RANDALL, R.J. (1951). Protein measurement with the Folin phenol reagent. *J. Biol. Chem.*, **193**, 265–275.

MAHLE, C.D., WIENER, H.L., YOCCA, F.D. & MAAYANI, S. (1992). Allosteric interactions between the binding sites of receptor agonists and guanine nucleotides: a comparative study of the 5-hydroxytryptamine$_{1A}$ and adenosine A_1 receptor systems in rat hippocampal membranes. *J. Pharmacol. Exp. Ther.*, **263**, 1275–1284.

MELLER, E., BOHMAKER, K., NAMBA, Y., FRIEDHOFF, A.J. & GOLDSTEIN, M. (1987). Relationship between receptor occupancy and response at striatal dopamine autoreceptors. *Mol. Pharmacol.*, **31**, 592–598.

MELLER, E., ENZ, A. & GOLDSTEIN, M. (1988). Absence of receptor reserve at striatal dopamine receptors regulating cholinergic neuronal activity. *Eur. J. Pharmacol.*, **155**, 151–154.

MELLER, E., GOLDSTEIN, M. & BOHMAKER, K. (1990). Receptor reserve for 5-hydroxytryptamine$_{1A}$-mediated inhibition of serotonin synthesis: possible relationship to anxiolytic properties of 5-hydroxytryptamine$_{1A}$ agonists. *Mol. Pharmacol.*, **37**, 231–237.

MIDDLEMISS, D.N. & FOZARD, J.R. (1983). 8-hydroxy-2-(di-n-propylamino)-tetralin discriminates between subtypes of the 5-HT$_1$ recognition site. *Eur. J. Pharmacol.*, **90**, 151–153.

MUNSON, P.J. & RODBARD, D. (1980). LIGAND: a versatile computerized approach for the characterization of ligand binding systems. *Anal. Biochem.*, **107**, 220–239.

NATHANSON, N.M. (1983). Binding of agonists and antagonists to muscarinic acetylcholine receptors on intact cultured heart cells. *J. Neurochem.*, **41**, 1545–1549.

NELSON, D.L., HERBERT, A., BOURGOIN, S., GLOWINSKI, J. & HAMON, M. (1978). Characteristics of central 5-HT receptors and adaptive changes following intracerebral 5,7-dihydroxytryptamine administration in the rat. *Mol. Pharmacol.*, **14**, 983–995.

OTT, S. & COSTA, T. (1989). Guanine nucleotide-mediated inhibition of opioid agonist binding. Modulatory effects of ions and of receptor occupancy. *Biochem. Pharmacol.*, **38**, 1931–1939.

PAZOS, A. & PALACIOS, J. (1985). Quantitative autoradiographic mapping of 5-HT receptors in the rat brain. I. Serotinin-1 receptors. *Brain Res.*, **346**, 205–230.

SENOGLES, S.E., SPIEGEL, A.M., PADRELL, E., IYENGAR, R. & CARON, M.G. (1990). Specificity of receptor-G protein interactions. *J. Biol. Chem.*, **265**, 4507–4514.

SPROUSE, J.S. & AGHAJANIAN, G.K. (1987). Electrophysiological responses of serotonergic dorsal raphe neurons to 5-HT$_{1A}$ and 5-HT$_{1B}$ agonists. *Synapse*, **1**, 3–9.

SPROUSE, J.S. & AGHAJANIAN, J.K. (1988). Response of hippocampal pyramidal cells to putative serotonin 5-HT$_{1A}$ and 5-HT$_{1B}$ agonists: A comparative study with dorsal raphe neurons. *Neuropharmacology*, **27**, 707–715.

VARRAULT, A., JOURNOT, L., AUDIGIER, Y. & BOCKAERT, J. (1992). Transfection of human 5-hydroxytryptamine receptors in NIH-3T$_3$ fibroblasts: effects of increasing receptor density on the coupling of 5-hydroxytryptamine$_{1A}$ receptors to adenyl cyclase. *Mol. Pharmacol.*, **41**, 999–1007.

YOCCA, F.D., IBEN, L. & MELLER, E. (1992). Lack of apparent receptor reserve at postsynaptic 5-hydroxytryptamine$_{1A}$ receptors negatively coupled to adenylylcyclase activity in rat hippocampal membranes. *Mol. Pharmacol.*, **14**, 1066–1072.

YOCCA, F.D., SMITH, D.W., HYSLOP, D.K. & MAAYANI, S. (1987). BMY 7378: a buspirone analog with high selectivity, affinity and low efficacy at 5-HT$_{1A}$ receptors in rat and guinea pig hippocampal membranes. *Eur. J. Pharmacol.*, **137**, 293–294.

(Received June 10, 1994
Revised July 20, 1994
Accepted July 22, 1994)

Br. J. Pharmacol. (1994), **113**, 1407–1415 © Macmillan Press Ltd, 1994

Differences in the distribution and characteristics of tachykinin NK_1 binding sites between human and guinea pig lung

[1]David A. Walsh*†, Michael Salmon*, Roland Featherstone‡, John Wharton*, Martin K. Church‡ & Julia M. Polak*

*Department of Histochemistry, Royal Postgraduate Medical School, Hammersmith Hospital, Du Cane Road, London W12 0NN, †Inflammation Group, Arthritis and Rheumatism Council Building, The London Hospital Medical College, Whitechapel, London, E1 2AD, and ‡Department of Immunopharmacology, Centre Block, Southampton General Hospital, Southampton SO9 4XY

1 The distribution and characteristics of tachykinin NK_1 binding sites have been compared in human and guinea pig lung using quantitative *in vitro* receptor autoradiography with [^{125}I]-Bolton Hunter-labelled substance P ([^{125}I]-BH-SP). In addition, the effects on these sites of ovalbumin sensitization and challenge have been determined in guinea pig lung.

2 [^{125}I]-BH-SP bound specifically and with high affinity to microvascular endothelium in both human and guinea pig lung, but to bronchial smooth muscle and pulmonary artery media in only guinea pig lung.

3 Specific binding of [^{125}I]-BH-SP to guinea pig bronchial smooth muscle was positively correlated with airway diameter in the range 150–800 μm and was less dense in trachea than in main bronchi.

4 [^{125}I]-BH-SP binding was inhibited by tachykinins with rank orders of affinity of SP > NKA > NKB (human microvessels) and SP > NKA = NKB (guinea pig bronchi and pulmonary arteries). NKA displayed a higher affinity for [^{125}]-BH-SP binding sites in human microvessels than in guinea pig tissues ($P<0.0001$), indicating differences in selectivity for tachykinins between human and guinea pig NK_1 receptors.

5 In both human and guinea pig lung, [^{125}I]-BH-SP binding was inhibited by the specific tachykinin receptor antagonists FK888 (NK_1 selective antagonist) and FK224 (mixed NK_1/NK_2 antagonist), with FK888 displaying equal affinity to SP and > 500 times higher affinity than FK224. SP, NKA, NKB and FK888 exhibited similar affinities for [^{125}I]-BH-SP binding sites in both guinea pig arteries and bronchi.

6 Similar distributions, densities and characteristics of [^{125}I]-BH-SP binding sites were demonstrated in ovalbumin-sensitized and -challenged guinea-pig lung and in naive animals.

7 Differences in the distribution and characteristics of NK_1 binding sites labelled with [^{125}I]-BH-SP between guinea pig and human lung suggest limitations in the use of guinea pig models for studying roles of tachykinins in pulmonary disease. However, the similar microvascular distributions of NK_1 binding sites in human and guinea pig lung suggest that the selective tachykinin receptor antagonists FK888 and FK224 may be useful in the management of airway inflammation in man.

Keywords: Substance P; receptor; autoradiography; asthma; bronchoconstriction; endothelium; tachykinin antagonists.

Introduction

Tachykinins, including substance P (SP) and neurokinin A (NKA), have been implicated in the regulation of airway tone and in the induction of oedema and mucous secretion, as well as in the control of inflammatory cell function and pulmonary vascular tone (Frossard & Advenier, 1991). Tachykinin receptors have been classified into three main types, referred to as NK_1, NK_2 and NK_3, for which SP, NKA and neurokinin B (NKB) are the preferred endogenous agonists respectively, although considerable cross-reactivity occurs (Frossard & Advenier, 1991).

Both NK_1 and NK_2 receptors can mediate bronchoconstriction in the guinea pig (Maggi *et al.*, 1991), although endogenous tachykinins, released by agents such as capsaicin or by nerve stimulation, cause bronchoconstriction predominantly via NK_2 receptors (Maggi *et al.*, 1991; Ballati *et al.*, 1992; Renzetti *et al.*, 1992). In human airways, tachykinin-induced bronchoconstriction is predominantly NK_2 receptor mediated (Advenier *et al.*, 1987; Joos *et al.*, 1987). By contrast, in animals, airway oedema induced by exogenous or endogenously released tachykinins is mediated almost entirely by NK_1 receptors (Lembeck *et al.*, 1992; Murai *et al.*, 1993), and NK_1 receptors have been implicated in airway oedema induced by environmental agents such as cigarette smoke and allergen challenge (Delay-Goyet *et al.*, 1992; Bertrand *et al.*, 1993). NK_1 receptor activation also increases mucous secretion in human and guinea pig airways (Rogers *et al.*, 1989; Kuo *et al.*, 1990).

Because of these widespread effects on pulmonary function, it has been suggested that tachykinins play a role in human airway diseases such as asthma (Barnes, 1991). Recently, metabolically stable, selective tachykinin receptor antagonists have been developed as potential therapeutic agents for the treatment of human airway disease. These include the macrocyclic peptide, mixed NK_1/NK_2 receptor antagonist FK224 (*N*-[N^2-[*N*-[*N*-[2,3-didehydro-*N*-methyl-*N*-[*N*-[3-(2-pentylphenyl)-propionyl]-L-threonyl]tyrosyl-L-leucynyl]-D-phenylalanyl]-L-*allo*-threonyl]-L-asparaginyl]-L-serine-*v*-lactone) (Morimoto *et al.*, 1992) and the selective dipeptide NK_1 receptor antagonist, FK888 (N^2-[(4*R*)-4-hydroxy-1-(1-methyl-1H-indol-3-yl)carbonyl-L-prolyl]-*N*- methyl-*N*-phenyl methyl-3-(2-naphthyl)-L-alaninamide) (Fujii *et al.*, 1992). However, differences between experimental models and man have made interpretation of data derived from animals difficult. SP, for example, is a more potent mediator of bronchoconstriction in the commonly used models of airway

[1] Author for correspondence.

hyperreactivity in guinea pigs than in man (Advenier *et al.*, 1987).

Such species differences may be attributable to different distributions or pharmacological specificities of tachykinin receptor subtypes between species. Initial reports suggested similar distributions of [^{125}I]-BH-SP binding sites in human and guinea pig lung (Carstairs & Barnes, 1986), although a subsequent study found abundant binding to guinea pig airway smooth muscle but little or none to that in human lung (Goldie, 1990). [^{125}I]-BH-SP binding to guinea pig lung membranes has characteristics of NK_1 receptors (Geraghty *et al.*, 1992), and interspecies differences have recently been observed in the pharmacological profile of NK_1 receptors (Beresford *et al.*, 1991; Fujii *et al.*, 1992; Walsh *et al.*, 1993). The pharmacological characteristics of [^{125}I]-BH-SP binding sites in human lung have not, however, previously been reported or compared with those in the guinea-pig.

In addition to interspecies differences, responsiveness to SP may change during pulmonary disease. Following allergen challenge, guinea pigs become more sensitive to the bronchoconstrictor actions of SP with a leftward shift of the dose–response curve (Nieri *et al.*, 1992). It is at present unknown, however, whether antigen challenge modulates tachykinin receptor expression or if this increased sensitivity is due to other factors such as changes in peptide degradation or concomitant changes in prostaglandin release.

Since guinea pigs are commonly used as models of airway hyperreactivity in the development of pharmacological agents, we have compared the distribution and characteristics of [^{125}I]-BH-SP binding sites between guinea pig and human lung and have compared naive with ovalbumin-sensitized and -challenged guinea pigs. We have, furthermore, investigated the interaction with these sites of two tachykinin receptor antagonists, FK224 and FK888, recently developed as potential therapeutic agents for the treatment of human airway disease.

Methods

Tissues

Normal human lung was obtained from regions which were both macroscopically and microscopically normal from pneumonectomy samples removed for bronchial carcinoma ($n = 11$) and at autopsy ($n = 2$). The autoradiographic localization of [^{125}I]-BH-SP binding sites was investigated in samples of trachea, main/hilar bronchus and peripheral lung from two, ten and five cases respectively, and quantitative analysis performed on main and hilar bronchi.

Male Dunkin–Hartley guinea pigs were killed by overdose with sodium pentobarbitone (60 mg kg^{-1}), their tracheae and both lungs rapidly removed, and the lungs inflated by intratracheal insufflation with Tissue-Tek (Miles, Elkhart, IN, U.S.A.) diluted 1:1 with phosphate-buffered saline. Unfixed tissues were mounted on cork blocks with Tissue-Tek, snap frozen in melting isopentane and stored at −20°C. Sections (10 μm) were thaw mounted onto Vectabond-pretreated slides (Vector laboratories, Peterborough, U.K.) and used immediately or stored at −20°C with silica gel for up to 4 days before use.

Hypersensitive guinea pig model

Male Dunkin–Hartley strain guinea pigs ($n = 9$) were sensitized and challenged to ovalbumin by a modification of the method of Hutson *et al.* (1988). Animals were sensitized on two occasions (day 0 and 7) by 3 min exposure to an aerosol of 1% ovalbumin solution (w/v) in 0.9% saline, generated by a Wright nebulizer. Exposure was performed via an endotracheal tube inserted under transient anaesthesia induced by an injection of hypnorm (fentanyl citrate 0.315, fluanisone 10 mg ml^{-1}, 0.1 ml kg^{-1} s.c.) followed by exposure to methoxyflurane vapour. The use of an endotracheal tube avoids nasal deposition of the allergen and so restricts responses to the lower airways (Varley *et al.*, 1991a). Challenge of sensitized animals was performed on day 14, when they were exposed to an aerosol of 2% ovalbumin solution for 5 min, also administered via endotracheal tube while under anaesthesia. Animals were pretreated with mepyramine (15 mg kg^{-1} i.p.) 30 min prior to challenge to prevent death due to anaphylactic shock. Control animals included guinea pigs which were not sensitized and were challenged with normal saline rather than ovalbumin (naive group, $n = 6$), sensitized but not challenged (sensitized group, $n = 6$), or were not sensitized but challenged with ovalbumin (challenged group, $n = 6$).

Following challenge, lower airways responses were measured in sensitized and challenged animals and in naive animals using an automated, computer-controlled whole-body plethysmograph (Varley *et al.*, 1991b). Measurements of lung function were taken at 15, 30, 45, 60 and 90 min after challenge, at which point the animals were killed by overdose of sodium pentobarbitone (60 mg kg^{-1}). The mean weight of animals at death was 621 g (95% CI 596–646).

[^{125}I]-BH-SP in vitro *autoradiography*

Quantitative *in vitro* autoradiography, using [^{125}I]-BH-SP, was performed as previously described (Wharton *et al.*, 1993). Sections of guinea pig lung (10 μm thick) were preincubated for 20 min in 10 mM HEPES buffer, pH 7.4, containing 130 mM NaCl, 4.7 mM KCl, 5 mM $MgCl_2$, 1 mM ethyleneglycol-bis-(β-aminoethyl ether)-*N*,*N*,*N*',*N*-tetraacetic acid (EGTA) and 0.005% (v/v) polyethylenimine (buffer A). Excess buffer was removed and sections were incubated for 45 min with [^{125}I]-BH-SP in buffer B (buffer A plus 1% bovine serum albumin, 0.1% bacitracin, 100 μM chymostatin, 100 μM leupeptin and 10 μM phosphoramidon). Radioligand comprised 0.25 nM [^{125}I]-BH-SP alone (total binding) or together with an excess (1 μM) of unlabelled SP (non-specific binding). Sections were subsequently washed twice for 5 min at 4°C in buffer A and rinsed in distilled water before being rapidly dried under a stream of cold air. Binding to 10-μm-thick sections of human lung was assessed using a modification of the method of Carstairs & Barnes (1986). Incubation times and ligand concentrations were as for guinea pig lung, but, for human lung, buffers comprised 50 mM Tris-HCl, pH 7.4, with 3 mM $MnCl_2$ and 0.0025% polyethylenimine (buffer A) with buffer B containing, in addition, 1% bovine serum albumin, 0.1% bacitracin, 100 μM chymostatin, 100 μM leupeptin and 10 μM phosphoramidon. Except where stated, incubations were performed at 22°C.

Quantification of autoradiographic images

Radiolabelled tissue sections were apposed to radiosensitive film (Hyperfilm-[^{3}H], Amersham International, U.K.) and exposed for 3 days (guinea pig lung) or 5 days (human lung) at 4°C. Films were developed in Kodak D19 for 3 min at 15°C. Autoradiographic images were analysed using an IBAS 386 image processing system (Kontron, Watford, U.K.). Bronchi and pulmonary arteries were distinguished by comparison of films with corresponding tissue sections stained with haematoxylin and eosin. Binding density was derived from grey values by comparison with 10-μm-thick ^{125}I-labelled standards (Amersham International, U.K.) co-exposed with each film and corrected for the activity date of the radioligand.

Bronchus and pulmonary artery diameters were measured interactively on autoradiograms using the IBAS 386 image processing system. Diameters were taken as the maximum width perpendicular to the long axis of the structure, measured between the mid-points of the muscle layers, as indicated by localization of specific binding.

Microautoradiography

Tissue sections labelled with [^{125}I]-BH-SP were fixed in modified Bouin solution for 1 h at room temperature, washed in phosphate-buffered saline, rinsed in distilled water and dried in a flow of cold air. Sections were dipped in radiosensitive emulsion (Ilford K5) at 42°C and dried at room temperature. Following exposure for 3–5 weeks at 4°C, dipped slides were developed as for film autoradiograms, then counterstained with haematoxylin and eosin, dehydrated and mounted in dibutylphthalate polystyrene xylene (DPX, Raymond Lamb, London, U.K.).

Pharmacological characterization of [^{125}I]-BH-SP binding sites

Specific binding of [^{125}I]-BH-SP was defined as total binding minus non-specific binding (in the presence of 1 μM SP). Saturability of binding was measured by 'cold' saturation using total SP concentrations over the range 0.25–10.25 nM. Sections were incubated with 0.25 nM [^{125}I]-BH-SP together with increasing concentrations of unlabelled SP and total bound ligand (radiolabelled plus unlabelled) calculated as $([*L] + [L]) \times *B/[*L]$, where [*L] is the concentration of free [^{125}I]-BH-SP, [L] is the concentration of free unlabelled SP, and *B is the measured bound [^{125}I]-BH-SP.

Specificity of [^{125}I]-BH-SP binding was measured by inhibition studies using unlabelled ligands, including SP and the related tachykinins NKA and NKB. In addition, inhibition studies were performed using the tachykinin receptor antagonists FK224 and FK888 (Fujisawa Pharmaceuticals, Osaka, Japan). NKB, FK224 and FK888 were each initially dissolved in dimethylsulphoxide (DMSO) and subsequently diluted in incubation buffer to give a maximum concentration of DMSO of 0.001%. In separate experiments, DMSO was found not to affect [^{125}I]-BH-SP binding at concentrations up to 0.005%.

Data analysis

Equilibrium constants were derived from specific binding data by iterative non-linear regression, assuming single-site models, using GraphPAD Inplot 4 (GraphPAD Software, San Diego, CA, U.S.A.). For guinea-pigs, equilibrium constants were derived for each of 2–6 bronchi and 1–4 pulmonary arteries per animal. Equilibrium binding densities (B_{eq}) were obtained with 0.25 nM [^{125}I]-BH-SP, and equilibrium dissociation constants (K_d) and maximal binding densities (B_{max}) were derived from binding inhibition studies using 0.25 nM [^{125}I]-BH-SP and 0–1000 nM unlabelled SP (DeBlasi *et al.*, 1989). Values for binding inhibition constants (K_i) and Hill coefficients were derived by fitting to sigmoid curves. K_i values were derived from IC_{50} values for each structure using the K_d value calculated for that structure in a consecutive series of sections (Cheng & Prusoff, 1973). Descriptive data are expressed as geometric means (95% confidence interval) of six guinea pigs per group. For human lung, the 12 microvessels per section with the most dense specific binding were quantified, and data are expressed as geometric means (95% confidence intervals) of 5–6 cases. The relationships between equilibrium binding density and structure diameter in peripheral lung tissues were determined for each case by linear regression. B_{eq} and B_{max} values were compared between naive and ovalbumin-challenged animals by stepwise multiple regression incorporating structure diameter and using the Statistical Package for Social Sciences (SPSS) software version 4.0 (Chicago, IL, U.S.A.). Comparisons of K_i values (which were not significantly correlated with structure diameter) and between different structures were made using analysis of variance (ANOVA) and Student's *t*-test with Bonferroni corrections on geometric data. Comparisons between bronchi and pulmonary arteries were made on data from separate experiments to those for comparisons between naive and ovalbumin-sensitized and -challenged animals.

Immunohistochemistry

To confirm the binding of [^{125}I]-BH-SP to bronchial microvessels, consecutive sections to microautoradiograms were immunostained for von Willebrand factor (vWF) or platelet–endothelial cell adhesion molecule (PECAM, CD31) using previously characterized rabbit polyclonal antibodies (A082; Dako, High Wycombe, U.K.) or mouse monoclonal antibodies (JC170; Dako, High Wycombe, U.K.) respectively, and the avidin–biotin complex (ABC) method of Hsu *et al.* (1981). Cryosat sections (10 μm) were fixed in acetone for 5 min at 4°C, incubated with primary antibody for 2 h at room temperature, then with biotinylated goat anti-rabbit IgG (for vWF) or biotinylated horse antimouse IgG (for PECAM) for 30 min, avidin–biotin complex for 30 min and finally developed in diaminobenzidine, dehydrated and mounted in DPX.

Materials

[^{125}I]-BH-SP (Specific activity 2000 Ci mmol^{-1}), ^{125}I-labelled standards and Hyperfilm-[^{3}H] were obtained from Amersham International, U.K. FK224 (*N*-[*N*^{2}-[*N*-[*N*-[2,3-didehydro-*N*-methyl-*N*-[*N*-[3-(2-pentylphenyl)-propionyl]-L-threonyl]tyrosyl-L-leucynyl]-D-phenylalanyl]-L-*allo*-threonyl]-L-asparaginyl]-L-serine-*v*- lactone) and FK888 (*N*^{2}-[(4R)-4-hydroxy-1-(1-methyl-1H-indol-3-yl)carbonyl-L-prolyl]-*N*-methyl-*N*-phenyl methyl-3-(2-naphthyl)-L-alaninamide) were kindly provided by Fujisawa Pharmaceuticals, Osaka, Japan. Other unlabelled peptides, enzyme inhibitors and enzyme-free bovine serum albumin were obtained from Sigma Chemical Co., Poole, U.K. Antibodies to vWF and PECAM were purchased from Dako, High Wycombe, U.K., and biotinylated goat anti-rabbit affinity-purified IgG biotinylated horse anti-mouse affinity-purified IgG and avidin–biotin complex were from Vector laboratories, Peterborough, U.K.

Results

Localisation of [^{125}I]-BH-SP binding sites

Human lung Specific binding of [^{125}I]-BH-SP was demonstrated to the endothelium of bronchial microvessels between the airway epithelium and smooth muscle, and in the connective tissue around cartilage (Figures 1a and 2a–d). Specific binding of [^{125}I]-BH-SP to microvessels was also observed in sections of human trachea and in main and hilar bronchus, but not in peripheral lung. No specific binding was observed to the smooth muscle of bronchus, trachea or pulmonary artery at any level. Specific binding of [^{125}I]-BH-SP in the region of bronchial and tracheal glands appeared to be localized to microvessels, as demonstrated by the distribution of vWF- and PECAM-like immunoreactivity, rather than to glandular elements themselves (Figure 2c and d). Binding of [^{125}I]-BH-SP to human lung under identical conditions to those used for guinea pig lung also revealed specific binding only to bronchial microvessels. Non-specific binding was, however, higher under these conditions.

Guinea pig lung Specific binding of [^{125}I]-BH-SP was localized in both naive and ovalbumin-challenged guinea pig lung to bronchial and tracheal smooth muscle (Figures 1c and e and 2e). On emulsion-dipped preparations, specific equilibrium binding of [^{125}I]-BH-SP to larger peripheral airways (diameter >500 μm) appeared denser than that to smaller peripheral airways (diameter <250 μm). Specific binding was observed to the endothelium of bronchial microvessels, both immediately beneath the epithelium and in connective tissue outside the cartilage of trachea and main bron-

chi. The distribution of [^{125}I]-BH-SP binding to bronchial microvessels corresponded to that of vWF-immunoreactive endothelia. Specific binding in the region of tracheal mucous glands was localized to microvessels rather than to glandular elements. Specific binding was also observed to the media of pulmonary arteries in peripheral lung (Figure 1e), but not in central pulmonary arteries. Specific binding was observed to ganglia in the oesophagus and intense non-specific binding was observed to airway epithelium and to eosinophils in some specimens. Polyethylenimine at 0.005% did not significantly inhibit specific [^{125}I]-BH-SP binding, but considerably reduced non-specific binding to eosinophils. Specific binding was not observed to airway epithelium.

Characterisation of [^{125}I]-BH-SP binding sites

Human lung Specific binding of [^{125}I]-BH-SP to human bronchial microvessels was saturable and of high affinity (Table 1 and Figure 3). Specific binding was inhibited by tachykinins with a rank order of affinities SP> NKA > NKB (Table 1 and Figure 4a). The selective tachykinin receptor antagonists inhibited specific binding, FK888 having > 500 times higher affinity than FK224 and equal affinity to SP (Table 1 and Figure 4b).

Guinea pig lung Specific binding of [^{125}I]-BH-SP to guinea pig bronchi and pulmonary arteries was also saturable and of

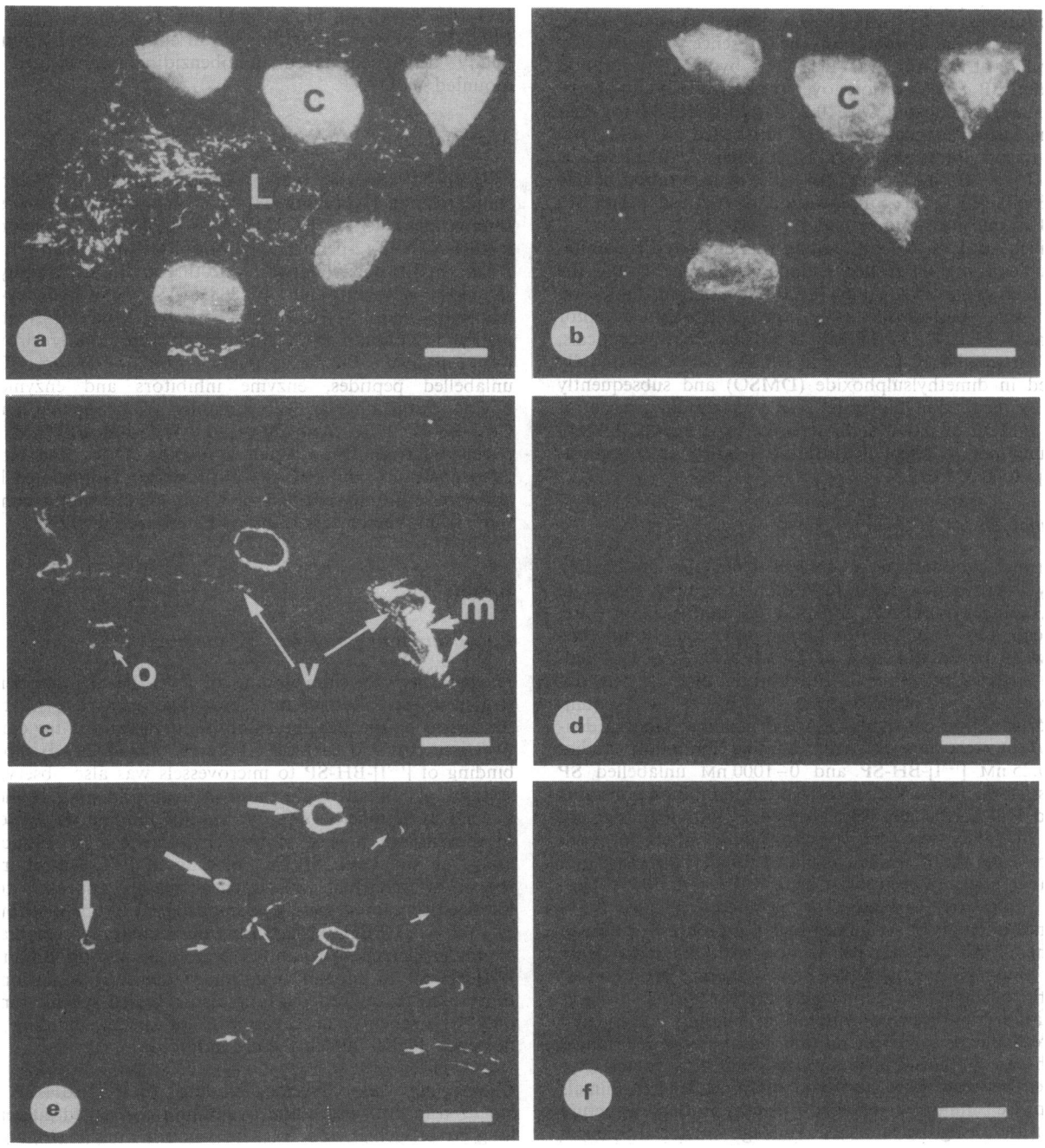


Figure 1 Binding of 0.25 nM [^{125}I]-Bolton Hunter-labelled substance P to human (a and b) and guinea-pig (c–f) lung. (a and b) Human bronchus showing specific punctate binding to microvessels in the submucosa and peribronchial regions. No specific binding is observed to bronchial smooth muscle. C, non-specific binding to bronchial cartilage; L, bronchial lumen. (c and d) Guinea pig trachea and hilar region showing specific binding to tracheal and hilar airway smooth muscle (m), to subepithelial microvessels (v) and to oesophagus (o). (e and f) Intrapulmonary structures in guinea pig lung with specific binding to bronchial smooth muscle (large arrows) and pulmonary artery media (small arrows). (a, c and e) Total binding and (b, d and f) non-specific binding in the presence of 1 μM unlabelled substance P. Reversal prints of film autoradiograms. Bars = 2 mm.

high affinity (Table 1 and Figure 3). Specific binding to each structure was inhibited by tachykinins with the rank order of affinities SP > NKA = NKB (Table 1 and Figures 4c and 5). Binding was also inhibited by the tachykinin receptor antagonists FK224 and FK888, with FK888 having > 500 times higher affinity than FK224 (Table 1 and Figure 4d). No significant differences were found between bronchi and pulmonary arteries for affinities of SP, NKA, NKB or FK888. Bronchial microvessels demonstrated a similar order of affinities for these compounds, as assessed subjectively on emulsion-dipped preparations, to that found by quantification for bronchi and pulmonary arteries.

No significant differences in K_i values were found between human bronchial microvessels and guinea pig bronchi for the antagonists FK224 and FK888, but the agonist NKA had higher affinity in human bronchial microvessels than in guinea pig bronchi (Table 1).

Equilibrium binding of [^{125}I]-BH-SP to airway smooth muscle varied through the bronchial tree, with most dense binding to large, central bronchi and less dense binding to trachea ($t = 3.19$, $P = 0.004$). Increasing bronchial diameter in peripheral lung sections was associated with increasing B_{eq} (Table 2) and with increasing maximal binding density [slope of log B_{max} vs. mean bronchial diameter = 0.7 (95% CI 0.02–1.4) (log amol mm^{-2}) mm^{-1}, $R^2 = 0.14$, $P = 0.04$]. No significant associations were observed between K_i values and bronchial diameter. Equilibrium binding of [^{125}I]-BH-SP to pulmonary arteries in peripheral lung was positively correlated with pulmonary artery diameter (Table 2).

Hypersensitive guinea pig model Ovalbumin challenge of sensitized guinea pigs induced significant and transient increases in airway resistance from 15 to 30 min after challenge, as compared with sensitized animals challenged

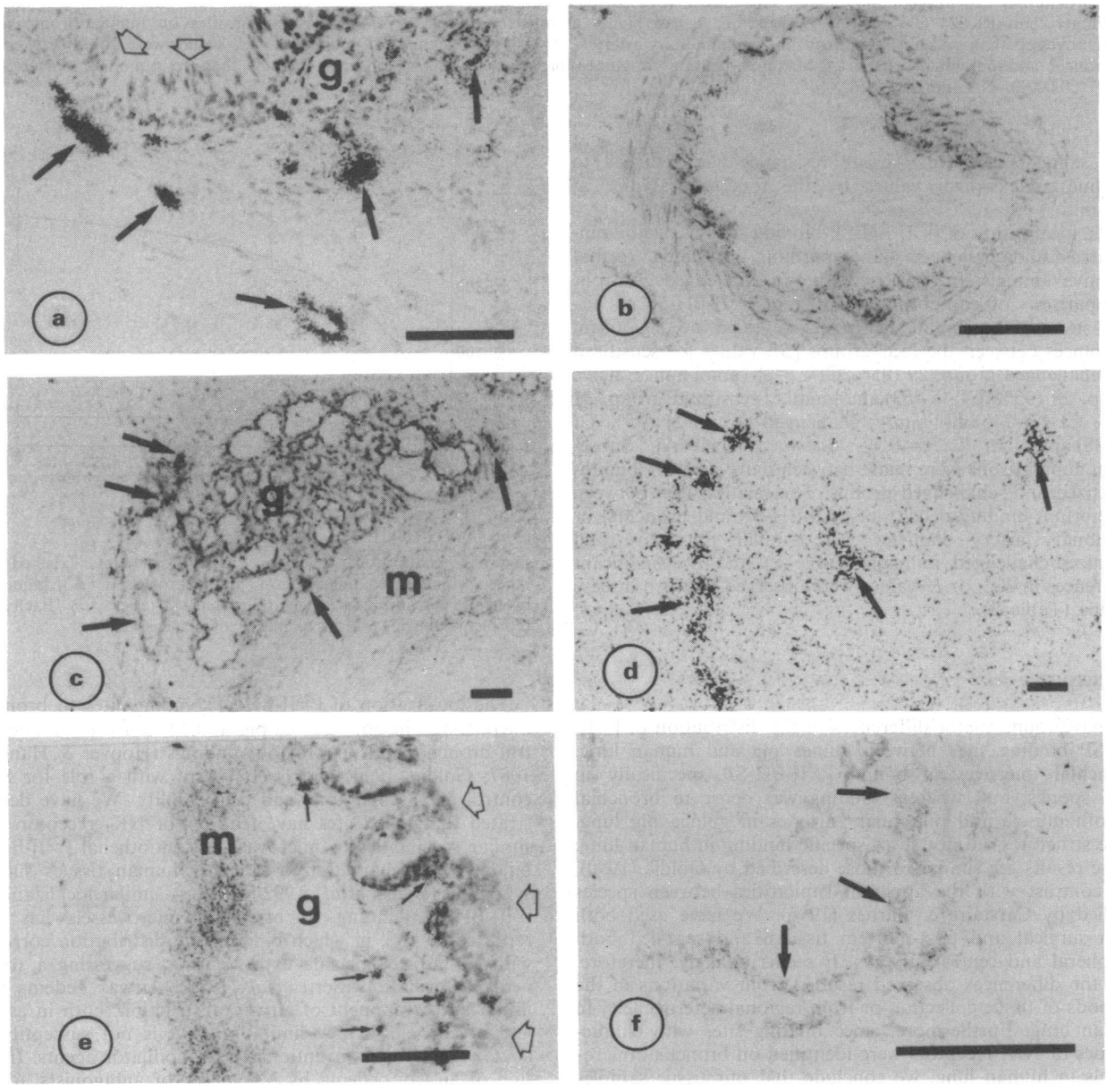


Figure 2 Microscopic localization of [^{125}I]-Bolton Hunter-labelled substance P binding in human (a–d) and guinea pig (e and f) lung. (a) Specific binding to submucosal microvessels (arrows) in human bronchus. No specific binding is observed to epithelium (open arrows) or bronchial glands (g). (b) Bronchial artery showing endothelial localization of binding. (c) Section of human lung showing bronchial microvessels (arrows), gland (g) and muscle (m). (d) Film autoradiogram corresponding to (c). Specific binding is restricted to microvessels, rather than to glandular elements or smooth muscle. (e) Specific binding to guinea pig bronchial smooth muscle (m), but not to bronchial glands or epithelium. Non-specific binding is observed over eosinophils (small arrows). (f) Specific binding to guinea pig bronchial microvessels (arrows). (a, b, e. and f) are emulsion-dipped preparations with haematoxylin counterstain. (c) shows immunostaining for PECAM with haematoxylin counterstain. Bars = 100 μm.

Table 1 Characteristics of [^{125}I]-Bolton Hunter-labelled substance P binding to human and naive guinea pig lung

	Human lung *Microvessels*	*Guinea pig lung* *Bronchus*	*Pulmonary artery*
B_{max} (amol mm^{-2})	96 (37 to 251)	916[d] (608 to 1377)	206[d] (131 to 324)
K_i values (nM)			
Substance P	0.8[ab] (0.5 to 1.1)	1.0[ab] (0.7 to 1.3)	0.5[ab] (0.3 to 0.7)
FK888	0.8[b] (0.3 to 1.7)	0.9[b] (0.7 to 1.3)	0.7[b] (0.3 to 1.7)
Neurokinin A	13.3[ac] (5.6 to 31.9)	336[ac] (231 to 488)	215[ac] (150 to 307)
Neurokinin B	439[a] (149 to 1294)	179[a] (114 to 284)	126[a] (74 to 213)
FK224	434[b] (263 to 714)	619[b] (408 to 938)	NA
Hill coefficients			
Substance P	−1.3 (−1.2 to −1.5)	−1.4 (−1.2 to −1.6)	−1.2 (−0.9 to −1.6)
FK888	−1.0 (−0.7 to −1.4)	−0.8 (−0.7 to −1.0)	−0.8 (−0.5 to −1.2)
Neurokinin A	−1.0 (−0.7 to −1.4)	−0.9 (−0.8 to −1.0)	−1.0 (−0.8 to −1.2)
Neurokinin B	−1.2 (−0.9 to −1.7)	−1.2 (−1.0 to −1.5)	−1.1 (−0.9 to −1.4)
FK224	−1.3 (−1.0 to −1.5)	−1.3 (−1.1 to −1.5)	NA

Values expressed as geometric means (95% CI) of six cases per group. In both human and guinea pig lung [a]neurokinin A and neurokinin B had lower affinities than substance P (SP) ($P<0.001$) and [b]SP and FK888 had equal affinities, and each had higher affinity than FK224 ($P<0.001$). [c]Neurokinin A had higher affinity for specific [^{125}I]-BH-SP binding sites on human bronchial microvessels than on guinea pig bronchus or pulmonary artery ($P<0.001$). No significant differences in K_i values were found between bronchi and pulmonary arteries. [d]Maximal binding to guinea pig bronchi was significantly greater than to pulmonary arteries ($P<0.0001$). NA, not assessed.

with saline (Figure 6). Airway resistance had returned to baseline and control values by the time of sacrifice at 90 min.

The localization of [^{125}I]-BH-SP binding sites in ovalbumin-sensitized and-challenged guinea pig lung was similar to that in naive animals, in sensitized and in challenged controls. Comparisons of equilibrium binding of [^{125}I]-BH-SP to airway smooth muscle at the carina revealed no significant differences between the four groups [B_{eq} values for sensitized and challenged group, 29 (95% CI 22–38) amol mm^{-2}; naive group, 28 (95% CI 15–53) amol mm^{-2}; sensitized group, 31 (95% CI 13–74) amol mm^{-2}; challenged group, 21 (95% CI 22–38) amol mm^{-2}; $P=0.59$, one-way ANOVA]. Subsequent comparisons were made between naive and ovalbumin-sensitized and -challenged groups. The relationships between equilibrium binding density of [^{125}I]-BH-SP and bronchial or pulmonary artery diameter were similar for naive and sensitized/challenged animals (Table 2) and no significant differences in B_{max} or K_i values were observed between disease groups (Table 3).

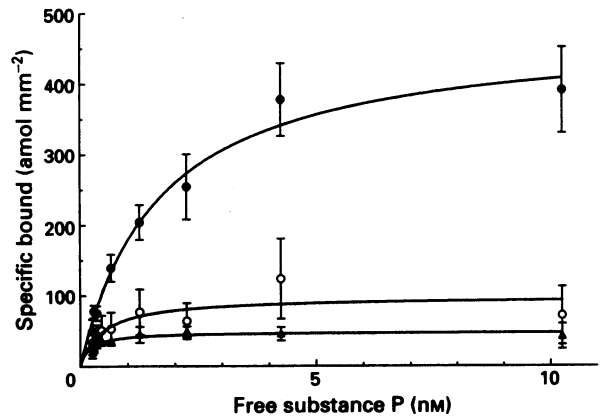


Figure 3 Saturation curves for [^{125}I]-Bolton Hunter-labelled substance P binding to human bronchial microvessels (▲), guinea pig bronchi (●) and guinea pig pulmonary arteries (○). Each point represents the mean (± s.e. mean) of six cases.

Discussion

We have found major differences in the distribution of [^{125}I]-BH-SP binding sites between guinea pig and human lung. Bronchial microvessels bound [^{125}I]-BH-SP specifically in both species, but, whereas binding was dense to bronchial smooth muscle and pulmonary arteries in guinea pig lung, these structures did not show specific binding in human lung. These results are similar to those described by Goldie (1990), but contrast with the apparent similarities between species implied by Carstairs & Barnes (1986). We have used both fresh surgical and post-mortem tissues, and sampled both peripheral and central airways. It seems unlikely, therefore, that the differences observed resulted from variations in the methods of tissue collection or from regional heterogeneity in human lung. Furthermore, since binding sites with characteristics of NK_1 receptors were identified on bronchial microvessels in human lung, we conclude that our tissue samples were adequately preserved for receptor autoradiography. It remains possible that human bronchi and pulmonary arteries possess NK_1 receptors, but at levels below the sensitivity of our autoradiographic method. However, our data are consistent with findings that human bronchi are less sensitive to NK_1 agonists than are guinea pig bronchi, and we suggest that such differences are due to lower levels of NK_1 receptors in human bronchial smooth muscle.

The localization of [^{125}I]-BH-SP binding sites to bronchial microvessels in both guinea-pig and human trachea and central bronchi confirms previous findings (Hoover & Hancock, 1987; Goldie, 1990) and is consistent with a role for SP in control of vascular tone and permeability. We have demonstrated that these sites have features of NK_1 receptors with similar specificities to microvascular endothelial [^{125}I]-BH-SP binding sites characterized in other human tissues such as synovium (Walsh *et al.*, 1992; 1993). A similar localization of [^{125}I]-BH-SP binding to bronchial microvessels has been reported in rats, in which binding site distribution correlates with SP-induced plasma extravasation, suggesting a role in oedema formation (Sertl *et al.*, 1988). Airway oedema is an important component of airway obstruction, both in asthma and in chronic airflow limitation, but is not susceptible to acute reversal by conventional bronchodilator agents. Inhibition of airway oedema by NK_1 receptor antagonists, including FK888, has been demonstrated in animal models (Eglezos *et al.*, 1991; Lei *et al.*, 1992; Delay-Goyet *et al.*, 1992; Hirayama *et al.*, 1993; Murai *et al.*, 1993). Our demonstration that human bronchial microvessels also possess NK_1 binding sites and that [^{125}I]-BH-SP binding is inhibited by the tachykinin receptor antagonists FK888 and FK224 suggests that NK_1 antagonists may be of value in the control of airway oedema in humans.

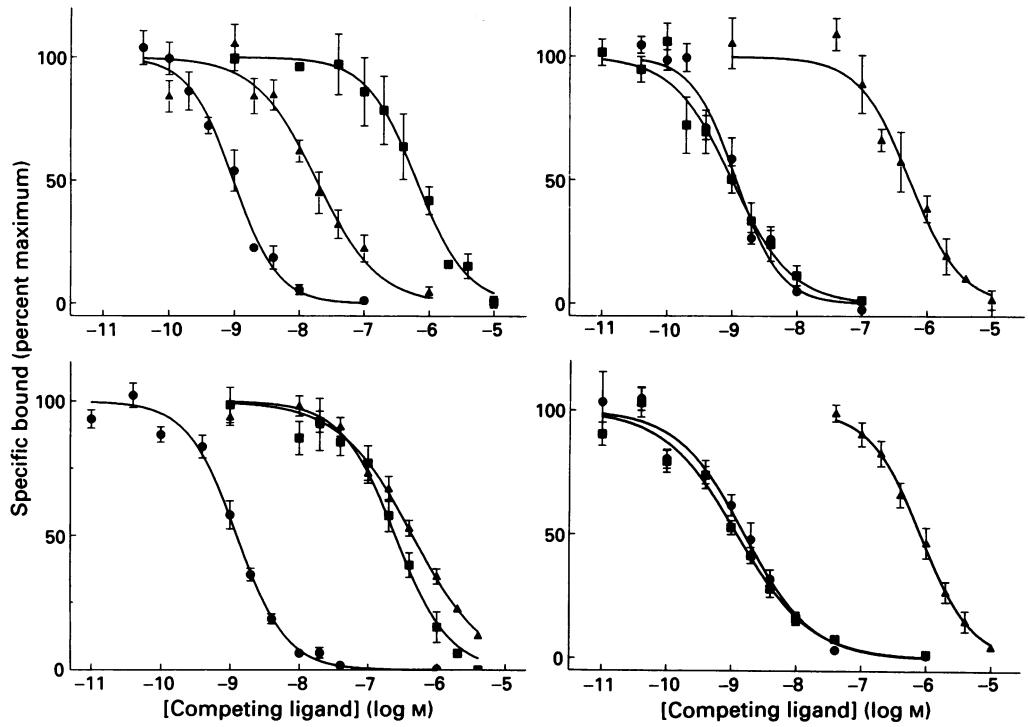


Figure 4 Inhibition of specific [^{125}I]-Bolton Hunter-labelled substance P binding to human bronchial microvessels (a and b) and to guinea-pig bronchi (c and d) by unlabelled agonists and antagonists. (a and c) the rank orders of affinities for substance P (SP, ●), neurokinin A (NKA, ▲) and neurokinin B (NKB, ■) are SP> NKA > NKB in human lung, and SP> NKB = NKA in guinea pig bronchi, NKA having significantly higher affinity in human microvessels than in the guinea pig ($P<0.0001$). (b and d) FK888 (■) and FK224 (▲) inhibit binding with similar affinities in both human microvessels and guinea pig bronchi, with FK888 having approximately equal affinity to SP (●) and higher affinity than FK224. Values represent means (± s.e. mean) of six cases, specific binding expressed as per cent of that in absence of unlabelled ligand.

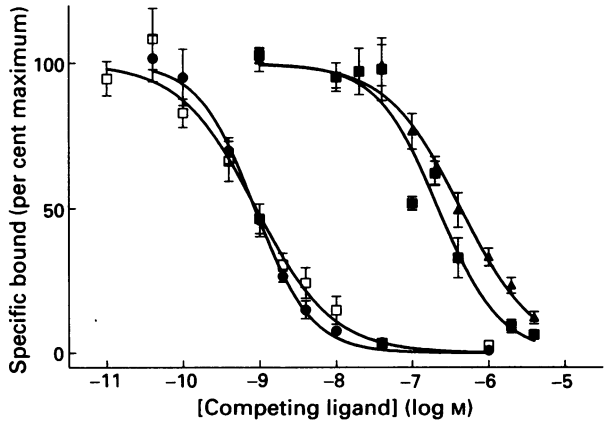


Figure 5 Inhibition of specific [^{125}I]-Bolton Hunter-labelled substance P binding to guinea pig pulmonary arteries by unlabelled substance P (●), neurokinin A (▲), neurokinin B (■) and FK888 (□). No significant differences were found between affinities between guinea pig pulmonary arteries and bronchi. Values represent means (± s.e. mean) of six cases, specific binding expressed as per cent of that in absence of unlabelled ligand.

Guinea pig bronchi, in contrast to human airways, demonstrate clear bronchoconstrictor responses to NK_1 receptor agonists. In some species, bronchial responsiveness to NK_1 receptor agonists is greater in peripheral rather than central segments of main bronchi, and greater in central than peripheral lung strips (Black *et al.*, 1990; Wong *et al.*, 1992). The regional distribution of [^{125}I]-BH-SP binding sites noted in the current study in guinea pig central airways is similar to that previously reported in the rabbit (Black *et al.*, 1990). Furthermore, the decrease in the density of [^{125}I]-BH-SP binding sites with decreasing intrapulmonary airway diameter indicates that regional heterogeneity in small- and medium-sized airway responses to SP may result from variations in NK_1 receptor densities. The biological importance of differential regulation of bronchial tone at different levels of the bronchial tree remains to be determined.

Guinea pig pulmonary vasculature responds to tachykinins *in vivo* through actions on multiple receptors (Maggi *et al.*, 1990). Endothelium-dependent vasodilation, as in the systemic circulation, is NK_1 receptor mediated, while endothelium-independent vasoconstriction is predominantly NK_2 receptor mediated. Specific binding of [^{125}I]-BH-SP to the media of guinea pig pulmonary arteries has previously been noted, but not characterized (Carstairs & Barnes, 1986; Burcher *et al.*, 1989). Our findings suggest that this binding is to NK_1 rather than to NK_2 receptors, and to sites very similar to NK_1 receptors present in bronchial smooth muscle. A precise functional role for NK_1 receptors in the media of pulmonary arteries remains to be determined, but the available data suggest differences in peptide regulation between systemic and pulmonary vascular beds.

NKA and NKB displayed similar affinities for [^{125}I]-BH-SP binding sites in guinea pig lung, as previously found in membrane preparations (Geraghty *et al.*, 1992). In human lung, however, NKA displayed higher affinity than NKB, suggesting that guinea pig and human NK_1 receptors differ in their sensitivity to agonists. The rank order of affinities of unlabelled tachykinins and antagonists for specific microvascular [^{125}I]-BH-SP binding sites in human lung was identical to that previously demonstrated for microvessels in human synovium (Walsh *et al.*, 1992; 1993). These latter studies used HEPES buffer containing the same concentrations of cations as those used for guinea pig lung in this study, suggesting that differences in selectivity between human and guinea pig [^{125}I]-BH-SP binding sites were not due to the different buffers used.

Table 2 Relationship between specific equilibrium binding density of [^{125}I]-Bolton Hunter-labelled substance P and bronchial or pulmonary artery diameter in naive and ovalbumin-sensitized and -challenged guinea pigs

	Bronchus		*Pulmonary artery*	
	Naive	*Ovalbumin-sensitized/ challenged*	*Naive*	*Ovalbumin-sensitized/ challenged*
R^2	0.48 (0.30 to 0.67)	0.41 (0.26 to 0.56)	0.29 (0.05 to 0.53)	0.26 (0.18 to 0.34)
Gradient [(log amol mm^{-1}) mm^{-1}]	2.1 (1.7 to 2.6)	2.3 (1.4 to 3.1)	2.1 (1.1 to 3.1)	1.8 (0.7 to 2.9)
y intercept (log amol mm^{-2})	0.8 (0.4 to 1.1)	0.7 (0.2 to 1.1)	0.1 (−0.2 to 0.4)	−0.2 (−0.5 to 0.1)

Values represent means (95% CI) of six cases per group. Values of R^2, gradient and y intercept were derived for each case in each group by linear regression analysis of $\log_{10}$ equilibrium binding density (abscissa) against structure diameter (in mm). All bronchial or pulmonary artery profiles with diameters between 0.2 and 0.8 mm were quantified ($n = 8-20$ per case). Significant positive relationships were observed between equilibrium binding density and bronchial and pulmonary artery diameters in both naive and experimental lung, with no overall differences between disease groups.

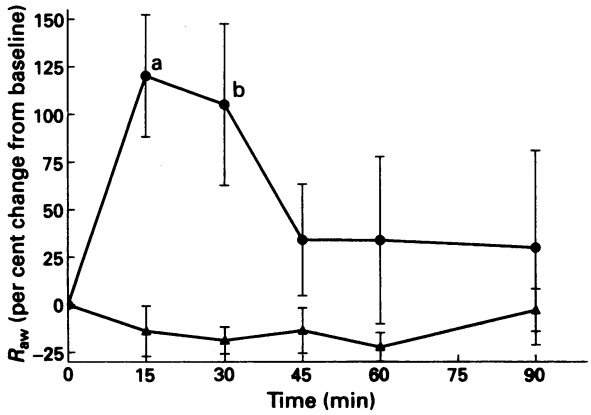


Figure 6 Changes in airway resistance (R_{aw}) in ovalbumin-sensitized guinea pigs following challenge via an intratracheal tube with aerosolized ovalbumin (●) or saline (▲). (a and b) The increase in R_{aw} was significantly greater 15 and 30 min following challenge with ovalbumin than following saline ($^aP<0.01$ and $^bP<0.05$).

Table 3 Characteristics of [^{125}I]-Bolton Hunter-labelled substance P binding to bronchi from naive and ovalbumin-sensitized and -challenged guinea pigs

	Naive	*Ovalbumin-sensitized/ challenged*
B_{max} (amol mm^{-2})	427 (275 to 676)	724 (386 to 1380)
K_i values (nM)		
Substance P	1.5 (0.9 to 2.3)	1.8 (1.2 to 2.7)
FK888	1.1 (0.6 to 1.8)	1.2 (0.7 to 2.0)
FK224	619 (408 to 938)	607 (472 to 847)
Hill coefficients		
Substance P	−1.0 (−0.9 to −1.2)	−1.2 (−1.0 to −1.5)
FK888	−1.1 (−1.0 to −1.2)	−1.3 (−1.0 to −1.6)
FK224	−1.3 (−1.1 to −1.5)	−1.4 (−1.2 to −1.7)

Values expressed as geometric means (95% CI) of six animals from each group. No significant differences in B_{max} or K_i values, or in Hill coefficients, were observed between naive and ovalbumin-sensitized and challenged animals.

The tachykinin receptor antagonists FK888 and FK224 displaced [^{125}I]-BH-SP binding from both human and guinea pig pulmonary tissues. Recently, Miyayasu *et al.* (1993) demonstrated that [^{3}H]-FK888 binds to guinea pig bronchial smooth muscle and to sites with characteristics of NK_1 receptors in guinea pig lung. In our studies, human and guinea pig [^{125}I]-BH-SP binding sites had similar affinities for the antagonists FK224 and FK888. By contrast, FK888 displays much lower affinity for [^{125}I]-BH-SP binding sites in rat tissues than in guinea pig lung and human synovial microvessels (Fujii *et al.*, 1992; Walsh *et al.*, 1993). Similar orders of affinities between species have been observed for the non-peptide NK_1 receptor antagonist CP-96,345 (Beresford *et al.*, 1991). It seems likely that further interspecies differences in NK_1 receptors may be uncovered by the development of novel ligands in the future, and testing of potential therapeutic compounds on human NK_1 receptors will remain an important aspect of drug development.

Intraspecies NK_1 receptor subtypes have been suggested by *in vivo* work performed in guinea pig ileum (Petitet *et al.*, 1992), but not, so far, confirmed in binding studies. Quantitative *in vitro* receptor autoradiography permits the independent characterization of multiple structures in a single tissue simultaneously incubated under identical conditions. We found no evidence, however, that [^{125}I]-BH-SP binds to different receptor subtypes in different structures in guinea pig lung.

The presence of [^{125}I]-BH-SP binding sites in hypersensitive and challenged guinea-pig airways suggests that these animals are, like naive animals, susceptible to the actions of NK_1 receptor agonists and antagonists on airway function. However, after taking account of regional variations in NK_1 receptor distribution in guinea pig lung, we found no significant differences in [^{125}I]-BH-SP binding to bronchial smooth muscle between naive and ovalbumin-challenged hypersensitive guinea pigs. In particular, we found no evidence for changes in equilibrium or maximal binding densities for [^{125}I]-BH-SP, or in affinity for SP, FK224 or FK888 following ovalbumin sensitization and challenge. The increased sensitivity to SP observed following ovalbumin challenge in hypersensitive guinea pigs (Neiri *et al.*, 1992) may not be caused by receptor up-regulation or changes in receptor affinity, but rather by changes in peptide-degrading enzymes, or by potentiation by other mediators released during the challenge.

In conclusion, [^{125}I]-BH-SP binds with high affinity to NK_1 binding sites present on human bronchial microvessels and, in the guinea pig, present on bronchi, pulmonary arteries and microvessels. Interspecies differences are apparent between the guinea pig and human in terms both of the distribution of binding sites and the affinities of tachykinin agonists for these sites, particularly NKA, but not the tachykinin antagonists tested here. Our data support a potential role for NK_1 receptor antagonists such as FK224 and FK888 in the therapeutic control of airway function, but suggest that NK_1 receptor antagonists are more likely in man to be of benefit in controlling airway microvascular function and inflammation rather than to have direct effects on airway tone.

We are grateful to Fujisawa Pharmaceuticals, Osaka, Japan, for their generous financial support and the provision of the tachykinin receptor antagonists used in these studies. D.A.W. is an Arthritis and Rheumatism Council Clinical Research Fellow.

References

ADVENIER, C., NALINE, E., DRAPEAU, G. & REGOLI, D. (1987). Relative potencies of neurokinins in guinea-pig trachea and human bronchus. *Eur. J. Pharmacol.*, **139**, 133–137.

BALLATI, L., EVANGELISTA, S., MAGGI, C.A. & MANZINI, S. (1992). Effects of selective tachykinin receptor antagonists on capsaicin-induced and tachykinin-induced bronchospasm in anaesthetized guinea-pigs. *Eur. J. Pharmacol.*, **214**, 215–221.

BARNES, P.J. (1991). Neurogenic inflammation in airways. *Int. Arch. Allergy Appl. Immunol.*, **94**, 303–309.

BERESFORD, I.J.M., BIRCH, P.J., HAGAN, R.M. & IRELAND, S.J. (1991). Investigation into species variants in tachykinin NK_1 receptors by use of the non-peptide antagonist, CP 96,345. *Br. J. Pharmacol.*, **104**, 292–293.

BERTRAND, C., GEPPETTI, P., BAKER, J., YAMAWAKI, I. & NADEL, J.A. (1993). Role of neurogenic inflammation in antigen-induced vascular extravasation in guinea-pig trachea. *J. Immunol.*, **150**, 1479–1485.

BLACK, J., DIMENT, L., ARMOUR, C., ALOUAN, L. & JOHNSON, P. (1990). Distribution of SP receptors in rabbit airways, functional and autoradiographic studies. *J. Pharmacol. Exp. Ther.*, **253**, 381–386.

BURCHER, E., WATKINS, D.J. & O'FLYNN, N.M. (1989). Both neurokinin A and substance P bind to NK_1 receptors in guinea-pig lung. *Pulm. Pharmacol.*, **1**, 201–203.

CARSTAIRS, J.R. & BARNES, P.J. (1986). Autoradiographic mapping of substance P receptors in lung. *Eur. J. Pharmacol.*, **127**, 295–296.

CHENG, Y.C. & PRUSOFF, W.H. (1973). Relationship between the inhibition constant (K_I) and the concentration of inhibitor which causes 50 per cent inhibition (I_{50}) of an enzymatic reaction. *Biochem. Pharmacol.*, **22**, 3099–3108.

DEBLASI, A., O'REILLY, K. & MOTULSKY, H.J. (1989). Calculating receptor number from binding experiments using same compound as radioligand and competitor. *Trends Pharmacol. Sci.*, **101**, 227–229.

DELAY-GOYET, P., FRANCO-CERECEDA, A., GONSALVES, S.F., CLINGAN, C.A., LOWE, J.A. & LUNDBERG, J.M. (1992). CP-96,345 antagonism of NK_1 receptors and smoke-induced protein extravasation in relation to its cardiovascular effects. *Eur. J. Pharmacol.*, **222**, 213–218.

EGLEZOS, A., GIULIANI, S., VITI, G. & MAGGI, C.A. (1991). Direct evidence that capsaicin-induced plasma protein extravasation is mediated through tachykinin NK_1 receptors. *Eur. J. Pharmacol.*, **209**, 277–279.

FROSSARD, N. & ADVENIER, C. (1991). Tachykinin receptors and the airways. *Life Sci.*, **49**, 1941–1953.

FUJII, T., MURAI, M., MORIMOTO, H., MAEDA, Y., YAMAOKA, M., HAGIWARA, D., MIYAKE, H., IKARI, N. & MATSUO, M. (1992). Pharmacological profile of a high affinity dipeptide NK_1 receptor antagonist, FK888. *Br. J. Pharmacol.*, **107**, 785–789.

GERAGHTY, D.P., MUSSAP, C.J. & BURCHER, E. (1992). Radioiodinated substance P, neurokinin A, and eledoisin bind predominantly to NK_1 receptors in guinea-pig lung. *Mol. Pharmacol.*, **41**, 147–153.

GOLDIE, R.G. (1990). Receptors in asthmatic airways. *Am. Rev. Respir. Dis.*, **141**, S151–S156.

HIRAYAMA, Y., LEI, Y.-H., BARNES, P.J. & ROGERS, D.F. (1993). Effects of two novel tachykinin antagonists, FK224 and FK888, on neurogenic airway plasma exudation, bronchoconstriction and systemic hypotension in guinea-pigs *in vivo*. *Br. J. Pharmacol.*, **108**, 844–851.

HOOVER, D.B. & HANCOCK, J.C. (1987). Autoradiographic localization of substance P binding sites in guinea-pig airways. *J. Autonom. Nerv. Syst.*, **19**, 171–174.

HSU, S.-M., RAINE, L. & FANGER, H. (1981). Use of avidin-biotin-peroxidase complex (ABC) method in immunoperoxidase techniques: a comparison between ABC and unlabelled antibody (PAP) procedures. *J. Histochem. Cytochem.*, **29**, 577–580.

HUTSON, P.A., CHURCH, M.K., CLAY, T.P., MILLER, P. & HOLGATE, S.T. (1988). Early and late-phase bronchoconstriction after allergen challenge of nonanesthetized guinea-pigs. I. The association of disordered airway physiology to leukocyte infiltration. *Am. Rev. Respir. Dis.*, **137**, 548–557.

JOOS, G., PAUWELS, R. & VAN DER STRAETEN, M. (1987). Effect of inhaled substance P and neurokinin A on the airways of normal and asthmatic subjects. *Thorax*, **42**, 779–783.

KUO, H.P., ROHDE, J.A., TOKUYAMA, K., BARNES, P.J. & ROGERS, D.F. (1990). Capsaicin and sensory neuropeptide stimulation of goblet cell secretion in guinea-pig trachea. *J. Physiol.*, **431**, 629–641.

LEI, Y.H., BARNES, P.J. & ROGERS, D.F. (1992). Inhibition of neurogenic plasma exudation in guinea-pig airways by CP-96,345, a new non-peptide NK_1 receptor antagonist. *Br. J. Pharmacol.*, **105**, 261–262.

LEMBECK, F., DONNERER, J., TSUCHIYA, M. & NAGAHISA, A. (1992). The non-peptide tachykinin antagonist, CP-96,345, is a potent inhibitor of neurogenic inflammation. *Br. J. Pharmacol.*, **105**, 527–530.

MAGGI, C.A., PATACCHINI, R., PERRETTI, F., TRAMONTANA, M., MANZINI, S., GEPPETTI, P. & SANTICIOLI, P. (1990). Sensory nerves, vascular endothelium and neurogenic relaxation of the guinea-pig isolated pulmonary artery. *Naunyn-Schmiedeberg's Arch. Pharmacol.*, **342**, 78–84.

MAGGI, C.A., PATACCHINI, R., ROVERO, P. & SANTICIOLI, P. (1991). Tachykinin receptors and noncholinergic bronchoconstriction in the guinea-pig isolated bronchi. *Am. Rev. Respir. Dis.*, **144**, 363–367.

MIYAYASU, K., MAK, J.C.W., NISHIKAWA, M. & BARNES, P.J. (1993). Characterization of guinea-pig pulmonary neurokinin type 1 receptors using a novel antagonist ligand, [^{3}H]FK888. *Mol. Pharmacol.*, **44**, 539–544.

MORIMOTO, H., MURAI, M., MAEDA, Y., YAMAOKA, M., NISHIKAWA, M., KIYOTOH, S. & FUJII, T. (1992). FK224, a novel cyclopeptide substance P antagonist with NK_1 and NK_2 receptor selectivity. *J. Pharmacol. Exp. Ther.*, **224**, 398–402.

MURAI, M., MAEDA, Y., HAGIWARA, D., MIYAKE, H., IKARI, N., MATSUO, M. & FUJII, T. (1993). Effects of an NK_1 receptor antagonist, FK888, on constriction and plasma extravasation induced in guinea-pig airway by neurokinins and capsaicin. *Eur. J. Pharmacol.*, **236**, 7–13.

NEIRI, P., DAFFONCHIO, L., OMINI, C., MARTINOTTI, E. & BRESCHI, M.C. (1992). Changes in airway reactivity to exogenous and endogenous acetylcholine and substance P after anaphylactic bronchoconstriction in anaesthetised guinea-pigs. *J. Autonom. Pharmacol.*, **12**, 403–409.

PETITET, F., SAFFROY, M., TORRENS, Y., LAVIELLE, S., CHASSAING, G., LOEUILLET, D., GLOWINSKI, J. & BEAUJOUAN, J.C. (1992). Possible existence of a new tachykinin receptor subtype in the guinea-pig ileum. *Peptides*, **13**, 383–388.

RENZETTI, L.M., SHENVI, A. & BUCKNER, C.K. (1992). Nonadrenergic, noncholinergic contractile responses of the guinea-pig bronchus involve the preferential activation of tachykinin neurokinin$_2$ receptors. *J. Pharmacol. Exp. Ther.*, **262**, 957–963.

ROGERS, D.F., AURSUDKIJ, B. & BARNES, P.J. (1989). Effects of tachykinins on mucus secretion in human bronchi in vitro. *Eur. J. Pharmacol.*, **174**, 283–286.

SERTL, K., WIDERMANN, C.J., KOWALSKI, M.L., HURTADO, S., PLUTCHOCK, J., LINNOILA, I., PERT, C.B. & KALINER, M.A. (1988). Substance P: the relationship between receptor distribution in rat lung and the capacity of substance P to stimulate vascular permeability. *Am. Rev. Respir. Dis.*, **138**, 151–159.

VARLEY, J.G., PERRING, S., SEMINARIO, M.-C., FLEMING, J., HOLGATE, S.T. & CHURCH, M.K. (1991a). Aerosol deposition in the guinea-pig. A comparison of two methods of exposure. *Am. Rev. Respir. Dis.*, **143**, A708.

VARLEY, J.G., HEATH, J.R., HOLGATE, S.T. & CHURCH, M.K. (1991b). Pulmonary function values using a new guinea-pig body plethysmograph. *Am. Rev. Respir. Dis.*, **143**, A354.

WALSH, D.A., MAPP, P.I., WHARTON, J., RUTHERFORD, R.A.D., KIDD, B.L., REVELL, P.A., BLAKE, D.R. & POLAK, J.M. (1992). Localisation and characterisation of substance P binding to human synovium in rheumatoid arthritis. *Ann. Rheum. Dis.*, **51**, 313–317.

WALSH, D.A., SALMON, M., MAPP, P.I., WHARTON, J., GARRETT, N., BLAKE, D.R. & POLAK, J.M. (1993). Microvascular substance P binding to normal and inflamed rat and human synovium. *J. Pharmacol. Exp. Ther.*, **267**, 951–960.

WHARTON, J., WALSH, D.A., RUTHERFORD, R.A.D., KNOCK, G.A. & POLAK, J.M. (1993). *In vitro* autoradiographic localization and characterization of binding sites. In *Receptor Autoradiography; Principles and Practice*. ed. Wharton, J. & Polak, J.M., pp. 79–105. Oxford: Oxford University Press.

WONG, W.S., BLOOMQUIST, S.L., BENDELE, A.M. & FLEISCH, J.H. (1992). Pharmacological and histological examinations of regional differences of guinea-pig lung: a role of pleural surface smooth muscle in lung strip contraction. *Br. J. Pharmacol.*, **105**, 620–626.

(Received May 5, 1994
Revised July 14, 1994
Accepted August 4, 1994)

Br. J. Pharmacol (1994), **113**, 1416–1422 © Macmillan Press Ltd, 1994

Dexamethasone-induced selective inhibition of the central μ opioid receptor: functional *in vivo* and *in vitro* evidence in rodents

S. Pieretti, A. Di Giannuario, M.R. Domenici, S. Sagratella, *A. Capasso, *L. Sorrentino & [1]A. Loizzo

Istituto Superiore di Sanita', V. le Regina Elena 299, 00161, Roma and *Facolta' di Farmacia, Universita' di Salerno, P.a. V. Emanuele 9, 88084, Penta di Fisciano, Fisciano, Salerno, Italy

1 Endogenous corticosteroids and opioids are involved in many functions of the organism, including analgesia, cerebral excitability, stress and others. Therefore, we considered it important to gain information on the functional interaction between corticosteroids and specific opioid receptor subpopulations.

2 We have found that systemic administration (i.p.) of the potent synthetic corticosteroid, dexamethasone, reduced the antinociception induced by the highly selective μ agonist, DAMGO or by less selective μ agonists morphine and β-endorphin administered i.c.v.. On the contrary dexamethasone exerted little or no influence on the antinociception induced by a δ_1 agonist, DPDPE and a δ_2 agonist deltorphin II. Dexamethasone potentiated the antinociception induced by the κ agonist, U50,488.

3 In experiments performed in an *in vitro* model of cerebral excitability in the rat hippocampal slice, dexamethasone strongly prevented both the increase of the duration of the field potential recorded in CA1, and the appearance and number of additional population spikes induced by μ receptor agonists.

4 In both models pretreatment with cycloheximide, a protein synthesis inhibitor, prevented the antagonism by dexamethasone of responses to the μ opioid agonists.

5 Our data indicate that in the rodent brain there is an important functional interaction between the corticosteroid and the opioid systems at least at the μ receptor level, while δ and κ receptors are modulated in different ways.

Keywords: Dexamethasone, opioid, analgesia, epilepsy, μ receptor

Introduction

In 1981 the characterisation of the molecular structure of Corticotropin Releasing Factor (CRF) was reported (Spiess *et al.*, 1981). The same authors also reported the CRF-induced release of adrenocorticotrophic hormone ACTH and β-endorphin from the anterior pituitary (Vale *et al.*, 1981). β-Endorphin and other natural and synthetic opioids are involved in a series of functions, such as pain, nerve cell excitability and epilepsy, immunomodulation, stress and others. Analgesia induced by opioids and opioid peptides is a well known phenomenon (Millan, 1986) and the role of endorphins in stress has also been studied (Amir *et al.*, 1980). Furthermore, in animals, opioids may have pro- and anticonvulsant effects (Ramabadran & Bansinath, 1990). Important effects are thought to be induced in the same functions by ACTH as well, and to a larger extent by corticosteroids. Many findings indicate that corticosteroids and ACTH play a role not only in stress, but also in pain modulation (Lewis *et al.*, 1980; MacLennan *et al.*, 1982) and in brain excitability (McEven *et al.*, 1986; Ortolani *et al.*, 1990). A series of investigations have indicated that corticosteroids such as dexamethasone exert consistent inhibition against the effects induced by morphine on pain sensitivity and hippocampal excitability. There is evidence that ACTH and corticosteroids reduce opioid analgesia (Winter & Flataker, 1951; Chatterjee *et al.*, 1982). We reported that dexamethasone pretreatment was able to reduce morphine analgesia both in the hot plate test (Pieretti *et al.*, 1991) and in the tail flick test (Capasso *et al.*, 1992). We also found that dexamethasone pretreatment was able to prevent the appearance of the epileptiform hippocampal electroencephalographic activity induced by central morphine administration in rabbits. Furthermore, dexamethasone pretreatment was also able to prevent the appearance of CA1 epileptiform bursting induced by morphine and DAMGO on rat hippocampal slices. Both these inhibitory effects were blocked by cycloheximide pretreatment performed before dexamethasone (Pieretti *et al.*, 1992). It is well known that opioids and opioid peptides administered intracerebroventricularly or intrathecally act at μ, δ and κ opioid receptors to produce analgesia or seizures (Millan, 1986; Pasternak, 1987; Hong *et al.*, 1993). In contrast no data are available, to our knowledge, on the effects exerted by glucocorticoids on the analgesic and epileptiform effects induced by selective opioid agonists. Since our recent paper indicated that both effects could be due to an interaction of the two drugs on some specific opioid receptors, we studied whether this could be verified, and, if this was the case, which mechanism of action could be suggested. In this paper two series of experiments were carried out. In the first series groups of mice were treated with dexamethasone followed by: the highly selective μ agonist (DAMGO) or less selective μ agonists (morphine and β-endorphin); selective δ_1 agonist (DPDPE); selective δ_2 agonist (deltorphin II) or selective κ agonist (U50,488H). The second series of experiments was performed in an *in vitro* model of hippocampal slices, perfused with various types of opioid drugs, according to a schedule analogous to the one used for the first series.

Methods

In vivo *experiments*

Male CD-1 mice (Charles River, Italy) weighing 25–30 g were used in the experiments. The animals were housed in colony cages (5 mice each) with free access to food and

[1] Author for correspondence.A. Loizzo, M.D. Istituto Superiore di Sanita', Via Regina Elena 299, 00161 Roma, Italy.

water. They were maintained in a climate and light controlled room (22 ± 1°C, 12/12 h dark/light cycle with light on at 07 h 00 min at least 7 days before testing. Testing took place during the light phase. The animals were brought to the test room for at least 3 h before testing. Each animal was used only in one experimental session. In all experiments attention was paid to the ethical guidelines for investigations of experimental pain in conscious animals (Zimmerman, 1983).

Analgesic assay Mice were tested with the hot plate as previously reported (Pieretti *et al.*, 1991). Briefly, the device (U. Basile, Italy) consisted of a metal plate (25 × 25 cm) heated to a constant temperature, on which a plexiglass cylinder (20 cm diameter × 16 cm height) was placed. The hot plate was set to 55 ± 0.5°C to give a hind paw licking latency of 15–17 s in controls. The measurement was terminated at the first paw lick or when the latency exceeded the cut-off time (60 s).

Tail flick latency (Capasso *et al.*, 1992) was obtained using a tail flick unit (U. Basile, Italy) consisting of an infrared source (100 W bulb), whose radiant light of adjustable intensity was focused by an aluminized parabolic mirror on a photocell. Radiant heat was focused on a blackened spot 1–2 cm from the tip of the tail, and the latency was recorded until the mouse flicked its tail away from the heat source. Beam intensity was adjusted to give a tail flick latency of 2–3 s in controls. The animals were restrained during the trials by means of a plexiglass cylinder (4 cm in diameter and 8 cm long). In order to avoid tissue damage the measurement was terminated if the latency exceeded the cut-off time (10 s).

In all experiments the response latencies were expressed as percentage of analgesia which were calculated as (post-opioid latency *minus* pre-drug latency)/(cut off latency *minus* pre-drug latency) × 100.

Drug administration and experimental procedure All drugs used in the experimental sessions were purchased from Sigma Chemical Co (St. Louis, U.S.A.) with the exception of morphine HCl which was purchased from Carlo Erba (Milan, Italy). They were dissolved in 0.9% NaCl solution for intraperitoneal (i.p.) administration, or in distilled water for intracerebroventricular (i.c.v.) administration, on the day of testing. These drugs were injected in a volume of 5 ml kg^{-1} or 5 µl per mouse, respectively. The i.c.v. injection was performed by the method described by Haley & McCormick (1957). In the preliminary experiments the time of the peak analgesic effect induced by opioid agonists (morphine, DAMGO, β-endorphin, DPDPE, deltophin II, U50,488H) administered i.c.v. was determined from time-response curves. Thereafter, dose-response curves of various i.c.v. doses of some opioid agonists alone or in the presence of dexamethasone-21-phosphate (0.1 mg kg^{-1}) administered i.p. 30 min before opioid treatment, was determined in the tail flick and in the hot plate tests. The ED_{50} and 95% confidence intervals were computed from the dose-response curve by the method of Litchfield & Wilcoxon (1949) with the aid of a computer programme.

In another series of experiments mice were pretreated with cycloheximide (15 mg kg^{-1}, administered i.p. 2 h before dexamethasone or 2.5 h before opioid agonist) plus dexamethasone (0.1 mg kg^{-1} administered i.p., 30 min before opioid agonists), plus the opioid agonist administered i.c.v. at the dose inducing 50% analgesia.

In vitro *experiments*

Transverse slices of hippocampus (450 µm thick) were prepared from male Wistar rats weighing 200–250 g, and immediately placed in a submerged recording chamber, where they were constantly perfused (at a rate of 2–3 ml min^{-1}) with an artificial cerebrospinal fluid (CSF) saturated with 95% O_2: 5% CO_2. The composition of the artificial CSF was as follows (mM): NaCl 122, KH_2PO_4 0.4, KCl 3, $MgSO_4$ 1.2, $NaHCO_3$ 25, $CaCl_2$ 1.3, and glucose 10 (pH 7.3). The temperature of the perfusion chamber was maintained at 33 ± 1°C. An interval of 60–90 min elapsed between the time the slices were cut and the start of the recording session. Dexamethasone-21-phosphate, morphine HCl, methadone HCl, morphiceptin, DAMGO ([D-Ala^2-N-methyl-Phe^4-Gly^5-ol]-enkephalin), DPDPE ([D-Pen^2-D-Pen^5]-enkephalin), deltorphin II, U50,488H (trans-(±)-3,4,Dichloro-N-methyl-N-[2-(1-pyrrolidinyl)-cyclohexyl]-benzene-acetamide methanesulphate salt) and cycloheximide were dissolved in the CSF and bath-applied. Somatic extracellular field potentials (FPs) were recorded through 3 M NaCl-filled glass microelectrodes (1–5 MΩ) in the CA1 area after electrical stimulation (0.1 Hz, 70 ms, 100–200 µA) of the stratum radiatum. Electrical potentials were amplified, recorded on tape (Racal 4DS), digitized at 10 kHz, and analysed on line, by an *ad hoc* software package on a PS2 IBM computer on averaged (five consecutive recordings) traces. A total of 112 slices were used, one slice for each experiment.

Experimental protocol The drugs were directly added to the perfused solution and after 60 min of perfusion their effects were evaluated on: (1) the amplitude of the primary CA1 population spike (PPSA); (2) the occurrence of additional epileptiform populations spikes per field potential (AEPS/FP); (3) the duration of the field potential (FPD measured from the first to the last population spike whose amplitude was higher than 0.2 mV). The following drugs were used: highly selective µ agonists (DAMGO, morphiceptin), less selective µ agonists (morphine, methadone), a highly selective δ_2 agonist (deltorphin II), a highly selective δ_1 agonist (DPDPE), a selective κ agonist (U50,488H), dexamethasone and the protein synthesis inhibitor, cycloheximide. The following treatments were performed: (1) morphine (300 µM), methadone (100 µM), DAMGO (0.5 µM), morphiceptin (10 µM), DPDPE (0.5 µM), deltorphin II (0.5 µM), U50,488H (150 µM), dexamethasone (100 µM) were perfused for 60 min; (2) dexamethasone (100 µM) followed 30 min later by perfusion with morphine (300 µM), or methadone (100 µM), or DAMGO (0.5 µM), or morphiceptin (10 µM), or DPDPE (0.5 µM), or deltorphin II (0.5 µM), or U50,488H (150 µM) plus dexamethasone (100 µM) for 60 min; (3) cycloheximide (1 µM) was perfused for 30 min; (4) cycloheximide (1 µM) plus dexamethasone (100 µM) followed 30 min later by perfusion with morphine (300 µM), or methadone (100 µM) or DAMGO (0.5 µM) plus dexamethasone (100 µM) for 60 min.

Statistical analysis

The results obtained in *in vivo* and *in vitro* experiments were analysed by using Student's test or by ANOVA. Statistical significance was assigned to a statistical probability of 5% or less.

Results

In vivo *experiments*

Figure 1 and Table 1 show that in both the tail flick and hot plate tests, dexamethasone pretreatment was able to induce a consistent shift of ED_{50} towards higher values i.e. to reduce strongly the analgesic potency of the drugs which have selective or prevalent µ effects. However, less evident effects were induced by dexamethasone on the antinociceptive potency of DPDPE, which has prevailing δ_1 effects. On the contrary, dexamethasone did not induce inhibitory influences on the κ drug U50,488H, but it did induce a slight, although significant potentiating effect. In the experiments performed with a drug which has highly selective δ_2 effects (deltorphin II), dexamethasone had no effect (Table 2). The antagonistic effect of dexamethasone on DAMGO or morphine antino-

ciception was completely prevented by pretreatment with cycloheximide, a protein synthesis inhibitor (Table 2).

In vitro *experiments*

Slice perfusion with 300 μM morphine ($n = 10$) or 100 μM methadone ($n = 10$) or 0.5 μM DAMGO ($n = 6$) or 10 μM morphiceptin ($n = 6$) in 100% of the experiments within 60 min changed the CA1 FP into an epileptiform bursting characterized by an increase of the amplitude of the CA1 PS from 2–5 to 7–11 mV, the appearance of some (1 to 3) additional population spikes and an increase in duration up to 8–15 ms (Sagratella *et al.*, 1987; Frank *et al.*, 1988). These effects completely disappeared within 30–60 min after the drug was withdrawn from the perfusing solution ($n = 6$). Within 60 min of slice perfusion with 0.5 μM of DPDPE ($n = 5$) or 0.5 μM of deltorphin II ($n = 10$) these drugs failed to produce the appearance of epileptiform bursting, but they induced only an increase of the amplitude of the CA1 PS (PPSA = + 51 ± 11%). Slice perfusion with 150 μM of the κ agonist, U50,488H ($n = 6$) induced a decrease of the amplitude of the CA1 PS (PPSA = to 40.5 ± 7%) within 60 min. Dexamethasone perfusion (100 μM, $n = 4$) for 60 min did not significantly affect the CA1 FP amplitude (PPSA = + 12 ± 6%) or duration (FPD = + 5 ± 3%). Dexamethasone per-

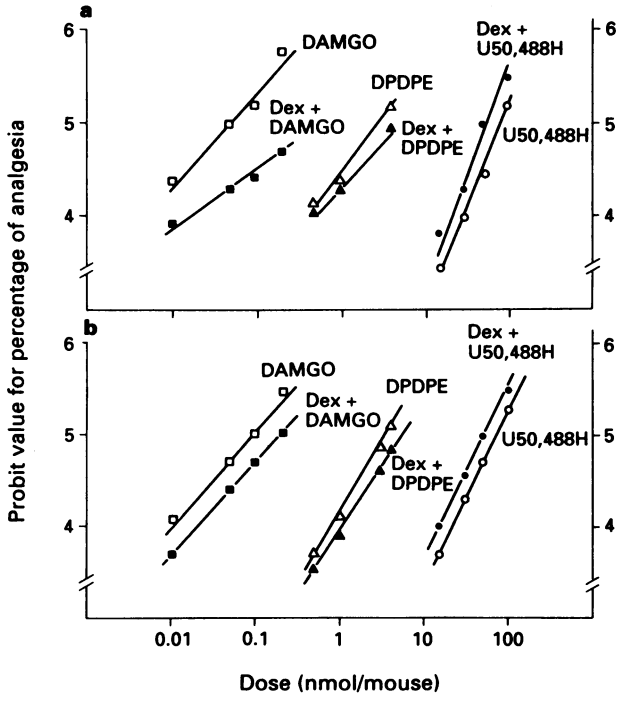


Figure 1 Dose-response curves of various i.c.v. doses of some opioid agonists alone or in the presence of dexamethasone pretreatment (Dex 0.1 mg kg^{-1} administered i.p. 30 min before opioid agonist) in the tail flick (a) and in the hot plate tests (b). The latency of the responses was expressed as percentage of analgesia. This was calculated as (post-opioid latency − pre-drug latency)/(cut latency − pre-drug latency) × 100, where the cut off time was 10 s in tail flick and 60 s in hot plate. In control animals the latency of the responses was 2–3 s in the tail flick test and 15–17 s in the hot plate test. The ED_{50} and 95% confidence intervals were computed from the dose-response curve by the method of Litchfield & Wilcoxon (1949) with the aid of a computer programme.

Table 2 Effects of dexamethasone pretreatment (Dex, 0.1 mg kg^{-1} administered 30 min before opioid agonist), cycloheximide pretreatment (Cyclo, 15 mg kg^{-1} administered 2 h before dexamethasone or 2.5 h before opioid agonist) on the analgesia induced by i.c.v. injection of some opioid agonists

Drugs	*Tail flick test* *Mean ± s.e.*		*Hot plate test* *Mean ± s.e.*	
Morphine				
1.6 nmol/mouse	69.1 ± 1.5	*	63.5 ± 1.7	*
Dex + morphine	43.5 ± 2.1		40.2 ± 1.7	
Cyclo + morphine	63.0 ± 2.0		70.0 ± 1.5	
Cyclo + Dex + morphine	72.3 ± 1.7		68.9 ± 2.5	
DAMGO				
0.05 nmol/mouse	65.0 ± 3.1	*	53.0 ± 4.0	*
Dex + DAMGO	33.6 ± 2.3		40.1 ± 1.7	
Cyclo + DAMGO	68.9 ± 2.7		55.0 ± 1.4	
Cyclo + Dex + DAMGO	70.0 ± 1.7		57.0 ± 2.0	
Deltorphin II				
1 nmol/mouse	50.0 ± 4.3		63.0 ± 2.1	
Dex + deltorphin II	43.0 ± 1.3		54.0 ± 4.0	

Changes in the latency were expressed as percentage of analgesia which was calculated as (post-opioid latency − pre-drug latency)/(cut-off latency − pre-drug latency) × 100, where the cut off time was 10 s in tail flick and 60 s in hot plate. Statistical analysis was performed by using the Student's test. Groups consisted of at least 20 animals; each animal was tested once.
*$P < 0.05$.

Table 1 Effects of dexamethasone pretreatment (Dex, 0.1 mg kg^{-1} i.p.) on the analgesia induced by i.c.v. injection of some opioid agonists

Drugs	*Tail flick test* ED_{50} *nmol/mouse* *(95% confidence limits)*		*Hot plate test* ED_{50} *nmol/mouse* *(95% confidence limits)*	
Morphine	0.92 (0.73–1.17)	*	1.42 (1.13–1.78)	*
Dex + morphine	3.20 (2.65–3.86)		4.51 (3.66–5.56)	
β-Endorphin	0.10 (0.078–0.14)	*	0.080 (0.058–0.11)	*
Dex + β-endorphin	0.36 (0.24–0.53)		0.200 (0.144–0.27)	
DAMGO	0.04 (0.029–0.055)	*	0.078 (0.056–0.10)	*
Dex + DAMGO	0.66 (0.35–1.23)		0.18 (0.128–0.268)	
DPDPE	3.33 (2.45–4.52)	*	3.44 (0.83–14.2)	
Dex + DPDPE	5.84 (3.99–8.56)		5.50 (4.15–7.29)	
U-50,488H	76.10 (63.2–91.6)	*	61.4 (50.4–74.7)	
Dex + U-50,488H	55.4 (46.6–65.8)		48.8 (22.6–105.5)	

Morphine (0.6–5.2 nmol), β-endorphin (0.015–0.6 nmol), DAMGO (0.01–0.2 nmol), DPDPE (0.5–4 nmol), U-50,488H (15–100 nmol) were administered 30 min after dexamethasone injection. Changes in the latency of the responses were expressed as percentage of analgesia which was calculated as (post-opioid latency − pre-drug latency)/(cut off latency − pre-drug latency) × 100, where the cut off time was 10 s in tail flick and 60 s in hot plate. The ED_{50} and 95% confidence intervals were computed from the dose-response curve by the method of Litchfield and Wilcoxon with the aid of the computer programme. Statistical analysis was carried out by Student's test. Groups consisted of at least 20 animals; each animal was tested only once.
*Significant ratio (at least $P < 0.05$).

fusion (100 μM) for 30 min followed by dexamethasone (100 μM) plus morphine (300 μM) or methadone (100 μM) ($n = 6$) or DAMGO (0.5 μM) ($n = 6$) or morphiceptin (10 μM) ($n = 6$) significantly reduced, within 60 min, the increase of the CA1 FP duration and the number of additional population spikes due to the μ opiate agonists. Dexamethasone perfusion (100 μM) for 30 min followed by dexamethasone (100 μM) application plus DPDPE (0.5 μM, $n = 6$) or deltorphin II (0.5 μM, $n = 6$) failed within 60 min to affect significantly the increase of the CA1 PS amplitude due to the δ opioid agonists.

Dexamethasone perfusion (100 μM) for 30 min followed by dexamethasone (100 μM), plus U50,488H (150 μM) ($n = 6$) failed within 60 min to affect significantly the decrease of the CA1 PS amplitude due to the κ opioid agonist.

Slice perfusion for 30 min with the protein synthesis inhibitor, cycloheximide, at a concentration of 1 μM ($n = 4$) did not significantly change CA1 FP amplitude (PPSA=

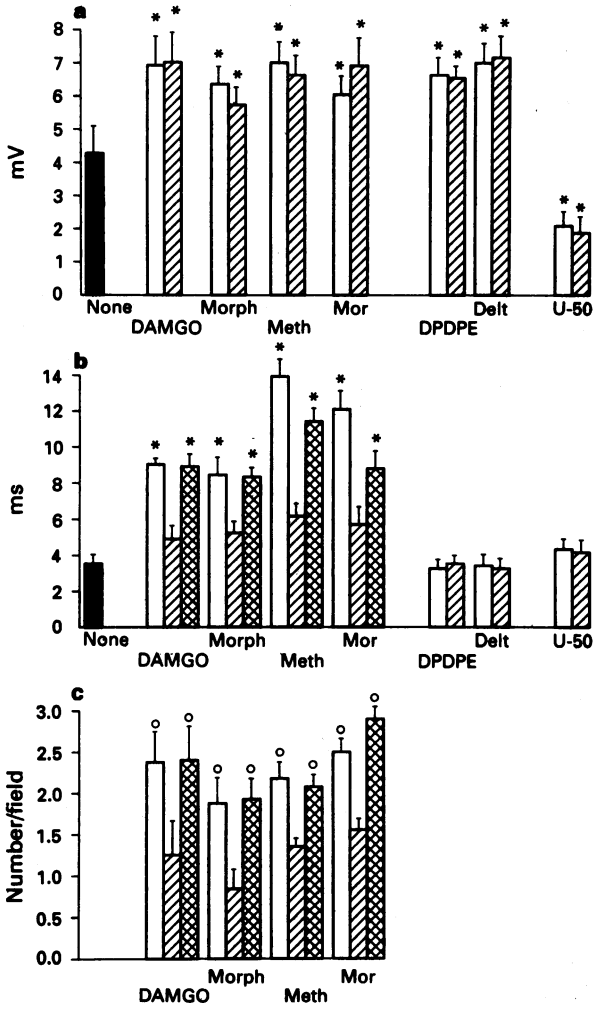


Figure 2 Influence of dexamethasone (Dex) on the electrophysiological effects of selected opioids on hippocampal CA1 pyramidal neurones. (a) Effects on CA1 PPSA: the histograms show the influence of Dex (100 μM) on opioid-induced effects on the amplitude of the CA1 primary population spike amplitude (measured from the beginning to the maximum of the negative deflection of the extracellular field potential). (b) Effects on CA1 FDP: the histograms show the influence of Dex (100 μM) on opioid-induced effects on the duration of the CA1 field potentials (measured from the first to the last population spike whose amplitude was higher than 0.2 mV). (c) Effects on CA1 AEPS: the histograms show the influence of Dex (100 μM) on opioid-induced occurrence of additional epileptiform population spikes. Abbreviations: DAMGO = 0.5 μM DAMGO slice perfused for 60 min; Morph = 10 μM morphiceptin slice perfused for 60 min; METh = 100 μM methadone slice perfused for 60 min; Mor = 300 μM morphine slice perfused for 60 min; DPDPE = 0.5 μM DPDPE slice perfused for 60 min Delt = 0.5 μM deltorphin II slice perfused for 60 min; U-50 = 150 μM U-50,488 H slice perfused for 60 min; + Dex = 30 min slice perfusion with 100 μM dexamethasone followed by 60 min slice perfusion with 100 μM dexamethasone plus the opioid; + Cyc = 30 min slice perfusion with 1 μM cycloheximide plus 100 μM dexamethasone followed by 60 min slice perfusion with 1 μM cycloheximide plus 100 μM dexamethasone plus the opioid; * = significantly different from control (NONE, $P<0.01$ according to Newman Keuls test); °Significantly different from + Dex ($P<0.01$ according to Newman Keuls test). Open columns: opioid; hatched columns: dexamethasone plus opioid; cross-hatched columns: cycloheximide plus dexamethasone plus opioid.

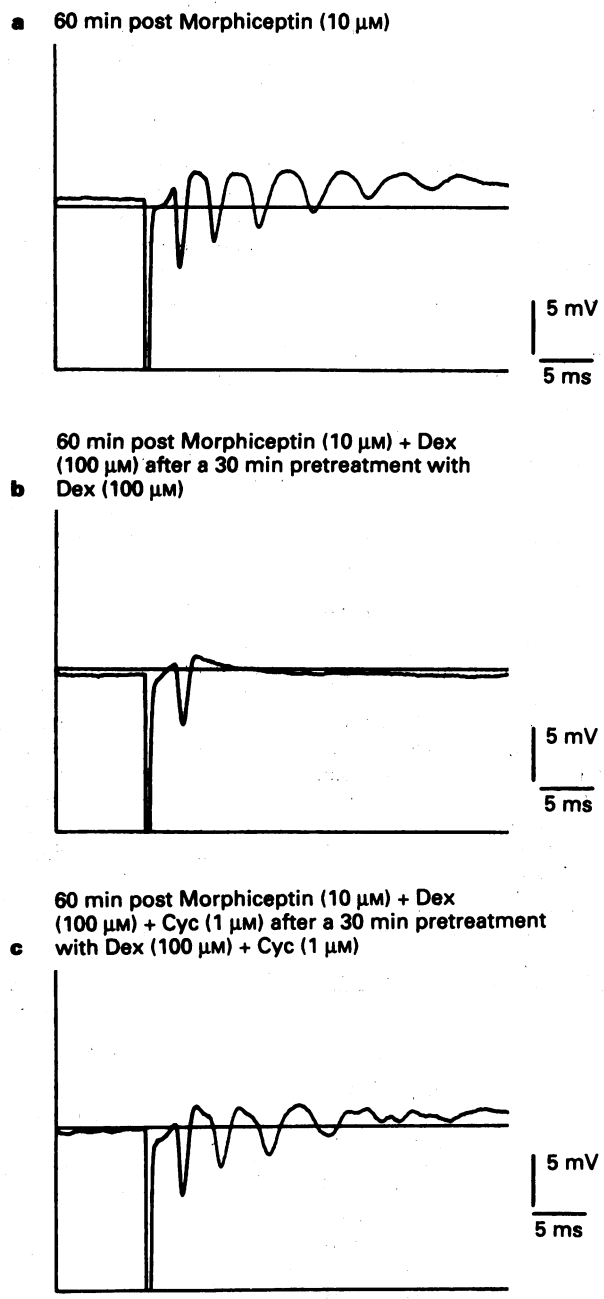


Figure 3 Influence of dexamethasone and cycloheximide on morphiceptine epileptiform bursting in rat hippocampal slices (a) The record shows the epileptiform bursting induced in rat hippocampal slices within 60 min from the perfusion of 10 μM morphiceptin; (b) 30 min after dexamethasone (Dex, 100 μM) pretreatment and 60 min after perfusion of morphiceptin (10 μM), continuing the dexamethasone (100 μM) perfusion, dexamethasone blocked the rise of epileptiform bursting induced by morphiceptin; (c) 60 min after perfusion of morphiceptin (10 μM) continuing the dexamethasone (100 μM) plus cycloheximide (Cyc 1 μM) perfusion, dexamethasone did not block the rise of epileptiform bursting induced by morphiceptin.

$-12 \pm 11\%$) or duration (FPD= $+2 \pm 8.6\%$). Adding cycloheximide (1 μM) ($n = 6$) for 30 min to the medium perfusing the slice containing dexamethasone (100 μM) followed by a 60 min perfusion of morphine (300 μM), methadone (100 μM) or DAMGO (0.5 μM) plus dexamethasone (100 μM) completely blocked the previously described dexamethasone effects on the μ agonists (Figures 2 and 3).

Discussion

These results confirm and extend previous findings that dexamethasone induces inhibition of two main effects related to the opioid system, i.e., analgesia and hippocampal excitability. Moreover, this inhibition is quite evident as an antagonism of the μ opioid receptor, as tested with the tail flick and hot plate antinociception tests, and with the *in vitro* hippocampal model.

The different influence of dexamethasone on opioid-induced effects is probably dependent on the different mechanisms that are activated after μ and δ opioid receptor stimulation. We should note that the inhibition exerted by dexamethasone on the μ opioid agonist is strong and highly reproducible. However the inhibition exerted by dexamethasone on effects induced by the highly specific δ_2 agonist, deltorphin II was not significant in both the tail flick and hot plate tests. The inhibition exerted by dexamethasone on the δ_1 agonist, DPDPE, was of borderline significance in the tail flick test and was not consistent in the hot plate test. Both DPDPE and deltorphin II in contrast to μ opioids failed to induce epileptiform bursting in the rat hippocampus model. The inability of the selective δ agonists to induce spontaneous or evoked epileptiform burstings, which was also shown in the dentate gyrus, is probably dependent on the inability of δ agonists to affect hippocampal recurrent inhibition (Lupica *et al.*, 1992). However, μ and δ agonists also affected hippocampal non-recurrent synaptic inhibition, an effect revealed in extracellular studies by an increase of the CA1 PS amplitude. Dexamethasone was not able to prevent it. Since hippocampal recurrent inhibition depends on the activity of GABAergic interneurones (Neumaier *et al.*, 1988), the specific influence of dexamethasone on opioid-induced epileptiform bursting (but not on the opioid-induced increase of the amplitude of the CA1 PS) might indicate a possible influence of dexamethasone on GABA-mediated opioid-induced effects. In agreement with this hypothesis, in preliminary experiments we noted that dexamethasone was able to prevent significantly the CA1 epileptiform bursting due to the GABA antagonists, penicillin but not due to 'magnesium free' solutions (Sagratella, unpublished observations).

Dexamethasone also induced a slight, but significant potentiation of the U50,488H-induced analgesia measured with the tail flick test, and a significant potentiation on the hot plate test. The potentiating effect of dexamethasone on the analgesic effects of U50,488H is not surprising. In fact, opposite interactions between μ and κ receptors have been reported in different assays of analgesia (Ramarao *et al.*, 1988; Craft & Dykstra, 1992) and discriminative stimulus effects (Negus *et al.*, 1991). In fact, in the rat hippocampal slice preparation, the κ opioid U50,488H by itself in contrast to μ and δ agonists induced a consistent diminution in amplitude of CA1 PS in rat hippocampal slices. This effect was not modified by dexamethasone pretreatment in *in vitro* experiments. Previous studies have also shown that κ agonists such as dynorphin produced depressive effects on hippocampal synaptic transmission *in vivo* and *in vitro* experiments (Brookes & Bradley, 1984; Moises & Walker, 1985; Iwama *et al.*, 1986). Recent studies also demonstrated that other high affinity κ agonists such as U-69593 and U-54494A showed depressant effects on the electrical synaptic response at the CA1 and CA3 hippocampal areas (Alzheimer & Bruggencate, 1990; Proietti *et al.*, 1991) and the discussion on the possible opioid nature of this phenomenon is still open. However, the discrepancy between *in vivo* and *in vitro* experiments might indicate that the influence of dexamethasone on κ opioid-induced analgesia did not involve the hippocampus.

Various electrophysiological effects of corticosteroids on hippocampal neurones are described in the literature. Prevalent short-lasting neuronal depressant or membrane hyperpolarising activity are described within a short time from hippocampal slice perfusion with cortisol succinate or corticosterone and, in agreement with our results, dexamethasone perfusion resulted in few effects (Vidal *et al.*, 1986; Joels & De Kloet, 1989; Chen *et al.*, 1991). Reports in the literature support the view that effects mediated by steroids involve intracellular mechanisms on the genome. Recently it has been shown that a high corticosterone concentration and the selective glucocorticoid RU 28362 1 h after application increase the amplitude of the afterhyperpolarisation of CA1 pyramidal neurones obtained from adrenalectomized rats resulting in a potential suppression of hippocampal excitability (Kerr *et al.*, 1989; Joels & de Kloet, 1989). This effect did not occur in the presence of the protein synthesis inhibitor, cycloheximide, thus suggesting a genomic action of steroids (Karst & Joels, 1991). Furthermore, it was reported that high levels of corticosterone also affect calcium action potentials other than the slow afterhyperpolarisation (Kerr *et al.*, 1989). Our results indicate that at least 15–30 min latency is necessary for the manifestation of the inhibitory properties exerted by dexamethasone on these opioid effects, and confirm also that these effects are prevented by pretreatment with the protein synthesis inhibitor, cycloheximide. All these findings suggest that the inhibitory effects that glucocorticoids exert on hippocampal excitability (Joels & de Kloet, 1992) *via* protein-synthesis mechanism may explain dexamethasone antagonism on opioid-induced effects. This antagonism has been reproduced without substantial modifications using two *in vivo* models for the evaluation of the analgesic effects, and one *in vitro* model for the evaluation of cerebral excitability. In our previous paper (Pieretti *et al.*, 1992) data very similar to those obtained *in vitro* (i.e., strong inhibition induced by dexamethasone on the epileptiform effects elicited by morphine) were obtained also *in vivo* in rabbits treated i.v. with dexamethasone followed by morphine injected i.c.v. On that occasion, deamethasone was also able to prevent consistently EEG background alterations as well as gross behavioural alterations induced by morphine. Therefore, there is sufficient evidence to hypothesize that the interference exerted by dexamethasone on some opioid effects depends on the capacity of dexamethasone to affect the μ-mediated effects throughout a mechanism involving protein synthesis. Recently Magnuson *et al.* (1990) investigated the electrophysiological action of cholecystokinin octapeptide on the reduction of the C-fibre evoked dorsal horn neurone activity elicited by transcutaneous electrical stimulation induced by DAMGO and DSTBULET (Tyr-D-Ser(otbu)-Gly-Phe-Leu-Thr), a δ opioid agonist. Magnuson reported that cholecystokinin selectively prevented the inhibition of C-fibre evoked activity induced by DAMGO whereas no effect was shown on the inhibition of C-fibre evoked activity induced by DSTBULET. Others reported that cholecystokinin octapeptide antagonized the analgesia mediated by the μ agonist, PL017 or morphine (Faris *et al.*, 1983) whereas the peptide did not change the analgesic effects induced by the δ agonist DPDPE (Wang *et al.*, 1990). Studies performed *in vivo* have shown that stress induced changes in cholecystokinin concentration in the rat hypothalamus, and that dexamethasone treatment increased the cellular content and secretion of some cholecystokinin peptides in a thyroid carcinoma cell line (Odum & Rehfeld, 1990). Dexamethasone treatment was also reported to be able to triple the number of cholecystokinin receptors per cell with little change in receptor affinity, and it was shown that dexamethasone increased the sensitivity of AR42J pancreatic acinar cells to cholecystokinin (Logsdon, 1986). The possibility that dexamethasone exerts its antagonism *versus* opioid-induced effects *via* cholecystokinin may be considered,

although some reports indicate that cholecystokinin may also reduce κ-induced analgesia (Wang *et al.*, 1990) or selectively antagonize only β-endorphin-induced analgesia (Itoh *et al.*, 1982; Tseng & Collins, 1991).

Finally, whatever the mechanism may be, our data indicated that glucocorticoid and opioid may exert inter-regulatory properties on pain and cerebral excitability.

This research was supported in part by grants from Consiglio Nazionale delle Richerche (CNR N:9301752). We thank Ms Susan Holt for the English revision of the manuscript.

References

ALZHEIMER, C. & BRUGGENCATE, G.T. (1990). Non-opioid actions of the k-opioid receptor agonist U50488H and U69593 on the electrophysiologic properties of hippocampal CA3 neurons in vitro. *J. Pharmacol. Exp. Ther.*, **255**, 900–905.

AMIR, S., BROWN, Z.W. & AMIT, Z. (1980). The role of endorphins in stress: evidence and speculations. *Neurosci. Behav. Rev.*, **4**, 77–87.

BROOKES, A. & BRADLEY, P.B. (1984). Electrophysiological evidence for a k-agonist activity of dynorphin in rat brain. *Neuropharmacology*, **23**, 207–210.

CAPASSO, A., DI GIANNUARIO, A., LOIZZO, A., PIERETTI, S. & SORRENTINO, L. (1992). Central interaction of dexamethasone and RU-38486 on morphine antinociception in mice. *Life Sci.*, **51**, 139–143.

CHATTERJEE, T.K., SUMANTRA, D., BANERJE, P. & GHOSH, J.J. (1982). Possible physiological role of adrenal and gonadal steroids in morphine analgesia. *Eur. J. Pharmacol.*, **77**, 119–121.

CHEN, Y.Z., HUA, S.Y., WANG, C.A., WU, L.G., GU, Q. & XING, B.R. (1991). An electrophysiological study on the membrane receptor-mediated action of glucocorticoids in mammalian neurons. *Neuroendocrinology*, **53**, 25–30.

CRAFT, R.M. & DYKSTRA, L.A. (1992). Agonist and antagonist activity of kappa opioids in the squirrel monkey: antinociception and urine output. *J. Pharmacol. Exp. Ther.*, **260**, 327–333.

FARIS, P.L., KOMISARUK, B.R., WATKINS, L.R. & MAYER, D.J. (1983). Evidence for the neuropeptide cholecystokinin as an antagonist of opiate analgesia. *Science*, **219**, 310–312.

FRANK, C., SAGRATELLA, S., BENEDETTI, M. & SCOTTI DE CAROLIS, A. (1988). Comparative influence of calcium blocker and purinergic drugs on epileptiform bursting in rat hippocampal slices. *Brain Res.*, **441**, 393–397.

HALEY, T.J. & MCCORMICK, W.G. (1957). Pharmacological effect produced by intracerebral injections of drugs in the conscious mouse. *Br. J. Pharmacol. Chemother.*, **12**, 12–15.

HONG, J.S., MCGINTY, J.F., LEE, P.H.K., XIE, C.W. & MICTHELL, C.L. (1993). Relationship between hippocampal opioid peptides and seizures. *Progr. Neurobiol.*, **40**, 507–528.

ITOH, S., KATSUURA, G. & MAEDA, Y. (1982). Caerulein and cholecystokinin suppress β-endorphin-induced analgesia in the rat. *Eur. J. Pharmacol.*, **80**, 421–425.

IWAMA, T., ISHIHARA, K., SATOH, M. & TAKAGI, H. (1986). Different effects of dynorphin on in vitro guinea pig hippocampal CA3 pyramidal cells with various degrees of paired-pulse facilitation. *Neurosci. Lett.*, **63**, 190–194.

JOELS, M. & DE KLOET, E.R. (1989). Effects of glucocorticoids and norepinephrine on the excitability in the hippocampus. *Science*, **245**, 1502–1505.

JOELS, M. & DE KLOET, E.R. (1992). Control of neuronal excitability by corticosteroid hormones. *Trends Neurosci.*, **15**, 25– 30.

KARST, H. & JOELS, M. (1991). The induction of corticosteroid actions on membrane properties of hippocampal CA1 neurons requires protein synthesis. *Neurosci. Lett.*, **130**, 27–31.

KERR, D.S., CAMPBELL, L.W., HAO, S.-Y., LANDFIELD, P.W. (1989). Corticosteroid modulation of hippocampal potentials: increased effects with aging. *Science*, **245**, 1505–1509.

LEWIS, J.W., CANNON, J.T. & LEIBESKIND, J.C. (1980). Opioid and non-opioid mechanisms of stress analgesia. *Science*, **208**, 623–625.

LITCHFIELD, J.T. & WILCOXON, F. (1949). A simplified method of evaluating dose effects experiments. *J. Pharmacol. Exp. Ther.*, **96**, 99–113.

LOGSDON, C.D. (1986). Glucocorticoids increase cholecystokinin receptors and amylase secretion in pancreatic acinar AR42J cells. *J. Biol. Chem.*, **261**, 2096–2101

LUPICA, C.R., PROCTOR, W.R. & DUNWIDDLE, T.V. (1992). Dissociation of μ and δ opioid receptor-mediated reduction in evoked and spontaneous synaptic inhibition in the rat hippocampus in vitro. *Brain Res.*, **593**, 226–238.

MACLENNAN, A.J., DRUGAN, C.R., HYSON, R.L., MAISER, S.F., MADDEN, IV, J. & BARCHAS, J.D. (1982). Corticosterone: a critical factor in an opioid form of stress-induced analgesia. *Science*, **215**, 1530–1532.

MAGNUSON, D.S.K., SULLIVAN, A.F., SIMONNET, G., ROQUES, B.P. & DICKENSON, A.H. (1990). Differential interactions of cholecystokinin and FLFQPQRF-NH_2 with μ and δ opioid antinociception in the rat spinal cord. *Neuropeptides*, **16**, 213–218.

MCEVEN, B.S., DE KLOET, E.R. & ROSTENE, W. (1986). Adrenal steroid receptors and actions in the nervous system. *Physiol. Rev.*, **66**, 1121–1188.

MILLAN, J.M. (1986). Multiple opioid system and pain. *Pain*, **27**, 303–347.

MOISES, H.C. & WALKER, M.J. (1985). Electrophysiological effects of dynorphin peptides on hippocampal pyramidal cells in rats. *Eur. J. Pharmacol.*, **108**, 85–88.

NEGUS, S.S., PICKER, M.J. & DYKSTRA, L.A. (1991). Interaction between the discriminative stimulus effects of mu and kappa opioid agonist in the squirrel monkey. *J. Pharmacol. Exp. Ther.*, **256**, 149–158.

NEUMAIER, J.F., MAILHEAU, S. & CHAVIKIN, C. (1988). Opioid receptor-mediated responses in the dentate gyrus and CA1 region of the rat hippocampus. *J. Pharmacol. Exp. Ther.*, **244**, 564–570.

ODUM, L. & REHFELD, J.F. (1990). Expression and processing of procholecystokinin in a rat medullary thyroid carcinoma cell line. *Biochem. J.*, **271**, 31–36.

ORTOLANI, E., DI GIANNUARIO, A., NEROZZI, D., ZAPPONI, G.A. & LOIZZO, A. (1990). Some endorphin derivatives and hydrocortisone prevent EEG limbic seizures induced by corticotropin-releasing factor in rabbits. *Epilepsia*, **31**, 702–707.

PASTERNAK, G.W. (1987). Opioid receptors. In *Psychopharmacology: the Third Generation of Progress*. ed. Meltzer, H.Y. pp. 281–288. New York: Raven Press.

PIERETTI, S., CAPASSO, A., DI GIANNUARIO, A., LOIZZO, A. & SORRENTINO, L. (1991). The interaction of peripherically and centrally administered dexamethasone and RU 38486 on morphine analgesia in mice. *Gen. Pharmacol.*, **22**, 929–933.

PIERETTI, S., DI GIANNUARIO, A., LOIZZO, A., SAGRATELLA, S., SCOTTI DE CAROLIS, A., CAPASSO, A. & SORRENTINO, L. (1992). Dexamethasone prevents epileptiform activity induced by morphine in *in vivo* and *in vitro* experiments. *J. Pharmacol. Exp. Ther.*, **263**, 830–839.

PROIETTI, M.L., SCOTTI DE CAROLIS, A., FRANK, C., ZENG, Y.C. & SAGRATELLA, S. (1991). In vitro depressant effects of U-54494A, an anticonvulsant related to kappa opioids in the hippocampus. *Neuropharmacol.*, **30**, 637–642.

RAMABADRAN, K. & BANSINATH, M. (1990). Endogenous opioid peptides and epilepsy. *Int. J. Clin. Pharmacol. Ther. Toxicol.*, **28**, 47–62.

RAMARAO, P., JABLONSKI, H.I., REHDER, K.R. & BHARGAVA, H.N. (1988). Effect of k-opioid receptor agonists on morphine analgesia in morphine-naive and morphine-tolerant rats. *Eur. J. Pharmacol.*, **156**, 239–246.

SAGRATELLA, S., FRANK, C. & SCOTTI DE CAROLIS, A. (1987). Effects of ketamine and (+) cyclazocine on 4-aminopyridine and 'magnesium free' epileptogenic activity in hippocampal slices of rats. *Neuropharmacology*, **26**, 1181–1184.

SPIESS, J., RIVIER, J., RIVIER, C. & VALE, W. (1981). Primary structure of corticotropin releasing factor from ovine hypothalamus. *Proc. Natl. Acad. Sci. U.S.A.*, **78**, 6517–6521.

TSENG, L.F. & COLLINS, K.A. (1991). Cholecystokinin administered intrathecally selectively antagonizes intracerebroventricular β-endorphin-induced tail flick inhibition in the mouse. *J. Pharmacol. Exp. Ther.*, **260**, 1086–1092.

VALE, W., SPIESS, J., RIVIER, C., RIVIER, J. (1981). Characterization of a 41-residue ovine hypothalamic peptide that stimulates the secretion of corticotropin and b-endorphin. *Science*, **231**, 1394–1397.

VIDAL, C., JORDAN, W. & ZIEGLAGANSBERGER, W. (1986). Corticosterone reduces the excitability of hippocampal pyramidal cells in vitro. *Brain Res.*, **383**, 54–59.

WANG, X.-J., WANG, X.-H. & HAN, J.-S. (1990). Cholecystokinin octapeptide antagonized opioid analgesia mediated by μ- and κ- but not δ-receptors in the spinal cord of the rat. *Brain Res.*, **523**, 5–10.

WINTER, C.A. & FLATAKER, J. (1951). The effect of corticosterone, desoxycorticosterone and adrenocorticotropic hormone upon the response of animals to analgesic drugs. *J. Pharmacol. Exp. Ther.*, **103**, 93–95.

ZIMMERMAN, M. (1983). Ethical guidelines for investigations of experimental pain in conscious animals. *Pain*, **16**, 109–110.

(Received April 12, 1994
Revised June 24, 1994
Accepted July 25, 1994)

Br. J. Pharmacol. (1994), **113**, 1423–1431 © Macmillan Press Ltd, 1994

Anti-inflammatory and bronchodilator properties of RP 73401, a novel and selective phosphodiesterase type IV inhibitor

[1]David Raeburn, Stephen L. Underwood, Susan A. Lewis, Valerie R. Woodman, Cliff H. Battram, Adrian Tomkinson, Steven Sharma, Roy Jordan, John E. Souness, Stephen E. Webber & Jan-Anders Karlsson

Rhône-Poulenc Rorer Ltd., Dagenham Research Centre, Rainham Road South, Dagenham, Essex RM10 7XS

1 We have investigated the effects of RP 73401, a novel, potent and highly selective cyclic nucleotide phosphodiesterase (PDE) type IV inhibitor, in guinea-pig and rat models of bronchoconstriction and allergic inflammation. In some models, the effects of RP 73401 have been compared with those of the standard PDE type IV inhibitor, rolipram.

2 RP 73401 (0.4–400 $\mu g\,kg^{-1}$, intratracheally (i.t.) on lactose) inhibited antigen-induced bronchospasm in previously sensitized conscious guinea-pigs (ID_{50}: $7 \pm 1\,\mu g\,kg^{-1}$) and in anaesthetized rats (ID_{50}: $100 \pm 25\,\mu g\,kg^{-1}$). Rolipram inhibited the antigen-induced bronchospasm in guinea-pigs with an ID_{50} of $5 \pm 1\,\mu g\,kg^{-1}$. In guinea-pig bronchoalveolar lavage (BAL) fluid, total inflammatory cell and eosinophil numbers were reduced by RP 73401 (ID_{50}s: $3.9 \pm 0.8\,\mu g\,kg^{-1}$ and $3.2 \pm 0.7\,\mu g\,kg^{-1}$, respectively). In the rat, inflammatory cell numbers are less affected. Only the highest dose of RP 73401 ($400\,\mu g\,kg^{-1}$) significantly inhibited eosinophil influx ($41 \pm 16\%$ inhibition).

3 RP 73401 (0.02–100 $\mu g\,kg^{-1}$, i.v.) inhibited PAF-induced bronchial hyperreactivity to bombesin in the anaesthetized guinea-pig (ID_{50}: $0.09 \pm 0.03\,\mu g\,kg^{-1}$) and inhibited (0.4–40 $\mu g\,kg^{-1}$, i.t.) histamine-induced airway microvascular leakage in the anaesthetized guinea-pig by approximately 60% at all doses.

4 RP 73401 relaxed guinea-pig isolated trachea under basal tone (EC_{50}: 9 nM) and when precontracted with histamine (IC_{50}: 2 nM), methacholine (IC_{50}: 29 nM) or leukotriene D_4 (LTD_4, IC_{50}: 4 nM).

5 RP 73401 (0.4–100 $\mu g\,kg^{-1}$, i.t.) inhibited bronchospasm induced by histamine (ID_{50}: $34 \pm 6\,\mu g\,kg^{-1}$), methacholine (ID_{50}: $66 \pm 12\,\mu g\,kg^{-1}$) and LTD_4 (ID_{50}: $<4\,\mu g\,kg^{-1}$) in the anaesthetized guinea-pig. Against these same bronchoconstrictors, rolipram (i.t.) had ID_{50} values of 44 ± 4, 72 ± 18 and $<4\,\mu g\,kg^{-1}$ respectively. RP 73401 (4 and 40 $\mu g\,kg^{-1}$, i.t.) increased the magnitude and duration of bronchodilatation produced by salbutamol in the anaesthetized guinea-pig. At doses producing significant bronchodilatation, RP 73401 was without effect on heart rate or blood pressure in the anaesthetized guinea-pig. RP 73401 (0.01–0.25 mg kg^{-1}, i.v.) did not affect heart rate and produced only a small fall in blood pressure in the anaesthetized rat.

6 These data demonstrate that RP 73401 and rolipram inhibit antigen- and mediator-induced bronchospasm in guinea-pigs with the same potency. Furthermore, RP 73401 administered directly into the airways, protects against allergic airway inflammation. These results indicate the importance of PDE IV in regulating smooth muscle and inflammatory cell activity. At doses suppressing the inflammatory response in the lung, RP 73401 had little effect in the cardiovascular system. RP 73401 may have a role as a bronchodilator and, more importantly, as a prophylactic anti-inflammatory agent in the treatment of asthma.

Keywords: Phosphodiesterase inhibitor; RP 73401; bronchospasm; bronchodilator; inflammation; anti-inflammatory; anti-asthmatic; salbutamol; rolipam

Introduction

At least five different cyclic nucleotide phosphodiesterase (PDE) isoenzymes have now been identified on the basis of their functional characteristics such as substrate specificity and susceptibility to selective inhibitors (Beavo & Reifsnyder, 1990). The realization that there are differences in the relative functional importance of the PDE isoenzymes in specific cell types has fuelled the search for isoenzyme-selective PDE inhibitors which can be targeted to the cells implicated in the pathophysiology of asthma (Torphy & Undem, 1991; Giembycz & Dent, 1992; Raeburn *et al.*, 1993; Karlsson *et al.*, 1993).

Granulocytes, mononuclear cells and mast cells/basophils contain principally the PDE type IV isoenzyme. Inhibition of this enzyme is associated with increased intracellular adenosine 3':5'-cyclic monophosphate (cyclic AMP) and suppression of cell activity (Torphy & Undem, 1991; Giembycz & Dent, 1992; Raeburn *et al.*, 1993; Karlsson *et al.*, 1993). Although human airways smooth muscle contains at least five isoenzyme families (see Raeburn *et al.*, 1993 and references therein), the PDE III and PDE IV isoenzymes are functionally the most important as modulators of contractility (De Boer *et al.*, 1992; Qian *et al.*, 1993). In animal studies the functional profile of PDE isoenzymes in airways smooth muscle preparations both *in vitro* and *in vivo* appears similar to that in human tissue (Raeburn *et al.*, 1993).

RP 73401 (3-cyclopentyloxy-*N*-(3,5-dichloro-4-pyridyl)-4-methoxybenzamide) is a novel, highly selective and very potent PDE type IV inhibitor (Karlsson *et al.*, 1993; Ashton *et al.*, 1994). PDE type IV isolated from various cell types is inhibited by RP 73401 with an IC_{50} of about 1 nM and it displays at least a 19,000 fold selectivity compared with the other PDE isoenzymes (Ashton *et al.*, 1994; Souness *et al.*, 1994b). We have now characterized the airways smooth muscle relaxant and anti-inflammatory effects of RP 73401 in the guinea-pig and rat. In some models, we have compared the

[1] Author for correspondence.

effects of RP 73401 with those of the standard PDE type IV inhibitor rolipram. This study demonstrates potent inhibitory effects on a range of bronchoconstrictor and inflammatory responses in the tracheobronchial tree by RP 73401 and indicates that this compound has potential as an anti-asthma agent.

Methods

Guinea-pig isolated trachea

Male, Dunkin-Hartley guinea-pigs (350–500 g) were killed by cervical dislocation and the tracheas removed and placed in Krebs-Ringer bicarbonate (KRB) solution. The epithelium was removed by gently rubbing the luminal surface with a cotton swab. Transverse tracheal strips were prepared and suspended under an applied load of 2 g in 5 ml tissue baths containing KRB solution at 37°C gassed with 5% CO_2 in O_2. The load was determined from preliminary experiments (data not shown) to give maximum force of contraction in response to methacholine. The composition of the KRB was as follows (mM): NaCl 118, KCl 4.7, $CaCl_2$ 2.5, $MgSO_4$ 1.2, KH_2PO_4 1.2, $NaHCO_3$ 25, glucose 10.1. Changes in isometric force of contraction were measured with force-displacement transducers (Grass FT03) connected to a pen recorder (Lectromed Multitrace 8).

To examine the effects of RP 73401 on basal tone, tracheal tissues were equilibrated for 60 min, washing at 10 min intervals with KRB solution. Isoprenaline (2 μM) was then added to the baths to determine zero tone. The isoprenaline was subsequently washed from the tissues and when tone was fully recovered, the relaxant effects of RP 73401 were assessed following its cumulative addition.

To examine effects on spasmogen-induced increases in the force of contraction tissues were equilibrated as above but KRB solution containing indomethacin (5.6 μM) was used. Tissues were contracted to an EC_{30} (concentration producing 30% maximal contraction) of histamine (0.49 μM, 0.94 ± 0.11 g), methacholine (0.10 μM, 0.82 ± 0.09 g) or leukotriene D_4 (LTD_4) (0.41 nM, 0.63 ± 0.04 g). Contractile responses to all agonists remained stable over the time-course of the experiment. When the contractile response to each agonist had plateaued, RP 73401 was added cumulatively. The vehicle for RP 73401 (dimethylsulphoxide, DMSO, 0.1%) produced less than 10% reduction in maintained force of contraction.

Responses to RP 73401 (mean ± s.e.mean from *n* animals) are expressed as % inhibition of spasmogen-induced contraction or % reduction in basal tone where appropriate. EC_{50} values (basal tone) or IC_{50} (precontracted tissues) were calculated by linear regression and are presented as geometric means with 95% confidence limits.

Spasmogen-induced bronchospasm in the anaesthetized guinea-pig

Male, Dunkin-Hartley guinea-pigs (350–450 g) were anaesthetized with sodium pentobarbitone (60 mg kg^{-1}, i.p.). The trachea was cannulated to allow mechanical ventilation (Harvard 683 rodent ventilator) at 60 strokes min^{-1} with a stroke volume of 1 ml 100 g^{-1}. Pulmonary inflation pressure (PIP) was measured with a Druck (model PDCR75) pressure transducer connected to a side arm from the tracheal cannula. Blood pressure was measured by a second pressure transducer connected to a cannula tied into the left carotid artery. Heart rate was derived from the blood pressure signal. PIP, blood pressure and heart rate were recorded on a Lectromed (Multitrace 8) pen recorder. A cannula was tied into the right jugular vein to allow administration of spasmogen solutions in saline. RP 73401 or rolipram (4–100 μg kg^{-1}) were administered as a dry powder formulation (particle size, 4–8 μm) on lactose. A bolus (10 mg kg^{-1}) dose was blown from a tube into the airways by a plastic bulb (Underwood *et al.*, 1991; Raeburn & Karlsson, 1993). Vehicle control animals received lactose carrier (10 mg kg^{-1}) alone. We have shown (data on file) that a uniform distribution of drug throughout the lung occurs following administration as a dry powder.

Spasmogens (histamine, methacholine or LTD_4) were administered (i.v. bolus) at 6 min intervals and the dose titrated so that each produced an increase in PIP equivalent to about 60% of the maximum obtained by manually occluding the tracheal cannula. After two stable responses had been obtained, RP 73401 or rolipram were administered into the airways 1 min before the next dose of spasmogen. Administration of spasmogen was continued at 6 min intervals until responses had returned to pretreatment amplitude or for a maximum of 48 min. Each animal received only a single dose of the PDE inhibitor. Results are expressed as percentage inhibition (mean ± s.e.mean) of bronchospasm and duration of action (min). The ID_{50} (the dose causing 50% inhibition of bronchospasm) in each case was calculated by linear regression.

Antigen-induced bronchospasm in vivo

Guinea-pigs were sensitized (i.p.) with ovalbumin (10 μg) and aluminium hydroxide (100 mg) in saline (1 ml). After 21–28 days, sensitization was confirmed by the intradermal injection of albumin (25 μl of 200 μg ml^{-1}) into the dorsal surface of the left ear. Animals not responding with marked erythema and oedema, maximal after 20–40 min, were excluded from the study. Sensitized animals were used 7–14 days later.

RP 73401 or rolipram (0.4–400 μg kg^{-1}) were administered intratracheally (i.t.). To facilitate dosing, animals were briefly anaesthetized with halothane (4% in oxygen) and placed in a dorsal recumbent position with the head elevated at an angle of 45°. A blunt-ended metal tube (external diameter 1.5 mm) was gently inserted through the larynx into the trachea. A bolus (10 mg kg^{-1}) of the dry powder formulation was blown from a tube into the airways as above. The dosing procedure took approximately 10 s, after which the animal rapidly recovered from anaesthesia. Vehicle control animals received lactose carrier (10 mg kg^{-1}) alone. Untreated control animals were not anaesthetized or dosed. Thirty min after administration of a PDE inhibitor or lactose, animals received mepyramine maleate (30 mg kg^{-1}, i.p.) to protect against fatal anaphylaxis during antigen challenge; 50 min after administration of a PDE inhibitor, animals were placed in a whole body, double chamber plethysmograph to allow measurement of specific airway resistance (sR_{aw}) by a method modified from that described by Pennock *et al.* (1979). A Buxco (model LS-14) respiratory mechanics analyser was used to measure the phase shift between nasal and thoracic air flows and compute sR_{aw} on a breath by breath basis. A bias flow of air (600 ml min^{-1}) was maintained through the nasal chamber to ensure a constant supply of fresh air to the animal. This flow was subtracted by the respiratory mechanics analyser from its calculations.

Sixty min after administration of RP 73401 or rolipram, animals were challenged by exposure for 5 min to an aerosol of ovalbumin, generated from a 20 mg ml^{-1} solution in saline by a nebulizer (deVilbiss Pulmosonic) and passed through the nasal chamber by an air pump operating at a flow rate of 12 l min^{-1}. The mean sR_{aw} was calculated for the 5 min period immediately before antigen challenge (baseline measurement) and for 3 consecutive 5 min periods after challenge. The post-challenge mean measurement obtained during the 5 min period of peak change was used for subsequent analysis. For each treatment group, results were expressed as mean ± s.e.mean percentage inhibition of bronchospasm compared with that in the vehicle control group.

Male, Brown Norway rats (250–300 g) were sensitized with ovalbumin (1 mg) and aluminium hydroxide (100 mg) in 1 ml saline s.c. plus *B. pertussis* vaccine (0.25 ml, nominally 1×10^{10} cells) i.p. After 21–28 days, rats were anaesthetized

with sodium pentobarbitone (60 mg kg^{-1}, i.p.). The trachea was cannulated to allow mechanical ventilation (Harvard 683 rodent ventilator) at 80 strokes min^{-1} with a stroke volume of 1 ml 100 g^{-1}. PIP was recorded as before. A cannula was placed in a tail vein to allow ovalbumin administration.

RP 73401 (4 to 400 $\mu g\ kg^{-1}$) was administered as described for the guinea-pig studies; 1 min after receiving RP 73401 or vehicle, rats were challenged with ovalbumin (1 mg in 0.1 ml saline, bolus i.v.). Bronchospasm was measured as an increase in PIP, which reached maximum within 3 min of challenge. This challenge dose was determined from preliminary experiments (data not shown) to give a bronchospasm of approximately 60% of maximum in vehicle control animals.

Antigen-induced inflammatory cell accumulation in vivo

Guinea-pigs used for studies of antigen-induced bronchospasm were concurrently assessed for pulmonary inflammatory cell accumulation. Rats were sensitized as before and used for experiments 28 days later. RP 73401 (4–400 $\mu g\ kg^{-1}$) was administered during halothane anaesthesia; 30 min after administration of RP 73401, rats were placed in a 3.5 l perspex chamber and challenged by exposure for 20 min to an aerosol of ovalbumin generated from a 10 mg ml^{-1} solution in saline by a nebulizer (deVilbiss Pulmosonic) and pumped into the chamber by a respiration pump operating at 100 × 5 ml min^{-1}. A further group of animals acted as untreated, unchallenged controls; 24 h after antigen exposure, animals were killed with sodium pentobarbitone (200 mg kg^{-1}, i.p.). This time-point was used because we have previously demonstrated that eosinophil influx into the airways is maximal at this time (Raeburn *et al.*, 1994). The trachea was immediately cannulated and the lungs lavaged with saline (2 × 5 ml, guinea-pigs; 2 × 4 ml, rats) at 37°C. Each aliquot was left in the lungs for 3 min. The aliquots were pooled and the total volume measured. The sample was centrifuged (800 r.p.m. for 10 min) and the cell pellet resuspended in Hank's balanced salt solution (10 ml). Total cell counts were made with a Coulter (model S-plus IV) cell counter. Differential counts were made from Cytospin preparations stained with Hema-Tek modified Wright's stain. At least 200 cells were differentiated according to standard morphological criteria by an operator unaware of the identity of the treatment groups. In addition, basal cell populations were determined in unchallenged animals. For each treatment group, results were expressed as percentage inhibition (mean ± s.e.mean) of cell influx compared with that in the vehicle control group.

PAF-induced bronchial hyperreactivity (BHR) in the anaesthetized guinea-pig

Guinea-pigs were anaesthetized and ventilated as before. Two responses to bombesin (100–300 ng kg^{-1}, i.v. bolus), equivalent to 15% of the maximum PIP were obtained 15 and 5 min before the start of an infusion of PAF (600 ng kg^{-1}, i.v.) or its vehicle (0.1% bovine serum albumin, BSA, i.v.) delivered (Harvard 2681 infusion pump) over a period of 60 min. PAF was administered as three consecutive infusions: 180 ng kg^{-1} for 10 min, 360 ng kg^{-1} for 20 min and 900 ng kg^{-1} for 30 min. Two further doses of bombesin were administered 5 and 15 min after the end of the PAF infusion. BHR was assessed by comparing the mean bombesin responses before and after PAF and expressing the difference as % change. To determine its inhibitory action on PAF-induced bronchial hyperreactivity, RP 73401 (0.02–100 $\mu g\ kg^{-1}$, i.v.) or vehicle (DMSO, 0.1%) was administered 1 min before infusion of PAF or its vehicle. RP 73401 was administered by the i.v. route because in preliminary experiments (data not shown) the duration of action following i.t. administration, but not i.v. administration, was such that there may have been residual bronchodilator activity at the time after dosing when responses to bombesin were reassessed. Further, we have found that, although i.t. lactose has no effect on bronchospasm, this vehicle may augment hyperreactivity. For each treatment group, results are expressed as percentage inhibition (mean ± s.e.mean) of PAF-induced BHR.

Histamine-induced microvascular leakage in the anaesthetized guinea-pig

Measurements of microvascular leakage (MVL) in guinea-pigs (400–500 g), anaesthetized with xylazine (0.8 mg kg^{-1}, s.c.) and ketamine (3 mg kg^{-1}, s.c.), were made as previously described (Raeburn & Karlsson, 1993). RP 73401 (0.4–40 $\mu g\ kg^{-1}$) was administered as a dry powder as for the cell influx studies. A fine bore polythene cannula (external diameter 0.63 mm) was introduced into the trachea via the metal tube which was then withdrawn. The end of the cannula was positioned just below the larynx; 10 min after drug or vehicle administration, fluorescein isothiocyanate (FITC)-dextran (mol.wt. 150,000, 50 mg kg^{-1}, i.v., marginal ear vein) was injected as a marker of plasma extravasation. After a further 10 min, histamine (60 nmol) was administered over a period of 2 min by superfusion of the airways via the polythene cannula. This dose was determined in preliminary studies to induce maximum MVL over basal levels without causing bronchospasm. Negative control animals received vehicle (saline, 0.02 ml min^{-1}) to establish basal leakage.

Ten min after histamine or vehicle challenge, blood samples were removed by cardiac puncture and the animals were killed with sodium pentobarbitone (200 mg kg^{-1}, i.v.). The trachea and bronchi were removed and lavaged with phosphate-buffered saline (PBS, 3 × 1 ml). FITC content of tracheal tissue and lavage fluid was measured by agitating the samples for 15 h in PBS (2 ml) and assaying FITC content by fluorimetry (Perkin Elmer LS5B fluorescence spectrophotometer set with excitation and emission wavelengths of 480 and 520 nm respectively). FITC content was expressed as ng FITC mg^{-1} tissue or μg FITC ml^{-1} lavage fluid. These values were calculated from a standard calibration curve of FITC-dextran concentration versus fluorescence intensity. Percentage inhibition of histamine-induced FITC extravasation was then calculated.

Effects on salbutamol-induced bronchodilatation in the anaesthetized guinea-pig

Guinea-pigs were anaesthetized and prepared to allow stable responses to histamine to be obtained as described above. After 2 consecutive, reproducible responses RP 73401 (4 or 40 $\mu g\ kg^{-1}$, i.t. on lactose) was administered into the airways as previously described; 2 min later, animals similarly received salbutamol (2 or 10 $\mu g\ kg^{-1}$, i.t. on lactose) and 1 min later the next dose of histamine was given. Administration of histamine was continued at 6 min intervals until responses had returned to pretreatment amplitude. For each dose group, results (mean ± s.e.mean) were expressed as percentage inhibition of bronchospasm duration of action (min).

Cardiovascular effects of RP 73401

Rats (300 ± 50 g, Sprague-Dawley CD) were anaesthetized, ventilated and cannulated for blood pressure measurement as before. Drugs were administered (i.v.) into the jugular vein. Mean arterial blood pressure and heart rate were determined with a Modular Instruments Signal Processing Centre (MI^2 system). Cardiovascular parameters were allowed to stabilize before drug administration. RP 73401 (0.01–0.25 mg kg^{-1}) was administered over 30 s in a dose volume of 1 ml kg^{-1} followed by a wash-in of saline (0.2 ml). The RP 73401 vehicle was polyethylene glycol 200/0.1 M HCl. Animals received only one dose of RP 73401. Cardiovascular

parameters were measured before (baseline) and from 5 to 60 min after drug treatment. Results are expressed as mean ± s.e.mean from n animals.

To assess cardiovascular effects following i.t. dosing in the anaesthetized guinea-pig, RP 73401 (ID_{50} against histamine-induced bronchospasm) was administered into the airways as before. Each animal received only a single dose of the PDE inhibitor. Baseline mean arterial blood pressure and heart rate were measured and expressed as group mean ± s.e.mean. The peak change in arterial blood pressure and heart rate in the 20 min period after dosing were each expressed as percent change from baseline values.

Drugs and solutions

Drugs used were: ovalbumin (chicken egg grade V), histamine diphosphate, methacholine chloride, salbutamol hemisulphate, bovine serum albumin, FITC-dextran and DMSO (Sigma, U.K.); aluminium hydroxide (M&B Labchem, U.K.); *Bordetella pertussis* vaccine (Wellcome, U.K.); mepyramine maleate and sodium pentobarbitone (Rhône-Poulenc Rorer, U.K.); xylazine (Bayer, U.K.); ketamine (Parke Davis, U.K.); PAF and bombesin (NovaBiochem, U.K.); Hank's balanced salt solution (Gibco, U.K.); lactose (median particle size 60 μm, Lactochem, U.K.). RP 73401 and rolipram were synthesized by Rhône-Poulenc Rorer, U.K. Saline was prepared as 0.9% sodium chloride solution. Dry powder formulations of RP 73401 and rolipram were prepared as described previously (Underwood *et al.*, 1991). Median particle size of RP 73401 and rolipram in all formulations was 4–8 μm.

Statistical analysis

The statistical significance of differences between treatment group means was determined by applying parametric (ANOVA and Dunnett's multiple comparison) or non-parametric (Kruskal-Wallis multiple comparison) tests as appropriate. $P<0.05$ was accepted as significant.

Results

Spasmogen-induced smooth muscle contraction

RP 73401 produced concentration-dependent relaxation of guinea-pig tracheal strips under basal tone and reversed contractions induced by histamine, methacholine and LTD_4 (Figure 1). RP 73401 vehicle was without effect. RP 73401 EC_{50} (basal tone) and IC_{50} (pre-contracted) values are given in Table 1. *In vivo*, RP 73401 and rolipram each caused a dose-related inhibition of bronchospasm induced by histamine (Figure 2a), methacholine (Figure 3a) or LTD_4 (Figure 4a) in the anaesthetized guinea-pig. Lactose alone had no significant effect. ID_{50} values for RP 73401 and rolipram against histamine, methacholine and LTD_4 are given in Table 2. Both RP 73401 and rolipram were more potent as inhibitors of LTD_4-induced bronchospasm than as inhibitors of either histamine or methacholine. In addition the degree of inhibition of LTD_4-induced bronchospasm was greater than that seen with the other spasmogens. Since the PIP induced by each agonist was similar, the greater effect of RP 73401 and rolipram on the LTD_4 response cannot be due to the smaller maximum contractile effects seen with this agent *in vitro*. RP 73401 and rolipram each had a similar duration of action against histamine (Figure 2b) and methacholine (Figure 3b) but a markedly longer duration of action against LTD_4 (Figure 4b).

Table 1 Effects of RP 73401 on basal tone (EC_{50}) and against spasmogen-induced contractions in guinea-pig tracheal preparation *in vitro* (IC_{50})

	n	IC_{50} (nM)
Histamine	7	2 (1–5)
Methacholine	6	29 (14–59)
LTD_4	8	4 (2–9)
Basal tone (EC_{50})	7	9 (3–24)

Results are presented as geometric mean (confidence limits).

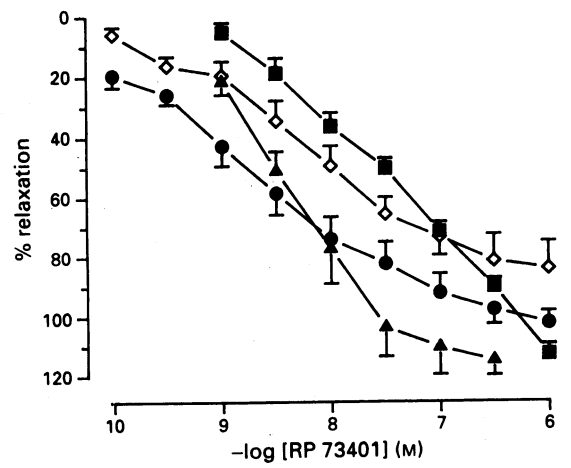


Figure 1 The relaxant effects of RP 73401 on guinea-pig trachealis under basal tone (◇) or contracted with histamine (●), methacholine (■) or leukotriene D_4 (▲). Results are expressed as mean ± s.e.mean, $n = 6–8$.

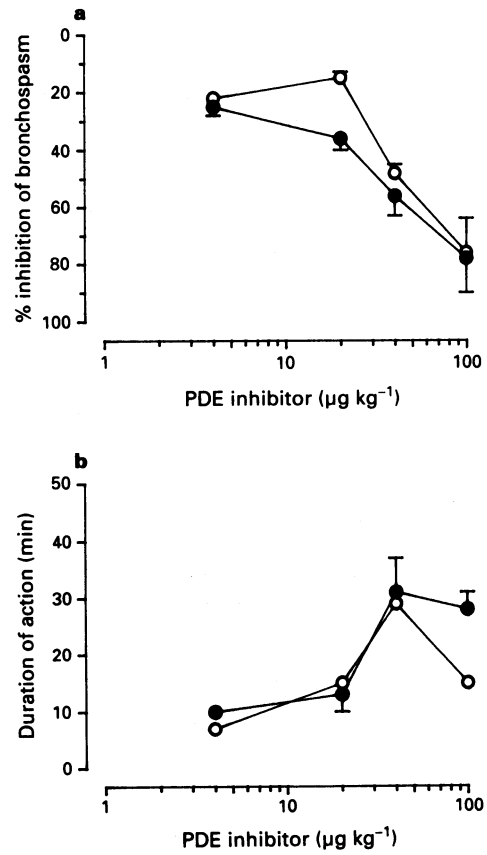


Figure 2 (a) The effects of RP 73401 (●) and rolipram (○) against bronchospasm induced by histamine in the anaesthetized guinea-pig. (b) Duration of action of RP 73401 (●) and rolipram (○) against bronchospasm induced by histamine in the anaesthetized guinea pig. Results are expressed as mean ± s.e.mean, $n = 3–5$.

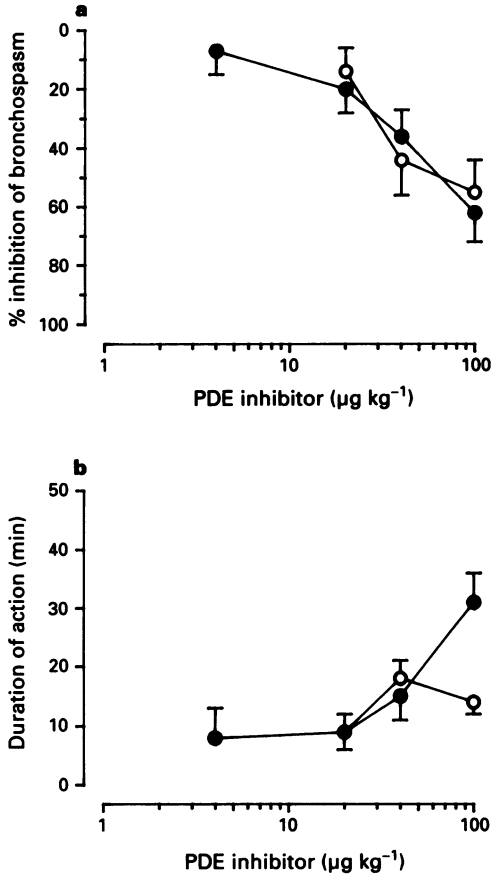


Figure 3 (a) The effects of RP 73401 (●) and rolipram (○) against bronchospasm induced by methacholine in the anaesthetized guinea-pig. (b) Duration of action of RP 73401 (●) and rolipram (○) against bronchospasm induced by methacholine in the anaesthetized guinea pig. Results are expressed as mean ± s.e.mean, $n = 3-5$.

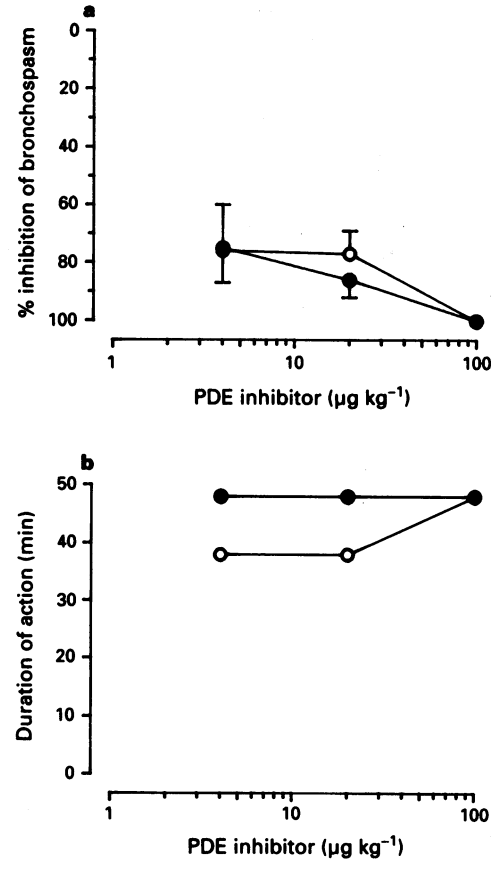


Figure 4 (a) The effects of RP 73401 (●) and rolipram (○) against bronchospasm induced by leukotriene D_4 (LTD_4) in the anaesthetized guinea-pig. (b) Duration of action of RP 73401 (●) and rolipram (○) against bronchospasm induced by LTD_4 in the anaesthetized guinea pig. Results are expressed as mean ± s.e.mean, $n = 3-5$.

Table 2 Effects of RP 73401 and rolipram against spasmogen-induced bronchospasm in the anaesthetized guinea-pig

	n	*RP 73401* ID_{50} (μg kg^{-1})	n	*Rolipram* ID_{50} (μg kg^{-1})
Histamine	5	34 ± 6	5	44 ± 4
Methacholine	5	66 ± 12	5	72 ± 18
LTD_4	5	<4	5	<4

Antigen-induced bronchospasm

Aerosolized antigen caused an acute bronchospasm which peaked within 15 min in conscious guinea-pigs. sR_{aw} increased from 4.7 ± 0.8 to 24.5 ± 2.9 ml cmH_2O^{-1} in vehicle control animals. RP 73401 and rolipram, but not lactose vehicle, caused a dose-related inhibition of antigen-induced bronchospasm (Figure 5). The ID_{50} values were RP 73401 7 ± 1 μg kg^{-1}, rolipram 5 ± 1 μg kg^{-1}.

In the anaesthetized rat bronchospasm induced by antigen (ovalbumin, 1 mg, i.v.) challenge was inhibited in a dose-dependent manner by RP 73401 (Figure 6). The calculated ID_{50} was 100 ± 25 μg kg^{-1}. Lactose alone had no significant effect on antigen-induced bronchospasm.

Antigen-induced cell influx

In guinea-pigs and rats, aerosolized antigen but not vehicle caused an increase in total cell and eosinophil numbers in bronchoalveolar lavage 24 h later (Tables 3–5). In the guinea-pig, RP 73401 (4 and 40 μg kg^{-1}) significantly inhibited eosinophil influx (Table 3). Eosinophil numbers were also lower in guinea-pigs treated with rolipram (4 and 40 μg kg^{-1}) but the difference did not achieve statistical significance (Table 4). In the rat only the highest dose of RP 73401 (400 μg kg^{-1}) significantly inhibited (41 ± 16%) antigen-induced airway eosinophilia (Table 5). In each study the drug vehicle was without effect.

PAF-induced bronchial hyperreactivity

PAF infusion significantly increased bronchoconstrictor responses to bombesin from 18 ± 3% of maximum PIP (before PAF infusion) to 39 ± 2% of maximum PIP. This represented an increase of 179 ± 5% over the pre-infusion response. Infusion of PAF vehicle (0.1% BSA) had no significant effect. RP 73401 (0.02–100 μg kg^{-1}, i.v.) produced a dose-dependent and potent (ID_{50}: 0.09 ± 0.03 μg kg^{-1}) inhibition of PAF-induced bronchial hyperreactivity (Figure 7). RP 73401 vehicle (DMSO) had no significant effect.

Histamine-induced microvascular leakage

Histamine (60 nmol) significantly increased microvascular leakage of FITC-dextran in tracheal tissue from a basal level of 13.2 ± 1.6 ng mg^{-1} to 84 ± 12 ng mg^{-1} and leakage into the airway lumen (as measured in lavage fluid) from a basal level of 0.66 ± 0.24 μg ml^{-1} to 3.2 ± 0.52 μg ml^{-1}. RP 73401 (0.4–40 μg kg^{-1}) significantly inhibited histamine-induced microvascular leakage into tracheal tissue (59–63% inhibition) and into the airway (87–95% inhibition) at each dose

($n = 5-11$) (Figure 8). Maximum inhibition was achieved with the smallest dose of RP 73401 which could be given by this technique. Lactose alone had no significant effect on leakage.

Effects on salbutamol-induced bronchodilatation

Salbutamol (2 or 10 $\mu g\,kg^{-1}$, i.t.) caused a dose-related inhibition of histamine-induced bronchospasm (Table 6). When given 2 min before salbutamol (2 $mg\,kg^{-1}$) RP 73401 (4 and 40 $\mu g\,kg^{-1}$) appeared to potentiate the effects of the β_2-adrenoceptor agonist in terms of magnitude (Table 6). With the higher dose of RP 73401 (40 $\mu g\,kg^{-1}$) both the response magnitude and duration of action of salbutamol (2 $mg\,kg^{-1}$) were significantly increased. Combining the larger doses of salbutamol (10 $\mu g\,kg^{-1}$) and RP 73401 (40 $\mu g\,kg^{-1}$) completely inhibited responses to histamine with a duration of about 1 h.

Cardiovascular effects of RP 73401

Baseline heart rate and mean arterial blood pressure in the anaesthetized rat were 426 ± 16 beats min^{-1} and 120 ± 2 mmHg respectively, $n = 20$. RP 73401 up to the top dose (0.25 $mg\,kg^{-1}$, i.v.) was without effect on heart rate whereas a small ($14 \pm 1\%$) fall, which was not dose-related, in mean arterial blood pressure was seen. This compares with the vehicle-induced fall of $6 \pm 1\%$. The effect of RP 73401 was maximal within 5 min of dosing.

In the anaesthetized guinea-pig, baseline mean arterial blood pressure was 46 ± 3 mmHg. Baseline heart rate was 258 ± 6 beats min^{-1}. When administered as a dry powder formulation into the airways at the ID_{50} against histamine-induced bronchospasm (ID_{50}: $34 \pm 6\,\mu g\,kg^{-1}$), RP 73401 ($n = 6$) had no significant effect on mean arterial blood pressure (% change: $+2 \pm 2\%$) or heart rate (% change: $+3 \pm 2\%$).

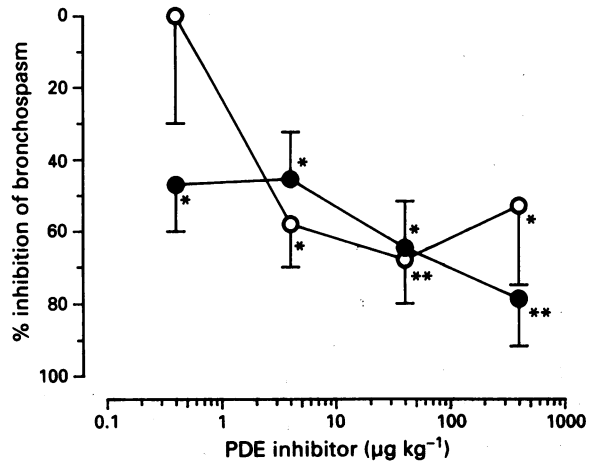


Figure 5 The effects of RP 73401 (●) and rolipram (○) against antigen-induced bronchospasm in the conscious guinea pig. Results are expressed as mean ± s.e.mean, $n = 5-8$. $^*P<0.05$; $^{**}P<0.01$ compared to vehicle control group.

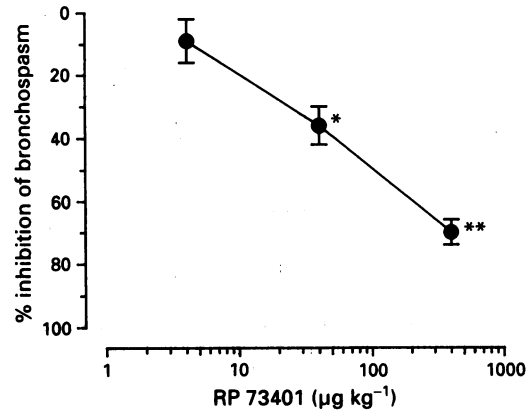


Figure 6 The effects of RP 73401 against antigen-induced bronchospasm in the anaesthetized rat. Results are expressed as mean ± s.e.mean, $n = 5-8$. $^*P<0.05$; $^{**}P<0.01$ compared to vehicle control group.

Table 3 Effect of RP 73401 on inflammatory cell influx into BAL fluid in the anaesthetized, antigen-challenged, guinea-pig

	Total cell numbers ($10^6\,ml^{-1}$)	*% inhibition of increase*	*Eosinophil numbers* ($10^6\,ml^{-1}$)	*% inhibition of increase*
Naive	10 ± 1	–	2 ± 1	–
Unchallenged	8 ± 2	–	2 ± 1	–
Challenged + vehicle	28 ± 2#	–	13 ± 1#	–
Challenged + RP73401 (0.4 $\mu g\,kg^{-1}$)	28 ± 3	0	14 ± 2	0
Challenged + RP73401 (4 $\mu g\,kg^{-1}$)	18 ± 2*	50 ± 6	7 ± 1*	55 ± 8
Challenged + RP73401 (40 $\mu g\,kg^{-1}$)	14 ± 2*	70 ± 10	5 ± 1*	73 ± 14

#$P<0.05$ versus unchallenged; *$P<0.05$ versus challenged plus vehicle. Data are presented as mean ± s.e.mean, $n = 5-10$ animals per group.

Table 4 Effect of rolipram on inflammatory cell influx into BAL fluid in the anaesthetized, antigen-challenged, guinea-pig

	Total cell numbers ($10^6\,ml^{-1}$)	*% inhibition of increase*	*Eosinophil numbers* ($10^6\,ml^{-1}$)	*% inhibition of increase*
Naive	10 ± 1	–	2 ± 1	–
Unchallenged	8 ± 2	–	2 ± 1	–
Challenged + vehicle	28 ± 2#	–	13 ± 1#	–
Challenged + rolipram (0.4 $\mu g\,kg^{-1}$)	27 ± 2	5 ± 2	14 ± 2	0
Challenged + rolipram (4 $\mu g\,kg^{-1}$)	21 ± 4	35 ± 11	10 ± 2	27 ± 19
Challenged + rolipram (40 $\mu g\,kg^{-1}$)	18 ± 3	50 ± 10	9 ± 2	36 ± 18

#$P<0.05$ versus unchallenged; *$P<0.05$ versus challenged plus vehicle. Data are presented as mean ± s.e.mean, $n = 5-10$ animals per group.

Table 5 Effect of RP 73401 on inflammatory cell influx into BAL fluid in the anaesthetized, antigen-challenged, rat

	Total cell numbers (10^6 ml^{-1})	*Eosinophil numbers* (10^3 ml^{-1})
Naive	171 ± 19	2 ± 2
Unchallenged	158 ± 6	3 ± 2
Challenged + vehicle	280 ± 26#	42 ± 19#
Challenged + RP 73401 (4 μg kg^{-1})	302 ± 54	53 ± 23
Challenged + RP 73401 (40 μg kg^{-1})	290 ± 35	72 ± 15
Challenged + RP 73401 (400 μg kg^{-1})	338 ± 89	26 ± 10* (41 ± 16% reduction)

#$P<0.05$ versus unchallenged; *$P<0.05$ versus challenged plus vehicle.
Data presented as mean ± s.e.mean, $n = 5$ animals per group.

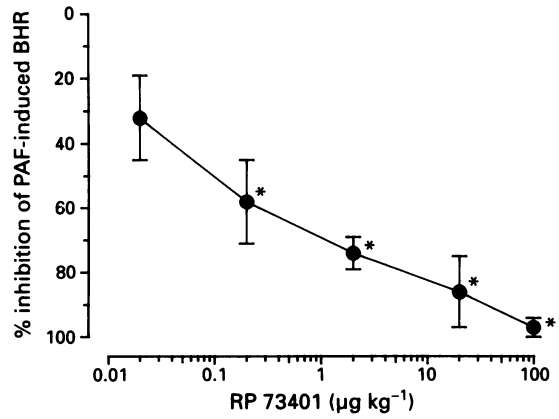


Figure 7 The effects of RP 73401 on PAF-induced bronchial hyperreactivity (BHR) to bombesin in the anaesthetized guinea-pig. Results are expressed as mean ± s.e.mean, $n = 3-12$. *$P<0.05$ compared to vehicle control group.

Discussion

RP 73401 is a very selective inhibitor of the PDE IV isoenzyme compared with its effects on other PDE isoenzymes. RP 73401 inhibits the activity of PDE IV isoenzyme isolated from pig aorta or guinea-pig eosinophils with IC_{50} values of about 1 nM (Karlsson *et al.*, 1993; Ashton *et al.*, 1994). It is at least 19,000 fold more selective for the type IV than for type I, II, III or V (Karlsson *et al.*, 1993; Ashton *et al.*, 1994; Souness *et al.*, 1994b). RP 73401 seems to interact with the PDE IV isoenzyme differently from rolipram since the potency of the latter depends on enzyme location, enzyme conformation and cell type (Karlsson *et al.*, 1993; Souness *et al.*, 1994b). The present study demonstrates potent anti-inflammatory and bronchodilator effects of RP 73401 in guinea-pigs and rats.

RP 73401 relaxed guinea-pig isolated tracheal preparations under basal tone or when precontracted by putative asthma mediators such as histamine, a muscarinic cholinoceptor agonist and LTD_4 indicating that RP 73401 acts as a functional antagonist. Comparison with previously reported data in this preparation (Souness *et al.*, 1994a) demonstrates that RP 73401 is approximately 16 fold more potent than rolipram as an inhibitor of histamine-induced contractions (RP 73401 IC_{50}: 2 nM; rolipram IC_{50} 32 nM), 3 fold more potent against methacholine (RP 73401 IC_{50}: 29 nM; rolipram IC_{50} 96 nM) and 5 fold more potent against LTD_4 (RP 73401 IC_{50}: 4 nM; rolipram IC_{50} 19 nM). Thus, both PDE inhibitors were more effective against contractions produced by histamine and LTD_4 than against those induced by methacholine. RP 73401 is less potent than the β_2-adrenoceptor agonist salbutamol (Tomkinson *et al.*, 1993) but considerably more potent than the non-selective PDE inhibitor theophylline (Karlsson & Persson, 1981). All agents produced complete relaxations of the induced tone.

Table 6 The effects of pretreatment with RP 73401 on salbutamol-induced inhibition of histamine-induced bronchospasm in the anaesthetized guinea pig

Treatment	*% inhibition of histamine-induced bronchospasm*	*Duration of action* (min)
RP 73401 4 μg kg^{-1}	25 ± 3	10 ± 2
RP 73401 40 μg kg^{-1}	56 ± 7	31 ± 6
Salbutamol 2 μg kg^{-1}	42 ± 4	18 ± 4
Salbutamol 10 μg kg^{-1}	71 ± 8	29 ± 6
RP 73401 4 μg kg^{-1} + salbutamol 2 μg kg^{-1}	61 ± 8*	24 ± 3
RP 73401 40 μg kg^{-1} + salbutamol 2 μg kg^{-1}	70 ± 14*	57 ± 3*
RP 73401 4 μg kg^{-1} + salbutamol 10 μg kg^{-1}	76 ± 10	25 ± 6
RP 73401 40 μg kg^{-1} + salbutamol 10 μg kg^{-1}	100 ± 0*	54 ± 6*

Results are expressed as mean ± s.e.mean of 4–6 experiments. *$P<0.05$ compared with salbutamol alone.

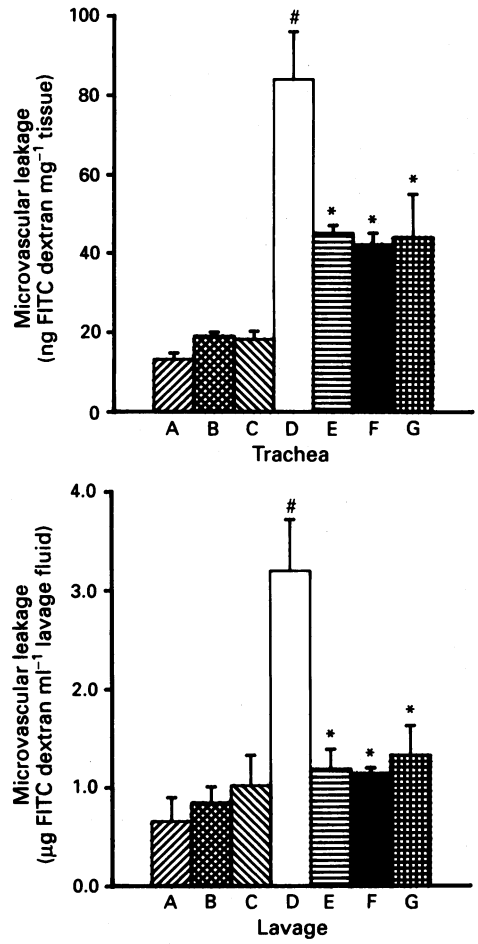


Figure 8 The effects of RP 73401 on histamine-induced microvascular leakage in the anaesthetized guinea pig lung. (A) Sham treated; (B) saline; (C) lactose + saline; (D) lactose + histamine (60 nmol); (E) RP 73401 (0.4 mg kg^{-1}, i.t.); (F) RP 73401 (4 mg kg^{-1}, i.t.); (G) RP 73401 (40 mg kg^{-1}, i.t.). Results are expressed as mean ± s.e.mean, $n = 5-8$. *$P<0.05$ compared to vehicle control group.

Consistent with the results *in vitro*, RP 73401 and rolipram each potently and dose-dependently inhibited bronchoconstriction induced by histamine, methacholine and LTD_4 in anaesthetized guinea-pigs, the contractions produced by LTD_4 being particularly sensitive (about 10 times more than the other spasmogens) to each of the PDE IV inhibitors. Furthermore, the duration of the inhibition of LTD_4 with RP 73401 or rolipram was significantly longer than with the other spasmogens. The prolonged duration was not dependent on the magnitude of the inhibition indicating that it is the mechanism of LTD_4-induced bronchospasm that is particularly sensitive to inhibition by the PDE inhibitors. Additionally in conscious animals, the bronchospasm produced by antigen aerosol (in the presence of a histamine (H_1) receptor antagonist) was suppressed by prior treatment with RP 73401 or rolipram. Interestingly, RP 73401 was 5 to 9 times more potent as an inhibitor of this allergic contraction, than of those produced by histamine and methacholine, supporting the view that leukotrienes indeed are major mediators of this immediate response. It is possible that suppression of mediator release from inflammatory cells (see below), in addition to a direct smooth muscle relaxant effect, also contributed to inhibition of this allergic response. Acute, antigen-induced bronchospasm in the rat was similarly inhibited by pretreatment with RP 73401.

RP 73401 and rolipram were equipotent inhibitors of bronchospasm in the guinea-pig, despite a 1000 fold difference in potency on the type IV enzyme isolated from pig aortic smooth muscle or bovine trachea (Karlsson *et al.*, 1993; Souness *et al.*, 1994b). This suggests that the *in vitro* data does not necessarily predict the *in vivo* potency against smooth muscle contraction. RP 73401 is more potent than rolipram in human cells such as monocytes (e.g. >100 fold more potent as an inhibitor of TNFα release, Souness *et al.*, unpublished data) perhaps suggesting that the potency difference between the two compounds may be more marked in man.

β_2-Adrenoceptor agonists are the most effective bronchodilators currently available for symptomatic relief. These agents act by raising intracellular levels of cyclic AMP, so the observation that pretreatment with RP 73401 increased the bronchodilator effects (potency and, particularly, duration) of salbutamol is to be expected. However, previously reported studies on the interaction between β_2 agonists and non-selective PDE inhibitors are contradictory (Karlsson & Persson, 1981).

The present data on the functional importance of the type IV PDE in regulating airways tone is in general agreement with earlier studies by us and others (see review by Raeburn *et al.*, 1993). It is worth noting, though, that selective inhibitors of the type III PDE relax guinea-pig trachealis *in vitro*, but with a lower potency (Tomkinson *et al.*, 1993). Similarities between guinea-pig and human airways preparations *in vitro* regarding PDE isoenzyme profiles and relative functional importance (Qian *et al.*, 1993; DeBoer *et al.*, 1993) predict that RP 73401 will also relax human isolated airways preparations.

RP 73401 significantly reduced the influx of eosinophils into the airways following antigen exposure in sensitized guinea-pigs and rats. RP 73401 was however twice as potent as rolipram (Karlsson *et al.*, 1993). PDE inhibitors may act in several ways to reduce cell trafficking into the airways (see review by Karlsson *et al.*, 1993). They may suppress antigen-induced release of chemotactic mediators from pro-inflammatory cells, inhibit endothelial cell contractility (thereby maintaining the integrity of the microvenular endothelium) or inhibit the expression of selectin and integrin adhesion molecules on either the endothelium or the leukocyte itself. It is not clear why RP 73401 was more effective in the guinea-pig than in the rat. This may have been a consequence of different challenge protocols, necessitated by the different sensitivities of the species to antigen challenge. In addition to this reduction in BAL fluid inflammatory cell numbers, preliminary data indicate that RP 73401 also reduces inflammatory cell numbers and their degree of activation in lung tissues (unpublished observations). The reduced cell influx would further reduce granulocyte-derived chemotactic and inflammatory mediator content in the lung thereby reducing inflammatory changes. This is likely to occur since RP 73401 potently inhibits superoxide generation and the release of cytotoxic proteins from human granulocytes and guinea-pig eosinophils *in vitro* (Karlsson *et al.*, 1993; Ashton *et al.*, 1994).

Plasma extravasation from postcapillary venules of the tracheobronchial microcirculation induced by histamine and other pro-inflammatory mediators, has been reported as a potent pro-inflammatory mechanism in human asthmatic airways (Persson, 1988). These mediators may act directly to produce contraction of endothelial cells, a prerequisite for plasma extravasation. RP 73401 inhibited microvascular leakage in the guinea-pig which is in agreement with our earlier findings that PDE IV (rolipram) and PDE V (zaprinast) inhibition prevents PAF-induced MVL in the guinea-pig lung (Raeburn & Karlsson, 1993). Interestingly, RP 73401 was more potent in inhibiting leakage (this study) than rolipram (no effect at 50 μg, i.t., Raeburn & Karlsson, 1993) although PAF was used as the stimulus in the latter study. MVL into the airway lumen (lavage fluid) was more readily inhibited than into the tracheobronchial tissues which suggests that RP 73401 more effectively inhibits epithelial than endothelial membrane permeability, possibly as a consequence of PDE isoenzyme distribution. The PDE isoenzyme profile in the endothelium of the airway microvasculature is not known but, in bovine and porcine aorta, PDE II and IV predominate whereas PDE III may be important in the pulmonary artery (see Raeburn & Karlsson, 1993 and references therein). Our data with RP 73401 indicate that PDE IV is of major importance in inhibiting endothelial cell contractility in the airway microcirculation.

In addition to the anti-inflammatory effects reported above, low doses of RP 73401 prevented PAF-induced BHR in the guinea-pig. PAF, a product of several inflammatory cell types, is a potent chemoattractant and activator of a range of inflammatory cells including eosinophils. It seems likely that the suppression of BHR reflects the potent inhibitory effects of RP 73401 on mediator release from granulocytes and monocytes (Karlsson *et al.*, 1993; Ashton *et al.*, 1994) rather than a direct antagonism of PAF itself. Even though PAF may not be an important mediator in human asthma, airway hyperresponsiveness is a characteristic feature and drugs such as RP 73401 with widespread anti-inflammatory actions may reduce BHR in asthmatic subjects.

Since RP 73401 is a selective inhibitor of type IV PDE, our results confirm that this isoenzyme is functionally important in modulating inflammation and bronchoconstriction in the guinea-pig and rat. Type III PDE also has a significant role in modulating airways smooth muscle contractility. However, PDE type III inhibitors have been shown to induce positive inotropism and vasodilatation whereas PDE type IV inhibitors are not often associated with such cardiovascular effects (Nicholson & Shahid, 1994). Indeed, whereas both type III and type IV PDE inhibitors have been shown to induce bronchodilatation in the dog, only the latter did not produce cardiovascular side-effects at doses which produced bronchodilatation (Heaslip *et al.*, 1991). In our study, RP 73401 did not cause significant changes in arterial blood pressure or heart rate when administered to anaesthetized rats or guinea-pigs at doses producing significant inhibition of bronchospasm. We have demonstrated that, following i.t. administration of RP 73401 ($500\,\mu g\,kg^{-1}$) to rats, peak plasma levels are reached after 5 min (97 ± 44 nM), remain high after 15 min (79 ± 40 nM) and thereafter decrease to 3 ± 1 nM after 6 h (data on file with Rhône-Poulenc Rorer Ltd.). This data demonstrates that, following i.t. administration, RP 73401 achieves a concentration in the systemic circulation which is greater than the IC_{50} for inhibition of

PDE type IV. The lack of cardiovascular effects in our studies would therefore seem to be due to tissue PDE subtype selectivity rather than low systemic availability. Thus, specific type IV PDE inhibitors such as RP 73401 may be more selective and useful for the treatment of asthma than specific type III inhibitors or mixed type III/IV inhibitors. Furthermore, PDE III inhibitors such as siguazodan have no effect on airways MVL (Raeburn & Karlsson, 1993) and only poorly inhibit antigen-induced cell influx into BAL fluid (Karlsson *et al.*, 1993).

Asthma is an inflammatory disease of the airways where the prominent symptoms are a reversible airflow obstruction combined with an increased responsiveness to non-specific bronchoconstrictor stimuli. Inflammatory changes in the asthmatic airway include microvascular plasma protein leakage and oedema, mucous gland hyperplasia, smooth muscle hypertrophy, sub-epithelial fibrosis, lumenal mucus and cellular debris, leukocyte (predominantly eosinophils) infiltration of the bronchial mucosa and epithelial cell damage and/or sloughing (Djukanovic *et al.*, 1990; Alexander *et al.*, 1991). Release of mast cell mediators such as histamine and possibly leukotrienes plays an important role in immediate bronchoconstriction; eosinophils, macrophages, lymphocytes and other inflammatory cells are more usually associated with late phase events and chronic disease (Djukanovic *et al.*, 1990; Alexander *et al.*, 1991).

Glucocorticosteroids are currently the most effective drugs available to treat airway inflammation. The number and activity of infiltrating inflammatory cells, particularly eosinophils, are reduced and microvascular leakage (and thereby oedema) and other signs of the inflammatory response are dampened (Barnes & Pedersen, 1993). Glucocorticosteroids do not however inhibit the release of mast cell mediators, have no direct bronchodilator activity and, when given for prolonged periods, are associated with significant systemic adverse effects (Barnes & Pedersen, 1993). A drug with combined anti-inflammatory and bronchodilator actions would therefore provide additional benefits in the treatment of asthma. The *in vitro* and *in vivo* studies described here demonstrate RP 73401 to possess many of these desirable actions at least in animal models of allergic inflammation.

In conclusion, RP 73401 has bronchodilator activity and is a functional antagonist of the bronchoconstriction produced by asthma mediators. More importantly, its potent anti-inflammatory actions reduce those facets of allergic pulmonary inflammation in the guinea-pig and rat which are characteristic of human asthma. Its potency and selectivity make RP 73401 an ideal tool to investigate the functional importance of the PDE IV isoenzyme in biological systems. RP 73401 is a promising new agent for the treatment of asthma and other inflammatory disease of human airways.

We thank Dr V. Facchini for kindly supplying previously unpublished data on plasma levels of RP 73401.

References

ALEXANDER, A.G., WILSON, J.W., HOLGATE, S.T. & KAY, A.B. (1991). The contribution of inflammatory cells to the pathogenesis of asthma. In *Pharmacology of Asthma*. ed. Page, C.P. & Barnes, P.J. pp. 27–51. London: Springer-Verlag.

ASHTON, M.J., COOK, D.C., FENTON, G., KARLSSON, J.-A., PALFREYMAN, M.N., RAEBURN, D., RATCLIFFE, A.J., SOUNESS, J.E., THURAIRAITNAM, S. & VICKER, N. (1994). Selective type IV phosphodiesterase inhibitors as anti-asthmatic agents. The synthesis and biological activities of 3-cyclopentyloxy-4-methoxybenzamides and analogues. *J. Med. Chem.*, **37**, 1696–1703.

BARNES, P.J. & PEDERSEN, S. (1993). Efficacy and safety oif inhaled corticosteroids in asthma. *Am. Rev. Respir. Dis.*, **148** (Suppl.), S1–S26.

BEAVO, J.A. & REIFSNYDER, D.H. (1990). Primary sequence of cyclic nucleotide phosphodiesterase isozymes and the design of selective inhibitors. *Trends Pharmacol. Sci.*, **11**, 150–155.

DE BOER, J., PHILPOTT, A.J., VAN AMSTERDAM, R.G.M., SHAHID, M., ZAAGSMA, J. & NICHOLSON, C.D. (1991). Human bronchial cyclic nucleotide phosphodiesterase isoenzymes: biochemical land pharmacological analysis using selective inhibitors. *Br. J. Pharmacol.*, **106**, 1028–1034.

DJUKANOVIC, R., ROCHE, W.R., WILSON, J.W., BEASLEY, C.R.W., TWENTYMAN, O.P., HOWARTH, P.H. & HOLGATE, S.T. (1990). Mucosal inflammation in asthma. *Am. Rev. Respir. Dis.*, **142**, 434–457.

GIEMBYCZ, M.A. & DENT, G. (1992). Prospects for selective cyclic nucleotide phosphodiesterase inhibitors in the treatment of bronchial asthma. *Clin. Exp. Allergy*, **22**, 337–344.

HEASLIP, R.J., BUCKLEY, S.K., SICKELS, B.D. & GRIMES, D. (1991). Bronchial vs. cardiovascular activities of selective phosphodiesterase inhibitors in the anaesthetized beta-blocked dog. *J. Pharmacol. Exp. Ther.*, **257**, 741–747.

KARLSSON, J.-A. & PERSSON, C.G.A. (1981). Influence of tracheal contraction on relaxant effects *in vitro* of theophylline and isoprenaline. *Br. J. Pharmacol.*, **74**, 73–79.

KARLSSON, J.-A., SOUNESS, J., RAEBURN, D., PALFREYMAN, M. & ASHTON, M. (1993). Anti-inflammatory effects of novel selective cyclic nucleotide phosphodiesterase inhibitors. In *T-lymphocyte and Inflammatory Cell Research in Asthma*. ed. Jolles, G., Karlsson, J.-A. & Taylor, J. pp. 323–351. London: Academic Press.

NICHOLSON, C.D. & SHAHID, M. (1994). Inhibitors of cyclic nucleotide phosphodiesterase isoenzymes – their potential utility in the therapy of asthma. *Pulm. Pharmacol.*, **7**, 1–17.

PENNOCK, B.E., COX, C.P., RODGERS, R.M., CAIN, W.A. & WELLS, J.H. (1979). A non-invasive technique for the measurement of changes in specific airway resistance. *J. Appl. Physiol.*, **46**, 399–406.

PERSSON, C.G.A. (1988). Plasma exudation and asthma. *Lung*, **166**, 1–23.

QIAN, Y., NALINE, E., KARLSSON, J.-A., RAEBURN, D. & ADVENIER, C. (1993). Effects of rolipram and siguazodan on the human isolated bronchus and their interaction with isoprenaline and sodium nitroprusside. *Br. J. Pharmacol.*, **109**, 774–778.

RAEBURN, D. & KARLSSON, J.-A. (1993). Effects of isoenzyme-selective inhibitors of cyclic nucleotide phosphodiesterase on microvascular leak in guinea pig airways *in vivo*. *J. Pharmacol. Exp. Ther.*, **267**, 1147–1152.

RAEBURN, D., SOUNESS, J.E., TOMKINSON, A. & KARLSSON, J.-A. (1993). Isozyme-selective cyclic nucleotide phosphodiesterase inhibitors: biochemistry, pharmacology and therapeutic potential in asthma. *Prog. Drug Res.*, **40**, 9–32.

RAEBURN, D., UNDERWOOD, S.L., FOSTER, M., WOODMAN, V. & KARLSSON, J.-A. (1994). Antigen-induced airway inflammation and hyperreactivity in the guinea pig: a time-course study. *Am. Rev. Respir. Dis.*, (in press).

SOUNESS, J.E., VILLAMIL, M.-E., SCOTT, L.C., TOMKINSON, A., GIEMBYCZ, M.A. & RAEBURN, D. (1994a). Possible role of cyclic AMP phosphodiesterases in the actions of ibudilast on eosinophil thromboxane generation and airways smooth muscle tone. *Br. J. Pharmacol.*, **111**, 1081–1088.

SOUNESS, J.E., WEBBER, S.E., POLLOCK, K., PALFREYMAN, M.N., ASHTON, M.J., RAEBURN, D. & KARLSSON, J.-A. (1994b). Comparison of the inhibitory actions of RP 73401 and rolipram on cAMP phosphodiesterase (PDE IV) from guinea-pig eosinophils and pig aorta. *FASEB J.*, **8**, A371.

TOMKINSON, A., KARLSSON, J.-A. & RAEBURN, D. (1993). Comparison of the effects of selective inhibitors of phosphodiesterase types III and IV in airway smooth muscle with differing b-adrenoceptor subtypes. *Br. J. Pharmacol.*, **108**, 57–61.

TORPHY, T.J. & UNDEM, B.J. (1991). Phosphodiesterase inhibitors: new opportunities for the treatment of asthma. *Thorax*, **46**, 512–523.

UNDERWOOD, S.L., LINGHAM, D., PEARSON, J. & RAEBURN, D. (1991). A novel technique for the administration of bronchodilator drugs formulated as dry powders to the anaesthetized guinea-pig. *J. Pharmacol. Methods*, **26**, 203–210.

(Received May 12, 1994
Revised August 11, 1994
Accepted August 15, 1994)

Br. J. Pharmacol. (1994), **113**, 1432–1438 © Macmillan Press Ltd, 1994

Pharmacological analysis of ecto-ATPase inhibition: evidence for combined enzyme inhibition and receptor antagonism in P_{2X}-purinoceptor ligands

*B.E. Crack, †M.W. Beukers, *K.C.W. McKechnie, †A.P. IJzerman & [1]*P. Leff

*Department of Pharmacology, Fisons R&D Labs, Bakewell Road, Loughborough, Leicestershire, LE11 ORH; †Division of Medicinal Chemistry, LACDR, Leiden, The Netherlands

1 Previous studies have shown that suramin and FPL 66301 are competitive antagonists at the P_{2X}-purinoceptor in the rabbit ear artery. Those studies employed α,β-methylene ATP, a poorly hydrolysable ATP analogue, as the agonist. In this study these compounds have been tested using ATP as the agonist.

2 Suramin, in the concentration range 30–1000 μM, *potentiated* the contractile effects of ATP, producing a 3-fold leftward shift of the ATP E/[A] curves. FPL 66301, in the concentration range 100–1000 μM, produced a significant but small (≈3-fold) rightward shift of the ATP curves. These results are in marked contrast with previous studies using α,β-methylene ATP in which 30-fold rightward shifts were achieved using the same concentration ranges of suramin and FPL 66301.

3 Suramin and FPL 66301 were tested as ecto-ATPase inhibitors in a human blood cell assay. Suramin inhibited the enzyme with a pIC_{50} of 4.3, FPL 66301 with a pIC_{50} of 3.3.

4 The pharmacological data were analysed using a theoretical model describing the action of a compound with dual enzyme inhibitory and receptor antagonistic properties on the effects of an agonist susceptible to enzymatic degradation. The model was found to fit the data well using the known pK_B estimates for suramin and FPL 66301 and similar relative (but not absolute) pK_I estimates to those obtained for the compounds in the enzyme assay.

5 From this analysis it was concluded that the limited shifts of ATP E/[A] curves produced by suramin and FPL 66301 were the result of 'self-cancellation' of the potentiating (enzyme inhibitory) and rightward-shifting (receptor antagonistic) properties.

6 The analysis also indicated that the presence of ecto-ATPase activity in the rabbit ear artery preparation has a marked effect on the apparent potency of ATP. The experimental $p[A_{50}]$ was 3.4, whereas the 'true' value, that is the value which would be obtained in the absence of ecto-ATPase activity, was 6.0, some 400-fold higher.

7 Two conclusions are drawn from this study. Firstly, caution must be exercised in the use of suramin and FPL 66301 as tools for receptor classification. Absence of overt antagonism by these compounds when metabolically unstable agonists are used could lead to erroneous claims for receptor subtypes. Secondly, the agonist potency order currently used to designate P_{2X}- purinoceptors may require modification.

Keywords: P_{2X}-purinoceptors; ATP; ecto-ATPase; suramin; FPL 66301; agonist potency orders; receptor classification

Introduction

A well-recognized issue in the classification of P_2-purinoceptors is the susceptibility of the natural agonists and some synthetic agonist analogues to enzymatic dephosphorylation in tissues used in pharmacological experiments. Previous studies have demonstrated the metabolic instability of agonists and determined their structure–activity dependence (Welford *et al.*, 1986; 1987). The potential pharmacological complications produced by such processes are generally 2-fold: to convert the applied agonist to other chemical species which may be active as agonists or antagonists at the receptor under study or at other receptors in the tissue preparation and to reduce the concentration of the agonist available to interact with the receptors under study so that the applied agonist concentration does not reflect the active one. Although there are a number of reports describing effects at purinoceptors of the former kind (Maguire & Satchell, 1981), evidence for the pharmacological impact of the latter is limited (Welford *et al.*, 1987). However, studies conducted in other receptor systems, for example adrenoceptors and muscarinic receptors, show that problems of this kind manifest as incorrect determination of agonist potency orders (Kenakin, 1980) and cause difficulties in the quantitative analysis of antagonist effects (Kenakin & Beek, 1985).

A particular problem that has received attention elsewhere is the pharmacological analysis of receptor antagonists which possess additional properties that confound the expression of simple competitive antagonism (Black *et al.*, 1986). When the additional property is inhibition of an enzyme which acts to degrade the experimental agonist, potentiation of agonist concentration effect (E/[A]) curves can occur (Kenakin & Beek, 1985). Combination of this property with receptor antagonism can result in 'self-cancellation' of E/[A] curve displacements in which neither the enzyme inhibitory nor receptor antagonistic components are fully expressed. In this study we address a problem of this kind affecting the pharmacological analysis of P_{2X}-purinoceptor antagonists.

In previous studies carried out in this laboratory, using the rabbit isolated ear artery preparation, suramin was shown to demonstrate simple competitive antagonism of P_{2X}-purinoceptors (Leff *et al.*, 1990). Significantly, those experiments were conducted using a α,β-methylene ATP and β,γ-methylene L-ATP, agonists which have been reported to be relatively stable to hydrolysis by ectonucleotidase (Welford *et al.*, 1986). A synthetic analogue of ATP, FPL 66301 (β,γ-methylenedibromo-2-methylthio-L-ATP) also demonstrates competitive antagonism under these conditions (Leff *et al.*, 1993). In the present paper we report further studies on these antagonists which demonstrate the presence of ecto-

[1] Author for correspondence.

ATPase-inhibitory properties in each of them and which quantify the extent to which these are expressed pharmacologically. The results of this study are considered in relation to the impact of ecto-ATPase activity on the pharmacological analysis of purinoceptors and in relation to the utility of compounds such as suramin and FPL 66301 in purinoceptor classification.

Methods

Rabbit ear artery

Male New Zealand White rabbits weighing 2–3.5 kg were killed with an overdose of pentobarbitone sodium (Euthatal) via the marginal ear vein. The ears were removed and the central ear artery located at the base of the ears. A small section of the artery was cleared of connective tissue and an incision was made to allow the insertion of a nylon cannula (external diameter 0.75 mm). The cannula was lightly scored with a scalpel blade prior to insertion into the vessel, to remove the vessel endothelium. The artery, mounted on the cannula, was then dissected from the ear, cleared of connective tissue and cut into 5 mm rings. These were mounted horizontally over tungsten wire hooks (0.25 mm diameter) in 10 ml organ baths. The lower hook was attached to a stationary support in the organ bath and the upper hook was connected to an Ormed transducer for recording changes in isometric force. Tissues were bathed in Krebs' buffer (pH 7.4) of the following composition (mM): NaCl 117.56; $NaH_2PO_4.2H_2O$ 0.89; $NaHCO_3$ 25.0; $MgSO_4.7H_2O$ 1.18; glucose 11.1; KCl 5.36 and $CaCl_2$ 2.55. The tissues were maintained at 37°C and gassed continuously with 95% O_2/5% CO_2. The Krebs' solution also contained indomethacin (2.8 μM) to prevent the formation of cyclo-oxygenase products and 8-sulphophenyltheophylline (300 μM) to exclude possible influence of P_1-purinoceptor activation.

The tissues were subjected to an initial force of 1.0 g and then allowed to equilibrate for a minimum of 1 h, during which time the force was adjusted to achieve a final value of 0.5–1.0 g. The tissues were then washed by exchange of the bath solution.

Tissue viability was assessed by treatment with KCl (80 mM). Only those tissues producing an increase in force of 0.5 g or more were included in the study. The functional state of the endothelium was tested by subsequent addition of acetylcholine (1 μM). In these studies, the vasorelaxation to acetylcholine was invariably less than 15% of the KCl-induced contraction. Tissues were then washed and allowed to re-equilibrate for 45 min.

Experimental protocols for the rabbit ear artery

A paired curve design was adopted in which all tissues were initially treated with cumulative additions of ATP at 0.5 log unit intervals. Following washout and re-equilibration, FPL 66301 or suramin (0–1000 μM) was applied. Subsequently, a second cumulative curve was constructed using ATP. In the case of FPL 66301, all concentrations were incubated for 45 min between paired curves. In the case of suramin, incubation times were chosen based on previous kinetic studies (Leff *et al.*, 1990) as follows: 30 μM (220 min); 100 μM (86 min); 300 μM (31 min); 1 mM (10 min). The interval between paired ATP curves was 70 min in the case of FPL 66301 and 240 min in the case of suramin. Contractile effects were expressed as percentages of the first curve maximum.

Ecto-ATPase assay

Human blood was obtained by venepuncture from healthy volunteers, heparinized then centrifuged (2000 g, 10 min). Plasma was removed, care being taken not to disturb the buffy coat. The remaining cells were washed twice with buffer of composition (mM) Tris 20.0, glucose 5.0, NaCl 140.0, KCl 5.0, adjusted with HCl to pH 7.4, 20°C. The cell suspensions were then diluted 7-fold with buffer.

[γ^{32}P]ATP assays were carried out at 37°C in a shaking water bath. The total incubation volume was 200 μl, of which the added volume of cells was 75 μl. The incubation medium contained, in addition to buffer, NaN_3 (5.0 mM) and $CaCl_2$ (0.5 mM). The substrate concentration of ATP was 10 μM containing 80,000–90,000 d.p.m. [γ^{32}P]ATP. This concentration was near the K_M determined in previous studies (Beukers *et al.*, 1993). Suramin or FPL 66301 was added to achieve final concentrations in the range 0.3–1000 μM. Their inhibitory effects were measured as percentages of the degradation achieved in the presence of 10 μM ATP alone, over a period of 30 min.

Incubations were terminated by addition of activated charcoal (400 μl of 40 mg ml^{-1} charcoal in 0.1 N HCl), then centrifugation (6500 G, 2 min). Supernatant samples of 350 μl were homogenized with 4 ml of emulsifier (Emulsifier Safe, Packard) and radioactivity was counted in an LKB-Wallace 1214 Rackbeta Excel Spectrometer. Controls, without cells, were processed identically.

Drugs and materials

The following drugs were used: acetylcholine bromide, adenosine 5'-triphosphate, disodium salt (ATP) (Sigma Chemical Co., Poole, U.K.); FPL 66301, tetrasodium salt (synthesized by P.A. Cage, Medicinal Chemistry Department, Fisons); 8(*p*-sulphophenyl)theophylline (8-SPT) (Research Biochemicals, St. Albans, U.K.); suramin (a gift from Bayer, U.K.); indomethacin (Sigma); activated charcoal, particle size 4–7 μM (Serva, Heidelberg, Germany); ATP (for ecto-ATPase studies) (Aldrich Chemie, Steinheim, Germany); [γ^{32}P]ATP (Amersham, U.K.).

For rabbit ear artery experiments, ATP, FPL 66301 and 8-SPT were dissolved in distilled water, suramin in Kreb's solution. Indomethacin was prepared as a 28 mM solution in Na_2CO_3 (0.35 M) and subsequently diluted in Krebs' solution.

Analysis of E/[A] curve data

Agonist concentration effect (E/[A]) data were fitted to the logistic function:

$$E = \frac{\alpha[A]^m}{[A_{50}]^m + [A]^m} \quad (1)$$

in which α, $[A_{50}]$ and m are respectively the asymptote, location and slope parameters. $[A_{50}]$ values were assumed to be log-normally distributed and are presented as their negative logarithms, $p[A_{50}]$.

Each E/[A] curve in an experimental pair was fitted and the effects of suramin and FPL 66301 were tested by analysing paired changes in the three parameters, i.e. $\Delta\alpha$, $\Delta p[A_{50}]$ and Δm. Preliminary analysis showed that variances of Δ values were not consistent among treatment groups. Therefore, non-parametric tests were adopted: the Kruskal–Wallis test for analysing group differences and the Mann–Whitney *U*-test for individual comparisons.

Analysis of ecto-ATPase inhibition

Data for the inhibitory effects of suramin and FPL 66301 on ATP degradation were fitted to equation (1). The concentrations which produced 50% inhibition of degradation (IC_{50}) were read from the fitted lines and quoted as negative logarithms (pIC_{50}). Since the concentration of ATP used was near its K_M (Beukers *et al.*, 1993), IC_{50} values were assumed to approximate to K_I values for the purposes of theoretical modelling.

Theoretical analysis of combined ecto-ATPase inhibition and receptor antagonism

The theoretical model of Furchgott (1972) was employed. In this model, agonist is applied to the organ bath at concentration $[A_o]$. The access of the agonist to biophase containing the receptors is considered to be diffusion rate limited, and it is catabolized by enzymatic activity within the biophase. Hence the concentration of agonist presented to its receptor within the biophase, $[A_i]$, may be substantially lower than $[A_o]$. The relationship between $[A_o]$ and $[A_i]$ can be determined from the following equations. The rate of entry of agonist is described by:

$$d[A_i]/dt = k_l([A_o] - [A_i]) \quad (2)$$

in which k_l is the diffusion constant for the agonist.

The degradation of agonist is assumed to follow Michaelis–Menten kinetics:

$$d[A_i]/dt = V_{max}[A_i]/(K_M + [A_i]) \quad (3)$$

At steady-state the rates of agonist entry and degradation are balanced. Under this condition, the right-hand sides of equations (2) and (3) can be equated, and the following relationship can be derived:

$$k_l[A_i]^2 + (V_{max} + k_l K_M - k_l[A_o])[A_i] - k_l K_M[A_o] = 0 \quad (4)$$

This is a quadratic equation in $[A_i]$. In theoretical simulations, values of k_l, V_{max} and K_M are chosen, then $[A_i]$, the active, biophase agonist concentration can be calculated in terms of $[A_o]$, the applied concentration, by numerical solution of equation (4).

To generate theoretical E/[A] curves, values of $[A_i]$ were substituted into a simple rectangular hyperbolic function, equivalent to equation (1) with m set to unity, thereby producing curves plotted against the applied agonist concentration, $[A_o]$.

To simulate the effect of enzyme inhibition, K_m was multiplied by the factor $(1 + [X]/K_I)$, in which X is a competitive inhibitor with a dissociation constant K_I. To simulate receptor antagonism, $[A_{50}]$ was multiplied by the factor $(1 + [X]/K_B)$, where K_B is the receptor dissociation constant of X. To simulate the combined properties, both factors were varied simultaneously.

Results

Figure 1 shows the effect of suramin on ATP E/[A] curves in the rabbit ear artery. For ease of display, the average second curve data are shown. Statistical analysis was carried out using the paired curve data (Table 1). Kruskal–Wallis analysis indicated that, as a group, the $\Delta p[A_{50}]$ estimates obtained in the presence of suramin were significantly greater than control values ($p = 0.022$), that is suramin had potentiated the effects of ATP. The average control $p[A_{50}]$ was 3.39 ± 0.13 (SE, $n = 11$) and suramin produced a 3-fold leftward shift of the curves. The Mann–Whitney U-test indicated that the leftward shifts obtained at 100 μM and 1 mM suramin were individually significant ($0.01 < P < 0.05$). No significant effect of suramin on the values of α or m of the E/[A] curves was detected.

Figure 2 shows the effect of FPL 66301 on ATP E/[A] curves. Again average second curves are displayed. Kruskal–Wallis analysis of the paired data indicated an overall significant rightward shift ($P = 0.031$; Table 1). Mann–Whitney-U analysis indicated that the effects of 100 μM and 300 μM FPL 66301 were individually significant. No significant effects on curve asymptotes or slopes were detected.

Figure 3 shows the effects of suramin and FPL 66301 on [γ^{32}P]ATP degradation by human blood cells. Clear concentration-dependent inhibition of degradation was obtained in both cases, with suramin evidently being more potent ($pIC_{50} = 4.33 \pm 0.03$, SE, $n = 3$) than FPL 66301 ($pIC_{50} = 3.33 \pm 0.06$, SE, $n = 3$).

Figure 4 illustrates theoretical analysis of the effects of suramin on ATP E/[A] curves using the model for combined receptor antagonism and ecto-ATPase inhibition. For clarity the effects of only the highest concentration of suramin (1 mM) have been simulated in the figure. Figure 4a shows the experimental data obtained using ATP as agonist, Figure 4b the computer simulation and Figure 4c experimental data previously obtained using α,β-methylene ATP as agonist (replotted from Leff *et al.*, 1990). The pK_B value (4.8) describing the receptor antagonism component used in the simulation was that found experimentally when α,β-methylene ATP was used (Leff *et al.*, 1990). This is indicated in Figure 4 by the quantitative correspondence between the rightward shift of α,β-methylene ATP curves obtained experimentally (Figure 4c) and the simulated rightward shift corresponding to the

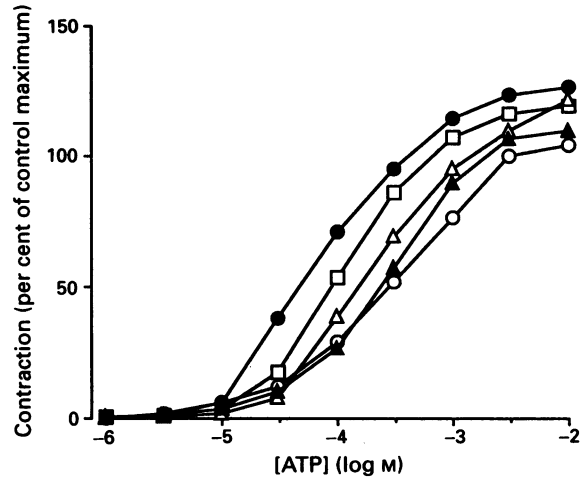


Figure 1 Effect of suramin on ATP E/[A] curves in the rabbit ear artery. Cumulative E/[A] curves to ATP were constructed in the presence of the following concentrations of suramin (μM): zero (○); 30 (▲); 100 (●); 300 (△); 1000 (□). A paired curve protocol was used (see Methods) but, for ease of display, the graph shows the average second-curve data, measured as percentages of the first-curve maximum ($n = 4$ or 5). The complete data together with statistical analyses are shown in Table 1.

Table 1 Statistical analysis of the effects of suramin and FPL 66301 on ATP E/[A] curves. Analysis of paired differences in asymptote (α), slope (m) and location ($p[A_{50}]$) of curves obtained in the absence and presence of the two compounds

	Δα		Δm		Δp[A_{50}]		
Antagonist	*Mean*	*SE*	*Mean*	*SE*	*Mean*	*SE*	n
Suramin (μM)							
0	2.9	12.0	0.08	0.05	−0.04	0.15	5
30	6.3	4.6	0.19	0.18	−0.21	0.05	5
100	17.8	11.6	0.28	0.10	−0.67*	0.13	4
300	22.7	10.5	0.21	0.36	−0.43	0.28	4
1000	11.6	8.5	0.45	0.18	−0.45*	0.11	5
FPL 66301 (μM)							
0	−2.1	4.2	−0.01	0.05	−0.04	0.07	6
100	−1.5	5.9	0.01	0.04	0.41*	0.10	5
300	3.6	7.2	0.03	0.15	0.38*	0.10	5
1000	3.3	7.1	−0.15	0.13	0.37	0.42	5

*Indicates difference between treatment group and control, ($P < 0.05$) by Mann–Whitney U-test.

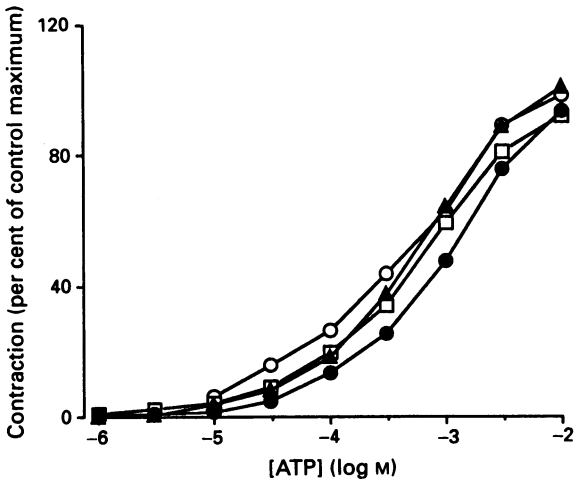


Figure 2 Effect of FPL 66301 on ATP E/[A] curves in the rabbit ear artery. Cumulative E/[A] curves to ATP were constructed in the presence of the following concentrations of FPL 66301 (μM): zero (○); 100 (□); 300 (●); 1000 (▲). A paired curve protocol was used (see Methods) but, for ease of display, the graph shows average second-curve data, measured as percentages of the first-curve maximum ($n = 5$ or 6). The full data together with statistical analyses are shown in Table 1.

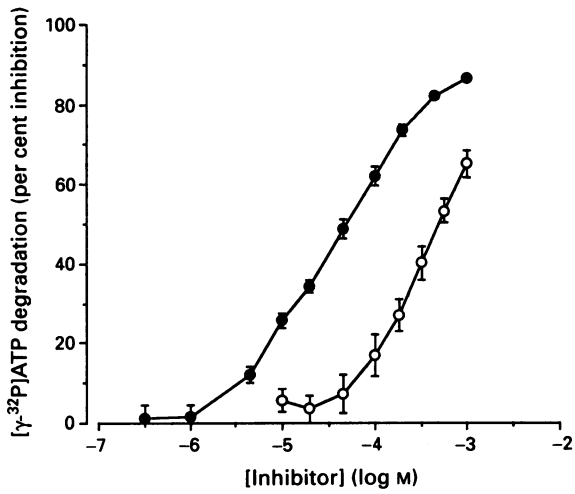


Figure 3 Effect of suramin and FPL 66301 on ATP degradation in human blood cells. Inhibition curves are shown for suramin (●) and FPL 66301 (○) (both $n = 3$) on [γ^{32}P]ATP dephosphorylation by ecto-ATPase in human blood cells. The estimated pIC_{50} values were 4.33 for suramin and 3.33 for FPL 66301.

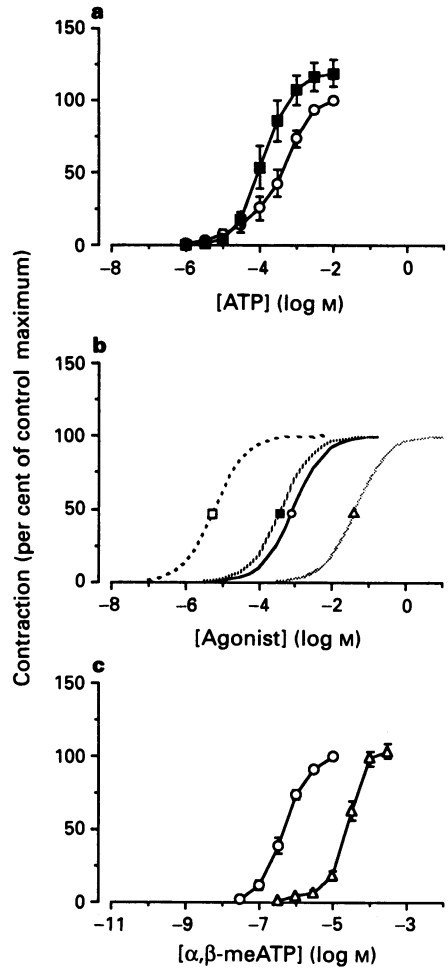


Figure 4 Theoretical analysis of combined ecto-ATPase inhibition and P_{2X}-purinoceptor antagonism by suramin. (a) ATP E/[A] curves obtained in the rabbit ear artery in the absence (○) and presence (■) of suramin (1 mM), redrawn from Figure 1. (b) A simulation of a theoretical model describing the effect of a compound with dual enzyme and receptor inhibitory properties on an agonist susceptible to enzymic degradation (see Methods section for details). The dual inhibitor was assumed to have a pK_B (receptor antagonism) of 4.8 and a pK_I (enzyme inhibition) of 5.2 and the simulation shows its predicted effects at 1 mM. Theoretical curves were generated under the conditions: control (○); receptor antagonism alone (△); enzyme inhibition alone (□); combined effects (■). (c) α,β-Methylene ATP curves obtained in the rabbit ear artery in the absence (○) and presence (△) of suramin (1 mM) (redrawn from Leff *et al.*, 1990).

receptor antagonism by suramin Figure 4b. Values of the other model parameters, including the pK_I value, were chosen to obtain reasonable correspondence between the theoretical curve simulating the combined effects of ATPase inhibition and receptor antagonism and the expermental data in Figure 4a.

Figure 5 shows a similar theoretical analysis of the effects of FPL 66301 on ATP. Again, the pK_B value (4.4) used in the simulation was that previously obtained for FPL 66301 as antagonist of α,β-methylene ATP (Leff *et al.*, 1993). The pK_I value required to simulate the experimental data was lower than in the case of suramin, but the remaining parameter values were set to the same values as in Figure 4.

Table 2 summarizes the parameter values used to generate the computer simulations shown in Figures 4 and 5. Of note is the $p[A_{50}]$ value for ATP used in the simulations. This value is the theoretical position of the ATP E/[A] curve that would be obtained in the absence of ecto-ATPase activity. It contrasts markedly with the experimental control $p[A_{50}]$ (3.39). Also note that the values of pK_I are higher than those found in the blood cell assay, though they maintain a similar ratio of K_I values.

Discussion

The present study has investigated the effects of suramin and FPL 66301 on ATP E/[A] curves in the rabbit isolated ear artery. The results obtained are in marked contrast with those previously reported from this laboratory when the two compounds were tested, in the same preparation and under the same experimental conditions, but using α,β-methylene ATP or β,γ-methylene L-ATP as agonists (Leff *et al.*, 1990; 1993). In those studies, both suramin and FPL 66301 were shown to behave as competitive antagonists of the P_{2X}-purinoceptors in this preparation, producing parallel rightward shifts of E/[A] curves which accorded with a Schild plot slope of unity. In the case of suramin a pK_B estimate of 4.8

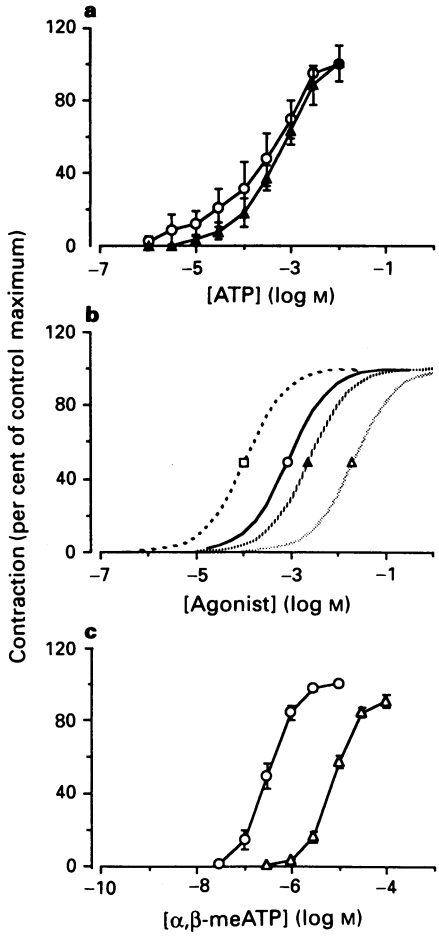


Figure 5 Theoretical analysis of combined ecto-ATPase inhibition and P_{2X}-purinoceptor antagonism by FPL 66301. (a) ATP E/[A] curves obtained in the rabbit ear artery in the absence (○) and presence (▲) of FPL 66301 (1 mM), redrawn from Figure 2. (b) A simulation of a theoretical model describing the effect of a compound with dual enzyme and receptor inhibitory properties on an agonist susceptible to enzymic degradation (see Methods section for details). The dual inhibitor was assumed to have a pK_B (receptor antagonism) of 4.4 and a pK_I (enzyme inhibition) of 3.9 and the simulation shows its predicted effects at 1 mM. Theoretical curves were generated under the conditions: control (○); receptor antagonism alone (△); enzyme inhibition alone (□); combined effects (▲). (c) α,β-Methylene ATP curves obtained in the rabbit ear artery in the absence (○) and presence (△) of suramin (1 mM) (redrawn from Leff *et al.*, 1993).

was reported and in the case of FPL 66301 an estimate of 4.4. In the present study, neither compound exhibited effects consistent with their P_{2X}-purinoceptor antagonist properties: suramin potentiated the effects of ATP rather than antagonized them; FPL 66301 produced only limited (no more than 3-fold) rightward shifts. In both cases the concentration range employed had produced rightward shifts of 30-fold in the previous study.

It was hypothesized that these differences were due to the susceptibility of ATP but not α,β-methylene ATP or β,γ-methylene L-ATP to metabolic degradation by ecto-ATPase in the tissue and that suramin and FPL 66301 could act as inhibitors of this enzyme as well as receptor antagonists. This combination of properties could, in theory, lead to a 'self-cancellation' of ATP E/[A] curve displacements in which the effects of receptor antagonism are offset by the potentiating influence of inhibiting the degradation of ATP. In contrast, when a metabolically stable agonist is used, only the receptor antagonism component would be apparent. In support of this hypothesis, *in vitro* studies on the metabolic degradation of

Table 2 Model parameter values used in theoretical simulations

Parameter	*Value*
Diffusion constant for ATP, k_1	0.1 min^{-1}
Ecto-ATPase, K_M	3×10^{-3} M
Ecto-ATPase, V_{max}	0.3 M min^{-1}
Location of ATP E/[A] curve, $p[A_{50}]$	6.0 (−log M)
Dissociation constant for ecto-ATPase inhibition, pK_I	
Suramin	5.2 (−log M)
FPL 66301	3.9 (−log M)
Dissociation constant for P_{2X}-purinoceptor antagonism*, pK_B	
Suramin	4.8 (−log M)
FPL 66301	4.4 (−log M)

*Values obtained experimentally with α,β-methylene ATP as agonist (Leff *et al.*, 1990; 1993).

nucleotides have shown triphosphates such as ATP to be susceptible to rapid hydrolysis. In contrast, phosphonates containing α,β- or β,γ-methylene substituents have been shown to be relatively stable. Thus, in a guinea pig taenia coli preparation ATP was dephosphorylated with a half-life of about 20 min, whereas α,β-methylene ATP degradation was less than 10% in 20 min and β,γ-methylene L-ATP appeared completely resistant to hydrolysis over this period (Welford *et al.*, 1986). Suramin has been reported to be an inhibitor, albeit at high concentrations, of ATP degradation in the guinea pig bladder (Hourani & Chown, 1989). Furthermore, in the present study, using the human blood assay, suramin and FPL 66301 have been clearly demonstrated to possess ecto-ATPase inhibitory properties, characterized by IC_{50} values in the concentration range relevant to the pharmacological studies.

However, as explained in the Introduction, another way in which the metabolism of agonists by tissues can lead to complications in pharmacological analysis is the production of metabolites which are active as agonists in their own right. In the present system, it was necessary to consider the possible conversion of ATP to ADP, AMP and adenosine. In particular, accumulation of adenosine may have resulted in the activation of P_1-purinoceptors mediating vasorelaxation, which would have opposed the P_{2X}-purinoceptor-mediated contractile effects of ATP. Inhibition of adenosine formation could have then led to potentiation of ATP effects. This explanation could be ruled out in this study because 8-SPT was present in all experiments at a concentration 30 to 100-fold higher than its dissociation constant for P_1-purinoceptors. Another potential complication may have been the local generation of ADP from ATP and its effects at P_{2X}-purinoceptors in the tissue. However, for this factor to explain the potentiation of ATP effects by inhibition of ecto-ATPase, ADP would had to have been acting as an antagonist of ATP under control conditions. In fact, ADP is an agonist at the receptors concerned, so we do not consider this to be a viable explanation. The possible effects of metabolites of ATP active at P_{2Y}-purinoceptors could also be excluded since these receptors are absent in this preparation (O'Connor *et al.*, 1990).

On the basis that the original hypothesis was plausible it was then necessary to assess whether it could account quantitatively for the E/[A] curve data. To do this a theoretical model proposed by Furchgott (1972) was applied. This model was originally developed to analyse the pharmacological influence of catecholamine metabolism and its inhibition on β-adrenoceptor agonist effects. Its application here showed it to be a valid description of the data, giving a quantitatively accurate fit to the E/[A] curves for ATP and α,β-methylene ATP obtained using both suramin and FPL 66301, as shown in Figures 4 and 5. It was considered, therefore, to be a

reasonable framework for assessing the influence of ecto-ATPase on the position of ATP E/[A] curves and for quantifying the effects of suramin and FPL 66301.

The choice of parameter values in the simulations requires some discussion. Firstly, the K_M value used was higher than that reported elsewhere for ATP dephosphorylation in human blood (Beukers *et al.*, 1993). This was considered necessary for the following reason. The E/[A] curves for ATP obtained in the rabbit ear artery in the presence and absence of suramin and FPL 66301 were evidently parallel. This indicated that, over the range of concentrations of ATP employed, the dephosphorylation mechanism was operating in a pseudo first-order manner, meaning in turn that the ATP concentrations used were less than the K_M. Had this not been the case, changes in slope of the E/[A] curves would have been expected (Furchgott, 1972). A value of K_M was chosen to ensure that this condition was fulfilled.

A key feature of the theoretical analysis was that it employed the known pK_B estimates for suramin and FPL 66301 as agonists of the P_{2X}-purinoceptors in the rabbit ear artery. These estimates fixed the degree of underlying shift associated with the receptor antagonism component of each compound when ATP was used as the agonist. On the basis that the experimental curves obtained in the presence of suramin and FPL 66301 represented the 'self-cancelled' position, the extent of underlying potentiation could be estimated. The magnitude of the potentiation determined the values of k_I and V_{max} used in the simulations because these are the model parameters which govern the difference between the ATP concentrations in the organ bath ($[A_o]$) and in the biophase ($[A_i]$) and, therefore, the impact of ecto-ATPase on the position of the ATP E/[A] curve. In the simulations, $[A_i]$ was some 1000-fold lower than $[A_o]$.

Regarding the pK_I values for suramin and FPL 66301 used in the simulations, these needed to be higher than the estimates made in the human blood assay. Bearing in mind the fact that the pharmacological and biochemical data were obtained in different tissues and under different conditions, this result is perhaps not surprising. Ideally, an ecto-ATPase assay using cells from the rabbit ear artery would have been employed but, to our knowledge, such an assay is not available. Another consideration here is that in the theoretical analysis suramin and FPL 66301 are treated as competitive enzyme inhibitors. This assumption may be questioned in the case of suramin (Hourani & Chown, 1989). However, as explained above, dephosphorylation of ATP in the ear artery appeared to operate in a pseudo first-order manner. Under this condition, the relationship between $[A_i]$ and $[A_o]$ is given by $[A_i] = (V_{max}K_M/k_I)[A_o]$, so that multiplying K_M by the factor $(1 + [X]/K_I)$, as for a competitive interaction, is technically identical to dividing V_{max} by the same factor, as for a non-competitive interaction. In this sense, the theoretical simulations and their ability to account for the experimental data are not dependent on the assumption that the inhibition of ecto-ATPase by either compound is truly competitive.

The pK_I estimates required to model the E/[A] curve displacements have similar relative values to those obtained in the ecto-ATPase assay. So there is at least qualitative accordance between the pharmacological and biochemical analyses. Moreover, from the point of view of pharmacological analysis, we would consider the relevant estimates to be the ones obtained in the tissue study since these reflect the extent of potentiation that the compounds are able to produce. In these respects therefore, the model parameter values used in simulating the data were deduced rather than chosen.

An important conclusion from this analysis is that, in order to allow for the extent of potentiation that was required to offset the antagonist effects, it was necessary to assume that the location of the ATP curve, in the absence of ecto-ATPase activity, would have been some 400-fold to the left of its experimental position. This is signified in the theoretical analysis by the $p[A_{50}]$ value of 6.0 (see Table 2), contrasted with the experimental value of 3.39. Attention has been drawn to the potential influence of ecto-ATPase on the location of E/[A] curves for ATP (and other metabolically unstable agonists) obtained in tissue preparations (for example, Burnstock & Kennedy, 1985) but, to our knowledge, the present study is the first to attempt to quantify this influence. This finding has some important implications for P_2-purinoceptor classification. The degree to which ecto-ATPase affects the position of the ATP E/[A] curve in this preparation means that the true potency of ATP is underestimated by over two orders of magnitude. This is particularly relevant in the context of agonist potency orders. In previous studies (O'Connor *et al.*, 1990) the following agonist potency order ($p[A_{50}]$ values in parentheses) was obtained: α,β-methylene ATP (6.47) > β,γ-methylene L-ATP (5.52) > β,γ-methylene ATP (4.37) ≥ 2-MeS-ATP (4.15) > ATP (3.14). This potency order was characteristic of that designated for P_{2X}-purinoceptors (Burnstock & Kennedy, 1985). However, if the true $p[A_{50}]$ value for ATP is taken as 6.0 then its position in the potency order changes markedly relative to the metabolically stable α,β- and β,γ-methylene-substituted compounds. It is also reasonable to suggest that the position of 2-MeS-ATP should change since it has been shown to be as susceptible as ATP to dephosphorylation by ectonucleotidases (Welford *et al.*, 1986). If its true potency is calculated on the same basis as that of ATP then there would be little difference between α,β-methylene ATP and 2-MeS-ATP. This implies that the agonist potency order currently held to characterize P_{2X}-purinoceptors may need to be re-evaluated.

It may be relevant to consider these conclusions in relation to radioligand binding studies on P_{2X}-purinoceptors. A notable feature of the results from such studies is the high apparent affinity values obtained for agonists compared with the potency values obtained in isolated tissues (e.g. Michel & Humphrey, 1993). It is possible that this difference may partly be explained by the absence of ecto-ATPase activity in the binding assays. However, it is to be noted that the difference also applies to poorly hydrolysable agonists such as α,β-methylene ATP and so additional explanations need to be sought.

Regarding suramin and FPL 66301, the present study indicates that caution should be adopted when using these compounds in receptor classification studies. The propensity for their receptor antagonistic and ecto-ATPase inhibitory properties to 'self-cancel' when metabolically unstable agonists are used is a basis for misinterpretation. For example, in the present system, the ability of each compound to antagonize the effects of α,β-methylene ATP in an apparently simple competitive manner, but their failure to displace ATP E/[A] curves could have led to the conclusion that ATP acted at a different receptor from the other agonists. This interpretation would clearly have been quite misleading and unhelpful in purinoceptor classification.

Obviously, experimental resolution of these issues would be greatly aided by the provision of a selective ecto-ATPase inhibitor. A compound of this kind has been discovered in our laboratory and studies are currently under way in which it is being used to elucidate problems of the kind described here.

References

BEUKERS, M.W., PIROVANO, I.M., VAN WEERT, A., KERKHOF, C.J.M., IJZERMAN, A.P. & SOUDIJN, W. (1993). Characterization of ecto-ATPase on human blood cells. *Biochem. Pharmacol.*, **46**, 1959–1966.

BLACK, J.W., GERSKOWITCH, V.P., LEFF, P. & SHANKLEY, N.P. (1986). Analysis of competitive antagonism when this property occurs as part of a pharmacological resultant. *Br. J. Pharmacol.*, **89**, 547–555.

BURNSTOCK, G. & KENNEDY, C. (1985). Is there a basis for distinguishing two types of P_2-purinoceptor? *Gen. Pharmacol.*, **16,** 433–440.

FURCHGOTT, R.F. (1972). The classification of adrenoceptors (adrenergic receptors). An evaluation from the standpoint of receptor theory. In *Handbook of Experimental Pharmacology,* Vol. 33, ed. Blaschko, H. & Muscholl, E., pp. 283–335. New York: Springer.

HOURANI, S.M.O. & CHOWN, J.A. (1989). The effects of some possible inhibitors of ectonucleotidases on the breakdown and pharmacological effects of ATP in the guinea-pig urinary bladder. *Gen. Pharmacol.*, **20,** 413–416.

KENAKIN, T.P. (1980). Errors in the measurement of agonist potency-ratios produced by uptake processes: a general model applied to β-adrenoceptor agonists. *Br. J. Pharmacol.*, **71,** 407–417.

KENAKIN, T.P. & BEEK, D. (1985). Self-cancellation of drug properties as a mode of organ selectivity: the antimuscarinic effects of ambenonium. *J. Pharmacol. Exp. Ther.*, **232,** 732–740.

LEFF, P., WOOD, B.E. & O'CONNOR, S.E. (1990). Suramin is a slowly-equilibrating but competitive antagonist at P_{2X}-receptors in the rabbit isolated ear artery. *Br. J. Pharmacol.*, **101,** 645–649.

LEFF, P., WOOD, B.E., O'CONNOR, S.E. & MCKECHNIE, K.C.W. (1993). Quantitative analysis of the agonist and antagonist actions of some ATP analogues at P_{2X}-purinoceptors in the rabbit ear artery. *Br. J. Pharmacol.*, **108,** 490–496.

MAGUIRE, M.H. & SATCHELL, D.G. (1981). Purinergic receptors in visceral smooth muscle. In *Purinergic Receptors. Receptors and Recognition, Series B,* Vol 12. ed. Burnstock, G. pp. 49–92. London: Chapman & Hall.

MICHEL, A.D. & HUMPHREY, P.P.A. (1993). Distribution and characterization of [^{3}H]α,β-methyleneATP binding sites in the rat. *Naunyn-Schmied. Arch. Pharmacol.*, **348,** 608–617.

O'CONNOR, S.E., WOOD, B.E. & LEFF, P. (1990). Characterization of P_{2X}-purinoceptors in rabbit isolated ear artery. *Br. J. Pharmacol.*, **101,** 640–644.

WELFORD, L.A., CUSACK, N.J. & HOURANI, S.M.O. (1986). ATP analogues and the guinea-pig taenia coli: a comparison of the structure–activity relationships of ectonucleotidases with those of the P_{2X}-purinoceptor. *Eur. J. Pharmacol.*, **129,** 217–224.

WELFORD, L.A., CUSACK, N.J. & HOURANI, S.M.O. (1987). The structure–activity relationships of ectonucleotidases and of excitatory P_2-purinoceptors: evidence that dephosphorylation of ATP analogues reduces pharmacological potency. *Eur. J. Pharmacol.*, **141,** 123–130.

(Received April 5, 1994
Revised July 15, 1994
Accepted August 4, 1994)

Br. J. Pharmacol. (1994), **113**, 1439–1447 © Macmillan Press Ltd, 1994

Modulation of dopamine and noradrenaline release and of intracellular Ca^{2+} concentration by presynaptic glutamate receptors in hippocampus

[1,*†]João O. Malva, *Arsélio P. Carvalho & *Caetana M. Carvalho

*Center for Neurosciences of Coimbra, Department of Zoology, University of Coimbra, 3049 Coimbra Codex, Portugal and †Department of Biology, University of Minho, Braga, Portugal

1 We studied the release of [^{3}H]-dopamine and [^{3}H]-noradrenaline (NA) from hippocampal synaptosomes induced by glutamate receptors and the associated Ca^{2+} influx through Ca^{2+} channels. The release of tritiated neurotransmitters was studied by use of superfusion system and the intracellular free Ca^{2+} concentration ($[Ca^{2+}]_i$) was determined by a fluorimetric assay with Indo-1 as a probe for Ca^{2+}.

2 Presynaptic glutamate receptor activation induced Ca^{2+}-dependent release of [^{3}H]-dopamine and [^{3}H]-NA from rat hippocampal synaptosomes. Thus, L-glutamate induced the release of both neurotransmitters in a dose-dependent manner ($EC_{50} = 5.62\,\mu M$), and the effect of 100 μM L-glutamate was inhibited by 83.8% in the presence of 10 μM 6-cyano-7-nitroquinoxaline-2,3-dioxine (CNQX), but was not affected by 1 μM (+)-5-methyl-10,11-dihydro-5H-dibenzo[a,d]-cyclohepten-5,10-imine (MK-801).

3 Other glutamate receptor agonists also stimulated the Ca^{2+}-dependent release of [^{3}H]-dopamine and [^{3}H]-NA as follows: N-methyl-D-aspartate (NMDA), at 200 μM, released $3.65 \pm 0.23\%$ of the total ^{3}H catecholamines, and this effect was inhibited by 81.2% in the presence of 1 μM MK-801; quisqualate (50 μM), S-α-amino-3-hydroxy-5-methyl-4-isoxazolopropionic acid (AMPA) (100 μM) or kainate (100 μM) released $1.57 \pm 0.26\%$, $1.93 \pm 0.17\%$ and $2.09 \pm 0.22\%$, of the total ^{3}H catecholamines, respectively.

4 The ionotropic glutamate receptor agonist, AMPA, induced an increase in the $[Ca^{2+}]_i$ which was inhibited by 58.6% in the presence of 10 μM CNQX. In contrast, the increase in $[Ca^{2+}]_i$ due to stimulation by glutamate was not sensitive to CNQX or MK-801.

5 Nitrendipine, at 1 μM, did not inhibit the neurotransmitter release induced by AMPA, but, both 0.5 μM ω-conotoxin GVIA (ω-CgTx) and 100 nM ω-Aga IVA reduced catecholamine release to $49.03 \pm 3.79\%$ and $46.06 \pm 10.51\%$ of the control, respectively. In the presence of both toxins the release was reduced to $12.58 \pm 4.64\%$ of the control.

6 The results indicate that activation of presynaptic glutamate receptors of the NMDA and non-NMDA type induces the release of [^{3}H]-dopamine and [^{3}H]-NA from rat hippocampal synaptosomes and that the release induced by AMPA involves the activation of N- and P-type Ca^{2+} channels which allow the influx of Ca^{2+} that triggers the ^{3}H catecholamines release.

Keywords: Hippocampus; catecholamines release; presynaptic glutamate receptors; calcium; synaptosomes; voltage-sensitive calcium channels

Introduction

The exocytotic release of neutrotransmitters depends on the Ca^{2+} influx into the cell (for review see: Carvalho, 1982; Augustine, 1987; Smith & Augustine, 1988; Knight *et al.*, 1989). The influx of Ca^{2+} is mediated by Ca^{2+} channels activated upon excitation of the nerve terminal, providing a mechanism for the coupling between stimulation and neurosecretion (Tsien *et al.*, 1988, 1991).

Voltage-sensitive Ca^{2+} channels (VSCCs) are activated by membrane depolarization and two groups of VSCC's can be distinguished on the basis of the different sensitivities to membrane depolarization. Low voltage-sensitive calcium channels or T-Type VSCCs are transiently activated by small decreases in membrane potential. High voltage-sensitive calcium channels are VSCCs which are activated after large depolarizations of the membrane. Three different types of high VSCCs can be distinguished on the basis of their sensitivity to specific antagonists. The L-type Ca^{2+} channels are a group of channels inhibited by dihydropyridines, like nitrendipine (Tsien *et al.*, 1991). The N-type Ca^{2+} channels are blocked by ω-conotoxin GVIA (ω-CgTx) (Kerr & Yoshikami, 1984; Tsien *et al.*, 1991). The P-type VSCCs are inhibited by the polyamine FTX (Llinás *et al.*, 1989) or by the peptide ω-Aga IVA (Mintz *et al.*, 1992b) which is a component of the venom of the funnel web spider, *Agenelopsis asperta*.

The excitatory neurotransmitter L-glutamate acts both at the postsynaptic and presynaptic membranes by interaction with its receptors. Glutamate receptors may be ionotropic, allowing the influx of ions through a receptor channel (Zorumski & Thio, 1992; Ruzicka & Jhamandas, 1993), or G protein-coupled metabotropic receptors, which are coupled to several second messenger systems (Schoepp & Conn, 1993). The metabotropic receptors are coupled to phospholipase C (Nicoletti *et al.*, 1986; Sugiyama *et al.*, 1987) and the activated phospholipase C catalyzes the hydrolysis of phosphatidyl inositols and produces inositol phosphate which releases Ca^{2+} from internal stores (Zorumski & Thio, 1992). The metabotropic receptor is activated by ACPD and also by quisqualate (Zorumski & Thio, 1992). The ionotropic glutamate receptors are the N-methyl-D-aspartate (NMDA), S-α-amino-3-hydroxy-5-methyl-4-isoxazolopropionic acid (AMPA) and kainate receptors (Zorumski & Thio, 1992; Ruzicka & Jhamandas, 1993). The NMDA receptor is very permeable to Ca^{2+} (MacDermott *et al.*, 1986; Iino *et al.*, 1990), reversibly blocked by Mg^{2+} (Nowak *et al.*, 1984) and potentiated by the co-agonist, glycine (Johnson & Ascher,

[1] Author for correspondence at: Department of Zoology, University of Coimbra, 3049 Coimbra Codex, Portugal.

1987; Kemp & Leeson, 1993). As compared to the NMDA receptor, AMPA and kainate receptors are less permeable to Ca^{2+} (Iino *et al.*, 1990; Ruzicka & Jhamandas, 1993). The AMPA- and kainate-induced depolarization activates VSCCs which allows the influx of Ca^{2+}, coupling the stimulation to neurosecretion (Ruzicka & Jhamandas, 1993).

The effectiveness of the Ca^{2+} entering the nerve terminal in releasing of neurotransmitters, following presynaptic glutamate receptors activation, depends on the spatial localization of the receptors and the Ca^{2+} channels in the active zones (Smith & Augustine, 1988). In this work we studied the role of presynaptic glutamate receptors of rat hippocampal synaptosomes in inducing the release of [^{3}H]-dopamine and [^{3}H]-noradrenaline ([^{3}H]-NA) and we determined which high voltage-sensitive Ca^{2+} channels mediate the coupling between glutamate receptor activation and catecholamine release in synaptosomes isolated from rat hippocampus.

A preliminary account of this work has been presented at the 14th International Society for Neurochemistry Meeting (Malva *et al.*, 1993).

Methods

Preparation of synaptosomes

A crude synaptosomal fraction (P_2) was isolated from hippocampi of two month-old male Wistar rats, essentially as described previously (McMahon *et al.*, 1992), with some modifications. Hippocampi were homogenized in 9 volumes of 0.32 M sucrose, 5 mM HEPES-Tris, pH 7.4, by using a Thomas B homogenizer, and centrifuged at 3000 g_{max} for 2 min. The pellet so obtained was washed by resuspension in approximately the original volume of the sucrose solution and centrifuged as above. The combined supernatants were centrifuged at 14600 g_{max}, for 12 min, and a P_2 pellet was obtained. The whiter and loosely packed layer of the pellet, which contains the majority of the synaptosomes, was carefully isolated with a spatula and resuspended in 0.32 M sucrose, 5 mM HEPES-Tris, pH 7.4, at a protein concentration of about 10 mg ml^{-1}. Aliquots of 1 mg of protein were diluted in 1 ml of sucrose medium and pelleted in a microfuge at 15800 g_{max}, for 2 min. The drained pellets were stored on ice and used within 3 h. Protein concentration was determined by the biuret method (Layne, 1957).

$[Ca^{2+}]_i$ measurements

Loading of synaptosomes with Indo-1 was carried out essentially as described previously (Duarte *et al.*, 1991). Synaptosomes (3.5 mg ml^{-1}) were incubated with 3 μM Indo-1-acetoxymethyl ester (Indo-1/AM) in a medium containing (mM): NaCl 132, KCl 1, $MgCl_2$ 1.4, $CaCl_2$ 100, H_3PO_4 1.2 fatty acid-free bovine serum albumin (BSA) 1 mg ml^{-1}, glucose 10 and HEPES-Na 10, pH 7.4, for 20 min, at 25°C, followed by 10 min at 30°C. The loading was stopped by pelleting the synaptosomes at 15800 *g*, for 10 s, and the supernatant, containing the nonhydrolyzed probe, was discarded. The synaptosomal pellet was resuspended (0.5 mg ml^{-1}) in a medium containing (mM): NaCl 132, KCl 1, $MgCl_2$ 1, glucose 10 and HEPES-Na 10, pH 7.4, and transferred into the cuvette. Fluorescence measurements were carried out at 30°C during stirring, in a Spex Fluoromax spectrofluorometer, at two emission wavelengths of 410 nm and 485 nm with a single excitation wavelength of 335 nm, using 5 nm slits. The maximal fluorescence ratio was obtained upon addition of 2 μM ionomycin, in the presence of 1 mM $CaCl_2$, and the minimal ratio was determined by adding 40 μl of 0.5 M EGTA solution at pH 10. The fluorescence intensities were converted into $[Ca^{2+}]_i$ values by using the calibration equation for double emission wavelength measurements and taking the dissociation constant of the Indo-1/Ca^{2+} complex at 250 nM (Grynkiewicz *et al.*, 1985). In all experiments, the synaptosomes were preincubated for 300 s before stimulation, in the presence or in the absence of drugs.

^{3}H-catecholamine release by synaptosomes

The uptake and release of ^{3}H catecholamines was performed as follows: synaptosomes were loaded (0.75 mg ml^{-1}) with 100 nM dopamine, containing 5 μCi of [^{3}H]-dopamine nmol^{-1}, in Na^+ medium (NaCl 132 mM, KCl 1 mM, $MgCl_2$ 1.4 mM, H_3PO_4 1.2 mM, $CaCl_2$ 100 μM, glucose 10 mM and HEPES-Tris 10 mM, pH 7.4) containing nialamide 12.5 μM, ascorbic acid 0.1% and fatty acid-free BSA 1 mg ml^{-1}. The loading of synaptosomes proceeded for 15 min at 30°C and was stopped by pelleting the synaptosomes at 15800 *g* for 30 s. The supernatant was discarded and the pellet resuspended in Na^+ medium (1.5 mg ml^{-1}). Samples of the synaptosomal suspension containing 0.75 mg of protein were aspirated and collected onto Whatman GF/B filters mounted in a superfusion system as described previously (Raiteri *et al.*, 1974). Synaptosomes were washed for 15 min with Na^+ medium containing 12.5 μM nialamide and 0.1% ascorbic acid, at a flow rate of 0.8 ml min^{-1}, using a peristaltic pump. By this time a stable basal release of ^{3}H catecholamines was obtained and the sample collection was started. Each sample was collected for 1 min and the total experiment proceeded for 10 min. All drugs used were added 1 min before starting the sample collection and the stimulation of synaptosomes was initiated at minute 3. At the end of the experiment, all the filters containing synaptosomes were dried and transferred into scintillation vials. The radioactivity present in the samples and in the filters was determined in vials after addition of a scintillation cocktail (Universol, ICN laboratories), using a liquid scintillation spectrometer (Packard, Tri-Carb 2000) provided with a d.p.m. correction programme.

Some of the results are presented as ^{3}H-catecholamines released in percentage of the total ^{3}H-catecholamines accumulated. To determine the ^{3}H-catecholamines effectively released upon stimulation, the following calculations were made: from the amount of ^{3}H-catecholamines released in each sample, the average value of basal release was subtracted. All individual values above basal release were summed and the obtained value was considered as the ^{3}H-catecholamines released by the stimulus. The total ^{3}H-catecholamines accumulated was calculated as the sum of ^{3}H-catecholamines released by stimulation of synaptosomes and the ^{3}H-catecholamines still present in the filters at the end of the experiment.

Catecholamine analysis by h.p.l.c.-e.d.

Dopamine, NA and dihydroxyphenylacetic acid (DOPAC) content of synaptosomes was compared in untreated synaptosomes (endogenous catecholamines) and in synaptosomes loaded with unlabelled dopamine in the conditions described in the previous section for the loading with tritiated dopamine. In both cases, 2 mg of synaptosomal protein was pelleted in order to determine the content of catecholamines. The obtained pellets were resuspended in 0.5 ml of a solution consisting of 10% acetic acid and 0.4 M perchloric acid. The samples were kept at −20°C for later high performance liquid chromatography (h.p.l.c.) analysis (Duarte *et al.*, 1993).

Dopamine and DOPAC analysis was performed as follows: the samples were injected into a 15 × 0.4 cm Spherisorb ODS-1 column with 5 μm particle size and eluted at a flow rate of 1 ml min^{-1} with a mobile phase consisting of 50 mM NaH_2PO_4, 1.24 mM heptanesulphonic acid, 0.24 mM EDTA, 10% methanol, pH 2.9. The electrochemical detector used was an ESA model Coulochem II.

The same samples were used to quantify NA levels in hippocampal synaptosomes by h.p.l.c. Samples were injected

in a column Ultrasphere ODS, 4.7 × 75 mm with 3 μm particle size. The mobile phase was 50 mM NaH_2PO_4, 0.02% trichloroacetic acid and 14% acetonitrile, pH 3.5 (Levine, 1986). The flow rate of the mobile phase and the conditions for electrochemical detection were the same used for dopamine and DOPAC analysis.

Analysis of released [^{3}H]-NA, [^{3}H]-dopamine and [^{3}H]-DOPAC by h.p.l.c.-e.d.

Hippocampal synaptosomes were loaded as described previously in this paper, but with the following modifications. The loading proceeded in the same Na^+ medium (1 mg ml^{-1} with 100 nM dopamine, containing 20 μCi of [^{3}H]-dopamine $nmol^{-1}$. One sample (1 min) of the basal release and another sample during the first min of stimulation, were collected. To each sample acetic acid (10% final concentration) and perchloric acid (0.4 M final concentration) were added, and the samples were stored at −20°C for latter h.p.l.c.-e.d. analysis (Duarte *et al.*, 1993).

The samples were injected in a column Ultrasphere ODS, 4.7 × 7.5 mm with 3 μm particle size with the same mobile phase and flow conditions as described in the previous section for NA quantification. The injected samples were prepared as following: 186 μl of tritiated sample were mixed with cold standards containing 100 pmol dopamine, 100 pmol NA and 50 pmol DOPAC, at a final volume of 200 μl. A volume of 100 μl of this mixture was injected into the column, using the appropriated loop. At the exit of the analytical cell, five of each 2 min samples were collected into scintillation vials and the radioactivity determined as previously described. The radioactivity in each sample was compared with the chromatogram of the cold standards (see Figure 1).

Materials

Nitrendipine was obtained from Research Biochemical International, Natick, U.S.A. The ω-conotoxin GVIA (ω-CgTx) was from Peninsula Laboratories Inc., Belmont, CA, U.S.A. The ω-AGA IVA was from Scientific Marketing Associates, U.K. and 6-nitro-7-cyano-quinoxaline-2,3-dione (CNQX) was obtained from NOVO, Nordisk, Denmark. (+)-5-Methyl-16,11-dihydro-5H-dibenzo [a,d] cyclohepten-5,10-imine maleate (MK-801) was purchased from Merck Sharp & Dohme Research Lab., Rahway, N.J., U.S.A. S-α-amino-3-hydroxy-5-methyl-4-isoxazolopropionic acid (AMPA) was obtained from Tocris Neuramin, Bristol, England. The acetoxymethyl ester of Indo-1 (Indo-1/AM) was obtained from Molecular Probes Inc. Eugene, OR, U.S.A. Ionomycin and fatty acid-free bovine serum albumin (BSA) were from Calbiochem-Boehringer Corp., San Diego, U.S.A. [7,8-^{3}H]-dopamine hydrochloride (40–60 Ci $mmol^{-1}$) was purchased from Amersham Laboratories, Buckinghamshire, England. All other reagents were from Sigma Chemical Co., St. Louis, MO, U.S.A. or from Merck-Schuchard, Germany. Stock solutions of Indo-1/AM, ionomycin, nitrendipine and CNQX were prepared in dimethyl sulphoxide.

Other methods

Results are presented as means ± s.e.mean of the number of experiments indicated. Statistical significance was determined by Student's two-tailed *t* test.

Results

Endogenous content of NA, dopamine and DOPAC in hippocampal synaptosomes

The hippocampal synaptosomes contain endogenous NA (2.94 ± 0.22 pmol mg^{-1} protein), dopamine (0.69 ± 0.16 pmol mg^{-1} protein) and small amounts of DOPAC (0.029 ± 0.027 pmol mg^{-1} protein) (Table 1). When we loaded the synaptosomes with exogenous dopamine, as described in Methods, we observed that the total content of NA was not significantly different from the content of endogenous NA (2.91 ± 0.21 pmol mg^{-1} protein) ($P > 0.05$). However, after the loading with dopamine, the synaptosomal content of this catecholamine increased to 4.40 ± 0.78 pmol mg^{-1} protein. The content of DOPAC in the synaptosomes observed after loading with exogenous dopamine was also significantly higher (2.28 ± 0.41 pmol mg^{-1} protein) (Table 1) than the content of the endogenous DOPAC in the synaptosomes.

Release of ^{3}H-catecholamines by hippocampal synaptosomes loaded with [^{3}H]-dopamine

After loading the hippocampal synaptosomes with [^{3}H]-dopamine, we observed that the main component of the tritium release in basal conditions was DOPAC (68.11 ± 2.17% of basal release), but also some dopamine (23.13 ± 1.89% of basal release) and NA (8.76 ± 0.64% of basal release) were released in the same conditions (Figure 1). However, after stimulation with L-glutamate, AMPA or KCl, the amount of DOPAC released did not increase as compared to basal conditions, some NA was released, and we observed a large increase in the tritium efflux with the retention time characteristic of dopamine (Figure 1). Thus, the increase in ^{3}H catecholamines release due to stimulation with 100 μM L-glutamate, 100 μM AMPA, 5 mM KCl or 30 mM KCl was mainly due to the release of [^{3}H]-dopamine (68.43 ± 4.03%, 74.05 ± 2.66, 69.53 ± 4.17 and 71.35 ± 3.19%, respectively of the total tritium released), but a significant part of [^{3}H]-NA was also released in the same conditions (31.58 ± 4.03%, 25.95 ± 2.66%, 30.48 ± 4.17% and 28.65 ± 3.19%, respectively). Thus, this methodology allow us to study in the same sample the release of both NA and dopamine induced by stimulating the glutamate receptors, although the major neurotransmitter in the efflux medium is dopamine (Figure 1c).

Stimulation of ^{3}H-catecholamines release from hippocampal synaptosomes by glutamate receptors agonists

Synaptosomes obtained from rat hippocampus released ^{3}H-catecholamines in response to stimulation with L-glutamate in a dose-dependent manner (Figure 2). Superfusion with medium containing 1 mM Ca^{2+} released 0.658 ± 0.171% ($n = 9$) of the total ^{3}H-catecholamines accumulated. The addition of L-glutamate released ^{3}H-catecholamines in a Ca^{2+}-dependent process, with the EC_{50} determined as 5.6 μM and the maximum ^{3}H-catecholamines release of 2.17% of the total tritium accumulated (Figure 2b). The release induced by L-glutamate was dependent on extracellular Ca^{2+}, since we did not observe [^{3}H]-catecholamines release in the absence of added Ca^{2+} (Figure 2a).

Table 1 Catecholamine levels in synaptosomes from rat hippocampus, determined by high performance liquid chromatography (h.p.l.c.)

	A	*B*
DOPAC	0.03 ± 0.03 ($n = 6$)	2.28 ± 0.41 ($n = 6$)*
NA	2.94 ± 0.22 ($n = 6$)	2.91 ± 0.21 ($n = 6$)
Dopamine	0.69 ± 0.16 ($n = 5$)	4.40 ± 0.78 ($n = 5$)*

A, Endogenous content of dihydroxyphenylacetic acid (DOPAC), noradrenaline (NA) and dopamine. **B** Contents of DOPAC, NA and dopamine observed after the loading of the synaptosomes with exogenous dopamine as described in the Methods Section. The values are expressed as pmol mg^{-1} protein.
*Significantly higher than endogenous, $P < 0.05$.

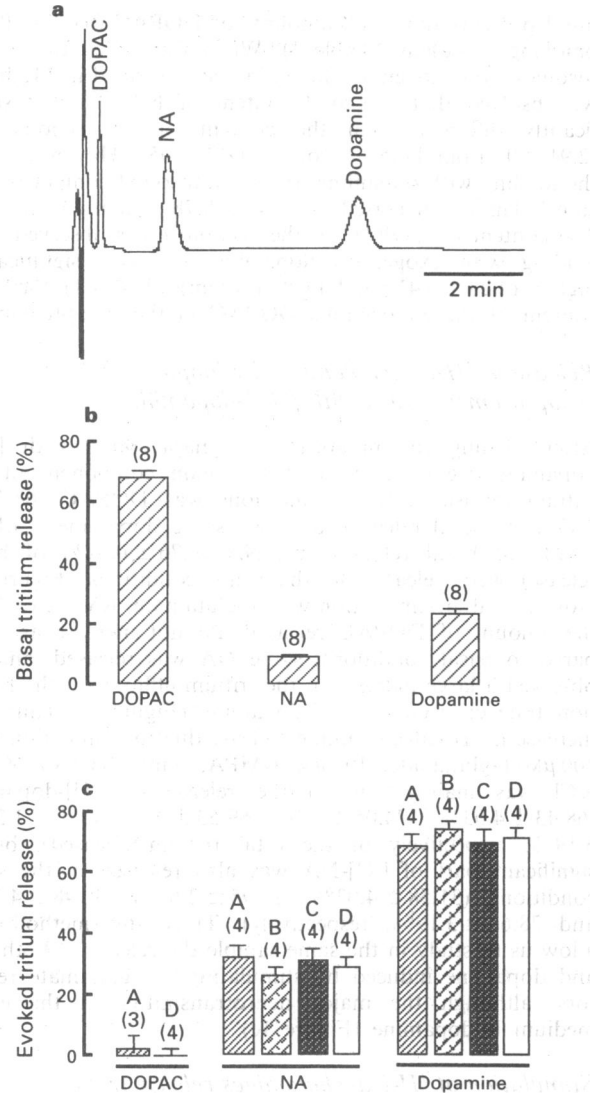


Figure 1 Release of tritiated catecholamines by hippocampal synaptosomes loaded with [^{3}H]-dopamine. (a) H.p.l.c. chromatogram of cold standards of 50 pmol of dihydroxyphenylacetic acid (DOPAC), 100 pmol noradrenaline (NA) and 100 pmol dopamine. (b) Separation of tritiated DOPAC, NA and dopamine released in basal conditions by h.p.l.c. The tritiated samples were supplemented with cold standards of DOPAC, NA and dopamine, and the 2 min samples correspondent to each standard were collected and the radioactivity counted. (c) Tritiated NA and dopamine released by stimulation of synaptosomes with 100 μM L-glutamate (A), 100 μM AMPA (B), 5 mM KCl (C) or 30 mM KCl (D). Only NA and dopamine release was evoked by the stimulation of the synaptosomes, whereas the release of DOPAC was the same before or after the stimulation. The results are the mean value ± s.e.mean of 4 to 8 experiments performed in duplicate. For abbreviations in this and subsequent figure legends, please see text.

We also observed that agonists of the ionotropic glutamate receptors induced the release of ^{3}H-catecholamines (Figures 2 and 3). Thus, the extent of tritium release by 100 μM AMPA was 1.93 ± 0.17% ($n = 9$) ($EC_{50} = 10.9$ μM and maximum ^{3}H-catecholamines release = 2.09%), and by 100 μM kainate was 2.09 ± 0.22% ($n = 6$) ($EC_{50} = 4.9$ μM and maximum ^{3}H-catecholamines release = 2.22%) (Figures 2b and 3b). Quisqualate (50 μM) released 1.57 ± 0.26% ($n = 5$) of the total ^{3}H accumulated. We also observed that NMDA, in the presence of 5 μM glycine and in the absence of added Mg^{2+}, was effective in releasing ^{3}H-catecholamines. Thus, NMDA (200 μM) released 3.65 ± 0.23% ($n = 13$) of the total ^{3}H-catecholamines (Figure 3).

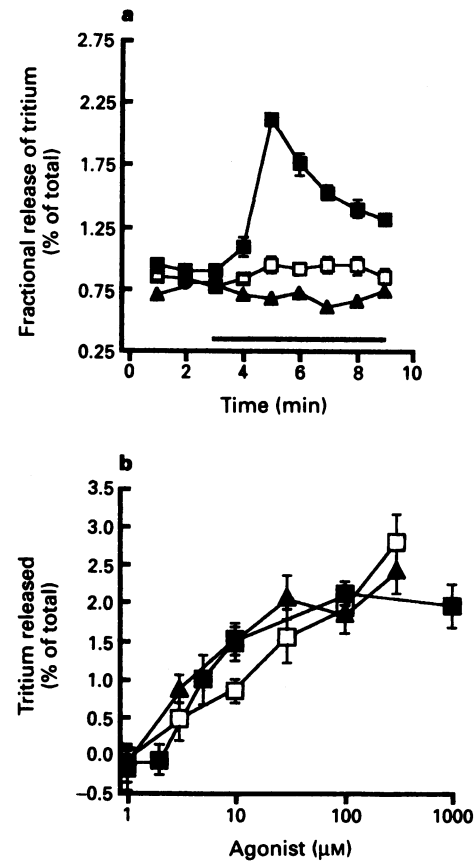


Figure 2 Effect of L-glutamate (Glu) on the release of ^{3}H-catecholamines in rat hippocampal synaptosomes. (a) Fractional release induced by Ca^{2+} (1 mM) alone (□), by 100 μM L-glutamate in medium without Ca^{2+} (▲), or by 10 μM L-glutamate (■) in the presence of 1 mM Ca^{2+}. The results are the mean value ± s.e.mean of 4 to 9 experiments performed in duplicate. (b) Dose-response curves for the release of ^{3}H-catecholamines induced by L-glutamate (■), AMPA (□) or kainate (▲). The curves were determined by the mean value ± s.e.mean of 4 to 5 independent experiments performed in duplicate.

Glutamate-induced release of ^{3}H-catecholamines is due to receptor activation

It has been described in various cell models that L-glutamate increases the $[Ca^{2+}]_i$ in part due to glutamate transport, which can cause membrane depolarization, and activate VSCCs (Heinonen *et al.*, 1989; McMahon *et al.*, 1989). Therefore, we investigated whether the observed Ca^{2+}-dependent release of ^{3}H-catecholamines induced by L-glutamate was mediated through the L-glutamate transport or by activation of presynaptic glutamate receptors.

We observed that the increase of the hippocampal synaptosomal $[Ca^{2+}]_i$ due to 100 μM L-glutamate was not inhibited by 10 μM CNQX or 1 μM MK-801 (Figure 4a). However, the 100 μM AMPA-induced increase in the $[Ca^{2+}]_i$ was strongly inhibited by 10 μM CNQX (58.6% inhibition) ($P < 0.05$) (Figure 4b). Interestingly, when we studied the effects of L-glutamate or AMPA on the release of ^{3}H-catecholamines, we observed that the release induced by L-glutamate or by AMPA was inhibited by CNQX (Figure 5a and b), but, in the presence of 1 μM MK-801, the observed release of [^{3}H]-catecholamines induced by 100 μM L-glutamate was not significantly different from the control ($P > 0.05$), indicating that the release evoked under these conditions did not involve the activation of NMDA receptors. However, in the presence of 10 μM CNQX, the release induced by 100 μM L-glutamate was reduced by 83.8% (Figure 5a), indicating

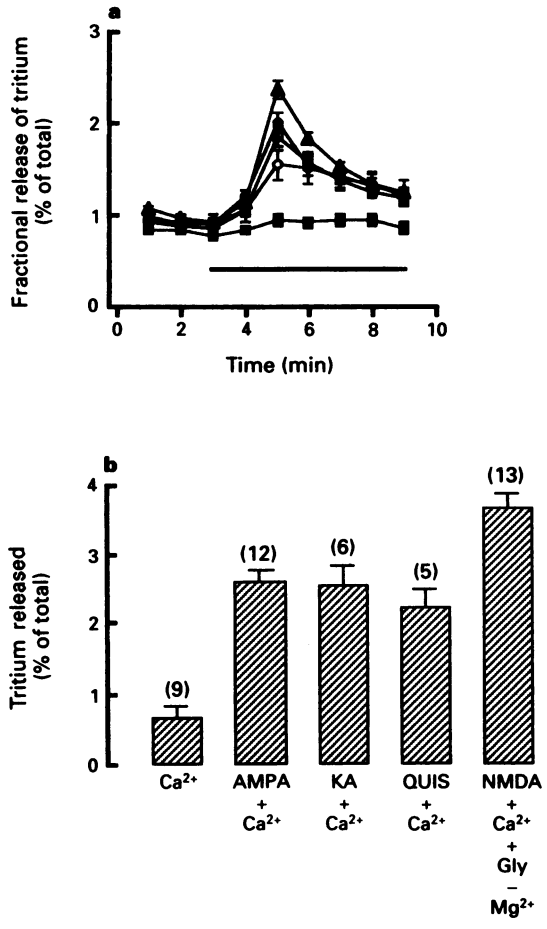


Figure 3 ^{3}H-catecholamine release induced by L-glutamate receptor agonists. (a) Fractional release induced by Ca^{2+} (1 mM) alone (■) or by 100 μM AMPA (□), 100 μM kainate (●), 50 μM quisqualate (○), in the presence of 1 mM Ca^{2+}; or 200 μM NMDA in the absence of Mg^{2+} and in the presence of 1 mM Ca^{2+} (▲). (b) ^{3}H-catecholamines released by L-glutamate receptor agonists (applied from min 3 to 9) as a percentage of the total tritium accumulated. The results are the mean value ± s.e.mean of 5 to 13 experiments performed in duplicate.

activation of ionotropic non-NMDA glutamate receptors coupled to [^{3}H]-dopamine and [^{3}H]-NA release. Further evidence that presynaptic non-NMDA glutamate receptors activation release ^{3}H-catecholamines was obtained in a study in which we observed that a specific non-NMDA glutamate receptor agonist (AMPA) induced the release of ^{3}H-catecholamines and that this release was significantly inhibited ($P<0.05$) by 10 μM CNQX (61.2% inhibition) (Figure 5b).

As reported above, we did not observe any inhibition of the 100 μM L-glutamate induced [^{3}H]-dopamine or [^{3}H]-NA release by 1 μM MK-801 (Figure 5a). However, we observed that 200 μM NMDA in the presence of 5 μM glycine, and in the absence of added Mg^{2+}, induced the release of 3.65 ± 0.23% ($n = 13$) of the total tritiated neurotransmitter accumulated (Figures 3 and 5c). The release of ^{3}H-catecholamines induced by NMDA was inhibited by 81.2% by 1 μM MK-801 (Figure 5c).

AMPA induced release of ^{3}H-catecholamines is mediated by N- and P-type VSCCs

The ionotropic glutamate receptors activated by AMPA allow the influx of cations, inducing membrane depolarization (Ruzicka & Jhamandas, 1993) which may activate VSCCs, allowing the influx of Ca^{2+} which may trigger the release of several neurotransmitters. In this work we observed that the L-type VSCCs blocker nitrendipine (Tsien *et al.*, 1988; 1991) did not inhibit the release of [^{3}H]-dopamine or [^{3}H]-NA, but the N-type calcium channel blocker, ω-CgTx (Kerr & Yoshikami, 1984; Reynolds *et al.*, 1986) inhibited the release of [^{3}H]-catecholamines to 49.03 ± 3.79% of the control whereas, the ω-Aga IVA, a blocker of the P-type VSCCs (Mintz *et al.*, 1992a,b) reduced the release of ^{3}H-catecholamines to 46.06 ± 10.51% the control. When both blockers were perfused simultaneously, the release of ^{3}H-catecholamines was inhibited to 12.76 ± 4.64% ($n = 4$) of the control. The release observed in the presence of ω-CgTx, in the presence of ω-Aga IVA or with both toxins were significantly different from the release observed in the absence of VSCC blockers ($P<0.05$) (Figure 6).

These results suggest that most of the Ca^{2+}-dependent release of [^{3}H]-dopamine and [^{3}H]-NA, due to activation of

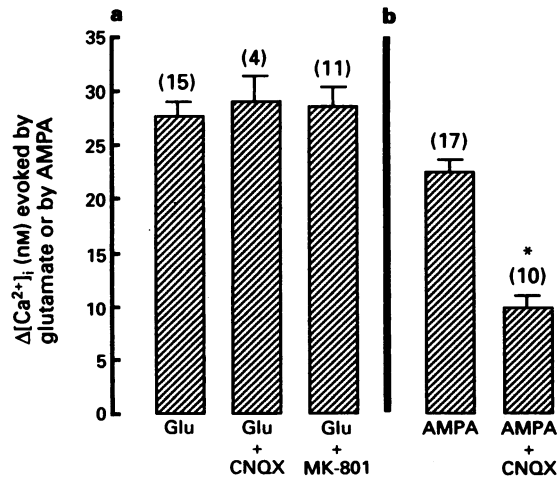


Figure 4 Increases in the $[Ca^{2+}]_i$ concentration in hippocampal synaptosomes induced by 100 μM L-glutamate or 100 μM AMPA. (a) Increase in the $[Ca^{2+}]_i$ induced by L-glutamate (Glu) is not sensitive to either 10 μM CNQX or 1 μM MK-801. (b) AMPA-induced increase in the $[Ca^{2+}]_i$ is sensitive to 10 μM CNQX. The results are the mean ± s.e.mean of 4 to 17 experiments. Significantly lower than control: $^*P<0.05$.

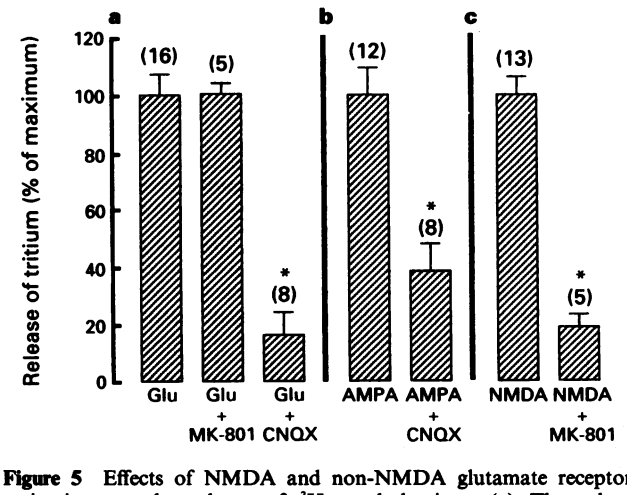


Figure 5 Effects of NMDA and non-NMDA glutamate receptors activation on the release of ^{3}H-catecholamines. (a) The release induced by 100 μM L-glutamate is inhibited by 10 μM CNQX and is not sensitive to the NMDA receptor antagonist MK-801 (1 μM). (b) The release of ^{3}H-catecholamines evoked by 100 μM AMPA is inhibited by 10 μM CNQX. (c) The release induced by 200 μM NMDA, in medium without Mg^{2+} and in the presence of 1 mM Ca^{2+} and 5 μM glycine, is inhibited by 1 μM MK-801. The results are the mean value ± s.e.mean of 5 to 16 experiments performed in duplicate. Significantly lower than control: $^*P<0.05$.

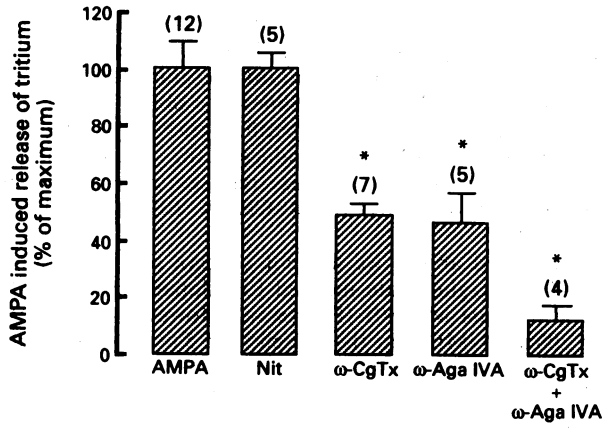


Figure 6 Characterization of VSCCs which couple the activation of the AMPA receptors with the release of ^{3}H-catecholamines. Addition of 100 μM AMPA in the absence or in the presence of nitrendipine (1 μM), ω-CgTx (0.5 μM), ω-Aga IVA (100 nM), or both ω-CgTx (0.5 μM) and ω-Aga IVA (100 nM). The results are the mean value ± s.e.mean of 4 to 12 experiments performed in duplicate. Significantly lower than control, $*P<0.05$.

presynaptic receptors with AMPA, is a consequence of activation of VSCCs due to membrane depolarization induced by activation of the AMPA receptors (Figures 5 and 6).

Discussion

Dopaminergic and noradrenergic terminals are present in the hippocampus (Wyss *et al.*, 1979; Lopes da Silva *et al.*, 1990). It was shown previously that synaptosomes isolated from rat hippocampus are endowed with endogenous dopamine and NA, and that they release catacholamines in response to depolarization (Verhage *et al.*, 1992). However, in spite of the presence of dopamine in the hippocampus, the physiological role of this neurotransmitter in this area of the brain is still unclear (Lopes da Silva *et al.*, 1990).

We have determined the endogenous content of NA and dopamine in the crude synaptosomal fraction of the hippocampus used in this work. The NA content of these synaptosomes is about four fold higher than the dopamine content (Table 1), in agreement with previous observations showing much higher levels of NA than of dopamine in purified hippocampus synaptosomes (Verhage *et al.*, 1992). However, we find a dopamine content about 3.5 fold higher than that reported (Verhage *et al.*, 1992). We also found that the NA content was about 18.3 fold lower than the levels described earlier (Verhage *et al.*, 1992). These differences are probably due to different isolation methods used for preparing the synaptosomes. Apparently, we used a crude synaptosomal fraction which is much richer in dopamine and poorer in NA than the purified synaptosomes used by Verhage *et al.* (1992).

We used h.p.l.c.-e.d. to analyze the nature of the ^{3}H-catecholamines released by hippocampal synaptosomes previously loaded with [^{3}H]-dopamine. In the hippocampus the catecholamine nerve terminals are less than 1% of the total nerve terminals (Lopes da Silva *et al.*, 1990), and the endogenous content of either NA or dopamine is too low to allow the study of endogenous catecholamines release stimulated by presynaptic glutamate receptors. Thus, we decided to use [^{3}H]-dopamine loaded synaptosomes since the high sensitivity of the tritium detection allowed us to detect very small amounts of neurotransmitters released.

Monoamine oxidase can transform dopamine in DOPAC, in an enzymatic reaction inhibited by nialamide. We observed in our preparation that after loading the synaptosomes with exogenous dopamine, the synaptosomal content of DOPAC increased (Table 1). We concluded that, in spite of the presence of nialamide throughout the experiment, some dopamine was metabolized to DOPAC. In this work, we also observed that DOPAC is released in basal conditions and that the increase in ^{3}H-catecholamines release observed after synaptosomal stimulation was mainly due to the release of dopamine and, to a smaller extent, to release of NA (Figure 1). After loading the synaptosomes with dopamine, we observed that the NA content of hippocampal synaptosomes did not increase (Table 1). However, we observed that after stimulation of the synaptosomes some [^{3}H]-NA was released, indicating that in hippocampal synaptosomes some [^{3}H]-dopamine can be transported into noradrenergic terminals and then be converted in [^{3}H]-NA (Figure 1).

The increase in [^{3}H]-NA release observed after [^{3}H]-dopamine loading and the finding that NA content of the synaptosomes did not increase after loading with dopamine may be explained by the rapid turnover of NA, which allows the conversion of [^{3}H]-dopamine in [^{3}H]-NA without affecting total NA levels. During the loading of hippocampal synaptosomes with [^{3}H]-dopamine the neurotransmitter can be transported into both dopaminergic and noradrenergic nerve terminals. In the dopaminergic nerve terminals this catecholamine is stored in dopaminergic synaptic vesicles (Henry & Scherman, 1989; Moriyama *et al.*, 1993), whereas in noradrenergic terminals the [^{3}H]-dopamine is transported into the nerve terminal and is accumulated in the noradrenergic synaptic vesicles where it is transformed to [^{3}H]-NA. In other brain regions with high ratios NA/dopamine, experimental evidence suggested that dopamine can also be accumulated into noradrenergic terminals and converted into NA (Kelly *et al.*, 1985; Carboni *et al.*, 1990).

We observed that the majority of the ^{3}H-catecholamines released after stimulation of the synaptosomes with 30 mM KCl (71.4 ± 3.2%), 5 M KCl (69.5 ± 4.2%), 100 μM L-glutamate (68.4 ± 4.0%) or 100 μM AMPA (74.1 ± 2.7%), was in fact [^{3}H]-dopamine, but that a significant portion of the ^{3}H-catecholamines was released as [^{3}H]-NA (28.7 ± 3.2% for 30 mM KCl, 30.5 ± 3.2% for 5 mM KCl, 31.6 ± 4.0% for 100 μM L-glutamate and 26.0 ± 2.7% for 100 μM AMPA). L-Glutamate induced the release of [^{3}H]-dopamine and [^{3}H]-NA from rat hippocampal synaptosomes in a process which depends on extracellular Ca^{2+} (Figure 2). The dependence on external Ca^{2+} of the dopamine release induced by depolarization (Raiteri *et al.*, 1978; Drapeau & Blaustein, 1983) is due to the requirement of Ca^{2+} for exocytosis, since this neurotransmitter is stored in synaptic vesicles within the synaptic terminal (Henry & Scherman, 1989; Moriyama *et al.*, 1993).

The release of ^{3}H-catecholamines induced by 100 μM L-glutamate in the presence of 1 mM Ca^{2+} and 1 mM Mg^{2+} was reduced by 83.8% by 10 μM CNQX, but it was insensitive to 1 μM MK-801 (Figure 5). The insensitivity of the L-glutamate induced [^{3}H]-dopamine and [^{3}H]-NA release to the NMDA receptor inhibitor, MK-801, probably reflects the blocking of the NMDA receptor channel by Mg^{2+} (Nowak *et al.*, 1984; Zorumski & Thio, 1992), and the depolarization which occurs after the non-NMDA receptors activation probably was not sufficient to remove the Mg^{2+} from the NMDA receptor channel. Another possibility is the localization of the NMDA and non-NMDA receptors in different synaptosomes, which could explain the finding that the activation of the non-NMDA receptors was not sufficient to release the NMDA channel from the blockade due to Mg^{2+}.

The 100 μM L-glutamate induced change in $[Ca^{2+}]_i$, which reflects the influx of Ca^{2+} following stimulation of synaptosomes, was insensitive to 10 μM CNQX or 1 μM MK-801 (Figure 4). The insensitivity of the L-glutamate induced increase in the $[Ca^{2+}]_i$ to the non-NMDA glutamate receptor antagonist, CNQX (Honoré *et al.*, 1988; Zorumski & Thio, 1992; Figure 4a), or to the NMDA glutamate receptor antagonist, MK-801 (Zorumski & Thio, 1992; Figure 4a) is compatible with the idea that L-glutamate transport through its carrier may lead to Ca^{2+} influx due to depolarization which activates VSCCs. These results are in agreement with pre-

vious observations that D-aspartate increases the $[Ca^{2+}]_i$ in synaptosomes from the guinea-pig cerebral cortices (McMahon *et al.*, 1989). However, the release of ^{3}H-catecholamines induced by glutamate does not appear to be mediated by a carrier-dependent process, since it is sensitive to CNQX. This observation indicates that presynaptic non-NMDA glutamate receptors mediate the release of ^{3}H-catecholamines in this preparation. We also observed that both NMDA and non-NMDA glutamate receptor agonists induced the release of ^{3}H-catecholamines (Figure 3). The release induced by 100 μM AMPA was sensitive to 10 μM CNQX and the release induced by 200 μM NMDA was inhibited by 1 μM MK-801 (Figure 5). These results are consistent with both presynaptic non-NMDA and NMDA receptor activation mediating the Ca^{2+}-dependent ^{3}H-catecholamine release.

Interestingly, NMDA (200 μM) is the glutamate receptor agonist which induces the highest release of ^{3}H-catecholamines (Figure 3). This result apparently is contradictory to the observation that NMDA is the least effective glutamate receptor agonist in elevating the $[Ca^{2+}]_i$ (not shown). Probably, the local Ca^{2+} concentrations attained in the active zones (Smith & Augustine, 1988) after the NMDA receptors activation are sufficient to induce ^{3}H-catecholamine release, without changing the bulk Ca^{2+} concentrations to any great extent. Another possible explanation is that only a subpopulation of synaptosomes respond to NMDA stimulation, inducing a large efflux of ^{3}H-catecholamines, without causing large average changes in the $[Ca^{2+}]_i$ of all the synaptosomes.

Glutamate receptors modulate the release of several neurotransmitters and neuromodulators (Ruzicka & Jhamandas, 1993). The ionotropic NMDA receptor stimulation was reported to induce the release of NA from rat hyppothalamus slices, but had no effect on the release of dopamine in this preparation (Blandina *et al.*, 1992). The presence of presynaptic NMDA receptors able to induce the release of NA was also demonstrated in synaptosomes isolated from rat cerebral cortex (Fink *et al.*, 1990). In the hippocampus, the presence of presynaptic glutamate receptors which modulate the release of NA was shown for both NMDA receptors (Pittaluga & Raiteri, 1990; Wang *et al.*, 1992) and non-NMDA receptors (Pittaluga & Raiteri, 1992; Wang *et al.*, 1992). Glutamate receptors also modulate the release of dopamine in rat mesencephalic cells in culture by both NMDA and non-NMDA subtypes (Mount *et al.*, 1990). Presynaptic glutamate receptors activated by kainate (Desce *et al.*, 1991; Wang, 1991), by AMPA (Desce *et al.*, 1991; Wang *et al.*, 1991; Desce *et al.*, 1992) or by NMDA (Krebs *et al.*, 1991; Wang, 1991; Desce *et al.*, 1992) also modulate the release of dopamine from synaptosomes isolated from the rat striatum.

The present work specifically addressed the mechanisms involved in the coupling between presynaptic glutamate receptor activation and catecholamine release. We showed that after stimulating hippocampal synaptosomes with glutamate or AMPA, an increase in the $[Ca^{2+}]_i$ was observed (Figure 4), due to presynaptic glutamate receptors stimulation. We further characterized the involvement of VSCCs in the Ca^{2+} influx coupled to dopamine and NA release. Thus, we observed that, nitrendipine, which blocks the L-type VSCCs (Tsien *et al.*, 1988; 1991) did not affect the AMPA induced catecholamines release (Figure 6), indicating that L-type calcium channels do not mediate the influx of Ca^{2+} following AMPA receptor activation. It was previously observed that 1 μM nitrendipine does not inhibit significantly the release of dopamine from cultured foetal rat ventral mesencephalon evoked by glutamate receptor agonists (Chadieu *et al.*, 1992), also indicating that the L-type VSCCs are not activated following glutamate receptor activation. However, it was observed in the same work that the activation of the L-type calcium channels by Bay K 8644 induces the release of [^{3}H]-dopamine and that this activation could be blocked by nitrendipine (Chadieu *et al.*, 1992).

The N-type calcium channels blocker, ω-CgTx (Kerr & Yoshikami, 1984; Reynolds *et al.*, 1986), strongly inhibited the 100 μM AMPA induced release of ^{3}H-catecholamines (Figure 6), and the same extent of inhibition by ω-CgTx was also observed on the elevation of the $[Ca^{2+}]_i$ induced by AMPA (not shown), indicating that the N-type VSCCs are important in mediating the effects between AMPA receptor activation and neurotransmitter release. It was shown previously that ω-CgTx inhibits the release of noradrenaline and 5-hydroxytryptamine, as well as the Ca^{2+} influx, in synaptosomes isolated from rat hippocampus or striatum (Reynolds *et al.*, 1986). Furthermore, the ability of ω-CgTx in inhibiting the KCl evoked release of NA and dopamine as well as the influx of Ca^{2+}, was shown to depend on stimulus intensity (Keith *et al.*, 1993; Turner *et al.*, 1993).

A dihydropyridine and ω-CgTx insensitive class of VSCCs, which is inhibited by FTX (Llinás *et al.*, 1989) and by ω-Aga IVA (Mintz *et al.*, 1992a,b) the P-type calcium channels, have been shown to be particularly important in mammalian nerve terminals (Mintz *et al.*, 1992a,b; Turner *et al.*, 1992; 1993; Tareilus *et al.*, 1993). We observed in the present study that the ^{3}H-catecholamines release induced by AMPA was also strongly inhibited by ω-Aga IVA (Figure 6). This observation indicates that P-type VSCCs are important in mediating the influx of Ca^{2+} following AMPA receptor activation, which induced the release of ^{3}H-catecholamines. We observed that ω-Aga IVA also inhibited the AMPA-induced increase in the $[Ca^{2+}]_i$ as well as the KCl induced increase in the $[Ca^{2+}]_i$ (not shown). When we applied ω-CgTx and ω-Aga IVA simultaneously, we observed that the inhibition of ^{3}H-catecholamine release was almost complete, supporting the idea that the influx of Ca^{2+} following AMPA receptor stimulation occurred mainly through N- and P-type VSCCs. Other authors have reported effects of ω-Aga IVA on $^{45}Ca^{2+}$ influx into synaptosomes (Mintz *et al.*, 1992b; Tareilus *et al.*, 1993). The release of glutamate by rat cortical or striatal synaptosomes is also sensitive to ω-Aga IVA (Turner *et al.*, 1992; 1993), also indicating the presence of P-type VSCCs in glutamatergic terminals. The release of dopamine in rat striatal synaptosomes induced by depolarization with KCl or 4-aminopyridine is inhibited by blockers of the P-type VSCCs (Turner *et al.*, 1993). A synergistic inhibition of KCl evoked [^{3}H]-dopamine release was observed by combining the effects of ω-Aga IVA and ω-CgTx, suggesting the coexistence of P- and N-type calcium channels in dopaminergic terminals of the striatum (Turner *et al.*, 1993).

In summary, we showed here that presynaptic glutamate receptors modulate the release of [^{3}H]-dopamine and [^{3}H]-NA in rat hippocampal synaptosomes, since glutamate receptors agonists were effective in releasing these catecholamines in a Ca^{2+}-dependent manner. The AMPA induced release of ^{3}H-catecholamines is mediated by VSCC activation of the N- and P-type, which allows the influx of Ca^{2+} and therefore the exocytosis of synaptic vesicles. These observations are in agreement with the current idea that the function of the N-type calcium channels can be closely related to the release of catecholamines (Reynolds *et al.*, 1986; Tsien *et al.*, 1988), and with the coexistence of both N- and P-type VSCCs in dopaminergic terminals (Turner *et al.*, 1993).

This work was supported by J.N.I.C.T.-Portugal. We thank E. Duarte and T. Morgadinho for important suggestions in the h.p.l.c. measurements.

References

AUGUSTINE, G.J. (1987). Calcium action in synaptic transmitter release. *Annu. Rev. Neurosci.*, **10**, 633–693.

BLANDINA, P., JOHNSON, D., WALCOTT, J. & GOLDFARB, J. (1992). Release of endogenous norepinephrine from rat hypothalamus by stimulation of the N-methyl-D-aspartic acid receptors. *J. Pharmacol. Exp. Ther.*, **263**, 61–68.

CARBONI, E., TANDA, G.L., FRAU, R. & DI CHIARA, G. (1990). Blockade of the noradrenaline carrier increases extracellular dopamine concentration in the prefrontal cortex: evidences that dopamine is taken up in vivo by noradrenergic terminals. *J. Neurochem.*, **55**, 1067–1070.

CARVALHO, A.P. (1982). Calcium in the nerve cell, In *Handbook of Neurochemistry* (2nd Ed.) ed. Lajtha, A., pp. 69–116. New York: Plenum Press.

CHADIEU, I., ALONSO, R., MOUNT, H., QUIRION, R. & BOKSA, P. (1992). Effect of L- and N-type Ca^{2+} channel antagonists on excitatory amino acid-evoked dopamine release. *Eur. J. Pharmacol.*, **220**, 203–209.

DESCE, J.M., GODEHEU, G., GALLI, T., ARTAUD, F., CHÉRAMY, A. & GLOWINSKI, J. (1991). Presynaptic facilitation of dopamine release through D,L-α-amino-3-hydroxy-5-methyl-4-isoxazole propionate receptors on synaptosomes from the rat striatum. *J. Pharmacol. Exp. Ther.*, **259**, 692–698.

DESCE, J.M., GODEHEU, G., GALLI, T., ARTAUD, F., CHÉRAMY, A. & GLOWINSKI, J. (1992). L-Glutamate-evoked release of dopamine from synaptosomes of the rat striatum: involvement of AMPA and N-methyl-D-aspartate receptors. *Neuroscience*, **47**, 333–339.

DUARTE, C.B., CARVALHO, C.A.M., FERREIRA, I.L. & CARVALHO, A.P. (1991). Synaptosomal $[Ca^{2+}]_i$ as influenced by Na^+/Ca^{2+} exchange and K^+ depolarization. *Cell Calcium*, **12**, 623–633.

DUARTE, C.B., ROSÁRIO, L.M., SENA, C.M. & CARVALHO, A.P. (1993). A toxin fraction (FTX) from the funnel-web spider poison inhibits dihydropyridine-insensitive Ca^{2+} channels coupled to catecholamine release in bovine adrenal chromaffin cells. *J. Neurochem.*, **60**, 908–913.

DRAPEAU, P. & BLAUSTEIN, M. (1983). Initial release of [^{3}H] dopamine from striatal synaptosomes: correlation with calcium entry. *J. Neurosci.*, **3**, 703–713.

FINK, K., BÖNISCH, H. & GÖTHERT, M. (1990). Presynaptic NMDA receptors stimulate noradrenaline release in the cerebral cortex. *Eur. J. Pharmacol.*, **185**, 115–117.

GRYNKIEWICZ, G., POENIE, M. & TSIEN, R.Y. (1985). A new generation of Ca^{2+} indicators with greatly improved fluorescence properties. *J. Biol. Chem.*, **260**, 3440–3450.

HENRY, J.-P. & SCHERMAN, D. (1989). Radioligands of the vesicular monoamine transporter and their use as markers of monoamine storage vesicles. *Biochem. Pharmacol.*, **38**, 2395–2404.

HEINONEN, E., ÅKERMAN, K.E.O. & PANULA, P. (1989). Changes of the membrane potential in striatal synaptoneurosome, synaptosome and membrane sac preparations induced by glutamate, kainate and aspartate with a cyanine dye DiS-C_2-(5). *Brain Res.*, **496**, 187–196.

HONORÉ, T., DAVIES, S.N., DREJER, J., FLETCHER, E.J., JACOBSEN, P., LODGE, D. & NIELSEN, F.E. (1988). Quinoxalinediones: potent competitive non-NMDA glutamate receptor antagonists. *Science*, **241**, 701–703.

IINO, M., OZAWA, S. & TSUZUKI, K. (1990). Permeation of calcium through excitatory amino acid receptor channels in cultured rat hippocampal neurones. *J. Physiol.*, **424**, 151–165.

JOHNSON, J.W. & ASCHER, P. (1987). Glycine potentiates the NMDA responses in cultured mouse brain neurons. *Nature*, **325**, 529–531.

KEITH, R.A., HORN, M.B., PISER, T.M. & MANGANO, T.J. (1993). Effects of stimulus intensity on the inhibition by ω-conotoxin GVIA and neomycin of K^+-evoked [^{3}H] norepinephrine release from hippocampal brain slices and synaptosomal calcium influx. *Biochem. Pharmacol.*, **45**, 165–171.

KEMP, J.A. & LEESON, P.D. (1993). The glycine site of the NMDA receptor-five years on. *Trends Pharmacol. Sci.*, **14**, 20–25.

KELLY, E., JENNER, P. & MARSDEN, C.D. (1985). Evidence that [^{3}H]-dopamine is taken up and released from nondopaminergic nerve terminals in the rat substantia nigra in vitro. *J. Neurochem.*, **45**, 137–144.

KERR, L.M. & YOSHIKAMI, D. (1984). A venom peptide with novel presynaptic blocking action. *Nature*, **308**, 282–284.

KNIGHT, D.E., VON GRAFENSTEIN, H. & ATHAYDE, C.M. (1989). Calcium-dependent and calcium-independent exocytosis. *Trends Neurosci.*, **12**, 451–458.

KREBS, M.O., DESCE, J.M., KEMEL, M.L., GAUCHY, C., GODEHEU, G., CHÉRAMY, A. & GLOWINSKI, J. (1991). Glutamatergic control of dopamine release in the rat striatum: evidence for presynaptic N-methyl-D-aspartate receptors on dopaminergic nerve terminals. *J. Neurochem.*, **56**, 81–85.

LAYNE, E. (1957). Spectrophotometric and turbidimetric method for measuring proteins. In *Methods in Enzymology*. ed Colowick, S.P. & Kaplan, N.O. pp. 447–451. New York: Academic Press.

LEVINE, M. (1986). Ascorbic acid specifically enhances dopamine monooxygenase activity in resting and stimulated chromaffin cells. *J. Biol. Chem.*, **261**, 7347–7356.

LLINÁS, R., SUGIMORI, M., LIN, J.-W. & CHERKSEY, B. (1989). Blocking and isolation of a calcium channel from neurons in mammals and cephalopods utilizing a toxin fraction (FTX) from funnel-web spider poison. *Proc. Natl. Acad. Sci. U.S.A.*, **86**, 1689–1693.

LOPES DA SILVA, F.H., WITTER, M.P., BOEIJINGA, P.H. & LOHMAN, A.A. (1990). Anatomic organization and physiology of the limbic cortex. *Physiol. Rev.*, **70**, 453–511.

MACDERMOTT, A.B., MAYER, M.L., WESTBROOK, G.L., SMITH, S.J. & BARKER, J.L. (1986). NMDA-receptor activation increases cytoplasmic calcium concentration in cultured spinal cord neurones. *Nature*, **321**, 519–522.

MCMAHON, H.T., BARRIE, A.P., LOWE, M. & NICHOLLS, D.G. (1989). Glutamate release from guinea-pig synaptosomes: stimulation by reuptake-induced depolarization. *J. Neurochem.*, **53**, 71–79.

MCMAHON, T.H., FORAN, P., DOLLY, J.O., VERHAGE, M., WIEGANT, V.M. & NICHOLLS, D.G. (1992). Tetanus toxin and botulinum toxins type A and B inhibit glutamate, γ-aminobutyric acid, aspartate, and Met-enkephalin release from synaptosomes. *J. Biol. Chem.*, **267**, 21338–21343.

MALVA, J.O., CARVALHO, A.P. & CARVALHO, C.A.M. (1993). Release of [^{3}H]-dopamine from hippocampal synaptosomes due to activation of non-NMDA receptors. *J. Neurochem.*, **61** (Suppl.), S-203C.

MINTZ, I.M., ADAMS, M.E. & BEAN, B.P. (1992a). P-Type calcium channels in rat central and peripheral neurons. *Neuron*, **9**, 85–95.

MINTZ, I.M., VENEMA, V.J., SWIDEREK, K.M., LEE, T.D., BEAN, B.P. & ADAMS, M.E. (1992b). P-type calcium channels blocked by the spider toxin ω-Aga-IVA. *Nature*, **335**, 827–829.

MORIYAMA, Y., TSAI, H. & FUTAI, M. (1993). Energy-dependent accumulation of neuron blockers causes selective inhibition of neurotransmitter uptake by brain synaptic vesicles. *Arch. Biochem. Biophys.*, **305**, 278–281.

MOUNT, H., QUIRION, R., CHADIEU, I. & BOKSA, P. (1990). Stimulation of dopamine release from cultured rat mesencephalic cells by naturally occurring excitatory amino acids: involvement of both N-methyl-D-aspartate (NMDA) and non-NMDA receptors subtypes. *J. Neurochem.*, **55**, 268–275.

NICOLETTI, F., MEEK, J.L., IADAROLA, M.J., CHUANG, D.M., ROTH, B.L. & COSTA, E. (1986). Coupling of inositol phospholipid metabolism with excitatory amino acid recognition sites in rat hippocampus. *J. Neurochem.*, **46**, 40–46.

NOWAK, L., BREGESTOVSKI, P., ASCHER, P., HERBET, A. & PROCHIANTZ, A. (1984). Magnesium gates glutamate-activated channels in mouse central neurones. *Nature*, **307**, 462–465.

PITTALUGA, A. & RAITERI, M. (1990). Release-enhancing glycine-dependent presynaptic NMDA receptors exist on noradrenergic terminals of hippocampus. *Eur. J. Pharmacol.*, **191**, 231–234.

PITTALUGA, A. & RAITERI, M. (1992). N-Methyl-D-aspartic acid (NMDA) and non-NMDA receptors regulating hippocampal norepinephrine release. I. Location on axon terminals and pharmacological characterization. *J. Pharmacol. Exp. Ther.*, **260**, 232–237.

RAITERI, M., ANGELINI, F. & LEVI, G. (1974). A simple apparatus for studying the release of neurotransmitters from synaptosomes. *Eur. J. Pharmacol.*, **25**, 411–414.

RAITERI, M., CERRITO, F., CERVONI, A.M., DEL CARMINE, R., RIBERA, M.T. & LEVI, G. (1978). Studies on dopamine uptake and release in synaptosomes. In *Advances in Biochemical Psychopharmacology*, Vol. 19, ed. Roberts P.J., Woodruff, G.N. & Iversen, L.L., pp. 35–53. New York: Raven Press.

REYNOLDS, I.J., WAGNER, J.A., SNYDER, S.H., THAYER, S.A., OLIVERA, B.M. & MILLER, R.J. (1986). Brain voltage-sensitive calcium channels subtypes differentiated by ω-conotoxin fraction GVIA. *Proc. Natl. Acad. Sci. U.S.A.*, **83**, 8804–8807.

RUZICKA, B.B. & JHAMANDAS, K.H. (1993). Excitatory amino acid action on the release of brain neurotransmitters and neuromodulators: biochemical studies. *Prog. Neurobiol.*, **40**, 223–247.

SCHOEPP, D.D. & CONN, P.J. (1993). Metabotropic glutamate receptors in brain function and pathology. *Trends Pharmacol. Sci.*, **14**, 13–20.

SMITH, S.J. & AUGUSTINE, G.J. (1988). Calcium ions, active zones and synaptic transmitter release. *Trends Neurosci.*, **11**, 458–464.

SUGIYAMA, H., ITO, I. & HIRONO, C. (1987). A new type of glutamate receptor linked to inositol phospholipid metabolism. *Nature*, **325**, 531–533.

TAREILUS, E., SCHOCH, J., ADAMS, M. & BREER, H. (1993). Analysis of rapid calcium signals in synaptosomes. *Neurochem. Int.*, **23**, 331–341.

TSIEN, R.W., ELLINOR, P.T. & HORNE, W.A. (1991). Molecular diversity of voltage-dependent Ca^{2+} channels. *Trends Pharmacol. Sci.*, **12**, 349–354.

TSIEN, R.W., LIPSCOMBE, D., MADISON, D.V., BLEY, K.R. & FOX, A.P. (1988). Multiple types of neuronal calcium channels and their selective modulation. *Trends Neurosci.*, **11**, 431–438.

TURNER, T.J., ADAMS, M.E. & DUNLAP, K. (1992). Calcium channels coupled to glutamate release identified by ω-Aga-IVA. *Science*, **258**, 310–313.

TURNER, T.J., ADAMS, M.E. & DUNLAP, K. (1993). Multiple Ca^{2+} channel types coexist to regulate synaptosomal neurotransmitter release. *Proc. Natl. Acad. Sci. U.S.A.*, **90**, 9518–9522.

VERHAGE, M., GHIJSEN, W.E.J.M., BOOMSMA, F. & LOPES DA SILVA, F.H.L. (1992). Endogenous noradrenaline and dopamine in nerve terminals of the hippocampus: differences in levels and release kinetics. *J. Neurochem.*, **59**, 881–887.

WANG, J.K.T. (1991). Presynaptic glutamate receptors modulate dopamine release from striatal synaptosomes. *J. Neurochem.*, **57**, 819–822.

WANG, J.K.T., ANDREWS, H. & THUKRAL, V. (1992). Presynaptic glutamate receptors regulate noradrenaline release from isolated nerve terminals. *J. Neurochem.*, **58**, 204–211.

WYSS, J.M., SWANSON, L.W. & COWAN, W.M. (1979). A study of subcortical afferents to the hippocampal formation in the rat. *Neuroscience*, **4**, 463–476.

ZORUMSKI, C.F. & THIO, L.L. (1992). Properties of vertebrate glutamate receptors: calcium mobilization and desensitization. *Progr. Neurobiol.*, **39**, 295–336.

(Received March 11, 1994
Revised August 1, 1994
Accepted August 17, 1994)

Br. J. Pharmacol. (1994), **113**, 1448–1454 © Macmillan Press Ltd, 1994

Inhibition of nitric oxide synthesis in vascular smooth muscle by retinoids

K. Hirokawa, K.M. O'Shaughnessy, P. Ramrakha & [1]M.R. Wilkins

Department of Clinical Pharmacology, Royal Postgraduate Medical School, Du Cane Road, London W12 ONN

1 These studies examine the effect of retinoids on interleukin 1β (IL-1β)-induced nitric oxide synthase (NOS) activity in cultured rat aortic vascular smooth muscle (VSM) cells and isolated rat aortic rings.

2 All-*trans*-retinoic acid (all-*trans*-RA, 0.1–10 μM) and its active analogues produced concentration-dependent inhibition of IL-1β (0.1–10 ng ml^{-1})-induced nitrite production in cultured VSM cells. In contrast, the inactive retinoid, Ro 14-6113 (0.1–10 μM), had no effect on IL-1β-induced nitrite production.

3 Since some of the actions of retinoids are mediated by induction of transforming growth factor beta (TGF-β), its effect on inducible NOS activity in VSM cells was examined. TGF-β produced concentration-dependent (0.1–10 ng ml^{-1}) inhibition of IL-1β-induced nitrite production and the maximum effect (approximately 90% inhibition) was significantly greater than that seen with all-*trans*-RA (approximately 70% with 10 μM). However, an anti-TGF-β antibody (50 μg ml^{-1}) which blocked the effect of exogenous TGF-β (5 ng ml^{-1}) did not significantly reverse the inhibitory action of all-*trans*-RA (10 μM).

4 In addition to inhibiting IL-1β-induced nitrite production, all-*trans*-RA (10 μM) reduced substantially inducible NOS mRNA and protein levels in IL-1β-induced VSM cells ($P<0.01$).

5 Incubation of isolated rat aortic rings with IL-1 β (10 ng ml^{-1}) caused a progressive resistance of the rings to the vasoconstrictor action of phenylephrine (10 nM to 10 μM). This effect was abolished by the addition of the nitric oxide synthase inhibitor L-N^G-monomethyl-L-arginine (L-NMMA, 1 mM). All-*trans*-RA (10 μM) also markedly and significantly reversed this IL-1β-induced vascular hyporeactivity ($P<0.01$).

6 These data show that all-*trans*-RA and other active retinoids are able to block cytokine-stimulated expression of inducible NOS in cultured VSM cells and isolated aortic rings.

Keywords: Retinoic acid; vascular smooth muscle; cytokine; nitric oxide synthase

Introduction

Nitric oxide (NO) is a potent vasodilator generated enzymatically from the guanidino nitrogen group of L-arginine by the action of nitric oxide synthase (NOS) (Moncada *et al.*, 1991). One isoform of NOS is calcium dependent, expressed constitutively in endothelium and produces picomolar amounts of NO (Rees *et al.*, 1989). A second isoform, whose synthesis is induced in endothelium and vascular smooth muscle (VSM) cells by endotoxin and some cytokines, is calcium independent and capable of generating substantially larger (nanomolar) amounts of NO (Radomski *et al.*, 1990). Stimulation of the synthesis of this inducible NOS (iNOS) isoform by endotoxin/cytokines is thought to play a key role in the hypotension of septic shock (Moncada *et al.*, 1991). The profound hypotension that often accompanies the use of cytokines in anti-tumour therapy is probably mediated by the same mechanism (Ochoa *et al.*, 1992).

Glucocorticoids have been shown to block the induction of iNOS in endothelial (Radomski *et al.*, 1990) and VSM (Hirokawa *et al.*, 1994) cells, but these agents are not clinically effective in patients with septic shock (Slotman *et al.*, 1993). Several other inhibitors of iNOS synthesis have been reported, including interleukin 10 (Cunha *et al.*, 1992), nicotinamide (Cetkovic-Cvrlje *et al.*, 1993), cyclosporin A (Muhl *et al.*, 1993), transforming growth factor β (TGF-β; Schini *et al.*, 1992), platelet-derived growth factor (PDGF; Scott-Burden *et al.*, 1992) and thrombin (Schini *et al.*, 1993). However, these compounds are generally of limited therapeutic potential.

The retinoids are a group of natural and synthetic analogues of vitamin A with potent effects on cell growth and differentiation and an important role in embryogenesis (Roberts & Sporn, 1984). In addition, they have been shown to exhibit both anti-inflammatory and immunomodulatory actions (Orfanos & Bauer, 1983), and it is relevant that retinoids can modify cytokine-induced responses (Ishii *et al.*, 1992). Recently, Mehta *et al.* (1994) have reported that all-*trans*-retinoic acid (all-*trans*-RA) blocks the release of tumour necrosis factor (TNF) from peritoneal macrophages stimulated with endotoxin and interferon-γ. Interestingly, they also noted an inhibitory effect on NO production in these cells. We have studied the effect of retinoids on cytokine induction of iNOS in VSM and found that all-*trans*-RA and a number of its analogues are inhibitors of iNOS expression in this tissue.

[1] Author for correspondence.

Methods

Isolation and primary culture of rat VSM cells

VSM cells were harvested from enzymatically dissociated rat thoracic aorta (male Wistar rats 300–350 g, in-house colony) according to the method of Beasley *et al.* (1991) with some minor modifications (Hirokawa *et al.*, 1994). The cells were suspended in Dulbecco's modified Eagle medium (DMEM) containing 20% fetal calf serum (FCS), L-glutamine 2 mM, penicillin 500 U ml^{-1}, streptomycin 0.5 mg ml^{-1} and amphotericin B 2.5 μg ml^{-1} and seeded into 25 cm^2 flasks. After reaching confluence, cells were passaged by harvesting with trypsin–EDTA, seeded at a ratio of 1:5 into 96-well plates and grown in DMEM supplemented with 10% FCS, L-glutamine 2 mM and antibiotics. The cells were characterized as smooth muscle cells by morphology and immunostaining with a monoclonal antibody to smooth muscle α-actin.

All studies were carried out on VSM cells obtained between the fourth and 20th passage. Cells were stimulated by incubation with interleukin 1β (IL-1β) at different concentrations for varying periods of time up to 24 h. In an earlier study we observed that IL-1β-stimulated nitrite production was reduced in the presence of FCS, which is known to stimulate mitosis (Hirokawa *et al.*, 1994). In order to maximize the nitrite signal and to study quiescent cells, all subsequent experiments were conducted in the absence of FCS. Thus, 24 h prior to study, the medium (100 μl per well) was changed to DMEM without phenol red containing 0.1% bovine serum albumin (BSA) (fatty acid free and low endotoxin) in place of FCS.

Measurement of NO production

NOS activity was assessed by measurement of nitrite production according to the method of Zembowicz & Vane (1992) (Griess reaction) with minor modifications. Supernatants (100 μl) were mixed with 100 μl of the Griess reagent (1% sulphanilamide in 5% H_3PO_4 and 0.1% naphthyl-ethylenediamine dihydrochloride in a ratio of 1:1). After a 10 min incubation at room temperature, the absorbance was read at 540 nm using a Titertek Multiscan Plus MKII 96-well plate spectrophotometer. Standard curves were determined using known concentrations of $NaNO_2$. Nitrite levels reflect NOS activity in this system since no other potential source of this ion exists (all media and solutions testing as blank), and NO in aqueous solution containing oxygen is oxidized primarily to nitrite with little or no formation of nitrate (Ignarro *et al.*, 1993).

This assay was used to examine the effect of a variety of agents on NOS activity. Unless indicated all experiments were carried out using IL-1β 10 ng ml^{-1}. Appropriate controls were included in each 96-well plate to overcome variation produced by differences in cell density since VSM cells continue to grow after confluency. All wells in each experiment were judged microscopically to be of similar confluence.

Western blot analysis of iNOS

VSM cells were cultured in 75 cm^2 culture flask with phenol red-free DMEM containing antibiotics, L-glutamine 2 mM and 0.1% BSA for 24 h, and then stimulated with IL-1β 10 ng ml^{-1} in the presence or absence of retinoids or TGF-β for 24 h. At the end of the experiments, culture supernatant was aliquoted and stored for the measurement of nitrite and the cells released using 2 ml of trypsin–EDTA. The cells were washed in phosphate-buffered saline (PBS) (NaCl 8 g l^{-1}, Na_2HPO4 1.15 g l^{-1}; KCl 0.2 g l^{-1}; KH_2PO_4 0.2 g l^{-1}), resuspended in 300 μl lysis buffer (50 mM Tris–HCl, pH 7.4) containing pepstatin A 5 μg ml^{-1}, chymostatin 1 μg ml^{-1}, aprotinin 5 μg ml^{-1}, leupeptin 1 μg ml^{-1}, dithiothreitol 1 mM and phenylmethylsulphonyl fluoride 100 μM, then lysed by freeze and thaw. The lysate was centrifuged at 16,000 *g* for 10 min and the supernatant stored at −70°C until blotted. The protein content of these supernatants were measured with the BCA protein assay reagent (Pierce, IL, USA).

VSM cell protein (12.5–400 μg) was electrophoresed on 7.5% SDS–PAGE, using prestained molecular weight markers as previously described (Hirokawa *et al.*, 1994). Proteins were electroblotted in 20% methanol, Tris 25 mM, glycine 192 mM (pH 8.3) onto nitrocellulose membranes (ECL-Hyperbond, Amersham International, Amersham, U.K.). The membranes were blocked with 4% low-fat milk (Marvel Original, Premier Brands, U.K.) in PBS for 2 h, washed three times in PBS containing 0.05% BSA and 0.05% Tween-20, then incubated with rabbit anti-rat iNOS antiserum (diluted 1:5000 in PBS, 0.1% BSA) (Riveros-Moreno *et al.*, 1993) for 2 h, washed and finally incubated with a 1:20,000 dilution of goat anti-rabbit IgG conjugated to horseradish peroxidase (ICN Flow, Oxford, U.K.) for 2 h. The immunocomplexes were visualized using an enhanced horseradish peroxidase/luminol chemiluminescence reaction (ECL Western blotting detection reagents, Amersham International) and Hyperfilm (Amersham International, Amersham, U.K.).

Extraction of total RNA from VSM cells and analysis of iNOS mRNA by reverse transcription–polymerase chain reaction (RT–PCR)

The RT–PCR method employed has been validated and described in full in previous publications (Brown *et al.*, 1993; Hirokawa *et al.*, 1994). Briefly, total RNA was extracted from VSM cells cultured in 96-well plates using a modified guanidium isothiocyanate method (Chomczynski & Sacchi, 1987). After ethanol precipitation the RNA was resuspended in 20 μl of nuclease-free water. The amount of mRNA in each RNA sample was quantified by dot-blot hybridization (of 2 μl aliquots) using an oligo-dT 30-mer probe 5'-labelled with [γ^{32}P]-dATP. Aliquots of 4 μl of total RNA were mixed with 25 pmol of a 15-mer random sequence primer, incubated for 2 h at 37°C with 10-U of Moloney murine leukaemia virus reverse transcriptase (Pharmacia, Milton Keynes, U.K.) and the final cDNA samples diluted with nuclease-free water to a volume of 100 μl and stored at 4°C. The primers used for iNOS were as follows: iNOS, sense 5'-CCTACCAAGGTGACCTGAAAG and antisense 5'-TAATGAATTCAATGGCTTGA (Nunokawa *et al.*, 1993). PCR was performed using 2.5 μl of the diluted cDNA sample in a total reaction volume of 25 μl with 1 μM iNOS primers, 1 unit of Taq DNA polymerase (Promega Corporation, Madison, WI, U.S.A.) and 0.25 μCi of [α-^{32}P]-dCTP (>5000 Ci mmol^{-1}; Amersham International). Preliminary experiments were performed to ensure that the PCR was terminated during the exponential phase of amplification (data not shown). The cycling conditions comprised 93°C for 30 s, 60°C for 30 s and 73°C for 1 min. A 15 μl aliquot of each PCR reaction was separated by electrophoresis through a 6% polyacrylamide gel. The gels were exposed to Kodak-X-Omat XAR5 autoradiography film to locate the specific product bands on the gel. These bands were then excised and the amount of incorporated ^{32}P quantified by liquid scintillation counting. The specificity of the iNOS band was verified by DNA sequencing using the dideoxy chain-termination method (Sanger *et al.*, 1977). The relative amounts of template cDNA at the start of the PCR were assessed by measuring the quantity of PCR product during the exponential phase of amplification. For each sample, the counts (in c.p.m.) incorporated into iNOS cDNA were divided by the counts in the oligo-dT dot blot to correct for variation in mRNA extraction.

Studies of iNOS induction in aortic rings

Thoracic arteries were excised from male Wistar rats (300–350 g, in-house colony) and placed in ice-cold Krebs–Henseleit buffer (pH 7.4) containing (mM) $NaHCO_3$ 25, glucose 11, NaCl 118, KCl 4.5, $NaH_2PO_4$1.2, $MgSO_4.7H_2O$ 1.2 and $CaCl_2$1.25) and cleaned of adherent tissue (Parsaee *et al.*, 1992). The arteries were cut into 4 mm rings and de-endothelialized by gentle rotation of the ring around a closed pair of forceps. The rings were transferred to a 96-well plate and covered with 0.2 ml of DMEM containing: L-glutamine 2 mM, penicillin 500 U ml^{-1}, streptomycin 0.5 mg ml^{-1}, 0.1% BSA and, where appropriate, IL-1β and/or all-*trans*-RA at final concentrations of 10 ng ml^{-1} and 10 μM respectively. The plates were incubated for 2 h at 37°C in 95% air and 5% CO_2. After incubation, the rings were suspended in 20 ml organ chambers filled with Krebs–Henseleit buffer (gassed with 95% O_2, 5% CO_2, pH 7.4, at 37°C) by means of two stainless-steel stirrups. The lower stirrup was fixed to the bottom of the chamber and the upper one was connected to a force transducer (Harvard Bioscience, Kent, U.K.) inter-

faced to a MacLab (AD Instruments, Castle Hill, Australia) to record changes in isometric tension. The rings were allowed to relax for 1 h and stretched to a resting tension of 1.5 g. After equilibration, the rings were contracted with phenylephrine (1 μM) several times until steady contraction was observed, and the lack of relaxation with acetylcholine (1 μM) confirmed the absence of endothelium. Contractility of the rings were assessed by tension generated in grams to cumulative concentrations of phenylephrine (10 nM to 10 μM). All experiments were performed in the presence of indomethacin (10 μM).

Materials

Recombinant human IL-1β, recombinant human TGF-β_1 and chicken anti-human TGF-β antibody were obtained from R&D Systems Europe Ltd (Oxford, U.K.) and L-NMMA from Calbiochem (Nottingham, U.K.). 9-*cis*-retinoic acid and RO 14-6113 were generous gifts from Dr Klaus, Hofmann-La Roche (Basle, Switzerland) and all other retinoids were from Sigma (Poole, U.K.). All culture media, antibiotics, antifungal agents and trypsin–EDTA were obtained from ICN Flow (Oxford, U.K.). Plastics for culture were purchased from Falcon (Oxford, U.K.). Fetal calf serum was from Imperial laboratories (West Portway, U.K.). Unless stated otherwise reagents for RT–PCR were from Sigma (Poole, U.K.).

Statistics

Where appropriate, data were analysed by ANOVA (Complete Statistical System, StatSoft software) and statistical significance assessed by unpaired two-tailed Student's *t*-test or variance analysis. Differences were considered statistically significant for $P<0.05$.

Results

Effect of retinoids on iNOS activity in cultured VSM cells

Exposure of cultured VSM cells to IL-1β increases nitrite concentration in the supernatant in both a concentration- and time-dependent manner (Hirokawa *et al.*, 1994). In these studies, mean (±s.e.mean) nitrite concentration in media from unstimulated VSM cells was 2.96 ± 0.40 μM ($n=17$ plates) and from cells cultured for 24 h with IL-1β (10 ng ml^{-1}) 24.6 ± 2.28 μM ($n=17$ plates; $P<0.001$). The IL-1β-induced increase in nitrite formation has been well characterized previously and is inhibited by cyclohexmide and L-NMMA (Hirokawa *et al.*, 1994). The variation between plates was largely due to differences in the density of plated cells; each 96-well plate contained controls appropriate to the treatment examined.

VSM cells were exposed to the following agents during incubation with IL-1β (10 ng ml^{-1} for 24 h: all-*trans*-RA (0.1–10 μM), 13-*cis*-RA (0.1–10 μM), 9-*cis*-RA (0.1–10 μM), all-*trans*-retinal (0.1–10 μM), all-*trans*-retinol (vitamin A, 0.1–10 μM), Ro 14-6113 (an inactive analogue of retinoic acid; 0.1–10 μM) or TGF-β (0.1–10 ng ml^{-1}). All five active retinoids and TGF-β exhibited concentration-dependent inhibition of IL-1β-induced elevation of nitrite levels (Figure 1 and Table 1). Maximum reduction in IL-1β-induced nitrite accumulation by the retinoids (approximately 60–70%) was observed at a concentration of 10 μM; it is noteworthy that TGF-β (10 ng ml^{-1}) produced significantly greater inhibition (approximately 90%) than the maximum effect of the retinoids (Table 1). The inactive analogue, Ro 14-6113, had no effect on IL-1β-induced nitrite production (data not shown).

To investigate the role of TGF-β in mediating the actions of retinoids, we examined the effect of an anti-TGF-β antibody (affinity-purified chicken anti-human TGF-β immunoglobulin; BDA 19, R&D Systems) on the inhibitory action of all-*trans*-RA on IL-1β stimulated cells. At 10 μg ml^{-1} this antibody completely neutralizes the biological activity of 10 ng ml^{-1} rat or human TGF-β assayed by inhibition of proliferation of VSM cells in 10% fetal calf serum (Kirschenlohr *et al.*, 1993; D.J. Grainger, personal communication). Control experiments were performed using

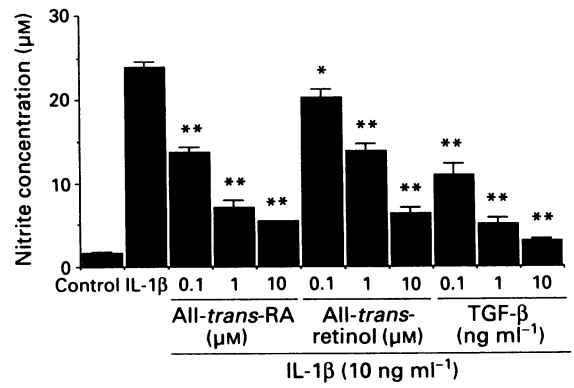


Figure 1 Retinoids and TGF-β inhibit IL-1β-induced NO production by VSM cells in a concentration-dependent manner. VSM cells were cultured with IL-1β (10 ng ml^{-1}) for 24 h in the presence or absence of retinoids or TGF-β. Control represents cells cultured with medium alone. Data are mean ± s.e.mean of four wells and are representative of three independent experiments. *$P<0.05$, **$P<0.001$ compared with control cells incubated with IL-1β alone.

Table 1 Effect of retinoids and TGF-β on IL-1β-induced changes in nitrite concentration

Agent	*Concentration*	*Nitrite concentration* (per cent of control)	n	*Agent*	*Concentration*	*Nitrite concentration* (per cent of control)	n
All-*trans* retinoic acid	0.1 μM	66 ± 3.9	9	All-*trans*-retinol	0.1 μM	90 ± 4.2	3
	1.0 μM	46 ± 4.4	10		1.0 μM	71 ± 10	3
	10	28 ± 2.3	11		10 μM	38 ± 11	3
13-*cis*-Retinoic acid	0.1 μM	72 ± 1.6	3	All-*trans*-retinol	0.1 μM	84 ± 8.9	3
	1.0 μM	52 ± 1.9	3		1.0 μM	72 ± 6.1	3
	10	31 ± 1.8	3		10 μM	43 ± 6.9	3
9-*cis*-retinoic acid	0.1 μM	59 ± 17	3	TGF-β	0.1 ng ml^{-1}	50 ± 6.1	3
	1.0 μM	34 ± 5.1	3		1.0 ng ml^{-1}	23 ± 4.8	4
	10 μM	29 ± 3.6	3		10 ng ml^{-1}	7.2 ± 1.4	6

VSM cells were cultured in 96-well plates for 24 h with IL-1β (10 ng ml^{-1}) ± different concentrations of retinoids (0.1–10 μM) or TGF-β (0.1–10 ng ml^{-1}). Nitrite levels in the supernatant from cells incubated with IL-1β + retinoids/TGF-β are expressed as percentage of levels in supernatant from cells incubated with IL-1β alone (mean ± s.e.mean; n = number of plates).

TGF-β and normal chicken immunoglobulin. In the concentrations employed (up to 50 ng ml^{-1}), anti-TGF-β antibody was able to reduce markedly the inhibitory effect of TGF-β on nitrite production (from approximately 90% to 30%) but the same concentrations had no effect on the action of all-*trans*-RA (Figure 2).

Further insight into the mechanisms underlying the inhibitory action of retinoic acid on IL-1β-induced NO production was provided by measurements of iNOS protein and mRNA levels. Immunoblotting of protein extract from IL-1β-induced cells with anti-iNOS antibody demonstrated a single band of approximately 130 kDa, appropriate for the molecular weight of iNOS (Figure 3). This band was not detected in control cells. Similarly, no band was seen in IL-1β-induced cells co-incubated with TGF-β (10 ng ml^{-1}), while a faint band was detected in IL-1β-induced cells exposed to all-*trans*-RA (10 μM) at the highest protein concentration blotted (400 μg per lane). Consistent with inhibition of iNOS protein synthesis, measurement of iNOS mRNA by RT–PCR showed marked reduction of IL-1β-induced elevation in iNOS mRNA levels (Figure 4).

Effect of retinoic acid on IL-1β-induced relaxation of aortic rings

Preincubation of aortic rings with IL-1β (10 ng ml^{-1}) for 2 h reduced markedly ($P<0.01$) the constrictor response to phenylephrine (Figure 5a). This vascular hyporeactivity was reversed by L-NMMA (1 mM), confirming its dependence on NO generation (Figure 5a). Co-incubation of the rings with all-*trans*-RA (10 μM) and IL-1β inhibited the vasorelaxant effect of the cytokine and restored the vasoconstrictor response to the α-agonist (Figure 5b).

Discussion

These studies demonstrate that all-*trans*-RA inhibits the induction of iNOS by IL-1β in rat VSM cells in culture and in aortic rings. The studies on cultured VSM cells show that this property is common to a number of retinoids and a specific effect of retinoid receptor binding since the inactive retinoid, Ro 14-6113, has no effect in our system. Furthermore, we have shown that the mechanism of action involves a reduction in iNOS mRNA and protein levels. These observations confirm and extend those of Mehta *et al.* (1994) using endotoxin and interferon-γ to induce NO production in mouse peritoneal macrophages.

Retinoids have been shown to influence (activate or inhibit) the expression of a number of genes, including those associated with cell growth and differentiation (Chytil & Haq, 1990), cell matrix turnover (Brinckerhoff *et al.*, 1986; Nicholson *et al.*, 1990; Schule *et al.*, 1991), growth factors such as PDGF (Wang *et al.*, 1990) and TGF-β (Roberts & Sporn, 1992) and co-factors of coagulation (Ishii *et al.*, 1992). They exert their biological effects through at least two distinct classes of intracellular receptors, namely the retinoic acid receptors (RARs), α, β and γ, and the retinoid X receptors (RXR), α, β and γ (Lohnes *et al.*, 1992). RARs in cell extracts exhibit high affinity for both all-*trans*-retinoic acid and 9-*cis*-retinoic acid (in the nanomolar range for both ligands), while RXRs bind 9-*cis*-retinoic acid only at nanomolar concentrations (Heyman *et al.*, 1992; Levin, 1992). These properties, together with the fact that retinoids undergo spontaneous isomerization within cells, has led to the suggestion that 9-*cis*-retinoic acid is the common mediator of the actions of retinoids. Studies of the tissue distribution of retinoic acid receptor mRNA show that RAR-α and RXR-β are expressed in almost all tissues, while RAR-β and RAR-γ and RXRα and RXR-γ display a more restricted pattern of distribution (Mangelsdorf *et al.*, 1992; Wan *et al.*, 1992). There are no data to date on the predominant receptor subtypes expressed in VSM cells.

An interesting observation is that, while the affinity of retinoid receptors for their ligands in cell extracts is in the

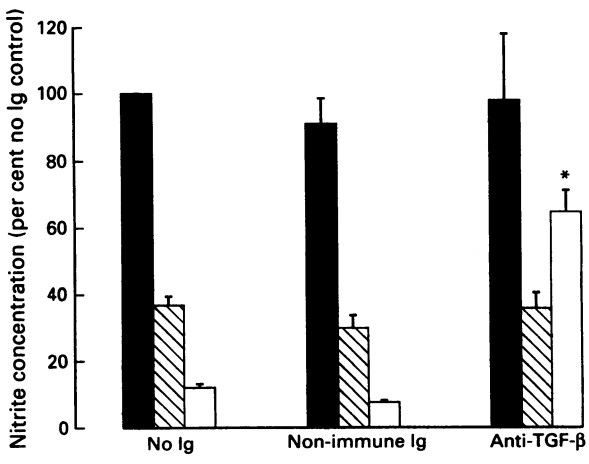


Figure 2 Anti-TGF-β antibody reverses TGF-β inhibition of IL-1β-induced nitrite production, while it fails to reverse the effect of all-*trans*-RA. VSM cells were incubated with IL-1β 10 ng ml^{-1} alone (solid column), IL-1β and all-*trans*-RA 10 μM (hatched column), or IL-1β and TGF-β 5 ng ml^{-1} (open column) in combination with normal chicken immunoglobulin 50 μg ml^{-1} (non-immune Ig) or anti-human-TGF-β chicken polyclonal antibody 50 μg ml^{-1} (anti-TGF-β) for 24 h. No Ig represents VSM cells incubated without immunoglobulin. Nitrite concentration of each well was normalized to mean value of that incubated with IL-1β alone (open column, No Ig). Data are mean ± s.e.mean of three wells and are representative of three independent experiments. *$P<0.05$ compared with cells incubated with IL-1β alone.

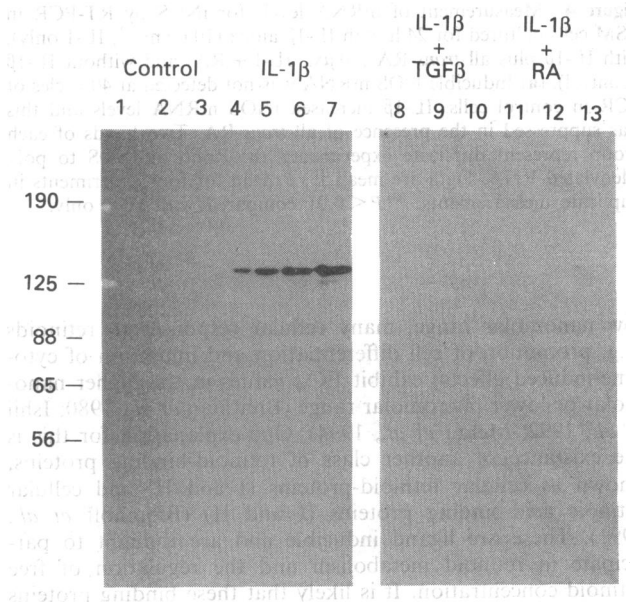


Figure 3 Western blot analysis of iNOS in VSM cells. Supernatant fraction of cell lysate was separated by SDS–PAGE, transferred to nitrocellulose and blotted with anti-iNOS antibody. A single band was seen approximately at 130 kDa, appropriate for the molecular weight of iNOS protein. VSM cells were incubated with medium alone (lanes 1–3) or IL-1β 10 ng ml^{-1} (lanes 4–7), IL-1β plus TGF-β 10 ng ml^{-1} (lanes 8–10) or IL-1β plus all-*trans*-RA (RA) 10 μM (lanes 11–13) for 24 h. Different amounts of protein were subjected to SDS–PAGE (25 μg, lane 4; 50 μg, lane 5; 100 μg, lanes 1,6,8 and 11; 200 μg, lanes 2,7,9 and 12; 400 μg, lanes 3,10 and 13) to enable semi-quantitation of iNOS protein. iNOS band was not detected in cells incubated with IL-1β plus TGF-β and only a faint band was detected in cells incubated with IL-1β plus all-*trans*-RA even at the highest protein concentration examined (400 μg per lane, lanes 10 and 13).

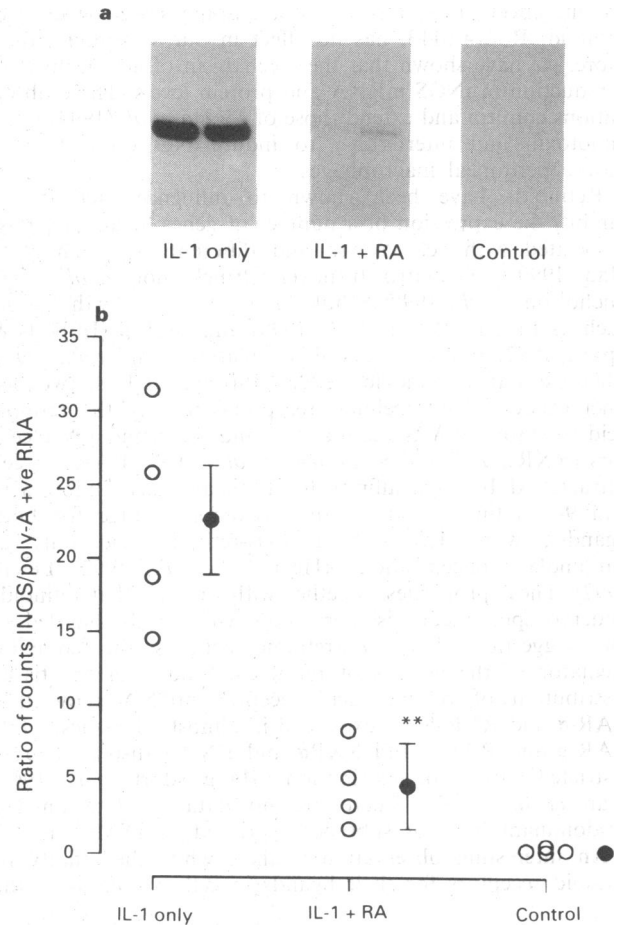


Figure 4 Measurement of mRNA levels for iNOS by RT-PCR in VSM cells cultured for 24 h with IL-1β alone (10 ng ml^{-1}; IL-1 only), with IL-1β plus all-*trans*-RA (10 μM, IL-1 + RA) and without IL-1β (Control). (**a**) Inducible NOS mRNA was not detected at 40 cycles of PCR in control cells. IL-1β increased iNOS mRNA levels and this was suppressed in the presence of all-*trans*-RA. Two bands of each group represent duplicate experiments. (**b**) Ratio of iNOS to poly adenylated RNA. Data are mean ± s.e.mean for four experiments in duplicate measurements. $^{**}P<0.01$ compared with IL-1 only.

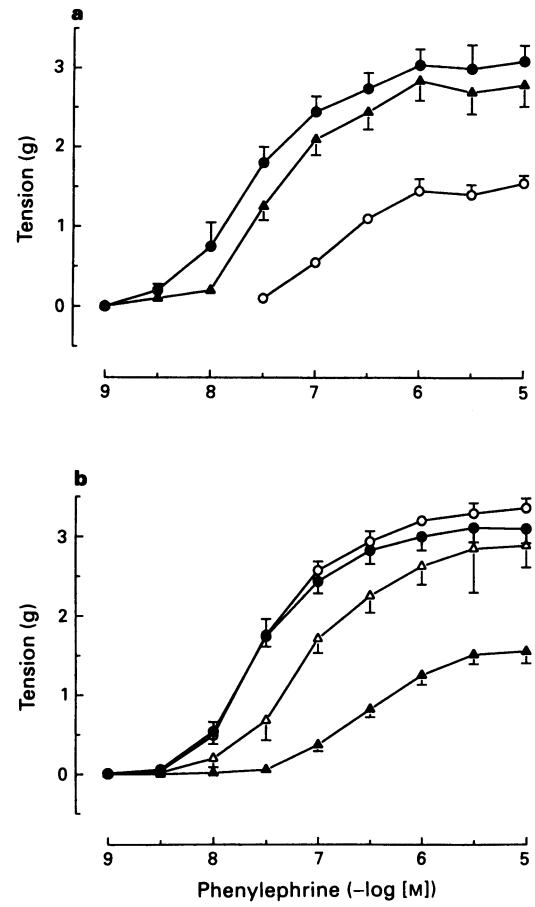


Figure 5 All-*trans*-RA attenuates IL-1β-induced relaxation of aortic rings. Rings, made from isolated rat thoracic aortae, were de-endothelialized and incubated with or without IL-1β (10 ng ml^{-1}) in the presence or absence of RA (10 μM) for 2 h at 37°C. The rings were then suspended in an organ bath and contracted by phenylephrine. (**a**) Rings incubated with IL-1β (○) showed markedly reduced contraction to phenylephrine ($P<0.01$) compared with control rings (●) which was reversed by the NOS inhibitor L-NMMA (1 mM, ▲). (**b**) Contraction of the rings incubated with IL-1β (▲) was again significantly ($P<0.01$) suppressed compared with that of control rings (●), while the rings incubated with all-*trans*-RA alone (○) were not significantly different from control rings. Incubation of rings with IL-1β + all-*trans*-RA (△) significantly restored the response to phenylephrine ($P<0.01$). Data points are mean ± s.e.mean of five rings isolated from 5 different rats.

low nanomolar range, many cellular responses to retinoids (e.g. promotion of cell differentiation and inhibition of cytokine-induced effects) exhibit EC_{50} values in the higher nanomolar or lower micromolar range (Breitman *et al.*, 1980; Ishii *et al.*, 1992; Mehta *et al.*, 1994). One explanation for this is the existance of another class of retinoid-binding proteins, known as cellular retinoid-proteins (I and II) and cellular retinoic acid-binding proteins (I and II) (Blomhoff *et al.*, 1991). These are ligand inducible and are thought to participate in retinoid metabolism and the regulation of free retinoid concentration. It is likely that these binding proteins modify the apparent retinoid concentration–response relationship in intact cells by reducing the free concentration of the ligand.

It is clear that retinoids can regulate gene expression at several different levels. Firstly, it is well established that heterodimers of RAR/RXR (and RXR homodimers) bind to specific DNA sequences known as retinoic response elements (RAREs) on target genes and act as transcription factors. Secondly, RARs, but not RXRs, have been shown to antagonize AP-1 dependent transcription through direct coupling between RAR and AP-1 (Nicholson *et al.*, 1990; Schule *et al.*, 1991). Thirdly, studies on the expression of TGF-β isoforms suggest that retinoids can also act by post-transcriptional mechanisms (Roberts & Sporn, 1992).

The molecular mechanism(s) by which retinoids inhibit the synthesis of iNOS protein remains to be elucidated. Sequence for the promoter region of rat iNOS is not available, but it is noteworthy that a 1749 bp fragment from the 5'-flanking region of the mouse macrophage iNOS gene contains AP-1 binding sites (Xie *et al.*, 1993). An important consideration, however, is that the effects of retinoids on iNOS may be mediated indirectly via its action on other factors. Retinoic acid has, for example, been reported to induce expression of TGF-β (Roberts & Sporn, 1992), which is a potent inhibitor of iNOS expression (data reported here and Schini *et al.*, 1992; 1993). Nevertheless, the effects of all-*trans*-RA in our study were not antagonized by an anti-TGF-β antibody which was able to block the actions of exogenous TGF-β.

In addition to its effects on iNOS expression in this study, RA has also been shown to inhibit cytokine-induced expression of tissue factor and down-regulation of thrombomodulin in endothelial cells (Ishii *et al.*, 1992). This could reduce the thrombotic properties of cytokines, and these properties taken together provide retinoids with a very attractive activity profile as possible therapeutic agents for septic shock.

There is now considerable experience with the use of high doses of all-*trans*-RA in patients with leukaemia (Vahlquist, 1992; Warrell *et al.*, 1993) and its effects on iNOS synthesis and activity could be examined in humans.

The authors are grateful to Dr V. Riveros-Moreno for anti-iNOS antibody and Dr Klaus for analogues of retinoic acid. This work was supported in part by a grant from Daiichi Pharmaceutical Co. Ltd.

References

BEASLEY, D., SCHWARTZ, J.H. & BRENNER, B.M. (1991). Interleukin 1 induces prolonged L-arginine-dependent cyclic guanosine monophosphate and nitrate production in rat vascular smooth muscle cells. *J. Clin. Invest.*, **87**, 602–698.

BLOMHOFF, R., GREEN, M.H., BERG, T. & NORUM, K. (1991). Vitamin A metabolism: new perspectives on absorption, transport and storage. *Physiol. Rev.*, **71**, 952–990.

BREITMAN, T.R., SELONICK, S.E. & COLLINS, S.J. (1980). Induction of differentiation of the human promyelocytic leukemia cell line (HL 60) by retinoic acid. *Proc. Natl. Acad. Sci. USA*, **77**, 2936–2940.

BRINCKERHOFF, C.E., PLUCINSKA, I.M., SHELDON, L.A. & O'CONNOR, G.T. (1986). Half-life of synovial cell collagense mRNA in modulated by phorbol myristate acetate but not all-trans-retinoic acid or dexamethasone. *Biochemistry*, **25**, 6378–6384.

BROWN, L.A., NUNEZ, D.J. & WILKINS, M.R. (1993). Differential regulation of natriuretic peptide receptor messenger RNAs during the development of cardiac hypertrophy in the rat. *J. Clin. Invest.*, **92**, 2702–2712.

CETKOVIC-CVRLJE, M., SANDLER, M. & EIZIRIK, D.L. Nicotinamide and dexamethasone inhibit IL-1 induced nitric oxide production by RINm5F without decreasing messenger ribonucleic acid expression for nitric oxide synthase. *Endocrinology*, **133**, 1739–1744.

CHOMCZYNSKI, P. & SACCHI, A. (1987). Single step method of RNA isolation by acid guanidium isothiocyanate-phenol-chloroform extraction. *Anal. Biochem.*, **162**, 156–159.

CHYTIL, F. & HAQ, R. (1990). Vitamin A mediated gene expression. *Crit. Rev. Eucaryotic Gene Expr.*, **1**, 61–73.

CUNHA, F.Q., MONCADA, S. & LIEW, F.Y. (1992). Interleukin-10 (IL-10) inhibits the induction of nitric oxide synthase by interleukin-Y in murine macrophages. *Biochem. Biophys. Res. Commun.*, **182**, 1155–1159.

HEYMAN, R.A., MANGELSDORF, D.J., DYCK, J.A., STEIN, R.B., EICHELE, G. EVANS, R.M. & THALLER, C. (1992). 9-Cis retinoic acid is a high affinity ligand for the retinoid X receptor. *Cell*, **68**, 397–406.

HIROKAWA, K., O'SHAUGHNESSY, K., MOORE, K., RAMRAKHA, P. & WILKINS, M.R. (1994). Induction of nitric oxide synthase in cultured vascular smooth muscle cells: The role of cyclic AMP. *B. J. Pharmacol.*, **108**, 786–792.

IGNARRO, L.J., FACADE, J.M., GRISCAVAGE, J.M., ROGERS, N.E. & BYRNS, R.E. (1993). Oxidization of nitric oxide in aqueous solution to nitrite but not nitrate: Comparison with enzymatically formed nitric oxide from L-arginine. *Proc. Natl. Acad. Sci. USA*, **90**, 8103–8107.

ISHII, H., HORIE, S., KIZAKI, K. & KAZAMA, M. (1992). Retinoic acid counteracts both the downregulation of thrombomodulin and the induction of tissue factor in cultured human endothelial cells exposed to tumour necrosis factor. *Blood*, **80**, 2556–2562.

KIRSCHENLOHR, H.L., METCALFE, J.C., WEISSBERG, P.L. & GRAINGER, D.J. (1993). Adult human aortic smooth muscle cells in culture productive active TGF-β. *Am. J. Physiol.*, **265**, C571–576.

LEVIN, A.A. (1992). 9-Cis retinoic acid stereoisomer binds and activates the nuclear receptor RXRa. *Nature*, **355**, 359–361.

LOHNES, D., DIERICH, A., GHYSELINCK, N., KASTNER, P., LAMPRON, C., LEMEUR, M., LUFKIN, T., MENDELSOHN, C., NAKSHATRI, H. & CHAMBON, P. (1992). Retinoid receptors and binding proteins. *J. Cell Sci.*, **16**, 69–76.

MANGELSDORF, D.J., BORGMEYER, U., HEYMAN, R.A., ZHOU, J.Y., ONG, E.S., ORO, A.E., KAKIZUKA, A. & EVANS, R.M. (1992). Characterization of three RXR genes that mediate the action of 9-cis retinoic acid. *J. Leukocyte Biol.*, **55**, 336–342.

MEHTA, K., MCQUEEN, T., TUCKER, S., PANDITA, R. & AGGARWAL, B.B. (1994). Inhibition of all-*trans*-retinoic acid of tumour necrosis factor and nitric oxide production by peritoneal macrophages. *J. Leukocyte Biol.*, **55**, 336–342.

MONCADA, S., PALMER, R.M.J. & HIGGS, E.A. (1991). Nitric oxide: Physiology, pathophysiology and pharmacology. *Pharmacol. Rev.*, **43**, 109–142.

MUHL, H., KUNZ, D., ROB, P. & PFEILSCHIFTER, J. (1993). Cyclosporin derivatives inhibit interleukin 1B induction of nitric oxide synthase in renal mesangial cells. *Eur. J. Pharmacol.*, **249**, 95–100.

NICHOLSON, R.C., MADER, S., NAGPAL, S., LEID, M., ROCHETTEEGLY, C. & CHAMBON, P. (1990). Negative regulation of the rat stromelysin gene promoter by retinoic acid is mediated by an AP1 binding site. *EMBO J.*, **9**, 4443–4454.

NUNOKAWA, Y., ISHIDA, N. & TANAKA, S. (1993). Cloning of inducible nitric oxide synthase in rat vascular smooth muscle cells. *Biochem. Biophys. Res. Commun.*, **191**, 89–94.

OCHOA, J.B., CURTI, B., PEITZMAN, A.B., SIMMONS, R.L. BILLIAR, T.R., HOFFMAN, R., RAULT, R., LONGO, D.L., URBA, W.J. & OCHOA, A.C. (1992). Increased circulating nitrogen oxides after human tumor immunotherapy: correlation with toxic hemodynamic changes, *J. Natl. Cancer Inst.*, **84**, 864–867.

ORFANOS, C.E. & BAUER, R. (1983). Evidence for antiflammatory activities for oral and synthetic retinoids: experimental findings and clinical experience. *B. J. Dermatol.*, **S25**, 55–60.

PARSAEE, H., MCEWAN, J.R., JOSEPH, S. & MACDERMOT, J. (1992). Differential sensitivities of the prostacylin and nitric oxide biosynthetic pathways to cytosolic calcium in bovine aortic endothelial cells. *B. J. Pharmacol.*, **107**, 1013–1019.

RADOMSKI, M.W., PALMER, R.M.J. & MONCADA, S. (1990). Glucocorticoids inhibit the expression of an inducible, but not the constitutive, nitric oxide synthase in vascular endothelial cells. *Proc. Natl. Acad. Sci. USA*, **87**, 10043–10047.

REES, D.D., PALMER, R.M.J. & MONCADA, S. (1989). Role of endothelium-derived nitric oxide in the regulation of blood pressure. *Proc. Natl. Acad. Sci. USA*, **86**, 3375–3378.

RIVEROS-MORENO, V., BEDDELL, C. & MONCADA, S. (1993). Nitric oxide synthase: structural studies using antipeptide antibodies. *Eur. J. Biochem.*, **215**, 801–808.

ROBERTS, A.B. & SPORN, M.B. (1984). Cellular biology and biochemistry of retinoids. In *The Retinoids*, Vol. 2. ed. Sporn, M.B., Roberts, A. & Goodman, D.S., pp. 210–287. New York: Academic Press.

ROBERTS, A.B. & SPORN, M.B. (1992). Mechanistic interrelationships between two superfamilies: The steroid/retinoid receptors and transforming growth factor-B. *Cancer Surv.*, **14**, 205–220.

SANGER, F., NICKLEN, S. & COULSEN, A.R. (1977). DNA sequencing with chain terminating inhibitors. *Proc. Natl. Acad. Sci. USA*, **74**, 5463–5467.

SCHINI, V.B., DURANTE, W., ELIZONDO, E., SCOTT-BURDEN, T., JUNQUERO, D.C., SCHAFER, A.I. & VANHOUTTE, P.M. (1992). The induction of nitric oxide synthase activity is inhibited by TGF-B1, PDGFab and PDGFbb in vascular smooth muscle cells. *Eur. J. Pharmacol.*, **216**, 379–383.

SCHINI, V.B., CATOVSKY, S., DURANTE, W., SCOTT-BURDEN, T., SCHAFER, A.I. & VANHOUTTE, P.M. (1993). Thrombin inhibits induction of nitric oxide synthase in vascular smooth muscle cells. *Am. J. Physiol.*, **264**, H611–H616.

SCHULE, R., RANGARAJAN, P., YANG, N., KLIEWER, S., RANSONE, L.J., BOLADO, J., VERMA, I.M. & EVANS, R.M. (1991). Retinoic acid is a negative regulator of AP-1 responsive genes. *Proc. Natl. Acad. Sci. USA*, **88**, 6092–6096.

SCOTT-BURDEN, T., SCHINI, V.B., ELIZONDO, E., JUNQUERO, D.C. & VANHOUTTE, P.M. (1992). Platelet-derived growth factor suppresses and fibroblast growth factor enhances cytokine-induced production of nitric oxide by cultured smooth muscle cells. *Circ. Res.*, **71**, 1088–1100.

SLOTMAN, G.J., FISHER, C.J., BONE, R.C., CLEMMER, T.P. & METZ, C.A. (1993). Detrimental effects of high-dose methylprednisolone sodium succinate on serum concentrations of hepatic and renal function indicators in severe sepsis and septic shock. The methylprednisolone severe sepsis study group. *Crit. Care Med.*, **21**, 191–195.

VAHLQUIST, A. (1992). Long-term safety of retinoid therapy. *J. Am. Acad. Dermatol.*, **27**, S29–S33.

WAN, Y.-J.Y., WANG, L. & WU, T.-C.J. (1992). Detection of retinoic acid receptor mRNA in rat tissues by reverse transcriptase-polymerase chain reaction. *J. Mol. Endocrinol.*, **9**, 291–294.

WANG, C., KELLY, J., BOWDEN-POPE, D.F. & STILES, C.D. (1990). Retinoic acid promotes transcription of the PDGFa-receptor gene. *Mol. Cell. Biol.*, **10,** 6781–6784.

WARRELL, Jr., R.P. DETHE, H., WANG, Z.-Y. & DEGOS, L. (1993). Acute promyelocytic leukemia. *N. Engl. J. Med.*, **329,** 177–189.

XIE, Q.-W., WHISNANT, R. & NATHAN, C. (1993). Promoter of the mouse gene encoding calcium-independent nitric oxide synthase confers inducibility by interferon Y and bacterial lipopolysaccharide. *J. Exp. Med.*, **177,** 1779–1784.

ZEMBOWICZ, A. & VANE, J.R. (1992). Induction of nitric oxide synthase activity by toxic shock syndrome toxin 1 in a macrophage-monocyte cell line. *Proc. Natl. Acad. Sci. USA*, **89,** 2051–2055.

(Received June 14, 1994
Revised August 5, 1994
Accepted August 11, 1994)

Br. J. Pharmacol. (1994), **113**, 1455–1463 © Macmillan Press Ltd, 1994

Stimulation by extracellular ATP and UTP of the mitogen-activated protein kinase cascade and proliferation of rat renal mesangial cells

Andrea Huwiler & [1]Josef Pfeilschifter

Department of Pharmacology, Biozentrum, University of Basel, Klingelbergstrasse 70, CH-4056 Basel, Switzerland

1 Extracellular ATP and UTP have been reported to activate a nucleotide receptor that mediates phosphoinositide and phosphatidylcholine hydrolysis by phospholipases C and D, respectively. Here we report that ATP and UTP potently stimulate mesangial cell proliferation.

2 Both nucleotides stimulate phosphorylation and activation of mitogen-activated protein kinase and a biphasic phosphorylation of the up-stream mitogen-activated protein kinase kinase.

3 When added at 100 μM, ATPγS, UTP and ATP were the most potent activators of mitogen-activated protein kinase. βγ-imido-ATP was somewhat less active and ADP and 2-methylthio-ATP caused a weak induction of enzyme activity. Activation of mitogen-activated protein kinase by both ATP and UTP is dose-dependently attenuated by the P_2-receptor antagonist, suramin.

4 The protein kinase C activator 12-0-tetradecanoylphorbol 13-acetate, but not the biologically inactive 4α-phorbol 12,13-didecanoate, increased mitogen-activated protein kinase activity in mesangial cells, suggesting that protein kinase C may mediate nucleotide-induced stimulation of mitogen-activated protein kinase.

5 Down-regulation of protein kinase C -α and-δ isoenzymes by 4 h or 8 h treatment with phorbol ester partially inhibited ATP- and UTP-triggered mitogen-activated protein kinase activation. Moreover, a 24 h treatment of mesangial cells with phorbol ester, a regimen that also causes depletion of protein kinase C-ε did not further reduce the level of mitogen-activated protein kinase stimulation.

6 The specific protein kinase C inhibitor, CGP 41251, which displayed a selectivity for the Ca^{2+}-dependent isoenzymes, as compared to the Ca^{2+}-independent isoenzymes did not inhibit nucleotide-stimulated mitogen-activated protein kinase phosphorylation, thus implicating the involvement of a Ca^{2+}-independent protein kinase C isoform.

7 In summary, these results suggest that ATP and UTP trigger the activation of the mitogen-activated protein kinase signalling cascade in mesangial cells and this may be responsible for the potent mitogenic activity of both nucleotides.

Keywords: Nucleotide receptor; mitogen-activated protein kinase; mitogen-activated protein kinase kinase; renal mesangial cells; protein kinase C.

Introduction

Renal mesangial cells are involved in the regulation of the glomerular circulation as well as in the preservation of the structural integrity of the glomerulus. In addition mesangial cells play an impotant role in most pathological processes of the renal glomerulus. The response of intrinsic glomerular cells, especially of mesangial cells, to external stimulation by invading macrophages, polymorphonuclear neutrophils and platelets is crucial in the pathogenesis of glomerular injury. Several important pro-inflammatory functions of mesangial cells have been established. The three most prominent include: (i) increased mediator production by mesangial cells; (ii) increased matrix production by mesangial cells; and (iii) mesangial cell proliferation (for review see Couser, 1993). A central feature of glomerular inflammation is that during the injurious process the normally quiescent mesangial cells become primed and activated. A considerable number of potent biological mediators are released by professional inflammatory cells, including interleukin 1, tumour necrosis factor α, transforming growth factor β, platelet-derived growth factor and eicosanoids, and may be responsible for the priming of mesangial cells. Especially platelets are a rich source for ATP, another important mediator present in the inflammatory glomerular microenvironment *in vivo*. ATP is stored in the dense bodies of platelets and secreted after activation (Gordon, 1986). We have reported that extracellular ATP triggers multiple signal transduction cascades which were activated when quiescent mesangial cells were exposed to well-known growth factors. These early signals generated include the activation of phospholipase C with a concomitant production of inositol trisphosphate and diacylglycerol, and a subsequent mobilization of intracellular Ca^{2+}, activation of protein kinase C and synthesis of prostaglandin E_2 (Pfeilschifter, 1990a,b; Pavenstädt *et al.*, 1993). Furthermore, we observed that extracellular ATP stimulates a phospholipase D-mediated phosphatidylcholine hydrolysis resulting in a sustained increase in the cellular levels of diacylglycerol (Pfeilschifter & Merriweather, 1993). These signalling responses are equally triggered by ATP and UTP and we have suggested that ATP and UTP activate a common nucleotide receptor (Pfeilschifter, 1990b; Pfeilschifter & Merriweather, 1993). Taken together these observations raise the possibility that extracellular nucleotides act as growth factors and thus may contribute to mesangial cell proliferation, a hallmark of progressive glomerular disease. Cellular responses to growth factors include a rapid increase of cellular protein phosphorylation accompanied by the sequential activation of a protein kinase cascade. Mitogen-activated protein kinases (MAP kinases) or extracellular signal-regulated kinases (ERKs) are a group of protein kinases having molecular masses of 42–45 kD which are phos-

[1] Author for correspondence.

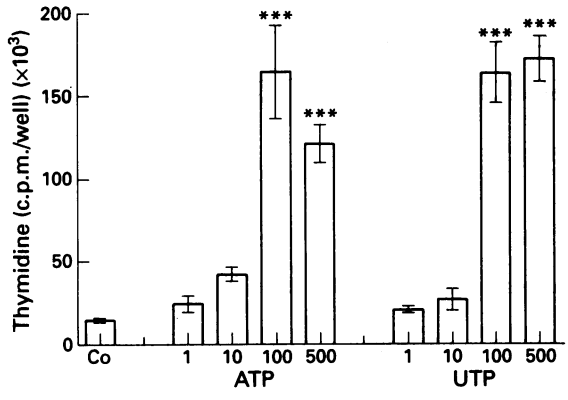


Figure 1 Dose-dependency of ATP- and UTP-stimulated DNA synthesis in mesangial cells. Mesangial cells were made quiescent by incubation for 3 days in serum-free medium and then stimulated for 24 h with the indicated concentration (μM) of ATP or UTP in the presence of [^{3}H]-thymidine. [^{3}H]-Thymidine incorporation into DNA was quantified as described in the Methods section. Results are expressed as [^{3}H]-thymidine uptake (c.p.m./well) and are means ± s.d. of 4 experiments. Significant differences from control. ***$P<0.001$; ANOVA.

phorylated on tyrosine and threonine and activated upon growth factor stimulation. Possible physiological targets of MAP kinase include the S6 ribosomal protein kinase p90^{rsk} and the transcription factors c-Jun and c-Myc (for review see Leevers & Marshall, 1992; Davis, 1993; Crews & Erikson, 1993). Thus, MAP kinase is thought to be directly involved in transmitting signals from growth factor receptors to the nucleus in order to regulate gene transcription and protein synthesis. The direct upstream activator of MAP kinase is a dual specificity protein kinase, MAP kinase kinase or MEK (mitogen-activated protein kinase or ERK kinase). Recent data have shown that at least two different signalling pathways converge to activate MEK, one is activated by G-protein-linked receptor agonists and involves MEK kinase, whereas the other pathway is triggered by receptor tyrosine-kinase agonists and utilizes the two proto-oncogene products Raf and Ras.

In this study, we demonstrate that ATP and UTP activate the MAP kinase cascade and stimulate mesangial cell proliferation.

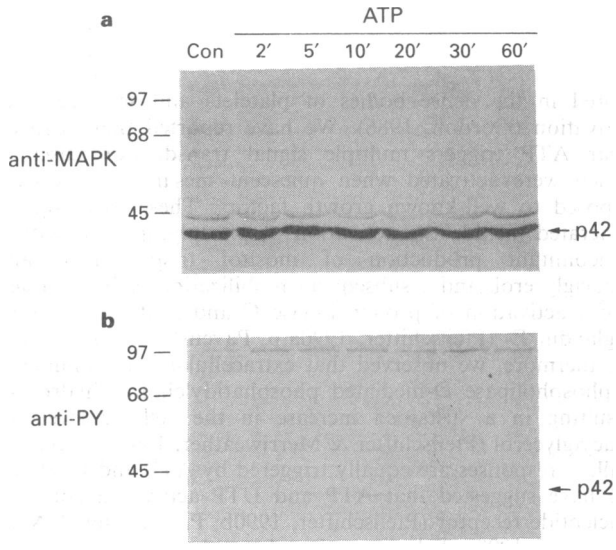


Figure 2 Immunodetection of 42 kDa MAP kinase (p42^{mapk}) and of tyrosine phosphorylated proteins in ATP-stimulated mesangial cells. Mesangial cells were treated for the indicated time periods with ATP (100 μM), and the cell homogenates (100 μg of protein) were subjected to SDS–PAGE (10% acrylamide gel), transferred to nitrocellulose and Western blot analysis was performed using an antiserum reactive with p42^{mapk} and p44^{mapk} (anti-MAPK) at a dilution of 1:500 (a) or using an anti-phosphotyrosine antibody (anti-PY) at a dilution of 1:1000 (b). Bands were visualized by horseradish peroxidase. Similar results were obtained in three independent experiments.

Methods

Cell-culture

Rat renal mesangial cells were cultured as described previously (Pfeilschifter, 1990a). In a second step, single cells were cloned by limited dilution on 96-microwell plates. Clones with apparent mesangial cell morphology were used for further processing. The cells were grown in RPMI 1640 supplemented with 10% (v/v) foetal-calf serum, penicillin (100 units ml^{-1}), streptomycin (100 μg ml^{-1}) and bovine insulin (0.66 units ml^{-1}). Mesangial cells exhibited the typical stellate morphology. Moreover, there was positive staining for the intermediate filaments desmin and vimentin, which is considered to be specific for myogenic cells, positive staining for Thy 1.1 antigen, and negative staining for factor VIII-related antigen and cytokeratin, which excludes endothelial and epithelial contaminations. Generation of inositol trisphosphate upon activation of the angiotensin II AT_1 receptor (Pfeilschifter, 1990c) was used as a funtional criterion for characterizing the cloned cell line. For the experiments, passages 9–16 of mesangial cells were used.

Cell labelling and immunoprecipitation

Confluent mesangial cells in 100 mm-diameter dishes were washed with PBS and incubated for 2 days in DMEM containing 0.1 mg of fatty acid-free BSA ml^{-1} and then washed 3 times with phosphate free DMEM in order to remove all phosphate. Then the cells were metabolically labelled for 4 h at 37°C with [^{32}P]-orthophosphate (1 mCi/plate) in phosphate-free DMEM. After labelling, cells were stimulated for the indicated time periods at 37°C with various agents. To stop the reaction, the medium was removed and the cells washed twice with ice cold buffer containing 50 mM Tris/HCl, pH 7.5 and 150 mM NaCl. Cells were then scraped directly into 1 ml of ice cold lysis buffer (50 mM Tris/HCl, pH 7.5, 150 mM-NaCl, 10% glycerol, 1% Triton X 100, 2 mM EDTA, 2 mM EGTA, 40 mM β-glycerophosphate,

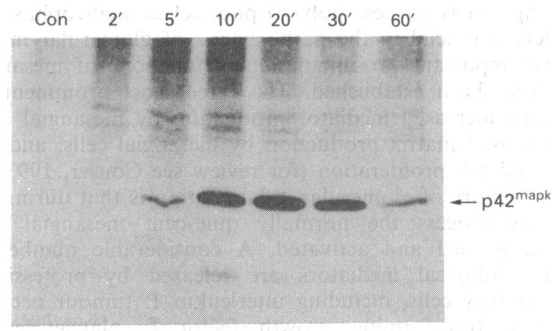


Figure 3 Time course of ATP-stimulated 42 kDa MAP kinase (p42^{mapk}) phosphorylation in mesangial cells. Mesangial cells were labelled with [^{32}P]-orthophosphate and were stimulated with vehicle (Con) or ATP (100 μM) for the indicated time periods. Cells were then lysed and p42^{mapk} was immunoprecipitated with a p42^{mapk}-specific antiserum at a dilution of 1:200. The immunoprecipitates were separated on SDS–PAGE (10% acrylamide gel) and exposed to Hyperfilm MP at −70°C. Similar results were obtained in three independent experiments.

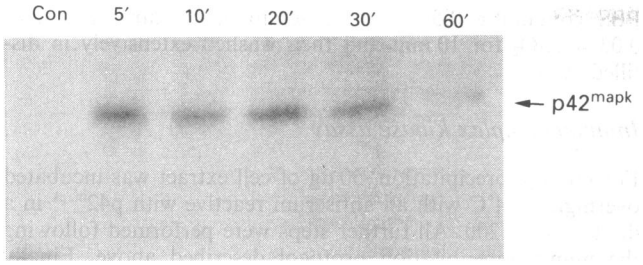


Figure 4 Time course of UTP-stimulated 42 kDa MAP kinase ($p42^{mapk}$) phosphorylation in mesangial cells. Mesangial cells were labelled with [^{32}P]-orthophosphate and were stimulated with vehicle (Con) or UTP (100 μM) for the indicated time periods. Cells were than lysed and $p42^{mapk}$ was immunoprecipitated with a $p42^{mapk}$-specific antiserum at a dilution of 1:200. The immunoprecipitates were separated on SDS–PAGE (10% acrylamide gel) and exposed to Hyperfilm MP at −70°C. Similar results were obtained in three independent experiments.

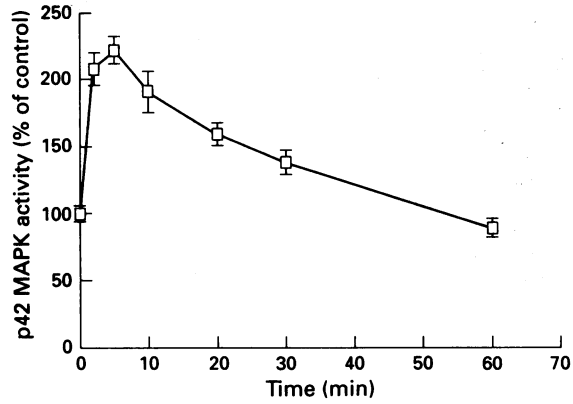


Figure 6 Time course of 42 kDa MAP kinase ($p42^{mapk}$) activation by ATP in mesangial cells. Mesangial cells were treated for the indicated time periods with vehicle or ATP (100 μM). Cells were then lysed and cell extracts were immunoprecipitated with a specific anti-$p42^{mapk}$ antiserum at a dilution of 1:200. MBP kinase activity in immuncomplexes were analysed by SDS–PAGE (14% acrylamide gel) and MBP bands were individually quantified by densitometry, and are expressed as % of control (in the absence of nucleotides). The data are means ± s.d. of three independent experiments.

50 mM sodiumfluoride, 10 mM sodium pyrophosphate, 200 μM sodium orthovanadate, 10 μg leupeptin ml^{-1}, 200 u aprotinin ml^{-1}, 1 μM pepstatin A, 1 mM phenylmethanesulphonyl fluoride, 100 nM ocadaic acid) and homogenized with 10 passes through a 26-gauge needle fitted to a 1 ml syringe. The homogenate was centrifuged for 10 min at 14,000 *g* and the supernatant taken for immunoprecipitation. Samples of 1 ml volume, containing 150×10^6 c.p.m. of labelled protein, 5% foetal calf serum and 1.5 mM iodoacetamide in lysis buffer, were incubated with different specific antisera for 3 h at room temperature, or overnight at 4°C. Then 100 μl of a 50% slurry of protein A-Sepharose 4B-CL in PBS was added and the mixture was incubated for 1.5 h at room temperature with mild shaking. After centrifugation for 5 min at 3000 *g* immunocomplexes were washed 3 times with 1 ml of a low saft buffer (50 mM-Tris/HCl, pH 7.5, 150 mM NaCl, 0.2%-Triton X100, 2 mM EDTA 2 mM EGTA, 0.1% SDS), 3 times with 1 ml of a high salt buffer (50 mM Tris/HCl, pH 7.5, 500 mM NaCl, 0.2% Triton X100, 2 mM EDTA, 2 mM EGTA, 0.1% SDS) and once with 1 ml of 10 mM Tris. Pellets were boiled for 5 min in 50 μl Laemmli dissociation buffer and subjected to SDS–PAGE (10% acrylamide gel). After fixing in 25% isopropanol, 10% acetic acid, the gels were dried and exposed to Hyperfilm MP at −70°C.

MBP kinase assay

Quiescent mesangial cells in 60 mm-diameter dishes were stimulated with the indicated concentration of agonists. To stop the reaction, the cells were washed with PBS and scraped into 0.5 ml of kinase buffer (20 mM-Tris/HCl, pH 7.5, 1 mM EGTA, 2 mM $MnCl_2$, 0.1 mM-sodiumorthovanadate, 1 mM-PMSF, 25 μg ml^{-1} leupeptin). Cells were then homogenized by passes through a 26G-needle, centrifuged for 5 min at 14'000 *g* and the supernatant was taken for determination of protein concentration. 50 μg of cell extracts were incubated for 15 min at 30°C in the presence of 20 μg MBP, 10 μM ATP and 4 μCi [γ^{32}P]-ATP. The reaction was terminated by adding 40 μl of Lämmli buffer and heated for 5 min at 95°C. The proteins were then separated by SDS–PAGE (14% acrylamide gel) following by autoradiography to visualize the phosphorylation of MBP.

Peptide synthesis and generation of antibodies

For $p44^{mapk}$ and $p42^{mapk}$ synthetic peptides based on the C-terminal sequences (IFQETARFQPGAPEAP for $p44^{mapk}$ and IFEETARFQPGYRS for $p42^{mapk}$) were synthesized, coupled to keyhole-limpet haemocyanin, and used to immunize rabbits. Whereas the anti-$p44^{mapk}$ antiserum recognized specially the p44-isoform, the anti-$p42^{mapk}$ antiserum recognized both p42- and p44-isoforms.

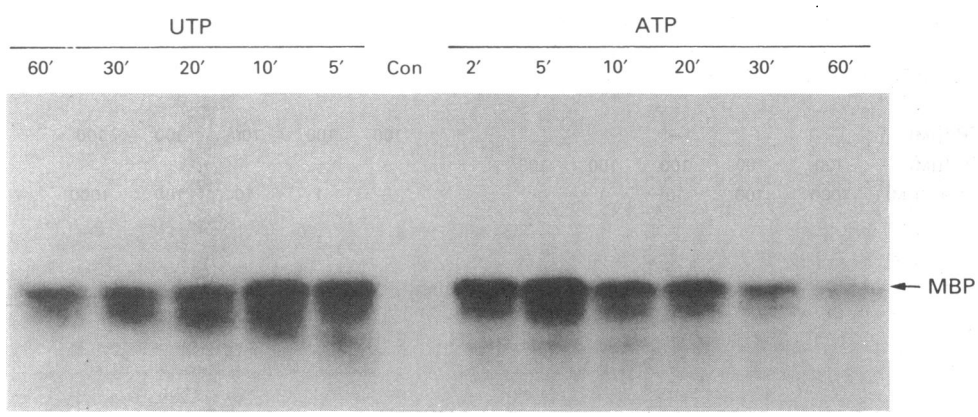


Figure 5 Time course of ATP- and UTP-stimulated MBP-kinase activity in mesangial cells. Mesangial cells were treated with vehicle (Con), ATP (100 μM) or UTP (100 μM) for the indicated time periods. Thereafter cells were harvested in kinase assay buffer and 50 μg of cell protein was used for MBP kinase activity assays as described in the Methods section. Similar results were obtained in four independent experiments.

An antiserum which specifically recognized the p42-isoform was kindly provided by Dr M.J. Dunn, Cleveland (αl, Cp42), U.S.A.

For MAPKK a synthetic peptide based on the N-terminal sequence of murine MEK-1 was synthesized and coupled to keyhole-limpet haemocyanin and used to immunize rabbits. The sequence of the peptide was CPKKKPTPIQLNPAPDG. Anti-MARCKS antiserum was generated by immunizing rabbits with a synthetic peptide of the sequence EAAEPEQPE-QPEQPAA which was coupled to keyhole-limpet haemocyanin. The affinity-purified antiphosphotyrosine antibodies were generously provided by Dr Paul Burn, Basel, Switzerland.

Western blot analysis

Cell extracts (100 μg) were subjected to SDS–PAGE (10% acrylamide gel), and proteins were transferred on to nitrocellulose paper for 1 h at 250 mA using a Bio-Rad Transblot apparatus. The blotting buffer used was 25 mM Tris-HCl, pH 7.4, 190 mM glycine in 20% (v/v) methanol. After the transfer, nitrocellulose filters were washed extensively in distilled water and blocked in blocking buffer (50 mM Tris-HCl, pH 7.4, 200 mM NaCl, 0.2% (v/v) Triton X-100 with 3% (w/v) BSA and 10% (v/v) horse serum) for 1 h at 25°C. Filters were then incubated for 4 h at 25°C with an antiserum reactive with $p42^{mapk}$ and $p44^{mapk}$, or an antiphosphotyrosine antiserum (diluted in blocking buffer as indicated in the figure legends). After washing in buffer A (50 mM Tris-HCl, pH 7.4, 200 mM NaCl, 0.2% (v/v) Triton X-100; 4 × 5 min), the filters were incubated for 1 h with hoseradish peroxidase-conjugated anti-rabbit IgG antibodies in blocking buffer. Thereafter, filters were washed again (4 × 5 min) in buffer A and finally, for colour reaction the filters were incubated in PBS containing 0.5 mg of 3,3′-diaminobenzidine ml^{-1} and 0.03% H_2O_2 for 10 min and then washed extensively in distilled water.

Immunocomplex kinase assay

For immunoprecipitation, 50 μg of cell extract was incubated overnight at 4°C with an antiserum reactive with $p42^{mapk}$ in a dilution of 1:200. All further steps were performed following the immunoprecipitation protocol described above. Finally the beads were incubated for 15 min at 30°C in 50 μl of kinase buffer including 20 μg MBP, 10 μM ATP and 4 μCi [γ^{32}P]-ATP. To stop the reaction 40 μl of Lämmli's buffer was added, the samples were heated and subjected to SDS–PAGE followed by autoradiography.

[^{3}H]-thymidine incorporation

Confluent mesangial cells in 24-well-plates were made quiescent by incubation for 3 days in serum-free DMEM supplemented with 0.1 mg ml^{-1} of fatty-acid-free BSA, and then stimulated for 24 h with [^{3}H]-thymidine 1 μCi ml^{-1} in the presence or absence of the different nucleotides. To stop the incubation, the medium was withdrawn and the cells washed twice with PBS and incubated for 30 min at 4°C with 5% trichloroacetic acid. Cells were then washed twice with 5% trichloroacetic acid and incubated for 30 min at 37°C in 1 M NaOH to solubilize the DNA, and the radioactivity, incorporated in DNA was counted in a β-scintillation counter.

Statistical analysis

Statistical analysis was performed by one way analysis of variance (ANOVA). For multiple comparisons with the same

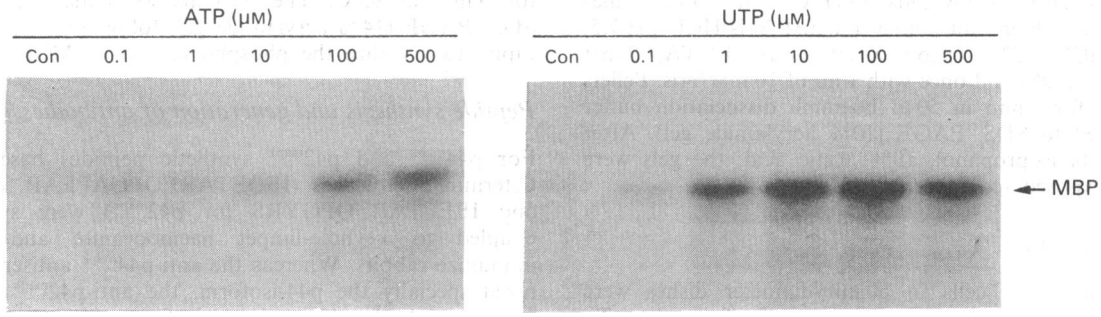


Figure 7 Dose-dependency of ATP- and UTP-stimulated MBP-kinase activity in mesangial cells. Mesangial cells were treated with vehicle (Con) or the indicated concentrations of ATP or UTP for 10 min. Cells were then harvested in kinase assay buffer and MBP kinase activity was measured as described in the Methods section. Similar results were obtained in four independent experiments.

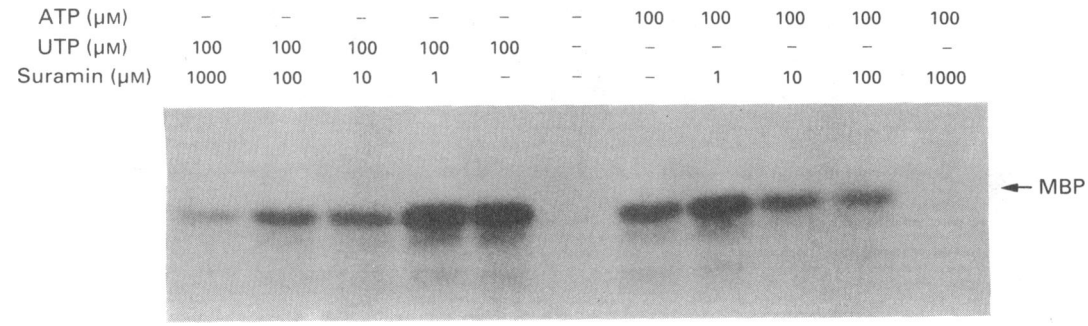


Figure 8 Inhibition of ATP- and UTP-stimulated MBP kinase activity by suramin. Mesangial cells were treated with vehicle or the indicated concentrations of ATP or UTP in the absence or presence of suramin as indicated. Cells were then harvested in kinase assay buffer and MBP kinase activity was measured as described in the Methods section. Similar results were obtained in two independent experiments.

control group, the limit of significance was divided by the number of comparisons according to Bonferroni.

Chemicals

ATP, ADP, ATP γS and UTP were from Boehringer Mannheim, Rotkreuz, Switzerland; βγ-imido-ATP was from Fluka Chemie, Buchs, Switzerland; 2-methylthio-ATP was from ANAWA, Wangen, Switzerland; suramin was from Bayer AG, Leverkusen, Germany; TPA was purchased from Calbiochem, Lucerne, Switzerland; [^{32}P]-orthophosphate, [γ^{32}P]-ATP (specific activity:4000 Ci mmol^{-1}), [methyl-^{3}H]-thymidine (specific activity:6.7 Ci mmol^{-1}) and hyperfilm MP were from Amersham International, Bucks, U.K.; protein A-sepharose 4B-CL was purchased from Pharmacia Fine Chemicals, Uppsala, Sweden; CGP 41251 was a kind gift of Dr G. Caravatti, Ciba-Geigy Ltd., Basel, Switzerland; all cell culture nutrients were from Gibco BRL, Basel, Switzerland; all other chemicals were from either Merck, Darmstadt, Germany, or Fluka, Buchs, Switzerland.

Results

Extracellular ATP and UTP stimulate DNA synthesis

To determine whether extracellular nucleotides are mitogenic for glomerular mesangial cells we measured the incorporation of [^{3}H]-thymidine into DNA of quiescent cells. Mesangial cells were first kept in serum-free medium for 3 days and cultures were then incubated with ATP or UTP at various concentrations for 24 h. As shown in Figure 1, ATP and UTP dose-dependently stimulated DNA synthesis in mesangial cells and maximum effects were obtained at 100 μM for both nucleotides. ATP and UTP stimulated [^{3}H]-thymidine incorporation to a comparable extent (Figure 1) thus suggesting that the common nucleotide receptor may be responsible for this effect.

Extracellular ATP and UTP stimulate MAP kinase activation

Western blot analysis of mesengial cell lysates with a polyclonal antiserum reactive with the 42 kDa and the 44 kDa MAP kinases confirms that both isoforms of MAP kinases are present in mesangial cells (Figure 2), thus confirming a previous report of Wang *et al.* (1992). Addition of ATP (100 μM) caused only a slight retardation of gel mobility of the 42 kDa MAP kinase (p42^{mapk}) which was maximal after 5 min and transient within 20 min (Figure 2a). In parellel, there was a transient tyrosine phosphorylation of a 42 kDa protein which was maximal after 10 min of ATP stimulation (Figure 2b) and most probably corresponds to p42^{mapk}. To assess phosphorylation of p42^{mapk} more directly we metabolically labelled mesangial cells with [^{32}P]-orthophosphate and after stimulation of the cells, p42^{mapk} was immunoprecipitated with a polyclonal antibody specific for p42^{mapk} and phosphorylation was quantitated after SDS–PAGE separation and autoradiography. Whereas basal phosphorylation was not visible, ATP stimulated a marked increase in the levels of p42^{mapk} phosphorylation within 5 min (Figure 3). Maximal levels of phosphorylation were observed after 10–20 min and then declined again, but were still slightly elevated at 60 min (Figure 3). Similar kinetics of p42^{mapk} phosphorylation were seen after stimulation of mesangial cells with UTP (Figure 4). Next we assessed MAP kinase activity after nucleotide stimulation by an *in vitro* assay using myelin basic protein (MBP) as a substrate. The data in Figure 5 show that ATP and UTP augmented p42^{mapk} activity with kinetics comparable to the time-course of p42^{mapk} phosphorylation (Figures 3 and 4). The time course of activation of immunoprecipitated p42^{mapk} was similar to that of the whole cell extract kinase assay (Figure 6). Figure 7 shows the concentration-dependency of MAP kinase activation by ATP and UTP. In this experiment UTP seems to be more potent than ATP and confirms previous observations where UTP always tended to be more potent than ATP in terms of phosphoinositide turnover and phosphatidylcholine hydrolysis (Pfeilschifter, 1990b; Pfeilschifter & Merriweather, 1993). Preincubation of the cells with the putative P_2-receptor antagonist, suramin, dose-dependently attenuated both ATP- and UTP-induced MAP kinase activity (Figure 8). Figure 9 shows the specificity for different nucleotides in stimulation of MBP phosphorylation in mesangial cells. ATP, UTP and ATPγS potently induced MAP kinase activity whereas βγ-imdio-ATP was somewhat less effective. ADP and 2-methylthio-ATP had only a weak effect on MBP phosphorylation. These data are compatible with a nucleotide receptor-mediated MAP kinase activation (Pfeilschifter, 1990b; O'Connor, 1992; Pfeilschifter & Merriweather, 1993).

Role of protein kinase C in ATP and UTP-stimulated MAP kinase activation

It has been previously demonstrated that ATP and UTP evoke an increased inositol 1,4,5-trisphosphate and diacylglycerol generation from phosphatidylinositol 4,5-bisphosphate which trigger Ca^{2+} mobilization and PKC activation, respectively (Pfeilschifter, 1990a,b; Pavenstädt *et al.*, 1993). Furthermore by phospholipase D-mediated hydrolysis of

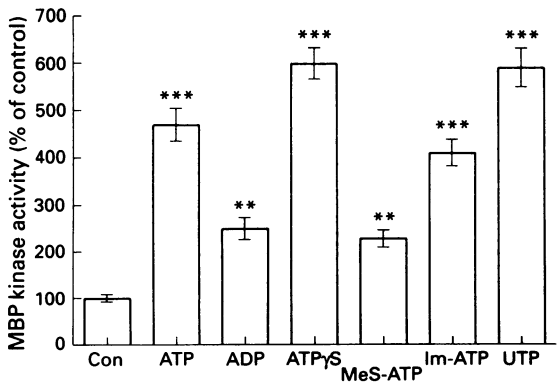


Figure 9 Effects of different nucleotide analogues on MBP kinase activity in mesangial cells. Mesangial cells were treated for 10 min with vehicle (Con), ATP, ADP, ATPγS, 2-methylthio-ATP (MeS-ATP); βγ-imido-ATP (Im-ATP) or UTP (100 μM each) and were then harvested in kinase assay buffer and MBP kinase activity was measured as described in the Methods section. The data are means ± s.d. of four independent experiments. Significant differences from control: $^{**}P<0.01$; $^{***}P<0.001$; ANOVA.

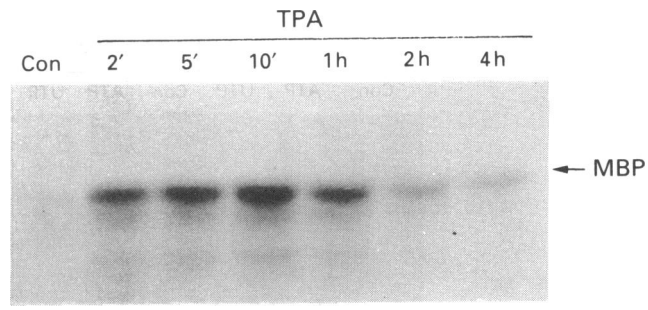


Figure 10 Time course of TPA-stimulated MBP kinase activity in mesangial cells. Mesangial cells were treated with vehicle (Con) or TPA (500 nM) for the indicated time periods. Cells were then harvested in kinase assay buffer and MBP kinase activity was measured as described in the Methods section. Similar results were obtained in four independent experiments.

phosphatidylcholine a sustained production of diacylglycerol is provided in mesangial cells (Pfeilschifter & Merriweather, 1993). Activation of MAP kinase has been reported in response to direct activators of PKC in a variety of cell lines (Leevers & Marshall, 1992).

We were, therefore interested to investigate what role, if any, PKC activation plays in ATP-and UTP-induced MAP kinase activation. The possible involvement of PKC in the nucleotide stimulation of MAP kinase was examined using phorbol esters, PKC down regulation experiments, as well as a specific inhibitor of PKC. As shown in Figure 10, the PKC activator TPA caused a rapid and transient increase in MAP kinase activity as assessed by MBP phosphorylation. In contrast, the biologically inactive phorbol ester 4α-phorbol 12,13-didecanoate did not activate MAP kinase (data not shown). Furthermore, PKC down-regulation by prolonged TPA treatment attenuated ATP- and UTP-stimulated MAP-kinase activity (Figure 11). A 4 h or 8 h treatment with TPA that causes complete depletion of α- and δ-isoenzymes of PKC in mesangial cells (Huwiler *et al.*, 1991; 1992; 1993) maximally suppressed nucleotide-induced MAP-kinase activity. Preincubation of the cells for 24 h with TPA, a regimen that also causes depletion of 80–90% of PKC-ε (Huwiler *et al.*, 1991) did not further reduce the remaining MAP kinase activity detected after ATP or UTP stimulation (Figure 11). However, there was a slight increase of MAP kinase activity under basal conditions in the absence of nucleotide stimulation when cells were treated with TPA for 24 h (Figure 11). These data suggest that both, PKC-dependent and PKC-independent pathways are involved in MAP kinase activation in nucleotide-stimulated mesangial cells. Surprisingly, the selective protein kinase C inhibitor CGP 41251 (Meyer *et al.*, 1989) did not suppress ATP- or UTP-triggered MAP kinase phosphorylation (Table 1) although it completely abolished ATP- or UTP-stimulated phosphorylation of MARCKS protein (Table 1), a specific PKC substrate (Aderem, 1992). In this context it is important to mention that CGP 41251 displays a strong preference for Ca^{2+}-dependent PKC isoenzymes such as PKC-α, -β and -γ (Ochsner *et al.*, 1993; Marte *et al.*, 1994).

Table 1 Effects of CGP 41251 on ATP- and UTP-stimulated 42 kDa MAP kinase ($p42^{mapk}$) and MARCKS protein phosphorylation in mesangial cells

Addition	*$p42^{mapk}$*	*MARCKS*
	(% of maximal phosphorylation)	
Control	7 ± 4	2 ± 1
ATP	74 ± 9**	84 ± 11***
ATP + CGP 41251	72 ± 8**	10 ± 5††
UTP	100 ± 12**	100 ± 9***
UTP + CGP 41251	94 ± 10**	9 ± 6†††

Mesangial cells were labelled with [^{32}P]-orthophosphate and were stimulated for 10 min with vehicle (control), ATP (100 μM) or UTP (100 μM) in the absence or presence of the specific proteinkinase C (PKC) inhibitor, CGP 41251 (1 μM) as indicated. Cells were then lysed and $p42^{mapk}$ and MARCKS protein were successively immunoprecipitated with antibodies specific for $p42^{mapk}$ (dilution 1:200) or MARCKS protein (dilution 1:100), respectively, as described in the Methods section. Data were evaluated densitometrically and are means ± s.d. of three independent experiments.

Significant differences from corresponding controls: $^{**}P<0.01$; $^{***}P<0.001$, ANOVA. Significant differences from corresponding ATP and UTP stimulation (without CGP 41251): $\dagger\dagger P<0.01$; $\dagger\dagger\dagger P<0.001$; ANOVA.

Extracellular ATP and UTP stimulate MEK activation

The MAP kinase-activating kinase, MEK, has recently been cloned from mouse, man, and *Xenopus* (Crews *et al.*, 1992; Seger *et al.*, 1992a; Wu *et al.*, 1993; Kosako *et al.*, 1993; Zheng *et al.*, 1993). Three different human MEK cDNAs (MEK1, MEK2 and MEK3) have been isolated (Seger *et al.*, 1992b; Zheng *et al.*, 1993). In this study, we have generated an antipeptide antibody against murine MEK1 and used this antibody to immunoprecipitate MEK from mesangial cell lysates. Figure 12a shows that mesangial cells express MEK that is slightly phosphorylated already under basal conditions. Addition of UTP triggers a marked increase is MEK phosphorylation that is biphasic with maximal levels at 10 min and a second peak at 90 min, the latest time point examined. The data have been quantified by laser densitometry (Figure 12b) and demonstrate that again both nucleotides cause a comparable phosphorylation of MEK in mesangial.

Discussion

There is considerable evidence suggesting that extracellular ATP and UTP at low μM concentrations can function as signalling molecules in a wide range of physiological responses of cells (Gordon, 1986; O'Connor, 1992; El-Moatassim *et al.*, 1992; Burnstock, 1993). ATP is secreted in central and peripheral synapses and mediates fast excitatory neurotransmission; ATP stimulates secretion from mast cells and platelets and stimulates transepithelial ion transport and in the vascular system, extracellular ATP has contractile or relaxant effects on many blood vessels. Moreover, extracellular ATP may be of importance in the growth regulation of mammalian cells. Stimulation of DNA synthesis has been reported for a variety of cultured cells including mouse

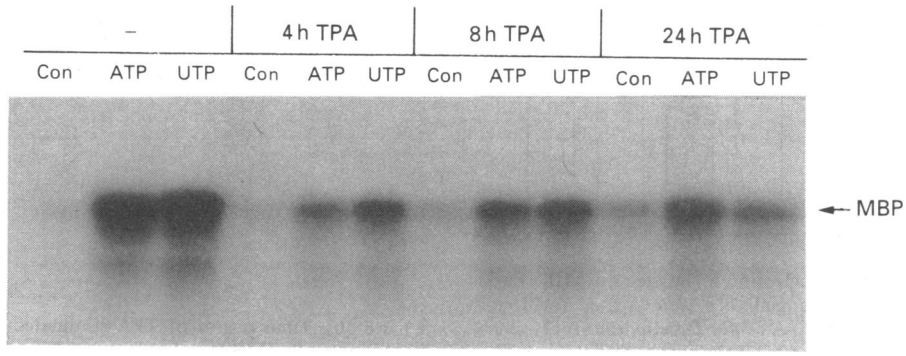


Figure 11 Effects of PKC downregulation on ATP- and UTP-stimulated MBP kinase activity in mesangial cells. Mesangial cells were pretreated for the indicated time periods with TPA (500 nM) and thereafter stimulated for 10 min with either vehicle (Con), ATP (100 μM) or UTP (100 μM) as indicated. Cells were harvested in kinase assay buffer and MBP kinase activity was measured as described in the Methods section. Similar results were obtained in three independent experiments.

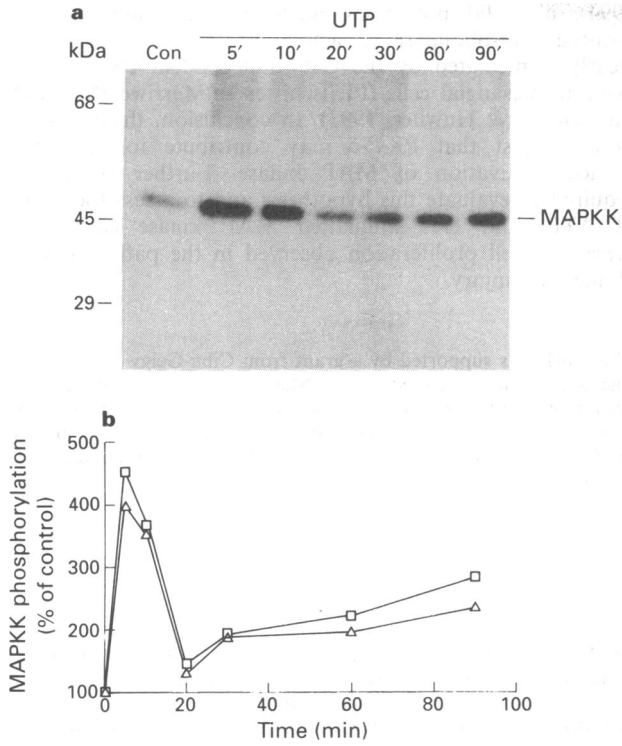


Figure 12 Time course of ATP- and UTP-stimulated phosphorylation of MAP kinase kinase (MAPKK) in mesangial cells. (a) Mesangial cells were labelled with [^{32}P]-orthophosphate and were stimulated with vehicle (Con) or UTP (100 μM) for the indicated time periods. Cells were then lysed and MAPKK was immunoprecipitated with a MAPKK-specific antiserum at a dilution of 1:100 as described in the Methods section. (b) Densitometrical evaluation of ATP- (Δ) and UTP- (□) stimulated MAPKK phosphorylation. Similar results were obtained in two independent experiments.

fibroblasts, A431 epidermoid carcinoma cells and DDT_1-MF-2 vas deferens cells (Huang *et al.*, 1989), in aortic smooth muscle cells (Malam-Souley *et al.*, 1993; Erlinge *et al.*, 1993), endothelial cells (Van Daele *et al.*, 1992) and mesangial cells (Schulze-Lohoff *et al.*, 1992). It has been reported that activation of PKC and phospholipase A_2 and subsequent production of prostaglandin E_2 and cyclic AMP formation are obligatory early steps in a pathway resulting in ATP-dependent mitogenesis (Wang *et al.*, 1991; Huang *et al.*, 1991). Recently a novel group of serine/threonine kinases, the MAP kinases, have been described that are activated commonly by various growth factors and PKC-activating tumour promoters. They are now considered to function as key enzymes in the signalling process leading from growth factor receptors to growth control of mammalian cells (Leevers & Marshall, 1992; Davis, 1993; Crewe & Erikson, 1993). We therefore investigated whether stimulation of MAP kinases is also important in nucleotide-stimulated post-receptor signalling in mesangial cells. Our data demonstrate for the first time that ATP and UTP activate the MAP kinase cascade. Addition of nucleotides to mesangial cells rapidly activated a kinase activity that phosphorylates exogenous MBP. This kinase was identified as $p42^{mapk}$ by immunoprecipitation with a specific antibody and by immunocomplex kinase assays. The time course and extent of activation of immunoprecipitated $p42^{mapk}$ was similar to the whole cell extract MBP kinase activity (compare Figures 5 and 6) and was paralleled by a phosphorylation of $p42^{mapk}$. Similar observations were reported for endothelin-stimulated MAP kinase activity in mesangial cells (Wang *et al.*, 1992). Whether ATP and UTP also activate $p44^{mapk}$ was not addressed in our experiments.

The responses observed after exposure of cells to extracellular ATP and UTP are most probably mediated by specific nucleotide receptors. The presence of a nucleotide receptor with pharmacological characteristics differing from those reported for P_2 purinoceptors was first described for rat mesangial cells (Pfeilschifter 1990b; Pfeilschifter & Merriweather, 1993) and sheep pituitary cells (Davidson *et al.*, 1990). For this putative nucleotide receptor, ATP and UTP are more potent agonists in triggering cell responses than classical P_{2y} agonists (2-methylthio-ATP, ADPβS) or P_{2x} agonists (α, β-methylene-ATP, βγ-methylene-ATP). The presence of such a nucleotide receptor has been reported for rat hepatocytes (Keppens *et al.*, 1992), the neuronal cell line N1E-115 (Iredale *et al.*, 1992), PC-12 phaeochromocytoma cells (Murrin & Boarder, 1991; Raha *et al.*, 1993) and a variety of other cell types (O'Connor, 1992). Very recently, Lustig *et al.* (1993) reported on the cloning of a mouse cDNA encoding an ATP receptor from neuroblastoma cells that upon expression in *Xenopus laevis* oocytes displayed the pharmacological profile of the nucleotide receptor. In the present study we have shown that ATP and UTP potently activate $p42^{mapk}$. Our data are compatible with a nucleotide-receptor-mediated $p42^{mapk}$ activation (Figure 9).

We have also addressed the question concerning the pathways leading to activation of MAP kinase in mesangial cells. MAP kinases are activated upon concurrent phosphorylation of tyrosine and of threonine. This double phosphorylation is mediated by the dual protein kinase, MEK, which itself is regulated by threonine phosphorylation. We now report for the first time that MEK is present in mesangial cells and is phosphorylated in a biphasic manner upon stimulation of the cells with extracellular ATP and UTP (Figure 12). We assume that this phosphorylation of MEK is accompanied by an activation of the enzyme. However, we are not in a position to prove this suggestion definitely, as we have no access to the necessary specific substrate required for a MEK activity assay (a kinase-negative mutant of MAP kinase).

The first peak of MEK phosphorylation at 10 min coincides with the phosphorylation and activation of $p42^{mapk}$ (Figures 3–6) and thus may mirror the chain of activation down the MAP kinase cascade. In contrast the second peak of MEK phosphorylation at 90 min is not paralleled by an increased $p42^{mapk}$ phosphorylation and activation. We only can speculate that this late phase of MEK phosphorylation may trigger $p44^{mapk}$ activation or, alternatively, is an expression of a negative feedback regulation exerted by MAP kinase or other kinases. Recently, Matsuda *et al.* (1993) reported that *Xenopus* MEK is phosphorylated on a threonine residue by its target kinase, MAP kinase. This site is different from the phosphorylation site catalyzed by MEK kinase, suggesting that the phosphorylation state of MEK is regulated not only by the upstream kinases (MEK kinase, Raf-1 kinase), but also by the downstream MAP kinases.

MEK acts as an integration point for at least three signalling pathways involving different protein kinase: (i) the serine-threonine kinase Raf-1, (ii) MEK kinase and (III) the *Xenopus* germ-cell specific serine/threonine kinase, MOS (Posada *et al.*, 1993). Thus, MEK would be activated by Raf-1 kinase after stimulation of receptor tyrosine kinases and by MEK kinase after triggering of receptors coupling to trimeric G-proteins and protein kinase C. Extracellular nucleotides couple to heterotrimeric G-proteins and have been shown to trigger phosphoinositide and phosphatidylcholine hydrolysis with the subsequent activation of PKC in mesangial cells. We therefore also addressed the role of PKC in triggering MAP kinase activation in mesangial cells. Short-term exposure of mesangial cells to TPA increased MAP kinase activity (Figure 10). By immunoblot analysis we have shown previously that mesangial cells express 4 PKC isoenzymes, PKC-α, -δ, -ε and -ζ. No PKC-β, -γ and -η isoforms were detected (Huwiler *et al.*, 1991; 1992; 1993). On exposure to TPA, these isoenzymes displayed distinctly different down-regulation kinetics. A 4–8 h treatment with TPA was sufficient to deplete mesangial cells completely of PKC-α and -δ isotypes, and a 24 h incubation with TPA was necessary to

down-regulate 80–90% of PKC-ε. In contrast, TPA treatment does not affect PKC-ζ. Treatment of mesangial cells with TPA for 4 h or 8 h, a regimen that depletes PKC-α and -δ isoforms, decreased by 50–60% the stimulation of MAP kinase induced by ATP or UTP (Figure 11). Pretreatment of the cells with TPA for 24 h, which also largely removes PKC-ε did not further reduce the stimulation of MAP kinase triggered by extracellular nucleotides (Figure 11). These data suggest that PKC-α and -δ are candidates that may mediate, at least in part, nucleotide-stimulated MAP kinase activation. In an attempt to elucidate further the contribution of PKC isoenzymes to MAP kinase activation we used the selective PKC inhibitor CGP 41251 (Meyer *et al.*, 1989). Surprisingly, CGP 41251 did not suppress ATP- or UTP-induced MAP kinase activation (Table 1), although the phosphorylation of the specific PKC substrate, MARCKS, was completely inhibited (Table 1). In this context it is worth noting that CGP 41251 which displays a selectivity for the Ca^{2+}-indepdent group B of PKC isoforms (Marte *et al.*, 1994), also did not block nucleotide- or angiotensin II-induced phospholipase D activation, a cell response that clearly is mediated by the Ca^{2+} independent PKC-ε isoenzyme in mesangial cells (Pfeilschifter & Merriweather, 1993; Pfeilschifter & Huwiler, 1993). In conclusion, these observations suggest that PKC-δ may contribute to nucleotide-induced activation of MAP kinase. Further studies are required to evaluate this hypothesis and to assess the impact of ATP- and UTP-stimualted MAP kinase cascade on mesangial cell proliferation observed in the pathogenesis of glomerular injury.

This work was supported by a grant from Ciba-Geigy Ltd. for A.H. The authors are indebted to Dr M.J. Dunn and Dr P. Burn for providing antibodies specific for $p42^{mapk}$ and phosphotyrosine, respectively. The authors gratefully acknowledge Dr D. Fabbro, Dr G. Caravatti and Dr T. Meyer for providing peptides and PKC inhibitors, respectively.

References

ADEREM, A.A. (1992). The role of myristoylated protein kinase C substrates in intracellular signalling pathways in macrophages. *Curr. Top. Microbiol. Immunol.*, **181**, 189–207.

BURNSTOCK, G. (1993). Physiological and pathological roles of purines: an update. *Drug Develop. Res.*, **28**, 195–206.

COUSER, W.G. (1993). Pathogenesis of glomerulonephritis. *Kidney Int.*, **44**, S19–S26.

CREWS, C.M., ALESSANDRINI, A. & ERIKSON, R.L. (1992). The primary structure of MEK, a protein kinase that phosphorylates the ERK gene product. *Science*, **258**, 478–480.

CREWS, C.M. & ERIKSON, R.L. (1993). Extracellular signals and reversible protein phosphorylation: what to MEK of it all. *Cell*, **74**, 215–217.

DAVIDSON, J.S., WAKEFIELD, I.K., SOHNIUS, U., VAN DER MERWE, P.A. & MILLAR, R.P. (1990). A novel extracellular nucleotide receptor coupled to phosphoinositidase-C in pituitary cells. *Endocrinology*, **126**, 80–87.

DAVIS, R.J. (1993). The mitogen-activated protein kinase signal transduction pathway. *J. Biol. Chem.*, **268**, 14553–14556.

EL-MOATASSIM, C., DORNAND, J. & MANI, J.C. (1992). Extracellular ATP and cell signalling. *Biochim. Biophys. Acta*, **1134**, 31–45.

ERLINGE, D., YOO, H., EDVINSSON, L., REIS, D.J. & WAHLESTEDT, C. (1993). Mitogenic effects of ATP on vascular smooth muscle cells vs. other growth factors and sympathetic cotransmitters. *Am. J. Physiol.*, **265**, H1089–H1097.

GORDON, J.L. (1986). Extracellular ATP: effects, sources and fate. *Biochem.*, **233**, 309–319.

HUANG, N., WANG, D. & HEPPEL, L.A. (1989). Extracellular ATP is a mitogen for 3T3, 3T6, and A431 cells and acts synergistically with other growth factors. *Proc. Natl. Acad. Sci. U.S.A.*, **86**, 7904–7908.

HUANG, N.N., WANG, D.-J., GONZALEZ, F. & HEPPEL, L.A. (1991). Multiple signal transduction pathways lead to extracellular ATP-stimulated mitogenesis in mammalian cells: II. A Pathway involving arachidonic acid release, prostaglandin synthesis, and cyclic AMP accumulation. *J. Cell. Physiol.*, **146**, 483–494.

HUWILER, A., FABBRO, D., STABEL, S. & PFEILSCHIFTER, J. (1992). Immunocharacterization of δ- and ζ-isoenzymes of protein kinase C in rat renal mesangial cells. *FEBS Lett.*, **300**, 259–262.

HUWILER, A., SCHULZE-LOHOFF, E., FABBRO, D. & PFEILSCHIFTER, J. (1993). Immunocharacterization of protein kinase C isoenzymes in rat kidney glomeruli, and cultured glomerular epithelial and mesangial cells. *Exp. Nephrol.*, **1**, 19–25.

HUWILER, A., FABBRO, D. & PFEILSCHIFTER, J. (1991). Possible regulatory functions of protein kinase C-α and -ε isoenzymes in rat renal mesangial cells. Stimulation of prostaglandin synthesis and feedback-inhibition of angiotensin II-stimulated phosphoinositide hydrolysis. *Biochem. J.*, **279**, 441–445.

IREDALE, P.A., MARTIN, K.F., ALEXANDER, S.P.H., HILL, S.J. & KENDALL, D.A. (1992). Inositol 1,4,5-trisphosphate generation and calcium mobilization via activation of an atypical P_2 receptor in the neuronal cell line, N1E-115. *Br. J. Pharmacol.*, **107**, 1083–1087.

KEPPENS, S.A., VANDEKERCKHOVE, A. & DE WULF, H. (1992). Extracellular ATP and UTP exert similar effects on rat isolated hepatocytes. *Br. J. Pharmacol.*, **105**, 475–479.

KOSAKO, H., NISHIDA, E. & GOTOH, Y. (1993). cDNA cloning of MAP kinase kinase reveals kinase cascade pathways in yeasts to vertebrates. *EMBO J.*, **12**, 787–794.

LEEVERS, S.J. & MARSHALL, C.J. (1992). MAP kinase regulation–the oncogene connection. *Trends Cell Biol.*, **2**, 283–286.

LUSTIG, K.D., SHIAU, A.K., BRAKE, A.J. & JULIUS, D. (1993). Expression cloning of an ATP receptor from mouse neuroblastoma cells. *Proc. Natl. Acad. Sci. U.S.A.*, **90**, 5113–5117.

MALAM-SOULEY, R., CAMPAN, M., GADEAU, A.-P. & DESGRANGES, C. (1993). Exogenous ATP induces a limited cell cycle progression of arterial smooth muscle cells. *Am. J. Physiol.*, **264**, C783–C788.

MARTE, B.M., MEYER, T., STABEL, S., STANDKE, G.J.R., JAKEN, S., FABBRO, D. & HYNES, N.E. (1994). Protein kinase C and mammary cell differentiation: involvement of PKC-α in the induction of β-casein expression. *Cell Growth Diff.*, **5**, 239–247.

MATSUDA, S., GOTOH, Y. & NISHIDA, E. (1993). Phosphorylation of *Xenopus* mitogen-activated protein (MAP) kinase kinase by MAP kinase kinase kinase and MAP kinase. *J. Biol. Cehm.*, **268**, 3277–3281.

MEYER, T., REGENASS, U., FABBRO, D., ALTERI, E. RÖSEL, J., MÜLLER, M., CARAVATTI, G. & MATTER, A. (1989). A derivative of staurosporine (CGP 41 251) shows selectivity for protein kinase C inhibition and *in vitro* anti-proliferative as well as *in vivo* anti-tumor activity. *Int. J. Cancer*, **43**, 851–856.

MURRIN, R.J.A. & BOARDER, M.R. (1991). Neuronal 'nucleotide' receptor linked to phospholipase C and phospholipase D? Stimulation of PC12 cells by ATP analogues and UTP. *Mol. Pharmacol.*, **41**, 561–568.

OCHSNER, M., HUWILER, A., FLECK, T. & PFEILSCHIFTER, J. (1993). Protein kinase C inhibitors potentiate angiotensin II-induced phosphoinositide hydrolysis and intracellular Ca^{2+}-mobilization in renal mesangial cells. *Eur. J. Pharmacol. Mol. Pharmacol.*, **245**, 15–21.

O'CONNOR, S.E. (1992). Recent development in the classification and functional significance of receptors for ATP and UTP, evidence for nucleotide receptors. *Life Sci.*, **50**, 1657–1664.

PAVENSTÄDT, H., GLOY, J., LEIPZIGER, J., KLÄR, B., PFEILSCHIFTER, J., SCHOLLMEYER, P. & GREGER, R. (1993). Effect of extracellular ATP on contraction, cytosolic calcium activity, membrane voltage and ion currents of rat mesangial cells in primary culture. *Br. J. Pharmacol.*, **109**, 953–959.

PFEILSCHIFTER, J. (1990a). Extracellular ATP stimulates polyphosphoinositide hydrolysis and prostaglandin synthesis in rat renal mesangial cells. Involvement of a pertussis toxin-sensitive guanine nucleotide binding protein and feedback inhibition by protein kinase C. *Cell Signalling*, **2**, 129–138.

PFEILSCHIFTER, J. (1990b). Comparison of extracellular ATP and UTP signalling in rat renal mesangial cells. No indications for the involvement of separate purino- and pyrimidino-ceptors. *Biochem. J.*, **272**, 469–472.

PFEILSCHIFTER, J. (1990c). Angiotensin II B-type receptor mediates phosphoinositide hydrolysis in mesangial cells. *Eur. J. Pharmacol.*, **184**, 201–202.

PFEILSCHIFTER, J. & HUWILER, A. (1993). A role for protein kinase C-ε in angiotensin II stimulation of phospholipase D in rat renal mesangial cells. *FEBS Lett.*, **331**, 267–271.

PFEILSCHIFTER, J. & MERRIWEATHER, C. (1993). Extracellular ATP and UTP activation of phospholipase D is mediated by protein kinase C-ε in rat renal mesangial cells. *Br. J. Pharmacol.*, **110**, 847–853.

POSADA, J., YEW, N., AHN, N.G., VANDE WOUDE, G.F. & COOPER, J.A. (1993). Mos stimulates MAP kinase in *Xenopus* oocytes and activates a MAP kinase kinase in vitro. *Mol. Cell. Biol.*, **13**, 2546–2553.

RAHA, S., DE SOUZA, L.R. & REED, J.K. (1993). Intracellular signalling by nucleotide receptors in PC12 pheochromocytoma cells. *J. Cell. Physiol*, **154**, 623–630.

SCHULZE-LOHOFF, E., ZANNER, S., OGILVIE, A. & STERZEL, R.B. (1992). Extracellular ATP stimulates proliferation of cultured mesangial cells via P_2-purinergic receptors. *Am. J. Physiol.*, **263**, F374–F383.

SEGER, R., SEGER, D., LOZEMAN, F.J., AHN, N.G., GRAVES, L.M., CAMPELL, J.S., ERICSSON, L., HARRYLOCK, M., JENSEN, A.M. & KREBS, E.G. (1992a). Human T-cell mitogen-activated protein kinase kinases are related to yeast signal transduction kinases. *J. Biol. Chem.*, **267**, 25628–25631.

SEGER, R., AHN, N.G., POSADA, J., MUNAR, E.S., JENSEN, A.M., COOPER, J.A., COBB, M.H. & KREBS, E.G. (1992b). Purification and characterization of mitogen-activated protein kinase activator(s) from epidermal growth factor-stimulated A431 cells. *J. Biol. Chem.*, **267**, 14373–14381.

VAN DAELE, P., VAN COEVORDEN, A., ROGER, P.P. & BOEYNAEMS, J.-M. (1992). Effects of adenine nucleotides on the proliferation of aortic endothial cells. *Circ. Res.*, **70**, 82–90.

WANG, D.J., HUANG, N.-N., GONZALEZ, F.A. & HEPPEL, L.A. (1991). Multiple signal transduction pathways lead to extracellular ATP-stimulated mitogenesis in mammalian cells: I. Involvement of protein kinase C-dependent and -independent pathways. *J. Cell. Physiol.*, **146**, 473–482.

WANG, Y., SIMONSON, M.S., POUYSSÉGUR, J. & DUNN, M.J. (1992). Endothelin rapidly stimulates mitogen-activated protein kinase activity in rat mesangial cells. *Biochem. J.*, **287**, 589–594.

WU, J., HARRISON, J.K., VINCENT, L.A., HAYSTEAD, C., HAYSTEAD, T.A.J., MICHEL, H., HUNT, D.F., LYNCH, K.R. & STURGILL, T.W. (1993). Molecular structure of a protein-tyrosine/threonine kinase activating p42 mitogen-activated protein (MAP)kinase: MAP kinase kinase. *Proc. Natl. Acad. Sci. U.S.A.*, **90**, 173–177.

ZHENG, C.-F. & GUAN, K.L. (1993). Cloning and characterization of two distinct human extracellular signal-regulated kinase activator kinases, MEK1 and MEK2. *J. Biol. Chem.*, **268**, 11435–11439.

(Received April 18, 1994
Revised July 4, 1994
Accepted August 18, 1994)

Br. J. Pharmacol. (1994), **113**, 1464–1470 © Macmillan Press Ltd, 1994

Antimuscarinic action of liriodenine, isolated from *Fissistigma glaucescens*, in canine tracheal smooth muscle

Chien-Huang Lin, *Chuen-Mao Yang, Feng-Nien Ko, †Yang-Chang Wu & [1]Che-Ming Teng

Pharmacological Institute, College of Medicine, National Taiwan University, Taipei, *Department of Pharmacology, Chang Gung Medical College, Tao-Yuan and †Graduate Institute of Natural Products, Kaohsiung Medical College, Kaohsiung, Taiwan

1 The antimuscarinic properties of liriodenine, isolated from *Fissistigma glaucescens*, were compared with methoctramine (cardioselective M_2 antagonist) and 4-diphenylacetoxy-*N*-methylpiperidine (4-DAMP, smooth muscle selective M_3 antagonist) by radioligand binding tests, functional tests and measurements of second messenger generation in canine cultured tracheal smooth muscle cells.

2 Liriodenine, pirenzepine, methoctramine and 4-DAMP displaced [^{3}H]-N-methyl scopolamine ([^{3}H]-NMS) binding in a concentration-dependent manner with K_i values of $2.2 \pm 0.4 \times 10^{-6}$, $3.3 \pm 0.7 \times 10^{-7}$, $8.9 \pm 2.3 \times 10^{-8}$ and $2.3 \pm 0.6 \times 10^{-9}$ M, respectively. The curves for competitive inhibition of [^{3}H]-NMS with liriodenine, methoctramine and 4-DAMP were best fitted according to a two site model of binding, but pirenzepine was best fitted according to a model with one site.

3 Liriodenine and 4-DAMP displayed a high affinity for blocking tracheal contraction ($pK_B = 5.9$ and 9.1, respectively) and inositol phosphate formation ($pK_B = 6.0$ and 8.9, respectively), but a low affinity for antagonism of cyclic AMP inhibition ($pK_B = 4.7$ and 7.8, respectively).

4 Methoctramine blocked cyclic AMP inhibition with a high affinity ($pK_B = 7.4$), but it antagonized tracheal contraction and inositol phosphate formation with a low affinity ($pK_B = 6.1$ and 6.0, respectively).

5 In conclusion, both M_2 and M_3 muscarinic receptor subtypes coexist in canine tracheal smooth muscle and are coupled to the inhibition of cyclic AMP formation and phosphoinositide breakdown, respectively. The antimuscarinic characteristics of liriodenine are similar to those of 4-DAMP. It may act as a selective M_3 receptor antagonist in canine tracheal smooth muscle.

Keywords: Liriodenine; muscarinic receptor antagonist; tracheal smooth muscle cells; *Fissistigma glaucescens*

Introduction

Various evidence indicates that muscarinic receptors are divisible into three categories on the basis of their selectivity for different antagonists (Caulfield, 1993). M_1 muscarinic receptors have high affinity for pirenzepine and are abundant in brain and sympathetic ganglia (Hammer & Giachetti, 1982; Watson *et al.*, 1983). The M_2 subtypes have high affinity for methoctramine and AF-DX 116 (11-[[2-(diethylamino)methyl]-1-piperidinyl]acetyl]-5, 11-dihydro-6H-pyrido-[2,3-b][1,4]benzodiazepin-6-one) and account for most, if not all, muscarinic receptors in the mammalian myocardium (Giachetti *et al.*, 1986; Waelbroeck *et al.*, 1987). M_3 muscarinic receptors have high affinity for 4-diphenylacetoxy-*N*-methylpiperidine methiodide (4-DAMP) and trigger responses in smooth muscles and exocrine glands (Mutschler & Lambrecht, 1984; Doods *et al.*, 1987). Five genes for the muscarinic receptors have been cloned and designated as m_1, m_2, m_3, m_4 and m_5 (Bonner, 1989; Buckley *et al.*, 1989). The different receptor subtypes coupled to various effector systems demonstrated that the expressed m_1, m_3 and m_5 subtypes are preferentially coupled to hydrolysis of phosphoinositide, whereas the m_2 and m_4 subtypes are coupled to attenuation of adenylate cyclase (Bonner *et al.*, 1988; Shapiro *et al.*, 1988; Peralta *et al.*, 1988; Bonner, 1989). Previous experiments demonstrated that M_2 and M_3 receptor subtypes exist in freshly isolated canine tracheal smooth muscle cells (TSMCs) as demonstrated by radioligand binding (Yang, 1991; Fernandes *et al.*, 1992) and receptor-mediated generation of second messengers (Yang *et al.*, 1991). Moreover, M_2 and M_3 receptor subtypes are also coexpressed in other types of smooth muscle including gastrointestinal smooth muscle, urinary bladder and vascular tissue (Eglen *et al.*, 1994).

In our previous experiments we have found that liriodenine (Figure 1), isolated from *Fissistigma glaucescens*, acts as a selective M_3 muscarinic receptor antagonist in guinea-pigs (Lin *et al.*, 1994). It possesses an equal affinity for tracheal and ileal muscarinic receptors ($pA_2 = 6.22 \pm 0.08$ and 6.36 ± 0.10, respectively). Moreover, it is ten times more potent for smooth muscle M_3 muscarinic receptors than for the cardiac M_2 muscarinic receptors that mediate negative inotropic and chronotropic effects (Lin *et al.*, 1994). The aim of the present work was to investigate the selectivity of liriodenine on M_2 and M_3 receptor subtypes in canine tracheal smooth muscle. Therefore, we tested the binding affinity of liriodenine, pirenzepine (selective M_1 antagonist), methoctramine (cardioselective M_2 antagonist) and 4-DAMP (smooth muscle selective M_3 antagonist) in canine cultured TSMCs. We compared the ability of these antagonists to block the receptor-mediated

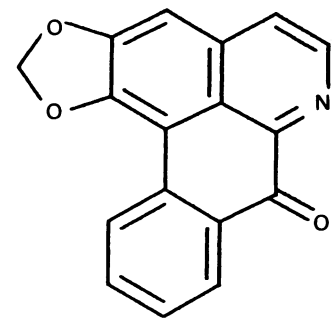


Figure 1 Chemical structure of liriodenine.

[1] Author for correspondence at: Pharmacological Institute, College of Medicine, National Taiwan University, No. 1, Jen-Ai Road, Section 1, Taipei 10018, Taiwan.

contraction of tracheal smooth muscle, and to block stimulation of phosphoinositide hydrolysis and inhibition of adenylate cyclase activity in canine cultured TSMCs.

Methods

Animals

Mongrel dogs of either sex, 20–30 kg, purchased from a local supplier, were used throughout this work. Dogs were housed indoors in animal facilities under automatically controlled temperature and light cycle and fed standard laboratory chow and tap water *ad libitum*. Dogs were anaesthesized with pentobarbitone (30 mg kg^{-1}, i.v.) and the lungs were ventilated mechanically via an orotracheal tube. The trachea was removed from the animal.

Mechanical response

The trachea, about 20 cm long from larynx to bifuraction, was quickly removed and transferred to oxygenated (95% O_2 plus 5% CO_2) Krebs-Henseleit solution (KHS) of the following composition (mM):NaCl 117, KCl 4.7, $MgSO_4$ 1.1, KH_2PO_4 1.2, $NaHCO_3$ 20, $CaCl_2$ 2.4, glucose 1, HEPES 20. The trachea was opened by cutting the cartilage rings opposite the smooth muscle. The muscle was cleaned in two steps. The initial step in each dissection involved removal of the epithelium and submucosal tissue with forceps. The connective tissue on the serosal surface was carefully cleaned under a microscope. In order to hook the muscle strips to the transducer, the section of cartilage up to the point of insertion of the muscle was maintained. Then the trachea was cut into separated individual rings. The tracheal preparations were mounted in an organ bath containing KHS (5 ml) and gassed with 95% O_2 plus 5% CO_2 at 37°C. The tracheal preparations were equilibrated in KHS for 60 min with three changes of KHS and maintained under an optimal tension of 0.5 g. Contractions were recorded isometrically via a force-displacement transducer connected to a recorder (Gould 3000, Cleveland, U.S.A.). The tracheal preparations were allowed to equilibrate for 15 min with liriodenine, methoctramine or 4-DAMP before the generation of cumulative concentration-response curves to carbachol at 5 min intervals. Results are expressed as percentages of maximal control response for carbachol before addition of muscarinic antagonists.

Isolation of tracheal smooth muscle cells

TSMCs were isolated according to the method described previously (Yang, 1991). In brief, the smooth muscle was dissected, minced and transferred to the dissociation medium containing collagenase I (0.02%), DNase I (0.01%) and elastase IV (0.01%) and antibiotics in a solution composed of (in mM): NaCl 137, KCl 5, $CaCl_2$ 1.1, $NaHCO_3$ 20, NaH_2PO_4 1, glucose 11, HEPES 25, pH 7.4. The tissue pieces were gently agitated at 37°C in a rotary shaker for 1 h; the released cells were collected and the residue was digested in the same fresh enzyme solution for an additional hour at 37°C. All released cells were collected and washed twice with DMEM/F-12 medium. The cells suspended in DMEM/F-12 containing foetal bovine serum (FBS, 10%) were preplated onto petri dishes (60 mm) and incubated at 37°C for 1 h to remove fibroblasts. The cells were then counted and diluted with DMEM/F-12 to 2×10^5 cells ml^{-1}. The cell suspension was plated onto 24-well culture plates for receptor binding and adenosine 3':5'-cyclic monophosphate (cyclic AMP) assay and 12-well culture plates for assay of inositol phosphate accumulation. The culture medium was changed after 24 h and then changed every three days. After five days in culture, the cells were removed to DMEM/F-12 containing FBS (1%) for 24 h at 37°C. Then, the cells were cultured in DMEM/F-12 containing FBS (1%) supplemented with IGF-I (10 ng ml^{-1}) and insulin (1 $\mu g\ ml^{-1}$) for 12–14 days. To characterize the isolated and cultured TSMCs and to exclude the possibility of contamination by epithelial cells and fibroblasts, we examined the preparations by means of an indirect immunofluorescence method using antibody of light chain myosin (Gown *et al.*, 1985). Over 95% of the cells isolated were found to be smooth muscle cells.

Receptor binding assay

The binding assay for muscarinic receptors was performed by using [^{3}H]-N-methylscopolamine ([^{3}H]-NMS) as described previously (Yamamura & Snyder, 1974; Yang, 1991). Saturation binding assays were carried out in triplicate with [^{3}H]-NMS in the presence (non-specific binding) and absence (total binding) of atropine (1 μM). In brief, cultured TSMCs were washed twice with Tris-Cl (300 mM) buffer solution (pH 7.4) and then incubated for 45 min at 37°C with [^{3}H]-NMS at various concentrations (20–1000 pM) in a total volume 0.25 ml of Tris-Cl buffer solution. Competitive binding experiments were performed in the presence of liriodenine, pirenzepine, methoctramine and 4-DAMP at various concentrations in triplicate with [^{3}H]-NMS (400 pM). The reaction was terminated by removing the medium and washing the cells three times with Tris-Cl buffer solution. Cells were solubilized in NaOH (0.1 N); the radioactivity was determined with a liquid scintillation counter (Beckman 5000 TC).

Accumulation of inositol phosphates

Cultured TSMCs were incubated with *myo*-[2-^{3}H]-inositol (5 $\mu Ci\ ml^{-1}$) at 37°C for two days. TSMCs were washed twice with KHS and incubated in KHS containing LiCl (10 mM) at 37°C for 30 min. After an agonist was added at the concentration indicated, incubation was continued for another 60 min. When an antagonist was used, it was added 15 min before the addition of the agonist. Reactions were terminated on addition of perchloric acid (5%) followed by sonication and centrifugation at 3000 *g* for 15 min.

Supernatants soluble in perchloric acid were extracted four times with diethyl ether, neutralized with potassium hydroxide, and applied to a column of anion exchange resin (AGI-X8, formate form, 100–200 mesh). The resin was washed successively with water (5 ml) and ammonium formate (60 mM)/sodium tetraborate (5 mM) in 5 ml to eliminate free [^{3}H]-*myo*-inositol and glycerophosphoinositol, respectively. A total inositol phosphate fraction was then eluted with ammonium formate (1 M)/formic acid (0.1 M) in 10 ml. The amount of [^{3}H]-inositol phosphates was determined by scintillation counting of samples (0.5 ml). Results are expressed as percentages of the maximal control response for carbachol in the absence of muscarinic antagonists.

Cyclic AMP assay

Cultured TSMCs were incubated with 3-isobutyl-1 methylxanthine (IBMX) (0.2 mM) at 37°C for 10 min and then exposed to isoprenaline (1 μM) alone or combined with the specific muscarinic agonist carbachol used at indicated concentrations and continuously incubated at 37°C for 10 min. When an antagonist was used, it was added at the indicated concentrations 15 min before addition of carbachol and/or isoprenaline. Reactions were stopped by adding the buffer solution (mM): Tris-Cl 50, theophylline 100, EDTA 4 (pH 13) and neutralized with HCl (0.1 N), followed by centrifugation at 10,000 *g* for 15 min at 4°C. Cyclic AMP was assessed with Amersham cyclic AMP RIA kits. Cyclic AMP levels are expressed as pmol mg^{-1} protein. Inhibition of cyclic AMP accumulation mediated by carbachol was evaluated as the difference between cyclic AMP due to isoprenaline and cyclic AMP obtained in the simultaneous presence of isoprenaline

and carbachol. Alternatively, inhibition was expressed as the percentage of inhibitory response to a maximally effective concentration of carbachol.

Materials

Liriodenine was isolated from the plant *Fissistigma glaucescens* as previously described (Lu *et al.*, 1985). The following drugs were used: carbachol, isoprenaline hydrochloride, 3-isobutyl-l-methylxanthine (IBMX), myoinositol, collagenase I, DNase I, elastase IV, Penstrep, gentamicin (Sigma Chemical Co., St. Louis, MO, U.S.A.), methoctramine hydrochloride and 4-diphenylacetoxy-*N*-methylpiperidine methiodide (4-DAMP) (RBI, Boston, MA, U.S.A.), AGl-X8 (Bio-Rad, Richmond, CA, U.S.A.), 1-[N-methyl-^{3}H]-scopolamine methyl chloride ([^{3}H]-NMS, 85 Ci mmol^{-1}), *myo*-[2-^{3}H]-inositol (18 Ci mmol^{-1}) and cyclic AMP RIA kits (Amersham, Buckinghamshire, England).

Data analysis

In radioligand binding tests, the maximal number of binding sites (B_{max}) and equilibrium dissociation constant (K_d) were obtained by Scatchard analysis (Scatchard, 1949) of saturation binding. IC_{50} values were transformed to K_i values, according to the method of Cheng & Prusoff (1973). From competitive experiments, data were analysed by means of the LIGAND programme of Munson & Rodbard (1980). To analyse subtypes we fitted competitive inhibition curves according to models with either one or two sites of binding using iterative least squares corrected for occupancy by [^{3}H]-NMS, with statistical significance established by Fisher's F test (Zar, 1974). The equation for displacements is

$$B/B_{max} = F_n/\{1 + (K_d/[L](1 + [I]/K_{in})\}$$

in which B and B_{max} represent observed and maximal (asymptotic) concentrations of binding sites, F_n is the fraction of sites of type n, K_d is the binding constant for the labelled ligand, measured for each preparation, [L] is the concentration of the ligand, [I] is the concentration of the inhibitor and K_{in} is the inhibitory constant for the competing ligand for type n. The model with two binding sites was preferred when, according to the F test, $P<0.05$.

The EC_{50} values of carbachol for tracheal contraction, inositol phosphates accumulation and inhibition of cyclic AMP formation were estimated with the Graph Pad programme (Graph Pad, San Diego, California, U.S.A.), sharing the same estimate of the maximum response between the control value and the value measured in the presence of muscarinic antagonists. When several concentrations of antagonists were used, the dissociation constants (K_B) of muscarinic antagonists were estimated by measurement of their abilities to antagonize carbachol-mediated contraction of tracheal smooth muscle, stimulation of phosphoinositide hydrolysis and inhibition of cyclic AMP formation. The K_B values were calculated as described by Furchgott (1972).

The experimental results are expressed as mean ± s.e.mean, and accompanied by the number of observations. Statistical significance was assessed with Student's t test and P values less than 0.05 are considered significant.

Results

Identification and characterization of [^{3}H]-NMS binding sites in cultured TSMCs

Muscarinic receptors were characterized by use of binding tests with [^{3}H]-NMS in cultured TSMCs. The binding of [^{3}H]-NMS was saturable and of high affinity. Scatchard plot analysis revealed that the muscarinic receptor binding sites in cultured TSMCs constituted a single population (Hill coefficients 0.99) (Figure 2). The equilibrium dissociation constant (K_d) and the maximal receptor density (B_{max}) for [^{3}H]-NMS binding was 336.1 ± 10.7 pM and 113.6 ± 11.2 fmol mg^{-1} protein, respectively.

Effects of liriodenine, pirenzepine, methoctramine and 4-DAMP on [^{3}H]-NMS binding in cultured TSMCs

Displacement curves for liriodenine, pirenzepine, methoctramine and 4-DAMP against [^{3}H]-NMS at a single concen-

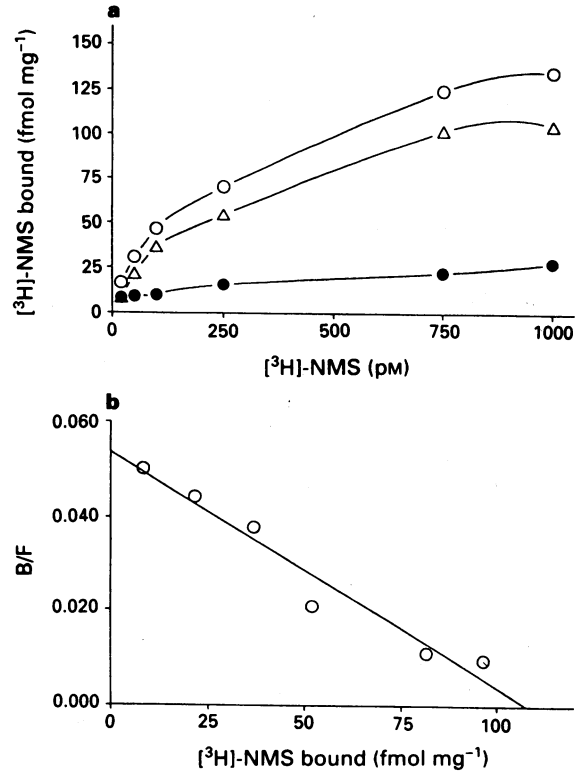


Figure 2 Saturation experimental data (a) and Scatchard plots (b) of [^{3}H]-N-methylscopolamine ([^{3}H]-NMS) binding to cultured canine tracheal smooth muscle cells. Specific binding (Δ) is the difference between total binding (O) and binding (●) in the presence of atropine (1 μM) (non-specific binding). The data shown are those from a single experiment of four experiments determined in triplicate in cultured canine tracheal smooth muscle cells.

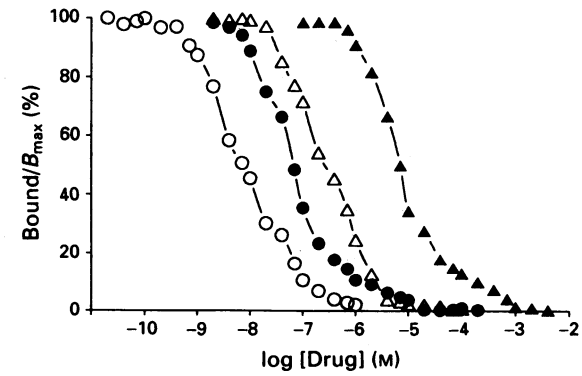


Figure 3 Displacement curves of specific [^{3}H]-N-methylscopolamine ([^{3}H]-NMS) binding to canine cultured tracheal smooth muscle cells. Cells were incubated with 4-diphenylacetoxy-*N*-methylpiperidine methiodide (4-DAMP, o), methoctramine (●), pirenzepine (Δ) or liriodenine (▲) at various concentrations in the presence of [^{3}H]-NMS (400 pM) at 37°C for 45 min. Non-specific binding determined in the presence of atropine (1 μM) was subtracted from the total binding. The typical data shown are those from a single experiment of four experiments determined in triplicate.

tration (400 pM) were examined in cultured TSMCs (Figure 3). Liriodenine, pirenzepine, methoctramine and 4-DAMP displaced [^{3}H]-NMS binding in a concentration-dependent manner with K_i values of $2.2 \pm 0.4 \times 10^{-6}$, $3.3 \pm 0.7 \times 10^{-7}$, $8.9 \pm 2.3 \times 10^{-8}$ and $2.3 \pm 0.6 \times 10^{-9}$ M, respectively. The model with one or two binding sites was chosen on the basis of a statistical test of goodness of fit ($P < 0.05$) according to Fisher's F test. The curves for competitive inhibition of [^{3}H]-NMS binding with liriodenine, methoctramine and 4-DAMP were shallow and best fitted with a model having two binding sites ($P < 0.05$) (Figure 3). The competition curves were steep and adequately described with a model for one site of binding of pirenzepine (Figure 3). Based on the binding parameters obtained from competitive inhibition experiments, the K_i of each competing ligand and the fraction of total receptor population represented by each subtype are given in Table 1.

Effects of liriodenine, methoctramine and 4-DAMP on carbachol-induced contraction of canine tracheal smooth muscle

Carbachol (0.03–30 μM) caused a concentration-dependent contraction in canine tracheal smooth muscle; the EC_{50} for carbachol was 0.41 ± 0.04 μM. The concentration-response curves for carbachol were shifted to the right by liriodenine (10 and 100 μM), methoctramine (10 and 100 μM) and 4-DAMP (0.1 and 1 μM) in a parallel fashion with no change in the maximal response (Figure 4). The dissociation constants (K_B) of each antagonist were calculated from dose-ratios according to the method of Furchgott (1972). As two concentrations of each antagonist were used in these experiments; consequently, two values of K_B were calculated for each antagonist. Table 2 lists these values of muscarinic antagonists. There was no distinction between these two values ($P > 0.05$). The pK_B values of liriodenine, methoctramine and 4-DAMP were 5.9, 6.0 and 9.1, respectively, which corresponded to a low affinity for methoctramine and a high affinity for liriodenine and 4-DAMP in this response (see Table 1 and review by Hulme *et al.*, 1990).

Effects of liriodenine, methoctramine and 4-DAMP on carbachol-mediated accumulation of inositol phosphates

Carbachol (0.3–100 μM) caused a concentration-dependent accumulation of inositol phosphates in cultured TSMCs, with the maximal effect being a seven fold increase over basal levels (9680 d.p.m./well). The EC_{50} value for carbachol-mediated inositol phosphate accumulation was approximately 6.4 ± 1.1 μM (Figure 5). Liriodenine (10 and 100 μM), methoctramine (10 and 100 μM) and 4-DAMP (0.1 and 1 μM) produced a parallel, rightward shift of the curve without diminution of maximal response (Figure 5). Table 2 lists K_B values for muscarinic antagonists used in these experiments. Two values of K_B were calculated for each antagonist, as two concentrations of each antagonist were used in this work. There was no distinction between these two K_B values ($P > 0.05$). The pK_B values of liriodenine, methoctramine and 4-DAMP for antagonizing the carbachol-mediated inositol phosphate accumulation were 6.0, 6.1 and 8.9, respectively, in satisfactory agreement with the low affinity for methoctramine and high affinity for liriodenine and 4-DAMP in this response (see Table 1 and review Hulme *et al.*, 1990).

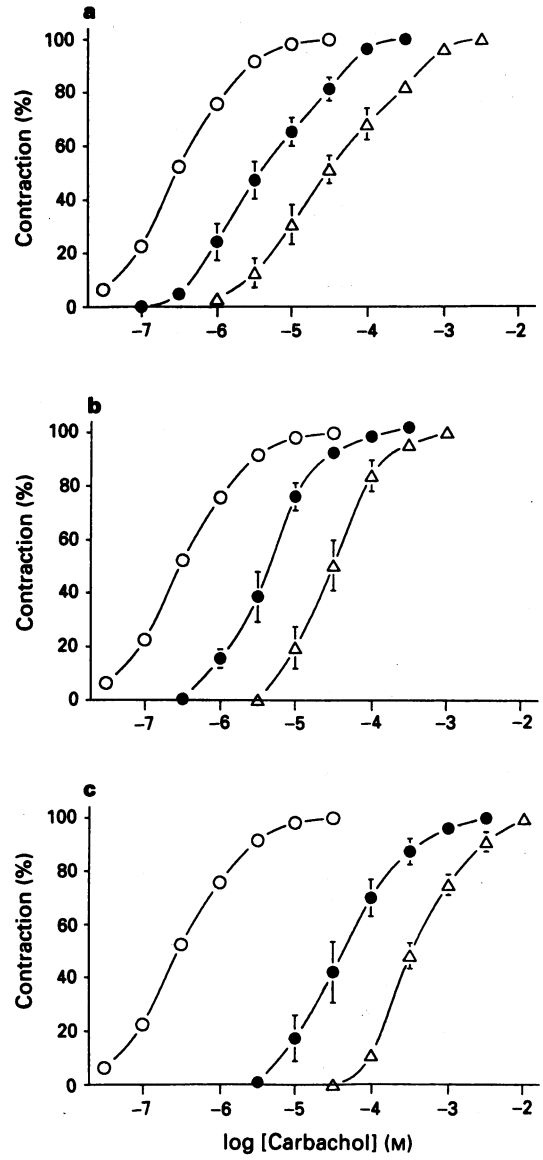


Figure 4 Antagonism of carbachol-mediated contraction by liriodenine (a), methoctramine (b) and 4-diphenylacetoxy-*N*-methylpiperidine (4-DAMP) (c) in canine tracheal smooth muscle. The concentration-response curve of carbachol-mediated smooth muscle contraction was constructed in the absence (control, o) and presence of liriodenine (●, 10 μM; Δ, 100 μM), methoctramine (●, 10 μM; Δ, 100 μM) and 4-DAMP (●, 0.1 μM; Δ, 1 μM) in a cumulative addition of carbachol at 5 min intervals. Results are expressed as percentage of the maximal control response of carbachol. Each point represents the mean ± s.e.mean of six or seven experiments.

Table 1 Binding parameters obtained in competitive experiments and analysis according to models with binding at one and two sites

	Low affinity		*High affinity*	
Drugs	K_{il} (M)	F_l (%)	K_{ih} (M)	F_h (%)
Liriodenine	$2.6 \pm 0.8 \times 10^{-5}$	21.3 ± 4.0	$1.4 \pm 0.3 \times 10^{-6}$	78.6 ± 4.0
Pirenzepine	$2.7 \pm 0.9 \times 10^{-7}$	–	–	–
Methoctramine	$1.8 \pm 0.4 \times 10^{-6}$	34.1 ± 6.0	$3.6 \pm 1.6 \times 10^{-8}$	65.9 ± 6.0
4-DAMP	$5.7 \pm 0.8 \times 10^{-9}$	45.8 ± 5.3	$4.4 \pm 1.3 \times 10^{-10}$	54.2 ± 5.4

Values are expressed as the means ± s.e.mean of four experiments. K_{il} and K_{ih} are the inhibitory constants of low and high affinity for the competing ligand, respectively. F_l and F_h are the fraction of sites of low and high affinity, respectively.

Table 2 Dissociation constants (K_B) for liriodenine, methoctramine and 4-diphenyl acetoxy-N-methylpiperidine (4-DAMP) to antagonize carbachol-mediated tracheal contraction, accumulation of inositol phosphates and inhibition of adenylate cyclase activity

	Tracheal contraction			*Accumulation of inositol phosphates*			*Inhibition of adenylate cyclase activity*		
Drugs (M)	EC_{50} (μM)	pK_B	*n*	EC_{50} (μM)	pK_B	*n*	EC_{50} (μM)	pK_B	*n*
Liriodenine									
10^{-5}	4.7 ± 1.0	5.9 ± 0.2	6	85.5 ± 24.1	6.1 ± 0.2	3	–	–	–
10^{-4}	37.0 ± 4.6	5.9 ± 0.1	6	945.6 ± 186.1	6.0 ± 0.1	3	1.32 ± 0.23	4.6 ± 0.1	4
3×10^{-4}	–	–	–	–	–	–	3.89 ± 0.68	4.7 ± 0.2	4
Methoctramine									
10^{-6}	–	–	–	–	–	–	8.1 ± 2.4	7.4 ± 0.2	3
10^{-5}	6.4 ± 1.4	6.1 ± 0.1	6	66.5 ± 11.4	6.0 ± 0.1	3	57.6 ± 10.9	7.3 ± 0.1	3
10^{-4}	43.1 ± 12.0	6.0 ± 0.1	7	1072.7 ± 178.6	6.2 ± 0.1	3	–	–	–
4-DAMP									
10^{-7}	68.9 ± 19.8	9.2 ± 0.1	6	642.9 ± 157.7	8.9 ± 0.1	3	2.1 ± 0.3	7.8 ± 0.1	3
10^{-6}	401.4 ± 14.5	9.0 ± 0.1	6	5933.9 ± 1588.2	8.9 ± 0.1	3	19.7 ± 0.4	7.8 ± 0.1	3

Values (mean ± s.e.mean for number (*n*) experiments) were calculated from the concentration-response curves for carbachol shown in Figures 4–6. EC_{50} values of carbachol-mediated tracheal contraction, inositol phosphates accumulation and inhibition of isoprenaline-stimulated cyclic AMP formation were 0.41 ± 0.04, 6.4 ± 1.1 and 0.27 ± 0.03 μM, respectively.

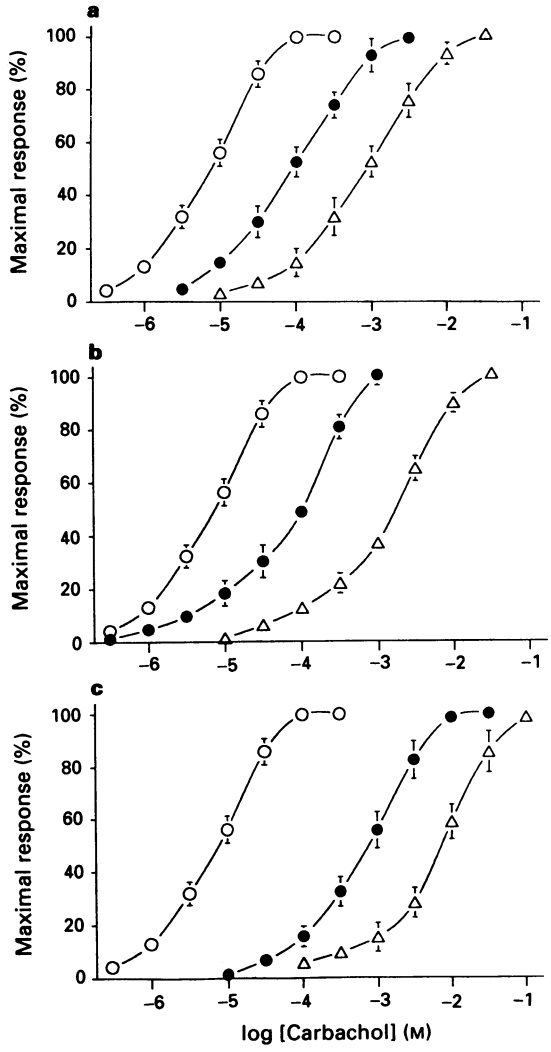


Figure 5 Antagonism of carbachol-mediated accumulation of inositol phosphates by liriodenine (a), methoctramine (b) and 4-diphenylacetoxy-*N*-methylpiperidine (4-DAMP) (c) in cultured canine tracheal smooth muscle cells. The concentration-response curve of carbachol-mediated inositol phosphate accumulation was constructed in the absence (control, o) and presence of liriodenine (●, 10 μM; △, 100 μM), methoctramine (●, 10 μM; △, 100 μM) and 4-DAMP (●, 0.1 μM; △, 1 μM) with non-cumulative addition of carbachol. Productions of inositol phosphates are expressed as the percentage of the inositol phosphate accumulation stimulated by a maximal concentration of carbachol in the absence of antagonists. Each point represents the mean ± s.e.mean of three experiments determined in triplicate.

Effects of liriodenine, methoctramine and 4-DAMP on carbachol-mediated inhibition of cyclic AMP formation

Carbachol (0.01–30 μM) inhibited isoprenaline-induced cyclic AMP formation in a concentration-dependent manner with maximal inhibition at 30 μM carbachol in cultured TSMCs (Figure 6). The basal levels of cyclic AMP, in the absence of isoprenaline, were 3.9 ± 0.6 and 4.2 ± 0.5 pmol mg^{-1} protein in the absence and presence of carbachol, respectively. The amount of cyclic AMP stimulated by isoprenaline (1 μM) was 41.1 ± 6.5 pmol mg^{-1} protein. The minimal level of cyclic AMP remaining after maximal inhibition by 30 μM carbachol was 4.5 ± 0.7 pmol mg^{-1} protein. The EC_{50} value for the inhibitory effect of carbachol on accumulation of cyclic AMP stimulated by isoprenaline was 0.27 ± 0.03 μM. Liriodenine (100 and 300 μM), methoctramine (1 and 10 μM) and 4-DAMP (0.1 and 1 μM) antagonized carbachol-mediated inhibition of cyclic AMP accumulation in cultured TSMCs. These antagonists caused parallel rightward shifts in the concentration-response curves of carbachol (Figure 6). Table 2 lists the K_B values for muscarinic antagonists used in these experiments. Two K_B values were calculated for each antagonist, as two concentrations of each antagonist were used in this work. There was no distinction between these two K_B values ($P > 0.05$). The pK_B values of liriodenine, methoctramine and 4-DAMP for antagonizing cyclic AMP inhibition were 4.7, 7.4 and 7.8, respectively, consistent with the low affinity of liriodenine and 4-DAMP and high affinity of methoctramine in this response (see Table 1 and review Hulme *et al.*, 1990).

Discussion

The present experiments demonstrate that liriodenine, isolated from *Fissistigma glaucescens*, depressed contractile responses to the muscarinic receptor agonist, carbachol and competed with [^{3}H]-NMS for binding sites. It also antagonized the accumulation of inositol phosphates and the inhibition of cyclic AMP formation caused by carbachol. These findings support the idea that liriodenine acts as a muscarinic receptor antagonist in canine tracheal smooth muscle.

The cultured TSMCs had [^{3}H]-NMS specific, saturable and high affinity muscarinic receptor binding sites. The K_d value for [^{3}H]-NMS was 336.1 ± 10.7 pM in cultured TSMCs. This value is similar to the K_d reported by Yang (1991), 320 ± 20 pM in freshly isolated canine TSMCs. Therefore, the cultured canine TSMC may express functional muscarinic receptors under these cultured conditions.

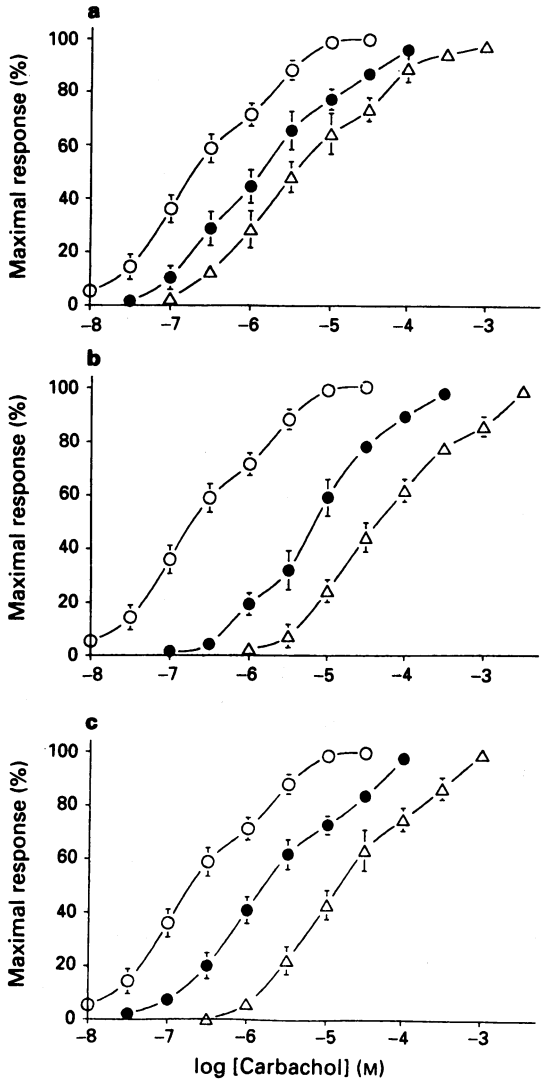


Figure 6 Antagonism of carbachol-mediated inhibition of isoprenaline-stimulated cyclic AMP formation by liriodenine (a), methoctramine (b) and 4-diphenylacetoxy-*N*-methylpiperidine (4-DAMP) (c) in canine cultured tracheal smooth muscle cells. The concentration-response curves were constructed in the presence of carbachol at various concentrations in the absence (control, o) and in the presence of liriodenine (●, 100 μM; Δ, 300 μM), methoctramine (●, 1 μM; Δ, 10 μM) and 4-DAMP (●, 0.1 μM; Δ, 1 μM) with non-cumulative addition of carbachol. Basal levels of cyclic AMP, in the absence of isoprenaline, were 3.9 ± 0.6 and 4.2 ± 0.5 pmol mg^{-1} protein in the absence and presence of carbachol, respectively. The amount of cyclic AMP inhibited by carbachol was calculated as the amount of cyclic AMP stimulated by isoprenaline (1 μM) alone (41.1 ± 6.5 pmol mg^{-1} protein) minus the amount of cyclic AMP generated by the simultaneous presence of isoprenaline and carbachol. Results are expressed as the percentage of the response to a maximally effective concentration of carbachol. Each point represents the mean ± s.e.mean of four experiments determined in triplicate.

It is increasingly clear that muscarinic receptors are not pharmacologically homogeneous in canine tracheal smooth muscle. Evidence from radioligand binding tests, functional studies of smooth muscle contraction and/or receptor-mediated second messenger accumulation show substantial variations in the affinities of antagonists for muscarinic receptors (Hulme *et al.*, 1990; Caulfield, 1993). Previous tests have demonstrated that M_2 and M_3 receptor subtypes exist in canine tracheal smooth muscle (Yang 1991; Yang *et al.*, 1991; Fernandes *et al.*, 1992) and other types of smooth muscle including gastrointestinal smooth muscle, urinary bladder and vascular tissue (Eglen *et al.*, 1994). Our results confirm these findings in the airways. The inhibition constants (K_i) obtained from pirenzepine, methoctramine and 4-DAMP inhibition of [^{3}H]-NMS binding are consistent with previously reported values in tracheal smooth muscle (Fryer & El-Fakahany, 1990; Yang, 1991). Analysis of competitive binding curves for pirenzepine yields a model of one binding site with low affinity (Hulme *et al.*, 1990), indicating the absence of M_1 muscarinic receptors in TSMC. The pK_B value of pirenzepine for inhibition of generation of inositol phosphates inhibition of contraction and reversal of cyclic AMP attenuation (7.0, 7.1 and 6.7, respectively) were of low affinity (Hulme *et al.*, 1990; Yang *et al.*, 1991). These results indicate that the M_1 receptor subtype is not involved in generation of second messengers in TSMC. The curves for competitive binding with methoctramine and 4-DAMP were shallow and best fitted according to a model with two binding sites. Furthermore, in the present work, the discrepancy in the concentration-response relationship for the effect of carbachol on the metabolism of cyclic AMP and phosphoinositide in cultured TSMCs is consistent with those reported by other authors using other tissues and cell preparations (Brown & Brown, 1984; Candell *et al.*, 1990; Yang *et al.*, 1991). We found that methoctramine (a selective M_2 antagonist) possessed a high affinity to antagonize cyclic AMP inhibition ($pK_B = 7.4$), whereas it antagonized inositol phosphate formation ($pK_B = 6.0$) and tracheal smooth muscle contraction ($pK_B = 6.1$) with low affinity. In contrast, 4-DAMP (selective M_3 antagonist) displayed a high affinity in blocking inositol phosphate formation ($pK_B = 8.9$) and tracheal smooth muscle contraction ($pK_B = 9.1$), but a low affinity in antagonizing cyclic AMP inhibition ($pK_B = 7.8$). These results support the earlier conclusion (Yang *et al.*, 1991; Eglen *et al.*, 1994) that M_2 and M_3 receptor subtypes are coupled to distinct effector systems in tracheal smooth muscle. Inhibition of adenylate cyclase seems to be coupled to the M_2 subtype and is distinct from the M_3 subtype coupled to phospholipase C activation. The M_3 muscarinic receptor is shown to mediate contraction of airway smooth muscle (Roffel *et al.*, 1990; Yang *et al.*, 1991), but a functional role of the M_2 subtype in this tissue remains unclear. Fernandes *et al.* (1992) suggested that stimulation of M_2 muscarinic receptors in canine airway smooth muscle may play an important role in functional antagonism by decreasing the relaxation caused by agents such as isoprenaline and forskolin.

In guinea-pigs, we found that liriodenine competitively antagonized carbachol-induced tracheal and ileal smooth muscle contraction with pA_2 values of 6.22 ± 0.08 and 6.36 ± 0.10, respectively. Moreover, it was ten times less potent in atrial preparations than in smooth muscle preparations. These results indicate that liriodenine is a selective M_3 receptor antagonist (Lin *et al.*, 1994). In the present work, liriodenine displaced [^{3}H]-NMS binding in a concentration-dependent manner in cultured TSMCs. Analysis of competitive binding curves for liriodenine yielded a two sites model of binding with a low affinity of 26 μM and a high affinity of 1.4 μM. The affinity of liriodenine for M_3 receptors mediating tracheal contraction and for receptors linked to inositol phosphate formation were equal ($pK_B = 5.9$ and 6.0, respectively), corresponding to a K_i value of high affinity, whereas it antagonized cyclic AMP inhibition ($pK_B = 4.7$) in agreement with a K_i value of low affinity. These results indicate that the antimuscarnic characteristics of liriodenine are similar to those of 4-DAMP. It acts as a selective M_3 receptor antagonist in canine tracheal smooth muscle.

In conclusion, the selective inhibitory action of liriodenine on M_3 receptors may be a useful tool to elucidate the M_3 receptor-mediated responses and to differentiate muscarinic receptor subtypes. Its structural novelty may provide an original chemical basis for the development of new M_3 muscarinic receptor antagonists.

This work was supported by research grants of the National Science Council (NSC83-0420-B002-004-M03, NSC83-0412-B002-172).

References

BONNER, T.I. (1989). The molecular basis of muscarinic receptor diversity. *Trends Neurosci.*, **12**, 148–151.

BONNER, T.I., YOUNG, A.C., BRANN, M.R. & BUCKLEY, N.J. (1988). Cloning and expression of the human and rat M_5 muscarinic acetylcholine receptor genes. *Neuron*, **1**, 403–410.

BROWN, J.H., & BROWN, S.L. (1984). Agonists differentiate muscarinic receptors that inhibit cyclic AMP formation from those that stimulate phosphoinositide metabolism. *J. Biol. Chem.*, **259**, 3777–3781.

BUCKLEY, N.J., BONNER, T.I., BUCKLEY, C.M. & BRANN, M.R. (1989). Antagonist binding properties of five cloned muscarinic receptors expressed in CHO K1 cells. *Mol. Pharmacol.*, **35**, 469–476.

CANDELL, L.M., YUN, S.H., TRAN, L.L.P. & EHLERT, F.J. (1990). Differential coupling of subtypes of the muscarinic receptor to adenylate cyclase and phosphoinositide hydrolysis in the longitudinal muscle of rat ileum. *Mol. Pharmacol.*, **38**, 689–697.

CAULFIELD, M.P. (1993). Muscarinic receptors-characterization, coupling and function. *Pharmacol. Ther.*, **58**, 319–379.

CHENG, Y.C. & PRUSOFF, W.H. (1973). Relationship between the inhibition constant (K_d) and the concentration of inhibitor which causes 50 percent inhibition (IC_{50}) of an enzymatic reaction. *Biochem. Pharmacol.*, **22**, 3099–3108.

DOODS, N.Y., MATHY, M.J., DAVIDESKO, D., VAN CHARLDORP, K.J., DE JONGE, A. & VAN ZWIETEN, P.A. (1987). Selectivity of muscarinic antagonists in radioligand and in vivo experiments for the putative M_1, M_2 and M_3 receptors. *J. Pharmacol. Exp. Ther.*, **242**, 257–262.

EGLEN, R.M., REDDY, H., WATSON, N. & JOHN CHALLISS, R.A. (1994). Muscarinic acetylcholine receptor subtype in smooth muscle. *Trends Pharmacol. Sci.*, **15**, 114–119.

FERNANDES, L.B., FRYER, A.D. & HIRSHMAN, C.A. (1992). M_2 muscarinic receptors inhibit isoproterenol-induced relaxation of canine airway smooth muscle. *J. Pharmacol. Exp. Ther.*, **262**, 119–126.

FRYER, A.D. & EL-FAKAHANY, E.E. (1990). Identification of three muscarinic receptor subtypes in rat lung using binding studies with selective antagonists. *Life Sci.*, **47**, 611–618.

FURCHGOTT, R.F. (1972). The classification of adrenoceptors (adrenergic receptors). An evaluation from the standpoint of receptor theory. In *Catecholamines*, Handbook of Experimental Pharmacology, Vol. 33, ed. Blaschko, H. & Muscholl, E. pp. 283–335. Berlin, Heidelberg, New York: Springer.

GIACHETTI, A., CHELETTI, A.R. & MONTAGNA, E. (1986). Cardioselective profile of AF-DX 116, a muscarinic M_2-receptor antagonist. *Life Sci.*, **38**, 1663–1672.

GOWN, A.M., VOGEL, A.N., GORDON, D. & LU, P.L. (1985). A smooth muscle-specific monoclonal antibody recognizes smooth muscle actin isozymes. *J. Cell Biol.*, **100**, 807–813.

HAMMER, R. & GIACHETTI, A. (1982). Muscarinic receptor subtypes M_1 and M_2: biochemical and functional characterization. *Life Sci.*, **31**, 2991–2999.

HULME, E.C., BIRDSALL, N.J.M. & BUCKLEY, N.J. (1990). Muscarinic receptor subtypes. *Annu. Rev. Pharmacol. Toxicol.*, **30**, 633–673.

LIN, C.H., CHANG, G.J., SU, M.J., WU, Y.C., TENG, C.M. & KO, F.N. (1994). Pharmacological characteristics of liriodenine, isolated from *Fissistigma glaucescens*, a novel muscarinic receptor antagonist in guinea-pigs. *Br. J. Pharmacol.*, **113**, 275–281.

LU, S.T., WU, Y.C. & LEOU, S.P. (1985). Alkaloids of Formosan Fissistigma and Goniothalamus species. *Phytochemistry*, **24**, 1829–1834.

MUNSON, P. & RODBARD, D. (1980). LIGAND: A versile computerized approach for characterization of ligand-binding system. *Anal. Chem.*, **107**, 220–239.

MUTSCHLER, E. & LAMBRECHT, G. (1984). Selective muscarinic agonists and antagonist in functional tests. *Trends Pharmacol. Sci.*, **5** (Suppl. I) 39–44.

PERALTA, E.G., ASHKENAZI, A., WINSLOW, J.W., RAMACHANDRAN, J. & CAPON, D.J. (1988). Differential regulation of PI hydrolysis and adenylyl cyclase by muscarinic receptor subtypes. *Nature*, **334**, 434–437.

ROFFEL, A.F., MEURS, H., ELZINGA, C.R.S. & ZAAGSMA, J. (1990). Characterization of the muscarinic receptor subtype involved in phosphoinositide metabolism in bovine tracheal smooth muscle. *Br. J. Pharmacol.*, **99**, 293–296.

SCATCHARD, G. (1949). The attractions of proteins or small molecules and ions. *Ann. NY Acad. Sci.*, **51**, 660–672.

SHAPIRO, R.A., SCHERER, N.M., HABECKER, B.A., SUBERS, E.M. & NATHANSON, N.M. (1988). Isolation, sequence and functional expression of the mouse M_1 muscarinic acetylcholine receptor gene. *J. Biol. Chem.*, **263**, 18397–18403.

WAELBROECK, M., GILLARD, M., ROBBERECHT, P. & CHRISTOPHE, J. (1987). Muscarinic receptor heterogeneity in rat central nervous system. I. Binding of four selective antagonists to three muscarinic receptor subclass: a comparison with M_2 cardiac muscarinic receptors of the C type. *Mol. Pharmacol.*, **32**, 91–99.

WATSON, M., YAMAMURA, H.I. & ROESKE, W.R. (1983). A unique regulatory profile and regional distribution of [^{3}H]pirenzepine binding in the rat provides evidence for distinct M_1 and M_2 muscarinic receptor subtypes. *Life Sci.*, **32**, 3001–3011.

YAMAMURA, H.I. & SYNDER, S.H. (1974). Muscarinic cholinergic binding in rat brain. *Proc. Natl. Acad. Sci. U.S.A.*, **71**, 1725–1729.

YANG, C.M. (1991). Characterization of muscarinic receptors in dog tracheal smooth muscle cells. *J. Auton. Pharmacol.*, **11**, 51–61.

YANG, C.M., CHOU, S.P. & SUNG, T.C. (1991). Muscarinic receptor subtypes coupled to generation of different second messengers in isolated tracheal smooth muscle cells. *Br. J. Pharmacol.*, **104**, 613–618.

ZAR, J.H. (1974). *Biostatistical Analysis: Multiple Regression and Correction.* p. 252. Englewood Cliffs, N.J: Prentice-Hall Inc.

(Received June 21, 1994
Accepted August 15, 1994)

Br. J. Pharmacol. (1994), **113**, 1471-1479 © Macmillan Press Ltd, 1994

Different endothelin receptors involved in endothelin-1- and sarafotoxin S6B-induced contractions of the human isolated coronary artery

[1]Willem A. Bax, *Zohara Aghai, *Corina L.J. van Tricht, *Claes Wassenaar & Pramod R. Saxena

Department of Pharmacology, Laboratory for Human Pharmacology and *Department of Thoracic Surgery, Thorax Centre, Faculty of Medicine and Health Sciences, Erasmus University Rotterdam, Post Box 1738, 3000 DR Rotterdam, The Netherlands

1 Endothelin receptors, that mediate contraction of the human isolated coronary artery, were characterized by use of a number of agonists and antagonists. Contraction induced by the non-selective agonists, endothelin (ET)-1 and sarafotoxin S6b, was compared in endothelium-intact and endothelium-denuded ring segments. The effects of ET-1 and BQ-123 (an ET_A receptor antagonist) were investigated both in ring segments and in spirally cut strips. Lastly, the effect of phosphoramidon was studied on contraction induced by big-ET-1.

2 The order of agonist potency (pD_2) in endothelium-intact coronary artery ring segments was: ET-1 (8.27)$\approx$sarafotoxin S6b (8.16)$>$big-ET-1 ($<$7.1)$\approx$ET-3 ($<$6.9). [$Ala^{1,3,11,15}$]ET-1 (ET_B receptor agonist) caused significant contraction only at 1 μM, whereas 0.3 μM big-ET-3 had no effect. Removal of the endothelium in ring segments did not affect the contractile response to ET-1 or to sarafotoxin S6b.

3 After a full concentration-response curve had been obtained to ET-1 or sarafotoxin S6b, further contractions of the endothelium-intact coronary artery segments could only be achieved by applying ET-1 in segments exposed to sarafotoxin S6b, and not the reverse.

4 BQ-123 (0.1 μM) antagonized contractions of endothelium-intact ring segments induced by sarafotoxin S6b (pK_B 7.86). Only 10 μM BQ-123 antagonized contractions induced by ET-1 (pK_B 5.75). FR139317 was also more potent against sarafotoxin S6b (pK_B 8.24- 8.47) than against ET-1 (pK_B 6.11). [$Ala^{1,3,11,15}$]ET-1 (1 μM) had no effect on the contractile response to ET-1 or to sarafotoxin S6b.

5 In strip preparations with intact endothelium, the pD_2 of ET-1 increased to 9.04 ± 0.16 (vs. 8.50 ± 0.07 in rings), and BQ-123 (1 μM) caused a rightward shift of the ET-1 induced concentration-response curve (pK_B 6.62 vs. 5.75 in rings).

6 Contractile responses to big-ET-1 of endothelium-intact coronary artery segments were attenuated in the presence of phosphoramidon (100 μM), indicating conversion of big-ET-1 to ET-1 within the coronary artery segment.

7 The present study indicates that ET-1 and sarafotoxin S6b contract the human isolated coronary artery via different receptors, which can probably be best characterized as subtypes of the ET_A receptor. Furthermore, it is demonstrated that the type of preparation (ring or strip) may affect the potency of ET-1 as an agonist and of BQ-123 as an antagonist.

Keywords: Human coronary artery; ET receptor subtypes; endothelin-1; sarafotoxin S6b; [$Ala^{1,3,11,15}$]ET-1; BQ-123; FR139317; big-ET-1; phosphoramidon

Introduction

The cloning of endothelin ET_A (Arai *et al.*, 1990) and ET_B (Sakurai *et al.*, 1990) receptors, and the subsequent development of relatively selective receptor agonists and antagonists, have stimulated the characterization of functional receptors, mediating vascular smooth muscle contraction to endothelin isopeptides. For instance, ET_A receptors have been shown to mediate contractile responses in the rat aorta (Sumner *et al.*, 1992), whereas ET_B receptors were found to mediate contraction of the rabbit saphenous vein (Moreland *et al.*, 1992). Other smooth muscle preparations were found to contract via a mixed receptor population, or via non-ET_A, non-ET_B receptors (e.g. the pig coronary artery: Harrison *et al.*, 1992; Schoeffter & Randriantsoa, 1993). In particular, the putative ET_A receptor antagonist BQ-123 (cyclo[D-Asp-L-Pro-D-Val-L-Leu-D-Trp-]: Ihara *et al.*, 1992a) was found to discriminate between contractions induced by endothelin-1 (ET-1) and contractions induced by ET-3 or sarafotoxin S6b in rat aorta (Sumner *et al.*, 1992), rat vas deferens (Eglezos *et al.*, 1993; Warner *et al.*, 1993) and goat cerebral artery (Salom *et al.*, 1993). Also in the human saphenous vein it was found that BQ-123 antagonized sarafotoxin S6b-induced contractions with higher affinity than ET-1-induced contractions (Bax *et al.*, 1993a). Similar data were obtained in the human umbilical artery (Bodelsson & Stjernquist, 1993). These apparently heterogeneous receptor populations could not be readily characterized as 'typical' ET_A or ET_B receptors.

In the human isolated coronary artery, Godfraind (1993) observed differential effects of BQ-123 against ET-1 and ET-3-induced contractile responses. Furthermore, the nature of the contractile endothelin receptors varied between proximal and distal coronary artery segments; distal segments were more sensitive to both the agonist effect of ET-1 (as was also observed by Chester *et al.*, 1992) and the antagonist effect of BQ-123. It was therefore concluded that distal parts of the artery contract via ET_A receptors only, but that other receptors are involved in the contractile response of proximal segments (Godfraind, 1993). Using quantitative receptor autoradiography in the human coronary artery, it was previously shown that [^{125}I]-ET-1 labelled a homogeneous receptor population in the media of proximal segments of the human coronary artery. [^{125}I]-sarafotoxin S6b labelled a

[1] Author for correspondence.

similar receptor, but also labelled a non-ET_A, non-ET_B receptor with relatively high affinity for BQ-123 and [$Ala^{1,3,11,15}$]ET-1 (ET_B receptor selective: Saeki *et al.*, 1991) (Bax *et al.*, 1993b).

In the present study, we have further characterized endothelin receptors that mediate contraction of the human isolated coronary artery, using BQ-123 and FR139317 (ET_A receptor selective: Sogabe *et al.*, 1992) as antagonists. We also examined whether the response to ET-1 or to sarafotoxin S6b is altered in the presence or absence of functionally intact endothelium (De Nucci *et al.*, 1988). We hypothesized that part of the differences found by Chester *et al.* (1992) and Godfraind (1993), between large proximal and small distal coronary artery segments, could be due to facilitated diffusion of the large peptide molecules to the receptors in distal coronary artery segments, rather than to a different receptor profile. To verify this hypothesis we compared the effect of ET-1 and BQ-123 on ring segments and on spirally cut coronary artery strips. Lastly, we investigated whether local conversion of big-ET-1 to ET-1 (Yanagisawa *et al.*, 1988; Okada *et al.*, 1990) is involved in the contractile response to big-ET-1. A part of this study was presented to the joint meeting of the British Pharmacological Society and the Società Italiana Farmacologia (Bax *et al.*, 1994).

Methods

Tissue preparation and experimental procedure

The right epicardial coronary artery was obtained from 43 hearts of organ donors, who had died of non-cardiac disorders less than 24 h before the tissue was taken to the laboratory (25 cerebrovascular accident, 16 polytrauna, 2 cerebral hypoxia; 24 male, 19 female; age 1–54 years). The hearts were provided by the Rotterdam Heart Valve Bank (Bio Implant Services Foundation/Eurotransplant Foundation) after removal of the aortic and pulmonary valves for homograft valve transplantation. The study was approved by the Joint Medical Ethics Committee of the Erasmus University Rotterdam and the University Hospital Rotterdam 'Dijkzigt'. The hearts were stored at 0–4°C in commonly used sterile organ protecting solutions (University of Wisconsin (UW) solution, HTK-Bretschneider solution, or EuroCollins solution, see Dreikorn, 1992), immediately following circulatory arrest. After arrival in the laboratory, the right coronary artery was removed and placed in a cold, oxygenated Krebs bicarbonate solution of the following composition (mM): NaCl 118, KCl 4.7, $CaCl_2$ 2.5, $MgSO_4$ 1.2, KH_2PO_4 1.2, $NaHCO_2$ 25 and glucose 8.3; pH 7.4. Segments 2 (mid segment) and 3 (distal segment: AHA Committee Report, 1975) of the coronary artery were cut into rings with similar diameter and approximately 4 mm in length. The rings were suspended on stainless steel hooks in 15 ml organ baths containing the Krebs bicarbonate solution, aerated with 95% O_2 and 5% CO_2 and maintained at 37°C. Vessel segments containing macroscopically visible atherosclerotic lesions were not used. In some ring segments, the endothelium was removed with a cotton swab and a watchmakers' forceps. However, if not mentioned otherwise, results refer to ring segments with intact endothelium. For the comparison of ring and strip segments, we made two such pairs from adjacent portions of the coronary artery with intact endothelium. The 4 mm rings were prepared as described above, while the strips were cut in a spiral manner (diameter 1 mm) and attached to silk threads.

All segments were allowed to equilibrate for at least 30 min and were washed every 15 min. Changes in tension were recorded with a Harvard isometric transducer. Preparations were stretched to a stable tension of approximately 20 mN. The tissue was exposed to K^+ (30 mM) twice. Subsequently, the functional integrity of the endothelium was verified by observing relaxation to substance P (1 nM) after precontraction with prostaglandin $F_{2\alpha}$ ($PGF_{2\alpha}$, 1 μM). After washout, the tissue was exposed to 100 mM K^+ to determine the maximal contractile response to K^+, which was expressed as mN. The tissue was allowed to equilibrate in the Krebs solution for a period of 30 min.

Determination of agonist and antagonist potency

After this period of equilibration, some segments were treated with vehicle only (controls), whereas others were incubated with an antagonist for 30 min. A cumulative concentration-response curve was then obtained on every segment. Responses were expressed as a percentage of the contractile response to 100 mM K^+. Curves obtained in the presence of a receptor antagonist were compared to the control curves. All curves were obtained in a paired, parallel experimental set-up. Some concentration–response curves were obtained in duplicate or triplicate. These curves were averaged and considered as a single curve in further analysis.

Analysis of data

Curves were analysed by means of a computerized curve fitting technique (De Lean *et al.*, 1978) to obtain E_{max} (maximal response), and pD_2 (− log of the molar concentration of an agonist needed to reach half of its maximal effect, i.e. $-\log EC_{50}$) values, which were averaged for the respective agonists. For antagonists against ET-1 or sarafotoxin S6b, a pK_B value was calculated, assuming the nature of antagonism to be competitive, using the equation described by Furchgott (1972):

$$pK_B = -\log[B] + \log\{([A_2]/[A_1]) - 1\},$$

where [B] is the antagonist concentration and $[A_1]$ and $[A_2]$ are respectively, the EC_{50} values of the agonist in the absence and presence of the antagonist. For calculation of pK_B values, only paired experiments were taken into account, pK_B values are given only when a more than 2 fold shift of the EC_{50} was obtained. All data are presented as mean ± s.e. mean. pD_2 and E_{max} of agonist-induced contractions without or in the presence of an antagonist were compared by Student's paired *t* test. Mean contractile reponses were compared by Analysis of Variance (ANOVA) followed by Student's *t* test, for paired data where appropriate. A correlation coefficient, *r*, was calculated according to Pearson. A *P* value less than 0.05 was assumed to denote a significant difference.

Compounds

The compounds used in this study were purchased from the sources indicated: Prostaglandin $F_{2\alpha}$ (tris salt), substance P acetate and phosphoramidon: Sigma Chemical Co. (St. Louis, U.S.A.); ET-1: Saxon Biochemicals GMBH (Hannover, Germany); ET-1, sarafotoxin S6b, FR139317 and BQ-123 (sodium salt): Neosystem S.A. (Strasbourg, France); sarafotoxin S6b, ET-3, big-ET-1 and BQ-123 (sodium salt): Novabiochem AG (Läufelfingen, Switzerland); sarafotoxin S6b, big-ET-3, and [$Ala^{1,3,11,15}$]ET-1: Peninsula Laboratories (Belmont, U.S.A.). It should be noted that due to non-availability of the compounds and/or cost factors, we had to order ET-1, sarafotoxin S6b, and BQ-123 from more than one source. Although direct comparisons were not made, the compounds obtained from different sources did not differ in potency. Stock solutions for [$Ala^{1,3,11,15}$]ET-1, and ET-1 (Saxon) were prepared in 0.1% acetic acid. Other compounds were dissolved in water.

Results

Basic properties of the preparations

All ring segments, when endothelium was left intact, relaxed to 1 nM substance P after precontraction to 1 μM $PGF_{2\alpha}$ (73 ± 5% of the contractile response to $PGF_{2\alpha}$; $n = 43$). This is in accordance with previous findings with substance P in the human isolated coronary artery obtained from patients undergoing cardiac transplantation (Bossaller *et al.*, 1987). K^+, 100 mM, caused a mean contractile response of 45 ± 3 mN ($n = 43$). Where the endothelium had been removed from the ring segments, the relaxant response to substance P was virtually abolished (2 ± 1% of the contractile response to 1 μM $PGF_{2\alpha}$; $n = 13$), and the contractile response to potassium was decreased from 37 ± 5 mN to 21 ± 3 mN. In strip preparations ($n = 5$) the relaxant response to substance P was 31 ± 12% of the contractile response to 1 μM $PGF_{2\alpha}$, and the contractile response to 100 mM K^+ was 20 ± 6 mN.

Effect of agonist peptides

In endothelium-intact coronary artery segments, sarafotoxin S6b, ET-1, big-ET-1, and ET-3 caused concentration-dependent contractions. [$Ala^{1,3,11,15}$]ET-1 caused a small contractile response at the highest concentration used (1 μM), whereas big-ET-3 had no effect at 0.3 μM (Figure 1). For big-ET-1, ET-3 and [$Ala^{1,3,11,15}$]ET-1 the highest concentration tested (1 μM) may not have reached the maximal contractile response, which could affect the given approximate pD_2 and E_{max} values. The order of potency of the agonists tested was: ET-1 ≈ sarafotoxin S6b > big-ET-1 ≈ ET-3 > [$Ala^{1,3,11,15}$]ET-1 ≥ big-ET-3 (for E_{max} and pD_2, see Table 1). The contractile response to ET-1 or sarafotoxin S6b in ring segments was not affected by removing the endothelium (Figure 2). Comparison of the E_{max} of 21 paired vessel segments, in which a concentration-response curve to both ET-1 and sarafotoxin S6b was constructed, revealed that the E_{max} but not the pD_2 of sarafotoxin is slightly but significantly different from that of ET-1 (105.7 ± 4.9% vs. 95.2 ± 3.9%, respectively, $P = 0.01$). No age-related variation was observed for the pD_2 of ET-1 ($n = 37$) and sarafotoxin S6b ($n = 26$) (correlation age, pD_2: $r = -0.12$ and -0.05, $P = 0.24$ and 0.40, respectively). Only the E_{max} of ET-1, but not of sarafotoxin S6b, was found to be somewhat higher in younger patients (correlation age, E_{max}, ET-1: $r = -0.36$, $P = 0.02$; sarafotoxin S6b: $r = 0.07$, $P = 0.37$).

Figure 3 shows experimental recordings of responses obtained with ET-1 and sarafotoxin S6b in endothelium-intact coronary artery segments. The addition of 0.1 μM sarafotoxin S6b at the end of a full concentration-response curve with ET-1 did not result in a further increase of tension (Figure 3a). However, in a parallel vessel segment, the addition of 0.1 μM ET-1 after a full concentration-response curve to sarafotoxin S6b, caused further increase of tension (Figure 3b and also 3d). Figure 3c shows that the maximal contractile response to sarafotoxin S6b (and also to ET-1: not shown) slowly faded after the highest concentration of agonist has been added. The mean contraction (as a percentage of contraction induced by 100 mM K^+), directly and 60 min after adding 0.3 μM ET-1 or 0.3 μM sarafotoxin S6b was: 84.0 ± 5.2% and 26.2 ± 3.5%, respectively, for ET-1 ($n = 18$ segments from 10 hearts), and 90.7 ± 10.0% and 56.3 ± 11.8%, respectively, for sarafotoxin S6b ($n = 10$ segments from 5 hearts). Sixty min after the maximal concentration of sarafotoxin S6b had been added (not shown in Figure 3), the subsequent addition of 0.03 μM ET-1 resulted in an increase of contractile force (from 33.0 ± 11.7% to 81.1 ± 6.0% of contraction induced by 100 mM K^+, $n = 5$), whereas the subsequent adding of 0.03 μM sarafotoxin S6b had no further effect (from 66.2 ± 3.2% to 64.3 ± 4.0% of contraction induced by 100 mM K^+, $n = 5$). When 0.1 μM ET-1 was added after this failure of 0.03 μM sarafotoxin S6b to produce further contraction, an increase of contractile force to 99.6 ± 3.1% of contraction induced by 100 mM K^+ was observed ($n = 5$; $P < 0.01$). Sixty min after the maximal concentration of ET-1 had been added, subsequent addition of neither 0.03 μM ET-1 nor 0.03 μM sarafotoxin S6b resulted in a further increase of contraction (from 22.1 ± 4.9% to 22.6 ± 5.0% ($n = 10$) and 31.3 ± 6.2% to 32.1 ± 6.1% ($n = 8$) of contraction induced by 100 mM K^+, respectively).

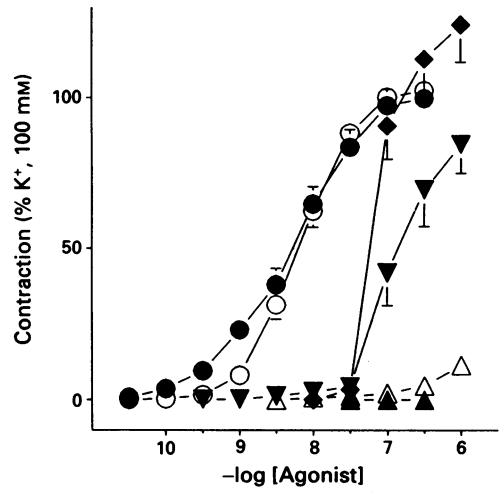


Figure 1 Contractions of the endothelium-intact human isolated coronary artery to endothelin (ET) receptor agonists; (●) ET-1 ($n = 37$); (○) sarafotoxin S6b ($n = 26$); (◆) big-ET-1 ($n = 4$); (▼) ET-3 ($n = 4$); (△) [$Ala^{1,3,11,15}$]ET-1 ($n = 7$); (▲) big-ET-3 ($n = 3$). Agonist concentration refers to mol l^{-1}. pD_2 and E_{max} are given in Table 1. Where no error bar is visible, error falls within the limits of the symbol.

Antagonist effects

In endothelium-intact coronary artery segments 0.1 μM BQ-123 antagonised contractions induced by sarafotoxin S6b resulting in a pK_B of 7.86 ± 0.08 ($n = 6$). This same concent-

Table 1 Potency (pD_2 (− log [EC_{50}, mol l^{-1}])) and maximal effect (E_{max}, expressed as a percentage of the contractile response to 100 mM K^+) of endothelin receptor agonists

Agonist	*Concentration-range studied*	n	*pD_2*	*E_{max}*
ET-1	30 pM–0.3 μM	37	8.27 ± 0.06	102.7 ± 5.4%
Sarafotoxin S6b	30 pM–0.3 μM	26	8.16 ± 0.05	104.5 ± 5.4%
Big-ET-1	0.1 nM–1 μM	4	< 7.1 ± 0.02[1]	> 124.3 ± 12.4%[1]
ET-3	0.1 nM–1 μM	4	< 6.9 ± 0.1[1]	> 84.4 ± 9.6%[1]
[$Ala^{1,3,11,15}$]ET-1	0.1 nM–1 μM	7	NC[1]	> 11.4 ± 3.6%[1]
Big-ET-3	0.1 nM–0.3 μM	3	No effect	

n, number of segments tested; NC, not calculated; [1]maximal effect possibly not reached at 1 μM.

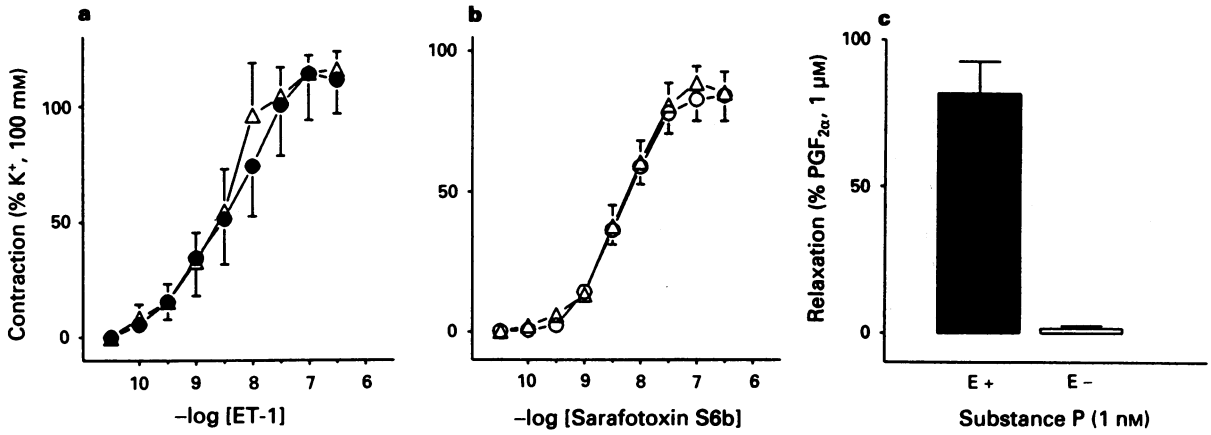


Figure 2 (a) Contractions of the human isolated coronary artery to endothelin-1 (ET-1) in endothelium-intact (●), or endothelium-denuded (Δ) ring segments ($n = 8$). (b) Contractions of the human isolated coronary artery to sarafotoxin S6b in endothelium-intact (○), or endothelium-denuded (Δ) ring segments ($n = 5$). The concentration of ET-1 and sarafotoxin S6b refers to mol l^{-1}. (c) Relaxant responses to 1 nM substance P in the same segments expressed as a percentage of precontraction with 1 μM prostaglandin F_α ($PGF_{2\alpha}$). E +, endothelium intact; E −, endothelium denuded. Where no error bar is visible, error falls within the limits of the symbol.

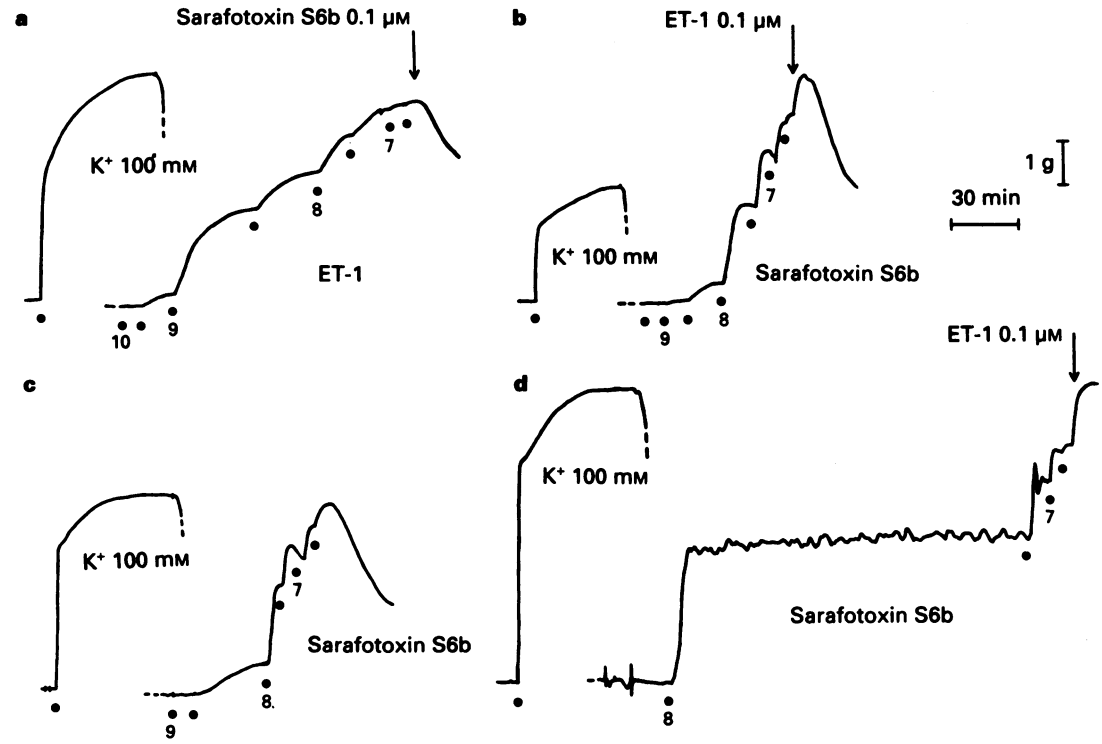


Figure 3 Experimental recordings of concentration-response curves, preceded by the reference contractile response to 100 mM K^+, in four endothelium-intact coronary artery segments obtained from a 41 year old male (a and b) and a 25 year old female (c and d). (a) After reaching the E_{max} in a concentration-response curve to ET-1, the addition of 0.1 μM sarafotoxin S6b (arrow) did not cause an additional response. (b) After reaching the E_{max} in a concentration-response curve to sarafotoxin S6b, the addition of 0.1 μM ET-1 (arrow) caused an additional contractile response. (c) After reaching the E_{max} of a concentration-response curve to sarafotoxin (but also to ET-1: not shown) contraction slowly faded away (also a and b). (d) Addition of a concentration of sarafotoxin S6b, causing a submaximal effect in a parallel segment, resulted in a sustained contractile response. After subsequently completing the concentration-response curve in this particular segment, a further contractile response could be induced by addition of 0.1 μM ET-1 (arrow).

ration of BQ-123 caused a small increase of contraction induced by ET-1 ($n = 7$). Only 10 μM BQ-123 antagonized contractions induced by ET-1 (pK_B: 5.75 ± 0.18; $n = 4$). FR139317 was also more potent against sarafotoxin S6b than against ET-1. This resulted in pK_B values for FR139317 against sarafotoxin S6b of 8.47 ± 0.17 (3 nM) and 8.24 ± 0.08 (0.3 μM) (both $n = 5$). However, 3 μM FR139317 applied against ET-1-induced contractions resulted in a pK_B of 6.11 ± 0.16 ($n = 6$). The small contractile response induced by 1 μM [$Ala^{1,3,11,15}$]ET-1 faded during the 30 min incubation when tested as an antagonist. [$Ala^{1,3,11,15}$]ET-1 (1 μM) did not affect the contractile response to ET-1 or to sarafotoxin S6b ($n = 6$) (Figure 4).

Comparison with strip preparations

ET-1 was more potent as an agonist on endothelium-intact strip preparations than on endothelium-intact ring segments (pD_2: 9.04 ± 0.16 in strips vs. 8.50 ± 0.07 in rings; $n = 5$). The pK_B of BQ-123 (1 μM) against ET-1-induced contractions

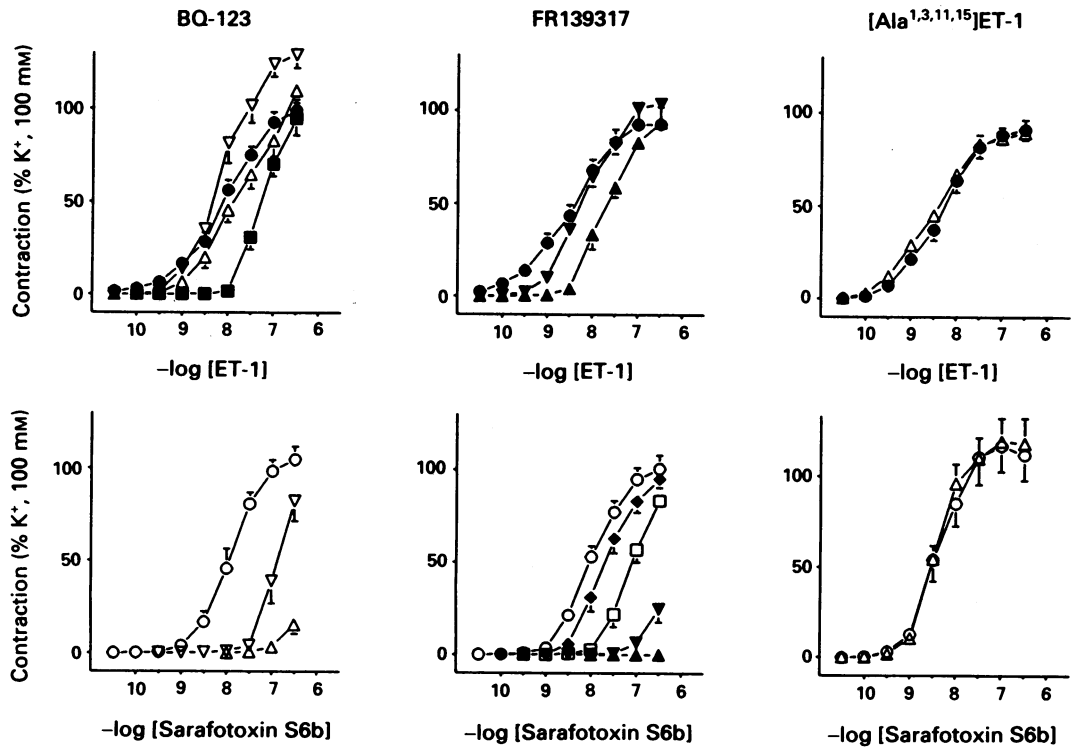


Figure 4 Contractions of the endothelium-intact human isolated coronary artery to endothelin-1 (ET-1) (upper panels), and sarafotoxin S6b (lower panels) in the absence (control ET-1: ●; control sarafotoxin S6b: ○) or presence of the endothelin receptor antagonist BQ-123 ($n = 4-13$), FR139317 ($n = 5-6$), or [Ala^{1,3,11,15}]ET-1 ($n = 6$). Concentrations of receptor antagonists were 3 nM (◆), 0.03 μM (□), 0.1 μM (▽), 0.3 μM (▼), 1 μM (△), 3 μM (▲) or 10 μM (■). Concentrations of ET-1 and sarafotoxin S6b refer to mol l^{-1}, pK_B values are mentioned in the text. Where no error bar is visible, error falls within the limits of the symbol.

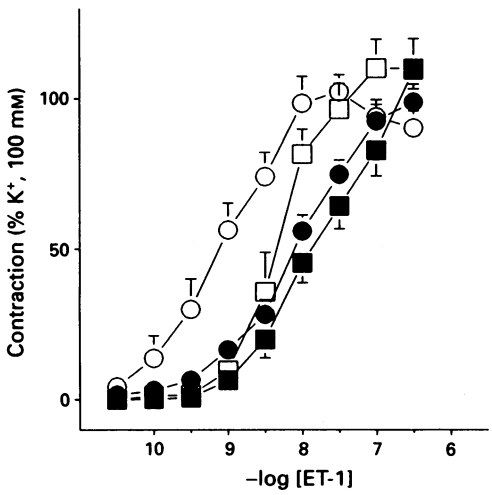


Figure 5 Contractions of the human isolated coronary artery to endothelin-1 (ET-1) in endothelium-intact ring preparations (closed symbols, $n = 12$) and endothelium-intact spiral strip preparations (open symbols, $n = 5$), in the absence (control, ● and ○) or presence of 1 μM BQ-123 (■ and □). For pD_2 and pK_B values, see text. The concentration of ET-1 refers to mol l^{-1}. Where no error bar is visible, error falls within the limits of the symbol.

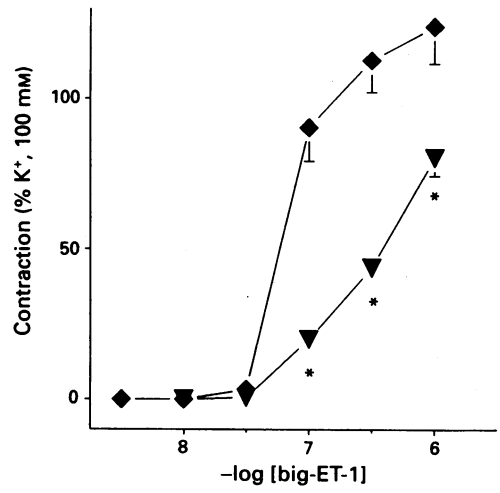


Figure 6 Contractions of the endothelium-intact human isolated coronary artery to big endothelin-1 (big-ET-1) in the absence (control, ◆) and presence of 100 μM phosphoramidon (▼). $n = 4$; *, $P < 0.05$ vs. control response. The concentration of big-ET-1 refers to mol l^{-1}. Where no error bar is visible, error falls within the limits of the symbol.

of strips was 6.62 ± 0.18 (Figure 5) vs. 5.75 ± 0.18 in rings (10 μM BQ-123).

Big-ET-1 and phosphoramidon

The concentration-response curve to big-ET-1 was remarkably steep in comparison with the other endothelin isopeptides (Figure 1). As shown in Figure 6, the pretreatment of the vessel segment with phosphoramidon (100 μM) resulted in significant attenuation of the contractile responses and in a non-parallel shift of the big ET-1-induced concentration-response curve.

Discussion

The main findings of the present study are the observed differences between contractions induced by ET-1 and sarafotoxin S6b. The ET_A receptor antagonists BQ-123 and FR139317 were clearly more potent against sarafotoxin S6b

than against ET-1. ET-1 and sarafotoxin S6b induced similar contractile responses in endothelium-intact and endothelium-denuded vessel segments. After a full concentration-response curve had been obtained to ET-1 or sarafotoxin S6b, further contractions of the endothelium-intact coronary artery segments could be achieved only by applying ET-1 in segments exposed to sarafotoxin S6b, and not in segments exposed to ET-1.

It is to be noted that most concentration-response curves were obtained in vessel segments in which the endothelium was left intact, due to the more frequent occurrence of spontaneous phasic oscillations in the absence of endothelium. These spontaneous rhythmic contractions would hinder detailed analysis of concentration-response curves (Kawasaki *et al.*, 1981). Destruction of the endothelium in a perfused mesenteric arterial bed of the rat increased the contractile response to ET-1, sarafotoxin S6b, ET-3 and big-ET-1 (Douglas & Hiley, 1990). We established for ET-1 and sarafotoxin S6b that removal of the endothelium in coronary artery segments in our model does not alter the contractile response (Figure 2). However, the possibility cannot be ruled out that contractile responses to the other agonists are modulated by the presence of endothelium.

Heterogeneity of receptors involved in the response to ET-1 and sarafotoxin S6b?

The present data supply evidence for heterogeneous mechanisms mediating the contractile response to ET-1 and sarafotoxin S6b. First, the ET_A receptor antagonists, BQ-123 and FR139317, had significantly different potencies against ET-1- and sarafotoxin S6b-induced contractile responses. Secondly, after a concentration-response curve ending with 0.3 μM ET-1 or 0.3 μM sarafotoxin S6b, further contractions could be achieved only with ET-1 in segments that had been exposed to sarafotoxin S6b and not in those exposed to ET-1. Also in view of the E_{max} of sarafotoxin S6b being slightly, but significantly, higher than that of ET-1, it is difficult to explain why ET-1, but not sarafotoxin S6b, caused further contraction of segments exposed to the other compound. Possibly, ET-1 caused desensitization of events beyond activation of the receptor for sarafotoxin S6b, without affecting this receptor itself. The latter was also suggested by Cardell *et al.* (1992), who made similar observations in the guinea-pig pulmonary artery, using ET-3 instead of sarafotoxin S6b. Hiley and co-workers (1992b) observed analogous cross-desensitization using ET-1 and ET-3, but suggested that ET-3 interacted with an ET-1-insensitive accessory binding site on the receptor used by ET-1 itself. This explanation of two agonists binding to different binding-sites on the same receptor also cannot be ruled out as the reason for the differences in antagonist potency observed against ET-1 and sarafotoxin S6b.

To characterize endothelin receptors in the present study, several complicating factors have to be kept in mind. First, we have no knowledge of possible differential metabolic- or uptake mechanisms of any of the endothelin receptor ligands. Indeed, contractile responses to high E_{max} concentrations of ET-1 or sarafotoxin S6b (with a magnitude of over 100% of the contractile response to 100 mM K^+) fade away partially. However, this decline is apparently not due to metabolic breakdown, since in our study the contractile response to lower concentrations of the peptides was sustained (Figure 3). Secondly, one may argue that receptor pharmacodynamics are not conventionally straightforward in interactions with endothelin receptors. After activating the receptor in human and porcine smooth muscle cells, the endothelin receptor-ligand complex was found to be internalized and, thus, possibly unavailable for competition (Resink *et al.*, 1990). It has also been reported that an endothelin receptor antagonist like BQ-123 may act either as a competitive, or non-competitive antagonist (Hiley *et al.*, 1992a), depending on whether or not equilibrium conditions are present (Vigne *et al.*, 1993). Lastly, the ligand-receptor kinetics for endothelins (e.g. different association/dissociation rates for different endothelin isopeptides, Galron *et al.*, 1991) could have implications for functional studies investigating the receptors involved. On the other hand, these conceivable, but yet theoretical pitfalls should not preclude comparison of the present observations with endothelin receptor characterizations in smooth muscle preparations as reported in previous studies. Furthermore, the involvement of heterogeneous receptors is supported by the observation of an additional non-ET_A, non-ET_B binding site in human coronary arteries labelled by [^{125}I]-sarafotoxin S6b, but not by [^{125}I]-ET-1, with particularly high affinity for BQ-123 (Bax *et al.*, 1993b). Also in support of the involvement of heterogeneous receptors are previous studies in human isolated saphenous veins in which BQ-123 biphasically inhibited sarafotoxin S6b-induced contractions. BQ-123 was more potent against high than against low concentrations of sarafotoxin S6b (Bax *et al.*, 1993a).

Are ET_A receptors involved in the contractile responses to ET-1 and sarafotoxin S6b?

Originally, ET_A receptors were differentiated from ET_B receptors by a high affinity of ET_A receptors for ET-1 compared to ET-3 (Arai *et al.*, 1990; Williams *et al.*, 1993). ET_B receptors, however, have similar affinity for ET-1 and ET-3 (Sakurai *et al.*, 1990; Williams *et al.*, 1993). Considering the difference in potency of ET-1 and ET-3 in the present study, it may be concluded that ET-1-induced responses in the present study are mediated by ET_A receptors. In addition, this order of potency virtually rules out the involvement of the putative ET_C receptor, which has higher affinity for ET-3 than for ET-1 (Masaki *et al.*, 1994). The presently observed agonist order of potency is similar to that in the rat thoracic aorta (Sumner *et al.*, 1992), the rabbit carotid artery (White *et al.*, 1993), and the guinea-pig aorta (Schoeffter & Randriantsoa, 1993). In all of these animal preparations, it was concluded that ET_A receptors mediate the contractile response. The fact that in the present study BQ-123 antagonized ET-1-induced contractions only at 10 μM ($pK_B = 5.75$) would however argue against involvement of the ET_A receptor, since BQ-123 has submicromolar (Ihara *et al.*, 1992a; Williams *et al.*, 1993) to nanomolar (Molenaar *et al.*, 1993; Davenport *et al.*, 1993) affinity for ET_A receptors in binding studies. In our experiments 0.1 μM BQ-123, if anything, caused a small potentiation of the contractile response. The pK_B value of BQ-123 against sarafotoxin S6b appears in better agreement with ET_A receptor involvement. It is however unlikely that sarafotoxin S6b activates an ET_A receptor, which is not activated by ET-1, since ET-1 has an even higher affinity for ET_A receptors than sarafotoxin S6b (Arai *et al.*, 1990).

The pK_B value (6.11) of FR139317 against ET-1 is in reasonable accordance with an ET_A receptor-mediated mechanism. Previously found pA_2 values for FR139317 include 6.0 in the rabbit femoral artery (Doherty *et al.*, 1993), 6.65 in the guinea-pig pulmonary artery (Cardell *et al.*, 1993) and 7.2 in the human coronary artery (Maguire *et al.*, 1994) and rabbit aorta (Sogabe *et al.*, 1993). A pK_B value of FR139317 as high as 8.2–8.5 against sarafotoxin S6b-induced responses (present results) has not yet been described for an ET_A receptor-mediated functional response in organ bath experiments and appears too high to point towards a 'typical' ET_A receptor-mediated mechanism.

Recent studies assessing the antagonist effects of BQ-123 against ET-1-induced contractions of human coronary artery rings (2 mm) report that, even at 0.1 μM, BQ-123 antagonized contractile responses to ET-1, resulting in pA_2 values of 6.4–7.5 (Godfraind, 1993; Davenport *et al.*, 1993). Both these studies concluded that ET_A receptors mediate the contractile responses to ET-1. It may be hypothesized that the difference in the potency of BQ-123 in those studies and our study, and also the discrepancies within other studies

between large proximal and small distal coronary artery segments (Chester *et al.*, 1992; Godfraind, 1993), could be due to differential diffusion of the large peptide molecules to the receptors in these two types of arterial segments. Indeed, we found in the present study that the type of preparation (4 mm ring or 1 mm spiral strip) made a difference in the observed potency of both ET-1 as an agonist and BQ-123 as an antagonist (Figure 5). Although the influence of the applied resting tension on strips and rings cannot be excluded, the observed discrepancy may be due to different drug concentrations in the receptor compartment, caused by differences in the diffusion barrier of large molecules (Kenakin, 1993), such as the endothelins. This could play a role in the observed divergence found between proximal and distal human coronary artery segments (Chester *et al.*, 1992; Godfraind, 1993), possibly in addition to a different receptor profile. One may argue that partial endothelial damage of the strip preparation affected the present results. However, it must be kept in mind that even a *complete* removal of the endothelium in ring segments did not affect the contractile response to ET-1 or sarafotoxin S6b (Figure 2). Similar diffussion-related differences may also play a role in the recently observed 3 fold leftward shift of the ET-1 concentration-response curve of human vertebral arteries of infants, when compared to vertebral arteries of adults (0–2 years vs. 38–71 years) (Charpie *et al.*, 1994). Our data from human coronary arteries do not support such age-dependent differences in the response to ET-1 or sarafotoxin S6b.

The pK_B value of 6.62 ± 0.18 for BQ-123, obtained here in strip preparations against ET-1, would not seem out of line when compared to a pA_2 of 6.93 in the rat aorta (Sumner *et al.*, 1992), of 6.5 in the rabbit femoral artery (Doherty *et al.*, 1993), of 6.8 and 6.9 in the rabbit caroitd artery and thoracic aorta, respectively (White *et al.*, 1993), and even compared to pA_2 values of 6.8–7.5 in the more distal parts of 2 mm human coronary artery rings (Godfraind, 1993). In all of these preparations the response was characterized as being mediated via ET_A receptors. Interestingly, Schoeffter & Randriantsoa (1993), using 3 mm ring preparations, found that ET-1-induced contractile responses of the porcine coronary artery were virtually insensitive to BQ-123 (pK_B:5.21) and concluded that these contractions were mediated by non-ET_A receptors. In contrast, an earlier study in the porcine coronary artery, using sprial strips (diameter 1 mm), found an apparently ET_A receptor-linked pA_2 value of 7.4 (Ihara *et al.*, 1992a). Also in the porcine coronary artery, the agonist potency of ET-1 in the strip preparation was clearly higher (pD_2:≈10; Ihara *et al.*, 1992a) than in the ring preparation studied by Schoeffter & Randriantsoa (1993) (pD_2:8.3).

The presence of mRNA encoding for ET_A receptors has been established in smooth muscle cells of the human coronary artery (Winkles *et al.*, 1993; Davenport *et al.*, 1993). In a receptor autoradiography analysis of endothelin receptors in the human coronary artery, it was shown that 30 pM [^{125}I]-ET-1 labelled a homogeneous receptor population in the human coronary artery with similar characteristics to the ET_A receptors identified in atrium and ventricle (Bax *et al.*, 1993b). Also Davenport *et al.* (1994), studying binding displacement of 100 pM [^{125}I]-PD151242, concluded that ET_A receptors were present in the media of (atherselerotic) human coronary artery.

Taking into account (*i*) the higher potency of ET-1 compared to ET-3, (*ii*) the pK_B value which we obtained (6.62 ± 0.18) for BQ-123 against ET-1 in strip preparations, (*iii*) the potency of FR139317 in coronary artery rings, and (*iv*) the previously obtained evidence from radioligand binding and molecular biology experiments for the presence of ET_A receptors in the human coronary artery, we have to conclude that contractile responses to ET-1 were most likely mediated via an ET_A receptor, despite a pK_B value of only 5.75 for BQ-123 against ET-1-induced responses in 4 mm coronary artery rings. We showed that the type of preparation can affect the potency of both ET-1 and BQ-123, which may have significant implications for the use of these compounds in other studies involving endothelin receptor characterization. Considering the associated high pK_B values of BQ-123 and especially FR139317, we propose that contractions to sarafotoxin S6b are mediated via another subtype of ET_A receptors. A similar suggestion has been made by Salom *et al.* (1993) for the effects of sarafotoxin S6b in the goat cerebral artery. Possibly, the effects of ET-3 (also extremely potently antagonized by BQ-123) are mediated via the same receptor, not only in the human isolated coronary artery (Godfraind, 1993), but also in the human small omental vein (Riezebos *et al.*, 1994), in the rat vas deferens (Eglezos *et al.*, 1993; Warner *et al.*, 1993), and in the guinea-pig left atrium (Hatton *et al.*, 1994). Although the above mentioned complicating receptor dynamics or kinetics cannot entirely be ruled out, no evidence is available as yet for such mechanisms.

Are ET_B receptors involved in contractile responses?

The very small contractile response elicited by high concentrations of [Ala^{1,3,11,15}]ET-1 in the human isolated coronary artery would argue against the involvement of ET_B receptors. Davenport *et al.* (1993) found a complete lack of agonist effect in the human coronary artery of both [Ala^{1,3,11,15}]ET-1 and BQ-3020, another ET_B receptor selective agonist (Ihara *et al.*, 1992b). In the pig coronary artery [Ala^{1,3,11,15}]ET-1 acted as a partial agonist with a pD_2 of 7.4 (Schoeffter & Randriantsoa, 1993). Furthermore, [Ala^{1,3,11,15}]ET-1 induced phosphoinositol turnover in human ET_B receptor-transfected COS-7 cells (K_D 20 nM, Stavros *et al.*, 1993), and caused relaxation of the porcine pulmonary artery (ED_{40} 4.4 nM, Saeki *et al.*, 1991). To verify whether [Ala^{1,3,11,15}]ET-1 acted as a partial agonist in this preparation, concentration-response curves to both ET-1 and sarafotoxin S6b were constructed in the presence and absence of 1 μM [Ala^{1,3,11,15}]ET-1, but no antagonism was observed (Figure 4). Thus, in the present study, no evidence was obtained to support functional involvement of contractile ET_B receptors. Also in our radioligand binding study, in which either 30 pM [^{125}I]-ET-1 or [^{125}I]-sarafotoxin S6b were used, no indication was found for the presence of ET_B receptors on the smooth muscle of the human coronary artery (Bax *et al.*, 1993b). However, in another investigation, where 100 pM [^{125}I]-ET-1 was used as a radioligand, it was concluded that a small proportion (13%) of ET_B receptors was present in the human coronary artery (Davenport *et al.*, 1993). The presence of mRNA encoding for ET_B receptors has been shown in human coronary artery smooth muscle cells (Davenport *et al.*, 1993; Winkles *et al.*, 1993). Possibly, these ET_B receptors do not play a major role in endothelin-induced vasoconstriction, but they may be involved in other yet unknown effects. Recently, however, it was shown in the human internal mammary artery and vein that ET-1 may induce contractions via a mixed ET_A/ET_B receptor population (Seo *et al.*, 1994).

Effects of big-ET-1 and phosphoramidon

The 21-amino acid peptide, ET-1, is formed after cleavage between Trp^{21} and Val^{22} of a 38 amino acid precursor peptide, big-ET-1 (Yanagisawa *et al.*, 1988; Okada *et al.*, 1990). The contractile response of big-ET-1 in isolated tissues may develop directly via binding of big-ET-1 to vascular smooth muscle receptors (Hirata *et al.*, 1990) as well as indirectly via ET-1 cleaved from big-ET-1 by the endothelin-converting-enzyme (ECE), which is reflected by the steep nature of the concentration-response curve. The activity of ECE was found to vary between different vascular beds (Auguet *et al.*, 1992), as shown by the ability of phosphoramidon, a metalloprotease inhibitor of ECE (Okada *et al.*, 1990), to inhibit the contractile response induced by big-ET-1. Since in the present study, pretreatment with 100 μM phosphoramidon partially reduced the contractile response to big-ET-1, we conclude that ECE, present in the coronary artery, contributed

to the contractile response induced by big-ET-1. It has been suggested that ECE has substrate specificity for big-ET-1 compared to big-ET-3 (Okada *et al.*, 1990). Apart from this explanation, the absence of contractile effects to big-ET-3 in the present study could also result from the lower contractile potency of ET-3 compared to ET-1 (Table 1), combined with, possibly, a low affinity of big-ET-3 itself for vascular contractile receptors.

In conclusion, the present study showed that ET-1 and sarafotoxin S6b contract the human isolated coronary artery via different receptor mechanisms, which can probably be characterized best as subtypes of the ET_A receptor. Responses to ET-1 and sarafotoxin S6b are not modified by endothelial denudation. This study also showed that the type of preparation (ring of strip) may affect the potency of ET-1 as an agonist, and of BQ-123 as an antagonist. Finally, the contractile response to big-ET-1 is mediated in part by conversion to ET-1, taking place within the vascular wall of the human isolated coronary artery.

We would like to thank Dr Philippe Schoeffter (Sandoz Pharma Ltd., Basel, Switzerland) for many fruitful discussions. Supported by the Netherlands Heart Foundation, grant 89.252 and 93.146.

References

AHA COMMITTEE REPORT (1975). A reporting system on patients evaluated for coronary artery disease. *Circulation*, **51**, (suppl. IV), IV.5–IV.40.

ARAI, H., HORI, S., ARAMORI, I., OHKUBO, H. & NAKANISHI, S. (1990). Cloning and expression of a cDNA encoding an endothelin receptor. *Nature*, **348**, 730–732.

AUGUET, M., DELAFLOTTE, S., CHABRIER, P.-E. & BRAQUET, P. (1992). The vasoconstrictor action of big endothelin-1 is phosphoramidon-sensitive in rabbit saphenous artery, but not in saphenous vein. *Eur. J. Pharmacol.*, **224**, 101–102.

BAX, W.A., BOS, E. & SAXENA, P.R. (1993a). Heterogeneity of endothelin/sarafotoxin receptors mediating contraction of the human isolated saphenous vein. *Eur. J. Pharmacol.*, **239**, 267–268.

BAX, W.A., BRUINVELS, A.T., VAN SUYLEN, R.-J., SAXENA, P.R. & HOYER, D. (1993b). Endothelin receptors in the human coronary artery, ventricle and atrium; A quantitative autoradiographic analysis. *Naunyn-Schmied Arch. Pharmacol.*, **348**, 403–410.

BAX, W.A., PETTERSON, R.W.G., INAN, T., BOS, E. & SAXENA, P.R. (1994). Heterogeneity of endothelin/sarafotoxin receptors mediating contractions of the human isolated coronary artery. *Br. J. Pharmacol.*, **111**, 15P (abstract).

BODELSSON, G. & STJERNQUIST, M. (1993). Characterization of endothelin receptors and localization of ^{125}I-endothelin-1 binding sites in human umbilical artery. *Eur. J. Pharmacol.*, **249**, 299–305.

BOSSALLER, C., HABIB, G.B., YAMAMOTO, H., WILLIAMS, C., WELLS, S. & HENRY, P.D. (1987). Impaired muscarinic endothelium-dependent relaxation and cyclic guanosine 5'-monophosphate formation in atherosclerotic human coronary artery and rabbit aorta. *J. Clin. Invest.*, **79**, 170–174.

CARDELL, L.O., UDDMAN, R. & EDVINSSON, L. (1992). Evidence for multiple endothelin receptors in the guinea-pig pulmonary artery and trachea. *Br. J. Pharmacol.*, **105**, 376–380.

CARDELL, L.O., UDDMAN, R. & EDVINSSON, L. (1993). A novel ET_A-receptor antagonist, FR 139317, inhibits endothelin-induced contractions of guinea-pig pulmonary arteries, but not trachea. *Br. J. Pharmacol.*, **108**, 448–452.

CHARPIE, J.R., SCHREUR, K.D., PAPADOPOULOS, S.M. & WEBB, R.C. (1994). Endothelium dependency of contractile activity differs in infant and adult vertebral arteries. *J. Clin. Invest.*, **93**, 1339–1343.

CHESTER, A.H., O'NEIL, G.S., ALLEN, S.P., LUU, T.N., TADJKARIMI, S. & YACOUB, M.H. (1992). Effect of endothelin on normal and diseased human coronary arteries. *Eur. J. Clin. Invest.*, **22**, 210–213.

DAVENPORT, A.P., O'REILLY, G., MOLENAAR, P., MAGUIRE, J.J., KUG, R.E., SHARKEY, A., BACON, C.R. & FERRO, A. (1993). Human endothelin receptors characterized using reverse transcriptase-polymerase chain reaction, in situ hybridization, and subtype-selective ligands BQ123 and BQ3020: Evidence for expression of ET_B receptors in human vascular smooth muscle. *J. Cardiovasc. Pharmacol.*, **22**, suppl. 8, S22–S25.

DAVENPORT, A.P., KUC, R.E., FITZGERALD, F., MAGUIRE, J.J., BERRYMAN, K. & 'OHERTY, A.M. (1994). [^{125}I]-PD151242: a selective radioligand for human ET_A receptors. *Br. J. Pharmacol.*, **111**, 4–6.

DE LEAN, A., MUNSON, P.J. & RODBARD, D. (1978). Simultaneous analysis of families of sigmoidal curves: application to bioassay, radioligand assay, and physiological dose-response curves. *Am. J. Physiol.*, **235**, E97–E102.

DE NUCCI, G., THOMAS, R., D'ORLÉANS-JUSTE, P., ANTUNES, E., WALDER, C., WARNER, T.D. & VANE, J.R. (1988). Pressor effects of circulating endothelin are limited by its removal in the pulmonary circulation and by the release of prostacyclin and endothelium-derived relaxing factor. *Proc. Natl. Acad. Sci. U.S.A.*, **85**, 9797–9800.

DOHERTY, A.M., CODY, W.L., HE, J.X., DEPUE, P.L., CHENG, X.-M., WELCH, K.M., FLYNN, M.A., REYNOLDS, E.E., LADOUCEUR, D.M., DAVIS, L.S., KEISER, J.A. & HALEEN, S.J. (1993). In vitro and in vivo studies with a series of hexapeptide endothelin antagonists. *J. Cardiovasc. Pharmacol.*, **22**, suppl. 8, S98–S102.

DOUGLAS, S.A. & HILEY, C.R. (1990). Endothelium-dependent vascular activities of endothelin-like peptides in the isolated superior mesenteric arterial bed of the rat. *Br. J. Pharmacol.*, **101**, 81–88.

DREIKORN, K. (1992). Organkonservierung. *Zentralbl. Chir.*, **117**, 642–647.

EGLEZOS, A., CUCCHI, P., PATACCHINI, R., QUARTARA, L., MAGGI, C.A. & MIZRAHI, J. (1993). Differential effects of BQ-123 against endothelin-1 and endothelin-3 on the rat vas deferens: evidence for an atypical endothelin receptor. *Br. J. Pharmacol.*, **109**, 736–738.

FURCHGOTT, R.F. (1972). The classification of adrenoceptors. An evaluation from the standpoint of receptor theory. In *Handbook of Experimental Pharmacology*, Vol. 33, *Catecholamines*. ed. Blaschko, H. & Muscholl, E. pp. 283–335. Berlin, Heidelberg, New York: Springer.

GALRON, R., BDOLAH, A., KOCHVA, E., WOLLBERG, Z., KLOOG, Y. & SOKOLOVSKY, M. (1991). Kinetic and cross-linking studies indicate different receptors for endothelins and sarafotoxins in the ileum and cerebellum. *FEBS Lett.*, **283**, 11–14.

GODFRAIND, T. (1993). Evidence for heterogeneity of endothelin receptor distribution in human coronary artery. *Br. J. Pharmacol.*, **110**, 1201–1205.

HARRISON, V.J., RANDRIANTSOA, A. & SCHOEFFTER, P. (1992). Heterogeneity of endothelin-sarafotoxin receptors mediating contraction of pig coronary artery. *Br. J. Pharmacol.*, **105**, 511–513.

HATTON, C.J., STOGGALL, S.M. & WILSON, C. (1994). Differential antagonism of the positive inotropic effects of ET-1 and ET-3 (abstract). *Br. J. Pharmacol.*, **112**, 158P.

HIRATA, Y., KANNO, K., WATANABE, T.X., KUMAGAYE, S., NAKAJIMA, K., KIMURA, T., SAKAKIBARA, S. & MARUMO, F. (1990). Receptor binding and vasoconstrictor activity of big endothelin. *Eur. J. Pharmacol.*, **176**, 225–228.

HILEY, C.R., COWLEY, D.J., PELTON, J.T. & HARGREAVES, A.C. (1992a). BQ-123, cyclo(D-Trp-D-Asp-Pro-D-Val-Leu), is a non-competitive antagonist of the actions of endothelin-1 in SK-N-MC human neuroblastoma cells. *Biochem. Biophys. Res. Commun.*, **184**, 504–510.

HILEY, C.R., MCSTAY, M.K.G., BOTTRILL, F.E. & DOUGLAS, S.A. (1992b). Cross-desensitization studies with endothelin isopeptides in the rat isolated superior mesenteric arterial bed. *J. Vasc. Res.*, **29**, 135 (abstract).

IHARA, M., NOGUCHI, K., SAEKI, T., FUKURODA, T., TSUCHIDA, S., KIMURA, S., FUKAMI, T., ISHIKAWA, K., NISHIKIBE, M. & YANO, M. (1992a). Biological profiles of highly potent novel endothelin antagonists selective for the ET_A receptor. *Life Sci.*, **50**, 247–255.

IHARA, M., SAEKI, T., FUKURODA, T., KIMURA, S., OZAKI, S., PATEL, A.C. & YANO, M. (1992b). A novel radioligand [^{125}I]BQ-3020 selective for endothelin (ET_B) receptors. *Life Sci.*, **51**, 47–52.

KAWASAKI, K., SEKI, K. & HOSODA, S. (1981). Spontaneous rhythmic contractions in isolated human coronary arteries. *Experientia*, **37**, 1291–1292.

KENAKIN, T. (1993). *Pharmacologic Analysis of Drug-Receptor Interaction*. 2nd edition, pp. 87–175. New York: Raven Press.

MAGUIRE, J.J. & DAVENPORT, A.P. (1994). Pre- or post-administration of BQ123 and FR139317 antagonizes endothelin-1 (ET-1)-induced contraction of human blood vessels *in vitro* (abstract). *Br. J. Pharmacol.*, **111**, 140P.

MASAKI, T., VANE, J.R. & VANHOUTTE, P.M. (1994). International Union of Pharmacology nomenclature of endothelin receptors. *Pharmacol. Rev.*, **46**, 137–142.

MOLENAAR, P., O'REILLY, G., SHARKEY, A., KUC, R.E., HARDING, D.P., PLUMPTON, C., GRESHAM, G.A. & DAVENPORT, A.P. (1993). Characterization and localization of endothelin receptor subtypes in the human atrioventricular conducting system and myocardium. *Circ. Res.*, **72**, 526–538.

MORELAND, S., MCCULLEN, D.M., DELANEY, C.L., LEE, V.G. & HUNT, J.T. (1992). Venous smooth muscle contains vasoconstrictor ET_B-like receptors. *Biochem. Biophys. Res. Commun.*, **184**, 100–106.

OKADA, K., MIYAZAKI, Y., TAKADA, J., MATSUYAMA, K., YAMAKI, T. & YANO, M. (1990). Conversion of big endothelin-1 by membrane-bound metalloendopeptidase in cultured bovine endothelial cells. *Biochem. Biophys. Res. Commun.*, **171**, 1192–1198.

RESINK, T.J., SCOTT-BURDEN, T., BOULANGER, C., WEBER, E. & BÜHLER, F.R. (1990). Internalization of endothelin by cultured human vascular smooth muscle cells: characterization and physiological significance. *Mol. Pharmacol.*, **38**, 244–252.

RIEZEBOS, J., WATTS, I.S. & VALLANCE, P.J.T. (1994). Endothelin receptors mediating functional responses in human small arteries and veins. *Br. J. Pharmacol.*, **111**, 609–615.

SAEKI, T., IHARA, M., FUKURODA, T., YAMAGIWA, M. & YANO, M. (1991). [$Ala^{1,3,11,15}$]Endothelin-1 analogs with ET_B agonistic activity. *Biochem. Biophys. Res. Commun.*, **179**, 286–292.

SAKURAI, T., YANAGISAWA, M., TAKUWA, Y., MIYAZAKI, H., KIMURA, S., GOTO, K. & MASAKI, T. (1990). Cloning of a cDNA encoding a non-isopeptide-selective subtype of the endothelin receptor. *Nature*, **348**, 732–735.

SALOM, J.B., TORREGROSA, G. BARBERÁ, M.D., JOVER, T. & ALBORCH, E. (1993). Endothelin receptors mediating contraction in goat cerebral arteries. *Br. J. Pharmacol.*, **109**, 826–830.

SCHOEFFTER, P. & RANDRIANTSOA, A. (1993). Differences between endothelin receptors mediating contraction of guinea-pig aorta and pig coronary artery. *Eur. J. Pharmacol.*, **249**, 199–206.

SEO, B., OEMAR, B.S., SIEBENMANN, R., VON SEGESSER, L. & LÜSCHER, T.F. (1994). Both ET_A and ET_B receptors mediate contraction to endothelin-1 in human blood vessels. *Circulation*, **89**, 1203–1208.

SOGABE, K., NIREI, H., SHOUBO, M., NOMOTO, A., AO, S., NOTSU, Y. & ONO, T. (1993). Pharmacological profile of FR139317, a novel, potent endothelin ET_A receptor antagonist. *J. Pharmacol. Exp. Ther.*, **264**, 1040–1046.

STAVROS, F.D., HASEL, K.W., OKUN, I., BALDWIN, J. & FRERIKS, K. (1993). COS-7 cells stably transfected to express the human ET_B receptor provide a useful screen for endothelin receptor antagonists. *J. Cardiovasc. Pharmacol.*, **22**, suppl. 8, S34–S37.

SUMNER, M.J., CANNON, T.R., MUNDIN, J.W., WHITE, D.G. & WATTS, I.S. (1992). Endothelin ET_A and ET_B receptors mediate vascular smooth muscle contraction. *Br. J. Pharmacol.*, **107**, 858–860.

VIGNE, P., BREITTMAYER, J.P. & FRELIN, C. (1993). Competitive and non competitive interactions of BQ-123 with endothelin ET_A receptors. *Eur. J. Pharmacol.*, **245**, 229–232.

WARNER, T.D., ALLCOCK, G.H., MICKLEY, E.J. & VANE, J.R. (1993). Characterization of endothelin receptors mediating the effects of the endothelin-sarafotoxin peptides on autonomic neurotransmission in the rat vas deferens and guinea-pig ileum. *Br. J. Pharmacol.*, **110**, 783–789.

WHITE, D.G., CANNON, T.R., GARRATT, H., MUNDIN, J.W., SUMNER, M.J. & WATTS, I.S. (1993). Endothelin ET_A and ET_B receptors mediate vascular smooth-muscle contraction. *J. Cardiovasc. Pharmacol.*, **22**, suppl. 8, S144–S148.

WILLIAMS, D.L., JONES, K.L., ALVES, K., CHAN, C.P., HOLLIS, G.F. & TUNG, J.-S. (1993). Characterization of cloned human endothelin receptors. *Life Sci.*, **53**, 407–414.

WINKLES, J.A., ALBERTS, G.F., BROGI, E. & LIBBY, P. (1993). Endothelin-1 and endothelin receptor mRNA expression in normal and atherosclerotic human arteries. *Biochem. Biophys. Res. Commun.*, **191**, 1081–1088.

YANAGISAWA, M., KURIHARA, H., KIMURA, S., TOMOBE, Y., KOBAYASHI, M., MITSUI, Y., YAZAKI, Y., GOTO, K. & MASAKI, T. (1988). A novel potent vasonconstrictor peptide produced by vascular endothelial cells. *Nature*, **332**, 411–415.

(Received February 21, 1994
Revised July 4, 1994
Accepted August 23, 1994)

Br. J. Pharmacol. (1994), 113, 1480–1486 © Macmillan Press Ltd, 1994

Possible roles of protein kinases in neutrophil chemotactic factor production by leucocytes in allergic inflammation in rats

Jun-ichi Tanabe, [1]Masako Watanabe, Sachiko Kondoh, *Suetsugu Mue & Kazuo Ohuchi

Department of Pathophysiological Biochemistry, Faculty of Pharmaceutical Sciences, Tohoku University, Aoba Aramaki, Aoba-ku, Sendai, Miyagi 980-77, Japan, and *College of Medical Sciences, Tohoku University, Seiryo-machi, Aoba-ku, Sendai, Miyagi 980-77, Japan

1 In an air pouch-type allergic inflammation model in rats, leucocytes that had infiltrated into the pouch fluid collected 4 h after the antigen challenge produced proteinaceous chemotactic factors for neutrophils when they were incubated in the medium.

2 To clarify the mechanism of activation of the infiltrated leucocytes in producing these factors, the effects of protein kinase inhibitors on neutrophil chemotactic factor production were examined.

3 When the infiltrated leucocytes were incubated for 4 h in medium containing the non-selective protein kinase inhibitor K-252a (1–100 ng ml^{-1}, 2.14–214 nM), the tyrosine kinase inhibitor genistein (1–50 μg ml^{-1}, 3.7–185 μM), and the more selective protein kinase C inhibitor H-7 (5–100 μg ml^{-1}, 13.7–274 μM); neutrophil chemotactic activity in the conditioned medium was decreased in a concentration-dependent manner, but the adenosine 3':5'-cyclic monophosphate (cAMP)-dependent protein kinase inhibitor H-89 (1–1000 ng ml^{-1}, 2.24–2240 nM) showed no effect.

4 Isoelectric focusing of the conditioned medium revealed that the leucocytes produced two neutrophil chemotactic factors, leucocyte-derived neutrophil chemotactic factor (LDNCF) 1 and LDNCF-2. Treatment of the leucocytes with K-252a, genistein, and H-7, but not H-89, inhibited production of both LDNCF-1 and LDNCF-2.

5 These results suggest that activation of tyrosine kinase and protein kinase C, but not cAMP-dependent protein kinase, is responsible for the production of LDNCF-1 and LDNCF-2.

6 The steroidal anti-inflammatory drug dexamethasone and the protein synthesis inhibitor cycloheximide inhibited neutrophil chemotactic factor production in a concentration-dependent manner. Time-course experiments showed that the inhibitory effect by dexamethasone was apparent even 30 min after the incubation.

7 Mechanism for inhibiting the production of LDNCF-1 and LDNCF-2 by dexamethasone is also discussed.

Keywords: Allergic inflammation; lecocyte; neutrophil chemotactic factor; protein kinase C; tyrosine kinase; cAMP-dependent protein kinase; dexamethasone

Introduction

Cytokines are protein mediators that play important roles in inflammation and immune response (Elias *et al.*, 1990; Antin & Ferrara, 1992). For example, in rheumatoid arthritis, granulocyte–macrophage colony-stimulating factor (GM-CSF) (Xu *et al.*, 1989), interleukin (IL) 1, IL-6, tumour necrosis factor α (Thorbecke *et al.*, 1992) and IL-8 (Koch *et al.*, 1991) exist in the synovial fluid. These cytokines are produced by such inflammatory cells as mononuclear cells, lymphocytes and fibroblasts in the synovial fluid and tissues, and are responsible for the development of rheumatoid arthritis. Many studies suggest that cytokines produced by infiltrated leucocytes regulate the production of each cytokine, and thus control the function of inflammatory cells (Elias *et al.*, 1990; Feldman *et al.*, 1990; Haworth *et al.*, 1991). Therefore, to further define the inflammatory reaction, it is important to clarify the regulatory mechanism of cytokine production by leucocytes infiltrated into inflammatory sites.

During the course of experiments to identify the difference between allergic and non-allergic inflammation employing an air pouch-type inflammation model in rats (Ohuchi *et al.*, 1982; 1985; Tsurufuji *et al.*, 1982; Hirasawa *et al.*, 1986; 1987; Watanabe *et al.*,1987; 1990), focused especially on the qualitative difference in the function of infiltrated leucocytes, we found (Watanabe *et al.*, 1994) that the leucocytes infiltrated into the pouch fluid in the allergic inflammation model are much more active than those in the non-allergic inflammation model with respect to neutrophil chemotactic factor production. When the infiltrated leucocytes in the pouch fluid were collected 4 h after injection of the antigen solution and incubated, leucocytes from the immunized rats produced a larger amount of neutrophil chemotactic factors than did leucocytes from the non-immunized rats, thereby suggesting that the leucocytes infiltrated into the pouch fluid in the immunized rats are much more active than those in the non-immunized rats (Watanabe *et al.*, 1994). Our present investigation was intended to clarify pharmacologically the mechanism of activation of leucocytes for the production of neutrophil chemotactic factors in the allergic inflammation. We have reported that the leucocytes infiltrated into the pouch fluid produce two neutrophil chemotactic proteins, leucocyte-derived neutrophil chemotactic factor (LDNCF) 1 and LDNCF-2 (Watanabe *et al.*, 1994). It is possible that the production of the two chemotactic proteins by the infiltrated leucocytes is induced after activation of leucocytes at the inflammatory sites. Because cytokine production by inflammatory cells is regulated through the signal transduction pathway of protein tyrosine phosphorylation (Muñoz *et al.*, 1992) or serine/threonine phosphorylation (Zhang *et al.*, 1992), we investigated whether the production of LDNCF-1 and LDNCF-2 by leucocytes infiltrated into the inflammatory locus is also associated with protein phosphorylation. Using several types of protein kinase inhibitors,

[1] Author for correspondence.

we found that the inhibitors of protein kinase C and tyrosine kinase, but not cAMP-dependent protein kinase, inhibit the production of both LDNCF-1 and LDNCF-2. These results suggest that protein kinase C and tyrosine kinase in the infiltrated leucocytes are activated by certain inflammatory stimuli to produce LDNCF-1 and LDNCF-2.

Several studies have demonstrated that the anti-inflammatory drug dexamethasone inhibits production of cytokines or expression of their genes by inflammatory cells *in vitro* (Lew *et al.*, 1988; Villiger *et al.*, 1992; Cassatella *et al.*, 1993). The present investigation also demonstrates that production of LDNCF-1 and LDNCF-2 by infiltrated leucocytes is inhibited by dexamethasone treatment.

Methods

Induction of allergic inflammation

The immunization and induction of air pouch-type allergic inflammation in rats were carried out as described previously (Tsurufuji *et al.*, 1982), with a slight modification. Male rats of the Sprague–Dawley strain, specific pathogen free and weighing 120–140 g (Charles River Japan, Kanagawa, Japan) were used. An antigen, azobenzenearsonate-conjugated acetyl bovine serum albumin (ABA-AcBSA) was synthesized according to the procedure described by Tabachnick & Sobotka (1962). The rats were immunized by i.d. injection of ABA-AcBSA and Freund's complete adjuvant (Difco Laboratories, Detroit, MI, U.S.A.). Nine days after immunization, 8 ml of air was injected s.c. in the dorsum to form an ellipsoid-shape air pouch. Twenty-four hours after the injection of air, 2 mg of the antigen dissolved in 4 ml of a sterilized solution of 0.8% (w/v) sodium carboxymethylcellulose (CMC-Na, Cellogen F3H; Daiichi Kogyo Seiyaku, Niigata, Japan) in 0.9% (w/v) NaCl solution was injected into the air pouch to provoke allergic inflammation. The CMC-Na solution was supplemented with penicillin G potassium and dihydrostreptomycin sulphate (Meiji Seika, Tokyo, Japan), each at a 0.1 mg ml^{-1} concentration.

Culture of leucocytes collected from the pouch fluid

Four hours after the injection of the antigen solution into the air pouch of the immunized rats, rats were sacrificed by cutting the carotid artery under diethyl ether anaesthesia and the entire pouch fluid was collected. The pouch fluid was diluted 4-fold with RPMI-1640 medium (Nissui Seiyaku, Tokyo, Japan) and leucocytes infiltrated into the pouch fluid were precipitated by centrifugation at 350 *g* and 4°C for 5 min. The precipitate was washed three times with the medium and suspended in RPMI-1640 medium containing 0.25% (w/v) bovine serum albumin (BSA, essentially fatty acid-free; Sigma, St Louis, MO, U.S.A.) at a concentration of 1×10^7 cells ml^{-1}. The rest of the cells were differentially counted for each type of cells after May–Gruenwald–Giemsa staining. Four millilitres of the cell suspension (4×10^7 cells) was incubated at 37°C for various lengths of time in the presence or absence of drugs. After appropriate incubation times, the cell suspension was centrifuged at 1,500 *g* and 4°C for 5 min. The supernatant fraction was obtained, finally diluted to 20-fold with RPMI-1640 medium containing 0.25% (w/v) BSA, and used for the measurement of neutrophil chemotactic activity.

Measurement of neutrophil chemotactic activity

Neutrophil chemotactic activity in the diluted supernatant fraction of the conditioned medium was assayed using modified Boyden chambers as described previously (Watanabe *et al.*, 1994).

Drug treatment

The non-specific protein kinase inhibitor K-252a (Elliott *et al.*, 1990; Nye *et al.*, 1992) (Kyowa Medex, Tokyo, Japan), the tyrosine kinase inhibitor genistein (Tremblay *et al.*, 1992) (Wako), the more selective protein kinase C inhibitor H-7 [1-(5-isoquinolinesulphonyl)-2-methylpiperazine dihydrochloride] (Hidaka *et al.*, 1991) (Seikagaku Kogyo, Tokyo, Japan), the protein kinase A inhibitor H-89 (*N*-[2-(*p*-bromocinnamylamino)ethyl]-5-isoquinoline-sulphonamide) (Chijiwa *et al.*, 1990) (Seikagaku Kogyo Co.), the protein synthesis inhibitor cycloheximide (Sigma) and the synthetic glucocorticoid dexamethasone (Sigma) were dissolved in ethanol and an aliquot of the ethanol solution was added to RPMI-1640 medium containing 0.25% (w/v) BSA. The final ethanol concentration in the medium was adjusted to 0.1% (v/v). After treatment with drugs, viability of the leucocytes was examined by trypan blue exclusion test, and no cytotoxic effect was observed.

Isoelectric focusing to separate neutrophil chemotactic activity in the conditioned medium

Leucocytes infiltrated into the pouch fluid of immunized rats were collected 4 h after the antigen challenge, and were incubated for 4 h at 37°C in RPMI-1640 medium containing 0.25% (w/v) BSA at a concentration of 1×10^7 cells ml^{-1} with or without drugs. After incubation, the cell suspension was centrifuged at 1,500 *g* and 4°C for 5 min. The supernatant fraction (49 ml) was dialysed against 10 mM NaCl and mixed with 1 ml of Bio-Lyte ampholytes (pH range 3–10, Bio-Rad, Richmond, CA, U.S.A.). The mixture was loaded into the focusing chamber of the Rotofor cell (Bio-Rad), and isoelectric focusing carried out at 12 W constant power for 3 h at 4°C (Watanabe *et al.*, 1994). Twenty fractions were harvested and their pH values measured. Each fraction (2.5 ml) was dialysed against 1 M NaCl to remove ampholytes, and further dialysed against phosphate-buffered saline (pH 7.4) at 4°C. Chemotactic activity in each fraction was then determined after a 10-fold dilution with RPMI-1640 medium containing 0.25% (w/v) BSA.

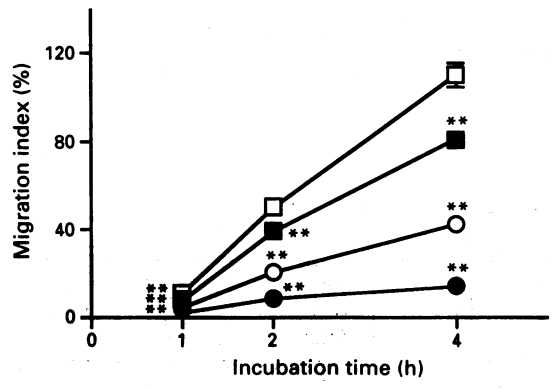


Figure 1 Effects of cycloheximide on chemotactic factor production by infiltrated leucocytes. Leucocytes (4×10^7 cells) in the pouch fluid collected 4 h after injection of the antigen solution into the air pouch of immunized rats were incubated for various periods at 37 °C in 4 ml of the medium containing cycloheximide at 0 μM (□), 0.018 μM (■), 0.18 μM (○) and 1.8 μM (●). A concentration of cycloheximide at 0.5 μg ml^{-1} corresponds to 1.8 μM. Neutrophil chemotactic activity in the conditioned medium was determined after 20-fold dilution. Values are the means from four samples in one experiment with s.e.mean shown by vertical bars. Where vertical bars are not depicted, s.e.mean is inside the symbol. Statistical significance: $^{**}P < 0.001$ vs the corresponding control. The results were confirmed by two separate experiments.

Statistical analysis

Results were analysed for statistical significance by Dunett's test for multiple comparisons and Student's *t*-test for unpaired observations.

Results

Production of neutrophil chemotactic factor by infiltrated leucocytes and its inhibition by cycloheximide

When leucocytes (4×10^7 cells) in the pouch fluid collected 4 h after injection of the antigen solution into the air pouch of immunized rats were incubated at 37°C in 4 ml of RPMI-1640 medium containing 0.25% (w/v) BSA, the chemotactic activity for neutrophils in the conditioned medium was increased time dependently (Figure 1). Differential cell count for the leucocytes collected at 4 h showed that 86.2% of the leucocytes were neutrophils, 9.9% were mononuclear cells and 3.9% were eosinophils (Table 1). Adding cycloheximide to the medium inhibited the production of neutrophil chemotactic factor in a concentration-dependent manner (Figure 1). Cycloheximide alone at these concentrations showed no direct effect on neutrophil chemotaxis towards 10 nM of platelet-activating factor (PAF) (Figure 2).

Effects of K-252a on chemotactic factor production by infiltrated leucocytes

To elucidate the significant roles of protein phosphorylation in neutrophil chemotactic factor production, the infiltrated leucocytes (4×10^7 cells) were incubated for 4 h in 4 ml of RPMI-1640 medium containing 0.25% (w/v) BSA and various concentrations of K-252a, a non-selective inhibitor of protein kinases. As shown in Figure 3, the neutrophil chemotactic activity in the conditioned medium was decreased in a concentration-dependent manner. A half-maximal effect was induced at a concentration of 17 ng ml^{-1} (36.4 nM). K-252a by itself, at these concentrations, showed no direct effect on neutrophil chemotaxis towards 10 nM PAF (data not shown).

Effects of specific inhibitor of protein kinases on chemotactic factor production by infiltrated leucocytes

To determine what types of protein kinases are associated with neutrophil chemotactic factor production by infiltrated leucocytes, the effects of the tyrosine kinase inhibitor genistein, the more selective protein kinase C inhibitor H-7 and the cAMP-dependent protein kinase inhibitor H-89 were examined. The infiltrated leucocytes (4×10^7 cells) were incubated for 4 h in 4 ml of the medium in the presence of various protein kinase inhibitors. Treatment with the tyrosine

Table 1 Differential cell count of leucocytes infiltrated into the pouch fluid at 4 h

Total cells (%)	*Neutrophils* (%)	*Mononuclear cells* (%)	*Eosinophils* (%)
100	86.2 ± 4.1	9.9 ± 0.4	3.9 ± 0.2

Leucocytes in the pouch fluid collected 4 h after challenge injection were collected and differential cell counts was performed after May–Gimsa–Grünwald staining. Values are percentages of total cells, and expressed as means ± s.e.mean from eight rats. The same results were obtained by three separate experiments.

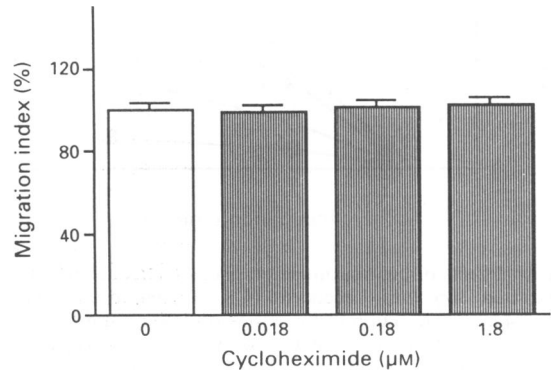


Figure 2 Effects of cycloheximide on PAF-induced neutrophil chemotaxis. Leucocytes (4×10^7 cells) in the pouch fluid were incubated at 37°C for 4 h in 4 ml of the medium containing 10 nM PAF and indicated concentrations of cycloheximide. A concentration of cycloheximide at 0.5 μg ml^{-1} corresponds to 1.8 μM. Values are the means from four samples with s.e.mean shown by vertical bars. The results were confirmed by three separate experiments.

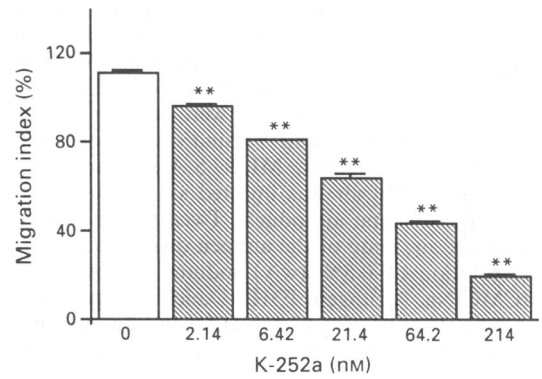


Figure 3 Effects of K-252a on chemotactic factor production by infiltrated leucocytes. Leucocytes (4×10^7 cells) in the pouch fluid were incubated at 37°C for 4 h in 4 ml of the medium containing indicated concentrations of K-252a. A concentration of K-252a at 1 ng ml^{-1} corresponds to 2.14 nM. Neutrophil chemotactic activity in the conditioned medium was determined after 20-fold dilution. Values are the means from four samples with s.e.mean shown by vertical bars. Statistical significance: $^{**}P < 0.001$ vs the control. The results were confirmed by three separate experiments.

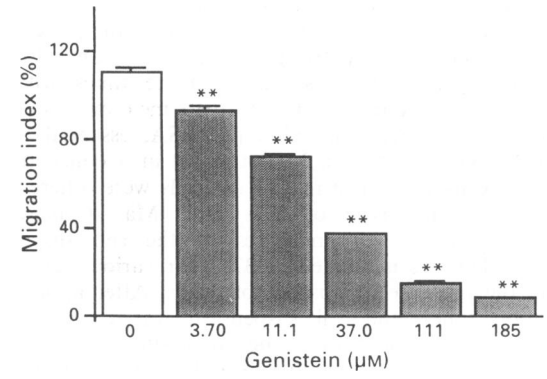


Figure 4 Effects of genistein on chemotactic factor production by the infiltrated leucocytes. Leucocytes (4×10^7 cells) in the pouch fluid were incubated at 37°C for 4 h in 4 ml of the medium containing indicated concentrations of genistein. A concentration of genistein at 1 μg ml^{-1} corresponds to 3.70 μM. Neutrophil chemotactic activity in the conditioned medium was determined after 20-fold dilution. Values are the means from four samples with s.e.mean shown by vertical bars. Statistical significance: $^{**}P < 0.001$ vs the control. The results were confirmed by three separate experiments.

kinase inhibitor genistein decreased neutrophil chemotactic activity in the conditioned medium in a concentration-dependent manner with a half-maximal effect at 5.6 $\mu g\ ml^{-1}$ (20.7 μM) (Figure 4). Similar results were obtained by the more selective protein kinase C inhibitor H-7 with a half-maximal effect at 8.9 $\mu g\ ml^{-1}$ (24.4 μM) (Figure 5). In contrast, treatment with the cAMP-dependent protein kinase inhibitor H-89 did not inhibit neutrophil chemotactic factor production at concentrations up to 1000 $ng\ ml^{-1}$ (2240 nM) (Figure 6). Each drug showed no direct effect on neutrophil chemotaxis toward 10 nM PAF (data not shown).

Effects of dexamethasone on chemotactic factor production by infiltrated leucocytes

When infiltrated leucocytes (4×10^7 cells) were incubated for 4 h in 4 ml of the medium containing various concentrations of dexamethasone, the neutrophil chemotactic activity in the conditioned medium was decreased in a concentration-dependent manner, with a half-maximal effect at 28 nM (Figure 7). Time-course experiments revealed that the inhibitory effect by dexamethasone was apparent even 30 min after incubation at 10 and 100 nM dexamethasone (Figure 8).

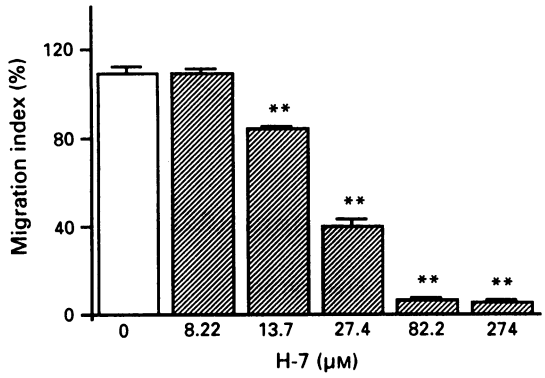


Figure 5 Effects of H-7 on chemotactic factor production by infiltrated leucocytes. Leucocytes (4×10^7 cells) in the pouch fluid were incubated at 37°C for 4 h in 4 ml of the medium containing indicated concentrations of H-7. A concentration of H-7 at 3 $\mu g\ ml^{-1}$ corresponds to 8.22 μM. Neutrophil chemotactic activity in the conditioned medium was determined after 20-fold dilution. Values are the means from four samples with s.e.mean shown by vertical bars. Statistical significance: $^{**}P < 0.001$ vs the control. The results were confirmed by three separate experiments.

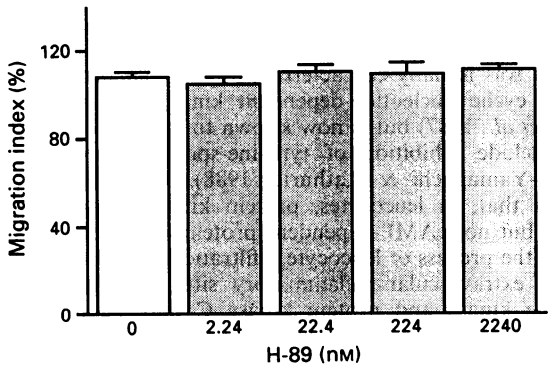


Figure 6 Effects of H-89 on chemotactic factor production by infiltrated leucocytes. Leucocytes (4×10^7 cells) in the pouch fluid were incubated at 37°C for 4 h in 4 ml of the medium containing indicated concentrations of H-89. A concentration of H-89 at 1 $ng\ ml^{-1}$ corresponds to 2.24 nM. Neutrophil chemotactic activity in the conditioned medium was determined after 20-fold dilution. Values are the means from four samples with s.e.mean shown by vertical bars. The results were confirmed by three separate experiments.

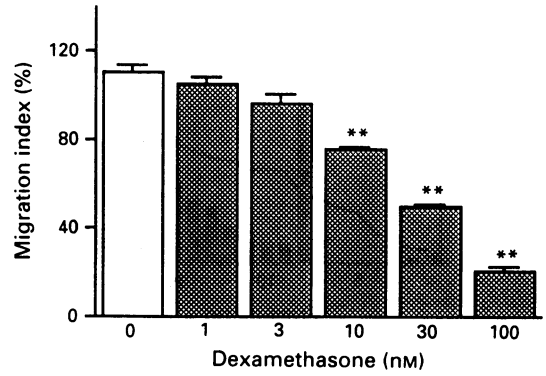


Figure 7 Effects of dexamethasone on chemotactic factor production by infiltrated leucocytes. Leucocytes (4×10^7 cells) in the pouch fluid were incubated at 37°C for 4 h in 4 ml of the medium containing indicated concentrations of dexamethasone. A concentration of dexamethasone at 0.39 $ng\ ml^{-1}$ corresponds to 1 nM. Neutrophil chemotactic activity in the conditioned medium was determined after 20-fold dilution. Values are the means from four samples with s.e.mean shown by vertical bars. Statistical significance: $^{**}P < 0.001$ vs the control. The results were confirmed by three separate experiments.

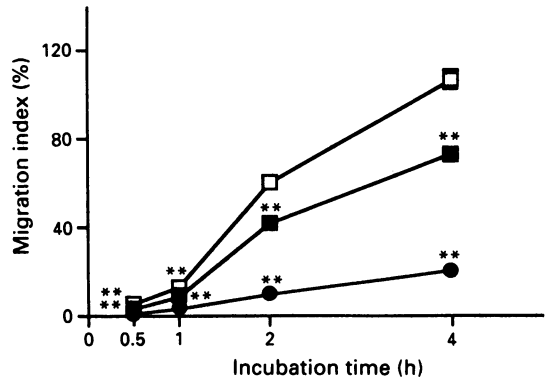


Figure 8 Time-course of effects of dexamethasone on neutrophil chemotactic factor production by infiltrated leucocytes. Leucocytes (4×10^7 cells) in the pouch fluid were incubated at 37°C for 4 h in 4 ml of the medium containing dexamethasone at 0 nM (□), 10 nM (■) and 100 nM (●). Neutrophil chemotactic activity in the conditioned medium was determined after 20-fold dilution. Values are the means from four samples with s.e.mean shown by vertical bars. Where vertical bars are not depicted, s.e.mean is inside the symbol. Statistical significance: $^{**}P < 0.001$ vs the control. The results were confirmed by three separate experiments.

Dexamethasone alone at these concentrations showed no direct effect on neutrophil chemotaxis towards 10 nM PAF (data not shown).

Effects of drugs on production of LDNCF-1 and LDNCF-2 by infiltrated leucocytes

Four hours after incubation of the infiltrated leucocytes in the medium with or without drugs, conditioned medium was obtained and the chemotactic activity for neutrophils in the conditioned medium was separated by isoelectric focusing. As shown in Figure 9a, neutrophil chemotactic activity was separated into two peaks: the first one is a sharp peak with a pI value around 6 (leucocyte-derived neutrophil chemotactic factor 1, LDNCF-1) and the second one is LDNCF-2 with a pI value above 8. Gradient analysis for neutrophil migration with LDNCF-1 or LDNCF-2 demonstrated that movement of neutrophils was not chemokinetic but chemotactic, because migrations in positive gradient were more effective than those in negative gradient (data not shown). When the

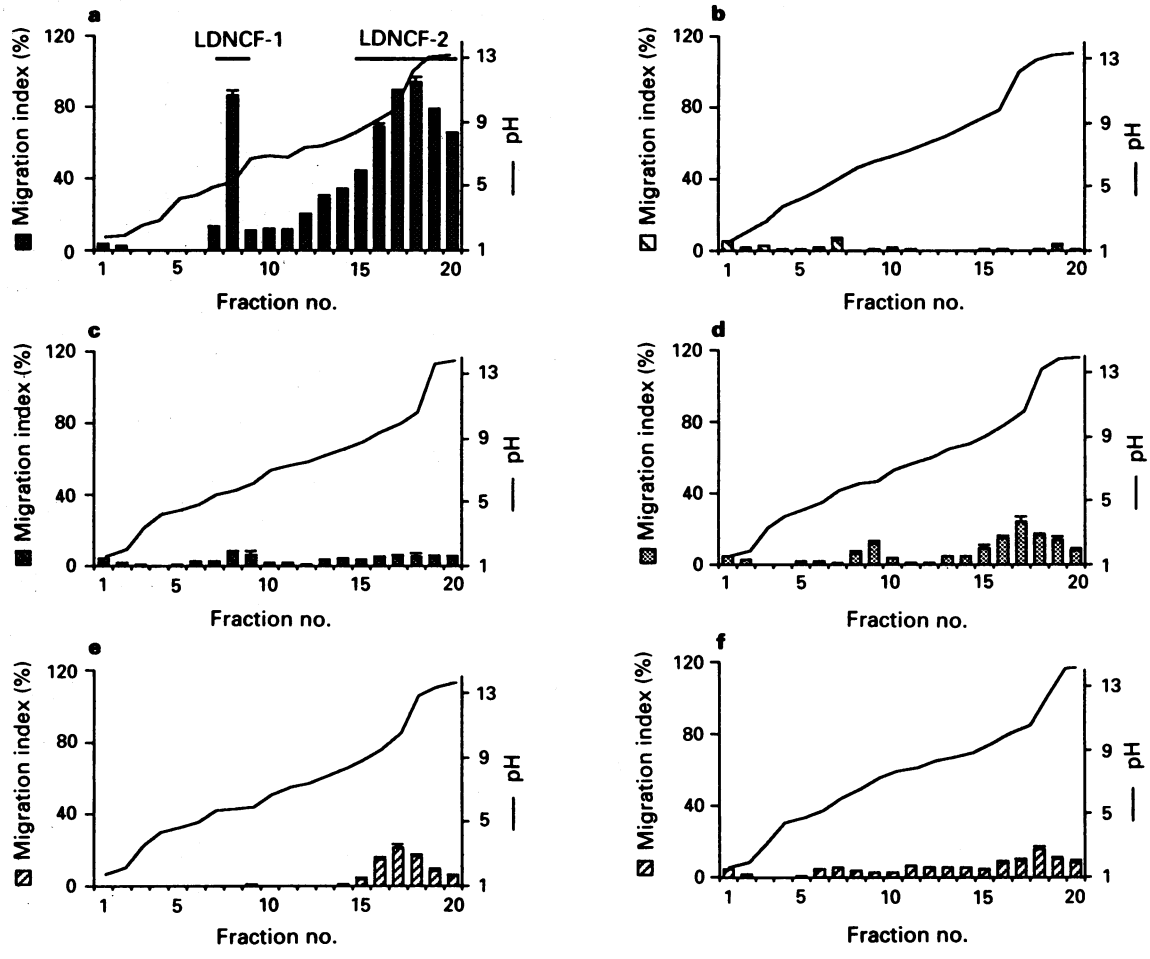


Figure 9 Separation profiles obtained by isoelectric focusing of the chemotactic activity for neutrophils in the conditioned medium. Leucocytes (5×10^8 cells) in the pouch fluid were incubated at 37 °C for 4 h in 50 ml of the medium containing (a) nothing, (b) cycloheximide (5 μg ml^{-1}, 17.8 μM), (c) K-252a (100 ng ml^{-1}, 214 nM), (d) genistein (50 μg ml^{-1}, 185 μM), (e) H-7 (30 μg ml^{-1}, 82.2 μM) or (f) dexamethasone (39.3 ng ml^{-1}, 100 nM). Neutrophil chemotactic activity in the conditioned medium was separated by isoelectric focusing. Chemotactic activity in each fraction was determined after 10-fold dilution. Values are the means with s.e.mean from four assays. In each group, one representative profile out of four separate experiments is shown.

infiltrated leucocytes were incubated in the presence of cycloheximide (5 μg ml^{-1}, 17.8 μM), K-252a (100 ng ml^{-1}, 214 nM), genistein (50 μg ml^{-1}, 185 μM), H-7 (30 μg ml^{-1}, 82.2 μM) or dexamethasone (39.3 ng ml^{-1}, 100 nM), production of both LDNCF-1 and LDNCF-2 was inhibited simultaneously (Figure 9b–f).

Discussion

Neutrophil chemotactic activity in the conditioned medium of leucocytes infiltrated into the inflammatory locus was decreased by treatment with the protein synthesis inhibitor cycloheximide (Figure 1). This treatment also inhibited production of LDNCF-1 and LDNCF-2 (Figure 9b). Therefore, the chemotactic factors in the conditioned medium are proteinaceous factors produced by the infiltrated leucocytes during the incubation period. The aim of the present investigation was to clarify the mechanism of the production of proteinaceous neutrophil chemotactic factors by leucocyte infiltrated into the inflammatory sites to gain further insight into the inflammatory reactions.

This study shows that production of chemotactic factor for neutrophils by leucocytes infiltrated into the inflammatory locus is inhibited by the non-selective inhibitor of protein kinases K-252a (Elliott *et al.*, 1990; Nye *et al.*, 1992), the more selective protein kinase C inhibitor H-7 (Hidaka *et al.*, 1991) and the tyrosine kinase inhibitor genistein (Tremblay *et al.*, 1992). However, the cAMP-dependent protein kinase inhibitor H-89 (Chijiwa *et al.*, 1990) did not inhibit the production of neutrophil chemotactic factor at concentrations great enough to inhibit the cAMP analogue-induced intercellular adhesion of JY cells (Haverstick & Gray, 1992). K-252a was initially characterized as a potent protein kinase C and cyclic nucleotide-dependent kinase inhibitor *in vitro* (Kase *et al.*, 1987) but is now known to have broader actions that include inhibition of tyrosine-specific protein kinases (Fujita-Yamaguchi & Kathuria, 1988). The present results suggest that, in leucocytes, protein kinase C and tyrosine kinase but not cAMP-dependent protein kinase are activated during the process of leucocyte infiltration from blood-stream to the extravascular inflammatory site. The activation of tyrosine kinase and protein kinase C may be induced by leucocyte–vascular endothelial cell interactions or by cytokines produced by inflammatory stimuli. Signalling cascades that initiate with tyrosine phosphorylations eventually also result in the serine/threonine phosphorylation of downstream molecules owing to the activation of serine/threonine kinases, such as Raf, protein kinase C and ribosomal S6 protein kinase (Ullrich & Schlessinger, 1990). For example, if tyrosine kinase in platelet-derived growth factor (PDGF) receptor is activated by the ligand, phospholipase C-γ associated with the PDGF receptor is activated (Kaplan *et al.*, 1990) and stimulates the canonical phosphatidyl inositol

turnover pathway, leading to elevation of cytosolic calcium and activation of protein kinase C (Whitman & Cantley, 1988). Other than GM-CSF, the association of tyrosine kinase with such receptors for cytokines as IL-2, IL-3, IL-5 and IL-6 has also been reported (Kishimoto *et al.*, 1994). On the other hand, 12-*O*-tetradecanoylphorbol 13-acetate (TPA), an activator of protein kinase C, induces protein tyrosine phosphorylation in neutrophils (Huang *et al.*, 1990). Actually, activation of protein kinase C of the infiltrated leucocytes by incubating the cells for 4 h with TPA at concentrations of $1-100\ ng\ ml^{-1}$ (1.62–162 nM) further stimulated the production of both LDNCF-1 and LDNCF-2 (J. Tanabe *et al.*, unpublished observations). This observation also indicates that production of LDNCF-1 and LDNCF-2 is mediated by activation of protein kinase C. Furthermore, the adhesion molecule component β1-integrin, which plays significant roles in leucocyte–endothelial cell and leucocyte–leucocyte interactions, is reported to induce protein tyrosine phosphorylation of $pp125^{FAK}$ (Kornberg *et al.*, 1992).

As to the characteristics of the neutrophil chemotactic factors produced by the leucocytes infiltrated into the inflammatory locus, we have reported that the major components of the neutrophil chemotactic factor are LDNCF-1 and LDNCF-2, of which the pI values are approximately 4 and >8 respectively (Watanabe *et al.*, 1994). During 4 h incubation of the leucocytes, leukotriene B_4 was produced, but the amount was less than the concentration needed to contribute to the chemotactic activity in the conditioned medium (Watanabe *et al.*, 1994). Determination of PAF in the conditioned medium after partial purification using immunoaffinity mini-columns (Watanabe *et al.*, 1992) and by radioimmunoassay revealed that the amount of PAF in the conditioned medium at 4 h was less than the detectable amount (<0.56 nM). Consequently, the proteinaceous chemotactic factors LDNCF-1 and LDNCF-2 are the major chemotactic factors produced by leucocytes infiltrated into the inflammatory locus. Further studies are necessary to clarify which type of cell (Table 1) is responsible for the production of LDNCF-1 and LDNCF-2. Production of both LDNCF-1 and LDNCF-2 was simultaneously inhibited by treatment with the non-selective protein kinase inhibitor K-252a, the more selective protein kinase C inhibitor H-7 and the tyrosine kinase inhibitor genistein, but was not inhibited by the cAMP-dependent protein kinase inhibitor H-89 (Figure 9), as was the case for the neutrophil chemotactic activity in the conditioned medium (Figures 3, 4, 5 and 6). These results indicate that the production of LDNCF-1 and LDNCF-2 is mediated by activation of tyrosine kinase and protein kinase C but not by cAMP-dependent protein kinase.

Production of LDNCF-1 and LDNCF-2 by the infiltrated leucocytes was inhibited by dexamethasone treatment (Figure 9). The time-course experiment revealed that the significant decrease in neutrophil chemotactic activity in the conditioned medium was observable even 30 min after incubation with dexamethasone at 10 and 100 nM (Figure 8). Dexamethasone binds to its receptor protein in the cytosol, moves into the nucleus, and the activated receptor–dexamethasone complex acts as the transcriptional factor, finally showing its biological effects under ongoing protein synthesis and RNA synthesis (Tobler *et al.*, 1992) or by suppression of gene expression (Jonat *et al.*, 1990; Schüle *et al.*, 1990; Yang-Yen *et al.*, 1990). In the present investigation, because the inhibitory effect of dexamethasone has appeared shortly after incubation (30 min), dexamethasone's inhibitory effect might not be mediated by induction of certain protein synthesis. As shown in Figures 1 and 9, production of the neutrophil chemotactic factor was inhibited by treatment with the protein synthesis inhibitor cycloheximide, so it is hard to prove that dexamethasone can inhibit the production of neutrophil chemotactic factors when protein synthesis is inhibited. Alternatively, dexamethasone might inhibit neutrophil chemotactic factor production by suppressing gene expression for LDNCF-1 and LDNCF-2. Inhibition by dexamethasone of IL-2 production in Jurkat T77 cells (Vacca *et al.*, 1990) and of IL-8 production in lipopolysaccharide-stimulated neutrophils (Weltheim *et al.*, 1993) is also reported to be mediated by the inhibition of gene expression.

Our recent work on the determination of amino acid sequence of LDNCF-1 and LDNCF-2 has revealed that the latter resembles murine macrophage inflammatory protein 2 (Wolpe *et al.*, 1989; Tekamp-Olson *et al.*, 1990) but not cytokine-induced neutrophil chemoattractant in rat (Watanabe *et al.*, 1989). Judging from the pI value, LDNCF-1 might be a new proteinaceous chemoattractant produced by leucocytes infiltrated into the inflammatory locus.

The mechanism of activation of protein kinase C and tyrosine kinase to produce LDNCF-1 and LDNCF-2 and the types of leucocytes that produce these factors remain to be elucidated. Further purification and characterization of LDNCF-1 are under investigation in our laboratories.

References

ANTIN, J.H. & FERRARA, J.L.M. (1992) Cytokine dysregulation and acute graft-versus-host disease. *Blood*, **80**, 2964–2968.

CASSATELLA, M.A., ASTE, M., CALZETTI, F., CONSTANTINS, G., GUASPARRI, I., CESKA, M. & ROSSI, F. (1993) Studies on the regulatory mechanisms of interleukin-8 gene expression in resting and IFN-γ-treated neutrophils: evidence on the capability of staurosporine of inducing the production of interleukin-8 by human neutrophils. (1993). *Biochem. Biophys. Res. Commun.*, **190**, 660–667.

CHIJIWA, T., MISHIMA, A., HAGIWARA, M., SANO, M., HAYASHI, K., INOUE, T., NAITO, K., TOSHIOKA, T. & HIDAKA, H. (1990). Inhibition of forskolin-induced neurite outgrowth and protein phosphorylation by a newly synthesized selective inhibitor of cyclic AMP-dependent protein kinase, *N*[2-(*p*-bromocinnamylamino)ethyl]-5-isoquinoline-sulfonamide (H-89), of PC12D pheochromocytoma cells. *J. Biol. Chem.*, **265**, 5267–5272.

ELIAS, J.A., FREUNDLICH, B., KERN, J.A. & ROSENBLOOM, J. (1990). Cytokine networks in the regulation of inflammation and fibrosis in lung. *Chest*, **97**, 1439–1445.

ELLIOTT, L.H., WILKINSON, S.E., SEDGWICK, A.D., HILL, C.H., LAWTON, G., DAVIS, P.D. & NIXON, J.S. (1990). K252a is a potent and selective inhibitor of phosphorylase kinase. *Biochem. Biophys. Res. Commun.*, **171**, 148–154.

FELDMANN, M., BRENNAN, F.M., CHANTRY, D., HAWORTH, C., TURNER, M., ABNEY, E., BUCHAN, G., BARRETT, K., BARKLEY, D., CHU, A., FIELD, M. & MAINI, R.N. (1990). Cytokine production in the rheumatoid joint: implications for treatment. *Ann. Rheum. Dis.*, **49**, 480–486.

FUJITA-YAMAGUCHI, Y. & KATHURIA, S. (1988). Characterization of receptor tyrosine-specific protein kinases by the use of inhibitors. Staurosporine is a 100-times more potent inhibitor of insulin receptor than IGF-1 receptor. *Biochem. Biophys. Res. Commun.*, **157**, 955–962.

HAVERSTICK, D.M. & GRAY, L.S. (1992) Lymphocyte adhesion mediated by lymphocyte function-associated antigen-1. I. Long term augmentation by transient increases in intracellular cAMP. *J. Immunol.*, **149**, 389–396.

HAWORTH, C., BRENNAN, F.M., CHANTRY, D., TURNER, M., MAINI, R.N. & FELDMANN, M. (1991). Expression of granulocyte-macrophage colony-stimulating factor in rheumatoid arthritis: regulation by tumor necrosis factor-α. *Eur. J. Immunol.*, **21**, 2575–2579.

HIDAKA, H., WATANABE, M, & KOBAYASHI, R. (1991) Properties and use of H-series compounds as protein kinase inhibitors. *Methods Enzymol.*, **201**, 328–339.

HIRASAWA, N., OHUCHI, K., SUGIO, K., TSURUFUJI, S., WATANABE, M. & YOSHINO, S. (1986). Vascular permeability responses and the role of prostaglandin E_2 in an experimental allergic inflammation in rats. *Br. J. Pharmacol.*, **87**, 751–756.

HIRASAWA, N., OHUCHI, K., WATANABE, M. & TSURUFUJI, S. (1987). Role of endogenous histamine in postanaphylactic phase of allergic inflammation in rats. *J. Pharmacol. Exp. Ther.*, **241**, 967–973.

HUANG, C.-K., BONAK, V., LARAMEE, G.R. & CASNELLIE, E. (1990). Protein tyrosine phosphorylation in rabbit peritoneal neutrophils. *Biochem. J.*, **269**, 431–436.

JONAT, C., RAHMSDORF, H.J., PARK, K.-K., CASTO, A.C.B., GEBEL, S., PONTA, H. & HERRLICH, P. (1990). Antitumor promotion and antiinflammation: down-modulation of AP-1 (Fos/Jun) activity by glucocorticoid hormone. *Cell*, **62**, 1189–1204.

KAPLAN, D.R., MORRISON, D.K., WONG, G., MCCORMICK, F. & WILLIAMS, L.T. (1990). PDGF β-receptor stimulates tyrosine phosphorylation of GAP and association of GAP with a signaling complex. *Cell*, **61**, 125–133.

KASE, H., IWAHASHI, K., NAKANISHI, S., MATSUDA, Y., YAMADA, K., TAKAHISHI, M., MURAKATA, C., SATO, A. & KANEKO, M. (1987). K-252a compounds, novel and potent inhibitors of protein kinase C and cyclic nucleotide-dependent protein kinases. *Biochem. Biophys. Res. Commun.*, **142**, 436–440.

KISHIMOTO, T., TAGA, T. & AKIRA, S. (1994). Cytokine signal transduction. *Cell*, **76**, 253–262.

KOCH, A.E., KUNKEL, S.L., BURROWS, J.C., EVANOFF, H.L., HAINES, G.K., POPE, R.M. & STRIETER, R.M. (1991). Synovial tissue macrophage as a source of the chemotactic cytokine IL-8. *J. Immunol.*, **147**, 2187–2195.

KORNBERG, L., EARP, H.S., PARSONS, J.T., SCHALLER, M. & JULIANO, R.L. (1992). Cell adhesion or integrin clustering increases phosphorylation of a focal adhesion-associated tyrosine kinase. *J. Biol. Chem.*, **267**, 23439–23442.

LEW, W., OPPENHEIM, J.J. & MATSUSHIMA, K. (1988). Analysis of the suppression of IL-1α and IL-1β production in human peripheral blood mononuclear adherent cells by a glucocorticoid hormone. *J. Immunol.*, **140**, 1895–1902.

MUÑOZ, E., ZUBIAGA, A., HUANG, C. & HUBER, B.T. (1992). Interleukin-1 induces protein tyrosine phosphorylation in T cells. *Eur. J. Immunol.*, **22**, 1391–1396.

NYE, S.H., SQUINTO, S.P., GLASS, D.J., STITT, T.N., HANTZOPOULOS, P., MACCHI, M.J., LINDSAY, N.S., IP, N.Y. & YANCOPOULOS, G.D. (1992). K-252a and staurosporine selectively block autophosphorylation of neurotrophin receptors and neurotrophin-mediated responses. *Mol. Biol. Cell.*, **3**, 677–686.

OHUCHI, K., YOSHINO, S., KANAOKA,K., TSURUFUJI, S. & LEVINE, L. (1982). A possible role of arachidonate metabolism in allergic air pouch inflammation in rats. Anti-inflammatory effect of indomethacin and dexamethasone and the level of prostaglandin E_2 in the exudate. *Int. Arch. Allergy Appl. Immunol.*, **68**, 326–331.

OHUCHI K., HIRASAWA, N., WATANABE, M. & TSURUFUJI, S. (1985). Pharmacological analysis of the vascular permeability response in the anaphylactic phase of allergic inflammation in rats. *Eur. J. Pharmacol.*, **117**, 337–345.

SCHÜLE, R., RANGARAJAN, P., KLIEWER, S., RANSONE, L.J., BOLADO, J., YANG, N., VERMA, I.M. & EVANS, R.M. (1990). Functional antagonism between oncoprotein c-Jun and the glucocorticoid receptor. *Cell*, **62**, 1217–1226.

TABACHNICK, M. & SOBOTKA, H. (1962). Azoprotein. II. A spectrophotometric study of the coupling on diazotized arsanilic acid with proteins. *J. Biol. Chem.*, **235**, 1051–1054.

TEKAMP-OLSON, P., GALLEGOS, C., MCCLAIN, J., SHERRY, B., FABRE, M., VAN-DEVENTER, S. & CERAMI, A. (1990). Cloning and characterization of cDNA for murine macrophage inflammatory protein 2 and its human homologues. *J. Exp. Med.*, **172**, 911–919.

THORBECKE, G.J., SHAH, R., LEU, C.H., KURUVILLA, A.P., HARDISON, A.M. & PALLADINO, M.A. (1992). Involvement of endogenous tumor necrosis factor α and transforming growth factor β during induction of collagen type II arthritis in mice. *Proc. Natl. Acad. Sci. USA*, **89**, 7375–7379.

TOBLER, A., MEIER, R. SEITZ, M., DEWALD, B., BAGGIOLINI, M. & FEY, M.F. (1992). Glucocorticoids downregulate gene expression of GM-CSF, NAP-1/IL-8, and IL-6, but not of M-CSF in human fibroblasts. *Blood*, **79**, 45–51.

TREMBLAY, L., GINGRAS, D., BOIVIN, D. & BE'LIVEAU, R. (1992). Tyrosine protein kinase activity in renal brushborder membrane. *Biochim. Biophys. Acta*, **1108**, 183–189.

TSURUFUJI, S., YOSHINO, S. & OHUCHI, K. (1982). Induction of an allergic air-pouch inflammation in rats. *Int. Arch. Allergy Appl. Immunol.*, **69**, 189–198.

ULLRICH, A. & SCHLESSINGER, J. (1990). Signal transduction by receptors with tyrosine kinase activity. *Cell*, **61**, 203–212.

VACCA, A., MARTINOTTI, S., SCREPANTI, I., MARODER, M., FELLI, M.P., FARINA, A.R., GISMONDI, A., SANTONI, A., FRATI, L. & GULINO, A. (1990). Transcriptional regulation of the interleukin 2 gene by glucocorticoid hormones. *J. Biol. Chem.*, **265**, 8075–8080.

VILLIGER, P.M., TERKELTAUB, R. & LOTZ, M. (1992). Production of monocyte chemoattractant protein-1 by inflamed synovial tissue and cultured synoviocytes. *J. Immunol.*, **149**, 722–727.

WATANABE, M. OHUCHI, K., SUGIDACHI, A., HIRASAWA, N., HAYASHI, Y. & TSURUFUJI, S. (1987). Platelet-activating factor in the inflammatory exudate in the anaphylactic phase of allergic inflammation in rats. *Int. Arch. Allergy Appl. Immunol.*, **84**, 396–403.

WATANABE, K., KONISHI, K., FUJIOKA, M., KINOSHITA, S. & NAKAGAWA, H. (1989). The neutrophil chemoattractant produced by the rat kidney epithelioid cell line NRK-52E is a protein related to the KC/gro protein. *J. Biol. Chem.*, **264**, 19559–19563.

WATANABE, M., SUGIDACHI, A., OMATA, M., HIRASAWA, N., MUE, S., TSURUFUJI, S., & OHUCHI, K. (1990). Possible role for platelet-activating factor in neutrophil infiltration in allergic inflammation in rats. *Int. Arch. Allergy Appl. Immunol.*, **92**, 396–403.

WATANABE, M., WATANABE, T., HIRASAWA, N., MUE, S., MURAMATSU, S., MATSUSHITA, Y., TAKAHAGI, H., BRAQUET, P., BROQUET, C., LEVINE, L. & OHUCHI, K. (1992). Preparation of immunoaffinity mini-columns for the analysis of platelet-activating factor (PAF) in biological samples. *J. Chromatogr.*, **597**, 309–314.

WATANABE, M., ARAKIDA, Y., TANABE, J., SUGIDACHI, A., HIRASAWA, N., MUE, S. & OHUCHI, K. (1994). Pharmacological analysis of neutrophil chemotactic factor production by leucocytes and roles of PAF in allergic inflammation in rats. *Br. J. Pharmacol.*, **111**, 123–130.

WELTHEIM, W.A., KUNKEL, S.L., STANDIFORD, T.J., BURDICK, M.D., BECKER, F.S., WILKE, C.A., GILBERT, A.R. & STRIETER, R.S. (1993). Regulation of neutrophil-derived IL-8: the role of prostaglandin E_2, dexamethasone, and IL-4. *J. Immunol.*, **151**, 2166–2175.

WHITMAN, M. & CANTLEY, L. (1988). Phosphoinositide metabolism and the control of cell proliferation. *Biochim. Biophys. Acta*, **948**, 327–344.

WOLPE, S.D., SHERRY, B., JUERS, D., DAVATELIS, G., YURT, R.W. & CERAMI, A. (1989). Identification of macrophage inflammatory protein 2. *Proc. Natl. Acad. Sci. USA*, **86**, 612–616.

XU, W.D., FIRESTEIN, G.S., TAETLE, R., KAUSHANSKY, K. & ZVAIFLER, N.J. (1989). Cytokines in chronic inflammatory arthritis II. Granulocyte-macrophage colony-stimulating factor in rheumatoid synovial effusions. *J. Clin. Invest.*, **83**, 876–882.

YANG-YEN, H.-F., CHAMBARD, J.-C., SUN, Y.-L., SMEAL, T., SCHMIDT, T.J., DROUIN, J. & KARIN, M. (1990). Transcriptional interference between c-Jun and the glucocorticoid receptor: mutual inhibition of DNA binding due to direct protein-protein interaction. *Cell*, **62**, 1205–1215.

ZHANG, Q.-Y., HAMMERBERG, C., BALDASSARE, J.J., HENDERSON, P.A., BURNS, D., CESKA, M., VOORHEES, J.J. & FISHER, G.J. (1992). Retinoic acid and phorbol ester synergistically up-regulate IL-8 expression and specifically modulate protein kinase C-ε in human skin fibroblasts. *J. Immunol.*, **149**, 1402–1408.

(Received May 9, 1994
Revised July 27, 1994
Accepted August 15, 1994)

Br. J. Pharmacol. (1994), **113**, 1487–1493 © Macmillan Press Ltd, 1994

Antinociceptive and toxic effects of (+)-epibatidine oxalate attributable to nicotinic agonist activity

[1]N.M.J. Rupniak, S. Patel, R. Marwood, J. Webb, J.R. Traynor*, J. Elliott*, S.B. Freedman, S.R. Fletcher & R.G. Hill

Merck Sharp and Dohme Research Laboratories, Neuroscience Research Centre, Terlings Park, Eastwick Road, Harlow, Essex, CM20 2QR and *Department of Chemistry, Loughborough University, Leicester, LE11 3TU

1 Epibatidine is an analgesic substance, isolated from the skin of the poisonous frog *Epipedobates tricolor*, for which the mechanism of action was previously unknown.

2 The IC_{50} of synthetic (+)-epibatidine oxalate (the naturally occurring isomer) for [^{3}H]-nicotine binding to rat whole-brain membranes was 0.1 nM. The (−)-isomer also exhibited high affinity (IC_{50} = 0.2 nM).

3 (+)- and (−)-Epibatidine exhibited much lower affinity for displacement of the muscarinic ligand [^{3}H]-N-methylscopolamine binding to rat cortical membranes (K_{app} = 6.9 μM and 16.0 μM respectively). The (+)-enantiomer of epibatidine had an antagonist/agonist (NMS/oxo-M) binding ratio of 4.2 This is consistent with a muscarinic antagonist profile.

4 (+)-Epibatidine oxalate (10 μM) did not cause significant (>30%) displacement of radioligand binding to opioid, excitatory amino acid, benzodiazepine, 5-HT, dopamine, adrenaline or peptide receptors.

5 (+)- and (−)-Epibatidine (5–20 μg kg^{-1} s.c.) doubled response latency in the mouse hot-plate test. Antinociception and behavioural depression induced by (+)-epibatidine (5 μg kg^{-1}) was fully blocked by the nicotinic antagonists mecamylamine (2 mg kg^{-1} s.c.) or dihydro-β-erythroidine (2 mg kg^{-1} s.c.). The muscarinic antagonist scopolamine (0.4 and 10 mg kg^{-1} s.c.) caused partial reversal of antinociception induced by (+)-epibatidine in mice, but not in rats.

6 These findings demonstrate that (+)-epibatidine oxalate salt is a highly selective and potent nicotinic analgesic agent.

Keywords: Antinociception; mouse; rat; nicotine

Introduction

Narcotic analgesics are the mainstay of therapy for severe pain but are frequently underprescribed because of side-effects including respiratory depression, emesis, sedation and dependence (Spence, 1990). Since the development of safe and efficacious non-opioid analgesics would represent a major breakthrough for the clinical management of pain, there has been great interest in the recent discovery of a natural product, epibatidine, with antinociceptive actions in rodents. Like morphine, epibatidine induced antinociception and Straub tail in mice, but in contrast to morphine these effects were not blocked by naloxone (Spande *et al.*, 1992). The mechanism by which epibatidine induces analgesia is not known, but a preliminary report has implicated nicotinic receptor agonist activity (Qian *et al.*, 1993). Like opioid analgesics, nicotinic receptor agonists have been shown to exhibit antinociceptive activity in simple rodent screens employing noxious thermal stimuli (Tripathi *et al.*, 1982).

Extracted in trace quantities from *Epipedobates tricolor*, native epibatidine is scarce and, like other skin alkaloids isolated from poisonous frogs and other amphibia (such as tetrodotoxin and batrachotoxin; Daly *et al.*, 1978), is highly toxic *in vivo*. The analgesia and toxicity induced by epibatidine would appear to be consistent with nicotinic agonist activity and/or some other unidentified mechanism of action, such as an interaction with ion channels (see Miranda *et al.*, 1992; Damaj *et al.*, 1993). Synthesis of the (+)- and (−)-exo-isomers of epibatidine oxalate (Fletcher *et al.*, 1993) has recently identified the natural product to be the (+)-isomer (Watt *et al.*, 1994). In the present study we have characterized both isomers of epibatidine in a number of radioreceptor binding assays to investigate the potential pharmacological properties of epibatidine which might contribute to the antinociceptive and toxic effects of this substance.

[1] Author for correspondence.

Methods

The species employed for *in vitro* and *in vivo* evaluation of epibatidine oxalate were rats, mice and guinea-pigs as detailed below.

Affinity of epibatidine for neurotransmitter recognition sites in vitro

The (+)-exo-isomer of epibatidine oxalate was submitted to Panlabs (WA, U.S.A.) to obtain a preliminary profile of receptor binding affinities. Details of the key radioligands used and methods for determining non-specific binding are summarized in Table 1. (+)-Epibatidine oxalate was screened at a single concentration of 10 μM dissolved in 0.5% dimethylsulphoxide (DMSO). Inhibition of ligand binding by less than 30% in any assay was considered not significant. (+)- and (−)-Epibatidine oxalate were subsequently submitted to detailed *in vitro* characterization using opioid, muscarinic and nicotinic receptor binding assays.

Opioid receptor binding

Homogenates were prepared in Tris–HCl buffer (pH 7.4, 50 mM) from the brains, without cerebella, of male CSI mice

Table 1 Summary of ligand-binding assays (Panlabs)

Recognition site	*Radioligand*	*Tissue*	*Inhibition at 10 μM (%)*
Opiate δ	[^{3}H]-DPDPE	Guinea pig whole brain	9
Opiate κ	[^{3}H]-U69593	Guinea pig whole brain	−5
Opiate μ	[^{3}H]-DAMGO	Guinea pig whole brain	−3
Muscarinic M_1	[^{3}H]-Pirenzepine	Rat cerebral cortex	70
Muscarinic M_2	[^{3}H]-NMS	Rat heart	−15
Nicotinic	[^{3}H]-Cytisine	Rat cerebral cortex	98
NMDA	[^{3}H]-CGS-19755	Rat cerebral cortex	18
AMPA (quisqualate)	[^{3}H]-AMPA	Rat cerebral cortex	13
Kainate	[^{3}H]-Kainate	Rat whole brain	28
Glycine (strychnine sensitive)	[^{3}H]-Strychnine	Rat spinal cord	10
Glycine (strychnine insensitive)	[^{3}H]-Glycine	Rat cerebral cortex	12
Benzodiazepine	[^{3}H]-Flunitrazepam	Rat whole brain	19
$GABA_A$	[^{3}H]-Muscimol	Rat whole brain	1
Serotonin 5-HT_1	[^{3}H]-5-HT	Rat cerebral cortex	8
Serotonin 5-HT_2	[^{3}H]-Ketanserin	Rat whole brain	−6
Dopamine D1	[^{3}H]-SCH23390	Rat striatum	−13
Dopamine D2	[^{3}H]-Raclopride	Rat striatum	3
Adrenergic α_1	[^{3}H]-Prazosin	Rat whole brain	−2
Adrenergic α_2	[^{3}H]-Rauwolscine	Rat cerebral cortex	13
β-Adrenergic	[^{3}H]-DHA	Rat whole brain	−7
Bradykinin BK_2	[^{3}H]-Bradykinin	Guinea pig ileum	3
CCK_A	[^{3}H]-L-364,718	Rat pancreas	−8
CCK_B	[^{3}H]-CCK-8	Mouse whole brain	−8
CGRP	[^{125}I]-CGRP	Rat whole brain	−10
Neurokinin NK_1	[^{3}H]-Substance P	Rat submaxillary gland	1
Calcium channel (L)	[^{3}H]-Nitrendipine	Rat cerebral cortex	20
Calcium channel (N)	[^{125}I]-ω-Conotoxin	Rat frontal lobes	−5

(25–35 g; Nottingham University Medical School) as previously described (Traynor *et al.*, 1990). Binding assays were performed in Tris–HCl buffer for 40 min at 25°C using 16 mg of tissue in a total volume of 1 ml, and terminated by rapid filtration (Traynor *et al.*, 1990). [^{3}H]-DAMGO ([D-Ala^2,MePhe^{4}Glyol^5]enkephalin; 1.95 nM) was used to label μ-sites, [^{3}H]-DPDPE ([D-Pen^2,D-Pen^5]enkephalin; 2.93 nM) to label δ-sites; and [^{3}H]-CI977 (5R-(5α,7a,8β)-N-methyl-N-[7-(pyrrolidinyl)-1-oxaspiro[4,5]dec-8-yl]-4-benzofuranoacetamide; 1.22 nM) to label κ-sites. Non-specific binding was defined using naloxone (10 μM).

Muscarinic receptor binding

The ability of (+)- and (−)-epibatidine oxalate to displace [^{3}H]-N-methylscopolamine (NMS) or [^{3}H]-oxotremorine-M (Oxo-M) binding was determined using methods described previously (Freedman *et al.*, 1988). Briefly, rat cerebral cortices were homogenized in ice-cold 0.32 M sucrose (1:10, w/v) and centrifuged at 1000 *g* for 15 min. The resulting supernatant was centrifuged at 17,000 *g* for 20 min to yield the crude synaptosomal mitochondrial pellet (P_2).

[^{3}H]-NMS P_2 fractions were homogenized and resuspended at a final dilution of 1:600 (wet w/v) in ice-cold Krebs HEPES buffer pH 7.4 (composition, mM: NaCl 118, KCl 4.7, $MgSO_4$ 1.2, $NaHCO_3$ 5, KH_2PO_4 1.2, $CaCl_2$ 2.5, glucose 11 and HEPES 20). Binding of [^{3}H]-NMS was determined using 0.01–1.0 nM ligand and non-specific binding defined with 1 μM atropine. Isomers of epibatidine were added in a volume of 10 μl to give a final assay volume of 1.0 ml. Incubations were initiated by adding 750 μl of membrane solution and were allowed to proceed for 60 min at 30°C. Assays were terminated by filtration. Filters were rinsed with 2 × 10 ml of ice-cold saline (0.9% NaCl, w/v).

[^{3}H]-Oxo-M P_2 fractions were washed by resuspending in 10 ml of 20 mM HEPES buffer pH 7.4 and centrifuged at 17,000 *g* for 15 min. The washed membranes were homogenized and resuspended at a final dilution of 1:100 (wet w/v) in ice-cold 20 mM HEPES buffer pH 7.4. Binding of [^{3}H]-Oxo-M was determined using 0.2–5 nM ligand and non-specific binding defined with 2 μM atropine. Displacing compounds were added in a volume of 10 μl to give a final assay volume of 1.0 ml. Incubations were initiated by adding 750 μl of membrane solution and were allowed to proceed for 40 min at 30°C. Assays were terminated by filtration over filters presoaked in 0.05% polyethyleneimine. Samples were washed with 10 ml of ice-cold saline and radioactivity estimated by liquid scintillation spectrometry.

Nicotinic receptor binding

High-affinity binding of [^{3}H]-(−)-nicotine was determined using modification of the method described by Romano & Goldstein (1980). Whole rat brains were homogenized in 1:10 (wet w/v) of 20 mM HEPES buffer pH 7.4 and centrifuged at 17,500 *g* for 30 min. The pellet was resuspended in ice-cold distilled water 1:20 (wet w/v) and incubated on ice for 1 h. This suspension was centrifuged at 17,500 *g* for 30 min and the pellet resuspended in ten volumes of buffer. After a final centrifugation (17,500 *g* for 30 min) the pellet was resuspended in buffer at a concentration of 15 mg ml^{-1}.

Binding assays were conducted in polypropylene tubes containing 100 μl of [^{3}H]-(−)-nicotine (final concentration 10 nM), 10 μl of displacing compound and 390 μl of buffer. Non-specific binding was defined by incorporation of 10 μl of carbachol (final concentration 1 mM). The reaction was initiated by adding 500 μl of the membrane suspension with vortex mixing. Samples were incubated for 60 min at 30°C. The reaction was terminated by filtration over filters presoaked in 0.05% polyethyleneimine followed by washing

with 10 ml of ice-cold saline. The radioactivity of filters was estimated by liquid scintillation spectrometry.

Determination of binding parameters Data from binding assays were subjected to non-linear least-squares regression analysis using RS1 (BBN Research Systems, Cambridge, MA, U.S.A.) and a computerized iterative procedure written by Dr A. Richardson, NRC Terlings Park.

Antinociceptive activity of isomers of epibatidine

Experiments conformed to ethical guidelines for investigation of nociception in conscious animals (Zimmermann, 1983). The number of animals and the intensity of noxious stimuli were the minimum necessary with which to demonstrate reliable effects of standard analgesic agents. Each animal was used once only and was humanely killed immediately following completion of testing or on appearance of adverse drug effects. Groups of 7–18 animals received each drug treatment or vehicle.

Mouse hot plate The subjects were male BKTO mice (20–40 g, Bantin & Kingman, U.K.). Nociception thresholds were determined using the method of Eddy & Leimbach (1953). Animals were placed in a glass beaker (internal diameter 10 cm) suspended in a water bath at 60°C. The sides of the water bath were made of clear Perspex to enable observation of the animals. The latency (s) for the mouse to react to the noxious heat, which usually involved licking the forepaws and occasionally jumping to escape from the beaker or thumping of the hindfeet, was recorded using a stop watch. If the mouse failed to respond after 30 s it was removed and a latency of 30 s was recorded.

Carrageenan-induced hyperalgesia The subjects were male Sprague–Dawley rats (90–110 g). Hyperalgesia to mechanical compression of the hindpaw was induced by intraplantar injection of carrageenan (4.5 mg per paw) 3 h previously. Test compounds were administered s.c. 2.5 h after carrageenan (i.e. 30 min before nociception testing). Paw oedema and the vocalization threshold for mechanical compression of the paw were measured using a Ugo Basile plethysmometer and algesiometer.

Drug preparation All test substances were dissolved in saline and administered subcutaneously in the mid-scapular region using an injection volume of 2.5 ml kg^{-1} for mice or 1 ml kg^{-1} for rats. Unless otherwise stated, analgesic agents given alone or in combination with selected antagonists were administered 30 min prior to nociception testing. The three isomers of epibatidine oxalate [(+)- and (−)-exo, and the endo-isomer] were synthesized by the Department of Medicinal Chemistry, Merck Sharp & Dohme, Harlow, U.K., as described by Fletcher *et al.* (1993). Initial doses for investigation were based on those reported for native epibatidine by Spande *et al.* (1992). Dihydro-β-erythroidine hydrobromide (DHE) was supplied by Merck Sharp & Dohme, Rahway, NJ, U.S.A. Morphine sulphate, naloxone hydrochloride, pilocarpine hydrochloride, scopolamine hydrobromide and mecamylamine hydrochloride were purchased from Sigma, U.K. All doses are expressed as the base equivalent.

Data analysis Where necessary, antinociception scores were subjected to square root transformation to achieve normality and homogeneity of variance followed by one-way analysis of variance (ANOVA) and Dunnett's or Newman–Keuls multiple comparison tests.

Results

Affinity of epibatidine for neurotransmitter recognition sites in vitro

Results from Panlabs screen At a concentration of 10 μM, the (+)-exo isomer of epibatidine oxalate markedly displaced specific binding of [^{3}H]-pirenzepine (1 nM) to muscarinic M_1-like receptors (70% inhibition) and specific binding of [^{3}H]-cytisine (2 nM) to nicotinic receptors (98% inhibition) to rat cerebral cortex membranes. Binding of [^{3}H]-*N*-methylscopolamine (NMS; 0.2 nM) to muscarinic M_2 receptors in rat heart was not displaced by (+)-epibatidine oxalate. Binding at recognition sites for opioids, excitatory amino acids, glycine, benzodiazepines, GABA, 5-HT, dopamine, noradrenaline, neuropeptides and calcium channels was displaced by less than 30% by (+)-epibatidine oxalate (10 μM; Table 1).

Opioid receptor binding Additional studies confirmed the absence of significant displacement of opioid receptor binding in whole mouse brain homogenates by either the (+)- or (−)-exo isomers of epibatidine oxalate (10 μM) using [^{3}H]-DAMGO (1.95 nM), [^{3}H]-DPDPE (2.93 nM) and [^{3}H]-CI977 (1.22 nM) as ligands for the μ-, δ- and κ-receptor respectively (Table 2).

Muscarinic receptor binding The (+)- and (−)-exo isomers of epibatidine oxalate were evaluated in muscarinic binding assays designed to measure the affinity and predict efficacy for muscarinic receptors in rat cerebral cortex (Freedman *et al.*, 1988). The results are shown in Table 3. Both isomers showed appreciable affinity for both [^{3}H]-*N*-methylscopolamine and [^{3}H]-oxotremorine-M binding. The (+)-isomer had slightly higher affinity (~3-fold) for the antagonist radioligand than the (−)-isomer. The activity in the [^{3}H]-*N*-methylscopolamine binding assay was similar to that observed with pilocarpine and carbachol. We have previously demonstrated that the ratio of affinities for muscarinic agents in the [^{3}H]-*N*-methylscopolamine and [^{3}H]-oxotremorine-M binding assays can be used to predict efficacy. The full agonist, carbachol (NMS/oxo-M ratio = 4500), has a significantly higher ratio than the partial agonist, pilocarpine (NMS/oxo-M ratio = 100), in this paradigm (Freedman *et al.*, 1988). The two isomers of epibatidine had very low NMS/oxo-M ratios (Table 3). Significantly higher activity was seen with the (−)-isomer (NMS/oxo-M ratio = 12), a value resembling the partial agonist profile of some muscarinic agonists described previously, e.g. L-687,306 (Freedman *et al.*, 1993). In contrast the (+)-isomer had a

Table 2 Inhibition of specific radioligand binding to μ, δ and κ opioid receptors in whole mouse brain homogenates by isomers of epibatidine oxalate (10 μM)

	Per cent of control binding		
Isomer	*[^{3}H]-DAMGO* (1.95 nM)	*[^{3}H]-DPDPE* (2.93 nM)	*[^{3}H]-CI977* (1.22 nM)
(+)-Epibatidine oxalate	93.1 + 4.2	88.4 + 3.3	74.4 + 4.0
(−)-Epibatidine oxalate	102.4 + 1.5	91.3 + 1.7	85.3 + 1.8

Values are the mean ± 1 s.e.mean from three separate determinations.

Table 3 Muscarinic receptor binding profile of isomers of epibatidine

	[^{3}H]-NMS K_{app} (μM)	[^{3}H]-Oxo-M K_{app} (μM)	NMS/Oxo-M ratio
Carbachol	22 (20–24)	0.0049 (0.0036–0061)	4500
Pilocarpine	4.0 (3.0;5.1)	0.040 (0.036–0.044)	100
Atropine	0.0010 (0.00094–0.0011)	0.00048 (0.00040–0.00057)	2.1
(+)-Epibatidine oxalate	6.9 (2.9;16)	1.6 (1.4;1.9)	4.2
(−)-Epibatidine oxalate	16 (11,25)	1.4 (1.4;1.9)	12

Values are expressed as an apparent affinity constant (K_{app}) which is corrected for ligand occupancy using the Cheng–Prussof relationship (Cheng & Prussoff, 1973). Each dose–response curve was typically performed in triplicate and consisted of 8–12 points. Values are the geometric means of at least three independent determinations. Numbers in parentheses indicate the low and high error value of the geometric mean. Studies were performed with 0.1 nM [^{3}H]-*N*-methylscopolamine ([^{3}H]-NMS) and 3.0 nM [^{3}H]-oxotremorine-M ([^{3}H]-Oxo-M) using tissue from rat whole brain.

Table 4 Nicotinic receptor binding of the isomers of epibatidine

Compound	IC_{50} (nM)
(−)-Nicotine	7.8
(+)-Epibatidine oxalate	0.10
(−)-Epibatidine oxalate	0.24

Each value is the geometric mean of five determinations. Studies were performed with 1 nM [^{3}H]-nicotine to rat cortical membranes.

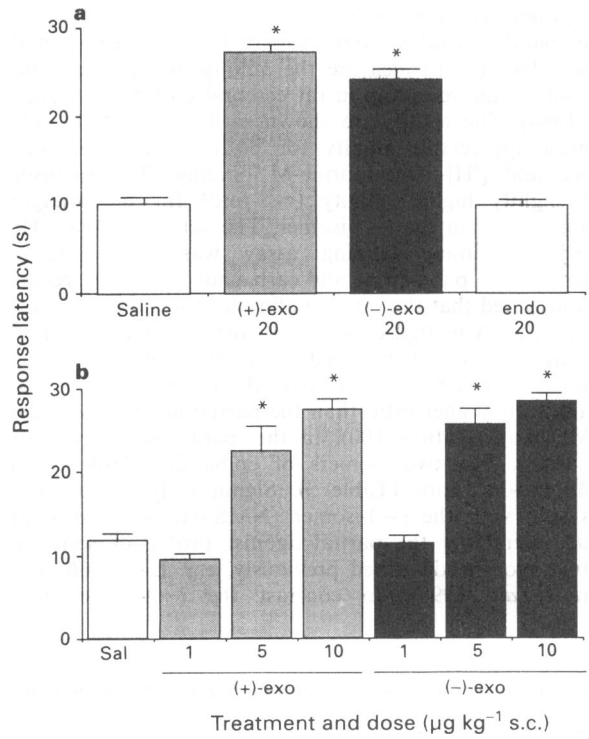


Figure 1 Effect of exo- and endo-isomers of epibatidine oxalate in the mouse hot-plate test. (**a**) Identification of active isomers and (**b**) comparison of potency of exo-isomers. Test compounds were administered 30 min before nociception testing. Values are the mean ± 1 s.e.mean for 8–16 animals per group. Data were subjected to square root transformation prior to one-way ANOVA and Dunnett's multiple comparison *t*-test. $^*P \leq 0.05$ compared with saline-treated animals.

significantly lower NMS/oxo-M binding ratio of 4.2, a profile more similar to the classic muscarinic antagonist atropine (Table 3).

[^{3}H]-Nicotine binding assay The two exo-isomers of epibatidine oxalate were also examined for their ability to displace [^{3}H]-nicotine binding to rat cerebral cortex membranes. Both isomers have subnanomolar affinity for this recognition site (Table 4). The more active compound was the (+)-isomer, although there was only minimal stereoselectivity. Both isomers were approximately 50-fold more active than (−)-nicotine (IC_{50} = 7.8 nM).

Antinociceptive activity of epibatidine

Identification of active isomers in mouse hot-plate test In saline-treated mice the nociceptive response typically involved licking the forepaws with a latency of approximately 10 s. After administration of the (+)- or (−)-exo-isomers of epibatidine oxalate (2 μg kg^{-1} s.c., 30 min previously), the response latency was more than doubled (Figure 1a). At this dose there was marked behavioural depression in mice treated with either (+)- or (−)-epibatidine. Animals were hypoactive, with a flattened body posture and laboured respiratory movements. During handling, limb movements were jerky. Full Straub tail was not observed in any animal, although partial elevation, rigidity and rattling of the tail was seen in approximately 50% of mice treated with either exo-isomer. Seizures were also induced at this dose [5 out of 16 mice receiving (+)-epibatidine and 6 out of 18 mice treated with the (−)-isomer]. In contrast, administration of the endo-isomer (20 μg kg^{-1} s.c., 30 min previously) did not increase response latency in the hot-plate test and induced no signs of behavioural toxicity (Figure 1a).

Administration of lower doses of the exo-isomers revealed a steep dose–response curve for antinociception and similar potency of the (+)- and (−)-isomer *in vivo*. Treatment with 5 or 10 μg kg^{-1} s.c. (30 min previously) of (+)- or (−)-epibatidine more than doubled response latency on the hot-plate (Figure 1b). Both doses of either isomer again caused marked motor suppression, flattened body posture and laboured respiratory movements. Convulsions were not observed in any mice receiving these doses of the (+)-isomer, but seizures were seen in two out of eight mice treated with 10 μg kg^{-1} of (−)-epibatidine. The frequency of tail rattling did not differ in saline or epibatidine-treated mice. Animals treated with the lowest dose examined (1 μg kg^{-1} s.c.) of either isomer did not exhibit antinociception or observable alteration in spontaneous behaviour (Figure 1b). Subsequent investigations therefore employed a dose of 5 μg kg^{-1} as the minimum effective dose with least toxicity.

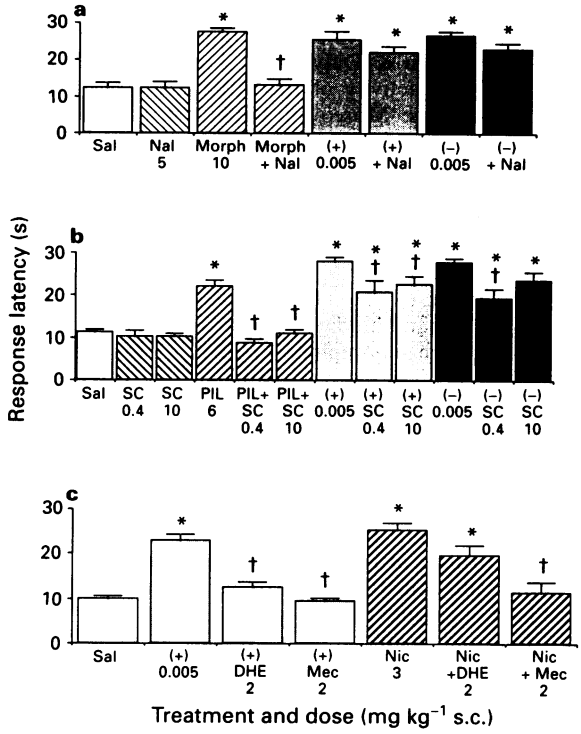


Figure 2 Effect of opioid and cholinergic receptor antagonists on epibatidine oxalate-induced antinociception in the mouse hot-plate test. (a) Naloxone (Nal; 5 mg kg^{-1}), (b) scopolamine (Scop; 0.4 and 10 mg kg^{-1}) and (c) mecamylamine (Mec; 2 mg kg^{-1}) or dihydro-β-erythroidine (DHE; 2 mg kg^{-1}). Values are the mean ± 1 s.e.mean for 8–17 animals per group. *$P<0.05$ compared with vehicle treatment, Dunnett's t-test. †$P<0.05$ compared with test compound alone, Newman–Keuls multiple comparison test.

Table 5 Effect of scopolamine and dihydro-β-erythroidine (DHE) on (+)-epibatidine-induced antinociception: carrageenan-induced hyperalgesia

Treatment and dose	*Paw pressure score (difference from baseline)* Test compound alone	Test compound + scopolamine 0.4 mg kg^{-1}
(a) Scopolamine		
Saline	−11.3 ± 0.4	−11.1 ± 1.4
Pilocarpine (3 mg kg^{-1})	6.9 ± 1.7*	−3.1 ± 1.3*†
(+)-Epibatidine oxalate (5 μg kg^{-1})	−4.1 ± 1.5*	−3.5 ± 1.8*
		Test compound + DHE (2 mg kg^{-1})
(b) Dihydro-β-Erythroidine		
Saline	−8.8 ± 0.5	−9.0 ± 1.2
Nicotine (1.5 mg kg^{-1})	−0.4 ± 1.6*	−5.7 ± 0.6†
(+)-Epibatidine oxalate (5 μg kg^{-1})	−3.4 ± 1.2*	−7.4 ± 1.7

Values are the mean ± 1 s.e.mean for 7–8 animals per group. *$P<0.05$ compared with vehicle treatment, Dunnett's t-test. †$P<0.05$ compared with test compound alone, Newman–Keuls multiple comparison test.

Effect of opioid and cholinergic receptor antagonists on epibatidine-induced antinociception

Naloxone Administration of morphine (10 mg kg^{-1} s.c., 30 min previously), like (+)- or (−)-epibatidine, caused an approximate doubling in response latency in the mouse hot-plate test (Figure 2a). Unlike epibatidine-treated mice, morphine-treated animals were hyperactive and all exhibited a prominent Straub tail response. Co-administration of naloxone (5 mg kg^{-1} s.c.) fully prevented the appearance of Straub tail and antinociception induced by morphine (10 mg kg^{-1}). In contrast, naloxone did not attenuate antinociception or other observable effects of either (+)- or (−)-epibatidine oxalate (5 μg kg^{-1}, 30 min previously; Figure 2a).

Scopolamine Treatment with the muscarinic receptor agonist pilocarpine (6 mg kg^{-1} s.c., 30 min previously) also doubled the response latency in the mouse hot-plate test (Figure 2b) and caused marked hypersalivation. These effects were fully blocked by co-administration of scopolamine (0.4 or 10 mg kg^{-1}). When given alone scopolamine did not alter response latency but caused hyperactivity and altered the behavioural end-point from licking of the forepaws to thumping of the hindfeet. In mice receiving (+)-epibatidine oxalate with scopolamine (0.4 or 10 mg kg^{-1}) there was a modest partial reversal of antinociception, such that response latency remained double that of control mice, but significantly shorter than that in mice treated with (+)-epibatidine oxalate alone. Scopolamine (0.4 mg kg^{-1}, but not 10 mg kg^{-1}) caused a similar partial attenuation of (−)-epibatidine-induced antinociception (Figure 2b).

In rats, administration of pilocarpine (3 mg kg^{-1} s.c., 30 min previously) reversed hyperalgesia to mechanical pressure induced by intraplantar injection of carrageenan (Table 5a) without reducing paw oedema (vehicle-treated animals, paw volume = 1.01 ± 0.04 ml compared with 0.89 ± 0.04 ml in pilocarpine-treated rats). The threshold for vocalization following compression of the non-injected paw was also increased by pilocarpine (paw pressure score in vehicle-treated rats = 1.6 ± 0.7 compared with 8.3 ± 1.3, $P<0.05$, Dunnett's t-test). Animals treated with pilocarpine exhibited chromodacryorrhoea, diarrhoea and hypersalivation. These peripheral effects were fully prevented by co-administration of scopolamine (0.4 mg kg^{-1}). The antialgesic effect of pilocarpine was markedly reduced by scopolamine, although paw pressure thresholds remained higher than those of vehicle-treated rats. By comparison with pilocarpine, (+)-epibatidine oxalate (5 μg kg^{-1} s.c., 30 min previously) caused a modest reduction in hyperalgesia (Table 5a). Paw pressure scores in the non-inflamed foot were not significantly increased by (+)-epibatidine oxalate (score = 3.4 ± 1.3; control value as stated above, $P>0.05$). Higher doses of (+)-epibatidine oxalate were not examined because of toxicity. Unlike pilocarpine, the antialgesic effect of (+)-epibatidine was not blocked by co-administration of scopolamine (Table 5a).

Dihydro-β-erythroidine (DHE) and mecamylamine

In the mouse hot-plate test, treatment with nicotine (3 mg kg^{-1} s.c., 5 min previously) markedly increased response latency. The antinociception induced by nicotine was accompanied by behavioural toxicity indistinguishable from that induced by the isomers of epibatidine: flattened body posture, hypoactivity and pronounced respiratory movements were all present. Limb movements were jerky during handling. Administration of the nicotinic receptor antagonist mecamylamine (2 mg kg^{-1} s.c.), but not DHE (2 mg kg^{-1} s.c., both given 25 min prior to nicotine), fully prevented nicotine-induced antinociception and other behavioural effects. Similarly, the effects of (+)-epibatidine were fully reversed by co-administration of either mecamylamine or DHE (Figure 2c).

In rats the antinociceptive effects of nicotine (1.5 mg kg^{-1} s.c., 30 min previously) were evident in both reversing carrageenan-induced hyperalgesia (Table 5b) and increasing paw pressure thresholds in the non-inflamed paw (vehicle-

treated rats, score = -0.1 ± 1.4 compared with 6.1 ± 1.2 in nicotine-treated animals, $P<0.05$). Rats receiving this dose of nicotine exhibited laboured respiration and flaccidity. Nicotine-induced antinociception was fully blocked by co-administration of DHE ($2\ mg\ kg^{-1}$; Table 5b). The less marked antialgesic effect of (+)-epibatidine oxalate ($5\ \mu g\ kg^{-1}$ s.c., 30 min previously) was also blocked by DHE in that paw pressure scores were similar to those seen in vehicle-treated rats. However, the scores were not significantly different from animals treated with (+)-epibatidine oxalate alone (Table 5b).

Discussion

The present study confirms that synthetic (+)-epibatidine oxalate, the naturally occurring isomer (Watt *et al.*, 1994), is responsible for the antinociceptive and toxic effects of the natural product and demonstrates that these effects are attributable to nicotinic agonist activity. (−)-Epibatidine oxalate, which does not occur naturally, exhibited extremely potent nicotinic receptor agonist activity similar to that of the (+)-isomer *in vitro* and *in vivo*: both displayed high affinity for displacement of [^{3}H]-nicotine binding [$IC_{50} = 0.1$ nM for (+)-epibatidine, 0.2 nM for (−)-isomer] and similar potency in reducing thermal nociception in mice (minimum effective dose = $5\ \mu g\ kg^{-1}$ s.c. for both isomers). These findings are in good agreement with observations from other laboratories (K_i values in the region of 20–50 pM for displacement of [^{3}H]-nicotine binding and an ED_{50} of $1-3\ \mu g\ kg^{-1}$ s.c. for antinociception obtained for both the (+)- and (−)-isomers; Badio & Daly, 1994: B.R. Martin *et al.*, unpublished data) and are consistent with the nicotinic receptor agonist activity reported for *I*-epibatidine by Qian *et al.* (1993). The toxic effects of (+)- and (−)-epibatidine oxalate (reduced activity, laboured respiration and convulsions) closely resembled those induced by nicotine; like the antinociceptive actions of epibatidine and nicotine, the toxicity was prevented by administration of the nicotinic receptor antagonists mecamylamine and dihydro-β-erythroidine (Qian *et al.*, 1993; Badio & Daly, 1994; present study).

In the report which first described the antinociceptive activity of native epibatidine (Spande *et al.*, 1992), the presence of a Straub tail reaction in mice suggested an opioid-mediated analgesia. However, the inability of naloxone to reverse antinociception induced by native (Spande *et al.*, 1992) or synthetic epibatidine (Qian *et al.*, 1993; present study) and the low affinity of epibatidine for opioid binding sites *in vitro* (Badio & Daly, 1994; present study) confirms that the analgesic activity of this substance is not mediated by opioid receptors. Moreover, unlike the natural product, Straub tail has not been reported in studies employing synthetic epibatidine. Possibly the phenomenon observed by Spande *et al.* (1992) was part of a preconvulsant, toxic syndrome induced by high doses; alternatively, other biologically active substances may have been present in the natural product extract.

(+)-Epibatidine oxalate (10 μM) was not active in a range of other radioligand-binding assays for excitatory amino acid, glycine, benzodiazepine, $GABA_A$, 5-HT, dopamine, adrenergic or peptide receptors, and did not exhibit affinity for ion channels. While (+)-and (−)-epibatidine did exhibit low (μM) affinity for muscarinic receptors, we do not believe that this is the primary mechanism underlying their antinociceptive activity. It is well known that muscarinic, as well as nicotinic, receptor agonists are antinociceptive (Brodie & Proudfit, 1984). However, the profile of (+)-epibatidine oxalate *in vitro* is more consistent with that of a muscarinic antagonist (NMS/oxo-M ratio of 4.2). Some reports have suggested that M_2-selective antagonists including AFDX-116 and methoctramine at low doses may have analgesic properties (Bartolini *et al.*, 1989; Gualtieri *et al.*, 1989). However, the binding studies with both enantiomers of epibatidine oxalate do not show any activity in the M-2 assay, and administration of a muscarinic receptor antagonist only partially attenuated antinociception induced by epibatidine, an effect which probably reflected the induction of hyperactivity by scopolamine, rather than a specific effect on nociception. Moreover, scopolamine or atropine did not block the antialgesic effect of epibatidine in paw pressure (present study) or tail-flick tests (Qian *et al.*, 1993).

Nicotinic receptor agonists are of potential interest for treating neurological disorders (Alzheimer's and Parkinson's disease) and as tobacco substitutes (Jarvik, 1991). Because of its toxicity it is unlikely that epibatidine can be developed as a therapeutic agent for use in man. Nevertheless, this compound may provide a valuable tool with which to investigate the diversity and function of neuronal nicotinic receptors.

We wish to thank Dr M. Chambers and Ms S. Hobbs for providing the isomers of epibatidine.

References

BADIO, B. & DALY, J.W. (1994). Epibatidine:a potent analgetic and nicotinic agonist. *Mol. Pharmacol.*, **45**, 563–569.

BARTOLINI, A., GHELARDINI, C., GUALTIERI, F., MALCANGIO, M., MALMBERG-AIELLO, P., ROMANELLI, N. & GIOTTI, A. (1989). ICV AFDX-116 induces the analgesia only when administered at very low doses. Subtypes of Muscarinic Receptors IV. *Trends Pharmacol. Sci.* (Suppl.), 99.

BRODIE, M.S. & PROUDFIT, H.K. (1984). Hypoalgesia induced by the local injection of carbachol into the nucleus raphe magnus. *Brain Res.*, **291**, 337–342.

CHENG, K.C. & PRUSSOFFF, W.H. (1973). Relationship between the inhibition constant (Ki) and the concentration of inhibitor which causes 50 per cent inhibition (I_{50}) of an enzymatic reaction. *Biochem. Pharmacol.*, **22**, 3099.

DALY, J.W., BROWN, G.B., MENSAH-DWUMAH, M. & MYERS, C.W. (1978). Classification of skin alkaloids from neotropical poison-dart frogs (*Dendrobatidae*). *Toxicon*, **16**, 163–188.

DAMAJ, M.I., WELCH, S.P. & MARTIN, B.R. (1993). Involvement of calcium and L-type channels in nicotine-induced antinociception. *J. Pharmacol. Exp. Ther.*, **266**, 1330–1338.

EDDY, N.B. & LEIMBACH, D. (1953). Synthetic analgesics. II. dithienylbutenyl- and dithienylbutylamines. *J. Pharmacol. Exp. Ther.*, **107**, 385–393.

FLETCHER, S.R., BAKER, R., CHAMBERS, M.S., HOBBS, S.C. & MITCHELL, P.J. (1993). The synthesis of (+)- and (−)-epibatidine. *J. Chem. Soc. Chem. Commun.*, **15**, 1216–1218.

FREEDMAN, S.B., HARLEY, E.A. & IVERSEN, L.L. (1988). Relative affinities of drugs acting at cholinoceptors in displacing agonist and antagonist radioligands: the NMS/Oxo-M radio as an index of efficacy at cortical muscarinic receptors. *Br. J. Pharmacol.*, **93**, 437–445.

FREEDMAN, S.B., DAWSON, G.R., IVERSEN, L.L., BAKER, R. & HARGREAVES, R.J. (1993). The design of novel muscarinic partial agonists that have functional selectivity in pharmacological preparations *in vitro* and have reduced side-effect profile *in vivo*. *Life Sci.*, **52**, 489–495.

GUALTIERI, F., GHELARDINI, C., GIOTTI, A., MALCANGIO, M., MALMBERG-AIELLO, P. & BARTOLINI, A. (1989). Analgesia induced by the M_2 antagonist methoctramine administered icv. Subtypes of Muscarinic Receptors IV. *Trends Pharmacol. Sci.* (Suppl.), 99.

JARVIK, M.E. (1991). Beneficial effects of nicotine. *Br. J. Addict.*, **86**, 571–579.

MIRANDA, H.F., BUSTAMANTE, D., KRAMER, V., PELISSIER, T., SAAVEDRA, H., PAEILE, C., FERNANDEZ, E. & PINARDI, G. (1992). Antinociceptive effects of Ca^{2+} channel blockers. *Eur. J. Pharmacol.*, **217**, 137–141.

QIAN, C., LI, T., SHEN, T.Y., LIBERTINE-GARAHAN, L., ECKMAN, J., BIFTU, T. & IP, S. (1993). Epibatidine is a nicotinic analgesic. *Eur. J. Pharmacol.*, **250**, R13–R14.

ROMANO, C. & GOLDSTEIN, A. (1980). Stereospecific nicotine receptors on rat brain membranes. *Science*, **210**, 647–650.

SPANDE, T.F., GARRAFFO, H.M., EDWARDS, M.W., YEH, H.J.C., PANNELL, ?. & DALY, J.W. (1992). Epibatidine: a novel (chloropyridyl) azabicycloheptane with potent analgesic activity from an Ecuadoran poison frog. *J. Am. Chem. Soc.*, **114**, 3475–3478.

SPENCE, A. (1990). *Report of the Working Party on Pain after Surgery*. London: The Royal College of Surgeons of England and College of Anaesthetists.

TRAYNOR, J.R., HUNTER, J.C., RODRIGUEZ, R.E., HILL, R.G. & HUGHES, J. (1990). δ-Opioid receptor binding sites in rodent spinal cord. *Br. J. Pharmacol.*, **100**, 319–323.

TRIPATHI, H.L., MARTIN, B.R. & ACETO, M.D. (1982). Nicotine-induced antinociception in rats and mice: correlation with nicotine brain levels. *J. Pharmacol. Exp. Ther.*, **221**, 91–96.

WATT, A.P., VERRIER, H.M. & O'CONNOR, D. (1994). Resolution of synthetic (+) and (−)-epibatidine by chiral high performance liquid chromatography and identification of the natural enantiomer. *J. Liq. Chromatogr.*, **17**, 1257–1264.

ZIMMERMANN, M. (1983). Ethical guidelines for investigations of experimental pain in conscious animals. *Pain*, **16**, 109–110.

(Received May 10, 1994
Accepted August 15, 1994)

Br. J. Pharmacol. (1994), **113**, 1494–1500 © Macmillan Press Ltd, 1994

Variable potency of nitrergic-nitrovasodilator relaxations of the mouse anococcygeus against different forms of induced tone

[1]A. Gibson, I. McFadzean, J.F. Tucker & C. Wayman

Smooth Muscle Pharmacology Group, Biomedical Sciences Division, King's College London, Manresa Road, London SW3 6LX

1 U46619 (thromboxane A_2 receptors; 0.002-1 μM), carbachol (muscarinic M_3 receptors; 0.1–100 μM), cyclopiazonic acid (CPA; Ca^{2+}-ATPase inhibitor; 0.1–30 μM) and K^+ (5–100 mM) produced concentration-dependent contractions of the mouse isolated anococcygeus muscle. Equi-effective, submaximal concentrations of each agent were used in further experiments (40 nM U46619; 5 μM carbachol; 5 μM CPA; 70 mM K^+).

2 Nifedipine (1 μM) totally abolished contractile responses to K^+; those to U46619, carbachol and CPA were reduced by only 20–30% in the presence of nifedipine, but were greatly reduced (>90%) by a combination of nifedipine and SKF 96365 (0.1–40 μM).

3 In Ca^{2+}-free medium, contractions to K^+ and CPA were abolished. Small residual responses remained to both carbachol and U46619; those to carbachol were transient, could not be repeated in the continued absence of Ca^{2+} and were prevented by pre-incubation with CPA, but unaffected by SKF 96365; those to U46619 were sustained, could be repeated in the absence of Ca^{2+}, and were resistant to CPA and SKF 96365.

4 Tone induced by all four agents could be relaxed by sodium nitroprusside (SNP), but with a clear order of potency. SNP (pIC_{40}) was most effective against U46619 (7.92), less so against carbachol (6.80) and CPA (6.68), and least potent against K^+ (5.94). A similar order of potency was observed with 8Br-cyclic GMP (50 μM) and nitrergic field stimulation (1–20 Hz).

5 The relaxant potency of SNP was similar in normal Krebs solution and in high K^+ (70 mM) Krebs containing 1 μM nifedipine.

6 Inclusion of SNP (0.01–1 μM) or 8Br-cyclic GMP (50 μM) in the Ca^{2+}-free medium inhibited the transient residual response to carbachol. Inclusion of similar concentrations of SNP or 8Br-cyclic GMP, during Ca^{2+} re-loading, increased the subsequent residual contraction to carbachol in Ca^{2+}-free medium.

7 At higher concentrations, SNP (0.1–10 μM) produced a partial relaxation of the sustained contraction to U46619 in Ca^{2+}-free medium.

8 Thus, the relaxant potency of the nitrergic stimuli was dependent on the agent and mechanism used to induce tone in the preparation. Examination of the contractile/relaxant interactions suggests that altered Ca^{2+} sequestration and inhibition of contractile protein function may underlie nitrergic relaxations of this tissue.

Keywords: Anococcygeus; 8Br-cyclic GMP; carbachol; cyclopiazonic acid; nifedipine; nitrergic stimulation; potassium; SKF 96365; sodium nitroprusside; U46619

Introduction

Anococcygeus muscles from rats and mice have proved useful models for the investigation of nitrergic neurotransmission in non-vascular smooth muscle (Rand, 1992). Field stimulation-induced relaxations are reduced by inhibitors of nitric oxide synthase (Gillespie *et al.*, 1989; Li & Rand, 1989; Ramagopal & Leighton, 1989; Gibson *et al.*, 1990) while relaxations to nitrovasodilator drugs, which mimic the effects of nitrergic stimulation via a postsynaptic action, are unaffected. Nitric oxide synthase has been detected in homogenates of the anococcygeus (Mitchell *et al.*, 1991) and has been localized by immunocytochemistry, to 6-hydroxydopamine-resistant nerves within the tissue (Brave *et al.*, 1993). Postsynaptically, nitrergic relaxations result from activation of the guanylyl cyclase/guanosine 3':5'-cyclic monophosphate (cyclic GMP) system since relaxations to field stimulation and nitrovasodilator drugs are reduced by inhibitors of guanylyl cyclase, enhanced by inhibitors of phosphodiesterase, and are associated with an increase in cyclic GMP within the tissue (Gibson & Mirzazadeh, 1989; Mirzazadeh *et al.*, 1991). However, the cellular mechanism(s) by which cyclic GMP effects relaxation is not known. In vascular smooth muscle, nitrovasodilator drugs also act through cyclic GMP (Waldman & Murad, 1987) and several mechanisms have been proposed for the relaxations observed in these tissues, including membrane hyperpolarization, inhibition of phospholipase C, increased removal of Ca^{2+} from the cytosol and direct inhibition of contractile protein function (for reviews see Lincoln, 1989; Lincoln & Cornwell, 1993). In contrast, the mechanisms underlying NO/cyclic GMP-induced relaxations of non-vascular smooth muscle have received much less attention, mainly because the controlling influence of nitrergic nerves in such tissues has only recently been recognised. We have therefore begun a series of experiments to investigate the cellular mechanisms associated with nitrergic relaxations of the anococcygeus and, in the present study, we have investigated whether the ability of nitrergic activation (presynaptically via field stimulation, or postsynaptically via application of sodium nitroprusside [SNP] or 8Br-cyclic GMP) to cause relaxations of the mouse anococcygeus is dependent on the agent and mechanism, used to induce tone in the preparation. Four contractile agents, with varying cellular mechanisms, were used: (1) carbachol, which acts on muscarinic (M_3) receptors (Sideso *et al.*, 1994) believed to be linked to the phospholipase C/inositol 1,4,5 trisphosphate (IP_3)/diacylglycerol pathway; (2)

[1] Author for correspondence.

U46619, a thromboxane A_2 receptor agonist, also believed to stimulate phospholipase C but which, in addition, directly sensitizes the contractile proteins to Ca^{2+}, possibly via a G-protein (Himpens *et al.*, 1990; Crichton *et al.*, 1993; Kurata *et al.*, 1993); (3) cyclopiazonic acid (CPA), a reversible inhibitor of the Ca^{2+}-ATPase of the sarcoplasmic reticulum (SR), which has been shown to increase cytosolic Ca^{2+} concentratrions in several cell types via a Ca^{2+}-release activated Ca^{2+}-entry (CRAC) pathway (Low *et al.*, 1991; Demaurex *et al.*, 1992; Missaien *et al.*, 1992) and (4) K^+, which depolarizes the tissue leading to opening of voltage operated Ca^{2+} channels (VOCCs). A preliminary account of some of these results has been published (Gibson *et al.*, 1994b).

Methods

Male mice (LACA strain; 25–35 g) were killed by stunning and exsanguination. The anococcygeus muscles were dissected and set up in 1 or 2 ml glass organ baths containing Krebs-bicarbonate buffer (mM: NaCl 118.1, KCl 4.7, $MgSO_4$ 1.0, KH_2PO_4 1.0, $NaHCO_3$ 25.0, glucose, 11.1 and $CaCl_2$ 2.5) which was maintained at 37°C and gassed continuously with 95% O_2:5% CO_2. A resting tension of 200–400 mg was placed on the tissue and changes in tension recorded with a Grass FT03 force-displacement transducer attached to a Graphtec pen recorder (WR3101). Muscles were allowed to equilibrate for 45 min before beginning the experiment. In all experiments, except those involving nitrergic field stimulation, the Krebs solution also contained 1 μM phentolamine and 50 μM N^G-nitro-L-arginine (L-NOARG), and the tissues were preincubated for 10 min with 30 μM guanethidine (during the 45 min equilibration period); these drugs were used to prevent any effects due to release of transmitter from either the motor noradrenergic or inhibitory nitrergic nerves within the tissue. In experiments involving nitrergic field stimulation L-NOARG was omitted. Field stimulation (1 ms; 70 V) was applied via two parallel platinum electrodes running down either side of the tissue.

Concentration-response curves to contractile agents were constructed in a non-cumulative manner. The agents were left in contact with the tissue until the contraction had reached a plateau and the succeeding concentration was not added until tone had returned to baseline following washout.

To obtain relaxations, tone was first raised by the appropriate concentration of contractile agent. Once the plateau contraction had been established the relaxant stimulus was applied. Concentration-response curves to SNP were obtained in a cumulative fashion. Relaxations to 8Br-cyclic GMP were obtained with a single concentration of 50 μM, which has been shown to relax carbachol-induced tone of the mouse anococcygeus by about 50% (Gibson & Mirzazadeh, 1989). Results were expressed as % relaxation of induced tone. pIC_{40} values ($-\log_{10}$ of the molar concentration of relaxant required to produce a 40% reduction of induced tone) were calculated by regression analysis of individual concentration-response curves.

K^+-rich solutions were prepared by substituting the appropriate amount of KCl for NaCl; Ca^{2+}-free solutions were prepared by omission of $CaCl_2$ and addition of EGTA (1mM). For experiments in Ca^{2+}-free solution, control contractions were first established in normal medium. The muscle was then bathed in Ca^{2+}-free medium for 5 min before challenging with contractile agent; 5 min was found to be the minimum time for complete loss of the response to 70 mM K^+. If Ca^{2+} was to be re-admitted, the muscle was returned to normal medium for 15 min.

Results are expressed as mean ± s.e.mean. Statistical analysis was by Student's *t* test (unpaired) with $P<0.05$ taken as indicating a significant difference.

The following drugs were used: 8-bromo-cyclic guanosine monophosphate (Sigma); carbachol (Aldrich); cyclopiazonic acid (Sigma); guanethidine sulphate (Ciba); nifedipine (Sigma); N^G-nitro-L-arginine (Sigma); phentolamine mesylate (Ciba); SKF 96365 (1-{β-[3-(4-methoxyphenyl) Propoxy]-4-methoxyphenethyl}-1H-imidazole HCl; Smithkline Beecham); sodium nitroprusside (Sigma); U46619 (9,11-dideoxy-11α,9α,-epoxymethano prostaglandin $F_{2\alpha}$; Sigma).

All drugs were dissolved in distilled water except: cyclopiazonic acid (10 mM stock in dimethyl sulphoxide); nifedipine (10 mM stock in ethanol); U46619 (1 mM stock in ethanol).

Results

Contractions to U46619, carbachol, CPA and K^+

U46619 (0.002–1 μM), carbachol (0.1–100 μM), CPA (0.1–30 μM) and K^+ (5–100 mM) produced concentration-related contractions of the mouse anococcygeus (Figure 1). The contractions to all four agents were sustained, and were reversed on washout. The onset of contraction following addition of U46619, carbachol and K^+ was much faster (2–3 s) than that observed with CPA (1–2 min). In all subsequent experiments, equi-effective sub-maximal concentrations of each agent were used: 40 nM U46619, 5 μM carbachol, 5 μM CPA and 70 mM K^+ (Figure 1).

A number of experiments were performed to determine the source of Ca^{2+} utilized by each of the agents to produce contraction. Following 5 min incubation in Ca^{2+}-free medium, contractions to both K^+ and CPA were absent (Figure 2a); in the case of both U46619 and carbachol small residual contractions remained which amounted to about 5% of those obtained in normal medium (Figures 2a and 3). Although of similar magnitude, the characteristics of the two responses were quite different (Figure 3). Those to carbachol were transient and could not be repeated in the continued absence

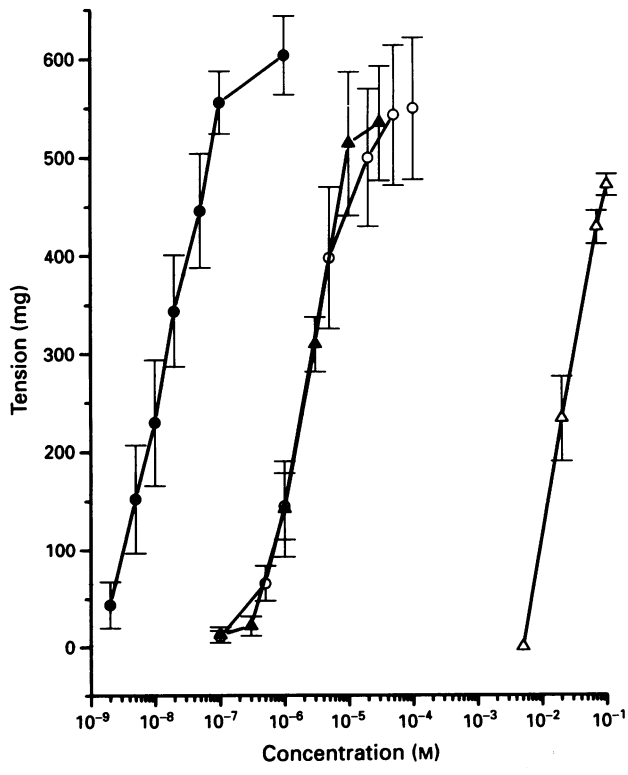


Figure 1 Concentration-response curves for contractions of the mouse anococcygeus in response to U46619 (●), carbachol (○), cyclopiazonic acid (▲) and K^+ (△). Each point represents the mean ± s.e.mean from at least five different muscle preparations.

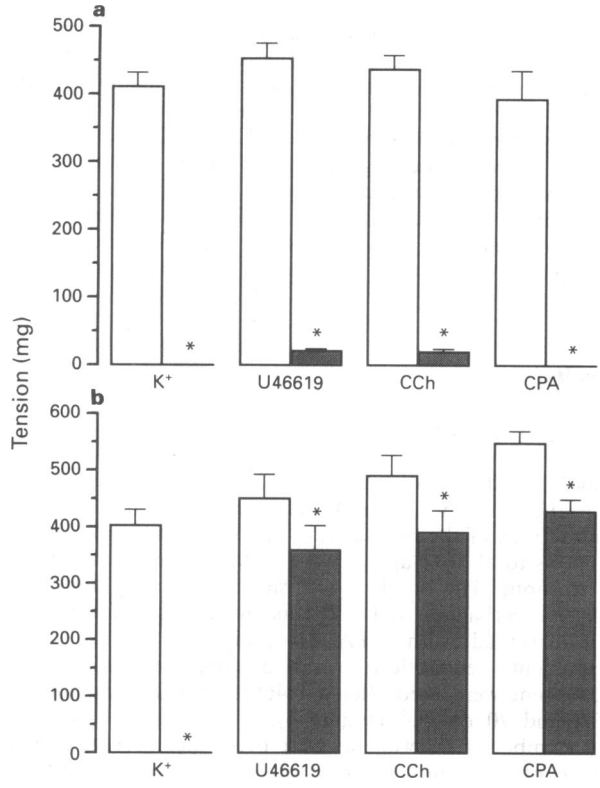


Figure 2 Histograms of contractions of the mouse anococcygeus to sub-maximal concentrations of K^+ (70 mM), U46619 (40 nM), carbachol (Cch; 5 μM) and cyclopiazonic acid (CPA; 5 μM) under control conditions (open columns), in Ca^{2+}-free medium (cross-hatched columns in a), or in the presence of 1 μM nifedipine (cross-hatched columns in b). Each point represents the mean ± s.e.mean from at least five different muscle preparations. *Significantly different from adjoining column.

of Ca^{2+} (not shown). However, after re-admission of Ca^{2+} for 15 min, a normal response to carbachol was obtained and, following a 5 min exposure to Ca^{2+}-free medium, a further transient contraction could be elicited (Figure 3a). Addition of 5 μM CPA, during the 5 min incubation in Ca^{2+}-free medium, greatly reduced the residual response to carbachol and this inhibition was reversed on washout of the CPA; a higher concentration of CPA (20 μM) completely blocked the contraction to carbachol in Ca^{2+}-free medium (Figure 3a). On the other hand, the residual responses to U46619 in Ca^{2+}-free medium were sustained, could be repeated (at least four times) in the continued absence of Ca^{2+}, and were unaffected by inclusion of 5 μM CPA (Figure 3b).

In the presence of 1 μM nifedipine, responses to K^+ were again totally blocked (Figure 2b), but those to U46619, carbachol and CPA were reduced by only 20–30% in each case. However, the nifedipine-resistant component of the contractions to U46619, carbachol and CPA was reduced, in a concentration-dependent manner, by SKF 96365 (0.1–40 μM; Figure 4), which inhibits both voltage- and non-voltage-dependent Ca^{2+}-entry processes (Merritt *et al.*, 1990); contractile responses to CPA were more sensitive to the inhibitory effect of SKF 96365 than those to either carbachol or U46619 (Figure 4). SKF 96365 had no effect on the residual responses to either carbachol or U46619 in Ca^{2+}-free medium (against carbachol, response in presence of 30 μM SKF 96365 was 96 ± 18% of that in its absence; against U46619, response in presence of 20 μM SKF 96365 was 109 ± 14% of that in its absence; $n = 5$, $P > 0.05$ in both cases).

Relaxations to SNP, 8Br-cyclic GMP and nitrergic field stimulation

In these experiments, tone was again raised by the equi-effective, sub-maximal concentrations of the contractile agents mentioned previously.

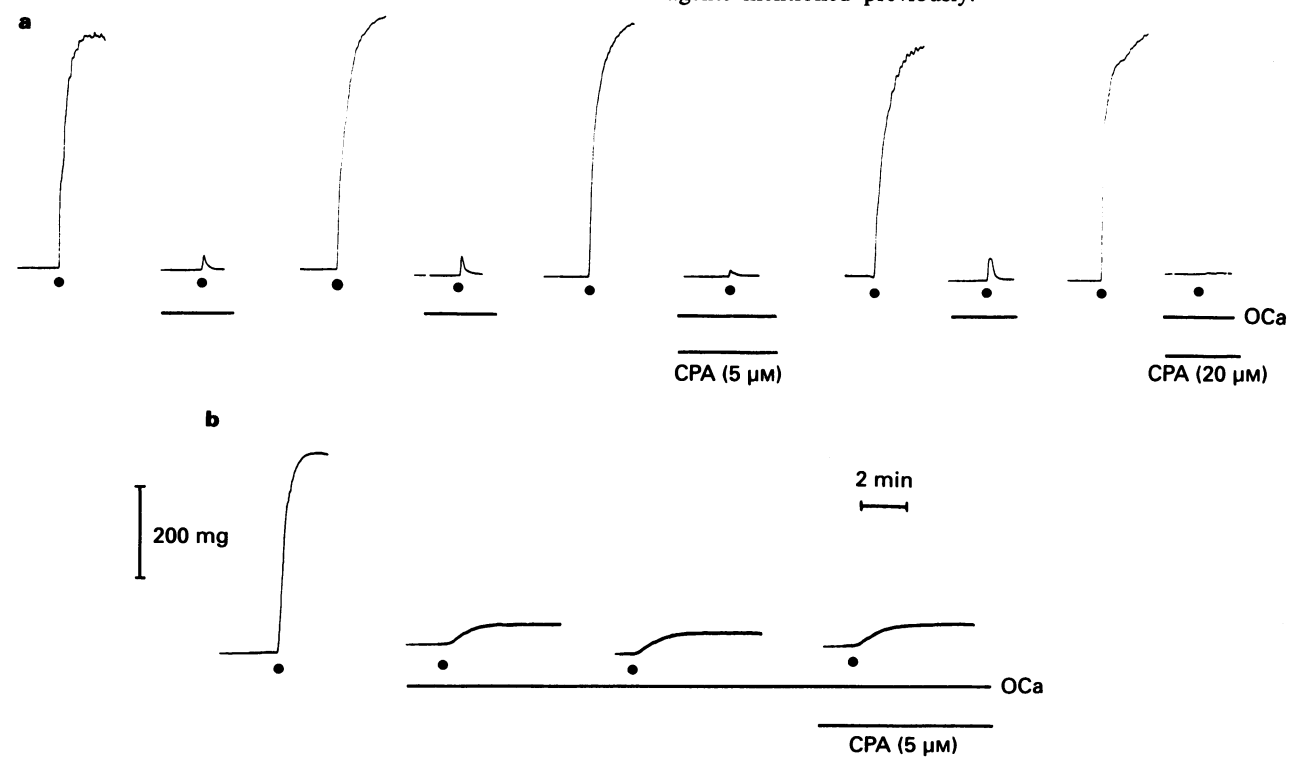


Figure 3 Traces showing contractions of the mouse anococcygeus muscle in response to carbachol (5 μM in a; ●) or U46619 (40 nM in b; ●). The first trace in each panel shows a control response in normal medium. In (a), the muscle was then bathed in Ca^{2+}-free medium (0Ca) for 5 min and then challenged with carbachol, which produced a small, transient contraction; following re-admission of Ca^{2+} for 15 min a normal response to carbachol was obtained. Inclusion of cyclopiazonic acid (CPA), during the 5 min incubation in Ca^{2+}-free medium, reduced the residual response to carbachol. In (b), following the control response, the muscle was bathed in Ca^{2+}-free medium for 5 min and then challenged with U46619, which produced a small, sustained contraction. This response to U46619 could be repeated in the continued absence of Ca^{2+}, and was unaffected by CPA.

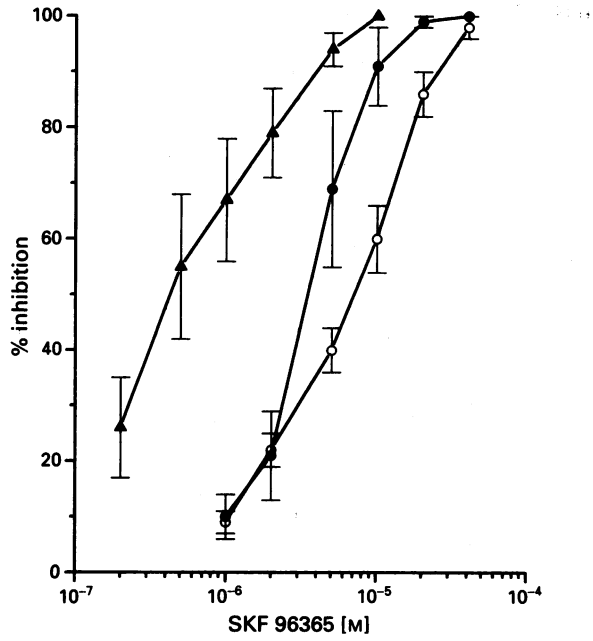


Figure 4 Concentration-response curves for inhibition by SKF 96365 of the nifedipine-resistant contraction to cyclopiazonic acid (5 μM; ▲), U46619 (40 nM; ●) and carbachol (5 μM; ○) in the mouse anococcygeus. Experiments were carried out in the presence of 1 μM nifedipine. Each point represents the mean ± s.e.mean from at least five different muscle preparations.

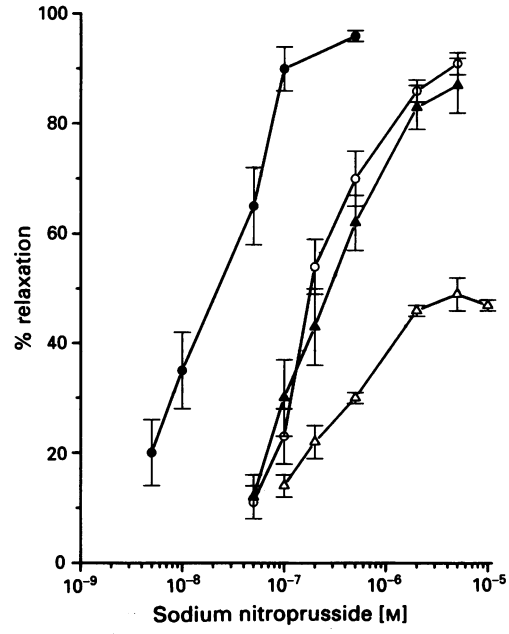


Figure 5 Concentration-response curves for relaxations of the mouse anococcygeus to sodium nitroprusside against tone induced by U46619 (40 nM; ●), carbachol (5 μM; ○), cyclopiazonic acid (5 μM; ▲) and K^+ (70 mM; △). Each point represents the mean ± s.e.mean from at least five different muscle preparations.

SNP produced concentration-related relaxations of tone induced by each agent (Figure 5), but with a clear order of potency; SNP was most potent against tone induced by U46619 (pIC_{40} 7.92 ± 0.13; $n = 5$), equipotent against tone induced by carbachol (pIC_{40} 6.80 ± 0.07; $n = 5$) and CPA (pIC_{40} 6.68 ± 0.10; $n = 5$), and least potent against tone induced by K^+ (pIC_{40} 5.94 ± 0.02; $n = 5$).

A similar order of potency was observed with 50 μM 8Br-cyclic GMP, which relaxed U46619-induced tone by 97 ± 1%, carbachol-induced tone by 55 ± 5%, CPA-induced tone by 52 ± 7% and K^+-induced tone by 34 ± 3% ($n > 5$ in each case).

Nitrergic field stimulation (10 s train every 100 s) also caused frequency-dependent relaxations of tone induced by U46619, carbachol and CPA (Figure 6) and again, was most potent against U46619. The $\log_{10}$ of the frequency-reducing tone by 40% was 0.5 ± 0.09 against U46619, 0.78 ± 0.09 against carbachol, and 0.81 ± 0.09 against CPA ($n = 5$ in each case). For obvious reasons, nitrergic relaxations of K^+-induced tone could not be studied.

Experiments were also carried out to determine the effects of SNP and 8Br-cyclic GMP on the contractions to carbachol and U46619 obtained in Ca^{2+}-free medium; the results of these are given in Figure 7. Addition of SNP (0.01–1 μM) during the incubation in Ca^{2+}-free medium, 1 min before challenge with carbachol, produced a concentration-related inhibition of the residual transient contraction to carbachol (Figure 7). However, if SNP (0.01–10 μM) was included during the 15 min period of Ca^{2+} re-admission, but omitted during the subsequent 5 min in Ca^{2+}-free medium, then a concentration-related potentiation of the residual response to carbachol was observed (Figure 7). Similar effects were observed with 8Br-cyclic GMP; inclusion of 50 μM 8Br-cyclic GMP during the 5 min incubation in Ca^{2+}-free medium (added 4 min before carbachol) reduced the residual response to carbachol by 79 ± 8% ($n = 5$), but inclusion of 50 μM 8Br-cyclic GMP during the period of Ca^{2+}-reloading enhanced the residual response to carbachol by 98 ± 18% ($n = 5$).

Addition of SNP (0.01–10 μM), during the sustained contraction to U46619 in Ca^{2+}-free medium, produced a concentration-related relaxation of tone (Figure 7), but it was considerably less potent against the residual response to U46619 than against that to carbachol.

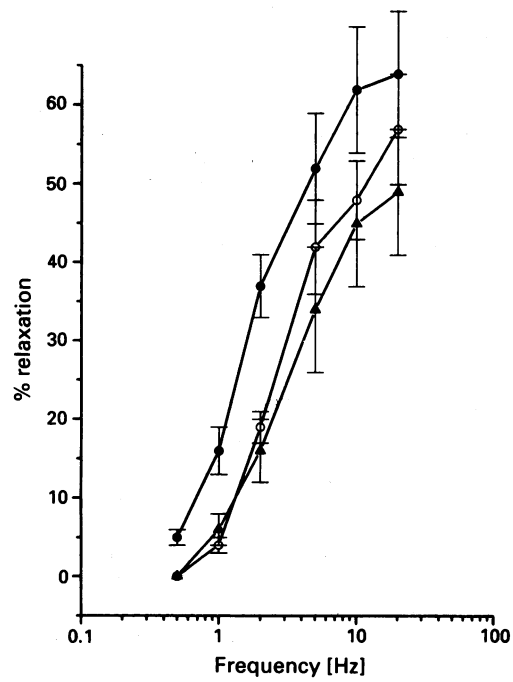


Figure 6 Frequency-response curves for relaxations of the mouse anococcygeus to field stimulation (10 s train) against tone induced by U46619 (40 nM; ●), carbachol (5 μM; ○) and cyclopiazonic acid (5 μM; ▲). Each point is the mean ± s.e.mean from at least five different muscle preparations.

A number of experiments were carried out to determine whether the potency of SNP varied in the presence of nifedipine and in depolarizing medium. In these experiments, tone was raised with 5μM carbachol. The potency of SNP

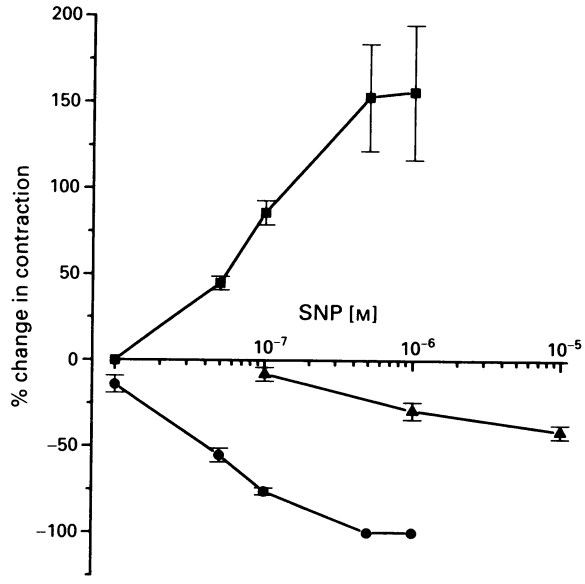


Figure 7 Concentration-response curves showing the effects of sodium nitroprusside (SNP) on contractions to carbachol (5 μM; ■ and ●) and U46619 (40 nM; ▲) in Ca^{2+}-free medium (see Figure 3); (■) show the potentiating effect of SNP, present during the duration of the 15 min Ca^{2+}-reloading period but omitted during the subsequent 5 min in Ca^{2+}-free medium, on the residual response to carbachol; (●) show the inhibitory effect of SNP added during the Ca^{2+}-free incubation, 1 min before challenge with carbachol; (▲) show the relaxant effect of SNP on the sustained response to U46619 in Ca^{2+}-free medium. Each point is the mean ± s.e.mean from at least five different muscle preparations.

(0.05–5μM) against carbachol was similar ($P > 0.05$) whether the experiments were carried out in normal Krebs (pIC_{40} 6.90 ± 0.10; maximum relaxation 92 ± 3%; $n = 6$), normal Krebs + 1μM nifedipine (pIC_{40} 7.05 ± 0.05; maximum relaxation 95 ± 1%; $n = 5$), or high K^+ (70 mM) Krebs + 1μM nifedipine (pIC_{40} 7.06 ± 0.07; maximum relaxation 96 ± 1%; $n = 6$).

Discussion

Actions of the contractile agents

K^+-induced contractions were clearly due to entry of Ca^{2+} through VOCCs since responses were abolished in Ca^{2+}-free medium and in the presence of nifedipine. Although K^+ can cause complex effects on tone of the anococcygeus, due to non-selective depolarization of both smooth muscle cells and nerve terminals (Gibson & James. 1977), the effects of the latter were negated by the use of sympatholytic drugs (phentolamine and guanethidine) and a nitric oxide synthase inhibitor (L-NOARG).

Both U46619 (thromboxane A_2 receptors) and carbachol (muscarinic M_3 receptors) are believed to activate the phospholipase C/IP_3/diacylglycerol system and thereby release Ca^{2+} from the SR. However, in other smooth muscles, it has been found that U46619 produces a relatively weak activation of phospholipase C, as reflected in a lower release of Ca^{2+} from the SR, but that it also possesses a marked ability to sensitize the contractile proteins, possibly by way of a G protein (Himpens *et al.*, 1990; Crichton *et al.*, 1993; Kurata *et al.*, 1993). This difference was apparent in our experiments in Ca^{2+}-free medium. Carbachol produced a transient contractile response which could not be repeated in the continued absence of Ca^{2+}. This transient contraction is likely to be due to the release of Ca^{2+} from the SR since it was reduced by CPA, which depletes the SR of Ca^{2+} by inhibiting Ca^{2+}-ATPase (Demaurex *et al.*, 1992); refilling of this store would occur during the period of Ca^{2+} re-admission. On the other hand, in Ca^{2+}-free medium, U46619 produced a sustained contraction which could be repeated in the continued absence of Ca^{2+} and which was unaffected by CPA. This contraction, therefore, is likely to be due to the sensitizing action of U46619 on the contractile proteins; it is not clear whether the U46619 sensitizes the contractile proteins to the low levels of cytoplasmic Ca^{2+} which would exist in Ca^{2+}-free medium or whether the effect is Ca^{2+} independent (Matsuo *et al.*, 1989; Ozaki *et al.*, 1990). The lack of a rapid, transient component in the response to U46619 in Ca^{2+}-free medium would be consistent with a low release of Ca^{2+} from the SR, insufficient to be detected as a contraction.

The contractions to both carbachol and U46619 in Ca^{2+}-free medium were only some 5% of those obtained in normal medium, suggesting that the major source of Ca^{2+} used by these agents comes from the extracellular space. Entry of Ca^{2+} through VOCCs contributes only in small part to the overall response since contractions were reduced by only 20–30% in the presence of nifedipine, at a concentration which completely blocked contractions to K^+. This suggests that U46619 and carbachol also activate a non-voltage-dependent Ca^{2+} entry process, a suggestion confirmed by the observation that the nifedipine-resistant contraction to both agents was greatly reduced by SKF 96365, which blocks both voltage- and non-voltage-dependent Ca^{2+} entry (Merritt *et al.*, 1990). The selectivity of SKF 96365 against Ca^{2+} entry processes was demonstrated by its lack of effect on contractions to U46619 and carbachol in Ca^{2+}-free medium. One possibility is that U46619 and carbachol, by reducing the Ca^{2+} content of the SR, stimulate the CRAC pathway which has been detected in several cell types (Penner *et al.*, 1993) including smooth muscle (Missaien *et al.*, 1992). Some evidence that this mechanism may exist in the anococcygeus was provided by the observation that CPA produced powerful, sustained contractions.

CPA inhibits the Ca^{2+}-ATPase of the SR, and thereby depletes the SR of Ca^{2+} and activates the CRAC pathway (Demaurex *et al.*, 1992); entry of Ca^{2+} through the CRAC pathway is prevented by SKF 96365. The contractions to CPA in the anococcygeus were dependent on extracellular Ca^{2+}, were only slightly reduced by nifedipine, but were completely blocked by a combination of nifedipine and SKF96365. The lack of contraction to CPA in Ca^{2+}-free medium, and the slower onset of contraction in normal medium, probably reflect the slower depletion of Ca^{2+} from the SR (Demaurex *et al.*, 1992). These results would therefore be consistent with CPA-induced opening of a CRAC pathway, but definitive evidence would come from patch-clamp studies of single smooth muscle cells, and such studies are in progress.

As mentioned, a small component of the contractions to U46619, carbachol and CPA was inhibited by nifedipine, suggesting a small contribution of Ca^{2+} entry through VOCCs. Opening of VOCCs probably results from depolarization caused by Ca^{2+}-activated Cl^- channels known to occur in several smooth muscle cell types (Hogg *et al.*, 1994), including the anococcygeus (Byrne & Large, 1987); any agent increasing cytosolic Ca^{2+} will tend to open such channels.

Despite the variety of mechanisms, and sources of Ca^{2+}, utilized by the four contractile agents, tone induced by each agent could be relaxed by nitrergic field stimulation, SNP and 8Br-cyclic GMP, although with a clear order of potency (U46619 > carbachol = CPA > K^+). These observations may be helpful in identifying the cellular mechanisms underlying nitrergic relaxations.

Actions of relaxant stimuli

Field stimulation, SNP and 8Br-cyclic GMP were potent relaxants of tone induced by U46619, carbachol and CPA, with SNP producing maximum relaxations of > 90% in each

case; contractions to these agents were, however, much less sensitive to block by nifedipine. In contrast, K^+-induced tone, which was totally blocked by nifedipine, was much less sensitive to relaxation by the nitrergic stimuli, with SNP producing a maximum relaxation of only 50%. In addition, both SNP and 8Br-cyclic GMP retained normal potency against carbachol in depolarizing medium. Although these results do not rule out a small contribution of membrane hyperpolarization to the overall relaxation to nitrergic activation such an action could be of only minor importance. In this respect, the mouse anococcygeus differs from the canine proximal colon in which membrane hyperpolarization is thought to be important for nitrergic relaxations (Thornbury *et al.*, 1991).

As discussed in the preceding section, CPA induces Ca^{2+} influx via inhibition of the Ca^{2+}-ATPase of the SR, an action which by-passes phospholipase C and which is not accompanied by an increased metabolism of inositol phosphates (Demaurex *et al.*, 1992; Fasolato *et al.*, 1994). The observation that nitrergic field stimulation, SNP and 8Br-cyclic GMP were potent relaxants of tone induced by CPA suggests that inhibition of phospholipase C is unlikely to underlie nitrergic relaxations of the mouse anococcygeus. This suggestion is supported by the recent finding that carbachol-induced inositol phosphate generation in the rat anococcygeus is unaffected by nitrergic field stimulation, SNP or 8Br-cyclic GMP (Gibson *et al.*, 1994a) and is consistent with observations in several other non-vascular smooth muscles in which it has been shown that inhibition of inositol phosphate metabolism does not underly relaxations to nitrovasodilators or cyclic GMP (Akhtar & Abdel-Latif, 1991; Chilvers *et al.*, 1991; Garcia-Pascual & Triguero, 1994).

In Ca^{2+}-free medium, the transient, residual contraction to carbachol is likely to reflect release of Ca^{2+} from the SR (see previous discussion). The observation that inclusion of SNP or 8Br-cyclic GMP during the period of Ca^{2+}-reloading increased the subsequent residual response to carbachol suggests that these relaxant drugs increased the carbachol-releasable store of Ca^{2+} in the SR. The concentrations of SNP required to increase the residual response to carbachol were similar to those which relaxed carbachol-induced tone in normal medium, and which inhibited the residual response to carbachol when included in the Ca^{2+}-free medium. Thus, modification of the cellular mobilization of Ca^{2+} may be an important mechanism of nitrergic relaxations of the mouse anococcygeus, which would be consistent with the observed reduction in cytosolic Ca^{2+} associated with nitrergic relaxations of the rat anococcygeus (Ramagopal & Leighton, 1989). There is considerable evidence that nitrovasodilators and cyclic GMP can increase the pumping of Ca^{2+} into the SR, possibly through phosphorylation of the regulatory protein phospholamban and consequent activation of Ca^{2+}-ATPase (Lincoln, 1989; Cornwell *et al.*, 1991; Lincoln & Cornwell, 1993). Pumping of Ca^{2+} into the SR would reduce cytosolic concentrations of the ion leading to relaxation; it would also indirectly affect any CRAC pathway, since filling of the SR would reduce the stimulus for CRAC opening. One difficulty in accepting that increased pumping of Ca^{2+} into the SR is important in nitrergic relaxations of the anococcygeus is the observation that field stimulation, SNP and 8Br-cyclic GMP were potent relaxants of tone induced by CPA, which is an inhibitor of the Ca^{2+}-ATPase of the SR. It may be that the nitrergic stimuli increase Ca^{2+} loading of the SR through a CPA-insensitive pathway (Bourreau *et al.*, 1993), or that other mechanisms are involved, such as reduced release of Ca^{2+} from the SR (Lincoln & Cornwell, 1993).

Also in Ca^{2+}-free medium, SNP could relax the residual, sustained contraction to U46619, which probably results from a direct action of the thromboxane-mimetic on the contractile proteins. SNP may, therefore, exert a direct inhibitory effect on the contractile proteins, as has been suggested in several vascular smooth muscle preparations (Pfitzer *et al.*, 1984; Nishimura & van Breemen, 1989). This effect, however, was observed with concentrations of SNP considerably higher that those which relaxed tone induced by U46619, carbachol or CPA in normal medium, although similar to those which relaxed K^+-induced tone. Thus, inhibition of contractile protein function may be more important against K^+-induced tone than against the other agents used. Experiments using chemically skinned preparations are in progress to examine this possibility.

In conclusion, the results of this study have shown that the relaxant potency of nitrergic stimuli in the mouse anococcygeus muscle is dependent on the cellular mechanisms activated to induce tone in the preparation. Analysis of the contractile/relaxant interactions suggests that neither membrane hyperpolarization nor inhibition of phospholipase C can play major roles in nitrergic relaxations of this tissue, but that further study of the effects of nitrergic activation on Ca^{2+} fluxes and on contractile protein function is warranted.

The authors thank the MRC for support.

References

AKHTAR, R.A. & ABDEL-LATIF, A.A. (1991). The effect of M&B 22948 on carbachol-induced inositol trisphosphate accumulation and contraction in iris sphincter smooth muscle. *Eur. J. Pharmacol.*, **206**, 291–295.

BOURREAU, J.P., KWAN, C.Y. & DANIEL. E.E. (1993). Distinct pathways to refill ACh-sensitive internal Ca^{2+} stores in canine airway smooth muscle. *Am. J. Physiol.*, **265**, C28–C35.

BRAVE, S.R., TUCKER, J.F., GIBSON, A., BISHOP, A.E., RIVEROS-MORENO, S., MONCADA, S. & POLAK, J.M. (1993). Localisation of nitric oxide synthase within non-adrenergic, non-cholinergic nerves in the mouse anococcygeus. *Neurosci. Lett.*, **161**, 93–96.

BYRNE, N.G. & LARGE, W.A. (1987). Membrane mechanism associated with muscarinic receptor activation in single cells freshly dispersed from the rat anococcygeus muscle. *Br. J. Pharmacol.*, **92**, 371–379.

CHILVERS, E.R., GIEMBYCZ, M.A., CHALLIS, R.A.J., BARNES, P.J. & NAHORSKI, S.R. (1991). Lack of effect of Zaprinast on methacholine-induced tone and inositol (1,4,5) trisphosphate accumulation in bovine airway smooth muscle. *Br. J. Pharmacol.*, **103**, 1119–1125.

CORNWELL, T.L., PRYZWANSKY, K.B., WYATT, T.A. & LINCOLN, T.M. (1991). Regulation of sarcoplasmic reticulum phosphorylation by localised cyclic GMP-dependent protein kinase in vascular smooth muscle cells. *Mol. Pharmacol.*, **40**, 923–931.

CRICHTON, C.A., TEMPLETON, A.G.B., McGRATH, J.C. & SMITH, G.I. (1993). Thromboxane A_2 analogue, U46619, potentiates calcium-activated force in human umbilical artery. *Am. J. Physiol.*, **264**, H1878–H1883.

DEMAUREX, N., LEW, D.P. & KRAUSE, K-H. (1992). Cyclopiazonic acid depletes intracellular Ca^{2+} stores and activates an influx pathway for divalent cations in HL-60 cells. *J. Biol. Chem.*, **267**, 2318–2324.

FASOLATO, C., INNOCENTI, B. & POZZAN, T. (1994). Receptor-activated Ca^{2+} influx: how many mechanisms for how many channels? *Trends Pharmacol. Sci.*, **15**, 77–83.

GARCIA-PASCUAL, A. & TRIGUERO, D. (1994). Relaxation mechanisms induced by stimulation of nerves and by nitric oxide in sheep urethral muscle. *J. Physiol.*, **476**, 333–348.

GIBSON, A., BRAVE, S.R., McFADZEAN, I., MIRZAZADEH, S., TUCKER, J.F. & WAYMAN, C. (1994a). Nitrergic stimulation does not inhibit carbachol-induced inositol phosphate generation in the rat anococcygeus. *Neurosci. Lett.*, **178**, 35–38.

GIBSON, A. & JAMES, T. (1977). The nature of potassium chloride-induced relaxations of the rat anococcygeus muscle. *Br. J. Pharmacol.*, **60**, 141–145.

GIBSON, A., McFADZEAN, I. & TUCKER, J.F. (1994b). Influence of contractile agent on relaxations of the mouse anococcygeus muscle to endogenous and exogenous nitrates. *J. Physiol.*, **475**, 47P–48P.

GIBSON, A. & MIRZAZADEH, S. (1989). N-methyl-hydroxylamine inhibits and M&B 22948 potentiates relaxations of the mouse anococcygeus to non-adrenergic, non-cholinergic field stimulation and to nitrovasodilator drugs. *Br. J. Pharmacol.*, **96,** 637–644.

GIBSON, A., MIRZAZADEH, S., HOBBS, A.J. & MOORE, P.K. (1990). L-N^G-monomethyl arginine and L-N^G-nitro arginine inhibit non-adrenergic, non-cholinergic relaxation of the mouse anococcygeus muscle. *Br. J. Pharmacol.*, **99,** 602–606.

GILLESPIE, J.S., LIU, X. & MARTIN, W. (1989). The effects of arginine and N^G-monomethyl-L-arginine on the responses of the rat anococcygeus muscle to NANC stimulation. *Br. J. Pharmacol.*, **98,** 1080–1082.

HIMPENS, B., KITAZAWA, T. & SOMLYO, A.P. (1990). Agonist-dependent modulation of Ca^{2+} sensitivity in rabbit pulmonary artery smooth muscle. *Pflügers Arch.*, **417,** 21–28.

HOGG, R.C., WANG, Q. & LARGE, W. (1994). Effects of Cl channel blockers on Ca-activated chloride and potassium currents in smooth muscle cells from rabbit portal vein. *Br. J. Pharmacol.*, **111,** 1333–1341.

KURATA, R., TAKAYANAGI, I. & HISAYAMA, T. (1993). Eicosanoid-induced Ca^{2+} release and sustained contraction in Ca^{2+}-free media are mediated by different signal transduction pathways in rat aorta. *Br. J. Pharmacol.*, **110,** 875–881.

LI, C.G. & RAND, M.J. (1989). Evidence for a role of nitric oxide in the neurotransmitter system mediating relaxation of the rat anococcygeus muscle. *Clin. Exp. Pharmacol. Physiol.*, **16,** 933–938.

LINCOLN, T.M. (1989). Cyclic GMP and mechanisms of vasodilatation. *Pharmacol. Ther.*, **41,** 479–502.

LINCOLN, T.M. & CORNWELL, T.L. (1993). Intracellular cyclic GMP receptor proteins. *FASEB J.*, **7,** 328–338.

LOW, A.M., GASPAR, V., KWAN, C.Y., DARBY, D.J., BOURREAU, J.P. & DANIEL, E.E. (1991). Thapsigargin inhibits repletion of phenylephrine-sensitive intracellular Ca^{2+} pool in vascular smooth muscles. *J. Pharmacol. Exp. Ther.*, **258,** 1105–1113.

MATSUO, K., GOKITA, T., KARIBE, H. & UCHIDA, M.K. (1989). Ca^{2+}-independent contraction of uterine smooth muscle. *Biochem. Biophys. Res. Commun.*, **165,** 722–727.

MERRIT, J.E., ARMSTRONG, W.P., BENHAM, C.D., HALLAM, T.J., JACOB, R., JAXA-CHAMIEC, A., LEIGH, B.K., MCCARTHY, S.E., MOORES, K.E. & RINK, T.J. (1990). SK&F 96365, a novel inhibitor of receptor-mediated calcium entry. *Biochem. J.*, **271,** 515–522.

MIRZAZADEH, S., HOBBS, A.J., TUCKER, J.F. & GIBSON, A. (1991). Cyclic nucleotide content of the rat anococcygeus during relaxations induced by drugs or by non-adrenergic, non-cholinergic field stimulation. *J. Pharm. Pharmacol.*, **43,** 247–257.

MISSAIEN, L., DE SMEDT, H.D., DROOGMANS, G., HIMPENS, B. & CASTEELS, R. (1992). Calcium ion homeostasis in smooth muscle. *Pharmacol. Ther.*, **56,** 191–231.

MITCHELL, J.A., SHENG, H., FORSTERMANN, U. & MURAD, F. (1991). Characterisation of nitric oxide synthases in non-adrenergic, non-cholinergic containing tissue from rat anococcygeus muscle. *Br. J. Pharmacol.*, **104,** 289–291.

NISHIMURA, J. & VAN BREEMEN, C. (1989). Direct regulation of smooth muscle contractile elements by second messengers. *Biochem. Biophys. Res. Commun.*, **163,** 929–935.

OZAKI, H., OHYAMA, T., SATO, K. & KARAKI, H. (1990). $Ca2^{+}$-dependent and independent mechanisms of sustained contraction in vascular smooth muscle of rat aorta. *Jpn. J. Pharmacol.*, **52,** 509–512.

PENNER, R., FASOLATO, C. & HOTH, M. (1993). Calcium influx and its control by calcium release. *Curr. Opin. Neurobiol.*, **3,** 368–374.

PFITZER, G., HOFMANN, F., DISALVO, J. & RUEGG, J.C. (1984). cGMP and cAMP inhibit tension development in skinned coronary artery. *Pflügers Arch.*, **401,** 277–280.

RAMAGOPAL. M.V. & LEIGHTON, H.J. (1989). Effects of N^G-monomethyl-L-arginine on field stimulation-induced decreases in cytosolic Ca^{2+} levels and relaxation in the rat anococcygeus muscle. *Eur. J. Pharmacol.*, **174,** 297–299.

RAND, M.J. (1992). Nitrergic transmission: nitric oxide as a mediator of non-adrenergic, non-cholinergic neuro-effector transmission. *Clin. Exp. Pharmacol. Physiol.*, **19,** 147–169.

SIDESO, E., TUCKER, J.F. & GIBSON, A. (1994). Lack of antagonist action of L-NAME on muscarinic (M_3) receptors in the mouse anococcygeus. *Br. J. Pharmacol.*, **112,** 233P.

THORNBURY, K.D., WARD, S.M., DALZIEL, H.H., CARL, A., WESTFALL, D.P. & SANDERS, K.M. (1991). Nitric oxide and nitrocysteine mimic nonadrenergic noncholinergic hyperpolarisation in canine proximal colon. *Am. J. Physiol.*, **261,** G553–G557.

WALDMAN, S.A. & MURAD, F. (1987). Cyclic GMP synthesis and function. *Pharmacol Rev.*, **39,** 163–196.

(Received May 10, 1994
Revised August 1, 1994
Accepted August 18, 1994)

Br. J. Pharmacol. (1994), **113**, 1501–1507 © Macmillan Press Ltd, 1994

A_1 adenosine receptor inhibition of cyclic AMP formation and radioligand binding in the guinea-pig cerebral cortex

[1]Stephen P.H. Alexander, Alistair R. Curtis, David A. Kendall & Stephen J. Hill

Department of Physiology & Pharmacology, University of Nottingham Medical School, Queen's Medical Centre, Nottingham, NG7 2UH

1 A_1 adenosine receptors were investigated by radioligand binding and functional studies in slices and particulate preparations from guinea-pig cerebral cortex.

2 Binding of the adenosine receptor antagonist radioligand, 8-cyclopentyl-[^{3}H]-1,3-dipropylxanthine (DPCPX) to guinea-pig cerebral cortical membranes exhibited high density (1410 ± 241 fmol mg^{-1} protein) and high affinity (K_d 3.8 ± 0.3 nM).

3 [^{3}H]-DPCPX binding to guinea-pig cerebral cortical membranes was displaced in a monophasic manner by adenosine receptor antagonists with the rank order of affinity (K_i values, nM): DPCPX (6) < xanthine amine congener (XAC, 153) < PD 115,199 (308).

4 Agonist displacement of [^{3}H]-DPCPX binding was biphasic and exhibited the following rank order at the low affinity site (K_i values): 2-chloro-N^6-cyclopentyl-adenosine (CCPA, 513 nM) = N^6-**R**-phenyl-isopropyladenosine (**R**-PIA, 526 nM) = N^6-cyclopentyladenosine (CPA, 532 nM) < 2-chloroadenosine (2CA, 3.2 μM) = 5'-N-ethylcarboxamidoadenosine (NECA, 4.6 μM) < N^6-S-phenylisopropyladenosine (S-PIA, 19.9 μM).

5 In cerebral cortical slices, [^{3}H]-DPCPX binding was displaced by antagonists and agonists in an apparently monophasic manner with the rank order of affinity (K_i values, nM): DPCPX (14) < XAC (45) < **R**-PIA (266) < PD 115,199 (666) < S-PIA (21000).

6 Cyclic AMP accumulation stimulated by 30 μM forskolin in guinea-pig cerebral cortical slices was inhibited by **R**-PIA, CCPA and CPA up to 1 μM in a concentration-dependent fashion with IC_{50} values of 14, 18, and 22 nM, respectively. All three analogues inhibited the forskolin response to a similar extent (82–93% inhibition). NECA, S-PIA and 2CA failed to inhibit the forskolin response, but rather enhanced the accumulation of cyclic AMP at concentrations of 100 nM or greater, presumably through activation of A_{2b} adenosine receptors coupled to stimulation of cyclic AMP accumulation in guinea-pig cerebral cortical slices.

7 The inhibition of forskolin-stimulated cyclic AMP accumulation by CPA was antagonized with the rank order of affinity (K_i values, nM): DPCPX (6) < XAC (52) < PD 115,199 (505).

8 Xanthine-based antagonists inhibited the adenosine receptor augmentation of histamine-induced phosphoinositide turnover in guinea-pig cerebral cortical slices with the rank order of affinity (K_i, nM): DPCPX (12) = XAC (17) < PD 155,199 (640).

9 In summary, we observe a good correlation between antagonist affinity at A_1 receptors defined by radioligand binding, inhibition of cyclic AMP generation or augmentation of histamine-evoked phosphoinositide turnover in guinea-pig cerebral cortex.

Keywords: A_1 adenosine receptor; xanthines; cyclic AMP; phosphoinositide turnover; guinea-pig cerebral cortex

Introduction

The role of extracellular adenosine as a neuromodulator in the central nervous system is now well established. Two classes of extracellular adenosine receptor were originally delineated from studies of the effects of adenosine in mouse astroglial primary culture, subserving an inhibition (A_1) and a stimulation (A_2 of adenosine 3':5'-cyclic monophosphate (cyclic AMP) levels (van Calker *et al.*, 1979; Londos *et al.*, 1980; Daly *et al.*, 1983). However, to date in the literature there exist relatively few examples (such as the work of Fredholm in the rat hippocampus: Fredholm *et al.*, 1982; 1986; Dunwiddie & Fredholm, 1985) of investigations of the pharmacological profile of A_1 adenosine receptor-evoked alterations in second messenger levels in tissue slice preparations from the CNS. Quantitative investigations of the A_1 adenosine receptor have in the main been limited to applying radioligand binding assays using either agonists (e.g. [^{3}H]-**R**-PIA: Schwabe & Trost, 1980) or antagonists (e.g. [^{3}H]-DPCPX: Bruns *et al.*, 1987; Lohse *et al.*, 1987). Studies of adenylyl cyclase activity in cell-free preparations from the CNS have also been carried out to investigate A_1 adenosine receptors (e.g. Schubert *et al.*, 1979). We are particularly interested in adenosine receptors of guinea-pig cerebral cortical slices since we have previously observed a selective enhancement of histamine H_1 receptor-stimulated phosphoinositide turnover in this tissue through activation of an adenosine receptor (Hill & Kendall, 1987). The agonist rank order of potency, whereby the N^6-derivative CPA was more potent than the 5'-derivative NECA could indicate mediation of this response through an A_1 adenosine receptor. However, the agonist potencies observed were relatively high (ca. micromolar), which is not entirely compatible with a typical A_1 receptor. We have additionally reported that the receptor mediating this potentiation is distinct from the A_{2b} adenosine receptor of guinea-pig cerebral cortical slices which mediates a stimulation of cyclic AMP levels (Alexander *et al.*, 1989). We have recently further characterized the latter A_{2b} adenosine receptor in guinea-pig cerebellum and cerebral cortex and identified a rank order of antagonist potency at this receptor of xanthine amino congener (XAC) > DPCPX > PD 115, 199 (Hernández *et al.*, 1993; Alexander *et al.*, 1994).

Comparisons between affinity constants estimated from functional and radioligand binding studies are relatively few in the adenosine receptor field, and are often conducted

[1] Author for correspondence.

across species (e.g. rat brain radioligand binding data compared with guinea-pig atrial preparations. This situation is obviously far from ideal. In the current paper, we present an investigation of the A_1 adenosine receptor-mediated inhibition of forskolin-stimulated cyclic AMP accumulation in guinea-pig cerebral cortical slices and compare data obtained from this approach with data from radioligand binding techniques.

Methods

Inhibition of forskolin-stimulated cyclic AMP accumulation

After equilibration of cerebral cortex slices (350 × 350 μm) for 60 min with several changes of Krebs-Henseleit medium, slices were exposed to [^{3}H]-adenine (74 kBq ml^{-1}) for 40 min, then washed to remove excess radioactivity. Aliquots of gravity-packed slices (25 μl) were placed in flat-bottomed vials to which Krebs-Henseleit solution was added to give a final volume of 300 μl. Adenosine deaminase (1 u ml^{-1}) was also included at this time in the assay, together with antagonist, where indicated. After an interval of at least 10 min, adenosine analogues were added in 10 μl, followed rapidly by the addition of forskolin to a final concentration of 30 μM. The slices were allowed to incubate for a further 10 min, before termination of the reaction with 200 μl of 1 M hydrochloric acid containing 30–35 Bq of [^{14}C]-cyclic AMP, followed by 750 μl of ice-cold water. Cyclic AMP was isolated by the Dowex-alumina method (Salomon *et al.*, 1974).

Augmentation of histamine-stimulated phosphoinositide turnover

Histamine-stimulated phosphoinositide turnover was assessed by measuring the accumulation of [^{3}H]-inositol phosphates over a 45 min incubation period in [^{3}H]-inositol pre-labelled cerebral cortex slices in the presence of 5 mM LiCl, as previously described (Alexander *et al.*, 1989).

Radioligand binding studies

[^{3}H]-DPCPX binding to a particulate fraction A particulate preparation was obtained from guinea-pig cerebral cortex by homogenization of tissue in 10 volumes of 1 mM EDTA in 50 mM Tris, pH 7.4 and centrifugation at 20 000 *g* for 15 min. The membranes were re-suspended by homogenization in 10 volumes of the same buffer and the centrifugation process repeated. After a second homogenization/centrifugation step the membranes were re-suspended in the same buffer to a protein concentration of approximately 1 mg ml^{-1}.

[^{3}H]-DPCPX binding was carried out in a final volume of 200 μl in 1 mM EDTA, 50 mM Tris pH 7.4 containing 1.25 u ml^{-1} adenosine deaminase and 0.01% Triton X-100. Non-displaceable binding was defined by the presence of 5 mM theophylline, and was typically 5–10%. The incubation was allowed to proceed for 90 min at room temperature before termination by rapid filtration over Whatman GF/B filters using a cell harvester (Brandel, Semat, Herts, UK). Filters were extracted overnight in scintillation cocktail prior to estimation of radioactivity by liquid scintillation spectrometry.

[^{3}H]-DPCPX binding in cerebral cortical slices [^{3}H]-DPCPX binding was carried out using 10 μl of gravity-packed cerebral cortical slices in a final volume of 2 ml, in Krebs Henseleit medium, pH 7.4 containing 1.25 u ml^{-1} adenosine deaminase. Non-displaceable binding was defined by the presence of 5 mM theophylline, and was typically 25–35% of total binding for 0.5–1.2 nM [^{3}H]-DPCPX. The incubation was allowed to proceed for 60–90 min at 37°C in a shaking water bath before termination by rapid filtration over Whatman GF/B filters using a 10 place manifold (Shearline, Cambridge, UK). Filters were extracted overnight in scintillation cocktail prior to estimation of radioactivity by liquid scintillation spectrometry.

Data analysis and statistics

Data are expressed as means ± s.e.mean. Saturation and competition data were analysed with the computer programme InPlot (GraphPad, California, U.S.A.) using non-linear equations for rectangular hyperbolae and sigmoidal curves, respectively. Apparent inhibition constants were calculated from radioligand binding data using the Cheng-Prusoff transformation (Cheng & Prusoff, 1973). Functional affinity constants were calculated as previously described (Alexander *et al.*, 1989).

Materials

8-cyclopentyl-[^{3}H]-1,3-dipropylranthine [^{3}H]-DPCPX, 4040 GBq mmol^{-1}) and [^{3}H]-adenine (880 GBq mmol^{-1}) were obtained from DuPont NEN, Herts. [^{14}C]-cyclic AMP (10.3 GBq mmol^{-1}) was from Amersham International, Bucks. Adenosine analogues (CPA, N^6-cyclopentyladenosine; CCPA, 2-chloro-N^6-cyclopentyladenosine; 2CA, 2-chloroadenosine; NECA, 5'-N-ethylcarboxamidoadenosine; **R**-PIA, **R**-N^6-phenylisopropyladenosine; and **S**-PIA, **S**-N^6-phenylisopropyladenosine) were obtained from Research Biochemicals Incorporated, Herts and were dissolved to 50 mM in dimethylsulphoxide. Adenosine receptor antagonists (DPCPX, 8-cyclopentyl-1,3-dipropylxanthine and XAC, xanthine amino congener) were also obtained from RBI (with the exception of PD 115,199, a gift from Warner-Lambert, U.S.A.), and were also initially dissolved in dimethylsulphoxide to 10 mM. Adenosine deaminase was obtained from Boehringer Mannheim (Sussex). All other chemicals were from Fisons (Leics) or Sigma Chemicals (Dorset).

Guinea-pigs of the Hartley strain, 200–600 g, of either sex were used throughout.

Results

[^{3}H]-DPCPX radioligand binding

Analysis of [^{3}H]-DPCPX binding to guinea-pig cerebral cortical membranes gave estimates of the maximal capacity for this tissue of 1410 ± 241 fmol mg^{-1} protein, with a K_d of 3.8 ± 0.3 nM. Antagonist competition curves for [^{3}H]-DPCPX binding showed a rank order of potency of DPCPX > XAC > PD 115,199, each of which exhibited Hill slopes near to unity (Figure 1a, Table 1). Displacement of [^{3}H]-DPCPX by agonists, in contrast, was biphasic exhibiting high and low affinity sites for all the agonists examined (e.g. **R**- and **S**-PIA, Figure 1a). At the low affinity site, constituting *c.* 66% of displaceable binding, displacement of [^{3}H]-DPCPX by adenosine receptor agonists showed the rank order of potency **R**-PIA = CCPA = CPA > 2CA > NECA > S-PIA (Table 1).

[^{3}H]-DPCPX bound to cerebral cortical slices in a time-dependent manner, reaching steady-state levels at 30–45 min, remaining constant for at least a further 45 min. Subsequent binding experiments were allowed to proceed over 60–90 min. The antagonists DPCPX, XAC and PD 115,199 and the agonists **R**-PIA and S-PIA competed for [^{3}H]-DPCPX binding (Figure 1b, Table 2). Radioligand binding in slices was observed to be somewhat more variable than the comparable particulate binding assays. B_{max} values estimated from DPCPX competition curves were 4078 ± 1285 fmol mg^{-1} protein. This value derives from an average protein content of 40 mg ml^{-1} slices (data not shown) which includes both soluble and particulate proteins and so must be taken to be

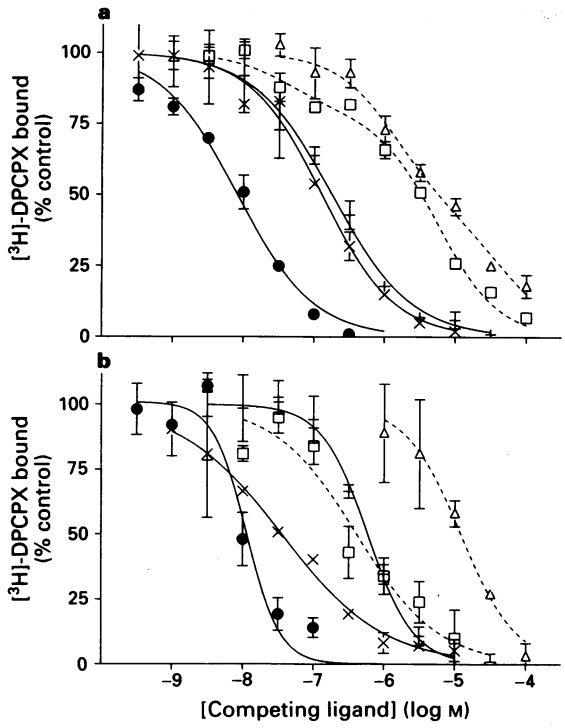


Figure 1 Displacement of [^{3}H]-DPCPX (0.5–1.2 nM binding to (a) a particulate preparation or (b) intact slices from guinea-pig cerebral cortex. Data are means and s.e.mean from single experiments conducted in triplicate (a) or quadruplicate (b) in the presence of increasing concentrations of DPCPX (●), XAC (×), PD 115,199 (+), R-PIA (□) or S-PIA (△). For abbreviations, see text.

Table 1 Inhibition constants, K_i, for displacement of [^{3}H]-DPCPX binding to a cerebral cortical particulate preparation by adenosine receptor antagonists and agonists

Antagonist	K_i (nM)	n_H
DPCPX	5.5 ± 1.6	− 1.14 ± 0.07
XAC	153 ± 30	− 1.07 ± 0.10
PD 115,199	264 ± 54	− 1.15 ± 0.08

Agonist	*Low affinity binding site* K_i (nM)	*% low affinity binding site*	*High affinity binding site* K_i (nM)
CPA	529 ± 123	70 ± 7	4 ± 1
CCPA	905 ± 430	59 ± 8	19 ± 4
R-PIA	1618 ± 101	75 ± 6	18 ± 12
2CA	4913 ± 1904	65 ± 7	37 ± 16
NECA	10580 ± 1320	52 ± 10	107 ± 15
S-PIA	22150 ± 538	62 ± 10	751 ± 344

Data are means ± s.e.mean of experiments conducted on at least four (up to eight) separate preparations of guinea-pig cerebral cortex membranes. Agonist competition data were fitted to a two-site model for competition of [^{3}H]-DPCPX binding (using the computer programme InPlot, in all cases $r^2 > 0.98$) to generate high and low affinity binding sites for the agonists. For abbreviations, see text.

an underestimate of binding capacity for comparison with data derived using the particulate preparation.

Forskolin-stimulated [^{3}H]-cyclic AMP accumulation

Since A_1 adenosine receptors are commonly associated with an inhibition of adenylyl cyclase activity (Jacobson *et al.*, 1992), we investigated the possible functional linkage of A_1 receptors in guinea-pig cerebral cortical slices using adenosine analogues and forskolin as a stimulus of cyclic AMP formation. When [^{3}H]-cyclic AMP accumulation was stimulated in the presence of 30 μM forskolin and 1 u ml^{-1} adenosine deaminase, a variety of responses was observed with adenosine analogues (Figure 2). The putative A_{2a}-selective agonist, CGS 21680 was without significant effect on basal (Alexander *et al.*, 1994) or forskolin-stimulated cyclic AMP generation at concentrations up to 10 μM (Figure 2). In contrast, the non-selective adenosine receptor agonists NECA and 2CA elicited concentration-dependent enhancements of the forskolin response (Figure 2) with EC_{50} values of 89 ± 47 nM and 1.5 ± 0.2 μM, and a maximal effect of 374 ± 59% and 352 ± 66% of the forskolin response, respectively ($n=3$). S-PIA also increased forskolin-induced cyclic AMP generation without reaching saturation. Assuming a similar maximal response to S-PIA compared with NECA and 2CA, an EC_{50} value could be estimated at 13 and 14 μM ($n=2$). In comparison, stimulation of cyclic AMP generation in the absence of forskolin is evoked by NECA and 2CA with EC_{50} values of 3.1 and 10 μM, respectively (Alexander *et al.*, 1994).

Certain N^6-derivatives of adenosine elicited biphasic effects on the forskolin response. Thus, at concentrations below micromolar, concentration-dependent inhibitions of [^{3}H]-cyclic AMP generation were observed, while at higher concentrations, increased cyclic AMP responses were apparent (e.g. R-PIA, Figure 2). Thus, R-PIA, CCPA and CPA in the concentration range 1–1000 nM all inhibited the forskolin response to a maximal level of 82 ± 3, 92 ± 4, and 91 ± 2% inhibition, respectively (Table 3). The stimulation of [^{3}H]cyclic AMP accumulation by NECA, 2CA and S-PIA

Table 2 Inhibition constants, K_i, for displacement of [^{3}H]-DPCPX binding to cerebral cortical slices adenosine receptor antagonists and agonists

	K_i (nM)	n_H
DPCPX	14 ± 4	− 1.37 ± 0.26
XAC	45 ± 10	− 0.80 ± 0.20
PD 115,199	666 ± 117	− 1.22 ± 0.26
R-PIA	266 ± 55	− 0.82 ± 0.16
S-PIA	21 000 ± 6000	− 1.15 ± 0.47

Data are means ± s.e.mean of experiments conducted on at least four separate preparations of guinea-pig cerebral cortical slices. Competition data were fitted to a sigmoidal using the computer programme InPlot (in all cases $r^2 > 0.98$). For abbreviations, see text.

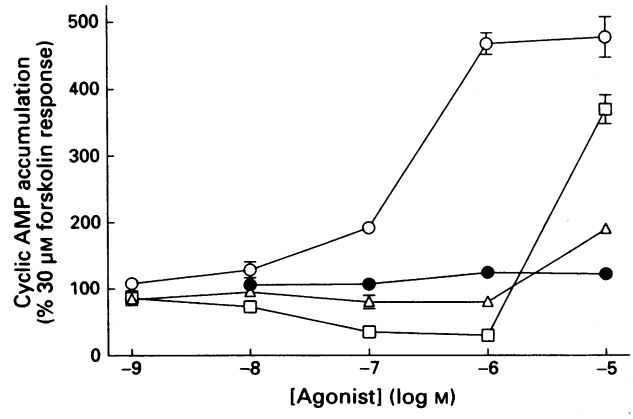


Figure 2 Modulation of forskolin-stimulated cyclic AMP accumulation in guinea-pig cerebral cortical slices by adenosine analogues. [^{3}H]-adenine-prelabelled slices were incubated with increasing concentrations of R-PIA (□), S-PIA (△), NECA (○) or CGS 21680 (●) immediately prior to addition of 30 μM forskolin. Results are means ± s.e.mean of single experiments expressed as a percentage of the forskolin response. The response to each agonist was investigated on at least two further occasions. For abbreviations, see text.

and higher concentrations of R-PIA, CCPA and CPA is presumably mediated through activation of A_{2b} adenosine receptors (Jacobson *et al.*, 1992; Alexander *et al.*, 1994). Since no selective antagonist for this receptor exists, however, it is not possible to assert unequivocally that these effects are A_{2b} receptor-mediated.

Estimation of antagonist apparent affinity constants

The CPA-elicited inhibition of forskolin-stimulated [^{3}H]cyclic AMP generation was investigated to determine the apparent affinity constants of the three antagonists (e.g. DPCPX, Figure 3). Using concentrations of antagonists at approximately one order of magnitude greater than the K_i calculated from the radioligand binding studies presented above, rightward shifts in the agonist concentration-inhibition curves were analysed in order to calculate antagonist apparent inhibition constants. The antagonist rank order of potency observed was DPCPX > XAC > PD 115,199 (Table 3).

Table 3 Agonist potency, IC_{50} or EC_{50} values (nM), and antagonist affinity, K_i (nM), at adenosine receptors of guinea-pig cerebral cortical slices

Agonist	*Cyclic AMP inhibition*	*PI turnover potentiation*
R-PIA	14 ± 2 (4)	815 ± 110[1]
CCPA	18 ± 7 (14)	573 ± 123 (4)
CPA	22 ± 3 (14)	410 ± 100[1]
NECA	–	920 ± 95[1]
2CA	–	1900 ± 150[1]
S-PIA	–	> 75 000 (3)[2]
CGS 21680	–	–

Antagonist	*Cyclic AMP inhibition*	*PI turnover potentiation*
DPCPX	6.0 ± 2.3 (3)	12 ± 3 (8)
XAC	52 ± 10 (3)	17 ± 8 (4)
PD 115,199	521 ± 109 (4)	640 ± 133 (3)

[1]Data taken from Hill & Kendall (1987). [2]The augmentatory response to S-PIA failed to reach an asymptote at concentrations up to 1 mM in two out of three experiments, while in the third an EC_{50} value of 75 μM could be calculated. Data are means ± s.e.mean of the number of experiments shown in parentheses. For abbreviations, see text.

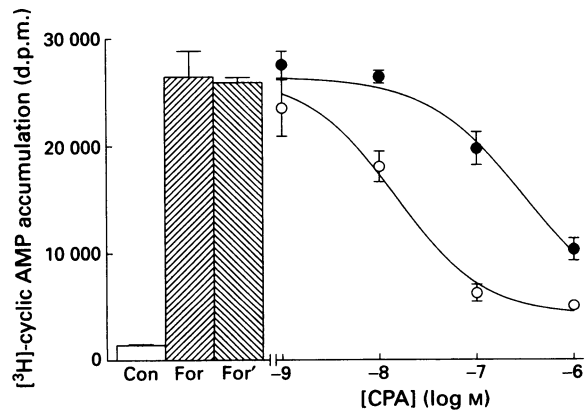


Figure 3 Antagonism by DPCPX of the CPA-elicited inhibition of forskolin-stimulated cyclic AMP accumulation. [^{3}H]-adenine-prelabelled slices were pre-incubated in the absence (○) or presence (●) of 50 nM DPCPX before the addition of increasing concentrations of CPA immediately prior to addition of 30 μM forskolin. Also shown are the basal response (Con) and the response to 30 μM forskolin in the absence (For) and presence (For') of 50 nM DPCPX. Results are means ± s.e.mean of a single experiment. Essentially identical results were obtained on two further occasions.

Augmentation of histamine-stimulated phosphoinositide turnover

We have previously reported potencies of a number of adenosine analogues for augmentation of H_1 histamine receptor-evoked phosphoinositide turnover in guinea-pig cerebral cortical slices (Hill & Kendall, 1987). In the present investigation, we further assayed the potency of a number of these agents together with two further analogues, CCPA and S-PIA. Using data from these two series of experiments, agonist potency at this adenosine receptor was observed to be CPA ≥ CCPA ≥ R-PIA = NECA > 2CA > S-PIA (Table 3). Antagonist apparent affinities at this receptor were in the rank order DPCPX ≥ XAC > PD 115,199 (Table 3).

Discussion

In this study, we compare the ability of adenosine receptor agonists and antagonists to displace binding of [^{3}H]-DPCPX to guinea-pig cerebral cortical membranes and slices, with their activity at functional adenosine receptor responses in intact tissue slices. The three antagonists show good correlation of receptor affinity estimates in these paradigms, while the agonists may be divided into A_1-selective and non-selective groups based on the functional responses to these agents.

Radioligand binding to membranes

Results presented here show that DPCPX exhibits high affinity for the A_1 receptor of guinea-pig cerebral cortex with a K_i of 4 nM and a maximal capacity of 1410 fmol mg^{-1} protein (Table 1). These values compare well with other investigations of [^{3}H]-DPCPX binding in guinea-pig cerebral cortex (Stroeher *et al.*, 1989; Klotz *et al.*, 1991). The xanthine-derived antagonists exhibited a monophasic displacement of [^{3}H]-DPCPX binding with a rank order of potency of DPCPX > XAC > PD 115,199, consistent with the binding site labelled being the A_1 adenosine receptor. Agonist displacement of [^{3}H]-DPCPX was biphasic, a phenomenon expected for a G-protein-coupled receptor, with a rank order of potency at the low affinity site of CCPA = CPA = R-PIA > 2CA = NECA > S-PIA. The higher potency of N^6-adenosine analogues CCPA, CPA and R-PIA compared to the 5'- derivative NECA, together with the high degree of stereoselectivity exhibited for the isomers of PIA, are consistent with the binding site being the A_1 adenosine receptor (Jacobson *et al.*, 1992).

Radioligand binding to cerebral cortical slices

In cerebral cortical slices, [^{3}H]-DPCPX was observed to bind with relatively high affinity (ca. 14 nM) and high capacity (ca. 4100 fmol mg^{-1} protein). This latter value is subject to some error, since protein content was not assayed in each tube, and was likely to be variable, no doubt increasing the variability of the parameters described for radioligand binding in slices. The binding capacity in slices is expressed relative to total protein content and not simply particulate protein as is the case for the binding carried out in cell-free preparations (see above, 1410 fmol mg^{-1} protein), and is therefore likely to be an underestimate of binding capacity expressed per unit membrane protein. Increases in affinity and capacity are commonly found when comparing binding data in slices and in cell-free preparations (Shaw & Wilkinson, 1994). Nevertheless, the competition data for radioligand binding in slices is in good agreement with data obtained with the particulate preparation. Significantly, binding parameters for the agonists, R- and S-PIA showed closer

agreement with K_is identified for the low affinity site in the particulate preparation, a phenomenon also observed for A_1 receptors in intact cells and particulate preparations of the DDT1 MF-2 cell line (Gerwins *et al.*, 1990). It is likely that the presence of intracellular GTP allows only the low affinity state of the A_1 receptor to be visualised using steady-state radioligand binding.

It should also be noted that the non-displaceable binding observed with this technique was rather higher than that obtained with membranes (typical values of 25–35% and 5–10% of total binding, respectively).

Inhibition of forskolin-stimulated cyclic AMP accumulation

Forskolin-stimulated cyclic AMP generation was inhibited by three adenosine analogues (CPA, CCPA and **R**-PIA) but not NECA, 2CA or S-PIA, although all six analogues competed for [^{3}H]-DPCPX binding. However, the three 'active' analogues were more potent at competing for [^{3}H]-DPCPX binding than the three 'inactive' compounds (Table 2). It appears likely that, since all six compounds stimulate cyclic AMP formation at higher concentrations, all six are agonists at the A_{2b} adenosine receptor linked to cyclic AMP generation in guinea-pig cerebral cortex (Alexander *et al.*, 1994). Thus, the 'active' analogues probably exhibit greater differences in potency for A_1 versus A_{2b} receptors than the 'inactive' analogues. The affinity of the three 'active' analogues for [^{3}H]-DPCPX binding to the high affinity site of the A_1 receptor is similar to the IC_{50}s for agonist inhibition of cyclic AMP generation. A similar observation was made in DDT_1 MF-2 cells (Gerwins *et al.*, 1990), where **R**-PIA inhibited β-adrenoceptor-stimulated cyclic AMP generation with an IC_{50} value of 0.4 nM, and competed for [^{3}H]-DPCPX binding in cell membranes with K_i values of 1.7 and 93 nM. Interestingly, however, inhibition of [^{3}H]-DPCPX binding to intact cells with **R**-PIA revealed only a single site with a K_i value of 77 nM. The low affinity of **R**-PIA in intact cells presumably reflects high intracellular levels of GTP leading to uncoupling of the G-protein from the receptor and formation of the low agonist affinity state.

The cyclic AMP response to 30 μM forskolin was inhibited by more than 80% by the three N^6-derivatives of adenosine, CPA, CCPA and **R**-PIA. A similar maximal inhibition (>90%) is observed when forskolin-stimulated cyclic AMP formation is inhibited by metabotropic glutamate receptor agonists (Cartmell *et al.*, 1992). The question therefore arises as to whether 90% of cells in the guinea-pig cerebral cortex express A_1 adenosine receptors or metabotropic glutamate receptors. Intuitively, one would suggest that this is unlikely, and that it is more likely that the stimulation of cyclic AMP by forskolin (which is not maximal at 30 μM, data not shown) may be selective, in that a subpopulation of cells and/or adenylyl cyclase isoforms may be activated by forskolin. These possibilities require further investigation.

It has been suggested that adenosine antagonists may have 'negative efficacy' effects on A_1 adenosine receptor function (Parsons *et al.*, 1988; Ramkumar & Stiles, 1988a,b). Also, GTP analogues have been observed to enhance antagonist radioligand binding to A_1 adenosine receptors (Stiles, 1988; Klotz *et al.*, 1990). If this were the case, then we would observe an enhancement of forskolin-stimulated cyclic AMP formation in guinea-pig cerebral cortical slices in the presence of DPCPX, XAC and PD 115,199. However, this was not the case (data not shown). Therefore, we would support the hypothesis of Prater *et al.* (1992), who suggested that the effects of guanine nucleotide on antagonist radioligand binding were due to release of endogenous adenosine from 'cryptic' binding sites in vesicles hidden from adenosine deaminase action. In the radioligand binding assays in the present study, we have included a low concentration of the detergent Triton X-100 to improve access of adenosine deaminase (Schiemann *et al.*, 1990).

Comparison of data from functional and radioligand binding assays

It is common for the selectivity of compounds to be inferred from radioligand binding assays, to the extent that agents may be given *in vivo* at relatively large doses, and functional responses ascribed to particular receptor subtypes. In the case of adenosine receptors, it is clear from the present results that CCPA, CPA and **R**-PIA are A_1 selective (eliciting an inhibition of forskolin-stimulated cyclic AMP generation) in their action at concentrations in the nanomolar range. However, at higher concentrations, these agents were able to enhance cyclic AMP generation, presumably through activating A_{2b} receptors. Thus, in different tissues exhibiting a higher relative density of A_{2b} receptors (at the present time it is not possible to define A_{2b} receptor density due to the lack of a radioligand for this receptor), it is possible that the functional inhibition of cyclic AMP generation by the three A_1-selective agents might be lost. This may possibly explain our recent findings that CPA fails to inhibit forskolin-stimulated cyclic AMP generation in slices from the guinea-pig cerebellum (Hernández *et al.*, 1993).

In the case of the adenosine receptor antagonists as opposed to the agonists, there should be greater parity between affinity defined by radioligand binding techniques compared to functional assays. Comparing antagonist affinities in the various assays, DPCPX affinity varies between 4–14 nM, while PD 115,199 and XAC exhibited greater variation (521–666 and 17–52 nM respectively). However, these variations appear to be within the experimental error of the assays conducted, and it appears justifiable to assume that the antagonist affinities are not different in the different assays. One potential explanation for the greater variation of PD 115,199 and XAC compared to DPCPX, concerns the charges of the sidechains of the compounds which are all based on a 1,3-dipropylxanthine core. The 8-substituent of DPCPX (a cyclopentyl group) is uncharged, while XAC and PD 115,199 are charged at neutral pH. Thus, although binding in both membranes and slices was carried out at pH 7.4, factors such as ionic strength and sequestration of antagonist in the tissues may lead to alterations in the distribution of XAC and PD 115,199 in the intact slice preparations, and hence their apparent affinity. Since the receptor is an integral membrane protein subject to influence by agents from both cytoplasmic and extracellular faces of the plasma membrane, it may not be possible to replicate the same conditions in the broken cell particulate preparation which the receptor experiences in the slice preparation.

A further difference between radioligand binding and functional approaches to establishing antagonist affinities is the concentrations of agents used relative to their affinities. Thus, in the radioligand binding assays, accurate determination of K_is relies heavily on the linear portion of the graph, which is most likely to be spread less than one log unit either side of the K_i (or IC_{50}). In the functional assays, accurate determinations of K_is can only be effected using concentrations of antagonists at least 10 fold the K_i value. Therefore, should sequestration of compounds occur it is more likely to underestimate the K_i determined using lower concentrations of antagonist, that is, the radioligand binding assay.

A further potential source of error arises from the assumption that these agents are competitive antagonists. Proper Schild analysis of the functional A_1 inhibition of cyclic AMP over a 2–3 log unit range of antagonist concentrations is not possible in this tissue, since a greater than 10 fold rightward shift of the agonist concentration-response curves will result in concentrations of agonist being required which are active in the A_{2b} activation range leading to stimulation of cyclic AMP generation, thereby confounding the experiment.

Modulation of histamine-stimulated phosphoinositide turnover

All the adenosine analogues tested exhibited the ability to enhance the accumulation of [^{3}H]-inositol phosphates stimulated by histamine H_1-receptor activation (Table 3, see also Hill & Kendall, 1987). When potencies for the N^6-analogues are compared for inhibition of forskolin-stimulated cyclic AMP generation and phosphoinositide turnover potentiation, it is apparent that these agents are approximately one order of magnitude more potent in the cyclic AMP assay. This was not a factor of the incubation period of the assay since preliminary results indicated a similar inhibitory response to 100 nM CPA after prolonged incubation in the presence of forskolin (data not shown). The rank order of agonist potency appears to suggest an A_1-type adenosine receptor since the N^6-derivatives of adenosine CPA and CCPA were more potent than NECA and 2CA. Similarly, the S-isomer of N^6-phenylisopropyladenosine was much less potent than the R-isomer, again indicating that the adenosine receptor responsible for the potentiation of the H_1 receptor response was of the A_1 class. Antagonist rank order of potency at these two adenosine receptors is identical for the three antagonists investigated.

The mechanism of potentiation of histamine-stimulated phosphoinositide turnover remains to be defined, but it is attractive to hypothesize that the G-protein through which the A_1 receptor couples to elicit inhibition of adenylyl cyclase also mediates the enhancement of the histamine response. The latter response may require the recruitment of more intermediary G-proteins than the latter, and this may therefore underlie the difference in agonist potency (and presumably occupancy) between the two systems. It is relevant to note, therefore, that A_1 receptors transfected into Chinese hamster ovary cells and in DDT1 MF-2 hamster vas deferens smooth muscle cells couple to phosphoinositide turnover and calcium mobilisation through a pertussis toxin-sensitive mechanism (Dickenson & Hill, 1993; Iredale *et al.*, 1994).

Concluding remarks

In the present study, we show that functional A_1 adenosine receptors may be demonstrated in intact brain slices from the guinea-pig and that using this method there is good coincidence of apparent antagonist affinity compared with radioligand binding studies. There is also good correlation in apparent antagonist affinity between the A_1 receptor-induced inhibition of cyclic AMP generation compared to the A_1-type receptor which is responsible for potentiation of histamine-evoked phosphoinositide turnover.

We thank the Wellcome Trust for financial support.

References

ALEXANDER, S.P.H., KENDALL, D.A. & HILL, S.J. (1989). Differences in the adenosine receptors modulating inositol phosphates and cyclic AMP accumulation in mouse and guinea pig brain. *Br. J. Pharmacol.*, **98**, 1241–1247.

ALEXANDER, S.P.H., LOSINSKI, A., KENDALL, D.A. & HILL, S.J. (1994). A comparison of adenosine receptor stimulated cyclic AMP generation in guinea-pig cerebral cortex and relaxation of pre-contracted aorta. *Br. J. Pharmacol.*, **111**, 185–190.

BRUNS, R.F., FERGUS, J.H., BADGER, E.W., BRISTOL, J.A., SANTAY, L.A., HARTMAN, J.D., HAYS, S.J. & HUANG, C.C. (1987). Binding of the A1-selective adenosine antagonist 8-cyclopentyl-1,3-dipropylxanthine to rat membranes. *Naunyn-Schmied. Arch. Pharmacol.*, **335**, 59–63.

CARTMELL, J., KEMP, J.A., ALEXANDER, S.P.H., HILL, S.J. & KENDALL, D.A. (1992). Inhibition of forskolin-stimulated cyclic AMP formation in guinea-pig cerebral cortical slices by ACPD. *J. Neurochem.*, **58**, 1964–1966.

CHENG, Y.-C. & PRUSOFF, W.H. (1973). Relationship between the inhibition constant (Ki) and the concentration of inhibitor which causes 50 per cent inhibition (I50) of an enzymatic reaction. *Biochem. Pharmacol.*, **22**, 3099–3108.

DALY, J.W., BUTTS-LAMB, P. & PADGETT, W. (1983). Subclasses of adenosine receptors in the central nervous system: interaction with caffeine and related methylxanthines. *Cell. Mol. Neurobiol.*, **3**, 69–80.

DICKENSON, J.M. & HILL, S.J. (1993). Intracellular cross-talk between receptors coupled to phospholipase C via pertussis toxin-sensitive and pertussis toxin-insensitive G-proteins in DDT1MF-2 cells. *Br. J. Pharmacol.*, **109**, 719–724.

DUNWIDDIE, T.V. & FREDHOLM, B.B. (1985). Adenosine modulation of synaptic responses in rat hippocampus: possible role of inhibition or activation of adenylate cyclase. *Adv. Cyc. Nuc. Prot. Phos. Res.*, **19**, 259–272.

FREDHOLM, B.B., JONZON, B., LINDGREN, E. & LINDSTROEM, K. (1982). Adenosine receptors mediating cyclic AMP production in the rat hippocampus. *J. Neurochem.*, **39**, 165–175.

FREDHOLM, B.B., JONZON, B. & LINDSTROEM, K. (1986). Effect of adenosine receptor agonists and other compounds on cyclic AMP accumulation in forskolin-treated hippocampal slices. *Naunyn-Schmied. Arch. Pharmacol.*, **332**, 173–178.

GERWINS, P., NORDSTEDT, C. & FREDHOLM, B.B. (1990). Characterization of adenosine A1 receptors in intact DDT1 MF-2 smooth muscle cells. *Mol. Pharmacol.*, **38**, 660–666.

HERNÁNDEZ, F., KENDALL, D.A. & ALEXANDER, S.P.H. (1993). Adenosine receptor-induced second messenger production in the adult guinea-pig cerebellum. *Br. J. Pharmacol.*, **110**, 1085–1100.

HILL, S.J. & KENDALL, D.A. (1987). Studies on the adenosine-receptor mediating the augmentation of histamine-induced inositol phospholipid hydrolysis in guinea-pig cerebral cortex. *Br. J. Pharmacol.*, **91**, 661–669.

IREDALE, P.A., ALEXANDER, S.P.H. & HILL, S.J. (1994). Coupling of a transfected human brain A1 adenosine receptor in CHO-K1 cells to calcium mobilisation via a pertussis toxin-sensitive mechanism. *Br. J. Pharmacol.*, **111**, 1252–1256.

JACOBSON, K.A., VAN GALEN, P.J.M. & WILLIAMS, M. (1992). Adenosine receptors: pharmacology, structure-activity relationships, and therapeutic potential. *J. Med. Chem.*, **35**, 407–422.

KLOTZ, K.-N., KEIL, R., ZIMMER, F.J. & SCHWABE, U. (1990). Guanine nucleotide effects on 8-cyclopentyl-1,3-[3H]dipropylxanthine binding to membrane-bound and solubilized A1 adenosine receptors of rat brain. *J. Neurochem.*, **54**, 1988–1994.

KLOTZ, K.-N., VOGT, H. & TAWFIK-SCHLIEPER, H. (1991). Comparison of A1 adenosine receptors in brain from different species by radioligand binding and photoaffinity labelling. *Naunyn-Schmied. Arch. Pharmacol.*, **343**, 196–201.

LOHSE, M.J., KLOTZ, K.-N., LINDENBORN-FOTINOS, J., REDDINGTON, M., SCHWABE, U. & OLSSON, R.A. (1987). 8-cyclopentyl-1,3-dipropylxanthine (DPCPX) – a selective high affinity antagonist radioligand for A1 adenosine receptors. *Naunyn-Schmied. Arch. Pharmacol.*, **336**, 204–210.

LONDOS, C., COOPER, D.M.F. & WOLFF, J. (1980). Subclasses of external adenosine receptors. *Proc. Natl. Acad. Sci. USA*, **77**, 2551–2554.

PARSONS, W.J., RAMKUMAR, V. & STILES, G.L. (1988). The new cardiotonic agent sulmazole is an A1 adenosine receptor antagonist and functionally blocks the inhibitory regulator, Gi. *Mol. Pharmacol.*, **33**, 441–448.

PRATER, M.R., TAYLOR, H., MUNSHI, R. & LINDEN, J. (1992). Indirect effect of guanine nucleotides on antagonist binding to A_1 adenosine receptors: occupation of cryptic sites by endogenous vesicular adenosine. *Mol. Pharmacol.*, **42**, 765–772.

RAMKUMAR, V. & STILES, G.L. (1988a). A novel site of action of a high affinity A1 adenosine receptor antagonist. *Biochem. Biophys. Res. Commun.*, **153**, 939–944.

RAMKUMAR, V. & STILES, G.L. (1988b). Reciprocal modulation of agonist and antagonist binding to A_1 adenosine receptors by guanine nucleotides is mediated via a pertussis toxin-sensitive G protein. *J. Pharmacol. Exp. Ther.*, **246**, 1194–1200.

SALOMON, Y., LONDOS, C. & RODBELL, M. (1974). A highly sensitive adenylate cyclase assay. *Anal. Biochem.*, **58**, 541–548.

SCHIEMANN, W.P., WALTHER, J.M. & BUXTON, I.L.O. (1990). On the ability of endogenous adenosine to regulate purine nucleoside receptor binding of antagonists in smooth muscle membranes. *J. Pharmacol. Exp. Ther.*, **255**, 886–892.

SCHUBERT, P., REDDINGTON, M. & KREUTZBERG, G.W. (1979). On the possible role of adenosine as a modulatory messenger in the hippocampus and other regions of the CNS. *Prog. Brain. Res.*, **51**, 149–165.

SCHWABE, U. & TROST, T. (1980). Characterization of adenosine receptors in rat brain by (−)[^{3}H]N6-phenylisopropyladenosine. *Naunyn-Schmied. Arch. Pharmacol.*, **313**, 179–187.

SHAW, C.A. & WILKINSON, M. (1994). Receptor characterization and regulation in intact tissue preparations. Pharmacological implications. *Biochem. Pharmacol.*, **47**, 1109–1119.

STILES, G.L. (1988). A_1 Adenosine receptor-G protein coupling in bovine brain membranes: effects of guanine nucleotides, salt and solubilization. *J. Neurochem.*, **51**, 1592–1598.

STROEHER, M., NANOFF, C. & SCHÜTZ, W. (1989). Differences in the GTP-regulation of membrane-bound and solubilised A_1-adenosine receptors. *Naunyn-Schmied. Arch. Pharmacol.*, **340**, 87–92.

VAN CALKER, D., MUELLER, M. & HAMPRECHT, B. (1979). Adenosine regulates via two different types of receptors, the accumulation of cyclic AMP in cultured brain cells. *J. Neurochem.*, **33**, 999–1005.

(Received November 29, 1993
Revised July 10, 1994
Accepted August 22, 1994)

Br. J. Pharmacol. (1994), **113**, 1508–1514 © Macmillan Press Ltd, 1994

Nitric oxide formation from glyceryl trinitrate by rabbit aortic strip: detection by rabbit taenia coli concurrent with vasorelaxation

Aman S. Hussain, Margo Poklewska-Koziell, James F. Brien, Gerald S. Marks & [1]Kanji Nakatsu

Department of Pharmacology and Toxicology, Faculty of Medicine, Queen's University, Kingston, Ontario, Canada K7L 3N6

1 The purpose of the present study was to assay NO formation from GTN biotransformation by the rabbit aortic strip (RAS) at times concurrent with its vasorelaxation. Such an assay is an important test of the prodrug hypothesis where it is postulated that glyceryl trinitrate (GTN) is biotransformed to nitric oxide (NO), the active species that initiates vascular smooth muscle relaxation. To test such a hypothesis, we propose that a sample of smooth muscle, poorly responsive to GTN, yet sensitive to the effects of NO could be used to detect RAS production of NO from GTN.

2 Muscle strips of rabbit taenia coli (RTCS) and RAS in close apposition, were mounted in tissue baths, and muscle relaxation was recorded with isometric force transducers. Tissues were submaximally precontracted with 30–35 mM K^+ depolarizing solution and exposed to increasing concentrations of GTN (0.1 nM–10 μM).

3 EC_{25} for GTN-induced relaxation of RTCS in the presence of RAS was significantly decreased to that for RTCS in the absence of RAS ($5.9 \pm 3.0 \times 10^{-8}$ M and $5.5 \pm 3.7 \times 10^{-6}$ M, respectively). Mean maximal levels of GTN-induced relaxation of similarly precontracted RTCS also differed in the presence and absence of RAS, viz., $80.8 \pm 2.1\%$ and $29.8 \pm 8.3\%$ respectively.

4 RTCS was found to relax upon administration of NO gas bubbled through the incubation medium. Analysis of tissue bath medium revealed that the NO concentration to which RTCS was exposed attained a maximum of 33 nM. Relaxation of RTCS by NO gas was inhibited by 1 μM reduced haemoglobin.

5 For GTN-incubation with intestinal and vascular smooth muscle preparations, NO formation was greater with RAS compared to RTCS. Thus, in the two-issue bioassay, the RAS was the predominant source of NO formation from GTN.

6 Reduced deoxyhaemoglobin (1 μM), a potent extracellular NO scavenger, was found to decrease the augmented GTN-induced relaxation in the RTCS-RAS sandwich preparation from $17.3 \pm 1.8\%$ to $8.0 \pm 0.8\%$. The augmented RTCS response was restored upon washout and subsequent addition of GTN, in the absence of reduced Hb.

7 These data indicate that nitric oxide or a closely related NO-donor is produced by vascular biotransformation of GTN as seen by the increased sensitivity of RTCS to GTN when in the presence of RAS. The results of this bioassay thus support the GTN-NO prodrug hypothesis.

Keywords: glyceryl trinitrate; biotransformation; nitric oxide; vasodilatation

Introduction

The vasodepressor action of organic nitrates, such as glyceryl trinitrate (GTN) have been well documented for over 130 years and they have been used successfully for treatment of angina, hypertensive emergencies and acute congestive heart failure. In spite of considerable progress in the last decade, our understanding of their exact mechanism of action remains incomplete.

Endothelium-independent mediated vasodilation by glyceryl trinitrate (GTN) is believed to effect its *in vivo* hypotensive action via intracellular biotransformation to nitric oxide (NO) in vascular smooth muscle (Ignarro *et al.*, 1981). This proposed prodrug hypothesis of GTN-induced vasorelaxation involves denitration of GTN to glyceryl-1,2-dinitrate and /or glyceryl-1,3-dinitrate with the attendant formation of the free radical NO. It is believed that NO activates soluble guanylyl cyclase (Diamond & Holmes, 1975; Katsuki *et al.*, 1977; Murad *et al.*, 1978; Gruetter *et al.*, 1981), thereby elevating guanosine 3':5'-cyclic monophosphate (cyclic GMP) levels and lowering intracellular free Ca^{2+} concentration, which results in smooth muscle relaxation. Although the actual bioactivation pathway of GTN to NO remains uncertain, several hypotheses have been put forward. These include enzymatic metabolism by cytosolic glutathione-*S*-transferases (Needleham *et al.*, 1969; Hill *et al.*, 1992), non-enzymatic formation of NO by thiol-containing compounds such as cysteine (Feelisch & Noack, 1987) and haemoprotein-mediated GTN biotransformation (Bennett *et al.*, 1986; Marks *et al.*, 1989).

Because of the uncertainty surrounding metabolic activation of GTN, substantial research has been conducted to test the original prodrug hypothesis proposed by Ignarro and colleagues (1981). Accordingly, previous studies from our laboratory have shown that rabbit aortic strip (RAS) biotransformation of [^{14}C]-GTN occurs concurrently with relaxation of vascular tissue (Brien *et al.*, 1986). Subsequent experiments using [^{3}H]-GTN of high specific activity demonstrated time-dependent biotransformation of [^{3}H]-GTN to [^{3}H]-GDN by isolated RAS during a 30 s time course, with a positive correlation between the incubation time of RAS with GTN and the magnitude of biotransformation of the organic nitrate. This study also showed that significant biotransformation of GTN as well as elevation of cylic GMP content occurs at least concurrently with the onset of vasodilatation

[1]Author for Correspondence.

(Brien *et al.*, 1988). This established a relationship between GTN biotransformation, tissue cyclic GMP elevation, and relaxation of rabbit aorta consistent with the proposed multistep action of GTN. A subsequent study by Kawamoto *et al.* (1990) confirmed this temporal relationship, in which biotransformation of GTN and cyclic GMP elevation preceded vasodilatation.

Although the above observations are consistent with the prodrug hypothesis, the critical observation of NO formation had not been tested. This was due mainly to technical problems; nitric oxide is a gas and has a short half-life in biological preparations (Palmer *et al.*, 1987). Additionally, it is necessary to analyse NO in the presence of other nitrogen oxides like NO_2^-, which are also produced during GTN metabolism. Nevertheless, the advent of a sensitive chemiluminescence method for NO revealed that the headspace gas in a flask containing bovine pulmonary artery incubated with GTN contained picomole quantities of nitric oxide (Marks *et al.*, 1992). This was the first direct chemical measurement of NO formation during the incubation of vascular tissue with GTN, and further supported the idea that organic nitrates elicit vascular smooth muscle relaxation via their biotransformation to NO.

The effects of NO are not limited to blood vessels, as non-vascular smooth muscle, including guinea-pig trachea, jejunum, rabbit colon, and bovine retractor penis appear to be relaxed by endogenously produced NO (Li & Rand, 1990; Stark *et al.*, 1993; Martin *et al.*, 1988). Such smooth muscle, if unresponsive to GTN yet sensitive to NO, can act as an assay for vascular conversion of GTN to NO *in vitro*. The GTN prodrug hypothesis predicts that NO generated in vascular tissue should diffuse out of the tissues in which it is formed and be subject to bioassay. To this end, a two tissue bioassay consisting of GTN-responsive and non-responsive tissue was used to test for NO formation during interaction of GTN with vascular tissue. We present data which demonstrate that NO or a NO-releasing intermediate was formed from GTN by vascular tissue. These findings are consistent with the prodrug hypothesis of GTN-induced vasodilatation.

Methods

Rabbit aortic strips (RAS) and rabbit taenia coli strips (RTCS)

Male New Zealand White rabbits (3.3–4.0 kg body weight) were killed by sodium pentobarbitone overdose (250 mg kg^{-1}) via rapid ear vein injection. The descending thoracic aorta was immediately removed and placed in ice cold Krebs solution. After adipose and connective tissue were gently removed, the aorta was then cut helically into a single strip from which smaller strips were obtained (5 mm wide by 30 mm long). In order to remove endothelium, the intimal surfaces of the aortic strips were gently rubbed for 30 s with a cotton swab moistened in Krebs solution. Endothelium-denuded rabbit aortic strips were found to contract in the presence of 1 μM acetylcholine. Taenia coli taken from the proximal portion of the large intestine was cut into smaller strips, 5 mm wide by 30 mm long. Animals used in this experiment were cared for in accordance with the principles and guidelines of the Canadian Council on Animal Care.

Cumulative concentration-response relationships for GTN, ISDN, SNP, SIN-1, and SNAP in RAS and RTCS

RAS and RTCS, were suspended by use of polyester sutures in individual tissue baths containing 10 ml Krebs solution at 37°C, through which 95% O_2:5% CO_2 was continuously bubbled. RAS and RTCS were maintained at preload tension of 2 g. Tissues were equilibrated for 1 h during which time the Krebs solution was replaced every 15 min. The maximum contraction for each tissue was elicited by exposure to 100 mM K^+, then the tissues were equilibrated further for 1 h. To determine the relaxant effects of the nitrovasodilator drugs, the tissues were first contracted submaximally (60–70% of maximum) with K^+ added in 5 mM increments to a final concentration 35–40 mM. Cumulative concentration-response curves were determined for RAS and RTCS with GTN, ISDN, SNP, SIN-1, and SNAP (0.1 nM to 10 μM). Isometric changes in tension of RAS and RTCS were recorded by force-displacement transducers (Grass FT03D) coupled to a Grass Model 7 polygraph (Quincy, Massachussetts, U.S.A.).

To determine the formation of NO or a NO derivative from a nitrovasodilator agent during incubation with RAS, a bioassay tissue, viz. RTCS, was mounted in close apposition to the vascular tissue strip such that the long axes of both strips were vertical, i.e. sandwich preparation (Furchott & Zawadzki, 1981). To avoid extraneous non-nitrovasodilator sources of NO, the endothelium was removed from the RAS. The sandwich preparation was incubated in a Krebs-filled tissue bath, kept at a constant temperature of 37°C and aerated with 95% O_2:5% CO_2. Controls consisted of individual RAS and RTCS strips treated with dilator agents in separate baths.

Preparation of reduced haemoglobin

A 250 mg mixture of reduced and oxidised beef haemoglobin (Type I, No. H-2500, Sigma Chemical Co., St. Louis, Missouri, U.S.A.) was dissolved in 5 ml of 0.05 M phosphate buffer, pH 7.4, containing 5×10^{-4} M EDTA. Phosphate buffer was deoxygenated with nitrogen gas and kept on ice. Reduced Hb solution was obtained by addition of sodium dithionite to the freshly prepared crude Hb solution until a colour change from reddish brown to purple occurred. Excess dithionite was removed via gel filtration on a Sephadex G-25-M column of 1.2 cm by 9 cm (Pharmacia Fine Chemicals, Dorval, Quebec, Canada). Dithionite removal was confirmed spectrophotometrically by monitoring absorbance at 312 to 314 nm. The concentration of Hb was determined spectrophotometrically at 540 nm by the method of Van Kampen & Zijlstra (1961), in which haemoproteins are converted to their cyanomet derivatives and assayed using an extinction coefficient of 44.0 $mM^{-1} \times cm^{-1}$.

Chemiluminescence measurement of NO

To detect NO formation chemically from RTCS and RAS incubated with GTN a modified chemiluminescence-headspace gas method was employed (Brien *et al.*, 1991). To a 6.2 ml micro-Fernbach flask (Kimax, Fisher Scientific, Toronto, Ontario, Canada) was added 3 ml Krebs buffer, 0.1 ml of 2000 units ml^{-1} SOD (final concentration 100 units ml^{-1}), 0.03 ml of 3 M KCl (final concentration of 30 mM), for strips of RAS and RTCS, and a micro-stir bar to stir the sample continually during deoxygenation and incubation with GTN. The flask was sealed with a rubber-sleeve septum (Aldrich Chemical Co. Inc., Milwaukee, Wisconsin, U.S.A.), and deoxygenation was achieved with a stream of 95% Ar:5% CO_2 positioned 1 cm above fluid level for 5 min. Eight 100 μl aliquots of GTN solution (diluted to 3 mM with Krebs solution), previously degassed for 3 min, was added to the flask via injection through the septum (final concentration of GTN, 1 mM). After 2, 5, 10, or 20 min, 400 μl aliquots of headspace gas were drawn via an air-tight syringe and injected into a model 270A Nitric Oxide Analyzer (Sievers Research, Inc., Boulder, Colorado, U.S.A.). A control experiment was performed following the same protocol except that GTN vehicle (propylene glycol, ethanol) was added instead of active drug. The amount of NO was calculated by interpolation of the chemiluminescence signal on a NO standard curve (52–1618 pmol, $r = 0.99$) and was corrected with the use of the appropriate blank. Separate stan-

dard curves were prepared for each experiment. NO content was expressed as picomol of NO per g wet weight tissue.

Drugs and solutions

Krebs solution contained the following (mM): NaCl 120, KCl 5.6, $MgSO_4$ 1.2, NaH_2PO_4 1.2, $CaCl_2$ 2.5, $NaHCO_3$ 25, and dextrose 10; 30 μM ethylenediaminetetraacetic acid (EDTA) also was added. The above solution was aerated with 95% O_2:5% CO_2 (medical grade: Union Carbide Canada Ltd., Linde Division, Toronto, Ontario, Canada). Stock soltuions of GTN (2.2×10^{-2} M) were obtained from Dupont (Toronto, Ontario, Canada) as Tridil. Sodium nitroprusside (SNP) and bovine liver superoxide dismutase (SOD) were obtained from Sigma Chemical Co. (St. Louis, Missouri, U.S.A.). Isosorbide dinitrate (ISDN) was obtained from Wyeth Ltd. (Toronto, Ontario, Canada) and 3-morpholino-sydnonimine (SIN-1, an active metabolite of molsidomine) was received as a gift from Cassella AG (Frankfurt, Germany). S-Nitroso acetylpenicillamine (SNAP) was obtained from Colour Your Enzyme (Bath, Ontario, Canada). Stock solutions of SNP, SNAP, and SIN-1 were prepared by dissolving in Krebs solution while the ISDN stock solution was prepared using acetone. All working dilutions of the above drugs were done on the day of experimentation using Krebs solution, and all stock solutions and dilutions were kept on ice. Authentic NO gas (5% NO:95% N_2) was obtained from Scotts Specialty Gases (Detroit, Michigan, U.S.A.). All other chemicals used were at least reagent grade and obtained from BDH Chemical Canada Ltd. (Toronto, Ontario, Canada).

Data analysis

The data are presented as the group means ± s.d. Statistical analysis of tissue relaxation, $EC_{25/50}$, and NO formation data was conducted by Student's uncorrelated sample *t* test where dependent variables RTCS relaxation or amounts of NO formed were considered to be statistically different from controls when $P \leqslant 0.05$ (Zivin & Bartko, 1976). Data from GTN, ISDN, SNP, SIN-1 and SNAP concentration-response curves of RTCS, and haemoglobin inhibition experiments were subject to randomized designed one-way analysis of variance (ANOVA) followed by *post hoc* Newman-Keuls test for a significant *F*-statistic ($P < 0.05$). In all analyses, homogeneity of variance was evaluated by *F*-statistic for Student's *t* test or by Bartlett's test for one-way ANOVA analyses.

Results

Nitrovasodilator-induced relaxation of rabbit taenia coli strips (RTCS)

Preliminary experiments involving tests of various smooth muscle preparations showed RTCS to be non-responsive to GTN relative to RAS. Cumulative concentration-response relationships for ISDN (Figure 1a) revealed that the maximal relaxation achieved was not statistically different from that elicited by GTN (35.4 ± 2.4% and 35.0 ± 2.4%, respectively). Thus, both these vasodilators which are believed to undergo similar bioactivation paths (Feelisch & Noack, 1991) were found to be similarly effective relaxants of rabbit taenia coli. Treatment of RTCS with nitrovasodilators such as SNP, SNAP, and SIN-1 (Figure 1b), agents that are thought to form NO in a manner different from organic nitrates, produced concentration-response profiles distinct from GTN and ISDN. SNP, SIN-1, and SNAP-treated samples induced maximal relaxations of 64.7 ± 3,2%, 70.1 ± 2.5%, and 66.2% ± 4.8% ($n = 4$), respectively, which were greater than that induced by GTN ($P < 0.01$).

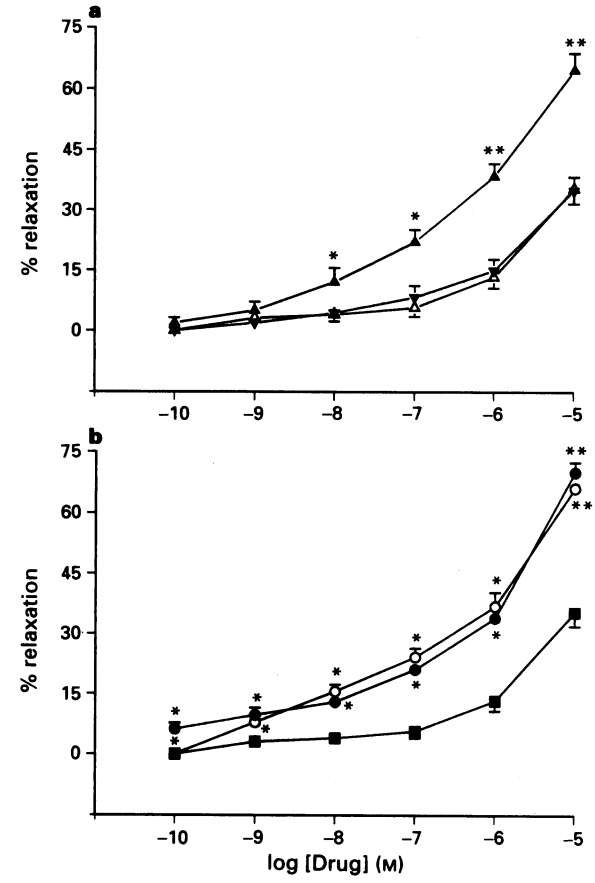


Figure 1 (a) Strips of rabbit taenia coli (RTCS) submaximally precontracted with K^+ relaxed to increasing concentrations of SNP (▲) and shifted concentration-response curve to the left relative to GTN (▼). ISDN (△), a nitrate ester, produced relaxations similar to GTN-treated RTCS as reflected by the similar concentration-response profiles. The submaximal levels of precontraction ± s.d. for GTN, ISDN and SNP treatments were 69 ± 3%, 73 ± 3% and 71 ± 5%, respectively. (b) Submaximally precontracted RTCS treated with increasing concentrations of SIN-1 (●) and SNAP (○) produced concentration-response profiles shifted to the left compared to that of RTCS treated with GTN (■). The submaximal levels of precontraction ± s.d. for GTN, SNAP and SIN-1 treatments were 68 ± 3%, 71 ± 2% and 67 ± 6% of maximal K^+ contraction, respectively. RTCS appears to be relatively non-responsive to nitrate esters, GTN and ISDN, requiring tissue biotransformation, yet responsive to direct NO-donors such as SNP, SNAP, and SIN-1. Mean relaxations for five experiments are shown with standard deviations. Significant differences in relaxation to SNP, SNAP, SIN-1, and ISDN from GTN response at each concentration were tested by randomized one-way ANOVA; $^*P < 0.05$, $^{**}P < 0.01$. For abbreviations, see text.

Effect of RAS on relaxation of RTCS by GTN

When RTCS was incubated in the presence of RAS, its responsiveness to GTN increased significantly. This increase in GTN-induced relaxation was concentration-related as shown in Figures 2a and 2b. Maximal GTN-induced relaxation were also observed to differ notably between RTCS of the bioassay and RTCS alone (80.8 ± 2.1% and 29.8 ± 8.0%, respectively ($P < 0.01$, $n = 5$)). Highly significant differences were also seen between the EC_{25} of GTN of RTCS of bioassay and its control ($5.9 \pm 3.0 \times 10^{-8}$ M versus $5.5 \pm 3.7 \times 10^{-6}$ M, $P < 0.01$, $n = 5$). EC_{25} instead of EC_{50} was analysed as GTN-treated RTCS could not attain 50% relaxation.

In contrast to GTN, the presence of RAS had no effect on the relaxation of RTCS induced by SNAP as seen in Figure 2c. Cumulative concentration-response profiles revealed no

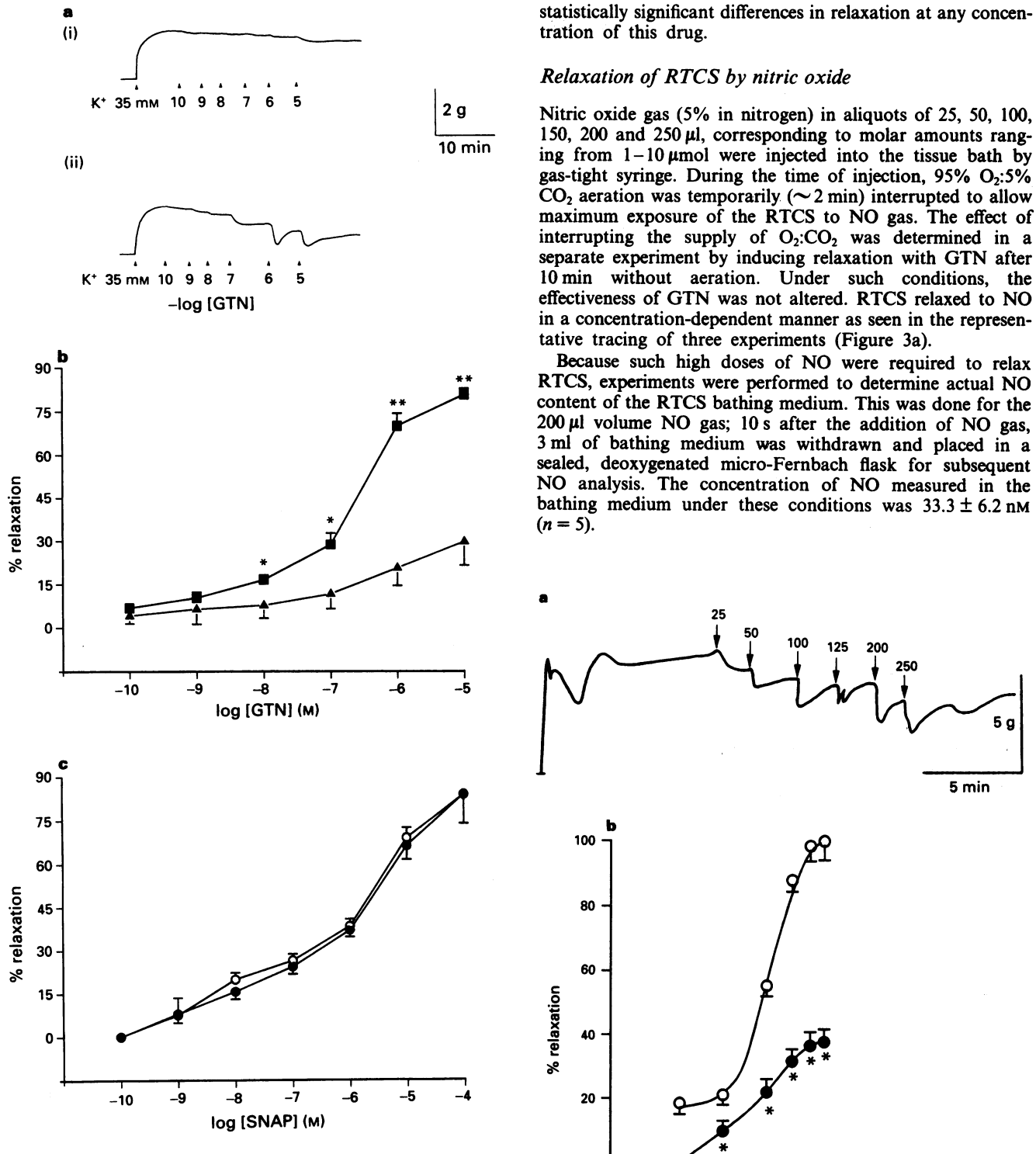


Figure 2 (a) Representative polygraph tracing of (i) strips of rabbit taenia coli (RTCS) in its own tissue bath and (ii) RTCS in the presence of rabbit aortic strip (RAS), viz. sandwich preparation. Both tissues submaximally precontracted with 35 mM K^+ with increasing concentrations of GTN (0.1 nM–10 μM) in a cumulative manner. Note different patterns of relaxation between the tissues. Each numbered event marker indicates logarithm of GTN concentration. (b) GTN concentration-response profiles of RTCS in the presence (■) and absence (▲) of RAS ($n = 5$). Levels of submaximal precontraction ± s.d. by K^+ for the treatment groups were 73 ± 6% and 71.5 ± 5% of maximal K^+ contraction, respectively. (c) SNAP concentration-response profiles of RTCS in the presence (●) (precontracted 63 ± 5% of KCl max) and absence (○) (precontracted 65 ± 2% of KCl max) of RAS representing the mean of four experiments with standard deviations. Significant differences in GTN-induced relaxation between RTCS with RAS and its control at each concentration were tested by randomized one-way ANOVA; $*P < 0.05$; $**P < 0.01$. For abbreviations, see text.

statistically significant differences in relaxation at any concentration of this drug.

Relaxation of RTCS by nitric oxide

Nitric oxide gas (5% in nitrogen) in aliquots of 25, 50, 100, 150, 200 and 250 μl, corresponding to molar amounts ranging from 1–10 μmol were injected into the tissue bath by gas-tight syringe. During the time of injection, 95% O_2:5% CO_2 aeration was temporarily (~2 min) interrupted to allow maximum exposure of the RTCS to NO gas. The effect of interrupting the supply of O_2:CO_2 was determined in a separate experiment by inducing relaxation with GTN after 10 min without aeration. Under such conditions, the effectiveness of GTN was not altered. RTCS relaxed to NO in a concentration-dependent manner as seen in the representative tracing of three experiments (Figure 3a).

Because such high doses of NO were required to relax RTCS, experiments were performed to determine actual NO content of the RTCS bathing medium. This was done for the 200 μl volume NO gas; 10 s after the addition of NO gas, 3 ml of bathing medium was withdrawn and placed in a sealed, deoxygenated micro-Fernbach flask for subsequent NO analysis. The concentration of NO measured in the bathing medium under these conditions was 33.3 ± 6.2 nM ($n = 5$).

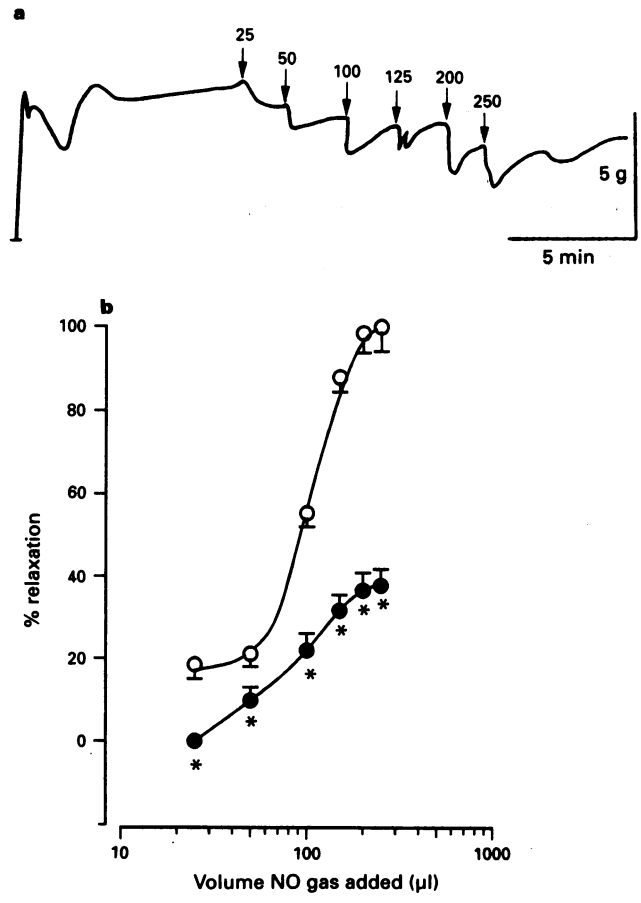


Figure 3 (a) Potassium (30–35 mM), precontracted strips of rabbit taenia coli (RTCS) relaxed in a dose-dependent manner to 5% NO gas. Each solid event marker indicates volume (μl) of NO bubbled directly into the tissue medium. These volumes of gas added to the bath represent a molar amount of NO ranging from (1–10 μmol). (b) NO gas dose-response curves of RTCS in the presence (●) and absence (○) of 1 μM Hb ($n = 3$). Significant differences in NO-induced relaxation between Hb treated and untreated RTCS at each concentration were tested by randomized one-way ANOVA; $*P < 0.01$. For abbreviations, see text.

Effect of haemoglobin on taenia coli

To test that the active agent that diffuses from the donor tissue to the recipient was indeed NO or some precursor thereof, reduced haemoglobin was used as a potent scavenger of NO. Reduced haemoglobin (1 μM) was added to the tissue bath of the RAS-RTCS sandwich preparation. After incubation with Hb for 2 min, 30 nM GTN was added to submaximally contracted tissue. Hb blunted the relaxation of the RTCS in the sandwich preparation (7.9 ± 0.8%, $n = 4$) compared with the Hb-free preparation (17.3 ± 1.8%, $n = 4$, $P < 0.01$) (Figure 4). However, when the Hb-treated preparation was washed, allowed to equilibrate for 1 h and treated with another concentration of GTN, the relaxation achieved was almost restored to the original level (14.51 ± 2.28%, $n = 4$) and found to be significantly different from the Hb-treated preparation ($P < 0.01$).

Hb inhibited the relaxation of RTCS induced by exposure of the tissue to authentic NO gas (Figure 3b). Relaxation of RTCS with isoprenaline, a NO-independent relaxant, was found to be unaffected by the presence of Hb; at a concentration of 10 nM, isoprenaline relaxed the RTCS of the sandwich preparation 33.1 ± 1.8% in the absence of Hb, and 32.2 ± 0.7% in the presence of 1 μM Hb.

Nitric oxide formation from incubation of GTN with RTCS and RAS

To test if NO from GTN was the active agent produced by the donor tissue to relax the recipient tissue, chemiluminescence analysis of the headspace gas in a sealed incubation system was conducted. The individual RAS and RTCS were suspended in tissue baths as described for the concentration-response protocol, and allowed to equilibrate for 1 h. The tissues were exposed to a maximal concentration of K^+, washed, allowed to equilibrate further and then treated with a submaximal concentration of K^+ (65-75% of maximal tone). Subsequently, each tissue was rinsed with Krebs solution and placed in a sealed micro-Fernbach flask for chemiluminescence determination of NO formation from GTN. NO formation profiles from the two smooth muscle samples differed significantly (Figure 5). At 2 min, there was no measurable NO formation in either RAS or RTCS. At 5 min, NO formation in the RAS sample was 205 pmol g^{-1} tissue (wet weight), whereas for RTCS there was still no measurable NO found. Only at 10 and 20 min sample points was there NO formation for the incubation of GTN with RTCS. At these time points, NO formation from GTN by the RAS was substantially greater than that for the RTCS (313, 564 pmol g^{-1} and 102, 322 pmol g^{-1}, respectively; $n = 3$, $P < 0.01$).

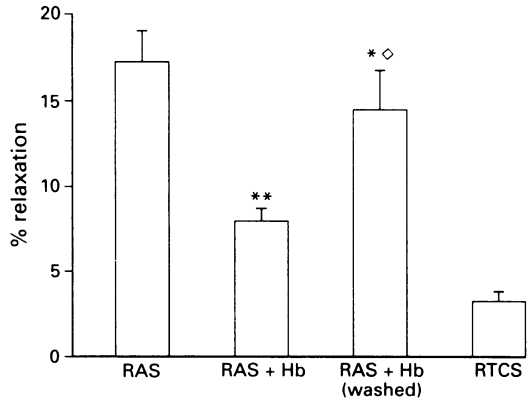


Figure 4 Effect of 30 nM GTN on strips of rabbit taenia coli (RTCS) in the presence of rabbit aortic strip (RAS) and reduced deoxyhaemoglobin (1 μM) and RTCS in the presence of RAS without of Hb. Inhibition of RTCS by Hb was partially restored upon washout, precontraction and exposure to 30 nM GTN. Relaxation of RTCS alone to the same concentration of GTN is shown for comparison. Mean levels of submaximal precontraction as % of KCl max ± s.d. for each group were as follows: RAS (72 ± 6%), RAS + Hb (73 ± 3%), RAS + Hb, washed (73 ± 6%) and RTCS alone (68 ± 3%). Mean relaxations for four experiments are shown with standard deviations. Significant differences in relaxation of Hb-treated bioassay, washed bioassay from the untreated control sandwich preparation were tested by randomized one-way ANOVA; $*P < 0.05$, $**P < 0.01$. Significant difference between Hb-treated sandwich preparation and the washed bioassay preparation were established by one-way ANOVA and denoted by $*P < 0.01$. For abbreviations, see text.

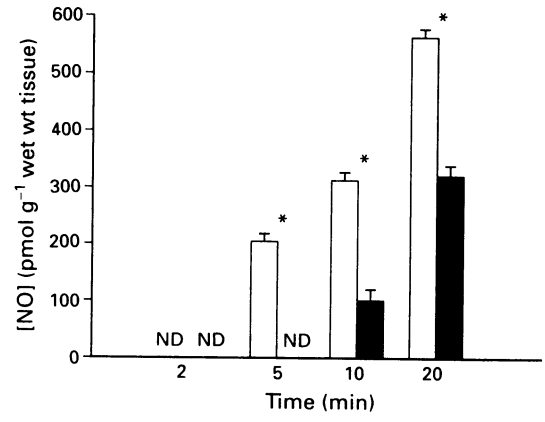


Figure 5 Comparison of NO release by strips of rabbit taenia coli (RTCS) (solid columns) and rabbit aortic strip (RAS) (open columns) as measured by headspace chemiluminescence detection at different times of incubation with GTN (100 μM). At 5, 10, and 20 min, greater levels of NO was detected in samples of GTN-treated RAS compared to GTN-treated RTCS. Levels of NO detected are expessed as pmol of NO g^{-1} tissue (wet weight). Time points at which no NO was detectable are denoted as ND. Data are presented as the mean of three experiments with standard deviations. Differences in NO release between RAS and RTCS at each sampling time point were tested by uncorrelated Student's t test and are denoted by $*P < 0.01$. For abbreviations, see text.

Discussion

One objective of the present work was to test further the prodrug hypothesis of organonitrate action. Specifically, the experiments were designed to determine if GTN was metabolically activated to form the putative ultimate drug, NO, or some derivative. Experiments conducted in our laboratory over the past several years have yielded observations that are consistent with the idea that GTN is biotransformed to an ultimate vascular smooth muscle relaxant and glyceryl-1,2-dinitrate and/or glyceryl-1,3-dinitrate (Brien *et al.*, 1986; 1988; Kawamoto *et al.*, 1990). Nevertheless, it has not been possible to demonstrate the formation of NO by vascular tissue prior to the onset of relaxation. Recently our laboratory was able to observe the formation of NO from GTN during incubation with bovine pulmonary artery (Marks *et al.*, 1992); the earliest time point at which NO was quantitated in that study was after 5 min of incubation. With chemiluminescence, part of the difficulty in being able to measure NO after its formation within isolated blood vessel strips is the fact that this small molecule must diffuse from the tissue into the aqueous bathing medium, and from there into the overlying headspace. The aim of the study described here was to determine if we could monitor vascular smooth muscle activation of GTN to NO within a shorter time frame and at lower concentrations of GTN than were required to observe NO formation by the headspace chemiluminescence assay.

The first requirement of the study was to identify a smooth muscle preparation that responded to agents that are known to release NO and yet do not respond to GTN. Preliminary experiments entailing tests of various samples of smooth muscle, including small intestine, trachea, and taenia coli, indicated that rabbit taenia coli precontracted with KCl was least responsive to the effects of GTN. KCl was the contracting agent of choice in tests with RTCS, as this agent produced a reproducible contraction whereas histamine, carbachol, and acetylcholine did not; unlike blood vessels, α-adrenoceptor agonists such as phenylephrine were not useful. To examine further the basis of this lack of response to GTN, rabbit taenia coli strips (RTCS) were tested with ISDN, another organic nitrovasodilator that appears to undergo metabolism similar to that of GTN (Johnson *et al.*, 1972), and SNP, a compound that forms NO by a mechanism different from GTN (Tinker & Michenfelder, 1976). Additionally, SIN-1 and SNAP, two chemically distinct releasers of NO, were tested on RTCS. While resistant to the effects of ISDN, RTCS was sensitive to SNP, SNAP, and SIN-1. These observations were taken to mean that rabbit taenia coli is non-responsive to the effects of GTN due to insufficient bioactivation rather than lack of sensitivity to NO. Of all nitrovasodilators tested, maximal RTCS relaxations were lowest with GTN and ISDN. This indicates that RTCS has a low capacity for metabolic activation of organic nitrate esters like GTN or ISDN, yet it was sensitive to compounds that release NO in solution. Thus, the RTCS was considered to be a suitable assay tissue for vascular smooth muscle biotransformation of GTN to NO.

The sandwich biassay preparation consisting of RAS and RTCS was treated with increasing concentrations of GTN, with RTCS in its own bath treated with GTN serving as a control. Such a setup was designed to test the prodrug hypothesis where such a paradigm predicts that the RAS can biotransform GTN to NO which then diffuses to the recipient assay tissue, eliciting relaxation. Observations that the presence of RAS enhanced GTN-induced relaxation of RTCS support the prodrug hypothesis. The inability of RAS to enhance the relaxant effects of SNAP, a nitrosothiol that generates NO without the requirement of vascular tissue activation (Feelisch & Noack, 1991), indicate that the liberation of an enhancing factor from RAS alone could not account for the ability of RAS to increase the relaxation response of RTCS to GTN. Thus, our observations do not support the possibility of functional antagonism due to the presence of RAS. Additional evidence to support this position arises from the observations that submaximal contractions to KCl were not significantly different in the presence of RAS (Figures 2b and 2c). Taking into consideration all of these results, we interpret this to mean that RAS acted by virtue of its ability to activate metabolically GTN.

To confirm that this GTN-derived relaxing factor diffusing from the donor tissue (RAS) to the recipient tissue (RTCS) was NO, it was important to show that RTCS could relax to authentic NO. Direct injection of NO (52–1400 pmol) produced no relaxant effects in the absence or presence of SOD, which increases NO-induced relaxation. However, higher doses of NO (1–10 μmol) did produce dose-dependent relaxation. Due to the volatile nature of NO gas, it is difficult to know exactly how much NO was delivered to the tissue. The present experiments indicate that only a small portion of the NO bubbled into the bathing medium dissolved therein and was available to effect relaxation. Furthermore, it is possible that RAS metabolizes GTN to a transport form of NO.

Another method used to assess whether the ultimate factor responsible for RTCS relaxation in the sandwich preparation is NO, was incubation with reduced deoxyhaemoglobin. Reduced haemoglobin (1 μM), a known extracellular haemoprotein scavenger of NO (Murad *et al.*, 1978; Gruetter *et al.*, 1979), was incubated with the sandwich preparation which was then treated with 30 nM GTN. This concentration of GTN demonstrated the greatest differences in relaxation between RTCS in the sandwich preparation and RTCS alone, which exhibited little or no independent GTN metabolizing activity. Haemoglobin eliminated the enhanced RTCS response to GTN in the presence of RAS. This inhibition was found to be reversible as washout and repeat of the protocol without Hb yielded augmented RTCS relaxation. These data indicate that Hb inhibited the RTCS response by binding to NO or a related compound that diffused from the RAS to RTCS and indicate that NO or an NO adduct was the active agent produced during GTN exposure to vascular smooth muscle. Furthermore, this interpretation is consistent with and supported by the finding that 1 μM Hb also inhibited RTCS relaxations induced by authentic NO gas.

Analysis of headspace gas from the RTCS and RAS incubated with GTN for 2, 5, 10 and 20 min, further implicates NO as the active species. There was no measurable NO for the incubation of RTCS with GTN for less than 5 min, but there was measurable NO for incubation of RAS with GTN at 5 min. At 10 and 20 min, RTCS was found to produce considerably less NO than RAS (Figure 5). These observations were taken to mean that most likely the relaxing factor was formed from GTN in the RAS, to relax the adjacent RTCS in the sandwich preparation.

The idea that the relaxing agent formed from GTN by RAS was NO is not entirely obvious upon initial examination of the data. Nevertheless, after administration of NO gas, the effective concentrations of NO in the bathing medium were similar to the effective concentrations of GTN, the putative NO prodrug. Furthermore, if NO is formed from GTN within vascular smooth muscle cells, the concentrations of NO in the region of its receptors would be higher that those measured outside the tissue. In comparison, the concentrations of NO inside vascular cells would be less than those outside the tissue whenever NO is delivered extracellularly. Another possible interpretation of our observations is that NO is transported as a sulphydryl adduct (Stamler *et al.*, 1992; Keaney *et al.*, 1993), which cannot be detected immediately by chemiluminescence, but later detection is possible due to a breakdown of the S-nitrosothiol to NO.

This study was able to exploit RTCS as bioassay of NO or congeners thereof produced by RAS treated with GTN. Such ability to measure NO produced from vascular smooth muscle has been difficult due to the problems of NO volatility. Using the bioassay sandwich preparation, we have been able to detect qualitatively NO formation from GTN in amounts below the lower limit of sensitivity of the chemiluminescence assay and for experimental times close to the onset of vascular smooth muscle relaxation. It is reasonable to conclude that NO or a similar NO precursor is acting to relax RTCS of the sandwich bioassay since it is inhibited by haemoglobin and chemiluminescence demonstrated that RAS is the predominant source of NO from GTN compared to RTCS. Although authentic NO gas was found to relax the RTCS, the large quantities required give rise to the prospect that one relaxant factor formed from GTN by RAS is a NO adduct, or a low molecular weight nitrosothiol that releases NO intracellularly activating guanylyl cyclase and effecting the cascade that results in vascular smooth muscle relaxation. Experiments of this study would not be capable of distinguishing between NO or a NO adduct, but such results would be consistent with the observations that prodrugs of NO like SIN-1, and particulary SNAP, act as carriers of NO and on a molar basis elicit the greatest levels of relaxation in RTCS. Current work in our laboratory and others would seem to support such an idea. Chemiluminescence analysis has shown (unpublished observations) that many drugs that liberate NO spontaneously in solution are less potent than GTN as vasorelaxants. Work by others has shown that nitrosothiols are as potent relaxants (Stamler & Loscalzo, 1992) and activators of guanylyl cyclase (Kukovetz *et al.*, 1991; Noack & Feelisch, 1991) as authentic NO. Such evidence also further supports the existence of a nitrosothiol as an intermediate in organonitrate relaxation.

In conclusion, results from this sandwich bioassay study have shown that rabbit aorta strip generates NO or some NO-labile compound which can be detected by taenia coli. Different RTCS relaxation profiles between GTN-treated sandwich preparation and RTCS alone exposed to NO raise some questions concerning whether or not some NO adduct may exist in organonitrate-mediated vasodilatation.

The authors gratefully acknowledge support from the Heart and Stroke Foundation of Ontario (B-2197). We also thank Mr Brian McLaughlin for his helpful discussion of this work.

References

BENNETT, B.M., KOBUS, S.M., BRIEN, J.F., NAKATSU, K. & MARKS, G.S. (1986). Requirement for reduced, unliganded hemoprotein for the haemoglobin- and myoglobin-mediated biotransformation of glyceryl trinitrate. *J. Pharmacol. Exp. Ther.*, **237**, 629–635.

BRIEN, J.F., MCLAUGHLIN, B.E., BREEDON, T.H., BENNETT, B.M., NAKATSU, K. & MARKS, G.S. (1986). Biotransformation of glyceryl trinitrate occurs concurrently with relaxation of rabbit aorta. *J. Pharmacol. Exp. Ther.*, **237**, 608–614.

BRIEN, J.F., MCLAUGHLIN, B.E., KOBUS, S.M., KAWAMOTO, J.H., NAKATSU, K. & MARKS, G.S. (1988). Mechanism of glyceryl trinitrate induced vasodilation. I. Relationship between drug biotransformation, tissue cGMP elevation and relaxation of rabbit aorta. *J. Pharmacol. Exp. Ther.*, **244**, 323–327.

BRIEN, J.F., MCLAUGHLIN, B.E., NAKATSU, K. & MARKS, G.S. (1991). Quantitation of nitric oxide formation from nitrovasodilator drugs by chemiluminescence analysis of headspace gas. *J. Pharmacol. Methods*, **25**, 19–27.

DIAMOND, J. & HOLMES, T.J. (1975). Effects of potassium chloride and smooth muscle relaxants on tension and cyclic nucleotide levels in rat myometrium. *Can. J. Physiol. Pharmacol.*, **53**, 1099–1107.

FEELISCH, M. & NOACK, E.A. (1987). Correlation between nitric oxide during degradation of organic nitrates and activation of guanylate cyclase. *Eur. J. Pharmacol.*, **139**, 19–30.

FURCHOTT, R.F. & ZAWADZKI, J.V. (1981). The obligatory role of endothelial cells in the relaxation of arterial smooth muscle by acetylcholine. *Nature*, **288**, 373–376.

GRUETTER, C.A., BARRY, B.I., MCNAMARA, D.B., GRUETTER, D.Y., KADOWITZ, P.J. & IGNARRO, L.J. (1979). Relaxation of bovine coronary artery and activation of coronary arterial guanylate cyclase by nitric oxide, nitroprusside and a carcinogenic nitrosamine. *J. Cyclic Nucleotide Res.*, **5**, 211–224.

GRUETTER, C.A., GRUETTER, D.Y., LYON, J.E., KADOWITZ, P.J. & IGNARRO, L.J. (1981). Relationship between cyclic guanosine 3':5'-monophosphate formation and relaxation of coronary smooth muscle by glyceryl trinitrate, nitroprusside, nitrite and nitric oxide: effects of methylene blue and methemoglobin. *J. Pharmacol. Exp. Ther.*, **219**, 181–186.

HILL, K.E., HUNT, R.W. Jr., JONES, R., HOOVER, R.L. & BURK, R.F. (1992). Metabolism of nitroglycerin by smooth muscle cells: Involvement of glutathionone and glutathionone-S-transferase. *Biochem. Pharmacol.*, **43**, 561–566.

IGNARRO, L.J., LIPPTON, H., EDWARDS, J.C., BARICOS, W.H., HYMAN, A.L., KADOWITZ, P.J. & GRUETTER, C.A. (1981). Mechanism of vascular smooth muscle relaxation by organic nitrates, nitrites, nitroprusside, and nitric oxide: Evidence for the involvement of S-nitrosothiols as active intermediates. *J. Pharmacol. Exp. Ther.*, **218**, 739–749.

JOHNSON, E.M. Jr., HARKEY, A.B., BLEHM, D.J. & NEEDLEMAN, P. (1972). Clearance and metabolism of organic nitrates. *J. Pharmacol. Exp. Ther.*, **182**, 56–62.

KATSUKI, S., ARNOLD, W.P. & MURAD, F. (1977). Effects of sodium nitroprusside, nitroglycerin, and sodium azide on levels of cyclic nucleotides and mechanical activity of various tissues. *Adv. Cyclic Nucleotide Res.*, **3**, 239–247.

KAWAMOTO, J.H., MCLAUGHLIN, B.E., BRIEN, J.F., MARKS, G.S. & NAKATSU, K. (1990). Biotransformation of glyceryl trinitrate and elevation of cGMP precede glyceryl trinitrate-induced relaxation of isolated blood vessels. *J. Cardiovasc. Pharmacol.*, **15**, 714–719.

KEANEY, J., SIMON, D.I., STAMLER, J.S., JARAKI, O., SCHARFESTEIN, D., VITA, J. & LOSCALZO, J. (1993). NO forms an adduct with serum albumin that has endothelium-derived relaxing factor-like properties. *J. Clin. Invest.*, **91**, 1582–1589.

KUKOVETZ, W.R., HOLZMANN, S. & SCHMIDT, K. (1991). Cellular mechanisms of action of therapeutic nitric oxide donors. *Eur. Heart J.*, **12**, (Supplement E), 16–24.

LI, C.G. & RAND, M.J. (1991). Evidence that part of the NANC relaxant response of guinea-pig trachea to electrical field stimulation is mediated by nitric oxide. *Br. J. Pharmacol.*, **102**, 91–94.

MARKS, G.S., MCLAUGHLIN, B.E., MACMILLAN, H.F., NAKATSU, K. & BRIEN, J.F. (1989). Differential biotransformation of glyceryl trinitrate by red blood cell-supernatant fraction and pulmonary homogenate. *Can. J. Physiol. Pharmacol.*, **67**, 417–422.

MARKS, G.S., MCLAUGHLIN, B.E., NAKATSU, K. & BRIEN, J.F. (1992). Direct evidence for nitric oxide formation from glyceryl trinitrate during incubation with intact bovine pulmonary artery. *Can. J. Physiol. Pharmacol.*, **70**, 308–311.

MARTIN, W., SMITH, J.A., LEWIS, M.J. & HENDERSON, A.H. (1988). Evidence that inhibitory factor extracted from bovine retractor penis is nitrite, whose acid-activated derivative is stabilized nitric oxide. *Br. J. Pharmacol.*, **93**, 579–586.

MURAD, F., MITTAL, C.K., ARNOLD, W.P., KATSUKI, S. & KIMURA, H. (1978). Guanylate cyclase: activation by azide, nitro compounds, nitric oxide, and hydroxyl radical and inhibition by hemoglobin and myoglobin. *Adv. Cyclic Nucleotide Res.*, **9**, 145–148.

NEEDLEMAN, P., BLEHM, D.J. & ROTSKOFF, K.S. (1969). Relationship between glutathionine-dependent denitration and the vasodilator effectiveness of organic nitrates. *J. Pharmacol. Exp. Ther.*, **237**, 286–288.

NOACK, E.M. & FEELISCH, M. (1991). Molecular mechanisms of nitrovasodilator bioactivation. *Basic Res. Cardiol.*, **86** (Supplement 2), 37–50.

PALMER, R.M.J., FERRIDGE, A.G. & MONCADA, S. (1987). Nitric oxide release accounts for the biological activity of endothelium-derived relaxing factor. *Nature*, **327**, 524–526.

STAMLER, J.S., JARAKI, O., OSBORNE, J., SIMON, D.I., KEANEY, J., VITA, J., SINGEL, D., VALERI, C.R. & LOSCALZO, J. (1992). Nitric oxide circulates in mammalian plasma primarily as an S-nitroso adduct of serum albumin. *Proc. Natl. Acad. Sci. U.S.A.*, **89**, 7674–7677.

STAMLER, J.S. & LOSCALZO, J. (1992). S-Nitrosylation of proteins with nitric oxide synthesis and characterization of biologically active compounds. *Proc. Natl. Acad. Sci. U.S.A.*, **89**, 444–448.

STARK, M.E., BAUER, A.J., SARR, M.G. & SZURSZEWSKI, J.H. (1993). Nitric oxide mediates inhibitory nerve input in human and canine jejunum. *Gastroenterology*, **104**, 398–409.

TINKER, J.H. & MICHENFELDER, J.D. (1976). Sodium nitroprusside: pharmacology, toxicology and therapeutics. *Anesthesiology*, **95**, 340–354.

VAN KAMPEN, E.J. & ZIJLSTRA, W.G. (1961). Standardization of hemoglobinometry II. the hemoglobincyanide method. *Clinica Chemica Acta*, **6**, 535–544.

ZIVIN, J.A. & BARTKO, J.J. (1976). Statistics for disinterested scientists. *Life Sci.*, **18**, 15–26.

(Received February 7, 1994
Revised July 4, 1994
Accepted August 22, 1994)

Br. J. Pharmacol. (1994), **113**, 1515–1521 © Macmillan Press Ltd, 1994

GABA and glutamate release affected by $GABA_B$ receptor antagonists with similar potency: no evidence for pharmacologically different presynaptic receptors

[1]Peter C. Waldmeier, Peter Wicki, Jean-Jacques Feldtrauer, Stuart J. Mickel, Helmut Bittiger & Peter A. Baumann

Research Department, Pharmaceuticals Division, K-125.607, Ciba-Geigy Ltd., CH-4002 Basel, Switzerland

1 The effects of a series of nine $GABA_B$ receptor antagonists of widely varying potencies on electrically stimulated release from cortical slices of [^{3}H]-GABA in the absence or presence of 10 μM of the $GABA_B$ agonist, (−)-baclofen and of endogenous glutamate in the presence of (−)-baclofen were compared.

2 The concentrations of the compounds half maximally increasing [^{3}H]-GABA release (EC_{50}'s) at a stimulation frequency of 2 Hz correlated well with the IC_{50} values obtained from the inhibition of the binding of the agonist, [^{3}H]-CGP 27492, to $GABA_B$ receptors in rat brain membranes (rank order of potency: CGP 56999 A ⩾ CGP 55845 A > CGP 52432 ⩾ CGP 56433 A > CGP 57034 A > CGP 57070 A ⩾ CGP 57976 > CGP 51176 > CGP 35348).

3 Likewise, the concentrations causing half-maximal increases of [^{3}H]-GABA in the absence or presence of (−)-baclofen, and of endogenous glutamate in the presence of (−)-baclofen, correlated well with each other. Reports in the literature suggesting the CGP 35348 exhibits a 70 fold preference for inhibition of (−)-baclofen's effects on glutamate over [^{3}H]-GABA release, and that CGP 52432 shows a 100 fold preference in the opposite sense, could not be confirmed in our model.

4 Therefore, our results suggest that, if there are pharmacological differences between $GABA_B$ autoreceptors and $GABA_B$ heteroreceptors on glutamatergic nerve endings in the rat cortex, they are not revealed by this series of compounds of widely different potencies.

5 In particular, our results with CGP 35348 and CGP 52432 do not support the hypothesis that $GABA_B$ autoreceptors and $GABA_B$ heteroreceptors on glutamatergic nerve endings represent subtypes with different pharmacology.

Keywords: $GABA_B$ autoreceptors; $GABA_B$ heteroreceptors; subtypes; [^{3}H]-GABA release; glutamate release; $GABA_B$ receptor antagonists

Introduction

Presynaptic $GABA_B$ receptors seem to modulate the release of several neurotransmitters. The $GABA_B$ agonist, baclofen, has been reported to inhibit the release of GABA itself via autoreceptors (Pittaluga *et al.*, 1987; Waldmeier *et al.*, 1988), and glutamate (Potashner, 1979), biogenic amines (Bowery *et al.*, 1980; Schlicker *et al.*, 1984; Gray & Green, 1987), cholecystokinin (Conzelmann *et al.*, 1986) and somatostatin (Bonanno *et al.*, 1991) via heteroreceptors. Recently, evidence for differential pharmacology of auto- and heteroreceptors has been presented. Thus, the $GABA_B$ receptor antagonist, phaclofen, was 10 times more potent in antagonizing the inhibitory effect of (−)-baclofen on the release of GABA and of somatostatin-like immunoreactivity (SRIF-LI) than of glutamate, whereas CGP 35348 was about 70 times more potent in inhibiting the effect of baclofen on glutamate and SRIF-LI than on GABA release (all from rat cortical synaptosomes and elicited by elevated K^+; Bonanno & Raiteri, 1992). The novel, more potent $GABA_B$ receptor antagonist, CGP 52432, inhibited the effect of baclofen on GABA release about 100 or 40 times more potently than its effects on glutamate or SRIF-LI release (Lanza *et al.*, 1993), respectively. From these results, the existence of multiple subtypes of $GABA_B$ receptors was inferred (Bonanno & Raiteri, 1993), an attractive hypothesis particularly with respect to drug development, because it offers the possibility of obtaining $GABA_B$ receptor antagonists which preferentially interact with the $GABA_B$ autoreceptor or certain heteroreceptors.

We have therefore investigated a series of new $GABA_B$ receptor antagonists, with markedly different potencies for the $GABA_B$ receptor as measured in *in vitro* radioligand binding assays, with respect to their relative potencies for antagonizing the inhibitory effect of (−)-baclofen on the electrically stimulated release of [^{3}H]-GABA and endogenous glutamate from rat cortical slices. The compounds were selected for this study because they are structurally related to CGP 35348 and CGP 52432, which reportedly affect GABA and glutamate release differentially. It seemed of interest to see whether relative potency differences with respect to $GABA_B$ auto- and heteroreceptors such as reported for the above two compounds, could also be found among structural relatives. CGP 35348 and CGP 52432 were included in the study for comparison.

Methods

Release experiments

Cross-chopped slices from rat (male Tif:RAlf(SPF) rats, Tierfarm Sisseln, Switzerland, weighing 180–240 g) cerebral cortex were prepared, loaded with [^{3}H]-GABA if appropriate and superfused as described previously (Baumann *et al.*, 1990; Waldmeier *et al.*, 1993a). Experiments in which [^{3}H]-GABA release was measured were done in the presence of the GABA transminase inhibitor, AOAA (50 μM), and the GABA uptake inhibitor, SK&F 89976 (10 μM), as described by Baumann *et al.* (1990). Three groups of 4 slice preparations each, were twice stimulated electrically at 2 Hz for 2 min (25 mA, 2 ms), at an interval of 36 min. One group

[1] Author for correspondence.

served as a control; in the remaining two, the $GABA_B$ antagonists were added at appropriate concentrations, 2 fractions after the first stimulation (S_1). In one series of experiments, (−)-baclofen (10 μM) was present throughout, in the control as well as in the test group; again, the $GABA_B$ receptor antagonists were added at appropriate concentrations, 2 fractions after S_1.

The release of endogenous glutamate was measured by an *o*-phthaldialdehyde/h.p.l.c./fluorescence detection method in the presence of the glutamate uptake inhibitor, L-*trans*-PDC, as described by Waldmeier *et al.* (1993b). Three groups of 4 slice preparations each were twice stimulated electrically at 1 Hz for 4 min (25 mA, 2 ms), at an interval of 36 min. One group served as a 'baclofen control', (−)-baclofen (10 μM) being present throughout. In the two others, the $GABA_B$ receptor antagonists were added at appropriate concentrations, 2 fractions after the first stimulation (S_1).

Data were calculated as a percentage of fractional release for each fraction. From this, the release evoked by electrical stimulation in S_1 and S_2 was calculated by subtraction of the basal release, assuming a linear decline between the fractions before and after stimulation. This integration was done for one fraction in the case of [^{3}H]-GABA and, due to the longer stimulation period, for two fractions in the case of glutamate. The data shown in the graphs are the effects of the $GABA_B$ receptor antagonists as percentages of controls ± s.e.mean obtained from a comparison of the S_2/S_1 ratios in each experiment.

Binding experiments

[^{3}H]-CGP 27492 was used as a radioligand to measure interactions of the compounds with $GABA_B$ receptors (Bittiger *et al.*, 1988; Olpe *et al.*, 1990). Membranes from rat cerebral cortex were used and the assay was performed in 2 ml Krebs-Henseleit buffer pH 7.4, containing 20 mM Tris buffer, 200–300 μg membrane protein, 2 nM [^{3}H]-CGP 27492 (15 Ci mmol^{-1}) and the compounds to be tested. The incubation was performed at room temperature for 40 min and terminated by rapid filtration on Whatman GF/B glass fibre filters, which were washed twice with 5 ml ice-cold buffer. Filter-bound radioactivity was counted in Irgascint A 300 (Ciba-Geigy). Incubations were performed in triplicate and nonspecific binding was determined in the presence of (−)-baclofen (10 μM).

Estimations of IC_{50} and K_i values and Hill coefficients of the radioligand binding data, and EC_{50} values and maximal increases of release

These calculations were performed by nonlinear (sigmoidal) fitting using a commercially available PC software programme (GraphPad Prism 1.0, GraphPad Software Inc., San Diego, Ca, U.S.A.). K_i values were calculated from the IC_{50}'s by means of the Cheng-Prusoff equation (Cheng & Prusoff, 1973).

Chemicals

L-Glutamate, S-carboxymethylcysteine and amino-oxyacetic acid (AOAA) were obtained from FLUKA AG (Buchs, Switzerland), L-*trans*-pyrrolidine-2,4-dicarboxylic acid (L-*trans*-PDC) from Tocris (Bristol, U.K.), and *o*-phthaldialdehyde solution from Pierce Europe (Oud Beijerland, The Netherlands). The hydrochloride of SK&F 89976 (1-(4,4-diphenyl-3-butenyl)-3-piperidine carboxylic acid hydrochloride) was prepared by Dr H. Allgeier in our Chemistry Department. (−)-Baclofen, CGP 35348 (3-aminopropyl-diethoxy-methylphosphinic acid), CGP 51176 (3-amino-2-(**R**)-hydroxy-propyl-cyclohexyl-methyl-phosphinic acid), CGP 52432 ([3-[[(3,4-dichlorophenyl)methyl]amino]propyl] (diethoxymethyl) phosphinic acid), CGP 55845 A (3-[1-(**S**)-(3,4-dichlorophenyl)-ethyl]amino-2(**S**)-hydroxy-propyl-benzyl-phosphinic acid (hydrochloride), CGP 56433 A ([3-[[1-(**S**)-(3-carboxyphenyl) ethyl]amino] 2-(**S**)-hydroxy-propyl]-cyclohexyl-methyl-phosphinic acid (lithium salt)), CGP 56999 A ([3[[1-(**R**)-(3-carboxyphenyl)ethyl]amino] 2-(**S**)-hydroxy-propyl]-cyclohexyl-methyl-phosphinic acid (lithium salt)), CGP 57034 A ([3-[[1-(**S**)-(4-carboxy-phenyl)ethyl]amino] 2-(**S**)-hydroxy-propyl]-cyclohexylmethyl-phosphinic acid (lithium salt)), CGP 57070 A ([3-[[1-(**R**)-(4-carboxyphenyl) ethyl]amino] 2-(**S**)-hydroxy-propyl]-cyclohexylmethyl-phosphinic acid (lithium salt)) and CGP 57976 ([3-[[1-(**R**)-(3,4,5-trimethoxyphenyl) ethyl]amino] 2-(**S**)-hydroxy-propyl]-cyclohexylmethyl-phosphinic acid) are experimental compounds of Ciba-Geigy. The chemical structures are given in the left column of Table 1. The $GABA_B$ radioligand, [^{3}H]-CGP 27492 was synthesized by Ciba-Geigy Horsham, U.K. High purity water (MilliQ water purification system, Waters Assoc., Milford, MA, U.S.A.) was used for all drug dilutions, buffers, mobile phases etc. [2,3-^{3}H(N)-Aminobutyric acid ([^{3}H]-GABA; NET-191, specific activity 25–40 Ci mmol^{-1}) was obtained from New England Nuclear, Boston, Mass, U.S.A.

Results

Inhibition of ^{3}H-CGP 27492 binding

All nine $GABA_B$ receptor antagonists displaced [^{3}H]-CGP 27492 concentration-dependently in a monophasic manner, and to completeness. The IC_{50} values and the corresponding Hill coefficients were estimated by sigmoidal fitting. Because the Hill coefficients were all close to unity, the corresponding K_i values were calculated by means of the Cheng-Prusoff equation (radioligand concentration used in the experiments = 2 nM, K_D = 7.4 nM, cf. Bittiger *et al.*, 1988). The negative logarithms of the K_i values (pK_i) are given in Table 1.

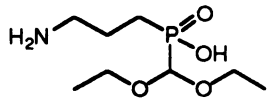
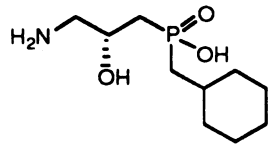
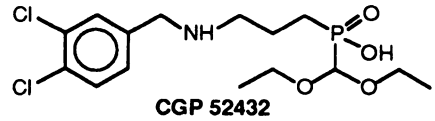
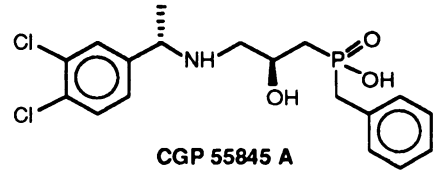
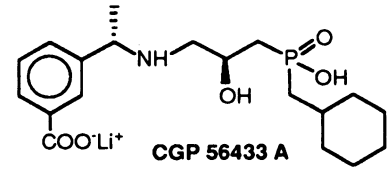
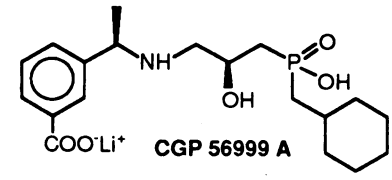
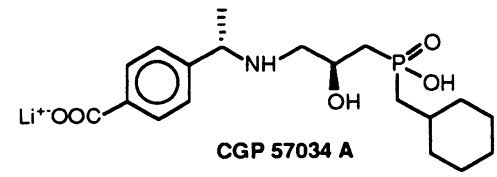
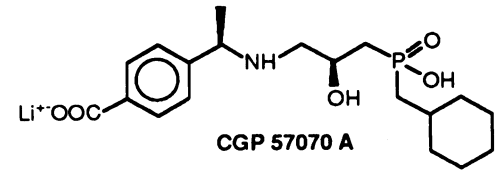
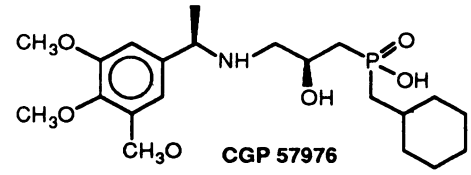
Effects on [^{3}H]-GABA release in the absence of (−)-baclofen

A typical example of an experiment, in this case with 1 μM CGP 56433 A, is given in Figure 1a. The increase in [^{3}H]-GABA release caused by this concentration of the drug was calculated as a percentage of control, comparing S_2/S_1 ratios. All the investigated compounds concentration-dependently increased the release of [^{3}H]-GABA elicited by electrical stimulation at 2 Hz, at which sufficient endogenous GABA is released to activate markedly the autoreceptor (Figures 2–4). The corresponding pEC_{50} values, (concentrations which increase control release half maximally), are summarized in Table 1. The data show that the selection of $GABA_B$ receptor antagonists investigated in this study covers a range of four orders of magnitude with respect to potency, from low nanomolar (CGP 56999 A) to micromolar (CGP 35348). The maximal increases of [^{3}H]-GABA release caused by these agents were approximately 300% of controls. This is in keeping with previous experience with a number of other $GABA_B$ receptor antagonists (Waldmeier *et al.*, 1993a).

Effects on [^{3}H]-GABA release in the presence of (−)-baclofen

Concentration-response curves of the effects of the $GABA_B$ receptor antagonists on [^{3}H]-GABA release were made in the presence of (−)-baclofen (10 μM), at a stimulation frequency of 2 Hz as above. A typical example of an experiment, in this case with 1 μM CGP 56433 A, is given in Figure 1b. The concentration-response data, also shown in Figures 2–4, differ little from those in the absence of (−)-baclofen, except that the maximal percentual increases are higher (approximately 450–500% of controls).

Table 1 IC_{50} values with respect to inhibition of binding of [^{3}H]-CGP 27492 to the GABA$_B$ receptor and concentrations causing half-maximal increases of the release of GABA, in the absence and presence of (−)-baclofen, and of glutamate in the presence of 10 μM (−)-baclofen

Compound		*[^{3}H]CGP 27492 binding* pKi A	*[^{3}H]-GABA release* pEC_{50} B	*[^{3}H]GABA rel. in presence of (−)-baclofen* pEC_{50} C	*Glu release in presence of (−)-baclofen* pEC_{50} D
	**CGP 35348**	4.71 ± 0.01 *Hill: 1.05 ± 0.03*	4.16 ± 0.33	3.98 ± 0.07	3.98 ± 0.11
	**CGP 51176**	5.47 ± 0.05 *Hill: 0.73 ± 0.06*	4.73 ± 0.38	4.83 ± 0.06	4.88 ± 0.10
	**CGP 52432**	7.35 ± 0.02 *Hill: 0.91 ± 0.04*	6.47 ± 0.07	6.49 ± 0.02	6.65 ± 0.25
	**CGP 55845 A**	8.35 ± 0.01 *Hill: 0.99 ± 0.02*	8.08 ± 0.26	7.60 ± 0.14	7.85 ± 0.08
	**CGP 56433 A**	7.20 ± 0.07 *Hill: 1.04 ± 0.17*	6.82 ± 0.01	6.59 ± 0.02	6.53 ± 0.14
	**CGP 56999 A**	8.70 ± 0.15 *Hill: 1.29 ± 0.04*	8.46 ± 0.09	8.20 ± 0.09	7.89 ± 0.15
	**CGP 57034 A**	6.75 ± 0.02 *Hill: 1.01 ± 0.04*	6.31 ± 0.01	6.31 ± 0.01	6.21 ± 0.01
	**CGP 57070 A**	6.27 ± 0.02 *Hill: 0.93 ± 0.04*	5.85 ± 0.01	5.66 ± 0.01	5.84 ± 0.25
	**CGP 57976**	6.05 ± 0.02 *Hill: 0.89 ± 0.03*	5.65 ± 0.01	5.55 ± 0.09	5.81 ± 0.04

Data are the negative logarithms ± s.e.mean of the K_i values (pK_i) of the compounds for the inhibition of [^{3}H]-CGP 27492 binding to GABA$_B$ receptors (**A**; Hill coefficients ± s.e.mean in italics) or of the half-maximal increases (pEC_{50}) of [^{3}H]-GABA release in the absence of (−)-baclofen (**B**), of [^{3}H]-GABA release in the presence of (−)-baclofen (**C**), and of the release of endogenous glutamate (Glu) in the presence of (−)-baclofen (**D**), respectively. They were determined by non-linear sigmoidal fitting of the binding data and the release data shown in Figures 2–4. Examination of the correlation between the different sets of data by means of linear regression yielded the following correlation coefficients: **A** vs. **B**: $r = 0.991$; **A** vs. **C**: $r = 0.994$; **A** vs. **D**: $r = 0.991$: **B** vs. **C**: $r = 0.994$; **B** vs. **D**: $r = 0.988$; **C** vs. **D**: $r = 0.990$.

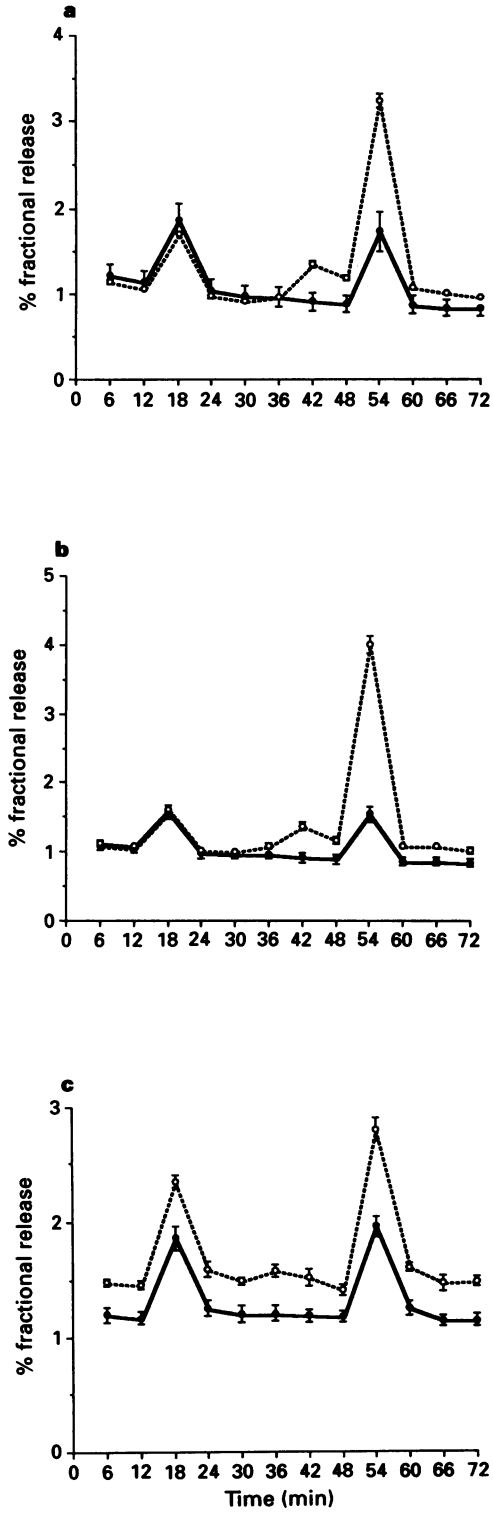


Figure 1 Examples of raw data used to calculate percentage increases given in Figures 2–4. Groups of 4 slice preparations were twice stimulated electrically, at 2 Hz for 2 min (25 mA, 2 ms) for measurements of the release of [^{3}H]-GABA, and at 1 Hz for 4 min (25 mA, 2 ms) for measurements of the release of endogenous glutamate (Glu). In the experiment with [^{3}H]-GABA in the absence (a) and presence of 10 μM (−)-baclofen (b), 50 μM AOAA and 10 μM SK&F 89976 were present as inhibitors of GABA transaminase and GABA uptake, respectively. In the experiments with endogenous glutamate (c), 100 μM *trans*-PDC was present as an inhibitor of glutamate uptake, and 10 μM (−)-baclofen was also present throughout. The test drug (in this case 1 μM CGP 56433 A) was added to the superfusion medium two fractions after the first stimulation (S_1). Data are means ± s.e.mean as a percentage of fractional release: (●—●) controls; (○—○) CGP 56433 A 1 μM.

Effects on endogenous glutamate release in the presence of (−)-baclofen

In analogy to the above, concentration-response curves of the effects of the $GABA_B$ receptor antagonists on the release of endogenous glutamate were made in the presence of (−)-baclofen (10 μM), at a stimulation frequency of 1 Hz. A typical example of an experiment, in this case with 1 μM CGP 56433 A, is given in Figure 1c. The data of the whole series of experiments are summarized in Figures 2–4. All the compounds concentration-dependently increased glutamate release as compared with that observed in the presence of (−)-baclofen alone. The maximal increases were approximately 170% of controls. It is important to note that there were no major differences between the concentration-response curves with respect to the release of [^{3}H]-GABA or endogenous glutamate (both in the presence of 10 μM (−)-baclofen) with any of the nine $GABA_B$ receptor antagonists studied.

The data of Figures 2–4 were used to estimate the concentrations of the compounds causing half-maximal responses (EC_{50}'s) with respect to [^{3}H]-GABA release in the absence or presence of (−)-baclofen, and to the release of endogenous glutamate in the presence of (−)-baclofen. The negative logarithms of the values obtained (pEC_{50}'s) are listed in Table 1. On the average, EC_{50}'s for [^{3}H]-GABA release without (−)-baclofen were about half those in its presence. The ratios [EC_{50} for [^{3}H]-GABA release]/[EC_{50} for glutamate release] in the presence of (−)-baclofen were on the average close to 1. The pEC_{50}'s all correlated with each other as well as with the pK_i's with respect to inhibition of [^{3}H]-CGP 27492 binding with correlation coefficients approaching unity (see footnote to Table 1). As examples, the correlation plots of the pK_i's with respect to [^{3}H]-CGP 27492 binding vs. pEC_{50}'s with respect to [^{3}H]-GABA release in the absence of (−)-baclofen (a) and of the pEC_{50}'s with respect to [^{3}H]-GABA vs. those of glutamate release, both in the presence of (−)-baclofen (b), are shown in Figure 5.

Discussion

There was an almost perfect correlation between the potencies of the nine $GABA_B$ receptor antagonists tested for inhibition of [^{3}H]-CGP 27492 binding to $GABA_B$ receptors in rat cortical membranes and for antagonism of the autoreceptor-mediated suppressing effect of endogenously released GABA on its own release, as measured by the overflow of [^{3}H]-GABA from preloaded rat cortical slices. Incidentally, the potencies of a different selection of $GABA_B$ receptor antagonists for increasing [^{3}H]-GABA release at 2 Hz have previously been found to correlate well with their potencies for inhibition of the binding of the agonist radioligand, [^{3}H]-CGP 27492 to $GABA_B$ receptors in rat brain membrane preparations (Waldmeier *et al.*, 1992). Such a result would be expected if (a) neither the agonist radioligand nor the antagonists discriminate between possible $GABA_B$ receptor subtypes, or (b) they are specific for a certain subtype.

Likewise, the correlation between binding data and those with respect to increasing [^{3}H]-GABA release in the presence of a large concentration of (−)-baclofen was almost perfect. Although the latter experimental conditions are complex, because the $GABA_B$ autoreceptor is activated both by endogenously released GABA and by the exogenous agonist, (−)-baclofen, these data were necessary to allow comparison with those on the effects of the $GABA_B$ receptor antagonists on glutamate release. The maximal increase of glutamate release from rat cortical slices elicited by a $GABA_B$ receptor antagonist is rather small, probably because there is little tonic activation by endogenous GABA of $GABA_B$ heteroreceptors on glutamatergic nerve endings in this area (Waldmeier *et al.*, 1993b). This makes potency comparisons with the effects of the compounds on [^{3}H]-GABA release difficult,

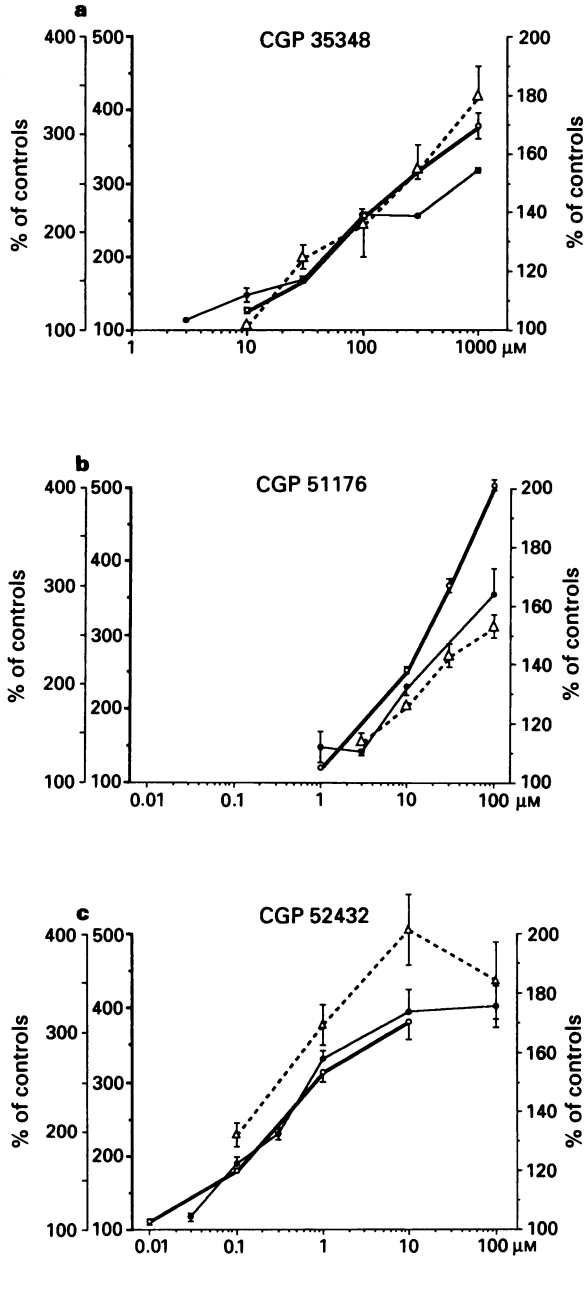


Figure 2 Effects of (a) CGP 35348, (b) CGP 51176 and (c) CGP 52432 on the release of [^{3}H]-GABA in the absence and presence of (−)-baclofen, and of endogenous glutamate (glutamate) in the presence of (−)-baclofen. Groups of 4 slice preparations were twice stimulated electrically, at 2 Hz for 2 min (25 mA, 2 ms) for measurements of the release of [^{3}H]-GABA, and at 1 Hz for 4 min (25 mA, 2 ms) for measurements of the release of endogenous glutamate. In the experiments with [^{3}H]-GABA, 50 μM AOAA and 10 μM SK&F 89976 were present as inhibitors of GABA transaminase and GABA uptake, respectively. In one series of experiments, 10 μM (−)-baclofen was also present throughout. In the experiments with endogenous glutamate, 100 μM *trans*-PDC was present as an inhibitor of glutamate uptake, and 10 μM (−)-baclofen was also present throughout.

Each experiment consisted of a control of 4 slice preparations which were stimulated twice under identical conditions, and two groups of 4 slice preparations where the test drugs were added to the superfusion medium two fractions after the first stimulation (S_1). The effects of the drugs were evaluated by expressing the corresponding S_2/S_1 ratios as a percentage of those of the controls ± s.e.mean ($n = 4$). When only the effects on [^{3}H]-GABA release were measured, these controls were not exposed to drugs other than AOAA and SK&F 89976. Otherwise, all groups in an experiment were exposed to 10 μM (−)-baclofen throughout (designated by 'GABA/baclofen' and 'glutamate/baclofen').

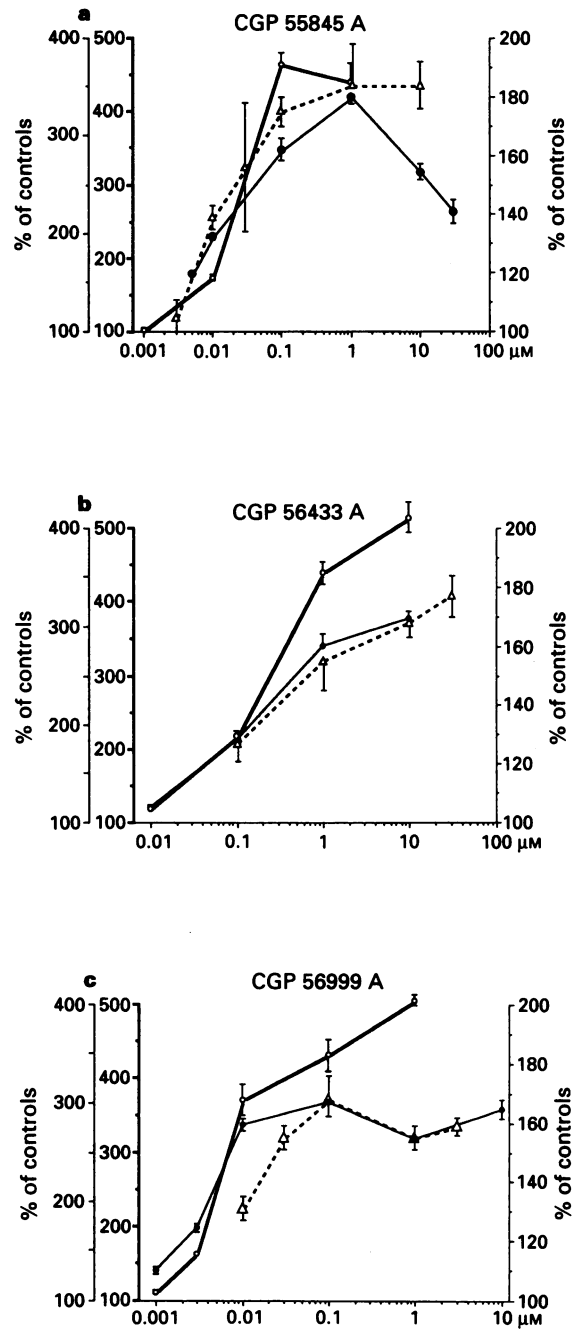


Figure 3 Effects of (a) CGP 55845 A, (b) CGP 56433 A and (c) CGP 56999 A on the release of [^{3}H]-GABA in the absence and presence of (−)-baclofen, and of endogenous glutamate in the presence of (−)-baclofen. Data are means ± s.e.mean as percentage of controls. For details see legend of Figure 2; (●—●) GABA; (○—○) GABA/baclofen; (Δ---Δ) Glu/baclofen.

Basal [^{3}H]-GABA release in the fraction immediately before S_1, S_1 and S_2/S_1 were 0.90–1.20% (fractional release), 0.725–1.165% (fractional release), and 0.938 and 1.165, respectively, in the absence of (−)-baclofen. In its presence, the corresponding figures were 0.95–1.05%, 0.507–0.644% and 1.142–1.366, respectively. Basal glutamate release, S_1, and S_2/S_1 were 0.746–1.187% (fractional release; absolute amounts of glutamate being between about 250–500 pmol/fraction), 0.605–0.893% (fractional release), and 1.122–1.299, respectively. These figures represented the lower and upper limits found in the experiments depicted in Figures 2–4.

The ordinates from left to right refer to [^{3}H]-GABA release in the absence and presence of (−)-baclofen, and to glutamate (Glu) release in the presence of (−)-baclofen, respectively: (●—●) GABA; (○—○) GABA/baclofen; (Δ---Δ) Glu/baclofen.

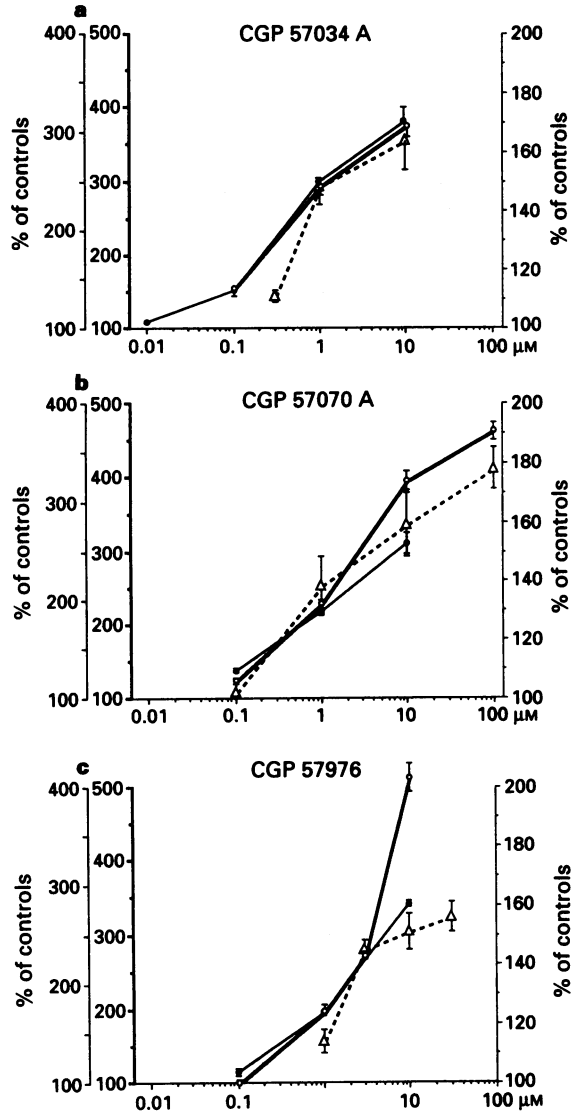


Figure 4 Effects of (a) CGP 57034 A, (b) CGP 57070 A and (c) CGP 57976 on the release of [^{3}H]-GABA in the absence and presence of (−)-baclofen, and of endogenous glutamate in the presence of (−)-baclofen. Data are means ± s.e.mean as percentage of controls. For details see legend of Figure 2; (●—●) GABA; (○—○) GABA/baclofen; (Δ---Δ) Glu/baclofen.

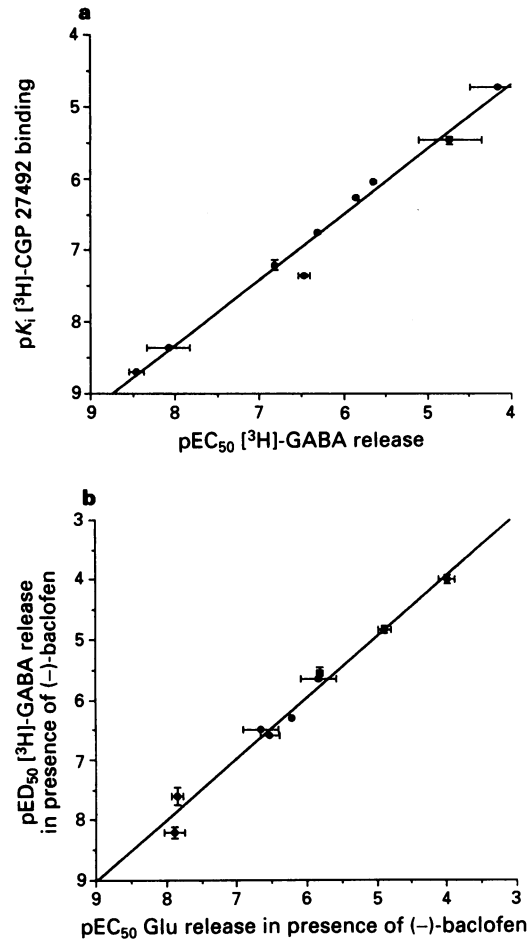


Figure 5 Examples of correlation plots: the negative logarithms ± s.e.mean of the K_i values (pK_i) of the compounds to inhibit [^{3}H]-CGP 27492 binding to the $GABA_B$ receptor were plotted against those of their EC_{50} values (pEC_{50}) to increase [^{3}H]-GABA release in the absence of (−)-baclofen (a) and the pEC_{50} values to increase [^{3}H]-GABA release in the presence of (−)-baclofen were plotted against those to increase glutamate (Glu) release in the presence of (−)-baclofen (b). Data taken from Table 1. The graphs serve to illustrate the correlations. Wherever error bars are absent, they are too small to be visible.

if not impossible. Much more useful data are obtained if antagonism by the compounds of the inhibitory effect of (−)-baclofen on glutamate release is considered. Consequently, a comparable set of data with respect to [^{3}H]-GABA release had to be generated.

There was little difference between the EC_{50}'s with respect to [^{3}H]-GABA and endogeneous glutamate release in the presence of (−)-baclofen given in Table 1. It seems even less impressive if one examines the concentration response-curves depicted in Figures 2–4. A less than twofold difference was observed with CGP 52432, in favour of increasing glutamate release. Interestingly, this compound was reported to exhibit a very marked, 100 fold specificity for the antagonism of the effects of (−)-baclofen on [^{3}H]-GABA vs endogenous glutamate release (Lanza *et al.*, 1993; Bonanno & Raiteri, 1993). Another prototypic compound on which these authors based their suggestion of the existence of multiple $GABA_B$ receptors is CGP 35348, which they found to be about 70 times more potent in antagonizing the effects of (−)-baclofen on glutamate than on [^{3}H]-GABA release (Bonanno & Raiteri, 1992; 1993). In our experiments, this factor was 1. Thus, some fundamental elements of Bonanno of Raiteri's hypothesis concerning multiple $GABA_B$ receptors could not be confirmed under our conditions. Moreover, a set of 9 $GABA_B$ receptor antagonists, structurally related to CGP 35348 and CGP 52432, did not show clearcut differences with respect to the antagonism of the effects of (−)-baclofen on [^{3}H]-GABA and glutamate release.

These differences between the findings of Raiteri's group and ours are unexpected. Notwithstanding the differences in the models (K^+ stimulation in synaptosomes vs. electrical stimulation in slices), there is reasonable agreement about the potencies of the inhibitory effects of the agonist, (−)-baclofen, on [^{3}H]-GABA (Baumann *et al.*, 1990; Bonanno & Raiteri, 1993) and glutamate release (Bonanno & Raiteri, 1993; Waldmeier *et al.*, 1993b). The differences begin with the effect of the antagonist CGP 35348 on [^{3}H]-GABA release in the presence of (−)-baclofen, where the Italian group finds a somewhat lower potency than we do. On the contrary, in their model, CGP 52432 is about 10 times more potent than in ours. The differences with respect to glutamate release in the presence of (−)-baclofen are even more marked: Bonanno & Raiteri (1993) find CGP 35348 about 30 times more potent and Lanza *et al.* (1993) find CGP 52432 about 60 times less potent than we do. The reasons for these

discrepancies between the results of Raiteri's group and ours are not clear.

Certainly, there are the above-mentioned experimental differences: i.e. K^+ vs. electrical stimulation, synaptosomes vs. slices. It is likely that, at the stimulation frequency of 2 Hz which we used for GABA, the antagonists must compete not only with the exogenous agonist but in addition with endogenously released GABA, and this may lead to somewhat higher EC_{50}'s than in synaptosomes. Also, the relations between effects on GABA and glutamate release might be systematically altered by a small factor because competition of the $GABA_B$ receptor antagonists with the endogenous ligand may play a lesser role in the case of glutamate release. This is because there seems to be little tonic activation of $GABA_B$ heteroreceptors on glutamate nerve endings (Waldmeier *et al.*, 1993b). However, these factors would affect the EC_{50}'s of every compound in the same manner and thus cause only a parallel shift of the correlations.

We have attempted to study the effects of the prototype drugs, CGP 35348 and CGP 52432, with respect to antagonism of the inhibitory effect of (−)-baclofen on K^+-evoked GABA and glutamate release in synaptosomes in much the same way as Raiteri's group. However, in our hands the maximal inhibition obtained with (−)-baclofen was too small (between 30 and 40%) and the variability too high to allow appropriate conclusions. Therefore, we are left at present with a quite unsatisfactory discrepancy with the Italian group, whose hypothesis on the pharmacological heterogenity of $GABA_B$ autoreceptors and heteroreceptors regulating glutamate release we cannot confirm in our model.

References

BAUMANN, P.A., WICKI, P., STIERLIN, C. & WALDMEIER, P.C. (1990). Investigations on $GABA_B$ receptor-mediated autoinhibition of GABA release. *Naunyn-Schmied. Arch. Pharmacol.*, **341**, 88–93.

BITTIGER, H., REYMANN, N., HALL, R. & KANE, P. (1988). CGP 27492, a new, potent and selective radioligand for $GABA_B$ receptors. *E. J. Neurosci* (Suppl: 11th ENA meeting, Zürich) Abstr. No. 16.10, 60.

BONANNO, G.. GEMIGNANI, A., FEDELE, E., FONTANA, G. & RAITERI, M. (1991). Gamma-aminobutyric $acid_B$ receptors mediate inhibition of somatostatin release from cerebrocortex nerve terminals. *J. Pharmacol. Exp. Ther.*, **259**, 1153–1157.

BONANNO, G. & RAITERI, M. (1992). Functional evidence for multiple gamma-aminobutyric $acid_B$ receptor subtypes in the rat cerebral cortex. *J. Pharmacol. Exp. Ther.*, **262**, 114–118.

BONANNO, G. & RAITERI, M. (1993). Multiple $GABA_B$ receptors. *Trends Pharmacol. Sci.*, **14**, 259–261.

BOWERY, N.G., HILL, D.R., HUDSON, A.L., DOBLE, A., MIDDLEMISS, D.N., SHAW, J. & TURNBULL, M. (1980). (−)-Baclofen decreases neurotransmitter release in the mammalian CNS by an action at a novel GABA receptor. *Nature*, **283**, 92–94.

CHENG, Y.C. & PRUSOFF, W.H. (1973). Relationship between the inhibition constant (K_i) and the concentration of inhibitor which causes 50 per cent inhibition (I_{50}) of an enzymatic reaction. *Biochem. Pharmacol.*, **22**, 3099–3108.

CONZELMANN, U., MEYER, D.K. & SPERK, G. (1986). Stimulation of receptors of γ-aminobutyric acid modulates the release of cholecystokinin-like immunoreactivity from slices of the rat neostriatum. *Br. J. Pharmacol.*, **89**, 845–852.

GRAY, J.A. & GREEN, A.R. (1987). $GABA_B$-receptor mediated inhibition of potassium-evoked release of endogenous 5-hydroxytryptamine from mouse frontal cortex. *Br. J. Pharmacol.*, **91**, 517–522.

LANZA, M., FASSIO, A., GEMIGNANI, A., BONANNO, G. & RAITERI, M. (1993). CGP 52432: a novel potent and selective $GABA_B$ autoreceptor antagonist in rat cerebral cortex. *Eur. J. Pharmacol.*, **237**, 191–195.

OLPE, H.-R., KARLSSON, G., POZZA, M.F., BRUGGER, F., STEINMANN, M., VAN RIEZEN, H., FAGG, G., HALL, R.G., FROESTL, W. & BITTIGER, H. (1990). CGP 35348: A centrally active blocker of $GABA_B$ receptors. *Eur. J. Pharmacol.*, **187**, 27–38.

PITTALUGA, A., ASARO, D., PELLEGRINI, G. & RAITERI, M. (1987). Studies on [^{3}H]GABA and endogenous GABA release in rat cerebral cortex suggest the presence of autoreceptors on $GABA_B$ type. *Eur. J. Pharmacol.*, **144**, 45–52.

POTASHNER, S.J. (1979). Baclofen: Effects on amino acid release and metabolism in slices of guinea-pig cerebral cortex. *J. Neurochem.*, **32**, 103–109.

SCHLICKER, E., CLASSEN, K. & GÖTHERT, M. (1984). $GABA_B$ receptor-mediated inhibition of serotonin release in the rat brain. *Naunyn-Schmied. Arch. Pharmacol.*, **326**, 99–105.

WALDMEIER, P.C., HERTZ, C., WICKI, P., GRUNENWALD, C. & BAUMANN, P.A. (1993a). Autoreceptor-mediated regulation of GABA release: role of uptake inhibition and effects of novel $GABA_B$ antagonists. *Naunyn-Schmied. Arch. Pharmacol.*, **347**, 514–520.

WALDMEIER, P.C., WICKI, P., BITTIGER, H. & BAUMANN, P.A. (1992). The regulation of GABA release by $GABA_B$ autoreceptors: some intriguing findings and their possible implications. *Pharmacol. Commun.*, **2**, 4–7.

WALDMEIER, P.C., WICKI, P. & FELDTRAUER, J.-J. (1993b). Release of endogenous glutamate from rat cortical slices in presence of the glutamate uptake inhibitor L-trans-pyrrolidine-2,4-dicarboxylic acid. *Naunyn-Schmied. Arch. Pharmacol.*, **348**, 478–485.

WALDMEIER, P.C., WICKI, P., FELDTRAUER, J.J. & BAUMANN, P.A. (1988). Potential involvement of a baclofen-sensitive autoreceptor in the modulation of the release of endogenous GABA from rat brain slices in vitro. *Naunyn-Schmied. Arch. Pharmacol.*, **337**, 289–295.

(Received July 7, 1994
Accepted August 28, 1994)

Br. J. Pharmacol. (1994), **113**, 1522–1528 © Macmillan Press Ltd, 1994

Involvement of tyrosine kinase in the induction of cyclo-oxygenase and nitric oxide synthase by endotoxin in cultured cells

P. Akarasereenont, [1]J.A. Mitchell, I. Appleton, [2]C. Thiemermann & J.R. Vane

The William Harvey Research Institute, St. Bartholomew's Hospital Medical College, Charterhouse Square, London EC1M 6BQ

1 Cyclo-oxygenase (COX) and nitric oxide synthase (NOS) are two enzymes which have distinct cytokine-inducible isoforms (COX-2 and iNOS). Many cytokine receptors have an intracellular tyrosine kinase domain. Here we have used the tyrosine kinase inhibitors, erbstatin and genistein, to investigate the potential role of tyrosine kinase activation in the induction on COX-2 and iNOS caused by endotoxin (lipopolysaccharide; LPS) in bovine aortic endothelial cells (BAEC) and J774.2 macrophages.

2 The main COX metabolites, 6-oxo-prostaglandin $F_{1\alpha}$ (6-oxo-$PGF_{1\alpha}$) (for BAEC) and $PGF_{2\alpha}$ (for 774.2 macrophages) were measured by radioimmunossay: (i) accumulation of COX metabolites from endogenous arachidonic acid was measured at 24 h after addition of LPS (1 $\mu g\,ml^{-1}$); (ii) in experiments designed to measure 'COX activity', COX metabolites generated by BAEC or J774.2 macrophages activated with LPS were assayed (at 12 h after LPS administration) after incubation of the washed cells with exogenous arachidonic acid (30 μM for 15 min). Western blot analysis with a specific antibody to COX-2 was used to determine the expression of COX-2 protein caused by LPS in cell extracts. Accumulation of nitrite (measured by the Griess reaction) was used as an indicator of NO formation and, hence, iNOS activity.

3 Erbstatin (0.05 to 5 $\mu g\,ml^{-1}$) or genistein (0.5 to 50 $\mu g\,ml^{-1}$) caused a dose-dependent inhibition of the accumulation of COX metabolites in the supernatant of BAEC or J774.2 macrophages activated with LPS. Erbstatin or genistein also caused a dose-dependent inhibition of 'COX activity' in both cell types. Western blot analysis showed that erbstatin (5 $\mu g\,ml^{-1}$) or genistein (50$\mu g\,ml^{-1}$) inhibited the expression of COX-2 protein in BAEC and J774.2 macrophages activated with LPS (1$\mu g\,ml^{-1}$ for 24 h).

4 Erbstatin or genistein also caused a dose-dependent inhibition of nitrite accumulation in J774.2 macrophages activated with LPS (1 $\mu g\,ml^{-1}$ for 24 h). In contrast to J774.2 macrophages, BAEC stimulated with LPS (1 $\mu g\,ml^{-1}$ for 24 h) did not produce detectable amounts ($< 1\mu M$) of nitrite.

5 These results suggest that tyrosine phosphorylation is part of the signal transduction mechanism that mediates (i) the induction of COX-2 and iNOS elicited by LPS in J774.2 macrophages, and (ii) the induction of COX-2 by LPS in BAEC.

Keywords: cytokines; lipopolysaccharide; prostaglandins; nitric oxide; tyrosine kinase receptor

Introduction

Bacterial lipopolysaccharide (LPS), derived from bacterial cell walls, is the fragment responsible for many of the symptoms of bacterial septicaemia. Exposure of cells in culture to LPS causes the release of inflammatory cytokines such as interleukin-1 (IL-1), IL-6 and tumour necrosis factor. In addition, LPS alone or in combination with such cytokines causes the synthesis of a growing list of adhesion proteins (see Cotran & Pober, 1990; see Dinerman & Mehta, 1990) and enzymes. These enzymes include nitric oxide synthase (NOS) and cyclo-oxygenase (COX).

Prostaglandins have numerous cardiovascular and inflammatory effects (Vane & Botting, 1992). COX is the first enzyme in the pathway in which arachidonic acid is converted to prostaglandins, prostacyclin and thromboxane A_2 (Vane & Botting, 1990; Smith & Marnett, 1991). The enzyme is localized primarily in the endoplasmic reticulum (Nugteren *et al.*, 1973; Rollins & Smith, 1980) and has been purified as a dimer of 70-kDa subunits (Roth *et al.*, 1975; Van der Ouderaa *et al.*, 1977). COX exists in at least 2 isoforms (Xie *et al.*, 1991). COX-1 is present constitutively in various types of cells including endothelial cells (Mitchell *et al.*, 1993), whereas the expression of COX-2 is induced by pro-inflammatory stimuli including mitogens (O'Banion *et al.*, 1992), cytokines (Maier *et al.*, 1990) and bacterial lipopolysaccharide (Lee *et al.*, 1992) in various cultured cells *in vitro* such as endothelial cells (Akarasereenont *et al.*, 1994) and macrophages (Mitchell *et al.*, 1993; Akarasereenont *et al.*, 1994). Moreover, induction of COX-2 was recently demonstrated in inflamed sites in a murine model of chronic granulomatous inflammation *in vivo* (Vane *et al.*, 1994).

Nitric oxide (NO) is a gaseous mediator with potent vasodilator and cytotoxic effects (see Moncada *et al.*, 1991; Thiemermann, 1994). The enzyme responsible for NO formation from L-arginine, NOS, exists as constitutive (cNOS; Bredt & Snyder, 1990, Pollock *et al.*, 1991) and inducible isoforms (iNOS; Förstermann *et al.*, 1991; Stuehr *et al.*, 1991). Like COX-2, the constitutive isoforms of NOS are present in many types of cells, while the inducible isoform (iNOS) is expressed after stimulation of cells with a variety of agents including LPS, as well as some cytokines and mitogens (see Nussler & Billiar, 1993). Thus, both COX and NOS have distinct cytokine-inducible isoforms (COX-2 and iNOS) and exposure of macrophages to LPS causes the co-induction of iNOS and COX-2 (Swierkosz *et al.*, 1993; Salvemini *et al.*, 1993; Akarasereenont *et al.*, 1994).

[1]Present address: Departments of Thoracic Medicine and Applied Pharmacology, The National Heart and Lung Institute, Dovehouse Street, London SW3 6LD
[2]Author for correspondence.

Many cytokine receptors have an intracellular tyrosine kinase domain (Ullrich & Schlessinger, 1990), activation of which results in the phosphorylation of proteins following ligand binding. Activation of tyrosine kinase by cytokines has been suggested as a key event in the signal transduction pathway that mediates some of the late cellular events afforded by cytokines (Ullrich & Schlessinger, 1990). More recently, the phosphorylation of tyrosine residues on cellular proteins leading to liberation of arachidonic acid (AA) metabolites and NO has been observed in macrophages (Weinstein *et al.*, 1991; Glaser *et al.*, 1993), neutrophils (Gomez-Cambronero *et al.*, 1989, 1991; Huang *et al*, 1990; Berklow & Dodson *et al.*, 1991; Connelly *et al.*, 1991), platelets (Nakashima *et al.*, 1991), basophilic cells (Connelly *et al.*, 1991; Yu *et al*, 1991; Eiseman *et al.*, 1992) and rat Kupffer cells (Chao *et al.*, 1992) in response to agents such as endotoxin and IL. Sodhi & Kumar (1994) used the tyrosine kinase inhibitors, genistein and lavendustin, to demonstrate the crucial role of tyrosine kinase phosphorylation in the induction of iNOS in murine peritoneal macrophages. We have used the tyrosine kinase inhibitors, erbstatin (Umezawa *et al.*, 1990) and genistein (Akiyama *et al.*, 1987) as pharmacological tools to investigate the potential role of tyrosine kinase phosphorylation in the induction of COX-2 caused by LPS in bovine aortic endothelial cells (BAEC) and J774.2 macrophages. For comparison, we have also investigated the effects of tyrosine kinase inhibition on the induction of iNOS in J774.2 macrophages.

Methods

Cell Culture

Murine macrophages (J774.2; The European Collection of Animal Cell Culture; Salisbury, UK) were cultured in 96-well plates with Dulbecco's Modified Eagle's Medium (DMEM; 200 µl/well) containing 10% foetal calf serum (Gibco) and 4 mM L-glutamine. Bovine aortic endothelial cells (BAEC) were obtained from fresh bovine aortae as previously described (de Nucci *et al.*, 1988) and cultured in 96-well plates as above. The agents, which were dissolved in distilled water, were sterilised by filtration through a filter (pore size: 0.22 micron) before being added to the cells under sterile conditions. Cells were incubated at 37°C in a humidified incubator.

Measurement of the release of cyclo-oxygenase metabolites

The main COX metabolites released after activation of cells with LPS (6-oxo-$PGF_{1\alpha}$ for BAEC and $PGF_{2\alpha}$ for J774.2 macrophages; Akarasereenont *et al.*, 1994) were measured by radioimmunoassay (Salmon, 1978). In experiments to measure the effects of tyrosine kinase inhibitors on the release of COX metabolites from endogenous arachidonic acid, cells were treated with LPS (1 µg ml^{-1}) together with the tyrosine kinase inhibitors erbstatin (0.05, 0.5, 1.5 or 5 µg ml^{-1}) or genistein (0.5, 5, 15 or 50 µg ml^{-1}) for 24 h, and the medium was subsequently removed for radioimmunoassay. In separate experiments designed to measure the effect of tyrosine kinase inhibitors (concentrations as above) on 'COX activity', to eliminate any effects of other enzymes induced or activated by LPS involved in the arachidonic cascade during LPS stimulation, cells were treated with LPS (1 µg ml^{-1}) together with the respective tyrosine kinase inhibitors (as above) for 12 h, after which time cells were washed and fresh medium containing arachidonic acid (30 µM) was added for 15 min at 37°C. The formation of COX-metabolites was then assessed by radioimmunoassay in the cell culture supernatant.

Immunoblot (Western blot) analysis

BAEC and J774.2 macrophages which were untreated (control), treated with LPS alone (1 µg ml^{-1}), treated with LPS (1 µg ml^{-1}) plus erbstatin (5 µg ml^{-1}) or with LPS plus genistein (50 µg ml^{-1}) were cultured in 6-well culture plates (37°C; for 24 h). After incubation, cells were washed with phosphate buffered saline (PBS; pH 7.4) and incubated (5 min) with 1 ml of extraction buffer (Tris, 50 mM; EDTA, 10 mM; Triton X-100, 1% v/v; phenylmethylsulphonyl fluoride (PMSF), 1 mM; pepstatin A, 0.05 mM and leupeptin, 0.2 mM) with gentle shaking. The cell extract was then boiled (10 min) in a ratio of 1:1 with gel loading buffer (Tris 50 mM, SDS 10% w/v, glycerol 10% v/v, 2-mercaptoethanol 10% v/v and bromphenol blue 2 mg ml^{-1}). Samples were centrifuged at 10,000 g for 2 min before being loaded onto gradient gels (4-10% Tris-glycine) and subjected to electrophoresis (1 h at 125 V). The separated proteins were transferred to nitrocellulose (BIORAD; 1 h at 200 V). After transfer to nitrocellulose, the blot was incubated in blocking solution (dried minimal-fat milk 5% w/v and Tween-20 0.25% v/v in PBS solution) for 1 h and then primed with primary antibody (dilution 1:1000), a rabbit antibody raised to murine COX-2 (Caymen Chemical Company, MI, USA; no detectable cross-reactivity with COX-1), for 1 h. The blot was then incubated with secondary antibody (dilution 1:1000), an anti-rabbit IgG developed in sheep, linked to alkaline phosphatase conjugate, for 1 h. Finally, the blot was developed for approximately 5 min with premixed solution containing 5-bromo-4-chloro-3-indolyl phosphate (BCIP) 0.56 mM, nitro blue tetrazolium (NBT) 0.48 mM, Tris. 10 mM, and $MgCl_2$ 59.3 mM; (pH 9.2). The detection limit of protein in cell extracts was 1–10 ng of protein.

Measurement of NOS activity

NOS activity was assessed by measuring the accumulation of nitrite in the culture medium by the Griess reaction adapted for a 96-well plate reader (Gross *et al.*, 1991). Nitrite levels were measured in aliquots of the same culture medium used to determine COX metabolites. Nitrite was measured by adding 100 µl of Griess reagent (1% sulphanilamide and 0.1% naphthylethylenediamide in 5% phosphoric acid) to 100 µl of sample culture medium. The optical density at 550 nm (OD_{550}) was measured with a Molecular Devices microplate reader (Richmond, CA, U.S.A.). Nitrite concentrations were calculated by comparison with OD_{550} of standard solutions of sodium nitrite prepared in culture medium. The detection limit for nitrite measurement in culture medium was 1 µM.

Measurement of cell viability

Cell respiration, an indicator of cell viability, was assessed by the mitochondrial dependent reduction of 3-(4,5-dimethylthiazol-2-yl)-2,5-diphenyltetrazolium bromide (MTT) to formazan (Gross & Levi, 1992). At the end of each experiment, cells in 96-well plates were incubated (37°C; 1 h) with MTT (0.2 mg ml^{-1}) dissolved in culture medium, after which time, the medium was removed by aspiration and cells were solubilized in dimethylsulphoxide (DMSO, 200 µl). The extent of reduction of MTT to formazan within cells was quantitated by measurement of optical density at 650 nm (OD_{650}) using a Molecular Devices microplate reader (Richmond, CA, U.S.A.).

Statistical analysis

Results shown are mean ± s.e.mean from triplicate determinations (wells) from 3 separate experimental days. Student's paired or unpaired *t* tests, as appropriate, were used to determine the significance of differences between means and a

P-value of less than 0.05 was taken as statistically significant.

Materials

Escherichia coli lipopolysaccharide (serotype: 0111:B4), DMSO, phosphate buffered saline (PBS; pH 7.4), Trizma base, EDTA, triton X-100, phenylmethylsulfonyl fluoride (PMSF), pepstatin A, Leupeptin, glycerol, 2-mercaptoethanol, bromphenol blue, sulphanilamide, naphthylethylenediamide, phosphoric acid, sodium nitrite, sodium dodecyl sulfate (SDS), anti-rabbit IgG antibody, premixed BCIP/NBT solution, 3-(4,5-dimethylthiazol-2-yl)-2,5-diphenyltetrazolium bromide (MTT), 6-oxo-$PGF_{1\alpha}$ and $PGF_{2\alpha}$ and their respective antibodies were supplied by Sigma Chemical Company (Poole, UK). Erbstatin and genistein were purchased from Calbiochem Novabiochem (Nottingham, U.K.). [^{3}H]-6-oxo-$PGF_{1\alpha}$ and [^{3}H]-$PGF_{2\alpha}$ were purchased from Amersham International (Buckinghamshire, U.K.). Dulbecco's modified Eagle's medium (DMEM) was obtained from Flow Laboratories. L-Glutamine was obtained from B.D.H. (Dagenham, U.K.) and foetal calf serum was obtained from Gibco BRL (U.K.). Pure nitrocellulose membrane (0.45 micron) and filter paper were purchased from BIO-RAD (Hertfordshire, U.K.).

Results

Effect of tyrosine kinase inhibitors on the release of cyclo-oxygenase metabolites from endogenous stores of arachidonic acid by BAEC or J774.2 macrophages activated by LPS

LPS (1 $\mu g\,ml^{-1}$) enhanced the accumulation of 6-oxo $PGF_{1\alpha}$ from BAEC by more than eighty fold (Figure 1a). This accumulation was inhibited by erbstatin or genistein in a dose-dependent manner as shown in Figure 1a. Activation of J774.2 macrophages with LPS similarly increased the accumulation of $PGF_{2\alpha}$ by more than ten-fold (Figure 1b). This enhanced formation of $PGF_{2\alpha}$ by macrophages activated with LPS was also inhibited by erbstatin or genistein in a dose-dependent manner (Figure 1b).

Incubation of either BAEC or J774.2 macrophages with LPS for 24 h did not result in any loss of cell viability as measured by the MTT assay. In addition, neither of the tyrosine kinase inhibitors used (up to 50 $\mu g\,ml^{-1}$) had any effect on cell viability, either alone or in combination with LPS.

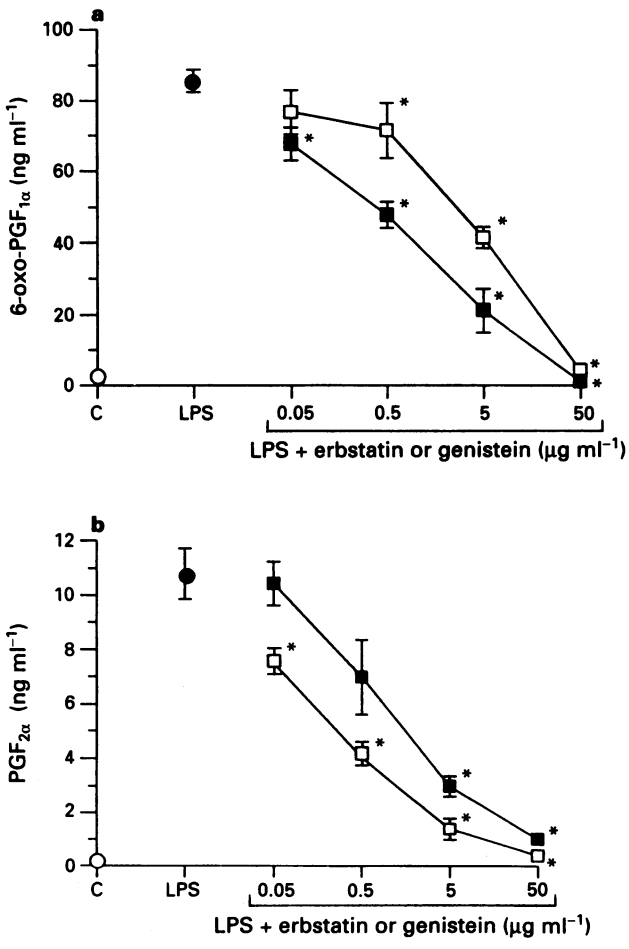


Figure 1 Effects of erbstatin and genistein on the accumulation of 6-oxo-$PGF_{1\alpha}$ from endothelial cells (a) and $PGF_{2\alpha}$ from J774.2 macrophages (b). Cells were treated with vehicle for 24 h (○, C) or LPS (1 $\mu g\,ml^{-1}$ for 24 h) in the absence (●) or presence of either erbstatin (□) or genistein (■). Data are expressed as mean ± s.e.mean from triplicate determinations (wells) from 3 separate experimental days ($n = 9$). *$P < 0.05$ when compared to LPS-treated cells at 24 h (LPS).

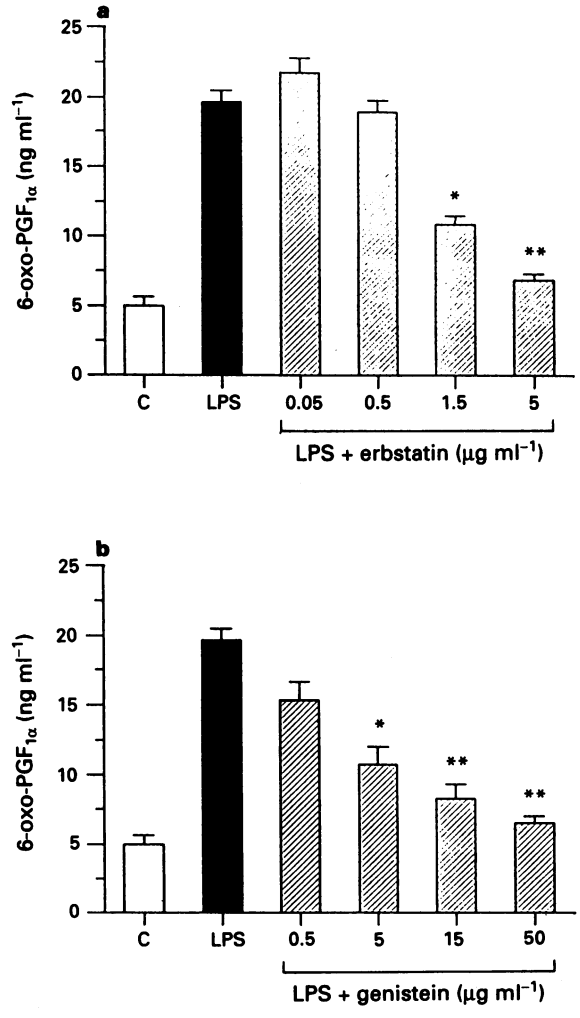


Figure 2 Dose-dependent inhibition of cyclo-oxygenase (COX) activity by erbstatin (a) or genistein (b) in LPS-activated BAEC measured at 12 h by the formation of the COX metabolites (6-oxo-$PGF_{1\alpha}$) in the presence of exogenous arachidonic acid (30 μM; 15 min). Data are expressed as mean ± s.e.mean from triplicate determinations (wells) from 3 separate experimental days ($n = 9$). *$P < 0.05$ and **$P < 0.01$ when compared to untreated cells at 12 h (C).

Effect of tyrosine kinase inhibitors on COX activity

In BAEC, the increase in COX activity afforded by LPS, measured in the presence of exogenous arachidonic acid, was almost four fold that of the control cells at 12 h. (Figure 2). This figure also shows the dose-dependent inhibition by erbstatin or genistein of this increase in COX activity, to almost control levels at the highest concentrations. The increase in COX activity afforded by LPS in J774.2 macrophages was inhibited to a similar extent by the same concentrations of erbstatin or genistein (Figure 3).

The effect of tyrosine kinase inhibitors on COX-2 protein in LPS-treated BAEC and J774.2 macrophages.

Untreated BAEC (Figure 4a) or J774.2 macrophages (Figure 4b) contained no detectable COX-2 protein (Figure 4; lane 1). In contrast, BAEC or J774.2 macrophages activated with LPS (1 $\mu g\,ml^{-1}$; 24 h) contained a protein of approximately 70 kDa, which was recognised by a specific antibody to COX-2 (Figure 4; lane 2). This induction of COX-2 protein by LPS in both BAEC and J774.2 macrophages was prevented by erbstatin (5 $\mu g\,ml^{-1}$ at 24 h; Figure 4; lane3) or genistein (50 $\mu g\,ml^{-1}$ at 24 h; Figure 4; lane 4).

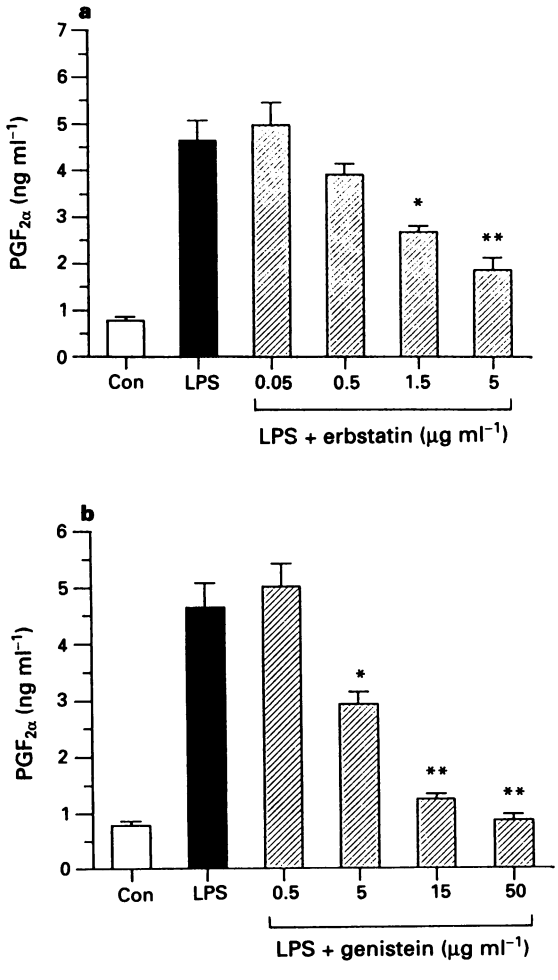


Figure 3 Dose-dependent inhibition of cyclo-oxygenase (COX) activity by erbstatin (a) or genistein (b) in LPS-activated J774.2 macrophages measured at 12 h by the formation of the COX metabolites ($PGF_{2\alpha}$) in the presence of exogenous arachidonic acid (30 μM; 15 min). Data are expressed as mean ± s.e.mean from triplicate determinations (wells) from 3 separate experimental days ($n = 9$). $^*P < 0.05$ and $^{**}P < 0.005$ when compared to untreated cells at 12 h (C).

The effect of tyrosine kinase inhibitors on the stimulation of nitric oxide synthesis by LPS in J774.2 macrophages

In J774.2 macrophages, incubation with LPS for 24 h caused a significant increase in nitrite from $< 1\,\mu M$ in untreated control cells at 24 h (detection limit) to $17.6 \pm 0.8\,\mu M$. This enhanced formation of nitrite was inhibited in a dose-dependent manner by erbstatin (Figure 5a; $n = 9$) or genistein (Figure 5b; $n = 9$). This inhibition of nitrite formation by the respective tyrosine kinase inhibitors was already significant at concentrations of erbstatin and genistein of 0.5 and 5 $\mu g\,ml^{-1}$, respectively.

Incubation of BAEC with LPS for 24 h did not result in any detectable accumulation of nitrite ($n = 9$; data not shown).

Discussion

LPS is known to cause co-induction of iNOS and COX-2 activity in J774.2 macrophages (Swierkosz *et al.*, 1993; Salvemini *et al.*, 1993). Here we show that the tyrosine kinase inhibitors, erbstatin and genistein, inhibit the induction by LPS of COX-2 activity and protein expression in J774.2 macrophages and also in BAEC. Although iNOS activity is not induced in BAEC under our conditions (MacNaul & Hutchinson, 1993; Marumo *et al.*, 1993; Akarasereenont *et al.*, 1994), in J774.2 cells, nitrite production is markedly increased by LPS. We also show that erbstatin or genistein inhibits the expression of iNOS activity caused by LPS in

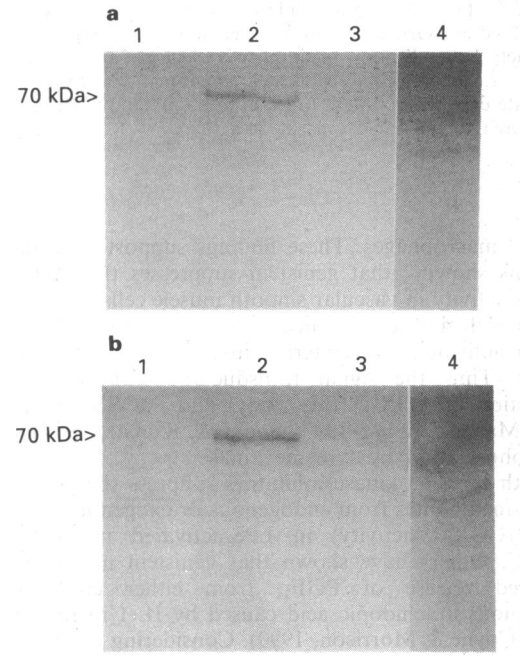


Figure 4 The figure shows Western blots using polyclonal antibodies to inducible cyclo-oxygenase (COX-2) of cell extracts from LPS-treated and untreated BAEC (a) and J774.2 macrophages (b). Equal amounts of protein were loaded in all lanes of BAEC (30 μg/lane) and J774.2 macrophages (60 μg/lane). Control untreated BAEC or J774.2 macrophages at 24 h (lane 1) contained no detectable COX-2 protein. In contrast, LPS-activated (1 $\mu g\,ml^{-1}$ for 24 h) BAEC or J774.2 macrophages contained COX-2 protein (lane 2). The induction of COX-2 protein by LPS in both BAEC and J774.2 macrophages was prevented by erbstatin (5 $\mu g\,ml^{-1}$; lane 3) or genistein (50 $\mu g\,ml^{-1}$; lane 4). Similar results were obtained with cell extracts from 3 separate batches of cells.

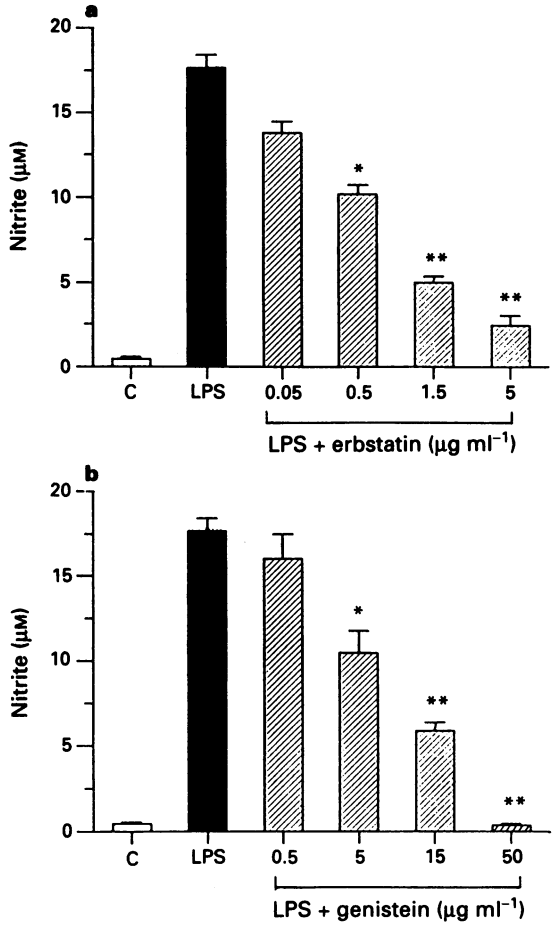


Figure 5 Dose-dependent inhibition of nitrite accumulation at 24 h (measured by Griess reaction) by erbstatin (a) or genistein (b) in LPS-activated J774.2 macrophages. Data are expressed as mean ± s.e.mean from triplicate determinations (wells) from 3 separate experimental days ($n = 9$). $^*P < 0.05$ and $^{**}P < 0.005$ when compared to untreated cells at 24 h (C).

J774.2 macrophages. These findings support previous observations showing that genistein suppresses the expression of iNOS activity in vascular smooth muscle cells (Marczin *et al.*, 1993) and murine peritoneal macrophages (Sodhi & Kumar, 1994) activated with interleukin-1 (IL-1) and LPS, respectively. Thus the signal transduction pathway leading to induction of COX-2 (this study) and iNOS (this study; see also Marczin *et al.*, 1993; Sodhi & Kumar, 1994) involves phosphorylation by tyrosine kinase.

Both tyrosine kinase inhibitors suppress the generation of COX-metabolites from endogenous or exogenous arachidonic acid (COX-2 activity) in LPS-activated macrophages or BAEC. Others have shown that genistein inhibits the IL-1 induced release of $PGF_{2\alpha}$ from either endogenous or exogenous arachidonic acid caused by IL-1 in rat mesangial cells (Coyne & Morrison, 1990). Considering our finding here that genistein abolishes the expression of COX-2 caused by LPS in J774.2 macrophages and bovine aortic endothelial cells, we propose that the IL-1 stimulated release of $PGF_{2\alpha}$ afforded by IL-1 in rat mesangial cells (Coyne & Morrison, 1990) is due to the induction of COX-2 by IL-1, a process which is prevented by genistein.

Bacterial lipopolysaccharide (LPS) has cytotoxic effects and is a potent activator of the immune system, induces local or systemic inflammation and septic shock (Morrison & Ryan, 1979). In addition to its cytotoxic effects, LPS stimulates the release of a variety of inflammatory mediators including cytokines *in vitro* and *in vivo* (Hewett & Roth, 1993; see Thiemermann, 1994). The signal transduction mechanisms by which LPS induces alterations in cell function or the expression of proteins such as COX-2 or iNOS are not completely understood.

It is well-documented that LPS binds to a number of different constituents on the surface of cells or in the plasma/serum (i.e. LPS-binding protein). These interactions can modulate cellular function *in vitro*. Two different cell surface molecules, CD14 and CD18, have been proposed as LPS receptors (Raetz *et al*, 1991; Bright *et al.*, 1990; Wright *et al.*, 1990) but their contribution to the cellular activation afforded by LPS is less well investigated. Recently, it has been proposed that the membrane form of CD14 functions as a receptor for LPS, while its soluble form acts as a co-ligand with LPS to activate endothelial cells (Haziot *et al.*, 1993). Even less is known about the early intracellular events that mediate specific LPS responses. A pertussis toxin-sensitive guanine nucleotide-binding protein (G protein) has been identified which couples the binding of LPS to the cell surface to the intracellular signal transduction pathways leading to the response such as altered gene expression of may cytokines (Jakway & DeFranco, 1986; Wang *et al.*, 1988; Daniel-Issakani *et al.*, 1989; Dziarski, 1989). However, some actions of LPS in cells are unaffected by pertussis toxin treatment (Dziarski, 1989; Forehand *et al.*, 1989), suggesting that some of the responses elicited by LPS do not occur through a single class of a G protein-dependent signalling mechanism. In terms of the intracellular signal transduction pathway, the phopsphorylation of tyrosine residues on cellular proteins, leading to formation of arachidonic acid (AA) metabolites or NO, has been observed in many cell types (see Introduction). Activation of tyrosine kinase may, therefore, be an integral part, either independently or in concert with Ser/Thr protein kinases (e.g. protein kinase C), of the signal transduction pathways leading to expression of COX-2 and iNOS in macrophages and smooth muscle cells. LPS stimulates the secretion of many cytokines and growth factors which have receptors with an intracellular tyrosine kinase domain, resulting in the phosphorylation of proteins following ligand binding (Ullrich & Schlessinger, 1990). Whether LPS causes COX-2 or iNOS induction by directly activating tyrosine kinase or indirectly via the release of cytokines remains the subject of investigation.

The demonstration that inhibitors of tyrosine kinase suppress the induction of both COX-2 and iNOS provides a possible explanation for the anti-inflammatory activities of such inhibitors in a variety of models (Williams *et al.*, 1992; Levitski, 1992; Bartlett *et al.*, 1993). However, these two enzymes are not expressed in parallel in all models. Thus, in the murine chronic granulomatous air pouch model, COX-2 and iNOS activity show a reciprocal relationship (Vane *et al.*, 1994). Furthermore, growth factors such as platelet-derived growth factor (PDGF), inhibit the induction of iNOS in vascular smooth muscle cells (Schini *et al.*, 1992), but induce the synthesis of COX-2 in fibroblasts (Lin *et al.*, 1989). These findings suggest that the cytokines which contribute to the induction of COX-2 and iNOS by LPS may well be different in different cells although the intracellular mechanisms may be similar. Although this and other studies (MacNaul & Hutchinson, 1993; Marumo *et al.*, 1993; Akarasereenont *et al.*, 1994) demonstrate that LPS alone does not cause a detectable increase in nitrite in endothelial cells, there is evidence that a mixture of cytokines can cause an induction of iNOS in these cells (Radomski *et al.*, 1990; Kilbourn & Belloni, 1990). The identification of the cytokines, which are ultimately responsible for the induction of COX-2 and iNOS in different cells, will lead to a better understanding of the mechanism(s) leading to an enhanced formation of COX-metabolites and NO as well as their interaction in inflammation or circulatory shock.

The authors are indebted to Ms Elizabeth Wood for supplying the cultured cells and Ms Ivana Vojnovic for technical assistance. We

thank Dr. Y.S. Bakhle for his comments and helpful discussion of this manuscript. The authors would also like to thank Dr. Jamie Croxtall and Dr. Tomas Hohlfield for helpful discussions. I.A. is a recipient of a Royal Society Smith and Nephew Research Fellowship.

References

AKARASEREENONT, P., MITCHELL, J.A., THIEMERMANN, C. & VANE, J.R. (1994). Lipopolysaccharide induces bovine aortic endothelial cells to synthesize cyclo-oxygenase but not nitric oxide synthase: a comparison with macrophages. *Br. J. Pharmacol.*, **111**, 33P.

AKIYAMA, T., ISHIDA, J., NAKAGAWA, S., OGAWARA, H., WATANABE, S.I., ITOH, N., SHIBUYA, M. & FUKAMI, Y. (1987). Genistein, a specific inhibitor of tyrosine-specific protein kinases. *J. Biol. Chem.*, **262**, 5592–5595.

BARTLETT, R.R., ANAGNOSTOPULOS, H., ZIELINSKI, T., MATTAR, T. & SCHLEYERBACH, R. (1993). Effects of leflunomide on immune responses and models of inflammation. *Spring. Semin. Immunopathol.*, **14**, 381–394.

BERKLOW, R.L. & DODSON, R.W. (1991). Alterations in tyrosine protein kinase activities upon activation of human neutrophils. *J. Leukoc. Biol.*, **49**, 599–604.

BREDT, D.S. & SNYDER, S.H. (1990). Isolation of nitric oxide synthetase, a calmodulin-requiring enzyme. *Proc. Natl. Acad. Sci. U.S.A.*, **87**, 682–685.

BRIGHT, S.W., CHEN, T.Y., FLEBBE. L.M., LEI, M.G. & MORRISON, D.C. (1990). Generation and characterization of hamster mouse hybridomas secreting monoclonal antibodies with specificity for lipopolysaccharide receptor. *J. Immunol.*, **145**, 1–7.

CHAO, W., LIU, H., HANAHAN, D.J. & OLSON, M.S. (1992). Platelet activating factor stimulated protein tyrosine phosphorylation and eicosanoid synthesis in rat Kupffer cells. Evidence for calcium-dependent and protein kinase C-dependent and -independent pathways. *J. Biol. Chem.*, **267**, 6725–6735.

CONNELLY, P.A., FARRELL, C.A., MERENDA, J.M., CONKLYN, M.J. & SHOWELL, H.J. (1991). Tyrosine phosphorylation is an early signaling event common to Fc receptor crosslinking in human neutrophils and rat basophilic leukemia cells (RBL-2H3). *Biochem. Biophys. Res. Commun.*, **177**, 192–201.

COTRAN, R.S. & POBER, J.S. (1990). Cytokine-endothelial interactions in inflammation, immunity, and vascular injury. *J. Am. Soc. Nephrol.*, **1**, 225–235.

COYNE, D.W. & MORRISON, A.R. (1990). Effect of the tyrosine kinase inhibitor, genistein, on interleukin-1 stimulated PGE_2 production in mesangial cells. *Biochem. Biophys. Res. Commun.*, **173**, 718–724.

DANIEL-ISSAKANI, S., SPIEGEL, A.M. & STRULOVICI, B. (1989). Lipopolysaccharide response is linked to the GTP binding protein, Gi_2, in the promonocytic cell line U937. *J. Biol. Chem.*, **264**, 20240–20247.

DE NUCCI, G., GRYGLEWSKI, R.J., WARNER, T.D. & VANE, J.R. (1988). Receptor mediated release of endothelium-derived relaxing factor and prostacyclin from bovine aortic endothelial cells is coupled. *Proc. Natl. Acad. Sci. U.S.A.*, **85**, 2334–2338.

DINERMAN, J.L. & MEHTA, J.L. (1990). Endothelial, platelet and leukocyte interactions in ischemic heart disease: insights into potential mechanisms and their clinical relevance. *J. Am. Coll. Cardiol.*, **16**, 207–222.

DZIARSKI, R. (1989). Correlation between ribosylation of pertussis toxin substrates and inhibition of peptidoglycan-, muramyl dipeptide- and lipopolysaccharide-induced mitogenic stimulation in B lymphocytes. *Eur. J. Immunol.*, **19**, 125–130.

EISEMAN, E. & BOLEN, J.B. (1992). Engagement of the high affinity IgE receptor activates *src* protein-related tyrosine kinases. *Nature*, **355**, 78–80.

FOREHAND, J.R., PABST. M.J., PHILLIPS, W.A. & JOHNSTON, R.B. (1989). Lipopolysaccharide priming of human neutrophils for an enhanced respiratory burst. Role of intracellular free calcium. *J. Clin. Invest.*, **83**, 74–83.

FÖRSTERMANN, U., SCHMIDT, H.H.H.W., POLLOCK, J., SHENG. H., MITCHELL, J.A., WARNER, T.D., NAKANE, M. & MURAD, F. (1991). Isoforms of nitric oxide synthase. Characterization and purification from different cell types. *Biochem. Pharmacol.*, **42**, 1849–1857.

GLASER, K.B., SUNG, A., BAUER, J. & WEICHMAN, B.M. (1993). Regulation of eicosanoid biosynthesis in the macrophage: involvement of protein tyrosine phosphorylation and modulation by selective protein tyrosine kinase inhibitors. *Biochem. Pharmacol.*, **45**, 711–721.

GOMEZ-CAMBRONERO, J., HUANG, C.K., BONAK, V.A., WANG, E., CASNELLIE, J.E., SHIRAISHI, J. & SHA'AFI, R.L. (1989). Tyrosine phosphorylation in human neutrophil. *Biochem. Biophys. Res. Commun.*, **162**, 1478–1485.

GOMEZ-CAMBRONERO, J., WANG, E., JOHNSON, G., HUANG, C.K. & SHA'AFI, R.L. (1991). Platelet activating factor induces tyrosine phosphorylation in the human neutrophil. *J. Biol. Chem.*, **266**, 6240–6245.

GROSS, S.S., JAFFE, E.A., LEVI, R. & KILBOURN, R.G., (1991). Cytokine-activated endothelial cells express an isotype of nitric oxide synthase which is tetrahydrobiopterin-dependent, calmodulin-independent and inhibited by arginine analogs with a rank-order of potency characteristic of activated macrophages. *Biochem. Biophys. Res. Commun.*, **187**, 823–829.

GROSS, S.S. & LEVI, R. (1992). Tetrahydrobiopterin synthesis: An absolute requirement for cytokine-induced nitric oxide generation by vascular smooth muscle. *J. Biol. Chem.*, **267**, 25722–25729.

HAZIOT, A., RONG, G.W., SILVER, J. & GOYERT, S.M. (1993). Recombinant soluble CD14 mediates the activation of endothelial cells by lipopolysaccharide. *J. Immunol.*, **151**, 1500–1507.

HEWETT, J.A., & ROTH, R.A. (1993). Hepatic and extrahepatic pathobiology of bacterial lipopolysaccharides. *Pharmacol. Rev.*, **45**, 381–411.

HUANG, C.K., BONAK, V.A., LARAMEE, G.R. & CASNELLIE, J.E. (1990). Protein tyrosine phosphorylation in rabbit peritoneal neutrophils. *Biochem. J.*, **269**, 431–436.

JAKWAY, J.P. & DeFRANCO, A.L. (1986). Pertussis toxin inhibition of B cell and macrophage responses to bacterial lipopolysaccharide. *Science*, **234**, 743–746.

KILBOURN, R.G. & BELLONI, P. (1990). Endothelial cell production of nitrogen oxides in response to interferon-γ in combination with tumor necrosis factor, interleukin-1, or endotoxin. *J. Natl. Cancer Inst.*, **82**, 772–776.

LEE, S.H., SOYOOLA, E., CHANMUGAM, P., HART, S., SUN, W., ZHONG, H., LIOU, S., SIMMONS, D. & HWANG, D. (1992). Selective expression of mitogen inducible cyclo-oxygenase in macrophages stimulated with lipopolysaccharide. *J. Biol. Chem.*, **267**, 25934–25938.

LEVITZKI, A. (1992). Tyrphostins: tyrosine kinase blockers as novel antiproliferative agents and dissectors of signal transduction. *FASEB. J.*, **6**, 3275–3282.

LIN, A.H., BIENKOWSKI, M.J. & GORMAN, R.R. (1989). Regulation of prostaglandin H synthase mRNA levels and prostaglandin biosynthesis by platelet-derived growth factor. *J. Biol. Chem.*, **264**, 17379–17383.

MACNAUL, K.L. & HUTCHINSON, N.L. (1993). Differential expression of iNOS and cNOS mRNA in human vascular smooth muscle cells and endothelial cells under normal and inflammatory conditions. *Biochem. Biophys. Res. Commun.*, **196**, 1330–1334.

MAIER, J.A., HLA, T. & MACIAG, T. (1990). Cyclo-oxygenase is an immediate early gene induced by interleukin-1 in human endothelial cells. *J. Biol. Chem.*, **265**, 10805–10808.

MARCZIN, N., PAPAPETROPOULOS, A. & CATRAVAS, J.D. (1993). Tyrosine kinase inhibitors suppress endotoxin- and I-$^1\beta$-induced NO synthesis in aortic smooth muscle cells. *Am. J. Physiol.*, **265**, H1014–H1018.

MARUMO, T., NAKAKI, T., ADACHI, H., ESUMI, H., SUZUKI, H., SARUTA, T. & KATO, R. (1993). Nitric oxide synthase mRNA in endothelial cells: synergistic induction by interferon-γ, tumor necrosis factor-α and lipopolysaccharide and inhibition by dexamethasone. *Jpn. J. Pharmacol.*, **63**, 327–334.

MITCHELL, J.A., AKARASEREENONT, P., THIEMERMANN, C., FLOWER, R.J. & VANE, J.R. (1993). Selectivity of nonsteroidal anti-inflammatory drugs as inhibitors of constitutive and inducible cyclo-oxygenase. *Proc. Natl. Acad. Sci. U.S.A.*, **90**, 11693–11697.

MONCADA, S., PALMER, R.M.J. & HIGGS, E.A. (1991). Nitric oxide: Physiology, pathophysiology, and pharmacology. *Pharmacol. Rev.*, **43**, 109–142.

MORRISON, D.C. & RYAN, J.L. (1979). Bacterial endotoxins and host immune responses. *Adv. Immunol.*, **28**, 293–450.

NAKASHIMA, S., KOIKE, T. & NOZAWA, Y. (1991). Genistein, a protein tyrosine kinase inhibitor, inhibits thromboxane A_2 mediated human platelet responses. *Mol. Pharmacol.*, **39**, 475–480.

NUGTEREN, D.H. & HAZELHOF, E. (1973). Isolation and properties of intermediates in prostaglandin biosynthesis. *Biochem. Biophys. Acta*, **326**, 448–461.

NUSSLER, A.K. & BILLIAR, T.R. (1993). Inflammation, immunoregulation, and inducible nitric oxide synthase. *J. Leukoc. Biol.*, **54**, 171–178.

O'BANION, M.K., WINN, V.D. & YOUNG, D.A. (1992). cDNA cloning and functional activity of glucocorticoid-regulated inflammatory cyclo-oxygenase. *Proc. Natl. Acad. Sci. U.S.A.*, **89**, 4888–4892.

POLLOCK, J.S., FÖRSTERMANN, U., MITCHELL, J.A., WARNER, T.D., SCHMIDT, H.H.H.W., NAKANE, M. & MURAD, F. (1991). Purification and characterization of particulate endothelium-derived relaxing factor synthase from cultured and native bovine aortic endothelial cells. *Proc. Natl. Acad. Sci. U.S.A.*, **88**, 10480–10484.

RADOMSKI, M.W., PALMER, R.M.J. & MONCADA, S. (1990). Glucocorticoids inhibit the expression of an inducible, but not the constitutive, nitric oxide synthase in vascular endothelial cells. *Proc. Natl. Acad. Sci. U.S.A.*, **87**, 10043–10047.

RAETZ, C.R.H., ULEVITCH, R.J., WRIGHT, S.D., SIBLEY, C.H., DING, A. & NATHAN, C.F. (1991). Gram-negative endotoxin: an extraordinary lipid with profound effects on eukaryotic signal transduction. *FASEB. J.*, **5**, 2652–2660.

ROLLINS, T.E. & SMITH, W.L. (1980). Subcellular localization of prostaglandin forming cyclo-oxygenase in Swiss mouse 3T3 fibroblasts by electron microscopic immunocytochemistry. *J. Biol. Dhem.*, **255**, 4872–4875.

ROTH, G.J., STANFORD, N. & MAJERUS, P.W. (1975). Acetylation of prostaglandin synthase by aspirin. *Proc. Natl. Acad. Sci. U.S.A.*, **72**, 3073–3076.

SALMON, J.A. (1978). A radioimmunoassay for 6-keto-prostaglandin $F_{1\alpha}\psi$ *Prostaglandins*, **15**, 383–397.

SALVEMINI, D., MISKO, T.P., MASFERRER, J.L., SEIBERT, K., CURRIE, M.G. & NEEDLEMAN, P. (1993). Nitric oxide activates cyclooxygenase enzymes. *Proc. Natl. Acad. Sci. U.S.A.*, **90**, 7240–7244.

SCHINI, V.B., DURANTE, W., ELIZONDO, E., SCOTT-BURDEN, T., JUNQUERO, D.C., SCHAFER, A.I. & VANHOUTTE, P.M. (1992). The induction of nitric oxide synthase activity is inhibited by TGF-β1, PDGF-AB and PDGF-BB in vascular smooth muscle cells. *Eur. J. Pharmacol.*, **216**, 379–383.

SMITH, W.L. & MARNETT, L.J. (1991). Prostaglandin endoperoxide synthase: sturcture and catalysis. *Biochem. Biophys. Acta*, **1083**, 1–17.

SODHI, A. & KUMAR, R. (1994). Production of nitric oxide and its regulation in murine peritoneal macrophages treated with cisplatin and lipopolysaccharide. *Int. J. Immunopathol. Pharmacol.*, **7**, 65–77.

STUEHR, D.J., CHO, H.J., KWON, N.S., WEISE, M.F. & NATHAN, C.F. (1991). Purification and characterization of the cytokine-induced macrophage nitric oxide synthase: an FAD- and FMN-containing flavoprotein. *Proc. Natl. Acad. Sci. U.S.A.*, **88**, 7773–7777.

SWIERKOSZ, T.A., MITCHELL, J.A., WOOD, E.G., WARNER, T.D., THIEMERMANN, C. & VANE, J.R. (1993). Co-release and interactions of nitric oxide and prostanoids *in vitro* and *in vivo* following exposure to bacterial lipopolysaccharide. *Endothelium*, **1** (Suppl.), 175.

THIEMERMANN, C. (1994). The role of arginine: nitric oxide pathway in circulatory shock. *Adv. Pharmacol.*, **28**, 49–75.

ULLRICH, A. & SCHLESSINGER, J. (1990). Signal transduction by receptors with tyrosine kinase activity. *Cell*, **61**, 203–212.

UMEZAWA, K., HORI, T., TAJIMA, H., IMOTO, M., ISSHIKI, K. & TAKEUCHI, T. (1990). Inhibition of epidermal growth factor-induced DNA synthesis by tyrosine kinase inhibitors. *FEBS. Lett.*, **260**, 198–200.

VAN DER OUDERAA, F.J., BUYTENHEK, M., NUGTEREM, D.H. & VAN DORP, P.A. (1977). Purification and characterisation of prostaglandin endoperoxide synthase from sheep vesicular glands. *Biochem. Biophys. Acta*, **487**, 315–333.

VANE, J.R. & BOTTING, R.M. (1990). Mediators from the endothelial cell. *Adv. Prostaglandin Thromb. Leukor. Res.*, **21**, 627–636.

VANE, J.R. & BOTTING, R.M. (1992). In *Aspirin and Other Salicylates: The Prostaglandins*, ed. Vane, J.R. & Botting, R.M., pp 17–34, London,Chapman & Hall.

VANE, J.R., MITCHELL, J.A., APPLETON, I., TOMLINSON, A., BISHHOP-BAILY, D., CROXTALL, J. & WILLOUGHBY, D. (1994). Inducible isoforms of cyclo-oxygenase and nitric oxide synthase in inflammation. *Proc. Natl. Acad. Sci. U.S.A.*, **91**, 2046–2050.

WANG, J., KESTER, M. & DUNN, M.J. (1988). Involvement of a pertussis toxin-sensitive G-protein-coupled phospholipase A_2 in lipopolysaccharide-stimulated prostaglandin E_2 synthesis in cultured rat mesangial cells. *Biochem. Biophys. Acta*, **963**, 429–435.

WEINSTEIN, S.L., GOLD, M.R. & DE FRANCO. A.L. (1991). Bacterial lipopolysaccharide stimulates protein tyrosine phosphorylation in macrophages. *Proc. Natl. Acad. Sci. U.S.A.*, **88**, 4148–4152.

WILLIAMS, W.V., VONFELDT, J.M., RAMANUJAM, T. & WEINER, D.B. (1992). Tyrosine kinase signal transduction in rheumatoid synovitis. *Semi. Arthritis Rheum.*, **21**, 317–329.

WRIGHT, S.D., RAMOS, R.A., TOBIAS, P.S., ULEVITCH, R.J. & MATHISON, J.C. (1990). CD14, a receptor for complexes of lipopolysaccharide (LPS) and LPS binding protein. *Science*, **249**, 1431–1433.

XIE, W.L., CHIPMAN, J.G., ROBERTSON, D.L., ERIKSON, R.L. & SIMMONS, D.L. (1991). Expression of a mitogen-responsive gene encoding prostaglandin synthase is regulated by mRNA splicing *Proc. Natl. Acad. Sci. U.S.A.*, **88**, 2692–2696.

YU, K.T., LYALL, R., JARIWALA, N., ZILBERSTEIN, A. & HAIMOVICH, J. (1991). Antigen- and ionophore-induced signal transduction in rat basophilic leukemia cells involves protein tyrosine phosphorylation. *J. Biol. Chem.*, **266**, 22564–22568.

(Received June 23, 1994
Revised August 8, 1994
Accepted August 26, 1994)

Br. J. Pharmacol. (1994), **113**, 1529–1537 © Macmillan Press Ltd, 1994

Two populations of muscarinic binding sites in the chick heart distinguished by affinities for ligands and selective inactivation

Jan Jakubík & [1]Stanislav Tuček

Institute of Physiology, Academy of Sciences of the Czech Republic, Vídeňská 1083, 14220 Prague, Czech Republic

1 By measuring the binding of N-[^{3}H-methyl]-scopolamine ([^{3}H]-NMS) and of unlabelled subtype-specific muscarinic antagonists, two populations of muscarinic binding sites can be distinguished in the membranes of cardiac ventricles taken from 1-day-old chicks. One of them, corresponding to approximately 80% of [^{3}H]-NMS binding sites, has higher affinities for AF-DX116 (pKi = 6.42) and methoctramine (pKi = 7.33); the rate of [^{3}H]NMS dissociation from these sites is fast. The other population, corresponding to approximately 20% of [^{3}H]-NMS binding sites, has lower affinities for AF-DX116 (pKi = 5.00) and methoctramine (pKi = 6.19); the rate of [^{3}H]-NMS dissociation from these sites is slow. Both populations have high affinities for pirenzepine, but the affinity of the former (major) population is lower (pKi = 7.99) than that of the latter (minor) population (pKi = 10.14).

2 Since it has been shown earlier that two mRNAs for muscarinic receptors are expressed in the chick heart, one of them close to the genetically defined m2 and the other to the m4 subtype, we propose that the major population of binding sites with high affinities for AF-DX116 and methoctramine and the lower affinity for pirenzepine represents the M_2-like receptors, while the minor population represents the M_4-like receptors.

3 It proved possible to obtain isolated samples of either population by selectively protecting the M_2-like sites with AF-DX116 and the M_4-like sites with pirenzepine, and by inactivating the unprotected sites with benzilylcholine mustard. The properties of the isolated populations corresponded to those derived from the analysis of [^{3}H]-NMS binding to the original mixed population.

4 Alcuronium exerted positive allosteric action on the binding of [^{3}H]-NMS both to the M_2-like and the M_4-like population and severely slowed down [^{3}H]-NMS dissociation from them; its affinity for the M_2-like sites was 3–10 times higher.

Keywords: Heart, muscarinic receptor subtypes; heart, chick; muscarinic receptors, binding properties; muscarinic receptors, allosteric control; alcuronium; pirenzepine; methoctramine; AF-DX116; M_2 muscarinic receptors; M_4 muscarinic receptors

Introduction

Five subtypes (m1–m5) of muscarinic acetylcholine receptors have been defined genetically, while only four subtypes (M_1–M_4) can be distinguished pharmacologically (Bonner, 1989; Hulme *et al.*, 1990; Caulfield, 1993). Mammalian cardiac muscarinic receptors belong to the M_2 (m2) subtype and can be distinguished from the other receptor subtypes by their low affinities for pirenzepine and 4-DAMP and high affinities for AF-DX116 and methoctramine (Mitchelson, 1988).

Another notable feature of mammalian cardiac muscarinic receptors is their high sensitivity to gallamine and several other neuromuscular blockers which have been found to inhibit allosterically muscarinic receptors in experiments with isolated organs (Clark & Mitchelson, 1976) and with radioligand binding to membranes (Stockton *et al.*, 1983; Lee & El-Fakahany, 1991a; Ellis *et al.*, 1991), and also in investigations of biochemical effects of muscarinic activation (Ehlert, 1988a; for reviews see Kharkevich & Shorr, 1986; Hulme *et al.*, 1990; Lee & El-Fakahany, 1991b). We have discovered recently that the neuromuscular blocker, alcuronium, allosterically *increases* the binding of N-methylscopolamine (NMS) to muscarinic receptors in rat heart (M_2), but not to those in rat salivary glands (M_3) and brain cortex (M_1) (Tuček *et al.*, 1990).

It has been noted that muscarinic receptors in the chick heart differ from those in the mammalian heart. They appear similar to the M_1 subtype because of their high affinity for pirenzepine (Brown *et al.*, 1985; Lindmar & Löffelholz, 1987; Jeck *et al.*, 1988), but the pattern of affinities of other subtype-specific muscarinic ligands does not support their classification as the M_1, M_2 or M_3 subtype (Michel & Whiting, 1989; Kwatra *et al.*, 1989). Based on the similarity between the binding properties of chick heart and rabbit lung muscarinic receptors, Lazareno *et al.* (1990) proposed that chick heart receptors belong to the M_4 category. A gene closely corresponding to mammalian m4 muscarinic AChR gene has indeed been found to be expressed in the chick heart (Tietje *et al.*, 1990), but it has been shown subsequently that a second gene, homologous to the mammalian m2 subtype, is also expressed in the chick heart (Tietje & Nathanson, 1991).

Using radioligand binding techniques, we have found that it is possible to discern the presence of two populations of muscarinic binding sites in the chick heart and to separate them by selectively protecting one of the subtypes and inactivating the other subtype with the irreversible muscarinic ligand, benzilylcholine mustard (BCM; Gill & Rang, 1966). The data we obtained permitted us to make estimates of the sizes of the two receptor populations in the chick heart, to describe some of their binding properties (which led us to describe them as 'M_2-like' and 'M_4-like') and to show that both of them are subject to the positive allosteric action of alcuronium on [^{3}H]-NMS binding.

Methods

Preparation of membranes

One-day-old Leghorn chicks were killed by decapitation while Wistar rats of either sex (body weight 180–230 g) were killed by cervical dislocation and exsanguination. Chick heart

[1] Author for correspondence.

ventricles and rat atria were homogenized in a medium consisting of (mM): NaCl 136, KCl 5, $MgSO_4$ 1, Na-phosphate (pH 7.4) 1, and Na-HEPES (pH 7.4) 10. A polytron-type homogenizer was used for the chick heart and a Potter-Elvehjem glass homogenizer for the rat atria. The homogenates were centrifuged at 600 *g* for 10 min, the sediments were suspended and recentrifuged at the same force, and the combined supernatants from the two centrifugations were used for subsequent work. The membranes were sedimented by 40 min centrifugation at 13,000 *g* and washed by resuspension in the homogenization medium and recentrifugation under the same conditions. The washing was repeated twice more. Washed resuspended membranes were kept at −20°C. Protein content was determined by the method of Peterson (1977).

Inactivation of [^{3}H]-NMS binding sites with benzilylcholine mustard (BCM)

BCM was kept in a refrigerator in an ethanolic stock solution (2 mM). Immediately before the experiment, it was diluted by the incubation medium to a concentration of 0.1 mM and kept for 60 min at room temperature. To protect specific subpopulations of receptors from alkylation by BCM membranes were preincubated (before the addition of BCM) for 60 min at 38°C in the presence of either 100 nM AF-DX116 or 5 nM pirenzepine. BCM was then added to a final concentration of 20 nM for 7 min in the presence of AF-DX116, or for 4 min in the presence of pirenzepine. The action of BCM was stopped by 1 mM sodium thiosulphate and the membranes were sedimented at 13,000 *g* and washed twice as described above.

General arrangement of radioligand binding experiments

Incubation was at 38°C and was terminated by vacuum filtration through Whatman GF/C glass fibre filters in a Brandel cell harvester. The composition of the incubation medium corresponded to that of the homogenization medium, with [^{3}H]-NMS and other compounds added as described for each type of experiment. Non-specific radioligand binding was measured in the presence of 5 μM atropine. Each incubation tube contained untreated membranes which corresponded to 2 mg of original tissue (close to 32 fmol binding sites/tube), or membranes which had been treated with BCM in the presence of AF-DX116 and corresponded to 4 mg of original tissue (close to 25 fmol binding sites/tube), or membranes which had been treated with BCM in the presence of pirenzepine and corresponded to 6 mg of original tissue (close to 9 fmol binding sites/tube). All incubations were performed in triplicate.

Data analysis

Saturation binding experiments and experiments with radioligand displacement were analysed using 'Ligand' (Munson & Rodbard, 1980). 'Enzfitter' (Leatherbarrow, 1987) was used to obtain preliminary estimates of the binding parameters in all experiments, to compute the Hill slope factor values (n_H) according to Equation 3, the K_d for alcuronium and the cooperativity factor α according to Equation 7, and to determine the dissociation rate constants according to equations 5 and 6. Proportional weighting was used throughout. To compare the suitability of the one-site and two-site models, the 'extra sum of squares' principle and the F statistics were employed as described by Munson & Rodbard (1980). Runs test as applied in the Ligand programme and Student's two-tailed *t*-test were used where indicated.

[^{3}H]-NMS saturation binding experiments

Membranes were incubated for 3 h in a total volume of 0.8 ml, with [^{3}H]-NMS added to final concentrations of 35–1200 pM. K_d and B_{max} values were computed by non-linear regression analysis, fitting the equations

$$B = (B_{max} \times F)/(K_d + F) \quad (1)$$

for a single population of binding sites, and

$$B = (B_{max1} \times F)/(K_{d1} + F) + (B_{max2} \times F)/(K_{d2} + F) \quad (2)$$

for two populations (1 and 2) of binding sites to the binding data. B denotes the amount of specifically bound radioligand and F the concentration of free radioligand.

Displacement of [^{3}H]-NMS binding by inhibitors

Membranes were incubated for 3 h in a total volume of 1.6 ml in the presence of 100 pM (chick heart) or 200 pM (rat atria) [^{3}H]-NMS and of increasing concentrations of pirenzepine, AF-DX116, or methoctramine. The IC_{50} and n_H values were obtained by fitting the equation

$$B/B_o = 1 - [I]^{nH}/(IC_{50}{}^{nH} + [I]^{nH}) \quad (3)$$

for a single population of binding sites, and

$$B/B_o = 1 - (f_l \times [I]/(IC_{50l} + [I]) - (f_h \times [I])/(IC_{50h} + [I]) \quad (4)$$

for two populations of binding sites, to the data on radioligand binding. [I] denotes the concentration of the inhibitor, B denotes the amount of specifically bound radioligand in the presence of the inhibitor, B_o the amount of specifically bound radioligand in the absence of the inhibitor, f the proportion of binding sites with high (f_h) or low (f_l) affinity to the inhibitor. For comparisons of the one-site and two-site models, n_H values were taken as equal to unity. K_i values were calculated from the IC_{50} values according to Cheng & Prusoff (1973).

[^{3}H]-NMS dissociation

Membranes were preincubated for 60 min at 38°C in the presence of 3 nM [^{3}H]-NMS in a volume of 1.6 ml. Dissociation was started by the addition of 5 μM atropine. In experiments investigating the effect of alcuronium on [^{3}H]-NMS dissociation, the preincubation lasted 120 min: after 60 min preincubation with 3 nM [^{3}H]-NMS alone, alcuronium was added and the preincubation was continued for a further 60 min before the addition of atropine. Dissociation rate constants (K_{off}) were computed by fitting the equation.

$$B_t = B_o \times e^{-K_{off} \times t} \quad (5)$$

for a single population of sites from which dissociation occurs, and

$$B_t = B_o \times f_1 \times e^{-K_{off1} \times t} + B_o \times f_2 \times e^{-K_{off2} \times t} \quad (6)$$

for two populations of sites (with relative proportions f_1 and f_2) from which dissociation occurs. In these equations, B_t is the amount of radioligand bound at time t after the addition of atropine and B_o is the amount of radioligand bound immediately before the addition of atropine.

Determination of the apparent dissociation constant for alcuronium binding to receptors (K_{dAlc}) and of the cooperativity factor, α

Membranes were incubated for 5 h in a total volume of 1.6 ml in the presence of 100 pM (chick) or 200 pM (rat) [^{3}H]-NMS and of increasing concentrations of alcuronium ([Alc]). The values of K_{dAlc} and α were obtained by fitting the function described by Ehlert (1988b):

$$B/B_o = \frac{[NMS] + K_{dNMS}}{[NMS] + K_{dNMS} \times (K_{dAlc} + [Alc])/(K_{dAlc} + [Alc]/\alpha)} \quad (7)$$

The cooperativity factor α corresponds to the ratio of [^{3}H]-NMS K_d values in the presence of a saturating concentration of alcuronium, and in the absence of alcuronium.

Reagents

N-[^{3}H-methyl]-scopolamine ([^{3}H]-NMS 80 Ci mmol^{-1}) was from Du Pont de Nemours (Bad Homburg, Germany), alcuronium chloride from Hoffmann-La Roche (Basel, Switzerland), AF-DX116 (11-2[[2-[(diethylamino)methyl]-1-piperidinyl]acetyl]-5,11-dihydro-6H-pyrido [2,3-b][1,4] benzodiazepin-6-one) and pirenzepine dihydrochloride from Dr H. Ladinsky (Milan, Italy), methoctramine tetrahydrochloride from Dr C. Melchiorre (Bologna, Italy), and BCM (N-2-chlorethyl-*N*-methyl-2-aminoethyl benzilate) from Dr S. Shelkovnikov (St. Petersburg, Russia).

Results

Inhibition of [^{3}H]-NMS binding to untreated rat and chick membranes by pirenzepine, AF-DX116, and methoctramine

Binding curves for AF-DX116, methoctramine and pirenzepine in rat atria membranes (circles in Figure 1) had Hill slopes of 0.96–0.99, not significantly different from 1 (Table 1). In chick heart membranes the Hill slopes were 0.75 with pirenzepine, 0.77 with AF-DX116, and 0.76 with methoctramime, all significantly different from unity (*t* test, $P<0.001$ for pirenzepine, $P<0.01$ for AF-DX116 and methoctramine); a significantly better fit (*F* statistic, $P<0.01$) was obtained with a two-site model. Two-site fits to data for chick heart showed that 83%, 81% and 23% of the binding sites had high affinity for AF-DX116, methoctramine, and pirenzepine, respectively (Table 1). Computations of K_{ih}, K_{il} and f_i values for untreated chick cardiac membranes were performed on the assumption that the K_d for [^{3}H]-NMS of binding sites with the high affinities for AF-DX116 and methoctramine and with the low affinity for pirenzepine corresponds to 416 pM, while that of the receptors with reverse affinities for these ligands corresponds to 801 pM (see Table 3). The dissociation constants (K_i) for AF-DX116 and methoctramine in rat atria membranes were of the same order of magnitude as the computed high-affinity dissociation constants (K_{ih}) for the same compounds in the chick heart. In the case of pirenzepine, both the K_{ih} and K_{il} values were considerably lower in the chick heart (*t* test, $P<0.001$) than the K_i value in the rat atria.

Inhibition of [^{3}H]-NMS binding to BCM-treated chick membranes by pirenzepine, AF-DX116, and methoctramine

To separate the two populations of binding sites apparently present in the chick heart, we inactivated muscarinic receptors with BCM, applied in the presence of either 100 nM AF-DX116 (preserving M_2-like sites) or 5 nM pirenzepine (preserving M_4-like sites). The conditions for inactivation described in Methods (i.e., the concentrations of BCM and of the protecting ligands, and the duration of incubation with BCM) were empirically selected to achieve homogeneous (single-site) equilibrium binding of pirenzepine, AF-DX116 and methoctramine, with a minimum extent of receptor inactivation. The competition curves for the binding of [^{3}H]-NMS in the presence of increasing concentrations of AF-DX116, methoctramine, and pirenzepine were steeper in the BCM-treated chick membranes as compared to the untreated chick membranes (Figure 1), which was reflected by their Hill slope factors of 0.94–1.00, not significantly different from unity (*t* test, $P<0.05$) (Table 1).

Dissociation of [^{3}H]-NMS from receptors

The time course of [^{3}H]-NMS dissociation from untreated chick cardiac membranes was better described (*F* statistic, $P<0.01$) by a model assuming dissociation from two populations of sites with fast and slow dissociation rates, rather than by a one-site model (Figure 2b and Table 2). Dissociation curves obtained on untreated membranes from rat atria and on BCM-treated M_2-like and M_4-like fractions from the chick heart were one-component exponentials (Figure 2a), but the K_{off} value for the M_4-like fraction was 5 times lower than the K_{off} values for the M_2-like fraction and for rat atria.

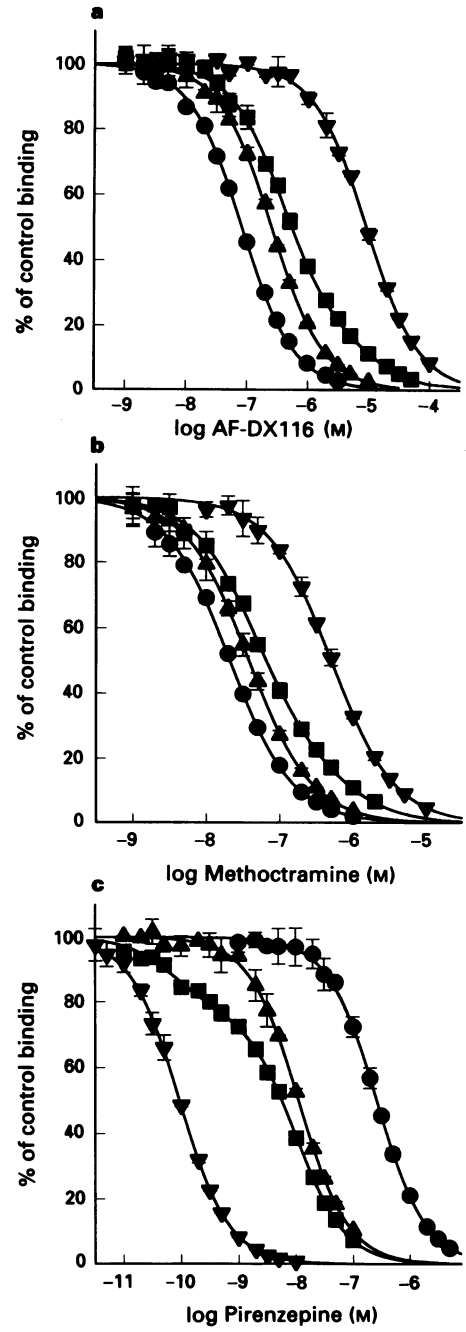


Figure 1 Binding of N-[^{3}H-methyl]-scopolamine ([^{3}H]-NMS) to cardiac membranes in the presence of increasing concentrations of (a) AF-DX116, (b) methoctramine, and (c) pirenzepine. Untreated rat atrial membranes (●); untreated chick ventricular membranes (■); chick ventricular membranes treated with benzilylcholine (BCM) in the presence of AF-DX116 (M_2-like sites) (▲); chick ventricular membranes treated with BCM in the presence of pirenzepine (M_4-like sites, (▼). Data are means ± s.e.mean of 4 experiments with incubations performed in triplicate, on membranes from two preparations. Curves are drawn according to a one-site model, except for untreated chick heart ventricular membranes, where a two-site model was used. Computed K_i and n_H values have been summarized in Table 1.

Table 1 Inhibition constants (K_i) and Hill slope factors (n_H) for AF-DX116, methoctramine and pirenzepine in rat atria and chick heart ventricular membranes

	Rat atria	*Chick heart ventricles*	*M_2-like sites*	*M_4-like sites*
Pirenzepine				
K_i [nM]	262 ± 3		11.2 ± 0.2	0.093 ± 0.007
K_{ih} [nM]		0.073 ± 0.007		
K_{il} [nM]		10.4 ± 0.3		
f_l%		77.1 ± 7.6		
n_H	0.99 ± 0.01		0.96 ± 0.03	0.94 ± 0.08
AF-DX116				
K_i [nM]	83.2 ± 1.1		256 ± 3	9240 ± 216
K_{ih} [nM]		379 ± 26		
K_{il} [nM]		9916 ± 1409		
f_l%		17.3 ± 2.9		
n_H	0.96 ± 0.01		1.00 ± 0.12	1.00 ± 0.12
Methoctramine				
K_i [nM]	21.1 ± 0.7		38.5 ± 6.6	508 ± 7
K_{ih} [nM]		46.9 ± 3.5		
K_{il} [nM]		639 ± 47		
f_l%		19.1 ± 3.4		
n_H	0.97 ± 0.04		1.00 ± 0.01	0.98 ± 0.01

Values in the Table are from rat atrial membranes, untreated chick ventricular membranes and chick ventricular membranes which had been pretreated with benzilylcholine mustard (BCM) in the presence of AF-DX116 (M_2-like sites) or pirenzepine (M_4-like sites). They are means ± s.e.mean of four experiments (see Figure 1) and were computed using a one-site model for all types of membranes except for the untreated chick ventricular membranes, for which the two-site model was applied. K_{ih} and K_{il} symbols denote the inhibition constants for the high- and low-affinity populations of binding sites, respectively, and f_l is the estimated proportion (%) of binding sites displaying low affinity for the inhibitor.

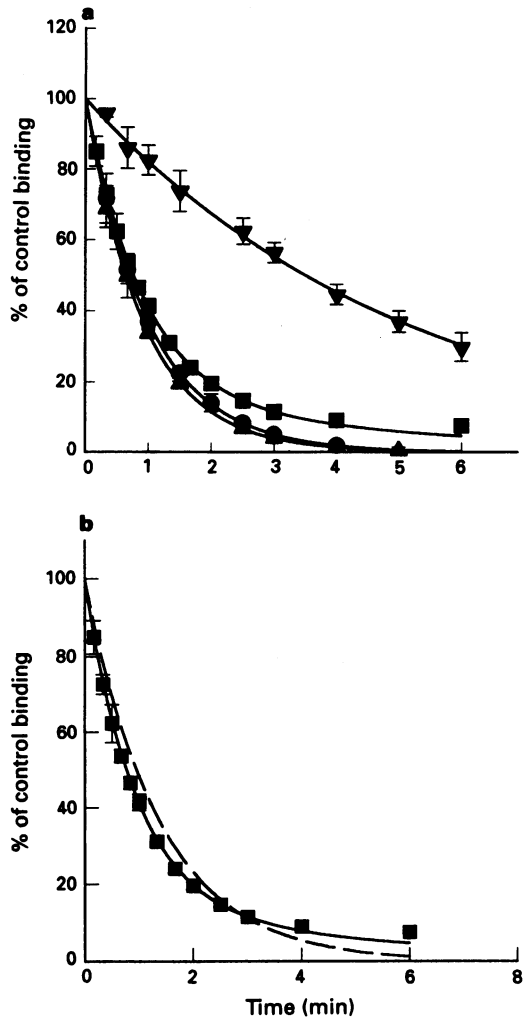


Table 2 N-[^{3}H-methyl]-scopolamine ([^{3}H]-NMS) dissociation rate constants

	K_{off1} (min^{-1})	f_2 %	K_{off2} (min^{-1})
Rat atria	0.993 ± 0.024		
Chick ventricles	1.10 ± 0.04	21.3 ± 0.8	0.178 ± 0.008
M_2-like sites	1.08 ± 0.02		
M_4-like sites	0.198 ± 0.005		

Values in the Table are means ± s.e.mean of four experiments (see Figure 2) and were computed for the model of [^{3}H]-NMS dissociation from a single population of binding sitets in rat atrial membranes and in chick ventricular membranes which had been pretreated with benzilylcholine mustard (BCM) in the presence of AF-DX116 (M_2-like sites) or pirenzepine (M_4-like sites) and from two populations of binding sites in untreated chick ventricular membranes. The fraction (%) of binding sites from which dissociation occurs at the slow rate is denoted as f_2.

Figure 2 Dissociation of N-[^{3}H-methyl]-scopolamine ([^{3}H]-NMS) from membranes. (a) Rat atrial membranes (●), untreated chick ventricular membranes (■), and chick ventricular membranes pretreated with benzilylcholine mustard (BCM) either in the presence of AF-DX116 (M_2-like sites, ▲), or in the presence of pirenzepine (M_4-like sites, ▼). Data are means ± s.e.mean of four experiments with incubations performed in triplicate, on membranes from two preparations. The curves were drawn according to models for dissociation from a single site (rat membranes, BCM-treated chick membranes) or from two binding sites (untreated chick membranes). Computed apparent dissociation rate constants have been summarized in Table 2. (b) Data for untreated chick ventricular membranes on which, for comparison, the lines were drawn both for a one-site model (dashed line) and for a two-site model (continuous line).

Effect of alcuronium on the binding of [^{3}H]-NMS at equilibrium

The effect of increasing concentrations of alcuronium on the binding of [^{3}H]-NMS at low concentrations is shown in Figure 3. The binding of [^{3}H]-NMS to cardiac membranes was augmented at alcuronium concentrations of 0.5–1 μM and higher. Saturation binding experiments (Figure 4) indicated that alcuronium increased the affinity of [^{3}H]-NMS binding sites for the radioligand without altering their maximum numbers available.

Table 3 gives a summary of K_d and B_{max} values for [^{3}H]-NMS obtained in saturation binding experiments performed in the absence and presence of alcuronium. Data on the binding of [^{3}H]-NMS to untreated chick heart membranes in the absence of alcuronium were better fitted by the two-site than the one-site model (F statistics: $P<0.05$; runs test: fit for two-site model, lack of fit for one-site model); in the presence of alcuronium, the difference between the fit with the one-site and two-site models was not significant ($0.05<P<0.1$). Only single populations of binding sites were seen in the M_2-like and M_4-like fractions and in rat atria, both in the absence and in the presence of alcuronium. Alcuronium diminished K_d values for both populations of binding sites in the untreated chick membranes (K_{d1} and K_{d2}), for the M_2-like and M_4-like fractions in BCM-treated chick membranes and for the binding sites in rat atria (t test, $P<0.01$).

Analysis of the binding curves obtained in the presence of increasing concentrations of alcuronium (Figure 3) by the

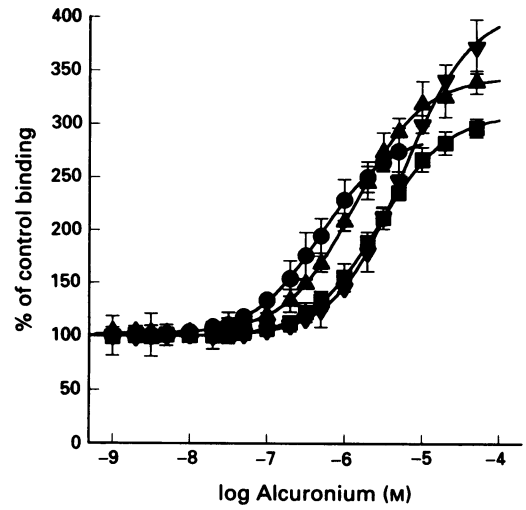


Figure 3 Effects of increasing concentrations of alcuronium on the binding of N-[^{3}H-methyl]-scopolamine ([^{3}H]-NMS) to membranes. Rat atrial membranes, (●); untreated chick heart ventricular membranes, (■); chick heart ventricular membranes pretreated with benzilylcholine mustard (BCM) in the presence of AF-DX116 (M_2-like sites), (▼); or in the presence of pirenzepine (M_4-like sites) (▲). Data are means ± s.e.mean of four experiments with incubations performed in triplicate on membranes from two preparations. Curves were drawn to fit Eqn. No. 7.

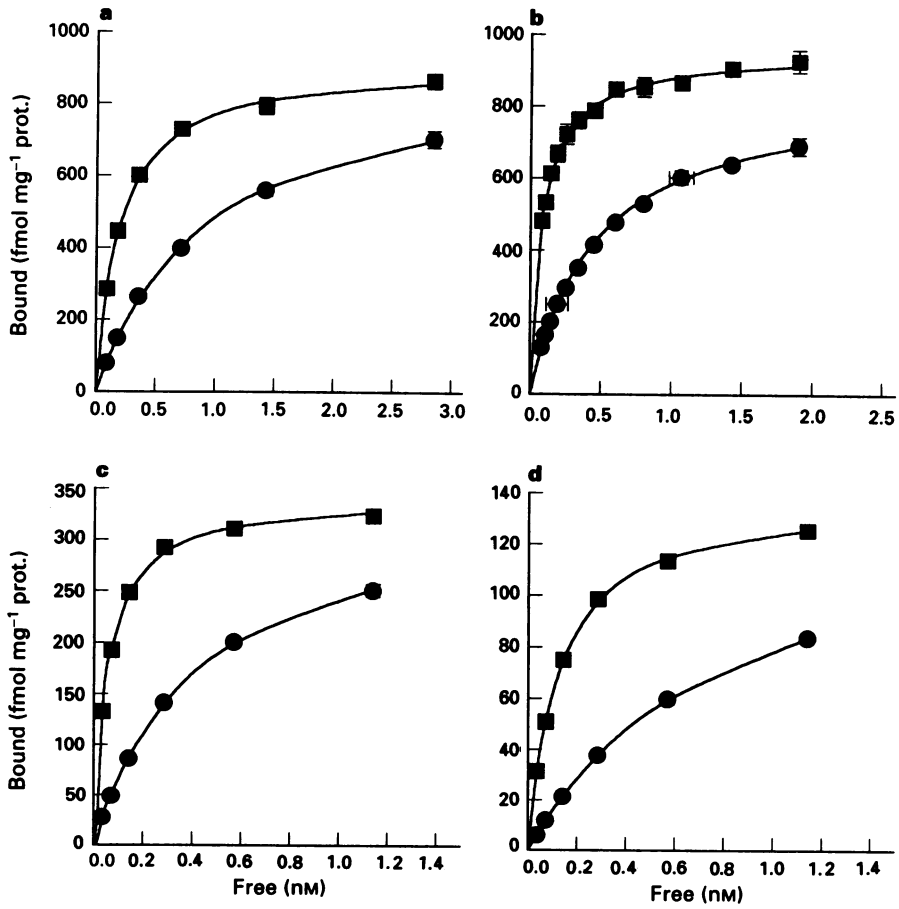


Figure 4 Specific N-[^{3}H-methyl]-scopolamine ([^{3}H]-NMS) binding at increasing radioligand concentrations, in the absence (●) and presence (■) of alcuronium. (a) Rat atrial membranes; (b) Untreated chick ventricular membranes: (c) Chick ventricular membranes pretreated with benzilylcholine mustard (BCM) in the presence of AF-DX116 (M_2-like); (d) Chick ventricular membranes pretreated with BCM in the presence of pirenzepine (M_4-like). Alcuronium was applied at concentrations of 10 μM (rat atrial membranes, untreated chick ventricular membranes and M_2-like sites) or 100 μM (M_4-like sites). Data are means ± s.e.mean of two experiments with incubations performed in triplicate on membranes from two preparations. In (a), (c) and (d), the best fits (full lines) were obtained for the one-site model and in (b) for the two-site model.

Table 3 Equilibrium dissociation constants (K_d) and B_{max} values for the binding of N-[^{3}H-methyl]-scopolamine ([^{3}H]-NMS) to membranes in the absence and in the presence of alcuronium

	Without alcuronium				*With alcuronium*			
	K_{d1}	B_{max1}	K_{d2}	B_{max2}	K_{d1}	B_{max1}	K_{d2}	B_{max2}
Rat atria	939 ± 86	885 ± 63			191 ± 8	879 ± 51		
Chick ventricles	416 ± 16	777 ± 38	801 ± 27	162 ± 45	72.2 ± 8.5	812 ± 27	148 ± 55	142 ± 37
M_2-like sites	413 ± 19	319 ± 23			54.8 ± 6.8	328 ± 15		
M_4-like sites	798 ± 54	131 ± 14			121 ± 7	127 ± 7		

K_d values are expressed as pM and B_{max} as fmol mg^{-1} protein. Data are means ± s.e.mean and were computed by non-linear regression from the results of saturation binding experiments shown in Figure 4. The concentration of alcuronium was 10 μM in experiments with rat atrial membranes, untreated chick ventricular membranes and chick ventricular membranes which had been pretreated with benzilylcholine mustard (BCM) in the presence of AF-DX116 (M_2-like sites), while it was 100 μM in experiments with chick ventricular membranes which had been pretreated with BCM in the presence of pirenzepine (M_4-like sites). The one-site [^{3}H]-NMS binding model was used except for untreated chick ventricular membranes, for which the two-site model was applied. The subscripts $_1$ and $_2$ denote the first (or the only) and the second population of binding sites.

method of Ehlert (1988b), showed that the affinity of alcuronium decreased in the order: rat atrial membranes > chick heart BCM-treated M_2-like fraction > chick heart BCM-treated M_4-like fraction. The cooperativity factor α was lowest in the M_2-like fraction (Table 4).

Effect of alcuronium on the dissociation of [^{3}H]-NMS

Comparison of Figure 2 and Figure 5 shows that the dissociation curves of rat atrial membranes and of the M_2-like and M_4-like chick heart fractions became biphasic in the presence of alcuronium: a comparatively rapid phase was followed by a very slow phase. As alcuronium concentration increased, the relative proportion of rapidly-dissociating sites diminished, and at the highest alcuronium concentration, almost all of the sites exhibited slow dissociation of [^{3}H]-NMS.

Computed apparent dissociation rate constants are shown in Table 5. With increasing concentrations of alcuronium, the K_{off1} values do not change, while the K_{off2} values slowly but consistently diminish (t test, $P<0.01$ for differences between neighbouring alcuronium concentrations). The K_{off2} values obtained in the presence of alcuronium do not represent true dissociation rate constants since, apparently, [^{3}H]-NMS can only dissociate from the alcuronium-receptor-[^{3}H]-NMS complexes after the dissociation of alcuronium (Proška & Tuček, 1994). About ten fold higher concentrations of alcuronium were needed to achieve the same slow rates of dissociation in the M_4-like fraction as compared to the M_2-like fraction (Table 5).

Discussion

Two types of experiments indicate that at least two populations of muscarinic binding sites are present in the membranes from cardiac ventricles of 1-day-old chicks: (a) displacement of [^{3}H]-NMS binding by pirenzepine, AF-DX116, and methoctramine indicated that about 80% of binding sites in the untreated membranes have high affinities for AF-DX116 and methoctramine and 23% have a high affinity for pirenzepine. (b) [^{3}H]-NMS dissociated rapidly from about 79% and slowly from about 21% of binding sites. The results of experiments with [^{3}H]-NMS saturation binding also suggested that the radioligand binds to two sites in untreated chick heart membranes.

Table 4 Values of equilibrium dissociation constants for the binding of alcuronium to membranes (K_{dAlc}) and of cooperativity factors α

	K_{dAlc} (μM)	α
Rat atria	0.835 ± 0.038	0.198 ± 0.015
Chick ventricles	5.38 ± 1.27	0.153 ± 0.029
M_2-like sites	3.24 ± 1.28	0.123 ± 0.014
M_4-like sites	9.15 ± 1.51	0.150 ± 0.016

Data are means ± s.e.mean and have been computed from the results of experiments shown in Figure 3.

In view of reports that two muscarinic receptor mRNAs are expressed in the chick heart, one of them close to the mammalian m2 and the other to the mammalian m4 subtype (Tietje *et al.*, 1990; Tietje & Nathanson, 1991), it seems apposite to compare the properties of the two subpopulations of binding sites revealed in the present binding experiments with the properties of the M_2 and M_4 receptors investigated in other locations. One of the distinguishing features of the M_2 receptors is their high affinity for AF-DX116. Compared to the M_2 subtype, the affinity of M_4 receptors for AF-DX116 was 6 times lower in experiments on the rat tissues (Waelbroeck *et al.*, 1990) and 5 times lower in a fibroblast cell line transfected with human m4 gene as compared to the rat heart (Doods *et al.*, 1994). In cells transfected with chick genes, M_4 receptors had a five fold lower affinity for AF-DX116 than the M_2 receptors (Tietje & Nathanson, 1991). The affinity for methoctramine of the M_4 as compared to the M_2 subtype was 2–3 times less in mammalian tissues (Waelbroeck *et al.*, 1990; Lazareno *et al.*, 1990) and the IC_{50} value for the inhibition of [^{3}H]-NMS binding to M_4 receptors was 43 times higher as compared to the M_2 receptors on cloned cells (Buckley *et al.*, 1989).

On the other hand, the affinity of the M_4 subtype for pirenzepine appeared 10 times (Waelbroeck *et al.*, 1990; Lazareno *et al.*, 1990), 6 times (Wess *et al.*, 1991) or 3 times higher (Doods *et al.*, 1994) than that of the M_2 subtype. The rate constant of the dissociation of [^{3}H]-NMS from the M_4 receptors was 29 times lower (Waelbroeck *et al.*, 1990), 8 times lower (Ellis *et al.*, 1991), or 7 times lower (Lazareno *et al.*, 1990) than that of [^{3}H]-NMS dissociation from the M_2 subtype.

Thus, it seems reasonable to suggest that the larger receptor population with the high affinity for AF-DX116 and with fast NMS dissociation, detected in the present work, corresponds to the chick M_2 and the smaller population to the chick M_4 subtype. This is supported by experiments in which receptors with high affinity for either pirenzepine or AF-DX116 had been protected and the remaining receptors were inactivated with BCM, where we demonstrated homogenous subpopulations with properties corresponding to those expected of the M_2-like or M_4-like sites.

Chick heart muscarinic receptors differ from their mammalian counterparts in at least two respects: (1) Their affinity for pirenzepine is comparatively high, and this holds for both subpopulations described. The K_d values for pirenzepine are 0.073 nM and 10.4 nM, compared to 262 nM in rat atrial

receptors. The high affinity of chick cardiac receptors for pirenzepine has been observed repeatedly (Brown *et al.*, 1985; Lindmar & Löffelholz, 1987; Jeck *et al.*, 1988; Choo *et al.*, 1988; Lazareno *et al.*, 1990; Tietje & Nathanson, 1991), although low affinity was found by Sorota *et al.* (1986). (2) The M_2-like sites in chick heart have a slightly lower K_d for NMS than the M_4-like population, while in mammalian tissues, the affinity of M_4 receptors for NMS is higher than that of M_2 receptors (Waelbroeck *et al.*, 1990; Lazareno *et al.*, 1990).

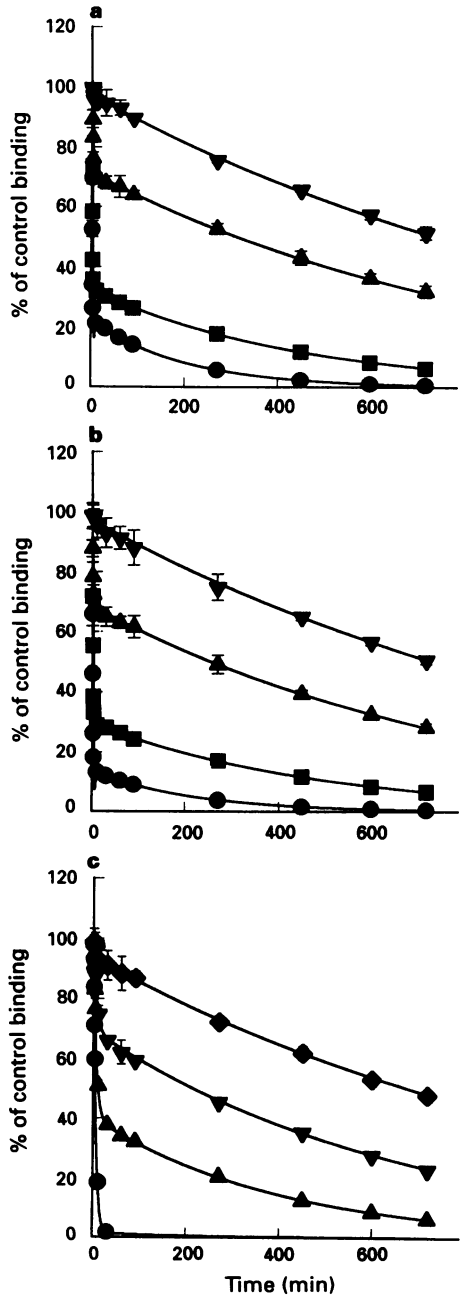


Figure 5 Effects of alcuronium on the rates of N-[^{3}H-methyl]-scopolamine ([^{3}H]-NMS) dissociation. (a) Rat atrial membranes; (b) Chick ventricular membranes pretreated with benzilylcholine mustard (BCM) in the presence of AF-DX116 (M_2-like sites); (c) Chick ventricular membranes pretreated with BCM in the presence of pirenzepine (M_4-like sites). The concentrations of alcuronium were 10^{-6} M (●), 3 × 10^{-6} M (■), 10^{-5} M (▲), 10^{-4} M (▼), or 10^{-3} M (◆). Data are means ± s.e.mean of four experiments with incubations performed in triplicate, on membranes from two preparations. The curves were drawn for the model of dissociation from two binding sites.

Table 5 N-[^{3}H-methyl]-scopolamine ([^{3}H]-NMS) dissociation rate constants (min^{-1}) in the presence of increasing concentrations of alcuronium ([Alc], M)

log [Alc]	*Rat atria*			*M_2-like sites*			*M_4-like sites*		
	K_{off1}	f_2 %	K_{off2}	K_{off1}	f_2 %	K_{off2}	K_{off1}	f_2 %	K_{off2}
–	0.993 ± 0.024			1.08 ± 0.02			0.198 ± 0.005		
–7	1.07 ± 0.26			1.11 ± 0.19			ND		
–6	0.959 ± 0.067	22.6 ± 1.0	(5.00 ± 0.80) × 10^{-3}	0.964 ± 0.460	13.8 ± 2.3	(4.67 ± 0.14) × 10^{-3}	0.175 ± 0.033		
–5.5	0.972 ± 0.049	32.6 ± 2.1	(2.23 ± 0.11) × 10^{-3}	1.02 ± 0.27	29.8 ± 4.3	(2.09 ± 0.49) × 10^{-3}	ND		
–5	0.939 ± 0.076	71.2 ± 5.3	(1.13 ± 0.15) × 10^{-3}	1.07 ± 0.09	68.4 ± 8.5	(1.24 ± 0.37) × 10^{-3}	0.164 ± 0.036	40.2 ± 3.1	(2.56 ± 0.19) × 10^{-3}
–4			(0.898 ± 0.012) × 10^{-3}			(0.913 ± 0.010) × 10^{-3}	0.153 ± 0.021	69.3 ± 1.6	(1.52 ± 0.06) × 10^{-3}
–3	ND			ND			0.198 ± 0.103	93.8 ± 2.1	(0.927 ± 0.064) × 10^{-3}

Data have been computed from the results shown in Figure 5 and are means ± s.e.mean. The subscripts 1 and 2 relate to the first and the second populations of sites from which dissociation occurred (f_2 being the site with the slower dissociation), and f_2 indicates the fraction (%) of binding sites with the slower dissociation. ND = not determined.

In contrast to our findings, heterogeneity of the binding properties of muscarinic receptors in chick heart was not seen in earlier investigations. One possible explanation is that the expression of individual subtypes varies in the course of embryonic and early postnatal development. While the present study was made on 1-day-old chicks, Michel & Whiting (1989) investigated 6–8-week-old chicks, Lazareno *et al.* (1990) 6–12-week-old chicks, and Brown *et al.* (1985) performed the bulk of their study on 13 day-old embryos.

We have found earlier that the neuromuscular blocker, alcuronium interacts allosterically with muscarinic receptors (Nedoma *et al.*, 1985; 1986) and increases the specific binding of [^{3}H]-NMS in rat heart, smooth muscle and cerebellum, but not in cerebral cortex and salivary gland (Tuček *et al.*, 1990). This variation in the effect of alcuronium with tissue location is consistent with the distribution of M_2 receptors and suggests that the drug's positive allosteric action is selective for the M_2 receptor subtype. We wondered if alcuronium also exerts positive cooperativity on the binding of [^{3}H]-NMS to chick heart receptors and what effects it has on the M_4 subtype, which was not represented in our earlier study (Tuček *et al.*, 1990). Present data indicate that alcuronium does increase the binding of [^{3}H]-NMS to chick heart muscarinic receptors and that it affects both the M_2-like and the M_4-like population, with a higher affinity for the M_2 subtype. The finding of positive allosteric effects of alcuronium on both the M_2 and the M_4 receptors (with no such effects being apparent on the M_1 and M_3 receptors) raises the question of whether there is any relation between receptor coupling mechanisms (M_2 and M_4 being similar in their preferential effects on adenylate cyclase) and the allosteric action of alcuronium.

Alcuronium had a strong inhibitory effect on the rate of [^{3}H]-NMS dissociation from either class of chick cardiac muscarinic binding sites. This is in good accord with what had been observed on mammalian tissues both with alcuronium (Tuček *et al.*, 1990) and with the allosteric effectors which display negative cooperativity vis-a-vis the binding of [^{3}H]-NMS (reviewed by Henis *et al.*, 1989; Lee & El. Fakahany, 1991b); presumably, alcuronium slows down [^{3}H]-NMS dissociation (and also association) by steric hindrance (Proška & Tuček, 1994).

We thank Dr J. Proška for fruitful discussions, Mrs Z. Kereškeni for technical help, and Drs H. Bachelard, H. Ladinsky, C. Melchiorre, S. Shelkovnikov, A. Kaiser, Mr P. Weber and The Wellcome Trust for assistance in providing drugs and reagents. The study was supported by grant No. 711103 of the Academy of Sciences of the Czech Republic.

References

BONNER, T.I. (1989). The molecular basis of muscarinic receptor diversity. *Trends Neurosci.*, **12**, 148–151.

BROWN, J.H., GOLDSTEIN, D. & MASTERS, S.B. (1985). The putative M_1 muscarinic receptor does not regulate phosphoinositide hydrolysis. Studies with pirenzepine and McN-A343 in chick heart and astrocytoma cells. *Mol. Pharmacol.*, **27**, 525–531.

BUCKLEY, N.J., BONNER, T.I., BUCKLEY, C.M. & BRANN, M.R. (1989). Antagonist binding properties of five cloned muscarinic receptors expressed in CHO-K1 cells. *Mol. Pharmacol.*, **35**, 469–476.

CAULFIELD, M.P. (1993). Muscarinic receptors – characterization, coupling and function. *Pharmacol. Ther.*, **58**, 319–379.

CHENG, Y. & PRUSOFF, W.H. (1973). Relationship between the inhibition constant (K_I) and the concentration of an inhibitor that causes a 50% inhibition (IC_{50}) of an enzymatic reaction. *Biochem. Pharmacol.*, **22**, 3099–3108.

CHOO, L.K., MITCHELSON, F. & NAPIER, P. (1988). Differences in antagonist affinities at muscarinic receptors in chick and guinea-pig. *J. Autonom. Pharmacol.*, **8**, 259–266.

CLARK, A.L. & MITCHELSON, F. (1976). The inhibitory effect of gallamine on muscarinic receptors. *Br. J. Pharmacol.*, **58**, 323–331.

DOODS, H.M., ENTZEROTH, M., ZIEGLER, H., MAYER, N. & HOLZER, P. (1994). Pharmacological profile of selective muscarinic receptor antagonists on guinea-pig ileal smooth muscle. *Eur. J. Pharmacol.*, **253**, 275–281.

EHLERT, F.J. (1988a). Gallamine allosterically antagonizes muscarinic receptor-mediated inhibition of adenylate cyclase activity in the rat myocardium. *J. Pharmacol. Exp. Ther.*, **247**, 596–602.

EHLERT, F.J. (1988b). Estimation of the affinities of allosteric ligands using radioligand binding and pharmacological null methods. *Mol. Pharmacol.*, **33**, 187–194.

ELLIS, J., HUYLER, J.H. & BRANN, M.R. (1991). Allosteric regulation of cloned m1–m5 muscarinic receptor subtypes. *Biochem. Pharmacol.*, **42**, 1927–1932.

GILL, E.W. & RANG, H.P. (1966). An alkylating derivative of benzilylcholine with specific and long-lasting parasympathetic activity. *Mol. Pharmacol.*, **2**, 284–297.

HENIS, Y.I., KLOOG, Y. & SOKOLOVSKY, M. (1989). Allosteric interactions of muscarinic receptors and their regulation by other membrane proteins. In *The Muscarinic Receptors*. ed. Brown, J.H. pp. 377–418. Clifton (NJ): The Humana Press.

HULME, E.C., BIRDSALL, N.J.M. & BUCKLEY, N.J. (1990). Muscarinic receptor subtypes. *Annu. Rev. Pharmacol. Toxicol.*, **30**, 633–673.

JECK, D., LINDMAR, R., LÖFFELHOLZ, K. & WANKE, M. (1988). Subtypes of muscarinic receptor on cholinergic nerves and atrial cells of chicken and guinea-pig hearts. *Br. J. Pharmacol.*, **93**, 357–366.

KHARKEVICH, D.A. & SHORR, V.A. (1986). Antimuscarinic and ganglion-blocking activity of neuromuscular blocking agents. In: *New Neurosmuscular Blocking Agents. Handbook of Experimental Pharmacology*, vol. 79. ed. Kharkevich, D.A. pp. 191–224. Berlin: Springer-Verlag.

KWATRA, M.M., PTASIENSKI, J. & HOSEY, M.M. (1988). The porcine heart M2 muscarinic receptor: agonist induced phosphorylation and comparison of properties with the chick heart receptor. *Mol. Pharmacol.*, **35**, 553–558.

LAZARENO, S., BUCKLEY, N.J. & ROBERTS, F. (1990). Characterization of muscarinic M_4 binding sites in rabbit lung, chicken heart, and NG1078-15 cells. *Mol. Pharmacol.*, **38**, 805–815.

LEATHERBARROW, R.J. (1987). *Enzfitter: A Non-linear Regression Data Analysis Program for the IBM PC.* Amsterdam: Elsevier Science Publishers BV.

LEE, N.H. & EL-FAKAHANY, E.E. (1991b). Allosteric interactions at the m1, m2 and m3 muscarinic receptor subtypes. *Biochem Pharmacol.*, **42**, 199–205.

LEE, N.H. & EL-FAKAHANY, E.E. (1991b). Allosteric antagonists of the muscarinic acetylcholine receptor. *J. Pharmacol. Exp. Ther.*, **256**, 468–479.

LINDMAR, R. & LÖFFELHOLZ, K. (1987). Muscarinic M_1-receptors mediate the negative inotropic effect of methacholine in chicken but not in guinea-pig atria. *Eur. J. Pharmacol.*, **139**, 359–360.

MICHEL, A.D. & WHITING, R.L. (1989). Radioligand binding characteristics of the chicken cardiac muscarinic receptor. *Naunyn-Schmied. Arch. Pharmacol.*, **340**, 279–284.

MITCHELSON, F. (1988). Muscarinic receptor differentiation. *Pharmacol. Ther.*, **37**, 357–423.

MUNSON, P.J. & RODBARD, D. (1980). Ligand: a versatile computerized approach for characterization of ligand-binding systems. *Analyt. Biochem.*, **107**, 220–239.

NEDOMA, J., DOROFEEVA, N.A., TUČEK, S., SHELKOVNIKOV, S.A. & DANILOV, A.F. (1985). Interaction of the neuromuscular blocking drugs alcuronium, decamethonium, gallamine, pancuronium, ritebronium, tercuronium and d-tubocurarine with muscarinic acetylcholine receptors in the heart and ileum. *Naunyn-Schmied. Arch. Pharmacol.*, **329**, 176–181.

NEDOMA, J., TUČEK, S., DANILOV, A.F. & SHELKOVNIKOV, S.A. (1986). Stabilization of antagonist binding to cardiac muscarinic acetylcholine receptors by gallamine and other neuromuscular blocking drugs. *J. Pharmacol. Exp. Ther.*, **236**, 219–223.

PETERSON, G.L. (1977). A simplification of the protein assay method of Lowry et al. which is more generally applicable. *Analyt. Biochem.*, **83**, 346–356.

PROŠKA, J. & TUČEK, S. (1994). Mechanisms of steric and cooperative actions of alcuronium on cardiac muscarinic acetylcholine receptors. *Mol. Pharmacol.*, **45**, 709–717.

SOROTA, S., ADAM, L.P. & PAPPANO, A.J. (1986). Comparison of muscarinic receptor properties in hatched chick heart atrium and ventricle. *J. Pharmacol. Exp. Ther.*, **236**, 602–609.

STOCKTON, J.M., BIRDSALL, N.J.M., BURGEN, A.S.V. & HULME, E.C. & (1983). Modification of the binding properties of muscarinic receptors by gallamine. *Mol. Pharmacol.*, **23**, 551–557.

TIETJE, K.M., GOLDMAN, P.S. & NATHANSON, N.M. (1990). Cloning and functional analysis of a gene encoding a novel muscarinic acetylcholine receptor expressed in chick heart and brain. *J. Biol. Chem.*, **265**, 2828–2834.

TIETJE, K.M. & NATHANSON, N.M. (1991). Embryonic chick heart expresses multiple muscarinic acetylcholine receptor subtypes. Isolation and characterization of a gene encoding a novel m2 muscarinic acetylcholine receptor with high affinity for pirenzepine. *J. Biol. Chem.*, **266**, 17382–17387.

TUČEK, S., MUSÍLKOVÁ, J., NEDOMA, J., PROŠKA, J., SHELKOVNIKOV, S. & VORLÍČEK, J. (1990). Positive cooperativity in the binding of alcuronium and N-methylscopolamine to muscarinic acetylcholine receptors. *Mol. Pharmacol.*, **38**, 674–680.

WAELBROECK, M., TASTENOY, M., CAMUS, J. & CHRISTOPHE, J. (1990). Binding of selective antagonists to four muscarinic receptors (M1 to M4) in rat forebrain. *Mol. Pharmacol.*, **38**, 267–273.

WESS, J., LAMBRECHT, G., MUTSCHLER, E., BRANN, M.R. & DÖRJE, F. (1991). Selectivity profile of the novel muscarinic antagonist UH-AH 37 determined by the use of cloned receptors and isolated tissue preparations. *Br. J. Pharmacol.*, **102**, 246–250.

(Received April 18, 1994
Revised June 24, 1994
Accepted July 14, 1994)

Br. J. Pharmacol. (1994), **113**, 1538–1547 © Macmillan Press Ltd, 1994

Ion channel modulation by NS 1619, the putative BK_{Ca} channel opener, in vascular smooth muscle

[1]G. Edwards, [2]A. Niederste-Hollenberg, [2]J. Schneider, *Th. Noack & A.H. Weston

School of Biological Sciences, G.38 Stopford Building, University of Manchester, Manchester M13 9PT, UK and *Department of Physiology, Philipps University, Deutschhausstrasse 2, 35033 Marburg, Germany

1 The effects of NS 1619, the putative BK_{Ca} channel opener, were investigated on rat intact portal veins and on single smooth muscle cells enzymatically separated from the same tissue.

2 Under whole-cell patch clamp conditions with K-rich pipettes, exposure of single cells held at −10 mV to NS 1619 (10–33 μM) induced a noisy, outward current which reached a maximum (33 μM NS 1619; mean 35.8 ± 17 pA, $n = 8$) within about 6 min.

3 On stepping to test potentials (range −50 to +50 mV) from a holding potential of −10 mV, the NS 1619-induced noisy current exhibited time-dependent activation and marked outward rectification.

4 The stimulation of outward currents by NS 1619 at −10 mV was independent of the presence of Ca^{2+} in the bath or pipette solutions but was antagonized by either charybdotoxin (250 nM) or penitrem A (100 nM) in the bath solution.

5 Stationary fluctuation analysis of the noisy current induced by NS 1619 at −10 mV yielded a value of 70 ± 8 pS ($n = 4$) (under the quasi-physiological conditions of the experiment) for the unitary conductance of the channel involved.

6 At −10 mV, NS 1619 (10–33 μM) rapidly inhibited spontaneous transient outward currents.

7 With a holding potential of −90 mV, NS 1619 (10–33 μM) produced a reduction of outward currents evoked by depolarizing steps to +50 mV, an effect associated with marked inhibition of the delayed rectifier current, $I_{K(V)}$.

8 NS 1619 (3–100 μM) produced a concentration-dependent inhibition of spontaneous activity in rat portal vein characterized by a reduction in the amplitude and duration of the tension waves. This inhibition was slightly potentiated in the presence of either charybdotoxin (250 nM) or penitrem A (1 μM). NS 1619 also totally inhibited contractions of rat aorta induced by KCl (both 20 mM and 80 mM).

9 Under whole-cell recording conditions and using Cs-rich pipettes, Ca-currents evoked in portal vein cells by stepping from a holding potential of −90 mV to test potentials in the range −30 to +50 mV were totally inhibited in the presence of 33 μM NS 1619.

10 NS 1619 (33 μM) inhibited the induction of $I_{K(ATP)}$ by levcromakalim (10 μM).

11 It is concluded that NS 1619 activates the large conductance, Ca^{2+}-sensitive channel, BK_{Ca} and over the same concentration range it inhibits both K_V and L-type Ca-channels. The observed NS 1619-induced mechanical inhibition in rat portal vein and aorta seems most likely to be due to the observed inhibition of Ca-currents.

Keywords: NS 1619; charybdotoxin; penitrem A; levcromakalim; B_{KCa}; K_V; L-type Ca-channels; K_{ATP}; rat blood vessels; whole-cell patch clamp; relaxation

Introduction

Over the past few years, many agents have been described which can open plasmalemmal potassium (K) channels. The best known of these constitute the diverse chemical entities known as the *K-channel openers*, typified by levcromakalim, pinacidil and aprikalim. The target for these agents is the ATP- and glibenclamide-sensitive K-channel, K_{ATP} (see Edwards & Weston, 1993).

More recently, however, openers of the large conductance Ca^{2+}-sensitive K-channel (BK_{Ca}) have been described. These include the dehydrosaponins, the prototypes of which were extracted from the herb *Desmodium adscendens* (McManus *et al.*, 1993) and the benzimidazoles, initially exemplified by NS004. This agent hyperpolarizes neuroblastoma cells and increases the open probability of charybdotoxin-sensitive BK_{Ca} channels in inside-out membrane patches (Olesen & Wätjen, 1992). NS 1619, a close chemical relative of NS004, was recently shown to hyperpolarize bovine aortic smooth muscle cells and to shift the voltage activation characteristics of charybdotoxin-sensitive whole cell currents in a hyperpolarizing direction (Olesen *et al.*, 1994b).

The objective of the present study was to investigate further the profile of action of NS 1619 in rat vascular smooth muscle. Using both whole portal veins and freshly isolated single cells from this tissue together with segments of rat aorta, it was hoped to clarify the effects of this agent on both mechanical activity and on whole-cell K-currents. In further experiments, the action of NS 1619 on whole-cell Ca currents was also evaluated since inhibition of such currents by the related molecule, NS004, has been reported (Sargent *et al.*, 1993). A preliminary account of our observations has been presented to the British Pharmacological Society (Schneider *et al.*, 1994).

Methods

All experiments were performed on tissues removed from male Sprague-Dawley rats (100–125 g body weight), previously killed by stunning and bleeding. The whole-cell

[1] Author for correspondence.
[2] Present address: Department of Physiology, Philipps University Deutschhausstrasse 2, 35033 Marburg, Germany.

voltage-clamp experiments were performed on single smooth muscle cells isolated from portal veins while mechanical studies were carried out on both whole portal veins and segments of aorta.

Cell separation

After dissection, the portal veins were placed in a physiological salt solution (PSS) containing 0.5 mM Ca^{2+} and carefully cleaned of fat and connective tissue with fine scissors in conjunction with a dissecting microscope. Each vein was then opened along its longitudinal axis and transferred to an identical PSS to which collagenase and pronase had been added. The tissue was agitated for 21 min at 37°C and then washed in Kraftbrühe (Klöckner & Isenberg, 1985). The veins were then cut into approximately six segments and triturated in Kraftbrühe with a wide bore, smooth-tipped pipette. The dispersed cells were used for experiments within 8 h of separation, during which time they were stored at 6°C in Kraftbrühe.

Single-cell electrophysiology

Experiments were performed at 23°C using the whole-cell configuration of the patch-clamp technique (Hamill *et al.*, 1981). Patch pipettes were pulled from Pyrex glass (H 15/10, Jencons, UK) and had resistances of 3–4MΩ when filled with the internal (intracellular) solution. Voltage commands and data acquisition were performed as described by Noack *et al.* (1992). For cell stimulation and for recording and analysing data, the pCLAMP 5.5 programme was used (Axon Instruments, U.S.A.). Data acquisition and storage were as described by Ibbotson *et al.* (1993b).

As in previous studies, we used a double holding potential protocol (see Noack *et al.*, 1992; Edwards *et al.*, 1993) to distinguish between the time-dependent currents, $I_{K(A)}$ and $I_{K(V)}$, and the time-independent current, $I_{BK(Ca)}$. With Ca-PSS in the bath, $I_{K(A)}$, $I_{K(V)}$ and $I_{BK(Ca)}$ were all available on stepping from a holding potential of −90 mV to more positive potentials up to +50 mV. However, when cells were clamped at a holding potential of −10 mV, $I_{K(A)}$ and $I_{K(V)}$ became inactivated allowing the characteristics of $I_{BK(Ca)}$ alone to be examined by stepping to a series of potentials in the range −50 mV to +50 mV. In all experiments, the currents evoked by 500 ms voltage steps from the stated holding potential were measured at their peak level.

The effects of NS 1619, levcromakalim, charybdotoxin and penitrem A were each investigated by adding the appropriate amount(s) of these agents to the main reservoir containing the external solution to ensure that responses were obtained under steady-state conditions. The bath (volume: 1 ml) was continuously perfused (0.7 ml min^{-1}) with fresh solution using a pump (Microperpex, Pharmacia LKB); a second identical pump was used to remove excess solution from the recording chamber.

Whole-tissue mechanical studies

Whole portal veins were mounted in a Krebs PSS at 37°C under 10 mN tension for isometric recording. Whole dorsal aortae were cut into 4 segments which were each opened longitudinally and similarly mounted for isometric tension recording.

The tissues were allowed to equilibrate for approximately 45 min before they were exposed at 15 min intervals to increasing concentrations of NS 1619 added cumulatively. Modification of the relaxant effect of NS 1619 was determined by preincubating portal veins with charybdotoxin or penitrem A for 20 min before exposure to NS 1619 in the continuing presence of the modifying agent. Aortic contractions to 20 mM or 80 mM KCl (which were substituted for equimolar concentrations of NaCl in the Krebs PSS) were allowed to plateau before further addition of NS 1619.

Mechanical responses were recorded and this activity was integrated with respect to time by use of an Apple Macintosh computer in conjunction with MacLab hardware (MacLab 8) and software (Chart, version 2.5) (Analog Digital Instruments).

Drugs and solutions

Electrophysiological studies The low-Ca^{2+} PSS used during cleaning of the veins comprised (mM): KCl 130, $CaCl_2$ 0.05, taurine 20, pyruvate 5, creatine 5, HEPES 10, fatty acid-free albumin 1 mg ml^{-1}, buffered with methanesulphonic acid to pH 7.4. Collagenase (Type VIII, Sigma) 1 mg ml^{-1} and pronase (Calbiochem) 0.2 mg ml^{-1} were added to this solution for cell separation. Kraftbrühe comprised (mM): KCl 85, KH_2PO_4 30, $MgSO_4$ 5, Na_2ATP 5, K-pyruvate 5, creatine 5, taurine 20, β-OH-butyrate 5, fatty acid-free albumin 1 mg ml^{-1}, pH adjusted to 7.2 with KOH.

Two bath (external) solutions were used for the measurement of K-currents. One of these was a calcium-containing PSS (Ca^{2+}-PSS) comprising (mM): NaCl 125, KCl 4.8, $CaCl_2$ 2.5, $MgCl_2$ 1.2, KH_2PO_4 1.2, glucose 11, HEPES 10, buffered with NaOH to pH 7.30; aerated with O_2. The composition of the Ca^{2+}-free bath solution (Ca^{2+}-free PSS) was similar except that the $CaCl_2$ was omitted. The $MgCl_2$ concentration was increased to 3.7 mM to compensate for the loss of divalent cations and 1.0 mM EGTA (ethylene glycol-*bis* β-aminoethyl ether tetraacetic acid) was also added. Ca-PSS was used during the measurement of Ca-currents.

Two pipette (internal) solutions differing in their respective Ca^{2+} concentrations were employed in the study of K-currents. The Ca-containing pipette solution contained (mM): NaCl 5, KCl 120, $MgCl_2$ 1.2, K_2HPO_4 1.2, HEPES 10, glucose 11, oxalacetic acid 5, sodium pyruvate 2, sodium succinate 5, buffered to pH 7.30 with KOH. Using fura-2 and atomic absorbtion spectrophotometry, the estimated free Ca^{2+} concentration of this solution was 1 μM derived from the Ca^{2+} contamination of the constituents. The Ca^{2+}-free pipette solution was prepared similarly but the addition of 1.2 mM EGTA which yielded a free Ca^{2+} concentration of <1 nM (fura-2). A third, caesium-rich pipette solution was used for measurement of Ca^{2+} currents. This was similar to the Ca^{2+}-free pipette solution, except that the KCl and K_2HPO_4 were each replaced by equimolar concentrations of CsCl and the pH of the solution was adjusted to pH 7.30 with CsOH.

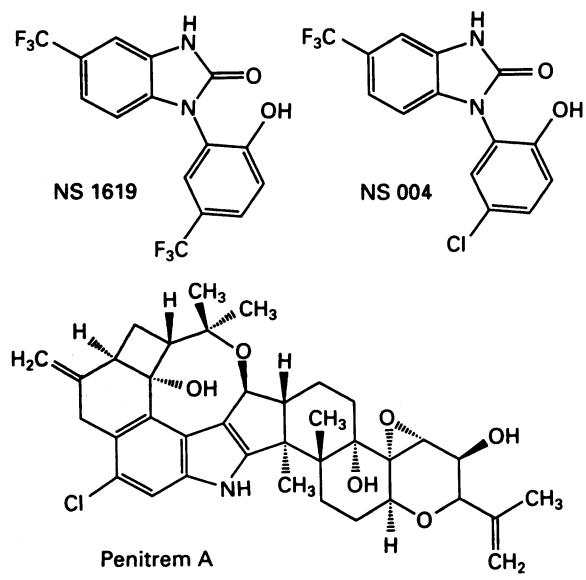


Figure 1 Structural formulae of some modulators of BK_{Ca} described in the text.

Organ bath studies The physiological salt solution used for the whole-tissue mechanical studies comprised (mM): NaCl 118, KCl 4.8, $CaCl_2$ 2.5, $MgSO_4$ 1.2, KH_2PO_4 1.2, $NaHCO_3$ 25 and glucose 11.1. This solution was gassed with a mixture of 95% O_2 and 5% CO_2 at 37°C.

NS 1619 (Figure 1, NeuroSearch), levcromakalim (Pfizer Central Research) and penitrem A (Figure 1) were each first dissolved in dimethyl sulphoxide (DMSO) to produce a concentrated stock solution (20 mM) from which dilutions were prepared with bath solution immediately before they were required. Synthetic charybdotoxin (Latoxan) was dissolved in glucose-free bath solution (pH 7.30) and used immediately. Unless otherwise stated, all reagents and compounds were obtained from Sigma.

Data analysis

Treatment effects were analysed by 2-way within subject (repeated measures) ANOVA (Statistica v.3.0a:Statsoft) or Student's two-tailed paired t test as appropriate. P values less than 0.05 were considered to be significant.

Results

Characteristics of NS 1619-induced changes at a holding potential of − 10 mV

General effects When the whole-cell recording mode was achieved with a pipette solution containing 1 μM Ca^{2+} and a Ca^{2+}-free PSS in the bath, the dominant currents observed on stepping from a holding potential of − 90 mV to a series of more positive test potentials were $I_{K(A)}$ and $I_{K(V)}$ (see methods). $I_{K(A)}$ activated and inactivated rapidly (within 200 ms at − 20 mV) and was only visible at test potentials within the range − 30 mV to 0 mV. At more positive voltages this current was masked by the larger current component, $I_{K(V)}$, which activated more slowly than $I_{K(A)}$ and which inactivated only slightly over the period of the test pulse (Figure 2a). At a holding potential of − 10 mV $I_{K(A)}$ and $I_{K(V)}$ inactivated, and under this condition these time-dependent currents were essentially abolished (Figure 2b). On changing the bath solution to Ca^{2+}-PSS, a larger, noisy, time-dependent, outwardly rectifying current was generated with an identical test protocol and a holding potential of − 10 mV (compare mean currents, Figures 2b and 3a). This current showed no signs of inactivation even after holding for several minutes at positive potentials (data not shown). Under these conditions, spontaneous transient outward currents (STOCs) were observed in approximately 20% of cells (Figure 3c).

Exposure to NS 1619 (10–33 μM) immediately abolished any STOCs which were present and there was a gradual increase in the level of outward current. This reached a maximum (33 μM NS 1619; mean 35.8 ± 17 pA, $n = 8$) within about 6 min and was associated with a marked increase in current noise (Figure 3c). On stepping to test potentials in the range − 40 mV to + 50 mV, the large, noisy, time-dependent, non-inactivating, outwardly rectifying current (Figure 3a) was markedly enhanced by NS 1619 in a concentration-dependent manner (mean currents in 33 μM NS 1619, Figure 3b; $I-V$ relationships for 10 and 33 μM NS 1619, Figure 4a). In the presence of 33 μM NS 1619, the zero current potential was shifted from − 35.5 ± 6.6 mV to − 38.4 ± 4.9 mV ($P < 0.05$, $n = 8$).

Since the noisy, outwardly-rectifying current was non-inactivating, the effects of NS 1619 cannot be attributed to modification of inactivation characteristics. Thus, to determine whether there was an NS 1619-induced shift in the *activation* threshold of the currents available on stepping from − 10 mV, the net effects of two concentrations of NS 1619 (10 μM and 33 μM) were calculated by subtracting the control currents (Figure 3a and open circles, Figure 4a) from the currents available in the presence of these two concentrations of NS 1619 (closed symbols, Figure 4a). It can be clearly seen that NS 1619 did indeed shift the activation threshold of the non-inactivating current to more negative values ($P < 0.05$, Figure 4b).

In the absence of Ca^{2+}, i.e. with Ca^{2+}-free PSS in the bath and a Ca^{2+}-free pipette solution, STOCs were never detected but the ability of NS 1619 to enhance outward currents was

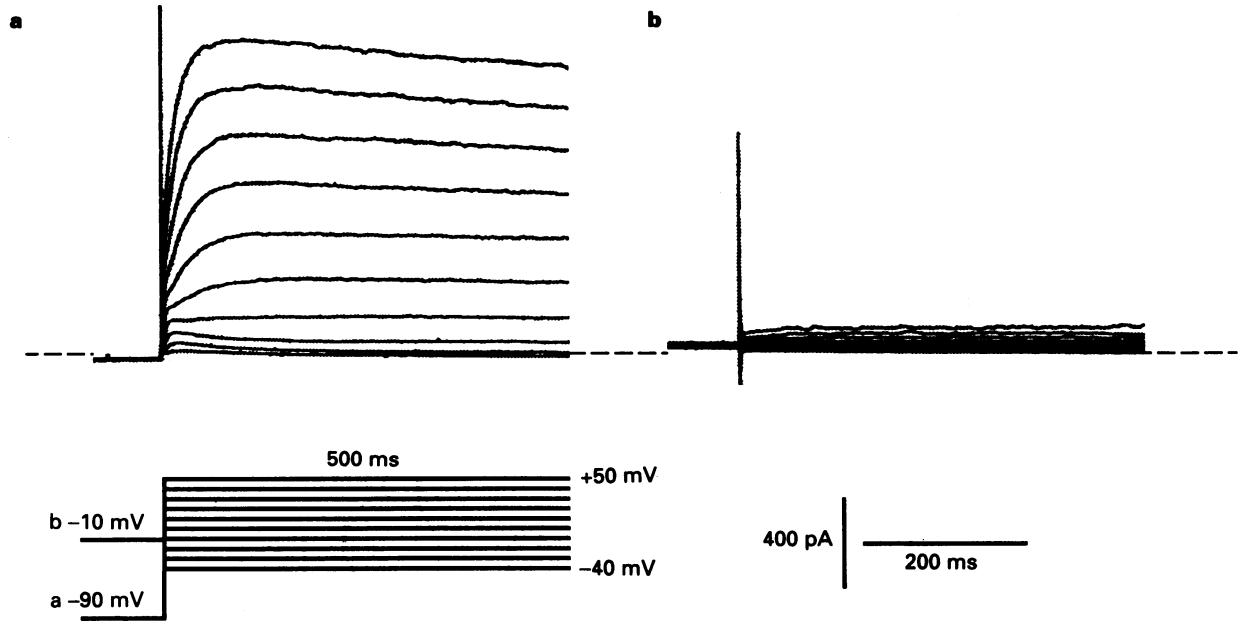


Figure 2 Effect of holding potential on whole-cell currents available in rat portal vein cells bathed in Ca-free PSS. The pipette solution contained approximately 1 μM calcium and no EGTA. (a) Cells were held at − 90 mV and stepped to test potentials from − 40 to + 50 mV in 10 mV increments. $I_{K(A)}$ activated and inactivated rapidly and was visible in the range − 30 mV to 0 mV. At more positive potentials, $I_{K(V)}$ masked all other currents and inactivated only slowly during the test pulse. (b) At a holding potential of − 10 mV, $I_{K(A)}$ and $I_{K(V)}$ inactivated leaving only low-amplitude, non-inactivating currents. Each trace represents the computer-derived mean from the same 5 cells under the two conditions. In all traces, zero current is indicated by a dashed line.

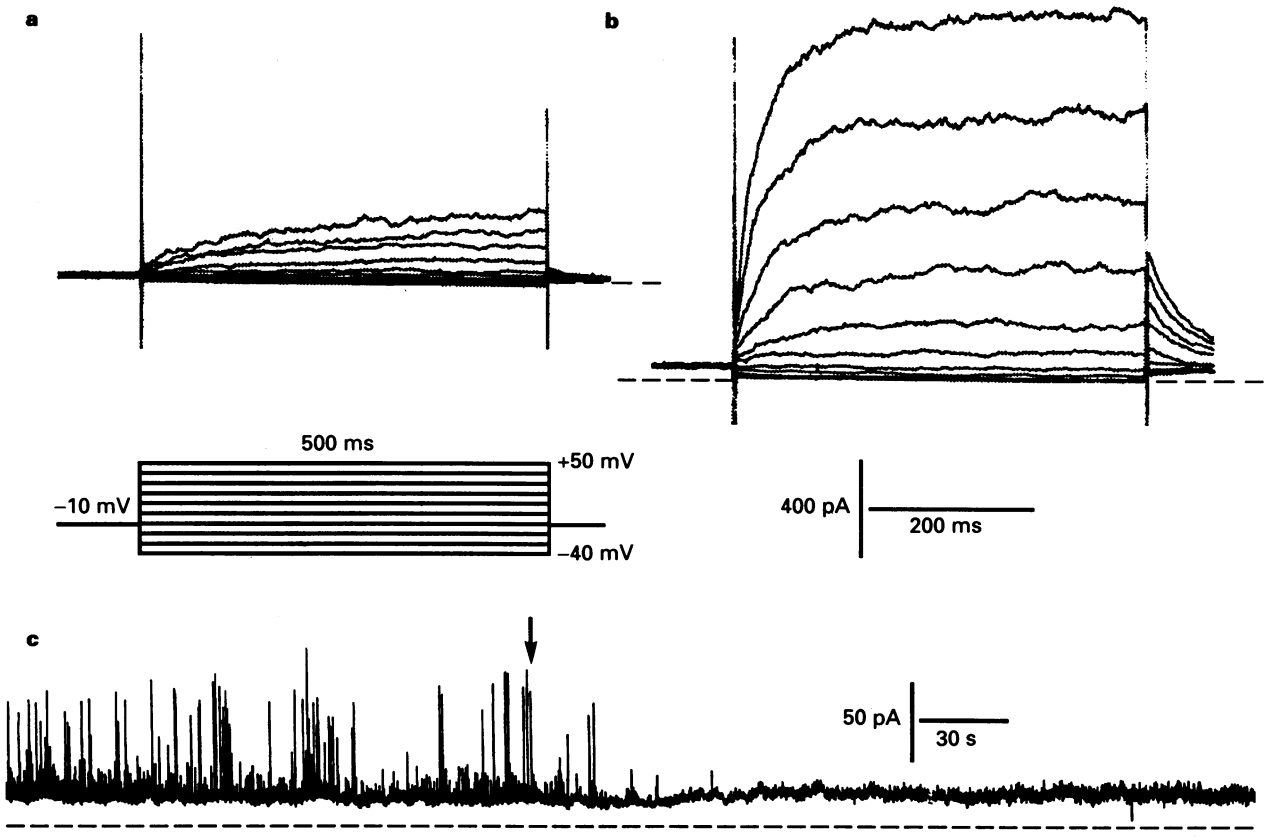


Figure 3 Effect of calcium and NS 1619 on whole-cell currents available from − 10 mV in rat portal vein cells. The pipette solution contained approximately 1 μM calcium and no EGTA. (a) When cells were bathed in Ca^{2+}- PSS, a noisy, outwardly-rectifying, time-dependent current was obtained on stepping from a holding potential of − 10 mV to test potentials from − 40 to + 50 mV in 10 mV increments. (b) Subsequent exposure to 33 μM NS 1619 produced a further increase in this current, an effect which was particularly striking at test potentials more depolarized than − 10 mV. Each trace represents the computer-derived mean from the same 5 cells under the various conditions. (c) In the presence of 2.5 mM calcium, spontaneous transient outward currents (STOCs) were evident in some cells under whole-cell recording conditions at a holding potential of − 10 mV. In the single example shown, exposure to 20 μM NS 1619 (arrow) rapidly inhibited the STOCs. The onset of the gradual development of a noisy, outward current is also visible. In all traces, zero current is indicated by a dashed line.

still observed. Thus, under these conditions, 33 μM NS 1619 produced an increase in the noisy, time-dependent, outwardly-rectifying current identical (ANOVA, $P>0.05$) to that seen in the presence of Ca^{2+} (compare the $I-V$ relationships, open and closed inverted triangles in Figure 4b).

Effects of charybdotoxin and penitrem A

With Ca^{2+}-PSS in the bath, exposure to 250 nM charybdotoxin abolished any STOCs which were present (data not shown) and totally inhibited the stimulation of the noisy, outwardly rectifying current by 10–33 μM NS 1619 ($I-V$ relationships for 20 μM NS 1619, Figure 4c). With Ca^{2+}-free PSS in the bath, the current induced by 33 μM NS 1619 was also abolished by 250 nM charybdotoxin (data not shown).

These results, together with the electrophysiological characteristics of the changes induced by NS 1619 strongly indicated that the current involved was $I_{BK(Ca)}$. To confirm this view, experiments were also carried out with 100 nM penitrem A, a recently-described, selective inhibitor of BK_{Ca} (Knaus *et al.*, 1994). In the presence of this agent, the currents induced by NS 1619 (33 μM) were totally inhibited ($I-V$ relationships, Figure 4d).

Effects of NS 1619 on currents available from a holding potential of − 90 mV

On stepping from a holding potential of − 90 mV, the evoked currents comprised $I_{K(A)} + I_{K(V)} + I_{BK(Ca)}$ but because of the very rapid inactivation of $I_{K(A)}$ (see Figure 2), this current did not contribute to the measured peak current which comprised approximately 74% $I_{K(V)}$ and 26% $I_{BK(Ca)}$. With Ca^{2+}-PSS as the bath solution and 1 μM Ca^{2+}-containing PSS in the pipette, NS 1619 (10–33 μM) *inhibited* the total currents evoked on stepping from − 90 mV to the range of test potentials ($I-V$ relationships, Figure 5a). Since NS 1619 increases $I_{BK(Ca)}$ (Figures 3 and 4), these inhibitory effects strongly indicate an inhibition of $I_{K(V)}$. This action was confirmed by exposing cells to 20 μM NS 1619 in the absence of Ca^{2+} from the bath and pipette together with the presence of charybdotoxin to eliminate any effects of NS 1619 on $I_{BK(Ca)}$ ($I-V$ relationships, Figure 5b). To clarify the *resultant* effect of NS 1619-induced inhibition of $I_{K(V)}$ and activation of $I_{BK(Ca)}$, difference curves were constructed from the data presented in Figure 5a (Figure 5c). These clearly show that 10 μM and 33 μM NS 1619 each produced an overall *inhibitory* effect on K-currents, the degree of which depended not only on the extent to which $I_{K(V)}$ was compromised but also on the degree of stimulation of $I_{BK(Ca)}$.

Noise analysis of current stimulated by NS 1619

Using stationary fluctuation analysis of the basal level of current noise and of that in the presence of 33 μM NS 1619, we estimated the unitary current and unitary conductance of those ionic channels which carried the NS 1619-induced outward current. This procedure was performed for a membrane potential of − 10 mV to allow a sufficient number of the

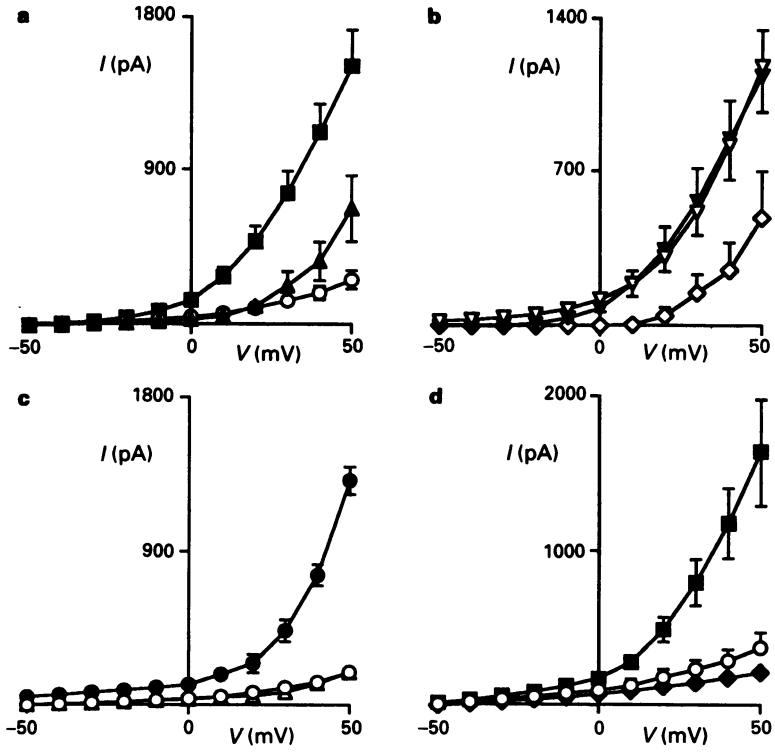


Figure 4 Effect of NS 1619 on currents available on stepping from − 10 mV. (a) with Ca-PSS in the bath a small outwardly-rectifying current was evident under control conditions (○; $n = 16$). This current was increased in a concentration-dependent manner by 10 μM (▲, $n = 5$) and 33 μM (■, $n = 8$) NS 1619. (b) Subtraction of the control current at each test potential from the corresponding current in the presence of NS 1619 (10 μM, ◇; 33 μM, ▼) shows the current, $I_{BK(CA)}$ induced by the drug. Note that increasing the concentration of NS 1619 shifts the activation potential of $I_{BK(Ca)}$ in a hyperpolarizing direction. The magnitude of $I_{BK(Ca)}$ in the presence of 33 μM NS 1619 but under calcium-free conditions (EGTA in bath and pipette solutions; ▽, $n = 5$) is shown for comparison. (c) With calcium in the bath and pipette solutions (control, ○), the effect of 20 μM NS 1619 (●) was completely inhibited when 250 nM charybdotoxin was present in the bath (△) ($n = 5$). (d) The effect of 33 μM NS 1619 was totally inhibited by 100 nM penitrem A (control, ○; 33 μM NS 1619, ■; NS 1619 + penitrem A, ◆; $n = 5$).

target channels to be opened by NS 1619 but to keep the total open probability relatively low (<0.1; see Figure 4 for the voltage-dependency). Interference between the NS 1619-induced outward current and the other currents modified by this drug ($I_{K(V)}$ and the calcium current, I_{Ca}; see Figure 5 and Figure 7, respectively) can be excluded since both $I_{K(V)}$ and I_{Ca} inactivate at − 10 mV and neither a shift of the mean current (μ) nor a change of the current variance (σ^2) would result from inhibition of either $I_{K(V)}$ or I_{Ca} or both of these currents.

Under control conditions, the background noise ranged from 2.5–3.5 pA, giving a current variance of 6.25–12.25 $(pA)^2$, respectively. In the presence of NS 1619, background current increased with an accompanying increase in noise and the mean quotient $(\Delta\sigma^2)/\Delta\mu)$ was 2.7 pA ($n = 4$). This value represents the mean current carried by the K-channels opened by NS 1619 under a normal K-gradient and at a potential of − 10 mV. Application of the Goldman-Hodgkin-Katz equation yielded a value for the single channel conductance of 70 ± 8 pS ($n = 4$).

Effects of NS 1619 on mechanical activity in rat blood vessels

The characteristic spontaneous mechanical activity of rat portal vein was inhibited by NS 1619 (3 to 100 μM) in a concentration-dependent manner. This was characterized by a gradual reduction in the amplitude and duration of the tension waves with little effect on their frequency. Attempts were made to antagonize the effects of NS 1619 with either charybdotoxin (250 nM) or penitrem A (1 μM). Both inhibitors increased the integrated spontaneous mechanical activity of the portal vein (by 140 ± 24%, charybdotoxin, $n = 4$ and by 82 ± 25%, penitrem A, $n = 4$). However, the relaxant effects of NS 1619 were not inhibited but were slightly potentiated by both inhibitors (Figure 6a,b), suggesting that NS 1619-induced activation of BK_{Ca} was not solely responsible for the observed mechano-inhibitory effects of this agent. We therefore investigated the possibility that NS 1619 might relax smooth muscle by a mechanism independent of K-channel opening using segments of rat aorta contracted with either 20 mM or 80 mM KCl. Under each of these conditions, NS 1619 produced full inhibition of the contractions induced by both 20 mM and 80 mM KCl (Figure 6c).

Effects of NS 1619 on calcium currents

The ability of NS 1619 to relax an 80 mM KCl-induced contraction together with the failure of either charybdotoxin or penitrem A to antagonize the mechano-inhibitory effects of this agent suggested that NS 1619 might inhibit calcium currents. This possibility was reinforced by the report that the closely-related molecule NS 004 (Figure 1) inhibits L-type calcium currents in cardiac myocytes (Sargent *et al.*, 1993).

With Ca^{2+}PSS in the bath and a Cs-rich pipette solution, Ca-currents (Figure 7) were evoked in portal vein cells by stepping from a holding potential of − 90 mV to test potential in the range − 30 mV to + 40 mV. These currents were totally inhibited by 1 μM nifedipine (data not shown) and thus almost certainly represent Ca^{2+} flux through L-type calcium channels. In the presence of 33 μM NS 1619 these currents were essentially totally inhibited by NS 1619 (33 μM) within a period of 10 min ($I-V$ relationship, Figure 7b).

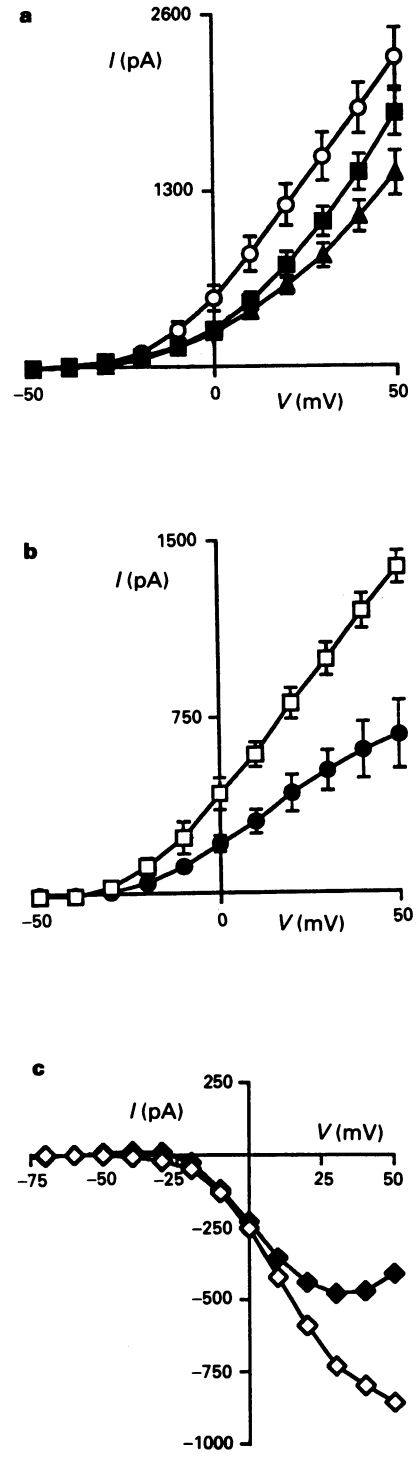


Figure 5 Effect of NS 1619 on currents available from − 90 mV with Ca-PSS in the bath. (a) An outwardly-rectifying current which activated at − 35 mV was evident under control conditions (○; $n = 16$). This total current was inhibited by 10 μM NS 1619 (▲, $n = 5$) although 33 μM NS 1619 (■, $n = 8$) produced a smaller inhibition. (b) In the presence of charybdotoxin (to eliminate $I_{BK(Ca)}$), the inhibitory effect of NS 1619 on $I_{K(V)}$ was evident (control, □; 20 μM NS 1619, ●, $n = 4$). (c) Transformation of data presented in (a) to illustrate more clearly the effect of NS 1619 on total currents. Subtraction of the control current at each test potential from the corresponding current in the presence of NS 1619 (10 μM, ◇; 33 μM, ◆) shows that the drug inhibited a current which activated at approximately − 35 mV. There was little difference in the magnitude of inhibition of current by 10 μM or 33 μM NS 1619 over the range of test potentials from − 40 mV to 0 mV. At more positive test potentials the inhibitory effect of 33 μM NS 1619 was reduced because of its comparatively larger stimulatory effect on $I_{BK(Ca)}$ (see Figure 4).

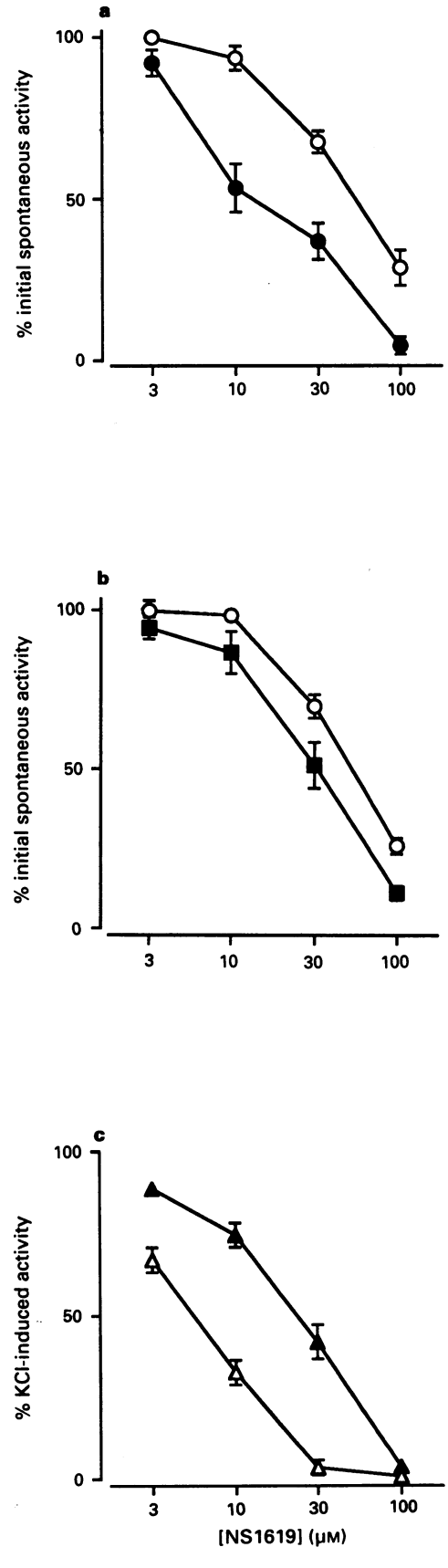


Figure 6 Mechano-inhibitory effect of NS 1619 in rat portal vein and aorta. NS 1619 produced a concentration-dependent inhibition of spontaneous activity in rat portal veins (○; a,b). This effect was not antagonized in the presence of either 250 nM charybdotoxin (●; a) or 1 μM penitrem A (■; b). (c) In rat aorta, NS 1619 fully inhibited contractions induced by either 20 mM (△) or 80 mM (▲) KCl ($n = 4$).

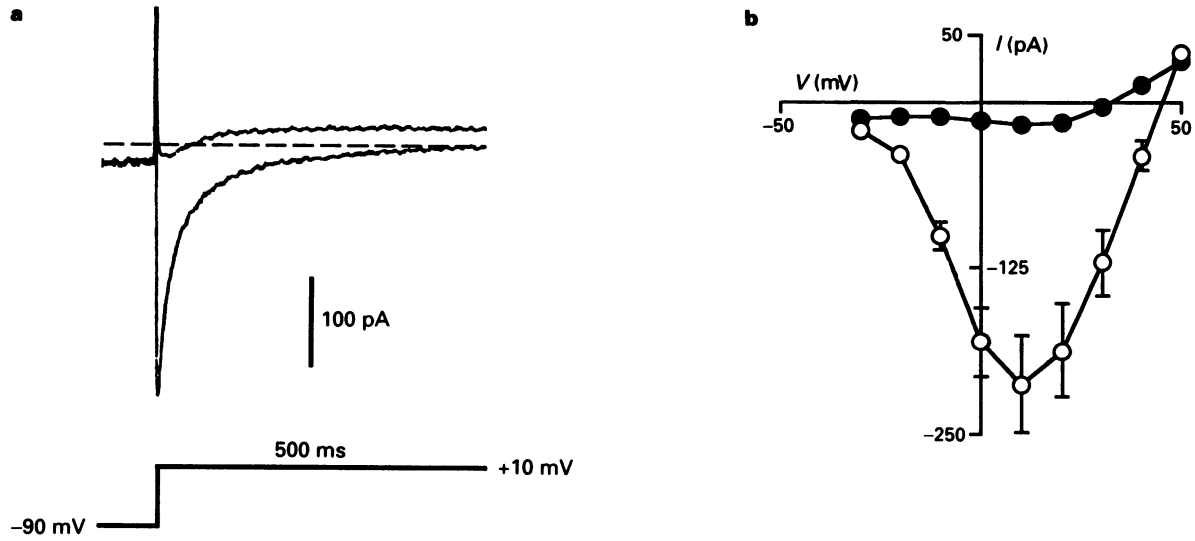


Figure 7 Effect of NS 1619 on calcium currents in rat portal vein cells. (a) When cells were held at − 90 mV then stepped to + 10 mV for 500 ms a rapidly-activating and -inactivating calcium current was observed (○). This current was abolished by exposure to 33 μM NS 1619 (●). (b) Current-voltage relationship for peak calcium currents evoked on stepping (at 8 s intervals) from a holding potential of − 90 mV to a series of test potentials in the absence (○) or presence (●) of 33 μM NS 1619 ($n = 3$).

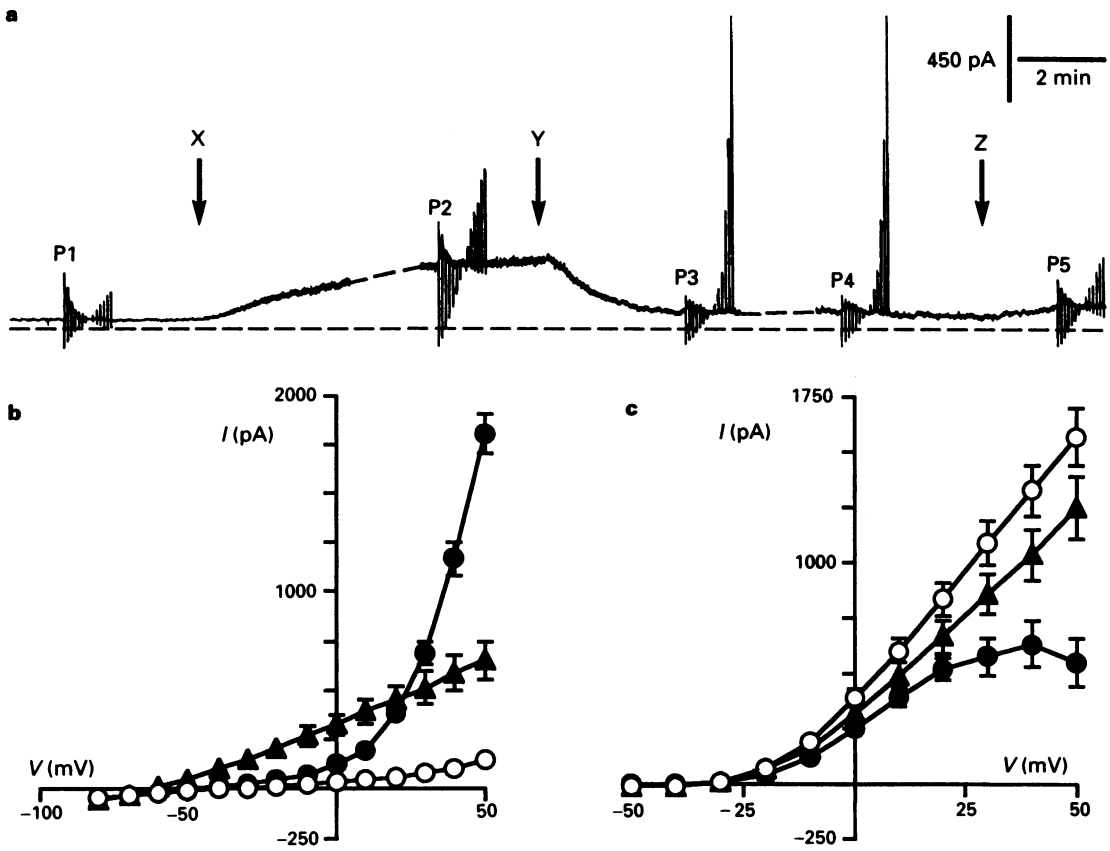


Figure 8 Inhibition of effects of levcromakalim by NS 1619. (a) Recording from a single cell clamped at a holding potential of − 10 mV under calcium-free whole-cell recording conditions. On stepping to a series of test potentials ranging from − 90 mV to + 50 mV in 10 mV increments (P1), a non-inactivating, voltage-insensitive current with a reversal potential of − 40 mV was obtained. On exposure to 10 μM levcromakalim (X) there was a marked increase in the holding current and application of the test potentials (P2) yielded larger, but still voltage-insensitive, currents with a reversal potential of approximately − 60 mV. In the continued presence of levcromakalim, 33 μM NS 1619 (Y) produced a rapid inhibition of the levcromakalim-induced increase in the holding current. The reversal potential became less negative and there was a marked increase in the voltage-dependent outward current component, $I_{BK(Ca)}$ (P3, P4). On washout (Z), the effects of NS 1619 on $I_{BK(Ca)}$ were rapidly reversed (P5). (b) Currents obtained at test potentials in 4 such experiments when cells were stepped from a holding potential of − 10 mV; (○) control, P1; (▲) levcromakalim, P2; (●) levcromakalim + NS1619, P4. (c) Shows inhibition of $I_{K(V)}$ (calculated by subtracting currents at each test potential after stepping from − 10 mV from those obtained on stepping from − 90 mV) by levcromakalim (▲) and further inhibition in the presence of levcromakalim + NS 1619 (●) ($n = 4$).

Interaction between NS 1619 and levcromakalim

Drugs like levcromakalim, which open the so-called ATP-sensitive K-channel (K_{ATP}) are inhibited by agents which inhibit $I_{K(V)}$ (Edwards & Weston, 1993, Ibbotson *et al.*, 1993a,b). Thus, the unexpected finding in the present study that NS 1619 was an inhibitor of $I_{K(V)}$ prompted an examination of the interaction between NS 1619 and levcromakalim.

As shown in Figure 8, cells were held at − 10 mV and first exposed to levcromakalim (10 μM) which produced a characteristic increase in current noise associated with the development of an outward current (Figure 8a). Stepping from the holding potential to a range of test potentials (P2, Figure 8a) confirmed that the levcromakalim-induced current was voltage- and time-independent with the previously-described characteristics of $I_{K(ATP)}$ ($I-V$ relationship, Figure 8b, see also Noack *et al.*, 1992; Edwards *et al.*, 1993). When this current had reached a peak, cells were additionally exposed to NS 1619 (33 μM) and after a short delay, $I_{K(ATP)}$ declined. Subsequent application of stepping voltage protocols (P3, P4, Figure 8a) confirmed that a current with the voltage-dependency and outwardly-rectifying characteristics characteristic of $I_{BK(Ca)}$ had indeed been activated $I-V$ relationship, Figure 8b). On wash-out of NS 1619, but in the continued presence of levcromakalim, the stimulation of $I_{BK(Ca)}$ was rapidly lost (within 2 to 3 min) whereas inhibition of the levcromakalim-induced current was maintained for up to 10 min (P5, Figure 8a). Consistent with our previously-described findings with levcromakalim (Noack *et al.*, 1992; Edwards *et al.*, 1993) and with NS 1619 (present study) use of depolarizing pulse protocols from a holding potential of − 90 mV (applied at the broken lines on the current trace in Figure 8a but removed for clarity) confirmed that both agents inhibited $I_{K(V)}$ ($I-V$ relationship, Figure 8c).

Discussion

Induction of $I_{BK(Ca)}$ by NS 1619

Exposure to NS 1619 of freshly-isolated portal vein cells, induced a noisy, time- and voltage-dependent, outwardly-rectifying current and stationary fluctuation analysis of the associated current noise was used to estimate the unitary conductance of the channel opened by NS 1619. This method may yield erroneous values unless the channel open probability is low and if other currents such as $I_{K(V)}$ and I_{Ca} are still present. We thus analysed current noise after holding at − 10 mV for several minutes under which conditions $I_{K(V)}$ and I_{Ca} are largely inactivated (see Figures 2 and 7). In addition, since − 10 mV was close to the activation threshold for BK_{Ca} in the present study, we estimate that the open probability of this channel would have been much less than 0.1 (see Figure 4 and Olesen *et al.*, 1994a). With this method an estimate for the unitary conductance underlying the NS 1619-induced current of 70 ± 8 pS were obtained (at − 10 mV and under the quasi-physiological conditions of the experiment, $n = 4$). When corrected for symmetrical (150 mM) K^+ conditions, this yielded a value of approximately 140 pS which lies within the range of values previously reported for BK_{Ca} in smooth muscle (Bolton & Beech, 1992). On the basis of this relatively large unitary conductance, together with its charybdotoxin and penitrem A sensitivity, we conclude that the NS 1619-induced current can be identified as $I_{BK(Ca)}$. This confirms the recent findings of Olesen *et al.* (1994a) obtained using cultured bovine aortic smooth muscle. As in these cultured cells, NS 1619 produced a concentration-dependent increase in $I_{BK(Ca)}$ in rat portal vein cells, apparently by shifting the $I_{BK(Ca)}$ − voltage relationship to more negative levels. This shift did not appear to be primarily due to a change in the calcium-sensitivity of BK_{Ca} since, in the present study, 33 μM NS 1619 stimulated similar increases in the magnitude of $I_{BK(Ca)}$ in the presence or absence of calcium.

Inhibition of $I_{K(V)}$ by NS 1619

In both the present investigation and in that of Olesen *et al.* (1994a), the effects of NS 1619 on $I_{BK(Ca)}$ were measured after optimising the conditions for the detection of this current. However, an important finding of the present study was that over a similar range of concentrations, NS 1619 not only enhanced $I_{BK(Ca)}$ but also inhibited $I_{K(V)}$. Thus, despite the magnitude of the stimulatory effect of NS 1619 on $I_{BK(Ca)}$ (measured from − 10 mV), a comparison of the total evoked currents before and after exposure to NS 1619 showed that the compound had a net *inhibitory* effect on the total outward current (measured after stepping from − 90 mV). Since BK_{Ca} is clearly opened by NS 1619, the inhibition of the total current strongly suggests a very substantial inhibition of $I_{K(V)}$ which was confirmed by experiments performed in the presence of charybdotoxin (in which $I_{BK(Ca)}$ was abolished), thus simplifying the determination of $I_{K(V)}$.

This inhibition contrasts with the reported lack of effect of NS 1619 on $I_{K(V)}$ in neuronal cells (Olesen *et al.*, 1994a) and the reasons for this discrepancy are not clear. However, numerous gene products have been identified which associate into homo- or heteromultimers to produce voltage-sensitive K-channels with differing gating properties (see Pongs, 1993). Thus, the marked difference between the very rapid activation of neuronal delayed reactifier currents (Olesen *et al.*, 1994a) and the slower time-course of activation of $I_{K(V)}$ in smooth muscle (present study) may reflect differences in the multimeric composition of neuronal and smooth muscle delayed rectifier channels. If so, it would not be surprising if the underlying channels exhibited different drug sensitivities.

Relaxant effects of NS 1619 in whole tissues

The rat portal vein exhibits spontaneous mechanical activity. This is generated by the discharge of electrical multi-spike complexes which at their peak shift the membrane potential into the range − 10 to 0 mV (Southerton *et al.*, 1988). Since inhibitors of both $I_{K(V)}$ (phentolamine; Ibbotson *et al.*, 1993b) and $I_{BK(Ca)}$ (charybdotoxin and penitrem A; present study) increase spontaneous activity in portal vein, both K_V and BK_{Ca} are probably involved in the repolarization phase of such complexes. Thus, it was of interest to study the effects of NS 1619 on spontaneous mechanical activity in whole portal veins.

NS 1619 produced a concentration-dependent inhibition of spontaneous mechanical activity characterized by a reduction in tension wave amplitude and duration with little effect on wave frequency. Despite the findings from the whole-cell clamp experiments which indicated a net inhibitory action on outward currents in single cells, we initially assumed that the mechanical inhibition of a whole vein must somehow reflect a dominant opening effect of NS 1619 on BK_{Ca} (since inhibition of K_V should depolarize cell membranes and produce conditions favourable for an increase in the frequency and magnitude of the spontaneous contractions). However, the relaxant effect of NS 1619 was not reduced following preincubation of the vessels with either charybdotoxin or penitrem A at concentrations identical to, or even greater than, those which totally inhibited $I_{BK(Ca)}$ in the presence of NS 1619 (whole-cell recording, present study.)

A further indication that the relaxant effect of NS 1619 was not due to the opening of K-channels was provided by the finding that NS 1619 produced a full relaxation of rat aorta precontracted with 80 mM KCl (see Hamilton *et al.*, 1986). Based on these observations, and the finding that NS 004 (a compound structually very similar to NS 1619; see Figure 1) inhibited L-type calcium channels (Sargent *et al.*, 1993), we considered the possibility that NS 1619 might also inhibit plasmalemmal calcium channels.

Inhibition of calcium-currents and STOCs by NS 1619

Using the whole-cell recording configuration, we found that NS 1619 (33 μM) was an effective inhibitor of nifedipine-sensitive calcium currents (I_{Ca}) in portal vein. This effect was not readily reversible, in contrast to the actions of NS 1619 on $I_{BK(Ca)}$ and $I_{K(V)}$ which were rapidly reversed on washout of the drug. In tissue-bath experiments, the inhibition of portal vein spontaneous mechanical activity by NS 1619 was also only slowly reversible and it thus seems likely that the observed inhibition of I_{Ca} rather than activation of $I_{BK(Ca)}$ plays the major role in the spasmolytic effect of NS 1619.

One interesting and unexpected observation was the rapid inhibition of STOCs by NS 1619. These currents are thought to be carried by BK_{Ca} channels which open in response to transient increases in $[Ca^{2+}]_i$ released spontaneously from inositol 1,4,5-trisphosphate (IP_3)-sensitive intracellular Ca-stores close to the membrane (Benham & Bolton, 1986; Ohya *et al.*, 1988; Bolton & Lim, 1989). STOCs are only observed when Ca^{2+} is present extracellularly (Hume & Leblanc, 1989) and they may represent a pathophysiological phenomenon associated with Ca^{2+} leak from the extracellular medium into the cell through the gigaseal between cell and patch pipette (Bolton, personal communication). In favour of this is the finding in intact single jejunal cells that the $[Ca^{2+}]_i$ measured by use of the dye Indo-1 was significantly lower than that in the same cells held under whole-cell clamp conditions (Pacaud & Bolton, 1991).

Irrespective of the mechanism involved in the induction of STOCs, the importance of Ca^{2+} release from stores in their production (Benham & Bolton, 1986; Ohya *et al.*, 1988; Bolton & Lim, 1989) makes these currents sensitive indicators of Ca^{2+} release from stores. Their inhibition by NS 1619 could indicate that this compound modifies intracellular Ca^{2+} release from, or sequestration into IP_3 sensitive Ca-stores. Alternatively, if Ca^{2+} entry *via* L-type Ca-channels is involved, inhibition of these by NS 1619 (see above) would inhibit STOC production. These alternatives and their possible contribution to the mechano-inhibitory action of NS 1619 are the subject of further study.

Interaction between NS 1619 and levcromakalim

In the present study, NS 1619 inhibited $I_{K(ATP)}$ induced by levcromakalim, a property shared by chemically-diverse inhibitors of the smooth muscle $I_{K(V)}$ such as phentolamine, guanethidine and ciclazindol (see Edwards & Weston, 1993). To account for this and for the finding that procedures designed to reduce intracellular ATP simultaneously inhibit $I_{K(V)}$ (rat portal vein, Noack *et al.*, 1992; rabbit atria, Ogbaghebriel & Shrier, 1994; frog skeletal muscle, Fink & Wettwer, 1978), we proposed that K_{ATP} and K_V might be different phosphorylated states of the same channel (Edwards *et al.*, 1993). Recently, however, an inwardly-rectifying K-channel inhibited by micromolar concentrations of intracellular ATP and opened by (50 μM) pinacidil has been cloned from rat heart (Ashford *et al.*, 1994). This channel, which seems likely to be the cardiac K_{ATP}, comprises α-subunits consisting of only two membrane-spanning segments linked by a pore region, a structure which shares homology with the S5-pore-S6 region of K_V (J. Adelman, personal communication). Thus the pharmacological features which led us to propose that K_{ATP} and K_V might be two states of a single channel (Edwards *et al.*, 1993) may rather indicate that modulators of K_{ATP} and K_V directly or indirectly interact with sites commmon to both channel types (and which probably lie in the vicinity of their respective pore-forming regions). In favour of this is the recent finding that deletion of four transmembrane segments (S1 to S4) of the *delayed rectifier*, K_V (leaving the S5-pore-S6 structure), produces subunits which associate to form K-selective, *inwardly-rectifying* channels (Tytgat *et al.*, 1994).

Conclusions

The present study has shown that the pharmacology of NS 1619 is more complex than originally described by Olesen *et al.* (1994a). Our observation that NS 1619 can inhibit calcium currents is perhaps not surprising in view of the fact that the closely-related benzimidazole NS 004 (Figure 1) exhibits this property (Sargent *et al.*, 1993). However, an unexpected finding was the NS 1619-induced inhibition of $I_{K(V)}$ and $I_{K(ATP)}$, a property shared by many structurally-diverse molecules (see Edwards & Weston, 1993). The ability of NS 1619 simultaneously to open BK_{Ca} and to *inhibit* L-type calcium channels is not unique but is also shared by niguldipine (Klöckner *et al.*, 1989). Furthermore, BK_{Ca} is activated by the chloride channel inhibitor, niflumic acid (Toro *et al.*, 1993). Other agents also exhibit similarly diverse properties. Thus, openers of K_{ATP} also inhibit K_V (levcromakalim, aprikalim, P1060: Edwards *et al.*, 1993; Ibbotson *et al.*, 1993b) and chloride channels (levcromakalim, P1075, minoxidil sulphate and diazoxide: Sheppard & Welsh, 1993; Holevinsky *et al.*, 1994). It is not yet clear whether the multiple excitatory and inhibitory effects of these agents result from their direct interaction with channel structural components or involve modulation of biochemical pathways which regulate channel gating.

Perhaps the most striking feature of NS 1619 was its ability to stimulate $I_{BK(Ca)}$ in smooth muscle although this action was almost certainly not responsible for a major component of the observed relaxant effects of this molecule in the intact vessels studied. Nevertheless, in those tissues such as bladder or trachea in which BK_{Ca} is perhaps more important (Suarez-Kurtz *et al.*, 1991; Small *et al.*, 1993) and in those experimental situations in which $I_{BK(Ca)}$ can be studied in isolation, NS 1619 would seem to be a useful tool for the investigation of the pharmacology of BK_{Ca}.

NS 1619 was a generous gift from Dr S.P. Olesen (NeuroSearch). Helpful discussions with Dr D.J. Beech, Professor T.B. Bolton, Dr G. Kaczorowski and Dr O.B. McManus are gratefully acknowledged. G.E. was supported by Pfizer Central Research.

References

ASHFORD, M.L.J., BOND, C.T., BLAIR, T.A. & ADELMAN, J.P. (1994). Cloning and functional expression of a rat heart K_{ATP} channel. *Nature*, **370**, 456–459.

BENHAM, C.D. & BOLTON, T.B. (1986). Spontaneous transient outward currents in single visceral and vascular smooth muscle cells of the rabbit. *J. Physiol.*, **381**, 385–406.

BOLTON, T.B. & BEECH, D.J. (1992). Smooth muscle potassium channels: their electrophysiology and function. In *Potassium Channel Modulators*. ed. Weston, A.H. & Hamilton, T.C. pp. 144–180. Oxford: Blackwell Scientific.

BOLTON, T.B. & LIM, S.P. (1989). Properties of calcium stores and transient outward currents in single smooth muscle cells of rabbit intestine. *J. Physiol.*, **409**, 385–401.

EDWARDS, G., IBBOTSON, T. & WESTON, A.H. (1993). Levcromakalim may induce a voltage-independent K-current in rat portal veins by modifying the gating properties of the delayed rectifier. *Br. J. Pharmacol.*, **110**, 1037–1048.

EDWARDS, G. & WESTON, A.H. (1993). The pharmacology of ATP-sensitive potassium channels. *Annu. Rev. Pharmacol. Toxicol.*, **33**, 597–637.

FINK, R. & WETTWER, E. (1978). Modified K-channel gating by exhaustion and the block by internally-applied TEA^+ and 4-aminopyridine in muscle. *Pflügers Arch.*, **374**, 289–292.

HAMILL, O.P., MARTY, A., NEHER, E., SAKMANN, B. & SIGWORTH, F.J. (1981). Improved patch clamp techniques for high-resolution current recording from cells and cell-free membrane patches. *Pflügers Arch.*, **391**, 85–100.

HAMILTON, T.C., WEIR, S.W. & WESTON, A.H. (1986). Comparison of the effects of BRL 34915 and verapamil on electrical and mechanical activity in rat portal vein. *Br. J. Pharmacol.*, **88**, 103–111.

HOLEVINSKY, K.O., FAN, Z., FRAME, M., MAKIELSKI, J.C., GROPPI, V. & NELSON, D.J. (1994). ATP-sensitive K^+ channel opener acts as a potent Cl^- channel inhibitor in vascular smooth muscle cells. *J. Membr. Biol.*, **137**, 59–70.

HUME, J.R. & LEBLANC, N. (1989). Macroscopic K^+ currents in single smooth muscle cells of the rabbit portal vein. *J. Physiol.*, **413**, 49–73.

IBBOTSON, T., EDWARDS, G., NOACK, Th. & WESTON, A.H. (1993a). Effects of P1060 and aprikalim on whole-cell currents in rat portal vein; inhibition by glibenclamide and phentolamine. *Br. J. Pharmacol.*, **108**, 991–998.

IBBOTSON, T., EDWARDS, G. & WESTON, A.H. (1993b). Antagonism of levcromakalim by imidazoline-derivatives and guanidine-derivatives in rat portal vein–involvement of the delayed rectifier. *Br. J. Pharmacol.*, **110**, 1556–1564.

KLÖCKNER, U. & ISENBERG, G. (1985). Action potentials and net membrane currents of isolated smooth muscle cells (urinary bladder of the guinea-pig). *Pflügers Arch.*, **405**, 329–339.

KLÖCKNER, U., TRIESCHMANN, U. & ISENBERG, G. (1989). Modulation of calcium and potassium channels in isolated vascular smooth muscle cells. *Drug Res.*, **39**, 120–126.

KNAUS, H.G., MCMANUS, O.B., LEE, S.H., SCHMALHOFER, W.A., GARCIACALVO, M., HELMS, L.M.H., SANCHEZ, M., GIANGIACOMO, K., REUBEN, J.P., SMITH, A.B., KACZOROWSKI, G.J. & GARCIA, M.L. (1994). Tremorgenic indole alkaloids potently inhibit smooth muscle high-conductance calcium-activated potassium channels. *Biochemistry*, **33**, 5819–5828.

MCMANUS, O.B., HARRIS, G.H., GIANGIACOMO, K.M., FEIGENBAUM, P., REUBEN, J.P., ADDY, M.E., BURKA, J.F., KACZOROWSKI, G.J. & GARCIA, M.L. (1993). An activator of calcium-dependent potassium channels isolated from a medicinal herb. *Biochemistry*, **32**, 6128–6133.

NOACK, Th., DEITMER, P., EDWARDS, G. & WESTON, A.H. (1992). Characterization of potassium currents modulated by BRL-38227 in rat portal vein. *Br. J. Pharmacol.*, **106**, 717–726.

OGBAGHEBRIEL, A. & SHRIER, A. (1994). Inhibition of metabolism abolishes transient outward current in rabbit atrial myocytes. *Am. J. Physiol.*, **266**, H182–H190.

OHYA, Y., TERADA, K., YAMAGACHI, K., INOUE, R., OKABE, K., KITAMURA, K., HIRATA, M. & KURIYAMA, H. (1988). Effects of inositol phosphates on the membrane activity of smooth muscle cells of the rabbit portal vein. *Pflügers Arch.*, **412**, 382–389.

OLESEN, S.P. & WÄTJEN, F. (1992). Benzimidazole derivatives, their preparation and use. European patent application, EP-477819-A.

OLESEN, S.P., MUNCH, E., MOLDT, P. & DREJER, J. (1994a). Selective activation of Ca^{2+}-dependent K^+ channels by novel benzimidazolone. *Eur. J. Pharmacol.*, **251**, 53–59.

OLESEN, S.P., MUNCH, E., WÄTJEN, F. & DREJER, J. (1994b). NS 004–an activator of Ca^{2+}-dependent K^+ channels in cerebellar granule cells. *Neuroreport*, **5**, 1001–1004.

PACAUD, P. & BOLTON, T.B. (1991). Relation between muscarinic receptor cationic current and internal calcium in guinea-pig jejunal smooth muscle cells. *J. Physiol.*, **441**, 477–499.

PONGS, O. (1993). Shaker related K channels. *Seminars Neurosci.*, **5**, 93–100.

SARGENT, C.A., GROVER, G.J., ANTONACCIO, M.J. & MCCULLOUGH, J.R. (1993). The cardioprotective, vasorelaxant and electrophysiological profile of the large conductance calcium-activated potassium channel opener. NS-004. *J. Pharmacol. Exp. Ther.*, **266**, 1422–1429.

SCHNEIDER, J., NIEDERSTE-HOLLENBERG, A., EDWARDS, G., NOACK, Th & WESTON. A.H. (1994). Potassium channel modulation by NS1619 in vascular smooth muscle. *Br. J. Pharmacol. Proc. Suppl.*, (in press)

SHEPPARD, D.N. & WELSH, M.J. (1993). Inhibition of the cystic fibrosis transmembrane conductance regulator by ATP-sensitive K^+ channel regulators. *Ann. N.Y. Acad. Sci.*, **707**, 275–284.

SMALL, R.C., BERRY, J.L., COOK, S.J., FOSTER, R.W., GREEN, K.A. & MURRAY, M.A. (1993). Potassium channels in airways. In *Pharmacology of the Respiratory Tract: Experimental and Clinical Research*. ed. Chung, K.F. & Barnes, P.J. pp. 137–176. New York: Marcel Dekker, Inc.

SOUTHERTON, J.S., WESTON, A.H., BRAY, K.M., NEWGREEN, D.T. & TAYLOR, S.G. (1988). The potassium channel opening action of pinacidil; studies using biochemical, ion flux and microelectrode techniques. *Naunyn-Schmied. Arch. Pharmacol.*, **338**, 310–318.

SUAREZ-KURTZ, G., GARCIA, M.L. & KACZOROWSKI, G.J. (1991). Effects of charybdotoxin and iberiotoxin on the spontaneous motility and tonus of different guinea pig smooth muscle tissues. *J. Pharmacol. Exp. Ther.*, **259**, 439–443.

TORO, L., OTTOLIA, R., OLCESE, R. & STEFANI, E. (1993). Niflumic acid activates large conductance K_{Ca} channels. *Biophys. J.*, **64**, A2.

TYTGAT, J., VEREECKE, J. & CARMELIET, E. (1994). A possible structural link between voltage-gated and inward rectifier K^+ channels. *Biophys. J.*, **66**, A425.

(Received July 15, 1994
Revised August 30, 1994
Accepted August 31, 1994)

Br. J. Pharmacol. (1994), **113**, 1548–1553 © Macmillan Press Ltd, 1994

Display of the characteristics of endothelium-derived hyperpolarizing factor by a cytochrome P450-derived arachidonic acid metabolite in the coronary microcirculation

Johann Bauersachs, [1]Markus Hecker & Rudi Busse

Center of Physiology, Johann Wolfgang Goethe University Clinic, Theodor-Stern-Kai 7, D-60590 Frankfurt am Main, Germany

1 In addition to nitric oxide (NO) and prostacyclin (PGI_2) an endothelium-derived factor, which hyperpolarizes vascular smooth muscle cells via activation of K^+ channels, contributes to the dilator effect of bradykinin in different vascular beds. Since this so-called endothelium-derived hyperpolarizing factor (EDHF) also seems to play an important role in the coronary circulation, we investigated its nature and mechanism of action in the rat isolated perfused heart (Langendorff preparation).

2 Bolus injections of bradykinin (1, 10, and 100 pmol) elicited a transient dose-dependent dilator response (e.g., 12 ± 2% decrease in coronary perfusion pressure (CPP) at 10 pmol bradykinin, $n = 41$). Administration of the cyclo-oxygenase inhibitor, diclofenac (1 μM), augmented the bradykinin-induced dilation approximately twofold ($n = 9$ $P < 0.01$). Combined treatment with the NO synthase inhibitor, N^G-nitro-L-arginine (30 μM) and diclofenac (1 μM) significantly reduced the duration, but increased the amplitude of the dilator response to bradykinin (27 ± 2% decrease in CPP, $n = 24$, $P < 0.01$).

3 The abolition of this N^G-nitro-L-arginine/diclofenac-insensitive dilator response to bradykinin by tetrabutylammonium (0.3 mM), an inhibitor of Ca^{2+}-dependent K^+ channels (4 ± 1% decrease in CPP, $n = 6$, $P < 0.01$), supports the view that the dilator compound released in the coronary microcirculation is EDHF.

4 This EDHF-type dilation was reversibly inhibited by the phospholipase A_2 inhibitor, quinacrine (3 μM, 9 ± 3% decrease in CPP, $n = 6$, $P < 0.01$) and by the cytochrome P450 inhibitor SKF525a (3 μM, 6 ± 1% decrease in CPP, $n = 6$, $P < 0.01$).

5 Tetrabutylammonium, quinacrine or SKF 525a did not affect the endothelium-independent dilator response to sodium nitroprusside (1 nmol), indicating that these compounds did not affect smooth muscle relaxation in a non-specific manner.

6 These findings suggest that in the coronary microcirculation bradykinin stimulates the release of a cytochrome P450-derived arachidonic acid metabolite, which exhibits the characteristic features of EDHF.

Keywords: Endothelium-derived hyperpolarizing factor; bradykinin; coronary microcirculation; cytochrome P450; arachidonic acid metabolite

Introduction

Apart from the release of nitric oxide (NO) and prostacyclin (PGI_2), other mechanisms contribute to the endothelium-dependent relaxation of coronary arteries (Richard *et al.*, 1990; Cowan & Cohen, 1991; Myers *et al.*, 1992). One candidate is the so-called endothelium-derived hyperpolarizing factor (EDHF) which causes hyperpolarization and subsequent relaxation of the vascular smooth muscle (Chen *et al.*, 1991; Nagao & Vanhoutte, 1992). This hyperpolarization is thought to be mediated by an increase in the K^+ conductance of the smooth muscle cell membranes (for review see Suzuki *et al.*, 1992). Recent studies demonstrated the inhibition of endothelium-dependent hyperpolarization and subsequent relaxation in coronary arteries by tetrabutylammonium (TBA), indicating that Ca^{2+}-activated K^+ channels (K_{Ca} channels) may mediate membrane hyperpolarization (Nagao & Vanhoutte, 1992; Holzmann *et al.*, 1994).

Although endothelium-dependent hyperpolarization has been demonstrated in bovine, porcine and human epicardial coronary arteries *in vitro* (Nagao & Vanhoutte, 1992; Nakashima *et al.*, 1993) the chemical nature of this factor is still unclear. Moreover, the role of EDHF in the coronary microcirculation remains to be established.

The aim of the present study was therefore to assess the relative contribution of NO, PGI_2 and EDHF to the dilator response to bradykinin in the microcirculation of the rat isolated perfused heart. EDHF-mediated dilation was taken as that component of the dilator response to bradykinin, which persisted after combined inhibition of NO synthase and cyclo-oxygenase, but was inhibited by TBA. Furthermore, the role of the cytochrome P450 pathway of arachidonic acid metabolism in the EDHF-mediated dilatations was investigated.

[1] Author for correspondence at the Zentrum der Physiologie, Klinikum der Johann Wolfgang Goethe-Universität, Theodor-Stern-Kai 7, D-60590 Frankfurt am Main, Germany.

Methods

Rat isolated perfused heart

Wistar rats (250–350 g) of either sex were anaesthetized with sodium pentobarbitone (60 mg kg^{-1}, intraperitoneally). After heparinization (500 units i.v.), the chests were opened and the hearts rapidly perfused *in situ* through a cannula inserted into the aortic stump (Langendorff preparation). After ligation of the superior and inferior vena cava close to the right atrium, the hearts were excised and perfused at constant flow with a roller pump (Heidolf RGL 85, Kelheim, Germany). The flow rate (15 ± 1 ml min^{-1}, $n = 41$) was adjusted to obtain a coronary perfusion pressure (CPP) of approximately 75 mmHg. A modified Krebs-Henseleit solution (pH 7.4 37°C, continuously gassed with 95% O_2 and 5% CO_2) con-

taining (in mM) NaCl 118.0, $NaHCO_3$ 24.0, glucose 5.0, $CaCl_2$ 2.5, KCl 4.0, KH_2PO_4 1.2, $MgSO_4$ 1.0, and pyruvate 2.0, was used as perfusate. CPP was monitored with a pressure transducer (Gould P2310, Oxnard, Calif., U.S.A.) connected to a sidearm of the aortic perfusion cannula. Isovolumetric left ventricular pressure (LVP) was measured with a fluid-filled latex balloon inserted into the left ventricle via the left atrium and connected to another pressure transducer (Gould CP-01). Balloon volume was adjusted to obtain a diastolic pressure of about 10 mmHg; heart rate was derived from the LVP signal by a cardiotachometer. Vasodilator agents (in 10 µl aliquots) were administered to the coronary vascular bed as bolus injections into the perfusate via an applicator. Infusions of compounds were given through a Y-connector in the aortic perfusion line at a rate of $1/100^{th}$ of the coronary flow rate to produce the final concentrations described in the results section.

Experimental protocols

The hearts were allowed to equilibrate for at least 20 min in order to obtain a stable CPP. Bolus injections of bradykinin (1, 10 and 100 pmol) were given under basal conditions and during treatment with the following drugs: (i) the cyclooxygenase inhibitor, diclofenac, (ii) the NO synthase inhibitor, N^G-nitro-L-arginine, (iii) the thromboxane-mimetic, 9,11-dideoxy-11α,9α-epoxymethano-prostaglandin $F_{2\alpha}$ (U46619), and (iv) diclofenac plus N^G-nitro-L-arginine. The diclofenac and N^G-nitro-L-arginine-insensitive effects of bradykinin were further analysed after pretreatment with the phospholipase A_2 inhibitor, quinacrine, the cytochrome P450 inhibitor, SKF 525a, or inhibitors of K_{Ca} channels, such as apamin and tetrabutylammonium. All compounds were infused for a minimum period of 15 min before bolus injections of bradykinin were given. Sodium nitroprusside, an endothelium-independent dilator compound was used in all experiments to monitor alterations in vascular smooth muscle dilator capacity following different pretreatments.

Radioimmunoassay of PGI_2

The concentration of 6-keto-$PGF_{1\alpha}$, the stable hydrolysis product of PGI_2, in the coronary effluent (collected for 60 s before and after application of 100 pmol bradykinin) was measured by a specific radioimmunoassay (Lamontagne *et al.*, 1992). Values were expressed as percentage increase over basal levels following stimulation with bradykinin.

Materials

Bradykinin was purchased from Bachem (Heidelberg, Germany), sodium nitroprusside, apamin, quinacrine and tetrabutylammonium from Sigma (Deisenhofen, Germany), N^G-nitro-L-arginine from Serva (Heidelberg, Germany) and diclofenac (Voltaren injection solution) from Ciba-Geigy (Wehr, Germany). U46619, SKF 525a and D-Arg[Hyp^3, Thi^5,D-Tic^7,Dic^8]-bradykinin (Hoe 140) were kind gifts from the Upjohn Co. (Kalamazoo, MI, U.S.A.), Cassella (Frankfurt/M., Germany) and Hoechst (Frankfurt/M., Germany) respectively.

Statistics

Dilator responses were calculated as percentage decrease in CPP, the duration of dilator responses is calculated as half-recovery time, i.e. the time taken for the vasodilator response to return to 50% of its maximum.

Statistical analysis was performed by one-way analysis of variance (ANOVA) followed by a Bonferroni t test. Results are expressed as means ± s.e.mean with P values < 0.05 considered statistically significant.

Results

Vasodilator action of bradykinin and sodium nitroprusside

After the equilibration period, CPP was 73 ± 1 mmHg, systolic LVP 67 ± 3 mmHg, and heart rate 275 ± 6 beats min^{-1} ($n = 41$). Bolus injections of the endothelium-dependent vasodilator bradykinin (1, 10 and 100 pmol) induced a dose-dependent decrease in CPP (Figures 1 and 2). This vasodilatation was sustained for over 10 min at the highest dose with a half-recovery time of 3 ± 0.2 min ($n = 41$), and bradykinin affected LVP and heart rate only at this dose (8 ± 1% decrease of LVP and a 4 ± 2% increase of the heart rate, $n = 41$). The endothelium-independent vasodilator sodium nitroprusside (1 nmol) elicited a decrease in CPP without affecting LVP or heart rate (Figures 1 and 2).

Treatment with the selective B_2 receptor antagonist (Hock *et al.*, 1991), Hoe 140 (0.1 µM), virtually abolished the dilator

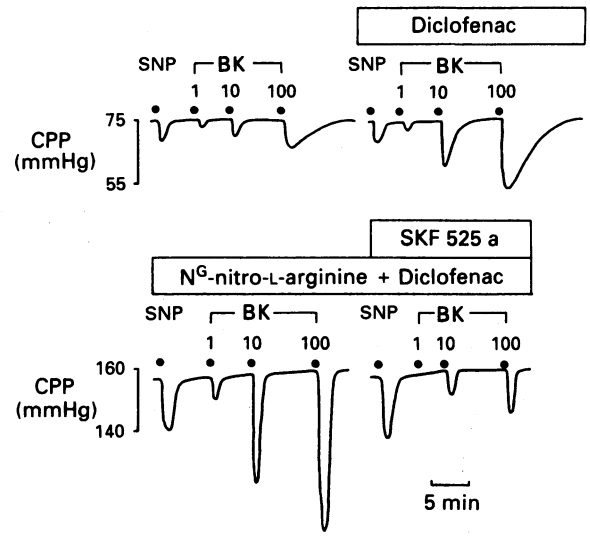


Figure 1 Typical tracing showing the effects of bolus injections of bradykinin (BK) (1, 10 and 100 pmol) and sodium nitroprusside (SNP) (1 nmol) on coronary perfusion pressure (CPP) under control conditions, during treatment with diclofenac (1 µM), N^G-nitro-L-arginine (30 µM) plus diclofenac and subsequent co-infusion of SKF 525a (0.3 µM). Note the marked increase in CPP following administration of N^G-nitro-L-arginine.

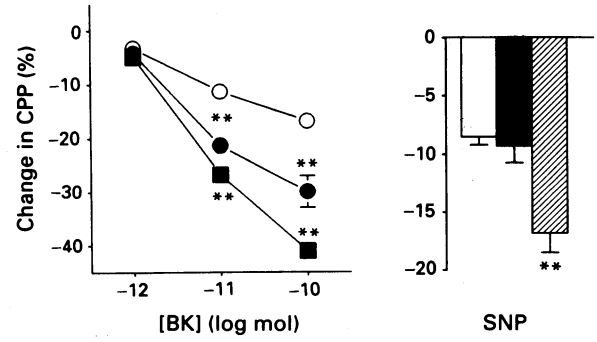


Figure 2 Decrease in coronary perfusion pressure (CPP) following bolus injections of bradykinin (BK) and sodium nitroprusside (SNP) (1 nmol) under control condition (○ and open column, $n = 31$), after pretreatment with diclofenac (1 µM, ● and solid column, $n = 9$) and during combined treatment with N^G-nitro-L-arginine (30 µM) and diclofenac (■ and hatched column, $n = 24$, $^{**}P < 0.01$ vs. control).

response to bradykinin (from 12 ± 2% to 0.3 ± 0.8% and from 17 ± 1% to 2 ± 1% decrease in CPP, $n = 10$, $P < 0.01$, for 10 pmol and 100 pmol bradykinin respectively).

Effects of diclofenac and N^G-nitro-L-arginine

During the infusion of diclofenac (1 μM) there was no significant change in either CPP, LVP or heart rate ($n = 9$). Under these conditions the dilator response to SNP (1 nmol) remained unaffected, while the bradykinin-induced dilatation was significantly enhanced following cyclo-oxygenase blockade (Figure 2).

Co-infusion of diclofenac (1 μM) and N^G-nitro-L-arginine (30 μM) elicited an increase in CPP reaching a plateau at 150 ± 3 mmHg ($n = 24$); LVP and heart rate however remained unaffected. The amplitude of the fall in CPP following bolus injections of bradykinin was further increased (Figure 2) by the combined treatment with diclofenac and N^G-nitro-L-arginine as compared to diclofenac alone, whereas the duration of the response was significantly shortened (decrease in half-recovery time from 3 ± 0.2 min to 1 ± 0.1 min at 100 pmol bradykinin, $n = 24$, $P < 0.01$). The dilator response to SNP was also significantly augmented in the presence of both diclofenac and N^G-nitro-L-arginine (Figure 2), while its time course remained unaffected.

Effects of N^G-nitro-L-arginine and U46619

To assess the influence of the increase in CPP elicited by N^G-nitro-L-arginine on the vasodilator action of bradykinin, the effects of bradykinin during treatment with N^G-nitro-L-arginine and U46619 (0.1 μM) were compared. The thromboxane-mimetic caused an identical increase in CPP to the NO synthase inhibitor (143 ± 6 mmHg and 145 ± 8 mmHg respectively, $n = 4$) without affecting either LVP or heart rate.

In U46619-treated hearts, the vasodilator response to bradykinin was similar to that observed in N^G-nitro-L-arginine-treated hearts (Figure 3), indicating that the N^G-nitro-L-arginine-mediated enhancement of bradykinin-induced dilation is due to an increase in coronary vascular tone and not due to a specific effect of N^G-nitro-L-arginine.

Effect of K_{Ca} channel blockers on the diclofenac/N^G-nitro-L-arginine-insensitive dilator response to bradykinin

The non-selective inhibitor of K_{Ca} channels, tetrabutylammonium (TBA, 0.3 mM), induced a transient increase in CPP, which remained slightly above control levels 10 min after starting infusion (165 ± 6 mmHg, $n = 6$, NS), had no influence on LVP, but significantly decreased heart rate (to 150 ± 31 beats min^{-1}, $n = 6$, $P < 0.05$). The dilator response to bradykinin was virtually abolished in the presence of TBA, whereas the dilator effect of SNP was unaffected (Figure 4a). These effects of TBA were reversible after a washout period of 30 min (data not shown). In contrast to TBA, the infusion of apamin (3 μM), a specific inhibitor of small conductance K_{Ca} channels, did not significantly affect the action of bradykinin (Figure 4a).

Role of cytochrome P450-derived arachidonic acid metabolite(s) in the diclofenac/N^G-nitro-L-arginine-resistant dilator response to bradykinin

During continuous infusion of diclofenac and N^G-nitro-L-arginine, treatment with the phospholipase A_2 inhibitor, quinacrine (3 μM), did not affect CPP, but decreased LVP (from 67 ± 3 mmHg to 43 ± 11 mmHg, $n = 6$, $P < 0.05$) and heart rate (from 275 ± 6 beats min^{-1} to 214 ± 17 beats min^{-1}, $n = 6$, $P < 0.05$). The response to SNP did not change significantly, whereas the dilator effect of bradykinin was strongly reduced (Figure 4b). After washout of quinacrine for 30 min, the responses to bradykinin were restored (data not shown).

The cytochrome P450-inhibitor SKF 525a (3 μM) had no significant effect on either CPP or LVP, but heart rate fell to 189 ± 13 beats min^{-1}, $n = 6$, $P < 0.05$. The dilator response to bradykinin was strongly inhibited in the presence of SKF 525a, whereas the effect of SNP remained virtually unchanged (Figure 4). These effects of SKF 525a were reversible after a washout period of 30 min (data not shown).

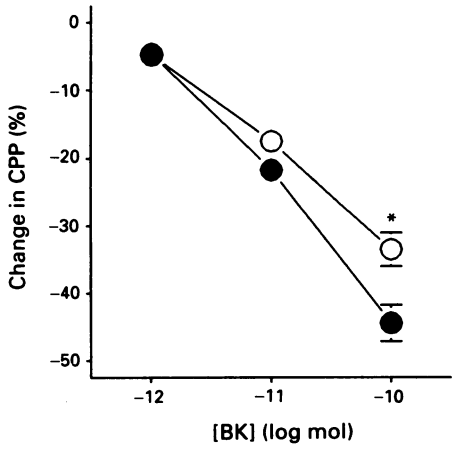


Figure 3 Decrease in coronary perfusion pressure (CPP) elicited by bolus injections of bradykinin (BK) after pretreatment with U46619 (0.1 μM, $n = 4$, ○) and N^G-nitro-L-arginine (30 μM, $n = 4$, ●, $^*P < 0.05$ vs N^G-nitro-L-arginine).

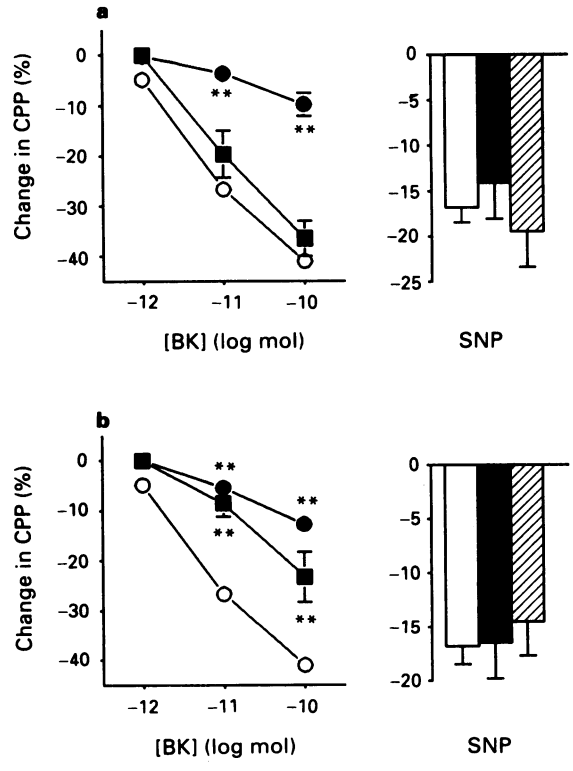


Figure 4 Decrease in coronary perfusion pressure (CPP) following bolus injections of bradykinin (BK) and sodium nitroprusside (SNP) (1 nmol) after pretreatment with N^G-nitro-L-arginine (30 μM) plus diclofenac (1 μM, $n = 24$, ○ and open columns), in the presence of (a) tetrabutylammonium (0.3 mM, $n = 6$, ● and solid column) or apamin (3 μM, $n = 4$, ■ and hatched column) and (b) in the presence of SKF 525a (3 μM, $n = 6$, ● and solid column) or quinacrine (3 μM, $n = 6$, ■ and hatched column, $^{**}P < 0.01$ vs. control).

Effect of quinacrine on the dilator response to bradykinin in the absence of diclofenac and N^G-nitro-L-arginine

In order to demonstrate the contribution of EDHF to the dilator response to bradykinin without previous inhibition of NO synthase and cyclo-oxygenase, quinacrine (3 μM) was applied after elevation of CPP with U46619 (1 μM) in an additional series of experiments without pretreatment with diclofenac or N^G-nitro-L-arginine. Treatment with quinacrine plus U46619 did not significantly change CPP and LVP as compared to U46619 alone, but decreased heart rate from 240 ± 10 beats min^{-1} to 200 ± 9 beats min^{-1} ($n = 4$, $P < 0.05$). The dilator response to bradykinin was significantly inhibited during treatment with quinacrine (Figure 5), whereas the SNP-induced dilatation was not affected ($8 \pm 2\%$ decrease in CPP as compared to $11 \pm 2\%$, $n = 4$).

Effect of quinacrine on PGI_2 formation by the rat heart

To confirm the ability of quinacrine to inhibit the release of arachidonic acid from phospholipids, the concentration of 6-keto-$PGF_{1\alpha}$ was determined in the coronary effluent from hearts which were not exposed to diclofenac. Quinacrine (3–10 μM) significantly reduced the bradykinin-induced (100 pmol bolus) increase in PGI_2 release (Figure 6).

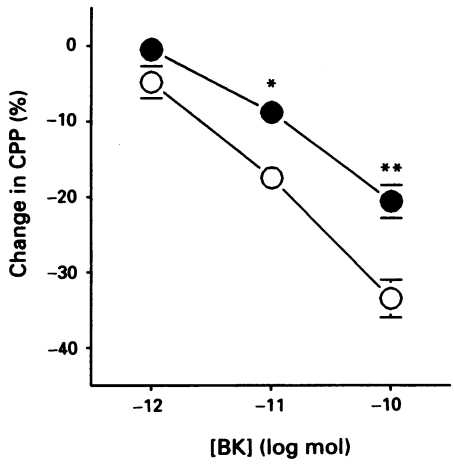


Figure 5 Effect of quinacrine (3 μM, $n = 4$, ●) on the dilator response to bradykinin ($n = 4$, ○) in hearts pretreated with U46619 (0.1 μM, $^*P < 0.05$, $^{**}P < 0.01$ vs. control).

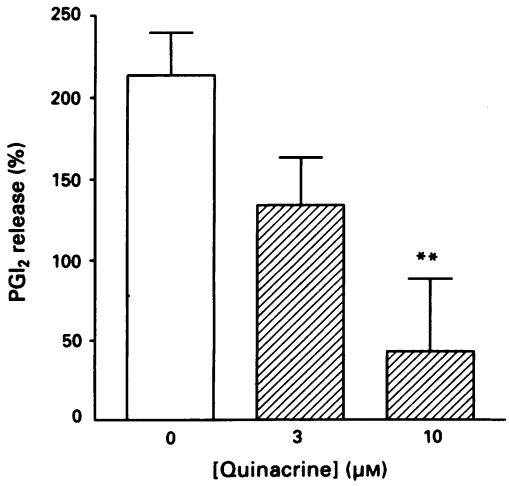


Figure 6 Prostacyclin (PGI_2) release measured as concentration of 6-keto-$PGF_{1\alpha}$ in the coronary effluent is inhibited during treatment with quinacrine. Data are expressed as percentage increase in PGI_2 release over basal levels following application of 100 pmol bradykinin ($n = 5$, $^{**}P < 0.01$ vs. control).

Discussion

The results of this study demonstrate that in the coronary microcirculation of the rat isolated perfused heart, a diclofenac and N^G-nitro-L-arginine-insensitive component substantially contributes to the endothelium-dependent vasodilatation in response to bradykinin. Activation of bradykinin B_2 receptors on the coronary endothelium mediates the dilator response, as confirmed by the inhibitory effect of the specific antagonist Hoe 140. The diclofenac/N^G-nitro-L-arginine-insensitive dilator response to bradykinin was abolished by TBA, a non-selective inhibitor of K_{Ca} channels, thus providing indirect evidence that the release of EDHF causes this component of relaxation. In addition, the strong inhibitory effects of quinacrine and SKF 525a suggest that a cytochrome P450-derived metabolite of arachidonic acid released from the endothelium displays the characteristics of EDHF in the coronary microcirculation.

In coronary arteries, bradykinin stimulates the release of three distinct endothelium-derived dilator compounds: NO, PGI_2 and EDHF. The significant contribution of basal and shear stress-dependent NO release to the maintenance of coronary tone is illustrated by the marked increase in CPP observed following inhibition of NO synthesis. However, treatment with N^G-nitro-L-arginine only diminished the duration of the dilator response but not the maximum decrease in CPP following administration of bradykinin, indicating that the agonist-induced NO release causes the sustained rather than the initial phase of the dilator response (Baydoun & Woodward, 1991). The greater amplitude of the bradykinin-stimulated dilatation in the presence of the NO synthase inhibitor can be attributed to the higher level of preconstriction, because elevation of CPP to the same extent by treatment with U46619 caused a similar amplification of the maximum dilator response.

Cyclo-oxygenase inhibition was without effect on CPP under control conditions, suggesting that the basal release of cyclo-oxygenase products, i.e. PGI_2, is too small to influence significantly the tone of the coronary arteries. The dilator response to bradykinin was significantly augmented following cyclo-oxygenase blockade, an effect that might be explained by a reduced formation of vasoconstrictor prostanoids, such as $PGF_{2\alpha}$. However, it is equally possible that inhibition of cyclo-oxygenase redirects the arachidonic acid metabolism towards an enhanced synthesis of vasodilator cytochrome P450 or lipoxygenase metabolites. Since the bradykinin-induced dilatations in the rat isolated heart are not attenuated by the dual cyclo-oxygenase and lipoxygenase inhibitor, BW755C (Baydoun & Woodward, 1991), cytochrome P450-derived rather than lipoxygenase-derived arachidonic acid metabolites seem to contribute to the dilator response.

An unspecific change in the responsiveness of the coronary microcirculation to vasodilator agents following cyclo-oxygenase inhibition is unlikely, since the basal CPP level and the dilator response to SNP remained unchanged. The further augmentation of the bradykinin-induced dilatation during combined treatment with diclofenac and N^G-nitro-L-arginine when compared to diclofenac alone is most likely based on the same mechanism as described before, i.e. the marked rise in CPP after NO synthase inhibition.

The failure to inhibit the maximum decrease in CPP following application of bradykinin after NO synthase and cyclo-oxygenase inhibition, demonstrates the crucial role of a third vasodilator principle in the coronary microcirculation, which has already been described in large coronary arteries as EDHF (Chen *et al.*, 1991; Nagao & Vanhoutte, 1992). Although the chemical nature of this factor has not yet been elucidated, recent studies suggest that the release of a diffusible substance from the endothelial cells mediates the hyperpolarization of the underlying smooth muscle cells and not a direct electrical coupling between endothelial and smooth muscle cells (Beny & Pacicca, 1994). A strictly

abluminal secretion of such a humoral factor could in fact account for the inability to detect EDHF by conventional bioassay techniques (Kauser & Rubanyi, 1992).

The hyperpolarization of the vascular smooth muscle cells elicited by EDHF is generated by an increase in the K^+ conductance of the cell membrane via activation of K^+ channels (Suzuki *et al.*, 1992). Recent studies have demonstrated that the endothelium-dependent hyperpolarization and subsequent relaxation are sensitive to inhibition by tetrabutylammonium in coronary arteries, thus implicating the activation of K_{Ca} channels in the hyperpolarization of smooth muscle (Nagao & Vanhoutte, 1992; Holzmann *et al.*, 1994). In the coronary microcirculation, the diclofenac and N^G-nitro-L-arginine-insensitive dilator response to bradykinin was virtually abolished in the presence of tetrabutylammonium, a non-selective inhibitor of K_{Ca} channels, suggesting that the remaining dilator effect of bradykinin is most likely caused by the release of EDHF, as described for large coronary conduit arteries (Nagao & Vanhoutte, 1992).

Apamin, a selective inhibitor of small conductance (6–14 pS) K_{Ca} channels (Blatz & Magleby, 1986), which blocks the diclofenac/N^G-nitro-L-arginine-resistant responses to bradykinin in the rabbit heart (Mülsch *et al.*, 1994) and in isolated porcine coronary arteries (Hecker *et al.*, unpublished observation), on the other hand, had no significant effect in the rat heart. Thus large conductance K_{Ca} channels seem to be involved in the endothelium-dependent hyperpolarization in the rat coronary microcirculation.

In order to characterize the nature of EDHF in the coronary microcirculation in more detail, we studied the role of non cyclo-oxygenase-dependent arachidonic acid metabolites. Bovine coronary artery endothelial cells metabolize arachidonic acid not only via cyclo-oxygenase and PGI_2 synthase to PGI_2, but also via the cytochrome P450 pathway to several regioisomeric epoxides (EETs). The relaxant effect of arachidonic acid in these arteries is only partially inhibited by treatment with indomethacin of SKF 525a, but completely abolished by the combined treatment with these agents, indicating that cytochrome P450-derived EETs mediate part of the dilator effect of arachidonic acid in this preparation (Rosolowsky & Campbell, 1993). Moreover, these EETs have been shown to activate large conductance K_{Ca} channels in cultured coronary smooth muscle cells (Hu & Kim, 1993). Taken together these observations imply that cytochrome P450-derived metabolites may account for the EDHF released by coronary arteries.

The strong inhibition of the diclofenac/N^G-L-arginine-resistant dilator response to bradykinin by SKF 525a in the rat isolated heart suggests that at least in the coronary microcirculation, EDHF may be a cytochrome P450-derived arachidonic acid metabolite. Moreover, inhibiting the release of arachidonic acid from phospholipids with the phospholipase A_2 inhibitor, quinacrine, also caused a significant reduction in the release of EDHF in the coronary microcirculation. To ensure that a decreased release of arachidonic acid, and not an unspecific action of quinacrine was responsible for this effect, the release of PGI_2 in the coronary effluent after the application of bradykinin was determined. Quinacrine effectively reduced the concentration of PGI_2 in the coronary effluent demonstrating inhibition of arachidonic acid release during treatment with quinacrine.

In view of these findings, the amplification of the dilator responses to bradykinin after cyclo-oxygenase inhibition may be explained by a redirection in arachidonic acid metabolism towards the synthesis of vasodilator cytochrome P450 metabolites.

Although the NO/PGI_2-independent agonist-induced vasodilatation is referred to as EDHF release (Nagao & Vanhoutte, 1992), it is still unclear to what extent EDHF contributes to the vasodilator response, when the synthesis of NO and PGI_2 is not inhibited. In our model of the coronary microcirculation, the bradykinin-induced dilatation was attenuated by quinacrine alone. This finding suggests that the EDHF-induced dilatation is not simply a response observed following inhibition of the synthesis of the other dilatory autacoids, but represents a substantial constitutive component of the dilator response to bradykinin in the coronary microcirculation under physiological conditions. Moreover, therapeutics such as angiotensin-converting enzyme inhibitors, which have been shown to restore impaired endothelium-dependent vasodilatations, enhance both the NO-mediated and the NO/PGI_2-independent dilator response to bradykinin in isolated coronary arteries (Mombouli *et al.*, 1992; Hecker *et al.*, 1993), indicating that part of the beneficial cardiovascular action of these drugs may be related to an enhanced synthesis and release of EDHF.

In conclusion, our data demonstrate that in the rat coronary microcirculation an endothelium-derived cytochrome P450 metabolite of arachidonic acid, which displays the characteristics of EDHF, is a fundamental component of the dilator response to bradykinin.

This work was supported by the Deutsche Forschungsgemeinschaft (Bu 436/4–3), the Commission of the European Community (BMH1-CT92-1893) and the Dr Paul and Cilli Weill-Stiftung. M.H. is recipient of a Heisenberg fellowship from the Deutsche Forschungsgemeinschaft. The expert technical assistance of Gabriele Hoch is gratefully acknowledged. The authors also wish to thank Dr Ingrid Fleming for expert and enthusiastic editorial assistance.

References

BAYDOUN, A.R. & WOODWARD, B. (1991). Effects of bradykinin in the rat isolated perfused heart: role of kinin receptors and endothelium-derived relaxing factor. *Br. J. Pharmacol.*, **103**, 1829–1833.

BENY, J.L. & PACICCA, C. (1994). Bidirectional electrical communication between smooth muscle and endothelial cells in the pig coronary artery. *Am. J. Physiol.*, **266**, H1465–H1472.

BLATZ, A.L. & MAGLEBY, K.L. (1986). Single apamin-blocked Ca^{2+}-activated K^+ channels of small conductance in cultured rat skeletal muscle. *Nature*, **323**, 718–720.

CHEN, G.F., YAMAMOTO, Y., MIWA, K. & SUZUKI, H. (1991). Hyperpolarization of arterial smooth muscle induced by endothelial humoral substances. *Am. J. Physiol.*, **260**, H1888–H1892.

COWAN, C.L. & COHEN, R.A. (1991). Two mechanisms mediate the relaxation by bradykinin of pig coronary artery: NO-dependent and -independent responses. *Am. J. Physiol.*, **261**, H830–H835.

HECKER, M., BARA, A.T. & BUSSE, R. (1993). Relaxation of isolated coronary arteries by angiotensin converting enzyme inhibitors: role of endothelium-derived kinins. *J. Vasc. Res.*, **30**, 257–262.

HOCK, F.J., WIRTH, K., ALBUS, U., LINZ, W., GERHARDS, H.J., WIEMER, G., HENKE, S., BREIPOHL, G., KÖNIG, W., KNOLLE, J. & SCHÖLKENS, B.A. (1991). Hoe 140, a new potent and long acting bradykinin-antagonist: *in vitro* studies. *Br. J. Pharmacol.*, **102**, 769–773.

HOLZMANN, S., KUKOVETZ, W.R., WINDISCHHOFER, W., PASCHKE, E. & GRAIER, W.F. (1994). Pharmacologic differentiation between endothelium-dependent relaxations sensitive and resistant to nitro-L-arginine in coronary arteries. *J. Cardiovasc. Pharmacol.*, **23**, 747–756.

HU, S. & KIM, H.S. (1993). Activation of K^+ channel in vascular smooth muscles by cytochrome P450 metabolites of arachidonic acids. *Eur. J. Pharmacol.*, **230**, 215–221.

KAUSER, K. & RUBANYI, G.M. (1992). Bradykinin-induced, nitro-L-arginine-insensitive endothelium-dependent relaxation of porcine coronary artery is not mediated by bioassayable substances. *J. Cardiovasc. Pharmacol.*, **20** (Suppl. 12), S101–S104.

LAMONTAGNE, D., KÖNIG, A., BASSENGE, E. & BUSSE, R. (1992). Prostacyclin and nitric oxide contribute to the vasodilator action of acetylcholine and bradykinin in the intact rabbit coronary bed. *J. Cardiovasc. Pharmacol.*, **20**, 652–657.

MOMBOULI, J.-V., ILLIANO, S., NAGAO, T., SCOTT-BURDEN, T. & VANHOUTTE, P.M. (1992). Potentiation of endothelium-dependent relaxations to bradykinin by angiotensin I converting enzyme inhibitors in canine coronary artery involves both endothelium-derived relaxing and hyperpolarizing factors. *Circ. Res.*, **71**, 137–144.

MÜLSCH, A., ZHENG, X., BUSSE, R. & BASSENGE, E. (1994). Initial relaxation to bradykinin in the coronary resistance bed is presumably mediated by endothelium-dependent hyperpolarization. *Pflügers Arch.*, **426**, (suppl), R126 (Abstract).

MYERS, P.R., GUERRA, R. & HARRISON, D.G. (1992). Release of multiple endothelium-derived relaxing factors from porcine coronary arteries. *J. Cardiovasc. Pharmacol.*, **20**, 392–400.

NAGAO, T. & VANHOUTTE, P.M. (1992). Hyperpolarization as a mechanism for endothelium-dependent relaxation in the porcine coronary artery. *J. Physiol.*, **445**, 355–367.

NAKASHIMA, M., MOMBOULI, J.-V., TAYLOR, A.A. & VANHOUTTE, P.M. (1993). Endothelium-dependent hyperpolarization caused by bradykinin in human coronary arteries. *J. Clin. Invest.*, **92**, 2867–2871.

RICHARD, V., TANNER, F.C., TSCHUDI, M., YANG, Z. & LÜSCHER, T.F. (1990). Different activation of the endothelial L-arginine pathway by bradykinin, serotonin and clonidine in porcine coronary arteries. *Am. J. Physiol.*, **259**, H1433– H1439.

ROSOLOWSKY, M. & CAMPBELL, W.B. (1993). Role of PGI_2 and epoxyeicosatrienic acids in relaxation of bovine coronary arteries to arachidonic acid. *Am. J. Physiol.*, **264**, H327–H335.

SUZUKI, H., CHEN, G. & YAMAMOTO, Y. (1992). Endothelium-derived hyperpolarizing factor (EDHF). *Jpn. Circ. J.*, **56**, 170–174.

(Received July 19, 1994
Accepted August 18, 1994)

Br. J. Pharmacol. (1994), **113**, 1554–1560 © Macmillan Press Ltd, 1994

Endogenous expression of histamine H_1 receptors functionally coupled to phosphoinositide hydrolysis in C6 glioma cells: regulation by cyclic AMP

Marie-Claire Peakman & [1]Stephen J. Hill

Department of Physiology & Pharmacology, Medical School, Queen's Medical Centre, Nottingham, NG7 2UH

1 The effects of histamine receptor agonists and antagonists on phospholipid hydrolysis in rat-derived C6 glioma cells have been investigated.

2 Histamine H_1 receptor-stimulation caused a concentration-dependent increase in the accumulation of total [^{3}H]-inositol phosphates in cells prelabelled with [^{3}H]-*myo*-inositol. The rank order of agonist potencies was histamine (EC_{50} = 24 μM) > N^{α}-methylhistamine (EC_{50} = 31 μM) > 2-thiazolylethylamine (EC_{50} = 91 μM).

3 The response to 0.1 mM histamine was antagonized in a concentration-dependent manner by the H_1-antagonists, mepyramine (apparent K_d = 1 nM) and (+)-chlorpheniramine (apparent K_d = 4 nM). In addition, (−)-chlorpheniramine was more than two orders of magnitude less potent than its (+)-stereoisomer.

4 Elevation of intracellular cyclic AMP accumulation with forskolin (10 μM, EC_{50} = 0.3 μM), isoprenaline (1 μM, EC_{50} = 4 nM) or rolipram (0.5 mM), significantly reduced the histamine-mediated (0.1 mM) inositol phosphate response by 37%, 43% and 26% respectively. In contrast, 1,9-dideoxyforskolin did not increase cyclic AMP accumulation and had no effect on the phosphoinositide response to histamine.

5 These data indicate the presence of functionally coupled, endogenous histamine H_1 receptors in C6 glioma cells. Furthermore, the results also indicate that H_1 receptor-mediated phospholipid hydrolysis is inhibited by the elevation of cyclic AMP levels in these cells.

Keywords: C6 glioma cells; cyclic AMP accumulation; histamine H_1 receptor; inositol phosphate turnover

Introduction

Histamine H_1 receptors in mammalian cells are generally coupled via a regulatory guanosine 5'-triphosphate (GTP)-binding protein to phospholipase C and mediate functional responses through the mobilization of intracellular free calcium ions (by inositol-1,4,5-trisphosphate) and the activation of protein kinase C (by diacylglycerol) (Hill, 1990). A notable feature of the histamine H_1 receptor-mediated inositol phosphate response in a number of smooth muscle preparations, such as bovine trachea (Hall & Hill, 1988; Hall *et al.*, 1989) and the hamster vas deferens smooth muscle cell line, DDT_1MF-2 (Dickenson *et al.*, 1993), is its inhibition by agents which can increase the intracellular levels of adenosine 3': 5'-cyclic monophosphate (cyclic AMP). In contrast, the inositol phosphate responses to histamine in guinea-pig and mouse cerebral cortical slices are insensitive to regulation by cyclic AMP elevating agents (Alexander *et al.*, 1989; Hollingsworth & Daly, 1985). Brain slice preparations, however, contain a heterogeneous population of different cell types and in this study we have investigated whether a modulation by cyclic AMP of the response to histamine can be demonstrated in brain-derived glial cells.

The presence of histamine H_1 receptors on glial cells was first indicated by studies of the binding of [^{3}H]-histamine and [^{3}H]-mepyramine to glial cells in explant cultures from rat brain (Hosli & Hosli, 1984). [^{3}H]-mepyramine binding studies have since revealed the presence of H_1 receptors on rat astrocytes *in vitro* (Inagaki *et al.*, 1989) and activation of these receptors has been shown to stimulate phosphoinositide hydrolysis (Arbones *et al.*, 1988). In primary cultures of astrocytes, two populations of cells can be identified which differ morphologically and biochemically (Raff *et al.*, 1983). Using single cell imaging techniques and cultures enriched in the different astrocyte types, it has become clear that H_1 receptors are present on 'type-2' but not 'type-1' astrocytes (Fukui *et al.*, 1991; Inagaki *et al.*, 1991a,b: Kondou *et al.*, 1991). C6 glioma cells grown in medium containing 10% foetal calf serum have many of the characteristics of type-2 rat astrocytes (Mangoura *et al.*, 1989). However, previous studies of phosphoinositide turnover in C6 rat glioma cells have only described responses to endothelins (Gusovsky, 1992; Lin *et al.*, 1992), ATP (Kitanaka *et al.*, 1992), bradykinin (Donie & Reiser, 1991), 5-hydroxytryptamine (Ananth *et al.*, 1987) and acetylcholine (DeGeorge *et al.*, 1987).

The apparent lack of endogenous histamine H_1 receptors in C6 cells has recently been exploited by researchers (Liu *et al.*, 1992; Fujimoto *et al.*, 1993) who have isolated the rat histamine H_1 receptor gene, transfected it into this cell line and examined H_1 receptor expression using [^{3}H]-mepyramine binding assays. However, in this paper we provide evidence for the presence of endogenous histamine H_1 receptors functionally linked to phosphoinositide turnover in rat C6 glioma cells and demonstrate that this response can be modulated by agents which elevate intracellular levels of cyclic AMP.

Methods

Cell culture

C6 glioma cells were maintained in Dulbecco's modified Eagle's medium (DMEM) supplemented with 2 mM L-glutamine and 10% foetal calf serum (FCS) at 37°C in a water saturated atmosphere of 10% CO_2 in air. Cells were cultured as monolayers in 75 cm^2 flasks (containing 15 ml growth medium) or 24 well cluster dishes (containing 1 ml per well growth medium). The cells reached confluence in 3

[1] Author for correspondence.

days and confluent cluster dishes were used for experiments at this stage. Confluent flasks of cells were passaged using trypsin-EDTA (ethylenediaminetetraacetic acid) solution (composition g l^{-1} trypsin 0.5, EDTA, 0.2, NaCl 0.85) and were reseeded using a 1:6 split ratio.

Inositol phospholipid hydrolysis

Inositol phospholipid hydrolysis was investigated by the method previously described by White *et al.* (1993). Confluent monolayers were incubated with 500 µl per well inositol-free DMEM containing 1 µCi per well *myo*-[2-^{3}H(N)]-inositol and antibiotic-antimycotic solution (penicillin 100u ml^{-1}, streptomycin 100 µg ml^{-1} and amphotericin B 0.25 µg ml^{-1}) for 24 h at 37°C in a water saturated atmosphere of 10% CO_2 in air.

The labelled cell monolayers were washed twice with 1 ml per well of Hanks HEPES (N-[2-hydroxyethyl] piperazine-N'-[2-ethanesulphonic acid]) buffer (composition mM: NaCl 137, KCl 5.4, Na_2HPO_4 0.03, KH_2PO_4 0.4, $CaCl_2$ 1.3, $MgSO_4$ 0.8, D-glucose 5.5, HEPES 20 and phenol red sodium salt 10 mg ml^{-1}; pH 7.4) and then incubated at 37°C for 30 min with 290 µl per well buffer containing 20 mM lithium chloride (LiCl). Where appropriate, antagonists in 10 µl buffer were also added at this stage. Agonists were added, in 10 µl buffer, and incubated with the cells for a further 10 min. Incubations were terminated by aspiration of the incubation medium and the addition of 1 ml cold (−20°C) methanol: hydrochloric acid, 0.12M (1:1 v/v).

Disrupted monolayers were left for at least 12 h at −20°C before isolation of total [^{3}H]-inositol phosphates from the supernatant by anion exchange chromatography (White *et al.*, 1993). Briefly, an 800 µl sample of supernatant was removed from each well of a cluster dish, neutralized by the addition of 3.1 ml distilled water, 1 ml Tris buffer (Tris-[hydroxymethyl]aminomethane, 25 mM, adjusted to pH 7 with hydrochloric acid) and 135 µl sodium hydroxide (0.5M) and added to chromatography columns containing Dowex 1 anion exchange resin (1 ml). Washes of 20 ml distilled water and 10 ml ammonium formate (25 mM) removed *myo*-[2-^{3}H(N)]-inositol and glycerophosphoinositol, respectively, and total [^{3}H]-inositol phosphates were then eluted into scintillation vials with 3 ml hydrochloric acid (1 M). Emulsifier scintillator (299, Packard) (10 ml) was added to each vial and radioactivity was quantified by scintillation counting in the gel phase.

Accumulation of [^{3}H]-cyclic AMP

Cyclic AMP accumulation was investigated by the method of Peakman & Hill (1994). Cells were washed twice with Hanks HEPES buffer and then incubated for 2 h at 37°C in 1 ml per well buffer containing 2 µCi per well 8-[^{3}H]-adenine.

The labelled cell monolayers were again washed twice with Hanks HEPES and incubated for 30 min at 37°C in 1 ml per well buffer with or without 100 µM rolipram, an inhibitor of the cyclic AMP selective (type IV) phosphodiesterase isoenzyme (Donaldson *et al.*, 1988). Where appropriate, adenosine deaminase, 1.2 u ml^{-1}, and antagonists in 10 µl buffer were also added at this stage. Agonists were added, in 10 µl buffer, and incubated with the cells for a further 10 min. Incubations were terminated by the addition of 50 µl concentrated hydrochloric acid and the cells were frozen overnight.

[^{3}H]-cyclic AMP was isolated by sequential dowex-alumina chromatography as described by Donaldson *et al.* (1988). [^{14}C]-cyclic AMP (~2000 d.p.m.) was added to each sample prior to elution to correct for percentage recovery of the columns. Eluted samples were collected, 500 µl, 1 M hydrochloric acid and 10 ml emulsifier scintillator (299, Packard) were added and levels of [^{3}H]- and [^{14}C]-cyclic AMP were quantified by scintillation counting in the gel phase.

[^{3}H]-mepyramine binding

Radioligand binding assays were performed by the method described by Dickenson & Hill (1994). C6 glioma cells were removed with a cell scraper from 4 confluent, 162 cm^2 flasks in the presence of 50 mM Tris buffer (pH 7.4) homogenized and centrifuged at 1300 r.p.m. for 5 min. The resulting pellets were resuspended in approximately 20 ml Tris buffer and centrifuged for a further 5 min at 1700 r.p.m. The final pellet was resuspended in 2.6 ml buffer.

[^{3}H]-mepyramine was diluted with Tris buffer to produce concentrations of 8 nM, 4 nM, 2 nM, 1 nM, 0.5 nM and 0.25 nM. Aliquots of membrane suspension (50 µl; 205 ± 10 µg protein) were incubated in triplicate with each concentration of [^{3}H]-mepyramine (940 µl) in the presence of (10 µl) buffer or promethazine (final concentration 2 µM). Non-specific binding was defined as the concentration of bound ligand in the presence of promethazine. Incubations lasted for 30 min at 37°C and the membrane suspensions were gently shaken throughout this period. The remaining membrane suspension was frozen for protein assay at a later date.

The incubations were each terminated by rapid filtration and 2 washes of approximately 5 ml ice cold Tris buffer over Whatman GF/B filters (pre-soaked for 1 h in 0.3% polyethylenimine to reduce non-specific binding) using a Brandel MR24 cell harvester. The filters were transferred to scintillation vial inserts and 5 ml emulsifier scintillator (299, Packard) was added. The inserts were allowed to stand at room temperature for at least 2 h before levels of [^{3}H]-mepyramine were quantified by scintillation counting in the gel phase.

The protein content of the membrane suspension was determined by the method of Bradford (1976). Sodium hydroxide (0.5 M) was used to digest the samples and bovine serum albumin was used as the standard.

Data analysis

Agonist concentration-response curves were fitted to a logistic equation using the non-linear regression program, GraphPAD (ISI). The equation fitted was:

$$\text{Response} = \frac{E_{max} \times [A]^n}{(EC_{50}{}^n + [A]^n}$$

where E_{max} is the maximal response, [A] is the agonist concentration, EC_{50} is the concentration of agonist producing half maximal stimulation, and n is the Hill coefficient.

Antagonist dissociation constants (K_d) were estimated by a modification of the null method described by Lazareno & Roberts (1987). Briefly, a concentration-response curve to histamine was generated and a concentration (C:0.1 mM) chosen which gave a response greater than 50% of the maximum agonist response. The concentration of antagonist (IC_{50}) required to reduce the response of this concentration (C) of histamine by 50% was then determined. The histamine concentration-response curve was fitted to the logistic equation as above and a concentration of histamine (C') identified which yielded a response equivalent to 50% of that produced by concentration C (in the absence of antagonist). The apparent K_d (assuming competitive antagonism) was then determined from the relationship:

$$C/C' = (IC_{50}/K_d) + 1$$

Statistical analysis was performed by use of Student's unpaired *t* test or 2 way analysis of variance (ANOVA) with *post-hoc* Newman-Keuls. Unless otherwise stated, each value given in the text represents mean ± s.e.mean of *n* separate experiments.

Materials

C6 glioma cells were obtained from European Cell Collection, Porton Down and tissue culture plastics from Costar.

DMEM and FCS were purchased from Biological Industries (Cumbernauld, U.K.). L-Glutamine and powdered, inositol-free DMEM, with glutamine were supplied by ICN Flow Laboratories. Antibiotic-antimycotic solution (100x) and trypsin-EDTA solution (10x) were obtained from Gibco Laboratories (Paisley, U.K.) (Irvine, U.K.). *Myo*-[2-^{3}H(N)]-inositol (23.45Ci mmol^{-1}) was purchased from NEN Research Products, Du Pont (U.K.) Ltd. (Stevenage, Herts.). 8-[^{3}H]-adenine (27Ci mmol^{-1}), [pyridinyl-5-^{3}H]-mepyramine (28 Ci mmol^{-1}) and 8-[^{14}C]-cyclic adenosine monophosphate (309 mCi mmol^{-1}) ammonium salt were purchased from Amersham International (Aylesbury, U.K.). Hanks Balanced Salts Solution (10x) was supplied by Northumbria Biologicals (Northumberland, U.K.) and HEPES Trizma base and Dowex 1 by Sigma Chemical Co. (Poole, U.K.). Rolipram was a gift from Schering (Berlin, Germany).

Results

In the presence of 20 mM LiCl, histamine (0.1 mM) produced an initial, rapid increase in the accumulation of total [^{3}H]-inositol phophates in C6 glioma cells. After 10 min of agonist stimulation, accumulation began to reach a steady state level (2.2 ± 0.3 fold over basal levels, $n = 5$, $P < 0.01$) and was maintained throughout the remaining 30 min of the experiment (Figure 1). This response to histamine (10 min stimulation) was concentration-dependent and the mean EC_{50} value calculated from 8 separate experiments was 23.9 ± 4.5 μM (Figure 2, Table 1). The maximal response, achieved at 1 mM histamine, was 2.9 ± 0.8 fold over basal levels ($n = 8$, $P < 0.01$). Similar responses were obtained from the H_1 receptor-selective agonist, 2-thiazolylethylamine (1 mM, 1.9 ± 0.2 fold over basal levels, $n = 3$, $P < 0.01$), and the non-selective agonist N^{α}-methylhistamine (1 mM, 1.9 ± 0.4 fold over basal levels, $n = 4$, $P < 0.01$) (Figure 2). The mean EC_{50} values obtained for these compounds were similar to values previously reported for the stimulation of inositol phosphate accumulation in the hamster vas deferens smooth muscle cell line, DDT$_1$MF-2 (Table 1).

The response to 0.1 mM histamine (10 min stimulation, 20 mM LiCl) was antagonized in a concentration-dependent manner by the H_1 receptor-selective antagonist, mepyramine (Figure 3). Furthermore, the addition of mepyramine (10 μM) immediately following a 10 min period of stimulation with 0.1 mM histamine significantly reduced phosphoinositide turnover over the next 5 min and had returned accumulation to basal levels within 30 min (Figure 1). These data suggest that inositol monophosphate breakdown has not been completely attenuated by 20 mM LiCl in these cells. This confirms the observations of Ananth *et al.* (1987) in C6 cells. Similar decreased sensitivities to lithium have been observed in N1E-115 neuroblastoma (Thompson & Fisher, 1990), HeLa cells (Bristow *et al.*, 1991) and DDT$_1$MF-2 cells (White *et al.*, 1993).

The histamine response (0.1 mM) was also antagonized by low concentrations of (+)-chlorpheniramine whereas (−)-chlorpheniramine was more than two orders or magnitude less potent than its (+)-stereoisomer (Figure 3). The apparent dissociation constants obtained for mepyramine and (+)-chlorpheniramine were similar to those reported for the inhibition of [^{3}H]-mepyramine binding to membranes from transfected C6 cells, cultured astrocytes and rat cerebral cortex (Table 2). Pretreatment with either the H_2 receptor-selective antagonist, tiotidine, at concentrations up to 10 μM (10 μM, 96.4 ± 9.9% of the control response to 0.1 mM his-

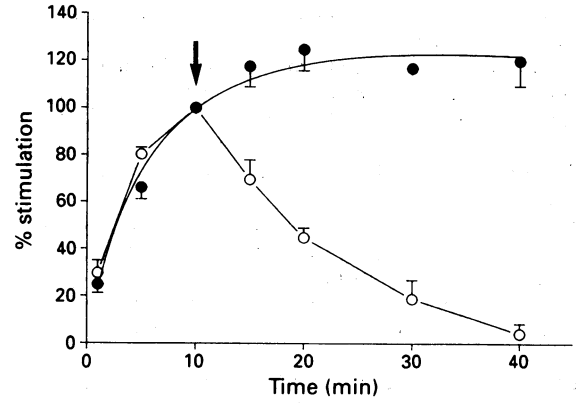


Figure 1 Time courses for the accumulation of total [^{3}H]-inositol phosphates in response to histamine, in the absence and presence of mepyramine, in rat C6 glioma cells. The control response obtained with histamine (0.1 mM, added at time zero) in the absence of mepyramine is indicated by (●). The effect of mepyramine addition (10 μM, added at the arrow) 10 min after stimulation with histamine (0.1 mM, added at time zero) is indicated by (○). Results are expressed as a percentage of the control response to 0.1 mM histamine after a 10 min stimulation period. Values represent means ± s.e.means from triplicate determinations in 5 separate experiments (in the absence if mepyramine) and 4 separate experiments (in the presence of mepyramine).

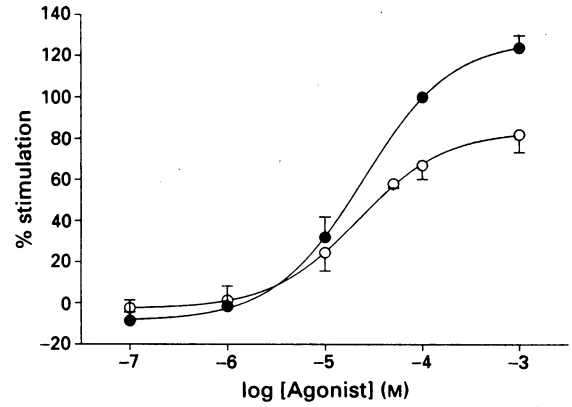


Figure 2 Effect of histamine receptor agonists on total [^{3}H]-inositol phosphates accumulation in rat C6 glioma cells. Results obtained from histamine (●) and N^{α}-methylhistamine (○) are expressed as a percentage of the response to 0.1 mM histamine which was measured in every experiment. Values represent the combined means ± s.e.means from quadruplicate determinations in 8 separate experiments (histamine) and triplicate determinations in 4(N^{α}-methylhistamine) separate experiments.

Table 1 Agonist properties of histamine analogues for stimulation of total [^{3}H]-inositol phosphates accumulation in C6 glioma cells

Agonist	*Maximal response expressed as mean % response to 0.1 mM histamine*	n	*Total [^{3}H]-inositol phosphates accumulation EC_{50} (μM)* *C6 cells*	*DDT$_1$MF-2 cells*[a]	*Type-2 astrocytes*[b]
Histamine	123.6 ± 5.6	8	23.9 ± 4.5	12.0	2.4
2-TE	98.5 ± 6.8	3	90.6 ± 18.3	42.7	
N^{α}MeHA	81.9 ± 8.6	4	30.8 ± 8.6	72.4	

The maximal response for each agonist is expressed as a mean percentage of the response to 0.1 mM histamine which was measured in each experiment. EC_{50} values are represented as means ± s.e.means for total [^{3}H]-inositol phosphates accumulation in n separate experiments. Data taken from [a]White *et al.* (1993) and [b]Kondou *et al.* (1991). Abbreviations2 2-TE, 2-thiazolylethylamine; N^{α}MeHist, N^{α}methylhistamine.

tamine, $n = 3$), or the H_3 receptor-selective antagonist, thioperamide, at concentrations up to 1 μM (1 μM, 92.3 ± 8.1% of the control response to 0.1 mM histamine, $n = 3$) did not significantly affect histamine-mediated inositol phosphate accumulation.

Despite the obvious presence of a functionally coupled histamine H_1 receptor in these cells, ligand binding experiments with [^{3}H]-mepyramine were unable to detect any significant specific binding to cell homogenates over the concentration range 0.5–8.0nM ($n = 4$).

Preincubation of the cells with forskolin (1 μM) for 10 min significantly reduced the inositol phosphate response to histamine (0.1 mM). A typical experiment is shown in Figure 4. The maximal percentage decrease in response was 37.4 ± 10.4% ($n = 3$, $P < 0.01$) and was obtained after 40 min co-incubation with histamine and forskolin. This effect was further investigated with a range of forskolin concentrations. At concentrations above 0.1 μM, forskolin produced a significant decrease in histamine-mediated (0.1 mM) inositol phosphate accumulation. A maximal percentage decrease of 37.2 ± 4.3% ($n = 6$, $P < 0.001$) was obtained with 10 μM agonist (Figure 5).

The possibility that the inhibitory effect of forskolin was mediated via alterations in [^{3}H]-cyclic AMP accumulation was considered. Forskolin alone (1 μM) caused a small but significant elevation of [^{3}H]-cyclic AMP accumulation. After 10 min stimulation, [^{3}H]-cyclic AMP levels had increased from a mean basal response of 1729 ± 173 d.p.m. to 4501 ± 461 d.p.m. (2.7 ± 0.4 fold over basal levels, $n = 6$, $P < 0.001$). This was much enhanced (12.8 ± 2.8 fold over basal levels, $n = 3$, $P < 0.001$) and proved to be concentration-dependent (mean $EC_{50} = 0.3 \pm 0.03$ μM) in the presence of 100 μM rolipram, an inhibitor of the cyclic AMP-selective (type IV) phosphodiesterase isoenzyme (Donaldson *et al.*, 1988). In contrast, 1,9-dideoxyforskolin, which does not elevate adenylyl cyclase activity, had no significant effect on the histamine response (Figure 5). Isoprenaline, in the absence of rolipram, caused

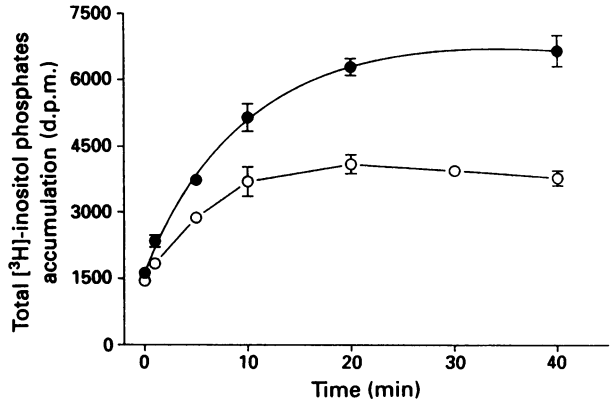


Figure 4 Time courses for the accumulation of total [^{3}H]-inositol phosphates in response to histamine, in the absence and presence of forskolin, in rat C6 glioma cells. The control response obtained with histamine (0.1 mM, added at time zero) in the absence of forskolin is indicated by (●). The response obtained with histamine (0.1 mM, added at time zero) after 10 min preincubation with forskolin (1 μM) is indicated by (○). Values represent means ± s.e.means of triplicate determinations in a single experiment. Similar data were obtained in two other experiments.

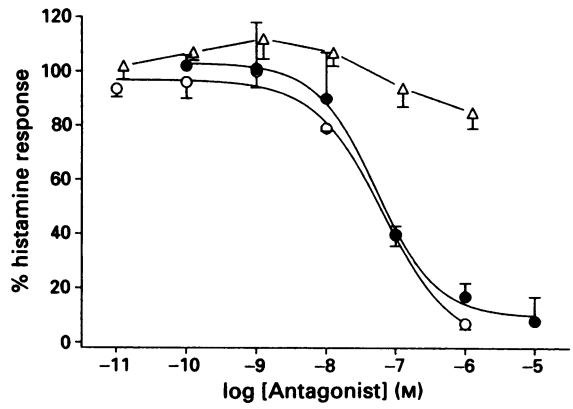


Figure 3 Effect of histamine receptor antagonists on histamine-mediated (0.1 mM) total [^{3}H]-inositol phosphates accumulation in rat C6 glioma cells. Results obtained from histamine (0.1 mM, 10 min stimulation) after 30 min preincubation with (+)-chlorpheniramine (○); (−)-chlorpheniramine (Δ); or mepyramine (●) are expressed as a percentage of the control response to 0.1 mM histamine alone, which was measured in every experiment. Values represent the combined means ± s.e.means from triplicate determinations in 4 ((+)-chlorpheniramine) and 3 ((−)-chlorpheniramine and mepyramine) separate experiments

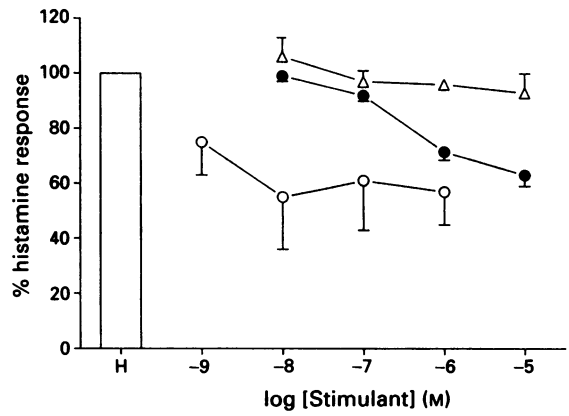


Figure 5 Effect of elevation of cyclic AMP accumulation on histamine-mediated (0.1 mM) total [^{3}H]-inositol phosphates accumulation in rat C6 glioma cells. Results obtained from histamine (0.1 mM, 10 min stimulation) after 10 min preincubation with isoprenaline (○); 1,9-dideoxyforskolkin (Δ); and forskolin (●) are expressed as a percentage of the control response to 0.1 mM histamine alone, which was measured in every experiment. Values represent the combined means ± s.e.means from quadruplicate determinations in 6 (forskolin) and 3 (1,9-dideoxyforskolin and isoprenaline) separate experiments

Table 2 Antagonism of histamine-stimulated total [^{3}H]-inositol phosphates accumulation in C6 glioma cells

	Inositol phosphate hydrolysis			*Histamine receptor* K_d (nM)[a]		
Antagonist	IC_{50} (nM)	*Apparent* K_d (nM)	n	*Transfected C6 cells*	*Astrocytes*	*Rat cerebral cortex*
Mepyramine	47.3 ± 11.1	1.0 ± 0.2	3	2	8	11
(+)-Chlorpheniramine	91.5 ± 34.8	4.4 ± 0.6	4	8	48	43
(−)-Chlorpheniramine	> 1000	> 620 ± 30	3	540	2100	1500

Values for inositol phosphate hydrolysis represent means ± s.e.means of the antagonist IC_{50} values obtained from inhibition of histamine-stimulated (0.1 mM) total [^{3}H]-inositol phosphates accumulation in n separate experiments. Apparent K_d values were calculated from these IC_{50} values as described under Methods. [a]Data obtained from antagonism of [^{3}H]-mepyramine binding to membranes from transfected C6 cells (Fujimoto *et al.*, 1993), cultured astrocytes and rat cerebral cortex (Fukui *et al.*, 1991).

signifiant, concentration-dependent (mean $EC_{50} = 4.3 \pm 2.5$nM) elevations in [^{3}H]-cyclic AMP accumulation (1 mM, 33.8 ± 5.7 fold over basal levels, $n = 3$, $P < 0.01$) in C6 cells and inhibited histamine-mediated inositol phosphate accumulation (1 μM, 42.7 ± 12.4% inhibition, $n = 3$, $P < 0.001$) (Figure 5). Rolipram (100 μM), in the absence of receptor stimulation, also significantly elevated basal levels of [^{3}H]-cyclic AMP accumulation. After 10 min incubation, [^{3}H]-cyclic AMP levels in C6 cells had increased from a mean basal response of 1441 ± 272 d.p.m. to 4607 ± 455 d.p.m. (4.0 ± 1.1 fold over basal levels, $n = 3$, $P < 0.001$). In addition, it produced a concentration-dependent (mean $IC_{50} = 42.0 \pm 7.8$ μM) reduction of histamine-mediated phosphoinositide turnover (0.5 mM, 26.4 ± 3.7% inhibition, $n = 4$, $P < 0.001$) (Figure 6).

Preincubation of C6 cells (30 min) with H89 (20 μM), a relatively selective inhibitor of the cyclic AMP-dependent protein kinase A (Chijiwa *et al.*, 1989), significantly reduced the attenuation of histamine (0.1 mM)-stimulated [^{3}H]-inositol phosphate accumulation produced by isoprenaline (10 nM) from 51 ± 4% to 27 ± 4% ($n = 4$; $P < 0.05$). An example of the data obtained in a single experiment is shown in Figure 7. Interestingly, H89 (20 μM) had no significant effect on either basal or histamine-stimulated [^{3}H]-inositol phosphate accumulation (Figure 7). Over 4 experiments, the mean response to histamine (0.1 mM) obtained in the presence of H89 was 99 ± 8% of that obtained in the absence of the protein kinase A inhibitor.

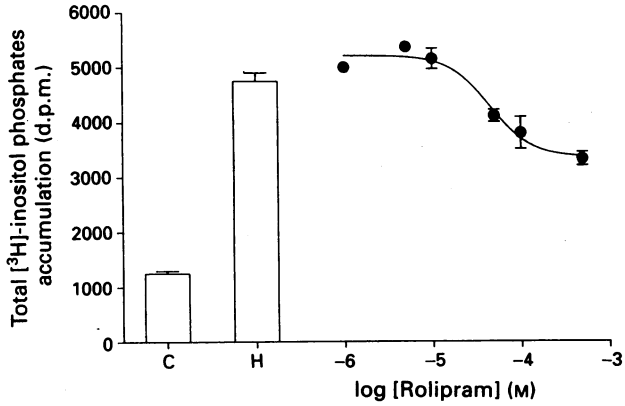


Figure 6 Effect of rolipram on histamine-mediated (0.1 mM) total [^{3}H]-inositol phosphates accumulation in rat C6 glioma cells column C represents the mean basal, and column H, the mean histamine-stimulated (0.1 mM) accumulation of total [^{3}H]-inositol phosphates. Values represent the means ± s.e.means from triplicate determinations in a single experiment. Similar data were obtained in 3 other experiments

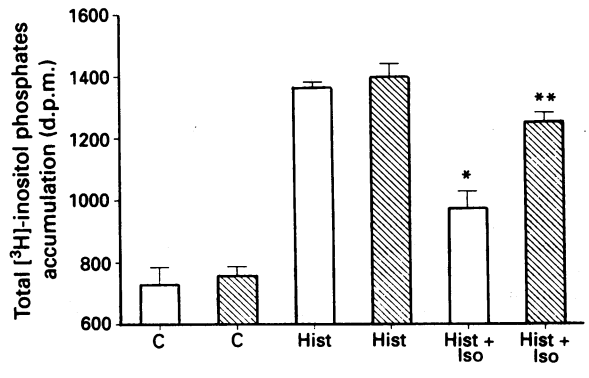


Figure 7 Effect of protein kinase A inhibition on the isoprenaline-mediated (10 nM) reduction of histamine-stimulated (0.1 mM) total [^{3}H]-inositol phosphates accumulation in rat C6 glioma cells. Results were obtained following stimulation with histamine (Hist, 0.1 mM) and a combination of histamine (0.1 mM) plus isoprenaline (10 nM) (Hist + Iso) in the presence (hatched columns) or absence (open columns) of 20 μM H89. Columns marked C represent the basal accumulation of total [^{3}H]-inositol phosphates obtained in the presence (hatched column) or absence of H89 (open column). Values represent the means ± s.e.means from quadruplicate determinations in a single experiment. Similar data were obtained in 7 other experiments. Statistical significance was calculated by one way analysis of variance: $^*P < 0.01$ with respect to Hist (open column); $^{**}P < 0.01$ with respect to Hist + Iso (open column).

Discussion

Histamine H_1 receptors are coupled to phospholipase C and mediate a variety of functional responses as a consequence of elevating intracellular free calcium ion concentration (Hill, 1990; 1992). Recently the rat H_1 receptor gene has been isolated by using the bovine H_1 receptor cDNA as a probe (Fujimoto *et al.*, 1993). The isolated gene encoded a protein of 486 amino acids which was 73% homologous with the bovine receptor sequence and exhibited the 7 putative transmembrane regions common to GTP-binding protein-coupled receptors. The rat H_1 receptor cDNA has been successfully transfected into rat glioma C6 cells and the binding characteristics of the transfected H_1 receptor determined with [^{3}H]-mepyramine (Fujimoto *et al.*, 1993). In the present study we have observed a histamine H_1 receptor-mediated elevation in total [^{3}H]-inositol phophates in untransfected C6 cells and its modification by cyclic AMP elevating agents, despite the fact that specific [^{3}H]-mepyramine binding could not be detected in these cells.

Histamine, 2-thiazolylethylamine and N^{α}-methylhistamine were able to elevate significantly total [^{3}H]-inositol phosphates accumulation in C6 glioma cells (Figure 2). The EC_{50} values for these compounds were similar to those calculated in DDT_1MF-2 cells, although, the potency of histamine was lower than has previously been reported in type-2 astrocytes (Table 1). This latter observation may be a consequence of the much lower H_1 receptor number in the C6 cells compared to type 2 astrocytes (Fukui *et al.*, 1991). From the agonist concentration-response curves, the rank order of agonist potencies was histamine > N^{α}-methylhistamine > 2-thiazolylmethylamine which is consistent with the presence of histamine H_1 receptors (Ganellin, 1982). In addition, the relative agonist potencies (expressed as the ratio, molar concentration of histamine/molar concentration of agonist necessary to produce equal effects; histamine = 100) were calculated to be N^{α}-methylhistamine = 77 and 2-thiazolylethylamine = 26. These values are in very close agreement with the values of N^{α}-methylhistamine = 72 and 2-thiazolylethylamine = 26 which have previously been calculated (Ganellin, 1982) for the activity of these compounds on guinea-pig ileum *in vitro*. Mepyramine and (+)-chlorpheniramine proved to be potent antagonists of histamine-stimulated [^{3}H]-inositol phosphates accumulation in C6 cells (Figure 3). The apparent dissociation constants calculated for these compounds were similar to values previously recorded at H_1 receptor sites (Table 2). (−)-Chlorpheniramine was at least two orders of magnitude less potent than its (+)-stereoisomer, a feature which has previously been noted in studies of H_1 receptor function in guinea-pig ileum and brain (Roth & Govier, 1958; Hill *et al.*, 1981) and in transformed cell lines (White *et al.*, 1993).

It, therefore, appears that, in spite of earlier work showing no specific binding of [^{3}H]-mepyramine to non-transfected C6 cells (Fujimoto *et al.*, 1993), this cell line can express functionally coupled endogenous histamine H_1 receptors. These results provide a warning which should be considered whenever transformed cell lines are used for transfection work. The selective subcloning, integral to transfections techniques, raises the possibility that resulting clonal characteristics may be partly the consequences of the selection and propagation of a cell expressing high levels of endogenous receptor. Thus a thorough pre-transfection screening incorporating both binding and functional assays is of paramount importance when

beginning clonal work. The lack of significant specific [^{3}H]-mepyramine binding to C6 cells in the present study would suggest a very efficient receptor-effector coupling of a low density of endogenous H_1 receptors to inositol phospholipid hydroysis in these cells. A similar observation has been made for the coupling of 5-HT_{1B} receptors to adenylyl cyclase in CHO cells (Giles *et al.*, 1994).

Forskolin and isoprenaline elevated intracellular cyclic AMP accumulation in C6 cells via direct activation of adenylyl cyclase and receptor stimulation, respectively. The EC_{50} values calculated for these responses were in close agreement with those estimated (from Figure 5) for the inhibition of histamine-mediated inositol phosphates accumulation by these compounds. A dose-dependent inhibition of the histamine response was also produced by the phosphodiesterase inhibitor, rolipram, which prevents breakdown and causes accumulation of cyclic AMP. In contrast, the forskolin analogue, 1,9-dideoxyforskolin, which does not stimulate adenylyl cyclase activity (Seamon & Daly, 1986) and hence does not elevate cyclic AMP levels, had no effect on the histamine response (Figure 5).

The inhibition of histamine-induced inositol phospholipid hydrolysis by cyclic AMP has been well documented in peripheral tissues although it has not been observed previously in brain tissues (for reviews see Hill, 1991; Hill & Kendall, 1992). The observations presented in this study indicate that inhibitory effects of cyclic AMP elevating agents on histamine-stimulated phosphoinositide hydrolysis in brain tissues may be restricted to certain cell populations (e.g. glial cells). One possible mechanism for this effect is a protein kinase A-mediated phosphorylation of some component(s) of the inositol phospholipid receptor-effector system. Studies using A-kinase inhibitors have supported this theory (Yada *et al.*, 1989). The cyclic AMP-mediated inhibition of phosphinositide hydrolysis, which was directly stimulated via the GTP-binding protein using fluoroaluminate complexes (Hall *et al.*, 1990; Tachado *et al.*, 1992) or guanosine 5'[3-O-thio]triphosphate (Yada *et al.*, 1989), has led to the suggestion that phosphorylation occurs at a post-receptor site (eg the GTP-binding protein or phospholipase C). On the other hand, in rat glomerulosa cells (Guillon *et al.*, 1988) cholera toxin-mediated increases in cyclic AMP inhibited angiotensin II-sensitive phosphoinositide turnover at the receptor level. The authors proposed that phosphorylation of the hormone receptors by protein kinase A resulted in uncoupling or desensitization, effectively reducing the receptor density and hence phospholipase C activation.

A potential role of protein kinase A in the effect of cyclic AMP elevating agents on histamine-stimulated inositol phospholipid hydrolysis in C6 cells is supported by the data obtained with H-89 (Figure 7). This relatively selective protein kinase A inhibitor (Chijiwa *et al.*, 1989) was able to attenuate significantly the inhibitory effects of isoprenaline on histamine-stimulated inositol phosphate accumulation. Interestingly, H-89 did not alter the basal or histamine-stimulated inositol phosphate accumulation in the absence of isoprenaline. These data suggest that there is not a high endogenous turnover of cyclic AMP in C6 cells which is producing a depression of the H_1 receptor-mediated inositol phosphate response.

It is now generally accepted that the phosphorylation site for a particular protein kinase possesses a specific 'consensus sequence', generally a short, linear sequence of amino acids, whose presence is required for and is sufficient for recognition by the enzyme (for review see Kenelly & Krebs, 1991). Activation of protein kinase A causes phosphorylation of substrate serine (preferentially) or threonine residues; however, the presence of basic amino acids, particularly arginine, N-terminal to the phosphoacceptor is of critical importance in substrate recognition (Zetterqvist *et al.*, 1976; Kemp *et al.*, 1977). The optimal sequence for protein kinase A recognition has been proposed to be arginine-arginine-X-serine*/threonine* (where * denotes the phosphoacceptor group,/denotes interchangeable amino acids and X denotes a site not important for recognition) (Kenelly & Krebs, 1991). In light of this, we have examined the amino acid sequence of the cloned, rat histamine H_1 receptor (Fujimoto *et al.*, 1993) and have identified a consensus sequence of, arginine-arginine-isoleucine-serine, which appears to be optimal for protein kinase A recognition, located at positions 339–342 in the third-putative intracellular loop of the receptor. This discrete region of GTP-binding protein-coupled receptors is thought to play a critical role in the receptor transduction mechanism (Lechleiter *et al.*, 1990; Wess *et al.*, 1990). Thus, it is possible that cyclic AMP-mediated inhibition of histamine-stimulated phosphoinositide turnover in C6 glioma cells involves protein kinase A-mediated uncoupling of the H_1 receptor via phosphorylation at a specific site in its third putative intracellular loop.

In conclusion, the data from this study provide evidence for the presence of endogenous histamine H_1 receptors, functionally linked to inositol phospholipid hydroysis, in rat C6 glioma cells. Additionally, we have shown that the histamine-mediated accumulation of inositol phosphates appears to be inhibited by the elevation of intracellular cyclic AMP levels, possibly via a mechanism involving protein kinase A-mediated phosphorylation of the receptor.

We would like to thank the Wellcome Trust for financial support. M-C.P. holds a Wellcome Trust Prize Studentship.

References

ALEXANDER, S.P.H., KENDALL, D.A. & HILL, S.J. (1989). Differences in the adenosine receptors modulating inositol phosphates and cyclic AMP accumulation in mammalian cerebral cortex. *Br. J. Pharmacol.*, **98**, 1241–1248.

ANANTH, U.S., LELI, U. & HAUSER, G. (1987). Stimulation of phosphoinositide hydrolysis by serotonin in C6 glioma cells. *J. Neurochem.*, **48**, 253–261.

ARBONES, L., PICATOSTE, F. & GARCIA, A. (1988). Histamine H_1-receptors mediate phosphoinositide hydrolysis in astrocyte-enriched primary cultures. *Brain Res.*, **450**, 144–152.

BRADFORD, M.M. (1976). A rapid and sensitive method for the quantitation of microgram quantities of protein using the principle of protein dye binding. *Anal. Biochem.*, **72**, 248–254.

BRISTOW, D.R., ARIAS-MONTANO, J.A. & YOUNG, J.M. (1991). Histamine-induced inositol phosphate accumulation in HeLa cells: lithium sensitivity. *Br. J. Pharmacol.*, **104**, 677–684.

CHIJIWA, T., MISHIMA, A., HAGIWARA, M. SANO, M., HAYASI, K., INOUE, T., NAITO, K., TOSHIOKA, T. & HIDAKA, H. (1990). Inhibition of forskolin-induced neurite outgrowth and protein phosphorylation by a newly synthesized selective inhibitor of cyclic AMP-dependent protein kinase, N-[2-(*P*-bromocinnamylamino)ethyl]-5-isoquinoline sulfonamide (H-89), of PC12D pheochromocytoma cells. *J. Biol. Chem.*, **265**, 5267–5272.

DEGEORGE, J.J., OUSLEY, A.H., MCCARTHY, K.D., LAPETINA, E.G. & MORELL, P. (1987). Acetylcholine stimulates selective liberation and re-esterification of arachidonate and accumulation of inositol phosphates and glycerophosphoinositol in C62B glioma cells. *J. Biol. Chem.*, **262**, 8077–8083.

DICKENSON, J.M. & HILL, S.J. (1994). Characteristics of [^{3}H]mepyramine binding in DDT_1MF-2 cells: Evidence for high affinity binding to a functional H_1 receptor. *Eur. J. Pharmacol.*, **268**, 257–262.

DICKENSON, J.M., WHITE, T.E. & HILL, S.J. (1993). The effects of elevated cyclic AMP levels on histamine-H_1-receptor-stimulated inositol phospholipid hydrolysis and calcium mobilization in the smooth-muscle cell line DDT_1MF-2. *Biochem. J.*, **292**, 409–417.

DONALDSON, J., BROWN, A.M. & HILL, S.J. (1988). Influence of rolipram on the cyclic 3'5',-adenosine monophosphate response to histamine and adenosine in slices of guinea-pig cerebral cortex. *Biochem. Pharmacol.*, **37**, 715–723.

DONIE, F. & REISER, G. (1991). Mass measurements of inositol 1,4,5-trisphosphate and inositol 1,3,4,5-tetrakisphosphate in a neuronal cell line stimulated with bradykinin: inositol phosphate response shows desensitization. *Biochem. Biophys. Res. Commun.*, **181**, 997–1003.

FUJIMOTO, K., HORIO, Y., SUGAMA, K., ITO, S., LIU, Y.Q. & FUKUI, H. (1993). Genomic cloning of the rat histamine H_1 receptor. *Biochem. Biophys. Res. Commun.*, **190**, 294–301.

FUKUI, H., INAGAKI, N., ITO, S., KUBO, H., KONDOU, H., YAMATODANI, A. & WADA, H. (1991). Histamine H_1-receptors on astrocytes in primary cultures: a possible target for histaminergic neurones. In *New Perspectives in Histamine Research*. ed. Timmerman, H. & van der Goot, H., AAS 33 pp. 161–180. Basel: Birkhauser Verlag.

GANELLIN, C.R. (1982). Chemistry and structure-activity relationships of drugs acting at histamine receptors. In *Pharmacology of Histamine Receptors*. ed. Ganellin, C.R. & Parsons, M.E. pp. 10–102. Bristol: Wright, PSG.

GILES, H., LANSDELL, S.J., FOX, P., LOCKYER, M., HALL, V. & MARTIN, G.R. (1994). Characterisation of a 5-HT_{1B} receptor on CHO cells: Functional responses in the absence of radioligand binding. *Br. J. Pharmacol.*, **112**, 317P.

GUILLON, G.N., GALLO-PAYET, N., BALESTRE, M.N. & LOMBARD, C. (1988). Cholera toxin and corticotrophin modulation of inositol phosphate accumulation induced by vasopressin and angiotensin II in rat glomerulosa cells. *Biochem. J.*, **253**, 765–775.

GUSOVSKY, F. (1992). Endothelin-elicited stimulation of phospholipase C is mediated by guanine nucleotide binding protein(s). *Eur. J. Pharmacol.*, **225**, 339–45.

HALL, I.P. & HILL, S.J. (1988). β-Adrenoceptor stimulation inhibits histamine-stimulated inositol phospholipid hydrolysis in bovine tracheal smooth muscle. *Br. J. Pharmacol.*, **95**, 1204–1212.

HALL, I.P., DONALDSON, J. & HILL, S.J. (1989). Inhibition of histamine-stimulated inositol phospholipid hydrolysis by agents which increase AMP levels in bovine tracheal smooth muscle. *Br. J. Pharmacol.*, **97**, 603–613.

HALL, I.P., DONALDSON, J. & HILL, S.J. (1990). Modulation of fluoroaluminate-induced inositol phosphate formation by increase in tissue cyclic AMP content in bovine tracheal smooth muscle. *Br. J. Pharmacol.*, **100**, 646–650.

HILL, S.J. (1990). Distribution, properties, and functional characteristics of three classes of histamine receptor. *Pharmacol. Rev.*, **42**, 45–83.

HILL, S.J. (1991). Histamine receptors and interactions between second messenger transduction systems. In *New Perspectives in Histamine Research*. ed. Timmerman, H. & van der Goot, H., AAS 33, pp. 145–159. Basel: Birkhauser Verlag.

HILL, S.J. (1992). Multiple histamine receptors: properties and functional characteristics. *Biochem. Soc. Trans.*, **20**, 122–125.

HILL, S.J., DAUM, P. & YOUNG, J.M. (1981). Affinities of histamine H_1-antagonists in guinea-pig brain: Similarity of values determined from [^{3}H]mepyramine binding and from inhibition of a functional response. *J. Neurochem.*, **37**, 1357–1360.

HILL, S.J. & KENDALL, D.A. (1992). Cross-talk between intracellular second messenger transduction systems. *Drugs, News and Perspectives*, **5**, 39–48.

HOLLINGSWORTH, E.B. & DALY, J.W. (1985). Accumulation of inositol phosphates and cyclic AMP in guinea-pig cerebral cortical preparations. Effects of norepinephrine, histamine, carbamylcholine and 2-chloroadenosine. *Biochim. Biophys. Acta*, **847**, 207–216.

HOSLI, E. & HOSLI, L. (1984). Autoradiographic localization of binding sites for [^{3}H]histamine and H_1- and H_2-antagonists on cultured neurones and glial cells. *Neurosci.*, **13**, 863–870.

INAGAKI, N., FUKUI, H., ITO, S. & WADA, H. (1991a). Type-2 astrocytes show intracellular Ca^{2+} elevation in response to various neuroactive substances. *Neurosci. Lett.*, **128**, 257–260.

INAGAKI, N., FUKUI, H., ITO, S., YAMATODANI, A. & WADA, H. (1991b). Single type-2 astrocytes show multiple independent sites of Ca^{2+} signaling in response to histamine. *Proc. Natl. Acad. Sci. U.S.A*, **88**, 4215–4219.

INAGAKI, N., FUKUI, H., TAGUCHI, Y., WANG, N.P., YAMATODANI, A. & WADA, H. (1989). Characterization of Histamine H_1-receptors on astrocytes in primary culture: [^{3}H]mepyramine binding studies. *Eur. J. Pharmacol.*, **173**, 43–51.

KEMP, B.E., GRAVES, D.J., BENJAMINI, E. & KREBS, E.G. (1977). Roles of multiple basic residues in determining the substrate specificity of cyclic AMP dependent protein kinase (porcine liver pyruvate kinase). *J. Biol. Chem.*, **252**, 4888–4894.

KENNELLY, P.J. & KREBS, E.G. (1991). Consensus sequences as substrate specificity determinants for protein kinases and protein phosphatases. *J. Biol. Chem.*, **266**, 15555–15558.

KITANAKA, J.-I., HASHIMOTO, H., GOTOH, M., MAYUMI, T. & BABA, A. (1992). Mechanism of extracellular ATP-stimulated phosphoinositide hydrolysis in rat C6 glioma cells. *J. Pharmacol. Exp. Ther.*, **263**, 1248–1252.

KONDOU, H., INAGAKI, N., FUKUI, H., KOYAMA, Y., KANAMURA, A. & WADA, H. (1991). Histamine-induced inositol phosphate accumulation in type-2 astrocytes. *Biochem. Biophys. Res. Commun.*, **177**, 734–738.

LAZARENO, S. & ROBERTS, F.F. (1987). Measuring muscarinic antagonist potency using phosphoinositide breakdown in rat cortex slices. *Br. J. Pharmacol.*, **92**, 677P.

LECHLEITER, J., HELLMISS, R., DUERSON, K., ENNULAT, D., DAVID, N., CLAPHAM, D. & PERALTA, E. (1990). Distinct sequence elements control the specificity of G protein activation by muscarinic acetylcholine receptor subtypes. *EMBO J.*, **9**, 4381–4390.

LIN, W.-W., KIANG, J.G. & CHUANG, D.M. (1992). Pharmacological characterization of endothelin-stimulated phosphoinositide breakdown and cytosolic free Ca^{2+} rise in rat C6 glioma cells. *J. Neurosci.*, **12**, 1077–1085.

LIU, Y.Q., HORIO, Y., MIZUGUCHI, H., FUJIMOTO, K., IMAMURA, I., ABE, Y. & FUKUHI, H. (1992). Re-examination of [^{3}H]mepyramine binding assay for histamine H_1 receptor using quinine. *Biochem. Biophys. Res. Commun.*, **189**, 378–384.

MANGOURA, D., SAKELLARIDIS, N., JONES, J. & VERNADAKIS, A. (1989). Early and late passage C6-glial cell growth: similarities with primary glial cells in culture. *Neurochem. Res.*, **14**, 941–947.

PEAKMAN, M.-C. & HILL, S.J. (1994). Adenosine A_{2B}-receptor-mediated cyclic AMP accumulation in primary rat astrocytes. *Br. J. Pharmacol.*, **111**, 191–198.

RAFF, M.C., ABNEY, E.R., COHEN, J., LINDSAY, R. & NOBLE, M. (1983). Two types of astrocytes in cultures of developing rat white matter: Differences in morphology, surface gangliosides and growth characteristics. *J. Neurosci.*, **3**, 1289–1300.

ROTH, F.E. & GOVIER, W.M. (1958). Comparative pharmacology of chlorpheniramine (chlor-trimeton) and its optical isomers. *J. Pharmacol. Exp. Ther.*, **124**, 347–349.

SEAMON, K.B. & DALY, J.W. (1986). Forskolin: its biological and chemical properties. *Adv. Cyclic Nucleotide Protein Phosphorylation Res.*, **20**, 1–150.

TACHADO, S.D., AKHTAR, R.A., ZHOU, C.-J. & ABDEL-LATIF, A.A. (1992). Effects of isoproterenol and forskolin on carbachol- and fluoroaluminate-induced polyphosphoinositide hydrolysis, inositol trisphosphate production and contraction on bovine iris sphincter smooth muscle: interaction between cAMP and IP_3 second messenger systems. *Cell. Signalling*, **4**, 61–75.

THOMPSON, A.K. & FISHER, S.K. (1990). Relationship between agonist-induced muscarinic receptor loss and desensitization of stimulated phosphoinositide turnover in two neuroblastomas: methodological considerations. *J. Pharmacol. Exp. Ther.*, **252**, 744–752.

WESS, J., BONNER, T.I., DORJE, F. & BRANN, M.R. (1990). Delineation of muscarinic receptor domains conferring selectivity of coupling to guanine nucleotide binding proteins and second messengers, *Mol. Pharmacol.*, **38**, 517–523.

WHITE, T.E., DICKENSON, J.M. & HILL, S.J. (1993). Histamine H_1-receptor-mediated inositol phospholipid hydrolysis in DDT_1MF-2 cells: agonist and antagonist properties. *Br. J. Pharmacol.*, **108**, 196–203.

YADA, Y., NAGAO, S., OKANA, Y. & NOZAWA, Y. (1989). Inhibition by cyclic AMP of guanine nucleotide-induced activation of phosphoinositide-specific phospholipase C in human platelets. *FEBS Lett.*, **242**, 368–372.

ZETTERQVIST, O., RAGNARSSON, U., HUMBLE, E., BERGLUND, L. & ENGSTROM, L. (1976). The minimum substrate of cyclic AMP-stimulated protein kinase, as studied by synthetic peptides representing the phosphorylatable site of pyruvate kinase (type L) of rat liver. *Biochem. Biophys. Res. Commun.*, **70**, 696–703.

(Received February 21, 1994
Revised July 22, 1994
Accepted September 6, 1994).

Br. J. Pharmacol. (1994), **113**, 1561–1566 © Macmillan Press Ltd, 1994

Spinal cord SP release and hyperalgesia in monoarthritic rats: involvement of the $GABA_B$ receptor system

[1]Marzia Malcangio & Norman G. Bowery

Department of Pharmacology, The School of Pharmacy, 29/39 Brunswick Square, London WC1N 1AX

1 Monoarthritis was induced in Lewis rats by interdermal injection in the left hind paw of a suspension of *Mycobacterium tubercolusis* in mineral oil (500 μg 100 μl^{-1}). Controls were injected with 100 μl mineral oil.

2 Withdrawal latencies to thermal stimuli of the inflamed paw, the contralateral and both paws of control rats were measured at daily intervals after injection by the plantar test.

3 After detection of the pain threshold, rat spinal cords were removed and horizontal dorsal slices were mounted in a 3-compartment bath to measure electrically-evoked release of substance P-like immunoreactivity (SP-LI).

4 The inflamed paw of monoarthritic rats exhibited a lower pain threshold to thermal stimuli than the contralateral paw of the same animals and both paws of control rats. Inflamed paw hyperalgesia was maximal two days after injection, and declined gradually between 7 to 21 days with no evidence of excitability of withdrawal reflexes after 28 days.

5 During the 28 days study, monoarthritic rats gained less weight than control rats.

6 Electrical stimulation of the dorsal roots attached to rat isolated spinal cord slices induced a significant increase (174 ± 18% of basal outflow which was 30.3 fmol 8 ml^{-1}, $n = 5$) in SP-LI release.

7 One-week after induction of inflammation no differences in the amount of SP-LI released from the spinal cord of incomplete Freund's adjuvant-treated rats (IFA) and Freund's adjuvant-treated rats (CFA) were detected. Two weeks after, CFA spinal cord tended to release more SP-LI than IFA cords and, 21 days after injection, the spinal cord of CFA rats released significantly more peptide than IFA rats (17.8 ± 2.8 fmol ml^{-1}, $n = 12$ and 6.9 ± 3.2 fmol ml^{-1}, $n = 9$, respectively).

8 Twenty-one days after treatment, the evoked release from monoarthritic rat spinal cords was increased by 263 ± 42% ($n = 3$) in the presence of the $GABA_B$ receptor antagonist, CGP 36742 (100 μM) which also significantly potentiated monoarthritis-induced hyperalgesia up to 45 min after injection (100 mg kg^{-1}, i.p.).

9 These findings may provide a basis for a novel approach to chronic pain therapy but also an explanation for the lack of analgesia produced by the $GABA_B$ agonist, baclofen, in chronic as compared to acute pain.

Keywords: Monoarthritis; chronic pain; $GABA_B$ receptor; SP-LI release

Introduction

Freund's adjuvant-induced arthritis in rats is associated with chronic pain (Colpaert, 1987). Inflammation of the paw induces a quantitative increase in the afferent input to the spinal cord (Levine *et al.*, 1984). High threshold peripheral afferent fibres respond even to gentle stimulation of the inflamed area (Schaible & Schmidt, 1988). It seems possible that changes in intraspinal mechanisms, which enhance the sensitivity of the spinal neurones, may be implicated in the increased nociception.

The transmission of afferent impulses within the spinal cord is possibly mediated, in part, via peptidergic mechanisms (see Sluka *et al.*, 1992) and among the peptide candidates proposed is the undecapeptide, substance P (SP). This is thought to be released from the central end of sensory fibres as well as from the peripheral terminals where it has been implicated in the genesis of neurogenic inflammation. Increased biosynthesis of SP in the dorsal root ganglia of adjuvant arthritic rats is reflected in an increase in the mRNA levels of preprotachykinin A, the precursor of SP (Minami *et al.*, 1989) and the number of SP-immunoreactive fibres increases in the dorsal horn of the lumbar spinal cord (Kar *et al.*, 1991). In polyarthritic rats, spontaneous release of SP from the spinal dorsal horn exceeds that in control rats (Oku *et al.*, 1987). Movement of the ankle joint which is innocuous and does not affect the release of SP in non-inflamed control rats, is converted into a noxious stimulus producing a significant increase in SP release in polyarthritic rats (Oku *et al.*, 1987).

It has been reported that adjuvant arthritic rats show an increase in the number of γ-aminobutyric acid (GABA)-immunoreactive cells due to an enhanced concentration of intracellular GABA in lamina I–III of the dorsal horn (L3–L5) (Castro-Lopes *et al.*, 1992). This increase in the amount of GABA occurs within the zone of projection of afferent nerves emanating from the inflamed foot, supporting the possibility that GABA modulates the nociceptive input at the segmental level (Castro-Lopes *et al.*, 1992).

GABA activates two receptor types, $GABA_A$ and $GABA_B$ and the latter may be involved in nociception within the spinal cord (see Sawynok, 1987). The $GABA_B$ agonist, baclofen, exhibits antinociceptive activity which stems, at least in part from an activaton of receptors within the spinal cord (Wilson & Yaksh, 1978).

We have recently demonstrated that baclofen can inhibit the electrically-evoked release of SP from the rat spinal cord and that this effect is mimicked by GABA and prevented by $GABA_B$ antagonists (Malcangio & Bowery, 1993). The aim of the present study was to evaluate the potential role of the GABAergic system within the spinal cord in the physiology or pathology of chronic pain associated with monoarthritis. Electrically-evoked release of SP from isolated spinal cords of

[1] Author for correspondence.

monoarthritic and control rats was evaluated and the effect of GABAergic drugs examined. The pain thresholds were determined in the same rats.

Methods

The present study was carried out on male Lewis rats (Perlik & Zidek, 1973) weighing 180–200 g at the time experiments were started. They were housed four to a cage and given food and water *ad libitum*. All behavioural tests were conducted in the morning.

Induction of monoarthritis

Monoarthritis was induced by intradermal injections into the left hind paw of 500 μg heat-killed and dried *Mycobacterium tubercolusis* (H37 Ra, Difco laboratories, U.K.) in 0.1 ml mineral oil (complete Freund's adjuvant) under halothane anaesthesia. Control animals were injected with 0.1 ml mineral oil (incomplete Freund's adjuvant) (Difco laboratories, U.K.). Five normal rats were injected with phosphate buffered saline (PBS) (into the left hind paw) and killed three weeks later to serve as naive controls. Arthritic rats were bedded on soft paper shavings. Rat body weight and pain threshold of both treated and non-treated paws were monitored for four weeks after inoculation, at two-day intervals.

Paw withdrawal test

Thermal hyperalgesia to radiant heat was assessed by using the paw-withdrawal test where the paw withdrawal latency is considered to be an index of the thermal nociceptive index (Hargreaves *et al.*, 1988). The choice of this test was based on its sensitivity for detecting hyperalgesia and we have used the Ugo Basile (Comerio, Italy) plantar test. It consists of a movable infrared (I.R.) generator placed below a glass pane upon which the operator places the rat. A perspex enclosure defines the space within which the animal is unrestrained. It is divided into three compartments so that up to three rats can be tested simultaneously. The radiant heat source is placed directly under the plantar surface of the rat hind paw. The paw-withdrawal latency to radiant heat stimulation is defined as the time from onset of radiant heat to withdrawal of the rat hind paw. The radiant heat source was adjusted to result in baseline latencies of 10–12 s. Three test trials (with an intertrial interval of 3 min) were made and scores from them were averaged to yield a mean withdrawal latency.

Rat spinal cord slice preparation and superfusion

Horizontal spinal cord slices were obtained from adult rats as previously described (Malcangio & Bowery, 1993; 1994). Briefly, hemisected dorsal lumbosacral slices with attached dorsal roots were cut with a Vibratome (Campden Instruments, London) and mounted in a three-compartment chamber. The tissue was positioned in the central compartment where it was continuously perfused with Krebs solution at 1 ml min^{-1} and the dorsal roots were placed across two pairs of bipolar electrodes and immersed in mineral oil in the lateral compartments. Leak-proof partition barriers of perspex and paraffin grease ensured electrical isolation. After 1 h wash, normal Krebs solution (composition in millimolar: NaCl 118, KCl 4, $MgSO_4$ 1.2, KH_2PO_4 1.2, $NaHCO_3$ 25, $CaCl_2$ 2.5 and glucose 11) was substituted with Krebs solution containing 0.1% bovine serum albumin, 100 μM captopril, 1 μM phosphoramidon, 20 μg ml^{-1} bacitracin and dithiothreitol (6 μM) to prevent metabolic breakdown of SP. Eight-minute fractions were collected in the following order: 3 fractions to measure basal outflow, one fraction to evaluate release following electrical stimulation at 20 V, 0.5 ms, 1 Hz either in the absence or presence of drugs and 3 fractions to evaluate recovery to basal levels. At the completion of each experiment, the slice was blotted, weighed and extracted. Samples (8 ml volume) were desalted by using 100 mg SEP-PAK C_{18} reverse phase silica gel cartridges (Millipore) as already described (Malcangio & Bowery, 1993; 1994). The eluates were dried by evaporation at 55°C under nitrogen and stored at −80°C until they could be assayed for SP-LI content by radioimmunoassay using the scintillation proximity assay bead technique (Amersham International, U.K.).

SP radioimmunoassay (RIA)

In each experiment, RIA standard curves were constructed for SP by using known amounts of synthetic peptides ranging between 1 and 100 fmol per tube. The dried samples were resuspended in 300 μl of 50 mM phosphate buffer (pH 7.4) containing bovine serum albumin and 10 mM ethylenediaminetetracetic acid (EDTA) and assayed in amounts of SP immunoreactivity sufficient to place them within the range of the standard curve. SP content was measured by using a polyclonal rabbit antiserum specific for the whole SP undecapeptide (Amersham International, U.K.). The incubation mixtures of each assay contained sample or standard (100 μl), tracer containing ~6000 c.p.m. of the isotope (100 μl), diluted antiserum (100 μl) and 50 μl of scintillation proximity assay protein A reagent. All samples were assayed in duplicate. The reaction mixture was vortexed and incubated at room temperature on a shaker for 48 h before being placed in the scintillation-counter.

Drugs

(−)-Baclofen (β-*p*-chlorophenyl-GABA) and CGP 36742 (3-aminopropyl-*n*-butyl-phosphinic acid) were a gift from Ciba-Geigy, Switzerland. Naloxone hydrochloride, bicuculline methiodide and SP were purchased from Sigma, U.K. Antiserum raised against SP and [^{125}]-Bolton-Hunter SP were obtained from Amersham, U.K. Drugs were dissolved in distilled water or saline immediately before use.

Statistical analysis

Student's *t* test was used throughout. *P* values <0.05 were considered to be statistically significant.

Results

Monoarthritis-induced hyperalgesia and loss of body weight in rats

In most rats, moderate inflammatory signs occurred 2–4 h after injection and rose quickly to reach the maximum score of 4 after 2–3 weeks. In every animal the inflammatory signs were restricted to the injected paw. The inflamed paw of Freund's adjuvant-treated (CFA) rats exhibited a lower withdrawal latency to thermal stimuli than the contralateral paw of the same animals and both paws of incomplete Freund's adjuvant-treated (IFA) rats (Figure 1). Inflamed paw hyperalgesia was maximal two days after injection, and declined gradually between 7 and 21 days with no evidence of any excitability of withdrawal reflexes after 28 days (Figure 1). It is worth noting that 21 days after injection, the contralateral paw of CFA rats also showed a significant hyperalgesia. Of course, when the degree of inflammation was so high to cause loss of use of the limb, paw withdrawal latency was not measured.

As expected, CFA rats lost body weight immediately after induction of inflammation and then gained less weight than control rats (IFA) (Figure 1 insert).

Electrically-evoked SP-LI release from the spinal cord of monoarthritic rats

After rats were tested for their threshold to thermal stimuli, their spinal cords were isolated to measured SP-LI release. Electrical stimulation (20 V, 0.5 ms, 1 Hz) of the dorsal roots for 8 min induced a significant release of substance P-like immunoreactivity (SP-LI), which was approximately twice the basal level, from rat spinal cord slices. This evoked release was Ca^{2+}-dependent and inhibited by tetrodotoxin (1 μM) as previously described (Malcangio & Bowery, 1993; 1994) (data not shown).

Electrical stimulation of the dorsal roots attached to control rat isolated spinal cord slices induced a significant increase (174 ± 18% of basal outflow which was 30.4 ± 3.1 fmol per fraction 8 ml^{-1}) in SP-LI release (Figure 2, open column).

One week after injection of CFA no differences in the amount of SP-LI released from the spinal cord of IFA and CFA rats were detected (Figure 2) whereas after two weeks the spinal cord from CFA-treated rats tended to release more SP-LI than IFA cords. Twenty-one days after injection, the spinal cord of CFA rats released significantly more peptide compared to IFA rats (Figure 2). By contrast, four weeks after injection, the release of SP-LI from the spinal cord of CFA rats was almost absent (Figure 2). Basal outflow of SP-LI, total content of SP-LI and SP-LI release induced by capsaicin were unaffected in CFA and IFA rats throughout the 28 days period (Table 1).

Effect of CGP 37642, naloxone and bicuculline on electrically-evoked SP-LI release from monoarthritic rat spinal cord slices

In view of the higher release of SP-LI from CFA spinal cords and the contralateral hyperalgesia which were both detectable 21 days after treatment, all subsequent experiments were performed at this time after injection.

Evoked release of SP-LI from the spinal cord of CFA rats was greatly increased by perfusion with the GABA$_B$ antagonist, CGP 36742 (10 and 100 μM) which did not alter the release from IFA spinal cord. The effect of this drug was dose-dependent, achieving statistical significance at 100 μM (Figure 3). The GABA$_A$ antagonist, bicuculline (100 μM),

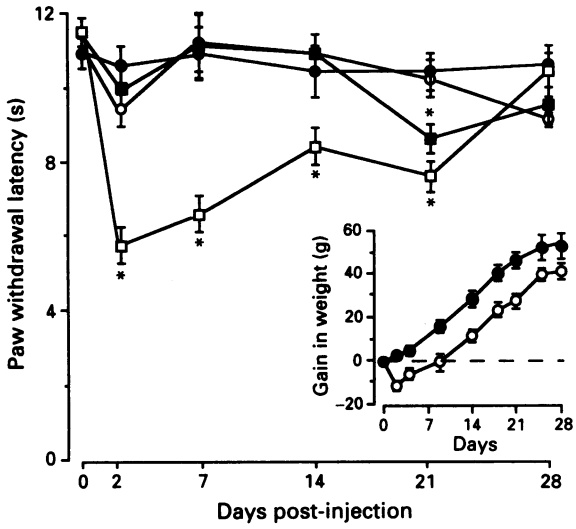


Figure 1 Freund's adjuvant-induced hyperalgesia in the rat paw detected by the paw withdrawal test, and cumulative weight gained by CFA rats and IFA rats (insert). Paw withdrawal latency to radiant heat was measured in the ipsilateral (open symbols) and contralateral (closed symbols) paws of IFA (circles) and CFA (squares) rats, respectively. Insert panel shows the cumulative weight gain in CFA (○) and IFA (●) rats from day 0 to day 28. Values are mean ± s.e.mean of 6–30 rats. *$P<0.05$ CFA ipsilateral vs. IFA ipsilateral (Student's t test).

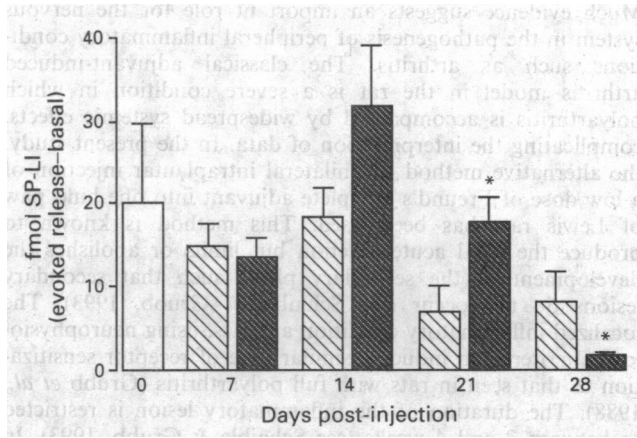


Figure 2 Effect of monoarthritis on substance P-like immunoreactivity (SP-LI) from Lewis rat spinal cord slices. Basal outflow of SP-LI from the spinal cord of saline-injected (open column) IFA (widely hatched column) and CFA (closely hatched column) rats was 36.7 ± 3.0 fmol 8 ml^{-1} per fraction, $n = 61$ (pooled means). SP-LI was released by electrical stimulation of the dorsal roots at 20 V, 0.5 ms, 1 Hz for 8 min. Values are mean ± s.e.mean. $n = 5$ spinal cords for open column, 9 spinal cords for IFA except at 28 days when they were 3; 8 spinal cords for CFA at 7 days; 12 spinal cords for CFA at 14 and 21 days; 3 spinal cords for CFA at 28 days. *$P<0.05$ CFA vs. IFA (Student's t test).

Table 1 Substance P-like immunoreactivity (SP-LI) basal outflow, SP-LI released by capsaicin and SP-LI total content from spinal cord slices of monoarthritic rats

Days after injection	*Injection*	n	*SP-LI basal outflow* (fmol 8 ml^{-1})	*SP-LI released by capsaicin* (1 μM) (fmol 8 ml^{-1})	*SP-LI total content* (fmol mg^{-1} tissue)
21	PBS	5	30.3 ± 3.1	110.8 ± 29.7	64.0 ± 11.0
7	IFA	6	34.7 ± 5.7	216.7 ± 82.5	103.0 ± 40.8
7	CFA	6	38.0 ± 7.3	214.0 ± 57.0	76.4 ± 5.4
14	IFA	9	42.2 ± 5.6	156.5 ± 40.8	84.6 ± 5.8
14	CFA	8	36.4 ± 4.4	146.6 ± 28.9	83.1 ± 13.8
21	IFA	9	38.2 ± 3.9	166.9 ± 72.0	56.4 ± 9.7
21	CFA	12	37.1 ± 3.5	156.7 ± 44.0	57.2 ± 3.8
28	IFA	3	30.9 ± 2.3	144.7 ± 53.1	78.4 ± 5.1
28	CFA	3	33.6 ± 0.3	100.3 ± 24.1	78.1 ± 9.0

Lewis rats were injected intradermally with 100 μl phosphate-buffered saline (PBS), complete or incomplete Freund's adjuvant (CFA or IFA) in the left hind paw. Their spinal cords were excised after the period indicated. SP-LI basal outflow was calculated as the mean of the first three 8 ml fraction collected before stimulation. Capsaicin (1 μM) was perfused over the spinal cord slices at the end of each experiment for 2 min out of 8 min collection time. Data are mean ± s.e.mean.

failed to enhance the peptide release from either the CFA or IFA rat spinal cord removed 21 days after injection (Figure 3). Naxolone (1 μM) increased the peptide release from both IFA and CFA spinal cord to the same extent (Figure 3) as well as from naive rat spinal cord (330 ± 157% of control evoked release, $n = 3$, $P < 0.05$).

Effect of CGP 37642 on monoarthritis-induced hyperalgesia

On the 21st day after injection, intraperitoneal injection of the $GABA_B$ antagonist, significantly decreased the withdrawal latency of both inflamed and contralateral paw of CFA rats up to 45 min after treatment (Figure 4a). CGP 36742 was not hyperalgesic in IFA rats (Figure 4a). The $GABA_B$ agonist, (−)-baclofen, could reverse the hyperalgesia in the inflamed paw but a high dose of 3 mg kg^{-1} was necessary to raise the paw withdrawal latency from 5.2 ± 0.8 s to 8.2 ± 0.5 s ($n = 6$, $P < 0.05$, Student's t test). Naloxone (3 mg kg^{-1}) did not modify monoarthritis-induced hyperalgesia (Figure 4b).

Discussion

Much evidence suggests an important role for the nervous system in the pathogenesis of peripheral inflammatory conditions such as arthritis. The classical adjuvant-induced arthritis model in the rat is a severe condition in which polyarthritis is accompanied by widespread systemic effects, complicating the interpretation of data. In the present study, the alternative method of unilateral intraplantar injection of a low dose of Freund's complete adjuvant into one hind paw of Lewis rats has been used. This method is known to produce the local acute reaction but limits or abolishes the development of the secondary phase such that secondary lesions do not occur (see Schaible & Grubb, 1993). The localized inflammatory condition appears, using neurophysiological criteria, to induce a similar type of receptor sensitization to that seen in rats with full polyarthritis (Grubb *et al.*, 1988). The duration of the inflammatory lesion is restricted to between 2 and 4 weeks (see Schaible & Grubb, 1993). In the present work, the injection of Freund's adjuvant in one paw led to a unilateral, localized inflammation which reached its peak between 2 and 3 weeks, as already reported (Stein *et al.*, 1988; Donaldson *et al.*, 1993).

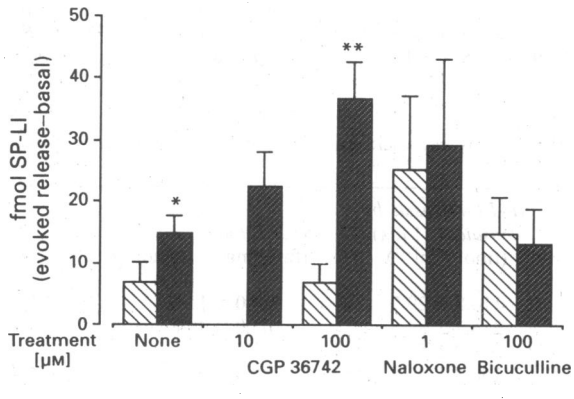


Figure 3 Effect of CGP 36742, naloxone and bicuculline on electrically-evoked substance P-like immunoreativity (SP-LI) release from the spinal cord of IFA and CFA rats. Basal outflow of SP-LI from IFA (widely hatched column) and CFA (closely hatched column) rat spinal cord slices was 6.5 ± 1.5 fmol 8 ml^{-1} per fraction, $n = 26$. Drugs were perfused 5 min prior to and during stimulation (20 V, 0.5 ms, 1 Hz for 8 min). Values are mean ± s.e.mean of 3–4 slices for each group. *$P < 0.01$ CFA in absence vs presence of drug (Student's t test).

Onset of monoarthritis-induced hyperalgesia in rats detected by the plantar test

Animals inoculated with Freund's adjuvant showed the decrease in threshold for nociceptive reflexes already observed in polyarthritic rats (Millan *et al.*, 1987) and rats bearing a carrageenin-induced hindlimb inflammation (Hargreaves *et al.*, 1988). Initial inflammation-induced elevation of paw threshold to heat, declined in the course of 4 weeks; thus it followed neither the time course nor the peak of severity of inflammation. This finding is consistent with data obtained in monoarthritic rats followed for only 1 week (Millan *et al.*, 1988). Interestingly, a significant hyperalgesia was also detected at the level of the contralateral paw, 3 weeks after treatment. This might suggest a spread of the inflammation even though no other major signs, like redness or swelling of the paw, were observed. It has been previously shown that the inflammatory process could, even within one week, significantly influence vascular responses and blood flow in the knee joint (Lam & Ferrell, 1993) involving alteration in sympathetic and neuropeptidergic actions (McDougall *et al.*, 1994). The inflammation induced by a low dose of Freund's adjuvant in the present study, would have very likely affected the blood flow in the inflamed paw and changed the skin temperature. However, in carrageenin-induced inflammation it has been demonstrated that the treated paw local erythema

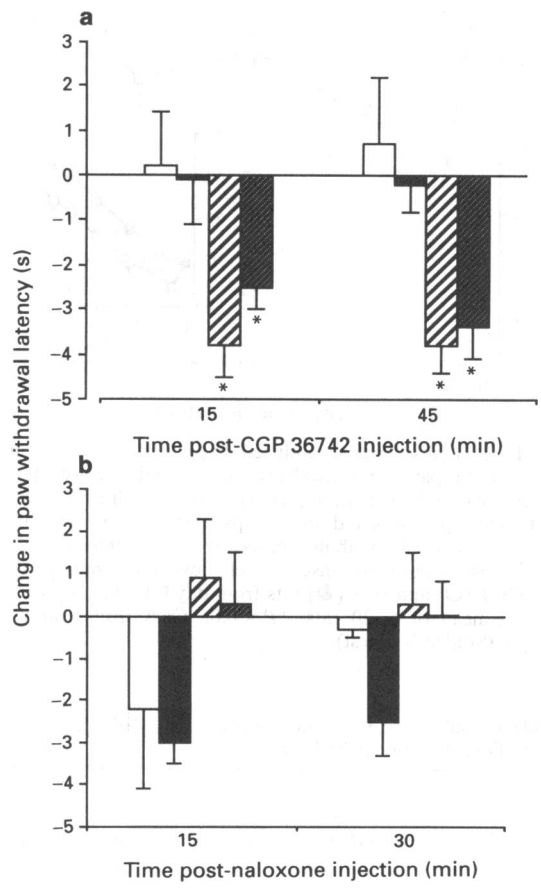


Figure 4 Effect of CGP 36742 (a) and naloxone (b) on monoarthritis-induced hyperalgesia. CGP 36742 (100 mg kg^{-1}, i.p.) and naloxone (3 mg kg^{-1}, i.p.) were injected to all rats immediately after determination of pre-injection paw withdrawal latency. Paw withdrawal latency was subsequently measured at 15 and 45 min after injection of CGP 36742 and at 15 and 30 min after injection of naloxone. Pre-injection values were subtracted from the 15, 30 and 45 min values and data are mean ± s.e.mean of 6 rats per group. Key to histograms: Contralateral paw IFA (open column); ipsilateral paw IFA (solid column); contralateral paw CFA (widely hatched column); ipsilateral paw CFA (closely hatched column). *$P < 0.05$ CFA vs. IFA (Student's t test).

and hypothermia, do not contribute to the decrease in paw withdrawal latency observed after carrageenin (Hargreaves *et al.*, 1988).

Monoarthritic rats displayed a diminished rate of body weight gain which is also normally observed in polyarthritic rats and could be due to factors released during stress like β-endorphin and corticotropin-releasing factor (Morley *et al.*, 1985) or simply to the fact that the motor activity which is required to obtain food causes discomfort and thus, the animals avoid such activities.

SP-LI release from the spinal cord of monoarthritic rats in vitro

Spinal cord slices from CFA rats released more SP-LI than those from IFA rats after electrical stimulation of the dorsal roots whereas the basal outflow of the peptide remained constant irrespective of treatment. However, the increase in SP-LI release was significant only 21 days after the treatment. By contrast, four weeks after injection, the release of SP-LI from the spinal cord of CFA rats was almost absent. This latter observation is in line with a previously reported decrease in the density of SP immunoreactive nerves in rat dorsal horn four weeks after induction of inflammation (Mapp *et al.*, 1993). The failure to detect SP-LI release earlier than 2–3 weeks after induction of monoarthritis, is in agreement with the delayed release of SP from the spinal cord of anaesthetized rats with an acute inflammation of the joint (Schaible *et al.*, 1990). This delay was suggested to be due to the period that fibres, which release the peptide, require to be sensitized by inflammatory mediators before they can be excited by joint stimuli (Schaible *et al.*, 1990).

On the basis of recent reports (Oku *et al.*, 1987; Schaible *et al.*, 1990; Kar *et al.*, 1991; Smith *et al.*, 1992), we were expecting a more pronounced release of SP-LI from the spinal cord of CFA rats. For example, it has been reported that in polyarthritic rats even spontaneous, basal release of SP from the dorsal horn exceeded that of control rats (Oku *et al.*, 1987). In our study, only one in 141 rats showed clear signs of polyarthritis, 21 days after injection. The spinal cord slice excised from this rat released the largest amount of SP-LI after electrical stimulation of the dorsal roots (759% of IFA evoked release) of any of the CFA rats, however, the basal outflow of the peptide was in the same range as controls. The lower increase in the amount of the peptide released by CFA cords might be attributed to the lesser severity of the monoarthritis model compared to polyarthritis. However, in view of the rapid reduction from the initial hyperalgesia developed in the chronically inflamed paw, we considered whether inhibitory influences develop rapidly within the spinal cord in response to chronic inflammation to reduce the release of the nociceptive peptide. The rapid rise in the threshold to heat does not appear to be opioid-mediated (Millan *et al.*, 1987; 1988).

Effect of GABAergic antagonists and naloxone on SP-LI release and monoarthritis-induced hyperalgesia at 21 days after treatment

The inhibitory neurotransmitter GABA is highly concentrated in interneurones of the superficial dorsal horn (Magoul *et al.*, 1987; Todd & McKenzie, 1989) which is also the main site of termination of the unmyelinated (C) fibres, containing SP (Hokfelt *et al.*, 1975), and of small myelinated (Aδ) fibres. Both of these systems convey nociceptive inputs arising in the periphery (see Perl, 1984). GABA levels increase 2–3 weeks after induction of monoarthritis and this has been attributed either to an enhancement of its synthesis or to a reduced release of the neurotransmitter (Castro-Lopes *et al.*, 1992). GABA can inhibit SP-LI release from rat spinal cord (Malcangio & Bowery, 1993), thus antagonists of both $GABA_A$ and $GABA_B$ receptors were tested in the paw withdrawal test and on SP-LI release from the spinal cord 21 days after injection. Evoked release of SP-LI from the spinal cord of CFA rats was greatly increased by perfusion with the $GABA_B$ antagonst, CGP 36742 (Olpe *et al.*, 1993). The range of CGP 36742 concentrations used in the present study has already been shown to antagonize the inhibition of electrically-evoked SP-LI release induced by either GABA or the $GABA_B$ agonist (−)-baclofen and not to modify the basal outflow of peptide (Malcangio & Bowery, 1993). Thus, the effect of CGP 36742 could be assumed to be due to blockade of $GABA_B$ receptors. The $GABA_B$ antagonist-induced release of SP-LI from monoarthritic rat spinal cord correlated with the potentiation of the paw hyperalgesia. CGP 36742 was not hyperalgesic in IFA rats, whereas it significantly decreased the withdrawal latency of both the inflamed and contralateral paw of CFA rats. The lack of any behavioural effect of the $GABA_B$ antagonist in control rats is not surprising (Olpe *et al.*, 1993) and augurs well for possible therapeutic use since adverse effects may be limited (Bowery, 1993). The $GABA_B$ agonist, (−)-baclofen, could reverse the hyperalgesia in the inflamed paw but a high dose of 3 mg kg^{-1} was necessary to raise the paw withdrawal latency. Chronically inflamed rats were less sensitive to the antinociceptive effect of baclofen than animals subjected to acute pain.

The $GABA_A$ antagonist, bicuculline, failed to enhance the peptide release from either the CFA or IFA rat spinal cord, thus supporting the concept that $GABA_A$ receptors are unlikely to mediate the GABA control of SP-LI release from primary afferent terminals either in normal rats (Malcangio & Bowery, 1993) or in rats with chronic inflammatory pain.

It has been reported that rats with unilateral chronic inflammation of the paw developed a supersentivity to morphine in the paw pressure withdrawal test (Kayser & Guilbaud, 1983; Millan *et al.*, 1988) even though naloxone is inactive in polyarthritic rats (Millan *et al.*, 1987) and unilaterally inflamed rats at 1 week (Millan *et al.*, 1988). As a consequence we tested the effect of naloxone on electrically-evoked SP-LI release. This drug was not specific in its action, increasing the peptide release from both IFA and CFA spinal cord to the same extent as well as from naive rat spinal cord. Furthermore, in contrast to the $GABA_B$ antagonists but in line with previous studies (Millan *et al.*, 1987; 1988), naloxone did not modify monoarthritis-induced hyperalgesia. These observations, support the concept of a role for opioids in the control of SP release from primary afferent fibres (Mudge *et al.*, 1979; Cesselin *et al.*, 1984; Go & Yaksh, 1987), and also support the idea that this system is not specifically activated when chronic pain develops (Przewlocka *et al.*, 1992; Millan *et al.*, 1987; 1988). On the contrary, it would seem that the GABAergic system within the spinal cord, during chronic pain, might be activated to counteract pain sensation. In our model it seems very likely that a tonic GABAergic control is activated in CFA rats since the selective block of $GABA_B$ receptors caused a significant increase in the release of SP from primary afferent fibres of monoarthritic rats coupled with an intense hyperalgesia. This could explain the low efficacy of baclofen as a therapeutic analgesic in chronic pain despite its effectiveness in acute pain models (Malcangio *et al.*, 1991) and in trigeminal neuralgia in man (Fromm & Terence, 1987). Thus activation of the GABAergic system which is strongly activated as a consequence of chronic pain would be expected to be little affected by the addition of a GABA agonist.

Conclusions

In conclusion, the induction of chronic inflammation appears to activate the GABAergic system within the spinal cord to counteract pain sensation. This increases presynaptic inhibition of the primary afferent input to the dorsal spinal cord via $GABA_B$ receptors reducing the sensation of painful stimuli. This endogenous pathological activation of $GABA_B$

receptors could explain the weak analgesic activity of baclofen in human chronic pain, and further information about this mechanism may provide a basis for a novel approach to alternative pain therapy.

We thank the Arthritis and Rheumatism Council for financial support (GRANT B 0196) and CIBA-Geigy for CGP 36742 and (−)-baclofen. We also thank Steve Coppard, Dave Zeraschi and Donna Howell for technical assistance.

References

BOWERY, N.G. (1993). $GABA_B$ receptor pharmacology. *Annu. Rev. Pharmacol. Toxicol.*, **33**, 109–147.

CASTRO-LOPES, J.M., TAVARES, I., TOLLE, T.R., COITO, A. & COIMBRA, A. (1992). Increase in GABAergic cells and GABA levels in the spinal cord in unilateral inflammation of the hindlimb of the rat. *Eur. J. Neurosci.*, **4**, 296–301.

CESSELIN, F., BOURGOIN, S., ARTAUD, F. & HAMON, M. (1984). Basic and regulatory mechanisms of *in vitro* release of Met-enkephalin from the dorsal zone of the rat spinal cord. *J. Neurochem.*, **43**, 763–773.

COLPAERT, F.C. (1987). Evidence that adjuvant arthritis in the rat is associated with chronic pain. *Pain*, **28**, 201–222.

DONALDSON, L.F., SECKL, J.R. & MCQUEEN, D.S. (1993). A discrete-induced monoarthritis in the rat: effects of adjuvant dose. *J. Neurosci. Methods*, **49**, 5–10.

FROMM, G.H. & TERENCE, C.F. (1987). Comparison of L-baclofen and racemic baclofen in trigeminal neuralgia. *Neurology*, **37**, 1725–1728.

GO, V.L.W. & YAKSH, T.L. (1987). Release of substance P from the cat spinal cord. *J. Physiol.*, **391**, 141–167.

GRUBB, B.D., MCQUEEN, D.S., IGGO, A., BIRRELL, G.J. & DUTIA, M.B. (1988). A study of 5-HT-receptors associated with afferent nerves located in normal and inflamed rat ankle joints. *Agents Actions*, **25**, 216–218.

HARGREAVES, K., DUBNER, R., BROWN, F., FLORES, C. & JORIS, J. (1988). A new and sensitive method for measuring thermal nociception in cutaneous hyperalgesia. *Pain*, **32**, 77–88.

HOKFELT, T., KELLERTH, J.O., NILSSON, G. & PERNOW, B. (1975). Substance P: localization in the central nervous system and in some primary sensory neurons. *Science*, **190**, 889–890.

KAR, S., GIBSON, S.J., REES, R.G., JURA, W.G.Z.O., BREWERTON, D.A. & POLAK, J.M. (1991). Increased calcitonin-gene-related peptide (CGRP), substance P and enkephalin immunoreactivities in dorsal spinal cord and loss of CGRP-immunoreactive motoneurons in arthritic rats depend on intact peripheral nerve supply. *J. Mol. Neurosci.*, **3**, 7–18.

KAYSER, V. & GUILBAUD, G. (1983). The analgesic effects of morphine, but not those of the enkephalinase inhibitor thiorphan, are enhanced in arthritic rats. *Brain Res.*, **267**, 131–138.

LAM, F.Y. & FERRELL, W.R. (1993). Acute inflammation in the rat knee joint attenuates sympathetic vasoconstriction but enhances neuropeptide-mediated vasodilatation assessed by laser doppler perfusion imaging. *Neuroscience*, **52**, 443–449.

LEVINE, J.D., CLARK, R., DEVOR, M., HELMS, C., MOSKOWITZ, M.A. & BASBAUM, A.I. (1984). Intraneuronal substance P contributes to the severity of experimental arthritis. *Science*, **226**, 547–549.

MAGOUL, R., ONTENIENTE, B., GEFFARD, M. & CALAS, S. (1987). Anatomical distribution and ultrastructural organization of the GABAergic system in the rat spinal cord. An immunocytochemical study using anti-GABA antibodies. *Neuroscience*, **20**, 1001–1009.

MALCANGIO, M. & BOWERY, N.G. (1993). γ-Aminobutyric $acid_B$, but not γ-aminobutyric $acid_A$ receptor activation, inhibits electrically-evoked substance P-like immunoreactivity from rat spinal cord in vitro. *J. Pharmacol. Exp. Ther.*, **266**, 1490–1496.

MALCANGIO, M. & BOWERY, N.G. (1994). Effect of the tachykinin antagonists, RP 67580 and SR 140333, on electrically-evoked substance P release from rat spinal cord. *Br. J. Pharmacol.*, **113**, 635–646.

MALCANGIO, M., GHELARDINI, C., GIOTTI, A., MALMBERG-AIELLO, P. & BARTOLINI, A. (1991). CGP 35348, a new $GABA_B$ antagonist, prevents antinociception and muscle-relaxant effect induced by baclofen. *Br. J. Pharmacol.*, **103**, 1303–1308.

MAPP, P.I., TERENGH, G., WALSH, D.A., CHEN, S.T., CRUWYS, S.C., GARRETT, N., KIDD, B.L., POLAK, J.M. & BLAKE, D.R. (1993). Monoarthritis in the rat knee induces bilateral and time-dependent changes in substance P and calcitonin gene-related peptide immunoreactivity in the spinal cord. *Neuroscience*, **57**, 1091–1096.

MCDOUGALL, J.J., KARIMIAN, S.M. & FERRELL, W.R. (1994). Alteration of substance P-mediated vasodilatation and sympathetic vasoconstriction in the rat knee joint by adjuvant-induced inflammation. *Neurosci. Lett.*, **174**, 127–129.

MILLAN, M.J., CZLONKOWSKI, A., MORRIS, B., STEIN, C., ARENDT, R., HUBER, A., HOLLT, V. & HERZ, A.J. (1988). Inflammation of the hind limb as a model of unilateral, localized pain: influence on multiple opioid systems in the spinal cord of the rat. *Pain*, **35**, 299–312.

MILLAN, M.J., CZLONKOWSKI, A., PILCHER, C.W.T., ALMEIDA, O.F.X., MILLAN, M.H., COLPAERT, F.C. & HERZ, A. (1987). A model of chronic pain in the rat: functional correlates of alterations in the activity of opioid system. *J. Neurosci.*, **7**, 77–87.

MINAMI, M., KURAISHI, Y., KAWAMURA, M., YAMAGUCHI, T., MASU, Y., NAKANISHI, S. & SATOH, M. (1989). Enhancement of preprotachykinin in the rat spinal cord: possible involvement of substance P-containing spinal neurons in nociception. *Neurosci. Lett.*, **98**, 105–110.

MORLEY, J.E., BARTNESS, T.J., GOSNELL, B.A. & LEVINE, A.S. (1985). Peptidergic regulation of feeding. *Int. Rev. Neurobiol.*, **27**, 207–298.

MUDGE, A.W., LEEMAN, S.E. & FISCHBACH, G.D. (1979). Enkephalin inhibits release of substance P from sensory neurons in culture and decreases action potential duration. *Proc. Natl. Acad. Sci. U.S.A.*, **76**, 526–530.

OKU, R., SATOH, M. & TAGAKI, H. (1987). Release of substance P from the spinal dorsal horn is enhanced in polyarthritic rats. *Neurosci. Lett.*, **74**, 315–319.

OLPE, H.-R., STEIMANN, M.W., FERRAT, T., POZZA, M.F., GREINER, K., BRUGGER, F., FROESTL, W., MICKEL, S.J. & BITTIGER, H. (1993). The actions of orally active $GABA_B$ receptor antagonists on GABAergic transmission in vivo and in vitro. *Eur. J. Pharmacol.*, **233**, 179–186.

PERL, E.R. (1984). Characterization of nociceptors and their activation of neurons in the superficial dorsal horn: first step for the sensation of pain. In *Neuronal Mechanism of Pain*. ed. Kruger, L. & Liebeskin, J.C. Vol. 6, pp. 23–51. New York: Raven Press.

PERLIK, F. & ZIDEK, Z. (1973). Breeding experiments on the frequency of adjuvant arthritis in the rat. *Ann. Rheum. Dis.*, **32**, 72–74.

PRZEWLOCKA, B., LASON, W. & PRZEWLOCKI, R. (1992). Time-dependent changes in the activity of opioid systems in the spinal cord of monoarthritic rats – a release and *in situ* hybridization study. *Neuroscience*, **46**, 209–216.

SAWYNOK, Y. (1987). GABAergic mechanism of analgesia: an update. *Pharmacol. Biochem. Behav.*, **26**, 463–474.

SCHAIBLE, H.-S. & GRUBB, B.D. (1993). Afferent and spinal mechanism of joint pain. *Pain*, **55**, 5–54.

SCHAIBLE, H.-S. & JARROTT, B., HOPE, P.J. & DUGGAN, A.W. (1990). Release of immunoreactive substance P in the spinal cord during development of acute arthritis in the knee joint of the cat: a study with antibody microprobes. *Brain Res.*, **529**, 214–223.

SCHAIBLE, H.-S. & SCHMIDT, R.F. (1988). Time course of mechanosensitivity changes in articular afferents during a developing experimental arthritis. *J. Neurophysiol.*, **60**, 2180–2195.

SLUKA, K.A., DOUGHERTY, P.M., OKIN, L.S., WILLIS, W.D. & WESTLUND, K.N. (1992). Neuronal changes in acute arthritis in monkeys III. Changes in substance P, CGRP and glutamate in the dorsal horn of the spinal cord. *Brain Res. Rev.*, **17**, 29–38.

SMITH, G.P., HARMAR, A.J., MCQUEEN, D.S. & SECKL, J.R. (1992). Increase in substance P and CGRP, but not somatostatin, content of innervating dorsal root ganglia in adjuvant monoarthritis in the rat. *Neurosci. Lett.*, **137**, 257–260.

STEIN, C., MILLAN, M.J. & HERZ, A. (1988). Unilateral inflammation of the hindpaw in rats as a model of prolonged noxious stimulation: alterations in behaviour and nociceptive threshold. *Pharmacol. Biochem. Behav.*, **31**, 445–451.

TODD, A.J. & MCKENZIE, J. (1989). GABA-immunoreactive neurons in the dorsal horn of the rat spinal cord. *Neuroscience*, **31**, 799–806.

WILSON, P.R. & YAKSH, A. (1978). Baclofen is antinociceptive in the spinal intrathecal space of animals. *Eur. J. Pharmacol.*, **51**, 323–330.

(Received June 24, 1994
Revised September 7, 1994
Accepted September 9, 1994)

Br. J. Pharmacol. (1994), **113**, 1567–1573 © Macmillan Press Ltd, 1994

The role of nitric oxide, adrenergic activation and kinin-degradation in blood pressure homeostasis following an acute kinin-induced hypotension

Anniken Bjørnstad-Østensen & [1]Torill Berg

Department of Physiology, Institute of Basic Medical Sciences, Medical faculty, University of Oslo, Blindern, 0317 Oslo, Norway

1 Nitric oxide (NO) has been suggested as the mediator of the vascular response to bradykinin. In the present study, we found that NO did not mediate the hypotensive response to bradykinin. In addition, the significance of kininase II in terminating a kinin-induced hypotension and the role of the adrenergic system in compensating for the acute fall in blood pressure (BP) was established.

2 In normal rats, the NO-synthase inhibitor Nω-nitro-L-arginine methyl ester (L-NAME) induced a rise in basal BP ($\Delta BP = 40 \pm 6$ mmHg, $P < 0.0014$) which was not altered by pretreatment with phentolamine ($\Delta BP = 50 \pm 6$ mmHg, NS). L-NAME did not attenuate the acute fall in BP in response to bradykinin (3–30 $\mu g\,kg^{-1}$) or kallikrein (6–300 $\mu g\,kg^{-1}$). However, a significant decrease was observed in the duration of the hypotensive response ($P < 0.027$). This shorter duration was not observed after pretreatment with phentolamine in addition to L-NAME. Phentolamine alone prolonged the hypotensive response to bradykinin ($P < 0.04$). These experiments confirm the role of NO-formation as a hypotensive component in BP homeostasis but not the role of NO as a mediator in kinin-induced hypotension. It further shows that the continuous NO-release also impedes the compensatory adrenergic hypertensive response following the acute fall in BP induced by bradykinin.

3 The hypertensive respose to intravenously administered phenylephrine was found to be unchanged by preadministration of L-NAME (NS) thus showing that L-NAME did not change the sensitivity to the adrenergic response. In a separate protocol on L-NAME-treated rats we found no difference in heart rate (NS) during the recovery period following bradykinin before as compared to after administration of phentolamine. It was therefore concluded that the observed alterations in the duration of the hypotensive response were most probably due to changes in peripheral vascular resistance.

4 To confirm further that NO is not a mediator in kinin-induced hypotension, we used an experimental model where the response to bradykinin was prolonged by preventing kinin degradation by kininase II-converting enzyme inhibitor (CEI). To produce a hypotensive response purely dependent on kinin, the studies were performed after removal of the renin-angiotensin system by nephrectomy (Nx). In this model, bradykinin (6 $\mu g\,kg^{-1}$, i.v.) induced a prolonged hypotensive response. Pretreatment with L-NAME did not alter the magnitude or the progression of the hypotensive response to bradykinin, thus confirming that NO was not a mediator in BK-induced hypotension.

5 To study the mechanisms involved in terminating the hypotensive response to bradykinin, the results from the Nx CEI-treated rats were compared with Nx animals not treated with CEI. In the latter group, bradykinin induced a short hypotensive response, i.e. 0.5 ± 0.1 min as compared to the 17 ± 1 min after CEI ($P < 0.003$). After kininase II-inhibition (and L-NAME), BP recovery was totally dependent on the adrenergic system, since phentolamine prevented a recovery in BP during the experimental period ($P < 0.01$, compared to the CEI/L-NAME group). These results demonstrate the importance of kininase II as the major agent in terminating a bradykinin-induced hypotension, whereas the adrenergic system plays a small, although significant role in compensating for the fall in BP. The continuous release of NO therefore not only lowers basal BP but also impedes the compensatory adrenergic response.

Keywords: Bradykinin; kallikrein; EDRF; NO, NO-synthase antagonist; sympathetic nervous system; blood pressure regulation; converting enzyme inhibitor; kininase II

Introduction

Bradykinin is a potent vasodilator peptide released by kallikrein (E.C. 3.4.21.35) from the precursor kininogen. Recent studies strongly indicate that kinin participates in the control of blood pressure (BP) (Kiowski *et al.*, 1992; Cachofeiro *et al.*, 1992; Pellacani *et al.*, 1992). It has been suggested that the hypotensive effect of bradykinin is mediated through the release of endothelium-derived relaxing factor (EDRF) or nitric oxide (NO): bradykinin has been shown to stimulate the release of NO from bovine pulmonary artery endothelial cells (O'Shaughnessy *et al.*, 1992) and from guinea-pig isolated hearts (Kelm & Schrader, 1988). Moreover, experiments in rats demonstrated a shorter hypotensive response to bradykinin after treatment with NO-synthase inhibitor, thus indicating a role of NO in the late phase of bradykinin-induced hypotension (Rees *et al.*, 1990). However, similar results were not obtained by O'Shaughnessy *et al.* (1992), thus questioning the role of NO as a mediator in bradykinin-induced hypotension.

Since BP is the result of the balance between hypotensive and hypertensive systems (Dzau, 1989; Burnstock, 1990), any change in BP may be counteracted and modulated by opposing systems. It is therefore possible that the observed shortening of the hypotensive response to bradykinin in rats treated with NO-synthase inhibitor may be explained by a hampered NO-modulation of a compensatory hypertensive response following an acute fall in BP. In the present work, the role of NO-formation in hypotension induced by bradykinin and

[1] Author for correspondence.

kallikrein was studied in protocols which in addition allowed us to study adrenergic involvement in the BP regulation. The results do not support the concept that bradykinin- and kallikrein-induced hypotension is mediated through NO-formation but indicate that an abbreviated kinin-induced hypotensive response after inhibition of NO-formation is due to the fact that the adrenergic response following the acute fall in blood pressure is no longer impeded by the vasodilator NO-system. Furthermore, the mechanisms involved in terminating the bradykinin-induced hypotension were elucidated.

Methods

Surgical procedures

Male Wistar rats (250–300 g) were anaesthetized with pentobarbitone (70 mg kg^{-1}, i.p., unless otherwise indicated) and tracheotomized. Arterial BP was recorded continuously through a catheter in the femoral artery connected to a Statham strain-gauge transducer and a Hewlett Packard 7402 A recorder. All drugs were administered as bolus injections (0.15 ml, 20 s) through a catheter in the femoral vein, unless otherwise indicated. After each injection, the catheter was flushed with 0.1 ml phosphate-buffered saline (PBS; 0.01 M Na-phosphate, pH 7.4, 0.14 M NaCl).

Experimental design

Protocol 1: The effect of L-NAME on bradykinin- and kallikrein-induced hypotension with and without pretreatment with phentolamine The rats were prepared as described above and divided into four groups: The control group ($n = 6$) received two sham injections of PBS 5 min apart; the second group ($n = 6$) received PBS and L-NAME (0.3 g kg^{-1}) at the same time intervals; the third group ($n = 6$), the α-adrenoceptor antagonist, phentolamine (2 mg kg^{-1}) and L-NAME (0.3 g kg^{-1}); and the fourth group ($n = 6$) received phentolamine (2 mg kg^{-1}) followed by PBS; 15 min later, all animals were given bradykinin (3, 6 and 30 μg kg^{-1}) and kallikrein (6, 30, 60 and 300 μg kg^{-1}) in consecutive injections administered 5 min apart. As a measure of the duration of the hypotensive response to bradykinin and kallikrein, the time when BP had returned to 75% of the maximum fall was recorded.

Protocol 2: The effect of L-NAME on the sensitivity to phenylephrine An experimental group ($n = 8$) and a control group ($n = 8$) received L-NAME (0.3 g kg^{-1}) or a sham injection with PBS, respectively; 15 min later, all rats received phenylephrine (0.3, 3, 13, 25, 50 and 150 μg kg^{-1}, 0.1 ml) injected 5 min apart, and the hypertensive response was recorded for each dose.

Protocol 3: The effect of bradykinin on heart rate before and after administration of phentolamine in the presence of L-NAME All rats ($n = 6$) were given an initial injection of L-NAME (0.3 g kg^{-1}); 15 min later, they received two injections of bradykinin (6 and 30 μg kg^{-1}) 5 min apart. After another 5 min, the rats were given phentolamine (2 mg kg^{-1}), and after 5 min, the injections of bradykinin were repeated. Heart rate was recorded before bradykinin and during the BP recovery period.

Protocol 4: The effect of L-NAME and phentolamine on bradykinin-induced hypotension in nephrectomized (Nx) rats pretreated with CEI All animals were nephrectomized 24 h prior to the experiment to prevent a hypotensive response due to the renal renin-angiotensin system when the CEI was administered. Binephrectomy was performed through flank incisions during anaesthesia (136 mg kg^{-1} chloralhydrate and 30 mg kg^{-1} pentobarbitone, i.p.). The following day the rats were anaesthetized with pentobarbitone (50 mg kg^{-1}), prepared as described above, and given an initial injection of CEI (10 mg in 0.5 ml 0.45% NaCl). The rats were divided into three groups; the control group ($n = 6$) was given two sham injections with PBS 5 and 20 min after CEI; the second group ($n = 6$) L-NAME (0.3 g kg^{-1}) followed by PBS; and the third group ($n = 6$), L-NAME followed by phentolamine (2 mg kg^{-1}) at the same time intervals. Five minutes later, all rats were given one dose of bradykinin (6 μg kg^{-1}). BP was recorded for another period of 30 min. The order in which L-NAME and phentolamine was administered was altered from that in protocol 1 because the initial BP was lower in Nx than in normal rats. If phentolamine was given first, BP in preliminary experiments was found to drop so low that a proper response to L-NAME and subsequently bradykinin could not be recorded.

Protocol 5: The effect of L-NAME on bradykinin- and kallikrein-induced hypotension with and without pretreatment with phentolamine in Nx rats All animals were nephrectomized 24 h prior to the experiment. On the day of the experiment, the rats were prepared as described above and treated as outlined in protocol 1, except that L-NAME was administered prior to phentolamine in group 3 for the same reasons as given above for protocol 4. Also for the same reasons, the fourth group (phentolamine and PBS) was omitted from this protocol. To determine the hypertensive response which in Nx rats followed the hypotension, the area exceeding the BP level before each injection of bradykinin and kallikrein was determined by computerized planimetry.

Materials

Heparin was obtained from Nycomed, Oslo, Norway; pentobarbitone from The National Hospital, Oslo, Norway; bradykinin acetate salt, N^{ω}-nitro-L-arginine methyl ester (L-NAME), and L-phenylephrine hydrochloride were from Sigma Chemical Co., St. Louis, MO, U.S.A.; Regitin (phentolamine) from Ciba-Geigy, Basel, Switzerland; and captopril (converting enzyme inhibitor, CEI) from Squibb, Princeton, NJ, U.S.A. Kallikrein was purified from the rat submandibular gland as previously described (Johansen *et al.*, 1987).

Statistics

The results are expressed as mean ± s.e.mean. Dose-response relationships were tested by two-way analysis of variance (ANOVA). One-way ANOVA was used to test for differences between the groups in protocol 1 and 5. When differences were observed, Student's two-sample t test were used to determine differences between groups at a particular dose. Student's two-sample t-test was also used to determine differences in heart rate in protocol 3. To analyse for differences between groups in protocol 2 and 4, Analysis of Variance and Covariance with Repeated Measures (BMDP) were used. A P value less than 0.05 was considered significant.

Results

Protocol 1: The effect of L-NAME on bradykinin- and kallikrein-induced hypotension with and without pretreatment with phentolamine

Bradykinin and kallikrein induced an immediate fall in BP which shortly (after 0.5 ± 0.1 min) returned to preinjection levels (Figure 1a). The immediate drop in BP was found to be dose-dependent ($P < 0.01$) and did not differ among the groups with the exception of the phentolamine-only group where the fall in BP in response to bradykinin was significantly less than the other three groups ($P < 0.02$) due to the lower starting BP (Figure 2). A dose-dependency was also

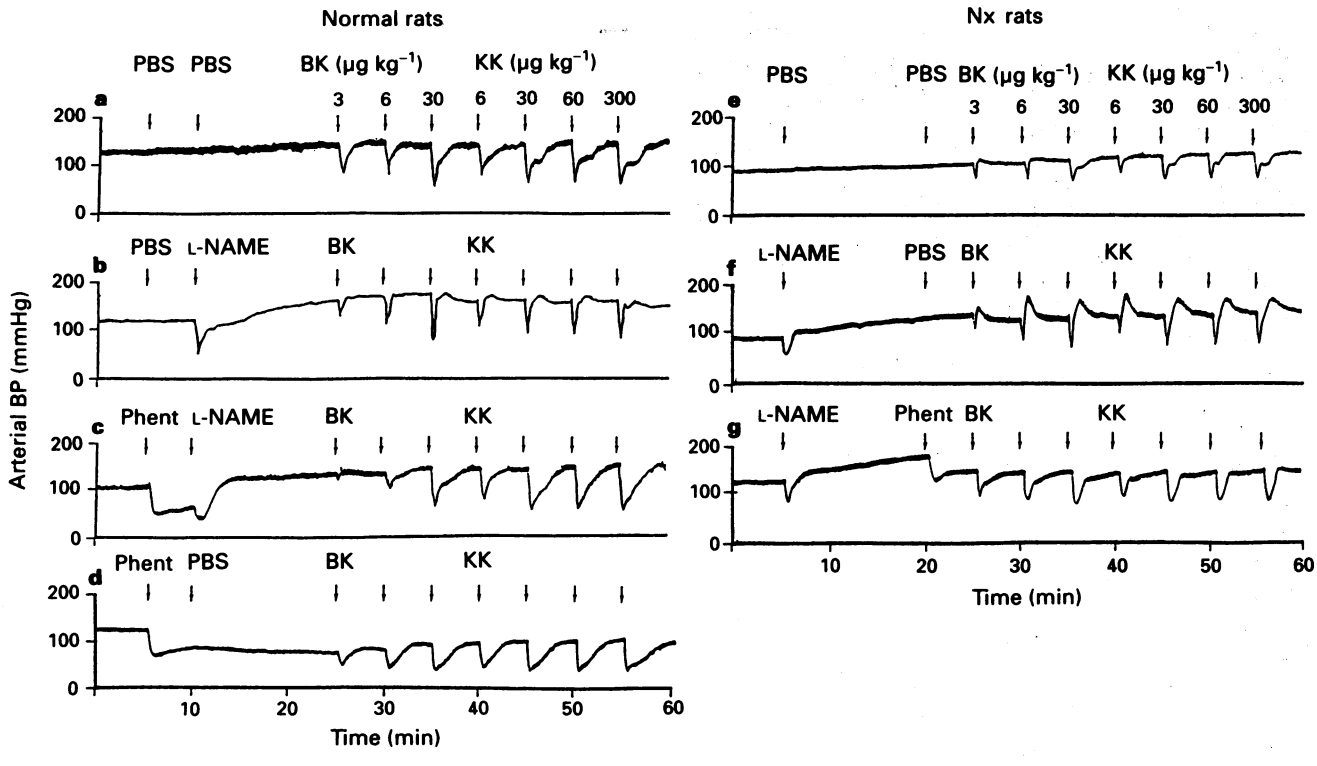


Figure 1 Typical recordings of the haemodynamic response in normal rats (a–d) and nephrectomized (Nx) rats (e–g) to bradykinin (BK) and kallikrein (KK) in a control rat (a and e), N^{ω}-nitro-L-arginine methyl ester (L-NAME)-treated rat (b and f), a rat pretreated with phentolamine (Phent) in addition to L-NAME (c and g), and a rat pretreated with phentolamine only (Phent) (d). L-NAME caused a decrease in the duration of the hypotensive response both in normal and nephrectomized rats, which was abolished by preadministration of phentolamine. In Nx L-NAME rats, hypotension was followed by hypertension which was also abolished by phentolamine.

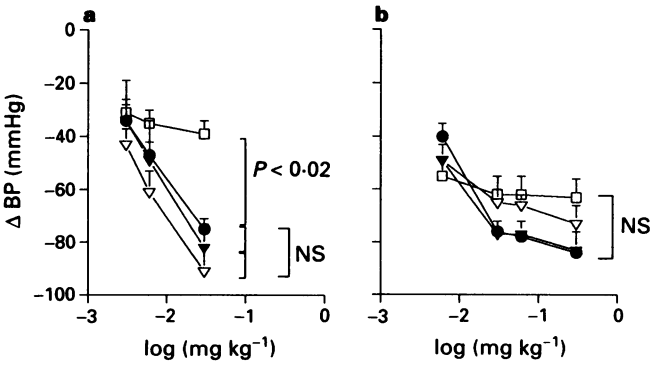


Figure 2 Graph showing the fall in mean arterial blood pressure (ΔBP) in normal rats immediately after administration of bradykinin (3, 6, 30 μg kg^{-1}) (a) or kallikrein (6, 3, 60, 300 μg kg^{-1}) (b) in the control group (●) ($n = 6$), in N^{ω}-nitro-L-arginine methyl ester (L-NAME)-treated rats (▽) ($n = 6$), in rats pretreated with phentolamine in addition to L-NAME (▼) ($n = 6$), and after pretreatment with phentolamine only (□) ($n = 6$). A dose-dependency was observed for all groups ($P < 0.01$). Differences between groups are indicated on the figure.

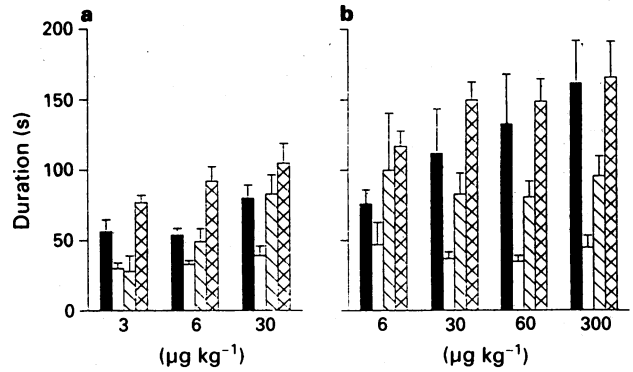


Figure 3 The duration of the hypotensive response in non-nephrectomized animals induced by bradykinin (3, 6, 30 μg kg^{-1}) (a) and kallikrein (6, 30, 60, 300 μg kg^{-1}) (b) in control rats (solid columns) ($n = 6$), in rats treated with N^{ω}-nitro-L-arginine methyl ester (L-NAME) (open columns) ($n = 6$), in rats treated with phentolamine in addition to L-NAME (hatched columns) ($n = 6$), and in rats treated with phentolamine (cross-hatched columns) ($n = 6$). As a measure of the duration of the hypotensive response to bradykinin and kallikrein, the time when BP had returned to 75% of the maximum fall, was recorded. There was a significant decrease in the duration of the hypotensive response in the presence of L-NAME ($P < 0.003$ and $P < 0.027$ respectively), whereas the duration in rats treated with phentolamine and L-NAME was not significantly different from that in the control group (NS). After pretreatment with phentolamine alone there was a significant increase in the duration of the hypotensive response after bradykinin compared to control rats and phentolamine/NAME-treated rats ($P < 0.04$). The same tendency was observed also for kallikrein although the differences were not statistically significant.

observed for the duration of the hypotensive response ($P < 0.03$) (Figure 3). In L-NAME-treated animals, the duration of the bradykinin-induced ($P < 0.003$) and the kallikrein-induced ($P < 0.027$) hypotensive response was significantly shorter than in the control group. However, in the group given phentolamine in addition to L-NAME no significant

difference (NS) was observed compared to the control group (Figure 3). In the fourth group after pretreatment with phentolamine alone, the duration of the hypotensive response to bradykinin was significantly prolonged compared to the control as well as the phentolamine/NAME-treated group ($P<0.04$). The same tendency was observed also after kallikrein although this difference was not statistically significant.

After the administration of L-NAME (group 2), BP increased from 119 ± 4 to 159 ± 5 mmHg ($P<0.001$). Injection of phentolamine (group 3) resulted in an initial fall in BP of 49 ± 6 mmHg ($P<0.0004$), but did not alter the increase in BP induced by the subsequent administration of L-NAME (from 95 ± 5 just prior to and 145 ± 7 mmHg 15 min after L-NAME (NS) compared to the group pretreated with L-NAME only).

Protocol 2: The effect of L-NAME on the sensitivity to phenylephrine

L-NAME did not alter the sensitivity to phenylephrine since there was no significant difference (NS) in the hypertensive response to increasing doses of phenylephrine in rats pretreated with L-NAME as compared to control animals (Figure 4).

Protocol 3: The effect of bradykinin on heart rate before and after administration of phentolamine in the presence of L-NAME

The change in heart rate from before to after injection of bradykinin was not altered by administration of phentolamine in L-NAME-treated rats: The change in heart rate following the first dose of bradykinin was -5 ± 4 strokes min^{-1} before compared to -7 ± 4 strokes min^{-1} after administration of phentolamine, and -4 ± 8 strokes min^{-1} compared to -5 ± 6 strokes min^{-1} for the second bradykinin dose (NS).

Protocol 4: The effect of L-NAME and phentolamine on bradykinin-induced hypotension in Nx rats pretreated with CEI

CEI itself induced a minor fall in BP (-4 ± 3, -2 ± 1 and -3 ± 2 mmHg in the three groups, respectively) (NS) indicating that the renin-angiotensin system had been successfully eliminated. In the control group, injection of bradykinin caused a fall in BP, which returned to pre-bradykinin levels after 17 ± 1 min (Figure 5). Administration of L-NAME induced an elevation of BP from 86 ± 7 to 125 ± 13 mmHg ($P<0.0018$), but the fall in BP in response to bradykinin equalled that of the control rats (NS) (Figure 5). In rats pretreated with phentolamine in addition to L-NAME, BP prior to administration of bradykinin equalled that of control rats (82 ± 8 and 90 ± 3 mmHg, respectively, NS). The immediate drop in BP following bradykinin was equal to that in control rats, whereas, in these rats, BP remained at the minimum value throughout the experimental period, and was in this respect significantly different from both the control and the L-NAME-treated animals ($P<0.01$) (Figure 5).

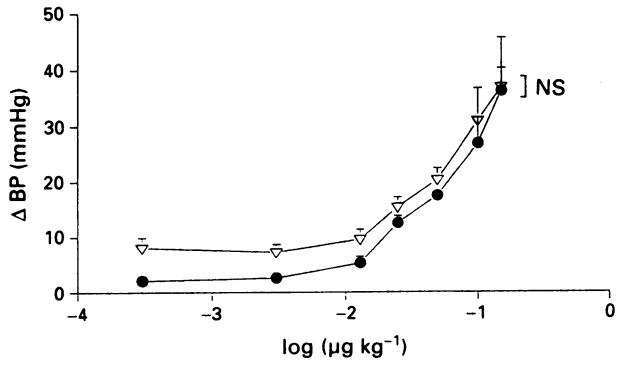


Figure 4 The hypertensive response to increasing doses of phenylephrine in control rats (●) ($n=8$) and N^{ω}-nitro-L-arginine methyl ester (L-NAME)-treated rats (▽) ($n=8$). No significant difference (NS) was observed between the two groups indicating that L-NAME did not change the sensitivity to phenylephrine.

Protocol 5: The effect of L-NAME on bradykinin- and kallikrein-induced hypotension with and without pretreatment with phentolamine in Nx rats

To determine the role of kininase II in terminating a bradykinin-induced hypotension, the response to bradykinin after CEI (protocol 4) was compared to that of the corresponding dose of bradykinin in Nx rats not treated with CEI (protocol 5). The duration of the hypotensive response was clearly longer lasting when kininase II was inhibited by CEI (17 ± 1 min) than without CEI (0.5 ± 0.1 min) ($P<0.003$) (Figures 5 and 1g).

The response pattern in Nx rats not treated with CEI (protocol 5) resembled that of non-Nx rats (protocol 1). In the untreated control group, bradykinin and kallikrein caused a dose-dependent fall in BP ($P<0.001$) and in the duration of the hypotensive response ($P<0.0003$) (Figure 6). However, the duration of the hypotensive response was significantly shorter than in non-Nx rats for bradykinin ($P<0.01$) (Figures 3 and 6). This was also observed for kallikrein, although the difference was not statistically significant. As in non-Nx rats L-NAME-treatment resulted in a shortening of the hypotensive period following kallikrein ($P<0.005$), whereas for bradykinin the same tendency was observed, although the difference was not significantly different from the control group (Figure 6). After administration of phentolamine in addition to L-NAME, we observed a significant prolongation of the hypotensive response as compared to that in the L-NAME-treated animals as well as the control animals ($P<0.017$) (Figure 6). On the other hand, in Nx rats, the hypotension was followed by a short period of hypertension which was enhanced by L-NAME ($P<0.025$) (Figures 1f and 7). This hypertensive response, which was barely observed in normal rats (Figure 1b), was almost totally abolished by phentolamine ($P<0.026$) (Figures 1f and 7).

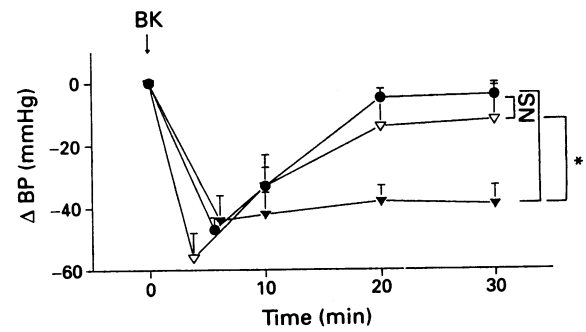


Figure 5 The fall in BP after an intravenous injection of bradykinin ($6\ \mu g\ kg^{-1}$) in nephrectomized rats pretreated with converting enzyme inhibitor (CEI) after a sham injection with vehicle (●) ($n=6$), after L-NAME (▽) ($n=6$), and after L-NAME and phentolamine (▼) ($n=6$). BP prior to administration of bradykinin did not differ significantly in control rats and rats treated with L-NAME and phentolamine, whereas BP in rats treated only with L-NAME was significantly higher ($P<0.02$). In the L-NAME-treated group, the fall in BP to bradykinin paralleled that in control rats (NS). In the group treated with L-NAME and phentolamine, the hypotensive response to bradykinin showed a significantly different development over time from the control group as well as from the L-NAME-treated group (*$P<0.01$). BP in this group remained at the minimum levels throughout the experimental period.

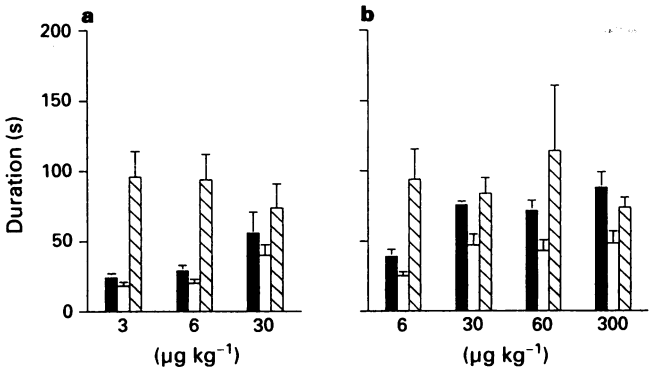


Figure 6 The duration of the hypotensive response in nephrectomized rats induced by bradykinin (3, 6, 30 μg kg^{-1}) and kallikrein (6, 30, 60, 300 μg kg^{-1}) in control rats (solid columns) ($n = 6$), in rats treated with N$^{\omega}$-nitro-L-arginine methyl ester (L-NAME) (open columns) ($n = 6$), and in rats treated with phentolamine in addition to L-NAME (hatched columns) ($n = 6$). As a measure of the duration of the hypotensive response to bradykinin and kallikrein, the time when BP had returned to 75% of maximum fall, was recorded. There was a significant decrease in the duration of the hypotensive response in the presence of L-NAME after injection of kallikrein ($P < 0.005$). This tendency was also observed after injection of bradykinin, although the change was not statistically significant. There was a significant increase in the duration of the hypotensive response after pretreatment with phentolamine in addition to L-NAME compared to both control and L-NAME-treated rats ($P < 0.017$).

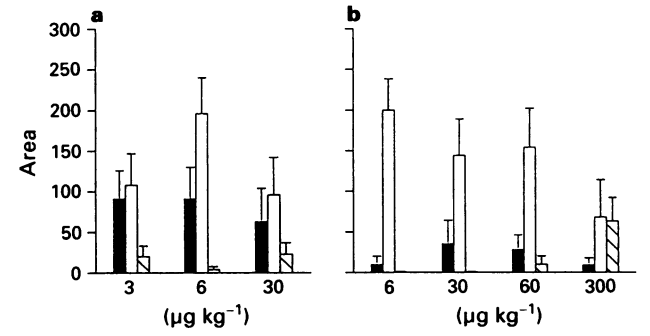


Figure 7 The hypertension following acute hypotension in nephrectomized rats in response to bradykinin (3, 6, 30 μg kg^{-1}) (a) and kallikrein (6, 30, 60, 300 μg kg^{-1}) (b) in control rats (solid columns) ($n = 6$), in rats treated with N$^{\omega}$-nitro-L-arginine methyl ester (L-NAME) (open columns) ($n = 6$), and rats treated with phentolamine in addition to L-NAME (hatched columns) ($n = 6$). The area under the BP curve exceeding the BP level before each injection of bradykinin and kallikrein was measured and determined by computerized planimetry. There was a significant increase in the hypertension following kallikrein-induced hypotension in L-NAME-treated rats compared to control rats ($P < 0.025$). After injection of bradykinin the same tendency was observed, although not statistically significant. Phentolamine almost abolished the hypertensive response ($P < 0.026$).

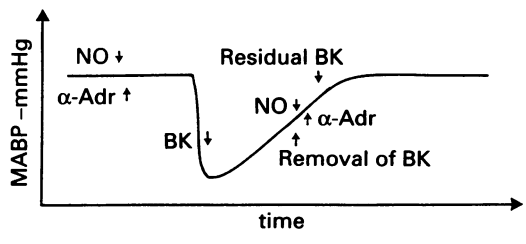


Figure 8 Illustration of the balance between hypotensive and hypertensive systems in the regulation of BP. The present results can easily be explained if the hypotensive response to bradykinin and kallikrein is divided into two phases; a first period where hypotensive systems predominate, in this case by a high concentration of plasma kinin, which is followed by a second period of recovery where hypertensive components, in this case adrenergic activation, takes over while plasma kinin is being removed. The NO system functions as a continuous hypotensive force, and the release of NO is not altered by either the kinin or the adrenergic system.

Discussion

In contrast to previous studies in whole animals, (Whittle *et al.*, 1989; Rees *et al.*, 1990) and what may be deduced from studies on cell cultures (Palmer *et al.*, 1988; Bogle *et al.*, 1991; O'Shaughnessy *et al.*, 1992) and isolated organs (Kelm & Schrader, 1988), the present results do not support a role for NO-formation in bradykinin- or kallikrein-induced hypotension. In studies on acetylcholine- and bradykinin-induced hypotension in rats (Rees *et al.*, 1990) and acetylcholine-induced hypotension in guinea-pig (Aisaka *et al.*, 1989), it was suggested that the hypotension could be divided into two phases, an immediate fall in BP which was resistant to NO-synthase blocker, and a late hypotensive phase which was sensitive to NO-synthase blocker. Although we, like Rees *et al.* (1990) did observe an abbreviation of the hypotensive response after injection of bradykinin in rats treated with L-NAME, we found this effect to be abolished by α-adrenoceptor blockade, thus indicating that NO-release normally modulates the adrenergic recovery response following an acute fall in BP. Furthermore, when the effect of the adrenergic system was removed by phentolamine but with the NO-system intact, a prolonged hypotensive response to bradykinin was observed. The present results can easily be explained if the hypotensive response to bradykinin and kallikrein is not interpreted as two phases of hypotension, but as a first period where hypotensive systems predominate, in this case by a high concentration of plasma kinin, which is followed by a second period of recovery where hypertensive components, in this case adrenergic activation, take over while plasma kinin is being removed (Figure 8). In this balance, the NO-system functions as a continuous hypotensive force not altered by either the kinin or the adrenergic system (Figure 8), and impedes the compensatory adrenergic response following the acute fall in BP. A NO-independent bradykinin-induced relaxation has been demonstrated in isolated coronary arteries of the pig (Kauser & Rubanyi, 1992), which is in agreement with the results of the present study.

To confirm our results that bradykinin-induced hypotension is not mediated through NO-release, we also used an experimental model known to represent a longer-lasting kinin-dependent hypotension, i.e. prevention of degradation of kinin by kininase II (angiotensin converting enzyme) inhibition. To make this a pure kinin-dependent response the influence of the renin-angiotensin sysem was excluded by nephrectomy (Ørstavik *et al.*, 1982). Also in this model, NO-synthase inhibition had no effect on the hypotensive response to bradykinin.

In non-Nx rats, the effect of phentolamine declined (although it was not abolished) by increasing doses of kallikrein but not bradykinin. This observation may be explained by a continuous release of kinin when kallikein was present in the circulation in unphysiologically high concentrations. This would probably result in a prolonged period of high plasma kinin concentration, thus counterbalancing the compensatory hypertensive response for a longer period of time.

It could be argued that the fall and return of BP following an acute injection of bradykinin may be altered by differences in starting BP induced by L-NAME. In this study, the difference in starting BP was eliminated by administration of the α-adrenoceptor blocker, phentolamine in addition to L-NAME, instead of increasing basal BP in the control group by adrenaline (see Rees *et al.*, 1990). If NO were a mediator in bradykinin-induced hypotension, an abbreviated hypotension should also have been expected to occur in this situation, which it did not. Furthermore, it is possible that the discrepancy between the *in vitro* studies showing bradykinin-dependent release of NO in cell cultures (Palmer *et al.*, 1988) and isolated organs (Kelm & Schrader, 1988) and our *in vivo* studies could have been explained by an enhanced adrenergic response due to an increased sensitivity to phenylephrine by L-NAME. However, this possibility was excluded since the

dose-response curve to phenylephrine was not altered by administration of L-NAME.

The present study did not allow us to conclude that the changes in BP were due to alterations in peripheral vascular resistance, since we did not measure cardiac output. However, phentolamine did not result in any change in heart rate during the recovery phase following bradykinin in L-NAME-treated non-nephrectomized rats, and it is therefore likely that the observed changes in BP were indeed a result of altered adrenergic control of peripheral vascular resistance.

Since bradykinin has been shown to be a potent inducer of adrenal gland medullary hormone release (Feldberg & Lewis, 1964), the increased adrenergic activity in L-NAME-treated rats may have been a result of a specific adrenaline release from the adrenal glands and not to adrenal adrenaline or peripheral nerve noradrenaline release induced by the fall in blood pressure as such. However, the recovery in L-NAME-treated rats occurred within 30 s after the injection of bradykinin or kallikrein. It therefore seems likely that the compensatory hypertensive response was induced by noradrenaline released from sympathetic nerves innervating resistance vessels in response to the acute fall in BP, and that this hypertensive response became apparent when it was no longer impeded by NO release. Similar studies with another hypotensive agent such as acetylcholine to test this hypothesis could not be done since the hypotensive effect of acetylcholine is mediated through NO synthesis (Furchgott & Zawadzki, 1980).

These studies also allowed us to draw some conclusions on the mechanisms involved in BP-recovery after a kinin-induced hypotension. In normal rats, the recovery of BP was rapid and only slightly dependent on adrenergic activation. However, BP-recovery was heavily dependent on removal of bradykinin by kininase II/converting enzyme as demonstrated by the markedly prolonged hypotensive response after administration of CEI. This was not due to the use of Nx rats in the latter protocol since the rapid return in BP was also observed in untreated Nx rats. On the other hand, when kininase II was inhibited by CEI in Nx rats, BP-recovery was totally dependent on the adrenergic system. Since a short duration pattern was observed in both Nx and non-Nx rats not treated with CEI, it could be concluded that the kidney was of little importance in the removal of kinin, even though the kidney is one of the richest sources of kininase II (Erdös, 1979). This is in accordance with studies by Ishida *et al.* (1989) showing that nephrectomy did not affect the concentration of endogenous plasma kinins. These results demonstrate that an acute bradykinin-induced hypotension is normally terminated by a rapid removal of the hypotensive agent by kininase II, and that this recovery response is to a small but significant extent enhanced by the adrenergic system (Figure 8).

To our surprise we found that Nx rats (not treated with CEI) seemed to have a stronger adrenergic response than non-Nx rats. This was concluded from the observed shorter duration of the hypotensive response and the subsequent period of overshoot of hypertension in Nx rats; both responses being α-adrenergically dependent since they were blocked by phentolamine. This enhanced adrenergic compensation in Nx rats seemed normally to be modulated and well balanced by the NO-system, since this observation was apparent only after NO-synthase inhibition. This was a side-observation arising from the need of a proper protocol for determining the role of kininase II in BP-recovery, and we have no explanation for why Nx rats should be more adrenergically active than non-Nx rats. However, it is possible that by removing the kidneys, we also removed a hypotensive agent which normally would balance the adrenergic compensatory response. Medullipin, an arachidonic acid metabolite released by the kidney and which functions through the release of NO (Gothberg & Karlstrom, 1991), may be the responsible agent.

As in previous studies (Rees *et al.*, 1990; O'Shaughnessy *et al.*, 1992), the present study showed that inhibition of NO-formation resulted in an elevated basal BP. It has therefore been suggested that basal release of NO may play an important role in BP regulation as a hypotensive system, similar to the role of the sympathetic nervous system in maintaining a vasoconstrictor tone (Figure 8). Since the response to L-NAME was not altered by pretreatment with phentolamine as demonstrated in the present study, the two systems under basal conditions seem to play a role in BP homeostasis independent of each other.

The acute hypotensive effect of bradykinin has also been reported to be mediated through synthesis of prostaglandin E_2 (PGE_2) and the duration of the hypotensive response by PGI_2 synthesis (Türker *et al.*, 1982). However, our experimental setup was identical to that of Rees *et al.* (1990), except that in their studies all rats were pretreated with indomethacin, and the hypotensive response to bradykinin as observed by Rees *et al.* (1990) was similar to that observed by us. Prostaglandins are therefore not likely to play a role in the observed hypotensive effect of bradykinin.

In conclusion, in spite of previous suggestions, the present results clearly demonstrate that NO is not a mediator of kinin-induced hypotension. Thus the mediator for the hypotensive action of kinins remains unknown. It further shows the importance of NO-formation in impeding the small, although significant, compensatory adrenergic hypertensive response following the acute fall in BP. The present study also demonstrates the importance of converting enzyme/kininase II as the major agent in terminating bradykinin-induced hypotension.

This work was supported by The Norwegian Research Council and The Norwegian Council on Cardiovascular Diseases.

References

AISAKA, K., GROSS, S.S., GRIFFITH, O.W. & LEVI, R. (1989). L-arginine availability determines the duration of acetylcholine-induced systemic vasodilatation in vivo. *Biochem. Biophys. Res. Commun.*, **163**, 710–717.

BOGLE, R.G., COADE, S.B., MONCADA, S., PEARSON, J.D. & MANN, G.E. (1991). Bradykinin and ATP stimulate L-arginine uptake and nitric oxide release in vascular endothelial cells. *Biochem. Biophys. Res. Commun.*, **180**, 926–932.

BURNSTOCK, G. (1990). Local mechanisms of blood flow control by perivascular nerves and endothelium. *J. Hypertens.*, **8** (Suppl 7), 95–106.

CACHOFEIRO, V., SAKAKIBARA, T. & NASJLETTI, A. (1992). Kinin, nitric oxide, and the hypotensive effect of Captopril and Ramiprilat in hypertension. *Hypertension*, **19**, 138–145.

DZAU, V.J. (1989). Multiple pathways of angiotensin production in the blood vessel wall: evidence, possibilities and hypotheses. *J. Hypertens.*, **7**, 933–936.

ERDÖS, E.G. (1979). Bradykinin, kallidin and kallikrein. In *Handbook of Experimental Pharmacology* ed. 2, Vol. 25, pp. 427–448. Berlin: Springer-Verlag.

FELDBERG, W. & LEWIS, G.P. (1964). The action of peptides on the adrenal medulla. Release of adrenaline by bradykinin and angiotensin. *J. Physiol.*, **171**, 98–108.

FURCHGOTT, R.F. & ZAWADZKI, J.V. (1980). The obligatory role of endothelial cells in the relaxation of arterial smooth muscle by acetylcholine. *Nature*, **288**, 373–376.

GOTHBERG, G. & KARLSTROM, G. (1991). Physiological effects of the humoral renomedullary antihypertensive system. *Am. J. Hypertens.*, **4**, (10 Pt 2), 569S–574S.

ISHIDA, H., SCILI, A.G. & CARRETERO, O.A. (1989). Role of angiotensin converting enzyme and other peptidases in vivo metabolism of kinins. *Hypertension*, **14**, 322–327.

JOHANSEN, L., BERGUNDHAUGEN, H. & BERG, T. (1987). Rapid purification of tonin, esterase B, antigen gamma and kallikrein from rat submandibular gland by fast protein liquid chromatography. *J. Chromatog.*, **387**, 347–359.

KAUSER, K. & RUBANYI, G.M. (1992). Bradykinin-induced, N^{A}-nitro-L-arginine-insensitive endothelium-dependent relaxation of porcine coronary arteries is not mediated by bioassayable relaxing substances. *J. Cardiovasc. Pharmacol.*, **20** (Suppl. 12), 101–104.

KELM, M. & SCHRADER, J. (1988). Nitric oxide release from the isolated guinea pig heart. *Eur. J. Pharmacol.*, **155**, 317–321.

KIOWSKI, W., LINDER, L., KLEINBLOESEM, C., VAN BRUMMELEN, P. & BÜHLER, F.R. (1992). Blood pressure control by the renin-angiotensin system in normotensive subjects. Assessment by angiotensin converting enzyme and renin inhibition. *Circulation*, **85**, 1–8.

ØRSTAVIK, T.B., CARRETERO, O.A., JOHANSEN, L. & SCICLI, A.G. (1982). Role of kallikrein in the hypotensive effect of captopril after sympathetic stimulation of the rat submandibular gland. *Circ. Res.*, **51**, 385–390.

O'SHAUGHNESSY, K.M., NEWMAN, C.M. & WARREN, J.B. (1992). Inhibition in the rat of nitric oxide synthesis in vivo does not attenuate the hypotensive action of acetylcholine, ATP or bradykinin. *Exp. Physiol.*, **77**, 285–292.

PALMER, R.M.Jan., ASHTON, D.S. & MONCADA, S. (1988). Vascular endothelial cells synthesize nitric oxide from L-arginine. *Nature*, **333**, 664–666.

PELLACANI, A., BRUNNER, H.R. & NUSSBERGER, J. (1992). Antagonizing and measurement: Approaches to understanding of hemodynamic effects of kinins. *J. Cardiovasc. Pharmacol.*, **20** (Suppl. 9), 28–34.

REES, D.D., PALMER, R.M.J., SHULZ, R., HODSON, H.F. & MONCADA, S. (1990). Characterization of three inhibitors of endothelial nitric oxide synthase *in vitro* and *in vivo*. *Br. J. Pharmacol.*, **101**, 746–752.

TÜRKER, R.K., ERCAN, Z.S., ERSOY, A. & ZENGIL, H. (1982). Inhibition by nicotine of the vasodilator effect of bradykinin: evidence for a prostacyclin-dependent mechanism. *Arch. Int. Pharmacodyn.*, **257**, 94–103.

WHITTLE, B.J.R., LOPEZ-BELMONTE, J. & REES, D.D. (1989). Modulation of the vasodepressor actions of acetylcholine, bradykinin, substance P and endothelin in the rat by a specific inhibitor of nitric oxide formation. *Br. J. Pharmacol.*, **98**, 646–652.

(Received January 12, 1994
Revised August 3, 1994
Accepted August 22, 1994)

British Journal of Pharmacology

VOLUME 113 (4) DECEMBER 1994

OBITUARY

W. Perry. Sir William Paton, CBE, DM FRCP FRS

SPECIAL REPORTS

A. Vegh, J.G. Papp & J.R. Parratt. Prevention by dexamethasone of the marked antiarrhythmic effects of preconditioning induced 20 h after rapid cardiac pacing **1081**

W. Song, B.L. Furman & J.R. Parratt. Attenuation by dexamethasone of endotoxin protection against ischaemia-induced ventricular arrhythmias **1083**

M. Neal & J. Cunningham. Modulation of endogenous ATP of the light-evoked release of ACh from retinal cholinergic neurones **1085**

PAPERS

H.H. Iversen, L.E. Gustafsson, A.M. Leone & N.P. Wiklund. Smooth muscle relaxing effects of NO, nitrosothiols and a nerve-induced relaxing factor released in guinea-pig colon **1088**

A.P. Stork & T.M. Cocks. Pharmacological reactivity of human epicardial coronary arteries: phasic and tonic responses to vasoconstrictor agents differentiated by nifedipine **1093**

A.P. Stork & T.M. Cocks. Pharmacological reactivity of human epicardial coronary arteries: characterization of relaxation responses to endothelium-derived relaxing factor **1099**

J.L. Morris. Blockade of noradrenaline-induced constrictions by yohimbine and prazosin differs between consecutive segments of cutaneous arteries in guinea-pig ears **1105**

D.H. Manicourt, A. Druetz-Van Egeren, L. Haazen & C. Nagant de Deuxchaisnes. Effects of tenoxicam and aspirin on the metabolism of proteoglycans and hyaluronan in normal and osteoarthritic human articular cartilage **1113**

J.S. Thompson, W. Sheedy & A.H. Morice. Neutral endopeptidase (NEP) inhibition in rats with established pulmonary hypertension secondary to chronic hypoxia **1121**

F. Capasso, N. Mascolo, A.A. Izzo & T.S. Gaginella. Dissociation of castor oil-induced diarrhoea and intestinal mucosal injury in rat: effect of N^G-nitro-L-arginine methyl ester **1127**

F. László, B.J.R. Whittle & S. Moncada. Interactions of constitutive nitric oxide with PAF and thromboxane on rat intestinal vascular integrity in acute endotoxaemia **1131**

Y. Kita, R. Ozaki, S. Sakai, T. Sugimoto, Y. Hirasawa, M. Ohtsuka, H. Senoh, K. Yoshida & K. Maeda. Antianginal effects of FK409, a new spontaneous NO releaser **1137**

R. Hosoki, M. Yanagisawa, J.-Z. Guo, K. Yoshioka, T. Maehara & M. Otsuka. Effects of RP 67580, a tachykinin NK_1 receptor antagonist, on a primary afferent-evoked response of ventral roots in the neonatal rat spinal cord **1141**

F.L.M. Ricciardolo, J.A. Nadel, S. Yoishihara & P. Geppetti. Evidence for reduction of bradykinin-induced bronchoconstriction in guinea-pigs by release of nitric oxide **1147**

F. Squadrito, D. Altavilla, P. Canale, M. Ioculano, G.M. Campo, L. Ammendolia, M. Ferlito, B. Zingarelli, G. Squadrito, A. Saitta & A.P. Caputi. Participation of tumour necrosis factor and nitric oxide in the mediation of vascular dysfunction in splanchnic artery occlusion shock **1153**

M.D. Berry, E. Scarr, M.-Y. Zhu, I.A. Paterson & A.V. Juorio. The effects of administration of monoamine oxidase-B inhibitors on rat striatal neurone responses to dopamine **1159**

A. Vegh, J.G. Papp & J. Paratt. Attenuation of the antiarrhythmic effects of ischaemic preconditioning by blockade of bradykinin B_2 receptors **1167**

M. Ushio-Fukai, K. Hirano & H. Kanaide. The effects of a noval vasodilator, LP-805, on cytosolic Ca^{2+} concentrations and on tension in rabbit isolated femoral arteries **1173**

S.I. Ramnarine, Y. Hirayama, P.J. Barnes & D.F. Rogers. 'Sensory-efferent' neural control of mucus secretion: characterization using tachykinin receptor antagonists in ferret trachea *in vitro* **1183**

C.R. Johnson & S.M.O. Hourani. Contractile effects of uridine 5'-triphosphate in the rat duodenum **1191**

K.M. Desai, T.D. Warner, A.E. Bishop, J.M. Polak & J.R. Vane. Nitric oxide, and not vasoactive intestinal peptide, as the main neurotransmitter of vagally induced relaxation of the guinea pig stomach **1197**

K. Shinozuka, M. Hashimoto, S. Masumura, R.A. Bjur, D.P. Westfall & K. Hattori. *In vitro* studies of release of adenine nucleotides and adenosine from rat vascular endothelium in response to α_1-adrenoceptor stimulation **1203**

C.N. Berry, D. Girard, S. Lochot & C. Lecoffre. Antithrombotic actions of argatroban in rat models of venous, 'mixed' and arterial thrombosis, and its effects on the tail transection bleeding time **1209**

M.E. Fundytus & T. J. Coderre. Effect of activity at metabotropic, as well as ionotropic (NMDA), glutamate receptors on morphine dependence **1215**

I. Wessler, T. Reinheimer, G. Brunn, G.P. Anderson, J. Maclagan & K. Racké. β-Adrenoceptors mediate inhibition of [^{3}H]-acetylcholine release from the rat and guinea-pig isolated trachea: role of the airway mucosa and prostaglandins **1221**

E. Santti, R. Huupponen, J. Rouru, V. Hänninen, U. Pesonen, M. Jhanwar-Uniyal & M. Koulu. Potentiation of the anti-obesity effect of the selective β_3-adrenoceptor agonist BRL 35135 in obese Zucker rats by exercise **1231**

L.C. Chopra, C.H.C. Twort & J.P.T. Ward. Differences in sensitivity to the specific protein kinase C inhibitor Ro31-8220 between small and large bronchioles of the rat **1237**

H.M. Cox & I.R. Tough. Calcitonin gene-related peptide receptors in human gastrointestinal epithelia **1243**

J.A. Peachey, S.M.O. Hourani & I. Kitchen. The binding of 1,3-[^{3}H]-dipropyl-8-cyclopentylxanthine to adenosine A_1 receptors in rat smooth muscle preparations **1249**

P. D'Orléans-Juste, A. Claing, S. Télémaque, M.-C. Maurice, M. Yano & J.-P. Gratton. Block of endothelin-1-induced release of thromboxane A_2 from the guinea pig lung and nitric oxide from the rabbit kidney by a selective ET_B receptor antagonist, BQ-788 **1257**

A.M. Low, D.M. Bowdish, T.R. Prashad & V. Gaspar. Interactions of chloroethylclonidine with rauwolscine- and prazosin-sensitive adrenoceptors in dog saphenous vein **1263**

M. Pestana & P. Soares-da-Silva. Effect of type A and B monoamine oxidase selective inhibition by Ro 41-1049 and Ro 19-6327 on dopamine outflow in rat kidney slices **1269**

S.J. W. Parsons, A. Hill, G.J. Waldron, F. Plane & C.J. Garland. The relative importance of nitric oxide and nitric oxide-independent mechanisms in acetylcholine-evoked dilatation of the rat mesenteric bed **1275**

F. Pérez-Vizcaíno, B. Fernández del Pozo, F. Zaragozá & J. Tamargo. Voltage- and time-dependent inhibitory effects on rat aortic and porcine coronary artery contraction induced by propafenone and quinidine **1281**

E. Kühberger, K. Groschner, W.R. Kukovetz & F. Brunner. The role of myoendothelial cell contact in non-nitric oxide-, non-prostanoid-mediated endothelium-dependent relaxation of porcine coronary artery **1289**

T.P. Obrenovitch, J. Urenjak & E. Zilkha. Intracerebral microdialysis combined with recording of extracellular field potential: a novel method for investigation of depolarizing drugs *in vivo* **1295**

A.P. Davenport, R.E. Kuc, S.L. Hoskins, F.E. Karet & F. Fitzgerald. [^{125}I]-PD151242: a selective ligand for endothelin ET_A receptors in human kidney which localizes to renal vasculature **1303**

R.J. Benschop, F.P. Nijkamp, R.E. Ballieux & C.J. Heijnen. The effects of β-adrenoceptor stimulation on adhesion of human natural killer cells to cultured endothelium **1311**

A. Barber, G.D. Bartoszyk, H.M. Bender, R. Gottschlich, H.E. Greiner, J. Harting, F. Mauler, K.-O. Minck, R.D. Murray, M. Simon & C.A. Seyfried. A pharmacological profile of the novel, peripherally-selective κ-opioid receptor agonist, EMD 61753 **1317**

J.E. Nally, R.A. Clayton, N.C. Thomson & J.C. McGrath. The interaction of α-human atrial natriuretic peptide (ANP) with salbutamol, sodium nitroprusside and isosorbide dinitrate in human bronchial smooth muscle **1328**

B.R. Lucchessi, W.E. Rote, E.M. Driscoll & D.-X. Mu. Prevention of thrombosis and rethrombosis and enhancement of the thrombolytic actions of recombinant tissue-type plasminogen activator in the canine heart by DMP728, a glycoprotein IIb/IIIa antagonist **1333**

D.C. Bolser, F.C. DeGennaro, S. O'Reilly, R.W. Chapman, W. Kreutner, R.W. Egan & J.A. Hey. Peripheral and central sites of action of $GABA_B$ agonists to inhibit the cough reflex in the cat and guinea-pig **1344**

W. Löscher & D. Hönack. Effects of the non-NMDA antagonists NBQX and the 2,3-benzodiazepine GYKI 52466 on different seizure types in mice: comparison with diazepam and interactions with flumazenil **1349**

A. Morán, C. Velasco, T. Salvador, M.L. Martín & L. San Román. Inhibitory 5-hydroxytryptamine receptors involved in pressor effects obtained by stimulation of sympathetic outflow from spinal cord in pithed rats **1358**

M.M. Teixeira, S.M. Fairbairn, K.E. Norman, T.J. Williams, A.G. Rossi & P.G. Hellewell. Studies on the mechanisms involved in the inflammatory response in a reversed passive Arthus reaction in guinea-pig skin: contribution of neutrophils and endogenous mediators **1363**

G. Brignola, A. Calignano & M. Di Rosa. Modulation of morphine antinociception in the mouse by endogenous nitric oxide **1372**

S. Chuliá, M.D. Ivorra, C. Lugnier, E. Vila, M.A. Noguera & P. D'Ocon. Mechanism of the cardiovascular activity of laudanosine: comparison with papaverine and other benzylisoquinoles **1377**

R. Anderson, M.J. Sheehan & P. Strong. Characterization of the adenosine receptors mediating hypothermia in the conscious mouse **1386**

F. Karoum, S.J. Chrapusta, R. Brinjak, A. Hitri & R.J. Wyatt. Regional effects of amphetamine, cocaine, nomifensine and GBR 12909 on the dynamics of dopamine release and metabolism in the rat brain **1391**

L.G. Iben, C.D. Mahle & F.D. Yocca. Differential sensitivity of ^{3}H-agonist binding to pre- and postsynaptic 5-HT_{1A} receptors in bovine brain **1400**

D.A. Walsh, M. Salmon, R. Featherstone, J. Wharton, M.K. Church & J.M. Polak. Differences in the distribution and characteristics of tachykinin NK_1 binding sites between human and guinea pig lung **1407**

S. Pieretti, A. Di Giannuario, M.R. Domenici, S. Sagratella, A. Capasso, L. Sorrentino & A. Loizzo. Dexamethasone-induced selective inhibition of the central μ opioid receptor: functional *in vivo* and *in vitro* evidence in rodents **1416**

D. Raeburn, S.L. Underwood, S.A. Lewis, V.R. Woodman, C.H. Battram, A. Tomkinson, S. Sharma, R. Jordan, J.E. Souness, S.E. Webber & J.-A. Karlsson. Anti-inflammatory and bronchodilator properties of RP 73401, a novel and selective phosphodiesterase type IV inhibitor **1423**

B.E. Crack, M.W. Beukers, K.C.W. McKechnie, A.P. IJzerman & P. Leff. Pharmacological analysis of ecto-ATPase inhibition: evidence for combined enzyme inhibition and receptor antagonism in P_{2X}-purinoceptor ligands **1432**

J.O. Malva, A.P. Carvalho & C.M. Carvalho. Modulation of dopamine and noradrenaline release and of intracellular Ca^{2+} concentration by presynaptic glutamate receptors in hippocampus **1439**

K. Hirokawa, K.M. O'Shaughnessy, P. Ramrakha & M.R. Wilkins. Inhibition of nitric oxide synthesis in vascular smooth muscle by retinoids **1448**

A. Huwiler & J. Pfeilschifter. Stimulation by extracellular ATP and UTP of the mitogen-activated protein kinase cascade and proliferation of rat renal mesangial cells **1455**

C.-H. Lin, C.-M. Yang, F.-N. Ko, Y.-C. Wu & C.-M. Teng. Anti-muscarinic action of liriodenine, isolated from *Fissistigma glaucescens*, in canine tracheal smooth muscle **1464**

W.A. Bax, Z. Aghai, C.L.J. van Tricht, C. Wassenaar & P.R. Saxena. Different endothelin receptors involved in endothelin-1- and sarafotoxin S6B-induced contractions of the human isolated coronary artery **1471**

J. Tanabe, M. Watanabe, S. Kondoh, S. Mue & K. Ohuchi. Possible roles of protein kinases in neutrophil chemotactic factor production by leucocytes in allergic inflammation in rats **1480**

N.M.J. Rupniak, S. Patel, R. Marwood, J. Webb, J.R. Traynor, J. Elliott, S.B. Freedman, S.R. Fletcher & R.G. Hill. Antinociceptive and toxic effects of (+)-epibatidine oxalate attributable to nicotinic agonist activity **1487**

A. Gibson, I. McFadzean, J.F. Tucker & C. Wayman. Variable potency of nitrergic-nitrovasodilator relaxations of the mouse anococcygeus against different forms of induced tone **1494**

S.P.H. Alexander, A.R. Curtis, D.A. Kendall & S.J. Hill. A_1 adenosine receptor inhibition of cyclic AMP formation and radioligand binding in the guinea-pig cerebral cortex **1501**

A.S. Hussain, M. Poklewska-Koziell, J.F. Brien, G.S. Marks & K. Nakatsu. Nitric oxide formation from glyceryl trinitrate by rabbit aortic strip: detection by rabbit taenia coli concurrent with vasorelaxation **1508**

P.C. Waldmeier, P. Wicki, J.-J. Feldtrauer, S.J. Mickel, H. Bittiger & P.A. Baumann. GABA and glutamate release affected by $GABA_B$ receptor antagonists with similar potency: no evidence for pharmacologically different presynaptic receptors **1515**

P. Akarasereenont, J.A. Mitchell, I. Appleton, C. Thiemermann & J.R. Vane. Involvement of tyrosine kinase in the induction of cyclo-oxygenase and nitric oxide synthase by endotoxin in cultured cells **1522**

J. Jakubík & S. Tuček. Two populations of muscarinic binding sites in the chick heart distinguished by affinities for ligands and selective inactivation **1529**

G. Edwards, A. Niederste-Hollenberg, J. Schneider, Th. Noack & A.H. Weston. Ion channel modulation by NS 1619, the putative BK_{Ca} channel opener, in vascular smooth muscle **1538**

J. Bauersachs, M. Hecker & R. Busse. Display of the characteristics of endothelium-derived hyperpolarizing factor by a cytochrome P450-derived arachidonic acid metabolite in the coronary microcirculation **1548**

M.-C. Peakman & S.J. Hill. Endogenous expression of histamine H_1 receptors functionally coupled to phosphoinositide hydrolysis in C6 glioma cells: regulation by cyclic AMP **1554**

M. Malcangio & N.C. Bowery. Spinal cord SP release and hyperalgesia in monoarthritic rats: involvement of the $GABA_B$ receptor system **1561**

A. Bjørnstad-Østensen & T. Berg. The role of nitric oxide, adrenergic activation and kinin-degradation in blood pressure homeostasis following an acute kinin-induced hypotension **1567**